Advances in Experimental Medicine and Biology 740

Md. Shahidul Islam *Editor*

Calcium Signaling

Springer

Calcium Signaling

ADVANCES IN EXPERIMENTAL MEDICINE AND BIOLOGY

For further volumes:
http://www.springer.com/series/5584

Md. Shahidul Islam

Calcium Signaling

Springer

Editor
Md. Shahidul Islam
Department of Clinical Sciences and Education, Ssödersjukhuset
Karolinska Institutet
SE 118 83 Stockholm, Sweden, and Department of Internal Medicine,
Uppsala University Hospital, Uppsala, Sweden

Please note that additional material for this book can be downloaded from http://extras.springer.com

ISSN 0065-2598
ISBN 978-94-007-2887-5 ISBN 978-94-007-2888-2 (eBook)
DOI 10.1007/978-94-007-2888-2
Springer Dordrecht Heidelberg New York London

Library of Congress Control Number: 2012934566

Printed on acid-free paper

Springer is part of Springer Science+Business Media (www.springer.com)

Dedicated to my father
A.T.M. Shamsul Islam

Preface

At the time of this writing, I feel tired. From my experience with "The Islets of Langerhans" [1], and "Transient Receptor Potential Channels" [2], I knew how much energy it takes to edit a book of this type. It steals time from other academic activities, destroys leisure and holidays, and it may affect your health. Why did I decide to edit this book? The answer is short: I like the field of Ca^{2+} signaling. I started measuring Ca^{2+}, by ion-selective mini-electrodes, first in 1990. Those experiments were so difficult that I do not like to think about those now. In the department I worked, there was another new, sensitive, and easier method for measuring the free Ca^{2+} concentration in the cytoplasm of living cells. Those days, the method was considered too expensive and too sophisticated for a beginner like me to use it. Two years later, I got access to this fura-2-based microfluorometry system for the first time, and since then I have stayed in the field of Ca^{2+} signaling. During the next two decades, I have listened to many pioneers, and many experts, in many conferences on Ca^{2+} signaling. I have invited many high profile scientists to give talks at the Karolinska Institutet. I have known who is doing what in this field. I have given many courses on Ca^{2+} signaling, and I have learnt a little bit of almost everything in this field. I am an enthusiast, not an expert in this field. I am convinced that discoveries in the field of Ca^{2+} signaling have saved numerous human lives. I wish that pioneer scientists, who have made breakthrough discoveries in this field, get Nobel Prize. I am a busy clinician, and I commute to and from my job about 80 min per day, every day. Surprisingly, these 80 min per day, turned out to be the most convenient time for me to work on this book.

I felt happy when I noticed that so many authors responded to my request to contribute to this book. Writing a book chapter is not an easy task. It takes almost six months to write a chapter. I apologize to the authors of this book for stressing them by sending repeated reminders. One chapter took longer time because of death of a family member of one of the authors. That was a reminder for reflection. Another chapter had to wait because the author had to get married. Some chapters needed repeated revisions. It has been a test of my patience, and of my skills in managing interpersonal relationships. Finally, at the time of this writing, I have received almost all the chapters. I missed five chapters because of time constraints,

but I cannot be too greedy. What worries me now is that I still have to do a lot of work. The manuscripts have only been sent to the printers. I know, numerous mistakes will crop up, and we will have to fix them. One thing I can tell you is that you will get the flavors of some Indian English, French English, Spanish English, or German English in many chapters in this book.

This book has the taste of a text book, but it is more than a text book. It is not an encyclopedia. We did not intend to cover all the molecules, and all the processes that regulate Ca^{2+} signaling, and Ca^{2+} homeostasis. Still the book covers diverse areas, and discusses many crucial issues at great depth. It describes cutting edge researches, contemporary thoughts, and numerous testable hypotheses for future research. It is not just a collection of papers; it is a complete book that represents the essence of the broad field of Ca^{2+} signaling. I believe that all categories of readers will find something useful in this book. For some, it may be an eye-opener.

I thank the authors for their hard work, and for timely submission of the chapters. I have not met most of the authors of this book. I cannot even correctly pronounce the names of some of them. But, I know what they are burning for. I wish we all could meet once somewhere, perhaps in a Ca^{2+} conference that we could organize. I thank the referees, about 150 of them, who have helped the authors see things from a different angle. I wish I could publish some of the comments made by some of the referees. Some chapters were not reviewed by external referees because of lack of time, but I do not think that this is a big problem. I thank Melania Ruiz, and Ilse Hansen of Springer. I thank my family, members of my research group, and my colleagues for their support, and spontaneous informal comments that I always listened to seriously. As always, I am grateful to the Karolinska Institutet, my Alma mater that has ensured infrastructures for my creative activities over more than two decades.

While editing the book, I have been forced to read and think, and I have learnt a lot. That is my biggest reward. I will read this book many more times.

Stockholm, Sweden Md. Shahidul Islam

References

1. Islam MS (2010) The islets of Langerhans. Springer, Dordrecht
2. Islam MS (2011) Transient receptor potential channels. Springer, Dordrecht

Contents

Chapter 1
The Regulation of a Cell's Ca^{2+} Signaling Toolkit: The Ca^{2+} Homeostasome

Beat Schwaller

Abstract The Ca^{2+} ion serves as a ubiquitous second messenger in eukaryotic cells and changes in the intracellular Ca^{2+} concentration regulate many responses within a cell, but also communication between cells. In order to make use of such an apparently simple signal, i.e. a change in the intracellular Ca^{2+} concentration, cells are equipped with sophisticated machinery to precisely regulate the shape (amplitude, duration) of Ca^{2+} signals in a localization-specific manner. To ascertain such a precise regulation, cells rely on the components of the Ca^{2+} signaling toolkit. This embraces Ca^{2+} entry systems including Ca^{2+} channels in the plasma membrane and organellar membranes, and Ca^{2+} extrusion/uptake systems including Ca^{2+}-ATPases (Ca^{2+} pumps) and Na^{+}/Ca^{2+} exchangers. Besides mitochondria, organelles implicated also in Ca^{2+} signaling, cytosolic Ca^{2+} buffers are cell-specific subtle modulators of Ca^{2+} signals. The Ca^{2+}-signaling components not only orchestrate their activity as to ascertain the high accuracy of intracellular Ca^{2+} signaling, but they are also implicated in the regulation of their own expression. The total of the molecules that build the network of Ca^{2+} signaling components, and that are involved in their own regulation as to maintain physiological Ca^{2+} homeostasis resulting in phenotypic stability is named the Ca^{2+} homeostasome. Mechanistic details on the functioning of the Ca^{2+} homeostasome are presented.

Keywords Calcium buffer • Calcium homeostasis • Calcium signaling • Calcium signaling toolkit • Homeostatic remodeling • Parvalbumin • Calbindin D-28k • Calretinin • EF-hand • Calcium ATPase • Calcium channel • Mitochondria • Subplasmalemmal ER • Calcium homeostasome

B. Schwaller (✉)
Unit of Anatomy, Department of Medicine, University of Fribourg,
Route Albert-Gockel 1, CH-1700, Fribourg, Switzerland
e-mail: Beat.Schwaller@unifr.ch

M.S. Islam (ed.), *Calcium Signaling*, Advances in Experimental Medicine and Biology 740, DOI 10.1007/978-94-007-2888-2_1,

Components of the Calcium Signaling Toolkit with a Special Focus on Ca^{2+}-Binding Proteins (CaBP) Classified as "Ca^{2+} Buffers"

General Considerations

Intracellular Ca^{2+} signals regulate many aspects of physiological responses within a cell, but also the communication between cells. Such processes include transcription, cell cycle regulation, differentiation, cell motility/migration, programmed cell death, muscle contraction/relaxation of skeletal muscle and heart, and neurotransmission. In order to make use of such an apparently simple signal, i.e. a change in the intracellular Ca^{2+} concentration $[Ca^{2+}]_i$, cells need to be equipped with sophisticated machinery to precisely regulate Ca^{2+} signals in a localization-specific and time-dependant manner. Obviously also the amplitude of Ca^{2+} signals contain essential information for inducing downstream signaling events. For such a precise regulation, cells rely on the components of the Ca^{2+} signaling toolkit [1], which are briefly summarized here. In the plasma membrane, the presence of receptor-operated (ROCC), voltage-operated (VOCC) and store-operated (SOCC) Ca^{2+} channels allows entry of Ca^{2+} ions from the extracellular space (Fig. 1.1). Additionally, an increase in $[Ca^{2+}]_i$ may be mediated by release from intracellular organelles, the most important one being the sarcoplasmic/endoplasmic reticulum expressing inositol 1,4,5-trisphosphate receptors ($InsP_3$-R) and/or their close relatives, ryanodine receptors (RyR) acting as Ca^{2+} release channels. In the lumen of these organelles, large amounts of Ca^{2+} are stored/buffered by organellar Ca^{2+} buffers that are distinct from another group of proteins called cytosolic Ca^{2+} buffers (see below). In most cases, the organellar Ca^{2+} buffers are considered as low-affinity, high-capacity Ca^{2+} buffers that in addition to Ca^{2+} buffering, have many other cellular functions [2]. For the return of $[Ca^{2+}]_i$ to basal, pre-activity levels, thus serving as so-called "off" mechanisms [1], Ca^{2+}-ATPases in the membranes of the endoplasmic reticulum (SERCA pumps) or in the plasma membrane (PMCAs) together with a plasmalemmal Na^+/Ca^{2+} exchanger (NCX) are activated via the increased $[Ca^{2+}]_i$. Also mitochondria, mostly associated with functions related to energy metabolism and oxidative phosphorylation, play an important role in the regulation/modulation of intracellular Ca^{2+} signals. An increase in $[Ca^{2+}]_i$ activates the mitochondrial Ca^{2+} uniporter, whose molecular identity has not yet been revealed (see note added in proof). The accumulated mitochondrial Ca^{2+} $[Ca^{2+}]_m$ is then extruded by the mitochondrial Na^+/Ca^{2+} exchanger (mNCX). Finally, mobile and immobile Ca^{2+} buffers modulate spatiotemporal aspects of intracellular Ca^{2+} signals. Historically, these proteins, generally termed calcium-binding proteins (abbreviated CaBPs) are classified as either Ca^{2+} buffers or Ca^{2+} sensors. The prototypical representative of the sensor group is calmodulin (CaM) ubiquitously expressed in all cells, while typical Ca^{2+} buffers including parvalbumin (PV), calbindin D-28k (CB-D28k), calbindin D-9k (CB-D9k) and calretinin (CR) have very distinct and most often non-overlapping expression patterns [3]. Other more tissue-specific Ca^{2+} sensors include the neuronal

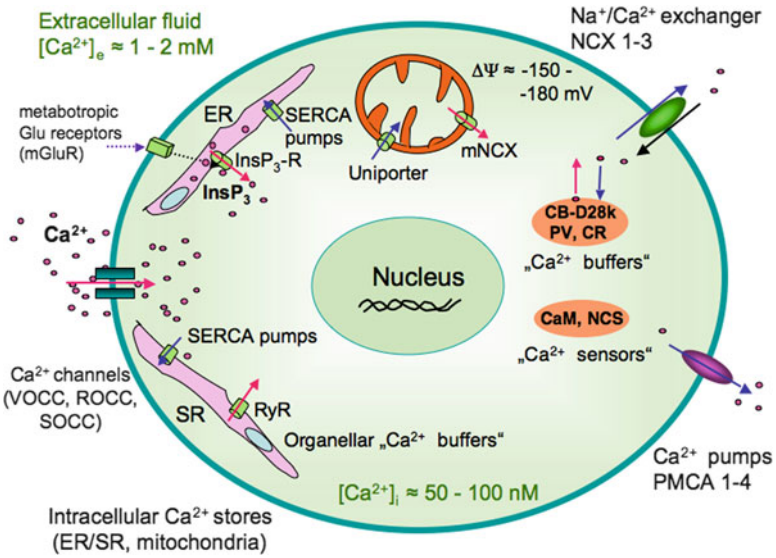

Fig. 1.1 Components of the Ca^{2+} signaling toolkit that govern the spatiotemporal aspects of intracellular Ca^{2+} signals. The extracellular $[Ca^{2+}]$ as well as the intraluminal $[Ca^{2+}]$ are in the order of 1–2 mM, while the intracellular (cytosolic) $[Ca^{2+}]$ is approximately 10,000-fold smaller (50–100 nM). *Red arrows* indicate systems that lead to a transient increase in $[Ca^{2+}]_i$. This includes several types of Ca^{2+} channels in the plasma membrane: voltage-operated (*VOCC*), receptor-operated (*ROCC*) and store-operated (*SOCC*) Ca^{2+} channels. Ca^{2+} ions are also released from organelles including the endoplasmic and sarcoplasmic reticulum (ER and SR), respectively, by activation of $InsP_3$ and ryanodine receptors ($InsP_3$-R and RyR, respectively). In the lumen of the ER/SR, large amounts of organellar Ca^{2+} buffers (*light blue*) including calreticulin are involved in the regulation of Ca^{2+} homoeostasis and ER Ca^{2+} buffering [2]. Also release of Ca^{2+} from mitochondria via the mitochondrial Na^+/Ca^{2+} exchanger (mNCX) and from Ca^{2+} buffers increases $[Ca^{2+}]_i$. Mechanisms that decrease $[Ca^{2+}]_i$ (*blue arrows*) include plasma membrane Ca^{2+}-ATPases (Ca^{2+} pumps; PMCAs), Na^+/Ca^{2+} exchangers, sarcoendoplasmic reticulum Ca^{2+}-ATPases (SERCA pumps), the mitochondrial uniporter and Ca^{2+} buffers such as calbindin-D28k (CB-D28k), parvalbumin (PV) and calretinin (CR). For most of the Ca^{2+} signaling components, many isoforms and splice variants exist, thus providing each cell with a unique set of components from the large toolkit. For more details, see text

Ca^{2+} sensor (NCS) family and proteins from the CaBPs/calneuron1/2 sub-family [4]. A word of caution concerning the nomenclature for the latter proteins (CaBP1-CaBP5): in many papers, textbooks and also in this review, the term CaBP is used as a generic name for all Ca^{2+}-binding proteins, most often for the ones belonging to the large family of EF-hand Ca^{2+}-binding proteins. A second important note: the distinction between Ca^{2+} sensors and Ca^{2+} buffers is slowly beginning to blur. At the structural level, Ca^{2+} sensors were characterized by having relatively large Ca^{2+}-dependant conformational changes, which then allows for the interaction with target proteins. On the other hand, the Ca^{2+}-dependant conformational changes observed in Ca^{2+} buffers are often of smaller magnitude indicating that these proteins may mainly serve as intracellular mobile modulators of intracellular Ca^{2+} signals. In the light of newer results, however, this notion may need to be changed. Additional

sensor functions have been reported for the Ca^{2+} buffer CB-D28k [5] and the "classical" Ca^{2+} sensor CaM might act as a very fast intracellular Ca^{2+} buffer [6], for details, see section "Ca^{2+} Buffers/Ca^{2+} Sensors are Components of the Ca^{2+} Homeostasome").

Ca^{2+} Buffers/Ca^{2+} Sensors Are Components of the Ca^{2+} Homeostasome

How a Ca^{2+} buffer affects an intracellular Ca^{2+} signal depends on several factors: (1) the Ca^{2+}-binding properties of the buffer, i.e. the affinity for Ca^{2+} and possibly other ions (e.g. Mg^{2+}) and the kinetics of Ca^{2+}-binding ($k_{on,Ca}$) and Ca^{2+}-release ($k_{off,Ca}$); (2) the intracellular concentration of the Ca^{2+} buffer and (3) the mobility of the Ca^{2+} buffer inside the cytosol. Reported values for some selected Ca^{2+} buffers are summarized in Table 1.1. Yet another subtlety derives from the fact that all physiological Ca^{2+} buffers have more than one, most often 2, 4 or 6 Ca^{2+}-binding sites, and thus show co-operativity to various degrees. Noteworthy, often not all of the putative Ca^{2+}-binding sites are functional (Table 1.1). A more detailed description of the relevant parameters related to Ca^{2+} binding is found in [5, 7]. For the understanding of the physiological roles of these Ca^{2+} buffers, their kinetic parameters have gained a place in the spotlight.

The prototypical "fast" and "slow" physiological Ca^{2+} buffers are CB-D9k and PV, respectively. The on rate for Ca^{2+} binding ($k_{on,Ca}$) is 2–3 orders of magnitude faster in CB-D9k than in PV (Table 1.1). In that respect, they closely match with the on rates for the synthetic Ca^{2+} chelators BAPTA (10^8–10^9 $M^{-1}s^{-1}$) and EGTA ($3–10 \times 10^6$ $M^{-1}s^{-1}$) [7]. Albeit differences in co-operativity of Ca^{2+} binding (strong for CB-D9k, weak, if any, for PV), the Ca^{2+}-induced conformational changes are rather small and so far, no interacting proteins for both, CB-D9k and PV have been identified yet, the latter two features are typical for so-called Ca^{2+} buffers. Interestingly, the slow Ca^{2+} buffer PV is expressed in several physiological settings; in a subset of mostly GABAergic (inhibitory) neurons in various brain regions [21], in fast-twitch muscles [22] and in epithelial cells of the kidney distal convoluted tubule, a segment of the nephron that is involved in the fine-tuning of Ca^{2+} resorption [23]. The expression of CB-D9k is restricted to non-excitable cells involved in Ca^{2+} resorption and also shows some species differences. In rat, CB-D9k is present in the epithelial cells of the loops of Henle, the distal convoluted tubule and in intercalated cells in the collecting duct. In the mouse kidney, CB-D9k is strongly expressed in distal convoluted tubules and to a lesser extent in the connecting tubules [24]. CB-D9k is thought to principally act as an intracellular Ca^{2+} shuttle implicated in the transport of the Ca^{2+} ions from the apical to the basolateral side of the epithelial cells, as also proposed for CB-D28k, a protein also expressed in specific kidney epithelial cells, for additional details, see [25, 26]. Additionally, in the mouse intestine, CB-D9k is highly expressed in the first 2 cm of the duodenum [27]. However, CB-D9k is likely to be absent either from muscle fibers or neurons, since no reports of CB-D9k in

Table 1.1 Properties of selected Ca^{2+}-binding proteins (Modified from [5, 7])

	PV	CB-D9k	CaM	CB-D28k	CR
Ca^{2+} binding sites (functional)	3 (2)	2 (2)	4 (4)	6 (4)	6 (5)
Ca^{2+} specific/mixed Ca^{2+}/Mg^{2+} sites	0/2	2/0	4/0	4/0[a]	5/0
$K_{D,Ca}$ (nM)	4–9[b]	$K_{D1} \approx 200–500$[c] $K_{D2} \approx 60–300$	N-lobe $K_{D(T)}$ 193 μM[f] $K_{D(R)}$ 0.788 μM $K_{D(app)}$ 12.7 μM C-lobe $K_{D(T)}$ 27.8 μM[f] $K_{D(R)}$ 0.264 μM $K_{D(app)}$ 2.7 μM	High aff. (h)[d] $K_{D1} \approx 180–240$ Medium aff. (m) $K_{D2} \approx 410–510$ $K_{D1\text{-}D4}$:393[g]	$K_{D(T)}$ 28 μM[e] $K_{D(R)}$ 68 $K_{D(app)}$ 1.4 μM EF5: 36 μM
$K_{D,Mg}$	≈30 μM[b]			714 μM[a]	4.5 mM[h]
$K_{D,Ca(app)}$ (nM) at $[Mg^{2+}]$ of 0.5–1 mM	150–250[i]				
$k_{on,Ca}$ ($\mu M^{-1}\ s^{-1}$)	6[b]	1,000[j]	N-lobe T site: 770[f] R sites: 32,000 C-lobe T site: 84[f] R sites: 25	h sites ≈ 12[d] m sites ≈ 82 All 4 sites: 75[g]	T sites: 1.8[e] R sites: 310 Site EF5: 7.3
$k_{on,Mg}$ ($\mu M^{-1}\ s^{-1}$)	0.1–1[i]				
Cooperativity	No[k]	Yes[l]	Yes N-lobe[l,f] $n_H \approx 1.9 \pm 0.1$[f] C-lobe[l,f] $n_H \approx 1.8 \pm 0.1$[f]	Yes/no? $n_H \approx 1.1–1.2$[a] $n_H \approx 1$[g]	Yes $n_H \approx 1.3–1.9$[e]

(continued)

Table 1.1 (continued)

	PV	CB-D9k	CaM	CB-D28k	CR
$D_{Cabuffer}$ ($\mu m^2\ s^{-1}$)	37–43[m]	n.d.	n.d.	>100[n]	≈25[o]
	~12			≈25	

n.d. not determined

[a]Although considered as Ca^{2+} specific, at physiological $[Mg^{2+}]_i$ the apparent Ca^{2+} affinity is ≈twofold lower [8]

[b][9]

[c][10]

[d]CB-D28k has high-affinity (h) and medium-affinity (m) sites, the stochiometry h/m is either 2/2 or 3/1 [11]

[e]For details on CR, see text and [12]

[f]For details on CaM's Ca^{2+}-binding properties, see text and [6]

[g]Newer result indicate that in CB-D28k all 4 Ca^{2+}-binding sites have the same binding properties [6]

[h][13]

[i]$K_{D,Ca}$ and k_{on} for PV are $[Mg^{2+}]$ dependent; calculated values are estimates at $[Mg^{2+}]_i$ 0.6–0.9 mM

[j]The value represents the diffusion limit, assuming a maximal Ca^{2+} diffusion rate of ≈200 $\mu m^2\ s^{-1}$ [14]

[k]PV has 2 essentially identical Ca^{2+}-binding sites with n_H close to 1

[l][15]

[m]The diffusion coefficients $D_{Cabuffer}$ for PV in muscle myoplasm (37 $\mu m^2\ s^{-1}$; [16]) and Purkinje cell dendrites of (43 $\mu m^2\ s^{-1}$; [17]); smaller values are measured in PC soma and axons (≈12 $\mu m^2\ s^{-1}$; [18])

[n]CB-D28k's mobility in PC dendrites is 26 $\mu m^2\ s^{-1}$ [19], clearly slower than in water [20] and also slower than PV in PC dendrites

[o]Estimation based on the similar size of CB-D28k and CR

these cell types have been published, to our best knowledge. This appears "to make sense" because the properties of CB-D9k, which are similar to those of BAPTA, would result in blunting the amplitude and prolong the duration of the fast Ca^{2+} signals in neurons and muscle cells. At first sight, CB-D28k and CR would be assumed to represent the neuron-specific fast buffers and there is ample evidence that they do so [5, 7]. The amplitude of climbing fiber-evoked $[Ca^{2+}]_i$ rises in Purkinje cell dendrites is significantly larger in dendrites from CB-D28K$^{-/-}$ mice and the kinetics of $[Ca^{2+}]_i$ decay is slower [28]. Thus, CB-D28k is fast enough to already affect the rising phase of the Ca^{2+} transient, but at later times acts as a Ca^{2+} source, thus prolonging the decay phase [29]. Indirect evidence, based on the measurement of the excitability of CR-expressing cerebellar granule cells, also supports the role of CR as a fast Ca^{2+} buffer [30]. This is further confirmed by the finding that in granule cells of CR$^{-/-}$ mice, the excitability is essentially restored to the situation in wild-type mice by the addition of 150 μM BAPTA and selective re-expression of CR in granule cells of CR$^{-/-}$ mice rescues the cerebellar CR$^{-/-}$ phenotype [31].

Although, CB-D28k and CR are mostly considered as Ca^{2+} buffers, several findings indicate that these two proteins have also additional sensor functions. The characteristics of Ca^{2+} sensors is (1) their interaction with specific targets and (2) the modulation of the function of these target proteins by either binding (in most cases) or unbinding from the target. A rare example for the latter case is DREAM (downstream regulatory element (DRE)-antagonist modulator). Binding of Ca^{2+} to the 4 EF-hand domains prevents the binding to the DRE and thus DREAM's repressor function [32]. Associated with these Ca^{2+} sensor/target interactions are rather distinct pronounced Ca^{2+}-induced conformational changes [33]. Several targets for CB-D28k have been identified and include Ran-binding protein M, caspase-3, plasma membrane ATPase, 3′,5′-cyclic nucleotide phosphodiesterase, L-type Ca^{2+} channel α subunit ($Ca_V1.2$), *myo*-inositol monophosphatase and TRPV5, for details, see [7]. Also for CR, there is increasing evidence that CR might have additional Ca^{2+} sensor function(s). CR shows relatively large Ca^{2+}-dependent conformational changes [34], is transiently associated with membranes in brainstem auditory neurons in the chick nucleus magnocellularis [35] and is also present in the particulate brain fraction [36], for more details on CR, see also [37].

While calmodulin (CaM) is undoubtedly the most ubiquitous Ca^{2+} sensor expressed in all cells, CaM is also an extremely fast Ca^{2+} buffer, in particular the EF-hand pair in the N-lobe [6]. Evidently all known Ca^{2+} sensors may function as Ca^{2+} buffers, if present at sufficiently high intracellular concentrations. It is generally assumed that the concentration of Ca^{2+} sensors is in the order of 1 to several tens of μM (on average 10 μM), the concentration of Ca^{2+} buffers is 1–2 orders of magnitude higher that is, in the range of 50 up to several hundreds of μM, for more details, see [5].

In many cells, the Ca^{2+} ions entering the cytosolic compartment are rapidly buffered by a fast buffer and it is thought that this buffered level of Ca^{2+} triggers the Ca^{2+}-activated downstream biochemical processes. The most important one is the activation of CaM and the associated Ca^{2+}/CaM-dependent signaling pathways. A recent *in vitro* study indicates that CaM binds Ca^{2+} ions faster than any of the

known Ca^{2+} buffers [6]. Based on their results, the authors propose that incoming Ca^{2+} is first bound to CaM, which then passes on the Ca^{2+} ion to the "slower" Ca^{2+} buffers instead of reacting to the lower $[Ca^{2+}]_i$ caused by the other buffers. As a consequence, other Ca^{2+}-binding proteins including Ca^{2+} buffers such as PV and CB-D28k may "have a previously undescribed role in regulating the lifetime of Ca^{2+} bound to CaM and thereby setting the gain of signal transduction" [6]. Whether this is the case inside a cell "*in vivo*" depends on the intracellular concentration of CaM. There is still a considerable uncertainty about [CaM] and values from 10 to 100 μM have been reported. Further studies are necessary to unequivocally demonstrate this novel role for CaM. In summary, in view of most recent findings, the distinction between Ca^{2+} buffers and Ca^{2+} sensors possibly needs to be re-defined, or with respect to the physiological role(s) may become even obsolete.

Adaptation/Compensation/Homeostatic Mechanisms

General Considerations

Based on the extremely precise control of intracellular Ca^{2+} signals, with respect to duration, the kinetics of $[Ca^{2+}]_i$ increase and decrease as well as intracellular localization, (e.g. axonal vs. somato-dendritic compartment), it is not surprising that malfunction, blocking or elimination of any one Ca^{2+} signaling component leads to modifications by the system. In order to explain these changes mechanistically, different terms are used and include: homeostatic changes, adaptations or compensation mechanisms. All terms imply (a) a certain redundancy in the system and (b) "sensing" mechanisms that result in subtle and specific changes to cope with the missing or malfunctioning component. Homeostasis is defined as a property of a system, here a living organism, to regulate itself in such a way as to maintain "stable", constant conditions, i.e. to keep the many parameters within a physiological range. This holds true for the processes taking place within single cells, but also among cells functionally linked in a "rather simple" way as in skeletal muscle or heart or in a highly complex fashion as in the brain. The term homeostasis is mostly applied when investigating changes occurring under physiological conditions, e.g. in response to altered energy demand or a different physiological/metabolic situation. In the brain, homeostasis of synaptic function is linked to vital processes such as learning or memory. On the other hand, adaptation or compensation often has the connotation of a process that occurs as the result of a pathological "insult" to the system. However, at the molecular level, the changes occurring under one or another condition might be very similar or even the same.

A classical procedure in Life Sciences to obtain mechanistic insight into a process is to perform perturbation experiments. For this, the component of interest is specifically blocked (e.g. by pharmacological tools), down-regulated by genetic approaches including antisense or siRNA methods, completely removed by genetic

methods (knock-out) or subtly modified by e.g. knock-in methods. With respect to the interpretation of the results obtained in all types of perturbation experiments, there is no fundamental difference with respect to adaptation and/or compensation. The principal difference is the allotted time, and thus the (biological) processes occurring in this time period, that would allow for adaptation/compensation mechanisms to take place. This may sound strange at first, but some examples are given to illustrate this point.

Temporally Overlapping Activities of Ca^{2+} Signaling Toolkit Components Impede the Precise Determination of Their Contribution to Intra- and Intercellular Ca^{2+} Signaling

As reported above, the intracellular processes governing changes in $[Ca^{2+}]_i$ operate on similar and often partially overlapping time scales. That is, as $[Ca^{2+}]_i$ rises in an excitable cell (skeletal muscle cell, myocyte, neuron) due to influx from the extracellular space and/or release from intracellular stores, Ca^{2+} buffering and reuptake/extrusion systems start to operate after a very short delay, often overlapping with the processes that lead to an increase in $[Ca^{2+}]_i$. If one wishes to determine the contribution of the various reuptake/extrusion systems by selectively blocking (one by one) all of the known components of the Ca^{2+} signaling toolkit (SERCA pumps, mitochondrial uptake, PMCAs and NCX) by specific inhibitors, such a measurement does NOT report how much is the contribution of a particular protein/component to the removal of $[Ca^{2+}]_i$. More precisely, the difference in the Ca^{2+} signal (with and without the component X) reports on the extent to which the remaining functional systems could not compensate for the inactivation/removal of protein/component X. Thus, not surprisingly, when the role of Ca^{2+} extrusion systems following depolarization-evoked $[Ca^{2+}]_i$ rises from the soma of cerebellar Purkinje cells was investigated in a quantitative manner, the sum of the contributions of all uptake/extrusion systems does not add up to 100% [38]. Moreover, the contribution of the different Ca^{2+} clearance systems clearly depends on the initial $[Ca^{2+}]_i$. At moderate elevations (0.5 μM Ca^{2+}), both SERCA and NCX contribute equally to the Ca^{2+} clearance, which accounts for approximately 80% of the removal. At higher $[Ca^{2+}]_i$ of 2 μM, the contribution of the two systems is "apparently" only in the order of 45%; at this higher $[Ca^{2+}]_i$ of 2 μM, PCMAs also contribute to Ca^{2+} extrusion and their contribution is approximately 6%. Although the contribution of mitochondrial Ca^{2+} uptake is also expected to increase in a $[Ca^{2+}]$-dependant manner, at higher $[Ca^{2+}]_i$ the extrusion/uptake by the non-blocked components is likely to be increased, leading to this apparent decrease of the contribution of the inhibited component in Ca^{2+} clearance. Thus, to account for this "competition" between the different Ca^{2+} clearance mechanism operating on similar time scales, one would have to determine the precise properties of each component in an artificial system where also the $[Ca^{2+}]_i$ dependence of the process would have to be determined. The drawback of such an approach is however

that if Ca^{2+} clearance would be additionally modulated by an interacting partner (e.g. a mobile protein), possibly in a $[Ca^{2+}]_i$ dependent way, then even the apparently simplest case is not trivial even longer. To make things even more complicated, for most of the components of the Ca^{2+} signaling toolkit, several isoforms exist (e.g. PMCA 1, 2, 3 and 4) and within one isoform several splice variants exist that differ (1) in their sensitivity to $[Ca^{2+}]_i$ elevations, (2) with respect to kinetics of $[Ca^{2+}]_i$ removal and (3) in the modulation by CaM [39, 40]. This complexity not only exists for components involved in Ca^{2+} clearance, but is equally present in components of the Ca^{2+} entry systems, including the various types of voltage-operated Ca^{2+} channels including L- ($Ca_V1.n$), P/Q-, N-, R- ($Ca_V2.n$) and T-type ($Ca_V3.n$) Ca^{2+} channels [41]. In addition, the modulatory subunits β and $\alpha_2-\delta$ affect the properties of the Ca^{2+} channels [42]. Thus, each neuron subtype or even individual neuron is equipped with a highly specialized set of Ca^{2+} signaling components likely necessary for its proper physiological function. The first level of homeostatic modulation is already "built-in", i.e. it results from the specific properties of the Ca^{2+} signaling components themselves. Hence, it does not require any processes such as intracellular redistribution of e.g. membrane proteins implicated in Ca^{2+} entry/removal, protein synthesis or even fast processes such as phosphorylation/dephosphorylation, myristoylation or other modifications. Few examples at the cellular level, but also affecting entire neuronal networks are summarized in the next chapter.

Cellular Modifications Caused by Ablation/Blocking of a Ca^{2+} Signaling Toolkit Component

The Ca^{2+} Homeostasome

Data summarized in this chapter are mostly obtained from knockout mice, where Ca^{2+} signaling components are (often completely) eliminated by genetic manipulation or in some instances, the functional impairment is the result of spontaneous mutations often leading to a loss-of-function phenotype. However, also some gain-of-function studies using transgenic mice are summarized. As stated before (section "General Considerations"), each individual cell's Ca^{2+} signaling components (expression levels, isoform patterns including splice variants, intracellular localization, e.g. axon, soma, dendrite, spine) finally determine the amplitude and spatiotemporal aspects of an intracellular Ca^{2+} signal elicited by an upstream signal, e.g. an action potential (AP) in a presynaptic terminal or neurotransmitter release-induced elevation in $[Ca^{2+}]_i$ in a postsynaptic compartment (e.g. spine, dendrite, soma). Components such as Ca^{2+} channels may show an even more restricted localization: e.g. concentrated in active zones of GABAergic presynaptic terminals of basket cells in the hippocampus [43] or axon initial segments (AIS) of dorsal cochlear nucleus interneurons [44]. The precise shape of a Ca^{2+} signal will then, in turn, elicit the "cor-

rect" downstream, Ca^{2+}-mediated response. This response may be manifold, from additional Ca^{2+} release from internal stores to reducing the mobility of mitochondria, to modulating the fission/fusion of vesicular compartments or to activating/inhibiting the transcriptional machinery in a cell's nucleus.

The Ca^{2+}-signaling components not only orchestrate their action to determine the high accuracy of intracellular Ca^{2+} signaling, but are also implicated in the regulation of the expression of the Ca^{2+}-signaling components [1, 7]. The total compliment of the molecules that build the network of Ca^{2+} signaling components, and that are involved in their own regulation resulting in physiological Ca^{2+} homeostasis (phenotypic stability) is named the Ca^{2+} homeostasome [5, 7]. The binding of Ca^{2+} ions to CaM and activation of Ca^{2+}/CaM-dependent kinases (CaMK) and/or binding to Ca^{2+}-regulated phosphatases (e.g. calcineurin; CaN) links changes in $[Ca^{2+}]_i$ to downstream transcriptional events, the so-called excitation-transcription (E-T) coupling. Ca^{2+}-dependent gene regulation controls several aspects of neuronal plasticity and also heart remodeling; details on the mechanisms of E-T coupling were investigated most often in relation to skeletal and heart muscle physiology/pathophysiology [45], but also in neurons [46]. A variety of genes is regulated by changes in $[Ca^{2+}]_i$: the promoter region of certain genes contain Ca^{2+}-responsive elements, examples are the genes *Calb1* coding for CB-D28k and *Calm2*, one of the genes coding for CaM [47]. Also a considerable number of transcription factors are regulated in a Ca^{2+}-dependent manner and include factors such as CREB (cyclic adenosine 3′,5′-monophosphate-responsive element binding protein), Elk-1 (an ETS family transcription factor), NFAT (nuclear factor of activated T cells) and NF-κB (nuclear factor kappa B). The fine-tuning of the Ca^{2+}-dependent expression of Ca^{2+}-signaling components is a typical trait during development and maturation of the nervous system. At the early stage of Purkinje cell (PC) maturation, somatic Ca^{2+} currents are essentially mediated by L-type channels ($Ca_V1.2$ and $Ca_V1.3$), which are then gradually replaced by P/Q-type ($Ca_V2.1$) channels [48]. In another cerebellar cell type, glutamatergic granule cells, their long-term survival *in vitro* is dependent on appropriate Ca^{2+} signals and this requires temporal changes in the transcription of Ca^{2+}-signaling components. In comparison to the freshly isolated cells, $InsP_3$-R and PMCAs 2 and 3 are upregulated, while a PMCA4 splice variant and plasma membrane NCX2 are downregulated in a CaN-dependent manner in the surviving granule cell population [49]. While developmental changes or changes resulting from physiological activity including e.g. neuronal plasticity clearly help to unravel the mechanisms implicated in the regulation of the Ca^{2+} homeostasome, also "non-physiological" situations as occurring due to a (spontaneous) genetic mutation or the deliberate elimination (e.g. in knockout mice) help to better understand the network of proteins implicated in Ca^{2+} signaling/regulation/homeostasis. As an example, the modulation of the Ca^{2+} homeostasome brought about by altered expression of CaBPs of the Ca^{2+} buffer family (PV, CB-D28k, CR), but also of few selected Ca^{2+} channels and pumps are discussed in detail in the next section ("The Cellular Ca^{2+} Homeostasome"), with a focus on the changes occurring at the level of a single cell; a more global view is presented in section "The "Global" Ca^{2+} Homeostasome".

The Cellular Ca^{2+} Homeostasome

Given the fact that for each Ca^{2+}-signaling component exists a considerable number of isoforms (e.g. PMCA1-4) or closely related proteins (in the case of EF-hand CaBPs more than 240 proteins with identified EF-hand motifs), then the most obvious compensation/adaptation mechanism in the case of malfunctioning or absence of a given component would be to replace it with a component that most closely matches its functional properties. As an example, one could imagine replacing the high-voltage activated (HVA) $Ca_V2.1$ (P/Q) Ca^{2+} channel by $Ca_V2.2$ (N) or to exchange the "fast" buffer CB-D28K by CR, etc. However, what is observed in almost all instances is that this appears not to be the general rule. In virtually all reported CaBP knockout mice and in the cell types expressing a particular CaBP, the ablated one is not compensated by another member of the huge EF-hand protein family. In the subset of the PV-expressing neurons including the Purkinje cells, stellate and basket cells in the cerebellum, the axo-axonic and basket cells in the hippocampus, the basket and chandelier neurons in the cortex as well as in the reticular thalamic neurons, none of the other "classical" Ca^{2+} buffers (CB-D28k, CB-D9k or CR) are expressed in the PVergic neurons of $PV^{-/-}$ mice [50]. Similarly in CB-D28k$^{-/-}$ and $CR^{-/-}$ mice [28, 51], global expression levels for the other Ca^{2+} buffers are not increased nor does one observe ectopic expression of the remaining Ca^{2+} buffers in the neuron subtypes with the deleted CaBPs. One could argue that certainly not all 240 other family members were tested. However, in a $^{45}Ca^{2+}$ overlay blot using cerebellar protein extracts from $PV^{-/-}$ and $PV^{-/-}$ CB-D28K$^{-/-}$ double knockout mice, no upregulation of other CaBPs occurs, at least not to expression levels close to the ones of the deleted protein(s), for details, see Fig. 6 in [29]. The situation is somewhat different with respect to Ca^{2+} channels. Most neurons express different types of Ca^{2+} channels that are often localized to different cellular compartments (axon, soma, dendrites) and are subjected to regulation during the normal maturation. Thus, in knockout mice lacking the α_{1A} subunit of the P/Q-type, its absence in PC is compensated by an increase in N- and L-type Ca^{2+} channels, the latter representing the channel isoform prevalent during earlier steps of cerebellar development [52]. An exception with respect to CaBPs is the upregulation of CB-D9k in epithelial kidney cells in CB-D28k$^{-/-}$ mice, but in this case, both proteins are normally expressed in the same cell type in a developmentally regulated manner [53]. The following conclusions can be drawn from the analyses of these mutant (knockout) mice:

1. In cells, selectively expressing only one type of a CaBP (PV, CB-D28K, CR), the remaining ones are neither globally up-regulated nor expressed in the neuron subpopulation of neurons, where the ablated one is normally expressed. This might be due to a neuron's inability to switch on the promoter for a closely related CaBP, i.e. the transcriptional machinery does not "allow" reactivation of the promoter for other Ca^{2+} buffers or "that the particular (Ca^{2+}-related) properties mentioned in section "General Considerations" (affinities, kinetics, co-operativity, mobility, binding partners) of other Ca^{2+} buffers would not be adequate to restore "normal" Ca^{2+} signaling" [7].

2. In neurons, where several "similar" Ca^{2+}-signaling components, e.g. different HVA Ca^{2+} channels are co-expressed, possibly in distinct cellular compartments, loss-of-function mutations or gene deletion may lead, in addition to other changes (see below), to the upregulation of the still functional component.
3. In most instances, the adaptation/compensation/homeostatic mechanisms take place at the level of the remaining cell-specific Ca^{2+}-signaling components and selected examples are presented here. Cerebellar Purkinje cells (PC) are particularly well suited to address such questions; they are characterized by extensive Ca^{2+} signaling in the dendrites and spines, as well as in the soma and express several Ca^{2+}-signaling components either in high concentrations, such as the Ca^{2+} buffers PV and CB-D28k, selectively express the Ca^{2+} pump isoform PMCA2 and also with respect to Ca^{2+} channels, in mature PC, most of the Ca^{2+} entry (>90%) is mediated via P/Q type Ca^{2+} channels.

In PC, PV and CB-D28k are localized in the soma, axon, dendrites and spines characteristic for mobile cytosolic proteins. PV is completely mobile in all compartments [18] and the slightly smaller diffusion coefficients (*D*) in the soma and the nucleus are likely due to different cytoplasmic properties such as viscosity, tortuosity and density of fibers or organelles in the different cellular compartments. While a large majority of CB-D28k is also freely mobile in PC compartments, a small proportion of CB-D28k molecules is immobilized in dendrites and spines by its binding to the enzyme *myo*-inositol monophosphatase (IMPase), a key enzyme of the $InsP_3$ signaling cascade [19]. Interestingly, the absence of either PV or CB-D28K in PC of the respective knockout mice, leads to very specific changes in Ca^{2+}-signaling components in combination, with CaBP-specific morphological changes. In the PC soma of $PV^{-/-}$ mice, the mitochondrial volume is increased by about 40% (Fig. 1.2); this increase is not randomly distributed throughout the cytosol, but is restricted to a narrow zone (≈1.5 μm width) underneath the plasma membrane [54]. Mitochondria are also Ca^{2+} sequestrating organelles that serve as transient Ca^{2+} stores [55, 56] and with respect to Ca^{2+} sequestrating/uptake, the kinetics appears to be similar as for the slow-onset buffer PV. A second morphological alteration in the PC soma is a decrease in the subplasmalemmal smooth ER compartment within a zone of 0.5 μm below the plasma membrane (Fig. 1.2). None of the above morphological changes occur in the absence of the "fast" buffer CB-D28k. Yet, in $CB\text{-}D28k^{-/-}$ PC spines, compartments characterized by brief Ca^{2+} signals in the subsecond range, the morphology is altered: spines are longer and the spine head volume is increased [57]. In spiny cortical pyramidal neurons characterized by low expression of Ca^{2+} buffers, spine heads are considered as "separate biochemical compartments with negligible Ca^{2+} diffusion via the spine neck" [58]. The situation is quite different in PC spines, where Ca^{2+} buffers are not only modulating the kinetics and amplitudes of Ca^{2+} transients within the spines, but in conjunction with the spine neck geometry also determine the amount of Ca^{2+} ions that reach the parental dendrite. This increase in dendritic $[Ca^{2+}]_i$ then leads to activation of Ca^{2+}/CaM-dependent signaling cascades [59]. Based on the results from $CB\text{-}D28K^{-/-}$ and $PV^{-/-}$ mice, it is hypothesized that mostly CB-D28k is involved in spino-dendritic coupling

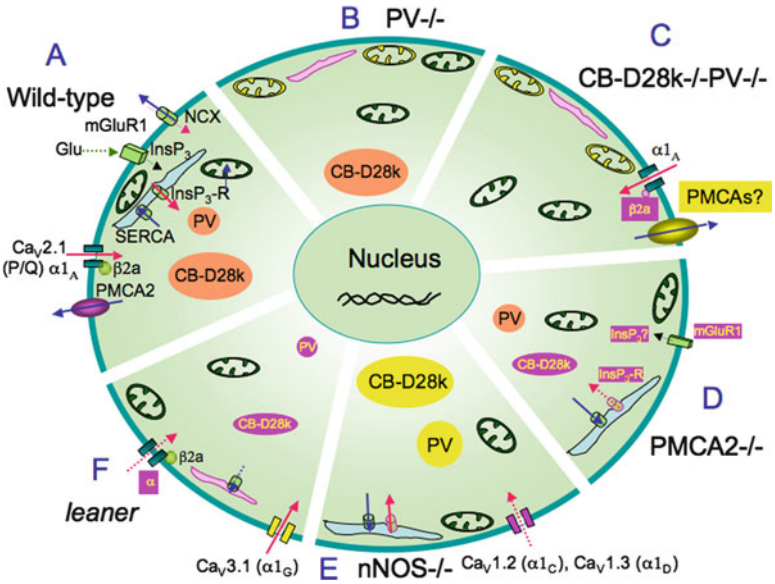

Fig. 1.2 The cellular Ca^{2+} homeostasome. Homeostatic/adaptive/compensatory changes in the soma of cerebellar Purkinje cells (PC) caused by genetic elimination or loss-of-function mutations of Ca^{2+}-signaling components (Modified from [5]). The most detailed situation is depicted for Purkinje cells from wild-type mice. (**a**) Entry of Ca^{2+} ions (*red arrows*) mostly via $Ca_V2.1$ (P/Q) type Ca^{2+} channels or resulting from the release from internal stores (ER, *light blue*) mediated by the $InsP_3$ receptor transiently increases $[Ca^{2+}]_i$. $InsP_3$ is generated through the activation of metabotropic glutamate receptors (mGluR). Ca^{2+} extrusion/re-uptake systems (*blue arrows*) include Ca^{2+} pumps (PMCA) and NCX in the plasma membrane, SERCA pumps in the ER and the Ca^{2+} uniporter in mitochondria (*green*). Changes in Ca^{2+}-signaling components including organelles implicated in Ca^{2+} homeostasis, which are up- or down-regulated in the PC soma of mutant mice are highlighted in yellow and magenta, respectively. Uncertain or hypothesized changes are marked by question marks. (**b**) In $PV^{-/-}$ PC, mitochondria are increased in a narrow zone (1.5 μm) underneath the plasma membrane and the subplasmalemmal ER volume is decreased. The remaining Ca^{2+} buffer, CB-D28k is not up-regulated in $PV^{-/-}$ PC. (**c**) In PC of $PV^{-/-}$ $CB\text{-}D28k^{-/-}$ mice, the mRNA level of auxiliary $Ca_V\beta2a$ subunit of $Ca_V2.1$ (P/Q) type Ca^{2+} channel is decreased leading to increased voltage-dependent inactivation of P/Q-type currents. Results from modeling studies suggest that additionally Ca^{2+} extrusion systems, possibly PMCAs could be increased in the double mutants [29]. (**d**) The expression of mGluR1 and of $InsP_3$ receptor type 1 ($InsP_3$-R1), the latter responsible for the Ca^{2+} release from ER stores is decreased in $PMCA2^{-/-}$ PC somata. Also the expression of the Ca^{2+} buffer CB-D28k is decreased likely reducing the "fast" Ca^{2+} buffering capacity. Whether also PV levels are affected, is currently unknown. (**e**) In mice deficient for the neuronal nitric oxide synthase ($nNOS^{-/-}$), the Ca^{2+} buffers CB-D28k and PV are up-regulated, in addition to a down-regulation of the VOCC $Ca_V1.2$ ($\alpha1_C$) and $Ca_V1.3$ ($\alpha1_D$) coding for L-type HVA Ca^{2+} channels (**f**) In *leaner* mice PC, $Ca_V2.1$ Ca^{2+} channel function is attenuated by approximately 60%. The result from a likely homeostatic/adaptive process is the prominent decrease in the rapid Ca^{2+} buffering/sequestering capacity mediated by CB-D28k and to a lesser extent, by PV. Also the subplasmalemmal ER is decreased and/or impaired leading to a reduction in Ca^{2+} uptake into these organelles. At the level of Ca^{2+} channels, $Ca_V3.1$ ($\alpha1_G$) is upregulated in *leaner* PC. The described changes occurring in the different mutants are the ones that have been investigated and published. This does not exclude that additional, yet not reported changes take place in the PC somata of the various mutants

by buffered Ca^{2+} diffusion, while the contribution of PV to this process is negligible. In line with the predictions of a minute contribution by PV, the spine morphology of $PV^{-/-}$ PC is indistinguishable from that of WT mice [57]. In mice deficient for PV, CB-D28K or both, additional changes at the level of Ca^{2+} signaling components are present in Purkinje cells. In adult PC, >90% of the whole-cell voltage-gated Ca^{2+} current is mediated by $Ca_v2.1$ (P/Q type) channels. As for most of the HVA channels, also $Ca_v2.1$ is regulated by Ca^{2+}-dependent feedback mechanisms: Ca^{2+}-dependent facilitation (CDF) and inactivation (CDI). However, it is the latter that is mostly dependent on Ca^{2+} buffers, whether brought about by the synthetic buffers EGTA and BAPTA or the physiological ones, PV and CB-D28k *in vitro* [60]. Importantly, already in this *in vitro* model, PV and CB-D28k affect $Ca_v2.1$ channel inactivation differently than the synthetic buffers EGTA and BAPTA. Thus, studies using the synthetic buffers in order to mimic the "real" ones have to be viewed with some caution, see also [37]. For the other process, CDF, Ca^{2+} sensors including CaM [61] and CaBP1 [4] play an important role. Interestingly, the effect of ectopic expression of PV and CB-D28 in HEK cells expressing $Ca_v2.1$ does not have the same effect as is observed in Purkinje cells of WT mice compared to $PV^{-/-}$ $CB\text{-}D28k^{-/-}$ mice. In transfected HEK cells, the presence of the Ca^{2+} buffers PV and CB-D28K decrease CDI, while CDI in PC of double knockout ($CB\text{-}D28k^{-/-}$ $PV^{-/-}$) mice is not increased indicative of an adaptation/compensation mechanism induced in the knockout mice. Unexpectedly, voltage-dependent inactivation (VDI) is increased; this is the result of a decreased expression of the auxiliary $Ca_v\beta2a$ subunit in double knockout mice compared to WT animals [62] (Fig. 1.2). Concomitant with the finding that spontaneous APs are not different in control and mutant Purkinje cells indicates that "increased inactivation due to molecular switching of $Ca_v2.1$ beta subunits may preserve normal activity-dependent Ca^{2+} signals in the absence of PV and CB-D28k" [5]. Additional adaptive/homeostatic changes in PC of $CB\text{-}D28k^{-/-}$ $PV^{-/-}$ mice are postulated, based on modeling studies [29]. The model also predicts that Ca^{2+} extrusion and/or Ca^{2+} uptake systems should be increased in the dendrites of these mutant mice and likely candidates are PMCAs, NCX and SERCA pumps.

The "global" effects of eliminating the pore-forming alpha subunit of $Ca_v2.1$ are discussed in section "The "Global" Ca^{2+} Homeostasome". Here, a brief summary about the effects of a mouse mutant with reduced $Ca_v2.1$ channel function, the *leaner* mouse is presented. The significantly decreased (≈40% compared to WT) Ca^{2+} influx is compensated by a diminished rapid Ca^{2+} buffering/sequestering capacity of Purkinje cells [63]. It is less than 50% compared to Purkinje cells from WT mice due to a reduction in PV and CB-D28k expression levels (Fig. 1.2). Furthermore, the reduced Ca^{2+} uptake capacity most likely caused by a decrease in subplasmalemmal ER additionally contributes to the reduced Ca^{2+} buffering ability of *leaner* mice Purkinje cells [64]. Modifications in PC Ca^{2+} signaling components are also observed in mice with a mutation in PMCA2 leading to a decreased rate of Ca^{2+} extrusion. In these neurons, the maximal amplitude in $[Ca^{2+}]_i$ during high K^+-induced depolarization is smaller than in WT PC and it was proposed "that voltage-gated Ca^{2+} channels were down-regulated in the mutant mice in order to regulate $[Ca^{2+}]_i$ toward the normal

homeostasis" [65]. In the complete absence of functional PMCA2 in PMCA2$^{-/-}$ mice, expression levels of CB-D28k [66], metabotropic glutamate receptor 1 (mGluR1) and of $InsP_3$-R type 1 [67] responsible for the Ca^{2+} release from ER stores are decreased in PC (Fig. 1.2). Thus, the impaired/reduced Ca^{2+} extrusion is the likely cause leading to a reduction in mGluR1-mediated $[Ca^{2+}]_i$ elevation. Although "the decrease in the expression of mGluR1 and its downstream effectors and perturbations in the mGluR1 signaling complex in the absence of PMCA2 may cumulatively result in aberrant mGluR signaling in Purkinje neurons leading to cerebellar deficits in the PMCA2-null mouse" [67], the severely distorted PMCA2$^{-/-}$ Purkinje cell morphology may also be a plausible explanation for the ataxic phenotype [68]. PMCA2$^{-/-}$ PCs have smaller somata and their dendritic trees are visibly distorted.

The "Global" Ca^{2+} Homeostasome

During synaptic transmission, Ca^{2+}-dependent processes are occurring in both, the presynaptic and the postsynaptic compartments. For its proper functioning, homeostatic mechanisms including feedback regulation ensure reliable and "meaningful" information transfer across synapses. The question arises how the system ascertains that synaptic transmission avoids the extremes of complete quiescence or excessive action potential firing, i.e. how it maintains synaptic transmission within a physiological range, in situations where one of the Ca^{2+} signaling components is impaired (e.g. due to genetic mutations) or completely eliminated as in knockout mice. While the previous section ("The Cellular Ca^{2+} Homeostasome") was focused on events occurring on the postsynaptic side, here a more global view of synaptic transmission and homeostatic mechanisms are discussed. In presynaptic terminals of hippocampal neurons from mice lacking the pore-forming alpha subunit of the P/Q type ($Ca_V2.1$) Ca^{2+} channel ($\alpha_{1A}^{-/-}$), synaptic release is almost identical as in WT neurons, although in the latter, a large part of the neurotransmission is dependent on P/Q channel function as evidenced by blocking it with ω-Agatoxin IVA in WT mice [69]. Identified homeostatic mechanisms at the presynaptic site include a larger number of docked vesicles and a slightly larger active recycling pool of synaptic vesicles without an increase in the total vesicle number per terminal. In addition, expression levels (mRNA and/or protein) of several proteins implicated in excitation-secretion coupling and the Ca^{2+}-dependent endocytic machinery are altered in $\alpha_{1A}^{-/-}$ mice. Dynamin levels are increased as well as mRNA levels of synaptogyrin 1, synaptophysin 1 and synaptotagmin 7, the latter being a plasma membrane-bound Ca^{2+}-sensing protein that functions together with the vesicle-associated Ca^{2+} sensors synaptotagmin 1 and 2, both members of the C2-family of Ca^{2+}-binding proteins [4]. These changes in the presynaptic exo-/endocytic machinery are also the likely cause for the two-fold increase in frequency of mEPSCs. Interestingly, there is no indication of an increase in α_{1B} nor in α_{1C} coding for the N- ($Ca_V2.2$) and L- ($Ca_V1.2$) type of Ca^{2+} channels, respectively. However, mRNA levels of α_{1G} ($Ca_V3.1$) coding for T-type channel are increased in the $\alpha_{1A}^{-/-}$ hippocampal neurons, a possible

explanation for the increased seizure sensitivity of $\alpha_{1A}^{-/-}$ mice. Altered expression of α_{1G} in the cerebellum of the *leaner* mouse (a mutant with a mutation in the α_{1A} subunit, for details, see below) is thought to be implicated in the movement disorder; α_{1G} is decreased in granule cells and increased in PC as revealed by quantitative in situ hybridization histochemistry [70]. In *rocker* mice characterized by a mutation in α_{1A} leading to a moderate reduction in Ca^{2+} channel current density, the number and density of AMPA-R at the parallel fiber (PF)-PC synapses is decreased and furthermore the arborization of the PC dendrites is impaired [71]. Morphological changes in PC caused by impaired P/Q type Ca^{2+} channel function is also seen in the *rolling mouse Nagoya* (tg^{rol}/tg^{rol}). The spine density and average spine length is reduced at PF-PC synapses, while on proximal dendritic spines reflecting climbing fiber (CF) inputs, the spine density is increased [72]. Based on these results the authors suggest that the "two major excitatory afferent systems may be regulated reciprocally in the cerebellum of these mutant mice". How the impaired function of the P/Q channel differently affects the spine morphology at proximal and distal dendrites remains to be determined. At the functional level, EPSC amplitudes at the PF-PC synapse are reduced [73]. In another P/Q channel mutant mouse, *tottering*, EPSCs at the same synapse (PF-PC) are normal in young mice, but reduced in the ataxic adult animals, thus showing a clear correlation between diminished EPSCs in the mutants and age-related ataxia. At the level of granule cells, CR gene expression in *tottering* is reduced possibly as a compensation/adaptive mechanism to cope with the reduced P/Q-type Ca^{2+} channel function, likely to be important for somatic Ca^{2+} signals and moreover modulation of $[Ca^{2+}]_i$ in the presynaptic PF terminals [74]. The absence of CR in granule cells of $CR^{-/-}$ mice increases the intrinsic neuronal excitability: APs are faster and granule cells generate repetitive spike discharges that show an enhanced frequency increase with injected currents [30]. In contrast, EPSCs at the CF-PC synapses are unaltered in *tottering* and even increased in *rolling mouse Nagoya*; this increase is linked to altered properties of postsynaptic Glu-R, but might be also correlated with the increased spine density in proximal dendrites of this mouse mutant [72].

While the above mutants are characterized by impaired (reduced) P/Q channel function, also gain-of function mutations (increased Ca^{2+} influx) are associated with diseases including Familial Hemiplegic Migraine type 1 (FHM-1). In FHM-1 mutant mice (knock-in mice carrying the human missense mutation), both forms of Ca^{2+}/CaM-dependent forms of modulation of synaptic plasticity, i.e. Ca^{2+}-dependent facilitation (CDF) and Ca^{2+}-dependent inactivation (CDI) are strongly reduced. The decreased CDF correlates with reduced short-term synaptic facilitation at PF-PC synapses [75]. Of note, these effects are mostly seen in the S218L mutant, which in human patients is associated with severe migraine and often also with ataxia. This mutation maintains the P/Q channel in an essentially facilitated state resulting in a larger Ca^{2+} influx during APs in presynaptic PF terminals. Also in the PCs of the ataxic *groggy* rat (GRY), a missense mutation in the α_{1A} subunit (M251K) is responsible for the increased current density mediated through HVA Ca^{2+} channels [76]. The fact that low voltage-activated (LVA) Ca^{2+} channel currents are not

different from the ones in WT PCs strongly indicates that increased, likely P/Q-mediated, Ca^{2+} channel function leads to the ataxic phenotype of GRY rats. How can one reconcile that both decreased and increased P/Q-type Ca^{2+} channel function results in an ataxic phenotype in the various species (human, rat, mouse)? PC display regular intrinsic pacemaking properties that are shaped by inhibitory and excitatory inputs. Subtle variations in the interspike interval from that of intrinsic regular pacemaking carry motor coordination-relevant information to the deep cerebellar nuclei (DCN). In PC of *leaner* (mutation in α_{1A}) and *ducky* [mutation in the α_2-$\delta-2$ (*Cacna2d2*) auxiliary subunit], both of which are characterized by reduced P/Q channel function, intrinsic pacemaking is highly irregular [77] and is probably caused by a reduction in the activation of Ca^{2+}-dependant potassium channels (K_{Ca}). The positive K_{Ca} channel-gating modulator 1-ethyl-2-benzimidazolinone (EIBO) restores the precision of the pacemaking and infusion of EIBO *in vivo* in mutant mice improves motor performance, i.e. reduces the ataxic phenotype. Whether in mutant mice with increased P/Q-type Ca^{2+} channel function, also a putatively increased activation of K_{Ca} channels is linked to the ataxic phenotype has, according to my best knowledge, not been investigated yet. However, also based on the results obtained in CaBP-KO mice ($CR^{-/-}$, CB-D28K$^{-/-}$ and $PV^{-/-}$), the motor coordination phenotype can only be understood at the level cerebellar network functioning (see below). Thus, an increase, a decrease and/or an alteration in the dynamics of excitatory and inhibitory inputs onto PCs are correlated with aberrant motor coordination phenotypes in several models of altered/modified Ca^{2+} signaling components.

A silencing mutation in the modulatory subunit γ2 of VOCC channels, named stargazin, also induces several changes in cerebellar and hippocampal synapses in the *stargazer* mouse [78]. In the cerebellum, it causes a down-regulation of postsynaptic α_{1C} L-type Ca^{2+} channels, but not affecting the presynaptic α_{1A} P/Q-type channels. Under physiological conditions, stargazin is also involved in the assembly and trafficking of AMPA receptors. Thus, the non-functional stargazin might prevent appropriate formation of AMPA-R/L-type Ca^{2+} channel complexes in the postsynaptic terminals. In hippocampal synapses from *stargazer* mice neither L-type nor P/Q-type Ca^{2+} channel expression is affected, possibly as the result of an upregulation of the γ8 subunit of VOCC.

The signaling molecule nitric oxide (NO) is produced by neuronal NO synthase (nNOS) in a Ca^{2+}/CaM-dependent manner, thus linking NO and Ca^{2+} signaling pathways. NO also modulates the activity of various channels and receptors: it decreases the activity of AMPA-R and N-methyl-D-aspartate (NMDA)-type glutamate receptor and inhibits voltage-gated Ca^{2+} channels (e.g. L-, N-type), for details, see [79] and refs therein. Analysis of nNOS$^{-/-}$ mice revealed also changes in the expression levels CB-D28K, CR and PV in the cerebellum of these knockout mice [80]. CR levels in granule cells are decreased, while CB-D28K and PV immunoreactivity (PV-ir) in PCs and PV-ir additionally in the molecular layer interneurons (stellate and basket cells) is increased (Fig. 1.2). At the level of VOCC, α_{1C} ($Ca_V1.2$) and α_{1D} ($Ca_V1.3$) immunoreactivity is decreased in PC somata as well as in the neuropil of nNOS$^{-/-}$ mice DCN [81]. Conversely, expression of nNOS is affected in the α_{1A}

channel mutants *leaner* and *tottering*, mice characterized by reduced Ca^{2+} influx (60% and 40% reduction, respectively) via the P/Q Ca^{2+} type channel, in a developmentally regulated manner. Alterations are specific for each mutant indicating that the gradual reduction in Ca^{2+} influx entails different compensatory/homeostatic mechanisms. At P12, nNOS expression in the cerebellum is increased only in *tottering* mice, but immunostaining in basket cells is stronger for both mutants compared to WT mice. However, in line with the Western blot results, the effect is more pronounced in *tottering* mice [82]; albeit the Ca^{2+} channel impairment is more severe in the *leaner* mutant. Additionally nNOS levels are decreased at P20 in granule cells of *leaner* mice. Most interestingly, cerebellar NO concentrations in P12 mice of all three groups are not different and the authors propose that "changes in nNOS expression in the l*eaner* and *tottering* cerebella are compensatory in nature with NO most likely functioning as a Ca^{2+}-regulated neuroprotective/neurotrophic factor in postnatal cerebellar development."

At the behavioral level, $nNOS^{-/-}$ mice show a mild phenotype with respect to nocturnal balance and motor coordination [83]. Thus, in some respect, this motor phenotype resembles the one observed in $CR^{-/-}$, but also in $PV^{-/-}$ and CB-$D28K^{-/-}$ mice [7]. All of these mice have problems to walk on a narrow bar with small obstacles evidenced by the increased rate of foot slips and $CR^{-/-}$ mice display abnormal wheel running [84]. At first glance, this similar phenotype seems surprising, since expression of PV and CB-D28K is increased in $nNOS^{-/-}$ mice, not completely absent as in $PV^{-/-}$ and CB-$D28K^{-/-}$ mice. However, the motor phenotype in all three CaBP knockout mice is likely a phenotype arising from the alterations in the functioning of the cerebellar network. In all three $CaBP^{-/-}$ strains, the emergence of 160 Hz oscillations is proposed to contribute to the motor coordination impairment [85]. Transient blocking of glutamatergic (via NMDA-R) and $GABA_A$ergic transmission as well as blocking of the gap junction between molecular layer interneurons (MLIs; stellate and basket cells) leads to a decrease of these oscillations, which reappear after washout of the blockers [86, 87]. Thus, the appearance of the 160 Hz oscillations and concomitantly the impairment of motor coordination is a cerebellar network phenotype that results from a modification in the function of granule cells ($CR^{-/-}$), PC (CB-$D28k^{-/-}$) and in $PV^{-/-}$ mice additionally from MLIs. Another spontaneous mutant mouse model, the *circling mouse*, shows a motor phenotype likely linked to altered cerebellar Ca^{2+} signaling/homeostasis. Although the precise genetic defect is currently unknown double-mutant mice with reduced PMCA2 function and a constitutive active form of the transient receptor potential channel TRPML3 leading to display circling behavior, have inner ear sensory hair cell degeneration as in the *circling mouse* [88]. In the cerebellum of the *circling mouse*, the immunoreactivity for CR in granule cells, for CB-D28k in PC and for PV in PC and MLI is decreased compared to control WT mice [89] indicative of a general impairment in neuronal Ca^{2+} signaling. Of interest, triple knockout mice for the three proteins (CB-$D28k^{-/-}$ $CR^{-/-}$ $PV^{-/-}$) neither show a circling behavior nor hair cell degeneration, the likely result from homeostatic/compensation mechanisms induced/activated in those mice (B. Schwaller, unpublished observation).

Conclusions, Hypotheses and Outlook

What is the bottom line from the results obtained in the various animal models and human patients with altered expression/function of Ca^{2+} signaling toolkit components and what hypotheses can be put forward? (1) Although the number of principal components responsible for intracellular Ca^{2+} signaling is relatively small (see Fig. 1.1; Ca^{2+} buffers, Ca^{2+} channels, Ca^{2+} pumps, exchangers, in the plasma membrane and in organelles), the complexity is massively increased by the many isoforms and splice variants of the different Ca^{2+}-signaling toolkit components. As a result, different neuron types and possibly each individual neuron has a "personalized" set of Ca^{2+} signaling components tuned to the specific physiological needs of that particular cell (type). (2) A high degree of plasticity with respect to Ca^{2+} signaling components is observed during development and this "latent" plasticity remains throughout the lifespan of a cell or the entire organism. (3) A defect or absence of a Ca^{2+} signaling component in a cell induces homeostatic/adaptive/compensatory mechanisms, both at the level of the affected cell and more often, within the entire network, in which the affected cell exerts its physiological function. In the case of the nervous system, this implies both, anterograde and retrograde signaling leading to modifications/adaptations of Ca^{2+} signaling components within the network, i.e. the activation of the Ca^{2+} homeostasome. (4) The precise nature of these homeostatic changes can only be understood by including the level of networks. (5) In all investigated cases, the homeostatic changes/compensations are never "perfect", even if there is a deletion/mutation of a single Ca^{2+} signaling component. While an organism, e.g. a knockout/knockin mouse may not show an evident phenotype under standard housing conditions, an often-subtle phenotype becomes generally apparent in conditions requiring more complex brain functions such as in cognition, behavior and experience-dependent modifications, such as learning and memory. Thus, it is the specific properties of each individual Ca^{2+} signaling component and the precise effects at a cellular level that form the basis of "normal/physiological" functioning. (6) The pathological phenotype (e.g. altered pain sensitivity, epilepsy, migraine, and schizophrenia) may not be the primary result of a defective/lacking Ca^{2+} signaling component, but may be the result of the global homeostatic "reorganization" of the entire network, leading to a disparity in the finely tuned excitation/inhibition balance. This may, at least in part, explain why defects in apparently functional-unconnected genes, finally merge to give raise to a common pathological phenotype. It is hypothesized that a better understanding of the Ca^{2+} homeostasome at the cellular level and even more importantly, at the network level may help to unravel the underlying cause for the many neurological diseases that have in one way or another been linked to disturbed Ca^{2+} signaling/homeostasis.

Note added in proof The mitochondrial Ca^{2+} uniporter protein (MCU), a 40-kDa transmembrane inner mitochondrial membrane protein is an essential component of the functionally defined "mitochondrial Ca^{2+} uniporter" and was described in 2 papers published in 2011: [90, 91].

Acknowledgements I would like to thank Walter-Vincent Blum, Laszlo Pecze and Thomas Henzi, University of Fribourg, Switzerland for their helpful comments. The fruitful discussions and comments from Michael Berridge, The Babraham Institute, Cambridge, UK are highly appreciated. I would also like to thank the reviewers that have helped to improve the manuscript.

References

1. Berridge MJ, Bootman MD, Roderick HL (2003) Calcium signalling: dynamics, homeostasis and remodelling. Nat Rev Mol Cell Biol 4:517–529
2. Prins D, Michalak M (2011) Organellar calcium buffers. Cold Spring Harb Perspect Biol 3:a004069
3. Schwaller B (2009) Ca^{2+}-buffers. In: Bradshaw RA, Dennis EA (eds) Handbook of cell signaling, 2nd edn. Academic, Oxford, pp 955–962
4. McCue HV, Haynes LP, Burgoyne RD (2010) The diversity of calcium sensor proteins in the regulation of neuronal function. Cold Spring Harb Perspect Biol 2:a004085
5. Schwaller B (2010) Cytosolic Ca^{2+} buffers. Cold Spring Harb Perspect Biol 2:a004051
6. Faas GC, Raghavachari S, Lisman JE, Mody I (2011) Calmodulin as a direct detector of Ca^{2+} signals. Nat Neurosci 14:301–304
7. Schwaller B (2009) The continuing disappearance of "pure" Ca^{2+} buffers. Cell Mol Life Sci 66:275–300
8. Berggard T, Miron S, Onnerfjord P, Thulin E, Akerfeldt KS, Enghild JJ, Akke M, Linse S (2002) Calbindin D28k exhibits properties characteristic of a Ca^{2+} sensor. J Biol Chem 277:16662–16672
9. Eberhard M, Erne P (1994) Calcium and magnesium binding to rat parvalbumin. Eur J Biochem 222:21–26
10. Linse S, Johansson C, Brodin P, Grundstrom T, Drakenberg T, Forsen S (1991) Electrostatic contributions to the binding of Ca^{2+} in calbindin D9k. Biochemistry 30:154–162
11. Nagerl UV, Novo D, Mody I, Vergara JL (2000) Binding kinetics of calbindin-D(28k) determined by flash photolysis of caged Ca(2+). Biophys J 79:3009–3018
12. Faas GC, Schwaller B, Vergara JL, Mody I (2007) Resolving the fast kinetics of cooperative binding: Ca^{2+} buffering by calretinin. PLoS Biol 5:e311. doi:310.1371/journal.pbio.0050311
13. Stevens J, Rogers JH (1997) Chick calretinin: purification, composition, and metal binding activity of native and recombinant forms. Protein Expr Purif 9:171–181
14. Martin SR, Linse S, Johansson C, Bayley PM, Forsen S (1990) Protein surface charges and Ca2+ binding to individual sites in calbindin D9k: stopped-flow studies. Biochemistry 29:4188–4193
15. Yang JJ, Gawthrop A, Ye Y (2003) Obtaining site-specific calcium-binding affinities of calmodulin. Protein Pept Lett 10:331–345
16. Maughan DW, Godt RE (1999) Parvalbumin concentration and diffusion coefficient in frog myoplasm. J Muscle Res Cell Motil 20:199–209
17. Schmidt H, Brown EB, Schwaller B, Eilers J (2003) Diffusional mobility of parvalbumin in spiny dendrites of cerebellar purkinje neurons quantified by fluorescence recovery after photobleaching. Biophys J 84:2599–2608
18. Schmidt H, Arendt O, Brown EB, Schwaller B, Eilers J (2007) Parvalbumin is freely mobile in axons, somata and nuclei of cerebellar Purkinje neurones. J Neurochem 100:727–735
19. Schmidt H, Schwaller B, Eilers J (2005) Calbindin D28k targets myo-inositol monophosphatase in spines and dendrites of cerebellar Purkinje neurons. Proc Natl Acad Sci USA 102:5850–5855

20. Gabso M, Neher E, Spira ME (1997) Low mobility of the Ca2+ buffers in axons of cultured Aplysia neurons. Neuron 18:473–481
21. Celio MR (1986) Parvalbumin in most gamma-aminobutyric acid-containing neurons of the rat cerebral cortex. Science 231:995–997
22. Heizmann CW, Berchtold MW, Rowlerson AM (1982) Correlation of parvalbumin concentration with relaxation speed in mammalian muscles. Proc Natl Acad Sci USA 79:7243–7247
23. Schneeberger PR, Heizmann CW (1986) Parvalbumin in rat kidney. Purification and localization. FEBS Lett 201:51–56
24. Lee GS, Choi KC, Jeung EB (2006) Glucocorticoids differentially regulate expression of duodenal and renal calbindin-D9k through glucocorticoid receptor-mediated pathway in mouse model. Am J Physiol Endocrinol Metab 290:E299–E307
25. Boros S, Bindels RJ, Hoenderop JG (2009) Active Ca(2+) reabsorption in the connecting tubule. Pflugers Arch 458:99–109
26. Choi KC, Jeung EB (2008) Molecular mechanism of regulation of the calcium-binding protein calbindin-D(9k), and its physiological role(s) in mammals: a review of current research. J Cell Mol Med 12:409–420
27. Huybers S, Naber TH, Bindels RJ, Hoenderop JG (2007) Prednisolone-induced Ca^{2+} malabsorption is caused by diminished expression of the epithelial Ca^{2+} channel TRPV6. Am J Physiol Gastrointest Liver Physiol 292:G92–G97
28. Airaksinen MS, Eilers J, Garaschuk O, Thoenen H, Konnerth A, Meyer M (1997) Ataxia and altered dendritic calcium signaling in mice carrying a targeted null mutation of the calbindin D28k gene. Proc Natl Acad Sci USA 94:1488–1493
29. Schmidt H, Stiefel KM, Racay P, Schwaller B, Eilers J (2003) Mutational analysis of dendritic Ca^{2+} kinetics in rodent Purkinje cells: role of parvalbumin and calbindin D28k. J Physiol 551:13–32
30. Gall D, Roussel C, Susa I, D'Angelo E, Rossi P, Bearzatto B, Galas MC, Blum D, Schurmans S, Schiffmann SN (2003) Altered neuronal excitability in cerebellar granule cells of mice lacking calretinin. J Neurosci 23:9320–9327
31. Bearzatto B, Servais L, Roussel C, Gall D, Baba-Aissa F, Schurmans S, de Kerchove d'Exaerde A, Cheron G, Schiffmann SN (2006) Targeted calretinin expression in granule cells of calretinin-null mice restores normal cerebellar functions. FASEB J 20:380–382
32. Carrion AM, Link WA, Ledo F, Mellstrom B, Naranjo JR (1999) DREAM is a Ca^{2+}-regulated transcriptional repressor. Nature 398:80–84
33. Skelton NJ, Kördel J, Akke M, Forsén S, Chazin WJ (1994) Signal transduction versus buffering activity in Ca++-binding proteins. Nat Struct Biol 1:239–245
34. Schwaller B, Durussel I, Jermann D, Herrmann B, Cox JA (1997) Comparison of the Ca^{2+}-binding properties of human recombinant calretinin-22k and calretinin. J Biol Chem 272:29663–29671
35. Hack NJ, Wride MC, Charters KM, Kater SB, Parks TN (2000) Developmental changes in the subcellular localization of calretinin. J Neurosci 20:RC67
36. Hubbard MJ, McHugh NJ (1995) Calbindin 28kDa and calbindin 30kDa (calretinin) are substantially localised in the particulate fraction of rat brain. FEBS Lett 374:333–337
37. Saftenku EE (2011) Effects of calretinin on Ca(2+) signals in cerebellar granule cells: implications of cooperative Ca(2+) binding. Cerebellum. 10.1007/s12311-011-0263-4
38. Fierro L, DiPolo R, Llano I (1998) Intracellular calcium clearance in Purkinje cell somata from rat cerebellar slices. J Physiol 510:499–512
39. Brini M, Carafoli E (2009) Calcium pumps in health and disease. Physiol Rev 89:1341–1378
40. Strehler EE, Filoteo AG, Penniston JT, Caride AJ (2007) Plasma-membrane Ca(2+) pumps: structural diversity as the basis for functional versatility. Biochem Soc Trans 35:919–922
41. Catterall WA (2010) Signaling complexes of voltage-gated sodium and calcium channels. Neurosci Lett 486:107–116
42. Dolphin AC (2009) Calcium channel diversity: multiple roles of calcium channel subunits. Curr Opin Neurobiol 19:237–244

43. Bucurenciu I, Kulik A, Schwaller B, Frotscher M, Jonas P (2008) Nanodomain coupling between Ca(2+) channels and Ca(2+) sensors promotes fast and efficient transmitter release at a cortical GABAergic synapse. Neuron 57:536–545
44. Bender KJ, Trussell LO (2009) Axon initial segment Ca^{2+} channels influence action potential generation and timing. Neuron 61:259–271
45. Bers DM (2008) Calcium cycling and signaling in cardiac myocytes. Annu Rev Physiol 70:23–49
46. Dolmetsch R (2003) Excitation-transcription coupling: signaling by ion channels to the nucleus. Sci STKE 2003:PE4
47. Arnold DB, Heintz N (1997) A calcium responsive element that regulates expression of two calcium binding proteins in Purkinje cells. Proc Natl Acad Sci USA 94:8842–8847
48. Gruol DL, Netzeband JG, Quina LA, Blakely-Gonzalez PK (2005) Contribution of L-type channels to Ca^{2+} regulation of neuronal properties in early developing purkinje neurons. Cerebellum 4:128–139
49. Carafoli E, Genazzani A, Guerini D (1999) Calcium controls the transcription of its own transporters and channels in developing neurons. Biochem Biophys Res Commun 266:624–632
50. Schwaller B, Tetko IV, Tandon P, Silveira DC, Vreugdenhil M, Henzi T, Potier MC, Celio MR, Villa AE (2004) Parvalbumin deficiency affects network properties resulting in increased susceptibility to epileptic seizures. Mol Cell Neurosci 25:650–663
51. Schiffmann SN, Cheron G, Lohof A, d'Alcantara P, Meyer M, Parmentier M, Schurmans S (1999) Impaired motor coordination and Purkinje cell excitability in mice lacking calretinin. Proc Natl Acad Sci USA 96:5257–5262
52. Jun K, Piedras-Renteria ES, Smith SM, Wheeler DB, Lee SB, Lee TG, Chin H, Adams ME, Scheller RH, Tsien RW, Shin HS (1999) Ablation of P/Q-type Ca(2+) channel currents, altered synaptic transmission, and progressive ataxia in mice lacking the alpha(1A)-subunit. Proc Natl Acad Sci USA 96:15245–15250
53. Zheng W, Xie Y, Li G, Kong J, Feng JQ, Li YC (2004) Critical role of calbindin-D28k in calcium homeostasis revealed by mice lacking both vitamin D receptor and calbindin-D28k. J Biol Chem 279:52406–52413
54. Chen G, Racay P, Bichet S, Celio MR, Eggli P, Schwaller B (2006) Deficiency in parvalbumin, but not in calbindin D-28k upregulates mitochondrial volume and decreases smooth endoplasmic reticulum surface selectively in a peripheral, subplasmalemmal region in the soma of Purkinje cells. Neuroscience 142:97–105
55. Murchison D, Griffith WH (2000) Mitochondria buffer non-toxic calcium loads and release calcium through the mitochondrial permeability transition pore and sodium/calcium exchanger in rat basal forebrain neurons. Brain Res 854:139–151
56. Billups B, Forsythe ID (2002) Presynaptic mitochondrial calcium sequestration influences transmission at mammalian central synapses. J Neurosci 22:5840–5847
57. Vecellio M, Schwaller B, Meyer M, Hunziker W, Celio MR (2000) Alterations in Purkinje cell spines of calbindin D-28k and parvalbumin knock-out mice. Eur J Neurosci 12:945–954
58. Sabatini BL, Oertner TG, Svoboda K (2002) The life cycle of Ca(2+) ions in dendritic spines. Neuron 33:439–452
59. Schmidt H, Eilers J (2009) Spine neck geometry determines spino-dendritic cross-talk in the presence of mobile endogenous calcium binding proteins. J Comput Neurosci 27:229–243
60. Kreiner L, Lee A (2005) Endogenous and exogenous Ca^{2+} buffers differentially modulate Ca^{2+}-dependent inactivation of Ca(v)2.1 Ca^{2+} channels. J Biol Chem 281:4691–4698
61. Lee A, Scheuer T, Catterall WA (2000) Ca^{2+}/calmodulin-dependent facilitation and inactivation of P/Q-type Ca^{2+} channels. J Neurosci 20:6830–6838
62. Kreiner L, Christel CJ, Benveniste M, Schwaller B, Lee A (2010) Compensatory regulation of Cav2.1 Ca^{2+} channels in cerebellar Purkinje neurons lacking parvalbumin and calbindin D-28k. J Neurophysiol 103:371–381
63. Dove LS, Nahm SS, Murchison D, Abbott LC, Griffith WH (2000) Altered calcium homeostasis in cerebellar Purkinje cells of leaner mutant mice. J Neurophysiol 84:513–524

64. Murchison D, Dove LS, Abbott LC, Griffith WH (2002) Homeostatic compensation maintains Ca^{2+} signaling functions in Purkinje neurons in the leaner mutant mouse. Cerebellum 1:119–127
65. Ueno T, Kameyama K, Hirata M, Ogawa M, Hatsuse H, Takagaki Y, Ohmura M, Osawa N, Kudo Y (2002) A mouse with a point mutation in plasma membrane Ca^{2+}-ATPase isoform 2 gene showed the reduced Ca^{2+} influx in cerebellar neurons. Neurosci Res 42:287–297
66. Hu J, Qian J, Borisov O, Pan S, Li Y, Liu T, Deng L, Wannemacher K, Kurnellas M, Patterson C, Elkabes S, Li H (2006) Optimized proteomic analysis of a mouse model of cerebellar dysfunction using amine-specific isobaric tags. Proteomics 6:4321–4334
67. Kurnellas MP, Lee AK, Li H, Deng L, Ehrlich DJ, Elkabes S (2007) Molecular alterations in the cerebellum of the plasma membrane calcium ATPase 2 (PMCA2)-null mouse indicate abnormalities in Purkinje neurons. Mol Cell Neurosci 34:178–188
68. Empson RM, Garside ML, Knopfel T (2007) Plasma membrane Ca^{2+} ATPase 2 contributes to short-term synapse plasticity at the parallel fiber to Purkinje neuron synapse. J Neurosci 27:3753–3758
69. Piedras-Renteria ES, Pyle JL, Diehn M, Glickfeld LL, Harata NC, Cao Y, Kavalali ET, Brown PO, Tsien RW (2004) Presynaptic homeostasis at CNS nerve terminals compensates for lack of a key Ca^{2+} entry pathway. Proc Natl Acad Sci USA 101:3609–3614
70. Nahm SS, Jung KY, Enger MK, Griffith WH, Abbott LC (2005) Differential expression of T-type calcium channels in P/Q-type calcium channel mutant mice with ataxia and absence epilepsy. J Neurobiol 62:352–360
71. Kodama T, Itsukaichi-Nishida Y, Fukazawa Y, Wakamori M, Miyata M, Molnar E, Mori Y, Shigemoto R, Imoto K (2006) A CaV2.1 calcium channel mutation rocker reduces the number of postsynaptic AMPA receptors in parallel fiber-Purkinje cell synapses. Eur J Neurosci 24:2993–3007
72. Oda SI, Lee KJ, Arii T, Imoto K, Hyun BH, Park IS, Kim H, Rhyu IJ (2010) Differential regulation of Purkinje cell dendritic spines in rolling mouse Nagoya (tg/tg), P/Q type calcium channel (alpha1(A)/Ca(v)2.1) mutant. Anat Cell Biol 43:211–217
73. Matsushita K, Wakamori M, Rhyu IJ, Arii T, Oda S, Mori Y, Imoto K (2002) Bidirectional alterations in cerebellar synaptic transmission of tottering and rolling Ca^{2+} channel mutant mice. J Neurosci 22:4388–4398
74. Cicale M, Ambesi-Impiombato A, Cimini V, Fiore G, Muscettola G, Abbott LC, de Bartolomeis A (2002) Decreased gene expression of calretinin and ryanodine receptor type 1 in tottering mice. Brain Res Bull 59:53–58
75. Adams PJ, Rungta RL, Garcia E, van den Maagdenberg AM, MacVicar BA, Snutch TP (2010) Contribution of calcium-dependent facilitation to synaptic plasticity revealed by migraine mutations in the P/Q-type calcium channel. Proc Natl Acad Sci USA 107:18694–18699
76. Tanaka K, Shirakawa H, Okada K, Konno M, Nakagawa T, Serikawa T, Kaneko S (2007) Increased Ca^{2+} channel currents in cerebellar Purkinje cells of the ataxic groggy rat. Neurosci Lett 426:75–80
77. Walter JT, Alvina K, Womack MD, Chevez C, Khodakhah K (2006) Decreases in the precision of Purkinje cell pacemaking cause cerebellar dysfunction and ataxia. Nat Neurosci 9:389–397
78. Leitch B, Shevtsova O, Guevremont D, Williams J (2009) Loss of calcium channels in the cerebellum of the ataxic and epileptic stargazer mutant mouse. Brain Res 1279:156–167
79. Steinert JR, Chernova T, Forsythe ID (2010) Nitric oxide signaling in brain function, dysfunction, and dementia. Neuroscientist 16:435–452
80. Lee JC, Chung YH, Cho YJ, Kim J, Kim N, Cha CI, Joo KM (2010) Immunohistochemical study on the expression of calcium binding proteins (calbindin-D28k, calretinin, and parvalbumin) in the cerebellum of the nNOS knock-out($^{-/-}$) mice. Anat Cell Biol 43:64–71
81. Kim MJ, Chung YH, Joo KM, Oh GT, Kim J, Lee B, Cha CI (2004) Immunohistochemical study of the distribution of neuronal voltage-gated calcium channels in the nNOS knock-out mouse cerebellum. Neurosci Lett 369:39–43

82. Frank-Cannon TC, Zeve DR, Abbott LC (2007) Developmental expression of neuronal nitric oxide synthase in P/Q-type voltage-gated calcium ion channel mutant mice, leaner and tottering. Brain Res 1140:96–104
83. Kriegsfeld LJ, Demas GE, Lee SE Jr, Dawson TM, Dawson VL, Nelson RJ (1999) Circadian locomotor analysis of male mice lacking the gene for neuronal nitric oxide synthase ($nNOS^{-/-}$). J Biol Rhythms 14:20–27
84. Cheron G, Schurmans S, Lohof A, d'Alcantara P, Meyer M, Draye JP, Parmentier M, Schiffmann SN (2000) Electrophysiological behavior of Purkinje cells and motor coordination in calretinin knock-out mice. Prog Brain Res 124:299–308
85. Servais L, Bearzatto B, Schwaller B, Dumont M, De Saedeleer C, Dan B, Barski JJ, Schiffmann SN, Cheron G (2005) Mono- and dual-frequency fast cerebellar oscillation in mice lacking parvalbumin and/or calbindin D-28k. Eur J Neurosci 22:861–870
86. Cheron G, Gall D, Servais L, Dan B, Maex R, Schiffmann SN (2004) Inactivation of calcium-binding protein genes induces 160 Hz oscillations in the cerebellar cortex of alert mice. J Neurosci 24:434–441
87. Cheron G, Servais L, Dan B, Gall D, Roussel C, Schiffmann SN (2005) Fast oscillation in the cerebellar cortex of calcium binding protein-deficient mice: a new sensorimotor arrest rhythm. Prog Brain Res 148:165–180
88. Grimm C, Jors S, Heller S (2009) Life and death of sensory hair cells expressing constitutively active TRPML3. J Biol Chem 284:13823–13831
89. Maskey D, Pradhan J, Kim HJ, Park KS, Ahn SC, Kim MJ (2010) Immunohistochemical localization of calbindin D28-k, parvalbumin, and calretinin in the cerebellar cortex of the circling mouse. Neurosci Lett 483:132–136
90. De Stefani D, Raffaello A, Teardo E, Szabo I, Rizzuto R (2011) A forty-kilodalton protein of the inner membrane is the mitochondrial calcium uniporter. Nature 476:336–340
91. Baughman JM, Perocchi F, Girgis HS, Plovanich M, Belcher-Timme CA, Sancak Y, Bao XR, Strittmatter L, Goldberger O, Bogorad RL, Koteliansky V, Mootha VK. Integrative genomics identifies MCU as an essential component of the mitochondrial calcium uniporter. Nature 476:341–345

Chapter 2
Methods to Detect Ca^{2+} in Living Cells

Joseph D. Bruton, Arthur J. Cheng, and Håkan Westerblad

Abstract Measurements of free cytosolic Ca^{2+} concentration ($[Ca^{2+}]_i$) or free Ca^{2+} concentration in cellular organelles have become more routine. The primary reason for this is the availability of membrane permeant forms of Ca^{2+} indicators that can easily enter cells. In this chapter, the properties required of an ideal Ca^{2+} indicator are identified and the advantages and disadvantages of available Ca^{2+} indicators are pointed out. The pitfalls associated with usage of Ca^{2+} indicators together with the clear advantages of ratiometric over non-ratiometric indicators are discussed. The excitation of Ca^{2+} indicators and detection of the emitted fluorescence light require dedicated equipment; epifluorescence or confocal microscopes are most frequently used for this purpose and the advantages and disadvantages of these are discussed. Calibration experiments are required to translate changes in the fluorescence of Ca^{2+} indicators into real $[Ca^{2+}]_i$ changes, but this procedure is non-trivial and potential sources of error are identified. Future developments in the field of Ca^{2+} detection are discussed.

Keywords Ca^{2+} • Confocal microscopy • Fluorescence • Ratiometric

Calcium (Ca^{2+}) has a key role in numerous cellular processes and measurements of Ca^{2+} are therefore routinely performed in a great variety of studies and experimental conditions. Such measurements are frequently referred to as measurements of cellular or intracellular Ca^{2+} concentration ($[Ca^{2+}]$). However, what is actually measured in most instances is the free Ca^{2+} concentration in the cytosol, although measurements of the Ca^{2+} concentration in different parts of the cell can also be performed. The free Ca^{2+} concentration in the cytosol is often alluded to as $[Ca^{2+}]_i$, which is somewhat misleading since the "i" can easily be interpreted to stand for

J.D. Bruton (✉) • A.J. Cheng • H. Westerblad
Department of Physiology & Pharmacology, Karolinska Institutet, 171 77 Stockholm, Sweden
e-mail: Joseph.Bruton@ki.se

M.S. Islam (ed.), *Calcium Signaling*, Advances in Experimental Medicine and Biology 740, DOI 10.1007/978-94-007-2888-2_2,

intracellular. It might then be asked whether the distinction between intracellular [Ca^{2+}] and free cytosolic [Ca^{2+}] really matters. The answer is: Yes, in many cases there is a large difference between the two. For instance, in this chapter we will give several examples of Ca^{2+} measurements in adult skeletal muscle cells. When these cells are activated, the free cytosolic [Ca^{2+}] (i.e. $[Ca^{2+}]_i$) may increase more than 100-fold in a few ms, whereas the intracellular [Ca^{2+}] remains virtually constant. The increase in $[Ca^{2+}]_i$ here occurs as a consequence of Ca^{2+} being released into the cytosol from an organelle, the sarcoplasmic reticulum. Thus, Ca^{2+} moves from one cellular compartment to another and the total intracellular [Ca^{2+}] is not changed.

The development of an astonishing range of fluorescent Ca^{2+} indicators that can be easily introduced into cells has given many the chance to measure $[Ca^{2+}]_i$ in their cells. Since many users are non-experts and simply follow the often sketchily described methods in earlier papers in their field of research, the likelihood of errors and misinterpretation of data has increased. The aim of this chapter is to point out what is and is not possible with available Ca^{2+} indicators and how pre-existing equipment can be used to acquire data.

Methods to Measure $[Ca^{2+}]_i$ Before the Era of Fluorescent Ca^{2+} Indicators

Measurements of $[Ca^{2+}]_i$ were rather complicated before the invention of the various fluorescent Ca^{2+} indicators that are commonplace today. Methods that were used include:

1. *Ca^{2+}-selective microelectrodes*. These electrodes are rather difficult to make, especially to make the tip of the electrode small enough so that not only very large cells can be penetrated without causing cell damage. The response time of Ca^{2+}-selective microelectrodes is also rather slow, on the order of seconds, and hence rapid $[Ca^{2+}]_i$ transients cannot be detected. However, microelectrodes with improved properties have been developed and are used in certain conditions [1].
2. *Ca^{2+}-activated photoproteins*. These proteins, of which aequorin was the most popular, emit blue light and the rate of light emission increases dramatically in response to increased $[Ca^{2+}]_i$ [2]. A major advantage with these photoproteins is that they do not require any stimulating light and hence the background signal is very low. In the high physiological range of $[Ca^{2+}]_i$ (0.5–10 μm), the light emission of aequorin increases as approximately the third power of [Ca^{2+}]. This means that translating the light signal into actual values of $[Ca^{2+}]_i$ is rather complicated and if $[Ca^{2+}]_i$ differs within the cell, the signal will be heavily dominated by the regions with the highest $[Ca^{2+}]_i$. Moreover, the light emitted by aequorin depends not only on $[Ca^{2+}]_i$, but also on factors such as the concentration of Mg^{2+} and the ionic strength. The Ca^{2+}-activated photoproteins can be seen as “precharged” and Ca^{2+} binding triggers an energy-consuming reaction where light is produced. Each molecule emits light only once, which means that

the light-emitting capacity declines over time. A major problem with photoproteins is to introduce them into the cell. In large cells this can be achieved by microinjection, but this method is not suitable for small cells. Various cell fusing techniques have been developed but these also have drawbacks. A more recent approach is to transfect cells to induce transient or stable expression of recombinant aequorin [3]. This technique can be easily used with various cultured cells, whereas transfection can be difficult in adult cells. A major advantage with this technique is that the usage of recombinant proteins allows targeting to different cellular compartments (e.g. mitochondria, endoplasmic reticulum or surface membrane) and the Ca^{2+} binding properties can be modified, for instance, in order to optimize the Ca^{2+} sensitivity or to enhance the kinetics. Thus, photoprotein-based methods to measure $[Ca^{2+}]_i$ are still being used because in some situations they can be advantageous as compared to fluorescent indicators. It should be noted that bioluminescence emitted is quite small and the need for an efficient optical system to collect the light is more stringent than for most of the currently used fluorescent indicators.

3. *Bis-azo metallochromic Ca^{2+} dyes*. There are two dyes in this class of Ca^{2+} indicators: arsenazo III and antipylazo III. The property that makes them useful as Ca^{2+} indicators is that their light absorbance depends on the $[Ca^{2+}]$. An advantages with these indicators is that they are fast and therefore can detect rapid $[Ca^{2+}]_i$ transients. They display a relatively low Ca^{2+} affinity, which means that they readily can detect high $[Ca^{2+}]_i$ levels and show little Ca^{2+} buffering. However, there are also major disadvantages, which include complex Ca^{2+}-binding properties, marked Mg^{2+} and pH sensitivity, and a large tendency to bind to intracellular proteins. Moreover, the metallochromic Ca^{2+} dyes cannot pass the cell membrane so when using intact cells, these dyes have to be e.g. microinjected. Thus, these dyes are seldom used now.

Fluorescent Ca^{2+} Indicators

By far the most common Ca^{2+} indicators in use today are derived from the Ca^{2+} chelators EGTA and BAPTA. These indicators have high affinity and one-to-one stoichiometry for Ca^{2+}. They display low affinity for Mg^{2+} and H^+ and when Ca^{2+} binds to them, there are large absorbance and fluorescence changes [4]. It should be remembered that even with their low affinity for Mg^{2+} and H^+, Ca^{2+} indicators will be affected by these ions in experiments that are designed to induce metabolic depletion or large changes in pH. The indicator molecule consists of two parts: the Ca^{2+}-binding part that changes its shape when Ca^{2+} binds to it and which in turn alters the conformation of the fluorescent part of the molecule. Much work has gone into developing different Ca^{2+}-binding properties and fluorescent tails that are optimised to work in defined ranges of $[Ca^{2+}]$ and with different types of detection systems.

Ca^{2+} indicators fall into one of two groups: dual-wavelength ratiometric indicators and single-wavelength non-ratiometric indicators. Most indicators have well-characterised absorption and emission spectra. The optimal excitation and emission wavelengths for individual indicators can generally be found in the papers where they were originally described. In addition, this information has been collected in the Molecular Probes Handbook, which can be found on the Invitrogen Life Technologies website, http://www.invitrogen.com/site/us/en/home/References/Molecular-Probes-The-Handbook.html.

Non-ratiometric indicators generally have very little fluorescence at low (<100 nm) $[Ca^{2+}]$ and show up to a 100-fold increase in fluorescence when $[Ca^{2+}]$ is increased so that the indicator becomes saturated with Ca^{2+}. Ratiometric indicators have the advantage that the Ca^{2+}-free and Ca^{2+}-bound forms of the indicator have distinct peaks at different wavelengths and thus measurements can be made at the two separate peaks and combined into a ratio. This ratio is mostly constructed so that the wavelength where the fluorescence shows a maximum at high $[Ca^{2+}]$ and minimum at low $[Ca^{2+}]$ is divided by the wavelength showing the opposite (i.e. maximum at low $[Ca^{2+}]$ and minimum at high $[Ca^{2+}]$). Between the two wavelength peaks there is an isosbestic point where the fluorescence does not depend on $[Ca^{2+}]$. In some cases it can be advantageous to use the wavelength at the isosbestic point in the ratio. For instance, the classical ratiometric indicator fura-2 requires excitation at two wavelengths while the emitted fluorescent light is measured at one wavelength (~510 nm). The isosbestic point for fura-2 excitation is ~360 nm and with increasing $[Ca^{2+}]$, the emitted light increases at shorter wavelengths and decreases at longer wavelengths. The ratio with maximal dynamic range is then obtained by excitation below (~340 nm) divided by above (~380 nm) the isosbestic point. However, this requires continuous alteration between 340 and 380 nm excitation, which is technically troublesome, especially if rapid $[Ca^{2+}]_i$ transient are being measured. An alternative is then to use the isosbestic point when constructing the ratio because the 360 nm signal does not depend on $[Ca^{2+}]$ and therefore only has to be measured at regular intervals to check for a general decline in signal. The preferred ratios will then be 340/360 or 360/380, which both will show an increase when $[Ca^{2+}]$ increases, albeit the ratio increase will not be as large as for the 340/380 ratio.

In the case of the non-ratiometric indicators, the property that is measured is the intensity of the emitted fluorescent light. The expectation is that this light signal mainly reflects $[Ca^{2+}]_i$, which is probably true under ideal conditions. However, to be able to directly compare signals from different experiments the following requirements have to be fulfilled: (1) cells exposed to similar loading conditions will have similar concentrations of indicator; (2) indicators remain in the cytosol and do not leak or get pumped out of the cytosol; (3) cell volume remains constant and there is no change in cell thickness; (4) the cell(s) does not move; (5) the indicator is not affected by repeated exposure to excitation light. Unfortunately all these requirements are almost never fulfilled and so the results obtained with non-ratiometric indicators have to be carefully assessed and possible errors have to be controlled for. The situation is less critical for ratiometric indicators, because changes in indicator

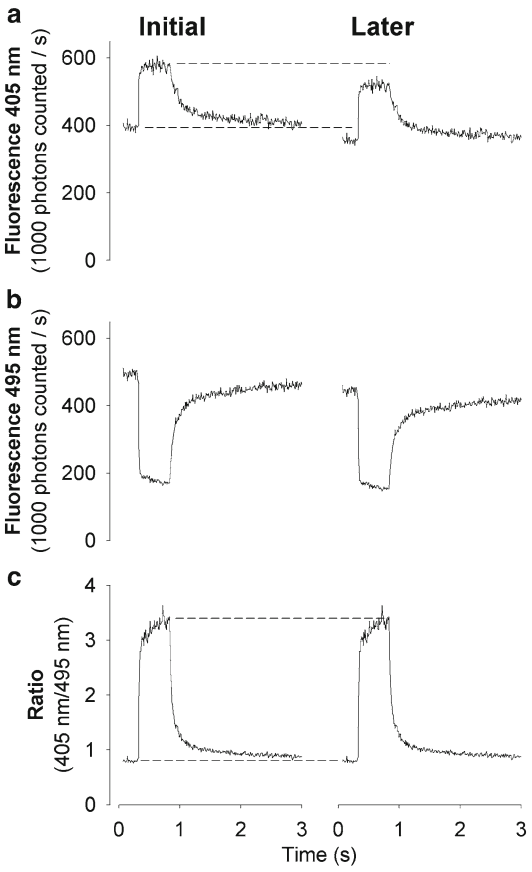

Fig. 2.1 *Ratiometric indicators show large advantages during prolonged experiments.* Indo-1 records obtained in a skeletal muscle cell stimulated to perform a tetanic contraction (70 Hz stimulation for 350 ms). Indo-1 was excited at 360 nm and the emitted light was measured simultaneously at 405 nm (**a**) and 495 nm (**b**) and the 405/495 ratio was constructed (**c**). Note that over time, the ratio signal remained constant (*dashed lines* in **c**) while the fluorescence intensity decreased for both the 405 nm (*dashed lines* in **a**) and 495 nm signal. Note that the decline in the 405 nm trace shown in **a** is qualitatively similar to what would be seen if fluo-3 or other non-ratiometric indicator was used

concentration and cell volume, as well as cell movement, will affect measurements at both wavelengths equally and will cancel each other out when a ratio is made. This fundamental advantage of ratiometric indicators is examplified in Fig. 2.1, which shows fluorescence records from a single skeletal muscle fiber at rest and during stimulation to produce a maximum contraction. Figure 2.1a shows the results as they would appear with a single wavelength indicator. As the experiments progressed, the fluorescent signal showed a general decline, which might then be interpreted as a decrease in $[Ca^{2+}]_i$ both in the basal state and during contraction. However, the ratiometric indicator indo-1 was used in the experiment. In contrast to fura-2, this indicator is excited at one wavelength (~360 nm) and the emitted light is measured at two wavelengths (405 nm (increased signal with increasing $[Ca^{2+}]_i$) and 495 nm (decreased signal with increasing $[Ca^{2+}]_i$) in the depicted experiment). Figure 2.1b shows that there was a general decrease also in 495 nm signal as the experiment progressed. This means that there was no change in the 405/495 ratio with time (Fig. 2.1c), which correctly reflects that there was no change in $[Ca^{2+}]_i$. Thus, this example clearly illustrates that uncritical usage of signals from

non-ratiometric indicators can result in completely erroneous conclusions. It should, however, be noted that not all problems are avoided by using ratiometric indicators. For instance, excessive light exposure can lead to qualitatively altered properties of the indicator, which cannot be corrected for by ratios.

How Does One Decide on Which Ca^{2+} Indicator to Use?

As explained above, ratiometric indicators have major advantages compared to non-ratiometric indicators and should therefore be used if this is possible. In addition there are several other aspects to consider. First one has to use an indicator with excitation and emission wavelengths that the available equipment can deal with. For ratiometric indicators this can be a serious problem because the most common of these (i.e. fura-2 and indo-1 and their close relatives mag-fura-2 and mag-indo-1) are excited by UV light, which is not available in many systems. For instance, lasers are the most common light source in confocal microscopes (see below) and UV lasers are not commonplace. On the other hand, finding a non-ratiometric indicator with suitable wavelengths is less of a problem, because these often come in many different versions with different excitation and emission wavelengths.

In principle, one would always like to use an indicator which gives a fluorescence signal with little noise that shows large changes when $[Ca^{2+}]_i$ is changing and which is fast enough to follow the changes in $[Ca^{2+}]_i$ under study. However, the perfect indicator does not exist because some properties are difficult, or even impossible, to combine. For instance, a Ca^{2+} indicator showing large changes in fluorescence with $[Ca^{2+}]_i$ changes in the low physiological range (~100 nm) is relatively slow and the opposite is also true. The relation between the intensity of the fluorescent signal (F) and $[Ca^{2+}]_i$ for a non-ratiometric indicator is given by the following Eq. 2.1:

$$\left[Ca^{2+}\right]_i = K_d * \left(F - F_{min}\right) / \left(F_{max} - F\right), \tag{2.1}$$

where F_{min} and F_{max} is the fluorescence intensity at virtually zero and saturating $[Ca^{2+}]_i$, respectively. K_d is the dissociation constant. In a plot of F against $[Ca^{2+}]_i$, K_d is the $[Ca^{2+}]$ where F is half-way between F_{min} and F_{max} and this is where the indicator displays its largest sensitivity. K_d is decided by the indicator's rate of Ca^{2+} binding (K_{on}) and dissociation (K_{off}), i.e. $K_d = K_{off}/K_{on}$. The rate that mainly differs between indicators is K_{off}. Accordingly, a slow indicator (low K_{off}) has a low K_d, which means that it is most sensitive at relatively low $[Ca^{2+}]_i$ and such indicators are therefore called high-affinity indicators. Conversely, a fast indicator has a high K_d and is referred to as a low-affinity indicator.

For ratiometric indicators, a slightly more complex equation describes the relation between fluorescence ratio (R) and $[Ca^{2+}]_i$ (Eq. 2.2):

$$\left[Ca^{2+}\right]_i = K_d * \beta * \left(R - R_{min}\right) / \left(R_{max} - R\right), \tag{2.2}$$

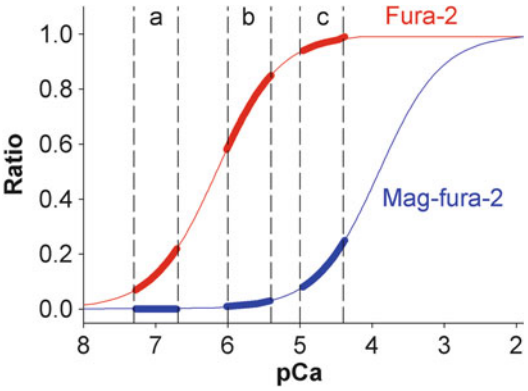

Fig. 2.2 *High-affinity Ca^{2+} indicators are more sensitive to stable changes in $[Ca^{2+}]_i$ within the normal physiological range.* The relation between $[Ca^{2+}]_i$ and fluorescence ratio (340 nm/380 nm excitation) for the high-affinity indicator fura-2 and the low-affinity indicator mag-fura-2. $[Ca^{2+}]_i$ expressed as pCa ($-\log[Ca^{2+}]_i$) in order to cover a larger range of concentrations. (*a*) 50–200 nM; (*b*) 1–4 μM; (*c*) 10–40 μM

where R_{min} and R_{max} is the fluorescence ratio at virtually zero and saturating $[Ca^{2+}]_i$, respectively. β is obtained by dividing the fluorescence intensity of the ratio's second wavelength (denominator) acquired at virtually zero and saturating $[Ca^{2+}]_i$, respectively. Thus, the mid-point between R_{min} and R_{max} occurs at a $[Ca^{2+}]_i$ that equals $K_d * \beta$.

Figure 2.2 illustrates how the properties of two different Ca^{2+} indicators affect the change in fluorescence signal observed when $[Ca^{2+}]_i$ is changed in different concentration intervals. The comparison is between one high-affinity indicator, fura-2, and a low-affinity indicator, mag-fura-2. The name mag-fura-2 comes from the fact that it was designed to measure $[Mg^{2+}]$, but it is mostly used as a low-affinity Ca^{2+} indicator since $[Mg^{2+}]$ seldom shows significant changes in the cytosol. $[Ca^{2+}]_i$ may vary dramatically between different physiological states. For instance, $[Ca^{2+}]_i$ peaks during contraction in a skeletal muscle cell may be up to 1,000-fold higher than resting $[Ca^{2+}]_i$. $[Ca^{2+}]_i$ is therefore often expressed as pCa, which equals $-\log[Ca^{2+}]_i$ (analogous to the concept of pH). In Fig. 2.2, the 340/380 ratio is used for both indicators and β is set to 4. This means that the mid-point between R_{min} and R_{max} occurs at a $[Ca^{2+}]_i$ of 0.56 μm for fura-2 (K_d assumed to be 0.14 μm) and 100 μm for mag-fura-2 (K_d assumed to be 25 μm). The interval (a) in Fig. 2.2 shows the change in ratio signal obtained when $[Ca^{2+}]_i$ is changed in the range of normal resting values, from 50 nM to 200 nM. Here the fura-2 ratio signal shows a substantial increase, whereas mag-fura-2 ratio signal is hardly affected at all. Thus, fura-2 readily detects changes in basal $[Ca^{2+}]_i$, whereas mag-fura-2 is not a good indicator in this respect. The interval (b) in Fig. 2.2 (1–4 μM) would reflect $[Ca^{2+}]_i$ in cells that are in an activated state. Again fura-2 is a rather sensitive indicator in this interval, whereas mag-fura-2 shows little change in the ratio signal. Finally (c) reflects $[Ca^{2+}]_i$ (10–40 μM)

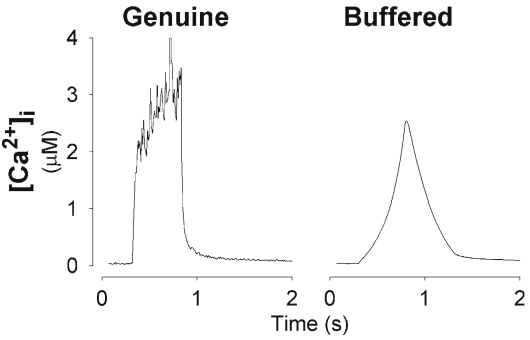

Fig. 2.3 *Excessive cytosolic loading of Ca^{2+} indicator results in noise-free but distorted $[Ca^{2+}]_i$ transients.* The records illustrate the genuine $[Ca^{2+}]_i$ response to tetanic stimulation of a skeletal muscle cell and the response as it would look like with an excessive amount of Ca^{2+} indicator that buffers the $[Ca^{2+}]_i$ changes

in a condition with maximal activation. In this case, fura-2 is reaching saturation, whereas mag-fura-2 readily detects the change in $[Ca^{2+}]_i$.

As a rule of thumb, Ca^{2+} indicators readily detects changes in $[Ca^{2+}]_i$ in an interval between about tenfold below and tenfold above the mid-point, i.e. K_d for non-ratiometric indicators and $K_d * \beta$ for indicators used in the ratiometric mode. This is also the $[Ca^{2+}]_i$ interval where Ca^{2+} most easily binds to the indicator, which introduces a problem with buffering. The noise in the detected fluorescent light signal decreases with increasing light intensity. From this perspective it is advantageous to have a large concentration of fluorescent indicator in the studied cell(s). However, a large concentration of indicator with a K_d in the physiological $[Ca^{2+}]_i$ range will also buffer $[Ca^{2+}]_i$ and this is illustrated in Fig. 2.3: with a relatively low concentration of indicator ("Genuine") a rapid and relatively large change in $[Ca^{2+}]_i$ is recorded but the signal contains some irregular fluctuations (noise); a markedly higher concentration of indicator ("Buffered") gives a virtually noise-free signal but the time course of the increase and decrease of $[Ca^{2+}]_i$ is slowed and the amplitude of the change decreased. Thus, with high-affinity Ca^{2+} indicators there is a delicate balance between a sufficiently high indicator concentration to obtain records with a low noise level and that producing cytosolic Ca^{2+} buffering, which leads to distorted $[Ca^{2+}]_i$ signals and often also to altered cell function.

Figure 2.2 shows that a high-affinity Ca^{2+} indicator is better than a low-affinity indicator at monitoring changes in $[Ca^{2+}]_i$ in the normal physiological range. However, the diagram in Fig. 2.2 refers to stable or slowly changing $[Ca^{2+}]_i$. As discussed above, a trade-off of high Ca^{2+} sensitivity is that the indicator may be too slow to follow rapid changes in $[Ca^{2+}]_i$. In Fig. 2.4 this is illustrated for $[Ca^{2+}]_i$ transients in a skeletal muscle cell. The $[Ca^{2+}]_i$ transient in response to a single stimulation pulse has a duration of ~10 ms. Figure 2.4a shows such a $[Ca^{2+}]_i$ transient as recorded with the high-affinity indicator indo-1. This indicator is not fast enough to accurately follow the rapid changes in $[Ca^{2+}]_i$ and the recorded transient is too slow and the amplitude too low. In Fig. 2.4b the signal has been corrected for the slow response of indo-1 and a $[Ca^{2+}]_i$ signal which better represents the true transient is then obtained. A low-affinity Ca^{2+} indicator would be able to follow the $[Ca^{2+}]_i$ transient more accurately and is therefore preferable in experiments where rapid $[Ca^{2+}]_i$ changes are being studied; the drawback though being the magnitude of change in fluorescent signal is going to be small and hence difficult to monitor. Figure 2.4c

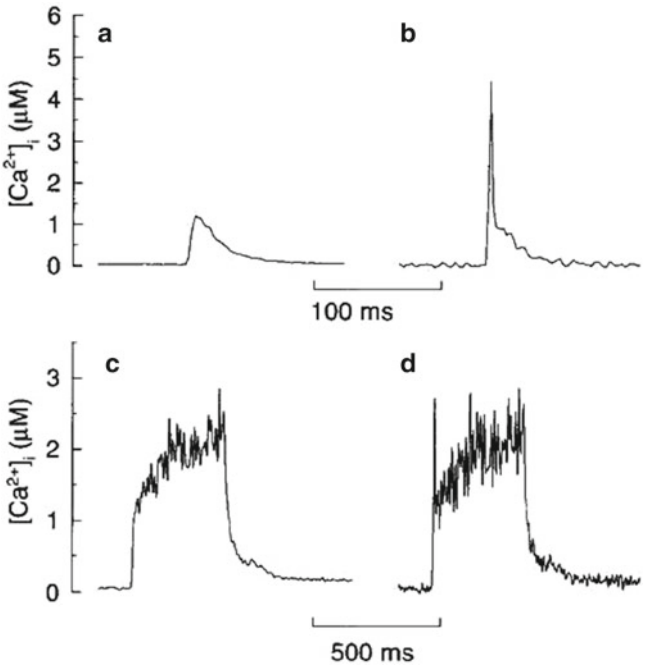

Fig. 2.4 *Fast low-affinity Ca^{2+} indicators are required to accurately follow rapid $[Ca^{2+}]_i$ transients.* $[Ca^{2+}]_i$ records measured with indo-1 in a skeletal muscle cell in response to a single stimulation pulse (**a**) and a tetanus (**c**). This high-affinity indicator is too slow to accurately follow the most rapid changes in $[Ca^{2+}]_i$. Kinetic correction reveals a faster and larger $[Ca^{2+}]_i$ transient with the single stimulation pulse (**b**) and a $[Ca^{2+}]_i$ spike at start of the tetanus (**d**) (Figure adapted from Westerblad and Allen [5])

shows $[Ca^{2+}]_i$ as recorded by indo-1 during tetanic stimulation (70 Hz, 350 ms duration) of the muscle cell; in Fig. 2.4d the record is corrected for the slow response of indo-1. It can be that the initial "spike" of $[Ca^{2+}]_i$ is missed without correction, but otherwise the records are rather similar. To sum up, Fig. 2.4 thus illustrates that problems with slow, high-affinity Ca^{2+} indicators are substantial when recording rapid $[Ca^{2+}]_i$ transients but much less so during more prolonged $[Ca^{2+}]_i$ changes. Thus, again there is a delicate balance, which in this case is between being able to follow large and rapid $[Ca^{2+}]_i$ changes (low-affinity indicators are preferable) and small prolonged changes (high-affinity indicators are better).

The signals from the detectors of the fluorescent light are nowadays almost always stored on a computer. The rate at which the signals are sampled is then another factor to consider. The sampling rate should be coordinated with the Ca^{2+} indicator used, i.e. a lower sampling rate with a slow high-affinity indicator than with a fast low-affinity indicator. Sampling theorems can be used to decide what the optimal sampling rate is. As a general rule, we use a sampling rate at least tenfold faster than the expected fastest speed of $[Ca^{2+}]_i$ transients under study. Also in this case there is a fine balance. A high sampling rate means that less light signal is integrated for each time point and hence the noise level is higher with fast than with

slow sampling. On the other hand, rapid $[Ca^{2+}]_i$ transients might be missed or distorted with a lower sampling rate.

How Does One Introduce Indicators into Cells?

Indicators are charged molecules and do not easily pass lipid membranes. While many cells display endocytotic behaviour, the amount of indicator that can enter the cell via this mechanism is insufficient to make meaningful measurements. Ca^{2+}-indicator can be introduced into cells by pressure injection or electrophoreses using a microelectrode or patch electrode. Alternatively, one could electroporate the cell membrane, which means using very brief, high voltage pulses to form transient small pores in the cell membrane through which the indicator can pass. Both of these techniques require specialised equipment and some skill, but they have the advantage that the charged indicator will be located in the cytosol and not penetrate into sub-cellular compartments, such as the mitochondria or sarco-endoplasmic reticulum.

Fortunately for users, there is a much easier method for introducing large quantities of fluorescent indicator into the cytoplasm of single or multiple cells. In fact, the existence of a simple method to transport fluorescent indicators into cells is a major reason behind the great success of these indicators. The principle behind the method is that lipophilic groups (e.g. acetoxymethyl (AM) groups) are added to the charged indicator molecule. In this way the charges are hidden and the indicator complex becomes lipophilic and hence membrane-permeant. Once the complex has entered into the cytosol, cytoplasmic esterases gradually cut off the lipophilic groups and the free indicator molecule is then trapped in the cytosol and ready to detect $[Ca^{2+}]_i$ [4].

The lipophilic indicator complex is typically dissolved in dimethylsulfoxide (usually written as DMSO) and the detergent Pluronic is often added to disperse the indicator molecules and aid loading. Typically, cells are bathed in a solution with a final indicator concentration of 1–10 μM and loaded for 10–30 min. After the loading period is finished, the cells must be washed to remove residual extracellular indicator and left for a further 30 min to ensure that all lipophilic groups have been cleaved off by cytoplasmic esterases.

The method with loading of lipophilic indicator complexes is not completely without problems. For instance, the amount loaded cannot be directly controlled and there is a risk of excessive loading. This may then results in additional buffering of $[Ca^{2+}]_i$, which affects $[Ca^{2+}]_i$ measurements as well as Ca^{2+}-dependent cellular signaling. Furthermore, the lipophilic indicator complex may pass across intracellular membranes into organelles and, if the lipophilic groups are cleaved off in the organelle, detect $[Ca^{2+}]$ in this organelle instead of in the cytosol. These problems seem to be minimised when cells are loaded at room temperature rather than at the higher physiological temperature of mammals. There are no universal guidelines for optimal loading of cells and the best loading procedures need to be established for

each new combination of indicator and cell. For example in our hands, indo-1 AM does not load while fluo-3 AM readily loads into mouse cardiac myocytes.

Equipment Overview

Typically, the instruments used are those that are available rather than those that are optimal for a given task. In order to detect the fluorescence emitted from selected cells containing an indicator, one needs a microscope with a light source that can be applied to excite the indicator and a detection device that is typically one or more photomultiplier tubes or a CCD camera; a simpler fluorometer system not based on a microscope can be used if one is working with e.g. cell suspensions and not interested in the response of individual cells. Filters can be inserted into the light path to limit the wavelength and intensity of the light that excites the indicator and also to limit the wavelengths of the light that are measured by the light detectors. The signals from the light detectors are generally stored on a computer. In most cases the experimental set-up used for measurements with fluorescent indicators comes with software controlling various parameters related both to light excitation and to detection of the emitted light.

The most important but often neglected part of the whole acquisition system is the objective lens. The lens is what allows one to magnify and focus on the cell or tissues. While magnification is important to see the sample, what is equally or more important is the ability of the lens to collect light and resolve fine specimen detail. The effectiveness to collect light is described by the numerical aperture (N.A.) written on the lens casing. In general, one should have the lens with the highest N.A. possible (for more details see http://micro.magnet.fsu.edu/primer/anatomy/numaperture.html). It should be noted that lenses that are optimised to work with ultraviolet (UV) light are not optimal for visible light and vice versa. The lens is exposed to the environment unlike most of the other elements of the system, which are encased in protective housing. Even if an acquisition system is handled carefully, the lens is liable to become dirty from the floating dust in the air. If the lens requires oil or water for its proper operation, the combination of liquid and dust can lead rather quickly to the formation of a film coating the lens surface and the light path deteriorates. Similarly if a superfusion system is used, leakage or overflow of fluid can lead to salt deposits on the lens or, in the worst case scenario, fluid enters the lens casing resulting in solution coating both the outside and inside of the lens. Problems of this kind will become apparent as increased noise in the fluorescence signal and in the worse cases result in difficulties in focussing on the cells or tissue. Thus, the lens should always be checked before and at the end of the experiment. It should become routine to use lens paper or an air spray to clean the lens before and after experiments or immediately one observes that solution has dripped on to the lens surface. If solution has dried on the lens, lens paper moistened with distilled water can be used to wipe the lens and finally lens paper moistened with ethanol is used to clear off residual water.

The two most common types of detection set-ups are epifluorescence microscopy and confocal microscopy. In epifluorescence microscopy, excitation light illuminates

the whole sample and emitted light from the indicator is collected not just from the section that is in focus but also from above and below this plane of focus. Emitted light travels to one or more photomultiplier tubes or a CCD camera. Epifluorescent microscopy has been used with ratiometric dyes such as indo-1 or fura-2 that are excited with light in the UV region. This type of set-up is ideal for measuring changes in $[Ca^{2+}]_i$ in virtually any cell type over extended periods of time while using mechanical, electrical or chemical stimulation. The area of interest can be limited to a single cell or data can be collected from a larger number of cells. While this method allows one to measure from the total volume of the cell, it is difficult (or with photomultiplier tubes basically impossible) to focus in on particular areas of the cell and visualise discrete events, such as, the entry of extracellular Ca^{2+} through surface membrane Ca^{2+} channels. However, when combined with special indicators, one can measure $[Ca^{2+}]$ changes in discrete organelles. For example, rhod-2 is a Ca^{2+}-indicator that loads preferentially into the mitochondria and indo-5N can be used for measurements in the endo-sarcoplasmic reticulum. Moreover, fatty chains have been attached to the indicator moiety and these preferentially anchor themselves into the surface membrane allowing the indicator molecule to dangle just below the surface membrane and measure changes in $[Ca^{2+}]$ close to the membrane rather than in the bulk of the cytoplasm (further details can be found here, http://www.teflabs.com/ion-indicators/near-membrane-indicators/).

Generally confocal microscopes rely on pretty much the same hardware and software as that used in epifluorescence microscopy with two important additions: a point light source to excite the indicator and a pinhole in the emission pathway that when opened to its optimal size allows passage only of light from the focal plane, i.e. blocking light from above and below the plane of focus. The fundamental advantage of the confocal microscope is that one limits the focus to a very narrow plane and can in this way detect discrete or rapid events such as localised release/entry of Ca^{2+} into the cytoplasm. A common misconception is that the light from a laser is essential for a confocal microscope to work. However, while most confocal microscopes use lasers as light sources, this is not essential and indeed the original patent did not use a laser light source (see http://web.media.mit.edu/~minsky/papers/ConfocalMemoir.html).

Laser confocal microscopes are made in three basic designs. These are (1) laser scanning, (2) the Nipkow or spinning disk, and (3) two- or multi-photon versions.

1. The laser scanning confocal microscope is a ubiquitous instrument in virtually every biological or medical science department. This device relies on the fact that a laser is a point source of light, which is moved rapidly from point to point (pixel to pixel) along a horizontal line. This movement is achieved by means of a galvanometer-controlled or resonant-oscillating pair of mirrors. To build up a two dimensional image, the laser beam is moved vertically to a new line using a second pair of mirrors. This procedure is then repeated until a full frame is obtained. This obviously takes a finite period of time and does not give an instantaneous view of what is happening in the cell. One can increase the scanning speed and obtain a full frame two to three times faster by reducing the “dwell time”, i.e. the time for which the laser illuminates each pixel. The disadvantage of doing this is

that the signal to noise ratio is reduced, which limits the ability to monitor small, spatially restricted changes in the fluorescence signal. If temporal resolution of a Ca^{2+} event in the cell is critical, the best approach is to abandon the two dimensional image acquisition approach and use the line scan mode instead. In this configuration, the laser beam scans the same line sequentially for a period of time. On the newer laser scanning confocal microscopes, line scans can be performed at over 1 kHz which probably is sufficiently fast to resolve even the fastest Ca^{2+} events in a cell. The trade-off for the increased speed of data acquisition with line scanning is that only a single plane in a portion of the cell or tissue can be monitored. The line scan mode is obviously extremely useful if one, for example, is monitoring localised transient releases of Ca^{2+} from the sarcoplasmic reticulum in muscle or trying to localise the sites of Ca^{2+} entry in a neuron.

2. The Nipkow or spinning disk laser confocal microscope uses a spinning disk (spins at several thousand revolutions per minute) with multiple pinholes (>1,000) through which parallel light beams pass. These beams excite the fluorescent indicator in the cell and the emitted light returns through the pinholes to the detection device, which is normally a very sensitive CCD camera operated at low temperatures to minimise noise. Commercial spinning disk confocal microscopes can now acquire images at rates of up to 50 frames per second, which makes them suitable for visualizing temporal and spatial $[Ca^{2+}]$ changes in cells. This may generate excessive amounts of data but the accompanying software is usually sophisticated enough so that regions that are decided to be of no interest can be masked or hidden and only data from defined areas will be acquired and saved. The limited popularity of these confocal microscopes may in part be due to the trade-off between spatial resolution and speed, i.e. greater spatial resolution generally requires a slower frame rate of acquisition.
3. The two- or multi-photon confocal microscopes limit problems occurring when deeper parts of cells or tissues are being studied. Virtually every confocal microscope is fitted with a motorised drive that allows one to move the plane of focus up or down in steps smaller than 1 μm. Thus, one can theoretically build up a three dimensional image of a cell or tissue and check for possible inhomogeneous change in $[Ca^{2+}]$ in response to a stimulus. However, in practice one finds that the image quality obtained with a simple laser confocal scanning microscope deteriorates as one penetrates deeper into a cell or tissue with a decline in both resolution and fluorescence intensity. In an ordinary laser confocal scanning microscope, the laser beam consists of a continuous stream of photons. When a single photon hits an indicator molecule, the indicator molecule is excited and transiently lifted from its ground state to a higher energy state. It remains in this higher energy state for a few picoseconds and then decays back to its original ground state by emitting a photon with a longer wavelength than the original photon. Unfortunately, light does not travel in an empty space as it passes through a cell. Instead the photons emitted by the fluorescent indicator will hit solid constituents (e.g. proteins and fats) and become deflected. The longer the distance that the photons must travel, the greater will be the number of photons from the focal plane that are lost. In addition, because of light deflection and scattering, some photons from areas that were not part of the original focus will be delivered to the light detector.

A two- or multi-photon laser confocal scanning microscope reduces these problems. This technique has long been used by physicists, but its usage in biological applications is relatively recent. The technique is based on the fact that the same excitation of an indicator molecule can be obtained by two photons each with twice the wavelength and half of the energy of a single photon. Longer wavelength light can penetrate deeper into tissues and cells. In a two- or multi-photon laser, the photons are sent out in femtosecond bursts. They do not have sufficient energy to excite indicator molecules on their travel to the focal point. At the focal point, on the other hand, there is a high density of photons and the probability of two or more photons colliding with an indicator molecule are high. Thus, it is only at the focal point that any indicator molecule can absorb two photons and be raised from its ground state to an excited, photon-emitting state.

As anybody who has been sunburnt knows, prolonged exposure to ultraviolet light causes skin damage. In a similar way, the experience of seeing cells die as one tries to obtain the best record or image emphasises that light energy is dangerous to cells. While this is an extreme example of photodamage, one should be aware that the energy that each photon of light contains may impact on the measurements being made and should try to limit the intensity of the light to the minimum possible. An additional potential problem with light and virtually all Ca^{2+} indicators is photodegradation or photobleaching whereby the indicator is converted into a fluorescent but Ca^{2+} insensitive form that results in false measurements of resting and transient changes in $[Ca^{2+}]_i$ [6]. Again, the problem can be avoided by minimising the intensity and duration of light exposure. One advantage of a multiphoton laser confocal microscope is that it reduces the energy load that a cell receives.

Calibration

Some kind of calibration is required in order to translate fluorescence signals into $[Ca^{2+}]_i$. The first thing that must be taken into account before any calibration is attempted is to recognise that there is always some background signal in fluorescence systems, e.g. because of imperfect filters and some of the excitation light reaching the detectors. Moreover, each tissue or cell displays intrinsic or auto-fluorescence. The autofluorescence arises predominantly from metabolites, nicotinamide adenine dinucleotide and to a far lesser extent from flavin adenine dinucleotide. The amount of background and intrinsic fluorescence depends on the excitation and emission wavelengths being used. It is advisible to measure the background and intrinsic fluorescence in a sample before loading the Ca^{2+} indicator and to subtract this value from all subsequent measurements. Failure to do this may have dramatic effects on the translation of the indicator signals into $[Ca^{2+}]_i$. Complete and accurate calibrations are generally very difficult, or even impossible, to perform and some simplifications must be allowed. However, there is an increasing tendency to completely ignore calibrations and simply take the viewpoint that the fluorescent light intensity (F, non-ratiometric indicators) or ratio (R, ratiometric indicators) of Ca^{2+}

indicators is linearly related to $[Ca^{2+}]_i$, which clearly is a severe oversimplification (e.g. see Fig. 2.2). Numerous papers erroneously state that $[Ca^{2+}]_i$ increased/decreased by x%, whereas what was actually measured was an increase/decrease in fluorescence intensity or ratio of x%, which can represent markedly different changes in $[Ca^{2+}]_i$. For instance, a minimal (<1%) change in fluorescence signal measured in a resting cell with a low-affinity indicator may represent a several-fold change in $[Ca^{2+}]_i$ (see Fig. 2.2). Similarly, a major increase in $[Ca^{2+}]_i$ may result in only a small increase in the fluorescence signal of a high-affinity indicator because the indicator was close to saturated with Ca^{2+} already before the increase.

Ca^{2+} indicators are affected by the fluid environment and hence their properties display major differences in the cytosolic milieu as compared to in simple salt solutions. The relationship between fluorescence signals and $[Ca^{2+}]_i$ also differs between different experimental set ups. This means that all parameters in Eqs. 2.1 and 2.2 required to translate fluorescence signals into $[Ca^{2+}]_i$ basically have to be established in the cell(s) using the same conditions and equipment as for the real experiments. This is of course easier said than done and some simplifications are necessary. In principle, the intracellular calibration is based on clamping $[Ca^{2+}]_i$ to a known value, without severe alterations of the cytosolic milieu, and then measure the fluorescence signal. The most important points relate to a minimum $[Ca^{2+}]_i$, to obtain F_{min} or R_{min}, and to a saturating $[Ca^{2+}]_i$, to establish F_{max} or R_{max}. For ratiometric indicators, β is also obtained if R_{min} and R_{max} can be established without any major general decrease in fluorescence intensity. In addition, establishing K_d requires some intermediate $[Ca^{2+}]_i$. The reason why F_{min} or R_{min} and F_{max} or R_{max} are most important is because they set the limits between which the fluorescence signal can vary. Serious errors in these parameters result in nonlinear errors when fluorescence signals are translated into $[Ca^{2+}]_i$. Erroneous estimates of F_{min} or R_{min} has the largest impact on the assessment of resting $[Ca^{2+}]_i$, whereas errors in F_{max} or R_{max} have the largest effects at high $[Ca^{2+}]_i$. On the other hand, K_d and β act as scaling factors and errors in these simply make the changes in $[Ca^{2+}]_i$ smaller or larger, whereas relative changes during an experiments are not affected.

Numerous methods have been used to perform a cytosolic calibration of $[Ca^{2+}]_i$. Most of these are based on introducing a strongly buffered solution with a set $[Ca^{2+}]$ to the cytosol. The solution can be introduced with methods similar to those described above for the introduction of the fluorescent indicator. In addition, so called Ca^{2+} ionophores are frequently used. Popular Ca^{2+} ionophores are ionomycin and A23187 and in principle they create small holes in the surface membrane through which Ca^{2+} can pass and in this way $[Ca^{2+}]_i$ will attain the same value as that in surrounding bath solution.

Future Directions

In the past few years, there have been marked improvements in the level of spatial resolution. It was known and accepted for more than a century that separation of two objects closer than 250 nm in the horizontal plane was not possible with a standard

single lens and light source. However, the use of two opposing and matched objective lenses and a complementary approach that relies on the photochemical properties of the indicators have led to at least a threefold improvement in both axial and horizontal resolution. While these technical improvements are still expensive and not trivial to set up and maintain, it appears feasible that the ordinary user will be able to visualise Ca^{2+} fluxes through groups of ion channels in the near future (for a non-technical description, see [7]).

In recent years, the development of genetically encoded calcium indicators (GECI's) has focussed on (i) targeting the indicator to specific organelles or to specific channel proteins, (ii) improving their Ca^{2+} sensitivity and (iii) increasing their dynamic range [8, 9]. The key to these developments was the recognition that the green fluorescent protein (GFP) in jellyfish could be genetically modified to produce variants in various colours. When the coloured variants of GFP were coupled to calmodulin, the result was a functional Ca^{2+} indicator that could be expressed in organelles such as the mitochondria or sarcoplasmic reticulum using a variety of transfection techniques. The best known of these are cameleons and pericams. Cameleons have a hairpin-like structure composed of two different coloured GFP's joined together by a spacer peptide and a calmodulin molecule which can bind Ca^{2+}. Excitation light is chosen that excites only one of the GFP pair that then emits a photon at longer wavelength. This photon can then excite the second GFP molecule of the pair only if they are very close together (<10 nm). When a stimulus increases $[Ca^{2+}]$, the increased Ca^{2+} binds to calmodulin and causes the whole complex of GFP's-peptide spacer-calmodulin to bend and bring the two GFP molecules into very close proximity and at this time excitation of the second of the GFP pair can occur. Pericams are more simple structures that consist of a circular construct of calmodulin linked to a GFP. Binding of calcium to pericam causes a shift of its excitation peak from 415 to 490 nm, while the emission spectrum remains unchanged and thus like fura-2 it can be used as a ratiometric indicator. Future refinements include reducing the sensitivity of cameleons and pericams to pH changes in the physiological range and increasing their dynamic ranges (to a level comparable to indo-1 or even fluo-3).

Acknowledgment Research reported from our laboratory was supported by the Swedish Research Council.

References

1. Hove-Madsen L, Baudet S, Bers DM (2010) Making and using calcium-selective mini- and microelectrodes. Methods Cell Biol 99:67–89
2. Blinks JR, Prendergast FG, Allen DG (1976) Photoproteins as biological calcium indicators. Pharmacol Rev 28:1–93
3. Eglen RM, Reisine T (2008) Photoproteins: important new tools in drug discovery. Assay Drug Dev Technol 6:659–671
4. Tsien RY (1983) Intracellular measurements of ion activities. Annu Rev Biophys Bioeng 12:91–116

5. Westerblad H, Allen DG (1996) Intracellular calibration of the calcium indicator indo-1 in isolated fibers of *Xenopus* muscle. Biophys J 71:908–917
6. Scheenen WJ, Makings LR, Gross LR, Pozzan T, Tsien RY (1996) Photodegradation of indo-1 and its effect on apparent Ca^{2+} concentrations. Chem Biol 3:765–774
7. Hell SW (2009) Microscopy and its focal switch. Nat Methods 6:24–32
8. Tian L, Hires SA, Mao T, Huber D, Chiappe ME, Chalasani SH, Petreanu L, Akerboom J, McKinney SA, Schreiter ER, Bargmann CI, Jayaraman V, Svoboda K, Looger LL (2009) Imaging neural activity in worms, flies and mice with improved GCaMP calcium indicators. Nat Methods 6:875–881
9. Piljić A, de Diego I, Wilmanns M, Schultz C (2011) Rapid development of genetically encoded FRET reporters. ACS Chem Biol 6:685–691

Chapter 3
Development and Optimization of FLIPR High Throughput Calcium Assays for Ion Channels and GPCRs

Irina Vetter

Abstract Ca^{2+} permeable ion channels and GPCRs linked to Ca^{2+} release are important drug targets, with modulation of Ca^{2+} signaling increasingly recognized as a valid therapeutic strategy in a range of diseases. The FLIPR is a high throughput imaging plate reader that has contributed substantially to drug discovery efforts and pharmacological characterization of receptors and ion channels coupled to Ca^{2+}. Now in its fourth generation, the FLIPR^{TETRA} is an industry standard for high throughput Ca^{2+} assays. With an increasing number of excitation LED banks and emission filter sets available; FLIPR Ca^{2+} assays are becoming more versatile. This chapter describes general methods for establishing robust FLIPR Ca^{2+} assays, incorporating practical aspects as well as suggestions for assay optimization, to guide the reader in the development and optimization of high throughput FLIPR assays for ion channels and GPCRs.

Keywords FLIPR • Ca^{2+} • High throughput screening • G protein-coupled receptor • Voltage-gated Ca^{2+} channel • Ligand-gated Ca^{2+} channel • Fluo-4 • Assay development • Optimization

Abbreviations

FLIPR	Fluorescent Imaging Plate Reader
Ca^{2+}	Calcium ion
ATP	Adenosine triphosphate
PMCA	Plasma Membrane Ca^{2+} ATPase
NCX	Na^{+}/Ca^{2+} exchanger

I. Vetter (✉)
Institute for Molecular Bioscience, The University of Queensland, St Lucia, QLD, Australia
e-mail: i.vetter@uq.edu.au

M.S. Islam (ed.), *Calcium Signaling*, Advances in Experimental Medicine and Biology 740, DOI 10.1007/978-94-007-2888-2_3,

SERCA	Sarco/endoplasmic reticulum Ca^{2+} ATPase
IP3	Inositol-1,4,5,-triphosphate
RyR	Ryanodine receptors
GPCR	G-protein coupled receptor
PIP_2	Phosphatidylinositol 4, 5 bisphosphate
DAG	Diacylglycerol
HTS	High throughput screening
VGCC	Voltage-gated Ca^{2+} channels
LGCC	Ligand-gated Ca^{2+} channels
EGTA	Ethylene glycol-bis(2-aminoethylether)-*N*,*N*,*N′*,*N′*-tetraacetic acid
APTRA	2-aminophenol-N,N,O-triacetic acid
BAPTA	1,2-bis(o-aminophenoxy)ethane-N,N,N′,N′-tetraacetic acid
K_d	Dissociation constant
AM	Acetoxymethyl
ER	Endoplasmic reticulum
LED	Light-emitting diode
CCD	Charge-coupled device
PDL	Poly-D-lysine
PLL	Poly-L-lysine
PLO	*Poly-L-ornithine*
nAChR	Nicotinic acetylcholine receptors
HEPES	4-(2-hydroxyethyl)-1-piperazineethanesulfonic acid
PAR2	Protease-activated receptor 2
RFU	Relative fluorescence unit.

Introduction

Calcium – A Universal Signaling Molecule

The calcium ion Ca^{2+} is often referred to as a “universal” signaling molecule; indeed, most biological processes involve Ca^{2+} signaling in one form or another [1, 2]. It is thus not surprising that Ca^{2+} is involved in diverse physiological functions ranging from differentiation, excitability and motility to apoptosis.

Because Ca^{2+} acts as a ubiquitous messenger molecule, a myriad of proteins are dedicated to its extrusion, chelation, sequestration and release, resulting in astonishingly precise temporal and spatial control of Ca^{2+} [1, 2]. At the cellular level, Ca^{2+} concentrations are extremely tightly controlled in the cytoplasm, where resting $[Ca^{2+}]$ is approximately 100 nM. It is maintained at this level by extrusion to the extracellular space through pumps such as the Plasma Membrane Ca^{2+} ATPase (PMCA) and the Na^+/Ca^{2+} exchanger (NCX) [3]. Ca^{2+} is also sequestered into intracellular stores such as the endoplasmic or sarcoplasmic reticulum by sarco/endoplasmic reticulum Ca^{2+} ATPases (SERCA). As a result, extracellular Ca^{2+}

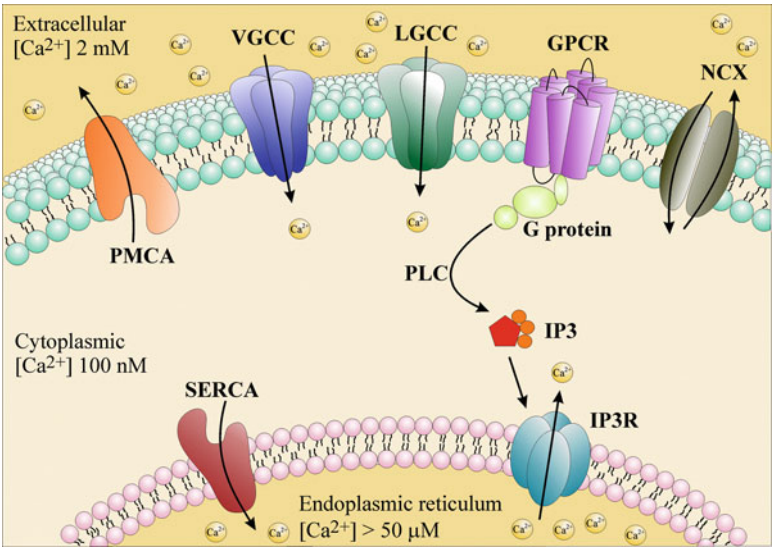

Fig. 3.1 Calcium signaling pathways. Cytoplasmic Ca^{2+} is maintained at approximately 100 nM by plasma membrane extrusion through the Plasma Membrane Ca^{2+} ATPase (PMCA) and the Na^{+}/Ca^{2+} (NCX). Ca^{2+} is also sequestered into the endoplasmic or sarcoplasmic reticulum by the sarco/endoplasmic reticulum Ca^{2+} ATPase (SERCA). Activation of voltage- (VGCC) or ligand-gated Ca^{2+} channels (LGCC) leads to influx of Ca^{2+} down its large concentration gradient. In addition, activation of G_q-coupled G-protein coupled receptors (GPCR) results in activation of phospholipase C which in turn leads to the generation of 1,4,5-inositol trisphosphate (IP3). IP3 then activates IP3 receptors (IP3R) located on the endoplasmic reticulum, causing release of Ca^{2+} into the cytoplasm

concentrations are significantly higher at approximately 1.8–2 mM, and a large Ca^{2+} reserve also occurs in intracellular compartments, where Ca^{2+} is stored in protein-bound form and also occurs at relatively high concentrations as free Ca^{2+} [4].

To initiate signaling events, Ca^{2+} can be derived from the extracellular space, where voltage- or ligand-gated ion channels permit flow of this extraordinary ion down its approximately 20,000-fold concentration gradient (Fig. 3.1). Ca^{2+} can also be released from intracellular stores such as the endoplasmic reticulum through activation of inositol-1,4,5,-triphosphate (IP3) receptors and ryanodine receptors (RyR), resulting in a net increase in cytoplasmic Ca^{2+}.

GPCRs

Activation of some G-protein coupled receptors (GPCR), in particular the $G_{q/11}$ subtypes, results in activation of phospholipase C which in turn facilitates cleavage of phosphatidylinositol 4, 5 bisphosphate (PIP_2) into 1,4,5-inositol trisphosphate (IP3) and diacylglycerol (DAG). IP3 then activates IP3 receptors located on the

endoplasmic reticulum, causing release of Ca^{2+} into the cytoplasm [5]. While $G_{\alpha s}$ and $G_{\alpha i}$-coupled GPCR do not signal through Ca^{2+} physiologically, co-expression of chimeric or promiscuous G-proteins, such as $G_{\alpha 15/16}$ [6–8], can couple activation of these receptors to increases in intracellular Ca^{2+} and thus allows development of functional high throughput (HTS) assays based on Ca^{2+} imaging.

Ca^{2+}-Permeable Ion Channels

Voltage-gated Ca^{2+} channels (VGCC), expressed in excitable cells, are large transmembrane proteins that undergo conformational changes in response to altered membrane potential [9]. As a result, activation of voltage-gated Ca^{2+} channels causes rapid influx of Ca^{2+} from the extracellular space, which controls processes such as muscle contractions or synaptic exocytosis. The properties of these channels can be exploited in the design of high throughput Ca^{2+} assays, where addition of extracellular KCl leads to membrane depolarization and thus channel opening [10, 11]. In addition, a plethora of Ca^{2+}-permeable transmembrane ion channels facilitate influx of extracellular Ca^{2+} along its concentration gradient in response to extra- or intracellular binding of ligands. These ligand-gated Ca^{2+} channels include, to name a few, ionotropic purinergic and glutamate receptors, nicotinic receptors and TRP channels and are indispensible to many physiological processes.

Accordingly, Ca^{2+} permeable ion channels and GPCRs linked to Ca^{2+} release are important drug targets, with modulation of Ca^{2+} signaling increasingly recognized as a valid therapeutic strategy in a range of diseases, including cardiac disease, neurological disorders such as Alzheimer's disease, and cancer [12–14].

Thus, the design and optimization of Ca^{2+} assays, particularly in high throughput format using state-of-the-art platforms such as the FLIPR^{TETRA}, is important not only to increase our understanding of the role of Ca^{2+} signaling in the pathophysiology of these diseases, but also to guide the identification of novel Ca^{2+} modulators with therapeutic potential.

Calcium Assays

Chemical Ca^{2+} Indicator Dyes

Assessment of calcium signaling has been greatly aided by development of Ca^{2+} dyes which exhibit changes in fluorescence spectra and/or intensity upon binding of free Ca^{2+} ions, enabling assessment of Ca^{2+} signals at the single cell level or in high throughput format. Most of these dyes were developed from the Ca^{2+} chelators EGTA, APTRA or BAPTA, and incorporate a fluorophore with the characteristic ion liganding groups of these molecules [15–19]. Continuous improvement of these compounds has resulted in a diverse array of dyes with unique properties (Table 3.1).

Table 3.1 Properties of chemical Ca^{2+} indicators

Dye	Excitation wavelength (nm)		Emission wavelength (nm)		K_d (nM)	F_{Max}/F_{min}	K_{on} 1/(M*s)	K_{off} 1/s	References
	Ca^{2+}-free	Ca^{2+}-bound	Ca^{2+}-free	Ca^{2+}-bound					
Quin-2	353	333	495	495	60	5–8			[18, 35]
Fura-2	363	335	512	505	135–258	13–25	4.0×10^8	103	[19, 27, 28, 35]
Bis-Fura-2	366	338	511	504	370		5.5×10^8	257	[28, 35]
Fura-4F	366	336	511	505	770				[35, 36]
Fura-5F					400				[35]
Fura-6F	364	336	512	505	5,300				[35, 36]
Fura-FF	364	335	510	506	5,500				[35, 36]
Fura-PE3	364	335	508	500	250	18			[35, 37]
FFP18	364	335	475	408	331	7			[37, 38]
Fura-Red	472	436	657	637	140	5–12			[35, 39]
Mag-Fura-2	369	329	511	508	50,000	6–30	7.5×10^8	26,760	[28, 36]
Indo-1	346	330	485	410	250	20–80	9.4×10^8	180	[19, 23, 99]
Indo 1-PE3	346	330	475	408	260				[35]
Mag-Indo-1	349	328	480	390	35,000	12	2.3×10^5	> 1,000	[23, 53]
Fluo-3	503	506	526	526	400	40–100	9.2×10^8	587/186	[16, 23, 55]
Fluo-4	491	494	–	516	345	100		350	[17, 61]
Mag-Fluo-4	490	493	–	516	22,000				[17, 35, 58]
Fluo-5F	491	494	–	518	2,300			300	[28, 59–61]
Fluo-5N	491	494	–	516	90,000				[28, 35, 59–61]
Fluo-4FF	491	494	–	516	9,700				[28, 35, 59–61]
Fluo-8	490			514	389	>200			[63]
Fluo-8H	490			514	232	>200			[63]
Fluo-8L	490			514	1,860	>200			[63]

(continued)

Table 3.1 (continued)

Dye	Excitation wavelength (nm)		Emission wavelength (nm)		K_d (nM)	F_{Max}/F_{min}	K_{on} 1/(M*s)	K_{off} 1/s	References
	Ca^{2+}-free	Ca^{2+}-bound	Ca^{2+}-free	Ca^{2+}-bound					
Rhod-2,	556	553	576	576	1,000	14–100			[35]
X-Rhod-1	576	580	–	602	700	4–100			[35]
Rhod-FF	551		556		19,000				[35]
X-Rhod-5F	576	580	–	602	1,600				[35]
X-Rhod-FF	568		605		17,000				[35]
Rhod-5N	547	549	–	576	320,000				[35]
Calcium-Green-1	506	506	532	532	190	38	0.79×10^9	178	[28, 72]
Calcium-Green-2	506	503	536	536	550	60–100			[35]
Calcium-Green-5N	506	506	532	532	4,000–19,000				[73–75]
Oregon green 488 BAPTA-1	494	494	523	523	170	14			[35, 76]
Oregon green 488 BAPTA-2	494	494	523	523	580	100			[35, 76]
Oregon green 488 BAPTA-6F	494	494	523	523	3,000				[35, 76]
Oregon green 488 BAPTA-5N	494	494	521	521	20,000	44			[35]
Calcium crimson	590	589	615	615	185	2.5	0.86×10^9	232	[35, 72]
Calcium ruby	579		598		30,000	32			[77]
Calcium orange	549	549	575	576	185	3	0.51×10^9	233	[35, 72]

Assessment of calcium signaling has been greatly aided by development of Ca^{2+} dyes which exhibit changes in fluorescence spectra and/or intensity upon binding of free Ca^{2+} ions, enabling assessment of Ca^{2+} signals at the single cell level or in high throughput format. Ratiometric dyes exhibit a spectral shift, either in excitation or emission wavelength, upon Ca^{2+} binding, often in conjunction with altered fluorescence intensity, while binding of Ca^{2+} to single wavelength dyes elicits an increase in quantum efficiency, resulting in brighter fluorescence in the absence of spectral excitation or emission shifts. Differences in their Ca^{2+} dissociation constant (K_d) and thus dynamic range, binding kinetics (K_{on} and K_{off}), and fluorescence characteristics (emission and excitation maxima, F_{Max}/F_{Min}) govern the usefulness of these compounds in a variety of applications

Differences in their Ca^{2+} dissociation constant (K_d) and thus dynamic range, binding kinetics, photostability, sequestration into intracellular compartments, fluorescence quenching characteristics as well as excitation and emission wavelengths govern the usefulness of these compounds in a variety of applications [20]. In particular, the K_d of chemical Ca^{2+} indicator dyes should be carefully matched to the expected Ca^{2+} concentration in the cellular environment, with the useful range over which changes in Ca^{2+} are most reliably detected approximating $0.1–10 \times K_d$ [21]. Thus, measurement of cytoplasmic Ca^{2+} events require high affinity Ca^{2+} dyes, while low affinity dyes will be useful in high Ca^{2+} cellular compartments such as the mitochondria or endoplasmic reticulum [22]. It is, however, important to take into consideration that the K_d of these compounds is affected by pH, temperature, viscosity, ionic strength, protein binding and the presence of other ions such as Mg^{2+} [17, 23–26]. Accordingly, the actual intracellular K_d of these dyes is frequently several orders of magnitude higher than the K_d determined *in vitro*, and can be expected to vary depending on the cell type and even the cellular compartment assessed [20, 25].

In addition, the binding kinetics of fluorescent Ca^{2+} indicators can affect temporal resolution of Ca^{2+} signals [21, 27, 28]. Ca^{2+} signals are generally transient, so that the binding kinetics of the dye need to be significantly faster than the change in Ca^{2+} concentration if Ca^{2+} signals are to be resolved with sufficient temporal precision [27]. Dyes with slow binding kinetics thus lead to substantial inaccuracies, particularly with respect to the temporal resolution of Ca^{2+} signals. This problem is further compounded by the Ca^{2+} buffering properties displayed by these compounds, especially if present at sufficiently high concentrations [27, 28]. Thus, bright fluorescent dyes which enable reduction in concentration are often preferable to dyes that require higher concentrations in order to achieve sufficient signal strength and similarly, dyes with fast dissociation kinetics are preferable for transient Ca^{2+} signals and in high throughput applications.

In addition to these key characteristics, the spectrometric properties of these compounds determine the selection of fluorescent Ca^{2+} indicators for specific applications. Principally, chemical Ca^{2+} indicators can be divided into ratiometric and single wavelength dyes.

Ratiometric Dyes

Ratiometric dyes exhibit a spectral shift, either in excitation or emission wavelength, upon Ca^{2+} binding, often in conjunction with altered fluorescence intensity. This effectively results in increased and decreased fluorescence intensity, respectively, at wavelengths on either side of the isosbestic point. Ratiometric dyes are advantageous for measurement of Ca^{2+} in application where uneven dye loading, dye leakage, photobleaching, compartmentalization, or cell thickness occur, as the fluorescence ratio is independent of the absolute signal strength, thus compensating for these variables [29]. However, these advantages come at the cost of increased

photodamage to cells by excitation wavelengths in the ultraviolet range, increased cellular autofluorescence as well as decreased compatibility with caged compounds. While the need for equipment capable of dual excitation or emission monitoring makes ratiometric dyes poorly suited for high throughput applications such as the FLIPR^{TETRA}, these dyes will be discussed here for completeness.

Quin-2

Quin-2 is a first generation Ca^{2+} dye developed by the research group of Roger Tsien [18]. It exhibits low quantum yield and absorptivity, necessitating high dye concentrations to achieve adequate signal strength. This is turn leads to problems with Ca^{2+} buffering [30] and has resulted in this dye being largely superseded by newer derivatives.

Fura-2

Fura-2 is a dual excitation, single emission ratiometric dye and has become the Ca^{2+} indicator of choice for fluorescent microscopy, where it is more practical to use dual excitation wavelengths and maintain a single emission wavelength [31]. Upon binding of Ca^{2+}, the maximum fluorescence excitation wavelength of Fura-2 shifts from 362 to 335 nm, with an accompanying twofold increase in fluorescence quantum efficiency [19]. In contrast, the fluorescence emission maxima of the free Fura-2 anion and Ca^{2+}-bound Fura-2 are, at 512 and 505 nm, virtually unaltered [19]. Thus, excitation of Fura-2 at 340 and 380 nm results in increased and decreased fluorescence, respectively, at an emission wavelength of ~510 nm. The fluorescence ratio of 340/380 nm therefore increases with increasing concentrations of Ca^{2+}. With a K_d of approximately 135–258 nM, a K_{on} (1/(M.s)) of 4.0×10^8 and a K_{off} (1/s) of 103, Fura-2 and its derivatives are suitable for rapid, time-resolved measurement of cytoplasmic Ca^{2+} signals [19, 28]. In addition, Fura-2 has been reported to be more resistant to photobleaching than Indo-1 [32, 33], although it tends to be more susceptible to intracellular departmentalization [34].

Bis-Fura-2

Bis-Fura-2 consists of two fluorophores incorporated with one BAPTA molecule, resulting in brighter signal strength with a slightly reduced K_d (370 nM). With excitation and emission spectra identical to Fura-2, Bis-Fura-2 is particularly suitable for applications which require better signal or tolerate Ca^{2+} buffering poorly and

thus require reduced dye concentrations. While on-rates are similar to Fura-2 with a K_{on} (1/(M.s)) of 5.5×10^8, off-rates are slightly higher for Bis-Fura-2 with a K_{off} of 257 (1/s) [28].

Fura-4F, Fura-5F, Fura-6F and Fura-FF

These analogues of Fura-2 exhibit similar excitation and emission spectra upon binding of Ca^{2+}, however, the K_d of these compounds has been significantly shifted by addition of one (Fura-4F, Fura-5F, Fura-6F) or two (Fura-FF) fluorine substitutes at varying positions. With K_ds of 400 nM (Fura-5F), 770 nM (Fura-4F), 5,300 nM (Fura-6F) and 5,500 nM (Fura-FF) [35, 36], these fluorescent Ca^{2+} indicators exhibit intermediate Ca^{2+} affinities and are useful for applications where Ca^{2+} concentration >1 μM occur.

Fura-PE3 (Fura-2 LeakRes)

Fura-PE3 was developed from an analogue of BAPTA, Fura-FF6, by addition of a positive charge in order to improve cytosolic retention of the dye and minimize compartmental sequestration [37]. The spectral properties of Fura-PE3 are identical to Fura-2, but this dye avoids problems associated with uneven loading and dye leakage.

FFP18

FFP18 is similar to Fura-PE3 but incorporates a hydrophobic tail that targets this dye to lipids such as cell membranes [37]. The spectral properties of FFP18 are similar to Fura-2, with a slightly decreased K_d of 331 nM [37] and improved hydrophilicity compared to other membrane-associating Ca^{2+} indicators. Thus, FFP18 appears suitable for measurement of membrane-associated Ca^{2+} events [38].

Fura-Red

Fura-Red is a Fura-2 analogue excited by visible light, with excitation maxima at approximately 450–500 nm, depending on the presence of Ca^{2+}, and a very long-wave emission maximum at approximately 660 nm. Fura-Red fluorescence decreases upon binding of Ca^{2+}, and in addition, the relatively low quantum efficiency of Fura-Red necessitates use of higher concentrations to achieve an adequate fluorescence signal. The *in vitro* K_d of Fura-Red is similar to Fura-2 at approximately 140 nM, although

the K_d of Fura-Red has been reported to be significantly higher (~1,100–1,600 nM) in myoplasm [39]. The large Stokes shift of Fura-Red permits simultaneous measurement of Ca^{2+} as well as other fluorophores excited at ~488 nm. Accordingly, Fura-Red has been used for ratiometric Ca^{2+} measurement in conjunction with the single wavelength Ca^{2+} indicator Fluo-3 [40–42], although ratiometric imaging is also possible with Fura-Red alone using excitation wavelengths of 420/480 nm or 457/488 nm [39, 43].

Mag-Fura-2

Mag-Fura-2 (Furaptra) was, as the name suggests, originally developed to measure changes in Mg^{2+} concentration, and exhibits spectral properties similar to Fura-2.

Its propensity for intracellular departmentalization, in combination with its low affinity for Ca^{2+} with a K_d of approximately 50 μM [28, 44, 45], have seen application of this fluorescent indicator to measurement of Ca^{2+} in intracellular IP3-sensitive Ca^{2+} stores [46]. In addition, Mag-Fura-2 retains fast binding kinetics with a K_{on} (1/(M.s)) of 7.5×10^8 and particularly fast off-rates [28], enabling measurement of Ca^{2+} responses with little or no kinetic delay [47–49].

Indo-1

Like Fura-2, Indo-1 was developed as a BAPTA analogue by the research group of Roger Tsien [19]. However, in contrast to Fura-2, Indo-1 displays shifts in emission wavelength upon Ca^{2+} binding, with emission maxima of 485 and 410 nm in the absence and presence of Ca^{2+}, respectively [19]. Thus, this probe is generally more practical in flow cytometry applications, where it easier to use a single excitation wavelength and monitor two emissions [50]. Indo-1 is also useful as it displays less compartmentalization than Fura-2, although it tends to photobleach more rapidly [34]. With a K_d of 250 nM, it displays slightly lower affinity for Ca^{2+} than Fura-2 and is useful for measurement of Ca^{2+} concentrations in the cytoplasmic range.

Indo-1-PE3 (Indo-1 LeakRes)

Like Fura-PE3, Indo-1-PE3 was developed as an Indo-1 analogue less prone to sequestration into intracellular compartments and dye extrusion [35]. Compared to the parent compound, Indo-1-PE3 displays the same spectral properties, but avoids problems with uneven loading, differences in cell thickness and uncontrolled loss of dye fluorescence due to extrusion or photobleaching [51, 52].

Mag-Indo-1

Mag-Indo-1 is a low affinity fluorescent Ca^{2+} indicator derived from Indo-1. Accordingly, its spectral properties are virtually identical to its parent compound, except that they occur at significantly higher Ca^{2+} concentrations ($K_d \sim 35$ μM) [21, 23, 53]. In combination with extremely fast kinetics [23], this compound is useful for measurement of Ca^{2+} kinetics in environments with high Ca^{2+} concentration.

Single Wavelength Dyes

In contrast to ratiometric fluorescent probes, binding of Ca^{2+} to single wavelength dyes elicits an increase in quantum efficiency, resulting in brighter fluorescence in the absence of spectral excitation or emission shifts. This eliminates the need for sophisticated equipment capable of dual excitation or dual emission monitoring and greatly simplifies experimental protocols. However, while single wavelength dyes generally exhibit large increases in fluorescence intensity upon binding of Ca^{2+}, brightness is also dependant on dye concentration. Thus, in addition to Ca^{2+} binding, fluorescence intensity of single wavelength Ca^{2+} probes is also affected by variables relating to the amount of dye present in cells. Most notably, differences in dye loading, extrusion, compartmentalization and photobleaching, as well as cell thickness and cellular environment can lead to apparent changes in dye concentration or fluorescence. Thus, because fluorescence intensity is the only measure for single wavelength dyes, quantitation of Ca^{2+}, particularly at the single cell level, tends to be less accurate than for ratiometric dyes. As an alternative to wavelength ratioing, time-based ratioing has been suggested as a viable strategy for single wavelength dyes, where the change in fluorescence intensity is expressed relative to a baseline fluorescence value [16, 54]. In circumstances where cell volume and shape changes as well as photobleaching have not been significant, this ratiometric $\Delta F/F$ value will approximate changes in Ca^{2+} [16]. Thus, single wavelength dyes have significantly advanced fluorescent Ca^{2+} imaging and are invaluable particularly for high throughput assessment of Ca^{2+} responses.

Fluo-3

Fluo-3 was developed by Roger Tsien and his research group from the calcium chelator BAPTA conjugated with a xanthene chromophore [16]. Fluo-3 is excited by visible light, with absorption and emission maxima at 506 and 526 nm, respectively [16]. While the AM ester of Fluo-3 is virtually non-fluorescent, emission intensity of Fluo-3 increases approximately 40-fold in the presence of Ca^{2+} [16]. With a K_d of 400 nM, this makes Fluo-3 well suited for high resolution of cytosolic

Ca^{2+} signals while at the same time being less prone to saturation and Ca^{2+} buffering at resting cytosolic Ca^{2+} than ratiometric dyes such as Fura-2 [55]. Fluo-3 – like all Ca^{2+}-dyes – is pH-sensitive, with an apparent pKa of 6.2, necessitating careful consideration of intracellular pH when measuring Ca^{2+} [16, 55]. In addition, Fluo-3 exhibits biphasic Ca^{2+} dissociation constants which, while also pH-dependent, are faster than Quin-2 and thus allow high time resolution of Ca^{2+} responses at neutral or physiological pH [55].

Fluo-4

Fluo-4 is a di-fluoro analogue of Fluo-3, and accordingly exhibits very similar spectral properties with absorption and emission maxima of 494 and 516 nm, respectively [17]. However, Fluo-4 is considerably brighter and more photostable than Fluo-3, and with a K_d of 345 nM [17], has become the dye of choice for measurement of cytosolic Ca^{2+} particularly in high throughput applications. Fluo-4 fluorescence, when excited at 488 nM, increases more than 100-fold upon binding of Ca^{2+}, permitting both use of lower dye concentrations and shorter loading times.

Mag-Fluo-4

Mag-Fluo-4 is a low affinity analogue of Fluo-4, and with a K_d of 22 μM, is particularly suitable for measurement of Ca^{2+} in the low μM – mM range. Accordingly, Mag-Fluo-4 has been used for measurement of Ca^{2+} responses in sarcoplasmic reticulum, and due to its affinity for Mg^{2+}, has also found applications in the measurement of intracellular Mg^{2+} [56, 57]. The spectral properties of Mag-Fluo-4, with an excitation maximum of 493 nm and an emission maximum of 516 nm, are very similar to Fluo-4 [17]. In addition, similar to Mag-Fura-2, Mag-Fluo-4 has fast dissociation kinetics which make this dye suitable for measurement of high resolution Ca^{2+} kinetics [58].

Fluo-5F, Fluo-5Cl, Fluo-5N and Fluo-4FF

These mono-or di-substituted Fluo-4 analogues exhibit similar spectral properties to Fluo-4 upon binding of Ca^{2+}, however, the addition of one or two fluorine, chlorine or NO_2 substitutes results in significantly decreased Ca^{2+} affinity. The relatively high K_d values of Fluo-5F (2.3 μM), Fluo-5Cl (6.2 μM), Fluo-4FF (9.7 μM) and Fluo-5N (90 μM) make these dyes suitable for measurement of Ca^{2+} under conditions which would result in saturation of higher affinity dyes [17]. The dissociation rate

constant for Fluo-4 and Fluo-5F were determined as approximately 200–300 $s-1$ *in vitro*, making these dyes kinetically similar to Fura-2 [28, 59–61].

Fluo-8, Fluo-8H and Fluo-8L

Fluo-8 and its analogues (AAT Bioquest) are a novel green-emitting Ca^{2+} probe (excitation/emission maxima ~ 490 nm/514 nm) that have been reported to be considerably brighter than Fluo-3 and even Fluo-4, resulting in improved signal-to-noise [62]. With K_ds of 389 nM (Fluo-8), 232 nM (Fluo-8H) and 1.86 μM (Fluo-8L), these dyes may prove to be viable alternatives to Fluo-3, Fluo-4 and their analogues [63].

Rhod-2, X-Rhod-1 and Low Affinity Derivatives

Rhod-2 was developed by the research group of Roger Tsien as a BAPTA analogue incorporating a rhodamine-like fluorophore [16]. This dye exhibits an excitation maximum of 553 nm and an emission maximum of 576 nm, with a K_d in the low μM range (~ 1.0 μM) [16]; while the analogue X-Rhod-1 has slightly shifted absorption and emission maxima (~580/602 nm, respectively) and a K_d of approximately 800 nM [64]. The cationic AM-esters of Rhod-2 and X-Rhod-1 can accumulate, using optimized loading protocols, in negatively charged mitochondria [65, 66], making Rhod-2, X-Rhod-1, and their derivatives useful for measurement of mitochondrial Ca^{2+} [64, 67, 68]. However, due to their relatively higher K_d values and thus lower potential for saturation in high Ca^{2+} environments, the low affinity Rhod-2 derivatives Rhod-FF (K_d 19 μM), X-Rhod-5F (K_d 1.9 μM), X-Rhod-FF (K_d 17 μM) and Rhod-5N (K_d 320 μM) are preferred for this application [22, 69–71].

Calcium-Green-1 and Calcium-Green-2 Indicators

The Calcium-Green indicators display increased fluorescence emission intensity with little spectral shift upon binding of Ca^{2+} [72]. With peak excitation at ~507 nm, peak emission at ~530 nm and K_ds of approximately 200 and 550 nM for Calcium-Green-1 and Calcium-Green-2, respectively, these dyes are well suited to measurement of fast cytosolic Ca^{2+} responses [72].

In addition, Calcium-Green dyes have a higher quantum yield than Fluo-3, particularly at saturating Ca^{2+} concentrations, which improves brightness of these dyes at high Ca^{2+} concentrations and provides an excellent dynamic range [72]. In contrast to Fluo-3, Ca^{2+} dissociation from Calcium-Green dyes is mono- rather than

bi-exponential with a K_{off} of approximately 180 s^{-1} [72]. Substitution of a NO_2 group in Calcium-Green-1 produced the low affinity analogue Calcium-Green-5N, which has similar spectral properties but considerably lower Ca^{2+} affinity with a K_d of approximately 4–19 μM, making this dye less prone to saturation [73–75].

Oregon Green 488 BAPTA Indicators

Oregon Green 488 BAPTA-1, Oregon Green 488 BAPTA-2 and their derivates are fluorinated analogues of Calcium-Green indicators that were developed to achieve increased excitation efficiencies by the 488 nm spectral line of an argon laser. Accordingly, peak excitation and emission wavelengths of these Oregon Ca^{2+} indicators are 494/523 nm. Like the Calcium-green dyes, Oregon Green 488 BAPTA indicators are bright dyes with higher quantum efficiencies than Fluo-3. Oregon Green 488 BATPA-1 in particular, with a K_d of 170 nM, may thus be particularly well suited for measuring small changes in Ca^{2+} near resting cytosolic Ca^{2+}, while the K_d of Oregon Green 488 BAPTA-2, at ~580 nM, more closely resembles the Ca^{2+} affinity of Fluo-4 [76]. Oregon Green 488 BAPTA-6F and Oregon Green 488 BAPTA-5N are the 6'-fluorine and 5'-nitro analogues of Oregon Green 488 BAPTA-1 with reduced Ca^{2+} affinities (Oregon Green 488 BAPTA-6F K_d for Ca^{2+} ~3 μM and Oregon Green 488 BAPTA-5N K_d for Ca^{2+} ~20 μM) and thus more suitable for measurement of larger Ca^{2+} responses.

Calcium Crimson, Calcium Ruby and Calcium Orange

Like other single wavelength dyes, Calcium Crimson, Ruby and Orange exhibit increased fluorescence emission intensity with little or no spectral shift in the presence of Ca^{2+}. As their names suggest, the excitation and emission spectra of these indicators are red-shifted with peak excitation/emission at 549/576 nm (Calcium Orange), 590/615 nm (Calcium Crimson) and 579/598 nm (Calcium Ruby) [77]. Calcium Ruby in particular displays large increases in fluorescence intensity upon Ca^{2+} binding, while all of these indicators are particularly useful where cellular autofluorescence is problematic [77]. The K_ds of these red-emitting Ca^{2+} indicators vary from ~300 nM (Calcium Crimson) and ~400 nM (Calcium Orange) to 30 μM (Calcium Ruby), allowing selection of Ca^{2+} dyes suitable for most imaging applications [72, 77].

In recent years, an increasing number of Ca^{2+} dyes have become available, expanding on pivotal work by Roger Tsien and his research group in the 1980s. These new and often improved Ca^{2+} probes include both ratiometric and single wavelength dyes; high and low affinity dyes; and Ca^{2+} probes with excitation and emission wavelengths spanning almost the entire UV-visible range. Currently,

however, the number of Ca^{2+} dyes suitable for use in high throughput FLIPR assays is limited. While the latest generation of HTS platforms such as the FLIPR^{TETRA} in principle provide the flexibility of measuring single wavelength as well as ratiometric dyes, the limited excitation/emission wavelengths available, as well as the cost associated with customising these settings, restricts the number of suitable dyes. In addition, interference from sample or plastic autofluorescence can pose particular problems with UV-excitable dyes such as Fura-2. Other dyes, while in principle suitable for FLIPR HTS assays, have not yet been extensively explored for this application. Thus, the most widely used fluorescent Ca^{2+} probe for HTS FLIPR assays currently remains Fluo-4. While we will most certainly see the development of new and improved probes for measurement of Ca^{2+} in future, this review will focus on Fluo-4 as the "gold-standard" Ca^{2+} probe for FLIPR assays.

Dye Loading

Several methods for introduction of these dyes into the cell cytoplasm have been developed; these include ATP-induced permeabilization, electroporation, hypoosmotic shock, cationic liposomes, chelators mediating dye uptake through pinocytosis, microinjection as well as loading of dyes coupled to acetoxymethyl (AM) ester [23–25, 46, 78–81]. Of these, the acetoxymethyl (AM) ester loading technique has become popular due to its simplicity, ease of use and low toxicity and is particularly well suited to high throughput applications.

AM Ester Loading Technique

As free poly-anionic, large fluorescent Ca^{2+} probes are unable to passively cross the cell membrane, these dyes can be conjugated to lipophilic acetoxymethyl (AM) groups to render them membrane permeable. Once in the cytoplasm, ubiquitous esterases hydrolyse these derivatized indicators, which again become unable to passively cross the plasma membrane, thus effectively trapping the free fluorescent Ca^{2+} probe. As an additional advantage, these AM derivatives are often non-fluorescent, thus reducing or eliminating fluorescence from non-hydrolysed extracellular dye.

No-Wash Extracellular Quenchers

Because physiologically, extracellular Ca^{2+} is high, fluorescence signals from the extracellular compartment generally need to be excluded to enable measurement of the often relatively small changes in cytosolic Ca^{2+}. This can be achieved either

by physically removing extracellular Ca^{2+} dyes by washing, or alternatively by incorporation of fluorescence quenchers in the extracellular media. Quenchers that have been used successfully include Trypan Blue, haemoglobin and brilliant black [82, 83]. In addition, several of these quenchers or "no-wash" kits are now commercially available, and they can provide significant improvements in assay performance particularly for cells that are only weakly adherent, or for cells that are prone to dye extrusion. However, as the composition and nature of these quenchers is largely proprietary information, it can be difficult to assess potential interference of quenchers with assays or to design protocols for assay optimization [83].

Problems with AM Ester Loading

Sequestration: Once introduced into the cell cytoplasm, fluorescent Ca^{2+} dyes start to accumulate into intracellular membrane-bound vacuoles and organelles such as the endoplasmic reticulum (ER) and mitochondria in a process commonly referred to as sequestration or compartmentalization [84]. This process is, however, not restricted to the AM ester loading technique and generally results in increasing baseline fluorescence readings as the free dye accumulates in high Ca^{2+} intracellular compartments, as well as accompanying decreases in cytosolic Ca^{2+} responses due to dye loss. To minimize dye sequestration, loading with the lowest AM ester concentration that produces reliable Ca^{2+} signals, as well as loading for the shortest possible time is beneficial. Loading and imaging cells at room temperature rather than 37°C can also help reduce dye sequestration, although restricting recordings to approximately 30 min largely avoids this problem. In addition, while for most applications, retention of the dye in the cell cytoplasm is desirable, dye sequestration can be exploited to assess calcium levels in organelles [85–88].

Incomplete AM ester hydrolysis: Residual cytosolic non-hydrolysed Ca^{2+} dyes, due to insufficient intracellular esterase activity or failure to completely remove AM ester dyes, can lead to signal artefacts, most notably an apparent decrease in intracellular Ca^{2+} response, as AM esters tend to be non-fluorescent [89, 90]. In addition, efficiency of ester hydrolysis can be highly variable and often depends on the cell type; incubation at 37°C generally improves ester hydrolysis but optimal conditions usually have to be determined empirically. In contrast, excessive extracellular ester hydrolysis leads to poor dye loading and as a result poor intracellular Ca^{2+} signals, while extracellular hydrolysed Ca^{2+} probes provide high fluorescence background [91].

Dye extrusion: Extrusion of hydrolysed intracellular Ca^{2+} probes by cellular anion transporters results in decreased available dye concentrations and thus, decreased signal strength. This problem is not restricted to the AM-loading technique, and can be a particular problem in certain cell types. Dye extrusion or leakage can be minimized by incorporation of anion transport inhibitors such as probenecid or sulphinpyrazone [84]. However, these compounds can alter cellular function and should

thus be used with caution. Loading cells and measuring fluorescence a quickly as possible, as well as performing experiments at room temperature rather than 37° generally also aid in minimising dye extrusion [21].

FLIPR

The FLIPR is a HTS imaging plate reader that has contributed substantially to drug discovery efforts and pharmacological characterization of receptors and ion channels coupled to Ca^{2+}. The main advantage of this system is its capability to measure fluorescence emission from 96,384 or 1,536 wells simultaneously with high temporal resolution. This in turn negates problems associated with conventional Ca^{2+} imaging that arise from uneven dye loading, extrusion, intracellular compartmentalization or photobleaching, as loading and imaging conditions are constant across all wells. Thus, the FLIPR is well suited for the primary identification of drug leads as well as detailed pharmacological characterization of compounds. Because functional responses are measured, pharmacological characterization of full or partial agonists as well as competitive and non-competitive antagonists at a range of targets can be accomplished using the FLIPR.

Excitation Optics

The latest generation of HTS platforms in the FLIPR family, the FLIPR^{TETRA}, uses up to two sets of customisable LED banks for excitation of the multi-well plates. In addition to standard LED bank with excitation wavelengths of 470–495 nm, suitable for HTS Ca^{2+} using Fluo-4, Fluo-3 or similar fluorescent Ca^{2+} probes, LED banks with excitation wavelengths from 360 to 626 nm are now available (Table 3.2), further increasing the possible complexity of FLIPR assays and the range of fluorescent Ca^{2+} probes which can be used at least in principle.

Emission Optics

The FLIPR^{TETRA} incorporates an EMCCD cooled charge-coupled device (CCD) camera for fluorescence detection, or optionally an ICCD intensified CCD camera capable of luminescence and fluorescence detection. In addition, to compensate for increased light-tightness of the system, an external thermo cube is required to maintain adequate camera temperatures. Measurements from an entire plate can be taken in as little as 1 s intervals, with up to 800 reads enabling prolonged real-time pre-incubation with antagonists as well as kinetics recordings for even the slowest Ca^{2+} responses.

Table 3.2 Available LED banks and emission filter sets for the FLIPR^{TETRAplus}

LED excitation (nm)	Emission filters (nm)
360–380	400–460
390–420	440–480
420–455	475–535
470–495	515–575
495–505	526–586
510–545	565–625
610–626	646–706

Emission Filters

In addition to a selection of LED banks, an increasing number of available emission filters, with wavelengths ranging from 400 to 706 nm (Table 3.2), permit selection of fluorescent dyes that are most suitable for individual applications. Up to three emission filters can be accommodated simultaneously. For Ca^{2+} assays using Fluo-4, the default emission filter of 515–575 is most appropriate.

Fluidics

In order to measure Ca^{2+} kinetics in response to stimulation accurately, it is imperative to incorporate a fluorescence plate reader with sophisticated liquid handling system. The FLIPR achieves this through high precision, user-exchangeable 96,384 or 1,534 pipettor heads which aspirate from 0.5 to 100 μl and simultaneously dispense test compounds, agonists or antagonists to the cell plate. This allows fluorescent readings to be taken both before and after compound addition. Furthermore, the ability to configure aspiration and dispense height and speed allows optimization of liquid handling to minimize disruption of cell monolayers and addition artefacts.

Plate Stage

Four plate positions accommodate up to three reagent plates containing test compounds, antagonists and agonists as well as one read plate containing cells.

As the FLIPR^{TETRA} is a bottom-reading instrument, use of clear-bottom imaging plates is required. The plate stage can be temperature-controlled from ambient up to 40°C, however, most Ca^{2+} assay perform well at ambient temperature.

Software and Optional Accessories

The FLIPR^{TETRA} utilized the ScreenWorks software (Molecular Devices), which features a drop-and-drag interface that enables easy definition of complex multi-step protocols. Parameters that can be user-defined include fluorescent or luminescent read modes, as well as excitation and emission wavelengths and single wavelength or ratiometric read modes. In addition, complex quadrant or multiple aspiration/dispensing fluid handling, aspiration and dispensing height and speed, tip washing and multiple read protocols can be customized to suit individual needs. To increase user-independent operation as well as throughput capacity, the FLIPR^{TETRA} can in addition include a cell dispensing system as well as plate robotics.

The following sections describe general methods for FLIPR Ca^{2+} assays, incorporating practical aspects as well as suggestions for assay optimization to guide the reader in the development and optimization of high throughput FLIPR assays for ion channels and GPCRs.

Materials and Methods

Design and Optimization of FLIPR Assays

FLIPR assays can be performed on cells either heterologously or endogenously expressing ion channels and GPCRs of interest [92]. While endogenously expressed targets may provide more physiologically relevant data owing to co-expression appropriate auxiliary subunits, little control over subtypes present or expression levels is possible [92]. In contrast, heterologously expressed ion channels and GPCRs allow control of both subtype expression as well as selection of cells with appropriate target expression levels, and are thus often the favoured approach particularly for primary identification of novel lead compounds.

FLIPR assays are generally possible with both adherent and suspension cell lines, though adherent cell lines tend to produce less addition artefacts. Suspension cell lines often require use of no-wash kits using extracellular quenchers, while this is optional for adherent cell lines. While no-wash kits are considerably more expensive, they also require less time due to omission of washing steps and can improve assay performance particularly for poorly adherent cell lines.

The most important aspect of a successful FLIPR assay is the quality of cells. For adherent cell lines, this optimally requires a 90–95% confluent monolayer of cells. As a rule of thumb, over-confluent cells tend to produce better assays than sub-confluent or patchy cells, although changes in cell morphology that occur as a result of confluency need to be considered. For example, some cancer cell lines differentiate when over-confluent, and receptor expression can also vary with cell confluency.

Table 3.3 Optimised cell plating parameters for FLIPR Ca^{2+} assays

Cell line	No of cells/well (96-well plate)	Culture time (h)	PDL required?
HEK293	30,000–50,000	24	Yes
HEK293	10,000–20,000	48	Yes
Cos-1	35,000–50,000	24	No
Cos-7	35,000–50,000	24	No
CHO	35,000–50,000	24	No
F11	50,000	24	Yes
50B11	100,000	24	No
ND7/23	50,000	24	Yes
Neuro2A	50,000	24	Yes
PC12	50,000	24	Yes
SH-SY5Y	120,000–150,000	48	No
MDA-MB-231	5,000–7,000	72	No

Cell plating densities and incubation times suggested to achieve 90–95% confluent monolayers on the day of the FLIPR experiment based on studies by Vetter et al. (unpublished and [92]). Cell adherence can be improved by coating plates with PDL and is required for some commonly used cell lines

It is also important that the cells adhere firmly so no disruption of the cell layer occurs even with multiple washing steps. If cells can be even partially dislodged from their tissue culture flask by mechanical means, cell adhesion probably needs to be optimized for successful FLIPR assays (Table 3.3).

Cell adherence can be improved by coating plates with poly-D-lysine (PDL), poly-L-lysine (PLL), collagen or similar substances. Adhesion-promoting plates such as Cell^{BIND} (Corning) plates can also help, though improvement appears generally less dramatic than with coating with PDL. Generally, cells should be plated at least 24 h prior to the FLIPR assay, although cell viability and morphology is often improved with plating 48 h prior to the assay.

As both fluorescence excitation and emission occur from below the read plate containing cells, selection of appropriate imaging plates is essential. For best performance, choose black-walled plates to minimize well-to-well cross-talk, as well as clear bottom imaging plates with optimized optics to minimize auto-fluorescence and light scatter.

Agonists

In order to design successful FLIPR assays, increases in intracellular Ca^{2+} need to be elicited by addition of suitable agonists; the choice of agonist is often crucial to the success of the assay and will need to be determined carefully.

In the case of ligand-gated ion channels or GPCRs, these will generally consist of endogenous or exogenous ligands. For example, addition of nicotine or acetylcholine could be utilized to elicit Ca^{2+} responses mediated through nicotinic acetylcholine receptors (nAChR) [92]. Similarly, membrane depolarization can be

induced through addition of KCl in order to activate voltage-gated Ca^{2+} channels, though in the case of N-type VGCC ($Ca_v2.2$), addition of extracellular Ca^{2+} is required to elicit sufficiently robust responses [10]. It may also be necessary to co-express inward rectifier K^+ channels to adequately control membrane potential [93], or to include allosteric modulators to delay inactivation or enhance signaling, as is the case for α7 nAChR [92].

Materials

- Poly-D-lysine (PDL, Sigma P6407-5 mg, optional)
- Sterile water (optional)
- 384- or 96-well cell/imaging microplates
  - e.g. Corning® 384 Well Flat Clear Bottom Black Polystyrene TC-Treated Microplates Cat No 3712;
  - e.g. Corning® 96 Well Flat Clear Bottom Black Polystyrene TC-Treated Microplates Cat No 3904
- Reagent microplates
  - e.g. Corning® 384 Well Clear Round Bottom Polypropylene Not Treated Microplate Cat No 3657;
  - e.g. Corning® 96 Well Elisa Plate Clear Round Bottom Polystyrene Not Treated Microplate Cat No 3797
- Confluent monolayer of cells (90–95%)
- Assay buffer
  - Based on HEPES-buffered Hank's Balanced Salt Solution
  - Ca^{2+}-free or with 1.8–2 mM extracellular Ca^{2+}
  - Phenol red-free
  - e.g. Physiological Salt Solution (PSS): NaCl 140 mM, glucose 11.5 mM, KCl 5.9 mM, $MgCl_2$ 1.4 mM, NaH_2PO_4 1.2 mM, $NaHCO_3$ 5 mM, $CaCl_2$ 1.8 mM, HEPES 10 mM (pH 7.4)
- Assay-specific agonists and antagonists
- positive control (optional)
  - e.g. Ionomycin
- Fluo-4-AM (e.g. Invitrogen F-14201)
  - Prepare 5 mM stock solution by dissolving 50 μg in 9.1 μl DMSO
  - *Alternatively*: Calcium 4 assay kit (Molecular Devices R8141)
- Probenecid (optional)
- Pluronic F-127 (optional)
- Fatty-acid free bovine serum albumin (BSA, optional)

– FLIPR^{TETRA} tips
  - e.g. 384-Well FLIPR^{TETRA} Pipet Tips (Molecular Devices 9000-0764)
  - e.g. 96-Well FLIPR^{TETRA} Pipet Tips, Black (Molecular Devices 9000-0762)

Methods

PDL Coating

1. If required (see Table 3.3), prepare PDL (e.g. Sigma, P6407-5 mg) by adding 25 ml s sterile filtered water to 5 mg vial of PDL.
   Optimal PDL concentrations should be determined empirically. For some applications, cell coating with other adhesion promoters such as poly-L-ornithine (PLO), PLL or collagen may be beneficial
2. Add approximately 40–50 µl of PDL solution/well of a 96-well plate
   It is possible to use as little as 30 µl of solution/well of a 96 well plate, by coating the well through light tapping of the plate
3. Incubate for 1 h at room temperature for plastic bottom plates or 24 h for glass-bottom plates
4. Remove PDL solution carefully
   The solution can be re-used up to five times. Some coating may be visible to the naked eye when the plate is held against the light, although this seems to be batch-dependent
5. Rinse plate at least once with 100 µl of sterile water or sterile PBS
   This is crucial as cell viability can be severely affected by residual PDL solution.
6. Remove residual water or PBS thoroughly
   If all liquid is removed by pipetting, it is not necessary to further dry the plate. Residual liquid can adversely affect cell viability and dilute growth media. It is usually best to prepare the plates fresh for each assay

Cell Plating

7. If assessing Ca^{2+} responses in transiently transfected cells, transfect cells in a tissue culture flask using standard protocols >48 h prior to FLIPR assay
   Transfecting in a tissue culture flask rather than directly in the imaging plate is preferred as this can decrease well-to-well variability. Optimal time for transfection needs to be determined for each assay.
8. 24–48 h prior to the FLIPR assay, split and count cells as usual.
   Some applications require plating of cells >48 h prior to the FLIPR assay, however, generally plating lower densities and increasing culture time leads to increased variability. Some GPCRs are sensitive to tryptic digest, resulting in decreased responses. Enzyme-free dissociation buffer may be used as an alternative.

9. Prepare cell solution to yield the required number of cells/volume in growth or differentiation medium as appropriate (see Table 3.3) and plate on imaging microplates.
   Optimal plating volume for 96-well plates is 100 ml and 20–40 ml for 384-well plates.
10. Incubate plates for 24–48 h in a 37°/5% CO2 incubator
    Optimal cell plating densities and incubation times should be determined for each assay. See Table 3.3 as a guide.

Reagent Plate Preparation

11. Prepare ligand solutions for reagent plate 1
    The test compounds will be dispensed into the cell imaging plate containing 100 µl (96-well plate) or 20 µl (384-well plate) assay buffer. The FLIPR^{TETRA} pipettor heads can add 5–200 µl (96-well pipettor) or 1–25 µl (384-well pipettor). The optimum volume to produce rapid mixing of solutions while minimising disruptions to the cell monolayer needs to be determined for each application. A good starting point for assays in 96-well format are 50 µl additions and 10 µl additions for 384-well plates.

    It is important to remember that addition of reagents to wells containing assay buffer will dilute the final reagent concentration. Therefore, reagents need to be prepared as appropriately concentrated stock solutions to achieve the desired final well concentration after addition, e.g. for addition of 50 µl reagent 1 to the cell plate containing 100 µl assay buffer, the reagent needs to be prepared as a 3× concentrated solution.
12. Prepare ligand solutions for reagent plate 2 (optional)
    Reagents for a second addition need to be prepared as appropriately concentrated stock solutions to yield the desired final well concentration.

    e.g. for addition of 50 µl reagent 2 to the cell plate now containing 150 µl, reagent 2 needs to be added as a 4× concentrated solution, containing 1× reagent 1 as appropriate.
13. Prepare ligand solutions for reagent plate 3 (optional)
    Reagents for a third addition need to be prepared as appropriately concentrated stock solutions to yield the desired final well concentration.

    e.g. for addition of 50 µl reagent 3 to the cell plate now containing 200 µl, reagent 3 needs to be added as a 5× concentrated solution, containing 1× reagent 1 and 1× reagent 2 as appropriate.
14. Pipette ligands in appropriate wells of reagent plates
    Inclusion of appropriate negative (i.e. buffer), solvent and positive (i.e. endogenous ligand or Ca^{2+} ionophores like ionomycin) controls is essential.

    While in principle the dead volume for aspiration, particularly if using U- or V-shaped reagent plates, is nil because the FLIPR^{TETRA} pipettor tracks down while aspirating, it is generally advisable to pipette some excess (i.e. 55–60 µl) reagent into the reagent plate to avoid air aspiration.

As preparation of the reagent plates can take considerable time, it is generally advisable to complete reagent plate preparation prior to commencing dye loading.

15. Place reagent plates and pipette tips in appropriate positions in FLIPR^{TETRA}

Dye Preparation

16. Prepare Fluo-4 AM (e.g. Invitrogen F14202 or F14201) by adding sufficient DMSO to produce a 5 mM stock solution

    Dye solution is best prepared as a 1,000 × stock solution in DMSO. While the usual range of dye concentration is between 1 and 10 μM, for most applications, final dye concentrations of 4–5 μM are optimal.

17. Aliquot in 20 μl aliquots and store, wrapped in foil, at −20°C

    It is best to aliquot dye stocks to avoid repeated freeze-thaw cycles. Fluorescent Ca^{2+} dyes are poorly water soluble and can form particulates which are prone to compartmentalization. However, if proper care is taken, dye stock solutions can be re-used at least three times.

18. Dilute Fluo-4-AM stock 1:1,000 in assay buffer to result in a 5 μM loading solution

    Addition of 0.3% fatty-acid free BSA to the loading solution can improve dye dissolution and reduce compartmentalization, although this is not essential.

    Pluronic F-127 is a detergent that has been used to enhance dye solubility. However, addition of Pluronic F-127, due to its detergent nature, can adversely affect cell viability. Thus, while Pluronic F-127 is required for larger sodium dyes such as CoroNa Green or Sodium Green, fluorescent Ca^{2+} probes such as Fluo-3 or Fluo-4 do not usually require addition of Pluronic F-127.

    Similarly, for the majority of applications, addition of probenecid to block dye efflux is not usually required. However, probenecid (0.5–5 mM) can improve loading in leaky cells such as PC12 or Neuro2A cells and if required should be added at this stage. Where possible, use of probenecid should be avoided as it may have unknown off-target effects and has been reported to affect cellular Ca^{2+} signaling [94].

    Dye solution is best prepared fresh, although it can also be prepared several hours in advance and stored at room temperature wrapped in aluminium foil.

Loading Cells with Dye

Dye loading should optimally be carried out under low light conditions, that is, with dimmed lights, although loading under light, if light exposure is minimized, does not appear to produce detrimental results. All incubation steps should be performed with the plate wrapped in foil and protected from light, as the dyes are light-sensitive and will photobleach.

19. Remove culture media carefully
Media can be removed initially by flicking the cell plate. If cell plates have been prepared appropriately, this should not adversely affect the cell monolayer.

It is important to completely remove culture media, as residual serum can lead to extracellular dye hydrolysis and thus poor loading. It is generally preferable to use an electronic multichannel pipette with adjustable speed setting to aspirate residual culture media at a low speed setting. In addition, positioning of pipette tips in the corner of the well avoids physical disruption of the cells and maintains a uniform cell monolayer.

If culture medium is aspirated thoroughly in this manner, no additional washing of cells is required at this stage.
20. Slowly dispense loading solution onto cell monolayer.
Ideally the plate is tilted, and an electronic pipette with adjustable speed setting at a low dispense speed is used. A volume of 40–50 μl /well of a 96-well plate is generally sufficient and will save costs by reducing the required amount of dye solution.

If using no-wash dyes, add the required final volume of dye, i.e. 100 μl for 96-well plates or 20 μl for 384-well plates.

Dye loading of suspension cells essentially occurs as for adherent cells, except that incubation and washing steps occur with bulk cells in suspension and plating of dye-loaded cells is the final step.
21. Incubate cells to allow uptake and de-esterification of dye.
Generally, incubation at 37°C for 30 min is sufficient for most cell types and a good starting point. Longer incubation times tend to increase dye sequestration into intracellular compartments, while shorter incubation times are not sufficient to achieve dye uptake and de-esterification. Incubation at room temperature can decrease dye sequestration but may require slightly longer incubation times, and can, depending on the cell type, compromise viability.

For suspension cells, after harvesting of cells, they are incubated for 30 min at 37°C with fluorescent Ca^{2+} dyes as for adherent cells.
22. Remove loading medium by flicking the plate and/or aspirating.
(If using no-wash dyes, this step is omitted).

It is important to completely dry the well, as residual dye solution will compromise washing and introduce artefacts due to residual extracellular dye.

For suspension cells, loading solution is removed by centrifugation at 500–800 g for 3–5 min.
23. Wash cells with assay buffer.
(If using no-wash dyes, this step is omitted.)

It is important to maintain integrity of the cell monolayer at this stage. Dispense 50–100 μl assay buffer at low speed setting into the well, holding the plate at an angle and positioning the pipette tips in the corner of the well.

This wash step can be repeated if desired. Washing twice will generally produce the best results and less addition artefacts due to residual extracellular dye. However, a single wash can be sufficient particularly if the cell monolayer is prone to dislodging.

For suspension cells, after centrifugation, cells are resuspended in dye-free assay buffer and again harvested by centrifugation at 500–800 g for 3–5 min.

24. Remove assay buffer and thoroughly dry the wells by aspirating residual buffer at slow speed.
(If using no-wash dyes, this step is omitted.)
25. Dispense the final volume of assay buffer
(If using no-wash dyes, this step is omitted.)
For 96-well plates, use 100 µl of assay buffer, or 20 µl for 384-well plates. It is important to maintain the integrity of the cell monolayer at this stage, so ideally use an electronic pipette with adjustable speed setting on a low setting and avoid physical disruption of the cell monolayer by holding the plate at an angle and positioning the pipette tips in the corner of the well.
For suspension cells, after the final wash, cells are harvested by centrifugation at 500–800 g for 3–5 min and resuspended in an appropriate amount of assay buffer for plating on the read plate. As a final step, the read plate is centrifuged to collect cells at the bottom of the well.
26. Transfer the cell plate to the FLIPR^{TETRA} read position.

Assay on FLIPR^{TETRA} (Table 3.4)

27. Setup **Read mode** to excitation 470–495 nm and emission to 515–575 nm
These settings are used for fluorescent Ca^{2+} probes like Fluo-3, Fluo-4 or Calcium Green. If using alternative dyes, excitation and emission wavelengths should be varied accordingly. It is also possible to define ratiometric imaging at this stage but selecting Read Mode 2 and defining appropriate excitation and emission wavelengths.
See Table 3.4 for a typical FLIPR protocol setup for 384 well plate with single addition.
28. Assign Plate to Position
It is necessary to define the precise dimensions of cell and reagent plates used to allow correct positioning of the pipettor head.
29. Define **Fluid Transfer** protocol as Single aspirate – Single dispense
For most applications, Single aspirate – Single dispense mode will be optimal as it allows detection of both agonism and antagonism in the same experiment. This usually involves addition of antagonists from reagent plate 1, followed by addition of agonists from reagent plate 2. For adherent cells, faster addition provides better mixing and is preferred, while fluid addition speeds may need to be decreased for suspension cells or poorly adherent cells to avoid disruption of the cell monolayer. As a guide, for adherent cells, dispensing the entire reagent volume in 1 s provides sufficient mixing while minimising addition artefacts.
Other options include 'Single aspirate – Multiple dispense', which allows dispensing in quadrants e.g. using a 96-well pipettor head can dispense into a

Table 3.4 Typical FLIPR protocol setup for 384 well plate with single addition using adherent cells

FLIPR parameter	Settings
Read mode	
Excitation wavelength	Excitation 470–495 nm
Emission wavelength	Emission 515–575 nm
Gain	Defined during protocol signal test
Exposure time	Defined during protocol signal test
Excitation intensity	Defined during protocol signal test
Gate open	0% or N/A
Assign plate to position	
Read plate	Corning
Source plate 1	Corning
Source plate 2	NONE
Source plate 3	N/A
Load tips position	Ticked
Data file name	
Include data	Ticked
User defined name	*The name of your experiment*
Temperature control	
Use manual	Ticked
Transfer Fluid	
Transfer fluid type	Single aspirate – single dispense
Aspirate	Source plate 1
Volume	10 µl
Height	Default 4.6 µl
Speed	10 µl/s
Tip up speed	20 mm/s
Hold volume	0 µl
Quadrant	NONE
Done	NO
Fill Res speed	N/A
Drain Res Dest	N/A
Drain Res speed	N/A
Put tips in well before read	Not ticked
Mix fluid before aspirate	Not ticked
Dispense	Ticked
Plate	Read plate
Volume	10 µl
Height	19 µl
Speed	10 µl/s
Expel volume	0 µl
Pause(s)	0
Removal speed	20 mm/s
Quadrant	None
Hold pipettor	No
Mix fluid after dispense	Not ticked

(continued)

Table 3.4 (continued)

FLIPR parameter	Settings
Unload tips after fluid transfer	Not ticked
Read with TF	
First interval	
Read time interval (s)	1
Number of reads before dispense	10
Number of reads after dispense	180
(total number of reads)	190
Save images	Ticked
Number of images before dispense	1
Number of images after dispense	19
Second interval	
Read time interval (s)	1
Number of reads	0

384-well plate using this setting. The "Multiple aspirate – single dispense" setting allows simultaneous addition of agonist and antagonists prepared in separate reagent plates (see Section: 'Applications')

30. Define **Read with TF** settings
In this section, the number of baseline reads, the read interval (fastest 1 s), as well as the total number of reads are defined. It is possible to divide the read time into two intervals, providing more flexibility.

In addition, the option to save plate images is available, which is very useful to assess the integrity of the cell monolayer during the experiment.

31. Protocol signal test
A protocol test signal needs to be determined in order to adjust excitation intensity and camera gain to achieve satisfactory basal fluorescence levels. Baseline starting fluorescence should ideally be ~1,000 RFU, with StDev < 5%. Using the cell plating and loading conditions given here, an exposure time of 0.8 s, excitation intensity of 80% and gain of approximately 150 will produce good signal. Checking the plate image at this stage helps to identify uneven cell plating, loading, or disruption to the cell monolayer.

32. Data analysis
ScreenWorks can be used for data analysis, although currently the software does not convert raw fluorescence to Δ F/F values. It is, however, possible to define pre-addition baselines, with data reported as response over baseline values. Another useful analysis feature is the negative control correction option, which allows correction for buffer addition artefacts. While it is also possible to define addition groups and plot concentration-response graphs, many users find it more practical to export the data and analyse using standard data analysis software.

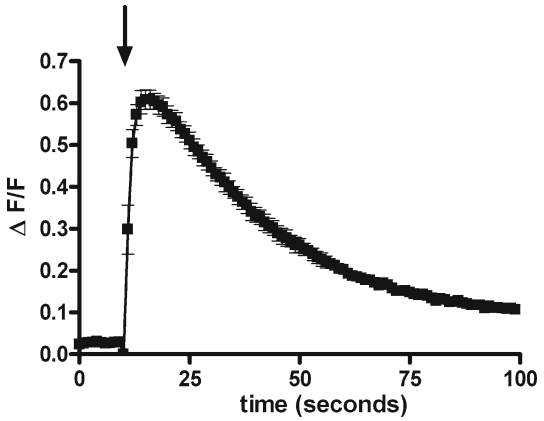

Fig. 3.2 Ca^{2+} response elicited by noradrenaline in Cos-1 cells transiently expressing the α1B adrenoreceptor. Ca^{2+} responses were monitored using the $FLIPR^{TETRA}$ in Cos-1 cells transiently transfected with the hamster α1B adrenoreceptors. Increases in intracellular Ca^{2+} in response to addition of 1 μM noradrenaline peaked 5–10 s after stimulation and returned to near-baseline levels over approximately 100 s. Shown is a representative Ca^{2+} response to addition of 1 μM noradrenaline. Data are presented as mean Δ F/F ± SEM of $n = 3$ wells

Applications

The kinetics of Ca^{2+} responses measured using the FLIPR result from a combination of the binding rate constants of the Ca^{2+} dye, the binding kinetics of agonists and antagonists used, the rate of inactivation or desensitization of receptors and ion channels as well as extrusion and sequestration of Ca^{2+} by pumps such as PMCA or SERCA [95, 96]. Nonetheless, Ca^{2+} kinetics obtained with the FLIPR can provide valuable information. Activation of IP3 receptors result in Ca^{2+} kinetics that are often quite distinct from those of voltage- or ligand ion channels. GPCR activation leads to relatively slow, concentration-dependent increases in intracellular Ca^{2+}, which peak approximately 5–20 s after ligand addition and return to baseline within ~100–180 s. In contrast, ion channels often display extremely rapid increases in Ca^{2+}, which, depending on the desensitization kinetics of the channel as well as the Ca^{2+} load, may or may not return to baseline (see Fig. 3.2, 3.4 and 3.5).

FLIPR Ca^{2+} assays can be used for drug screening or the primary identification of novel drug leads, as well as for detailed pharmacological characterization of known or novel agonists and antagonists. However, while the most commonly used protocol involves addition of antagonists first, followed by addition of agonists, this setup can lead to ambiguous pharmacological profiles due to the kinetics of receptor binding and the Ca^{2+} response. As an example, pre-incubation for a short period with the competitive α1B adrenoreceptor antagonist prazosin, followed by stimulation with noradrenaline, leads to a pseudo-noncompetitive profile (Fig. 3.3a and b). In the presence of increasing concentrations of prazosin, the noradrenaline concentration-response curve is not shifted to the right, as could be expected for a competitive

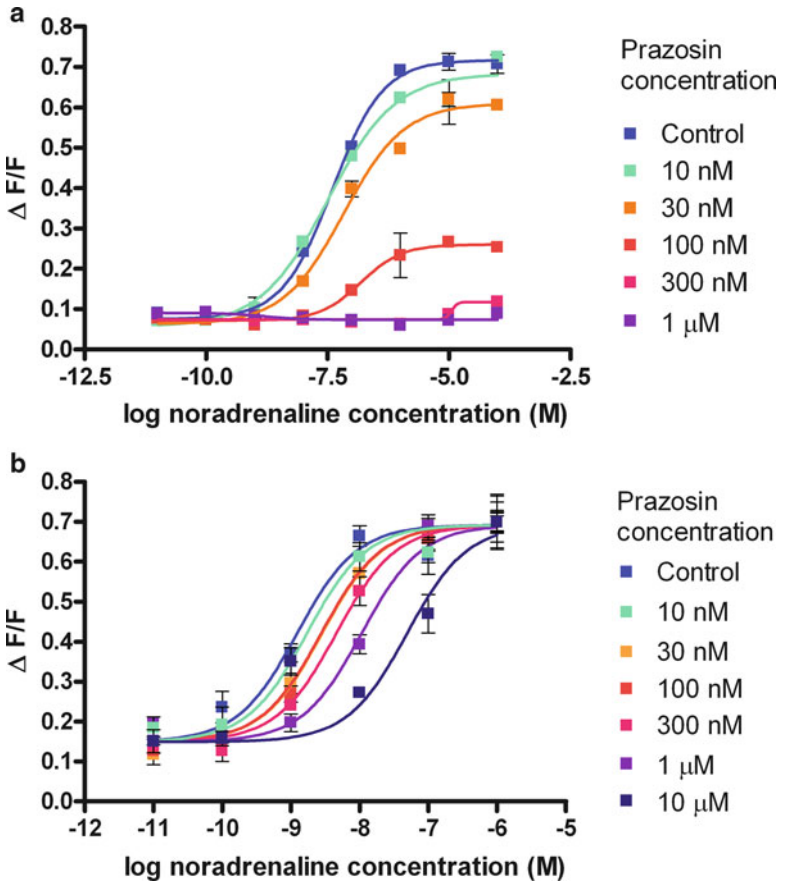

Fig. 3.3 Pharmacological profiles of α1B adrenoreceptor inhibition by prazosin using pre-incubation and co-addition FLIPR protocols. Ca^{2+} responses to increasing concentrations of noradrenaline were measured in Cos-1 cells transiently expressing the α1B adrenoreceptor using the $FLIPR^{TETRA}$. (**a**) Pre-incubation for a 5 min with the competitive α1B adrenoreceptor antagonist prazosin, followed by stimulation with noradrenaline, leads to a pseudo-noncompetitive profile with decreased maximal Ca^{2+} responses in the presence of prazosin. (**b**) Co-addition of prazosin and noradrenaline at the same time results in a rightward shift of the noradrenaline concentration-response curve as expected for a competitive antagonist like prazosin

antagonist like prazosin. Instead, the maximal responses are decreased in a manner typical for non-competitive antagonists. This seeming discrepancy arises from the fact that the Ca^{2+} response occurs before the receptor occupancy can achieve equilibrium, thus leading to pseudo-noncompetitive inhibition at non-equilibrium state [97, 98]. In contrast, when prazosin and noradrenaline are applied at the same time,

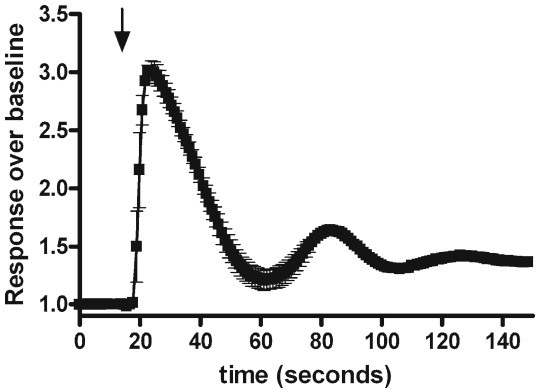

Fig. 3.4 Ca^{2+} response elicited by SLIGRL in HEK293 cells endogenously expressing PAR2. Ca^{2+} responses to addition of the PAR2 agonist SLIGR (1 μM) were measured in HEK-293 cells endogenously expressing PAR2 receptors using the $FLIPR^{TETRA}$. SLIGRL elicited transient increases in intracellular Ca^{2+} which initially peaked approximately 10 s after compound addition and elicited prolonged Ca^{2+} oscillations. Shown is a representative Ca^{2+} response to addition of 1 μM SLIGRL. Data are presented as mean response over baseline ± SEM of $n = 3$ wells

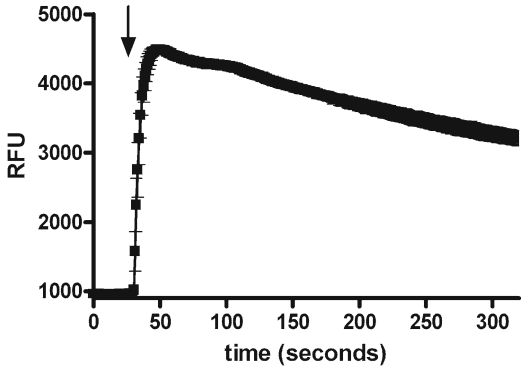

Fig. 3.5 The α7 nAChR agonist choline elicits Ca^{2+} responses in SH-SY5Y cells in the presence of the α7 nAChR allosteric modulator PNU120596. In the presence of the α7 nAChR allosteric modulator PNU120596, addition of choline elicited large, rapid increases in intracellular Ca^{2+} that were sustained, with Ca^{2+} not returning to baseline levels even after 300 s. Shown is a representative Ca^{2+} response to addition of 30 μM choline. Data are presented as mean RFU ± SEM of $n = 3$ wells

a classical rightward shift for competitive antagonism is observed. Thus, when using FLIPR Ca^{2+} assays for pharmacological characterization of compounds, the possibility of complex pharmacological behaviour based on Ca^{2+} and binding kinetics should be considered carefully.

Examples

α1B Adrenoreceptor Transiently Expressed in Cos-1 Cells (Figs. 3.2 and 3.3)

Transfection

Cos-1 cells were transfected with the hamster α1B adrenoreceptors in a T75 tissue culture flask using Fugene. In brief, 18 μg of DNA were mixed with 50 μl Fugene and added to 900 μl OptiMEM serum-free medium. After 20 min incubation at room temperature, the DNA/Fugene mix was added to the cell flask containing 10 ml s of normal growth media (DMEM + 10% FCS) and incubated in a 37°/5% CO2 incubator for 24 h.

Cell Plating

Transfected cells were harvested, plated at a density of 15,000 cells/well on uncoated 384-well imaging plates and incubated in a 37°/5% CO2 incubator for 24 h.

Dye Loading

Calcium 4 assay kit solution (1×) was prepared as recommended by the manufacturer. Growth media was removed and cells were incubated with 20 μl of dye solution for 30 min at 37°.

FLIPR Assay

After transfer of the cell plate to the read position of the FLIPR^{TETRA}, Cos-1 cells expressing the α1B adrenoreceptor were exposed to varying concentration of prazosin for 300 s prior to stimulation with noradrenaline (pre-incubation protocol). For co-administration of compounds, prazosin and noradrenaline were added to the cells simultaneously by using the multiple aspirate – single dispense function.

Data Analysis

Raw fluorescence values were converted to Δ F/F by subtracting baseline fluorescence values from subsequent fluorescence reads and dividing the resulting value by

baseline fluorescence. To establish concentration-response curves, the maximum increase in Δ F/F after addition of agonist was plotted against agonist concentration using GraphPad Prism Version 4.01 and a 4-parameter Hill equation was fitted to the data.

PAR2 Endogenously Expressed in HEK293 Cells (Fig. 3.4)

Cell Plating

HEK293 cells were plated at a density of 50,000 cells/well on PDL-coated, black-walled 96-well imaging plates and incubated in a 37°/5% CO2 incubator for 24 h.

Dye Loading

Fluo-4-AM (Invitrogen) was prepared as a 5 mM stock solution in DMSO and diluted to final concentration of 5 μM in PSS containing 0.3% BSA. Cells were incubated with 45 μl of the loading solution in a 37°/5% CO2 incubator for 30 min. After removal of dye solution, cells were washed twice with PSS prior to addition of 100 μl PSS/well and transfer to the FLIPR^{TETRA}.

FLIPR Assay

HEK293 cells endogenously expressing PAR2 were stimulated by addition of 50 μl SLIGR prepared as a 3 × concentrated stock solution in PSS.

Data Analysis

Raw fluorescence values were converted to response over baseline values using the analysis tool of ScreenWorks 3.1 by subtracting baseline reads (read 1–10) from subsequent fluorescent reads.

α7 nAChR Endogenously Expressed in SH-SY5Y Cells (Fig 3.5)

Cell Plating

SH-SY5Y cells were plated at a density of 50,000 cells/well on uncoated, black-walled 384-well imaging plates and incubated in a 37°/5% CO2 incubator for 48 h.

Dye Loading

Fluo-4-AM (Invitrogen) was prepared as a 5 mM stock solution in DMSO and diluted to a final concentration of 5 μM in PSS containing 0.3% BSA. Cells were incubated with 20 μl of the loading solution in a 37°/5% CO2 incubator for 30 min and washed once with PSS to remove extracellular dye. PSS (20 μl) containing 10 μM of the allosteric modulator PNU120596 was then added to each well and the plate was transferred to the FLIPR^{TETRA}.

FLIPR Assay

SH-SY5Y cells endogenously expressing α7 nAChR were stimulated with 30 μM choline in the presence of PNU120596 (10 μM). Choline was prepared as a 3 × concentrated stock solution in PSS containing 10 μM PNU120596, added to the cells in a volume of 10 μl and responses were measured for 300 s after 10 baseline reads.

Data Analysis

Data is presented as raw fluorescence values with n = 3 wells.

References

1. Clapham DE (2007) Calcium signaling. Cell 131:1047–1058
2. Berridge MJ, Lipp P, Bootman MD (2000) The versatility and universality of calcium signalling. Nat Rev Mol Cell Biol 1:11–21
3. Brini M, Carafoli E (2011) The plasma membrane Ca2+ ATPase and the plasma membrane sodium calcium exchanger cooperate in the regulation of cell calcium. Cold Spring Harb Perspect Biol 3. doi:10.1101/cshperspect.a004168
4. Bygrave FL, Benedetti A (1996) What is the concentration of calcium ions in the endoplasmic reticulum? Cell Calcium 19:547–551
5. Berridge MJ (1993) Inositol trisphosphate and calcium signalling. Nature 361:315–325
6. Liu AM, Ho MK, Wong CS, Chan JH, Pau AH, Wong YH (2003) Galpha(16/z) chimeras efficiently link a wide range of G protein-coupled receptors to calcium mobilization. J Biomol Screen 8:39–49
7. Zhu T, Fang LY, Xie X (2008) Development of a universal high-throughput calcium assay for G-protein- coupled receptors with promiscuous G-protein Galpha15/16. Acta Pharmacol Sin 29:507–516
8. Kostenis E, Waelbroeck M, Milligan G (2005) Techniques: promiscuous Galpha proteins in basic research and drug discovery. Trends Pharmacol Sci 26:595–602
9. Catterall WA (2000) Structure and regulation of voltage-gated Ca2+ channels. Annu Rev Cell Dev Biol 16:521–555
10. Benjamin ER, Pruthi F, Olanrewaju S, Shan S, Hanway D, Liu X, Cerne R, Lavery D, Valenzano KJ, Woodward RM, Ilyin VI (2006) Pharmacological characterization of recombinant N-type calcium channel (Cav2.2) mediated calcium mobilization using FLIPR. Biochem Pharmacol 72:770–782

11. Belardetti F, Tringham E, Eduljee C, Jiang X, Dong H, Hendricson A, Shimizu Y, Janke DL, Parker D, Mezeyova J, Khawaja A, Pajouhesh H, Fraser RA, Arneric SP, Snutch TP (2009) A fluorescence-based high-throughput screening assay for the identification of T-type calcium channel blockers. Assay Drug Dev Technol 7:266–280
12. Monteith GR, McAndrew D, Faddy HM, Roberts-Thomson SJ (2007) Calcium and cancer: targeting Ca2+ transport. Nat Rev Cancer 7:519–530
13. Duncan RS, Goad DL, Grillo MA, Kaja S, Payne AJ, Koulen P (2010) Control of intracellular calcium signaling as a neuroprotective strategy. Molecules 15:1168–1195
14. Talukder MA, Zweier JL, Periasamy M (2009) Targeting calcium transport in ischaemic heart disease. Cardiovasc Res 84:345–352
15. Otten PA, London RE, Levy LA (2001) A new approach to the synthesis of APTRA indicators. Bioconjug Chem 12:76–83
16. Minta A, Kao JP, Tsien RY (1989) Fluorescent indicators for cytosolic calcium based on rhodamine and fluorescein chromophores. J Biol Chem 264:8171–8178
17. Gee KR, Brown KA, Chen WN, Bishop-Stewart J, Gray D, Johnson I (2000) Chemical and physiological characterization of fluo-4 Ca(2+)-indicator dyes. Cell Calcium 27:97–106
18. Tsien RY (1980) New calcium indicators and buffers with high selectivity against magnesium and protons: design, synthesis, and properties of prototype structures. Biochemistry 19:2396–2404
19. Grynkiewicz G, Poenie M, Tsien RY (1985) A new generation of Ca2+ indicators with greatly improved fluorescence properties. J Biol Chem 260:3440–3450
20. Thomas D, Tovey SC, Collins TJ, Bootman MD, Berridge MJ, Lipp P (2000) A comparison of fluorescent Ca2+ indicator properties and their use in measuring elementary and global Ca2+ signals. Cell Calcium 28:213–223
21. Paredes RM, Etzler JC, Watts LT, Zheng W, Lechleiter JD (2008) Chemical calcium indicators. Methods 46:143–151
22. Yasuda R, Nimchinsky EA, Scheuss V, Pologruto TA, Oertner TG, Sabatini BL, Svoboda K (2004) Imaging calcium concentration dynamics in small neuronal compartments. Sci STKE 2004:pl5
23. Lattanzio FA Jr (1990) The effects of pH and temperature on fluorescent calcium indicators as determined with Chelex-100 and EDTA buffer systems. Biochem Biophys Res Commun 171:102–108
24. Oliver AE, Baker GA, Fugate RD, Tablin F, Crowe JH (2000) Effects of temperature on calcium-sensitive fluorescent probes. Biophys J 78:2116–2126
25. O'Malley DM, Burbach BJ, Adams PR (1999) Fluorescent calcium indicators: subcellular behavior and use in confocal imaging. Methods Mol Biol 122:261–303
26. Poenie M (1990) Alteration of intracellular Fura-2 fluorescence by viscosity: a simple correction. Cell Calcium 11:85–91
27. Kao JP, Tsien RY (1988) Ca2+ binding kinetics of fura-2 and azo-1 from temperature-jump relaxation measurements. Biophys J 53:635–639
28. Naraghi M (1997) T-jump study of calcium binding kinetics of calcium chelators. Cell Calcium 22:255–268
29. Dustin LB (2000) Ratiometric analysis of calcium mobilization. Clin Appl Immunol Rev 1:5–15
30. Hesketh TR, Bavetta S, Smith GA, Metcalfe JC (1983) Duration of the calcium signal in the mitogenic stimulation of thymocytes. Biochem J 214:575–579
31. O'Connor N, Silver RB (2007) Ratio imaging: practical considerations for measuring intracellular Ca2+ and pH in living cells. Methods Cell Biol 81:415–433
32. Becker PL, Fay FS (1987) Photobleaching of fura-2 and its effect on determination of calcium concentrations. Am J Physiol 253:C613–C618
33. Scheenen WJ, Makings LR, Gross LR, Pozzan T, Tsien RY (1996) Photodegradation of indo-1 and its effect on apparent Ca2+ concentrations. Chem Biol 3:765–774
34. Wahl M, Lucherini MJ, Gruenstein E (1990) Intracellular Ca2+ measurement with Indo-1 in substrate-attached cells: advantages and special considerations. Cell Calcium 11:487–500

35. Spence MTZ, Johnson ID (2010) Molecular probes handbook, a guide to fluorescent probes and labeling technologies. Invitrogen, Carlsbad
36. Wokosin DL, Loughrey CM, Smith GL (2004) Characterization of a range of fura dyes with two-photon excitation. Biophys J 86:1726–1738
37. Vorndran C, Minta A, Poenie M (1995) New fluorescent calcium indicators designed for cytosolic retention or measuring calcium near membranes. Biophys J 69:2112–2124
38. Etter EF, Minta A, Poenie M, Fay FS (1996) Near-membrane [Ca2+] transients resolved using the Ca2+ indicator FFP18. Proc Natl Acad Sci USA 93:5368–5373
39. Kurebayashi N, Harkins AB, Baylor SM (1993) Use of fura red as an intracellular calcium indicator in frog skeletal muscle fibers. Biophys J 64:1934–1960
40. Floto RA, Mahaut-Smith MP, Somasundaram B, Allen JM (1995) IgG-induced Ca2+ oscillations in differentiated U937 cells; a study using laser scanning confocal microscopy and co-loaded fluo-3 and fura-red fluorescent probes. Cell Calcium 18:377–389
41. Lipp P, Niggli E (1993) Ratiometric confocal Ca(2+)-measurements with visible wavelength indicators in isolated cardiac myocytes. Cell Calcium 14:359–372
42. Schild D, Jung A, Schultens HA (1994) Localization of calcium entry through calcium channels in olfactory receptor neurones using a laser scanning microscope and the calcium indicator dyes Fluo-3 and Fura-Red. Cell Calcium 15:341–348
43. Lohr C (2003) Monitoring neuronal calcium signalling using a new method for ratiometric confocal calcium imaging. Cell Calcium 34:295–303
44. Martinez-Zaguilan R, Parnami J, Martinez GM (1998) Mag-Fura-2 (Furaptra) exhibits both low (microM) and high (nM) affinity for Ca2+. Cell Physiol Biochem 8:158–174
45. Zhao M, Hollingworth S, Baylor SM (1996) Properties of tri- and tetracarboxylate Ca2+ indicators in frog skeletal muscle fibers. Biophys J 70:896–916
46. Hofer AM (2005) Measurement of free [ca(2+)] changes in agonist-sensitive internal stores using compartmentalized fluorescent indicators. Methods Mol Biol 312:229–247
47. Claflin DR, Morgan DL, Stephenson DG, Julian FJ (1994) The intracellular Ca2+ transient and tension in frog skeletal muscle fibres measured with high temporal resolution. J Physiol 475:319–325
48. Konishi M, Hollingworth S, Harkins AB, Baylor SM (1991) Myoplasmic calcium transients in intact frog skeletal muscle fibers monitored with the fluorescent indicator furaptra. J Gen Physiol 97:271–301
49. Berlin JR, Konishi M (1993) Ca2+ transients in cardiac myocytes measured with high and low affinity Ca2+ indicators. Biophys J 65:1632–1647
50. MacFarlane AW 4th, Oesterling JF, Campbell KS (2010) Measuring intracellular calcium signaling in murine NK cells by flow cytometry. Methods Mol Biol 612:149–157
51. Takahashi A, Camacho P, Lechleiter JD, Herman B (1999) Measurement of intracellular calcium. Physiol Rev 79:1089–1125
52. Overholt JL, Ficker E, Yang T, Shams H, Bright GR, Prabhakar NR (2000) HERG-Like potassium current regulates the resting membrane potential in glomus cells of the rabbit carotid body. J Neurophysiol 83:1150–1157
53. Launikonis BS, Zhou J, Royer L, Shannon TR, Brum G, Rios E (2005) Confocal imaging of [Ca2+] in cellular organelles by SEER, shifted excitation and emission ratioing of fluorescence. J Physiol 567:523–543
54. Smith SJ, Augustine GJ (1988) Calcium ions, active zones and synaptic transmitter release. Trends Neurosci 11:458–464
55. Eberhard M, Erne P (1989) Kinetics of calcium binding to fluo-3 determined by stopped-flow fluorescence. Biochem Biophys Res Commun 163:309–314
56. Lee S, Lee HG, Kang SH (2009) Real-time observations of intracellular Mg2+ signaling and waves in a single living ventricular myocyte cell. Anal Chem 81:538–542
57. Shmigol AV, Eisner DA, Wray S (2001) Simultaneous measurements of changes in sarcoplasmic reticulum and cytosolic. J Physiol 531:707–713
58. Hollingworth S, Gee KR, Baylor SM (2009) Low-affinity Ca2+ indicators compared in measurements of skeletal muscle Ca2+ transients. Biophys J 97:1864–1872

59. Scott R, Rusakov DA (2006) Main determinants of presynaptic Ca2+ dynamics at individual mossy fiber-CA3 pyramidal cell synapses. J Neurosci 26:7071–7081
60. Woodruff ML, Sampath AP, Matthews HR, Krasnoperova NV, Lem J, Fain GL (2002) Measurement of cytoplasmic calcium concentration in the rods of wild-type and transducin knock-out mice. J Physiol 542:843–854
61. Goldberg JH, Tamas G, Aronov D, Yuste R (2003) Calcium microdomains in aspiny dendrites. Neuron 40:807–821
62. Bioquest A (2011) Quest Fluo-8™ calcium reagents and screen quest™ Fluo-8 NW calcium assay kits
63. Falk S, Rekling JC (2009) Neurons in the preBotzinger complex and VRG are located in proximity to arterioles in newborn mice. Neurosci Lett 450:229–234
64. Gerencser AA, Adam-Vizi V (2005) Mitochondrial Ca2+ dynamics reveals limited intramitochondrial Ca2+ diffusion. Biophys J 88:698–714
65. Tao J, Haynes DH (1992) Actions of thapsigargin on the Ca(2+)-handling systems of the human platelet. Incomplete inhibition of the dense tubular Ca2+ uptake, partial inhibition of the Ca2+ extrusion pump, increase in plasma membrane Ca2+ permeability, and consequent elevation of resting cytoplasmic Ca2+. J Biol Chem 267:24972–24982
66. Trollinger DR, Cascio WE, Lemasters JJ (1997) Selective loading of Rhod 2 into mitochondria shows mitochondrial Ca2+ transients during the contractile cycle in adult rabbit cardiac myocytes. Biochem Biophys Res Commun 236:738–742
67. Davidson SM, Yellon D, Duchen MR (2007) Assessing mitochondrial potential, calcium, and redox state in isolated mammalian cells using confocal microscopy. Methods Mol Biol 372:421–430
68. Gerencser AA, Adam-Vizi V (2001) Selective, high-resolution fluorescence imaging of mitochondrial Ca2+ concentration. Cell Calcium 30:311–321
69. Pologruto TA, Yasuda R, Svoboda K (2004) Monitoring neural activity and [Ca2+] with genetically encoded Ca2+ indicators. J Neurosci 24:9572–9579
70. David G, Talbot J, Barrett EF (2003) Quantitative estimate of mitochondrial [Ca2+] in stimulated motor nerve terminals. Cell Calcium 33:197–206
71. Simpson AW (2006) Fluorescent measurement of [Ca2+]c: basic practical considerations. Methods Mol Biol 312:3–36
72. Eberhard M, Erne P (1991) Calcium binding to fluorescent calcium indicators: calcium green, calcium orange and calcium crimson. Biochem Biophys Res Commun 180:209–215
73. Stout AK, Reynolds IJ (1999) High-affinity calcium indicators underestimate increases in intracellular calcium concentrations associated with excitotoxic glutamate stimulations. Neuroscience 89:91–100
74. Rajdev S, Reynolds IJ (1993) Calcium green-5N, a novel fluorescent probe for monitoring high intracellular free Ca2+ concentrations associated with glutamate excitotoxicity in cultured rat brain neurons. Neurosci Lett 162:149–152
75. Eilers J, Callewaert G, Armstrong C, Konnerth A (1995) Calcium signaling in a narrow somatic submembrane shell during synaptic activity in cerebellar Purkinje neurons. Proc Natl Acad Sci USA 92:10272–10276
76. Agronskaia AV, Tertoolen L, Gerritsen HC (2004) Fast fluorescence lifetime imaging of calcium in living cells. J Biomed Opt 9:1230–1237
77. Gaillard S, Yakovlev A, Luccardini C, Oheim M, Feltz A, Mallet JM (2007) Synthesis and characterization of a new red-emitting Ca2+ indicator, calcium ruby. Org Lett 9: 2629–2632
78. Roe MW, Lemasters JJ, Herman B (1990) Assessment of Fura-2 for measurements of cytosolic free calcium. Cell Calcium 11:63–73
79. Tsien RY (1981) A non-disruptive technique for loading calcium buffers and indicators into cells. Nature 290:527–528
80. Williams DA, Bowser DN, Petrou S (1999) Confocal Ca2+ imaging of organelles, cells, tissues, and organs. Methods Enzymol 307:441–469
81. Johnson I (1998) Fluorescent probes for living cells. Histochem J 30:123–140

82. Cronshaw DG, Kouroumalis A, Parry R, Webb A, Brown Z, Ward SG (2006) Evidence that phospholipase-C-dependent, calcium-independent mechanisms are required for directional migration of T-lymphocytes in response to the CCR4 ligands CCL17 and CCL22. J Leukoc Biol 79:1369–1380
83. Mehlin C, Crittenden C, Andreyka J (2003) No-wash dyes for calcium flux measurement. Biotechniques 34:164–166
84. Di Virgilio F, Steinberg TH, Silverstein SC (1990) Inhibition of Fura-2 sequestration and secretion with organic anion transport blockers. Cell Calcium 11:57–62
85. Vetter I, Cheng W, Peiris M, Wyse BD, Roberts-Thomson SJ, Zheng J, Monteith GR, Cabot PJ (2008) Rapid, opioid-sensitive mechanisms involved in transient receptor potential vanilloid 1 sensitization. J Biol Chem 283:19540–19550
86. Kabbara AA, Allen DG (2001) The use of the indicator fluo-5N to measure sarcoplasmic reticulum calcium in single muscle fibres of the cane toad. J Physiol 534:87–97
87. Rehberg M, Lepier A, Solchenberger B, Osten P, Blum R (2008) A new non-disruptive strategy to target calcium indicator dyes to the endoplasmic reticulum. Cell Calcium 44:386–399
88. Solovyova N, Verkhratsky A (2002) Monitoring of free calcium in the neuronal endoplasmic reticulum: an overview of modern approaches. J Neurosci Methods 122:1–12
89. Oakes SG, Martin WJ 2nd, Lisek CA, Powis G (1988) Incomplete hydrolysis of the calcium indicator precursor fura-2 pentaacetoxymethyl ester (fura-2 AM) by cells. Anal Biochem 169:159–166
90. Gillis JM, Gailly P (1994) Measurements of [Ca2+]i with the diffusible Fura-2 AM: can some potential pitfalls be evaluated? Biophys J 67:476–477
91. Jobsis PD, Rothstein EC, Balaban RS (2007) Limited utility of acetoxymethyl (AM)-based intracellular delivery systems, in vivo: interference by extracellular esterases. J Microsc 226:74–81
92. Vetter I, Lewis RJ (2010) Characterization of endogenous calcium responses in neuronal cell lines. Biochem Pharmacol 79:908–920
93. Dai G, Haedo RJ, Warren VA, Ratliff KS, Bugianesi RM, Rush A, Williams ME, Herrington J, Smith MM, McManus OB, Swensen AM (2008) A high-throughput assay for evaluating state dependence and subtype selectivity of Cav2 calcium channel inhibitors. Assay Drug Dev Technol 6:195–212
94. Di Virgilio F, Fasolato C, Steinberg TH (1988) Inhibitors of membrane transport system for organic anions block fura-2 excretion from PC12 and N2A cells. Biochem J 256:959–963
95. Redondo PC, Rosado JA, Pariente JA, Salido GM (2005) Collaborative effect of SERCA and PMCA in cytosolic calcium homeostasis in human platelets. J Physiol Biochem 61:507–516
96. Brini M, Bano D, Manni S, Rizzuto R, Carafoli E (2000) Effects of PMCA and SERCA pump overexpression on the kinetics of cell Ca(2+) signalling. EMBO J 19:4926–4935
97. Kaler G, Otto M, Okun A, Okun I (2002) Serotonin antagonist profiling on 5HT2A and 5HT2C receptors by nonequilibrium intracellular calcium response using an automated flow-through fluorescence analysis system, HT-PS 100. J Biomol Screen 7:291–301
98. Miller TR, Witte DG, Ireland LM, Kang CH, Roch JM, Masters JN, Esbenshade TA, Hancock AA (1999) Analysis of apparent noncompetitive responses to competitive H(1)-histamine receptor antagonists in fluorescent imaging plate reader-based calcium assays. J Biomol Screen 4:249–258
99. Westerblad H, Allen DG (1996) Intracellular calibration of the calcium indicator indo-1 in isolated fibers of Xenopus muscle. Biophys J 71:908–917

Chapter 4
Two-Photon Calcium Imaging in the Intact Brain

Marco Dal Maschio, Riccardo Beltramo, Angela Michela De Stasi, and Tommaso Fellin

Abstract The calcium ion is a fundamental second messenger that plays crucial roles in the pathophysiology of brain cells. In this chapter, we will focus on the measurement of calcium fluctuations as a reporter of cellular excitability of both neurons and glial cells in the intact central nervous system. We will first describe the methodological aspects of *in vivo* two-photon fluorescence calcium imaging and then review recent data highlighting the ways in which this technique is revolutionizing our understanding of brain circuits at the cellular level. Finally, we will discuss recent technical advancements that promise to open new horizons in the optical investigation of brain function in awake, behaving animals.

Keywords Calcium imaging • Calcium indicators • Non-linear microscopy • Fluorescence microscopy • *In vivo* • Cortex • Neuronal networks • Cortical microcircuits • Glia • Astrocytes

Introduction

Although electrophysiology has long been the preferred method for studying the central nervous system, the use of fluorescent indicators in combination with two-photon microscopy is now recognized as an equally fundamental tool for brain circuit analysis *in vivo*. The development of fluorescent calcium indicators [1, 2] not only revealed the importance and complexity of the biochemical pathways that are controlled by this second messenger but also allowed the monitoring of the activity of different brain cells. For example, in neurons, the depolarization that underlies an

M.D. Maschio • R. Beltramo • A.M. De Stasi • T. Fellin (✉)
Department of Neuroscience and Brain Technologies, Italian Institute of Technology, Via Morego 30, 16163 Genoa, Italy
e-mail: marco.dalmaschio@iit.it; riccardo.beltramo@iit.it; angela.destasi@iit.it; tommaso.fellin@iit.it

M.S. Islam (ed.), *Calcium Signaling*, Advances in Experimental Medicine and Biology 740, DOI 10.1007/978-94-007-2888-2_4,

action potential opens voltage-gated calcium channels, leading to significant calcium accumulation in the intracellular space [3–5]. The intracellular calcium concentration can thus be used as an indirect measure of the suprathreshold activity of neurons. Moreover, fluorescence calcium imaging is useful for investigating the activity of non-neuronal cells, in particular astrocytes, which are a sub-type of glial cell [6, 7]. Primarily due to their non-electrically excitable nature, astrocytes have long been regarded as merely supporting elements in the brain. However, recent studies are changing this traditional view and demonstrating that astrocytes do exhibit a form of excitability that is based on oscillations in the cell's intracellular calcium concentration [8–10]. Thus, by using a combination of two-photon microscopy and calcium imaging it is now possible to monitor the excitability of both neurons and glia in the intact central nervous system.

The value of this optical approach in studying the functional properties of cellular networks is not difficult to appreciate. Because the interactions between different cells generate the complex ensemble dynamics that are believed to form the basis of higher brain functions, preserving the structure and function of the network circuitry is of paramount importance. Because light penetrates the tissue without causing mechanical disturbances, fluorescence calcium imaging allows one to investigate the function of brain cells and their interactions with the external world with minimal invasiveness. From this point of view, imaging confers distinct advantages over electrophysiology. Furthermore, *in vivo* fluorescence microscopy allows the simultaneous visualization of the function and structure of hundreds of cells with single-cell resolution [11, 12], which is not possible with current electrophysiological approaches.

In this chapter, we will first describe the principles of fluorescence microscopy using two-photon excitation and briefly review the molecules that are most commonly used as *in vivo* fluorescent calcium indicators. We will then discuss recent results that have been obtained with this technique, focusing on studies of the ensemble dynamics of neuronal and glial networks, primarily in intact mammalian sensory cortices.

Two-Photon Microscopy for *In Vivo* Fluorescence Imaging

From an optical point of view, recording fluorescent signals that are generated deep within the brain is not a trivial task. The presence of many molecules and compartments with different optical properties renders the brain optically non-homogeneous with large variations in its refractive index [13]. These differences in optical homogeneity cause the deflection of light rays from their original path in a phenomenon termed scattering. Light scattering plays a fundamental role in the progressive degradation of fluorescence imaging at increasing depths below the brain surface, which renders the signal generally impossible to detect in regions deeper than 1 mm [13]. Most importantly, light scattering is inversely related to the wavelength of the light that is used; thus, blue-shifted light (of a shorter wavelength) is highly scattered,

whereas red-shifted light (of a longer wavelength) is scattered to a lesser extent. The success of two-photon microscopy in *in vivo* fluorescence imaging relies heavily on using infrared-shifted light to significantly decrease light scattering when compared to imaging using the visible wavelength range [13–17]. This approach permits the detection of fluorescent signals from deeper (up to 900–1,000 μm) regions of the brain [18] compared to imaging using single-photon excitation (up to 50–100 μm) while providing sufficient spatial resolution to monitor cellular and subcellular structures [13, 19–21].

Two-photon excitation requires the near-simultaneous (0.5×10^{-15} s) absorption of two photons in order for their energy to efficiently sum, thereby causing the transition of an electron to an excited state (Fig. 4.1a). Given that the probability of absorption is quadratic [13], the high probability of excitation is constrained to a small, three-dimensional volume at the objective focus (Fig. 4.1b). The intrinsic spatial confinement of two-photon excitation overcomes the limitations of the single-photon approach, which causes significant fluorescence excitation in the out-of-focus planes as well (Fig. 4.1b). Because two-photon excitation is spatially confined, all emitted photons that are collected by the microscope objective can be directly deflected by a dichroic mirror to the photo-detector. This optical configuration, named non-descanned mode, leads to a net increase in the signal-to-noise ratio of the fluorescent signal [13]. Moreover, the intrinsic "confocal nature" of two-photon excitation prevents phototoxicity and photobleaching in out-of-focus planes, which can cause significant deterioration of the sample as occurs during single-photon imaging [17]. However, efficient two-photon excitation requires a high temporal density of photons at the focal plane. This is obtained by using mode-locked laser sources that emit ultrashort (~140 fs duration) pulses with a large peak power and a fast (~80 MHz) repetition rate. Typical two-photon sources include Ti:sapphire lasers, which can be tuned over a relatively large spectral range (700–1,100 nm). Although the peak power that is reached during a single ultrashort pulse is high, the average power is low, which limits the photo-damaging effects at the focal plane.

The basic design of a two-photon microscope is shown in Fig. 4.1c [13, 17, 22]. The laser beam is directed onto a fast deflection system which is usually based on galvanometric mirrors [14, 22] or acousto-optic devices [23, 24] that allows image formation through the sequential illumination of the field of view. A beam expander composed by the scan and the tube lens, positioned in the optical path before the objective, matches the dimension of the laser beam with that of the back-aperture of the objective. To compensate for the progressive loss of power at increasing depths below the surface of the brain, an intensity modulator that is based on acousto-optic or electro-optic effects can be inserted downstream of the laser source (Pockels cell; see Fig. 4.1c). Because of the strong light absorbing properties of the tissue and the fact that two-photon microscopy is usually (but not always) used in *in vivo* applications, the preferred configuration for detecting the emitted fluorescence is the episcopic mode. In this configuration, a single objective is used to both deliver the excitation light and collect the emitted photons. The maximum signal-to-noise ratio is achieved by using a high numerical aperture and low-magnification objective combined with a detection strategy that is based on

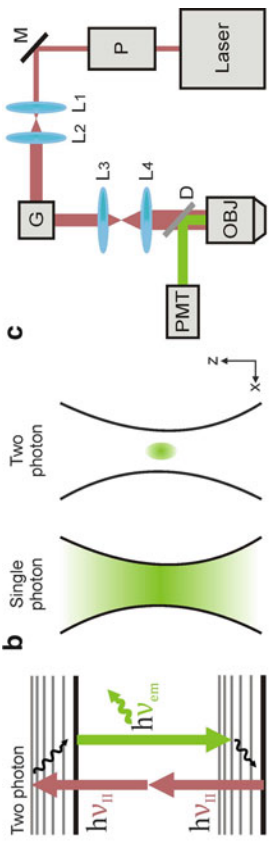

Fig. 4.1 (**a**) Jablonsky diaghram showing the transitions of an electron through two energy levels (s_0 and s_1) following the absorbtion of one photon of energy $h\nu_I$ (*blue arrow, left*) or following the simultaneous absorption of two photons of half energy $h\nu_{II}$ (*red arrow, right*). Once in the excited state, the electron undergoes transitions through vibrational levels (*dark arrow*) and then to the ground state, which is accompanied by the emission of a photon (*green arrow*) of energy $h\nu_{em}$ with $\nu_{II} < \nu_{em} < \nu_I$. (**b**) x-z profiles of the volume excited with single-photon (*left*) or two-photon (*right*) excitation. (**c**) Schematic of the optical layout of a typical two-photon scanning microscope. *P* Pockels cell, *M* turning mirror, *G* galvanometric mirrors, L_1, L_2, L_3, L_4 telescope lenses, *D* dichroic mirror, *OBJ* objective, *PMT* photomultiplier tube

photo-conversion devices (e.g., avalanche photodiodes or photomultiplier tubes) in the non-descanned configuration.

Fluorescent Calcium Indicators

Fluorescent calcium dyes are calcium-binding molecules that change their fluorescent properties upon binding calcium. There are two broad classes of indicators, chemically engineered and genetically encoded molecules. Chemically engineered indicators can be used to measure calcium over a wide concentration range [25–27]; in general, these indicators are relatively easy to use and load into the cells *in vivo* (see below). In contrast, genetically encoded sensors require the coding DNA to be inserted into the cells by methods that include electroporation, virus injection and the generation of a transgenic animal.

Synthetic calcium indicators were developed by Roger Tsien and coworkers about 30 years ago [1, 2] and currently comprise a large family of molecules with high dynamic ranges, various affinities and fast binding dynamics [28]. Because they were originally developed for single-photon excitation, many fluorophores are less suited to two-photon illumination [17]. Nonetheless, some (e.g. Fluo-4 and Oregon Green BAPTA) have sufficient two-photon cross sections and are largely used in imaging experiments *in vivo* [11, 29, 30]. An advantage of two-photon illumination is that the excitation spectra are usually broader than with single-photon excitation; thus, a single wavelength can excite two different dyes, the fluorescent signals of which are then separated by a dichroic mirror in the emission path [31].

Indicators can be made in either a hydrophilic or hydrophobic form, with the latter being created by binding an acetoxymethyl (AM) group to the hydrophilic form with an ester bond. *In vivo*, the AM form can be loaded into many cells using a bulk loading approach [11, 31] (see Fig. 4.2a–c). A glass pipette containing the AM indicator is lowered into the cortex, and upon reaching the desired depth, a pressure pulse is applied inside the pipette to eject the indicator into the extracellular space. Because the AM form of the indicator permeates lipid membranes, the indicator enters cells that are in the vicinity of the injection site. Once in the cytoplasm, the ester bond is cleaved by the activity of intracellular esterases, and the hydrophobic indicator becomes hydrophilic and trapped within the cell. As a result, the intracellular concentration of the dye becomes higher than that of the injected solution [31]. However, a limitation of this approach is that all of the cells near the injection site (neurons, interneurons and glia) are labeled, and thus it becomes difficult to differentiate the responses of various cell types. This problem has been partly circumvented by the use of sulforhodamine 101 (SR101), a fluorescent dye that selectively stains astrocytes [32]. It should be noted, however, that sulforhodamine has recently been reported to affect synaptic plasticity [33], and thus should be used cautiously. Another efficient strategy for cell identification is the use of the bulk loading approach in combination with genetically modified mice expressing a fluorescent reporter in specific subclasses of cells. If a mouse line carrying a red-emitting

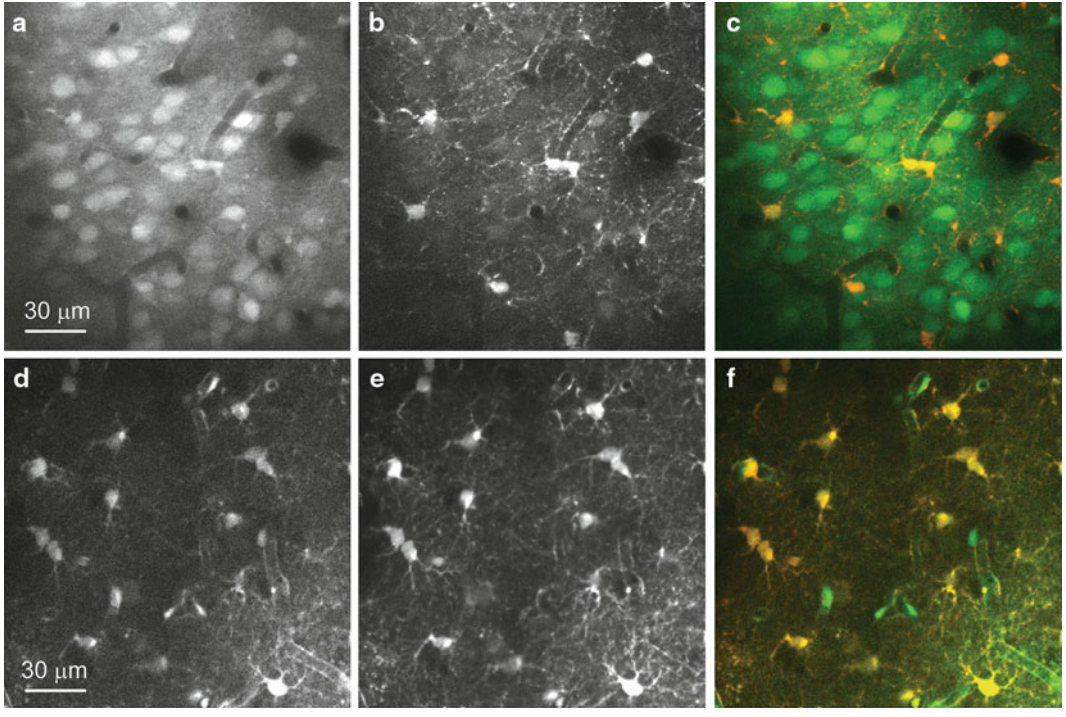

Fig. 4.2 (**a**–**c**) Bulk loading of layer II/III cells in the somatosensory cortex of an anesthetized mouse using Oregon Green BAPTA-AM (**a**) and sulforhodamine 101 (**b**). Oregon Green BAPTA-AM stains all cells, whereas sulforhodamine 101 selectively enters astrocytes. The two images are merged in (**c**). (**d**–**f**) Topical loading of Fluo-4-AM (**d**) and sulforhodamine 101 (**e**) results in the selective loading of astrocytes. The two images are merged in (**f**)

reporter is available, Fluo-4 and Oregon Green BAPTA are the indicators of choice. If, in contrast, mice with a green-emitting reporter (e.g. GFP) are used, functional imaging can be performed with a red-shifted calcium indicator as for example, Fura-2 or Rhod-2 [34]. As an alternative, by analyzing the green and orange components of the emitted fluorescence it is also possible to use GFP in combination with green-emitting dyes as, for example, Oregon Green BAPTA [35]. In contrast to using a bulk loading approach, the AM dye can be applied to the surface of the cortex, where it will enter superficial cells and then spread via the astrocytic syncytium to deeper layers [30, 32], resulting in the selective labeling of astroglial cells (Fig. 4.2d–f).

The hydrophilic version of an indicator is usually loaded into individual cells using an intracellular [36] or patch-clamp electrode [37] or through local electroporation [38, 39]. As discussed in the introduction, synthetic calcium indicators can be used to record the suprathreshold activity of neuronal cells. For superficial cortical neurons, which generally fire at a low frequency [40], a one-to-one relationship between the fluorescent signal and neuronal action potentials has been demonstrated using combined optical and electrophysiological recordings [23, 29, 41–43].

The Tsien laboratory also developed the genetically encoded group of calcium indicators [44, 45], which (compared to synthetic dyes) have the significant advantage of being targeted to either specific cells in the brain or specific subcellular compartments [46], thus facilitating the identification of the cellular source of the signal. Moreover, since their expression is stable, functional imaging of calcium signals over extended periods of time (from weeks to months) is possible [47]. Nonetheless, the methods for delivering the DNA that codes for these indicators present some disadvantages. First, injecting viral particles is invasive and can cause inflammation in the surrounding tissue. Moreover, *in utero* electroporation targets only certain regions and cell types. Lastly, generating a transgenic animal is time-consuming and maybe unsuccessful because of low expression levels of the transgene.

Genetically encoded calcium indicators are generally chimeric proteins comprised of a calcium-binding protein (for example, calmodulin in the case of YC3.6 and D3CPV or Troponin-C in the case of TN-XXL) that is fused to a spectral variant of the Green Fluorescent Protein (GFP). The resulting protein is engineered either in tandem configuration for Förster Resonance Energy Transfer (FRET) or as a single-molecule fluorophore molecule. FRET-based indicators [45, 48, 49], for example members of the Chameleon family, rely on the increase in resonance efficiency between donor and acceptor fluorescent moieties that is induced by a conformational change in the indicator that occurs upon a calcium binding event. This approach allows ratiometric measures, thus minimizing signal fluctuations that can arise from either a change in pH or movement artifacts such as breathing and heart beating. Single-fluorophore indicators [50, 51], for example members of the Camgaroo family, exhibit stronger changes in fluorescence than FRET-based dyes in terms of both brightness and signal-to-noise ratio but generally display slow kinetics [52].

Although genetic sensors generally have a decreased signal-to-noise ratio and slower kinetics compared to synthetic indicators [52], some of these indicators can detect individual action potentials [53].

Spatial and Temporal Mapping of Neuronal Network Activity at Single-Cell Resolution

The capability of two-photon calcium imaging to detect the activity of individual cells (see above) coupled with the possibility to simultaneously monitor hundreds of cells offer researchers the opportunity to map neuronal activity in the intact brain at unprecedented spatial resolution. Cortical layer II/III neurons are the preferred target for two-photon calcium imaging studies, as they are among the most superficial cells in the cortex and exhibit low-frequency action potential firing rates [29]. Calcium transients in these neurons display relatively fast rise-times and slow decay-times (on the order of hundreds of milliseconds) [11]. Simultaneous imaging and electrophysiological recording showed that these calcium signals are due to action potential discharge [29] and thus report the supra-threshold activity of neurons. In the remaining part of this section, we will highlight recent studies that used two-photon fluorescence microscopy to functionally map network activity primarily in the somatosensory and visual cortices.

The somatosensory cortex is a preferred model for the study of sensory integration and input processing [54–57]. Rodents rely primarily on the movement of their vibrissae (or whiskers) for exploration. At the base of each vibrissa, tactile receptors relay sensory information to a sub-region of the somatosensory cortex called the barrel field. This region is composed of highly ordered functional columns (called barrel columns) that contain neurons that primarily respond to the movement of one specific vibrissa. At the center of each column, positioned across layer IV, is the barrel [58], an anatomical dark-stained structure that is composed of neurons innervated by ascending thalamic fibers that relay information from one specific whisker. The barrels are separated by narrow regions called septa. Using this brain area as a model system in combination with two-photon calcium imaging, various investigators have measured the *in vivo* response of cortical networks to sensory stimulation at unprecedented spatial resolution [29, 41, 59]. Whisker-evoked activity is both sparse and highly variable in superficial layers, which is in agreement with previous intracellular patch-clamp recordings [56, 60–63]. Within a given barrel column, an average of ~20% of the neurons respond to a whisker deflection [41, 59]. Importantly, evoked activity displays a high level of spatial organization [41], with barrel-related neurons having a higher probability of firing than septa-related neurons. The highest neuronal spiking probability is at the center of the barrel, and this probability decreases with increasing radial distance from the center. Evoked activity widely fluctuates from trial to trial, and the activity of responding neurons are generally weakly correlated [41]. The correlation of activity between different neurons is a function of the position within the barrel column,

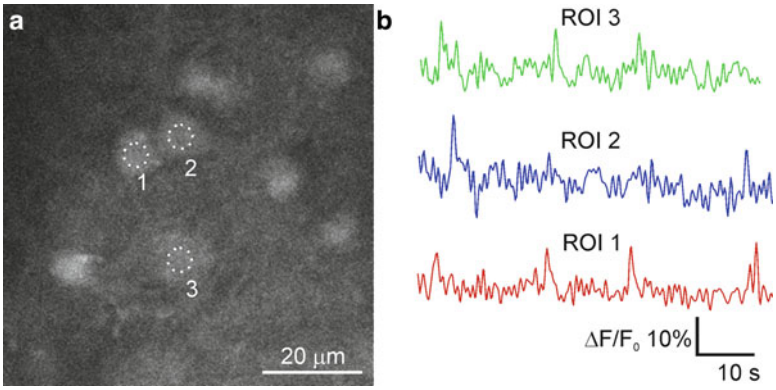

Fig. 4.3 (**a**) Two-photon image of Oregon Green BAPTA-loaded cells in layer II/III of the neocortex. (**b**) Time course of the $\Delta F/F_0$ signal showing calcium elevations in three distinct cells during spontaneous cortical activity

i.e., highest at the center and lowest at the borders of the barrel [41]. In the absence of sensory input, the somatosensory cortex is not silent but exhibits recurrent spontaneous activity. Using two-photon microscopy, spontaneous activity in the somatosensory cortex has also been observed and was found to be sparse and highly variable (Fig. 4.3). Around 10% of the neurons in layer II/III fire APs during up-states as shown using two-photon calcium imaging, a result that is in agreement with previous electrophysiological data [56]. The latency between AP firing and the onset of the up-state is highly variable, and spontaneous activity displays a smaller degree of spatial organization than whisker-evoked activity [29].

In addition to the barrel cortex, other brain regions (including the visual cortex) have been extensively studied with two-photon microscopy [42, 64–66]. When a moving bar is used as a visual stimulus, neurons in the visual cortex respond preferentially to a specific orientation or movement direction of the bar. Traditional imaging approaches that utilize voltage-sensitive dyes or metabolic-related signals have demonstrated that domains of direction and orientation preference are present in higher mammals. These domains involve ample cortical regions with sharp transitions from one domain to another [67–69]. Nonetheless, due to the limited spatial resolution (~100 μm) of these traditional approaches, the precise borders between domains could not be resolved. Using two-photon calcium imaging, it is possible to map the function of orientation and direction domains within the visual cortex at cellular resolution [64, 65]. Using this approach, direction preference domains are found to be rather uniform, with all of the cells within a domain showing a similar response to the stimulus. No interspersed cells that are tuned to opposite directions have been observed. At the border of domains that have different orientations (called pinwheel centers), the boundaries are (at the cellular level) extremely sharp, with neighboring neurons having different direction preferences [64, 65]. Interestingly and in contrast to the rodent somatosensory cortex, neurons that respond similarly to a given stimulus orientation are also more likely to be spontaneously co-active, which suggests

that functionally-related cells might be organized in distinct sub-networks [66]. This concept has recently received a direct experimental validation [70]. The response of neurons to visual stimuli was first recorded with functional calcium imaging *in vivo*. The connectivity of the same cells recorded *in vivo* was then determined in brain slices using multi patch-clamp recordings. Neurons that responded similarly to visual stimulation were found to form connections at higher rates than neurons with uncorrelated responses [70]. By combining two-photon calcium imaging with genetic- or immuno-labeling of cortical interneurons in layer II/III, these studies were recently expanded to the interneuronal network [71–75]. Different types of interneurons (e.g., positive for parvalbumin, somatostatin and vasoactive intestinal peptide) have a broader selectivity for orientation than excitatory neurons [72], although heterogeneity of responses, even within parvalbumin-positive interneurons, has been observed [74].

Imaging Calcium at Subcellular Resolution

Besides the cell soma the multi-bolus bulk loading approach described in the previous sections leads to staining of the neuropil, which includes dendritic, axonal and glial processes. The fluorescence emitted by the neuropil is mainly generated by axons and thus reflect local input activity [29]. Nonetheless, given that the background neuropil signal is strong, diffuse and contains fluorescence generated in processes that belong to several different cells, individual processes cannot be resolved. As originally shown with Golgi staining, visualizing these fine cellular structures can be achieved only by sparse labeling of a small number of cells. Visualizing one or a few neurons can be achieved by intracellular loading via a glass pipette, using either a sharp [4] or tight-seal electrode [76] or by local electroporation [38, 39]. Alternatively, the use of genetically-encoded calcium probes has also proved successful for visualizing calcium signals in small neuronal processes [77, 78].

The combination of these labeling approaches with the development of improved scanning systems for two-photon microscopy [37, 79] has made it possible to visualize the complexity of intracellular calcium signaling in the dendritic tree of cells while they are embedded in their natural context during sensory stimulation. Initial experiments demonstrated that single action potential-mediated calcium transients are strong in proximal and absent in the distal dendrites of layer II/III neurons [36, 76]. However, when the action potential coincides with a synaptic input, either driven by extracellular stimulation [76] or by spontaneous ongoing activity [80], a supralinear response occurs in distal dendrites. The calcium signal that is generated by the combined stimulation of synaptic activity and action potential back-propagation has higher amplitude than the sum of each individual stimulus. In the case of layer II/III neurons, this supralinear summation has been proposed to represent a mechanism that links ascending sensory inputs from layer IV with the associative inputs to layer I via local cortical microcircuits [76]. Using a fiber-optic microendoscope to image calcium signals in layer V dendrites, two studies provided remarkable

insight into the functional interactions, at dendritic resolution, of cortical excitatory and inhibitory circuits [81] among various brain states [82] in both anesthetized and awake animals. More recently, using *in vivo* high-speed image acquisition, subthreshold calcium signals in layer II/III dendrites in the visual cortex were visualized, and a map of the spatial distribution of orientation-selective synaptic inputs was generated [37]. Afferents with the same orientation specificity are widely scattered throughout the dendritic tree, whereas inputs with different orientation preferences can be located in adjacent dendritic regions [37].

Astrocytes Display Complex Spontaneous and Activity-Evoked Calcium Signals

Because they lack electrical excitability, the functional importance of astrocytes has long been underestimated. However, recent studies demonstrated that astrocytes can sense changes in the extracellular concentration of many molecules and neurotransmitters [6]. Experiments with cultured cells [83, 84] and slice preparations [85, 86] demonstrated that astrocytes exhibit spontaneous and neuronal activity-driven oscillations in their intracellular calcium concentration. The advent of two-photon fluorescence microscopy has expanded these initial studies and has made it possible to investigate *in vivo* astrocytic calcium signaling. In 2004, Hirase and coworkers described spontaneous calcium oscillations in cortical astrocytes of anesthetized rats [87]. Three principal patterns of intracellular calcium elevation were identified: extremely low frequency (< 0.025 Hz) oscillations in baseline calcium levels; brief (5–50 s) calcium spikes and prolonged (>50 s) plateaus. Spontaneous calcium transients are sporadic events that typically occur in individual astrocytes, with limited correlation with the activity of neighboring glial cells [32, 87]. On the other hand, a more recent study found that a subset (around 10%) of spontaneous calcium increases occurred in locally synchronized cell groups: dynamic clusters containing 2–5 cortical astrocytes in a volume of ~80 μm in diameter were simultaneously activated within 2 s [88]. These spontaneous events are independent of neuronal activity, as they are unaffected by the voltage-gated sodium channel blocker tetrodotoxin [89].

In addition to spontaneous calcium fluctuations, there is a large body of *in vivo* evidence showing that neuronal activity can trigger calcium oscillations in astrocytes. For example, applying the $GABA_A$ antagonists bicuculline or picrotoxin to enhance the activity of the excitatory network boosts calcium oscillations and the level of correlation of astrocytic calcium signals [12, 87]. Sensory stimuli also trigger increased astrocytic calcium signaling. Whisker deflection or toe pinch, visual stimuli and odor stimuli each reliably induces calcium oscillations in astrocytes within the somatosensory cortex [90, 91], the visual cortex [92] and the olfactory bulb [93], respectively. Whereas spontaneous calcium oscillations are rare and primarily involve individual astrocytes ([87], but see [88]), activity-evoked Ca^{2+} fluctuations synchronously involve clusters of neighboring cells [92]. Astrocytic

calcium responses measured in the cell body are usually delayed by 1–6 s relative to neuronal responses [90, 92–94]. However, in some cases, the astrocytic response can be as fast as the neuronal one. For example, a small subset (5%) of astrocytes in the somatosensory cortex has a short (0.5 s) latency response following sensory stimulation [91]. Sensory-evoked calcium responses in astrocytes are spatially coordinated in a manner that is very similar to neurons (see also the previous sections). For example, in the visual cortex, the presentation of moving bars with different orientations causes different groups of astrocytes to respond in topologically ordered maps. Compared to neurons, astrocytes have spatially limited receptive fields and even sharper spatial frequency tuning and orientation preference [92]. Calcium waves that propagate through the astrocytic network have been observed *in vivo* in the cerebellum [95] and in the dorsal hippocampus after surgical removal of the overlying cortex [96].

The mechanisms that underlie sensory-evoked calcium oscillations in astrocytes are not fully understood. Because the processes of one astrocyte contact over 10^5 synapses [97, 98], and because a broad repertoire of receptors for distinct neurotransmitters are available on their cell membrane [6], these glial cells are well suited to sense synaptic activity. mGluR agonists cause calcium elevations (Fig. 4.4a–b), whereas the mGluR1 and mGluR5 antagonists LY367385 and MPEP, respectively, attenuate sensory-evoked astrocytic responses, thereby suggesting that metabotropic glutamate receptors may initiate the astrocytic Ca^{2+} response to whisker stimulation [90]. In the olfactory bulb [93], odor-evoked calcium transients in glomerular astrocytes are suppressed by topical application of MPEP and the group I/II mGluR antagonist MCPG, confirming that the neurotransmitter glutamate (acting through metabotropic receptors) is involved in driving astrocytic calcium transients. The observation that application of the glutamate transporter antagonist TBOA significantly reduces sensory-evoked astrocytic responses [92] also suggests that glutamate may drive calcium signaling in astrocytes by multiple pathways. Moreover, molecules other than glutamate are likely involved in the generation of calcium responses in astrocytes. For example, in the somatosensory cortex, footshock stimulation causes astrocytic calcium transients that are mediated by long-range noradrenergic inputs from the locus ceruleus and are significantly reduced by local administration of the α-adrenergic antagonist yohimbine [94]. Experiments performed in brain slices suggest that Ca^{2+} ions are primarily released by the activation of IP3 receptors located in intracellular stores [6]. In support of this hypothesis, spontaneous and, Gq-linked, GPCR mediated calcium increases are significantly prevented in IP3R2 knockout mice [99], and these results have been recently confirmed by *in vivo* experiments [100]. Taken together, these *in vivo* studies demonstrate that astrocytes exhibit a complex pattern of excitability that is based on changes in the intracellular calcium concentration. These oscillations can be either spontaneous or driven by neuronal activity and are likely generated by separate mechanisms.

Researchers studying glial cells are now faced with a number of fundamental questions: What is the role of calcium signaling in astrocytes? What are the functional implications of astrocytic calcium signals in the brain? Given that astrocytes

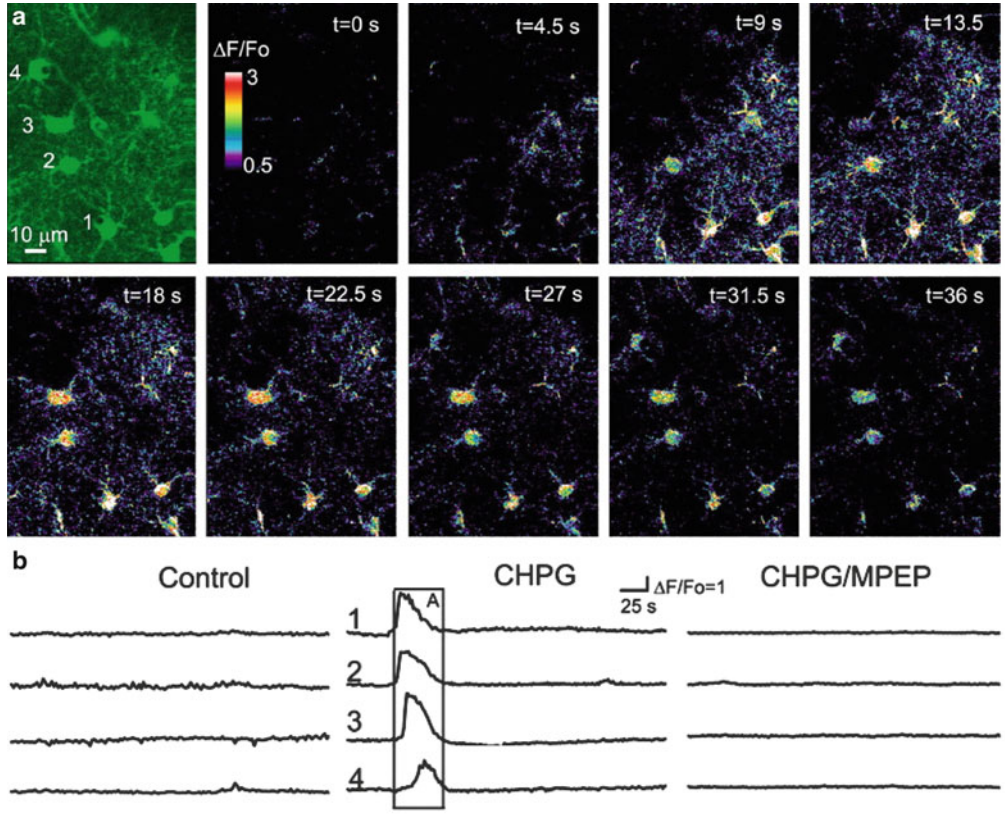

Fig. 4.4 (**a–b**) *in vivo* application of the mGluR agonist 2-chloro-5-hydroxyphenylglycine (*CHPG*) causes propagating calcium waves in astrocytes. Astrocyte-specific loading is achieved by topical application of Fluo-4-AM (Reproduced with permission from Ding et al. [30])

can respond to neuronal activity with calcium elevations, can they also signal back to neurons? Several lines of evidence obtained from various groups over the past 15 years demonstrate crucial roles of astrocytic calcium signaling in brain physiology and pathology. Astrocytic calcium signals trigger the release of various neuroactive molecules that have been shown *in vivo* to regulate local blood microcirculation [101–103], neuronal excitability [104, 105], network activity [106] and behavior [107]. This bi-directional communication between neurons and astrocytes forms the basis of the so-called "tripartite synapse" [8, 108], in which astrocytes are considered the third active synaptic element together with the pre- and post-synaptic compartments. This third element modulates the function of neurons by releasing various molecules called "gliotransmitters". How are distinct astrocytic calcium patterns linked to the release of different gliotransmitters, and how do distinct molecules modulate synaptic function and behavior *in vivo* are outstanding questions that have only recently begun to be addressed.

Present and Future Perspectives

The investigation of electrical activity in the intact central nervous system ideally requires a wide range of temporal resolutions from milliseconds to days and even months and spatial resolution ranging from a few microns to centimeters. Optical approaches, in particular two-photon calcium imaging, have the potential to fulfill this requirement of spatiotemporal resolutions; however, major technical advancements on multiple levels must be made to achieve this goal. For example, a major limitation of currently available scanning microscopes that use a galvanometric mirror is that image acquisition is time-consuming and has a maximum full frame rate of only a few frames per second. The use of resonant scanning mirrors has increased the acquisition rate to as fast as 30 fps but does not overcome the intrinsic limitation of raster scanning [37]. A promising solution to this problem is to use an acousto-optic deflector (AOD). An AOD-based microscope was recently used for *in vivo* fluorescence imaging, achieving an increase in frame rate of nearly two orders of magnitude (up to 1,000 fps). Using this approach, a map was generated of the suprathreshold activity of several tens of neurons in the somatosensory and visual cortices during sensory stimulation [23]. Another promising approach is the use of spatial light modulators [109]; however, to date, this technique has only been used to study cultured cells and slices [110–113], and its applicability in *in vivo* applications has not yet been validated.

Furthermore, since network responses can be deeply influenced by anesthetics [114, 115], it is increasingly evident that physiological studies will more and more require the recording from awake, behaving animals. Researchers have developed two different strategies to tackle the hurdles typically associated with an awake animal preparation, particularly those that are linked to mechanical instability and movement artifacts. On the one side, microfabricated fiber optic-based microscopes have been developed [116, 117]; these portable microscopes can be secured to

the skull of small rodents and can image cellular activity during active behavior at sufficiently high resolution [118, 119]. On the other side, following on the footsteps of experimental paradigms that are used in experiments involving flies, imaging techniques in head-restrained, awake rodents have been developed [120]. In this paradigm, the mouse is kept awake with its head secured under the two-photon microscope. Head-fixed mice can perform certain behavioral tasks [121–123] such as running on a treadmill in front of a virtual environment that is projected on a screen [124, 125]. These innovative approaches, together with the development of new calcium indicators and the use of genetics to obtain reporter expression in specific cell subpopulations, will allow researchers to study learning-correlated activity in hundreds of neurons and glial cells. These experiments promise to provide fundamental clues regarding sensory and motor processing in the brain under both physiological and pathological conditions.

Acknowledgments This work was supported by grants from Telethon-Italy (GGP10138) and San Paolo "Programma in Neuroscienze".

References

1. Tsien RY (1980) New calcium indicators and buffers with high selectivity against magnesium and protons: design, synthesis, and properties of prototype structures. Biochemistry 19:2396–2404
2. Tsien RY (1981) A non-disruptive technique for loading calcium buffers and indicators into cells. Nature 290:527–528
3. Helmchen F, Imoto K, Sakmann B (1996) Ca2+ buffering and action potential-evoked Ca2+ signaling in dendrites of pyramidal neurons. Biophys J 70:1069–1081
4. Svoboda K, Denk W, Kleinfeld D, Tank DW (1997) In vivo dendritic calcium dynamics in neocortical pyramidal neurons. Nature 385:161–165
5. Borst JG, Helmchen F (1998) Calcium influx during an action potential. Methods Enzymol 293:352–371
6. Haydon PG (2001) GLIA: listening and talking to the synapse. Nat Rev Neurosci 2:185–193
7. Volterra A, Meldolesi J (2005) Astrocytes, from brain glue to communication elements: the revolution continues. Nat Rev Neurosci 6:626–640
8. Fellin T (2009) Communication between neurons and astrocytes: relevance to the modulation of synaptic and network activity. J Neurochem 108:533–544
9. Halassa MM, Fellin T, Haydon PG (2007) The tripartite synapse: roles for gliotransmission in health and disease. Trends Mol Med 13:54–63
10. Halassa MM, Haydon PG (2010) Integrated brain circuits: astrocytic networks modulate neuronal activity and behavior. Annu Rev Physiol 72:335–355
11. Stosiek C, Garaschuk O, Holthoff K, Konnerth A (2003) In vivo two-photon calcium imaging of neuronal networks. Proc Natl Acad Sci USA 100:7319–7324
12. Gobel W, Kampa BM, Helmchen F (2007) Imaging cellular network dynamics in three dimensions using fast 3D laser scanning. Nat Methods 4:73–79
13. Helmchen F, Denk W (2005) Deep tissue two-photon microscopy. Nat Methods 2:932–940
14. Denk W, Strickler JH, Webb WW (1990) Two-photon laser scanning fluorescence microscopy. Science 248:73–76
15. Denk W, Svoboda K (1997) Photon upmanship: why multiphoton imaging is more than a gimmick. Neuron 18:351–357

16. Zipfel WR, Williams RM, Webb WW (2003) Nonlinear magic: multiphoton microscopy in the biosciences. Nat Biotechnol 21:1369–1377
17. Svoboda K, Yasuda R (2006) Principles of two-photon excitation microscopy and its applications to neuroscience. Neuron 50:823–839
18. Theer P, Hasan MT, Denk W (2003) Two-photon imaging to a depth of 1000 microm in living brains by use of a Ti:Al2O3 regenerative amplifier. Opt Lett 28:1022–1024
19. Diaspro A (1999) Introduction to two-photon microscopy. Microsc Res Tech 47:163–164
20. Diaspro A, Sheppard C (2002) Confocal and two-photon microscopy: foundations, applications, and advances. Wiley-Liss, New York
21. So PT, Dong CY, Masters BR, Berland KM (2000) Two-photon excitation fluorescence microscopy. Annu Rev Biomed Eng 2:399–429
22. Majewska A, Yiu G, Yuste R (2000) A custom-made two-photon microscope and deconvolution system. Pflugers Arch 441:398–408
23. Grewe BF, Langer D, Kasper H, Kampa BM, Helmchen F (2010) High-speed in vivo calcium imaging reveals neuronal network activity with near-millisecond precision. Nat Methods 7:399–405
24. Helmchen F, Denk W (2002) New developments in multiphoton microscopy. Curr Opin Neurobiol 12:593–601
25. Tsien RY (1988) Fluorescence measurement and photochemical manipulation of cytosolic free calcium. Trends Neurosci 11:419–424
26. Tsien RY (1989) Fluorescent indicators of ion concentrations. Methods Cell Biol 30:127–156
27. Tsien RY (1989) Fluorescent probes of cell signaling. Annu Rev Neurosci 12:227–253
28. Paredes RM, Etzler JC, Watts LT, Zheng W, Lechleiter JD (2008) Chemical calcium indicators. Methods 46:143–151
29. Kerr JN, Greenberg D, Helmchen F (2005) Imaging input and output of neocortical networks in vivo. Proc Natl Acad Sci USA 102:14063–14068
30. Ding S, Fellin T, Zhu Y, Lee SY, Auberson YP, Meaney DF, Coulter DA, Carmignoto G, Haydon PG (2007) Enhanced astrocytic Ca2+ signals contribute to neuronal excitotoxicity after status epilepticus. J Neurosci 27:10674–10684
31. Garaschuk O, Milos RI, Konnerth A (2006) Targeted bulk-loading of fluorescent indicators for two-photon brain imaging in vivo. Nat Protoc 1:380–386
32. Nimmerjahn A, Kirchhoff F, Kerr JN, Helmchen F (2004) Sulforhodamine 101 as a specific marker of astroglia in the neocortex in vivo. Nat Methods 1:31–37
33. Kang J, Kang N, Yu Y, Zhang J, Petersen N, Tian GF, Nedergaard M (2010) Sulforhodamine 101 induces long-term potentiation of intrinsic excitability and synaptic efficacy in hippocampal CA1 pyramidal neurons. Neuroscience 169:1601–1609
34. Rubart M, Pasumarthi KB, Nakajima H, Soonpaa MH, Nakajima HO, Field LJ (2003) Physiological coupling of donor and host cardiomyocytes after cellular transplantation. Circ Res 92:1217–1224
35. Gandhi SP, Yanagawa Y, Stryker MP (2008) Delayed plasticity of inhibitory neurons in developing visual cortex. Proc Natl Acad Sci USA 105:16797–16802
36. Svoboda K, Helmchen F, Denk W, Tank DW (1999) Spread of dendritic excitation in layer 2/3 pyramidal neurons in rat barrel cortex in vivo. Nat Neurosci 2:65–73
37. Jia H, Rochefort NL, Chen X, Konnerth A (2010) Dendritic organization of sensory input to cortical neurons in vivo. Nature 464:1307–1312
38. Nevian T, Helmchen F (2007) Calcium indicator loading of neurons using single-cell electroporation. Pflugers Arch 454:675–688
39. Nagayama S, Zeng S, Xiong W, Fletcher ML, Masurkar AV, Davis DJ, Pieribone VA, Chen WR (2007) In vivo simultaneous tracing and Ca(2+) imaging of local neuronal circuits. Neuron 53:789–803
40. Brecht M, Roth A, Sakmann B (2003) Dynamic receptive fields of reconstructed pyramidal cells in layers 3 and 2 of rat somatosensory barrel cortex. J Physiol 553:243–265

41. Kerr JN, de Kock CP, Greenberg DS, Bruno RM, Sakmann B, Helmchen F (2007) Spatial organization of neuronal population responses in layer 2/3 of rat barrel cortex. J Neurosci 27:13316–13328
42. Smith SL, Hausser M (2010) Parallel processing of visual space by neighboring neurons in mouse visual cortex. Nat Neurosci 13:1144–1149
43. Cheng A, Goncalves JT, Golshani P, Arisaka K, Portera-Cailliau C (2011) Simultaneous two-photon calcium imaging at different depths with spatiotemporal multiplexing. Nat Methods 8:139–142
44. Miyawaki A, Llopis J, Heim R, McCaffery JM, Adams JA, Ikura M, Tsien RY (1997) Fluorescent indicators for Ca2+ based on green fluorescent proteins and calmodulin. Nature 388:882–887 [see comments]
45. Miyawaki A, Griesbeck O, Heim R, Tsien RY (1999) Dynamic and quantitative Ca2+ measurements using improved cameleons. Proc Natl Acad Sci USA 96:2135–2140
46. Kotlikoff MI (2007) Genetically encoded Ca2+ indicators: using genetics and molecular design to understand complex physiology. J Physiol 578:55–67
47. Mank M, Santos AF, Direnberger S, Mrsic-Flogel TD, Hofer SB, Stein V, Hendel T, Reiff DF, Levelt C, Borst A, Bonhoeffer T, Hubener M, Griesbeck O (2008) A genetically encoded calcium indicator for chronic in vivo two-photon imaging. Nat Methods 5:805–811
48. Pologruto TA, Yasuda R, Svoboda K (2004) Monitoring neural activity and [Ca2+] with genetically encoded Ca2+ indicators. J Neurosci 24:9572–9579
49. Griesbeck O, Baird GS, Campbell RE, Zacharias DA, Tsien RY (2001) Reducing the environmental sensitivity of yellow fluorescent protein mechanism and applications. J Biol Chem 276:29188–29194
50. Nakai J, Ohkura M, Imoto K (2001) A high signal-to-noise Ca(2+) probe composed of a single green fluorescent protein. Nat Biotechnol 19:137–141
51. Nagai T, Sawano A, Park ES, Miyawaki A (2001) Circularly permuted green fluorescent proteins engineered to sense Ca2+. Proc Natl Acad Sci USA 98:3197–3202
52. Hendel T, Mank M, Schnell B, Griesbeck O, Borst A, Reiff DF (2008) Fluorescence changes of genetic calcium indicators and OGB-1 correlated with neural activity and calcium in vivo and in vitro. J Neurosci 28:7399–7411
53. Wallace DJ, Meyer zum Alten BS, Astori S, Yang Y, Bausen M, Kugler S, Palmer AE, Tsien RY, Sprengel R, Kerr JN, Denk W, Hasan MT (2008) Single-spike detection in vitro and in vivo with a genetic Ca2+ sensor. Nat Methods 5:797–804
54. Petersen CC (2003) The barrel cortex–integrating molecular, cellular and systems physiology. Pflugers Arch 447:126–134
55. Petersen CC (2007) The functional organization of the barrel cortex. Neuron 56:339–355
56. Brecht M (2007) Barrel cortex and whisker-mediated behaviors. Curr Opin Neurobiol 17:408–416
57. Diamond ME, von Heimendahl M, Knutsen PM, Kleinfeld D, Ahissar E (2008) 'Where' and 'what' in the whisker sensorimotor system. Nat Rev Neurosci 9:601–612
58. Woolsey TA, Van der Loos H (1970) The structural organization of layer IV in the somatosensory region (SI) of mouse cerebral cortex. The description of a cortical field composed of discrete cytoarchitectonic units. Brain Res 17:205–242
59. Sato TR, Gray NW, Mainen ZF, Svoboda K (2007) The functional microarchitecture of the mouse barrel cortex. PLoS Biol 5:e189
60. Margrie TW, Brecht M, Sakmann B (2002) In vivo, low-resistance, whole-cell recordings from neurons in the anaesthetized and awake mammalian brain. Pflugers Arch-Eur J Physiol 444:491–498
61. Petersen CC, Grinvald A, Sakmann B (2003) Spatiotemporal dynamics of sensory responses in layer 2/3 of rat barrel cortex measured in vivo by voltage-sensitive dye imaging combined with whole-cell voltage recordings and neuron reconstructions. J Neurosci 23:1298–1309
62. Petersen CCH, Hahn TTG, Mehta M, Grinvald A, Sakmann B (2003) Interaction of sensory responses with spontaneous depolarization in layer 2/3 barrel cortex. Proc Natl Acad Sci USA 100:13638–13643

63. Waters J, Helmchen F (2006) Background synaptic activity is sparse in neocortex. J Neurosci 26:8267–8277
64. Ohki K, Chung S, Ch'ng YH, Kara P, Reid RC (2005) Functional imaging with cellular resolution reveals precise micro-architecture in visual cortex. Nature 433:597–603
65. Ohki K, Chung S, Kara P, Hubener M, Bonhoeffer T, Reid RC (2006) Highly ordered arrangement of single neurons in orientation pinwheels. Nature 442:925–928
66. Ch'ng YH, Reid RC (2010) Cellular imaging of visual cortex reveals the spatial and functional organization of spontaneous activity. Front Integr Neurosci 4:20
67. Bonhoeffer T, Grinvald A (1991) Iso-orientation domains in cat visual cortex are arranged in pinwheel-like patterns. Nature 353:429–431
68. Shmuel A, Grinvald A (1996) Functional organization for direction of motion and its relationship to orientation maps in cat area 18. J Neurosci 16:6945–6964
69. Shoham D, Glaser DE, Arieli A, Kenet T, Wijnbergen C, Toledo Y, Hildesheim R, Grinvald A (1999) Imaging cortical dynamics at high spatial and temporal resolution with novel blue voltage-sensitive dyes. Neuron 24:791–802
70. Ko H, Hofer SB, Pichler B, Buchanan KA, Sjostrom PJ, Mrsic-Flogel TD (2011) Functional specificity of local synaptic connections in neocortical networks. Nature 473:87–91
71. Sohya K, Kameyama K, Yanagawa Y, Obata K, Tsumoto T (2007) GABAergic neurons are less selective to stimulus orientation than excitatory neurons in layer II/III of visual cortex, as revealed by in vivo functional Ca2+ imaging in transgenic mice. J Neurosci 27:2145–2149
72. Kerlin AM, Andermann ML, Berezovskii VK, Reid RC (2010) Broadly tuned response properties of diverse inhibitory neuron subtypes in mouse visual cortex. Neuron 67:858–871
73. Kameyama K, Sohya K, Ebina T, Fukuda A, Yanagawa Y, Tsumoto T (2010) Difference in binocularity and ocular dominance plasticity between GABAergic and excitatory cortical neurons. J Neurosci 30:1551–1559
74. Runyan CA, Schummers J, Van WA, Kuhlman SJ, Wilson NR, Huang ZJ, Sur M (2010) Response features of parvalbumin-expressing interneurons suggest precise roles for subtypes of inhibition in visual cortex. Neuron 67:847–857
75. Zariwala HA, Madisen L, Ahrens KF, Bernard A, Lein ES, Jones AR, Zeng H (2011) Visual tuning properties of genetically identified layer 2/3 neuronal types in the primary visual cortex of cre-transgenic mice. Front Syst Neurosci 4:162
76. Waters J, Larkum M, Sakmann B, Helmchen F (2003) Supralinear Ca2+ influx into dendritic tufts of layer 2/3 neocortical pyramidal neurons in vitro and in vivo. J Neurosci 23:8558–8567
77. Lutcke H, Murayama M, Hahn T, Margolis DJ, Astori S, Zum Alten Borgloh SM, Gobel W, Yang Y, Tang W, Kugler S, Sprengel R, Nagai T, Miyawaki A, Larkum ME, Helmchen F, Hasan MT (2010) Optical recording of neuronal activity with a genetically-encoded calcium indicator in anesthetized and freely moving mice. Front Neural Circuits 4:9
78. Heim N, Garaschuk O, Friedrich MW, Mank M, Milos RI, Kovalchuk Y, Konnerth A, Griesbeck O (2007) Improved calcium imaging in transgenic mice expressing a troponin C-based biosensor. Nat Methods 4:127–129
79. Gobel W, Helmchen F (2007) New angles on neuronal dendrites in vivo. J Neurophysiol 98:3770–3779
80. Waters J, Helmchen F (2004) Boosting of action potential backpropagation by neocortical network activity in vivo. J Neurosci 24:11127–11136
81. Murayama M, Perez-Garci E, Nevian T, Bock T, Senn W, Larkum ME (2009) Dendritic encoding of sensory stimuli controlled by deep cortical interneurons. Nature 457:1137–1141
82. Murayama M, Larkum ME (2009) Enhanced dendritic activity in awake rats. Proc Natl Acad Sci USA 106:20482–20486
83. Cornell-Bell AH, Finkbeiner SM, Cooper MS, Smith SJ (1990) Glutamate induces calcium waves in cultured astrocytes: long-range glial signaling. Science 247:470–473
84. Charles AC, Merrill JE, Dirksen ER, Sanderson MJ (1991) Intercellular signaling in glial cells: calcium waves and oscillations in response to mechanical stimulation and glutamate. Neuron 6:983–992

85. Porter JT, McCarthy KD (1996) Hippocampal astrocytes *in situ* respond to glutamate released from synaptic terminals. J Neurosci 16:5073–5081
86. Pasti L, Volterra A, Pozzan T, Carmignoto G (1997) Intracellular calcium oscillations in astrocytes: a highly plastic, bidirectional form of communication between neurons and astrocytes in situ. J Neurosci 17:7817–7830
87. Hirase H, Qian L, Bartho P, Buzsaki G (2004) Calcium dynamics of cortical astrocytic networks in vivo. PLoS Biol 2:E96
88. Sasaki T, Kuga N, Namiki S, Matsuki N, Ikegaya Y (2011) Locally synchronized astrocytes. Cereb Cortex 21:1889–1900
89. Takata N, Hirase H (2008) Cortical layer 1 and layer 2/3 astrocytes exhibit distinct calcium dynamics in vivo. PLoS One 3:e2525
90. Wang XH, Lou NH, Xu QW, Tian GF, Peng WG, Han XN, Kang J, Takano T, Nedergaard M (2006) Astrocytic Ca2+ signaling evoked by sensory stimulation in vivo. Nat Neurosci 9:816–823
91. Winship IR, Plaa N, Murphy TH (2007) Rapid astrocyte calcium signals correlate with neuronal activity and onset of the hemodynamic response in vivo. J Neurosci 27:6268–6272
92. Schummers J, Yu H, Sur M (2008) Tuned responses of astrocytes and their influence on hemodynamic signals in the visual cortex. Science 320:1638–1643
93. Petzold GC, Albeanu DF, Sato TF, Murthy VN (2008) Coupling of neural activity to blood flow in olfactory glomeruli is mediated by astrocytic pathways. Neuron 58:897–910
94. Bekar LK, He W, Nedergaard M (2008) Locus coeruleus alpha-adrenergic-mediated activation of cortical astrocytes in vivo. Cereb Cortex 18:2789–2795
95. Nimmerjahn A, Mukamel EA, Schnitzer MJ (2009) Motor behavior activates Bergmann glial networks. Neuron 62:400–412
96. Kuga N, Sasaki T, Takahara Y, Matsuki N, Ikegaya Y (2011) Large-scale calcium waves traveling through astrocytic networks in vivo. J Neurosci 31:2607–2614
97. Bushong EA, Martone ME, Jones YZ, Ellisman MH (2002) Protoplasmic astrocytes in CA1 stratum radiatum occupy separate anatomical domains. J Neurosci 22:183–192
98. Halassa MM, Fellin T, Takase H, Dong JH, Haydon PG (2007) Synaptic islands defined by the territory of a single astrocyte. J Neurosci 27:6473–6477
99. Petravicz J, Fiacco TA, McCarthy KD (2008) Loss of IP3 receptor-dependent Ca2+ increases in hippocampal astrocytes does not affect baseline CA1 pyramidal neuron synaptic activity. J Neurosci 28:4967–4973
100. Takata N, Mishima T, Hisatsune C, Ebisui E, Mikoshiba K, Hirase H (2010) Astrocytic contribution of a sensory induced synaptic plasticity in the somatosensory cortex (Abstract). Soc Neurosci San Diego, CA
101. Takano T, Tian GF, Peng W, Lou N, Libionka W, Han X, Nedergaard M (2006) Astrocyte-mediated control of cerebral blood flow. Nat Neurosci 9:260–267
102. Iadecola C, Nedergaard M (2007) Glial regulation of the cerebral microvasculature. Nat Neurosci 10:1369–1376
103. Giaume C, Koulakoff A, Roux L, Holcman D, Rouach N (2010) Astroglial networks: a step further in neuroglial and gliovascular interactions. Nat Rev Neurosci 11:87–99
104. Gradinaru V, Mogri M, Thompson KR, Henderson JM, Deisseroth K (2009) Optical deconstruction of parkinsonian neural circuitry. Science 324:354–359
105. Gourine AV, Kasymov V, Marina N, Tang F, Figueiredo MF, Lane S, Teschemacher AG, Spyer KM, Deisseroth K, Kasparov S (2010) Astrocytes control breathing through pH-dependent release of ATP. Science 329:571–575
106. Fellin T, Halassa MM, Terunuma M, Succol F, Takano H, Frank M, Moss SJ, Haydon PG (2009) Endogenous nonneuronal modulators of synaptic transmission control cortical slow oscillations in vivo. Proc Natl Acad Sci USA 106:15037–15042
107. Halassa MM, Florian C, Fellin T, Munoz JR, Lee SY, Abel T, Haydon PG, Frank MG (2009) Astrocytic modulation of sleep homeostasis and cognitive consequences of sleep loss. Neuron 61:213–219

108. Araque A, Parpura V, Sanzgiri RP, Haydon PG (1999) Tripartite synapses: glia, the unacknowledged partner. Trends Neurosci 22:208–215
109. Watson BO, Nikolenko V, Araya R, Peterka DS, Woodruff A, Yuste R (2010) Two-photon microscopy with diffractive optical elements and spatial light modulators. Front Neurosci 4:29
110. Lutz C, Otis TS, DeSars V, Charpak S, DiGregorio DA, Emiliani V (2008) Holographic photolysis of caged neurotransmitters. Nat Methods 5:821–827
111. Nikolenko V, Watson BO, Araya R, Woodruff A, Peterka DS, Yuste R (2008) SLM microscopy: scanless two-photon imaging and photostimulation with spatial light modulators. Front Neural Circuits 2:5–19
112. Dal Maschio M, Difato F, Beltramo R, Blau A, Benfenati F, Fellin T (2010) Simultaneous two-photon imaging and photo-stimulation with structured light illumination. Opt Express 18:18720–18731
113. Papagiakoumou E, Anselmi F, Begue A, de Sars V, Gluckstad J, Isacoff EY, Emiliani V (2010) Scanless two-photon excitation of channelrhodopsin-2. Nat Methods 7:848–854
114. Ferezou I, Bolea S, Petersen CC (2006) Visualizing the cortical representation of whisker touch: voltage-sensitive dye imaging in freely moving mice. Neuron 50:617–629
115. Greenberg DS, Houweling AR, Kerr JN (2008) Population imaging of ongoing neuronal activity in the visual cortex of awake rats. Nat Neurosci 11:749–751
116. Helmchen F, Fee MS, Tank DW, Denk W (2001) A miniature head-mounted two-photon microscope. High-resolution brain imaging in freely moving animals. Neuron 31:903–912
117. Jung JC, Schnitzer MJ (2003) Multiphoton endoscopy. Opt Lett 28:902–904
118. Flusberg BA, Nimmerjahn A, Cocker ED, Mukamel EA, Barretto RP, Ko TH, Burns LD, Jung JC, Schnitzer MJ (2008) High-speed, miniaturized fluorescence microscopy in freely moving mice. Nat Methods 5:935–938
119. Sawinski J, Wallace DJ, Greenberg DS, Grossmann S, Denk W, Kerr JN (2009) Visually evoked activity in cortical cells imaged in freely moving animals. Proc Natl Acad Sci USA 106:19557–19562
120. Dombeck DA, Khabbaz AN, Collman F, Adelman TL, Tank DW (2007) Imaging large-scale neural activity with cellular resolution in awake, mobile mice. Neuron 56:43–57
121. O'Connor DH, Clack NG, Huber D, Komiyama T, Myers EW, Svoboda K (2010) Vibrissa-based object localization in head-fixed mice. J Neurosci 30:1947–1967
122. Komiyama T, Sato TR, O'Connor DH, Zhang YX, Huber D, Hooks BM, Gabitto M, Svoboda K (2010) Learning-related fine-scale specificity imaged in motor cortex circuits of behaving mice. Nature 464:1182–1186
123. O'Connor DH, Peron SP, Huber D, Svoboda K (2010) Neural activity in barrel cortex underlying vibrissa-based object localization in mice. Neuron 67:1048–1061
124. Dombeck DA, Harvey CD, Tian L, Looger LL, Tank DW (2010) Functional imaging of hippocampal place cells at cellular resolution during virtual navigation. Nat Neurosci 13:1433–1440
125. Andermann ML, Kerlin AM, Reid RC (2010) Chronic cellular imaging of mouse visual cortex during operant behavior and passive viewing. Front Cell Neurosci 4:3

Chapter 5
Signaling Through the Extracellular Calcium-Sensing Receptor (CaSR)

Bandana Chakravarti, Naibedya Chattopadhyay, and Edward M. Brown

Abstract The extracellular calcium (Ca^{2+}_o)-sensing receptor (CaSR) was the first GPCR identified whose principal physiological ligand is an ion, namely extracellular Ca^{2+}. It maintains the near constancy of Ca^{2+}_o that complex organisms require to ensure normal cellular function. A wealth of information has accumulated over the past two decades about the CaSR's structure and function, its role in diseases and CaSR-based therapeutics. This review briefly describes the CaSR and key features of its structure and function, then discusses the extracellular signals modulating its activity, provides an overview of the intracellular signaling pathways that it controls, and, finally, briefly describes CaSR signaling both in tissues participating in Ca^{2+}_o homeostasis as well as those that do not. Factors controlling CaSR signaling include various factors affecting the expression of the CaSR gene as well as modulation of its trafficking to and from the cell surface. The dimeric cell surface CaSR, in turn, links to various heterotrimeric and small molecular weight G proteins to regulate intracellular second messengers, lipid kinases, various protein kinases, and transcription factors that are part of the machinery enabling the receptor to modulate the functions of the wide variety of cells in which it is expressed. CaSR signaling is impacted by its interactions with several binding partners in addition to signaling elements per se (i.e., G proteins), including filamin-A and caveolin-1. These latter two proteins act as scaffolds that bind signaling components and other

B. Chakravarti, M.Sc. • N. Chattopadhyay, Ph.D.
Division of Endocrinology, CSIR-Central Drug Research Institute, Lucknow, India
e-mail: vandanaks@gmail.com; n_chattopadhyay@cdri.res.in

E.M. Brown, M.D. (✉)
Division of Endocrinology, Diabetes and Hypertension,
Brigham and Women's Hospital and Harvard Medical School,
EBRC223A, 221 Longwood Ave., Boston, MA 02115, USA
e-mail: embrown@partners.org

M.S. Islam (ed.), *Calcium Signaling*, Advances in Experimental Medicine and Biology 740, DOI 10.1007/978-94-007-2888-2_5,

key cellular elements (e.g., the cytoskeleton). Thus CaSR signaling likely does not take place randomly throughout the cell, but is compartmentalized and organized so as to facilitate the interaction of the receptor with its various signaling pathways.

Keywords Calcium • Calcium-sensing receptor • Parathyroid • Kidney • Bone • Intestine • C-cell • Extracellular fluid • Protein kinase • Phospholipase • Adenylate cyclase • Second messenger • Calmodulin • Tyrosine kinase • Thick ascending limb • Distal convoluted tubule • Inner medullary collecting duct

Introduction

The extracellular calcium (Ca^{2+}_o)-sensing receptor (CaSR) was the first GPCR identified whose principal physiological ligand is an ion, namely extracellular Ca^{2+} [1]. It ensures the nearly constant level of Ca^{2+}_o that complex organism need to ensure normal cellular function [2]. Since its cloning in 1993, a great deal of information has accumulated concerning the CaSR's structure and function, its role in diseases and CaSR-based therapeutics, and these areas are covered in recent reviews [3–6]. Key aspects of the CaSR impacting its biological roles are its intra- and extracellular signaling, which comprise both the numerous extracellular ligands in addition to Ca^{2+} to which it responds as well as the plethora of intracellular signaling cascades that it regulates. This review briefly describes the CaSR and key features of its structure and function, then discusses the extracellular signals modulating its activity, provides an overview of the intracellular signaling pathways that it controls, and, finally, briefly describes CaSR signaling both in tissues participating in Ca^{2+}_o homeostasis (e.g., parathyroid and kidney) as well as those that do not (e.g., normal skin cells and various malignant cell types). Because of space constraints this discussion will not be exhaustive and in some instances the reader will be referred to other reviews rather than to original articles.

Structure and Function of the CaSR

To maintain near constancy of the level of blood Ca^{2+}, there must be a mechanism that senses small changes in Ca^{2+}_o and responds appropriately so as to normalize Ca^{2+}_o [7]. The CaSR serves this function. It is a G protein-coupled receptor (GPCR) with Ca^{2+}_o as its principal physiological ligand. The CaSR was first cloned from bovine parathyroid [1], then from human parathyroid [8] and, subsequently, from a variety of other species (e.g., chicken [9] or dogfish shark [10]).

The CaSR belongs to family C of the GPCRs [11], which is comprised of eight metabotropic glutamate receptors (mGluRs), two $GABA_B$ receptors, receptors for taste and pheromones, and a putative amino acid- and divalent cation-sensing receptor [11, 12]. The human CaSR's 612 amino acid extracellular domain (ECD) is

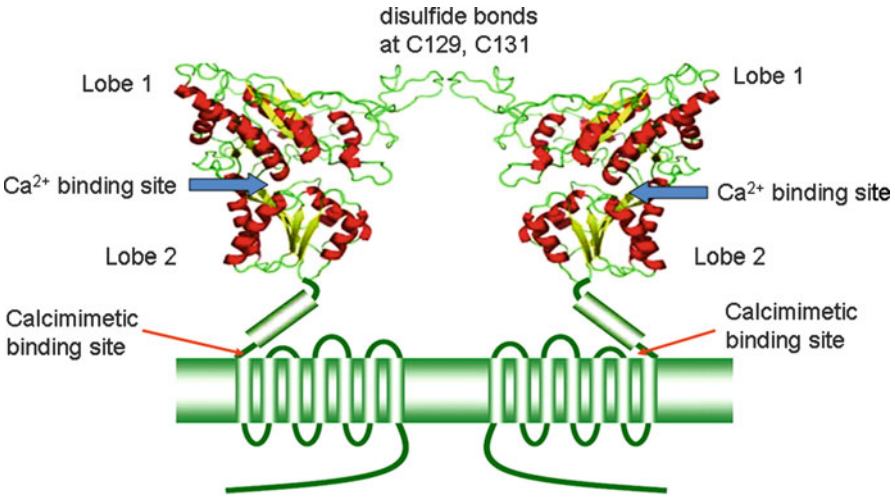

Fig. 5.1 Schematic representation of the ECD of the CaSR based on the known structure of the ECDs of several mGluRs. Note the dimeric structure of the ECD, with each monomer assuming a Venus flytrap-like conformation and having a binding site for Ca^{2+} in the crevice between the two lobes. Additional binding sites for Ca^{2+} are likely present elsewhere in the ECD, while a binding site for amino acids (e.g., phenylalanine) resides close to the binding site for Ca^{2+}_o that is shown. Calcimimetics, in contrast, bind to a site within the TMD, with the amino group of the drug in the linker between the two hydrophobic ends anchored to Glu837 (Reproduced in modified form with permission from Huang et al. [14])

followed by a 250 amino acid transmembrane domain (TMD) of 7 transmembrane helices, a signature of the GPCRs, and, finally, by a 216 residue carboxyterminal (C)-tail [8]. Between the first ~500 amino acids of the ECD and the first transmembrane helix is a cysteine-rich domain that serves as a linker between the ECD and TMD [4]. The CaSR's signaling capacity is lost if the cysteine-rich domain is removed [13]. The heavily glycosylated CaSR resides on the cell surface as a disulfide-linked dimer, involving cysteines 129 and 131 of each monomer [4].

Molecular modeling, utilizing known 3-dimensional structures of several mGluR ECDs, strongly suggests that the CaSR's ECD assumes a bilobed, venus flytrap (VFT)-like structure with a crevice between the lobes [4] (Fig. 5.1). The CaSR responds over a narrower range of Ca^{2+}_o than would be anticipated for a protein with a single binding site for Ca^{2+}_o. This positive cooperativity likely results from the CaSR having at least two binding sites for Ca^{2+}_o on each monomer [14]. One resides in the crevice between the two lobes of each monomeric VFT, while additional putative binding pockets have been predicted to reside within other regions of the ECD [15]. There may also be a calcium binding site in the receptor's TMD, as a "headless" receptor lacking the ECD still has some capacity to signal [16]. The cleft in the VFT is presumed to be open when no agonist is bound and to close upon binding Ca^{2+}_o. Concomitant conformational changes in the TMD and intracellular domains are likely to occur that initiate signal transduction. As noted later, clinically

useful, allosteric CaSR activators (calcimimetics) and antagonists (calcilytics) are thought to bind to overlapping sites within the CaSR's TMD [17, 18], where, through unknown mechanisms, they sensitize or inhibit, respectively, the receptor's response to Ca^{2+}_o.

Role of CaSR in Ca^{2+}_o Homeostasis

The Ca^{2+}_o homeostatic system has three key elements: (1) cells transporting Ca^{2+} into or out of the extracellular fluid (ECF) (kidney, bone and intestine); (2) hormones regulating these fluxes {parathyroid hormone (PTH), calcitonin (CT), and 1,25-dihydroxyvitamin D_3 ($1,25(OH)_2D_3$)}; and (3) one or more Ca^{2+}_o-sensors (e.g., the CaSR) controlling the secretion/production of those hormones or the Ca^{2+} fluxes themselves [7, 19]. Of these hormones, PTH is a Ca^{2+}_o-elevating hormone whose secretion is stimulated by low and inhibited by high Ca^{2+}_o. $1,25(OH)_2D_3$ is the other important Ca^{2+}_o-elevating hormone and is produced in the renal proximal tubule in response to PTH, hypocalcemia or hypophosphatemia [19]. $1,25(OH)_2D_3$ also feeds back to inhibit its own synthesis. CT is a Ca^{2+}_o-lowering hormone secreted by the thyroidal C-cells during hypercalcemia [20]. It inhibits osteoclastic bone resorption and helps to maintain bone mass during lactation, when skeletal stores of calcium are drawn upon for the growing neonate [19]. A more recently discovered hormone regulating both calcium and phosphate homeostasis is fibroblast growth factor (FGF)-23. It is a phosphaturic hormone produced by osteocytes (osteoblasts encased in bone during bone formation) in response to $1,25(OH)_2D_3$ and hyperphosphatemia [21]. FGF-23 inhibits both $1,25(OH)_2D_3$ production and PTH secretion. The rapid developments regarding the roles of FGF-23 in phosphorus and calcium metabolism are detailed in recent reviews [21, 22].

The Ca^{2+}_o homeostatic system functions as follows: Low Ca^{2+}_o directly stimulates both PTH secretion and $1,25(OH)_2D_3$ synthesis by reducing the activity of the CaSR, indirectly enhances $1,25(OH)_2D_3$ synthesis by increasing PTH, and decreases CT secretion [7]. The hormone-like role of Ca^{2+}_o, acting as a first messenger, contrasts with calcium's much better known function as a key intracellular messenger, which is covered later in this review. The increase in PTH stimulates the formation and activity of the bone-resorbing osteoclasts [23] and produces a net movement of Ca^{2+} out of bone over a time frame of about 1–3 h [24, 25]. Recent studies [26] also emphasize more rapid, PTH-independent fluxes of Ca^{2+} into and out of bone during induced hyper- and hypocalcemia, respectively. These are perhaps mediated, in part, by the CaSR in bone, and appear to "buffer" short term changes in Ca^{2+}_o [27]. Concomitantly, PTH increases renal tubular Ca^{2+} reabsorption in both the cortical thick ascending limb (cTAL) [7] and distal convoluted tubule (DCT) [28]. The hypocalcemia-induced elevation in $1,25(OH)_2D_3$ levels also enhances Ca^{2+} reabsorption in the DCT [28], increases $1,25(OH)_2D_3$-stimulated bone resorption, and stimulates intestinal Ca^{2+} absorption [7, 28]. The resulting increase in intestinal

Ca^{2+} absorption and renal tubular Ca^{2+} reabsorption, and net movement of Ca^{2+} out of bone normalize Ca^{2+}_o. The homeostatic response to hypercalcemia comprises essentially opposite changes in the parameters just described [7].

Overview of CaSR Signaling

Signaling by the CaSR is complex, both because of the variety of ligands that modulate its activity as well as because of the diversity of intracellular signal transduction pathways that it regulates (Table 5.1) [3, 6].

Table 5.1 Mechanisms regulating intracellular signaling by the CaSR[a]

1. Diverse extracellular ligands (di-, trivalent cations, organic polyvalent cations, amino acids, calcimimetics, calcilytics, etc.)
2. Changes in CaSR gene expression
3. Changes in CaSR desensitization, internalization, and degradation
4. Changes in forward trafficking of CaSR to the plasma membrane
5. Interaction of CaSR with scaffold proteins (caveolin-1, filamin) that bind signaling molecules (MAPK components, G proteins, etc.)
6. Activation of G proteins
   a. Heterotrimeric G proteins ($G_{i/o}$, $G_{q/11}$, $G_{12/13}$, G_s)
   b. Low molecular weight G proteins (Arf6, RhoA, Ras, Rab1, Rab11a)
7. Generation of second messengers
   a. Adenylate cyclase (cAMP)
   b. Phospholipase A_2 (arachidonic acid)
   c. Phospholipase C (IP_3, DAG)
   d. Phospholipase D (phosphatidic acid)
   e. Sphingomyelinase (ceramide)
8. Activation of lipid kinases
   a. PI-3 kinase (forms PIP_3)
   b. PI-4 kinase (forms inositol 4-phosphate))
9. Activation of protein kinases
   a. Protein kinase A
   b. Protein kinase B (Akt)
   c. Protein kinase C
   d. Calmodulin-dependent kinases (CaMKII)
   e. Tyrosine kinases (Src, EGFR)
   f. Mitogen-activated protein kinases (ERK1/2, P38 MAPK, JNK)
   g. Phospholipid-dependent kinase 1
10. Activation/inhibition of transcription factors
    a. Growth/proliferation-related (cyclins D1, 2, and 3, c-Myc, c-Fos, Egr1)
    b. NFAT and NFκB
    c. ATF2
    d. PTTG
    e. VDR

[a]See text for details and abbreviations

Extracellular Signals for the CaSR Other Than Ca^{2+}_o

A variety of agents in addition to Ca^{2+}_o modulate the CaSR's activity, including other divalent (e.g., Mg^{2+} and Sr^{2+}) and trivalent cations (e.g., La^{3+} and Gd^{3+}) [29], as well as organic polycations, such as polylysine, polyarginine [30], and neomycin [31]. These so-called type I agonists directly activate the receptor (do not require the concomitant presence of Ca^{2+}_o or any other agonist), perhaps by binding to the orthosteric site(s) (the site where the primary ligand is bound) to which Ca^{2+} is bound. As a result, signaling via the CaSR must be thought of in the context of the particular environment in which it is expressed. That is, the concentration of the polycationic CaSR agonist, spermine, for example, could be high enough in certain tissues, such as the pancreas [32], to activate the CaSR by itself or in concert with Ca^{2+}_o. The level of Ca^{2+}_o also varies from that measured in blood in specific microenvironments in which the CaSR is present. In the immediate vicinity of a resorbing osteoclast, for instance, the level of Ca^{2+}_o is several-fold higher than that in blood (as high as 40 mM underneath such active osteoclasts) [33]. Moreover, cells in the lumen of the gastrointestinal (GI) tract expressing the CaSR presumably encounter a range of concentrations of Ca^{2+}_o as a function of the fasted or fed state and the constituents of a recent meal and their bioavailability.

Type II agonists, in contrast, require the presence of Ca^{2+}_o in order to act and do so allosterically by interacting with binding sites distinct from those for Ca^{2+}_o, thereby sensitizing the receptor to activation by Ca^{2+}_o. The two best-characterized classes of type II agonists are L-amino acids {especially aromatic amino acids [34]} and the calcimimetic CaSR activators [5], viz., cinacalcet HCl. The latter is currently in use in the clinic as a means of suppressing overactive parathyroid glands in patients receiving dialysis therapy for end stage renal disease [35]. The receptor's activity is also altered by extracellular pH [36] and ionic strength [37], which may also be thought of as acting by a type II mechanism, since they modulate the CaSR's EC_{50} for Ca^{2+}_o. The CaSR is likely to encounter a range of amino acid concentrations as well as of pH and ionic strength in sites such as the GI tract or within the tubular fluid of the kidney. Calcilytics are allosteric CaSR antagonists, which have not yet reached the clinic, but can increase PTH secretion by "fooling" the parathyroid gland into responding as though Ca^{2+}_o were low [5]. They are thought to bind to a pocket within the receptor's TMD that overlaps with that for the calcimimetics but is not identical [17].

Regulation of CaSR Signaling Through Changes in Cell Surface CaSR Expression

Regulation of CaSR Gene Expression

Factors that modify the level of cell surface expression of the CaSR can modify CaSR signaling by changing receptor occupancy at a given level of Ca^{2+}_o. Four

agents have been identified that enhance receptor-mediated CaSR expression by increasing the expression of its gene and two that modulate its trafficking to the plasma membrane. The former are $1,25(OH)_2D_3$ [38], interleukin (IL)-1β [39], IL-6 [40], and increases in Ca^{2+}_o {which acts upon the CaSR to upregulate the receptor's expression (CaSR) [41]}, while the latter two are macrophage chemotactic protein (MCP)-1 and stromal-derived factor (SDF)-1 [42]. CaSR expression is downregulated in various hyperparathyroid states by poorly understood mechanisms, which may include a decrease in $1,25(OH)_2D_3$ in states with impaired renal function owing to reduced renal synthesis of this active form of vitamin D_3 [43].

Cellular Mechanisms Regulating CaSR Trafficking, Desensitization and Degradation: The Importance of CaSR Binding Partners

Additional mechanisms by which the level of cell surface CaSR expression can be modified are by regulation of its: (1) forward-trafficking during its biosynthesis, (2) internalization from the cell surface and/or (3) degradation. These three processes all involve for the most part interactions of the receptor with binding partners that impact the receptor's fate. Three proteins that promote movement of the CaSR forward in the biosynthetic pathway in model systems in vitro and ultimately to the cell surface are the cargo receptor p24A [44], receptor-activity-modifying-proteins (RAMPs) [45] and the small GTP-binding protein Rab1 [46]. The CaSR in poorly expressed in cos7 cells, for example, unless it is co-expressed with RAMP 1 or 3 but not RAMP 2, while overexpressing Rab1 strongly enhances cell surface expression of the CaSR in transfected HEK293 cells [45]. Rab11a participates in recycling of endocytosed CaSR to the cell surface, thereby ensuring the continued availability of receptor on the plasma membrane that is needed for ongoing signaling [47].

GPCRs have complex regulatory mechanisms involving a balance between agonist-induced desensitization, whereby G protein-receptor kinases (GRKs) phosphorylate the receptor's C-tail, promoting binding of so-called β-arrestins, which inhibit G protein coupling. Binding of β-arrestin can be followed by internalization of the receptor by endocytosis, and the internalized receptor can either be recycled to the plasma membrane or degraded [48, 49]. In the case of the CaSR, one study showed that the receptor's C-tail can be phosphorylated by GRK4, accompanied by binding of β-arrestin [50]. GRK2, however, can inhibit signaling by a different mechanism, namely by binding directly to $G_{q/11}$, thereby interfering with its function [50]. In another study, GRK2 inhibited CaSR signaling in a similar manner, while GRK3 inhibited CaSR signaling by ~70% apparently in a β-arrestin-dependent manner that required prior phosphorylation of the CaSR by PKC (rather than GRKs) [51]. There was little agonist-induced internalization in either case, however, indicating that the function of the cell surface CaSR could be effectively inhibited by these two GRK-dependent mechanisms without alterations in its trafficking [51]. The CaSR's limited agonist-induced internalization and its resistance against degradation in the course of its usual signaling activities [52] may be important in ensuring that sufficient cell surface receptor is available to enable to receptor to continuously monitor Ca^{2+}_o in the course of its homeostatic functions.

Recent studies have shown further mechanisms that regulate CaSR surface expression, signaling and degradation, which involve the interaction of the CaSR with additional important binding partners. First, agonist-stimulated, intracellular Ca^{2+} (Ca^{2+}_o)-dependent binding of calmodulin (CaM) to the CaSR's proximal C-terminus, stabilizes cell surface expression of the receptor and enhances intracellular calcium (Ca^{2+}_i) signaling [53]. Second, the actin-binding protein, filamin A (also see next section), binds to the CaSR C-terminus and stabilizes the receptor against degradation [52]. Finally, dorfin, an E-2 ubiquitin ligase that binds to the CaSR's C-terminus, likely provides a mechanism by which degradation of the receptor by the proteasomal pathway can be regulated [54]. The ubiquitin isopeptidase, AMSH (associated molecule with the SH3 domain of STAM), can also reduce CaSR signaling by redirecting internalized receptor from recycling back to the plasma membrane to down-regulation instead [55, 56].

CaSR-Interacting Proteins and CaSR-Signaling

In addition to its role in protecting the CaSR against degradation, filamin-A plays additional important roles in CaSR signaling. Filamin A was the first molecular binding partner of the CaSR identified [57, 58]. The CaSR binds to filamin A via an element within amino acids 962–981 in its C-terminus [52]. This interaction is functionally relevant, since blocking it by overexpressing a peptide comprising this region of the C-tail [58], using a membrane-permeant peptide comprising this region of the C-tail [57], or utilizing knockdown with siRNA [59] inhibits CaSR-mediated stimulation of extracellular signal regulated kinases 1 and 2 (ERK1/2) {and c-jun N-terminal kinase (JNK) [59]}, as noted above. While originally identified as a large, dimeric, actin-binding protein, filamin A {one of three related filamins (A, B, and C) in the human genome} acts as a scaffold that binds numerous other proteins relevant to cell signaling. The latter include GPCRs in addition to the CaSR (dopamine receptors, mGluRs), low molecular weight, monomeric G proteins (CDC42, RhoA), the Rho guanine nucleotide exchange protein, Trio, beta-arrestins 1/2, protein kinase Cα (PKCα), Src, components of the mitogen-activated protein kinase (MAPK) pathways, and SMADs 3 and 5 (http://www.ncbi.nlm.nih.gov/gene/2316).

Another binding partner of filamin A relevant to CaSR signaling is caveolin-1, a small cholesterol-binding protein that is a key component of caveolae, small flask-shaped invaginations in the plasma membrane that serve numerous cellular functions, including vesicular transport (e.g., transcytosis, endocytosis), cellular cholesterol homeostasis, and signal transduction [60]. With regard to the last of these, caveolae contain abundant signaling elements, such as receptor and non-receptor tyrosine kinases (i.e., EGFR, Src), GPCRs, heterotrimeric G proteins (G_s, G_i, G_q), Ca^{2+}-ATPase, and Ser/Thr protein kinases {protein kinase A (PKA), PKCα, δ, and ε, as well as the mitogen-activated protein kinases, ERK1/2, and G protein receptor kinases (GRK)}, as well as the lipid kinase, phosphatidylinositol 3-kinase

(PI3K) [60]. Some of these proteins interact directly with caveolin-1 though the latter's so-called scaffold domain (amino acids 82–101). Notably, the CaSR in bovine parathyroid cells is located predominantly within caveolae, at least in part through its interaction with caveolin-1's binding partner, filamin A. Parathyroid cell caveolae also contain $G_{q/11}$, endothelial nitric oxide synthase (eNOS) and PKCα, δ, and ζ and are closely associated with filamin A and actin [61]. No doubt additional signaling elements reside within parathyroid caveolae, but have not been identified to date. Caveolin-1 may have an additional direct functional effects on the CaSR, as downregulation of caveolin-1 in the human osteosarcoma cell line, Saos-2, decreased CaSR signaling [62]. Moreover, a reduction in caveolin-1 expression in parathyroid cells from parathyroid tumors is associated with decreased CaSR expression, which may contribute to abnormal Ca^{2+}_o-sensing in these tumors [63]. Thus caveolin-1-based caveolae in parathyroid cells likely provide a microenvironment where signaling molecules linked to the CaSR are concentrated and organized in a way that facilitates cellular signaling.

Initiation of CaSR Signaling

Based on modeling by homology with the conformational changes known to occur upon binding of glutamate to the ECD of several mGluRs [64], binding of Ca^{2+} (and likely of other polycations) to its binding site (s) within the CaSR ECD following an increase in Ca^{2+}_o is thought to shut the Venus flytrap, closing the crevice between the two lobes of each monomer [4, 15]. In the mGluRs, there is an additional 70° rotation of one monomer relative to the other about an axis perpendicular to the dimer interface, which is presumed to occur in the CaSR as well. Transduction of this conformational "message" to the TMD, and ultimately the receptor's cytoplasmic domains, requires the presence of the CaSR's cysteine-rich linker present in the ECD just before the first transmembrane domain [13]. Transmembrane signaling by GPCRs following agonist binding is thought to involve alterations in the orientation of the transmembrane helices relative to one another, but there are no data addressing this point for the CaSR.

Proximal Elements in CaSR Signaling

Heterotrimeric G Proteins

The CaSR is known to interact directly with several heterotrimeric G proteins [3, 6], notably $G_{q/11}$, $G_{i/o}$ (probably primarily isoforms of G_i), $G_{12/13}$ and, rarely, G_s. These couple the activated receptor to the control of the downstream signaling pathways

that are described below. For example, CaSR-mediated formation of active (GTP-bound) $G\alpha_{q/11}$ and $G\alpha_{i}$ subunits activates phosphoinositide-specific phospholipase Cβ (PI-PLCβ) by releasing free $G\alpha_{q/11}$, thereby producing diacylglycerol and inositol trisphosphate (IP_3), and inhibits adenylate cyclase, lowering cellular cAMP levels, respectively. Activation of $G_{12/13}$ by the CaSR stimulates PLD, which produces phosphatidic acid, by activating the low molecular weight G protein Rho in some cell types (see below) [65]. Amino acids within the second and third intracellular loop and the proximal portion of the C-tail are important for the receptor's ability to couple efficiently to activation of PLC by $G_{q/11}$ [3, 6, 66], while there is little information related to the structural requirements for the CaSR's coupling to G_i and $G_{12/13}$.

Not only are α-subunits liberated from heterotrimeric G proteins that have been activated by the CaSR (and other GPCRs), but also $G_{\beta\gamma}$ subunits, which exert numerous biological actions of their own [67]. For instance, $G_{\beta\gamma}$ subunits have been shown in a variety of cell type to activate PLCβ, directly modulate inwardly rectifying potassium channels and some calcium channels, regulate GRK2 and 3, activate or inhibit specific adenylate cyclase isoforms, and activate Src, PI3K, Raf-1, PLCβ and PLD [67]. Actions of $G_{\beta\gamma}$ subunits relevant to CaSR signaling will be discussed further in the next section.

Low Molecular Weight G Proteins

Low molecular weight, monomeric G proteins can function downstream of GPCRs and participate in a wide variety of biological processes {for review, see [68]}. They are GTPases, which serve as switches that are activated by proteins facilitating the replacement of bound GDP by GTP (guanine nucleotide exchange factors or GEFs). Some require initial activation of a heterotrimeric G protein, which then activates the small GTP-binding protein through a separate GEF. In other cases, the monomeric G protein can interact directly with a GPCR, which sometimes can itself serve as a GEF for the monomeric G protein [68]. Five low molecular weight G proteins have been shown to act downstream of the CaSR: ARF6, RhoA, Ras, Rab1 and Rab11A. ARF6 (ADP-ribosylating factor 6) has been implicated as a mediator of CaSR-elicited changes in cell shape and plasma membrane ruffling [69] by a process that involves binding of beta-arrrestin-1 to the CaSR, followed by the action of ARNO (Arf nucleotide binding site opener) to activate ARF6 and produce downstream effects on plasma membrane structure and motility.

Rho participates in the CaSR-mediated activation of PLD and several other processes. Activation of Rho by the CaSR appears to involve the participation of filamin serving as a scaffold that facilitates activation of Rho by the Rho guanine nucleotide exchange factor (RhoGEF) Lbc, which stimulates the exchange of GDP for GTP to activate Rho [70]. Biological actions of Rho, acting downstream of the CaSR, include regulation of cell-cell adhesion [71], modulation on Ca^{2+}_{i} oscillations

induced by amino acids [72], activation of choline kinase and phosphatidylinositol 4-kinase (PI4K) [73], and regulation of stress fiber assembly and cell shape [74].

Ras mediates actions of the CaSR on cell growth and proliferation. For instance, it mediates CaSR-induced stimulation of proliferation of ovarian surface cells by a mechanism involving activation of the tyrosine kinase, Src, and subsequent tyrosine phosphorylation of the protein, Shc, which then binds to the adaptor protein, GRB-2, and the guanine nucleotide exchange protein, SOS [75]. By enhancing the replacement of GTP for GDP, SOS activates Ras, leading, in turn, to activation of Raf1, MEK and, finally, ERK1/2. In some cases, the CaSR stimulates this pathway by transactivating the epidermal growth factor receptor (EGFR), which then stimulates the pathway just described following autophosphorylation of tyrosine residues within its intracellular domains [76–78].

Rab1 and Rab11a both participate in the trafficking of the CaSR to and from the plasma membrane. Rab1, which regulates protein transport from the ER to the Golgi, promotes cell surface expression of the CaSR when co-transfected in HEK293 cells, indicating that it can enhance forward trafficking of the receptor to the cell surface [46]. Rab11a, in contrast, participates in the constitutive endocytosis of the CaSR and its recycling to the plasma membrane [56]. The Rab11a-mediated recycling of the CaSR to the plasma membrane, which is needed to ensure adequate cell surface expression, can be interfered with by the binding of AMSH to the CaSR C-terminus, as AMSH redirects the CaSR from slow recycling to down-regulation [56]. These latter studies were performed in HEK293 cells and have not been replicated in a cell type expressing the CaSR endogenously.

Generation of Second Messengers

Adenylate Cyclase

In addition to lowering cellular cAMP levels via G_i-mediated inhibition of adenylate cyclase, the CaSR can also lower cAMP indirectly by elevating Ca^{2+}_i, which can inhibit a Ca^{2+}-inhibitable isoform of adenylate cyclase (type 6) or stimulate cAMP hydrolysis by activating phosphodiesterase(s) [56, 79]. Uncommonly, the CaSR stimulates adenylate cyclase via $G\alpha_s$ (through a switch in G protein coupling from G_i to G_s in PTHrP-secreting breast cancer cell lines, for instance) [80]. Examples of CaSR-regulated biological processes known to be mediated by the cAMP/PKA pathway include: stimulation or inhibition of PTHrP secretion by mammary epithelial cells [80], as just noted, and of PTH by parathyroid cells [81], inhibition of lipolysis in an adipocyte cell line [82], and suppression of chloride reabsorption in the thick ascending limb of the rat kidney [83]. These actions of cAMP are mediated by PKA. There is only a limited amount of work that has taken place in the regulation of PKA activity per se by the CaSR and how it regulates downstream biological functions, and PKA in CaSR-expressing tissues will not be discussed further.

Phospholipase C

Activation of PLCβ by $G\alpha_{q/11}$ hydrolyzes phosphatidylinositol bisphosphate (PIP_2) to form diacylglycerol and IP_3. CaSR-mediated activation of PLCβ is a key signaling pathway through which the CaSR regulates the functions of a variety of cell types [3, 6]. For example, knocking out both $G\alpha_q$ and $G\alpha_{11}$ in a mouse model produces severe hyperparathyroidism, indicating that these two G proteins, presumably through their actions on PLC and/or other downstream mediators, play a key role in the inhibition of parathyroid function by the CaSR, e.g., PTH secretion and parathyroid cellular proliferation [84]. Activation of $G_{q/11}$ is not sensitive to inhibition by pertussis toxin. In occasional cell types (such as pituitary-derived Att20 cells), however, CaSR-induced activation of PLC takes place by a pertussis toxin-sensitive pathway [41], likely involving activation of PLC by Gβγ subunits liberated from G_i. Additional examples of actions mediated by CaSR-elicited activation of PLC include chemotaxis of MC3T3-E1 osteoblastic cells [85], upregulation of cyclooxygenase-2 (COX-2) in fibroblasts [86], and stimulation of PLA_2 in some cell types (see below) [87].

Diacylglycerol formed by PLC activates the so-called "conventional" PKC isoforms (PKCα, β_I, β_{II} and γ) in combination with IP_3-mediated elevations in Ca^{2+}_i, which induces translocation of these PKC isoforms to anionic phospholipids (e.g., phosphatidylserine) in the plasma membrane [6, 88]. The novel PKC isoforms (PKCs δ, ε, η, and θ) in contrast, are activated by diacylglycerol but do not require an increase in Ca^{2+}_i, while the atypical PKCs (e.g., PKCs ι and ς) are activated by different mechanisms altogether [89]. These various PKC isoforms participate in some key CaSR-mediated biological actions, such as activation of ERK1/2, PLA_2, and PLD [90], although other signaling elements participating in CaSR-elicited activation of these pathways have been identified in other studies (see below). PKC is an important feedback regulator of CaSR signaling via PLC through its phosphorylation of PKC sites (especially T888) in the CaSR's C-tail [91–93]. For instance, the functional consequence of activating PKC in parathyroid cells by brief exposure to phorbol myristate acetate is inhibition of inositol phosphate generation in response to high Ca^{2+}_o, while downregulating PKC produces a substantial increase in inositol phosphate levels [91]. The elevation in Ca^{2+}_i, in addition to participating in activation of PKC can stimulate calmodulin (CaM)-dependent processes [3, 6].

CaSR-Evoked Ca^{2+}_i Signaling

IP_3 produced from PIP_2 by PLC releases Ca^{2+} from endoplasmic reticulum (ER) stores and initiates Ca^{2+}_i signaling [3, 6]. When examined at the single cell level by imaging using Ca^{2+}-sensitive dyes, IP_3 can cause an initial "spike" in Ca^{2+}_i owing to Ca^{2+} release from the ER, followed by a sustained increase in Ca^{2+}_i produced by Ca^{2+} entry from the extracellular space through calcium release-activated calcium channels. Sensors of the level of calcium in the ER (STIM1 and 2) are now known to couple the IP_3-mediated decrease in ER Ca^{2+} to influx of extracellular calcium through a channel complex which includes the pore-forming, Orai1 channel [94].

Ca^{2+} influx in this setting can also take place via the so-called classical transient receptor potential C (TRPC) plasma membrane channels [95]. Several studies have documented the presence of TRPC isoforms in CaSR-expressing cells [96, 97], especially TRPC1, which has been implicated in CaSR-evoked Ca^{2+}_i oscillations in human colonic epithelial cell lines [97], proliferation of the breast cancer cell line, MCF-7 [98], and differentiation of keratinocytes [99]. Human parathyroid cells express STIM1, Orai1 and TRPC1, and the latter two may likewise serve as a calcium-influx channels in this cell type in response to CaSR activation [100]. The CaSR not only activates but also upregulates the expression of TRPC1 in breast cancer cells [98]. TRPC6, in contrast, contributes to calcium influx in rat neonatal cardiomyocytes [101] and human aortic smooth muscle cells [96].

In a number of cells, however, including bovine and human parathyroid cells and CaSR-transfected human embryonic kidney (HEK) 293 cells, activation of the CaSR initiates slow oscillations in Ca^{2+}_i [6, 102]. Amino acids in the CaSR's proximal C-terminus, including T876 and T888, play important roles in oscillatory Ca^{2+}_i signaling via the CaSR [102]. It has been suggested that repetitive phosphorylation of T888 by PKC, coupled with release of Ca^{2+} from thapsigargin-sensitive pools in the ER, may participate in generating CaSR-induced Ca^{2+}_i oscillations [103]. Amino acids (e.g., phenylalanine) activating the CaSR sensitize the receptor to the initiation of Ca^{2+}_i oscillations stimulated by increases in Ca^{2+}_o [6]. The mechanisms underlying amino acid-evoked oscillations may differ in their details from those elicited by high Ca^{2+}_o, with the former involving $G_{12/13}$, Rho, filamin-A and TRPC1 [72].

PLA_2

High Ca^{2+}_o stimulates cytosolic phospholipase A_2 ($cPLA_2$) in bovine parathyroid cells and CaSR-transfected HEK293 cells [90]. Unlike PLC, this enzyme is not directly activated by the CaSR through a G protein but is stimulated by phosphorylation of the enzyme by ERK1/2 in one study [90] or by calmodulin-dependent protein kinase II (CaMKII) in another [87]. The reason(s) underlying the differing results in these two studies have not been elucidated, although both pathways are known to mediate GPCR-stimulated activation of $cPLA_2$ in other cell types. Additional sources of AA other than through activation of PLA_2 are cleavage of AA from the 2 position of the glycerol backbone of diacylglycerol or of phosphatidic acid [3].

Arachidonic acid (AA), formed in response to CaSR-mediated activation of PLA_2, has biological functions in CaSR-expressing tissues, inhibiting PTH release, for example, when added to dispersed parathyroid cells [104]. Furthermore, AA arising in this manner can be metabolized to produce additional biologically relevant products. These include a metabolite of the P450 pathway {20-hydroxyeicosatetraenoic acid (20-HETE)}, which has been implicated in the regulation of Ca^{2+} reabsorption in the renal thick ascending limb (TAL) [105], as well as 12- and 15-lipoxygenase products, e.g., 12- and 15-HETE, which have been suggested to mediate high Ca^{2+}_i -induced inhibition of PTH secretion [106]. High Ca^{2+}_i, acting

via the CaSR, also activates COX-2 in the TAL [107], generating prostaglandins such as PGE_2, which stimulates the production of tumor necrosis factor alpha (TNFα) [108], thereby activating the transcription factor nuclear factor of activated T-cells 5 (NFAT5) and, in turn, stimulating oxygen consumption and inhibiting apical chloride entry [109].

PLD

The CaSR has been shown to activate phospholipase D in two studies, one using the Madin-Darby canine kidney cell line (MDCK) [65] and the other utilizing both bovine parathyroid cells and CaSR-transfected HEK293 cells [90]. In the first, activation of PLD involved $G_{12/13}$ and subsequent activation of Rho [65]. In the second, CaSR-mediated activation of PLD was a PKC-dependent process [90]. Given the differences in the cell types used in the two studies, it is difficult to make detailed mechanistic comparisons between them that could account for the differences in how the CaSR activates PLD. Of the two mammalian forms of PLD, PLD1 and PLD2, the former best explains the observations in the two studies just quoted. PLD1 requires PIP_2 as a cofactor and is activated by PKC and by low molecular G proteins, including Rho, whereas PLD2 is insensitive to both classes of activators [110]. Activation of PLD results in formation of phosphatidic acid, which can be reversibly converted to diacylglycerol. PA and PLD have been linked to multiple signaling pathways, including vesicle trafficking, actin cytoskeletal dynamics, and cell proliferation, differentiation, migration and survival {for review, see [110]}, although their involvement in CaSR-mediated control of cellular function is largely unexplored.

Other Lipid Mediators: Ceramide

The CaSR can either stimulate or inhibit apoptosis in different cell types. Wu, et al. showed the involvement of the CaSR in stimulating apoptosis in HEK293 cells stably expressing the CaSR through a pathway that involves $G\alpha_i$-dependent ceramide accumulation and activation of c-Jun N-terminal kinase, followed by caspase-3 activation, and DNA cleavage and programmed cell death [111]. The results of this report contrast with those of an earlier one in which the CaSR protected stably transfected HEK 293 cells, but not non-transfected cells, against apoptosis induced by simian virus [112], perhaps because of the difference in the methods used to induce apoptosis in the two studies.

Lipid Kinases: Phosphatidylinositol 3-Kinase (PI3K) and PI4K

The CaSR activates two lipid kinases, phosphoinositide 3-kinase (PI3K) [71, 113, 114], which adds a phosphate group to the 3 position of the inositol ring of PIP_2 to form PIP_3, and phosphoinositide 4-kinase (PI4K) [73], which phosphorylates the 4 position of the inositol moiety as part of the synthesis of PIP_2. Protein kinase B

(PKB; also known as Akt) binds to PIP_3 through a sequence motif termed a pleckstrin homology domain (PHD), resulting in translocation of PKB to PIP_3 bound to the plasma membrane [115]. PKB is then activated by the phosphoinositide-dependent protein kinase 1 (PDK1), which binds to PIP_3 by its own PHD, physically approximating PDK1 and PKB and promoting the phosphorylation and activation of the latter by PDK1 [115]. PI3K and PDK1 have been shown to participate in the CaSR-mediated stimulation of serotonin secretion from sheep parafollicular cells [116]. In addition, CaSR-induced activation of PI3K has been implicated in the stimulation of cell proliferation in H-500 leydig cells [113], osteoblastic cells [117], and ovarian surface cells as well the differentiation and survival of keratinocytes [71]. CaSR-mediated activation of PI4K, which involves formation of a complex that includes the CaSR and PI4K, occurs through a Rho-dependent mechanism downstream of $G_{12/13}$ [73]. Activation of this enzyme by the CaSR is likely important as a means of ensuring ongoing availability of PIP_2 and its 4-phosphorylated precursors.

Protein Kinase C (PKC)

The CaSR activates several isoforms of protein kinase C (PKC), including PKCα, PKCβI, PKCβII, PKCδ, PKCε, and PKCζ [3, 6]. Examples of CaSR-regulated processes proven to be PKC-dependent include phosphorylation of the CaSR itself during prolonged increases in or oscillations in Ca^{2+}_i [92, 93], activation of ERK1/2 [90] (see below) and of $cPLA_2$ [87], as well as stimulation of the renal Ca^{2+}-permeable channel, TRPV5 [118], apoptosis of osteoclasts [119], induction of COX-2 [120], serotonin secretion by thyroidal parafollicular cells, which also secrete calcitonin [116], and acid secretion by gastric parietal cells [121]. Additional details can be found in recent reviews [3, 6, 89].

Calmodulin-Dependent Protein Kinases

Calmodulin-dependent protein kinases, particularly CaMKII, are important mediators of some of the biological actions of calmodulin [122]. The role of calmodulin in stabilizing the cell surface expression of the CaSR described earlier was an example of a direct action of calmodulin mediated by the binding of CaM to its target protein (in this case the CaSR) [53]. Additional actions of the CaSR, on the other hand, are mediated by the actions of the Ca^{2+}- and CaM-dependent kinase, CaMKII. For example, the use of CaMKII inhibitors has implicated CaMKII in that activation of cytosolic PLA_2 described earlier [87], as well as CaSR-mediated stimulation of insulin secretion [123].

Tyrosine Kinases

As noted above, two tyrosine kinases activated by the CaSR are upstream of the mitogen-activated protein kinases, ERK1/2. These tyrosine kinases are the

epidermal growth factor (EGF) receptor (EGFR), a receptor tyrosine kinase, and the non-receptor tyrosine kinase, c-Src [3, 6]. The former can be activated by the CaSR through a "triple membrane-spanning" mechanism, whereby the CaSR is thought to activate a matrix metalloproteinase, cleaving heparin-binding EGF to its active form, which can then activate the EGFR [77]. The EGFR, in turn, is upstream of the ERK1/2 pathway (see next section for additional details). The CaSR has been shown to activate this pathway in H-500 leydig cancer cells [124] and prostate cancer cells [77] in association with stimulation of PTHrP secretion. In the MCF-7 breast cancer cell line, CaSR-mediated stimulation of proliferation has been shown to involve the EGFR, ERK1/2 and TRPC1 [98].

In CaSR-expressing rat-1 fibroblasts [125] and ovarian surface cells [75], activation of the receptor increased c-Src activity, which, in turn, activated ERK1/2. A tyrosine kinase inhibitor, which would inhibit Src, prevented the stimulation of ERK1/2, suggesting that c-Src activation was upstream of ERK1/2 [75]. However, in a subsequent study, transactivation of the EGFR was also implicated in ERK1/2 activation in rat-1 fibroblasts [78]. Tyrosine kinase(s) also participate in the stimulation of ERK1/2 in CaSR-transfected HEK-293 cells and bovine parathyroid cells, as assessed by the use of Src kinase inhibitor, herbimycin, although other pathways (e.g., PKC) were also active [126].

Mitogen-Activated Protein Kinases: ERK1/2

ERK1/2 are activated by growth factors, {e.g., EGF and platelet-derived growth factor (PDGF)}, insulin, diverse GPCRs, cytokines and osmotic stress, and they exert numerous biological actions in a variety of cell types, such as regulating gene expression, differentiation, proliferation, and cell survival/apoptosis {For review, see [127]}. High Ca^{2+}_o, acting via the CaSR, activates ERK1/2 in a variety of cell types, thereby modulating diverse cellular processes. These include: (a) stimulation of the proliferation of ovarian surface cells [75], rat-1 fibroblasts [125] and MC-3T3-E1 murine osteoblastic cells [128], (b) inducing apoptosis of cardiomyocytes [129], (c) activating cytosolic PLA_2 [90], (d) upregulating the expression of the vitamin D receptor (VDR) (in parathyroid cells) [130], COX-2 [86], and PTHrP (as well as its secretion) [131], and (e) mediating CaSR-induced suppression of PTH secretion from parathyroid cells in one [114] but not in another study [132].

The CaSR activates ERK1/2 by several different mechanisms similar to those utilized by other GPCRs and other types of cell surface receptors. The original scenario described by Rodland, et al. for the CaSR in ovarian surface cells utilized a mechanism by which Src phosphorylated Shc and engaged the well-known downstream signaling cascade in which Ras, Raf, MEK and then ERK1/2 are sequentially activated [75]. In this pathway, Raf and MEK serve as MAPK kinase (MAPKKK) and MAPK kinase (MAPKK), respectively, for ERK1/2 [127]. The same authors subsequently showed in CaSR-transfected HEK293 cells that the CaSR activated ERK1/2 by a Ras-dependent pathway that could be blocked by inhibitors of PI3K but not of tyrosine kinases [133]. PI3K can be activated by Gβγ

submits liberated from G_i-coupled receptors, a mechanism that likely was the basis for CaSR-induced activation of PI3K in this latter study. The involvement of G_i in CaSR-stimulated activation of ERK1/2 is also supported by the inhibitory action of pertussis toxin on ERK1/2 activation in this setting [90].

A third mechanism by which the CaSR can activate the ERK1/2 signaling pathway is transactivation of the EGFR by the CaSR, which was described above and has been demonstrated in several studies [77, 78, 124]. The final way in which the CaSR can activate ERK1/2 utilizes a PKC-dependent mechanism that in other cells can entail phosphorylation and activation of Raf by PKC.

Mitogen-Activated Protein Kinases: P38 MAPK

The p38 MAPKs (there are 4 isoforms) are activated by environmental stresses (e.g., oxidative stress, UV irradiation, hypoxia, etc.) and inflammatory cytokines (IL-1, TNF-α) [127]. The principal modes of activation of p38 MAPK involve MAPKKs, primarily MKK3 and MKK6, as well as upstream MAPKKKs. As is the case for the MAPKK activating ERK1/2 (MEK), the MAPKKs activating p38 MAPK phosphorylate both threonine and tyrosine residues in a conserved motif within their target kinases (Thr-Pro-Tyr) [127]. p38 MAPK has been shown to mediate biological actions of the CaSR in several different cell types. These include: stimulation of proliferation in the mouse osteoblastic MC3T3-E1 cell line [134], rat calvarial osteoblasts [135], and H-500 rat leydig cancer cells [113], inhibition of proliferation in pancreatic cancer cells [136], and stimulation of PTHrP secretion by H-500 cells [131]. Additional p38-mediated processes include activation of a potassium channel in U87 astrocytoma cells [137], enhanced expression of the vitamin D receptor (VDR) in the renal proximal tubular cell line, HK-2 G [138], and stimulation of COX-2 in fibroblasts [86]. There has been very limited investigation of the mechanism(s) underlying CaSR-mediated activation of p38 MAPK, except that it was PKC-independent in H-500 cells [131].

Mitogen-Activated Protein Kinases: c-jun N-Terminal Kinases

Members of the JNK family (there are 3 isoforms) belong to another MAPK family and also participate in cellular responses to various stresses (e.g., stress-activated protein kinase) similar to those activating the p38 MAPKs, as well as heat shock, inhibitors of DNA and protein synthesis, growth factor deprivation, etc. [127]. Their activation requires dual threonine and tyrosine phosphorylation by MKK4/MKK7 of the same Thr-Pro-Tyr motif that is present in the ERK1/2 and p38 MAPKs. As with ERK1/2 and p38 MAPK, there are also MAPKKKs upstream of these two MAPKK. The CaSR has been shown to activate JNK in several different cell types, where it stimulates (1) PTHrP secretion from CaSR-transfected HEK293 cells [131], (2) cellular proliferation in rat calvarial osteoblasts [135], and (3) expression of COX-2 in fibroblasts [86]. There are very limited data on the mechanism by

which the receptor activates JNK. In MDCK cells, activation of JNK was pertussis toxin-sensitive, implicating a pathway involving G_i, while in H-500 leydig cell tumor cells [131], activation of SEK-1, which is upstream of JNK, was not dependent on PKC as assessed by the use of the PKC inhibitor, GF 109203X.

Transcription Factors Participating in CaSR Signaling

Transcription factors are important targets of the CaSR transduction pathways described to this point. It is likely that numerous transcription factors mediate the actions of the CaSR on gene expression. For instance, several thousand genes are either up- or downregulated in the kidney by high dietary calcium intake and concomitant increases in serum calcium concentration in mice with knockout of the 1-hydroxylase gene [139]. However, these actions have not been proven to be CaSR-mediated, and this discussion will be limited to changes in the expression or activity of transcription factors known to be mediated by the CaSR. Activation of the CaSR modulates the expression of transcription factors associated with the control of cellular proliferation, including cyclins D1 [140], D2 and D3 [135], c-Fos [135], c-Myc [141] and Egr-1 [135]. The CaSR upregulates these genes in cells in which it stimulates proliferation (e.g., osteoblasts) [135] and downregulates them (e.g., c-Myc) in cells in which it inhibits proliferation (e.g., colonic epithelial cells) [141]. The transcription factors, NFAT and NFκB mediate the actions of the CaSR on tumor necrosis factor production in cells from the murine TAL [142] and on apoptosis in osteoclasts in vitro [143], respectively. The CaSR also upregulates activating transcription factor 2 (ATF2) in H-500 leydig cells [144], which is known to bind to the cAMP responsive element and also has histone acetyltransferase activity. In H-500 cells, activation of the CaSR gene likewise upregulates the pituitary tumor transforming gene (PTTG) [144]. Finally, the CaSR upregulates the vitamin D receptor (VDR) in parathyroid [145], which could contribute not only to high Ca_o^{2+}- but also to vitamin D-induced inhibition of parathyroid function.

CaSR Signaling in Tissues Participating in Ca_o^{2+} Homeostasis

Parathyroid

In the parathyroid, the CaSR controls three important parameters of parathyroid function, inhibiting (a) PTH secretion, (b) PTH synthesis and (c) parathyroid cellular proliferation [7]. However, the molecular mechanisms by which the CaSR regulates PTH secretion remain elusive. Knocking out both G_q and G_{11} [84] in a mouse model results in a phenotype reminiscent of neonatal severe hyperparathyroidism (NSHPT), which in mice and humans results from homozygous knock out of the CaSR gene [146, 147]. These two G proteins, therefore, must be key downstream effectors of the CaSR in the regulation of PTH secretion and parathyroid cellular

proliferation, presumably by activating PLC. Production of AA by phospholipase A_2 has also been suggested to be a key downstream mediator of calcium-induced inhibition of PTH secretion [104], owing, at least in part, to conversion of arachidonic acid to products of the 12- and 15-lipoxygenease pathways [106]. The CaSR can activate $cPLA_2$ either by ERK1/2- [90] or CaMKII-mediated phosphorylation [87] of the phospholipase, as noted earlier. CaSR-evoked, ERK1/2-mediated stimulation of $cPLA_2$ and the ensuing generation of arachidonic acid metabolites that inhibit PTH secretion could explain the blockade of high Ca^{2+}_o-induced suppression of PTH secretion by inhibitors of ERK1/2 observed in one [114] but not another study [132]. The mechanistic basis underlying the inverse relationship between Ca^{2+}_i and PTH secretion remains unclear, but the presence of a calcium-independent synaptosomal-associated protein 23 (SNAP-23) in the parathyroid [148] instead of a calcium dependent one, namely SNAP-25, which normally promotes secretory vesicle fusion when Ca^{2+}_i is high, may be a clue to this riddle. Also the cytoskeleton in bovine parathyroid cells undergoes changes that may enable it to serve as a physical barrier to secretion at high Ca^{2+}_o [149]. Figure 5.2 schematically illustrates mechanisms proposed to underlie the regulation of PTH secretion by Ca^{2+}_o.

Elevated levels of Ca^{2+}_o produce a CaSR-mediated decrease the levels of the mRNA encoding preproPTH [150, 151]. The CaSR-mediated change in the level of PTH mRNA is the result of a change in preproPTH mRNA stability rather than in PTH gene transcription by a pathway involving stimulation of calmodulin (CaM) and protein phosphatase 2B [152] {for review, see [153]}. The CaSR-mediated inhibition of parathyroid cellular proliferation is thought to be the result of induction of the cyclin-dependent kinase inhibitor, $p21^{WAF1}$, and downregulation of both the growth factor, TGF-α, and its receptor, the EGFR [154]. An endothelin-1-mediated stimulation of parathyroid cellular proliferation has also been described [155]. The signaling pathways by which the CaSR controls parathyroid growth are not well understood.

The CaSR in the C-Cell

Studies carried out prior to the cloning of the CaSR showed that high Ca^{2+}_i depolarized C-cells [156], resulting in the activation of voltage-dependent calcium channels (VDCC) [157] and stimulation of CT secretion by the classical mechanism of stimulus-secretion coupling, whereby an increase in Ca^{2+}_i directly stimulates the exocytotic machinery [158]. The control of CT secretion by high Ca^{2+}_o was not thought at that time to involve the CaSR regulating PTH secretion [159]. The cloning of the CaSR enabled direct documentation that C-cells do, in fact, express the receptor [160, 161]. Studies in CaSR knock out mice subsequently documented the mediatory role of the CaSR in high Ca^{2+}_o-stimulated CT secretion by showing near total loss of Ca^{2+}-elicited CT secretion in CaSR knockout mice rescued from the lethal hyperparathyroidism of this genotype by concomitant deletion of the PTH gene [162]. A model for how the CaSR stimulates CT secretion [163] involves CaSR-induced activation of a nonselective cation channel,

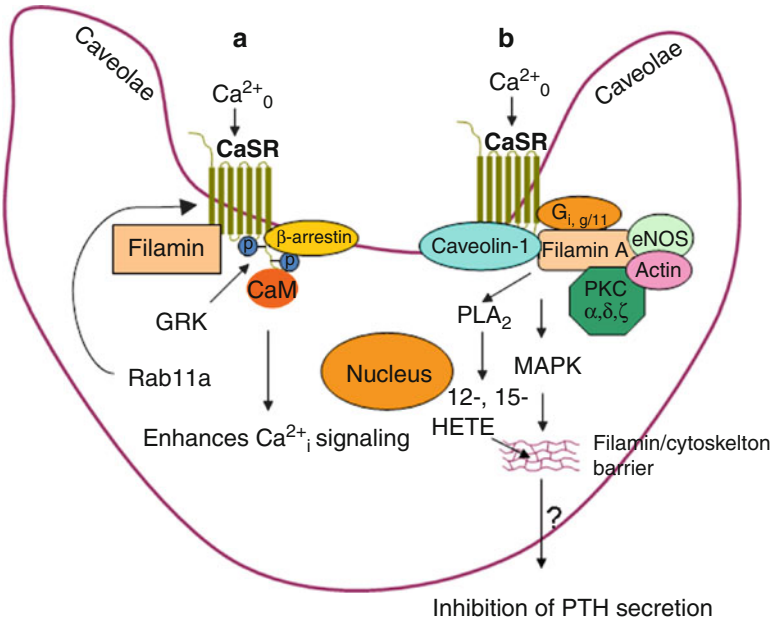

Fig. 5.2 Schematic diagram showing subcellular localization of CaSR, mechanisms governing its cell surface expression/activity, and signaling pathways postulated to *inhibit PTH secretion*. (**a**) Regulation of CaSR on cell membrane: CaSR is located in the caveolae of the cell membrane. *Rab11a* promotes recycling of the CaSR to the cell surface and binding of the receptor to filamin protects it from degradation. *Rab1* (not shown) stimulates movement of the CaSR to the cell surface during its biosynthesis. High Ca^{2+}_O activates the CaSR and induces binding of calmodulin (*CaM*) to the receptor's C-terminus, which stabilizes the receptor on the cell surface and enhances signaling. Following activation of the CaSR, *GRK2* inhibits $G_{q/11}$ binding, while GRK3/4 phosphorylate the CaSR's C-tail, facilitating binding of *β-arrestin*, which downregulates receptor activity. (**b**) The CaSR, coupled to G_i and/or $G_{q/11}$, is also bound to *caveolin-1* and *Filamin*, both of which can serve as scaffolds for various signaling molecules. The activated CaSR, acting through G proteins and signaling elements bound to these scaffolding partners stimulates *MAPK* activation and the generation of lipoxygenase products from arachidonic acid formed by PLA_2. These and perhaps additional, as yet poorly characterized, signaling pathways produce inhibition of secretion, resulting, at least in part, from the formation of a cytoskeletal barrier at the vascular/secretory pole of parathyroid cells. See text for additional details

which causes cellular depolarization, thereby stimulating VDCC, elevating Ca^{2+}_i, and activating exocytosis. The signaling pathway involved in this model has subsequently been shown to comprise CaSR-mediated increases in free Gβγ subunits, which activate PI3Kβ, leading to stimulation of PDK1, which in turn, phosphorylates and activates PKCζ [116]. How PKCζ activates non-selective cation channels to initiate cellular depolarization and opening of VDCC in this cell type has not been elucidated.

The CaSR in Kidney

In the kidney three key locations of the CaSR where the receptor's signaling pathways will be addressed here are the proximal tubule, the TAL, and the inner medullary collecting duct (IMCD) [164–166]. The interested reader is referred to recent reviews of additional locations and functions of the receptor in the kidney [167]. In the proximal tubule the receptor antagonizes the phosphaturic action of PTH and inhibits the synthesis of $1,25(OH)_2D_3$ in a proximal tubule cell line, at least in part by upregulating the VDR [168]. In the cortical TAL the CaSR directly suppresses renal tubular Ca^{2+} reabsorption [7] and in the IMCD it antagonizes vasopressin-stimulated water flow, thereby reducing urinary concentrating ability [165, 166]. A second mechanism by which the CaSR reduces urinary concentration is by inhibiting salt transport in the medullary TAL, thereby reducing the medullary hypertonicity needed for passive reabsorption of water in the medulla [167].

CaSR signaling in the proximal tubule has not been studied in any detail. Recent studies have implicated CaSR-induced activation of p38 MAPK as mediating the attendant increase in VDR expression in the human proximal tubular cell line, HK-2G [138]. There was concurrent activation of ERK1/2, but this did not mediate the effect of the CaSR on the VDR based on the use of ERK1/2 inhibitors. Comparable studies have not been carried out in native tubular cells. In contrast, ERK1/2 mediates the CaSR-evoked increase in VDR expression in the parathyroid gland [130].

Studies utilizing tubules from the TAL have shown a pertussis toxin-sensitive inhibition of hormone-stimulated cAMP accumulation by high Ca^{2+}_o presumably acting through coupling of the CaSR via G_i to inhibition of adenylate cyclase, while in the proximal tubule, high Ca^{2+}_o had no such effect on cAMP levels [169, 170]. A different mechanism for CaSR-evoked lowering of cAMP in TAL is by stimulating a PLC-dependent increase in Ca^{2+}_i, which both inhibited a Ca^{2+}-inhibitable form of adenylate cyclase (type 6) and increased cAMP breakdown by phosphodiesterase [83]. These changes in cAMP could reduce Ca^{2+} reabsorption both by the paracellular and transepithelial routes by inhibiting the actions of cAMP-elevating hormones (e.g., PTH) stimulating Ca^{2+} reabsorption [171].

A second transduction pathway stimulated by the CaSR in the TAL is activation of phospholipase A_2 and subsequent metabolism of the AA by the P450 ω-hydroxylase to 20-HETE [105], which has potent inhibitory actions on channels and transporters participating in the paracellular pathway for Ca^{2+} reabsorption in the TAL. These include a potassium channel and the Na^+-K^+-$2Cl^-$ cotransporter (NKCC2) {for review see [172]}. The K^+ channel and NKCC2, both located in the apical membrane, are key participants in the generation of the lumen-positive potential driving the paracellular reabsorption of not only Ca^{2+}, but also Mg^{2+} and, to some extent, Na^+ in the TAL [172]. The importance of this mechanism has been abundantly proven by experiments in nature in humans that knock out these and other participating genes, producing the wasting of sodium chloride, K^+, Mg^{2+} and Ca^{2+} characteristic of Bartter syndrome [173]. In fact, some activating mutations of the CaSR are the cause for type 5 Bartter syndrome through the mechanism just described [174, 175].

Abdullah and co-workers have described another signal transduction pathway in the TAL that links the CaSR to enhanced production of prostaglandin E_2, which has potent diuretic and natriuretic actions on the kidney. The CaSR couples to activation of PLC via both $G_{q/11}$ and, to a lesser extent, G_i [120]. The resultant increases in diacylglycerol levels and Ca^{2+}_i activate PKC, which stimulates the protein phosphatase, calcineurin (CaN), resulting in dephosphorylation and activation of NFAT5 [120]. NFAT5 then stimulates the production of TNFα, which acts on its receptor in an autocrine/paracrine manner to upregulate COX-2 and stimulate the production of PGE_2 [176]. The CaSR, in addition to inhibiting cAMP accumulation through the type 6 adenylate cyclase and by activating phosphodiesterase in the TAL, activates PLC in the rat TAL [83], while in the rabbit TAL, CaSR-evoked increases in Ca^{2+}_i occur solely by calcium influx [177].

Vasopressin normally stimulates translocation of the water channel, aquaporin-2 (AQP-2), to the plasma membrane by a cAMP-dependent process that phosphorylates serine 236 in AQP-2 [178]. In the collecting duct cell line, CD8, the CaSR decreases cAMP accumulation and activates PKC, both of which would be expected to reduce the expression of aquaporin-2 (AQP-2) water channels on the plasma membrane, the former by decreasing PKA-mediated translocation to the membrane and the latter by stimulating endocytosis of AQP-2 [179]. In addition to AQP-2, endosomes isolated from the inner medullary collecting duct of the rat kidney contain CaSR, $G_{q/11}$, G_i, and PKCs δ and ζ, which may facilitate signal transduction by bringing these signaling elements together to promote efficient signaling [166].

CaSR Signaling in Tissues Not Participating in Ca^{2+}_o Homeostasis

The CaSR is expressed in numerous tissues in addition to those involved in Ca^{2+}_o homeostasis {for review, see [180]}. Its many roles in these diverse cell types are still being unraveled and Table 5.2 presents examples of some of these normal tissues/cells in which information is available related to the receptor's signaling pathways therein. This general area is also discussed in recent comprehensive reviews [3, 6].

CaSR Signaling in Cancer

CaSR and Cancer

The CaSR is expressed (or over-expressed) in diverse types of cancer, and may participate in the development of many types of benign or malignant tumors, from parathyroid adenomas to breast, prostate, colon cancers, ovarian cancer and gastrinoma [218]. Humoral hypercalcemia of malignancy (HHM) is an important paraneoplastic syndrome that is caused by the secretion from the tumor of a humoral factor that acts systemically on target organs of bone, kidney, and intestine to disrupt normal calcium homeostasis and produce hypercalcemia [219].

Table 5.2 Role of CaSR in normal cells not participating in Ca^{2+}_O homeostasis[a]

Normal cells	Role of CaSR	CaSR signaling
Keratinocytes	For a number of years prior to the cloning of the CaSR, calcium was recognized as a critical regulator of the proliferation and differentiation of keratinocytes both in vivo and in vitro [181]. Thus not all of these effects were initially formally proven to be mediated by the CaSR	IP_3 and DAG levels increase in response to elevated Ca^{2+}_o, owing to activation of the phospholipase C-γ1 (PLC-γ1) pathway, which is critical for keratinocyte differentiation, which express CaSR [182–184]
	Primary keratinocytes are a model for epidermal differentiation in response to changes in Ca^{2+}_o[185]	The increase in Ca^{2+}_i and prolonged elevation of DAG stimulate the PKC pathway (mainly PKCα) [182, 186]
	At low Ca^{2+}_o, below 0.07 mM, There is proliferation of keratinocytes, which express a basal cell phenotype but fail or are slow to form cornified envelopes [187]	Activated PKC leads to the induction and activation of AP-1 transcription factors, which regulate the transcription of a number of differentiation genes [188]
	At higher Ca^{2+}_o(~0.1 mM), there is differentiation of keratinocytes, associated with increases in Ca^{2+}_i, leading to formation of desmosomes, stratification and cornification and activation of differentiation-related genes, including keratins K1, K10, involucrin, transglutaminase I, profilaggrin and loricrin [181, 185]	
Central nervous system	CaSR participates in GnRH-mediated neuronal migration [189]	CaSR stimulates of CXCL-10 by activating charybdotoxin-sensitive, calcium-activated potassium channels [189]. CaSR stimulates NCC and/or calcium-activated potassium channels in hippocampal pyramidal neurons [190, 191]
	CaSR modulates synaptic plasticity, neurotransmission [190, 192]	
	CaSR has been suggested to participate in neurodegeneration with long term memory loss in Alzheimer's disease [193] and has been implicated in the development of sporadic and late-onset Alzheimer's disease [194]. CaSR serves as a cellular target for amyloid β peptides (Aβ) in hippocampal neurons and stimulates non-selective cation channels (NCCs) [193, 195]	Promotes downstream elevation of Ca^{2+}_i, IP_3 and diacylglycerol by activating PLC, thereby stimulating PKC. Individuals lacking the Apo E4 allele are particularly susceptible to factors promoting the development of Alzheimer's disease, e.g., Aβ) [196]
	CaSR affects differentiation of astrocytes and progression of malignant tumors (U373 cells) [198]	CaSR stimulates PTHrP [197] and activates mitogenesis with the involvement of non-selective cation channels via an attendant rise in Ca^{2+}_i [197]
		CaSR promotes upregulation of cytokines, reactive oxygen species (ROS) and nitric oxide (NO) [194]

(continued)

Table 5.2 (continued)

Normal cells	Role of CaSR	CaSR signaling
Chondrocyte	CaSR plays critical role in cartilage development and growth in conditional knockout mouse model [200]	Differentiation program is regulated by the PTHrP-Indian hedgehog (IHH) feedback loop [199] and acts cooperatively with canonical BMP pathway [199]
	Ca_o^{2+} modulates chondrocyte differentiation, including expression of alkaline phosphatase, types I, II, X collagen, osteonectin and osteopontin [201, 202]	
	CaSR stimulates PTHrP secretion by growth plate chondrocytes [203]	
Heart	CaSR is expressed in neonatal as well as adult rat cardiomyocytes [204]	CaSR activates ERK1/2 in neonatal cardiomyocytes [205, 206]
	Ca_o^{2+} promotes increases in Ca_i^{2+} and inositol phosphates (IPs) [205, 206]. CaSR is involved in regulation of cardiac hypertrophy [207], cell cycle [206] and apoptosis/cell survival [208]	CaSR is linked to the PLC pathway [205, 206, 209]
GI tract	CaSR modulates fluid secretion and absorption along the intestine [79, 210]	Increased $[Ca^{2+}]_i$ activates Ca^{2+}-calmodulin-sensitive phosphodiesterases, thereby lowering intracellular cAMP and abrogating fluid secretion [210]. A concomitant rise in intracellular Ca^{2+} is mediated through a PLC/PKC-dependent pathway [210]
	CaSR maintains G-cell number and stimulates gastrin and gastric acid secretion [211–214]	
	CaSR stimulates cholecystokinin secretion by intestinal enterochromaffin cells in response to increases in Ca_o^{2+} or amino acid concentrations [216, 217]	CaSR in G cells stimulates PLC and PKC and activates NCC to enhance gastrin secretion [212, 215]. CaSR in gastric glands activates a pertussis toxin-sensitive G protein, PLC, calcium influx, PKC isoforms, ERK1/2 and H^+-K^+-ATPase, thereby stimulating proton secretion [121, 214]
		CaSR stimulates Ca_i^{2+} mobilization in ST-C, cholecystokinin-secreting cells [216]

[a]In some cases, effects of Ca_o^{2+} are described that are not formally proven to be CaSR-mediated, either because they were carried out prior to the cloning of the CaSR or before the routine availability of CaSR activators/inhibitors, dominant negative CaSR constructs and/or knockdown of the CaSR (e.g., by RNAi)

Bone Metastases in Cancer

The frequent bony metastases seen in patients with certain forms of cancer, e.g., multiple myeloma and breast cancer, including those with HHM, can be explained by the 'seed and soil' hypothesis proposed by Paget [220]. Bone is not simply the depot for 99% of the body's calcium but is also a rich storage site for immobilized growth factors such as transforming growth factor (TGF)-β, insulin-like growth factors (IGF) I and II, fibroblast growth factor (FGF)-1 and −2, and platelet-derived growth factors (PDGF). These growth factors can be released during normal bone resorption as well as by osteolytic metastases [221]. Bony metastases can be osteoblastic, osteolytic, or mixed [222]. Osteoblastic metastases are commonly associated with prostate and breast cancer, but mixed osteolytic–osteoblastic metastases are also seen in these two types of cancer [223]. Trabecular regions, such as the proximal ends of the long bones, ribs, and vertebral column, are preferential sites of prostate cancer metastasis [224]. Endothelin-1 (ET-1) is a potent osteoblast-stimulatory factor that is involved in osteoblastic bone metastases through its activation of the ET A receptor (ETAR) in breast cancer [225, 226]. TGF-β plays an integral role in promoting the development and progression of osteolytic bone metastases by inducing production by the metastatic cancer cells of parathyroid hormone-related protein (PTHrP), a known stimulator of osteoclastic bone resorption [227]. This is typically described as a vicious cycle between the tumor cells and bone.

One of the direct effects of increased bone resorption during HHM is an increase in Ca^{2+}_o, both locally and systemically. The levels of Ca^{2+}_o in the vicinity of resorbing osteoclasts are many-fold higher than the level of systemic Ca^{2+}_o (i.e., ranging from 8 to 40 mM) [228]. In this regard, buffering of Ca^{2+}_i becomes crucial for avoiding the toxicity of large (micromolar) sustained increases in Ca^{2+}_i [229]. However, the CaSR could enable Ca^{2+}_o to contribute directly to this vicious cycle by stimulating the production of PTHrP by the cancer cells instead of released Ca^{2+} merely entering the local and then systemic ECF. Under these circumstances, the CaSR could serve as a central element in a physiologically inappropriate "feed-forward" mechanism. Examples of the roles of the CaSR in various cancers and its associated signaling pathways are presented in Table 5.3.

Table 5.3 Role of CaSR in cancer and its signaling[a]

Type of cancer	Role of CaSR	CaSR signaling
Breast cancer	Ca^{2+}_o stimulates normal breast epithelial cell proliferation; high Ca^{2+}_o promotes differentiation [230]	PKC/MEK-1/ERK1/2 and p38 MAPK pathways activated and have been implicated in production of PTHrP by MCF-7 breast cancer cells [231, 232]
	CaSR detected along the epithelial cells of the ducts in normal, fibrocystic breast tissue, and ductal carcinoma as a biomarker of breast cancer [233]	
	CaSR stimulates the synthesis and secretion of PTHrP in MCF-7 and MDA-MB-231 breast cancer cells [231]	
	CaSR exerts estrogen-like effects in MCF-7 cells at 15–20 mM Ca^{2+}_o [231]	
Prostate cancer	PC-3 prostate cancer cells (highly tumorigenic and androgen-independent) have higher levels of CaSR mRNA than LNCaP cells (androgen dependent) cells [234, 235]	CaSR acts via a pertussis toxin-sensitive G protein to inhibit cAMP accumulation, activate the MEK/ERK and PI3K-Akt pathways and stabilize Cyclin D1 in PC-3 cells, thereby enhancing cell growth and adherence [235]
	Increasing Ca^{2+}_o from 0.5 mM to 2.5 mM increases cellular growth of PC-3 cells but not of LnCaP cells [235]	CaSR transactivates the EGFR to stimulate the MEK/ERK pathway and enhance PTHrP release [77]
	Knockdown of CaSR expression reduces cell growth of PC-3 cells both in vitro and in vivo in a murine model of prostate cancer metastasis [235]	
Leydig cells (model of HHM)	The Rice H-500 rat leydig cell tumor is a widely used model of HHM, which secretes PTHrP and produces a PTHrP-dependent form of hypercalcemia [113, 236, 237]	CaSR activates several mitogen-activated protein kinases (MEK1/2, ERK1/2, p38MAPK and SEK-1) in H-500 cells [113]. PTHrP release is PKC-dependent and PLC-independent and inactivation of conventional PKC isoforms with GF-109203X partially attenuates high Ca^{2+}-induced, CaSR-mediated PTHrP release [131]
	Elevated levels of Ca^{2+}_o produce a concentration-dependent increase in PTHrP release, while changes in Ca^{2+}_i do not modify PTHrP release [237, 238]	Ca^{2+}_o-induced, CaSR-mediated SEK-1 activation is independent of PKC in H-500 cells [131]
	Elevated Ca^{2+}_o increases uptake of [^{3}H]-thymidine in H-500 cells via the PI-3-kinase/Akt pathway [239]	CaSR activates the PKC and MEK/ERK1/2 pathways in H-500 cells in parallel [113]
	High Ca^{2+}_o also increases expression by H-500 cells of the angiogenic factor, vascular endothelial growth factor, and stimulates inducible nitric oxide (NO) synthase with attendant NO production [240]	
	CaSR increases expression in H-500 cells of the proliferative and angiogenic oncogene, pituitary tumor-transforming gene (PTTG) [144]	

Gastrointestinal tract	CaSR is highly expressed in well-differentiated regions of colonic neoplasms and nearly lacking in poorly differentiated regions [241] CaSR inhibits proliferation of colonic crypt cells and calcium is considered a chemo-protective agent [243] In colorectal carcinogenesis, there is frequently mutation of the adenomatous polyposis coli (APC) gene [244] Elevated Ca_o^{2+} increases E-cadherin expression in colonic cells via CaSR [248, 249] Reduction of Ca_o^{2+} to 0.025 mM on the luminal surface of confluent Caco-2 cell monolayers reduces c-myc RNA expression, but 0.025 mM Ca^{2+} had no effect on basolateral surface; at low Ca_o^{2+} proliferation of normal intestinal epithelial cells is highest in the bases of crypts [141]	Mutation of APC causes nuclear accumulation of β-catenin which binds with a member of the T-cell receptor family of transcription factors (TCF) and activates genes required for cellular proliferation [242]. There is commonly defective Wnt signaling in colon cancer [245]. Wnts are cysteine-rich glycoproteins that interact with their receptors, lipoprotein receptor-related proteins 5 and 6 (LRP5/6) and Frizzled [246]. Wnts (Wnt1, Wnt3, Wnt3a) activate β-catenin signaling in the nucleus by dephosphorylating and stabilizing β-catenin [246]. Wnt4, Wnt5a, and Wnt11 signal non-canonically without liberating β-catenin. In some cases, wnt5a can promote β-catenin degradation [247]. Wnt5a acts via either the orphan tyrosine kinase Ror2 or an uncharacterized Frizzled receptor to increase E-ubiquitin ligase, called seven in absentia homolog 2 (Siah2) [247]. c-Myc is a key target gene in the β-catenin signaling pathway and is a major factor regulating cell cycle progression [141] High Ca_o^{2+} via CaSR stimulates Wnt5a secretion by colon cancer cell lines, which interacts with Ror2 to inhibit β-catenin signaling by upregulating Siah2 [250]. High levels of Ca_o^{2+} also inhibit β-catenin/TCF4 complex formation [249]

[a]In some cases, effects of Ca_o^{2+} are described that are not formally proven to be CaSR-mediated, either because they were carried out prior to the cloning of the CaSR or before the routine availability of CaSR activators/inhibitors, dominant negative CaSR constructs and/or knockdown of the CaSR (e.g., by RNAi)

References

1. Brown EM, Gamba G, Riccardi D, Lombardi M, Butters R, Kifor O, Sun A, Hediger MA, Lytton J, Hebert SC (1993) Cloning and characterization of an extracellular Ca(2+)-sensing receptor from bovine parathyroid. Nature 366:575–580
2. Tfelt-Hansen J, Brown EM (2005) The calcium-sensing receptor in normal physiology and pathophysiology: a review. Crit Rev Clin Lab Sci 42:35–70
3. Magno AL, Ward BK, Ratajczak T (2011) The calcium-sensing receptor: a molecular perspective. Endocr Rev 32:3–30
4. Hu J, Spiegel AM (2007) Structure and function of the human calcium-sensing receptor: insights from natural and engineered mutations and allosteric modulators. J Cell Mol Med 11:908–922
5. Nemeth EF (2004) Calcimimetic and calcilytic drugs: just for parathyroid cells? Cell Calcium 35:283–289
6. Brennan SC, Conigrave AD (2009) Regulation of cellular signal transduction pathways by the extracellular calcium-sensing receptor. Curr Pharm Biotechnol 10:270–281
7. Brown EM (2007) Clinical lessons from the calcium-sensing receptor. Nat Clin Pract Endocrinol Metab 3:122–133
8. Garrett JE, Capuano IV, Hammerland LG, Hung BC, Brown EM, Hebert SC, Nemeth EF, Fuller F (1995) Molecular cloning and functional expression of human parathyroid calcium receptor cDNAs. J Biol Chem 270:12919–12925
9. Diaz R, Hurwitz S, Chattopadhyay N, Pines M, Yang Y, Kifor O, Einat MS, Butters R, Hebert SC, Brown EM (1997) Cloning, expression, and tissue localization of the calcium-sensing receptor in chicken (Gallus domesticus). Am J Physiol 273:R1008–R1016
10. Nearing J, Betka M, Quinn S, Hentschel H, Elger M, Baum M, Bai M, Chattopadyhay N, Brown EM, Hebert SC, Harris HW (2002) Polyvalent cation receptor proteins (CaRs) are salinity sensors in fish. Proc Natl Acad Sci USA 99:9231–9236
11. Brauner-Osborne H, Wellendorph P, Jensen AA (2007) Structure, pharmacology and therapeutic prospects of family C G-protein coupled receptors. Curr Drug Targets 8:169–184
12. Pi M, Faber P, Ekema G, Jackson PD, Ting A, Wang N, Fontilla-Poole M, Mays RW, Brunden KR, Harrington JJ, Quarles LD (2005) Identification of a novel extracellular cation-sensing G-protein-coupled receptor. J Biol Chem 280:40201–40209
13. Hu J, Hauache O, Spiegel AM (2000) Human Ca^{2+} receptor cysteine-rich domain. Analysis of function of mutant and chimeric receptors. J Biol Chem 275:16382–16389
14. Huang Y, Zhou Y, Yang W, Butters R, Lee HW, Li S, Castiblanco A, Brown EM, Yang JJ (2007) Identification and dissection of Ca^{2+} −binding sites in the extracellular domain of Ca^{2+} -sensing receptor. J Biol Chem 282:19000–19010
15. Huang Y, Zhou Y, Castiblanco A, Yang W, Brown EM, Yang JJ (2009) Multiple Ca(2+)-binding sites in the extracellular domain of the Ca(2+)-sensing receptor corresponding to cooperative Ca(2+) response. Biochemistry 48:388–398
16. Hu J, Reyes-Cruz G, Chen W, Jacobson KA, Spiegel AM (2002) Identification of acidic residues in the extracellular loops of the seven-transmembrane domain of the human Ca^{2+} receptor critical for response to Ca^{2+} and a positive allosteric modulator. J Biol Chem 277: 46622–46631
17. Miedlich SU, Gama L, Seuwen K, Wolf RM, Breitwieser GE (2004) Homology modeling of the transmembrane domain of the human calcium sensing receptor and localization of an allosteric binding site. J Biol Chem 279:7254–7263
18. Petrel C, Kessler A, Dauban P, Dodd RH, Rognan D, Ruat M (2004) Positive and negative allosteric modulators of the Ca^{2+}−sensing receptor interact within overlapping but not identical binding sites in the transmembrane domain. J Biol Chem 279:18990–18997
19. Bringhurst FR, Demay MB, Kronenberg HM (1998) Hormones and disorders of mineral metabolism. In: Wilson JD, Foster DW, Kronenberg HM, Larsen PR (eds) Williams textbook of endocrinology, 9th edn. W.B. Saunders, Philadelphia, pp 1155–1209

20. Inzerillo AM, Zaidi M, Huang CL (2004) Calcitonin: physiological actions and clinical applications. J Pediatr Endocrinol Metab 17:931–940
21. Juppner H (2007) Novel regulators of phosphate homeostasis and bone metabolism. Ther Apher Dial 11(Suppl 1):S3–S22
22. Berndt T, Kumar R (2009) Novel mechanisms in the regulation of phosphorus homeostasis. Physiology (Bethesda) 24:17–25
23. Matsuo K, Irie N (2008) Osteoclast-osteoblast communication. Arch Biochem Biophys 473: 201–209
24. Robertson WG, Peacock M, Atkins D, Webster LA (1972) The effect of parathyroid hormone on the uptake and release of calcium by bone in tissue culture. Clin Sci 43:714–718
25. Raisz LG, Niemann I (1967) Early effects of parathyroid hormone and thyrocalcitonin on bone in organ culture. Nature 214:486–487
26. Wang W, Lewin E, Olgaard K (1999) Parathyroid hormone is not a key hormone in the rapid minute-to-minute regulation of plasma Ca^{2+} homeostasis in rats. Eur J Clin Invest 29:309–320
27. Lewin E, Wang W, Olgaard K (1999) Rapid recovery of plasma ionized calcium after acute induction of hypocalcaemia in parathyroidectomized and nephrectomized rats. Nephrol Dial Transplant 14:604–609
28. Hoenderop JG, Nilius B, Bindels RJ (2005) Calcium absorption across epithelia. Physiol Rev 85:373–422
29. Brown EM, Fuleihan GE-H, Chen CJ, Kifor O (1990) A comparison of the effects of divalent and trivalent cations on parathyroid hormone release, 3',5'-cyclic-adenosine monophosphate accumulation, and the levels of inositol phosphates in bovine parathyroid cells. Endocrinology 127:1064–1071
30. Brown EM, Katz C, Butters R, Kifor O (1991) Polyarginine, polylysine, and protamine mimic the effects of high extracellular calcium concentrations on dispersed bovine parathyroid cells. J Bone Miner Res 6:1217–1225
31. Brown EM, Butters R, Katz C, Kifor O (1991) Neomycin mimics the effects of high extracellular calcium concentrations on parathyroid function in dispersed bovine parathyroid cells. Endocrinology 128:3047–3054
32. Larsson LI, Morch-Jorgensen L, Hougaard DM (1982) Cellular and subcellular localization of polyamines cytochemical methods providing new clues to polyamine function in normal and neoplastic cells. Histochemistry 76:159–174
33. Silver IA, Murrils RJ, Etherington DJ (1988) Microlectrode studies on the acid microenvironment beneath adherent macrophages and osteoclasts. Exp Cell Res 175:266–276
34. Conigrave AD, Mun HC, Brennan SC (2007) Physiological significance of L-amino acid sensing by extracellular Ca(2+)-sensing receptors. Biochem Soc Trans 35:1195–1198
35. Brown EM (2010) Clinical utility of calcimimetics targeting the extracellular calcium-sensing receptor (CaSR). Biochem Pharmacol 80:297–307
36. Quinn SJ, Bai M, Brown EM (2004) pH Sensing by the calcium-sensing receptor. J Biol Chem 279:37241–37249
37. Quinn SJ, Kifor O, Trivedi S, Diaz R, Vassilev P, Brown E (1998) Sodium and ionic strength sensing by the calcium receptor. J Biol Chem 273:19579–19586
38. Canaff L, Hendy GN (2002) Human calcium-sensing receptor gene. Vitamin D response elements in promoters P1 and P2 confer transcriptional responsiveness to 1,25-dihydroxyvitamin D. J Biol Chem 277:30337–30350
39. Canaff L, Hendy GN (2005) Calcium-sensing receptor gene transcription is up-regulated by the proinflammatory cytokine, interleukin-1beta. Role of the NF-kappaB PATHWAY and kappaB elements. J Biol Chem 280:14177–14188
40. Canaff L, Zhou X, Hendy GN (2008) The proinflammatory cytokine, interleukin-6, up-regulates calcium-sensing receptor gene transcription via Stat1/3 and Sp1/3. J Biol Chem 283:13586–13600
41. Emanuel RL, Adler GK, Kifor O, Quinn SJ, Fuller F, Krapcho K, Brown EM (1996) Calcium-sensing receptor expression and regulation by extracellular calcium in the AtT-20 pituitary cell line. Mol Endocrinol 10:555–565

42. Olszak IT, Poznansky MC, Evans RH, Olson D, Kos C, Pollak MR, Brown EM, Scadden DT (2000) Extracellular calcium elicits a chemokinetic response from monocytes in vitro and in vivo. J Clin Invest 105:1299–1305
43. Goodman WG, Quarles LD (2008) Development and progression of secondary hyperparathyroidism in chronic kidney disease: lessons from molecular genetics. Kidney Int 74:276–288
44. Stepanchick A, Breitwieser GE (2010) The cargo receptor p24A facilitates calcium sensing receptor maturation and stabilization in the early secretory pathway. Biochem Biophys Res Commun 395:136–140
45. Bouschet T, Martin S, Henley JM (2005) Receptor-activity-modifying proteins are required for forward trafficking of the calcium-sensing receptor to the plasma membrane. J Cell Sci 118:4709–4720
46. Zhuang X, Adipietro KA, Datta S, Northup JK, Ray K (2010) Rab1 small GTP-binding protein regulates cell surface trafficking of the human calcium-sensing receptor. Endocrinology 151:5114–5123
47. Revillion F, Vandewalle B, Hornez L, Lefebvre J (1993) Influence of cAMP on E-cadherin expression and cell surface heparan sulfate proteoglycan synthesis in human breast cancer cells. Anticancer Res 13:1625–1629
48. Gainetdinov RR, Premont RT, Bohn LM, Lefkowitz RJ, Caron MG (2004) Desensitization of G protein-coupled receptors and neuronal functions. Annu Rev Neurosci 27:107–144
49. Lefkowitz RJ, Whalen EJ (2004) Beta-arrestins: traffic cops of cell signaling. Curr Opin Cell Biol 16:162–168
50. Pi M, Oakley RH, Gesty-Palmer D, Cruickshank RD, Spurney RF, Luttrell LM, Quarles LD (2005) Beta-arrestin- and G protein receptor kinase-mediated calcium-sensing receptor desensitization. Mol Endocrinol 19:1078–1087
51. Lorenz S, Frenzel R, Paschke R, Breitwieser GE, Miedlich SU (2007) Functional desensitization of the extracellular calcium-sensing receptor is regulated via distinct mechanisms: role of G protein-coupled receptor kinases, protein kinase C and beta-arrestins. Endocrinology 148:2398–2404
52. Zhang M, Breitwieser GE (2005) High affinity interaction with filamin A protects against calcium-sensing receptor degradation. J Biol Chem 280:11140–11146
53. Huang Y, Zhou Y, Wong HC, Castiblanco A, Chen Y, Brown EM, Yang JJ (2010) Calmodulin regulates Ca^{2+} −sensing receptor-mediated Ca^{2+} signaling and its cell surface expression. J Biol Chem 285:35919–35931
54. Huang C, Wu Z, Hujer KM, Miller RT (2006) Silencing of filamin A gene expression inhibits its Ca^{2+} −sensing receptor signaling. FEBS Lett 580:1795–1800
55. Herrera-Vigenor F, Hernandez-Garcia R, Valadez-Sanchez M, Vazquez-Prado J, Reyes-Cruz G (2006) AMSH regulates calcium-sensing receptor signaling through direct interactions. Biochem Biophys Res Commun 347:924–930
56. Reyes-Ibarra AP, Garcia-Regalado A, Ramirez-Rangel I, Esparza-Silva AL, Valadez-Sanchez M, Vazquez-Prado J, Reyes-Cruz G (2007) Calcium-sensing receptor endocytosis links extracellular calcium signaling to parathyroid hormone-related peptide secretion via a Rab11a-dependent and AMSH-sensitive mechanism. Mol Endocrinol 21:1394–1407
57. Hjalm G, MacLeod RJ, Kifor O, Chattopadhyay N, Brown EM (2001) Filamin-A binds to the carboxyl-terminal tail of the calcium-sensing receptor, an interaction that participates in CaR-mediated activation of mitogen-activated protein kinase. J Biol Chem 276:34880–34887
58. Awata H, Huang C, Handlogten ME, Miller RT (2001) Interaction of the calcium-sensing receptor and filamin, a potential scaffolding protein. J Biol Chem 276:34871–34879
59. Miller GD, Groziak SM, DiRienzo D (1996) Age considerations in nutrient needs for bone health. J Am Coll Nutr 15:553–555
60. Razani B, Woodman SE, Lisanti MP (2002) Caveolae: from cell biology to animal physiology. Pharmacol Rev 54:431–467
61. Kifor O, Diaz R, Butters R, Kifor I, Brown EM (1998) The calcium-sensing receptor is localized in caveolin-rich plasma membrane domains of bovine parathyroid cells. J Biol Chem 273:21708–21713

62. Jung SY, Kwak JO, Kim HW, Kim DS, Ryu SD, Ko CB, Cha SH (2005) Calcium sensing receptor forms complex with and is up-regulated by caveolin-1 in cultured human osteosarcoma (Saos-2) cells. Exp Mol Med 37:91–100
63. Kifor O, Kifor I, Moore FD Jr, Butters RR Jr, Cantor T, Gao P, Brown EM (2003) Decreased expression of caveolin-1 and altered regulation of mitogen-activated protein kinase in cultured bovine parathyroid cells and human parathyroid adenomas. J Clin Endocrinol Metab 88:4455–4464
64. Kunishima N, Shimada Y, Tsuji Y, Sato T, Yamamoto M, Kumasaka T, Nakanishi S, Jingami H, Morikawa K (2000) Structural basis of glutamate recognition by a dimeric metabotropic glutamate receptor. Nature 407:971–977
65. Huang C, Hujer KM, Wu Z, Miller RT (2004) The Ca^{2+} −sensing receptor couples to Galpha12/13 to activate phospholipase D in Madin-Darby canine kidney cells. Am J Physiol Cell Physiol 286:C22–C30
66. Chang W, Chen TH, Pratt S, Shoback D (2000) Amino acids in the second and third intracellular loops of the parathyroid Ca^{2+} −sensing receptor mediate efficient coupling to phospholipase C. J Biol Chem 275:19955–19963
67. Smrcka AV (2008) G protein betagamma subunits: central mediators of G protein-coupled receptor signaling. Cell Mol Life Sci 65:2191–2214
68. Bhattacharya M, Babwah AV, Ferguson SS (2004) Small GTP-binding protein-coupled receptors. Biochem Soc Trans 32:1040–1044
69. Bouschet T, Martin S, Kanamarlapudi V, Mundell S, Henley JM (2007) The calcium-sensing receptor changes cell shape via a beta-arrestin-1 ARNO ARF6 ELMO protein network. J Cell Sci 120:2489–2497
70. Pi M, Spurney RF, Tu Q, Hinson T, Quarles LD (2002) Calcium-sensing receptor activation of rho involves filamin and rho-guanine nucleotide exchange factor. Endocrinology 143:3830–3838
71. Tu CL, Chang W, Xie Z, Bikle DD (2008) Inactivation of the calcium sensing receptor inhibits E-cadherin-mediated cell-cell adhesion and calcium-induced differentiation in human epidermal keratinocytes. J Biol Chem 283:3519–3528
72. Rey O, Young SH, Yuan J, Slice L, Rozengurt E (2005) Amino acid-stimulated Ca^{2+} oscillations produced by the Ca^{2+} −sensing receptor are mediated by a phospholipase C/inositol 1,4,5-trisphosphate-independent pathway that requires G12, Rho, filamin-A, and the actin cytoskeleton. J Biol Chem 280:22875–22882
73. Huang C, Handlogten ME, Miller RT (2002) Parallel activation of phosphatidylinositol 4-kinase and phospholipase C by the extracellular calcium-sensing receptor. J Biol Chem 277:20293–20300
74. Davies SL, Gibbons CE, Vizard T, Ward DT (2006) Ca^{2+} −sensing receptor induces Rho kinase-mediated actin stress fiber assembly and altered cell morphology, but not in response to aromatic amino acids. Am J Physiol Cell Physiol 290:C1543–C1551
75. Hobson SA, McNeil SE, Lee F, Rodland KD (2000) Signal transduction mechanisms linking increased extracellular calcium to proliferation in ovarian surface epithelial cells. Exp Cell Res 258:1–11
76. MacLeod RJ, Yano S, Chattopadhyay N, Brown EM (2004) Extracellular calcium-sensing receptor transactivates the epidermal growth factor receptor by a triple-membrane-spanning signaling mechanism. Biochem Biophys Res Commun 320:455–460
77. Yano S, Macleod RJ, Chattopadhyay N, Tfelt-Hansen J, Kifor O, Butters RR, Brown EM (2004) Calcium-sensing receptor activation stimulates parathyroid hormone-related protein secretion in prostate cancer cells: role of epidermal growth factor receptor transactivation. Bone 35:664–672
78. Tomlins SA, Bolllinger N, Creim J, Rodland KD (2005) Cross-talk between the calcium-sensing receptor and the epidermal growth factor receptor in Rat-1 fibroblasts. Exp Cell Res 308:439–445
79. Geibel J, Sritharan K, Geibel R, Geibel P, Persing JS, Seeger A, Roepke TK, Deichstetter M, Prinz C, Cheng SX, Martin D, Hebert SC (2006) Calcium-sensing receptor abrogates

secretagogue- induced increases in intestinal net fluid secretion by enhancing cyclic nucleotide destruction. Proc Natl Acad Sci USA 103:9390–9397
80. Mamillapalli R, Wysolmerski J (2010) The calcium-sensing receptor couples to Galpha(s) and regulates PTHrP and ACTH secretion in pituitary cells. J Endocrinol 204:287–297
81. Brown EM, Hurwitz S, Aurbach GD (1977) Beta-adrenergic stimulation of cyclic AMP content and parathyroid hormone release from isolated bovine parathyroid cells. Endocrinology 100:1696–1702
82. Cifuentes M, Rojas CV (2008) Antilipolytic effect of calcium-sensing receptor in human adipocytes. Mol Cell Biochem 319:17–21
83. de Jesus Ferreira MC, Helies-Toussaint C, Imbert-Teboul M, Bailly C, Verbavatz JM, Bellanger AC, Chabardes D (1998) Co-expression of a Ca^{2+} -inhibitable adenylyl cyclase and of a Ca^{2+} -sensing receptor in the cortical thick ascending limb cell of the rat kidney. Inhibition of hormone-dependent cAMP accumulation by extracellular Ca^{2+}. J Biol Chem 273:15192–15202
84. Wettschureck N, Lee E, Libutti SK, Offermanns S, Robey PG, Spiegel AM (2007) Parathyroid-specific double knockout of Gq and G11 alpha-subunits leads to a phenotype resembling germline knockout of the extracellular Ca^{2+} −sensing receptor. Mol Endocrinol 21:274–280
85. Godwin SL, Soltoff SP (1997) Extracellular calcium and platelet-derived growth factor promote receptor-mediated chemotaxis in osteoblasts through different signaling pathways. J Biol Chem 272:11307–11312
86. Ogata S, Kubota Y, Satoh S, Ito S, Takeuchi H, Ashizuka M, Shirasuna K (2006) Ca^{2+} stimulates COX-2 expression through calcium-sensing receptor in fibroblasts. Biochem Biophys Res Commun 351:808–814
87. Handlogten ME, Huang C, Shiraishi N, Awata H, Miller RT (2001) The Ca^{2+} −sensing receptor activates cytosolic phospholipase A2 via a Gqalpha -dependent ERK-independent pathway. J Biol Chem 276:13941–13948
88. Newton AC (2008) Protein kinase C. IUBMB Life 60:765–768
89. Newton AC (2010) Protein kinase C: poised to signal. Am J Physiol Endocrinol Metab 298:E395–E402
90. Kifor O, Diaz R, Butters R, Brown EM (1997) The Ca^{2+} −sensing receptor (CaR) activates phospholipases C, A2, and D in bovine parathyroid and CaR-transfected, human embryonic kidney (HEK293) cells. J Bone Miner Res 12:715–725
91. Kifor O, Congo D, Brown EM (1990) Phorbol esters modulate the high Ca^{2+} −stimulated accumulation of inositol phosphates in bovine parathyroid cells. J Bone Miner Res 5: 1003–1011
92. Jiang YF, Zhang Z, Kifor O, Lane CR, Quinn SJ, Bai M (2002) Protein kinase C (PKC) phosphorylation of the Ca^{2+}_o-sensing receptor (CaR) modulates functional interaction of G proteins with the CaR cytoplasmic tail. J Biol Chem 277:50543–50549
93. Davies SL, Ozawa A, McCormick WD, Dvorak MM, Ward DT (2007) Protein kinase C-mediated phosphorylation of the calcium-sensing receptor is stimulated by receptor activation and attenuated by calyculin-sensitive phosphatase activity. J Biol Chem 282:15048–15056
94. Varnai P, Hunyady L, Balla T (2009) STIM and Orai: the long-awaited constituents of store-operated calcium entry. Trends Pharmacol Sci 30:118–128
95. Gees M, Colsoul B, Nilius B (2010) The role of transient receptor potential cation channels in Ca^{2+} signaling. Cold Spring Harb Perspect Biol 2:a003962
96. Chow JY, Estrema C, Orneles T, Dong X, Barrett KE, Dong H (2011) Calcium sensing receptor modulates extracellular Ca^{2+} entry via TRPC-encoded receptor-operated channels in human aortic smooth muscle cells. Am J Physiol Cell Physiol 301(2):C461–C468
97. Rey O, Young SH, Jacamo R, Moyer MP, Rozengurt E (2010) Extracellular calcium sensing receptor stimulation in human colonic epithelial cells induces intracellular calcium oscillations and proliferation inhibition. J Cell Physiol 225:73–83
98. El Hiani Y, Lehen'kyi V, Ouadid-Ahidouch H, Ahidouch A (2009) Activation of the calcium-sensing receptor by high calcium induced breast cancer cell proliferation and TRPC1

cation channel over-expression potentially through EGFR pathways. Arch Biochem Biophys 486:58–63
99. Cai S, Fatherazi S, Presland RB, Belton CM, Roberts FA, Goodwin PC, Schubert MM, Izutsu KT (2006) Evidence that TRPC1 contributes to calcium-induced differentiation of human keratinocytes. Pflugers Arch 452:43–52
100. Lu M, Branstrom R, Berglund E, Hoog A, Bjorklund P, Westin G, Larsson C, Farnebo LO, Forsberg L (2010) Expression and association of TRPC subtypes with Orai1 and STIM1 in human parathyroid. J Mol Endocrinol 44:285–294
101. Sun YH, Li YQ, Feng SL, Li BX, Pan ZW, Xu CQ, Li TT, Yang BF (2010) Calcium-sensing receptor activation contributed to apoptosis stimulates TRPC6 channel in rat neonatal ventricular myocytes. Biochem Biophys Res Commun 394:955–961
102. Breitwieser GE (2006) Calcium sensing receptors and calcium oscillations: calcium as a first messenger. Curr Top Dev Biol 73:85–114
103. McCormick WD, Atkinson-Dell R, Campion KL, Mun HC, Conigrave AD, Ward DT (2010) Increased receptor stimulation elicits differential calcium-sensing receptor (T888) dephosphorylation. J Biol Chem 285:14170–14177
104. Bourdeau A, Souberbielle J-C, Bonnet P, Herviaux P, Sachs C, Lieberherr M (1992) Phospholipase-A2 action and arachidonic acid metabolism in calcium-mediated parathyroid hormone secretion. Endocrinology 130:1339–1344
105. Wang WH, Lu M, Hebert SC (1996) Cytochrome P-450 metabolites mediate extracellular Ca(2+)-induced inhibition of apical K+ channels in the TAL. Am J Physiol 271:C103–C111
106. Bourdeau A, Moutahir M, Souberbielle J, Bonnet P, Herviaux P, Sachs C, Lieberherr M (1994) Effects of lipoxygenase products of arachidonate metabolism on parathyroid hormone secretion. Endocrinology 135:1109–1112
107. Wang D, An SJ, Wang WH, McGiff JC, Ferreri NR (2001) CaR-mediated COX-2 expression in primary cultured mTAL cells. Am J Physiol Renal Physiol 281:F658–F664
108. Wang D, Pedraza PL, Abdullah HI, McGiff JC, Ferreri NR (2002) Calcium-sensing receptor-mediated TNF production in medullary thick ascending limb cells. Am J Physiol Renal Physiol 283:F963–F970
109. Abdullah HI, Pedraza PL, McGiff JC, Ferreri NR (2008) CaR activation increases TNF production by mTAL cells via a Gi-dependent mechanism. Am J Physiol Renal Physiol 294: F345–F354
110. Peng X, Frohman MA (2012) Mammalian phospholipase D physiological and pathological roles. Acta Physiol (Oxf) 204(2):219–226
111. Wu Z, Tandon R, Ziembicki J, Nagano J, Hujer KM, Miller RT, Huang C (2005) Role of ceramide in Ca^{2+} –sensing receptor-induced apoptosis. J Lipid Res 46:1396–1404
112. Lin KI, Chattopadhyay N, Bai M, Alvarez R, Dang CV, Baraban JM, Brown EM, Ratan RR (1998) Elevated extracellular calcium can prevent apoptosis via the calcium- sensing receptor. Biochem Biophys Res Commun 249:325–331
113. Tfelt-Hansen J, Chattopadhyay N, Yano S, Kanuparthi D, Rooney P, Schwarz P, Brown EM (2004) Calcium-sensing receptor induces proliferation through p38 mitogen-activated protein kinase and phosphatidylinositol 3-kinase but not extracellularly regulated kinase in a model of humoral hypercalcemia of malignancy. Endocrinology 145:1211–1217
114. Corbetta S, Lania A, Filopanti M, Vincentini L, Ballare E, Spada A (2002) Mitogen-activated protein kinase cascade in human normal and tumoral parathyroid cells. J Clin Endocrinol Metab 87:2201–2205
115. Fayard E, Xue G, Parcellier A, Bozulic L, Hemmings BA (2010) Protein kinase B (PKB/Akt), a key mediator of the PI3K signaling pathway. Curr Top Microbiol Immunol 346:31–56
116. Liu KP, Russo AF, Hsiung SC, Adlersberg M, Franke TF, Gershon MD, Tamir H (2003) Calcium receptor-induced serotonin secretion by parafollicular cells: role of phosphatidylinositol 3-kinase-dependent signal transduction pathways. J Neurosci 23:2049–2057
117. Dvorak MM, Siddiqua A, Ward DT, Carter DH, Dallas SL, Nemeth EF, Riccardi D (2004) Physiological changes in extracellular calcium concentration directly control osteoblast function in the absence of calciotropic hormones. Proc Natl Acad Sci USA 101:5140–5145

118. Topala CN, Schoeber JP, Searchfield LE, Riccardi D, Hoenderop JG, Bindels RJ (2009) Activation of the Ca^{2+} –sensing receptor stimulates the activity of the epithelial Ca^{2+} channel TRPV5. Cell Calcium 45:331–339
119. Hurtel-Lemaire AS, Mentaverri R, Caudrillier A, Cournarie F, Wattel A, Kamel S, Terwilliger EF, Brown EM, Brazier M (2009) The calcium-sensing receptor is involved in strontium ranelate-induced osteoclast apoptosis. New insights into the associated signaling pathways. J Biol Chem 284:575–584
120. Abdullah HI, Pedraza PL, McGiff JC, Ferreri NR (2008) Calcium-sensing receptor signaling pathways in medullary thick ascending limb cells mediate COX-2-derived PGE2 production: functional significance. Am J Physiol Renal Physiol 295:F1082–F1089
121. Remy C, Kirchhoff P, Hafner P, Busque SM, Mueller MK, Geibel JP, Wagner CA (2007) Stimulatory pathways of the Calcium-sensing receptor on acid secretion in freshly isolated human gastric glands. Cell Physiol Biochem 19:33–42
122. Wayman GA, Tokumitsu H, Davare MA, Soderling TR (2011) Analysis of CaM-kinase signaling in cells. Cell Calcium, Epub ahead of print
123. Gray E, Muller D, Squires PE, Asare-Anane H, Huang GC, Amiel S, Persaud SJ, Jones PM (2006) Activation of the extracellular calcium-sensing receptor initiates insulin secretion from human islets of Langerhans: involvement of protein kinases. J Endocrinol 190:703–710
124. Tfelt-Hansen J, Yano S, John Macleod R, Smajilovic S, Chattopadhyay N, Brown EM (2005) High calcium activates the EGF receptor potentially through the calcium-sensing receptor in Leydig cancer cells. Growth Factors 23:117–123
125. McNeil SE, Hobson SA, Nipper V, Rodland KD (1998) Functional calcium-sensing receptors in rat fibroblasts are required for activation of SRC kinase and mitogen-activated protein kinase in response to extracellular calcium. J Biol Chem 273:1114–1120
126. Kifor O, MacLeod RJ, Diaz R, Bai M, Yamaguchi T, Yao T, Kifor I, Brown EM (2001) Regulation of MAP kinase by calcium-sensing receptor in bovine parathyroid and CaR-transfected HEK293 cells. Am J Physiol Renal Physiol 280:F291–F302
127. Cargnello M, Roux PP (2011) Activation and function of the MAPKs and their substrates, the MAPK-activated protein kinases. Microbiol Mol Biol Rev 75:50–83
128. Yamaguchi T, Chattopadhyay N, Kifor O, Butters RR Jr, Sugimoto T, Brown EM (1998) Mouse osteoblastic cell line (MC3T3-E1) expresses extracellular calcium (Ca^{2+}_o)-sensing receptor and its agonists stimulate chemotaxis and proliferation of MC3T3-E1 cells. J Bone Miner Res 13:1530–1538
129. Lu F, Tian Z, Zhang W, Zhao Y, Bai S, Ren H, Chen H, Yu X, Wang J, Wang L, Li H, Pan Z, Tian Y, Yang B, Wang R, Xu C (2010) Calcium-sensing receptors induce apoptosis in rat cardiomyocytes via the endo(sarco)plasmic reticulum pathway during hypoxia/reoxygenation. Basic Clin Pharmacol Toxicol 106:396–405
130. Canadillas S, Canalejo R, Rodriguez-Ortiz ME, Martinez-Moreno JM, Estepa JC, Zafra R, Perez J, Munoz-Castaneda JR, Canalejo A, Rodriguez M, Almaden Y (2010) The up-regulation of the parathyroid VDR expression by extracellular calcium is mediated by the ERK1/2-MAPK signaling pathway. Am J Physiol Renal Physiol 298:F1197–F1204
131. Tfelt-Hansen J, MacLeod RJ, Chattopadhyay N, Yano S, Quinn S, Ren X, Terwilliger EF, Schwarz P, Brown EM (2003) Calcium-sensing receptor stimulates PTHrP release by pathways dependent on PKC, p38 MAPK, JNK, and ERK1/2 in H-500 cells. Am J Physiol Endocrinol Metab 285:E329–E337
132. Sakwe AM, Larsson M, Rask L (2004) Involvement of protein kinase C-alpha and -epsilon in extracellular Ca(2+) signalling mediated by the calcium sensing receptor. Exp Cell Res 297:560–573
133. Hobson SA, Wright J, Lee F, McNeil SE, Bilderback T, Rodland KD (2003) Activation of the MAP kinase cascade by exogenous calcium-sensing receptor. Mol Cell Endocrinol 200:189–198
134. Yamaguchi T, Chattopadhyay N, Kifor O, Sanders JL, Brown EM (2000) Activation of p42/44 and p38 mitogen-activated protein kinases by extracellular calcium-sensing receptor agonists induces mitogenic responses in the mouse osteoblastic MC3T3-E1 cell line. Biochem Biophys Res Commun 279:363–368

135. Chattopadhyay N, Yano S, Tfelt-Hansen J, Rooney P, Kanuparthi D, Bandyopadhyay S, Ren X, Terwilliger E, Brown EM (2004) Mitogenic action of calcium-sensing receptor on rat calvarial osteoblasts. Endocrinology 145:3451–3462
136. Morgan R, Fairfax B, Pandha HS (2006) Calcium insensitivity of FA-6, a cell line derived from a pancreatic cancer associated with humoral hypercalcemia, is mediated by the significantly reduced expression of the Calcium Sensitive Receptor transduction component p38 MAPK. Mol Cancer 5:51
137. Ye CP, Yano S, Tfelt-Hansen J, MacLeod RJ, Ren X, Terwilliger E, Brown EM, Chattopadhyay N (2004) Regulation of a Ca^{2+} −activated K+ channel by calcium-sensing receptor involves p38 MAP kinase. J Neurosci Res 75:491–498
138. Maiti A, Hait NC, Beckman MJ (2008) Extracellular calcium-sensing receptor activation induces vitamin D receptor levels in proximal kidney HK-2G cells by a mechanism that requires phosphorylation of p38alpha MAPK. J Biol Chem 283:175–183
139. Hoenderop JG, Dardenne O, Van Abel M, Van Der Kemp AW, Van Os CH, St-Arnaud R, Bindels RJ (2002) Modulation of renal Ca^{2+} transport protein genes by dietary Ca^{2+} and 1,25-dihydroxyvitamin D3 in 25-hydroxyvitamin D3-1alpha-hydroxylase knockout mice. FASEB J 16:1398–1406
140. Corbetta S, Eller-Vainicher C, Vicentini L, Lania A, Mantovani G, Beck-Peccoz P, Spada A (2007) Modulation of cyclin D1 expression in human tumoral parathyroid cells: effects of growth factors and calcium sensing receptor activation. Cancer Lett 255:34–41
141. Kallay E, Kifor O, Chattopadhyay N, Brown EM, Bischof MG, Peterlik M, Cross HS (1997) Calcium-dependent c-myc proto-oncogene expression and proliferation of Caco-2 cells: a role for a luminal extracellular calcium-sensing receptor. Biochem Biophys Res Commun 232:80–83
142. Abdullah HI, Pedraza PL, Hao S, Rodland KD, McGiff JC, Ferreri NR (2006) NFAT regulates calcium-sensing receptor-mediated TNF production. Am J Physiol Renal Physiol 290:F1110–F1117
143. Mentaverri R, Yano S, Chattopadhyay N, Petit L, Kifor O, Kamel S, Terwilliger EF, Brazier M, Brown EM (2006) The calcium sensing receptor is directly involved in both osteoclast differentiation and apoptosis. FASEB J 20:2562–2564
144. Tfelt-Hansen J, Schwarz P, Terwilliger EF, Brown EM, Chattopadhyay N (2003) Calcium-sensing receptor induces messenger ribonucleic acid of human securin, pituitary tumor transforming gene, in rat testicular cancer. Endocrinology 144:5188–5193
145. Mendoza FJ, Lopez I, Canalejo R, Almaden Y, Martin D, Aguilera-Tejero E, Rodriguez M (2009) Direct upregulation of parathyroid calcium-sensing receptor and vitamin D receptor by calcimimetics in uremic rats. Am J Physiol Renal Physiol 296:F605–F613
146. Ho C, Conner DA, Pollak MR, Ladd DJ, Kifor O, Warren HB, Brown EM, Seidman JG, Seidman CE (1995) A mouse model of human familial hypocalciuric hypercalcemia and neonatal severe hyperparathyroidism [see comments]. Nat Genet 11:389–394
147. Egbuna OI, Brown EM (2008) Hypercalcaemic and hypocalcaemic conditions due to calcium-sensing receptor mutations. Best Pract Res Clin Rheumatol 22:129–148
148. Lu M, Forsberg L, Hoog A, Juhlin CC, Vukojevic V, Larsson C, Conigrave AD, Delbridge LW, Gill A, Bark C, Farnebo LO, Branstrom R (2008) Heterogeneous expression of SNARE proteins SNAP-23, SNAP-25, Syntaxin1 and VAMP in human parathyroid tissue. Mol Cell Endocrinol 287:72–80
149. Quinn SJ, Kifor O, Kifor I, Butters RR Jr, Brown EM (2007) Role of the cytoskeleton in extracellular calcium-regulated PTH release. Biochem Biophys Res Commun 354:8–13
150. Nechama M, Ben-Dov IZ, Silver J, Naveh-Many T (2009) Regulation of PTH mRNA stability by the calcimimetic R568 and the phosphorus binder lanthanum carbonate in CKD. Am J Physiol Renal Physiol 296:F795–F800
151. Ritter CS, Pande S, Krits I, Slatopolsky E, Brown AJ (2008) Destabilization of parathyroid hormone mRNA by extracellular Ca^{2+} and the calcimimetic R-568 in parathyroid cells: role of cytosolic Ca and requirement for gene transcription. J Mol Endocrinol 40: 13–21

152. Bell O, Gaberman E, Kilav R, Levi R, Cox KB, Molkentin JD, Silver J, Naveh-Many T (2005) The protein phosphatase calcineurin determines basal parathyroid hormone gene expression. Mol Endocrinol 19:516–526
153. Naveh-Many T, Nechama M (2007) Regulation of parathyroid hormone mRNA stability by calcium, phosphate and uremia. Curr Opin Nephrol Hypertens 16:305–310
154. Cozzolino M, Lu Y, Finch J, Slatopolsky E, Dusso AS (2001) p21WAF1 and TGF-alpha mediate parathyroid growth arrest by vitamin D and high calcium. Kidney Int 60:2109–2117
155. Jara A, von Hoveling A, Jara X, Burgos ME, Valdivieso A, Mezzano S, Felsenfeld AJ (2006) Effect of endothelin receptor antagonist on parathyroid gland growth. PTH values and cell proliferation in azotemic rats. Nephrol Dial Transplant 21:917–923
156. Scherubl H, Schultz G, Hescheler J (1991) Electrophysiological properties of rat calcitonin-secreting cells. Mol Cell Endocrinol 82:293–301
157. Cooper CW (1997) Parathyroid hormone-related protein and its role in pregnancy, lactation, and neonatal growth and development. Eur J Endocrinol 136:465–466
158. Fried R, Tashjian AJ (1986) Unusual sensitivity of cytosolic free Ca^{2+} to changes in extracellular Ca^{2+} in rat C-cells. J Biol Chem 261:7669–7674
159. Scherubl H, Kleppisch T, Zink A, Raue F, Krautwurst D, Hescheler J (1993) Major role of dihydropyridine-sensitive Ca^{2+} channels in Ca^{2+} –induced calcitonin secretion. Am J Physiol 264:E354–E360
160. Garrett JE, Tamir H, Kifor O, Simin RT, Rogers KV, Mithal A, Gagel RF, Brown EM (1995) Calcitonin-secreting cells of the thyroid express an extracellular calcium receptor gene. Endocrinology 136:5202–5211
161. Freichel M, Zink-Lorenz A, Holloschi A, Hafner M, Flockerzi V, Raue F (1996) Expression of a calcium-sensing receptor in a human medullary thyroid carcinoma cell line and its contribution to calcitonin secretion. Endocrinology 137:3842–3848
162. Kantham L, Quinn SJ, Egbuna OI, Baxi K, Butters R, Pang JL, Pollak MR, Goltzman D, Brown EM (2009) The calcium-sensing receptor (CaSR) defends against hypercalcemia independently of its regulation of parathyroid hormone secretion. Am J Physiol Endocrinol Metab 297:E915–E923
163. McGehee DS, Aldersberg M, Liu KP, Hsuing S, Heath MJ, Tamir H (1997) Mechanism of extracellular Ca^{2+} receptor-stimulated hormone release from sheep thyroid parafollicular cells. J Physiol (Lond) 502:31–44
164. Riccardi D, Hall AE, Chattopadhyay N, Xu JZ, Brown EM, Hebert SC (1998) Localization of the extracellular Ca^{2+}/polyvalent cation-sensing protein in rat kidney. Am J Physiol 274:F611–F622
165. Sands JM, Flores FX, Kato A, Baum MA, Brown EM, Ward DT, Hebert SC, Harris HW (1998) Vasopressin-elicited water and urea permeabilities are altered in IMCD in hypercalcemic rats. Am J Physiol 274:F978–F985
166. Sands JM, Naruse M, Baum M, Jo I, Hebert SC, Brown EM, Harris HW (1997) Apical extracellular calcium/polyvalent cation-sensing receptor regulates vasopressin-elicited water permeability in rat kidney inner medullary collecting duct. J Clin Invest 99:1399–1405
167. Riccardi D, Brown EM (2009) Physiology and pathophysiology of the calcium-sensing receptor in the kidney. Am J Physiol Renal Physiol 298:F485–F499
168. Maiti A, Beckman MJ (2007) Extracellular calcium is a direct effecter of VDR levels in proximal tubule epithelial cells that counter-balances effects of PTH on renal Vitamin D metabolism. J Steroid Biochem Mol Biol 103:504–508
169. Takaichi K, Kurokawa K (1988) Inhibitory guanosine triphosphate-binding protein-mediated regulation of vasopressin action in isolated single medullary tubules of mouse kidney. J Clin Invest 82:1437–1444
170. Takaichi K, Kurokawa K (1986) High Ca^{2+} inhibits peptide hormone-dependent cAMP production specifically in thick ascending limbs of Henle. Miner Electrolyte Metab 12:342–346
171. Ba J, Friedman PA (2004) Calcium-sensing receptor regulation of renal mineral ion transport. Cell Calcium 35:229–237

172. Gamba G, Friedman PA (2009) Thick ascending limb: the Na(+):K (+):2Cl (−) co-transporter, NKCC2, and the calcium-sensing receptor, CaSR. Pflugers Arch 458:61–76
173. Simon DB, Lifton RP (1996) The molecular basis of inherited hypokalemic alkalosis: Bartter's and Gitelman's syndromes. Am J Physiol 271:F961–F966
174. Vezzoli G, Arcidiacono T, Paloschi V, Terranegra A, Biasion R, Weber G, Mora S, Syren ML, Coviello D, Cusi D, Bianchi G, Soldati L (2006) Autosomal dominant hypocalcemia with mild type 5 Bartter syndrome. J Nephrol 19:525–528
175. Watanabe S, Fukumoto S, Chang H, Takeuchi Y, Hasegawa Y, Okazaki R, Chikatsu N, Fujita T (2002) Association between activating mutations of calcium-sensing receptor and Bartter's syndrome. Lancet 360:692–694
176. Hao S, Zhao H, Darzynkiewicz Z, Battula S, Ferreri NR (2009) Expression and function of NFAT5 in medullary thick ascending limb (mTAL) cells. Am J Physiol Renal Physiol 296:F1494–F1503
177. Desfleurs E, Wittner M, Pajaud S, Nitschke R, Rajerison RM, Di Stefano A (1999) The Ca^{2+} −sensing receptor in the rabbit cortical thick ascending limb (CTAL) is functionally not coupled to phospholipase C. Pflugers Arch 437:716–723
178. Valenti G, Procino G, Tamma G, Carmosino M, Svelto M (2005) Minireview: aquaporin 2 trafficking. Endocrinology 146:5063–5070
179. Procino G, Carmosino M, Tamma G, Gouraud S, Laera A, Riccardi D, Svelto M, Valenti G (2004) Extracellular calcium antagonizes forskolin-induced aquaporin 2 trafficking in collecting duct cells. Kidney Int 66:2245–2255
180. Brown EM, MacLeod RJ (2001) Extracellular calcium sensing and extracellular calcium signaling. Physiol Rev 81:239–297
181. Hennings H, Michael D, Cheng C, Steinert P, Holbrook K, Yuspa SH (1980) Calcium regulation of growth and differentiation of mouse epidermal cells in culture. Cell 19:245–254
182. Jaken S, Yuspa SH (1988) Early signals for keratinocyte differentiation: role of Ca^{2+} −mediated inositol lipid metabolism in normal and neoplastic epidermal cells. Carcinogenesis 9:1033–1038
183. Yuspa SH, Hennings H, Tucker RW, Jaken S, Kilkenny AE, Roop DR (1988) Signal transduction for proliferation and differentiation in keratinocytes. Ann NY Acad Sci 548:191–196
184. Xie Z, Bikle DD (1999) Phospholipase C-gamma1 is required for calcium-induced keratinocyte differentiation. J Biol Chem 274:20421–20424
185. Eckert RL, Crish JF, Robinson NA (1997) The epidermal keratinocyte as a model for the study of gene regulation and cell differentiation. Physiol Rev 77:397–424
186. Denning MF, Dlugosz AA, Williams EK, Szallasi Z, Blumberg PM, Yuspa SH (1995) Specific protein kinase C isozymes mediate the induction of keratinocyte differentiation markers by calcium. Cell Growth Differ 6:149–157
187. Hennings H, Holbrook KA (1983) Calcium regulation of cell-cell contact and differentiation of epidermal cells in culture. An ultrastructural study. Exp Cell Res 143:127–142
188. Yang LC, Ng DC, Bikle DD (2003) Role of protein kinase C alpha in calcium induced keratinocyte differentiation: defective regulation in squamous cell carcinoma. J Cell Physiol 195:249–259
189. Bandyopadhyay S, Jeong KH, Hansen JT, Vassilev PM, Brown EM, Chattopadhyay N (2007) Calcium-sensing receptor stimulates secretion of an interferon-gamma-induced monokine (CXCL10) and monocyte chemoattractant protein-3 in immortalized GnRH neurons. J Neurosci Res 85:882–895
190. Phillips CG, Harnett MT, Chen W, Smith SM (2008) Calcium-sensing receptor activation depresses synaptic transmission. J Neurosci 28:12062–12070
191. Vassilev PM, Ho-Pao CL, Kanazirska MP, Ye C, Hong K, Seidman CE, Seidman JG, Brown EM (1997) Cao-sensing receptor (CaR)-mediated activation of K+ channels is blunted in CaR gene-deficient mouse neurons. Neuroreport 8:1411–1416
192. Vassilev PM, Mitchel J, Vassilev M, Kanazirska M, Brown EM (1997) Assessment of frequency-dependent alterations in the level of extracellular Ca^{2+} in the synaptic cleft. Biophys J 72:2103–2116

193. Scallet AC, Ye X (1997) Excitotoxic mechanisms of neurodegeneration in transmissible spongiform encephalopathies. Ann NY Acad Sci 825:194–205
194. Chiarini A, Dal Pra I, Marconi M, Chakravarthy B, Whitfield JF, Armato U (2009) Calcium-sensing receptor (CaSR) in human brain's pathophysiology: roles in late-onset Alzheimer's disease (LOAD). Curr Pharm Biotechnol 10:317–326
195. Ye C, Ho-Pao CL, Kanazirska M, Quinn S, Rogers K, Seidman CE, Seidman JG, Brown EM, Vassilev PM (1997) Amyloid-beta proteins activate Ca(2+)-permeable channels through calcium-sensing receptors. J Neurosci Res 47:547–554
196. Bandyopadhyay S, Tfelt-Hansen J, Chattopadhyay N (2010) Diverse roles of extracellular calcium-sensing receptor in the central nervous system. J Neurosci Res 88:2073–2082
197. Chattopadhyay N, Evliyaoglu C, Heese O, Carroll R, Sanders J, Black P, Brown EM (2000) Regulation of secretion of PTHrP by Ca(2+)-sensing receptor in human astrocytes, astrocytomas, and meningiomas. Am J Physiol Cell Physiol 279:C691–C699
198. Chattopadhyay N, Ye CP, Yamaguchi T, Kerner R, Vassilev PM, Brown EM (1999) Extracellular calcium-sensing receptor induces cellular proliferation and activation of a non-selective cation channel in U373 human astrocytoma cells. Brain Res 851:116–124
199. Kobayashi T, Chung UI, Schipani E, Starbuck M, Karsenty G, Katagiri T, Goad DL, Lanske B, Kronenberg HM (2002) PTHrP and Indian hedgehog control differentiation of growth plate chondrocytes at multiple steps. Development 129:2977–2986
200. Chang W, Tu C, Chen TH, Bikle D, Shoback D (2008) The extracellular calcium-sensing receptor (CaSR) is a critical modulator of skeletal development. Sci Signal 1:ra1
201. Chang W, Tu C, Bajra R, Komuves L, Miller S, Strewler G, Shoback D (1999) Calcium sensing in cultured chondrogenic RCJ3.1C5.18 cells. Endocrinology 140:1911–1919
202. Linsenmayer TF, Chen QA, Gibney E, Gordon MK, Marchant JK, Mayne R, Schmid TM (1991) Collagen types IX and X in the developing chick tibiotarsus: analyses of mRNAs and proteins. Development 111:191–196
203. Burton DW, Foster M, Johnson KA, Hiramoto M, Deftos LJ, Terkeltaub R (2005) Chondrocyte calcium-sensing receptor expression is up-regulated in early guinea pig knee osteoarthritis and modulates PTHrP, MMP-13, and TIMP-3 expression. Osteoarthritis Cartilage 13:395–404
204. Wang R, Xu C, Zhao W, Zhang J, Cao K, Yang B, Wu L (2003) Calcium and polyamine regulated calcium-sensing receptors in cardiac tissues. Eur J Biochem 270:2680–2688
205. Smajilovic S, Hansen JL, Christoffersen TE, Lewin E, Sheikh SP, Terwilliger EF, Brown EM, Haunso S, Tfelt-Hansen J (2006) Extracellular calcium sensing in rat aortic vascular smooth muscle cells. Biochem Biophys Res Commun 348:1215–1223
206. Tfelt-Hansen J, Hansen JL, Smajilovic S, Terwilliger EF, Haunso S, Sheikh SP (2006) Calcium receptor is functionally expressed in rat neonatal ventricular cardiomyocytes. Am J Physiol Heart Circ Physiol 290:H1165–H1171
207. Wang LN, Wang C, Lin Y, Xi YH, Zhang WH, Zhao YJ, Li HZ, Tian Y, Lv YJ, Yang BF, Xu CQ (2008) Involvement of calcium-sensing receptor in cardiac hypertrophy-induced by angiotensinII through calcineurin pathway in cultured neonatal rat cardiomyocytes. Biochem Biophys Res Commun 369:584–589
208. Sun YH, Liu MN, Li H, Shi S, Zhao YJ, Wang R, Xu CQ (2006) Calcium-sensing receptor induces rat neonatal ventricular cardiomyocyte apoptosis. Biochem Biophys Res Commun 350:942–948
209. Smajilovic S, Tfelt-Hansen J (2008) Novel role of the calcium-sensing receptor in blood pressure modulation. Hypertension 52:994–1000
210. Geibel JP, Hebert SC (2009) The functions and roles of the extracellular Ca^{2+} –sensing receptor along the gastrointestinal tract. Annu Rev Physiol 71:205–217
211. Chakravarti B, Dwivedi SK, Mithal A, Chattopadhyay N (2009) Calcium-sensing receptor in cancer: good cop or bad cop? Endocrine 35:271–284
212. Buchan AM, Squires PE, Ring M, Meloche RM (2001) Mechanism of action of the calcium-sensing receptor in human antral gastrin cells. Gastroenterology 120:1128–1139
213. Ceglia L, Harris SS, Rasmussen HM, Dawson-Hughes B (2009) Activation of the calcium sensing receptor stimulates gastrin and gastric acid secretion in healthy participants. Osteoporos Int 20:71–78

214. Dufner MM, Kirchhoff P, Remy C, Hafner P, Muller MK, Cheng SX, Tang LQ, Hebert SC, Geibel JP, Wagner CA (2005) The calcium-sensing receptor acts as a modulator of gastric acid secretion in freshly isolated human gastric glands. Am J Physiol Gastrointest Liver Physiol 289:G1084–G1090
215. Buchan AM, Meloche RM (1994) Signal transduction events involved in bombesin-stimulated gastrin release from human G cells in culture. Can J Physiol Pharmacol 72:1060–1065
216. Hira T, Nakajima S, Eto Y, Hara H (2008) Calcium-sensing receptor mediates phenylalanine-induced cholecystokinin secretion in enteroendocrine STC-1 cells. FEBS J 275:4620–4626
217. Liou AP, Sei Y, Zhao X, Feng J, Lu X, Thomas C, Pechhold S, Raybould HE, Wank SA (2011) The extracellular calcium-sensing receptor is required for cholecystokinin secretion in response to L-phenylalanine in acutely isolated intestinal I cells. Am J Physiol Gastrointest Liver Physiol 300:G538–G546
218. Saidak Z, Mentaverri R, Brown EM (2009) The role of the calcium-sensing receptor in the development and progression of cancer. Endocr Rev 30:178–195
219. Grill V, Martin TJ (2000) Hypercalcemia of malignancy. Rev Endocr Metab Disord 1:253–263
220. Paget S (1889) The distribution of secondary growths in cancer of the breast. Lancet 1:571–572
221. Kakonen SM, Selander KS, Chirgwin JM, Yin JJ, Burns S, Rankin WA, Grubbs BG, Dallas M, Cui Y, Guise TA (2002) Transforming growth factor-beta stimulates parathyroid hormone-related protein and osteolytic metastases via Smad and mitogen-activated protein kinase signaling pathways. J Biol Chem 277:24571–24578
222. Chirgwin JM, Mohammad KS, Guise TA (2004) Tumor-bone cellular interactions in skeletal metastases. J Musculoskelet Neuronal Interact 4:308–318
223. Chattopadhyay N (2006) Effects of calcium-sensing receptor on the secretion of parathyroid hormone-related peptide and its impact on humoral hypercalcemia of malignancy. Am J Physiol Endocrinol Metab 290:E761–E770
224. Parkinson IH, Fazzalari NL (2003) Interrelationships between structural parameters of cancellous bone reveal accelerated structural change at low bone volume. J Bone Miner Res 18:2200–2205
225. Guise TA, Yin JJ, Mohammad KS (2003) Role of endothelin-1 in osteoblastic bone metastases. Cancer 97:779–784
226. Guise TA, Kozlow WM, Heras-Herzig A, Padalecki SS, Yin JJ, Chirgwin JM (2005) Molecular mechanisms of breast cancer metastases to bone. Clin Breast Cancer 5(Suppl 2):S46–S53
227. Kozlow W, Guise TA (2005) Breast cancer metastasis to bone: mechanisms of osteolysis and implications for therapy. J Mammary Gland Biol Neoplasia 10:169–180
228. Chattopadhyay N, Brown EM (2006) Role of calcium-sensing receptor in mineral ion metabolism and inherited disorders of calcium-sensing. Mol Genet Metab 89:189–202
229. Lambers TT, Mahieu F, Oancea E, Hoofd L, de Lange F, Mensenkamp AR, Voets T, Nilius B, Clapham DE, Hoenderop JG, Bindels RJ (2006) Calbindin-D28K dynamically controls TRPV5-mediated Ca^{2+} transport. EMBO J 25:2978–2988
230. McGrath CM, Soule HD (1984) Calcium regulation of normal human mammary epithelial cell growth in culture. In Vitro 20:652–662
231. Sanders JL, Chattopadhyay N, Kifor O, Yamaguchi T, Butters RR, Brown EM (2000) Extracellular calcium-sensing receptor expression and its potential role in regulating parathyroid hormone-related peptide secretion in human breast cancer cell lines. Endocrinology 141:4357–4364
232. Mamillapalli R, VanHouten J, Zawalich W, Wysolmerski J (2008) Switching of G-protein usage by the calcium-sensing receptor reverses its effect on parathyroid hormone-related protein secretion in normal versus malignant breast cells. J Biol Chem 283:24435–24447
233. Cheng I, Klingensmith ME, Chattopadhyay N, Kifor O, Butters RR, Soybel DI, Brown EM (1998) Identification and localization of the extracellular calcium-sensing receptor in human breast. J Clin Endocrinol Metab 83:703–707

234. Sanders JL, Chattopadhyay N, Kifor O, Yamaguchi T, Brown EM (2001) Ca(2+)-sensing receptor expression and PTHrP secretion in PC-3 human prostate cancer cells. Am J Physiol Endocrinol Metab 281:E1267–E1274
235. Liao J, Schneider A, Datta NS, McCauley LK (2006) Extracellular calcium as a candidate mediator of prostate cancer skeletal metastasis. Cancer Res 66:9065–9073
236. Tam CS, Heersche JNM, Murray TM, Parsons JA (1982) Parathyroid hormone stimulates the bone apposition rate independently of its resorptive action. Differential effects of intermittent and continuous administration. Endocrinology 110:506–512
237. Sanders JL, Chattopadhyay N, Kifor O, Yamaguchi T, Brown EM (2000) Extracellular calcium-sensing receptor (CaR) expression and its potential role in parathyroid hormone-related peptide (PTHrP) secretion in the H-500 rat Leydig cell model of humoral hypercalcemia of malignancy. Biochem Biophys Res Commun 269:427–432
238. Liu B, Goltzman D, Rabbani SA (1993) Regulation of parathyroid hormone-related peptide production in vitro by the rat hypercalcemic Leydig cell tumor H-500. Endocrinology 132:1658–1664
239. Rabbani SA, Gladu J, Liu B, Goltzman D (1995) Regulation in vivo of the growth of Leydig cell tumors by antisense ribonucleic acid for parathyroid hormone-related peptide. Endocrinology 136:5416–5422
240. Tfelt-Hansen J, Ferreira A, Yano S, Kanuparthi D, Romero JR, Brown EM, Chattopadhyay N (2005) Calcium-sensing receptor activation induces nitric oxide production in H-500 Leydig cancer cells. Am J Physiol Endocrinol Metab 288:E1206–E1213
241. Sheinin Y, Kallay E, Wrba F, Kriwanek S, Peterlik M, Cross HS (2000) Immunocytochemical localization of the extracellular calcium-sensing receptor in normal and malignant human large intestinal mucosa. J Histochem Cytochem 48:595–602
242. Sparks AB, Morin PJ, Vogelstein B, Kinzler KW (1998) Mutational analysis of the APC/beta-catenin/Tcf pathway in colorectal cancer. Cancer Res 58:1130–1134
243. Lamprecht SA, Lipkin M (2003) Chemoprevention of colon cancer by calcium, vitamin D and folate: molecular mechanisms. Nat Rev Cancer 3:601–614
244. Powell SM, Zilz N, Beazer-Barclay Y, Bryan TM, Hamilton SR, Thibodeau SN, Vogelstein B, Kinzler KW (1992) APC mutations occur early during colorectal tumorigenesis. Nature 359:235–237
245. Logan CY, Nusse R (2004) The Wnt signaling pathway in development and disease. Annu Rev Cell Dev Biol 20:781–810
246. Sancho E, Batlle E, Clevers H (2004) Signaling pathways in intestinal development and cancer. Annu Rev Cell Dev Biol 20:695–723
247. Topol L, Jiang X, Choi H, Garrett-Beal L, Carolan PJ, Yang Y (2003) Wnt-5a inhibits the canonical Wnt pathway by promoting GSK-3-independent beta-catenin degradation. J Cell Biol 162:899–908
248. Semb H, Christofori G (1998) The tumor-suppressor function of E-cadherin. Am J Hum Genet 63:1588–1593
249. Chakrabarty S, Radjendirane V, Appelman H, Varani J (2003) Extracellular calcium and calcium sensing receptor function in human colon carcinomas: promotion of E-cadherin expression and suppression of beta-catenin/TCF activation. Cancer Res 63:67–71
250. MacLeod RJ, Hayes M, Pacheco I (2007) Wnt5a secretion stimulated by the extracellular calcium-sensing receptor inhibits defective Wnt signaling in colon cancer cells. Am J Physiol Gastrointest Liver Physiol 293:G403–G411

Chapter 6
Ca^{2+} Signaling: An Outlook on the Characterization of Ca^{2+} Channels and Their Importance in Cellular Functions

Jordan Karlstad, Yuyang Sun, and Brij B. Singh

Abstract Calcium (Ca^{2+}) is essential in regulating a plethora of cellular functions that includes cell proliferation and differentiation, axonal guidance and cell migration, neuro/enzyme secretion and exocytosis, development/maintenance of neural circuits, cell death and many more. Since Ca^{2+} regulates so many fundamental processes, it could be anticipated that numerous Ca^{2+} channels and transporters will assist in regulating Ca^{2+} entry across the plasma membrane. Towards this several Ca^{2+} channels such as voltage-gated channels, store-operated Ca^{2+} entry (SOCE) channels, NMDA, AMPA and other ligand gated channels have been identified. In recent years research focus has been targeted towards identification of the precise function of these essential channels. Furthermore, characterization of these individual Ca^{2+} channels has also gained much attention, since specific Ca^{2+} channels have been shown to influence a particular cellular response. Moreover, perturbations in these Ca^{2+} channels have also been implicated in a spectrum of pathological conditions. Hence, understanding the precise involvement of these Ca^{2+} channels in disease conditions would presumably unveil avenues for plausible therapeutic interventions. We thus review the role of Ca^{2+} signaling in select disease conditions and also provide experimental evidence as how they can be characterized in a given cell.

Keywords Cell signaling • Calcium channels and currents • Neurodegenerative diseases • Congestive heart failure

J. Karlstad • Y. Sun • B.B. Singh (✉)
Department of Biochemistry and Molecular Biology,
School of Medicine and Health Sciences, University of North Dakota, Grand Forks, ND, USA
e-mail: brij.singh@med.und.edu

M.S. Islam (ed.), *Calcium Signaling*, Advances in Experimental Medicine and Biology 740, DOI 10.1007/978-94-007-2888-2_6,

Introduction

Ca^{2+} Signaling

Most of us see the word Ca^{2+} daily, whether it is read on the label of a multivitamin or seen on a carton of milk, but do not realize the complexity and vast array of functions that this simple divalent cation plays on a molecular level. The majority of people know Ca^{2+} is involved in bone development and in the prevention of diseases such as osteoporosis; however, Ca^{2+} is one of the most abundant signaling molecules found in the human body which regulate functions ranging from the cell cycle and embryogenesis to cell death. Disruptions in Ca^{2+} signaling has been linked to the pathogenesis of numerous diseases such as, but not limited to Huntington's disease, Alzheimer's disease, Cancer, Congenital Heart Failure, and Diabetes. The focus of this chapter is to give an appreciation for Ca^{2+} signaling, characterization of Ca^{2+} channel activity, and how certain diseases arise due to disruptions or remodeling of the Ca^{2+} signaling cascade.

Many cellular responses act like factory machines, and their efficiency depends on a delicate balance between the input and output signal. The same can be said for Ca^{2+} signaling where the concentration of Ca^{2+} acts as the signal. One of the most important parts of Ca^{2+} signaling is the cell's ability to regulate this signal, since cells use the concentration of Ca^{2+} as a mechanism to drive many cellular processes. In order for a cell to elicit a cellular response due to Ca^{2+} signaling, it must be able to regulate the concentration of Ca^{2+} in different cellular locations. In any given cell, Ca^{2+} concentrations can range from its basal cytosolic concentration of 100 nM to as much as 1–10 μM when the cell is ready to produce a signaling cascade [1]. Importantly, certain cellular responses have an optimum Ca^{2+} concentration which once reached, signaling proteins can create a signal cascade which act on downstream effectors to activate transcription factors or other proteins to aid in the regulation of that response (Fig. 6.1). Before the cell is able to elicit a Ca^{2+} signal to activate certain processes required to maintain a healthy cell, it must be able to sustain a steady level of Ca^{2+} within its stores and in the cytoplasm. Since cells and their corresponding responses are sensitive to varying levels of Ca^{2+}, they must create a mechanism to keep Ca^{2+} at its basal cytosolic concentration except to elicit a cellular response. Thus, cell have developed a sophisticated mechanism that balances the Ca^{2+} levels, by several methods that include compartmentalization, chelation, or expulsion of Ca^{2+} from the cell (Fig. 6.1) [1].

Ca^{2+} Influx Channels and Cellular Homeostasis

The plasma membrane and endoplasmic reticulum are two of the most basic barriers for the compartmentalization of Ca^{2+}. The cell adapts Ca^{2+} channels to aid in the compartmentalization, expulsion, and transport of Ca^{2+} (Fig. 6.1) [1]. The plasma membrane acts as a divider to keep intracellular and extracellular Ca^{2+} concentrations

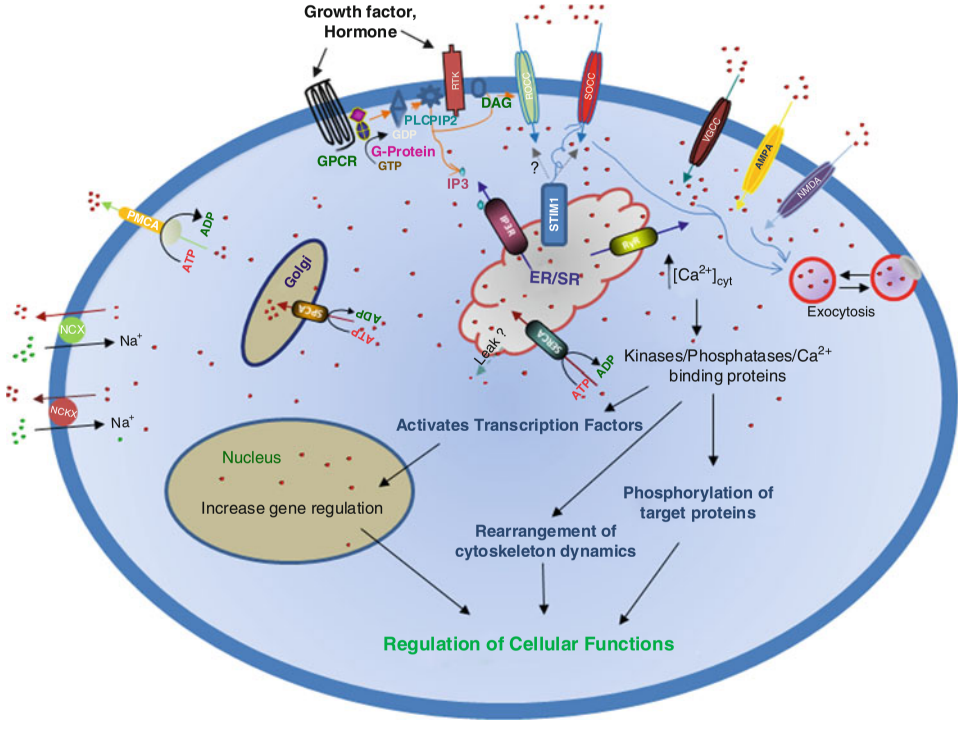

Fig. 6.1 Ca^{2+} signaling: This cartoon illustrates the intricate balance between several channels and proteins that regulate Ca^{2+} signaling. Activation of Ca^{2+} signaling initiates either via agonist binding to the receptors (GPCR/RTK) that results in the generation of cellular messenger IP_3 or by alterations in the membrane potential that activates the voltage-gated Ca^{2+} channels (VGCC). Binding of the ligand to the AMPA and NMDA receptors also directly activate these channels that bring Ca^{2+}. IP_3 binding to its receptor (IP_3R) in the ER depletes ER Ca^{2+} stores and activates store/receptor operated Ca^{2+} channels (SOCC/ROCC). Activation of these Ca^{2+} channels raises the $[Ca^{2+}]_{cyt}$ which not only aid in the SERCA pump-mediated ER store refilling but also promotes the regulation of several cellular functions as highlighted in the figure. Additionally, other transporters (such as NCX, NCKX) along with the activity of PMCA further remove Ca^{2+} from the cytosol and assist in maintaining low $[Ca^{2+}]_{cyt}$ levels

separate. ATPase pumps on the plasma membrane known as plasma membrane Ca^{2+} ATPases (PMCA pumps) push Ca^{2+} out of the cell against its concentration gradient at the expense of ATP^2. Other proteins such as Na^+/Ca^{2+} (NCX) and Na^+/Ca^{2+} -K^+ (NCKX) exchangers use the concentration gradient of other ions such as sodium to extrude one Ca^{2+} ion for three sodium ions or cotransport one Ca^{2+} and potassium ion to the outside of the cell for four sodium ions into the cell, respectively [2]. The endoplasmic reticulum is another organelle that acts as a barrier to aid in the separation of concentration. The endoplasmic reticulum can also act as a storage unit for Ca^{2+} to be used later when the cell needs to elicit a Ca^{2+} dependent response. ATPases on the endoplasmic reticulum known as sarcoendoplasmic reticular Ca^{2+} ATPases (SERCA pumps) push Ca^{2+} into the endoplasmic reticulum at the expense of ATP^2. Due to the actions of the plasma membrane, endoplasmic reticulum, and their corresponding Ca^{2+} channels, the cell is able to transport Ca^{2+} into the extracellular space or into the endoplasmic reticulum for storage to be release in response to certain agonist binding which will be discussed later.

Ca^2 expulsion from the cell is only applicable when dealing with large increases in the intracellular concentration of Ca^{2+}. As mentioned earlier, Ca^{2+} signaling occurs in response to changes in Ca^{2+} concentration ranging from minute to large increases in intracellular Ca^{2+}. Cells are able to regulate the amount of Ca^{2+} entering the cell much the same way they control the amount of Ca^{2+} leaving the cell. Ca^{2+} channels such as voltage-gated Ca^{2+} selective channels, store/receptor operated Ca^{2+} entry channels, and NMDA/AMPA channels coordinate the amount of Ca^{2+} entering the cell at any given time (Fig. 6.1).

Voltage-Gated $Ca^{2\pm}$ Channels

Voltage-gated Ca^{2+} selective channels (CaV) are found on the plasma membrane where they function in Ca^{2+} entry elevating the intracellular concentration of Ca^{2+}. These channels function by predominantly using the electrochemical gradient that is created by the separation of charges between the intracellular and extracellular space thus creating a polarized cell [3]. The channel opens due to a helix-turn-helix loop containing positively charged amino acids that is able to sense voltage changes allowing Ca^{2+} to enter the cell [1]. Voltage-gated Ca^{2+} selective channels are able to create vast increases in intracellular Ca^{2+} concentrations in a matter of milliseconds making these types of channels the fastest and most efficient channel to elicit a Ca^{2+} signaling response [3]. Since the regulation of the amount of Ca^{2+} entering and exiting the cell is controlled by plasma membrane channels; the cell is able to create an efficient mechanism for maintaining Ca^{2+}-dependent processes.

Store/Receptor-Operated $Ca^{2\pm}$ Channels

Store-operated Ca^{2+} entry (SOCE) is a unique mechanism for Ca^{2+} entry, since it involves many channels and proteins throughout the cell, which is unlike voltage-gated channels which rely solely on the separation of charges between the

intracellular and extracellular space. Ca^{2+} in the ER is continuously leaking out into the cytosol (due to concentration gradient), which is constantly pumped back into the ER by the high activity of SERCA pumps and avoids emptying of the ER Ca^{2+} stores. However, upon agonist stimulation second messengers are generated that eventually depletes ER Ca^{2} that relays the signal to the plasma membrane and initiate Ca^{2+} entry via the SOCE mechanism [4]. One of the long lasting question in the field was as how does a cell respond when these pumps are blocked or the cytosol doesn't have enough Ca^{2+} to sustain the repletion of ER by SERCA pumps? The answer to the question came by the identification of the SOCE, which satisfies this requirement by acting as a response mechanism through crosstalk between the ER and Ca^{2+} channels on the plasma membrane, thereby allowing Ca^{2+} to enter the cell from the extracellular space and refill the Ca^{2+} stores in the ER [4].

Changes in ER [Ca^{2+}] are sensed through a single transmembrane ER Ca^{2+} sensing protein known as stromal interacting molecule 1 (STIM1), via an EF hand which is located on the luminal C-terminal tail [4]. Upon ER Ca^{2+} store depletion, Ca^{2+} dissociates from the EF hand causing STIM1 to aggregate on the ER through the assistance of its cytosolic N terminus sterile α-motif forming puncta near the plasma membrane [5]. These puncta translocate close to the plasma membrane where it interacts with a four transmembrane spanning plasma membrane protein, Orai or TRPCs or both, to allow Ca^{2+} to enter the cell and refill the ER stores. Although recent research has put forth a plausible working model, several issues such as how STIM1 is regulated and how it is translocated to the plasma membrane still remains a mystery today. Thus, further scientific inquiries into the regulation of STIM1 can hopefully yield interesting results that will open further areas of research in the field of Ca^{2+} signaling.

SOCE function is not only limited to refilling of the intracellular Ca^{2+} stores, but can elicit a Ca^{2+} response itself propagating the signal downstream to its effectors and yielding a specific cellular action. It can accomplish this by using the phosphatidylinositol signaling pathway that is also known as receptor-operated Ca^{2+} entry. When an agonist binds to a G protein-coupled receptor (GPCR) causing hydrolysis of the receptors subunits, Gα and Gβ/Gγ, Gα moves downstream to activate phospholipase C (PLC) which in turn cleaves phosphatidylinositol 4,5 bisphosphate (PIP2) into 1,4,5 inositol triphosphate (IP_3) and diacylglycerol (DAG) [6]. IP_3 is able to bind to an ER receptor named 1, 4, 5 inositol triphosphate receptors (IP_3Rs) where it causes a conformational change in the receptor allowing Ca^{2+} to exit the ER stores and raise the cytosolic Ca^{2+} ($[Ca^{2+}]_i$) from its basal level of 100 nM to as much as 1 μM in a matter of seconds priming the cell for a Ca^{2+} dependent cellular response [6].

How does the cell recognize an elevation in Ca^{2+} concentration? How is the cell able to translate the increase in [Ca^{2+}] to a signal for downstream proteins to activate a cellular process such as apoptosis or transcription? A cell's answer to these questions is the creation of Ca^{2+} binding protein. Many proteins within the cell contain Ca^{2+} binding domains such as calmodulin whose EF hand, like the one seen in STIM1, is able to bind Ca^{2+} to regulate cellular functions [4]. Upon Ca^{2+} binding, calmodulin is able to undergo a conformational change which causes inhibitory proteins to dissociate from calmodulin making it accessible to interact with other proteins. The conformational change that has occurred upon Ca^{2+} binding allows

active sites to emerge that have previously been hidden by the closed conformation [7]. The Ca^{2+} bound calmodulin has numerous roles in the cell. One such role is the ability to aid in certain phosphylation pathways such as the calmodulin kinase family (CAMK). Once Ca^{2+} bound calmodulin binds to calmodulin kinase, autoinhibitory proteins dissociate allowing CAMK to experience autophosphorylation. Autophosphorylation allows kinase activity to be active for a longer duration [8] and this extended kinase activity exerts its effect on many downstream proteins which participate in numerous cellular processes. In addition, Ca^{2+} binding proteins are also able to propagate the Ca^{2+} signal to a wide array of different proteins found in different areas of the cell which are responsible for triggering precise cell specific tasks.

Characterization of Ca^{2+} Channels

Measurement of $Ca^{2\pm}$ Currents

Patch clamping is a technology that is widely used to record multiple ion currents including Ca^{2+} currents. Using a glass microelectrode it is possible to record Ca^{2+} channel activity, since it seals the surface of cells by over 10^{10}□ resistance, thereby electrically isolating this tip-touched small region on the plasma membrane from its vicinity, thus maintaining membrane potential to monitor and record the single- and whole cell-channel Ca^{2+} currents [9].

SOCE Currents

SOCE currents are generally pretty small, for example, in HEK293 cells and in HSG (human submandibular gland) I_{soc} are only 0.5pA/pF and 2pA/pF respectively. In addition, the current and voltage (IV) relationship of I_{soc} is slightly different in different cell types. For example, in HSG and RBL cells, the IV curve exhibit inward rectification (however the amount of inward rectification is different in both cells). Meanwhile in HSY cells, the IV cure is close to linear, suggesting that different channels could contribute to the same current [10]. In addition, the reversal potential of I_{soc} also varies in different cells and is close to 0 or +40 mV in most cell types (Fig. 6.2).

Measurement of SOCE Currents

For the recording of I_{soc}, the basic protocol is as follows: In standard whole cell mode, every 4 s, a voltage ramp is applied that ranges from −90 to 90 mV over a period of 1 s with a holding potential of 0 mV. Using this protocol, it's easy to monitor the development of I_{soc} over time as well as establishing the IV relationship of the $I_{soc.}$

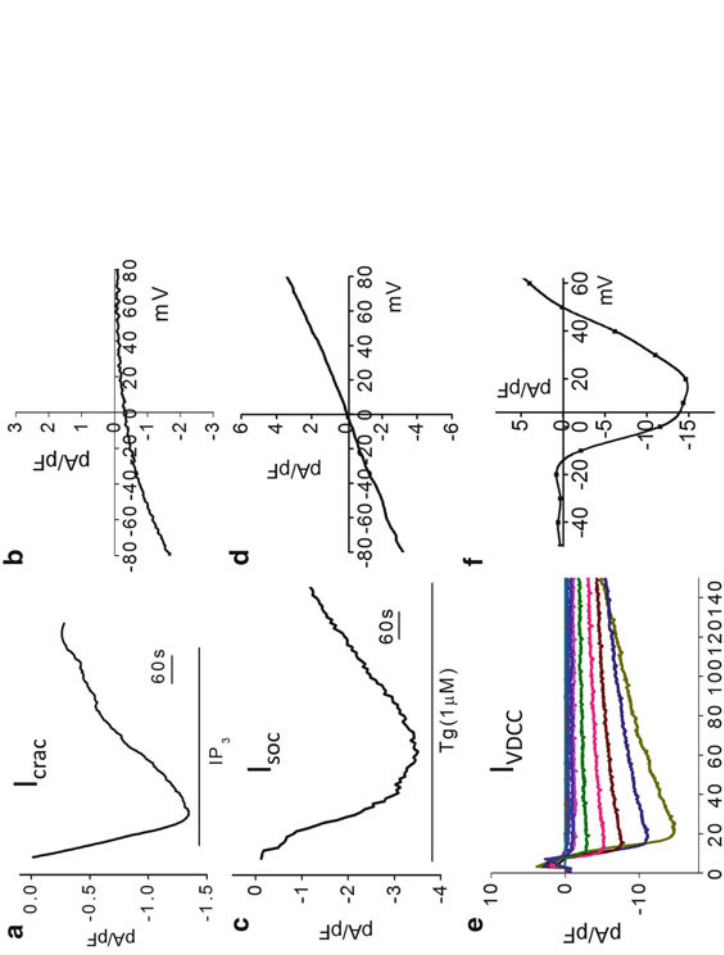

Fig. 6.2 Characterization of Ca^{2+} channels: IP_3- and EGTA-induced currents in macrophage cells. 10 μM IP_3 and 10 mM EGTA were introduced through patch pipette into the cells. (**a**), indicated the inward currents measured at −80 mV and (**b**), indicates the I-*V* curve exhibiting inward rectification. Tg induced currents in SH-SY5Y cells are shown in (**c**) and the I-*V* curve is close to linear which is different from macrophage cells (**d**). A representative current trace from primary hippocampal neurons, elicited by 150 ms test pulses in 10 mV increments from a holding potential of −70 mV to potentials between −50 and +50 mV is shown in (**e**). I_{Ca}-voltage relationship of the voltage-gated channels is shown in (**f**). Current amplitudes were normalized to cell capacitance and plotted as mean values

The external solution used is the modified Ringer's solution with the exception of using a high concentration of Ca^{2+}. Internal solution consists of Cs^{+} along with Ca^{2+} chelators. Importantly, I_{soc} can be activated by several ways, which includes: (i) Intracellular dialysis with high concentration of the chelators (10 mM EGTA, or 10 mM BAPTA) that can activate an inward Ca^{2+} current after a short delay. (ii) In contrast, addition of IP_3 along with Ca^{2+} chelators in the internal solution develops a current, which is relatively fast. (iii) SERCA pump inhibitors such as thapsigargin or ionomycin can also deplete Ca^{2+} stores in order to active the I_{soc} currents (Fig. 6.2).

Facilitation of SOCE

In most cell types, I_{soc} is so small that it is important to enlarge the current amplitude by several ways. Ca^{2+} has a positive effect on I_{soc}, since its potentiation depends on external Ca^{2+} concentrations [11]. Thus, increasing Ca^{2+} concentration of the external solution (10–20 mM) is generally sufficient to experimentally record I_{soc}. However, Ca^{2+} regulation of I_{soc} is complex and besides having a positive effect, it is also involved in Ca^{2+}-dependent inactivation, which is further characterized by either fast or slow inactivation [12, 13]. Thus, exposing the cells to a normal solution can minimize the period of cells that are exposed to high Ca^{2+} concentration before initiating patch clamping experiment is important. Another way to reduce the inactivation is to use Ca^{2+} chelators. EGTA has been shown to be less effective on fast inactivation, whereas BAPTA is a more rapid chelator and reduces fast inactivation. In addition, to increase the conductance of I_{soc} it is also advisable to use DVF (divalent cation-free) solution, where removal of all extracellular divalent cation, results in a large Na^{+} currents through SOCE channels.

Voltage Dependent $Ca^{2\pm}$ Currents

Voltage dependent Ca^{2+} currents (VDCC) are present especially in excitable cells. For recording VDCC, K^{+} current have to be blocked by the addition of Cs^{+} or by applying 4-aminopyridine. Similarly, Na^{+} is also blocked by either replacing Na^{+} from the solution or by adding tetrodotoxin in the solution. In whole cell mode, current is elicited from a holding potential of −70 mV by 150-ms depolarizing voltage step that range between −70 and +70 mV. A typical VDCC and IV relationship in hippocampus cells is shown in Fig. 6.2. There is a remarkable rundown effect, which will affect recording of the VDCC and including 10 mM ATP intracellularly can decrease the rundown effect. However, the best solution for abolishing rundown of VDCC is using perforated patch recordings, with nystatin (100 ug/ml) or amphotericin B (30 ug/ml) in the intracellular solution. These polyene antibiotics form pores to allow small ion to permeate in a cell-attached patch mode, thereby abolishing rundown by preventing the leak. However, a potential problem for perforated path recording is that sometimes the access resistance is large that will decrease the amplitude of VDCC.

$Ca^{2\pm}$ Activated $K^{\pm}$ Currents

Ca^{2+} activated K^{+} current is another way to monitor the changes in Ca^{2+} concentrations especially in the subplasma membrane region for its tight regulation by Ca^{2+} concentration [14]. To record these currents in a whole cell configuration, gap-free mode is used with a holding potential of 0 mV, and addition of Ca^{2+} activators (such as IP_3, Carbachol) can induce K_{Ca} that are much larger and are easy to record. For recording the IV relationship, the membrane potential is changed from −120 to 80 mV using a 20 mV step protocol.

Ca^{2+} Channels and Their Implication in Various Diseases

To the human eye, diseases present themselves as a collection of signs and symptoms varying in the degree of severity. For instance, Alzheimer's disease can only be viewed by the symptoms it presents such as a progressive decline in cognitive function. This cognitive dysfunction manifests itself as memory loss, trouble understanding visual and spatial relationships, and a decrease in judgment. However, on a molecular scale, diseases arise due to cellular dysfunctions and different diseases correlate do different abnormalities in cellular functions. Cellular abnormities can vary from the level of transcription to protein localization and regulation. Thus, the rest of this chapter is going to be focused on cellular dysfunctions and its correlation to the progression of different diseases with respect to Ca^{2+} signaling. As mentioned previously, Ca^{2+} play a vital role in numerous cell functions; therefore, the diseases that arise from disruptions in Ca^{2+} signaling range from neurodegenerative diseases such as Huntington's disease to cardiomyopathies such as congestive heart failure.

$Ca^{2\pm}$ Channels in Alzheimer's Disease

A disruption in Ca^{2+} signaling is not known to be the cause of Alzheimer's disease (AD). On the other hand, there is growing evidence supporting the hypothesis that a remodeling of the Ca^{2+} signaling is involved in the slow decline in cognitive thinking seen in AD. Within the scientific community, AD has been studied extensively leading to the discovery of amyloid fibrils and plaques which aggregate outside never terminals [15]. The cause of this buildup in amyloid plaques is the hydrolysis of β-amyloid precursor protein (APP) by the β- and γ-secretase complex. The product of the hydrolysis, β-amyloid protein (Aβ protein), tends to polymerize into the plaques and fibrils seen in the pathology of Alzheimer's disease [16]. Although many factors can play a role in the pathogenesis of AD, all factors essentially affect this amyloid cascade hypothesis leading to abnormal amounts of amyloid production. There are two forms of Alzheimer's disease, sporadic and familiar, that have been studied. However, both of these disease forms affect the amyloid cascade hypothesis and the only difference lies between the two is as how the hypothesis is

affected. Sporadic AD is the most widely known as it is this form which is the most common among people who develop AD. Sporadic AD is generally characterized by a slow severe decline in cognitive functions [17]. On the other hand, familiar Alzheimer's disease (FAD) is developmentally a faster form than sporadic AD as it involves mutations in the amyloid pathway. Some examples of the more commonly mutated proteins that are involved in FAD are APP, members of the presenilin family, and apolipoproteins [17]. Sporadic and familiar Alzheimer's disease are under extensive scientific studies trying to elucidate the link between the development of AD and the neuronal cell abnormalities and degeneration leading to cognitive dysfunction.

There are many current hypotheses proposing the involvement of Ca^{2+} in Alzheimer's disease. Most of these hypotheses involve the amyloidogenic pathway remodeling the Ca^{2+} signal in cells exhibiting amyloid plaques and fibrils. One such role includes α-secretase cleavage of the membrane bound APP into a soluble portion sAPPα and the C terminus membrane bound portion (CTFα). ℘-secretase is able to hydrolyze (CTFα) into an APP intracellular domain (AICD), which translocates to the nucleus and act as a transcription factor and may have an effect on the expression of ryanodine, a receptor on the SR that when activated releases Ca^{2+} from the SR stores, and calbindin proteins [16, 18]. It has been shown that individuals with AD have a down regulation of the expression of the Ca^{2+} buffering protein calbindin which aids in restricting the Ca^{2+} amplitude thus regulating Ca^{2+} signaling [16]. Another important hypothesis that is being studied suggests that a specific amyloid plaque, $A\alpha_{42}$, may act as a ligand for the membrane bound cellular prion protein receptor, which when activated may carry out Ca^{2+} cellular responses such as activating NMDA receptors allowing Ca^{2+} into the cell that induces excitotoxicity [19]. Taken together, these current hypotheses drastically change the overall levels of $[Ca^{2+}]_i$ throughout the cell leading to a remodeling of the Ca^{2+} signal that can activate processes, which are involved in neuronal cell death (such as caspases or cytochrome C) to assist in the neurodegenerative damages present in AD.

The role of Ca^{2+} in Alzheimer's disease also extends its reach into the symptomatic manifestations of learning and memory deficiencies. Memories are either stored or erased according to varying levels of Ca^{2+} which effects the phosphorylation and trafficking of the α-amino-3-hydroxy-5-methyl-4-isoxazolepropionic receptors (AMPA) [20]. Long-term potentiation (LTP) occurs at high $[Ca^{2+}]_i$, which can signal the phosphorylation and membrane insertion of the AMPA receptor, thereby, allowing memories to be stored for a short term [21]. On the other hand, long-term depression (LTD) occurs at lower $[Ca^{2+}]_i$ which allows activation of phosphatases such as Ca^{2+}-dependent calcineurins to remove phosphates from the AMPA receptor, thus, removing it from the plasma membrane by the process of endocytosis [22]. LTD leads to the elimination of temporary memories previously stored by LTP. Thus, overall, LTP and LTD occur at varying Ca^{2+} levels and are associated with different times throughout the day. LTP occurs while learning during the day leading to a quick spike in Ca^{2+}, while LTD occurs during sleep when a low steady level of Ca^{2+} is maintained [21]. In contrast, permanent memory storage occurs during different stages of sleep when LTP and permanent memory storage overlap, it is when that

the brain transfers memories from short term to storage for long term, however, any memories that did not overlap during this transition are erased by LTD. Interestingly, in AD, remodeling of the Ca^{2+} signal causes changes in $[Ca^{2+}]_i$ which can affect memory storage by the LTP and LTD mechanisms. One possible explanation for memory loss seen in AD is the change in Ca^{2+} levels that leads to the continuous activation of LTD, thereby causing memories stored by LTP to be constantly erased before the transfer to permanent storage can begin [21].

$Ca^{2\pm}$ Channels in Huntington's Disease

Huntington's disease (HD) is an autosomal dominant neurodegenerative disease characterized by disruptions in motor skills and cognitive functions such as the development of chorea and dementia. On a molecular level, HD appears due to a trinucleotide expansion, CAG, in the gene encoding for a 350 kDa cytosolic protein [23]. In HD, the expanded CAG repeats enable the protein to be translated with an expanded polyglutamine (polyQ) tract on its amino terminus. The length of the polyQ tract reveals an inverse relationship between the age of onset of the disease and the number of glutamines present in the amino terminus [24]. Symptomatic manifestations of HD most commonly occur with individuals presenting at least a 35Q stretch in huntingtin gene (Htt) [25]. Individuals with the mutated form of Htt start to exhibit symptoms later in life, most commonly become symptomatic anywhere from 35 to 45. However, symptoms may arise earlier in life depending on the severity of the polyQ tracts [26]. Mutated Htt may play several roles in the disruption of numerous cellular functions such as axonal transport, proteasomes, and endocytosis [26]. In addition, Ca^{2+} signaling involving the NMDA receptor, mitochondrial Ca^{2+} homeostasis, and the regulation of the inositol (1,4,5)-triphosphate receptor ($InsP_3R$) may also play a role in HD [27].

NMDAR is one of the three classes of ionotropic glutamate receptors that lead to a drastic increase in Ca^{2+} influx upon the activation of NMDAR. A possible outcome of the over activation of NMDAR is Ca^{2+} overload leading to cell death in these neurons. Experiments have been developed to ascertain whether there is a causal role in the activation of NMDAR and neuronal cell death as seen in HD. In one of the classical experiment overexpression of the expanded Htt (Htt-138Q), but not the wild type Htt (Htt-15Q) was able to activate NMDAR [28]. A possible role in expanded Htt activating NMDAR was then established which was mediated through its interaction with PSD95. Htt is able to bind to PSD95, a modular adaptor protein; however, expanded Htt has been shown to have a decreased interaction with PSD95 [29]. PSD95 is known to associate with NR2 subunits which assist in the recruitment of Src tyrosine kinase that phosphorylates NMDAR receptors leading to an increase in NMDAR activation [30]. Due to the decreased association between expanded Htt and PSD95, PSD95 interaction with NR2 increases leading to Src kinase to phosphorylate NMDAR.

IP_3R is intimately involved in the release of Ca^{2+} from the ER stores (as mentioned earlier), but how does this receptor play a role in neuronal cell death seen in

HD is a new concept? Several investigators have studied the relationship between Htt and IP_3R. It has been shown that expanded Htt is able to sensitize IP_3R1, the neuronal isoform of IP_3R, to IP_3 due to a tertiary interaction with Htt-associated protein 1A (HAP1A) [31]. Further evidence has been discovered indicating Htt-138Q, but not the normal length Htt-23Q, leading to the sensitization of IP_3R, thereby increasing cytosolic Ca^{2+} levels [31]. Taken together, the evidence indicate that increased cytosolic Ca^{2+} concentration due to the sensitization of IP_3R and activation of NMDAR could lead to cytosolic and mitochondrial Ca^{2+} overload causing neuronal death as observed in HD.

Expanded Htt is also able to interfere in many pathways involving Ca^{2+} signaling leading to progressive decline in cellular function due to Ca^{2+} mishandling. Proapoptotic pathways are sensitive to changes in Ca^{2+} in the mitochondria and cytosol. A raise in cytosolic Ca^{2+}, due to activation of NMDAR and IP_3R by expanded Htt, can lead to the activation of a family of proapoptotic proteins such as Bcl-2 [32]. During times of Ca^{2+} overload, the mitochondria can act as a Ca^{2+} sink relieving the cytosol of Ca^{2+}. If the mitochondrial Ca^{2+} increases to the point where the mitochondria can no longer withstand the Ca^{2+} overload, the permeability transition pore (PTP) in the mitochondria opens, thereby releasing Ca^{2+} and other proapoptotic factors such as cytochrome C [33]. Ca^{2+} mishandling as seen in HD is an extensively researched area in the scientific community, and through this research, novel drugs may be developed to regulate the amount of Ca^{2+} entering the cell or exiting the ER. Thus, novel compounds could be developed that can alleviate neuronal cell death by HD.

$Ca^{2\pm}$ Channels in Congestive Heart Failure

Congestive heart failure is a condition characterized by a slow progression of fatigue and breathlessness that eventually leads to death of an individual. The cause of these symptoms is a heart defect in which the heart cannot provide the body's tissue with a sufficient amount of blood. Insufficient blood supply to body tissue triggers a cascade of events such as neurohormone stimulation and intracellular signaling to compensate for the loss of cardiac performance. However, as the disease progresses, these events act in concert leading to complete organ failure. Disruptions in Ca^{2+} handling are a major factor in the progression of congestive heart failure. A heart contraction begins due an action potential caused mainly by an influx of Na^+ ion to depolarize the sarcolemma. The depolarization of the membrane activates L-type Ca^{2+} channels, which increases Ca^{2+} entry. Furthermore, this increased cytosolic Ca^{2+} also allows Ca^{2+} to be extruded from the sacroplasmic reticulum (SR) through Ca^{2+}-induced Ca^{2+} release mechanism, thereby further raising the cytosolic $[Ca^{2+}]_i$ levels [34]. An increase in cytosolic $[Ca^{2+}]_i$ allows Ca^{2+} to bind to troponin C, a myofilament protein, that then leads to muscle contraction. Heart relaxation occurs by the activation of SERCA pumps, sarcolemma Na^+-Ca^{2+} exchangers (NCX), sarcolemma Ca^{2+}ATPases, and mitochondrial Ca^{2+} uniporters [35]. These channels act together to decrease the cyotosolic $[Ca^{2+}]$ by either extruding Ca^{2+} from the cell,

i.e. sarcolemma Na^{+}-Ca^{2+} exchangers and Ca^{2+}ATPase's, or refilling the SR, via the SERCA pumps. The majority of the cytosolic $[Ca^{2+}]_i$ is taken to refill the SR while the rest is extruded from the cell. The important thing is that Ca^{2+} must be kept at a steady state, meaning the Ca^{2+} entering the cytoplasm, either from the SR or extracellular space, during the contraction phase must equal the amount of Ca^{2+} leaving the cytoplasm during the relaxation phase [35], since an unbalance in the steady state of Ca^{2+} leads to congestive heart failure.

Although Ca^{2+} mishandling can occur due to many reasons, it is the decrease in the SR Ca^{2+} stores that often leads to congestive heart failure. The decrease in SR Ca^{2+} can be caused by several abnormalities in the influx and efflux Ca^{2+} mechanisms. Down regulation of SERCA and up regulation of NCX are two of the most common affect seen in heart failure [36]. The upregulation of NCX seen in heart failure is mainly attributed to increased mRNA and protein levels. On the other hand, the downregulation of SERCA is only partially credited to reduced levels of SERCA2a. The down regulated SERCA may also be caused by a decrease in the phosphorylation of phospholambin which inhibits SERCA until phosphorylation occurs [37]. Up regulation of NCX causes the majority of Ca^{2+} to exit the cell disrupting the steady state balance of Ca^{2+} within the myocytes. The down regulated SERCA further struggles to refill its stores due to the decrease in cytosolic $[Ca^{2+}]_i$ by NCX. In the typical model of heart failure, diminished cytosolic $[Ca^{2+}]_i$ causes inadequate Ca^{2+} binding to troponin C which fails to illicit a heart contraction. However, studies have demonstrated that the decrease in SERCA can be overcome by a significant increase in NCX function leading normal diastolic function [38].

Another area of research being investigated is the effect of Ca^{2+} leakage through the ryanodine receptors on the SR. The ryanodine receptor is often hyperphosphorylated at Ser-2809 by PKA in heart failure, which is mainly due to a decrease in phosphatases and phosphodiesterases activity which remove phosphates groups from proteins [39]. Phosphorylation of the ryanodine receptor causes dissociation of the protein calstabin allowing ryanodine to leak Ca^{2+} from its internal SR stores. In addition, ryanodine receptors can also be phosphorylated by CAMKII at Ser 2815 which allows calstabin to dissociate and initiate Ca^{2+} leakage [40]. These two areas of research are being investigated as possible drug therapies for heart failure. The use of small-molecule inhibitors of CAMKII and stabilizers of calstabin may aid in the regulation ryanodine receptors by maintaining the complex that holds ryanodine in the closed conformation, thus inhibiting Ca^{2+} leakage [41].

Conclusion

Ca^{2+} is one of the most diverse and well researched second messenger molecules found in the cell. Ca^{2+} function varies greatly depending on cell type and local Ca^{2+} concentrations, which can initiate many physiological functions, such as muscle contractions to apoptosis. Similarly, several mechanisms are present that can regulate Ca^{2+} homeostasis. Disruptions in Ca^{2+} handling can contribute to the pathogenesis of

many diseases such as Alzheimer's disease, Huntington's disease, and congestive heart failure. Thus, identification of the unique Ca^{2+} channels and research on proteins that are involved in Ca^{2+} signaling and its deficiencies in Ca^{2+} handling may lead to the development of drug therapy to combat the symptoms or possibly the disease itself.

References

1. Clapham DE (2007) Calcium signaling. Cell 131(6):1047–1058, Dec 14
2. Guerini D, Coletto L, Carafoli E (2005) Exporting calcium from cells. Cell Calcium 38 (3–4):281–289, Sep-Oct
3. Benarroch EE (2010) Neuronal voltage-gated calcium channels: brief overview of their function and clinical implications in neurology. Neurology 74(16):1310–1315, Apr 20
4. Cahalan MD (2009) STIMulating store-operated ca(2+) entry. Nat Cell Biol 11(6):669–677
5. Kurosaki T, Baba Y (2010) Ca2+ signaling and STIM1. Prog Biophys Mol Biol 103(1):51–58, Sep
6. Berridge MJ (2009) Inositol trisphosphate and calcium signalling mechanisms. Biochim Biophys Acta 1793(6):933–940, Jun
7. Skelding KA, Rostas JA (2009) Regulation of CaMKII in vivo: the importance of targeting and the intracellular microenvironment. Neurochem Res 34(10):1792–1804, Oct
8. Dobrev D, Wehrens XH (2010) Calmodulin kinase II, sarcoplasmic reticulum Ca2+ leak, and atrial fibrillation. Trends Cardiovasc Med 20(1):30–34, Jan
9. Neher E, Sakmann B (1976) Single-channel currents recorded from membrane of denervated frog muscle fibres. Nature 260:799–802
10. Liu X, Groschner K, Ambudkar IS (2004) Distinct Ca(2+)-permeable cation currents are activated by internal Ca(2+)-store depletion in RBL-2H3 cells and human salivary gland cells, HSG and HSY. J Membr Biol 200(2):93–104
11. Christian EP, Spence KT, Togo JA, Dargis PG, Warawa E (1996) Extracellular site for econazole-mediated block of Ca2+ release activated Ca2+ current (Icrac) in T lymphocytes. Br J Pharmacol 119:647–654
12. Zweifach A, Lewis RS (1995) Rapid inactivation of depletion-activated calcium current (ICRAC) due to local calcium feedback. J Gen Physiol 105:209–226
13. Fierro L, Parekh AB (1999) Fast calcium-dependent inactivation of calcium release-activated calcium current (CRAC) in RBL-1 cells. J Membr Biol 168:9–17
14. Liu X, Rojas E, Ambudkar IS (1998) Regulation of KCa current by store-operated Ca2+ influx depends on internal Ca2+ release in HSG cells. Am J Physiol 275(2 Pt 1):C571–C580, Aug
15. Mattson MP (2004) Pathways towards and away from Alzheimer's disease. Nature 430(7000):631–639, Aug 5
16. Berridge MJ (2010) Calcium hypothesis of Alzheimer's disease. Pflugers Arch 459(3):441–449, Feb
17. Bezprozvanny I, Hayden MR (2004) Deranged neuronal calcium signaling and huntington disease. Biochem Biophys Res Commun 322(4):1310–1317, Oct 1
18. Supnet C, Bezprozvanny I (2010) The dysregulation of intracellular calcium in Alzheimer disease. Cell Calcium 47:183–189, Jan 15
19. Green KN, LaFerla FM (2008) Linking calcium to abeta and Alzheimer's disease. Neuron 59(2):190–194, Jul 31
20. Citri A, Malenka RC (2008) Synaptic plasticity: multiple forms, functions, and mechanisms. Neuropsychopharmacology 33(1):18–41, Jan
21. Berridge MJ (2010) Calcium signalling and Alzheimer's disease. Neurochem Res 36:1149–1156, Dec 24

22. Hsieh H, Boehm J, Sato C, Iwatsubo T, Tomita T, Sisodia S, Malinow R (2006) AMPAR removal underlies abeta-induced synaptic depression and dendritic spine loss. Neuron 52(5):831–843, Dec 7
23. Lynch G, Kramar EA, Rex CS, Jia Y, Chappas D, Gall CM, Simmons DA (2007) Brain-derived neurotrophic factor restores synaptic plasticity in a knock-in mouse model of huntington's disease. J Neurosci 27(16):4424–4434, Apr 18
24. Quintanilla RA, Johnson GV (2009) Role of mitochondrial dysfunction in the pathogenesis of huntington's disease. Brain Res Bull 80(4–5):242–247, Oct 28
25. Milnerwood AJ, Raymond LA (2010) Early synaptic pathophysiology in neurodegeneration: insights from huntington's disease. Trends Neurosci 33(11):513–523, Nov
26. Moller T (2010) Neuroinflammation in huntington's disease. J Neural Transm 117(8):1001–1008, Aug
27. Carafoli E (2004) Calcium-mediated cellular signals: a story of failures. Trends Biochem Sci 29(7):371–379, Jul
28. Chen N, Luo T, Wellington C, Metzler M, McCutcheon K, Hayden MR, Raymond LA (1999) Subtype-specific enhancement of NMDA receptor currents by mutant huntingtin. J Neurochem 72(5):1890–1898, May
29. Sun Y, Savanenin A, Reddy PH, Liu YF (2001) Polyglutamine-expanded huntingtin promotes sensitization of N-methyl-D-aspartate receptors via post-synaptic density 95. J Biol Chem 276(27):24713–24718, Jul 6
30. Ali DW, Salter MW (2001) NMDA receptor regulation by src kinase signalling in excitatory synaptic transmission and plasticity. Curr Opin Neurobiol 11(3):336–342, Jun
31. Tang TS, Tu H, Chan EY, Maximov A, Wang Z, Wellington CL, Hayden MR, Bezprozvanny I (2003) Huntingtin and huntingtin-associated protein 1 influence neuronal calcium signaling mediated by inositol-(1,4,5) triphosphate receptor type 1. Neuron 39(2):227–239, Jul 17
32. Rizzuto R, Pinton P, Ferrari D, Chami M, Szabadkai G, Magalhaes PJ, Di Virgilio F, Pozzan T (2003) Calcium and apoptosis: facts and hypotheses. Oncogene 22(53):8619–8627, Nov 24
33. Hajnoczky G, Davies E, Madesh M (2003) Calcium signaling and apoptosis. Biochem Biophys Res Commun 304(3):445–454, May 9
34. Bers DM (2008) Calcium cycling and signaling in cardiac myocytes. Annu Rev Physiol 70:23–49
35. Bers DM (2006) Altered cardiac myocyte Ca 2+ regulation in heart failure. Physiology (Bethesda) 21:380–387, Dec
36. Pogwizd SM, Schlotthauer K, Li L, Yuan W, Bers DM (2001) Arrhythmogenesis and contractile dysfunction in heart failure: roles of sodium-calcium exchange, inward rectifier potassium current, and residual beta-adrenergic responsiveness. Circ Res 88(11):1159–1167, Jun 8
37. MacLennan DH, Asahi M, Tupling AR (2003) The regulation of SERCA-type pumps by phospholamban and sarcolipin. Ann NY Acad Sci 986:472–480, Apr
38. Lehnart SE, Maier LS, Hasenfuss G (2009) Abnormalities of calcium metabolism and myocardial contractility depression in the failing heart. Heart Fail Rev 14(4):213–224, Dec
39. Stange M, Xu L, Balshaw D, Yamaguchi N, Meissner G (2003) Characterization of recombinant skeletal muscle (ser-2843) and cardiac muscle (ser-2809) ryanodine receptor phosphorylation mutants. J Biol Chem 278(51):51693–51702, Dec 19
40. Wehrens XH, Lehnart SE, Marks AR (2005) Intracellular calcium release and cardiac disease. Annu Rev Physiol 67:69–98
41. Mudd JO, Kass DA (2008) Tackling heart failure in the twenty-first century. Nature 451(7181):919–928, Feb 21

Chapter 7
Ryanodine Receptor Calcium Release Channels: An Evolutionary Perspective

John J. Mackrill

Abstract Ryanodine receptors (RyRs), along with the related inositol 1,4,5-trisphosphate receptors (IP_3Rs), mediate the release of Ca^{2+} from intracellular organelles of eukaryotes. As discussed in other chapters, such increases in intracellular Ca^{2+} levels act a fundamental second messenger, regulating a diverse array of cellular processes. For over two decades, it has been reported that vertebrates express multiple *RYR* genes, whereas non-vertebrate multicellular organisms possess a single homologue within their genomes. Recently, the existence of RyR-like channels in unicellular organisms has also been reported. This chapter exploits recent expansions in available genome data to generate an overview of the expression of RyR-like genes in organisms representing a broad range of viral, archaeal, bacterial and eukaryotic taxa. Analyses of the multidomain structures and phylogenetic relationships of these proteins has lead to a model in which, early during eukaryotic evolution, IP_3R-like ancestral Ca^{2+} release channels were converted to RyR proteins via the addition of promiscuous protein domains, possibly via horizontal gene transfer mechanisms.

Keywords Calcium • Calcium release channel • Evolution • Inositol 1,4,5-trisphosphate receptor • Protein domains • Ryanodine receptor

J.J. Mackrill, Ph.D. (✉)
Department of Physiology, University College Cork, Western Gateway Building, Western Road, Cork, Ireland
e-mail: j.mackrill@ucc.ie

M.S. Islam (ed.), *Calcium Signaling*, Advances in Experimental Medicine and Biology 740, DOI 10.1007/978-94-007-2888-2_7,

Introduction

Calcium ions (Ca^{2+}) have long been recognised as a pivotal second messenger in eukaryotic organisms. Core tenets for this role include that Ca^{2+} is neither created nor destroyed within cellular systems; that, under unstimulated conditions, the concentrations of this ion are several orders of magnitude lower in the cytosol than they are in the extracellular environment; and that intrinsic and extrinsic cues can trigger rises in cellular Ca^{2+} levels. Increased levels of this ion are detected by various calcium binding effectors, to elicit appropriate intracellular responses. In order to terminate these effects, Ca^{2+} can be expelled from the cell by active transport and ion exchange mechanisms, buffered by anionic biomolecules, or accumulated into membrane delimited organelles. Biological membranes are essential barriers employed in such signal transduction processes. Since it is energetically unfavourable for Ca^{2+} to cross the hydrophobic environment of lipid membranes, cation channel and transporter proteins have evolved to regulate fluxes of this ion across these barriers. It is likely that the evolution of Ca^{2+}-conducting channels and transporters coincided with the emergence of cellular life and the requirement of a cell-surface membrane [1]. Bacteria and archaea are modern-day representatives possessing this "primeval" Ca^{2+} signaling arrangement, in which the cell-surface membrane represents the key barrier across which calcium fluxes are regulated. Bacteria are endowed with a variety of Ca^{2+} signaling proteins, many of which resemble their eukaryotic counterparts. The concentration of Ca^{2+} within the cytosol of bacteria is typically in the range of 100–300 nM, or about 10,000-fold lower than most extracellular environments; and the levels of this ion can change in response to extracellular stimuli [2, 3]. Like eukaryotes, prokaryotes possess multiple Ca^{2+}-binding proteins that can act as buffers or effectors for Ca^{2+} signals. In bacteria, changes in cytosolic Ca^{2+} concentration are coupled to alterations in cellular function, such as the release of proteins from inclusion bodies [4], indicating that Ca^{2+} has a true second messenger role in bacteria.

Diverse organelles are employed for Ca^{2+} signaling: the cell-surface or plasma membrane is common to all cellular organisms, but in eukaryotes intracellular structures such as the endoplasmic reticulum (ER), nuclear envelope, sarcoplasmic reticulum (SR), Golgi apparatus, mitochondria, plastids, lysosomes, endosomes, peroxisomes, secretory vesicles and vacuoles are also widely utilised for this role. Such organelles actively accumulate Ca^{2+} to concentrations similar to those in the extracellular environment, in the order of 200 μM to 1 mM. Two main hypotheses on the evolution of such intracellular membrane systems have been put forward. The endosymbiosis hypothesis proposes that these organelles were derived by the capture of bacteria by proto-eukaryotes, followed by the evolution of these trapped organisms into intracellular systems, no longer capable of free living [5, 6]. The autogenesis hypothesis suggests mechanisms by which organelles are derived by specialisation of existing membranes, in processes which do not directly involve the capture of other organisms [7]. It should be pointed out that these mechanisms are not mutually exclusive and that certain organelles might have been generated by a combination of these processes [6].

Employment of intracellular organelles as Ca^{2+} stores offers several advantages in signal transduction processes, compared to systems relying solely on fluxes of this ion across the cell-surface membrane. Firstly, it allows independence from extracellular Ca^{2+} levels, which is of importance in environments where the concentration of this ion can vary greatly. Secondly, exchange of Ca^{2+} between the cytosol and intracellular stores can be an order of magnitude more rapid than that between the cytosol and extracellular medium. For example, in gastric parietal cells, Ca^{2+} fluxes across the ER membrane are approximately tenfold faster than those across the plasma membrane either under resting conditions, or during stimulation with an acetylcholine receptor agonist [8]. Rapid alterations in levels of cytosolic Ca^{2+} permit swift and efficient regulation of downstream cellular responses. This is typified by the process of excitation contraction-(EC-) coupling in vertebrate skeletal muscle fibres: a rapid process that is Ca^{2+}-regulated but which is largely independent of extracellular Ca^{2+} [9]. A third key advantage of intracellular Ca^{2+} stores is that they enhance compartmentalisation of signals. For example, in mammalian cardiomyocytes both hypertrophic gene expression and EC-coupling are Ca^{2+}-regulated processes, but normal contraction of the heart does not result in hypertrophy. This is because hypertrophic responses are coupled to Ca^{2+} release from the nuclear envelope (a form of ER) via inositol 1,4,5-trisphosphate receptors (IP_3Rs), activated by the second messenger IP_3; whereas the contractile apparatus is activated by Ca^{2+} released from the SR, via ryanodine receptor (RyR) Ca^{2+} channels [10]. Finally, in multicellular organisms, such organelles can provide a route for the vectorial transport of Ca^{2+} across cells, avoiding exposure of cytoplasmic systems to toxic concentrations of this ion [11]. In mammals, such processes are likely to play roles in the transport of Ca^{2+} across epithelial cells of the intestine during uptake of dietary calcium and those of the placenta, for mineralisation of the fetal skeleton.

Mechanisms that expel Ca^{2+} from the cytosol are utilised by even the most primitive bacteria [1, 2]. Bacterial P-type Ca^{2+} ATPase pumps [12] structurally and functionally resemble their plasmalemmal Ca^{2+} ATPase (PMCA) and SR/ER Ca^{2+} ATPase (SERCA) pump counterparts in eukaryotes. Bacteria are also endowed with secondary calcium transport mechanisms that couple expulsion of Ca^{2+} to the energy stored in electrochemical gradients of other ions across the cell-surface membrane. These mechanisms include Ca^{2+}/H^+-exchangers and Ca^{2+}/Na^+ exchangers, which are related to proteins in metazoan systems [13]. Prokaryotes express multiple channel families that allow the influx of Ca^{2+} down its electrochemical gradient, from the extracellular environment into the cytosol [14]. In eukaryotes, key functional superfamilies of Ca^{2+}-conducting channels are the voltage-gated calcium channels (VGCC), whose opening is control by membrane potential; ligand-gated channels, which contain an intrinsic receptor that can respond to ions, small compounds, or biomolecules; and channels gated by physical stimuli, including light, temperature and mechanical forces. In many cases, prokaryotes express "primitive" forms of these channels, from which many eukaryotic forms probably evolved. It is likely that ion channels originated at multiple times during evolution, with channel diversity increasing via processes like genome duplication, domain insertion, duplication and divergence [15]. Cation channels that appear to be absent from prokaryotes, presumably having

originated during eukaryotic evolution, include the store-operated Ca^{2+} channel Orai family, that mediate Ca^{2+} influx in response to ER Ca^{2+}-store depletion; the ATP gated purinoreceptor family P2X; and the IP_3R and RyR Ca^{2+} release channels that are the focus of this chapter.

Evolution of Ryanodine Receptor Calcium Release Channels

The Pre-genomic Era: Identification of RyRs

RyRs were first identified as pivotal components of EC-coupling mechanisms in striated muscles, with research particularly focussed on the myocytes of vertebrates and especially those of mammals. In vertebrate skeletal muscle, nerve impulses depolarise the sarcolemma (the cell-surface membrane). Action potentials propagate into muscle fibres via invaginations of the sarcolemma known as t-tubules, which contain a voltage-sensing protein called the α1S-subunit of the dihydropyridine receptor, a VGCC also known as $Ca_v1.1$. Like RyRs, dihydropyridine receptors operate as high molecular weight, multi-subunit complexes. Within these complexes, the α1 subunit contains both the voltage-sensor and ion permeation pathway, with the auxiliary subunits (β, α2δ and sometimes γ) being crucial for channel regulation and membrane targeting [16]. Upon sensing depolarisation, the dihydropyrine receptor α1 subunit transmits a conformational signal to type 1 RyRs (RyR1) in the terminal cisternae of the SR located at specialised interfaces with the t-tubule known as triad junctions, thereby initiating Ca^{2+} release. This mode of EC-coupling is often termed conformationally coupled Ca^{2+}-release (CCCR). Triads are so called because each t-tubule interacts with paired terminal cisternae along its length, appearing as three interacting membrane profiles in transmission electron micrographs of skeletal muscle [17]. In cardiomyocytes analogous structures, termed dyads because they contain t-tubular interfaces with single terminal cisternae, participate in EC-coupling [18]. In addition to these dyad junctions, extracorbular SR interacts with unspecialised sarcolemma in cardiomyocytes. At both dyad and extracorbular subplasmalemmal junctions in the heart, a distinct member of the dihydropyridine receptor family called α1C or $Ca_v1.2$ responds to surface membrane depolarisation [19]. In contrast to $Ca_v1.1$ in skeletal muscle, $Ca_v1.2$ acts as both a voltage-sensor and a Ca^{2+} channel, gating to allow the entry of this ion down its electrochemical gradient. This Ca^{2+} influx directly opens type 2 RyR (RyR2) channels in the closely abutted junctional SR, in an amplification process termed Ca^{2+}-induced Ca^{2+}-release (CICR). In transmission electron micrographs of triad, dyad and extracorbular junctions, electron-dense structures appear to span the gap (in the order of 10–20 nm) between these apposing membrane systems. These structures are proteinaceous in nature and because of their appearance, were named junctional "feet" [20, 21].

During much of its infancy, research into nature of these "feet" proteins and their roles in EC-coupling centred on vertebrate striated muscles. However, key steps in

the identification of RyR proteins relied on use of the plant alkaloid ryanodine and related compounds, which were originally employed as insecticides [22]. Given that ryanodine induces paralysis in muscle fibres from both vertebrates and insects, this implied that arthropods possess a similar type of Ca^{2+} release channel. Other agonists that gate RyRs include millimolar caffeine, micromolar Ca^{2+} and micromolar concentrations of the putative second messenger, cyclic ADP ribose (cADPr). "Diagnostic" RyR antagonists include millimolar ryanodine, millimolar Ca^{2+} and Mg^{2+}, micromolar dantrolene, ruthenium red and procaine [23]. During the mid-1980s, the availability of tritiated ryanodine facilitated monitoring of the solubilisation and purification of the binding protein for this toxin from striated muscles, by several laboratories [24–26]. All preparations of this ryanodine binding protein contained a protein of extremely high apparent molecular weight, of at least 300 kDa. Purification, transmission electron microscopy and functional reconstitution of this high molecular weight protein demonstrated that the skeletal muscle RyR and the SR Ca^{2+} release channel were one and the same [24]. The RyR complex is homotetrameric, displaying fourfold symmetry in transmission electron micrographs and forming complexes of fourfold greater molecular weight than monomers in chemical cross-linking experiments [27].

Proteolytic digestion and peptide sequencing of RyR1 protein purified from rabbit skeletal muscle facilitated the isolation of the cDNA encoding it, using a "reverse cloning" library screening strategy [28]. This ~16 kb cDNA encodes a protein of 565 kDa, the N-terminal ~80% of which was predicted to reside in the cytoplasm, with the remainder forming multiple transmembrane segments containing the ion permeation pathway, lumenal regions and a cytoplasmic C-terminus. The primary structure of rabbit RyR1 was reported to display limited identity to other proteins known at the time, being most similar to Na^+ channels, K^+ channels and VGCCs. Rabbit RyR1 represented the first member of a new family of intracellular cation channel proteins. In the same year, two independent laboratories deduced the primary structures of the rat and mouse type 1 IP_3R, a class intracellular Ca^{2+} channel gated by the second messenger IP_3 [29, 30]. It was noted that the 313 kDa IP_3R1 protein displayed limited amino acid identity (~17%) to the RyR, with greatest identity (~35%) within the predicted transmembrane/ion channel domain.

The "Peri-genomic" Era: RyRs Are Present in Animals, But Not Other Eukaryotes

During the 1990s, following deduction of the primary structure of rabbit RyR1 and rodent IP_3R1s, cDNAs encoding RyR1 orthologues from other species and paralogues produced from distinct *RYR* genes were subsequently isolated and sequenced. This was generally achieved using cDNA library screening approaches with oligonucleotide probes derived from conserved RyR1 sequences. Rabbit type 2 RyR (RyR2) cDNA is of similar size to that of RyR1 and encodes a protein of 565 kDa. Rabbit RyR2 shares 66% amino acid identity with rabbit RyR1 and has a similar

predicted transmembrane topology. Mammalian RyR1 is expressed at high levels in skeletal muscle and is present, but less abundant, in a number of tissues and cells including smooth muscle [31], B-lymphocytes [32], dendritic cells [33] and in certain regions of the brain [34]. In contrast, mammalian RyR2 is expressed at high density in the heart, but is also abundant in the nervous system and in smooth muscle [31, 34]. Type 3 RyR (RyR3) was original identified as a transforming growth factor-β inducible transcript in mink lung epithelial cells [35]. It is encoded by a cDNA of ~15 kb and is about 65% identical to RyR1 and RyR2 paralogues at the protein level. RyR3 displays a low-level, ubiquitous tissue distribution, being most abundant in the nervous system and in certain skeletal muscle fibres, particularly those of the diaphragm [34].

Concurrently with the identification of the three mammalian RyR subtypes, two distinct channel proteins called RyR-α and RyR-β were characterised in the skeletal muscles of fish, amphibians and birds [36]. A third non-mammalian RyR subtype, termed "cardiac" RyR was found in avian heart and skeletal muscle [37]. It transpired that the α, cardiac and β RyR subtypes are homologues of mammalian RyR1, RyR2 and RyR3 and that these channel proteins display broadly similar tissue distribution patterns to their mammalian counterparts [38]. In addition to the three RyR genes present in other vertebrates, it has recently been found that teleost fish express a fourth RyR gene in certain skeletal muscle groups, that is most similar to RyR1 and is termed RyR1b [39]. Since they also express additional, functionally specialised forms of non-Ca^{2+}-conducting L-type VGCCs which conformationally couple to RyRs [40], it has been postulated that euteleosts have evolved the most advanced form of vertebrate skeletal muscle EC-coupling.

Characterisation of RyRs in vertebrates was rapidly preceded by determination of their primary structures in invertebrates. The fruit fly *Drosophila melanogaster* expresses a single *RYR* gene encoding a protein of approximately 5,200 amino acid residues, that is ~46% identical to the three vertebrate family members [41, 42]. This gene is expressed at high levels in somatic muscles and lower levels in the nervous system [41]. Mutant fruit flies lacking *RYR* expression display deficits in larval development, with impairment of muscle EC-coupling being a major phenotype. However, analysis of mutants in which *RYR* expression was selectively deleted in the adult eye demonstrated that this channel does not play a role in phototransduction [43]. Together with biochemical, pharmacological and physiological data from crustaceans such as crayfish [44] and the lobster *Homarus americanus* [45], this indicated that ryanodine-sensitive Ca^{2+} release channels are present in vertebrates and a range of arthropods. A single *RYR* gene is also present in the nematode worm *Caenorhaditis elegans* and encodes a high molecular weight protein sharing about 40% amino acid identity with vertebrate RyRs [46]. Unlike the case in *Drosophila*, mutant worms (*unc-68*) lacking the *RYR* gene maintain muscle EC-coupling but show deficits in certain muscle groups. This implies that RyR channels are not essential in nematode EC-coupling, but can amplify Ca^{2+} influx via VGCCs by CICR in this process [47].

Biochemical, pharmacological and physiological evidence also suggested the presence of RyR channels in a variety other organisms. For example, SR from a

mollusc, the scallop *Pecten megellanicus*, bears feet structures, contains high affinity binding sites for tritiated ryanodine and a Ca^{2+}- and ryanodine-sensitive cation channel [48]. Membrane fractions from the trematode worm *Schistosoma mansoni* contain high affinity ryanodine binding sites and release $^{45}Ca^{2+}$ in response to this alkaloid [49]. The chromoalveolate protozoan parasite *Toxoplasma* uses a specialised secretory structure called the microneme to invade host cells. In *T. gondii*, both microneme secretion and Ca^{2+} release from intracellular stores are stimulated by the RyR agonists caffeine and ryanodine [50]. Functional evidence suggests the presence of RyR-like channels in higher plants. For example, caffeine or ryanodine pretreatment inhibits cADPr-induced Ca^{2+} release from microsomal membranes isolated from the red beet, *Beta vulgaris* [51]. In the mouse ear-cress *Arabidopsis thaliana*, a higher plant, the RyR antagonists dantrolene and 8-bromo-cADPr inhibit increases in cytoplasmic Ca^{2+} levels and stomatal closure elicited by the hormone abscisic acid [52].

Overall, these studies support the utilisation of RyR-like cation channels in diverse animal phyla, including vertebrates, molluscs, arthropods, nematodes and platyhelminthes. Functional data also supported the presence of RyRs in higher plants and in unicellular eukaryotes such as *T. gondii*. However, the primary structures of many of these channel proteins awaited characterisation. Furthermore, there was no published evidence supporting the existence of RyR-like channels in prokaryotic organisms, which is not unexpected given their lack of intracellular membrane systems. During the 1990s, one consensus view was that RyR channels of a "classical" primary structure are only expressed in animals possessing a nervous system [53]. This is consistent with roles of RyRs in rapid stimulus-response coupling: the high conductance and long open duration of these channels, in combination with their large cytoplasmic domain permitting interactions with various modulatory proteins [54], provides the means to produce large changes in cytoplasmic Ca^{2+} concentration in response to external cues, such as action potentials. Somatic muscle EC-coupling is perhaps the best example of a signal transduction process that is dependent on both the nervous system and the unique properties of RyR channels.

The Post-genomic Era: RyRs Are Present in Some Unicellular Eukaryotes

In the first decade of the second millennium, DNA sequences of genomes from viruses, prokaryotes and eukaryotes became available in ever increasing numbers and quality. This information has had fundamental impacts on fields such as medicine and evolutionary biology. In order to identify RyR homologues and paralogues, the full-length amino acid sequence of *Homo sapiens* RyR2 (Acc. No. NP_001026.2) was searched against a suite of databases at the National Centre for Biotechnology Information (http://blast.ncbi.nlm.nih.gov/Blast.cgi/) using the BLAST algorithm [55]. As of April 2011, this search generated 309 hits: however, exclusion of partial,

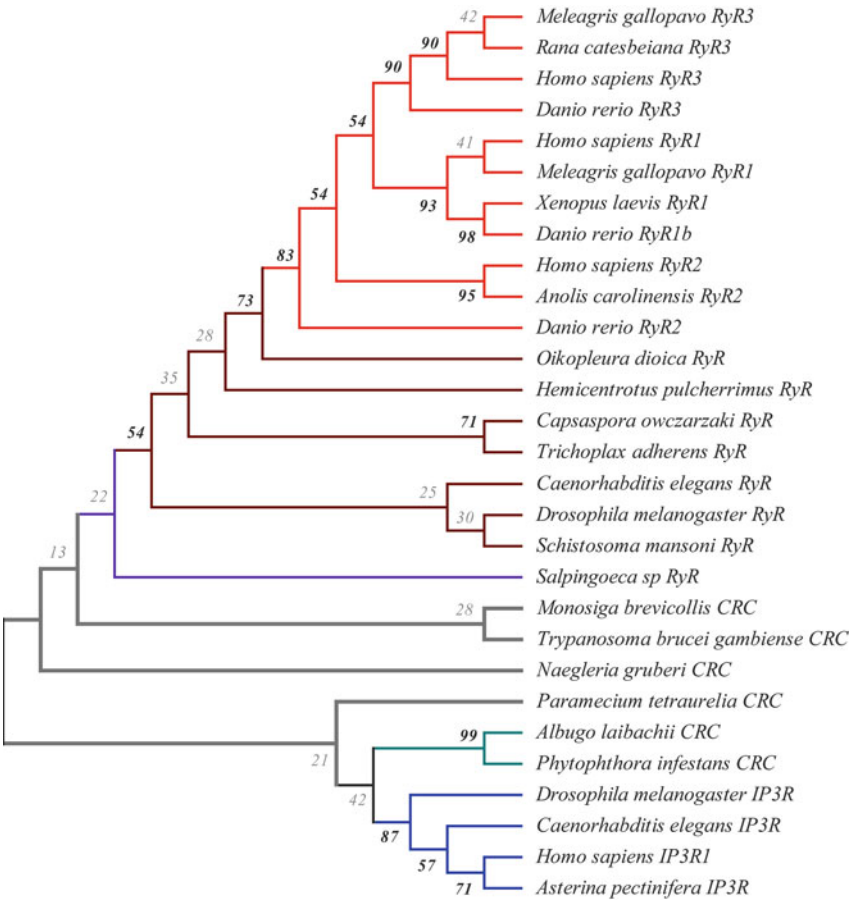

Fig. 7.1 *Phylogenetic analysis of CRC proteins.* The evolutionary history of CRC proteins related to human RyR2 was inferred using the Maximum Likelihood method, based on the Jones-Taylor-Thorton matrix-based model [56]. Branches coloured *red* represent vertebrate RyRs; those in *brown* are non-vertebrate metazoan and capsasporan RyRs; the *purple* branch is an RyR from the choanoflagellate *Salpingoeca*; the *green* branches are oomycete CRCs; the *grey* branches are other unicellular eukaryotic CRCs; and the *blue* branches are IP_3R proteins from various taxa. Bootstrap values inferred from 500 replicates are taken to represent the evolutionary history of CRC proteins in the taxa analyzed [57]. The percentage of replicate trees in which the associated taxa clustered together in the bootstrap test (500 replicates) are shown next to the branches [57], with values above a threshold value for significant grouping of 50% indicated in *bold font*. The analysis involved 29 amino acid sequences. All positions containing gaps and missing data were eliminated. There were a total of 304 positions in the final dataset. Evolutionary analyses were conducted in MEGA5 [58]

redundant or very closely related sequences (within the same taxonomic class) resulted in a set of 29 primary structures for further examination. Figure 7.1 shows a phylogenetic tree generated by analyses of these sequences generated using MEGA5 software [58]: details of the methods employed are presented in the figure caption.

It should be born in mind that some genome data utilised are incomplete, or are of low quality. Furthermore, certain groups of organism are under-represented, in particular unicellular eukaryotes; whereas others, particularly organisms that are of importance in health and agriculture, are over-represented. However, this tree reiterates many of the earlier deductions made about RyR evolutionary biology [53]. For example, it seems likely that the expansion of *RYR* genes per genome occurred early in vertebrate evolution: without exception to date, single *RYR* genes are present in invertebrates, whereas at least three genes are present in fish, amphibia, birds and mammals. Currently, only one full-length *RYR* gene (*RYR2*) has been identified a reptile, *Anolis carolinensis*, but it is more likely that this is due to limited sequencing of reptilian genomes, rather than these vertebrates possessing just a single *RYR* gene. This concept is supported by the identification of three partial DNA sequences in the draft genome of an archetypal cephalochordate, the lancelet *Branchiostoma floridae*, encoding proteins of greatest identity to RyR1, RyR2 and RyR3. Biochemical and electrophysiological studies of myotomes from these protochordates indicate that they utilise a vertebrate-like, CCCR mode of EC-coupling [21, 59]. In contrast, the genome of the sea squirt *Oikopleura dioica* [60], which as a urochordate is generally considered to be more primitive than the cephalochordate *B. floridae*, possesses a single *RYR* gene.

The absence of recognisable *RYR* or *IP3R* genes in any higher plant genome also supports earlier observations [61]. This view holds in very high quality, well annotated plant genomes, such as that of *Arabidopsis thaliana*. This represents a major paradox, since functional and biochemical evidence indicates that these organisms utilise both ryanodine- and IP_3-sensitive cation channels. As mentioned earlier, Ca^{2+} channels that are sensitive to either ryanodine or dantrolene are present in the higher plants *Beta vulagaris*, *Arabidopsis thaliana* and others [52, 61, 62]. One explanation for this paradox is that the structures of plant RyRs and IP_3Rs have diverged drastically from a common ancestor shared with animal calcium release channels (CRCs), such that these homologues display no detectable amino acid identity. A related possibility is that the components of plant RyR complexes that are sensitive to "classical" RyR agonists or antagonists reside in subunits that are distinct from the channel-forming protein. This would exacerbate the difficulties in identification of plant RyRs. Indirect evidence for this possibility has been reported for plant IP_3R Ca^{2+} channels. The cytosolic plant enzyme phytase can both bind IP_3 and trigger Ca^{2+} mobilisation from vacuolar membranes [63], despite its lack of transmembrane segments. This implies the IP_3-phytase complex binds to and gates a distinct, unidentified CRC protein located in the plant vacuole. Alternatively, the apparent lack of RyRs in higher plants could reflect a simple loss of this channel family, as may have occurred with other calcium signaling components in higher plants. It is speculated that the loss or extreme structural divergence of RyRs in higher plants could reflect the action of selection pressures that are distinct from those acting on animals [62, 64, 65].

None of the multiple high quality fungal genomes available contain "classical" *RYR* or *IP3R* genes [66]. RyRs also seem to be absent from certain animal groups,

such as poriferans (sponges), cnidarians (including corals, jellyfish and anemones) and ctenophorans (comb jellies or sea gooseberries). With the exception of poriferans, these animal taxa appear to possess *IP3R* genes. However, absence of *RYR* genes should be interpreted with caution, given the low quality or quantity of genome data available from these taxa. Many of these organisms, particularly fungi and poriferans are predominantly sedentary, indicating that RyRs are dispensable for this mode of life. However, jellyfish and ctenophorans are predominantly motile. Another possibility is that loss of RyRs has enabled the evolution of novel mechanisms of defence against predation. For example, the sponge *Ianthella basta* produces macrocyclic toxins termed bastadins, that are derived from bromotyrosine. One of these compounds, bastadin-5, modulates RyR1 channels present in rabbit skeletal muscle SR, increasing their open duration [67], thus providing protection against predators that utilise RyR channels in their neuromuscular systems.

A novel observation from the current search was the detection of a single predicted *RYR* gene within the genome of the placozoan *Trichoplax adhaerens* [68]. This organism possibly represents the simplest free-living animal, with a body plan consisting of a central core of fibre cells ensheathed within an epithelial layer. It lacks neurons and muscle cells [69], suggesting that RyR channels were first employed by animals prior to the development of a nervous system, or of EC-coupling. However, the position of placozoans in metazoan evolution is highly contentious at present. Some analyses place these animals at a branch after sponges but before eumetazoans (cnidaria, ctenophora and bilateria), whereas other studies place them prior to the poriferans [70].

The current searches have also revealed that RyR channels might be employed by certain unicellular eukaryotes. Choanoflagellates, or "collared flagellates", are protozoans that are considered to be the closest living relatives to animals [71, 72]. They are single-celled, sedentary or motile, solitary or colonial and employ a single flagellum to drive water through their collar, thereby trapping prey bacteria. A single putative *RYR* gene is present in the genome of the choanoflagellate *Salpingoeca sp.* ATCC 50818. This gene is predicted to encode of protein of similar size (5,340 amino acid residues), primary structure (~36% identity, E-values $<1 \times 10^{-80}$) and protein domain organisation (see section "Protein Domains Shared by RyRs and IP3Rs") to metazoan RyR proteins, with closest identity to RyR1. Note that E-values give any estimate of the probability that a sequence of amino residues arose in a pair of proteins by chance, rather than by evolutionary relationship: the lower the E-value, the greater possibility of common ancestry. Other predicted CRCs in the *Salpingoeca* genome are incorrectly annotated as RyR2 homologues: BLAST searches indicated that these proteins are more closely related to IP_3Rs than to RyRs. Another choanoflagellate, *Monosiga brevicollis*, possesses IP_3R channel homologues, but lacks detectable RyRs [73].

Capsaspora owczarzaki is a unicellular eukaryotic symbiont of the snail *Biomphalaria glabrata*, that forms an opisthokont lineage distinct from metazoa, fungi, choanoflagellates and ichthyosporeans [74]. The *C. owczarzaki* genome

contains a gene predicted to encode a protein of 6,625 amino acid residues that displays a highly similar primary structure (E-values $<1 \times 10^{-80}$) and domain organisation to metazoan RyRs. Homologues of this protein are apparently absent from ichthyosporeans, such as *Sphaeroforma artica*, although this could be a consequence of low quality or incomplete genome data. Overall, this hints that RyRs evolved prior to the divergence of choanoflagellates and metazoans, but could have been subsequently lost from certain taxa, including land plants, fungi, sponges and possibly ichthyosporeans. The presence of "metazoan" transcription factor genes in the unicellular *C.owczarzaki*, provides a precedent for the evolution of "metazoan" CRCs, such as RyRs, prior to the evolution of multicellularity in eukaryotes [75].

The relationships between metazoan RyRs and other CRCs present in unicellular eukaryotes more primitive than the choanoflagellates, are less clear. For example, the genome of the ciliated protozoan *Paramecium tetraurelia* contains at least 34 genes predicted to encode proteins of limited identity (20–30%) to metazoan IP_3R and RyR channels [76]. Certain members of this family form IP_3-gated Ca^{2+} channels and participate in osmoregulation in this organism [77]. Knockdown of another member of this family, CRC-IV-1, inhibited stimulus-secretion responses in *P. tetraurelia* [76]. Twenty three hypothetical proteins of similar primary structure (E-values of $<1 \times 10^{-30}$) to the *P. tetraurelia* CRCs are encoded within the genome of another ciliated protozoan, *Tetrahymena thermophila* [78]. The large number of CRC genes in these ciliated protozoans is surprising, but could be explained by the inability of these organisms to generate structural diversity in proteins by mRNA splicing mechanisms: gene expansion might be used as an alternative strategy [76].

Other CRC genes are present in chlorophytes such as *Volvox* and *Chlamydomonas*. Brown algae (Class: Phaeophyceae) are heterokont eukaryotes that evolved multicellularity independently of animals and land plants. The nuclear genome of one of these brown algae, *Ectocarpus siliculosus*, has been deduced and is predicted to encode a member of the RyR-IP_3R CRC family [79]. Chlorophyte, protozoan and brown algal CRC proteins might represent ancestral eukaryotic CRCs, since they appear to be intermediate in primary structure between IP_3Rs and RyRs, although they share greatest identity with the former channel family. In addition, as discussed in section "Protein Domains Present in RyRs But Not IP3Rs", these proteins lack domains that are definitive of "genuine" RyR channels.

In the current survey, genes encoding RyR-like proteins were detected in one other branch of the eukaryotic tree, known as oomycetes. This class of organism belong to a distinct phylum of eukaryotes known as the heterokonts: these are defined by possession of two flagellae of differing morphology during the motile stage of their life cycle. Oomycetes, or "water moulds" are filamentous microorganisms, many of which are plant pathogens. They include *Phytophthora infestans*, the causative agent of late potato blight, a disease of major historical significance in western Europe, particularly in Ireland. The genomes of *Phytophthora infestans* and *Albugo laibachii* (causative agent of white rust plant disease) each contain two

genes encoding CRC-like proteins. All four of these proteins have similar domain architectures, share considerable identity with metazoan RyRs (E-values of $<1 \times 10^{-28}$) and are of high calculated molecular weight (1,293 and 1,420 amino acid residues for *P. infestans*; 1,160 and 2,549 residues for the *A. laibachii* CRCs). However, they display distinct domain organisation compared with metazoan RyRs. Since these oomycete RyR-like proteins differ from the RyRs of other metazoans, they might represent an attractive target for the development of pesticides [80]. The RyR-like CRC from *P. infestans* might represent a particularly attractive target for pesticide development, since the mRNA encoding this protein is upregulated more than 150-fold during zoosporogenesis, a process that generates a motile stage responsible for the spread of this disease [81].

Small domains (~100 amino acid residues) present in proteins from prokaryotes and viruses share high levels of identity (E-values of $<1 \times 10^{-5}$) with so-called "RyR domains" and "SPRY domains" present in eukaryotic RyRs, section "The RyR Domain". However, bacteria and archaea lack recognisable IP_3R homologues. Furthermore, many of these non-eukaryotic RyR domain-containing proteins lack predicted transmembrane segments and so cannot be ion channel homologues. This leads to the question: what features constitute a "genuine" RyR channel protein? An attempt will be made to address this question in the next section, by analysing the domain architectures of candidate CRC proteins.

Domain Structures of Ryanodine Receptor Proteins

To generate insights into RyR channel evolution, a novel alternative to phylogenetic analyses was comparison of the domain architectures of these proteins. Domains are defined as self-folding structural units of proteins, typically of 50–200 residues in length. These units are considered to play key roles in the evolution of novel protein functions, via mechanisms including generation of new combinations within multi-domain proteins, particularly via the incorporation or loss of "mobile" protein domains [82, 83]. Furthermore, protein three dimensional structures tend to be more conserved than their corresponding linear sequences, making the assessment of evolution of proteins via analyses of their domains architectures a valid approach, particularly when combined with "classical" phylogenetic methods [84]. In order to facilitate this in the current overview, candidate RyR protein sequences indentified in the earlier BLAST searches were analysed using the Conserved Domain Database [85], part of the suite of software tools at the National Center for Biotechnology Information website (http://www.ncbi.nlm.nih.gov/Structure/cdd/). Domain matches with E-values of less than 1×10^{-5} were subjected to further comparisons between proteins. On the basis of these findings, the protein domains present in RyRs can be grouped into two categories: those shared with the IP_3Rs and those shared with other proteins, but not with IP_3Rs, Fig. 7.2.

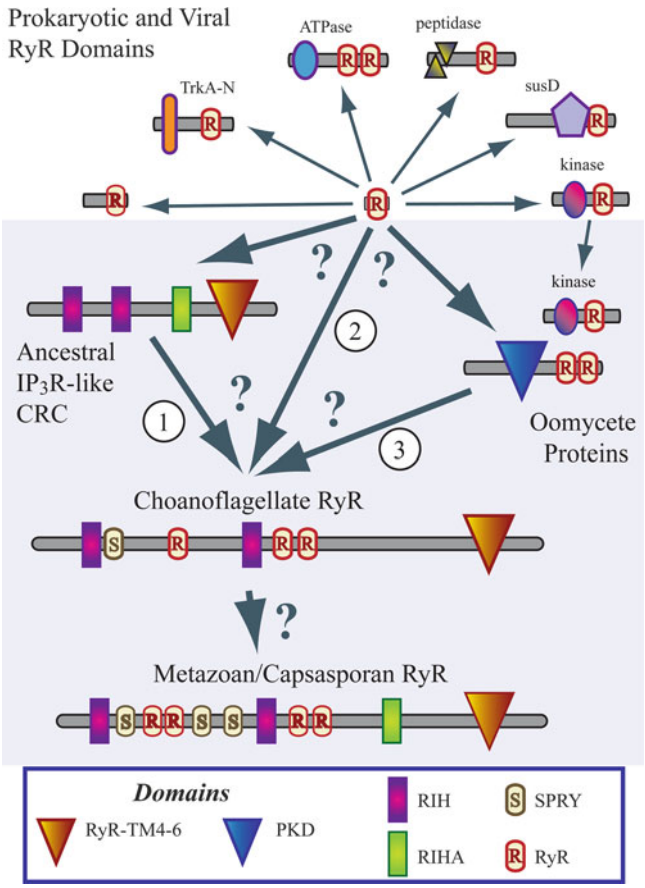

Fig. 7.2 *Multidomain organisation of RyR-related proteins.* A range of bacterial, archaeal and viral proteins contain the RyR domain, either as a single structural unit, or in combination with other domains. In eukaryotes, RyR domains are only present in CRC proteins and in oomycete protein kinases that are structurally related to bacterial RyR domain-containing kinases. IP_3Rs and ancestral CRCs do not contain the RyR domain. In combination with phylogenetic analyses, three routes for the evolution of metazoan/capsasporan RyRs are proposed: *1* promiscuous prokaryote domains such as the SPRY and RyR domains were incorporated into an ancestral IP_3R-like CRC; these domains were then duplicated and diverged to generate the "modern" RyR architecture; *2* choanoflagellate RyRs evolved directly from prokaryotic ancestors, which then developed into metazoan/capsasporan forms; or *3* choanoflagellate RyRs evolved from precursors unrelated to ancestral IP_3R-like channels. Of these, mechanism *1* is best supported by the available evidence

Protein Domains Shared by RyRs and IP_3Rs

Following the determination of sequences of multiple mammalian RyR and IP_3R proteins, several domains common to both CRCs were identified [53]. These are the MIR (protein mannosyltransferase, IP_3R and RyR), the RIH (RyR and IP_3R homology) and

RIHA (RIH Associated) domains. In addition, the candidate permeation pathways, transmembrane domains and selectivity filters of these channels share similar conserved features [86].

The Protein Mannosyltransferase, IP_3R and RyR (MIR) Domain

MIR domains were first identified using a PSI-BLAST based approach with the N-terminal, IP_3-binding region of rat IP_3R1 as a query sequence [87]. This strategy identified a domain of nearly 200 amino acid residues, repeated four times at the N-termini of both rat IP_3R1 and human RyR1. Three MIR domains were also detected in a protein o-mannosyltransferase from the yeast *Saccharomyces cerevisiae*, in stromal cell-derived factor 2-like protein precursor from higher plants and as a single copy in the membrane attack complex/perforin domain protein CT153, from the bacterium *Chlamydia trachomatis*. Although these domains are present in an IP_3-binding region, they do not form a discrete binding unit for inositol phosphates. It was suggested that MIR domains are involved in protein-protein interactions, since they are present in a region of mammalian IP_3Rs that can interact with plasmalemmal TRPC3 (hTrp3) channels [87, 88]. Mammalian RyRs also interact with TRPC3, modulating the gating of this surface channel [89]. However, the current analyses indicate that MIR domains might not be a conserved unit within IP_3R and RyR proteins: they are either absent, or below the E-value threshold of 1×10^{-5}, in CRCs of all unicellular eukaryotes examined and are present a single copy in non-vertebrate RyRs. The numbers of these units in vertebrate RyRs varies between channel subtypes and between species: in general, RyR1 contains 3–4, RyR2 possesses 1 and RyR3 has 2 MIR domains. These observations suggest that multiple MIR domains are not essential for basic RyR channel functions, but their incorporation into and expansion in vertebrate RyRs might have permitted specialisation of function, for example, during the evolution of different modes of EC-coupling.

The RyR and IP_3R Homology (RIH) and RIH Associated Domains

Another conserved domain identified in the PSI-BLAST analysis of the N-terminus of rat IP_3R1 was termed the RyR and IP_3R homology (RIH) domain [87, 88]. Two copies of this structural unit, each of ~200 amino acid residues in length, are found close to the N-termini of many CRC proteins. These domains are often combined with an additional conserved structure, just over 100 residues in length, closer to the C-termini of these proteins. This is termed the RIH associated (RIHA) domain owing to its coexistence with the RIH domains, rather than it sharing any major structural identity to them. The RIH-RIH-RIHA arrangement is also found in many "ancestral CRC" eukaryotic proteins, with exceptions being those from the non-IP_3R/non-RyR CRCs present in oomycetes. This multidomain architecture and its constituent parts are undetectable in any prokaryotic protein. This implies that development of the RIH-RIH-RIHA multidomain architecture underpinned the evolution of the IP_3R/RyR CRC family. However, the functional properties that this

arrangement endows a channel protein with awaits characterisation: presumably, some "special" property of this channel family, such as very high cation conductance, gating by cytoplasmic second messengers, or the ability to interact with multiple accessory proteins [54].

The Permeation Pathway and Selectivity Filter

During its initial characterisation, it was noted that the primary structure of rabbit RyR1 shares a region of identity to other cation channels, towards the C-terminus of this protein [28]. Determination of the primary structures of rodent type 1 IP_3Rs also revealed extensive homology with the RyRs in this region [29, 30]. Atomic structures are currently only available for a limited number of domains within RyR and IP_3R channel complexes, with the majority of 3-dimensional structures being based on low resolution reconstructions from images obtained by transmission cryoelectron microscopy techniques. This limits the direct, atomic resolution understanding of gating and ion permeation in IP_3Rs and RyRs [90]. However, modelling of RyR/IP_3R proteins based on detailed atomic resolution structures of distantly related bacterial cation channels has generated useful insights into the structure-function relationships of their channel pores and selectivity filters. Furthermore, predictions based on these models can be tested using a variety of strategies, including functional analyses of channels mutated at critical amino acid residues. Such strategies have lead to the identification of consensus features likely to be essential for RyR channel function.

The selectivity filter of a channel enables it to discriminate between ions, allowing conductance of some to be more favourable than of others. Both RyRs and IP_3Rs are poorly selective cation channels: a range of monovalent and divalent cations can pass through their permeation pathway. However, it should be noted that, at least in higher eukaryotes, of all ions, Ca^{2+} displays the largest electrochemical gradient between the lumen of organelles and the cytoplasm. Consequently, relatively non-selective cation channels in intracellular membranes will conduct mainly Ca^{2+}. In both IP_3Rs and RyRs, a conserved GGGXGD motif acts as the selectivity filter, with the carbonyl groups of the glycine (G) residues co-ordinating with the permeating cations and the aspartic acid (D) attracting positive charges and repelling anions [86, 90]. Based on the atomic resolution structures of bacterial potassium channels, the predicted pore-forming transmembrane helices of RyRs also bear conserved, negatively charged residues that participate in both cation selectivity and conduction [91].

BLAST searches of the conserved selectivity filter and pore helices of RyRs listed in the current correlated well with the phylogenetic findings presented in section "The Post-genomic Era: RyRs Are Present in Some Unicellular Eukaryotes". Related RyR pore-filter structures are present in all eukaryotic IP_3Rs, metazoan, capsasporan and choanoflagellate RyRs, and in "ancestral" CRC proteins. Notable exceptions to this are the hypothetical RyR-like CRC proteins of oomycetes. The predicted pores of these proteins are related to those of the polycystic kidney disease-2 (PKD2) cation channels, members of the TRP channel superfamily [92]. In addition to the eukaryotic RyR/IP_3R CRCs listed, searching of the so-called "RR-TM4-6 domain" containing four conserved predicted transmembrane segments of

RyR1, identified a single prokaryotic protein that displays a partial threshold (E-value 1.24×10^{-3}) relationship with this structural unit. This is a hypothetical protein from the genome of the firmicute bacterium *Bacillus cellulosilyticus*. It displays limited identity with a range of other transmembrane proteins, including bacterial chloride and potassium channels, eukaryotic potassium channels and vertebrate RyR1 proteins. This threshold E-value is likely to be due to the small size of the predicted transmembrane domain concerned: a 16 residue overlap with RyR1, displaying 69% identity. Consequently, it is difficult to draw inferences about the evolutionary relationships between RyRs and the single transmembrane segment *B. cellulosilyticus* protein: these molecules could be related or could resemble each other by chance. The absence of RyR-TM4-6 domain containing proteins encoded in any other prokaryotic genome favours the latter possibility.

Protein Domains Present in RyRs But Not IP_3Rs

To date, two domains have been identified in RyRs and other proteins which are not present in IP_3Rs. These are known as the Spore Lysis A and RyR (SPRY) domain and the RyR domain. It is likely that these domains confer unique properties to RyRs, distinct from those of the IP_3Rs.

The Spore Lysis A and RyR (SPRY) Domain

SPRY domains are structural units that were originally identified in the *Dictyostelium discoideum* tyrosine kinase spore lysis A (SplA) protein and in mammalian RyRs [93]. Subsequent analyses indicated that such domains are "promiscuous", being present in diverse proteins from most taxa from eukaryotes to bacteria, archaea and viruses. SPRY domains display limited identity at the level of their amino acid sequences, but share a common three dimensional structure consisting of a sandwich of two beta sheets [94]. In the current study, consistent with earlier observations, three SPRY (SPRY1, SPRY2, SPRY3) domains are located towards the N-termini of all metazoan/capsaporan RyRs identified. The candidate RyR from the choanoflagellate *Salpingoeca* contains a single SPRY domain, of similar location to and sharing greatest identity with SPRY1 from mammalian RyRs. However, these structural units are absent from the IP_3Rs and oomycete RyR-like CRC proteins. Despite this, SPRY domains are present in other oomycete proteins.

SPRY domains are generally involved in protein-protein interactions. For example, a SPRY domain protein termed BSPRY binds to and inhibits the gating of the cation channel TRPV5 [95]. In the case of mammalian RyR1 channels, the SPRY2 domain interacts with the II–III cytoplasmic loop of the dihydropyridine receptor α1S-subunit [96], a region critical for the CCCR mode of EC-coupling in skeletal muscle. Roles for the other two SPRY domains in RyR1, or indeed of any SPRY domain in other RyR proteins, have not been reported.

The RyR Domain

During the first determinations of mammalian RyR primary structures, a fourfold repeated domain was noted [28, 97, 98]. These structural units are typically of about 100 amino acid residues in length. In metazoan and capsasporan RyRs, the four RyR domains are arranged in two tandem repeats (RyR domain I/II, RyR domain III/IV): one towards the N-terminus (between SPRY1 and SPRY2) and the other close to the central region. In the hypothetical *Salpingoeca* RyR, only three RyR domains are present; one of the N-terminal pair is missing. In oomycete CRCs, a conserved pair of RyR domains is located to the C-terminus of the PKD-like predicted channel domain. In addition, the genomes of the oomycetes *Albugo laibachii* and *Phytophthora infestans* both encode hypothetical proteins consisting of a single RyR domain paired with a candidate protein kinase domain.

RyR domains are not detectable in IP_3Rs, nor in any other eukaryotic protein family, hinting that they might play specialised roles in RyR-like channels and in certain protein kinases. However, RyR domains are present in a plethora of bacterial, archaeal and bacteriophage proteins, Fig. 7.2. Such RyR domains are found as single units, or in pairs. In some cases, they are associated with other protein domains, but in other cases they do not appear to be joined with any other conserved structural unit. For example, a hypothetical protein from the marine gamma proteobacterium HTCC2148 displays a similar domain organisation to the protein kinase-RyR domain proteins of oomycetes. This demonstrates the possibility of eukaryotic RyR domain containing proteins evolving directly from prokaryotic ones.

A protein composed of a single RyR domain combined with a peptidase C39-like domain is encoded within the genomes of at least six commensal bacteroidete bacteria, including *Bacteroides ovatus* and *Prevotella ruminicola*. In the bacterium *Chlorobium ferrooxidans*, an ATPase domain is present in a hypothetical protein in association with a pair of RyR domains. A peripheral membrane component of bacterial K^+ uptake systems known as TrkA [99] contains a nicotinamide adenine dinucleotide binding domain called TrkA-N, that is conserved in a number of prokaryotic and eukaryotic proteins [100, 101]. Hypothetical proteins containing a TrkA-N domain paired with an RyR domain are present in various proteobacteria, such as *Delsulfuromonas acetoxidans*; actinobacteria including *Streptosporangium roseum* and *Catenulispora acidiphila*; and archaea, such as *Methanocella paludicola.* In the proteobacterium *Desulfovibrio desulfuricans*, a hypothetical protein contains a single RyR domain associated with the starch-binding outer membrane protein domain, SusD.

To date, 51 proteins have been identified that contain the RyR domain in the absence of any other known structural unit. These are found in the genomes of bacteria from the phyla Proteobacteria (*Pasteurella*, *Hirschia*, *Pseudomonas*, *Methylobacterium* and *Stenotrophomonas*), Firmicutes (*Bacillus, Butyrivibrio, Clostridium, Coprococcus* and *Eubacterium*), Bacteriodetes (*Bacteroides, Odoribacter* and *Geobacter*), Chlorobia (*Pelodictyon*), Actinobacteria (*Frankia, Mycobacteria* and *Slackia*) and in archaea of the phylum Euryarchaeota (*Methanosphaerula*). In addition, such "RyR domain only" proteins are present in

viruses including Aeromonas bacteriophage 65, phiAS5, Aeh1 and PX29; Roseophage DSS3P2; Ralstonia phage RSL1; and Pseudomonas phage F116.

The crystal structure of a single RyR domain protein from the bacterium *Bacteroides thetaiotaomicron* VPI-5482 has been deduced at 2.54 Å resolution by Ruiying *et al* at the Midwest Center for Structural Genomics, USA (http://www.rcsb.org/pdb/explore/explore.do?structureId=3NRT/). This 100 residue protein adopts a helix-sheet-sheet-helix structure and potentially self-associates into dimers or hexamers. The presence of the RyR domain in multiple prokaryotic and viral proteins, often in combination with a various of other domains, suggest that it is a "promiscuous" domain. Such units play critical roles in the evolution of novel domain structures and often participate in protein-protein interactions or small molecule binding, as exemplified by the Src Homology 3 (SH3) domains of eukaryotic proteins [82].

Detection of RyR domains encoded in bacteriophage genomes hints at a possible lateral or horizontal gene transfer (HGT) of genes encoding these structural units between unrelated species. The "conventional" mode of transfer of genetic material between individuals is vertical, from parent(s) to offspring. A distinct mechanism in eukaryotes involves the endosymbiotic route, in which genes from the captured "organelle" organisms are incorporated into the host cell nucleus. In contrast, HGT involves transfer of genes between unrelated species and occurs by processes in which individual domains, single genes or groups of genes, rather than a whole organism, are captured. HGT provides a mechanism for rapid evolution of novel multidomain combinations under circumstances where the newly incorporated domains are positively selected. Viruses, uptake from the environment and phagocytosis represent mechanisms by which HGT could occur [102]. Phylogenetic evidence indicates the occurrence of HGT from marine bacteria to gut bacteria [103]; proteobacteria to choanoflagellates/capsasporans [104, 105]; prokaryotes to ascomycete fungi and from ascomycetes to oomycetes [106]; and from humans to the commensal, enterotoxigenic gut bacterium *Bacteroides fragilis* [107]. It is tempting to speculate that the RyR domains present in eukaryotic RyR channel proteins are derived by HGT from prokaryotes. This is not without precedent, since similar mechanisms are thought to have operated during the evolution of other proteins, such as the incorporation of TrkA domains into bacterial K^+-channels during the evolution of eukaryotic nucleotide-gated K^+ channels [99]. Evidence for HGT-dependent evolution of RyRs awaits more extensive phylogenetic investigations, based on a greater number of genomes from more taxa.

Perspectives on RyR Evolution

Consensus mechanisms for the evolution of RyR channel proteins, based on both direct phylogenetic analyses and on interpretation of multidomain structures, are represented in Fig. 7.2. RyR domains are present in diverse prokaryotic and viral proteins, but among eukaryotic proteins are only represented in RyR-like channels

and putative oomycete protein kinases. Although eukaryotic RyRs could have evolved directly from prokaryotic ancestors, it seems more likely they arose via modification of pre-existing, ancestral IP_3R-like channels present in prokaryotes or in proto-eukaryotes. Evidence for this is that proteins containing RIH, RIHA and channel domains evolved in a broad range of simple eukaryotes, including chlorophytes, alveolates, choanoflagellates and amoebazoids. However, these proteins represent a range of multidomain structures, namely RIH-RIH-RIHA-channel, RIH-RIH-channel and RIH-RIHA-channel domain arrangements. It is tempting to speculate that incorporation of promiscuous domains, such as the RyR and SPRY domains, into such prototypical eukaryotic CRCs lead to the evolution of metazoan/capsasporan forms of RyR channel proteins. Such incorporation events could have potentially arisen as a result of HGT of such promiscuous domains from prokaryotes to eukaryotes. It is of note that the "simplest" eukaryotes in which RyR and SPRY domain-containing channels are encoded are choanoflagellates, which prey on bacteria and could have potentially captured such structural units via phagocytic HGT [104, 105].

One intriguing aspect of CRC evolution re-iterated in the current review is the absence of RyR-like proteins in certain eukaryotes, particularly in higher forms such as land plants and fungi. This could be explained either by selective losses of genes encoding RyR-like proteins from certain eukaryotic taxa (section "The Post-genomic Era: RyRs are Present in Some Unicellular Eukaryotes"), or by multiple HGT transfer events resulting the incorporation of promiscuous domains into pre-existing CRC protein structures in certain groups of organisms, but not others. These processes are not mutually exclusive. There is scant evidence to support either mechanism: however, the presence of RyR domains in oomycyte CRCs that are not highly related to other eukaryotic RyRs is suggestive of the latter mechanism. The preservation of promiscuous RyR and SPRY domains in eukaryotic channel proteins infers that they confer selective advantages over the unmodified, IP_3R-like ancestors. These advantages probably relate to the unique features of RyR channels relative to IP_3Rs, such as their greater unitary conductance, longer open times or the capability of interacting with a distinct set of accessory proteins [54]. It is expected that continued analyses of genomic data from an increasing numbers of organisms, particularly from unicellular eukaryotes, will unveil RyR evolution and function in greater detail.

References

1. Case RM, Eisner D, Gurney A, Jones O, Muallem S, Verkhratsky A (2007) Evolution of calcium homeostasis: from birth of the first cell to an omnipresent signalling system. Cell Calcium 42:345–350
2. Dominguez DC (2004) Calcium signalling in bacteria. Mol Microbiol 54:291–297
3. Norris V, Grant S, Freestone P, Canvin J, Sheikh FN, Toth I, Trinei M, Modha K, Norman RI (1996) Calcium signalling in bacteria. J Bacteriol 178:3677–3682
4. Naseem R, Davies SR, Jones H, Wann KT, Holland IB, Campbell AK (2007) Cytosolic Ca^{2+} regulates protein expression in E. coli through release from inclusion bodies. Biochem Biophys Res Commun 360:33–39

5. Gray MW, Doolittle WF (1982) Has the endosymbiont hypothesis been proven? Microbiol Rev 46:1–42
6. Roger AJ (1999) Reconstructing early events in eukaryotic evolution. Am Nat 154:S146–S163
7. Cavalier-Smith T (1975) The origin of nuclei and of eukaryotic cells. Nature 256:463–468
8. Negulescu PA, Machen TE (1993) Ca transport by plasma membrane and intracellular stores of gastric cells. Am J Physiol 264:C843–C851
9. Endo M (2006) Calcium ion as a second messenger with special reference to excitation-contraction coupling. J Pharmacol Sci 100:519–524
10. Wu X, Zhang T, Bossuyt J, Li X, McKinsey TA, Dedman JR, Olson EN, Chen J, Brown JH, Bers DM (2006) Local InsP3-dependent perinuclear Ca^{2+} signaling in cardiac myocyte excitation-transcription coupling. J Clin Invest 116:675–682
11. Liang W, Buluc M, van Breemen C, Wang X (2004) Vectorial Ca^{2+} release via ryanodine receptors contributes to Ca^{2+} extrusion from freshly isolated rabbit aortic endothelial cells. Cell Calcium 36:431–443
12. Berkelman T, Garret-Engele P, Hoffman NE (1994) The pacL gene of Synechococcus sp. strain PCC 7942 encodes a Ca(2+)-transporting ATPase. J Bacteriol 176:4430–4436
13. Shigaki T, Rees I, Nakhleh L, Hirschi KD (2006) Identification of three distinct phylogenetic groups of CAX cation/proton antiporters. J Mol Evol 63:815–825
14. Kung C, Blount P (2004) Channels in microbes: so many holes to fill. Mol Microbiol 53:373–380
15. Jegla TJ, Zmasek CM, Batalov S, Nayak SK (2009) Evolution of the human ion channel set. Comb Chem High Throughput Screen 12:2–23
16. Dolphin AC (2009) Calcium channel diversity: multiple roles of calcium channel subunits. Curr Opin Neurobiol 19:237–244
17. Flucher BE, Takekura H, Franzini-Armstrong C (1993) Development of the excitation-contraction coupling apparatus in skeletal muscle: association of sarcoplasmic reticulum and transverse tubules with myofibrils. Dev Biol 160:135–147
18. Franzini-Armstrong C, Protasi F, Tijskens P (2005) The assembly of calcium release units in cardiac muscle. Ann NY Acad Sci 1047:76–85
19. Meissner G (2002) Regulation of mammalian ryanodine receptors. Front Biosci 7:d2072–d2080
20. Franzini-Armstrong C (1970) STUDIES OF THE TRIAD: I. Structure of the junction in frog twitch fibers. J Cell Biol 47:488–499
21. Di Biase V, Franzini-Armstrong C (2005) Evolution of skeletal type e-c coupling: a novel means of controlling calcium delivery. J Cell Biol 171:695–704
22. Rogers EF, Koniuszy FR et al (1948) Plant insecticides; ryanodine, a new alkaloid from Ryania speciosa Vahl. J Am Chem Soc 70:3086–3088
23. West DJ, Williams AJ (2007) Pharmacological regulators of intracellular calcium release channels. Curr Pharm Des 13:2428–2442
24. Lai FA, Erickson HP, Rousseau E, Liu QY, Meissner G (1988) Purification and reconstitution of the calcium release channel from skeletal muscle. Nature 331:315–319
25. Campbell KP, Knudson CM, Imagawa T, Leung AT, Sutko JL, Kahl SD, Raab CR, Madson L (1987) Identification and characterization of the high affinity [3H]ryanodine receptor of the junctional sarcoplasmic reticulum Ca^{2+} release channel. J Biol Chem 262:6460–6463
26. Inui M, Saito A, Fleischer S (1987) Purification of the ryanodine receptor and identity with feet structures of junctional terminal cisternae of sarcoplasmic reticulum from fast skeletal muscle. J Biol Chem 262:1740–1747
27. Lai FA, Misra M, Xu L, Smith HA, Meissner G (1989) The ryanodine receptor-Ca^{2+} release channel complex of skeletal muscle sarcoplasmic reticulum. Evidence for a cooperatively coupled, negatively charged homotetramer. J Biol Chem 264:16776–16785
28. Takeshima H, Nishimura S, Matsumoto T, Ishida H, Kangawa K, Minamino N, Matsuo H, Ueda M, Hanaoka M, Hirose T et al (1989) Primary structure and expression from complementary DNA of skeletal muscle ryanodine receptor. Nature 339:439–445

29. Mignery GA, Sudhof TC, Takei K, De Camilli P (1989) Putative receptor for inositol 1,4,5-trisphosphate similar to ryanodine receptor. Nature 342:192–195
30. Furuichi T, Yoshikawa S, Miyawaki A, Wada K, Maeda N, Mikoshiba K (1989) Primary structure and functional expression of the inositol 1,4,5-trisphosphate-binding protein P400. Nature 342:32–38
31. Coussin F, Macrez N, Morel JL, Mironneau J (2000) Requirement of ryanodine receptor subtypes 1 and 2 for Ca(2+)-induced Ca(2+) release in vascular myocytes. J Biol Chem 275:9596–9603
32. Sei Y, Gallagher KL, Basile AS (1999) Skeletal muscle type ryanodine receptor is involved in calcium signaling in human B lymphocytes. J Biol Chem 274:5995–6002
33. O'Connell PJ, Klyachko VA, Ahern GP (2002) Identification of functional type 1 ryanodine receptors in mouse dendritic cells. FEBS Lett 512:67–70
34. Giannini G, Conti A, Mammarella S, Scrobogna M, Sorrentino V (1995) The ryanodine receptor/calcium channel genes are widely and differentially expressed in murine brain and peripheral tissues. J Cell Biol 128:893–904
35. Giannini G, Clementi E, Ceci R, Marziali G, Sorrentino V (1992) Expression of a ryanodine receptor-Ca^{2+} channel that is regulated by TGF-beta. Science 257:91–94
36. Olivares EB, Tanksley SJ, Airey JA, Beck CF, Ouyang Y, Deerinck TJ, Ellisman MH, Sutko JL (1991) Nonmammalian vertebrate skeletal muscles express two triad junctional foot protein isoforms. Biophys J 59:1153–1163
37. Airey JA, Grinsell MM, Jones LR, Sutko JL, Witcher D (1993) Three ryanodine receptor isoforms exist in avian striated muscles. Biochemistry 32:5739–5745
38. Ottini L, Marziali G, Conti A, Charlesworth A, Sorrentino V (1996) Alpha and beta isoforms of ryanodine receptor from chicken skeletal muscle are the homologues of mammalian RyR1 and RyR3. Biochem J 315(Pt 1):207–216
39. Darbandi S, Franck JP (2009) A comparative study of ryanodine receptor (RyR) gene expression levels in a basal ray-finned fish, bichir (Polypterus ornatipinnis) and the derived euteleost zebrafish (Danio rerio). Comp Biochem Physiol B Biochem Mol Biol 154:443–448
40. Schredelseker J, Shrivastav M, Dayal A, Grabner M (2010) Non-Ca^{2+}-conducting Ca^{2+} channels in fish skeletal muscle excitation-contraction coupling. Proc Natl Acad Sci USA 107:5658–5663
41. Hasan G, Rosbash M (1992) Drosophila homologs of two mammalian intracellular Ca(2+)-release channels: identification and expression patterns of the inositol 1,4,5-triphosphate and the ryanodine receptor genes. Development 116:967–975
42. Takeshima H, Nishi M, Iwabe N, Miyata T, Hosoya T, Masai I, Hotta Y (1994) Isolation and characterization of a gene for a ryanodine receptor/calcium release channel in Drosophila melanogaster. FEBS Lett 337:81–87
43. Sullivan KM, Scott K, Zuker CS, Rubin GM (2000) The ryanodine receptor is essential for larval development in Drosophila melanogaster. Proc Natl Acad Sci USA 97:5942–5947
44. Formelova J, Hurnak O, Novotova M, Zachar J (1990) Ryanodine receptor purified from crayfish skeletal muscle. Gen Physiol Biophys 9:445–453
45. Seok JH, Xu L, Kramarcy NR, Sealock R, Meissner G (1992) The 30S lobster skeletal muscle Ca^{2+} release channel (ryanodine receptor) has functional properties distinct from the mammalian channel proteins. J Biol Chem 267:15893–15901
46. Sakube Y, Ando H, Kagawa H (1993) Cloning and mapping of a ryanodine receptor homolog gene of Caenorhabditis elegans. Ann NY Acad Sci 707:540–545
47. Maryon EB, Coronado R, Anderson P (1996) unc-68 encodes a ryanodine receptor involved in regulating C. elegans body-wall muscle contraction. J Cell Biol 134:885–893
48. Quinn KE, Castellani L, Ondrias K, Ehrlich BE (1998) Characterization of the ryanodine receptor/channel of invertebrate muscle. Am J Physiol 274:R494–R502
49. Silva CL, Cunha VM, Mendonca-Silva DL, Noel F (1998) Evidence for ryanodine receptors in Schistosoma mansoni. Biochem Pharmacol 56:997–1003
50. Lovett JL, Marchesini N, Moreno SN, Sibley LD (2002) Toxoplasma gondii microneme secretion involves intracellular Ca(2+) release from inositol 1,4,5-triphosphate (IP(3))/ryanodine-sensitive stores. J Biol Chem 277:25870–25876

51. Muir SR, Sanders D (1996) Pharmacology of Ca^{2+} release from red beet microsomes suggests the presence of ryanodine receptor homologs in higher plants. FEBS Lett 395:39–42
52. Meimoun P, Vidal G, Bohrer AS, Lehner A, Tran D, Briand J, Bouteau F, Rona JP (2009) Intracellular Ca^{2+} stores could participate to abscisic acid-induced depolarization and stomatal closure in Arabidopsis thaliana. Plant Signal Behav 4:830–835
53. Sorrentino V, Barone V, Rossi D (2000) Intracellular Ca(2+) release channels in evolution. Curr Opin Genet Dev 10:662–667
54. Mackrill JJ (1999) Protein-protein interactions in intracellular Ca^{2+}-release channel function. Biochem J 337(Pt 3):345–361
55. Altschul SF, Madden TL, Schaffer AA, Zhang J, Zhang Z, Miller W, Lipman DJ (1997) Gapped BLAST and PSI-BLAST: a new generation of protein database search programs. Nucleic Acids Res 25:3389–3402
56. Jones DT, Taylor WR, Thornton JM (1992) The rapid generation of mutation data matrices from protein sequences. Comput Appl Biosci 8:275–282
57. Felsenstein J (1985) Confidence-limits on phylogenies – an approach using the bootstrap. Evolution 39:783–791
58. Tamura K, Peterson D, Peterson N, Stecher G, Nei M, Kumar S (2011) MEGA5: molecular evolutionary genetics analysis using maximum likelihood, evolutionary distance, and maximum parsimony methods. Mol Biol Evol 28:2731–2739
59. Benterbusch R, Herberg FW, Melzer W, Thieleczek R (1992) Excitation-contraction coupling in a pre-vertebrate twitch muscle: the myotomes of Branchiostoma lanceolatum. J Membr Biol 129:237–252
60. Seo HC, Kube M, Edvardsen RB, Jensen MF, Beck A, Spriet E, Gorsky G, Thompson EM, Lehrach H, Reinhardt R, Chourrout D (2001) Miniature genome in the marine chordate Oikopleura dioica. Science 294:2506
61. Nagata T, Iizumi S, Satoh K, Ooka H, Kawai J, Carninci P, Hayashizaki Y, Otomo Y, Murakami K, Matsubara K, Kikuchi S (2004) Comparative analysis of plant and animal calcium signal transduction element using plant full-length cDNA data. Mol Biol Evol 21:1855–1870
62. Krinke O, Novotna Z, Valentova O, Martinec J (2007) Inositol trisphosphate receptor in higher plants: is it real? J Exp Bot 58:361–376
63. Dasgupta S, Dasgupta D, Sen M, Biswas S, Biswas BB (1996) Interaction of myoinositoltrisphosphate-phytase complex with the receptor for intercellular Ca^{2+} mobilization in plants. Biochemistry 35:4994–5001
64. Verret F, Wheeler G, Taylor AR, Farnham G, Brownlee C (2010) Calcium channels in photosynthetic eukaryotes: implications for evolution of calcium-based signalling. New Phytol 187:23–43
65. Wheeler GL, Brownlee C (2008) Ca^{2+} signalling in plants and green algae – changing channels. Trends Plant Sci 13:506–514
66. Zelter A, Bencina M, Bowman BJ, Yarden O, Read ND (2004) A comparative genomic analysis of the calcium signaling machinery in Neurospora crassa, Magnaporthe grisea, and Saccharomyces cerevisiae. Fungal Genet Biol 41:827–841
67. Mack MM, Molinski TF, Buck ED, Pessah IN (1994) Novel modulators of skeletal muscle FKBP12/calcium channel complex from Ianthella basta. Role of FKBP12 in channel gating. J Biol Chem 269:23236–23249
68. Srivastava M, Begovic E, Chapman J, Putnam NH, Hellsten U, Kawashima T, Kuo A, Mitros T, Salamov A, Carpenter ML, Signorovitch AY, Moreno MA, Kamm K, Grimwood J, Schmutz J, Shapiro H, Grigoriev IV, Buss LW, Schierwater B, Dellaporta SL, Rokhsar DS (2008) The Trichoplax genome and the nature of placozoans. Nature 454:955–960
69. Schierwater B (2005) My favorite animal, Trichoplax adhaerens. Bioessays 27:1294–1302
70. Philippe H, Derelle R, Lopez P, Pick K, Borchiellini C, Boury-Esnault N, Vacelet J, Renard E, Houliston E, Queinnec E, Da Silva C, Wincker P, Le Guyader H, Leys S, Jackson DJ, Schreiber F, Erpenbeck D, Morgenstern B, Worheide G, Manuel M (2009) Phylogenomics revives traditional views on deep animal relationships. Curr Biol 19:706–712

71. Moreira D, von der Heyden S, Bass D, Lopez-Garcia P, Chao E, Cavalier-Smith T (2007) Global eukaryote phylogeny: combined small- and large-subunit ribosomal DNA trees support monophyly of Rhizaria, Retaria and Excavata. Mol Phylogenet Evol 44:255–266
72. King N (2005) Choanoflagellates. Curr Biol 15:R113–R114
73. Cai X (2008) Unicellular Ca^{2+} signaling 'toolkit' at the origin of metazoa. Mol Biol Evol 25:1357–1361
74. Ruiz-Trillo I, Inagaki Y, Davis LA, Sperstad S, Landfald B, Roger AJ (2004) Capsaspora owczarzaki is an independent opisthokont lineage. Curr Biol 14:R946–R947
75. Sebe-Pedros A, de Mendoza A, Lang BF, Degnan BM, Ruiz-Trillo I (2011) Unexpected repertoire of metazoan transcription factors in the unicellular holozoan Capsaspora owczarzaki. Mol Biol Evol 28:1241–1254
76. Ladenburger EM, Sehring IM, Korn I, Plattner H (2009) Novel types of Ca^{2+} release channels participate in the secretory cycle of Paramecium cells. Mol Cell Biol 29:3605–3622
77. Ladenburger EM, Korn I, Kasielke N, Wassmer T, Plattner H (2006) An Ins(1,4,5)P3 receptor in Paramecium is associated with the osmoregulatory system. J Cell Sci 119:3705–3717
78. Eisen JA, Coyne RS, Wu M, Wu D, Thiagarajan M, Wortman JR, Badger JH, Ren Q, Amedeo P, Jones KM, Tallon LJ, Delcher AL, Salzberg SL, Silva JC, Haas BJ, Majoros WH, Farzad M, Carlton JM, Smith RK Jr, Garg J, Pearlman RE, Karrer KM, Sun L, Manning G, Elde NC, Turkewitz AP, Asai DJ, Wilkes DE, Wang Y, Cai H, Collins K, Stewart BA, Lee SR, Wilamowska K, Weinberg Z, Ruzzo WL, Wloga D, Gaertig J, Frankel J, Tsao CC, Gorovsky MA, Keeling PJ, Waller RF, Patron NJ, Cherry JM, Stover NA, Krieger CJ, del Toro C, Ryder HF, Williamson SC, Barbeau RA, Hamilton EP, Orias E (2006) Macronuclear genome sequence of the ciliate Tetrahymena thermophila, a model eukaryote. PLoS Biol 4:e286
79. Cock JM, Sterck L, Rouze P, Scornet D, Allen AE, Amoutzias G, Anthouard V, Artiguenave F, Aury JM, Badger JH, Beszteri B, Billiau K, Bonnet E, Bothwell JH, Bowler C, Boyen C, Brownlee C, Carrano CJ, Charrier B, Cho GY, Coelho SM, Collen J, Corre E, Da Silva C, Delage L, Delaroque N, Dittami SM, Doulbeau S, Elias M, Farnham G, Gachon CM, Gschloessl B, Heesch S, Jabbari K, Jubin C, Kawai H, Kimura K, Kloareg B, Kupper FC, Lang D, Le Bail A, Leblanc C, Lerouge P, Lohr M, Lopez PJ, Martens C, Maumus F, Michel G, Miranda-Saavedra D, Morales J, Moreau H, Motomura T, Nagasato C, Napoli CA, Nelson DR, Nyvall-Collen P, Peters AF, Pommier C, Potin P, Poulain J, Quesneville H, Read B, Rensing SA, Ritter A, Rousvoal S, Samanta M, Samson G, Schroeder DC, Segurens B, Strittmatter M, Tonon T, Tregear JW, Valentin K, von Dassow P, Yamagishi T, Van de Peer Y, Wincker P (2010) The Ectocarpus genome and the independent evolution of multicellularity in brown algae. Nature 465:617–621
80. Mackrill JJ (2010) Ryanodine receptor calcium channels and their partners as drug targets. Biochem Pharmacol 79:1535–1543
81. Tani S, Yatzkan E, Judelson HS (2004) Multiple pathways regulate the induction of genes during zoosporogenesis in Phytophthora infestans. Mol Plant Microbe Interact 17:330–337
82. Basu MK, Poliakov E, Rogozin IB (2009) Domain mobility in proteins: functional and evolutionary implications. Brief Bioinform 10:205–216
83. Long M, Betran E, Thornton K, Wang W (2003) The origin of new genes: glimpses from the young and old. Nat Rev Genet 4:865–875
84. Valas RE, Yang S, Bourne PE (2009) Nothing about protein structure classification makes sense except in the light of evolution. Curr Opin Struct Biol 19:329–334
85. Marchler-Bauer A, Lu S, Anderson JB, Chitsaz F, Derbyshire MK, DeWeese-Scott C, Fong JH, Geer LY, Geer RC, Gonzales NR, Gwadz M, Hurwitz DI, Jackson JD, Ke Z, Lanczycki CJ, Lu F, Marchler GH, Mullokandov M, Omelchenko MV, Robertson CL, Song JS, Thanki N, Yamashita RA, Zhang D, Zhang N, Zheng C, Bryant SH (2011) CDD: a Conserved Domain Database for the functional annotation of proteins. Nucleic Acids Res 39:D225–D229
86. Welch W, Rheault S, West DJ, Williams AJ (2004) A model of the putative pore region of the cardiac ryanodine receptor channel. Biophys J 87:2335–2351
87. Ponting CP (2000) Novel repeats in ryanodine and IP3 receptors and protein O-mannosyltransferases. Trends Biochem Sci 25:48–50

88. Kiselyov K, Mignery GA, Zhu MX, Muallem S (1999) The N-terminal domain of the IP3 receptor gates store-operated hTrp3 channels. Mol Cell 4:423–429
89. Kiselyov KI, Shin DM, Wang Y, Pessah IN, Allen PD, Muallem S (2000) Gating of store-operated channels by conformational coupling to ryanodine receptors. Mol Cell 6:421–431
90. Schug ZT, da Fonseca PC, Bhanumathy CD, Wagner L 2nd, Zhang X, Bailey B, Morris EP, Yule DI, Joseph SK (2008) Molecular characterization of the inositol 1,4,5-trisphosphate receptor pore-forming segment. J Biol Chem 283:2939–2948
91. Mead-Savery FC, Wang R, Tanna-Topan B, Chen SR, Welch W, Williams AJ (2009) Changes in negative charge at the luminal mouth of the pore alter ion handling and gating in the cardiac ryanodine-receptor. Biophys J 96:1374–1387
92. Montell C (2001) Physiology, phylogeny, and functions of the TRP superfamily of cation channels. Sci STKE 2001:re1
93. Ponting C, Schultz J, Bork P (1997) SPRY domains in ryanodine receptors (Ca(2+)-release channels). Trends Biochem Sci 22:193–194
94. Tae H, Casarotto MG, Dulhunty AF (2009) Ubiquitous SPRY domains and their role in the skeletal type ryanodine receptor. Eur Biophys J 39:51–59
95. van de Graaf SF, van der Kemp AW, van den Berg D, van Oorschot M, Hoenderop JG, Bindels RJ (2006) Identification of BSPRY as a novel auxiliary protein inhibiting TRPV5 activity. J Am Soc Nephrol 17:26–30
96. Cui Y, Tae HS, Norris NC, Karunasekara Y, Pouliquin P, Board PG, Dulhunty AF, Casarotto MG (2009) A dihydropyridine receptor alpha1s loop region critical for skeletal muscle contraction is intrinsically unstructured and binds to a SPRY domain of the type 1 ryanodine receptor. Int J Biochem Cell Biol 41:677–686
97. Otsu K, Willard HF, Khanna VK, Zorzato F, Green NM, MacLennan DH (1990) Molecular cloning of cDNA encoding the Ca^{2+} release channel (ryanodine receptor) of rabbit cardiac muscle sarcoplasmic reticulum. J Biol Chem 265:13472–13483
98. Zorzato F, Fujii J, Otsu K, Phillips M, Green NM, Lai FA, Meissner G, MacLennan DH (1990) Molecular cloning of cDNA encoding human and rabbit forms of the Ca^{2+} release channel (ryanodine receptor) of skeletal muscle sarcoplasmic reticulum. J Biol Chem 265:2244–2256
99. Durell SR, Hao Y, Nakamura T, Bakker EP, Guy HR (1999) Evolutionary relationship between K(+) channels and symporters. Biophys J 77:775–788
100. Aravind L, Koonin EV (1998) A novel family of predicted phosphoesterases includes Drosophila prune protein and bacterial RecJ exonuclease. Trends Biochem Sci 23:17–19
101. Anantharaman V, Koonin EV, Aravind L (2001) Regulatory potential, phyletic distribution and evolution of ancient, intracellular small-molecule-binding domains. J Mol Biol 307:1271–1292
102. Andersson JO (2005) Lateral gene transfer in eukaryotes. Cell Mol Life Sci 62:1182–1197
103. Hehemann JH, Correc G, Barbeyron T, Helbert W, Czjzek M, Michel G (2010) Transfer of carbohydrate-active enzymes from marine bacteria to Japanese gut microbiota. Nature 464:908–912
104. Whitaker JW, McConkey GA, Westhead DR (2009) The transferome of metabolic genes explored: analysis of the horizontal transfer of enzyme encoding genes in unicellular eukaryotes. Genome Biol 10:R36
105. Torruella G, Suga H, Riutort M, Pereto J, Ruiz-Trillo I (2009) The evolutionary history of lysine biosynthesis pathways within eukaryotes. J Mol Evol 69:240–248
106. Richards TA, Soanes DM, Foster PG, Leonard G, Thornton CR, Talbot NJ (2009) Phylogenomic analysis demonstrates a pattern of rare and ancient horizontal gene transfer between plants and fungi. Plant Cell 21:1897–1911
107. Goulas T, Arolas JL, Gomis-Ruth FX (2011) Structure, function and latency regulation of a bacterial enterotoxin potentially derived from a mammalian adamalysin/ADAM xenolog. Proc Natl Acad Sci USA 108:1856–1861

Chapter 8
Techniques and Methodologies to Study the Ryanodine Receptor at the Molecular, Subcellular and Cellular Level

Cedric Viero, N. Lowri Thomas, Joanne Euden, Sammy A. Mason, Christopher H. George, and Alan J. Williams

Abstract In excitable tissues, the ryanodine receptor Ca^{2+} release channel (RyR) protein complex regulates excitation-contraction coupling, exocytosis, gene expression and apoptosis. Defects in RyR function, in genetic or acquired pathologies, lead to massive disruptions of Ca^{2+} release that can be lethal. Therefore, RyR has emerged as a putative therapeutic target and an increasing number of RyR-targeting drugs are currently being tested.

Nonetheless this large-size channel is still a mystery in terms of structure, which hinders full characterization of the properties of this central protein. This chapter is dedicated to the methods available to examine RyR structure and function. The aim of the article is to concentrate on contemporary methodologies rather than focusing overtly on the progress that has been achieved using these techniques. Here we review a series of reliable approaches that are routinely employed to investigate this channel. Technical limitations are discussed, and technological developments are presented. This work is not a handbook, but it can be used as a resource and a starting point for the investigation of RyR at different levels of resolution.

Keywords Ryanodine • Calcium channel • Lipid bilayer • Single channel recording • Cardiac myocyte • Transfection • HEK293 • Sparks • Cryo-EM • Recombinant expression

C. Viero (✉) • N.L. Thomas • J. Euden • S.A. Mason • C.H. George • A.J. Williams
Department of Cardiology, Wales Heart Research Institute, School of Medicine, Cardiff University, Heath Park, Cardiff CF14 4XN, UK
e-mail: VieroCL@cardiff.ac.uk; thomasnl1@Cardiff.ac.uk; Eudenj@cardiff.ac.uk; MasonSA@cardiff.ac.uk; georgech@cf.ac.uk; WilliamsAJ9@cardiff.ac.uk

M.S. Islam (ed.), *Calcium Signaling*, Advances in Experimental Medicine and Biology 740, DOI 10.1007/978-94-007-2888-2_8,

Introduction

The Role of the Ryanodine Receptor (RyR)

Cell signaling pathways involving calcium ions (Ca^{2+}) require stimulators, receptors, transducers (or 2nd messengers) and effectors. In excitable tissues (nerves and muscles), the ryanodine receptor calcium release channel (RyR) holds a unique position, playing at the same time the role of receptor, amplifier and effector, thus enabling the propagation and regulation of Ca^{2+} signals.

Upon plasma membrane depolarization, voltage-gated L-type Ca^{2+} channels open, leading to the activation of RyRs either by entry of a small amount of Ca^{2+} into the cytosol (Ca^{2+}-induced Ca^{2+} release (CICR) in cardiac muscle cells) or mechanically (in skeletal muscles). RyR channels sit in the membrane of the endo/sarcoplasmic reticulum (ER/SR) and control the release of Ca^{2+} from intracellular stores. The resultant massive Ca^{2+} flux from the ER/SR into the cytosol through clusters of RyRs throughout the cell eventually produces a global increase in the intracellular Ca^{2+} concentration ($[Ca^{2+}]_i$) that is necessary for contraction in muscles, exocytosis in neurones or apoptosis if the Ca^{2+} level reaches the corresponding threshold. In muscles this phenomenon is referred to as excitation-contraction coupling (ECC) [1]. Hence RyR is a pivotal protein at the interface between plasma membrane and ER/SR which is able to decode these two environments and integrate signals between the extracellular space and the intracellular stores. Moreover, depending on the cell model, RyR can modulate or be modulated by Ca^{2+} signals initiated by other channels, such as inositol trisphosphate receptors ($InsP_3R$) [2] and transient receptor potential (TRP) channels [3]. Therefore RyRs serve as cell signaling integration centres that are at the origin of various types of Ca^{2+} signals (different in terms of size, spread and frequency).

So far three isoforms have been identified for the human RyR. RyR1 is expressed in skeletal muscle and Purkinje neurones [4], RyR2 is abundant in cardiac muscle and can be found in brain and pancreatic cells [5], and RyR3 is the predominant isoform in smooth muscle, brain and is detected in the testis [6]. Their different level of expression in various organs correlates to distinct functions in physiological and pathological processes, and that variation impinges on the characterisation of these receptors. Indeed the abundance of RyR1 and RyR2 in muscles and the critical role they play in these tissues have contributed to detailed investigations of the structure and function of these isoforms, whereas our understanding of RyR3 function is still unclear. Therefore we will concentrate in this chapter on techniques developed to study RyR in muscular tissues.

Why Study RyR (dys)function?

The finely orchestrated process of ECC involves a number of exquisitely regulated protein components. Intrinsic alteration of these proteins, or the environment in which

they function optimally is known to cause contractile impairment, arrhythmia, or other pathological consequences. The dysfunction of RyRs, usually apparent as enhanced Ca^{2+} release at rest appears to underlie several inherited and acquired skeletal muscle and cardiac diseases (for review see [7]).

In skeletal muscle, malignant hyperthermia (MH) and central core disease (CCD) result from mutations in RyR1. MH is a pharmacogenetic disease triggered by exposure to halogenated anaesthetics and characterised by muscle rigidity, respiratory and metabolic acidosis and a sudden rise in body temperature [8]. CCD is a related but distinct disorder which generally presents as nonprogressive muscle weakness and hypotonia and some patients are also MH susceptible [9]. The disorder derives its name from the finding of amorphous central areas or cores that lack mitochondria in skeletal muscle fibres. Both conditions are thought to result from RyR1 dysfunction, causing excessive mobilisation of Ca^{2+} from the SR with cores being explained by the fact that, with such perturbation of Ca^{2+} regulation, central mitochondria go into Ca^{2+} overload and die [7]. There has been speculation that the severity of the pathophysiological responses seen with MH and CCD could depend upon the mutational locus. It has been noted that MH susceptible patients who lack clinical myopathies are more likely to carry a mutation at the N-terminus of the RyR protein, while those who present with clinical myopathy exhibit a C-terminal bias [10]. Some CCD mutations are also thought to affect the Ca^{2+} permation pathway of the channel, making them unresponsive to activation by agonists and by depolarization of the sarcolemma. Thus it appears that two distinct molecular mechanisms can lead to muscle weakness in CCD patients: (i) some mutations cause "leaky channels" which exhibit sensitized activation, leading to depletion of the Ca^{2+} store and impairment of muscle function, (ii) whereas "EC uncoupling" is characterized by a deficit in ECC [11].

Mutations in RyR2 are associated with catecholaminergic polymorphic ventricular tachycardia (CPVT), a disorder associated with stress/exercise-induced arrhythmia leading to possible sudden cardiac death (SCD) in the absence of any structural heart disease [12]. These symptoms are again attributed to inappropriate Ca^{2+} release from hypersensitive, "leaky" mutant channels. However, the precise molecular mechanisms responsible for hypersensitivity have not yet been fully resolved (reviewed in [13]) and there does not seem to be any relationship between the severity of phenotype and mutational locus, as is evident in MH/CCD. One putative mechanism proposed to account for dysfunctional channel behaviour in MH/CCD and CPVT is that mutation weakens intra-molecular interactions between key domains that stabilize the closed channel conformation [14]. In particular, it has been shown *in vitro* that exposure to a peptide corresponding to a small portion of the central domain (residues in RyR1: 2442–2477 and RyR2: 2460–2945) causes competitive binding to the N-terminal domain of the channel. This leads to the disruption ("unzipping") of an important stabilizing interaction between these regions of the polypeptide. Eventually it results in channel hypersensitisation and Ca^{2+} leak. These effects are abolished with the introduction of a known pathological mutation (RyR1: R2458C and RyR2: R2474S), leading the authors to suggest that these domains are involved in the mechanism of channel regulation, and that mutation causes instability of the closed state causing the hypersensitisation effects seen [15, 16].

In addition, these authors and others have hypothesized that dantrolene (used to treat MH), and K201 (a new drug potentially useful in the treatment of CPVT) remedy channel dysfunction by somehow "re-zipping" these weakened domain interactions [17, 18]. The "unzipping" theory has been extended to explain proarrhythmic Ca^{2+} leak from RyR2 in heart failure (HF) [19]. Work by Yamamoto et al. [20] implies that RyR2 activity is increased as a result of catecholaminergic stimulation, which is known to be upregulated in the HF state [21]. Marks and colleagues proposed that in HF, with beta-adrenergic activation, RyR2 is phosphorylated by protein kinase A (PKA), which results in the dissociation of the channel stabilizing protein FKBP12.6 (sometimes referred to as calstabin2), hence leading to diastolic SR Ca^{2+} leak [21]. A similar mechanism, with nitrosylation rather than phosphorylation as the culprit, has been proposed for RyR1 dysfunction in muscular dystrophy [22]. However, the mechanism itself has been the subject of much controversy [23–25] and has been deconstructed elsewhere [26, 27].

As RyR dysfunction has been implicated in so many disorders of skeletal and cardiac muscle it is not surprising that its study has become an ever-expanding area of research and the design of therapeutic agents to correct the abnormal channel function underlying these pathologies is a major goal for all working in this field. New drugs aim at normalizing RyR function at rest, preventing aberrant opening and Ca^{2+} leakage, as discussed in the recent review by Thireau and co-workers [28]. This chapter will focus on the techniques used to investigate multiple aspects of RyR structure and function. While study of the channel in its native muscle is the most physiological approach to take, it is not always the most useful or convenient and the use of cloned RyR isoforms and recombinant expression techniques, as well as biophysical study of the channel outside the cell have greatly facilitated the elucidation of the molecular basis of Ca^{2+} release functionality. However, due to the vast size of RyR and the complexity of its three dimensional architecture [29], the use of heterologous expression systems to generate full-length, functional recombinant protein in sufficient quantity has been a challenge (see section "Heterologous Cell Systems to Study RyR Function" and [30–33]). This has meant that dissection of the protein into smaller fragments in order to ease recombinant manipulation and expression has been beneficial, especially in the elucidation of the crystal structure of RyR domains (see section "Crystal Structure of the N-Terminus" and [34, 35]) and more recently in the engineering of knock in mouse models of RyR-related disease [25, 36, 37].

RyR Structure

To understand RyR function, it is essential to know the structural determinants of the different elements of RyR that make the channel stable, allow interaction with other proteins, and cause opening to release huge amounts of ions in short periods of time.

The use of electron microscopy (EM) has been pivotal in elucidating structural components of RyRs. Many reviews have outlined the challenges of obtaining high-resolution structures and progress in the last few years has seen structures reaching subnanometer resolutions bringing greater insight into the organisation of RyRs. This section will merely introduce the various methods that can be used in conjunction with electron microscopy and will not necessarily detail results, which is outside the scope of the current chapter. For more in depth reviews see the following references [38–40].

RyR Domain Architecture

The functional RyR channel is a homotetramer. RyRs are composed of two main domains: the cytoplasmic assembly (CA) which adopts a large square-prism shape (also referred to as the "foot" domain [41] measuring 280 × 120 × 60 Å) and a smaller square-tapering prism region which corresponds to the transmembrane assembly (TM), measuring 120 × 120 × 60 Å [29] (Shown in Fig. 8.1).

Negative Staining

As mentioned above, the enormous size and structural complexity of RyRs has greatly impeded their detailed structural analysis. Until a 3D crystal structure has been obtained for the RyRs, electron microscopy (negative stain-EM and cryo-EM) remains a relatively simple means of obtaining vast amounts of structural information, albeit at a much lower resolution. The first images of purified RyRs were from RyR1 and were generated over 20 years ago from negative-stain electron micrographs [42]. In this technique, molecules are adsorbed to a carbon grid and coated in an electron-dense heavy film, such as uranyl acetate, generating a high contrast image. Although a simple procedure, and ideal for initial characterisation, the major disadvantage of negative stain is collapse of macromolecular structure due to dehydration during preparation of samples, resulting in distortion of the sample and therefore loss of resolution. Incomplete embedding of stain can also lead to artefacts in the final structure obtained. The resolution limit of negative stain EM is around 20 Å therefore other methods to gain structural information are often used in conjunction with this technique.

Cryo-EM

In cryo-EM the sample always remains in solution, preventing collapse or distortion of the sample as seen in negative stain-EM. In this technique the sample is vitrified which involves applying a few drops of the aqueous sample onto an EM grid

containing a carbon support film and rapidly plunging into liquid ethane. This results in thin layers of vitreous ice in which the macromolecules are embedded. Until relatively recently continuous carbon substrate grids were used for vitrification, which meant that RyRs adsorbed to the support film possibly in a preferred orientation. Current techniques in single particle cryo-EM analysis use holey carbon grids so that the RyRs are suspended in the ice over the holes. This allows for greater resolution of the 3D reconstruction of the protein due to an increase in random orientations of the sample within the vitreous ice [43, 44].

The advances in techniques for sample preparation have enhanced our knowledge of RyR structure dramatically from early low-resolution structures (30 Å) with RyR1 to cryo-EM reconstructions reaching subnanometer resolutions [45, 46]. Image reconstruction has also greatly improved by increasing the numbers of single particles chosen for image analysis to several thousand, and new approaches use several hundreds of thousands. This serves to generate a higher number of structures with similar conformations enabling structures with higher signal to noise ratios to be obtained from class averages. Cheng and Walz provide an excellent review on the methodologies used in processing of cryo-EM images and final image reconstruction [43]. As no crystal structures for the complete RyR tetramer exist, density maps must be interpreted by visual analysis or by using atomic coordinates of other proteins thought to be similar in structure. The two crystal structures most commonly used for this purpose are those of the K^+ channels KcsA [47] and MthK [48]. Although both are very similar in overall architecture KcsA is known to be in a closed conformation whereas MthK is thought to resemble an open conformation. The main structural differences in these two crystal structures are attributable to the absence or presence of an observed kink in the inner helices respectively. The atomic coordinates which best fit the cryo-EM data are then used for image reconstruction.

Despite differences in methods of data collection, image processing and 3D reconstruction, published structures are mostly in good agreement with one another with some differences in the interpretation of higher resolution structures particularly the helices visualised in the TM domain. Figure 8.1 shows the 9.6 Å cryo-EM structure published by Serysheva et al. Very small differences, as determined by cryo-EM difference maps, can be observed in the structures of the RyR isoforms [45, 46].

Building a Picture of RyR Domain Localisation

Although vast in size, the CA contains numerous cavities and areas of empty space where accessory proteins and protein modulators are thought to bind and interact with RyR to modulate function. Radermacher et al. [49] were the first to identify different globular regions in the CA and divided it into 10 subdomains based on cryo-EM reconstructions (see Fig. 8.1). Each domain is thought to interact with various modulators of RyR, as outlined in section "Functional Study *In Situ*: Ca^{2+} Sparks".

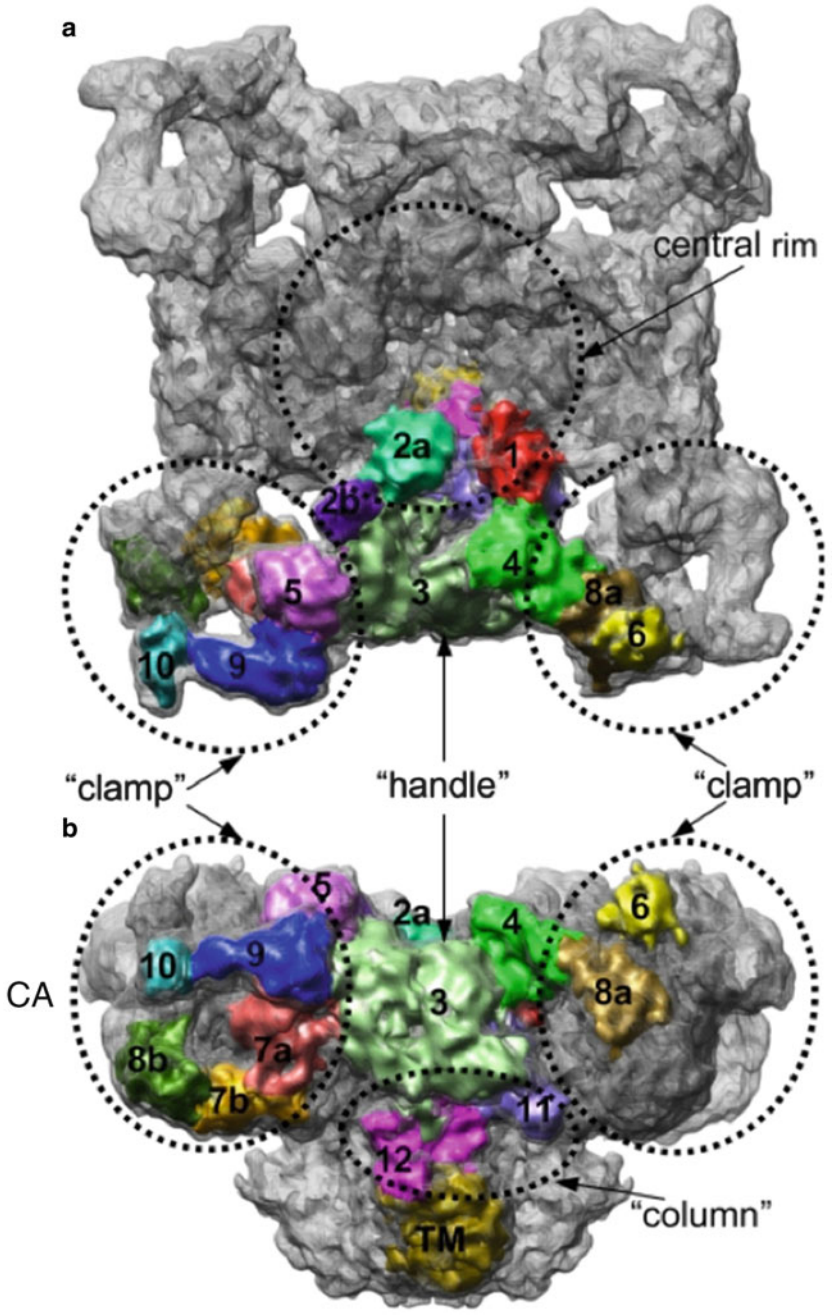

Fig. 8.1 Closed structure of RyR1 at 9.6 Å highlighting the clamp, handle and central rim domains [29] (Copyright 2008 National Academy of Sciences, U.S.A.). (**a**) Shows the cytoplasmic view and (**b**) the side view. *Coloured/numbered* regions relate to subdomains originally mapped by Radermacher et al. [49]

Mapping the 3D Structure in Terms of Binding Sites

Although current cryo-EM structures have achieved 1 nm resolutions, tracing the polypeptide backbone is still not possible in these structures. Several approaches have been used to identify where specific sequences are located in the 3D structure or where accessory proteins bind. These can be divided into two main strategies. The first involves a biochemical identification of peptide regions in the RyR sequence that interact with other accessory proteins (i.e. co-immunoprecipitation (IP) of peptides or GST-fusion proteins containing RyR or accessory protein sequences). The second is based on difference mapping of WT and mutant RyR cryo-EM structures, either with or without bound modulators, antibodies or with green fluorescent protein (GFP) inserted at defined positions in the primary sequence. As this section discusses structure, biochemical identification of binding sequences will not be further elaborated upon here and accessory protein interaction sites are reviewed in [50]. The reader can also refer to [51, 52] for particular examples of measurements of RyR biochemical status (co-IP analysis and phosphorylation-site antibodies respectively).

Difference Mapping of cryo-EM Structures Using Ligands/Modulators

Information regarding binding sites of various modulators of RyR function has been derived from cryo-EM difference maps. By adding protein modulators, toxins or RyR accessory proteins, the cryo-EM maps obtained in the absence of the chosen ligand can be subtracted from the map in the presence of the ligand. This generates a difference map with the additional positive density most likely attributable to the bound ligand. Examples of RyR ligand binding sites determined by cryo-EM difference mapping include: FKBP12 [53], calmodulin (CaM) [54], CLIC2 [55], imperatoxin A [56] and natrin [57].

Difference Mapping of cryo-EM Structures Using GFP Tags

GFP is a well-established and reliable reporter of protein folding, as fluorescence only occurs when the protein is in its correct conformation. The technique of using GFP fusion proteins in conjunction with cryo-EM to ascertain the location of surface exposed residues was first demonstrated using chimeric GFP-virus particles [58]. As well as being visualized by fluorescence microscopy, GFP is also large enough to be detected in cryo-EM maps.

Generating GFP chimeras of RyRs is relatively simple and involves inserting the DNA sequence of GFP at defined positions into the cDNA of RyR, usually at positions that are thought to be solvent exposed. As the CA of RyR is full of cavities and crevices this particular technique has enabled the precise locations of numerous amino acids in the primary sequence of RyR to be mapped to the three dimensional structure. Such examples include the localization of the three divergent regions of

RyRs [59–61], serine phosphorylation sites [62, 63], regions that contain mutations resulting in MH and CCD in RyR1 [64], and in CPVT in RyR2 [65] (see section "Why Study RyR (dys)function?" and Figs. 8.2 and 8.3). However, caution should be taken in the interpretation of GFP insertions as they can potentially affect overall protein folding and thus give rise to false interpretation of amino acid or domain localization. Functional characterisation of chimeric RyRs, compared to wild type RyRs, should be carried out in conjunction with this technique to determine whether global conformation has been compromised. Van Petegem's group has recently shown that the GFP localization determined by cryo-EM is ambiguous (see sections "Crystal Structure of the N-Terminus" and "Heterologous Cell Systems to Study RyR Function") highlighting the need for caution in analysis.

Intrinsic Lattice Formation

As well as using techniques to study structure of single RyR particles, electron microscopy has been used to study the phenomenon of lattice formation. This refers to the unique way in which RyRs may assemble in the membrane to enhance the signaling capability upon ligand binding [67]. Yin et al. [68] first showed that RyRs possess an intrinsic ability to associate into large two-dimensional (2D) arrays to form a chequerboard-like pattern. Following purification of RyR1 from rabbit skeletal muscle, concentrated protein was dialysed against buffers of various ionic strengths and mounted onto carbon grids for electron microscopy. The reader is referred to the paper for full details of this technique. Recently, the use of positively charged lipid membranes to capture RyR in reconstituted arrays has enabled small crystals to be obtained. They are consistent with the previously observed 2D arrays seen in native SR of muscle tissues. For more detail on the use of lipid membranes in crystallographic trials, information can be found in the article by Yin et al. [69].

Crystal Structure of the N-Terminus

A recent approach used to gain structural insights into RyR has been to express separate domains and attempt the crystallisation of smaller fragments of around 200 amino acids. By subcloning smaller RyR constructs into pET vectors and expressing in bacteria, higher yields of protein can be generated resulting in the recent crystal structures of the N-terminal domain (NTD) of rabbit RyR1 and mouse RyR2 at subnanometer resolutions [35, 70]. This approach has also enabled the structural investigation of several disease causing mutations in both RyR1 and RyR2. Although the expression of the NTD in isolation represents a static picture, separate from the whole protein, this technique has allowed an insight into how mutations in this region can affect function and overall protein stability. Discrete differences between the isoforms can also be detected when comparing crystal structures.

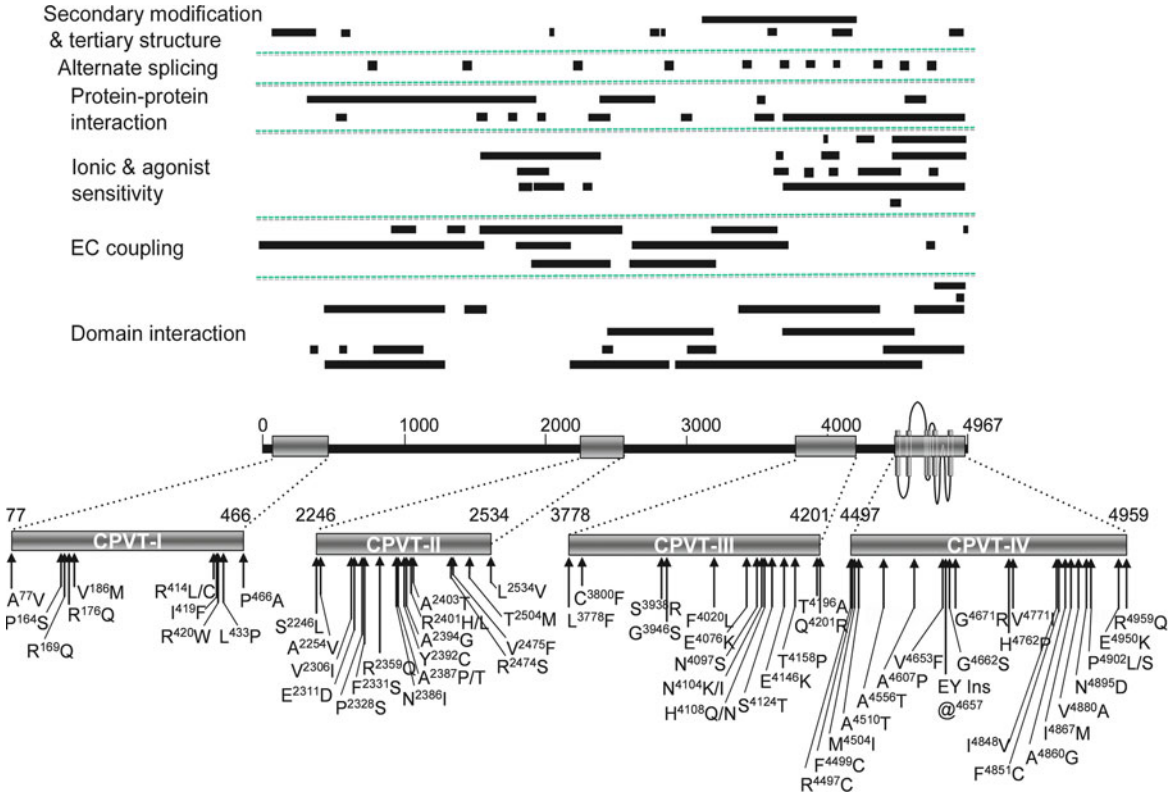

Fig. 8.2 RyR2 polypeptide domain organization. The diagram depicts ligand binding sites, localization of regulatory regions, and sites of mutations. Clusters of CPVT mutations can here clearly be identified. The reader is referred to the article by George and colleagues published in 2007 (figure used and minimally adapted with permission from Elsevier) to understand how these domains were mapped [27]

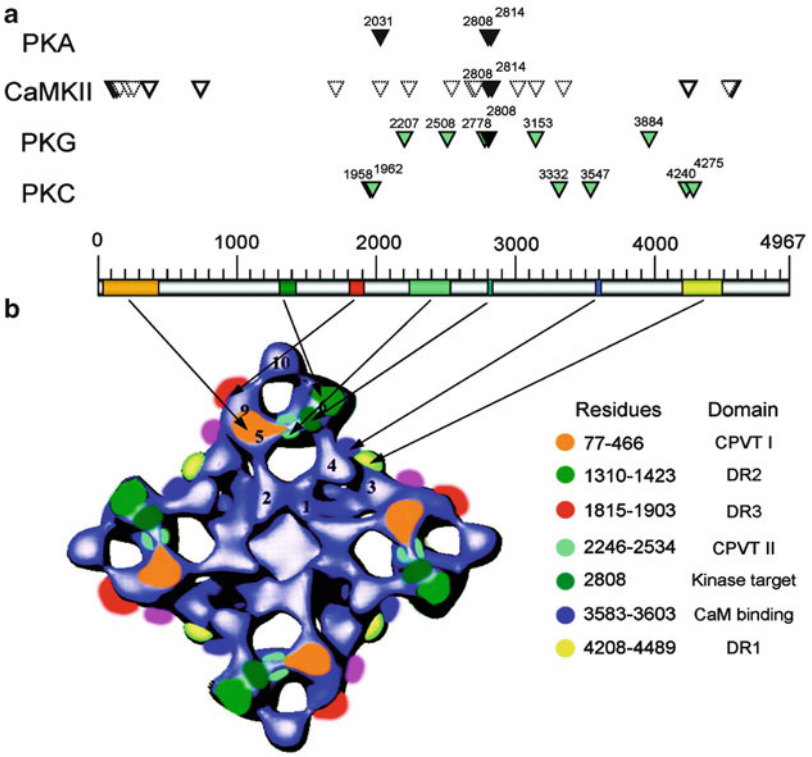

Fig. 8.3 RyR2 is modulated by phosphorylation. These panels illustrate the schematic phosphorylation site map (**a**) as well as the localization of critical regions for RyR conformation and (dys)function (**b**) as presented by George in 2008, and used with permission from Oxford University Press [66]. This localization of functional domains was based on data from the cryo-EM work of Chen and Wagenknecht (see 58). Newer data from Van Petegem's group though suggest that at least some of these domains are probably mislocalized using cryo-EM [134]

Structural Influences of RyR Mutations – Protein Stability Assays

Other methods to assess protein stability and overall protein secondary structure include circular dichroism (CD) and nuclear magnetic resonance (NMR) assays. As NMR is a useful tool for small molecules, the expression of recombinant sub-fragments of RyR opens up these additional methodologies as a means of assessing possible effects of mutations on channel domain function compared to the full-length RyRs.

A relatively recent method in protein characterisation is the ThermoFluor assay, a fluorescence based thermal shift assay which utilises the environmentally sensitive dye, Sypro-Orange [71]. This is a simple technique and uses very small amounts of protein sample (10 μg per sample of protein [35]). Results using this technique, in conjunction with recently obtained crystallographic data, have identified a region rich in disease-associated mutations within the NTD [35]. Together with thermal melts, NMR and CD information it seems that mutations cause only local changes in structure with no loss to overall protein stability. This

has led to the proposal that disease causing mutations affect the interaction of RyRs with various modulators without causing any global change in protein structure [35, 70]. However, different data have suggested otherwise, such as the results obtained by Ikemoto and co-workers [72].

The characterization of the whole structure of RyR is still a challenge because of the size of the channel. Further technical progress should be made in the near future to allow improvements of our understanding of the structure-function relationship in this protein.

RyR Function

Based on our knowledge of the structural components that form the homotetrameric RyR protein, the study of its behaviour in terms of function can be approached in two different but complementary ways. First the investigator can look at native proteins to examine RyR activity in a physiological-like environment where the interactions with accessory proteins can be preserved, the level of phosphorylation and redox state can be conserved and the natural cellular influences can still be intact if it is required. However this approach increases the level of complexity and is dependent on the amount of native material. Alternatively the use of recombinant expression techniques for RyR enables both the characterization of the isolated protein in a simplified system and the introduction of straightforward genetic manipulations (for example single-point mutations). To overcome the issue of the loss of the physiological relevance, it is possible to add back the elements that participate in the regulation of RyR functionality. This section will discuss issues concerning these methods, and describe how they have been adapted for working with RyR.

Functional Study In Situ: Ca^{2+} Sparks

Due to their intracellular location, techniques developed to study the function of RyR *in situ* (primary cells and tissues) are based on the visualization of Ca^{2+} flux passing from the ER/SR into the cytosol. This has been rendered possible by the use of membrane-permeable Ca^{2+} sensitive fluorescent dyes also known as fluorescent Ca^{2+} probes or indicators, such as the ratiometric fura-2 which is appropriate to measure overall intracellular Ca^{2+} changes. These molecules share a similar structure with Ca^{2+} binding compounds or Ca^{2+} chelators such as EGTA (ethylene glycol tetraacetic acid) and BAPTA (1,2-bis(o-aminophenoxy)ethane-N,N,N′,N′-tetraacetic acid) [73]. To introduce these fluorescent Ca^{2+} indicators into cells, acetoxymethyl (AM) ester derivatives of these compounds are employed. Changes in fluorescence intensity reflect the changes in binding of free Ca^{2+} to the indicator. Hence it becomes possible to monitor global variations of the $[Ca^{2+}]_i$ that mainly result from the release from intracellular stores through RyR during ECC for

instance. Nonetheless since different types of Ca^{2+} signals can then be mixed together (Ca^{2+} influx, Ca^{2+} extrusion, Ca^{2+} reuptake, involvement of other channels such as $InsP_3R$ and TRP channels), it is difficult to identify the precise contribution made by RyR. Of course, there are broadly selective drugs that are able to activate or inhibit RyR in myocytes or neurones. The most well-known are caffeine (agonist), ryanodine (agonist within the nanomolar range and antagonist within the micromolar range), 4-chloro-m-cresol (agonist), dantrolene (antagonist), ruthenium red (antagonist), tetracaine (antagonist) and procaine (antagonist). While these drugs can be useful in giving an estimation of the involvement of RyR in $[Ca^{2+}]_i$ responses, they are not able to provide information on the localization and the number of active RyRs. In addition, we know that most of these compounds are not specific. Moreover caffeine interacts with some of the fluorescent Ca^{2+} indicators inducing a quenching of the fluorescence signal intensity [74].

To examine the participation of RyRs within a myocyte, a Ca^{2+} imaging method using confocal microscopy has been established to detect, monitor and analyze brief Ca^{2+} events arising from RyR clusters also referred to as Ca^{2+} release units (CRU). These elementary events as visualized by their corresponding fluorescence intensity change were first described by Cheng and collaborators in 1993 who coined the term "Ca^{2+} sparks" [75]. The discovery of these confined (~2 μm diameter), brief (~50 ms), small amplitude (twofold increase in fluorescence intensity) Ca^{2+} transients [76] provided an insight into the complex Ca^{2+} signaling involved in ECC. Measurements of Ca^{2+} sparks require the combination of confocal microscopy with a high acquisition rate and the use of fluorescent Ca^{2+} indicators displaying a large dynamic range. Indicators of choice are the non-ratiometric fluo-3 and fluo-4 dyes, due to their convenient Kd, visible spectrum wavelengths of excitation and emission, and their enhanced intensity compared to more traditional ratiometric dyes (for review on the topic of Ca^{2+} dye comparison, see [77, 78]).

Preparation of Cells and Spark Recording

To date Ca^{2+} sparks or spark-like events have been observed in cardiac cells, skeletal muscle cells, smooth muscle myocytes, neuroendocrine cells, and neurones (for review, see [76]). Depending on the cell type and on the culturing conditions, spark properties may change over time due to structural and functional cell remodelling (mainly the ER/SR content is subject to variation) [79].

Unlike the loading protocol necessary to record global $[Ca^{2+}]_i$ changes (i.e. incubation with the esterified-form of the Ca^{2+}-dependent fluorescent indicator for >30 min), Ca^{2+} spark detection requires a "gentle" dye loading step. It is critical to minimize the basal fluorescence intensity and the loading of organelles. For this, the concentration of esterified dye (to enable the crossing of the plasma membrane) and the loading time should be reduced (for example see [79]). Alternatively, investigators have carried out experiments on permeabilized myocytes (often using the natural detergent saponin) which is a reliable method to control the intracellular environment [80, 81]. Moreover both spontaneous [82, 83] and induced (by agonists

of RyRs for example or electrical stimulation; [84]) Ca^{2+} sparks can be examined, depending on the type of cellular phenomenon and on the level of "physiological relevance" one is interested in.

Dissection of Ca^{2+} spark kinetics requires millisecond resolution and many confocal systems are nowadays equipped with resonant scanning mirrors able to collect images at above 30 frames per second. A useful way of monitoring these rapid spatially-restricted Ca^{2+} events at suitably high frame rates is to create line scan images (usually x axis versus time t). However the recording of line scans presents limitations in the study of Ca^{2+} spark diffusion and does not afford an effective assessment of an entire population of elementary events within a cell. Therefore, encouraged by improvements in temporal and spatial resolutions of newer confocal systems, researchers tend to monitor sparks in 2D over time (3D: x, y, t). This approach allows a more complete picture of the spark activity within one confocal slice of a cell (Fig. 8.4) or within one cell [87]. From this, it is even possible to produce and analyze pseudo line scans with the help of specific spark detection and analysis softwares (for example see [88]).

Analysis of the Data

The classical manner of detecting and analyzing Ca^{2+} spark events consists of manually selecting Ca^{2+} spark sites that were visibly apparent on the fluorescence-dependent Ca^{2+} imaging recording. Usually a circular "region of interest" is drawn (of sufficient diameter to preserve spatial resolution) and the resultant plot of the fluorescence intensity level versus time is expressed as the change in fluorescence (ΔF) divided by the basal fluorescence (F_0). Any increase of the fluorescence intensity above a determined threshold (typically 1–2 standard deviations depending on the signal-to-noise ratio) will be considered to be a potential Ca^{2+} spark, provided the amplitude and the lifetime of the event are within the range of the "normally" accepted values mentioned above. Measurement of Ca^{2+} sparks is quite time-consuming since spark analysis requires the detection of hundreds of events to ensure statistical power.

The development of powerful algorithms has been a huge advance in this field and nowadays a plethora of Ca^{2+} spark detection and analysis programs are available. These automated programs first filter the normalized raw image (by setting the threshold criterion described above) to obtain a binary image for easy detection of sparks. The conventional parameters studied (Fig. 8.5) include: amplitude, duration (full duration at half maximum of the fluorescence intensity), spatial spread (full width at half maximum of the fluorescence intensity), and frequency (at spark sites, of spark events per cell) [93, 94]. Moreover according to the temporal resolution of the confocal system employed, kinetics of Ca^{2+} sparks can be examined in details leading to the determination of complementary parameters such as rise time and decay time constant [95, 96]. For example, an acquisition speed >100 frames per second should give a sufficient number of data points.

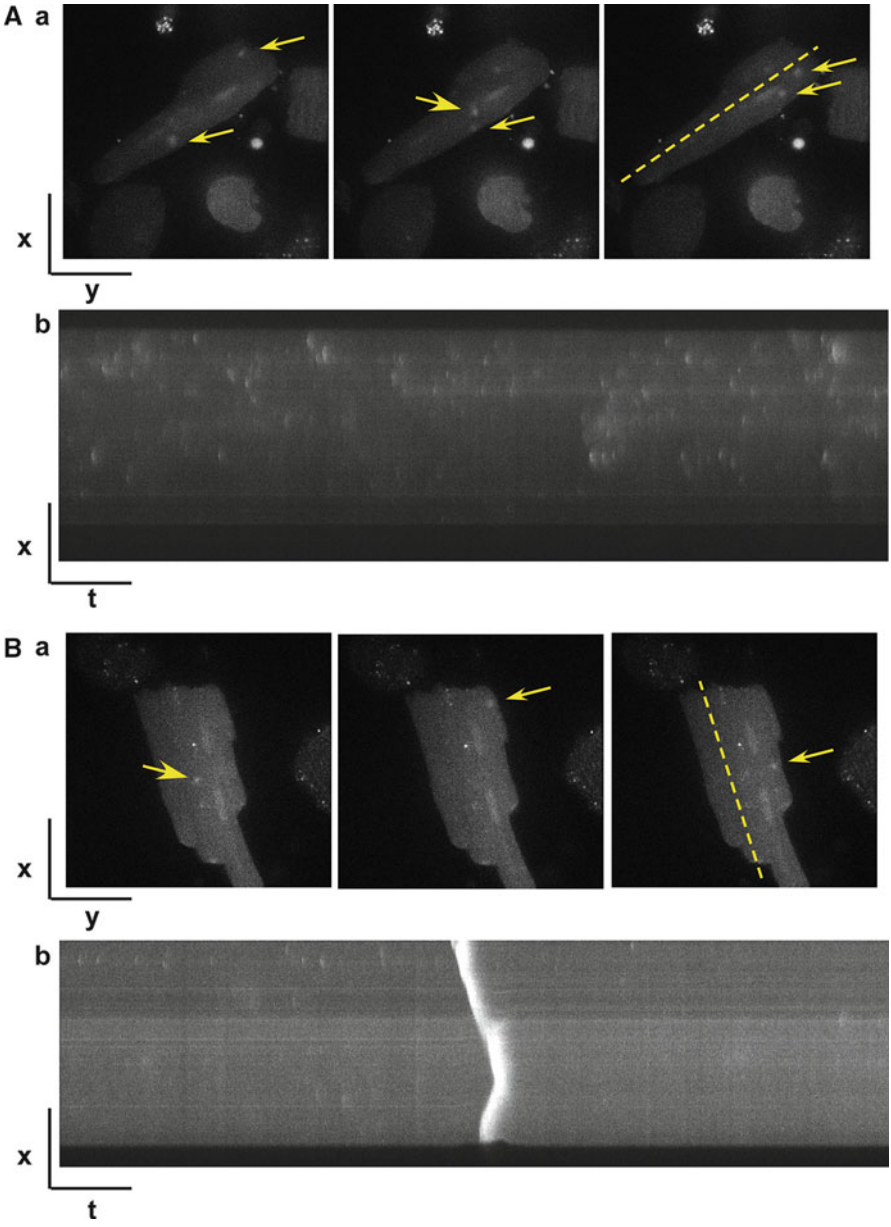

Fig. 8.4 Examples of elementary Ca^{2+} event recordings. Freshly isolated adult rat cardiac ventricular myocytes were loaded with fluo-4 and 2D (x, y) confocal pictures were collected over time (t). Spontaneous localised Ca^{2+} events, occurring at different time points, are indicated by *yellow arrows* (Aa and Ba). Images of these two representative myocytes were processed in ImageJ software (W. Rasband, NIH, USA). In both cases, longitudinal lines were drawn across each myocyte (see *dashed yellow lines*) to produce pseudo line scans (x, t; Ab and Bb), as can be seen below each row of xy images (Aa and Ba). While the top cell (**a**) is spontaneously active in terms of Ca^{2+} sparks, the bottom cell (**b**) displays a global Ca^{2+} wave across the entire cell (Viero, *unpublished*). Detailed protocols of spark imaging can be found in the excellent manuals written by Cannell and colleagues [85, 86]

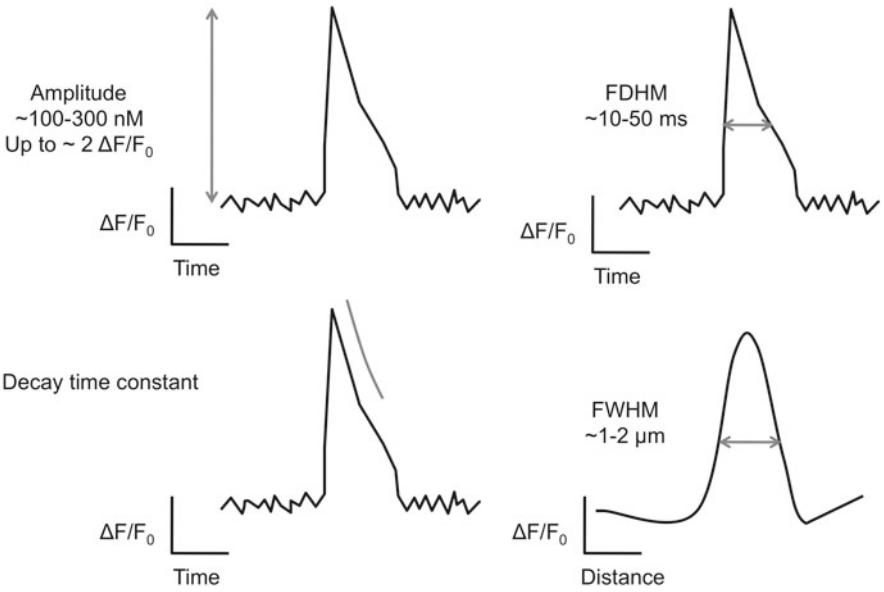

Fig. 8.5 Ca^{2+} spark analysis: typical parameters studied. This panel depicts four of the most representative parameters conventionally investigated to describe Ca^{2+} spark characteristics: amplitude (expressed as $[Ca^{2+}]_i$ increase or $\Delta F/F_0$ where ΔF is the fluorescence level subtracted from the background and F_0 is the basal fluorescence), full duration at half maximum (FDHM), decay time constant and full width at half maximum (FWHM, presented here as an averaged spatial profile). Important parameters that can be further examined are for example rise time and frequency (in a cell or at a spark site). The values reported here were taken from Niggli and Shirokova [89]. Powerful algorithms have been developed to automatically detect and analyze elementary Ca^{2+} events [90–92]

Ideally it is advisable to compare the output parameters coming from different programs and compare them with the "manual" method. The investigator should ensure that the program does not entail too strong a filtering step that might blunt the peak of the elementary transients. Another issue comes from the occurrence of out-of-focus Ca^{2+} sparks. When detected, they tend to reduce the global fluorescence intensity of elementary event populations and therefore lead to an underestimation of the mean amplitude distributions [97]. To overcome this problem, alternative methods are available such as the loose-seal patch clamp method that allows in-focus Ca^{2+} sparks to be repeatedly evoked and thus minimizes the blunting effect due to the out-of-focus Ca^{2+} events [98]. Another technique involves the local photorelease of caged Ca^{2+} [99]. Interestingly these methods revealed that even in such optimized conditions, the amplitude of sparks is quite variable and several populations of events co-exist at the same spark sites.

Many studies have tried to correlate Ca^{2+} spark and RyR gating [100]. Recently Porta and collaborators have suggested that only long (>6 ms) spontaneous openings of single RyRs could evoke sparks [101]. However the number of open RyRs within a cluster necessary to generate Ca^{2+} sparks is still the object of extensive

investigation. Furthermore, whether Ca^{2+} sparks are the ultimate physiological elementary release events or whether smaller release from one or a very small number of RyRs does take place *in situ* is under debate [102].

Genetically encoded Ca^{2+} indicators could potentially revolutionize the functional study of RyR and Ca^{2+} signaling in living cells, but their kinetics and other properties, such as pH sensitivity and dynamic range, require improvements [103]. Their kinetic features are being enhanced in such a way that rapid genetically encoded Ca^{2+} probes will be able to monitor brief confined events as well as global transients in the cytosol and in specific organelles [104], in addition to intact native tissues [105].

Heterologous Cell Systems to Study RyR Function

Heterologous expression approaches are used to introduce wild type or mutant RyR into a cell that typically does not express RyR and then isolate/purify membrane fractions containing RyR for downstream molecular, biochemical or biophysical analysis.

The open reading frames (ORF) of full-length RyR isoforms 1, 2 and 3 are enormous (approximately 15 kb) [106–111] and this poses a technical challenge when working with this scale of cDNA in conventional plasmid vectors. Specifically, the ORF of human cardiac RyR (hRyR2) exhibits a remarkable fragility that frequently leads to spontaneous deletion/recombination events within the sequence under non-optimised conditions. To this end, painstaking efforts were needed to optimize the conditions for the bona fide handling and propagation of the full-length ORF sequence [31]. To date, we have only found two bacterial strains (Stratagene's XL-10 Gold and Invitrogen's Stbl2) that are useful for this purpose, and all propagative steps are done at 30°C for precise time periods [31]. Even minor deviations from our stringent protocols (e.g. liquid culture of bacteria for approximately 90 min beyond optimal time) may lead to catastrophic rearrangement of the plasmid.

One of the consequences of such a massive protein coding sequence is that the introduction of experimental or disease-linked mutations requires the adoption of a cassette-based strategy in which fragments must be excised (usually using polymerase chain reaction (PCR) or restriction endonucleases), mutated (routinely using Stratagene's Quikchange system) and re-inserted back into the host vector [112]. Given the size and fragility of the cDNA that is being manipulated here, the propensity for non-specific sequence errors is large and we routinely sequence the RyR2 ORF following these preparative manoeuvres.

Once the vector-contained cDNA sequence encoding wild type or engineered mutant RyR2 is propagated and validated, the next step is to transfect mammalian cells with the aim of either isolating recombinant protein or to investigate the functional behaviour of the channel in a cellular context. As would be anticipated from studies with other large Ca^{2+} ion channels, bacterial expression strains (e.g. BL21 and its derivatives such as Rosetta), insect cells (e.g. SF9) and yeast (e.g. DSY-6,

DualSystems Biotech) typically will not express the full-length recombinant RyR [113]. The cells routinely used for heterologous expression of RyR (e.g. CHO and HEK cells) are endogenously RyR-deficient and lack many of the regulatory co-proteins that would associated with RyR *in situ* [114]. Consequently there is often a profound cellular toxicity associated with appreciable levels of recombinant RyR expression. There are many modalities for introducing the cDNA into cells. Traditional $CaPO_4$ procedures are very useful because they enable extremely high-level protein expression in a wide variety of cells [115] but the procedure itself, coupled with the immense over-driving of recombinant protein expression, is usually associated with significant cellular toxicity. $CaPO_4$-mediated transfection is useful primarily for obtaining high yields of recombinant protein for use in *in vitro* biophysical and biochemical studies. Lipid-based technologies for introducing RyR2 cDNA (e.g. Roche's Fugene, Qiagen's Effectene, Invitrogen's Lipofectamine, Peqlab's jetPei etc.) usually give more transfected cells than $CaPO_4$ offset by much lower levels of protein expression per cell. This overall reduction in recombinant protein yield is typically associated with higher cell viability and is more useful in terms of functional assessment of channel behaviour in a cellular context (e.g. determination of Ca^{2+} cycling in living cells) [31, 112, 116]. The efficiency of both $CaPO_4$ and lipid-mediated transfection is capped at around 40% although sub-populations of cells that exhibit nearly 100% transfection are frequently observed. In order to improve the efficiency of expression, making permanently-expressing cells (i.e. genetic integration of the ORF at a random locus in the cellular genome and subsequent antibiotic selection) is normally the preferred route. However, the generation of stable cell lines that robustly express RyR is difficult to achieve because cytotoxicity issues mean that only very low levels of recombinant protein expression are tolerated. To counter this, we have developed a strategy in which those cells expressing higher levels of recombinant protein are positively selected using FACS and subsequently re-cultured. This is enabled by tagging the RyR2 with enhanced GFP (eGFP, see below) [112, 117, 118]. This FACS-enriching process is cumbersome and time-consuming. Furthermore there is a progressive and heterogeneous loss of recombinant expression in the cell population between rounds of sorting that means it has to be frequently repeated. One technological development that goes some way to circumventing this cell-to-cell heterogeneity in permanently-expressing populations is the Flp-In system (Invitrogen). Here, the RyR sequence is cloned into a vector containing the Frt locus that enables integration at a discrete single site in pre-adapted cell lines and it appears to work well for RyR [119].

Inducible gene technologies have successfully been used to control the timing and graded extent of recombinant protein expression (e.g. ponasterone A/steroid receptor-based inducible expression system) [120] and these have been augmented by the availability of "TetOn/Off" systems in which tetracycline is used to regulate recombinant expression in an all-or-none fashion. However these systems are not entirely satisfactory and are prone to a background "leak" of expression. Consequently, most laboratories have resorted to frequent, high-volume transient transfection that requires huge amounts of DNA and this approach necessitates the full validation of the protocols used in deriving the full-length RyR2 cDNA.

An alternative mode of recombinant protein production is virally-driven expression systems. Although the large size of the RyR2 gene precludes easy co-option into viral-based strategies such as adenoviral-mediated expression, RyR1 and RyR3 have been robustly expressed using a herpes-simplex virus (HSV)-based system [121]. So far, it has not been possible to express RyR2 using this methodology.

An effective alternative system is the nuclear microinjection of RyR cDNA. Whilst amazingly laborious and low throughput, it remains unsurpassed as a technique for controlling the precise timing and amount of cDNA to be transduced. However, the amount of material generated is typically insufficient for anything beyond microscopy-based imaging or single cell electrophysiology [122].

In view of the above considerations, the most important decision is what cell type to use. Clearly this choice must be predicated on the ultimate purpose of expression. As discussed above, the most common scenario is that heterologous expression is performed in RyR-null cells that enable the recombinant protein to be studied in a background not complicated by endogenous expression of RyR. For example, this is very useful in studies that aim to determine the stoichiometry of RyR subunit heteromerisation [123]. However, there are drawbacks to this approach since the cellular machinery is not appropriately equipped to express RyR and there are real problems with cellular toxicity and non-specific phenotypic changes. Moreover, these cell types do not recreate the native skeletal- and cardiac-muscle specific environments and their utility as investigative platforms should be interpreted with due caution. One important development was Allen and colleagues skeletal muscle-cell model system, the 1B5 myotube, that genetically lacks RyR [121]. This has enabled the HSV-driven expression of RyR1 and RyR3 in an engineered cellular environment that is fully competent to handle this protein.

However, in situations in which RyR expression is driven in cells that do express endogenous protein (e.g. HL-1, myotubes) it is advantageous to be able to discriminate between the exogenous recombinant RyR and the endogenous channel. This is commonly done via the use of genetically introduced tags including engineered fluorescent protein derivatives from Aequorea *sp.* (e.g. enhanced GFP) [124] and Discosoma *sp.* (e.g. DsRed, mCherry) [124, 125], or by the use of epitopes to high-titre antibodies (e.g. c-myc, V5). Early studies suggested that the functionality of RyR was compromised by the fusion tags [126], and it is certainly true that the cytoplasmic C-terminal tail is extremely prone to adverse modification [127]. However in our hands the fusion of eGFP to the N-terminus of the full-length RyR2 produces a recombinant protein that is indistinguishable from the untagged version in every experimental assay so far performed [112]. Such fusion is not limited to the terminal ends either; Chen and colleagues have robustly shown that intra-sequence fusion of GFP is compatible with retention of protein function, although the introduction of GFP at some sites within the polypeptide produces a brilliantly green, non functional channel [27, 128]. We have also used the DsRed to probe the heteromerization status of RyR2 [117, 120] although the drawbacks of using this fluorescent protein, that includes its obligate tetramerisation, are acknowledged [129]. One advantageous downstream application of being able to introduce fluorescent proteins into

RyR is the ability to perform fluorescence energy resonance transfer (FRET) between and within subunits [130, 131]. However, these experiments require very cautious extrapolation because the mapping of the linear polypeptide sequence to the structural domains of RyR (identifiable by cryo-EM, see section "Difference Mapping of Cryo-EM Structures Using GFP Tags") has not been fully elucidated [114]. Indeed a recent study has shown that a GFP-based domain mapping approach may be of limited use in determining the structural architecture of the folded protein at atomic resolution [34] (see section "Building a Picture of RyR Domain Localisation" above).

New genetic (mouse) models of RyR-associated disease are enabling the next generation of molecular insights into RyR function to be determined [36, 132–136]. However, it is anticipated that in view of their almost endless configuration and utility for providing material for the *in vitro* study of RyR, heterologous expression models will remain an important strategy in the foreseeable future.

Subcellular Assays to Measure RyR Function

Among the macroscopic techniques established to look at the behaviour of large numbers of channels, a valuable approach involves the isolation of intracellular vesicles to monitor Ca^{2+} release from RyR stores independently of the various cellular constituents.

Since the emergence of methods for the subcellular fractionation of functional SR vesicles from myocytes, assays have been developed to quantify Ca^{2+} release via populations of RyRs. The earliest method used to study Ca^{2+} flux from vesicles involved monitoring of the $^{45}Ca^{2+}$ radioisotope [137–139], which was used even before the discovery of RyR as the Ca^{2+} release channel. This method involves either active or passive loading of the vesicles with the isotope before initiation of efflux using rapid mixing or filtration devices and quantification of the remaining vesicular radioisotope by scintillation counting. This assay has been further developed with the advent of Ca^{2+} sensitive colorimetric, and latterly fluorescent indicators; from murexide/tetramethylmurexide [140, 141] and arsenazo/antipyrylazo III [20, 55, 139, 142] to fura-2 [143, 144] and fluo-3 [72, 145]. This enabled experiments to be carried out with smaller amounts of vesicles and in real time. In fact, this technique has been invaluable in the peptide studies of Ikemoto and colleagues that suggest key domain-domain interactions stabilise the resting conformation of the channel [146] (see section "Why Study RyR (dys)function?").

In terms of the study of RyR function, one of the most important contributions has been the discovery of the plant alkaloid ryanodine (reviewed in [147]), more precisely the production of radiolabelled ryanodine [148], which has introduced a new approach in RyR characterisation. Ryanodine binds with high-affinity to the open conformation of the channel [149], hence it follows that changes in [^{3}H] ryanodine binding levels reflect changes in functional state [150]. Therefore [^{3}H] ryanodine binding is enhanced by activators of RyR-mediated Ca^{2+} release and decreased by channel inhibitors. This is a straightforward assay, where any number

of conditions can be manipulated. For instance it is possible to buffer Ca^{2+} in the assay medium without compromising the assay itself, allowing quantification of Ca^{2+} sensitivity of channel populations – a feature which cannot be accurately investigated in whole cells or using Ca^{2+} flux. The main disadvantage of this assay is that it can produce misleading results when mutant channels are being studied. This is because some mutations affect the ability of the channel to bind ryanodine, without affecting gating [151–153]. In other cases, complications may arise because the mutation may cause RyR instability that renders the channel non-functional, or to have altered function outside the environment of the cell [154], in this case complementary Ca^{2+} imaging studies in intact cells are invaluable.

Subcellular assays provide a considerable advantage in the characterization of RyR function over the study of single channels (see section "Monitoring the Function of Individual RyR Channels"), as they provide more representative data, since the kinetic behaviour of a large number of channels acting together is averaged, though this can in no way be as precise. In addition, a possible loss or alteration of function during channel purification and reconstitution into a foreign lipid environment is less likely. Moreover, the use of vesicles means that assay conditions may be modified to a greater extent than in whole cell systems, although removal from the intracellular milieu may in some cases produce spurious results. In conclusion, we find that these assays are useful and straightforward, but are best used in conjunction with complementary techniques.

Monitoring the Function of Individual RyR Channels

The assays of RyR function described in preceding sections of this chapter provide valuable information on the properties of populations of Ca^{2+}-release channels either within the cell or within the isolated SR membrane. To gain information on the mechanisms governing the function of RyR as a channel (interaction of an activating ligand regulating the channel open probability or discrimination between cations), we need to study the behaviour of individual channels. RyR is located in an intracellular membrane network and consequently is not amenable to conventional electrophysiological procedures such as patch-clamping [155, 156]. To study the function of single RyR channels they must be removed from the cell and incorporated into artificial planar phospholipid bilayers.

Membrane Isolation and RyR Purification

The starting material for these experiments can be native tissue such as mammalian skeletal [157] or cardiac muscle [158] or cells in culture expressing wild type or mutant recombinant RyR (see section "Heterologous Cell Systems to Study RyR Function"). RyR channels from these sources can be incorporated into planar phospholipid bilayers either by the fusion of isolated membrane vesicles or following the purification of the channel tetramer from the membrane.

Following cell disruption, populations of intracellular membrane vesicles containing RyR are separated from other cellular components by differential and density gradient centrifugation [159]. In addition to RyR, membrane vesicles isolated from either native tissue or cells in culture will contain other species of ion channel and the presence of these in the bilayer will severely restrict the range of experiments that can be carried out to characterise RyR function. To overcome this limitation RyR channels can be separated from other membrane proteins following solubilisation of the membrane with a suitable detergent. Once liberated from the membrane RyR is conventionally isolated from other solubilised proteins using density gradient centrifugation [160, 161].

Planar Phospholipid Bilayers and Incorporation of RyR

The artificial membrane into which single RyR channels are incorporated for characterisation is formed from a suspension of purified phospholipids in n-decane across a small hole in a partition that separates two chambers containing appropriate ionic solutions. This system provides a very flexible environment in which the composition of the bilayer can be defined, the ionic composition of the media on either side of the channel can be controlled and modified during the experiment and current flow through the channel can be monitored under voltage clamp conditions [162, 163].

To measure the function of RyR channels either isolated native membrane vesicles (for example muscle SR) or purified RyR channels are added to the solution at one side of the bilayer (defined as *cis*). Fusion with the planar membrane is induced by creating an osmotic gradient such that the solution in the *cis* chamber is hyperosmotic with respect to the solution at the other (*trans*) side of the membrane. Both SR membranes and purified channels incorporate into the bilayer in only one orientation so that following fusion the cytosolic face of RyR is exposed to the *cis* chamber and the luminal face to the *trans* chamber [164].

Characterisation of RyR Single Channel Function

Incorporation of an individual RyR channel into a planar bilayer permits detailed characterisation of the two fundamental properties of RyR – gating and ion translocation. A functional RyR channel oscillates between closed and open conformations and the equilibrium between these states can be controlled by the interaction of a wide range of physiological and pharmacological ligands. The states are distinguished by monitoring current movement across the bilayer. With RyR closed no current flows, when the channel opens permeant ions move through the channel down their electrochemical gradient. The current amplitude of the open state is a measure of the number of ions moving per unit time and will vary with the electrochemical driving force.

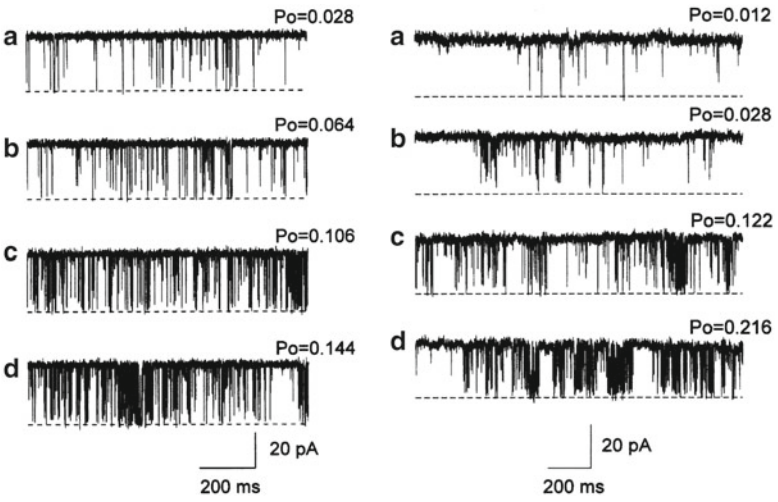

Fig. 8.6 Representative bilayer experiment and cytosolic Ca^{2+} activation. The traces represent current fluctuations over time through a single Ca^{2+} release channel recorded at a holding potential of +40 mV. The open state is indicated by *dashed lines*. Increasing Ca^{2+} concentrations (from a to d) raise channel open probability in sheep purified (*left panel*) and native RyR2 proteins (*right panel*) [164]

The response of RyR to a ligand can be determined by monitoring variations in the probability of a single channel being open in response to different concentrations of the ligand. Information on the mechanisms underlying changes in open probability can be obtained from measurements of dwell times in the closed and open states. As an example, cytosolic Ca^{2+} has been shown to increase open probability (Fig. 8.6) via a decrease in the closed dwell times, as opposed to an increase in the open dwell times, signifying that the channel opens more frequently under conditions of increasing Ca^{2+} concentration rather than remaining open for a longer duration [164].

The conditions used to characterise function and the range of information that can be obtained depend on the nature of the material incorporated into the bilayer. As outlined above, the fusion of an SR vesicle with the bilayer will transfer not only RyR but also a number of other species of ion channel, including those permeable to monovalent cations and anions. The incorporation of more than one species of channel into a bilayer limits the characterisation of RyR function, however this can, to some extent, be overcome by chemically isolating RyR. This is achieved by excluding from the recording solutions at either side of the bilayer ions that are permeant in the unwanted channels [157]. In practice this means that in these studies RyR function can be monitored with either Ca^{2+} or Ba^{2+} as the only potential charge-carrying ion in the system. Under these conditions RyR single channel current amplitude is small (4–7 pA) and, as a consequence, data must be severely

low-pass filtered to resolve events. This in turn limits the temporal resolution of RyR activity. Nevertheless the effects of both physiological and pharmacological modulators of RyR gating have been characterised using this approach [165]. To improve resolution, RyR single channel current amplitude can be increased by the use of Cs^+ as the only permeant ion in the system [166]. While the SR monovalent cation channel is permeable to Cs^+ [167], unitary conductance is low leading to only minimal corruption of the RyR signal.

A potential advantage of RyR characterisation following fusion of native membrane vesicles is that regulatory proteins that form part of the *in situ* RyR complex may remain associated with the channel in the bilayer [168], however separation of RyR from other native membrane channels greatly increases the scope for characterisation of function. Important properties of ion-handling in RyR have been monitored in channels incorporated from SR vesicles [169, 170]. However, with a purified single RyR in the bilayer the ionic environment on either side of the channel can be changed dramatically so that the ability of RyR to discriminate between ions, the affinity of RyR for specific cations, the ability of cations and larger molecules to block permeant ion movement and even some dimensions of the conduction pathway of the channel can be determined [171]. Detailed investigations of ion-handling have revealed that, while RyR excludes anions, it is permeable to many divalent and monovalent cations. Importantly rates of translocation of monovalent cations are roughly five fold greater than those of divalents [171]. As a result, with K^+, for example, as the permeant ion temporal resolution of RyR gating is much improved.

The efficiency of RyR as an intracellular Ca^{2+}-release channel is underpinned by tight regulation of gating and by very high rates of Ca^{2+} movement through the open channel. Characterisation of the function of individual RyR channels has revealed details of the mechanisms involved in the regulation of gating and has established that high rates of Ca^{2+} are achieved at the expense of discrimination. Characterisation of the function of individual RyR channels in which the properties of specific residues that are predicted to play a role in gating or ion translocation are altered is beginning to reveal the structural basis of function of this important channel [151, 153, 172–176].

Concluding Remarks

With this review, we explored different methods that are routinely employed to measure different facets of RyR function. As a complex molecule, it needs to be approached from a multidisciplinary angle. Structural biology, mutagenesis, fluorescence imaging and electrophysiology techniques have been developed to provide an increasing amount of information that ultimately broadens our knowledge of the mechanisms involved in the very efficient Ca^{2+} release mediated by RyR.

Both functional and structural data will be required in order to properly elucidate the exact nature of RyR (dys)function.

Acknowledgements We are very much obliged to the British Heart Foundation, which provides the financial support for all researchers involved in this work. Moreover we would like to thank Prof. Peter Lipp and Dr. Lars Kaestner from the Institute of Molecular Cell Biology (Medical Faculty, Saarland University, Homburg/Saar, Germany) for their great support and help in monitoring Ca^{2+} dynamics in rat heart muscle cells and the use of confocal microscopy.

References

1. Bers DM (2002) Cardiac excitation-contraction coupling. Nature 415:198–205
2. Lipp P, Laine M, Tovey SC, Burrell KM, Berridge MJ, Li W, Bootman MD (2000) Functional InsP3 receptors that may modulate excitation-contraction coupling in the heart. Curr Biol 10:939–942
3. Gustafsson AJ, Ingelman-Sundberg H, Dzabic M, Awasum J, Nguyen KH, Ostenson CG, Pierro C, Tedeschi P, Woolcott O, Chiounan S, Lund PE, Larsson O, Islam MS (2005) Ryanodine receptor-operated activation of TRP-like channels can trigger critical Ca^{2+} signalling events in pancreatic beta-cells. FASEB J 19:301–303
4. Berridge MJ (1997) Elementary and global aspects of calcium signalling. J Exp Biol 200:315–319
5. Islam MS (2002) The ryanodine receptor calcium channel of beta-cells: molecular regulation and physiological significance. Diabetes 51:1299–1309
6. Giannini G, Conti A, Mammarella S, Scrobogna M, Sorrentino V (1995) The ryanodine receptor/calcium channel genes are widely and differentially expressed in murine brain and peripheral tissues. J Cell Biol 128:893–904
7. Benkusky NA, Farrell EF, Valdivia HH (2004) Ryanodine receptor channelopathies. Biochem Biophys Res Commun 322:1280–1285
8. Mickelson JR, Louis CF (1996) Malignant hyperthermia: excitation-contraction coupling, Ca^{2+} release channel, and cell Ca^{2+} regulation defects. Physiol Rev 76:537–592
9. Lyfenko AD, Goonasekera SA, Dirksen RT (2004) Dynamic alterations in myoplasmic Ca^{2+} in malignant hyperthermia and central core disease. Biochem Biophys Res Commun 322: 1256–1266
10. Mathews KD, Moore SA (2004) Multiminicore myopathy, central core disease, malignant hyperthermia susceptibility, and RYR1 mutations: one disease with many faces? Arch Neurol 61:27–29
11. Brini M (2004) Ryanodine receptor defects in muscle genetic diseases. Biochem Biophys Res Commun 322:1245–1255
12. Priori SG, Napolitano C, Tiso N, Memmi M, Vignati G, Bloise R, Sorrentino V, Danieli GA (2001) Mutations in the cardiac ryanodine receptor gene (hRyR2) underlie catecholaminergic polymorphic ventricular tachycardia. Circulation 103:196–200
13. Thomas NL, Maxwell C, Mukherjee S, Williams AJ (2010) Ryanodine receptor mutations in arrhythmia: the continuing mystery of channel dysfunction. FEBS Lett 584:2153–2160
14. Ikemoto N, Yamamoto T (2000) Postulated role of inter-domain interaction within the ryanodine receptor in Ca(2+) channel regulation. Trends Cardiovasc Med 10:310–316
15. Yamamoto T, El-Hayek R, Ikemoto N (2000) Postulated role of interdomain interaction within the ryanodine receptor in Ca(2+) channel regulation. J Biol Chem 275:11618–11625
16. Yamamoto T, Ikemoto N (2002) Peptide probe study of the critical regulatory domain of the cardiac ryanodine receptor. Biochem Biophys Res Commun 291:1102–1108
17. Kobayashi S, Bannister ML, Gangopadhyay JP, Hamada T, Parness J, Ikemoto N (2005) Dantrolene stabilizes domain interactions within the ryanodine receptor. J Biol Chem 280:6580–6587
18. Tateishi H, Yano M, Mochizuki M, Suetomi T, Ono M, Xu X, Uchinoumi H, Okuda S, Oda T, Kobayashi S, Yamamoto T, Ikeda Y, Ohkusa T, Ikemoto N, Matsuzaki M (2009) Defective

domain-domain interactions within the ryanodine receptor as a critical cause of diastolic Ca^{2+} leak in failing hearts. Cardiovasc Res 81:536–545
19. Oda T, Yano M, Yamamoto T, Tokuhisa T, Okuda S, Doi M, Ohkusa T, Ikeda Y, Kobayashi S, Ikemoto N, Matsuzaki M (2005) Defective regulation of interdomain interactions within the ryanodine receptor plays a key role in the pathogenesis of heart failure. Circulation 111: 3400–3410
20. Yamamoto T, Yano M, Kohno M, Hisaoka T, Ono K, Tanigawa T, Saiki Y, Hisamatsu Y, Ohkusa T, Matsuzaki M (1999) Abnormal Ca^{2+} release from cardiac sarcoplasmic reticulum in tachycardia-induced heart failure. Cardiovasc Res 44:146–155
21. Marx SO, Reiken S, Hisamatsu Y, Jayaraman T, Burkhoff D, Rosemblit N, Marks AR (2000) PKA phosphorylation dissociates FKBP12.6 from the calcium release channel (ryanodine receptor): defective regulation in failing hearts. Cell 101:365–376
22. Bellinger AM, Reiken S, Carlson C, Mongillo M, Liu X, Rothman L, Matecki S, Lacampagne A, Marks AR (2009) Hypernitrosylated ryanodine receptor calcium release channels are leaky in dystrophic muscle. Nat Med 15:325–330
23. Curran J, Hinton MJ, Rios E, Bers DM, Shannon TR (2007) Beta-adrenergic enhancement of sarcoplasmic reticulum calcium leak in cardiac myocytes is mediated by calcium/calmodulin-dependent protein kinase. Circ Res 100:391–398
24. Stange M, Xu L, Balshaw D, Yamaguchi N, Meissner G (2003) Characterization of recombinant skeletal muscle (Ser-2843) and cardiac muscle (Ser-2809) ryanodine receptor phosphorylation mutants. J Biol Chem 278:51693–51702
25. Liu N, Colombi B, Raytcheva-Buono EV, Bloise R, Priori SG (2007) Catecholaminergic polymorphic ventricular tachycardia. Herz 32:212–217
26. Currie S, Elliott EB, Smith GL, Loughrey CM (2011) Two candidates at the heart of dysfunction: the ryanodine receptor and calcium/calmodulin protein kinase II as potential targets for therapeutic intervention – an in vivo perspective. Pharmacol Ther 131:204–220
27. George CH, Jundi H, Thomas NL, Fry DL, Lai FA (2007) Ryanodine receptors and ventricular arrhythmias: emerging trends in mutations, mechanisms and therapies. J Mol Cell Cardiol 42:34–50
28. Thireau J, Pasquie JL, Martel E, Le Guennec JY, Richard S (2011) New drugs vs. old concepts: a fresh look at antiarrhythmics. Pharmacol Ther. doi:10.1016/j.pharmthera.2011.03.003
29. Serysheva II, Ludtke SJ, Baker ML, Cong Y, Topf M, Eramian D, Sali A, Hamilton SL, Chiu W (2008) Subnanometer-resolution electron cryomicroscopy-based domain models for the cytoplasmic region of skeletal muscle RyR channel. Proc Natl Acad Sci USA 105: 9610–9615
30. Bhat MB, Hayek SM, Zhao J, Zang W, Takeshima H, Wier WG, Ma J (1999) Expression and functional characterization of the cardiac muscle ryanodine receptor Ca(2+) release channel in Chinese hamster ovary cells. Biophys J 77:808–816
31. George CH, Sorathia R, Bertrand BM, Lai FA (2003) In situ modulation of the human cardiac ryanodine receptor (hRyR2) by FKBP12.6. Biochem J 370:579–589
32. Rossi D, Simeoni I, Micheli M, Bootman M, Lipp P, Allen PD, Sorrentino V (2002) RyR1 and RyR3 isoforms provide distinct intracellular Ca^{2+} signals in HEK 293 cells. J Cell Sci 115:2497–2504
33. Xu X, Bhat MB, Nishi M, Takeshima H, Ma J (2000) Molecular cloning of cDNA encoding a drosophila ryanodine receptor and functional studies of the carboxyl-terminal calcium release channel. Biophys J 78:1270–1281
34. Tung CC, Lobo PA, Kimlicka L, Van Petegem F (2010) The amino-terminal disease hotspot of ryanodine receptors forms a cytoplasmic vestibule. Nature 468:585–588
35. Lobo PA, Van Petegem F (2009) Crystal structures of the N-terminal domains of cardiac and skeletal muscle ryanodine receptors: insights into disease mutations. Structure 17:1505–1514
36. Uchinoumi H, Yano M, Suetomi T, Ono M, Xu X, Tateishi H, Oda T, Okuda S, Doi M, Kobayashi S, Yamamoto T, Ikeda Y, Ohkusa T, Ikemoto N, Matsuzaki M (2010) Catecholaminergic polymorphic ventricular tachycardia is caused by mutation-linked defective conformational regulation of the ryanodine receptor. Circ Res 106:1413–1424

37. Kannankeril PJ, Mitchell BM, Goonasekera SA, Chelu MG, Zhang W, Sood S, Kearney DL, Danila CI, De Biasi M, Wehrens XH, Pautler RG, Roden DM, Taffet GE, Dirksen RT, Anderson ME, Hamilton SL (2006) Mice with the R176Q cardiac ryanodine receptor mutation exhibit catecholamine-induced ventricular tachycardia and cardiomyopathy. Proc Natl Acad Sci USA 103:12179–12184
38. Lanner JT, Georgiou DK, Joshi AD, Hamilton SL (2010) Ryanodine receptors: structure, expression, molecular details, and function in calcium release. Cold Spring Harb Perspect Biol 2:a003996
39. Hamilton SL, Serysheva II (2009) Ryanodine receptor structure: progress and challenges. J Biol Chem 284:4047–4051
40. Wagenknecht TC, Liu Z (2010) Electron microscopy of ryanodine receptors. In: Serysheva I (ed) Structure and function of calcium release channels, Current topics in membranes. Elsevier/Academic, Amsterdam, pp 28–47
41. Franzini-Armstrong C (2004) Functional implications of RyR-dHPR relationships in skeletal and cardiac muscles. Biol Res 37:507–512
42. Wagenknecht T, Grassucci R, Frank J, Saito A, Inui M, Fleischer S (1989) Three-dimensional architecture of the calcium channel/foot structure of sarcoplasmic reticulum. Nature 338:167–170
43. Cheng Y, Walz T (2009) The advent of near-atomic resolution in single-particle electron microscopy. Annu Rev Biochem 78:723–742
44. Wagenknecht TC, Liu Z (2010) Electron microscopy of ryanodine receptors. In: Serysheva I (ed) Structure and function of calcium release channels. Academic Press, San Diego, CA. Curr Top Membr, Vol 66, pp 27–47
45. Ludtke SJ, Serysheva II, Hamilton SL, Chiu W (2005) The pore structure of the closed RyR1 channel. Structure 13:1203–1211
46. Samso M, Wagenknecht T, Allen PD (2005) Internal structure and visualization of transmembrane domains of the RyR1 calcium release channel by cryo-EM. Nat Struct Mol Biol 12:539–544
47. Doyle DA, Cabral JM, Pfuetzner RA, Kuo A, Gulbis JM, Cohen SL, Chait BT, MacKinnon R (1998) The structure of the potassium channel: molecular basis of K^+ conduction and selectivity. Science 280:69–77
48. Jiang Y, Lee A, Chen J, Cadene M, Chait BT, MacKinnon R (2002) The open pore conformation of potassium channels. Nature 417:523–526
49. Radermacher M, Rao V, Grassucci R, Frank J, Timerman AP, Fleischer S, Wagenknecht T (1994) Cryo-electron microscopy and three-dimensional reconstruction of the calcium release channel/ryanodine receptor from skeletal muscle. J Cell Biol 127:411–423
50. Capes EM, Loaiza R, Valdivia HH (2011) Ryanodine receptors. Skeletal Muscle 1:1–13
51. Zissimopoulos S, Lai FA (2005) Interaction of FKBP12.6 with the cardiac ryanodine receptor C-terminal domain. J Biol Chem 280:5475–5485
52. Yang D, Zhu WZ, Xiao B, Brochet DX, Chen SR, Lakatta EG, Xiao RP, Cheng H (2007) Ca^{2+}/calmodulin kinase II-dependent phosphorylation of ryanodine receptors suppresses Ca^{2+} sparks and Ca^{2+} waves in cardiac myocytes. Circ Res 100:399–407
53. Samso M, Shen X, Allen PD (2006) Structural characterization of the RyR1-FKBP12 interaction. J Mol Biol 356:917–927
54. Samso M, Wagenknecht T (2002) Apocalmodulin and Ca^{2+}-calmodulin bind to neighboring locations on the ryanodine receptor. J Biol Chem 277:1349–1353
55. Meng X, Wang G, Viero C, Wang Q, Mi W, Su XD, Wagenknecht T, Williams AJ, Liu Z, Yin CC (2009) CLIC2-RyR1 interaction and structural characterization by cryo-electron microscopy. J Mol Biol 387:320–334
56. Samso M, Trujillo R, Gurrola GB, Valdivia HH, Wagenknecht T (1999) Three-dimensional location of the imperatoxin A binding site on the ryanodine receptor. J Cell Biol 146:493–499
57. Zhou Q, Wang QL, Meng X, Shu Y, Jiang T, Wagenknecht T, Yin CC, Sui SF, Liu Z (2008) Structural and functional characterization of ryanodine receptor-natrin toxin interaction. Biophys J 95:4289–4299

58. Kratz PA, Bottcher B, Nassal M (1999) Native display of complete foreign protein domains on the surface of hepatitis B virus capsids. Proc Natl Acad Sci USA 96:1915–1920
59. Liu Z, Zhang J, Li P, Chen SR, Wagenknecht T (2002) Three-dimensional reconstruction of the recombinant type 2 ryanodine receptor and localization of its divergent region 1. J Biol Chem 277:46712–46719
60. Liu Z, Zhang J, Wang R, Chen SRW, Wagenknecht T (2004) Location of divergent region 2 on the three-dimensional structure of cardiac muscle ryanodine receptor/calcium release channel. J Mol Biol 338:533–545
61. Zhang J, Liu Z, Masumiya H, Wang R, Jiang D, Li F, Wagenknecht T, Chen SR (2003) Three-dimensional localization of divergent region 3 of the ryanodine receptor to the clamp-shaped structures adjacent to the FKBP binding sites. J Biol Chem 278:14211–14218
62. Jones PP, Meng X, Xiao B, Cai S, Bolstad J, Wagenknecht T, Liu Z, Chen SR (2008) Localization of PKA phosphorylation site, Ser (2030), in the three-dimensional structure of cardiac ryanodine receptor. Biochem J 410:261–270
63. Meng X, Xiao B, Cai S, Huang X, Li F, Bolstad J, Trujillo R, Airey J, Chen SR, Wagenknecht T, Liu Z (2007) Three-dimensional localization of serine 2808, a phosphorylation site in cardiac ryanodine receptor. J Biol Chem 282:25929–25939
64. Liu Z, Wang R, Zhang J, Chen SR, Wagenknecht T (2005) Localization of a disease-associated mutation site in the three-dimensional structure of the cardiac muscle ryanodine receptor. J Biol Chem 280:37941–37947
65. Wang R, Chen W, Cai S, Zhang J, Bolstad J, Wagenknecht T, Liu Z, Chen SR (2007) Localization of an NH(2)-terminal disease-causing mutation hot spot to the "clamp" region in the three-dimensional structure of the cardiac ryanodine receptor. J Biol Chem 282: 17785–17793
66. George CH (2008) Sarcoplasmic reticulum Ca^{2+} leak in heart failure: mere observation or functional relevance? Cardiovasc Res 77:302–314
67. Bray D, Levin MD, Morton-Firth CJ (1998) Receptor clustering as a cellular mechanism to control sensitivity. Nature 393:85–88
68. Yin CC, Lai FA (2000) Intrinsic lattice formation by the ryanodine receptor calcium-release channel. Nat Cell Biol 2:669–671
69. Yin CC, Han H, Wei R, Lai FA (2005) Two-dimensional crystallization of the ryanodine receptor Ca^{2+} release channel on lipid membranes. J Struct Biol 149:219–224
70. Amador FJ, Liu S, Ishiyama N, Plevin MJ, Wilson A, MacLennan DH, Ikura M (2009) Crystal structure of type I ryanodine receptor amino-terminal beta-trefoil domain reveals a disease-associated mutation "hot spot" loop. Proc Natl Acad Sci USA 106:11040–11044
71. Nettleship JE, Brown J, Groves MR, Geerlof A (2008) Methods for protein characterization by mass spectrometry, thermal shift (ThermoFluor) assay, and multiangle or static light scattering. Methods Mol Biol 426:299–318
72. Kobayashi S, Yamamoto T, Parness J, Ikemoto N (2004) Antibody probe study of Ca^{2+} channel regulation by interdomain interaction within the ryanodine receptor. Biochem J 380:561–569
73. Grynkiewicz G, Poenie M, Tsien RY (1985) A new generation of Ca^{2+} indicators with greatly improved fluorescence properties. J Biol Chem 260:3440–3450
74. Muschol M, Dasgupta BR, Salzberg BM (1999) Caffeine interaction with fluorescent calcium indicator dyes. Biophys J 77:577–586
75. Cheng H, Lederer WJ, Cannell MB (1993) Calcium sparks: elementary events underlying excitation-contraction coupling in heart muscle. Science 262:740–744
76. Cheng H, Lederer WJ (2008) Calcium sparks. Physiol Rev 88:1491–1545
77. Thomas D, Tovey SC, Collins TJ, Bootman MD, Berridge MJ, Lipp P (2000) A comparison of fluorescent Ca^{2+} indicator properties and their use in measuring elementary and global Ca^{2+} signals. Cell Calcium 28:213–223
78. Rudolf R, Mongillo M, Rizzuto R, Pozzan T (2003) Looking forward to seeing calcium. Nat Rev Mol Cell Biol 4:579–586

79. Hammer K, Ruppenthal S, Viero C, Scholz A, Edelmann L, Kaestner L, Lipp P (2010) Remodelling of Ca^{2+} handling organelles in adult rat ventricular myocytes during long term culture. J Mol Cell Cardiol 49:427–437
80. Farrell EF, Antaramian A, Rueda A, Gomez AM, Valdivia HH (2003) Sorcin inhibits calcium release and modulates excitation-contraction coupling in the heart. J Biol Chem 278: 34660–34666
81. Pereira L, Matthes J, Schuster I, Valdivia HH, Herzig S, Richard S, Gomez AM (2006) Mechanisms of $[Ca^{2+}]_i$ transient decrease in cardiomyopathy of db/db type 2 diabetic mice. Diabetes 55:608–615
82. Rodney GG, Schneider MF (2003) Calmodulin modulates initiation but not termination of spontaneous Ca^{2+} sparks in frog skeletal muscle. Biophys J 85:921–932
83. Remillard CV, Zhang WM, Shimoda LA, Sham JS (2002) Physiological properties and functions of Ca(2+) sparks in rat intrapulmonary arterial smooth muscle cells. Am J Physiol Lung Cell Mol Physiol 283:L433–L444
84. Shorofsky SR, Izu L, Wier WG, Balke CW (1998) Ca^{2+} sparks triggered by patch depolarization in rat heart cells. Circ Res 82:424–429
85. Cannell MB, McMorland AJC, Soeller C (2005) Imaging microscopic calcium signals in excitable cells. In: Yuste AKR (ed) Imaging in neuroscience and development: a laboratory manual. Cold Spring Harbor Labortory Press, Cold Spring Harbor, pp 299–305
86. Cannell MB, Cody SH (2006) Fluorescent ion measurement. In: Pawley JB (ed) Handbook of biological confocal microscopy, 3rd edn. Springer Science+Business Media, New York, pp 736–745
87. Lipp P, Hammer KP, Flockerzi A, Zeug A, Kaestner L (2009) Automatic calcium spark detection and analysis in time series of two-dimensional confocal images. Biophys J 96:278a
88. Picht E, Zima AV, Blatter LA, Bers DM (2007) SparkMaster: automated calcium spark analysis with ImageJ. Am J Physiol Cell Physiol 293:C1073–C1081
89. Niggli E, Shirokova N (2007) A guide to sparkology: the taxonomy of elementary cellular Ca^{2+} signalling events. Cell Calcium 42:379–387
90. Sebille S, Cantereau A, Vandebrouck C, Balghi H, Constantin B, Raymond G, Cognard C (2005) Calcium sparks in muscle cells: interactive procedures for automatic detection and measurements on line-scan confocal images series. Comput Methods Programs Biomed 77:57–70
91. Wegner FV, Both M, Fink RH (2006) Automated detection of elementary calcium release events using the a trous wavelet transform. Biophys J 90:2151–2163
92. Bray MA, Geisse NA, Parker KK (2007) Multidimensional detection and analysis of Ca^{2+} sparks in cardiac myocytes. Biophys J 92:4433–4443
93. Cheng H, Song LS, Shirokova N, Gonzalez A, Lakatta EG, Rios E, Stern MD (1999) Amplitude distribution of calcium sparks in confocal images: theory and studies with an automatic detection method. Biophys J 76:606–617
94. Apostol S, Ursu D, Lehmann-Horn F, Melzer W (2009) Local calcium signals induced by hyper-osmotic stress in mammalian skeletal muscle cells. J Muscle Res Cell Motil 30:97–109
95. Ferrier GR, Smith RH, Howlett SE (2003) Calcium sparks in mouse ventricular myocytes at physiological temperature. Am J Physiol Heart Circ Physiol 285:H1495–H1505
96. Zahradnikova A Jr, Polakova E, Zahradnik I, Zahradnikova A (2007) Kinetics of calcium spikes in rat cardiac myocytes. J Physiol 578:677–691
97. Pratusevich VR, Balke CW (1996) Factors shaping the confocal image of the calcium spark in cardiac muscle cells. Biophys J 71:2942–2957
98. Wang SQ, Stern MD, Rios E, Cheng H (2004) The quantal nature of Ca^{2+} sparks and in situ operation of the ryanodine receptor array in cardiac cells. Proc Natl Acad Sci USA 101:3979–3984
99. Lipp P, Niggli E (1998) Fundamental calcium release events revealed by two-photon excitation photolysis of caged calcium in Guinea-pig cardiac myocytes. J Physiol 508(Pt 3): 801–809

100. Zahradnikova A, Valent I, Zahradnik I (2010) Frequency and release flux of calcium sparks in rat cardiac myocytes: a relation to RYR gating. J Gen Physiol 136:101–116
101. Porta M, Zima AV, Nani A, Diaz-Sylvester PL, Copello JA, Ramos-Franco J, Blatter LA, Fill M (2011) Single ryanodine receptor channel basis of caffeine's action on Ca^{2+} sparks. Biophys J 100:931–938
102. Brochet DX, Xie W, Yang D, Cheng H, Lederer WJ (2011) Quarky calcium release in the heart. Circ Res 108:210–218
103. Tallini YN, Ohkura M, Choi BR, Ji G, Imoto K, Doran R, Lee J, Plan P, Wilson J, Xin HB, Sanbe A, Gulick J, Mathai J, Robbins J, Salama G, Nakai J, Kotlikoff MI (2006) Imaging cellular signals in the heart in vivo: cardiac expression of the high-signal Ca^{2+} indicator GCaMP2. Proc Natl Acad Sci USA 103:4753–4758
104. Canato M, Scorzeto M, Giacomello M, Protasi F, Reggiani C, Stienen GJ (2010) Massive alterations of sarcoplasmic reticulum free calcium in skeletal muscle fibers lacking calsequestrin revealed by a genetically encoded probe. Proc Natl Acad Sci USA 107:22326–22331
105. Horikawa K, Yamada Y, Matsuda T, Kobayashi K, Hashimoto M, Matsu-ura T, Miyawaki A, Michikawa T, Mikoshiba K, Nagai T (2010) Spontaneous network activity visualized by ultrasensitive Ca(2+) indicators, yellow Cameleon-Nano. Nat Methods 7:729–732
106. Takeshima H, Nishimura S, Matsumoto T, Ishida H, Kangawa K, Minamino N, Matsuo H, Ueda M, Hanaoka M, Hirose T, Numa S (1989) Primary structure and expression from complementary-DNA of skeletal- muscle ryanodine receptor. Nature 339:439–445
107. Otsu K, Willard HF, Khanna VK, Zorzato F, Green NM, MacLennan DH (1990) Molecular-cloning of cDNA-encoding the Ca^{2+} release channel (ryanodine receptor) of rabbit cardiac-muscle sarcoplasmic-reticulum. J Biol Chem 265:13472–13483
108. Zorzato F, Fujii J, Otsu K, Phillips M, Green NM, Lai FA, Meissner G, MacLennan DH (1990) Molecular cloning of cDNA encoding human and rabbit forms of the Ca^{2+} release channel (ryanodine receptor) of skeletal muscle sarcoplasmic reticulum. J Biol Chem 265: 2244–2256
109. Leeb T, Brenig B (1998) cDNA cloning and sequencing of the human ryanodine receptor type 3 (RyR3) reveals a novel alternative splice site in the RyR3 gene. FEBS Lett 423:367–370
110. Marziali G, Rossi D, Giannini G, Charlesworth A, Sorrentino V (1996) cDNA cloning reveals a tissue specific expression of alternatively spliced transcripts of the ryanodine receptor type 3 (RyR3) calcium release channel. FEBS Lett 394:76–82
111. Tunwell REA, Wickenden C, Bertrand BMA, Shevchenko VI, Walsh MB, Allen PD, Lai FA (1996) The human cardiac muscle ryanodine receptor-calcium release channel: identification, primary structure and topological analysis. Biochem J 318:477–487
112. George CH, Higgs GV, Lai FA (2003) Ryanodine receptor mutations associated with stress-induced ventricular tachycardia mediate increased calcium release in stimulated cardiomyocytes. Circ Res 93:531–540
113. Niu TK, Ashley RH (2000) Expression of full-length and truncated recombinant human brain type I inositol 1,4,5-trisphosphate receptors in mammalian and insect cells. Biochem Biophys Res Commun 273:123–128
114. George CH, Yin CC, Lai FA (2005) Toward a molecular understanding of the structure:function of ryanodine receptor Ca^{2+} release channels: perspectives from recombinant expression systems. Cell Biochem Biophys 42:197–222
115. Chen C, Okayama H (1987) High efficiency transformation of mammalian cells by plasmid DNA. Mol Cell Biol 7:2745–2752
116. George CH, Higgs GV, Mackrill JJ, Lai FA (2003) Dysregulated ryanodine receptors mediate cellular toxicity: restoration of normal phenotype by FKBP12.6. J Biol Chem 278:28856–28864
117. George CH, Rogers SA, Bertrand BMA, Tunwell REA, Thomas NL, Steele DS, Cox EV, Pepper C, Hazeel CJ, Claycomb WC, Lai FA (2007) Alternative splicing of ryanodine receptors modulates cardiomyocyte Ca^{2+} signalling and susceptibility to apoptosis. Circ Res 100:874–883

118. George CH, Jundi H, Thomas NL, Walters N, West RR, Lai FA (2006) Arrhythmogenic mutation-linked defects in ryanodine receptor autoregulation reveal a novel mechanism of Ca^{2+} release channel dysfunction. Circ Res 98:88–97
119. Jiang D, Chen W, Wang R, Zhang L, Chen SRW (2007) Loss of luminal Ca^{2+} activation in the cardiac ryanodine receptor is associated with ventricular fibrillation and sudden death. Proc Natl Acad Sci USA 104:18309–18314
120. George CH, Jundi H, Thomas NL, Scoote M, Walters N, Williams AJ, Lai FA (2004) Ryanodine receptor regulation by intramolecular interaction between cytoplasmic and transmembrane domains. Mol Biol Cell 15:2627–2638
121. Moore RA, Nguyen H, Galceran J, Pessah IN, Allen PD (1998) A transgenic myogenic cell line lacking ryanodine receptor protein for homologous expression studies: reconstitution of Ry1R protein and function. J Cell Biol 140:843–851
122. Nakai J, Dirksen RT, Nguyen HT, Pessah IN, Beam KG, Allen PD (1996) Enhanced dihydropyridine receptor channel activity in the presence of ryanodine receptor. Nature 380:72–75
123. Xiao B, Masumiya H, Jiang D, Wang R, Sei Y, Zhang L, Murayama T, Ogawa Y, Lai FA, Wagenknecht T, Chen SRW (2002) Isoform dependent formation of heteromeric Ca^{2+} release channels (ryanodine receptors). J Biol Chem 277:41778–41785
124. Heim R, Tsien RY (1996) Engineering green fluorescent protein for improved brightness, longer wavelengths and fluorescence resonance energy transfer. Curr Biol 6:178–182
125. Shaner NC, Campbell RE, Steinbach PA, Giepmans BNG, Palmer AE, Tsien RY (2004) Improved monomeric red, orange and yellow fluorescent proteins derived from Discosoma sp. red fluorescent protein. Nat Biotechnol 22:1567–1572
126. Lorenzon NM, Grabner M, Suda N, Beam KG (2001) Structure and targeting of RyR1: implications from fusion of green fluorescent protein and the amino-terminal. Arch Biochem Biophys 388:13–17
127. Stewart R, Zissimopoulos S, Lai FA (2003) Oligomerization of the cardiac ryanodine receptor C-terminal tail. Biochem J 376:795–799
128. George CH (2008) Sarcoplasmic reticulum Ca^{2+} leak in heart failure: mere observation or functional relevance? Cardiovasc Res 77:302–314
129. Gross LA, Baird GS, Hoffman RC, Baldridge KK, Tsien RY (2000) The structure of the chromophore within dsRed, a red fluorescent protein from coral. Proc Natl Acad Sci USA 97:11990–11995
130. Liu Z, Wang R, Tian X, Zhong X, Gangopadhyay JP, Cole R, Ikemoto N, Chen SRW, Wagenknecht T (2010) Dynamic, inter-subunit interactions between the N-terminal and central mutation regions of cardiac ryanodine receptor. J Cell Sci 123:1775–1784
131. George CH, Yeung WY, Walters N, Thomas NL, Claycomb WC, Lai FA (2006) A novel cardiomyocyte FRET-based bioassay for investigating the molecular basis of RyR2 dysfunction in arrhythmogenesis. Biophys J (Suppl.S) 90:264a
132. Cerrone M, Colombi B, Santoro M, di Barletta MR, Scelsi M, Villani L, Napolitano C, Priori SG (2005) Bidirectional ventricular tachycardia and fibrillation elicited in a knock-in mouse model carrier of a mutation in the cardiac ryanodine receptor (RyR2). Circ Res 96: e77–e82
133. Kannankeril PJ, Mitchell BM, Goonasekera SA, Chelu MG, Zhang W, Subeena S, Kearney DL, Danila CI, De Biasi M, Wehrens XHT, Pautler RG, Roden DM, Taffet GE, Dirksen RT, Anderson ME, Hamilton SL (2006) Mice with R176Q cardiac ryanodine receptor mutation exhibit catecholamine-induced ventricular tachycardia and cardiomyopathy. Proc Natl Acad Sci USA 32:12179–12184
134. Goddard CA, Ghais NS, Zhang Y, Williams AJ, Colledge WH, Grace AA, Huang CL-H (2008) Physiological consequences of the P2328S mutation in the ryanodine receptor (RyR2) gene in genetically modified murine hearts. Acta Physiol (Oxf) 194:123–140
135. Giulivi C, Ross-Inta C, Omanska-Klusek A, Napoli E, Sakaguchi D, Barrientos G, Allen PD, Pessah IN (2011) Basal bioenergetic abnormalities in skeletal muscle from ryanodine receptor malignant hyperthermia-susceptible R163C knock-in mice. J Biol Chem 286:99–113

136. Lehnart SE, Mongillo M, Bellinger AM, Lindegger N, Chen B-X, Hseuh W, Reiken S, Wronska A, Drew LJ, Ward CW, Lederer WJ, Kass RS, Morley G, Marks AR (2008) Leaky Ca^{2+} release channel/ryanodine receptor 2 causes seizures and sudden cardiac death in mice. J Clin Invest 118:2230–2245
137. Hidalgo C, Gonzalez ME, Garcia AM (1986) Calcium transport in transverse tubules isolated from rabbit skeletal muscle. Biochim Biophys Acta 854:279–286
138. Meissner G, Henderson JS (1987) Rapid calcium release from cardiac sarcoplasmic reticulum vesicles is dependent on Ca^{2+} and is modulated by Mg^{2+}, adenine nucleotide, and calmodulin. J Biol Chem 262:3065–3073
139. Palade P (1987) Drug-induced Ca^{2+} release from isolated sarcoplasmic reticulum. II. Releases involving a Ca^{2+}-induced Ca^{2+} release channel. J Biol Chem 262:6142–6148
140. Ohnishi T, Ebashi S (1963) Spectrophotometrical measurement of instantaneous calcium binding of the relaxing factor of muscle. J Biochem 54:506–511
141. Ogawa Y, Harafuji H, Kurebayashi N (1980) Comparison of the characteristics of four metallochromic dyes as potential calcium indicators for biological experiments. J Biochem 87:1293–1303
142. El-Hayek R, Yano M, Antoniu B, Mickelson JR, Louis CF, Ikemoto N (1995) Altered E-C coupling in triads isolated from malignant hyperthermia-susceptible porcine muscle. Am J Physiol 268:C1381–C1386
143. Currie S, Smith GL (1999) Enhanced phosphorylation of phospholamban and downregulation of sarco/endoplasmic reticulum Ca^{2+} ATPase type 2 (SERCA 2) in cardiac sarcoplasmic reticulum from rabbits with heart failure. Cardiovasc Res 41:135–146
144. Smith GL, Duncan AM, Neary P, Bruce L, Burton FL (2000) P(i) inhibits the SR Ca^{2+} pump and stimulates pump-mediated Ca^{2+} leak in rabbit cardiac myocytes. Am J Physiol Heart Circ Physiol 279:H577–H585
145. Ikemoto N, Yano M, El-Hayek R, Antoniu B, Morii M (1994) Chemical depolarization-induced SR calcium release in triads isolated from rabbit skeletal muscle. Biochemistry 33:10961–10968
146. Ikemoto N, Yamamoto T (2002) Regulation of calcium release by interdomain interaction within ryanodine receptors. Front Biosci 7:d671–d683
147. Zucchi R, Ronca-Testoni S (1997) The sarcoplasmic reticulum Ca^{2+} channel/ryanodine receptor: modulation by endogenous effectors, drugs and disease states. Pharmacol Rev 49:1–51
148. Pessah IN, Waterhouse AL, Casida JE (1985) The calcium-ryanodine receptor complex of skeletal and cardiac muscle. Biochem Biophys Res Commun 128:449–456
149. Lai FA, Meissner G (1989) The muscle ryanodine receptor and its intrinsic Ca^{2+} channel activity. J Bioenerg Biomembr 21:227–246
150. Chu A, Diaz-Munoz M, Hawkes MJ, Brush K, Hamilton SL (1990) Ryanodine as a probe for the functional state of the skeletal muscle sarcoplasmic reticulum calcium release channel. Mol Pharmacol 37:735–741
151. Zhao M, Li P, Li X, Zhang L, Winkfein RJ, Chen SR (1999) Molecular identification of the ryanodine receptor pore-forming segment. J Biol Chem 274:25971–25974
152. Chen SR, Li P, Zhao M, Li X, Zhang L (2002) Role of the proposed pore-forming segment of the Ca^{2+} release channel (ryanodine receptor) in ryanodine interaction. Biophys J 82:2436–2447
153. Gao L, Balshaw D, Xu L, Tripathy A, Xin C, Meissner G (2000) Evidence for a role of the lumenal M3-M4 loop in skeletal muscle Ca^{2+} release channel (ryanodine receptor) activity and conductance. Biophys J 79:828–840
154. Fessenden JD, Feng W, Pessah IN, Allen PD (2004) Mutational analysis of putative calcium binding motifs within the skeletal ryanodine receptor isoform, RyR1. J Biol Chem 279:53028–53035
155. Gibb AJ (1995) Patch-clamp recording. In: Ashley RH (ed) Ion channels: a practical approach. IRL Press, Oxford, pp 1–42
156. Mortensen M, Smart TG (2007) Single-channel recording of ligand-gated ion channels. Nat Protoc 2:2826–2841

157. Smith JS, Coronado R, Meissner G (1986) Single channel measurements of the calcium release channel from skeletal muscle sarcoplasmic reticulum. Activation by Ca^{2+} and ATP and modulation by Mg2+. J Gen Physiol 88:573–588
158. Holmberg SR, Williams AJ (1989) Single channel recordings from human cardiac sarcoplasmic reticulum. Circ Res 65:1445–1449
159. Ashley RH, Williams AJ (1990) Divalent cation activation and inhibition of single calcium release channels from sheep cardiac sarcoplasmic reticulum. J Gen Physiol 95:981–1005
160. Lai FA, Erickson HP, Rousseau E, Liu QY, Meissner G (1988) Purification and reconstitution of the calcium release channel from skeletal muscle. Nature 331:315–319
161. Lindsay AR, Williams AJ (1991) Functional characterisation of the ryanodine receptor purified from sheep cardiac muscle sarcoplasmic reticulum. Biochim Biophys Acta 1064:89–102
162. Williams AJ (1995) The measurement of the function of ion channels reconstituted into artificial membranes. In: Ashley RH (ed) Ion channels: a practical approach. IRL Press, Oxford, pp 43–67
163. Favre I, Sun YM, Moczydlowski E (1999) Reconstitution of native and cloned channels into planar bilayers. Methods Enzymol 294:287–304
164. Sitsapesan R, Williams AJ (1994) Gating of the native and purified cardiac SR Ca(2+)-release channel with monovalent cations as permeant species. Biophys J 67:1484–1494
165. Fill M, Copello JA (2002) Ryanodine receptor calcium release channels. Physiol Rev 82:893–922
166. Laver D (2001) The power of single channel recording and analysis: its application to ryanodine receptors in lipid bilayers. Clin Exp Pharmacol Physiol 28:675–686
167. Cukierman S, Yellen G, Miller C (1985) The K^+ channel of sarcoplasmic reticulum. A new look at Cs+ block. Biophys J 48:477–484
168. Tester DJ, Dura M, Carturan E, Reiken S, Wronska A, Marks AR, Ackerman MJ (2007) A mechanism for sudden infant death syndrome (SIDS): stress-induced leak via ryanodine receptors. Heart Rhythm 4:733–739
169. Tu Q, Velez P, Brodwick M, Fill M (1994) Streaming potentials reveal a short ryanodine-sensitive selectivity filter in cardiac Ca^{2+} release channel. Biophys J 67:2280–2285
170. Tomaskova Z, Gaburjakova M (2008) The cardiac ryanodine receptor: looking for anomalies in permeation properties. Biochim Biophys Acta 1778:2564–2572
171. Williams AJ, West DJ, Sitsapesan R (2001) Light at the end of the Ca^{2+}-release channel tunnel: structures and mechanisms involved in ion translocation in ryanodine receptor channels. Q Rev Biophys 34:61–104
172. Du GG, Guo X, Khanna VK, MacLennan DH (2001) Functional characterization of mutants in the predicted pore region of the rabbit cardiac muscle Ca^{2+} release channel (ryanodine receptor isoform 2). J Biol Chem 276:31760–31771
173. Wang R, Bolstad J, Kong H, Zhang L, Brown C, Chen SR (2004) The predicted TM10 transmembrane sequence of the cardiac Ca^{2+} release channel (ryanodine receptor) is crucial for channel activation and gating. J Biol Chem 279:3635–3642
174. Mead-Savery FC, Wang R, Tanna-Topan B, Chen SR, Welch W, Williams AJ (2009) Changes in negative charge at the luminal mouth of the pore alter ion handling and gating in the cardiac ryanodine-receptor. Biophys J 96:1374–1387
175. Wang Y, Xu L, Pasek DA, Gillespie D, Meissner G (2005) Probing the role of negatively charged amino acid residues in ion permeation of skeletal muscle ryanodine receptor. Biophys J 89: 256–265
176. Xu L, Wang Y, Gillespie D, Meissner G (2006) Two rings of negative charges in the cytosolic vestibule of type-1 ryanodine receptor modulate ion fluxes. Biophys J 90:443–453

Chapter 9
Ryanodine Receptor Physiology and Its Role in Disease

Johanna T. Lanner

Abstract The ryanodine receptors (RyRs) is the major intracellular Ca^{2+} release channel localized in the plasma membrane of the endoplasmatic/sarcoplasmatic reticulum. RyR-mediated Ca^{2+} release is crucial for every heart beat and skeletal muscle contraction and also important in learning and memory. Given the important role RyR has in physiological functions it is not surprising that dysregulation and impaired RyR channel function contributes to severe pathologies e.g. cardiac arrhythmias and Alzheimer's disease. Mutations in the RyR channels are associated with a number of human disorders e.g. malignant hyperthermia (MH) and central core disease (CCD), catecholaminergic polymorphic ventricular tachycardia (CPVT), and arrhythmogenic right ventricular dysplasia (ARVD). RyRs are modulated directly and indirectly by various ions, small molecules and proteins and RyR structure and function are expected to be defined within this macromolecular set of interactions. This article discusses the physiological function of RyR and examines its role in disorders and diseases.

Keywords Ryanodine receptor • Ca^{2+} • Skeletal muscle • Cardiac muscle • Sarcoplasmatic reticulum • Ca^{2+} leak • Ca^{2+} channel • RyR gene mutation • Malignant hyperthermia • Central core disease • Catecholaminergic polymorphic ventricular tachycardia • Diabetic cardiomyopathy • Alzheimer's disease

J.T. Lanner (✉)
Department of Physiology & Pharmacology, Karolinska Institutet,
von Eulersväg 8, 171 77 Stockholm, Sweden
e-mail: johanna.lanner@ki.se

M.S. Islam (ed.), *Calcium Signaling*, Advances in Experimental Medicine and Biology 740, DOI 10.1007/978-94-007-2888-2_9,

Ca^{2+} Dynamics and Ryanodine Receptors

Ca^{2+} is a multifaceted messenger and apart from enabling activation of contraction it also regulates other cellular events such as fertilization, synaptic transmission, gene transcription, memory and learning, hormonal signaling, metabolism, and cell death. Duration, amplitude, and spatial distribution of Ca^{2+} play a significant role in facilitating these diverse effects of Ca^{2+} [1–3]. The Ca^{2+}-signaling time scale spans from milliseconds, e.g. in exocytosis of neurotransmitters and in skeletal muscle contractions [1, 2, 4, 5], up to minutes and hours as observed in fertilization and immune responses [6–8]. Furthermore, free cytosolic Ca^{2+} can vary markedly in various cellular loci depending on the nature of the stimulus (i.e. microdomains of concentration gradients). These gradients can change with time and have completely different effects on various cellular events. For example, local hot spots at the mouth of Ca^{2+} channels enable neurotransmitter release and global prolonged oscillations can effect fertilization of oocytes and gene transcription [1, 2, 4, 6–8]. An increase in cytosolic Ca^{2+} is either derived from intracellular stores by opening of the endoplasmatic/sarcoplasmatic reticulum (ER/SR) Ca^{2+} release channels, or from the extracellular medium via Ca^{2+} influx channels sitting in the plasma membrane [1, 3, 9].

Ryanodine Receptor Isoforms, Expression and Modulators

The ryanodine receptor (RyR) is the largest known ion channel; it is a homotetramer with a total mass of >2 MDa (each subunit is >550 kDa) [10–15]. RyR is localized in the plasma membrane of ER/SR and is a large conductance channel capable of creating rapid transient increase in cytosolic Ca^{2+} [16, 17]. Four-fifths of the RyR protein is cytoplasmic and remaining, one-fifth, consists of luminal and membrane spanning domains. Three mammalian isoforms of RyR have been isolated and the terminology, RyR1-3, is based on in which order the isoforms were isolated and tissue of initial purification. However, none of the isoforms are entirely tissue-specific; RyR1 is predominantly expressed in skeletal muscle and in cerebellar Purkinje neurons [11, 14, 18, 19]; RyR2 is greatly expressed in cardiac muscle [12, 13], and is considered to be the most abundant isoform in the brain [19, 20]; RyR3 was first identified in the brain and is mainly found in cortical and hippocampal regions involved in learning and memory [15, 19, 21]. RyR3 is also expressed in the diaphragm [22].

RyR exist predominantly in the closed state, but it has been noted that they open randomly in the absence of any stimulus. Furthermore, it has been determined that the number of open RyR, and the frequency and duration can be modulated by many physiological agents. RyRs are modulated directly and indirectly by DHPR and by various ions, small molecules and proteins (e.g. Ca^{2+}, Mg^{2+}, protein kinase A (PKA), FK506 binding proteins (FKBP12 and 12.6), calmodulin (CaM), Ca^{2+}/CaM-dependent kinase II (CaMKII), calsequestrin (CSQ), triadin, and junctin) (Fig. 9.1).

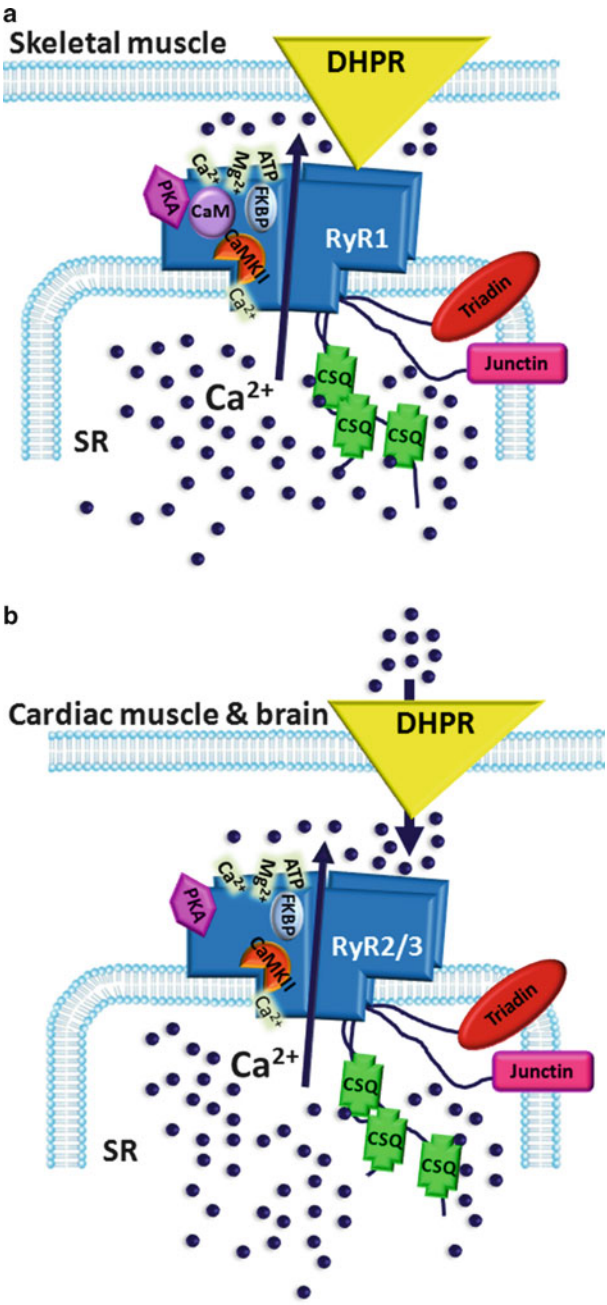

Fig. 9.1 ***Schematic illustration of the RyR complex in skeletal muscle, cardiac muscle, and brain.*** RyRs is modulated directly and indirectly by DHPR and by various ions, small molecules and proteins. Together they form a macromolecular complex that regulates Ca^{2+} release. (**a**) Illustrates the mechanic coupling between DHPR and RyR1 that occurs in skeletal muscle and (**b**) exemplifies Ca^{2+}-induced Ca^{2+} release that is found in cardiac muscle and in brain. Modulators bind to each monomer of the RyR tetramer, but are only depicted on one monomer for simplicity

These together form the core of the macromolecular complex that regulates RyR structure and function and hence Ca^{2+} release will be defined by this macromolecular set of interactions [23]. RyR1-3 have a similar sequence homology (~65%), but despite this the isoforms differ markedly in their response to modulators. For instance, each subtype show different Ca^{2+} binding affinities with RyR1 > RyR2 > RyR3. RyR1 activity shows a bell-shaped response curve; activated by low Ca^{2+} concentrations (~1 μM) and inhibition by high Ca^{2+} concentrations (~1 mM). RyR2 and RyR3, however, require substantially higher Ca^{2+} concentrations for feedback inhibition [24–27].

RyR in Skeletal and Cardiac Muscle Contraction

Every heart beat and skeletal muscle contraction is dependent on Ca^{2+}. The activation of the Ca^{2+}-dependent contractile machinery is similar in skeletal and cardiac muscle, with exception of the Ca^{2+} release process from SR [28, 29] (see Fig. 9.2 for schematic picture). In skeletal muscle, action potentials travel along an α-motor neuron to a group of muscle fibers. When the action potential reaches the muscle fibers, the neurotransmitter acetylcholine is released into the neuro-muscular cleft, which results in depolarization of the muscular membrane. This depolarization gives rise to an action potential, which propagates in all direction at the surface membrane and down to the inner parts of the muscle fiber via the transverse tubular (t-tubular) system. The t-tubules are narrow invaginations of the plasma membrane (sarcolemma) located in the A- and I-band interface in mammalian muscle, resulting in a branched network [30–32]. The action potential in the t-tubules activates voltage sensitive dihydropyridine receptors (DHPRs), also known as L-type Ca^{2+} channels ($Ca_{v1.1}$), located in the t-tubular wall. The DHPR are in close physical contact with the RyR1 in the SR membrane. When activated, DHPR opens RyR1 by mechanical interaction. The free cytoplasmic (myoplasmic) Ca^{2+} concentration is very low (~50 nM) under resting conditions, whereas [Ca^{2+}] inside SR is high (~1 mM). The low myoplasmic Ca^{2+} is maintained mainly by the adenosine trisphosphate (ATP) consuming SR Ca^{2+}-ATPase (SERCA) [33, 34]. Following of the action potential, RyR1 opens which results in release of Ca^{2+} from SR and a transient increase in myoplasmic Ca^{2+}. The myoplasmic Ca^{2+} binds to troponin C, initiating movement of tropomyosin, which allows actin and myosin interaction, and force development. After the action potential the SR Ca^{2+} release terminates. SERCA pumps Ca^{2+} back into SR and myoplasmic Ca^{2+} returns to resting levels and that stops myosin actin interaction [28, 30, 35]. In cardiac muscle, action potentials are initiated by pace maker cells. The action potential is longer (~200 ms) compared to skeletal muscle (~3 ms) [29, 36]. The longer action potential allows for the DHPRs ($Ca_{v1.2}$) to be open for a sufficient duration to permit Ca^{2+} influx to occur. Influx of Ca^{2+} ions induce the opening of the RyR2 and Ca^{2+} release from SR, a process known as Ca^{2+}-induced Ca^{2+} release. The increase in myoplasmic Ca^{2+} enables actin and myosin interaction (as described for skeletal muscle),

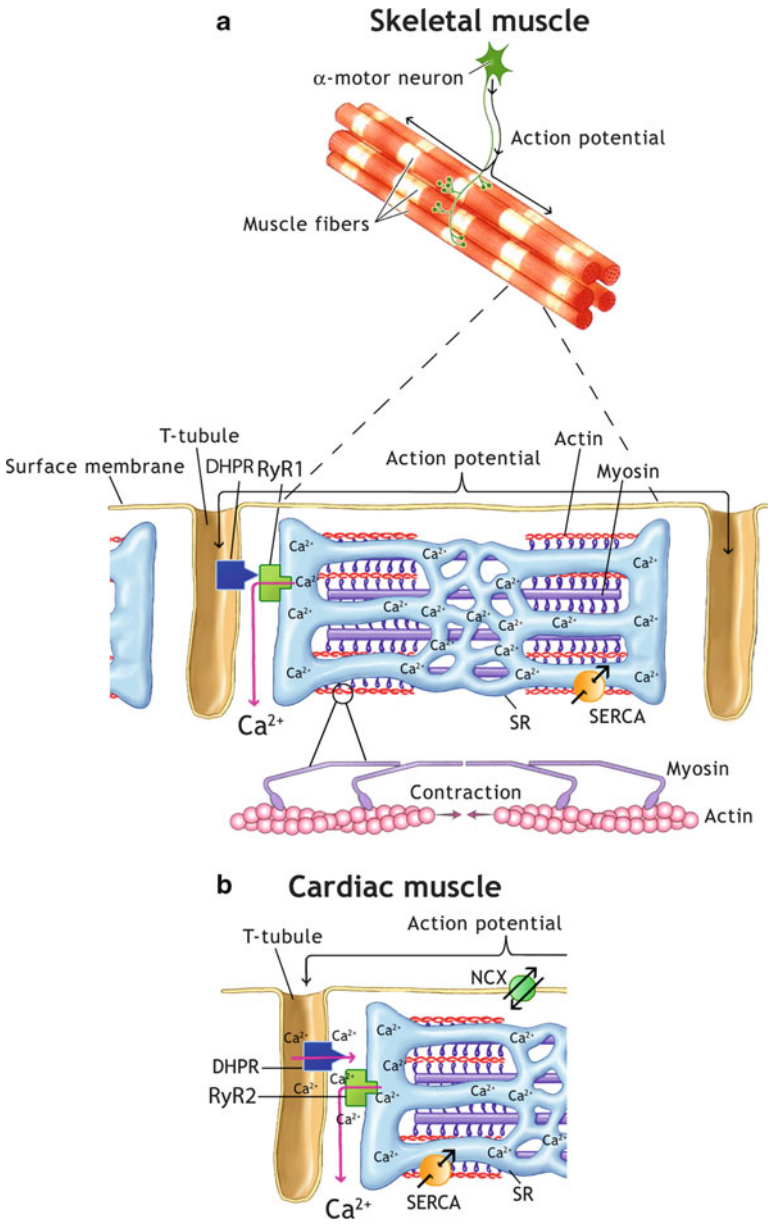

Fig. 9.2 ***Activation of the contractile machinery in skeletal and cardiac muscles.*** (**a**) An action potential travels along an α-motor neuron to a group of skeletal muscle fibers and triggers an action potential in each of the muscle fibers. The action potential in turn activates DHPR. The DHPR opens RyR by mechanical interaction resulting in release of Ca^{2+} from SR and a transient increase in myoplasmic Ca^{2+}, which enables actin and myosin interaction, and force development. SERCA pumps Ca^{2+} back into SR and myoplasmic Ca^{2+} returns to resting levels and the contraction ceases. (**b**) The activation of the Ca^{2+}-dependent contractile machinery is almost identical in cardiac muscle, with exception of the Ca^{2+} release process. The cardiac action potentials last longer compared to skeletal muscle, which results in Ca^{2+} influx through DHPRs and these Ca^{2+} ions induce opening of the RyR and Ca^{2+} release from SR. The increase in myoplasmic Ca^{2+} enables actin and myosin interaction. Myoplasmic Ca^{2+} return to resting levels by SERCA-mediated pumping of Ca^{2+} into SR and extrusion of Ca^{2+} via NCX

which eventually results in contraction. In cardiac muscle, myoplasmic Ca^{2+} returns to resting levels by SERCA-mediated pumping of Ca^{2+} to SR and by extrusion of Ca^{2+} via the Na^{+}-Ca^{2+} exchanger (NCX) [29].

Role of RyRs in Human Skeletal and Cardiac Muscle Disorders

Dysregulation and impaired RyR channel function can lead to severe muscle pathologies, which is not surprising given the important role RyR has in Ca^{2+} release and skeletal and cardiac muscle contraction. Several mutations in both RyR1 and RyR2 are associated with human disorders. For example, the first of these to be identified in 1960 was malignant hyperthermia (MH) [37] and later central core disease (CCD), catecholaminergic polymorphic ventricular tachycardia (CPVT), and arrhythmogenic right ventricular dysplasia (ARVD) [23]. More recently, it has been demonstrated that alterations in post-translational modifications of RyR e.g. phosphorylation, oxidation and nitrosylation also cause significant remodeling of the large RyR channel macromolecular complex and have been suggested to be involved in muscle pathologies including skeletal muscle fatigue and cardiac arrhythmias [38–41].

Changes in phosphorylation levels by kinases and phosphatases, and in the redox state by reactive oxygen/nitrogen species (ROS/RNS) constitutes a basal signaling system for the cell and is a reversible way for proteins to interact and modulate the RyR channels. However, hyperphosphorylation and/or high levels of ROS/RNS can cause deleterious and irreversible modifications of the RyR, which is associated with impaired muscle function and cardiac arrhythmias [38–42]. Precisely which phosphorylation sites are phosphorylated and which kinases are responsible for the hyperphosphorylation i.e. protein kinase A (PKA) [43–45] and/or calmodulin kinase II (CamKII) [46–49] has been a topic of debate. The overall hypothesis as to how this leads to altered RyR function is, however, generally accepted: in the heart increased phosphorylation is associated with increased SR Ca^{2+} leak, which contributes to reduced contractile function and increased propensity for arrhythmias [45–49]. In skeletal muscle, increased SR Ca^{2+} leak is linked to impaired muscle functions and exercise tolerance in mice [40, 41]. How hyperphosphorylation makes the RyR channels “leaky” is not fully understood but Marks and colleagues have suggested that hyperphosphorylation causes FKBP12/12.6s to dissociate from RyR, which results in “leaky” channels or larger numbers of spontaneous RyR openings, resulting in increased cytosolic Ca^{2+} levels, decreased SR Ca^{2+} load and decreased Ca^{2+} release [43, 44]. Disorders such as MH and CPVT which are caused by mutation in RyR1 and RyR2, respectively, are also associated with increased SR Ca^{2+} leak [45, 50–52]. FKBP12/12.6 are small cytosolic proteins (named according to their molecular mass) that physically interact with all three RyR isoforms but have different expression levels and binding affinity in different tissues [53–56]. In mammals FKBP12/12.6 binds four FKBPs per RyR homotetramer [57, 58]. FKBPs are considered to bind to RyR with high affinity and stabilize the closed state of the channel [43, 54, 59].

Alteration in the redox state of RyR is known to both increase and decrease its activity [60, 61]. RyR has approximately 100 cysteine residues per subunit and about 20 of them have been estimated to be available for redox modifications [62, 63]. Hypernitrosylation is also considered to produce RyR-mediated SR Ca^{2+} leak that is suggested to contribute to muscle weakness and decreased exercise endurance [39, 40]. Pharmacological treatment to stabilize RyR1, by preventing depletion of FKBPs from the RyR1 complex and hence decrease SR Ca^{2+}, has been shown to reduce muscle damage and improve muscle function in the mouse model of muscular dystrophy (*mdx*) [40]. Furthermore, increased RyR1 nitrosylation has been observed in mice with MH. The increased nitrosylation is suggested to sensitize the RyR1 channel and hence make it more prone to open spontaneously and to trigger heat stroke and MH crisis [41]. Moreover, comparable to CCD muscles MH muscles have been shown to demonstrate an additional associated myopathy characterized by central cores lacking mitochondria and increased SR Ca^{2+} leak combined with increased ROS/RNS production, which is believed to impact the structure and function of the muscle [41]. Durham et al. showed that treating MH mice with the antioxidant N-acetylcysteine (NAC) or with the nitric oxide synthase inhibitor, NG-nitro-L-arginine methyl ester (L-NAME), reduced the SR Ca^{2+} leak and improved the muscle function [41]. Together, attempts to reduce RyR-mediated SR Ca^{2+} leak seems beneficial for muscle function in both cardiac and skeletal muscle. Noteworthy, although altered RyR-mediated Ca^{2+} release caused by hyperphosphorylation and hypernitrosylations appears to play a central role in the process of cardiac arrhythmias and skeletal muscle function, it is important to remember that other targets of theses kinases and ROS/RNS could also alter the Ca^{2+} handling and Ca^{2+} effects in cardiac and skeletal muscles e.g. troponin I, sarcolemmal Ca^{2+} channels, and phospholamban.

Malignant Hyperthermia (MH)

MH is a potentially life-threatening disorder typically caused by mutations in the RyR1 channel. MH mutations predispose an affected individual to potentially fatal hypermetabolic reactions triggered by anesthetics (e.g. isoflurane and halothane), depolarizing muscle relaxants (e.g. succinylcholine) and exertion and heat challenge [23, 64–67]. The incidence of MH ranges from as high as 1:5,000 to as low as 1:50,000–100,000. However, the prevalence of genetic abnormalities in the *RyR1 gene* may be as great as 1:3,000 [67]. It is difficult to exactly determine the MH prevalence since it often is a silent disorder until the human or animal undergoes surgery or is exposed to high ambient temperatures (~37°C) [67, 68]. An MH episode is characterized by elevations in body core temperature, metabolic acidosis, hypoxia, tachycardia, skeletal muscle rigidity and rhabdamyolysis [37, 69, 70]. MH has also been described in pigs, cats, dogs and horses [37]. The overall underlying physiological consequence of MH is abnormal intracellular Ca^{2+} homeostasis with increased susceptibly of RyR1 channel opening in response to activators [41, 71].

Durham et al. recently showed in a knock-in mouse model of MH ($RyR1^{Y524S+/-}$) that the MH mutation makes RyR1 leak more Ca^{2+}, especially at higher temperatures [41]. The elevated intracellular Ca^{2+} and the associated increase in the ATP consuming SERCA pump generated increased oxidative/nitrosative stress and one effect of this was S-nitrosylation/oxidation of RyR1. The RyR1 S-nitrosylation in turn rendered the channel to become even more sensitive to temperature, activators, and leak even more Ca^{2+}. Together this produces a vicious feed-forward cycle that drives both MH episodes and the myopathy associated with the disease [41]. MH episodes are life-threatening if not immediately treated with the muscle relaxant dantrolene, which is currently the only clinically approved treatment for MH [72–74]. Dantrolene was introduced in the 1960s and decreased the mortality of MH from 80% to <10% today. The precise mechanism of dantrolene's action is still not completely understood. RyR1 is considered to be the major molecular target for dantrolene [73, 75, 76] and direct or indirect binding of dantrolene to RyR1 is believed to decrease SR Ca^{2+} release and thereby halt the MH episode [73]. However, adverse side-effects of dantrolene e.g. drowsiness, hepatoxicity, and significant muscle weakness preclude it from prophylactic usage [72–74]. Furthermore, Durham et al. tried to treat MH mice with the antioxidant NAC or the nitric oxide synthase inhibitor, L-NAME. This improved Ca^{2+} homeostasis and delayed the heat-induced increase in body core temperature but it did not prevent the MH response and hypermetabolism upon exposure of the mice to high temperatures [41].

Central Core Disease (CCD)

In addition to MH, mutations in *RyR1* are associated with the rare congenital myopathy CCD and the related multiminicore disease and nemaline myopathy [77–79]. CCD exhibits autosomal dominant and recessive models of inheritance [79]. CCD is believed to be the most common congenital myopathy and the total incidence of congenital myopathies is estimated to be around 6/100,000 live births [77]. Many patients with CCD also test positive for MH susceptibility in the characteristic *in vitro* caffeine contracture test (IVCT). Thus, they should be considered at risk of developing malignant hyperthermia episodes during general anesthesia [80]. Common clinical features of CCD in humans include muscle atrophy, lower limb skeletal muscle weakness leading to delayed motor developmental, and skeletal deformities e.g. scoliosis. However, significant clinical variability is observed, even within the same families [79]. CCD typically follows a static or only slow progressive course and almost all CCD patients achieve the ability to walk independently except the most severe neonatal cases. No curative treatment is currently available for CCD and presently the best available treatment is to preserve muscle power and function by regular physiotherapy [81].

Slow-twitch (type I) skeletal muscles (e.g. soleus) of CCD patients exhibit amorphous areas or "cores" that lack mitochondria and oxidative enzymes. The cores can be central or peripheral, single or multiple but what is consistent is that most of

them run along the length of the myofiber. The affected fibers also exhibit fibrosis and ectopic fat accumulation [77, 82]. Nevertheless, the knowledge of core formation and their pathological feature in muscle weakness and CCD is not well understood. The muscle weakness and core development in CCD are suggested to arise from two aberrant types of RyR1 channel behaviors. First, mutations in RyR1 results in constitutively overactive channels, which permits excessive SR Ca^{2+} leak as described in MH [83, 84]. Second, that RyR1 mutations may reduce the coupling between DHPR and RyR1 during the excitation and contraction process ("uncoupling"), which results in decreased RyR1-mediated Ca^{2+} release from the SR and leads to muscle weakness [84, 85]. Functional analysis of different CCD mutant RyR1 proteins has provided compelling support for both of these mechanisms and it appears to be dictated by the location of the particular disease-causing mutation [84, 86]. A total of 63 different mutations within the *RyR1 gene* are known to be associated with CCD in humans [23]. Of the six reported different RyR1 mutations in CCD that has been reconstituted in myotubes five have exhibited varying degrees of the leaky-channel phenotype (R164C, I404M, Y5523S, R2163H, R2435H) and only one (I4897T) function as an uncoupled channel [84, 86].

Catecholaminergic Polymorphic Ventricular Tachycardia (CPVT)

CPVT was first described in the 1970s as a familial tachyarrhythmia disorder induced by exercise and emotional stress leading to sudden death in individuals with structurally normal hearts [87]. CPVT is a rare but severe form of cardiac arrhythmia caused by mutations in RyR2 and CSQ2 [88–90]. CSQ2 is a low-affinity, high-capacity Ca^{2+} binding protein. CSQ2 is considered to be present in the SR as a mixture of monomers, dimers, and multimers. CSQ2 monomers interact with the RyR2 multicomplex via triadin and junctin [91]. The CSQ2-triadin-junctin complex is believed to serve as a luminal Ca^{2+} sensor for RyR2 by inhibiting RyR2 opening at low luminal Ca^{2+} levels [91, 92]. Approximately 10 times more RyR2 mutations linked to CPVT are known compared to identified CSQ2 mutations [87] and thus I will focus on RyR2. Several studies have demonstrated that CPVT linked RyR2 mutations respond to sympathetic activation with an abnormal diastolic Ca^{2+} leak from the SR which is suggested to be the basis of the arrhythmias. However, the pathways that mediate the response to adrenergic stimulation have not been completely defined but both PKA and CamKII phosphorylation are suggested to be involved [45, 51, 52]. For instance, recently CaMKII inhibition was shown to counteract the effects of adrenergic stimulation resulting in antiarrhythmic activity in the $RyR2^{R4496C+/-}$ knock-in mouse model of CPVT [50]. The results suggest that CaMKII inhibition attenuated SR Ca^{2+} leak and blunted catecholaminergic-mediated SERCA activation and could be considered a new therapeutic target for CPVT [50].

As it is recognized that β-adrenergic stimulation triggers ventricular tachycardia in CPVT, β-blockers are the considered first-line therapy today, but unfortunately they are not completely effective in preventing life-threatening arrhythmias [93, 94].

Recent reports show that flecainide treatment completely prevents adrenergic-induced arrhythmias in a mouse model of CPVT and in humans with *CSQ2* and *RyR2* mutations [95–97]. Flecainide is an approved antiarrhythmic drug known to block sodium channels but has showed remarkable efficacy in preventing spontaneous SR Ca^{2+} release by inhibiting RyR2 opening [96]. Lidocaine is another Na^{+} blocker that does not inhibit RyR2 and has very low clinical effect on CPVT [98]. Thus, flecinide appears to be a promising mechanism-based therapy in CPVT and an adjunct or alternative to β-blockers [95–97]. RyR2 mutations in CPVT have been detected at three regions that are homologous to those where the mutations in RyR1 associated with MH and CCD are found [23, 99]. The only known treatment for MH, dantrolene, which is thought to prevent the induction of MH crisis by reducing RyR1-mediated SR Ca^{2+} leak has been shown to also significantly inhibit epinephrine and exercise induced arrhythmias in the $RyR2^{R2474S+/-}$ mouse model of CPVT [100]. Thus, dantolene appears to bind to both RyR1 and RyR2. Dantrolene is a muscle relaxant and hence not suitable for long-term treatment but shows mechanistic confirmation that SR Ca^{2+} leak is involved in the pathogenesis of CPVT, and offers hope of future targeted dantrolene derivatives.

Arrhythmogenic Right Ventricular Dysplasia (ARVD)

ARVD is also a rare inherited disorder caused by RyR2 mutation located in same regions as CPVT and homologous with RyR1 mutations in MH and CCD [23, 99]. ARVD is characterized by substitution of the right ventricular myocardium with fibrofatty tissue, which appears to be a result of progressive death of cardiomyocytes resulting from apoptosis and inflammation [101]. Clinical presentation of ARVD is characterized by arrhythmias of right ventricular origin, ranging from premature beats to sustained ventricular fibrillation, often leading to sudden cardiac death [101]. It is believed that both ARVD and CPVT involve a functional defect in RyR2 resulting in increased SR Ca^{2+} leak [99]. Analogous to CPVT, ARVD patients also exhibit exercise- and adrenergic-induced fatal arrhythmias [99, 101]. Therapeutic options for ARVD remain limited, antiarrhythmic drug therapy e.g. β-blockers has been used but is not completely effective in preventing life-threatening arrhythmias [102]. Today implantable cardioverter/defibrillator appears to be the best treatment; it is an invasive method which is a risk itself, but has shown to be successful in averting sudden cardiac death [102]. Thus, given that CPVT and ARVD appear to have common features suggests that flecinide and dantrolene derivatives can be potential therapeutical options in the future.

Ryanodine Receptors in Diabetic Cardiomyopathy

Diabetes mellitus (type I and type II) is one major risk factor for cardiovascular disease which is the leading cause of death in United States [103, 104]. The cellular

and molecular mechanism for diabetes-induced reduction in myocyte and cardiac contractility remains not fully understood. As Ca^{2+} release and uptake are at the root of contraction and relaxation, defects in intracellular Ca^{2+} handling have been suggested as the source of cardiomyopathy [105–110]. Decreased Ca^{2+} release, Ca^{2+} transient amplitude, and SR Ca^{2+} load together with abnormal SERCA activity and impaired mitochondrial Ca^{2+} handling are all reported factors that result in depressed contractile function in diabetic cardiomyocytes [105, 109, 110]. Moreover, RyR2 from diabetic hearts is known to exhibit increased phosphorylation at Ser2809 and Ser2814 and reduced levels of FKBP12.6 [106, 107, 109]. These RyR2 serine residues are the same that are observed to be hyperphosphorylated in stress/exercise-induced cardiac arrhythmias and CPVT [38, 45, 99]. Diabetic hearts also have shown a reduction in the number of functional RyR2 channels, however, the functional ones showed increased sensitivity to Ca^{2+} activation [106, 107]. Field stimulation of the diabetic ventricular myocytes caused non-uniform intracellular Ca^{2+} release that was independent of Ca^{2+} influx via DHPR, which might be caused by reduced FKBP12.6 binding [106]. Thus, it appears as RyR2 can become 'leaky' both via specific phosphorylation events and/or by dissociation of FKBP12.6 from RyR2 during diabetes. This defect may partly be responsible for the increased incidence of arrhythmias, decreased contractility and sudden cardiac death in diabetes.

Ryanodine Receptors in Learning, Memory and Alzheimer's Disease

Neuronal Ca^{2+} signaling is usually strictly controlled to ensure proper function of the pleotropic Ca^{2+}-dependent processes including learning and memory. In the brain, activation of both inositol-1,4,5-trisphosphate receptors (IP_3R) and RyR channels is driven by Ca^{2+}-induced Ca^{2+} release. Long-term potentiation (LTP) is widely considered to be a major component that underlies learning and memory [111]. Dendritic spines from CA1 pyramidal cells where LTP is encoded have been shown to require RyR-mediated Ca^{2+} release [111]. Blocking RyRs with ryanodine (20 μM) blocks LTP induction [111] whereas application of a RyR agonist, caffeine (10 mM), has shown to facilitate LTP induction [112]. Thus, this suggests that RyR opening and resultant Ca^{2+} release play a role in the mechanism underlying learning and memory and furthermore it also seems to be involved in the pathogenesis of neurological disorders.

Growing evidence implicates Ca^{2+} signaling disruption in the origination of neurological diseases including Alzheimer's disease (AD) [113–115]. AD is a progressive neurodegenerative disorder characterized clinically by cognitive impairments and histopathologically by amyloid plaques, neurofibrillary tangles, and synaptic loss [116]. Biochemical mechanisms responsible for plaque formation are reasonable well understood, but it is still not clear why this leads to progressive degenerations of synapses and death of neurons [113, 116]. The Ca^{2+} hypothesis of AD is becoming more prominent since there is more and more evidence pointing to

involvement of IP_3R and RyR in the pathophysiology of AD [111, 114, 117, 118]. The basics of the AD Ca^{2+} hypothesis is that remodeling of Ca^{2+} signal changes the neuronal pathways, which distorts the normal Ca^{2+}-dependent mechanisms responsible for learning and memory. This normally occurs by an upregulation of signaling although downregulation has been described. Recently RyR-mediated Ca^{2+} release was shown to be greatly increased in pyramidal neurons from the 3xTg-AD mouse model of AD compared to non-transgenic mice [111]. The increased RyR-mediated Ca^{2+} release was suggested to be caused by reduced Ca^{2+}-induced Ca^{2+} release threshold, indicative of remodeling of Ca^{2+} signals in AD neurons [111].

One consistent finding in mouse models of AD is increased expression of RyR e.g. relative to control mice was a five-fold increase in protein expression of RyR2 found in the hippocampus of the 3xTg-AD mouse model of AD and this resulted in changes in both synaptic transmission and plasticity [117]. One function of RyR is to exaggerate the release of Ca^{2+} which has been demonstrated to be increased in neurons from AD compared to normal mice [119]. This could lead to increased neuronal intracellular Ca^{2+} levels which has previously been shown in AD mice and is intimately linked to apoptosis and cell death [120, 121]. Further studies are needed in order to understand the role of RyR in Alzheimer's disease but current evidence points towards a potential role of RyR in the pathogenesis of the disease. This also suggests that RyRs might be potential drug targets to reverse the Ca^{2+} remodeling of AD affected neuronal cells.

Concluding Remarks

Accurate Ca^{2+} signaling is required for proper physiological functions ranging from learning a new language to walking up the stairs. RyR mediated Ca^{2+} release plays an intriguing role in several of these physiological processes. Therefore, it is not unexpected that RyR malfunction results in severe diseases and disorders as described in this review. Although many questions still remain to be answered, it appears that RyR-mediated SR Ca^{2+} leak is a common feature in several disorders and diseases which may predispose for cardiac arrhythmias and skeletal muscle weakness. In Alzheimer's disease, gain-of-function of RyR and potentiation of Ca^{2+} release appears to remodel Ca^{2+} signals which in turn may contribute to the progression of the disease. Further understanding about these mechanisms is important in the development of therapeutics for treatment of diseases associated with RyR and Ca^{2+} dysfunction.

References

1. Rizzuto R, Pozzan T (2006) Microdomains of intracellular Ca^{2+}: molecular determinants and functional consequences. Physiol Rev 86:369–408
2. Sudhof TC (2002) Synaptotagmins: why so many? J Biol Chem 277:7629–7632

3. Berridge MJ, Bootman MD, Roderick LH (2003) Calcium signalling: dynamics, homeostasis and remodelling. Nat Rev Mol Cell Biol 4:517–529
4. Bootman MD, Lipp P, Berridge MJ (2001) The organisation and functions of local Ca^{2+} signals. J Cell Sci 114:2213–2222
5. Westerblad H, Lee JA, Lännergren J, Allen DG (1991) Cellular mechanisms of fatigue in skeletal muscle. Am J Physiol 261:C195–C209
6. Ozil JP, Swann K (1995) Stimulation of repetitive calcium transients in mouse eggs. J Physiol 483:331–346
7. Lewis RS (2001) Calcium signaling mechanisms in T lymphocytes. Annu Rev Immunol 19:497–521
8. Dolmetsch RE, Xu K, Lewis RS (1998) Calcium oscillations increase the efficiency and specificity of gene expression. Nature 392:933–936
9. Smyth JT, Hwang S-Y, Tomita T, DeHaven WI, Mercer JC, Putney JW (2010) Activation and regulation of store-operated calcium entry. J Cell Mol Med 14:2337–2349
10. Inui M, Saito A, Fleischer S (1987) Purification of the ryanodine receptor and identity with feet structures of junctional terminal cisternae of sarcoplasmic reticulum from fast skeletal muscle. J Biol Chem 262:1740–1747
11. Takeshima H, Nishimura S, Matsumoto T, Ishida H, Kangawa K, Minamino N, Matsuo H, Ueda M, Hanaoka M, Hirose T et al (1989) Primary structure and expression from complementary DNA of skeletal muscle ryanodine receptor. Nature 339:439–445
12. Nakai J, Imagawa T, Hakamat Y, Shigekawa M, Takeshima H, Numa S (1990) Primary structure and functional expression from cDNA of the cardiac ryanodine receptor/calcium release channel. FEBS Lett 271:169–177
13. Otsu K, Willard HF, Khanna VK, Zorzato F, Green NM, MacLennan DH (1990) Molecular cloning of cDNA encoding the Ca^{2+} release channel (ryanodine receptor) of rabbit cardiac muscle sarcoplasmic reticulum. J Biol Chem 265:13472–13483
14. Zorzato F, Fujii J, Otsu K, Phillips M, Green NM, Lai FA, Meissner G, MacLennan DH (1990) Molecular cloning of cDNA encoding human and rabbit forms of the Ca^{2+} release channel (ryanodine receptor) of skeletal muscle sarcoplasmic reticulum. J Biol Chem 265: 2244–2256
15. Hakamata Y, Nakai J, Takeshima H, Imoto K (1992) Primary structure and distribution of a novel ryanodine receptor/calcium release channel from rabbit brain. FEBS Lett 312: 229–235
16. Smith JS, Coronado R, Meissner G (1985) Sarcoplasmic reticulum contains adenine nucleotide-activated calcium channels. Nature 316:446–449
17. Smith J, Coronado R, Meissner G (1986) Single channel measurements of the calcium release channel from skeletal muscle sarcoplasmic reticulum: activation by Ca^{2+} and ATP and modulation by Mg^{2+}. J Gen Physiol 88:573–588
18. Furuichi T, Furutama D, Hakamata Y, Nakai J, Takeshima H, Mikoshiba K (1994) Multiple types of ryanodine receptor/Ca^{2+} release channels are differentially expressed in rabbit brain. J Neurosci 14:4794–4805
19. Hertle DN, Yeckel MF (2007) Distribution of inositol-1,4,5-trisphosphate receptor isotypes and ryanodine receptor isotypes during maturation of the rat hippocampus. Neuroscience 150:625–638
20. Lai FA, Dent M, Wickenden C, Xu L, Kumari G, Misra M, Lee HB, Sar M, Meissner G (1992) Expression of a cardiac Ca^{2+}-release channel isoform in mammalian brain. Biochem J 288:553–564
21. Futatsugi A, Kato K, Ogura H, Li S-T, Nagata E, Kuwajima G, Tanaka K, Itohara S, Mikoshiba K (1999) Facilitation of NMDAR-independent LTP and spatial learning in mutant mice lacking ryanodine receptor type 3. Neuron 24:701–713
22. Marks AR, Tempst P, Hwang KS, Taubman MB, Inui M, Chadwick C, Fleischer S, Nadal-Ginard B (1989) Molecular cloning and characterization of the ryanodine receptor/junctional channel complex cDNA from skeletal muscle sarcoplasmic reticulum. Proc Natl Acad Sci USA 86:8683–8687

23. Lanner JT, Georgiou DK, Joshi AD, Hamilton SL (2010) Ryanodine receptors: structure, expression, molecular details, and function in calcium release. Cold Spring Harb Perspect Biol 2:a003996
24. Meissner G (1986) Ryanodine activation and inhibition of the Ca^{2+} release channel of sarcoplasmic reticulum. J Biol Chem 261:6300–6306
25. Meissner G (1994) Ryanodine receptor/Ca^{2+} release channels and their regulation by endogenous effectors. Annu Rev Physiol 56:485–508
26. Meissner G, Rios E, Tripathy A, Pasek DA (1997) Regulation of skeletal muscle Ca^{2+} release channel (ryanodine receptor) by Ca^{2+} and monovalent cations and anions. J Biol Chem 272:1628–1638
27. Györke I, Györke S (1998) Regulation of the cardiac ryanodine receptor channel by luminal Ca^{2+} involves luminal Ca^{2+} sensing sites. Biophys J 75:2801–2810
28. Melzer W, Herrmann-Frank A, Lüttgau HC (1995) The role of Ca^{2+} ions in excitation-contraction coupling of skeletal muscle fibres. Biochim Biophys Acta 1241:59–116
29. Bers DM (2002) Cardiac excitation-contraction coupling. Nature 415:198–205
30. Dulhunty AF (1992) The voltage-activation of contraction in skeletal muscle. Prog Biophys Mol Biol 57:181–223
31. Franzini-Armstrong C (1991) Simultaneous maturation of transverse tubules and sarcoplasmic reticulum during muscle differentiation in the mouse. Dev Biol 146:353–363
32. Franzini-Armstrong C, Jorgensen AO (1994) Structure and development of E-C coupling units in skeletal muscle. Annu Rev Physiol 56:509–534
33. Carafoli E (1987) Intracellular calcium homeostasis. Annu Rev Biochem 56:395–433
34. Maclennan DH, Abu-Abed M, Kang C (2002) Structure-function relationships in Ca^{2+} cycling proteins. J Mol Cell Cardiol 34:897–918
35. Stephenson DG, Lamb GD, Stephenson GM (1998) Events of the excitation-contraction-relaxation (E-C-R) cycle in fast- and slow-twitch mammalian muscle fibres relevant to muscle fatigue. Acta Physiol Scand 162:229–245
36. Campbell DT (1983) Sodium channel gating currents in frog skeletal muscle. J Gen Physiol 82:679–701
37. Denborough M (1998) Malignant hyperthermia. Lancet 352:1131–1136
38. Lehnart SE, Mongillo M, Bellinger A, Lindegger N, Chen B-X, Hsueh W, Reiken S, Wronska A, Drew LJ, Ward CW, Lederer WJ, Kass RS, Morley G, Marks AR (2008) Leaky Ca^{2+} release channel/ryanodine receptor 2 causes seizures and sudden cardiac death in mice. J Clin Invest 118:2230–2245
39. Bellinger AM, Reiken S, Dura M, Murphy PW, Deng S-X, Landry DW, Nieman D, Lehnart SE, Samaru M, LaCampagne A, Marks AR (2008) Remodeling of ryanodine receptor complex causes "leaky" channels: a molecular mechanism for decreased exercise capacity. Proc Natl Acad Sci USA 105:2198–2202
40. Bellinger AM, Reiken S, Carlson C, Mongillo M, Liu X, Rothman L, Matecki S, Lacampagne A, Marks AR (2009) Hypernitrosylated ryanodine receptor calcium release channels are leaky in dystrophic muscle. Nat Med 15:325–330
41. Durham WJ, Aracena-Parks P, Long C, Rossi AE, Goonasekera SA, Boncompagni S, Galvan DL, Gilman CP, Baker MR, Shirokova N, Protasi F, Dirksen R, Hamilton SL (2008) RyR1 *S*-nitrosylation underlies environmental heat stroke and sudden death in Y522S RyR1 knockin mice. Cell 133:53–65
42. Ferdinandy P, Schulz R (2003) Nitric oxide, superoxide, and peroxynitrite in myocardial ischaemia-reperfusion injury and preconditioning. Br J Pharmacol 138:532–543
43. Marx SO, Reiken S, Hisamatsu Y, Jayaraman T, Burkhoff D, Rosemblit N, Marks AR (2000) PKA phosphorylation dissociates FKBP12.6 from the calcium release channel (Ryanodine receptor): defective regulation in failing hearts. Cell 101:365–376
44. Reiken S, Lacampagne A, Zhou H, Kherani A, Lehnart SE, Ward C, Huang F, Gaburjakova M, Gaburjakova J, Rosemblit N, Warren MS, He K-l, Yi G-h, Wang J, Burkhoff D, Vassort G, Marks AR (2003) PKA phosphorylation activates the calcium release channel (ryanodine receptor) in skeletal muscle: defective regulation in heart failure. J Cell Biol 160:919–928

45. Wehrens XH, Lehnart SE, Huang F, Vest JA, Reiken SR, Mohler PJ, Sun J, Guatimosim S, Song LS, Rosemblit N, D'Armiento JM, Napolitano C, Memmi M, Priori SG, Lederer WJ, Marks AR (2003) FKBP12.6 deficiency and defective calcium release channel (ryanodine receptor) function linked to exercise-induced sudden cardiac death. Cell 113:829–840
46. Ai X, Curran JW, Shannon TR, Bers DM, Pogwizd SM (2005) Ca^{2+}/calmodulin-dependent protein kinase modulates cardiac ryanodine receptor phosphorylation and sarcoplasmic reticulum Ca^{2+} leak in heart failure. Circ Res 97:1314–1322
47. Chelu MG, Sarma S, Sood S, Wang S, van Oort RJ, Skapura DG, Li N, Santonastasi M, Muller FU, Schmitz W, Schotten U, Anderson ME, Valderrabano M, Dobrev D, Wehrens XHT (2009) Calmodulin kinase II-mediated sarcoplasmic reticulum Ca^{2+} leak promotes atrial fibrillation in mice. J Clin Invest 119:1940–1951
48. Neef S, Dybkova N, Sossalla S, Ort KR, Fluschnik N, Neumann K, Seipelt R, Schondube FA, Hasenfuss G, Maier LS (2010) CaMKII-dependent diastolic SR Ca^{2+} leak and elevated diastolic Ca^{2+} levels in right atrial myocardium of patients with atrial fibrillation. Circ Res 106:1134–1144
49. Curran J, Brown KH, Santiago DJ, Pogwizd S, Bers DM, Shannon TR (2010) Spontaneous Ca waves in ventricular myocytes from failing hearts depend on Ca^{2+}-calmodulin-dependent protein kinase II. J Mol Cell Cardiol 49:25–32
50. Liu N, Ruan Y, Denegri M, Bachetti T, Li Y, Colombi B, Napolitano C, Coetzee WA, Priori SG (2011) Calmodulin kinase II inhibition prevents arrhythmias in $RyR2^{R4496C+/-}$ mice with catecholaminergic polymorphic ventricular tachycardia. J Mol Cell Cardiol 50:214–222
51. Kashimura T, Briston SJ, Trafford AW, Napolitano C, Priori SG, Eisner DA, Venetucci LA (2010) In the $RyR2^{R4496C+/-}$ mouse model of CPVT, β-adrenergic stimulation induces Ca^{2+} waves by increasing SR Ca^{2+} content and not by decreasing the threshold for Ca^{2+} waves. Circ Res 107:1483–1489
52. Jiang D, Xiao B, Zhang L, Chen SR (2002) Enhanced basal activity of a cardiac Ca^{2+} release channel (ryanodine receptor) mutant associated with ventricular tachycardia and sudden death. Circ Res 91:218–225
53. Chelu MG, Danila CI, Gilman CP, Hamilton SL (2004) Regulation of ryanodine receptors by FK506 binding proteins. Trends Cardiovasc Med 14:227–234
54. Brillantes AB, Ondrias K, Scott A, Kobrinsky E, Ondriasova E, Moschella MC, Jayaraman T, Landers M, Ehrlich BE, Marks AR (1994) Stabilization of calcium release channel (ryanodine receptor) function by FK506-binding protein. Cell 77:513–523
55. Jayaraman T, Brillantes AM, Timerman AP, Fleischer S, Erdjument-Bromage H, Tempst P, Marks AR (1992) FK506 binding protein associated with the calcium release channel (ryanodine receptor). J Biol Chem 267:9474–9477
56. Timerman AP, Onoue H, Xin H-B, Barg S, Copello J, Wiederrecht G, Fleischer S (1996) Selective binding of FKBP12.6 by the cardiac ryanodine receptor. J Biol Chem 271:20385–20391
57. Timerman AP, Ogunbumni E, Freund E, Wiederrecht G, Marks AR, Fleischer S (1993) The calcium release channel of sarcoplasmic reticulum is modulated by FK-506-binding protein. Dissociation and reconstitution of FKBP-12 to the calcium release channel of skeletal muscle sarcoplasmic reticulum. J Biol Chem 268:22992–22999
58. Qi Y, Ogunbunmi EM, Freund EA, Timerman AP, Fleischer S (1998) FK-binding protein is associated with the ryanodine receptor of skeletal muscle in vertebrate animals. J Biol Chem 273:34813–34819
59. Marx SO, Ondrias K, Marks AR (1998) Coupled gating between individual skeletal muscle Ca^{2+} release channels (Ryanodine Receptors). Science 281:818–821
60. Eager KR, Dulhunty AF (1998) Activation of the cardiac ryanodine receptor by sulfhydryl oxidation is modified by Mg^{2+} and ATP. J Membr Biol 163:9–18
61. Stoyanovsky D, Murphy T, Anno PR, Kim YM, Salama G (1997) Nitric oxide activates skeletal and cardiac ryanodine receptors. Cell Calcium 21:19–29
62. Zable AC, Favero TG, Abramson JJ (1997) Glutathione modulates ryanodine receptor from skeletal muscle sarcoplasmic reticulum. Evidence for redox regulation of the Ca^{2+} release mechanism. J Biol Chem 272:7069–7077

63. Xu L, Eu JP, Meissner G, Stamler JS (1998) Activation of the cardiac calcium release channel (ryanodine receptor) by poly-S-nitrosylation. Science 279:234–237
64. Bouchama A, Knochel JP (2002) Heat Stroke. N Engl J Med 346:1978–1988
65. Hopkins PM, Ellis FR, Halsall PJ (1991) Evidence for related myopathies in exertional heat stroke and malignant hyperthermia. Lancet 338:1491–1492
66. Capacchione JF, Muldoon SM (2009) The relationship between exertional heat illness, exertional rhabdomyolysis, and malignant hyperthermia. Anesth Analg 109:1065–1069
67. Rosenberg H, Davis M, James D, Pollock N, Stowell K (2007) Malignant hyperthermia. Orphanet J Rare Dis 2:21
68. Jurkat-Rott K, McCarthy T, Lehmann-Horn F (2000) Genetics and pathogenesis of malignant hyperthermia. Muscle Nerve 23:4–17
69. Pamukcoglu T (1988) Sudden death due to malignant hyperthermia. Am J Forensic Med Pathol 9:161–162
70. Ryan JF, Tedeschi LG (1997) Sudden unexplained death in a patient with a family history of malignant hyperthermia. J Clin Anesth 9:66–68
71. Tong J, McCarthy TV, MacLennan DH (1999) Measurement of resting cytosolic Ca^{2+} concentrations and Ca^{2+} store size in HEK-293 cells transfected with malignant hyperthermia or central core disease mutant Ca^{2+} release channels. J Biol Chem 274:693–702
72. Brandom BW, Larach MG, Chen MSA, Young MC (2011) Complications associated with the administration of dantrolene 1987 to 2006: a report from the North American malignant hyperthermia registry of the malignant hyperthermia association of the United States. Anesth Analg 112:1115–1123
73. Krause T, Gerbershagen MU, Fiege M, Weishorn R, Wappler F (2004) Dantrolene – a review of its pharmacology, therapeutic use and new developments. Anaesthesia 59:364–373
74. Ward A, Chaffman MO, Sorkin EM (1986) Dantrolene. A review of its pharmacodynamic and pharmacokinetic properties and therapeutic use in malignant hyperthermia, the neuroleptic malignant syndrome and an update of its use in muscle spasticity. Drugs 32:130–168
75. Palnitkar SS, Bin B, Jimenez LS, Morimoto H, Williams PG, Paul-Pletzer K, Parness J (1999) [3 H]Azidodantrolene: synthesis and use in identification of a putative skeletal muscle dantrolene binding site in sarcoplasmic reticulum. J Med Chem 42:1872–1880
76. Parness J, Palnitkar SS (1995) Identification of dantrolene binding sites in porcine skeletal muscle sarcoplasmic reticulum. J Biol Chem 270:18465–18472
77. Jungbluth H (2007) Central core disease. Orphanet J Rare Dis 2:25
78. Jungbluth H (2007) Multi-minicore disease. Orphanet J Rare Dis 2:31
79. Robinson R, Carpenter D, Shaw MA, Halsall J, Hopkins P (2006) Mutations in RYR1 in malignant hyperthermia and central core disease. Hum Mutat 27:977–989
80. Robinson RL, Brooks C, Brown SL, Ellis FR, Halsall PJ, Quinnell RJ, Shaw M-A, Hopkins PM (2002) RYR1 mutations causing central core disease are associated with more severe malignant hyperthermia in vitro contracture test phenotypes. Hum Mutat 20:88–97
81. Jungbluth H, Müller CR, Halliger-Keller B, Brockington M, Brown SC, Feng L, Chattopadhyay A, Mercuri E, Manzur AY, Ferreiro A, Laing NG, Davis MR, Roper HP, Dubowitz V, Bydder G, Sewry CA, Muntoni F (2002) Autosomal recessive inheritance of RYR1 mutations in a congenital myopathy with cores. Neurology 59:284–287
82. Sewry CA, Müller C, Davis M, Dwyer JSM, Dove J, Evans G, Schröder R, Fürst D, Helliwell T, Laing N, Quinlivan RCM (2002) The spectrum of pathology in central core disease. Neuromuscul Disord 12:930–938
83. Zhang Y, Chen HS, Khanna VK, De Leon S, Phillips MS, Schappert K, Britt BA, Browell AK, MacLennan DH (1993) A mutation in the human ryanodine receptor gene associated with central core disease. Nat Genet 5:46–50
84. Dirksen RT, Avila G (2002) Altered ryanodine receptor function in central core disease: leaky or uncoupled Ca^{2+} release channels? Trends Cardiovasc Med 12:189–197
85. Quane KA, Healy JM, Keating KE, Manning BM, Couch FJ, Palmucci LM, Doriguzzi C, Fagerlund TH, Berg K, Ording H et al (1993) Mutations in the ryanodine receptor gene in central core disease and malignant hyperthermia. Nat Genet 5:51–55

86. Avila G, Dirksen RT (2001) Functional effects of central core disease mutations in the cytoplasmic region of the skeletal muscle ryanodine receptor. J Gen Physiol 118:277–290
87. Napolitano C, Priori SG (2007) Diagnosis and treatment of catecholaminergic polymorphic ventricular tachycardia. Heart Rhythm 4:675–678
88. Laitinen PJ, Swan H, Kontula K (2004) Molecular genetics of exercise-induced polymorphic ventricular tachycardia: identification of three novel cardiac ryanodine receptor mutations and two common calsequestrin 2 amino-acid polymorphisms. Eur J Hum Genet 11: 888–891
89. Eldar M, Pras E, Lahat H (2003) A missense mutation in the CASQ2 gene is associated with autosomal-recessive catecholamine-induced polymorphic ventricular tachycardia. Trends Cardiovasc Med 13:148–151
90. Priori SG, Napolitano C, Tiso N, Memmi M, Vignati G, Bloise R, Sorrentino V, Danieli GA (2001) Mutations in the cardiac ryanodine receptor gene (hRyR2) underlie catecholaminergic polymorphic ventricular tachycardia. Circulation 103:196–200
91. Györke I, Hester N, Jones LR, Györke S (2004) The role of calsequestrin, triadin, and junctin in conferring cardiac ryanodine receptor responsiveness to luminal calcium. Biophys J 86: 2121–2128
92. Terentyev D, Kubalova Z, Valle G, Nori A, Vedamoorthyrao S, Terentyeva R, Viatchenko-Karpinski S, Bers DM, Williams SC, Volpe P, Gyorke S (2008) Modulation of SR Ca release by luminal Ca and calsequestrin in cardiac myocytes: effects of CASQ2 mutations linked to sudden cardiac death. Biophys J 95:2037–2048
93. Hayashi M, Denjoy I, Extramiana F, Maltret A, Buisson NR, Lupoglazoff J-M, Klug D, Hayashi M, Takatsuki S, Villain E, Kamblock J, Messali A, Guicheney P, Lunardi J, Leenhardt A (2009) Incidence and risk factors of arrhythmic events in catecholaminergic polymorphic ventricular tachycardia. Circulation 119:2426–2434
94. Haugaa KH, Leren IS, Berge KE, Bathen J, Loennechen JP, Anfinsen O-G, Früh A, Edvardsen T, Kongsgård E, Leren TP, Amlie JP (2010) High prevalence of exercise-induced arrhythmias in catecholaminergic polymorphic ventricular tachycardia mutation-positive family members diagnosed by cascade genetic screening. Europace 12:417–423
95. van der Werf C, Kannankeril PJ, Sacher F, Krahn AD, Viskin S, Leenhardt A, Shimizu W, Sumitomo N, Fish FA, Bhuiyan ZA, Willems AR, van der Veen MJ, Watanabe H, Laborderie J, Haïssaguerre M, Knollmann BC, Wilde AAM (2011) Flecainide therapy reduces exercise-induced ventricular arrhythmias in patients with catecholaminergic polymorphic ventricular tachycardia. J Am Coll Cardiol 57:2244–2254
96. Watanabe H, Chopra N, Laver D, Hwang HS, Davies SS, Roach DE, Duff HJ, Roden DM, Wilde AAM, Knollmann BC (2009) Flecainide prevents catecholaminergic polymorphic ventricular tachycardia in mice and humans. Nat Med 15:380–383
97. Hwang HS, Hasdemir C, Laver D, Mehra D, Turhan K, Faggioni M, Yin H, Knollmann BC (2011) Inhibition of cardiac Ca^{2+} release channels (RyR2) determines efficacy of class I antiarrhythmic drugs in catecholaminergic polymorphic ventricular tachycardia. Circ Arrhythm Electrophysiol 4:128–135
98. De Rosa G, Delogu A, Piastra M, Chiaretti A, Bloise R, Priori S (2004) Cathecolaminergic polymorphic ventricular tachycardia: successful emergency treatment with intravenous propranolol. Pediatr Emerg Care 20:175–177
99. Marks AR, Priori S, Memmi M, Kontula K, Laitinen PJ (2002) Involvement of the cardiac ryanodine receptor/calcium release channel in catecholaminergic polymorphic ventricular tachycardia. J Cell Physiol 190:1–6
100. Kobayashi S, Yano M, Suetomi T, Ono M, Tateishi H, Mochizuki M, Xu X, Uchinoumi H, Okuda S, Yamamoto T, Koseki N, Kyushiki H, Ikemoto N, Matsuzaki M (2009) Dantrolene, a therapeutic agent for malignant hyperthermia, markedly improves the function of failing cardiomyocytes by stabilizing interdomain interactions within the ryanodine receptor. J Am Coll Cardiol 53:1993–2005
101. Corrado D, Basso C, Thiene G (2000) Arrhythmogenic right ventricular cardiomyopathy: diagnosis, prognosis, and treatment. Heart 83:588–595

102. Muthappan P, Calkins H (2008) Arrhythmogenic right ventricular dysplasia. Prog Cardiovasc Dis 51:31–43
103. Gleissner CA, Galkina E, Nadler JL, Ley K (2007) Mechanisms by which diabetes increases cardiovascular disease. Drug Discov Today Dis Mech 4:131–140
104. Gu K, Cowie CC, Harris MI (1998) Mortality in adults with and without diabetes in a national cohort of the U.S. population, 1971–1993. Diabetes Care 21:1138–1145
105. Pereira L, Matthes J, Schuster I, Valdivia HH, Herzig S, Richard S, Gomez AM (2006) Mechanisms of $[Ca^{2+}]_i$ transient decrease in cardiomyopathy of *db/db* type 2 diabetic mice. Diabetes 55:608–615
106. Shao C-H, Rozanski GJ, Patel KP, Bidasee KR (2007) Dyssynchronous (non-uniform) Ca^{2+} release in myocytes from streptozotocin-induced diabetic rats. J Mol Cell Cardiol 42: 234–246
107. Shao C-H, Wehrens XHT, Wyatt TA, Parbhu S, Rozanski GJ, Patel KP, Bidasee KR (2009) Exercise training during diabetes attenuates cardiac ryanodine receptor dysregulation. J Appl Physiol 106:1280–1292
108. Tian C, Shao CH, Moore CJ, Kutty S, Walseth T, DeSouza C, Bidasee KR (2011) Gain of function of cardiac ryanodine receptor in a rat model of type 1 diabetes. Cardiovasc Res 91:300–309
109. Yaras N, Ugur M, Ozdemir S, Gurdal H, Purali N, Lacampagne A, Vassort G, Turan B (2005) Effects of diabetes on ryanodine receptor Ca^{2+} release channel (RyR2) and Ca^{2+} homeostasis in rat heart. Diabetes 54:3082–3088
110. Fauconnier J, Lanner JT, Zhang SJ, Tavi P, Bruton JD, Katz A, Westerblad H (2005) Insulin and inositol 1,4,5-trisphosphate trigger abnormal cytosolic Ca^{2+} transients and reveal mitochondrial Ca^{2+} handling defects in cardiomyocytes of *ob/ob* mice. Diabetes 54:2375–2381
111. Goussakov I, Chakroborty S, Stutzmann GE (2011) Generation of dendritic Ca^{2+} oscillations as a consequence of altered ryanodine receptor function in AD neurons. Channels (Austin) 5:9–13
112. Sajikumar S, Li Q, Abraham WC, Xiao ZC (2009) Priming of short-term potentiation and synaptic tagging/capture mechanisms by ryanodine receptor activation in rat hippocampal CA1. Learn Mem 16:178–186
113. Berridge M (2010) Calcium hypothesis of Alzheimer's disease. Pflugers Arch 459:441–449
114. Stutzmann GE, Caccamo A, LaFerla FM, Parker I (2004) Dysregulated IP3 signaling in cortical neurons of knock-in mice expressing an Alzheimer's-linked mutation in presenilin1 results in exaggerated Ca^{2+} signals and altered membrane excitability. J Neurosci 24:508–513
115. Guo Q, Fu W, Sopher BL, Miller MW, Ware CB, Martin GM, Mattson MP (1999) Increased vulnerability of hippocampal neurons to excitotoxic necrosis in presenilin-1 mutant knock-in mice. Nat Med 5:101–106
116. Mattson MP (2004) Pathways towards and away from Alzheimer's disease. Nature 430:631–639
117. Chakroborty S, Goussakov I, Miller MB, Stutzmann GE (2009) Deviant ryanodine receptor-mediated calcium release resets synaptic homeostasis in presymptomatic 3xTg-AD mice. J Neurosci 29:9458–9470
118. Goussakov I, Miller MB, Stutzmann GE (2010) NMDA-mediated Ca^{2+} influx drives aberrant ryanodine receptor activation in dendrites of young Alzheimer's disease mice. J Neurosci 30:12128–12137
119. Stutzmann GE, Smith I, Caccamo A, Oddo S, LaFerla FM, Parker I (2006) Enhanced ryanodine receptor recruitment contributes to Ca^{2+} disruptions in young, adult, and aged Alzheimer's disease mice. J Neurosci 26:5180–5189
120. Lopez JR, Lyckman A, Oddo S, LaFerla FM, Querfurth HW, Shtifman A (2008) Increased intraneuronal resting $[Ca^{2+}]$ in adult Alzheimer's disease mice. J Neurochem 105:262–271
121. Ruiz A, Matute C, Alberdi E (2010) Intracellular Ca^{2+} release through ryanodine receptors contributes to AMPA receptor-mediated mitochondrial dysfunction and ER stress in oligodendrocytes. Cell Death Dis 1:e54

Chapter 10
Phospholipase C

Charlotte M. Vines

Abstract Phospholipase C (PLC) family members constitute a family of diverse enzymes. Thirteen different family members have been cloned. These family members have unique structures that mediate diverse functions. Although PLC family members all appear to signal through the bi-products of cleaving phospholipids, it is clear that each family member, and at times each isoform, contributes to unique cellular functions. This chapter provides a review of the current literature. In addition, references have been provided for more in depth information regarding areas that are discussed. Ultimately, understanding the roles of the individual PLC enzymes, and their distinct cellular functions, will lead to a better understanding of the development of diseases and the maintenance of homeostasis.

Keywords Calcium • Diacyl glycerol • Heterotrimeric G protein • Inositol triphosphate • Isoforms • Isozymes • Phosphatidyl inositol • Phospholipase C • Signal transduction • Structure

Discovery

In 1953, it was reported that the addition of acetylcholine or carbamylcholine to pancreatic cells led to the production of phospholipids [1]. In these studies, ^{32}P was used to detect a seven-fold increase in the levels of phospholipids in the samples treated with the drugs, when compared with control slices, which had remained unstimulated. Although unrecognized at that time, this was the first evidence of the presence of phospholipase C (PLC) function in cells. More than 20 years later, in 1975, it was shown that impure preparations of PLC could be used to cleave phos-

C.M. Vines, Ph.D. (✉)
Department of Microbiology, Molecular Genetics and Immunology,
University of Kansas Medical Center, 3901 Rainbow Blvd,
MSN 3029, Kansas City, KS 66160, USA
e-mail: cvines@kumc.edu

M.S. Islam (ed.), *Calcium Signaling*, Advances in Experimental Medicine and Biology 740, DOI 10.1007/978-94-007-2888-2_10,

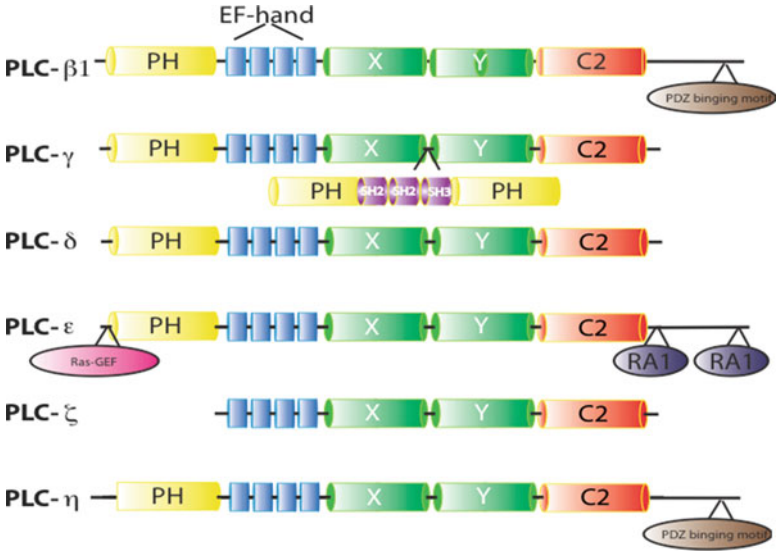

Fig. 10.1 Structures of the 6 different identified members of the PLC family. Relative positions of pleckstrin homology domain (PH), EF hand, X and Y domains and the C2 domains are shown. Unique domains found in individual family members include the following: Post synaptic density (PSD)-95, Drosophila disc large tumor suppressor (DlgA), and Zonula occludens-1 protein (zo-1) (PDZ), src homology 2 (SH2) and src homology 3 (SH3), Ras-GEF binding, and Ras associated (RA) domains. The PDZ domain is only found in one spliced form of PLCη

phatidylinositol [2]. In 1981, the first purified preparation of PLC was isolated [3]. A couple of years later it was found that the inositol trisphosphate (IP_3) generated from the cleavage of phosphatidylinositol 4,5 bisphosphate (also known as PI(4,5) P_2 or PIP_2) could induce the release of Ca^{2+} from intracellular stores [4] (Fig. 10.1). This important observation provided new insight into the function of PLC in living organisms. Eventually, the PLCβ, PLCγ, PLCδ, PLCε, PLCη and PLCζ cDNAs were cloned [5–10]. Although PIP_2 is a minor phospholipid in the plasma membrane, it plays a central role in regulating a host of cellular processes. PLC is activated following stimulation of cells with G protein-coupled receptor ligands including neurotransmitters, histamine, and hormones ([11–14] and as reviewed by [15]). Signaling through PLC family members regulates diverse functions, which will be outlined within this chapter. In addition, we will discuss PLC mediated signaling, common structural domains found in this family of enzymes, current knowledge about the isoforms and areas that have yet to be explored.

Cleavage of PIP_2 and Signaling

PLC is a cytoplasmic protein that controls the levels of PIP_2 in cells by localizing to the plasma membrane and catalyzing the hydrolysis of phosphorylated forms of phosphatidylinositol in response to cellular stimuli (Figs. 10.1 and 10.2). Therefore,

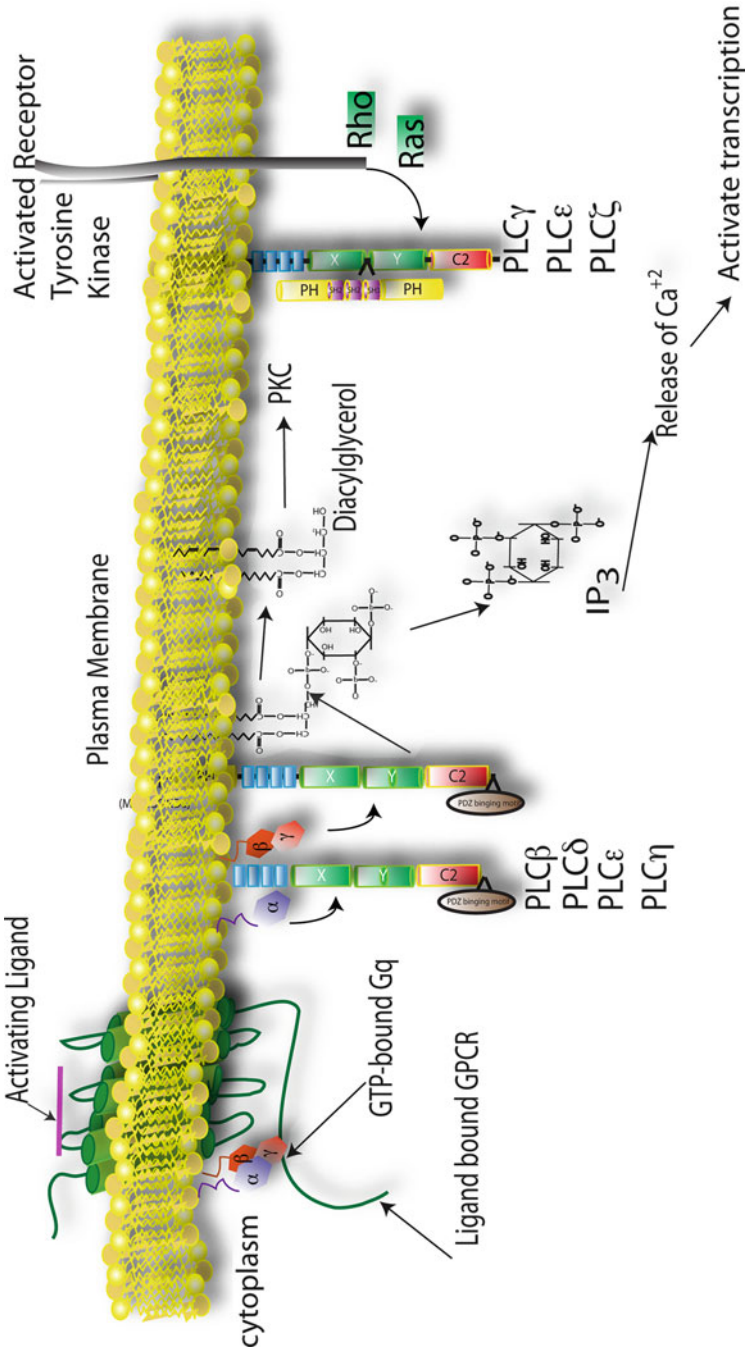

Fig. 10.2 Different effectors activate signaling through PLC to induce cleavage of PIP2 to yield diacylglycerol and inositol trisphosphate

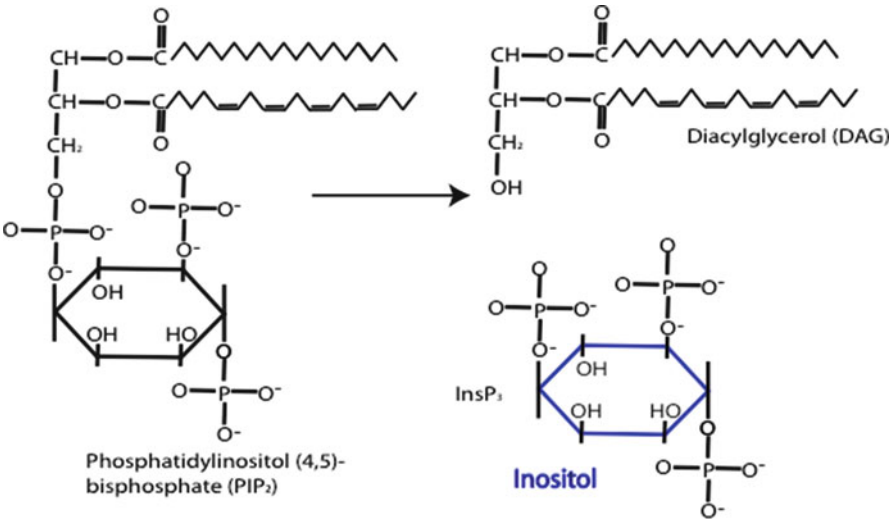

Fig. 10.3 PLC family members cleave PIP_2 to produce diacylglycerol and inositol trisphosphate

targeting of PLC to the plasma membrane plays a critical role in the functioning of this enzyme. The preferred substrate of PLC is PIP_2, followed by phosphatidyl inositol phosphate (PIP), and then phosphatidyl inositol (PI). Cleavage of PIP_2 leads to the generation of two products. One product, diacylglycerol (DAG), activates the calcium dependent protein kinase C (PKC), which then phosphorylates downstream effectors to activate an array of cellular functions including regulating cell proliferation, cell polarity, learning, memory and spatial distribution of signals [16, 17]. DAG, which remains membrane bound, can then be cleaved to produce another signaling molecule, arachidonic acid (Fig. 10.3). The second product, IP_3, is a small water-soluble molecule, which diffuses away from the membrane and through the cytosol to induce the release of Ca^{2+} from intracellular stores found within the endoplasmic reticulum [4]. In turn, the cytoplasmic calcium levels are quickly elevated and cause the characteristic calcium spike that signals cell activation. Once the endoplasmic reticulum stores have been used up, they are replenished through the store-operated calcium channels. Ca^{2+} activates downstream transcription factors resulting in a plethora of gene activation pathways. Signaling through PLC can regulate proliferation, differentiation, fertilization, cell division, growth, sensory transduction, modification of gene expression, activation, degranulation, secretion and motility [15, 18–25].

Structure of PLC

Thirteen different PLC family members have been identified in humans, which can be subdivided into six classes, β, γ, δ, ε, η and ζ (Fig. 10.2) [26, 27]. Different isoforms have been discovered in a wide range of species including mouse, rat and bovine.

PLC-like isozymes have been found in *Drosophila melanogaster*, *Glycine max* (soybean), *A. Thaliana*, *Saccharomyces cerevisiae,* and *Schizosaccharomyces pombe.* Overall, there is a low level of amino acid conservation between the family members; however, the similarity of the pleckstrin homology domains, the EF hand motifs, the X and Y domains and the C2 domains is greater than 40–50% [15]. With the exception of the PH domain, which is not expressed on PLCζ, each family member shares all of the core domains. A description of each domain [28] follows.

Pleckstrin Homology (PH) Domains

As mentioned, with the exception of PLCζ, the PLC family members have an N-terminal pleckstrin homology (PH) domain, which consists of approximately 120 amino acids. PH domains are common elements found in a large number of distinct protein families involved in signal transduction [29]. PH domains can mediate recruitment of the PLC family members to the plasma membrane. Unlike the PH domain of PLCδ1, which uses the PH domain to bind to the phosphatidylinositol 4,5-bisphosphate [PtdIns(4,5)P2] in the membrane, the PH domain of PLCβ2 cannot bind to phosphoinositides [30, 31]. Early on, it was found that the carboxy-terminal region of the PH domains of PLCγ, PLCβ2 and PLCβ3 controls the binding of the βγ subunits of G proteins to PLC following activation of G protein-coupled receptors [32]. Interestingly, the binding of the PH domain to Gβγ and the binding of the PH domain to Gα is mutually exclusive [32] and implicates PLC activation in preventing the regeneration of the Gα/Gβγ heterotrimeric G proteins. In this way [30] the binding may regulate the signaling of proteins that are activated following stimulation of G protein-coupled receptors.

EF Hand Motifs

The EF hands are helix-loop-helix motifs present in a number of calcium-binding proteins, such as calmodulin, calreticulin and troponin [33]. EF hand motifs were first described for PLC when the crystal structure analysis of PLCδ1 revealed the characteristic helix-loop-helix motifs [34]. Within PLC, the EF hand is part of the catalytic core that consists of an EF-hand, the X and Y and the C2 domains [34]. Upon binding to Ca^{2+}, the structure of PLC is stabilized as the EF-hand motifs undergo a conformational change to activate calcium-regulated functions, by exposing sites that become ligands for other proteins [35]. For example, in PLCβ, the EF hands contain sites that mediate association with subunits of heterotrimeric G proteins, while in PLCγ, the EF hands contain regions that lead to binding of tyrosine kinases [36]. Deletion of the EF hands in the enzyme reduces PLC function, independent of the Ca^{2+} concentration [37]; however, binding of Ca^{2+} to the EF-hand motifs can promote binding of PLC to PtdIns(4,5)P2 via the PH domain.

X and Y Domains

So far, PLCδ1, PLCβ2 and PLCβ3 have been crystallized and their structures analyzed [30, 34, 38]. The X and Y domains consist of approximately 300 amino acids and lie at the C-terminus of the EF-hand motifs. These domains consist of alternating α-helices and β-sheets that form a βαβαβαβ motif with a triosephosphate isomerase (TIM) barrel-like structure [34]. The X-region, containing all of the catalytic residues, is somewhat conserved across the PLC family members [27, 34]. The X-region forms one half of the TIM-barrel like structure. Within the X-region lies histidine residues that support the generation of the 1,2 cyclic inositol 4,5-bisphosphate [39]. The catalytic activity of this domain increases as the concentration of Ca^{2+} rises from 0.01 to 10 μM. Mutational analysis of rat PLCδ1 revealed that histidine^{311} and histidine^{356}, which are crucial for catalyzing the hydrolysis of PIP_2, have an important role within the X domain [39]. These residues are well conserved in PLC family members [39].

Structurally, the Y-domain (residues 489–606) forms the second half of the TIM-barrel-like architecture. This eightfold barrel structure is almost always found within an enzyme that regulates metabolism [40], although the functions of the enzymes are quite diverse. The Y-domain of PLC is found in the second half of the TIM-barrel-like structure, and contains an extended loop instead of a helix, which connects the β5 and β6 strand. This Y-domain is important for substrate recognition and regulates the preference of PLC for PIP2, PIP and PI [41, 42].

PLCγ contains a unique region that splits the X and Y domains. This region consists of two N-terminal src homology (SH2) domains followed by an SH3 domain. The SH2 domains provide docking sites for tyrosine kinase growth factor receptors such as the platelet derived growth factor receptors (PDGF-Rs) and the epidermal growth factor receptors (EGFRs) to promote activation of this PLC family member [43–45]. The binding of tyrosine kinase receptors to PLCγ results in phosphorylation and activation of PLCγ [46, 47]. The SH3 domain directs the cellular localization of signaling proteins such as dynamin and the actin cytoskeleton. In addition, the SH3 domains have been found to mediate nerve growth factor-induced cell proliferation through activation of a guanine nucleotide exchange factor for PI3K [48, 49].

C2 Domains

C2 domains are formed [50] from about 120 amino acids and can be found in more than 40 different proteins [34]. These motifs have several binding targets and have been implicated in signal transduction and membrane interactions. The C2 domains found within PLC family members are formed by an eight-stranded anti-parallel β-sandwich [34]. There are between three and four C2 domains found within PLCδ family members. In combination with Ca^{2+}, the C2 domain mediates the binding of PLCδ1 to anionic phospholipids. In this way, C2 domains mediate signal transduction and membrane trafficking [36]. C2 domains have common structural motifs,

which are found in PKCβ, rabphilin 3A [51, 52], and synaptotagmin I [53]. High cooperativity of Ca^{2+}-dependent phospholipid binding sites implies that there are multiple sites that bind Ca^{2+}, which function synergistically [36].

PDZ Domains

PDZ (Post synaptic density (PSD)-95, Drosophila disc large tumor suppressor (DlgA), and Zonula occludens-1 protein (zo-1)) binding motifs are separate from C2 domains, and are found in the C-terminal tails of PLCβ and PLCη lipases (Fig. 10.1) [50]. These motifs are thought to bind PDZ domains, which are formed by 5 of 6 β-strands and 2 or 3 α-helices [54]. The PDZ domain motif is found in many signaling proteins, where it functions as a scaffold for large molecular complexes [55]. In this way, the motif links many proteins to signaling from the cytoskeletal membranes. It has been postulated that each PLCβ form may be used by different G protein-coupled receptors in regulating signaling events [56].

Roles of Each PLC

Thirteen different PLCs have been identified, which fall into six classes based on structure (Fig. 10.2). There is no alpha form of PLC, since the protein that was originally described as the α form turned out to be a protein disulfide isomerase without phospholipase activity [57]. Under most conditions, PLC is a cytoplasmic protein that moves to the plasma membrane following activation catalyzing the hydrolysis of phosphatidyl inositol. There are exceptions to this rule, however, that will be discussed below. With the exception of PLCγ2, there have been spliced versions reported for each PLC isoform (as reviewed by [37, 26]). A different gene encodes each isoform. The diversity of the isoforms is created with splice variants. Using ESTs, different PLC family members have been proposed to associate with different tissues (as reviewed by [26]). For the purposes of this chapter, we will focus on the general properties described for each isoform.

PLCβ1,2,3,4

There are four isoforms of PLCβ that range in size from 130 kDa for PLCβ4, 140 kDa for PLCβ2, 150 kDa for PLCβ1 and 152 kDa for PLCβ3. In addition, although splice variants have been reported for each of these isoforms, it remains unclear why the multiple forms of PLCβ exist [58–60]. These well-characterized isoforms of PLC are classically activated by G protein-coupled receptors and their catalytic activity is entirely dependent upon Ca^{2+}. $PLC\beta_1$ serves as a GTPase-activating protein (GAP) for $G\alpha_q$ [61], while $G\alpha_q$, $G\alpha_{11}$, and $G\alpha_{16}$ can activate

PLCβ1, PCLβ2 and PLCβ3 family members [62]. In this case, the G protein-coupled receptor is stimulated by binding to its ligand, undergoing a conformational change to release $G\alpha_q$ or $G\alpha_{i/o}$ and Gβ/γ [61, 63, 64]. The PLCβ family members have an additional 450 amino acid residues in the C-terminus (Fig. 10.2). While all PLCβ family members have been found in the nucleus, PLCβ1 is the major nuclear PLC [65–67]. Within this C-terminal 450 amino acid region lies the greatest dissimilarity between PLC family members. In this region of the PLCβ1a and 1b splicing variants is a nuclear localization signal, which directs localization of PLCβ1 isoforms, mostly to the nucleus while a nuclear export signal allows PLCβ1a to remain in the cytosol [59]. In addition, the binding site for Gq is found within a region that mediates activation of Gαq by regulator of G protein signaling 4 (RGS4) and G alpha interacting protein (GAIP), which are GTPase-activating proteins (GAPs). This binding site blocks activation of PLCβ [68]. PLCβ1 is expressed at high levels in the cerebral cortex, retina, hippocampus and cardiomyocytes [69–71]. PLCβ2 can be activated by a member of the Rho-family of kinases, Rac [72].

The PH domain of PLCβ2 mediates binding of active forms of Rac (Rac1, Rac2 and Rac3), which leads to activation [73]. Unlike PLCβ1 and PLCβ2, PLCβ3 lacks 10–20 amino acids within its C-terminus [74], although the significance of this difference is unknown. This PLC isoform is expressed by liver, brain and parotid gland [74]. In contrast, the expression of PLCβ2, which shares 48% identity with PLCβ1, appears to be restricted to cells of the hematopoietic lineages [75].

Studies of $PLC\beta1^{-/-}$ mice revealed roles for PLCβ1 in regulating vision and central nervous system homeostasis. Loss of PLCβ1 can lead to seizures and sudden death [76]. PLCβ is recruited to the membranes through interactions with Gβγ, but not Gαq [77]. In addition, PLCβ is recruited only through specific Gα subunits and the Gβγ subunits. These studies demonstrate that the PLC family members respond specifically not only for Gα but for Gβγ as well [78, 79].

PLCγ1,2

There are two isoforms of PLCγ, PLCγ1 and PLCγ2. These family members are activated by both receptor and non-receptor protein tyrosine kinases [80] and play important roles in differentiation, proliferation, transformation, Ca^{2+} flux and tumorigenesis [21, 24, 81, 82]. Homozygous disruption of PLCγ1 in a mouse model revealed that this family member plays an essential role in growth and development [83]. In the absence of PLCγ1, the mice die at day E9.0, although until that stage of development the embryos appear normal. This mouse model revealed that although other PLCγ family members might be available, the role of PLCγ1 is essential and is not compensated by other proteins. In contrast, homozygous deletion of PLCγ2 leads to defects in platelet functions that are stimulated through β1 and β3 integrin adhesion proteins [84, 85]. PLCγ2 plays an essential role in B cell development, and function [19, 25]. Similar to PLCβ2, Rac, a member of the Rho-family of GTPases, can bind to and activate PLCγ2 [72]. This PLC family member can be activated

through interactions with the cytoplasmic tails of growth factor receptors by binding phosphorylated tyrosines within their intracellular tyrosine activation motifs (ITAMs). PLCγ2 also regulates Ca^{2+} oscillations induced by the transcription factor, nuclear factor of activated T cells (NFAT). Additionally, the SH2 domains can mediate activation of NFAT.

PLCγ1 is expressed ubiquitously [86], while PLCγ2 is found primarily in cells of the hematopoietic lineage [87]. PLCγ can regulate proliferation by functions that are independent of its lipase activity. One example is that DNA synthesis does not require phospholipase function, but instead is regulated through src homology 3 (SH3) recruitment of a Ras exchange factor, son-of-sevenless (SOS)1 [88]. In addition to the PH domain which is found in the N-terminus of most PLCg family members, these PLC family members have a second PH domain. This second PH domain is separated into two domains that flank two SH2 domains followed by an SH3 domain (Fig. 10.2). This C-terminal is thought to bind directly to the transient receptor potential cation channel (TRPC)3 Ca^{2+} channel, which then leads to agonist-induced Ca^{2+} entry into the cell [89]. T cells express more PLCγ1 than PLCγ2. PLCγ1 is activated by ligation of the T cell antigen receptor [90] and recruitment of PLCγ1 by linker of activated T cells (LAT) to the plasma membrane [91]. Phosphorylated LAT, in turn, serves as the primary docking site for the amino terminal SH2 domain of PLCγ1 to the membrane [92, 93]. All three SH domains of PLCγ1, however, are required to stabilize association of PLCγ1 with LAT, which is required to activate T cells [90]. Vav1, c-Cbl and SH2 domain-containing protein of 76 kDa (Slp76), via interactions with either the SH3 domain or the C-terminal SH2 domain, are also required to help stabilize the recruitment of PLCγ1 to the plasma membrane [90]. Following engagement of the T cell receptor (TCR), PLCγ1 production of DAG leads to activation of not only PKC, but also Ras guanyl releasing protein (GRP)-dependent signaling events [94, 95].

PLCγ1 is also activated by certain G protein-coupled receptors. Recently, we have shown that PLCγ1 can also be activated following stimulation of the C-C chemokine Receptor 7, a $G\alpha_{i/o}$ receptor, to mediate activation of β1 integrin, heterodimeric adhesion receptors [96]. In addition, PLCγ1 and PLCγ2 are both activated by the angiotensin and bradykinin G protein coupled receptors.

PLCδ1,3,4

There are three identified isoforms of PLCδ [97]. The isoform originally identified from bovine as PLCδ2 was found to be a homologue of mouse and human PLCδ4 [98]. This isoform of PLC has an absolute requirement for Ca^{+2} in order to carry out its role in the cell. The PLCδ family members are activated by levels of Ca^{2+} that are normally found in the cytoplasm (10^{-7} to 10^{-5} M) [99, 100]. While PLCδ1 is localized to the cytoplasm in quiescent cells, this PLC isoform can shuttle between the nucleus and the cytoplasm following activation [101]. Depletion of PLCδ1 leads to a block in the cell cycle [102]. PLCδ family members are thought to have a role in

potentiating calcium signaling [99]. This form of PLC is similar to non-mammalian forms of PLC [15, 103]. Gi/o and Ga_q can activate PLCδ1 following stimulation of coupled G protein-coupled receptors [104]. PLCδ is involved in regulating the activation of the actin cytoskeleton.

Misregulation of PLCδ1 has been linked to Alzheimer's disease [105]. In these patients, using a PLCδ specific antibody, the family member was found at high concentration within the neurofibrilary tangles, the neuritis that surround the senile plaque cores and within neuropil threads of the brains of patients with Alzheimer's disease. Interestingly, this function of this PLC is inhibited by sphingomyelin, a membrane lipid that is found in high concentrations in neurons. PLCδ1 is also misregulated in rat models of hypertension [106].

PLCδ1 is expressed at high levels in hair follicles. Homozygous deletion of PLCδ1 leads to hair loss [107, 108]. It was found that hair loss was due to an increase in leukocytes, specifically macrophages, neutrophils and T cells within the hair follicle [108]. These observations led to speculation that PLCδ1 can regulate the degree of inflammation as marked by leukocyte infiltration, within the hair follicle. Homozygous deletion of PLCδ3 or PLCδ4 had no apparent effect and the mice appeared normal.

During fertilization, a transient increase in Ca^{2+} precedes oocyte activation. Like other forms of PLC, this isoform appears to play a role in fertilization. Notably, PLCδ4$^{-/-}$ male mice are sterile [109, 110]. Even when PLCδ4$^{-/-}$ sperm were injected into oocytes, few viable embryos developed. These studies implicate this family member in the regulation of fertilization [109]. In the same study, sperm isolated from PLCδ4 knockout mice were found to be inferior to sperm isolated from wild type mice in that the Ca^{2+} oscillations in these mice were delayed or did not occur at all [109].

PLCε

PLCε is the largest of the PLC family members cloned to date, with an apparent molecular weight of 250 kDa. This PLC isoform is expressed at the highest levels in the heart, liver and lung, but can also be found in the skeletal muscle, spleen, brain, lungs, kidneys, pancreas, testis and uterus, thymus and intestine [7, 111, 112]. This class of PLC, which was originally identified in *Caenorhabditis elegans* and was later cloned in humans [7, 111–113], is activated through association of its Ras-binding (RA) domains, by Ras. The RA domains consist of approximately 100 amino acids that interact directly with the Ras-family GTPases, Ras [7, 112] and Rho [114]. Subsequently, it was found that PLCε could also be activated by the $G\alpha_{12}$ and Gβ/γ released by activated G protein coupled receptors [112, 115]. Receptors that activate PLCε include the adrenergic and PGE receptors. In addition, Gαs has been shown to stimulate activation of phospholipase Ce [116], whereas $G\alpha_{12}$ and $G\alpha_{13}$ can activate RhoA, which can stimulate PLCε [116, 117]. Not only was this PLC family member found to be activated by Ras and Rho, it was also shown to

be able to function as a guanine nucleotide exchange factor (GEF) for the Ras superfamily of GTPases [112]. In a contrasting study, the CDC25 domain of PLCε was found to serve as a GEF for Rap1 but not for other Ras family members [118]. These characteristics of PLCε reveal that, unlike any other PLC family member, the PLCε enzyme can be activated not only by subunits of heterotrimeric G proteins, but also by small GTPases.

This ability of PLCε to be regulated by Ras as well as Rho suggests that this family member can contribute to both proliferation and migration. More interestingly, since PLCβ can be activated by Rho, both PLC family members may work together to regulate signal transduction pathways that are activated following stimulation of cells by Rho to control cell migration. Similarly, since PLCε can be regulated by Ras, a downstream effector of PLCγ signaling following activation of growth factor receptors such as the epidermal growth factor (EGF) receptor, the signaling pathways may work together to promote proliferation. The ability of PLCε to coordinate signaling through these pathways points to regulatory mechanisms that may be more complex than originally thought.

PLCζ

To date, PLCζ expression has been confined to mammalian sperm heads [10, 119, 120] where it serves to activate oocytes during fertilization [10, 121]. Although this is the only isoform of PLC identified that lacks the N-terminal PH domain, it shares the closest homology with PLCδ1 [122]. The absence of the PH domain demonstrates that its presence is not required for membrane localization of PLCζ. It is unclear, however, how PLCζ targets the plasma membrane in the absence of the PH domain. There is some indication that the C2 domain may contribute to targeting PLCζ to membrane-bound PIP_2. Following fusion of sperm with the oocyte, PLCζ is released into an oocyte, which until that point, is arrested at the second meiotic division. Ca^{2+} oscillations that mediate activation of an oocyte are due to IP_3 mediated Ca^{2+} release. The presence of PLCζ within the cytoplasm leads to Ca^{2+} oscillations, which are classically observed during activation of the oocyte and release from the meiotic arrest [123]. In addition, immuno-depletion of PLCζ suppresses Ca^{2+} release. After the oocyte is fertilized, the Ca^{2+} oscillations end when the pronuclei form [124, 125]. It is unclear how PLCζ function is attenuated at this point.

PLCη1,2

The sequence homology between PLCη1 and PLCη2 is ~50%. PLCη1 has an apparent molecular weight of 115 kDa in mouse and humans, while PLCη2 is larger

at 125 kDa. The PLCη$_1$ and PLCη$_2$ isoforms are localized to the brain and neurons and are extremely sensitive to changes in Ca^{2+} levels [8, 9, 126, 127]. Like PLCδ, this form of PLC responds to the 100 nM Ca^{2+} concentrations found inside the cell [9]. However, PLCη is more sensitive than PLCδ [8]. PLCη2 is expressed in the infant brain, specifically in the hippocampus, cerebral cortex and olfactory bulb [9], where it may play an important role in Ca^{2+} mobilization required for axon growth and retraction, growth cone guidance, the generation of synapses and neurological responses [9]. PLCη signaling has been linked to activation of G protein-coupled receptors in neurons, where it is activated by Ca^{2+} and in this way functions to amplify signaling [128]. In humans, loss of the human chromosomal region, which encodes PLCη2, has been linked to mental retardation [129].

Methods to Inhibit PLC

Several chemical inhibitors can be used to block PLC function. A commonly used pan inhibitor, 1-[6-((17β-3-methoxyestra-1,3,5(10)trien-17-yl)amino)hexyl]-1H-pyrrole-2,5-dione, (U71322), of phospholipase C, is thought to function by blocking translocation of the enzyme to the membrane [130]. For example, using 2 μM U73122, we found that stimulation of CCR7 through one of its ligands, CCL21 [96], but not CCL19, promoted PLCγ1 dependent migration of T cells via β1 integrin adhesion proteins. These data suggest that one G protein-coupled receptor can activate PLCγ1 through two different ligands to control migration in T cells. In this case, we speculate that PLCγ1 mediates integrin activation through inside-out signaling, leading to activation of β1-integrins.

Recently, it has been shown that U73122 forms covalent associations with human PLCβ3, when the phospholipase is associated with mixed micelles [131]. U73122 has been used as a pan inhibitor of PLC in numerous studies [20, 96, 132–136]. However, in the study by Klein et al., instead of inhibiting PLC, U73122 activated human PLCγ1, human PLCβ2 and human PLCβ3, which had been incorporated into micelles, by differing magnitudes. Since the PLC used in these studies was in a purified form, it is unclear how U73122 functions to regulate the extent of PLC activation. In a second study, 1 μM U73122 was found to directly inhibit G protein-activated inwardly rectifying potassium channels. This was in contrast to a second PLC inhibitor, 2-Nitro-4-carboxyphenylN,N -diphenylcarbamate (NCDC), which did not have that effect [137]. NCDC, however, is also thought to have non-specific effects that are not related to PLC functions [138]. Other inhibitors such as PLC inhibitor, 1-O-octadecyl-2-O-methyl-rac-glycero-3-phosphorylcholine (ET-18-OCH3), have been described as selective [139, 140].

The use of heterozygous deletion of siRNA, or shRNA, however, can yield targeted results [96]. In these studies, PLCγ1 specific siRNA was used to confirm the role of this PLC isoform in the regulation of β1 integrins during the adhesion of primary T cells. In the future, it may be advisable to determine the specific PLC family member involved in a cellular response by using siRNAs.

Future Directions

It is unclear how the different isoforms of PLC are activated in cells receiving multiple stimuli from different receptors. With 13 identified isoforms expressed in multiple cell types, it will be important to define how the different signaling events that are linked to each isoform are controlled. Since PLC activation leads to release of IP_3 and DAG in response to activation, it will be necessary to determine how cells discriminate between multiple PLC signals in order to understand the hierarchy, intensity and duration of signaling events. As mentioned, PLCβ2 and PLCγ2 are activated by Rac, while PLCε is activated by RhoA. These observations suggest that key regulators of cell motility function through different PLC family members, and may have pivotal roles in defining where and when a cell migrates.

Phospholipase C enzymes are found in every cell in the body, where they play critical roles in regulating diverse cellular responses (as reviewed in [26]). As mentioned, some family members serve as scaffolds for other signaling proteins, while others can serve as GAPs or GEFs for secondary signaling proteins. Other PLCs function to amplify the Ca^{2+} oscillations in the cell. Certain PLC family members can travel to the nucleus to control signaling there. With PLC family members playing key roles in numerous cell functions, it will be important to define how each PLC is regulated and how the cellular environment affects the duration and intensity of the response.

References

1. Hokin MR, Hokin LE (1953) Enzyme secretion and the incorporation of P32 into phospholipides of pancreas slices. J Biol Chem 203:967–977
2. Michell RH, Allan D (1975) Inositol cyclis phosphate as a product of phosphatidylinositol breakdown by phospholipase C (Bacillus cereus). FEBS Lett 53:302–304
3. Takenawa T, Nagai Y (1982) Effect of unsaturated fatty acids and Ca^{2+} on phosphatidylinositol synthesis and breakdown. J Biochem 91:793–799
4. Streb H, Irvine RF, Berridge MJ, Schulz I (1983) Release of Ca^{2+} from a nonmitochondrial intracellular store in pancreatic acinar cells by inositol-1,4,5-trisphosphate. Nature 306:67–69
5. Suh PG, Ryu SH, Moon KH, Suh HW, Rhee SG (1988) Inositol phospholipid-specific phospholipase C: complete cDNA and protein sequences and sequence homology to tyrosine kinase-related oncogene products. Proc Natl Acad Sci USA 85:5419–5423
6. Suh PG, Ryu SH, Moon KH, Suh HW, Rhee SG (1988) Cloning and sequence of multiple forms of phospholipase C. Cell 54:161–169
7. Kelley GG, Reks SE, Ondrako JM, Smrcka AV (2001) Phospholipase C(epsilon): a novel Ras effector. EMBO J 20:743–754
8. Hwang JI, Oh YS, Shin KJ, Kim H, Ryu SH, Suh PG (2005) Molecular cloning and characterization of a novel phospholipase C, PLC-eta. Biochem J 389:181–186
9. Nakahara M, Shimozawa M, Nakamura Y, Irino Y, Morita M, Kudo Y, Fukami K (2005) A novel phospholipase C, PLC(eta)2, is a neuron-specific isozyme. J Biol Chem 280:29128–29134
10. Saunders CM, Larman MG, Parrington J, Cox LJ, Royse J, Blayney LM, Swann K, Lai FA (2002) PLC zeta: a sperm-specific trigger of Ca(2+) oscillations in eggs and embryo development. Development 129:3533–3544

11. Albuquerque EX, Thesleff S (1967) Influence of phospholipase C on some electrical properties of the skeletal muscle membrane. J Physiol 190:123–137
12. Macchia V, Pastan I (1967) Action of phospholipase C on the thyroid. Abolition of the response to thyroid-stimulating hormone. J Biol Chem 242:1864–1869
13. Portela A, Perez JC, Stewart P, Perez R, Vicente JA, Luchelli MA, Paris MN (1966) Membrane response to phospholipase C and acetylcholine in cesium and potassium Ringer. Acta Physiol Lat Am 16:380–386
14. Trifaro JM, Lejen T, Rose SD, Pene TD, Barkar ND, Seward EP (2002) Pathways that control cortical F-actin dynamics during secretion. Neurochem Res 27:1371–1385
15. Fukami K, Inanobe S, Kanemaru K, Nakamura Y (2010) Phospholipase C is a key enzyme regulating intracellular calcium and modulating the phosphoinositide balance. Prog Lipid Res 49:429–437
16. Sun MK, Alkon DL (2010) Pharmacology of protein kinase C activators: cognition-enhancing and antidementic therapeutics. Pharmacol Ther 127:66–77
17. Rosse C, Linch M, Kermorgant S, Cameron AJ, Boeckeler K, Parker PJ (2010) PKC and the control of localized signal dynamics. Nat Rev Mol Cell Biol 11:103–112
18. Akutagawa A, Fukami K, Banno Y, Takenawa T, Kannagi R, Yokoyama Y, Oda K, Nagino M, Nimura Y, Yoshida S, Tamiya-Koizumi K (2006) Disruption of phospholipase Cdelta4 gene modulates the liver regeneration in cooperation with nuclear protein kinase C. J Biochem 140:619–625
19. Hashimoto A, Takeda K, Inaba M, Sekimata M, Kaisho T, Ikehara S, Homma Y, Akira S, Kurosaki T (2000) Cutting edge: essential role of phospholipase C-gamma 2 in B cell development and function. J Immunol 165:1738–1742
20. Hong J, Behar J, Wands J, Resnick M, Wang LJ, Delellis RA, Lambeth D, Cao W (2010) Bile acid reflux contributes to development of esophageal adenocarcinoma via activation of phosphatidylinositol-specific phospholipase Cgamma2 and NADPH oxidase NOX5-S. Cancer Res 70:1247–1255
21. Li M, Edamatsu H, Kitazawa R, Kitazawa S, Kataoka T (2009) Phospholipase Cepsilon promotes intestinal tumorigenesis of Apc(Min/+) mice through augmentation of inflammation and angiogenesis. Carcinogenesis 30:1424–1432
22. Sun C, Wang N, Huang J, Xin J, Peng F, Ren Y, Zhang S, Miao J (2009) Inhibition of phosphatidylcholine-specific phospholipase C prevents bone marrow stromal cell senescence in vitro. J Cell Biochem 108:519–528
23. Varela D, Simon F, Olivero P, Armisen R, Leiva-Salcedo E, Jorgensen F, Sala F, Stutzin A (2007) Activation of H2O2-induced VSOR Cl- currents in HTC cells require phospholipase Cgamma1 phosphorylation and Ca^{2+} mobilisation. Cell Physiol Biochem 20:773–780
24. Wahl MI, Olashaw NE, Nishibe S, Rhee SG, Pledger WJ, Carpenter G (1989) Platelet-derived growth factor induces rapid and sustained tyrosine phosphorylation of phospholipase C-gamma in quiescent BALB/c 3T3 cells. Mol Cell Biol 9:2934–2943
25. Wang D, Feng J, Wen R, Marine JC, Sangster MY, Parganas E, Hoffmeyer A, Jackson CW, Cleveland JL, Murray PJ, Ihle JN (2000) Phospholipase Cgamma2 is essential in the functions of B cell and several Fc receptors. Immunity 13:25–35
26. Suh PG, Park JI, Manzoli L, Cocco L, Peak JC, Katan M, Fukami K, Kataoka T, Yun S, Ryu SH (2008) Multiple roles of phosphoinositide-specific phospholipase C isozymes. BMB Rep 41:415–434
27. Bunney TD, Katan M (2011) PLC regulation: emerging pictures for molecular mechanisms. Trends Biochem Sci 36:88–96
28. Gifford JL, Walsh MP, Vogel HJ (2007) Structures and metal-ion-binding properties of the Ca^{2+}-binding helix-loop-helix EF-hand motifs. Biochem J 405:199–221
29. Harlan JE, Hajduk PJ, Yoon HS, Fesik SW (1994) Pleckstrin homology domains bind to phosphatidylinositol-4,5-bisphosphate. Nature 371:168–170
30. Jezyk MR, Snyder JT, Gershberg S, Worthylake DK, Harden TK, Sondek J (2006) Crystal structure of Rac1 bound to its effector phospholipase C-beta2. Nat Struct Mol Biol 13: 1135–1140

31. Yamamoto T, Takeuchi H, Kanematsu T, Allen V, Yagisawa H, Kikkawa U, Watanabe Y, Nakasima A, Katan M, Hirata M (1999) Involvement of EF hand motifs in the Ca(2+)-dependent binding of the pleckstrin homology domain to phosphoinositides. Eur J Biochem 265:481–490
32. Touhara K, Inglese J, Pitcher JA, Shaw G, Lefkowitz RJ (1994) Binding of G protein beta gamma-subunits to pleckstrin homology domains. J Biol Chem 269:10217–10220
33. Kawasaki H, Kretsinger RH (1994) Calcium-binding proteins. 1: EF-hands. Protein Profile 1:343–517
34. Essen LO, Perisic O, Cheung R, Katan M, Williams RL (1996) Crystal structure of a mammalian phosphoinositide-specific phospholipase C delta. Nature 380:595–602
35. Rhee SG, Choi KD (1992) Regulation of inositol phospholipid-specific phospholipase C isozymes. J Biol Chem 267:12393–12396
36. Essen LO, Perisic O, Lynch DE, Katan M, Williams RL (1997) A ternary metal binding site in the C2 domain of phosphoinositide-specific phospholipase C-delta1. Biochemistry 36:2753–2762
37. Otterhag L, Sommarin M, Pical C (2001) N-terminal EF-hand-like domain is required for phosphoinositide-specific phospholipase C activity in Arabidopsis thaliana. FEBS Lett 497:165–170
38. Waldo GL, Ricks TK, Hicks SN, Cheever ML, Kawano T, Tsuboi K, Wang X, Montell C, Kozasa T, Sondek J, Harden TK (2010) Kinetic scaffolding mediated by a phospholipase C-beta and Gq signaling complex. Science 330:974–980
39. Ellis MV (1995) U S, Katan M: Mutations within a highly conserved sequence present in the X region of phosphoinositide-specific phospholipase C-delta 1. Biochem J 307(Pt 1):69–75
40. Nagano N, Orengo CA, Thornton JM (2002) One fold with many functions: the evolutionary relationships between TIM barrel families based on their sequences, structures and functions. J Mol Biol 321:741–765
41. Williams RL (1999) Mammalian phosphoinositide-specific phospholipase C. Biochim Biophys Acta 1441:255–267
42. Ryu SH, Suh PG, Cho KS, Lee KY, Rhee SG (1987) Bovine brain cytosol contains three immunologically distinct forms of inositolphospholipid-specific phospholipase C. Proc Natl Acad Sci USA 84:6649–6653
43. Margolis B, Zilberstein A, Franks C, Felder S, Kremer S, Ullrich A, Rhee SG, Skorecki K, Schlessinger J (1990) Effect of phospholipase C-gamma overexpression on PDGF-induced second messengers and mitogenesis. Science 248:607–610
44. Meisenhelder J, Suh PG, Rhee SG, Hunter T (1989) Phospholipase C-gamma is a substrate for the PDGF and EGF receptor protein-tyrosine kinases in vivo and in vitro. Cell 57:1109–1122
45. Wahl MI, Daniel TO, Carpenter G (1988) Antiphosphotyrosine recovery of phospholipase C activity after EGF treatment of A-431 cells. Science 241:968–970
46. Ronnstrand L, Mori S, Arridsson AK, Eriksson A, Wernstedt C, Hellman U, Claesson-Welsh L, Heldin CH (1992) Identification of two C-terminal autophosphorylation sites in the PDGF beta-receptor: involvement in the interaction with phospholipase C-gamma. EMBO J 11: 3911–3919
47. Kim HK, Kim JW, Zilberstein A, Margolis B, Kim JG, Schlessinger J, Rhee SG (1991) PDGF stimulation of inositol phospholipid hydrolysis requires PLC-gamma 1 phosphorylation on tyrosine residues 783 and 1254. Cell 65:435–441
48. Gout I, Dhand R, Hiles ID, Fry MJ, Panayotou G, Das P, Truong O, Totty NF, Hsuan J, Booker GW et al (1993) The GTPase dynamin binds to and is activated by a subset of SH3 domains. Cell 75:25–36
49. Bar-Sagi D, Rotin D, Batzer A, Mandiyan V, Schlessinger J (1993) SH3 domains direct cellular localization of signaling molecules. Cell 74:83–91
50. van Huizen R, Miller K, Chen DM, Li Y, Lai ZC, Raab RW, Stark WS, Shortridge RD, Li M (1998) Two distantly positioned PDZ domains mediate multivalent INAD-phospholipase C interactions essential for G protein-coupled signaling. EMBO J 17:2285–2297
51. Yamaguchi T, Shirataki H, Kishida S, Miyazaki M, Nishikawa J, Wada K, Numata S, Kaibuchi K, Takai Y (1993) Two functionally different domains of rabphilin-3A, Rab3A p25/smg

p25A-binding and phospholipid- and Ca(2+)-binding domains. J Biol Chem 268: 27164–27170
52. Luo JH, Weinstein IB (1993) Calcium-dependent activation of protein kinase C. The role of the C2 domain in divalent cation selectivity. J Biol Chem 268:23580–23584
53. Davletov BA, Sudhof TC (1993) A single C2 domain from synaptotagmin I is sufficient for high affinity Ca^{2+}/phospholipid binding. J Biol Chem 268:26386–26390
54. Fanning AS, Anderson JM (1996) Protein-protein interactions: PDZ domain networks. Curr Biol 6:1385–1388
55. Wang CK, Pan L, Chen J, Zhang M (2010) Extensions of PDZ domains as important structural and functional elements. Protein Cell 1:737–751
56. Kim JK, Lim S, Kim J, Kim S, Kim JH, Ryu SH, Suh PG (2011) Subtype-specific roles of phospholipase C-beta via differential interactions with PDZ domain proteins. Adv Enzyme Regul 51:138–151
57. Charnock-Jones DS, Day K, Smith SK (1996) Cloning, expression and genomic organization of human placental protein disulfide isomerase (previously identified as phospholipase C alpha). Int J Biochem Cell Biol 28:81–89
58. Lagercrantz J, Carson E, Phelan C, Grimmond S, Rosen A, Dare E, Nordenskjold M, Hayward NK, Larsson C, Weber G (1995) Genomic organization and complete cDNA sequence of the human phosphoinositide-specific phospholipase C beta 3 gene (PLCB3). Genomics 26: 467–472
59. Mao GF, Kunapuli SP, Rao AK (2000) Evidence for two alternatively spliced forms of phospholipase C-beta2 in haematopoietic cells. Br J Haematol 110:402–408
60. Kim MJ, Min DS, Ryu SH, Suh PG (1998) A cytosolic, galphaq- and betagamma-insensitive splice variant of phospholipase C-beta4. J Biol Chem 273:3618–3624
61. Berstein G, Blank JL, Jhon DY, Exton JH, Rhee SG, Ross EM (1992) Phospholipase C-beta 1 is a GTPase-activating protein for Gq/11, its physiologic regulator. Cell 70:411–418
62. Runnels LW, Scarlata SF (1999) Determination of the affinities between heterotrimeric G protein subunits and their phospholipase C-beta effectors. Biochemistry 38:1488–1496
63. Hwang JI, Heo K, Shin KJ, Kim E, Yun C, Ryu SH, Shin HS, Suh PG (2000) Regulation of phospholipase C-beta 3 activity by Na+/H+ exchanger regulatory factor 2. J Biol Chem 275:16632–16637
64. Camps M, Carozzi A, Schnabel P, Scheer A, Parker PJ, Gierschik P (1992) Isozyme-selective stimulation of phospholipase C-beta 2 by G protein beta gamma-subunits. Nature 360: 684–686
65. Martelli AM, Gilmour RS, Bertagnolo V, Neri LM, Manzoli L, Cocco L (1992) Nuclear localization and signalling activity of phosphoinositidase C beta in Swiss 3 T3 cells. Nature 358:242–245
66. Kim CG, Park D, Rhee SG (1996) The role of carboxyl-terminal basic amino acids in Gqalpha-dependent activation, particulate association, and nuclear localization of phospholipase C-beta1. J Biol Chem 271:21187–21192
67. Payrastre B, Nievers M, Boonstra J, Breton M, Verkleij AJ, Van Bergen en Henegouwen PM (1992) A differential location of phosphoinositide kinases, diacylglycerol kinase, and phospholipase C in the nuclear matrix. J Biol Chem 267:5078–5084
68. Wang HL (1997) Basic amino acids at the C-terminus of the third intracellular loop are required for the activation of phospholipase C by cholecystokinin-B receptors. J Neurochem 68:1728–1735
69. Adamski FM, Timms KM, Shieh BH (1999) A unique isoform of phospholipase Cbeta4 highly expressed in the cerebellum and eye. Biochim Biophys Acta 1444:55–60
70. Min DS, Kim DM, Lee YH, Seo J, Suh PG, Ryu SH (1993) Purification of a novel phospholipase C isozyme from bovine cerebellum. J Biol Chem 268:12207–12212
71. Alvarez RA, Ghalayini AJ, Xu P, Hardcastle A, Bhattacharya S, Rao PN, Pettenati MJ, Anderson RE, Baehr W (1995) cDNA sequence and gene locus of the human retinal phosphoinositide-specific phospholipase-C beta 4 (PLCB4). Genomics 29:53–61

72. Harden TK, Hicks SN, Sondek J (2009) Phospholipase C isozymes as effectors of Ras superfamily GTPases. J Lipid Res 50:S243–S248
73. Snyder JT, Singer AU, Wing MR, Harden TK, Sondek J (2003) The pleckstrin homology domain of phospholipase C-beta2 as an effector site for Rac. J Biol Chem 278: 21099–21104
74. Jhon DY, Lee HH, Park D, Lee CW, Lee KH, Yoo OJ, Rhee SG (1993) Cloning, sequencing, purification, and Gq-dependent activation of phospholipase C-beta 3. J Biol Chem 268: 6654–6661
75. Park D, Jhon DY, Kriz R, Knopf J, Rhee SG (1992) Cloning, sequencing, expression, and Gq-independent activation of phospholipase C-beta 2. J Biol Chem 267:16048–16055
76. Kim D, Jun KS, Lee SB, Kang NG, Min DS, Kim YH, Ryu SH, Suh PG, Shin HS (1997) Phospholipase C isozymes selectively couple to specific neurotransmitter receptors. Nature 389:290–293
77. Lee SB, Shin SH, Hepler JR, Gilman AG, Rhee SG (1993) Activation of phospholipase C-beta 2 mutants by G protein alpha q and beta gamma subunits. J Biol Chem 268:25952–25957
78. Wang T, Pentyala S, Elliott JT, Dowal L, Gupta E, Rebecchi MJ, Scarlata S (1999) Selective interaction of the C2 domains of phospholipase C-beta1 and -beta2 with activated Galphaq subunits: an alternative function for C2-signaling modules. Proc Natl Acad Sci USA 96: 7843–7846
79. Wang T, Pentyala S, Rebecchi MJ, Scarlata S (1999) Differential association of the pleckstrin homology domains of phospholipases C-beta 1, C-beta 2, and C-delta 1 with lipid bilayers and the beta gamma subunits of heterotrimeric G proteins. Biochemistry 38:1517–1524
80. Cockcroft S, Thomas GM (1992) Inositol-lipid-specific phospholipase C isoenzymes and their differential regulation by receptors. Biochem J 288(Pt 1):1–14
81. Rivas M, Santisteban P (2003) TSH-activated signaling pathways in thyroid tumorigenesis. Mol Cell Endocrinol 213:31–45
82. Kroczek C, Lang C, Brachs S, Grohmann M, Dutting S, Schweizer A, Nitschke L, Feller SM, Jack HM, Mielenz D (2010) Swiprosin-1/EFhd2 controls B cell receptor signaling through the assembly of the B cell receptor, Syk, and phospholipase C gamma2 in membrane rafts. J Immunol 184:3665–3676
83. Ji QS, Winnier GE, Niswender KD, Horstman D, Wisdom R, Magnuson MA, Carpenter G (1997) Essential role of the tyrosine kinase substrate phospholipase C-gamma1 in mammalian growth and development. Proc Natl Acad Sci USA 94:2999–3003
84. Wonerow P, Pearce AC, Vaux DJ, Watson SP (2003) A critical role for phospholipase Cgamma2 in alphaIIbbeta3-mediated platelet spreading. J Biol Chem 278:37520–37529
85. Inoue O, Suzuki-Inoue K, Dean WL, Frampton J, Watson SP (2003) Integrin alpha2beta1 mediates outside-in regulation of platelet spreading on collagen through activation of Src kinases and PLCgamma2. J Cell Biol 160:769–780
86. Rhee SG, Kim H, Suh PG, Choi WC (1991) Multiple forms of phosphoinositide-specific phospholipase C and different modes of activation. Biochem Soc Trans 19:337–341
87. Homma Y, Takenawa T, Emori Y, Sorimachi H, Suzuki K (1989) Tissue- and cell type-specific expression of mRNAs for four types of inositol phospholipid-specific phospholipase C. Biochem Biophys Res Commun 164:406–412
88. Kim MJ, Chang JS, Park SK, Hwang JI, Ryu SH, Suh PG (2000) Direct interaction of SOS1 Ras exchange protein with the SH3 domain of phospholipase C-gamma1. Biochemistry 39:8674–8682
89. Wen W, Yan J, Zhang M (2006) Structural characterization of the split pleckstrin homology domain in phospholipase C-gamma1 and its interaction with TRPC3. J Biol Chem 281:12060–12068
90. Braiman A, Barda-Saad M, Sommers CL, Samelson LE (2006) Recruitment and activation of PLCgamma1 in T cells: a new insight into old domains. EMBO J 25:774–784
91. Finco TS, Kadlecek T, Zhang W, Samelson LE, Weiss A (1998) LAT is required for TCR-mediated activation of PLCgamma1 and the Ras pathway. Immunity 9:617–626

92. Stoica B, DeBell KE, Graham L, Rellahan BL, Alava MA, Laborda J, Bonvini E (1998) The amino-terminal Src homology 2 domain of phospholipase C gamma 1 is essential for TCR-induced tyrosine phosphorylation of phospholipase C gamma 1. J Immunol 160:1059–1066
93. Zhang W, Trible RP, Zhu M, Liu SK, McGlade CJ, Samelson LE (2000) Association of Grb2, Gads, and phospholipase C-gamma 1 with phosphorylated LAT tyrosine residues. Effect of LAT tyrosine mutations on T cell angigen receptor-mediated signaling. J Biol Chem 275:23355–23361
94. Dower NA, Stang SL, Bottorff DA, Ebinu JO, Dickie P, Ostergaard HL, Stone JC (2000) RasGRP is essential for mouse thymocyte differentiation and TCR signaling. Nat Immunol 1:317–321
95. Ebinu JO, Stang SL, Teixeira C, Bottorff DA, Hooton J, Blumberg PM, Barry M, Bleakley RC, Ostergaard HL, Stone JC (2000) RasGRP links T-cell receptor signaling to Ras. Blood 95:3199–3203
96. Shannon LA, Calloway PA, Welch TP, Vines CM (2010) CCR7/CCL21 migration on fibronectin is mediated by phospholipase Cgamma1 and ERK1/2 in primary T lymphocytes. J Biol Chem 285:38781–38787
97. Meldrum E, Kriz RW, Totty N, Parker PJ (1991) A second gene product of the inositol-phospholipid-specific phospholipase C delta subclass. Eur J Biochem 196:159–165
98. Irino Y, Cho H, Nakamura Y, Nakahara M, Furutani M, Suh PG, Takenawa T, Fukami K (2004) Phospholipase C delta-type consists of three isozymes: bovine PLCdelta2 is a homologue of human/mouse PLCdelta4. Biochem Biophys Res Commun 320:537–543
99. Allen V, Swigart P, Cheung R, Cockcroft S, Katan M (1997) Regulation of inositol lipid-specific phospholipase cdelta by changes in Ca^{2+} ion concentrations. Biochem J 327(Pt 2):545–552
100. Kim YH, Park TJ, Lee YH, Baek KJ, Suh PG, Ryu SH, Kim KT (1999) Phospholipase C-delta1 is activated by capacitative calcium entry that follows phospholipase C-beta activation upon bradykinin stimulation. J Biol Chem 274:26127–26134
101. Yamaga M, Fujii M, Kamata H, Hirata H, Yagisawa H (1999) Phospholipase C-delta1 contains a functional nuclear export signal sequence. J Biol Chem 274:28537–28541
102. Stallings JD, Tall EG, Pentyala S, Rebecchi MJ (2005) Nuclear translocation of phospholipase C-delta1 is linked to the cell cycle and nuclear phosphatidylinositol 4,5-bisphosphate. J Biol Chem 280:22060–22069
103. Yoko-o T, Matsui Y, Yagisawa H, Nojima H, Uno I, Toh-e A (1993) The putative phosphoinositide-specific phospholipase C gene, PLC1, of the yeast Saccharomyces cerevisiae is important for cell growth. Proc Natl Acad Sci USA 90:1804–1808
104. Murthy KS, Zhou H, Huang J, Pentyala SN (2004) Activation of PLC-delta1 by Gi/o-coupled receptor agonists. Am J Physiol Cell Physiol 287:C1679–C1687
105. Shimohama S, Homma Y, Suenaga T, Fujimoto S, Taniguchi T, Araki W, Yamaoka Y, Takenawa T, Kimura J (1991) Aberrant accumulation of phospholipase C-delta in Alzheimer brains. Am J Pathol 139:737–742
106. Yagisawa H, Tanase H, Nojima H (1991) Phospholipase C-delta gene of the spontaneously hypertensive rat harbors point mutations causing amino acid substitutions in a catalytic domain. J Hypertens 9:997–1004
107. Nakamura Y, Ichinohe M, Hirata M, Matsuura H, Fujiwara T, Igarashi T, Nakahara M, Yamaguchi H, Yasugi S, Takenawa T, Fukami K (2008) Phospholipase C-delta1 is an essential molecule downstream of Foxn1, the gene responsible for the nude mutation, in normal hair development. FASEB J 22:841–849
108. Ichinohe M, Nakamura Y, Sai K, Nakahara M, Yamaguchi H, Fukami K (2007) Lack of phospholipase C-delta1 induces skin inflammation. Biochem Biophys Res Commun 356:912–918
109. Fukami K, Yoshida M, Inoue T, Kurokawa M, Fissore RA, Yoshida N, Mikoshiba K, Takenawa T (2003) Phospholipase Cdelta4 is required for Ca^{2+} mobilization essential for acrosome reaction in sperm. J Cell Biol 161:79–88

110. Fukami K, Nakao K, Inoue T, Kataoka Y, Kurokawa M, Fissore RA, Nakamura K, Katsuki M, Mikoshiba K, Yoshida N, Takenawa T (2001) Requirement of phospholipase Cdelta4 for the zona pellucida-induced acrosome reaction. Science 292:920–923
111. Lopez I, Mak EC, Ding J, Hamm HE, Lomasney JW (2001) A novel bifunctional phospholipase c that is regulated by Galpha 12 and stimulates the Ras/mitogen-activated protein kinase pathway. J Biol Chem 276:2758–2765
112. Song C, Hu CD, Masago M, Kariyai K, Yamawaki-Kataoka Y, Shibatohge M, Wu D, Satoh T, Kataoka T (2001) Regulation of a novel human phospholipase C, PLCepsilon, through membrane targeting by Ras. J Biol Chem 276:2752–2757
113. Shibatohge M, Kariya K, Liao Y, Hu CD, Watari Y, Goshima M, Shima F, Kataoka T (1998) Identification of PLC210, a Caenorhabditis elegans phospholipase C, as a putative effector of Ras. J Biol Chem 273:6218–6222
114. Wing MR, Snyder JT, Sondek J, Harden TK (2003) Direct activation of phospholipase C-epsilon by Rho. J Biol Chem 278:41253–41258
115. Wing MR, Bourdon DM, Harden TK (2003) PLC-epsilon: a shared effector protein in Ras-, Rho-, and G alpha beta gamma-mediated signaling. Mol Interv 3:273–280
116. Schmidt M, Evellin S, Weernink PA, Von Dorp F, Rehmann H, Lomasney JW, Jakobs KH (2001) A new phospholipase-C calcium signaling pathway mediated by cyclic AMP and a Rap GTPase. Nat Cell Biol 3:1020–1024
117. Evellin S, Nolte J, Tysack K, vom Dorp F, Thiel M, Weernink PA, Jakobs KH, Webb EJ, Lomasney JW, Schmidt M (2002) Stimulation of phospholipase C-epsilon by the M3 muscarinic acetylcholine receptor mediated by cyclic AMP and the GTPase Rap2B. J Biol Chem 277:16805–16813
118. Jin TG, Satoh T, Liao Y, Song C, Gao X, Kariya K, Hu CD, Kataoka T (2001) Role of the CDC25 homology domain of phospholipase Cepsilon in amplification of Rap1-dependent signaling. J Biol Chem 276:30301–30307
119. Fujimoto S, Yoshida N, Fukui T, Amanai M, Isobe T, Itagaki C, Izumi T, Perry AC (2004) Mammalian phospholipase Czeta induces oocyte activation from the sperm perinuclear matrix. Dev Biol 274:370–383
120. Cox LJ, Larman MG, Saunders CM, Hashimoto K, Swann K, Lai FA (2002) Sperm phospholipase Czeta from humans and cynomolgus monkeys triggers Ca^{2+} oscillations, activation and development of mouse oocytes. Reproduction 124:611–623
121. Jones KT, Matsuda M, Parrington J, Katan M, Swann K (2000) Different Ca^{2+}-releasing abilities of sperm extracts compared with tissue extracts and phospholipase C isoforms in sea urchin egg homogenate and mouse eggs. Biochem J 346(Pt 3):743–749
122. Swann K, Saunders CM, Rogers NT, Lai FA (2006) PLCzeta(zeta): a sperm protein that triggers Ca^{2+} oscillations and egg activation in mammals. Semin Cell Dev Biol 17:264–273
123. Nomikos M, Blayney LM, Larman MG, Campbell K, Rossbach A, Saunders CM, Swann K, Lai FA (2005) Role of phospholipase C-zeta domains in Ca^{2+}-dependent phosphatidylinositol 4,5-bisphosphate hydrolysis and cytoplasmic Ca^{2+} oscillations. J Biol Chem 280: 31011–31018
124. Halet G, Marangos P, Fitzharris G, Carroll J (2003) Ca^{2+} oscillations at fertilization in mammals. Biochem Soc Trans 31:907–911
125. Marangos P, FitzHarris G, Carroll J (2003) Ca^{2+} oscillations at fertilization in mammals are regulated by the formation of pronuclei. Development 130:1461–1472
126. Stewart AJ, Mukherjee J, Roberts SJ, Lester D, Farquharson C (2005) Identification of a novel class of mammalian phosphoinositol-specific phospholipase C enzymes. Int J Mol Med 15:117–121
127. Zhou Y, Wing MR, Sondek J, Harden TK (2005) Molecular cloning and characterization of PLC-eta2. Biochem J 391:667–676
128. Kim JK, Choi JW, Lim S, Kwon O, Seo JK, Ryu SH, Suh PG (2011) Phospholipase C-eta1 is activated by intracellular Ca(2+) mobilization and enhances GPCRs/PLC/Ca(2+) signaling. Cell Signal 23:1022–1029

129. Lo Vasco VR (2011) Role of Phosphoinositide-Specific Phospholipase C eta2 in Isolated and Syndromic Mental Retardation. Eur Neurol 65:264–269
130. Wang C, Du XN, Jia QZ, Zhang HL (2005) Binding of PLCdelta1PH-GFP to PtdIns(4,5)P2 prevents inhibition of phospholipase C-mediated hydrolysis of PtdIns(4,5)P2 by neomycin. Acta Pharmacol Sin 26:1485–1491
131. Klein RR, Bourdon DM, Costales CL, Wagner CD, White WL, Williams JD, Hicks SN, Sondek J, Thakker DR (2011) Direct activation of human phospholipase C by its well known inhibitor u73122. J Biol Chem 286:12407–12416
132. Dwyer L, Kim HJ, Koh BH, Koh SD (2010) Phospholipase C-independent effects of 3M3FBS in murine colon. Eur J Pharmacol 628:187–194
133. Frei E, Hofmann F, Wegener JW (2009) Phospholipase C mediated Ca^{2+} signals in murine urinary bladder smooth muscle. Eur J Pharmacol 610:106–109
134. Xu S, Huo J, Lee KG, Kurosaki T, Lam KP (2009) Phospholipase Cgamma2 is critical for Dectin-1-mediated Ca^{2+} flux and cytokine production in dendritic cells. J Biol Chem 284:7038–7046
135. Shi TJ, Liu SX, Hammarberg H, Watanabe M, Xu ZQ, Hokfelt T (2008) Phospholipase C{beta}3 in mouse and human dorsal root ganglia and spinal cord is a possible target for treatment of neuropathic pain. Proc Natl Acad Sci USA 105:20004–20008
136. Ibrahim S, Calzada C, Pruneta-Deloche V, Lagarde M, Ponsin G (2007) The transfer of VLDL-associated phospholipids to activated platelets depends upon cytosolic phospholipase A2 activity. J Lipid Res 48:1533–1538
137. Sickmann T, Klose A, Huth T, Alzheimer C (2008) Unexpected suppression of neuronal G protein-activated, inwardly rectifying K^+ current by common phospholipase C inhibitor. Neurosci Lett 436:102–106
138. Kim DD, Ramirez MM, Duran WN (2000) Platelet-activating factor modulates microvascular dynamics through phospholipase C in the hamster cheek pouch. Microvasc Res 59:7–13
139. Naito Y, Okada M, Yagisawa H (2006) Phospholipase C isoforms are localized at the cleavage furrow during cytokinesis. J Biochem 140:785–791
140. Grotterod I, Maelandsmo GM, Boye K (2010) Signal transduction mechanisms involved in S100A4-induced activation of the transcription factor NF-kappaB. BMC Cancer 10:241

Chapter 11
Inositol 1,4,5-Trisphosphate and Its Receptors

Jan B. Parys and Humbert De Smedt

Abstract Activation of cells by many extracellular agonists leads to the production of inositol 1,4,5-trisphosphate (IP_3). IP_3 is a global messenger that easily diffuses in the cytosol. Its receptor (IP_3R) is a Ca^{2+}-release channel located on intracellular membranes, especially the endoplasmic reticulum (ER). The IP_3R has an affinity for IP_3 in the low nanomolar range. A prime regulator of the IP_3R is the Ca^{2+} ion itself. Cytosolic Ca^{2+} is considered as a co-agonist of the IP_3R, as it strongly increases IP_3R activity at concentrations up to about 300 nM. In contrast, at higher concentrations, cytosolic Ca^{2+} inhibits the IP_3R. Also the luminal Ca^{2+} sensitizes the IP_3R. In higher organisms three genes encode for an IP_3R and additional diversity exists as a result of alternative splicing mechanisms and the formation of homo- and heterotetramers. The various IP_3R isoforms have a similar structure and a similar function, but due to differences in their affinity for IP_3, their variable sensitivity to regulatory parameters, their differential interaction with associated proteins, and the variation in their subcellular localization, they participate differently in the formation of intracellular Ca^{2+} signals and this affects therefore the physiological consequences of these signals.

Keywords Ca^{2+} signaling • Endoplasmic reticulum • Inositol 1,4,5-trisphosphate • Inositol 1,4,5-trisphosphate receptor • Intracellular Ca^{2+}-release channel

Inositol 1,4,5-Trisphosphate (IP_3) as Second Messenger

Cells can be activated at their extracellular surface by a multitude of signal molecules as hormones, growth factors and neurotransmitters. These signal molecules do not need to cross themselves the plasma membrane but are sensed by specific

J.B. Parys (✉) • H. De Smedt
Laboratory of Molecular and Cellular Signaling, Department of Cellular and Molecular Medicine, KU Leuven, Campus Gasthuisberg O/N1 – Bus 802, Herestraat 49, B-3000 Leuven, Belgium
e-mail: Jan.Parys@med.kuleuven.be

M.S. Islam (ed.), *Calcium Signaling*, Advances in Experimental Medicine and Biology 740, DOI 10.1007/978-94-007-2888-2_11,

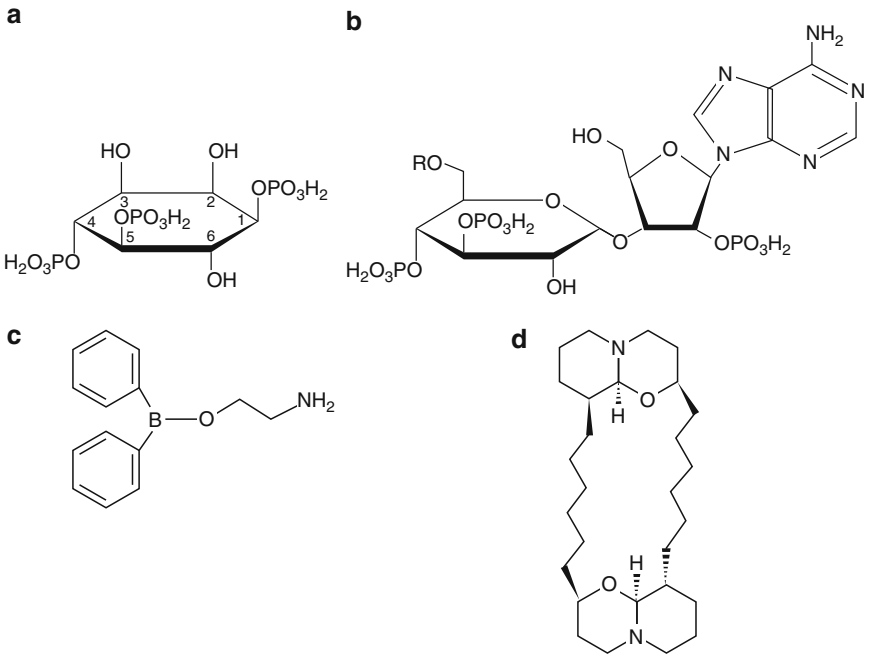

Fig. 11.1 Molecular structure of important compounds affecting the IP_3R. (**a**) IP_3. The numbering of the C-atoms is indicated. (**b**) Adenophostin A (R=H) and B (R=$COCH_3$). (**c**) 2APB. (**d**) Xestospongin C

receptors which convey the signal to the cell interior where it is converted to an intracellular message. There are several of these so-called second messenger molecules (e.g. cAMP, cGMP, cADP ribose, NAADP, …), but in the framework of this review we will focus on the unique role of IP_3. Early work by Hokin and Hokin already indicated that agonist stimulation could lead to an increased phosphatidyl inositol turnover [1]. Michell in turn proposed that lipid metabolism could be linked to intracellular Ca^{2+} signaling [2]. The exact nature of this link remained for a long time obscure, until Berridge and collaborators demonstrated in a series of elegant experiments that IP_3 (Fig. 11.1a) was the linking molecule [3–5]. This discovery, further discussed below, was the starting point of a completely new field in signal transduction, the $IP_3 \rightarrow IP_3$ receptor (IP_3R) $\rightarrow Ca^{2+}$ signal pathway, which will be the topic of this chapter.

IP_3 Metabolism

The direct precursor of IP_3 is the phospholipid phosphatidylinositol 4,5-bisphosphate, which is cleaved by phospholipase C (PLC) to 1,2-diacylglycerol (DAG), an activator of several effector proteins including the protein kinase C isoforms, and IP_3.

The various PLCs form six families (PLCβ, PLCγ, PLCδ, PLCε, PLCξ and PLCη) containing several members and/or different splice isoforms. The various PLC isoforms differ in their activation mechanisms and in their regulatory properties, allowing for a controlled production of IP_3 (and DAG) after cell stimulation by agonists acting on different types of receptors [6].

IP_3 is a H_2O-soluble molecule that diffuses away from its production site at the plasma membrane. IP_3 has a diffusion coefficient of 283 $\mu m^2/s$ and a life time of about 1 s, which accounts for an effective range of 24 μm, while Ca^{2+} has a much more limited range of action [7]. Therefore, IP_3 acts in cells as a global messenger. IP_3 is however not stable and its degradation contributes to the limitation of the signal. IP_3 5-phosphatase and IP_3 3-kinase are the main IP_3-metabolizing enzymes [8]. Heterologous overexpression of in particular the IP_3 5-phosphatase can have a dramatic effect on the subsequent cellular response [9].

Discovery of the IP_3R

As indicated above, Berridge and co-workers demonstrated the importance of IP_3 in Ca^{2+} signaling. Their seminal paper published in 1983 in Nature [4] provided direct evidence that in permeabilized pancreatic acinar cells IP_3 induced Ca^{2+} release from non-mitochondrial Ca^{2+} stores corresponding to the endoplasmic reticulum (ER). Soon after this publication, the universality of the mechanism was demonstrated as similar results were obtained in various other cell types, as e.g. neutrophils [10], hepatocytes [11], oocytes [12], platelets [13], insulinoma cells [14], and renal epithelial cells [15, 16]. Among those various cellular models however, the amount of Ca^{2+} that could be released by IP_3 varied widely (between 10% and nearly 100%), which indicates at the one hand that regulatory mechanisms may act on the IP_3-induced Ca^{2+}-release system and at the other that several types of Ca^{2+} stores likely co-exist in the same cell.

The molecular mechanism responsible for IP_3-induced Ca^{2+} release was however not yet identified at that time. Labeling of the receptor with $[^3H]IP_3$ or $[^{32}P]IP_3$ allowed first its biochemical identification and characterization [17–19] followed by its purification, first from cerebellum [20], a tissue with a very high IP_3R density, and subsequently from other tissues [21–23]. The results were concordant: in all cell types a high molecular mass glycoprotein (224–273 kDa after SDS-PAGE) was identified with a nanomolar affinity for IP_3 and a high specificity for it over other inositol phosphates. Electron microscopy, gel filtration, cross-linking experiments and migration on density gradients indicated a molecular mass of about 1,000 kDa and thus a tetrameric assembly [21–27]. A partial cDNA clone showed that the protein had a certain homology with an already known Ca^{2+}-release channel, the ryanodine receptor (RyR) [24]. Finally, antibodies demonstrated both at the immunocytochemistry level and at the electron microscopy level that this protein (mainly) localized to the ER [24, 28]. In parallel, P_{400}, a protein of similar molecular mass,

similar biochemical properties and similar expression pattern was independently purified and characterized [29].

The first full-length cloning of an IP_3R was performed, starting from mouse cerebellum cDNA libraries, by Mikoshiba and co-workers; the deduced amino acid (a.a.) sequence was 2,749 a.a. long, corresponding to a calculated molecular mass of 313 kDa, and had a significant homology with the RyR [30]. Importantly, heterologous expression of this protein in NG108–15 cells indicated a correlation with the IP_3-binding activity and an identity with the previously purified and characterized P_{400}. Furthermore, functional experiments demonstrated that this protein also possessed Ca^{2+}-channel properties [31, 32]. As indicated above, the functional properties of the IP_3R/Ca^{2+}-release channel were already investigated in various preparations, including intact cells, permeabilized cells and microsomes. Once the identity of the channel was ascertained, further characterization by electrophysiological techniques could be performed, first by reconstitution in artificial bilayers [27, 33–35] and later also by patch-clamp experiments. The latter were predominantly performed on the *Xenopus laevis* oocyte nucleus allowing the measurement of the IP_3R activity in its native environment [36, 37]. From these various measurements it clearly appeared that the IP_3R forms a large conductance cation channel, with a quite limited selectivity for Ca^{2+}. P_{Ca}/P_K values were typically found between 6 and 8 and single-channel slope conductances followed the sequence $Ba^{2+} > Sr^{2+} > Ca^{2+} > Mg^{2+}$ [38]. This does however not affect its function as a Ca^{2+}-release channel, as Ca^{2+} is the only ion which is actively accumulated in the ER and for which a driving force exist [39].

Finally, further immunolocalization studies, analysis by electron microscopy and biochemical methods, indicated that although most of the IP_3Rs are located in the ER and in the perinuclear membrane, IP_3Rs are also present in the Golgi apparatus, in some types of secretory vesicles and to a low extent also in the plasma membrane (reviewed in [40, 41]).

Taken together these results clearly demonstrated that the IP_3R is a large, tetrameric protein, that forms a Ca^{2+}-release channel in the ER and that is activated by IP_3.

IP_3R Isoform Diversity

Shortly after cloning of the murine IP_3R [30], an IP_3R was also cloned from rat [42] and subsequently from human and other organisms (reviewed in [43, 44]). It became clear that in Mammalia and other higher organisms, IP_3Rs are encoded by three different genes giving rise in addition to the originally cloned receptor, now termed IP_3R1, to an IP_3R2, first fully cloned in 1991 [45], and an IP_3R3, first fully cloned in 1993 [46]. Diversity is further increased by the existence of splice isoforms (e.g. for IP_3R1, see [47–49]), and by the fact that the tetrameric nature of the IP_3R allows for homo- as well as heterotetramer formation [50–52]. It however appeared that due to kinetic constraints in their formation, heterotetramers are less prevalent than would be expected if the monomers randomly interacted [53].

The interspecies homology is very high: e.g. at the amino acid level the similarity between mouse, rat and human IP_3R1 is greater than 99% [43, 44]. Although all IP_3R isoforms have a very similar size (between 2,670 and 2,848 amino acids) and a high similarity at the amino acid level (around 75% for higher organisms, around 50% for *C. elegans*) [44], they harbour significant differences in specific domains [43, 44]. These differences lead to a different affinity for IP_3 ($IP_3R2 > IP_3R1 > IP_3R3$) [54–58] as well as a different sensitivity to various regulatory mechanisms (e.g. phosphorylation, activation by ATP and interaction with regulatory proteins), leading to IP_3R isoform-specific Ca^{2+} signals [59].

Most cell types express more than one IP_3R isoform but their expression patterns vary between cell and tissues [54, 60, 61]. The various IP_3R isoforms expressed in a same cell can thereby have very distinct subcellular localizations, allowing to set up specific intracellular Ca^{2+} signals. Furthermore, IP_3R distribution is subjected to a dynamic regulation as not only the IP_3R expression levels but also the subcellular localization of each IP_3R isoform can depend on the physiological state of the cell [40]. Finally, an important feature of the IP_3Rs is that they are not uniformly distributed over the ER but can form clusters of about 20–30 units. Also the formation of these IP_3R clusters can be dynamically regulated, and may depend on the IP_3 concentration [62]. These clustered IP_3Rs have not only a higher probability to be exposed to higher Ca^{2+} concentrations but also the gating of the IP_3Rs in the clusters becomes coupled at increasing local Ca^{2+} concentration [62, 63]. The intracellular Ca^{2+} signals demonstrate a complex spatio-temporal behavior, and local Ca^{2+} signals form the building blocks for global Ca^{2+} signals [64–67]. IP_3R clusters are thereby important for setting up local Ca^{2+} signals, named puffs, which depending on the local IP_3 and Ca^{2+} concentration may eventually lead to the formation of regenerative Ca^{2+} waves propagating throughout the cell [41, 68–70].

IP_3R Activators and Inhibitors

Although the IP_3R can bind several synthetic IP_3 analogs [71], in a cellular context the selectivity for IP_3 over other (naturally-occurring) inositol phosphates is high [18, 19, 72]. Apart from IP_3, the only other compounds used to experimentally activate the IP_3R are adenophostin A and adenophostin B, which are isolated from the culture broth of *Penicillium brevicompactum* [73]. These both compounds, which have a structure displaying features of both IP_3 and adenine nucleotides (Fig. 11.1b), bind and activate the IP_3R with a much higher affinity than IP_3 itself without being subjected to metabolic degradation as is IP_3 [73–75]. A strong IP_3R sensitization can also be obtained by the sulphydryl reagent thimerosal, as evidenced by the appearance of Ca^{2+} oscillations in oocytes [76]. It is assumed that this effect can only occur in the presence of (low concentrations of) IP_3 and therefore represents a sensitization, and not an activation, of the IP_3R [77]. This sensitization is however isoform-dependent (e.g. prominent in IP_3R1, absent in IP_3R3; [78]), while high thimerosal

concentrations stimulate the Ca^{2+} leak from the ER, and inhibit both IP_3Rs and Ca^{2+} pumps [77, 79], limiting the use of this compound.

A problem in the IP_3R field is the lack until now of specific inhibitors [80]. The most-used inhibitory compounds are heparin, 2-aminoethoxydiphenyl borate (2APB) and xestospongins. Heparins are sulfated glycosaminoglycans which competitively inhibit the IP_3R by binding to the IP_3-binding site [19, 81, 82]. Their efficacy is determined by both size and presence of negatively charged sulfate groups [83]. Problems are the non-specific interactions of heparins with other proteins and their cell impermeability.

2APB (Fig. 11.1c) is a small membrane-permeable molecule inhibiting the IP_3R without interacting with the IP_3-binding site [84]. Its cellular mode of action is however complex as it was later shown not only to activate the IP_3R at low concentrations, but also to affect store-operated Ca^{2+} influx in a biphasic fashion and to inhibit Ca^{2+} pumps (reviewed in [80, 85]). 2APB analogs with higher specificity towards the store-operated Ca^{2+}-influx mechanism were recently developed, but similar compounds directed towards the IP_3R are not yet available [86].

Finally, xestospongins (Fig. 11.1d) form a family of macrocyclic bis-1-oxaquinolizidine alkaloids that could be isolated from the Australian sponge *Xestospongia* and of which several inhibit the IP_3R [87]. Also in this case, the specificity has been questioned, though it may depend on the exact molecule used and on the cell type under investigation [88–90].

A lot of work had been performed by several groups in order to develop new IP_3 analogs, including membrane-permeant IP_3 and caged IP_3 [71] and it can be anticipated that compounds with either strong activating or inhibiting power will ultimately become available. Some of those already developed compounds however also affect IP_3-metabolizing enzymes as the IP_3 5-phosphatase [91].

IP_3R Structure

For describing and understanding the IP_3R structure-function relations, different models have been proposed. In the simplest one, the IP_3R was divided in three regions: the N-terminal ligand-binding region consisting of the first 600 amino acids, a very large regulatory and coupling region of about 1,600 amino acids and finally the C-terminal region consisting of six transmembrane helices (TM1–6) and a short cytosolic tail (Fig. 11.2a) [45]. Interestingly, the N-terminal and C-terminal regions demonstrated a higher level of homology between the isoforms than the central region.

Subsequent experimental work refined this model, and five distinct functional domains were recognized: the N-terminal coupling domain usually called the suppressor domain (for IP_3R1: a.a. 1–225), the IP_3-binding core (a.a. 226–578), the internal coupling domain or modulatory and transducing domain (a.a. 579–2,275), the channel domain containing TM1–6 and including the pore site and the N-glycosylation sites (a.a. 2,276–2,589) and finally the C-terminal tail also named gatekeeper domain (a.a. 2,590–2,749) (Fig. 11.2c) [92, 93].

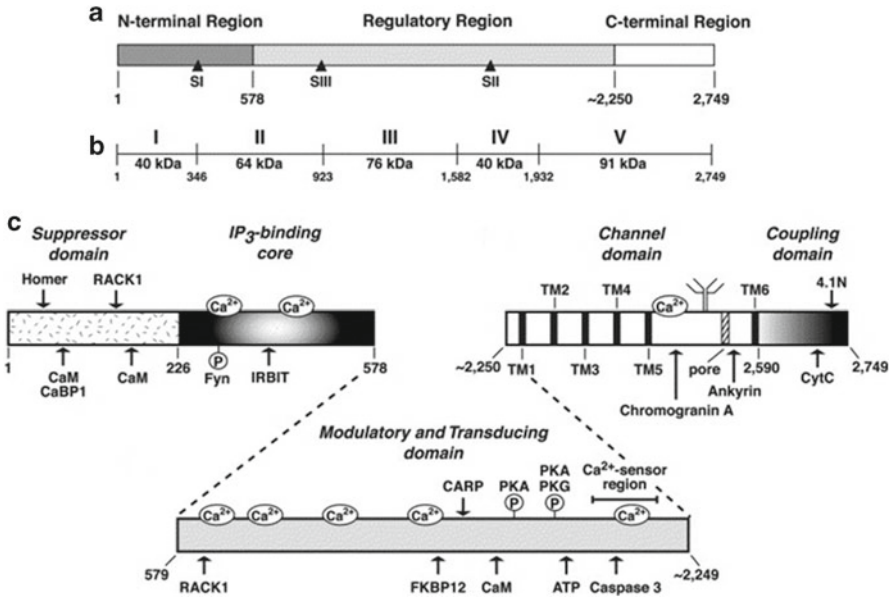

Fig. 11.2 Structure of the IP_3R. (**a**) Linear representation of IP_3R1. The three main regions and the location of the three splice sites (SI–SIII) are shown. (**b**) The five domains as obtained by limited proteolysis are indicated. (**c**) The five functional domains of the IP_3R are shown: the suppressor domain (also called N-terminal coupling domain), the IP_3-binding core, the modulatory and transducing domain (corresponding to the regulatory and coupling region), the channel domain and the C-terminal tail acting as coupling and gatekeeper domain. Transmembrane helices (TM1–TM6), the pore domain (*striped box*), glycosylation sites (*tree-like structure*), Ca^{2+}-binding sites, and a number of important protein-protein interaction sites as well as phosphorylation sites are indicated [92]. Please note the important number of regulatory sites on the N- and C-terminal domains (Reprinted from Bosanac et al. [92], with permission from Elsevier)

The N-terminal coupling domain was proposed to have two separate functions, at the one hand it attenuates IP_3 binding to the IP_3-binding core – and therefore its name suppressor domain [94] – leading to the difference in IP_3 affinity observed between the various IP_3R isoforms [58], and at the other it transmits the binding signal to the channel domain by interacting with the C-terminal tail [93, 95, 96]. The importance of the N-terminal coupling domain is apparent from the fact that deletion of this domain leads to an IP_3R with increased affinity for IP_3, but completely inactive as a Ca^{2+} channel [93]. Moreover, it is noteworthy that many regulatory proteins perform their regulatory function, not by binding to the modulatory and transducing domain, but by interacting specifically either with the N-terminal coupling domain (suppressor domain) or the gatekeeper domain (C-terminal tail) (Table 11.1). Recent data indicate that interactions as well between the N-terminal coupling domain (suppressor domain) and the cytosolic loop between TM4 and TM5 as well as conformational changes in the modulatory and transducing domain contribute in relaying the IP_3 signal to the Ca^{2+} channel (Fig. 11.3) [131, 132].

Table 11.1 Regulatory proteins acting on the IP_3R (in alphabetical order)

Regulatory protein acting on the IP_3R	General role of the protein	Interaction with the IP_3R	Effect on IP_3R	Selected references
80K-H	Protein kinase C substrate	Interacts with C-terminal tail of all IP_3R isoforms	Stimulation of IP_3R	[97]
Ataxin-2 and -3	Cytosolic proteins; polyQ extension in ataxia disorders	Interact with the C-terminal tail of IP_3R1	Sensitization of the IP_3R to IP_3 by polyQ form of ataxins	[98]
Bcl-2 and Bcl-Xl	Anti-apoptotic proteins	Interact with all IP_3R isoforms. Two sites of interactions: one in the middle of the modulatory and transducing domain and another in the C-terminal tail	Inhibitory and stimulatory effects on the IP_3R described, possibly due to a differential action of Bcl-2 and Bcl-Xl	[99–102]
Beclin-1	Autophagic protein	Interacts with the ligand-binding domain of IP_3R1 and IP_3R3	Sensitization of the IP_3R to IP_3	[103, 188]
BiP/GRP78	ER chaperone	Interacts under oxidized conditions with the third luminal loop of IP_3R1 only	Regulate IP_3R1 activity via the stabilization of its tetrameric assembly	[104]
CaBP family members and CIB1	Neuronal (CaBP) and ubiquitously expressed (CIB1) Ca^{2+}-sensor proteins	Interact with the suppressor domain of all IP_3R isoforms	Activatory and inhibitory role have been described	[105–108]
Calmodulin	Ubiquitous Ca^{2+}-sensor protein	Interacts with all IP_3R isoforms. Several binding sites are reported: a complex site in the suppressor domain, and two others in the modulatory and transducing domain, of which one only occurs in a splice isoform of IP_3R1	Inhibits the IP_3R	[109–112]

Carbonic anhydrase-related protein	Protein specifically expressed in Purkinje cells	Interacts with the modulatory and transducing domain of IP_3R1	Reduces the affinity of IP_3R1 for IP_3	[113]
Chromogranin A and B	Low-affinity, high-capacity Ca^{2+}-binding proteins, mainly but not exclusively in secretory granules	Interact in a pH-dependent manner with IP_3R1 between the pore region and TM6	Stimulate IP_3R activity	[114–116]
Cytochrome c	Mitochondrial protein, released under stress conditions to induce apoptosis	Interacts with the C-terminal tail of IP_3R1 and IP_3R3	Suppression of IP_3R inhibition by high cytosolic Ca^{2+} concentration	[117]
DANGER	Membrane-associated protein	Interacts with the modulatory and transducing domain of IP_3R1 and IP_3R3	Enhancement of the Ca^{2+}-dependent inhibition of the IP_3R	[118]
ERp44	Protein of the thioredoxin family	Interacts under reduced conditions with the third luminal loop of IP_3R1 only	Inhibits IP_3R1	[119]
Gβγ	Transducer protein	Interacts with IP_3R1	Inhibition of IP_3 binding but activation of IP_3R	[120]
GAPDH	Glycolytic enzyme	Interacts with the modulatory and transducing domain of IP_3R1	Local generation of NADH that may stimulate the IP_3R	[121]
GIT1 and GIT2	GRK-interacting proteins	Interact in a Ca^{2+}-dependent manner with the C-terminal tail of all IP_3R isoforms	Inhibit IP_3R	[122]
HSP90	Heat shock protein	Interacts with IP_3R3	Inhibits IP_3R	[123]
Huntingtin	Cytosolic protein; polyQ extension in neurological disorder	Interacts with the C-terminal tail of IP_3R1	Sensitization of the IP_3R to IP_3 depending on the polyQ extension and the presence of Huntingtin-associated protein 1	[124]
IRBIT	Regulatory protein in various signal transduction pathways	Interacts with the IP_3-binding site	Reduction of IP_3R sensitivity	[125, 126]

(continued)

Table 11.1 (continued)

Regulatory protein acting on the IP_3R	General role of the protein	Interaction with the IP_3R	Effect on IP_3R	Selected references
KRAS-induced actin interacting protein	Actin-interacting protein	Interacts with the ligand-binding domain of all IP_3R isoforms	Affects localization and activity of the IP_3R	[127]
Na/K-ATPase	Ubiquitous ion pump	Interacts with the ligand-binding domain of all IP_3R isoforms	Stimulation of IP_3R in the presence of ouabain, especially in the presence of ankyrin B	[128]
RACK1	Adapter protein, binds to protein kinase C	Two interaction sites: one in the suppressor domain, another at the end of the IP_3-binding core	Increases affinity for IP_3 and potentiates Ca^{2+} release.	[129]

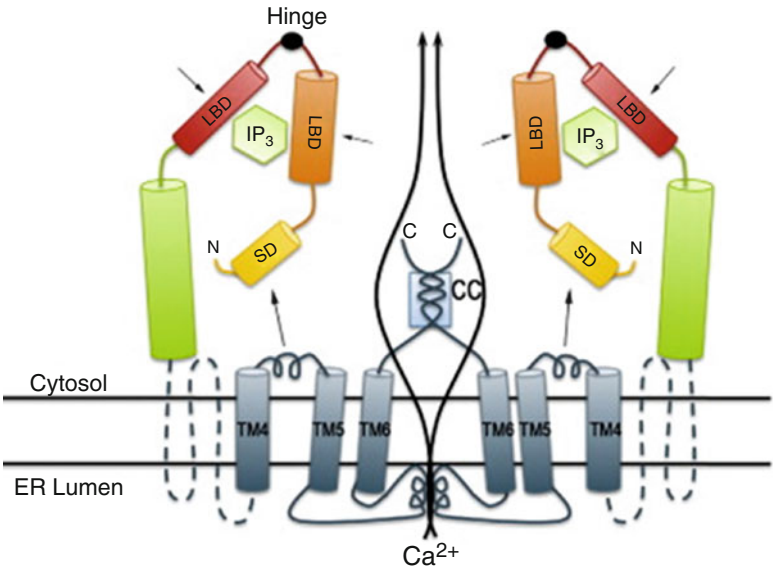

Fig. 11.3 Model of IP_3R channel activation. The IP_3R forms a tetramer, but for clarity, only two IP_3R1 subunits are depicted here. The colored parts indicate the first three functional domains: *yellow*, the suppressor domain (also called N-terminal coupling domain); *orange* and *red*, the two parts of the IP_3-binding core, linked by a hinge, and forming a cleft for IP_3; *green*, the modulatory and transducing domain (corresponding to the regulatory and coupling region). The subsequent channel domain and the C-terminal tail together contain the six transmembrane helices (TM1–6) linked by three luminal loops and two cytosolic loops, and a coiled-coil (CC) segment that participates in tetramer assembly. The channel pore is formed by TM5 and TM6 and the intervening luminal loop [130]. IP_3 binding is relayed to the channel as well by a direct interaction between suppressor domain and the cytosolic loop between TM4 and TM5 as through the modulatory and transducing domain (Reprinted from Wojcikiewicz et al. [130], with permission from Elsevier)

The channel domain consists of the six transmembrane helices, with two relatively small luminal loops, and a much larger third luminal loop (i.e. between TM5 and TM6), which supposedly intrudes in the membrane and forms the pore region of the IP_3R [133, 134]. This pore region has the same structure as the pore of the RyR and could be modelled based on the structure of the bacterial KcsA channel [92].

Finally, in order to avoid confusion, it should be mentioned here that independently of the above discussed functional subdivision, another subdivision in five domains could be made, based on the access of the IP_3R1 to proteolytic enzymes (Fig. 11.2b). Degradation of the IP_3R1 by low concentrations of trypsin or chymotrypsin does indeed deliver a finite number of fragments that remain aggregated and functional [135]. It was therefore assumed that these fragments largely corresponded to native, functional parts of the IP_3R. Although further structural analysis indicated this might not be completely accurate [39], the proteolytic products or their recombinant counterparts have been successfully used by various groups for

analysis of IP_3R1 (and IP_3R3) activation and their regulation by various compounds and proteins (e.g. [93–95, 99, 118, 136]).

More information on the action and regulation of the IP_3R is expected to originate from the knowledge of the 3-dimensional structure of the IP_3R. Due to its huge size, X-ray crystallographic analysis was until now limited to the N-terminal part of the IP_3R, allowing to resolve the N-terminal coupling domain (at 1.8 Å resolution; [137]) and the IP_3-binding core (at 2.2 Å resolution; [138]). The structure of these domains can be represented as follows: two successive β-trefoil domains (1–223 and 224–434) separated by a short hinge from an α-helical domain containing armadillo repeats (438–604). Those three domains interact with each other, whereby the latter two form together a cleft with positively charged amino acids in which IP_3 can bind [92, 94]. A schematic model of the IP_3R structure and of those interactions is shown in Fig. 11.3. In addition, a unusual helix-turn-helix extension between the β4 and β5 strands of the first β-trefoil domain is observed, which can act as a binding site for regulatory proteins as RACK1 [137].

The full-size IP_3R was investigated by several groups by cryo-electron microscopy at a resolution of about 30 Å, describing all a structure with fourfold symmetry and a lateral dimension of about 200 Å though with considerable variability between them at the level of the more detailed physical structure [139]. Subsequent analysis performed at a resolution of <20 Å demonstrated for the purified cerebellar IP_3R1, after single-particle analysis and 3D reconstruction, a height of 231 Å. Further, the diameter of the spherical cytosolic part was found to be 175 Å while the luminal part formed a square with sides of 96 Å [140]. The observed structure contained large cavities, allowing for the interaction of many regulatory components. This high-resolution analysis was performed in the absence of IP_3 and Ca^{2+}. Changes in Ca^{2+} concentration however provoke a drastic rearrangement of the IP_3R from a square-like conformation to a windmill-like conformation, as observed by proteolysis experiments and transmission electron microscopy [141], but this conformational change could not yet be investigated at higher resolution.

IP_3R Regulation by Ca^{2+}

As may already be inferred from the large conformational changes occurring in the IP_3R by changes in Ca^{2+} concentration [141], the Ca^{2+} ion is an important regulator of IP_3R activity. The basal Ca^{2+} concentrations in the cytosol is about 50–100 nM, but may be much higher in localized microdomains, e.g. between ER and mitochondria [142, 143]. From early on, it was observed that increases in the cytosolic Ca^{2+} concentration up to about 300 nM stimulate IP_3-induced Ca^{2+} release while at a higher concentration Ca^{2+} becomes inhibitory [23, 34, 144, 145]. As in the absence of Ca^{2+}, IP_3 is nearly completely inactive for inducing Ca^{2+} release, Ca^{2+} is considered a co-agonist of the IP_3R [145, 146]. This biphasic or bell-shaped dependence on Ca^{2+} also occurs for the RyR and was demonstrated for the various IP_3R isoforms [147, 148]. Some differences in Ca^{2+} sensitivity were observed between the IP_3R isoforms, which may be due either to intrinsic properties of the various IP_3R

isoforms but also to the presence of modulators (e.g. regulatory proteins such as calmodulin). The cytosolic Ca^{2+} concentration also affects the affinity for IP_3 binding to the IP_3R; in hepatocytes Ca^{2+} induced a switch between a low-affinity and a high-affinity state of the IP_3R [149]. The biphasic effect of Ca^{2+} on the IP_3R is indubitably important for explaining hierarchical Ca^{2+} signaling including the occurrence of Ca^{2+} oscillations and Ca^{2+}-wave propagation [64, 146, 150–153] but is at the molecular level mechanistically still not completely understood.

From the functional data it may be anticipated that multiple sites are involved [154]. $^{45}Ca^{2+}$ overlay techniques indicated the existence of seven cytosolic Ca^{2+}-binding sites [155, 156], of which two are located in the IP_3-binding core [138]. Subsequently, an additional site (E2100) was discovered on IP_3R1 which mutation significantly decreased the Ca^{2+} sensitivity and modified the biphasic Ca^{2+}-dependency curve [157, 158]. It is however not yet clear whether this site participates to a Ca^{2+}-binding site itself or whether it allosterically couples to it [39, 154]. In addition to direct Ca^{2+} binding to the IP_3R, there is also evidence that indirect effects via Ca^{2+}-binding proteins may also be involved. A prime candidate for this regulation would be calmodulin. Calmodulin inhibits the various IP_3R isoforms in a Ca^{2+}-dependent way [109, 110, 159, 160]. Although a modulation of IP_3R activity by calmodulin is not disputed, it is probably not the physiological mediator of the Ca^{2+}-dependent inhibition during the inhibitory phase of the biphasic regulation of the IP_3R by Ca^{2+} [39, 154].

Independently of its regulation by cytosolic Ca^{2+}, the IP_3R appears also to be regulated by the luminal Ca^{2+} concentration. The Ca^{2+} concentration in the lumen of the ER is about 200–500 μM [161]. It is now mostly accepted that not only the extent of IP_3-induced Ca^{2+} release is dependent on the Ca^{2+} store content, but that the luminal Ca^{2+} concentration has also a regulatory effect on the IP_3R [162–169]. This regulation, characterized by a decreased sensitivity of the IP_3R at lower filling levels of the ER, prevents an excessive Ca^{2+} depletion of the ER, which could be detrimental for other ER functions, as e.g. protein folding, and can even lead to ER stress. The regulation by luminal Ca^{2+} can also explain the phenomenon of graded or "quantal" Ca^{2+} release [170, 171], originally described by Muallem and colleagues [172] and by Meyer and Stryer [173]. The mechanism by which luminal Ca^{2+} affects the sensitivity of the IP_3R remains however elusive, and may involve either a luminal Ca^{2+} binding site on the IP_3R [155] or on a luminal, associated Ca^{2+}-binding protein as for example ERp44 [119]. Alternatively, the possibility that (part of) the effect, reflects an interaction of the released Ca^{2+} with a regulatory site at the cytosolic side of the IP_3R can not be completely excluded [174].

Regulatory Proteins Acting on the IP_3R

More than 50 different proteins were already shown to interact with the IP_3R. Included in this number are not only regulatory proteins but also scaffolding proteins, structural proteins and motor proteins. Moreover, not all those interactions are as extensively documented and in many cases the exact binding site is not known.

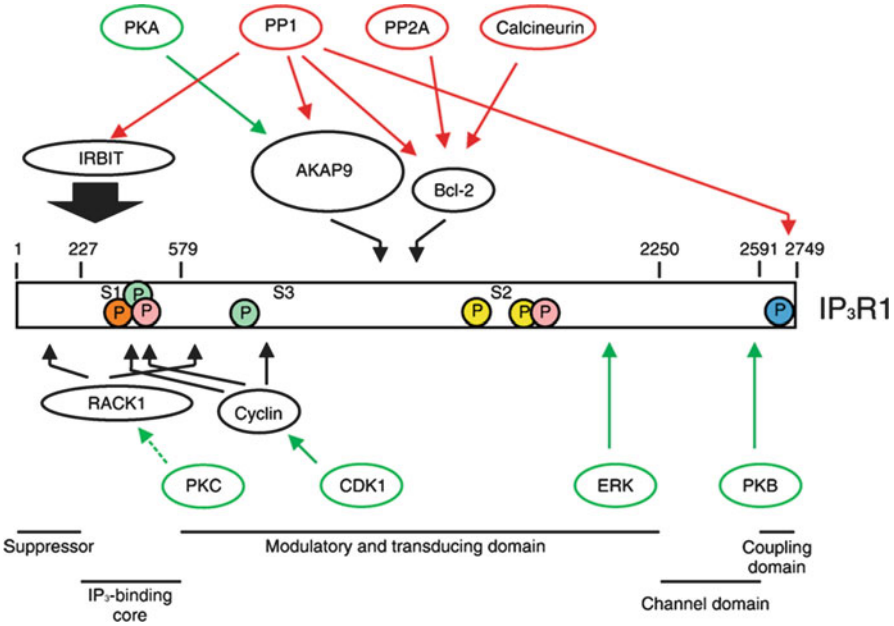

Fig. 11.4 Regulation of IP_3R1 by phosphorylation/dephosphorylation. Identified phosphorylation sites are shown in *yellow* (phosphorylation by protein kinase A and G), *blue* (by protein kinase B), *pale green* (by cyclin-dependent kinase 1), *pink* (by extracellular-signal regulated kinase) and *orange* (by the tyrosine kinase Fyn). Docking proteins (*black*), protein kinases (*green*) and protein phosphatases (*red*) are also shown. Splice sites (S1, S2 and S3) are indicated. Functional domains are indicated at the *bottom* of the figure [178] (Reprinted from Vanderheyden et al. [178]. With permission from Elsevier)

In addition, it is not always clear which interactions are direct, and which are indirect and may involve multiprotein complexes. A full account on all interacting proteins is beyond the scope of this article and for more details we refer to some recent reviews on the subject [39, 175–177]. The best documented regulatory proteins are listed in Table 11.1, with their action on the IP_3R.

Kinases and phosphatases have a complex pattern of action, as they can modulate the IP_3R and IP_3-induced Ca^{2+} release both in a direct (phosphorylation sites on the IP_3R, see Fig. 11.4) or in an indirect way (phosphorylation sites on regulatory proteins) and we therefore here refer to a recent review [178].

IP_3R Degradation

Persistent activation of plasma membrane receptors coupled to IP_3 production leads to IP_3R down-regulation by protein degradation [179, 180]. The process occurs for all three IP_3R isoforms, though with different kinetics [61]. This down-regulation

corresponds to a rapid decrease in the density of the IP_3Rs and is mediated by the ubiquitin-proteasome pathway. Interestingly, only activated IP_3Rs, i.e. which have bound IP_3 (or adenophostin), are the target of the ubiquitin-conjugating enzymes [181] but also the Ca^{2+} released by the IP_3R plays a role [182]. This down-regulation is probably part of homeostatic mechanisms that protect cells against excessive stimulation [130]. Multiple ubiquitinylation sites on the various IP_3R isoforms were detected, all localized in the modulatory and transducing domain [183]. As different forms of conjugated ubiquitin can be detected, and not all seem implicated in IP_3R degradation, other functions, maybe related to regulation of signaling activity, are conceivable.

Additionally, the various IP_3R isoforms can be differentially degraded by calpains and caspases [184, 185]. Importantly, degradation by caspase-3 is limited to IP_3R1 and this process is thought to play a role in apoptotic cell death [186, 187].

Conclusions

The IP_3R acts as a sensor and integrator of many cellular parameters and converts these inputs into a Ca^{2+} signal. In this way the IP_3R plays a crucial role in controlling a multiplicity of cellular functions. Due to its multiple regulatory sites, its isoform diversity, and its expression pattern and differential subcellular localizations, the IP_3R can fine tune Ca^{2+} release from the ER, and thereby generate complex spatio-temporal Ca^{2+} signals in a very precise way. Despite the large number of studies during the last quarter of a century, its exact activation mechanism and its regulation by the Ca^{2+} ion itself are not yet fully understood. The structure of the IP_3R is still not fully elucidated but it is expected that the availability of such information will boost the further unravelling of the molecular and cellular mechanisms.

Acknowledgments The authors want to acknowledge all their past and present collaborators, and in particular Profs. L. Missiaen and G. Bultynck, for stimulating discussions and continuous support.

References

1. Hokin MR, Hokin LE (1953) Enzyme secretion and the incorporation of P^{32} into phospholipides of pancreas slices. J Biol Chem 203:967–977
2. Michell RH (1975) Inositol phospholipids and cell surface receptor function. Biochim Biophys Acta 415:81–147
3. Berridge MJ, Dawson RM, Downes CP, Heslop JP, Irvine RF (1983) Changes in the levels of inositol phosphates after agonist-dependent hydrolysis of membrane phosphoinositides. Biochem J 212:473–482
4. Streb H, Irvine RF, Berridge MJ, Schulz I (1983) Release of Ca^{2+} from a nonmitochondrial intracellular store in pancreatic acinar cells by inositol-1,4,5-trisphosphate. Nature 306: 67–69

5. Berridge MJ (1983) Rapid accumulation of inositol trisphosphate reveals that agonists hydrolyse polyphosphoinositides instead of phosphatidylinositol. Biochem J 212:849–858
6. Bunney TD, Katan M (2011) PLC regulation: emerging pictures for molecular mechanisms. Trends Biochem Sci 36:88–96
7. Allbritton NL, Meyer T, Stryer L (1992) Range of messenger action of calcium ion and inositol 1,4,5-trisphosphate. Science 258:1812–1815
8. Erneux C, Takazawa K (1991) Intracellular control of inositol phosphates by their metabolizing enzymes. Trends Pharmacol Sci 12:174–176
9. De Smedt F, Missiaen L, Parys JB, Vanweyenberg V, De Smedt H, Erneux C (1997) Isoprenylated human brain type I inositol 1,4,5-trisphosphate 5-phosphatase controls Ca^{2+} oscillations induced by ATP in Chinese hamster ovary cells. J Biol Chem 272:17367–17375
10. Prentki M, Wollheim CB, Lew PD (1984) Ca^{2+} homeostasis in permeabilized human neutrophils. Characterization of Ca^{2+}-sequestering pools and the action of inositol 1,4,5-triphosphate. J Biol Chem 259:13777–13782
11. Burgess GM, Godfrey PP, McKinney JS, Berridge MJ, Irvine RF, Putney JW Jr (1984) The second messenger linking receptor activation to internal Ca release in liver. Nature 309: 63–66
12. Oron Y, Dascal N, Nadler E, Lupu M (1985) Inositol 1,4,5-trisphosphate mimics muscarinic response in Xenopus oocytes. Nature 313:141–143
13. O'Rourke FA, Halenda SP, Zavoico GB, Feinstein MB (1985) Inositol 1,4,5-trisphosphate releases Ca^{2+} from a Ca^{2+}-transporting membrane vesicle fraction derived from human platelets. J Biol Chem 260:956–962
14. Prentki M, Corkey BE, Matschinsky FM (1985) Inositol 1,4,5-trisphosphate and the endoplasmic reticulum Ca^{2+} cycle of a rat insulinoma cell line. J Biol Chem 260:9185–9190
15. Thévenod F, Streb H, Ullrich KJ, Schulz I (1986) Inositol 1,4,5-trisphosphate releases Ca^{2+} from a nonmitochondrial store site in permeabilized rat cortical kidney cells. Kidney Int 29:695–702
16. Parys JB, De Smedt H, Borghgraef R (1986) Calcium transport systems in the LLC-PK_1 renal epithelial established cell line. Biochim Biophys Acta 888:70–81
17. Spät A, Bradford PG, McKinney JS, Rubin RP, Putney JW Jr (1986) A saturable receptor for ^{32}P-inositol-1,4,5-triphosphate in hepatocytes and neutrophils. Nature 319:514–516
18. Guillemette G, Balla T, Baukal AJ, Catt KJ (1987) Inositol 1,4,5-trisphosphate binds to a specific receptor and releases microsomal calcium in the anterior pituitary gland. Proc Natl Acad Sci USA 84:8195–8199
19. Worley PF, Baraban JM, Supattapone S, Wilson VS, Snyder SH (1987) Characterization of inositol trisphosphate receptor binding in brain. Regulation by pH and calcium. J Biol Chem 262:12132–12136
20. Supattapone S, Worley PF, Baraban JM, Snyder SH (1988) Solubilization, purification, and characterization of an inositol trisphosphate receptor. J Biol Chem 263:1530–1534
21. Chadwick CC, Saito A, Fleischer S (1990) Isolation and characterization of the inositol trisphosphate receptor from smooth muscle. Proc Natl Acad Sci USA 87:2132–2136
22. Mourey RJ, Verma A, Supattapone S, Snyder SH (1990) Purification and characterization of the inositol 1,4,5-trisphosphate receptor protein from rat vas deferens. Biochem J 272: 383–389
23. Parys JB, Sernett SW, DeLisle S, Snyder PM, Welsh MJ, Campbell KP (1992) Isolation, characterization, and localization of the inositol 1,4,5-trisphosphate receptor protein in Xenopus laevis oocytes. J Biol Chem 267:18776–18782
24. Mignery GA, Südhof TC, Takei K, De Camilli P (1989) Putative receptor for inositol 1,4,5-trisphosphate similar to ryanodine receptor. Nature 342:192–195
25. Guillemette G, Favreau I, Boulay G, Potier M (1990) Solubilization and partial characterization of inositol 1,4,5-trisphosphate receptor of bovine adrenal cortex reveal similarities with the receptor of rat cerebellum. Mol Pharmacol 38:841–847
26. Mignery GA, Südhof TC (1990) The ligand binding site and transduction mechanism in the inositol-1,4,5-triphosphate receptor. EMBO J 9:3893–3898

27. Maeda N, Kawasaki T, Nakade S, Yokota N, Taguchi T, Kasai M, Mikoshiba K (1991) Structural and functional characterization of inositol 1,4,5-trisphosphate receptor channel from mouse cerebellum. J Biol Chem 266:1109–1116
28. Ross CA, Meldolesi J, Milner TA, Satoh T, Supattapone S, Snyder SH (1989) Inositol 1,4,5-trisphosphate receptor localized to endoplasmic reticulum in cerebellar Purkinje neurons. Nature 339:468–470
29. Maeda N, Niinobe M, Nakahira K, Mikoshiba K (1988) Purification and characterization of P_{400} protein, a glycoprotein characteristic of Purkinje cell, from mouse cerebellum. J Neurochem 51:1724–1730
30. Furuichi T, Yoshikawa S, Miyawaki A, Wada K, Maeda N, Mikoshiba K (1989) Primary structure and functional expression of the inositol 1,4,5-trisphosphate-binding protein P_{400}. Nature 342:32–38
31. Ferris CD, Huganir RL, Supattapone S, Snyder SH (1989) Purified inositol 1,4,5-trisphosphate receptor mediates calcium flux in reconstituted lipid vesicles. Nature 342:87–89
32. Miyawaki A, Furuichi T, Maeda N, Mikoshiba K (1990) Expressed cerebellar-type inositol 1,4,5-trisphosphate receptor, P_{400}, has calcium release activity in a fibroblast L cell line. Neuron 5:11–18
33. Ehrlich BE, Watras J (1988) Inositol 1,4,5-trisphosphate activates a channel from smooth muscle sarcoplasmic reticulum. Nature 336:583–586
34. Bezprozvanny I, Watras J, Ehrlich BE (1991) Bell-shaped calcium-response curves of Ins(1,4,5)P_3- and calcium-gated channels from endoplasmic reticulum of cerebellum. Nature 351:751–754
35. Mayrleitner M, Chadwick CC, Timerman AP, Fleischer S, Schindler H (1991) Purified IP_3 receptor from smooth muscle forms an IP_3 gated and heparin sensitive Ca^{2+} channel in planar bilayers. Cell Calcium 12:505–514
36. Mak DO, Foskett JK (1994) Single-channel inositol 1,4,5-trisphosphate receptor currents revealed by patch clamp of isolated Xenopus oocyte nuclei. J Biol Chem 269: 29375–29378
37. Mak DO, Foskett JK (1997) Single-channel kinetics, inactivation, and spatial distribution of inositol trisphosphate (IP_3) receptors in Xenopus oocyte nucleus. J Gen Physiol 109:571–587
38. Bezprozvanny I, Ehrlich BE (1994) Inositol (1,4,5)-trisphosphate ($InsP_3$)-gated Ca channels from cerebellum: conduction properties for divalent cations and regulation by intraluminal calcium. J Gen Physiol 104:821–856
39. Foskett JK, White C, Cheung KH, Mak DO (2007) Inositol trisphosphate receptor Ca^{2+} release channels. Physiol Rev 87:593–658
40. Vermassen E, Parys JB, Mauger JP (2004) Subcellular distribution of the inositol 1,4,5-trisphosphate receptors: functional relevance and molecular determinants. Biol Cell 96:3–17
41. Taylor CW, Taufiq UR, Pantazaka E (2009) Targeting and clustering of IP_3 receptors: key determinants of spatially organized Ca^{2+} signals. Chaos 19:037102
42. Mignery GA, Newton CL, Archer BTd, Südhof TC (1990) Structure and expression of the rat inositol 1,4,5-trisphosphate receptor. J Biol Chem 265:12679–12685
43. Patel S, Joseph SK, Thomas AP (1999) Molecular properties of inositol 1,4,5-trisphosphate receptors. Cell Calcium 25:247–264
44. Taylor CW, Genazzani AA, Morris SA (1999) Expression of inositol trisphosphate receptors. Cell Calcium 26:237–251
45. Sudhof TC, Newton CL, Archer BT 3rd, Ushkaryov YA, Mignery GA (1991) Structure of a novel $InsP_3$ receptor. EMBO J 10:3199–3206
46. Blondel O, Takeda J, Janssen H, Seino S, Bell GI (1993) Sequence and functional characterization of a third inositol trisphosphate receptor subtype, IP_3R-3, expressed in pancreatic islets, kidney, gastrointestinal tract, and other tissues. J Biol Chem 268:11356–11363
47. Nakagawa T, Okano H, Furuichi T, Aruga J, Mikoshiba K (1991) The subtypes of the mouse inositol 1,4,5-trisphosphate receptor are expressed in a tissue-specific and developmentally specific manner. Proc Natl Acad Sci USA 88:6244–6248

48. Danoff SK, Ferris CD, Donath C, Fischer GA, Munemitsu S, Ullrich A, Snyder SH, Ross CA (1991) Inositol 1,4,5-trisphosphate receptors: distinct neuronal and nonneuronal forms derived by alternative splicing differ in phosphorylation. Proc Natl Acad Sci USA 88:2951–2955
49. Nucifora FC Jr, Li SH, Danoff S, Ullrich A, Ross CA (1995) Molecular cloning of a cDNA for the human inositol 1,4,5-trisphosphate receptor type 1, and the identification of a third alternatively spliced variant. Brain Res Mol Brain Res 32:291–296
50. Monkawa T, Miyawaki A, Sugiyama T, Yoneshima H, Yamamoto-Hino M, Furuichi T, Saruta T, Hasegawa M, Mikoshiba K (1995) Heterotetrameric complex formation of inositol 1,4,5-trisphosphate receptor subunits. J Biol Chem 270:14700–14704
51. Joseph SK, Lin C, Pierson S, Thomas AP, Maranto AR (1995) Heteroligomers of type-I and type-III inositol trisphosphate receptors in WB rat liver epithelial cells. J Biol Chem 270:23310–23316
52. Nucifora FC Jr, Sharp AH, Milgram SL, Ross CA (1996) Inositol 1,4,5-trisphosphate receptors in endocrine cells: localization and association in hetero- and homotetramers. Mol Biol Cell 7:949–960
53. Joseph SK, Bokkala S, Boehning D, Zeigler S (2000) Factors determining the composition of inositol trisphosphate receptor hetero-oligomers expressed in COS cells. J Biol Chem 275:16084–16090
54. Newton CL, Mignery GA, Südhof TC (1994) Co-expression in vertebrate tissues and cell lines of multiple inositol 1,4,5-trisphosphate ($InsP_3$) receptors with distinct affinities for $InsP_3$. J Biol Chem 269:28613–28619
55. Miyakawa T, Maeda A, Yamazawa T, Hirose K, Kurosaki T, Iino M (1999) Encoding of Ca^{2+} signals by differential expression of IP_3 receptor subtypes. EMBO J 18:1303–1308
56. Vanlingen S, Sipma H, De Smet P, Callewaert G, Missiaen L, De Smedt H, Parys JB (2000) Ca^{2+} and calmodulin differentially modulate myo-inositol 1,4, 5-trisphosphate (IP_3)-binding to the recombinant ligand-binding domains of the various IP3 receptor isoforms. Biochem J 346:275–280
57. Tu H, Wang Z, Nosyreva E, De Smedt H, Bezprozvanny I (2005) Functional characterization of mammalian inositol 1,4,5-trisphosphate receptor isoforms. Biophys J 88:1046–1055
58. Iwai M, Michikawa T, Bosanac I, Ikura M, Mikoshiba K (2007) Molecular basis of the isoform-specific ligand-binding affinity of inositol 1,4,5-trisphosphate receptors. J Biol Chem 282:12755–12764
59. Zhang S, Fritz N, Ibarra C, Uhlen P (2011) Inositol 1,4,5-trisphosphate receptor subtype-specific regulation of calcium oscillations. Neurochem Res 36:1175–1185
60. De Smedt H, Missiaen L, Parys JB, Bootman MD, Mertens L, Van Den Bosch L, Casteels R (1994) Determination of relative amounts of inositol trisphosphate receptor mRNA isoforms by ratio polymerase chain reaction. J Biol Chem 269:21691–21698
61. Wojcikiewicz RJ (1995) Type I, II, and III inositol 1,4,5-trisphosphate receptors are unequally susceptible to down-regulation and are expressed in markedly different proportions in different cell types. J Biol Chem 270:11678–11683
62. Rahman TU, Skupin A, Falcke M, Taylor CW (2009) Clustering of $InsP_3$ receptors by $InsP_3$ retunes their regulation by $InsP_3$ and Ca^{2+}. Nature 458:655–659
63. Rahman T, Taylor CW (2009) Dynamic regulation of IP_3 receptor clustering and activity by IP_3. Channels (Austin) 3:226–232
64. Parker I, Choi J, Yao Y (1996) Elementary events of $InsP_3$-induced Ca^{2+} liberation in Xenopus oocytes: hot spots, puffs and blips. Cell Calcium 20:105–121
65. Bootman MD, Berridge MJ, Lipp P (1997) Cooking with calcium: the recipes for composing global signals from elementary events. Cell 91:367–373
66. Berridge MJ (1997) Elementary and global aspects of calcium signalling. J Physiol (Lond) 499:290–306
67. Marchant JS, Parker I (2001) Role of elementary Ca^{2+} puffs in generating repetitive Ca^{2+} oscillations. EMBO J 20:65–76

68. Berridge MJ, Lipp P, Bootman MD (2000) The versatility and universality of calcium signalling. Nat Rev Mol Cell Biol 1:11–21
69. Diambra L, Marchant JS (2009) Localization and socialization: experimental insights into the functional architecture of IP_3 receptors. Chaos 19:037103
70. Diambra L, Marchant JS (2011) Inositol (1,4,5)-trisphosphate receptor microarchitecture shapes Ca^{2+} puff kinetics. Biophys J 100:822–831
71. Conway SJ, Miller GJ (2007) Biology-enabling inositol phosphates, phosphatidylinositol phosphates and derivatives. Nat Prod Rep 24:687–707
72. DeLisle S, Radenberg T, Wintermantel MR, Tietz C, Parys JB, Pittet D, Welsh MJ, Mayr GW (1994) Second messenger specificity of the inositol trisphosphate receptor: reappraisal based on novel inositol phosphates. Am J Physiol 266:C429–C436
73. Takahashi M, Kagasaki T, Hosoya T, Takahashi S (1993) Adenophostins A and B: potent agonists of inositol-1,4,5-trisphosphate receptor produced by Penicillium brevicompactum. Taxonomy, fermentation, isolation, physico-chemical and biological properties. J Antibiot (Tokyo) 46:1643–1647
74. Morris SA, Nerou EP, Riley AM, Potter BV, Taylor CW (2002) Determinants of adenophostin A binding to inositol trisphosphate receptors. Biochem J 367:113–120
75. Rossi AM, Sureshan KM, Riley AM, Potter VL, Taylor CW (2010) Selective determinants of inositol 1,4,5-trisphosphate and adenophostin A interactions with type 1 inositol 1,4,5-trisphosphate receptors. Br J Pharmacol 161:1070–1085
76. Swann K (1991) Thimerosal causes calcium oscillations and sensitizes calcium-induced calcium release in unfertilized hamster eggs. FEBS Lett 278:175–178
77. Bootman MD, Taylor CW, Berridge MJ (1992) The thiol reagent, thimerosal, evokes Ca^{2+} spikes in HeLa cells by sensitizing the inositol 1,4,5-trisphosphate receptor. J Biol Chem 267:25113–25119
78. Missiaen L, Parys JB, Sienaert I, Maes K, Kunzelmann K, Takahashi M, Tanzawa K, De Smedt H (1998) Functional properties of the type-3 $InsP_3$ receptor in 16HBE14o- bronchial mucosal cells. J Biol Chem 273:8983–8986
79. Parys JB, Missiaen L, De Smedt H, Droogmans G, Casteels R (1993) Bell-shaped activation of inositol-1,4,5-trisphosphate-induced Ca^{2+} release by thimerosal in permeabilized A7r5 smooth-muscle cells. Pflugers Arch 424:516–522
80. Bultynck G, Sienaert I, Parys JB, Callewaert G, De Smedt H, Boens N, Dehaen W, Missiaen L (2003) Pharmacology of inositol trisphosphate receptors. Pflugers Arch 445:629–642
81. Hill TD, Berggren PO, Boynton AL (1987) Heparin inhibits inositol trisphosphate-induced calcium release from permeabilized rat liver cells. Biochem Biophys Res Commun 149:897–901
82. Ghosh TK, Eis PS, Mullaney JM, Ebert CL, Gill DL (1988) Competitive, reversible, and potent antagonism of inositol 1,4,5-trisphosphate-activated calcium release by heparin. J Biol Chem 263:11075–11079
83. Tones MA, Bootman MD, Higgins BF, Lane DA, Pay GF, Lindahl U (1989) The effect of heparin on the inositol 1,4,5-trisphosphate receptor in rat liver microsomes. Dependence on sulphate content and chain length. FEBS Lett 252:105–108
84. Maruyama T, Kanaji T, Nakade S, Kanno T, Mikoshiba K (1997) 2APB, 2-aminoethoxydiphenyl borate, a membrane-penetrable modulator of $Ins(1,4,5)P_3$-induced Ca^{2+} release. J Biochem 122:498–505
85. Bootman MD, Collins TJ, Mackenzie L, Roderick HL, Berridge MJ, Peppiatt CM (2002) 2-aminoethoxydiphenyl borate (2-APB) is a reliable blocker of store-operated Ca^{2+} entry but an inconsistent inhibitor of InsP3-induced Ca^{2+} release. FASEB J 16:1145–1150
86. Goto J, Suzuki AZ, Ozaki S, Matsumoto N, Nakamura T, Ebisui E, Fleig A, Penner R, Mikoshiba K (2010) Two novel 2-aminoethyl diphenylborinate (2-APB) analogues differentially activate and inhibit store-operated Ca^{2+} entry via STIM proteins. Cell Calcium 47:1–10

87. Gafni J, Munsch JA, Lam TH, Catlin MC, Costa LG, Molinski TF, Pessah IN (1997) Xestospongins: potent membrane permeable blockers of the inositol 1,4,5-trisphosphate receptor. Neuron 19:723–733
88. De Smet P, Parys JB, Callewaert G, Weidema AF, Hill E, De Smedt H, Erneux C, Sorrentino V, Missiaen L (1999) Xestospongin C is an equally potent inhibitor of the inositol 1,4,5- trisphosphate receptor and the endoplasmic-reticulum Ca^{2+} pumps. Cell Calcium 26:9–13
89. Jaimovich E, Mattei C, Liberona JL, Cárdenas C, Estrada M, Barbier J, Debitus C, Laurent D, Molgó J (2005) Xestospongin B, a competitive inhibitor of IP_3-mediated Ca^{2+} signalling in cultured rat myotubes, isolated myonuclei, and neuroblastoma (NG108–15) cells. FEBS Lett 579:2051–2057
90. Haak LL, Song LS, Molinski TF, Pessah IN, Cheng H, Russell JT (2001) Sparks and puffs in oligodendrocyte progenitors: cross talk between ryanodine receptors and inositol trisphosphate receptors. J Neurosci 21:3860–3870
91. Vandeput F, Combettes L, Mills SJ, Backers K, Wohlkönig A, Parys JB, De Smedt H, Missiaen L, Dupont G, Potter BV, Erneux C (2007) Biphenyl 2,3',4,5',6-pentakisphosphate, a novel inositol polyphosphate surrogate, modulates Ca^{2+} responses in rat hepatocytes. FASEB J 21:1481–1491
92. Bosanac I, Michikawa T, Mikoshiba K, Ikura M (2004) Structural insights into the regulatory mechanism of IP_3 receptor. Biochim Biophys Acta 1742:89–102
93. Uchida K, Miyauchi H, Furuichi T, Michikawa T, Mikoshiba K (2003) Critical regions for activation gating of the inositol 1,4,5-trisphosphate receptor. J Biol Chem 278:16551–16560
94. Yoshikawa F, Iwasaki H, Michikawa T, Furuichi T, Mikoshiba K (1999) Cooperative formation of the ligand-binding site of the inositol 1,4, 5-trisphosphate receptor by two separable domains. J Biol Chem 274:328–334
95. Boehning D, Joseph SK (2000) Direct association of ligand-binding and pore domains in homo- and heterotetrameric inositol 1,4,5-trisphosphate receptors. EMBO J 19:5450–5459
96. Bultynck G, Szlufcik K, Kasri NN, Assefa Z, Callewaert G, Missiaen L, Parys JB, De Smedt H (2004) Thimerosal stimulates Ca^{2+} flux through inositol 1,4,5-trisphosphate receptor type 1, but not type 3, via modulation of an isoform-specific Ca^{2+}-dependent intramolecular interaction. Biochem J 381:87–96
97. Kawaai K, Hisatsune C, Kuroda Y, Mizutani A, Tashiro T, Mikoshiba K (2009) 80K-H interacts with inositol 1,4,5-trisphosphate (IP_3) receptors and regulates IP_3-induced calcium release activity. J Biol Chem 284:372–380
98. Liu J, Tang TS, Tu H, Nelson O, Herndon E, Huynh DP, Pulst SM, Bezprozvanny I (2009) Deranged calcium signaling and neurodegeneration in spinocerebellar ataxia type 2. J Neurosci 29:9148–9162
99. Rong YP, Aromolaran AS, Bultynck G, Zhong F, Li X, McColl K, Matsuyama S, Herlitze S, Roderick HL, Bootman MD, Mignery GA, Parys JB, De Smedt H, Distelhorst CW (2008) Targeting Bcl-2-IP3 receptor interaction to reverse Bcl-2's inhibition of apoptotic calcium signals. Mol Cell 31:255–265
100. Chen R, Valencia I, Zhong F, McColl KS, Roderick HL, Bootman MD, Berridge MJ, Conway SJ, Holmes AB, Mignery GA, Velez P, Distelhorst CW (2004) Bcl-2 functionally interacts with inositol 1,4,5-trisphosphate receptors to regulate calcium release from the ER in response to inositol 1,4,5-trisphosphate. J Cell Biol 166:193–203
101. White C, Li C, Yang J, Petrenko NB, Madesh M, Thompson CB, Foskett JK (2005) The endoplasmic reticulum gateway to apoptosis by Bcl-X_L modulation of the $InsP_3R$. Nat Cell Biol 7:1021–1028
102. Monaco G, Decrock E, Akl H, Ponsaerts R, Vervliet T, Luyten T, De Maeyer M, Missiaen L, Distelhorst CW, De Smedt H, Parys JB, Leybaert L, Bultynck G (2012) Selective regulation of IP_3-receptor-mediated Ca^{2+} signaling and apoptosis by the BH4 domain of Bcl-2 versus Bcl-Xl. Cell Death and Differentiation 19:295–309. doi:10.1038/cdd.2011.97
103. Vicencio JM, Ortiz C, Criollo A, Jones AW, Kepp O, Galluzzi L, Joza N, Vitale I, Morselli E, Tailler M, Castedo M, Maiuri MC, Molgó J, Szabadkai G, Lavandero S, Kroemer G (2009) The inositol 1,4,5-trisphosphate receptor regulates autophagy through its interaction with Beclin 1. Cell Death Differ 16:1006–1017

104. Higo T, Hamada K, Hisatsune C, Nukina N, Hashikawa T, Hattori M, Nakamura T, Mikoshiba K (2010) Mechanism of ER stress-induced brain damage by IP_3 receptor. Neuron 68: 865–878
105. Yang J, McBride S, Mak DO, Vardi N, Palczewski K, Haeseleer F, Foskett JK (2002) Identification of a family of calcium sensors as protein ligands of inositol trisphosphate receptor Ca^{2+} release channels. Proc Natl Acad Sci USA 99:7711–7716
106. Nadif Kasri N, Holmes AM, Bultynck G, Parys JB, Bootman MD, Rietdorf K, Missiaen L, De Smedt H, Conway SJ, Holmes AB, Berridge MJ, Roderick HL (2004) Regulation of $InsP_3$ receptor activity by neuronal Ca^{2+} binding proteins. EMBO J 23:312–321
107. Haynes LP, Tepikin AV, Burgoyne RD (2004) Calcium-binding protein 1 is an inhibitor of agonist-evoked, inositol 1,4,5-trisphosphate-mediated calcium signaling. J Biol Chem 279:547–555
108. White C, Yang J, Monteiro MJ, Foskett JK (2006) CIB1, a ubiquitously expressed Ca^{2+}-binding protein ligand of the $InsP_3$ receptor Ca^{2+} release channel. J Biol Chem 281: 20825–20833
109. Michikawa T, Hirota J, Kawano S, Hiraoka M, Yamada M, Furuichi T, Mikoshiba K (1999) Calmodulin mediates calcium-dependent inactivation of the cerebellar type 1 inositol 1,4,5-trisphosphate receptor. Neuron 23:799–808
110. Missiaen L, Parys JB, Weidema AF, Sipma H, Vanlingen S, De Smet P, Callewaert G, De Smedt H (1999) The bell-shaped Ca^{2+} dependence of the inositol 1,4, 5-trisphosphate-induced Ca^{2+} release is modulated by Ca^{2+}/calmodulin. J Biol Chem 274:13748–13751
111. Sienaert I, Nadif Kasri N, Vanlingen S, Parys JB, Callewaert G, Missiaen L, De Smedt H (2002) Localization and function of a calmodulin-apocalmodulin-binding domain in the N-terminal part of the type 1 inositol 1,4,5-trisphosphate receptor. Biochem J 365:269–277
112. Kang S, Kwon H, Wen H, Song Y, Frueh D, Ahn HC, Yoo SH, Wagner G, Park S (2011) Global dynamic conformational changes in the suppressor domain of IP_3 receptor by stepwise binding of the two lobes of calmodulin. FASEB J 25:840–850
113. Hirota J, Ando H, Hamada K, Mikoshiba K (2003) Carbonic anhydrase-related protein is a novel binding protein for inositol 1,4,5-trisphosphate receptor type 1. Biochem J 372:435–441
114. Yoo SH, Lewis MS (1995) Thermodynamic study of the pH-dependent interaction of chromogranin A with an intraluminal loop peptide of the inositol 1,4,5-trisphosphate receptor. Biochemistry 34:632–638
115. Yoo SH (2000) Coupling of the IP_3 receptor/Ca^{2+} channel with Ca^{2+} storage proteins chromogranins A and B in secretory granules. Trends Neurosci 23:424–428
116. Thrower EC, Park HY, So SH, Yoo SH, Ehrlich BE (2002) Activation of the inositol 1,4,5-trisphosphate receptor by the calcium storage protein chromogranin A. J Biol Chem 277: 15801–15806
117. Boehning D, Patterson RL, Sedaghat L, Glebova NO, Kurosaki T, Snyder SH (2003) Cytochrome c binds to inositol (1,4,5) trisphosphate receptors, amplifying calcium-dependent apoptosis. Nat Cell Biol 5:1051–1061
118. van Rossum DB, Patterson RL, Cheung KH, Barrow RK, Syrovatkina V, Gessell GS, Burkholder SG, Watkins DN, Foskett JK, Snyder SH (2006) DANGER, a novel regulatory protein of inositol 1,4,5-trisphosphate-receptor activity. J Biol Chem 281:37111–37116
119. Higo T, Hattori M, Nakamura T, Natsume T, Michikawa T, Mikoshiba K (2005) Subtype-specific and ER lumenal environment-dependent regulation of inositol 1,4,5-trisphosphate receptor type 1 by ERp44. Cell 120:85–98
120. Zeng W, Mak DO, Li Q, Shin DM, Foskett JK, Muallem S (2003) A new mode of Ca^{2+} signaling by G protein-coupled receptors: gating of IP3 receptor Ca^{2+} release channels by $G\beta\gamma$. Curr Biol 13:872–876
121. Patterson RL, van Rossum DB, Kaplin AI, Barrow RK, Snyder SH (2005) Inositol 1,4,5-trisphosphate receptor/GAPDH complex augments Ca^{2+} release via locally derived NADH. Proc Natl Acad Sci USA 102:1357–1359
122. Zhang S, Hisatsune C, Matsu-Ura T, Mikoshiba K (2009) G-protein-coupled receptor kinase-interacting proteins inhibit apoptosis by inositol 1,4,5-triphosphate receptor-mediated Ca^{2+} signal regulation. J Biol Chem 284:29158–29169

123. Nguyen N, Francoeur N, Chartrand V, Klarskov K, Guillemette G, Boulay G (2009) Insulin promotes the association of heat shock protein 90 with the inositol 1,4,5-trisphosphate receptor to dampen its Ca^{2+} release activity. Endocrinology 150:2190–2196
124. Tang TS, Tu H, Chan EY, Maximov A, Wang Z, Wellington CL, Hayden MR, Bezprozvanny I (2003) Huntingtin and huntingtin-associated protein 1 influence neuronal calcium signaling mediated by inositol-(1,4,5) triphosphate receptor type 1. Neuron 39:227–239
125. Ando H, Mizutani A, Kiefer H, Tsuzurugi D, Michikawa T, Mikoshiba K (2006) IRBIT suppresses IP_3 receptor activity by competing with IP_3 for the common binding site on the IP_3 receptor. Mol Cell 22:795–806
126. Devogelaere B, Sammels E, De Smedt H (2008) The IRBIT domain adds new functions to the AHCY family. Bioessays 30:642–652
127. Fujimoto T, Machida T, Tsunoda T, Doi K, Ota T, Kuroki M, Shirasawa S (2011) KRAS-induced actin-interacting protein regulates inositol 1,4,5-trisphosphate-receptor-mediated calcium release. Biochem Biophys Res Commun 408:214–217
128. Zhang S, Malmersjo S, Li J, Ando H, Aizman O, Uhlen P, Mikoshiba K, Aperia A (2006) Distinct role of the N-terminal tail of the Na, K-ATPase catalytic subunit as a signal transducer. J Biol Chem 281:21954–21962
129. Patterson RL, van Rossum DB, Barrow RK, Snyder SH (2004) RACK1 binds to inositol 1,4,5-trisphosphate receptors and mediates Ca^{2+} release. Proc Natl Acad Sci USA 101:2328–2332
130. Wojcikiewicz RJ, Pearce MM, Sliter DA, Wang Y (2009) When worlds collide: IP_3 receptors and the ERAD pathway. Cell Calcium 46:147–153
131. Yamazaki H, Chan J, Ikura M, Michikawa T, Mikoshiba K (2010) Tyr-167/Trp-168 in type 1/3 inositol 1,4,5-trisphosphate receptor mediates functional coupling between ligand binding and channel opening. J Biol Chem 285:36081–36091
132. Chan J, Yamazaki H, Ishiyama N, Seo MD, Mal TK, Michikawa T, Mikoshiba K, Ikura M (2010) Structural studies of inositol 1,4,5-trisphosphate receptor: coupling ligand binding to channel gating. J Biol Chem 285:36092–36099
133. Michikawa T, Hamanaka H, Otsu H, Yamamoto A, Miyawaki A, Furuichi T, Tashiro Y, Mikoshiba K (1994) Transmembrane topology and sites of N-glycosylation of inositol 1,4,5-trisphosphate receptor. J Biol Chem 269:9184–9189
134. Galvan DL, Borrego-Diaz E, Perez PJ, Mignery GA (1999) Subunit oligomerization, and topology of the inositol 1,4, 5-trisphosphate receptor. J Biol Chem 274:29483–29492
135. Yoshikawa F, Iwasaki H, Michikawa T, Furuichi T, Mikoshiba K (1999) Trypsinized cerebellar inositol 1,4,5-trisphosphate receptor. Structural and functional coupling of cleaved ligand binding and channel domains. J Biol Chem 274:316–327
136. Maes K, Missiaen L, Parys JB, De Smet P, Sienaert I, Waelkens E, Callewaert G, De Smedt H (2001) Mapping of the ATP-binding sites on inositol 1,4,5-trisphosphate receptor type 1 and type 3 homotetramers by controlled proteolysis and photoaffinity labeling. J Biol Chem 276:3492–3497
137. Bosanac I, Yamazaki H, Matsu-Ura T, Michikawa T, Mikoshiba K, Ikura M (2005) Crystal structure of the ligand binding suppressor domain of type 1 inositol 1,4,5-trisphosphate receptor. Mol Cell 17:193–203
138. Bosanac I, Alattia JR, Mal TK, Chan J, Talarico S, Tong FK, Tong KI, Yoshikawa F, Furuichi T, Iwai M, Michikawa T, Mikoshiba K, Ikura M (2002) Structure of the inositol 1,4,5-trisphosphate receptor binding core in complex with its ligand. Nature 420:696–700
139. Taylor C, da Fonseca P, Morris E (2004) IP_3 receptors: the search for structure. Trends Biochem Sci 29:210–219
140. Sato C, Hamada K, Ogura T, Miyazawa A, Iwasaki K, Hiroaki Y, Tani K, Terauchi A, Fujiyoshi Y, Mikoshiba K (2004) Inositol 1,4,5-trisphosphate receptor contains multiple cavities and L-shaped ligand-binding domains. J Mol Biol 336:155–164
141. Hamada K, Miyata T, Mayanagi K, Hirota J, Mikoshiba K (2002) Two-state conformational changes in inositol 1,4,5-trisphosphate receptor regulated by calcium. J Biol Chem 277:21115–21118

142. Csordás G, Várnai P, Golenar T, Roy S, Purkins G, Schneider TG, Balla T, Hajnóczky G (2010) Imaging interorganelle contacts and local calcium dynamics at the ER-mitochondrial interface. Mol Cell 39:121–132
143. Giacomello M, Drago I, Bortolozzi M, Scorzeto M, Gianelle A, Pizzo P, Pozzan T (2010) Ca^{2+} hot spots on the mitochondrial surface are generated by Ca^{2+} mobilization from stores, but not by activation of store-operated Ca^{2+} channels. Mol Cell 38:280–290
144. Iino M (1990) Biphasic Ca^{2+} dependence of inositol 1,4,5-trisphosphate-induced Ca release in smooth muscle cells of the guinea pig taenia caeci. J Gen Physiol 95:1103–1122
145. Finch EA, Turner TJ, Goldin SM (1991) Calcium as a coagonist of inositol 1,4,5-trisphosphate-induced calcium release. Science 252:443–446
146. Dupont G, Goldbeter A (1993) One-pool model for Ca^{2+} oscillations involving Ca^{2+} and inositol 1,4,5-trisphosphate as co-agonists for Ca^{2+} release. Cell Calcium 14:311–322
147. Mak DO, McBride S, Foskett JK (2001) Regulation by Ca^{2+} and inositol 1,4,5-trisphosphate ($InsP_3$) of single recombinant type 3 $InsP_3$ receptor channels. Ca^{2+} activation uniquely distinguishes types 1 and 3 $InsP_3$ receptors. J Gen Physiol 117:435–446
148. Tu H, Wang Z, Bezprozvanny I (2005) Modulation of mammalian inositol 1,4,5-trisphosphate receptor isoforms by calcium: a role of calcium sensor region. Biophys J 88:1056–1069
149. Pietri F, Hilly M, Mauger JP (1990) Calcium mediates the interconversion between two states of the liver inositol 1,4,5-trisphosphate receptor. J Biol Chem 265:17478–17485
150. De Young GW, Keizer J (1992) A single-pool inositol 1,4,5-trisphosphate-receptor-based model for agonist-stimulated oscillations in Ca^{2+} concentration. Proc Natl Acad Sci USA 89:9895–9899
151. Atri A, Amundson J, Clapham D, Sneyd J (1993) A single-pool model for intracellular calcium oscillations and waves in the Xenopus laevis oocyte. Biophys J 65:1727–1739
152. Hajnóczky G, Thomas AP (1997) Minimal requirements for calcium oscillations driven by the IP_3 receptor. EMBO J 16:3533–3543
153. Berridge MJ (2006) Calcium microdomains: organization and function. Cell Calcium 40:405–412
154. Taylor CW, Tovey SC (2010) IP_3 receptors: toward understanding their activation. Cold Spring Harb Perspect Biol 2:a004010
155. Sienaert I, De Smedt H, Parys JB, Missiaen L, Vanlingen S, Sipma H, Casteels R (1996) Characterization of a cytosolic and a luminal Ca^{2+} binding site in the type I inositol 1,4,5-trisphosphate receptor. J Biol Chem 271:27005–27012
156. Sienaert I, Missiaen L, De Smedt H, Parys JB, Sipma H, Casteels R (1997) Molecular and functional evidence for multiple Ca^{2+}-binding domains in the type 1 inositol 1,4,5-trisphosphate receptor. J Biol Chem 272:25899–25906
157. Miyakawa T, Mizushima A, Hirose K, Yamazawa T, Bezprozvanny I, Kurosaki T, Iino M (2001) Ca^{2+}-sensor region of IP_3 receptor controls intracellular Ca^{2+} signaling. EMBO J 20:1674–1680
158. Tu H, Nosyreva E, Miyakawa T, Wang Z, Mizushima A, Iino M, Bezprozvanny I (2003) Functional and biochemical analysis of the type 1 inositol (1,4,5)-trisphosphate receptor calcium sensor. Biophys J 85:290–299
159. Missiaen L, De Smedt H, Bultynck G, Vanlingen S, Desmet P, Callewaert G, Parys JB (2000) Calmodulin increases the sensitivity of type 3 inositol-1,4, 5-trisphosphate receptors to Ca^{2+} inhibition in human bronchial mucosal cells. Mol Pharmacol 57:564–567
160. Adkins CE, Morris SA, De Smedt H, Sienaert I, Török K, Taylor CW (2000) Ca^{2+}-calmodulin inhibits Ca^{2+} release mediated by type-1, -2 and -3 inositol trisphosphate receptors. Biochem J 345:357–363
161. Sienaert I, De Smedt H, Parys JB, Missiaen L (1998) Regulation of Ca^{2+} release channels by luminal Ca^{2+}. In: Verkhratsky A, Toescu E (eds) Integrative aspects of calcium signalling. Plenum Press, New York, pp 131–161
162. Missiaen L, Taylor CW, Berridge MJ (1991) Spontaneous calcium release from inositol trisphosphate-sensitive calcium stores. Nature 352:241–244

163. Missiaen L, De Smedt H, Droogmans G, Casteels R (1992) Ca^{2+} release induced by inositol 1,4,5-trisphosphate is a steady-state phenomenon controlled by luminal Ca^{2+} in permeabilized cells. Nature 357:599–602
164. Parys JB, Missiaen L, De Smedt H, Casteels R (1993) Loading dependence of inositol 1,4,5-trisphosphate-induced Ca^{2+} release in the clonal cell line A7r5. Implications for the mechanism of quantal Ca^{2+} release. J Biol Chem 268:25206–25212
165. Missiaen L, De Smedt H, Parys JB, Casteels R (1994) Co-activation of inositol trisphosphate-induced Ca^{2+} release by cytosolic Ca^{2+} is loading-dependent. J Biol Chem 269:7238–7242
166. Tanimura A, Turner RJ (1996) Calcium release in HSY cells conforms to a steady-state mechanism involving regulation of the inositol 1,4,5-trisphosphate receptor Ca^{2+} channel by luminal [Ca^{2+}]. J Cell Biol 132:607–616
167. Caroppo R, Colella M, Colasuonno A, DeLuisi A, Debellis L, Curci S, Hofer AM (2003) A reassessment of the effects of luminal [Ca^{2+}] on inositol 1,4,5-trisphosphate-induced Ca^{2+} release from internal stores. J Biol Chem 278:39503–39508
168. Yamasaki-Mann M, Demuro A, Parker I (2010) Modulation of endoplasmic reticulum Ca^{2+} store filling by cyclic ADP-ribose promotes inositol trisphosphate (IP_3)-evoked Ca^{2+} signals. J Biol Chem 285:25053–25061
169. Yamasaki-Mann M, Parker I (2011) Enhanced ER Ca^{2+} store filling by overexpression of SERCA2b promotes IP_3-evoked puffs. Cell Calcium 50:36–41
170. Parys JB, Missiaen L, Smedt HD, Sienaert I, Casteels R (1996) Mechanisms responsible for quantal Ca^{2+} release from inositol trisphosphate-sensitive calcium stores. Pflugers Arch 432:359–367
171. McCarron JG, Olson ML, Rainbow RD, MacMillan D, Chalmers S (2007) Ins(1,4,5)P_3 receptor regulation during 'quantal' Ca^{2+} release in smooth muscle. Trends Pharmacol Sci 28:271–279
172. Muallem S, Pandol SJ, Beeker TG (1989) Hormone-evoked calcium release from intracellular stores is a quantal process. J Biol Chem 264:205–212
173. Meyer T, Stryer L (1990) Transient calcium release induced by successive increments of inositol 1,4,5-trisphosphate. Proc Natl Acad Sci USA 87:3841–3845
174. McCarron JG, Chalmers S, Muir TC (2008) "Quantal" Ca^{2+} release at the cytoplasmic aspect of the Ins(1,4,5)P_3R channel in smooth muscle. J Cell Sci 121:86–98
175. Bezprozvanny I (2005) The inositol 1,4,5-trisphosphate receptors. Cell Calcium 38: 261–272
176. Choe CU, Ehrlich BE (2006) The inositol 1,4,5-trisphosphate receptor (IP_3R) and its regulators: sometimes good and sometimes bad teamwork. Sci STKE 2006:re15
177. Mikoshiba K (2007) IP_3 receptor/Ca^{2+} channel: from discovery to new signaling concepts. J Neurochem 102:1426–1446
178. Vanderheyden V, Devogelaere B, Missiaen L, De Smedt H, Bultynck G, Parys JB (2009) Regulation of inositol 1,4,5-trisphosphate-induced Ca^{2+} release by reversible phosphorylation and dephosphorylation. Biochim Biophys Acta 1793:959–970
179. Wojcikiewicz RJ, Nahorski SR (1991) Chronic muscarinic stimulation of SH-SY5Y neuroblastoma cells suppresses inositol 1,4,5-trisphosphate action. Parallel inhibition of inositol 1,4,5-trisphosphate-induced Ca^{2+} mobilization and inositol 1,4,5-trisphosphate binding. J Biol Chem 266:22234–22241
180. Wojcikiewicz RJ, Furuichi T, Nakade S, Mikoshiba K, Nahorski SR (1994) Muscarinic receptor activation down-regulates the type I inositol 1,4,5-trisphosphate receptor by accelerating its degradation. J Biol Chem 269:7963–7969
181. Zhu CC, Wojcikiewicz RJ (2000) Ligand binding directly stimulates ubiquitination of the inositol 1, 4,5-trisphosphate receptor. Biochem J 348:551–556
182. Alzayady KJ, Wojcikiewicz RJ (2005) The role of Ca^{2+} in triggering inositol 1,4,5-trisphosphate receptor ubiquitination. Biochem J 392:601–606

183. Sliter DA, Aguiar M, Gygi SP, Wojcikiewicz RJ (2011) Activated inositol 1,4,5-trisphosphate receptors are modified by homogeneous Lys-48- and Lys-63-linked ubiquitin chains, but only Lys-48-linked chains are required for degradation. J Biol Chem 286:1074–1082
184. Magnusson A, Haug LS, Walaas SI, Østvold AC (1993) Calcium-induced degradation of the inositol (1,4,5)-trisphosphate receptor/Ca^{2+}-channel. FEBS Lett 323:229–232
185. Diaz F, Bourguignon LY (2000) Selective down-regulation of IP_3 receptor subtypes by caspases and calpain during TNF alpha-induced apoptosis of human T-lymphoma cells. Cell Calcium 27:315–328
186. Hirota J, Furuichi T, Mikoshiba K (1999) Inositol 1,4,5-trisphosphate receptor type 1 is a substrate for caspase-3 and is cleaved during apoptosis in a caspase-3-dependent manner. J Biol Chem 274:34433–34437
187. Assefa Z, Bultynck G, Szlufcik K, Nadif Kasri N, Vermassen E, Goris J, Missiaen L, Callewaert G, Parys JB, De Smedt H (2004) Caspase-3-induced truncation of type 1 inositol trisphosphate receptor accelerates apoptotic cell death and induces inositol trisphosphate-independent calcium release during apoptosis. J Biol Chem 279:43227–43236
188. Decuypere JP, Welkenhuyzen K, Luyten T, Ponsaerts R, Dewaele M, Molgo J, Agostinis P, Missiaen L, De Smedt H, Parys JB, Bultynck G (2011) IP3 receptor-mediated Ca^{2+} signaling and autophagy induction are interrelated. Autophagy 7:1472–1489

Chapter 12
The Discovery and Structural Investigation of the IP_3 Receptor and the Associated IRBIT Protein

Katsuhiko Mikoshiba

Abstract The IP_3 receptor (IP_3R) is a Ca^{2+} channel that releases Ca^{2+} from the endoplasmic reticulum (ER) and plays a variety of roles in cell functions. This receptor was discovered as a developmentally regulated glyco-phosphoprotein, known as P400, which was absent in cerebellar mutant mice. The IP_3R has three different isoforms in vertebrates, and each IP_3R is composed of different subdomains. The affinities of the IP_3-binding core of the three isoforms of the IP_3R for IP_3 are similar. The N-terminal IP_3-binding suppressor region of each isoform is responsible for its isoform-specific IP_3-binding affinity. IP_3 binding to the IP_3-binding core leads to a conformational change, resulting in direct interactions of tyrosine-168 (in IP_3R1)/tryptophane-168 (in IP_3R2 and 3) in the N-terminal suppressor region with the loop region of transmembrane 4–5. The suppressor region and C-terminal portion which associate with nearly 20 signaling molecules are located at the areas near the channel pore. The area including suppressor region and C-terminal portion are regarded as hot spots for the regulating opening and closing of the channel pore. A pseudo-ligand of the IP_3R, known as IRBIT (IP_3R binding protein released with inositol 1,4,5-trisphosphate), that interacts with the IP_3-binding core domain of the IP_3R was discovered. IRBIT not only regulates Ca^{2+} release by binding to the IP_3-binding core domain but also regulates the acid-base balance by binding to various ion transporters, such as pancreas-type NBC1 (pNBC1) and CFTR. Most of the associated proteins bind to these areas and regulate IP_3R channel gating. Cryo-electron microscopy shows a balloon-like structure, which has vacancy inside the IP_3R with multi-porous surface area. The unique 3-dimensional structure of the IP_3R is convenient for associating with many IP_3R-associated proteins. Therefore, the IP_3R serves as a signaling hub, which forms macromolecular complex with various molecules.

K. Mikoshiba (✉)
Laboratory for Developmental Neurobiology, RIKEN Brain Science Institute and Calcium Oscillation Project, ICORP-SORST, JST 2-1 Hirosawa, Wako-shi, Saitama 351-0198, Japan
e-mail: mikosiba@brain.riken.jp

M.S. Islam (ed.), *Calcium Signaling*, Advances in Experimental Medicine and Biology 740, DOI 10.1007/978-94-007-2888-2_12,

Keywords IP_3 • IP_3 receptor • Ca^{2+} • Ca^{2+} channel • Ca^{2+} signaling • P400 • Gating mechanism • IRBIT • Signaling hub

Abbreviations

IP_3R	IP_3 receptor
ER	endoplasmic reticulum
SDS-PAGE	SDS polyacrylamide gel electrophoresis
SAHH	S-adenosylhomocysteine hydrolase

The IP_3R and Protein Kinase C (PKC) Signaling Cascade System

Inositol phosphates and inositol lipids are known to bind to their target molecules, triggering signaling cascades that accomplish various physiological functions (Fig. 12.1). The IP_3 receptor (IP_3R) and protein kinase C (PKC) signaling cascades are among the most well-known signaling cascades (Fig. 12.2). IP_3 and DAG are hydrolysed from phosphatidylinositol 4,5-bisphosphate (PIP2). This bifurcating signaling system is of fundamental importance in regulating in regulating a wide range of cellular processes. IP_3 and DAG have different functions by binding to different type of molecules specific to IP_3 and DAG. IP_3 has been shown to be responsible for Ca^{2+} release from non-mitochondrial stores [1]. IP_3-induced Ca^{2+} release plays a role in regulation of secretion of hormones, growth factors, neurotransmitters, neurotrophins, perception of odorants and light and gene expression. DAG activates PKC to phosphorylate various proteins, leading to various cellular responses.

Discovery of the IP_3R as the Missing P400 in the Mutant Cerebellum

IP_3 was originally found to increase cytosolic Ca^{2+} [1]. The source of the Ca^{2+} was not known with certainty but has been speculated to be non-mitochondrial stores. Furthermore, whether solely the IP_3R is an IP_3-binding protein or a Ca^{2+}-release channel remains to be determined [1].

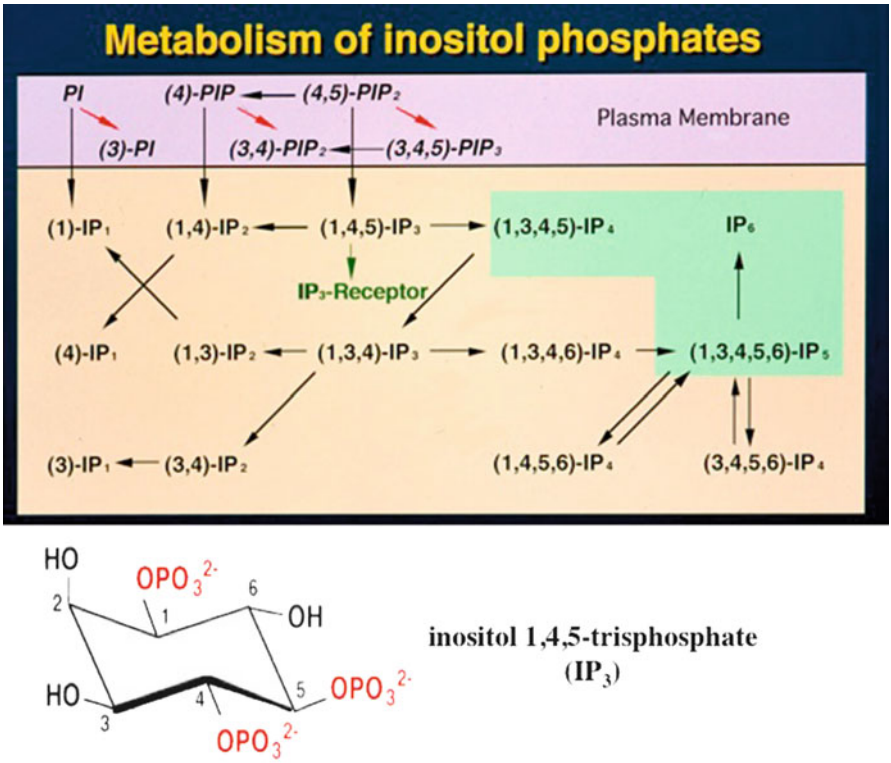

Fig. 12.1 Metabolism of inositol phosphates. Among the various kinds of signaling cascades, inositol phosphates are important signaling molecules which are linked with phosphatidyl inositol (*PI*), phosphatidyl inositol monophosphate (*PIP1*), and phosphatidylinositol bisphosphates (*PIP2*). Importance of phosphatidylinositol trisphophate is also recognized. Inositol 7 phosphates or inositol 8 phosphates are reported and they may play an important role for supplying the high energy from the high-energy phosphate bond. Among these inositol phosphates, IP_3 is the only inositol phosphate molecule whose target is a channel

Studies on P400

We studied the expression of protein P400 and observed an increase in expression during mouse development. However, in the cerebellum of mutant mice, P400 expression is greatly reduced or almost absent (Fig. 12.3). A marked decrease in P400 expression was observed in *pcd(Purkinje cell deficient)* mutant mice with degenerated and lost Purkinje cells (Fig. 12.3). P400 was also observed to be missing in *staggerer* mutant mice that have poor dendritic arborization and lack spines on the dendrites of the neurons in the cerebellum [2, 3]. P400 is a highly phosphorylated membrane protein with increased expression during the development of animals.

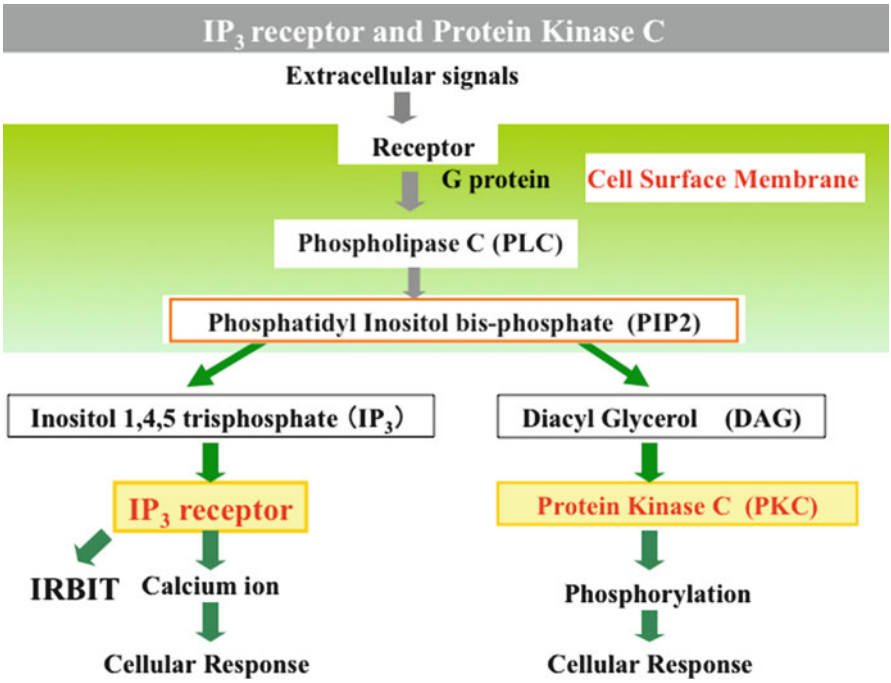

Fig. 12.2 The IP_3R and protein kinase C. The IP_3R and protein kinase C (*PKC*) signaling cascade system. Both IP_3 and diacylglycerol (*DAG*) are produced from phosphatidylinositol 4,5-bisphosphate, but they have completely different functions: IP_3 releases Ca^{2+} from intracellular stores and also releases IRBIT from IP_3 binding core of IP_3R, whereas DAG activates PKC to phosphorylate various proteins. IP_3 is the only one among the various inositol lipids and phosphates whose target molecule is a channel to release Ca^{2+} [92]

Furthermore, a hypothesis was proposed linking inositol lipids to Ca^{2+} signaling [4]. We later discovered that P400 was an IP_3-binding protein and realized that we had been working on an IP_3 binding protein for several years before IP_3 was even identified as an important second messenger for Ca^{2+} release from intracellular stores.

We were able to identify P400 as an IP_3R based on several reports that were published on IP_3. While we were studying P400, a report was published demonstrating that IP_3 released Ca^{2+} from non-mitochondrial stores [1].

A year later, another report was published describing the absence of Ca^{2+} spikes in Purkinje cells of the cerebellum of *staggerer* mutant mice [5]. Subsequently, another group reported high IP_3-binding activity in the cerebellum compared with other parts of the mouse brain [6]. P400 is also highly enriched in the cerebellum. The expression profile of P400 matched the IP_3 binding profile [7] and we were able to find a link between P400 and IP_3 binding. These data enabled us to consider the possibility that P400 might be related to IP_3 and Ca^{2+}. One hypothesis we considered was that P400 might be an IP_3R.

P400 was highly enriched in both isolated Purkinje cells and in the microsomal fraction of the cerebellum. Various detergents were used in the attempts to purify

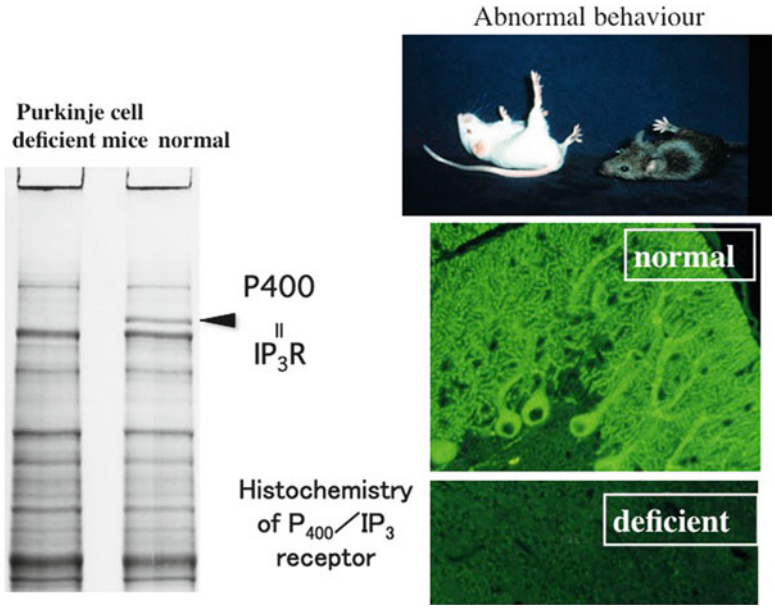

Fig. 12.3 SDS-polyacrylamide gel electrophoresis (SDS-PAGE) of the membrane fraction from the cerebella from wild type and Purkinje-cell-deficient mutant mice and its immunohistochemical staining of the cerebellar sections from the wild type and the mutant mice cerebella using anti-P400/IP_3R antibody. Left panel: SDS-PAGE of membrane fraction of the normal mice (right side) and that of Purkinje cell deficient mice (*left side*). High molecular weight membrane protein called P400 is greatly reduced in the Purkinje cell deficient mutant *pcd (Purkinje cell deficient)* cerebellum. Three monoclonal antibodies were screened by western-blotting using the cerebellar membrane fractions from the wild type and Purkinjce cell deficient mutant mice or wild type brain tissue without the cerebellum. *Upper right panel*: Various cerebellar mutant mice with cerebellar ataxia. *Lower right panel*: Immunohistochemical staining of the P400/IP_3R. P400/IP_3R is absent in Purkinje cell deficient mice (*indicated as deficient*) but is present in wild mice cerebella (*indicated as normal*). Specific monoclonal antibodies against P400 were used to analyse if the IP_3 binding activity exist in the immunoprecipated fraction of the solubilized fraction from the cerebellum. Monoclonal antibodies immunoprecipitated the IP_3 binding activity in the immunoprecipitates fraction. By using the three monoclonal antibodies, cDNA from the mouse cerebellum were screened by expression vector system and whole cDNA sequence of P400/IP_3R was cloned and whole sequence was determined [10, 11]

P400 to homogeneity [8, 9] to determine its biochemical properties. After purification, the purified fraction was used to raise specific monoclonal antibodies and also to sequence amino acids. The cloning and sequencing of P400 cDNA were also completed successfully.

To obtain the primary amino acid sequence of P400, two strategies were adopted. The first strategy involved purifying P400 and analyzing the primary amino acid sequence using an amino acid analyzer. The second strategy was to obtain specific antibodies against P400, use these antibodies in an expression vector system, and immunoscreen a cDNA library prepared from whole mouse cerebellum. In addition, by generating antibodies, we were able to determine the location of P400 and characterize the biochemical property of P400. Highly specific antibodies are required

for this immunoscreen, immunocytochemical and biochemical studies. Therefore, we injected purified IP_3R as an antigen. Specific monoclonal antibodies were obtained by western blot screening of more than 10,000 hybridoma clones using the cerebellum comparing with other part of the brain tissue. If antibodies from any clone interacted with any other protein band except the P400 250 KD band, then the antibodies were discarded. After almost two and a half years, three specific monoclonal antibodies that recognized different region of P400 were obtained [3].

The Identification of P400 as an IP_3R

The monoclonal antibodies efficiently interacted with P400 in every step of the purification procedure of the IP_3-binding protein and clearly interacted with the purified IP_3-binding protein. Notably, the P400 monoclonal antibody (18A10) immunoprecipitated with the IP_3-binding protein when added to the solubilized purified IP_3-binding fraction. In Fig. 12.3 immunostaining was performed using the monoclonal antibodies which we raised. No immuno positive reaction was observed in the microsomal fraction from Purkinje cell deficient mutant mice. Based on the above evidence, in 1989, we concluded that P400 was the IP_3-binding protein/receptor [10].

cDNA Cloning of the IP_3R by Immunoscreening

The successful strategy was to use an expression vector system to immunoscreen a cDNA library prepared from the whole tissue of mouse cerebellum to obtain the amino acid sequence of the P400/IP_3-binding protein. In 1988, immunoscreening the entire P400/IP_3 binding protein cDNA sequence was completed, which was faster than determining the amino acid sequence of the fragments of the IP_3-binding protein. However, we later found that some of the amino sequence fragments of the type 1 IP_3R obtained via sequencing were clearly identical to the sequences identified by immunoscreening.

The lengths of the amino acid sequence and those of mouse P400/IP_3R type 1 were approximately 2,700 amino acids and approximately 10 kb [11–13], respectively. Rat IP_3R type 2 was also the same size [10]. At the time of this work, IP_3Rs were the second longest sequence ever reported. The longest sequence was determined as the ryanodine receptor, another important Ca^{2+} channel, first cloned by Prof. Shosaku Numa [14]. Since whole cDNA of IP_3R was cloned, cDNA of other isoforms of IP_3Rs and those of other species were also cloned from their homology and their sequences were determined [15–19].

Another approach was by differential subtraction analyses of cerebellar cDNAs between wild-type and *pcd(Purkinje cell deficient)* mutant were performed [20]. The partial sequence (PCD6) obtained by differential subtraction [20] was determined to be different from that of the ryanodine receptor. Mignery et al. hypothesized that the partial sequence could be part of the sequence of the putative IP_3R

[21] based on immunostaining results obtained by using the antibody against the reported sequence of the clone obtained by Nordquist et al. [20].

Although we cloned the full length cDNA of P400/IP_3 receptor, many other researchers were still attempting to purify the protein [10, 22, 23]. The IP_3 binding protein was purified from rat cerebellum [22], bovine cerebellum [24, 25] bovine aorta smooth muscle [26], rat vas deferens [27] and *Xenopus laevis* oocytes [28].

The IP_3R Is a Ca^{2+} Channel

The purified type 1 IP_3R was determined to function as a Ca^{2+} channel when incorporated into a lipid bilayer [12, 29] or liposome [30, 31]. Additionally, the overexpression of type 1 IP_3R cDNA enhanced IP_3-binding activity and Ca^{2+} release activity [30, 31]. Based on the aforementioned reasons, the IP_3R was identified as a Ca^{2+} channel. The IP_3R is a cationic channel located in the membrane of the endoplasmic reticulum [29]. Channel opening is regulated in a dual manner by two second messengers, IP_3 and Ca^{2+}[32–34].

Structure and Functional Analyses Demonstrate the Diverse Functions of the IP_3R

Three isoforms of the IP_3R have been cloned and sequenced in vertebrates. Each isoform has different affinities for IP_3 [16, 35–38]. A detailed analysis of the affinities of the IP_3-binding core for IP_3 revealed that these three isoforms exhibited similar affinities [39]. The IP_3-binding suppressor domain linked to the N-terminal side of the binding core of each of the three isoforms was found to be responsible for the isoform-specific tuning of IP_3-binding affinity [39]. There are three isoforms in vertebrates such as human [16, 36], mouse [12, 38], rat, Xenopus laevis [15], but single isoform in ascidian egg(unpublished), star fish [17], drosophila [40]. Type 1 isoform is highly expressed in neurons particularly in high amount in the Purkinje cells in the cerebellum, and smooth muscle cell and very low amount ubiquitously. Type 2 is highly expressed in astrocytes in the brain and heart and secretory organs [41–43]. Type 3 is expressed in secretory organs and ubiquitously in other immuno systems.

Unique Structural Properties

The three IP_3R isoforms have different IP_3-binding affinities and cooperativities [10, 35, 38, 44–47].

The IP_3-binding core domain is the minimum region required for specific IP_3 binding and has been mapped to within residues 226–578 of the mouse type-1 IP_3R (Fig. 12.4). The type 1 IP_3R is a polypeptide composed of 2,749 residues.

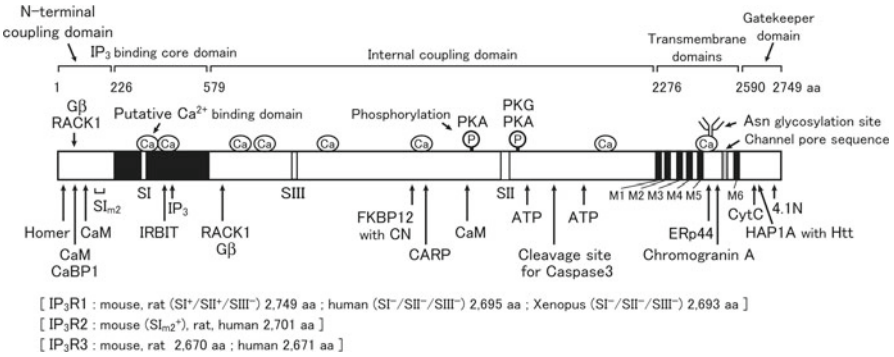

Fig. 12.4 Structure of the IP_3R and associated molecules. This figure shows the primary structure of the IP_3R. The IP_3R has a long N-terminal, short C-terminal, and transmembrane domains near the C-terminal region. IP_3R1 associates with Ca^{2+} and with many functional signaling molecules, like a signaling hub [92]. *M1–M6* transmembrane domain located at the C-terminus, *the pore* channel pore site, *SI, SII, SIII* splicing sites, *branched bars at the channel domain* N-glycosylation sites, *PKA* cAMP-dependent protein kinase, *PKG* cGMP-dependent protein kinase, *CaM* calmodulin-binding site, *ATP* ATP-binding site, *FKBP* FK506-binding protein, *CN* calcineurin, *Htt* Huntingtin, *HAPIA* Http-associated protein–IA, *CytC* cytochrome C, *CARP* carbonic anhydrase-related protein, *IRBIT* IP_3R binding protein released with inositol 1,4,5-trisphosphate

The crystal structure of the IP_3-binding core domain (residues 224–604) in complex with IP_3 at a resolution of 2.2 Å [48] exhibits an asymmetric, boomerang-like structure consisting of an N-terminal beta-trefoil domain and a C-terminal alpha-helical domain containing an armadillo repeat-like fold (Fig. 12.5). Eleven amino acid residues within the IP_3-binding core domain are responsible for the strict recognition of IP_3. All of these residues except Gly268 are conserved in the other IP_3R isoforms [10, 36]. We cloned the mouse type-2 and type-3 IP_3R genes [38] and compared the IP_3-binding affinities of the IP_3-binding core domains of all three IP_3R isoforms. The IP_3-binding core domains of the three isoforms shared approximately 70% amino acid sequence identity. Surprisingly, the IP_3-binding affinities of the three IP_3-binding core domains were indistinguishable [48].

The N-Terminal IP_3-Binding Suppressor Domain Is Responsible for Isoform-Specific IP_3-Binding

The 225 amino acid residues at the N-terminus of IP_3R1 function as a suppressor of IP_3 binding. Deletion of these residues results in a significant increase in IP_3-binding affinity [49, 50]. The suppressor domain physically interacts with the IP_3-binding core domain of IP_3R1 [51]. We determined the structure of the suppressor domain of mouse IP_3R1 by X-ray crystallography at a resolution of 1.8 Å [52] (Fig. 12.5). The N-terminal region comprises head and arm subdomains, which form a beta-trefoil

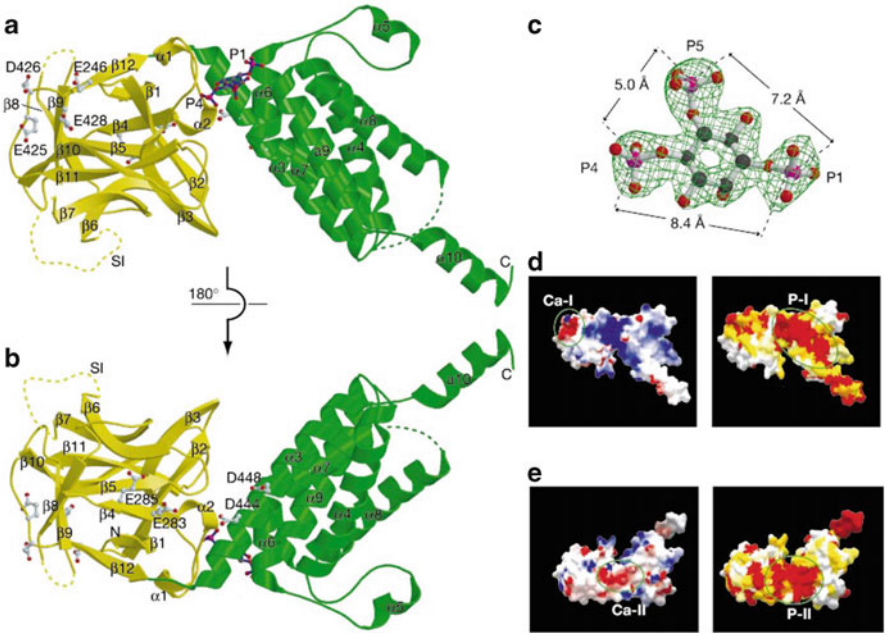

Fig. 12.5 Structure of IP_3 binding core domain of mouse IP_3R type 1 in complex with IP_3 [48]. (**a**) The β-domain (*yellow*) and the α-domain (*green*) with the IP_3 molecule at the interface. Residues in the Ca-I and Ca-II sites and the splicing site (SI) are shown. (**b**) View in a rotated by 180°. (**c**) Electron density map around the IP_3 molecule. (**d**, **e**) Molecular surface representations of IP_3 binding core domain of mouse IP_3R type 1 in the same orientations as (**a**) and (**b**), respectively. Surface electrostatic potential (*left panel* with Ca-I and Ca-II sites) and conserved surface residues (*right panel* with P-I, P-II sites; identical residues are shown in *red*, and least-conserved residues in *white*)

fold and a helix-turn-helix structure that protrudes from the globular head subdomain, respectively. The N-terminal 604 residues of the three IP_3R isoforms, which contain both suppressor and IP_3-binding core domains, exhibited K_d values of 49.5 ± 10.5 nM (IP_3R1), 14.0 ± 3.5 nM (IP_3R2) and 163.0 ± 44.4 nM (IP_3R3) [39]. These values are close to the values of the intrinsic IP_3-binding affinities of full-length IP_3Rs [38], suggesting that the suppression of IP_3 binding generates the isoform-specific IP_3-binding affinities of the three IP_3R isoforms. Site-directed mutagenesis analyses of the suppressor domain of mouse IP_3R1 showed that seven conserved amino acid residues (Leu30, Leu32, Val33, Asp34, Arg36, Arg54 and Lys127) were critical for the suppression of IP_3 binding [52]. Moreover, mutagenesis analyses demonstrated that 11 type 3-specific residues (Glu39, Ala41, Asp46, Met127, Ala154, Thr155, Leu162, Trp168, Asn173, Asn176 and Val179) were critical for the type-3 receptor-specific IP_3-binding affinity [39]. All of these conserved and nonconserved residues, with the exception of Leu162, are located on the surface of the head subdomain of the suppressor domain, indicating that the head subdomain is responsible for the tuning of isoform-specific IP_3-binding affinity (Fig. 12.6).

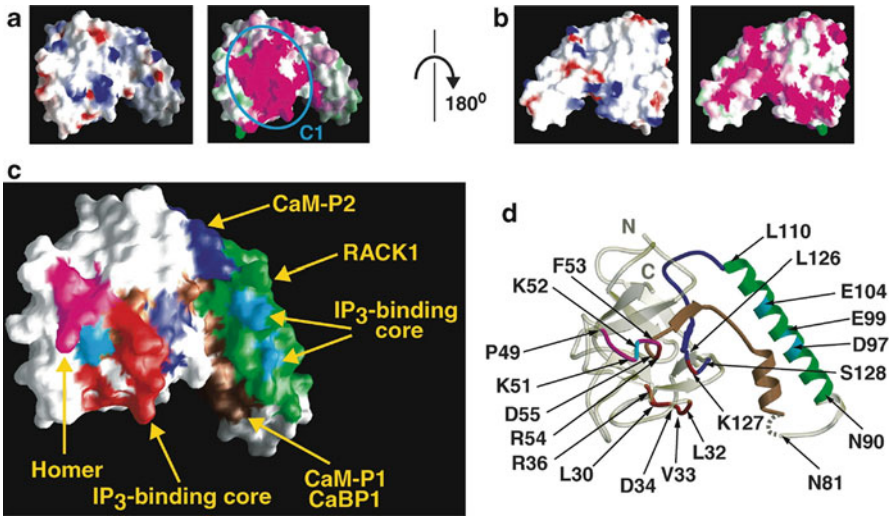

Fig. 12.6 Molecular Surface Characteristics of N-terminal suppressor domain of IP_3R type 1 [52]. (**a**) *Left panel* surface shows the surface electrostatic potential with positive charge depicted in *blue* and negative charge in *red*. *Right panel* shows the surface residue conservation determined from sequence alignment is plotted with color gradient from magenta (identical residues) to green (least conserved residues) and is presented in the *right panel*. The highly conserved surface region (*C1*) is labeled. (**b**) View in (**a**) is rotated by 180°. (**c** and **d**) Surface and ribbon diagram representations of key sites on N-terminal suppressor domain of IP_3R for binding other proteins. Residues involved in IP_3 suppression are shown in *red*. Residues in cyan are not involved in IP_3 suppression but play a part in interaction of N-terminal suppressor domain of IP_3R with IP_3 binding core domain of IP_3R. Docking sites for Homer (*magenta*, residues P49–F53) [91] and RACK1 (*green*, residues N90–L110) [87] are shown. Due to the overlap with Homer, RACK1, and the IP3 binding core, not all residues responsible for binding CaM-P1 and CaBP1 (*brown*, residues P49–N81) [93, 94] and CaM-P2 (*blue*, residues E106–S128) [94] are colored. Conservation was determined with ConSurf [95] and surface representation was presented (**a**–**c**)

The 3-Dimensional Structure of the Type 1 IP_3R

The tetrameric structure of the type 1 IP_3R determined by electron microscopy (EM) has been reported by our group and several other groups [53–58]. We succeeded in purifying type 1 IP_3R in its native form. EM analyses revealed a reversible transition between two distinct structures with four-fold symmetry between a windmill and a square structure. We demonstrated that Ca^{2+} promotes the transition from square to windmill structures via the relocation of four peripheral IP_3-binding domains, which were identified by binding to heparin-gold [54]. We collected additional biochemical and EM evidence of a structural change in the 3-dimensional (3D) architecture of the type 1 IP_3R (Fig. 12.7) regulated by the physiological Ca^{2+} concentration [56]. In the absence of Ca^{2+}, the type 1 IP_3R structure was observed to be "mushroom-like" with a large square-shaped head and a small channel domain linked by four thin bridges. In the presence of Ca^{2+}, the structure was in a "windmill-like" form, containing four bridges that connected the IP_3-binding domain with the channel

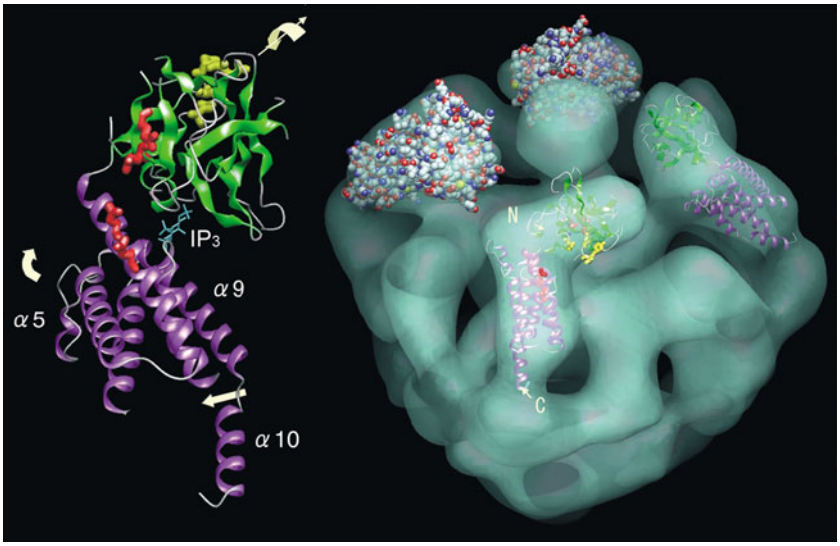

Fig. 12.7 The IP_3R contains multiple cavities and L-shaped ligand-binding domains [58]**.** Three-dimensional structure of IP_3 receptor in the IP_3-unbound state has also been resolved at high resolution (15 Å) using electron microscopic images of the receptor. The tetrameric IP_3 receptors have a *hot-air balloon like shape* (total height of 231 Å) with the *spherical* cytoplasmic domain (diameter of 175 Å) and the *square-shaped* luminal domain (side length of 96 Å). The transmembrane domain is 30 Å in thickness. A prominent *L-shaped* densities were found in the *spherical* cytoplasmic region of the three dimensional structure, and estimated as the *L-shaped* IP_3 binding core domains determined by X-ray crystalographic analysis [48]

domain, thereby verifying the Ca^{2+}-dependence of the 3D structural change of the IP_3R. We succeeded in visualizing the structure of the IP_3R using atomic force microscopy (AFM) to examine individual IP_3R particles in aqueous solution [59]. AFM or photometric analyses can be used to monitor real-time changes caused by dynamic conformational changes in aqueous solutions and in living cells.

The precise 3D structure of the Ca^{2+}-free tetrameric IP_3R was determined by cryo-EM on a helium-cooled specimen stage using an automatic particle selection system. At a resolution of 15 Å, structural analyses revealed a multi-porous architecture and L-shaped densities that were assigned according to the X-ray structure of the IP_3-binding domains (Fig. 12.7) [58].

The Gating Mechanism of the IP_3R Channel

The structure of the IP_3R has traditionally been divided into the following functional domains: the N-terminal ligand-binding domain, the modulatory/coupling domain and the C-terminal transmembrane/channel-forming domain [12, 44, 60]. When the C-terminal channel-forming domain or the caspase-3-cleaved form of mouse IP_3R1 was expressed in HeLa and COS-7 cells, both ATP and thapsigargin failed to induce an

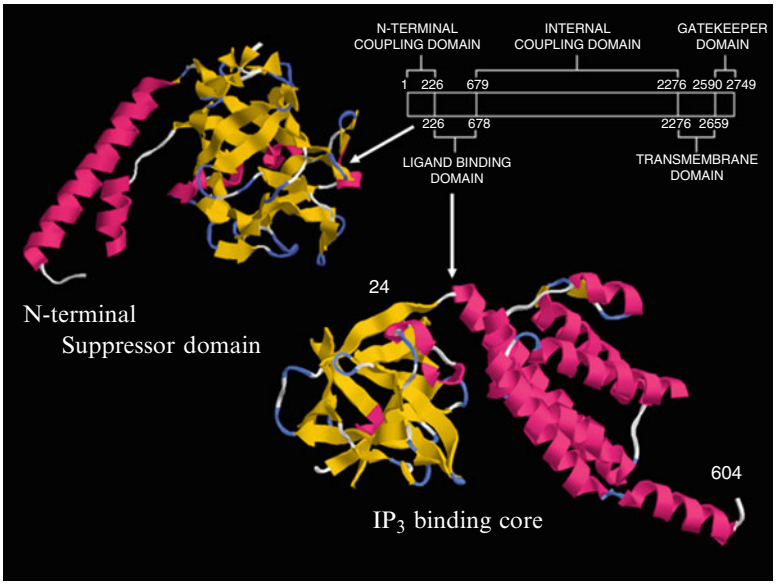

Fig. 12.8 Alignment of the N-terminal suppressor domain of mouse IP_3R1 and IP_3-binding core domain. (*Right*) Ribbon diagram of the IP_3-binding core complex, comprising a beta-trefoil domain (*yellow*), an alpha-helical domain (*orange*), and a hinge region (*purple*) (see Fig. 12.5). (*Left*) Structure of the suppressor domain. The ribbon diagram shows the head subdomain (*yellow*) and the arm subdomain alpha-helical (*red*) of the suppressor domain (see Fig. 12.6). The N-terminal suppressor domain and IP_3-binding core domain interact each other to regulate the IP_3 binding affinity. Binding affinity of IP_3 to each IP_3 binding core domain isolated from type 1, 2 and 3 are higher than whole IP_3R. In addition it is interesting that of IP_3 binding core domain from each isoform showed very high IP_3 binding affinity. From the analysis of the chimera work of different combination of N-terminal suppressor domain with the IP_3-binding core domain, we found that N-terminal suppressor domain regulates isoform-specific IP_3 binding affinity of each isoform of IP_3R [39]

increase in cytosolic Ca^{2+} [61]. Normal entry of Ca^{2+} after store depletion (store-operated Ca^{2+} entry) was observed in these cells, indicating that the Ca^{2+} stores of the cells expressing the truncated IP_3R were nearly empty in the resting state and that these proteins continuously leaked Ca^{2+}. We hypothesize that the large cytoplasmic N-terminal region that covers the channel domain is necessary to keep the channel closed [61].

To understand the mechanism of IP_3-induced gating of the channel, we analyzed the channel properties of deletion mutants that retained both the IP_3-binding domain and the channel-forming domain of IP_3R1 [62]. The results showed that mutants lacking the 223 N-terminal residues, which correspond to the IP_3-binding suppressor domain, or residues 651–1,130 did not exhibit any measurable Ca^{2+} release activity in response to the addition of IP_3. However, both mutants retained their IP_3-binding activity. These results suggest that residues within the 1–223 and 651–1,130 regions are critical for the functional coupling of IP_3 binding and channel opening (Fig. 12.8). When the cysteine residue in the C-terminal portion is mutated, no Ca^{2+} release activity is observed. Therefore, we proposed a novel 5-domain structural

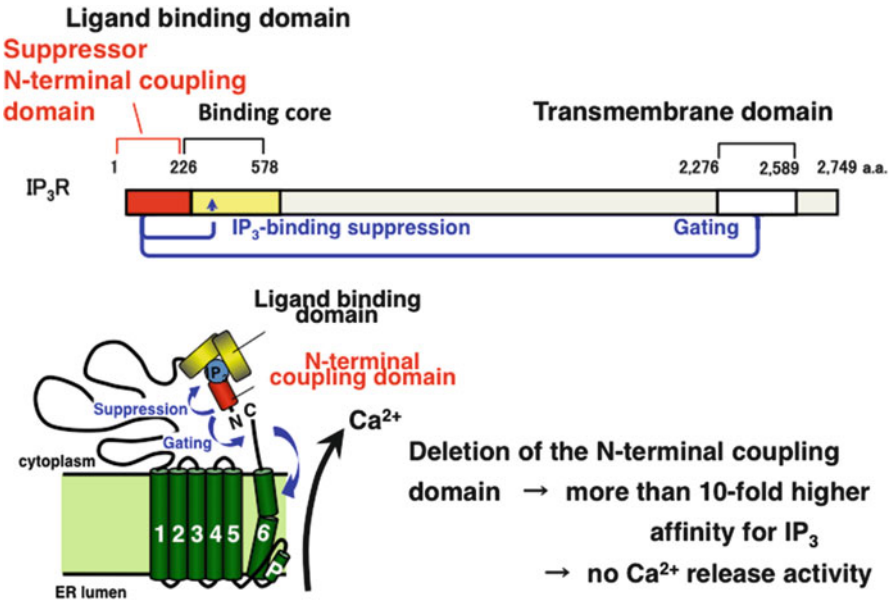

Fig. 12.9 Five-domain structure model of mouse IP_3R1. The structure of IP_3R1 is divided into five functional domains: an N-terminal coupling/suppressor domain, an IP_3-binding core domain, an internal coupling domain, a transmembrane/channel-forming domain, and a gatekeeper domain. The IP_3 binding signal is transferred through both the N-terminal and internal coupling domains to the gatekeeper domain, which triggers a conformational change in the activation gate formed within the transmembrane/channel-forming domain (see in detail the Ref. [62]). There are two functions in suppressor N-terminal coupling domain: One is to suppress the IP_3 binding activity. Second is directly related to gating since when suppressor domain is deleted Ca^{2+} releasing activity is lost even in the presence of IP_3 binding core and channel region is present [96]

model in which conformational changes in the IP_3-binding core domain caused by IP_3 binding are transmitted through both the N-terminal coupling/suppressor domain and the internal coupling domain to the C-terminal tail, triggering channel opening (Fig. 12.9). The unique gating machinery comprised of the N-terminal ligand-binding and C-terminal channel-forming domains may account for the characteristic behavior of IP_3R channels, such as quantal Ca^{2+} release without desensitization. Recently, we found that the tyrosine 167 (in type 1 IP_3R) and tryptophan 168 (in both type 2 and type 3 IP_3R) bind to the loop [63] region of transmembrane domains 4 and 5. When tyrosine 167 and tryptophan 168 are mutated, channel activity is lost. Based on these results, the gating mechanism of the IP_3R could be initiated by binding IP_3 to the IP_3-binding core, resulting in the conformational change of the N-terminal suppressor region to bind to the loop region of transmembrane domains 4 and 5 that are associated with the C-terminal portion. Subsequently, the channel pore is opened (Fig. 12.8).

Various Roles of the IP_3R in Cell Functions

Developmental studies on the role of the IP_3R showed that the receptor is involved in fertilization by playing roles in both the egg [15, 64, 65] and sperm (Fig. 12.10) [66, 67]. The IP_3R has been shown to function as a Ca^{2+} oscillator [64] and to be essential for dorsoventral axis formation [65, 68] and cell cleavage [69]. Additionally, the IP_3R has been observed to be involved in neurite extension using the CALI (chromophore-assisted laser inactivation) technique [70] and IP_3 indicator [71]. The IP_3R has also been found to be important for neuronal plasticity in the cerebellum [72] and hippocampus [63, 73, 74]. Although most of the Ca^{2+} release channel is a ryanodine receptor and is highly enriched in the heart, the IP_3 receptor has recently been shown to play an essential role in cardiogenesis [42, 75–77]. Due to different expression levels of the IP_3R in different cell types, which have different properties, it will be interesting to discover how these unique and specific properties are produced (Fig. 12.11).

We examined the biochemical and biophysical properties of the IP_3R extensively, focusing on structure-function relationships and the identification of molecules associated with the IP_3R. Numerous molecules associated with the IP_3R have been reported by our laboratory as well as several other laboratories. Together, these molecules form a macromolecular complex that is capable of functioning as a signaling hub. The properties of this complex depend on the unique structural properties of the IP_3R.

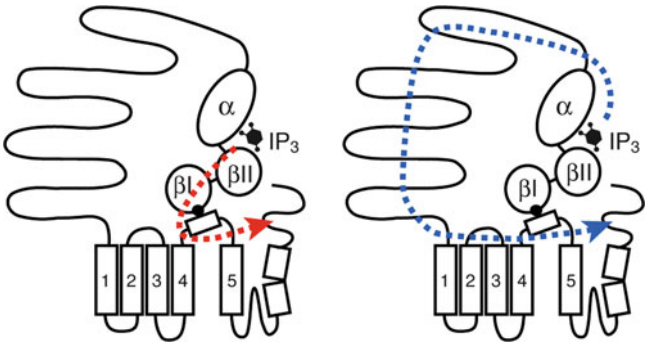

Fig. 12.10 Schematic models of the unliganded and liganded states of the IP_3R. A model of the IP_3R in the liganded state [88]. Tyrosine-168 (in IP_3R1)/tryptophane-168 (in IP_3R2 and 3) of the N-terminal suppressor region interacts with loop region of transmembrane 5 and 6 (M4-M5) linker and maintains the conformation of the gatekeeper domain in a low trypsin sensitive form in the wild-type channel. The Tyr/Trp contact region is composed of Tyr-167/Trp-168 (*Y/W*) plus Glu-20/Glu19 (*E*), Lys-168/Lys-169 (*K*), Leu-169/Leu-170 (*L*), and Ser-217/Ser-218 (*S*) of IP_3R1/IP_3R3. Substitution of Tyr-167 or Trp-168 into alanine (*right*, *open circle*) disrupts the interaction with the M4-M5 linker, and the gatekeeper domain is maintained in a high trypsinsensitive form (Y167A/W168A). A model for the liganded state of IP_3R shows two routes that relay IP_3 binding signals to the gatekeeper domain demonstrated by *red* and *blue arrows*. The gating hinge is assumed to be within the sixth membrane- spanning helix. Channel gating is associated with C-terminal portion. Since C-terminal side next to IP_3 binding core is deleted [62], channel activity is lost. Therefore, the two routes that relay IP_3 binding signals to the gatekeeper domain are indicated by a *red arrow* and a *blue arrow*, respectively

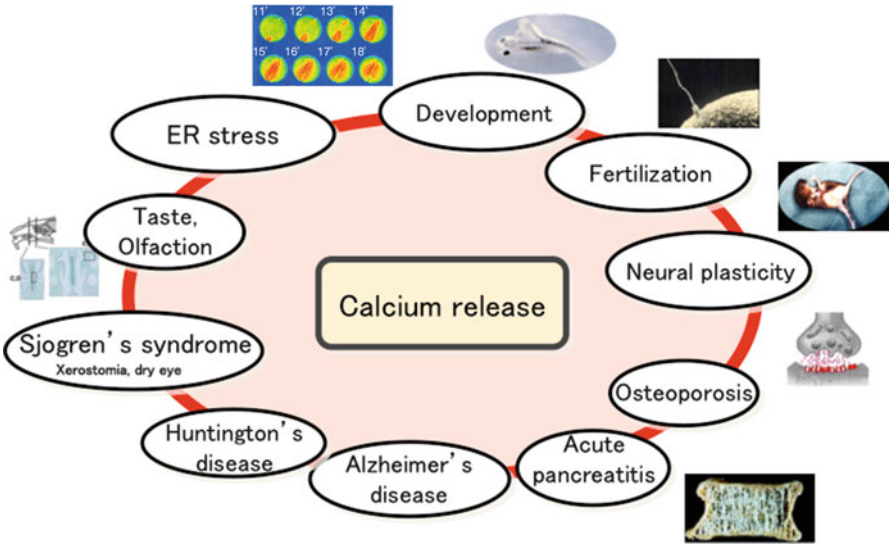

Fig. 12.11 The variety of physiological and pathological phenomena regulated by the IP_3R. IP_3R is involved in various developmental events including fertilization in both egg side and sperm side, cell division, dorso-ventral axis formation. Since type 1 IP_3R is highly enriched in the neurons, abnormal expression causes severe cerebellar ataxia accompanied with abnormal neural plasticity. In addition, IP_3R was found to be involved in osteoclast function in bone formation, pancreatic secretion, sensory functions such as taste or olfaction. Role of IP_3 receptor in exocrine function of type 2 and 3 are found by producing double knock out mice which is related to Sjogren's syndrome. Recently, in heart, although most of the Ca^{2+} release channel is ryanodine receptor, IP_3R is found to be involved in cardiogenesis [42, 75–77]. It is found that ER stress caused apoptosis of neurons accompanied by the degradation of IP_3R type 1, suggesting that IP_3R is protecting neuronal cells from ER stress. This phenomena is a collaborative work with the GRP78 chaperone particularly associated with type 1 IP_3R (see more detail to [97])

IRBIT, a Pseudo-Ligand of the IP_3R

To isolate all the proteins associated with the IP_3R, this receptor was attached to a column, which associates with solubilized proteins, and eluted using a stepwise salt solution followed by a high-salt solution. In order to isolate more proteins, a high-salt solution containing IP_3 was used. We were able to obtain a single protein (residues 1–2,217). Using this method, a novel protein, IRBIT (IP_3R Binding protein released with Inositol 1,4,5-Trisphosphate), was identified. IRBIT consists of 530 amino acids and has a domain homologous to *S*-adenosylhomocysteine hydrolase near the C-terminus and a 104-amino-acid appendage containing multiple potential phosphorylation sites near the N-terminus (Fig. 12.12). *In vitro* binding experiments demonstrated that the N-terminal region of IRBIT is essential for its interaction with the IP_3R1 and that IRBIT binds to the IP_3-binding core domain. The amino acids required for the recognition of IP_3 are also required for IRBIT recognition (Fig. 12.13). IP_3-dissociated IRBIT from IP_3R1 with an EC_{50} of approximately 0.5 μM. IP_3 was 50-times more

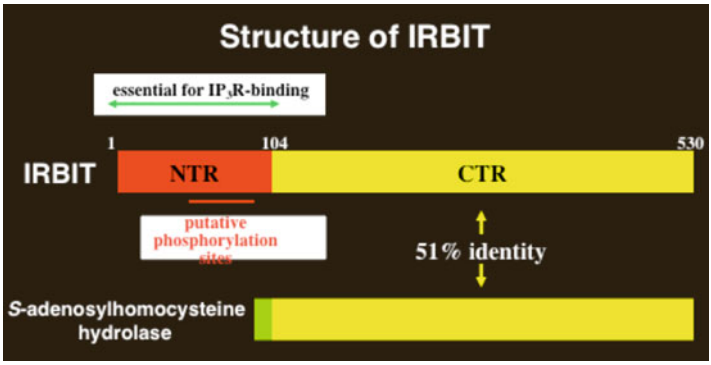

Fig. 12.12 IRBIT (IP_3R binding protein released with Inositol 1,4,5- Trisphosphate), a pseudoligand of IP_3R. IRBIT was a homologue of S-adenosylhomocysteine hydrolase (*SAHH*), but has no enzyme activity of SAHH. Multiserine phosphorylation of IRBIT was essential for the binding, and 10 of the 12 key amino acids in IP_3R for IP_3 recognition participated in binding to IRBIT. Therefore a unique mode of IP_3R regulation in which IP_3 sensitivity is regulated by IRBIT acting as an endogenous "pseudoligand" whose inhibitory activity can be modulated by its phosphorylation status [78]

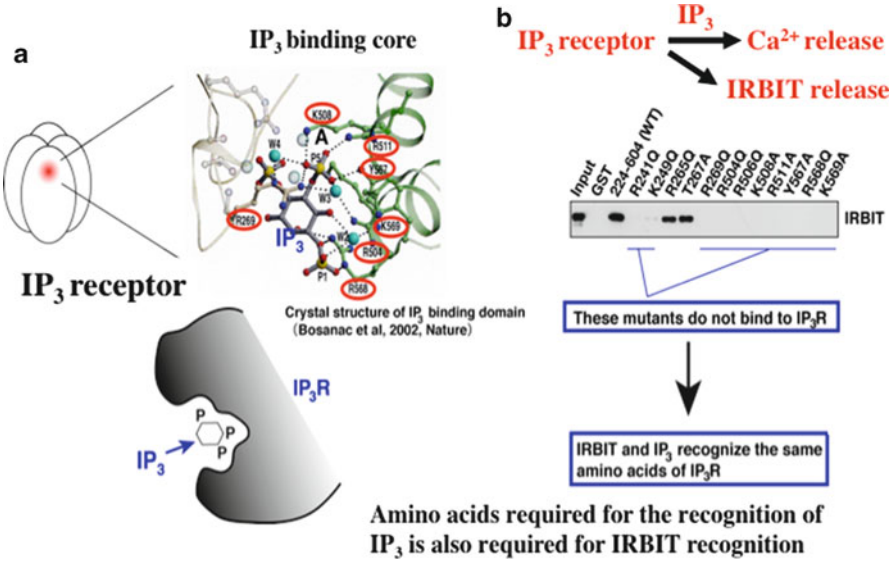

Fig. 12.13 Amino acids required for the recognition of IP_3 are also required for IRBIT recognition. There are several amino acids in the IP_3 binding core domain of the IP_3R which are essential for the recognition of IP_3. These are also required for the recognition of IRBIT since when one of these are mutated to another amino acid, IRBIT cannot bind to IP_3R [78]

potent than other inositol polyphosphates, including inositol 1,3,4,5-tetrakisphosphate and inositol 1,4-bisphosphate. Alkaline phosphatase treatment abolished the interaction, suggesting that the interaction was regulated by both IP_3 and phosphorylation. Immunohistochemical studies and co-immunoprecipitation assays showed the relevance of the interaction in a physiological context [78]. These findings suggested that IRBIT has at least two biological functions, an IP_3R-bound state and release from the IP_3R. The state that IRBIT assumes is determined by the intracellular IP_3 concentration.

The Effect of IRBIT on the IP_3-Binding Activity and IP_3-Induced Ca^{2+} Release Activity of the IP_3R

The phosphorylation sites of IRBIT essential for IP_3R binding were identified. The results of $[^3H]IP_3$ binding assays, *in vitro* Ca^{2+} release assays and Ca^{2+} imaging of intact cells revealed that IRBIT suppresses the activation of the IP_3R by competing with IP_3. The phosphorylation of four Ser residues (Ser 68, 71, 74 and 77) of IRBIT was determined to be essential for its interaction with the IP_3R (Fig. 12.12). Ten of the 12 amino acids residues essential for IP_3 recognition by the IP_3R participated in binding to IRBIT. Based on these findings, we hypothesized that IRBIT acts as an endogenous "pseudo-ligand" in its IP_3R-bound state [78]. To determine whether IRBIT suppresses IP_3R-mediated Ca^{2+} release in intact cells, we utilized RNA interference to suppress the expression of IRBIT in HeLa cells. The expression of IRBIT was observed to be suppressed by siRNA IRBIT in HeLa cells but had no effect on IP_3R expression. The depletion of IRBIT resulted in an increase in the number of cells that responded to the threshold dose of ATP stimulation and an enhancement of the amplitude and frequency of Ca^{2+} oscillation, demonstrating that IRBIT regulates IP_3-induced Ca^{2+} release.

IRBIT Functions as a Messenger to Regulate Acid-Base Balance and Protein Synthesis

To determine the functions of IRBIT after its release from the IP_3R, we screened for target molecules of IRBIT. Na^+/HCO^{3-} cotransporter 1 (NBC1) was identified as an IRBIT-binding protein. Of the two major splicing variants of NBC1, pancreas-type NBC1 (pNBC1) and kidney-type NBC1 (kNBC1), IRBIT was found to bind specifically to pNBC1 and not bind to kNBC1 at all. IRBIT binds to the N-terminal pNBC1-specific domain of NBC1 depending on the phosphorylation of several serine residues of IRBIT. Moreover, an electrophysiological analysis in *Xenopus*

oocytes revealed that pNBC1 requires coexpression of IRBIT to have substantial activity comparable to that of kNBC1, which exhibits substantial activity independently of IRBIT. These findings strongly suggest that pNBC1 is the target molecule of IRBIT and that IRBIT plays an important role in pH regulation via pNBC1. Our findings suggest that regulation through IRBIT enables NBC1 variants to have different physiological roles [79]. Notably, many hereditary human diseases involve NBC1 and IRBIT is likely to be involved in their pathogenesis.

In addition, IRBIT binds the cleavage and polyadenylation specificity factor (CPSF) that regulates the elongation of poly A nucleotide sequence IRBIT regulates protein synthesis [80].

IP_3Rs Form Macro-Signal Complexes That Act as a Signaling Hub

The IP_3R isoforms have unique three-dimensionally constructed structures demonstrated in Fig. 12.14. Surprisingly, most proteins associate with IP_3Rs at a site near the channel pore region of the IP_3R. Cytochrome c [81], GIT 1 [82], 80H [83] and a disease-related protein, Huntington (Htt)-associated protein (HAPIA), were determined to bind to the C-terminus of IP_3R1 [84, 85]. The activation of IP_3R1 by IP_3 is sensitized by the polyglutamine expansion of Htt caused by Huntington disease. Protein phosphatases (PPI and PP2A) [85, 86], RACK1 [87], ankyrin [88] and chromogranin have been reported to bind to the channel region and regulate channel

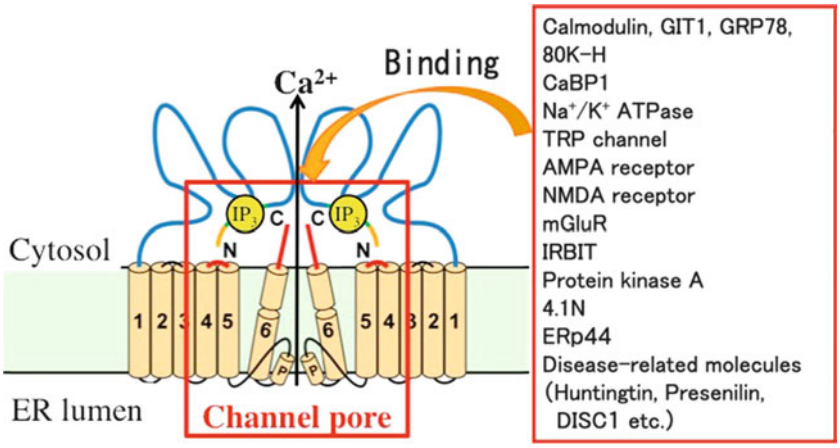

Fig. 12.14 Protein-complex formation endows the IP_3R with its functional diversity as a signaling hub. Many different molecules bind to the hot spot around the channel pore and control channel gating in a cooperative manner. Since the listed molecules are the list of molecules which were already reported. A particular cell expresses some of these molecules and associate with the each type of IP_3R expressed in a cell. The combination enables the functional diversity of the IP_3R in a cell

activity [89]. CARP (carbonic anhydrase-related protein) has been found to bind to a central part of the molecule between the IP_3-binding core and the channel region to regulate channel activity [90]. Additionally, Homer [91] has been determined to bind to the N-terminal suppressor region of the IP_3R. IRBIT is a pseudo-ligand of the IP_3R that appears to bind to the IP_3-binding pocket in a resting state and is released when cell stimulation triggers the release of a large amount of IP_3. Chaperones, such as ERp44, a redox sensor and GRP78, bind to the internal loop region between transmembrane [domains] 5 and 6. The physiological relevance of these interactions is expected to be important.

IP_3 binding to the IP_3-binding core results in a conformational change of the N-terminal suppressor region, which can then bind to the loop region of transmembrane domains 4 and 5 that are associated with C-terminal portion, resulting in the opening of the channel pore (Fig. 12.9).

The areas near the channel pore region that are associated with N-terminal site and the C-terminal region are regarded as hot spots for channel opening and closing. Most of the aforementioned associated proteins bind to these hot spots to regulate IP_3R channel gating. The unique 3-dimensional structure obtained by cryo-EM demonstrating a vacancy inside the balloon-like receptor with multi-porous architecture on the surface serves as a signaling hub for interactions with many of the associated molecules.

References

1. Streb H, Irvine RF, Berridge MJ, Schulz I (1983) Release of Ca2+ from a nonmitochondrial intracellular store in pancreatic acinar cells by inositol-1,4,5-trisphosphate. Nature 306:67–69
2. Mikoshiba K, Okano H, Tsukada Y (1985) P400 protein characteristic to Purkinje cells and related proteins in cerebella from neuropathological mutant mice: autoradiographic study by 14C-leucine and phosphorylation. Dev Neurosci 7:179–187
3. Maeda N, Niinobe M, Inoue Y, Mikoshiba K (1989) Developmental expression and intracellular location of P400 protein characteristic of Purkinje cells in the mouse cerebellum. Dev Biol 133:67–76
4. Michell RH (1975) Inositol phospholipids and cell surface receptor function. Biochim Biophys Acta 415:81–147
5. Crepel F, Dupont JL, Gardette R (1984) Selective absence of calcium spikes in Purkinje cells of staggerer mutant mice in cerebellar slices maintained in vitro. J Physiol 346:111–125
6. Snyder SH, Supattapone S (1989) Isolation and functional characterization of an inositol trisphosphate receptor from brain. Cell Calcium 10:337–342
7. Maeda N, Niinobe M, Mikoshiba K (1990) A cerebellar Purkinje cell marker P400 protein is an inositol 1,4,5-trisphosphate (InsP3) receptor protein. Purification and characterization of InsP3 receptor complex. EMBO J 9:61–67
8. Mikoshiba K, Huchet M, Changeux JP (1979) Biochemical and immunological studies on the P400 protein, a protein characteristic of the Purkinje cell from mouse and rat cerebellum. Dev Neurosci 2:254–275
9. Maeda N, Niinobe M, Nakahira K, Mikoshiba K (1988) Purification and characterization of P400 protein, a glycoprotein characteristic of Purkinje cell, from mouse cerebellum. J Neurochem 51:1724–1730
10. Sudhof TC, Newton CL, Archer BT 3rd, Ushkaryov YA, Mignery GA (1991) Structure of a novel $InsP_3$ receptor. EMBO J 10:3199–3206

11. Furuichi T, Yoshikawa S, Mikoshiba K (1989) Nucleotide sequence of cDNA encoding P400 protein in the mouse cerebellum. Nucleic Acids Res 17:5385–5386
12. Furuichi T, Yoshikawa S, Miyawaki A, Wada K, Maeda N, Mikoshiba K (1989) Primary structure and functional expression of the inositol 1,4,5-trisphosphate-binding protein P400. Nature 342:32–38
13. Mignery GA, Newton CL, Archer BT, Sudhof TC (1990) Structure and expression of the rat inositol 1,4,5-trisphosphate receptor. J Biol Chem 265:12679–12685
14. Takeshima H, Nishimura S, Matsumoto T, Ishida H, Kangawa K, Minamino N, Matsuo H, Ueda M, Hanaoka M, Hirose T et al (1989) Primary structure and expression from complementary DNA of skeletal muscle ryanodine receptor. Nature 339:439–445
15. Kume S, Muto A, Aruga J, Nakagawa T, Michikawa T, Furuichi T, Nakade S, Okano H, Mikoshiba K (1993) The Xenopus IP3 receptor: structure, function, and localization in oocytes and eggs. Cell 73:555–570
16. Yamada N, Makino Y, Clark RA, Pearson DW, Mattei MG, Guenet JL, Ohama E, Fujino I, Miyawaki A, Furuichi T et al (1994) Human inositol 1,4,5-trisphosphate type-1 receptor, $InsP_3R1$: structure, function, regulation of expression and chromosomal localization. Biochem J 302:781–790
17. Iwasaki H, Chiba K, Uchiyama T, Yoshikawa F, Suzuki F, Ikeda M, Furuichi T, Mikoshiba K (2002) Molecular characterization of the starfish inositol 1,4,5-trisphosphate receptor and its role during oocyte maturation and fertilization. J Biol Chem 277:2763–2772
18. Baylis HA, Furuichi T, Yoshikawa F, Mikoshiba K, Sattelle DB (1999) Inositol 1,4,5-trisphosphate receptors are strongly expressed in the nervous system, pharynx, intestine, gonad and excretory cell of Caenorhabditis elegans and are encoded by a single gene (itr-1). J Mol Biol 294:467–476
19. Blondel O, Takeda J, Janssen H, Seino S, Bell GI (1993) Sequence and functional characterization of a third inositol trisphosphate receptor subtype, IP3R-3, expressed in pancreatic islets, kidney, gastrointestinal tract, and other tissues. J Biol Chem 268:11356–11363
20. Nordquist DT, Kozak CA, Orr HT (1988) cDNA cloning and characterization of three genes uniquely expressed in cerebellum by Purkinje neurons. J Neurosci 8:4780–4789
21. Mignery GA, Sudhof TC, Takei K, De Camilli P (1989) Putative receptor for inositol 1,4,5-trisphosphate similar to ryanodine receptor. Nature 342:192–195
22. Supattapone S, Worley PF, Baraban JM, Snyder SH (1988) Solubilization, purification, and characterization of an inositol trisphosphate receptor. J Biol Chem 263:1530–1534
23. Prentki M, Biden TJ, Janjic D, Irvine RF, Berridge MJ, Wollheim CB (1984) Rapid mobilization of Ca2+ from rat insulinoma microsomes by inositol-1,4,5-trisphosphate. Nature 309:562–564
24. Hingorani SR, Agnew WS (1991) A rapid ion-exchange assay for detergent-solubilized inositol 1,4,5- trisphosphate receptors. Anal Biochem 194:204–213
25. Hingorani SR, Agnew WS (1992) Assay and purification of neuronal receptors for inositol 1,4,5- trisphosphate. Methods Enzymol 207:573–591
26. Chadwick CC, Saito A, Fleischer S (1990) Isolation and characterization of the inositol trisphosphate receptor from smooth muscle. Proc Natl Acad Sci USA 87:2132–2136
27. Mourey RJ, Verma A, Supattapone S, Snyder SH (1990) Purification and characterization of the inositol 1,4,5- trisphosphate receptor protein from rat vas deferens. Biochem J 272:383–389
28. Parys JB, Sernett SW, DeLisle S, Snyder PM, Welsh MJ, Campbell KP (1992) Isolation, characterization, and localization of the inositol 1,4,5- trisphosphate receptor protein in Xenopus laevis oocytes. J Biol Chem 267:18776–18782
29. Maeda N, Kawasaki T, Nakade S, Yokota N, Taguchi T, Kasai M, Mikoshiba K (1991) Structural and functional characterization of inositol 1,4,5-trisphosphate receptor channel from mouse cerebellum. J Biol Chem 266:1109–1116
30. Ferris CD, Huganir RL, Snyder SH (1990) Calcium flux mediated by purified inositol 1,4,5-trisphosphate receptor in reconstituted lipid vesicles is allosterically regulated by adenine nucleotides. Proc Natl Acad Sci USA 87:2147–2151

31. Nakade S, Maeda N, Mikoshiba K (1991) Involvement of the C-terminus of the inositol 1,4,5-trisphosphate receptor in Ca2+ release analysed using region-specific monoclonal antibodies. Biochem J 277:125–131
32. Iino M (1990) Biphasic Ca2+ dependence of inositol 1,4,5-trisphosphate-induced Ca release in smooth muscle cells of the guinea pig taenia caeci. J Gen Physiol 95:1103–1122
33. Finch EA, Turner TJ, Goldin SM (1991) Calcium as a coagonist of inositol 1,4,5-trisphosphate-induced calcium release. Science 252:443–446
34. Bezprozvanny I, Watras J, Ehrlich BE (1991) Bell-shaped calcium-response curves of Ins(1,4,5)P3- and calcium-gated channels from endoplasmic reticulum of cerebellum. Nature 351:751–754
35. Newton CL, Mignery GA, Sudhof TC (1994) Co-expression in vertebrate tissues and cell lines of multiple inositol 1,4,5-trisphosphate (InsP3) receptors with distinct affinities for InsP3. J Biol Chem 269:28613–28619
36. Yamamoto-Hino M, Sugiyama T, Hikichi K, Mattei MG, Hasegawa K, Sekine S, Sakurada K, Miyawaki A, Furuichi T, Hasegawa M, Mikoshiba K (1994) Cloning and characterization of human type 2 and type 3 inositol 1, 4, 5-trisphosphate receptors. Receptors Channels 2(1):9–22
37. Blondel O, Moody MM, Depaoli AM, Sharp AH, Ross CA, Swift H, Bell GI (1994) Localization of inositol trisphosphate receptor subtype 3 to insulin and somatostatin secretory granules and regulation of expression in islets and insulinoma cells. Proc Natl Acad Sci USA 91:7777–7781
38. Iwai M, Tateishi Y, Hattori M, Mizutani A, Nakamura T, Futatsugi A, Inoue T, Furuichi T, Michikawa T, Mikoshiba K (2005) Molecular cloning of mouse type 2 and type 3 inositol 1,4,5-trisphosphate receptors and identification of a novel type 2 receptor splice variant. J Biol Chem 280:10305–10317
39. Iwai M, Michikawa T, Bosanac I, Ikura M, Mikoshiba K (2007) Molecular basis of the isoform-specific ligand-binding affinity of inositol 1,4,5-trisphosphate receptors. J Biol Chem 282:12755–12764
40. Yoshikawa S, Tanimura T, Miyawaki A, Nakamura M, Yuzaki M, Furuichi T, Mikoshiba K (1992) Molecular cloning and characterization of the inositol 1,4,5-trisphosphate receptor in Drosophila melanogaster. J Biol Chem 267:16613–16619
41. Futatsugi A, Nakamura T, Yamada MK, Ebisui E, Nakamura K, Uchida K, Kitaguchi T, Takahashi-Iwanaga H, Noda T, Aruga J, Mikoshiba K (2005) IP3 receptor types 2 and 3 mediate exocrine secretion underlying energy metabolism. Science 309:2232–2234
42. Nakayama H, Bodi I, Maillet M, DeSantiago J, Domeier T, Mikoshiba K, Lorenz J, Blatter L, Bers D, Molkentin J (2010) The IP_3 receptor regulates cardiac hypertrophy in response to select stimuli. Circ Res 107:659–666
43. Takata N, Mishima T, Hisatsune C, Nagai T, Ebisui E, Mikoshiba K, Hirase H (2011) Astrocyte calcium signaling transforms cholinergic modulation to cortical plasticity in vivo. J Neurosci 31:18155–18165
44. Furuichi T, Kohda K, Miyawaki A, Mikoshiba K (1994) Intracellular channels. Curr Opin Neurobiol 4:294–303
45. Miyakawa T, Maeda A, Yamazawa T, Hirose K, Kurosaki T, Iino M (1999) Encoding of Ca2+ signals by differential expression of IP3 receptor subtype. EMBO J 18:1303–1308
46. Tu H, Wang Z, Bezprozvanny I (2005) Modulation of mammalian inositol 1,4,5-trisphosphate receptor isoforms by calcium: a role of calcium sensor region. Biophys J 88:1056–1069
47. Tu H, Wang Z, Nosyreva E, De Smedt H, Bezprozvanny I (2005) Functional characterization of mammalian inositol 1,4,5-trisphosphate receptor isoform. Biophys J 88:1046–1055
48. Bosanac I, Alattia JR, Mal TK, Chan J, Talarico S, Tong FK, Tong KI, Yoshikawa F, Furuichi T, Iwai M, Michikawa T, Mikoshiba K, Ikura M (2002) Structure of the inositol 1,4,5-trisphosphate receptor binding core in complex with its ligand. Nature 420:696–700
49. Yoshikawa F, Morita M, Monkawa T, Michikawa T, Furuichi T, Mikoshiba K (1996) Mutational analysis of the ligand binding site of the inositol 1,4,5- trisphosphate receptor. J Biol Chem 271:18277–18284

50. Yoshikawa F, Iwasaki H, Michikawa T, Furuichi T, Mikoshiba K (1999) Cooperative formation of the ligand-binding site of the inositol 1,4, 5- trisphosphate receptor by two separable domains. J Biol Chem 274:328–334
51. Bultynck G, Szlufcik K, Kasri NN, Assefa Z, Callewaert G, Missiaen L, Parys JB, De Smedt H (2004) Thimerosal stimulates Ca2+ flux through inositol 1,4,5-trisphosphate receptor type 1, but not type 3, via modulation of an isoform-specific Ca2+-dependent intramolecular interaction. Biochem J 381:87–96
52. Bosanac I, Yamazaki H, Matsu-Ura T, Michikawa T, Mikoshiba K, Ikura M (2005) Crystal structure of the ligand binding suppressor domain of type 1 inositol 1,4,5-trisphosphate receptor. Mol Cell 17:193–203
53. Jiang QX, Thrower EC, Chester DW, Ehrlich BE, Sigworth FJ (2002) Three-dimensional structure of the type 1 inositol 1,4,5-trisphosphate receptor at 24 A resolution. EMBO J 21:3575–3581
54. Hamada K, Miyata T, Mayanagi K, Hirota J, Mikoshiba K (2002) Two-state conformational changes in inositol 1,4,5-trisphosphate receptor regulated by calcium. J Biol Chem 277:21115–21118
55. da Fonseca PC, Morris SA, Nerou EP, Taylor CW, Morris EP (2003) Domain organization of the type 1 inositol 1,4,5-trisphosphate receptor as revealed by single-particle analysis. Proc Natl Acad Sci USA 100:3936–3941, Epub 2003 Mar 3921
56. Hamada K, Terauchi A, Mikoshiba K (2003) Three-dimensional rearrangements within inositol 1,4,5-trisphosphate receptor by calcium. J Biol Chem 278:52881–52889
57. Serysheva II, Bare DJ, Ludtke SJ, Kettlun CS, Chiu W, Mignery GA (2003) Structure of the type 1 inositol 1,4,5-trisphosphate receptor revealed by electron cryomicroscopy. J Biol Chem 278:21319–21322
58. Sato C, Hamada K, Ogura T, Miyazawa A, Iwasaki K, Hiroaki Y, Tani K, Terauchi A, Fujiyoshi Y, Mikoshiba K (2004) Inositol 1,4,5-trisphosphate receptor contains multiple cavities and L-shaped ligand-binding domains. J Mol Biol 336:155–164
59. Suhara W, Kobayashi M, Sagara H, Hamada K, Goto T, Fujimoto I, Torimitsu K, Mikoshiba K (2006) Visualization of inositol 1,4,5-trisphosphate receptor by atomic force microscopy. Neurosci Lett 391:102–107
60. Mignery GA, Sudhof TC (1990) The ligand binding site and transduction mechanism in the inositol-1,4,5-triphosphate receptor. EMBO J 9:3893–3898
61. Nakayama T, Hattori M, Uchida K, Nakamura T, Tateishi Y, Bannai H, Iwai M, Michikawa T, Inoue T, Mikoshiba K (2004) The regulatory domain of the inositol 1,4,5-trisphosphate receptor is necessary to keep the channel domain closed: possible physiological significance of specific cleavage by caspase 3. Biochem J 377:299–307
62. Uchida K, Miyauchi H, Furuichi T, Michikawa T, Mikoshiba K (2003) Critical regions for activation gating of the inositol 1,4,5-trisphosphate receptor. J Biol Chem 278:16551–16560
63. Itoh S, Ito K, Fujii S, Kaneko K, Kato K, Mikoshiba K, Kato H (2001) Neuronal plasticity in hippocampal mossy fiber-CA3 synapses of mice lacking the inositol-1,4,5-trisphosphate type 1 receptor. Brain Res 901:237–246
64. Miyazaki S, Yuzaki M, Nakada K, Shirakawa H, Nakanishi S, Nakade S, Mikoshiba K (1992) Block of Ca2+ wave and Ca2+ oscillation by antibody to the inositol 1,4,5-trisphosphate receptor in fertilized hamster eggs [published erratum appears in Science 1992 Oct 9;258(5080):following 203]. Science 257:251–255
65. Saneyoshi T, Kume S, Amasaki Y, Mikoshiba K (2002) The Wnt/calcium pathway activates NF-AT and promotes ventral cell fate in Xenopus embryos. Nature 417:295–299
66. Fukami K, Nakao K, Inoue T, Kataoka Y, Kurokawa M, Fissore RA, Nakamura K, Katsuki M, Mikoshiba K, Yoshida N, Takenawa T (2001) Requirement of phospholipase Cdelta4 for the zona pellucida-induced acrosome reaction. Science 292:920–923
67. Fukami K, Yoshida M, Inoue T, Kurokawa M, Fissore RA, Yoshida N, Mikoshiba K, Takenawa T (2003) Phospholipase Cdelta4 is required for Ca2+ mobilization essential for acrosome reaction in sperm. J Cell Biol 161:79–88
68. Kume S, Muto A, Inoue T, Suga K, Okano H, Mikoshiba K (1997) Role of inositol 1,4,5-trisphosphate receptor in ventral signaling in Xenopus embryos. Science 278:1940–1943

69. Muto A, Kume S, Inoue T, Okano H, Mikoshiba K (1996) Calcium waves along the cleavage furrows in cleavage-stage Xenopus embryos and its inhibition by heparin. J Cell Biol 135:181–190
70. Takei K, Shin RM, Inoue T, Kato K, Mikoshiba K (1998) Regulation of nerve growth mediated by inositol 1,4,5-trisphosphate receptors in growth cones. Science 282:1705–1708
71. Matsu-ura T, Michikawa T, Inoue T, Miyawaki A, Yoshida M, Mikoshiba K (2006) Cytosolic inositol 1,4,5-trisphosphate dynamics during intracellular calcium oscillations in living cells. J Cell Biol 173:755–765
72. Inoue T, Kato K, Kohda K, Mikoshiba K (1998) Type 1 inositol 1,4,5-trisphosphate receptor is required for induction of long-term depression in cerebellar Purkinje neurons. J Neurosci 18:5366–5373
73. Nishiyama M, Hong K, Mikoshiba K, Poo MM, Kato K (2000) Calcium stores regulate the polarity and input specificity of synaptic modification. Nature 408:584–588
74. Fujii S, Matsumoto M, Igarashi K, Kato H, Mikoshiba K (2000) Synaptic plasticity in hippocampal CA1 neurons of mice lacking type 1 inositol-1,4,5-trisphosphate receptors [In Process Citation]. Learn Mem 7:312–320
75. Uchida K, Aramaki M, Nakazawa M, Yamagishi C, Makino S, Fukuda K, Nakamura T, Takahashi T, Mikoshiba K, Yamagishi H (2010) Gene knock-outs of inositol 1,4,5-trisphosphate receptors types 1 and 2 result in perturbation of cardiogenesis. PLoS One 5:e12500
76. Nakazawa M, Uchida K, Aramaki M, Kodo K, Yamagishi C, Takahashi T, Mikoshiba K, Yamagishi H (2011) Inositol 1,4,5-trisphosphate receptors are essential for the development of the second heart field. J Mol Cell Cardiol 51:58–66
77. Nakamura TY, Jeromin A, Mikoshiba K, Wakabayashi S (2011) Neuronal calcium sensor-1 promotes immature heart function and hypertrophy by enhancing Ca2+ signals. Circ Res 109(5):512–523
78. Ando H, Mizutani A, Kiefer H, Tsuzurugi D, Michikawa T, Mikoshiba K (2006) IRBIT suppresses IP3 receptor activity by competing with IP3 for the common binding site on the IP3 receptor. Mol Cell 22:795–806
79. Shirakabe K, Priori G, Yamada H, Ando H, Horita S, Fujita T, Fujimoto I, Mizutani A, Seki G, Mikoshiba K (2006) IRBIT, an inositol 1,4,5-trisphosphate receptor-binding protein, specifically binds to and activates pancreas-type Na+/HCO3- cotransporter 1 (pNBC1). Proc Natl Acad Sci USA 103:9542–9547, Epub 2006 Jun 9512
80. Kiefer H, Mizutani A, Iemura S, Natsume T, Ando H, Kuroda Y, Mikoshiba K (2009) Inositol 1,4,5-triphosphate receptor-binding protein released with inositol 1,4,5-triphosphate (IRBIT) associates with components of the mRNA 3′ processing machinery in a phosphorylation-dependent manner and inhibits polyadenylation. J Biol Chem 284:10694–10705
81. Boehning D, Patterson RL, Sedaghat L, Glebova NO, Kurosaki T, Snyder SH (2003) Cytochrome c binds to inositol (1,4,5) trisphosphate receptors, amplifying calcium-dependent apoptosis. Nat Cell Biol 5:1051–1061
82. Zhang S, Hisatsune C, Matsu-Ura T, Mikoshiba K (2009) G-protein-coupled receptor kinase-interacting proteins inhibit apoptosis by inositol 1,4,5-triphosphate receptor-mediated Ca2+ signal regulation. J Biol Chem 284:29158–29169
83. Kawaai K, Hisatsune C, Kuroda Y, Mizutani A, Tashiro T, Mikoshiba K (2009) 80K-H interacts with inositol 1,4,5-trisphosphate (IP3) receptors and regulates IP3-induced calcium release activity. J Biol Chem 284:372–380
84. Bezprozvanny I, Hayden MR (2004) Deranged neuronal calcium signaling and Huntington disease. Biochem Biophys Res Commun 322:1310–1317
85. Tang TS, Tu H, Chan EY, Maximov A, Wang Z, Wellington CL, Hayden MR, Bezprozvanny I (2003) Huntingtin and huntingtin-associated protein 1 influence neuronal calcium signaling mediated by inositol-(1,4,5) triphosphate receptor type 1. Neuron 39:227–239
86. DeSouza N, Reiken S, Ondrias K, Yang YM, Matkovich S, Marks AR (2002) Protein kinase A and two phosphatases are components of the inositol 1,4,5-trisphosphate receptor macromolecular signaling complex. J Biol Chem 277:39397–39400
87. Patterson RL, van Rossum DB, Barrow RK, Snyder SH (2004) RACK1 binds to inositol 1,4,5-trisphosphate receptors and mediates Ca2+ release. Proc Natl Acad Sci USA 101:2328–2332

88. Bourguignon LY, Jin H, Iida N, Brandt NR, Zhang SH (1993) The involvement of ankyrin in the regulation of inositol 1,4,5- trisphosphate receptor-mediated internal Ca2+ release from Ca2+ storage vesicles in mouse T-lymphoma cells. J Biol Chem 268:7290–7297
89. Yoo SH, So SH, Kweon HS, Lee JS, Kang MK, Jeon CJ (2000) Coupling of the inositol 1,4,5-trisphosphate receptor and chromogranins A and B in secretory granules. J Biol Chem 275:12553–12559
90. Hirota J, Ando H, Hamada K, Mikoshiba K (2003) Carbonic anhydrase-related protein is a novel binding protein for inositol 1,4,5-trisphosphate receptor type 1. Biochem J 372:435–441
91. Tu JC, Xiao B, Yuan JP, Lanahan AA, Leoffert K, Li M, Linden DJ, Worley PF (1998) Homer binds a novel proline-rich motif and links group 1 metabotropic glutamate receptors with IP3 receptors. Neuron 21:717–726
92. Mikoshiba K (2007) IP3 receptor/Ca2+ channel: from discovery to new signaling concepts. J Neurochem 102:1426–1446
93. Kasri NN, Holmes AM, Bultynck G, Parys JB, Bootman MD et al (2004) Regulation of InsP3 receptor activity by neuronal Ca2+-binding proteins. EMBO J 23:312–321
94. Sienaert I, Nadif Kasri N, Vanlingen S, Parys JB, Callewaert G, Missiaen L, de Smedt H (2002) Localization and function of a calmodulin-apocalmodulin-binding domain in the N-terminal part of the type 1 inositol 1,4,5-trisphosphate receptor. Biochem J 365:269–277
95. Armon A, Graur D, Ben-Tal N (2001) ConSurf: an algorithmic tool for the identification of functional regions in proteins by surface mapping of phylogenetic information. J Mol Biol 307:447–463
96. Yamazaki H, Chan J, Ikura M, Michikawa T, Mikoshiba K (2010) Tyr-167/Trp-168 in type 1/3 inositol 1,4,5-trisphosphate receptor mediates functional coupling between ligand binding and channel opening. J Biol Chem 285:36081–36091
97. Higo T, Hamada K, Hisatsune C, Nukina N, Hashikawa T, Hattori M, Nakamura T, Mikoshiba K (2010) Mechanism of ER stress-induced brain damage by IP(3) receptor. Neuron 68:865–878

Chapter 13
Pyridine Nucleotide Metabolites and Calcium Release from Intracellular Stores

Antony Galione and Kai-Ting Chuang

Abstract Ca^{2+} signals are probably the most common intracellular signaling elements, controlling an extensive range of responses in virtually all cells. Many cellular stimuli, often acting at cell surface receptors, evoke Ca^{2+} signals by mobilizing Ca^{2+} from intracellular stores. Inositol trisphosphate (IP_3) was the first messenger shown to link events at the plasma membrane to release of Ca^{2+} from the endoplasmic reticulum (ER), through activation of IP_3-gated Ca^{2+} release channels (IP_3 receptors). Subsequently, two additional Ca^{2+} mobilizing messengers were discovered, cADPR and NAADP. Both are metabolites of pyridine nucleotides, and may be produced by the same class of enzymes, ADP-ribosyl cyclases, such as CD38. Whilst cADPR mobilizes Ca^{2+} from the ER by activation of ryanodine receptors (RyRs), NAADP releases Ca^{2+} from acidic stores by a mechanism involving the activation of two pore channels (TPCs).

Keywords Calcium • Cyclic ADP-ribose • NAADP • CD38 • Ryanodine • Two-pore channel • Inositol trisphosphate • Lysosome • Endoplasmic reticulum • Calcium microdomain

Introduction

Studies of cardiac contractility in 1876 by Sidney Ringer showed dependence on Ca^{2+} ions in the perfusion solutions [1]. Use of jellyfish photoproteins, such as aequorin, provided the first measurements of cytosolic Ca^{2+} in muscle cells. Importantly, Ca^{2+} transients were found to precede contractions and this realization was important in generating the concept of a messenger role for Ca^{2+} ions [2].

A. Galione (✉) • K.-T. Chuang
Department of Pharmacology, University of Oxford,
Mansfield Road, Oxford, OX1 3QT, UK
e-mail: antony.galione@pharm.ox.ac.uk; kai-ting_chuang@hms.harvard.edu

M.S. Islam (ed.), *Calcium Signaling*, Advances in Experimental Medicine and Biology 740, DOI 10.1007/978-94-007-2888-2_13,

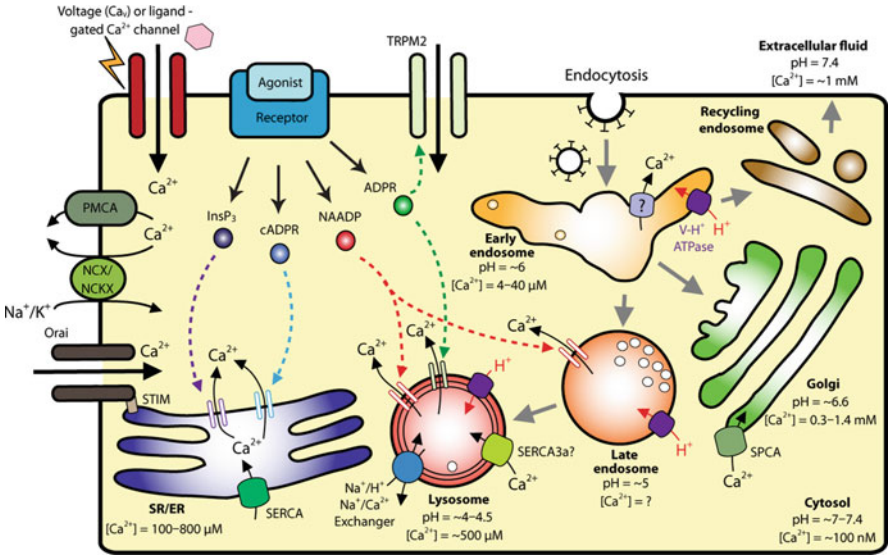

Fig. 13.1 Schematic representation of intracellular Ca^{2+} signaling and homeostasis in animal cells. Ca^{2+} can enter the cytosol from the extracellular space via plasma membrane ion channels, or from intracellular Ca^{2+} sequestering stores such as the ER or the acidic Ca^{2+} stores in response to second messengers: IP3, cADPR and NAADP. Ca^{2+} released to the cytosol is then exchanged or actively transported back to the Ca^{2+} stores or the extracellular space to restore a low cytosolic concentration of Ca^{2+}

Contemporary work studying transmitter release from neurons and hormone secretion [3], also led to a growing appreciation of the role of Ca^{2+} ions in stimulus-response coupling. An important source of Ca^{2+} was that mobilized from internal stores in response to hormones and neurotransmitters [4]. In the mid-1970s it was hypothesized that receptors could stimulate cellular Ca^{2+} signals by activating the hydrolysis of inositol lipids [5]. Importantly, the initial lipid hydrolysed was found to be phosphatidylinositol 4,5 bisphosphate [6]. The enzyme involved, phospholipase C thus generated diacylglycerol which activates protein kinase C, and inositol 1,4,5 trisphosphate (IP_3). A pivotal finding was that IP_3 added to permeabilized pancreatic acinar cells released Ca^{2+} from a non-mitochondrial fraction in a way that was mimicked by activating plasma membrane muscarinic acetylcholine receptors [7]. Thus IP_3 was proposed as a Ca^{2+} mobilizing messenger linking the activation of cell surface receptors to mobilization of Ca^{2+} from intracellular stores. Biochemical purification studies [8, 9] and molecular cloning experiments [10, 11] defined the principal targets for IP_3 on intracellular stores as homo-tetrameric Ca^{2+} release channels termed IP_3 receptors (IP_3Rs). The IP_3 signaling pathway is now well established, ubiquitous and plays key roles in mediating many of the actions of a variety of cellular stimuli [12].

The first intact cell in which IP_3 was shown to evoke a cellular response was the sea urchin egg [13]. IP_3 microinjection induced exocytosis of cortical granules resulting in the raising of the fertilization envelope which acts as a barrier to polyspermy. At around

the same time, sea urchin egg homogenates containing Ca^{2+} sequestering vesicles were found to be sensitive to IP_3 which discharged Ca^{2+} from non-mitochondrial stores [14]. Following the establishment of egg homogenates to study Ca^{2+} release mechanisms, Lee and colleagues found that in addition to IP_3, the pyridine nucleotides, NAD and NADP, at micromolar concentrations, were also found to release Ca^{2+} by mechanisms independent from those regulated by IP_3 [15]. NAD released Ca^{2+} from a subcellular fraction which was also sensitive to IP_3, but after a delay of several seconds. In contrast, NADP rapidly released Ca^{2+} from a denser fraction of vesicles. Subsequent analysis revealed that the Ca^{2+} mobilizing properties of NAD was due to an enzyme-produced metabolite identified as cyclic ADP-ribose (cADPR) [16], and that evoked by NADP was due to a contaminant, nicotinic acid adenine dinucleotide phosphate (NAADP) [17]. An abbreviated summary of our current understanding of Ca^{2+} homeostasis in animal cells is shown in Fig. 13.1.

Enzymology of cADPR and NAADP Synthesis and Metabolism

A family of multifunctional enzymes, termed ADP-ribosyl cyclases have been characterized that are capable of both the synthesis and metabolism of both cADPR and NAADP. An enzyme activity responsible for the synthesis of cADPR was first indicated by the finding that NAD mobilized Ca^{2+} from sea urchin egg homogenates but not purified microsomes, indicating that egg homogenate supernatant contained an activity responsible for the conversion of NAD to an active metabolite [15], later identified as cADPR [16]. This enzyme activity was also widespread in rat tissues and shown to be a enzyme showing stereo-specificity for substrate, pH and temperature-dependence as well as protease-sensitivity [18]. The first ADP-ribosyl cyclase that was purified and characterized at the molecular level was that from Aplysia ovotestis [19–21]. The rationale for this was that during the study of ADP-ribosylation of G proteins by endotoxins in this tissue, a protein factor was uncovered that inhibited this reaction by competing for NAD as a substrate. This protein factor, which was localized to ovotestis granules, was subsequently purified and cloned and found to catalyse the cyclization of NAD to cADPR (Fig. 13.2). Aplysia ADP-ribosyl cyclase was the founding member of a class of enzymes that by sequence homology was found to include the mammalian proteins CD38 and CD157 [22]. In contrast to Aplysia ADP-ribosyl cyclase, CD38 is a multifunctional enzyme. Not only does it cyclize NAD to cADPR, it also has a hydrolase activity that converts cADPR to ADP-ribose [23]. Furthermore, CD38 may also use the alternate substrate NADP and in the presence of nicotinic acid may catalyse a base-exchange reaction generating NAADP too (Fig. 13.3) [24]. Recent evidence has also emerged that CD38 may also hydrolyse NAADP to ADP-ribose 2′-phosphate [25], although cellular phosphatases may also convert NAADP to inactive NAAD [26]. Thus CD38 is responsible for both the synthesis of a number of Ca^{2+} signaling regulators and may also catalyse their metabolism.

Detailed mechanistic studies following the crystallization of both Aplysia ADP-ribosyl cyclase and CD38 have emerged in recent years to explain the various activities of these proteins (reviewed in [27]).

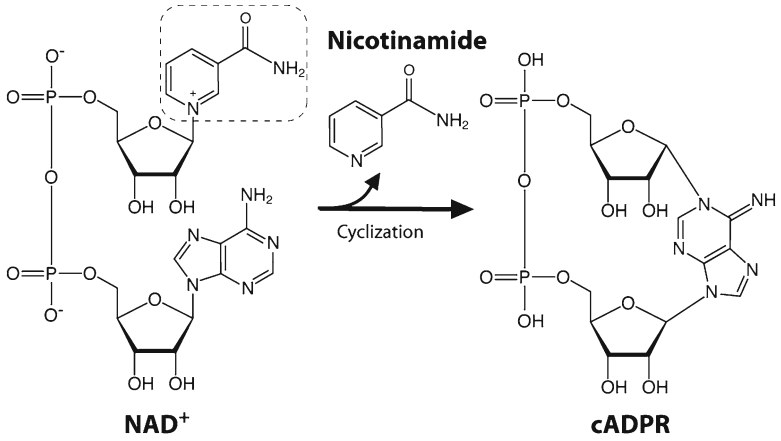

Fig. 13.2 cADPR synthesis. Synthesis of cADPR by cyclization of NAD^+ catalyzed by ADP-ribosyl cyclases

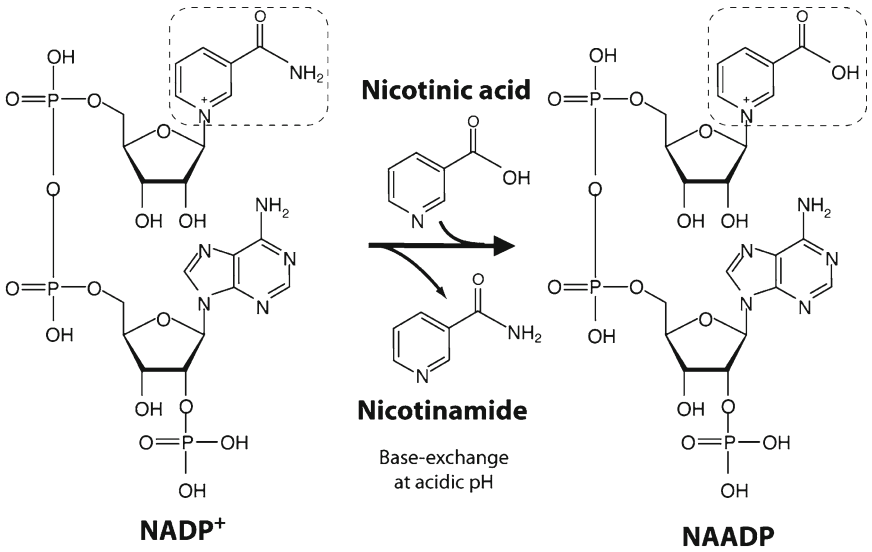

Fig. 13.3 NAADP synthesis. Synthesis of NAADP from NADP by base-exchange of the nicotinamide moiety for nicotinic acid at acidic pH catalyzed by ADP-ribosyl cyclases

cADPR-Mediated Ca^{2+} Release

The initial descriptions showed that IP_3, cADPR and NAADP likely released Ca^{2+} by activating distinct mechanisms in sea urchin eggs, since all three compounds independently self-desensitized their respective Ca^{2+} release mechanisms to a second challenge [17].

Pharmacological analysis of cADPR-evoked Ca^{2+} release in sea urchin egg homogenates and intact eggs showed that the target for cADPR was likely ryanodine receptors (RyRs) [28]. This is also the case in mammalian cells, where cADPR is now recognized as a widespread Ca^{2+} mobilizing messenger [29]. RyRs along with IP_3Rs, with which they share degrees of homology in both primary sequence and structure, were discovered as the principal Ca^{2+} release channels of the sarcoplasmic reticulum of striated muscle [30]. However, like IP_3Rs they are also widely expressed in most cell types, including sea urchin eggs [31–33], where they are often both present in the membranes of the endoplasmic reticulum (ER).

A key property of RyRs and indeed IP_3Rs are that they are also regulated by Ca^{2+} itself in a complex manner [34]. This may lead to Ca^{2+}-induced Ca^{2+} release (CICR), a phenomenon responsible for globalization of local Ca^{2+} signals as propagating Ca^{2+} waves or repetitive Ca^{2+} spiking, hallmarks of Ca^{2+} signaling in all cells [35]. Increases in cytoplasmic Ca^{2+} were found to potentiate cADPR-evoked Ca^{2+} release both in cell free systems, and also in intact cells [36]. Thus it has been proposed that cADPR sensitizes RyRs to activation by Ca^{2+}. This hypothesis has a pleasing symmetry with the way in which IP_3 is thought to regulate IP_3R gating by also modulating Ca^{2+} sensitivity of a Ca^{2+} release channel.

The exact mechanism by which cADPR regulates RyRs is currently unclear. However, pivotal roles for additional accessory proteins which interact with the large cytoplasmic domains of RyR subunits have been suggested. The radiolabelled photoaffinity cADPR derivative, [^{32}P]8-azido-cADPR, labels a 100 kDa and a 140 kDa protein in sea urchin egg extracts, too small for RyRs, but these have not been identified. A key finding was that in the sea urchin egg microsomal system a soluble protein factor was required to confer cADPR-sensitivity of RyRs [37]. This was found to be calmodulin, a well-known component of RyR macromolecular complexes [38]. Furthermore, it was found that cycles of dissociation and re-association of calmodulin could account for the desensitization and resensitization of cADPR-evoked Ca^{2+} release from sea urchin egg homogenates [39]. In mammalian systems a role for FKBP12.6, an immunophilin with prolyl isomerase activity, has been proposed as important for RyR cADPR sensitivity [40–45]. cADPR has been suggested to effect the dissociation of FKBP12.6 from RyRs which destabilizes the channel causing an increased probability in their openings. The dependence of accessory proteins on the cADPR-sensitivity of RyRs may explain in part the variations in cADPR sensitivity of purified RyRs reconstituted in planar lipid bilayers [46].

The development of 8-substituted analogues of cADPR as highly selective cADPR antagonists have been invaluable in dissecting cADPR-dependent signaling pathways [47, 48].

NAADP-Mediated Ca^{2+} Release

Of the three major Ca^{2+} releasing messengers, NAADP is the most potent, often effective in cells at concentrations as low as 1–10 nM [49]. Its mode of action intrigued researchers from its very discovery, since it appeared not to target the two

principal Ca^{2+} release channels, IP_3Rs/RyRs, but rather a novel Ca^{2+} release channel. In sea urchin eggs and homogenates, NAADP-evoked Ca^{2+} release, which is rapid and likely mediated by a channel [50], is not affected by IP_3Rs/RyRs or cADPR inhibitors such as heparin, ryanodine or 8-amino-cADPR [17], but is selectively antagonized by voltage-gated cation channel blockers such as certain dihydropyridines [51]. In addition, in contrast with IP_3Rs or RyRs, the NAADP-sensitive Ca^{2+} release mechanism was not potentiated by divalent cations leading to the proposal that it does not function as a CICR channel [52, 53]. Furthermore the NAADP-sensitive channel appeared not to reside on the ER [53, 54]. Fractionation of sea urchin egg homogenates showed that the NAADP-sensitive store was generally denser than IP_3 or cADPR-sensitive microsomes [15]. Treatment of homogenates with the SERCA pump inhibitor, thapsigargin, whilst completely abolishing Ca^{2+} release to either IP_3 or cADPR, did not prevent NAADP-evoked Ca^{2+} release [53]. In studies in stratified eggs where ER accumulates near the nucleus, IP_3 and cADPR were found to mobilize Ca^{2+} from this region, whilst NAADP released Ca^{2+} from structures at the opposite pole. In detailed studies of NAADP-evoked Ca^{2+} release from sea urchin eggs, NAADP was found to induce an initial Ca^{2+} release which was followed by a series of further Ca^{2+} spikes [55, 56]. The initial Ca^{2+} release was insensitive to thapsigargin, whereas subsequent Ca^{2+} spikes were abolished by thapsigargin or IP_3 and RyR inhibitors [56]. It was proposed that NAADP was initially releasing Ca^{2+} from a distinct organelle which then triggered further rounds of Ca^{2+} signals by stimulating Ca^{2+} release from the ER [56]. Further purification of the sea urchin egg NAADP-sensitive stores revealed them as rich in lysosomal markers and acidic in nature, since they stained with lysotracker red [57]. Furthermore, Ca^{2+} uptake whilst insensitive to thapsigargin, was dependent on proton gradients created by the action of bafilomycin-sensitive vacuolar proton pumps. In intact eggs, the lysomolytic agent, glycyl-L-phenylalanine 2-naphthylamide (GPN) was found to lyse lysotracker stained vesicles, which also caused bursts of localized Ca^{2+} release. Treatment with GPN also selectively abolished NAADP-evoked Ca^{2+} release whilst having no effect on either IP_3 or cADPR-induced Ca^{2+} signals. From this study it was proposed that NAADP selectively targets lysosome-like organelles in the sea urchin egg.

Building on these results from sea urchin eggs, the action of NAADP as a Ca^{2+} mobilizing molecule was investigated in a variety of mammalian cells. In the first study, pancreatic acinar cells were found to be exquisitely sensitive to NAADP which produced effects at considerably lower concentrations than either IP_3 or cADPR [58]. Several important principles for mammalian NAADP signaling were proposed from this study. First the concentration-response curve for NAADP-evoked Ca^{2+} release (assessed by activation of Ca^{2+}-activated currents) is bell-shaped, with high concentrations of NAADP causing no effect on account of induction of rapid desensitization of NAADP receptors. Secondly, the response to NAADP required functional IP_3Rs/RyRs, and thirdly, Ca^{2+} release by the secretagogue, cholecystokinin (CCK) required functional NAADP receptors. Until the development of selective NAADP antagonists such as Ned-19 [59], use of high, desensitizing, NAADP concentrations was the major way in which to implicate NAADP in Ca^{2+} signaling processes such as CCK signal transduction here [58]. The finding

that NAADP required functional IP_3Rs/RyRs indicated that as in the sea urchin egg, one major action of NAADP-evoked Ca^{2+} release in mammalian cells is to trigger further Ca^{2+} release by recruiting ER-based CICR channels [60].

NAADP has now been shown to have a widespread if not universal action in cells as a mobilizer of Ca^{2+} from acidic stores such as lysosomes [61]. Although these organelles contain considerably smaller amounts of Ca^{2+} than the ER, they nevertheless may play an important role in Ca^{2+} signaling by locally targeting Ca^{2+} to specific effectors. Questions still remain about the precise way in which Ca^{2+} is sequestered into lysosomes and related organelles. The proton gradient across organellar membranes is required and direct or indirect Ca^{2+}/H^+ exchange has been proposed [57]. In addition, SERCA3 has been proposed to mediate Ca^{2+} uptake in part, in NAADP-sensitive acidic Ca^{2+} stores of platelets [62]. Interestingly, in cells from patients with the lysosomal storage disease, Niemann Pick C, lysosomes have defects in Ca^{2+} sequestration, have a low intralysosomal Ca^{2+} concentration, and show a much reduced response to NAADP [63].

Two Pore Channels as NAADP Targets

Two principles for NAADP-mediated Ca^{2+} release have emerged in recent years. The first was that NAADP-gated channels have distinct properties from known Ca^{2+} release channels such as IP_3Rs and RyRs, and their pharmacology more closely resembled that of voltage-gated cation and TRP channels [51]. Secondly, the NAADP-sensitive release mechanism principally resides on acidic stores such as lysosomes and lysosome-related organelles [57].

Inspection of genomic sequences emerging from a variety of organisms including that of sea urchins, pointed to two families of channels as possible targets. The first was mucolipin-1, a lysosomal TRP channel whose mutations may lead to the lysosomal storage disease, mucolipidosis IV [64–66], and second, a poorly characterized family of channels termed Two-pore channels (TPCs) [67]. TPCs are members of the superfamily of voltage-gated channels which comprise of around 150 members with predicted molecular weights ranging between 80 and 100 kDa. TPCs are predicted to have two domains each containing six transmembrane segments and a single pore loop for each domain. As such they represent a proposed evolutionary intermediate between single domain α subunits which tetramerise to form shaker-like K^+ channels, and the single pore-forming four homologous domain α subunits of voltage-gated Ca^{2+} and Na^+ channels. These channels are thought to have evolved by successive rounds of gene duplication.

A two pore channel (TPC1) had first been identified from sequences homologous to voltage-gated ion Ca^{2+} channels from rat kidney cDNA [68]. This was followed by the identification of a TPC1 from the genome of the plant *Arabidopsis* [69]. Thus it was the plant channel that was most intensively investigated initially. Importantly, it was shown to be localized to the plant vacuole, the principal acidic organelle in plants, and to act as a Ca^{2+} release channel [70]. On account of a pair of EF hands in

the region between the two 6 transmembrane domain (TMD) repeats, not seen in mammalian TPCs, it was also proposed to function as a CICR channel. Electrophysiological analysis of AtTPC1 showed that it likely accounts for the slow vacuolar current and likely to play a key role in plant physiology [71].

At this time Michael Zhu cloned a novel mammalian TPC sequence termed TPC2, and heterologous expression showed that it largely localized to lysosomes, and thus TPCs emerged as plausible candidates as NAADP-gated channels. These data were finally reported in 2009 [72], as described below.

Both mucoplin-1 and TPCs have now been proposed as NAADP-gated channels.

Although there has been some evidence presented for mucoplin-1 as an NAADP-gated channel [73, 74], this has been balanced by opposing data [75, 76]. In contrast, a number of papers have emerged over the last 2 years firmly implicating TPCs as central components of NAADP-sensitive Ca^{2+} release channels [77, 78]. Heterologous expression of HsTPC2 in HEK293 cells greatly increased the responsiveness of these cells to NAADP so that now NAADP evoked biphasic Ca^{2+} signals [72]. Pharmacological analysis revealed that the initial Ca^{2+} release is due to Ca^{2+} release from acidic stores whilst the second larger release is mediated by activation of IP_3Rs. This coupling between lysosomes and ER nicely mirrors previous studies of NAADP mediated Ca^{2+} release through organellar cross-talk with NAADP acting in a triggering role [56, 58]. Indeed in pulmonary arteriolar smooth muscle cells, both endothelin-1 and NAADP mediated Ca^{2+} signals initiate in a subcellular region where lysosomes and ER are closely apposed [79, 80]. In contrast, expression of TPC1, which localizes to endosomal vesicles, when activated by NAADP, mediates localized Ca^{2+} signals apparently uncoupled from ER-based Ca^{2+} release mechanisms [72, 81]. Importantly, sea urchins also express TPC isoforms, and expression of both TPC1 and TPC2 also enhance the responsiveness of cells to NAADP generating characteristic biphasic Ca^{2+} signals [82, 83]. Sea urchins, in common with many animals, express three isoforms, although TPC3 is not expressed in man, mouse or rats. In one report, TPC3 appeared to act as a dominant negative suppressing the effects of NAADP on both small endogenous Ca^{2+} release or enhanced release due to TPC2 overexpression [82]. Another important finding is that immunopurified endogenous TPCs bind [^{32}P]NAADP with nanomolar affinity and recapitulates key properties of NAADP binding to native egg membrane fractions [82]. Electrophysiological studies either from isolated lysosomes [84], immunopurified TPC2 reconstituted into lipid bilayers [85] or channels redirected to the plasma membrane by mutating lysosomal targeting sequences [86], have shown that TPCs are indeed NAADP-gated cation channels which can pass Ca^{2+} ions. Interestingly, TPC2 channel activity is modulated by luminal pH, and increased luminal Ca^{2+} greatly increases their sensitivity to activation by NAADP [85].

Evidence from cells derived from TPC2 knockout mice also supports a key role for TPC2 in mediating NAADP-evoked Ca^{2+} release. In pancreatic beta cells, NAADP evokes Ca^{2+} activated plasma membrane currents which are absent in those from *Tpcn2*$^{-/-}$ mice [72]. In bladder smooth muscle, whilst NAADP contracts permeabilised myocytes, it fails to do so in cells from *Tpcn2*$^{-/-}$ mice, and now agonist-mediated contractions are due entirely to SR-mediated Ca^{2+} release since

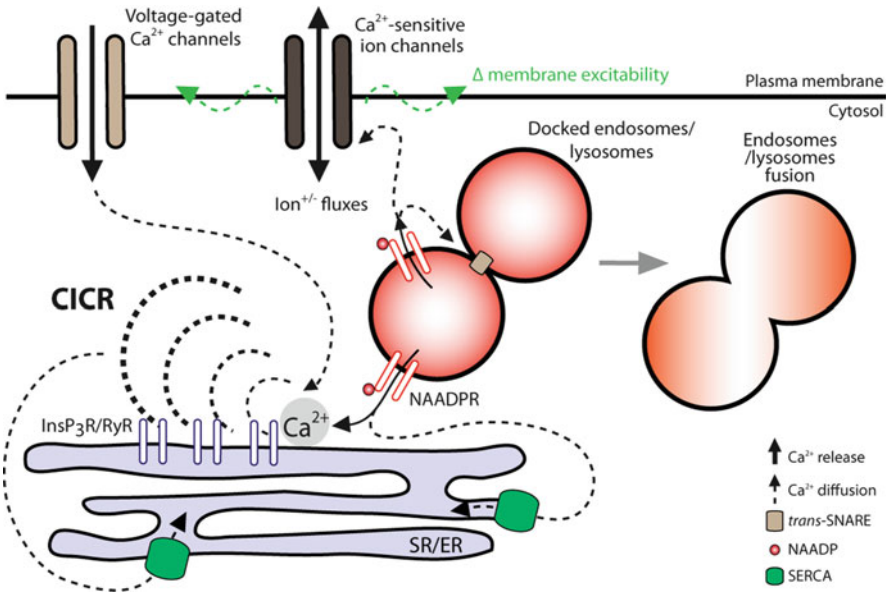

Fig. 13.4 Local to global Ca^{2+} responses mediated by NAADP. Locally, the Ca^{2+} release from acidic stores is likely to be important for normal functions of the endo-lysosomal system such as vesicle fusion or fission in lysosomal biogenesis. Small local Ca^{2+} release evoked by NAADP from lysosomes may also act as a trigger to initiate CICR from the SR/ER and generate global signals. NAADP-mediated Ca^{2+} release near the plasma membrane modulates membrane excitability (excitable cells), or ion fluxes (non-excitable cells) by opening Ca^{2+}-activated channels. Changes in the membrane potential could further activate, for example, voltage-gated Ca^{2+} channels, to allow Ca^{2+} influx and initiate a global response via CICR

agonist-coupling to Ca^{2+} release from acidic stores is now abolished [87]. RNA interference approaches are now emerging. For example, knockdown of TPC2 with siRNA has revealed important specific roles for the NAADP/TPC signaling pathway in striated muscle differentiation [88]. Importantly, this effect is phenocopied by use of the membrane-permeant NAADP antagonist, Ned-19 or disruption of Ca^{2+} storage by lysosomes/acidic stores by bafilomycin [88].

Taken together, there is now compelling evidence that TPCs are key components of the NAADP-sensitive Ca^{2+} release mechanism. A recent paper shows clearly that in HEK293 cells, that expression of RyRs confers cADPR-sensitivity, but TPC expression is needed for NAADP-evoked Ca^{2+} release [81] crystallizing the hypotheses that cADPR targets RyRs whilst NAADP targets TPCs. RyRs themselves have been proposed as direct targets for NAADP in some cell types [89, 90], although indirect activation of RyRs by local Ca^{2+} release from acidic stores is not trivial to discount.

NAADP-evoked Ca^{2+} release from acidic stores has been proposed to work in three major ways to regulate cellular processes (Fig. 13.4) [91]. The first is to coordinate Ca^{2+} release by organelle cross-talk at junctions between lysosomes and the ER. The second is to produce local Ca^{2+} signals in the sub-plasma membrane

space to control Ca^{2+}-activated plasma membrane channels and thus regulate processes such as fluid secretion in non-excitable cells such as exocrine gland cells [58], or membrane excitability in excitable cells. Examples of the latter are the polyspermy blocking cortical flash in sea urchin eggs [92] or activation of membrane currents in starfish oocytes [93], and depolarization of pancreatic beta cells [72] or neurones [94]. Thirdly, local Ca^{2+} release via TPCs may regulate endolysosomal trafficking and organelle biogenesis by regulating membrane fission and fusion processes. Overexpression of TPCs or their block by the NAADP antagonist Ned-19 induces deregulation of endocytosis, lysosome biogenesis and trafficking mimicking features of lysosomal storage diseases [82].

ADP-Ribose and Other Metabolites

As mentioned above, cADPR is metabolized to ADPR by CD38's intrinsic hydrolase activity. Other NADases may directly form ADPR. ADPR although inactive at releasing Ca^{2+} from the ER, was found to stimulate Ca^{2+} influx. This was first observed in ascidian oocytes where low ADPR concentrations may activate plasma membrane currents [95]. An important target for ADPR is TRPM2. TRPM2 channels are polymodal-gated channels responding to not only pyridine nucleotides but also to calcium, oxidants and raised temperature [96]. They are also chanzymes in that they express an intrinsic enzyme activity, ADPR pyrophosphate conferred by a nudix box containing domain at their C-terminus [97]. Both cADPR and NAADP have also been reported to activate TRPM2, but at high micromolar concentrations, substantially higher than reported concentrations of these molecules in cells and tissues [98]. In a T cell line, a second messenger role for ADP-ribose in mediating concanavalin A-activated Ca^{2+} influx via TRPM2 channels has been proposed [99]. Interestingly, although TRPM2 channels are mainly found in the plasma membrane, they have also been reported in lysosomes [100].

In addition to ADPR, ADP-ribosyl cyclases may also generate additional nucleotides including cADPR-phosphate, and adenine dinucleotides [101] which may also be active in some cells at generating Ca^{2+} signals.

Receptor-Mediated NAADP and cADPR-Mediated Ca^{2+} Signaling

Both cADPR and NAADP have satisfied all the criteria originally mandated by Sutherland, to be unambiguously assigned as second or intracellular messengers [102].

Endogenous levels of both cADPR and NAADP are found in a wide range of tissues and cells from across the phyla. Similarly, increases in levels of cADPR [29] and NAADP [61] have been reported in response to cell activation by a variety of

stimuli and cell surface receptor families. There have been two principal ways in which cADPR and NAADP levels have been measured [103]. The first are radioreceptor assays based on the high affinity binding sites for these molecules on sea urchin egg membranes [104], and the second is a cycling assay using ADP-ribosyl cyclase in reverse to generate NAD which is then coupled to the generation of a fluorescent product [105, 106]. The latter requires initial treatment with enzymes to completely remove endogenous NAD before proceeding. An additional important development was the use of NGD as an alternative substrate to NAD. True ADP-ribosyl cyclase as opposed to most ADP glycohydrolases tend to cyclise NGD to cGDPR which is fluorescent [107], and this assay has been extensively used to demonstrate ADP-ribosyl cylase activities in many preparations, and in some cases regulation of activities by various stimuli.

The first indication that cADPR levels could be regulated by phosphorylation processes was the finding that cGMP via G kinase stimulates Ca^{2+} release via cADPR synthesis in sea urchin eggs [108, 109]. cAMP on the other hand may selectively enhance NAADP forming base-exchange activity by PKA or EPAC [110], thus differential phosphorylation or regulation by cGMP or cAMP may dictate which messenger is generated on enzyme stimulation [111].

As a general principle, NAADP increases rapidly and transiently on cell stimulation, whilst cADPR remains elevated for many minutes [112, 113]. From this it has been proposed that NAADP plays a major role in triggering Ca^{2+} signals, whilst cADPR may have a longer term role in producing a long lasting increase in sensitivity of RyRs to CICR. Indeed prolonged elevations of cADPR have been associated with the circadian clock in plants as well as increased proliferative state of cells in culture [114].

CD38 knockout mice are providing important insights into the role of CD38 in agonist-mediated Ca^{2+} signaling mediated by both cADPR and NAADP. Several studies have indicated that various tissues from *Cd38*$^{-/-}$ mice have substantially reduced endogenous cADPR levels. In addition, the ability of a number of stimuli to elevate cADPR levels is impaired. Concomittantly, a number of important physiological processes are abrogated [22]. Defects include reduced insulin secretion from pancreatic beta cells [115], abolition of Ca^{2+} mobilization in pancreatic acinar cells [116, 117], cardiac hypertrophy [118], changes in airway [119] and vascular smooth muscle [120] pharmaco-mechanical coupling, defects in neutrophil chemotaxis with increased susceptibility to bacterial infection [121], impaired oxytocin signaling with associated behavioral correlates [122].

A recent report has suggested a novel way in which cADPR signaling is regulated in sperm. These cells with minimal signaling machineries apparently acquire CD38 and RyRs from secreted prostasomes from prostate gland cells and competence in cADPR signaling is required for sperm motility and thus ability to fertilize ova [123].

The finding that, at least in vitro, CD38 can synthesise NAADP [25], has also led to the investigation of this enzyme in receptor-mediated NAADP production. Using cells from *Cd38*$^{-/-}$ mice it was found that in pancreatic acinar cells, NAADP production stimulated by physiological concentrations of CCK is

abolished, and in hepatic stellate cells angiotensin II [124], and in IL8-stimulated lymphokine-activated killer cells [125], these agonist now fail to stimulate NAADP production. However, agonist-induced NAADP production has been reported in tissues from *Cd38*$^{-/-}$ mouse tissues, raising the possibility of alternate synthetic pathways [126].

The great plasticity of Ca^{2+} signaling pathways is exemplified by the ability of high affinity CCK receptors in Cd38$^{-/-}$ pancreatic acinar cells now to switch from NAADP production to IP_3-mediated Ca^{2+} signaling [117]. Conversely, CCK evoked Ca^{2+} signals in the ADP-ribosyl cyclase-deficient AR42J rat pancreatic cell line switch from IP_3-mediated Ca^{2+} signaling to NAADP signaling and Ca^{2+} release from acidic stores on transfection with CD38 cDNA [117].

A major question concerning the notion that CD38 is the major synthetic enzyme for cADPR and NAADP synthesis is the membrane topology of this protein [127]. It was originally noted as a plasma membrane ectoenzyme with its active site facing the extracellular space. De Flora and colleagues presented evidence that NAD may leak from the cell via connexins which is acted upon by extracellular CD38 to yield extracellular cADPR. cADPR may be transported back into the cell via nucleoside transporters [127]. However, an appreciable amount of CD38 is intracellular and associated with organelles such as secretory granules or endosomes, and this may increase on cell stimulation. This appears to be the case in sea urchin eggs, and evidence has been provided that NAD may be transported into organelles, converted to cADPR, which is transported into the cytoplasm to its site of action [128]. This also raises the possibility that cADPR and NAADP may also be stored in intracellular compartments, and cell stimuli may act to regulate the egress of these molecules into the cytoplasm as for Ca^{2+} mobilization from intracellular stored. Another possibility, recently proposed, is that CD38 may exist in two topologies with the active site of one form actually facing the cytoplasm [129]. Whatever the situation, more clarification is needed to understand how cellular stimuli are coupled to increases in ADP-ribosyl cyclase activities.

Conclusions

The emergence of cADPR and NAADP as Ca^{2+} mobilizing messengers and the elucidation of their place in signaling pathways and the identification of their molecular targets over the last two decades has provided many surprises and advances in our understanding of cellular regulatory processes. The field has moved on from the role of these molecules at fertilization of invertebrate eggs to central players in mammalian Ca^{2+} homeostasis and signaling. We can expect more surprises and answers in the years to come.

References

1. Ringer S (1882) Concerning the influence exerted by each of the constituents of the blood on the contraction of the ventricle. J Physiol 3:380–393
2. Ashley CC, Ridgway EB (1968) Simultaneous recording of membrane potential, calcium transient and tension in single muscle fibers. Nature 219:1168–1169
3. Douglas WW, Poisner AM (1964) Stimulus-secretion coupling in a neurosecretory organ: the role of calcium in the release of vasopressin from the neurohypophysis. J Physiol 172:1–18
4. Nielsen SP, Petersen OH (1972) Transport of calcium in the perfused submandibular gland of the cat. J Physiol 223:685–697
5. Michell RH (1975) Inositol phospholipids and cell surface receptor function. Biochim Biophys Acta 415:81–147
6. Berridge MJ (1983) Rapid accumulation of inositol trisphosphate reveals that agonists hydrolyse polyphosphoinositides instead of phosphatidylinositol. Biochem J 212:849–858
7. Streb H, Irvine RF, Berridge MJ, Schulz I (1983) Release of Ca^{2+} from a nonmitochondrial intracellular store in pancreatic acinar cells by inositol-1,4,5-trisphosphate. Nature 306:67–69
8. Supattapone S, Worley PF, Baraban JM, Snyder SH (1988) Solubilization, purification, and characterization of an inositol trisphosphate receptor. J Biol Chem 263:1530–1534
9. Maeda N, Niinobe M, Mikoshiba K (1990) A cerebellar Purkinje cell marker P400 protein is an inositol 1,4,5-trisphosphate ($InsP_3$) receptor protein. Purification and characterization of InsP3 receptor complex. EMBO J 9:61–67
10. Furuichi T, Yoshikawa S, Miyawaki A, Wada K, Maeda N, Mikoshiba K (1989) Primary structure and functional expression of the inositol 1,4,5-trisphosphate-binding protein P400. Nature 342:32–38
11. Mignery GA, Sudhof TC, Takei K, De Camilli P (1989) Putative receptor for inositol 1,4,5-trisphosphate similar to ryanodine receptor. Nature 342:192–195
12. Berridge MJ (1993) Inositol trisphosphate and calcium signalling. Nature 361:315–325
13. Whitaker MJ, Irvine RF (1984) lnositol (1,4,5) trisphosphate microinjection activates sea urchin eggs. Nature 312:636–639
14. Clapper DL, Lee HC (1985) Inositol trisphosphate induces calcium release from nonmitochondrial stores i sea urchin egg homogenates. J Biol Chem 260:13947–13954
15. Clapper DL, Walseth TF, Dargie PJ, Lee HC (1987) Pyridine nucleotide metabolites stimulate calcium release from sea urchin egg microsomes desensitized to inositol trisphosphate. J Biol Chem 262:9561–9568
16. Lee HC, Walseth TF, Bratt GT, Hayes RN, Clapper DL (1989) Structural determination of a cyclic metabolite of NAD with intracellular calcium-mobilizing activity. J Biol Chem 264:1608–1615
17. Lee HC, Aarhus R (1995) A derivative of NADP mobilizes calcium stores insensitive to inositol trisphosphate and cyclic ADP-ribose. J Biol Chem 270:2152–2157
18. Rusinko N, Lee HC (1989) Widespread occurrence in animal tissues of an enzyme catalyzing the conversion of NAD into a cyclic metabolite with intracellular calcium-mobilizing activity. J Biol Chem 264:11725–11731
19. Hellmich MR, Strumwasser F (1991) Purification and characterization of a molluscan egg-specific NADase, a second-messenger enzyme. Cell Regul 2:193–202
20. Glick DL, Hellmich MR, Beushausen S, Tempst P, Bayley H, Strumwasser F (1991) Primary structure of a molluscan egg-specific NADase, a second-messenger enzyme. Cell Regul 2:211–218
21. Lee HC, Aarhus R (1991) ADP-ribosyl cyclase: an enzyme that cyclizes NAD^+ into a calcium-mobilizing metabolite. Cell Regul 2:203–209
22. Malavasi F, Deaglio S, Funaro A, Ferrero E, Horenstein AL, Ortolan E, Vaisitti T, Aydin S (2008) Evolution and function of the ADP ribosyl cyclase/CD38 gene family in physiology and pathology. Physiol Rev 88:841–886

23. Howard M, Grimaldi JC, Bazan JF, Lund FE, Santosargumedo L, Parkhouse RME, Walseth TF, Lee HC (1993) Formation and hydrolysis of cyclic ADP ribose catalyzed by lymphocyte antigen-CD38. Science 262:1056–1059
24. Aarhus R, Graeff RM, Dickey DM, Walseth TF, Lee HC (1995) ADP-ribosyl cyclase and CD38 catalyze the synthesis of a calcium- mobilizing metabolite from NADP. J Biol Chem 270:30327–30333
25. Graeff R, Liu Q, Kriksunov IA, Hao Q, Lee HC (2006) Acidic residues at the active sites of CD38 and ADP-ribosyl cyclase determine nicotinic acid adenine dinucleotide phosphate (NAADP) synthesis and hydrolysis activities. J Biol Chem 281:28951–28957
26. Berridge G, Cramer R, Galione A, Patel S (2002) Metabolism of the novel Ca^{2+}-mobilizing messenger nicotinic acid-adenine dinucleotide phosphate via a 2'-specific Ca^{2+}-dependent phosphatase. Biochem J 365:295–301
27. Lee HC (2000) Enzymatic functions and structures of CD38 and homologs. Chem Immunol 75:39–59
28. Galione A, Lee HC, Busa WB (1991) Ca^{2+}-induced Ca^{2+} release in sea urchin egg homogenates: modulation by cyclic ADP-ribose. Science 253:1143–1146
29. Galione A, Churchill G (2000) Cyclic ADP-ribose as a calcium mobilizing messenger. Science STKE 1–6. www.stke.org/cgi/content/full/OC_sigtrans;2000/41/pe1
30. Fill M, Copello JA (2002) Ryanodine receptor calcium release channels. Physiol Rev 82:893–922
31. McPherson SM, McPherson PS, Mathews L, Campbell KP, Longo FJ (1992) Cortical localization of a calcium release channel in sea urchin eggs. J Cell Biol 116:1111–1121
32. Lokuta AJ, Darszon A, Beltran C, Valdivia HH (1998) Detection and functional characterization of ryanodine receptors from sea urchin eggs. J Physiol (Lond) 510:155–164
33. Shiwa M, Murayama T, Ogawa Y (2002) Molecular cloning and characterization of ryanodine receptor from unfertilized sea urchin eggs. Am J Physiol Regul Integr Comp Physiol 282:R727–R737
34. Taylor CW (1998) Inositol trisphosphate receptors: Ca^{2+}-modulated intracellular Ca^{2+} channels. Biochim Biophys Acta 1436:19–33
35. Roderick HL, Berridge MJ, Bootman MD (2003) Calcium-induced calcium release. Curr Biol 13:R425
36. Lee HC (1993) Potentiation of calcium- and caffeine-induced calcium release by cyclic ADP-ribose. J Biol Chem 268:293–299
37. Lee HC, Aarhus R, Graeff RM (1995) Sensitization of calcium-induced calcium release by cyclic ADP-ribose and calmodulin. J Biol Chem 270:9060–9066
38. Zhu X, Ghanta J, Walker JW, Allen PD, Valdivia HH (2004) The calmodulin binding region of the skeletal ryanodine receptor acts as a self-modulatory domain. Cell Calcium 35:165–177
39. Thomas JM, Summerhill RJ, Fruen BR, Churchill GC, Galione A (2002) Calmodulin dissociation mediates desensitization of the cADPR-induced Ca^{2+} release mechanism. Curr Biol 12:2018–2022
40. Noguchi N, Takasawa S, Nata K, Tohgo A, Kato I, Ikehata F, Yonekura H, Okamoto H (1997) Cyclic ADP-ribose binds to FK506-binding protein 12.6 to release Ca^{2+} from islet microsomes. J Biol Chem 272:3133–3136
41. Tang WX, Chen YF, Zou AP, Campbell WB, Li PL (2002) Role of FKBP12.6 in cADPR-induced activation of reconstituted ryanodine receptors from arterial smooth muscle. Am J Physiol Heart Circ Physiol 282:H1304–H1310
42. Wang YX, Zheng YM, Mei QB, Wang QS, Collier ML, Fleischer S, Xin HB, Kotlikoff M (2004) FKBP12.6 and cADPR regulation of Ca^{2+} release in smooth muscle cells. Am J Physiol Cell Physiol 286:C538–C546
43. Morita K, Kitayama T, Kitayama S, Dohi T (2006) Cyclic ADP-ribose requires FK506-binding protein to regulate intracellular Ca^{2+} dynamics and catecholamine release in acetylcholine-stimulated bovine adrenal chromaffin cells. J Pharmacol Sci 101:40–51

44. Zheng J, Wenzhi B, Miao L, Hao Y, Zhang X, Yin W, Pan J, Yuan Z, Song B, Ji G (2010) Ca^{2+} release induced by cADP-ribose is mediated by FKBP12.6 proteins in mouse bladder smooth muscle. Cell Calcium 47:449–457
45. Zhang X, Tallini YN, Chen Z, Gan L, Wei B, Doran R, Miao L, Xin HB, Kotlikoff MI, Ji G (2009) Dissociation of FKBP12.6 from ryanodine receptor type 2 is regulated by cyclic ADP-ribose but not beta-adrenergic stimulation in mouse cardiomyocytes. Cardiovasc Res 84:253–262
46. Copello JA, Qi Y, Jeyakumar LH, Ogunbunmi E, Fleischer S (2001) Lack of effect of cADP-ribose and NAADP on the activity of skeletal muscle and heart ryanodine receptors. Cell Calcium 30:269–284
47. Walseth TF, Lee HC (1993) Synthesis and characterization of antagonists of cyclic-ADP-ribose-induced Ca^{2+} release. Biochim Biophys Acta 1178:235–242
48. Sethi JK, Empson RM, Bailey VC, Potter BV, Galione A (1997) 7-Deaza-8-bromo-cyclic ADP-ribose, the first membrane-permeant, hydrolysis-resistant cyclic ADP-ribose antagonist. J Biol Chem 272:16358–16363
49. Guse AH, Lee HC (2008) NAADP: a universal Ca^{2+} trigger. Sci Signal 1:re10
50. Genazzani AA, Mezna M, Summerhill RJ, Galione A, Michelangeli F (1997) Kinetic properties of nicotinic acid adenine dinucleotide phosphate- induced Ca^{2+} release. J Biol Chem 272:7669–7675
51. Genazzani AA, Mezna M, Dickey DM, Michelangeli F, Walseth TF, Galione A (1997) Pharmacological properties of the Ca^{2+}-release mechanism sensitive to NAADP in the sea urchin egg. Br J Pharmacol 121:1489–1495
52. Chini EN, Dousa TP (1996) Nicotinate-adenine dinucleotide phosphate-induced Ca^{2+}-release does not behave as a Ca^{2+}-induced Ca^{2+}-release system. Biochem J 316:709–711
53. Genazzani AA, Galione A (1996) Nicotinic acid-adenine dinucleotide phosphate mobilizes Ca^{2+} from a thapsigargin-insensitive pool. Biochem J 315:721–725
54. Lee HC, Aarhus R (2000) Functional visualization of the separate but interacting calcium stores sensitive to NAADP and cyclic ADP-ribose. J Cell Sci 113:4413–4420
55. Aarhus R, Dickey DM, Graeff RM, Gee KR, Walseth TF, Lee HC (1996) Activation and inactivation of Ca^{2+} release by $NAADP^{+}$. J Biol Chem 271:8513–8516
56. Churchill GC, Galione A (2001) NAADP induces Ca^{2+} oscillations via a two-pool mechanism by priming IP_3 – and cADPR-sensitive Ca^{2+} stores. EMBO J 20:2666–2671
57. Churchill GC, Okada Y, Thomas JM, Genazzani AA, Patel S, Galione A (2002) NAADP mobilizes Ca^{2+} from reserve granules, a lysosome-related organelle, in sea urchin eggs. Cell 111:703–708
58. Cancela JM, Churchill GC, Galione A (1999) Coordination of agonist-induced Ca^{2+}-signalling patterns by NAADP in pancreatic acinar cells. Nature 398:74–76
59. Naylor E, Arredouani A, Vasudevan SR, Lewis AM, Parkesh R, Mizote A, Rosen D, Thomas JM, Izumi M, Ganesan A, Galione A, Churchill GC (2009) Identification of a chemical probe for NAADP by virtual screening. Nat Chem Biol 5:220–226
60. Patel S, Churchill GC, Galione A (2001) Coordination of Ca^{2+} signalling by NAADP. Trends Biochem Sci 26:482–489
61. Galione A, Morgan AJ, Arredouani A, Davis LC, Rietdorf K, Ruas M, Parrington J (2010) NAADP as an intracellular messenger regulating lysosomal calcium-release channels. Biochem Soc Trans 38:1424–1431
62. Jardin I, Lopez JJ, Pariente JA, Salido GM, Rosado JA (2008) Intracellular calcium release from human platelets: different messengers for multiple stores. Trends Cardiovasc Med 18:57–61
63. Lloyd-Evans E, Morgan AJ, He X, Smith DA, Elliot-Smith E, Sillence DJ, Churchill GC, Schuchman EH, Galione A, Platt FM (2008) Niemann-Pick disease type C1 is a sphingosine storage disease that causes deregulation of lysosomal calcium. Nat Med 14:1247–1255
64. Bargal R, Avidan N, Ben-Asher E, Olender Z, Zeigler M, Frumkin A, Raas-Rothschild A, Glusman G, Lancet D, Bach G (2000) Identification of the gene causing mucolipidosis type IV. Nat Genet 26:118–123

65. Sun M, Goldin E, Stahl S, Falardeau JL, Kennedy JC, Acierno JS Jr, Bove C, Kaneski CR, Nagle J, Bromley MC, Colman M, Schiffmann R, Slaugenhaupt SA (2000) Mucolipidosis type IV is caused by mutations in a gene encoding a novel transient receptor potential channel. Hum Mol Genet 9:2471–2478
66. Bach G (2001) Mucolipidosis type IV. Mol Genet Metab 73:197–203
67. Galione A, Evans AM, Ma J, Parrington J, Arredouani A, Cheng X, Zhu MX (2009) The acid test: the discovery of two-pore channels (TPCs) as NAADP-gated endolysosomal $Ca^{(2+)}$ release channels. Pflugers Arch 458:869–876
68. Ishibashi K, Suzuki M, Imai M (2000) Molecular cloning of a novel form (two-repeat) protein related to voltage-gated sodium and calcium channels. Biochem Biophys Res Commun 270:370–376
69. Furuichi T, Cunningham KW, Muto S (2001) A putative two pore channel AtTPC1 mediates Ca^{2+} flux in Arabidopsis leaf cells. Plant Cell Physiol 42:900–905
70. Peiter E, Maathuis FJ, Mills LN, Knight H, Pelloux J, Hetherington AM, Sanders D (2005) The vacuolar Ca^{2+}-activated channel TPC1 regulates germination and stomatal movement. Nature 434:404–408
71. Hedrich R, Marten I (2011) TPC1 – SV channels gain shape. Mol Plant 4:428–441
72. Calcraft PJ, Ruas M, Pan Z, Cheng X, Arredouani A, Hao X, Tang J, Rietdorf K, Teboul L, Chuang KT, Lin P, Xiao R, Wang C, Zhu Y, Lin Y, Wyatt CN, Parrington J, Ma J, Evans AM, Galione A, Zhu MX (2009) NAADP mobilizes calcium from acidic organelles through two-pore channels. Nature 459:596–600
73. Zhang F, Li PL (2007) Reconstitution and characterization of a nicotinic acid adenine dinucleotide phosphate (NAADP)-sensitive Ca^{2+} release channel from liver lysosomes of rats. J Biol Chem 282:25259–25269
74. Zhang F, Jin S, Yi F, Li PL (2009) TRP-ML1 functions as a lysosomal NAADP-sensitive Ca^{2+} release channel in coronary arterial myocytes. J Cell Mol Med 13:3174–3185
75. Pryor PR, Reimann F, Gribble FM, Luzio JP (2006) Mucolipin-1 Is a lysosomal membrane protein required for intracellular lactosylceramide traffic. Traffic 7:1388–1398
76. Yamaguchi S, Jha A, Li Q, Soyombo AA, Dickinson GD, Churamani D, Brailoiu E, Patel S, Muallem S (2011) TRPML1 and two-pore channels are functionally independent organellar ion channels. J Biol Chem 286:22934–22942
77. Zong X, Schieder M, Cuny H, Fenske S, Gruner C, Rotzer K, Griesbeck O, Harz H, Biel M, Wahl-Schott C (2009) The two-pore channel TPCN2 mediates NAADP-dependent Ca^{2+}-release from lysosomal stores. Pflugers Arch 458:891–899
78. Brailoiu E, Churamani D, Cai X, Schrlau MG, Brailoiu GC, Gao X, Hooper R, Boulware MJ, Dun NJ, Marchant JS, Patel S (2009) Essential requirement for two-pore channel 1 in NAADP-mediated calcium signaling. J Cell Biol 186:201–209
79. Kinnear NP, Boittin FX, Thomas JM, Galione A, Evans AM (2004) Lysosome-sarcoplasmic reticulum junctions. A trigger zone for calcium signaling by nicotinic acid adenine dinucleotide phosphate and endothelin-1. J Biol Chem 279:54319–54326
80. Kinnear NP, Wyatt CN, Clark JH, Calcraft PJ, Fleischer S, Jeyakumar LH, Nixon GF, Evans AM (2008) Lysosomes co-localize with ryanodine receptor subtype 3 to form a trigger zone for calcium signalling by NAADP in rat pulmonary arterial smooth muscle. Cell Calcium 44:190–201
81. Ogunbayo OA, Zhu Y, Rossi D, Sorrentino V, Ma J, Zhu MX, Evans AM (2011) Cyclic adenosine diphosphate ribose activates ryanodine receptors, whereas NAADP activates two-pore domain channels. J Biol Chem 286:9136–9140
82. Ruas M, Rietdorf K, Arredouani A, Davis LC, Lloyd-Evans E, Koegel H, Funnell TM, Morgan AJ, Ward JA, Watanabe K, Cheng X, Churchill GC, Zhu MX, Platt FM, Wessel GM, Parrington J, Galione A (2010) Purified TPC isoforms form naadp receptors with distinct roles for Ca^{2+} signaling and endolysosomal trafficking. Curr Biol 20:703–709
83. Brailoiu E, Hooper R, Cai X, Brailoiu GC, Keebler MV, Dun NJ, Marchant JS, Patel S (2010) An ancestral deuterostome family of two-pore channels mediates nicotinic acid adenine dinucleotide phosphate-dependent calcium release from acidic organelles. J Biol Chem 285: 2897–2901

84. Schieder M, Rotzer K, Bruggemann A, Biel M, Wahl-Schott CA (2010) Characterization of Two-pore channel 2 (TPCN2)-mediated Ca^{2+} currents in isolated lysosomes. J Biol Chem 285:21219–21222
85. Pitt SJ, Funnell TM, Sitsapesan M, Venturi E, Rietdorf K, Ruas M, Ganesan A, Gosain R, Churchill GC, Zhu MX, Parrington J, Galione A, Sitsapesan R (2010) TPC2 is a novel NAADP-sensitive Ca^{2+} release channel, operating as a dual sensor of luminal pH and Ca^{2+}. J Biol Chem 285:35039–35046
86. Brailoiu E, Rahman T, Churamani D, Prole DL, Brailoiu GC, Hooper R, Taylor CW, Patel S (2010) An NAADP-gated two-pore channel targeted to the plasma membrane uncouples triggering from amplifying Ca^{2+} signals. J Biol Chem 285:38511–38516
87. Tugba Durlu-Kandilci N, Ruas M, Chuang KT, Brading A, Parrington J, Galione A (2010) TPC2 proteins mediate nicotinic acid adenine dinucleotide phosphate (NAADP)- and agonist-evoked contractions of smooth muscle. J Biol Chem 285:24925–24932
88. Aley PK, Mikolajczyk AM, Munz B, Churchill GC, Galione A, Berger F (2010) Nicotinic acid adenine dinucleotide phosphate regulates skeletal muscle differentiation via action at two-pore channels. Proc Natl Acad Sci USA 107:19927–19932
89. Gerasimenko JV, Maruyama Y, Yano K, Dolman NJ, Tepikin AV, Petersen OH, Gerasimenko OV (2003) NAADP mobilizes Ca^{2+} from a thapsigargin-sensitive store in the nuclear envelope by activating ryanodine receptors. J Cell Biol 163:271–282
90. Dammermann W, Guse AH (2005) Functional ryanodine receptor expression is required for NAADP-mediated local Ca^{2+} signaling in T-lymphocytes. J Biol Chem 280:21394–21399
91. Galione A (2011) NAADP receptors. Cold Spring Harb Perspect Biol 3:a004036
92. Churchill GC, O'Neill JS, Masgrau R, Patel S, Thomas JM, Genazzani AA, Galione A (2003) Sperm deliver a new second messenger: NAADP. Curr Biol 13:125–128
93. Moccia F, Lim D, Kyozuka K, Santella L (2004) NAADP triggers the fertilization potential in starfish oocytes. Cell Calcium 36:515–524
94. Brailoiu GC, Brailoiu E, Parkesh R, Galione A, Churchill GC, Patel S, Dun NJ (2009) NAADP-mediated channel 'chatter' in neurons of the rat medulla oblongata. Biochem J 419:91–97, 92 p following 97
95. Wilding M, Russo GL, Galione A, Marino M, Dale B (1998) ADP-ribose gates the fertilization channel in ascidian oocytes. Am J Physiol 275:C1277–C1283
96. Sumoza-Toledo A, Penner R (2010) TRPM2: a multifunctional Ion channel for calcium signaling. J Physiol 589:1515–1525
97. Perraud AL, Fleig A, Dunn CA, Bagley LA, Launay P, Schmitz C, Stokes AJ, Zhu Q, Bessman MJ, Penner R, Kinet JP, Scharenberg AM (2001) ADP-ribose gating of the calcium-permeable LTRPC2 channel revealed by Nudix motif homology. Nature 411:595–599
98. Beck A, Kolisek M, Bagley LA, Fleig A, Penner R (2006) Nicotinic acid adenine dinucleotide phosphate and cyclic ADP-ribose regulate TRPM2 channels in T lymphocytes. FASEB J 20:962–964
99. Gasser A, Glassmeier G, Fliegert R, Langhorst MF, Meinke S, Hein D, Krueger S, Weber K, Heiner I, Oppenheimer N, Schwarz JR, Guse AH (2006) Activation of T cell calcium influx by the second messenger ADP-ribose. J Biol Chem 281:2489–2496
100. Lange I, Yamamoto S, Partida-Sanchez S, Mori Y, Fleig A, Penner R (2009) TRPM2 functions as a lysosomal Ca^{2+}-release channel in beta cells. Sci Signal 2:ra23
101. Basile G, Taglialatela-Scafati O, Damonte G, Armirotti A, Bruzzone S, Guida L, Franco L, Usai C, Fattorusso E, De Flora A, Zocchi E (2005) ADP-ribosyl cyclases generate two unusual adenine homodinucleotides with cytotoxic activity on mammalian cells. Proc Natl Acad Sci USA 102:14509–14514
102. Sutherland E (1971) Studies on the mechanism of hormone action. Nobel Prize Lecture 1–17
103. Morgan AJ, Galione A (2008) Investigating cADPR and NAADP in intact and broken cell preparations. Methods 46:194–203
104. Lewis AM, Masgrau R, Vasudevan SR, Yamasaki M, O'Neill JS, Garnham C, James K, Macdonald A, Ziegler M, Galione A, Churchill GC (2007) Refinement of a radioreceptor binding assay for nicotinic acid adenine dinucleotide phosphate. Anal Biochem 371:26–36

105. Graeff R, Lee HC (2002) A novel cycling assay for cellular cADP-ribose with nanomolar sensitivity. Biochem J 361:379–384
106. Graeff R, Lee HC (2002) A novel cycling assay for nicotinic acid-adenine dinucleotide phosphate with nanomolar sensitivity. Biochem J 367:163–168
107. Graeff RM, Walseth TF, Fryxell K, Branton WD, Lee HC (1994) Enzymatic synthesis and characterizations of cyclic GDP-ribose: a procedure for distinguishing enzymes with ADP-ribosyl cyclase activity. J Biol Chem 269:30260–30267
108. Galione A, White A, Willmott N, Turner M, Potter BV, Watson SP (1993) cGMP mobilizes intracellular Ca^{2+} in sea urchin eggs by stimulating cyclic ADP-ribose synthesis [see comments]. Nature 365:456–459
109. Graeff RM, Franco L, De Flora A, Lee HC (1998) Cyclic GMP-dependent and -independent effects on the synthesis of the calcium messengers cyclic ADP-ribose and nicotinic acid adenine dinucleotide phosphate. J Biol Chem 273:118–125
110. Kim BJ, Park KH, Yim CY, Takasawa S, Okamoto H, Im MJ, Kim UH (2008) Generation of nicotinic acid adenine dinucleotide phosphate and cyclic ADP-ribose by glucagon-like peptide-1 evokes Ca^{2+} signal that is essential for insulin secretion in mouse pancreatic islets. Diabetes 57:868–878
111. Wilson HL, Galione A (1998) Differential regulation of nicotinic acid-adenine dinucleotide phosphate and cADP-ribose production by cAMP and cGMP. Biochem J 331:837–843
112. Yamasaki M, Thomas JM, Churchill GC, Garnham C, Lewis AM, Cancela JM, Patel S, Galione A (2005) Role of NAADP and cADPR in the induction and maintenance of agonist-evoked Ca^{2+} spiking in mouse pancreatic acinar cells. Curr Biol 15:874–878
113. Gasser A, Bruhn S, Guse AH (2006) Second messenger function of nicotinic acid adenine dinucleotide phosphate (NAADP) revealed by an improved enzymatic cycling assay. J Biol Chem 281:16906–16913
114. Dodd AN, Gardner MJ, Hotta CT, Hubbard KE, Dalchau N, Love J, Assie JM, Robertson FC, Jakobsen MK, Goncalves J, Sanders D, Webb AA (2007) The Arabidopsis circadian clock incorporates a cADPR-based feedback loop. Science 318:1789–1792
115. Kato I, Yamamoto Y, Fujimura M, Noguchi N, Takasawa S, Okamoto H (1999) CD38 disruption impairs glucose-induced increases in cyclic ADP-ribose, $[Ca^{2+}]i$, and insulin secretion. J Biol Chem 274:1869–1872
116. Fukushi Y, Kato I, Takasawa S, Sasaki T, Ong BH, Sato M, Ohsaga A, Sato K, Shirato K, Okamoto H, Maruyama Y (2001) Identification of cyclic ADP-ribose-dependent mechanisms in pancreatic muscarinic Ca^{2+} signaling using CD38 knockout mice. J Biol Chem 276:649–655
117. Cosker F, Cheviron N, Yamasaki M, Menteyne A, Lund FE, Moutin MJ, Galione A, Cancela JM (2010) The ecto-enzyme CD38 is a nicotinic acid adenine dinucleotide phosphate (NAADP) synthase that couples receptor activation to Ca^{2+} mobilization from lysosomes in pancreatic acinar cells. J Biol Chem 285:38251–38259
118. Takahashi J, Kagaya Y, Kato I, Ohta J, Isoyama S, Miura M, Sugai Y, Hirose M, Wakayama Y, Ninomiya M, Watanabe J, Takasawa S, Okamoto H, Shirato K (2003) Deficit of CD38/cyclic ADP-ribose is differentially compensated in hearts by gender. Biochem Biophys Res Commun 312:434–440
119. Deshpande DA, White TA, Guedes AG, Milla C, Walseth TF, Lund FE, Kannan MS (2005) Altered airway responsiveness in CD38-deficient mice. Am J Respir Cell Mol Biol 32:149–156
120. Mitsui-Saito M, Kato I, Takasawa S, Okamoto H, Yanagisawa T (2003) CD38 gene disruption inhibits the contraction induced by alpha-adrenoceptor stimulation in mouse aorta. J Vet Med Sci 65:1325–1330
121. Partida-Sanchez S, Cockayne DA, Monard S, Jacobson EL, Oppenheimer N, Garvy B, Kusser K, Goodrich S, Howard M, Harmsen A, Randall TD, Lund FE (2001) Cyclic ADP-ribose production by CD38 regulates intracellular calcium release, extracellular calcium influx and chemotaxis in neutrophils and is required for bacterial clearance in vivo. Nat Med 7:1209–1216

122. Jin D, Liu HX, Hirai H, Torashima T, Nagai T, Lopatina O, Shnayder NA, Yamada K, Noda M, Seike T, Fujita K, Takasawa S, Yokoyama S, Koizumi K, Shiraishi Y, Tanaka S, Hashii M, Yoshihara T, Higashida K, Islam MS, Yamada N, Hayashi K, Noguchi N, Kato I, Okamoto H, Matsushima A, Salmina A, Munesue T, Shimizu N, Mochida S, Asano M, Higashida H (2007) CD38 is critical for social behaviour by regulating oxytocin secretion. Nature 446:41–45
123. Park KH, Kim BJ, Kang J, Nam TS, Lim JM, Kim HT, Park JK, Kim YG, Chae SW, Kim UH (2011) Ca^{2+} signaling tools acquired from prostasomes are required for progesterone-induced sperm motility. Sci Signal 4:ra31
124. Kim SY, Cho BH, Kim UH (2010) CD38-mediated Ca^{2+} signaling contributes to angiotensin II-induced activation of hepatic stellate cells: attenuation of hepatic fibrosis by CD38 ablation. J Biol Chem 285:576–582
125. Rah SY, Mushtaq M, Nam TS, Kim SH, Kim UH (2010) Generation of cyclic ADP-ribose and nicotinic acid adenine dinucleotide phosphate by CD38 for Ca^{2+} signaling in interleukin-8-treated lymphokine-activated killer cells. J Biol Chem 285:21877–21887
126. Soares S, Thompson M, White T, Isbell A, Yamasaki M, Prakash Y, Lund F, Galione A, Chini EN (2006) NAADP as a second messenger: Neither CD38 nor the base-exchange reaction are necessary for the in vivo generation of the NAADP in myometrial cells. Am J Physiol Cell Physiol 292:C227–C239
127. De Flora A, Guida L, Franco L, Zocchi E (1997) The CD38/cyclic ADP-ribose system: a topological paradox. Int J Biochem Cell Biol 29:1149–1166
128. Davis LC, Morgan AJ, Ruas M, Wong JL, Graeff RM, Poustka AJ, Lee HC, Wessel GM, Parrington J, Galione A (2008) Ca^{2+} signaling occurs via second messenger release from intraorganelle synthesis sites. Curr Biol 18:1612–1618
129. Lee HC (2011) Cyclic ADP-ribose and NAADP: fraternal twin messengers for calcium signaling. Sci China Life Sci 54:699–711

Chapter 14
NAADP on Target

Robert Hooper and Sandip Patel

Abstract Nicotinic acid adenine dinucleotide phosphate (NAADP) is a potent intracellular Ca^{2+}-mobilising messenger. Much evidence indicates that NAADP targets novel Ca^{2+} channels located on acidic organelles but the identity of these channels has remained obscure. Recent studies have converged on a novel class of ion channels, the two-pore channels (TPCs) as likely molecular targets. The location of these channels to the endo-lysosomal system and their sensitivity to NAADP match closely those of endogenous NAADP-sensitive channels in both mammalian cells and sea urchin eggs, where the effects of NAADP were discovered. Moreover, the functional coupling of TPCs to archetypal endoplasmic reticulum (ER) Ca^{2+} channels is also matched. Biophysical analysis in conjunction with site-directed mutagenesis demonstrates that TPCs are pore-forming subunits of NAADP-gated ion channels. TPCs have a unique two-repeat structure, are regulated by N-linked glycosylation and harbor an endo-lysosomal targeting motif in their N-terminus. Knockdown studies have shown TPCs to regulate smooth muscle contraction, differentiation and endothelial cell activation consistent with previous studies implicating NAADP in these processes. Thus multiple lines of evidence indicate that TPCs are the likely long sought targets for NAADP.

Keywords NAADP • Two-pore channel • Calcium • Acidic Ca^{2+} store • Lysosome • Endosome • Sea urchin • Ca^{2+}-mobilising second messenger • Inositol trisphosphate receptor • Ryanodine receptor

R. Hooper (✉) • S. Patel
Department of Cell and Developmental Biology, University College London, Gower Street, London, WC1E 6BT, UK
e-mail: r.hooper@ucl.ac.uk; patel.s@ucl.ac.uk

M.S. Islam (ed.), *Calcium Signaling*, Advances in Experimental Medicine and Biology 740, DOI 10.1007/978-94-007-2888-2_14,

Introduction

Changes in the concentration of cytosolic Ca^{2+} are effected by a multitude of external stimuli and drive a range of disparate cellular events [1]. A potent second messenger that links cell surface stimulation to the release of Ca^{2+} from intracellular Ca^{2+} stores is nicotinic acid adenine dinucleotide phosphate (NAADP) [2–4]. Less is known concerning its mechanism of action relative to the messengers, inositol trisphosphate and cyclic ADP-ribose which are known to target well-defined Ca^{2+} channels located on ER Ca^{2+} stores [5, 6]. Here, we highlight some of the initial studies that defined the unusual properties of the NAADP signaling pathway, and attempt to rationalise these findings in light of the recent identification of the two-pore channels (TPCs) as likely targets for NAADP [7–9].

NAADP-Mediated Ca^{2+} Signaling in the Sea Urchin Egg: The Early Days

For many years the sea urchin has been used extensively by both Ca^{2+} "signalers" and developmental biologists alike providing much insight in to the mechanisms of Ca^{2+} homeostasis and early development. The sea urchin emerged as a model system for intracellular Ca^{2+} signaling after it was shown by Lee that inositol trisphosphate could release Ca^{2+} from non-mitochondrial stores in a cell-free homogenate prepared from eggs [10]. In a subsequent land-mark paper, he also showed that the pyridine nucleotides NAD and NADP could stimulate Ca^{2+} release from preparations that had been desensitised to inositol trisphosphate [11]. The effect of NAD was ascribed to its conversion to a Ca^{2+}-mobilising derivative later identified as cyclic ADP-ribose [12] and now known to be produced via cyclisation reaction catalyzed by the multifunctional ADP-ribosyl cyclases [13–16]. The effect of NADP, which was more rapid than NAD, turned out to be due to a minor contaminant of commercial NADP. High resolution mass spectroscopy showed the active molecule mass to be one atomic unit higher than NADP which led to its identification as NAADP [17]. The lack of heterologous desensitisation between inositol trisphosphate, cyclic ADP-ribose and NAADP [11, 17] coupled with the inability of inositol trisphosphate and cyclic ADP-ribose antagonists to block NAADP responses [17] strongly pointed to the existence of a novel NAADP receptor. In support, the Ca^{2+} mobilizing properties of NAADP were unaffected by cytosolic Ca^{2+} [18] which contrasts sharply to the biphasic effects of Ca^{2+} on inositol trisphosphate and cyclic ADP-ribose-evoked Ca^{2+} release. Moreover, pre-treatment of homogenates with *sub-threshold* concentrations of NAADP rendered homogenates completely refractory to subsequent NAADP [19, 20] – a bizarre feature not shared by inositol trisphosphate or cyclic ADP-ribose.

It was also clear from the outset that NAADP mobilized Ca^{2+} from a novel Ca^{2+} store [11]. Thus, fractionation of egg homogenates on density gradients resulted in

a broad distribution of vesicles sensitive to NAADP whereas inositol trisphosphate and cyclic ADP-ribose mobilized Ca^{2+} from a smaller subset of vesicles enriched in ER markers [17]. This was subsequently confirmed in intact cells [21]. Moreover, unlike inositol trisphosphate and cyclic ADP-ribose, NAADP signaling was insensitive to the SERCA pump inhibitor thapsigargin, which depletes the ER of Ca^{2+} [22, 23]. A major step in the identification of the target NAADP-sensitive Ca^{2+} stores came in 2002 when Churchill and colleagues showed that the effects of NAADP could be selectively abolished by treatment of eggs with the lysomotropic agent, GPN [24]. GPN (Glycyl-L-phenylalanine 2-naphthylamide) is a peptide substrate of the acid hydrolase cathepsin C – a marker for lysosomes [25]. GPN causes osmotic lysis of cathepsin-C containing organelles as it hydrolyzed. Thus, it appeared that NAADP mobilized Ca^{2+} not from the ER but instead from an acidic lysosome-like organelle [24]. Further fractionation studies yielded subcellular preparations that were responsive to NAADP but not inositol trisphosphate/cyclic ADP-ribose, enriched in other lysosomal markers such as β-galactosidase and most likely corresponding to reserve granules – the functional equivalent of the lysosome in the egg [24]. Ca^{2+} uptake in to these vesicles was thapsigargin-insensitive but inhibited by the V-H^+-ATPase pump inhibitor bafilomycin-A1 [26], consistent with the notion that a proton gradient is required for Ca^{2+} loading presumably through a Ca^{2+}/H^+ exchanger [24, 27].

Despite the very discrete properties of the Ca^{2+} channels and stores targeted by NAADP compared to inositol trisphosphate/cyclic ADP-ribose in the broken egg preparation, the distinction becomes blurred in the intact cell. Thus, NAADP-evoked Ca^{2+} signals are partially sensitive to combined blockade of ER Ca^{2+} channels and depletion of ER stores with thapsigargin [28]. Moreover, NAADP evoked long lasting Ca^{2+} oscillations in intact eggs [19, 29] despite the lack of feedback effects of cytosolic Ca^{2+} on NAADP-evoked Ca^{2+} release and the potent self-desensitization apparent in homogenates – features perhaps more conducive to a "one-shot" mechanism of action. Notably, the oscillations were completely blocked by interfering with ER Ca^{2+} release [29]. Such observations were rationalized in a two-pool model whereby NAADP-evoked Ca^{2+} release from acidic Ca^{2+} stores is amplified by ER Ca^{2+} stores. Such a model necessitated a precise geometry of stores thereby explaining lack of functional coupling in homogenates where such geometry would be disrupted.

Sea Urchin NAADP Receptors

Whereas momentum gathered on the identification of the target Ca^{2+} store and the relationship between these stores and the better established ER, the target channels remained relatively poorly characterized. The use of radiolabelled NAADP however did provide insight in to the basic pharmacological and biochemical properties of the elusive target protein.

NAADP was shown to bind to a single class of sites in crude sea urchin egg homogenate with high nanomolar "affinity" [19, 30, 31]. Importantly, the rank order

of potency of NAADP analogues in competing with NAADP [32] and their ability to mobilize Ca^{2+} [33] were similar indicating that the identified binding site was closely associated with Ca^{2+} release. Moreover, binding was unaffected by Ca^{2+} and pH consistent with functional studies [30]. Additional studies identified a requirement for phospholipids for NAADP binding [34]. Intriguingly, kinetic analysis revealed that [^{32}P]NAADP did not substantially dissociate from its receptor under physiological conditions suggesting that binding was to all intents irreversible [19, 30, 31]. The binding site may therefore correspond to a desensitized conformation. Interestingly, the receptor appeared to be modulated by K^+ ions as ligand binding in media lacking K^+ was largely reversible revealing multiple binding sites [35]. Further evidence for multiple NAADP binding sites on the target protein(s) was recently provided by the use of analogues of the NAADP antagonist, Ned-19, identified in an elegant virtual screen [36]. One such molecule; Ned-20, inhibited NAADP binding and desensitisation of Ca^{2+} release by sub-threshold concentrations of NAADP but was without effect on Ca^{2+} release evoked by activating concentrations of NAADP [37]. Conversely, Ned-19.4 inhibited Ca^{2+} release but was without effect on NAADP binding [37]. These data support the hypothesis for high affinity (inactivating) and low-affinity (activating) binding sites.

The biochemical properties of the endogenous receptor were probed by exploiting the irreversible nature of ligand binding. Thus, homogenate preparations labelled with [^{32}P]NAADP could be effectively solubilized with mild detergents without appreciable ligand dissociation thereby allowing the target protein to be conveniently tracked during various fractionation procedures [38]. Results from electrophoresis on native and pH gradient gels indicated that NAADP bound to a protein with a isolelectric point of ~6 [38]. The apparent molecular weight of the labelled protein when analysed by gel filtration was 400–470 kDa. However, the protein appeared much smaller (120–150 kDa) on sucrose density gradients. The reasons for this anomalous migration are unclear but association of the receptor with lipids [34] may reduce its buoyant molar mass thereby underestimating its weight on sucrose gradients. During the course of our gel filtration analysis it became clear that the stability of the protein-ligand complex was dependent on the time that the receptor had been exposed to NAADP [20, 39]. Thus receptors labelled with NAADP for short periods dissociated more readily than those labelled for longer [20, 39]. Intriguingly, stabilization of NAADP receptors by their ligand was delayed by minutes relative to ligand binding and abolished at low temperature [20, 39]. These data point to a simple temperature-sensitive molecular “memory” endowing NAADP receptors to detect the duration of their activation [20, 39].

NAADP as a Wide-Spread Signaling Molecule

Following the initial studies in sea urchin eggs, the Ca^{2+} mobilizing activity of NAADP was documented in other echinoderms (starfish) [40], ascidians [41], gastropods (aplysia) [42] amphibians (frogs) [43] and mammals including humans

[44]. The first mammalian cell type in which NAADP was shown to be active was the pancreatic acinar cell [45]. A key feature that has emerged from study of this cell type and found applicable to other mammalian cells is that, similar to the sea urchin, NAADP appears to target acidic Ca^{2+} stores (lysosomes and endosomes), and that Ca^{2+} release from these stores is amplified by the ER likely through Ca^{2+}-induced Ca^{2+} release. This was termed the "trigger" hypothesis [45]. One difference noted between mammalian and sea urchin NAADP-sensitive Ca^{2+} channels related to their inactivation. In mammalian cells, high (micromolar) concentrations of NAADP resulted in diminished Ca^{2+} release relative to lower (nanomolar) concentrations, giving rise to unusual "bell-shaped" concentration-effect relationships [44, 45]. Direct measurements of cellular NAADP using a radioreceptor assay [46, 47] have identified many Ca^{2+} mobilizing agonists that are coupled to production of NAADP, consistent with a messenger role for NAADP (reviewed in [48]). Importantly, NAADP has been implicated in a diverse range of physiological processes summarised in Table 14.1. Of note, is the finding by several independent labs that NAADP participates in contraction of smooth muscle in a variety of tissues. More recently, NAADP has also been also been implicated in muscle relaxation through its action within neighbouring endothelial cells in which down-stream Ca^{2+}-dependent outputs including hyper-polarization and NO production were identified [63]. NAADP-evoked Ca^{2+} signals also appear to be sufficient to mediate differentiation of PC12 cells whereas interestingly, inositol trisphosphate-evoked Ca^{2+} signals were insufficient [56]. This suggests that selectivity in Ca^{2+}-dependent output may be driven by different intracellular messengers. Thus, it is clear that NAADP-mediated Ca^{2+} signaling is of major physiological significance.

Candidate NAADP-Sensitive Ca^{2+} Channels

Despite extensive characterisation of NAADP-mediated Ca^{2+} signaling and the identification of a host of physiological outcomes assigned to this messenger, the molecular identity of the NAADP-sensitive Ca^{2+} release channel remained elusive.

A bulk of the published data is consistent with an action of NAADP on acidic organelles. However, there is also evidence to suggest that NAADP directly mobilizes Ca^{2+} from the ER through activation of ryanodine receptors [73–76]. For example, single channel recordings of purified type 1 ryanodine receptors in artificial bilayers showed that NAADP increased the open-probability of these channels in a concentration-dependent manner [74], consistent with direct action of NAADP on ryanodine receptors. However, no such regulation was observed in other studies using similar methods [77]. It might be that there is a close, perhaps even physical association between ryanodine receptors and NAADP-sensitive channels that make disentanglement of the two difficult [78]. In arterial myocytes for example, type 3 ryanodine receptors form dense perinuclear clusters that colocalise with lysosomal markers [79]. These may constitute highly localized "trigger zones" for NAADP mediated signaling perhaps coincident with membrane contact sites involved in inter-organelle lipid transfer [80].

Table 14.1 NAADP physiology. Examples of cellular processes, grouped by organ system, that have been shown to be regulated by NAADP

Organ	Tissue/cell	Physiological process	References
Reproductive system	Eggs (starfish)	Fertilisation potential	[49]
	Eggs (sea urchin)	Cortical flash	[50]
	Eggs (sea urchin)	Luminal pH regulation	[51]
	Oocytes (ascidian)	Ca^{2+} current inhibition	[41]
	Leydig cells	Testosterone secretion	[52]
	Uterine smooth muscle	Contraction	[53]
Nervous System	Neuromuscular junction (frog)	Neurotransmitter release	[54]
	Cortical neurons	Neurite extension	[55]
	PC12 cells	Differentiation	[56]
	Astrocytes	Autophagy	[57]
	Medulla neurons	Depolarisation	[58]
	Buccal ganglion (aplysia)	Neurotransmitter release	[42]
Cardiovascular System	Platelets	Cell surface phosphatidyl-serine exposure	[59]
	Cardiac myocytes	Contraction	[60]
	Coronary artery smooth muscle	Contraction	[61]
	Pulmonary artery smooth muscle	Contraction	[62]
	Endothelial cells	NO production	[63]
		Hyperpolarisation	[63]
		vWF secretion	[64]
	Aorta	Relaxation	[63]
Immune System	T cells	Proliferation	[65]
	Lymphokine-activated killer cells	NFAT translocation	[65]
		Cytokine production	[65, 66]
		Stable arrests	[66]
		Invasive capacity	[66]
		Migration	[67]
Pancreas	Beta cells	Insulin secretion	[68]
		Insulin-stimulated ERK phosphorylation	[69]
Other			
Gut	Taenia caecum smooth muscle	Contraction	[70]
Bladder	Detrusor smooth muscle	Contraction	[70]
Skeletal Muscle	C2C12 cells	Differentiation	[71]
Connective Tissue	Fibroblasts	Endo-lysosomal lipid transfer	[72]

Members of the TRP channel super-family have also been proposed to be regulated by NAADP. Several lines of evidence provided by Zhang and colleagues suggest that the endo-lysosomal protein TRPML1 (the protein defective in the lysosomal storage disorder, Mucolipidosis IV) is an NAADP-sensitive Ca^{2+} channel [65, 72, 81, 82]. Electrophysiological recordings from planar lipid bilayers into which lysosomal proteins had been reconstituted revealed the presence of NAADP-gated ion channel activity that could be attenuated by a TRPML1 polyclonal antibody in a

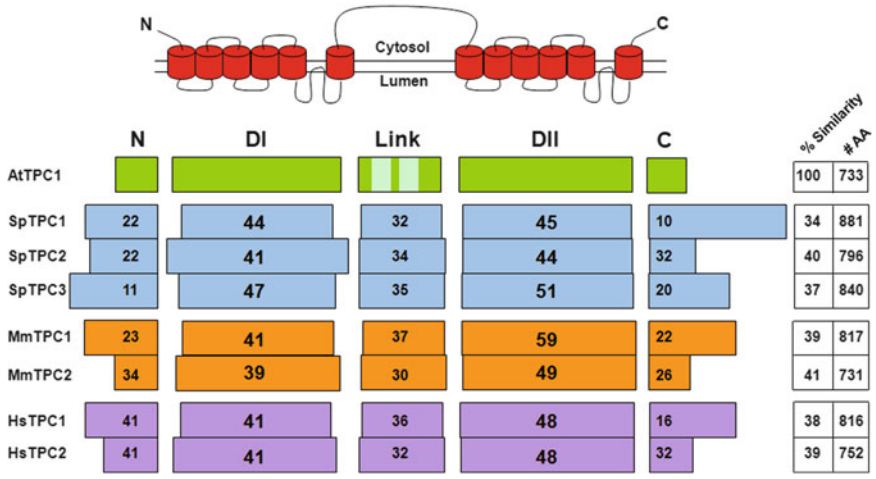

Fig. 14.1 Two-pore channels. *Top*, Schematic depiction of the two-pore channel highlighting the presence of a cytosolic N-terminus (N), two hydrophobic domains (DI and DII) each comprising six trans-membrane regions (*cylinders*) and a pore, a connecting cytosolic linker (Link) and a cytosolic C-terminus (C). *Bottom*, Percentage amino acid sequence similarity of the individual domains (*boxes*) within sea urchin (*blue*), mouse (*orange*) and human (*pink*) TPCs compared to plant TPCs (*green*). Boxes are scaled according to the number of residues. Note the presence of EF hands in plant TPCs. The overall percentage amino acid sequence similarity and the number of amino acids within each isoform is shown to the right. Abbreviations used; *At Arabidopsis thaliana*, *Sp Strongylocentrotus purpuratus*, *Mm Mus musculus*, *Hs Homo sapiens*

dose-dependent manner [82]. These most interesting findings, supported by TRPML1 knockdown studies [72], have yet to be independently verified and a recent study found no evidence for involvement of TRPML1 in NAADP action [83]. NAADP has also been shown to regulate TRPM2-mediated currents across the plasma membrane [84]. The specificity of this effect has been questioned given similar effects with NAAD which is unable to mobilize Ca^{2+} [85]. Nevertheless, in light of a possible lysosomal location of TRPM2 [86], it would be of major interest to determine whether NAADP can selectively mobilize lysosomal Ca^{2+} stores through TRPM2.

Plant TPCs Show the Way

The two-pore channel was first cloned from rat kidney by Ishibashi et al. in 2000 [87]. The channel had an estimated molecular weight of 94 kDa and comprised two homologous domains each consisting of six predicted trans-membrane regions with a putative pore between the fifth and sixth membrane spanning regions (Fig. 14.1). The structure was thus similar to voltage-gated Ca^{2+} and Na^{+} channels except that TPCs contained two as opposed to four repeated domains, leading to speculation that the two-pore channels may form dimers. However, no currents were recorded upon heterologous expression of rat TPCs in *Xenopus* oocytes [87]. The function of the animal TPCs was therefore unknown.

A year after publication describing the rat TPC, a plant TPC was cloned from *Arabidopsis* [88]. The protein had the same basic overall two-repeat structure as its rat homologue (Fig. 14.1). One difference in domain architecture was the presence of two putative EF hand Ca^{2+} binding domains in plant TPCs first noted for the rice protein [89]. Although several reports suggested a plasma membrane location for plant TPCs [88], in many cases, the conclusions relied on indirect methods such as yeast complementation assays. A re-examination by Peiter et al. however provided compelling evidence for location of plant TPC to the vacuole [90]. Moreover, using both overexpression and knockdown approaches, they showed that the plant TPC was a Ca^{2+} permeable channel and likely the molecular correlate of the well established "slow vacuolar" current [90]. Plant TPCs have now been implicated in a variety of cellular processes including stomatal movement [91].

The vacuole is the largest Ca^{2+} store in plant cells, with a typical luminal [Ca^{2+}] of 1.5–2.3 mM [92]. It is also acidic. The plant vacuole can therefore be classified as an acidic Ca^{2+} store [91, 93, 94]. The localisation of Ca^{2+}-permeable plant TPCs to vacuolar membranes, raised the possibility that animal TPCs may localize to the analogous lysosomes and thus serve as NAADP-mediated Ca^{2+} release channels.

The TPC Family in Animals

In contrast to plants which possess either one or two closely related TPC genes, there is evidence for both gene loss and multiplication in the animal kingdom. Animals can be classified as protostomes or deuterostomes according to whether the initial opening in the developing embryo forms the mouth or anus. Protostomes such as the flies and worms appear not to possess TPC genes [8, 95]. In contrast, gene duplication is evident in the deuterostome lineage with most animals possessing three TPC genes. These genes encode isoforms that display remarkably low sequence similarity (<40%) [7] compared to other intracellular channels such as inositol trisphosphate [5] and ryanodine [6] receptors (~70%). The three member family is present in sea urchins (basal deuterostomes), birds, frogs and most mammals [95]. It is intriguing in this context that we (humans) and rodents (rats and mice) appear to possess only two TPC genes that encode for proteins with molecular masses of ~94 kDa (TPC1) and ~85 kDa (TPC2). Ion channel genes are rarely degenerated in the primate lineage leading to humans. Loss of human TPC3 is a relatively recent event. Indeed, syntenic analysis of chromosomal regions equivalent to those in other mammals (such as dogs) that possess TPC3, revealed partial and degenerated sequences corresponding to human TPC3 [95]. Interestingly, the TPC3 pseudogene is abundantly expressed in a sequence tag cluster found in the reproductive organs, perhaps echoing an ancient functional role for TPC3 in these tissues [96]. Further analysis of genomes within other primates reveals that degeneration of TPC3 probably occurred ~25–40 Ma ago in the common ancestor of Apes and Old World monkeys [96]. Thus, TPC3 is likely functional in the closely related New World Monkeys and Prosimians. TPC3 is the first example of an intracellular ion channel subject to relaxed functional constraints [96].

2009: Animal TPCs as NAADP Targets – Initial Characterisation

It was within a short period in 2009 that three publications appeared demonstrating that animal TPCs were likely NAADP-sensitive Ca^{2+} channels. Our work [7] concentrated on TPC1 whereas Calcraft et al. [8] and Zong et al. [9] focussed primarily on TPC2.

Ishibashi et al. had already demonstrated by Northern blot analysis that transcripts for TPC1 were detectable in a range of rat tissues [87]. TPC1 expression in animal cells was confirmed by us using PCR in three NAADP-responsive cell types namely sea urchin eggs, rat PC12 cells and human SKBR3 cells (derived from a breast carcinoma) [7]. Quantitative analysis indicated that TPC1 was likely the major isoform. As anticipated, based on the localisation of plant TPC1 to the vacuole, both human TPC1 and TPC2 localized to the endo-lysosomal system when overexpressed in SKBR3 cells. Interestingly, TPC1 showed part colocalisation with both lysosomal and endosomal markers whereas TPC2 colocalized exclusively with a lysosomal marker. In SKBR3 cells loaded with fura-2 to measure cytosolic Ca^{2+} levels, microinjection of NAADP at a concentration that was sub-threshold in wild type cells evoked robust responses in cells over-expressing TPC1. These results provided molecular evidence that TPCs were indeed NAADP-sensitive Ca^{2+} channels. The responses were abolished by bafilomycin-A1 (consistent with the location of TPCs to acidic organelles) and also significantly inhibited by ryanodine (consistent with amplification by ER Ca^{2+} stores). Importantly, RNA interference of TPC1 diminished typical responses evoked by higher concentrations of NAADP in wild type cells thereby demonstrating the contribution of the endogenous TPC1 to NAADP-evoked Ca^{2+} signals. An alignment of amino acid sequences of the putative pore regions of TPCs identified a highly conserved leucine residue. Mutation of this residue (leucine 273) within the first domain of TPC1 to a helix-breaking proline eliminated the potentiating effects of TPC1 over-expression on NAADP-mediated Ca^{2+} signals. This mutant also diminished endogenous NAADP responses. The latter finding suggests the pore-mutant acts in a dominant-negative manner possibly by forming oligomers with endogenous TPCs (see below). Both gain and loss of function approaches thus provided evidence that TPC1 was an NAADP-sensitive Ca^{2+} channel [7].

Calcraft et al. [8] reported that similar to rat TPC1 [87], human TPC2 showed a wide tissue distribution. Subcellular localisation studies of both endogenous TPC2 in HEK cells and heterologously expressed TPC2 indicated a lysosomal distribution. The lysosomal location of TPC2 was further confirmed by subcellular fractionation. In contrast, heterologously expressed TPC1 and TPC3 (chicken) were shown to localize to endosomes although quantitative co-localization analysis suggested part localisation to lysosomes [8] similar to the distribution of TPC1 in SKBR3 cells [7]. Flash photolysis of caged NAADP in HEK293 cells over-expressing TPC2 revealed a remarkable biphasic Ca^{2+} response comprising a slow, low amplitude "pacemaker"-like response followed by an abrupt larger Ca^{2+} elevation that was not observed in wild type cells. Both phases were abolished by bafilomycin-A1 while

the inositol trisphosphate antagonist heparin only inhibited the larger second phase. Thus, in HEK cells TPC2 appears to evoke Ca^{2+} release from acidic organelles which is subsequently amplified by inositol trisphosphate receptors. The biphasic response to NAADP was also observed upon delivery of NAADP by a patch pipette. This analysis revealed the characteristic bell-shaped concentration-effect relationship for NAADP. The group also characterized Ca^{2+}-dependent electrical responses in mouse pancreatic β-cells upon whole-cell intracellular dialysis of NAADP. Whereas oscillatory responses were observed in wild type cells no such responses were observed in cells from TPC2 knockout mice. Thus, again both overexpression and knockdown studies were consistent with a role for TPCs in mediating NAADP-evoked Ca^{2+} release [8]. Radioligand binding studies also revealed enhanced binding in membranes from TPC2-overexpressing cells [8] although the effect of over-expression was modest and radioligand binding was not characterized in the TPC2 knock-out mice.

Zong et al. characterized the role of mouse TPCs in NAADP-mediated Ca^{2+} release [9]. Both TPC1 and TPC2 were found to be ubiquitously expressed in a range of tissues with a seemingly greater abundance of TPC1 mRNA transcripts. Subcellular localization of heterologously expressed TPC2 in HEK293 cells showed colocalization with a lysosomal marker but part ER localisation was also noted. Ca^{2+} transients in fura-2 loaded HEK cells were recorded upon whole cell patch dialysis of NAADP. The Ca^{2+} signals were substantially greater in TPC2-expressing cells. As in the study of Calcraft et al. [8], the group found that TPC2 expressing cells exhibited a bell-shaped concentration-effect relationship for NAADP-evoked Ca^{2+} release [9]. Moreover, NAADP-evoked Ca^{2+} signals were abolished by pre-treatment with bafilomycin-A1 again suggesting that Ca^{2+} release by TPC2 arises from acidic organelles. Zong et al. also found that heterologously expressed TPCs could form oligomers based on the results of co-immunoprecipitation. This finding offers a molecular basis for the dominant negative effect of a mutant TPC1 reported by Brailoiu et al. [7].

Thus, three independent groups were in overall agreement that TPCs were NAADP-sensitive Ca^{2+} channels. However, the studies threw up a few differences worthy of discussion. In our hands, TPC1-supported rapid global NAADP-evoked Ca^{2+} signals [7]. In contrast Calcraft reported highly localised Ca^{2+} transients in TPC1-expressing cells [8] and Zong et al. failed to record any responses [9]. Additionally in our hands, NAADP-evoked Ca^{2+} signals were rapid in onset peaking within a few seconds and therefore similar in kinetics to endogenous NAADP-evoked Ca^{2+} signals. In contrast Calcraft and Zong et al. reported Ca^{2+} transients that took >1 min to peak. The reason for these discrepancies is not clear at present. It has been suggested that microinjection of NAADP may induce mechanical artefacts thereby confounding our analysis [97]. It should be stressed however that microinjection of buffer alone in TPC-expressing cells does not evoke a significant Ca^{2+} signal [7], and that the similar sensitivity to TPC1 and TPC2 was achieved using cell permeable NAADP analogue [83]. Of note is a recent re-examination [98] of the sensitivity to NAADP, of TPC1-expressing cells used by Calcfraft et al. that reports global Ca^{2+} signals more comparable to ours.

Return to the Sea Urchin

Following the identification of mammalian TPCs as likely NAADP targets, attention turned to the sea urchin, in which NAADP-mediated Ca^{2+} release had been extensively characterized. Would the properties of endogenous NAADP-sensitive Ca^{2+} channels be recapitulated by sea urchin TPCs?

Brailoiu et al. characterised TPCs from the purple sea urchin, *Strongylocentrotus purpuratus*, (Sp) [95]. In a previous study, transcripts for SpTPCs had been detected in eggs and prism-stage embryos with notably higher levels of SpTPC3 in embryos suggesting that its expression was likely developmentally regulated [7]. The full length nucleotide sequences for all three isoforms were determined. The predicted molecular masses of the isoforms ranged from 92 to 101 kDa and sequence similarity between isoforms was typically low (30–40%) [95]. SpTPCs, when heterologously expressed in SKBR3 cells localised to acidic organelles as evidenced by colocalisation with LysoTracker Red. Additionally, SpTPC1 and SpTPC2 were shown to colocalise with their human orthologues when heterologously expressed. As with human TPCs, cytosolic Ca^{2+} responses to NAADP were substantially enhanced upon overexpression of all three isoforms. Moreover these responses were blocked by bafilomycin-A1. Thus as in sea urchin eggs, NAADP-evokes Ca^{2+} release from acidic organelles in cells expressing sea urchin TPCs [95].

An independent study by Ruas et al. [99] also reported the molecular cloning of SpTPCs. The sequence similarity between clones isolated by Ruas et al. [99] and Brailoiu et al. [95] were 97–100% – variation accountable by the high level of polymorphisms in sea urchins [100]. Heterologous expression of SpTPCs in HEK293 cells again suggested localization of TPCs to acidic organelles. Colocalization studies of TPCs with markers for lysosomes and recycling endosomes were ambiguous although subcellular fractionation of endogenous TPC2 and TPC3 in sea urchin eggs suggested differences in location. Heterologous localisation of the channels was also examined in starfish oocytes (not sea urchin for technical reasons) and shown to localise to puncta in the oocyte cortex, a region where the greatest sensitivity to NAADP had been demonstrated [40]. Similar to results obtained with human TPC2 [8], overexpression of both sea urchin TPC1 and TPC2 was associated with slow, biphasic Ca^{2+} responses to intracellular dialysis of NAADP in the whole-cell patch clamp configuration – effects that were abolished by bafilomycin-A1 treatment. However SpTPC3 appeared to be inactive and rather acted in a dominant negative manner. This result was in contrast to over-expression of an independent TPC3 clone in SKBR3 cells [95] due perhaps to polymorphic variation between the two. Importantly, immunoprecipitation of endogenous TPCs from sea urchin using anti-TPC antibodies to all three isoforms recovered NAADP binding sites [99]. Notably, the binding properties of SpTPC1 and SpTPC3 were similar to those characterized in egg preparations as NAADP bound with nanomolar affinity and dissociation of the ligand was sensitive to K^+. Thus, several properties of sea urchin TPCs (location, sensitivity to NAADP, pharmacology and binding characteristics), matched those reported for endogenous NAADP-sensitive Ca^{2+} channels a decade before [101]. These studies [95, 99] provided further evidence that TPCs were indeed NAADP targets.

Electrophysiology: The Gold Standard of Ion Channel Status

The three research groups that had initially identified TPCs as NAADP-mediated release channels published again in rapid succession to define the electrophysiological properties of TPCs. The intracellular location of TPCs to small vesicles represents a technical challenge in terms of accessibility for patch clamp analysis. The three groups employed different methodology, each with its own advantages and disadvantages (reviewed in [78]) to successfully circumvent these difficulties and provide biophysical insight in to TPCs.

Our collaborative study, took advantage of the ability to redirect human TPC2 to the plasma membrane by mutation of an endo-lysosomal targeting sequence (see below) thereby rendering the protein accessible to conventional patch-clamp recording [102]. In whole cell recordings, NAADP was shown to evoke currents using either symmetrical Cs^+ or Ca^{2+} as the charge carrier. Recordings from inside-out patches revealed rapid and reversible single channel activity (often manifest as "bursts") which could be blocked by the addition of the NAADP antagonist, *trans*-Ned-19. Interestingly the channel appeared to be largely voltage-insensitive. This was despite the presence of several basic residues within the fourth transmembrane regions of domains I and II, which confer voltage sensitivity in other channels. The unitary conductance was ~130 pS and 40 pS in the presence of symmetrical Cs^+ and Ca^{2+} solutions respectively. Importantly, the conductance of the channel could be significantly reduced by the mutation of a conserved leucine residue within the first putative pore region to a helix-breaking proline. This result indicates that TPC2 is the pore-forming subunit of the NAADP-activated cation channel [102].

Schieder et al. used a novel method to record NAADP-mediated currents through mouse TPC2 [103, 104]. In their approach, HEK293 cells over-expressing TPC2 were treated with vacuolin to enlarge the lysosomes. Isolated lysosomes were then attached to a <1 μm hole in a planar glass chip to enable "whole lysosome" recordings. NAADP-dependent currents (which they termed I_{NAADP}) were recorded at a low (60 nM) but not high (5 μM) concentration of NAADP, again indicative of self-inactivation [104]. Additionally, site-directed mutagenesis provided evidence that TPC2 is the pore-forming subunit. Thus, mutation of an asparagine residue with the first pore region substantially inhibited the currents. Moreover, the group identified an acidic residue within the second pore of TPC2 that is conserved in TRPV channels and shown previously to modulate cation selectivity. Mutation of this residue markedly decreased the permeability ratio of Ca^{2+} to K^+. These data suggest that this residue is key for the high level of selectivity for Ca^{2+} observed with TPC2.

Pitt et al. [105] reconstituted immunopurified human TPC2 into artificial lipid bilayers for electro-physiological analysis. Single channel activity in response to sub-micromolar concentrations NAADP were successfully recorded with either K^+ or Ca^{2+} as the permeant ion. The conductances were determined as ~300 pS and ~15 pS, respectively. Interestingly, the presence of luminal Ca^{2+} sensitized the channel to NAADP. NAADP was inactive at higher concentrations although interestingly such inactivation was only revealed in cumulative concentration-effect curves at low luminal pH.

Overall, the above three studies demonstrated that TPC2 was an NAADP-gated ion channel but as with Ca^{2+} release measurements there were some differences. The marked Ca^{2+} selectivity reported by Schieder et al. [104] was not observed by Pitt et al. [105]. Moreover, opposing effects of low luminal pH (corresponding to that within the lysosome) were reported by Schieder et al. (stimulatory) and Pitt et al. (inhibitory). Additionally, whereas channel activity was rapidly reversed upon washout of NAADP in our study [102], this was not the case at comparable neutral pH in the study by Pitt et al. [105]. The reasons for these discrepancies remain unknown but may well relate to the very different methodologies employed.

Structure-Function Analysis of TPCs

As mentioned previously, based on homology of TPCs to voltage-sensitive Ca^{2+} channels, TPCs were predicted to comprise two homologous domains each containing six trans-membrane regions (Fig. 14.1) [87]. Unbiased topology predictions using several algorithms however failed to reach consensus regarding the number and positions of the putative trans-membrane regions [106]. This promoted a series of experiments to address the topology of TPCs [106]. The use of fluorescence protease protection assays [107] showed that N and C termini of TPCs were cytosolic indicating an even number of transmembrane regions [106]. Additional analysis using truncated constructs placed residues 225 and 347 of TPC1 in the cytosol, and residue 628 in the lumen, consistent with a 12 transmembrane region model. Further, use of anti-TPC antibodies confirmed the cytosolic location of the C-termini and further defined residues 240–254 in TPC2 as luminal in accord with predicted position of this region prior the first putative pore.

TPCs had previously been shown to be glycoproteins based on their sensitivity to PNGase F treatment [8, 9]. This was confirmed by mutation of a cluster of predicted N-linked glycosylation sites in human TPC1 [106] and mouse TPC2 [9] prior to the second pore which abolished glycosylation thereby placing these sites within the lumen. N-glycosylation is known to regulate trafficking and activity of other ion channels such as K_v12.2 [108]. The N-glycosylation defective human TPC1 mutant was shown to traffic to the same intracellular compartments as wild-type TPC1 however NAADP-evoked Ca^{2+} signals were potentiated approximately two-fold in cells over-expressing the mutant compared to wild-type channel [106]. Glycosylation therefore seems to dampen NAADP-mediated Ca^{2+} release through TPCs, perhaps by inducing a conformational change in the channel or the influence of the negatively charged oligosaccharide chains on Ca^{2+} or H^+ interaction with the channel.

Many trans-membrane proteins are targeted to the endo-lysosomal system through dileucine motifs [109]. Vertebrate TPCs possess a conserved dileucine motif within the N-terminus. Deletion or mutation of this site in TPC2 resulted in its re-direction to the plasma membrane thereby providing evidence that this motif is responsible for targeting TPC2 to the endo-lysosomal system [102]. Intriguingly, NAADP-evoked Ca^{2+} signals were still resolvable in cells expressing plasma

membrane TPC2. However, the properties of the Ca^{2+} signal differed markedly compared to wild-type TPC2. Thus, NAADP-evoked Ca^{2+} signals in cells expressing wild-type TPC2 were blocked by both bafilomycin-A1 and ryanodine, similar to cells expressing TPC1 and consistent with the functional coupling of acidic and ER Ca^{2+} stores. In contrast, NAADP-evoked Ca^{2+} signals in cells expressing plasma-membrane targeted TPC2 were largely insensitive to bafilomycin-A1 and ryanodine, much slower in onset, and completely abolished be removal of external Ca^{2+}. Thus, redirecting TPC2 to the plasma membrane effectively dissociated NAADP-evoked Ca^{2+} release from subsequent amplification by the ER converting TPC2 into a Ca^{2+} influx channel. In essence, the recorded Ca^{2+} signal represents a "trigger" release event (albeit stemming from the extracellular space) that is unpolluted from ER Ca^{2+} release. Lack of amplification perhaps explains the slower kinetics relative to the wild type channel. These findings underscore the importance of the location of TPC2 in coupling to ER Ca^{2+} release in the generation of global Ca^{2+} signals [102].

Coming Full Circle: Physiological Roles for TPCs

In light of the identification of the TPCs as the molecular target of NAADP, three recent studies have examined the role of TPCs in physiological effects in which NAADP had been previously implicated.

Tugba Durlu-Kandilci et al. examined the role of TPC2 in smooth muscle contraction [70]. As mentioned previously, a role for NAADP in mediating contraction of smooth muscle had been reported in several preparations (Table 14.1). Accordingly, NAADP-evoked contractions were abolished in detrusor smooth muscle from TPC2 knock-out mice [70]. Interestingly, agonist-evoked contractions became insensitive to depletion of acidic stores although the amplitudes were not markedly reduced compared to muscle from wild-type animals. These data suggests that TPC2 contributes to agonist-evoked contractions [70] but that perhaps there has been compensation in the transgenic animals to maintain agonist-evoked contractions in the absence of TPC2 [110].

Aley et al. examined the role of TPC1 and TPC2 in differentiation of skeletal muscle [71]. Previous studies had demonstrated a messenger-specific role for NAADP in differentiation of PC12 cells [56]. In accord, cell permeable NAADP-AM was found to be capable of stimulating early- and late-stage differentiation of C2C12 cells in a Ned-19-sensitive manner [71]. Importantly, siRNA downregulation of either TPC1 or TPC2 was manifested as a decrease in differentiation index score. These studies highlight an important role for both TPC1 and TPC2 in differentiation.

Finally, a recent study has provided evidence that in endothelial cells, histamine is an NAADP-linked agonist coupled to the secretion of von Willebrand factor [64]. Prior studies had implicated NAADP in the response to activation of endothelial cells by acetylcholine [63]. Combined knock down of TPC1 and TPC2 by siRNA was found to inhibit histamine-induced von Willebrand factor secretion thus providing

further molecular evidence for a role for TPCs in a down-stream Ca^{2+}-dependent event [64]. The relative role of TPC isoforms in this response however was not examined.

A potential physiological role for the TPCs in pigmentation also emerged independently before the identification of TPCs as NAADP-sensitive Ca^{2+}-release channels [111]. A genome-wide association study identified two non-synonymous mutations within the human TPC2 gene that associated with blond versus brown hair colour [111]. A link between Ca^{2+} homeostasis and pigmentation had previously been proposed when a polymorphism in the potassium-dependent sodium-Ca^{2+} exchanger SLC24A5 was correlated to light skin pigmentation [112]. How Ca^{2+} regulates pigmentation is not known but it is possible that TPC2 and SLC24A5 may control Ca^{2+} flux across the melanosome – a lysosome-related organelle. This may in turn regulate pigment synthesis perhaps directly or indirectly through changes in luminal pH. Alternatively Ca^{2+} fluxes may regulate trafficking within the endo-lysosomal system. Indeed, a role for Ca^{2+} in vesicle fusion through an unidentified mechanism had been appreciated for some time [113], and it is notable that over-expression of TPCs disrupts retrograde trafficking from the plasma membrane to the Golgi [99]. A recent study has also indicated a role for local NAADP-mediated Ca^{2+} signals via TPC2 in regulating autophagy [57]. Thus, several functions of the endo-lysosomal system likely involve TPCs.

Concluding Remarks and Future Directions

NAADP was first described as a Ca^{2+}-mobilising molecule in 1995 [17]. The cloning of the first animal TPC followed 5 years later [87] but it was nearly a decade before the two were linked [7–9]. Since the initial identification of TPCs as NAADP targets in 2009, the pace of progress in the field has been impressive. Much however remains to be learned! Further localisation studies particularly of endogenous TPCs are required to pinpoint their subcellular distribution within the endo-lysosomal system which in turn may inform of their function. Why the sensitivity to NAADP of the various TPC isoforms (in particular TPC3) and the spatio-temporal nature of the resulting NAADP-mediated Ca^{2+} signals differs between labs is not clear and worthy of further investigation. The basic topology of the channel has been defined and we are beginning to identify residues important for targeting, conductance and regulation. More work however is required to clarify the effects of luminal pH and Ca^{2+} on TPCs and relating these effects to the primary sequence. Another area of investigation relates to the quaternary structure of TPCs which at present is unknown. If viewed as an intermediate between one-repeat and four-repeat channels, then it is possible that TPCs form dimers but experimental evidence to support this is currently lacking. Also many ion channels exist in protein complexes. Voltage-gated Ca^{2+} channels for example comprise the alpha (pore-forming) subunit and several tightly associated regulatory subunits such as the β-subunit [114]. It is therefore not unreasonable to suppose that TPCs might represent the pore-forming subunit of a

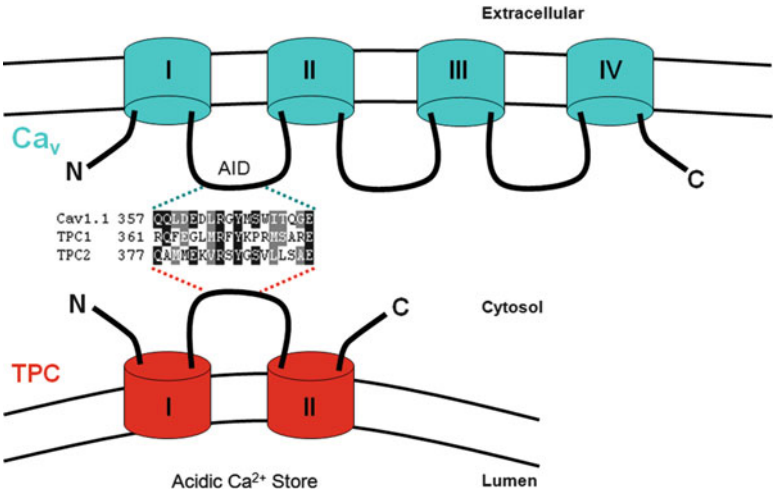

Fig. 14.2 A putative protein-protein interaction site in TPCs. Schematic depiction of voltage-sensitive Ca^{2+} channels (Ca_v) highlighting the AID domain within the cytosolic linker connecting domains I and II. Note sequence similarity (*middle*) between this domain and the equivalent region within human TPCs (*bottom*)

similar channel complex. Interestingly, the α subunit in voltage-sensitive Ca^{2+} channels interacts with β-subunits via the α1-interaction domain (AID) within the linker region connecting the first two domains [115]. We note here a surprising degree of sequence similarity between the AID and a similarly situated region within the cytosolic loop connecting the two domains in TPCs (Fig. 14.2). This perhaps indicates a site of interaction with an accessory protein or more radically the possibility that β-subunits of voltage-sensitive Ca^{2+} channels are more promiscuous than thought. Defining the TPC interactome is therefore of major importance, since this will more than likely provide new insight in to their regulation. This is underscored by the increasing range of physiological processes in which TPCs are directly implicated. With the tight functional coupling of NAADP-mediated Ca^{2+} release and Ca^{2+} release from the ER, it is likely that this list will grow. Perhaps functional roles for TPCs will emerge that are independent of ER Ca^{2+} release. It is notable that mutation of TRPML1, another endo-lysosomal ion channel results in pathology [116]. Thus it is conceivable that diseases may be identified due to aberrant TPC function particularly given their widespread distribution. Interest in these channels is thus likely to grow.

Acknowledgements The authors wish to thank Chi Li and Taufiq Rahman for useful discussion and the BBSRC for supporting their research (BB/G013721/1).

References

1. Berridge MJ, Lipp P, Bootman MD (2000) The versatility and universality of calcium signalling. Nat Rev Mol Cell Biol 1:11–21
2. Patel S, Churchill GC, Galione A (2001) Coordination of Ca^{2+} signalling by NAADP. Trends Biochem Sci 26:482–489
3. Lee HC (1997) Mechanisms of calcium signaling by cyclic ADP-ribose and NAADP. Physiol Rev 77:1133–1164
4. Guse AH, Lee HC (2008) NAADP: a universal Ca^{2+} trigger. Sci Signal 1:re10
5. Patel S, Joseph SK, Thomas AP (1999) Molecular properties of inositol 1,4,5-trisphosphate receptors. Cell Calcium 25:247–264
6. Fill M, Copello JA (2002) Ryanodine receptor calcium release channels. Physiol Rev 82:893–922
7. Brailoiu E, Churamani D, Cai X, Schrlau MG, Brailoiu GC, Gao X, Hooper R, Boulware MJ, Dun NJ, Marchant JS, Patel S (2009) Essential requirement for two-pore channel 1 in NAADP-mediated calcium signaling. J Cell Biol 186:201–209
8. Calcraft PJ, Ruas M, Pan Z, Cheng X, Arredouani A, Hao X, Tang J, Rietdorf K, Teboul L, Chuang KT, Lin P, Xiao R, Wang C, Zhu Y, Lin Y, Wyatt CN, Parrington J, Ma J, Evans AM, Galione A, Zhu MX (2009) NAADP mobilizes calcium from acidic organelles through two-pore channels. Nature 459:596–600
9. Zong X, Schieder M, Cuny H, Fenske S, Gruner C, Rotzer K, Griesbeck O, Harz H, Biel M, Wahl-Schott C (2009) The two-pore channel TPCN2 mediates NAADP-dependent Ca^{2+}-release from lysosomal stores. Pflugers Arch 458:891–899
10. Clapper DL, Lee HC (1985) Inositol trisphosphate induces calcium release from nonmitochondrial stores in sea urchin egg homogenates. J Biol Chem 260:13947–13954
11. Clapper DL, Walseth TF, Dargie PJ, Lee HC (1987) Pyridine nucleotide metabolites stimulate calcium release from sea urchin egg microsomes desensitized to inositol trisphosphate. J Biol Chem 262:9561–9568
12. Lee HC, Walseth TF, Bratt GT, Hayes RN, Clapper DL (1989) Structural determination of a cyclic metabolite of NAD^+ with intracellular Ca^{2+}-mobilizing activity. J Biol Chem 264:1608–1615
13. Lee HC, Aarhus R (1991) ADP-ribosyl cyclase: an enzyme that cyclizes NAD^+ into a calcium-mobilizing metabolite. Cell Regul 2:203–209
14. Churamani D, Boulware MJ, Geach TJ, Martin AC, Moy GW, Su YH, Vacquier VD, Marchant JS, Dale L, Patel S (2007) Molecular characterization of a novel intracellular ADP-ribosyl cyclase. PLoS One 2:e797
15. Davis LC, Morgan AJ, Ruas M, Wong JL, Graeff RM, Poustka AJ, Lee HC, Wessel GM, Parrington J, Galione A (2008) Ca^{2+} signaling occurs via second messenger release from intraorganelle synthesis sites. Curr Biol 18:1612–1618
16. Ramakrishnan L, Muller-Steffner H, Bosc C, Vacquier VD, Schuber F, Moutin MJ, Dale L, Patel S (2010) A single residue in a novel ADP-ribosyl cyclase controls production of the calcium-mobilizing messengers cyclic ADP-ribose and nicotinic acid adenine dinucleotide phosphate. J Biol Chem 285:19900–19909
17. Lee HC, Aarhus R (1995) A derivative of NADP mobilizes calcium stores insensitive to inositol trisphosphate and cyclic ADP-ribose. J Biol Chem 270:2152–2157
18. Chini EN, Dousa TP (1996) Nicotinate-adenine dinucleotide phosphate-induced Ca^{2+}-release does not behave as a Ca^{2+}-induced Ca^{2+}-release system. Biochem J 316(Pt 3):709–711
19. Aarhus R, Dickey DM, Graeff RM, Gee KR, Walseth TF, Lee HC (1996) Activation and inactivation of Ca^{2+} release by NAADP+. J Biol Chem 271:8513–8516
20. Genazzani AA, Empson RM, Galione A (1996) Unique inactivation properties of NAADP-sensitive Ca^{2+} release. J Biol Chem 271:11599–11602
21. Lee HC, Aarhus R (2000) Functional visualization of the separate but interacting calcium stores sensitive to NAADP and cyclic ADP-ribose. J Cell Sci 113(Pt 24):4413–4420

22. Genazzani AA, Galione A (1996) Nicotinic acid-adenine dinucleotide phosphate mobilizes Ca^{2+} from a thapsigargin-insensitive pool. Biochem J 315(Pt 3):721–725
23. Thastrup O, Cullen PJ, Drobak BK, Hanley MR, Dawson AP (1990) Thapsigargin, a tumor promoter, discharges intracellular Ca^{2+} stores by specific inhibition of the endoplasmic reticulum Ca^{2+}-ATPase. Proc Natl Acad Sci USA 87:2466–2470
24. Churchill GC, Okada Y, Thomas JM, Genazzani AA, Patel S, Galione A (2002) NAADP mobilizes Ca^{2+} from reserve granules, lysosome-related organelles, in sea urchin eggs. Cell 111:703–708
25. Jadot M, Colmant C, Wattiaux-De CS, Wattiaux R (1984) Intralysosomal hydrolysis of glycyl-L-phenylalanine 2-naphthylamide. Biochem J 219:965–970
26. Bowman EJ, Siebers A, Altendorf K (1988) Bafilomycins: a class of inhibitors of membrane ATPases from microorganisms, animal cells, and plant cells. Proc Natl Acad Sci USA 85:7972–7976
27. Docampo R, Moreno SN (1999) Acidocalcisome: A novel Ca^{2+} storage compartment in trypanosomatids and apicomplexan parasites. Parasitol Today 15:443–448
28. Churchill GC, Galione A (2000) Spatial control of Ca^{2+} signaling by nicotinic acid adenine dinucleotide phosphate diffusion and gradients. J Biol Chem 275:38687–38692
29. Churchill GC, Galione A (2001) NAADP induces Ca^{2+} oscillations via a two-pool mechanism by priming IP3- and cADPR-sensitive Ca^{2+} stores. EMBO J 20:2666–2671
30. Patel S, Churchill GC, Galione A (2000) Unique kinetics of nicotinic acid-adenine dinucleotide phosphate (NAADP) binding enhance the sensitivity of NAADP receptors for their ligand. Biochem J 352(Pt 3):725–729
31. Billington RA, Genazzani AA (2000) Characterization of NAADP(+) binding in sea urchin eggs. Biochem Biophys Res Commun 276:112–116
32. Patel S, Churchill GC, Sharp T, Galione A (2000) Widespread distribution of binding sites for the novel Ca^{2+}-mobilizing messenger, nicotinic acid adenine dinucleotide phosphate, in the brain. J Biol Chem 275:36495–36497
33. Lee HC, Aarhus R (1997) Structural determinants of nicotinic acid adenine dinucleotide phosphate important for its calcium-mobilizing activity. J Biol Chem 272:20378–20383
34. Churamani D, Dickinson GD, Patel S (2005) NAADP binding to its target protein in sea urchin eggs requires phospholipids. Biochem J 386:497–504
35. Dickinson GD, Patel S (2003) Modulation of NAADP (nicotinic acid-adenine dinucleotide phosphate) receptors by K^+ ions: evidence for multiple NAADP receptor conformations. Biochem J 375:805–812
36. Naylor E, Arredouani A, Vasudevan SR, Lewis AM, Parkesh R, Mizote A, Rosen D, Thomas JM, Izumi M, Ganesan A, Galione A, Churchill GC (2009) Identification of a chemical probe for NAADP by virtual screening. Nat Chem Biol 5:220–226
37. Rosen D, Lewis AM, Mizote A, Thomas JM, Aley PK, Vasudevan SR, Parkesh R, Galione A, Izumi M, Ganesan A, Churchill GC (2009) Analogues of the NAADP antagonist NED-19 indicate two binding sites on the NAADP receptor. J Biol Chem 284(50):34930–34934
38. Berridge G, Dickinson G, Parrington J, Galione A, Patel S (2002) Solubilization of receptors for the novel Ca^{2+}-mobilizing messenger, nicotinic acid adenine dinucleotide phosphate. J Biol Chem 277:43717–43723
39. Churamani D, Dickinson GD, Ziegler M, Patel S (2006) Time sensing by NAADP receptors. Biochem J 397:313–320
40. Santella L, Kyozuka K, Genazzani AA, De RL, Carafoli E (2000) Nicotinic acid adenine dinucleotide phosphate-induced Ca^{2+} release. Interactions among distinct Ca^{2+} mobilizing mechanisms in starfish oocytes. J Biol Chem 275:8301–8306
41. Albrieux M, Lee HC, Villaz M (1998) Calcium signaling by cyclic ADP-ribose, NAADP, and inositol trisphosphate are involved in distinct functions in ascidian oocytes. J Biol Chem 273:14566–14574
42. Chameau P, Van de Vrede Y, Fossier P, Baux G (2001) Ryanodine-, IP3- and NAADP-dependent calcium stores control acetylcholine release. Pflugers Arch 443:289–296

43. Brailoiu E, Miyamoto MD, Dun NJ (2001) Nicotinic acid adenine dinucleotide phosphate enhances quantal neurosecretion at the frog neuromuscular junction: possible action on synaptic vesicles in the releasable pool. Mol Pharmacol 60:718–724
44. Berg I, Potter BV, Mayr GW, Guse AH (2000) Nicotinic acid adenine dinucleotide phosphate (NAADP(+)) is an essential regulator of T-lymphocyte Ca^{2+}-signaling. J Cell Biol 150:581–588
45. Cancela JM, Churchill GC, Galione A (1999) Coordination of agonist-induced Ca^{2+}-signalling patterns by NAADP in pancreatic acinar cells. Nature 398:74–76
46. Churamani D, Carrey EA, Dickinson GD, Patel S (2004) Determination of cellular nicotinic acid-adenine dinucleotide phosphate (NAADP) levels. Biochem J 380:449–454
47. Lewis AM, Masgrau R, Vasudevan SR, Yamasaki M, O'Neill JS, Garnham C, James K, Macdonald A, Ziegler M, Galione A, Churchill GC (2007) Refinement of a radioreceptor binding assay for nicotinic acid adenine dinucleotide phosphate. Anal Biochem 371:26–36
48. Galione A, Morgan AJ, Arredouani A, Davis LC, Rietdorf K, Ruas M, Parrington J (2010) NAADP as an intracellular messenger regulating lysosomal calcium-release channels. Biochem Soc Trans 38:1424–1431
49. Moccia F, Lim D, Kyozuka K, Santella L (2004) NAADP triggers the fertilization potential in starfish oocytes. Cell Calcium 36:515–524
50. Churchill GC, O'Neill JS, Masgrau R, Patel S, Thomas JM, Genazzani AA, Galione A (2003) Sperm deliver a new second messenger: NAADP. Curr Biol 13:125–128
51. Morgan AJ, Galione A (2007) Fertilization and nicotinic acid adenine dinucleotide phosphate induce pH changes in acidic Ca^{2+} stores in sea urchin eggs. J Biol Chem 282: 37730–37737
52. Hwang GS, Jian CY, Chen TJ, Chen ST, Wang SW (2009) Effects of hypoxia on testosterone release in rat Leydig cells. Am J Physiol Endocrinol Metab 297:1039–1045
53. Aley PK, Noh HJ, Gao X, Tica AA, Brailoiu E, Churchill GC (2010) A functional role for nicotinic acid adenine dinucleotide phosphate in oxytocin-mediated contraction of uterine smooth muscle from rat. J Pharmacol Exp Ther 333:726–735
54. Brailoiu E, Patel S, Dun NJ (2003) Modulation of spontaneous transmitter release from the frog neuromuscular junction by interacting intracellular Ca^{2+} stores: critical role for nicotinic acid-adenine dinucleotide phosphate (NAADP). Biochem J 373:313–318
55. Brailoiu E, Hoard JL, Filipeanu CM, Brailoiu GC, Dun SL, Patel S, Dun NJ (2005) Nicotinic acid adenine dinucleotide phosphate potentiates neurite outgrowth. J Biol Chem 280: 5646–5650
56. Brailoiu E, Churamani D, Pandey V, Brailoiu GC, Tuluc F, Patel S, Dun NJ (2006) Messenger-specific role for nicotinic acid adenine dinucleotide phosphate in neuronal differentiation. J Biol Chem 281:15923–15928
57. Pereira GJ, Hirata H, Fimia GM, do Carmo LG, Bincoletto C, Han SW, Stilhano RS, Ureshino RP, Bloor-Young D, Churchill G, Piacentini M, Patel S, Smaili SS (2011) Nicotinic acid adenine dinucleotide phosphate (NAADP) regulates autophagy in cultured astrocytes. J Biol Chem 286(32):27875–27881
58. Brailoiu GC, Brailoiu E, Parkesh R, Galione A, Churchill GC, Patel S, Dun NJ (2009) NAADP-mediated channel 'chatter' in neurons of the rat medulla oblongata. Biochem J 419:91–97, 2
59. Mushtaq M, Nam TS, Kim UH (2011) Critical role for CD38-mediated Ca^{2+} signaling in thrombin-induced procoagulant activity of mouse platelets and hemostasis. J Biol Chem 286:12952–12958
60. Macgregor A, Yamasaki M, Rakovic S, Sanders L, Parkesh R, Churchill GC, Galione A, Terrar DA (2007) NAADP controls cross-talk between distinct Ca^{2+} stores in the heart. J Biol Chem 282:15302–15311
61. Zhang F, Zhang G, Zhang AY, Koeberl MJ, Wallander E, Li PL (2006) Production of NAADP and its role in Ca^{2+} mobilization associated with lysosomes in coronary arterial myocytes. Am J Physiol Heart Circ Physiol 291:H274–H282

62. Boittin FX, Galione A, Evans AM (2002) Nicotinic acid adenine dinucleotide phosphate mediates Ca^{2+} signals and contraction in arterial smooth muscle via a two-pool mechanism. Circ Res 91:1168–1175
63. Brailoiu GC, Gurzu B, Gao X, Parkesh R, Aley PK, Trifa DI, Galione A, Dun NJ, Madesh M, Patel S, Churchill GC, Brailoiu E (2010) Acidic NAADP-sensitive calcium stores in the endothelium: agonist-specific recruitment and role in regulating blood pressure. J Biol Chem 285:37133–37137
64. Esposito B, Gambara G, Lewis AM, Palombi F, D'Alessio A, Taylor LX, Genazzani AA, Ziparo E, Galione A, Churchill GC, Filippini A (2011) NAADP links histamine H1 receptors to secretion of von Willebrand factor in human endothelial cells. Blood 117:4968–4977
65. Dammermann W, Zhang B, Nebel M, Cordiglieri C, Odoardi F, Kirchberger T, Kawakami N, Dowden J, Schmid F, Dornmair K, Hohenegger M, Flugel A, Guse AH, Potter BV (2009) NAADP-mediated Ca^{2+} signaling via type 1 ryanodine receptor in T cells revealed by a synthetic NAADP antagonist. Proc Natl Acad Sci USA 106:10678–10683
66. Cordiglieri C, Odoardi F, Zhang B, Nebel M, Kawakami N, Klinkert WE, Lodygin D, Luhder F, Breunig E, Schild D, Ulaganathan VK, Dornmair K, Dammermann W, Potter BV, Guse AH, Flugel A (2010) Nicotinic acid adenine dinucleotide phosphate-mediated calcium signalling in effector T cells regulates autoimmunity of the central nervous system. Brain 133:1930–1943
67. Rah SY, Mushtaq M, Nam TS, Kim SH, Kim UH (2010) Generation of cyclic ADP-ribose and nicotinic acid adenine dinucleotide phosphate by CD38 for Ca^{2+} signaling in interleukin-8-treated lymphokine-activated killer cells. J Biol Chem 285:21877–21887
68. Kim BJ, Park KH, Yim CY, Takasawa S, Okamoto H, Im MJ, Kim UH (2008) Generation of nicotinic acid adenine dinucleotide phosphate and cyclic ADP-ribose by glucagon-like peptide-1 evokes Ca^{2+} signal that is essential for insulin secretion in mouse pancreatic islets. Diabetes 57:868–878
69. Alejandro EU, Kalynyak TB, Taghizadeh F, Gwiazda KS, Rawstron EK, Jacob KJ, Johnson JD (2010) Acute insulin signaling in pancreatic beta-cells is mediated by multiple Raf-1 dependent pathways. Endocrinology 151:502–512
70. Durlu-Kandilci NT, Ruas M, Chuang KT, Brading A, Parrington J, Galione A (2010) TPC2 proteins mediate nicotinic acid adenine dinucleotide phosphate (NAADP)- and agonist-evoked contractions of smooth muscle. J Biol Chem 285:24925–24932
71. Aley PK, Mikolajczyk AM, Munz B, Churchill GC, Galione A, Berger F (2010) Nicotinic acid adenine dinucleotide phosphate regulates skeletal muscle differentiation via action at two-pore channels. Proc Natl Acad Sci USA 107:19927–19932
72. Zhang F, Xu M, Han WQ, Li PL (2011) Reconstitution of lysosomal NAADP-TRP-ML1 signaling pathway and its function in TRP-ML1$^{-/-}$ cells. Am J Physiol Cell Physiol 301(2):C421–C430
73. Mojzisova A, Krizanova O, Zacikova L, Kominkova V, Ondrias K (2001) Effect of nicotinic acid adenine dinucleotide phosphate on ryanodine calcium release channel in heart. Pflugers Arch 441:674–677
74. Hohenegger M, Suko J, Gscheidlinger R, Drobny H, Zidar A (2002) Nicotinic acid-adenine dinucleotide phosphate activates the skeletal muscle ryanodine receptor. Biochem J 367:423–431
75. Gerasimenko JV, Maruyama Y, Yano K, Dolman NJ, Tepikin AV, Petersen OH, Gerasimenko OV (2003) NAADP mobilizes Ca^{2+} from a thapsigargin-sensitive store in the nuclear envelope by activating ryanodine receptors. J Cell Biol 163:271–282
76. Steen M, Kirchberger T, Guse AH (2007) NAADP mobilizes calcium from the endoplasmic reticular Ca^{2+} store in T-lymphocytes. J Biol Chem 282:18864–18871
77. Copello JA, Qi Y, Jeyakumar LH, Ogunbunmi E, Fleischer S (2001) Lack of effect of cADP-ribose and NAADP on the activity of skeletal muscle and heart ryanodine receptors. Cell Calcium 30:269–284
78. Patel S, Marchant JS, Brailoiu E (2010) Two-pore channels: regulation by NAADP and customized roles in triggering calcium signals. Cell Calcium 47:480–490

79. Kinnear NP, Wyatt CN, Clark JH, Calcraft PJ, Fleischer S, Jeyakumar LH, Nixon GF, Evans AM (2008) Lysosomes co-localize with ryanodine receptor subtype 3 to form a trigger zone for calcium signalling by NAADP in rat pulmonary arterial smooth muscle. Cell Calcium 44:190–201
80. Patel S, Brailoiu E (2011) Triggering of Ca^{2+} signals by NAADP-gated two-pore channels. A role for membrane contact sites? Biochem Soc Trans 40:153–157
81. Zhang F, Jin S, Yi F, Li PL (2009) TRP-ML1 functions as a lysosomal NAADP-sensitive Ca^{2+} release channel in coronary arterial myocytes. J Cell Mol Med 13(9B):3174–3185
82. Zhang F, Li PL (2007) Reconstitution and characterization of a nicotinic acid adenine dinucleotide phosphate (NAADP)-sensitive Ca^{2+} release channel from liver lysosomes of rats. J Biol Chem 282:25259–25269
83. Yamaguchi S, Jha A, Li Q, Soyombo AA, Dickinson GD, Churamani D, Brailoiu E, Patel S, Muallem S (2011) Transient receptor potential mucolipin 1 (TRPML1) and Two-pore channels Are functionally independent organellar Ion channels. J Biol Chem 286:22934–22942
84. Lange I, Penner R, Fleig A, Beck A (2008) Synergistic regulation of endogenous TRPM2 channels by adenine dinucleotides in primary human neutrophils. Cell Calcium 44:604–615
85. Toth B, Csanady L (2010) Identification of direct and indirect effectors of the transient receptor potential melastatin 2 (TRPM2) cation channel. J Biol Chem 285:30091–30102
86. Lange I, Yamamoto S, Partida-Sanchez S, Mori Y, Fleig A, Penner R (2009) TRPM2 functions as a lysosomal Ca^{2+}-release channel in beta cells. Sci Signal 2:ra23
87. Ishibashi K, Suzuki M, Imai M (2000) Molecular cloning of a novel form (two-repeat) protein related to voltage-gated sodium and calcium channels. Biochem Biophys Res Commun 270:370–376
88. Furuichi T, Cunningham KW, Muto S (2001) A putative two pore channel AtTPC1 mediates Ca^{2+} flux in Arabidopsis leaf cells. Plant Cell Physiol 42:900–905
89. Hashimoto K, Saito M, Matsuoka H, Iida K, Iida H (2004) Functional analysis of a rice putative voltage-dependent Ca^{2+} channel, OsTPC1, expressed in yeast cells lacking its homologous gene CCH1. Plant Cell Physiol 45:496–500
90. Peiter E, Maathuis FJ, Mills LN, Knight H, Pelloux J, Hetherington AM, Sanders D (2005) The vacuolar Ca^{2+}-activated channel TPC1 regulates germination and stomatal movement. Nature 434:404–408
91. Peiter E (2011) The plant vacuole: emitter and receiver of calcium signals. Cell Calcium 50(2):120–128
92. Pottosin II, Schonknecht G (2007) Vacuolar calcium channels. J Exp Bot 58:1559–1569
93. Patel S, Docampo R (2010) Acidic calcium stores open for business: expanding the potential for intracellular Ca^{2+} signaling. Trends Cell Biol 20:277–286
94. Patel S, Muallem S (2011) Acidic Ca^{2+} stores come to the fore. Cell Calcium 50(2):109–112
95. Brailoiu E, Hooper R, Cai X, Brailoiu GC, Keebler MV, Dun NJ, Marchant JS, Patel S (2010) An ancestral deuterostome family of two-pore channels mediates nicotinic acid adenine dinucleotide phosphate-dependent calcium release from acidic organelles. J Biol Chem 285:2897–2901
96. Cai X, Patel S (2010) Degeneration of an intracellular ion channel in the primate lineage by relaxation of selective constraints. Mol Biol Evol 27:2352–2359
97. Zhu MX, Ma J, Parrington J, Galione A, Evans AM (2010) TPCs: endolysosomal channels for Ca^{2+} mobilization from acidic organelles triggered by NAADP. FEBS Lett 584:1966–1974
98. Ogunbayo OA, Zhu Y, Rossi D, Sorrentino V, Ma J, Zhu MX, Evans AM (2011) Cyclic adenosine diphosphate ribose activates ryanodine receptors, whereas NAADP activates two-pore domain channels. J Biol Chem 286:9136–9140
99. Ruas M, Rietdorf K, Arredouani A, Davis LC, Lloyd-Evans E, Koegel H, Funnell TM, Morgan AJ, Ward JA, Watanabe K, Cheng X, Churchill GC, Zhu MX, Platt FM, Wessel GM, Parrington J, Galione A (2010) Purified TPC isoforms form NAADP receptors with distinct roles for Ca^{2+} signaling and endolysosomal trafficking. Curr Biol 20(8):703–709
100. Sodergren E, Weinstock GM, Davidson EH, Cameron RA, Gibbs RA, Angerer RC, Angerer LM, Arnone MI, Burgess DR, Burke RD, Coffman JA, Dean M, Elphick MR, Ettensohn CA, Foltz KR, Hamdoun A, Hynes RO, Klein WH, Marzluff W, McClay DR, Morris RL,

Mushegian A, Rast JP, Smith LC, Thorndyke MC, Vacquier VD, Wessel GM, Wray G, Zhang L, Elsik CG, Ermolaeva O, Hlavina W, Hofmann G, Kitts P, Landrum MJ, Mackey AJ, Maglott D, Panopoulou G, Poustka AJ, Pruitt K, Sapojnikov V, Song X, Souvorov A, Solovyev V, Wei Z, Whittaker CA, Worley K, Durbin KJ, Shen Y, Fedrigo O, Garfield D, Haygood R, Primus A, Satija R, Severson T, Gonzalez-Garay ML, Jackson AR, Milosavljevic A, Tong M, Killian CE, Livingston BT, Wilt FH, Adams N, Belle R, Carbonneau S, Cheung R, Cormier P, Cosson B, Croce J, Fernandez-Guerra A, Geneviere AM, Goel M, Kelkar H, Morales J, Mulner-Lorillon O, Robertson AJ, Goldstone JV, Cole B, Epel D, Gold B, Hahn ME, Howard-Ashby M, Scally M, Stegeman JJ, Allgood EL, Cool J, Judkins KM, McCafferty SS, Musante AM, Obar RA, Rawson AP, Rossetti BJ, Gibbons IR, Hoffman MP, Leone A, Istrail S, Materna SC, Samanta MP, Stolc V, Tongprasit W, Tu Q, Bergeron KF, Brandhorst BP, Whittle J, Berney K, Bottjer DJ, Calestani C, Peterson K, Chow E, Yuan QA, Elhaik E, Graur D, Reese JT, Bosdet I, Heesun S, Marra MA, Schein J, Anderson MK, Brockton V, Buckley KM, Cohen AH, Fugmann SD, Hibino T, Loza-Coll M, Majeske AJ, Messier C, Nair SV, Pancer Z, Terwilliger DP, Agca C, Arboleda E, Chen N, Churcher AM, Hallbook F, Humphrey GW, Idris MM, Kiyama T, Liang S, Mellott D, Mu X, Murray G, Olinski RP, Raible F, Rowe M, Taylor JS, Tessmar-Raible K, Wang D, Wilson KH, Yaguchi S, Gaasterland T, Galindo BE, Gunaratne HJ, Juliano C, Kinukawa M, Moy GW, Neill AT, Nomura M, Raisch M, Reade A, Roux MM, Song JL, Su YH, Townley IK, Voronina E, Wong JL, Amore G, Branno M, Brown ER, Cavalieri V, Duboc V, Duloquin L, Flytzanis C, Gache C, Lapraz F, Lepage T, Locascio A, Martinez P, Matassi G, Matranga V, Range R, Rizzo F, Rottinger E, Beane W, Bradham C, Byrum C, Glenn T, Hussain S, Manning G, Miranda E, Thomason R, Walton K, Wikramanayke A, Wu SY, Xu R, Brown CT, Chen L, Gray RF, Lee PY, Nam J, Oliveri P, Smith J, Muzny D, Bell S, Chacko J, Cree A, Curry S, Davis C, Dinh H, Dugan-Rocha S, Fowler J, Gill R, Hamilton C, Hernandez J, Hines S, Hume J, Jackson L, Jolivet A, Kovar C, Lee S, Lewis L, Miner G, Morgan M, Nazareth LV, Okwuonu G, Parker D, Pu LL, Thorn R, Wright R (2006) The genome of the sea urchin strongylocentrotus purpuratus. Science 314:941–952

101. Galione A, Patel S, Churchill GC (2000) NAADP-induced calcium release in sea urchin eggs. Biol Cell 92:197–204
102. Brailoiu E, Rahman T, Churamani D, Prole DL, Brailoiu GC, Hooper R, Taylor CW, Patel S (2010) An NAADP-gated two-pore channel targeted to the plasma membrane uncouples triggering from amplifying Ca^{2+} signals. J Biol Chem 285:38511–38516
103. Schieder M, Rotzer K, Bruggemann A, Biel M, Wahl-Schott C (2010) Planar patch clamp approach to characterize ionic currents from intact lysosomes. Sci Signal 3:l3
104. Schieder M, Rotzer K, Bruggemann A, Biel M, Wahl-Schott CA (2010) Characterization of two-pore channel 2 (TPCN2)-mediated Ca^{2+} currents in isolated lysosomes. J Biol Chem 285:21219–21222
105. Pitt SJ, Funnell TM, Sitsapesan M, Venturi E, Rietdorf K, Ruas M, Ganesan A, Gosain R, Churchill GC, Zhu MX, Parrington J, Galione A, Sitsapesan R (2010) TPC2 is a novel NAADP-sensitive Ca^{2+} release channel, operating as a dual sensor of luminal pH and Ca^{2+}. J Biol Chem 285:35039–35046
106. Hooper R, Churamani D, Brailoiu E, Taylor CW, Patel S (2011) Membrane topology of NAADP-sensitive two-pore channels and their regulation by N-linked glycosylation. J Biol Chem 286:9141–9149
107. Lorenz H, Hailey DW, Wunder C, Lippincott-Schwartz J (2006) The fluorescence protease protection (FPP) assay to determine protein localization and membrane topology. Nat Protoc 1:276–279
108. Noma K, Kimura K, Minatohara K, Nakashima H, Nagao Y, Mizoguchi A, Fujiyoshi Y (2009) Triple N-glycosylation in the long S5-P loop regulates the activation and trafficking of the Kv12.2 potassium channel. J Biol Chem 284:33139–33150
109. Bonifacino JS, Traub LM (2003) Signals for sorting of transmembrane proteins to endosomes and lysosomes. Annu Rev Biochem 72:395–447

110. Patel S, Ramakrishnan L, Rahman T, Hamdoun A, Marchant JS, Taylor CW, Brailoiu E (2011) The endo-lysosomal system as an NAADP-sensitive acidic Ca^{2+} store: role for the two-pore channels. Cell Calcium 50(2):157–167
111. Sulem P, Gudbjartsson DF, Stacey SN, Helgason A, Rafnar T, Jakobsdottir M, Steinberg S, Gudjonsson SA, Palsson A, Thorleifsson G, Palsson S, Sigurgeirsson B, Thorisdottir K, Ragnarsson R, Benediktsdottir KR, Aben KK, Vermeulen SH, Goldstein AM, Tucker MA, Kiemeney LA, Olafsson JH, Gulcher J, Kong A, Thorsteinsdottir U, Stefansson K (2008) Two newly identified genetic determinants of pigmentation in Europeans. Nat Genet 40:835–837
112. Lamason RL, Mohideen MA, Mest JR, Wong AC, Norton HL, Aros MC, Jurynec MJ, Mao X, Humphreville VR, Humbert JE, Sinha S, Moore JL, Jagadeeswaran P, Zhao W, Ning G, Makalowska I, McKeigue PM, O'donnell D, Kittles R, Parra EJ, Mangini NJ, Grunwald DJ, Shriver MD, Canfield VA, Cheng KC (2005) SLC24A5, a putative cation exchanger, affects pigmentation in zebrafish and humans. Science 310:1782–1786
113. Luzio JP, Bright NA, Pryor PR (2007) The role of calcium and other ions in sorting and delivery in the late endocytic pathway. Biochem Soc Trans 35:1088–1091
114. Dolphin AC (2009) Calcium channel diversity: multiple roles of calcium channel subunits. Curr Opin Neurobiol 19:237–244
115. Richards MW, Butcher AJ, Dolphin AC (2004) Ca^{2+} channel beta-subunits: structural insights AID our understanding. Trends Pharmacol Sci 25:626–632
116. Lloyd-Evans E, Waller-Evans H, Peterneva K, Platt FM (2010) Endolysosomal calcium regulation and disease. Biochem Soc Trans 38:1458–1464

Chapter 15
Store-Operated Ca^{2+} Entry

Alejandro Berna-Erro, Pedro C. Redondo, and Juan A. Rosado

Abstract Store-operated Ca^{2+} entry (SOCE) is an ubiquitous and major mechanism for Ca^{2+} influx in mammalian cells with important physiological relevance. Since the discovery of SOCE in 1986 both, the mechanism that communicates the amount of Ca^{2+} accumulated in the intracellular Ca^{2+} stores to the plasma membrane channels and the nature of the capacitative channels, have been a matter of intense investigation. During the last decade, two of the major elements of SOCE, STIM1, the Ca^{2+} sensor of the intracellular Ca^{2+} compartments, and Orai1, the protein forming the channel that conducts the capacitative Ca^{2+} release-activated current I_{CRAC}, were identified. Together with these proteins, different homologues, including STIM2, Orai2 and Orai3, were identified, although their relevance in SOCE has not been fully characterized yet. Before the identification of STIM1 and Orai1, TRPC proteins were found to be involved in SOCE in different cell types, more likely conducting the non-selective capacitative current described as I_{SOC}. Current evidence indicates that STIM1, Orai1 and TRPC proteins dynamically interact forming a ternary complex that mediates SOCE in a number of cellular models. The dynamic interaction of STIM1 with Orai1, TRPCs or both might provide an explanation to the distinct capacitative currents described in different cell types.

Keywords SOCE • Transient receptor potential (TRP) channels • Orai • STIM • CRAC • Store-operated Ca^{2+} entry • STIM1 • Orai1 • STIM2 • Orai2 • Orai3 • TRPC channels • Conformational coupling • $Ca_v1.2$ channels • SOAR/CAD

A. Berna-Erro • P.C. Redondo • J.A. Rosado (✉)
Department of Physiology, Cell Physiology Research Group, University of Extremadura, Cáceres 10003, Spain
e-mail: jarosado@unex.es

M.S. Islam (ed.), *Calcium Signaling*, Advances in Experimental Medicine and Biology 740, DOI 10.1007/978-94-007-2888-2_15,

Abbreviations

$[Ca^{2+}]_i$	Intracellular free Ca^{2+} concentration
CAD	CRAC-activating domain
CMD	CRAC modulatory domain
CRAC	Ca^{2+} release-activated Ca^{2+} channel
ER	Endoplasmic reticulum
IP_3	Inositol 3,4,5-trisphosphate
OASF	Orai-activating small fragment
PM	Plasma membrane
PMCA	Plasma membrane Ca^{2+}-ATPase
RACK1	Receptor for activated C-kinase-1
ROC	Receptor-operated Ca^{2+} channels
ROCE	Receptor-operated Ca^{2+} entry
SCID	Severe combined immune deficiency
SERCA	Sarcoplasmic/endoplasmic-reticulum Ca^{2+}-ATPase
SMOC	Second messenger-operated Ca^{2+} channels
SOC	Store-operated Ca^{2+} channel
SOAR	STIM1 Orai-activating region
SOCE	Store-operated Ca^{2+} entry
STIM1	Stromal interaction molecule 1
TRP	Transient receptor potential
VOC	Voltage-operated channels

Receptor-Operated Calcium Entry Mechanisms

Ca^{2+} is a ubiquitous second messenger that regulate a large number of cellular processes, ranging from short term responses, such as muscle contraction, exocytosis or platelet aggregation, to long term events, including gene transcription or cell proliferation [1]. The ability of Ca^{2+} to play an essential role in cell biology can be attributed to the facility that cells have to shape Ca^{2+} signals in time, space and amplitude depending on the stimulating agonist.

Physiological agonists elevate cytosolic free Ca^{2+} concentration ($[Ca^{2+}]_i$) by releasing compartmentalized Ca^{2+} or by facilitating the entry of extracellular Ca^{2+} through plasma membrane (PM) permeable channels. Once cellular stimulation is terminated, $[Ca^{2+}]_i$ should return to the low resting levels in order to allow further Ca^{2+} signals and to prevent cytosolic Ca^{2+} overload, which results in deleterious effects. Ca^{2+} clearance from the cytosol and thus reduction in $[Ca^{2+}]_i$ mainly occurs by Ca^{2+} sequestration into the intracellular organelles, especially relevant are agonist-sensitive Ca^{2+} compartments and mitochondria, and extrusion across the PM through the collaborative actions of different Ca^{2+}-ATPases and exchangers, including the plasma membrane Ca^{2+}-ATPase (PMCA) and the Na^+/Ca^{2+} exchanger. Ca^{2+} reuptake into the intracellular stores is mediated by the sarco/endoplasmic reticulum

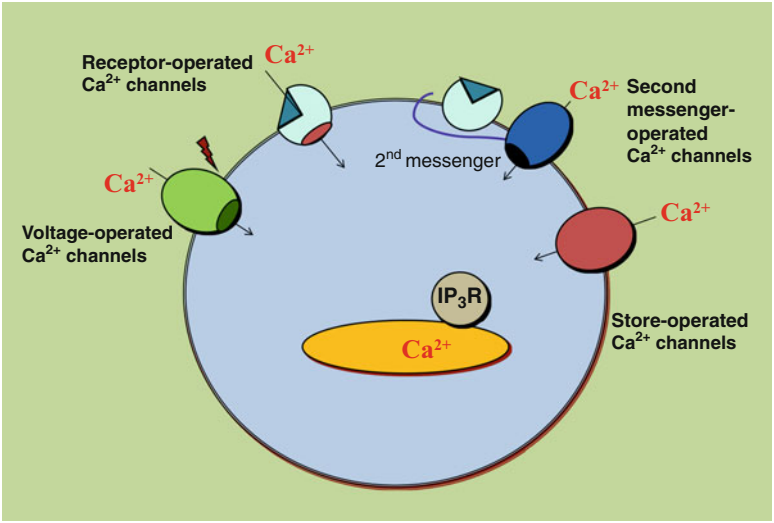

Fig. 15.1 Mechanisms for Ca^{2+} entry into cells. Ca^{2+} might enter the cells either through voltage-gated Ca^{2+} channels (electrically excitable cells), receptor-operated Ca^{2+} channels, second-messenger operated Ca^{2+} channels or store-operated Ca^{2+} channels. IP_3R, inositol 1,4,5-trisphosphate receptors

Ca^{2+}-ATPases [2], which are also responsible to maintain a low $[Ca^{2+}]_i$ in resting cells by working against Ca^{2+} leakage into the cytosol from the intracellular stores probably mediated by translocons [3].

Agonist-releasable intracellular Ca^{2+} compartments are localized in the endoplasmic reticulum (ER) and acidic organelles, including lysosomes, lysosomal-related organelles (melanosomes, lytic granules in lymphocytes, platelet dense granules, basophilic granules, neutrophil azurophil granules), secretary vesicles or the Golgi apparatus [4, 5]. Ca^{2+} release from intracellular compartments by agonists occurs via generation of a number of second messengers that gate Ca^{2+} channels located in the membrane of the Ca^{2+} stores, including the inositol 1.4.5-trisphosphate (IP_3), nicotinic acid adenine dinucleotide phosphate (NAADP), cyclic ADP ribose or sphingosine 1-phosphate [6–9].

While Ca^{2+} release from finite intracellular Ca^{2+} stores is transient and sometimes insufficient for full activation of cellular processes, Ca^{2+} entry through PM Ca^{2+}-permeable channels leads to a more sustained and usually greater increase in $[Ca^{2+}]_i$, which is essential for intracellular Ca^{2+} stores refilling and the activation of certain cellular processes. Ca^{2+} entry is a universal event that might occur through a number of processes in different cell types, including voltage-operated and receptor-operated Ca^{2+} entry mechanisms (Fig. 15.1).

Voltage-operated Ca^{2+} entry occurs in electrically excitable cells, where neurotransmitters or hormones induce membrane depolarization, with the consequential opening of voltage-operated Ca^{2+} channels (VOC). VOCs are members of the superfamily of voltage-gated ion channels, which also includes Na^+ and K^+-permeable

channels, and are mostly involved in the excitation-contraction coupling in skeletal cardiac and smooth muscle cells or in the excitation-secretion coupling and post-synaptic Ca^{2+} influx in neurons [10]. Ten VOCs have been cloned, which can be grouped into three categories: the high-voltage activated dihydropyridine-sensitive (L-type) Ca^{2+} channels, including $Ca_v1.1$, $Ca_v1.2$, $Ca_v1.3$ and $Ca_v1.4$; the high-voltage activated dihydropyridine-insensitive (P, Q, N and R-type) Ca^{2+} channels, including $Ca_v2.1$, $Ca_v2.2$ and $Ca_v2.3$ and the low-voltage activated (T-type) Ca^{2+} channels, including $Ca_v3.1$, $Ca_v3.2$ and $Ca_v3.3$ [11].

In non-electrically excitable cells, lacking VOCs, as well as in excitable cells, receptor-operated Ca^{2+} entry is an important mechanism for Ca^{2+} influx from the extracellular medium. Receptor-operated Ca^{2+} entry groups the mechanism for Ca^{2+} entry activated by receptor occupation, from the Ca^{2+} currents that occurs through the receptor-channel itself, the properly known receptor-operated Ca^{2+} channels (ROC), to cationic currents through channels operated by second messengers (SMOC) or discharge of the intracellular Ca^{2+} pools via store-operated Ca^{2+} channels (SOC).

ROC includes a number of PM resident receptor channels activated by different ligands that mediate Ca^{2+} entry without the participation of receptor-generated diffusible messengers, such as the P2X receptors, which have three α-helical transmembrane domains and conduct Na^+, K^+ and Ca^{2+} [11] or the N-methyl-D-aspartate (NMDA) and alpha-amino-3-hydroxy-5-methylisoxazole-4-propionate (AMPA) receptors that respond to glutamate [12, 13] (Fig. 15.1). This classification might also include Ca^{2+} entry via channels activated by physical stimuli, such as certain TRPV and TRPM channels activated by heat or cooling [14–16].

Second messenger-operated Ca^{2+} entry is mediated by Ca^{2+}-permeable SMOCs gated via diffusible messengers generated by receptor occupation (Fig. 15.1). There is a body of evidence supporting Ca^{2+} influx activated that diacylglycerol, or its membrane permeant analog 1-oleoyl-2-acetyl-sn-glycerol (OAG) [17–25], PKC [26], cyclic ADP ribose [27], reactive oxygen species [28–30] or epoxyeicosatrienoic acids derived from cytochrome P450 activity [31, 32], and a number of SMOCs are regulated by the cellular level of phosphatidylinositol 4,5-bisphosphate [33, 34].

Finally, store-operated Ca^{2+} entry (SOCE) is an ubiquitous mechanism for Ca^{2+} influx in mammalian cells that occurs via the activation of SOCs, and represents an important Ca^{2+} influx pathway. SOCE is a mechanism controlled by the filling state of the intracellular Ca^{2+} stores identified by James Putney in 1986 [35] (Fig. 15.1). In the last two decades SOCE has been extensively investigated and researchers have mostly focused on three major aspects: the functional role of SOCE in the different cell types investigated, the mechanism by which information is transmitted from the intracellular Ca^{2+} stores to the PM Ca^{2+} channels and the nature and regulation of SOCs.

There is a body of evidence supporting a physiological role for SOCE in the different cell types investigated, including cell proliferation, neutrophil-mediated inflammatory responses [36], regulation of smooth muscle tone [37], platelet aggregation and secretion [38–40] or lymphocyte function [41]. In addition, SOCE has been found to support Ca^{2+} oscillations in mammalian cells [42], Ca^{2+} signals consisting on oscillatory changes of $[Ca^{2+}]_i$ in response to agonist stimulation, which are thought to control a wide variety of cellular functions, although it has been

found that SOCE is not essential for certain oscillatory Ca^{2+} signaling events and for Ca^{2+} refilling in *Caenorhabditis elegans* [43]. This chapter summarizes the most relevant findings concerning the SOCE pathway and the key elements involved.

Proposed Mechanisms of Activation for SOC Entry

The mechanism by which the filling state of the intracellular Ca^{2+} stores is communicated to the PM Ca^{2+} permeable channels has been a matter of intense investigation and debate since the identification of SOCE. Hypotheses presented can be mainly grouped into three categories: those that propose the generation of a diffusible molecule with ability to induce SOC gating, those that assume a physical (constitutive or *de novo*) interaction between SOCs in the PM and an element of the ER membrane, and those suggesting the insertion of preformed SOCs in the PM upon depletion of the intracellular Ca^{2+} stores.

Among the diffusible messengers that have been proposed to be generated upon discharge of the stores, the still uncharacterized and non-protein molecule known as Ca^{2+} influx factor (CIF) focused much interest in the 1990s [44]. In addition, other signaling molecules have been reported to play an essential role in the activation of SOCE in different cell types, including cGMP [45], tyrosine kinases [46–48], products of the cytochrome P450 [49] and small GTP-binding proteins [50, 51] among others.

An alternative to this hypothesis consist in the translocation and insertion of preformed SOCs into the PM by vesicle trafficking and fusion. This model was originally presented by Penner's team [52] and latter on supported by studies performed in Roger Tsien's lab [53] where it was clearly demonstrated that SOCE requires the function of the SNARE (*S*oluble *N*SF *A*ttachment protein *RE*ceptor) protein, SNAP-25, a protein involved in the trafficking, docking and fusion of secretory vesicles with the PM. The named "secretion-like coupling mechanism" shares a number of events with the activation of exocytosis, especially concerning the dual role of the actin cytoskeleton both facilitating vesicle transport but also preventing constitutive activation of these processes [54, 55]. More recently, the channel insertion hypothesis for the activation of SOCE received support from studies reporting that agonists induce the expression of stored TRPC5 in the PM in cultured hippocampal neurons [56], TRPC6 in stably transfected HEK 293 cells [57], TRPC3 exogenously expressed in neuronal and epithelial cells [58] or Orai1 in HEK-293 and HeLa cells [59].

The last two hypotheses for the activation of SOCE are based on the association of proteins in the plasma and ER membranes. The physical or conformational coupling between elements in the ER and SOCs in the PM was initially proposed by Robin Irvine soon after the identification of SOCE [60]. The early studies mostly focused on the association of the IP_3 receptor with the SOCs in the PM, as a mechanism that resembles the excitation-contraction coupling between ryanodine receptors and dihydropyridine receptors in the skeletal muscle [61]. The classical conformational coupling postulated that portions of the ER must be close enough to the PM to allow a constitutive protein-protein interaction between the IP_3 receptors

and SOCs [38]. This hypothesis received support from studies demonstrating that, under resting conditions, TRPC1, TRPC3 and TRPC6 can be co-immunoprecipitated with IP_3 receptors, which modulates SOC gating through its N-terminal region [62–64]. In addition, more recent studies have revealed a role the protein junctate, which has been reported to induce and stabilize the coupling between IP_3 receptors and TRPC3, in the activation of SOCE [65].

An alternative to the classic "constitutive" conformational coupling hypothesis proposes a dynamic and reversible conformational coupling model for the activation of SOCE. The so called *de novo* conformational coupling mechanism proposes that elements in the ER, initially slightly distant from the PM, might interact with SOCs by a *de novo* protein coupling. This mechanism might require trafficking of portions of the ER towards the PM to allow a reversible interaction between elements in both membranes, a process where the actin cytoskeleton and microtubules might play a relevant role both inhibiting and facilitating the coupling, acting as a negative cortical clamp that prevents constitutive coupling but also providing support for the *de novo* coupling between elements in the ER and SOCs [39, 66–70]. In support of this hypothesis we found *de novo* coupling of naturally expressed TRPC1 and the type II IP_3 receptor following Ca^{2+} store depletion but not under resting conditions in human platelets [71], which occurs with the same latency as agonist-evoked stimulation as Ca^{2+} entry [72].

In 2005 the Ca^{2+} sensor of the ER was identified as the *S*tromal *I*nteraction *M*olecule-1 (STIM1) protein [73, 74], and 1 year later, Orai1 was identified as the channel conducting the Ca^{2+} selective CRAC (Ca^{2+} release-activated Ca^{2+} current), which have focused much attention concerning the activation of SOCE [75, 76]. STIM1 and Orai1 have been reported to associate by a reversible and physical coupling mechanism upon depletion of the intracellular Ca^{2+} stores, as reported below. Later on, functional interactions between the IP_3 receptors and TRPC or Orai1 proteins have been reported to play an important role in Ca^{2+} signaling in different cell types [77–79].

STIM Proteins

STIM1

One of the most significant advances in the mechanism underlying the communication between the Ca^{2+} stores and the SOCs was the identification of STIM1 as the intraluminal Ca^{2+} sensor. Based on RNAi screen to identify genes that alter thapsigargin-evoked Ca^{2+} influx, and the generation of STIM1 mutants that lack the ability to bind Ca^{2+}, the group of Cahalan and Stauderman demonstrated that STIM1 is the ER sensor that communicates information concerning the filling state of the ER to SOCs in the PM [73, 74]. Recently, STIM1 has been reported to act as the Ca^{2+} sensor of the agonist-sensitive acidic Ca^{2+} stores [80]. STIM1 knockdown in different mammalian cell types have revealed the relevant role of this protein in SOCE

[73, 81, 82] and I_{CRAC} [83]. Consistently, attenuation of dStim expression by RNAi in *Drosophila* S2 cells reduced SOCE [73, 81].

STIM1 contains a single transmembrane domain, with the N-terminal region within the ER lumen, or the extracellular medium, according to the protein location, and a cytosolic C-terminal region. Structurally, STIM1 N-terminal region includes a sterile-alpha motif (SAM), which facilitates protein interactions with different signaling molecules [84], a canonical, Ca^{2+}-binding, EF-hand domain, which shows a low Ca^{2+}-binding affinity (Kd ≈ 0.5 mM) [85], and a 'hidden' non-Ca^{2+}-binding EF-hand motif that stabilizes the intramolecular interaction between the canonical EF-hand and the SAM domain [86]. The cytosolic region contains two coiled-coil regions, several ezrin/radixin/moesin-like domains, and proline rich domains in the C terminus [87, 88]. In particular, the C-terminal region contains the SOAR/CAD domain that has an important functional role due to its relevance in the association with Orai1 subunits (see below).

The location of STIM1 is mostly intracellular, located in the membranes of the ER and the agonist-sensitive acidic Ca^{2+} stores; however, and a minor STIM1 pool has also been located in the PM [74, 81, 82, 89–91]. The location of STIM1 in the PM is not circumstantial, since the EF-hand motif of PM-resident STIM1 faces the extracellular medium, which suggests that STIM1 might act as a sensor of the extracellular free Ca^{2+} concentration. A number of studies have demonstrated that STIM1 located at the PM might regulate SOCE through the interaction with SOCs in different cell types. External application of an antibody specifically addressed towards the STIM1 EF-hand motif blocks both CRAC channels in hematopoietic cells and SOC channels in HEK293 cells [83]. In agreement with this, a similar experimental manoeuvre has been found to abolish the inhibition of SOCE induced by increasing extracellular Ca^{2+} concentrations in human platelets probably via STIM1 interaction with Orai1 but not with TRPC1 [90], an effect that was not mimicked by a non-specific mouse IgG (Lopez et al., personal communication). Therefore, the current evidence indicates that PM-located STIM1 might be involved in the regulation of SOCE by extracellular Ca^{2+}, probably providing a protective effect to avoid Ca^{2+} overload. The regulatory role of PM-resident STIM1 requires the integrity of the lipid raft domains [91], which is a common feature with Ca^{2+} signaling events such as SOCE [92].

STIM1 has been suggested to interact with several PM channels, including Orai1, which has been reported to mediate the activation of the highly selective Ca^{2+} current I_{CRAC} [93]. Expression of both STIM1 and Orai1 proteins in a number of cellular models potentiates I_{CRAC}; however, individual overexpression of either protein fails to amplify this current, even expression of Orai1 alone strongly reduces SOCE and I_{CRAC} in RBL cells [89], thus indicating that STIM1 and Orai1 mutually limit store-operated currents and that a correct stoichiometric expression is necessary for the activation of I_{CRAC} [94]. STIM1 has also been found to interact with the cation-permeable protein TRPC1 [95], an event that is probably associated to the activation of I_{SOC}. For further information concerning STIM1 the reader is referred to the specific chapter of this book.

Recent studies have provided evidence for a role of STIM1 in the regulation of the voltage-gated Ca^{2+} channel $Ca_v1.2$. In cells expressing both Orai1 and $Ca_v1.2$

channels, STIM1 interacts with and reciprocally controls both channels, activating Orai1 and inducing both inhibition of $Ca_v1.2$ channel gating, as well as long-term internalization of the channel from the membrane [96, 97], which is the first description of a role for STIM1 in the regulation of voltage-operated Ca^{2+} channels.

STIM2

STIM2 was identified together with STIM1 by Williams et al. in 2001 as a two member family, which apparently evolved from a single gene in lower multicellular eukaryotes and conserves a high homology in their aminoacid sequence and structure [98]. *Stim2* gene comprises 12 exons located on chromosome 4 and 5 in human and mouse, respectively [98]. STIM2 is a type I transmembrane protein of 833 residues (105–115 kDa) size in human. The N-terminal region (first 577 residues) shows 66% homology with STIM1 and the most C-terminal region, which participates in interactions with SOC channels [99, 100], shows a significant sequence divergence in contrast, indicating functional differences between both STIM isoforms [98]. Mouse STIM2 shares a 92% identity with human STIM2 (http://blast.ncbi.nlm.nih.gov/), indicating conserved structure along the evolution. Finally, human STIM2 protein undergoes maturation by cleavage of N-terminal ER signaling peptide (14 aa_s), and post-translational modifications by glycosylation and variable degrees of phosphorylation [98], but their functional consequences are still poorly understood. However, studies on phosphorylation in STIM1 reported modulation of SOCE by alteration of STIM1 interactions with SOC channels [101, 102], suggesting similar mechanisms in STIM2 regarding the high homology found in their structure.

STIM2 is almost ubiquitously expressed in human and mouse tissues [98, 103–105], being the dominant isoform in mouse brain, pancreas, placenta, heart but almost absent in skeletal muscle, kidney, liver and lung. It is found co-expressed together with STIM1 in many human cell lines [98] and cell types [106–109], indicating that both isoforms co-exist in the same cell. At intracellular level, STIM2 has been observed located in the ER membrane and in acidic intracellular stores [80, 81, 89, 110], but not in the plasma membrane in contrast to STIM1 [110–112]. Activated STIM2 form clusters in punctate structures only when coexpressed with STIM1, indicating an interaction between both isoforms as a mechanism to regulate SOCE or themselves [81, 89, 110].

Similar to STIM1, the N-terminal region of STIM2 contains a canonical EF-hand Ca^{2+}-binding motif necessary to detect changes in Ca^{2+} concentration inside the ER [73, 74, 81, 98], a "hidden" EF-hand Ca^{2+}-binding motif and a protein–protein interaction motif referred to as sterile α-motif (SAM) domain [113], which are located in the ER lumen. The SAM and the "hidden" EF-hand domain, which does not bind Ca^{2+}, are critical for stabilization of the entire EF-SAM region and STIM oligomerization [114–117]. The release of the Ca^{2+} bound to the EF-hand motif as consequence of decreases in ER Ca^{2+} content switches STIM2 to the active form [81, 89].

Despite the similar affinity to Ca^{2+} displayed by the EF-hand motif of both STIM isoforms (STIM2 Kd ~0.5 mM; STIM1 Kd ~0.2–0.6 mM), the full STIM2 protein showed a lower [Ca^{2+}] sensitivity compared to STIM1 in transfected cells *in vitro* [85], which might be explained by the contribution of other protein regions, such as the SAM domain in STIM2 [117, 118]. As consequence, STIM2 can be active at higher [Ca^{2+}] (0.4 mM) in contrast to STIM1 (0.2 mM) or already partially activated at basal ER [Ca^{2+}] (0.3–0.5 mM) [119–121] in unstimulated cells, becoming therefore active earlier than STIM1 during ER store depletion [85]. Separated from the N-terminal region by a highly conserved single-pass transmembrane motif, the C-terminal region contains a ezrin/radixin/moesin (ERM) domain that contains two coiled-coil domains [122], which mediates the homo and heteromultimerization of STIMs, a critical step for SOCE activation [99, 110, 112, 116]. Adjacent to this region, STIM2 contains a proline- and histidine-rich motif instead of the proline-rich region found in STIM1 [98], whose function is still not known. Finally, a lysine-rich motif of 17 residues is located at the very end of the C-terminal region, similarly to those found in STIM1 [98]. This region might interact with calmodulin (CaM), with high or low affinity in presence or absence of Ca^{2+} respectively, inhibiting STIM2 function [123, 124]. Moreover, STIM2 lysine-rich region might be necessary for the interaction with TRPC1 and Orai channels [95, 99, 100].

The function of STIM2 is controversial and still under discussion. In contrast to those observed in STIM1, Brandman et al. suggested that STIM2 could act as a regulator that stabilizes basal [Ca^{2+}] in the cytosol and in the ER, since knockdown of STIM2 expression using techniques of RNA interference (siRNA), but not STIM1, altered these parameters in different cell lines [85]. As explained before, this function would relies in the lower sensitivity to [Ca^{2+}] showed by STIM2 as compared to STIM1. STIM2 might be active in response to small decreases of Ca^{2+} stored in the ER, generated as consequence of weak receptor stimuli or passive leak into the cytosol, and promote SOCE probably through interaction with Orai1, which in turn would correct low $[Ca^{2+}]_i$ and refill Ca^{2+} pools stored in the ER [85]. Since [Ca^{2+}] values observed in ER lumen in resting conditions are very close to values in which STIM2 is active, STIM2 would be partially active when Ca^{2+} pools in the ER are also filled, and might correct spontaneous [Ca^{2+}] oscillations generated in the cytosol and ER [85]. Later, this hypothesis was confirmed by *in vitro* studies in human breast cancer cells, myoblasts [108, 125] and murine neuronal cells [103]. However, other studies performed in murine T cells, breast cancer cells and arterial smooth muscle did not observe such alterations in the absence of STIM2 [106, 126, 127], indicating that the ability of STIM2 to control Ca^{2+} homeostasis in the cytosol and ER might be highly dependent of the cell type. It is also conceivable that STIM1 might compensate the absence of STIM2 in these cells by partially controlling Ca^{2+} homeostasis. Studies in murine platelets and macrophages for instance, also observed that the absence of STIM1 altered the amount of Ca^{2+} stored in the ER [128, 129], indicating that the function of STIM1 concerning regulation of Ca^{2+} homeostasis and refilling of Ca^{2+} stores in the ER could overlap with STIM2. If so, the function of STIM2 might be also dependent of STIM1 abundance in the cell type.

The participation of STIM2 in Ca^{2+} entry into the cell by SOCE is more controversial. Functional studies demonstrated that STIM2 is able to interact with Orai [1–3] and TRPC1 channels [89, 124], indicating a potential role in SOCE. However, *in vitro* studies reported no change in SOCE upon overexpression or downregulation of STIM2 in murine platelets, neutrophil-like HL-60 cells or airway smooth muscle [130–132]. Moreover, studies performed by Soboloff et al. suggested that STIM2 inhibits SOCE when expressed alone [110], but could cause substantial constitutive SOCE when coexpressed with Orai1 [89]. Parvez et al. reported that STIM2 might mediate SOCE via two store-dependent and store-independent modes in HEK293 cells [124]. Other studies observed a minor decrease of SOCE in the absence of STIM2 function in murine embryonic fibroblasts (MEF), B and T cells, rat pulmonary arterial smooth muscle cells and some cell lines such as breast cancer, HeLa or HEK293 cells [81, 106, 107, 109, 125, 127, 133], while recent reports suggested a prominent function of STIM2 in SOCE in murine neurons, HEK293 and dendritic cells [103, 134, 135]. Thus, STIM2 showed an involvement in SOCE in different degrees depending of the cell type, which might be explained by partial compensation of STIM1, probably depending of the endogenous level of both STIMs in these cells. Indeed, studies in murine T cells and human myoblasts demonstrated that decreases of SOCE produced by the lack of STIM2 or STIM1 can be partially compensated by overexpression of STIM1 or STIM2, respectively [107, 136], indicating overlapping functions. Additionaly, they can act synergistically to regulate Ca^{2+} influx when both are expressed together, indicating cooperating functions between these isoforms [85, 108]. Taken together, these results indicate that STIM proteins might have differential or specialized roles in Ca^{2+} homeostasis. However, they might have partial overlapping functions and cooperate together to regulate SOCE, Ca^{2+} levels in the cytosol, store refilling and therefore Ca^{2+} levels stored inside the ER. As consequence, the decrease or absence of one isoform could be compensated by the other isoform and affect one or more of these parameters, which might be dependent of their abundance in the cell type. Evidences suggest that SOCE could be highly sensitive to the stoichiometric ratio of Ca^{2+} channels and molecules involved in this mechanism [89]; however, further studies are necessary to clarify these points.

Concerning the activation dynamics of SOCE, differences in STIM2 compared to STIM1 have been also observed. STIM1 can be active and aggregate fast in response to stimulation and produce transient and large *I*crac currents, while STIM2 gives slow responses and promote smaller but more sustained *I*crac currents [137]. These divergences might be explained by structural differences found in both isoforms. The short variable N-terminal region of STIM2 would attenuate Orai1-mediated SOCE, drastically slow their coupling and therefore Orai channel activation [137], further supporting the idea of specialized but overlapping functions.

Finally, recent reports suggested a role of STIM2 in HEK293 cell proliferation *in vitro* [135], *in vivo* secretion of cytokines in murine T and B cells [106, 107, 109], neuronal cell death during hypoxic conditions [103] and development of autoimmune responses [106, 109], thus indicating the importance of STIM2 function in basic cellular functions and in development of pathologic conditions.

Orai Proteins

Orai1

In 2006, the channel conducting the Ca^{2+} selective capacitative current, I_{CRAC}, was identified as the protein Orai1, through whole-genome screening of *Drosophila* S2 cells and gene mapping in patients with the hereditary severe combined immune deficiency (SCID) syndrome induced by I_{CRAC} deficiency [75, 138, 139]. The Orai family includes three human homologs, Orai1, Orai2 and Orai3. Orai1 is a protein containing 301 amino acids that shows four predicted transmembrane domains and cytosolic N- and C-terminal tails [75, 138, 140]. Orai1 presents a single putative channel pore and has been found as a tetramer. The reconstruction of the three-dimensional structure from negatively stained electron microscopic images reported that Orai1 channels show an elongated teardrop-shape 150 Å in height and 95 Å in width [141].

The cytosolic N-terminus of Orai1 contains proline/arginine-rich regions and a membrane-proximal domain (between residues 68 and 91) with the ability to bind calmodulin in a Ca^{2+}-dependent manner [142]. The calmodulin-binding domain has been reported to be involved in fast Ca^{2+}-dependent inactivation of I_{CRAC}, an event that occurs within the first 100 ms upon CRAC channel opening induced by a local increase in the $[Ca^{2+}]_i$ close to the channel pore [143, 144], that protects against cellular damage by limiting Ca^{2+} influx. The C-terminal region of all three Orais contains a putative coiled-coil sequence that plays a key role for dynamic interaction with STIM1 [145, 146]. A deletion or single point mutation (L273S) within this region has been shown to disrupt the functional communication of Orai1 with STIM1 [145]. All three Orai isoforms are gated by store depletion when co-expressed with STIM1 [146, 147]. Orai isoforms show slightly different sensitivity to 2-aminoethoxydiphenyl borate (2-APB). This agent acts as a direct Orai3 activator. In addition, low 2-APB concentrations activate Orai1 and Orai2 currents when co-expressed with STIM1. By contrast, at high concentrations, 2-APB is a potent antagonist or Orai1-conducted currents. This action might be attributed to direct block at the channel level, uncoupling from STIM1 or impairment of the store-dependent STIM1 multimerization [148].

Orai1 has been reported to form Ca^{2+} selective channels. The ion selectivity of Orai1 has been attributed to two conserved negatively charged glutamate residues located in the first and the third transmembrane regions (E106 and E190) [149–152]. Consistently, mutations at E106 and E190 reduced the Ca^{2+} selectivity of Orai1 characteristic of I_{CRAC} [151, 152]. Despite all three Orai isoforms are highly selective for Ca^{2+}, Orais have also been reported to be permeable to Na^+ in a medium free of divalent cations, and Na^+ currents through Orais, as well as the endogenous store-operated Na^+ currents in HEK293 cells, have been shown to be inhibited by extracellular Ca^{2+} with a half-maximal concentration of approximately 20 μM [140].

Orai channels show different fast Ca^{2+}-dependent inactivation profiles [147]. Orai3 currents exhibit a marked fast inactivation within the first 100 ms, while that

of Orai2 or Orai1 show less robust feedback regulation [147]. Current studies attribute the fast Ca^{2+}-dependent inactivation of Orai1 to the calmodulin-binding site, since a mutation in this region has been reported to abrogate fast inactivation of I_{CRAC} [142]. In addition, substitutions of an alanine residue within the second loop of Orai1 impairs fast inactivation [153], thus suggesting that the second loop is also involved in channel inactivation. In the case of Orai2 and Orai3, fast Ca^{2+}-dependent inactivation has been attributed to three conserved glutamates located at the C-terminus [154]. In addition, fast inactivation of I_{CRAC} also involves the pore region. This finding is based on the effects of mutations of negatively charged residues within the pore of Orai, which result in attenuation of Ca^{2+}-dependent inactivation [155], as well as in the observation that the fast Ca^{2+} buffer BAPTA is more effective attenuating fast inactivation than the slow Ca^{2+} buffer EGTA, which indicates that domains that control fast inactivation must to be close to the channel pore [154]. Fast Ca^{2+}-dependent inactivation of Orai channels also requires the CRAC modulatory domain (CMD) of STIM1, a regulatory domain at amino acids 474–485 of STIM1, which contains seven negatively charged residues [154, 156]. Mutations in the CMD, which is located C-terminal to the SOAR region, results in Orai1 currents with attenuated or even abolished Ca^{2+}-dependent inactivation, and similar results were reported to Orai3 [156]. Conversely, expression of cytosolic C-terminal fragments of STIM1 in RBL-2H3 mast cells expressing CRAC channels resulted in more pronounced fast Ca^{2+}-dependent inactivation than that characteristic of Orai1. Altogether, these findings suggest that the CMD region of STIM1 provides a negative feedback to Ca^{2+} entry by inducing fast inactivation of CRAC channels [156]. More recent studies have reported that the interaction between the three cytosolic domains of all Orai isoforms marks the subtype specific gating mode, including inactivation and reactivation processes [157]. For further information concerning Orai1 the reader is referred to the specific chapter in this book.

Orai2 and Orai3

In addition to Orai1, other two homologues were indentified in mammals Orai2 and Orai3 [75, 138, 147, 149]. In mouse, *Orai2* gene gives rise to two splice variants, Orai2 long (Orai2L) and Orai2 short (Orai2S) subunits, which are prominently expressed in T cells, brain, lung, spleen, and intestine [158]. Orai2S can be inactivated by the intracellular Ca^{2+}, and seems to play a negative dominant role in the formation of Orai channels [159]. Orai3 seems to be ubiquitously expressed in human and mouse, showing a minor presence in spleen and colon [104, 105, 159–163]. Orai2 also seems to be widely expressed in different human and mouse tissues, prominently expressed in neurons, kidney, lung and spleen [103, 161–163]. Orai subunits showed a high conserved structure, consisting in four transmembrane segments (TM) located in the plasma membrane and containing both N- and C-termini in the cytosol [149, 164]. It has been reported that Orai3 subunits could be essential components of arachidonic acid-regulated Ca^{2+} (ARC) channels, and that its N-terminal domain could determine their selectivity for activation by

arachidonic acid [165–167]. The C-terminal region of Orai interacts with the C-terminal region of STIM1 while the N-terminal region is critical for STIM1-mediated gating [100, 145, 168, 169]. The N-terminal region also contains a putative CaM-binding domain, indicating a possible role of CaM in Ca^{2+}-dependent inactivation of Orai channels [142, 168].

Studies using siRNA to knockdown gene expression in diverse cell lines revealed greatly reduced SOCE in the absence of Orai1, while only a minor decrease or unaltered SOCE was observed in the absence of Orai2 or Orai3 [136, 170–172], indicating a minor function of Orai2 or Orai3 and suggesting compensation mechanisms between isoforms. However, Orai3 has been found highly expressed in breast cancer cells, and knockdown of Orai3 substantially reduced SOCE, inhibited proliferation and arrested their cell cycle at G1 phase [126, 173], indicating a dominance of Orai3 function in cell proliferation and possible specialized functions of Orai subunits. Moreover, Orai3 seems to be insensitive to inactivation by hydrogen peroxide (H_2O_2) in contrast to Orai1 [174]. Increased expression of Orai3 by T-helper (T_H) cells correlated with their decreased redox sensitivity after differentiation into effector cells. Since Orai-mediated SOCE has demonstrated to be essential for T cell function [75, 175, 176], the replacement of Orai1 by a less redox sensitive SOC channel such as Orai3 might protect them from highly oxidizing environments generated during inflammation [174].

Similar to Orai1, Orai2 and Orai3 function is inhibited by extracellular Ca^{2+} [140]. Orai subunits also differ in their activation kinetics and selectivity to Ca^{2+} [147]. Orai1 and Orai2 show similarly fast activation kinetics while Orai3 shows slower activation, which is dependent of $[Ca^{2+}]$. All three isoforms are quite selective to Ca^{2+}, being Orai3 more permeant to monovalent cations such as Na^+ [147]. Co-transfection of STIM1 and Orai channels increased SOCE with different efficacies (Orai1 > Orai2) in HEK293 cells [76] and mouse [169], indicating that Orai2 and Orai3 interact and are activated by STIM1. No significant increases in SOCE were observed in cells coexpressing Stim1 and Orai3. However, Orai3 could rescue decreased SOCE in cells lacking Orai1 [76], indicating a cooperation between Orai isoforms during regulation of SOCE. This difference might rely in structural differences between isoforms. Orai1 and Orai3 chimeras with exchanged N-terminal regions, which is critical for STIM1-mediated gating, also showed exchanged characteristics in terms of Ca^{2+} currents and activation kinetics, indicating that this region determines in a great stent the gating to STIM1 and the properties of Orai channels [168]. Moreover, coexpression of a dominant negative Orai1 mutant (E106Q) abrogated SOCE mediated by all Orai homologues, suggesting heteromultimeric Orai channel formation.

The TRP Proteins

The transient receptor potential (TRP) proteins are non-selective cation channels identified in 1989 in the *trp* mutant of *Drosophila* [177]. In *Drosophila* photoreceptors the sustained light-sensitive ionic current due to Na^+ and Ca^{2+} influx is conducted by

two Ca^{2+}-permeable channels encoded by the *trp* and *trpl* genes [178, 179]. In contrast, the *trp* mutant exhibited transient, rather than sustained, light-sensitive receptor potential, which gave the name to TRP channels [180]. *Drosophila* TRP channels are receptor operated, activated by diacylglycerol (DAG) as well as by phosphatidylinositol 4,5-bisphosphate (PIP_2) depletion [181]. Soon after the identification of *Drosophila* TRP proteins, the first mammalian TRP protein was identified, the canonical transient receptor potential protein-1 (TRPC1), both in human [182, 183] and in mouse [184]. Several TRP proteins have been identified in vertebrates, which are classified into seven subfamilies: four are closely related to *Drosophila* TRP (TRPC, TRPV, TRPA and TRPM), two groups more distantly related subfamilies (TRPP and TRPML), and the TRPN group is solely expressed in fish, flies and worms [185]. These subfamilies, in turn, group different members, the TRPC subfamily comprises seven members (TRPC1-TRPC7), the vanilloid TRP subfamily (TRPV) includes six members (TRPV1–TRPV6), the TRPA (ankyrin) subfamily includes only one mammalian protein, TRPA1, the melastatin TRP subfamily (TRPM) groups eight members (TRPM1-TRPM8) and both the TRPP (polycystin) and the TRPML (mucolipin) subfamilies comprise three members each. No TRPN subfamily member is expressed in mammals [186].

TRP channels are mostly permeable to monovalent and divalent cations and exhibit a Ca^{2+} to Na^{+} permeability ratio <10 [187], with a number of exceptions such as those of TRPM4 and TRPM5, which are selective for monovalent cations, and TRPV5 and TRPV6, which are highly Ca^{2+} selective showing a Ca^{2+} to Na^{+} permeability ratio over 100 [188, 189]. The lack of Ca^{2+} selectivity for TRP channels excludes the possibility that these channels mediate the more Ca^{2+} selective I_{CRAC} currents, probably mediated by Orai proteins [149]; however, several store-operated currents, with diverse Ca^{2+} to Na^{+} permeability ratios have been reported, which can be defined as I_{SOC} to differentiate them from I_{CRAC} [190], where TRP channels might play an important role.

The TRP proteins share a common architecture, including six transmembrane domains, with cytosolic N- and C-termini and a pore loop region between the transmembrane domains 5 and 6 [184]. The C-terminal region of TRPs includes a characteristic TRP signature motif (EWKFAR) of unknown function and a CIRB (calmodulin/IP_3 receptor-binding) region, involved in the regulation of TRP channel gating [191]. Certain TRP subfamilies exhibit differential features such as the N-terminal ankyrin repeats present in TRPA or a kinase domain found in TRPM, [189, 192, 193].

Since the identification of the mammalian homologues of the *Drosophila* TRP members, the TRP channels have been proposed as candidates to conduct SOCE. The role of TRP proteins in SOCE has been challenged by the different ion selectivity of TRP forming channels and I_{CRAC}, the best characterized and Ca^{2+} selective store-operated current [144]. In addition, TRP channels in *Drosophila* were found to behave as non store-operated channels but, instead, as receptor-operated channels [181, 188, 194], as it has been described for a number of mammalian members [18, 19, 79, 195, 196]. Nevertheless, in addition to the involvement of TRP members in receptor-operated Ca^{2+} entry (ROCE), there is a body of evidence supporting a role

for mammalian TRP channels in the conduction of SOCE. Particular attention has been focused on the TRPC subfamily members, which have been found to be gated by Ca^{2+} store depletion in different cell types by using distinct experimental manoeuvres, from overexpression of specific TRPC proteins to knockdown of endogenous TRPs and knockout studies [99, 197–204]. Reports for store depletion induced activation of TRPC channels have been presented for all TRPC subfamily members, including TRPC1 [71, 197, 198, 204, 205], TRPC3 [206, 207], TRPC4 [208, 209], TRPC5 [209, 210], TRPC6 [17, 34, 211] and TRPC7 [212].

The most widely investigated TRPC member is, undoubtedly, TRPC1, whose involvement in the conduction of SOCE has been demonstrated by antisense experiments in human salivary glands [197, 213, 214] and vascular endothelial cells [215] and by functional knockdown, using antibodies directed to the pore region, in vascular smooth muscle cells and human platelets [198, 205]. The attenuation of SOCE by anti-TRPC1 antibodies directed towards the pore region has been questioned by authors claiming an effect mediated by the antibody preservative, sodium azide, rather by the antibody itself [216]; however, control experiments done with the highest concentration of the antibody neutralized by incubation with the control antigen peptide, which displayed no effect on SOCE in human platelets, clearly exclude this possibility [198].

In addition to their involvement in ROCE and SOCE, a role for TRPC3 in agonist-induced Ca^{2+} mobilization has been described to involve the assembly of a macromolecular complex including the scaffolding protein RACK-1 (receptor for activated C-kinase-1), the type I IP_3 receptor, as well as Orai1 and STIM1 [78, 79]; thus suggesting that TRPC proteins might act as a point of convergence between a number of Ca^{2+} signaling mechanisms.

Interaction Between STIM and Orai and TRP Proteins

Current evidence supports that Orai proteins form the Ca^{2+} selective CRAC channels. The permeability of Orai-forming channels to monovalent cations has been reported to be inhibited by the presence of Ca^{2+} in the extracellular medium [140], which raises the question of whether these channels might be involved in the conduction of the non-Ca^{2+} selective store-operated cation currents I_{SOC}. Channels formed by TRPC family members, alone or in combination with other ionic channel subunits, such as Orai proteins, are good candidates to mediate the I_{SOC} currents. Evidence has shown several store-operated currents with different biophysical properties in distinct cell types, operated through different signaling pathways, and suggest that these currents might be conducted through homo or heteromeric combinations of the different channel subunits identified with the participation of STIM1 to confer store-operated behaviour. STIM1 has been reported to interact physically both with Orai1 and TRPC channels (Fig. 15.2). The region involved in the association of STIM1 with Orai1 was identified almost at the same time by four independent groups. This region, located in the cytosolic region of STIM1, received

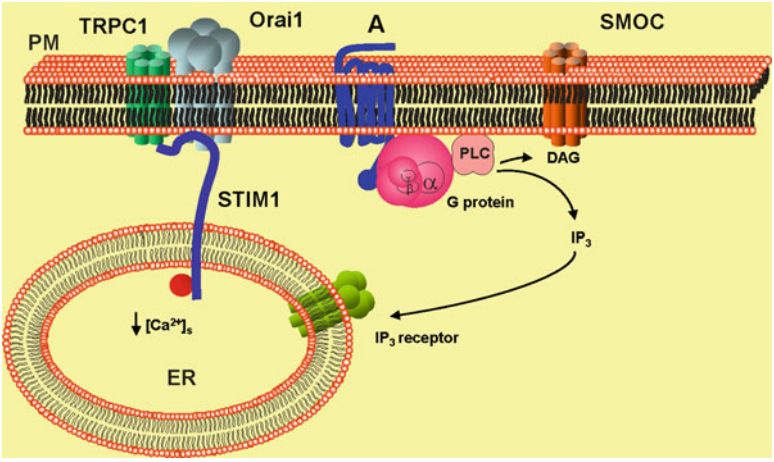

Fig. 15.2 Dynamic association of STIM1, Orai1 and TRPC1 for the activation of SOCE. Agonist receptor occupation leads to the activation of PLC through the heterotrimeric G-proteins. PLC hydrolyses phosphatidylinositol 4,5-bisphosphate leading to the generation of DAG and IP_3. DAG is a well known activator of SMOC, probably involving proteins of the TRPC subfamily and IP_3 leads to the activation of Ca^{2+} release from intracellular compartments by the occupation of IP_3 receptors. A reduction in $[Ca^{2+}]_s$ results in dissociation of Ca^{2+} from STIM1 and thus association of STIM1 with Orai1, TRPC forming channels or Orai1/TRPC1 channels to activate SOCE. $[Ca^{2+}]_s$ Ca^{2+} concentration in the agonist-sensitive stores, A agonist, DAG diacylglycerol, ER endoplasmic reticulum, IP_3 inositol 1,4,5-trisphosphate, PLC phospholipase C, PM plasma membrane, SMOC second messenger-operated Ca^{2+} channel, TRPC1 canonical transient receptor potential 1 protein

several names SOAR (STIM1 Orai-activating region) [218], OASF (Orai-activating small fragment) [218], CAD (CRAC-activating domain) [219] and CCb9 [220], although the most commonly used are SOAR and CAD, which from now on will be referred as SOAR/CAD region. The pioneer studies provide overlapping sequences for the newly identified regions: SOAR (amino acids 344–442), OASF (amino acids 233–450/474), CAD (amino acids 342–448) and CCb9 (amino acids 339–444). At resting state, acidic residues of the cytosolic coiled-coil domain of STIM1 have been reported to mask the basic residues of the SOAR/CAD domain, thus maintaining STIM1 in an inactive configuration; however, upon depletion of the intracellular Ca^{2+} stores, Ca^{2+} dissociates from the STIM1 EF-hand domain leading to dissociation between the coiled-coil domain and SOAR/CAD, whose positive charges now can interact with the acidic residues within the C-terminal domain of Orai1 and activate the SOCs [221]. In agreement with the proposed interaction between the STIM1 SOAR/CAD and the C-terminal region of Orai1, the Orai1 R91W mutant associated to the SCID syndrome did not alter the association of Orai1 with STIM1, although it has been shown to alter the activation of capacitative currents [145]. Association of Orai1 with the STIM1 SOAR/CAD region has recently been reported to be sufficient to induce an intramolecular transition into an extended conformation that might lead to activation of Orai1 [222].

Expression of STIM1 and any of the Orai isoforms has been found to be sufficient to activate I_{CRAC} [76, 89, 94, 147, 150]. Interestingly, an adequate stoichiometrical relationship between STIM1 and Orai1 has been reported to be essential for the activation of I_{CRAC} [89, 223]. Orai1 and STIM1 expression at different ratios (from 4:1 to 1:4) has revealed that low Orai1:STIM1 ratios result in I_{CRAC} with strong fast Ca^{2+}-dependent inactivation, while high Orai1:STIM1 ratios leads to I_{CRAC} with strong activation at negative potentials. In addition, the Orai1:STIM1 expression ratio affects Ca^{2+}, Ba^{2+} and Sr^{2+} conductance [224]; thus suggesting that the stoichiometry between STIM1 and Orai1 is important for the biophysical properties of the channel formed.

On the other hand, STIM1 has also been shown to associate with, and gate TRPC1 and TRPC3 by electrostatic interaction between two conserved, negatively charged aspartates in TRPC1 (D^{639} and D^{640}) and TRPC3 (D^{697} and D^{698}) with the positively charged STIM1 (K^{684} and K^{685}) located in the C-terminal STIM1 polybasic domain [225]. The association of STIM1 and TRPC1 has been demonstrated in a variety of cell types and models including rat basophilic leukaemia cells [226], HEK293 cells [227, 228] and human platelets, which express TRPC1 and STIM1 endogenously [82]. STIM1 has also been reported to associate with other members of the TRPC subfamily including TRPC4, TRPC5 [95] and TRPC6 [17]. The association of STIM1 with TRPC proteins has been reported to require the integrity of the lipid raft domains, plasma membrane microdomains enriched in cholesterol and sphingolipids [229], where STIM1-associated TRPC1 functions as a SOC channel [228, 230, 231]. STIM1 confers TRPC1 store-operated behaviour; in the absence of STIM1, TRPC1 participates in the formation of receptor-operated Ca^{2+} channels, which supports the key role of STIM1 in the activation mode of TRPC1 channels [202, 230, 232].

Despite co-expression of Orai and STIM1 proteins has been found to be sufficient to induce and activate I_{CRAC} [76, 89, 94, 147, 150], current evidence suggest a functional interactions between Orai1 and different TRPC subfamily members under the influence of STIM1. Studies performed in HEK293 cells reported that, in STIM1-expressing cells, TRPC3 and TRPC6, which initially operate in a store-independent manner, become sensitive to store depletion upon expression of exogenous Orai1 [233]. These findings are in agreement with reports in human salivary gland cells, where knockdown of Orai1 significantly reduces I_{SOC} [226], a current where TRPC1 plays a relevant role [197, 213, 214]. Similarly, in human platelets naturally expressing STIM1, Orai1 and TRPC1, selective impairment of the interplay between STIM1 and Orai1 after Ca^{2+} store depletion modifies the mode of activation of TRPC1 from store-operated to store independent, thus suggesting that Orai1 mediates the communication between STIM1 and TRPC1 in these cells [202]. In the same cell type, TRPC6 acts as a point of convergence between store-operated and -independent Ca^{2+} entry pathways. The activation mode is regulated by its interaction with the Orai1-STIM1 complex or hTRPC3, for store-dependent or -independent pathways, respectively [17]. The functional cooperation between STIM1, Orai1 and TRPC1 was further revealed by studies where the expression of TRPC1 was enhanced in the mouse myoblast cell line C2C12, which resulted in enhancement of SOCE and

downregulation of the STIM1-Orai1 pathway [204]. Furthermore, a recent study has reported that Ca^{2+} entry through Orai1-forming channels activates plasma membrane insertion of TRPC1, as demonstrated by knockdown of Orai1 and expression of the dominant negative mutant Orai1 lacking a functional pore Orai1(E106Q) in human salivary gland cells [234]. Therefore, current evidence suggests that store depletion results in a dynamic interplay between STIM1, Orai1 and TRPC proteins, where STIM1 communicates information from the Ca^{2+} stores to the SOCs. Orai proteins might participate in SOCE either independently of the TRPC proteins, leading to the activation of the Ca^{2+} selective I_{CRAC} current [94, 149, 152, 235], or they might participate in the conduction of the non-selective I_{SOC} current in combination with TRPC proteins, where Orai might be a component of the channel itself or might communicate the information of the Ca^{2+} stores from STIM1 to the TRPC subunits [202, 226, 232, 233]. In addition, Orai1 participates in ROCE, as demonstrated by the findings that the SCID Orai1 mutant (R91W) not only impairs SOCE, but, more interestingly, attenuates ROCE in cells expressing TRPC3 [236]. The coordination of STIM1, Orai1 and TRPC1 to mediate Ca^{2+} entry, as well as their possible regulatory role on other ionic channels deserves further investigations.

SOCE and Disease

Altered Ca^{2+} homeostasis and SOCE have been found associated to some pathological conditions in human and murine models of disease, indicating a critical role of SOCE in many cellular functions and for normal life. In human, patients lacking functional Orai1 and STIM1 suffered from compromised immune responses very early in their lives, similar to severe combined immune deficiency (SCID), which supposed a threat for their lives unless treated by hematopoietic stem cell transplantation [75, 175, 237–242], for review see [176, 243, 244]. The similarity of phenotypes found in Orai1- and STIM1-deficient cells indicated participation in similar signaling pathways. Normal numbers of T, B cells and natural killer (NK) cytotoxic cells were found in peripheral blood from these patients, but showed defective responses as consequence of impaired SOCE and cytokine production [75, 175, 176, 237–239, 243–246]. Despite the normal immunoglobulin (Ig) levels found in blood serum, Orai1-deficient patients failed to mount antigen-specific antibody responses [176, 243, 244]. These results indicated that STIM1- or Orai1-mediated SOCE is essential for cell function in the immune system but not for their development. STIM1-deficient patients also presented reduced blood platelet numbers as consequence of autoimmune responses against these cells [239], presumably due to the reduced number of $FoxP3^{+}$ regulatory T cells (Tregs) found in these patients, which are involved in inhibition of autoimmune responses [176, 239, 243, 244]. Orai1- and STIM1-deficient patients also presented myophaties characterized by global muscular hypotonia, chronic pulmonary disease as consequence of defective respiratory muscle function and impaired sweat production [175, 176, 239, 243, 244]. Taken together, these results indicated a predominant function of Orai1- and

STIM1-mediated SOCE in the immune system and in other tissues such as skeletal muscle and endodermal tissues. The localized phenotype found restricted to certain tissues contrast to the ubiquitous expression of Orai1 or STIM1, suggesting compensation mechanisms in the unaffected tissues, presumably by their homologues Orai2, Orai3 and STIM2 [176, 243, 244]. In human, other studies found strong correlation between presence of certain single nucleotide polymorphisms (rs12313273) in *Orai1* alleles and risk or recurrence of stone generation in kidney, referred to as calcium nephrolithiasis [247]. Diseases associated to absence of Orai2, Orai3 or STIM2 function have not been identified in human yet.

The phenotypic analysis of mice lacking Orai1, STIM1, and STIM2 function also helped to elucidate the role of SOCE in different cellular functions and pathologic conditions [103, 106, 107, 128–130, 158, 248–251]. The analysis of Orai1 and STIM deficiency in murine models already evidenced additional potential roles of SOCE mediated by these proteins in autoimmune and inflammatory responses. A crucial function of STIM1 and STIM2 has been reported in experimental autoimmune encephalomyelitis (EAE) [106, 252]. The absence of STIM1 function abrogated T cell autoimmune responses against neuronal tissue and impaired EAE in mice, while the lack of STIM2 only attenuated EAE, indicating an essential function of STIMs for development of autoinmune disorders. Mast cells isolated from Orai1-deficient mice showed defective degranulation and cytokine secretion, which impaired in turn allergic reactions elicited in these mutant mice [158], indicating an essential role of Orai1 in the development of allergic responses. Thus, Orai1 and STIMs molecules might be key molecules involved in cases of augmented autoreactive and allergic responses and therefore, attractive therapeutic targets for the treatment of these disorders. SOCE also has demonstrated a key role in blood platelet function, thrombosis and hemostasis. Orai1- and STIM1-deficient mice showed abrogated SOCE, impaired platelet function and procoagulant activity due to a reduced glycoprotein VI- and thrombin-dependent surface exposure of phosphatidylserine (PS), and were protected against ischemic brain infarction or pulmonary thromboembolism [128, 130, 248, 251], indicating that Orai1- and STIM1-mediated SOCE might play critical roles in the pathogenesis of ischemic cardio- and cerebrovascular diseases. Interestingly, STIM2-deficient mice showed normal platelet function but were also protected against ischemic brain infarction [103]. In this case, lack of STIM2 impaired SOCE and conferred protection to neurons against ischemic neuronal death, presumably by prevention of excessive Ca^{2+} entry and cytotoxic overload into the cytosol, indicating the STIM2 might play an active role in mechanisms underlying ischemic brain damage generated during pathologic conditions. Altered Ca^{2+} homeostasis has been also linked to neuronal damage caused by brain aging or Alzheimer's disease. A recent study suggested that the physiological role of amyloid-β precursor protein (APP), whose altered metabolism has been associated with Alzheimer's disease, is the regulation of TRPC1/Orai1-mediated SOCE which is critical for Ca^{2+} signaling in astrocytes [253]. In line with this report, impaired SOCE was also observed in fibroblasts bearing mutated presenilin-1 and 2 genes, which has been associated to autosomal dominant familial Alzheimer's disease (FAD), while absence of this protein led to increased SOCE

and augmented expression of STIM1 [254–257]. Similarly, the cellular prion protein (PrP^C), whose structural conversion is well known for generate the agent causing transmissible spongiform encephalopathies, has been also involved in regulation of SOCE in cerebellar granule neurons [258, 259]. Thus, altered SOCE might be also involved in these diseases, but its contribution still remains to be elucidated. Reduced SOCE was observed in platelets from type 2 diabetic patients, probably as consequence of impaired association between STIM1 and Orai1, hTRPC1 or hTRPC6, which might be involved in the altered platelet function observed in diabetic patients [260]. In the other hand, augmented vasoconstriction observed in diabetic mice was associated to increased SOCE and intracellular Ca^{2+} in endothelial cell of the vascular system, which might stimulate endothelial synthesis of thromboxane A2 and contractile prostaglandins and would contribute to arterial stiffness associated with diabetes [261].

Finally, emerging evidences suggest the involvement of the STIM/Orai-mediated SOCE in cancer. STIM1 was initially identified as a molecule which induces growth arrest and degeneration of certain human cancer cell lines, such as G401 and RD, suggesting a role in the pathogenesis of tumors [262]. Increased expression of STIM2 has been found in glioblastoma multiforme tumors [263]. Analysis of 295 breast cancers showed an altered relationship between STIM1 and STIM2, specially STIM1 high/STIM2 low expression ratios were found in cells from breast tumors with the poorest prognosis [125]. Recent studies reported the involvement of STIM1/2 and Orai3-dependent SOCE in estrogen receptor-positive ER(+)-breast cancer cells, while SOCE involved the STIM1/Orai1 pathway in ER(−) breast cancer cells [126]. Indeed, siRNA downregulation of Orai3 in MCF-7 breast cancer cell line, which expresses high levels of this SOC channel subunit, attenuated cell proliferation and arrested their cell cycle at G1 phase [173], indicating a critical implication of Orai3-mediated SOCE in cancer cell growth. Thus, these results indicate a potential use of STIM/Orai as therapeutic targets in certain types of cancer.

Acknowledgements This work was supported by M.E.C. grants BFU2010-21043-C02-01 and Junta de Extremadura-FEDER (PRIBS10020 and GR10010). PCR is supported by MEC "Ramón y Cajal program" (RYC2007-00349) and AB held a contract from the University of Extremadura.

References

1. Bootman MD, Lipp P, Berridge MJ (2001) The organisation and functions of local Ca^{2+} signals. J Cell Sci 114:2213–2222
2. O'Neill SC, Miller L, Hinch R, Eisner DA (2004) Interplay between SERCA and sarcolemmal Ca^{2+} efflux pathways controls spontaneous release of Ca^{2+} from the sarcoplasmic reticulum in rat ventricular myocytes. J Physiol 559:121–128
3. Van Coppenolle F, Vanden Abeele F, Slomianny C, Flourakis M, Hesketh J, Dewailly E, Prevarskaya N (2004) Ribosome-translocon complex mediates calcium leakage from endoplasmic reticulum stores. J Cell Sci 117:4135–4142
4. Patel S, Docampo R (2010) Acidic calcium stores open for business: expanding the potential for intracellular Ca^{2+} signaling. Trends Cell Biol 20:277–286

5. Meldolesi J, Pozzan T (1998) The endoplasmic reticulum Ca^{2+} store: a view from the lumen. Trends Biochem Sci 23:10–14
6. Cancela JM, Charpentier G, Petersen OH (2003) Co-ordination of Ca^{2+} signalling in mammalian cells by the new Ca^{2+}-releasing messenger NAADP. Pflugers Arch 446:322–327
7. Patel S, Churchill GC, Galione A (2001) Coordination of Ca^{2+} signalling by NAADP. Trends Biochem Sci 26:482–489
8. Streb H, Irvine RF, Berridge MJ, Schulz I (1983) Release of Ca^{2+} from a nonmitochondrial intracellular store in pancreatic acinar cells by inositol-1,4,5-trisphosphate. Nature 306:67–69
9. Galione A, Lee HC, Busa WB (1991) Ca^{2+}-induced Ca^{2+} release in sea urchin egg homogenates: modulation by cyclic ADP-ribose. Science 253:1143–1146
10. Sher E, Biancardi E, Passafaro M, Clementi F (1991) Physiopathology of neuronal voltage-operated calcium channels. FASEB J 5:2677–2683
11. Alexander SP, Mathie A, Peters JA (2006) Guide to receptors and channels, 2nd edition. Br J Pharmacol 147(Suppl 3):S1–S168
12. Kyrozis A, Goldstein PA, Heath MJ, MacDermott AB (1995) Calcium entry through a subpopulation of AMPA receptors desensitized neighbouring NMDA receptors in rat dorsal horn neurons. J Physiol 485:373–381
13. Matsuda K, Fletcher M, Kamiya Y, Yuzaki M (2003) Specific assembly with the NMDA receptor 3B subunit controls surface expression and calcium permeability of NMDA receptors. J Neurosci 23:10064–10073
14. McKemy DD, Neuhausser WM, Julius D (2002) Identification of a cold receptor reveals a general role for TRP channels in thermosensation. Nature 416:52–58
15. Caterina MJ, Rosen TA, Tominaga M, Brake AJ, Julius D (1999) A capsaicin-receptor homologue with a high threshold for noxious heat. Nature 398:436–441
16. Valente P, Garcia-Sanz N, Gomis A, Fernandez-Carvajal A, Fernandez-Ballester G, Viana F, Belmonte C, Ferrer-Montiel A (2008) Identification of molecular determinants of channel gating in the transient receptor potential box of vanilloid receptor I. FASEB J 22:3298–3309
17. Jardin I, Gomez LJ, Salido GM, Rosado JA (2009) Dynamic interaction of hTRPC6 with the Orai1/STIM1 complex or hTRPC3 mediates its role in capacitative or non-capacitative Ca^{2+} entry pathways. Biochem J 420:267–276
18. Hofmann T, Obukhov AG, Schaefer M, Harteneck C, Gudermann T, Schultz G (1999) Direct activation of human TRPC6 and TRPC3 channels by diacylglycerol. Nature 397:259–263
19. Vazquez G, Wedel BJ, Kawasaki BT, Bird GS, Putney JW Jr (2004) Obligatory role of Src kinase in the signaling mechanism for TRPC3 cation channels. J Biol Chem 279:40521–40528
20. Moneer Z, Pino I, Taylor EJ, Broad LM, Liu Y, Tovey SC, Staali L, Taylor CW (2005) Different phospholipase-C-coupled receptors differentially regulate capacitative and non-capacitative Ca^{2+} entry in A7r5 cells. Biochem J 389:821–829
21. Soboloff J, Spassova M, Xu W, He LP, Cuesta N, Gill DL (2005) Role of endogenous TRPC6 channels in Ca^{2+} signal generation in A7r5 smooth muscle cells. J Biol Chem 280:39786–39794
22. Chakrabarti R, Chakrabarti R (2006) Calcium signaling in non-excitable cells: Ca^{2+} release and influx are independent events linked to two plasma membrane Ca^{2+} entry channels. J Cell Biochem 99:1503–1516
23. Vazquez G, Bird GS, Mori Y, Putney JW Jr (2006) Native TRPC7 channel activation by an inositol trisphosphate receptor-dependent mechanism. J Biol Chem 281:25250–25258
24. Berra-Romani R, Mazzocco-Spezzia A, Pulina MV, Golovina VA (2008) Ca^{2+} handling is altered when arterial myocytes progress from a contractile to a proliferative phenotype in culture. Am J Physiol Cell Physiol 295:C779–C790
25. Wang Y, Deng X, Hewavitharana T, Soboloff J, Gill DL (2008) Stim, orai and trpc channels in the control of calcium entry signals in smooth muscle. Clin Exp Pharmacol Physiol 35:1127–1133
26. Rosado JA, Sage SO (2000) Protein kinase C activates non-capacitative calcium entry in human platelets. J Physiol 529(Pt 1):159–169

27. Togashi K, Hara Y, Tominaga T, Higashi T, Konishi Y, Mori Y, Tominaga M (2006) TRPM2 activation by cyclic ADP-ribose at body temperature is involved in insulin secretion. EMBO J 25:1804–1815
28. Redondo PC, Salido GM, Pariente JA, Rosado JA (2004) Dual effect of hydrogen peroxide on store-mediated calcium entry in human platelets. Biochem Pharmacol 67:1065–1076
29. Rosado JA, Redondo PC, Salido GM, Gomez-Arteta E, Sage SO, Pariente JA (2004) Hydrogen peroxide generation induces pp 60src activation in human platelets: evidence for the involvement of this pathway in store-mediated calcium entry. J Biol Chem 279:1665–1675
30. Zhang W, Tong Q, Conrad K, Wozney J, Cheung JY, Miller BA (2007) Regulation of TRP channel TRPM2 by the tyrosine phosphatase PTPL1. Am J Physiol Cell Physiol 292: C1746–C1758
31. Amor NB, Redondo PC, Bartegi A, Pariente JA, Salido GM, Rosado JA (2006) A role for 5,6-epoxyeicosatrienoic acid in calcium entry by de novo conformational coupling in human platelets. J Physiol 570:309–323
32. Loot AE, Popp R, Fisslthaler B, Vriens J, Nilius B, Fleming I (2008) Role of cytochrome P450-dependent transient receptor potential V4 activation in flow-induced vasodilatation. Cardiovasc Res 80:445–452
33. Rohacs T, Nilius B (2007) Regulation of transient receptor potential (TRP) channels by phosphoinositides. Pflugers Arch 455:157–168
34. Jardin I, Redondo PC, Salido GM, Rosado JA (2008) Phosphatidylinositol 4,5-bisphosphate enhances store-operated calcium entry through hTRPC6 channel in human platelets. Biochim Biophys Acta 1783:84–97
35. Putney JW Jr (1986) A model for receptor-regulated calcium entry. Cell Calcium 7:1–12
36. Lee C, Xu DZ, Feketeova E, Kannan KB, Fekete Z, Deitch EA, Livingston DH, Hauser CJ (2005) Store-operated calcium channel inhibition attenuates neutrophil function and post-shock acute lung injury. J Trauma 59:56–63
37. Leung FP, Yung LM, Yao X, Laher I, Huang Y (2008) Store-operated calcium entry in vascular smooth muscle. Br J Pharmacol 153:846–857
38. Berridge MJ (1995) Capacitative calcium entry. Biochem J 312(Pt 1):1–11
39. Redondo PC, Harper MT, Rosado JA, Sage SO (2006) A role for cofilin in the activation of store-operated calcium entry by de novo conformational coupling in human platelets. Blood 107:973–979
40. Galan C, Zbidi H, Bartegi A, Salido GM, Rosado JA (2009) STIM1, Orai1 and hTRPC1 are important for thrombin- and ADP-induced aggregation in human platelets. Arch Biochem Biophys 490:137–144
41. Feske S (2007) Calcium signalling in lymphocyte activation and disease. Nat Rev Immunol 7:690–702
42. Wedel B, Boyles RR, Putney JW Jr, Bird GS (2007) Role of the store-operated calcium entry proteins Stim1 and Orai1 in muscarinic cholinergic receptor-stimulated calcium oscillations in human embryonic kidney cells. J Physiol 579:679–689
43. Yan X, Xing J, Lorin-Nebel C, Estevez AY, Nehrke K, Lamitina T, Strange K (2006) Function of a STIM1 homologue in C. elegans: evidence that store-operated Ca^{2+} entry is not essential for oscillatory Ca^{2+} signaling and ER Ca^{2+} homeostasis. J Gen Physiol 128:443–459
44. Randriamampita C, Tsien RY (1993) Emptying of intracellular Ca^{2+} stores releases a novel small messenger that stimulates Ca^{2+} influx. Nature 364:809–814
45. Pandol SJ, Schoeffield-Payne MS (1990) Cyclic GMP mediates the agonist-stimulated increase in plasma membrane calcium entry in the pancreatic acinar cell. J Biol Chem 265:12846–12853
46. Sargeant P, Farndale RW, Sage SO (1993) ADP- and thapsigargin-evoked Ca^{2+} entry and protein-tyrosine phosphorylation are inhibited by the tyrosine kinase inhibitors genistein and methyl-2,5-dihydroxycinnamate in fura-2-loaded human platelets. J Biol Chem 268: 18151–18156

47. Sargeant P, Farndale RW, Sage SO (1994) Calcium store depletion in dimethyl BAPTA-loaded human platelets increases protein tyrosine phosphorylation in the absence of a rise in cytosolic calcium. Exp Physiol 79:269–272
48. Rosado JA, Graves D, Sage SO (2000) Tyrosine kinases activate store-mediated Ca^{2+} entry in human platelets through the reorganization of the actin cytoskeleton. Biochem J 351: 429–437
49. Alvarez J, Montero M, Garcia-Sancho J (1992) Cytochrome P450 may regulate plasma membrane Ca^{2+} permeability according to the filling state of the intracellular Ca^{2+} stores. FASEB J 6:786–792
50. Bird GS, Putney JW Jr (1993) Inhibition of thapsigargin-induced calcium entry by microinjected guanine nucleotide analogues. Evidence for the involvement of a small G-protein in capacitative calcium entry. J Biol Chem 268:21486–21488
51. Rosado JA, Sage SO (2000) Farnesylcysteine analogues inhibit store-regulated Ca^{2+} entry in human platelets: evidence for involvement of small GTP-binding proteins and actin cytoskeleton. Biochem J 347(Pt 1):183–192
52. Fasolato C, Hoth M, Penner R (1993) A GTP-dependent step in the activation mechanism of capacitative calcium influx. J Biol Chem 268:20737–20740
53. Yao Y, Ferrer-Montiel AV, Montal M, Tsien RY (1999) Activation of store-operated Ca^{2+} current in Xenopus oocytes requires SNAP-25 but not a diffusible messenger. Cell 98:475–485
54. Muallem S, Kwiatkowska K, Xu X, Yin HL (1995) Actin filament disassembly is a sufficient final trigger for exocytosis in nonexcitable cells. J Cell Biol 128:589–598
55. Patterson RL, van Rossum DB, Gill DL (1999) Store-operated Ca^{2+} entry: evidence for a secretion-like coupling model. Cell 98:487–499
56. Bezzerides VJ, Ramsey IS, Kotecha S, Greka A, Clapham DE (2004) Rapid vesicular translocation and insertion of TRP channels. Nat Cell Biol 6:709–720
57. Cayouette S, Lussier MP, Mathieu EL, Bousquet SM, Boulay G (2004) Exocytotic insertion of TRPC6 channel into the plasma membrane upon Gq protein-coupled receptor activation. J Biol Chem 279:7241–7246
58. Singh BB, Lockwich TP, Bandyopadhyay BC, Liu X, Bollimuntha S, Brazer SC, Combs C, Das S, Leenders AG, Sheng ZH, Knepper MA, Ambudkar SV, Ambudkar IS (2004) VAMP2-dependent exocytosis regulates plasma membrane insertion of TRPC3 channels and contributes to agonist-stimulated Ca^{2+} influx. Mol Cell 15:635–646
59. Woodard GE, Salido GM, Rosado JA (2008) Enhanced exocytotic-like insertion of Orai1 into the plasma membrane upon intracellular Ca^{2+} store depletion. Am J Physiol Cell Physiol 294:C1323–C1331
60. Irvine RF (1990) 'Quantal' Ca^{2+} release and the control of Ca^{2+} entry by inositol phosphates – a possible mechanism. FEBS Lett 263:5–9
61. Block BA, Imagawa T, Campbell KP, Franzini-Armstrong C (1988) Structural evidence for direct interaction between the molecular components of the transverse tubule/sarcoplasmic reticulum junction in skeletal muscle. J Cell Biol 107:2587–2600
62. Kiselyov K, Mignery GA, Zhu MX, Muallem S (1999) The N-terminal domain of the IP_3 receptor gates store-operated hTrp3 channels. Mol Cell 4:423–429
63. Boulay G, Brown DM, Qin N, Jiang M, Dietrich A, Zhu MX, Chen Z, Birnbaumer M, Mikoshiba K, Birnbaumer L (1999) Modulation of Ca^{2+} entry by polypeptides of the inositol 1,4, 5-trisphosphate receptor (IP_3R) that bind transient receptor potential (TRP): evidence for roles of TRP and IP_3R in store depletion-activated Ca^{2+} entry. Proc Natl Acad Sci USA 96:14955–14960
64. Birnbaumer L, Boulay G, Brown D, Jiang M, Dietrich A, Mikoshiba K, Zhu X, Qin N (2000) Mechanism of capacitative Ca^{2+} entry (CCE): interaction between IP_3 receptor and TRP links the internal calcium storage compartment to plasma membrane CCE channels. Recent Prog Horm Res 55:127–161
65. Treves S, Franzini-Armstrong C, Moccagatta L, Arnoult C, Grasso C, Schrum A, Ducreux S, Zhu MX, Mikoshiba K, Girard T, Smida-Rezgui S, Ronjat M, Zorzato F (2004) Junctate is a

key element in calcium entry induced by activation of $InsP_3$ receptors and/or calcium store depletion. J Cell Biol 166:537–548
66. Rosado JA, Jenner S, Sage SO (2000) A role for the actin cytoskeleton in the initiation and maintenance of store-mediated calcium entry in human platelets. Evidence for conformational coupling. J Biol Chem 275:7527–7533
67. Rosado JA, Sage SO (2001) Activation of store-mediated calcium entry by secretion-like coupling between the inositol 1,4,5-trisphosphate receptor type II and human transient receptor potential (hTrp1) channels in human platelets. Biochem J 356:191–198
68. Rosado JA, Sage SO (2002) The ERK cascade, a new pathway involved in the activation of store-mediated calcium entry in human platelets. Trends Cardiovasc Med 12:229–234
69. Redondo PC, Harper AG, Sage SO, Rosado JA (2007) Dual role of tubulin-cytoskeleton in store-operated calcium entry in human platelets. Cell Signal 19:2147–2154
70. Xie Q, Zhang Y, Zhai C, Bonanno JA (2002) Calcium influx factor from cytochrome P-450 metabolism and secretion-like coupling mechanisms for capacitative calcium entry in corneal endothelial cells. J Biol Chem 277:16559–16566
71. Rosado JA, Sage SO (2000) Coupling between inositol 1,4,5-trisphosphate receptors and human transient receptor potential channel 1 when intracellular Ca^{2+} stores are depleted. Biochem J 350(Pt 3):631–635
72. Brownlow SL, Sage SO (2003) Rapid agonist-evoked coupling of type II $Ins(1,4,5)P_3$ receptor with human transient receptor potential (hTRPC1) channels in human platelets. Biochem J 375:697–704
73. Roos J, DiGregorio PJ, Yeromin AV, Ohlsen K, Lioudyno M, Zhang S, Safrina O, Kozak JA, Wagner SL, Cahalan MD, Velicelebi G, Stauderman KA (2005) STIM1, an essential and conserved component of store-operated Ca^{2+} channel function. J Cell Biol 169:435–445
74. Zhang SL, Yu Y, Roos J, Kozak JA, Deerinck TJ, Ellisman MH, Stauderman KA, Cahalan MD (2005) STIM1 is a Ca^{2+} sensor that activates CRAC channels and migrates from the Ca^{2+} store to the plasma membrane. Nature 437:902–905
75. Feske S, Gwack Y, Prakriya M, Srikanth S, Puppel SH, Tanasa B, Hogan PG, Lewis RS, Daly M, Rao A (2006) A mutation in Orai1 causes immune deficiency by abrogating CRAC channel function. Nature 441:179–185
76. Mercer JC, Dehaven WI, Smyth JT, Wedel B, Boyles RR, Bird GS, Putney JW Jr (2006) Large store-operated calcium selective currents due to co-expression of Orai1 or Orai2 with the intracellular calcium sensor, Stim1. J Biol Chem 281:24979–24990
77. Jardin I, Lopez JJ, Salido GM, Rosado JA (2008) Functional relevance of the de novo coupling between hTRPC1 and type II IP_3 receptor in store-operated Ca^{2+} entry in human platelets. Cell Signal 20:737–747
78. Bandyopadhyay BC, Ong HL, Lockwich TP, Liu X, Paria BC, Singh BB, Ambudkar IS (2008) TRPC3 controls agonist-stimulated intracellular Ca^{2+} release by mediating the interaction between inositol 1,4,5-trisphosphate receptor and RACK1. J Biol Chem 283: 32821–32830
79. Woodard GE, Lopez JJ, Jardin I, Salido GM, Rosado JA (2010) TRPC3 regulates agonist-stimulated Ca^{2+} mobilization by mediating the interaction between type I inositol 1,4,5-trisphosphate receptor, RACK1, and Orai1. J Biol Chem 285:8045–8053
80. Zbidi H, Jardin I, Woodard GE, Lopez JJ, Berna-Erro A, Salido GM, Rosado JA (2011) STIM1 and STIM2 are located in the acidic Ca^{2+} stores and associates with Orai1 upon depletion of the acidic stores in human platelets. J Biol Chem 286:12257–12270
81. Liou J, Kim ML, Heo WD, Jones JT, Myers JW, Ferrell JE Jr, Meyer T (2005) STIM is a Ca^{2+} sensor essential for Ca^{2+}-store-depletion-triggered Ca^{2+} influx. Curr Biol 15:1235–1241
82. Lopez JJ, Salido GM, Pariente JA, Rosado JA (2006) Interaction of STIM1 with endogenously expressed human canonical TRP1 upon depletion of intracellular Ca^{2+} stores. J Biol Chem 281:28254–28264
83. Spassova MA, Soboloff J, He LP, Xu W, Dziadek MA, Gill DL (2006) STIM1 has a plasma membrane role in the activation of store-operated Ca^{2+} channels. Proc Natl Acad Sci USA 103:4040–4045

84. Schultz J, Ponting CP, Hofmann K, Bork P (1997) SAM as a protein interaction domain involved in developmental regulation. Protein Sci 6:249–253
85. Brandman O, Liou J, Park WS, Meyer T (2007) STIM2 is a feedback regulator that stabilizes basal cytosolic and endoplasmic reticulum Ca^{2+} levels. Cell 131:1327–1339
86. Huang Y, Zhou Y, Wong HC, Chen Y, Wang S, Castiblanco A, Liu A, Yang JJ (2009) A single EF-hand isolated from STIM1 forms dimer in the absence and presence of Ca^{2+}. FEBS J 276:5589–5597
87. Soboloff J, Spassova MA, Dziadek MA, Gill DL (2006) Calcium signals mediated by STIM and Orai proteins – a new paradigm in inter-organelle communication. Biochim Biophys Acta 1763:1161–1168
88. Schindl R, Muik M, Fahrner M, Derler I, Fritsch R, Bergsmann J, Romanin C (2009) Recent progress on STIM1 domains controlling Orai activation. Cell Calcium 46:227–232
89. Soboloff J, Spassova MA, Tang XD, Hewavitharana T, Xu W, Gill DL (2006) Orai1 and STIM reconstitute store-operated calcium channel function. J Biol Chem 281:20661–20665
90. Jardin I, Lopez JJ, Redondo PC, Salido GM, Rosado JA (2009) Store-operated Ca^{2+} entry is sensitive to the extracellular Ca^{2+} concentration through plasma membrane STIM1. Biochim Biophys Acta 1793:1614–1622
91. Dionisio N, Galan C, Jardin I, Salido GM, Rosado JA (2011) Lipid rafts are essential for the regulation of SOCE by plasma membrane resident STIM1 in human platelets. Biochim Biophys Acta 1813:431–437
92. Pani B, Ong HL, Liu X, Rauser K, Ambudkar IS, Singh BB (2008) Lipid rafts determine clustering of STIM1 in endoplasmic reticulum-plasma membrane junctions and regulation of store-operated Ca^{2+} entry (SOCE). J Biol Chem 283:17333–17340
93. Luik RM, Wu MM, Buchanan J, Lewis RS (2006) The elementary unit of store-operated Ca^{2+} entry: local activation of CRAC channels by STIM1 at ER-plasma membrane junctions. J Cell Biol 174:815–825
94. Peinelt C, Vig M, Koomoa DL, Beck A, Nadler MJ, Koblan-Huberson M, Lis A, Fleig A, Penner R, Kinet JP (2006) Amplification of CRAC current by STIM1 and CRACM1 (Orai1). Nat Cell Biol 8:771–773
95. Yuan JP, Zeng W, Huang GN, Worley PF, Muallem S (2007) STIM1 heteromultimerizes TRPC channels to determine their function as store-operated channels. Nat Cell Biol 9:636–645
96. Park CY, Shcheglovitov A, Dolmetsch R (2010) The CRAC channel activator STIM1 binds and inhibits L-type voltage-gated calcium channels. Science 330:101–105
97. Wang Y, Deng X, Mancarella S, Hendron E, Eguchi S, Soboloff J, Tang XD, Gill DL (2010) The calcium store sensor, STIM1, reciprocally controls Orai and CaV1.2 channels. Science 330:105–109
98. Williams RT, Manji SS, Parker NJ, Hancock MS, Van Stekelenburg L, Eid JP, Senior PV, Kazenwadel JS, Shandala T, Saint R, Smith PJ, Dziadek MA (2001) Identification and characterization of the STIM (stromal interaction molecule) gene family: coding for a novel class of transmembrane proteins. Biochem J 357:673–685
99. Huang GN, Zeng W, Kim JY, Yuan JP, Han L, Muallem S, Worley PF (2006) STIM1 carboxyl-terminus activates native SOC, I(crac) and TRPC1 channels. Nat Cell Biol 8:1003–1010
100. Li Z, Lu J, Xu P, Xie X, Chen L, Xu T (2007) Mapping the interacting domains of STIM1 and Orai1 in Ca^{2+} release-activated Ca^{2+} channel activation. J Biol Chem 282:29448–29456
101. Pozo-Guisado E, Campbell DG, Deak M, Alvarez-Barrientos A, Morrice NA, Alvarez IS, Alessi DR, Martin-Romero FJ (2010) Phosphorylation of STIM1 at ERK1/2 target sites modulates store-operated calcium entry. J Cell Sci 123:3084–3093
102. Smyth JT, Petranka JG, Boyles RR, DeHaven WI, Fukushima M, Johnson KL, Williams JG, Putney JW Jr (2009) Phosphorylation of STIM1 underlies suppression of store-operated calcium entry during mitosis. Nat Cell Biol 11:1465–1472
103. Berna-Erro A, Braun A, Kraft R, Kleinschnitz C, Schuhmann MK, Stegner D, Wultsch T, Eilers J, Meuth SG, Stoll G, Nieswandt B (2009) STIM2 regulates capacitive Ca^{2+} entry in neurons and plays a key role in hypoxic neuronal cell death. Sci Signal 2:ra67

104. Cordeiro S, Strauss O (2011) Expression of Orai genes and I(CRAC) activation in the human retinal pigment epithelium. Graefes Arch Clin Exp Ophthalmol 249:47–54
105. Gao YD, Hanley PJ, Rinne S, Zuzarte M, Daut J (2010) Calcium-activated K^+ channel (K(Ca)3.1) activity during Ca^{2+} store depletion and store-operated Ca^{2+} entry in human macrophages. Cell Calcium 48:19–27
106. Schuhmann MK, Stegner D, Berna-Erro A, Bittner S, Braun A, Kleinschnitz C, Stoll G, Wiendl H, Meuth SG, Nieswandt B (2010) Stromal interaction molecules 1 and 2 are key regulators of autoreactive T cell activation in murine autoimmune central nervous system inflammation. J Immunol 184:1536–1542
107. Oh-hora M, Yamashita M, Hogan PG, Sharma S, Lamperti E, Chung W, Prakriya M, Feske S, Rao A (2008) Dual functions for the endoplasmic reticulum calcium sensors STIM1 and STIM2 in T cell activation and tolerance. Nat Immunol 9:432–443
108. Darbellay B, Arnaudeau S, Ceroni D, Bader CR, Konig S, Bernheim L (2010) Human muscle economy myoblast differentiation and excitation-contraction coupling use the same molecular partners, STIM1 and STIM2. J Biol Chem 285:22437–22447
109. Matsumoto M, Fujii Y, Baba A, Hikida M, Kurosaki T, Baba Y (2011) The calcium sensors STIM1 and STIM2 control B cell regulatory function through interleukin-10 production. Immunity 34:703–714
110. Soboloff J, Spassova MA, Hewavitharana T, He LP, Xu W, Johnstone LS, Dziadek MA, Gill DL (2006) STIM2 is an inhibitor of STIM1-mediated store-operated Ca^{2+} Entry. Curr Biol 16:1465–1470
111. Manji SS, Parker NJ, Williams RT, Van SL, Pearson RB, Dziadek M, Smith PJ (2000) STIM1: a novel phosphoprotein located at the cell surface. Biochim Biophys Acta 1481: 147–155
112. Williams RT, Senior PV, Van SL, Layton JE, Smith PJ, Dziadek MA (2002) Stromal interaction molecule 1 (STIM1), a transmembrane protein with growth suppressor activity, contains an extracellular SAM domain modified by N-linked glycosylation. Biochim Biophys Acta 1596:131–137
113. Kim CA, Bowie JU (2003) SAM domains: uniform structure, diversity of function. Trends Biochem Sci 28:625–628
114. Stathopulos PB, Zheng L, Li GY, Plevin MJ, Ikura M (2008) Structural and mechanistic insights into STIM1-mediated initiation of store-operated calcium entry. Cell 135: 110–122
115. Stathopulos PB, Li GY, Plevin MJ, Ames JB, Ikura M (2006) Stored Ca^{2+} depletion-induced oligomerization of stromal interaction molecule 1 (STIM1) via the EF-SAM region: an initiation mechanism for capacitive Ca^{2+} entry. J Biol Chem 281:35855–35862
116. Baba Y, Hayashi K, Fujii Y, Mizushima A, Watarai H, Wakamori M, Numaga T, Mori Y, Iino M, Hikida M, Kurosaki T (2006) Coupling of STIM1 to store-operated Ca^{2+} entry through its constitutive and inducible movement in the endoplasmic reticulum. Proc Natl Acad Sci USA 103:16704–16709
117. Zheng L, Stathopulos PB, Schindl R, Li GY, Romanin C, Ikura M (2011) Auto-inhibitory role of the EF-SAM domain of STIM proteins in store-operated calcium entry. Proc Natl Acad Sci USA 108:1337–1342
118. Stathopulos PB, Zheng L, Ikura M (2009) Stromal interaction molecule (STIM) 1 and STIM2 calcium sensing regions exhibit distinct unfolding and oligomerization kinetics. J Biol Chem 284:728–732
119. Barrero MJ, Montero M, Alvarez J (1997) Dynamics of $[Ca^{2+}]$ in the endoplasmic reticulum and cytoplasm of intact HeLa cells. A comparative study. J Biol Chem 272:27694–27699
120. Demaurex N, Frieden M (2003) Measurements of the free luminal ER Ca^{2+} concentration with targeted "cameleon" fluorescent proteins. Cell Calcium 34:109–119
121. Yu R (2000) Hinkle PM: rapid turnover of calcium in the endoplasmic reticulum during signaling. Studies with cameleon calcium indicators. J Biol Chem 275:23648–23653
122. Parry DA, Fraser RD, Squire JM (2008) Fifty years of coiled-coils and alpha-helical bundles: a close relationship between sequence and structure. J Struct Biol 163:258–269

123. Bauer MC, O'Connell D, Cahill DJ, Linse S (2008) Calmodulin binding to the polybasic C-termini of STIM proteins involved in store-operated calcium entry. Biochemistry 47: 6089–6091
124. Parvez S, Beck A, Peinelt C, Soboloff J, Lis A, Monteilh-Zoller M, Gill DL, Fleig A, Penner R (2008) STIM2 protein mediates distinct store-dependent and store-independent modes of CRAC channel activation. FASEB J 22:752–761
125. McAndrew D, Grice DM, Peters AA, Davis FM, Stewart T, Rice M, Smart CE, Brown MA, Kenny PA, Roberts-Thomson SJ, Monteith GR (2011) ORAI1-mediated calcium influx in lactation and in breast cancer. Mol Cancer Ther 10:448–460
126. Motiani RK, Abdullaev IF, Trebak M (2010) A novel native store-operated calcium channel encoded by Orai3: selective requirement of Orai3 versus Orai1 in estrogen receptor-positive versus estrogen receptor-negative breast cancer cells. J Biol Chem 285: 19173–19183
127. Lu W, Wang J, Peng G, Shimoda LA, Sylvester JT (2009) Knockdown of stromal interaction molecule 1 attenuates store-operated Ca^{2+} entry and Ca^{2+} responses to acute hypoxia in pulmonary arterial smooth muscle. Am J Physiol Lung Cell Mol Physiol 297:L17–L25
128. Varga-Szabo D, Braun A, Kleinschnitz C, Bender M, Pleines I, Pham M, Renne T, Stoll G, Nieswandt B (2008) The calcium sensor STIM1 is an essential mediator of arterial thrombosis and ischemic brain infarction. J Exp Med 205:1583–1591
129. Braun A, Gessner JE, Varga-Szabo D, Syed SN, Konrad S, Stegner D, Vogtle T, Schmidt RE, Nieswandt B (2009) STIM1 is essential for Fcgamma receptor activation and autoimmune inflammation. Blood 113:1097–1104
130. Gilio K, van Kruchten R, Braun A, Berna-Erro A, Feijge MA, Stegner D, van der Meijden PE, Kuijpers MJ, Varga-Szabo D, Heemskerk JW, Nieswandt B (2010) Roles of platelet STIM1 and Orai1 in glycoprotein VI- and thrombin-dependent procoagulant activity and thrombus formation. J Biol Chem 285:23629–23638
131. Brechard S, Plancon S, Melchior C, Tschirhart EJ (2009) STIM1 but not STIM2 is an essential regulator of Ca^{2+} influx-mediated NADPH oxidase activity in neutrophil-like HL-60 cells. Biochem Pharmacol 78:504–513
132. Peel SE, Liu B, Hall IP (2006) A key role for STIM1 in store operated calcium channel activation in airway smooth muscle. Respir Res 7:119
133. Decuypere JP, Monaco G, Kiviluoto S, Oh-hora M, Luyten T, De Smedt H, Parys JB, Missiaen L, Bultynck G (2010) STIM1, but not STIM2, is required for proper agonist-induced Ca^{2+} signaling. Cell Calcium 48:161–167
134. Bandyopadhyay BC, Pingle SC, Ahern GP (2011) Store-operated Ca^{2+} signaling in dendritic cells occurs independently of STIM1. J Leukoc Biol 89:57–62
135. El Boustany C, Katsogiannou M, Delcourt P, Dewailly E, Prevarskaya N, Borowiec AS, Capiod T (2010) Differential roles of STIM1, STIM2 and Orai1 in the control of cell proliferation and SOCE amplitude in HEK293 cells. Cell Calcium 47:350–359
136. Darbellay B, Arnaudeau S, Konig S, Jousset H, Bader C, Demaurex N, Bernheim L (2009) STIM1- and Orai1-dependent store-operated calcium entry regulates human myoblast differentiation. J Biol Chem 284:5370–5380
137. Zhou Y, Mancarella S, Wang Y, Yue C, Ritchie M, Gill DL, Soboloff J (2009) The short N-terminal domains of STIM1 and STIM2 control the activation kinetics of Orai1 channels. J Biol Chem 284:19164–19168
138. Vig M, Peinelt C, Beck A, Koomoa DL, Rabah D, Koblan-Huberson M, Kraft S, Turner H, Fleig A, Penner R, Kinet JP (2006) CRACM1 is a plasma membrane protein essential for store-operated Ca^{2+} entry. Science 312:1220–1223
139. Zhang SL, Yeromin AV, Zhang XH, Yu Y, Safrina O, Penna A, Roos J, Stauderman KA, Cahalan MD (2006) Genome-wide RNAi screen of Ca^{2+} influx identifies genes that regulate Ca^{2+} release-activated Ca^{2+} channel activity. Proc Natl Acad Sci USA 103:9357–9362
140. DeHaven WI, Smyth JT, Boyles RR, Putney JW Jr (2007) Calcium inhibition and calcium potentiation of Orai1, Orai2, and Orai3 calcium release-activated calcium channels. J Biol Chem 282:17548–17556

141. Maruyama Y, Ogura T, Mio K, Kato K, Kaneko T, Kiyonaka S, Mori Y, Sato C (2009) Tetrameric Orai1 is a teardrop-shaped molecule with a long, tapered cytoplasmic domain. J Biol Chem 284:13676–13685
142. Mullins FM, Park CY, Dolmetsch RE, Lewis RS (2009) STIM1 and calmodulin interact with Orai1 to induce Ca^{2+}-dependent inactivation of CRAC channels. Proc Natl Acad Sci USA 106:15495–15500
143. Fierro L, Lund PE, Parekh AB (2000) Comparison of the activation of the Ca^{2+} release-activated Ca^{2+} current ICRAC to $InsP_3$ in Jurkat T-lymphocytes, pulmonary artery endothelia and RBL-1 cells. Pflugers Arch 440:580–587
144. Zweifach A, Lewis RS (1995) Rapid inactivation of depletion-activated calcium current (ICRAC) due to local calcium feedback. J Gen Physiol 105:209–226
145. Muik M, Frischauf I, Derler I, Fahrner M, Bergsmann J, Eder P, Schindl R, Hesch C, Polzinger B, Fritsch R, Kahr H, Madl J, Gruber H, Groschner K, Romanin C (2008) Dynamic coupling of the putative coiled-coil domain of ORAI1 with STIM1 mediates ORAI1 channel activation. J Biol Chem 283:8014–8022
146. Frischauf I, Muik M, Derler I, Bergsmann J, Fahrner M, Schindl R, Groschner K, Romanin C (2009) Molecular determinants of the coupling between STIM1 and Orai channels: differential activation of Orai1-3 channels by a STIM1 coiled-coil mutant. J Biol Chem 284:21696–21706
147. Lis A, Peinelt C, Beck A, Parvez S, Monteilh-Zoller M, Fleig A, Penner R (2007) CRACM1, CRACM2, and CRACM3 are store-operated Ca^{2+} channels with distinct functional properties. Curr Biol 17:794–800
148. Peinelt C, Lis A, Beck A, Fleig A, Penner R (2008) 2-Aminoethoxydiphenyl borate directly facilitates and indirectly inhibits STIM1-dependent gating of CRAC channels. J Physiol 586:3061–3073
149. Prakriya M, Feske S, Gwack Y, Srikanth S, Rao A, Hogan PG (2006) Orai1 is an essential pore subunit of the CRAC channel. Nature 443:230–233
150. Schindl R, Bergsmann J, Frischauf I, Derler I, Fahrner M, Muik M, Fritsch R, Groschner K, Romanin C (2008) 2-aminoethoxydiphenyl borate alters selectivity of Orai3 channels by increasing their pore size. J Biol Chem 283:20261–20267
151. Vig M, Beck A, Billingsley JM, Lis A, Parvez S, Peinelt C, Koomoa DL, Soboloff J, Gill DL, Fleig A, Kinet JP, Penner R (2006) CRACM1 multimers form the ion-selective pore of the CRAC channel. Curr Biol 16:2073–2079
152. Yeromin AV, Zhang SL, Jiang W, Yu Y, Safrina O, Cahalan MD (2006) Molecular identification of the CRAC channel by altered ion selectivity in a mutant of Orai. Nature 443:226–229
153. Srikanth S, Jung HJ, Ribalet B, Gwack Y (2010) The intracellular loop of Orai1 plays a central role in fast inactivation of Ca^{2+} release-activated Ca^{2+} channels. J Biol Chem 285:5066–5075
154. Lee KP, Yuan JP, Zeng W, So I, Worley PF, Muallem S (2009) Molecular determinants of fast Ca^{2+}-dependent inactivation and gating of the Orai channels. Proc Natl Acad Sci USA 106:14687–14692
155. Yamashita M, Navarro-Borelly L, McNally BA, Prakriya M (2007) Orai1 mutations alter ion permeation and Ca^{2+}-dependent fast inactivation of CRAC channels: evidence for coupling of permeation and gating. J Gen Physiol 130:525–540
156. Derler I, Fahrner M, Muik M, Lackner B, Schindl R, Groschner K, Romanin C (2009) A Ca^{2+} release-activated Ca^{2+} (CRAC) modulatory domain (CMD) within STIM1 mediates fast Ca^{2+}-dependent inactivation of ORAI1 channels. J Biol Chem 284:24933–24938
157. Frischauf I, Schindl R, Bergsmann J, Derler I, Fahrner M, Muik M, Fritsch R, Lackner B, Groschner K, Romanin C (2011) Cooperativeness of Orai cytosolic domains tunes subtype-specific gating. J Biol Chem 286:8577–8584
158. Vig M, DeHaven WI, Bird GS, Billingsley JM, Wang H, Rao PE, Hutchings AB, Jouvin MH, Putney JW, Kinet JP (2008) Defective mast cell effector functions in mice lacking the CRACM1 pore subunit of store-operated calcium release-activated calcium channels. Nat Immunol 9:89–96

159. Gross SA, Wissenbach U, Philipp SE, Freichel M, Cavalie A, Flockerzi V (2007) Murine ORAI2 splice variants form functional Ca^{2+} release-activated Ca^{2+} (CRAC) channels. J Biol Chem 282:19375–19384
160. Ohana L, Newell EW, Stanley EF, Schlichter LC (2009) The Ca^{2+} release-activated Ca^{2+} current (I_{CRAC}) mediates store-operated Ca^{2+} entry in rat microglia. Channels (Austin) 3:129–139
161. Gwack Y, Srikanth S, Feske S, Cruz-Guilloty F, Oh-hora M, Neems DS, Hogan PG, Rao A (2007) Biochemical and functional characterization of Orai proteins. J Biol Chem 282:16232–16243
162. Su AI, Wiltshire T, Batalov S, Lapp H, Ching KA, Block D, Zhang J, Soden R, Hayakawa M, Kreiman G, Cooke MP, Walker JR, Hogenesch JB (2004) A gene atlas of the mouse and human protein-encoding transcriptomes. Proc Natl Acad Sci USA 101:6062–6067
163. Wissenbach U, Philipp SE, Gross SA, Cavalie A, Flockerzi V (2007) Primary structure, chromosomal localization and expression in immune cells of the murine ORAI and STIM genes. Cell Calcium 42:439–446
164. Prakriya M (2009) The molecular physiology of CRAC channels. Immunol Rev 231:88–98
165. Thompson J, Mignen O, Shuttleworth TJ (2010) The N-terminal domain of Orai3 determines selectivity for activation of the store-independent ARC channel by arachidonic acid. Channels (Austin) 4:398–410
166. Mignen O, Thompson JL, Shuttleworth TJ (2009) The molecular architecture of the arachidonate-regulated Ca^{2+}-selective ARC channel is a pentameric assembly of Orai1 and Orai3 subunits. J Physiol 587:4181–4197
167. Mignen O, Thompson JL, Shuttleworth TJ (2008) Both Orai1 and Orai3 are essential components of the arachidonate-regulated Ca^{2+}-selective (ARC) channels. J Physiol 586:185–195
168. Lis A, Zierler S, Peinelt C, Fleig A, Penner R (2010) A single lysine in the N-terminal region of store-operated channels is critical for STIM1-mediated gating. J Gen Physiol 136:673–686
169. Takahashi Y, Murakami M, Watanabe H, Hasegawa H, Ohba T, Munehisa Y, Nobori K, Ono K, Iijima T, Ito H (2007) Essential role of the N-terminus of murine Orai1 in store-operated Ca^{2+} entry. Biochem Biophys Res Commun 356:45–52
170. Baryshnikov SG, Pulina MV, Zulian A, Linde CI, Golovina VA (2009) Orai1, a critical component of store-operated Ca^{2+} entry, is functionally associated with Na^{+}/Ca^{2+} exchanger and plasma membrane Ca^{2+} pump in proliferating human arterial myocytes. Am J Physiol Cell Physiol 297:C1103–C1112
171. Potier M, Gonzalez JC, Motiani RK, Abdullaev IF, Bisaillon JM, Singer HA, Trebak M (2009) Evidence for STIM1- and Orai1-dependent store-operated calcium influx through I_{CRAC} in vascular smooth muscle cells: role in proliferation and migration. FASEB J 23:2425–2437
172. Bisaillon JM, Motiani RK, Gonzalez-Cobos JC, Potier M, Halligan KE, Alzawahra WF, Barroso M, Singer HA, Jourd'heuil D, Trebak M (2010) Essential role for STIM1/Orai1-mediated calcium influx in PDGF-induced smooth muscle migration. Am J Physiol Cell Physiol 298:C993–C1005
173. Faouzi M, Hague F, Potier M, Ahidouch A, Sevestre H, Ouadid-Ahidouch H (2011) Down-regulation of Orai3 arrests cell-cycle progression and induces apoptosis in breast cancer cells but not in normal breast epithelial cells. J Cell Physiol 226:542–551
174. Bogeski I, Kummerow C, Al-Ansary D, Schwarz EC, Koehler R, Kozai D, Takahashi N, Peinelt C, Griesemer D, Bozem M, Mori Y, Hoth M, Niemeyer BA (2010) Differential redox regulation of ORAI ion channels: a mechanism to tune cellular calcium signaling. Sci Signal 3:ra24
175. McCarl CA, Picard C, Khalil S, Kawasaki T, Rother J, Papolos A, Kutok J, Hivroz C, Ledeist F, Plogmann K, Ehl S, Notheis G, Albert MH, Belohradsky BH, Kirschner J, Rao A, Fischer A, Feske S (2009) ORAI1 deficiency and lack of store-operated Ca^{2+} entry cause immunodeficiency, myopathy, and ectodermal dysplasia. J Allergy Clin Immunol 124:1311–1318, e1317
176. Feske S (2009) ORAI1 and STIM1 deficiency in human and mice: roles of store-operated Ca^{2+} entry in the immune system and beyond. Immunol Rev 231:189–209

177. Montell C, Rubin GM (1989) Molecular characterization of the Drosophila trp locus: a putative integral membrane protein required for phototransduction. Neuron 2:1313–1323
178. Hardie RC, Minke B (1992) The trp gene is essential for a light-activated Ca^{2+} channel in Drosophila photoreceptors. Neuron 8:643–651
179. Phillips AM, Bull A, Kelly LE (1992) Identification of a Drosophila gene encoding a calmodulin-binding protein with homology to the trp phototransduction gene. Neuron 8:631–642
180. Hardie RC, Reuss H, Lansdell SJ, Millar NS (1997) Functional equivalence of native light-sensitive channels in the Drosophila trp301 mutant and TRPL cation channels expressed in a stably transfected Drosophila cell line. Cell Calcium 21:431–440
181. Hardie RC (2003) Regulation of TRP channels via lipid second messengers. Annu Rev Physiol 65:735–759
182. Wes PD, Chevesich J, Jeromin A, Rosenberg C, Stetten G, Montell C (1995) TRPC1, a human homolog of a Drosophila store-operated channel. Proc Natl Acad Sci USA 92:9652–9656
183. Zhu X, Chu PB, Peyton M, Birnbaumer L (1995) Molecular cloning of a widely expressed human homologue for the Drosophila trp gene. FEBS Lett 373:193–198
184. Petersen CC, Berridge MJ, Borgese MF, Bennett DL (1995) Putative capacitative calcium entry channels: expression of Drosophila trp and evidence for the existence of vertebrate homologues. Biochem J 311(Pt 1):41–44
185. Montell C, Birnbaumer L, Flockerzi V, Bindels RJ, Bruford EA, Caterina MJ, Clapham DE, Harteneck C, Heller S, Julius D, Kojima I, Mori Y, Penner R, Prawitt D, Scharenberg AM, Schultz G, Shimizu N, Zhu MX (2002) A unified nomenclature for the superfamily of TRP cation channels. Mol Cell 9:229–231
186. Pedersen SF, Owsianik G, Nilius B (2005) TRP channels: an overview. Cell Calcium 38: 233–252
187. Zhu X, Jiang M, Peyton M, Boulay G, Hurst R, Stefani E, Birnbaumer L (1996) trp, a novel mammalian gene family essential for agonist-activated capacitative Ca^{2+} entry. Cell 85(5): 661–671
188. Montell C (2003) The venerable inveterate invertebrate TRP channels. Cell Calcium 33:409–417
189. Montell C, Birnbaumer L, Flockerzi V (2002) The TRP channels, a remarkably functional family. Cell 108:595–598
190. Parekh AB, Putney JW Jr (2005) Store-operated calcium channels. Physiol Rev 85:757–810
191. Wedel BJ, Vazquez G, McKay RR, St JBG, Putney JW Jr (2003) A calmodulin/inositol 1,4,5-trisphosphate (IP_3) receptor-binding region targets TRPC3 to the plasma membrane in a calmodulin/IP_3 receptor-independent process. J Biol Chem 278:25758–25765
192. Vannier B, Zhu X, Brown D, Birnbaumer L (1998) The membrane topology of human transient receptor potential 3 as inferred from glycosylation-scanning mutagenesis and epitope immunocytochemistry. J Biol Chem 273:8675–8679
193. Vazquez G, Wedel BJ, Aziz O, Trebak M, Putney JW Jr (2004) The mammalian TRPC cation channels. Biochim Biophys Acta 1742:21–36
194. Montell C (2005) Drosophila TRP channels. Pflugers Arch 451:19–28
195. Liu X, Bandyopadhyay BC, Singh BB, Groschner K, Ambudkar IS (2005) Molecular analysis of a store-operated and 2-acetyl-sn-glycerol-sensitive non-selective cation channel. Heteromeric assembly of TRPC1-TRPC3. J Biol Chem 280:21600–21606
196. Thebault S, Zholos A, Enfissi A, Slomianny C, Dewailly E, Roudbaraki M, Parys J, Prevarskaya N (2005) Receptor-operated Ca^{2+} entry mediated by TRPC3/TRPC6 proteins in rat prostate smooth muscle (PS1) cell line. J Cell Physiol 204:320–328
197. Liu X, Wang W, Singh BB, Lockwich T, Jadlowiec J, O'Connell B, Wellner R, Zhu MX, Ambudkar IS (2000) Trp1, a candidate protein for the store-operated Ca^{2+} influx mechanism in salivary gland cells. J Biol Chem 275:3403–3411
198. Rosado JA, Brownlow SL, Sage SO (2002) Endogenously expressed Trp1 is involved in store-mediated Ca^{2+} entry by conformational coupling in human platelets. J Biol Chem 277:42157–42163
199. Zagranichnaya TK, Wu X, Villereal ML (2005) Endogenous TRPC1, TRPC3, and TRPC7 proteins combine to form native store-operated channels in HEK-293 cells. J Biol Chem 280:29559–29569

200. Ambudkar IS, Ong HL, Liu X, Bandyopadhyay B, Cheng KT (2007) TRPC1: the link between functionally distinct store-operated calcium channels. Cell Calcium 42:213–223
201. Fatherazi S, Presland RB, Belton CM, Goodwin P, Al-Qutub M, Trbic Z, Macdonald G, Schubert MM, Izutsu KT (2007) Evidence that TRPC4 supports the calcium selective I_{CRAC}-like current in human gingival keratinocytes. Pflugers Arch 453:879–889
202. Jardin I, Lopez JJ, Salido GM, Rosado JA (2008) Orai1 mediates the interaction between STIM1 and hTRPC1 and regulates the mode of activation of hTRPC1-forming Ca^{2+} channels. J Biol Chem 283:25296–25304
203. Salido GM, Sage SO, Rosado JA (2008) TRPC channels and store-operated Ca^{2+} entry. Biochim Biophys Acta 1793:223–230
204. Olah T, Fodor J, Ruzsnavszky O, Vincze J, Berbey C, Allard B, Csernoch L (2011) Overexpression of transient receptor potential canonical type 1 (TRPC1) alters both store operated calcium entry and depolarization-evoked calcium signals in C2C12 cells. Cell Calcium 49(6):415–425
205. Xu SZ, Beech DJ (2001) TrpC1 is a membrane-spanning subunit of store-operated Ca^{2+} channels in native vascular smooth muscle cells. Circ Res 88:84–87
206. Vazquez G, Wedel BJ, Trebak M, St John Bird G, Putney JW Jr (2003) Expression level of the canonical transient receptor potential 3 (TRPC3) channel determines its mechanism of activation. J Biol Chem 278:21649–21654
207. Yildirim E, Kawasaki BT, Birnbaumer L (2005) Molecular cloning of TRPC3a, an N-terminally extended, store-operated variant of the human C3 transient receptor potential channel. Proc Natl Acad Sci USA 102:3307–3311
208. Philipp S, Cavalie A, Freichel M, Wissenbach U, Zimmer S, Trost C, Marquart A, Murakami M, Flockerzi V (1996) A mammalian capacitative calcium entry channel homologous to Drosophila TRP and TRPL. EMBO J 15:6166–6171
209. Brownlow SL, Sage SO (2005) Transient receptor potential protein subunit assembly and membrane distribution in human platelets. Thromb Haemost 94:839–845
210. Philipp S, Hambrecht J, Braslavski L, Schroth G, Freichel M, Murakami M, Cavalie A, Flockerzi V (1998) A novel capacitative calcium entry channel expressed in excitable cells. EMBO J 17:4274–4282
211. Brechard S, Melchior C, Plancon S, Schenten V, Tschirhart EJ (2008) Store-operated Ca^{2+} channels formed by TRPC1, TRPC6 and Orai1 and non-store-operated channels formed by TRPC3 are involved in the regulation of NADPH oxidase in HL-60 granulocytes. Cell Calcium 44:492–506
212. Lievremont JP, Bird GS, Putney JW Jr (2004) Canonical transient receptor potential TRPC7 can function as both a receptor- and store-operated channel in HEK-293 cells. Am J Physiol Cell Physiol 287:C1709–C1716
213. Singh BB, Liu X, Ambudkar IS (2000) Expression of truncated transient receptor potential protein 1alpha (Trp1alpha): evidence that the Trp1 C terminus modulates store-operated Ca^{2+} entry. J Biol Chem 275:36483–36486
214. Liu X, Singh BB, Ambudkar IS (2003) TRPC1 is required for functional store-operated Ca^{2+} channels. Role of acidic amino acid residues in the S5-S6 region. J Biol Chem 278:11337–11343
215. Brough GH, Wu S, Cioffi D, Moore TM, Li M, Dean N, Stevens T (2001) Contribution of endogenously expressed Trp1 to a Ca^{2+}-selective, store-operated Ca^{2+} entry pathway. FASEB J 15:1727–1738
216. Varga-Szabo D, Authi KS, Braun A, Bender M, Ambily A, Hassock SR, Gudermann T, Dietrich A, Nieswandt B (2008) Store-operated Ca^{2+} entry in platelets occurs independently of transient receptor potential (TRP) C1. Pflugers Arch 457:377–387
217. Yuan JP, Zeng W, Dorwart MR, Choi YJ, Worley PF, Muallem S (2009) SOAR and the polybasic STIM1 domains gate and regulate Orai channels. Nat Cell Biol 11:337–343
218. Muik M, Fahrner M, Derler I, Schindl R, Bergsmann J, Frischauf I, Groschner K, Romanin C (2009) A cytosolic homomerization and a modulatory domain within STIM1 C terminus determine coupling to ORAI1 channels. J Biol Chem 284:8421–8426
219. Park CY, Hoover PJ, Mullins FM, Bachhawat P, Covington ED, Raunser S, Walz T, Garcia KC, Dolmetsch RE, Lewis RS (2009) STIM1 clusters and activates CRAC channels via direct binding of a cytosolic domain to Orai1. Cell 136:876–890

220. Kawasaki T, Lange I, Feske S (2009) A minimal regulatory domain in the C terminus of STIM1 binds to and activates ORAI1 CRAC channels. Biochem Biophys Res Commun 385:49–54
221. Wang Y, Deng X, Gill DL (2010) Calcium signaling by STIM and Orai: intimate coupling details revealed. Sci Signal 3:pe42
222. Muik M, Fahrner M, Schindl R, Stathopulos P, Frischauf I, Derler I, Plenk P, Lackner B, Groschner K, Ikura M, Romanin C (2011) STIM1 couples to ORAI1 via an intramolecular transition into an extended conformation. EMBO J 30:1678–1689
223. Xu P, Lu J, Li Z, Yu X, Chen L, Xu T (2006) Aggregation of STIM1 underneath the plasma membrane induces clustering of Orai1. Biochem Biophys Res Commun 350:969–976
224. Scrimgeour N, Litjens T, Ma L, Barritt GJ, Rychkov GY (2009) Properties of Orai1 mediated store-operated current depend on the expression levels of STIM1 and Orai1 proteins. J Physiol 587:2903–2918
225. Zeng W, Yuan JP, Kim MS, Choi YJ, Huang GN, Worley PF, Muallem S (2008) STIM1 gates TRPC channels, but not Orai1, by electrostatic interaction. Mol Cell 32:439–448
226. Ong HL, Cheng KT, Liu X, Bandyopadhyay BC, Paria BC, Soboloff J, Pani B, Gwack Y, Srikanth S, Singh BB, Gill DL, Ambudkar IS (2007) Dynamic assembly of TRPC1-STIM1-Orai1 ternary complex is involved in store-operated calcium influx. Evidence for similarities in store-operated and calcium release-activated calcium channel components. J Biol Chem 282:9105–9116
227. Cheng KT, Liu X, Ong HL, Ambudkar IS (2008) Functional requirement for Orai1 in store-operated TRPC1-STIM1 channels. J Biol Chem 283:12935–12940
228. Galan C, Woodard GE, Dionisio N, Salido GM, Rosado JA (2010) Lipid rafts modulate the activation but not the maintenance of store-operated Ca^{2+} entry. Biochim Biophys Acta 1803:1083–1093
229. Simons K, Toomre D (2000) Lipid rafts and signal transduction. Nat Rev Mol Cell Biol 1:31–39
230. Sampieri A, Zepeda A, Saldaña C, Salgado A, Vaca L (2008) STIM1 converts TRPC1 from a receptor-operated to a store-operated channel: moving TRPC1 in and out of lipid rafts. Cell Calcium 44:479–491
231. Jardin I, Salido GM, Rosado JA (2008) Role of lipid rafts in the interaction between hTRPC1, Orai1 and STIM1. Channels (Austin) 2:401–403
232. Liao Y, Erxleben C, Abramowitz J, Flockerzi V, Zhu MX, Armstrong DL, Birnbaumer L (2008) Functional interactions among Orai1, TRPCs, and STIM1 suggest a STIM-regulated heteromeric Orai/TRPC model for SOCE/Icrac channels. Proc Natl Acad Sci USA 105:2895–2900
233. Liao Y, Erxleben C, Yildirim E, Abramowitz J, Armstrong DL, Birnbaumer L (2007) Orai proteins interact with TRPC channels and confer responsiveness to store depletion. Proc Natl Acad Sci USA 104:4682–4687
234. Cheng KT, Liu X, Ong HL, Swaim W, Ambudkar IS (2011) Local Ca^{2+} entry via Orai1 regulates plasma membrane recruitment of TRPC1 and controls cytosolic Ca^{2+} signals required for specific cell functions. PLoS Biol 9:e1001025
235. Lorin-Nebel C, Xing J, Yan X, Strange K (2007) CRAC channel activity in C. elegans is mediated by Orai1 and STIM1 homologues and is essential for ovulation and fertility. J Physiol 580:67–85
236. Liao Y, Plummer NW, George MD, Abramowitz J, Zhu MX, Birnbaumer L (2009) A role for Orai in TRPC-mediated Ca^{2+} entry suggests that a TRPC:Orai complex may mediate store and receptor operated Ca^{2+} entry. Proc Natl Acad Sci USA 106:3202–3206
237. Partiseti M, Le Deist F, Hivroz C, Fischer A, Korn H, Choquet D (1994) The calcium current activated by T cell receptor and store depletion in human lymphocytes is absent in a primary immunodeficiency. J Biol Chem 269:32327–32335
238. Le Deist F, Hivroz C, Partiseti M, Thomas C, Buc HA, Oleastro M, Belohradsky B, Choquet D, Fischer A (1995) A primary T-cell immunodeficiency associated with defective transmembrane calcium influx. Blood 85:1053–1062

239. Picard C, McCarl CA, Papolos A, Khalil S, Luthy K, Hivroz C, LeDeist F, Rieux-Laucat F, Rechavi G, Rao A, Fischer A, Feske S (2009) STIM1 mutation associated with a syndrome of immunodeficiency and autoimmunity. N Engl J Med 360:1971–1980
240. Byun M, Abhyankar A, Lelarge V, Plancoulaine S, Palanduz A, Telhan L, Boisson B, Picard C, Dewell S, Zhao C, Jouanguy E, Feske S, Abel L, Casanova JL (2010) Whole-exome sequencing-based discovery of STIM1 deficiency in a child with fatal classic Kaposi sarcoma. J Exp Med 207:2307–2312
241. Feske S, Giltnane J, Dolmetsch R, Staudt LM, Rao A (2001) Gene regulation mediated by calcium signals in T lymphocytes. Nat Immunol 2:316–324
242. Feske S, Prakriya M, Rao A, Lewis RS (2005) A severe defect in CRAC Ca^{2+} channel activation and altered K^+ channel gating in T cells from immunodeficient patients. J Exp Med 202:651–662
243. Feske S, Picard C, Fischer A (2010) Immunodeficiency due to mutations in ORAI1 and STIM1. Clin Immunol 135:169–182
244. Feske S (2010) CRAC channelopathies. Pflugers Arch 460:417–435
245. Feske S, Muller JM, Graf D, Kroczek RA, Drager R, Niemeyer C, Baeuerle PA, Peter HH, Schlesier M (1996) Severe combined immunodeficiency due to defective binding of the nuclear factor of activated T cells in T lymphocytes of two male siblings. Eur J Immunol 26:2119–2126
246. Maul-Pavicic A, Chiang SC, Rensing-Ehl A, Jessen B, Fauriat C, Wood SM, Sjoqvist S, Hufnagel M, Schulze I, Bass T, Schamel WW, Fuchs S, Pircher H, McCarl CA, Mikoshiba K, Schwarz K, Feske S, Bryceson YT, Ehl S (2011) ORAI1-mediated calcium influx is required for human cytotoxic lymphocyte degranulation and target cell lysis. Proc Natl Acad Sci USA 108:3324–3329
247. Chou YH, Juo SH, Chiu YC, Liu ME, Chen WC, Chang CC, Chang WP, Chang JG, Chang WC (2011) A polymorphism of the ORAI1 gene is associated with the risk and recurrence of calcium nephrolithiasis. J Urol 185:1742–1746
248. Bergmeier W, Oh-Hora M, McCarl CA, Roden RC, Bray PF, Feske S (2009) R93W mutation in Orai1 causes impaired calcium influx in platelets. Blood 113:675–678
249. Gwack Y, Srikanth S, Oh-Hora M, Hogan PG, Lamperti ED, Yamashita M, Gelinas C, Neems DS, Sasaki Y, Feske S, Prakriya M, Rajewsky K, Rao A (2008) Hair loss and defective T- and B-cell function in mice lacking ORAI1. Mol Cell Biol 28:5209–5222
250. Beyersdorf N, Braun A, Vogtle T, Varga-Szabo D, Galdos RR, Kissler S, Kerkau T, Nieswandt B (2009) STIM1-independent T cell development and effector function in vivo. J Immunol 182:3390–3397
251. Braun A, Varga-Szabo D, Kleinschnitz C, Pleines I, Bender M, Austinat M, Bosl M, Stoll G, Nieswandt B (2009) Orai1 (CRACM1) is the platelet SOC channel and essential for pathological thrombus formation. Blood 113:2056–2063
252. Ma J, McCarl CA, Khalil S, Luthy K, Feske S (2010) T-cell-specific deletion of STIM1 and STIM2 protects mice from EAE by impairing the effector functions of Th1 and Th17 cells. Eur J Immunol 40:3028–3042
253. Linde CI, Baryshnikov SG, Mazzocco-Spezzia A, Golovina VA (2011) Dysregulation of Ca^{2+} signaling in astrocytes from mice lacking amyloid precursor protein. Am J Physiol Cell Physiol 300:C1502–C1512
254. Leissring MA, Akbari Y, Fanger CM, Cahalan MD, Mattson MP, LaFerla FM (2000) Capacitative calcium entry deficits and elevated luminal calcium content in mutant presenilin-1 knockin mice. J Cell Biol 149:793–798
255. Bojarski L, Pomorski P, Szybinska A, Drab M, Skibinska-Kijek A, Gruszczynska-Biegala J, Kuznicki J (2009) Presenilin-dependent expression of STIM proteins and dysregulation of capacitative Ca^{2+} entry in familial Alzheimer's disease. Biochim Biophys Acta 1793: 1050–1057
256. Zatti G, Ghidoni R, Barbiero L, Binetti G, Pozzan T, Fasolato C, Pizzo P (2004) The presenilin 2 M239I mutation associated with familial Alzheimer's disease reduces Ca^{2+} release from intracellular stores. Neurobiol Dis 15:269–278

257. Giacomello M, Barbiero L, Zatti G, Squitti R, Binetti G, Pozzan T, Fasolato C, Ghidoni R, Pizzo P (2005) Reduction of Ca^{2+} stores and capacitative Ca^{2+} entry is associated with the familial Alzheimer's disease presenilin-2 T122R mutation and anticipates the onset of dementia. Neurobiol Dis 18:638–648
258. Sorgato MC, Bertoli A (2009) From cell protection to death: may Ca^{2+} signals explain the chameleonic attributes of the mammalian prion protein? Biochem Biophys Res Commun 379:171–174
259. Lazzari C, Peggion C, Stella R, Massimino ML, Lim D, Bertoli A, Sorgato MC (2011) Cellular prion protein is implicated in the regulation of local Ca^{2+} movements in cerebellar granule neurons. J Neurochem 116:881–890
260. Jardin I, Lopez JJ, Zbidi H, Bartegi A, Salido GM, Rosado JA (2011) Attenuated store-operated divalent cation entry and association between STIM1, Orai1, hTRPC1 and hTRPC6 in platelets from type 2 diabetic patients. Blood Cells Mol Dis 15(46):252–260
261. Okon EB, Golbabaie A, Breemen C (2008) Paracrine effects of endothelial cells in a diabetic mouse model: capacitative calcium entry stimulated thromboxane release. Horm Metab Res 40:645–650
262. Sabbioni S, Veronese A, Trubia M, Taramelli R, Barbanti-Brodano G, Croce CM, Negrini M (1999) Exon structure and promoter identification of STIM1 (alias GOK), a human gene causing growth arrest of the human tumor cell lines G401 and RD. Cytogenet Cell Genet 86:214–218
263. Ruano Y, Mollejo M, Ribalta T, Fiano C, Camacho FI, Gomez E, de Lope AR, Hernandez-Moneo JL, Martinez P, Melendez B (2006) Identification of novel candidate target genes in amplicons of Glioblastoma multiforme tumors detected by expression and CGH microarray profiling. Mol Cancer 5:39

Chapter 16
Structure, Regulation and Biophysics of I_{CRAC}, STIM/Orai1

Isabella Derler, Josef Madl, Gerhard Schütz, and Christoph Romanin

Abstract Ca^{2+} release activated Ca^{2+} (CRAC) channels mediate robust Ca^{2+} influx when the endoplasmic reticulum Ca^{2+} stores are depleted. This essential process for T-cell activation as well as degranulation of mast cells involves the Ca^{2+} sensor STIM1, located in the endoplasmic reticulum and the Ca^{2+} selective Orai1 channel in the plasma membrane. Our review describes the CRAC signaling pathway, the activation of which is initiated by a drop in the endoplasmic Ca^{2+} level sensed by STIM1. This in term induces multimerisation and puncta-formation of STIM1 proteins is followed by their coupling to and activation of Orai channels. Consequently Ca^{2+} entry is triggered through the Orai pore into the cytosol with subsequent closure of the channel by Ca^{2+}-dependent inactivation. We will portray a mechanistic view of the events coupling STIM1 to Orai activation based on their structure and biophysics.

Keywords (STIM1) stromal interaction molecule 1 • (CRAC) Ca^{2+} release-actived Ca^{2+} current • (SOC) store-operated current • (CMD) CRAC modulatory domain • (SCID) severe combined immune deficiency • (HEK) human embryonal kidney • (ARC) arachidonate regulated Ca^{2+} • (SHD) STIM1 homomerization domain • (CAD) CRAC activating domain • (SOAR) STIM1 Orai activating region • FRET Förster Resonance Energy Transfer • (ROS) reactive oxygen species • (TM) transmembrane • (2-APB) 2-aminoethoxydiphenyl borate

I. Derler (✉) • J. Madl • C. Romanin (✉)
Institute of Biophysics, University of Linz, A-4040 Linz, Austria
e-mail: isabella.derler@jku.at; christoph.romanin@jku.at

G. Schütz
Institute of Biophysics, University of Linz, A-4040 Linz, Austria

Institute of Applied Physics, Vienna University of Technology, A-1040 Vienna, Austria

M.S. Islam (ed.), *Calcium Signaling*, Advances in Experimental Medicine and Biology 740, DOI 10.1007/978-94-007-2888-2_16,

Store-Operated Ca^{2+} Channels

A variety of cellular processes ranging from short-term to long-term responses of immune cells such as mast cells and lymphocytes is controlled by changes in cytosolic Ca^{2+} levels [1]. Activation of immune receptors like T-, B-cell- or Fc-receptors initiates a signaling cascade which triggers the depletion of intracellular Ca^{2+} stores. Thereby the so called store-operated calcium (SOC) channels are activated and let Ca^{2+} pass into the cell. Among these ion channels the calcium release-activated Ca^{2+} (CRAC) channel is best characterized [1–5]. Biophysical characterization reveals a high Ca^{2+} selectivity, very low single channel conductance and a pronounced inward-rectifying current/voltage relationship [2]. For more than two decades, the molecular identity of CRAC channels has remained elusive. In 2005 and 2006, the two key players of the CRAC channel – STIM and Orai – have been identified as sufficient to fully reconstitute CRAC currents [6–10].

STIM1, the Ca^{2+} Sensor in the ER Membrane

STIM1 (Fig. 16.1) represents the ER-located Ca^{2+} sensor [6, 7] which includes a pair of luminal EF-hands and a sterile-alpha motif (SAM) in its N-terminus followed by a single transmembrane domain [11]. The C-terminal portion contains three coiled-coil domains [12], a CRAC modulatory domain (CMD), a serine-/proline- and a lysine-rich region [6, 13–16]. The STIM1 C-terminal second and third coiled-coil domains extended by ~20 amino acids have been elucidated as the smallest fragment sufficient for binding to and activating Orai1 [17–20]. STIM2, the second STIM protein, is structurally 61% homologous to STIM1. The two proteins diverge significantly in their N-terminal sequence [21] as well as in their C-terminal portion subsequent to the ERM/coiled-coil region [22].

Orai Proteins, the Pore Forming Subunits of CRAC Channels

Function-based genetic screens by systematic RNA interference and analysis of single nucleotide polymorphism arrays of patients with severe combined immune deficiency (SCID) syndrome who exhibit a defect in CRAC channel function, have led to the identification of Orai1 [8–10]. Orai1 localizes to the plasma membrane and functions as a Ca^{2+}-selective ion channel [8–10, 23]. Co-expression of STIM1 and Orai1 allows coupling of these two proteins upon store-depletion resulting in currents with biophysical and pharmacological properties similar to endogenous CRAC currents in RBL mast or Jurkat T cells [24]. Thus the two proteins are supposed to be sufficient for CRAC channel activation. Orai2 and Orai3 represent two additional homologues of the Orai family (Fig. 16.2), which all contain a cytosolic N- and C-terminus and in-between four transmembrane segments [9]. Only the

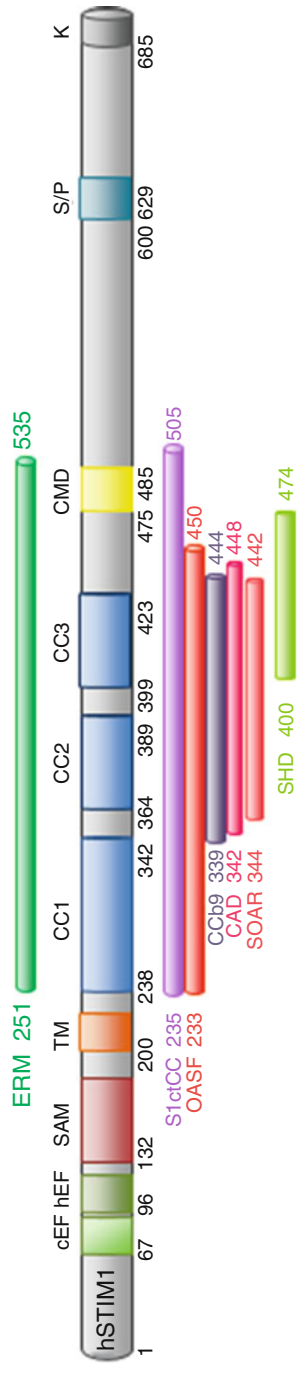

Fig. 16.1 Predicted domains within hSTIM1. CAD CRAC Activating Domain, CMD CRAC modulatory domain, CC Coiled Coil domain, CMD CRAC Modulatory Domain, EF EF-hand motif, ERM Ezrin Radixin Moesin like domain, K polybasic cluster, OASF Orai Activating Small Fragment, SAM Sterile Alpha Motif, SHD STIM1 Homomerization Domain, SOAR Stim Orai Activating Region, S/P Serine/Proline rich region, TM transmembrane domain

Orai1 N-terminus contains a proline-/arginine-rich region [25], while a cluster of positively charged amino acids close to the first transmembrane region is fully conserved among all three Orai channels. Moreover, each Orai protein consists of a C-terminal putative coiled-coil domain [26–28]. All three Orai channels are highly selective for Ca^{2+} and are activated upon store-depletion via coupling to STIM1. Moreover the respective Orai channels display distinct inactivation profiles, permeability properties and 2-aminoethyldiphenyl borate (2-APB) sensitivities [29].

Physiological Relevance of STIM1 and Orai Proteins

Upon the discovery of STIM1 and Orai1 diverse studies have focused on their physiological role in immune cells and diverse tissues. The most important ones will be described in this paragraph, however, further details are beyond of the scope of this study. The direct link between the immune system and Orai1 has been originally discovered by the SCID mutant Orai1 R91W. Its loss of store-operated function occurs together with functional defects of diverse lymphocytes, such as T-, B-cells and lymphocytes in patients containing this SCID mutant [30–32]. Mast cells which lack either STIM1 or Orai1 exhibit a considerable defect in degranulation. Moreover FcεRI-induced in vivo anaphylaxis is inhibited in Orai1-knockout mice and significantly reduced in $STIM1^{+/-}$ mice, which express much less STIM1 than $STIM1^{+/+}$ mice [33, 34]. T-cells and fibroblasts which lack STIM1 have displayed severely impaired store-operated Ca^{2+} influx. Moreover the lack or mutation of Orai1, lack of STIM1 or deficiency in store-operated Ca^{2+} entry in lymphocytes are associated with immunodeficiency, myopathy and ectodermal dysplasia [35, 36]. Recently, it has been demonstrated that Orai1-mediated Ca^{2+} influx is critical for granule exocytosis, for lymphocyte cytotoxicity as well as for cytokine production induced by target cell recognition. Besides the role of STIM1 in lymphocytes, STIM1 has been identified to be essential for SOCE in VSMC [37] as well as to be required for development and contractile function in skeletal muscle. Additionally STIM1 is involved in platelet activation and bleeding in mice [38] and an essential mediator of arterial thrombosis and ischemic brain infarction. Regarding Orai1, Bergmeier et al. [39] have shown that the SCID mutant in mice Orai1 R93W induces loss of calcium influx in platelets.

Structure

Structure of the STIM1/Orai Complex

Stoichiometry of Orai Channels and Their Assembly

Orai represents the pore-forming subunit of the CRAC channel. An individual subunit (Fig. 16.2) consists of four transmembrane domains, two cytosolic strands, two extracellular and one intracellular loops. Orai proteins have been found to form

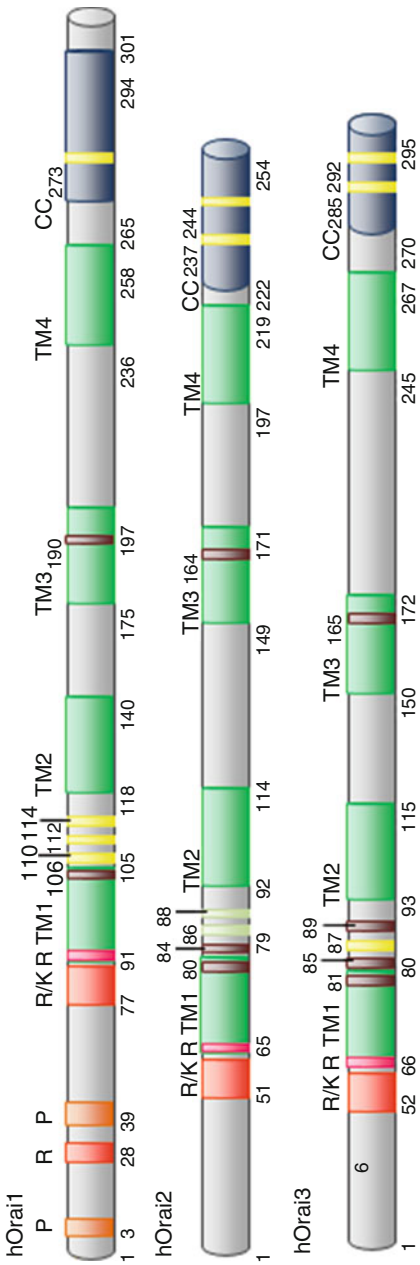

Fig. 16.2 Predicted domains of hOrai1, 2 and 3. *P* proline-rich region, *R* arginin-rich region, R/K arginine-lysine-rich region, TM transmembrane domain, CC coiled-coil domain

homomeric as well as heteromeric assemblies [29, 40–42]. They multimerize mainly via their transmembrane regions as truncation of the cytosolic strands does not influence aggregation of Orai subunits [28, 43]. However, Orai1 N-terminus has still been assumed to be involved in Orai assembly as it affects SOC channels in a dominant negative manner [25, 44]. Hitherto, crucial regions especially within the transmembrane segments mediating Orai subunit aggregation have not yet been mapped in detail.

As Orai channels exhibit no known homology to other calcium channels, speculations have emerged concerning their stoichiometry. Initially, biochemical approaches have disclosed that Orai1 forms at least stable dimers; while tetramers have been obtained by chemical cross-linking [41]. Disulfide cross-linking assays have approved tetrameric or higher order Orai1 aggregates [45]. Electron microscopy studies have visualized a tetrameric stoichiometry of purified Orai1 proteins [46]. Functional assays further underline a tetrameric subunit stoichiometry of activated and conducting Orai channels as store-operated Ca^{2+} currents mediated by expressed tetrameric Orai1 concatamers remain unaffected by co-expression with a dominant-negative Orai1 mutant [47].

We and other groups have recently addressed the resting state stoichiometry of Orai1 channels by single molecule fluorescence microscopy, which allows for counting subunits within the channel complex. This technique has been already successfully applied to bacterial flagellar motors [48] or ion channels [49], or for determination of the load of mobile molecular nano-platforms [50, 51]. Subunit stoichiometry can be inferred from counting the photobleaching steps of fluorescent dyes attached to the subunits [48, 49]. For this, the Orai1 proteins have to be labeled in a defined stoichiometric manner with GFP [52]; the number of individual bleaching steps then directly yield the oligomeric state. Fluorescent fusion proteins have the advantage of an inherent 1:1 labeling stoichiometry without the need for invasive labeling procedures. However, fluorescent proteins are rather dim compared to organic dyes [53]. Also, the photophysical properties are quite complex, e.g. phenomena such as photo-induced on/off-blinking have been reported [54]. In living cells, reliable counting of single photobleaching events for mobile complexes is extremely difficult even when using very bright organic dyes [53]: during the excursions of the molecule, the local background level changes, rendering precise brightness measurements difficult. Consequently, in the case of GFP, stepwise photobleaching analysis is usually restricted to immobile or slowly moving proteins [49].

For the determination of the Orai1 stoichiometry, stepwise photobleaching studies [55, 56] have been only applied to immobile [55] or immobilized [56] aggregates, respectively and have conformed the tetrameric subunit composition of the STIM1-activated, conducting CRAC channels. Under resting cell conditions, Ji et al. [56] have observed Orai1 tetramers in fixed HEK 293 cells. In contrast, Penna et al. [55] have reported a dimeric state for immobile Orai aggregates in *Xenopus levis* oocytes proposing that STIM1 causes dimerization of two Orai dimers, which finally results in full CRAC activation [55]. The discrepancy between the two studies might arise from the restriction to the analysis of immobile or immobilized proteins.

An alternative approach to stepwise photobleaching is direct single molecule brightness analysis. Schmidt et al. have introduced a brightness analysis method

that allows to measure the fluorescent load of individual mobile entities by comparing the signal of the fully labeled aggregate to the signal of a single fluorophore [57]. This method has been shown to be suitable for analyzing highly mobile entities in lipid bilayers [50] and for studying lipid nano-platforms in living cells [58]. We have extended this approach to study the stoichiometry of mobile, resting-state Orai1 in living HEK 293 cells [59], where the majority of Orai1 is mobile [19, 59]. By exclusively measuring the stoichiometry of mobile GFP-Orai1 proteins, we have been able to analyze the largest Orai1 fraction. Our results indicate a purely tetrameric assembly of Orai1 [59] under resting cell conditions.

Besides the homomeric and tetrameric assembly of Orai subunits, Shuttleworth's lab [60] has reported that Orai1 and Orai3 subunits form pentameric aggregates respresenting arachidonate regulated Ca^{2+} (ARC) channels. An oligomer composed of three Orai1 and two Orai3 subunits forms the functional ARC channel pore [47, 61–63]. The Orai3 N-terminus appears critical for switching a store-operated channel to an exclusively arachidonate regulated one [64].

STIM1 Oligomerization

The Ca^{2+} sensor STIM1 is uniformly distributed within the ER membrane at resting state [7, 65]. It interacts with the microtubule-plus-end-tracking protein EB1 at those sites where microtubule ends come in close contact with the ER [66]. Moreover, STIM1 co-localizes with endogenous α-tubulin [67].

STIM1 (see Fig. 16.1) senses, via its N-terminal EF-hands, the luminal Ca^{2+} content which is approximately 300–500 μM at resting state [6, 7]. Upon store-depletion, STIM1 proteins oligomerize at junctional ER sites close to the plasma membrane (20 nm) [6, 13, 65, 68–71] resulting in puncta-formation thereby activating CRAC channels. STIM1 oligomerization is strictly dependent on ER Ca^{2+} levels [72] and occurs with an EC_{50} of 210 μM Ca^{2+} [73]. Recently, it has been found that also an increase in temperature induces clustering of STIM1 [74] even when the stores are full.

N- as well as C-terminal domains of STIM1 contribute to its oligomerization, while for CRAC/Orai activation the cytosolic C-terminal portion plays a major role. The loss of Ca^{2+} at the N-terminal EF-hand upon store-depletion triggers the aggregation of STIM1 proteins. In accordance, oligomerization of a STIM1 fragment containing the EF-hand and the SAM domain is observed in the absence of Ca^{2+} [75, 76]. In support, a STIM1 deletion mutant devoid of the whole cytosolic C-terminus oligomerizes via the N-terminal EF-SAM domain, however, these aggregates are unstable [77]. The "hidden" EF-hand located between the EF-hand and the SAM domain is unable to bind Ca^{2+} [75]. The two EF-hands together interact with the SAM domain by hydrophobic amino acids [75]. Their mutation abolishes Ca^{2+} sensitivity and oligomerization via destabilization of the entire EF-SAM fragment which leads to puncta formation and constitutive activation of SOC channels [75].

Within the C-terminus of STIM1 (see Fig. 16.1), the Orai activation domain (CAD, SOAR) comprising the second and third coiled-coil domains and ~20 additional amino acids is sufficient for aggregation [77]. The amino acid region

420–450, located C-terminal to the coiled-coil regions has been suggested to contribute to STIM1 oligomerization and has been consequently named STIM1 homomerization domain (SHD) [17, 77, 78]. The first coiled-coil domain is reported to support oligomerization of STIM1 [77]. However, aggregates of STIM1 proteins that lack domains after the first coiled-coil domain remain unstable [77]. Moreover, C-terminal STIM1 fragments (233–420) including only coiled-coil domains are unable to form stable di-/oligo-mers [17].

In summary, STIM1 oligomerization and subsequent Orai activation are achieved by the second and third coiled-coil domains extended by ~20 residues.

Stoichiometric and Conformational Requirements Within a STIM1/Orai Complex

Aggregation of STIM1 and Orai1 following store-depletion is sufficient to reconstitute CRAC currents [6–10, 65, 79]. STIM1/Orai complexes form co-clustered puncta in the plasma membrane [6, 68, 71, 80] thereby initiating Ca^{2+} entry into the cell. Electrophysiological recordings of Orai1 currents induced by covalently-linked dimeric STIM1 constructs have revealed that eight STIM1 molecules allow maximal CRAC current activation [81]. Less than eight STIM1 molecules generate smaller Orai1 currents, suggesting that CRAC channel activation occurs in a graded but not in an "all-or-none" fashion [81]. In line, Hoover et al. [82] have recently shown by combined whole-cell recordings with single cell fluorescence measurements that a STIM1:Orai1 expression ratio of ~2 – thus eight STIM1 molecules – allows maximal Orai channel activation. In aggregate, four Orai molecules apparently couple to eight STIM1 molecules for maximal Ca^{2+} entry activation.

A novel STIM1-derived Förster Resonance Energy Transfer- (FRET-) sensor has enabled to visualize that the C-terminal portion of STIM1 switches into an extended conformation upon activation of Orai1 [83]. This conformational switch involves both hydrophobic [83] as well as electrostatic [84] interactions of the coiled-coil domains.

Direct Interaction of STIM1 and Orai1, and Modulatory Proteins

After discovery of the two molecular key players of CRAC channel, a series of labs has suggested that STIM1 and Orai1 couple indirectly to each other [41, 80, 85, 86]. Meanwhile, however, there is ample evidence in support of a direct interaction of STIM1 and Orai1 in response to store-depletion based on FRET as well as biochemistry studies [19, 28, 87–89] as described in detail in the next chapter [18–20, 27, 28]. Expression of STIM1 and Orai1 in yeast has additionally shown that STIM1 and Orai1 are sufficient to fully reconstitute CRAC currents [90], without the need of further proteins. Various other proteins and lipids have been identified to couple or interplay with either STIM1 or Orai1 or both. Among them are CaM [91, 92],

CRACR2A/B [93], MS4A4B [94], Golli [95], adenylyl cyclase type 8 (AC8) [96], the polycystin-1 cleavage product P100 [97], caveolin [98], SPCA2 [99] and the L-type Ca^{2+} channel (Cav1.2) [100, 101] or the phospholipids PIP_2 and PIP_3 [102–104]. However, these additional components rather function in a modulatory manner within the store-operated Ca^{2+} entry pathway.

Regulation

Domains Mediating Coupling and Regulation of STIM1 and Orai

The complex signaling cascade of STIM1/Orai involves a series of coupling steps including STIM1 multimerization, Orai oligomerization as well as STIM1/Orai interaction. These processes are controlled by several cytosolic domains of both proteins (see Fig. 16.3).

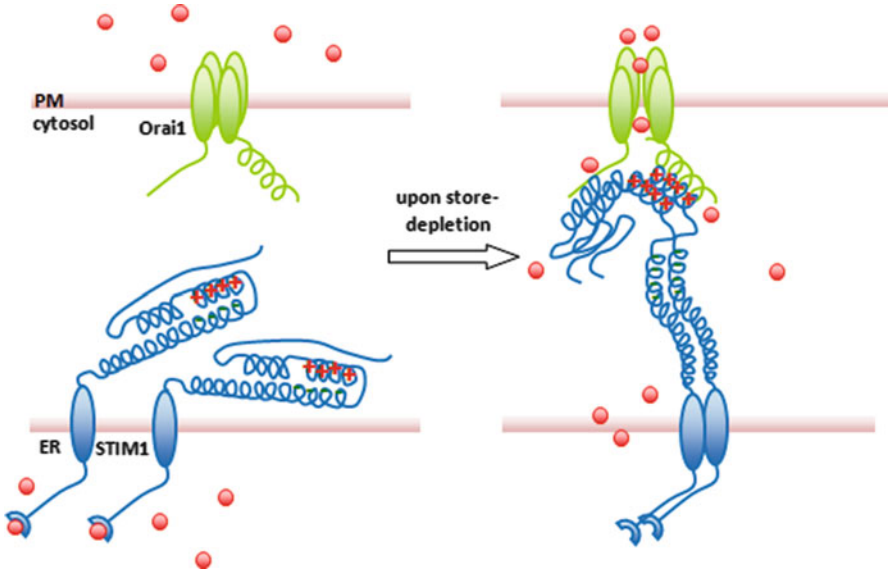

Fig. 16.3 Model for STIM1-Orai1 coupling. Under resting state conditions, STIM1 proteins are more uniformly distributed within the ER membrane and its C-terminus is locked in a closed conformation. Upon Ca^{2+}-store-depletion STIM1 oligomerizes which is mediated by luminal SAM as well as cytosolic SHD domain and rearranges STIM1 into punctate clusters in regions close to the plasma membrane. There STIM1 attracts almost uniformly distributed Orai1 via a direct interaction of their C-termini involving putative coiled-coil domains. Thereby STIM1 is switched to an open conformation where STIM1's second coiled-coil domain attached to the C-terminal coiled-coil domain of Orai. Coclustering together with additional involvement of Orai1 N-terminus culminates in the Orai1/CRAC activation. This model emphasizes domain interactions rather than stoichiometry of the STIM–Orai coupling

Within STIM1 C-terminus, regions for intramolecular as well as intermolecular interactions have been identified. The recently [84] reported intramolecular interaction involves a basic amino acid stretch within the second coiled-coil domain of STIM1 that is proposed to interact with an acidic domain in the first coiled-coil domain. This basic segment in the second coiled-coil domain of STIM1 is able to couple to acidic residues within the C-terminal coiled-coil region of Orai1 [84].

The main interaction region within STIM1 C-terminus for intermolecular coupling represents the second coiled-coil domain [27]. Small fragments of STIM1 C-terminus (CAD (aa 342–448), SOAR (aa 344–442), OASF (aa 233–450), Ccb9 (aa 339–444)) which all contain the second and third coiled-coil domains together with some further amino acids downstream have been sufficient for coupling to and activation of Orai proteins [17–20].

The structure within Orai interacting with the second coiled-coil domain of STIM1 has been localized to a C-terminal single, putative coiled-coil domain. Contrary to Orai1, both Orai2 and Orai3 exhibit a 15–17 fold higher coiled-coil probability [27]. A single point mutation in the Orai1 coiled-coil domain (L273S) abrogates communication with STIM1 C-terminus [27, 28]. In Orai2 as well as Orai3 a second point mutation in their coiled-coil domain is required to fully disrupt coupling to STIM1 probably reflecting the higher coiled-coil probability compared to Orai1. Accordingly, reducing the probability of the putative, second coiled-coil domain of STIM1 C-terminus by a single mutation has still allowed partial activation of Orai2 and Orai3 channels but not of Orai1. A double mutation within this region fully disrupts communication with all three Orai channels. Hence, coiled-coil regions are crucial structures for the coupling of STIM1 and Orai [27].

The C-terminal coiled-coil domain of Orai1 contains a series of acidic residues, while the second coiled-coil domain of STIM1 includes a highly conserved cluster of basic residues (KIKKKR – aa 382–387 of human STIM1). These charged amino acids have been proposed to mediate STIM1/Orai coupling [88, 105, 106]. However, respective charge swap in these coiled-coil domains somewhat disturbed the coupling of STIM1/Orai1 [106] suggesting the involvement of further structures in the coupling process. In aggregate, hydrophobic as well as charged residues contribute to a heteromeric coiled-coil interaction between the C-termini of STIM1 and Orai1 [107, 108].

Besides an interaction of STIM1/CAD with Orai1 C-terminus, the Orai1 N-terminus additionally functions as binding partner for STIM1/CAD, though to a weaker extent [19, 28, 43]. The N-terminus includes a region aa 74–91 close to the first transmembrane segment, which is fully conserved among all Orai proteins. Upon truncation of the whole N-terminus of Orai1, SOCE is completely abolished. In contrast, a partial deletion up to the residue 74 retaining the conserved region maintains Orai1 channel activity [43]. Co-immunoprecipitation studies have revealed that CAD couples to this N-terminal conserved domain of Orai1. A detailed mapping of residues within this conserved region regarding their contribution to STIM1 interaction and Orai1 gating is so far lacking, although a single lysine (K85) plays an important role in Orai1 gating [109]. Nevertheless, both N- and C-terminus of Orai1 are essential in triggering CRAC channel activation [19].

In addition to the coupling domains, N- as well as C-termini of STIM1 and Orai include regions that play regulatory roles. Orai1, but not Orai2 and Orai3 contain a polybasic and proline-rich region at the beginning of the N-terminus [78]. Its mutation or deletion [18, 25, 43] has revealed significantly reduced Ca^{2+} currents suggesting a role on the initial portion of the N-terminus in regulating the extent of maximum current density.

Furthermore, a CaM binding domain is located within the conserved N-terminal region adjacent to the first transmembrane segment. Mutation of CaM-specific residues has caused loss of CaM binding and abolished fast inactivation [91] (see below section Biophysics). Moreover, the conserved aa K85 in Orai1 (K60 in Orai3) within this N-terminal conserved region is a crucial determinant for Orai channel gating [109]. Upon its point mutation (K85E, K60E), Orai channels have completely lost store-operated activation, despite retaining STIM1 coupling. These results suggest that this single residue determines CRAC channel gating [109].

This conserved N-terminal region of Orai additionally exhibits a series of positively charged amino acids resembling a PH-domain known for PIP_2 binding. STIM1 similarly includes a polybasic region at the very end of its C-terminus that has been hypothesized to function as another PIP_2 binding domain. Its deletion in STIM1 impairs puncta formation although STIM1 homomerization as well store-operated activation of Orai are maintained. Thus, it is essential for redistribution of STIM1 to ER-plasma membrane junctions [6, 19, 43, 110] where puncta-formation is directed by phosphoinositides in the plasma membrane [70] even in the absence of Orai. The functional role of phosphoinositides that has been elucidated so far will be further discussed below.

Another regulatory component within STIM1 C-terminus represents the CRAC modulatory domain, termed CMD (aa 474–485). It comprises seven negatively charged residues and their mutation or deletion has strongly enhanced coupling to Orai1 together with two to three fold increased Ca^{2+} inward currents [16, 91, 111]. These larger currents additionally exhibit loss of fast inactivation, as described below in detail. Hence, CMD acts in an inhibitory manner on STIM1/Orai coupling, current activation as well as inactivation.

Despite STIM1 and Orai1 have been shown to be sufficient for the reconstitution of CRAC currents, several further cellular components regulate their interplay. Here, phosphoinositides, phosphorylation sites and oxidative stress apparently play a significant role.

STIM1/Orai1 and Plasma Membrane Phosphoinositides

A lysine-rich domain at the very end of STIM1 C-terminus resembles a PIP_2 binding domain [70]. STIM2, that includes an even larger lysine-rich region at the end of its C-terminus, exhibits preferential binding to PIP_2 [112]. Reduction of PIP_2 and also PIP_3 levels has been shown to affect puncta-formation of STIM1-Orai1 clusters [70, 102], targeting of STIM1 to ER-PM junctions [113] as well as stabilization of STIM1-PM interaction [103]. In contrast, store-operated currents have remained

preserved upon depletion of PIP_2 [103, 113]. Ecran et al. [112] have demonstrated preferential binding of STIM2 to liposomes containing PIP_2 suggesting a specific contribution of for recruitment of STIM2 C-terminus to the plasma membrane. However, reduction of PIP_2 levels has only a minor effect on STIM1 translocation, although STIM1/Orai1-mediated or CRAC currents are strongly inhibited [103].

In summary, phosphoinositides exhibit a regulatory impact on the STIM1/Orai signaling cascade, however, other components besides STIM1 might be additionally involved.

Phosphorylation Sites in STIM1 and Orai Proteins

During meiosis as well as mitosis store-operated currents are suppressed. During meiosis Orai proteins get internalized in intracellular vesicles [114], while during mitosis phosphorylation of STIM1 results in SOCE reduction. STIM1 represents a phospho-protein as it includes a series of phosphorylation sites in its C-terminus [115]. Mutation of the phophorylation sites within STIM1 C-terminus (Ser486, Ser 668) relevant for suppression of Orai1 currents during mitosis [116] rescues mitotic SOCE [116].

Moreover STIM1 functions as a probable target of the extracellular-signal-regulated kinases 1 and 2 (ERK1/2) [117]. Phosphorylation of ERK1/2 target sites on STIM1 has decreased SOCE by reduction of STIM1/Orai coupling [117].

Besides STIM1, also Orai1 contains putative phosphorylation sites within its N-terminus: S27 and S30 [118]. Their mutation has increased store-operated Ca^{2+} entry as well as CRAC currents which lets assume that PKC suppresses SOCE and CRAC channel activation by phosphorylation of Orai1 at these residues.

Hence, the function of STIM1 and Orai is additionally modulated by phosphorylation.

Regulation of STIM1/Orai Signaling by Oxidative Stress

Many physiological and patho-physiological processes like cell growth, differentiation, and cell death are mediated by reactive oxygen species (ROS) [119, 120]. They are generated in intracellular as well as extracellular compartments by redox-active proteins [119, 121, 122]. Antioxidants clear ROS and maintain the physiological redox state within the cells [119, 123]. Hydrogen peroxide (H_2O_2) appears biologically most relevant among the ~20 types of ROS [119]. It is relatively stable, diffuses across the plasma membrane and acts primarily by oxidizing cysteine residues in target proteins [119]. Several recent publications have provided evidence that STIM1/Orai signaling is modulated by oxidative stress [124–126].

Native CRAC currents have been shown to be stimulated by micromolar concentrations of H_2O_2 [125, 126], which requires STIM1. Mechanistically, activation by oxidative stress has been attributed to a reduction in the Ca^{2+}-binding affinity of STIM1 that involves cysteine 56 near the EF-hand within STIM1 N-terminus [126]. It is S-glutathionylated [126] upon addition of ROS and triggers STIM1 oligomerization.

In contrast, another study [124] has reported that oxidation via H_2O_2 blocks the activation of Orai1 channels, while Orai3 channels remain unaffected. The reason for this divergent redox sensitivity of Orai1 and Orai3 channels is attributed to an extracellularly-located reactive cysteine, which is missing in Orai3. Oxidation of cysteine may lock the pore in the closed conformation. The controversial stimulatory or inhibitory effects on CRAC currents by oxidative stress probably depend on the different expression ratios of the three Orai homologues compared to the sole Orai1 expression in HEK cells. Additionally, distinct concentrations of H_2O_2 have been utilized in these reports [124–126]. Alternatively, these findings may point to several potential target sites on STIM1 and Orai proteins within the CRAC machinery.

In summary, oxidative stress provides an additional pathway for modulating STIM1/Orai activation thereby opening new perspectives on a cross talk between Ca^{2+} homeostasis and ROS.

Biophysics

Permeation of CRAC and Orai Channels

Whole cell CRAC currents with Ca^{2+} as a charge carrier exhibit a current–voltage relationship with a strong inward rectification and a high reversal potential of +60 mV [127]. CRAC channels are more than 1,000 times higher selective for Ca^{2+} over Na^+ at physiological conditions [128]. Thus, CRAC channels represent one of the most Ca^{2+} selective channels. In comparison to endogenous CRAC currents, all three Orai channels exhibit similar permeation properties [29, 129]. Ba^{2+} instead of Ca^{2+} in the extracellular solution causes transient current increases which lets assume that CRAC/Orai channels prefer to conduct Ba^{2+} over Ca^{2+} [29, 130]. In contrast, maximally activated Ca^{2+} currents are decreased upon perfusion of Ba^{2+} [131–133]. Only in the absence of any divalent ions [24, 29, 127, 128, 130, 133–135] CRAC/Orai currents get also permeable for Na^+ and Li^+. Although the narrowest pore region of Orai/CRAC channels has been estimated as ~3.8–3.9 Å [133, 136, 137], Cs^+ ions displaying a slightly smaller diameter are impermeable for these channels, in contrast to findings on other Ca^{2+} selective channels like TRPV6 or L-type Ca^{2+} channels [138, 139]. Moreover, CRAC and Orai channels exhibit an extremely small unitary conductance of 9–24 fS, and 6 fS respectively, in a 2–110 mM Ca^{2+} solution [133, 140, 141].

Orai proteins exhibit a distinct transmembrane architecture and permeation profile compared to other Ca^{2+} channels suggesting a unique selectivity filter for these channels (Fig. 16.4). They form tetrameric assemblies of Orai subunits [47, 55, 56] that either include the same isoforms or a heteromeric combination [29, 41, 42]. The negatively charged amino acids within the first (human: E106 in Orai1, E80 in Orai2, E81 in Orai3, drosophila: E180 Orai) and third (human: E190 in Orai1, E164 in Orai2, E165 in Orai3 and drosophila: E262 Orai) transmembrane (TM) segments and the first loop (D110/112/114 for Orai1; E84/Q86/Q88 for Orai2; E85/D87/E89 for Orai3, D182/D184/N186 for drosophila Orai) [23, 85, 133, 137, 142] have been proposed to attract Ca^{2+} ions. Their mutation to glutamates or aspartates alters per-

meation profiles and reduces Ca^{2+} selectivity, while permeation for monovalent cations increases [23, 85, 133, 137, 142]. A glutamine or alanine substitution at position E106 of Orai1 generates a non-permeant channel that acts in a dominant negative manner on all three Orai-mediated [29, 85, 142] and native CRAC currents in T-cells [23, 41]. In line with the reduced Ca^{2+} selectivity of Orai1-E106D and Orai1-E190Q they display an enlarged minimum pore size of 5.3 and 7 Å, respectively [133]. The increase in Orai1 channel pore diameter enables Cs^{+} permeation probably by relief of steric hindrance [133].

Cysteine scanning mutagenesis and cysteine accessibility method [45, 143] reveal that the first extracellular loop forms a flexible outer vestibule of the CRAC channel with negative residues functioning as a Ca^{2+} sink. The selectivity filter forming the tight pore attracts Ca^{2+} at position E106 [85, 143] that curtails the pore by the glutamate side chain up to 3.8 Å. The third transmembrane domain especially E190 plays less likely a role as pore region or selectivity filter [45, 143] but rather affects the pore allosterically as mutations at this position reduce Ca^{2+} selectivity.

Within an Orai channel the first loops of distinct subunits come close to each other during Ca^{2+} permeation. As the three Orai homologues differ in their amino acid sequence in the first loop, within an Orai heteromer glutamates and aspartates in the first loop are asymmetrically arranged. Consequently, pore properties are affected and heteromeric channel yield reduced Ca^{2+} selectivity and robust Cs^{+} permeation in contrast to their homomeric isoforms [40]. Another lab has reported heteromeric Orai1/Orai3 channels as the molecular basis of the ARC channel that responds to arachidonic acid rather than store-depletion [60, 62]. Hence, analysis of native heteromeric Orai1/Orai3 channels [45, 144–146] may help to determine the intrinsic function of the proteins.

In aggregate, the extracellular loop between TM1 and TM2 forms a flexible outer pore vestibule providing a sink for Ca^{2+} ions (see Fig. 16.4). Then Ca^{2+} enters the narrow and rigid segment of the pore encompassing amino acids 99–105 of the first transmembrane segments with glutamate 106 representing the selectivity filter [143]. A second constriction site may be additionally found at the smaller N-terminal packing of TM1 segment. Ca^{2+} is allowed to pass into the cytosol via the hydrophilic side-chain of lysine 91 in Orai1 that is directly located at the interface between TM1 and the N-terminus. Its mutation to a hydrophobic residue inhibits Ca^{2+} entry and Orai activation [147].

Distinct Effects of the CRAC Channel Modulator 2-APB on the Three Orai Isoforms

STIM1/Orai channels have been already examined for the effects of various compounds that block CRAC currents as recently reviewed [148, 149]. 2-aminoethoxydiphenyl borate (2-APB) represents the pharmacologically best characterised modulator of CRAC/Orai currents. Its effects on CRAC/Orai currents are complex and depend on the Orai isoform. STIM1-mediated Orai1 and Orai2 currents display

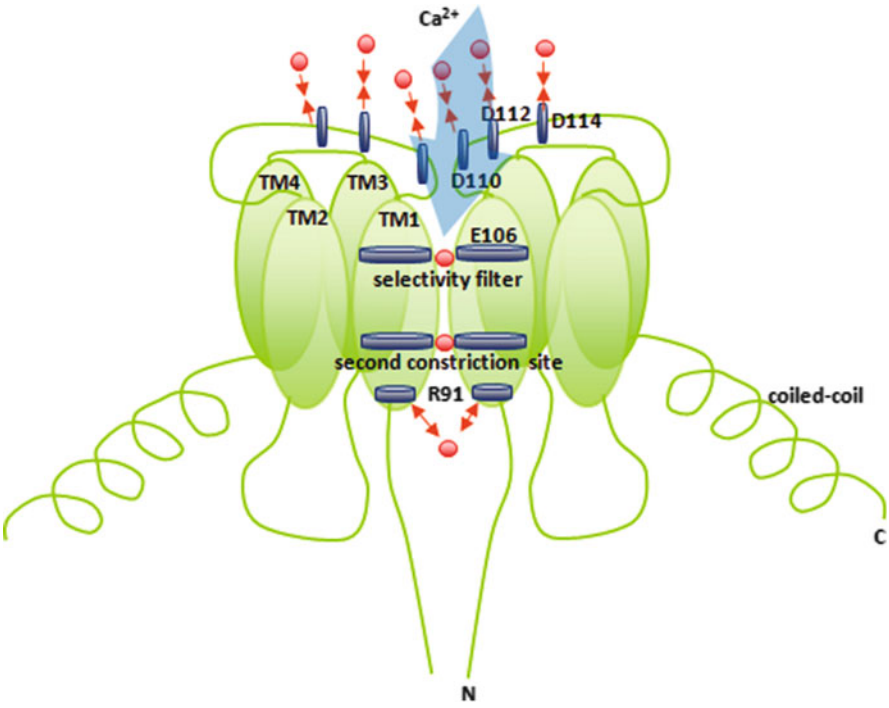

Fig. 16.4 The permeation pathway of Orai1. The extracellular loop between TM1 and TM2 forms a flexible outer pore vestibule providing a sink for Ca^{2+} ions. Afterwards Ca^{2+} enters the narrow and rigid segment of the pore encompassing amino acids 99–105 of the first transmembrane segments with glutamate 106 representing the selectivity filter. Additionally a second constriction site may be found at the smaller N-terminal packing of TM1 segment. Ca^{2+} is able to pass into the cytosol via the hydrophilic side-chain of lysine 91 in Orai1 that is directly located at the interface between TM1 and the N-terminus

transient activation upon low (~5 μM) concentrations of 2-APB and are inhibited at high (~50 μM) concentrations, while Orai3 currents are exclusively enhanced [150].

The temporary increase of Orai1 currents at low concentrations of 2-APB is due to an increased coupling of STIM1 with Orai channels as evaluated by FRET microscopy [89, 151]. The Orai1 current block by 2-APB has been shown to be accompanied by a reversal of STIM1 puncta formation in store-depleted cells [129, 150]. Alternatively, Navarro-Borelly et al. [89] have reported that 2-APB changed the FRET between two labelled Orai1 proteins, suggesting an interference with channel gating [89]. Further, STIM1 apparently interferes with the 2-APB activation of Orai channels, as derived from [152] 2-APB specific outward currents which develop with a ~14 s delay compared to inward currents. Accordingly, in the absence of STIM1 inward and outward currents activated at a parallel time-course upon 2-APB application. Hence, STIM1 seems to act in an inhibitory manner on the gating of Orai channels by 2-APB [152].

Moreover, 2-APB modulates the permeation characteristics of Orai3 channels, pointing to an interaction with the channels' pore. Robust activation of Orai3 by 2-APB occurs in a STIM1-independent manner [42, 130, 137, 150]. Even Orai1 can be stimulated by 2-APB in the absence of STIM1 though to a minor extent than Orai3 [150]. In contrast to store-dependent Orai3 currents, which display a Ca^{2+}-selective inward-rectifying current, those stimulated by 2-APB yield a double-rectifying current–voltage relationship. Thus, 2-APB mediated Orai3 currents are less Ca^{2+} selective and also permeable for other monovalent cations [137, 150] which correlates with an increase in the pore diameter to more than 5 Å [137]. The second as well as third transmembrane segment and the second loop of Orai3 have been mapped to interact with 2-APB [42]. In accordance, an Orai3 chimera with a substituted second loop of Orai1 has shown a dramatically decreased sensitivity to 2-APB (unpublished results; R. Schindl, I. Frischauf, C. Romanin).

In addition, heteromeric Orai1/Orai3 concatemers exhibit substantially diminished 2-APB activation [40]. Thus, homomeric Orai3 channels include unique structures for 2-APB sensitivity [42]. A glutamate in the third TM (E190Q in Orai1, E165Q in Orai3) has been mapped as an essential site affecting 2-APB interaction besides other Orai3 subtype specific regions [23, 137, 142, 150].

The Orai1 R91W Mutant Linked to Severe Combined Immune Deficiency (SCID)

SCID represents a genetic disorder causing defective T cell signaling and arises besides other gene defects by the single point mutation R91W in Orai1 [153–155]. Upon passive store-depletion, this Orai1 R91W mutant exhibits complete loss of current activation [8, 147, 156]. Corresponding point mutations of this conserved arginine in Orai2 and Orai3 have induced a similar loss of function [137, 147, 157]. Whether the Orai SCID mutant acts in a dominant negative manner, is still a controversial issue. One reason for this might arise from distinct ratios of wild-type Orai1 to R91W mutant expression levels possibly affecting the dominant negative action in the various studies [28, 63, 158, 159].

Despite loss of store-operated function of Orai1 R91W, its coupling to STIM1 is largely retained. An increase in the degree of hydrophobicity of residue 91 typically yields non-functional Orai channels [147], which assumedly alters the orientation/flexibility of TM1. Furthermore Orai channels with an increased pore size [133] such as Orai1 E106D or Orai3 in the presence of 2-APB [137] that additionally include the R91W or R66W mutation, respectively, have also remained non-functional. In conclusion, the Orai1 R91W mutant lack of function is linked to a substantial impairment of permeation/gating [147].

A decline in Orai1–Orai1 homomeric FRET which is similarly obtained with Orai1 R91W–Orai1 R91W homomers upon store-depletion, has been supposed to reflect gating rearrangements within the Orai channel [89]. Therefore, Orai1 R91W lack of function has been interpreted as a defect in permeation rather than channel gating [89].

As Orai mutants with increased pore sizes do not recover function, a potential constriction or collapse of the pore appears unlikely. As permeation and gating are processes that are somehow coupled [133], both might be defect in Orai1 R91W. Nevertheless, an ultimate proof for the proposed defect in permeation/gating structures requires resolution at the atomic level by crystallizing the respective Orai1 proteins.

Inactivation of Orai and CRAC Channels

Orai/CRAC channel inactivation represents an important feedback mechanism to control cytosolic Ca^{2+} levels. During a hyperpolarizing voltage step inactivation takes place over tens of milliseconds and follows from feedback inhibition of channel activity by high cytoplasmic Ca^{2+} concentrations close to the channels pore mouth [128, 160].

Fast inactivation of all Orai channels occurs within the first 100 ms of a voltage step and is for Orai3 three times stronger than for Orai1 or Orai2 [29, 40, 111]. Orai1 channels exhibit a late reactivation phase, while Orai2 and Orai3 currents further inactivate slowly [29, 40]. In contrast to ectopically expressed Orai proteins, inactivation of native CRAC channels [16, 160] is much more pronounced and the characteristic reactivation phase seen with Orai1 is lacking. Obviously, further components contribute to the inactivation of native CRAC channels. Moreover it has been reported that distinct expression ratios of STIM1 to Orai1 affect the extent of fast inactivation [161].

Diverse cytosolic regions of the Orai and STIM1 C-terminus have been elucidated as molecular determinants for inactivation of Orai channels. Orai1 and Orai3 N-termini include a calmodulin (CaM) binding domain close to the first transmembrane region which binds CaM in a Ca^{2+}-dependent manner [91, 162]. Transient CaM binding is assumed to mediate fast inactivation. It is tempting to speculate that CaM transiently competes with STIM1 for the N-terminal interaction site on Orai essential for channel gating. The Orai1 specific proline/arginine-rich region in the N-terminus has been shown to mediate reactivation [162].

The intracellular loop of Orai between TM2 and TM3 modulates fast and slow inactivation as revealed by chimeric and mutational approaches [163].

The relevance of the Orai C-terminus for fast inactivation appears complex. Orai2 and Orai3 chimeras with the C-terminus substituted by that of Orai1 exhibit diminished fast inactivation [111] attributed to three conserved glutamates in the C-termini of Orai2 and Orai3 channels [111]. However, fast inactivation is not affected by swapping Orai1/3 C-termini. Remarkably, not only the C- but also the N-terminus and the second intracellular loop contribute to Orai inactivation/gating in a cooperative manner [162]. Moreover fast inactivation is controlled by negatively charged residues within the outer pore vestibule of Orai1 channels [133]. Thus, Orai channels utilize multiple domains controlling fast inactivation.

STIM1 C-terminus includes an acidic cluster (aa 475–483) termed CRAC Modulatory Domain (CMD) that is indispensable for fast Orai/CRAC channel inactivation [16, 91, 111]. Accordingly, fast inactivation of native CRAC currents in

RBL cells has been diminished upon an overexpression of STIM1 C-terminus with all negatively charged residues within CMD mutated to alanines [16] compared to wild-type STIM1 C-terminus while the reactivation phase has remained unaffected. Unique slow reactivation phase of Orai1 has remained unaffected upon mutation or deletion of CMD in full-length STIM1 as well as STIM1 C-terminal fragments (unpublished results). The inactivation of all Orai1-3 channels is inhibited or reduced upon alanine substitution of these negatively charged residues within CMD [16, 111]. In summary, fast inactivation of Orai channels involves negative residues in both STIM1 and Orai as well as its second intracellular loop together with CaM acting on Orai N-terminus.

Additionally, 2-APB has been shown to modulate inactivation of native CRAC currents of T-lymphocytes. Low 2-APB concentrations enhance while high 2-APB concentrations abolish inactivation [131, 136, 160, 164]. As CRAC current inhibition occurs together with loss of inactivation, it has been supposed that these processes are possibly linked [136] in as that 2-APB interrupts a potential coupling between the CRAC channel activation and fast inactivation. The component mediating inactivation of CRAC currents may be represented by STIM1. To resolve the mechanism in detail further studies are still required. The intriguing strong activation of Orai3 currents by high concentrations of 2-APB occurs along a loss of fast inactivation with the appearance of a robust reactivation phase [165]. In this case, 2-APB probably has affected both activation and inactivation together with the geometry of the pore. Based on the findings that 2-APB stimulated Orai3 channels display an increased pore size, it appears likely that the pore is somewhat linked to the gating of Orai channels.

Conclusions

Over the last 20 years store-operated Ca^{2+} channels have been examined in detail, until the two essential key players of CRAC channels, i.e. Orai1 and STIM1, have been identified [8]. Their discovery has enabled characterization of the molecular events and structure-function relationships governing CRAC current activation, permeation and inactivation. Nevertheless, several processes within this signaling cascade are less well understood.

The store-operated coupling via the Orai1 C-terminus and CAD/SOAR within STIM1 C-terminus has already been extensively examined. An essential role for Orai gating via its N-terminus has also been suggested [166], yet the molecular mechanism within the STIM1/Orai signaling cascade is not fully resolved. The hypothesis that Orai N- and C-termini are bridged via STIM1 has still to be proven. Thereby the minimal essential domains need to be identified within the cytosolic stretches involved. It is remarkable that all three Orai proteins contain a highly conserved region within the N-terminal portion close to the first transmembrane segment. However, it is not yet clear whether this domain mediates a similar role within all Orai homologues or acts together with other domains that are distinct

between the Orai isoforms. Moreover it still remains open where the respective site(s) on STIM1 cytosolic portion is (are) that interacts with Orai N-terminal conserved region.

Further, the transformation of STIM1 interaction with Orai1 into opening the channels gate requires detailed analysis. So far FRET microscopy studies have shown that the cytosolic Orai N- and C-termini undergo a conformational change upon binding to STIM1 [89]. These arrangements may be coupled to movements of the gate and supply the energy required for CRAC channel opening. Conformational rearrangements within STIM1 C-terminal portion have been also visualized by a STIM1-based FRET-sensor when it couples to Orai1. Thus, it is tempting to conclude that the intramolecular switching within STIM1 C-terminus mirrors the opening of the CRAC channel [84].

Furthermore diverse proteins have been elucidated to interplay with or couple to either STIM1 or Orai1. However, STIM1 and Orai1 alone have been shown to be sufficient to reconstitute CRAC activation at least based on expression studies. Hence, the role of additional proteins may play a more important role in native systems modulating the STIM1/Orai signaling machinery.

Above all, STIM1 and Orai proteins are involved in a series of cellular processes and have an impact in autoimmune and inflammatory immune disorders [2]. Thus, the identification of STIM1 and Orai1-3 offers potential specific targets for drug development targeting immune diseases like rheumatoid arthritis, inflammatory disorders, allograft rejection [148].

Finally, a 3D atomic resolution of Orai and STIM1 proteins is most awaited, potentially providing the ultimate insight in the gating process, the unusual selectivity filter of this ligand-gated Ca^{2+} channel and allow for novel structure-based rational drug design [84].

Acknowledgements Isabella Derler (T466) is a Hertha-Firnberg scholarship holder. This work was supported by the Austrian Science Foundation (FWF): project P22565 to C.R., Ph.D. Program W1201 “Molecular Bioanalytics” and project Y250-B3 to G.J.S.

References

1. Berridge MJ, Bootman MD, Roderick HL (2003) Calcium signalling: dynamics, homeostasis and remodelling. Nat Rev Mol Cell Biol 4:517–529
2. Parekh AB, Putney JW Jr (2005) Store-operated calcium channels. Physiol Rev 85:757–810
3. Spassova MA, Soboloff J, He LP, Hewavitharana T, Xu W, Venkatachalam K, van Rossum DB, Patterson RL, Gill DL (2004) Calcium entry mediated by SOCs and TRP channels: variations and enigma. Biochim Biophys Acta 1742:9–20
4. Dutta D (2000) Mechanism of store-operated calcium entry. J Biosci 25:397–404
5. Chakrabarti R, Chakrabarti R (2006) Calcium signaling in non-excitable cells: Ca^{2+} release and influx are independent events linked to two plasma membrane Ca^{2+} entry channels. J Cell Biochem 99:1503–1516
6. Liou J, Kim ML, Heo WD, Jones JT, Myers JW, Ferrell JE Jr, Meyer T (2005) STIM is a Ca^{2+} sensor essential for Ca^{2+}-store-depletion-triggered Ca^{2+} influx. Curr Biol 15:1235–1241

7. Roos J, DiGregorio PJ, Yeromin AV, Ohlsen K, Lioudyno M, Zhang S, Safrina O, Kozak JA, Wagner SL, Cahalan MD, Velicelebi G, Stauderman KA (2005) STIM1, an essential and conserved component of store-operated Ca^{2+} channel function. J Cell Biol 169:435–445
8. Feske S, Gwack Y, Prakriya M, Srikanth S, Puppel SH, Tanasa B, Hogan PG, Lewis RS, Daly M, Rao A (2006) A mutation in Orai1 causes immune deficiency by abrogating CRAC channel function. Nature 441:179–185
9. Vig M, Peinelt C, Beck A, Koomoa DL, Rabah D, Koblan-Huberson M, Kraft S, Turner H, Fleig A, Penner R, Kinet JP (2006) CRACM1 is a plasma membrane protein essential for store-operated Ca^{2+} entry. Science 312:1220–1223
10. Zhang SL, Yeromin AV, Zhang XH, Yu Y, Safrina O, Penna A, Roos J, Stauderman KA, Cahalan MD (2006) Genome-wide RNAi screen of Ca^{2+} influx identifies genes that regulate Ca^{2+} release-activated Ca^{2+} channel activity. Proc Natl Acad Sci USA 103:9357–9362
11. Soboloff J, Spassova MA, Dziadek MA, Gill DL (2006) Calcium signals mediated by STIM and Orai proteins - A new paradigm in inter-organelle communication. Biochim Biophys Acta 1763:1161–1168
12. Hogan PG, Lewis RS, Rao A (2010) Molecular basis of calcium signaling in lymphocytes: STIM and ORAI. Annu Rev Immunol 28:491–533
13. Baba Y, Hayashi K, Fujii Y, Mizushima A, Watarai H, Wakamori M, Numaga T, Mori Y, Iino M, Hikida M, Kurosaki T (2006) Coupling of STIM1 to store-operated Ca^{2+} entry through its constitutive and inducible movement in the endoplasmic reticulum. Proc Natl Acad Sci USA 103:16704–16709
14. Smyth JT, Dehaven WI, Jones BF, Mercer JC, Trebak M, Vazquez G, Putney JW Jr (2006) Emerging perspectives in store-operated Ca^{2+} entry: roles of Orai, Stim and TRP. Biochim Biophys Acta 1763:1147–1160
15. Huang GN, Zeng W, Kim JY, Yuan JP, Han L, Muallem S, Worley PF (2006) STIM1 carboxyl-terminus activates native SOC, I(crac) and TRPC1 channels. Nat Cell Biol 8:1003–1010
16. Derler I, Fahrner M, Muik M, Lackner B, Schindl R, Groschner K, Romanin C (2009) A Ca^{2+}release-activated Ca^{2+} (CRAC) modulatory domain (CMD) within STIM1 mediates fast Ca^{2+}-dependent inactivation of ORAI1 channels. J Biol Chem 284:24933–24938
17. Muik M, Fahrner M, Derler I, Schindl R, Bergsmann J, Frischauf I, Groschner K, Romanin C (2009) A Cytosolic Homomerization and a Modulatory Domain within STIM1 C Terminus Determine Coupling to ORAI1 Channels. J Biol Chem 284:8421–8426
18. Yuan JP, Zeng W, Dorwart MR, Choi YJ, Worley PF, Muallem S (2009) SOAR and the polybasic STIM1 domains gate and regulate Orai channels. Nat Cell Biol 11:337–343
19. Park CY, Hoover PJ, Mullins FM, Bachhawat P, Covington ED, Raunser S, Walz T, Garcia KC, Dolmetsch RE, Lewis RS (2009) STIM1 clusters and activates CRAC channels via direct binding of a cytosolic domain to Orai1. Cell 136:876–890
20. Kawasaki T, Lange I, Feske S (2009) A minimal regulatory domain in the C terminus of STIM1 binds to and activates ORAI1 CRAC channels. Biochem Biophys Res Commun 385:49–54
21. Zhou Y, Mancarella S, Wang Y, Yue C, Ritchie M, Gill DL, Soboloff J (2009) The short N-terminal domains of STIM1 and STIM2 control the activation kinetics of Orai1 channels. J Biol Chem 284:19164–19168
22. Zheng L, Stathopulos PB, Li GY, Ikura M (2008) Biophysical characterization of the EF-hand and SAM domain containing Ca^{2+} sensory region of STIM1 and STIM2. Biochem Biophys Res Commun 369:240–246
23. Prakriya M, Feske S, Gwack Y, Srikanth S, Rao A, Hogan PG (2006) Orai1 is an essential pore subunit of the CRAC channel. Nature 443:230–233
24. Peinelt C, Vig M, Koomoa DL, Beck A, Nadler MJ, Koblan-Huberson M, Lis A, Fleig A, Penner R, Kinet JP (2006) Amplification of CRAC current by STIM1 and CRACM1 (Orai1). Nat Cell Biol 8:771–773
25. Takahashi Y, Murakami M, Watanabe H, Hasegawa H, Ohba T, Munehisa Y, Nobori K, Ono K, Iijima T, Ito H (2007) Essential role of the N-terminus of murine Orai1 in store-operated Ca^{2+} entry. Biochem Biophys Res Commun 356:45–52

26. Cahalan MD, Zhang SL, Yeromin AV, Ohlsen K, Roos J, Stauderman KA (2007) Molecular basis of the CRAC channel. Cell Calcium 42:133–144
27. Frischauf I, Muik M, Derler I, Bergsmann J, Fahrner M, Schindl R, Groschner K, Romanin C (2009) Molecular determinants of the coupling between STIM1 and Orai channels: differential activation of Orai1-3 channels by a STIM1 coiled-coil mutant. J Biol Chem 284:21696–21706
28. Muik M, Frischauf I, Derler I, Fahrner M, Bergsmann J, Eder P, Schindl R, Hesch C, Polzinger B, Fritsch R, Kahr H, Madl J, Gruber H, Groschner K, Romanin C (2008) Dynamic Coupling of the Putative Coiled-coil Domain of ORAI1 with STIM1 Mediates ORAI1 Channel Activation. J Biol Chem 283:8014–8022
29. Lis A, Peinelt C, Beck A, Parvez S, Monteilh-Zoller M, Fleig A, Penner R (2007) CRACM1, CRACM2, and CRACM3 are store-operated Ca^{2+} channels with distinct functional properties. Curr Biol 17:794–800
30. Feske S, Giltnane J, Dolmetsch R, Staudt LM, Rao A (2001) Gene regulation mediated by calcium signals in T lymphocytes. Nat Immunol 2:316–324
31. Feske S (2007) Calcium signalling in lymphocyte activation and disease. Nat Rev Immunol 7:690–702
32. Le Deist F, Hivroz C, Partiseti M, Thomas C, Buc HA, Oleastro M, Belohradsky B, Choquet D, Fischer A (1995) A primary T-cell immunodeficiency associated with defective transmembrane calcium influx. Blood 85:1053–1062
33. Baba Y, Nishida K, Fujii Y, Hirano T, Hikida M, Kurosaki T (2008) Essential function for the calcium sensor STIM1 in mast cell activation and anaphylactic responses. Nat Immunol 9:81–88
34. Vig M, Dehaven WI, Bird GS, Billingsley JM, Wang H, Rao PE, Hutchings AB, Jouvin MH, Putney JW, Kinet JP (2008) Defective mast cell effector functions in mice lacking the CRACM1 pore subunit of store-operated calcium release-activated calcium channels. Nat Immunol 9:89–96
35. McCarl CA, Picard C, Khalil S, Kawasaki T, Rother J, Papolos A, Kutok J, Hivroz C, Ledeist F, Plogmann K, Ehl S, Notheis G, Albert MH, Belohradsky BH, Kirschner J, Rao A, Fischer A, Feske S (2009) ORAI1 deficiency and lack of store-operated Ca^{2+} entry cause immunodeficiency, myopathy, and ectodermal dysplasia. J Allergy Clin Immunol 124:1311–1318, e1317
36. Feske S, Picard C, Fischer A (2010) Immunodeficiency due to mutations in ORAI1 and STIM1. Clin Immunol 135:169–182
37. Takahashi Y, Watanabe H, Murakami M, Ono K, Munehisa Y, Koyama T, Nobori K, Iijima T, Ito H (2007) Functional role of stromal interaction molecule 1 (STIM1) in vascular smooth muscle cells. Biochem Biophys Res Commun 361:934–940
38. Grosse J, Braun A, Varga-Szabo D, Beyersdorf N, Schneider B, Zeitlmann L, Hanke P, Schropp P, Muhlstedt S, Zorn C, Huber M, Schmittwolf C, Jagla W, Yu P, Kerkau T, Schulze H, Nehls M, Nieswandt B (2007) An EF hand mutation in Stim1 causes premature platelet activation and bleeding in mice. J Clin Invest 117:3540–3550
39. Bergmeier W, Oh-Hora M, McCarl CA, Roden RC, Bray PF, Feske S (2009) R93W mutation in Orai1 causes impaired calcium influx in platelets. Blood 113:675–678
40. Schindl R, Frischauf I, Bergsmann J, Muik M, Derler I, Lackner B, Groschner K, Romanin C (2009) Plasticity in Ca^{2+} selectivity of Orai1/Orai3 heteromeric channel. Proc Natl Acad Sci USA 106:19623–19628
41. Gwack Y, Srikanth S, Feske S, Cruz-Guilloty F, Oh-hora M, Neems DS, Hogan PG, Rao A (2007) Biochemical and functional characterization of Orai proteins. J Biol Chem 282:16232–16243
42. Zhang SL, Kozak JA, Jiang W, Yeromin AV, Chen J, Yu Y, Penna A, Shen W, Chi V, Cahalan MD (2008) Store-dependent and -independent modes regulating Ca^{2+} release-activated Ca^{2+} channel activity of human Orai1 and Orai3. J Biol Chem 283:17662–17671
43. Li Z, Lu J, Xu P, Xie X, Chen L, Xu T (2007) Mapping the interacting domains of STIM1 and Orai1 in Ca^{2+} release-activated Ca^{2+} channel activation. J Biol Chem 282:29448–29456

44. Fahrner M, Muik M, Derler I, Schindl R, Fritsch R, Frischauf I, Romanin C (2009) Mechanistic view on domains mediating STIM1-Orai coupling. Immunol Rev 231:99–112
45. Zhou Y, Ramachandran S, Oh-Hora M, Rao A, Hogan PG (2010) Pore architecture of the ORAI1 store-operated calcium channel. Proc Natl Acad Sci USA 107:4896–4901
46. Maruyama Y, Ogura T, Mio K, Kato K, Kaneko T, Kiyonaka S, Mori Y, Sato C (2009) Tetrameric Orai1 is a teardrop-shaped molecule with a long, tapered cytoplasmic domain. J Biol Chem 284:13676–13685
47. Mignen O, Thompson JL, Shuttleworth TJ (2008) Orai1 subunit stoichiometry of the mammalian CRAC channel pore. J Physiol 586:419–425
48. Leake MC, Chandler JH, Wadhams GH, Bai F, Berry RM, Armitage JP (2006) Stoichiometry and turnover in single, functioning membrane protein complexes. Nature 443:355–358
49. Ulbrich MH, Isacoff EY (2007) Subunit counting in membrane-bound proteins. Nat Methods 4:319–321
50. Moertelmaier M, Brameshuber M, Linimeier M, Schutz GJ, Stockinger H (2005) Thinning out clusters while conserving stoichiometry of labeling. Appl Phys Lett 87:263903
51. Ruprecht V, Brameshuber M, Schutz GJ (2010) Two-color single molecule tracking combined with photobleaching for the detection of rare molecular interactions in fluid biomembranes. Soft Matter 6:568–581
52. Shaner NC, Steinbach PA, Tsien RY (2005) A guide to choosing fluorescent proteins. Nat Methods 2:905–909
53. Simonson PD, Deberg HA, Ge P, Alexander JK, Jeyifous O, Green WN, Selvin PR (2010) Counting bungarotoxin binding sites of nicotinic acetylcholine receptors in mammalian cells with high signal/noise ratios. Biophys J 99:L81–L83
54. Dickson RM, Cubitt AB, Tsien RY, Moerner WE (1997) On/off blinking and switching behaviour of single molecules of green fluorescent protein. Nature 388:355–358
55. Penna A, Demuro A, Yeromin AV, Zhang SL, Safrina O, Parker I, Cahalan MD (2008) The CRAC channel consists of a tetramer formed by Stim-induced dimerization of Orai dimers. Nature 456:116–120
56. Ji W, Xu P, Li Z, Lu J, Liu L, Zhan Y, Chen Y, Hille B, Xu T, Chen L (2008) Functional stoichiometry of the unitary calcium-release-activated calcium channel. Proc Natl Acad Sci USA 105:13668–13673
57. Schmidt T, Schutz GJ, Gruber HJ, Schindler H (1996) Local stoichiometries determined by counting individual molecules. Anal Chem 68:4397–4401
58. Brameshuber M, Weghuber J, Ruprecht V, Gombos I, Horvath I, Vigh L, Eckerstorfer P, Kiss E, Stockinger H, Schutz GJ (2010) Imaging of mobile long-lived nanoplatforms in the live cell plasma membrane. J Biol Chem 285:41765–41771
59. Madl J, Weghuber J, Fritsch R, Derler I, Fahrner M, Frischauf I, Lackner B, Romanin C, Schutz GJ (2010) Resting-state Orai1 diffuses as homotetramer in the plasma membrane of live mammalian cells. J Biol Chem 285(52):41135–41142
60. Mignen O, Thompson JL, Shuttleworth TJ (2009) The molecular architecture of the arachidonate-regulated Ca^{2+}-selective ARC channel is a pentameric assembly of Orai1 and Orai3 subunits. J Physiol 587:4181–4197
61. Mignen O, Thompson JL, Shuttleworth TJ (2007) STIM1 regulates Ca^{2+} entry via arachidonate-regulated Ca^{2+}-selective (ARC) channels without store depletion or translocation to the plasma membrane. J Physiol 579:703–715
62. Mignen O, Thompson JL, Shuttleworth TJ (2008) Both Orai1 and Orai3 are essential components of the arachidonate-regulated Ca^{2+}-selective (ARC) channels. J Physiol 586:185–195
63. Thompson JL, Mignen O, Shuttleworth TJ (2009) The Orai1 severe combined immune deficiency mutation and calcium release-activated Ca^{2+} channel function in the heterozygous condition. J Biol Chem 284:6620–6626
64. Thompson J, Mignen O, Shuttleworth TJ (2010) The N-terminal domain of Orai3 determines selectivity for activation of the store-independent ARC channel by arachidonic acid. Channels (Austin) 4:398–410

65. Zhang SL, Yu Y, Roos J, Kozak JA, Deerinck TJ, Ellisman MH, Stauderman KA, Cahalan MD (2005) STIM1 is a Ca^{2+} sensor that activates CRAC channels and migrates from the Ca^{2+} store to the plasma membrane. Nature 437:902–905
66. Grigoriev I, Gouveia SM, van der Vaart B, Demmers J, Smyth JT, Honnappa S, Splinter D, Steinmetz MO, Putney JW Jr, Hoogenraad CC, Akhmanova A (2008) STIM1 Is a MT-Plus-End-Tracking Protein Involved in Remodeling of the ER. Curr Biol 18:177–182
67. Smyth JT, DeHaven WI, Bird GS, Putney JW Jr (2007) Role of the microtubule cytoskeleton in the function of the store-operated Ca^{2+} channel activator STIM1. J Cell Sci 120:3762–3771
68. Luik RM, Wu MM, Buchanan J, Lewis RS (2006) The elementary unit of store-operated Ca^{2+} entry: local activation of CRAC channels by STIM1 at ER-plasma membrane junctions. J Cell Biol 174:815–825
69. Xu P, Lu J, Li Z, Yu X, Chen L, Xu T (2006) Aggregation of STIM1 underneath the plasma membrane induces clustering of Orai1. Biochem Biophys Res Commun 350:969–976
70. Liou J, Fivaz M, Inoue T, Meyer T (2007) Live-cell imaging reveals sequential oligomerization and local plasma membrane targeting of stromal interaction molecule 1 after Ca^{2+} store depletion. Proc Natl Acad Sci USA 104:9301–9306
71. Wu MM, Buchanan J, Luik RM, Lewis RS (2006) Ca^{2+} store depletion causes STIM1 to accumulate in ER regions closely associated with the plasma membrane. J Cell Biol 174:803–813
72. Luik RM, Wang B, Prakriya M, Wu MM, Lewis RS (2008) Oligomerization of STIM1 couples ER calcium depletion to CRAC channel activation. Nature 454:538–542
73. Brandman O, Liou J, Park WS, Meyer T (2007) STIM2 Is a Feedback Regulator that Stabilizes Basal Cytosolic and Endoplasmic Reticulum Ca^{2+} Levels. Cell 131:1327–1339
74. Xiao B, Coste B, Mathur J, Patapoutian A (2011) Temperature-dependent STIM1 activation induces Ca^{2+} influx and modulates gene expression. Nat Chem Biol 7:351–358
75. Stathopulos PB, Zheng L, Li GY, Plevin MJ, Ikura M (2008) Structural and mechanistic insights into STIM1-mediated initiation of store-operated calcium entry. Cell 135: 110–122
76. Stathopulos PB, Li GY, Plevin MJ, Ames JB, Ikura M (2006) Stored Ca^{2+} depletion-induced oligomerization of stromal interaction molecule 1 (STIM1) via the EF-SAM region: An initiation mechanism for capacitive Ca^{2+} entry. J Biol Chem 281:35855–35862
77. Covington ED, Wu MM, Lewis RS (2010) Essential role for the CRAC activation domain in store-dependent oligomerization of STIM1. Mol Biol Cell 21:1897–1907
78. Fahrner M, Muik M, Derler I, Schindl R, Fritsch R, Frischauf I, Romanin C (2009) Mechanistic view on domains mediating STIM1-Orai coupling. Immunol Rev 231:99–112
79. Spassova MA, Soboloff J, He LP, Xu W, Dziadek MA, Gill DL (2006) STIM1 has a plasma membrane role in the activation of store-operated Ca^{2+} channels. Proc Natl Acad Sci USA 103:4040–4045
80. Varnai P, Toth B, Toth DJ, Hunyady L, Balla T (2007) Visualization and manipulation of plasma membrane-endoplasmic reticulum contact sites indicates the presence of additional molecular components within the STIM1-Orai1 Complex. J Biol Chem 282:29678–29690
81. Li Z, Liu L, Deng Y, Ji W, Du W, Xu P, Chen L, Xu T (2011) Graded activation of CRAC channel by binding of different numbers of STIM1 to Orai1 subunits. Cell Res 21(2):305–315
82. Hoover PJ, Lewis RS (2011) Stoichiometric requirements for trapping and gating of Ca^{2+} release-activated Ca^{2+} (CRAC) channels by stromal interaction molecule 1 (STIM1). Proc Natl Acad Sci USA 108(32):13299–13304
83. Muik M, Fahrner M, Schindl R, Stathopulos P, Frischauf I, Derler I, Plenk P, Lackner B, Groschner K, Ikura M, Romanin C (2011) STIM1 couples to ORAI1 via an intramolecular transition into an extended conformation. EMBO J 30:1678–1689
84. Korzeniowski MK, Manjarres IM, Varnai P, Balla T (2010) Activation of STIM1-Orai1 Involves an Intramolecular Switching Mechanism. Sci Signal 3:ra82

85. Yeromin AV, Zhang SL, Jiang W, Yu Y, Safrina O, Cahalan MD (2006) Molecular identification of the CRAC channel by altered ion selectivity in a mutant of Orai. Nature 443: 226–229
86. Csutora P, Peter K, Kilic H, Park KM, Zarayskiy V, Gwozdz T, Bolotina VM (2008) Novel role for STIM1 as a trigger for calcium influx factor production. J Biol Chem 283:14524–14531
87. Barr VA, Bernot KM, Srikanth S, Gwack Y, Balagopalan L, Regan CK, Helman DJ, Sommers CL, Oh-Hora M, Rao A, Samelson LE (2008) Dynamic Movement of the Calcium Sensor STIM1 and the Calcium Channel Orai1 in Activated T-Cells: Puncta and Distal Caps. Mol Biol Cell 19:2802–2817
88. Calloway N, Vig M, Kinet JP, Holowka D, Baird B (2009) Molecular clustering of STIM1 with Orai1/CRACM1 at the plasma membrane depends dynamically on depletion of Ca^{2+} stores and on electrostatic interactions. Mol Biol Cell 20:389–399
89. Navarro-Borelly L, Somasundaram A, Yamashita M, Ren D, Miller RJ, Prakriya M (2008) STIM1-Orai1 interactions and Orai1 conformational changes revealed by live-cell FRET microscopy. J Physiol 586:5383–5401
90. Zhou Y, Meraner P, Kwon HT, Machnes D, Oh-hora M, Zimmer J, Huang Y, Stura A, Rao A, Hogan PG (2010) STIM1 gates the store-operated calcium channel ORAI1 in vitro. Nat Struct Mol Biol 17:112–116
91. Mullins FM, Park CY, Dolmetsch RE, Lewis RS (2009) STIM1 and calmodulin interact with Orai1 to induce Ca^{2+}-dependent inactivation of CRAC channels. Proc Natl Acad Sci USA 106:15495–15500
92. Parvez S, Beck A, Peinelt C, Soboloff J, Lis A, Monteilh-Zoller M, Gill DL, Fleig A, Penner R (2008) STIM2 protein mediates distinct store-dependent and store-independent modes of CRAC channel activation. FASEB J 22:752–761
93. Srikanth S, Jung HJ, Kim KD, Souda P, Whitelegge J, Gwack Y (2010) A novel EF-hand protein, CRACR2A, is a cytosolic Ca^{2+} sensor that stabilizes CRAC channels in T cells. Nat Cell Biol 12:436–446
94. Howie D, Nolan KF, Daley S, Butterfield E, Adams E, Garcia-Rueda H, Thompson C, Saunders NJ, Cobbold SP, Tone Y, Tone M, Waldmann H (2009) MS4A4B is a GITR-associated membrane adapter, expressed by regulatory T cells, which modulates T cell activation. J Immunol 183:4197–4204
95. Walsh CM, Doherty MK, Tepikin AV, Burgoyne RD (2010) Evidence for an interaction between Golli and STIM1 in store-operated calcium entry. Biochem J 430:453–460
96. Martin AC, Willoughby D, Ciruela A, Ayling LJ, Pagano M, Wachten S, Tengholm A, Cooper DM (2009) Capacitative Ca^{2+} entry via Orai1 and stromal interacting molecule 1 (STIM1) regulates adenylyl cyclase type 8. Mol Pharmacol 75:830–842
97. Woodward OM, Li Y, Yu S, Greenwell P, Wodarczyk C, Boletta A, Guggino WB, Qian F (2010) Identification of a polycystin-1 cleavage product, P100, that regulates store operated Ca entry through interactions with STIM1. PLoS One 5:e12305
98. Yu F, Sun L, Machaca K (2010) Constitutive recycling of the store-operated Ca^{2+} channel Orai1 and its internalization during meiosis. J Cell Biol 191:523–535
99. Feng M, Grice DM, Faddy HM, Nguyen N, Leitch S, Wang Y, Muend S, Kenny PA, Sukumar S, Roberts-Thomson SJ, Monteith GR, Rao R (2010) Store-independent activation of Orai1 by SPCA2 in mammary tumors. Cell 143:84–98
100. Park CY, Shcheglovitov A, Dolmetsch R (2010) The CRAC channel activator STIM1 binds and inhibits L-type voltage-gated calcium channels. Science 330:101–105
101. Wang Y, Deng X, Mancarella S, Hendron E, Eguchi S, Soboloff J, Tang XD, Gill DL (2010) The calcium store sensor, STIM1, reciprocally controls Orai and CaV1.2 channels. Science 330:105–109
102. Chvanov M, Walsh CM, Haynes LP, Voronina SG, Lur G, Gerasimenko OV, Barraclough R, Rudland PS, Petersen OH, Burgoyne RD, Tepikin AV (2008) ATP depletion induces translocation of STIM1 to puncta and formation of STIM1-ORAI1 clusters: translocation and re-translocation of STIM1 does not require ATP. Pflugers Arch 457:505–517

103. Korzeniowski MK, Popovic MA, Szentpetery Z, Varnai P, Stojilkovic SS, Balla T (2009) Dependence of STIM1/Orai1-mediated calcium entry on plasma membrane phosphoinositides. J Biol Chem 284:21027–21035
104. Walsh CM, Chvanov M, Haynes LP, Petersen OH, Tepikin AV, Burgoyne RD (2009) Role of phosphoinositides in STIM1 dynamics and store-operated calcium entry. Biochem J 425:159–168
105. Hull JJ, Lee JM, Kajigaya R, Matsumoto S (2009) Bombyx mori homologs of STIM1 and Orai1 are essential components of the signal transduction cascade that regulates sex pheromone production. J Biol Chem 284:31200–31213
106. Calloway N, Holowka D, Baird B (2010) A basic sequence in STIM1 promotes Ca^{2+} influx by interacting with the C-terminal acidic coiled coil of Orai1. Biochemistry 49:1067–1071
107. Woolfson DN (2005) The design of coiled-coil structures and assemblies. Adv Protein Chem 70:79–112
108. Fairman R, Chao HG, Lavoie TB, Villafranca JJ, Matsueda GR, Novotny J (1996) Design of heterotetrameric coiled coils: evidence for increased stabilization by Glu(-)-Lys(+) ion pair interactions. Biochemistry 35:2824–2829
109. Lis A, Zierler S, Peinelt C, Fleig A, Penner R (2010) A single lysine in the N-terminal region of store-operated channels is critical for STIM1-mediated gating. J Gen Physiol 136:673–686
110. Carrasco S, Meyer T (2011) STIM Proteins and the Endoplasmic Reticulum-Plasma Membrane Junctions. Annu Rev Biochem 80:973–1000
111. Lee KP, Yuan JP, Zeng W, So I, Worley PF, Muallem S (2009) Molecular determinants of fast Ca^{2+}-dependent inactivation and gating of the Orai channels. Proc Natl Acad Sci USA 106:14687–14692
112. Ercan E, Momburg F, Engel U, Temmerman K, Nickel W, Seedorf M (2009) A conserved, lipid-mediated sorting mechanism of yeast Ist2 and mammalian STIM proteins to the peripheral ER. Traffic 10:1802–1818
113. Walsh CM, Chvanov M, Haynes LP, Petersen OH, Tepikin AV, Burgoyne RD (2010) Role of phosphoinositides in STIM1 dynamics and store-operated calcium entry. Biochem J 425:159–168
114. Yu F, Sun L, Machaca K (2009) Orai1 internalization and STIM1 clustering inhibition modulate SOCE inactivation during meiosis. Proc Natl Acad Sci USA 106:17401–17406
115. Manji SS, Parker NJ, Williams RT, van Stekelenburg L, Pearson RB, Dziadek M, Smith PJ (2000) STIM1: a novel phosphoprotein located at the cell surface. Biochim Biophys Acta 1481:147–155
116. Smyth JT, Petranka JG, Boyles RR, DeHaven WI, Fukushima M, Johnson KL, Williams JG, Putney JW Jr (2009) Phosphorylation of STIM1 underlies suppression of store-operated calcium entry during mitosis. Nat Cell Biol 11:1465–1472
117. Pozo-Guisado E, Campbell DG, Deak M, Alvarez-Barrientos A, Morrice NA, Alvarez IS, Alessi DR, Martin-Romero FJ (2010) Phosphorylation of STIM1 at ERK1/2 target sites modulates store-operated calcium entry. J Cell Sci 123:3084–3093
118. Kawasaki T, Ueyama T, Lange I, Feske S, Saito N (2010) Protein kinase C-induced phosphorylation of Orai1 regulates the intracellular Ca^{2+} level via the store-operated Ca^{2+} channel. J Biol Chem 285:25720–25730
119. Droge W (2002) Free radicals in the physiological control of cell function. Physiol Rev 82:47–95
120. Rhee SG (2006) Cell signaling. H2O2, a necessary evil for cell signaling. Science 312:1882–1883
121. Lambeth JD (2004) NOX enzymes and the biology of reactive oxygen. Nat Rev Immunol 4:181–189
122. Starkov AA (2008) The role of mitochondria in reactive oxygen species metabolism and signaling. Ann NY Acad Sci 1147:37–52
123. Fridovich I (1999) Fundamental aspects of reactive oxygen species, or what's the matter with oxygen? Ann NY Acad Sci 893:13–18

124. Bogeski I, Kummerow C, Al-Ansary D, Schwarz EC, Koehler R, Kozai D, Takahashi N, Peinelt C, Griesemer D, Bozem M, Mori Y, Hoth M, Niemeyer BA (2010) Differential redox regulation of ORAI ion channels: a mechanism to tune cellular calcium signaling. Sci Signal 3:ra24
125. Grupe M, Myers G, Penner R, Fleig A (2010) Activation of store-operated I(CRAC) by hydrogen peroxide. Cell Calcium 48:1–9
126. Hawkins BJ, Irrinki KM, Mallilankaraman K, Lien YC, Wang Y, Bhanumathy CD, Subbiah R, Ritchie MF, Soboloff J, Baba Y, Kurosaki T, Joseph SK, Gill DL, Madesh M (2010) S-glutathionylation activates STIM1 and alters mitochondrial homeostasis. J Cell Biol 190:391–405
127. Hoth M, Penner R (1992) Depletion of intracellular calcium stores activates a calcium current in mast cells. Nature 355:353–356
128. Hoth M, Penner R (1993) Calcium release-activated calcium current in rat mast cells. J Physiol 465:359–386
129. DeHaven WI, Smyth JT, Boyles RR, Bird GS, Putney JW Jr (2008) Complex actions of 2-aminoethyldiphenyl borate on store-operated calcium entry. J Biol Chem 283:19265–19273
130. DeHaven WI, Smyth JT, Boyles RR, Putney JW Jr (2007) Calcium inhibition and calcium potentiation of Orai1, Orai2, and Orai3 calcium release-activated calcium channels. J Biol Chem 282:17548–17556
131. Prakriya M (2009) The molecular physiology of CRAC channels. Immunol Rev 231:88–98
132. Su Z, Shoemaker RL, Marchase RB, Blalock JE (2004) Ca^{2+} modulation of Ca^{2+} release-activated Ca^{2+} channels is responsible for the inactivation of its monovalent cation current. Biophys J 86:805–814
133. Yamashita M, Navarro-Borelly L, McNally BA, Prakriya M (2007) Orai1 mutations alter ion permeation and Ca^{2+}-dependent fast inactivation of CRAC channels: evidence for coupling of permeation and gating. J Gen Physiol 130:525–540
134. Lepple-Wienhues A, Cahalan MD (1996) Conductance and permeation of monovalent cations through depletion-activated Ca^{2+} channels (ICRAC) in Jurkat T cells. Biophys J 71:787–794
135. Prakriya M, Lewis RS (2006) Regulation of CRAC channel activity by recruitment of silent channels to a high open-probability gating mode. J Gen Physiol 128:373–386
136. Prakriya M, Lewis RS (2001) Potentiation and inhibition of Ca^{2+} release-activated Ca^{2+} channels by 2-aminoethyldiphenyl borate (2-APB) occurs independently of IP(3) receptors. J Physiol 536:3–19
137. Schindl R, Bergsmann J, Frischauf I, Derler I, Fahrner M, Muik M, Fritsch R, Groschner K, Romanin C (2008) 2-aminoethoxydiphenyl borate alters selectivity of Orai3 channels by increasing their pore size. J Biol Chem 283:20261–20267
138. Voets T, Prenen J, Fleig A, Vennekens R, Watanabe H, Hoenderop JG, Bindels RJ, Droogmans G, Penner R, Nilius B (2001) CaT1 and the calcium release-activated calcium channel manifest distinct pore properties. J Biol Chem 276:47767–47770
139. Hess P, Lansman JB, Tsien RW (1986) Calcium channel selectivity for divalent and monovalent cations. Voltage and concentration dependence of single channel current in ventricular heart cells. J Gen Physiol 88:293–319
140. Zweifach A, Lewis RS (1993) Mitogen-regulated Ca^{2+} current of T lymphocytes is activated by depletion of intracellular Ca^{2+} stores. Proc Natl Acad Sci USA 90:6295–6299
141. Prakriya M, Lewis RS (2002) Separation and characterization of currents through store-operated CRAC channels and Mg^{2+}-inhibited cation (MIC) channels. J Gen Physiol 119:487–507
142. Vig M, Beck A, Billingsley JM, Lis A, Parvez S, Peinelt C, Koomoa DL, Soboloff J, Gill DL, Fleig A, Kinet JP, Penner R (2006) CRACM1 multimers form the ion-selective pore of the CRAC channel. Curr Biol 16:2073–2079

143. McNally BA, Yamashita M, Engh A, Prakriya M (2009) Structural determinants of ion permeation in CRAC channels. Proc Natl Acad Sci USA 106:22516–22521
144. Peel SE, Liu B, Hall IP (2008) ORAI and store-operated calcium influx in human airway smooth muscle cells. Am J Respir Cell Mol Biol 38:744–749
145. Motiani RK, Abdullaev IF, Trebak M (2010) A novel native store-operated calcium channel encoded by Orai3: selective requirement of Orai3 versus Orai1 in estrogen receptor-positive versus estrogen receptor-negative breast cancer cells. J Biol Chem 285:19173–19183
146. Jones BF, Boyles RR, Hwang SY, Bird GS, Putney JW (2008) Calcium influx mechanisms underlying calcium oscillations in rat hepatocytes. Hepatology 48:1273–1281
147. Derler I, Fahrner M, Carugo O, Muik M, Bergsmann J, Schindl R, Frischauf I, Eshaghi S, Romanin C (2009) Increased hydrophobicity at the N terminus/membrane interface impairs gating of the severe combined immunodeficiency-related ORAI1 mutant. J Biol Chem 284:15903–15915
148. Derler I, Fritsch R, Schindl R, Romanin C (2008) CRAC inhibitors: identification and potential. Expert Opin Drug Disc 3:787–800
149. Putney JW (2010) Pharmacology of Store-operated Calcium Channels. Mol Interv 10:209–218
150. Peinelt C, Lis A, Beck A, Fleig A, Penner R (2008) 2-Aminoethoxydiphenyl borate directly facilitates and indirectly inhibits STIM1-dependent gating of CRAC channels. J Physiol 586:3061–3073
151. Wang Y, Deng X, Zhou Y, Hendron E, Mancarella S, Ritchie MF, Tang XD, Baba Y, Kurosaki T, Mori Y, Soboloff J, Gill DL (2009) STIM protein coupling in the activation of Orai channels. Proc Natl Acad Sci USA 106:7391–7396
152. Yamashita M, Somasundaram A, Prakriya M (2011) Competitive modulation of Ca^{2+} release-activated Ca^{2+} channel gating by STIM1 and 2-aminoethyldiphenyl borate. J Biol Chem 286:9429–9442
153. Buckley RH (2004) The multiple causes of human SCID. J Clin Invest 114:1409–1411
154. Carroll HP, McNaull BB, Gadina M (2006) Immunodeficiency is a tough nut to CRAC: the importance of calcium flux in T cell activation. Mol Interv 6:253–256
155. Gaspar HB, Thrasher AJ (2005) Gene therapy for severe combined immunodeficiencies. Expert Opin Biol Ther 5:1175–1182
156. Feske S (2005) A severe defect in CRAC Ca^{2+} channel activation and altered K^+ channel gating in T cells from immunodeficient patients. J Exp Med 202:651–662
157. Soboloff J, Spassova MA, Dziadek MA, Gill DL (2006) Calcium signals mediated by STIM and Orai proteins–a new paradigm in inter-organelle communication. Biochim Biophys Acta 1763:1161–1168
158. Liao Y, Erxleben C, Yildirim E, Abramowitz J, Armstrong DL, Birnbaumer L (2007) Orai proteins interact with TRPC channels and confer responsiveness to store depletion. Proc Natl Acad Sci USA 104:4682–4687
159. Cheng KT, Liu X, Ong HL, Ambudkar IS (2008) Functional requirement for Orai1 in store-operated TRPC1-STIM1 channels. J Biol Chem 283:12935–12940
160. Zweifach A, Lewis RS (1995) Rapid inactivation of depletion-activated calcium current (ICRAC) due to local calcium feedback. J Gen Physiol 105:209–226
161. Scrimgeour N, Litjens T, Ma L, Barritt GJ, Rychkov GY (2009) Properties of Orai1 mediated store-operated current depend on the expression levels of STIM1 and Orai1 proteins. J Physiol 587(Pt 12):2903–2918
162. Frischauf I, Schindl R, Bergsmann J, Derler I, Fahrner M, Muik M, Fritsch R, Lackner B, Groschner K, Romanin C (2011) Cooperativeness of Orai cytosolic domains tunes subtype-specific gating. J Biol Chem 286:8577–8584
163. Srikanth S, Jung HJ, Ribalet B, Gwack Y (2010) The intracellular loop of Orai1 plays a central role in fast inactivation of Ca^{2+} release-activated Ca^{2+} channels. J Biol Chem 285:5066–5075

164. Prakriya M, Lewis RS (2003) CRAC channels: activation, permeation, and the search for a molecular identity. Cell Calcium 33:311–321
165. Yamashita M, Somasundaram A, Prakriya M (2011) Competitive modulation of CRAC channel gating by STIM1 and 2-aminoethyldiphenyl borate (2-APB). J Biol Chem 286(11):9429–9442
166. Lis A, Zierler S, Peinelt C, Fleig A, Penner R (2010) A single lysine in the N-terminal region of store-operated channels is critical for STIM1-mediated gating. J Gen Physiol 136:673–686

Chapter 17
Mitochondria-Associated Membranes (MAMs) as Hotspot Ca^{2+} Signaling Units

Angela Bononi, Sonia Missiroli, Federica Poletti, Jan M. Suski, Chiara Agnoletto, Massimo Bonora, Elena De Marchi, Carlotta Giorgi, Saverio Marchi, Simone Patergnani, Alessandro Rimessi, Mariusz R. Wieckowski, and Paolo Pinton

Abstract The tight interplay between endoplasmic reticulum (ER) and mitochondria is a key determinant of cell function and survival through the control of intracellular calcium (Ca^{2+}) signaling. The specific sites of physical association between ER and mitochondria are known as mitochondria-associated membranes (MAMs). It has recently become clear that MAMs are crucial for highly efficient transmission of Ca^{2+} from the ER to mitochondria, thus controlling fundamental processes involved in energy production and also determining cell fate by triggering or preventing apoptosis. In this contribution, we summarize the main features of the Ca^{2+}-signaling toolkit, covering also the latest breakthroughs in the field, such as the identification of novel candidate proteins implicated in mitochondrial Ca^{2+} transport and the recent

A. Bononi • S. Missiroli • F. Poletti • C. Agnoletto • M. Bonora • E. De Marchi • C. Giorgi • S. Marchi • S. Patergnani • A. Rimessi • P. Pinton (✉)
Laboratory for Technologies of Advanced Therapies (LTTA), Department of Experimental and Diagnostic Medicine, Section of General Pathology, Interdisciplinary Center for the Study of Inflammation (ICSI), University of Ferrara, Via Borsari, 46, 44121 Ferrara, Italy
e-mail: angela.bononi@unife.it; sonia.missiroli@unife.it; federica.poletti@unife.it; chiara.agnoletto@unife.it; massimo.bonora1@unife.it; elena.demarchi@unife.it; carlotta.giorgi@unife.it; saverio.marchi@unife.it; simone.patergnani@unife.it; alessandro.rimessi@unife.it; pnp@unife.it

J.M. Suski
Laboratory for Technologies of Advanced Therapies (LTTA), Department of Experimental and Diagnostic Medicine, Section of General Pathology, Interdisciplinary Center for the Study of Inflammation (ICSI), University of Ferrara, Via Borsari, 46, 44100 Ferrara, Italy

Nencki Institute of Experimental Biology, Warsaw, Poland
e-mail: j.suski@nencki.gov.pl

M.R. Wieckowski
Nencki Institute of Experimental Biology, Warsaw, Poland
e-mail: m.wieckowski@nencki.gov.pl

M.S. Islam (ed.), *Calcium Signaling*, Advances in Experimental Medicine and Biology 740, DOI 10.1007/978-94-007-2888-2_17,

direct characterization of the high-Ca^{2+} microdomains between ER and mitochondria. We review the main functions of these two organelles, with special emphasis on Ca^{2+} handling and on the structural and molecular foundations of the signaling contacts between them. Additionally, we provide important examples of the physiopathological role of this cross-talk, briefly describing the key role played by MAMs proteins in many diseases, and shedding light on the essential role of mitochondria-ER interactions in the maintenance of cellular homeostasis and the determination of cell fate.

Keywords Akt • Apoptosis • Bap31 • Bip • Ca^{2+} signaling • Calcium ions • Endoplasmic Reticulum • Ero1α • ERp44 • GM1-ganglioside • grp75 • IP3Rs • MCU • Microdomains • MICU1 • Mitochondria • Mitochondria-Associated Membranes • Mitofusin-1 and -2 • p66Shc • PACS-2 • Plasma Membrane Associated Membranes • PML • PP2a • Presenilin-1 and -2 • Sig-1R • VDAC

Abbreviations

$\Delta\Psi_m$	Mitochondrial membrane potential difference
AD	Alzheimer's disease
ANT	Adenine nucleotide translocase
Bap31	(B-cell receptor-associated protein 31)
BFP	Blue fluorescent protein
BiP	Binding immunoglobulin Protein
Ca^{2+}	Calcium ions
$[Ca^{2+}]$	Ca^{2+} concentration
$[Ca^{2+}]_c$	Cytosolic Ca^{2+} concentration
$[Ca^{2+}]_m$	Mitochondrial Ca^{2+} concentration
CABPs	Intraluminal Ca^{2+}-binding proteins
CaMKII	Calmodulin-dependent protein kinase II
CCE	Capacitative Ca^{2+} entry
Cyp D	Cyclophilin D
Drp1	Dynamin-related protein 1
ER	Endoplasmic reticulum
ERp44	(Endoplasmic reticulum resident protein 44)
FACL4	Long-chain fatty acid-CoA ligase type 4
FAD	Familial Alzheimer's disease
Fhit	Fragile histidine triad
Fis1	Fission 1 homologue
FRET	Fluorescence resonance energy transfer
GFP	Green fluorescent protein
GM1	GM1-ganglioside
grp75	Glucose-regulated protein 75
HK	Hexokinase

IMM	Inner mitochondrial membrane
IMS	Intermembrane space
IP3	Inositol 1,4,5-trisphosphate
IP3R	Inositol 1,4,5-trisphosphate receptor
Letm1	Leucine zipper-EF-hand containing transmembrane protein 1
MAMs	Mitochondria-associated membranes
MCU	Mitochondrial Ca^{2+} uniporter
MICU1	Mitochondrial calcium uptake 1
Mfn	Mitofusin
mHCX	Mitochondrial H^+/Ca^{2+} exchanger
MMP	Mitochondrial membrane permeabilization
mNCX	Mitochondrial Na^{2+}/Ca^{2+} exchanger
MOMP	Mitochondrial outer membrane permeabilization
NADH	Nicotinamide adenine dinucleotide
NCX	Na^{2+}/Ca^{2+} exchanger
NE	nuclear envelope
OMM	Outer mitochondrial membrane
OPA1	Optic atrophy 1
OXPHOS	Oxidative phosphorylation
p66shc	66-kDa isoform of the growth factor adapter shc
PACS-2	Phosphofurin acidic cluster sorting protein 2
PAMs	Plasma membrane associated membranes
PDH	Pyruvate dehydrogenase
PKA	Protein kinase A
PKC	Protein kinase C
PLC	Phospholipase C
PMCA	Plasma membrane Ca^{2+} ATPase
PML	Promyelocytic leukemia protein
PP2a	Protein phosphatase 2a
PS1	Presenilin-1
PS2	Presenilin-2
PSS-1	Phosphatidylserine synthase-1
PTP	Permeability transition pore
ROCs	Receptor operated Ca^{2+} channels
ROS	Reactive oxygen species
RyR	Ryanodine receptor
SERCA	Sarco-endoplasmic reticulum Ca^{2+} ATPase
Sig-1R	Sigma-1 receptor
SMOCs	Second messenger operated Ca^{2+} channels
SR	Sarcoplasmic reticulum
TIRF	Total internal reflection fluorescence
TpMs	Trichoplein/Mitostatin
UCP	Uncoupling protein
VDAC	Voltage-dependent anion channel
VOCs	Voltage operated Ca^{2+} channels.

The Ca^{2+}-Signaling Toolkit

Calcium ions (Ca^{2+}) are ubiquitous intracellular messengers that can set up and/or regulate many different cellular functions, including gene expression, cellular contraction, secretion, synaptic transmission, metabolism, differentiation and proliferation, as well as cell death. The universality of Ca^{2+}-based signaling depends on its enormous versatility in terms of amplitude, duration, frequency and localization. The formation of the correct spatio-temporal Ca^{2+} signals is dependent on an extensive cellular machinery named the Ca^{2+} toolkit, which includes the various cellular Ca^{2+}-binding and Ca^{2+}-transporting proteins, present mainly in the cytosol, plasma membrane, endoplasmic reticulum (ER), and mitochondria [1].

The resting cytosolic Ca^{2+} concentration ($[Ca^{2+}]_c$) is maintained around the value of 100 nM, significantly lower than extracellular [Ca^{2+}] (1 mM). This condition is achieved through active extrusion of Ca^{2+} by the plasma membrane Ca^{2+} ATPase (PMCA) and the Na^+/Ca^{2+} exchanger (NCX) [2, 3]. The increase of intracellular [Ca^{2+}] can be elicited by two fundamental mechanisms (or a combination of both). The first involves Ca^{2+} entry from the extracellular milieu, through the opening of plasma membrane Ca^{2+} channels (traditionally grouped into three classes: voltage operated Ca^{2+} channels (VOCs) [4], receptor operated Ca^{2+} channels (ROCs) [5] and second messenger operated Ca^{2+} channels (SMOCs) [6]); the second mechanism involves Ca^{2+} release from intracellular stores, mainly the ER and its specialized form in muscle, the sarcoplasmic reticulum (SR). In these intracellular stores, two main Ca^{2+}-release channels exist that, upon stimulation, release Ca^{2+} into the cytosol, thus triggering Ca^{2+} signaling: the inositol 1,4,5-trisphosphate (IP3) receptors (IP3Rs) and the ryanodine receptors (RyRs) [7, 8]. IP3Rs are ligand-gated channels that function in releasing Ca^{2+} from ER Ca^{2+} stores in response to IP3 generation initiated by agonist binding to cell-surface G protein-coupled receptor [9, 10]. The subsequent rise in $[Ca^{2+}]_c$ results in various Ca^{2+}-dependent intracellular events. The exact cellular outcome depends on the spatiotemporal characteristics of the generated Ca^{2+} signal [11]. Once its downstream targets are activated, basal $[Ca^{2+}]_c$ levels are regained by the combined activity of Ca^{2+} extrusion mechanisms, such as PMCA and NCX, and mechanisms that refill the intracellular stores, like sarco-endoplasmic reticulum Ca^{2+} ATPases (SERCAs) [2]. Due to SERCA activity and intraluminal Ca^{2+}-binding proteins (CABPs), *i.e.*, calnexin and calreticulin [12], the ER can accumulate Ca^{2+} more than a thousand-fold excess as compared to the cytosol.

While the role of the ER as a physiologically important Ca^{2+} store has long been recognized, a similar role for mitochondria have seen a reappraisal only in the past two decades [13]. The studies of Rizzuto, Pozzan and colleagues revealed that IP3-mediated Ca^{2+} release from the ER results in cytosolic Ca^{2+} increases that are accompanied by similar or even larger mitochondrial ones [14], driven by the large electrochemical gradient (mitochondrial membrane potential difference, $\Delta\Psi_m = -180$ mV, negative inside) generated by the respiratory chain [15]. The uptake of the Ca^{2+} ions into the mitochondrial matrix implies different transport systems

responsible for the transfer of Ca^{2+} across the outer and the inner mitochondrial membrane (OMM and IMM respectively). Despite the surprisingly low affinity of the mitochondrial uptake systems (Kd around 10–20 μM) and the submicromolar global $[Ca^{2+}]_c$ (which rarely exceed 2–3 μM) evoked by IP3-mediated Ca^{2+} release, mitochondrial Ca^{2+} concentration ($[Ca^{2+}]_m$) can undergo rapid changes upon cell stimulation, because their low affinity uptake systems are exposed to microdomains of high $[Ca^{2+}]$ in proximity to ER or plasma membrane Ca^{2+} channels [16–18]. The hypothesis, called "microdomain hypothesis" [19], was initially supported by a large body of indirect evidence, and its direct determination was carried out only very recently by two complementary studies that demonstrated the existence and amplitude of high Ca^{2+} microdomains on the surface of mitochondria. Giacomello et al. [20] targeted a new generation of FRET-based Ca^{2+} sensors [21] to the OMM and, through a sophisticated statistical analysis of the images, revealed the existence of small OMM regions whose $[Ca^{2+}]$ reaches values as high as 15–20 μM. The probe detected Ca^{2+} hotspots on about 10% of the OMM surface that were not observed in other parts of the cell. The Ca^{2+} hotspots were not uniform, and their frequency varied among mitochondria of the same cell. Moreover, classical epifluorescence and total internal reflection fluorescence (TIRF) microscopy experiments were combined in order to monitor the generation of high Ca^{2+} microdomains in mitochondria located near the plasma membrane. With this approach, it could be shown that Ca^{2+} hotspots on the surface of mitochondria occur upon opening of VOCs, but not upon capacitative Ca^{2+} entry (CCE). Csordás et al. [22] used a complementary approach in which they generated genetically encoded bifunctional linkers consisting of OMM and ER targeting sequences connected through a fluorescent protein, including a low-Ca^{2+}-affinity pericam, and coupled with the two components of the FKBP-FRB heterodimerization system [23], respectively. Using rapamycin-assembled heterodimerization of the FKBP-FRB-based linker, they detected ER/OMM and plasma membrane/OMM junctions (the latter at a much lower frequency). In addition, the recruited low-Ca^{2+}-affinity pericam reported Ca^{2+} concentrations as high as 25 μM at the ER/OMM junctions in response to IP3-mediated Ca^{2+} release, which is in excellent agreement with the values obtained by Giacomello et al..

The Ca^{2+}-import system across the OMM occurs through the so-called voltage-dependent anion channels (VDAC) [24], traditionally considered as a large voltage-gated channel, fully opened with high-conductance and weak anion-selectivity at zero and low transmembrane potentials (<20–30 mV), but switching to cation selectivity and lower conductance at higher potentials (the so-called "closed" state) [25–27]. In contrast, the molecular identity of the IMM Ca^{2+}-transport system, the mitochondrial Ca^{2+} uniporter (MCU), has been identified only very recently, preceded last year by the discovery of mitochondrial calcium uptake 1 (MICU1), an uniporter regulator which appears essential for mitochondrial Ca^{2+} uptake [28]. MICU1 has been identified in silico in the MitoCarta database [29]; it is a single-pass transmembrane protein which does not seem to participate in channel pore formation, so it is not known whether it actually forms (part of) a Ca^{2+} channel, or functions as Ca^{2+} buffer, or as a Ca^{2+}-dependent regulatory protein acting as a Ca^{2+}

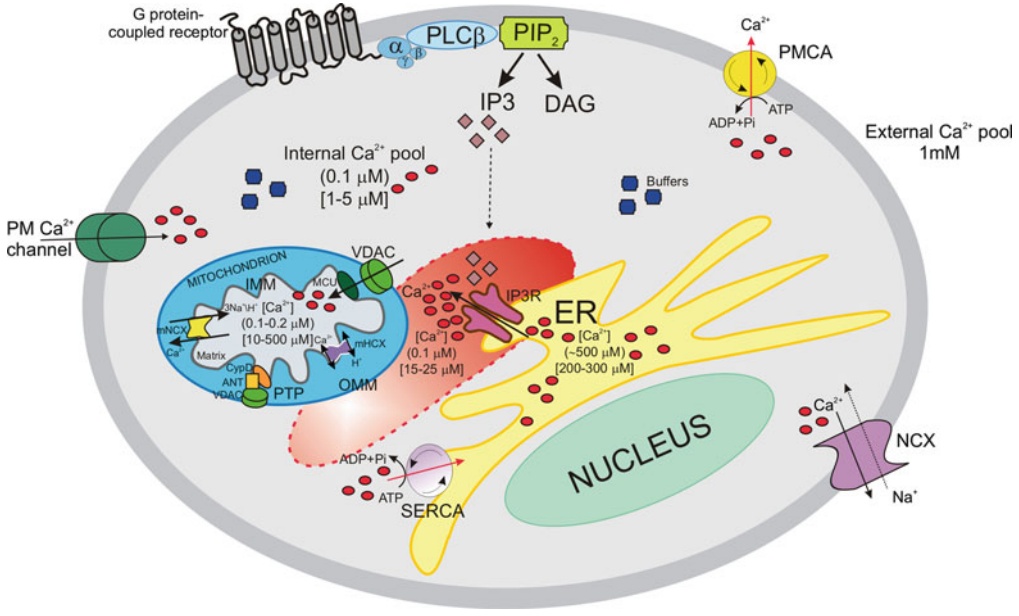

Fig. 17.1 Intracellular Ca^{2+} signaling. Schematic model of intracellular Ca^{2+} homeostasis. Plasma membrane G-protein coupled receptors activate phospholipase C-β (PLC-β) to promote the generation of inositol 1,4,5-trisphosphate (IP3) and the release of Ca^{2+} from the endoplasmic reticulum (ER) into the cytosol. Mitochondrial surface directly interacts with the ER through contact sites defining hotspots Ca^{2+} signaling units. Ca^{2+} import across the outer mitochondrial membrane (OMM) occurs by the voltage-dependent anion channel (VDAC), and then enters the matrix through the mitochondrial Ca^{2+} uniporter (MCU), the main inner mitochondrial membrane (IMM) Ca^{2+}-transport system (Ca^{2+} levels reached upon stimulation are indicated in square brackets). Mitochondrial Ca^{2+}exchangers present in the IMM export Ca^{2+} from the matrix once mitochondrial Ca^{2+} has carried its function; another mechanism for Ca^{2+} efflux from mitochondria is the permeability transition pore (PTP). Ca^{2+} levels return to resting conditions (indicated in round brackets) through the concerted action of cytosolic Ca^{2+} buffers, plasma membrane Ca^{2+}-ATPase (PMCA) and the Na^{+}/Ca^{2+} exchanger (NCX) that permit the ion extrusion in the extracellular milieu. Sarco-endoplasmic reticulum Ca^{2+} ATPase (SERCA) restablishes basal Ca^{2+} levels in intracellular stores. *ANT* adenine nucleotide translocase, *Cyp D* cyclophilin D, *DAG* diacylglycerol, PIP_2 phosphatidylinositol 4,5-bisphosphate

sensor (it has a pair of Ca^{2+}-binding EF-hand domains, the mutation of which eliminates the mitochondrial Ca^{2+} uptake). Then, this year, two independent papers identified the same protein, termed CCDC109A and renamed MCU, as the channel responsible for ruthenium-red-sensitive mitochondrial Ca^{2+} uptake. This protein shares the same tissue distribution with its regulator MICU1, and possesses two predicted transmembrane helices, which are separated by a highly conserved linker facing the intermembrane space. Just the protein's orientation is the mainly discrepancy between the two papers, one affirming a C-terminus localization in the intermembrane space [30], the other in the matrix [31]. Further experiments have to be performed to solve this question. Interestingly, MCU can form multimers and blue native gel separation experiment shows how MCU migrates as a large complex, with an apparent molecular weight of 40 kDa [31].

In the IMM are also present the mitochondrial Na^+/Ca^{2+} exchanger (mNCX) and the H^+/Ca^{2+} exchanger (mHCX). Their main function is probably to export Ca^{2+} from the matrix, once mitochondrial Ca^{2+} has carried out its function, to reestablish resting conditions [32]. They have yet to be identified, although recently strong evidence has been provided that the Na^+/Ca^{2+} exchanger isoform NCLX is the long-sought protein responsible for the mitochondrial Na^+-dependent Ca^{2+} efflux [33]. Finally, the low conductance mode of the permeability transition pore (PTP), a channel of still debated nature localized in the IMM [34], can be also considered as a non-saturating mechanism for Ca^{2+} efflux from mitochondria. When open, PTP allows the passage of ions and molecules with a molecular weight up to 1.5 kDa, including Ca^{2+}. Short-time openings may have a physiological function but its long-time activation leads to the demise of the cell, either by apoptosis or by necrosis, depending on whether PTP opening occurs in only a small fraction of the mitochondria or in all of them [35, 36].

The many efforts to better understand the Ca^{2+} toolkit and the role played by the relationship between ER and mitochondria in this elaborate signaling, are yielding a deeper understanding of how aberrant Ca^{2+} homeostasis is implicated in many diseases. A schematic view of the various processes described above is presented in Fig. 17.1.

Mitochondrial Functions and Ca^{2+} Handling

Mitochondrial Ca^{2+} homeostasis has a key role in the regulation of aerobic metabolism and cell survival.

The first role assigned to the Ca^{2+} ions taken up into the mitochondrial matrix was the stimulation of the mitochondrial ATP production since important metabolic enzymes localized in the matrix, the pyruvate-, α-ketoglutarate- and isocitrate-dehydrogenases are activated by Ca^{2+}, with different mechanisms: the first through a Ca^{2+}-dependent dephosphorylation step, the others via direct binding to a regulatory site [37, 38]. Those three enzymes represent rate-limiting steps of the Krebs cycle thus controlling the feeding of electrons into the respiratory chain and the

generation of the proton gradient across the inner membrane, in turn necessary for ATP production through oxidative phosphorylation (OXPHOS). As the ATP produced by mitochondria is subsequently transferred to the cytosol, mechanisms that control ATP production will not only affect overall cell life but, more specifically, will regulate the activity of ATP-sensitive proteins localized in the close vicinity of mitochondria, such as IP3Rs and SERCA which are stimulated by ATP [39, 40]. The bidirectional relation between Ca^{2+} release and ATP production allows for a positive feedback regulation between ER and mitochondria during increased energetic demand [41]. The uptake of Ca^{2+} in mitochondria will also affect Ca^{2+} signaling at both the local and the global level. Assuming the microdomain concept [16, 17], the local [Ca^{2+}] will depend on both the amount of Ca^{2+} released by IP3Rs and that taken up by mitochondria. Since both SERCA pumps and IP3Rs are also regulated by Ca^{2+}, the local [Ca^{2+}] in the vicinity of mitochondria will determine the refilling of the ER and eventually the spatiotemporal characteristics of the subsequent Ca^{2+} signals [42]. This will in turn depend on the efficiency of the coupling between the ER and the mitochondrial network, as well as on the exact subcellular localization of mitochondria [43].

The connection between mitochondria and the ER can be highly dynamic as the local Ca^{2+} concentration can also affect mitochondrial motility and ER–mitochondria associations in various ways [44]. Mitochondrial movement may increase the chance of dynamic interactions between organelles and aid in the transportation of molecules between the cytoplasm and the organelle. Proteins involved in mitochondrial movement along microtubules, dynein and kinesin, are prone to high $[Ca^{2+}]_c$ mediated by a Ca^{2+} sensor. Moreover, as the mitochondrial motility is inhibited by Ca^{2+} levels in the low micromolar range, it means that mitochondria will be trapped in the neighbourhood of active Ca^{2+}-release sites, allowing for a more efficient uptake of Ca^{2+} by these mitochondria [45, 46].

Apart from organelles movement, mitochondria also continuously remodel their shape. Many of the gene products mediating the fission and fusion processes have been identified in yeast screens, and most are conserved in mammals, including the fission mediators dynamin-related protein 1 (Drp1, Dnm1 in yeast) and Fis1 (Fission 1 homologue), as well as the fusion mediators mitofusins (Mfn) 1 and 2 (Fzo1 in yeast) and optic atrophy 1 (OPA1, Mgm1 in yeast) [47]. Several previous studies have indicated that elevation of $[Ca^{2+}]_c$ perturbs mitochondrial dynamics [48], and more recent works have clearly demonstrated that mitochondrial shape can be controlled by an ER-dependent signaling pathway [49, 50]. Mitochondria also undergo a more “macroscopic” remodelling of their shape during programmed cell death: after apoptosis induction, mitochondria become largely fragmented, resulting in small, rounded and numerous organelles. However, the relationship between mitochondrial fusion/fission and apoptosis is complex and mitochondrial fragmentation is not necessarily related to apoptosis [51]. Defects in fusion and fission processes are not to be underestimated, as they may have deleterious consequences on bioenergetic parameters and are likely to contribute to the pathogenesis of neurodegenerative diseases [52].

The mitochondrial Ca^{2+} signal also control the choice between cell survival and cell death, as it can participate in the induction and progression of apoptosis [53, 54]. Although the extrinsic pathway for apoptosis may or may not involve mitochondria, in the intrinsic pathway these organelles perform a pivotal role: they can release a number of proapototic factors - such as cytochrome *c*, apoptosis-inducing factor, Smac/Diablo, HtrA2/Omi and endonuclease G – from the intermembrane space (IMS) to the cytosol, which initiate the executor caspase cascade steering the cell towards the execution phase of apoptosis (for a review see [55]). Ca^{2+} uptake in mitochondria is crucial for multiple important cellular functions, but the risk of mitochondrial Ca^{2+} overload exists, and this may result in the induction of cell death. At a high concentration, mitochondrial Ca^{2+} favours the opening of the PTP, a mitochondrial megachannel likely to be located in the inner-outer contact sites of the mitochondrial membranes [35]. This event, also known as mitochondrial membrane permeabilization (MMP), leads to the subsequent release of various apoptogenic factors [56, 57]. MMP can also result from a distinct, yet partially overlapping process known as mitochondrial outer membrane permeabilization (MOMP) [55]. In MOMP, pro-apoptotic members of the Bcl-2 protein family may form protein-permeable pores in the OMM, and consequently release of IMS proteins into the cytosol. Bcl-2 family members function as regulators of Ca^{2+} signaling will be discussed later in this review (the interested reader should also refer to [58]).

Mitochondria are also an important source of ROS produced during OXPHOS. ROS can locally affect other systems, including Ca^{2+}-signaling mechanisms, and increased levels of ROS within mitochondria are the principal trigger not only for mitochondrial dysfunctions but, more generally, for diseases associated with ageing. One of the key regulators of ROS production, mitochondrial dysfunction, and ageing is the 66-kDa isoform of the growth factor adapter shc (p66shc) [59]. The mechanisms by which p66shc increases intracellular ROS levels, inducing apoptosis and the deleterious effects of ageing have recently been clarified by Pinton et al.. Once imported into mitochondria, p66Shc causes alterations of organelle Ca^{2+} responses and three-dimensional structure, thus inducing apoptosis [60].

ER Functions and Ca^{2+} Handling

The ER is possibly the largest individual intracellular organelle comprising a three dimensional network of endomembranes arranged in a complex grid of microtubules and cisternae. It is made up of functionally and structurally distinct domains (reviewed extensively by a number of authors [61–64]), in relation to the variety of cellular functions played by the organelle, primarily concerning protein synthesis, maturation and delivery to their destination [65, 66]. Moreover, the ER is a dynamic reservoir of Ca^{2+} ions, which can be activated by both electrical and chemical cell stimulation [67, 68] making this organelle an indispensable component of Ca^{2+} signaling [69–71].

Modern analysis methods enabled the determination of the molecular profile of the ER. This profile reflects the ER's role in signaling, as it comprises a number of components constituting the Ca^{2+} signaling pathway. It contains IP3Rs, RyRs, SERCAs, and in addition to these release channels and pumps, there are buffers (calnexin, calreticulin) and a number of ancillary proteins (FK 506-binding proteins, sorcin, triadin, phosholamban) that contribute to the ER Ca^{2+} signaling system [72].

The IP3Rs are activated after cell stimulation and play a crucial role in the initiation and propagation of the complex spatio-temporal Ca^{2+} signaling that control a myriad of cellular processes [73]. To achieve these various functions, often in a single cell, exquisite control of the Ca^{2+} release is needed. Ca^{2+} itself regulates channel activity in a biphasic manner: at low [Ca^{2+}], the ion exerts an activating role while, at high [Ca^{2+}], it has an opposite inhibitory effect, thus providing a fine dynamic feedback regulation during Ca^{2+} release [74]. In addition, also the ER Ca^{2+} content retains the capability to regulate the channel opening [75, 76]. Whereas IP3 and Ca^{2+} are essential for IP3R channel activation, other physiological ligands, such as ATP, are not necessary but can finely modulate the Ca^{2+}-sensitivity of the channel [77]. As for Ca^{2+}, the modulation of IP3R by ATP is biphasic: at micromolar concentrations, ATP exerts a stimulatory effect, while inhibiting channel opening in the millimolar range [78, 79]. Moreover, IP3R isoforms contain on their sequences multiple phosphorylation consensus sites and many docking sites for protein kinases and phosphatases. Currently, at least 12 different protein kinases are known to directly phosphorylate the IP3R [80], among them: Akt [81], protein kinase A (cAMP-dependent) [82], protein kinase G (cGMPdependent) [83], calmodulin-dependent protein kinase II (CaMKII) [84], protein kinase C (PKC) [85], and various protein tyrosine kinases [86].

Despite controlling many processes essential for life, Ca^{2+} arising from the ER can be a potent death-inducing signal [87, 88]. A clear impetus in the study of Ca^{2+} homeostasis in apoptosis came from the observation that important regulators of apoptosis, the proteins of the Bcl-2 family, are localized to ER and mitochondria, organelles deeply involved in Ca^{2+} handling. The role of the ER in supporting the mitochondrial apoptosis pathway is demonstrated by several findings, among which: (i) over-expression of anti-apoptotic proteins, such as Bcl-2, reduce the ER Ca^{2+} level, making the cells resistant to apoptosis [89–92]; (ii) genetic ablation of the pro-apoptotic proteins Bax and Bak (that drastically increases the resistance to death signals) also results in a dramatic reduction in ER Ca^{2+} content and consequently in a reduction of the Ca^{2+} that can be transferred to mitochondria [93, 94]; (iii) several different approaches resulting in decreases of ER Ca^{2+} content protect cells from apoptosis while, conversely, an increase in Ca^{2+} within the ER favours apoptosis triggered by a number of stimuli [95].

Hence, IP3R-mediated release of Ca^{2+} from ER appears to be a key sensitizing step in various apoptotic routes, but the precise molecular definition of this process still awaits a fine clarification of the macromolecular complex assembled at the interphase between the two organelles. As will be discussed shortly, significant research efforts have been made to shed some light on this signaling pathway.

ER and Mitochondria Physically and Functionally Interact at MAMs

Intracellular organelles coordinate complex pathways for signal transduction and metabolism in the cell through their functional or physical interactions with one another. The association between ER and mitochondria was first described by Copeland and Dalton over 50 years ago in pseudobranch gland cells [96]. By the beginning of the 1970s, the contacts between mitochondria and ER had been visualized by several groups [97, 98]. Electron micrograph images of quickly frozen samples [99] and experiments in living cells with the two organelles labelled by means of targeted spectral variants of GFP (mtBFP and erGFP) [17] demonstrated conclusively that such physical interactions between the two organelles indeed exist. These experiments revealed the presence of overlapping regions of the two organelles and allowed to estimate the area of the contact sites as 5–20% of the total mitochondrial surface. The distance between the ER and the OMM was originally estimated to be approximately 100 nm [100, 101]. More detailed morphological studies, carried out by Achleitner et al. in 1999, indicated that the distance between the ER and mitochondria in the areas of interaction varied between 10 and 60 nm [102]. Importantly, a direct fusion between membranes of the ER and mitochondria was not observed in any case, and the membranes invariably maintained their separate structures. The authors of this pioneering paper proposed that a distance of less than 30 nm between the two organelles could be considered as an association. More recently, electron tomography techniques allowed to estimate that the minimum distance is even shorter (e.g., 10–25 nm) [103]. This distance thus enables ER proteins to associate directly with proteins and lipids of the OMM. Further development of microscopic techniques enabled detailed analysis of such contacts with high resolution in three dimensions [104].

The interactions between these organelles at the contact sites are so tight and strong, that upon subcellular fractionation (at the step of mitochondria purification), a unique fraction, originally named "mitochondria-associated membranes" (MAMs) fraction, can be isolated [105, 106]. More recently, the isolation procedures was improved and adapted to isolate the MAMs fraction from yeast, different organs, tissues, and various cell lines [102, 107, 108]. Interestingly, the molecular analysis of both "crude" mitochondria and MAMs fractions demonstrated that, apart from specific ER and mitochondrial proteins, they also contain proteins which are abundant in the plasma membrane.

Research on the morphological organization of mitochondria and ER with respect to the plasma membrane is much less extensive. Modifications in the subcellular fractionation procedure enabled the isolation of the "plasma membrane associated membranes" (PAMs) fraction. In general, PAMs fractions have been described as the center of interactions between plasma membrane and the ER [109, 110], but the presence of mitochondrial proteins in these fractions indicates that mitochondria interact actively also with the plasma membrane [111, 112].

The MAMs have a pivotal role in several cellular functions related to bioenergetics and cell survival. MAMs have been originally shown to be enriched in enzymes

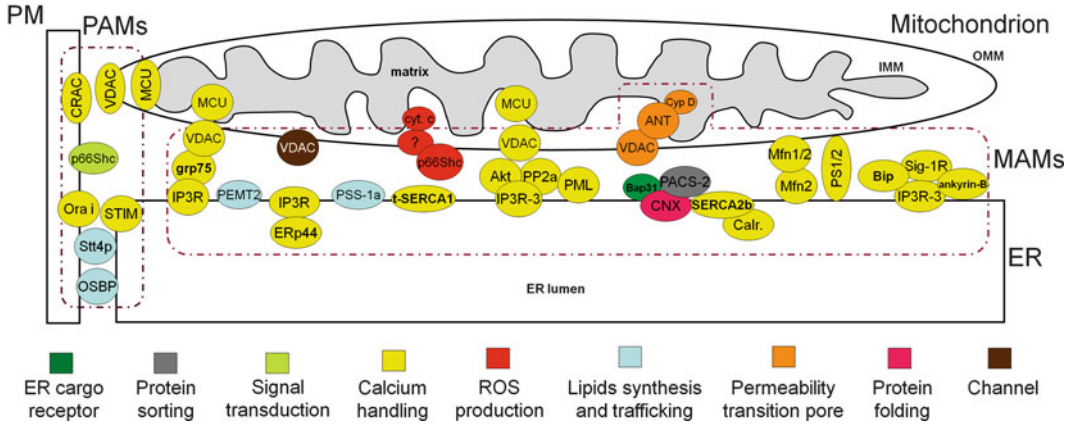

Fig. 17.2 Schematic view of the interorganelle interactions and protein composition of the membranes contact sites. *Possible contact sites between organelles are marked in dotted brown line. ER* endoplasmic reticulum, *ER* lumen endoplasmic reticulum lumen, *IMM* inner mitochondrial membrane, *MAMs* mitochondria-associated membranes, *OMM* outer mitochondrial membrane, *PAMs* plasma membrane associated membranes, *PM* plasma membrane.*The color indicates the function/role of the protein.* Akt, the serine-threonine protein kinase Akt; *ANT* adenine nucleotide translocase, *Bap31* B-cell receptor-associated protein 31 (or endoplasmic reticulum resident cargo receptor), *Calr* carleticulin, *CRAC* Ca^{2+} release-activated calcium channel, *Cyp D* cyclophilin D, *cyt. c* cytochrome c, *ERp44* endoplasmic reticulum resident protein 44, *grp75* glucose-regulated protein 75 (or mortalin), *BiP* Binding immunoglobulin Protein (or 78 kDa glucose-regulated protein (GRP78)), *IP3R* inositol 1,4,5-triphosphate receptor, *MCU* mitochondrial calcium uniporter, *Mfn1/2* mitofusin-1/2, *Ora i* ORAI calcium release-activated calcium modulator, *OSBP* oxysterol binding protein, *p66Shc* 66-kDa isoform of the growth factor adapter shc, *PACS-2* phosphofurin acidic cluster sorting protein 2, *PEMT2* phosphatidylethanolamine N-methyltransferase 2, *PP2a* protein phosphatase 2a, *PML* promyelocytic leukemia protein, *PS1/2* presenilin-1/2, *PSS-1a* phosphatidylserine synthase-1a, *SERCA2b* sarco-endoplasmic reticulum calcium ATPase 2b, *Sig-1R* Sigma-1 receptor, *STIM1* stromal-interacting molecule 1, *Stt4p* phosphatidylinositol-4-kinase, *t SERCA1* truncated sarco-endoplasmic reticulum Ca^{2+} ATPase, *VDAC* voltage-dependent anion channel, ?, unknown protein

involved in lipid synthesis and trafficking between ER and mitochondrial membranes, including long-chain fatty acid-CoA ligase type 4 (FACL4) and phosphatidylserine synthase-1 (PSS-1) [106, 113, 114]. The MAMs have since been shown to be enriched in functionally diverse enzymes involved not only in lipid metabolism but also in glucose metabolism (for recent reviews, see [115, 116]).

More recently, the same subcellular fraction has been shown to contain Ca^{2+}-sensing ER chaperones and oxidoreductases, as well as key Ca^{2+} handling proteins of both organelles [117, 118] (a schematic representation of the interorganelle interactions and some of these proteins with the assigned functions is presented in Fig. 17.2). Together, these data have led to the conclusion that the MAMs are not only a site of lipid synthesis and transfer, but also function as a fundamental hub of cellular signaling that controls a growing number of processes associated with both organelles, ranging from ER chaperone-assisted folding of newly synthesized proteins to the fine-tuning of physiological and pathological Ca^{2+} signals from ER to mitochondria.

MAMs Proteins and Ca^{2+} Homeostasis in Health and Disease

The aspect of functional interaction between the ER and mitochondria that has received most attention in recent decades is undoubtedly that involving Ca^{2+} ions. Ca^{2+}-handling proteins such as IP3Rs (especially type 3 IP3Rs) are highly compartmentalized at MAMs [119], identifying these zones as "hotspots" of Ca^{2+} transfer from the ER to the closely adjacent mitochondrial network [17, 18]. Ca^{2+} signals arising from the ER are vital for regulating Ca^{2+} levels in mitochondria. Mitochondrial Ca^{2+} spikes and oscillations play a central role in energy production by regulating Ca^{2+}-dependent enzymes involved in the ATP-producing Krebs cycle reactions [120, 121] and thus are important for cellular survival, although a mitochondrial Ca^{2+} overload will lead to the opening of the PTP, permeabilization of the OMM, eventually triggering cell death [122–124]. It remains unclear how the rise in mitochondrial Ca^{2+} (that has probably evolved to couple cell signaling to metabolic activation) can be transformed into a trigger of cell death. Both the amplitude and, most importantly, the duration of the Ca^{2+} rise in mitochondria, and perhaps even the concomitant insults that affect mitochondrial functions, play a major role in this transition. Therefore, ER Ca^{2+} handling on the MAMs acts as a double-edged sword, suggesting the existence of still not fully elucidated regulatory mechanisms, that are capable of discriminating between signals of life or death.

The connection between the ER and mitochondria is known to be highly dynamic as the local $[Ca^{2+}]$ itself can regulate ER-mitochondrial association in different ways [125], and increased $[Ca^{2+}]_c$ blocks the motility of both organelles, enhancing their interaction [46]. Recently Hajnoczky et al. demonstrated that exposure to TGFβ affects Ca^{2+} transfer to the mitochondria through an impairment of the ER–mitochondrial coupling, further supporting the notion of a highly dynamic regulation of inter-organelle communication [126].

Several proteins may participate in the stabilization of those MAMs and, through this stabilization, affect Ca^{2+} transfer between ER and mitochondria, while other proteins may be directly involved in regulating the Ca^{2+}-transport proteins described above. During the last years, research has focused on the identification of connecting structures between the ER and mitochondria at the MAMs, revealing that the interactions between the two organelles seem to be modulated both by a family of chaperone proteins and by a family of "mitochondria-shaping proteins". One of the first advances was made in 2006, when Csordás et al. showed by electron tomography that ER and mitochondria are adjoined by tethers seemingly composed of proteins, since the *in vitro* incubation with proteinase not only detached the ER from mitochondria, but also disrupted Ca^{2+} transfer. Tightening of the connections sensitized mitochondria to Ca^{2+} overloading, ensuing permeability transition, and seemed relevant for several mechanisms of cell death. Thus, these results revealed an unexpected dependence of cell function and survival on the maintenance of a proper spacing between the ER and mitochondria [103].

At the same time, Szabadkai et al. found that the mitochondrial chaperone grp75 (glucose-regulated protein 75) mediates the molecular interaction of VDAC with the ER Ca^{2+}-release channel IP3R. It was demonstrated that grp75 not only induces a chaperone-mediated conformational coupling of the proteins, but also allowed for a better transfer of the Ca^{2+} ions from the ER to the mitochondrial matrix [127]. In support of this view, we previously demonstrated that the overexpression of VDAC enhances Ca^{2+} signal propagation into the mitochondria, increasing the extent of mitochondrial Ca^{2+} uptake (also leading to a higher susceptibility for ceramide-induced cell death), acting at the ER–mitochondria contact sites [128]. Moreover, we have recently established that VDAC1, but not VDAC2 and VDAC3 isoforms, selectively interacts with IP3Rs; this interaction is further strengthened by apoptotic stimuli and thus VDAC1 is preferentially involved in the transmission of the low-amplitude apoptotic Ca^{2+} signals to mitochondria [129].

Subsequently, ER chaperones, particularly the Ca^{2+}-binding chaperones calnexin, calreticulin, Sigma-1 receptor (Sig-1R) and Binding immunoglobulin Protein (BiP, also known as the glucose-regulated protein GRP78), were also found to be compartmentalized at the MAMs, yielding a new picture whereby chaperone machineries at both ER and mitochondria orchestrate the regulation of Ca^{2+} signaling between these two organelles. For instance, calnexin reversibly interacts with SERCA2b to block Ca^{2+} import [130]. Similarly, calreticulin inhibits uptake of Ca^{2+} by inhibiting the affinity for Ca^{2+} of the SERCA2b pump, but also regulates IP3-induced Ca^{2+} release [12, 131]. *In vivo*, these functions of calreticulin may very well be more crucial for survival than its chaperone activity, since calreticulin-deficient cells have impaired Ca^{2+} homoeostasis [132, 133].

Back in 2005, Simmen et al. reported the identification of a multifunctional cytosolic sorting protein, PACS-2 (phosphofurin acidic cluster sorting protein 2), that partially resides in the MAMs and maintains its integrity [134]. PACS-2 depletion induces mitochondria fragmentation and uncouples these organelles from the ER, raising the possibility that, in addition to mediating MAMs formation, PACS-2 might also influence Ca^{2+} homeostasis and apoptosis. Indeed, it has been shown that

IP3Rs (and RyRs) possess potential PACS-2-binding sites [135]; hence, disruption of PACS-2 may cause mislocalization of IP3Rs, resulting in reduced Ca^{2+} transfer from the ER to mitochondria. Moreover, in response to apoptotic stimuli, PACS-2 has been demonstrated to be capable of inducing Bid recruitment to mitochondria, an event that leads to cytochrome *c* release and caspase 3 activation [134]. PACS-2 also interacts with and regulates the distribution and activity of calnexin. Under control conditions, >80% of calnexin localizes to the ER, mainly at the MAMs. However, through a protein–protein interaction, PACS-2 causes calnexin to distribute between the ER and the plasma membrane, affecting the homeostasis of ER Ca^{2+} [136]. PACS-2 and calnexin also interact with the MAMs-resident ER cargo receptor Bap31 (B-cell receptor-associated protein 31) and regulate its cleavage during the triggering of apoptosis [137]. Despite these observations, the exact role of PACS-2 in the regulation of Ca^{2+} transfer from the ER to the mitochondria remains to be further investigated.

Recently, Simmen's group have also shown that the GTPase Rab32, a member of the Ras-related protein family of Rab, localizes to the ER and mitochondria and identified this protein as a regulator of MAMs properties. Its activity levels control MAMs composition, destroying the specific enrichment of calnexin at the MAMs, and consequently ER calcium handling. Furthermore, as a PKA-anchoring protein, Rab32 determines the targeting of PKA to mitochondrial and ER membranes, resulting in modulated PKA signaling. Together, these functions result in a delayed apoptosis onset with high Rab32 levels and, conversely, accelerated apoptosis with low Rab32 levels, explaining the possible mechanism by which it could act as an oncogene [138].

Also Sig-1R, an ER chaperone serendipitously identified in cellular distribution studies by Hayashi and Su, is enriched in the MAMs and seems to be involved in Ca^{2+}-mediated stabilization of IP3Rs [139]. Under normal conditions in which the ER lumenal Ca^{2+} concentration is at 0.5–1.0 mM, it selectively resides at the MAMs and forms complexes with the ER Ca^{2+}-binding chaperone BiP. Upon the activation of IP3Rs, which causes the decrease of the Ca^{2+} concentration at the MAMs, Sig-1R dissociates from BiP to chaperone IP3R, which would otherwise be degraded by proteasomes. Thus, Sig-1R appears to be involved in maintaining, on the ER luminal side, the integrity of the ER-mitochondrial Ca^{2+} cross-talk, as demonstrated by the fact that its silencing leads to impaired ER-mitochondrial Ca^{2+} transfer. Sig-1R has been implicated in several neuronal and non-neuronal pathological conditions [140], and is also upregulated in a wide variety of tumour cell lines [141]. Therefore, degenerative neurons or tissue might benefit by Sig-1R agonists which promote cell survival [142, 143]; conversely, its antagonists inhibit tumour-cell proliferation [144].

Another example of a folding enzyme regulating ER Ca^{2+} content is the oxidoreductase ERp44 (endoplasmic reticulum resident protein 44) that interacts with cysteines of the type 1 IP3R, thereby inhibiting Ca^{2+} transfer to mitochondria when ER conditions are reducing [145]. Recent results suggest that another oxidoreductase, Ero1α, might also perform such a function, since Ero1α interacts with the IP3R and potentiates the release of Ca^{2+} during ER stress [146]. This function of Ero1α could

impact the induction of apoptosis that critically depends on ER-mitochondria Ca^{2+} communication [119, 147]. Gilady et al. showed that, despite Ero1α being an ER luminal protein, the targeting of Ero1α to the MAMs is quite stringent (>75%), consistent with its role in the regulation of Ca^{2+} homeostasis. Moreover, they found that localization of Ero1α on the MAMs is dependent on oxidizing conditions within the ER; indeed, hypoxia leads to a rapid and eventually complete depletion of Ero1α from the MAMs [148].

In the increasingly clear but complex picture that is emerging for MAMs, also the mitochondrial fusion protein Mfn2 has been shown to be enriched at contact sites between the ER and mitochondria. Mfn2 on the ER appeared to link the two organelles together: the connection depended on the interaction of the ER Mfn2 with either Mfn1 or Mfn2 on the OMM [104]. Moreover, its absence changes not only the morphology of the ER but also decreased by 40% the interactions between ER and mitochondria, thus affecting the transfer of Ca^{2+} signals to mitochondria. This may contribute to the Charcot-Marie-Tooth neuropathy type 2a in which missense mutations occur in Mfn2 [149]. A too strong ER–mitochondria interaction, and the concomitant improved Ca^{2+} transfer between the two organelles, may also be detrimental as overexpression of Mfn2 led to apoptosis in vascular smooth-muscle cells [150]. A recent report also propose the keratin-binding protein Trichoplein/mitostatin (TpMs), often downregulated in epithelial cancers [151], as a new regulator of mitochondria–ER juxtaposition in a Mfn2-dependent manner [152].

Also the mitochondrial fission protein Fis1 has been involved in ER-mitochondria coupling. Fis1 physically interacts with Bap31, an integral membrane protein expressed ubiquitously and highly enriched at the outer ER membrane), to bridge the mitochondria and the ER, setting up a platform for apoptosis induction. It appeared that the Fis1–Bap31 complex is required for the activation of procaspase-8. Importantly, as this signaling pathway can be initiated by Fis1, the Fis1-Bap31 complex establishes a feedback loop by releasing Ca^{2+} from the ER that is able to transmit an apoptosis signal from the mitochondria to the ER [153].

As described, it is now widely accepted that Ca^{2+} transfer between ER and mitochondria is a topic of major interest in physiology and pathology (Fig. 17.3). The release of Ca^{2+} from ER stores by IP3Rs has been implicated in multiple models of apoptosis as being directly responsible for mitochondrial Ca^{2+} overload. Apoptosis is a process of major biomedical interest, since its deregulation is involved in the pathogenesis of a broad variety of disorders (neoplasia, autoimmune disorders, viral and neurodegenerative diseases, to name a few).

Mitochondrial Ca^{2+} is therefore a central player in multiple neurodegenerative diseases such as Alzheimer's disease (AD), Parkinson's disease and Huntington's disease [154]. It is noteworthy that alteration in Ca^{2+} homeostasis in sporadic AD patients started being reported in the middle of the 1980s, albeit in contrasting ways. Interestingly, very recent data have revealed that presenilin-1 (PS1) and presenilin-2 (PS2), two proteins that, when mutated, cause familial AD (FAD), have a strong effect on Ca^{2+} signaling (sometimes yielding contradictory experimental findings, as recently reviewed in [155]). Of particular interest on this topic, is the report that MAMs are the predominant subcellular location for PS1 and PS2, and for γ-secretase

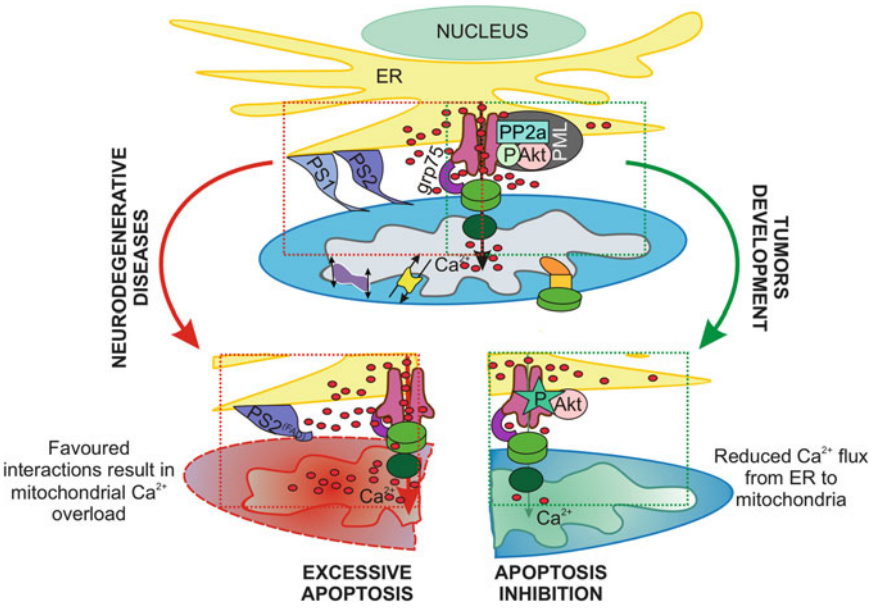

Fig. 17.3 Representation of MAMs proteins involved in ER-mitochondria Ca^{2+} cross-talk and perturbations implicated in cell survival and cell death. Ca^{2+} release from the endoplasmic reticulum (ER) results in high-Ca^{2+} hot spots at the mitochondrial surface to allow efficient Ca^{2+} uptake through voltage-dependent anion channel - which is coupled to inositol 1,4,5-trisphosphate receptor by the chaperone glucose-regulated protein 75 (grp75) - and the mitochondrial Ca^{2+} uniporter. Mitochondrial Ca^{2+} activates organelle metabolism and ATP synthesis but also, when in excess, triggers apoptosis. Apoptosis deregulation is involved in the pathogenesis of neurodegenerative diseases as well as tumors development. Presenelin-1 (PS1) and Presenelin-2 (PS2), two proteins that when mutated cause familial Alzheimer's disease (AD), have been recently found at MAMs, and familial AD (FAD) variants of PS2 ($PS2^{FAD}$) seem to increase ER and mitochondria interaction; this could result in mitochondrial Ca^{2+} overload and subsequent excessive apoptosis. In addition, controlled apoptosis is likely to be important to eliminate cells, thereby avoiding tumor genesis. In this process the recently identified localization of the tumor suppressor promyelocytic leukemia protein (PML) at ER/MAMs plays a crucial role as it promotes IP3R-mediated Ca^{2+} transfer from ER into mitochondria. While Akt is known to suppress IP3R-channel activity by its phosphorylation, the recruitment of protein phosphatase PP2a via PML in a specific multi-protein complex (comprising PML, IP3R-3, PP2a, and Akt), dephosphorylates and inactivates Akt. This suppresses Akt-dependent phosphorylation of IP3R-3 and thus promotes Ca^{2+} release through this channel and Ca^{2+} transfer into the mitochondria. In cancer cells, where PML is often missing, IP3R-3 are hyper-phosphorylated due to an impaired PP2a activity, as a result the Ca^{2+} flux from ER to mitochondria is reduced and cells become resistant to apoptosis

activity [156]. Moreover, it has recently been found that PS2 over-expression increases the interaction between ER and mitochondria and consequently Ca^{2+} transfer between these two organelles, an effect that is greater FAD variants [157]. It is possible to speculate that this favoured interaction could potentially result in a toxic mitochondrial Ca^{2+} overload (Fig. 17.3). A defect in Ca^{2+} signaling due to altered MAMs function could explain the well-known disturbances in Ca^{2+} homeostasis

in AD [158, 159]. It also opens the door to new ways of thinking about complementary treatment; in addition, it may be possible to exploit aberrant MAMs function as a useful marker for the development of a diagnostic tool for AD [160].

Sano et al. also demonstrated that in GM1-gangliosidosis, a neurodegenerative disease, GM1-ganglioside (GM1) accumulates in brain within the MAMs, where it specifically interacts with phosphorylated IP3R-1, influencing its activity [161]. GM1 has been previously shown to modulate intracellular Ca^{2+} flux [162, 163]. As such, the recent discovery that MAMs are the sites where GM1 accumulates and influences ER-to-mitochondria Ca^{2+} flux, leading to Ca^{2+} overload and activation of the mitochondrial apoptotic pathway, explains the neuronal apoptosis and neurodegeneration that occurs in patients with GM1-gangliosidosis [161]. These findings may have important implications for targeting checkpoints of the GM1-mediated apoptotic cascade in the treatment of this catastrophic disease.

Modulation of the progression of cell death may therapeutically be also very important for the inhibition of tumour growth. Specific stimulation of the Ca^{2+} transfer between the IP3R and mitochondria could lead to increased cell death and so form a supplementary pathway to combat cancer. Our group has recently described that the tumor suppressor promyelocytic leukemia protein (PML) modulates the ER–mitochondria Ca^{2+}-dependent cross-talk due to its unexpected and fundamental role at MAMs, highlighting a new extra-nuclear PML function critical for regulation of cell survival. This was demonstrated to be mediated by a specific multi-protein complex, localized at MAMs, including PML, IP3R-3, the protein phosphatase PP2a, and Akt. More than 50 different proteins can interact with and regulate the IP3Rs [80]; among these, a key role is played by the anti-apoptotic protein kinase Akt, which also phosphorylates IP3Rs, significantly reducing their Ca^{2+} release activity [81, 164]. In a previous work, we demonstrated that cells with the active form of Akt have a reduced cellular sensitivity to Ca^{2+}-mediated apoptotic stimuli through a mechanism that involved diminished Ca^{2+} flux from the ER to mitochondria [165]. Our recent data show that PML mediates PP2a retention in the MAMs, which dephosphorylates and inactivates Akt. Thus, in the absence of PML, the unopposed action of Akt at ER, due to an impaired PP2a activity, leads to a hyperphosphorylation of IP3R-3 and in turn a reduced Ca^{2+} flux from ER to mitochondria, rendering cells resistant to apoptotic Ca^{2+}-dependent stimuli [166] (Fig. 17.3). These findings may reveal a novel pharmacological target in apoptosis [167].

Interestingly, p66Shc, a cytosolic adaptor protein which is involved in the cellular response to oxidative stress (see above), has been found also in the MAMs fraction. In particular, we found that the level of p66Shc in MAMs fraction is age-dependent and corresponds well to the mitochondrial ROS production which is found to increase with age [168]. Finally, the functional significance of MAMs resident proteins in the regulation of ER-mitochondrial cross-talk is further supported by the finding that several viral proteins, such as the human cytomegalovirus vMIA [169], as well as the p7 and NS5B proteins of hepatitis C virus [170], are targeted to the MAMs and exert anti- or pro-apoptotic effects, respectively.

To conclude, whether or not mitochondria and MAMs contribute also to the Ca^{2+}-dependent activation of autophagy is still unknown. If mitochondria actively contribute to the activation of autophagy through Ca^{2+} handling remains to be solved, but the close interaction between IP3Rs and mitochondria, on the one hand, and between IP3Rs and autophagy proteins, on the other hand, led to the hypothesis that IP3Rs could participate in the induction of this process [171, 172]. The study of the relation between IP3Rs, Ca^{2+} and the autophagic processes may become very important, since autophagy can protect the organism against various pathologies, including cancer and neurodegenerative diseases [118, 173].

The deeper understanding at the molecular level of the structural and functional links that are established at MAMs and the possibility to modulate them may in the future be of great importance in the treatment of many different human pathologies.

Acknowledgements A.B. was supported by a research fellowship FISM – Fondazione Italiana Sclerosi Multipla – Cod. 2010/B/1. SP was supported by a training fellowship FISMJ.M.S. was supported by a PhD fellowship from The Foundation for Polish Science (FNP), EU, European Regional Development Fund and Operational Programme "Innovative economy". This research was supported by: the Polish Ministry of Science and Higher Education under grant NN407 075 137 to M.R.W. and by Telethon (GGP09128), local funds from the University of Ferrara, the Italian Ministry of Education, University and Research (COFIN), the Italian Cystic Fibrosis Research Foundation and Italian Ministry of Health to P.P.

References

1. Berridge MJ, Lipp P, Bootman MD (2000) The versatility and universality of calcium signalling. Nat Rev Mol Cell Biol 1:11–21
2. Brini M, Carafoli E (2009) Calcium pumps in health and disease. Physiol Rev 89:1341–1378
3. Blaustein MP, Lederer WJ (1999) Sodium/calcium exchange: its physiological implications. Physiol Rev 79:763–854
4. Bertolino M, Llinas RR (1992) The central role of voltage-activated and receptor-operated calcium channels in neuronal cells. Annu Rev Pharmacol Toxicol 32:399–421
5. McFadzean I, Gibson A (2002) The developing relationship between receptor-operated and store-operated calcium channels in smooth muscle. Br J Pharmacol 135:1–13
6. Meldolesi J, Pozzan T (1987) Pathways of Ca2+ influx at the plasma membrane: voltage-, receptor-, and second messenger-operated channels. Exp Cell Res 171:271–283
7. Foskett JK, White C, Cheung KH, Mak DO (2007) Inositol trisphosphate receptor Ca2+ release channels. Physiol Rev 87:593–658
8. Sutko JL, Airey JA (1996) Ryanodine receptor Ca2+ release channels: does diversity in form equal diversity in function? Physiol Rev 76:1027–1071
9. Patel S, Joseph SK, Thomas AP (1999) Molecular properties of inositol 1,4,5-trisphosphate receptors. Cell Calcium 25:247–264
10. Patterson RL, Boehning D, Snyder SH (2004) Inositol 1,4,5-trisphosphate receptors as signal integrators. Annu Rev Biochem 73:437–465
11. Berridge MJ (2006) Calcium microdomains: organization and function. Cell Calcium 40:405–412
12. John LM, Lechleiter JD, Camacho P (1998) Differential modulation of SERCA2 isoforms by calreticulin. J Cell Biol 142:963–973

13. Carafoli E (2003) Historical review: mitochondria and calcium: ups and downs of an unusual relationship. Trends Biochem Sci 28:175–181
14. Rizzuto R, Simpson AW, Brini M, Pozzan T (1992) Rapid changes of mitochondrial Ca2+ revealed by specifically targeted recombinant aequorin. Nature 358:325–327
15. Nicholls DG, Crompton M (1980) Mitochondrial calcium transport. FEBS Lett 111:261–268
16. Rizzuto R, Brini M, Murgia M, Pozzan T (1993) Microdomains with high Ca2+ close to IP3-sensitive channels that are sensed by neighboring mitochondria. Science 262:744–747
17. Rizzuto R, Pinton P, Carrington W, Fay FS, Fogarty KE, Lifshitz LM, Tuft RA, Pozzan T (1998) Close contacts with the endoplasmic reticulum as determinants of mitochondrial Ca2+ responses. Science 280:1763–1766
18. Csordas G, Thomas AP, Hajnoczky G (1999) Quasi-synaptic calcium signal transmission between endoplasmic reticulum and mitochondria. EMBO J 18:96–108
19. Rizzuto R, Pozzan T (2006) Microdomains of intracellular Ca2+: molecular determinants and functional consequences. Physiol Rev 86:369–408
20. Giacomello M, Drago I, Bortolozzi M, Scorzeto M, Gianelle A, Pizzo P, Pozzan T (2010) Ca2+ hot spots on the mitochondrial surface are generated by Ca2+ mobilization from stores, but not by activation of store-operated Ca2+ channels. Mol Cell 38:280–290
21. Palmer AE, Giacomello M, Kortemme T, Hires SA, Lev-Ram V, Baker D, Tsien RY (2006) Ca2+ indicators based on computationally redesigned calmodulin-peptide pairs. Chem Biol 13:521–530
22. Csordas G, Varnai P, Golenar T, Roy S, Purkins G, Schneider TG, Balla T, Hajnoczky G (2010) Imaging interorganelle contacts and local calcium dynamics at the ER-mitochondrial interface. Mol Cell 39:121–132
23. Inoue T, Heo WD, Grimley JS, Wandless TJ, Meyer T (2005) An inducible translocation strategy to rapidly activate and inhibit small GTPase signaling pathways. Nat Methods 2:415–418
24. Simamura E, Shimada H, Hatta T, Hirai K (2008) Mitochondrial voltage-dependent anion channels (VDACs) as novel pharmacological targets for anti-cancer agents. J Bioenerg Biomembr 40:213–217
25. De Pinto V, Reina S, Guarino F, Messina A (2008) Structure of the voltage dependent anion channel: state of the art. J Bioenerg Biomembr 40:139–147
26. Colombini M (2009) The published 3D structure of the VDAC channel: native or not? Trends Biochem Sci 34:382–389
27. Shoshan-Barmatz V, De Pinto V, Zweckstetter M, Raviv Z, Keinan N, Arbel N (2010) VDAC, a multi-functional mitochondrial protein regulating cell life and death. Mol Aspects Med 31:227–285
28. Perocchi F, Gohil VM, Girgis HS, Bao XR, McCombs JE, Palmer AE, Mootha VK (2010) MICU1 encodes a mitochondrial EF hand protein required for Ca(2+) uptake. Nature 467:291–296
29. Pagliarini DJ, Calvo SE, Chang B, Sheth SA, Vafai SB, Ong SE, Walford GA, Sugiana C, Boneh A, Chen WK, Hill DE, Vidal M, Evans JG, Thorburn DR, Carr SA, Mootha VK (2008) A mitochondrial protein compendium elucidates complex I disease biology. Cell 134: 112–123
30. De Stefani D, Raffaello A, Teardo E, Szabo I, Rizzuto R (2011) A forty-kilodalton protein of the inner membrane is the mitochondrial calcium uniporter. Nature 476:336–340
31. Baughman JM, Perocchi F, Girgis HS, Plovanich M, Belcher-Timme CA, Sancak Y, Bao XR, Strittmatter L, Goldberger O, Bogorad RL, Koteliansky V, Mootha VK (2011) Integrative genomics identifies MCU as an essential component of the mitochondrial calcium uniporter. Nature 476:341–345
32. Bernardi P (1999) Mitochondrial transport of cations: channels, exchangers, and permeability transition. Physiol Rev 79:1127–1155
33. Palty R, Silverman WF, Hershfinkel M, Caporale T, Sensi SL, Parnis J, Nolte C, Fishman D, Shoshan-Barmatz V, Herrmann S, Khananshvili D, Sekler I (2010) NCLX is an essential component of mitochondrial Na+/Ca2+ exchange. Proc Natl Acad Sci USA 107:436–441

34. Baines CP (2009) The molecular composition of the mitochondrial permeability transition pore. J Mol Cell Cardiol 46:850–857
35. Rasola A, Bernardi P (2007) The mitochondrial permeability transition pore and its involvement in cell death and in disease pathogenesis. Apoptosis 12:815–833
36. Rasola A, Sciacovelli M, Pantic B, Bernardi P (2010) Signal transduction to the permeability transition pore. FEBS Lett 584:1989–1996
37. McCormack JG, Halestrap AP, Denton RM (1990) Role of calcium ions in regulation of mammalian intramitochondrial metabolism. Physiol Rev 70:391–425
38. Carafoli E (2010) The fateful encounter of mitochondria with calcium: how did it happen? Biochim Biophys Acta 1797:595–606
39. Maes K, Missiaen L, De Smet P, Vanlingen S, Callewaert G, Parys JB, De Smedt H (2000) Differential modulation of inositol 1,4,5-trisphosphate receptor type 1 and type 3 by ATP. Cell Calcium 27:257–267
40. Betzenhauser MJ, Wagner LE 2nd, Iwai M, Michikawa T, Mikoshiba K, Yule DI (2008) ATP modulation of Ca2+ release by type-2 and type-3 inositol (1, 4, 5)-triphosphate receptors. Differing ATP sensitivities and molecular determinants of action. J Biol Chem 283:21579–21587
41. Walsh C, Barrow S, Voronina S, Chvanov M, Petersen OH, Tepikin A (2009) Modulation of calcium signalling by mitochondria. Biochim Biophys Acta 1787:1374–1382
42. Arnaudeau S, Kelley WL, Walsh JV Jr (2001) Demaurex N: mitochondria recycle Ca(2+) to the endoplasmic reticulum and prevent the depletion of neighboring endoplasmic reticulum regions. J Biol Chem 276:29430–29439
43. Tinel H, Cancela JM, Mogami H, Gerasimenko JV, Gerasimenko OV, Tepikin AV, Petersen OH (1999) Active mitochondria surrounding the pancreatic acinar granule region prevent spreading of inositol trisphosphate-evoked local cytosolic Ca(2+) signals. EMBO J 18:4999–5008
44. Goetz JG, Genty H, St-Pierre P, Dang T, Joshi B, Sauve R, Vogl W, Nabi IR (2007) Reversible interactions between smooth domains of the endoplasmic reticulum and mitochondria are regulated by physiological cytosolic Ca2+ levels. J Cell Sci 120:3553–3564
45. Wang HJ, Guay G, Pogan L, Sauve R, Nabi IR (2000) Calcium regulates the association between mitochondria and a smooth subdomain of the endoplasmic reticulum. J Cell Biol 150:1489–1498
46. Yi M, Weaver D, Hajnoczky G (2004) Control of mitochondrial motility and distribution by the calcium signal: a homeostatic circuit. J Cell Biol 167:661–672
47. Westermann B (2010) Mitochondrial fusion and fission in cell life and death. Nat Rev Mol Cell Biol 11:872–884
48. Rintoul GL, Filiano AJ, Brocard JB, Kress GJ, Reynolds IJ (2003) Glutamate decreases mitochondrial size and movement in primary forebrain neurons. J Neurosci 23:7881–7888
49. Germain M, Mathai JP, McBride HM, Shore GC (2005) Endoplasmic reticulum BIK initiates DRP1-regulated remodelling of mitochondrial cristae during apoptosis. EMBO J 24: 1546–1556
50. Alirol E, James D, Huber D, Marchetto A, Vergani L, Martinou JC, Scorrano L (2006) The mitochondrial fission protein hFis1 requires the endoplasmic reticulum gateway to induce apoptosis. Mol Biol Cell 17:4593–4605
51. Szabadkai G, Simoni AM, Chami M, Wieckowski MR, Youle RJ, Rizzuto R (2004) Drp-1-dependent division of the mitochondrial network blocks intraorganellar Ca2+ waves and protects against Ca2+-mediated apoptosis. Mol Cell 16:59–68
52. Lu B (2009) Mitochondrial dynamics and neurodegeneration. Curr Neurol Neurosci Rep 9:212–219
53. Giorgi C, Romagnoli A, Pinton P, Rizzuto R (2008) Ca2+ signaling, mitochondria and cell death. Curr Mol Med 8:119–130
54. Harr MW, Distelhorst CW (2010) Apoptosis and autophagy: decoding calcium signals that mediate life or death. Cold Spring Harb Perspect Biol 2:a005579
55. Kroemer G, Galluzzi L, Brenner C (2007) Mitochondrial membrane permeabilization in cell death. Physiol Rev 87:99–163

56. Tait SW, Green DR (2010) Mitochondria and cell death: outer membrane permeabilization and beyond. Nat Rev Mol Cell Biol 11:621–632
57. Armstrong JS (2006) The role of the mitochondrial permeability transition in cell death. Mitochondrion 6:225–234
58. Rong Y, Distelhorst CW (2008) Bcl-2 protein family members: versatile regulators of calcium signaling in cell survival and apoptosis. Annu Rev Physiol 70:73–91
59. Trinei M, Berniakovich I, Beltrami E, Migliaccio E, Fassina A, Pelicci P, Giorgio M (2009) P66Shc signals to age. Aging (Albany NY) 1:503–510
60. Pinton P, Rimessi A, Marchi S, Orsini F, Migliaccio E, Giorgio M, Contursi C, Minucci S, Mantovani F, Wieckowski MR, Del Sal G, Pelicci PG, Rizzuto R (2007) Protein kinase C beta and prolyl isomerase 1 regulate mitochondrial effects of the life-span determinant p66Shc. Science 315:659–663
61. Voeltz GK, Prinz WA, Shibata Y, Rist JM, Rapoport TA (2006) A class of membrane proteins shaping the tubular endoplasmic reticulum. Cell 124:573–586
62. Shibata Y, Voeltz GK, Rapoport TA (2006) Rough sheets and smooth tubules. Cell 126:435–439
63. English AR, Zurek N, Voeltz GK (2009) Peripheral ER structure and function. Curr Opin Cell Biol 21:596–602
64. Shibata Y, Shemesh T, Prinz WA, Palazzo AF, Kozlov MM, Rapoport TA (2010) Mechanisms determining the morphology of the peripheral ER. Cell 143:774–788
65. Chevet E, Cameron PH, Pelletier MF, Thomas DY, Bergeron JJ (2001) The endoplasmic reticulum: integration of protein folding, quality control, signaling and degradation. Curr Opin Struct Biol 11:120–124
66. Palade G (1975) Intracellular aspects of the process of protein synthesis. Science 189:347–358
67. Bootman MD, Petersen OH, Verkhratsky A (2002) The endoplasmic reticulum is a focal point for co-ordination of cellular activity. Cell Calcium 32:231–234
68. Verkhratsky A, Petersen OH (2002) The endoplasmic reticulum as an integrating signalling organelle: from neuronal signalling to neuronal death. Eur J Pharmacol 447:141–154
69. Jobsis FF, O'Connor MJ (1966) Calcium release and reabsorption in the sartorius muscle of the toad. Biochem Biophys Res Commun 25:246–252
70. Ridgway EB, Ashley CC (1967) Calcium transients in single muscle fibers. Biochem Biophys Res Commun 29:229–234
71. Ashley CC, Ridgway EB (1970) On the relationships between membrane potential, calcium transient and tension in single barnacle muscle fibres. J Physiol 209:105–130
72. MacKrill JJ (1999) Protein-protein interactions in intracellular Ca2+-release channel function. Biochem J 337(Pt 3):345–361
73. Rizzuto R, Marchi S, Bonora M, Aguiari P, Bononi A, De Stefani D, Giorgi C, Leo S, Rimessi A, Siviero R, Zecchini E, Pinton P (2009) Ca(2+) transfer from the ER to mitochondria: when, how and why. Biochim Biophys Acta 1787:1342–1351
74. Iino M, Endo M (1992) Calcium-dependent immediate feedback control of inositol 1,4,5-triphosphate-induced Ca2+ release. Nature 360:76–78
75. Missiaen L, Taylor CW, Berridge MJ (1992) Luminal Ca2+ promoting spontaneous Ca2+ release from inositol trisphosphate-sensitive stores in rat hepatocytes. J Physiol 455: 623–640
76. Nunn DL, Taylor CW (1992) Luminal Ca2+ increases the sensitivity of Ca2+ stores to inositol 1,4,5-trisphosphate. Mol Pharmacol 41:115–119
77. Smith JB, Smith L, Higgins BL (1985) Temperature and nucleotide dependence of calcium release by myo-inositol 1,4,5-trisphosphate in cultured vascular smooth muscle cells. J Biol Chem 260:14413–14416
78. Bezprozvanny I, Ehrlich BE (1993) ATP modulates the function of inositol 1,4,5-trisphosphate-gated channels at two sites. Neuron 10:1175–1184
79. Iino M (1991) Effects of adenine nucleotides on inositol 1,4,5-trisphosphate-induced calcium release in vascular smooth muscle cells. J Gen Physiol 98:681–698

80. Vanderheyden V, Devogelaere B, Missiaen L, De Smedt H, Bultynck G, Parys JB (2009) Regulation of inositol 1,4,5-trisphosphate-induced Ca2+ release by reversible phosphorylation and dephosphorylation. Biochim Biophys Acta 1793:959–970
81. Khan MT, Wagner L 2nd, Yule DI, Bhanumathy C, Joseph SK (2006) Akt kinase phosphorylation of inositol 1,4,5-trisphosphate receptors. J Biol Chem 281:3731–3737
82. Bugrim AE (1999) Regulation of Ca2+ release by cAMP-dependent protein kinase. A mechanism for agonist-specific calcium signaling? Cell Calcium 25:219–226
83. Murthy KS, Zhou H (2003) Selective phosphorylation of the IP3R-I in vivo by cGMP-dependent protein kinase in smooth muscle. Am J Physiol Gastrointest Liver Physiol 284:G221–G230
84. Bagni C, Mannucci L, Dotti CG, Amaldi F (2000) Chemical stimulation of synaptosomes modulates alpha -Ca2+/calmodulin-dependent protein kinase II mRNA association to polysomes. J Neurosci 20:RC76
85. Vermassen E, Fissore RA, Nadif Kasri N, Vanderheyden V, Callewaert G, Missiaen L, Parys JB, De Smedt H (2004) Regulation of the phosphorylation of the inositol 1,4,5-trisphosphate receptor by protein kinase C. Biochem Biophys Res Commun 319:888–893
86. Jayaraman T, Ondrias K, Ondriasova E, Marks AR (1996) Regulation of the inositol 1,4,5-trisphosphate receptor by tyrosine phosphorylation. Science 272:1492–1494
87. Joseph SK, Hajnoczky G (2007) IP3 receptors in cell survival and apoptosis: Ca2+ release and beyond. Apoptosis 12:951–968
88. Pinton P, Giorgi C, Siviero R, Zecchini E, Rizzuto R (2008) Calcium and apoptosis: ER-mitochondria Ca2+ transfer in the control of apoptosis. Oncogene 27:6407–6418
89. Pinton P, Ferrari D, Magalhaes P, Schulze-Osthoff K, Di Virgilio F, Pozzan T, Rizzuto R (2000) Reduced loading of intracellular Ca(2+) stores and downregulation of capacitative Ca(2+) influx in Bcl-2-overexpressing cells. J Cell Biol 148:857–862
90. Foyouzi-Youssefi R, Arnaudeau S, Borner C, Kelley WL, Tschopp J, Lew DP, Demaurex N, Krause KH (2000) Bcl-2 decreases the free Ca2+ concentration within the endoplasmic reticulum. Proc Natl Acad Sci USA 97:5723–5728
91. Palmer AE, Jin C, Reed JC, Tsien RY (2004) Bcl-2-mediated alterations in endoplasmic reticulum Ca2+ analyzed with an improved genetically encoded fluorescent sensor. Proc Natl Acad Sci USA 101:17404–17409
92. White C, Li C, Yang J, Petrenko NB, Madesh M, Thompson CB, Foskett JK (2005) The endoplasmic reticulum gateway to apoptosis by Bcl-X(L) modulation of the InsP3R. Nat Cell Biol 7:1021–1028
93. Scorrano L, Oakes SA, Opferman JT, Cheng EH, Sorcinelli MD, Pozzan T, Korsmeyer SJ (2003) BAX and BAK regulation of endoplasmic reticulum Ca2+: a control point for apoptosis. Science 300:135–139
94. Oakes SA, Scorrano L, Opferman JT, Bassik MC, Nishino M, Pozzan T, Korsmeyer SJ (2005) Proapoptotic BAX and BAK regulate the type 1 inositol trisphosphate receptor and calcium leak from the endoplasmic reticulum. Proc Natl Acad Sci USA 102:105–110
95. Pinton P, Rizzuto R (2006) Bcl-2 and Ca2+ homeostasis in the endoplasmic reticulum. Cell Death Differ 13:1409–1418
96. Copeland DE, Dalton AJ (1959) An association between mitochondria and the endoplasmic reticulum in cells of the pseudobranch gland of a teleost. J Biophys Biochem Cytol 5: 393–396
97. Lewis JA, Tata JR (1973) A rapidly sedimenting fraction of rat liver endoplasmic reticulum. J Cell Sci 13:447–459
98. Morre DJ, Merritt WD, Lembi CA (1971) Connections between mitochondria and endoplasmic reticulum in rat liver and onion stem. Protoplasma 73:43–49
99. Mannella CA, Buttle K, Rath BK, Marko M (1998) Electron microscopic tomography of rat-liver mitochondria and their interaction with the endoplasmic reticulum. Biofactors 8:225–228
100. Soltys BJ, Gupta RS (1992) Interrelationships of endoplasmic reticulum, mitochondria, intermediate filaments, and microtubules–a quadruple fluorescence labeling study. Biochem Cell Biol 70:1174–1186

101. Mannella CA, Marko M, Penczek P, Barnard D, Frank J (1994) The internal compartmentation of rat-liver mitochondria: tomographic study using the high-voltage transmission electron microscope. Microsc Res Tech 27:278–283
102. Achleitner G, Gaigg B, Krasser A, Kainersdorfer E, Kohlwein SD, Perktold A, Zellnig G, Daum G (1999) Association between the endoplasmic reticulum and mitochondria of yeast facilitates interorganelle transport of phospholipids through membrane contact. Eur J Biochem 264:545–553
103. Csordas G, Renken C, Varnai P, Walter L, Weaver D, Buttle KF, Balla T, Mannella CA, Hajnoczky G (2006) Structural and functional features and significance of the physical linkage between ER and mitochondria. J Cell Biol 174:915–921
104. de Brito OM, Scorrano L (2008) Mitofusin 2 tethers endoplasmic reticulum to mitochondria. Nature 456:605–610
105. Dennis EA, Kennedy EP (1972) Intracellular sites of lipid synthesis and the biogenesis of mitochondria. J Lipid Res 13:263–267
106. Vance JE (1990) Phospholipid synthesis in a membrane fraction associated with mitochondria. J Biol Chem 265:7248–7256
107. Vance JE, Stone SJ, Faust JR (1997) Abnormalities in mitochondria-associated membranes and phospholipid biosynthetic enzymes in the mnd/mnd mouse model of neuronal ceroid lipofuscinosis. Biochim Biophys Acta 1344:286–299
108. Wieckowski MR, Giorgi C, Lebiedzinska M, Duszynski J, Pinton P (2009) Isolation of mitochondria-associated membranes and mitochondria from animal tissues and cells. Nat Protoc 4:1582–1590
109. Pichler H, Gaigg B, Hrastnik C, Achleitner G, Kohlwein SD, Zellnig G, Perktold A, Daum G (2001) A subfraction of the yeast endoplasmic reticulum associates with the plasma membrane and has a high capacity to synthesize lipids. Eur J Biochem 268:2351–2361
110. Wu MM, Buchanan J, Luik RM, Lewis RS (2006) Ca2+ store depletion causes STIM1 to accumulate in ER regions closely associated with the plasma membrane. J Cell Biol 174:803–813
111. Frieden M, Arnaudeau S, Castelbou C, Demaurex N (2005) Subplasmalemmal mitochondria modulate the activity of plasma membrane Ca2+-ATPases. J Biol Chem 280:43198–43208
112. Koziel K, Lebiedzinska M, Szabadkai G, Onopiuk M, Brutkowski W, Wierzbicka K, Wilczynski G, Pinton P, Duszynski J, Zablocki K, Wieckowski MR (2009) Plasma membrane associated membranes (PAM) from Jurkat cells contain STIM1 protein is PAM involved in the capacitative calcium entry? Int J Biochem Cell Biol 41:2440–2449
113. Piccini M, Vitelli F, Bruttini M, Pober BR, Jonsson JJ, Villanova M, Zollo M, Borsani G, Ballabio A, Renieri A (1998) FACL4, a new gene encoding long-chain acyl-CoA synthetase 4, is deleted in a family with Alport syndrome, elliptocytosis, and mental retardation. Genomics 47:350–358
114. Stone SJ, Vance JE (2000) Phosphatidylserine synthase-1 and -2 are localized to mitochondria-associated membranes. J Biol Chem 275:34534–34540
115. Lebiedzinska M, Szabadkai G, Jones AW, Duszynski J, Wieckowski MR (2009) Interactions between the endoplasmic reticulum, mitochondria, plasma membrane and other subcellular organelles. Int J Biochem Cell Biol 41:1805–1816
116. Hayashi T, Rizzuto R, Hajnoczky G, Su TP (2009) MAM: more than just a housekeeper. Trends Cell Biol 19:81–88
117. Giorgi C, De Stefani D, Bononi A, Rizzuto R, Pinton P (2009) Structural and functional link between the mitochondrial network and the endoplasmic reticulum. Int J Biochem Cell Biol 41:1817–1827
118. Decuypere JP, Monaco G, Bultynck G, Missiaen L, De Smedt H, Parys JB (2011) The IP(3) receptor-mitochondria connection in apoptosis and autophagy. Biochim Biophys Acta 1813:1003–1013
119. Mendes CC, Gomes DA, Thompson M, Souto NC, Goes TS, Goes AM, Rodrigues MA, Gomez MV, Nathanson MH, Leite MF (2005) The type III inositol 1,4,5-trisphosphate receptor preferentially transmits apoptotic Ca2+ signals into mitochondria. J Biol Chem 280:40892–40900

120. Hajnoczky G, Robb-Gaspers LD, Seitz MB, Thomas AP (1995) Decoding of cytosolic calcium oscillations in the mitochondria. Cell 82:415–424
121. Rizzuto R, Duchen MR, Pozzan T (2004) Flirting in little space: the ER/mitochondria Ca2+ liaison. Sci STKE 2004:re1
122. Walter L, Hajnoczky G (2005) Mitochondria and endoplasmic reticulum: the lethal interorganelle cross-talk. J Bioenerg Biomembr 37:191–206
123. Green DR, Kroemer G (2004) The pathophysiology of mitochondrial cell death. Science 305:626–629
124. Bernardi P, Rasola A (2007) Calcium and cell death: the mitochondrial connection. Subcell Biochem 45:481–506
125. Garcia-Perez C, Hajnoczky G, Csordas G (2008) Physical coupling supports the local Ca2+ transfer between sarcoplasmic reticulum subdomains and the mitochondria in heart muscle. J Biol Chem 283:32771–32780
126. Pacher P, Sharma K, Csordas G, Zhu Y, Hajnoczky G (2008) Uncoupling of ER-mitochondrial calcium communication by transforming growth factor-beta. Am J Physiol Renal Physiol 295:F1303–F1312
127. Szabadkai G, Bianchi K, Varnai P, De Stefani D, Wieckowski MR, Cavagna D, Nagy AI, Balla T, Rizzuto R (2006) Chaperone-mediated coupling of endoplasmic reticulum and mitochondrial Ca2+ channels. J Cell Biol 175:901–911
128. Rapizzi E, Pinton P, Szabadkai G, Wieckowski MR, Vandecasteele G, Baird G, Tuft RA, Fogarty KE, Rizzuto R (2002) Recombinant expression of the voltage-dependent anion channel enhances the transfer of Ca2+ microdomains to mitochondria. J Cell Biol 159:613–624
129. De Stefani D, Bononi A, Romagnoli A, Messina A, De Pinto V, Pinton P, Rizzuto R (2011) VDAC1 selectively transfers apoptotic Ca(2+) signals to mitochondria. Cell Death Differ 2011 Jul 1. doi: 10.1038/cdd.2011.92. [Epub ahead of print]
130. Roderick HL, Lechleiter JD, Camacho P (2000) Cytosolic phosphorylation of calnexin controls intracellular Ca(2+) oscillations via an interaction with SERCA2b. J Cell Biol 149: 1235–1248
131. Camacho P, Lechleiter JD (1995) Calreticulin inhibits repetitive intracellular Ca2+ waves. Cell 82:765–771
132. Michalak M, Groenendyk J, Szabo E, Gold LI, Opas M (2009) Calreticulin, a multi-process calcium-buffering chaperone of the endoplasmic reticulum. Biochem J 417:651–666
133. Molinari M, Eriksson KK, Calanca V, Galli C, Cresswell P, Michalak M, Helenius A (2004) Contrasting functions of calreticulin and calnexin in glycoprotein folding and ER quality control. Mol Cell 13:125–135
134. Simmen T, Aslan JE, Blagoveshchenskaya AD, Thomas L, Wan L, Xiang Y, Feliciangeli SF, Hung CH, Crump CM, Thomas G (2005) PACS-2 controls endoplasmic reticulum-mitochondria communication and Bid-mediated apoptosis. EMBO J 24:717–729
135. Kottgen M, Benzing T, Simmen T, Tauber R, Buchholz B, Feliciangeli S, Huber TB, Schermer B, Kramer-Zucker A, Hopker K, Simmen KC, Tschucke CC, Sandford R, Kim E, Thomas G, Walz G (2005) Trafficking of TRPP2 by PACS proteins represents a novel mechanism of ion channel regulation. EMBO J 24:705–716
136. Myhill N, Lynes EM, Nanji JA, Blagoveshchenskaya AD, Fei H, Carmine Simmen K, Cooper TJ, Thomas G, Simmen T (2008) The subcellular distribution of calnexin is mediated by PACS-2. Mol Biol Cell 19:2777–2788
137. Breckenridge DG, Stojanovic M, Marcellus RC, Shore GC (2003) Caspase cleavage product of BAP31 induces mitochondrial fission through endoplasmic reticulum calcium signals, enhancing cytochrome c release to the cytosol. J Cell Biol 160:1115–1127
138. Bui M, Gilady SY, Fitzsimmons RE, Benson MD, Lynes EM, Gesson K, Alto NM, Strack S, Scott JD, Simmen T (2010) Rab32 modulates apoptosis onset and mitochondria-associated membrane (MAM) properties. J Biol Chem 285:31590–31602
139. Hayashi T, Su TP (2007) Sigma-1 receptor chaperones at the ER-mitochondrion interface regulate Ca(2+) signaling and cell survival. Cell 131:596–610

140. Maurice T, Su TP (2009) The pharmacology of sigma-1 receptors. Pharmacol Ther 124:195–206
141. Aydar E, Palmer CP, Djamgoz MB (2004) Sigma receptors and cancer: possible involvement of ion channels. Cancer Res 64:5029–5035
142. Marrazzo A, Caraci F, Salinaro ET, Su TP, Copani A, Ronsisvalle G (2005) Neuroprotective effects of sigma-1 receptor agonists against beta-amyloid-induced toxicity. Neuroreport 16:1223–1226
143. Vagnerova K, Hurn PD, Bhardwaj A, Kirsch JR (2006) Sigma 1 receptor agonists act as neuroprotective drugs through inhibition of inducible nitric oxide synthase. Anesth Analg 103:430–434, table of contents
144. Spruce BA, Campbell LA, McTavish N, Cooper MA, Appleyard MV, O'Neill M, Howie J, Samson J, Watt S, Murray K, McLean D, Leslie NR, Safrany ST, Ferguson MJ, Peters JA, Prescott AR, Box G, Hayes A, Nutley B, Raynaud F, Downes CP, Lambert JJ, Thompson AM, Eccles S (2004) Small molecule antagonists of the sigma-1 receptor cause selective release of the death program in tumor and self-reliant cells and inhibit tumor growth in vitro and in vivo. Cancer Res 64:4875–4886
145. Higo T, Hattori M, Nakamura T, Natsume T, Michikawa T, Mikoshiba K (2005) Subtype-specific and ER lumenal environment-dependent regulation of inositol 1,4,5-trisphosphate receptor type 1 by ERp44. Cell 120:85–98
146. Li G, Mongillo M, Chin KT, Harding H, Ron D, Marks AR, Tabas I (2009) Role of ERO1-alpha-mediated stimulation of inositol 1,4,5-triphosphate receptor activity in endoplasmic reticulum stress-induced apoptosis. J Cell Biol 186:783–792
147. Szalai G, Krishnamurthy R, Hajnoczky G (1999) Apoptosis driven by IP(3)-linked mitochondrial calcium signals. EMBO J 18:6349–6361
148. Gilady SY, Bui M, Lynes EM, Benson MD, Watts R, Vance JE, Simmen T (2010) Ero1alpha requires oxidizing and normoxic conditions to localize to the mitochondria-associated membrane (MAM). Cell Stress Chaperones 15:619–629
149. Cartoni R, Martinou JC (2009) Role of mitofusin 2 mutations in the physiopathology of Charcot-Marie-Tooth disease type 2A. Exp Neurol 218:268–273
150. Guo X, Chen KH, Guo Y, Liao H, Tang J, Xiao RP (2007) Mitofusin 2 triggers vascular smooth muscle cell apoptosis via mitochondrial death pathway. Circ Res 101:1113–1122
151. Vecchione A, Fassan M, Anesti V, Morrione A, Goldoni S, Baldassarre G, Byrne D, D'Arca D, Palazzo JP, Lloyd J, Scorrano L, Gomella LG, Iozzo RV, Baffa R (2009) MITOSTATIN, a putative tumor suppressor on chromosome 12q24.1, is downregulated in human bladder and breast cancer. Oncogene 28:257–269
152. Cerqua C, Anesti V, Pyakurel A, Liu D, Naon D, Wiche G, Baffa R, Dimmer KS, Scorrano L (2010) Trichoplein/mitostatin regulates endoplasmic reticulum-mitochondria juxtaposition. EMBO Rep 11:854–860
153. Iwasawa R, Mahul-Mellier AL, Datler C, Pazarentzos E, Grimm S (2011) Fis1 and Bap31 bridge the mitochondria-ER interface to establish a platform for apoptosis induction. EMBO J 30:556–568
154. Celsi F, Pizzo P, Brini M, Leo S, Fotino C, Pinton P, Rizzuto R (2009) Mitochondria, calcium and cell death: a deadly triad in neurodegeneration. Biochim Biophys Acta 1787:335–344
155. Contreras L, Drago I, Zampese E, Pozzan T (2010) Mitochondria: the calcium connection. Biochim Biophys Acta 1797:607–618
156. Area-Gomez E, de Groof AJ, Boldogh I, Bird TD, Gibson GE, Koehler CM, Yu WH, Duff KE, Yaffe MP, Pon LA, Schon EA (2009) Presenilins are enriched in endoplasmic reticulum membranes associated with mitochondria. Am J Pathol 175:1810–1816
157. Zampese E, Fasolato C, Kipanyula MJ, Bortolozzi M, Pozzan T, Pizzo P (2011) Presenilin 2 modulates endoplasmic reticulum (ER)-mitochondria interactions and Ca2+ cross-talk. Proc Natl Acad Sci USA 108:2777–2782
158. Smith IF, Green KN, LaFerla FM (2005) Calcium dysregulation in Alzheimer's disease: recent advances gained from genetically modified animals. Cell Calcium 38:427–437
159. Small DH (2009) Dysregulation of calcium homeostasis in Alzheimer's disease. Neurochem Res 34:1824–1829

160. Yu JT, Chang RC, Tan L (2009) Calcium dysregulation in Alzheimer's disease: from mechanisms to therapeutic opportunities. Prog Neurobiol 89:240–255
161. Sano R, Annunziata I, Patterson A, Moshiach S, Gomero E, Opferman J, Forte M, d'Azzo A (2009) GM1-ganglioside accumulation at the mitochondria-associated ER membranes links ER stress to Ca(2+)-dependent mitochondrial apoptosis. Mol Cell 36:500–511
162. d'Azzo A, Tessitore A, Sano R (2006) Gangliosides as apoptotic signals in ER stress response. Cell Death Differ 13:404–414
163. Wu G, Lu ZH, Obukhov AG, Nowycky MC, Ledeen RW (2007) Induction of calcium influx through TRPC5 channels by cross-linking of GM1 ganglioside associated with alpha5beta1 integrin initiates neurite outgrowth. J Neurosci 27:7447–7458
164. Szado T, Vanderheyden V, Parys JB, De Smedt H, Rietdorf K, Kotelevets L, Chastre E, Khan F, Landegren U, Soderberg O, Bootman MD, Roderick HL (2008) Phosphorylation of inositol 1,4,5-trisphosphate receptors by protein kinase B/Akt inhibits Ca2+ release and apoptosis. Proc Natl Acad Sci USA 105:2427–2432
165. Marchi S, Rimessi A, Giorgi C, Baldini C, Ferroni L, Rizzuto R, Pinton P (2008) Akt kinase reducing endoplasmic reticulum Ca2+ release protects cells from Ca2+-dependent apoptotic stimuli. Biochem Biophys Res Commun 375:501–505
166. Giorgi C, Ito K, Lin HK, Santangelo C, Wieckowski MR, Lebiedzinska M, Bononi A, Bonora M, Duszynski J, Bernardi R, Rizzuto R, Tacchetti C, Pinton P, Pandolfi PP (2010) PML regulates apoptosis at endoplasmic reticulum by modulating calcium release. Science 330:1247–1251
167. Pinton P, Giorgi C, Pandolfi PP (2011) The role of PML in the control of apoptotic cell fate: a new key player at ER-mitochondria sites. Cell Death Differ 18:1450–1456
168. Lebiedzinska M, Duszynski J, Rizzuto R, Pinton P, Wieckowski MR (2009) Age-related changes in levels of p66Shc and serine 36-phosphorylated p66Shc in organs and mouse tissues. Arch Biochem Biophys 486:73–80
169. Bozidis P, Williamson CD, Colberg-Poley AM (2008) Mitochondrial and secretory human cytomegwalovirus UL37 proteins traffic into mitochondrion-associated membranes of human cells. J Virol 82:2715–2726
170. Sheikh MY, Choi J, Qadri I, Friedman JE, Sanyal AJ (2008) Hepatitis C virus infection: molecular pathways to metabolic syndrome. Hepatology 47:2127–2133
171. Criollo A, Maiuri MC, Tasdemir E, Vitale I, Fiebig AA, Andrews D, Molgo J, Diaz J, Lavandero S, Harper F, Pierron G, di Stefano D, Rizzuto R, Szabadkai G, Kroemer G (2007) Regulation of autophagy by the inositol trisphosphate receptor. Cell Death Differ 14:1029–1039
172. Cardenas C, Miller RA, Smith I, Bui T, Molgo J, Muller M, Vais H, Cheung KH, Yang J, Parker I, Thompson CB, Birnbaum MJ, Hallows KR, Foskett JK (2010) Essential regulation of cell bioenergetics by constitutive InsP3 receptor Ca2+ transfer to mitochondria. Cell 142:270–283
173. Levine B, Kroemer G (2008) Autophagy in the pathogenesis of disease. Cell 132:27–42

Chapter 18
Calcium Around the Golgi Apparatus: Implications for Intracellular Membrane Trafficking

Massimo Micaroni

Abstract As with other complex cellular functions, intracellular membrane transport involves the coordinated engagement of a series of organelles and machineries; in the last couple of decades more importance has been given to the role of calcium (Ca^{2+}) in the regulation of membrane trafficking, which is directly involved in coordinating the endoplasmic reticulum-to-Golgi-to-plasma membrane delivery of cargo. Consequently, the Golgi apparatus (GA) is now considered not just the place proteins mature in as they move to their final destination(s), but it is increasingly viewed as an intracellular Ca^{2+} store. In the last few years the mechanisms regulating the homeostasis of Ca^{2+} in the GA and its role in membrane trafficking have begun to be elucidated. Here, these recent discoveries that shed light on the role Ca^{2+} plays as of trigger of different steps during membrane trafficking has been reviewed. This includes recruitment of proteins and SNARE cofactors to the Golgi membranes, which are both fundamental for the membrane remodeling and the regulation of fusion/fission events occurring during the passage of cargo across the GA. I conclude by focusing attention on Ca^{2+} homeostasis dysfunctions in the GA and their related pathological implications.

Keywords ATPase calcium pump • Calcium • COPI • Golgi apparatus • Hailey-Hailey disease • Intracellular membrane trafficking • Secretory pathway • SNARE • SPCA

M. Micaroni (✉)
Division of Molecular Cell Biology, Institute for Molecular Bioscience,
The University of Queensland, 306 Carmody Road, 4072 Brisbane, St. Lucia, QLD, Australia
e-mail: m.micaroni@imb.uq.edu.au

M.S. Islam (ed.), *Calcium Signaling*, Advances in Experimental Medicine and Biology 740, DOI 10.1007/978-94-007-2888-2_18,

Abbreviations

Ca^{2+}	Calcium ions
$[Ca^{2+}]_{cyt}$	Free calcium ion concentration in the cell cytosol
$[Ca^{2+}]_{ext}$	Free extracellular calcium ion concentration
$[Ca^{2+}]_{GA}$	Free calcium ion concentration in the Golgi apparatus
CaR	Ca^{2+} receptor
CGN	*Cis*-Golgi network
COPI	Coat protein I
ER	Endoplasmic reticulum
GA	Golgi apparatus
HDD	Hailey-Hailey disease
IGF1R	Insulin-like growth factor receptor
IP3R	Inositol 1,4,5-trisphospahate receptor
NCS-1	Neuronal calcium sensor 1
PLA2	Phospholipase A2
PM	Plasma membrane
SERCA	Sarco/endoplasmic reticulum Ca^{2+}-transport ATPase pump
SNARE	Soluble N-ethylmaleimide-sensitive fusion factor attachment protein receptor
SPCA1	Secretory pathway Ca^{2+}-ATPase isoform 1
TGN	*Trans*-Golgi network
VSMCs	Vascular smooth muscle cells
VSVG	Temperature sensitive variant of the G protein of vesicular stomatitis virus

Introduction

Ever since Camillo Golgi discovered a new cellular organelle in 1898 [1], the mechanism proteins use to cross the Golgi apparatus (GA), and reach their final destination, has remained an issue of debate [2–4]. The first of the two prevailing models is the cisternal maturation/progression model where cargo remains in a given compartment and different enzymes arrive to convert a *cis*-cisterna into a medial one, or a medial cisterna into a *trans*-cisterna. In the second of the two prevailing models, cargo moves from one Golgi compartment to the next, encountering different enzymes in each subsequent compartment, until it reaches the most *trans*-cisterna, where it is then sorted into carriers bound for post-Golgi destinations. This second model could use vesicles and/or compartment-connecting tubules through which cargo could pass, to transport cargo from one compartment to the next. Indeed, several thousand vesicles, some of which carry proteins back to the endoplasmic reticulum (ER), surround the GA. However, large protein like procollagen cannot physically enter the vesicles [5], casting doubts on the universality of the vesicular model. Membrane tubules have been detected between Golgi cisternae under conditions of active secretion [6]; this would permit cargo movement from one side

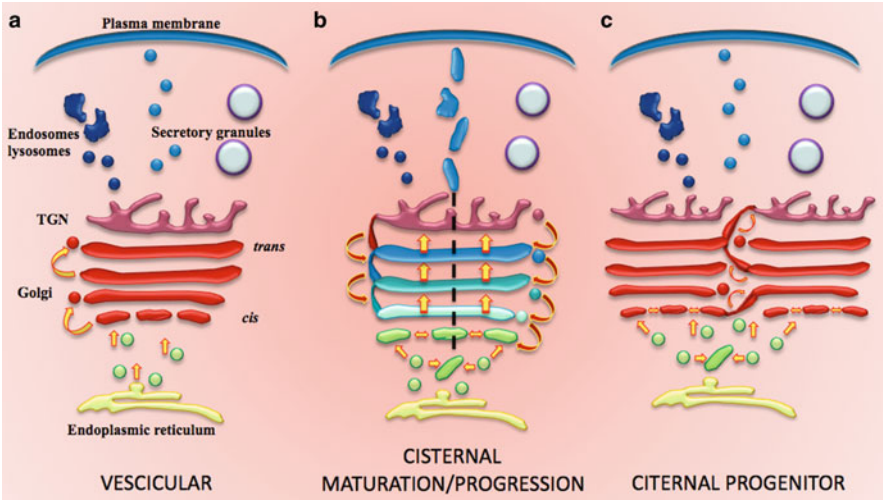

Fig. 18.1 Current models for protein transport across the GA. (**a**) In the vesicular model, cargo protein is delivered from the ER to the *cis*-Golgi via COPII vesicles. Once in the GA, the cargoes move in the *cis*-to-*trans* direction via COPI vesicles. In fact, the vesicular transport model assumes that the Golgi cisternae consist of stable compartments and the COPI vesicles convey cargo in the anterograde direction. (**b**) In the cisternal maturation/progression model the Golgi cisternae are transient structures that form *de novo* from ER-derived carriers (COPII vesicles). A new cisterna matures and progresses from the *cis* to the *trans*-Golgi pole. At the *trans*-most face (TGN), cisternae disassemble into transport carriers. Alternatively, the *trans*-cisterna delivers cargo to a post-Golgi compartment (TGN) where cargo accumulates before export. Cisternal maturation is driven by the retrograde transport of resident GA proteins/enzymes. This retrograde transport might involve COPI vesicles within the GA. (**c**) Cisternal progenitor model involves stable compartments that possess the capacity to generate subsequent compartments of the GA. This is distinct from a maturation/progression model whereby one compartment is turned into another, because in this model the original compartment is maintained. *cis*-Golgi homotypic fusion events can occur with another *cis* compartment or perhaps a medial compartment (or both). Similarly, a medial cisterna may be able to fuse with a trans cisterna. In this manner, a large cargo may be able to encounter all Golgi-processing enzymes without entering a transport vesicle

of the stack to the next, without maturation or vesicle transfer. What looks like cisternal maturation has been imaged directly in yeast, and reported in three independent works that describe an apparent conversion of one Golgi compartment to another by high-resolution and live-cell video microscopy [7–9]. A minor limitation of these studies is that it has not yet been possible to image cargo simultaneously and some (but not all) of the compartment markers monitored are capable of reversibly binding to and releasing from the surface of the GA.

In addition to the two prevailing models, a third "cisternal progenitor" model was recently proposed which suggests stable compartments possess the capacity to generate subsequent compartments of the GA [10]. This is distinct from a conversion model whereby one compartment is turned into another (cisternal maturation/progression model), because in the "cisternal progenitor" model the original compartment is maintained. These above described models are resumed in Fig. 18.1.

The high level of evolutionary conservation of the GA, from lower organisms (i.e. yeast) to humans, strongly suggests that despite their morphological differences, intra-Golgi transport will occur by similar mechanisms. Irrespective of which model is more accurate, membrane fusion and fission events are a central theme shared by all of them. These processes are now well characterized and are driven by SNAREs (soluble N-ethylmaleimide-sensitive factor attachment protein receptors) [11]. SNAREs are now generally accepted to be major players in the final stage of the docking and the subsequent fusion of diverse vesicle-mediated transport events [12]. In the presence of calcium (Ca^{2+}), SNAREs in opposing bilayers have been shown to interact and self-assemble in a circular pattern, forming conducting channels [13]. Recently, some colleagues and I reported a temporary increase of the Ca^{2+} concentration ($[Ca^{2+}]$) in the cytosol ($[Ca^{2+}]_{cyt}$), during a pulse of protein traffic; this temporary fluctuation of the $[Ca^{2+}]_{cyt}$ was shown to be necessary to allow the cargo movement through the GA [14]. This Ca^{2+} comes from within the GA positioned centrally, at least during trafficking, as an organelle able to regulate the $[Ca^{2+}]_{cyt}$, releasing Ca^{2+} itself and regulating the Ca^{2+} signaling in the cytosol.

Here, I will discuss the role of Ca^{2+} signaling in regulating the intracellular membrane trafficking, triggering the SNARE and the membrane remodeling protein (like the cytosolic phospholipase A2, hereafter cPLA2) functions and the consequences of altered Ca^{2+} homeostasis on membrane trafficking.

Ca^{2+} and Ras, Signaling Triggers of the Membrane Trafficking

Ca^{2+} is the most ubiquitous second messengers in vertebrates, and even slight variations in its levels can greatly affect cell behavior. Extracellular $[Ca^{2+}]$ ($[Ca^{2+}]_{ext}$) is usually in the low millimolar range, while resting free $[Ca^{2+}]_{cyt}$ is in the order of 100 nM. A large amount of intracellular Ca^{2+} is stored inside the ER and the GA; both of these organelles can accumulate millimolar levels of luminal Ca^{2+} [15, 16] (Fig. 18.2). These steep Ca^{2+} gradients between the organelle lumens and the cytosol, and between the cytosol and the extracellular space, are maintained by a series of ATP-dependent pumps and channels that fine-tune this homeostasis.

According to the classical paradigm, receptor activation at the plasma membrane (PM) stimulates the release of Ca^{2+} from the ER stores into the cell cytosol, which then activates downstream signaling proteins. More recently, the GA has also been considered as part of the intracellular Ca^{2+} response that can be triggered by extracellular stimuli [16]. The ER and GA release Ca^{2+} upon activation of the IP3Rs (inositol 1,4,5-trisphospate receptors) in their membranes [16, 17], while Ca^{2+} uptake involves two classes of Ca^{2+}-ATPase pumps, the sarcoplasmic and ER Ca^{2+}-ATPase (SERCA) present in the ER and the membranes of the *cis*-Golgi network (CGN), and the Golgi specific Ca^{2+}-ATPase SPCA (type 1 and 2) [18]. As well as pumping Ca^{2+}, SPCA1 also supplies Mn^{2+} as a cofactor for the GA glycosyltransferases [19]. The importance of the GA in cellular Ca^{2+} homeostasis is highlighted by the skin disorder Hailey-Hailey disease, a keratinocyte disorder that is characterized

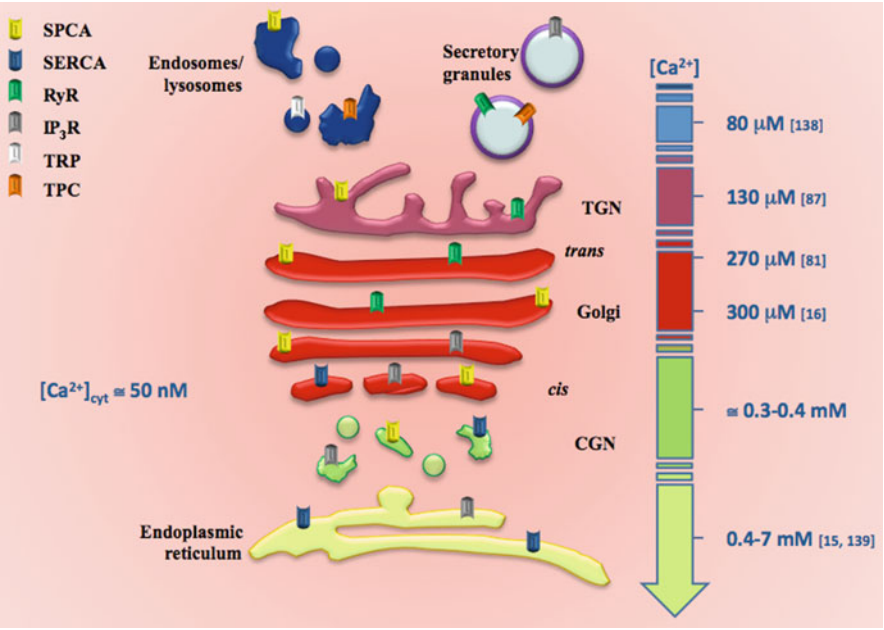

Fig. 18.2 Distribution of Ca^{2+} pumps and channels and luminal $[Ca^{2+}]$ along the secretory pathway. All the organelles along the secretory pathway have their own proper combination of Ca^{2+} pumps and channels, making them a unique Ca^{2+} storage compartment. The value of luminal $[Ca^{2+}]$ in each compartment decreases from the ER-to-PM direction, as reported on the right of the cartoon [138, 139], even if the luminal $[Ca^{2+}]$ of the organelles along the secretory pathway has been quantified with different methods and in different cells types, making the relative values sometimes discordant, but being in the order of at least 1,000 times bigger than the $[Ca^{2+}]_{cyt}$. This model is based on quantitative data for the ER and GA obtained in HeLa cells, while the data on the secretory vesicles have been extrapolated from experiments carried out in insulin secreting cells

by defects in cell-cell adhesion and differentiation, caused by an inactivating mutation in the SPCA1 Ca^{2+}-ATPase gene [20] (see also below). The contributions of SERCA and SPCA1 to the homeostasis of Ca^{2+} in the GA is also cell-type dependent. Indeed, as keratinocytes rely almost exclusively on SPCA1, this indicates why Hailey-Hailey disease is cell specific [21].

Fluctuations in the $[Ca^{2+}]_{ext}$ are also monitored by the Ca^{2+}-receptor (CaR). This is a low affinity, seven transmembrane domains GPCR that is coupled to various heterotrimeric G proteins of the Gi, Gq and G12/13 classes [22]. In keratinocytes, CaR coupling to the PLC signaling pathway can trigger the release of Ca^{2+} from intracellular stores, and hence promote cell differentiation. A recent study showed that CaR is also present on the TGN (*trans*-Golgi network), where it can sense the luminal $[Ca^{2+}]$ of the GA ($[Ca^{2+}]_{GA}$) and regulate the Ca^{2+} uptake into the GA by acting in concert with PLCγ1 and SPCA1 [23]. If this finding can be confirmed in future studies, it represents the first evidence of a Golgi-initiated signaling circuit.

Changes in Ca^{2+} homeostasis within the lumen of the GA or in the cytosol proximal to this organelle can affect the functions of the GA and cell signaling. Indeed,

there is evidence that variations in the levels of $[Ca^{2+}]_{cyt}$ are involved in different transport steps [24]. Specifically, a role for Ca^{2+} in endosomal fusion has been reported, as well as in homotypic vacuolar fusion in yeast [25–27]. In addition, a Ca^{2+}-dependent ER-to-Golgi transport step has been identified [28], and in a reconstituted intra-Golgi transport assay it was demonstrated that Ca^{2+} released from the GA is required for intra-Golgi transport of VSVG (temperature sensitive variant of the G protein of vesicular stomatitis virus) [29]. These data therefore suggest that Golgi transport is controlled by a micro-signaling circuit triggered by the arrival of cargo at the GA and that leads to the regulation of transport flow.

There is also clear evidence for a role for Ca^{2+} in constitutive exocytosis and endocytosis in whole cells, in agreement with previous studies performed with purified organelle membranes and semi-intact cell systems; Ca^{2+} chelator BAPTA impaired VSVG transport in NRK cells from the intermediate compartment-to-GA and the GA-to-PM transport steps [24]. When probed with Shiga toxin b fragment, the functioning of the endocytic/retrograde pathway was blocked by BAPTA treatment at the endosomal-to-GA and GA-to-ER interfaces. Ca^{2+} chelators also promoted the detachment of the COPI (coat protein I) from membranes, providing the first mechanistic explanation of how Ca^{2+} regulates transport throughout the constitutive exocytic pathway [24].

As well as these effects on the COPI machinery, Ca^{2+} can affect membrane trafficking by several means. In the first instance, an impairment of membrane trafficking could result from changes in the $[Ca^{2+}]_{GA}$. This hypothesis is supported by the presence of a number of Ca^{2+}-binding proteins (CALNUC, P54/NEFA and Cab45, all luminal GA resident proteins) that appear to be devoted to the control of the $[Ca^{2+}]_{GA}$ [30–33]. Secondly, changes in peri-Golgi $[Ca^{2+}]_{cyt}$ can affect the activities of Golgi-localized Ca^{2+}-dependent proteins and/or result in the recruitment of cytosolic signaling proteins that are involved in the initiation of signaling cascades similar to those seen at the PM. For example, Ca^{2+} increases in the proximity of the Golgi membranes can activate L-CaBP1, a Ca^{2+}-binding protein that negatively modulates Ca^{2+} release from the intracellular Ca^{2+} stores via the IP3R [34]. Recently, interactions have also been seen between L-CaBP1 and the AP-1 adaptor, suggesting a specific role of L-CaBP1 in the regulation of transport [35].

Furthermore, Ca^{2+} activates neuronal calcium sensor 1 (NCS-1), a protein that can stimulate PI4KIIIb at the TGN, leading to an increase in constitutive and stimulated transport from the TGN to the PM [36]. NCS-1 binding to Arf1 can also compete with Arf1 in the activation of PI4KIIIb, suggesting the presence of two mutually exclusive pathways acting upstream of PI4KIIIb in the regulation of exit from the TGN [36]. A peri-Golgi $[Ca^{2+}]_{cyt}$ increase can also activate the cysteine protease calpain, which is involved in many different cellular processes, including cell adhesion and migration. However, a recent study showed that calpain proteolyses the β subunit of the COPI coatomer [37]. This suggests that the activation of calpain by Ca^{2+}, which could be released from the GA during the transport of cargo, modulates its own transport by promoting the disassembly of the COPI coatomer.

There is a second class of proteins that although not generally localized on the Golgi membranes, are recruited to the GA in response to a $[Ca^{2+}]_{cyt}$ increase.

These proteins include other neuronal Ca^{2+}-sensor family proteins (hippocalcin, Vilip-1 and neurocalcin-d), cPLA2 (see also below in the text), K-Ras and Ras-GRP [38–41]. Hippocalcin has been recently reported to be involved in the activation of Ras mediated Raf1-activation along the MAPK pathway initiated by N-methyl-D aspartate (NMDA) and KCl [42]. As the GA hosts the Ras-dependent MAPK activation pathway, it can be assumed that the translocation of hippocalcin to the GA upon increased $[Ca^{2+}]_{cyt}$ allows it to participate in this signaling cascade from this Golgi location. This scenario opens the possibility of cross talk between the observed Ca^{2+} release from the GA during membrane trafficking [14] with signaling coming from the PM.

The Ras proteins are the founding members of a large family of small GTP-binding proteins, which now includes Arf, Rab and Rho. Ras itself comprises three proteins, N-Ras, H-Ras and K-Ras, which are involved in the regulation of cell proliferation and cell death promoted by PM receptors. The Ras family members are involved in cell signaling via three main pathways: Raf1/Erk, PI3K/AKT and RalGDS [43, 44]. Mutations in these Ras proteins that impair their GTPase activities are responsible for several human diseases, including cancer. Recent studies have reported a substantial bidirectional trafficking of H-Ras and N-Ras between the GA and the PM [45]. Indeed, using genetically encoded fluorescent probes that can sense Ras activation, Philips and colleagues have demonstrated that growth factor stimulation transiently activates Ras on the PM, while its activation is sustained on the Golgi membranes where Ras can promote cell growth or differentiation [46, 47]. Ras activation on the GA could be due to the retrograde transport of Ras from the PM, or it could rely on a diffusible mediator that transduces the message from the PM to the GA. Although both hypotheses might be valid, the most convincing experimental data indicate that Ca^{2+} is the diffusible signal involved in the activation of Ras that is already on Golgi membranes. Specifically, an increase in $[Ca^{2+}]_{cyt}$ recruits the Ca^{2+}-dependent Ras exchange factor Ras-GRP1 to the GA and the RAS GTPase-activating protein CAPRI to the PM, leading to Ras activation at the GA and its inactivation at the PM [48].

From these examples, it is evident that Ca^{2+} released from the GA (and/or the ER) can activate the Ras-GRP1/Ras signaling pathway. It would therefore be important to investigate whether the Ca^{2+} in the peri-Golgi area during membrane trafficking could also activate Ras signaling.

Membrane Trafficking Needs SNAREs, and SNAREs Need Ca^{2+}

Precise mechanisms are required to govern protein transport between different organelles, particularly in the secretory and endocytic pathways. Small shuttling vesicles (such as synaptic vesicles of neurons) or larger transport containers (such as zymogen granules of pancreatic acinar cells) are the major intermediates in anterograde or retrograde translocation of proteins between various compartments in the secretory and endocytic pathways. The basic steps underlying vesicle-mediated

transport are vesicle/container formation from a donor compartment, translocation of transport intermediates to a target compartment, tethering of transport intermediates with the target compartment, and, finally, the docking and fusion of vesicles/containers with the target compartment [49].

SNAREs function in the final event of docking of vesicles/containers with the target compartment and catalyze the fusion of the opposing membranes of the transport intermediate and the target compartment [50]. Functionally, SNAREs can be classified into v-SNAREs, associated with the vesicle/container, and t-SNAREs, associated with the target compartment. Specific interaction of v-SNARE on the transport intermediate with the cognate t-SNARE on the receiving target compartment underlies the central event of docking and fusion processes of vesicle-mediated transport. v-SNAREs usually consist of a tail-anchored SNARE having a single SNARE motif, while t-SNAREs consist of either (two or) three polypeptides [51]. Interaction between v-SNARE and t-SNARE leads to the formation of the *trans*-SNARE complex, in which the four SNARE motifs assemble as a twisted parallel four-helical bundle, which catalyzes the apposition and fusion of the vesicle with the target compartment [52, 53].

The crystal structure of the synaptic SNARE complex revealed that the four SNARE domains form a twisted parallel four-helical bundle with each SNARE domain contributing one helix [54]. The formation of the *trans*-SNARE complex, due to the contribution of three helical bundle form one membrane and one from the opposing membrane, will serve "to zip the two opposing membranes together" from the N- to the C-terminal end [55]. All this process requires energy to allow the membrane to come closer and fuse; the energy generated during the formation of the four-helical bundle has been proposed to be the driving force for the fusion process [55]. However, *trans*-SNARE complex needs Ca^{2+} and SNARE cofactors Ca^{2+}-dependent to be released. An example is the Munc13 (1–4) proteins, as SNARE cofactors contain several Ca^{2+}-binding C2 domains implicated in interactions with diacylglycerol, Ca^{2+}, and phospholipids [56]. Knockout of both Munc13-1 and Munc13-2 abolishes spontaneous and evoked synaptic transmissions. Munc13-1/2 is proposed to be essential for the priming process for synaptic vesicles tethered onto the presynaptic PM [57]. The priming process empowers the tethered/docked vesicles with the competence of evoked fusion.

Furthermore, synaptotagmin I (a member of the synaptotagmin protein family consisting of at least 13 members [58]), which is preferentially expressed in neurons, is associated with the synaptic vesicle as a type I membrane protein with its short N-terminal region oriented towards the lumen of the synaptic vesicle. Its larger C-terminal cytoplasmic domain contains two tandem Ca^{2+}-binding C2 (C2A and C2B) domains. Exocytosis of synaptic vesicles in the synapse is strictly regulated by changes in cytosolic $[Ca^{2+}]$ ($[Ca^{2+}]_{cyt}$), whereas synaptotagmin I is probably the Ca^{2+} sensor that couples this ion flux to the exocytosis of synaptic vesicles in response to an action potential [59–61].

Synaptotagmin I binds directly to Syn1 and SNAP-25 of the t-SNARE. The tandem C2 (C2A and C2B) domains cooperate to enhance the penetration of some hydrophobic residues into the lipid bilayer of the target compartment in response to Ca^{2+}.

The C2B domain apparently also interacts with phosphatidyl inositol 4,5-biphosphate (PtdIns4,5P) in response to Ca^{2+} binding, thus steering the penetration of hydrophobic residues of C2A and C2B into the target membrane [61, 62]. Several acidic residues in the C-terminal region of SNAP-25 are known to be important for its Ca^{2+}-triggered interaction with synaptotagmin-1 [63]. Through the simultaneously enhanced interactions with t-SNARE, PtdIns4,5P, and the lipid bilayer, synaptotagmin I triggers the complexin-stabilized *trans*-SNARE complex to catalyze the fusion process in the presynaptic membrane in response to a rise in Ca^{2+} levels [61, 64]. Mice lacking synaptotagmin I develop normally as embryos, but die within 48 h after birth [59]. Electrophysiological analysis of hippocampal neurons derived from these synaptotagmin I-null mice reveals severe impairment of synaptic transmission. Ca^{2+}-triggered synchronized synaptic exocytosis is specifically decreased, whereas asynchronous slow release processes, such as spontaneous synaptic activity and release triggered by hypertonic solution or alpha-latrotoxin, are unaffected. This demonstrates a physiological role for synaptotagmin I in Ca^{2+}-evoked synchronous neurotransmitter release.

cPLA2: Make-Up Artist for the Golgi Membranes to Be Ready for Trafficking

Four main subfamilies of PLA2 have been identified: secretory PLA2 (sPLA2); cytosolic, Ca^{2+}-dependent PLA2 (cPLA2); intracellular, Ca^{2+}-independent PLA2 (iPLA2); and platelet-activating factor acetylhydrolases (PAF-AHs) [65]. cPLA2 catalyzes the first step in the arachidonic acid (AA) cascade leading to the synthesis of important lipid mediators, the prostaglandins and leukotrienes; the isoform cPLA2α hydrolyses the fatty acids (FA) at the middle ester bond of cylindrical phospholipids to form wedge-shaped lysophospholipids [66, 67]. cPLA2 contains a Ca^{2+}-dependent membrane-binding domain (C2 domain). The activation of plasma-membrane receptors coupled to intracellular Ca^{2+} stimulation promotes the association of cPLA2 with the ER and with Golgi membranes [40]. The recruitment cPLA2 to these membranes could simply suggest that they act as relay stations along a plasma-membrane-initiated signaling cascade. The formation of wedge-shaped lysophospholipids favors the generation of spontaneous membrane curvature and transformation of flat cisternae-like membranes into highly curved tubular membranes, which serve as intermediates for transport across the Golgi stack or to generate and maintain tubular membranes [65, 67], that connect neighboring stacks. These highly curved membranes are where fusion/fission events occur and where the *trans*-SNARE complex forms. *Trans* interactions between SNAREs on opposing membranes have been proposed to facilitate or trigger $[Ca^{2+}]$ signals in response to docking [68, 69]. In fact, now we know that local increases in $[Ca^{2+}]_{cyt}$ near the GA are necessary to recruit SNARE cofactors, which force the release of the *trans*-SNARE complex helping the fusion of the two opposing bilayers, as well as recruit membrane remodeling enzymes, like the isoform cPLA2α, on the GA [67, 70].

Membrane trafficking involves the formation of tubular-shaped membranes that can act as carriers or as structural elements in specific compartments, including in the CGN and TGN [71]. Brown and co-workers [72] found that when the enzymatic activity of PLA2 is inhibited, the Brefeldin A-induced tubules that emanate from the GA are impaired, and redistribute Golgi proteins to the ER. Along the same lines, *in vitro* experiments performed on purified GA have indicated that activators of PLA2 promote tubule formation [73]. The mechanisms proposed for these PLA2-mediated effects rely on the local production of inverted cone-shaped lysophospholipids that drive the formation of positive curvature, a process that is involved in tubule formation [74]; however, a role for arachidonic acid as a signaling mechanism cannot be ruled out. PLA2 inhibitors are also able to block endosomal fusion *in vivo* [72]. Similar to that hypothesized for tubule formation, PLA2 could participate in membrane fusion by changing the local membrane composition through the production of lysolipids and free fatty acids, and/or via signaling cascades. From a physiological standpoint, PLA2 regulates the retrograde transport of proteins between the GA and the ER. The PLA2 inhibitors impair the retrograde transport of a chimeric KDEL receptor-VSVG [72]. Similar approaches have shown that PLA2 activity is important for the recycling of the transferrin receptor from the recycling endosomes towards the plasma membrane [75], and for the maintenance of the Golgi ribbon [76], with PLA2 inhibitors promoting the formation of separate Golgi stacks that remain in the perinuclear area [76].

Secretory Pathway Ca^{2+}-ATPase: New Family of Ca^{2+} Pump

The GA possesses mechanisms for Ca^{2+} accumulation (Ca^{2+} pumps), storage (Ca^{2+}-binding proteins) and release (i.e. IP3R) making this organelle a true Ca^{2+} store, playing a role in intracellular Ca^{2+} signaling [77] (Fig. 18.2).

A new class of Ca^{2+}-ATPase pump localized to the GA was identified for the first time about two decades ago [78]; more recently, its yeast homolog was investigated [79]. Only during the last few years interesting studies on its role and distribution at tissue and subcellular level has been reported. The secretory pathway Ca^{2+}/Mn^{2+}-ATPase protein (SPCA) type 1 (SPCA1) and type 2 (SPCA2) have different tissue distribution and apparently different roles on Ca^{2+} homeostasis and implications in trafficking, and both are excluded from the ER [80, 81] (Fig. 18.2). Here, the recent advances in understanding the role and functioning of this new family of Ca^{2+} pumps has been reviewed.

SPCA1

ATP2C1 encodes for the human SPCA1 protein, with four known mRNA splice variants [82]. Gene silencing of *ATP2C1* inhibits the correct organization of the GA [83] and affects the subsequent development of the affected tissue [83]. Like all

cellular Ca^{2+}-ATPase pumps, SPCA1, which probably has a main role in the GA, acts to reduce this otherwise "toxic" level of Ca^{2+} from the cytosol. Moreover, it also seems to be critical for maintenance of the GA ultrastructure organization [81, 84].

SPCA1 is distributed along the secretory pathway and mostly in the GA [81] (Fig. 18.2); however, SPCA1 has also been detected in pancreatic β-cell lines in both microsomal and dense-core secretory vesicle-enriched fraction [85]. This distribution of SPCA1 along the secretory pathway in this secreting cell lines (MIN6 and INS1) was coupled with a higher efficiency in insulin secretion in SPCA1 depleted cells. The authors proposed a new role of SPCA1 in the ER (and secretory vesicles), where SPCA1 "plays a significant role in the accumulation of Ca^{2+} by the ER" [85]. This is contrary to the recent reports where SPCA1 depletion induces a severe fragmentation of the GA with drastic reduction of protein secretion, resulting in an inefficient protein trafficking [81, 83, 84, 86]. Interestingly, in SPCA1-depleted cells the exit of enzymes from the ER is not affected [81], suggesting a minor role for SPCA1 in ER-to-GA trafficking, even if it does not completely exclude a role in ER Ca^{2+} homeostasis [85]. However, a prevalent role for SPCA1 in the GA was supported by the prevalent distribution on the *trans*-GA of the SPCA1, and complete exclusion from the most CGN [87, 88], even if it contradicts a recent report in which SPCA1 was not completely excluded from the CGN [81]. TGN is depleted in SERCA or IP3R, and it was shown that it accumulates Ca^{2+} via SPCA1, using a fluorescent FRET-based Ca^{2+} probe directly targeted to the TGN lumen [87]. Clearly, further investigations are needed to clarify the precise role of SPCA1 in trafficking.

As SPCA1 can transport Mn^{2+} in addition to Ca^{2+}, the alteration of neural polarity after SPCA1 depletion involves a deficiency of Ca^{2+} and/or Mn^{2+} uptake into the GA, and the subsequent reduction of its Ca^{2+} and/or Mn^{2+} content [84]. Ca^{2+} and Mn^{2+} are critical cofactors in many Golgi activities, which include the correct processing and trafficking of newly synthesized proteins and membranes required for neural polarity; proteins such as glycosyltransferases [19], sulfotransferases [89, 90], and prohormone convertases [91, 92] that need Ca^{2+} and/or Mn^{2+} for their activity. In fact, down regulation of SPCAs interferes with glycosylation of thyroglobulin in rat thyrocytes [93]. Disturbed Ca^{2+} handling by the GA function could however be compensated by the ER activity, even if the total SERCA number was not increased [84]. Recently, a new role for SPCA1 in Mn^{2+} detoxification in hepatic cells has been reported [94]. The authors showed "a prominent novel localization of SPCA1 to an endosomal population close to, but not on the basolateral membranes" [94]. This data confirmed a dual distribution of SPCA1 to the GA/TGN and the early endosomal compartment [81]. The localization on endosomal compartment may serve to sequester Mn^{2+} as it enters from the sinusoidal/basolateral domains [94], suggesting a role for SPCA1 in Mn^{2+} detoxification in liver.

Mutated SPCA1 Causes Hailey-Hailey Disease

Hailey-Hailey disease (HHD), also known as familial benign chronic pemphigus, is a rare, autosomal and dominantly inherited dermatosis. The genetic defect in HHD

causes the skin cells to become unstuck from one another, and not adhering together properly; it is characterized by suprabasal separation (acantholysis) of the epidermis resulting in recurrent blisters, crusted erosions, and warty papules; painful erosions may become hypertrophic, and even mild disease can affect quality of life [95]. In occasional cases, the lesions may develop into squamous cell carcinomas [96].

Molecular studies showed that HHD carried heterozygous mutations in the *ATP2C1* gene on 3q22.1, encoding the SPCA1 [97], which localize along the secretory pathway, mainly in the GA [80, 81, 98]. To date, 117 pathological mutations have been described scattered throughout the *ATP2C1* gene with no indication of mutational hotspot or clustering of mutations [99]. Moreover, different cutaneous diseases etiologically related to the HHD have been shown to be a variant of HHD [100]. This supports the view that histology, coupled with genetic testing is critical to diagnose this dermatological pathology.

The skin cells (keratinocytes) stick together via structures called desmosomes and it seems the desmosomes do not assemble properly if there is insufficient Ca^{2+} [20, 101], even if their secretion seems not to be altered [83]. Normally the cells are packed together tightly much like bricks. This could be the reason why depletion of SPCA1 affects mostly the skin and not other tissues. For further details see a recent, excellent review on SPCA1 and HHD [102] and the chapter "Calcium and skin" of this book.

SPCA1 and Diabetes

SPCA1 is also highly expressed in VSMCs (vascular smooth muscle cells) [103]; unfortunately it has not been investigated in relation to diabetes-related cardiovascular pathology. It is unlikely that the other isoform, SPCA2, plays a substantial role in cardiovascular pathology, as it is weakly expressed in vascular tissue [104]. However, previous studies have linked SPCA1 expression to diabetes in pancreatic cells [85]. Furthermore, alterations in the GA, with hypertrophy and partly vacuolized cisternal stacks, have also been observed in VSMCs treated with kinase inhibitors to block proliferation [105]. The store of Ca^{2+} ions in the GA operated by SPCA1 is required by Ca^{2+}-dependent enzymes essential for post-translational modification of proteins in transit through the secretory pathway [106] as well as to recruit membrane-remodeling enzymes necessary to sort the cargo out of the GA [67]. Recently, an excellent study revealed increased levels of expression of the SPCA1 (both at the mRNA and protein levels) in enriched glucose diet, to mimic the hyperglycemia, suggesting a central role for SPCA1 in the etiology of diabetes mellitus-associated vascular disease, due to alterations in Ca^{2+} homeostasis within the GA of VSMCs cells [107]. Interestingly, the authors also evaluated the possibility of an increased activity of the SPCA1 that also increased the total number of Ca^{2+}-pumps. This supports previous observation of abnormal expression and/or activity of proteins that participate in Ca^{2+} signaling and homeostasis which were linked to diabetes. These include Ca^{2+}-dependent enzymes, such as calpain in rat endothelial cells [108] and CaMKII (Ca^{2+}/calmodulin-dependent protein kinase II) in rat whole carotid arteries [109]. In addition, it was shown that Ca^{2+} transporters

may be influenced by the diabetic state in vascular cells. Examples of these include the inhibition of store-operated Ca^{2+} channels in rat micro VSMCs [110] and increased activity of T-type Ca^{2+} channels in rat cardiomyocytes [111].

SPCA1 and Cancer

The level of the $[Ca^{2+}]_{cyt}$ control a variety of cellular processes relevant to tumorigenesis such as proliferation, migration, and apoptosis [112, 113]. Although cellular Ca^{2+} homeostasis is precisely controlled, there is an emerging appreciation that it is remodelled during cancer with downstream consequences on cellular function [114]. Deregulation of Ca^{2+} homeostasis may arise via changes in Ca^{2+}-transporting proteins such as channels and pumps whose expression can be up- or down-regulated in cancers [113]. Changes to the expression of these Ca^{2+} transporters may modulate global $[Ca^{2+}]_{cyt}$ and/or due to their location may alter the Ca^{2+} levels, in particular intracellular Ca^{2+} stores, *e.g.* the GA [112–114]. Interestingly, the effects of SPCA1 inhibition in MDA-MB-231 cells reside in altered regulation of Ca^{2+}-dependent enzymes located in the secretory pathway, such as proprotein convertases. Inhibition of SPCA1 produced a pronounced alteration in the processing of insulin-like growth factor receptor (IGF1R), with significantly reduced levels of functional IGF1R and accumulation of the inactive TGN pro-IGF1R form [115]. This finding associated a Ca^{2+} transporter with the basal-like breast cancer subtype, and highlighted the role for Ca^{2+} transporters as regulators for the processing of proteins important in tumor progression without major alterations in cytosolic Ca^{2+} signaling.

SPCA2

Unlike to ubiquitously expressed SPCA1, SPCA2 expression is restricted to the brain, testis, gastrointestinal and respiratory tracts, prostate, thyroid, salivary, and mammary glands [18, 104] and in principle could define a Ca^{2+}-ATPase pump activity with a specific physiological role in secretory cells. Recently, a new finding from the Rao lab [115] highlighted a new role for SPCA2, assuming a link between Ca^{2+} and cancer, and highlighted SPCA2 as a potentially new therapeutic target for certain breast cancers. They found that the Ca^{2+} levels rose dramatically in human breast cancer-derived cells where SPCA2 was up-regulated; their data showed that SPCA2 moves from its normal location inside cells (mostly the GA) to the PM, where it interacts with the Ca^{2+} channel Orai1, the pore subunit of the Ca^{2+} release-activated Ca^{2+} (also termed CRAC) channel [116]. Direct binding of the SPCA2 amino terminus to Orai1 enabled access of its carboxyl terminus to Orai1 and activation of Ca^{2+} influx [115]. SPCA2 activated the channels, essentially calling all Ca^{2+} into the cells. This signaling role was overriding its pumping and scavenging function by overwhelming the pump's ability to put away the Ca^{2+} and the net effect was an elevation of $[Ca^{2+}]_{cyt}$ [115].

Furthermore, support for SPCA2's role in regulating protein secretion come from the studies of milk secretion. Human milk is extremely high in Ca^{2+}, due in part to the action of SPCA2, which along with an elaborate network of other proteins, is turned on during lactation [117] and goes off when the breast feeding stops [118]. SPCA2's normal purpose is to signal Ca^{2+} channels to open and allow a large influx of Ca^{2+} into mammary tissue cells, to be packaged and pumped out in the milk [117, 119]. Furthermore, in cells taken from human breast tumors the *ATP2C2* gene, encoding for SPCA2 normally turned off (except during lactation), was on [117, 119]. When SPCA2 is mis-regulated breast cancer can form, probably because the lack of regulation of the pump/signaling mechanism allows vast and constant influxes of Ca^{2+} into the cells, which stimulates the cell cycle, and triggers high levels of cell proliferation.

Most recently, using a positional fine-mapping approach has been demonstrated an association between *ATP2C2* and *CMIP* genes and non-word repetition performance across two independent language-impaired populations [120]. Both genes are expressed in the brain and represent good candidates for language- and memory-related processes. In fact, Ca^{2+} homeostasis is important for the regulation of many neuronal processes, including working memory, synaptic plasticity, and neuronal motility [121], and Mn^{2+}-dysregulation has been linked to Parkinsonism (MIM #168,600), Alzheimer disease (MIM #104,300), and disordered memory [122]. These evidences make SPCA2 a potential candidate to be further investigated to better understand the evolution of neurological disorders.

Remarks and Conclusions

The role played by the GA as a key organelle involved in the Ca^{2+} signaling during intracellular trafficking has been recently highlighted [77, 123]. Here, more attention has been done highlighting recent evidences of Ca^{2+} homeostasis and the physiology of the GA, which has to be considered as another piece of the membrane trafficking puzzle. The recent discovery of the new family of the SPCA Ca^{2+} pumps specifically localized to the secretory pathway, mainly in the GA, shed new light on the role of Ca^{2+} as trigger of the cargo delivery throughout the GA. Fluctuation of the $[Ca^{2+}]_{cyt}$, more than the absolute $[Ca^{2+}]_{cyt}$, have a critical role in recruiting remodeling proteins of the Golgi membranes (e.g. cPLA2α) necessary to prepare the delivery of cargo protein from the *trans*-GA; furthermore, this membrane remodeling enzyme also seems to be important in the reorganization of the different compartments of GA, when cargo moves through the GA. As mentioned above (Sect. 4), the membranes need to be remodeled to prepare the departure of cargo from the GA, or simply to be reorganized during the passage of cargo through the GA itself. The analysis of the SPCA1 subcellular distribution along the secretory pathway reveals its presence on the lateral rims of the GA [81]; this peculiar distribution is indicative of a role in generating local release of Ca^{2+} in the proximity of this suborganellar

region where the membranes need to be remodeled before cargo departure, and subsequent reuptake of the Ca^{2+} allows the release of the *trans*-SNARE complex, to induce the fusion/fission events. If we combine these observations, we can have a clear view of the role of this new family of Ca^{2+} pumps mainly regarding the regulation of trafficking more than the GA homeostasis.

The newly proposed role for SPCA2 as a direct regulator of the extracellular protein release in specific secreting cells with its own redistribution on the PM, reveals a completely new role for Ca^{2+} pumps in regulating not only the level of $[Ca^{2+}]_{cyt}$ but also in turning on/off the activity and redistribution of this pump according to the physiological status of the cell/tissue [115]. This reflects the differential distribution of membrane components between different lipid phases that has been well documented for the PM. Microdomains enriched in sphingomyelin and cholesterol function as platforms to concentrate different molecules and assemble them into efficient signal transduction machineries, including processes involving Ca^{2+} signals. Indeed, many Ca^{2+} influx channels and their regulators have been found in lipid raft domains (e.g. GPCRs, G proteins, PLC, PIP2, IP3R, and store-operated Ca^{2+} entry channels). It was suggested that lipid rafts probably regulate these processes by controlling Ca^{2+} signaling [124–127]. More recently, rafts were shown to be components of membranes of the secretory pathway organelles; furthermore, sphingomyelin- and cholesterol-enriched domains form in the GA [128–130]. These micro-regions function as partitioning sites for specific post-GA trafficking by forming molecular assemblies separated from GA resident proteins [128, 131, 132]. SPCA1 associated with raft-like domains in the GA might contribute to its retention in the upstream compartments of the secretory pathway [133]. Likewise, the seemingly weaker association of SPCA2 with these membrane phases suggests SPCA2 has been observed also outside the GA in presumably post-GA compartments [134] and PM [115]. In addition, the raft association of GA resident Ca^{2+} pumps could generate local Ca^{2+} signals around the GA [39, 135, 136], eventually via association with other components of the Ca^{2+} signaling pathway. However, the cholesterol-rich environment is essential for the proper functioning of SPCA1, while SPCA2 appears to be less tightly associated with raft-like domains [133].

From this new scenario, it seems much more clear that both SPCAs have distinct roles in regulating the homeostasis of Ca^{2+} of the GA as well as maintaining the levels of the $[Ca^{2+}]_{cyt}$, fundamental for regulating cargo moving through and exiting from the GA (SPCA1), and the subsequent release via the PM (SPCA2). These recent discoveries open a new era of Ca^{2+} signaling in the secretory pathway, where the SPCAs are the main players, but ones with much more to reveal about their functions in the future which will contribute to a deeper understanding of cancer, genetic disease and other pathologies linked to the secretory dysfunction with altered Ca^{2+} physiology.

Acknowledgments The author thanks Dr. Joshua S. Mylne for proofreading of the manuscript, Dr. Parashuraman Seetharaman for discussion and critical reading, and Dr. Giada Giacchetti for assistance with manuscript preparation and artworks.

References

1. Golgi C (1898) Intorno alla struttura delle cellule nervose. Boll Soc Med Chir Pavia 13:3–16
2. Pelham HR, Rothman JE (2000) The debate about transport in the Golgi – two sides of the same coin? Cell 102:713–719
3. Emr S, Glick BS, Linstedt AD, Lippincott-Schwartz J, Luini A, Malhotra V, Marsh BJ, Nakano A, Pfeffer SR, Rabouille C, Rothman JE, Warren G, Wieland FT (2009) Journeys through the Golgi – taking stock in a new era. J Cell Biol 187:449–453
4. Glick BS, Nakano A (2009) Membrane traffic within the Golgi apparatus. Annu Rev Cell Dev Biol 25:113–132
5. Bonfanti L, Mironov AA Jr, Martinez-Menarguez JA, Martella O, Fusella A, Baldassarre M, Buccione R, Geuze HJ, Mironov AA, Luini A (1998) Procollagen traverses the Golgi stack without leaving the lumen of cisternae: evidence for cisternal maturation. Cell 95:993–1003
6. Marsh BJ, Volkmann N, McIntosh JR, Howell KE (2004) Direct continuities between cisternae at different levels of the Golgi complex in glucose-stimulated mouse islet beta cells. Proc Natl Acad Sci USA 101:5565–5570
7. Losev E, Reinke CA, Jellen J, Strongin DE, Bevis BJ, Glick BS (2006) Golgi maturation visualized in living yeast. Nature 441:1002–1006
8. Matsuura-Tokita K, Takeuchi M, Ichihara A, Mikuriya K, Nakano A (2006) Live imaging of yeast Golgi cisternal maturation. Nature 441:1007–1010
9. Rivera-Molina FE, Novick PJ (2009) A Rab GAP cascade defines the boundary between two Rab GTPases on the secretory pathway. Proc Natl Acad Sci USA 106:14408–14413
10. Pfeffer SR (2010) How the Golgi works: a cisternal progenitor model. Proc Natl Acad Sci USA 107:19614–19618
11. Hong W (2005) SNAREs and traffic. Biochim Biophys Acta 1744:493–517
12. Jena BP (2009) Membrane fusion: role of SNAREs and calcium. Protein Pept Lett 16:712–717
13. Jeremic A, Kelly M, Cho JA, Cho SJ, Horber JK, Jena BP (2004) Calcium drives fusion of SNARE-apposed bilayers. Cell Biol Int 28:19–31
14. Micaroni M, Perinetti G, Di Giandomenico D, Bianchi K, Spaar A, Mironov AA (2010) Synchronous intra-Golgi transport induces the release of Ca^{2+} from the Golgi apparatus. Exp Cell Res 316:2071–2086
15. Montero M, Brini M, Marsault R, Alvarez J, Sitia R, Pozzan T, Rizzuto R (1995) Monitoring dynamic changes in free Ca2+ concentration in the endoplasmic reticulum of intact cells. EMBO J 14:5467–5475
16. Pinton P, Pozzan T, Rizzuto R (1998) The Golgi apparatus is an inositol 1,4,5-trisphosphate-sensitive Ca2+ store, with functional properties distinct from those of the endoplasmic reticulum. EMBO J 17:5298–5308
17. Berridge MJ (2002) The endoplasmic reticulum: a multifunctional signaling organelle. Cell Calcium 32:235–249
18. Missiaen L, Dode L, Vanoevelen J, Raeymaekers L, Wuytack F (2007) Calcium in the Golgi apparatus. Cell Calcium 41:405–416
19. Roseman S (2001) Reflections on glycobiology. J Biol Chem 276:41527–41542
20. Hu Z, Bonifas JM, Beech J, Bench G, Shigihara T, Ogawa H, Ikeda S, Mauro T, Epstein EH Jr (2000) Mutations in ATP2C1, encoding a calcium pump, cause Hailey-Hailey disease. Nat Genet 24:61–65
21. Callewaert G, Parys JB, De Smedt H, Raeymaekers L, Wuytack F, Vanoevelen J, Van Baelen K, Simoni A, Rizzuto R, Missiaen L (2003) Similar Ca(2+)-signaling properties in keratinocytes and in COS-1 cells overexpressing the secretory-pathway Ca(2+)-ATPase SPCA1. Cell Calcium 34:157–162
22. Ward DT (2004) Calcium receptor-mediated intracellular signalling. Cell Calcium 35:217–228
23. Tu CL, Chang W, Bikle DD (2007) The role of the calcium sensing receptor in regulating intracellular calcium handling in human epidermal keratinocytes. J Invest Dermatol 127: 1074–1083

24. Chen JL, Ahluwalia JP, Stamnes M (2002) Selective effects of calcium chelators on anterograde retrograde protein transport in the cell. J Biol Chem 277:35682–35687
25. Mayorga LS, Colombo MI, Lennartz M, Brown EJ, Rahman KH, Weiss R, Lennon PJ, Stahl PD (1993) Inhibition of endosome fusion by phospholipase A2 (PLA2) inhibitors points to a role for PLA2 in endocytosis. Proc Natl Acad Sci USA 90:10255–10259
26. Peters C, Mayer A (1998) Ca2+/calmodulin signals the completion of docking and triggers a late step of vacuole fusion. Nature 396:575–580
27. Pryor PR, Mullock BM, Bright NA, Gray SR, Luzio JP (2000) The role of intraorganellar Ca(2+) in late endosome–lysosome heterotypic fusion in the reformation of lysosomes from hybrid organelles. J Cell Biol 149:1053–1062
28. Beckers CJ, Balch WE (1989) Calcium and GTP: essential components in vesicular trafficking between the endoplasmic reticulum and Golgi apparatus. J Cell Biol 108:1245–1256
29. Porat A, Elazar Z (2000) Regulation of intra-Golgi membrane transport by calcium. J Biol Chem 275:29233–29237
30. Scherer PE, Lederkremer GZ, Williams S, Fogliano M, Baldini G, Lodish HF (1996) Cab45, a novel (Ca2+)-binding protein localized to the Golgi lumen. J Cell Biol 133:257–268
31. Lin P, Yao Y, Hofmeister R, Tsien RY, Farquhar MG (1999) Overexpression of CALNUC (nucleobindin) increases agonist and thapsigargin releasable Ca2+ storage in the Golgi. J Cell Biol 145:279–289
32. Kawano J, Kotani T, Ogata Y, Ohtaki S, Takechi S, Nakayama T, Sawaguchi A, Nagaike R, Oinuma T, Suganuma T (2000) CALNUC (nucleobindin) is localized in the Golgi apparatus in insect cells. Eur J Cell Biol 79:208–217
33. Morel-Huaux VM, Pypaert M, Wouters S, Tartakoff AM, Jurgan U, Gevaert K, Courtoy PJ (2002) The calcium-binding protein p54/NEFA is a novel luminal resident of medial Golgi cisternae that traffics independently of mannosidase II. Eur J Cell Biol 81:87–100
34. Haynes LP, Tepikin AV, Burgoyne RD (2004) Calcium-binding protein 1 is an inhibitor of agonist-evoked, inositol 1,4,5-trisphosphate-mediated calcium signaling. J Biol Chem 279: 547–555
35. Haynes LP, Fitzgerald DJ, Wareing B, O'Callaghan DW, Morgan A, Burgoyne RD (2006) Analysis of the interacting partners of the neuronal calcium-binding proteins L-CaBP1, hippocalcin, NCS-1 and neurocalcin delta. Proteomics 6:1822–1832
36. Haynes LP, Thomas GM, Burgoyne RD (2005) Interaction of neuronal calcium sensor-1 and ADP-ribosylation factor 1 allows bidirectional control of phosphatidylinositol 4-kinase beta trans-Golgi network-plasma membrane traffic. J Biol Chem 280:6047–6054
37. Hata S, Koyama S, Kawahara H, Doi N, Maeda T, Toyama-Sorimachi N, Abe K, Suzuki K, Sorimachi H (2006) Stomach-specific calpain, nCL-2, localizes in mucus cells and proteolyzes the beta-subunit of coatomer complex, beta-COP. J Biol Chem 281:11214–11224
38. O'Callaghan DW, Ivings L, Weiss JL, Ashby MC, Tepikin AV, Burgoyne RD (2002) Differential use of myristoyl groups on neuronal calcium sensor proteins as a determinant of spatio-temporal aspects of Ca^{2+} signal transduction. J Biol Chem 277:14227–14237
39. Bivona TG, Perez-De Castro I, Ahearn IM, Grana TM, Chiu VK, Lockyer PJ, Cullen PJ, Pellicer A, Cox AD, Philips MR (2003) Phospholipase Cgamma activates Ras on the Golgi apparatus by means of RasGRP1. Nature 424:694–698
40. Evans JH, Leslie CC (2004) The cytosolic phospholipase A2 catalytic domain modulates association and residence time at Golgi membranes. J Biol Chem 279:6005–6016
41. Lopez-Alcala C, Alvarez-Moya B, Villalonga P, Calvo M, Bachs O, Agell N (2008) Identification of essential interacting elements in K-Ras/Calmodulin binding and its role in K-Ras localization. J Biol Chem 283:10621–10631
42. Noguchi H, Kobayashi M, Miwa N, Takamatsu K (2007) Lack of hippocalcin causes impairment in Ras/extracellular signal-regulated kinase cascade via a Raf-mediated activation process. J Neurosci Res 85:837–884
43. Rodriguez-Viciana P, Sabatier C, McCormick F (2004) Signaling specificity by Ras family GTPases is determined by the full spectrum of effectors they regulate. Mol Cell Biol 24:4943–4954

44. Rodriguez-Viciana P, McCormick F (2005) RalGDS comes of age. Cancer Cell 7:205–206
45. Quatela SE, Philips MR (2006) Ras signaling on the Golgi. Curr Opin Cell Biol 18:162–167
46. Chiu VK, Bivona T, Hach A, Sajous JB, Silletti J, Wiener H, Johnson RL 2nd, Cox AD, Philips MR (2002) Ras signalling on the endoplasmic reticulum and the Golgi. Nat Cell Biol 4:343–350
47. Michaelson D, Ahearn I, Bergo M, Young S, Philips M (2002) Membrane trafficking of heterotrimeric G proteins via the endoplasmic reticulum and Golgi. Mol Biol Cell 13:3294–3302
48. Bivona TG, Philips MR (2003) Ras pathway signaling on endomembranes. Curr Opin Cell Biol 15:136–142
49. Bonifacino JS, Glick BS (2004) The mechanisms of vesicle budding and fusion. Cell 116:153–166
50. Sollner T, Whiteheart SW, Brunner M, Erdjument-Bromage H, Geromanos S, Tempst P, Rothman JE (1993) SNAP receptors implicated in vesicle targeting and fusion. Nature 362:318–324
51. Fukuda R, McNew JA, Weber T, Parlati F, Engel T, Nickel W, Rothman JE, Sollner TH (2000) Functional architecture of an intracellular membrane t-SNARE. Nature 407:198–202
52. Weber T, Zemelman BV, McNew JA, Westermann B, Gmachl M, Parlati F, Sollner TH, Rothman JE (1998) SNAREpins: minimal machinery for membrane fusion. Cell 92:759–772
53. Antonin W, Fasshauer D, Becker S, Jahn R, Schneider TR (2002) Crystal structure of the endosomal SNARE complex reveals common structural principles of all SNAREs. Nat Struct Biol 9:107–111
54. Sutton RB, Fasshauer D, Jahn R, Brunger AT (1998) Crystal structure of a SNARE complex involved in synaptic exocytosis at 2.4 A resolution. Nature 395:347–353
55. Fasshauer D (2003) Structural insights into the SNARE mechanism. Biochim Biophys Acta 1641:87–97
56. Brose N, Hofmann K, Hata Y, Sudhof TC (1995) Mammalian homologues of Caenorhabditis elegans Munc-13 gene define novel family of C2-domain proteins. J Biol Chem 270: 25273–25280
57. Sudhof TC (2004) The synaptic vesicle cycle. Annu Rev Neurosci 27:509–547
58. Sudhof TC (2002) Synaptotagmins: why so many? J Biol Chem 277:7629–7632
59. Geppert M, Goda Y, Hammer RE, Li C, Rosahl TW, Stevens CF, Sudhof TC (1994) Synaptotagmin I: a major Ca2+ sensor for transmitter release at a central synapse. Cell 79:717–727
60. Fernandez-Chacon R, Konigstorfer A, Gerber SH, Garcia J, Matos MF, Stevens CF, Brose N, Rizo J, Rosenmund C, Sudhof TC (2001) Synaptotagmin I functions as a calcium regulator of release probability. Nature 410:41–49
61. Bai J, Chapman ER (2004) The C2 domains of synaptotagmin – partners in exocytosis. Trends Biochem Sci 29:143–151
62. Bai J, Tucker WC, Chapman ER (2004) PIP2 increases the speed of response of synaptotagmin and steers its membrane-penetration activity toward the plasma membrane. Nat Struct Mol Biol 11:36–44
63. Zhang X, Kim-Miller MJ, Fukuda M, Kowalchyk JA, Martin TF (2002) Ca2+-dependent synaptotagmin binding to SNAP-25 is essential for Ca2+-triggered exocytosis. Neuron 34:599–611
64. Tucker WC, Weber T, Chapman ER (2004) Reconstitution of Ca2+-regulated membrane fusion by synaptotagmin and SNAREs. Science 304:435–438
65. Brown WJ, Chambers K, Doody A (2003) Phospholipase A_2 (PLA_2) enzymes in membrane trafficking: mediators of membrane shape and function. Traffic 4:214–221
66. Six DA, Dennis EA (2000) The expanding superfamily of phospholipase A(2) enzymes: classification and characterization. Biochim Biophys Acta 1488:1–19
67. San Pietro E, Capestrano M, Polishchuk EV, Di Pentima A, Trucco A, Zizza P, Mariggio' S, Pulvirenti T, Sallese M, Tete' S, Mironov AA, Leslie CC, Corda D, Luini A, Polishchuk RS

(2009) Group IV phospholipase A(2)alpha controls the formation of inter-cisternal continuities involved in intra-Golgi transport. PLoS Biol 7:e1000194
68. Bezprozvanny I, Scheller RH, Tsien RW (1995) Functional impact of syntaxin on gating of N-type and Q-type calcium channels. Nature 378:623–626
69. Schekman R (1998) Membrane fusion. Ready…aim…fire! Nature 396:514–515
70. Ghosh M, Tucker DE, Burchett SA, Leslie CC (2006) Properties of the Group IV phospholipase A2 family. Prog Lipid Res 45:487–510
71. Lippincott-Schwartz J, Snapp E, Kenworthy A (2001) Studying protein dynamics in living cells. Nat Rev Mol Cell Biol 2:444–456
72. de Figueiredo P, Drecktrah D, Polizotto RS, Cole NB, Lippincott-Schwartz J, Brown WJ (2000) Phospholipase A2 antagonists inhibit constitutive retrograde membrane traffic to the endoplasmic reticulum. Traffic 1:504–511
73. Polizotto RS, de Figueiredo P, Brown WJ (1999) Stimulation of Golgi membrane tubulation and retrograde trafficking to the ER by phospholipase A(2) activating protein (PLAP) peptide. J Cell Biochem 74:670–683
74. de Figueiredo P, Drecktrah D, Katzenellenbogen JA, Strang M, Brown WJ (1998) Evidence that phospholipase A2 activity is required for Golgi complex and trans Golgi network membrane tubulation. Proc Natl Acad Sci USA 95:8642–8647
75. de Figueiredo P, Doody A, Polizotto RS, Drecktrah D, Wood S, Banta M, Strang MS, Brown WJ (2001) Inhibition of transferrin recycling and endosome tubulation by phospholipase A2 antagonists. J Biol Chem 276:47361–47370
76. de Figueiredo P, Polizotto RS, Drecktrah D, Brown WJ (1999) Membrane tubule-mediated reassembly and maintenance of the Golgi complex is disrupted by phospholipase A2 antagonists. Mol Biol Cell 10:1763–1782
77. Micaroni M (2010) The role of calcium in intracellular trafficking. Curr Mol Med 10:763–773
78. Gunteski-Hamblin AG, Clarke DM, Shull GE (1992) Molecular cloning and tissue distribution of alternatively spliced mRNAs encoding possible mammalian homologs of the yeast secretory pathway calcium pump. Biochemistry 31:7600–7608
79. Park CS, Kim JY, Crispino C, Chang CC, Ryu DD (1998) Molecular cloning of YIPMR1, a S. cerevisiae PMR1 homologue encoding a novel P-type secretory pathway Ca2+-ATPase, in the yeast Yarrowia lipolytica. Gene 206:107–116
80. Behne MJ, Tu CL, Aronchik I, Epstein E, Bench G, Bikle DD, Pozzan T, Mauro TM (2003) Human keratinocyte ATP2C1 localizes to the Golgi and controls Golgi Ca^{2+} stores. J Invest Dermatol 121:688–694
81. Micaroni M, Perinetti G, Berrie CP, Mironov AA (2010) The SPCA1 Ca^{2+} pump and intracellular membrane trafficking. Traffic 11:1315–1333
82. Fairclough RJ, Dode L, Vanoevelen J, Andersen JP, Missiaen L, Raeymaekers L, Wuytack F, Hovnanian A (2003) Effect of Hailey-Hailey disease mutations on the function of a new variant of human secretory pathway Ca2+/Mn2+-ATPase (hSPCA1). J Biol Chem 278: 24721–24730
83. Van Baelen K, Vanoevelen J, Callewaert G, Parys JB, De Smedt H, Raeymaekers L, Rizzuto R, Missiaen L, Wuytack F (2003) The contribution of the SPCA1 Ca2+ pump to the Ca2+ accumulation in the Golgi apparatus of HeLa cells assessed via RNA-mediated interference. Biochem Biophys Res Commun 306:430–436
84. Sepulveda RM, Vanoevelen J, Raeymakers L, Mata AM, Wuytack F (2009) Silencing the SPCA1 (Secretory Pathway Ca^{2+}-ATPase isoform 1) impairs Ca^{2+} homeostasis in the Golgi and disturbs neural polarity. J Neurosci 29:12174–12182
85. Mitchell KJ, Tsuboi T, Rutter GA (2004) Role for plasma membrane-related Ca^{2+}-ATPase-1 (ATP2C1) in pancreatic beta-cell Ca^{2+} homeostasis revealed by RNA silencing. Diabetes 53:393–400
86. Okunade GW, Miller ML, Azhar M, Andringa A, Sanford LP, Doetschman T et al (2007) Loss of the ATP2C1 secretory pathway Ca(2+)-ATPase (SPCA1) in mice causes Golgi stress, apoptosis, and mid-gestational death in homozygous embryos and squamous cell tumours in adult heterozygotes. J Biol Chem 282:26517–26527

87. Lissandron V, Podini P, Pizzo P, Pozzan T (2010) Unique characteristics of Ca2+ homeostasis of the trans-Golgi compartment. Proc Natl Acad Sci USA 107:9198–9203
88. Pizzo P, Lissandron V, Pozzan T (2010) The trans-Golgi compartment: a new distinct intracellular Ca^{2+} store. Commun Integr Biol 3:462–464
89. Mishiro E, Liu MY, Sakakibara Y, Suiko M, Liu MC (2004) Zebrafish tyrosylprotein sulfotransferase: molecular cloning, expression, and functional characterization. Biochem Cell Biol 82:295–303
90. Seko A, Sumiya J, Yamashita K (2005) Porcine, mouse and human galactose 3-O-sulphotransferase-2 enzymes have different substrate specificities; the porcine enzyme requires basic compounds for its catalytic activity. Biochem J 391:77–85
91. Anderson ED, VanSlyke JK, Thulin CD, Jean F, Thomas G (1997) Activation of the furin endoprotease is a multiple-step process: requirements for acidification and internal propeptide cleavage. EMBO J 16:1508–1518
92. LaFerla FM (2002) Calcium dyshomeostasis and intracellular signalling in Alzheimer's disease. Nat Rev Neurosci 3:862–872
93. Ramos-Castaneda J, Park YN, Liu M, Hauser K, Rudolph H, Shull GE, Jonkman MF, Mori K, Ikeda S, Ogawa H, Arvan P (2005) Deficiency of ATP2C1, a Golgi ion pump, induces secretory pathway defects in endoplasmic reticulum (ER)-associated degradation and sensitivity to ER stress. J Biol Chem 280:9467–9473
94. Leitch S, Feng M, Muend S, Braiterman LT, Hubbard AL, Rao R (2011) Vesicular distribution of secretory pathway Ca^{2+}-ATPase isoform 1 and a role in manganese detoxification in liver-derived polarized cells. Biometals 24:159–170
95. Harris A, Burge SM, Dykes PJ, Finlay AY (1996) Handicap in Darier's disease and Hailey-Hailey disease. Br J Dermatol 135:959–963
96. Chun SI, Wang KC, Su WP (1988) Squamous cell carcinoma arising in Hailey-Hailey disease. J Cutan Pathol 15:234–237
97. Sudbrak R, Brown J, Dobson-Stone C, Carter S, Ramser J, White J, Healy E, Dissanayake M, Larregue M, Perrussel M, Lehrach H, Munro CS, Strachan T, Burge S, Hovnanian A, Monaco AP (2000) Hailey-Hailey disease is caused by mutation in ATP2C1 encoding a novel Ca(2+) pump. Hum Mol Genet 9:1131–1140
98. Micaroni M, Mironov AA (2010) Roles of Ca^{2+} and secretory pathway Ca^{2+}-ATPase pump type 1 (SPCA1) in intra-Golgi transport. Commun Integr Biol 3:504–507
99. Tian H, Yan X, Liu H, Yu Y, Zhang F (2010) Six novel mutations identified in Chinese patients with Hailey-Hailey disease. J Dermatol Sci 58:80–82
100. Lipoff JB, Mudgil AV, Young S, Chu P, Cohen SR (2009) Acantholytic dermatosis of the crural folds with APT2C1mutation is a possible variant of Hailey-Hailey disease. J Cutan Med Surg 13:151–154
101. Vasioukhin V, Bauer C, Yin M, Fuchs E (2000) Directed actin polymerization is the driving force for epithelial cell-cell adhesion. Cell 100:209–219
102. Missiaen L, Raeymakers L, Dode L, Vanoevelen J, Van Baelen K, Parys JB, Callewaert G, De Smedt H, Segaert S, Wuytack F (2004) SPCA1 pumps and Hailey-Hailey disease. Biochem Biophys Res Commun 322:1204–1213
103. Wootton LL, Argent CCH, Wheatley M, Michelangeli F (2004) The expression, activity and localization of the secretory pathway Ca^{2+}-ATPase (SPCA1) in different mammalian tissues. Biochim Biophys Acta 1664:189–197
104. Vanoevelen J, Dode L, Van Baelen K, Fairclough RJ, Missiaen L, Raeymaekers L, Wuytack F (2005) The secretory pathway Ca^{2+}/Mn^{2+}-ATPase 2 is Golgi-localized pump with high affinity for Ca^{2+} ions. J Biol Chem 280:22800–22808
105. Thyberg J (1998) Tyrphostin A9 and wortmannin perturb the Golgi complex and block proliferation of vascular smooth muscle cells. Eur J Cell Biol 76:33–42
106. Shahbazi S, Lenting PJ, Fribourg C, Terraube V, Denis CV, Christophe OD (2007) Characterization of the interaction between von Willebrand factor and osteoprotegerin. J Thromb Haemost 5:1956–1962

107. Lai P, Michelangeli F (2009) Changes in expression and activity of the secretory pathway Ca^{2+} APTase 1 (SPCA1) in A7r5 vascular smooth muscle cells cultured at different glucose concentrations. Biosci Rep 29:397–404
108. Stalker TJ, Gong Y, Scalia R (2005) The calcium-dependent protease calpain causes endothelial dysfunction in type 2 diabetes. Diabetes 54:1132–1140
109. Yousif MH, Akhtar S, Walther T, Benter IF (2008) Role of Ca2+/calmodulin-dependent protein kinase II in development of vascular dysfunction in diabetic rats with hypertension. Cell Biochem Funct 26:256–263
110. Curtis TM, Major EH, Trimble ER, Scholfield CN (2003) Diabetes-induced activation of protein kinase C inhibits store-operated Ca^{2+} uptake in rat retinal microvascular smooth muscle. Diabetologia 46:1252–1259
111. Li M, Zhang M, Huang LP, Zhou J, Zhuang H, Taylor JT, Keyser BM, Whitehurst RM Jr (2005) T-type Ca^{2+} channels are involved in high glucose-induced rat neonatal cardiomyocyte proliferation. Pediatr Res 57:550–556
112. Berridge MJ, Bootman MD, Roderick HL (2003) Calcium signalling: dynamics, homeostasis and remodelling. Nat Rev Mol Cell Biol 4:517–529
113. Monteith GR, McAndrew D, Faddy HM, Roberts-Thomson SJ (2007) Calcium and cancer: targeting Ca2+ transport. Nat Rev Cancer 7:519–530
114. Roderick HL, Cook SJ (2008) Ca2+ signalling checkpoints in cancer: remodelling Ca2+ for cancer cell proliferation and survival. Nat Rev Cancer 8:361–375
115. Feng M, Grice DM, Faddy HM, Nguyen N, Leitch S, Wang Y, Muend S, Kenny PA, Sukumar S, Roberts-Thomson SJ, Monteith GR, Rao R (2010) Store-independent activation of Orai1 by SPCA2 in mammary tumors. Cell 143:84–98
116. Cahalan MD, Zhang SL, Yeromin AV, Ohlsen K, Roos J (2007) Stauderman KA Molecular basis of the CRAC channel. Cell Calcium 42:133–144
117. Anantamongkol U, Takemura H, Suthiphongchai T, Krishnamra N, Horio Y (2007) Regulation of Ca2+ mobilization by prolactin in mammary gland cells: possible role of secretory pathway Ca2+-ATPase type 2. Biochem Biophys Res Commun 352:537–542
118. Reinhardt TA, Lippolis JD (2009) Mammary gland involution is associated with rapid down regulation of major mammary Ca2+-ATPases. Biochem Biophys Res Commun 378: 99–102
119. Faddy HM, Smart CE, Xu R, Lee GY, Kenny PA, Feng M, Rao R, Brown MA, Bissell MJ, Roberts-Thomson SJ, Monteith GR (2008) Localization of plasma membrane and secretory calcium pumps in the mammary gland. Biochem Biophys Res Commun 369:977–981
120. Newbury DF, Winchester L, Addis L, Paracchini S, Buckingham LL, Clark A, Cohen W, Cowie H, Dworzynski K, Everitt A, Goodyer IM, Hennessy E, Kindley AD, Miller LL, Nasir J, O'Hare A, Shaw D, Simkin Z, Simonoff E, Slonims V, Watson J, Ragoussis J, Fisher SE, Seckl JR, Helms PJ, Bolton PF, Pickles A, Conti-Ramsden G, Baird G, Bishop DV, Monaco AP (2009) CMIP and ATP2C2 modulate phonological short-term memory in language impairment. Am J Hum Genet 85:264–272
121. Zheng JQ, Poo MM (2007) Calcium signaling in neuronal motility. Annu Rev Cell Dev Biol 23:375–404
122. Normandin L, Hazell AS (2002) Manganese neurotoxicity: an update of pathophysiologic mechanisms. Metab Brain Dis 17:375–387
123. Pizzo P, Lissandron V, Capitanio P, Pozzan T (2011) Ca(2+) signalling in the Golgi apparatus. Cell Calcium 50:184–192
124. Isshiki M, Anderson RG (1999) Calcium signal transduction from caveolae. Cell Calcium 26:201–208
125. Brown DA, London E (2000) Structure and function of sphingolipid- and cholesterol-rich membrane rafts. J Biol Chem 275:17221–17224
126. Simons K, Toomre D (2000) Lipid rafts and signal transduction. Nat Rev Mol Cell Biol 1:31–39
127. Pani B, Singh BB (2009) Lipid rafts/caveolae as microdomains of calcium signaling. Cell Calcium 45:625–633

128. Bagnat M, Kernen S, Shevchenko A, Shevchenko A, Simons K (2000) Lipid rafts function in biosynthetic delivery of proteins to the cell surface in yeast. Proc Natl Acad Sci USA 97:3254–3259
129. Heino S, Lusa S, Somerharju P, Ehnholm C, Olkkonen VM, Ikonen E (2000) Dissecting the role of the Golgi complex and lipid rafts in biosynthetic transport of cholesterol to the cell surface. Proc Natl Acad Sci USA 97:8375–8380
130. Simons K, Ehehalt R (2002) Cholesterol, lipid rafts, and disease. J Clin Invest 110:597–603
131. Hirschberg K, Miller CM, Ellenberg J, Presley JF, Siggia ED, Phair RD, Lippincott-Schwartz J (1998) Kinetic analysis of secretory protein traffic and characterization of Golgi to plasma membrane transport intermediates in living cells. J Cell Biol 143:1485–1503
132. Patterson GH, Hirschberg K, Polishchuk RS, Gerlich D, Phair RD, Lippincott-Schwartz J (2008) Transport through the Golgi apparatus by rapid partitioning within a two-phase membrane system. Cell 133:1055–1067
133. Baron S, Vangheluwe P, Sepulveda MR, Wuytack F, Raeymakers L, Vanoevelen J (2010) The secretory pathway Ca^{2+}-ATPase 1 is associated with cholesterol-rich microdomains of human colon adenocarcinoma cells. Biochim Biophys Acta 1798:1512–1521
134. Xiang M, Mohamalawari D, Rao R (2005) A novel isoform of the secretory pathway Ca2+, Mn2+-ATPase, hSPCA2, has unusual properties and is expressed in the brain. J Biol Chem 280:11608–11614
135. Dolman NJ, Tepikin AV (2006) Calcium gradients and the Golgi. Cell Calcium 40:505–512
136. Baron S, Struyf S, Wuytack F, Van Damme J, Missiaen L, Raeymaekers L, Vanoevelen J (2009) Contribution of intracellular Ca2+ stores to Ca2+ signaling during chemokinesis of human neutrophil granulocytes. Biochim Biophys Acta 1793:1041–1049
137. Grice DM, Vetter I, Faddy HM, Kenny PA, Roberts-Thomson SJ, Monteith GR (2010) Golgi calcium pump secretory pathway calcium ATPase 1 (SPCA1) is a key regulator of insulin-like growth factor receptor (IGF1R) processing in the basal-like breast cancer cell line MDA-MB-231. J Biol Chem 285:37458–37466
138. Mitchell KJ, Pinton P, Varadi A, Tacchetti C, Ainscow EK, Pozzan T, Rizzuto R, Rutter GA (2001) Dense core secretory vesicles revealed as a dynamic Ca(2+) store in neuroendocrine cells with a vesicle-associated membrane protein aequorin chimaera. J Cell Biol 155:41–51
139. Meldolesi J, Pozzan T (1998) The endoplasmic reticulum Ca2+ store: a view from the lumen. Trends Biochem Sci 23:10–14

Chapter 19
Calcium Binding Proteins

Matilde Yáñez, José Gil-Longo, and Manuel Campos-Toimil

Abstract The role of Ca^{2+} as a key and pivotal second messenger in cells depends largely on a wide number of heterogeneous so-called calcium binding proteins (CBP), which have the ability to bind this ion in specific domains. CBP contribute to the control of Ca^{2+} concentration in the cytosol and participate in numerous cellular functions by acting as Ca^{2+} transporters across cell membranes or as Ca^{2+}-modulated sensors, i.e., decoding Ca^{2+} signals. In this chapter we review the main Ca^{2+}-modulated CBP, starting with those intracellular CBP that contain the structural EF-hand domain: parvalbumin, calmodulin, S100 proteins and calcineurin. Then, we address intracellular CBP lacking the EF-hand domain: CBP within intracellular Ca^{2+} stores (paying special attention to calreticulin and calsequestrin), annexins and proteins that contain a C2 domain, such as protein kinase C (PKC) or sinaptotagmin. Finally, extracellular CBP have been classified in six groups, according to their Ca^{2+} binding structures: (i) EF-hand domains; (ii) EGF-like domains; (iii) γ-carboxyl glutamic acid (GLA)-rich domains; (iv) cadherin domains; (v) Ca^{2+}-dependent (C)-type lectin-like domains; (vi) Ca^{2+}-binding pockets of family C G-protein-coupled receptors. For all proteins, we briefly review their structure, location and function and additionally their potential as pharmacological targets in several human diseases.

Keywords Ca^{2+} binding proteins • EF-hand domain • Ca^{2+} sensors

M. Yáñez • J. Gil-Longo • M. Campos-Toimil (✉)
Departamento de Farmacoloxía. Facultade de Farmacia, Universidade de Santiago de Compostela, Campus Vida, E-15782, Santiago de Compostela, Spain
e-mail: manuel.campos@usc.es

M.S. Islam (ed.), *Calcium Signaling*, Advances in Experimental Medicine and Biology 740, DOI 10.1007/978-94-007-2888-2_19,

Introduction

Ca^{2+} binding proteins (CBP) are a heterogeneous and wide group of proteins that participate in numerous cellular functions (e.g. Ca^{2+} homeostasis and Ca^{2+} signaling pathways), thus regulating animal and plant cell function. Although they have different structures and properties, most CBP selectively and reversibly bind Ca^{2+} in specific domains, the kinetics of this interaction being very fast. It has been suggested by Carafoli et al. [1] that CBP could be subdivided into two categories: membrane-intrinsic CBP that modulate Ca^{2+} concentration in the environment by transporting it across cell membranes and Ca^{2+}-modulated proteins. This last group includes proteins that not only contribute to the control of Ca^{2+} concentration, but also to decode Ca^{2+} signals, acting as Ca^{2+} sensors. According to this classification, in this chapter we have briefly reviewed the main Ca^{2+}-modulated CBP, focussing on their respective structures, location and functions and, in some cases, on their potential role as therapeutic targets in several pathologies [1, 2]. Ca^{2+} transporters and channels have been reviewed in other chapters of this book.

We have divided this chapter into three main sections. The first section deals with intracellular CBP presenting EF-hand domains. This domain is found in a large family of proteins that includes some of the most important and ubiquitous CBP, such as calmodulin, troponin C or calcineurin. The second section presents the intracellular CBP lacking EF-hand domains. Here, we have included some of the most important CBP within cell organelles, such as calsequestrin and calreticulin, the large family of proteins called annexins and some of the proteins that share a Ca^{2+}-binding domain called C2, such as PKC or synaptotagmin. In the last section, we have reviewed the main extracellular CBP (ECBP), grouping them according to their Ca^{2+} binding structures.

Intracellular Ca^{2+} Binding Proteins with EF-Hand Domains

The term EF-hand was coined in 1973 as a graphical description of the calcium-binding domain observed in parvalbumin [3]. It is descriptive not only of the polypeptide fold, but also of the potential motion that the binding of calcium can induce.

The classical EF-hand is a helix-loop-helix motif characterized by a sequence of, usually, 12 residues flanked with two alpha helices positioned perpendicular to one another in a spatial arrangement that mimicks the spread thumb and the index finger of a human hand. The loop integrated in this sequence can accommodate Ca^{2+} or Mg^{2+} with distinct geometries and the affinity for these ions is a determining factor for the function of the protein (Fig. 19.1) [4].

Commonly, EF-hand motifs occur in adjacent pairs. The minimal domain, with two motifs separated by a flexible linker, can be found in parvalbumin and the S100 subfamily. Calmodulin and troponin C both have four EF-hand motifs. One exception to the rule of EF-hand pairing is calpain, which has five EF-hand motifs in the

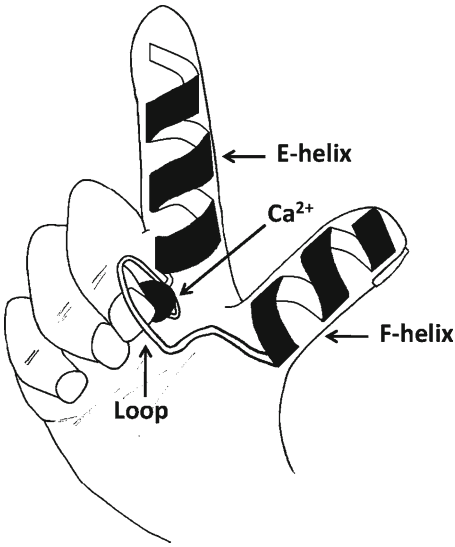

Fig. 19.1 Illustrative representation of the EF-hand motif

C-terminal part of its large subunit. However, these motifs are coupled with a small subunit composed of another five EF-hand motifs forming a heterodimer [4].

About 30 residues form the canonical sequence of the EF-hand domain, which appears in small proteins (e.g. calmodulin or S100), but also in much larger complex proteins (e.g. myosin or calpain). The sequence has also been identified in proteins in which it was not really expected, such as cholinesterases and neuroligins [5], the oncogenic protein MDM2 [6] and *Escherichia coli* lytic transglycosidase Slt35 [7].

This structural motif has been found in a large number of protein families: more than 66 subfamilies are known [8], possessing diverse functions that include calcium buffering in the cytosol, signal transduction between cellular compartments [9] and muscle contraction [10].

Parvalbumin Family Proteins

The parvalbumin family of Ca^{2+} binding proteins plays a pivotal role in the cell by keeping a check on calcium switching [11]. Parvalbumin was the first Ca^{2+} binding protein to have its amino acid sequence and atomic 3D-structure resolved [3], although Deuticke first reported its occurrence in the skeletal muscle fibers of fishes and amphibians [12]. Due to its low molecular weight (12 kDa) and high solubility in water, it was called parvalbumin (*parvus* is Latin for small), although it has no functional resemblance with serum albumin [13].

Two isoforms, alpha and beta parvalbumin, exist in vertebrates on the basis of isoelectric point and lineage-specific sequence differences. Beta parvalbumin is also

called oncomodulin as it was first found in tumour tissues. Parvalbumin contains three homologous EF-hand motifs, but only the two located at the C-terminal region are able to bind calcium with high affinity [14].

In general, the proteins of the parvalbumin family are highly water-soluble and have an isoelectric point between 4.1 and 5.2 and they are believed to function primarily as cytosolic calcium buffers [15]. They are associated with several calcium mediated cellular activities and physiological processes. It has been suggested that parvalbumin facilitates the relaxation process in fast-contracting muscles by shuttling calcium from troponin C to the sarcoplasmic reticulum [16]. But parvalbumins are also present in non-muscle tissues like bone, teeth, skin, brain, prostate, seminal vesicles, testes and ovaries, and play such different functional roles as chemotactic ligands, endocrine regulation and renal transport of NaCl [11]. It has been observed that parvalbumin deficiency alters neuronal activity, because parvalbumin-expressing interneurons contribute to its maintenance and synchronize cortical neurons through GABAergic synapses [17].

Calmodulin Family Proteins

The calmodulin family is very large and has been extensively characterized amongst the EF-hand Ca^{2+} sensor proteins. This subfamily of CBP is called CTER, an acronym composed from the first character of four of their most representative members: calmodulin, troponin C and essential and regulatory myosin light chains. Much of what is known today regarding the mode of action of EF-hand Ca^{2+} sensors is based on the structural analysis of the parent protein in this subfamily, calmodulin, and its interactions with various targets.

Calmodulin (CALcium MODULated proteIN) was discovered by Cheung [18] and Kakiuchi and Yamazaki [19] in the bovine brain and rat brain respectively, and it can be found in all eukaryotic organisms [20]. It is composed of 148 amino acids organized into two canonical EF-hand pairs separated by a flexible helical linker. The two domains share high overall sequence homology (75%), as well as structural similarity in the presence and absence of Ca^{2+} ions. However, the differences in the two domains are significant enough to result in distinct biochemical properties [20].

Calmodulin exists in at least two different configurations: apocalmodulin, which lacks Ca^{2+} and Ca^{2+}-calmodulin, which has four Ca^{2+} ions bound per molecule [21]. The shift from apo- to Ca^{2+}-calmodulin upon binding of submicromolar concentrations involves substantial structural changes. Therefore, protein interactions that depend on submicromolar Ca^{2+} are frequently mediated by calmodulin [22].

Calmodulin mediates a wide range of cellular processes including cell division and differentiation, gene transcription, DNA synthesis, membrane fusion and muscle contraction [23]. More than a 100 targets are regulated by calmodulin both in plants and animal cells, amongst them several cyclic nucleotide phosphodiesterases, nitric oxide synthase, adenylate cyclases 1 and 8, several ion channels and a number of cytoskeleton proteins [24].

Due to its crucial role as Ca^{2+} sensor in all types of cells, it is assumed that calmodulin may be involved in many pathological processes, such as Parkinson disease [25], Alzheimer disease [26] or rheumatoid arthritis [27].

Troponin C, as a part of the troponin complex, is present in all striated muscle, being the trigger that initiates the myocyte contraction. It was discovered by Perry and Corsi [28] in rabbit myofibrils as the mysterious factor along with actin and tropomyosin required to generate muscle contraction. Two isoforms of this protein have been described: fast skeletal muscle troponin C, which is activated by Ca^{2+} binding to two low-affinity sites on the N-terminal domain and cardiac and slow skeletal muscle troponin C, which is activated by Ca^{2+} binding to a single affinity site [29].

Troponin C has a very specific function in the initiation of the cascade events of conformational changes through the component proteins of the thin filament, leading to the formation of cross bridges between actin and myosin and the generation of force by the myocyte [29].

S100 Family Proteins

The 25 members of the S100 proteins are expressed exclusively in vertebrates and constitute the major family of EF-hand calcium sensor proteins. The S100 name does not indicate any functional aspect, but refers to their solubility in 100% ammonium sulphate [30].

The basic structural and functional unit of the S100 proteins is a symmetric dimer comprised of two EF-hand pairs, which are organized into an eight-helix bundle. Usually, S100 proteins form homodimers, although some of them are known to form heterodimers with other S100 isoforms. This subfamily displays unique properties in the EF-hand family: at the primary sequence level, S100 proteins are distinguished from all other EF-hand proteins by a unique 14-residue S100-specific Ca^{2+}-binding loop in the N-terminal EF-hand of each motif, named "pseudo EF-hand" [31]. It has been hypothesized that pseudo EF hands are phylogenetically younger than canonical EF hands and appear later in biological evolution as an additional adaptation to spatial and temporal tissue-specific requirements [32].

Another distinctive characteristic of S100 proteins is their binding of additional divalent metal ions such as Zn^{2+} and Cu^{2+} at sites that are remote from the Ca^{2+} binding sites. Binding of these divalent ions with high affinity plays a role in chemotactic activity and the homeostasis of toxic metal ions. It has not been firmly established how the binding of divalent ions supports or antagonizes the interaction with targets [33, 34].

S100s are associated with multiple targets that promote cell growth and differentiation, cell cycle regulation, transcription and cell surface receptor activities [35]. For example, S100A1, S100A2, S100A4 and S100B interact with the tumour suppressor p53, S100A12 participates in inflammatory processes due to its interaction with the receptor for advanced glycation end products (RAGE) and S100B stimulates

guanylyl cyclase [36]. The calcium signaling activities of these proteins are tailored in part by a distinct pattern of subcellular localization and tissue specific expression.

The detection of abnormal S100 gene expression in different disease states including chronic inflammation, tumour progression, cardiomyopathy, Alzheimer's and psoriasis has fuelled further clinical interest in this multigene family of proteins [37].

Calcineurin

Calcineurin is classified as a calmodulin-dependent serine/threonine phosphatase. Since its initial discovery in bovine brain [38], it has been found to be ubiquitously expressed in lower and higher eukaryotes, including plants and mammals [39].

Calcineurin plays a pivotal role in the information flow from local or global calcium signals to effectors that control immediate cellular responses and alter gene transcription. It is a heterodimer protein consisting of a catalytic A subunit (CNA), which is highly homologous to protein phosphatases 1 and 2, and a regulatory B subunit (CNB), that contains four EF-hand motifs and binds to CNA to regulate its phosphatase activity even in the absence of Ca^{2+} [40]. Calcineurin can dephosphorylate serine residues of transcription factor, nuclear factor of activated T cells (NFAT), initiating a cascade of transcriptional events involved in physiological and development processes [39]. A malfunction in calcineurin-NFAT signaling can engender several pathologies, such as cardiac hypertrophy, autoimmune diseases, osteoporosis, Alzheimer's disease, Down's syndrome and cancer [41].

Neuronal Ca^{2+} Sensor (NCS) Proteins

Frequenin was the first NCS protein discovered and designated NCS-1, due to its distribution in neuronal cell types [42]. Today, five classes of NCS proteins have been identified, and named A-E on the basis of their amino acid sequences. Most of them are expressed only in neurons, where they have different roles in the regulation of neuronal function [43]. Recoverins and guanylyl-cyclase-activating proteins are restricted to retinal photoreceptors.

Members of NCS protein family show four EF-hand motifs although the first of them cannot bind Ca^{2+} due to inactivating substitutions in the EF-hand loop [43]. Structurally they are quite homogeneous and differ from other four EF-hand motifs proteins, like calmodulin, in many aspects. For example, they are more compact and globular even when Ca^{2+} is bound. They also have motifs that allow membrane association and display different subcellular localizations determined by the interactions with specific phosphoinositides [44].

Dysregulation of NCS proteins have been observed in several CNS disorders, such as Alzheimer's disease, schizophrenia, and cancer [45].

Differences in Ca^{2+} Affinities Between Families

In order to optimize a response in Ca^{2+} signaling, both the activation and the inactivation kinetics for a specific pathway must be carefully fine-tuned. In the EF-hand motifs, residues 1, 3, 5, 7, 9 and 12 of the loop region provide the oxygen ligands required for the Ca^{2+} binding. The nature of the amino acid at position 9 in this loop seems to be a crucial factor in the steric and electrostatic parameters that determine equilibrium dissociation constants among the EF-hand family proteins [46]. The variability in the affinity of an EF-hand motif to bind Ca^{2+} is also dependent of two additional factors: the selectivity over Mg^{2+} and the interaction with a protein target [47]. Ca^{2+} buffer proteins, like parvalbumin, show the slowest off-rates (K_d for parvalbumin is 10^{-8} M) whereas most of the S100 members display a dissociation constant up to 10^{-4} M. Calmodulin presents different off-rates for the EF-hands in the amino- and in the carboxy-terminal lobe, which allows independent regulation for each lobe. The dissociation constants for this protein can range from 10^{-7} to 10^{-5} M depending on the interaction of calmodulin with its target proteins [43].

In summary, the structure of the EF-hand loop region dictates the calcium binding parameters of a particular protein and consequently the extent, the speed and the duration of its activation after a Ca^{2+} transient, that is critical for its physiological role.

Intracellular Ca^{2+} Binding Proteins Without EF-Hand Domains

There are several important intracellular CBP lacking the EF-hand domain. Calreticulin, calsequestrin and some other proteins play a key role in the regulation of intracellular Ca^{2+} homeostasis through the binding of Ca^{2+} within the endoplasmic reticulum (ER) and the sarcoplasmic reticulum (SR), thereby allowing these organelles to act as intracellular Ca^{2+} reservoirs. A large group of CBP without EF-hand domains is constituted by the so-called annexins, which are characterised by their ability to bind phospholipids. Some other proteins, among which are protein kinase C (PKC) and synaptotagmin, share a domain named C2, whose Ca^{2+} binding ability serves as a regulatory mechanism for their function.

Ca^{2+} Binding Proteins at Intracellular Ca^{2+} Stores

In eukaryotic cells, the ER and SR (in smooth and striated muscle) participate in the regulation of intracellular Ca^{2+} levels, acting as intracellular stores of readily-releasable Ca^{2+} ions. The presence of various CBP inside these organelles is essential for this function.

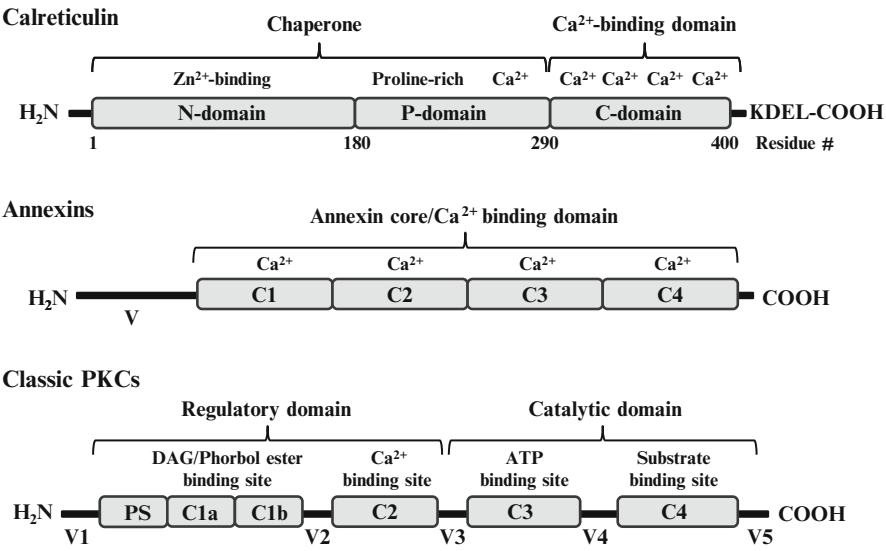

Fig. 19.2 Domain structure of calreticulin, annexins and classic PKCs. Calreticulin contains a KDEL signal that is responsible for the retrieval of ER proteins from the Golgi complex; *C* conserved regions, *V* variable regions, *PS* pseudosubstrate binding site. For more details, see text

Smooth Muscle Sarcoplasmic and Endoplasmic Reticulum

Several CBP have been reported to participate in ER-dependent Ca^{2+} homeostasis, including calreticulin, calnexin, glucose-regulated protein 94 (Grp 94), BiP/Grp78 and protein disulfide isomerase (PDI) [48]. These proteins also act as protein chaperones since they have the ability to bind mis-folded proteins [48, 49].

Amongst these CBP, calreticulin is undoubtedly the most important. It consists of three distinct structural and functional domains (Fig. 19.2). The N-terminal domain (residues 1–180) binds heavy metals and forms the chaperone (folding unit) together with a proline-rich domain or P-domain (residues 181–290). This P-domain includes a high-affinity ($K_d = 1$ μM), low-capacity (1 mol Ca^{2+}/mol of protein) Ca^{2+}-binding site [50]. The C-terminal domain (residues 291–400) accounts for the high capacity (~20 mol Ca^{2+}/mol of protein) and low affinity (K_d ~2 mM) Ca^{2+}-binding activity of this protein [51–53].

It has been described that calreticulin regulates Ca^{2+} uptake and release within the ER and mitochondria and that an enhanced expression of this CBP is directly related to a significant augmentation of the capacity of the ER to retain Ca^{2+} [54]. In accordance with this, it has been reported that lack of calreticulin significantly reduces ER Ca^{2+} capacity [52]. Apart from its capacity to bind high amounts of Ca^{2+}, calreticulin is a central component of the folding quality control system of glycoproteins, since it has the capacity to bind monoglucosylated high mannose oligosaccharides [51, 55].

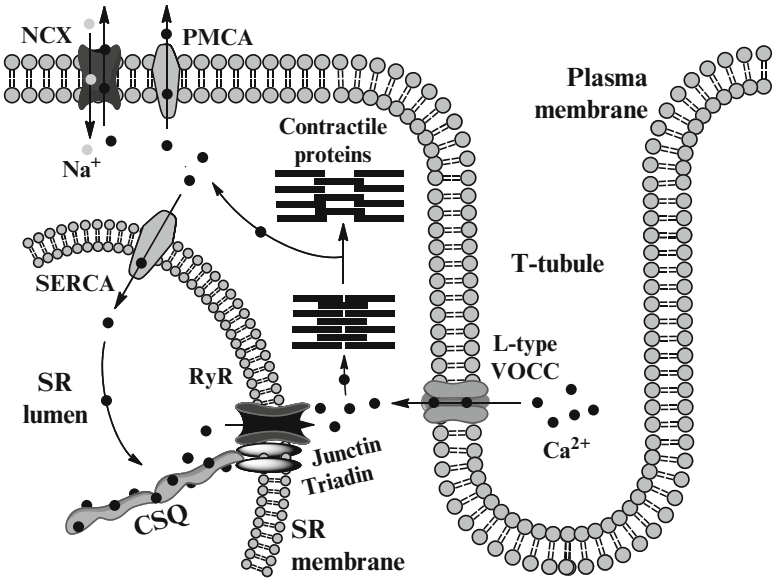

Fig. 19.3 Calsequestrin (CSQ) binds Ca^{2+} within the SR of cardiac myocytes. It is attached to the ryanonide receptor through the junctin-triadin protein complex. *NCX* Na^{2+}/Ca^{2+} exchanger; *PMCA* plasma membrane Ca^{2+} ATPase, *VOCC* voltage-operated Ca^{2+} channel, *SERCA* sarcoplasmic/endoplasmic reticulum Ca^{2+} ATPase, *RyR* ryanodine receptor

A possible role of calreticulin in the development of several human pathologies, including congenital arrhythmias and some cancers, has been described [51, 52, 56].

Striated Muscle Sarcoplasmic Reticulum

The storage and rapid release of Ca^{2+} from the skeletal and cardiac SR has been associated with calsequestrin [57, 58]. Calsequestrin is an acidic protein that binds Ca^{2+} with low affinity (K_d in the mM range), but with high capacity (see below), thus allowing a rapid release of this ion from the SR of striated muscle.

In mammals, two isoforms of calsequestrin have been described. Skeletal muscle calsequestrin or calsequestrin 1 (CASQ1 gene) is located in the SR of fast-twitch and slow-twitch skeletal muscles. Cardiac calsequestrin or calsequestrin 2 (CASQ2 gene) is found in the SR of cardiac muscle and adult slow-twitch skeletal muscle [58, 59]. They both act as SR luminal sensors for the skeletal or cardiac ryanodine receptors together with the proteins triadin and junctin (Fig. 19.3) [60, 61].

Structurally, calsequestrin isoforms differ in the acidic C-terminal tail which is highly extended in the cardiac isoform although, as reported by Novák and Soukup [58], most of our knowledge about differences of molecular interactions between skeletal and cardiac calsequestrin comes from studies of isolated systems. Thus, it

has been reported that canine cardiac calsequestrin binds 35–40 mol of Ca^{2+}/mol of protein [62] and that Ca^{2+} binding to sheep cardiac calsequestrin is 50% lower than to rabbit skeletal calsequestrin [63].

Apart from its role as a readily accessible reservoir of Ca^{2+} in cardiac muscle, cardiac calsequestrin participates in the regulation of the opening/closing of the SR Ca^{2+} release channels [64]. Although the role of skeletal calsequestrin in skeletal muscle as a primary Ca^{2+} store is not completely understood [58, 65], it has been demonstrated, using CASQ1-null mice, that a lack of this CBP causes important structural changes in the SR and alters the storage and release of appropriate amounts of SR Ca^{2+} [66]. Additionally, an alteration in calsequestrin expression is involved in the pathogenesis of Duchenne progressive muscular dystrophy [67]. In fact, some patients with Duchenne muscular dystrophy lacked a CBP of the mitochondrial matrix named calmitine, which was found to be identical to calsequestrin [68].

Annexins

Annexins, also known as lipocortins, are a multigene superfamily of Ca^{2+}-dependent phospholipid- and membrane-binding proteins that are expressed in a wide variety of animal and plant tissues and that are implicated in various extracellular and intracellular processes, including vesicle trafficking, membrane scaffolding or regulation of ion channel activity. The name “annexin” was proposed for the superfamily in 1990 and the annexins have been classified in five families [69–71].

The annexin A family includes 12 annexins common to humans and vertebrates (human gene symbols AXA1 to AXA13, leaving A12 unassigned in the official nomenclature). The annexin B family includes those present in invertebrates. The annexin C family includes proteins present in fungi and some groups of unicellular eukaryotes, such as mycetozoa. Plant and protist annexins are included in the annexin D and E families, respectively [71].

All annexins are structurally related and have a highly conserved C terminal domain named the annexin core and an N terminal region that varies greatly. The annexin core is a structural fold formed by four annexin repeats of 70 amino acids (Fig. 19.2), except annexin VI that contains 8 repeats. Each repeat is packed into a compact domain consisting of five α-helices wound in a right-handed superhelix. The Ca^{2+}- and phospholipid-binding sites correspond to a 17 amino acid sequence contained in each of the four repeats. Three of the repeats bind Ca^{2+} with moderate affinity (K_d in the μM to mM range), but the third repeat does not appear to bind Ca^{2+} at low concentrations due to deviations from the canonical sequence and structure [1, 69, 70, 72]. The N terminal region regulates the interactions with protein ligands and the annexin-membrane association [69, 73].

Annexins locate intracellularly, mainly in the cytosol, both in a soluble form or associated with components of the cytoskeleton or matricellular proteins [71]. However, some of them have been reported to be expressed at the cell surface in certain circumstances, as is the case for annexin 1 [74] and annexin 2 [75].

In humans, it has been suggested that annexins may be involved in the origin of a diverse range of diseases, including cancer, diabetes or inflammatory pathologies [76].

Ca^{2+} Binding Proteins with C2 Domain

The C2 domain is a Ca^{2+}-binding motif originally identified in protein kinase C (PKC) [77]. It comprises approximately 130 residues and consists of a compact β-sandwich composed of two four-stranded β-sheets. Three loops at the top of the domain and four at the bottom connect the eight β-strands. Ca^{2+} binding occurs exclusively at the top three loops with low affinity ($K_d > 1$ mM) [1, 78].

The C2 domain is widely distributed in eukaryotes and, besides Ca^{2+}, it has the ability to bind phospholipids, inositol polyphosphates and some other intracellular proteins. It mediates a wide range of intracellular processes, such as membrane trafficking, generation of lipid-second messengers, activation of GTPases, and control of protein phosphorylation [79]. Amongst the best known proteins presenting the C2 domain are PKC, synaptotagmins, phospholipase C (PLC) and phospholipase A (PLA).

PKC is composed of a large family of lipid-activated enzymes that regulate the function of other proteins via phosphorylation of serine and threonine residues. Multiple isoforms of PKC, ten of them found in mammals, may exist in the cytosol in a soluble form or bind to the plasma membrane, participating in many functions, such as intracellular signaling, secretion, cell growth and differentiation [80, 81].

In order to fulfil its function, PKC needs the presence of several lipid cofactors and Ca^{2+}, although these requirements may vary for different isozymes. In mammalian PKC, three categories have been established: classical, novel and atypical isoforms, the last lacking the C2 domain [80, 82]. Classical isozymes contain a C2 type I Ca^{2+}- and phospholipid-binding domain and they need to bind Ca^{2+} in order to stabilize their interaction with the plasma membrane (Fig. 19.2) [81]. On the other hand, novel isozymes contain a variant of the C2 domain (type 2) that lacks key residues that coordinate Ca^{2+} and, as a result, the novel isozymes are not sensitive to Ca^{2+} [83]. In consequence, the classical PKC isoforms are activated by Ca^{2+} and diacylglycerol (DAG), whereas the novel PKC isoforms are activated by DAG, but not Ca^{2+}. Atypical PKC isoforms require neither Ca^{2+} nor DAG for activation [84].

Synaptotagmins are a family of transmembrane Ca^{2+} sensors found in synaptic vesicles and in secretory granules of endocrine cells that have a main role in exocytosis [1, 85]. They bind Ca^{2+} with low affinity by means of two C2 domains: C2A and C2B [86]. There are multiple known isoforms of synaptotagmins [87]. The best known is synaptotagmin I, which function as a sensor for evoked, synchronous neurotransmitter release in neurons [88].

Two other proteins that are involved in the modification of lipids also contain Ca^{2+} binding C2 domains that contribute to regulate their function: phosphoinositide-specific PLC, which liberates IP_3 and DAG in response to mitogenic signals that raise intracellular Ca^{2+} levels [89] and PLA2, which liberates arachidonic acid from glycerophospholipids to initiate production of leukotrienes and prostaglandins, potent mediators of inflammation [90].

Extracellular Ca^{2+} Binding Proteins

The Ca^{2+} concentration in human serum is maintained at about 1.4 mM [91]. Deviations in this concentration lead to severe pathological malfunctions. Different organs and hormones must cooperate to regulate the uptake, excretion and recycling of calcium in the body and, as a consequence, serum Ca^{2+} concentration. The study of extracellular Ca^{2+} as a messenger has probably been hampered by the generally accepted idea that Ca^{2+} concentration in the extracellular space does not fluctuate and by the technical difficulties of measuring spatial and temporal changes in extracellular Ca^{2+} concentration.

Several extracellular Ca^{2+} binding proteins (ECBP) have been discovered and their roles investigated. If it is assumed that the Ca^{2+} concentration in the extracellular space does not differ from that measured in serum, Ca^{2+} would not play an extracellular messenger role. ECBP would use Ca^{2+} for static roles (e.g. formation of active sites in enzymes or active conformations in receptors, structure protein stabilization and formation of supramolecular structures with other proteins or carbohydrates) or to maintain the extracellular Ca^{2+} homeostasis. Despite the constant concentration of serum Ca^{2+}, there are clear examples that show that local extracellular Ca^{2+} levels may differ from those usually measured in serum and may indeed fluctuate (e.g., fluctuations are very likely to occur during intracellular Ca^{2+} signaling events) [92]. Therefore, extracellular Ca^{2+} could fulfil a more dynamic function participating as a messenger in extracellular signal transduction pathways. Several membrane and soluble Ca^{2+} sensor proteins have been identified. These proteins undergo a conformational change in response to physiological fluctuations in extracellular Ca^{2+} concentrations; the conformational change allows interactions with a specific target protein, ultimately modulating its function.

ECBP are modulators of numerous cellular functions (e.g. blood-clotting, complement activation, cell-cell interactions, cell-matrix interactions, receptor-ligand interactions, Ca^{2+} transport and Ca^{2+} homeostasis) and may serve as important therapeutic targets. In this section we review the main ECBP, focussing on some proteins that can potentially have a role as extracellular Ca^{2+} sensors. We grouped the ECBP by Ca^{2+}-binding domain structures (see also Table 19.1).

Extracellular Ca^{2+} Binding Proteins with EF-Hand Domains

Ca^{2+}-binding proteins containing EF-hand domains are present within cells and also in the extracellular environment, or matrix. These proteins do not contribute directly to the architecture of the matrix, nor do they act as structural proteins [93].

Osteonectin, also known as SPARC (secreted protein acidic and rich in cysteines) or BM-40, is a matrix protein that serves as the prototype of the osteonectin family. Other members of this family are hevin, QR1, testicans 1-3, tsc 36, SMOC-1 and SMOC-2. The osteonectin family is characterized by a follistatin-like, cysteine rich

Table 19.1 Main extracellular Ca^{2+}-binding domain structures. All of the Ca^{2+}-binding domain structures have in common a high negative surface potential usually associated with Asp or Glu residues

Group and calcium-binding domain structure	Main proteins	Possible role of Ca^{2+}-binding to proteins
EF-hand domains	Osteonectin family: osteonectin, hevin, QR1, testicans 1–3, tsc 36, SMOC-1 and SMOC-2	Formation of binding sites for extracellular ligands Ca^{2+} signal transmission?
EGF-like domains	Coagulation factors VII, IX and X, protein C and protein S Fibrillin Notch and delta receptors LDL receptors	Induction of protein conformation required for biological activity Stabilization of proteins Ca^{2+} signal transmission?
γ-Carboxyl glutamic acid-rich domains	Coagulation factors II, VII, IX and X, protein C and protein Z	Anchoring of proteins to membrane
	Osteocalcin, matrix GLA protein and periostin Growth arrest-specific protein 6	Activation of proteins
Cadherin domains	Cadherin family: classical cadherins, protocadherins, and atypical cadherins (Fat, Dachsous, and Flamingo)	Modulation of mechanical integrity and mechanotransduction capability of proteins (using an adaptor complex cadherins connect to the cytoskeleton) Ca^{2+} signal transmission
(C)-type lectin-like domains	Selectins Mannose receptor family Dendritic cell-specific ICAM-3 grabbing non-integrin molecule Several collectins (e.g. mannose-binding protein)	Modulation of ligand binding Stabilization of proteins
Ca^{2+}-binding pockets of family C GPCRs	Ca^{2+}-sensing receptor Metabotropic glutamate receptors $GABA_B$ receptors	Change of receptor conformation Ca^{2+} signal transmission through G-proteins

domain and a C-terminal module with two EF-hand Ca^{2+}-binding domains (each EF-hand domain is predicted to bind one Ca^{2+} ion) [94–96]. The EF-hand pair is very similar to those of intracellular EF-hand proteins such as calmodulin. The affinity of the Ca^{2+}-binding domain for Ca^{2+} is high; for example, osteonectin binds 2 Ca^{2+} with a K_{d1} of 490 nM and K_{d2} of 26 nM [95]. Thus, the EF-hand domains should always be in the Ca^{2+}-saturated form in the extracellular space and Ca^{2+} would fulfil a structural role rather a regulatory role transmitting a signal [95, 97]. The osteonectin-like proteins modulate cell function by interacting with cell-surface receptors,

metalloproteinases, growth factors and other bioeffector molecules and proteins of the matrix such as collagens [93, 96]. Different lines of evidence link osteonectin-like proteins with human cancer progression [96].

Extracellular Ca^{2+} Binding Proteins with EGF-Like Domains

The epidermal growth factor (EGF)-like domain is one of the most widely distributed protein modules. A subset of EGF-like domains also contain a Ca^{2+}-binding domain that binds one Ca^{2+}, making this type of module one of the most prevalent extracellular Ca^{2+}-binding sites. The Ca^{2+}-binding domains have a wide range of Ca^{2+} affinities, with K_d from 0.1 mM to nM values [98, 99]. Among the proteins containing Ca^{2+}-binding EGF-like domains are proteins involved in blood coagulation, fibrinolysis and the complement system (e.g. factors VII, IX and X, protein C and protein S), matrix proteins (e.g. fibrillin) and cell surface receptors (e.g. low density lipoprotein receptor and Notch receptor and their homologues) [99]. The coagulation enzymes, factors VII, IX and X and protein C, all have two EGF-like domains, whereas the cofactor of activated protein C, protein S, has four EGF-like domains in tandem. Fibrillin, low density lipoprotein receptor and the developmentally important receptor Notch have numerous EGF-like domains in tandem [99, 100].

Ca^{2+}-binding to an EGF-like domain is important to orient neighbouring domains and to induce the protein conformation required for biological activity [99, 101]. Ca^{2+} binding to an EGF-like domain also stabilizes the proteins [100]. The EGF-like domains are involved in protein-protein interactions, receptor-ligand interactions and blood coagulation [98, 99].

Extracellular Ca^{2+} Binding Proteins with γ-Carboxyl Glutamic Acid-Rich Domains

Several human proteins have a γ-carboxyl glutamic acid (GLA)-rich domain that binds Ca^{2+}. They play key roles in the regulation of blood coagulation (factors II -prothrombin- VII, IX, X, protein C, protein S, and protein Z), bone metabolism (osteocalcin, matrix GLA protein and periostin) and vascular biology (growth arrest-specific protein 6) [102]. In addition to the GLA-rich domain, several blood-clotting proteins have EGF-like domains (see above; [2]). The GLA-rich domain consists of about 45 amino acids, of which the 10–12 glutamic acids are carboxylated to GLA by a vitamin K dependent carboxylase [97]. In coagulation factors VII, IX and X and protein C, the GLA-rich domain occupies the N-terminal half of the molecule and is followed by two EGF-like domains; in protein S, the GLA-rich domain also occupies the N-terminal half of the molecule and is followed by a thrombin-sensitive domain and four EGF-like domains [99]. According to different structural studies, the number of Ca^{2+} ions associated with the GLA domains seems

to be variable; specifically in the GLA domain of human FVIIa, nine of the ten GLA residues bind seven Ca^{2+} [103]. Ca^{2+} binding to blood-clotting proteins is required for the initiation of the coagulation cascade at sites of injury. The GLA domains of most of the coagulation factors have similar Ca^{2+} affinities, the average K_d being ~0.5 mM [104]. Thus, coagulation factors should generally be in the Ca^{2+}-saturated form in the extracellular space and Ca^{2+} would play a structural role rather a regulatory role. However, local fluctuations of Ca^{2+} levels have been described and a regulatory role of Ca^{2+} may occur in some circumstances. 4-hydroxycoumarin anticoagulants are currently used in clinical practice because they indirectly inhibit the vitamin K dependent carboxylation of several blood-clotting proteins; as a consequence, clotting proteins cannot bind Ca^{2+} and they cannot participate in the coagulation cascade.

Extracellular Ca^{2+} Binding Proteins with Cadherin Domains

As their name implies, cadherins are Ca^{2+}-dependent adherent receptors. The cadherin family includes classical cadherins, protocadherins and atypical cadherins. They all are single membrane-spanning proteins with the exception of flamingo, an atypical cadherin that is a seven-pass membrane protein. The different types of cadherins have diverse protein structures, but all possess Ca^{2+}-binding extracellular repeats [105]. For example, C-cadherin contains five extracellular domains (ectodomains) and each interdomain region can bind 3 Ca^{2+} ions, such that the entire ectodomain is capable of binding 12 Ca^{2+} ions [106]. High and low affinity Ca^{2+} binding sites have been identified in cadherins with a wide range of Ca^{2+} affinities, K_d from μM to mM. The cadherin extracellular domains may behave as a Ca^{2+}-switched "mechanical antenna", as suggested by Oroz et al. [107]; in particular, the Ca^{2+} concentration would affect its mechanical integrity and its mechanotransduction capability (cadherins connect to the cytoskeleton using an adaptor complex). Therefore, cadherins may act as Ca^{2+} sensors that respond to external Ca^{2+} fluctuations. Cadherins are involved in development, morphogenesis, synaptogenesis, differentiation and carcinogenesis [105].

Extracellular Ca^{2+} Binding Proteins with Ca^{2+}-Dependent (C)-Type Lectin-Like Domains

Ca^{2+}-dependent (C)-type lectin-like domains (CTLD) are present not only in the C-type lectins, but also in other extracellular proteins. C-type lectins are either produced as transmembrane proteins (e.g. selectins, the mannose receptor family and the dendritic cell-specific ICAM-3 grabbing non-integrin molecule) or secreted as soluble proteins (e.g. mannose-binding protein and other collectins) [108]. The CTLD structure has a characteristic double-loop ("loop-in-a-loop"): the secondary

loop is involved in Ca^{2+}-dependent carbohydrate binding, the main CTLD function, and in the interaction with other ligands. Four Ca^{2+}-binding sites are detected consistently in the CTLD domain, but depending on the particular CTLD sequence and on experimental conditions, zero, one, two or three sites are occupied [109]. Ca^{2+} is involved in ligand binding to C-type lectins and also serves to stabilize their molecular structure [108, 109]. Since changes in Ca^{2+} concentration dramatically enhance carbohydrate binding by C-type lectins, it was suggested that physiological fluctuations of extracellular Ca^{2+} have a regulatory effect on ligand binding by C-type lectins [97]. C-type lectins mediate many cell surface carbohydrate recognition events, e.g. cell to cell contact and recognition of pathogens [108].

Ca^{2+}-Binding Pockets of Family C G-Protein-Coupled Receptors

The family C of the superfamily of G protein-coupled receptors (GPCRs), also referred to as family 3 GPCRs, include the Ca^{2+}-sensing receptor (CaR), metabotropic glutamate receptors (mGluRs), $GABA_B$ receptors, taste receptors and putative pheromone receptors. Some of these receptors alter their function in response to small fluctuations of external Ca^{2+} and may behave as Ca^{2+} sensors.

Ca^{2+}-Sensing Receptor (CaR)

The CaR was initially identified on the bovine parathyroid as a plasma membrane-located GPCR. Later, the CaR was also identified on the surface of other cell types: bone-forming and bone-resorbing cells, kidney cells, intestine and haematopoietic stem cells [98].

The CaR has a long extracellular amino-terminal domain called a Venus flytrap module, containing the ligand binding pocket that gives the receptor the necessary sensitivity to detect small fluctuations of external Ca^{2+}. According to Silve et al. [110], the Ca^{2+}-binding site in the CaR involves a set of polar residues directly involved in Ca^{2+} coordination (Ser-170, Asp-190, Gln-193, Ser-296, and Glu-297), and an additional set of residues that contributes to complete the coordination sphere of the cation (Phe-270, Tyr-218, and Ser-147). The activity of the CaR is modulated by changes in the Ca^{2+} concentrations occurring in the mM range. CaR is coupled to intracellular signal transduction pathways through G-proteins, especially to phospholipase C, cytosolic phospholipase A_2 and various MAP kinase proteins [91].

The main function of CaR is to regulate the secretion of PTH (an increase in serum Ca^{2+} level negatively regulates PTH secretion). The vital role of the CaR maintaining normal systemic Ca^{2+} homeostasis is illustrated by human hypocalcemic and hypercalcemic disorders related to specific mutations of CaR and by mouse knockout models: complete ablation of functional CaR is lethal, resulting in severe skeletal demineralization, extremely high Ca^{2+} serum concentration, growth defects and ultrastructural changes in the epidermis [92].

In vitro experiments have revealed that CaR on cells responds to Ca^{2+} exported from the same or a neighbouring cell during Ca^{2+} signaling events; extracellular Ca^{2+} might thus act as an autocrine/paracrine messenger via CaR [92]. CaR also displays sensitivity to amino acids, especially aromatic amino acids, and other divalent and trivalent ions. Therefore, it is not surprising that CaR can play other roles than maintaining the systemic Ca^{2+} homeostasis, e.g. regulation of hormonal secretion and the activities of various ion channels, control of gene expression, programmed cell death (apoptosis) and cellular proliferation [91].

Direct activators of CaR (termed type I calcimimetics), synthetic allosteric activators of CaR (termed type II calcimimetics) and inhibitors of CaR (termed calcilytics) have been developed. Strontium, which may be considered a type I calcimimetic, is currently used in osteoporosis in the form of strontium ranelate; cinnacalcet, a type II calcimimetic, is currently used in primary and secondary hyperparathyroidism and parathyroid carcinoma; calcilytics are currently in clinical trials for the treatment of osteoporosis. Sustained elevations of PTH, as in hyperparathyroid states, have a net catabolic effect on bone, favouring resorption, whereas short bursts are anabolic, favouring formation [111]. Therefore, continuous administration of a calcimimetic or intermittent administration of a calcilytic could promote anabolic over catabolic actions.

Metabotropic Glutamate Receptors (mGluRs) and $GABA_B$ Receptors

Metabotropic glutamate receptors are family C GPCRs and structurally similar to CaR. On the basis of sequence homology to CaR, it was postulated that some mGluRs can respond to external Ca^{2+} fluctuations [92]. mGluRs are expressed principally in the brain, where the levels of external Ca^{2+} are highly dynamic. A Ca^{2+}-binding site in the mGluR1α was recently identified: it comprises Asp-318, Glu-325 and Asp-322 and the carboxylate side chain of the main receptor agonist, L-glutamate [112]. External Ca^{2+} has been proposed: (i) to directly activate mGluRs; (ii) to increase mGluRs sensitivity to L-glutamate; and (iii) to modulate mGluRs synergistically with L-glutamate [92, 112]. External Ca^{2+} also modulates other type C GPCRs, namely $GABA_B$ receptors, although external Ca^{2+} does not directly activate this class of receptors [91].

Concluding Remarks

In the last few decades, research on CBP has brought important advances. Cristallography, molecular biology, microscopy and other techniques have given us more knowledge about the sequences and structures of CBP. Many new proteins with the ability to bind Ca^{2+} have been discovered and there has been a great effort to rationally classify them. However, there is still much work to do, for example, trying to better establish the physiological role of many of these proteins. For some

of them, it is difficult to differentiate between structural and regulatory roles for Ca^{2+} binding (this is especially true in the case of extracellular CBP). It is also unclear where is a difference between proteins acting exclusively as Ca^{2+} sensors and those acting uniquely as Ca^{2+} buffers, since in some CBP, both roles are observed. A deeper knowledge of the structure and function of CBP, together with a better definition of their physiological role, will allow us to further investigate targeting of these proteins in novel therapeutic strategies.

References

1. Carafoli E, Santella L, Branca D, Brini M (2001) Generation, control, and processing of cellular calcium signals. Crit Rev Biochem Mol Biol 36:107–260
2. Permyakov EA, Kretsinger RH (2011) Calcium binding proteins. Wiley, Hoboken
3. Kretsinger RH, Nockolds CE (1973) Carp muscle calcium-binding protein. II. Structure determination and general description. J Biol Chem 248:3313–3326
4. Lewit-Bentley A, Rety S (2000) EF-hand calcium-binding proteins. Curr Opin Struct Biol 10:637–643
5. Tsigelny I, Shindyalov IN, Bourne PE, Sudhof TC, Taylor P (2000) Common EF-hand motifs in cholinesterases and neuroligins suggest a role for Ca^{2+} binding in cell surface associations. Protein Sci 9:180–185
6. Milner-White EJ (1999) The N-terminal domain of MDM2 resembles calmodulin and its relatives. J Mol Biol 292:957–963
7. van Asselt EJ, Dijkstra AJ, Kalk KH, Takacs B, Keck W, Dijkstra BW (1999) Crystal structure of Escherichia coli lytic transglycosylase Slt35 reveals a lysozyme-like catalytic domain with an EF-hand. Structure 7:1167–1180
8. Nakayama N, Kawasaki H, Kretsinger R (2000) Evolution of EF-hand proteins. In: Carafoli E, Krebs J (eds) Calcium homeostasis, topics in biological inorganic chemistry. Springer, Berlin, pp 29–58
9. Skelton NJ, Kordel J, Akke M, Forsen S, Chazin WJ (1994) Signal transduction versus buffering activity in Ca^{2+}-binding proteins. Nat Struct Biol 1:239–245
10. Holmes KC (1996) Muscle proteins–their actions and interactions. Curr Opin Struct Biol 6:781–789
11. Arif SH (2009) A Ca^{2+}-binding protein with numerous roles and uses: parvalbumin in molecular biology and physiology. Bioessays 31:410–421
12. Deuticke HJ (1934) Über die Sedimentationskonstante von Muskelproteinen. Hoppe Seylers Z Physiol Chem 224:216–228
13. Pechere JF (1968) Muscular parvalbumins as homologous proteins. Comp Biochem Physiol 24:289–295
14. Schaub MC, Heizmann CW (2008) Calcium, troponin, calmodulin, S100 proteins: from myocardial basics to new therapeutic strategies. Biochem Biophys Res Commun 369:247–264
15. Heizmann CW (1984) Parvalbumin, an intracellular calcium-binding protein; distribution, properties and possible roles in mammalian cells. Experientia 40:910–921
16. Gerday C, Gillis JM (1976) Proceedings: the possible role of parvalbumins in the control of contraction. J Physiol 258:96P–97P
17. Baude A, Bleasdale C, Dalezios Y, Somogyi P, Klausberger T (2007) Immunoreactivity for the GABAA receptor alpha1 subunit, somatostatin and connexin36 distinguishes axoaxonic, basket, and bistratified interneurons of the rat hippocampus. Cereb Cortex 17:2094–2107
18. Cheung WY (1970) Cyclic 3′,5′-nucleotide phosphodiesterase. Demonstration of an activator. Biochem Biophys Res Commun 38:533–538

19. Kakiuchi S, Yamazaki R (1970) Calcium dependent phosphodiesterase activity and its activating factor (PAF) from brain studies on cyclic 3′,5′-nucleotide phosphodiesterase (3). Biochem Biophys Res Commun 41:1104–1110
20. Cohen P, Klee CB (1988) Calmodulin. Elsevier, Amsterdam
21. Jurado LA, Chockalingam PS, Jarrett HW (1999) Apocalmodulin. Physiol Rev 79:661–682
22. Igarashi M, Watanabe M (2007) Roles of calmodulin and calmodulin-binding proteins in synaptic vesicle recycling during regulated exocytosis at submicromolar Ca^{2+} concentrations. Neurosci Res 58:226–233
23. Kawasaki H, Kretsinger RH (1994) Calcium-binding proteins. 1: EF-hands. Protein Profile 1:343–517
24. Toutenhoofd SL, Strehler EE (2000) The calmodulin multigene family as a unique case of genetic redundancy: multiple levels of regulation to provide spatial and temporal control of calmodulin pools? Cell Calcium 28:83–96
25. Iwatsubo T, Nakano I, Fukunaga K, Miyamoto E (1991) Ca^{2+}/calmodulin-dependent protein kinase II immunoreactivity in Lewy bodies. Acta Neuropathol 82:159–163
26. McLachlan DR, Wong L, Bergeron C, Baimbridge KG (1987) Calmodulin and calbindin D28K in Alzheimer disease. Alzheimer Dis Assoc Disord 1:171–179
27. Ali M, Ponchel F, Wilson KE, Francis MJ, Wu X, Verhoef A, Boylston AW, Veale DJ, Emery P, Markham AF, Lamb JR, Isaacs JD (2001) Rheumatoid arthritis synovial T cells regulate transcription of several genes associated with antigen-induced anergy. J Clin Invest 107:519–528
28. Perry SV, Corsi A (1958) Extraction of proteins other than myosin from the isolated rabbit myofibril. Biochem J 68:5–12
29. Gillis TE, Marshall CR, Tibbits GF (2007) Functional and evolutionary relationships of troponin C. Physiol Genomics 32:16–27
30. Moore BW, McGregor D (1965) Chromatographic and electrophoretic fraction of soluble proteins of brain and liver. J Biol Chem 240:1647–1653
31. Marenholz I, Heizmann CW, Fritz G (2004) S100 proteins in mouse and man: from evolution to function and pathology (including an update of the nomenclature). Biochem Biophys Res Commun 322:1111–1122
32. Zhou Y, Yang W, Kirberger M, Lee HW, Ayalasomayajula G, Yang JJ (2006) Prediction of EF-hand calcium-binding proteins and analysis of bacterial EF-hand proteins. Proteins 65:643–655
33. Fritz G, Botelho HM, Morozova-Roche LA, Gomes CM (2010) Natural and amyloid self-assembly of S100 proteins: structural basis of functional diversity. FEBS J 277:4578–4590
34. Nishikawa T, Lee IS, Shiraishi N, Ishikawa T, Ohta Y, Nishikimi M (1997) Identification of S100b protein as copper-binding protein and its suppression of copper-induced cell damage. J Biol Chem 272:23037–23041
35. Donato R (2003) Intracellular and extracellular roles of S100 proteins. Microsc Res Tech 60:540–551
36. Santamaria-Kisiel L, Rintala-Dempsey AC, Shaw GS (2006) Calcium-dependent and -independent interactions of the S100 protein family. Biochem J 396:201–214
37. Heizmann CW, Ackermann GE, Galichet A (2007) Pathologies involving the S100 proteins and RAGE. Subcell Biochem 45:93–138
38. Klee CB, Krinks MH (1978) Purification of cyclic 3′,5′-nucleotide phosphodiesterase inhibitory protein by affinity chromatography on activator protein coupled to Sepharose. Biochemistry 17:120–126
39. Rusnak F, Mertz P (2000) Calcineurin: form and function. Physiol Rev 80:1483–1521
40. Li J, Jia Z, Zhou W, Wei Q (2009) Calcineurin regulatory subunit B is a unique calcium sensor that regulates calcineurin in both calcium-dependent and calcium-independent manner. Proteins 77:612–623
41. Li H, Rao A, Hogan PG (2011) Interaction of calcineurin with substrates and targeting proteins. Trends Cell Biol 21:91–103
42. Pongs O, Lindemeier J, Zhu XR, Theil T, Engelkamp D, Krah-Jentgens I, Lambrecht HG, Koch KW, Schwemer J, Rivosecchi R, Mallart A, Galceran J, Canal I, Barbas JA, Ferrús A (1993)

Frequenin -a novel calcium-binding protein that modulates synaptic efficacy in the Drosophila nervous system. Neuron 11:15–28
43. Burgoyne RD (2007) Neuronal calcium sensor proteins: generating diversity in neuronal Ca^{2+} signalling. Nat Rev Neurosci 8:182–193
44. McCue HV, Haynes LP, Burgoyne RD (2010) The diversity of calcium sensor proteins in the regulation of neuronal function. Cold Spring Harb Perspect Biol 2:a004085
45. Braunewell KH (2005) The darker side of Ca^{2+} signaling by neuronal Ca^{2+}-sensor proteins: from Alzheimer's disease to cancer. Trends Pharmacol Sci 26:345–351
46. Renner M, Danielson MA, Falke JJ (1993) Kinetic control of Ca(II) signaling: tuning the ion dissociation rates of EF-hand Ca(II) binding sites. Proc Natl Acad Sci USA 90:6493–6497
47. Gifford JL, Walsh MP, Vogel HJ (2007) Structures and metal-ion-binding properties of the Ca^{2+}-binding helix-loop-helix EF-hand motifs. Biochem J 405:199–221
48. Coe H, Michalak M (2009) Calcium binding chaperones of the endoplasmic reticulum. Gen Physiol Biophys 28 Spec No Focus:F96–F103
49. Ashby MC, Tepikin AV (2001) ER calcium and the functions of intracellular organelles. Semin Cell Dev Biol 12:11–17
50. Baksh S, Michalak M (1991) Expression of calreticulin in Escherichia coli and identification of its Ca^{2+} binding domains. J Biol Chem 266:21458–21465
51. Gelebart P, Opas M, Michalak M (2005) Calreticulin, a Ca^{2+}-binding chaperone of the endoplasmic reticulum. Int J Biochem Cell Biol 37:260–266
52. Nakamura K, Zuppini A, Arnaudeau S, Lynch J, Ahsan I, Krause R, Papp S, De Smedt H, Parys JB, Muller-Esterl W, Lew DP, Krause KH, Demaurex N, Opas M, Michalak M (2001) Functional specialization of calreticulin domains. J Cell Biol 154:961–972
53. Villamil Giraldo AM, Lopez Medus M, Gonzalez Lebrero M, Pagano RS, Labriola CA, Landolfo L, Delfino JM, Parodi AJ, Caramelo JJ (2010) The structure of calreticulin C-terminal domain is modulated by physiological variations of calcium concentration. J Biol Chem 285:4544–4553
54. Arnaudeau S, Frieden M, Nakamura K, Castelbou C, Michalak M, Demaurex N (2002) Calreticulin differentially modulates calcium uptake and release in the endoplasmic reticulum and mitochondria. J Biol Chem 277:46696–46705
55. Trombetta ES (2003) The contribution of N-glycans and their processing in the endoplasmic reticulum to glycoprotein biosynthesis. Glycobiology 13:77R–91R
56. Zhu N, Wang Z (1999) Calreticulin expression is associated with androgen regulation of the sensitivity to calcium ionophore-induced apoptosis in LNCaP prostate cancer cells. Cancer Res 59:1896–1902
57. MacLennan DH, Wong PT (1971) Isolation of a calcium-sequestering protein from sarcoplasmic reticulum. Proc Natl Acad Sci USA 68:1231–1235
58. Novák P, Soukup T (2011) Calsequestrin distribution, structure and function, its role in normal and pathological situations and the effect of thyroid hormones. A review. Physiol Res 60: 439–452
59. Milstein ML, Houle TD, Cala SE (2009) Calsequestrin isoforms localize to different ER subcompartments: evidence for polymer and heteropolymer-dependent localization. Exp Cell Res 315:523–534
60. Gyorke I, Hester N, Jones LR, Gyorke S (2004) The role of calsequestrin, triadin, and junctin in conferring cardiac ryanodine receptor responsiveness to luminal calcium. Biophys J 86: 2121–2128
61. Qin J, Valle G, Nani A, Nori A, Rizzi N, Priori SG, Volpe P, Fill M (2008) Luminal Ca^{2+} regulation of single cardiac ryanodine receptors: insights provided by calsequestrin and its mutants. J Gen Physiol 131:325–334
62. Mitchell RD, Simmerman HK, Jones LR (1988) Ca^{2+} binding effects on protein conformation and protein interactions of canine cardiac calsequestrin. J Biol Chem 263:1376–1381
63. Wei L, Hanna AD, Beard NA, Dulhunty AF (2009) Unique isoform-specific properties of calsequestrin in the heart and skeletal muscle. Cell Calcium 45:474–484

64. Gyorke S, Gyorke I, Terentyev D, Viatchenko-Karpinski S, Williams SC (2004) Modulation of sarcoplasmic reticulum calcium release by calsequestrin in cardiac myocytes. Biol Res 37: 603–607
65. Royer L, Rios E (2009) Deconstructing calsequestrin. Complex buffering in the calcium store of skeletal muscle. J Physiol 587:3101–3111
66. Paolini C, Quarta M, Nori A, Boncompagni S, Canato M, Volpe P, Allen PD, Reggiani C, Protasi F (2007) Reorganized stores and impaired calcium handling in skeletal muscle of mice lacking calsequestrin-1. J Physiol 583:767–784
67. Pertille A, de Carvalho CL, Matsumura CY, Neto HS, Marques MJ (2010) Calcium-binding proteins in skeletal muscles of the mdx mice: potential role in the pathogenesis of Duchenne muscular dystrophy. Int J Exp Pathol 91:63–71
68. Lestienne P, Bataille N, Lucas-Heron B (1995) Role of the mitochondrial DNA and calmitine in myopathies. Biochim Biophys Acta 1271:159–163
69. Rescher U, Gerke V (2004) Annexins -unique membrane binding proteins with diverse functions. J Cell Sci 117:2631–2639
70. Gerke V, Moss SE (2002) Annexins: from structure to function. Physiol Rev 82:331–371
71. Moss SE, Morgan RO (2004) The annexins. Genome Biol 5:219
72. Geisow MJ, Fritsche U, Hexham JM, Dash B, Johnson T (1986) A consensus amino-acid sequence repeat in Torpedo and mammalian Ca^{2+}-dependent membrane-binding proteins. Nature 320:636–638
73. Mishra S, Chander V, Banerjee P, Oh JG, Lifirsu E, Park WJ, Kim dH, Bandyopadhyay A (2011) Interaction of annexin A6 with alpha actinin in cardiomyocytes. BMC Cell Biol 12:7
74. Solito E, Nuti S, Parente L (1994) Dexamethasone-induced translocation of lipocortin (annexin) 1 to the cell membrane of U-937 cells. Br J Pharmacol 112:347–348
75. Brownstein C, Falcone DJ, Jacovina A, Hajjar KA (2001) A mediator of cell surface-specific plasmin generation. Ann N Y Acad Sci 947:143–155
76. Fatimathas L, Moss SE (2010) Annexins as disease modifiers. Histol Histopathol 25:527–532
77. Nishizuka Y (1988) The molecular heterogeneity of protein kinase C and its implications for cellular regulation. Nature 334:661–665
78. Rizo J, Sudhof TC (1998) C2-domains, structure and function of a universal Ca^{2+}-binding domain. J Biol Chem 273:15879–15882
79. Nalefski EA, Falke JJ (1996) The C2 domain calcium-binding motif: structural and functional diversity. Protein Sci 5:2375–2390
80. Newton AC (2010) Protein kinase C: poised to signal. Am J Physiol Endocrinol Metab 298:E395–E402
81. Steinberg SF (2008) Structural basis of protein kinase C isoform function. Physiol Rev 88: 1341–1378
82. Newton AC, Johnson JE (1998) Protein kinase C: a paradigm for regulation of protein function by two membrane-targeting modules. Biochim Biophys Acta 1376:155–172
83. Giorgione JR, Lin JH, McCammon JA, Newton AC (2006) Increased membrane affinity of the C1 domain of protein kinase Cdelta compensates for the lack of involvement of its C2 domain in membrane recruitment. J Biol Chem 281:1660–1669
84. Breitkreutz D, Braiman-Wiksman L, Daum N, Denning MF, Tennenbaum T (2007) Protein kinase C family: on the crossroads of cell signaling in skin and tumor epithelium. J Cancer Res Clin Oncol 133:793–808
85. Perin MS, Fried VA, Mignery GA, Jahn R, Sudhof TC (1990) Phospholipid binding by a synaptic vesicle protein homologous to the regulatory region of protein kinase C. Nature 345:260–263
86. Fernandez I, Arac D, Ubach J, Gerber SH, Shin O, Gao Y, Anderson RG, Sudhof TC, Rizo J (2001) Three-dimensional structure of the synaptotagmin 1 C2B-domain: synaptotagmin 1 as a phospholipid binding machine. Neuron 32:1057–1069
87. Craxton M (2004) Synaptotagmin gene content of the sequenced genomes. BMC Genomics 5:43
88. Fernández-Chacón R, Konigstorfer A, Gerber SH, García J, Matos MF, Stevens CF, Brose N, Rizo J, Rosenmund C, Sudhof TC (2001) Synaptotagmin I functions as a calcium regulator of release probability. Nature 410:41–49

89. Bunney TD, Katan M (2011) PLC regulation: emerging pictures for molecular mechanisms. Trends Biochem Sci 36:88–96
90. Lee JC, Simonyi A, Sun AY, Sun GY (2011) Phospholipases A2 and neural membrane dynamics: implications for Alzheimer's disease. J Neurochem 116:813–819
91. Brown EM, MacLeod RJ (2001) Extracellular calcium sensing and extracellular calcium signaling. Physiol Rev 81:239–297
92. Hofer AM (2005) Another dimension to calcium signaling: a look at extracellular calcium. J Cell Sci 118:855–862
93. Bornstein P (2009) Matricellular proteins: an overview. J Cell Commun Signal 3:163–165
94. Brekken RA, Sage EH (2001) SPARC, a matricellular protein: at the crossroads of cell-matrix communication. Matrix Biol 19:816–827
95. Busch E, Hohenester E, Timpl R, Paulsson M, Maurer P (2000) Calcium affinity, cooperativity, and domain interactions of extracellular EF-hands present in BM-40. J Biol Chem 275: 25508–25515
96. Podhajcer OL, Benedetti L, Girotti MR, Prada F, Salvatierra E, Llera AS (2008) The role of the matricellular protein SPARC in the dynamic interaction between the tumor and the host. Cancer Metastasis Rev 27:523–537
97. Maurer P, Hohenester E, Engel J (1996) Extracellular calcium-binding proteins. Curr Opin Cell Biol 8:609–617
98. Krebs J, Heizmann CW (2007) Calcium-binding proteins and the EF-hand principle. In: Krebs J, Michalak M (eds) Calcium: a matter of life or death. Elsevier, Amsterdam, pp 51–93
99. Stenflo J, Stenberg Y, Muranyi A (2000) Calcium-binding EGF-like modules in coagulation proteinases: function of the calcium ion in module interactions. Biochim Biophys Acta 1477:51–63
100. Handford PA (2000) Fibrillin-1, a calcium binding protein of extracellular matrix. Biochim Biophys Acta 1498:84–90
101. Pena F, Jansens A, van Zadelhoff G, Braakman I (2010) Calcium as a crucial cofactor for low density lipoprotein receptor folding in the endoplasmic reticulum. J Biol Chem 285:8656–8664
102. Cranenburg EC, Schurgers LJ, Vermeer C (2007) Vitamin K: the coagulation vitamin that became omnipotent. Thromb Haemost 98:120–125
103. Ohkubo YZ, Tajkhorshid E (2008) Distinct structural and adhesive roles of Ca^{2+} in membrane binding of blood coagulation factors. Structure 16:72–81
104. Hansson K, Stenflo J (2005) Post-translational modifications in proteins involved in blood coagulation. J Thromb Haemost 3:2633–2648
105. Halbleib JM, Nelson WJ (2006) Cadherins in development: cell adhesion, sorting, and tissue morphogenesis. Genes Dev 20:3199–3214
106. Boggon TJ, Murray J, Chappuis-Flament S, Wong E, Gumbiner BM, Shapiro L (2002) C-cadherin ectodomain structure and implications for cell adhesion mechanisms. Science 296:1308–1313
107. Oroz J, Valbuena A, Vera AM, Mendieta J, Gomez-Puertas P, Carrion-Vazquez M (2011) Nanomechanics of the cadherin ectodomain: "canalization" by Ca^{2+} binding results in a new mechanical element. J Biol Chem 286:9405–9418
108. Cambi A, Koopman M, Figdor CG (2005) How C-type lectins detect pathogens. Cell Microbiol 7:481–488
109. Zelensky AN, Gready JE (2005) The C-type lectin-like domain superfamily. FEBS J 272: 6179–6217
110. Silve C, Petrel C, Leroy C, Bruel H, Mallet E, Rognan D, Ruat M (2005) Delineating a Ca^{2+} binding pocket within the venus flytrap module of the human calcium-sensing receptor. J Biol Chem 280:37917–37923
111. Steddon SJ, Cunningham J (2005) Calcimimetics and calcilytics -fooling the calcium receptor. Lancet 365:2237–2239
112. Jiang Y, Huang Y, Wong HC, Zhou Y, Wang X, Yang J, Hall RA, Brown EM, Yang JJ (2010) Elucidation of a novel extracellular calcium-binding site on metabotropic glutamate receptor 1{alpha} (mGluR1{alpha}) that controls receptor activation. J Biol Chem 285:33463–33474

Chapter 20
Cytoplasmic Calcium Buffering

Juan A. Gilabert

Abstract Calcium buffering is one of the mechanisms to control calcium (Ca^{2+}) persistence in the cytosol and hence, Ca^{2+} dependence of many intracellular processes. Compared with Ca^{2+} sequestration into intracellular Ca^{2+} stores, Ca^{2+} buffering is a rapid process occurring in sub-second scale.

Ca^{2+} buffers can be mobile or fixed depending of their molecular weight, but other parameters as their concentration, affinity for Ca^{2+} or Ca^{2+} binding and releasing kinetics are important to know their role in Ca^{2+} signaling.

This process determines Ca^{2+} diffusion and spatiotemporal Ca^{2+} signaling in the cell and is one of the basis of the versatility and complexity of Ca^{2+} as intracellular messenger.

Keywords Ca^{2+} buffering • Mobile and immobile buffers • Modeling Ca^{2+} signaling

Introduction

In the previous chapters the reader has had opportunity to explore the properties and characteristics making of calcium the essential and more versatile ion messenger in the cells. But, how its concentration is so closely regulated within the cells and for what reason?.

Calcium (Ca^{2+}) ions are involved in many processes along vital cycle of the cells but they also are cytotoxic at all phylogenetic stages (from bacteria to eukaryotic cells) making necessary an universal Ca^{2+} homeostasis system [1].

J.A. Gilabert (✉)
Department of Toxicology and Pharmacology, Faculty of Veterinary Medicine, Complutense University of Madrid, Avda. Puerta de Hierro, s/n. 28040, Madrid, Spain
e-mail: jagilabe@vet.ucm.es

M.S. Islam (ed.), *Calcium Signaling*, Advances in Experimental Medicine and Biology 740, DOI 10.1007/978-94-007-2888-2_20,

Thus, primitive cells needed to face a massive, constant and toxic pressure due to Ca^{2+} gradient. The appearance of a plasma membrane in the primitive cell was the border between extra- and intracellular spaces leading to the need to a tight control of this cation concentration in the cytoplasm, with low concentrations inside against high concentrations in the extracellular milieu. This generates a huge gradient in terms of concentration and also in terms of net charge considering the negative net charge of the intracellular milieu.

Since primitive cells successful mechanisms were developed very early in the evolution process to precisely regulate the cellular concentrations of free and sequestered Ca^{2+} both in time and space. These mechanisms are essentially the same in prokaryotes and eukaryotes organisms [2].

At a single cell level, Ca^{2+} homeostasis determines that cytosolic Ca^{2+} concentration ($[Ca^{2+}]_c$) is tightly regulated around 100 nM (10^{-7} M). This is crucial for a proper signaling process mediated by Ca^{2+} which as any other effective signal, must be fast, with an adequate magnitude (to exceed a threshold) and finite in spatial and/or temporal terms.

This resting $[Ca^{2+}]_c$ works as a threshold to switch on any signaling processes mediated by Ca^{2+} against an electrochemical gradient due to the 10,000 times higher concentration in the extracellular milieu (around 1 mM or 10^{-3} M). This threshold is kept by different mechanisms as active transport involving energy (i.e. ATP-dependent) for Ca^{2+} fluxes out the cell or into the organelles, antiport systems, Ca^{2+} buffering (mobile and immobile buffers) or ion condensation.

Ca^{2+} buffering at the cytosol can be mediated by mobile or immobile buffers keeping under control the diffusion of free Ca^{2+} ions inside the cytoplasm and reducing its diffusion spread. In other words, Ca^{2+} changes can occurs in the whole cell space or restricted to small areas around those elements involved in Ca^{2+} fluxes.

The importance of Ca^{2+} control mechanisms can be also seen at intercellular and multicellular level in higher organisms, where Ca^{2+} homeostasis is also found in the extracellular fluid. Thus, control of Ca^{2+} homeostasis in the cell and its role in different physiological processes reflects an integrative function of Ca^{2+} considering a whole organism point of view.

Next, we will review these mechanisms with special attention to the role of cytoplasmic Ca^{2+} buffering in the generation of different spatiotemporal Ca^{2+} signals and its physiological relevance at a single cell (eukaryote) level.

Ca^{2+} Buffering: An Overview

Control of $[Ca^{2+}]_c$ at the resting levels involves several mechanisms as Ca^{2+} influx (from the extracellular space), Ca^{2+} release (from internal Ca^{2+} stores), Ca^{2+} sequestration (towards internal Ca^{2+} stores), Ca^{2+} efflux (to the extracellular space) or Ca^{2+} buffering. Hence, Ca^{2+} persistence in the cytosol and derived Ca^{2+}-mediated actions are determined by two main processes: Ca^{2+} removal and Ca^{2+} diffusion (Fig. 20.1).

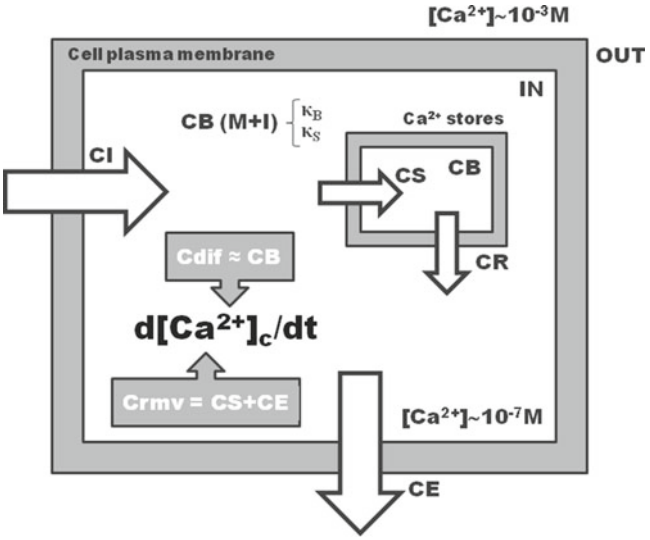

Fig. 20.1 Processes involved in the control of calcium concentration in the cytosol ($[Ca^{2+}]_c$). *CI* calcium influx, *CR* calcium release, *CS* calcium sequestration, *CE* calcium efflux, *CB* calcium buffering (*M* mobile and *I* immobile buffers). κ_B and κ_S: Ca^{2+}-binding ratios (ratio of bound to free Ca^{2+}) for mobile and fixed buffers, respectively. Ca^{2+} removal from the cytosol (*Crmv*) is a combined action of CS and CE. Ca^{2+} diffusion (*Cdif*) is mainly determined by CB. The combined action of these fluxes determines how $[Ca^{2+}]_c$ changes with the time ($d[Ca^{2+}]_c/dt$) to generate different patterns of spatiotemporal signaling

Ca^{2+} removal from the cytosol is a combined action of Ca^{2+} sequestration and Ca^{2+} efflux while Ca^{2+} diffusion is mainly determined by Ca^{2+} buffering. Ca^{2+} buffering is the rapid binding of Ca^{2+} ions entering to cytosolic space to different cellular binding sites. Ca^{2+} buffering is an important process in Ca^{2+} signaling because have been estimated that only about 1–5% of Ca^{2+} ions entering into the cell remains as free Ca^{2+}, their physiologically active form [3–7].

In 1992, Neher and Augustine showed that Ca^{2+} buffering was a rapid process kinetically distinct of Ca^{2+} sequestration, which is slower and occurs in tens of seconds scale. They also were able to determine at a single-cell level, using a combination of fura-2 microfluorimetry and Ca^{2+} current measurements, the Ca^{2+} binding capacity of cytoplasm (κ_s) [8]. The κ_s value was approximately 75, which did not change during prolonged whole cell recording (with a disrupted cell membrane). Thus, they concluded that the majority of cellular Ca^{2+} binding sites were immobile [9].

Immobile buffers are represented by molecules of high molecular weight or anchored to intracellular structures. Mobile buffers are molecules of low molecular size, typically less than 20–25 kDa, as soluble proteins or small organic anions and metabolites but mainly ATP. Their contribution can be difficult to estimate in some experiments involving whole cell recordings where washout phenomena lead to the loss of some of these small molecules. Mobile buffers are estimated to have a Ca^{2+} binding capacity about one tenth of the cytosol Ca^{2+} binding capacity.

One of main mobile Ca^{2+} buffers is ATP. ATP concentration in the cytosol is estimated to be around 2–3 mM from which 0.4 mM is in a free form. ATP is a highly mobile and effective Ca^{2+} chelator [10, 11].

But, how important is the mobility of buffers in the cell? When a signal opens a Ca^{2+} channel a fast and steep Ca^{2+} flux enters into the cytoplasm from extracellular space or from organelles driven by a large electrochemical gradient. Thus, more than 95% of the Ca^{2+} ions are immediately bound to the buffers within a distance of 10–50 nm from the point of Ca^{2+} entry [12, 13]. A mobile Ca^{2+} buffer will act to disperse such domains of elevated $[Ca^{2+}]_c$ whereas fixed Ca^{2+} buffers will tend to prolong them.

Therefore, commonly used exogenous buffers/chelators for experimental purposes (as EGTA or BAPTA or fluorescent indicators as fura-2) must be also considered due they reduce the effect of endogenous buffers increasing the transport of Ca^{2+} across the cell [14].

The presence of mobile and immobile buffers greatly reduces the diffusion spread of Ca^{2+}. The effective diffusion constant for Ca^{2+} free is around 300 $\mu m^2/s$ being reduced more than 20 times (<16 $\mu m^2/s$) by cytoplasmic buffering [15]. This fact was already described by Hodgkin and Keynes in 1957 in squid giant axon where the retardation factor of radioactivity-labeled Ca^{2+} was about 40 [3]. However, the timescale of those experiments was of minutes when Ca^{2+} buffering and Ca^{2+} sequestration can be already equilibrated.

One parameter that offers us one idea of Ca^{2+} diffusion is the mean distance covered by Ca^{2+} ions in one dimension. This distance can be calculated as $(2D_{eff}\,t)^{1/2}$, where D_{eff} is the effective diffusion coefficient for Ca^{2+} and t is the uptake time constant.

A stationary state situation (determining the threshold, usually around 100 nM) will be reached with Ca^{2+} influx or Ca^{2+} release to the cytosol space become equals to Ca^{2+} efflux plus Ca^{2+} sequestration to organelles and plus the buffered Ca^{2+} [16, 17].

Correspondingly the results of previous simulations on the spatial and temporal pattern of Ca^{2+} changes following stimulation depended very much on the assumptions made about mobility of buffers [18, 19]. Thus, it is important to have experimental data on mobility of cellular Ca^{2+} buffers. The result, showed by Neher and Augustine [8], that there is very little mobile buffer, would mean that addition of even minute concentrations of an exogenous mobile Ca^{2+} buffer, such as fura-2 (as in Ca^{2+} imaging experiments) should alter the temporal pattern of Ca^{2+} redistribution.

Ca^{2+} Buffers

Ca^{2+} role as intracellular messenger is highly dependent of the maintenance of their levels in the extracellular and intracellular spaces and the resulting high electrochemical driving force. Thus, minor changes in plasma membrane permeability to Ca^{2+} can make possible significant changes in the intracellular Ca^{2+} levels.

Any molecule (or process) with the ability to bind Ca^{2+} ions could be considered at least in principle as a buffer. However, the term Ca^{2+} buffer is applied only a small subset of Ca^{2+} binding proteins containing acidic side-chain residues.

The Ca^{2+} binding proteins can be found in the cytosol (as soluble proteins); but also inside organelles (intraluminal proteins) as in the endoplasmic reticulum (ER) or as intrinsic proteins in membranes (plasma or organellar membranes) (see Calcium Binding Proteins chapter on this volume). Ca^{2+} buffers are Ca^{2+} binding proteins which can bind the most of free Ca^{2+} at the cytosol [20]. The first of these proteins to be described was troponin C [21].

Several proteins families are able to bind Ca^{2+} thanks to different structural motifs as EF-hands [22] or other Ca^{2+} bindings sites [23]. However, the term Ca^{2+} buffer is applied only to a small subset of proteins of the EF-hand family, including parvalbumins (α and β isoforms), calbindin-D9k, calbindin D-28k and calretinin in the cytosol [20].

In the ER, main intraluminal Ca^{2+} buffers are calsequestrin and calreticulin (which can operate also in the cytosol). These organellar Ca^{2+} buffers play an important role as modulators in a dynamic network of organellar Ca^{2+} signaling [24].

Another Ca^{2+} binding proteins play a role as Ca^{2+} sensors more than as Ca^{2+} buffers due to its low concentration in the cell [20]. Ca^{2+} ions bind to Ca^{2+} sensors inducing a conformational change, which permits them to interact with specific targets in a Ca^{2+}-regulated manner. A prototype Ca^{2+} sensor is calmodulin [25].

On the other hand, depending on their diffusion characteristics, buffers can be considered as mobile or immobile. Therefore, their rate constants of Ca^{2+} binding and dissociation cover a wide range from slow buffers (with constants values about 1 s^{-1}) to fast buffers (constant values about 100 s^{-1}) [26].

An obvious consequence of the presence of Ca^{2+} buffers in the cells is Ca^{2+} buffering capacity of the cytoplasm, which will be directly dependent of their concentration and spatial location of the Ca^{2+} buffers. However, other parameters as affinity for Ca^{2+}, Ca^{2+} binding and releasing kinetics, or diffusional mobility contributes to make of Ca^{2+} signaling one of the most complex signaling activities of the cell.

Intracellular Concentration of Ca^{2+} Buffers

Intracellular Ca^{2+} buffering capacity (κ_s) is directly related to the concentration of Ca^{2+} buffers expressed in the cytosol [13]. However, this parameter is quite variable (μM to mM ranges) amongst different types of cells or even in the same cell depending of host tissue or species [13, 20].

An adequate approximation to the endogenous Ca^{2+} binding ratio is to estimate the ratio of buffer-bound Ca^{2+} changes over free Ca^{2+} changes ($\kappa_s \sim [Ca^{2+}\ \text{buffer}]/K_{D,Ca}$]) [13, 27]. We can also use this ratio to compare the Ca^{2+} buffering capacity κ_s of different cells whose values can be ranged from low (below 50) for motor neurons [28] to very high (around 1,000–2,000) as that found in cerebellar Purkinje neurons [29] (Table 20.1). It indicates that low values are probably needed in cells for a rapid Ca^{2+} signaling [30].

Table 20.1 Values of Ca^{2+} binding ratio (κ_S) in different cell types. More details (as experimental conditions of measurements) can be founded in the respective original references

Cell type	κ_s	References
Motor neurons	<50	[28]
Adrenal chromaffin cells	40–75	[8, 9]
Hippocampal neurons	60	[83]
Dopaminergic neurons	110–179	[30]
Smooth muscle from coronary artery	150	[84]
PV-expressing interneurons	150	[32]
Cerebellar Purkinje cells	900–2,000	[29]
Pancreatic acinar cells	1,500–2,000	[85]

Ca^{2+} Binding and Kinetics by Ca^{2+} Buffers

The EF-hands motifs are Ca^{2+}-binding sites with different selectivity and affinity for Ca^{2+} and Mg^{2+} ions [31]. The Ca^{2+}-specific sites display affinities for Ca^{2+} (K_{Ca}) of 10^{-3} to 10^{-7} M and significant lower ones for Mg^{2+} ($K_{Mg} = 10^{-1}$ to 10^{-2} M). The Ca^{2+} and Mg^{2+} sites bind Ca^{2+} with high ($K_{Ca} = 10^{-7}$ to 10^{-9} M) and Mg^{2+} with moderate (10^{-3} to 10^{-5} M) affinities (see [20]).

The majority of Ca^{2+} buffers have values of dissociation constants ($K_{D,Ca}$) in the low micromolar range. For it, in a resting cell Ca^{2+} buffers are mostly in a Ca^{2+}-free form. Another parameter to be considered is the kinetics of this binding (k_{on}). Ca^{2+} buffers considered as fast have k_{on} rates $> 10^8$ M^{-1} s^{-1} while those considered as slow have k_{on} rates around 10^6 M^{-1} s^{-1}. It is due to presence of Mg^{2+} (0.5–1.0 mM in physiological conditions) which determines the Ca^{2+}-binding due to the slow Mg^{2+} off rate [32]. Endogenous Ca^{2+} buffers posses several Ca^{2+} binding sites with different affinities and kinetics. The ratio between high:intermediate affinity can be 3:1 or 2:2 [33]. Therefore, Ca^{2+} binding sites (EF-hands) show allosterism in function of the occupied sites resulting in a non-linear Ca^{2+} buffering [34, 35].

Intracellular Mobility of Ca^{2+} Buffers

Ca^{2+} buffering is, at least in mechanistic terms, a different process of Ca^{2+} sequestration. The majority of Ca^{2+} entering ions to the cytoplasm space will be rapidly bound by Ca^{2+} buffers and later on sequestered into Ca^{2+} storing organelles by slower kinetically process [8]. Mobility of Ca^{2+} buffers is also an important determinant of the Ca^{2+} signaling due to a mobile Ca^{2+} buffer will disperse a local increment of Ca^{2+}.

Mobility of a Ca^{2+} buffer is expressed by its diffusion coefficient (D) which is proportional to the molecular weight but it is also influenced by some other factors. Molecular diffusion is a complex process determined by a dynamic and out-of equilibrium environment as the cytoplasm. The rate of the diffusion movement of a molecule

or particle is a function of temperature (thermal Brownian movement), viscosity and its radius (i.e. mass) (see [36]). Therefore, a same molecule can have different D values in different cellular compartments as occurs as parvalbumin with a D around 12 $\mu m^2/s$ in axons, somata and nuclei [37] versus 43 $\mu m^2/s$ in dendrites [38].

Physiological Relevance of Cytosolic Ca^{2+} Buffering

Ca^{2+} signaling can be observed and described in different levels of organization ranging from the whole organism to subcellular level but they are closely related [39, 40]. Most of Ca^{2+} in higher organisms is bound to bones and teeth forming hydroxyapatite. In humans, from the total amount of Ca^{2+} (1,250 g) only a few grams are in the extracellular and intracellular fluids, this level is controlled by the movements in and out of the bone deposits [41] and maintained by vitamin D and parathyroid hormone actions. Plasma concentration of Ca^{2+} is quite variable in animals from 1 to 15 mM (2.1–2.6 mM in man) but levels under 0.9 mM can produce uncontrollable muscle spasm (i.e. tetany).

As discussed above, extracellular (plasma) levels determines the electrochemical gradient respect to intracellular levels and Ca^{2+} fluxes from extracellular fluid to inside the cells are the signals and sources of Ca^{2+} for subcellular organelles as the ER, mitochondrion or nucleus. Thus, the extracellular pool acts as a large reservoir of free Ca^{2+}.

An increase of cytoplasmic $[Ca^{2+}]$ is the key signal to initiate many physiological actions as synaptic transmission, muscle contraction, hormonal secretion or gene expression [42]. Moreover, Ca^{2+} signaling is also present throughout the life history of the cell from its birth (mitosis) to death (apoptosis) [16, 43]. Alterations of Ca^{2+} homeostasis and signaling from systemic to subcellular levels also play a pivotal role in the pathogenesis of many diseases [44–49].

But, Ca^{2+} signaling is based not only in changes in their concentration at the cytoplasm levels. Cells have developed a complex code of signals based in the modulation of Ca^{2+} concentration on spatial and temporal basis [50]. Thus, Ca^{2+} signals can be graded from unitary and spatially located signals, with a very limited diffusion through the cell, to whole cell signals as Ca^{2+} waves or Ca^{2+} oscillations with Ca^{2+} changes travelling across the cell. These global signals are possible due to a coordinated activity of Ca^{2+} release and Ca^{2+} sequestration.

But, a signal to be an effective messenger must be finite. Ca^{2+} buffering and Ca^{2+} sequestration are crucial mechanisms to make intracellular Ca^{2+} changes transients, permitting to the cell recover the threshold and to be ready again for a new signaling round.

Ca^{2+} buffering changes can affect signaling patterns and modulate Ca^{2+} dependent physiological process. Thus, neuronal excitability can be modulated by Ca^{2+} buffering changing from an spike-based pattern to a bursting signaling [51].

Spatiotemporal Signaling

Intracellular Ca^{2+}signaling, as occurs with other second messengers-mediated signaling, can be also coded by changes in amplitude and frequency. Thus, the quality and quantity of an extracellular incoming signal is reflected at different domains in the cell [52]. Amplitude may be proportional to the strength of extracellular stimulus and the frequency to the strength and quality of the signal. But, local increase of Ca^{2+} in restricted domains represents an additional way of coding the signal at a spatial level. The combination of all these mechanisms make possible a huge variety of signals originated by intracellular Ca^{2+} changes [16, 50].

Ca^{2+} dynamics can be analyzed at several levels from unitary or elementary events (restricted to subcellular spaces) to global events (as waves or oscillations) occurring at whole cell level.

The basic phenomena involved in Ca^{2+} dynamics at a cytosolic level is the opening of a single channel in the plasma membrane or in an intracellular Ca^{2+}-store organelle leading to Ca^{2+} entry or Ca^{2+} release. They are elementary events which can be the starters of whole cell events (e.g. Ca^{2+} sparks and Ca^{2+} induced Ca^{2+} release from SR). Many other different elementary Ca^{2+} signaling events have been described from many cell and tissues types [53].

In an elementary event, opening is usually brief in duration and leads to a small and local increase of Ca^{2+} concentration. This local and spatially restricted increase of intracellular Ca^{2+} concentration results in the formation of submicron sharp Ca^{2+} concentration profile in the vicinity of the channel [54]. The temporal collapse of these Ca^{2+} domains after channel closing is believed to be achieved in the microsecond time scale.

Microdomain Ca^{2+} increases are restrained by a strong buffering and slow diffusion. The microdomain size is obviously a function of several parameters as the conductivity and opening time of the channel (i.e. how many ions can pass through channel pore by time unit) and the electrochemical driving force for Ca^{2+} (i.e. free Ca^{2+} concentration at both sides of channel) but it is strongly influenced by the buffer properties.

Ca^{2+} Buffering and Organelles

Ca^{2+} diffusion throughout the cell is not only restrained by Ca^{2+} buffering. Pumping (i.e. Ca^{2+} fluxes against the electrochemical gradients) removes Ca^{2+} from cytoplasm towards the extracellular space (plasma membrane Ca^{2+}-ATPases and Na/Ca^{2+} exchanger) into the ER (by SERCA pumps) and into the mitochondria (by the uniporter). In a resting state or for small Ca^{2+} changes the dominant pumping fluxes are into the ER and to the extracellular space. Whereas larger Ca^{2+} signals (micromolar range) involves mitochondrial participation [55].

The SERCA pumps are in charge of Ca^{2+} sequestration from the cytosol to inside of ER. This Ca^{2+} binds to intraluminal Ca^{2+} binding proteins with high capacity (10 mol per mol of protein) but low affinity (Kd around 1 μM) which permit to the ER stores huge amounts of Ca^{2+} which can rapidly exchange with cytosol. Many proteins in the ER can bind Ca^{2+}, Ca^{2+} is stored bound to Ca^{2+} binding proteins including calreticulin, protein disulfide isomerase (PDI), Glucose regulated protein 94 (Grp94), Immunoglobulin binding protein (BiP), and ERp57. In the sarcoplasmic reticulum (SR) the most abundant Ca^{2+} binding protein is calsequestrin next to sarcolumenin, a histidine-rich protein, junctin, junctate, and triadin (unique to the SR membrane) [56].

ER plays a dynamic role in Ca^{2+} signaling due it can exchange their intraluminal Ca^{2+} with the cytosol in a rapid manner by means of different stimuli of Ca^{2+} release through InsP3 or ryanodine receptors or by means of a passive leak channel.

The total concentration in the ER have been estimated between 5 and 50 mM [57]. The majority of this Ca^{2+} is bound with low affinity to proteins (Kd = 1–4 mM) as calreticulin/calsequestrin and other intraluminal proteins with Ca^{2+} binding capacity as chaperones. The high intraluminal content of Ca^{2+} and the low affinity of ER Ca^{2+} buffers suggest that Ca^{2+} free concentration inside the ER could be in the micromolar range (300–800 μM depending of cell type) [58].

Mitochondria is the another crucial organelle in the Ca^{2+} homeostasis in the cell, as the ER, mitochondria can store huge amounts of Ca^{2+}. Moreover the cation also plays an important role linking Ca^{2+} signaling with mitochondrial energetic status and cell death by apoptosis [59].

The Ca^{2+} entry way to the mitochondria occurs throughout the uniporter located in the organelle's inner membrane. Mitochondrial Ca^{2+} uniporter is a selective Ca^{2+} channel with very low affinity (K_m = 20 μM) and high capacity [60, 61].Thus, mitochondria is the predominant system of Ca^{2+} sequestration only when the $[Ca^{2+}]_c$ is well above of those reached during activation (around 1 μM) where PMCA and SERCA are the main Ca^{2+} transport systems [62].

An additional mechanism of Ca^{2+} entry into the mitochondria known as rapid uptake mode or RaM was described in hepatocytes [63]. RaM function could be to create a brief but high free Ca^{2+} concentration signal inside mitochondria which may activate intramitochondrial metabolic reactions with relatively small amounts of Ca^{2+} uptake reducing the probability to open Ca^{2+}-induced mitochondrial membrane permeability transition (MPT) [64]. Thus, mitochondria are the decoder between intensity of signaling and metabolic activity but also the place where the regulated process of death starts when Ca^{2+} homeostasis is lost.

An interesting point in order to understand Ca^{2+} dynamics in the cytoplasm is the crosstalk between organelles and plasma membrane. In fact, high resolution techniques have permitted to observe that the mitochondrial network inside the cells can be very close or even in contact with the ER membrane or plasma membrane channels. Thus, mitochondria could be able to sense large but spatially limited Ca^{2+} increments derived from InsP3 receptor activation or other Ca^{2+} fluxes from plasma membrane channels as VDCC or SOCE [11, 65, 66]. But, also increasing Ca^{2+} buffering capacity by a local release of ATP [11].

Elements for Modeling Ca^{2+} Buffering and Signaling

Ca^{2+} signaling processes share a common feature: they are a single (or repetitive) transient increase of their intracellular concentration. However, Ca^{2+} signaling has evolved towards many different signals in different cell types from local to global (whole cell) scales.

Ca^{2+} dynamics can be seen as a process of extremely complexity due to cells have the machinery to encode multiple Ca^{2+} signals with many different spatiotemporal patterns involving many different structural elements (e.g. pumps, channels, Ca^{2+} buffers, organelles,…) [16]. But, to understand Ca^{2+} dynamics in the cell also implies to know the influence of Ca^{2+} buffering in the control of this spatiotemporal code.

In the beginning, modeling of intracellular Ca^{2+} dynamics focused in the entry ways of Ca^{2+} (i.e. channels) considering the inside of cells as a continuous medium. Later, more descriptive models were proposed to explain activation kinetics of a single channel or spatial arrangements of a group of channel and the role of mobile and immobile buffers or even the alterations due to the exogenous buffers presence.

On the other hand, modeling permits a predictive analysis from experimental results and to study the particular contribution of different elements in a complex system. Mathematics behinds Ca^{2+} modeling can be hard for some of us (a comprehensive review about this issue have been written by Martin Falcke [67]). Thus, only the main elements (variables) and their role in the control of cytoplasmic Ca^{2+} will be shortly described below.

A valuable tool to study the contribution of buffers and its properties to Ca^{2+} signaling have been the single-cell techniques using Ca^{2+} indicators (as fura-2) and microfluorimetry. They have also permitted to study the contribution of exogenous Ca^{2+} buffers (i.e. fluorescent Ca^{2+} probes) competing with endogenous Ca^{2+} buffers [13]. The known as "added-buffer method" (see below) is based in the study of changes in fluorescent signals due to additions of exogenous buffer to compete with endogenous buffer in order to calculate binding capacity.

The basis to understand complex Ca^{2+} cellular signals as waves or oscillations is to describe Ca^{2+} fluxes through a single channel and to estimate their contribution to the global Ca^{2+} signal. For it, we need to know how Ca^{2+} buffering processes affect the intracellular diffusion of a Ca^{2+} wave entering by a single channel. The free Ca^{2+} increase from a single channel opening (or elementary event as blips or quarks) will depend of Ca^{2+} current and buffering characteristics of the cytosol, mainly.

In the early works, the aim was to estimate the cytosolic Ca^{2+} rise near the inner side of a single Ca^{2+} channel [68, 69] or by different arrays of single channels [70] and they have permitted us to understand mechanisms controlled by local Ca^{2+} signals; as Ca^{2+}-dependent inactivation of Ca^{2+} channels or activation of Ca^{2+}-dependent potassium channels [71] or highly specialized physiological processes as neurosecretion by regulated exocytosis [72].

The unitary Ca^{2+} signal mediated by a single channel is a nanodomain which produces a Ca^{2+} elevation until 50 nm from channel pore in neurons [73]. Thus, any potential Ca^{2+}-dependent process controlled by a nanodomain must have a Ca^{2+} sensor in that distance range as occurs in rapid release neurotransmitter release or the Ca^{2+}

dependent modulation of ionic channels commented above. Small groups or clusters of single channels can lead to a summation phenomenon of nanodomains producing some stronger signals or microdomains. These microdomains require Ca^{2+} sensors that are placed within a fraction of a micrometer from the Ca^{2+} channel cluster, to allow detection of summed signals.

The spread of Ca^{2+} during elemental events is the process most directly affected by buffer properties [19]. Thus, many efforts have been done to understand the cytosolic buffer dynamics and their influence in Ca^{2+} signaling from elementary events.

However, Ca^{2+} nano or microdomains occurs in spatial and temporal scales that requires highly sensitive optical imaging techniques [74]. An alternative is the theoretical approach to study the influence of buffering on Ca^{2+} microdomains formation and diffusion [8, 10, 14, 75, 76].

At this level some other phenomena can be considered, as the stochastic behavior or the spatial grouping of Ca^{2+} permeating channels forming clusters [26], much more complex and demanding in order to design a reliable mathematical approach.

An additional level of complexity of Ca^{2+} signaling occurring in the cytosol is represented by global phenomena as waves or oscillations. They reflect a synchronically coordinated activity between release and diffusion processes involving several fluxes among different cellular compartments and organelles. These fluxes are usually visualized as a periodic behavior of the Ca^{2+} concentration levels travelling across the cell.

Ca^{2+} waves were first observed in fertilized fish oocytes [77], now we know different patterns from one-way linear displacement to spiral waves with a synchronous or asynchronous behavior depending of cell types [78, 79]. Ca^{2+} wave propagation can be modified by changing InsP3 or buffer concentration, mitochondrial Ca^{2+} uptake or overexpressing SERCA pumps (see [67]). Repetitive Ca^{2+} spikes were instead first time observed in agonist-stimulated hepatocytes [80]. Ca^{2+} oscillations reflect an alternative exchange of Ca^{2+} between the buffers and the ER mediated by InsP3R and the SERCA [26] with dependence of external Ca^{2+} in the majority of cells. Ca^{2+} oscillations and waves can be found in many cells from intra- to intercellular level of signaling (coordinated and cooperative responses in multicellular systems). These transient events can permit to the cell a communication based in frequency instead of amplitude avoiding longed exposures to high Ca^{2+} concentrations potentially toxic for cells.

The mathematical description of global phenomena can be very complex (in function of the number of variables considered, see [81]). However, Ca^{2+} signaling involves a complex system with many elements and multiple interactions and models are useful tools to understand the spatiotemporal behavior of Ca^{2+} signaling in a particular system.

There are three basic types of models: qualitative, phenomenological and quantitative or mechanistic. Qualitative models are presented in a diagrammatic rather than mathematical form; they are easy to do and can serve to support an initial hypothesis. Phenomenological models are based and expressed in a mathematical form to explain the experimental observations. One of main disadvantage is that widely differing mathematical models can behave in a similar way. Finally, the quantitative or mechanistic are based as far as possible on known mechanisms and experimentally validated parameters [82].

Calculating Changes in Free Ca^{2+} Concentration

The most basic scenario to model Ca^{2+} transients is to consider that they occurs in a single compartment model [8]. Consider a cell (or subcellular location, e.g. dendritic segment) with a volume V and a Ca^{2+} influx (j_{in}) as consequence of a stimulus which will produce an increase in the total Ca^{2+} concentration. These Ca^{2+} ions will be partitioned in the cytoplasm between the endogenous Ca^{2+} buffer component (S) and the exogenous Ca^{2+} indicator/buffer (B) with constant Ca^{2+}-binding ratios κ_S and κ_B, respectively. The Ca^{2+} removal (j_{out}) is modeled as a linear extrusion mechanism with rate constant γ.

The next equation describes the kinetics of Ca^{2+} changes (with conservation of total Ca^{2+}) [27]:

$$\frac{d[Ca^{2+}]_i}{dt} + \frac{d[BCa]}{dt} + \frac{d[SCa]}{dt} = \frac{(j_{in} - j_{out})}{V} \tag{20.1}$$

where [BCa] is the concentration of a mobile buffer (such as fura-2) in its Ca^{2+}-bound form, [SCa] is the concentration of fixed (endogenous) Ca^{2+} buffer in the Ca^{2+}-bound form, and V is the accessible volume of the cell (or compartment).

The Eq. 20.1 can be expressed in function of calcium binding capacities of B and S as

$$\frac{d[Ca^{2+}]_i}{dt}\left(1 + \kappa_B + \kappa_S\right) = \frac{(j_{in} - j_{out})}{V}$$

where

$$\kappa_B = \frac{d[BCa]}{[Ca^{2+}]_i}$$

and

$$\kappa_S = \frac{d[SCa]}{[Ca^{2+}]_i}$$

Thus, to calculate changes in free Ca^{2+} concentration we need to know the proportion of current carried by calcium, the accessible cell volume, and the cellular Ca^{2+} binding ratio.

Ca^{2+}-Binding Ratio

Several experimental approaches have been employed to estimate Ca^{2+} fluxes and free Ca^{2+} concentration in cells being the most popular the combination of fluorescent imaging using Ca^{2+} indicators dyes with the electrophysiological measurements. But, these Ca^{2+} indicators are exogenous Ca^{2+} buffers that contribute to cytoplasmic Ca^{2+} binding capacity.

In 1995, E. Neher developed the "added buffer method" to estimate the endogenous component of Ca^{2+} buffering [13]. It consists to measure the Ca^{2+} transient in response to different exogenous Ca^{2+} indicator concentration making possible to extrapolate to zero concentration of added exogenous indicator to estimate endogenous Ca^{2+} buffering.

The differential Ca^{2+}-binding ratio of a Ca^{2+} buffer X (previously termed Ca^{2+}-binding capacity) is defined as $\kappa_X = d[XCa]/d[Ca^{2+}]_i$. In the practice, to calculate κ_S we need to measure changes in both the fluorescent signal and in the total calcium entering into the cytosol (valid for short time intervals and small incremental elevations in $[Ca^{2+}]_c$). As explained before, κ_S can be estimated by different approaches like the analysis of Ca^{2+} signal or the amount of Ca^{2+} bound to buffer (see [8, 13] for alternative methods and problems measuring Ca^{2+}-binding ratio).

References

1. Dominguez DC (2004) Calcium signalling in bacteria. Mol Microbiol 54:291–297
2. Case RM, Eisner D, Gurney A, Jones O, Muallem S, Verkhratsky A (2007) Evolution of calcium homeostasis: from birth of the first cell to an omnipresent signalling system. Cell Calcium 42:345–350
3. Hodgkin AL, Keynes RD (1957) Movements of labelled calcium in squid giant axons. J Physiol 138:253–281
4. Smith SJ, Zucker RS (1980) Aequorin response facilitation and intracellular calcium accumulation in molluscan neurones. J Physiol 300:167–196
5. Gorman AL, Thomas MV (1980) Intracellular calcium accumulation during depolarization in a molluscan neurone. J Physiol 308:259–285
6. McBurney RN, Neering IR (1985) The measurement of changes in intracellular free calcium during action potentials in mammalian neurones. J Neurosci Methods 13:65–76
7. Ahmed Z, Connor JA (1988) Calcium regulation by and buffer capacity of molluscan neurons during calcium transients. Cell Calcium 9:57–69
8. Neher E, Augustine GJ (1992) Calcium gradients and buffers in bovine chromaffin cells. J Physiol 450:273–301
9. Zhou Z, Neher E (1993) Mobile and immobile calcium buffers in bovine adrenal chromaffin cells. J Physiol 469:245–273
10. Naraghi M, Neher E (1997) Linearized buffered Ca2+ diffusion in microdomains and its implications for calculation of [Ca2+] at the mouth of a calcium channel. J Neurosci 17: 6961–6973
11. Montalvo GB, Artalejo AR, Gilabert JA (2006) ATP from subplasmalemmal mitochondria controls Ca2+–dependent inactivation of CRAC channels. J Biol Chem 281:35616–35623
12. Augustine GJ, Neher E (1992) Calcium requirements for secretion in bovine chromaffin cells. J Physiol 450:247–271
13. Neher E (1995) The use of fura-2 for estimating Ca buffers and Ca fluxes. Neuropharmacology 34:1423–1442
14. Wagner J, Keizer J (1994) Effects of rapid buffers on Ca2+ diffusion and Ca2+ oscillations. Biophys J 67:447–456
15. Gabso M, Neher E, Spira ME (1997) Low mobility of the Ca2+ buffers in axons of cultured Aplysia neurons. Neuron 18:473–481
16. Berridge MJ, Lipp P, Bootman MD (2000) The versatility and universality of calcium signalling. Nat Rev Mol Cell Biol 1:11–21

17. Berridge MJ, Bootman MD, Roderick HL (2003) Calcium signalling: dynamics, homeostasis and remodelling. Nat Rev Mol Cell Biol 4:517–529
18. Sala F, Hernandez-Cruz A (1990) Calcium diffusion modeling in a spherical neuron. Relevance of buffering properties. Biophys J 57:313–324
19. Nowycky MC, Pinter MJ (1993) Time courses of calcium and calcium-bound buffers following calcium influx in a model cell. Biophys J 64:77–91
20. Schwaller B (2010) Cytosolic Ca2+ buffers. Cold Spring Harb Perspect Biol 2:a004051
21. Ebashi S (1963) Third component participating in the superprecipitation of 'Natural Actomyosin'. Nature 200:1010
22. Gifford JL, Walsh MP, Vogel HJ (2007) Structures and metal-ion-binding properties of the Ca2+−binding helix-loop-helix EF-hand motifs. Biochem J 405:199–221
23. Bindreither D, Lackner P (2009) Structural diversity of calcium binding sites. Gen Physiol Biophys 28 Spec No Focus:F82–F88
24. Prins D, Michalak M (2011) Organellar calcium buffers. Cold Spring Harb Perspect Biol 3:a004069, http://www.ncbi.nlm.nih.gov/pubmed/21421925
25. Chin D, Means AR (2000) Calmodulin: a prototypical calcium sensor. Trends Cell Biol 10:322–328
26. Falcke M (2003) Buffers and oscillations in intracellular Ca2+ dynamics. Biophys J 84:28–41
27. Mathias RT, Cohen IS, Oliva C (1990) Limitations of the whole cell patch clamp technique in the control of intracellular concentrations. Biophys J 58:759–770
28. Lips MB, Keller BU (1998) Endogenous calcium buffering in motoneurones of the nucleus hypoglossus from mouse. J Physiol 511(Pt 1):105–117
29. Fierro L, Llano I (1996) High endogenous calcium buffering in Purkinje cells from rat cerebellar slices. J Physiol 496(Pt 3):617–625
30. Foehring RC, Zhang XF, Lee JC, Callaway JC (2009) Endogenous calcium buffering capacity of substantia nigral dopamine neurons. J Neurophysiol 102:2326–2333
31. Celio M, Pauls T, Schwaller B (1996) Guidebook to the calcium-binding proteins. Oxford University Press, Oxford
32. Lee SH, Schwaller B, Neher E (2000) Kinetics of Ca2+ binding to parvalbumin in bovine chromaffin cells: implications for [Ca2+] transients of neuronal dendrites. J Physiol 525(2):419–432
33. Nagerl UV, Novo D, Mody I, Vergara JL (2000) Binding kinetics of calbindin-D(28 k) determined by flash photolysis of caged Ca(2+). Biophys J 79:3009–3018
34. Schwaller B (2009) The continuing disappearance of "pure" Ca2+ buffers. Cell Mol Life Sci 66:275–300
35. Faas GC, Schwaller B, Vergara JL, Mody I (2007) Resolving the fast kinetics of cooperative binding: Ca2+ buffering by calretinin. PLoS Biol 5:e311
36. Brangwynne CP, Koenderink GH, MacKintosh FC, Weitz DA (2008) Cytoplasmic diffusion: molecular motors mix it up. J Cell Biol 183:583–587
37. Schmidt H, Arendt O, Brown EB, Schwaller B, Eilers J (2007) Parvalbumin is freely mobile in axons, somata and nuclei of cerebellar Purkinje neurones. J Neurochem 100:727–735
38. Schmidt H, Brown EB, Schwaller B, Eilers J (2003) Diffusional mobility of parvalbumin in spiny dendrites of cerebellar Purkinje neurons quantified by fluorescence recovery after photobleaching. Biophys J 84:2599–2608
39. Williams RJ (1998) Calcium: outside/inside homeostasis and signalling. Biochim Biophys Acta 1448:153–165
40. Williams RJ (2006) The evolution of calcium biochemistry. Biochim Biophys Acta 1763:1139–1146
41. Carafoli E (1987) Intracellular calcium homeostasis. Annu Rev Biochem 56:395–433
42. Carafoli E (2002) Calcium signaling: a tale for all seasons. Proc Natl Acad Sci USA 99:1115–1122
43. Krebs J, Michalak M (2007) Calcium: a matter of life or death. Elsevier B.V., Amsterdam

44. Peacock M (2010) Calcium metabolism in health and disease. Clin J Am Soc Nephrol 5(1):S23–S30
45. Chan CS, Gertler TS, Surmeier DJ (2009) Calcium homeostasis, selective vulnerability and Parkinson's disease. Trends Neurosci 32:249–256
46. Blair HC, Schlesinger PH, Huang CL, Zaidi M (2007) Calcium signalling and calcium transport in bone disease. Subcell Biochem 45:539–562
47. Feske S (2007) Calcium signalling in lymphocyte activation and disease. Nat Rev Immunol 7:690–702
48. Duchen MR, Verkhratsky A, Muallem S (2008) Mitochondria and calcium in health and disease. Cell Calcium 44:1–5
49. Lloyd-Evans E, Waller-Evans H, Peterneva K, Platt FM (2010) Endolysosomal calcium regulation and disease. Biochem Soc Trans 38:1458–1464
50. Bootman MD, Collins TJ, Peppiatt CM, Prothero LS, MacKenzie L, De Smet P, Travers M, Tovey SC, Seo JT, Berridge MJ, Ciccolini F, Lipp P (2001) Calcium signalling – an overview. Semin Cell Dev Biol 12:3–10
51. Roussel C, Erneux T, Schiffmann SN, Gall D (2006) Modulation of neuronal excitability by intracellular calcium buffering: from spiking to bursting. Cell Calcium 39:455–466
52. Lipp P, Niggli E (1996) A hierarchical concept of cellular and subcellular Ca(2+)-signalling. Prog Biophys Mol Biol 65:265–296
53. Niggli E, Shirokova N (2007) A guide to sparkology: the taxonomy of elementary cellular Ca2+ signaling events. Cell Calcium 42:379–387
54. Stern MD (1992) Buffering of calcium in the vicinity of a channel pore. Cell Calcium 13:183–192
55. Saris NE, Carafoli E (2005) A historical review of cellular calcium handling, with emphasis on mitochondria. Biochemistry (Mosc) 70:187–194
56. Lee D, Michalak M (2010) Membrane associated Ca2+ buffers in the heart. BMB Rep 43:151–157
57. Meldolesi J, Pozzan T (1998) The endoplasmic reticulum Ca2+ store: a view from the lumen. Trends Biochem Sci 23:10–14
58. Alvarez J, Montero M, Garcia-Sancho J (1999) Subcellular Ca(2+) Dynamics. News Physiol Sci 14:161–168
59. Gunter TE, Gunter KK, Sheu SS, Gavin CE (1994) Mitochondrial calcium transport: physiological and pathological relevance. Am J Physiol 267:C313–C339
60. Palmero M, Gutierrez LM, Hidalgo MJ, Reig JA, Ballesta JJ, Viniegra S (1995) The low-affinity dihydropyridine receptor and Na+/Ca2+ exchanger are associated in adrenal medullary mitochondria. Biochem Pharmacol 50:879–883
61. Kirichok Y, Krapivinsky G, Clapham DE (2004) The mitochondrial calcium uniporter is a highly selective ion channel. Nature 427:360–364
62. Alonso MT, Villalobos C, Chamero P, Alvarez J, Garcia-Sancho J (2006) Calcium microdomains in mitochondria and nucleus. Cell Calcium 40:513–525
63. Sparagna GC, Gunter KK, Sheu SS, Gunter TE (1995) Mitochondrial calcium uptake from physiological-type pulses of calcium. A description of the rapid uptake mode. J Biol Chem 270:27510–27515
64. Buntinas L, Gunter KK, Sparagna GC, Gunter TE (2001) The rapid mode of calcium uptake into heart mitochondria (RaM): comparison to RaM in liver mitochondria. Biochim Biophys Acta 1504:248–261
65. Rizzuto R, Brini M, Murgia M, Pozzan T (1993) Microdomains with high Ca2+ close to IP3-sensitive channels that are sensed by neighboring mitochondria. Science 262:744–747
66. Rizzuto R, Pinton P, Carrington W, Fay FS, Fogarty KE, Lifshitz LM, Tuft RA, Pozzan T (1998) Close contacts with the endoplasmic reticulum as determinants of mitochondrial Ca2+ responses. Science 280:1763–1766
67. Falcke M (2004) Reading the patterns in living cells - the physics of Ca2+ signaling. Adv Phys 53:255–440

68. Chad JE, Eckert R (1984) Calcium domains associated with individual channels can account for anomalous voltage relations of CA-dependent responses. Biophys J 45:993–999
69. Neher E (1986) Concentration profiles of intracellular calcium in the presence of a diffusible chelator. In: Klee M, Neher E, Singer W, Heinemann U (eds) Calcium electrogenesis and neuronal functioning. Springer, Berlin, pp 80–96
70. Fogelson AL, Zucker RS (1985) Presynaptic calcium diffusion from various arrays of single channels. Implications for transmitter release and synaptic facilitation. Biophys J 48:1003–1017
71. Fakler B, Adelman JP (2008) Control of K(Ca) channels by calcium nano/microdomains. Neuron 59:873–881
72. Klingauf J, Neher E (1997) Modeling buffered Ca2+ diffusion near the membrane: implications for secretion in neuroendocrine cells. Biophys J 72:674–690
73. Augustine GJ, Santamaria F, Tanaka K (2003) Local calcium signaling in neurons. Neuron 40:331–346
74. Demuro A, Parker I (2006) Imaging single-channel calcium microdomains. Cell Calcium 40:413–422
75. Smith GD, Wagner J, Keizer J (1996) Validity of the rapid buffering approximation near a point source of calcium ions. Biophys J 70:2527–2539
76. Neher E (1998) Usefulness and limitations of linear approximations to the understanding of Ca++ signals. Cell Calcium 24:345–357
77. Gilkey JC, Jaffe LF, Ridgway EB, Reynolds GT (1978) A free calcium wave traverses the activating egg of the medaka Oryzias latipes. J Cell Biol 76:448–466
78. Jaffe LF (2008) Calcium waves. Philos Trans R Soc Lond B Biol Sci 363:1311–1316
79. Jaffe LF (1993) Classes and mechanisms of calcium waves. Cell Calcium 14:736–745
80. Woods NM, Cuthbertson KS, Cobbold PH (1987) Agonist-induced oscillations in cytoplasmic free calcium concentration in single rat hepatocytes. Cell Calcium 8:79–100
81. Schuster S, Marhl M, Hofer T (2002) Modelling of simple and complex calcium oscillations. From single-cell responses to intercellular signalling. Eur J Biochem 269:1333–1355
82. Sneyd J, Keizer J, Sanderson MJ (1995) Mechanisms of calcium oscillations and waves: a quantitative analysis. FASEB J 9:1463–1472
83. Lee SH, Rosenmund C, Schwaller B, Neher E (2000) Differences in Ca2+ buffering properties between excitatory and inhibitory hippocampal neurons from the rat. J Physiol 525(2):405–418
84. Ganitkevich V, Isenberg G (1995) Efficacy of peak Ca2+ currents (ICa) as trigger of sarcoplasmic reticulum Ca2+ release in myocytes from the guinea-pig coronary artery. J Physiol 484(Pt 2): 287–306
85. Mogami H, Gardner J, Gerasimenko OV, Camello P, Petersen OH, Tepikin AV (1999) Calcium binding capacity of the cytosol and endoplasmic reticulum of mouse pancreatic acinar cells. J Physiol 518(Pt 2):463–467

Chapter 21
Elementary Calcium Release Events from the Sarcoplasmic Reticulum in the Heart

Didier X.P. Brochet, Dongmei Yang, Heping Cheng, and W. Jonathan Lederer

Abstract Ca^{2+} release events underlie global Ca^{2+} signaling yet they are regulated by local, subcellular signaling features. Here we review the latest developments of different elementary Ca^{2+} release features that include Ca^{2+} sparks, Ca^{2+} blinks (the corresponding depletion of Ca^{2+} in the sarcoplasmic reticulum (SR) during a spark) and the recently identified small Ca^{2+} release events called quarky SR Ca^{2+} release (QCR). QCR events arise from the opening of only a few type 2 ryanodine receptors (RyR2s) – possibly only one. Recent reports suggest that QCR events can be commingled with Ca^{2+} sparks and may thus explain some variations observed in Ca^{2+} sparks. The Ca^{2+} spark termination mechanism and the number of RyR2 channels activated during a Ca^{2+} spark will be discussed with respect to both Ca^{2+} sparks and QCR events.

Keywords Ca^{2+} blink • Ca^{2+} spark • Heart • Quarky SR Ca^{2+} release • Ryanodine receptor

D.X.P. Brochet (✉) • W.J. Lederer
Center for Biomedical Engineering and Technology (BioMET), Department of Physiology, University of Maryland School of Medicine, University of Maryland, 725 W. Lombard Street, Baltimore, MD 21201, USA
e-mail: dbrochet@umaryland.edu

D. Yang
Laboratory of Cardiovascular Science, National Institute on Aging, Baltimore, MD 21224, USA

H. Cheng
Institute of Molecular Medicine, National Laboratory of Biomembrane and Membrane Biotechnology, Peking University, Beijing 100871, China

M.S. Islam (ed.), *Calcium Signaling*, Advances in Experimental Medicine and Biology 740, DOI 10.1007/978-94-007-2888-2_21,

Abbreviations

AP	Action potential
CICR	Ca^{2+}-induced Ca^{2+} release
CRU	Ca^{2+} release unit
EC coupling	Excitation-contraction coupling
ER	Endoplasmic reticulum
FWHM	Full-width at half maximum
LCC	L-type Ca^{2+} channel
QCD	Quarky SR Ca^{2+} depletion
QCR	Quarky SR Ca^{2+} release
RyR2	Type 2 ryanodine receptor
SR	Sarcoplasmic reticulum
fSR	Free SR
jSR	Junctional SR
SERCA2a	SR/ER Ca^{2+} ATPase2a
TT	T-tubule

Introduction

Cardiac contraction underlies the pumping of blood needed to perfuse tissues and thereby deliver nutrients and oxygen. The cardiac action potential (AP) regulates contraction through the process of excitation-contraction (EC) coupling. Invaginations of the plasma membrane extend the surface membrane into the cardiomyocytes through the T-tubule (TT) network found in mammalian ventricular myocytes, enabling the AP to control EC coupling throughout the cell. The intracellular Ca^{2+}-rich organelle, the sarcoplasmic reticulum (SR), is organized so that the primary Ca^{2+} release component, the junctional SR (jSR), forms a thin pancake like structure that wraps around the TT and that remains within 15 nm of the TT membranes. The Ca^{2+} release channels (RyR2s) reside in the jSR and span the gap (the subspace) between the TT and jSR membranes. During EC coupling, activation of L-type Ca^{2+} channel (LCC) by the AP enables a small "puff" of Ca^{2+} to enter the subspace and activate RyR2s. The activated RyR2s open and permit Ca^{2+} to move from the jSR lumen into the cytosol. The local $[Ca^{2+}]_{subspace}$ bathes the other RyR2s in the same subspace and they in turn are activated. This process is called Ca^{2+}-induced Ca^{2+}-release (CICR) and it amplifies the initial Ca^{2+} entry into the cytosol. The measured increase of cytosolic $[Ca^{2+}]_i$ due to the activation of RyR2s in one jSR is seen as a Ca^{2+} spark. The unit of such Ca^{2+} release, including the LCC, the jSR with its cluster of RyR2s and local structures are called a Ca^{2+} release unit (CRU). Depending on species, 70–90% of the Ca^{2+} released during EC coupling is through the SR [3]. CICR is therefore an important part of the EC coupling. During EC coupling, a $[Ca^{2+}]_i$ transient is actually composed of thousands of Ca^{2+} sparks [6, 7, 19].

Ca^{2+} Spark

Ca^{2+} sparks can arise when the LCC are opened by depolarization, when local $[Ca^{2+}]_i$ is elevated by some other mechanisms but they can also open "spontaneously". Such spontaneous openings occur because each RyR2 has a finite probably of opening even when the diastolic $[Ca^{2+}]_i$ is low. While that probably is low, it is sufficient in rat heart cells to underlie a spontaneous Ca^{2+} spark rate of about 100 per cell per second. In all cases of Ca^{2+} spark occurrence, there is a component of CICR. Given that $[Ca^{2+}]_i$ in the subspace is elevated by the opening of a local LCC or the probabilistic RyR2, this elevated $[Ca^{2+}]_{subspace}$ increases the likelihood that another RyR2 opens. In this manner, CICR is a key element in the generation of a Ca^{2+} spark [21].

Ca^{2+} sparks typically are small with a diameter at the peak $[Ca^{2+}]_i$ of the spark characterized by the "full width at half-maximum" or FWHM (2–2.5 μm). They also have a variable amplitude ($\Delta F/F_0$ up to about 4) and a short duration (half time of decay of about 20–30 ms, [9]), suggesting a strong termination mechanism [25, 30] (Fig. 21.1a). The kinetics of Ca^{2+} sparks reflect the duration of release, the local diffusion of the released Ca^{2+} and the cytosolic buffering of Ca^{2+}. In the steady-state, the Ca^{2+} that is released by Ca^{2+} sparks is balanced by restorative mechanisms such as reuptake of Ca^{2+} into the SR by the SR/endoplasmic reticulum (ER) Ca^{2+}-ATPase2a (SERCA2a) and extrusion of Ca^{2+} from the cell into the extracellular compartment by the plasmalemmal sodium-calcium exchanger and the plasmalemmal Ca^{2+}-ATPase. The mitochondria takes up virtually no Ca^{2+} [1].

Ca^{2+} Blink

In cardiac cells, even if the volume of the SR accounts only for a few percent of the total volume of the cell, it has a major role, essentially as a dynamic Ca^{2+} store. It releases Ca^{2+} when the RyR2s open and reacquires Ca^{2+} by means of SERCA2a. The $[Ca^{2+}]_{SR}$ is around 1 mM, about 10,000 times higher than $[Ca^{2+}]_i$ in the cytosol. The SR is composed of two compartments: the jSR at the z-bands and the free SR (fSR) that connects the jSRs. In rabbit heart cells, the fSR is connected to the jSR by 4–5 diffusional strictures of only 30 nm in diameter [4], slowing down Ca^{2+} diffusion into the jSR during a spark and thereby allowing isolation of Ca^{2+} signaling in the jSR (also relevant for spark termination). The fSR and jSR are interconnected within the cell and form a single network that includes the ER and the nuclear envelope [31]. The fSR forms a diffuse network composed of interconnected narrow tubules whereas the jSR is composed of enlarged cisternae (as much as about 592 nm in diameter and 30 nm in thickness). The RyR2s in the jSR face the TT and LCC. The number of RyR2s at a jSR is comprised between 30 and 300 and forms a 2D paracrystalline array [12] although recent findings [2, 16] suggest that these arrays are incomplete and may arise from an assemblage of incomplete subclusters.

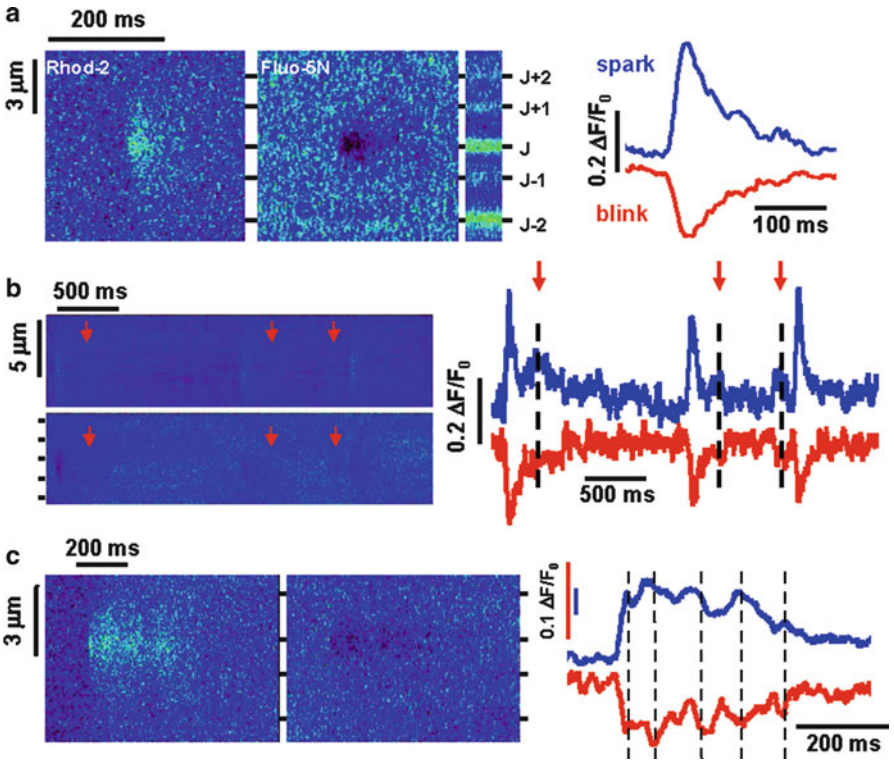

Fig. 21.1 Examples of different elementary Ca^{2+} release events. (**a**) Spark-blink pair. Linescan images of a Ca^{2+} spark (*left panel*) and its companion Ca^{2+} blink (*mid left panel*) after background subtraction with the corresponding time courses (*right*) in an intact rabbit ventricular myocyte. The enrichment of the fluo-5N dye in the junctional sarcoplasmic reticulum (*jSR*) can be seen on the unsubtracted fluo-5N image (*mid-right*). The spark-blink pair is centered on the jSR band identified as "J". (**b**) Quarky SR Ca^{2+} release (*QCR*) events. Succession of Ca^{2+} sparks and QCR events on the same jSR (*top left*) and their companion Ca^{2+} blinks and quarky SR Ca^{2+} depletion (*QCD*) events (*bottom left*), with the corresponding time courses (*right*). The arrows indicate the position of QCR and QCD events on the images and time course plots. (**c**) Long spark-blink pair. An example of a long spark (*left*) and long blink (*middle*), with the corresponding time courses (*right*). The *dashed lines* on the traces show the correspondence between bumps on the spark and dips on the blink

The jSR not only contains the RyR2s but also the high capacity Ca^{2+} buffer calsequestrin [11].

The use of the low affinity Ca^{2+} indicator fluo-5N which can be targeted to the SR by "loading protocols", has allowed the visualization of Ca^{2+} within the SR (when the dye can be accumulated preferentially in the jSR) [17, 24]. The visualization of the depletion of Ca^{2+} within a jSR during a spark, called Ca^{2+} blink, was possible because of the diffusional strictures between the fSR and jSR [4]. The simultaneous visualization of sparks (on the cytosolic side) and blinks (on the intra-SR side) has allowed a better understanding of the Ca^{2+} dynamics during a spark [5]. The sharpness

of blinks (FWHM = 1 μm), suggests that SR Ca^{2+} depletion is largely confined to a single jSR during a spark and therefore that Ca^{2+} sparks are the result of the activation of a single CRU. The amplitude of jSR Ca^{2+} depletion during a Ca^{2+} blink was about 80–85% of the SR Ca^{2+} depletion during a full-fledged transient, indicating that the jSR was largely depleted of Ca^{2+} during a spark.

Quarky SR Ca^{2+} Release (QCR) Event

Activation of a Single or a Few RyR2s During a QCR Event

The simultaneous recording of cytosolic [Ca^{2+}] and intra-SR [Ca^{2+}] was the tool needed for a more adequate understanding of the Ca^{2+} release process. This approach allowed us to examine the distinction between genuine small Ca^{2+} release events and out of focus sparks. An out of focus Ca^{2+} spark does not reveal Ca^{2+} blink signal since the jSR from which the Ca^{2+} blink signal arises is out of the plane of focus. Indeed, because of the localized FWHM of Ca^{2+} blinks, this technique has allowed the detection of very small Ca^{2+} release events (from 1/3 to 1/10 of a spark) with very rapid kinetics (t_{67} = 20 ms, [5]) (Fig. 21.1b). Interestingly, these small spontaneous events look similar to previously described sparkless Ca^{2+} release (quarks) triggered by CICR in guinea-pig under two photon photolysis of caged Ca^{2+} [18].

How Can a Single RyR2 Be Activated Without Activating the Array of RyR2s?

The smallest of the SR Ca^{2+} release events, now identified as "quarky SR Ca^{2+} release events" or QCR events, reflect the release of Ca^{2+} from a range of RyR2s – one to a few RyR2s. This raises the question of how can a single RyR2 or a very few RyR2s be activated within a full array of RyR2s without activating the rest of the array by CICR. One possibility is that not all RyR2s behave the same way within an array of RyR2s. For example, it is possible, in principle, that there is a mixture of naive RyR2s and inactivated RyR2s that exist within a cluster of RyR2s at the jSR. If such a condition could occur, then one or a few RyR2s could be activated while the remaining RyR2s may be "pre-inactivated". However, Ca^{2+} spark properties can be fully modeled without inactivation [26]. Another possibility is that RyR2s within the large array may not be activated by opening of a single (or few) RyR2 because of the weak negative allosteric effect of the binding of Mg^{2+} to RyR2 on the transition of the RyR2 to the open state [34]. The most likely explanation, however, is that one RyR2 may activate the RyR2 cluster with a probability significantly less than one [30]. Our preference for the Williams model arises because it so nicely reproduces diverse experimental findings (e.g. Ca^{2+} spark rate, variability and modulation as well as SR Ca^{2+} leak through RyR2s).

In addition to the explanation of Williams et al. [30], the geometry of the RyR2s within the jSR may importantly contribute to Ca^{2+} spark features including QCR. Using EM tomography and PALM (photo-activated light microscopy), it has been shown that the organization of the RyR2s within the RyR2 cluster at the jSR is one that is not fully packed [2, 16]. Instead, RyR2s at a jSR appear to be grouped in large numbers of small arrays of RyR2s of different sizes (from 1 to >100 RyR2s) close one from another. The average RyR2s per array was 14 with larger arrays of 25 RyR2s on average and some superclusters (association of clusters within 100 nm of each other) averaging 22 RyR2s. The physical distance between these arrays of RyR2s of different sizes may then contribute to the diversity in QCR events and Ca^{2+} sparks.

Spark Initiation

The existence of these QCR events raises the question of Ca^{2+} spark initiation. As one RyR2 within a CRU opens, the probability of other RyR2s opening is increased due to CICR [8, 30]. The amount of Ca^{2+} flux into the subspace is roughly the same as the amount of Ca^{2+} influx into the subspace due to the opening of the LCC. The probability of a Ca^{2+} spark increases significantly as additional RyR2s are activated and as the $[Ca^{2+}]_{subspace}$ increases. We imagine that QCR events would initiate Ca^{2+} sparks in a similar manner. However, it would be very difficult experimentally to observe QCR initiated Ca^{2+} sparks because of the rapidity of successive activation of RyR2s within the CRU and the signal-to-noise ratio.

During diastole and in the absence of a triggering LCC, Ca^{2+} sparks and QCR events still occur. This can happen because there is a finite opening rate of RyR2s that depends on many factors including the phosphorylation state [13, 20, 29, 33], $[Mg^{2+}]_i$, RyR2 oxidation and nitrosylation states, $[Ca^{2+}]_{SR}$ and many more [22, 28]. The estimated opening rate of RyR2s under diastolic physiologic conditions is about 10^{-4} s^{-1} which corresponds to a diastolic Ca^{2+} spark rate of about 100 sparks per cell per second in rat ventricular myocytes. During diastole, Ca^{2+} sparks are initiated by the opening rate of the RyR2s. Briefly, then, Ca^{2+} sparks are initiated by LCC during an AP. As noted above, however, and as modeled by Williams et al. [30], neither LCC nor RyR2s entrain Ca^{2+} sparks with 100% fidelity. QCRs arise when the Ca^{2+} sparks are not triggered.

Complex Features of Ca^{2+} Sparks

Mixture of Activation of Array and Rogue RyR2s During a Spark

The simultaneous measurement of spark and blink allows a more comprehensive understanding of the Ca^{2+} release process during a spark. Recent experiments have shown that the duration of Ca^{2+} release during a spark could be similar to the phase

of Ca^{2+} depletion within the SR during a blink [5]. Differences in the kinetics of cytosolic and SR Ca^{2+} diffusion and Ca^{2+} buffering may have led to differences in the signals. Importantly, when EGTA was increased in the buffer, the duration of the trailing part of a spark and recovering part of a blink became shorter, suggesting a CICR mechanism during the tail of a spark enabling the Ca^{2+} spark to last longer. However the rising phase of the Ca^{2+} sparks was invariant in the presence or absence of EGTA. These results suggest that during the rising phase of a spark, the main array of RyR2s produced enough Ca^{2+} to sustain the activation. Sobie et al. [26] suggested that large arrays of RyR2s would be less sensitive to Ca^{2+} at low Ca^{2+} than single RyR2 but more sensitive to Ca^{2+} at high Ca^{2+}. This depended on the cooperativity of RyR2s in a cluster. The large clusters would thus flicker less at low $[Ca^{2+}]_i$ and be more constantly activated at high $[Ca^{2+}]_i$. Therefore, despite the decrease of Ca^{2+} within the jSR during a spark, rogue RyR2s could be repetitively activated during the tail of a spark, prolonging the spark duration, whereas the probability of a large array of RyR2s to be re-activated would be minimal (Fig. 21.2). Thus QCR would have greater variability in Ca^{2+} spark duration than Ca^{2+} sparks that originate from within a cluster and that could then explain the variability observed in spark duration (90% of spark t_{67} between 25 and 95 ms [5]).

This phenomenon may also contribute to the explanation of the occurrence of rare sparks with long kinetics characterized most of the time by a peak followed by an extended plateau [5, 9, 32, 35] (Fig. 21.1c). The variation in the amplitude of the plateau suggests that this plateau could correspond to the maintaining of a varying number of opened RyR2s corresponding to small clusters of RyR2s (and not the main cluster anymore) for an extended period of time. Indeed, the absence of these long events in the presence of high EGTA (2 mM) further reinforces the notion of a CICR mechanism in the plateau phase of these long sparks. The similar and simultaneous variation in the amplitude of sparks and blinks during the plateau phase also indicates quick Ca^{2+} dynamics between the release and refilling of Ca^{2+}, suggesting that the SR is not fully depleted of Ca^{2+} during the plateau phase of these long events.

Spark Termination and Refractoriness

The possible opening of small array or rogue RyR2s on the tail of Ca^{2+} sparks suggests that I_{spark} is not a square function but rather a triangle function or decreasing function of time [25, 30]. How can then one explain the duration of sparks and its powerful termination scheme? Several mechanisms of spark termination have been proposed over the years. These different mechanisms include the jSR Ca^{2+} depletion during a spark (Ca^{2+} blink) that could lead to reduced Ca^{2+} efflux and RyR2 activation or that may underlie deactivation of the RyR2s from the intra-SR side [14]. Furthermore, it has been shown that addition of a Ca^{2+} buffer within the SR prolonged the spark duration, suggesting that SR Ca^{2+} depletion is an important factor for spark termination [27]. Therefore, a possible mechanism for spark termination

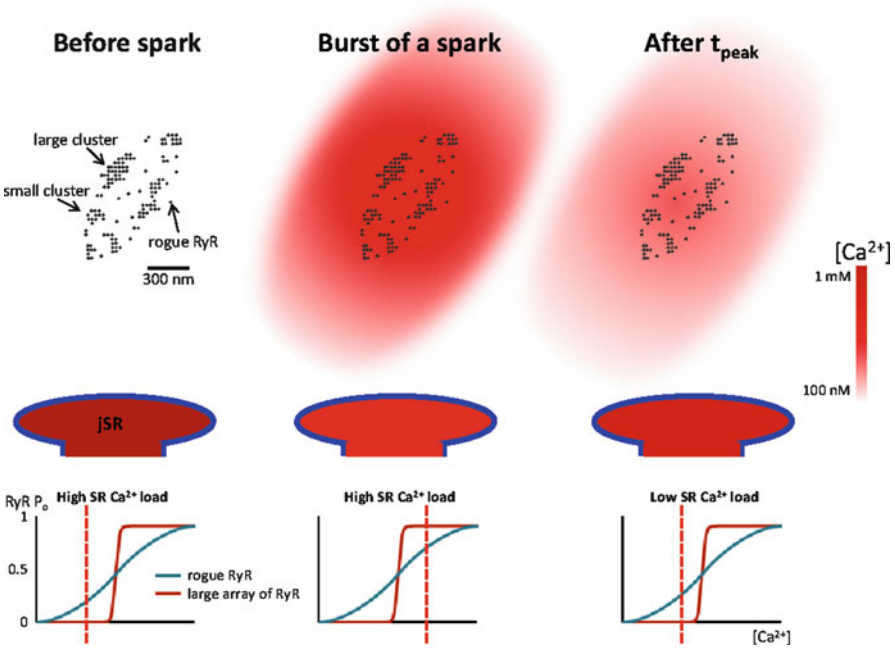

Fig. 21.2 Chronology of the events happening during the time course of a Ca^{2+} spark. Organization of the different clusters of type 2 ryanodine receptors (*RyR2s*) at a jSR (*top*). Before the burst of a Ca^{2+} spark, all the RyR2s are in a closed state (*top left column*). The jSR is fully loaded of Ca^{2+} (*mid left column*) and the open probability of RyR2s is very low for large array and below 0.5 for rogue RyR2s (*bottom left column*). During the burst of a Ca^{2+} spark, the increase in cytosolic Ca^{2+} activates the large array of RyR2s (open probability very high) and most of the small arrays or rogue RyR2s (open probability superior at 0.5, bottom middle column). The $[Ca^{2+}]$ at the jSR reaches its nadir (*mid middle column*) whereas the $[Ca^{2+}]$ in the cytosol attains its peak (*top middle column*). Once the Ca^{2+} blink has reached its nadir, the low SR $[Ca^{2+}]$ has shifted the activation curves of the large array and rogue RyR2s to the right. The open probability of RyR2s is then very low for large array and below 0.5 for rogue RyR2s (*bottom right column*). Therefore, only some small array or rogue RyR2s will be activated during the tail of a spark (the large array also become refractory). The $[Ca^{2+}]$ in the SR will then increase (*mid right column*) at the same time as $[Ca^{2+}]$ in the cytosol will diminish (*top right column*)

could be that as depletion of the SR Ca^{2+} occurs during a spark, the RyR2s become deactivated from the intra-SR side [25]. Rogue RyR2s or small clusters of RyR2s being less sensitive to Ca^{2+} alterations [30] could then shape the kinetics of a spark by being reactivated during the tail of a spark. The plateau phase of long sparks could also be explained by re-activation of small array(s) of RyR2s and rogue RyR2s because of their apparent reduced refractoriness (see below). According to Williams et al. [30], spark termination could be explained by the reduction of Ca^{2+} in the jSR (affecting RyR2 Ca^{2+} sensitivity and Ca^{2+} efflux) and also by the RyR2 cooperativity (a stochastic version of coupled gating).

However, there are several counter-examples that raise important questions. In our experiments, spark restitution can be longer than blink recovery – as much as three times in rabbit [4, 5]. Complex Ca^{2+} spark restitution can also arise when RyR2 behavior is changed [9] and spark termination and refractoriness may also be affected by "adaptation" of the RyR2s [15, 29]. Phosphorylation of RyR2s can depend on PKA and CaMKII and these changes may occur dynamically and affect termination and refractoriness [23]. Recent experiments also show that Ca^{2+} spark rate can change when RyR2s are oxidized or nitrosylated [10, 22]. Thus, refractoriness of local CICR and of Ca^{2+} sparks will vary as diverse spatial, sensitivity, chemical and triggering features of the CRU may change – including those of rogue RyR2s or small arrays of RyR2s [4, 5]. In this manner repetitive QCR events may be observed during long sparks [5] and the kinetics of restitution may be dynamic and complex.

How Many RyR2s Are Activated During a Spark?

The existence of QCR events suggest that there may be diversity of SR Ca^{2+} release events and that, in addition to Ca^{2+} sparks which are the classic SR Ca^{2+} release event at the 20,000 CRUs per cell, there is an additional population of smaller events with diverse kinetics. As noted above, new imaging approaches that include EM and super-resolution imaging suggest that in addition to the "classic" CRU [12], there are additional organization themes in the CRU [2, 16]. These themes include RyR2 arrays that are spread out as well as those with missing elements. How rogue RyR2s contribute to QCR and normal Ca^{2+} sparks must still be investigated by those of us examining Ca^{2+} release by all experimental means and by mathematical modeling.

This brings up the question of how many RyR2s open to produce a spark. With the initial Sobie model of the Ca^{2+} spark [25], a very broad range of RyR2s could underlie a Ca^{2+} spark (e.g. 10–100). In order to better characterize the quantitative nature of Ca^{2+} sparks, Williams et al. [30] have recently investigated how Ca^{2+} sparks may arise, how individual RyR2s within the CRU may open and fail to activate a Ca^{2+} spark and how Ca^{2+} sparks terminate. This model was based on the latest set of information characterizing RyR2 behavior and information on cardiac ion channels and ion transporters. As with the earlier Sobie model, a wide range of RyR2s may contribute to the Ca^{2+} spark but the character of the "Ca^{2+} leak" was better shown with the Williams model. Depending on the spatial geometry, the sensitivity of the RyR2s and the dynamics of the signal regulation, this modeling may help us understand QCR and their dynamics.

In conclusion, our understanding of RyR2 geometry in the CRU (with both tight clusters and loose clusters and with rogue RyR2s) provides an important background. It complements new information on the dynamic modulation of RyR2 sensitivity. Together they provide a background that will enable us to account for QCR events and organize experiments to investigate how QCRs contribute to Ca^{2+} sparks, normal Ca^{2+} signaling and pathological behavior.

Sources of Funding

This work was supported in part by the Intramural Research Program of the NIH, National Institute on Aging (to D.Y.); National Institute of Heart Lung and Blood grants (R01 HL106059, R01 105239 and P01 HL67849), Leducq North American-European Atrial Fibrillation Research Alliance, European Community's Seventh Framework Programme FP7/2007–2013 under grant agreement No. HEALTH-F2-2009-241526, EUTrigTreat, and support from the Maryland Stem Cell Commission (to W.J.L.); the Chinese Natural Science Foundation (30630021) and the Major State Basic Science Development Program (2007CB512100, 2011CB809100) (to H.C.).

References

1. Andrienko TN, Picht E, Bers DM (2009) Mitochondrial free calcium regulation during sarcoplasmic reticulum calcium release in rat cardiac myocytes. J Mol Cell Cardiol 46:1027–1036
2. Baddeley D, Jayasinghe ID, Lam L, Rossberger S, Cannell MB, Soeller C (2009) Optical single-channel resolution imaging of the ryanodine receptor distribution in rat cardiac myocytes. Proc Natl Acad Sci USA 106:22275–22280
3. Bassani JW, Bassani RA, Bers DM (1994) Relaxation in rabbit and rat cardiac cells: species-dependent differences in cellular mechanisms. J Physiol 476:279–293
4. Brochet DX, Yang D, Di Maio A, Lederer WJ, Franzini-Armstrong C, Cheng H (2005) Ca^{2+} blinks: rapid nanoscopic store calcium signaling. Proc Natl Acad Sci USA 102:3099–3104
5. Brochet DX, Xie W, Yang D, Cheng H, Lederer WJ (2011) Quarky calcium release in the heart. Circ Res 108:210–218
6. Cannell MB, Cheng H, Lederer WJ (1994) Spatial non-uniformities in $[Ca^{2+}]_i$ during excitation-contraction coupling in cardiac myocytes. Biophys J 67:1942–1956
7. Cannell MB, Cheng H, Lederer WJ (1995) The control of calcium release in heart muscle. Science 268:1045–1049
8. Cheng H, Lederer WJ (2008) Calcium sparks. Physiol Rev 88:1491–1545
9. Cheng H, Lederer WJ, Cannell MB (1993) Calcium sparks: elementary events underlying excitation-contraction coupling in heart muscle. Science 262:740–744
10. Fauconnier J, Thireau J, Reiken S, Cassan C, Richard S, Matecki S, Marks AR, Lacampagne A (2010) Leaky RyR2 trigger ventricular arrhythmias in Duchenne muscular dystrophy. Proc Natl Acad Sci USA 107:1559–1564
11. Franzini-Armstrong C (1980) Structure of sarcoplasmic reticulum. Fed Proc 39:2403–2409
12. Franzini-Armstrong C, Protasi F, Ramesh V (1999) Shape, size, and distribution of $Ca^{(2+)}$ release units and couplons in skeletal and cardiac muscles. Biophys J 77:1528–1539
13. Guo T, Zhang T, Mestril R, Bers DM (2006) Ca^{2+}/Calmodulin-dependent protein kinase II phosphorylation of ryanodine receptor does affect calcium sparks in mouse ventricular myocytes. Circ Res 99:398–406
14. Gyorke I, Gyorke S (1998) Regulation of the cardiac ryanodine receptor channel by luminal Ca^{2+} involves luminal Ca^{2+} sensing sites. Biophys J 75:2801–2810
15. Gyorke S, Fill M (1993) Ryanodine receptor adaptation: control mechanism of $Ca^{(2+)}$-induced Ca^{2+} release in heart. Science 260:807–809
16. Hayashi T, Martone ME, Yu Z, Thor A, Doi M, Holst MJ, Ellisman MH, Hoshijima M (2009) Three-dimensional electron microscopy reveals new details of membrane systems for Ca^{2+} signaling in the heart. J Cell Sci 122:1005–1013

17. Kabbara AA, Allen DG (2001) The use of the indicator fluo-5N to measure sarcoplasmic reticulum calcium in single muscle fibres of the cane toad. J Physiol 534:87–97
18. Lipp P, Niggli E (1998) Fundamental calcium release events revealed by two-photon excitation photolysis of caged calcium in Guinea-pig cardiac myocytes. J Physiol 508:801–809
19. Lopez-Lopez JR, Shacklock PS, Balke CW, Wier WG (1995) Local calcium transients triggered by single L-type calcium channel currents in cardiac cells. Science 268:1042–1045
20. Marx SO, Reiken S, Hisamatsu Y, Jayaraman T, Burkhoff D, Rosemblit N, Marks AR (2000) PKA phosphorylation dissociates FKBP12.6 from the calcium release channel (ryanodine receptor): defective regulation in failing hearts. Cell 101:365–376
21. Prosser BL, Ward CW, Lederer WJ (2010) Subcellular Ca^{2+} signaling in the heart: the role of ryanodine receptor sensitivity. J Gen Physiol 136:135–142
22. Prosser BL, Ward CW, Lederer WJ (2011) X-ROS signaling: rapid mechano-chemo transduction in heart. Science 333:1440–1445
23. Ramay HR, Liu OZ, Sobie EA (2011) Recovery of cardiac calcium release is controlled by sarcoplasmic reticulum refilling and ryanodine receptor sensitivity. Cardiovasc Res 91:598–605
24. Shannon TR, Guo T, Bers DM (2003) Ca^{2+} scraps: local depletions of free [Ca^{2+}] in cardiac sarcoplasmic reticulum during contractions leave substantial Ca^{2+} reserve. Circ Res 93:40–45
25. Sobie EA, Dilly KW, dos Santos CJ, Lederer WJ, Jafri MS (2002) Termination of cardiac $Ca^{(2+)}$ sparks: an investigative mathematical model of calcium-induced calcium release. Biophys J 83:59–78
26. Sobie EA, Guatimosim S, Gomez-Viquez L, Song LS, Hartmann H, Saleet JM, Lederer WJ (2006) The Ca^{2+} leak paradox and rogue ryanodine receptors: SR Ca^{2+} efflux theory and practice. Prog Biophys Mol Biol 90:172–185
27. Terentyev D, Viatchenko-Karpinski S, Valdivia HH, Escobar AL, Gyorke S (2002) Luminal Ca^{2+} controls termination and refractory behavior of Ca^{2+}-induced Ca^{2+} release in cardiac myocytes. Circ Res 91:414–420
28. Tocchetti CG, Wang W, Froehlich JP, Huke S, Aon MA, Wilson GM, Di BG, O'Rourke B, Gao WD, Wink DA, Toscano JP, Zaccolo M, Bers DM, Valdivia HH, Cheng H, Kass DA, Paolocci N (2007) Nitroxyl improves cellular heart function by directly enhancing cardiac sarcoplasmic reticulum Ca^{2+} cycling. Circ Res 100:96–104
29. Valdivia HH, Kaplan JH, Ellis-Davies GC, Lederer WJ (1995) Rapid adaptation of cardiac ryanodine receptors: modulation by Mg^{2+} and phosphorylation. Science 267:1997–2000
30. Williams GS, Chikando AC, Tuan HT, Sobie EA, Lederer WJ, Jafri MS (2011) Dynamics of calcium sparks and calcium leak in the heart. Biophys J 101:1287–1296
31. Wu X, Bers DM (2006) Sarcoplasmic reticulum and nuclear envelope are one highly interconnected Ca^{2+} store throughout cardiac myocyte. Circ Res 99:283–291
32. Xiao RP, Valdivia HH, Bogdanov K, Valdivia C, Lakatta EG, Cheng H (1997) The immunophilin FK506-binding protein modulates Ca^{2+} release channel closure in rat heart. J Physiol 500:343–354
33. Yang D, Zhu WZ, Xiao B, Brochet DX, Chen SR, Lakatta EG, Xiao RP, Cheng H (2007) Ca^{2+}/calmodulin kinase II-dependent phosphorylation of ryanodine receptors suppresses Ca^{2+} sparks and Ca^{2+} waves in cardiac myocytes. Circ Res 100:399–407
34. Zahradnikova A, Valent I, Zahradnik I (2010) Frequency and release flux of calcium sparks in rat cardiac myocytes: a relation to RYR gating. J Gen Physiol 136:101–116
35. Zima AV, Picht E, Bers DM, Blatter LA (2008) Termination of cardiac Ca^{2+} sparks: role of intra-SR [Ca^{2+}], release flux, and intra-SR Ca^{2+} diffusion. Circ Res 103:105–115

Chapter 22
Calcium Oscillations and Pacemaking

Mohammad S. Imtiaz

Abstract Calcium plays important role in biological systems where it is involved in diverse mechanisms such as signaling, muscle contraction and neuromodulation. Action potentials are generated by dynamic interaction of ionic channels located on the plasma-membrane and these drive the rhythmic activity of biological systems such as the smooth muscle and the heart. However, ionic channels are not the only pacemakers; an intimate interaction between intracellular Ca^{2+} stores and ionic channels underlie rhythmic activity. In this review we will focus on the role of Ca^{2+} stores in regulation of rhythmical behavior.

Keywords Ca^{2+} oscillations • Ca^{2+} stores • Synchronization • Coupled oscillators • Slow waves • Lymphatics • Pacemaking • Long-range signaling • Smooth muscle • Sinoatrial node

Abbreviations

IP_3	Inositol 1,4,5-trisphosphate
CICR	Ca^{2+}-induced-Ca^{2+} release
ER	Endoplasmic reticulum

M.S. Imtiaz (✉)
Department of Physiology & Pharmacology, Faculty of Medicine, University of Calgary, Health Sciences Centre, 3330 Hospital Drive NW, Calgary, AB T2N 4N1, Canada
e-mail: mimtiaz@ucalgary.ca

M.S. Islam (ed.), *Calcium Signaling*, Advances in Experimental Medicine and Biology 740, DOI 10.1007/978-94-007-2888-2_22,

Introduction

Maintenance of Dynamic of Ca^{2+} Concentration

Ca^{2+} concentration in the extracellular space is in the millimolar range, while Ca^{2+} concentration inside the cell is maintained within nanomolar range [1]. Transient elevations in cytosolic Ca^{2+} are employed by the cell as a signaling mechanism. A system of pumps, stores, receptors and ionic channels are involved in controlling Ca^{2+} concentration in the cell [1–4]. A Ca^{2+} "event" or signal is generated when an increase in cytosolic Ca^{2+} is followed by subsequent resolution to resting level. Ca^{2+} is elevated in the cytosol by influx from extracellular space or through release of Ca^{2+} from intracellular stores.

Influx of extracellular Ca^{2+} can occur through voltage operated Ca^{2+} channels, such as L-type and T-type Ca^{2+} channels. These ionic channels open in response to membrane depolarization and allow influx of Ca^{2+} into the cytosol. Sodium-calcium exchanger (NCX) is a pump located on the membrane which also can allow influx of Ca^{2+} when working in reverse mode. The other source of cytosolic Ca^{2+} increase is release of Ca^{2+} from intracellular Ca^{2+} stores located in the endoplasmic/sarcoplasmic reticulum (ER/SR). A store operated Ca^{2+} influx through membrane located channel can also be a source of cytosolic Ca^{2+} increase.

Removal of Ca^{2+} occurs when (1) Ca^{2+} is pumped to the extracellular space via membrane located channels, such as the NCX and Ca^{2+} ATPase, (2) by uptake into the Ca^{2+} stores and mitochondria through ATPase pumps (SERCA) located in the membrane of the endoplasmic reticulum or through the mitochondrial uniporter in mitochondria.

Ca^{2+} Stores

High concentration (milliMolars range) of Ca^{2+} is found within intracellular Ca^{2+} stores. Ca^{2+} is released from these stores upon second messenger binding through two types of receptors, (1) inositol 1,4,5-trisphosphate (IP_3) receptor (IP_3R) and (2) ryanodine receptor (RyR). The IP_3R is regulated by both Ca^{2+} and IP3 [5, 6], while the RyR is regulated by Ca^{2+} [7–10].

Cyclical Ca^{2+} Release from Ca^{2+} Store

An interesting feature of both the IP_3R and RyR is a bell shaped open probability. This causes the receptors to open regeneratively to release Ca^{2+} and then close when cytosolic Ca^{2+} reaches high concentration around the receptor, thus resulting in a Ca^{2+} spike. Ca^{2+} release from the store is also terminated due to decrease of Ca^{2+} within the store. Ca^{2+} is pumped back into the store through the SERCA raising the

store Ca^{2+} concentration while lowering Ca^{2+} cytosolic concentration. This primes the store for the next release, and this cycle can continue if sufficient Ca^{2+} and IP_3 are present in the cytosol. Ryanodine receptor operated stores also release Ca^{2+} cyclically if sufficient Ca^{2+} is present in the cytosol.

Ca^{2+} released from store through IP_3R or RyR can diffuse in the cytosol, raise local Ca^{2+} concentration and cause adjacent receptors to release Ca^{2+}. This process is called Ca^{2+}-induced-Ca^{2+} release (CICR) [9, 11, 12]. The Ca^{2+} dependence of Ca^{2+} release from stores can result in propagation of Ca^{2+} concentration wave within and across cells. Events have been variously named blips, sparks [13] and puffs [14] based on the type of receptor involved, duration and spatial resolution. Longer lasting events that span larger regions can appear as propagating waves [9, 13, 15] showing spiral or longitudinal forms.

Intracellular Ca^{2+} Store – Ionic Channel Interaction

Some ER/SR are located in close proximity to the cell membrane, within nanometers, resulting in very small local spaces known as nanodomains or microdomains [16–22]. Due to the small volume of the microdomain, even minuscule flux of Ca^{2+} can result in large changes in Ca^{2+} concentrations. Thus these microdomains provide an effective environment for interaction between processes that are sensitive to Ca^{2+} concentration. Although changes in Ca^{2+} concentration in the bulk of cytosol are responsible for a large number of biological processes, such as muscle contraction, we will limit the remainder of our discussion to Ca^{2+} changes within the microdomain.

Ca^{2+} entry during opening of voltage operated Ca^{2+} channels (VOCC) such as L-type and T-type Ca^{2+} channels cause increase in cytosolic Ca^{2+} concentration. VOCC-dependent cytosolic Ca^{2+} increase can trigger Ca^{2+} release from the store because both IP_3 and ryanodine receptors are sensitive to cytosolic Ca^{2+}. In this way VOCC can drive or pace the store Ca^{2+} release (Fig. 22.1).

Ca^{2+} released from the stores can interact with ionic channels, causing changes in the membrane potential. Store operated Ca^{2+} increase in the microdomain can either hyperpolarize or depolarize the membrane depending on the proximity of ionic channels. When store interact with Ca^{2+}-activated potassium channels, a transient outward current is generated which produce transient membrane hyperpolarizations [23–25]. In contrast, when store released Ca^{2+} activate inward current, such as by acting on Ca^{2+}-activated chloride channel, a transient membrane depolarization is generated [26, 27].

Role of Ca^{2+} Store in Pacemaking

Many single and multicellular systems display activities that are rhythmic, such as the heart, gut, vascular vasomotion, and insulin secretion. On the cellular level, cyclical membrane potential depolarization or action potentials underlie such rhythms.

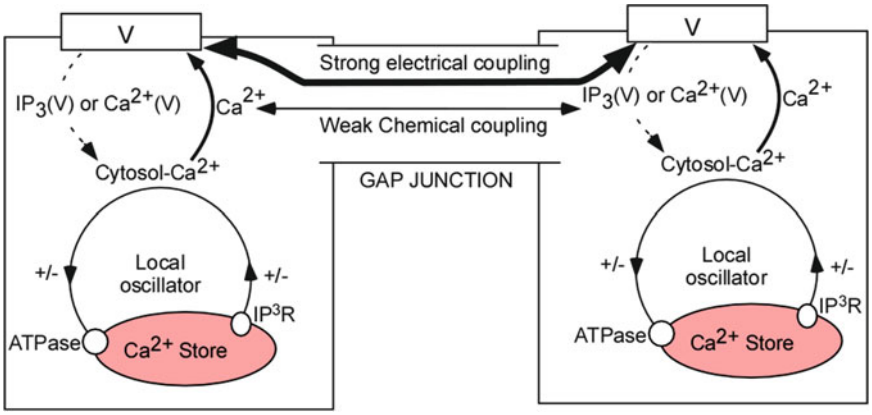

Fig. 22.1 A schematic showing interaction of store and membrane oscillator. Two cells are shown where each cell is a local oscillator composed of a cytosolic-store Ca^{2+} excitable system. The cytosolic Ca^{2+} of each oscillator is transformed into membrane potential (V) oscillations by a Ca^{2+}-activated inward current. The membrane potentials of the cells are strongly linked. Each local oscillator is weakly linked to the membrane potential by a voltage-dependent feedback loop such as voltage-dependent IP_3 synthesis or voltage-dependent Ca^{2+} influx. IP_3R is the IP_3 receptor, ATPase is the ATPase pump (Adapted from Imtiaz [76])

Action potential is generated due to the interaction of various voltage and/or Ca^{2+} activated membrane currents [28–30]. We call this the membrane oscillator which arises due dynamic action of membrane located ionic channels.

As discussed earlier, Ca^{2+} stores can release Ca^{2+} cyclically due to the intrinsic properties of the store receptors and SERCA pumps. We call this the store oscillator. A crosstalk exists between the membrane ionic channels and intracellular Ca^{2+} stores due to which the store and membrane oscillator can influence each other. This crosstalk occurs in the microdomain, as discussed in the last section; e.g. Ca^{2+} entry through VOCC can cause release of Ca^{2+} from the Ca^{2+} store through CICR, and Ca^{2+} release from store can polarize the membrane through activation of Ca^{2+} sensitive ionic channels. Given the restricted space in the microdomain, these interaction occur without significant delays. Below we discuss a few rhythms that occur as a result of interaction between the store and membrane oscillators.

Smooth Muscle

Ca^{2+} store have been shown to drive spontaneous contractions in various smooth muscle, such as the blood and lymphatic vessels, gastrointestinal system, prostate and urethra [31–36]. The current generated by store release is not sufficient to depolarize the membrane to threshold for opening of voltage activated channels. Thus a question arises as to how stores can act in a concerted manner to achieve effective depolarization [37, 38]. The manner in which stores achieve synchrony varies in different systems, the details are discussed below.

Gastric

Rhythmic electrical depolarizations, called slow waves, control the mechanical activity of many smooth muscles [34, 39–41]. It has been shown that release of Ca^{2+} from IP_3-sensitive Ca^{2+} stores underlie generation of slow waves [33, 34, 41, 42]. Ca^{2+} released from the stores depolarize the membrane and generate rhythmic pacemaker depolarization [38, 43–45].

Ca^{2+} stores can couple by diffusion of IP_3 or Ca^{2+} (CICR) or by voltage coupling where membrane depolarization activates store release [46, 47]. Ca^{2+} and IP_3 coupling is weak due to their limited effective diffusion (~5 μm) [48], however, voltage coupling is sufficiently strong to provide functional store pacemaking in cellular syncytia [47, 49].

A coupling mechanism has been proposed that combines the Ca^{2+}/IP_3 dependent excitability of Ca^{2+} stores and electrical coupling across cells to generate an effective pacemaker, Fig. 22.1. In this mechanism oscillatory store Ca^{2+} release generates inward current and resultant depolarization, the conducted depolarization in turn leads to activation of other Ca^{2+} stores, Fig. 22.2. This latter step could be mediated by depolarization-induced Ca^{2+} entry and/or production of IP_3 [49, 50]. Thus, a synchronized action of Ca^{2+} stores through an electrochemical coupling acts a pacemaker.

Lymphatic Smooth Muscle

Lymphatic vessels propel fluid by a rhythmic constriction-dilation cycle, a process known as lymphatic pumping. Lymphatic vessels are divided into chambers by interconnecting valves. Constriction and relaxation of these chambers propels lymph fluid through the lymphatic vessels.

IP_3-receptor operated Ca^{2+} release from intracellular Ca^{2+} stores has been found to generate a pacemaker mechanism that drives these rhythmic constrictions [37]. Spontaneous Ca^{2+} release events from IP_3R operated Ca^{2+} stores activate a transient inward current causing a spontaneous transient depolarization (STD). The coupling mechanism of store release is similar to that described above for the gastric smooth muscle, except Ca^{2+} entry through voltage operated Ca^{2+} channel activates further store release and a summation of STDs occur resulting in activation of action potential [51]. This same mechanism appears to be involved in vasomotion in both blood and lymphatic vessels [46, 49, 52, 53].

Cardiac Pacemaking: Sinoatrial Node

Earlier models of sinoatrial node (SAN) pacemaking in the heart were based on interaction of various voltage-activated membrane currents [28, 29], i.e. the membrane oscillator model. In this model pacemaker currents such as the hyperpolarization-activated HCN current (I_f), along with other low threshold voltage-activated currents such as the T-type Ca^{2+} channel current (IT-Ca) triggered action potential [54, 55].

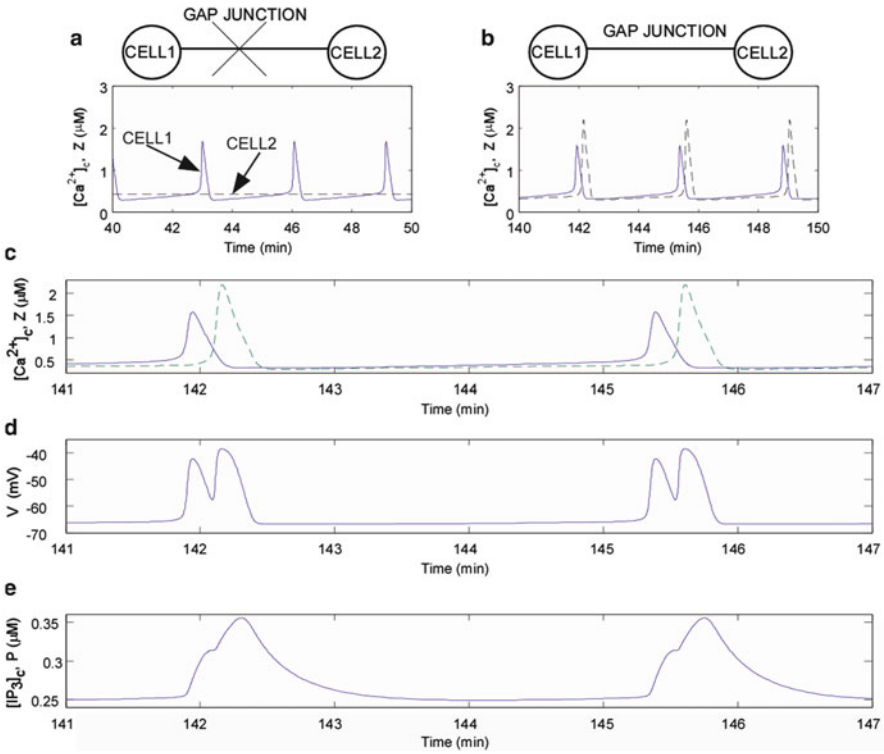

Fig. 22.2 Model illustration of cell pair synchronization. A two-cell system shows how synchrony can be achieved through voltage-dependent modulation of store release. $[Ca^{2+}]_c$ plot of Cell 1 and Cell 2 before (**a**) and after (**b**) coupling. Panels (**c**) and (**e**) show $[Ca^{2+}]_c$ and $[IP_3]_c$ respectively for the two cells after they are coupled. Note that the membrane potential (**d**) for both cells are same due to large electrical coupling. Note that changes in $[IP_3]_c$ for both cells follow changes in the membrane potential (Adapted from Imtiaz et al. [77])

Studies from various groups have now shown that SAN rhythm is generated by a cooperative interaction between the ryanodine receptor operated Ca^{2+} stores and the classical membrane oscillator [56–65]. Ca^{2+} release from ryanodine receptor operated Ca^{2+} stores depolarize the membrane through the NCX, which then accelerates the diastolic potential towards threshold for generation of action potential. Thus along with the I_f and T-type Ca^{2+} channel, store release acts as a pacemaker mechanism.

Future Directions

Store Operated Ca^{2+} Entry

Store operated Ca^{2+} entry (SOCE) has been found in various cell types [66–70]. Since Ca^{2+} release from stores is sensitive to Ca^{2+}, SOCE can influence cell dynamics. Furthermore, under pathological conditions SOCE could alter pacemaking significantly.

Capacitive Store Coupling Mechanism

Recent studies by M. Yamashita and colleagues [71, 72] shows that coupling between stores can occur though capacitive coupling across cell membrane without the need for gap junctions. It is possible that such coupling occurs in many cell types and augments coupling through gap junctions.

Ca^{2+} Stores in Pathology

Altered store Ca^{2+} release dynamics can significantly alter normal physiology, for example in the heart muscle, increased Ca^{2+} store excitability can cause emergence of unwanted pacemakers that result in pathological waves of contractions known as arrhythmias [73, 74]. Similarly, changes in intracellular buffers can create abnormal store release resulting in pathological heart conditions [65, 75]. Studies that increase our understanding of store dynamics and its interaction with the membrane oscillator are critical to finding treatments for such diseases.

References

1. Berridge MJ, Bootman MD, Roderick HL (2003) Calcium signalling: dynamics, homeostasis and remodelling. Nat Rev Mol Cell Biol 4:517–529
2. Sammels E, Parys JB, Missiaen L, De Smedt H, Bultynck G (2010) Intracellular Ca^{2+} storage in health and disease: a dynamic equilibrium. Cell Calcium 47:297–314
3. Wray S, Burdyga T (2010) Sarcoplasmic reticulum function in smooth muscle. Physiol Rev 90:113–178
4. Berridge MJ (2002) The endoplasmic reticulum: a multifunctional signaling organelle. Cell Calcium 32:235–249
5. Foskett JK, White C, Cheung K-H, Mak D-OD (2007) Inositol trisphosphate receptor Ca^{2+} release channels. Physiol Rev 87:593–658
6. Mikoshiba K (2007) IP3 receptor/Ca^{2+} channel: from discovery to new signaling concepts. J Neurochem 102:1426–1446
7. Zalk R, Lehnart SE, Marks AR (2007) Modulation of the ryanodine receptor and intracellular calcium. Annu Rev Biochem 76:367–385
8. Woods NM, Cuthbertson KS, Cobbold PH (1986) Repetitive transient rises in cytoplasmic free calcium in hormone-stimulated hepatocytes. Nature 319:600–602
9. Berridge MJ (1993) Inositol trisphosphate and calcium signalling. Nature 361:315–325
10. Meissner G (2002) Regulation of mammalian ryanodine receptors. Front Biosci 7:2072–2080
11. Endo M (1977) Calcium release from the sarcoplasmic reticulum. Physiol Rev 57:71–108
12. Iino M (1990) Biphasic Ca^{2+} dependence of inositol 1,4,5-trisphosphate-induced Ca^{2+} release in smooth muscle cells of the guinea pig taenia caeci. J Gen Physiol 95:1103–1122
13. Parker I, Yao Y (1991) Regenerative release of calcium from functionally discrete subcellular stores by inositol trisphosphate. Proc R Soc Ser B 246:269–274
14. Cheng H, Lederer WJ, Cannell MB (1993) Calcium sparks: elementary events underlying excitation-contraction coupling in heart muscle. Science 262:740–744
15. Lechleiter J, Girard S, Peralta E, Clapham D (1991) Spiral calcium wave propagation and annihilation in Xenopus laevis oocytes. Science 252:123–126
16. Devine CE, Somlyo AV, Somlyo AP (1972) Sarcoplasmic reticulum and excitation-contraction coupling in mammalian smooth muscles. J Cell Biol 52:690–718

17. Kuo KH, Herrera AM, Seow CY (2003) Ultrastructure of airway smooth muscle. Respir Physiol Neurobiol 137:197–208
18. van Breemen C, Chen Q, Laher I (1995) Superficial buffer barrier function of smooth muscle sarcoplasmic reticulum. Trends Pharmacol Sci 16:98–105
19. Yoshikawa A, van Breemen C, Isenberg G (1996) Buffering of plasmalemmal Ca^{2+} current by sarcoplasmic reticulum of guinea pig urinary bladder myocytes. Am J Physiol 271:C833–C841
20. White C, McGeown JG (2000) Ca^{2+} uptake by the sarcoplasmic reticulum decreases the amplitude of depolarization-dependent $[Ca^{2+}]_i$ transients in rat gastric myocytes. Pflugers Arch 440:488–495
21. Young RC, Schumann R, Zhang P (2001) Intracellular calcium gradients in cultured human uterine smooth muscle: a functionally important subplasmalemmal space. Cell Calcium 29:183–189
22. Shmigol AV, Eisner DA, Wray S (1999) The role of the sarcoplasmic reticulum as a Ca2+ sink in rat uterine smooth muscle cells. J Physiol 520 Pt 1:153–163
23. ZhuGe R, Tuft RA, Fogarty KE, Bellve K, Fay FS, Walsh JV Jr (1999) The influence of sarcoplasmic reticulum Ca^{2+} concentration on Ca^{2+} sparks and spontaneous transient outward currents in single smooth muscle cells. J Gen Physiol 113:215–228
24. Ganitkevich V, Hasse V, Pfitzer G (2002) Ca^{2+}-Dependent and Ca^{2+}-independent regulation of smooth muscle contraction. J Muscle Res Cell Motil 23:47–52
25. Benham CD, Bolton TB (1986) Spontaneous transient outward currents in single visceral and vascular smooth muscle cells of the rabbit. J Physiol 381:385–406
26. van Helden DF (1991) Spontaneous and noradrenaline-induced transient depolarizations in the smooth muscle of guinea-pig mesenteric vein. J Physiol 437:511–541
27. Wang Q, Hogg RC, Large WA (1992) Properties of spontaneous inward currents recorded in smooth muscle cells isolated from the rabbit portal vein. J Physiol 451:525–537
28. Brown HF (1982) Electrophysiology of the sinoatrial node. Physiol Rev 62:505–530
29. Noble D, Noble SJ (1984) A model of sino-atrial node electrical activity based on a modification of the DiFrancesco-Noble (1984) equations. Proc R Soc Lond B Biol Sci 222:295–304
30. Hodgkin AL, Rushton WAH (1946) The passive electrical properties of nerve axons. Proc R Soc Ser B 133:444–456
31. Berridge MJ (2008) Smooth muscle cell calcium activation mechanisms. J Physiol 586: 5047–5061
32. Van Helden DF (1993) Pacemaker potentials in lymphatic smooth muscle of the guinea-pig mesentery. J Physiol 471:465–479
33. Liu LW, Thuneberg L, Huizinga JD (1995) Cyclopiazonic acid, inhibiting the endoplasmic reticulum calcium pump, reduces the canine colonic pacemaker frequency. J Pharmacol Exp Ther 275:1058–1068
34. Hashitani H, van Helden DF, Suzuki H (1996) Properties of spontaneous depolarizations in circular smooth muscle cells of rabbit urethra. Br J Pharmacol 118:1627–1632
35. Sergeant GP, Hollywood MA, McCloskey KD, McHale NG, Thornbury KD (2001) Role of IP(3) in modulation of spontaneous activity in pacemaker cells of rabbit urethra. Am J Physiol Cell Physiol 280:C1349–C1356
36. Lang RJ, Nguyen DT, Matsuyama H, Takewaki T, Exintaris B (2006) Characterization of spontaneous depolarizations in smooth muscle cells of the Guinea pig prostate. J Urol 175:370–380
37. van Helden DF (1993) Pacemaker potentials in lymphatic smooth muscle of the guinea-pig mesentery. J Physiol (Lond) 471:465–479
38. van Helden DF, Imtiaz MS, Nurgaliyeva K, von der Weid P-Y, Dosen PJ (2000) Role of calcium stores and membrane voltage in the generation of slow wave action potentials in the guinea-pig gastric pylorus. J Physiol 524.1:245–265
39. Sanders KM (1996) A case for Interstitial cells of Cajal as pacemakers and mediators of neurotransmission in the gastrointestinal tract. Gastroenterology 111:492–515
40. Daniel EE, Bardakjian BL, Huizinga JD, Diamant NE (1994) Relaxation oscillator and core conductor models are needed for understanding of GI electrical activities. Am J Physiol 266:G339–G349

41. Exintaris B, DT TN, Lam M, Lang RJ (2009) Inositol trisphosphate-dependent Ca(2+) stores and mitochondria modulate slow wave activity arising from the smooth muscle cells of the guinea pig prostate gland. Br J Pharmacol 156:1098–1106
42. Suzuki H, Takano H, Yamamoto Y, Komuro T, Saito M, Kato K, Mikoshiba K (2000) Properties of gastric smooth muscles obtained from mice which lack inositol trisphosphate receptor. J Physiol 525:105–111
43. Suzuki H, Hirst GD (1999) Regenerative potentials evoked in circular smooth muscle of the antral region of guinea-pig stomach. J Physiol 517(Pt 2):563–573
44. Hirst GD, Bramich NJ, Teramoto N, Suzuki H, Edwards FR (2002) Regenerative component of slow waves in the guinea-pig gastric antrum involves a delayed increase in [Ca(2+)](i) and Cl(-) channels. J Physiol 540:907–919
45. von der Weid PY, Rahman M, Imtiaz MS, van Helden DF (2008) Spontaneous transient depolarizations in lymphatic vessels of the guinea pig mesentery: pharmacology and implication for spontaneous contractility. Am J Physiol Heart Circ Physiol 295:H1989–H2000
46. Peng H, Matchkov V, Ivarsen A, Aalkjaer C, Nilsson H (2001) Hypothesis for the initiation of vasomotion. Circ Res 88:810–815
47. van Helden DF, Imtiaz MS (2003) Ca2+ phase waves: a basis for cellular pacemaking and long- range synchronicity in the guinea-pig gastric pylorus. J Physiol 548.1:271–296
48. Allbritton NL, Meyer T, Stryer L (1992) Range of messenger action of calcium ion and inositol 1,4,5-trisphosphate. Science 258:1812–1815
49. Imtiaz MS, Zhao J, Hosaka K, von der Weid PY, Crowe M, van Helden DF (2007) Pacemaking through Ca^{2+} stores interacting as coupled oscillators via membrane depolarization. Biophys J 92:3843–3861
50. Imtiaz MS, Smith DW, van Helden DF (2002) A theoretical model of slow wave regulation using voltage-dependent synthesis of inositol 1,4,5-trisphosphate. Biophys J 83:1877–1890
51. Imtiaz MS, Zhao J, Hosaka K, Von Der Weid P-Y, Crowe M, van Helden D (2007) Pacemaking through Ca2+ stores interacting as coupled oscillators via membrane depolarization. Biophys 92:3843–3861
52. Koenigsberger M, Sauser R, Lamboley M, Beny JL, Meister JJ (2004) Ca^{2+} dynamics in a population of smooth muscle cells: modeling the recruitment and synchronization. Biophys J 87:92–104
53. Kapela A, Bezerianos A, Tsoukias NM (2008) A mathematical model of Ca^{2+} dynamics in rat mesenteric smooth muscle cell: agonist and NO stimulation. J Theor Biol 253:238–260
54. Mangoni ME, Nargeot J (2008) Genesis and regulation of the heart automaticity. Physiol Rev 88:919–982
55. DiFrancesco D (1985) The cardiac hyperpolarizing-activated current, if. Origins and developments. Prog Biophys Mol Biol 46:163–183
56. Maltsev VA, Lakatta EG (2009) Synergism of coupled subsarcolemmal Ca^{2+} clocks and sarcolemmal voltage clocks confers robust and flexible pacemaker function in a novel pacemaker cell model. Am J Physiol Heart Circ Physiol 296:H594–H615
57. Lakatta EG, Vinogradova T, Lyashkov A, Sirenko S, Zhu W, Ruknudin A, Maltsev VA (2006) The integration of spontaneous intracellular Ca^{2+} cycling and surface membrane ion channel activation entrains normal automaticity in cells of the Heart's pacemaker. Ann N Y Acad Sci 1080:178–206
58. Imtiaz MS, von der Weid PY, van Helden DF (2010) Synchronization of Ca^{2+} oscillations: a coupled oscillator-based mechanism in smooth muscle. FEBS J 277:278–285
59. Huser J, Blatter LA, Lipsius SL (2000) Intracellular Ca^{2+} release contributes to automaticity in cat atrial pacemaker cells. J Physiol 524:415–422
60. Lipsius SL, Huser J, Blatter LA (2001) Intracellular Ca^{2+} release sparks atrial pacemaker activity. News Physiol Sci 16:101–106
61. Rubenstein DS, Lipsius SL (1989) Mechanisms of automaticity in subsidiary pacemakers from cat right atrium. Circ Res 64:648–657
62. Zhou Z, Lipsius SL (1993) Na(+)-Ca^{2+} exchange current in latent pacemaker cells isolated from cat right atrium. J Physiol 466:263–285

63. Rigg L, Heath BM, Cui Y, Terrar DA (2000) Localisation and functional significance of ryanodine receptors during beta-adrenoceptor stimulation in the guinea-pig sino-atrial node. Cardiovasc Res 48:254–264
64. Rigg L, Terrar DA (1996) Possible role of calcium release from the sarcoplasmic reticulum in pacemaking in guinea-pig sino-atrial node. Exp Physiol 81:877–880
65. Imtiaz MS, von der Weid PY, Laver DR, van Helden DF (2010) SR Ca2+ store refill–a key factor in cardiac pacemaking. J Mol Cell Cardiol 49:412–426
66. Kurebayashi N, Ogawa Y (2001) Depletion of Ca2+ in the sarcoplasmic reticulum stimulates Ca^{2+} entry into mouse skeletal muscle fibres. J Physiol 533:185–199
67. Casteels R, Droogmans G (1981) Exchange characteristics of the noradrenaline-sensitive calcium store in vascular smooth muscle cells or rabbit ear artery. J Physiol 317:263–279
68. Launikonis BS, Barnes M, Stephenson DG (2003) Identification of the coupling between skeletal muscle store-operated Ca2+ entry and the inositol trisphosphate receptor. Proc Natl Acad Sci USA 100:2941–2944
69. Huang J, van Breemen C, Kuo KH, Hove-Madsen L, Tibbits GF (2006) Store-operated Ca^{2+} entry modulates sarcoplasmic reticulum Ca^{2+} loading in neonatal rabbit cardiac ventricular myocytes. Am J Physiol Cell Physiol 290:C1572–C1582
70. Ju YK, Huang W, Jiang L, Barden JA, Allen DG (2003) ATP modulates intracellular Ca^{2+} and firing rate through a P2Y1 purinoceptor in cane toad pacemaker cells. J Physiol 552:777–787
71. Yamashita M, Sugioka M, Ogawa Y (2006) Voltage- and Ca^{2+}-activated potassium channels in Ca^{2+} store control Ca^{2+} release. FEBS J 273:3585–3597
72. Yamashita M (2008) Synchronous Ca^{2+} oscillation emerges from voltage fluctuations of Ca^{2+} stores. FEBS J 275:4022–4032
73. Eisner DA, Kashimura T, Venetucci LA, Trafford AW (2009) From the ryanodine receptor to cardiac arrhythmias. Circ J 73:1561–1567
74. Eisner DA, Kashimura T, O'Neill SC, Venetucci LA, Trafford AW (2009) What role does modulation of the ryanodine receptor play in cardiac inotropy and arrhythmogenesis? J Mol Cell Cardiol 46:474–481
75. MacLennan DH, Chen SR (2009) Store overload-induced Ca^{2+} release as a triggering mechanism for CPVT and MH episodes caused by mutations in RYR and CASQ genes. J Physiol 587:3113–3115
76. Imtiaz MS (2003) Distributed pacemaking through coupled oscillator-based mechanisms: a basis for long-range signaling in smooth muscle. Newcastle, Australia, The University of Newcastle
77. Imtiaz MS, Katnik CP, Smith DW, van Helden DF (2006) Role of voltage-dependent modulation of store Ca^{2+} release in synchronization of Ca^{2+} oscillations. Biophys J 90:1–23

Chapter 23
Calcium Oscillations and Waves in Cells

Jai Parkash and Kamlesh Asotra

Abstract From beginning of the life to final moment of the life, Ca^{2+} functions as an important signaling messenger. The intracellular Ca^{2+} concentration, $[Ca^{2+}]_i$, in resting cells is normally maintained at around 100 nM with a very steep ~20,000 times concentration gradient of Ca^{2+} between extracellular and intracellular compartments. Ca^{2+} signals in the form of time-dependent changes in $[Ca^{2+}]_i$ appear as brief spikes that are organized into regenerative Ca^{2+} waves. The release of Ca^{2+} from internal stores plays a key role in regulating such Ca^{2+} signals. Since global Ca^{2+} oscillations arise from Ca^{2+} waves initiated locally, it results in generation of stochastic Ca^{2+} oscillations. In addition, the hierarchical organization of signaling structures translate the molecular fluctuations of single channels to the whole cell leading to formation of stochastic media. Several recent observations indicate that $[Ca^{2+}]_i$ changes are fluctuation driven as opposed to a typical deterministic intracellular reaction–diffusion system model. Elucidation of this signaling mechanism can provide detailed knowledge of relationship between cell signaling and cell physiology of living systems.

Keywords Calcium ions • Calcium wave • Deterministic • Endoplasmic reticulum • G-protein coupled receptor • GPCR • Inositol-3-phosphate • Inositol-3-phosphate receptors • Mitochondria • Oscillations • Signaling • Stochastic

J. Parkash (✉)
Department of Environmental and Occupational Health, Robert Stempel College of Public Health and Social Work, Florida International University, 11200 SW 8th Street, HLS-594, Miami, FL 33199, USA
e-mail: parkashj@fiu.edu

K. Asotra
GaneShiva Consultants, 10944 Rose Avenue, Suite 3, Los Angeles, CA 90034, USA
e-mail: kamlesh.asotra@gmail.com

M.S. Islam (ed.), *Calcium Signaling*, Advances in Experimental Medicine and Biology 740, DOI 10.1007/978-94-007-2888-2_23,

Introduction

Ca^{2+} regulates several processes such as egg fertilization, cell differentiation, energy transduction, secretions, apoptosis, muscle contraction, chemotaxis and neuronal synaptic plasticity in learning and memory [1–7]. The intracellular Ca^{2+} concentration, $[Ca^{2+}]_i$, in resting cells is normally maintained very low at around 100 nM which is approximately 10,000–20,000 times lower than the extracellular Ca^{2+} ions concentration [1–7]. Ca^{2+} signaling in cells is generally presented as changes in Ca^{2+} concentration as brief spikes which are often organized as regenerative Ca^{2+} waves [5–7]. The intracellular Ca^{2+} waves can induce changes in the gene expression and thus regulate several signal-transduction pathways [8–17].

The general mechanism for Ca^{2+} signaling involves the release of Ca^{2+} from intracellular Ca^{2+} stores such as the endoplasmic reticulum (ER) or the sarcoplasmic reticulum (SR). The binding of various agonists to the G-protein coupled receptors (GPCRs) can activate phospholipase C (PLC) which then cleaves phosphatidylinositol 4, 5-bisphosphate (PIP_2) into 1,4,5-inositol trisphosphate (IP_3) and diacylglycerol (DAG). IP_3 binding to the IP_3R channels causes efflux of Ca^{2+} from the ER or SR to the cytoplasm resulting in increase in $[Ca^{2+}]_i$ from ~100 nM to ~1 μM for several seconds [5, 7]. The higher cytoplasmic levels of Ca^{2+} stimulate rapid uptake of the Ca^{2+} ion by mitochondria, and oscillations in Ca^{2+} levels in mitochondria can be observed in response to those in the cytoplasm [18–20].

Generation of Calcium Oscillation and Waves

Direct visualization of a Ca^{2+} rise at fertilization has been shown in the medaka fish, sea urchin, and *Xenopus oocytes* [21–24]. Ca^{2+} rise in the form of oscillatory Ca^{2+} signal have also been observed in other cell types such as astrocytes, articular chondrocytes, and cardiac myocytes [25–28]. As shown in Fig. 23.1, the stimulation of a single astrocyte in an acutely isolated rat retina caused increases in $[Ca^{2+}]_i$ in the stimulated cell as well as in neighboring astrocytes and Muller cells [25]. This in turn caused the outward propagation of Ca^{2+} wave from the site of stimulation to the entire retinal surface (Fig. 23.1). Similarly, in the egg of the medaka fish, *Oryzias latipes,* the fertilization-induced Ca^{2+} increases in the form of a propagating wave swept through the entire egg [29]. Further studies characterized the fertilization-dependent Ca^{2+} release in mammals and other vertebrates and showed specificity in the spatial and temporal pattern of these signals. In mammals, an oscillatory Ca^{2+} signal lasting several hours is observed, whereas in the frog *X. laevis*, for example, only a single Ca^{2+} transient is induced at fertilization and takes the form of a sweeping Ca^{2+} wave [30].

As mentioned above, the binding of a specific agonist to its plasma membrane receptor activates PLC resulting in production of IP_3 that diffuses from the plasma membrane into the cytoplasm and then binds to IP_3R channels located on the ER [31–34].

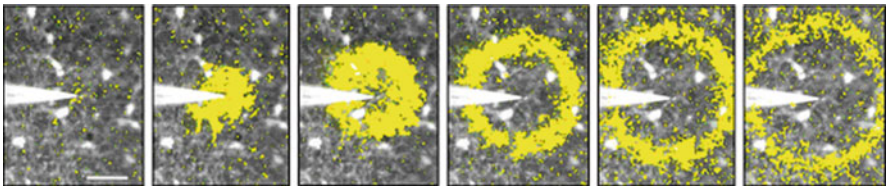

Fig. 23.1 Calcium wave propagation in glial cells of acutely isolated rat retina. The confocal fluorescence image of the vitreal surface of the rat retina labeled with a fluorescent probe Calcium Green-1. The application of mechanical/chemical/electrical stimulus resulted in the spread of a Ca^{2+} wave propagating at 23 μm/s. The fluorescence image shown in *black* and *white* with superimposed *yellow rings* indicating the leading edge of the Ca^{2+} wave. The interval between panels was 0.93 s and the scale bar shown is 50 μm. The confocal fluorescence images were acquired at the video rate using video-rate confocal microscopy (Adapted with permission from Newman and Zahs [25])

The binding of IP_3 and Ca^{2+} to an IP_3R, opens the channel and Ca^{2+} diffuses from the ER into the cytoplasm that is primarily driven by the large concentration difference of approximately three orders of magnitudes between the ER and the cytoplasm. The Ca^{2+} release from internal stores like the ER into the cytoplasm is a nonlinear process. In addition, the biphasic dependence of the IP_3R open probability on the cytoplasmic Ca^{2+} concentration leads to Ca^{2+} induced Ca^{2+} release (CICR) [35]. The open probability of the IP_3R increases nonlinearly with the IP_3 concentration as well as the Ca^{2+} concentration [36]. Hence, Ca^{2+} released by one IP_3R channel increases the open probability for neighboring IP_3R channels thereby initiating a self-amplifying release mechanism. Very high Ca^{2+} concentrations can inhibit the IP_3R channel and terminate the Ca^{2+} release from the ER.

In the cytoplasm not only do Ca^{2+} ions bind to several Ca^{2+} buffers but also these Ca^{2+} ions diffuse to adjacent channels and increase their open probability resulting in further Ca^{2+} release throughout the whole cell. The inhibition of IP_3R by high cytoplasmic Ca^{2+} concentrations and depletion of the ER Ca^{2+} store finally terminates the release of Ca^{2+}. The cytoplasmic Ca^{2+} is removed from the cytoplasm by the action of sarcoplasmic endoplasmic reticulum Ca^{2+}-ATPase (SERCA) pumps that pump in Ca^{2+} into the ER as well as by the activity of plasma membrane Ca^{2+}-ATPase (PMCA) that pump out Ca^{2+} into the extracellular space.

In cells, the IP_3R channels form clusters of 1–30 Ca^{2+} channels that are separated by 1–7 μm and these clusters are inhomogeneously distributed in space resulting in a typical hierarchal organization of Ca^{2+} signals [37, 38]. Since the open probability of the IP_3R Ca^{2+} release channels depends on the cytoplasmic Ca^{2+} concentration, the interactions between the channels results in the formation of hierarchal spatio-temporal patterns of intracellular Ca^{2+} release. The triggering of the smallest event is the opening of a single channel, called a "blip" as shown in Fig. 23.2. The blip in turn can activate other channels within the same channel cluster leading to the formation of the next larger event called "puff". This results in a large concentration increase in Ca^{2+} that is restricted to a small region close to the active cluster because of presence of SERCA pumps and Ca^{2+} buffers which can cause steep concentration gradients of up to four orders of magnitudes within 2 μm. The local self-amplified

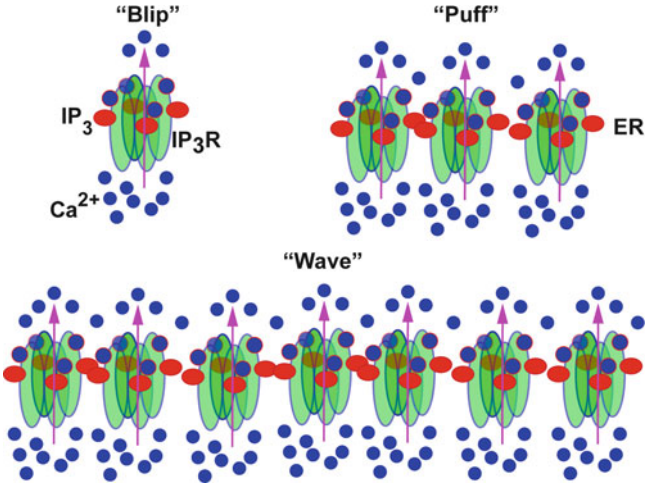

Fig. 23.2 The generation of Ca^{2+} wave in cells. The binding of IP_3 and Ca^{2+} to an IP_3R, opens the IP_3R channel and Ca^{2+} diffuses from the ER into the cytoplasm in a nonlinear process. The open probability of the IP_3R increases nonlinearly with the IP_3 concentration as well as the Ca^{2+} concentration. At lower IP_3 concentrations, the release of Ca^{2+} from an open IP_3R channel produces a stochastic event called "blip". At higher concentrations of IP_3, the "blip" can activate other IP_3R channels within the same channel cluster leading to the formation of "puff". At further higher concentrations of IP_3, the local self-amplified signal of a "puff" can be sensed by the neighboring IP_3R clusters and "puffs" cooperate to produce a Ca^{2+} wave travelling through the cell

signal of a "puff" can be detected by neighboring IP_3R clusters and "puffs" can cooperate to set off a wave travelling through the cell. The resulting waves appear as an elevation of the Ca^{2+} concentration engulfing the whole volume in cells. The periodic occurrence of such waves result in global oscillations.

Several theoretical studies have shown that the hierarchical organization of the structure of Ca^{2+} signals and the random behavior of IP_3R channels can cause spiking events and such spiking events have also been observed experimentally [39]. Such spiking events are formed from the wave nucleation in a stochastic medium due to simultaneous opening of several IP_3R clusters resulting in the formation of a critical nucleus that then forms a global wave [40–42]. Marchant and Parker [43] have observed this experimentally in *Xenopus oocytes*.

Falcke et al. [44] have proposed a model that takes into account the Ca^{2+} uptake and release by mitochondria to explain the role of increased mitochondrial activity on Ca^{2+} wave patterns.

It is assumed that the IP_3R channel has a binding site for IP_3, an activating binding site for Ca^{2+} and an inhibiting binding site for Ca^{2+}. The channel opens upon binding of IP_3 to its binding site on IP_3R channel and binding of Ca^{2+} to the activating binding site for Ca^{2+} of the IP_3R channel. The binding of Ca^{2+} to the inhibiting site closes the IP_3R channel. However, the binding of Ca^{2+} to the inhibiting site occurs slowly with a lower affinity as compared to the activating site. The IP_3 molecules bind to four receptor sites on the IP_3R, one on each subunit of the tetramer

resulting in opening of the IP_3R and consequently highly co-operative nonlinear release of Ca^{2+} from the ER [7]. Small perturbations in ambient $[Ca^{2+}]_i$, $[IP_3]$, and various regulators can cause uncoordinated bursts of local release of Ca^{2+} across a cell. Such uncoordinated bursts of Ca^{2+} are called "sparks" due to their appearance in Ca^{2+} imaging fluorescence microscopy as shown in Fig. 23.2 [45]. The brief opening of these channels produces localized Ca^{2+} pulses (Fig. 23.2) such as the sparks or blips and puffs [46]. Such a production of sparks or blips and puffs causes increase in the $[Ca^{2+}]_i$ [46, 47]. At higher concentrations of IP_3, these blips grow into larger puffs that then act as initiation sites for the onset of Ca^{2+} waves (Fig. 23.2). Upon sufficient sensitization of the IP_3Rs, these IP_3Rs respond by diffusing the Ca^{2+} from a puff site and thereby propagating the signal through a process of CICR as shown in Fig. 23.2. These Ca^{2+} waves are the mechanisms that coordinate the release of Ca^{2+} by all the IP_3Rs. Therefore, increasing spark frequency can cascade and become regenerative and is seen as two- or three- dimensional waves of changes in $[Ca^{2+}]_i$ that propagate within cells (Fig.23.2). Ca^{2+} oscillations, therefore, depend upon both the spatial organization of IP_3Rs and their regulation by Ca^{2+} although the links between IP_3R activities and Ca^{2+} oscillations are not fully understood.

Stochasticity of Calcium Waves

As a result of the coordinated action of many stochastic elemental events such as puffs and sparks, the released Ca^{2+} from intracellular storage compartments generate spatiotemporal patterns called Ca^{2+} concentration spikes. For the last more than 20 years, the sequences of such Ca^{2+} concentration spikes have been described using deterministic rate laws. However, recent experiments in five different cell types have shown that the Ca^{2+} concentration spikes are driven by fluctuations causing the formation of stochastic media thereby suggesting stochastic resonance phenomena [43, 48–53].

But how are random molecular events such as blips and puffs presented as global intracellular Ca^{2+} oscillations in the cells? It is generally assumed that if many IP_3 molecules are involved in these processes, the cell behaves like a continuously stirred reactor and the law of large numbers can be used to predict such Ca^{2+} oscillations [54]. Although most models of the dynamics of intracellular Ca^{2+} release use the law of large numbers, it is not consistent with experimental analyses that show that global oscillations arise from Ca^{2+} waves initiated locally [43]. Hence such a local initiation of Ca^{2+} waves is predicted to lead to stochastic oscillations because although each cell has many IP_3Rs and Ca^{2+} ions, the law of large numbers is not applicable to the initiating event, which is restricted to very few IP_3Rs and a very steep concentration gradients of Ca^{2+} [39]. These IP_3R channels are closely packed into clusters on the ER membrane [55]. The maximal number of channels in a cluster is not known but is estimated to be in the range of 20–30 [56]. The clusters are randomly distributed with areas of high cluster density called focal sites. Average distance of clusters outside focal sites in *Xenopus* oocytes has been determined as 7.3 μm and inside focal sites as 5 μm. Opening and closing of IP_3R channels occur

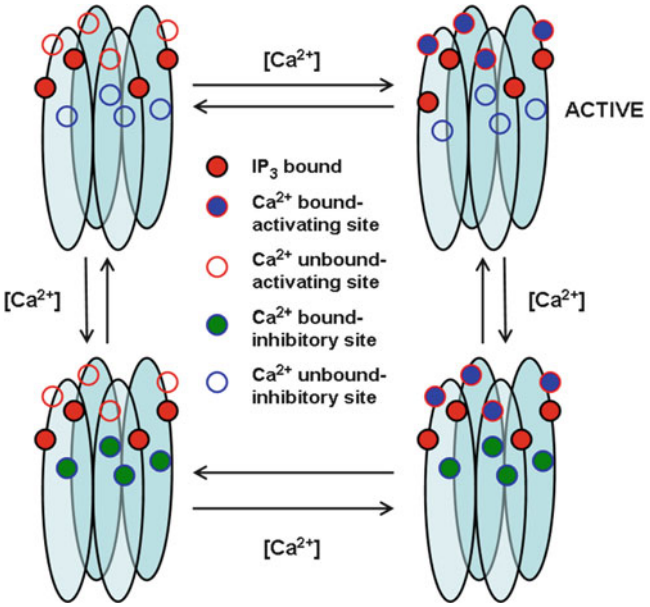

Fig. 23.3 The four Ca^{2+} binding states model of the stochasticity of Ca^{2+} wave. In this model it is presumed that each IP_3R channel has a binding site for IP_3, an activating binding site for Ca^{2+}, and an inhibiting binding site for Ca^{2+}. The IP_3R channel opens upon binding of IP_3, binding of Ca^{2+} to the activating site, and when Ca^{2+} is not bound to the inhibiting site. The binding of Ca^{2+} to the inhibiting site closes the IP_3R channel. However, the binding of Ca^{2+} to the inhibiting site occurs slowly with a lower affinity as compared to the activating site. In this model the stochastic events are binding of Ca^{2+} and IP_3 to and dissociation from the IP_3R channel subunits. The model also assumes that the rates of IP_3 binding occur with a two orders of magnitude faster than the other reaction rates

stochastically. Such a stochastic behavior of IP_3R channels results in spontaneous release events through single channels or several channels in a cluster [56].

Marchant and Parker [43] have investigated such hierarchal pattern of spatio-temporal structures in detail in *Xenopus* oocytes whereas Bootman et al. have carried out studies in HeLa cells [57, 58]. Marchant and Parker [43] have suggested that the elapsed time between two consecutive waves is determined by two processes namely the recovery from inhibition caused by the first wave and the creation of a supercritical nucleus for the second wave. Therefore, the probabilistic character of such nucleation processes introduces significant variations in the wave period.

The processes that produce random behavior in intracellular Ca^{2+} dynamics are the transitions between the different states of the IP_3R channel subunits in the IP_3R channel. Since the IP_3R channels open and close randomly, the opening and closing probability depends on the state of the IP_3R channel subunits. The opening probability of IP_3R channel is the highest when a minimum number of subunits are activated with an assumption that subunits of IP_3R channel are identical and independent of each other. In this model shown in Fig. 23.3, the stochastic events are binding of

Ca^{2+} and IP_3 to and dissociation from the channel subunits. In addition, there is a timescale separation between IP_3 binding and dissociation on one side and Ca^{2+} binding and dissociation on the other. This suggests that the binding state of IP_3 will be in a stationary distribution most of the time and pairs of states with identical Ca^{2+} binding configuration can be combined into one state. Such a combination of binding produces four different states of IP_3R channel subunits (see Fig. 23.3) that correspond to Ca^{2+} bound or not bound to the activating and inhibiting binding sites. Given one of these four states, the subunit is in one of the substates of IP_3 binding with the probability given by the stationary distribution. The probability for transitions corresponding to binding of Ca^{2+} ions depends on the concentration of free Ca^{2+} at the location of the IP_3R channel.

Conclusions

The intracellular Ca^{2+} waves generated as a result of concerted activities of several cellular Ca^{2+} channels and pumps provides for a very effective and fast signaling that is needed at every step of the way in the day-to-day life of a living organism. The intracellular Ca^{2+} dynamics show both the stochastic and deterministic features. Stochasticity appears in global events as well in the form of period distributions instead of regular oscillations and as the wave creation mechanism. The results of deterministic and stochastic modeling can complement each other.

Acknowledgements JP would like to thank the NIH/NIGMS for support. The content is solely the responsibility of the author and does not necessarily represent the official views of the National Institute of General Medical Sciences or the National Institute of Health.

Competing interests The authors declare that they have no competing interests.

Authors' contributions JP and KA wrote the manuscript and drafted figures. All authors read and approved the final manuscript.

References

1. Jaiswal JK (2001) Calcium-how and why? J Biosci 26:357–363
2. Shemarova IV, Nesterov VP (2005) Evolution of mechanisms of calcium signaling: the role of calcium ions in signal transduction in prokaryotes. Zh Evol Biokhim Fiziol 41:12–17
3. Parkash J, Asotra K (2010) Calcium wave signaling in cancer cells. Life Sci 87:587–595
4. Strunker T, Goodwin N, Brenker C, Kashikar ND, Weyand I, Seifert R, Kaupp UB (2011) The CatSper channel mediates progesterone-induced Ca^{2+} influx in human sperm. Nature 471: 382–386
5. Berridge MJ (2009) Inositol trisphosphate and calcium signaling mechanisms. Biochim Biophys Acta 1793:933–940
6. Clapham D (2007) Calcium signaling. Cell 131:1047–1058

7. Mikoshiba K (2007) IP3 receptor/Ca^{2+} channel: from discovery to new signaling concepts. J Neurochem 102:1426–1446
8. De Koninck P, Schulman H (1998) Sensitivity of CaM kinase II to the frequency of Ca^{2+} oscillations. Science 279:227–230
9. Dolmetsch R (2003) Excitation-transcription coupling: signaling by ion channels to the nucleus. Sci STKE 2003:PE4
10. Dolmetsch RE, Lewis RS, Goodnow CC, Healy JI (1997) Differential activation of transcription factors induced by Ca^{2+} response amplitude and duration. Nature 386:855–858
11. Cai L, Dalal C, Elowitz M (2008) Frequency-modulated nuclear localization bursts coordinate gene regulation. Nature 455:485–490
12. Ramsey IS, Delling M, Clapham DE (2006) An introduction to TRP channels. Ann Rev Physiol 68:619–647
13. Schwaller B (2010) Cytosolic Ca^{2+} buffers. Cold Spring Harb Perspect Biol 2:a004051, originally published online October 13, 2010
14. Long SB, Campbell EB, MacKinnon R (2005) Voltage sensor of Kv1.2: structural basis of electromechanical coupling. Science 309:903–908
15. Hajnoczky G, Csord'as G, Das S et al (2006) Mitochondrial calcium signalling and cell death: approaches for assessing the role of mitochondrial Ca^{2+} uptake in apoptosis. Cell Calcium 40:553–560
16. Chami M, Oul'es B, Szabadkai G, Tacine R, Rizzuto R, Paterlini-Br'echot P (2008) Role of SERCA1 truncated isoform in the proapoptotic calcium transfer from ER to mitochondria during ER stress. Mol Cell 32:641–651
17. Taylor CW, Rahman TU, Pantazaka E (2009) Targeting and clustering of IP3 receptors: key determinants of spatially organized Ca^{2+} signals. Chaos 19:037102-1-10
18. Putney JW Jr (2005) Capacitative calcium entry: sensing the calcium stores. J Cell Biol 169:381–382
19. Parekh AB, Penner R (1997) Store depletion and calcium influx. Physiol Rev 77:901–930
20. Trenker M, Malli R, Fertschai I, Levak-Frank S, Graier WF (2007) Uncoupling proteins 2 and 3 are fundamental for mitochondrial Ca^{2+} uniport. Nat Cell Biol 9:445–452
21. Ridgway EB, Gilkey JC, Jaffe LF (1977) Free calcium increases explosively in activating medaka eggs. Proc Natl Acad Sci USA 74:623–627
22. Steinhardt RA, Zucker R, Schatten G (1977) Intracellular calcium release at fertilization in the sea urchin egg. Dev Biol 58:185–196
23. Fontanilla RA, Nuccitelli R (1998) Characterization of the sperm-induced calcium wave in Xenopus eggs using confocal microscopy. Biophys J 75:2079–2087
24. Lechleiter JD, Girard S, Peralta E, Clapham D (1991) Spiral calcium wave propagation and annihilation in *Xenopus laevis* oocytes. Science 252:123–126
25. Newman EA, Zahs KR (1997) Calcium waves in retinal glial cells. Science 275:844–846
26. D'Andrea P, Vittur F (1995) Spatial and temporal Ca^{2+} signaling in articular chondrocytes. Biochem Biophys Res Commun 75:129–135
27. Orchard CH, Mustafa MR, White K (1995) Oscillations and waves of intracellular [Ca^{2+}] in cardiac muscle cells. Chaos Soliton Fract 5:447–458
28. Wussling MHP, Salz H (1996) Nonlinear propagation of spherical calcium waves in rat cardiac myocytes. Biophys J 70:1144–1153
29. Gilkey JC, Jaffe LF, Ridgway EB, Reynolds GT (1978) A free calcium wave traverses the activating egg of the Medaka, Oryzias latipes. J Cell Biol 76:448–466
30. Miyazaki S (2006) Thirty years of calcium signals at fertilization. Semin Cell Dev Biol 17:233–243
31. Vergara J, Tsien RY, Delay M (1985) Inositol 1,4,5-trisphosphate: a possible chemical link in excitation-contraction coupling in muscle. Proc Natl Acad Sci USA 82:6352–6356
32. Vergara J, Asotra K, Delay M (1987) A chemical link in excitation-contraction coupling in skeletal muscle. Soc Gen Physiol Ser 42:133–151
33. Vergara J, Asotra K (1987) A chemical transmission mechanism of excitation-contraction coupling in muscle. News Physiol Sci 2:182–186

34. Asotra K, Lagos N, Vergara J (1991) Synthesis of polyphosphoinositides in transverse tubule and sarcoplasmic reticulum membranes of frog skeletal muscle. Biochim Biophys Acta 1081:229–237
35. Williams G, Huertas M, Sobic E, Jafri M, Smith G (2007) A probability density approach to modeling local control of calcium-induced calcium release in cardiac myocytes. Biophys J 92:2311–2328
36. Patel S, Joseph SK, Thomas AP (1999) Molecular properties of inositol 1,4,5-trisphosphate receptors. Cell Calcium 25:247–264
37. Tateishi Y, Hattori M, Nakayama T et al (2005) Cluster formation of inositol 1,4,5-trisphosphate receptor requires its transition to open state. J Biol Chem 280:6816–6822
38. Rahman T, Skupin A, Falcke M, Taylor C (2009) Clustering of InsP3 receptors by InsP3 retunes their regulation by InsP3 and Ca^{2+}. Nature 458:655–659
39. Falcke M (2003) On the role of stochastic channel behavior in intracellular Ca^{2+} dynamics. Biophys J 84:42–56
40. Beato V, Sendina-Nadal I, Gerdes I, Engel H (2005) Noise-induced wave nucleations in an excitable chemical reaction. Phys Rev E71:035204, Epub 2005 Mar 28
41. Coombes S, Timofeeva Y (2003) Sparks and waves in a stochastic fire-diffuse-fire model of Ca^{2+} release. Phys Rev E68:021915, Epub 2003 Aug 25
42. Jung P, Mayer-Kress G (1995) Spatiotemporal stochastic resonance in excitable media. Phys Rev Lett 74:2130–2133
43. Marchant J, Parker I (2001) Role of elementary Ca^{2+} puffs in generating repetitive Ca^{2+} oscillations. EMBO J 20:65–76
44. Falcke M, Hudson JL, Camacho P, Lechleiter JD (1999) Impact of mitochondrial Ca^{2+} cycling on pattern formation and stability. Biophys J 77:37–44
45. Guatimosim S, Dilly K, Santana LF, Saleet Jafri M, Sobie EA, Lederer WJ (2002) Local Ca^{2+} signaling and EC coupling in heart: Ca^{2+} sparks and the regulation of the $[Ca^{2+}]i$ transient. J Mol Cell Cardiol 34:941–950
46. Parker I, Yao Y (1996) Ca^{2+} transients associated with openings of inositol trisphosphate-gated channels in *Xenopus* oocytes. J Physiol (Lond) 491:663–668
47. Parker I, Choi J, Yao Y (1996) Elementary events of InsP3-induced Ca^{2+} liberation in *Xenopus oocytes*: hot spots, puffs and blips. Cell Calcium 20:105–121
48. Skupin A, Kettenmann H, Winkler U, Wartenberg M, Sauer H, Tovey SC, Taylor CW, Falcke M (2008) How does intracellular Ca^{2+} oscillate: by chance or by the clock? Biophys J 94:2404–2411
49. Perc M, Green AK, Dixon CJ, Marhl M (2008) Establishing the stochastic nature of intracellular calcium oscillations from experimental data. Biophys Chem 132:33–38
50. Shuai JW, Jung P (2002) Optimal intracellular calcium signaling. Phys Rev Lett 88:068102
51. Skupin A, Falcke M (2009) From puffs to global Ca^{2+} signals: how molecular properties shape global signals. Chaos 19:037111
52. Dupont G, Combettes L (2009) What can we learn from the irregularity of Ca^{2+} oscillations? Chaos 19:037112
53. Perc M, Rupnik M, Gosak M, Mahrl M (2009) Prevalence of stochasticity in experimentally observed responses of pancreatic acinar cells to acetylcholine. Chaos 19:037113
54. van Kampen NG (2001) Stochastic processes in physics and chemistry. North-Holland, Amsterdam
55. Thomas D, Lipp P, Berridge MJ, Bootman MD (1998) Hormone-evoked elementary Ca^{2+} signals are not stereotypical, but reflect activation of different size channel clusters and variable recruitment of channels within a cluster. J Biol Chem 273:27130–27136
56. Falcke M (2003) Deterministic and stochastic models of intracellular Ca^{2+} waves. New J Phys 5:96.1–96.28
57. Bootman M, Berridge M, Lipp P (1997) Cooking with calcium: the recipes for composing global signals from elementary events. Cell 91:367–373
58. Bootman M, Niggli E, Berridge M, Lipp P (1997) Imaging the hierarchical Ca^{2+} signaling in HeLa cells. J Physiol 499:307–314

Chapter 24
Calcium Signaling: From Single Channels to Pathways

Alexander Skupin and Kevin Thurley

Abstract Ca^{2+} is not only one of the most versatile and ubiquitous second messengers but also a well-established representative example of cell signaling. The identification of most key elements involved in Ca^{2+} signaling enables a mechanistic and quantitative understanding of this particular pathway. Cellular behavior relies in general on the orchestration of molecular behavior leading to reliable cellular responses that allow for regulation and adaptation. Ca^{2+} signaling uses a hierarchical organization to transform single molecule behavior into cell wide signals. We have recently shown experimentally that this organization carries single channel signatures onto the whole cell level and renders Ca^{2+} oscillations stochastic. Here, we briefly review the co-evolution of experimental and theoretical studies in Ca^{2+} signaling and show how dynamic bottom-up modeling can be used to address biological questions and illuminate biological principles of cell signaling.

Keywords Calcium signaling • Hierarchical modeling • Noise induced spiking • Emergent behavior • Spatial properties of pathways

Introduction

In 1883, Sidney Ringer was the first who found that Ca^{2+} is not only needed as a structural element for bones and teeth, but it also has a crucial physiological role in heart contraction. From this coincidental empirical observation, it took more than

A. Skupin (✉)
Luxembourg Centre of Systems Biomedicine, University Luxembourg, 162a, avenue de la Faiencerie, L-1511 Luxembourg, Luxembourg

Institute for Systems Biology, 401 Terry Avenue North, 98103-8904 Seattle, WA, USA
e-mail: alexander.skupin@uni.lu

K. Thurley
Max Delbrück Center for Molecular Medicine (MDC), Robert-Rössle-Str. 10, 13092 Berlin, Germany

M.S. Islam (ed.), *Calcium Signaling*, Advances in Experimental Medicine and Biology 740, DOI 10.1007/978-94-007-2888-2_24,

60 years until the molecular link from Ca^{2+} liberation to ATP induced activity of myosin and the subsequent contraction of muscle fibers was found. Today, we know that Ca^{2+} is one of the most versatile and universal second messengers in eukaryotic cells, serving as a critical link between extracellular signals and intracellular responses. It plays a major role in many signaling pathways throughout physiology and development and has led to the paradigm of Ca^{2+} being a "life and death" signal [1–4].

The most astonishing property of Ca^{2+} signaling is that such a simple bivalent ion is involved in such a huge number of different signaling cascades. It is generally assumed that this versatility is achieved by a rich spatiotemporal spectrum of the intracellular concentration dynamics that allows triggering different physiological processes. Due to its frequent appearance and importance, Ca^{2+} signaling has been under intensive scientific investigation for many decades, and most of the molecular key elements are identified and referred to as the Ca^{2+} signaling tool kit. Despite these large efforts and the increasing molecular knowledge, the dynamic interplay of the different kit elements and their regulation are only rarely understood.

This discrepancy makes Ca^{2+} a highly interesting objective for interdisciplinary research. On the one hand, the complexity and diversity of the biological system can hardly be deciphered by pure experimental investigations, since some aspects are out of the experimental possibilities. On the other hand, the detailed studies of the isolated building blocks offer the opportunity for detailed modeling approaches and theoretical analyses. The cross-disciplinary research relies on the repeated comparison between model based hypotheses and experimental validations. Thereby the well-established experimental methods in Ca^{2+} imaging and the plethora of pharmacologic antagonists and modifiers allow for efficient connections between the two different disciplines. Moreover, mechanisms identified in Ca^{2+} signaling may hold for other pathways as well and may guide experiments in less accessible biological systems and thereby illuminate biological design principles in general.

The Ca^{2+} pathway translates external signals into intracellular responses by increasing the cytosolic Ca^{2+} concentration in a stimulus dependent pattern. The concentration increase can be caused by Ca^{2+} entry through plasma-membrane channels from the extracellular space, where the Ca^{2+} concentration is in the range of mM and thus much larger compared to the cytosolic resting concentration of tens of nM. Another main mechanism is Ca^{2+} release from internal storage compartments. While the vacuole is the major Ca^{2+} store in plant cells, muscle cells use mainly the sacroplasmic reticulum (SR) for Ca^{2+} storage. In the following, we'll focus on the inositol 1,4,5-trisphosphate (IP_3) pathway which is the most predominant Ca^{2+} release mechanism in many cell types and depicted in Fig. 24.1a. The main Ca^{2+} storage compartment in this pathway is the endoplasmic reticulum (ER). The signal cascade starts typically at a plasma-membrane receptor, which is most often a G-protein coupled receptor. Due to binding of an agonist, the receptor activates phospholipase C (PLC) that produces IP_3 at the cell membrane. From there IP_3 diffuses into the cytosol and can bind to IP_3 receptor (IP_3R) channels. These channels connect the cytosol and the endoplasmic reticulum. Once an IP_3R is activated by IP_3 and Ca^{2+}, it opens and induces a Ca^{2+} influx into the cytosol due to the large concentration differences between the two compartments, which is in the

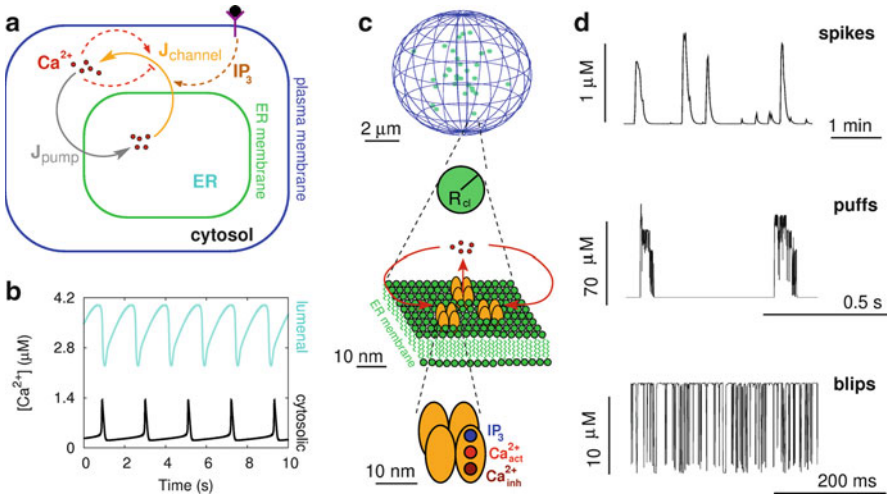

Fig. 24.1 Mechanism of Ca^{2+} signaling. (**a**) Ca^{2+} signals are generated by the release and uptake of Ca^{2+}. The main mechanism is Ca^{2+}-induced Ca^{2+} release from the endo/sarcoplasmic reticulum (ER) into the cytosol. This is typically initiated by a G-protein coupled plasma membrane receptor (magenta) that leads to IP_3 production after binding its corresponding agonist. IP_3 favors Ca^{2+} release from the ER by IP_3R channels. Early models assumed that the cell is a well-stirred reactor and thus described Ca^{2+} dynamics mainly by the interplay of spatially homogeneous release ($J_{channel}$) and uptake (J_{pump}) fluxes, which obey non-linear dependencies on the cytosolic Ca^{2+} concentration enabling the large dynamical spectrum of Ca^{2+} signals. (**b**) Concentration dynamics of the Goldbeter model [20]. The oscillatory behavior of the cytosolic Ca^{2+} concentration (*black line*) is caused by the repetitive emptying and refilling of the endoplasmic reticulum shown by the luminal concentration (*cyan line*). This kind of oscillation relies on well-tuned parameter sets and produces a specific kind of signals only. (**c**) Hierarchical organization of the Ca^{2+} pathway. The elementary building block of IP_3 induced Ca^{2+} signals is the IP_3R channel (*bottom*). It opens and closes stochastically due to the random binding of signaling molecules. An open channel induces a Ca^{2+} influx into the cytosol by the large concentration difference between the ER and the cytosol. Since channels are clustered, opening of a single channel, which is called a blip, leads to activation of other channels in the cluster (*middle*). The resulting puff corresponds to a source region with a radius R_{cl} that depends on the number of open channels. The stochastic local events are orchestrated by diffusion and self-amplification by channel properties in cell wide Ca^{2+} waves, which correspond to spikes on the level of the cell (*top*). (**d**) Corresponding simulated Ca^{2+} signals. The Green's Cell simulations [29] are able to model all corresponding levels of a Ca^{2+} signal – from single channel dynamics (*bottom*) to puffs (*middle*) and whole cell behavior (*top*). This bottom – up approach is able to resolve the different scales of the pathway. The hierarchical mechanism generates Ca^{2+} signals in a more robust way compared to the homogeneous models described in (**a**) and (**b**) and points to general principles how to produce reliable signals from molecular fluctuations

range of 3–4 orders of magnitude. The released Ca^{2+} is removed from the cytosol either by Sarco-Endoplasmic Reticulum Ca^{2+} ATPases (SERCAs) into the ER or by Ca^{2+} ATPases into the extracellular space. A similar scenario occurs in muscle cells where Ca^{2+} release from the SR is induced by Ryanodine receptors.

In the IP_3 pathway, the major elementary building block of a Ca^{2+} signal is the IP_3R channel [5, 6]. It consists of 4 identical subunits with many different regulatory

binding sites. Most mathematical models (see [7, 8] for review) consider one site for IP_3 binding that sensitizes the subunit, one for Ca^{2+} that activates the subunit and another one for Ca^{2+} that inhibits the subunit dominantly. In the DeYoung-Keizer-model [9], it is assumed that a channel opens if at least 3 subunits are in the active state. The different affinities for Ca^{2+} binding to the activating and inhibiting binding sites lead to a bell shaped stationary open probability of an IP_3R [7, 10]. It is low for small Ca^{2+} concentrations, increases for moderate concentrations due to Ca^{2+} binding to the activating site and decreases again for large concentrations due to inhibition by Ca^{2+}. The biphasic dependence on Ca^{2+} is the mechanism of Ca^{2+}-induced Ca^{2+} release (CICR) since Ca^{2+} released from one channel increases the open probability of others. This self-amplifying mechanism is enhanced by IP_3R clustering. The channels form clusters on the membrane of the ER, which are separated by some μm and contain up to a few tens of channels [11–16].

This sketch of the Ca^{2+} pathway already demonstrates the challenge we are faced to in understanding cell signaling: How do cells organize their molecular building blocks to form a functional, i.e. adaptive and reliable machine? This question is strongly related to the dynamic interactions of the diverse components. From a theoretical perspective, we know that systems with a wide dynamical range rely on specific internal structures. Thus, as a rule of thumb, regulatory mechanisms can be more versatile and robust when they obey non-linear interactions. As a simple illuminating example we might consider enzyme activity. The simplest assumption is that the activity is linearly dependent on the substrate concentration. This is indeed a reasonable assumption for small substrate concentrations but would lead to non-physiologically high production rates for large substrate concentrations. This can be compensated for by the Michaelis-Menten kinetics [17], which exhibit a saturated behavior due to non-linear dynamics.

The versatility of Ca^{2+} signaling is based on the rich dynamics of the cytosolic Ca^{2+} concentration. From the theory of complex systems we know that this kind of dynamics is only achievable by non-linear and dynamic feedback mechanisms. Thus, the described biphasic dependence of the channel opening on the cytosolic Ca^{2+} concentration is an essential component of the Ca^{2+} pathway since it carries non-linear feedback mechanisms required for Ca^{2+} dynamics. We will demonstrate in the following how integrative experimental and theoretical approaches can be used to understand cell signaling by Ca^{2+}.

The Rich Spectrum of Ca^{2+} Dynamics

After a long and successful period of identifying experimentally the most important elements of the Ca^{2+} pathway and its different downstream targets, it was in 1986 when Woods et al. [18] reported a first example of non-trivial temporal Ca^{2+} signals. They measured, by means of aequorin measurements, cytosolic free Ca^{2+} in hepatocytes stimulated by noradrenaline. They observed series of transients in the Ca^{2+} concentration. Moreover, they found that the frequency of transients depends on

the concentration of the agonist. This oscillatory-like behavior gave first evidence as to how Ca^{2+} may control many different physiological processes by frequency encoding.

This milestone experiment raised the interest of the modeling community and was the starting point for the ongoing interdisciplinary research. From a rather simple perspective, Ca^{2+} oscillations occur by the repeated release and uptake of Ca^{2+} as depicted in Fig. 24.1a. The interplay between the release flux $J_{channel}$ caused by open channels and the Ca^{2+} uptake by pumps determine the dynamics of the system. One of the first theoretical considerations was done by Meyer and Stryer in 1988 [19], in which they used a non-linear dependence of the release flux and invented the necessary feedback by IP_3 oscillations. This kind of hypothesized feedback could not be verified experimentally and led to further model developments.

One of the most successful and popular model was already introduced 1990 by Goldbeter, Dupont and Berridge [20]. Their model relies on the repeated emptying and refilling of the ER and introduced a feedback of the luminal concentration on the release current $J_{channel}$. A typical behavior of the luminal (cyan) and cytosolic (black) Ca^{2+} concentration dynamics is shown in Fig. 24.1b. The model is able to mimic a variety of experimental conditions; it gave some hypotheses about the influence of stimulation strength on the Ca^{2+} signal and predicted downstream dynamics like Ca^{2+} controlled protein phosphorylation dynamics. Despite its success, the model could not cover all experimental observations. Moreover, the essential model assumption of strong coupling between ER and cytosol could not be verified experimentally, and the dependency of channel opening on the luminal Ca^{2+} concentration is still under debate today.

A next major step regarding the diversity of Ca^{2+} dynamics was the characterization of intracellular Ca^{2+} waves that emphasized the spatial aspect of Ca^{2+} dynamics. Although observed already in the 1950s by secretion studies in large cells, Ca^{2+} waves were better described after the invention of Ca^{2+} dyes in the 1980s. In 1991, Cornell-Bell and Finkbeiner [21] observed, while measuring glutamate induced Ca^{2+} oscillations in astrocytes, a spatial structure in the Ca^{2+} concentration within the cell during a spike. They reported that Ca^{2+} increase begins in one part of the cell and spreads through the rest of the cell as a wave even in such a small cell type. Nearly simultaneously, Lechleiter and coworkers found propagating spiral waves in *Xenopus laevis* oocytes by confocal microscopy [22]. In their analysis of the observed pattern they used also modeling approaches related to spatially homogeneous regenerative excitable media. With this integrative approach they were able to estimate internal parameters like the refractory period for Ca^{2+} stores by comparison of experiments with modeling results. In the same year, Lionel Jaffe [23] found a temperature dependence of wave speed and already hypothesized that intracellular calcium pulses generally take the form of cytosolic Ca^{2+} waves. This perspective was often dropped in the following years since the diffusion of Ca^{2+} was assumed to be fast enough to describe the concentration homogeneously in models for small cells. The wave propagation mechanism in larger cells was analyzed by a variety of spatially resolved modeling concepts under the assumptions of continuously distributed Ca^{2+} release sites. For a more detailed review see [7].

The increased imaging technology has led to better resolution with which subcellular structures as well concentration dynamics and in particular Ca^{2+} concentration dynamics could be visualized. This has revealed the hierarchical organization of the Ca^{2+} pathway depicted in Fig. 24.1c. The molecular structure of IP_3R channels could be determined by X-ray experiments and atomic force microscopy. Thus, Taylor and coworkers and Suhara et al. have identified independently the 4 subunits of isolated IP_3Rs [24, 25]. Mikoshiba et al. have shown the channel clustering in COS7 cells by antibody staining [26]. While these studies determined stationary morphological properties, Marchant and Parker have shown the functional consequences for the cytosolic Ca^{2+} dynamics induced by these two key features. They measured the free concentration in *Xenopus oocytes* by line scans to obtain a fine temporal solution [12, 27]. In their experiments, they could follow the signal generation from its origin at a single channel cluster to the cell wide Ca^{2+} wave, which corresponds to a concentration spike. Thereby they observed very steep concentration differences close to an open cluster. A consequence of these gradients is that a cell is not describable as a homogenous medium. But global Ca^{2+} release relies on the concerted opening of many IP_3Rs, which is achieved by Ca^{2+}-induced Ca^{2+} release and thus by the coupling of the different release sites. This emphasizes the key role of IP_3Rs as the elementary building blocks of the Ca^{2+} pathway, as described more completely e.g. in reviews by Berridge and Taylor [2, 5, 28].

The small number of subunits of a channel with only a few binding sites each renders single channel opening (often referred to as a blip) highly random since stochastic binding of a few IP_3 molecules and Ca^{2+} ions can induce state changes. This discreteness prevents smearing out fluctuations by the law of large numbers. The strong coupling between channels in a cluster by Ca^{2+} leads to almost simultaneous opening of all channels in a cluster, which is called a puff. Marchant et al. [12, 27] characterized the puff-to-wave nucleation by high-resolution fluorescence microscopy: Several channel clusters have to open in synchrony in order to activate all other IP_3R clusters. This leads to the three levels of a cell wide Ca^{2+} signal shown in Fig. 24.1c, d – the triggering event is opening of a single channel (blip) that is amplified to a puff on the channel cluster level. The orchestrated opening of several clusters leads to a cellular (or global) Ca^{2+} spike. Figure 24.1d exhibits typical signal forms with their different characteristic scales for each level obtained by detailed simulations as described in [29] and below.

These experiments shed new light on the mechanistic question about the spike generating process raised by Jaffe. The concentration gradients induced by clustering, SERCA pumps and Ca^{2+} buffers suggest that Ca^{2+} dynamics cannot be described by homogeneous models. This was further emphasized by detailed numerical studies about the cytosolic concentration dynamics induced by single channels [30]. Furthermore, the feedback mechanism of Ca^{2+}-induced Ca^{2+} release on the single IP_3R level and its stochastic opening led to the assumption that cytosolic Ca^{2+} behaves like a stochastic medium even in smaller cells. The theoretical framework of a stochastic medium corresponds to the puff-to-wave experiment. In contrast to homogeneous models where all channels feel the same Ca^{2+} concentration

instantaneously, a stochastic medium takes the spatial dimension into account on which diffusion occurs. The stochasticity is described by excitable elements that can be activated by noise. The channel clustering emphasizes the random characteristics since even if one cluster is activated it does not necessarily lead to a wave throughout the whole cell but may also lead to an isolated local event that corresponds to a puff. Moreover, the spatial heterogeneity challenges spatially continuous model approaches even more.

Ca^{2+} Oscillations Are Stochastic

A direct consequence of this perspective is that described oscillations should not carry characteristics of periodic signals but of stochastic single channel dynamics. Recent studies have focused on this hypothesis by analyzing variations in Ca^{2+} signals of single cells. Marhl and coworkers used methods from time series analysis to test for stochasticity in hepatocytes stimulated by phenylephrine and ATP [31]. Their results give strong evidence for noise induced excitation dynamics of a Ca^{2+} spike but do not give a mechanistic picture of the underlying process. We used a more mechanistic approach in relation to the above described puff-to-wave nucleation process. We analyzed interspike intervals (ISIs) of individual cells in a variety of cell types. This is depicted in Fig. 24.2a exemplarily for a single human embryonic kidney (HEK) cell stimulated with 30 μM CCh. The upper panel exhibits the fluorescent signal measured with FURA2, and the lower panel shows the time between two specific concentration spikes defining the interspike intervals (ISIs). Although the fluorescent signal seems not to be too noisy at all, the variation in the ISIs appears rather random even by simple visual inspection.

For a systematic analysis, we analyzed the dependence of the standard deviation σ on the average ISI T_{av} [32, 33]. For complete deterministic oscillatory dynamics, we expect no standard deviation at all. The general assumption of an oscillatory system with an additional noise term should lead to an unspecific pattern of this dependency since unspecific noise should not correlate with the dynamical process. In Fig. 24.2b, c the relation between σ and T_{av} is shown for astrocytes and HEK cells, respectively, where each dot corresponds to the spike sequence of a single cell. The relation obeys four main features. First, the standard deviation σ exhibits a linear dependence on the average ISI as indicated by large linear correlation coefficients close to values of 0.9. Second, we observe an offset on the T_{av} axis, which corresponds to a refractory period following a spike. This time is needed to bring the cell into the excitable state again by removing the released Ca^{2+} form the cytosol and to recover channels from inhibition. Furthermore, we see that σ is in the same range as the average spiking period T_{av}, which is typical for stochastically driven excitation processes. A more careful inspection of the linear shapes reveals different slopes of the relation for the different cell types. This fourth feature may reflect differences of the internal signaling networks in terms of feedbacks and different environments cells are exposed to.

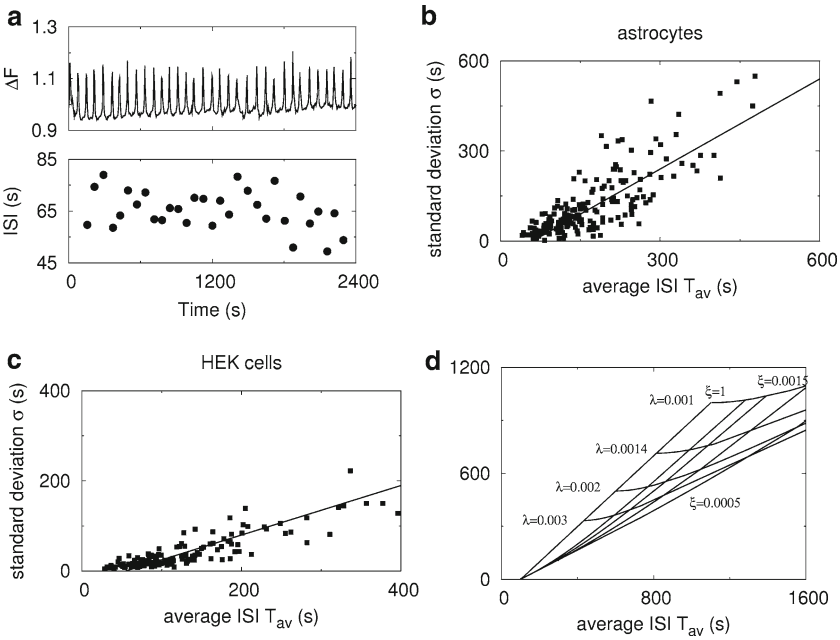

Fig. 24.2 Ca^{2+} oscillations are stochastic. (**a**) Representative time series of a single HEK cell stimulated by 30 μM CCh. The upper panel exhibits the fluorescent signal, which looks rather regular. By analyzing the individual interspike intervals (ISI) defined as the time between 2 fluorescent maxima, we see that also this quite regular signal includes fluctuations. (**b**), (**c**) Dependence of standard deviation σ on the average ISI T_{av} of individual cells. The standard deviation depends linearly on the average period and is in the same range for both spontaneously spiking astrocytes (**b**) and HEK cells stimulated with 30 μM CCh (**c**). This demonstrates the stochastic nature of Ca^{2+} spiking. (**d**) Theoretical prediction of the $\sigma - T_{av}$ relation by the heuristic spiking model using a time dependent Poisson process. The model includes spatial coupling and stimulation strength by the asymptotical nucleation rate λ and the recovery process by the regeneration rate ξ. From this model we see that stronger coupling and higher stimulation lead to faster coupling by large λ values. Furthermore, we observe that the slope of the relation depends on the regeneration rate ξ. For fast regeneration rates the slope is close to one corresponding to a pure Poisson process. The slope decreases with decreasing ξ leading to more regular spiking. This illustrates how feedback mechanisms may tune Ca^{2+} signals for different downstream targets. For more details see [32]

In order to understand these observed features in a more mechanistic way, we built a heuristic model that starts from the puff-to-wave nucleation mechanism and takes the experimentally observed refractory time into account [32]. A simple nucleation process obeys the features of a Poisson process, which describes random processes with rare events. To reflect the observed recovery process of cells, we extend the stationary rate of a pure Poisson process by recovery dynamics leading to a time dependent probability of observing a spike at time t after the previous one. The resulting probability distribution has two parameters λ and ξ. While λ is the asymptotic nucleation rate and depends on coupling between release sites as well as on stimulation strength, the regeneration rate ξ describes the dynamics of the recovery

process. With this probabilistic model, we are able to predict the relation between the standard deviation and the average period as shown in Fig. 24.2d. If regeneration is fast ($\xi >> 1$) the $\sigma - T_{av}$ relation has a slope close to one and corresponds to a pure Poisson process. For small values of the regeneration rate, the slope decreases which corresponds to a more regular spiking behavior. Thus, cells can tune their spike pattern by the dynamic interplay between excitation and recovery.

One prediction obtained from the probabilistic model above is that changing the spatial coupling between channel clusters should shift cells along straight lines in the $\sigma - T_{av}$ plane since coupling does not influence the recovery process. This hypothesis was tested in Ca^{2+} buffer experiments where spiking of specific cells was first measured under constant conditions for reference values [32]. Subsequently, an additional Ca^{2+} buffer was loaded to the cells before restarting the measurement with the same cells. In these experiments, we used again a variety of cell types and both BAPTA-AM as well as EGTA-AM buffers in smaller concentrations than usually used to suppress any Ca^{2+} signal. Indeed, we found that the slope of the shifting relation of individual cells coincides with the one of the $\sigma - T_{av}$ relation of the cell population. This demonstrates that the wave nucleation mechanism occurs also in smaller cells and that the spatial dimension is an important property of the Ca^{2+} pathway.

In similar experiments, Dupont and coworkers [34–36] have analyzed the stochastic aspects of oscillatory Ca^{2+} in hepatocytes stimulated with norepinephrine (NOR). They characterize the fluctuation by the coefficient of variation (*CV*) which is the normalized standard deviation $CV = \sigma / T_{av}$. Also these experiments exhibit a significant noise level of around 10% for the *CV*. They complement their study by a modeling approach in which they use a spatially homogeneous model of the form depicted in Fig. 24.1a. The model uses non-linear relations for the fluxes and molecular fluctuations are incorporated by the use of a discrete Markov chain gating scheme for the channel induced flux $J_{channel}$. This model fits the experiments and is able to analyze the dependence on stimulations strength and channel numbers. Thus, they show that the *CV*, in correspondence to their experiments, decreases from 35% to 17% with increasing NOR concentration from 85 to 95 nM. These results emphasize the role of the discrete channel opening further. The decrease in *CV* can be understood by the interplay of the recovery period and the nucleation time which is needed to initiate a global wave [33]. While the recovery period is rather independent of the stimulation strength, the nucleation time decreases for higher stimulations. This means that for higher stimulation the deterministic recovery period contributes with a relatively larger amount to an ISI compared to smaller stimulation levels where the nucleation time represents the main part of an ISI and thus leads to higher values of *CV*. Moreover the study quantitatively analyzed how the *CV* decreases with increasing number of release sites in simulations. Since they use a spatially homogeneous model, they do not describe the puff-to-wave nucleation mechanism and their analysis is mainly valid for the case of strong coupling between release sites. This is the case for tiny SERCA activity and Ca^{2+} buffering effects as well as for very fast diffusion of Ca^{2+}. Under these circumstances, the law of large numbers leads to more regular spiking for more release sites.

These experiments have led to a new perspective in modeling Ca^{2+} dynamics. While earlier models described Ca^{2+} spiking in a pendulum manner as self-sustained oscillations, recent experimental and modeling results indicate that Ca^{2+} signals occur by the hierarchical organization channel – cluster – cell as illustrated in Fig. 24.1c, d. Thus, mechanistic modeling must take the stochastic channel behavior as well as the spatial dimension of the Ca^{2+} pathway into account.

Change of Modeling Paradigm – Ca^{2+} Signals as a Hierarchical System

A mechanistic approach raises a couple of challenges since a large range of spatial and temporal dimensions must be covered. First, the steep spatial concentration gradients close to open channels require a tiny spatial discretization in order to guarantee numerical stability of partial differential equation solvers. Even with more sophisticated methods like finite elements solver this leads to extremely high computational costs [30]. On the temporal dimension, the stochastic binding and unbinding of IP_3 and Ca^{2+} to the subunits of IP_3R and the induced state changes lead to very small time steps of the Gillespie algorithm.

This is even strengthened by the locally high Ca^{2+} concentrations at the (open) channel's locations. Solovey et al. [37] use a coarse-grained approach, which separates the active channel cluster regions from the bulk. Within the cluster region a fine numerical grid is used and the dynamics are simplified to the main release terms. For the concentration outside a cluster region they use a full reaction–diffusion system where open channel clusters act as source terms. The separation of the two regions leads to matching conditions at the boundary where spatial discontinuities occur.

We avoid this kind of inconsistency by our recently developed *Green's Cell* (GC) algorithm combining several multi-scale techniques as depicted in Fig. 24.1c [29, 33]. We describe a single channel by a Markov chain according to the DeYoung-Keizer model. Thus, binding of an IP_3 molecule or Ca^{2+} ion is explicitly determined by a hybrid version of a Gillespie algorithm in dependence on the local concentration. An open channel leads to a blip and might activate other channels in the cluster. The resulting local puff concentration is determined by a quasi-steady state approximation derived in ref. [38]. On the cell level, the concentration dynamics are described by a spherical reaction–diffusion system, which describes free Ca^{2+} as well as a mobile and immobile Ca^{2+} buffer. For this 3-component system we derived an analytical mathematical solution in terms of a multicomponent Green's function where open clusters act as stochastic source terms. The analytical solution has the advantage that we do not have to deal with any discontinuities and that we only have to calculate the concentrations at cluster locations for possible channel transitions whereas numerical solvers always have to update the concentration at each grid point due to numerical stability criteria.

The model is able to reproduce all experimentally known Ca^{2+} signals in dependence on physiological parameters including diffusion and buffer properties, cell

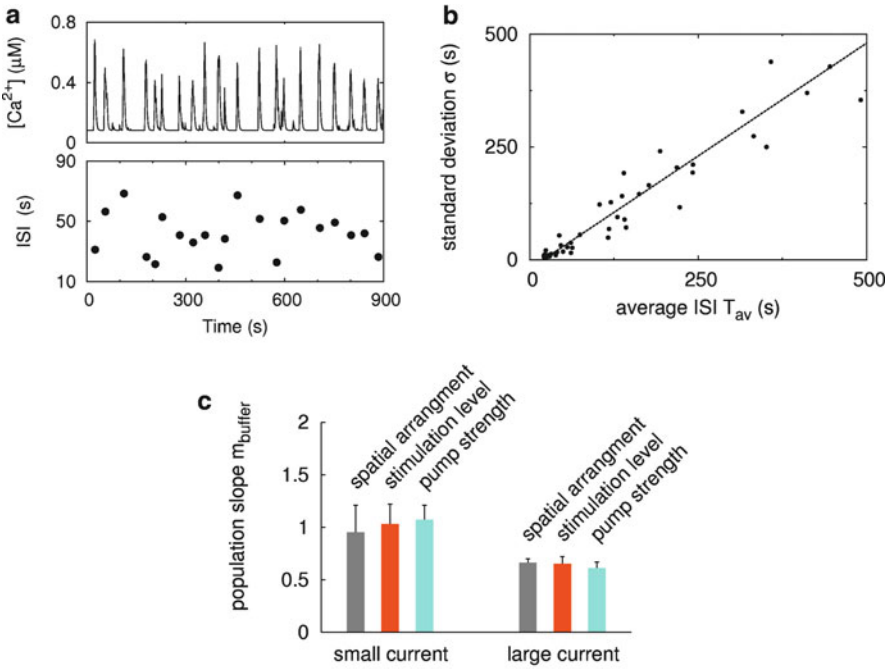

Fig. 24.3 Modeling the hierarchy of the Ca^{2+} pathway by the Green's cell algorithm. (**a**) The simulated Ca^{2+} dynamics of a Green's cell exhibit a behavior similar to typical experimental time series. Analogously to Fig. 24.2a, the *upper panel* shows the free cytosolic Ca^{2+} concentration and the *lower panel* the individual interspike intervals. (**b**) The $\sigma - T_{av}$ relation obtained from simulations. By varying IP_3, buffer and cytosolic calcium resting concentration, the Green's cell method produces a variety of different spike patterns from nearly regular oscillations to slow and random spiking. From the resulting spike trains, the standard deviation σ and the average period T_{av} were determined. The obtained linear dependence has a slope close to one and thus corresponds to spontaneously spiking cells in experiments. The coincidence of this bottom-up approach with experiments indicates further that the puff-to-wave nucleation mechanism produces reliable relations between statistical quantities. (**c**) Evidence for functional robustness. In extensive parameter scans, we analyzed the behavior of the $\sigma - T_{av}$ relation. Interestingly, we found that the slope of the relation is rather robust for variations over one magnitude regarding the spatial cluster arrangement, IP_3 concentration and SERCA activity. For standard values leading to a single channel current of 0.12 pA the slope was always close to 1 whereas a ten times higher current of 1.2 pA leads to a slope of around 0.6 what is comparable to the one observed in stimulated HEK cells (Fig. 24.2c). For more details see [29]

radius and cluster arrangement as well as SERCA activity and IP_3R properties [29]. The mechanistic approach allows us to follow a Ca^{2+} spike from its triggering event, the stochastic opening of a first channel, all the way along the CICR pathway as shown in Fig. 24.1c. Since we can control and monitor all dynamic processes in the model we can estimate the role of the different building blocks for the different signal forms. Figure 24.3a exhibits a representative time series obtained by GC simulation, which is in good agreement to experimental measurements shown in Fig. 24.3a. By varying parameters, this rather regular spiking can be tuned into more

irregular and slower spiking or into a plateau response with superimposed oscillations. In this way we produced a variety of different Ca^{2+} spiking signals and determined analogously to experiments the dependence of the standard deviation σ on the average period T_{av} of the resulting spike trains. This is shown in Fig. 24.3b where again each dot corresponds to such a spike train of one *in silico* cell. Like in the experimental analysis, we observe an offset on the T_{av} axis that corresponds to the deterministic recovery period. The slope of this relation is close to one and is thus in accordance to spontaneous oscillation in astrocytes and obeys the characteristics of a Poisson process with a regeneration period. Moreover, we could reproduce the experimentally observed effect that loading additional Ca^{2+} buffer renders spiking slower and more irregular. This consistent incidence emphasizes the spatial character of the Ca^{2+} pathway further.

In extensive simulations, we used fixed cellular setups and varied only one specific parameter leading to parameter specific $\sigma - T_{av}$ relations. Interestingly, it turns out that the slope of the $\sigma - T_{av}$ dependency seems to be highly conserved. Thus, varying the spatial distance between channel clusters, the stimulation level in terms of the IP_3 concentration or the pump strength over one magnitude has always led to a similar slope for a population of cells that only differs in the mobile buffer concentration. For standard values leading to corresponding single channel fluxes of 0.12 pA, the slope was always close to 1 and therefore in the range of spontaneous oscillation as shown in Fig. 24.3c. When we used a ten times larger channel current, either by increasing the concentration difference between the ER and the cytosol or by increasing the channel permeability, the slope decreased to around 0.6 what is comparable to experiments with stimulated HEK cells. We call this conserved relation between the statistical moments "functional robustness" [29]. This integrative approach may give first evidence how intrinsic feedbacks may be used to tune the Ca^{2+} pathway in dependence on diverse external signals and corresponding downstream targets.

The detailed physiological model can also be used to analyze phenomena, which are not easily accessible by experiments. Thus, the Green's cell method was used to study the effect of the experimental observation that the open time of IP_3Rs depends on their location [16]. We found in patch clamp experiments that isolated channels have a mean open time of 10 ms whereas open times of single channels located in a channel cluster have a halved open time of 5 ms. The question arose if such a change on a very fast time scale can influence the global dynamics which occurs on a time scale which is 3 order of magnitudes larger. This question is hard to answer in experiments since channel arrangement is not easy, if at all, to control. Moreover, such a study would have to monitor besides the channel arrangement also the opening behavior of each channel as well as to measure the global Ca^{2+} dynamics. This is out of the experimental possibilities but can be done with the bottom-up approach of the Green's cell algorithm. We performed parallel simulations of identical *in silio* cells with different IP_3R properties. We compared global Ca^{2+} signals from cells with only isolated channels with cells having the same number of channels arranged in clusters and obeying the different opening times. It turns out that clustering and the change on a microscopic time scale have major impacts on the global dynamics. For isolated and diffusively arranged channels no global Ca^{2+} spikes were observed in the physiological parameter range. Due to clustering

of these channels, the cell exhibits Ca^{2+} spikes even with a halved open time. The corresponding cellular setups with a hypothetical doubled open time lead to more frequent spiking with a on average 4 times faster mean period.

These examples demonstrate how mechanistic modeling of physiologic systems can be used to address biological questions. Here the hierarchical modeling framework was first used to test the hypothesis of the oscillation mechanism. The agreement of the simulation with experimental results strongly supports the validity of the puff-to-wave nucleation process being the general mechanism to generate cytosolic Ca^{2+} concentration spikes. Moreover, the modeling framework allows for estimation of internal cell properties by comparing simulations with experimental results. The overall message of this interdisciplinary approach is that understanding Ca^{2+} signals requires both analyses of the local IP_3R properties as well the cellular dynamics building a hierarchical cell signaling system.

A Closed Stochastic Theory Reveals Robustness and Adaptivity of the Calcium Signal

Although the Green's cell approach enables very detailed simulations and allows for studies that are beyond the experimental possibilities, it does not provide a closed mathematical framework. But such a framework is needed to uniquely proof assumed mechanisms of cell signaling. Moreover, even with the thoughtful implementation of the Green's cell model (see above), solving the concentration dynamics of a hierarchical system remains numerically extensive. In this section, we describe a recently developed strategy to obtain a closed theory of the core process generating stochastic Ca^{2+} signals [39].

For a reduced, but realistic description of the core process, we need to ask: Which are the key ingredients that determine the type of dynamics? For IP_3-induces Ca^{2+} signals, it is clear that clustered IP_3Rs are the most important molecules. Single IP_3Rs are activated by IP_3, and the activation strength is biphasically regulated by the cytosolic Ca^{2+} concentration [2, 7]. This mechanism is experimentally accessible by patch-clamping and is well understood in terms of mathematical models like the DeYoung-Keizer model [9]. But how can we incorporate the spatial organisation, i.e. the clustering? Standard techniques fail due to specific properties of the system. On the one hand, we cannot consider each IP_3R-subunit individually, because this leads to an astronomically high number of possible system states. On the other hand, methods based on the assumption of a large number of clusters are not appropriate, because the number of clusters is only of the order of 10 [7, 13].

The challenge encountered here is not at all exceptional in biology: It is an instance of the principle of emergent behavior [40, 41] – coupling and spatial arrangement of single molecules induce a new type of dynamics that cannot be inferred from the single molecules. This type of complex behavior leads us to a new strategy to gain a mathematical description. We switch to the next higher level of the dynamics and directly consider the channel clusters, not the individual channels (Fig. 24.4a). In fact, for the cytosolic Ca^{2+} dynamics in the whole cell, it is only

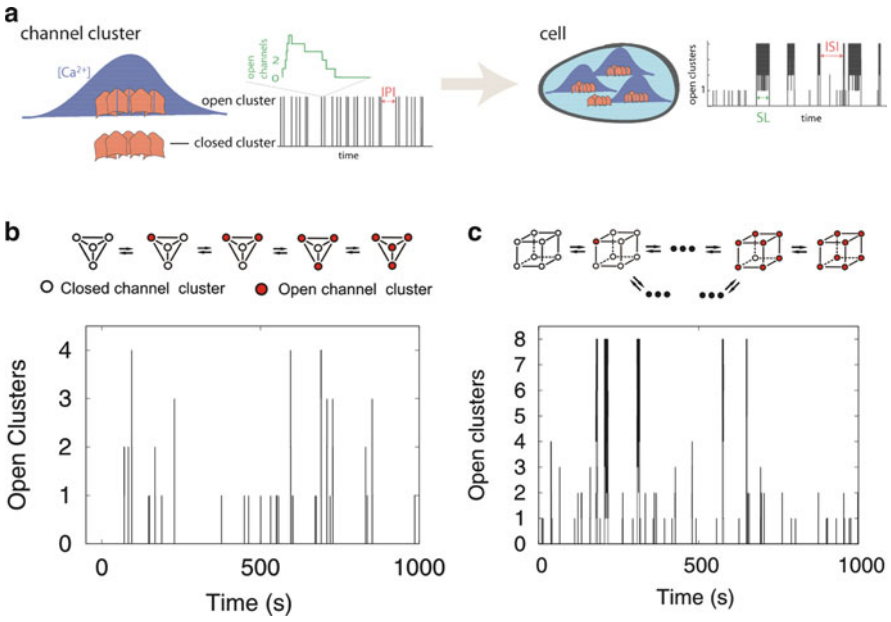

Fig. 24.4 Hierarchic stochastic modeling of Ca^{2+} spikes. (**a**) The new modeling strategy subsumes the dynamics of the lower structural level into waiting time distributions on the next higher level. Thus, we follow emergent behavior over three levels, from single Ca^{2+} channels over single clusters to coupled clusters. The waiting time distributions on the cluster level can be measured in vivo. That circumvents the problem arising from using parameter values from in vitro experiments for cell simulations, as rate equation models usually do. (**b**) The model with 4 clusters arranged as the vertices of a tetrahedron is the simplest non-trivial implementation, because all configurations with the same number of open clusters are equivalent. Events with one open cluster correspond to puffs, and with 4 open clusters to spikes. (**c**) In the model with 8 clusters forming the vertices of a cube, although the number of possible system configurations is much larger, the number of events with all clusters open (Ca^{2+} spikes) is similar to the tetrahedron model. Reprinted from Ref. [39]

important whether a cluster is open and releases Ca^{2+} ions into the cytosol or not at a given time. We do not need to know which particular subunit of which channel binds which regulatory molecule. Even though we are not interested in the full microscopic dynamics, we cannot neglect them: Of course, the state of the whole cluster (open or closed) depends on the states of all subunits. However, not every microscopic state-change (like unbinding of Ca^{2+} from an IP_3R-subunit) causes the whole cluster to start or stop releasing Ca^{2+} ions. Therefore, we can focus on the macroscopic cluster dynamics, if we keep in mind that the shape of the functions determining cluster state transitions depends on the microscopic dynamics. This leads to a mathematically more complex model as compared to many other stochastic descriptions in biology since it is non-Markovian, which means that a process does also depend on the history of the system and not only on the recent state [42]. But still we can obtain a full analytical description of the core process. We call this strategy hierarchic stochastic modeling [39, 43].

To gain a specific model from the new strategy, we need to specify the cluster arrangement and some other system parameters (see Ref. [39] for details).

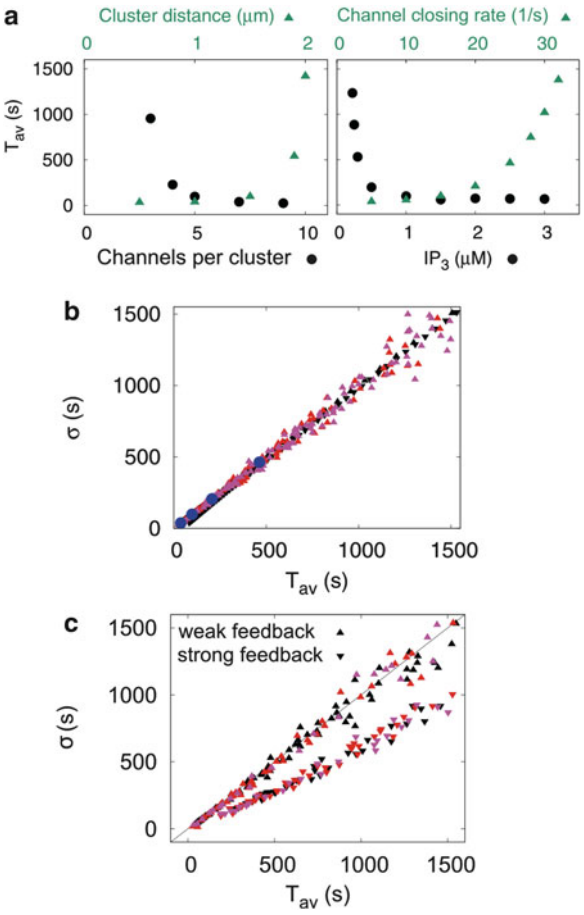

Fig. 24.5 Ca^{2+} spikes are functionally robust despite the high variability in the spike frequency. (**a**) The average interspike interval T_{av} depends sensitively on cellular parameters. (**b**) The slope of the $\sigma - T_{av}$ relation is one for all values of model parameters. *Upper triangles*: cluster distance a = 1.5 μm; *lower triangles*: a = 5 μm; *black symbols*: tetrahedron model; *red symbols*: regular cube model; *pink symbols*: irregular cube model with randomly shifted vertex positions; *blue circles*: analytical solution of the tetrahedron model with a = 1.5 μm. (**c**) The $\sigma - T_{av}$ relation can be adapted by global feedback, implemented here by inhibition of the puff-rate after a global spike and recovery with rate ξ. All *upper triangles*: $\xi = 0.1\ s^{-1}$; all *lower triangles*: $\xi = 10^{-3}\ s^{-1}$. The relations are identical for the tetrahedron model (*black symbols*), the cube model (*red*) and the irregular cube model (*pink*). Reprinted from Ref. [39]

Importantly, the qualitative dynamics arising from the model are independent of the detailed cluster arrangement (though they depend on the next-neighbour distance between clusters): For the same set of system parameters, events with most of the clusters open, calcium spikes occur at almost the same frequency in the tetrahedron model and in the cube model (Fig. 24.4b, c, see also Fig. 24.5b). The reason for this is that once a critical number of clusters is open, the cytosolic Ca^{2+} concentration

reaches such high values that the other clusters open as well with high probability, due to Ca^{2+}-induced Ca^{2+} release. Therefore, we can do most calculations with the simpler tetrahedron model.

With hierarchic stochastic modeling, we have developed a strategy to fully describe stochastic dynamics arising by emergent behavior of subsystems. Apart from the conceptual advantage for the mathematical model, a description in terms of cluster dynamics also has practical implications: Opening events of single clusters can be followed by live cell fluorescence microscopy, even in mammalian cells [13–15, 44]. Therefore, not only the model output (whole-cell Ca^{2+} dynamics), but also the model input in form of the cluster dynamics are experimentally accessible, and thus we have the unique opportunity to follow emergent behavior of an important biological process over several levels of molecular organisation. Indeed, by statistical analysis of Ca^{2+} puffs in two mammalian cell lines, we found that cellular Ca^{2+} dynamics are a consequence of true emergent behavior [45], providing further evidence that a hierarchic stochastic modeling strategy is appropriate.

We have seen that Ca^{2+} spikes can be characterized by the relation of standard deviation σ and average interspike interval T_{av}. In the hierarchic stochastic model, we find that T_{av} depends sensitively on details like cluster size and cluster distance, which are different from cell to cell (Fig. 24.5a). This is consistent with experiments showing huge cell-to-cell variability in T_{av} (Fig. 24.2a). The same experiments revealed that the $\sigma - T_{av}$ relation is not an individual cell property, but contains information on the cell population (Fig. 24.2b, c): All cells in a clonal population scatter along one straight line in the $\sigma - T_{av}$ plot, i.e. the relation is robust to cell-to-cell variability. Although the experimental results could be reproduced with the detailed modeling of the Green's cell algorithm, this framework does not give a sound explanation of this phenomenon. The most exciting result of the hierarchic stochastic model was that it shows this robustness in respect to all relevant system parameters, like stimulation strength, cluster size and even cluster distance (Fig. 24.5b) independently of explicit noise realizations of the Gillespie algorithm used in the Green's cell method. This strongly supports the modeling strategy, and more important – we have found a mathematical formulation that allows us to study and rationalise robustness arising from molecular fluctuations.

We did not postulate any assumptions about robustness to cell-to-cell variability when formulating the model. In the contrary, we assumed the highest possible irregularity (Poisson statistics [42]) for the dynamics of the single clusters [39]. An important assumption was however the coupling of the individual active elements, the IP3Rs. More specifically, we assumed that microscopic dynamics of channels in a cluster generate relatively simple probability distributions, which govern the dynamics of channel clusters. This assumption could be supported by analysis of data from live cell imaging [45]. Thus, we find that highly stochastic molecular dynamics in combination with emergent behavior can result in robustness.

Ca^{2+} signals carry information in their frequency [2, 7], which in our analysis translates to the distribution of stochastic interspike intervals. What is then the advantage of a robust $\sigma - T_{av}$ relation for Ca^{2+} signaling? The slope of this relation is identical to the coefficient of variation, which is a measure for the noise-to-signal ratio.

Therefore, a robust slope means robust signal quality, and thus *functional robustness* [46–48] of the mechanism, as its function is signal transduction. In the basic hierarchic stochastic model, the slope is always one (Fig. 24.5b), but in many experiments, the slope is smaller than one (Fig. 24.2c) corresponding to better signal quality. How can cells improve signal quality? We found only one possibility – global negative feedback. In the basic model, we only considered local feedback on the level of the individual clusters, namely Ca^{2+}-induced Ca^{2+} release and Ca^{2+}-mediated inhibition. However, real Ca^{2+} signaling pathways also contain global feedbacks from a cellular spike onto the activity of the clusters, like Ca^{2+}-activated Protein kinase C inhibiting G-protein coupled receptors [49]. Including such global negative feedback into the model substantially reduced the slope of the $\sigma - T_{av}$ relation (Fig. 24.5c).

Thus, the stochastic Ca^{2+} signaling pathway is not only functionally robust, it is also *adaptive*: In many cases it might be sufficient for downstream signaling to obtain a rather noisy and unspecific Ca^{2+} signal, which is the most economic mode of signaling. However, if more regular spike frequencies are required, this can be achieved by strengthening global negative feedback in the pathway, in the course of evolution. This conclusion is in agreement with the experimental finding that the slope is cell-type specific as indicated in Fig. 24.2b, c. Functional studies pointing into this direction are still missing. Nevertheless, it has been shown that small and unidirectional changes in the genetic code can be realised in time-frames which are short for evolution (~100 generations) in the appropriate conditions [50, 51]. Furthermore, it has been argued that functionally robust and adaptive core units are the pacemakers of evolution on the larger scale [52]. Since the analyses above reveal that stochastic Ca^{2+} signals are functional and robust, this could be an explanation for the universality of the Ca^{2+} signaling toolkit in cell physiology [2].

Conclusion

To persist in evolution, eukaryotes, and especially multicellular organisms, need precise signaling mechanisms to synchronise and adjust action of different cellular compartments or different cells. There is a variety of signaling pathways transmitting signals from the plasma membrane to the nucleus, and Ca^{2+} signaling is an integral part of many of those [4]. Biological pathways are always embedded in an environment largely determined by molecular fluctuations [53, 54]. Signaling pathways on the scale of single cells can be tuned to high accuracy only at very high costs in terms of energy consumption [55]. Therefore, apart from precise function, evolutionarily conserved biological systems also must be robust to noisy fluctuations [46–48]. Indeed, it recently became evident that intracellular Ca^{2+} signals exhibit huge variability [32, 34]. Therefore, it can be expected that the Ca^{2+} signaling mechanism is not only specific, but also robust: Its biological function should not depend on high precision. In this context, a mechanistic understanding of Ca^{2+} signals is indispensable. In this chapter, we have shown how interdisciplinary research is able to understand the essential mechanisms. While early studies have

revealed the general architecture of a cellular feedback mechanism, more recent studies go after a complete molecular description. The enhanced experimental techniques of the last decade have identified the hierarchy of the Ca^{2+} signaling pathway. This basis enables detailed modeling approaches and theoretical hypotheses, which may initiate further experimental studies.

A mechanistic understanding of the hierarchical organization has led to the assumption that single channel fluctuation should be carried up on the cell level by the nucleation process. Indeed, our experimental analysis has demonstrated that Ca^{2+} oscillations are stochastic and depend on the spatial coupling between release sites. Moreover, we found that it is probably not the frequency itself that is conserved, but the relation between the noise level in form of the standard deviation σ and the average period T_{av}. Interestingly, a heuristic 2-parameter model can explain this empirical observation. The model is based on the interplay between excitability and regeneration. While excitability relates to spatial coupling between release sites and stimulation level, the regeneration processes may reflect additional pathway interactions. This point of view is emphasized by the experimental observation that different cells of one type differ in their excitability whereas different cell types exhibit distinct regeneration characteristics. By decomposing the Ca^{2+} pathway into its elements and compiling it into a mechanistic model, we could illuminate this behavior. The bottom-up approach of the Green's cell method is able to reproduce experimental observations in a nearly perfect manner and clearly demonstrates that the Ca^{2+} pathway has a spatial dimension. It shows how the puff-to-wave nucleation process leads to a conserved $\sigma - T_{av}$ relation for a large parameter regime, and facilitates detailed analyses of the dependency of this process on biological parameters like buffer concentrations.

With the closed model of the hierarchic stochastic system, we have a mathematical formulation at hand, which allowed us to prove functional robustness of the Ca^{2+} signaling pathway based only on basic principles like Ca^{2+}-induced Ca^{2+} release and channel clustering. This demonstrates that functional robustness is a generic property of the system, which naturally emerges from the stochastic dynamics.

Signaling mechanisms like the Ca^{2+} signaling toolkit are not only functional and robust, but they also must be adaptive to changing needs in a changing world, a property sometimes referred to as evolvability [46, 56]. We found that the signal quality can be adjusted by modification of global feedback processes in the pathway, and that signal quality is a cell type specific property. This suggests that the Ca^{2+} system is indeed highly adaptive to specific needs in a specific pathway, which underpins its importance for intracellular signal transduction.

The results presented in this chapter illustrate how theory and experiment can complement each other to decipher the cascade of emergent behavior from single molecules to pathways. We found that the hierarchic structure of the Ca^{2+} system allows for functional robustness despite high variability of its components. It has to be elucidated by future research how this property affects specific signaling cascades and how far it applies to other biological mechanisms.

Acknowledgments We would like to thank Rüdiger Thul for helpful comments on the manuscript.

References

1. Berridge MJ, Bootman MD, Lipp P (1998) Calcium – a life and death signal. Nature 395: 645–648
2. Berridge MJ, Lipp P, Bootman MD (2000) The versatility and universality of calcium signalling. Nat Rev Mol Cell Biol 1:11–21
3. Taylor CW (2002) Controlling calcium entry. Cell 111:767–769
4. Lodish H, Berk A, Kaiser CA, Krieger M, Scott MP, Bretscher A (2007) Molecular cell biology. Palgrave Macmillan, Basingstoke
5. Taylor CW, Tovey SC (2010) IP3 receptors: toward understanding their activation. Cold Spring Harb Perspect Biol 2:a004010
6. Taylor CW, Laude AJ (2002) IP_3 receptors and their regulation by calmodulin and cytosolic Ca^{2+}. Cell Calcium 32:321–334
7. Falcke M (2004) Reading the patterns in living cells – the physics of Ca^{2+} signaling. Adv Phys 53:255–440
8. Schuster S, Marhl M, Hofer T (2002) Modelling of simple and complex calcium oscillations. From single-cell responses to intercellular signalling. Eur J Biochem 269:1333–1355
9. De Young GW, Keizer J (1992) A single-pool inositol 1,4,5-trisphosphate-receptor-based model for agonist-stimulated oscillations in Ca^{2+} concentration. Proc Natl Acad Sci USA 89:9895–9899
10. Bezprozvanny I, Watras J, Ehrlich BE (1991) Bell-shaped calcium-response curves of Ins(1,4,5)P3- and calcium-gated channels from endoplasmic reticulum of cerebellum. Nature 351:751–754
11. Yao Y, Choi J, Parker I (1995) Quantal puffs of intracellular Ca^{2+} evoked by inositol trisphosphate in Xenopus oocytes. J Physiol 482(Pt 3):533–553
12. Marchant JS, Callamaras N, Parker I (1999) Initiation of IP_3-mediated Ca^{2+} waves in *Xenopus* oocytes. EMBO J 18:5285–5299
13. Smith IF, Wiltgen SM, Parker I (2009) Localization of puff sites adjacent to the plasma membrane: functional and spatial characterization of Ca^{2+} signaling in SH-SY5Y cells utilizing membrane-permeant caged IP_3. Cell Calcium 45:65–76
14. Bootman MD, Berridge MJ, Lipp P (1997) Cooking with calcium: the recipes for composing global signals from elementary events. Cell 91:367–373
15. Tovey SC, de Smet P, Lipp P, Thomas D, Young KW, Missiaen L, De Smedt H, Parys JB, Berridge MJ, Thuring J, Holmes A, Bootman MD (2001) Calcium puffs are generic InsP(3)-activated elementary calcium signals and are downregulated by prolonged hormonal stimulation to inhibit cellular calcium responses. J Cell Sci 114:3979–3989
16. Taufiq Ur R, Skupin A, Falcke M, Taylor CW (2009) Clustering of $InsP_3$ receptors by $InsP_3$ retunes their regulation by $InsP_3$ and Ca^{2+}. Nature 458:655–659
17. Heinrich R, Schuster S (1996) The regulation of cellular systems. Chapman & Hall, New York
18. Woods NM, Cuthbertson KS, Cobbold PH (1986) Repetitive transient rises in cytoplasmic free calcium in hormone-stimulated hepatocytes. Nature 319:600–602
19. Meyer T, Stryer L (1988) Molecular model for receptor-stimulated calcium spiking. Proc Natl Acad Sci USA 85:5051–5055
20. Goldbeter A, Dupont G, Berridge MJ (1990) Minimal model for signal-induced Ca^{2+} oscillations and for their frequency encoding through protein phosphorylation. Proc Natl Acad Sci USA 87:1461–1465
21. Cornell-Bell AH, Finkbeiner SM (1991) Ca^{2+} waves in astrocytes. Cell Calcium 12:185–204
22. Lechleiter J, Girard S, Peralta E, Clapham D (1991) Spiral calcium wave propagation and annihilation in Xenopus laevis oocytes. Science 252:123–126
23. Jaffe LF (1991) The path of calcium in cytosolic calcium oscillations: a unifying hypothesis. Proc Natl Acad Sci USA 88:9883–9887
24. Taylor CW, da Fonseca PC, Morris EP (2004) IP(3) receptors: the search for structure. Trends Biochem Sci 29:210–219

25. Suhara W, Kobayashi M, Sagara H, Hamada K, Goto T, Fujimoto I, Torimitsu K, Mikoshiba K (2006) Visualization of inositol 1,4,5-trisphosphate receptor by atomic force microscopy. Neurosci Lett 391:102–107
26. Tateishi Y, Hattori M, Nakayama T, Iwai M, Bannai H, Nakamura T, Michikawa T, Inoue T, Mikoshiba K (2005) Cluster formation of inositol 1,4,5-trisphosphate receptor requires its transition to open state. J Biol Chem 280:6816–6822
27. Marchant JS, Parker I (2001) Role of elementary Ca^{2+} puffs in generating repetitive Ca^{2+} oscillations. EMBO J 20:65–76
28. Berridge MJ (2009) Inositol trisphosphate and calcium signalling mechanisms. Biochim Biophys Acta 1793:933–940
29. Skupin A, Kettenmann H, Falcke M (2010) Calcium signals driven by single channel noise. PLoS Comput Biol 6:e1000870
30. Rudiger S, Shuai JW, Huisinga W, Nagaiah C, Warnecke G, Parker I, Falcke M (2007) Hybrid stochastic and deterministic simulations of calcium blips. Biophys J 93:1847–1857
31. Perc M, Green AK, Dixon CJ, Marhl M (2008) Establishing the stochastic nature of intracellular calcium oscillations from experimental data. Biophys Chem 132:33–38
32. Skupin A, Kettenmann H, Winkler U, Wartenberg M, Sauer H, Tovey SC, Taylor CW, Falcke M (2008) How does intracellular Ca^{2+} oscillate: by chance or by the clock? Biophys J 94: 2404–2411
33. Skupin A, Falcke M (2009) From puffs to global Ca^{2+} signals: how molecular properties shape global signals. Chaos 19:037111
34. Dupont G, Abou-Lovergne A, Combettes L (2008) Stochastic aspects of oscillatory Ca^{2+} dynamics in hepatocytes. Biophys J 95:2193–2202
35. Dupont G, Combettes L (2009) What can we learn from the irregularity of Ca^{2+} oscillations? Chaos 19:037112
36. Dupont G, Erneux C (1997) Simulations of the effects of inositol 1,4,5-trisphosphate 3-kinase and 5-phosphatase activities on Ca^{2+} oscillations. Cell Calcium 22:321–331
37. Solovey G, Fraiman D, Pando B, Ponce Dawson S (2008) Simplified model of cytosolic Ca^{2+} dynamics in the presence of one or several clusters of Ca^{2+} -release channels. Phys Rev E Stat Nonlin Soft Matter Phys 78:041915
38. Bentele K, Falcke M (2007) Quasi-steady approximation for ion channel currents. Biophys J 93:2597–2608
39. Thurley K, Falcke M (2011) Derivation of Ca^{2+} signals from puff properties reveals that pathway function is robust against cell variability but sensitive for control. Proc Natl Acad Sci USA 108:427–432
40. Penzlin H (2009) The riddle of "life," a biologist's critical view. Naturwissenschaften 96:1–23
41. Laughlin RB, Pines D (2000) The theory of everything. Proc Natl Acad Sci USA 97:28–31
42. Van Kampen NG (2002) Stochastic processes in physics and chemistry. Elsevier Science B.V., Amsterdam
43. Thul R, Thurley K, Falcke M (2009) Toward a predictive model of Ca^{2+} puffs. Chaos 19: 037108
44. Smith IF, Parker I (2009) Imaging the quantal substructure of single IP3R channel activity during Ca^{2+} puffs in intact mammalian cells. Proc Natl Acad Sci USA 106:6404–6409
45. Thurley K, Smith IF, Tovey SC, Taylor CW, Parker I, Falcke M (2011) Timescales of IP_3-evoked Ca^{2+} spikes emerge from Ca^{2+} puffs only at the cellular level. Biophys J 101:2638–2644
46. Wagner A (2005) Robustness and evolvability in living systems. Princeton University Press, Princeton
47. Kitano H (2004) Biological robustness. Nat Rev Genet 5:826–837
48. Stelling J, Sauer U, Szallasi Z, Doyle FJ 3rd, Doyle J (2004) Robustness of cellular functions. Cell 118:675–685
49. Taylor CW, Thorn P (2001) Calcium signalling: IP3 rises again…and again. Curr Biol 11: R352–R355
50. Dekel E, Alon U (2005) Optimality and evolutionary tuning of the expression level of a protein. Nature 436:588–592

51. Kashtan N, Noor E, Alon U (2007) Varying environments can speed up evolution. Proc Natl Acad Sci USA 104:13711–13716
52. Gerhart J, Kirschner M (2007) The theory of facilitated variation. Proc Natl Acad Sci USA 104(Suppl 1):8582–8589
53. Rao CV, Wolf DM, Arkin AP (2002) Control, exploitation and tolerance of intracellular noise. Nature 420:231–237
54. Delbruck M (1945) The burst size distribution in the growth of bacterial viruses (bacteriophages). J Bacteriol 50:131–135
55. Lestas I, Vinnicombe G, Paulsson J (2010) Fundamental limits on the suppression of molecular fluctuations. Nature 467:174–178
56. Kirschner M, Gerhart J (1998) Evolvability. Proc Natl Acad Sci USA 95:8420–8427

Chapter 25
Simulation Strategies for Calcium Microdomains and Calcium-Regulated Calcium Channels

Frederic von Wegner, Nicolas Wieder, and Rainer H.A. Fink

Abstract In this article, we present an overview of simulation strategies in the context of subcellular domains where calcium-dependent signaling plays an important role. The presentation follows the spatial and temporal scales involved and represented by each algorithm. As an exemplary cell type, we will mainly cite work done on striated muscle cells, i.e. skeletal and cardiac muscle. For these cells, a wealth of ultrastructural, biophysical and electrophysiological data is at hand. Moreover, these cells also express ubiquitous signaling pathways as they are found in many other cell types and thus, the generalization of the methods and results presented here is straightforward.

The models considered comprise the basic calcium signaling machinery as found in most excitable cell types including Ca^{2+} ions, diffusible and stationary buffer systems, and calcium regulated calcium release channels. Simulation strategies can be differentiated in stochastic and deterministic algorithms. Historically, deterministic approaches based on the macroscopic reaction rate equations were the first models considered. As experimental methods elucidated highly localized Ca^{2+} signaling events occurring in femtoliter volumes, stochastic methods were increasingly considered. However, detailed simulations of single molecule trajectories are rarely performed as the computational cost implied is too large. On the mesoscopic level, Gillespie's algorithm is extensively used in the systems biology community and with increasing frequency also in models of microdomain calcium signaling. To increase computational speed, fast approximations were derived from Gillespie's exact algorithm, most notably the chemical Langevin equation and the τ-leap algorithm. Finally, in order to integrate deterministic and stochastic effects in multiscale simulations, hybrid algorithms are increasingly used. These include stochastic models of ion channels combined with deterministic descriptions of the calcium buffering

F. von Wegner (✉) • N. Wieder • R.H.A. Fink
Medical Biophysics Group, Institute of Physiology and Pathophysiology,
University of Heidelberg, Heidelberg, Germany
e-mail: fwegner@physiologie.uni-heidelberg.de

M.S. Islam (ed.), *Calcium Signaling*, Advances in Experimental Medicine and Biology 740, DOI 10.1007/978-94-007-2888-2_25,

and diffusion system on the one hand, and algorithms that switch between deterministic and stochastic simulation steps in a context-dependent manner on the other. The basic assumptions of the listed methods as well as implementation schemes are given in the text. We conclude with a perspective on possible future developments of the field.

Keywords Calcium • Calcium channel • Microdomains • Intracellular signaling • Stochastic simulation • Deterministic simulation • Gillespie algorithm • Chemical Langevin equation • Tau-Leap • Binomial leap

Canonical Models of Calcium Microdomains

Identical subcellular compartments and systems have been modelled using different stragtegies. Synaptic activation including vesicle release at the neuronal synapse, for instance, has been modelled with different approaches [1, 2] ranging from simulations at the scale of individual molecules to deterministic reaction rate equations. Similarly, different model classes of subcellular calcium dynamics in cardiomyocytes and skeletal muscle fibers are still being evaluated for their explanatory and predictive power. The simulated volume and average reactant concentrations can help to decide which simulation strategy is the most adequate for a given problem.

Virtually all cell types share a common family of molecules involved in the regulation of the local, subcellular calcium concentration and many cell lines even share common modules, i.e. small signaling networks that regulate key processes such as cell cycle regulation, adaptation of the metabolic rate, vesicle secretion, motility and excitability [3]. In order to keep the presentation of simulation strategies compact, we here focus on some key molecular species, in particular calcium buffers and calcium channels, from where the transfer to more specific problems should be easy.

The presentation and the implementation of the models used here is further facilitated by the fact that it is sufficient to take into account chemical reactions of second order, at most. In this context, zero-order reactions model the constant generation or degradation of a molecular species at a fixed rate, for instance, when a molecule is assumed to be unstable on time scales relevant for the simulation. Zero-order reactions also come into play when certain reaction networks are not simulated in detail but one of their products (resp. educts) appears as a reaction partner in the system that is simulated in detail. Also ion channel currents can be modeled as zero-order reactions occurring in time intervals when the channel is in an open state. Modeling ion channel currents as chemical reaction events has the advantage that the inclusion of channel currents does not require major modifications of the computational model but only the addition of another reaction type. First-order reactions are mainly concerned when a calcium-bound molecular complex dissociates and thereby liberates a calcium ion. Second-order reactions describe the corresponding association reaction of a calcium ion and a calcium-binding molecule such as buffer proteins, calcium-sensitive enzymes, membrane constituents, ion channels or fluorescent

dye molecules. In principle, any of these calcium-binding molecules can be considered a calcium buffer.

The molecular species used in this presentation are calcium ions (Ca^{2+}), a set of calcium buffers (B_i, $i = 1,\ldots,N_B$) that can be either diffusible or immobile and calcium-regulated ion channels (Ch). In the case of ion channels, those regulated by calcium ions but conducting another ionic species (e.g. calcium regulated chloride or potassium channels) must be distinguished from calcium-regulated calcium channels. The latter, e.g. IP_3- and RyR-channels, provide a highly localized, nonlinear calcium-sensitive feedback system since these channels have activating as well as inhibitory calcium binding sites.

Microscopic Simulation

To achieve a maximum of spatial detail, one has to simulate the Brownian motion of all molecules and introduce reaction events whenever a molecular collision of sufficiently high energy (the activation energy of the reaction) occurs [4]. The price of this level of detail is paid in computation time. Runtime scales unfavorably with increasing simulation volume and increasing number of reactants as diffusion events occur at much higher rates than chemical reactions and the number of trajectories grows linearly with the number of reactants. In the context of calcium dynamics, simulations of individual molecular trajectories are used less frequently than the approaches explained below. They can be found mainly in the context of calcium-regulated synaptic signaling [1, 5, 6]. Practically, these systems can be implemented with the freely available software package MCell developed by the Salk Institute (www.mcell.cnl.salk.edu).

Mesoscopic Stochastic Simulation

Mesoscopic simulation approaches have been the fastest growing area in computational cell biology in the past 15 years [7]. Using the mecoscopic perspective, the fluctuating number of molecules of each type is tracked by one of several stochastic algorithms.

To better understand different mesoscopic algorithms, it is necessary to introduce some notation and a few definitions. The state of a given model system of N molecular species $S_1,\ldots,S_N$ will from here on be described by the time-dependent ***state vector*** $x(t) = [x_1(t),\ldots,x_N(t)]$ that contains the ***copy number*** $x_i(t)$ of each species (index i) at time t. By copy number, we understand the number of molecules of a certain molecular species in a defined volume at a given time, e.g. a Ca^{2+} concentration of 100 nM in a 1 fl volume yields a copy number of 60. The term copy number is mostly used in the context of small reaction volumes and low molar concentrations resulting in relatively few molecules of each type. The N chemical species in our model system interact through M types of chemical reactions $R_j, j = 1,\ldots,M$. Next, a ***state change vector*** v_j is introduced for each reaction R_j.

The component v_{ji} describes the change in the copy number of species S_i caused by a single reaction R_j. After a reaction R_j occurs, the state vector is updated according to $x(t) \leftarrow x(t) + v_j$. Furthermore, we assume that given a state $x(t)$, there is a defined probability for each reaction R_j to occur within a small (infinitesimal) time interval $[t, t+dt]$. In the context of chemical reactions, this probability equals $a_j(x)dt$ and $a_j(x)$ is called the ***reaction propensity*** of reaction R_j. As the state vector $x(t)$ is time-dependent, the reaction propensity $a_j(x)$ is also time-dependent, however, this notation is often suppressed for the sake of simplicity.

The following stochastic algorithms can all be derived from the chemical master equation (CME). The CME is a differential (or difference) equation that describes the temporal evolution of the probability density $p(x,t)$, i.e. the multivariate distribution of the state vector $x(t)$. Using the notation introduced above, the CME reads:

$$\partial_t p(x,t) = \sum_{j=1}^{M} \left[a_j\left(x - v_j\right) p\left(x - v_j, t\right) - a_j(x) p(x,t) \right]. \tag{25.1}$$

In words, the CME states that the change in $p(x,t)$ is calculated as the net probability flow conveyed by flows from state $x - v_j$ into state x (via reaction R_j) and the reverse flows out of state x. A closed-form, analytical solution for $p(x,t)$ is only accessible for very simple systems [8]. As for many other stochastic systems, this is where Monte Carlo sampling schemes come into play.

Gillespie's Algorithm

Gillespie's algorithm provides a Monte Carlo simulation scheme that samples the time-dependent probability density $p(x,t)$ exactly [9]. The crucial point in Gillespie's algorithm is the insight that the evolution of the state vector $x(t)$ follows a multivariate Markov process on the N-dimensional integer lattice Z^N The transition rate between the lattice points x and $x + v_j$ is given by the reaction propensity a_j. As Markov processes are characterized by exponential waiting time distributions, the waiting time until the next reaction event can be calculated in a single step. The waiting time distribution is parametrized by the cumulative reaction rate

$$a_0(x) = \sum_{j=1}^{M} a_j(x). \tag{25.2}$$

The rate $a_0(x)$ determines the probability $p(\tau, j \mid x, t)$ that, given state x at time t, the next reaction event will be of type R_j and will occur in the small time interval $[t+\tau, t+\tau+dt]$:

$$p\left(\tau, j \mid x, t\right) = a_j(x) \exp\left(-a_0(x)\tau\right). \tag{25.3}$$

In the actual algorithm, the probability is factored in two parts. First, the waiting times τ for the next event are obtained as samples from an exponential distribution with parameter $a_0(x)$ according to

$$\tau = \frac{-\ln(r)}{a_0(x)} \tag{25.4}$$

where $r \sim U_{[0,1]}$ is a uniformly distributed random variable. Next, the reaction type R_j is determined according to the ratio $\frac{a_j(x)}{a_0(x)}$. Thus, the complete Gillespie algorithm reads:

1. ***Initialization***: initialize the state vector components $x_i(t=0)$ with the copy number of chemical species S_i expected in equilibrium or any other desired initial condition. Calculate all individual reaction propensities $a_j(x)$ and the cumulative propensity $a_0(x)$.
2. ***Waiting time and reaction selection***: sample a waiting time τ and a reaction index j from the distribution Eq. 25.3.
3. ***Update state and time***: $x(t) \leftarrow x(t) + v_j$ and $t \leftarrow t + \tau$.
4. ***Exit condition***: if $t > T_{max}$ where T_{max} is the desired length of the simulation.
5. ***Update propensities***: recalculate the propensities of all reactions affected by the last state change.
6. goto step 2.

An efficient implementation based on the dependency structure between reactions and the reuse of random numbers was developed later [10]. The result of Gillespie's algorithm is a set of N time series reflecting the fluctuating copy number of each molecular species S_i. The advantage of the algorithm becomes most clear when compared to earlier approaches. An alternative approach to simulate the reaction process relies on the fact that the probability of reaction R_j to occur in a small interval $[t, t+dt]$ equals $a_j(x)dt$. If dt is chosen small enough to ensure that $a_j(x)dt << 1$ one can iteratively advance the simulation time by dt and accept or reject reaction events by comparison with the value of a uniformly distributed random variable r. This strategy is not recommended however, as one will find that most time steps dt will pass without any reaction event happening. The problem becomes even worse when the desired precision demands a small time step dt. Gillespie's algorithm overcomes the problem by sampling the exponential waiting time distribution directly and by jumping to the next event time without further checks. Moreover, no fixed integration time step dt has to be chosen and therefore, the algorithm is stochastically "exact".

Though widely used in systems biology, there are comparatively few examples for the use of Gillespie's algorithm in the modeling of intracellular calcium dynamics. Gillespie's algorithm has been used to model stochastic resonance effects in whole cells [11, 12], calmodulin-dependent synaptic plasticity in dendritic spine microdomains [2] and to model calcium microdomains in the vicinity of individual L-type calcium channels [13]. Although the algorithm can be used for arbitrary simulation volumes, computation time quickly increases for larger

volumes because the copy numbers enter the propensity terms in a combinatorial way. Therefore, several approximations of the exact simulation algorithm have been developed.

The Binomial and the τ-Leap Methods

For small time steps dt, the probability for a reaction R_j to occur in the next time interval $[t, t+dt]$ is given by $a_j(x)dt$. Assuming that the propensity a_j remains approximately constant during the time span τ, the number of times the reaction R_j occurs during the span τ is a Poisson-distributed random variable with expected value $a_j(x)\tau$ [14]. Now, if τ is small enough to guarantee approximately constant reaction propensities a_j and at the same time large enough so that $a_j(\mathbf{x})\ \tau >> 1$, i.e. a significant number of reactions will occur during the time interval of length τ,then Gillespie's algorithm can be accelerated by using the larger time step τ and by sampling the number of reactions from Poissonian distributions with parameters $a_j(x)\tau$ directly. This procedure is called the ***τ-leap method*** [7]. Obviously, the main task is to set the right time step τ adaptively throughout the simulation. Small time steps will produce low numbers of reactions (even zero), and in this situation the exact Gillespie algorithm could be used instead. Too large time steps however, lead to a larger error compared to the exact solution and furthermore, can lead to negative molecule numbers. A detailed discussion of τ-selection procedures can be found in the literature [15]. Using Poisson random numbers, there is always a risk of producing negative entries in the state vector as Poisson variables range from zero to infinity. As an alternative, the ***binomial leap method*** has been proposed. Instead of Poisson variables, appropriately parametrized binomial random variables are used, the main advantage being that the range of the variable can be bounded by the current copy number of each molecule [16].

Irrespective of the method used, the update rule can be written as

$$x_i(t+\tau) = x_i(t) + \sum_{j=1}^{M} v_{ji}\xi_j\left(a_j(x)\right) \tag{25.5}$$

where ξ_j represents either a Poissonian or a binomial random variable. Applications and systematic evaluations of these methods for the simulation of calcium microdomains are still scarce, a comparative study can be found in [17].

The Chemical Langevin and Fokker-Planck Equations

The approximation of the number of reactions that occur in a given time interval by samples from a defined probability density can be taken a step further. In the case of the chemical Langevin equation (CLE), the number of reactions R_j occurring in a

small time interval of length dt is sampled from a normal distribution with mean and variance equal to $a_j(x)dt$. From a statistical point of view, this approach is justified as the Poisson random variable introduced in the last paragraph converges to a normal distribution in the case of a large mean value. When the expected number of reactions is too small, the symmetric normal distribution does not yield a good approximation of the corresponding right-skewed Poisson distribution and negative molecule counts can be obtained. The most important differences of the CLE approach are (i) that the time interval dt is fixed, and (ii) that, due to the normally distributed random variable, the copy numbers are real numbers rather than integers. The updating rule is given by

$$x_i\left(t+dt\right)=x_i(t)+\sum_{j=1}^{M}v_{ji}a_j(x)dt+\sum_{j=1}^{M}v_{ji}\sqrt{a_j(x)}dB(t) \tag{25.6}$$

where $dB(t)$ are the increments of a standard Brownian motion [8]. The first sum in Eq. 25.6 contains the deterministic dynamics that will be discussed in the following paragraph while the second sum adds appropriately scaled stochastic fluctuations. Compared to the algorithms discussed so far, the CLE provides an extremely fast way to obtain an approximate solution of the CME. A basic result in the theory of stochastic processes allows a transformation of the Langevin equation to an associated Fokker-Planck equation (FPE) that describes the temporal evolution of the probability density $p(x,t)$ [8].

As most applications are interested in sample paths of the modeled system rather than in probability distributions, the CLE approach is more widely used. Implementations of the CLE approach have been presented for calcium-dependent signaling pathways in neurons [18] and IP_3-mediated calcium sensitive pathways in non-excitable cells [11, 19, 20]. An example of the FPE method to calcium dynamics in the dyadic cleft of cardiomyocytes is given in [21].

Deterministic Simulation

When stochastic effects in the dynamics of the modeled system are ignored, the classical deterministic reaction-rate equations are recovered. These correspond to the deterministic terms found in the chemical Langevin Eq. 25.6. From a statistical physics point of view, the deterministic dynamics reflect the limit of an infinitely large simulation volume while keeping all reactant concentrations constant.

$$x_i(t+dt)=x_i(t)+\sum_{j=1}^{M}v_{ji}a_j(x)dt \tag{25.7}$$

As stochastic effects are no longer present, a set of ordinary differential equations is obtained that can be conveniently integrated using standard schemes as implemented

in most numerical software packages. If diffusion is included in the model, an additional term arises for each diffusible species with diffusion constant D_i

$$x_i(t+dt) = x_i(t) + \sum_{j=1}^{M} v_{ji} a_j(x)dt + D_i \nabla^2 x_i(t) \tag{25.8}$$

and the model is now described by set of partial differential equations. Deterministic methods represent the major part of the literature on calcium dynamics in excitable and non-excitable cells. In the context of microdomain calcium dynamics in cardiac and skeletal muscle cells, we list only a small selection of representative and landmark studies [22–26].

Hybrid Simulation

Complex subcellular systems often generate patterns across several temporal scales, especially when the participating reactions have rate constants that span several orders of magnitude. In these cases, it may happen that Gillespie's exact algorithm performs quite slowly due to the exact tracking of effectively irrelevant fluctuations while the system's dynamics may perform in an almost deterministic way. Moreover, models of subcellular calcium dynamics often contain plasma membrane or endoplasmic reticulum ion channels that modulate the local calcium concentration or are modulated by Ca^{2+} ions. As ion channel gating is almost exclusively described with stochastic methods, mainly with Markov chain models, the introduction of ion channels in deterministic models is not obvious. For these cases, hybrid models combining several of the aforementioned techniques have been developed. For instance, hybrid models using deterministic reaction dynamics for the subset of calcium diffusion, permeation and buffering reactions and stochastic models of ion channel gating have successfully been used for the modeling of skeletal and cardiac muscle cells [27, 28] as well as for generic cell types with an IP_3 regulated calcium signaling system [29]. Other approaches switch adaptively between deterministic dynamics and the CLE-approximation [30], or between the Gillespie algorithm, the CLE-approximation and the τ-leap method [17].

Reaction Propensities for Calcium Microdomains

In the preceding sections, reaction propensities were introduced in an abstract way to calculate certain probability densities. Now, we will give some explicit expressions for reaction types essential to microdomain calcium signaling.

1. ***Chemical reactions***. $a_j(x,t) = c_j \times h_j(x,t)$ where c_j is the stochastic reaction rate and $h_j(x,t)$ denotes the number of possible molecular combinations available for reaction R_j at time t. The stochastic rates are calculated from the macroscopic reaction rate constants k_j and the system volume Ω, for monomolecular reac-

tions we get $c_j = k_j$, for bimolecular reactions $c_j = k_j / \Omega$. Calcium buffering reactions consist of a pair of reactions, a second-order association reaction and a first-order dissociation reaction. Calcium pumps can be modeled in the same way.

2. ***Ion channel gating***. Given a gating scheme and the associated transition rates, transitions between channel substates can be treated as first-order chemical reactions where the different channel states are seen as different chemical species that are transformed into each other as specified by the gating scheme. Calcium-sensitive gating steps are modeled as a second-order association reaction between a calcium ion and the unbound channel state. The propensity terms are identical to the preceding case.
3. ***Ion channel currents***. If the mean channel current amplitude is known, the process of ion conduction and release from the channel pore can be simplified as a zero-order reaction, i.e. a Poisson process with a fixed rate [13]. Even though a constant release rate may only be a rough approximation of the real permeation process [31], the model yields the correct mean current and furthermore takes into account the quantal nature (release of a single ion at a time) and stochasticity inherent to ion channel currents. Conversion of the current amplitude I_{ch} to a stochastic rate constant is achieved by

$$c_j = \left(\frac{I_{ch}}{e \times z_{ion}} \right)$$

where e is the elementary charge and z_{ion} is charge of the permeating ion. A calcium current of $1pA$, for instance, has an "event rate" of $c_j \approx 3000 / ms$. The factor $h_j(x,t)$ is equal to the number of *open* channels at time t, which is easily implemented as each channel state is regarded as a separate chemical species.
4. ***Diffusion***. Assuming a multivoxel simulation, diffusion at the mesoscopic level can also be implemented using the concept of stochastic event rates [32]. In analogy to the previously introduced techniques, the diffusion event rate of species S_i is calculated from the macroscopic diffusion constant D_i in order to yield the correct behavior in the deterministic limit. At the microscopic level, the diffusion event constant controls the speed of the molecular random walk. Assuming a voxel side length δx, the rate is given by

$$a_j = \frac{D_i}{(\delta x)^2} \times x_i(t)$$

where x_i is the copy number of species S_i at time t. In practice, diffusion rates of small molecules often lie several orders of magnitude above the common reaction rates. This can lead to a significant increase in computation time. However, even in single voxel simulations the implementation of diffusion may be necessary to avoid accumulation of e.g. calcium ions released from calcium channels [13]. In the single voxel case, this reduces to a fixed efflux rate of the ion.

Working Examples

Example 1: We consider a simple system that contains Ca^{2+} ions and two buffers, called B_1 and B_2. The model geometry is given by a cube with a side length of 1 μm, i.e. the system volume is 1 fl. The copy numbers of the five molecular species, in the order $Ca^{2+}, B_1, B_2, CaB_1, CaB_2$ are stored in the state vector $x(t) = [x_1(t), ..., x_5(t)]$. We assume an equilibrium concentration of $[Ca^{2+}]_{eq} = 0.1\mu M$ (free Ca^{2+}), and total buffer concentrations of $[B_1]_T = [B_2]_T = 100\mu M$. The rate constants are set to $k_1^+ = 0.1\mu M^{-1} ms^{-1}$, $k_1^- = 0.1 ms^{-1}$ for the reaction of Ca^{2+} and the first buffer B_1, and to $k_2^+ = 0.01\mu M^{-1} ms^{-1}$, $k_2^- = 0.01 ms^{-1}$ for the reaction of Ca^{2+} with the second buffer B_2.

Thus, the four reactions read as follows.

Buffer 1:

$$Ca^{2+} + B_1 \rightarrow CaB_1$$
$$CaB_1 \rightarrow Ca^{2+} + B_1$$

Buffer 2:

$$Ca^{2+} + B_2 \rightarrow CaB_2$$
$$CaB_2 \rightarrow Ca^{2+} + B_2$$

The corresponding state change matrix $V = (v_{ji})$ with state change vector v_j in the $j-th$ row can be read off the stoichiometric coefficients directly:

$$V = \begin{pmatrix} -1 & -1 & 0 & 1 & 0 \\ 1 & 1 & 0 & -1 & 0 \\ -1 & 0 & -1 & 0 & 1 \\ 1 & 0 & 1 & 0 & -1 \end{pmatrix}$$

If we want to start the system in equilibrium, we obtain the initial state vector (after rounding) $x(0) = [60, 54755, 54755, 5476, 5476]$. The stochastic rate constants c_j are calculated as explained in the preceding paragraph and yield $c_1^+ = 1.66 \times 10^{-4} ms^{-1}$, $c_1^- = 0.1 ms^{-1}$, $c_2^+ = 1.66 \times 10^{-5} ms^{-1}$ and $c_2^- = 0.01 ms^{-1}$. For convenience, we adapted the notation using superscripts in order to better recognize the relation with macroscopic rate constants, i.e. c_1^+ is the stochastic rate constant associated with the macroscopic rate k_1^+.

The time and state dependent propensities a_j are given by: $a_1(x,t) = c_1^+ x_1(t) x_2(t)$, $a_2(x,t) = c_1^- x_4(t)$, $a_3(x,t) = c_2^+ x_1(t) x_3(t)$ and $a_4(x,t) = c_2^- x_5(t)$. Finally, using the cumulative propensity $a_0(x,t) = a_1(x,t) + ... + a_4(x,t)$ and the initial state vector $x(0)$, all parameters to run the Gillespie algorithm as defined above are given.

Using the state change matrix and the propensities defined above, we obtain the corresponding chemical Langevin Eq. 25.6:

$$
\begin{aligned}
dx_1(t) &= -c_1^+ x_1(t)x_2(t)dt - \sqrt{c_1^+ x_1(t)x_2(t)}\xi_1(t) \\
&\quad + c_1^- x_4(t)dt + \sqrt{c_1^- x_4(t)}\xi_2(t) \\
&\quad - c_2^+ x_1(t)x_3(t)dt - \sqrt{c_2^+ x_1(t)x_3(t)}\xi_3(t) \\
&\quad + c_2^- x_5(t)dt + \sqrt{c_2^- x_5(t)}\xi_4(t) \\
dx_2(t) &= -c_1^+ x_1(t)x_2(t)dt - \sqrt{c_1^+ x_1(t)x_2(t)}\xi_1(t) \\
&\quad + c_1^- x_4(t)dt + \sqrt{c_1^- x_4(t)}\xi_2(t) \\
dx_3(t) &= -c_2^+ x_1(t)x_3(t)dt - \sqrt{c_2^+ x_1(t)x_3(t)}\xi_3(t) \\
&\quad + c_2^- x_5(t)dt + \sqrt{c_2^- x_5(t)}\xi_4(t) \\
dx_4(t) &= c_1^+ x_1(t)x_2(t)dt - \sqrt{c_1^+ x_1(t)x_2(t)}\xi_1(t) \\
&\quad - c_1^- x_4(t)dt - \sqrt{c_1^- x_4(t)}\xi_2(t) \\
dx_5(t) &= c_2^+ x_1(t)x_3(t)dt - \sqrt{c_2^+ x_1(t)x_3(t)}\xi_3(t) \\
&\quad - c_2^- x_5(t)dt - \sqrt{c_2^- x_5(t)}\xi_4(t)
\end{aligned}
$$

Here, the random variables $\xi_j(t)$ represent the increments of four independent Brownian motions, i.e. each $\xi_j(t)$ is an independent and identically distributed Gaussian random variable with mean zero and variance dt. A first-order, explicit Euler integration scheme is often satisfactory and allows a straightforward implementation of the above formulas in virtually any programming language. Sample code (Matlab®, Octave) can be obtained from the authors.

Example 2: We consider a 1 fl single voxel system of diffusible Ca^{2+} ions and a single, immobile buffer B_1. The simulation volume is surrounded by a "constant pool", i.e. an infinite volume with constant (equilibrium) calcium concentration. The state vector $x(t) = [x_1(t), x_2(t), x_3(t)]$ represents the copy numbers of Ca^{2+}, B_1, CaB_1. We again set $[Ca^{2+}]_{eq} = 0.1\mu M$, $[B_1]_T = 100\mu M$ and $k_1^+ = 0.1\mu M^{-1} ms^{-1}$, $k_1^- = 0.1 ms^{-1}$ and set the diffusion coefficient of free calcium ions to $D_{Ca} = 200\mu m^2 / s$. Including the diffusion reactions of Ca^{2+} ions out of the simulation volume and influx of Ca^{2+} ions from the constant pool into the simulation volume, we get the following set of reactions.

Buffer 1:

$$
\begin{aligned}
Ca^{2+} + B_1 &\rightarrow CaB_1 \\
CaB_1 &\rightarrow Ca^{2+} + B_1
\end{aligned}
$$

Diffusion:

$$Ca^{2+} \rightarrow \varnothing$$
$$\varnothing \rightarrow Ca^{2+}$$

The state change matrix V now reads:

$$V = \begin{pmatrix} -1 & -1 & 1 \\ 1 & 1 & -1 \\ -1 & 0 & 0 \\ 1 & 0 & 0 \end{pmatrix}$$

Under equilibrium conditions, we obtain the initial state vector $x(0) = [60,54755,5476]$. The stochastic rate constants c_1^+ and c_1^- have the same magnitude as in the preceding example, and the stochastic diffusion rate c_D, calculated as explained in the preceding paragraph, evaluates to $c_D = 0.2ms^{-1}$. The diffusion propensities a_j are $a_3(x,t) = c_D x_1(t)$ and $a_4(x,t) = c_D x_1(0)$. Note that the rate a_4 is constant as the surrounding calcium concentration is assumed to be fixed. The according chemical Langevin equation is

$$\begin{aligned} dx_1(t) = & -c_1^+ x_1(t) x_2(t) dt - \sqrt{c_1^+ x_1(t) x_2(t)} \xi_1(t) \\ & + c_1^- x_3(t) dt + \sqrt{c_1^- x_3(t)} \xi_2(t) \\ & - c_D x_1(t) dt - \sqrt{c_D x_1(t)} \xi_3(t) \\ & + c_D x_1(0) dt + \sqrt{c_D x_1(0)} \xi_4(t) \end{aligned}$$

$$\begin{aligned} dx_2(t) = & -c_1^+ x_1(t) x_2(t) dt - \sqrt{c_1^+ x_1(t) x_2(t)} \xi_1(t) \\ & + c_1^- x_3(t) dt + \sqrt{c_1^- x_3(t)} \xi_2(t) \end{aligned}$$

$$\begin{aligned} dx_3(t) = & c_1^+ x_1(t) x_2(t) dt + \sqrt{c_1^+ x_1(t) x_2(t)} \xi_1(t) \\ & - c_1^- x_3(t) dt - \sqrt{c_1^- x_3(t)} \xi_2(t) \end{aligned}$$

Example 3: In the last example, we extend the system considered in Example 2 by a single ion channel that has a closed (C) and an open open substate (O) and conducts Ca^{2+} ions. It is convenient to model the two substates as different molecular species that can be transformed into each other. Obviously, the channel substate species are not diffusible. The state vector $x(t) = [x_1(t),...,x_5(t)]$ represents the copy numbers of $Ca^{2+}, B_1, CaB_1, C, O$. As we consider a single ion channel, both $x_4(t)$ and $x_5(t)$ must be equal to either zero or one and $x_4(t) + x_5(t) = 1$ must be fulfilled at all times *t*.

Introducing an extra reaction that models Ca^{2+} ion release from the O state (reaction 5), we extend the set of reactions introduced in the Example 2 by three ion channel related reactions.

Channel gating:

$$C \rightarrow O$$
$$O \rightarrow C$$

Calcium permeation:

$$O \rightarrow O + Ca^{2+}$$

The state change matrix V now reads:

$$V = \begin{pmatrix} -1 & -1 & 1 & 0 & 0 \\ 1 & 1 & -1 & 0 & 0 \\ -1 & 0 & 0 & 0 & 0 \\ 1 & 0 & 0 & 0 & 0 \\ 0 & 0 & 0 & -1 & 1 \\ 0 & 0 & 0 & 1 & -1 \\ 1 & 0 & 0 & 0 & 0 \end{pmatrix}$$

Reaction propensities for the new reactions are derived from the assumed channel kinetics and the channel permeability, respectively. As channel substate transitions are first-order reactions, we write $a_5(x,t) = c^+_{Ch} x_4(t)$ and $a_6(x,t) = c^-_{Ch} x_5(t)$ where $c^+_{Ch} = k^+_{Ch}$ and $c^-_{Ch} = k^-_{Ch}$ and k^+_{Ch}, k^-_{Ch} are the macroscopic rate constants for channel opening and closing as determined from electrophysiological measurements for instance. Finally, Ca^{2+} ion release is modelled by $a_7(x,t) = c_P x_5(t)$ with $c_P = I_{ch} / (2e)$.

In this case, it is important to note that a chemical Langevin equation approach cannot be applied because the system contains only a single ion channel and due to the use of normally distributed random numbers, negative values for x_4 or x_5 are highly probable. Negative copy numbers in turn lead to negative reaction propensities and render the square root terms in the CLE undefined.

Outlook

Stochastic methods have received an increasing amount of attention in the modeling of subcellular signaling systems. Given the central role of calcium ions in the regulation of many cellular functions and the very low number of calcium ions present in the relevant volumes, e.g. a calcium concentration of 100 nM translates to some

60 calcium ions in a $1\mu m^3$ volume, surprisingly few studies model the stochastic effects of calcium diffusion and buffering in small volumes [13, 21]. Here, it is important to note that possibly important effects such as bistability of a signaling pathway can even be missed completely when only deterministic dynamics are modeled [33]. The rising interest in simulating large systems with several interacting subsystems in some of which deterministic dynamics may dominate while in others stochastic effects may be important will lead to novel approaches combining deterministic and stochastic simulations. Most importantly, the validity of different approaches on a given scale will have to be evaluated for numerous experimental systems. At the same time, stochastic models of subcellular reactions will help to estimate the parameters of experimentally recorded signals, in which stochastic effects are uncovered thanks to technical advances such as high-resolution laser microscopy.

References

1. Keller DX, Franks KM, Bartol TM, Sejnowski TJ (2008) Calmodulin activation by calcium transients in the postsynaptic density of dendritic spines. PLoS One 3:e2045
2. Zeng S, Holmes WR (2010) The effect of noise on CaMKII activation in a dendritic spine during LTP induction. J Neurophysiol 103:1798–1808
3. Berridge MJ (2009) Inositol trisphosphate and calcium signalling mechanisms. Biochim Biophys Acta 1793(6):933–940
4. Andrews SS, Bray D (2004) Stochastic simulation of chemical reactions with spatial resolution and single molecule detail. Phys Biol 1:137–151
5. Franks KM, Bartol TM, Sejnowski TJ (2002) A Monte Carlo model reveals independent signaling at central glutamatergic synapses. Biophys J 83:2333–2348
6. Shahrezaei V, Delaney KR (2004) Consequences of molecular-level Ca^{2+} channel and synaptic vesicle colocalization for the Ca^{2+} microdomain and neurotransmitter exocytosis: A Monte Carlo study. Biophys J 87:2352–2364
7. Gillespie DT (2007) Stochastic simulation of chemical kinetics. Annu Rev Phys Chem 58:35–55
8. Gardiner C (2004) Handbook of stochastic methods for physics, chemistry and the natural sciences, 3rd edn, Springer series in synergetics. Springer, New York
9. Gillespie DT (1977) Exact stochastic simulation of coupled chemical reactions. J Phys Chem 81:2340–2361
10. Gibson MA, Bruck J (2000) Efficient exact stochastic simulation of chemical systems with many species and many channels. J Phys Chem A 104:1876–1889
11. Li H, Hou Z, Xin H (2005) Internal noise stochastic resonance for intracellular calcium oscillations in a cell system. Phys Rev E 71:061916
12. Kummer U, Krajnc B, Pahle J, Green AK, Dixon CJ, Marhl M (2005) Transition from stochastic to deterministic behavior in calcium oscillations. Biophys J 89:1603–1611
13. von Wegner F, Fink RHA (2010) Stochastic simulation of calcium microdomains in the vicinity of an L-type calcium channel. Eur Biophys J 39:1079–1088
14. Gillespie DT (2000) The chemical Langevin equation. J Chem Phys 113:297–306
15. Cao Y, Gillespie DT, Petzold LR (2006) Efficient step size selection for the tau-leaping simulation method. J Chem Phys 124:044109
16. Tian T, Burrage K (2004) Binomial leap methods for simulating stochastic chemical kinetics. J Chem Phys 121:10356–10364

17. Choi T, Maurya MR, Tartakovsky DM, Subramaniam S (2010) Stochastic hybrid modeling of intracellular calcium dynamics. J Chem Phys 133:165101
18. Manninen T, Linne M-L, Ruohonen K (2006) Developing Ito stochastic differential equation models for neuronal signal transduction pathways. Comput Biol Chem 30:280–291
19. Zhang J, Hou Z, Xin H (2004) System-size biresonance for intracellular calcium signaling. Chemphyschem 5:1041–1045
20. Zhu C-L, Jia Y, Liu Q, Yang L-J, Zhan X (2006) A mesoscopic stochastic mechanism of cytosolic calcium oscillations. Biophys Chem 125:201–212
21. Winslow RL, Tanskanen A, Chen M, Greenstein JL (2006) Multiscale modeling of calcium signaling in the cardiac dyad. Ann NY Acad Sci 1080:362–375
22. Cannell MB, Soeller C (1997) Numerical analysis of ryanodine receptor activation by L-type channel activity in the cardiac muscle diad. Biophys J 73:112–122
23. Soeller C, Cannell MB (1997) Numerical simulation local calcium movements during L-type calcium channel gating in the cardiac diad. Biophys J 73:97–111
24. Smith GD, Keizer JE, Stern MD, Lederer WJ, Cheng H (1998) A simple numerical model of calcium spark formation and detection in cardiac myocytes. Biophys J 75:15–32
25. Jiang YH, Klein MG, Schneider MF (1999) Numerical simulation of Ca^{2+} "sparks" in skeletal muscle. Biophys J 77:2333–2357
26. Baylor SM, Hollingworth S (2007) Simulation of Ca^{2+} movements within the sarcomere of fast-switch mouse fibers stimulated by action potentials. J Gen Physiol 130(3):283–302
27. Stern MD, Pizarro G, Rios E (1997) Local control model of excitation-contraction coupling in skeletal muscle. J Gen Physiol 110:415–440
28. Greenstein JL, Winslow RL (2002) An integrative model of the cardiac ventricular myocyte incorporating local control of Ca^{2+} release. Biophys J 83:2918–2945
29. Rüdiger S, Shuai JW, Huisinga W, Nagaiah C, Warnecke G, Parker I, Falcke M (2007) Hybrid stochastic and deterministic simulations of calcium blips. Biophys J 93:1847–1857
30. Kalantzis G (2009) Hybrid stochastic simulations of intracellular reaction–diffusion systems. Comput Biol Chem 33:205–215
31. Krishnamurty V, Chung SH (2007) Large scale dynamical models and estimation for permeation in biological membrane ion channels. Proc IEEE 95:853–880
32. Elf J, Doncic A, Ehrenberg M (2003) Mesoscopic reaction–diffusion in intracellular signaling. SPIE Proc 5110:114–125
33. Artyomov MN, Das J, Kardar M, Chakraborty AK (2007) Purely stochastic binary decisions in cell signaling models without underlying deterministic bistabilities. Proc Natl Acad Sci USA 104(48):18958–18963

Chapter 26
Combined Computational and Experimental Approaches to Understanding the Ca^{2+} Regulatory Network in Neurons

Elena É. Saftenku and David D. Friel

Abstract Ca^{2+} is a ubiquitous signaling ion that regulates a variety of neuronal functions by binding to and altering the state of effector proteins. Spatial relationships and temporal dynamics of Ca^{2+} elevations determine many cellular responses of neurons to chemical and electrical stimulation. There is a wealth of information regarding the properties and distribution of Ca^{2+} channels, pumps, exchangers, and buffers that participate in Ca^{2+} regulation. At the same time, new imaging techniques permit characterization of evoked Ca^{2+} signals with increasing spatial and temporal resolution. However, understanding the mechanistic link between functional properties of Ca^{2+} handling proteins and the stimulus-evoked Ca^{2+} signals they orchestrate requires consideration of the way Ca^{2+} handling mechanisms operate together as a *system* in native cells. A wide array of biophysical modeling approaches is available for studying this problem and can be used in a variety of ways. Models can be useful to explain the behavior of complex systems, to evaluate the role of individual Ca^{2+} handling mechanisms, to extract valuable parameters, and to generate predictions that can be validated experimentally. In this review, we discuss recent advances in understanding the underlying mechanisms of Ca^{2+} signaling in neurons via mathematical modeling. We emphasize the value of developing realistic models based on experimentally validated descriptions of Ca^{2+} transport and buffering that can be tested and refined through new experiments to develop increasingly accurate biophysical descriptions of Ca^{2+} signaling in neurons.

E.É. Saftenku (✉)
Department of General Physiology of Nervous System, State Key Laboratory of Molecular and Cellular Biology, A. A. Bogomoletz Institute of Physiology,
4 Bogomoletz St., 01024 Kyiv, Ukraine
e-mail: esaft@biph.kiev.ua

D.D. Friel
Department of Neurosciences, Case Western Reserve University,
10900 Euclid Avenue, 44106-4975 Cleveland, OH, USA
e-mail: david.friel@case.edu

M.S. Islam (ed.), *Calcium Signaling*, Advances in Experimental Medicine and Biology 740, DOI 10.1007/978-94-007-2888-2_26,

Keywords Calcium dynamics • Mathematical modeling • Endogenous buffers • Fluorescent indicators • Calcium diffusion • Ca^{2+} microdomains • Monte Carlo simulation • Ca^{2+} handling systems • Heterogeneous distribution • Computer simulations • Experimental data

Introduction

Intracellular calcium dynamics are critical in the regulation of virtually all known cell functions. Calcium ions (Ca^{2+}) act as both charge carriers and chemical messengers that bind to and alter the conformational states of different Ca^{2+}-sensitive proteins. At each instant in time, the probability of Ca^{2+} ions to activate sufficient number of specific target proteins depends on the occupancy of their Ca^{2+}-binding sites and transition probabilities between states. Some of these transition probabilities are a function of the local calcium concentration ($[Ca^{2+}]$) in the vicinity of each Ca^{2+}-binding site. The $[Ca^{2+}]$, in turn, is determined by the properties and spatial distribution of all Ca^{2+} regulatory systems that control Ca^{2+} entry, removal, buffering, and diffusion. Since multiple systems of Ca^{2+} handling are interdependent and their activities depend nonlinearly on $[Ca^{2+}]$, understanding the generation and evolution of Ca^{2+} signals requires consideration of the way these systems operate together at different spatial and temporal scales.

Mathematical modeling as a quantitative way to predict and explain the behavior of a complex system provides a powerful tool for addressing this problem. All mathematical models are idealizations that are based on a priori assumptions about the mechanisms under study and make simplifications about some issues in order to be able to explore other ones. The nature of the simplifications depends on the research objective and limitations in available information. When only few data are available or some particular behaviors, such as oscillations, are investigated, simple models of Ca^{2+} dynamics that ignore spatial heterogeneity of Ca^{2+} transport can, nevertheless, help build intuition regarding conditions that need to be imposed to observe certain qualitative patterns. More complex models can be used to design and interpret experiments, e.g., to determine if a particular collection of Ca^{2+} handling systems arranged with a particular geometry can reproduce a given set of observations. A concise description of the experimental data by itself does not guarantee the veracity of the model and may be consistent with multiple models. Thus, a model always is "a collection of hypotheses and facts" [1]. Models generate predictions that can be validated with new measurements under different experimental conditions (i.e., different from those that the model was designed to account for) when this is possible. When considering multiple competing models, a practical approach is to select the simplest available model that is consistent with available information. The ability of the model to predict the results of new experiments gives us confidence in its usefulness. In this case, usually the simplest model that is consistent with available data is chosen. If model predictions do not match experiment, it demonstrates incompleteness of our understanding and suggests new experiments.

Through cycles of experiment and model refinement, a progressively more accurate description of Ca^{2+} signal generation with increasing predictive power can be achieved. Clearly, one major challenge is to explain how measured Ca^{2+} signals are defined by the Ca^{2+} handling systems operating in the cell under study. Linking measured Ca^{2+} responses to the underlying Ca^{2+} transport and buffering systems requires information about the properties of these systems, including the way they contribute to $[Ca^{2+}]$ and their spatial distribution within the cell. Until recently, approaches to characterizing these systems in intact cells have been limited, but recent developments in imaging and biology have provided new methods and information. Models also can be helpful to estimate some valuable parameters, which are not accessible experimentally, and to extrapolate measured Ca^{2+} kinetics to the case where exogenous buffers are absent. The interpretation of fluorescence transients is especially important, because along with the development of Ca^{2+}-imaging techniques that permit measurements of $[Ca^{2+}]$ measurements with a high (nanoscale) resolution *in vitro* [2, 3] and with greatly improved temporal resolution *in vivo* [4] and optimization of synthetic and genetically encoded calcium indicators [5–9], the introduction of these indicators may significantly disrupt Ca^{2+} signaling and break down the compartmentalization of microdomains [10].

The review focuses on recent advances in the development of biophysical models to describe Ca^{2+} dynamics in neurons and does not include phenomenological models, which are usually used in the models of neuronal activity to simulate the activation of large conductance Ca^{2+}-activated K^+ channels. The reviewed models differ in their spatial (and temporal) resolution, from Ca^{2+} nanodomains around single open Ca^{2+} channels to models of Ca^{2+} dynamics in neurons with complex morphology. In the following paper, we aim first to discuss general features of Ca^{2+} dynamics in neurons and non-neuronal cells and describe different types of models, including deterministic and stochastic models of Ca^{2+} microdomains, spatial and compartmental models with uniform Ca^{2+} entry, models with uniform and heterogeneous distribution of Ca^{2+} handling systems, showing how the choice of the model structure depends on the characteristics of the system and available experimental methods. Then, we will show the distinction between phenomenological and experimentally determined descriptions of transport and buffering mechanisms that coexist in real cells and outline the importance of constraining models with experimental measurements and the use of models for designing new experiments. The most successful models that were obtained through a combination of experimental and theoretical approaches (e.g., [11, 12]) will be described in a more detail.

General Features of Cellular Ca^{2+} Signaling in Neurons and Non-neuronal Cells – Requirements for Model Development

Molecular systems responsible for cellular Ca^{2+} handling are limited to several protein families (Ca^{2+} channels, exchangers, transporters, and buffers), which are expressed within virtually all cells [13]. Eucaryotic cells contain multiple

membrane-surrounded intracellular compartments, including the cytoplasm, mitochondria, endoplasmic reticulum (ER) or the equivalent organelle sarcoplasmic reticulum (SR) of muscle cells, acidic secretory vesicles, such as endosomes and lysosomes, nucleus, and Golgi apparatus, each with distinctive Ca^{2+}-transport pathways. There is still incomplete agreement regarding contribution of some of these compartments to cytosolic Ca^{2+} signaling and cell type specificity of this contribution, although the nucleus is thought to have an autonomous Ca^{2+} signaling system that can generate its own Ca^{2+} transients [14]. Within each intracellular compartment, the total calcium concentration changes at a rate that depends on the net Ca^{2+} flux entering this compartment and the compartmental volume. The dynamics of the free Ca^{2+} concentration depends additionally on buffering. Thus, at a minimum, to understand the spatiotemporal properties of the Ca^{2+} concentration within a given membrane-delimited compartment, it is necessary to have information about the Ca^{2+} transporters that regulate Ca^{2+} movement into and out of that compartment, as well as the Ca^{2+} buffering systems that determine the relationship between free and bound Ca^{2+} levels. Understanding Ca^{2+} dynamics at the whole-cell level requires such information for *all* relevant compartments. This especially complicated because Ca^{2+} dynamics in all compartments are functionally coupled. The net Ca^{2+} flux that drives changes in Ca^{2+} concentration within the cytosol depends on Ca^{2+} transport across the plasma membrane (PM) and between the cytosol and organelles, such as mitochondria and the ER, which in turn depend on intraluminal Ca^{2+} concentration within these organelles. In neurons, the net flux across the PM may include Ca^{2+} influx through voltage-sensitive, synaptic, and leak channels and Ca^{2+} efflux via PM Ca^{2+}-ATPases and Na^{+}–Ca^{2+} exchangers. The dynamics of Ca^{2+} within the organelles depend on their own specific collections of transporters and buffers (Fig. 26.1).

Although Ca^{2+} signaling in various cell types shows many common features, there are differences in channel and receptor composition (different isoforms) as well as in the relative contribution of the various Ca^{2+} handling systems not only between different cell types, but even between species. In addition, studies over the last few decades have revealed the enormous diversity of proteins contributing to Ca^{2+} signals [15–17]. Neurons along with muscle cells and some secretory cells, such as the cells in anterior pituitary gland and pancreatic β-cells, are electrically excitable, and their Ca^{2+} dynamics are largely controlled by generated membrane potential and Ca^{2+} entry through voltage-dependent Ca^{2+} channels. In contrast, store-operated Ca^{2+} entry is thought to be a major Ca^{2+} entry mechanism in non-excitable cells [18]. Mechanisms fundamental to the control of Ca^{2+} release from the ER (SR), which are executed mainly by two families of Ca^{2+} channels, the ryanodine receptors (RyRs) and inositol-1,4,5-trisphosphate (IP3) receptors, are distinctly different in different cell types. RyR isoform in skeletal muscles can be activated solely by membrane depolarization due to a direct link with the plasmalemmal L-type Ca^{2+} voltage-dependent channels. Cardiac cells use a related L-type channel to activate ryanodine receptors through Ca^{2+}-induced Ca^{2+} release (CICR). Neurons express multiple types of Ca^{2+} channels and both pathways of Ca^{2+} release via RyR and IP3 receptor channels. The main function of neurons is to process and transmit information. This transmission occurs via chemical and, in few locations, via electrical

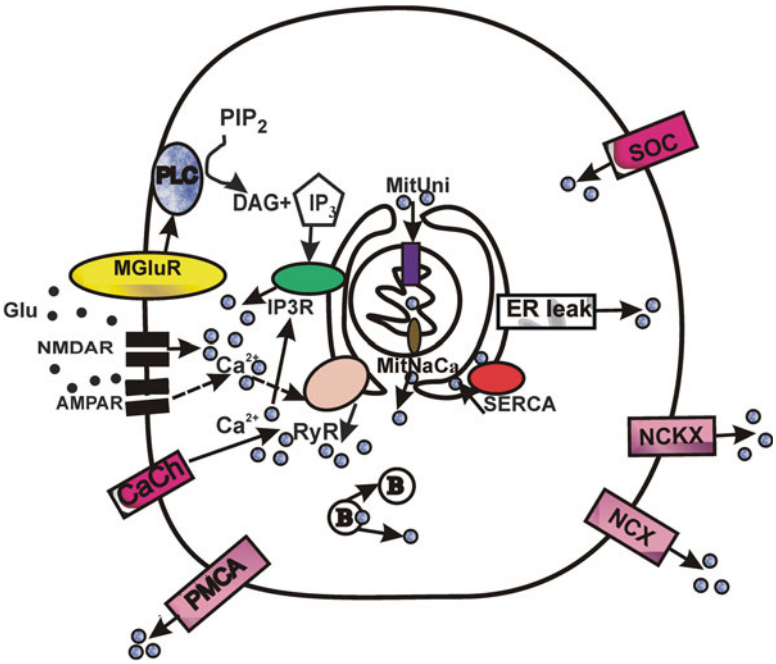

Fig. 26.1 Calcium handling in a neuron. *CaCh* voltage-gated Ca^{2+} channels, *NMDAR* NMDA receptors, *AMPAR* AMPA receptors,*Glu* glutamate, *MGluR* metabotropic glutamate receptors, *PMCA* plasma membrane (PM) Ca^{2+} ATPase, *NCX* PM sodium–calcium exchangers, *NCKX* PM potassium-dependent sodium–calcium exchangers, *PLC* phospholipase C, PIP_2 phosphatidylinositol-4,5-bisphosphate, IP_3 inositol-1,4,5-trisphosphate, *DAG* diacylglycerol, IP_3R IP_3 receptors, *RyR* ryanodine receptors, *SERCA* sarco/endoplasmic reticulum Ca^{2+}-transporting ATPases, *ER leak* leak pathways from the endoplasmic reticulum, *MitUni* mitochondrial electrogenic Ca^{2+} uniporters, *MitNaCa* mitochondrial Na^+–Ca^{2+} exchangers, *SOC* store-operated channels, *B* endogenous buffers. Although most non-NMDA-type glutamate receptors exhibit minimal Ca^{2+} permeability, Ca^{2+} influx via AMPARs has been directly demonstrated in some types of neurons

synapses. A typical neuron has complex morphology and possesses a soma, branched dendrites, and a long axon. Moreover, spatial compartmentalization may result in local [Ca^{2+}] gradients within extremely confined spaces (e.g., dendritic spines). Ca^{2+} entry in neurons is generated also by Ca^{2+} activation of synaptic (mainly, NMDA) receptors. Local calcium signaling is especially prominent at presynaptic active zones where calcium triggers neurotransmitter release and at postsynaptic densities where calcium signaling proteins are localized. Therefore, detailed neuronal models often have multiple electrical and several intracellular compartments. Other cell types, with the exception of skeletal muscle, are connected through gap junctions that allow direct electrical and chemical communication. For these cells, multicellular models coupled through the gap junction diffusion of Ca^{2+} and IP_3 can be created to study the propagation of intercellular Ca^{2+} waves [19–21].

Development of neuronal Ca^{2+} dynamics models was strongly influenced by comprehensive biophysical models of muscle, pancreatic β-cells, and non-excitable cells. For example, models in cardiac myocytes have included a time-dependent description of Ca^{2+} fluxes across the sarcoplasmic reticulum with descriptions of electrical activity [22, 23]. Integrated models of calcium dynamics and mitochondrial energy metabolism have been developed for both cardiac myocytes [24] and pancreatic β-cells [25–28]. Three-dimensional finite-element methods have been employed to model intracellular calcium responses in non-excitable cells using physiologically realistic ER geometry [29]. The latter models have no parallels in neurons. However, since intracellular Ca^{2+} fluxes were not measured in these studies, only semiqualitative comparisons between measured and simulated [Ca^{2+}] responses were possible, making it difficult to rigorously evaluate the corresponding models. Numerous models of Ca^{2+} oscillations have also been developed mainly for non-excitable cells (e.g., [30–38]), cardiac myocytes (e.g., [39–45]) and pituitary gonadotrophs [46, 47]. Moreover, experimental and theoretical analyses of Ca^{2+} oscillations in these cells have shown that global oscillations arise from locally initiated Ca^{2+} waves, and that such a local mechanism leads to stochastic oscillations [48–51]. The dynamic compartmentalization of the cell by concentration gradients (microdomains) may prevent the establishment of deterministic dynamics by the law of large numbers [52]. The multiplicity of length and time scales in such processes poses specific demands on the development of modeling tools that can deal efficiently with the large concentration gradients and with the time scale range from molecular transitions to cell behavior. One of the recently developed approaches in this direction is to simulate active molecules individually as stochastic Markov chains while describing diffusion and bulk reactions deterministically [52, 53]. This modeling paradigm [54] may be useful also in neurons where spontaneous elementary Ca^{2+} release events at dendritic branch points and locally initiated Ca^{2+} waves were reported [55]. For now, such modeling platforms as NEURON [56], GENESIS [57], Virtual Cell [58, 59], and MCell [60] are available for simulating of deterministic and/or stochastic Ca^{2+} dynamics in neurons.

Neuronal Ca^{2+} Models: From Microdomains to the Whole Neurons

Computational modeling of Ca^{2+} signaling in neurons dates from the works of Hodgkin and colleagues [61, 62] where Ca^{2+} diffusion and binding with immobile targets were modeled in the squid axon. Some later Ca^{2+} diffusion, buffering and extrusion processes were simulated in the spherical neurons [63–65] and in the presynaptic terminal ([66, 67]; see [65] for more comprehensive list of early models of Ca^{2+} diffusion).

Microdomain Models

Deterministic Models

Ca^{2+} microdomains, or local elevations of $[Ca^{2+}]_i$ generated around the mouth of open ion channels, represent the basic building blocks of cytosolic Ca^{2+} signals. Many computational models, the so-called "microdomain models", have been developed to describe Ca^{2+} signals produced by Ca^{2+} entry restricted to discrete points. A very high Ca^{2+} concentration of more than 100 μM in the immediate neighborhood of open Ca^{2+} channels was first postulated on the basis of numerical simulations of Ca^{2+} diffusion at the presynaptic terminal [68, 69]. The existence of nanoscale coupling between Ca^{2+} and Ca^{2+}-activated K^+ channels was soon experimentally demonstrated by Roberts [70] in saccular hair cells. Despite progress in improving the resolution of optical microscopes [3], many features of neurons such as thin dendritic spines and the organization of presynaptic terminals as well as the very localized Ca^{2+} transients within nanodomains caused by the influx of Ca^{2+} through a single Ca^{2+} channel and within microdomains arising from the spatial summation of Ca^{2+} entering from multiple channels [71] are still inaccessible to direct experimental measurements. Therefore, investigation of local $[Ca^{2+}]_i$ dynamics in these cases still relies on quantitative models. Extensive theoretical work has been done to obtain analytical steady-state solutions and approximations to Ca^{2+} buffering and diffusion [72–79]. The simplest numerical models were developed for simulation of buffered Ca^{2+} diffusion in a hemisphere around a source of Ca^{2+} entry [80–85]. Similar model geometry was utilized for simulating local $[Ca^{2+}]_i$ dynamics in a spine head following Ca^{2+} entry through a cluster of NMDA receptor channels [86]. A number of comprehensive deterministic models examined buffered Ca^{2+} diffusion near an array of voltage-dependent Ca^{2+} channels or separate active zones in hair cells [80, 87, 88], chromaffin cells [89], neuromuscular junctions [90–97], and the calyx of Held [98]. Integrating the three-dimensional reaction–diffusion problem in Ca^{2+} microdomains was facilitated by development of the CalC ("Calcium Calculator") software [93]. These models did not include intracellular stores. Indeed, experimental studies show that synaptic microdomains do not depend on mitochondrial transport or Ca^{2+}-induced Ca^{2+} release (CICR; [99, 100]).

Microdomains were modeled to help investigate the effects of free cytosolic $[Ca^{2+}]$ ($[Ca^{2+}]_i$) on vesicle release or activation of large-conductance Ca^{2+}-activated K^+ channels. For example, the model of Roberts [80] successfully predicted millimolar concentrations of a mobile endogenous buffer in frog saccular hair cells [101], although the kinetic properties of calbindin significantly differed from the values determined later by flash-photolysis of caged Ca^{2+} [102]. The differential ability of the fast chelator BAPTA and slow chelator EGTA to buffer Ca^{2+} in the vicinity of channel pore, which was first simulated by Stern et al. [73], has been widely used for estimating the distance between the Ca^{2+} channels and their targets (e.g., [74, 83, 84, 98, 103]). A Ca^{2+} balance across the entire cell after Ca^{2+} entry

through an array of individual Ca^{2+} channels and its influence on vesicle release was examined in a model introduced by Klingauf and Neher [89]. To reproduce some properties of Ca^{2+} transients at a release site, only a small fraction of the release-ready pool was suggested to be colocalized with Ca^{2+} channels. The model correctly predicted the observation that single action potentials (APs) evoke near-synchronous transmitter release with low quantal yield, whereas AP trains lead to desynchronized release, but with severalfold increased quantal yield. Proposed on purely theoretical grounds, a mechanism for facilitation of AP-evoked Ca^{2+} transients caused by the gradual saturation of endogenous buffers [89] was later shown to underlie facilitation in neocortical terminals [104]. Matveev et al. [105] used three-dimensional modeling of buffered Ca^{2+} diffusion to analyze the sensitivity of exocytosis to Ca^{2+} influx probed by different experimental protocols and demonstrated the distinction between the Ca^{2+} current cooperativity, defined by the relationship between exocytosis rate and the whole-terminal Ca^{2+} current magnitude, and the underlying Ca^{2+} channel cooperativity, defined as the average number of channels involved in the release of a single vesicle.

Some microdomain models were used for testing hypothesis. Cooper et al. [90] tested the hypothesis that two active zones of a single synapse in close proximity can enhance the local increase in $[Ca^{2+}]_i$. However, uncertainties in the values of endogenous buffering implied uncertainties in the estimation of the mean diffusional distance between the fusion machinery and Ca^{2+} channels and attempts to derive the topography of release sites in these studies was unsuccessful. In the model of Meinrenken et al. [98], Ca^{2+} influx, three-dimensional buffered Ca^{2+} diffusion, and the binding of Ca^{2+} to the release sensor for the calyx of Held were simulated. Parameters in the simulations were constrained by electrophysiological and morphological measurements of the calyx. The concentration and the binding kinetics of the endogenous buffers and ATP were varied in the model to estimate the sensitivity of the predicted release probability to these parameters. The only crucial unknown parameters were the conductance of single Ca^{2+} channels and the channel-vesicle topography at release sites. Initially, topography was assumed and subsequently the single Ca^{2+} channel conductance was set to obtain the experimentally observed release probability. Release was then simulated under nonphysiological conditions, including added exogenous Ca^{2+} buffers, lowered $[Ca^{2+}]$ in the extracellular solution, and reduced open probability of Ca^{2+} channels. The results of the model were compared with the experimental data and used to infer which topography was likely to be present at the calyx. Several other modeling studies focused on biophysically realistic implementation of mechanisms of synaptic facilitation. Using computer models of a crayfish motor bouton, the phenomenons of facilitation of Ca^{2+} transients resulting from the two-site mechanism [92, 93], the saturation of an endogenous Ca^{2+} buffer [87], and from slow Ca^{2+} unbinding [94] were examined. All these models can successfully reproduce the magnitude and the time course of facilitation recorded in the crayfish inhibitor neuromuscular junction as well as the reduction of facilitation by fast Ca^{2+} buffers. However, the third hypothesis is most consistent with the experimental data and better reproduces the biphasic decay of facilitation.

Stochastic Models

Given the relatively small number of Ca^{2+} ions and buffer molecules involved, the stochastic nature of signaling becomes important, and Monte Carlo methods that rely on the simulation of random numbers and probabilities, are usually used. Simulating the Brownian motion of all individual molecules provides an accurate model of Ca^{2+} dynamics, but for more than 10,000 molecules, this method becomes very time consuming. For a large number of molecules, it is sufficient to integrate the reaction–diffusion equations directly, to use Monte Carlo methods that follow the fate of mass elements instead of individual molecules [106], or to perform hybrid stochastic and deterministic simulations [53, 107]. The stochastic motion of Ca^{2+} ions, their binding to fixed buffers and their release can also be described by the stochastic differential equations (Langevin equations; [108]).

A stochastic approach was applied to modeling buffered diffusion of calcium ions near channel pores [109], quantal vesicle secretion near microdomains [92, 96, 110–119], and calcium dynamics within single spines [120, 121]. In these studies, Monte Carlo methods were used to simulate the random-walk Brownian motion of individual molecules or groups of molecules, stochastic chemical interactions, and the stochastic flickering of channels. Stochastic simulations have shown that deterministic calculations describe sufficiently accurately average calcium concentrations in the submembrane domain, at least for regions of 50–100 nm thickness, but stochastic channel openings and the possibility to study different configurations of channels gives a more realistic description of calcium dynamics near Ca^{2+} channels [98, 105]. Moreover, the fluctuations arising from the diffusion process only play a significant role when the concentration of Ca^{2+} at the calcium sensor is small, whereas stochastic openings of the Ca^{2+} channels within the cluster have a large effect on the vesicle release probability when the cluster is located close to the sensor [117].

Gil and Gonzalez-Velez [119] simulated a set of experimental depolarizing-pulse protocols adopting a stochastic computational approach for determining the kinetic cooperativity of secretion at the calyx of Held where calcium thresholds are low in comparison to other presynaptic terminals and a low cooperativity for $[Ca^{2+}]_i$ was observed. The authors found that a reduction of the apparent value of the kinetic cooperativity can be obtained for a non-uniform spatial distribution of channels and for low calcium influx. Keller et al. [121] used Monte Carlo simulations to develop an advanced model of Ca^{2+} dynamics in such a spine (Fig. 26.2) that included voltage-gated Ca^{2+} channels, NMDA receptors, Ca^{2+} pumps, buffering by endogenous and exogenous buffers and extrusion by PM Ca^{2+}-ATPases and Na^{+}-Ca^{2+}- exchangers. In such a spine with the volume 0.125 fL, a resting calcium concentration of 50 nM entails an average of only 4 free calcium ions. The model simulated the time series of open-closed transitions of voltage-dependent calcium channels and NMDA receptors, the random-walk Brownian motion of discrete diffusing molecules and concomitant chemical reactions in a complex three-dimensional environment reflecting realistic cell geometry. The simulations reproduced fluorescence recordings in spines following both an AP and an excitatory postsynaptic potential. After matching

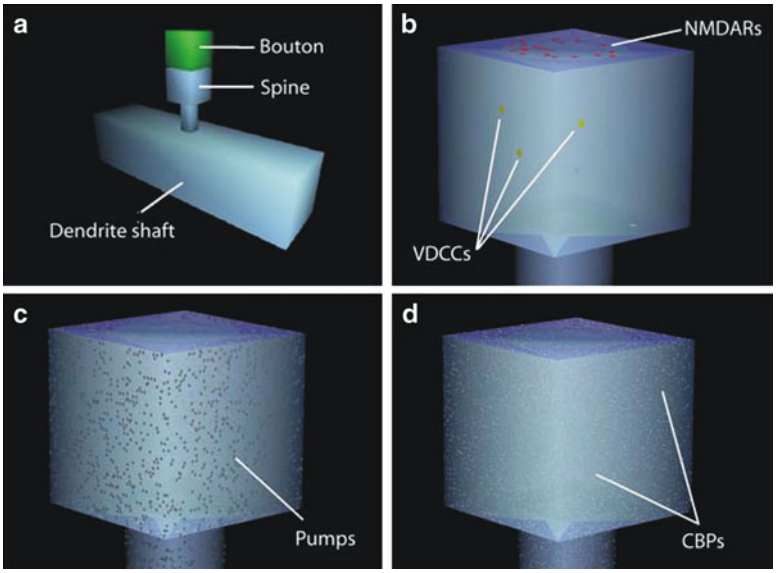

Fig. 26.2 Schematic representation of the model of Keller et al. [121]. To model a system with MCell, it is necessary to specify: (1) the geometry of the sub-cellular structures of the system, (2) the diffusion constants and initial locations of diffusing molecules, (3) the locations of transmembraneous molecules, (4) the reaction mechanisms and kinetic rate constants governing the interaction of diffusing molecules with each other and effector molecules (**a**) A segment of dendrite with a single spine (*grey*). A presynaptic bouton (*green*) was separated from the synaptic face of the spine by a 20 nm cleft. (**b**) Voltage-dependent calcium channels (*yellow*) were randomly distributed at low densities across the spine and dendrite membranes, whereas NMDA receptors (*red*) and AMPA receptors (not shown) were restricted to a patch centered on the synaptic face of the spine. (**c**) Calcium pumps were distributed evenly on the cell membrane. (**d**) Ca^{2+} binding proteins were uniformly distributed in the interior (Reprinted from Keller et al. [121] in accordance with open-access publication policy of PLoS ONE journal)

measurements at larger spatial scales, the model was used to investigate calcium dynamics at higher spatial and temporal resolution. The simulation results showed that approximations based on the assumption that calcium is well mixed within the spines are invalid. Strong calcium gradients can persist long enough to activate calmodulin in microdomains under conditions that lead to long-term depression or potentiation. This suggests a possible mechanism underlying the induction of long-term changes in synaptic strength.

Monte Carlo methods are also useful for simulating with great accuracy three-dimensional diffusion of large numbers of molecules with realistic cell geometries. Bortolozzi et al. [122] recently developed a novel method that combines electrophysiological recordings, fluorescence imaging, and numerical simulations to deconvolve Ca^{2+} signals within cytoplasmic microdomains that are not directly observable using available techniques. The method relies on the comparison of experimental data with calculations obtained using Monte Carlo simulation of diffusion and chemical reactions and a realistic reconstruction of the relevant cell boundaries in three dimensions.

Ca^{2+} Dynamics in Compartmental and Spatial Models with Uniform Ca^{2+} Entry and Uniform Distribution of Ca^{2+}-Handling Systems

In this section we shall consider models with uniform Ca^{2+} entry everywhere on the cell surface, which is not restricted to discrete points, and with uniformly distributed Ca^{2+}-handling systems. Models with heterogeneous distribution of Ca^{2+}-handling systems will be presented in a separate section below. If the processes under investigation are slow compared to the time required for diffusion and spatial equilibration of Ca^{2+} and mobile buffers within cellular compartments, it may be feasible to use the spatial average of $[Ca^{2+}]$ within compartments modeling a system by ordinary differential equations that contain functions of only one independent variable (time). A compartmental model contains one or several compartments, each containing well-mixed material. If Ca^{2+} gradients are not negligible for time and spatial scale of signal development, a system is described by partial differential equations. In spatial models, an area is divided into a large number of similar units. The three choices for the numerical solution of partial differential equations are the finite difference method, the finite element method, and the finite volume method. The latter two methods are better suited to handle complicated geometry.

Compartmental Models of Ca^{2+} Oscillations

If the goal is to investigate a particular behavior, e.g., Ca^{2+} oscillations, developing a model that displays similar behavior may be useful even if precise knowledge of parameter values is lacking. A traditional approach is to consider a simplified system and seek conditions and parameters that produce the behavior of interest. To simulate self-sustained Ca^{2+} oscillations by a system of kinetic equations, at least two variables are needed. Several models [123, 124], utilizing a single Ca^{2+} pool to represent the ER, produced $[Ca^{2+}]_i$ oscillations and rhythmic membrane hyperpolarization like those observed in bullfrog sympathetic ganglion cells in the presence of caffeine. The models included CICR via ryanodine receptors, active uptake into the ER, and Ca^{2+} entry and extrusion across the PM. The model of Kuba and Takeshita [123] employed nonlinear descriptions of Ca^{2+} transport based on studies in other cells. The model of Friel [124] was based on analysis of measured $[Ca^{2+}]_i$ relaxations following small perturbations that altered Ca^{2+} entry across the PM and Ca^{2+} release from the caffeine-sensitive pool. It was found [124] that these relaxations were quantitatively consistent with a one-pool model that described transport equations that are linear functions of the cytosolic and ER $[Ca^{2+}]$ to approximate Ca^{2+} transport near the resting state. With the addition of a nonlinear $[Ca^{2+}]_i$-sensitive Ca^{2+} permeability to represent the caffeine-sensitive CICR pathway, it was possible to account for $[Ca^{2+}]_i$ oscillations. It was found that three measured components of the net Ca^{2+} flux varied during the oscillatory cycle in a way that agreed with the corresponding fluxes in the model. These results indicated that the oscillations are consistent with the interplay between a nonlinear CICR mechanism and a collection

of Ca^{2+} transport and buffering systems operating within a range of the cytosolic and ER $[Ca^{2+}]$ around the resting state. However, since the experimental observations that provided the basis for the modeling effort were spatial averages of cytosolic $[Ca^{2+}]$, the results did not address subcellular non-uniformities in $[Ca^{2+}]_i$ during the oscillations. Subsequent studies revealed radial Ca^{2+} gradients during the oscillations, indicating spatial non-uniformity of Ca^{2+} transport in these cells [125, 126].

Several other studies in neurons have shown that slow subcellular dynamics, i.e., the exchange of calcium between an intracellular store and the cytoplasm, may be responsible for the origin and control of the chaotic bursting activity in stomatogastric neurons [127, 128]. The models incorporated membrane conductances with intracellular Ca^{2+} dynamics in the soma involving IP_3-induced Ca^{2+} release, Ca^{2+} uptake into the ER, leak from the ER and extrusion across the PM. These models had a speculative character since the properties and the role of IP_3 receptors in stomatogastric neurons are still unknown.

Models as a Tool for Interpretation of Fluorescence Measurements

Ca^{2+} indicators can significantly disrupt normal Ca^{2+} signaling since they directly bind Ca^{2+} and, thus, act as Ca^{2+} buffers. They decrease the amplitude, prolong the time course, and extend the spatial spread of intracellular $[Ca^{2+}]_i$ in comparison to the unperturbed state. If the Ca^{2+} indicator is diffusible, even the localized detection of its signal does not report the local $[Ca^{2+}]$. Therefore, as long as synthetic Ca^{2+} indicators are used, Ca^{2+} measurements have to rely on computer simulations to predict Ca^{2+} diffusion in the absence of exogenous buffers. Genetically encoded indicators have the great advantage that they can be targeted to sites of interest with the means of molecular biology [129]. An ideal strategy to measure local $[Ca^{2+}]_i$ signals would be to target genetically encoded, non-diffusible Ca^{2+} indicators, but the use of such indicators may create even more complicated problem since they can potentially interact not only with Ca^{2+}, but also with other endogenous proteins [130].

A number of models have been developed for interpretation of raw fluorescence measurements. Some of these models represented a cell body subdivided into well-mixed concentric shells (so-called, shell models) and a uniform calcium influx over the cell surface. These models were used to study distortions introduced by synthetic Ca^{2+} indicators on Ca^{2+} signals, the role of immobile and mobile buffers, and the formation and dissipation of radial Ca^{2+} gradients in the soma [131–133] and presynaptic terminal [134] as well as of axial Ca^{2+} transients in dendrites [135]. To create a model with a realistic three-dimensional geometry for prediction of calcium signals in the absence of indicator dye not only in the cytosol, but also in the nucleus, a uniform three-dimensional array of cubical voxels in the Virtual Cell modeling environment was used [136]. However, this model did not include intracellular Ca^{2+} stores. In contrast, Ca^{2+} changes in sympathetic neurons were simulated using compartmental and spatial shell models that included both the cytosol and intracellular pools. Some of these models were homogeneous, i.e. the cytosol, ER and mitochondria were assumed to coexist at every spatial point (e.g., [12]; see for

details below). In the other type of models (e.g., [137]), the cytosol and ER were treated as separate spatial domains.

Because of the resolution limits of confocal microscopy, models with uniform Ca^{2+} changes in a small cell compartment, e.g., presynaptic bouton, spine, or dendritic segment, have been used to translate experimental fluorescence measurements into underlying calcium dynamics [138] or to explore non-equilibrium dynamics of Ca^{2+} binding [85, 139]. When the volume of the region of interest is substantially larger than the resolution limits of optical recordings, such a region has been represented by several well-mixed compartments, e.g. the spine and the region of the parent dendrite [140–145]. This approach could be applied only to well-mixed systems, such as Purkinje neurons, which have a high Ca^{2+} buffering capacity and, therefore, a large number of molecules, buffers and Ca^{2+} ions within small volumes [142]. Compartmental models were also used to understand how different factors interact to determine Ca^{2+} decay kinetics in the spines and dendrites of neocortical pyramidal [143] and Purkinje cells [142] and to extrapolate measured Ca^{2+} kinetics to the case where exogenous buffers are absent.

Models as Tools for Analyzing the Role of Ca^{2+} in the Induction of Synaptic Plasticity

For predicting Ca^{2+} signals in hippocampal spines during different stimulation patterns that lead to long-term synaptic changes, the simulation of Ca^{2+} diffusion in the spine head and neck [146, 147] or in the spine head, neck, and dendritic shaft [148, 149] was performed. In these models, Ca^{2+} entered through NMDA receptor-gated channels on the distal part of a spine head, diffused along the length of the spine to the dendritic shaft, and was also buffered and pumped out in each compartment. Ca^{2+} diffusion was modeled using a one-dimensional diffusion equation. In some of the models, intracellular Ca^{2+} stores [147, 150] were included and/or diffusion of Ca^{2+} and buffers was modeled in a three-dimensional space using finite element methods [141, 150]. Schmidt et al. [141] showed that, as long as detailed information on the localization of the Ca^{2+}-dependent downstream signaling processes is unavailable, a two-compartmental model of Ca^{2+} dynamics in the spine and the adjacent dendritic compartment and a spatially resolved finite element model yield strongly overlapping results. Cornelisse et al. [151] measured both rise and decay kinetics of calcium in neocortical spines and dendrites by focusing a two-photon laser specifically on spines and their adjacent dendrites. The spine was modeled as a separate sphere and the dendrite was modeled as a separate cylinder. Radial diffusion, buffering and extrusion were included in each cell compartment. The model showed that diffusion cannot explain faster Ca^{2+} dynamics in spines and confirmed the experimental findings that a higher surface-to-volume ratio and a lower buffer capacity in spines both contribute to faster rise time kinetics.

Another spectacular modeling achievement is the simulation of signaling pathways in neurons. Because many signal transduction pathways interact with each other and often exhibit nonlinear dynamics, it is difficult to understand complex

cellular information processing on the basis of experiments alone. Computational kinetic simulation may make it possible to determine whether known signaling pathways are sufficient to reproduce cellular events of interest. A kinetic model of Ca^{2+} dynamics within a Purkinje dendritic spine [152] contained 21 species, such as sarco/endoplasmic reticulum Ca^{2+}-ATPases (SERCA), PM Ca^{2+}-ATPases, Na^{+}–Ca^{2+} exchanger, IP_3 receptor, AMPA receptors, etc. Ca^{2+} signal transduction pathways, including release from the ER through IP_3 receptors, were simulated in full detail. A mature Purkinje dendritic spine was divided into three compartments, i.e. the cytosol, postsynaptic density, and ER. Because of the small volume of the spine, all compartments were assumed to be well-mixed and contain uniform concentration. From 96 parameters, only 13 were taken from the studies of Purkinje cells, while the others were estimated from experimental studies obtained in other cells, chemical reactions in test tubes and other molecular subtypes, or were simply assumed. The simulations reproduced the supralinear Ca^{2+} response to conjunctive parallel fiber and climbing fiber stimulation and predicted that IP_3 receptors themselves may detect the temporal order of the changes in IP_3 and Ca^{2+}. But this model did not take into consideration the diffusion out of the spine into the adjacent dendritic shaft or the unique *in vivo* sensitivity and density of IP_3 receptors in Purkinje cells. Certainly, with tens of equations and kinetic parameters, it is difficult to assess the reliability of the model. Recently, considerable progress has been made in the use of optimization algorithms to automatically explore the whole model parameter space [153]. For example, the complex electrical activity of neurons can be reproduced with very different combinations of ionic channel maximum conductances, suggesting that a large parameter space is available for homeostatic mechanisms [153]. In the future, different parameter combinations will have to be tested systematically. However, parameter optimization is best carried out after establishing by experiment the validity of the descriptions of all transporters and buffers.

Simulations of the supralinear calcium spike observed experimentally during coincident activation of the parallel and climbing fibers were carried out also in the spatial and compartmental models by Hernjak et al. [144]. All parameters describing IP_3-induced Ca^{2+} release, ER Ca^{2+} uptake, and PM Ca^{2+} extrusion were taken from neuroblastoma and chromaffin cells. However, such properties of IP_3 receptors, which are expressed in Purkinje cells, as a high density and a low sensitivity, were included in the models and the supralinear calcium response was successfully simulated. It was concluded that the features of Purkinje cells that contribute to the ability to generate localized Ca^{2+} spikes in dendritic spines range from the biochemical effects of buffer capacity and the unique properties of the IP_3 receptors to the diffusional barrier imposed by the spine neck. Volfovsky et al. [150] in cultured hippocampal neurons and Schmidt and Eilers [142] in Purkinje cells tested different spine-neck lengths and showed that a long neck isolates Ca^{2+} signaling and calmodulin activation to the spine while stubby spines produce strong coupling between spines and the dendrite.

Simulation of Calcium Dynamics in Large Neuronal Models

The construction of biophysical models of Ca^{2+} dynamics in Purkinje cells, which have very complex morphology of their dendritic trees, was attempted by De Schutter and Smolen [154]. Their model included Ca^{2+} influx through voltage-dependent Ca^{2+} channels, an immobile endogenous Ca^{2+} buffer, an indicator dye, Ca^{2+} extrusion by Ca^{2+} pumps and Na^{+}–Ca^{2+} exchangers across the PM, CICR, IP_3-induced Ca^{2+} release, Ca^{2+} uptake, and leak from the ER. Some model parameters were taken from cardiomyocytes and most of the parameters of the CICR model were simply estimated. Moreover, Ca^{2+} uptake compensated Ca^{2+} release since its affinity was lower whereas the experimental findings show quite the opposite [155]. Only radial Ca^{2+} diffusion was modeled. This model was considered as the same first step towards understanding the Ca^{2+} dynamics in Purkinje cells. Anwar et al. [156] showed in their study that detailed Ca^{2+} dynamics models that include endogenous Ca^{2+} buffers identified in Purkinje cells, calbindin and parvalbumin [140], have significantly better control over Ca^{2+}-activated K^{+} channels and lead to physiologically more realistic simulations of Ca^{2+} spikes and bursting than phenomenological models. However, even without inclusion of CICR and IP_3-induced Ca^{2+} release, computations of detailed models including various buffers and pumps appeared to be very time-consuming because of the radial diffusion in large cell compartments. Using a compensation mechanism to replace radial diffusion by an additional buffer largely eliminates the effect of removing diffusion from the model and reduces significantly the program run time [156].

Distinction Between Phenomenological and Experimentally Determined Descriptions of Transport and Buffering

Rigorously tested models require information about the quantitative properties of Ca^{2+} handling in the cell under study. Unfortunately, a general problem in most existing models of Ca^{2+} dynamics is a lack of experimental data that specify the properties and distribution of all Ca^{2+} transport systems in the same cell type. Model parameters that have not been directly measured are usually taken from other cells or chemical reactions in test tubes. Using descriptions of Ca^{2+} handling from multiple sources is potentially problematic, because due to the nonlinear nature of the Ca^{2+} regulatory systems, errors arising from combining transport description from different cell types and from extrapolating measurements in reduced preparations to intact cells may result in different qualitative features of simulated Ca^{2+} dynamics as compared with Ca^{2+} dynamics in intact cells [157]. Transport parameters may be estimated from experimental results, but this requires that the correct Ca^{2+} handling systems are included in the model, since otherwise the physical interpretation of

the fitted parameters may be ambiguous. For example, Ca^{2+} extrusion across the PM by Ca^{2+}-ATPases and Na^{+}-Ca^{2+} exchangers is often modeled as one lumped process that may include Ca^{2+} uptake into intracellular Ca^{2+} pools (e.g., [89, 138–140]). In this section, achievements in the realistic description of Ca^{2+} handling systems and in the development of realistic integrated models of Ca^{2+} dynamics will be described.

Realistic Description of Endogenous Ca^{2+} Buffers

Much information has accumulated indicating that it may be unreasonable to model endogenous Ca^{2+} buffers as a single buffer with a fast Ca^{2+}-binding kinetics (e.g., [89, 132]) or to model buffering implicitly using a fast buffering approximation [75]. First, such a simplification may miss important time-dependent events controlled by the kinetics of buffering. Second, the effects of Ca^{2+} buffers during rapid neuronal Ca^{2+} signaling are determined by nonequilibrium Ca^{2+} dynamics, and it is possible to speak only about dynamic Ca^{2+}-binding ratio in the nonequlibrium phase of Ca^{2+} transients. All endogenous Ca^{2+} buffers have more than one Ca^{2+}-binding site. Parvalbumin, one of the three most abundant Ca^{2+}-binding proteins in neurons [158], is a slow-onset buffer at physiological concentrations of Mg^{2+}; the other two proteins, calbindin-D28k and calretinin, have Ca^{2+}-binding sites with slow and fast kinetics and bind Ca^{2+} cooperatively [159]. Calmodulin and neuronal Ca^{2+} sensors, which may also function as Ca^{2+} buffers if present at sufficiently high concentrations, also bind Ca^{2+} cooperatively [17]. For now, the fast kinetics of cooperative Ca^{2+} binding has been resolved only for calretinin [160]. Recent simulations have shown that an essential property of calretinin is a delayed equilibration with Ca^{2+}, which occurs only in several tens of milliseconds after a single AP ([85]; Fig. 26.3). This happens because of the competition for Ca^{2+} ions between Ca^{2+}-binding sites with different kinetics. The buffering effect of calretinin depends on the initial $[Ca^{2+}]_i$ [160], speed of Ca^{2+} influx, stimulus conditions, localization and presence of other buffers and can be mimicked, although incompletely, by a very wide range of the concentrations of fast synthetic indicators under different conditions [85]. The model predictions can be easily verified by substituting known concentrations of recombinant calretinin in patch pipettes. Previously, the implications of nonequilibrium dynamics of Ca^{2+} binding to numerous Ca^{2+}-binding proteins for dendritic Ca^{2+} signaling following APs were explored numerically by Markram et al. [139]. It was suggested that nonequilibrium calcium dynamics is a potential mechanism for differential and conditional activation of intradendritic targets. Competitive Ca^{2+} binding was then demonstrated experimentally using Ca^{2+} indicators with different kinetic properties [139]. In the study of Bortolozzi et al. [122], it was shown that equilibrium conditions for an average whole-cell $[Ca^{2+}]_i$ are heavily perturbed by Ca^{2+} influx in response to 50 ms depolarization even in the presence of millimolar concentrations of fast buffers. Therefore, simulation of all endogenous Ca^{2+} buffers with realistic kinetics is an important, but quite challenging task since the identification

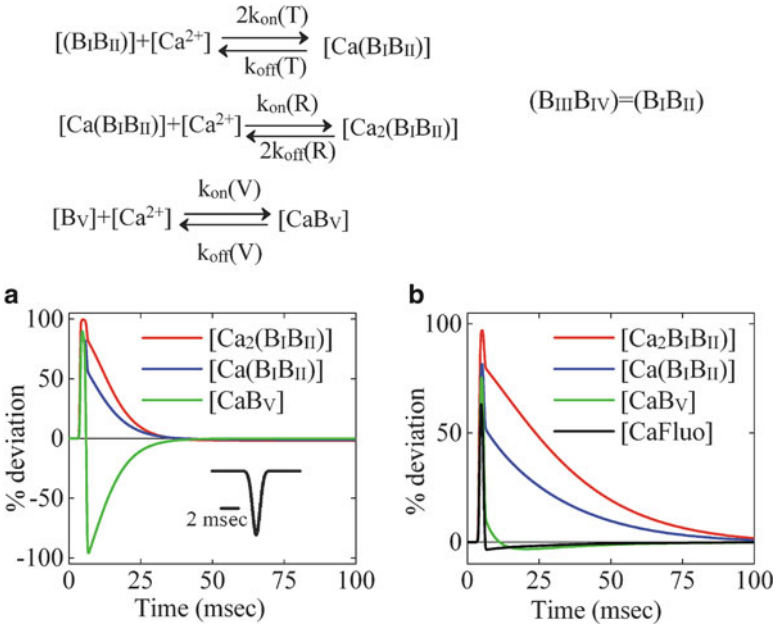

Fig. 26.3 Simulation of the equilibration of Ca^{2+} with calretinin during and after a brief Ca^{2+} influx evoked by an action potential in the presynaptic boutons of cerebellar granule cells. (**a**) Deviation of the calretinin Ca^{2+}-bound sites from the instantaneous equilibrium with $[Ca^{2+}]_i$ in the absence of exogenous buffers. (**b**) Deviation of the Ca^{2+}-bound sites of calretinin and Fluo-5F from the instantaneous equilibrium with $[Ca^{2+}]_i$ in the presence of 250 μM Fluo-5F. The concentration of calretinin was set at 700 μM. The kinetic schemes of Ca^{2+} binding with calretinin are shown in the *upper panel*. Calretinin is a Ca^{2+}-binding protein with two pairs of cooperative binding sites (I-IV) with indistinguishable properties and one independent binding site (V) for Ca^{2+}. The percentage deviation from equilibrium of a given species of buffer at a given time was calculated as 100% $(1-[CaB]/[CaB]_{EQ})$, where [CaB] is the concentration of the buffer or Ca^{2+}-binding sites and $[CaB]_{EQ}$ is the concentration of the buffer or Ca^{2+}-binding sites that would be bound with the $[Ca^{2+}]_i$ under equilibrium conditions. $[Ca_2(B_IB_{II})]$ is the concentration of all cooperative pairs of the Ca^{2+}-binding sites of calretinin with two Ca^{2+} bound, $[Ca(B_IB_{II})]$ is the concentration of the cooperative pairs with one Ca^{2+} bound, $[CaB_V]$ is the concentration of the Ca^{2+}-bound form of independent Ca^{2+}-binding sites of calretinin, *[CaFluo]* is the concentration of Ca^{2+}-bound Fluo-5F, k_{on} (R and T) and k_{off} (R and T) are the association and dissociation rate constants for two identical pairs of cooperative binding sites $((B_IB_{II})=(B_{III}B_{IV}))$ depending on their Ca^{2+}-binding status ("tensed" with a low affinity for Ca^{2+} or "relaxed" with a high affinity for Ca^{2+}) and k_{on}(V) and k_{off}(V) are the rate constants for the independent site (B_V) (Adapted from Saftenku [85]. With permission from Springer)

and localization of all Ca^{2+} buffers as well as the concentrations and properties of identified Ca^{2+} buffers are not currently available for any neuronal types.

Nevertheless, considerable progress has been made by characterizing experimentally the Ca^{2+}-binding properties of calbindin-D28k and parvalbumin [102, 161], estimating their diffusion constants from fluorescence recovery after photobleaching recordings [162, 163], and estimating the concentrations of these buffers in Purkinje cells [162, 164] and the concentration of calbindin-D28k in hippocampal neurons [82].

These buffers were explicitly included in the models of Ca^{2+} dynamics in dendrites and spines of Purkinje cells [140–142, 144, 145, 152, 165] and in the model of Ca^{2+} microdomains in hippocampal neurons [82]. Although the exact quantity and localization of the ubiquitous Ca^{2+} sensor calmodulin remains poorly-characterized experimentally, the kinetics of cooperative Ca^{2+} binding of this buffer is sufficiently well established, and this buffer was included, together with calbindinn-D28k, in the model of Ca^{2+} dynamics in the spines of neocortical pyramidal cells [121].

At present, uncertainties remain regarding uncharacterized Ca^{2+} buffers. Another problem that may be important for realistic description of endogenous Ca^{2+}-binding proteins is that the kinetic parameters of endogenous buffers and Ca^{2+} indicators are often obtained in a test cuvette. There are only a few examples where the forward binding rate constants and dissociation constants of Ca^{2+} indicators and lumped endogenous buffers were obtained experimentally *in vivo* (e.g., [166, 167]), but factors that influence indicator performance, such as ionic strength, osmolarity, pH, and protein environment, may differ from conditions *in vivo* [168]. Cooperativity of Ca^{2+} binding *in vivo* also may differ from the cooperativity of Ca^{2+} binding *in vitro* [168].

Models Based on Separation of Ca^{2+} Fluxes in Intact Cells

Only a limited number of studies have addressed how Ca^{2+} responses are defined by the Ca^{2+} transport and buffering systems that operate in the same cells. It would seem that the simplest way to carry out an *in situ* characterization of Ca^{2+} fluxes generated by individual transport pathways would be to inhibit them selectively and observe the resulting changes in evoked Ca^{2+} signals. However, because Ca^{2+} handling systems are functionally coupled through their dependence on the $[Ca^{2+}]$, blocking one system has the potential to influence transport by other systems. A similar problem encountered in the study of membrane potential dynamics was solved by the introduction of the voltage-clamp technique. This technique made it possible to measure ionic currents at a constant membrane potential, thereby uncoupling the activity of different populations of voltage-sensitive ion channels and greatly facilitating analysis of the currents carried by these channels. Ideally, an analogous technique would make it possible to measure the net Ca^{2+} flux across a cell membrane while fixing the Ca^{2+} concentration on both sides of that membrane. If this were possible, the component of the total flux generated by a particular transporter could be determined based on the difference in the total flux before and after applying a specific Ca^{2+} transport inhibitor. Moreover, by measuring the flux at different $[Ca^{2+}]$ levels, it would be possible to characterize how Ca^{2+} transport rate depends on $[Ca^{2+}]$. Unfortunately, such a technique has yet to be devised. Nevertheless, the formal similarity between Ca^{2+} and voltage dynamics is strong enough to suggest that pursuing this line of reasoning might be productive. Just as the total charge flux (current) that drives changes in membrane potential is the sum of macroscopic currents carried by different populations of ion channels, the total Ca^{2+} flux that changes the $[Ca^{2+}]$ in a given cellular compartment is the sum of macroscopic Ca^{2+} fluxes representing the activity of different transporters.

Therefore, given specific Ca^{2+} transport inhibitors, it should be possible to eliminate individual components of the total Ca^{2+} flux, using the consequences to provide information about the corresponding flux component. Indeed, these ideas served as a foundation for classical work on Ca^{2+} dynamics in skeletal [169–172] and cardiac muscle [173]. However, the question remains: how can one measure Ca^{2+} flux components in intact cells without a "Ca^{2+} clamp"?

One approach to characterizing the component of current carried by voltage-sensitive ion channels under voltage clamp is to start with a measure of the "leak" current carried by voltage-insensitive channels. The leak current can be measured based on the total current that flows when voltage-sensitive ion channels do not conduct current, either because they are blocked or permeant ions are absent. The critical property of the leak current that makes it useful for characterizing voltage-sensitive currents is that it depends only on voltage and not explicitly on time. This could happen if the underlying conductances are insensitive to voltage, or more generally, depend on voltage but adjust rapidly (or instantaneously) as the voltage changes. If the leak current has this property (the term "leak current" means that this property is satisfied), the component of the total current carried by voltage-sensitive channels at a particular voltage can be determined by measuring the total current before and after blocking the voltage-sensitive channels and taking the difference between the two. Such a current component may vary with voltage, and with time in a way that provides information about channel gating kinetics. This method requires that the leak current measured in the presence of channel blockers is the same as the current that flows via the same pathway in the absence of blockers, i.e. that the treatment used to block voltage-sensitive channels is selective. In much the same way, if there were a "leak" Ca^{2+} flux that depends only on $[Ca^{2+}]$ but not explicitly on time (e.g., because the underlying Ca^{2+} transporters adjust rapidly to changes in $[Ca^{2+}]$), it would greatly simplify characterization of other components of the net Ca^{2+} flux, e.g. those generated by Ca^{2+} uptake and release by intracellular stores. These other flux components could be determined as the difference between the total Ca^{2+} flux before and after blocking the "other" fluxes, at corresponding values of $[Ca^{2+}]$.

An approach motivated by these concepts was used for separation and characterization of Ca^{2+} fluxes in fura-2 loaded sympathetic neurons [12, 155, 174–177]. Flux characterizations were based on analysis of spatially averaged $[Ca^{2+}]_i$ during the recovery after depolarization-induced Ca^{2+} entry. The net flux representing the rate at which Ca^{2+} enters or leaves the cytoplasm per unit time per unit volume (scaled by a factor describing buffering strength) was determined by calculating the time derivative of $[Ca^{2+}]_i$, which provides a measure of the net Ca^{2+} flux entering the cytosol, and plotting this flux versus $[Ca^{2+}]_i$ throughout the response; this is analogous to current–voltage relations used to characterize membrane currents. To study Ca^{2+} dynamics without contributions from Ca^{2+} uptake and release by internal stores, cells were stimulated after inhibiting mitochondrial and ER Ca^{2+} uptake. Cells were depolarized under voltage clamp to open voltage sensitive Ca^{2+} channels, leading to Ca^{2+} entry and a rise in $[Ca^{2+}]_i$. Following repolarization and Ca^{2+} channel closure, the Ca^{2+} current fell to zero, followed by a slower decline in $[Ca^{2+}]_i$ reflecting a net flux that was uniquely defined by $[Ca^{2+}]_i$ at each point in time, making it suitable as a "leak Ca^{2+} flux" for measuring other flux components ([175]; Fig. 26.4).

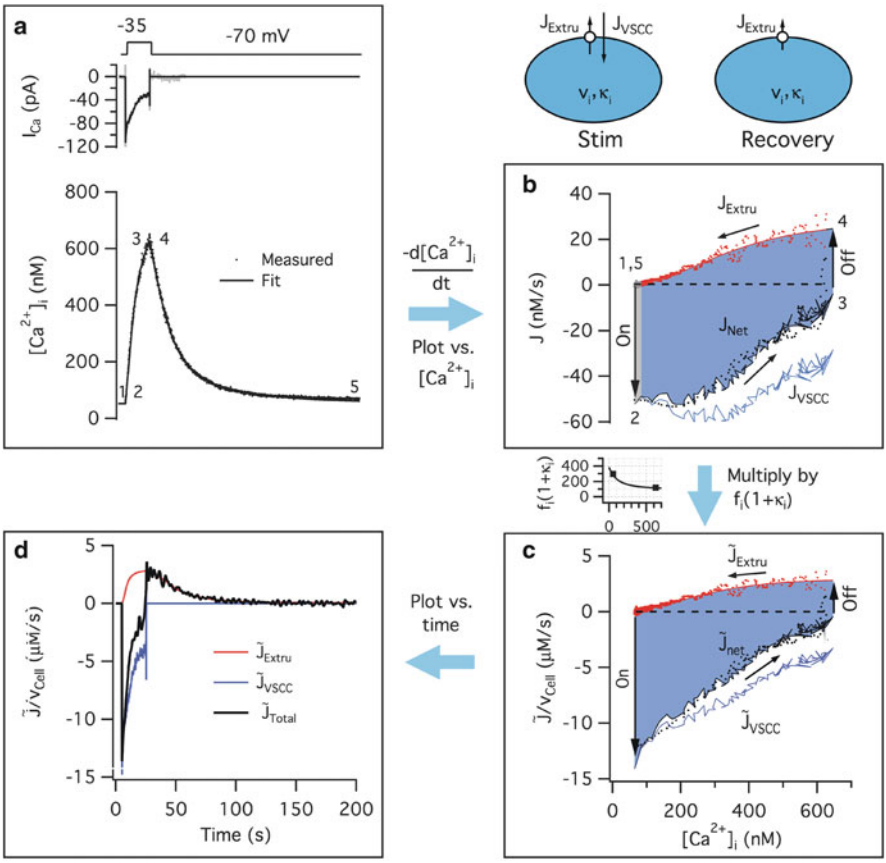

Fig. 26.4 Analysis of a measured Ca^{2+} response elicited by membrane depolarization in a sympathetic neuron under voltage clamp when $[Ca^{2+}]_i$ dynamics depend on voltage-sensitive Ca^{2+} entry, Ca^{2+} extrusion and cytoplasmic Ca^{2+} buffering strength (see diagrams, *top right*). Ca^{2+} uptake by mitochondria and endoplasmic reticulum were inhibited with the protonophore FCCP and thapsigargin, respectively. (**a**) Depolarization-induced $[Ca^{2+}]_i$ response, illustrating from top to bottom, voltage protocol, Ca^{2+} current (I_{Ca}) and time course of $[Ca^{2+}]_i$. Points show $[Ca^{2+}]_i$ based on fura-2 fluorescence measurements. Numbers 1–5 indicate stages of the response that can be related to the underlying fluxes. Continuous curve is a reconstruction of the response based on measurements of Ca^{2+} handling in the same cell. (**b**) Plot of net Ca^{2+} flux versus $[Ca^{2+}]_i$. Net flux (J_{Net}) was measured from the Ca^{2+} response by taking the time derivative of $[Ca^{2+}]_i$ at each time with the negative sign. The derivative represents the net cytoplasmic Ca^{2+} flux ($\hat{J}_{net}$, mol/s) divided by compartmental volume (v_i) scaled by $(1+\kappa_i)$, where κ_i is the cytoplasmic Ca^{2+} buffer ratio describing the relationship between changes in bound and free calcium concentrations. During the recovery, measurement of J_{Net} provides a quantitative description of the rate of Ca^{2+} extrusion (J_{Extru}, *red*) and its dependence on $[Ca^{2+}]_i$. Fitting a smooth curve to J_{Net} during the recovery (*top*) provides a quantitative description of the $[Ca^{2+}]_i$ dependence of J_{Extru}. This can be used to calculate the Ca^{2+} flux component (J_{VSCC}) representing Ca^{2+} entry via voltage sensitive Ca^{2+} channels as the difference between J_{Net} during depolarization and after repolarization at corresponding values of $[Ca^{2+}]_i$. (**c**) Plot of $\hat{J}_{net}/v_{Cell}$ and its components versus $[Ca^{2+}]_i$. These fluxes were obtained from the flux measurements in (**b**) by multiplication with the measured buffering factor $f_i(1+\kappa_i)$. $\hat{J}_{net}/v_{Cell}$ follows I_{Ca} during depolarization. (**d**) Time course of $\hat{J}_{net}/v_{Cell}$ and its components during the response, illustrating how the

The net mitochondrial Ca^{2+} flux was determined as the difference between the net cytosolic Ca^{2+} flux before and after blocking mitochondrial Ca^{2+} transport, at corresponding values of $[Ca^{2+}]_i$, under conditions where ER transport is blocked. An analogous approach was used to characterize the net ER Ca^{2+} flux, during cells were exposed to an inhibitor of mitochondrial Ca^{2+} transport.

To study components of the net mitochondrial Ca^{2+} flux, this flux was measured under conditions that prevent Ca^{2+} release by the mitochondrial Na^+–Ca^{2+} exchanger, using either Na^+-free pipette solutions or treatment with the specific Na^+–Ca^{2+} exchange inhibitor CGP 37157. The remaining Ca^{2+} flux showed a steep $[Ca^{2+}]_i$-dependence as expected for the mitochondrial uniporter. One intriguing finding was that mitochondrial Ca^{2+} uptake occurs at low Ca^{2+} levels, as low as 200–300 nM. The rate of Ca^{2+} release via the mitochondrial Na^+–Ca^{2+} exchanger was measured as the CGP-sensitive component of the total mitochonrial Ca^{2+} flux in cells where the exchanger was enabled by including Na^+ in the pipette solution. This flux was found to increase in a saturable manner as the mitochondrial Ca^{2+} load increeased, as expected based on known properties of the exchanger [175, 176]. Descriptions of ER Ca^{2+} uptake and release fluxes can be obtained in a similar manner [177].

The next step was to determine whether characterizations of the Ca^{2+} fluxes are sufficient, when taken together, to account quantitatively for depolarization-induced Ca^{2+} responses in the absence of transport inhibitors. In each case, measured Ca^{2+} responses were compared with calculated responses deduced through simulation using quantitative descriptions of Ca^{2+} transport and buffering. Since the predominant cytosolic buffer in the experiments was fura-2, which acts as a fast, mobile buffer, the fast buffering approximation was implemented, and quantified based on the relationship between the rate at which $[Ca^{2+}]_i$ rises under the influence of Ca^{2+} entry at different $[Ca^{2+}]_i$ levels. It was shown [12] that when these characterizations were incorporated into a model that assumes cytoplasmic Ca^{2+} is uniformly distributed, it was possible to account quantitatively for responses to weak depolarization, but not responses to stronger depolarization when radial $[Ca^{2+}]_i$ gradients are expected to be steep. However, a diffusion model that incorporated the same transport and buffering descriptions but considered radially non-uniform Ca^{2+} signals accounted for the observed responses elicited by strong depolarization.

Fig. 26.4 (continued) interplay between these fluxes accounts for the dynamics of $[Ca^{2+}]_i$ during and after depolarization. (Inset between (**b**) and (**c**)) Plot of buffering factor $f_i(1+\kappa_i)$ versus $[Ca^{2+}]_i$. Smooth curve shows fit by an equation describing the $[Ca^{2+}]_i$ dependence of buffering strength derived using the fast buffer approximationthat includes both endogenous and exogenous (fura-2) Ca^{2+} buffers. The measure of buffering strength is the product of $(1+\kappa_i)$ and the fraction of cell volume (f_i) occupied by cytoplasm. Using the $[Ca^{2+}]$ dependencies of J_{Extru} (**b**) and buffering strength (inset), along with the measured time course of I_{Ca} (**a**) to describe Ca^{2+} entry, it is possible to reconstruct the entire response (see smooth curve, (**a**)). This provides validation for the methods used to measure and characterize the flux and buffering systems (J_{Extru}, JVSCC and buffering strength) and the use of the same description of J_{Extru} throughout the response (Reprinted from Friel and Chiel [157]. With permission from Elsevier)

This approach for measuring and characterizing Ca^{2+} fluxes in intact cells can be applied to other cells, subject to the conditions that (i) the Ca^{2+} concentration is approximately spatially uniform within membrane delimited compartments, which can be promoted by inclusion of a fast, rapidly diffusing, Ca^{2+} indicator/buffer, (ii) the fast buffer approximation applies, and (iii) a component of the net Ca^{2+} flux can be isolated that depends on $[Ca^{2+}]$ but not explicitly on time. Extension to the more general case where $[Ca^{2+}]$ is spatially non-uniform within compartments, buffering is slow, and transport systems are non-uniformly distributed, is possible as long at measurements of $[Ca^{2+}]_i$ at the sites of transport and buffering are available. For adequate description of Ca^{2+} transport pathways on high Ca^{2+} microdomains [178], e.g., between the ER and mitochondrial membranes, more complex models combining a detailed model of a microdomain with a model of entire cell may be necessary.

Models of Ca^{2+} Dynamics with Heterogeneous Distribution of Ca^{2+} Handling Systems

There is mounting evidence that selective triggering of neuronal functions is achieved through spatial localization of Ca^{2+} signals [19, 71, 179]. The heterogenous subcellular distribution of Ca^{2+} channels, pumps, exchangers, ER, and mitochondria allows extracellular stimuli to induce Ca^{2+} signals with highly defined spatial and temporal patterns [180]. However, the distribution of all Ca^{2+} handling systems is rarely known. Moreover, it is necessary to predict how all these systems will interact to obtain a specific Ca^{2+} response.

Several models studied the formation of localized Ca^{2+} transients in dendrites. Goldberg et al. [181] examined which parameters most profoundly affect spatial localization of Ca^{2+} transients in aspiny dendrites of neocortical interneurons, and found that it is most sensitive to fast calcium influx through calcium-permeable AMPA receptors, calcium extrusion, and fixed buffer capacity. In cerebellar stellate cells, the diffusion of Ca^{2+} is severely retarded due to interactions with parvalbumin and a general restriction of small molecule mobility [182]. The calculation of the Ca^{2+} spread showed that, in the absence of Ca^{2+} indicators, Ca^{2+} is highly localized to small stretches of dendrite near the active synapse even during prolonged, repetitive stimulation. By combining two-photon calcium imaging experiments in acute slices with computer simulations, Schmidt et al.[165] studied the formation of a standing gradient of Ca^{2+} in distal dendrites of Purkinje cells evoked by a stimulation paradigm, which is known to induce parallel fiber-mediated long-term depression. The numerical simulations suggested that Ca^{2+} extrusion and calbindin-based Ca^{2+} transport balance each other and determine the steepness of the gradient over a distance of ~13 μm, while the amplitude of the plateau Ca^{2+} and the Ca^{2+} buffer parvalbumin are of minor importance. The predicted role of buffered diffusion was tested by performing experiments with a substantially increased amount of exogenous buffer in the pipette solution. Saftenku [183] examined whether heterogeneities in the distribution of Ca^{2+}-handling systems or cell morphology can account for the

formation of $[Ca^{2+}]_i$ gradients in the dendrites of cerebellar granule cells during depolarization and synaptic stimulation, exploiting various combinations of Ca^{2+} handling systems (endogenous buffers, calcium channels, extrusion mechanisms, and mitochondria). For this purpose, the following integrated approach was applied [184]: (i) investigating the cases of increasing complexity, comparing the measured and simulated $[Ca^{2+}]_i$ responses; (ii) testing various hypotheses about the distribution and properties of Ca^{2+} handling systems in the context of a realistic description of cell morphology and model parameters and rejecting those hypotheses that do not match experimental results; (iii) simulations within all the space of allowable ranges of uncertain parameters and their combinations; (iv) in the case of the absence of experimental data, the use of the least favorable for a particular hypothesis parameters. This approach is likely to be useful for the initial stage of spatial modeling in the absence of complete experimental data. The results of simulations supported the hypothesis that fixed Ca^{2+} buffers and Ca^{2+} channels are very heterogeneously distributed in granule cells. The critical measurements to discriminate between different hypotheses were proposed.

The model of Fink et al. [11, 185] represents one of the most successful examples of combined experimental and computational approaches for explanation of the spatial and temporal patterns of intracellular calcium signals. In neuroblastoma cells, saturating levels of bradykinin stimulate robust and reproducible calcium waves that always follow the geometric pattern of initiating in the neurite and propagating to the growth cone and soma. To understand how a particular agonist triggers a specific cellular calcium response, a series of calcium imaging experiments were performed. At first a model with the simplest possible set of assumptions was built. This model suggested that bradikynin receptors were evenly distributed along the PM, the ER was uniformly distributed within the cytosol, and the SERCA and IP_3 receptors were both evenly distributed within the ER membrane. This initial model produced a much higher calcium signal in the neurite than in the soma (Fig. 26.5). This result was a consequence of the higher levels of IP_3 in the neurite compared to the soma and this, in turn, was a consequenceof the higher surface to volume ratio in the neurite. Then, it was suggested that higher transient levels of IP_3 in the neurite are compensated by a higher density of the ER in the soma. This hypothesis was tested by extensive immunofluorescence imaging of ER markers, IP_3 receptors, bradykinin receptors, and pumps. It was found that the ER density was, indeed, approximately twofold higher in the soma than in the neurite, while SERCA and IP_3 receptors appeared to be evenly distributed along the ER membrane. The concentration of bradykinin receptors was the highest in the neurite.

Although the distribution of bradykinin receptors initially seemed strikingly correlated with the initiation point of the calcium wave, the ER distribution was demonstrated to bias the initiation point toward the soma. Additionally, the simulations predicted the high surface-to-volume ratio in the thinnest part of the cell and most rapid IP_3 accumulation in this part of the cell. The hypothesis that the concentration of IP_3 in the cytosol ($[IP_3]_i$) is biased toward the neurite was supported by uncaging experiments. When uniform $[IP_3]_i$ was produced throughout the cell by global

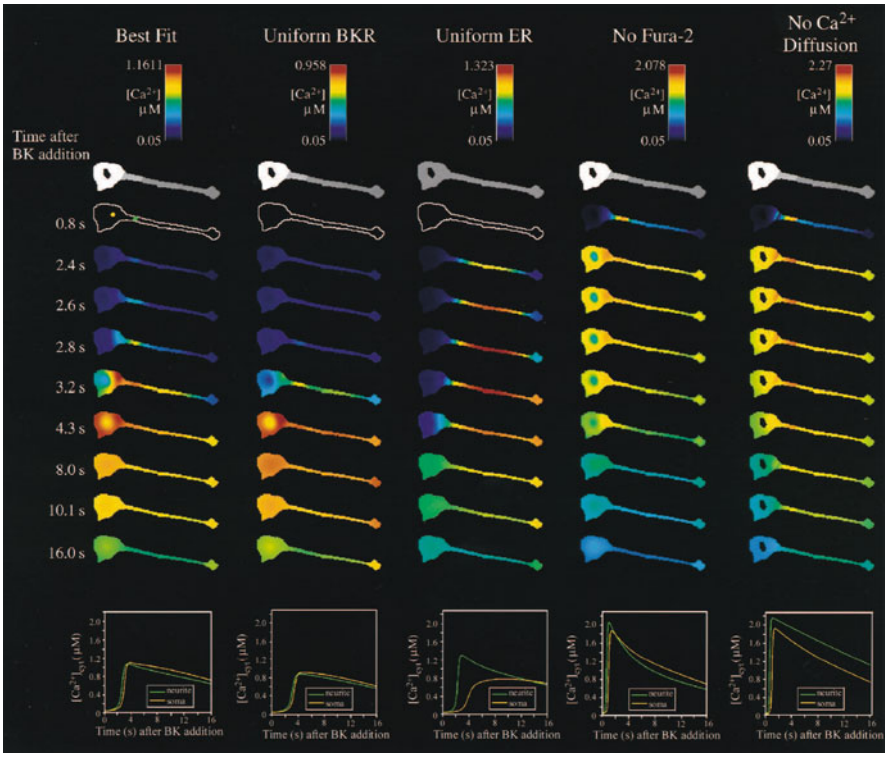

Fig. 26.5 Simulation results for the cytosolic [Ca^{2+}] following stimulation by external application of 500 nM bradykinin. Simulations were run for the best-fit parameters to match experimental results, and four variations of this simulation (with all other features being identical): uniform bradykinin receptor distribution across the plasma membrane, uniform endoplasmic reticulum (ER) (and inositol 1,4,5-trisphosphate and sarcoplasmic/endoplasmic reticulum Ca^{2+} ATPases) distribution throughout the cytosol, absence of calcium indicator (fura-2), and no calcium diffusion (which entails the absence of calcium indicator along with setting the diffusion coefficient of calcium to zero). [Ca^{2+}] has been pseudocolor-scaled with each column so that the maximum value is *red*. The first row shows the ER distribution that pertains to each column . The lower is the ER distribution, the darker is the *gray* scale. Below each column are plots of the cytosolic [Ca^{2+}] versus time for a point in the soma or neurite (indicated by the *yellow* or *green dots* on the 0.8 s image of the first column) (Reprinted from Fink et al. [11]. With permission from Elsevier)

uncaging, $[Ca^{2+}]_i$ was significantly higher in the soma than in the neurite. The simulations suggested the possibility of estimating experimentally inaccessible components (such as $[IP_3]_i$ and open probability of the IP_3-gated channel) and showed that literature-based estimates of IP_3 concentration for the bradykinin-induced IP_3 signals were too low to evoke calcium release in the model. Therefore, the measurements using standard radioligand binding assays on a cell population were carried out. The basal IP_3 concentration was measured to be 15-fold higher than the previous estimate, and the maximum stimulated level was almost two orders of magnitude higher. These levels provided a sufficient stimulus for calcium release in the

model and were later confirmed via quantitative IP_3 uncaging experiments. Results from the simulations supported the hypothesis that an interplay of cell shape (surface-to-volume ratio of neurite versus soma) and intracellular distribution of ER is sufficient to explain the pattern of calcium release. The model was able to predict a number of experimental results, e.g., the altered spatial pattern of the calcium signal for uncaging IP_3, the spatiotemporal pattern of calcium dynamics for cells with different morphologies, and the calcium responses to focal applications of bradykinin. This study clearly demonstrated the power of image-based spatial modeling when used together with measurements based on Ca^{2+} imaging.

Conclusions

The use of detailed computational models with biologically realistic features is fruitful for interpreting optical imaging data and understanding how the specific Ca^{2+} regulatory mechanisms define $[Ca^{2+}]$ elevations in the cells. Many models have been developed to account for Ca^{2+} dynamics in neurons, but a general problem of most of these models is a lack of parameters derived from the experiments with the same whole cells. Recently developed methods for measuring and characterizing Ca^{2+} fluxes *in situ* can be used to provide rate descriptions of Ca^{2+} transport in isolated neurons [157]. This approach helps to explain how the distribution and interplay between Ca^{2+} transport systems described in the same cells orchestrate measured Ca^{2+} responses. Moreover, it gives the possibility to predict the influence of pharmacological perturbations or specific mutations linked to human genetic diseases on calcium levels in the cell. Although the application of this approach is still limited when Ca^{2+}-handling systems are distributed heterogeneously and when neurons, especially with large dendritic trees, are studied in slices, the development of optogenetic techniques provides a promising tool for determining distributions of Ca^{2+}-handling systems and properties of endogenous calcium buffers and other proteins *in vitro* and *in vivo*. Future models, probably, will incorporate detailed structural information about an entire cellular cytosol, organelles, and about the properties and distribution of the sets of regulators of Ca^{2+} handling. Considerable progress of making faster and higher resolution Ca^{2+} measurements, on the one hand, and continual growth in computer power and creation of new integrated simulation algorithms that can run realistic models within reasonable computation time, on the other hand, result in merging of theory with experiment. This process is accelerated by the development of model description languages based on XML (Extensible Markup Language) that enables interoperability across multiple simulation environments [186]. Hopefully, computational science and cell biology will develop with a close interdependence, such that model predictions will inspire new experiments with discrepancies between theory and experiment serving as the impetus for model refinement.

Acknowledgements This work was supported by the Ukrainian grant SFFR F 46.2/001 to ES.

References

1. Schaff J, Loew LM (1999) The virtual cell. Pac Symp Biocomput 4:228–239
2. Iyer V, Hoogland TM, Saggau P (2006) Fast functional imaging of single neurons using random-access multiphoton (RAMP) microscopy. J Neurophysiol 95:535–545
3. Grewe BF, Langer D, Kasper H, Kampa BM, Helmchen F (2010) High-speed in vivo calcium imaging reveals neuronal network activity with near-millisecond precision. Nat Methods 7:399–405
4. Ding JB, Takasaki KT, Sabatini BL (2009) Supraresolution imaging in brain slices using stimulated-emission depletion two-photon laser scanning microscopy. Neuron 63:429–437
5. Knöpfel T, Lin MZ, Levskaya A, Tian L, Lin JY, Boyden ES (2010) Toward the second generation of optogenetic tools. J Neurosci 30:14998–15004
6. Grewe BF, Helmchen F (2009) Optical probing of neuronal ensemble activity. Curr Opin Neurobiol 19:520–529
7. Wallace DJ, Meyer zum Alten Borgloh S, Astori S, Yang Y, Bausen M, Kügler S, Palmer AE, Tsien RY, Sprengel R, Kerr JN, Denk W, Hasan MT (2008) Single-spike detection in vitro and in vivo with a genetic Ca^{2+} sensor. Nat Methods 5:797–804
8. Tian L, Hires SA, Mao T, Huber D, Chiappe ME, Chalasani SH, Petreanu L, Akerboom J, McKinney SA, Schreiter ER, Bargmann CI, Jayaraman V, Svoboda K, Looger LL (2009) Imaging neuronal activity in worms, flies and mice with improved GCaMP calcium indicators. Nat Methods 6:875–881
9. Lütcke H, Murayama M, Hahn T, Margolis DJ, Astori S, Zum Alten Borgloh SM, Göbel W, Yang Y, Tang W, Kügler S, Sprengel R, Nagai T, Miyawaki A, Larkum ME, Helmchen F, Hasan MT (2010) Optical recording of neuronal activity with a genetically-encoded calcium indicator in anesthetized and freely-moving mice. Front Neural Circuits 4:9
10. Higley MJ, Sabatini BL (2008) Calcium signaling in dendrites and spines: practical and functional considerations. Neuron 59:902–913
11. Fink CC, Slepchenko B, Moraru II, Watras J, Schaff JC, Loew LM (2000) An image-based model of calcium waves in differentiated neuroblastoma cells. Biophys J 79:163–183
12. Patterson M, Sneyd J, Friel DD (2007) Depolarization-induced calcium responses in sympathetic neurons: relative contributions from Ca^{2+} entry, extrusion, ER/mitochondrial Ca^{2+} uptake and release, and Ca^{2+} buffering. J Gen Physiol 129:29–56
13. Petersen OH, Michalak M, Verkhratsky A (2005) Calcium signalling: past, present and future. Cell Calcium 38:161–169
14. Bootman MD, Fearnley C, Smyrnias I, MacDonald F, Roderick HL (2009) An update on nuclear calcium signalling. J Cell Sci 122:2337–2350
15. Piedras-Rentería ES, Barrett CF, Cao YQ, Tsien RW (2007) Voltage-gated calcium channels, calcium signaling, and channelopathies. In: Krebs J, Michalak M (eds) Calcium: a matter of life and death. Elsevier, Amsterdam pp 127–166
16. Strehler EE, Filoteo AG, Penniston JT, Caride AJ (2007) Plasma-membrane Ca^{2+} pumps: structural diversity as the basis for functional versatility. Biochem Soc Trans 35(Pt 5):919–922
17. Burgoyne RD (2007) Neuronal calcium sensor proteins: generating diversity in neuronal Ca^{2+} signaling. Nat Rev Neurosci 8:182–193
18. Parekh AB, Putney JW Jr (2005) Store-operated calcium channels. Physiol Rev 85:757–810
19. Goldberg M, De Pità M, Volman V, Berry H, Ben-Jacob E (2010) Nonlinear gap junctions enable long-distance propagation of pulsating calcium waves in astrocyte networks. PLoS Comput Biol 6:e1000909
20. Kang M, Othmer HG (2009) Spatiotemporal characteristics of calcium dynamics in astrocytes. Chaos 19:037116
21. Kapela A, Nagaraja S, Tsoukias NM (2010) A mathematical model of vasoreactivity in rat mesenteric arterioles. II. Conducted vasoreactivity. Am J Physiol Heart Circ Physiol 298:H52–H65
22. Jafri MS, Rice JJ, Winslow RL (1998) Cardiac Ca^{2+} dynamics: the roles of ryanodine receptor adaptation and sarcoplasmic reticulum load. Biophys J 74:1149–1168

23. Shannon TR, Wang F, Puglisi J, Weber C, Bers DM (2004) A mathematical treatment of integrated Ca^{2+} dynamics within the ventricular myocyte. Biophys J 87:3351–3371
24. Cortassa S, Aon MA, Marbán E, Winslow RL, O'Rourke B (2003) An integrated model of cardiac mitochondrial energy metabolism and calcium dynamics. Biophys J 84:2734–2755
25. Magnus G, Keizer J (1997) Minimal model of β-cell Ca^{2+} mitochondrial Ca^{2+} handling. Am J Physiol 273:C717–C733
26. Magnus J, Keizer J (1998) Model of β-cell mitochondrial calcium handling and electrical activity. I. Cytoplasmic variables. Am J Physiol 274:C1158–C1173
27. Magnus J, Keizer J (1998) Model of β-cell mitochondrial calcium handling and electrical activity. II. Mitochondrial variables. Am J Physiol 274:C1174–C1184
28. Fall CP, Keizer JE (2001) Mitochondrial modulation of intracellular Ca^{2+} signaling. J Theor Biol 210:151–165
29. Means S, Smith AJ, Shepherd J, Shadid J, Fowler J, Wojcikiewicz RJ, Mazel T, Smith GD, Wilson BS (2006) Reaction diffusion modeling of calcium dynamics with realistic ER geometry. Biophys J 91:537–557
30. Goldbeter A, Dupont G, Berridge MG (1990) Minimal model for signal-induced Ca^{2+} oscillations and for their frequency encoding through protein phosphorylation. Proc Natl Acad Sci USA 87:1461–1465
31. Dupont G, Goldbeter A (1993) One-pool model for Ca^{2+} oscillations involving Ca^{2+} and inositol 1,4,5-trisphosphate as co-agonists for Ca^{2+} release. Cell Calcium 14:311–322
32. De Young GW, Keizer J (1992) A single-pool inositol 1,4,5-trisphosphate-receptor-based model for agonist-stimulated oscillations in Ca^{2+} concentration. Proc Natl Acad Sci USA 89:9895–9899
33. Keizer J, De Young GW (1992) Two roles of Ca^{2+} in agonist stimulated Ca^{2+} oscillations. Biophys J 61:649–660
34. Atri A, Amundson J, Clapham D, Sneyd J (1993) A single-pool model for calcium oscillations and waves in the Xenopus laevis oocyte. Biophys J 65:1727–1739
35. Jafri MS (1995) A theoretical study of cytosolic calcium waves in Xenopus oocytes. J Theor Biol 172:209–216
36. Falcke M, Li Y, Lechleiter JD, Camacho P (2003) Modeling the dependence of the period of intracellular Ca^{2+} waves on SERCA expression. Biophys J 85:1474–1481
37. Sneyd J, Tsaneva-Atanasova K, Yule DI, Thompson JL, Shuttleworth TJ (2004) Control of calcium oscillations by membrane fluxes. Proc Natl Acad Sci USA 101:1392–1396
38. Higgins ER, Cannell MB, Sneyd J (2006) A buffering SERCA pump in models of calcium dynamics. Biophys J 91:151–163
39. Tang Y, Othmer HG (1994) A model of calcium dynamics in cardiac myocytes based on the kinetics of ryanodine-sensitive calcium channels. Biophys J 67:2223–2235
40. Roth BJ, Yagodin SV, Holtzclaw L, Russell JT (1995) A mathematical model of agonist-induced propagation of calcium waves in astrocytes. Cell Calcium 17:53–64
41. Sneyd J, Keizer J, Sanderson MJ (1995) Mechanisms of calcium oscillations and waves: a quantitative analysis. FASEB J 9:1463–1472
42. Keizer J, Levine L (1996) Ryanodine receptor adaptation and Ca^{2+}-induced Ca^{2+} release-dependent Ca21 oscillations. Biophys J 71:3477–3487
43. Kupferman R, Mitra PP, Hohenberg PC, Wang SS (1997) Analytical calculation of calcium wave characteristics. Biophys J 72:2430–2444
44. Thul R, Smith GD, Coombes S (2008) A bidomain threshold model of propagating calcium waves. J Math Biol 56:435–463
45. Swietach P, Spitzer KW, Vaughan-Jones RD (2010) Modeling calcium waves in cardiac myocytes: importance of calcium diffusion. Front Biosci 15:661–680
46. Li YX, Rinzel J (1994) Equations for InsP3 receptor-mediated $[Ca^{2+}]_i$ oscillations derived from a detailed kinetic model: a Hodgkin–Huxley-like formalism. J Theor Biol 166:461–473
47. Li YX, Rinzel J, Vergara L, Stojilcović SS (1995) Spontaneous electrical and calcium oscillations in unstimulated pituitary gonadotrophs. Biophys J 69:785–795

48. Coombes S, Timofeeva Y (2003) Sparks and waves in a stochastic fire-diffuse-fire model of Ca^{2+} release. Phys Rev E Stat Nonlin Soft Matter Phys 68:021915
49. Keener JP (2006) Stochastic calcium oscillations. Math Med Biol 23:1–25
50. Dupont G, Abou-Lovergne A, Combettes L (2008) Stochastic aspects of oscillatory Ca^{2+} dynamics in hepatocytes. Biophys J 95:2193–2202
51. Skupin A, Kettenmann H, Winkler U, Wartenberg M, Sauer H, Tovey SC, Taylor CW, Falcke M (2008) How does intracellular Ca^{2+} oscillate: by chance or by the clock? Biophys J 94: 2404–2411
52. Skupin A, Kattenmann H, Falcke M (2010) Calcium signals driven by single channel noise. PLoS Comput Biol 6:e1000870
53. Rüdiger S, Shuai JW, Huisinga W, Nagaiah C, Warnecke G, Parker I, Falcke M (2007) Hybrid stochastic and deterministic simulations of calcium blips. Biophys J 93:1847–1857
54. Falcke M (2009) Introduction to focus issue: intracellular Ca^{2+} dynamics – a change of modelling paradigm? Chaos 19:037101
55. Manita S, Ross WN (2009) Synaptic activation and membrane potential changes modulate the frequency of spontaneous elementary Ca^{2+} release events in the dendrites of pyramidal cells. J Neurosci 29:7833–7845
56. Hines ML, Carnevale NT (1997) The NEURON simulation environment. Neural Comput 9:1179–1209
57. Bower JM, Beeman D (1998) The book of GENESIS: exploring realistic neural models with the General Neural Simulation System, 2nd edn. Springer, New York
58. Schaff J, Fink CC, Slepchenko B, Carson JH, Loew LM (1997) A general computational framework for modeling cellular structure and function. Biophys J 73:1135–1146
59. Moraru II, Schaff JC, Slepchenko BM, Blinov ML, Morgan F, Lakshminarayana A, Gao F, Li Y, Loew LM (2008) The Virtual Cell modelling and simulation software environment. IET Syst Biol 2:353–362
60. Stiles JR, Bartol TM Jr, Salpeter EE, Salpeter MM (1998) Monte Carlo simulation of neurotransmitter release using MCell, a general simulator of cellular physiological processes. In: Bower JM (ed) Computational neuroscience. Plenum Press, New York, pp 279–284
61. Blaustein MP, Hodgkin AL (1969) The effect of cyanide on the efflux of calcium from squid axons. J Physiol 200:497–527
62. Baker PF, Hodgkin AL, Ridgway EB (1971) Depolarization and calcium entry in squid giant axons. J Physiol 218:709–755
63. Smith SJ, Zucker RS (1980) Aequorin response facilitation and intracellular calcium accumulation in molluscan neurones. J Physiol 300:167–196
64. Connor JA, Nikolakopoulou G (1982) Calcium diffusion and buffering in nerve cytoplasm. Lect Math Life Sci 15:79–101
65. Sala F, Hernández-Cruz A (1990) Calcium diffusion modeling in a spherical neuron. Relevance of buffering properties. Biophys J 57:313–324
66. Zucker RS, Stockbridge N (1983) Presynaptic calcium diffusion and the time courses of transmitter release and synaptic facilitation at the squid giant synapse. J Neurosci 3:1263–1269
67. Fogelson AL, Zucker RS (1985) Presynaptic calcium diffusion from various arrays of single channels. Implications for transmitter release and synaptic facilitation. Biophys J 48:1003–1017
68. Simon SM, Llinás RR (1985) Compartmentalization of the submembrane calcium activity during calcium influx and its significance in transmitter release. Biophys J 48:485–498
69. Yamada WM, Zucker RS (1992) Time course of transmitter release calculated from simulations of a calcium diffusion model. Biophys J 61:671–682
70. Roberts WM (1993) Spatial calcium buffering in saccular hair cells. Nature 363:74–76
71. Augustine GJ, Santamaria F, Tanaka K (2003) Local calcium signaling in neurons. Neuron 40:331–346
72. Neher E (1986) Concentration profiles of intracellular Ca^{2+} in the presence of a diffusible chelator. Exp Brain Res Ser 14:80–96

73. Stern MD (1992) Buffering of calcium in the vicinity of a channel pore. Cell Calcium 13:183–192
74. Naraghi M, Neher E (1997) Linearized buffered Ca^{2+} diffusion in microdomains and its implications for calculation of $[Ca^{2+}]$ at the mouth of a calcium channel. J Neurosci 17:6961–6973
75. Wagner J, Keizer J (1994) Effects of rapid buffers on Ca^{2+} diffusion and Ca^{2+} oscillations. Biophys J 67:447–456
76. Smith GD (1996) Analytical steady-state solution to the rapid buffering approximation near an open Ca^{2+} channel. Biophys J 71:3064–3072
77. Sherman A, Smith GD, Dai L, Miura RM (2001) Asymptotic analysis of buffered calcium diffusion near a point source. SIAM J Appl Math 61:1816–1831
78. Trommershäuser J, Schneggenburger R, Zippelius A, Neher E (2003) Heterogeneous presynaptic release probabilities: functional relevance for short-term plasticity. Biophys J 84:1563–1579
79. Mironova LA, Mironov SL (2008) Approximate analytical time-dependent solutions to describe large-amplitude local calcium transients in the presence of buffers. Biophys J 94:349–358
80. Roberts WM (1994) Localization of calcium signals by a mobile calcium buffer in frog saccular hair cells. J Neurosci 14:3246–3262
81. Smith GD, Wagner J, Keizer J (1996) Validity of the rapid buffering approximation near a point source of calcium ions. Biophys J 70:2527–2539
82. Műller A, Kukley M, Stausberg P, Beck H, Műller W, Dietrich D (2005) Endogenous Ca^{2+} buffer concentration and Ca^{2+} microdomains in hippocampal neurons. J Neurosci 25:558–565
83. Műller A, Kukley M, Uebachs M, Beck H, Dietrich D (2007) Nanodomains of single Ca^{2+} channels contribute to action potential repolarization in cortical neurons. J Neurosci 27:483–495
84. Bucurenciu I, Kulik A, Schwaller B, Frostcher M, Jonas P (2008) Nanodomain coupling between Ca^{2+} channels and Ca^{2+} sensors promotes fast and efficient transmitter release at a cortical GABAergic synapse. Neuron 57:536–545
85. Saftenku EE (2011) Effects of calretinin on Ca^{2+} signals in cerebellar granule cells: implications of cooperative Ca^{2+} binding. Cerebellum Epub ahead of print
86. Naoki H, Sakumura Y, Ishii S (2005) Local signaling with molecular diffusion as a decoder of Ca^{2+} signals in synaptic plasticity. Mol Syst Biol 1:0027
87. Wu YC, Tucker T, Fettiplace R (1996) A theoretical study of calcium microdomains in turtle hair cells. Biophys J 71:2256–2275
88. Hall JD, Betarbet S, Jaramillo F (1997) Endogenous buffers limit the spread of free calcium in hair cells. Biophys J 73:1243–1252
89. Klingauf J, Neher E (1997) Modeling buffered Ca^{2+} diffusion near the membrane: implications for secretion in neuroendocrine cell. Biophys J 72:674–690
90. Cooper RL, Winslow JL, Govind CK, Atwood HL (1996) Synaptic structural complexity as a factor enhancing probability of calcium-mediated transmitter release. J Neurophysiol 75:2451–2466
91. DiGregorio DA, Peskoff A, Vergara JL (1999) Measurement of action potential-induced presynaptic calcium domains at a cultured neuromuscular junction. J Neurosci 19:7846–7859
92. Tang Y, Schlumpberger T, Kim T, Lueker M, Zucker RS (2000) Effects of mobile buffers on facilitation: experimental and computational studies. Biophys J 78:2735–2751
93. Matveev V, Sherman A, Zucker RS (2002) New and corrected simulations of synaptic facilitation. Biophys J 83:1368–1373
94. Matveev V, Zucker RS, Sherman A (2004) Facilitation through buffer saturation: constraints on endogenous buffering properties. Biophys J 86:2691–2709
95. Matveev V, Bertram R, Sherman A (2006) Residual bound Ca^{2+} can account for the effects of Ca^{2+} buffers on synaptic facilitation. J Neurophysiol 96:3389–3397
96. Bennett MR, Farnell L, Gibson WG (2004) The facilitated probability of quantal secretion within an array of calcium channels of an active zone at the amphibian neuromuscular junction. Biophys J 86:2674–2690

97. Lin JW, Fu Q, Allana T (2005) Probing the endogenous Ca^{2+} buffers at the presynaptic terminals of the crayfish neuromuscular junction. J Neurophysiol 94:377–386
98. Meinrenken CJ, Borst JG, Sakmann B (2002) Calcium secretion coupling at calyx of Held governed by nonuniform channel-vesicle topography. J Neurosci 22:1648–1667
99. Meinrenken CJ, Borst JG, Sakmann B (2003) Local routes revisited: the space and time dependence of the Ca^{2+} signal for phasic transmitter release at the rat calyx of Held. J Physiol 547(Pt 3):665–689
100. Frank T, Khimich D, Neef A, Moser T (2009) Mechanisms contributing to synaptic Ca^{2+} signals and their heterogeneity in hair cells. Proc Natl Acad Sci USA 106:4483–4488
101. Edmonds B, Reyes R, Schwaller B, Roberts WM (2000) Calretinin modifies presynaptic calcium signaling in frog saccular hair cells. Nat Neurosci 3:786–790
102. Nägerl UV, Novo D, Mody I, Vergara JL (2000) Binding kinetics of calbindin-D28k determined by flash photolysis of caged Ca^{2+}. Biophys J 79:3009–3018
103. Fakler B, Adelman JP (2008) Control of K_{Ca} channels by calcium nano/microdomains. Neuron 59:873–881
104. Blatow M, Caputi A, Burnashev N, Monyer H, Rozov A (2003) Ca^{2+} buffer saturation underlies paired pulse facilitation in calbindin-D28k-containing terminals. Neuron 38:79–88
105. Matveev V, Bertram R, Sherman A (2009) Ca^{2+} current versus Ca^{2+} channel cooperativity of exocytosis. J Neurosci 29:12196–12209
106. Bormann J, Brosens F, De Schutter E (2001) Modeling molecular diffusion. In: Bower JM, Bolouri H (eds) Computational methods in molecular and cellular biology: from genotype to phenotype. MIT, Boston, pp 189–224
107. Vasudeva K, Bhalla US (2004) Adaptive stochastic-deterministic chemical kinetic simulations. Bioinformatics 20:78–84
108. Holcman S, Schuss Z, Korkotian E (2004) Calcium dynamics in dendritic spines and spine motility. Biophys J 87:81–91
109. Gil A, Segura J, Pertusa JA, Soria B (2000) Monte Carlo simulation of 3-D buffered Ca^{2+} diffusion in neuroendocrine cells. Biophys J 78:13–33
110. Segura J, Gil A, Soria B (2000) Modeling study of exocytosis in neuroendocrine cells: influence of the geometrical parameters. Biophys J 79:1771–1786
111. Bennett MR, Farnell L, Gibson WG (2000) The probability of quantal secretion near a single calcium channel of an active zone. Biophys J 78:2201–2221
112. Bennett MR, Farnell L, Gibson WG (2000) The probability of quantal secretion within an array of calcium channels of an active zone. Biophys J 78:2222–2240
113. Shahrezaei V, Delaney KR (2004) Consequences of molecular-level Ca^{2+} channel and synaptic vesicle colocalization for the Ca^{2+} microdomain and neurotransmitter exocytosis: a Monte Carlo study. Biophys J 87:2352–2364
114. Shagrezaei V, Delaney KR (2005) Brevity of the Ca^{2+} microdomain and active zone geometry prevent Ca^{2+}-sensor saturation for neurotransmitter release. J Neurophysiol 94: 1912–1919
115. Shahrezaei V, Cao A, Delaney KR (2006) Ca^{2+} from one or two channels controls fusion of a single vesicle at the frog neuromuscular junction. J Neurosci 26:13240–13249
116. Gilmanov IR, Samigullin DV, Vyskocil F, Nikolsky EE, Bukharaeva EA (2008) Modeling of quantal neurotransmitter release kinetics in the presence of fixed and mobile calcium buffers. J Comput Neurosci 25:296–307
117. Modchang C, Nadkarni S, Bartol TM, Triampo W, Sejnowski TJ, Levine H, Rappel WJ (2010) A comparison of deterministic and stochastic simulations of neuronal vesicle release models. Phys Biol 7:026008
118. Nadkarni S, Bartol TM, Sejnowski TJ, Levine H (2010) Modelling vesicular release at hippocampal synapses. PLoS Comput Biol 6:e1000983
119. Gil A, González-Vélez V (2010) Exocytotic dynamics and calcium cooperativity effects in the calyx of Held synapse: a modelling study. J Comput Neurosci 28:65–76
120. Franks KM, Sejnowski TJ (2002) Complexity of calcium signaling in synaptic spines. Bioessays 24:1130–1144

121. Keller DX, Franks KM, Bartol TM Jr, Sejnowski TJ (2008) Calmodulin activation by calcium transients in the postsynaptic density of dendritic spines. PLoS One 3:e2045
122. Bortolozzi M, Lelli A, Mammano F (2008) Calcium microdomains at presynaptic active zones of vertebrate hair cells unmasked by stochastic deconvolution. Cell Calcium 44:158–168
123. Kuba K, Takeshita S (1981) Simulation of intracellular Ca^{2+} oscillation in a sympathetic neurone. J Theor Biol 93:1009–1031
124. Friel DD (1995) $[Ca^{2+}]_i$ oscillations in sympathetic neurons: an experimental test of a theoretical model. Biophys J 68:1752–1766
125. Hua SY, Liu C, Lu FM, Nohmi M, Kuba K (2000) Modes of propagation of Ca^{2+}-induced Ca^{2+} release in bullfrog sympathetic ganglion cells. Cell Calcium 27:195–204
126. McDonough SI, Cseresnyés Z, Schneider MF (2000) Origin sites of calcium release and calcium oscillations in frog sympathetic neurons. J Neurosci 20:9059–9070
127. Falcke M, Huerta R, Rabinovich MI, Abarbanel HD, Elson RC, Selverston AI (2000) Modeling observed chaotic oscillations in bursting neurons: the role of calcium dynamics and IP3. Biol Cybern 82:517–527
128. Varona P, Torres JJ, Huerta R, Abarbanel HD, Rabinovich MI (2001) Regularization mechanisms of spiking–bursting neurons. Neural Netw 14:865–875
129. Miyawaki A, Llopis J, Heim R, McCaffery JM, Adams JA, Ikura M, Tsien RY (1997) Fluorescent indicators for Ca^{2+} based on green fluorescent proteins and calmodulin. Nature 388:882–887
130. Palmer AE, Giacomello M, Kortemme T, Hires SA, Lev-Ram V, Baker D, Tsien RY (2006) Ca^{2+} indicators based on computationally redesigned calmodulin-peptide pairs. Chem Biol 13:521–530
131. Blumenfeld H, Zablow L, Sabatini B (1992) Evaluation of cellular mechanisms for modulation of calcium transients using a mathematical model of fura-2 Ca^{2+} imaging in Aplysia sensory neurons. Biophys J 63:1146–1164
132. Nowycky MC, Pinter MJ (1993) Time course of calcium and calcium-bound buffers following calcium influx in a model cell. Biophys J 64:77–91
133. Marengo FD, Monck JR (2000) Development and dissipation of Ca^{2+} gradients in adrenal chromaffin cells. Biophys J 79:1800–1820
134. Sinha SR, Wu LG, Saggau P (1997) Presynaptic calcium dynamics and transmitter release evoked by single action potentials at mammalian central synapses. Biophys J 72:637–651
135. Gabso M, Neher E, Spira ME (1997) Low mobility of the Ca^{2+} buffers in axons of cultured Aplysia neurons. Neuron 18:473–481
136. Coatesworth W, Bolsover S (2008) Calcium signal transmission in chick sensory neurones is diffusion based. Cell Calcium 43:236–249
137. Hernández-Cruz A, Escobar AL, Jiménez N (1997) Ca^{2+}-induced Ca^{2+} release phenomena in mammalian sympathetic neurons are critically dependent on the rate of rise of trigger Ca^{2+}. J Gen Physiol 109:147–167
138. Rusakov DA, Saitow F, Lehre KP, Konishi S (2005) Modulation of presynaptic Ca^{2+} entry by AMPA receptors at individual GABAergic synapses in the cerebellum. J Neurosci 25: 4930–4940
139. Markram H, Roth A, Helmchen F (1998) Competitive calcium binding: implications for dendritic calcium signaling. J Comput Neurosci 5:331–348
140. Schmidt H, Stiefel KM, Racay P, Schwaller B, Eilers J (2003) Mutational analysis of dendritic Ca^{2+} kinetics in rodent Purkinje cells: role of parvalbumin and calbindin D28k. J Physiol 551:13–32
141. Schmidt H, Kunerth S, Wilms C, Strotmann R, Eilers J (2007) Spino-dendritic cross-talk in rodent Purkinje neurons mediated by endogenous Ca^{2+}-binding proteins. J Physiol 581:619–629
142. Schmidt H, Eilers J (2009) Spine neck geometry determines spino-dendritic cross-talk in the presence of mobile endogenous calcium binding proteins. J Comput Neurosci 27:229–243
143. Holthoff K, Tsay D, Yuste R (2002) Calcium dynamics of spines depend on their dendritic location. Neuron 33:425–437

144. Hernjak N, Slepchenko BM, Fernald K, Fink CC, Fortin D, Moraru II, Watras J, Loew LM (2005) Modeling and analysis of calcium signaling events leading to long-term depression in cerebellar Purkinje cells. Biophys J 89:3790–3806
145. Canepari M, Vogt KE (2008) Dendritic spike saturation of endogenous calcium buffer and induction of postsynaptic cerebellar LTP. PLoS One 3:e4011
146. Gold JI, Bear MF (1994) A model of dendritic spine Ca^{2+} concentration exploring possible bases for a sliding synaptic modification threshold. Proc Natl Acad Sci USA 91:3941–3945
147. Schiegg A, Gerstner W, Ritz R, van Hemmen JL (1995) Intracellular Ca^{2+} stores can account for the time course of LTP induction: a model of Ca^{2+} dynamics in dendritic spines. J Neurophysiol 74:1046–1055
148. Zador A, Koch C, Brown TH (1990) Biophysical model of a Hebbian synapse. Proc Natl Acad Sci USA 87:6718–6722
149. Holmes WR, Levy WB (1990) Insights into associative long-term potentiation from computational models of NMDA receptor-mediated calcium influx and intracellular calcium concentration changes. J Neurophysiol 63:1148–1168
150. Volfovsky N, Parnas H, Segal M, Korkotian E (1999) Geometry of dendritic spines affects calcium dynamics in hippocampal neurons: theory and experiments. J Neurophysiol 82:450–462
151. Cornelisse LN, van Elburg RA, Meredith RM, Yuste R, Mansvelder HD (2007) High speed two-photon imaging of calcium dynamics in dendritic spines: consequences for spine calcium kinetics and buffer capacity. PLoS One 2:e1073
152. Doi T, Kuroda S, Michikawa T, Kawato M (2005) Inositol 1,4,5-trisphosphate-dependent Ca^{2+} threshold dynamics detect spike timing in cerebellar Purkinje cells. J Neurosci 25:950–961
153. Achard P, De Schutter E (2008) Calcium, synaptic plasticity and intrinsic homeostasis in Purkinje neuron models. Front Comput Neurosci 2:8
154. De Schutter E, Smolen P (1998) Calcium dynamics in large neuronal models. In: Koch C, Segev I (eds) Methods in neuronal modeling: from ions to networks, 2nd edn. MIT, Cambridge, pp 211–250
155. Albrecht MA, Colegrove SL, Hongpaisan J, Pivovarova NB, Andrews SB, Friel DD (2001) Multiple modes of calcium-induced calcium release in sympathetic neurons I: attenuation of endoplasmic reticulum Ca^{2+} accumulation at low $[Ca^{2+}]_i$ during weak depolarization. J Gen Physiol 118:83–110
156. Anwar H, Hong S, De Schutter E (2010) Controlling Ca^{2+}-activated K^+ channels with models of Ca^{2+} buffering in Purkinje cells. Cerebellum Epub ahead of print
157. Friel DD, Chiel HJ (2008) Calcium dynamics: analyzing the Ca^{2+} regulatory network in intact cells. Trends Neurosci 31:8–19
158. Baimbridge KG, Celio MR, Rogers JH (1992) Calcium-binding proteins in the nervous system. Trends Neurosci 15:303–308
159. Schwaller B (2010) Cytosolic Ca^{2+} buffers. Cold Spring Harb Perspect Biol 2:a004051
160. Faas GC, Schwaller B, Vergara JL, Mody I (2007) Resolving the fast kinetics of cooperative binding: Ca^{2+} buffering by calretinin. PLoS Biol 5:e311
161. Eberhard M, Erne P (1994) Calcium and magnesium binding to rat parvalbumin. Eur J Biochem 222:21–26
162. Schmidt H, Schwaller B, Eilers J (2005) Calbindin D28k targets myo-inositol monophosphatase in spines and dendrites of cerebellar Purkinje neurons. Proc Natl Acad Sci USA 102:5850–5855
163. Schmidt H, Brown EB, Schwaller B, Eilers J (2003) Diffusional mobility of parvalbumin in spiny dendrites of cerebellar Purkinje neurons quantified by fluorescence recovery after photobleaching. Biophys J 84:2599–2608
164. Kosaka T, Kosaka K, Nakayama T, Hunziker W, Heizmann CW (1993) Axons and axon terminals of cerebellar Purkinje cells and basket cells have higher levels of parvalbumin immunoreactivity than somata and dendrites: quantitative analysis by immunogold labeling. Exp Brain Res 93:483–491
165. Schmidt H, Arendt O, Eilers J (2010) Diffusion and extrusion shape standing calcium gradients during ongoing parallel fiber activity in dendrites of Purkinje neurons Cerebellum Epub ahead of print

166. Xu T, Naraghi M, Kang H, Neher E (1997) Kinetic studies of Ca^{2+} binding and Ca^{2+} clearance in the cytosol of adrenal chromaffin cells. Biophys J 73:532–545
167. Maeda H, Ellis-Davies GC, Ito K, Miyashita Y, Kasai H (1999) Supralinear Ca^{2+} signaling by cooperative and mobile Ca^{2+} buffering in Purkinje neurons. Neuron 24:989–1002
168. Hendel T, Mank M, Schnell B, Griesbeck O, Borst A, Reiff D (2008) Fluorescence changes of genetic calcium indicators and OGB-1 correlated with neural activity and calcium in vivo and in vitro. J Neurosci 28:7399–7411
169. Baylor SM, Chandler WK, Marshall MW (1983) Sarcoplasmic reticulum calcium release in frog skeletal muscle fibres estimated from Arsenazo III calcium transients. J Physiol 344:625–666
170. Kovacs L, Rios E, Schneider MF (1983) Measurement and modification of free calcium transients in frog skeletal muscle fibres by a metallochromic indicator dye. J Physiol 343:161–196
171. Melzer W, Rios E, Schneider MF (1987) A general procedure for determining the rate of calcium release from the sarcoplasmic reticulum in skeletal muscle fibers. Biophys J 51:849–863
172. Schuhmeier RP, Melzer W (2004) Voltage-dependent Ca^{2+} fluxes in skeletal myotubes determined using a removal model analysis. J Gen Physiol 123:33–51
173. Sipido KR, Wier WG (1991) Flux of Ca^{2+} across the sarcoplasmic reticulum of guinea-pig cardiac cells during excitation-contraction coupling. J Physiol 435:605–630
174. Hongpaisan J, Pivovarova NB, Colegrove SL, Leapman RD, Friel DD, Andrews SB (2001) Multiple modes of calcium-induced calcium release in sympathetic neurons II: a $[Ca^{2+}]_i$- and location-dependent transition from endoplasmic reticulum Ca^{2+} accumulation to net release Ca^{2+} release. J Gen Physiol 118:101–112
175. Colegrove SL, Albrecht MA, Friel DD (2000) Dissection of mitochondrial Ca^{2+} uptake and release fluxes in situ after depolarization-evoked $[Ca^{2+}]_i$ elevations in sympathetic neurons. J Gen Physiol 115:351–370
176. Colegrove SL, Albrecht MA, Friel DD (2000) Quantitative analysis of mitochondrial Ca^{2+} uptake and release pathways in sympathetic neurons. Reconstruction of the recovery after depolarization-evoked $[Ca^{2+}]_i$ elevations. J Gen Physiol 115:371–388
177. Albrecht MA, Colegrove SL, Friel DD (2002) Differential regulation of ER Ca^{2+} uptake and release rates accounts for multiple modes of Ca^{2+}-induced Ca^{2+} release. J Gen Physiol 119:211–233
178. Higgins ER, Goel P, Puglisi JL, Bers DM, Cannell M, Sneyd J (2007) Modelling calcium microdomains using homogenisation. J Theor Biol 247:623–644
179. Rizzuto R, Pozzan T (2006) Microdomains of intracellular Ca^{2+}: molecular determinants and functional consequences. Physiol Rev 86:369–408
180. Rizzuto R, Marchi S, Bonora M, Aguiari P, Bononi A, De Stefani D, Giorgi C, Leo S, Rimessi A, Siviero R, Zecchini E, Pinton P (2009) Ca^{2+} transfer from the ER to mitochondria: when, how and why. Biochim Biophys Acta 1787:1342–1351
181. Goldberg JH, Tamas G, Aronov D, Yuste R (2003) Calcium microdomains in aspiny dendrites. Neuron 40:807–821
182. Soler-Llavina GJ, Sabatini BL (2006) Synapse-specific plasticity and compartmentalized signaling in cerebellar stellate cells. Nat Neurosci 9:798–806
183. Saftenku EE (2009) Computational study of non-homogeneous distribution of Ca^{2+} handling systems in cerebellar granule cells. J Theor Biol 257:228–244
184. Saftenku EE (2010) Models of calcium dynamics in cerebellar granule cells. Cerebellum Epub ahead of print
185. Fink CC, Slepchenko B, Moraru II, Schaff J, Watras J, Loew LM (1999) Morphological control of inositol-1,4,5-trisphosphate-dependent signals. J Cell Biol 147:929–936
186. Gleeson P, Crook S, Cannon RC, Hines ML, Billings GO, Farinella M, Morse TM, Davison AP, Ray S, Bhalla US, Barnes SR, Dimitrova YD, Silver RA, Neuro ML (2010) A language for describing data driven models of neurons and networks with a high degree of biological data. PLoS Comput Biol 6:e1000815

Chapter 27
α7 Nicotinic ACh Receptors as a Ligand-Gated Source of Ca^{2+} Ions: The Search for a Ca^{2+} Optimum

Victor V. Uteshev

Abstract The spatiotemporal distribution of cytosolic Ca^{2+} ions is a key determinant of neuronal behavior and survival. Distinct sources of Ca^{2+} ions including ligand- and voltage-gated Ca^{2+} channels contribute to intracellular Ca^{2+} homeostasis. Many normal physiological and therapeutic neuronal functions are Ca^{2+}-dependent, however an excess of cytosolic Ca^{2+} or a lack of the appropriate balance between Ca^{2+} entry and clearance may destroy cellular integrity and cause cellular death. Therefore, the existence of optimal spatiotemporal patterns of cytosolic Ca^{2+} elevations and thus, optimal activation of ligand- and voltage-gated Ca^{2+} ion channels are postulated to benefit neuronal function and survival. Alpha7 nicotinic acetylcholine receptors (nAChRs) are highly permeable to Ca^{2+} ions and play an important role in modulation of neurotransmitter release, gene expression and neuroprotection in a variety of neuronal and non-neuronal cells. In this review, the focus is placed on α7 nAChR-mediated currents and Ca^{2+} influx and how this source of Ca^{2+} entry compares to NMDA receptors in supporting cytosolic Ca^{2+} homeostasis, neuronal function and survival.

Keywords α7 nAChR • NMDA • Ca^{2+} • Permeability • Ion channel • Receptor • ACh • Choline • Nicotinic • Positive allosteric modulator • PNU-120596 • Neuroprotection • Cognitive • Cognition • Dementia • Neurotoxicity • Synaptic • Extrasynaptic • Alzheimer • Schizophrenia • Trauma • Auditory • Gating

V.V. Uteshev (✉)
Department of Pharmacology & Neuroscience,
University of North Texas Health Science Center,
3500 Camp Bowie Blvd, Fort Worth, 76107 TX, USA
e-mail: Victor.Uteshev@unthsc.edu

M.S. Islam (ed.), *Calcium Signaling*, Advances in Experimental Medicine and Biology 740, DOI 10.1007/978-94-007-2888-2_27,

Ligand- and Voltage-Gated Sources of Ca^{2+} Ions

Background

Changes in cytosolic Ca^{2+} levels act as a messenger relaying information from the cellular membrane to the cellular cytoplasm and the nucleus. In neurons and other excitable cells, this message encodes the amplitude and duration of activation of voltage- and/or ligand-gated ion channels. The cellular response then includes a sequence of intracellular biochemical reactions that alter the expression and function of genes and proteins. In healthy neurons, the expression of different Ca^{2+} sources and the spatiotemporal patterns of Ca^{2+} entry are well-balanced and an adequate match between Ca^{2+} demand and supply is usually observed. However, when Ca^{2+} sources become dysfunctional due to age, disease, or trauma, persistent imbalance in Ca^{2+} entry and clearance destroys cellular integrity, leading to cellular damage, dysfunction, and excessive proliferation or death depending on the type of cells and the strength of the insult. Neuronal damage or loss may result in severe chronic neurodegenerative conditions including sensorimotor deficits and dementia. Therefore, a tight but subtle control of cytosolic Ca^{2+} levels is required for neuronal health, development and function. Understanding the pharmacology and mechanisms of cytosolic Ca^{2+} messaging is essential for developing successful preventative strategies and treatments for neurodegenerative conditions associated with aging, dementia and brain trauma.

Inadequate vs. Optimal Ca^{2+} Entries and Neuronal Fate

An important common motif in the livelihood of central neurons is the existence of an optimum in the cytosolic Ca^{2+} concentration ($[Ca^{2+}]_i$) and the spatiotemporal patterns of cytosolic Ca^{2+} elevations. This optimum promotes neuronal survival and delivers functional benefits to neurons. The farther $[Ca^{2+}]_i$ is from its optimum, the greater is the likelihood of neuronal damage and death. Accordingly, excessive elevations in $[Ca^{2+}]_i$ mediated by excessive activation of ligand- and/or voltage-gated Ca^{2+} ion channels have been associated with a loss of neuronal function and neuronal death (see, for instance, [1–11]). Moreover, in a number of *in vivo* and *in vitro* experimental models of normal aging and Alzheimer's disease (AD), elevated levels of cytosolic Ca^{2+} have been linked to age- and disease-related dysregulations in the function of voltage-gated Ca^{2+} ion channels (VGCCs) and N-Methyl-D-Aspartate (NMDA) receptor-mediated ion channels [2, 3, 6, 7, 10–17]. Conversely, moderate elevations in $[Ca^{2+}]_i$, for example, via a K^+-induced depolarization or weak persistent activation of highly Ca^{2+}-permeable $\alpha 7$ nicotinic acetylcholine receptors (nAChRs) have been shown to protect neurons from death in a variety of toxicity models [18–28]. In addition, some biologically active compounds (e.g., estrogen,

insulin-related growth factor 1 and positive allosteric modulators of α7 nAChRs) potentiate Ca^{2+} permeable voltage- or ligand-gated ion channels and increase Ca^{2+} influx [29–37] which can be neuroprotective and cognitively beneficial.

Originally, the concept of excitotoxicity linked neuronal injury to excessive elevations in $[Ca^{2+}]_i$ which resulted from activation of a variety of Ca^{2+} sources including ligand- and voltage-gated Ca^{2+} ion channels [38]. As such, the "Ca^{2+} set-point" hypothesis was introduced, proposing four stages of neuronal responsiveness to elevation in $[Ca^{2+}]_i$ elicited by K^+-dependent depolarization or electrical stimulation [1, 22, 39]: (1) a lack of neuroprotection in the near absence of cytosolic Ca^{2+} regardless of neurotrophic support (stage 1); (2) neuronal survival in the presence of normal cytosolic Ca^{2+} (~100 nM) with neurotrophic support (stage 2); (3) neuronal survival in the presence of moderate elevation in cytosolic Ca^{2+} (~200 nM) regardless of neurotrophic support (stage 3) and (4) an excess (>1 μM) of Ca^{2+} and neuronal death (stage 4). Although the Ca^{2+} set-point hypothesis supported the concept of Ca^{2+} optimum for neuronal survival and function, it did not explain the role of specific pathways of Ca^{2+} entry leaving a key question unanswered: can an elevation in $[Ca^{2+}]_i$ be optimal regardless of the pathway of Ca^{2+} entry?

Role of NMDARs

Further studies revealed that elevations in $[Ca^{2+}]_i$ are derivatives of a more elementary chain of events consisting of Ca^{2+} entry and intracellular Ca^{2+} processing. According to this concept, neuronal fate (i.e., survival or death) is predominantly determined by the source of Ca^{2+} entry rather than $[Ca^{2+}]_i$ [40]: i.e., Ca^{2+} ions entering the cell via NMDARs are much more likely to cause damage to the cell than similar amounts of Ca^{2+} ions entering the cell via VGCCs. In fact, VGCC-mediated elevations in $[Ca^{2+}]_i$ are more likely to be neuroprotective than neurotoxic (see above and [1, 20, 22, 24, 39, 41]). However, moderate activation of NMDARs during preconditioning in low concentrations of glutamate (<50 μM) as well as activation of nAChRs by nicotine have also been found to promote neuronal survival (see below and [41–44]). In general, a proper investigation of neuroprotective and neurotoxic effects of individual Ca^{2+} sources requires selective pharmacological tools because multiple Ca^{2+} sources often act in conjunction resulting in a cumulative elevation in $[Ca^{2+}]_i$ and emergent response properties [45–48].

The NMDAR-dependent pathways of cytosolic Ca^{2+} regulation are complex as both excessive activation and blockade of NMDARs promote neuronal death [5, 49–51], while moderate activation of NMDARs is absolutely required for normal neuronal development and function. As a result, a key challenge in development of NMDAR-based therapies is introduced by a possibility that the same agent (e.g., NMDAR antagonist) or process (e.g., NMDAR activation) can be both neuroprotective and neurotoxic depending on the neuronal status and the phase, intensity and

duration of ongoing neuronal damage. Therefore, the therapeutic index (i.e., the ratio of the lethal dose to the therapeutic dose) of many NMDAR agents would be expected to be variable, case-dependent and ≤1 on average.

A pool of functional NMDARs can be subdivided into synaptic and extrasynaptic based on their location relative to the synaptic cleft. Recent studies have started to explore an intriguing possibility that activity of synaptic and extrasynaptic NMDARs defines neuronal fate [50, 51]: activation of synaptic NMDARs leads to neuroprotection, while activation of extrasynaptic NMDARs is neurotoxic. Therefore, the overall intensity of NMDAR activation may not be as defining for the fate of neurons as the fraction of synaptic vs. extrasynaptic NMDAR activation. According to this hypothesis, Ca^{2+} ions entering neurons through extrasynaptic NMDARs are the most harmful. The basis for differences between the effects of synaptic and extrasynaptic NMDARs is not well-understood, but may include at least three factors, as discussed by [50]: (1) differences in the intracellular signaling pathways; (2) differences in the NMDAR subunit composition; and (3) differences in the activation profiles (e.g., synaptic NMDARs are typically activated by high transient concentrations of synaptic glutamate (~1 mM); while extrasynaptic NMDARs are activated by persistent, but relatively low concentrations (≤1 μM) of ambient glutamate). However, the division of NMDARs into synaptic and extrasynaptic may be rather provisional because NMDARs can move laterally between synaptic and extrasynaptic sites [52]. This behavior is not unique to NMDARs and has also been observed in α-amino-3-hydroxy-5-methyl-4-isoxazolepropionic acid receptors (AMPARs) [53] and α3-/α7-containing nAChRs [54].

Moreover, direct measurements of extracellular glutamate levels [55] as well as experimental and computer modeling of glutamatergic synaptic transmission and spillover [56–58] suggest that even after relocation to extrasynaptic sites (i.e., up to several micrometers away from presynaptic release site), NMDARs do not become independent of synaptic stimulation as they can still be activated by synchronous glutamate spillovers originating from multiple active glutamatergic synapses [59, 60]. The effectiveness of glutamate spillover in activation of extrasynaptic NMDARs and cross-talk between adjacent synapses directly results from morphological and release properties of central punctate glutamatergic synapses [56, 61] and kinetic properties of NMDARs: i.e., high potency (EC_{50} ~ 3 μM, [62]) and incomplete desensitization [63, 64]. Consistent with these views, the otherwise low levels of extracellular glutamate in hippocampal slices (e.g., ~25 nM; [65]) can be substantially enhanced in the vicinity of active glutamatergic synapses [55] or during the reversal of neuronal/glial glutamate transporters that may take place under ischemia and other pathological conditions [66, 67]. However, what happens to intracellular pathways linked to an individual receptor as it switches teams (i.e., from synaptic to extrasynaptic) remains unknown (see more discussions on this topic in [50, 68, 69]).

This apparent ambiguity in the role of NMDARs in neuronal death and survival should not derail the ongoing search for a therapeutic optimum in the level of NMDAR activation and Ca^{2+} entry while the fact that, to date, clinical trials have

been mostly unsuccessful in identifying effective NMDAR-based therapies against ischemia and other neurodegenerative conditions invites discoveries of new approaches and nontrivial solutions like never before. One of these promising emergent approaches termed "pathologically activated therapeutics" [70] makes use of low-potency open-channel NMDAR blockers, such as memantine [71]. These compounds may have neuroprotective properties as their inhibitory effects do not preclude the physiologically beneficial low-intensity activation of NMDARs, but substantially reduce the excessive activation of NMDARs which is neurotoxic. However, memantine has been also shown to inhibit α7 nAChRs with a similar or even greater potency (IC_{50} ~ 0.3–5 μM) than NMDARs (IC_{50} ~ 1–10 μM) [72–74]. In some cases, inhibition of α7 nAChRs by memantine may be counterproductive because moderate activation of α7 nAChRs is usually neuroprotective and cognitively beneficial (see below). Despite numerous reports of positive effects of memantine on patients with AD, non-AD dementias and other neurodegenerative disorders [75–81], the effectiveness, consistency and safety of memantine-based therapies have been questioned on multiple occasions [72, 82–85] and neurotoxic effects of therapeutic doses of memantine (~20 mg/kg) have been reported, for example, due to a drug interaction between memantine and common acetylcholine esterase inhibitors, such as donepezil [82, 86]. Accordingly, targeting intracellular sites downstream of NMDAR activation may present an alternative and possibly, more promising therapeutic approach [87].

α7 nAChRs

Background

Neuronal nicotinic AChRs are cation-selective and Ca^{2+} permeable ion channel complexes. Twelve genes encoding for neuronal nAChR subunits have been identified to date [88]. Four of these genes encode for α7, α8, α9, and α10 subunits that may form functional homomeric nAChRs when expressed alone. The family of functional heteromeric nAChRs is more diverse: these functional receptors are required to have two principal α subunits (i.e., α2, α3, α4 or α6) and two or three complementary β subunits (i.e., β2 or β4). In addition, one structural subunit (i.e., α5 or β3) may also be present [89]. Among nAChRs, the α7 nAChR exhibits the highest permeability ratio of Ca^{2+} over Na^{+} ions (P_{Ca}/P_{Na}) [90–97]. The high Ca^{2+} permeability of α7 nAChRs suggests important roles for this receptor in modulation of neurotransmitter release, gene expression, neuroprotection and neurotoxicity [98–101]. The existing evidence indicates that α7 nAChRs maintain a high degree of functional homology, including Ca^{2+} permeability, across species and preparations [102, 103]. Therefore, the properties of α7 nAChRs expressed in heterologous systems are expected to be comparable to native α7 nAChRs expressed in various

brain regions. However, although α7 nAChRs can form functional homomeric nAChRs, there is a growing pool of evidence for the existence of functional heteromeric α7-containing nAChRs resulting from co-expression of α7 and non-α7 subunits (e.g., α5, β2 and β3 subunits). These native α7-containing heteromeric receptor ion channel complexes exhibit pharmacological, kinetic and desensitization properties somewhat different from those of homomeric α7 nAChRs expressed in heterologous systems [104–112].

The early studies of Ca^{2+} permeability of α7 nAChRs used primarily heterologous systems expressing homomeric α7 nAChRs and reported the permeability ratios for Ca^{2+} over Na^{+} ions substantially greater than those for NMDARs: P_{Ca}/P_{Na} (α7R) ~ 15–20 vs. P_{Ca}/P_{Na} (NMDAR) ~ 8–10 [93–95, 113]. However, more recent studies used hippocampal cultured neurons and acutely dissociated hippocampal and hypothalamic neurons to report more modest values: P_{Ca}/P_{Na}(α7R) ~ 6 vs. P_{Ca}/P_{Na} (NMDAR) ~ 8–10 [90, 97]. Moreover, in these experiments the Ca^{2+} permeability of NMDARs was found to be significantly greater than that of α7 nAChRs [97]. The observed discrepancies between the early and more recent studies may have resulted from differences in agonist application techniques, data analysis and estimates of ionic activities and liquid junction potentials. Alternatively, it is possible that native, possibly heteromeric, α7-containing nAChRs exhibit a lower Ca^{2+} permeability than homomeric α7 nAChRs. However, a direct comparison of Ca^{2+} permeabilities of native and heterologous α7 nAChRs using identical experimental techniques and data analysis has not been conducted.

Because of their high permeability to Ca^{2+} ions, NMDARs and α7 nAChRs form excellent examples of ligand-gated Ca^{2+} ion channels. As discussed, moderate activation of these receptors and thus, moderate elevation in $[Ca^{2+}]_i$ have been found to be neuroprotective in a number of *in vitro* and *ex vivo* toxicity models as well as *in vivo* settings [18, 21, 23, 25–27, 41–44, 114–116]. Moreover, both types of receptors appear to employ Ca^{2+}-PI3K-Akt-dependent pathways for mediation of neuroprotective effects [41–43, 49, 101, 117]. However, despite these important similarities, NMDARs and α7 nAChRs belong to different families of ligand-gated receptors [62, 118] and their kinetic and pharmacological properties are quite different. For instance, the mean open time of α7 nAChR-mediated channels (~100–400 μs, [119–121]) is at least tenfold shorter than that of NMDAR channels [63, 122]. In addition, in the continuous presence of agonist, α7 nAChR-mediated currents (but not NMDAR-mediated currents) can be completely inhibited by desensitization and/or agonist-mediated open channel block [123, 124]. The short open time and rapid desensitization act as mechanisms that protect α7 nAChR-expressing cells from excessive and thus, damaging Ca^{2+} influx. The open channel Mg^{2+} block plays an analogous role for NMDAR-mediated ion channels. By contrast, Mg^{2+} ions do not significantly alter the function of α7 nAChRs at negative membrane potentials, although they induce rectification at depolarized membrane potentials [125].

Ca^{2+} Permeability of α7 nAChRs and NMDARs

The sensitivity of α7 nAChR- and NMDAR-mediated whole-cell responses to external Ca^{2+} ions (i.e., $[Ca^{2+}]_o$) have also been found to be different (Fig. 27.1, [97]). The whole-cell conductance of α7 nAChR-mediated responses in tuberomammillary (TM) neurons was significantly greater at low $[Ca^{2+}]_o$ (i.e., 2 mM) than at high $[Ca^{2+}]_o$ (i.e., 20 mM) [97]. This difference was not due to a current rundown because experiments in low $[Ca^{2+}]_o$ that gave larger currents were conducted after experiments in high $[Ca^{2+}]_o$ that gave smaller currents [97]. By contrast, a tenfold increase in $[Ca^{2+}]_o$ from 2 to 20 mM did not significantly reduce the whole-cell conductance of NMDAR-mediated responses near their reversal potential in acutely dissociated hippocampal CA1 neurons [97]. Similar observations have been made in single-channel [126] and whole-cell [90, 127] experiments in cultured hippocampal neurons. However, a 67-fold increase in $[Ca^{2+}]_o$ from 0.3 to 20 mM has been reported to reduce the whole-cell conductance of NMDAR-mediated currents by 32% in cultured spinal cord and hippocampal neurons [128]. These differences in Ca^{2+} sensitivity of α7 nAChR- and NMDAR-mediated ion channels may reflect different affinities with which Ca^{2+} ions block monovalent permeation [129], and/or a potential Ca^{2+}-dependent modulation of α7 nAChR-channel kinetics and/or binding. All of these effects would be expected to make excessive activation of α7 nAChRs somewhat less damaging than equivalent activation of NMDARs. These views are consistent with recent experimental results [41, 43]: in these experiments, preconditioning of retinal ganglion cells in very high concentrations of nicotine (i.e., <500 μM), but not glutamate, was neuroprotective against glutamate toxicity.

In addition to Ca^{2+} permeability, the impact of activation of ligand-gated Ca^{2+} channels on cellular behavior and survival is affected by the channel distribution within the cell and the cell surface [50, 54, 130–132]. As mentioned, synaptic NMDARs promote neuroprotection, while extrasynaptic NMDARs may be neurotoxic [133]. By contrast, functional neuronal α7 nAChRs are predominantly pre- or extrasynaptic with only a handful of known exceptions [134–137] and yet, moderate activation of α7 nAChRs is usually neuroprotective. The reason for this important difference between NMDARs and α7 nAChRs is unknown and it is likely that other receptor properties (e.g., kinetic and desensitization properties) in addition to receptor location and ion channel Ca^{2+} permeability contribute to determining the receptor role in neuronal survival.

Desensitization vs. Open-Channel Block of α7 nAChRs

In the continuous presence of nicotinic agonists, activation of α7 nAChRs is reduced naturally by two independent processes: desensitization and open channel block by agonist molecules. It is important to distinguish between these processes, especially if high concentrations of agonists are used (e.g., >2 mM ACh). At negative membrane voltages, positively charged agonists (e.g., ACh, choline) elicit both desensitization

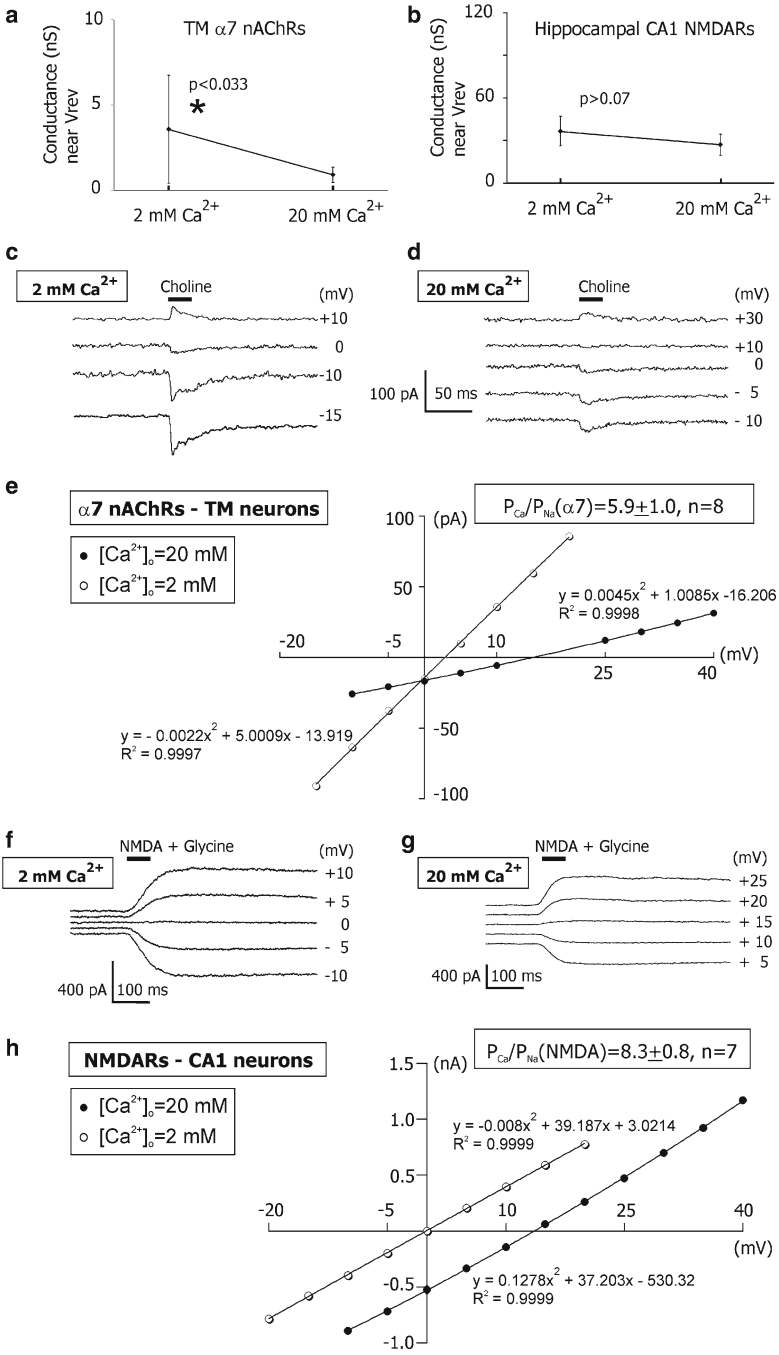
a
TM α7 nAChRs
Conductance (nS) near Vrev
10
5
0
p<0.033
*
2 mM Ca2+
20 mM Ca2+
b
Hippocampal CA1 NMDARs
120
60
0
p>0.07
c
2 mM Ca2+
Choline
(mV)
+10
0
-10
-15
d
20 mM Ca2+
+30
+10
0
- 5
- 10
100 pA
50 ms
e
α7 nAChRs - TM neurons
• [Ca2+]o=20 mM
○ [Ca2+]o=2 mM
PCa/PNa(α7)=5.9±1.0, n=8
100
(pA)
50
-50
-100
y = 0.0045x2 + 1.0085x -16.206
R2 = 0.9998
y = - 0.0022x2 + 5.0009x - 13.919
R2 = 0.9997
-20
-5
10
25
40
(mV)
f
NMDA + Glycine
+ 5
400 pA
100 ms
g
+25
+20
+ 15
+ 10
h
NMDARs - CA1 neurons
PCa/PNa(NMDA)=8.3±0.8, n=7
1.5
(nA)
1.0
0.5
-0.5
-1.0
y = -0.008x2 + 39.187x + 3.0214
R2 = 0.9999
y = 0.1278x2 + 37.203x - 530.32
R2 = 0.9999

and open channel block of α7 nAChR ion channels [123]. The desensitization component of α7 nAChR-mediated responses elicited by ACh or choline can be isolated by conducting electrophysiological experiments at positive membrane voltages [123]. At negative membrane voltages, when high agonists concentrations are used (e.g., >2 mM ACh), open channel block is nearly complete although fully reversible. To minimize open channel block at negative membrane voltages, lower agonist concentrations should be used (e.g., <200 μM ACh) because the block is low-potency. By contrast, if weakly charged agonists are used (e.g., [3-(2,4-dimethoxybenzylidene)-anabaseine, i.e., DMXBA, the code name GTS-21], $pK_a \sim 7.4$, [138]), the separation of desensitization from open channel block is more challenging as open channel block is less dependent on the membrane voltage. In these cases, low agonist concentrations (e.g., <30 μM DMXBA) need to be used to reduce the contribution of open channel block to current decay [123].

Effects of Activation and Inactivation of α7 nAChRs

While in some models of neurotoxicity high concentrations of α7 nAChR agonists caused cellular death [25]; in other models, even very high concentrations of nicotine (e.g., 500 μM) promoted neuronal survival [41]. These discrepancies in results

Fig. 27.1 The whole-cell conductances of α7 nAChR- and NMDAR-mediated responses near the reversal potential. The mean and standard deviation of the slope conductance near V_{rev} built for TM α7 nAChR- (**a**) and hippocampal CA1 pyramidal NMDAR-mediated responses (**b**). A significant $[Ca^{2+}]_o$–dependent decrease in the whole-cell conductance of TM α7 nAChR-, but not CA1 NMDAR-mediated responses was observed [97]. This decrease was not due to a current rundown because it persisted in experiments where high (i.e., 20 mM) $[Ca^{2+}]_o$ was used before low (i.e., 2 mM) $[Ca^{2+}]_o$ [97]. Examples of TM α7 nAChR-mediated currents obtained by applications of choline at various positive and negative membrane voltages in voltage-clamp in 2 mM $[Ca^{2+}]_o$ (**c**) and 20 mM $[Ca^{2+}]_o$ (**d**). The whole-cell conductance of TM α7 nAChR channels in high $[Ca^{2+}]_o$ was always lower than that in low $[Ca^{2+}]_o$, presumably due to a Ca^{2+}-dependent block of monovalent ion permeation. (**e**) The current–voltage relationship for responses illustrated in (**c**) and (**d**). No considerable current rectification was observed owing to Mg^{2+}-free external and internal solutions and the presence of F^- ions in the internal solution. The I-V curves were fitted with second-order polynomial equations. Panels (**c**–**e**) illustrate data obtained from the same acutely dissociated TM neuron. Examples of CA1 NMDAR-mediated currents obtained by applications of NMDA plus glycine at various positive and negative membrane voltages in voltage-clamp in 2 mM $[Ca^{2+}]_o$ (**f**) and 20 mM $[Ca^{2+}]_o$ (**g**). (**h**) The current–voltage relationship for responses illustrated in (**f**) and (**g**). The whole-cell conductance of NMDAR channels in 20 mM $[Ca^{2+}]_o$ was similar to that in 2 mM $[Ca^{2+}]_o$, indicating a lack of significant Ca^{2+}-dependent block of monovalent ion permeation. The I-V curves were fitted with second-order polynomial equations. Panels (**f**–**h**) illustrate data obtained from the same acutely dissociated hippocampal CA1 neuron. Note that although the application pipettes were filled with 40 mM choline or 200 μM NMDA + 20 μM glycine, the effective concentrations of choline or NMDA+glycine near the recorded neurons were unknown and considerably lower than the concentrations of agonists in application pipettes. However, in each given experiment these concentrations were very stable evidenced by stable responses [97] (Reprinted from Uteshev [97] with permission from Blackwell Publishing in the format Journal via Copyright Clearance Center)

may be linked to differences in the agonist concentration and time course of agonist application, as well as inactivation, desensitization and other kinetic properties of α7 nAChRs, e.g., open channel block by nicotinic agonists [123, 124, 139, 140]. Notably, low concentrations of nicotinic agonists such as those observed in the cerebrospinal fluid (CSF) *in vivo* (e.g., <1 μM nicotine or <100 μM choline) are more likely to cause desensitization than activation of α7 nAChRs [124, 140]. Accordingly, it has been hypothesized that it is desensitization or inhibition and not activation of α7 nAChRs that may trigger intracellular events responsible for neuroprotection and cognitive benefits [141–143]. This hypothesis, however, cannot explain a number of recent experimental findings. For instance, systemic administration of PNU-120596, a nicotinic agent that considerably reduces α7 nAChR desensitization (see below), produced positive behavioral effects restoring auditory gating deficit in a mouse model of schizophrenia [32]. Moreover, a direct testing of this hypothesis using structurally similar high-efficacy (i.e., full) and low-efficacy (i.e., partial) α7 nAChR agonists clearly demonstrated that activation of α7 nAChRs is essential for cognitive enhancement in a rat model of inhibitory avoidance [144]. Similarly, the eye-blink conditioning response is improved by α7 nAChR agonists, but impaired by antagonists [145–147] and in α7 knock-out animals [148]. Finally, cell death induced by excessive, but not moderate activity of α7 nAChRs in the NGF/serum-withdrawal toxicity model in pheochromocytoma-12 (PC-12) cells expressing functional α7 nAChRs supports the need for activation rather than desensitization of α7 nAChRs for survival of PC-12 cells [25].

By contrast, the role of α7 nAChRs in the pathophysiology of AD is less defined, primarily because of the limited understanding of how α7 nAChRs interact with $A\beta_{1\text{-}42}$. For example, both activation and blockade of α7 nAChRs inhibits $A\beta_{1\text{-}42}$-induced phosphorylation of tau proteins in PC-12 cells [143]. One hypothesis is that although activation of α7 nAChRs is neuroprotective and cognitively beneficial in some experimental models [23, 149–153], in mouse models of late stages of AD, which correlate with an excessive accumulation of $A\beta_{1\text{-}42}$, the role of α7 nAChRs reverses. The mechanism of this role reversal may include continuing high-affinity binding of $A\beta_{1\text{-}42}$ to α7 nAChRs and formation of α7-$A\beta_{1\text{-}42}$ complexes which inhibit and even reverse the physiological function of α7 nAChRs and thus, the neuroprotective binding of nicotinic agonists to α7 nAChRs becomes impaired [150, 154–161]. This hypothesis received additional support from a number of recent studies that demonstrated that blocking or eliminating α7 nAChRs could alleviate some symptoms of AD. Specifically, (1) deletion of the α7 nAChR gene ameliorates certain behavioral deficits in a transgenic mouse model of AD [162]; (2) intracellular accumulation of $A\beta_{1\text{–}42}$ that occurs predominantly in α7 nAChR-expressing neurons is blocked by α-bungarotoxin, a selective α7 nAChRs antagonist and by phenylarsine, an inhibitor of endocytosis [163]; and (3) α7 nAChRs mediate $A\beta_{1\text{-}42}$-induced phosphorylation of tau proteins [154, 155]. These experiments supported the idea of high-affinity binding of $A\beta_{1\text{–}42}$ to α7 nAChRs on neuronal cell surfaces [164], subsequent endocytosis of the resulting α7-$A\beta_{1\text{-}42}$ complex and its accumulation within the lysosomal compartment provoking intracellular toxicity [163, 165].

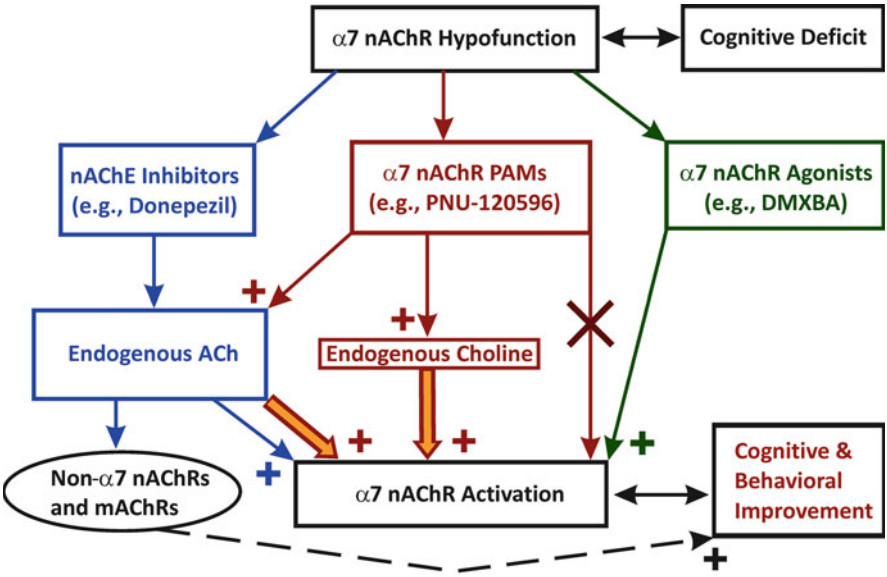

Fig. 27.2 Therapeutic approaches aimed at rescuing the brain α7 nAChR activation. The left most pathway: ACh esterase inhibitors (e.g., donepezil) increase the CSF level of ACh and promote activation of both nAChRs and mAChRs. Despite cognitive benefits (*dashed line*), the lack of selectivity may cause considerable side effects (e.g., autonomic). The right most pathway: α7 nAChR agonists. A moderate activation of α7 nAChRs by selective agonists (e.g., DMXBA) protects neurons, benefits cognition and appears to be clinically safe. The middle pathway: positive allosteric modulators (PAMs) of α7 nAChRs. Choline is a low-potency endogenous selective agonist of α7 nAChRs, but its potency can be considerably increased by Type-II α7-PAMs, such as PNU-120596. α7-PAMs do not activate α7 nAChRs in the absence of nicotinic agonists. Instead, α7-PAMs lower the energy barrier, allowing lower concentrations of nicotinic agonists to activate the receptor. In the presence of Type-II α7-PAMs, endogenous choline may become effective in producing moderate persistent activation of native α7 nAChRs. This type of activation of α7 nAChRs may promote neuroprotection and benefit cognition

α7 nAChRs as a Therapeutic Tool

There is a substantial body of supportive evidence linking age-, disease- and trauma-related alterations in the expression and function of α7 nAChRs to neurodegenerative, sensorimotor and psychiatric disorders associated with cognitive decline and attention deficits [101, 166–180]. By contrast, activation of α7 nAChRs by nicotine and selective α7 nAChR agents has been shown to produce neuroprotection *in vivo* [26, 150, 181], *ex vivo* and *in vitro* [18, 21, 23, 25–27, 182–189] and enhance cognitive performance in patients and animal models of neurodegenerative disorders including AD, schizophrenia, brain trauma and aging [32, 101, 148, 181, 183, 189–209].

Deficits in hippocampal α7 nAChR activation are a key accompanying factor in certain cognitive disorders and enhancing this activation by nicotinic agonists has been shown to produce neuroprotection and cognitive benefits. Currently available therapeutic approaches aimed at rescuing the brain α7 nAChR activation include (Fig. 27.2): (1) ACh esterase inhibitors (AChE; e.g., donepezil) – the left most

pathway; (2) α7 nAChR agonists – the right most pathway; and (3) positive allosteric modulators (PAMs) of α7 nAChRs – the middle pathway. The rationale for therapeutic use of α7 nAChR agonists and modulators arrives from observations that in neurological disorders such as dementia and schizophrenia as well as after brain trauma, functional α7 nAChRs expressed in central neurons do not vanish but their number may decline in a region-specific manner [167, 168, 171, 173, 177, 178, 180, 210]. Therefore, a moderately enhanced activation of α7 nAChRs can be achieved by pharmacological tools and this enhancement may benefit patients with neurodegeneration and cognitive decline (see Sects. 3.1, 3.2, 3.3, 3.4, 3.5).

Positive cognitive effects of inhibitors of AChE result from inhibition of the hydrolysis of ACh and thus, enhanced activation of both muscarinic AChRs (i.e., mAChRs) and nAChRs, including α7 subtype (Fig. 27.2, the left most pathway). Similar to α7 nAChRs, activation of mAChRs and non-α7 nAChRs has been reported to be cognitively beneficial (horizontal dashed path, Fig. 27.2) [211–217]. However, the lack of specificity may cause autonomic adverse effects. For example, donepezil and other AChE inhibitors have been reported to cause centrally-mediated nausea, vomiting and diarrhea [218, 219].

As discussed earlier, a moderate activation of α7 nAChRs by selective agonists (e.g., DMXBA, the right most pathway, Fig. 27.2) protects neurons, benefits cognition and appears to be clinically safe. For example, no major central side effects have been linked to oral administration of large doses of DMXBA (e.g., <450 mg/day, [138, 192]). In hippocampal slices, activation of α7 nAChRs by therapeutic nicotinic agonists, such as DMXBA, can be potentiated by PAMs [220]. PAMs would also be expected to enhance activation of α7 nAChRs by physiological levels of endogenous nicotinic agonists (i.e., ACh and choline) [34, 35] released naturally as needed.

Effects of PAMs on α7 nAChR Activation and Ca^{2+} Influx

PAM Hypothesis

Choline is an endogenous selective agonist of α7 nAChRs [221, 222]. The cerebrospinal fluid (CSF) contains choline at concentrations much lower (~5–10 μM, [169, 223–227]) than its EC_{50} (~0.5–1.5 mM; [222, 228]). Moreover, choline exhibits a much greater potency for desensitization (IC_{50} ~ 40 μM, [124]) than activation of α7 nAChRs. Therefore, the endogenous concentration of choline in the CSF appears to be too low to activate α7 nAChRs [34, 35, 124] and in the past, endogenous choline has not been seriously considered as a therapeutic candidate [186]. However, the ambient levels of choline can be elevated 3–4-fold under conditions associated with ischemia, stroke, and substantial plasma membrane damage [223, 224, 226, 227, 229]. Cell death also creates a large source of choline causing a breakdown of phosphatidylcholine, the principle plasma membrane phospholipid, into choline and diacylglycerol. Given the low ambient concentrations of choline

in the CSF under physiological conditions [169, 225], it is unlikely that in the absence of cholinergic synaptic inputs or exogenous nicotinic agents, native α7 nAChRs are persistently activated by endogenous choline [124]. However, the effects of endogenous choline may be notably different in the presence of Type-II α7-PAMs, such as PNU-120596, which significantly enhances the responsiveness of α7 nAChRs to nicotinic agents (see Sects. 3.2, 3.3, 3.4). PNU-120596 is a positive allosteric modulator of α7 nAChRs that reduces desensitization of α7 nAChRs and thus, increases the potency of nicotinic agonists enhancing the responsiveness of functional α7 nAChRs [32, 34, 220, 230, 231] and producing behavioral improvements in animal models [32]. PNU-120596 has been shown to increase the mean open time of α7 nAChR channels without producing significant changes in ion channel selectivity, single channel conductance and Ca^{2+} permeability [32]. PNU-120596 does not activate α7 nAChRs in the absence of nicotinic agonists. Instead, it lowers the energy barrier, allowing lower concentrations of nicotinic agonists to activate the receptor [232]. Intravenous administration of 1 mg/kg PNU-120596 elevates the concentration of PNU-120596 in the brains of rats to ~1.5 μM [32]. This value falls near the EC_{50} for potentiating effects of PNU-120596 (EC_{50} ~ 1.5 μM) [233, 234]. Concentrations slightly lower than the EC_{50} (i.e., 1 μM PNU-120596) have been shown to enhance the effects of sub-threshold concentrations of choline allowing physiological levels of choline to become effective in activation of native α7 nAChRs in the absence of exogenous nicotinic agents [34, 35]. Therefore, in the presence of PNU-120596, endogenous choline may become effective in producing moderate persistent activation of α7 nAChRs and the corresponding elevation in the Ca^{2+} influx and neuronal excitability (see Sects. 3.3 and 3.4) supporting neuroprotection and cognition (see Sect. 2.5).

There are two types of PAMs [235]: Type I – these compounds enhance the amplitude of α7 nAChR-mediated currents without affecting the current duration; and Type II – these compounds dramatically reduce desensitization and thus, prolong the duration of activation of α7 nAChRs in the constant presence of agonists (Fig. 27.3). The Type-II PAMs (e.g., PNU-120596) are most interesting because these compounds not only reduce desensitization of α7 nAChRs but also allow nicotinic agonists to activate already desensitized α7 nAChRs [32]. Therefore, in the presence of Type-II α7-PAMs, desensitization does not contribute to α7 nAChR activation deficits and previously desensitized α7 nAChRs can be successfully recruited for activation. Recent studies have also demonstrated that PNU-120596 is able to increase the activation potency of choline, allowing low sub-threshold (for activation) physiological concentrations of choline (~10 μM) to become effective in activation of α7 nAChRs [34, 35]. This finding suggests an intriguing possibility of using endogenous choline (in the presence of Type-II α7-PAMs) as a therapeutic agent for enhancing activation of α7 nAChRs and thus, Ca^{2+} influx in neuronal systems characterized by cholinergic deficiency.

A reduced version of this hypothesis has been tested in *ex vivo* electrophysiological experiments using hypothalamic and hippocampal brain slices [34, 35]. Under this scenario, endogenous levels of choline were modeled by the addition of physiological concentrations of choline (5–10 μM) to artificial cerebrospinal solution

(ACSF) and whole-cell voltage- and current-clamp recordings were conducted in the presence and absence of 1–5 μM PNU-120596 to determine the effects of enhanced activation of native α7 nAChRs by choline on the electrical activity of hypothalamic and hippocampal neurons in brain slices (Figs. 27.4 and 27.5).

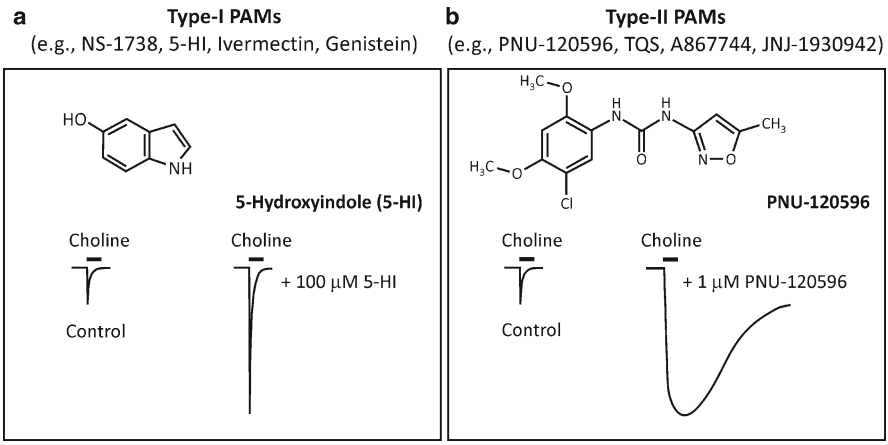

Fig. 27.3 Examples and illustrative effects of Type-I and Type-II α7-PAMs. (**a**) NS-1738, 5-HI, Invermectin and Genistein represent the family of Type-I α7-PAMs. Schematic current traces illustrate the effects of Type-I α7-PAMs on α7 nAChRs: Type-I α7-PAMs increase the peak of α7 nAChR-mediated responses but do not alter the rate of desensitization of α7 nAChRs. (**b**) PNU-120596, TQS, A867744, JNJ-1930942 represent the family of Type-II α7-PAMs. Schematic current traces illustrate the effects of Type-II α7-PAMs on α7 nAChRs: Type-II α7-PAMs increase the peak of α7 nAChR-mediated responses and considerably reduce the desensitization of α7 nAChRs

Fig. 27.4 Step-like current and voltage deviations in the presence of 10 μM choline and 1 μM PNU-120596 in ACSF. (**a**–**c**) Current deviations were completely and reversibly blocked by 20 nM MLA, confirming the involvement α7 nAChRs. All current traces in (**a**–**c**) were obtained from the same TM neuron. (**d, e**) Step-like responses were observed in both voltage- (**d**) and current-clamp (**e**) recordings. Traces in (**d**) and (**e**) were obtained from the same TM neuron 1 min apart. In these experiments, the frequency of step-like current events appeared to be sensitive and rapidly responsive to changes in the ACSF concentrations of choline and PNU-120596 [34, 35]. Activation of α7 nAChRs in current-clamp elicited transient repetitive step-like depolarizations: ~4 mV for individual events and ~25 mV for simultaneous multiple events (**e**). The bottom trace in (**d**) and the top trace in (**e**) share the same time scale shown between these traces. The vertical scale bar indicates either 20 pA (for traces in **d**) or 20 mV (for traces in **e**). In experiments shown in (**d, e**), 0.3 μM TTX was continuously present in ACSF and the internal pipette solution contained $CsMeSO_3$. In voltage-clamp experiments, the membrane voltage was held at −60 mV. (**f**) To visualize individual step-like depolarizations, a small continuous hyperpolarizing current (−5 pA) was injected into the recorded neuron resulting in cessation of spontaneous firing. Under these silent conditions, transient step-like depolarizations triggered short trains of action potentials (*open arrows*). However, occasionally, depolarizations did not trigger action potentials or triggered only a single action potential per depolarization (*filled arrows*). Step-like voltage and current deviations were resistant to 20 μM gabazine, 15 μM DNQX, 50 μM AP-5, 40 μM picrotoxin, and 0.3 μM TTX applied to ACSF (Reprinted from Gusev and Uteshev [34] with permission from ASPET)

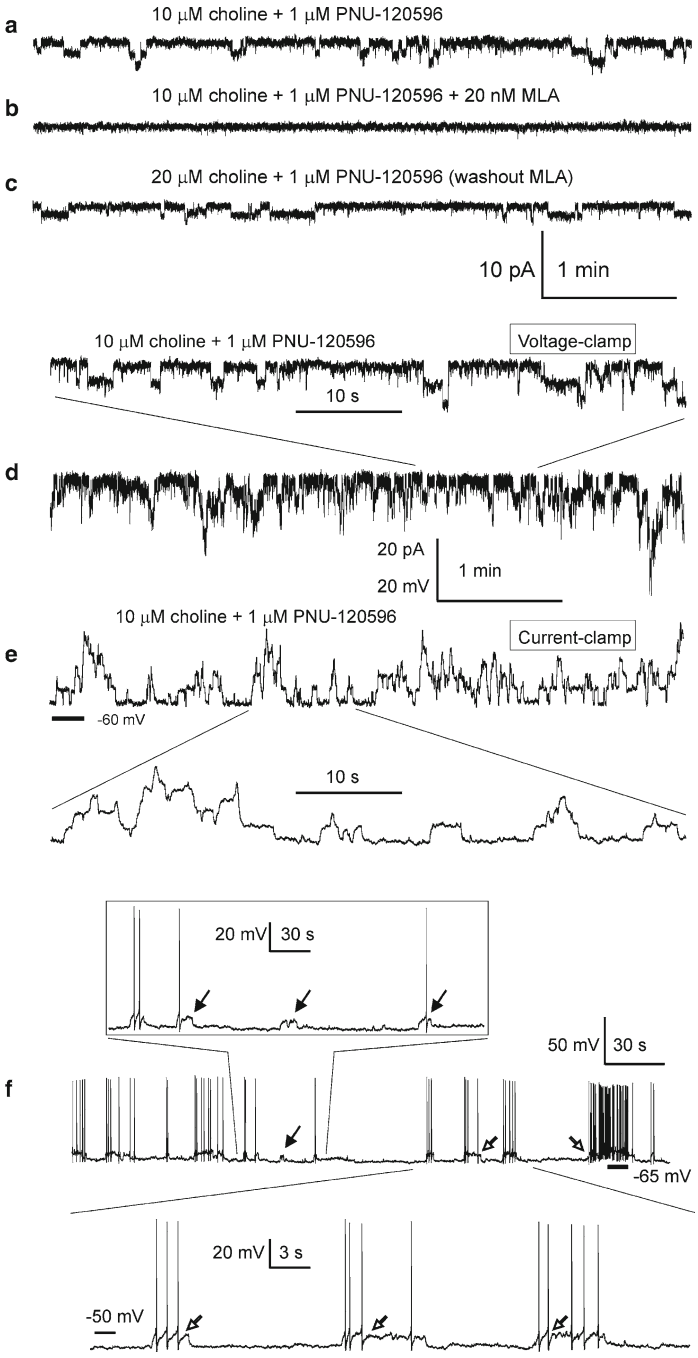
a
10 μM choline + 1 μM PNU-120596
b
10 μM choline + 1 μM PNU-120596 + 20 nM MLA
c
20 μM choline + 1 μM PNU-120596 (washout MLA)
10 pA
1 min
10 μM choline + 1 μM PNU-120596
Voltage-clamp
10 s
d
20 pA
20 mV
1 min
10 μM choline + 1 μM PNU-120596
Current-clamp
e
-60 mV
10 s
20 mV
30 s
50 mV
30 s
f
-65 mV
20 mV
3 s
-50 mV

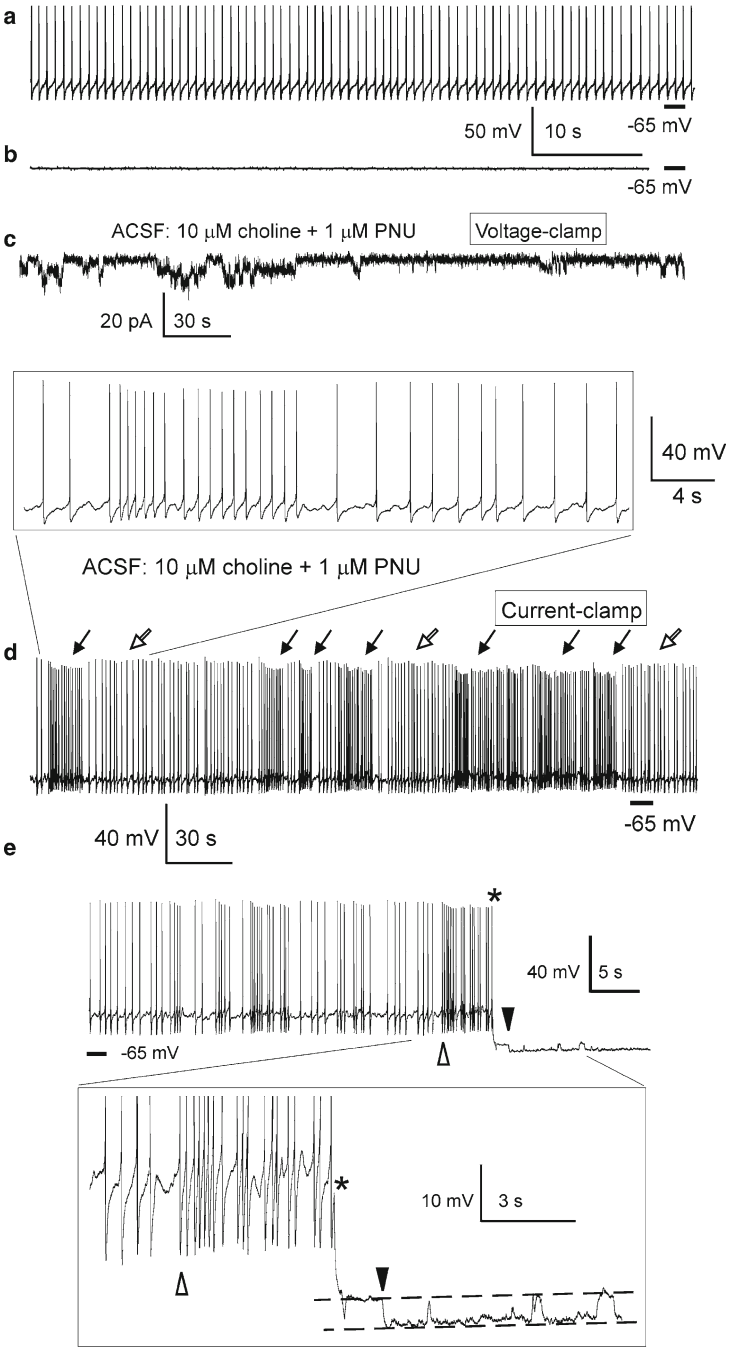
a
50 mV
10 s
-65 mV
b
-65 mV
c
ACSF: 10 μM choline + 1 μM PNU
Voltage-clamp
20 pA
30 s
40 mV
4 s
ACSF: 10 μM choline + 1 μM PNU
Current-clamp
d
-65 mV
e
40 mV
30 s
40 mV
5 s
-65 mV
10 mV
3 s

Synergistic Action of Physiological Choline and PNU-120596

Intriguingly, current and voltage deviations recorded in voltage- and current-clamp, respectively, resulting from a synergistic action of 10 μM choline plus 1–2 μM PNU-120596 were step-like and thus, reminiscent of and postulated to be single α7 nAChR ion channel openings detectable in whole-cell patch-clamp configuration (Fig. 27.4a–e). These experiments revealed that in the presence of PNU-120596 and 5–10 μM choline, even very low densities of α7 nAChRs such as the expression found in hippocampal CA1 pyramidal neurons (only ~5% of that found in hippocampal CA1 interneurons [35]) generate persistent step-like currents which cause transient step-like depolarizations and occasionally, trigger bursts of action potentials. This persistent current would be expected to generate a persistent Ca^{2+} influx (see Sects. 3.4 and 3.5). A similar activity was detected under slightly hyperpolarized conditions in hypothalamic TM neurons (Fig. 27.4f). Moreover, activation of TM α7 nAChRs by 10 μM choline plus 1 μM PNU-120596 enhances spontaneous firing of TM neurons (Fig. 27.5a–d). In current-clamp, when a hyperpolarizing current (~ −40 pA) was injected in the recorded TM neuron (the injection time is marked by * (Fig. 27.5e)) during a prolonged interval of increased frequency (the interval between open and filled triangles), it resulted in cessation of spontaneous firing, allowing detection of the final portion of an underlying step-like depolarization. Therefore, a prolonged step-like depolarization was observed as an increase in

Fig. 27.5 Activation of TM α7 nAChRs by 10 μM choline plus 1 μM PNU-120596 enhances spontaneous firing of TM neurons in current-clamp. The spontaneous firing of TM neurons was native as current injections were not applied (i.e., 0 pA). Horizontal bars indicate −65 mV. In current-clamp, in the absence of PNU-120596 and choline, TM neurons exhibited regular patterns of spontaneous firing (**a**). In these control experiments, when the membrane voltage was hyperpolarized to −65 mV by injections of a small current, step-like depolarizations were not observed (**b**). Recordings in (**a**) and (**b**) were obtained from the same TM neuron 1 min apart. After the sustained repetitive activation of TM nAChRs was observed in voltage-clamp upon administration of 10 μM choline plus 1 μM PNU-120596 (**c**), current-clamp recordings were conducted using the same TM neuron (**d**). In current clamp, activation of TM α7 nAChRs resulted in transient repetitive increases in the frequency of spontaneous firing of TM neurons (**d**, *filled arrows*). Traces shown in (**c**) and (**d**) were obtained from the same TM neuron 1 min apart. The framed insert in (**d**) illustrates at a higher time resolution a portion of recording containing one transient excitation. (**e**) The effects of individual step-like depolarizations in current clamp. When a hyperpolarizing current (~ −40 pA) was injected in the recorded TM neuron (the injection time is marked by *) during a prolonged interval of increased frequency (the interval between *open* and *filled triangles*), it resulted in cessation of spontaneous firing, allowing detection of the final portion of an underlying step-like depolarization. Therefore, a prolonged depolarization was observed as both an increase in spontaneous firing in the beginning of depolarization (*open triangle*) and a depolarizing step at the end of depolarization (*filled triangle*). Subsequent step-like depolarizations are also seen between the two dashed lines in insert. The insert illustrates this transition process at a higher resolution. In these experiments, ACSF contained 20 μM, gabazine, 15 μM DNQX, 50 μM AP-5 and 40 μM picrotoxin. The internal solution was K-gluconate-based (Reprinted from Gusev and Uteshev [34]. With permission from ASPET)

spontaneous firing in the beginning of depolarization (Fig. 27.5e, open triangle) and a depolarizing step at the end of depolarization (Fig. 27.5e, filled triangle).

In these experiments, the frequency of step-like current events appeared to be sensitive and rapidly responsive to changes in the ACSF concentrations of choline and PNU-120596 [34, 35]. Therefore, the synergistic action of endogenous choline and Type-II α7-PAMs may cause a sustained activation of α7 nAChRs and the corresponding persistent Ca^{2+} influx (see Sects. 3.4 and 3.5). These observations suggest that the net depolarization, excitation and Ca^{2+} influx could be modulated and optimized by tuning the administration doses of dietary choline [189] and Type-II α7-PAMs [34, 35].

Detection of Activity of Individual α7 nAChRs in Whole-Cell

It is this capability of as few as only one individual functional α7 nAChR to depolarize and excite the entire neuron that makes it possible for a low density expression of functional α7 nAChRs to be effective in enhancing the excitability of hippocampal CA1 pyramidal neurons in the presence of PNU-120596 [35]. Therefore, high levels of expression of α7 nAChRs and synchronization of their activity may not be required for significant depolarizing and excitatory effects of physiological concentrations of choline in the presence of PNU-120596. The excitability of hippocampal CA1 pyramidal neurons positively correlate with cognitive performance and has been shown to decline with age likely due to an age-dependent enhancement of inhibitory effects of the Ca^{2+}-dependent potassium conductance [236, 237]. Therefore, therapeutic approaches that provide neuroprotection and restore excitability of hippocampal CA1 pyramidal neurons may benefit patients with various forms of dementia and brain trauma.

Detecting activity of individual α7 nAChR ion channels in whole-cell patch-clamp experiments appears to be possible if the probability of ion channel openings is sufficiently low and the channels remain open for a prolonged period of time during which the ionic gradient across the membrane and thus, the ionic current, remain relatively constant. These requirements appear to be fulfilled for α7 nAChRs activated by physiological concentrations of choline in the presence of 1–5 μM PNU-120596 in hippocampal CA1 pyramidal neurons [35], hippocampal CA1 interneurons (Kalappa and Uteshev, unpublished observations) and hypothalamic TM α7 nAChRs [34].

In current-clamp patch-clamp experiments using hippocampal CA1 pyramidal neurons that express a very low density of functional α7 nAChRs [35], individual step-like voltage deviations triggered action potentials in 7 out of 13 cells tested (Fig. 27.4b, c). When these deviations failed to cause action potentials, they generated small step-like depolarizations whose amplitudes (~3–5 mV) could be predicted from the neuronal input resistance (~500 MΩ), the amplitude of step-like currents (~8 pA) and the Ohm's law (500 MΩ × 8 pA ~4 mV). These estimates support the hypothesis that the observed single channel openings were most likely

generated by α7 nAChRs expressed in both proximal and distal regions of the neuronal membrane and not generated only by α7 nAChRs located in the immediate vicinity of the recording patch electrode. An additional support to this hypothesis comes from the observation that in current-clamp experiments with hippocampal CA1 pyramidal neurons, recorded action potentials were triggered by α7 nAChR-mediated step-like depolarizations, while action potentials in between step-like depolarizations were not detected [35]. Therefore, it is unlikely that step-like depolarizations generated by distal α7 nAChRs (e.g., located far away from the recording pipette) have been routinely undetected (due to, for example, electrotonic filtering) because action potentials generated by distal α7 nAChRs would have occurred randomly including in between detected step-like depolarizations and this has not been observed.

These findings support the hypothesis that in the presence of PNU-120596, whole-cell patch-clamp recordings are able to detect α7 nAChR-mediated single ion channel openings from the entire cell surface. This conclusion justifies use of this approach for estimation of the total whole-cell influx of Ca^{2+} ions (see Sect. 3.4).

Current Net Charge and Ca^{2+} Influx

The mean net charge per min generated by hippocampal CA1 pyramidal α7 nAChR ion channels in response to 10 μM choline plus 2 μM PNU-120596 was estimated to be ~9.3 pC/min = 0.16 pA [35]. This value is nearly tenfold smaller than the mean net charge of TM α7 nAChR-mediated responses elicited by 10 μM choline plus 1 μM PNU-120596 which was estimated to be ~84 pC/min = 1.4 pA [34]. Therefore, given the 10% fractional Ca^{2+} current, Ca^{2+} ions would be expected to enter hippocampal and TM neurons at a rate of ~0.93 pC/min and ~8.4 pC/min, respectively, which translates into a sustained Ca^{2+} current ~0.016 pA and ~0.14 pA, respectively. These Ca^{2+} currents were elicited by physiological concentrations of choline and concentrations of PNU-120596 that restored the auditory gating deficit in mice [32]. Therefore, it is reasonable to expect that in *in vivo* settings, similar rates of Ca^{2+} entry in neurons expressing very low (such as hippocampal CA1 pyramidal neurons) and very high (such as hypothalamic TM neurons) densities of functional α7 nAChRs would contribute to behavioral improvements. However, a prolonged exposure of neurons to nicotinic agonists in the presence of Type-II α7-PAMs may be cytotoxic because of excessive accumulation of Ca^{2+} in the cytosol and possible activation of Ca^{2+}-dependent apoptotic pathways (see Sects. 1.1 and 1.2).

The mean number of α7 nAChR ion channels opened in hippocampal CA1 pyramidal and hypothalamic TM neurons at any given time were estimated to be $N_{pyr}P_{open} \sim 0.029$ (i.e., 0.16 pA/5.5 pA) and $N_{TM}P_{open} \sim 0.27$ (i.e., 1.4 pA/5.1 pA), respectively, where N_{pyr} and N_{TM} are the total number of detectable functional α7 nAChRs in a pyramidal and TM neuron, respectively. Note that in experiments with TM neurons, 10 μM choline plus 1 μM PNU-120596 were used [34], whereas in the

hippocampal study, the concentration of PNU-120596 was increased to 2 μM because of the substantially lower levels of expression of functional α7 nAChRs in hippocampal CA1 pyramidal neurons compared to TM neurons [35].

Direct Measurements of α7 nAChR-Mediated Ca^{2+} Influx in the Presence of PNU-120596

Openings of individual α7 nAChR-mediated ion channels recorded in whole-cell configuration would be expected to produce transient focal entries of Ca^{2+} ions. These near-membrane Ca^{2+} blinks have indeed been observed in fluorescent Ca^{2+} imaging experiments conducted in filopodia of human neuroblastoma SH-SY5Y cells and in chick retinal ganglion cells expressing α7-nAChR [238]. In the presence of PNU-120596, activation of individual and/or clusters of α7 nAChRs by nicotine resulted in transient and very focal elevations of $[Ca^{2+}]_i$ (Fig. 27.6). These Ca^{2+} blinks lasted for a few seconds and were clearly observed in the presence and absence of PNU-120596, but in the presence of PNU-120596, the frequency and the duration of Ca^{2+} blinks were considerably increased [238]. The Ca^{2+} blinks were resistant to hyperpolarization induced by valinomycin (a K^+ ionophore), but vanished upon removal of external Ca^{2+} [238]. Ryanodine (1 μM) failed to inhibit the Ca^{2+} blinks indicating that Ca^{2+} ions do not enter cells from ryanodine-sensitive cytosolic Ca^{2+} stores [238]. Figure 27.6 illustrates that, although the location and amplitudes of the Ca^{2+} blinks were variable in the presence of PNU-120596, spatiotemporally discrete Ca^{2+} blinks could be clearly resolved in the same filopodia during nicotine application. While certain distinct regions (#2 and #4) produced repetitive Ca^{2+} blinks, neighboring regions (#1, #3, and #5) did not display any Ca^{2+} events (Fig. 27.6a, b). The regions of brief Ca^{2+} elevations were localized to a submicron dimension (Fig. 27.6c). These observations further support the novel concept (see Sects. 3.1–3.4) that in the presence of Type-II α7-PAMs, individual functional α7 nAChRs generate distinct current events that may affect the behavior of the entire neuron [34, 35, 238].

Fig. 27.6 The spatiotemporal profile of the unitary Ca^{2+} events ("blinks"). (**a**) Sequential images from a time series showing two Ca^{2+} blinks separated by 1.1 μm in a single filopodia. Top left image shows the regions used for measurements overlaid on the fluorescence image, subsequent F/F0 images were captured every second during application of nicotine + PNU-120596. (**b**) Time-course of the F/F0 in two regions (#2 and #4) that exhibit repetitive Ca^{2+} elevations lasting ~3 s and in contiguous regions (#1, #3, and #5) that did not display considerable Ca^{2+} activity. (**c**) Intensity profile of the F/F0 signal at $t = 1$ s in regions #2 and #4, showing the spatial spread of the Ca^{2+} elevations. The cross-section at >20% of the peak fluorescence averaged 0.67 μm and 0.64 μm for regions #1 and #2, respectively. Cell calcium by CHURCHILL LIVINGSTONE (Reproduced from (Gilbert et al., 2009) [238] with permission of CHURCHILL LIVINGSTONE in the format Journal via Copyright Clearance Center)

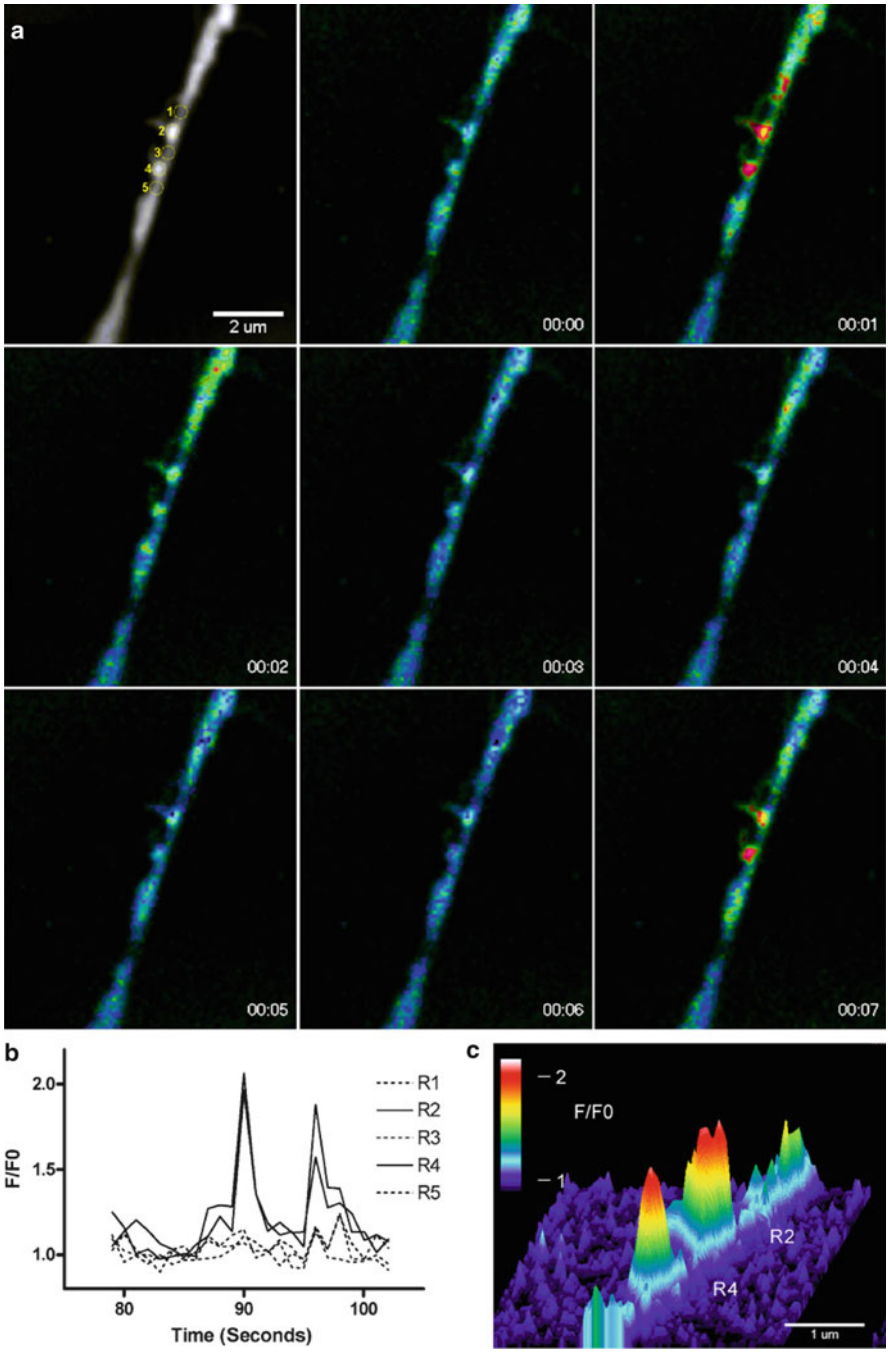
a
1
2
3
4
5
2 um
00:00
00:01
00:02
00:03
00:04
00:05
00:06
00:07
b
F/F0
2.0
1.5
1.0
80
90
100
Time (Seconds)
R1
R2
R3
R4
R5
c
2
F/F0
1
R2
R4
1 um

Non-neuronal NMDARs and α7 nAChRs

In addition to being broadly expressed in the central and peripheral nervous systems of mammals, functional NMDARs and α7 nAChRs are expressed in the immune system [186, 239–250], cancer cells [251–257] and other non-neuronal cells that promote angiogenesis and proliferation of cancer. Activation of α7 nAChRs in non-neuronal systems inhibits inflammation and promotes development of cancer. Although the exact role of NMDARs and α7 nAChRs in immune and cancer cells is not well understood, the high permeability of these receptor ion channels to Ca^{2+} ions suggest important implications for cellular function, survival and proliferation. Therefore, activation, inhibition and modulation of NMDARs and α7 nAChRs in immune and cancer cells can be used for therapeutic purposes to regulate immune defense mechanisms, reduce inflammation, inhibit proliferation or induce apoptosis of cancer cells.

Conclusions and Future Directions

In central neurons, there appear to be multiple ways of achieving optimal levels of Ca^{2+} entrance and $[Ca^{2+}]_i$ to support neuronal function and survival. Among these are inhibition of excessive Ca^{2+} influx through NMDAR channels by low-potency use-dependent blockers, such as memantine, and enhancement of deficient Ca^{2+} influx through α7 nAChR channels by partial agonists of α7 nAChRs, such as DMXBA. Moderate activation of highly Ca^{2+}-permeable NMDAR- and α7 nAChR-mediated ion channels has been shown to support neuronal function and is crucial for neuronal survival. Recently, positive allosteric modulators (PAMs) of α7 nAChRs have been identified as a promising pharmacological tool that can be used to enhance deficient activation of α7 nAChRs associated with certain neurodegenerative disorders. α7-PAMs do not activate α7 nAChRs and thus, α7 nAChRs are activated by endogenous cholinergic agonists released naturally as needed. Activation of functional α7 nAChRs is neuroprotective and thus, beneficial to neurons that express these receptors. Although some neurons that experience age- or trauma-related deficits in excitability (e.g., hippocampal CA1 pyramidal neurons [236, 237, 258]) express only very low densities of functional α7 nAChRs [35], in the presence of Type-II α7-PAMs, these neurons may also become eligible for benefits from expression and activation of functional α7 nAChRs [35].

Recent experimental results indicated that Type-II α7-PAMs may convert endogenous choline and ACh into efficacious therapeutic agents by enhancing their potency for activation of α7 nAChRs. Therefore, in the presence of Type-II PAMs, such as 1 mg/kg PNU-120596, endogenous choline may produce moderate persistent activation of α7 nAChRs and thus, moderately enhance Ca^{2+} influx and neuronal excitability in the absence of exogenous nicotinic agonists – effects that in *in vivo* settings may produce neuroprotection and cognitive benefits. Treatments involving endogenous choline may be safer than those involving synthetic α7

nAChR agonists. Hypothetically, activation of α7 nAChRs by endogenous nicotinic agonists can be moderately enhanced by optimal doses of α7-PAMs and a balanced choline diet [189]. Ideally, α7-PAM-based therapeutic interventions should be able to deliver neuroprotective and cognitive benefits by optimizing activation of α7 nAChRs and α7 nAChR-mediated Ca^{2+} influx in neuronal systems characterized by deficient activation of α7 nAChRs. In addition, an intriguing possibility exists for α7-PAMs to join a cohort of projected drug candidates for enhancement of cognition in healthy individuals [259].

Interestingly, only ~10% of hippocampal α7 proteins are surface-expressed [132] and therefore, the CA1 hippocampal region may contain a large pool of unused α7 proteins. It is intriguing to speculate that under certain physiological conditions, this pool of dormant α7 proteins could be recruited to become functional and cell surface-expressed. It is also reasonable to expect that certain endogenous compounds could enhance α7 nAChR activity in a manner similar to α7-PAMs. Finding these conditions and mechanisms of regulation of α7 nAChR surface expression and function may have a very positive impact on the future of cholinergic therapies aimed at restoring and boosting cognition in dementia patients and healthy individuals.

Acknowledgements I thank Dr. William Kem and Dr. Hong Xing for providing images of chemical structures of PNU-120596 and 5-HI. This work was supported by the NIH grant R01 DK082625 to VU.

References

1. Franklin JL, Johnson EM Jr (1992) Suppression of programmed neuronal death by sustained elevation of cytoplasmic calcium. Trends Neurosci 15:501–508
2. Freir DB, Herron CE (2003) Inhibition of L-type voltage dependent calcium channels causes impairment of long-term potentiation in the hippocampal CA1 region in vivo. Brain Res 967:27–36
3. Fu H, Li W, Lao Y, Luo J, Lee NT, Kan KK, Tsang HW, Tsim KW, Pang Y, Li Z, Chang DC, Li M, Han Y (2006) Bis(7)-tacrine attenuates beta amyloid-induced neuronal apoptosis by regulating L-type calcium channels. J Neurochem 98:1400–1410
4. Harkany T, Abraham I, Timmerman W, Laskay G, Toth B, Sasvari M, Konya C, Sebens JB, Korf J, Nyakas C, Zarandi M, Soos K, Penke B, Luiten PG (2000) Beta-amyloid neurotoxicity is mediated by a glutamate-triggered excitotoxic cascade in rat nucleus basalis. Eur J Neurosci 12:2735–2745
5. Ikonomidou C, Stefovska V, Turski L (2000) Neuronal death enhanced by N-methyl-D-aspartate antagonists. Proc Natl Acad Sci USA 97:12885–12890
6. Lopez JR, Lyckman A, Oddo S, Laferla FM, Querfurth HW, Shtifman A (2008) Increased intraneuronal resting [Ca2+] in adult Alzheimer's disease mice. J Neurochem 105:262–271
7. Mattson MP (1990) Antigenic changes similar to those seen in neurofibrillary tangles are elicited by glutamate and Ca 2+ influx in cultured hippocampal neurons. Neuron 4: 105–117
8. Nimmrich V, Grimm C, Draguhn A, Barghorn S, Lehmann A, Schoemaker H, Hillen H, Gross G, Ebert U, Bruehl C (2008) Amyloid beta oligomers (A beta(1–42) globulomer) suppress spontaneous synaptic activity by inhibition of P/Q-type calcium currents. J Neurosci 28:788–797

9. Papadia S, Hardingham GE (2007) The dichotomy of NMDA receptor signaling. Neuroscientist 13:572–579
10. Pierrot N, Ghisdal P, Caumont AS, Octave JN (2004) Intraneuronal amyloid-beta1-42 production triggered by sustained increase of cytosolic calcium concentration induces neuronal death. J Neurochem 88:1140–1150
11. Scragg JL, Fearon IM, Boyle JP, Ball SG, Varadi G, Peers C (2005) Alzheimer's amyloid peptides mediate hypoxic up-regulation of L-type Ca2+ channels. FASEB J 19:150–152
12. Bezprozvanny I, Mattson MP (2008) Neuronal calcium mishandling and the pathogenesis of Alzheimer's disease. Trends Neurosci 31:454–463
13. Davare MA, Hell JW (2003) Increased phosphorylation of the neuronal L-type Ca(2+) channel Ca(v)1.2 during aging. Proc Natl Acad Sci USA 100:16018–16023
14. Thibault O, Hadley R, Landfield PW (2001) Elevated postsynaptic [Ca2+]i and L-type calcium channel activity in aged hippocampal neurons: relationship to impaired synaptic plasticity. J Neurosci 21:9744–9756
15. Thibault O, Landfield PW (1996) Increase in single L-type calcium channels in hippocampal neurons during aging. Science 272:1017–1020
16. Ueda K, Shinohara S, Yagami T, Asakura K, Kawasaki K (1997) Amyloid beta protein potentiates Ca2+ influx through L-type voltage-sensitive Ca2+ channels: a possible involvement of free radicals. J Neurochem 68:265–271
17. Weiss JH, Pike CJ, Cotman CW (1994) Ca2+ channel blockers attenuate beta-amyloid peptide toxicity to cortical neurons in culture. J Neurochem 62:372–375
18. Akaike A, Tamura Y, Yokota T, Shimohama S, Kimura J (1994) Nicotine-induced protection of cultured cortical neurons against N-methyl-D-aspartate receptor-mediated glutamate cytotoxicity. Brain Res 644:181–187
19. Bok J, Wang Q, Huang J, Green SH (2007) CaMKII and CaMKIV mediate distinct prosurvival signaling pathways in response to depolarization in neurons. Mol Cell Neurosci 36:13–26
20. Collins F, Schmidt MF, Guthrie PB, Kater SB (1991) Sustained increase in intracellular calcium promotes neuronal survival. J Neurosci 11:2582–2587
21. Egea J, Rosa AO, Sobrado M, Gandia L, Lopez MG, Garcia AG (2007) Neuroprotection afforded by nicotine against oxygen and glucose deprivation in hippocampal slices is lost in alpha7 nicotinic receptor knockout mice. Neuroscience 145:866–872
22. Franklin JL, Johnson EM (1998) Control of neuronal size homeostasis by trophic factor-mediated coupling of protein degradation to protein synthesis. J Cell Biol 142:1313–1324
23. Kihara T, Shimohama S, Sawada H, Kimura J, Kume T, Kochiyama H, Maeda T, Akaike A (1997) Nicotinic receptor stimulation protects neurons against beta-amyloid toxicity. Ann Neurol 42:159–163
24. Koike T, Martin DP, Johnson EM Jr (1989) Role of Ca2+ channels in the ability of membrane depolarization to prevent neuronal death induced by trophic-factor deprivation: evidence that levels of internal Ca2+ determine nerve growth factor dependence of sympathetic ganglion cells. Proc Natl Acad Sci USA 86:6421–6425
25. Li Y, Papke RL, He YJ, Millard WJ, Meyer EM (1999) Characterization of the neuroprotective and toxic effects of alpha7 nicotinic receptor activation in PC12 cells. Brain Res 830:218–225
26. Shimohama S, Greenwald DL, Shafron DH, Akaike A, Maeda T, Kaneko S, Kimura J, Simpkins CE, Day AL, Meyer EM (1998) Nicotinic à7 receptors protect against glutamate neurotoxicity and neuronal ischemic damage. Brain Res 779:359–363
27. Shimohama S, Kihara T (2001) Nicotinic receptor-mediated protection against beta-amyloid neurotoxicity. Biol Psychiatry 49:233–239
28. Vaillant AR, Mazzoni I, Tudan C, Boudreau M, Kaplan DR, Miller FD (1999) Depolarization and neurotrophins converge on the phosphatidylinositol 3-kinase-Akt pathway to synergistically regulate neuronal survival. J Cell Biol 146:955–966
29. Sarkar SN, Huang RQ, Logan SM, Yi KD, Dillon GH, Simpkins JW (2008) Estrogens directly potentiate neuronal L-type Ca2+ channels. Proc Natl Acad Sci USA 105:15148–15153
30. Blair LA, Bence-Hanulec KK, Mehta S, Franke T, Kaplan D, Marshall J (1999) Akt-dependent potentiation of L channels by insulin-like growth factor-1 is required for neuronal survival. J Neurosci 19:1940–1951

31. Smith CC, McMahon LL (2006) Estradiol-induced increase in the magnitude of long-term potentiation is prevented by blocking NR2B-containing receptors. J Neurosci 26:8517–8522
32. Hurst RS, Hajos M, Raggenbass M, Wall TM, Higdon NR, Lawson JA, Rutherford-Root KL, Berkenpas MB, Hoffmann WE, Piotrowski DW, Groppi VE, Allaman G, Ogier R, Bertrand S, Bertrand D, Arneric SP (2005) A novel positive allosteric modulator of the alpha7 neuronal nicotinic acetylcholine receptor: in vitro and in vivo characterization. J Neurosci 25:4396–4405
33. Timmermann DB, Gronlien JH, Kohlhaas KL, Nielsen EO, Dam E, Jorgensen TD, Ahring PK, Peters D, Holst D, Christensen JK, Malysz J, Briggs CA, Gopalakrishnan M, Olsen GM (2007) An allosteric modulator of the alpha7 nicotinic acetylcholine receptor possessing cognition-enhancing properties in vivo. J Pharmacol Exp Ther 323:294–307
34. Gusev AG, Uteshev VV (2010) Physiological concentrations of choline activate native alpha7-containing nicotinic acetylcholine receptors in the presence of PNU-120596 [1-(5-chloro-2,4-dimethoxyphenyl)-3-(5-methylisoxazol-3-yl)-urea]. J Pharmacol Exp Ther 332:588–598
35. Kalappa BI, Gusev AG, Uteshev VV (2010) Activation of functional alpha7-containing nAChRs in hippocampal CA1 pyramidal neurons by physiological levels of choline in the presence of PNU-120596. PLoS One 5:e13964
36. Malysz J, Gronlien JH, Anderson DJ, Hakerud M, Thorin-Hagene K, Ween H, Wetterstrand C, Briggs CA, Faghih R, Bunnelle WH, Gopalakrishnan M (2009) In vitro pharmacological characterization of a novel allosteric modulator of alpha 7 neuronal acetylcholine receptor, 4-(5-(4-chlorophenyl)-2-methyl-3-propionyl-1H-pyrrol-1-yl)benzenesulfonamide(A-867744), exhibiting unique pharmacological profile. J Pharmacol Exp Ther 330:257–267
37. Dinklo T, Shaban H, Thuring JW, Lavreysen H, Stevens KE, Zheng L, Mackie C, Grantham C, Vandenberk I, Meulders G, Peeters L, Verachtert H, De Prins E, Lesage AS (2011) Characterization of 2-[[4-fluoro-3-(trifluoromethyl)phenyl]amino]-4-(4-pyridinyl)-5-thiazoleme thanol (JNJ-1930942), a novel positive allosteric modulator of the {alpha}7 nicotinic acetylcholine receptor. J Pharmacol Exp Ther 336:560–574
38. Choi DW (1988) Calcium-mediated neurotoxicity: relationship to specific channel types and role in ischemic damage. Trends Neurosci 11:465–469
39. Mennerick S, Zorumski CF (2000) Neural activity and survival in the developing nervous system. Mol Neurobiol 22:41–54
40. Tymianski M, Charlton MP, Carlen PL, Tator CH (1993) Source specificity of early calcium neurotoxicity in cultured embryonic spinal neurons. J Neurosci 13:2085–2104
41. Brandt SK, Weatherly ME, Ware L, Linn DM, Linn CL (2011) Calcium preconditioning triggers neuroprotection in retinal ganglion cells. Neuroscience 172:387–397
42. Soriano FX, Papadia S, Hofmann F, Hardingham NR, Bading H, Hardingham GE (2006) Preconditioning doses of NMDA promote neuroprotection by enhancing neuronal excitability. J Neurosci 26:4509–4518
43. Asomugha CO, Linn DM, Linn CL (2010) ACh receptors link two signaling pathways to neuroprotection against glutamate-induced excitotoxicity in isolated RGCs. J Neurochem 112:214–226
44. Ogita K, Okuda H, Yamamoto Y, Nishiyama N, Yoneda Y (2003) In vivo neuroprotective role of NMDA receptors against kainate-induced excitotoxicity in murine hippocampal pyramidal neurons. J Neurochem 85:1336–1346
45. Nakazawa H, Murphy TH (1999) Activation of nuclear calcium dynamics by synaptic stimulation in cultured cortical neurons. J Neurochem 73:1075–1083
46. Hardingham GE, Arnold FJ, Bading H (2001) A calcium microdomain near NMDA receptors: on switch for ERK-dependent synapse-to-nucleus communication. Nat Neurosci 4:565–566
47. Pokorska A, Vanhoutte P, Arnold FJ, Silvagno F, Hardingham GE, Bading H (2003) Synaptic activity induces signalling to CREB without increasing global levels of cAMP in hippocampal neurons. J Neurochem 84:447–452
48. Uteshev VV, Knot HJ (2005) Somatic Ca(2+) dynamics in response to choline-mediated excitation in histaminergic tuberomammillary neurons. Neuroscience 134:133–143

49. Papadia S, Soriano FX, Leveille F, Martel MA, Dakin KA, Hansen HH, Kaindl A, Sifringer M, Fowler J, Stefovska V, McKenzie G, Craigon M, Corriveau R, Ghazal P, Horsburgh K, Yankner BA, Wyllie DJ, Ikonomidou C, Hardingham GE (2008) Synaptic NMDA receptor activity boosts intrinsic antioxidant defenses. Nat Neurosci 11:476–487
50. Hardingham GE, Bading H (2010) Synaptic versus extrasynaptic NMDA receptor signalling: implications for neurodegenerative disorders. Nat Rev Neurosci 11:682–696
51. Hardingham GE, Bading H (2003) The Yin and Yang of NMDA receptor signalling. Trends Neurosci 26:81–89
52. Tovar KR, Westbrook GL (2002) Mobile NMDA receptors at hippocampal synapses. Neuron 34:255–264
53. Borgdorff AJ, Choquet D (2002) Regulation of AMPA receptor lateral movements. Nature 417:649–653
54. Fernandes CC, Berg DK, Gomez-Varela D (2010) Lateral mobility of nicotinic acetylcholine receptors on neurons is determined by receptor composition, local domain, and cell type. J Neurosci 30:8841–8851
55. Okubo Y, Sekiya H, Namiki S, Sakamoto H, Iinuma S, Yamasaki M, Watanabe M, Hirose K, Iino M (2010) Imaging extrasynaptic glutamate dynamics in the brain. Proc Natl Acad Sci USA 107:6526–6531
56. Uteshev VV, Pennefather PS (1997) Analytical description of the activation of multi-state receptors by continuous neurotransmitter signals at brain synapses. Biophys J 72:1127–1134
57. Rusakov DA, Wuerz A, Kullmann DM (2004) Heterogeneity and specificity of presynaptic Ca2+ current modulation by mGluRs at individual hippocampal synapses. Cereb Cortex 14:748–758
58. Zheng K, Scimemi A, Rusakov DA (2008) Receptor actions of synaptically released glutamate: the role of transporters on the scale from nanometers to microns. Biophys J 95:4584–4596
59. Asztely F, Erdemli G, Kullmann DM (1997) Extrasynaptic glutamate spillover in the hippocampus: dependence on temperature and the role of active glutamate uptake. Neuron 18: 281–293
60. Kullmann DM (2000) Spillover and synaptic cross talk mediated by glutamate and GABA in the mammalian brain. Prog Brain Res 125:339–351
61. Uteshev VV, Pennefather PS (1996) A mathematical description of miniature postsynaptic current generation at central nervous system synapses. Biophys J 71:1256–1266
62. Traynelis SF, Wollmuth LP, McBain CJ, Menniti FS, Vance KM, Ogden KK, Hansen KB, Yuan H, Myers SJ, Dingledine R (2010) Glutamate receptor ion channels: structure, regulation, and function. Pharmacol Rev 62:405–496
63. Lester RA, Jahr CE (1992) NMDA channel behavior depends on agonist affinity. J Neurosci 12:635–643
64. Clements AM, Westbrook GL (1991) Activation kinetics reveal the number of glutamate and glycine binding sites on the N -methyl-D-aspartate receptor. Neuron 7:605–613
65. Herman MA, Jahr CE (2007) Extracellular glutamate concentration in hippocampal slice. J Neurosci 27:9736–9741
66. Rossi DJ, Oshima T, Attwell D (2000) Glutamate release in severe brain ischaemia is mainly by reversed uptake. Nature 403:316–321
67. Camacho A, Massieu L (2006) Role of glutamate transporters in the clearance and release of glutamate during ischemia and its relation to neuronal death. Arch Med Res 37:11–18
68. Groc L, Heine M, Cousins SL, Stephenson FA, Lounis B, Cognet L, Choquet D (2006) NMDA receptor surface mobility depends on NR2A-2B subunits. Proc Natl Acad Sci USA 103:18769–18774
69. Groc L, Bard L, Choquet D (2009) Surface trafficking of N-methyl-D-aspartate receptors: physiological and pathological perspectives. Neuroscience 158:4–18
70. Lipton SA (2007) Pathologically activated therapeutics for neuroprotection. Nat Rev Neurosci 8:803–808
71. Chen HS, Pellegrini JW, Aggarwal SK, Lei SZ, Warach S, Jensen FE, Lipton SA (1992) Open-channel block of N-methyl-D-aspartate (NMDA) responses by memantine: therapeutic advantage against NMDA receptor-mediated neurotoxicity. J Neurosci 12:4427–4436

72. Aracava Y, Pereira EF, Maelicke A, Albuquerque EX (2005) Memantine blocks alpha7* nicotinic acetylcholine receptors more potently than n-methyl-D-aspartate receptors in rat hippocampal neurons. J Pharmacol Exp Ther 312:1195–1205
73. Maskell PD, Speder P, Newberry NR, Bermudez I (2003) Inhibition of human alpha 7 nicotinic acetylcholine receptors by open channel blockers of N-methyl-D-aspartate receptors. Br J Pharmacol 140:1313–1319
74. Kotermanski SE, Johnson JW (2009) Mg2+ imparts NMDA receptor subtype selectivity to the Alzheimer's drug memantine. J Neurosci 29:2774–2779
75. Aarsland D, Ballard C, Walker Z, Bostrom F, Alves G, Kossakowski K, Leroi I, Pozo-Rodriguez F, Minthon L, Londos E (2009) Memantine in patients with Parkinson's disease dementia or dementia with Lewy bodies: a double-blind, placebo-controlled, multicentre trial. Lancet Neurol 8:613–618
76. Atri A, Shaughnessy LW, Locascio JJ, Growdon JH (2008) Long-term course and effectiveness of combination therapy in Alzheimer disease. Alzheimer Dis Assoc Disord 22:209–221
77. Leroi I, Overshott R, Byrne EJ, Daniel E, Burns A (2009) Randomized controlled trial of memantine in dementia associated with Parkinson's disease. Mov Disord 24:1217–1221
78. Levin OS, Batukaeva LA, Smolentseva IG, Amosova NA (2009) Efficacy and safety of memantine in Lewy body dementia. Neurosci Behav Physiol 39:597–604
79. Parsons CG, Danysz W, Quack G (1999) Memantine is a clinically well tolerated N-methyl-D-aspartate (NMDA) receptor antagonist–a review of preclinical data. Neuropharmacology 38:735–767
80. Plosker GL, Lyseng-Williamson KA (2005) Memantine: a pharmacoeconomic review of its use in moderate-to-severe Alzheimer's disease. Pharmacoeconomics 23:193–206
81. Reisberg B, Doody R, Stoffler A, Schmitt F, Ferris S, Mobius HJ (2003) Memantine in moderate-to-severe Alzheimer's disease. N Engl J Med 348:1333–1341
82. Creeley CE, Wozniak DF, Nardi A, Farber NB, Olney JW (2008) Donepezil markedly potentiates memantine neurotoxicity in the adult rat brain. Neurobiol Aging 29:153–167
83. Schugens MM, Egerter R, Daum I, Schepelmann K, Klockgether T, Loschmann PA (1997) The NMDA antagonist memantine impairs classical eyeblink conditioning in humans. Neurosci Lett 224:57–60
84. Swerdlow NR, van Bergeijk DP, Bergsma F, Weber E, Talledo J (2009) The effects of memantine on prepulse inhibition. Neuropsychopharmacology 34:1854–1864
85. Vercelletto M, Boutoleau-Bretonniere C, Volteau C, Puel M, Auriacombe S, Sarazin M, Michel BF, Couratier P, Thomas-Anterion C, Verpillat P, Gabelle A, Golfier V, Cerato E, Lacomblez L (2011) Memantine in behavioral variant frontotemporal dementia: negative results. J Alzheimers Dis 23:749–759
86. Schneider LS, Insel PS, Weiner MW (2011) Treatment with cholinesterase inhibitors and memantine of patients in the Alzheimer's Disease neuroimaging initiative. Arch Neurol 68:58–66
87. Aarts M, Liu Y, Liu L, Besshoh S, Arundine M, Gurd JW, Wang YT, Salter MW, Tymianski M (2002) Treatment of ischemic brain damage by perturbing NMDA receptor- PSD-95 protein interactions. Science 298:846–850
88. Hogg RC, Raggenbass M, Bertrand D (2003) Nicotinic acetylcholine receptors: from structure to brain function. Rev Physiol Biochem Pharmacol 147:1–46
89. Corringer PJ, Le Novere N, Changeux JP (2000) Nicotinic receptors at the amino acid level. Annu Rev Pharmacol Toxicol 40:431–458
90. Castro NG, Albuquerque EX (1995) à-Bungarotoxin-sensitive hippocampal nicotinic receptor channel has a high calcium permeability. Biophys J 68:516–524
91. Fucile S (2004) Ca2+ permeability of nicotinic acetylcholine receptors. Cell Calcium 35:1–8
92. Seguela P, Wadiche J, Dinely-Miller K, Dani JA, Patrick JW (1993) Molecular cloning, functional properties and distribution of rat brain alpha 7: a nicotinic cation channel highly permeable to calcium. J Neurosci 13(2):596–604
93. Sands SB, Costa ACS, Patrick JW (1993) Barium permeability of neuronal nicotinic acetylcholine receptor alpha 7 expressed in Xenopus oocytes. Biophys J 65:2614–2621

94. Vernino S, Amador M, Luetje CW, Patrick J, Dani JA (1992) Calcium modulation and high calcium permeability of neuronal nicotinic acetylcholine receptors. Neuron 8:127–134
95. Bertrand D, Galzi JL, Devillers-Thiery A, Bertrand S, Changeux JP (1993) Mutations at two distinct sites within the channel domain M2 alter calcium permeability of neuronal alpha 7 nicotinic receptor. Proc Natl Acad Sci USA 90:6971–6975
96. Nutter TJ, Adams DJ (1995) Monovalent and divalent cation permeability and block of neuronal nicotinic receptor channels in rat parasympathetic ganglia. J Gen Physiol 105:701–723
97. Uteshev VV (2010) Evaluation of Ca2+ permeability of nicotinic acetylcholine receptors in hypothalamic histaminergic neurons. Acta Biochim Biophys Sin (Shanghai) 42:8–20
98. Meyer EM, Tay ET, Zoltewicz JA, Papke RL, Meyers C, King M, Fiebre CMd (1998) Neuroprotective and memory-related actions of novel à7 nicotinic agents with different mixed agonist/antagonist properties. J Pharmacol Exp Ther 284:1026–1032
99. Role LW, Berg DK (1996) Nicotinic receptors in the development and modulation of CNS synapses. Neuron 16:1077–1085
100. Dajas-Bailador F, Wonnacott S (2004) Nicotinic acetylcholine receptors and the regulation of neuronal signalling. Trends Pharmacol Sci 25:317–324
101. Thomsen MS, Hansen HH, Timmerman DB, Mikkelsen JD (2010) Cognitive improvement by activation of alpha7 nicotinic acetylcholine receptors: from animal models to human pathophysiology. Curr Pharm Des 16:323–343
102. Albuquerque EX, Pereira EF, Mike A, Eisenberg HM, Maelicke A, Alkondon M (2000) Neuronal nicotinic receptors in synaptic functions in humans and rats: physiological and clinical relevance. Behav Brain Res 113:131–141
103. Fucile S, Renzi M, Lax P, Eusebi F (2003) Fractional Ca(2+) current through human neuronal alpha7 nicotinic acetylcholine receptors. Cell Calcium 34:205–209
104. El-Hajj RA, McKay SB, McKay DB (2007) Pharmacological and immunological identification of native alpha7 nicotinic receptors: evidence for homomeric and heteromeric alpha7 receptors. Life Sci 81:1317–1322
105. Khiroug SS, Harkness PC, Lamb PW, Sudweeks SN, Khiroug L, Millar NS, Yakel JL (2002) Rat nicotinic ACh receptor alpha7 and beta2 subunits co-assemble to form functional heteromeric nicotinic receptor channels. J Physiol 540:425–434
106. Listerud M, Brussaard AB, Devay P, Colman DR, Role LW (1991) Functional contribution of neuronal AChR subunits revealed by antisense oligonucleotides. Science 254:1518–1521
107. Palma E, Maggi L, Barabino B, Eusebi F, Ballivet M (1999) Nicotinic acetylcholine receptors assembled from the alpha7 and beta3 subunits. J Biol Chem 274:18335–18340
108. Ramirez-Latorre J, Yu CR, Qu X, Perin F, Karlin A, Role L (1996) Functional contributions of alpha5 subunit to neuronal acetylcholine receptor channels. Nature 380:347–351
109. Sudweeks SN, Yakel JL (2000) Functional and molecular characterization of neuronal nicotinic ACh receptors in rat CA1 hippocampal neurons. J Physiol 527(Pt 3):515–528
110. Virginio C, Giacometti A, Aldegheri L, Rimland JM, Terstappen GC (2002) Pharmacological properties of rat alpha 7 nicotinic receptors expressed in native and recombinant cell systems. Eur J Pharmacol 445:153–161
111. Yu CR, Role LW (1998) Functional contribution of the alpha5 subunit to neuronal nicotinic channels expressed by chick sympathetic ganglion neurones. J Physiol 509(Pt 3):667–681
112. Yu CR, Role LW (1998) Functional contribution of the alpha7 subunit to multiple subtypes of nicotinic receptors in embryonic chick sympathetic neurones. J Physiol 509(Pt 3):651–665
113. Patrick J, Sequela P, Vernino S, Amador M, Luetje C, Dani JA (1993) Functional diversity of neuronal nicotinic acetylcholine receptors. Prog Brain Res 98:113–120
114. Levin ED (2002) Nicotinic receptor subtypes and cognitive function. J Neurobiol 53:633–640
115. Marini AM, Rabin SJ, Lipsky RH, Mocchetti I (1998) Activity-dependent release of brain-derived neurotrophic factor underlies the neuroprotective effect of N-methyl-D-aspartate. J Biol Chem 273:29394–29399
116. Valera E, Sanchez-Martin FJ, Ferrer-Montiel AV, Messeguer A, Merino JM (2008) NMDA-induced neuroprotection in hippocampal neurons is mediated through the protein kinase A and CREB (cAMP-response element-binding protein) pathway. Neurochem Int 53:148–154

117. Akaike A, Takada-Takatori Y, Kume T, Izumi Y (2010) Mechanisms of neuroprotective effects of nicotine and acetylcholinesterase inhibitors: role of alpha4 and alpha7 receptors in neuroprotection. J Mol Neurosci 40:211–216
118. Lester HA, Dibas MI, Dahan DS, Leite JF, Dougherty DA (2004) Cys-loop receptors: new twists and turns. Trends Neurosci 27:329–336
119. Fucile S, Palma E, Martinez-Torres A, Miledi R, Eusebi F (2002) The single-channel properties of human acetylcholine alpha 7 receptors are altered by fusing alpha 7 to the green fluorescent protein. Proc Natl Acad Sci USA 99:3956–3961
120. Mike A, Castro NG, Albuquerque EX (2000) Choline and acetylcholine have similar kinetic properties of activation and desensitization on the alpha7 nicotinic receptors in rat hippocampal neurons. Brain Res 882:155–168
121. Shao Z, Yakel JL (2000) Single channel properties of neuronal nicotinic ACh receptors in stratum radiatum interneurons of rat hippocampal slices. J Physiol 527(Pt 3):507–513
122. Ascher P, Bregestovski P, Nowak L (1988) N -methyl-D-aspartate-activated channels of mouse central neurones in magnesium-free solutions. J Physiol 399:207–226
123. Uteshev VV, Meyer EM, Papke RL (2002) Activation and inhibition of native neuronal alpha-bungarotoxin-sensitive nicotinic ACh receptors. Brain Res 948:33–46
124. Uteshev VV, Meyer EM, Papke RL (2003) Regulation of neuronal function by choline and 4OH-GTS-21 through alpha 7 nicotinic receptors. J Neurophysiol 89:1797–1806
125. Alkondon M, Reinhardt S, Lobron C, Hermsen B, Maelicke A, Albuquerque EX (1994) Diversity of nicotinic acetylcholine receptors in rat hippocampal neurons. II. The rundown and inward rectification of agonist-elicited whole cell currents and identification of receptor subunits by in situ hybridization. J Pharmacol Exp Ther 271:494–506
126. Jahr CE, Stevens CF (1993) Calcium permeability of the N-methyl-D-aspartate receptor channel in hippocampal neurons in culture. Proc Natl Acad Sci USA 90:11573–11577
127. Iino M, Ozawa S, Tsuzuki K (1990) Permeation of calcium through excitatory amino acid receptor channels in cultured rat hippocampal neurons. J Physiol 424:151–165
128. Mayer ML, Westbrook GL (1987) Permeation and block of N -methyl-D-aspartic acid receptor channels by divalent cations in mouse cultured central neurons. J Physiol 394:501
129. Lyford LK, Lee JW, Rosenberg RL (2002) Low-affinity Ca(2+) and Ba(2+) binding sites in the pore of alpha7 nicotinic acetylcholine receptors. Biochim Biophys Acta 1559:69–78
130. Conroy WG, Liu Z, Nai Q, Coggan JS, Berg DK (2003) PDZ-containing proteins provide a functional postsynaptic scaffold for nicotinic receptors in neurons. Neuron 38:759–771
131. Ehlers MD, Heine M, Groc L, Lee MC, Choquet D (2007) Diffusional trapping of GluR1 AMPA receptors by input-specific synaptic activity. Neuron 54:447–460
132. Mielke JG, Mealing GA (2009) Cellular distribution of the nicotinic acetylcholine receptor alpha7 subunit in rat hippocampus. Neurosci Res 65:296–306
133. Hardingham GE, Fukunaga Y, Bading H (2002) Extrasynaptic NMDARs oppose synaptic NMDARs by triggering CREB shut-off and cell death pathways. Nat Neurosci 5:405–414
134. Zhang Z, Coggan JS, Berg DK (1996) Synaptic currents generated by neuronal acetylcholine receptors sensitive to alpha-bungarotoxin. Neuron 17:1231–1240
135. Frazier CJ, Buhler AV, Weiner JL, Dunwiddie TV (1998) Synaptic potentials mediated via alpha-bungarotoxin-sensitive nicotinic acetylcholine receptors in rat hippocampal interneurons. J Neurosci 18:8228–8235
136. Hefft S, Hulo S, Bertrand D, Muller D (1999) Synaptic transmission at nicotinic acetylcholine receptors in rat hippocampal organotypic cultures and slices. J Physiol 515(Pt 3): 769–776
137. Hatton GI, Yang QZ (2002) Synaptic potentials mediated by alpha 7 nicotinic acetylcholine receptors in supraoptic nucleus. J Neurosci 22:29–37
138. Kem WR (2000) The brain alpha7 nicotinic receptor may be an important therapeutic target for the treatment of Alzheimer's disease: studies with DMXBA (GTS-21). Behav Brain Res 113:169–181
139. Uteshev VV, Stevens DR, Haas HL (1996) Alpha-Bungarotoxin-sensitive nicotinic responses in rat tuberomammillary neurons. Pflugers Arch 432:607–613

140. Alkondon M, Pereira EF, Almeida LE, Randall WR, Albuquerque EX (2000) Nicotine at concentrations found in cigarette smokers activates and desensitizes nicotinic acetylcholine receptors in CA1 interneurons of rat hippocampus. Neuropharmacology 39:2726–2739
141. Fujii S, Ji Z, Sumikawa K (2000) Inactivation of alpha7 ACh receptors and activation of non-alpha7 ACh receptors both contribute to long term potentiation induction in the hippocampal CA1 region. Neurosci Lett 286:134–138
142. Ferchmin PA, Perez D, Eterovic VA, de Vellis J (2003) Nicotinic receptors differentially regulate N-methyl-D-aspartate damage in acute hippocampal slices. J Pharmacol Exp Ther 305:1071–1078
143. Hu M, Gopalakrishnan M, Li J (2009) Positive allosteric modulation of alpha7 neuronal nicotinic acetylcholine receptors: lack of cytotoxicity in PC12 cells and rat primary cortical neurons. Br J Pharmacol 158:1857–1864
144. Briggs CA, Gronlien JH, Curzon P, Timmermann DB, Ween H, Thorin-Hagene K, Kerr P, Anderson DJ, Malysz J, Dyhring T, Olsen GM, Peters D, Bunnelle WH, Gopalakrishnan M (2009) Role of channel activation in cognitive enhancement mediated by alpha7 nicotinic acetylcholine receptors. Br J Pharmacol 158:1486–1494
145. Leon SF, Suwazono S, Takenaga S, Arimura K, Osame M (1997) The effects of tobacco smoking on the short, middle, and long latency responses of the blink reflex in humans. J Clin Neurophysiol 14:144–149
146. Woodruff-Pak DS, Green JT, Coleman-Valencia C, Pak JT (2000) A nicotinic cholinergic agonist (GTS-21) and eyeblink classical conditioning: acquisition, retention, and relearning in older rabbits. Exp Aging Res 26:323–336
147. Woodruff-Pak DS (2003) Mecamylamine reversal by nicotine and by a partial alpha7 nicotinic acetylcholine receptor agonist (GTS-21) in rabbits tested with delay eyeblink classical conditioning. Behav Brain Res 143:159–167
148. Brown KL, Comalli DM, Biasi MD, Woodruff-Pak DS (2010) Trace eyeblink conditioning is impaired in alpha7 but not in beta2 nicotinic acetylcholine receptor knockout mice. Front Behav Neurosci 4:166
149. Hernandez CM, Kayed R, Zheng H, Sweatt JD, Dineley KT (2010) Loss of alpha7 nicotinic receptors enhances beta-amyloid oligomer accumulation, exacerbating early-stage cognitive decline and septohippocampal pathology in a mouse model of Alzheimer's disease. J Neurosci 30:2442–2453
150. Ren K, King MA, Liu J, Siemann J, Altman M, Meyers C, Hughes JA, Meyer EM (2007) The alpha7 nicotinic receptor agonist 4OH-GTS-21 protects axotomized septohippocampal cholinergic neurons in wild type but not amyloid-overexpressing transgenic mice. Neuroscience 148:230–237
151. Jonnala RR, Buccafusco JJ (2001) Relationship between the increased cell surface alpha7 nicotinic receptor expression and neuroprotection induced by several nicotinic receptor agonists. J Neurosci Res 66:565–572
152. Hu M, Schurdak ME, Puttfarcken PS, El Kouhen R, Gopalakrishnan M, Li J (2007) High content screen microscopy analysis of A beta 1-42-induced neurite outgrowth reduction in rat primary cortical neurons: neuroprotective effects of alpha 7 neuronal nicotinic acetylcholine receptor ligands. Brain Res 1151:227–235
153. Qi XL, Nordberg A, Xiu J, Guan ZZ (2007) The consequences of reducing expression of the alpha7 nicotinic receptor by RNA interference and of stimulating its activity with an alpha7 agonist in SH-SY5Y cells indicate that this receptor plays a neuroprotective role in connection with the pathogenesis of Alzheimer's disease. Neurochem Int 51:377–383
154. Wang HY, Li W, Benedetti NJ, Lee DH (2003) Alpha 7 nicotinic acetylcholine receptors mediate beta-amyloid peptide-induced tau protein phosphorylation. J Biol Chem 278: 31547–31553
155. Dineley KT, Westerman M, Bui D, Bell K, Ashe KH, Sweatt JD (2001) Beta-amyloid activates the mitogen-activated protein kinase cascade via hippocampal alpha7 nicotinic acetylcholine receptors: in vitro and in vivo mechanisms related to Alzheimer's disease. J Neurosci 21:4125–4133

156. Dineley KT, Bell KA, Bui D, Sweatt JD (2002) Beta -Amyloid peptide activates alpha 7 nicotinic acetylcholine receptors expressed in Xenopus oocytes. J Biol Chem 277: 25056–25061
157. Dineley KT (2007) Beta-amyloid peptide–nicotinic acetylcholine receptor interaction: the two faces of health and disease. Front Biosci 12:5030–5038
158. Clifford PM, Siu G, Kosciuk M, Levin EC, Venkataraman V, D'Andrea MR, Nagele RG (2008) Alpha7 nicotinic acetylcholine receptor expression by vascular smooth muscle cells facilitates the deposition of Abeta peptides and promotes cerebrovascular amyloid angiopathy. Brain Res 1234:158–171
159. Soderman A, Thomsen MS, Hansen HH, Nielsen EO, Jensen MS, West MJ, Mikkelsen JD (2008) The nicotinic alpha7 acetylcholine receptor agonist ssr180711 is unable to activate limbic neurons in mice overexpressing human amyloid-beta1-42. Brain Res 1227:240–247
160. Wang HY, Stucky A, Liu J, Shen C, Trocme-Thibierge C, Morain P (2009) Dissociating beta-amyloid from alpha 7 nicotinic acetylcholine receptor by a novel therapeutic agent, S 24795, normalizes alpha 7 nicotinic acetylcholine and NMDA receptor function in Alzheimer's disease brain. J Neurosci 29:10961–10973
161. Martin SE, de Fiebre NE, de Fiebre CM (2004) The alpha7 nicotinic acetylcholine receptor-selective antagonist, methyllycaconitine, partially protects against beta-amyloid1-42 toxicity in primary neuron-enriched cultures. Brain Res 1022:254–256
162. Dziewczapolski G, Glogowski CM, Masliah E, Heinemann SF (2009) Deletion of the alpha 7 nicotinic acetylcholine receptor gene improves cognitive deficits and synaptic pathology in a mouse model of Alzheimer's disease. J Neurosci 29:8805–8815
163. Nagele RG, D'Andrea MR, Anderson WJ, Wang HY (2002) Intracellular accumulation of beta-amyloid(1–42) in neurons is facilitated by the alpha 7 nicotinic acetylcholine receptor in Alzheimer's disease. Neuroscience 110:199–211
164. Wang HY, Lee DH, D'Andrea MR, Peterson PA, Shank RP, Reitz AB (2000) Beta-Amyloid(1–42) binds to alpha7 nicotinic acetylcholine receptor with high affinity. Implications for Alzheimer's disease pathology. J Biol Chem 275:5626–5632
165. D'Andrea MR, Nagele RG (2006) Targeting the alpha 7 nicotinic acetylcholine receptor to reduce amyloid accumulation in Alzheimer's disease pyramidal neurons. Curr Pharm Des 12:677–684
166. Jenden DJ, Scremin OU, Roch M, Li G (1996) The influence of aging on whole body choline release and clearance. Life Sci 58:2003–2009
167. Guan ZZ, Zhang X, Ravid R, Nordberg A (2000) Decreased protein levels of nicotinic receptor subunits in the hippocampus and temporal cortex of patients with Alzheimer's disease. J Neurochem 74:237–243
168. Nordberg A (2001) Nicotinic receptor abnormalities of Alzheimer's disease: therapeutic implications. Biol Psychiatry 49:200–210
169. Sarter M, Parikh V (2005) Choline transporters, cholinergic transmission and cognition. Nat Rev Neurosci 6:48–56
170. Martin LF, Freedman R (2007) Schizophrenia and the alpha7 nicotinic acetylcholine receptor. Int Rev Neurobiol 78:225–246
171. Leonard S, Breese C, Adams C, Benhammou K, Gault J, Stevens K, Lee M, Adler L, Olincy A, Ross R, Freedman R (2000) Smoking and schizophrenia: abnormal nicotinic receptor expression. Eur J Pharmacol 393:237–242
172. Freedman R, Adams CE, Leonard S (2000) The alpha7-nicotinic acetylcholine receptor and the pathology of hippocampal interneurons in schizophrenia. J Chem Neuroanat 20: 299–306
173. Stevens KE, Freedman R, Collins AC, Hall M, Leonard S, Marks MJ, Rose GM (1996) Genetic correlation of inhibitory gating of hippocampal auditory evoked response and alpha-bungarotoxin-binding nicotinic cholinergic receptors in inbred mouse strains. Neuropsychopharmacology 15:152–162
174. Felix R, Levin ED (1997) Nicotinic antagonist administration into the ventral hippocampus and spatial working memory in rats. Neuroscience 81:1009–1017

175. Wevers A, Witter B, Moser N, Burghaus L, Banerjee C, Steinlein OK, Schutz U, de Vos RA, Steur EN, Lindstrom J, Schroder H (2000) Classical Alzheimer features and cholinergic dysfunction: towards a unifying hypothesis? Acta Neurol Scand Suppl 176:42–48
176. Freedman R, Hall M, Adler LE, Leonard S (1995) Evidence in postmortem brain tissue for decreased numbers of hippocampal nicotinic receptors in schizophrenia. Biol Psychiatry 38:22–33
177. Perry EK, Morris CM, Court JA, Cheng A, Fairbairn AF, McKeith IG, Irving D, Brown A, Perry RH (1995) Alteration in nicotine binding sites in Parkinson's disease. Lewy body dementia and Alzheimer's disease: possible index of early neuropathology. Neuroscience 64:385–395
178. Nordberg A, Winblad B (1986) Reduced number of [3H]nicotine and [3H]acetylcholine binding sites in the frontal cortex of Alzheimer brains. Neurosci Lett 72:115–119
179. Shimohama S, Taniguchi T, Fujiwara M, Kameyama M (1986) Changes in nicotinic and muscarinic cholinergic receptors in Alzheimer-type dementia. J Neurochem 46:288–293
180. London ED, Ball MJ, Waller SB (1989) Nicotinic binding sites in cerebral cortex and hippocampus in Alzheimer's dementia. Neurochem Res 14:745–750
181. Takeuchi H, Yanagida T, Inden M, Takata K, Kitamura Y, Yamakawa K, Sawada H, Izumi Y, Yamamoto N, Kihara T, Uemura K, Inoue H, Taniguchi T, Akaike A, Takahashi R, Shimohama S (2009) Nicotinic receptor stimulation protects nigral dopaminergic neurons in rotenone-induced Parkinson's disease models. J Neurosci Res 87:576–585
182. Kaneko S, Maeda T, Kume T, Kochiyama H, Akaike A, Shimohama S, Kimura J (1997) Nicotine protects cultured cortical neurons against glutamate-induced cytotoxicity via alpha7-neuronal receptors and neuronal CNS receptors. Brain Res 765:135–140
183. Meyer EM, King MA, Meyers C (1998) Neuroprotective effects of 2,4-dimethoxybenzylidene anabaseine (DMXB) and tetrahydroaminoacridine (THA) in neocortices of nucleus basalis lesioned rats. Brain Res 786:252–254
184. Li Y, Meyer EM, Walker DW, Millard WJ, He YJ, King MA (2002) Alpha7 nicotinic receptor activation inhibits ethanol-induced mitochondrial dysfunction, cytochrome c release and neurotoxicity in primary rat hippocampal neuronal cultures. J Neurochem 81:853–858
185. Verbois SL, Scheff SW, Pauly JR (2003) Chronic nicotine treatment attenuates alpha 7 nicotinic receptor deficits following traumatic brain injury. Neuropharmacology 44:224–233
186. Buccafusco JJ, Beach JW, Terry AV Jr, Doad GS, Sood A, Arias E, Misawa H, Masai M, Fujii T, Kawashima K (2004) Novel analogs of choline as potential neuroprotective agents. J Alzheimers Dis 6:S85–S92
187. Fucile S, Renzi M, Lauro C, Limatola C, Ciotti T, Eusebi F (2004) Nicotinic cholinergic stimulation promotes survival and reduces motility of cultured rat cerebellar granule cells. Neuroscience 127:53–61
188. Rosa AO, Egea J, Gandia L, Lopez MG, Garcia AG (2006) Neuroprotection by nicotine in hippocampal slices subjected to oxygen-glucose deprivation: involvement of the alpha7 nAChR subtype. J Mol Neurosci 30:61–62
189. Guseva MV, Hopkins DM, Scheff SW, Pauly JR (2008) Dietary choline supplementation improves behavioral, histological, and neurochemical outcomes in a rat model of traumatic brain injury. J Neurotrauma 25:975–983
190. Buccafusco JJ, Letchworth SR, Bencherif M, Lippiello PM (2005) Long-lasting cognitive improvement with nicotinic receptor agonists: mechanisms of pharmacokinetic-pharmacodynamic discordance. Trends Pharmacol Sci 26:352–360
191. Buccafusco JJ, Terry AV Jr, Decker MW, Gopalakrishnan M (2007) Profile of nicotinic acetylcholine receptor agonists ABT-594 and A-582941, with differential subtype selectivity, on delayed matching accuracy by young monkeys. Biochem Pharmacol 74:1202–1211
192. Kitagawa H, Takenouchi T, Azuma R, Wesnes KA, Kramer WG, Clody DE, Burnett AL (2003) Safety, pharmacokinetics, and effects on cognitive function of multiple doses of GTS-21 in healthy, male volunteers. Neuropsychopharmacology 28:542–551
193. Leiser SC, Bowlby MR, Comery TA, Dunlop J (2009) A cog in cognition: how the alpha 7 nicotinic acetylcholine receptor is geared towards improving cognitive deficits. Pharmacol Ther 122:302–311

194. Olincy A, Stevens KE (2007) Treating schizophrenia symptoms with an alpha7 nicotinic agonist, from mice to men. Biochem Pharmacol 74:1192–1201
195. Arendash GW, Sengstock GJ, Sanberg PR, Kem WR (1995) Improved learning and memory in aged rats with chronic administration of the nicotinic receptor agonist GTS-21. Brain Res 674:252–259
196. Meyer EM, Tay ET, Papke RL, Meyers C, Huang G, de Fiebre CM (1997) Effects of 3-[2,4-dimethoxybenzylidene]anabaseine (DMXB) on rat nicotinic receptors and memory-related behaviors. Brain Res 768:49–56
197. Ross RG, Stevens KE, Proctor WR, Leonard S, Kisley MA, Hunter SK, Freedman R, Adams CE (2010) Research review: cholinergic mechanisms, early brain development, and risk for schizophrenia. J Child Psychol Psychiatry 51:535–549
198. Olincy A, Harris JG, Johnson LL, Pender V, Kongs S, Allensworth D, Ellis J, Zerbe GO, Leonard S, Stevens KE, Stevens JO, Martin L, Adler LE, Soti F, Kem WR, Freedman R (2006) Proof-of-concept trial of an alpha7 nicotinic agonist in schizophrenia. Arch Gen Psychiatry 63:630–638
199. Martin EJ, Panikar KS, King MA, Deyrup M, Hunter B, Wang G, Meyer E (1994) Cytoprotective actions of 2,4-dimethoxybenzylidene anabaseine in differentiated PC12 cells and septal cholinergic cells. Drug Dev Res 31:134–141
200. Briggs CA, Anderson DJ, Brioni JD, Buccafusco JJ, Buckley MJ, Campbell JE, Decker MW, Donnelly-Roberts D, Elliot RL, Gopalakrishnan M, Holladay MW, Hui Y, Jackson W, Kim DJB, Marsh KC, O'Neill AO, Pendergast MA, Ryther KB, Sullivan JP, Arneric SP (1997) Functional characterization of the novel nicotinic receptor ligand GTS-21 in vitro and in vivo. Pharmacol Biochem Behav 57:231–241
201. Van Kampen M, Selbach K, Schneider R, Schiegel E, Boess F, Schreiber R (2004) AR-R 17779 improves social recognition in rats by activation of nicotinic alpha7 receptors. Psychopharmacology 172:375–383
202. Woodruff-Pak DS, Li Y, Kem WR (1994) A nicotinic agonist (GTS-21), eyeblink classical conditioning, and nicotinic receptor binding in rabbit brain. Brain Res 645:309–317
203. Wishka DG, Walker DP, Yates KM, Reitz SC, Jia S, Myers JK, Olson KL, Jacobsen EJ, Wolfe ML, Groppi VE, Hanchar AJ, Thornburgh BA, Cortes-Burgos LA, Wong EH, Staton BA, Raub TJ, Higdon NR, Wall TM, Hurst RS, Walters RR, Hoffmann WE, Hajos M, Franklin S, Carey G, Gold LH, Cook KK, Sands SB, Zhao SX, Soglia JR, Kalgutkar AS, Arneric SP, Rogers BN (2006) Discovery of N-[(3R)-1-azabicyclo[2.2.2]oct-3-yl]furo[2,3-c] pyridine-5-carboxamide, an agonist of the alpha7 nicotinic acetylcholine receptor, for the potential treatment of cognitive deficits in schizophrenia: synthesis and structure-activity relationship. J Med Chem 49:4425–4436
204. Bitner RS, Bunnelle WH, Decker MW, Drescher KU, Kohlhaas KL, Markosyan S, Marsh KC, Nikkel AL, Browman K, Radek R, Anderson DJ, Buccafusco J, Gopalakrishnan M (2010) In vivo pharmacological characterization of a novel selective alpha7 neuronal nicotinic acetylcholine receptor agonist ABT-107: preclinical considerations in Alzheimer's disease. J Pharmacol Exp Ther 334:875–886
205. Bitner RS, Bunnelle WH, Anderson DJ, Briggs CA, Buccafusco J, Curzon P, Decker MW, Frost JM, Gronlien JH, Gubbins E, Li J, Malysz J, Markosyan S, Marsh K, Meyer MD, Nikkel AL, Radek RJ, Robb HM, Timmermann D, Sullivan JP, Gopalakrishnan M (2007) Broad-spectrum efficacy across cognitive domains by alpha7 nicotinic acetylcholine receptor agonism correlates with activation of ERK1/2 and CREB phosphorylation pathways. J Neurosci 27:10578–10587
206. Boess FG, De Vry J, Erb C, Flessner T, Hendrix M, Luithle J, Methfessel C, Riedl B, Schnizler K, van der Staay FJ, van Kampen M, Wiese WB, Koenig G (2007) The novel alpha7 nicotinic acetylcholine receptor agonist N-[(3R)-1-azabicyclo[2.2.2]oct-3-yl]-7-[2-(methoxy)phenyl]-1-benzofuran-2- carboxamide improves working and recognition memory in rodents. J Pharmacol Exp Ther 321:716–725
207. Pichat P, Bergis OE, Terranova JP, Urani A, Duarte C, Santucci V, Gueudet C, Voltz C, Steinberg R, Stemmelin J, Oury-Donat F, Avenet P, Griebel G, Scatton B (2007) SSR180711, a novel selective alpha7 nicotinic receptor partial agonist: (II) efficacy in experimental models

predictive of activity against cognitive symptoms of schizophrenia. Neuropsychopharmacology 32:17–34
208. Tatsumi R, Fujio M, Takanashi S, Numata A, Katayama J, Satoh H, Shiigi Y, Maeda J, Kuriyama M, Horikawa T, Murozono T, Hashimoto K, Tanaka H (2006) (R)-3'-(3-methylbenzo[b]thiophen-5-yl)spiro[1-azabicyclo[2,2,2]octane-3,5′ -oxazolidin]-2′-one, a novel and potent alpha7 nicotinic acetylcholine receptor partial agonist displays cognitive enhancing properties. J Med Chem 49:4374–4383
209. Ren K, Thinschmidt J, Liu J, Ai L, Papke RL, King MA, Hughes JA, Meyer EM (2007) Alpha7 Nicotinic receptor gene delivery into mouse hippocampal neurons leads to functional receptor expression, improved spatial memory-related performance, and tau hyperphosphorylation. Neuroscience 145:314–322
210. Banerjee C, Nyengaard JR, Wevers A, de Vos RA, Jansen Steur EN, Lindstrom J, Pilz K, Nowacki S, Bloch W, Schroder H (2000) Cellular expression of alpha7 nicotinic acetylcholine receptor protein in the temporal cortex in Alzheimer's and Parkinson's disease-a stereological approac. Neurobiol Dis 7:666–672
211. Loughead J, Ray R, Wileyto EP, Ruparel K, Sanborn P, Siegel S, Gur RC, Lerman C (2010) Effects of the alpha4beta2 partial agonist varenicline on brain activity and working memory in abstinent smokers. Biol Psychiatry 67:715–721
212. Furey ML, Pietrini P, Haxby JV, Alexander GE, Lee HC, VanMeter J, Grady CL, Shetty U, Rapoport SI, Schapiro MB, Freo U (1997) Cholinergic stimulation alters performance and task-specific regional cerebral blood flow during working memory. Proc Natl Acad Sci USA 94:6512–6516
213. Kirrane RM, Mitropoulou V, Nunn M, Silverman J, Siever LJ (2001) Physostigmine and cognition in schizotypal personality disorder. Schizophr Res 48:1–5
214. Koller G, Satzger W, Adam M, Wagner M, Kathmann N, Soyka M, Engel R (2003) Effects of scopolamine on matching to sample paradigm and related tests in human subjects. Neuropsychobiology 48:87–94
215. Green A, Ellis KA, Ellis J, Bartholomeusz CF, Ilic S, Croft RJ, Phan KL, Nathan PJ (2005) Muscarinic and nicotinic receptor modulation of object and spatial n-back working memory in humans. Pharmacol Biochem Behav 81:575–584
216. Ellis JR, Ellis KA, Bartholomeusz CF, Harrison BJ, Wesnes KA, Erskine FF, Vitetta L, Nathan PJ (2006) Muscarinic and nicotinic receptors synergistically modulate working memory and attention in humans. Int J Neuropsychopharmacol 9:175–189
217. Dunbar G, Kuchibhatla R, Lee G (2011) A randomized double-blind study comparing 25 and 50 mg TC-1734 (AZD3480) with placebo, in older subjects with age-associated memory impairment. J Psychopharmacol 25:1020–1029
218. Farlow MR, Salloway S, Tariot PN, Yardley J, Moline ML, Wang Q, Brand-Schieber E, Zou H, Hsu T, Satlin A (2010) Effectiveness and tolerability of high-dose (23 mg/d) versus standard-dose (10 mg/d) donepezil in moderate to severe Alzheimer's disease: a 24-week, randomized, double-blind study. Clin Ther 32:1234–1251
219. Alva G, Cummings JL (2008) Relative tolerability of Alzheimer's disease treatments. Psychiatry (Edgmont) 5:27–36
220. Lopez-Hernandez GY, Thinschmidt JS, Morain P, Trocme-Thibierge C, Kem WR, Soti F, Papke RL (2009) Positive modulation of alpha7 nAChR responses in rat hippocampal interneurons to full agonists and the alpha7-selective partial agonists, 4OH-GTS-21 and S 24795. Neuropharmacology 56:821–830
221. Papke RL, Bencherif M, Lippiello P (1996) An evaluation of neuronal nicotinic acetylcholine receptor activation by quaternary nitrogen compounds indicates that choline is selective for the alpha 7 subtype. Neurosci Lett 213:201–204
222. Alkondon M, Pereira EF, Cortes WS, Maelicke A, Albuquerque EX (1997) Choline is a selective agonist of alpha7 nicotinic acetylcholine receptors in the rat brain neurons. Eur J Neurosci 9:2734–2742
223. Bertrand N, Ishii H, Spatz M (1996) Cerebral ischemia in young and adult gerbils: effects on cholinergic metabolism. Neurochem Int 28:293–297

224. Jope RS, Gu X (1991) Seizures increase acetylcholine and choline concentrations in rat brain regions. Neurochem Res 16:1219–1226
225. Parikh V, Sarter M (2006) Cortical choline transporter function measured in vivo using choline-sensitive microelectrodes: clearance of endogenous and exogenous choline and effects of removal of cholinergic terminals. J Neurochem 97:488–503
226. Rao AM, Hatcher JF, Dempsey RJ (2000) Lipid alterations in transient forebrain ischemia: possible new mechanisms of CDP-choline neuroprotection. J Neurochem 75:2528–2535
227. Scremin OU, Jenden DJ (1991) Time-dependent changes in cerebral choline and acetylcholine induced by transient global ischemia in rats. Stroke 22:643–647
228. Papke RL, Papke JKP (2002) Comparative pharmacology of rat and human alpha7 nAChR conducted with net charge analysis. Br J Pharmacol 137:49–61
229. Klein J, Koppen A, Loffelholz K (1998) Regulation of free choline in rat brain: dietary and pharmacological manipulations. Neurochem Int 32:479–485
230. Faghih R, Gfesser GA, Gopalakrishnan M (2007) Advances in the discovery of novel positive allosteric modulators of the alpha7 nicotinic acetylcholine receptor. Recent Patents CNS Drug Discov 2:99–106
231. Roncarati R, Seredenina T, Jow B, Jow F, Papini S, Kramer A, Bothmann H, Dunlop J, Terstappen GC (2008) Functional properties of alpha7 nicotinic acetylcholine receptors coexpressed with RIC-3 in a stable recombinant CHO-K1 cell line. Assay Drug Dev Technol 6:181–193
232. Barron SC, McLaughlin JT, See JA, Richards VL, Rosenberg RL (2009) The allosteric modulator of {alpha}7 nicotinic receptors, PNU-120596, causes conformational changes in the extracellular ligand binding domain similar to acetylcholine. Mol Pharmacol 76:253–263
233. Young GT, Zwart R, Walker AS, Sher E, Millar NS (2008) Potentiation of alpha7 nicotinic acetylcholine receptors via an allosteric transmembrane site. Proc Natl Acad Sci USA 105:14686–14691
234. Gronlien JH, Hakerud M, Ween H, Thorin-Hagene K, Briggs CA, Gopalakrishnan M, Malysz J (2007) Distinct profiles of alpha7 nAChR positive allosteric modulation revealed by structurally diverse chemotypes. Mol Pharmacol 72:715–724
235. Bertrand D, Bertrand S, Cassar S, Gubbins E, Li J, Gopalakrishnan M (2008) Positive allosteric modulation of the alpha7 nicotinic acetylcholine receptor: ligand interactions with distinct binding sites and evidence for a prominent role of the M2-M3 segment. Mol Pharmacol 74:1407–1416
236. Disterhoft JF, Oh MM (2007) Alterations in intrinsic neuronal excitability during normal aging. Aging Cell 6:327–336
237. Kaczorowski CC, Disterhoft JF (2009) Memory deficits are associated with impaired ability to modulate neuronal excitability in middle-aged mice. Learn Mem 16:362–366
238. Gilbert D, Lecchi M, Arnaudeau S, Bertrand D, Demaurex N (2009) Local and global calcium signals associated with the opening of neuronal alpha7 nicotinic acetylcholine receptors. Cell Calcium 45:198–207
239. De Rosa MJ, Dionisio L, Agriello E, Bouzat C, Esandi Mdel C (2009) Alpha 7 nicotinic acetylcholine receptor modulates lymphocyte activation. Life Sci 85:444–449
240. Hao J, Simard AR, Turner GH, Wu J, Whiteaker P, Lukas RJ, Shi FD (2010) Attenuation of CNS inflammatory responses by nicotine involves alpha7 and non-alpha7 nicotinic receptors. Exp Neurol 227:110–119
241. Kawashima K, Fujii T (2003) The lymphocytic cholinergic system and its contribution to the regulation of immune activity. Life Sci 74:675–696
242. Koval L, Lykhmus O, Zhmak M, Khruschov A, Tsetlin V, Magrini E, Viola A, Chernyavsky A, Qian J, Grando S, Komisarenko S, Skok M (2011) Differential involvement of alpha-4beta2, alpha7 and alpha9alpha10 nicotinic acetylcholine receptors in B lymphocyte activation in vitro. Int J Biochem Cell Biol 43:516–524
243. Mashkina AP, Cizkova D, Vanicky I, Boldyrev AA (2010) NMDA receptors are expressed in lymphocytes activated both in vitro and in vivo. Cell Mol Neurobiol 30:901–907

244. Mashkina AP, Tyulina OV, Solovyova TI, Kovalenko EI, Kanevski LM, Johnson P, Boldyrev AA (2007) The excitotoxic effect of NMDA on human lymphocyte immune function. Neurochem Int 51:356–360
245. Nizri E, Hamra-Amitay Y, Sicsic C, Lavon I, Brenner T (2006) Anti-inflammatory properties of cholinergic up-regulation: a new role for acetylcholinesterase inhibitors. Neuropharmacology 50:540–547
246. Nizri E, Irony-Tur-Sinai M, Lory O, Orr-Urtreger A, Lavi E, Brenner T (2009) Activation of the cholinergic anti-inflammatory system by nicotine attenuates neuroinflammation via suppression of Th1 and Th17 responses. J Immunol 183:6681–6688
247. Sharma G, Vijayaraghavan S (2002) Nicotinic receptor signaling in nonexcitable cells. J Neurobiol 53:524–534
248. Skok MV, Grailhe R, Agenes F, Changeux JP (2007) The role of nicotinic receptors in B-lymphocyte development and activation. Life Sci 80:2334–2336
249. Wang H, Yu M, Ochani M, Amella CA, Tanovic M, Susarla S, Li JH, Yang H, Ulloa L, Al-Abed Y, Czura CJ, Tracey KJ (2003) Nicotinic acetylcholine receptor alpha7 subunit is an essential regulator of inflammation. Nature 421:384–388
250. Yawata I, Takeuchi H, Doi Y, Liang J, Mizuno T, Suzumura A (2008) Macrophage-induced neurotoxicity is mediated by glutamate and attenuated by glutaminase inhibitors and gap junction inhibitors. Life Sci 82:1111–1116
251. Catassi A, Paleari L, Servent D, Sessa F, Dominioni L, Ognio E, Cilli M, Vacca P, Mingari M, Gaudino G, Bertino P, Paolucci M, Calcaterra A, Cesario A, Granone P, Costa R, Ciarlo M, Alama A, Russo P (2008) Targeting alpha7-nicotinic receptor for the treatment of pleural mesothelioma. Eur J Cancer 44:2296–2311
252. Catassi A, Servent D, Paleari L, Cesario A, Russo P (2008) Multiple roles of nicotine on cell proliferation and inhibition of apoptosis: implications on lung carcinogenesis. Mutat Res 659:221–231
253. Davis R, Rizwani W, Banerjee S, Kovacs M, Haura E, Coppola D, Chellappan S (2009) Nicotine promotes tumor growth and metastasis in mouse models of lung cancer. PLoS One 4:e7524
254. Egleton RD, Brown KC, Dasgupta P (2008) Nicotinic acetylcholine receptors in cancer: multiple roles in proliferation and inhibition of apoptosis. Trends Pharmacol Sci 29:151–158
255. North WG, Gao G, Memoli VA, Pang RH, Lynch L (2010) Breast cancer expresses functional NMDA receptors. Breast Cancer Res Treat 122:307–314
256. Paleari L, Catassi A, Ciarlo M, Cavalieri Z, Bruzzo C, Servent D, Cesario A, Chessa L, Cilli M, Piccardi F, Granone P, Russo P (2008) Role of alpha7-nicotinic acetylcholine receptor in human non-small cell lung cancer proliferation. Cell Prolif 41:936–959
257. Tachibana N, Shirakawa T, Ishii K, Takahashi Y, Tanaka K, Arima K, Yoshida T, Ikeda S (2010) Expression of various glutamate receptors including N-methyl-D-aspartate receptor (NMDAR) in an ovarian teratoma removed from a young woman with anti-NMDAR encephalitis. Intern Med 49:2167–2173
258. Oh MM, Wu WW, Power JM, Disterhoft JF (2006) Galantamine increases excitability of CA1 hippocampal pyramidal neurons. Neuroscience 137:113–123
259. Lynch G, Palmer LC, Gall CM (2011) The likelihood of cognitive enhancement. Pharmacol Biochem Behav 99:116–129

Chapter 28
The Biology of Protein Kinase C

Lily Zeng, Samuel V. Webster, and Philip M. Newton

Abstract This review gives a basic introduction to the biology of protein kinase C, one of the first calcium-dependent kinases to be discovered. We review the structure and function of protein kinase C, along with some of the substrates of individual isoforms. We then review strategies for inhibiting PKC in experimental systems and finally discuss the therapeutic potential of targeting PKC. Each aspect is covered in summary, with links to detailed resources where appropriate.

Keywords Kinases • PKC Alpha • PKC Beta • PKC Gamma • PKC Delta • PKC Epsilon • PKC Eta • PKC Theta • PKC Iota • PKC Zeta • PKC Inhibitors

Introduction

Intracellular protein phosphorylation and dephosphorylation is a major mechanism by which external stimuli are transformed into cellular events. Phosphorylation is performed by protein kinases which phosphorylate their substrates on serine, threonine or tyrosine residues. The effect of phosphorylation is to stabilize certain conformational states of substrate molecules and thus alter their biological activity [1].

Protein Kinase C (PKC) was one of the very first kinases to be discovered [2] and we now know that "Protein Kinase C" is actually a family of closely related serine/threonine kinases with at least ten different isoforms having been discovered to date. The isoforms can be split into three families according to their requirement for different co-factors: The conventional, or classical (c)PKCs: α, βI, βII and γ, the

L. Zeng
School of Medicine, University of California, San Francisco, CA, USA

S.V. Webster • P.M. Newton (✉)
College of Medicine, Swansea University, Swansea, Wales SA2 8PP, UK
e-mail: p.newton@swansea.ac.uk

M.S. Islam (ed.), *Calcium Signaling*, Advances in Experimental Medicine and Biology 740, DOI 10.1007/978-94-007-2888-2_28,

novel (n)PKCs: δ, ε, η and θ, and the atypical (a) PKCs: ζ and λ (referred to as PKCι in murine systems). Differential splicing gives rise to the two forms of β: βI and βII, which differ only in their extreme *C*-terminal ends [3], while a, shortened, constitutively active form of PKCzeta is expressed from an internal promoter within the PKCzeta gene and is known as PKMzeta [4]. A further isoform, PKCμ, was originally thought to belong to the PKC family but is now referred to as protein kinase D and will not be discussed further [5].

The principal co-factors required for PKC activity are Ca^{2+}, phosphatidylserine (PS) and diacylglycerol (DAG), although the requirement for these co-factors varies by isoform as discussed below. The activation of certain PKC isoforms by DAG can be exploited in experimental systems by the use of DAG mimics, typically a class of molecules known as the phorbol esters. Distribution of different PKC subtypes varies greatly among different tissues and cell types. For example, the expression patterns of the α, δ and ζ isoforms are fairly widespread [6], whereas PKCγ expression is restricted to tissues of the central nervous system [7, 8] and PKCθ is predominantly found in T-cells [9].

PKC Domain Function

Each PKC family contains slightly different domains, resulting in the aforementioned differences in co-factor requirements. For a detailed review of the different domains please see [10]. The function of some of the key relevant domains of PKC are summarised below and represented in Fig. 28.1.

PS: Pseudosubstrate Domain. The PS region interacts with the kinase domain, forming a hairpin structure which blocks kinase activity in the unactivated molecule. The pseudosubstrate site contains a PKC phosphorylation consensus sequence except that the phosphorylatable serine/threonine residue is replaced with an unphosphorylatable alanine [11]. The kinase-blocking property of the pseudosubstrate domain has been exploited in the development of specific PKC inhibitors. The PKMzeta form of PKCzeta lacks this pseudosubstrate domain and so is thought to be constitutively active [4].

C1: DAG/Phorbol Ester Binding Domain. These domains confer upon cPKCs and nPKCs the ability to bind diacylglycerol/phorbol esters, with the C1b region being critical for this function. These domains were originally discovered in PKCs but are now known to be found in multiple other DAG-binding proteins (reviewed in [12]). In cPKCs and in nPKCs the C1 domain is present as a tandem repeat (C1a and C1b). In the atypical PKCs, the ligand-binding pocket of the C1 domain does not allow the entry of DAG nor phorbol esters [13, 14]. C1b also appears to be the key region involved in the stereospecific interaction of PKC with phosphatidylserine (PS) [15] although the C2 domain interacts with anionic phospholipids in a Ca^{2+}-dependent manner. In PKCepsilon there is a 22 amino acid actin-binding sequence located between the C1a and C1b domains that is unique to this PKC isoform, although other isoforms bind to, and are activated by, F-actin. Both the affinity for F-actin, and the activity induced as a result of PKC binding to F-actin, are potentiated by the presence of PMA/Ca^{2+} [16].

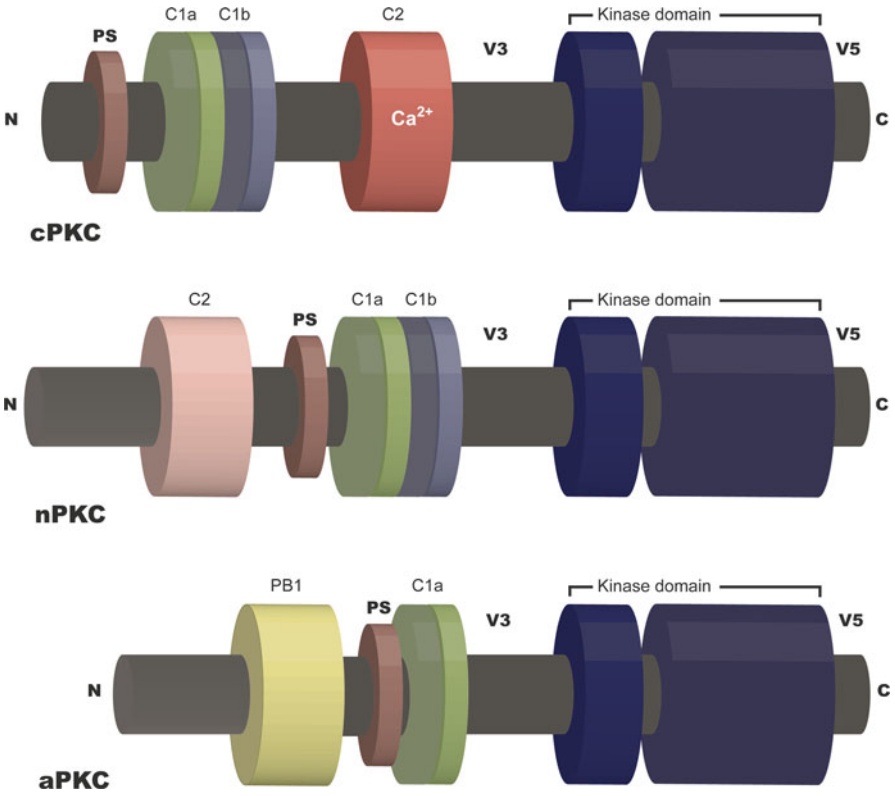

Fig. 28.1 Domain structure of the different subgroups of the PKC family. Classical (cPKCs): α, βI, βII and γ, novel (nPKCs): δ, ε, η and θ, and atypical (aPKCs): ζ and λ (referred to as PKCι in murine systems). For detail of domain function please refer to section "Introduction". Adapted from references cited in the text

C2: Binds Ca^{2+} and phospholipids. A detailed review of the C2 domain by Farah and Sossin can be found in Chap. 28 of this book. Briefly, the presence of aspartate residues in the C2 domain of cPKCs confers upon them the ability to bind Ca^{2+}, which is then crucial for activation. In the novel PKCs, these aspartate residues are absent and the nPKCs do not require Ca^{2+} for activation. Perhaps related to this, nPKCs have a two-fold greater affinity for DAG than cPKCs [17, 18].

Both the C2 and C1 domains are involved in the interaction of activated PKC with the plasma membrane: C1 in a DAG/PMA and phospholipid dependent manner and C2 in a Ca^{2+} dependent manner. aPKCs do not have a C2 domain (Fig. 28.1).

PB1: aPKCs differ from other PKC types in containing a PB1 domain (Fig. 28.1). This scaffolding domain of approximately 80 amino acids is found in many different protein types and is thus thought to facilitate the formation of aPKC-containing complexes, perhaps providing a means by which target specificity is achieved [19].

V3: Hinge Region. The V3 region forms the "hinge" of the molecule, allowing the pseudosubstrate to interact with the kinase domain (see above). The V3 region is

susceptible to proteolytic cleavage [7], which frees the catalytic domain and, for some isoforms, generates a constitutively active form of the kinase [10]. The V3 region may also be important for the targeting of certain isoforms to specific intracellular locations [20].

Catalytic Domain: This domain is highly conserved between the PKCs, indeed it is highly conserved between many families of kinase, meaning that reagents which target this region have poor specificity (see section "Strategies for Developing PKC Inhibitors").

V5: This region contains some of these sites which are phosphorylated as part of the activation of PKC (section "Regulation of PKC"). It is the principal region which varies between the βI and βII isoforms [21], in fact the extreme C-terminus of the domain is the most variable between isoforms and as a consequence it is often a region against which isoform specific antibodies are raised [10].

Regulation of PKC

Regulation by Phosphorylation

PKC undergoes a highly regulated sequence of phosphorylation steps which must occur before it can become fully active and thus able to transduce extracellular signals [22, 23]. Phosphorylation occurs at three sites: the activation loop, which is in the kinase domain, and the "turn" and "hydrophobic" motifs, which are in the V5 region. [24, 25]. When PKC is first synthesized, it is weakly attached to the membrane in an open conformation, meaning that the pseudosubstrate is not in the active site and the activation loop is exposed and can be phosphorylated [26]. Phosphoryation of the activation loop is achieved by PDK1 [27–29] and is essential to the survival of the PKC. Unphosphorylated PKCs are quickly degraded, and it has been demonstrated that cells deficient in PDK1 have reduced levels of PKC [30]. Phosphorylation of the activation loop by PDK1 is followed by the phosphorylation of the turn motif which turns PKC into a thermally stable, closed state [25]. This phosphorylation is critical for the enzymatic function of PKCs, as dephosphorylation abolishes activity [25, 31]. Although the mechanistic detail has not been fully elucidated, it has been shown that the mTORC2 complex, comprising of mTOR kinase, rictor, mLST8, and Sin1, is required for this phosphorylation [26, 32, 33]. Cells lacking any protein within the mTORC2 complex cannot process PKC and unphosphorylated species of PKC are degraded [33, 34]. Additionally, cells lacking mTORC2 have significantly reduced PKC levels [33–35], demonstrating the important role that phosphorylation plays in stabilizing the peptide. The last step in the maturation process is phosphorylation of the hydrophobic motif. The hydrophobic motif is situated at the C terminal and is a ser/thr that is flanked by lipophilic residues. The mechanisms by which phosphorylation of the hydrophobic motif is achieved have not been fully determined, although roles have been postulated for autophosphorylation and for mTORC2, among other kinases [24, 33, 36].

It is important to note that this applies only to cPKCs and nPKCs because aPKCs are not phosphorylated at the hydrophobic motif.

The activity of the mature PKC is regulated by secondary messengers, namely calcium, DAG and phosphatidylserine (PS). The hydrolysis of phosphatidylinositol 4,5-bisphosphate (PIP2) generates inositol 1,4,5-trisphosphate (IP3) and DAG. IP3 translocates to the cytosol to unlock a pool of intracellular calcium while DAG remains at the plasma membrane. Calcium binds to the C2 domain of cPKCs and targets them to the plasma membrane, where they bind to anionic phospholipids such as PS. Once tethered to the membrane, the C1 domain binds with membrane DAG, and interaction with the plasma membrane thermodynamically shifts the autoinhibitory PKC pseudosubstrate out of the active site. As previously mentioned, the C1 domain of nPKCs has twice the affinity for DAG as that of cPKCs, which significantly localizes nPKCs to the Golgi apparatus where the membrane is rich in DAG [37].

The function and targeting to substrates of activated PKC is facilitated by Receptors for Activated C Kinase (RACKs). Pioneering work from the laboratory of Daria Mochly-Rosen identified RACKs, to which PKCs bind once activated [38]. RACKs appear to be isoform-specific and serve to anchor PKC in close proximity to its substrates [39]. Short peptides based upon the RACK-interacting motifs of the different PKCs have proved to be useful tools to inhibit the translocation, and thus the activation, of PKC in an isoform specific manner. This is an active area of drug-discovery, targeting PKC for therapeutic benefit [40] (see also sections “Strategies for Developing PKC Inhibitors” and “PKC as a Therapeutic Target”).

PKC Targets, Substrates and Binding Partners

Substrates of PKC contain a consensus phosphorylation sequence which varies slightly among isoforms [41], but generally requires that there to be a basic residue in close proximity to the serine/threonine being phosphorylated [42]. Identification of a substrate *in vitro* does not necessarily mean that the same protein is a PKC substrate *in vivo.* In fact, to conclusively demonstrate *in vivo* phosphorylation is very difficult. Nevertheless a broad range of putative substrates have been identified and their regulation by individual isoforms is discussed below. The list is broad and includes a wide range of receptors, regulatory enzymes, and cytoskeletal proteins.

Only a handful of examples are included for each isoform, to give an idea of the range of potential substrates. Some additional substrates are discussed in section “PKC as a Therapeutic Target”.

PKC Alpha

DGK zeta. PKCalpha phosphorylation negatively regulates diacylglycerol kinase (DGK) zeta. DGK converts DAG to phosphatidic acid, thereby terminating DAG signaling. Activation of PKCalpha attenuates DGK zeta activity. Creating a

phospho-mimic of DGK zeta by converting a phosphorylatable serine to an aspartate residue results in increased cell growth [43]. **Filamin A** is a structural component of the cytoskeleton, anchoring membrane proteins to the actin filament network. Filamin A was identified as a phosphorylation target for PKC alpha by yeast two-hybrid analysis [44]. Filamin A is indispensible to normal development [45]. A consistent theme in the biology of cell signaling is the inter-regulation of different protein kinases and their pathways. **Raf-1** is a kinase which is part of the MAPK/ERK signaling pathway. PKCalpha directly phosphorylates and activates Raf-1 *in vitro* and *in vivo*. PKCalpha phosphorylates Raf-1 at multiple sites, of which serine 499 seems to be the most important. Activation of Raf-1 induces activation of a protein kinase cascade by the direct phosphorylation of MAP kinase resulting in the phosphorylation of ternary complex factor and Jun by MAP kinase. This pathway is crucial to cell proliferation [46]. PKC alpha, along with the beta I and II, and eta isoforms, phosphorylates the protein-tyrosine-phosphatase (PTP) **SHP2** on serine residues 576 and 591 [47]. SHP2 is thought to play a role in many disease states, including cancer [48], diabetes and obesity [49].

PKC Beta

F1/GAP 43, is a cytoskeletal regulator which is highly enriched in neuronal growth cones mutation of GAP 43 at ser 41, a PKC phosphorylation site, demonstrates that phosphorylation of GAP 43 regulates the biology of neurons [50]. *In vitro* phosphorylation experiments suggest that F1/GAP 43 is selectively phosphorylated by PKC beta [51]. PKC beta phosphorylates serine residues 505 and 509 in the cytoplasmic domain of **tyrokinase** to activate it. Tyrokinase is the rate-limiting enzyme in melanogenesis [52]. **Phospholipase D** – sustained stimulation of PKC alpha and beta II leads to localization of these isoforms to the juxtanuclear region. PKCbeta II activates PLD during the translocation and inhibition of PLD using a dominant negative construct prevents this translocation [53].

PKC Gamma

RC3 is a neural specific protein that is phosphorylated by PKC following the postsynaptic activation of metabotropic glutamate receptors. The failure of PKC stimulation to increase phosphorylated RC3 in PKCgamma knockout mice suggests that RC3 may be a substrate of PKCgamma. This could contribute to the spatial learning deficits and impaired hippocampal LTP seen in PKCgamma knockout mice [54]. A form of spinocerebellar ataxia (SCA14) arises from mutations in the gene encoding PKCgamma. In one family of sufferers it has been determined that a deletion mutation in PKCgamma elongates the enzyme by 13 amino acids. The resulting enzyme is hyperactive and results in a hyperphosphorylation, on Thr 111, of the DNA repair enyzme **aprataxin**. Phosphorylation of aprataxin prevents its entry into the nucleus

and results in increased cell death, establishing a putative mechanism by which PKC gamma mutation contributes to spinocerebellar ataxia [55].

PKC Delta

PKC delta has many roles in cell growth, survival, differentiation and apoptosis. Many of the substrates which mediate these effects have been identified and include transcription activators such as STATs (Signal Transducer and Activator of Transcription) and heat-shock proteins (HSPs).

Treatment with Interferon-alpha triggers the phosphorylation of **STAT1** on serine 727 via a process which requires PKCdelta, although it is not clear that PKCdelta directly phosphorylates STAT1 *in vivo*. This phosphorylation is essential to the transcriptional activity of Stat1 and is a crucial part of Type 1 Interferon signaling [56]. **STAT3** is also phosphorylated on ser 727 through a process which is induced by interleukin-6 (IL-6) and again appears to be mediated by PKCdelta. In several cell types, stimulation by IL-6 leads to the association of Stat3 with PKCdelta. Also, PKCdelta phosphorylates Stat3 *in vitro*, and *in vivo* phosphorylation of Stat3 is inhibited by expression of dominant negative PKCdelta. This phosphorylation negatively regulates the transcriptional activity of STAT3 [57]. **HSP25** interacts with PKCdelta to inhibit apoptosis. HSP25 binds to the V5 region of PKCdelta and inhibits both its kinase activity and membrane translocation. The interaction between PKCdelta and HSP25 induces the phosphorylation of HSP25 at serine 15 and serine 86, allowing the HSP to then "unbind" PKCdelta. This helps explain the cytoprotective role of HSP25 [58]. PKCdelta also interacts with HSP27 through the carboxyl terminus of PKCdelta, hindering the activity of PKCdelta and its role in cell death [59].

P47 Phox. The phosphorylation and translocation of p47 phox in activated human monocytes requires PKCdelta. P47phox is an important component of NADPH oxidase activity in monocytes and is part of the complex that produces the superoxide O2- [60]. **P60TNFR** is a proinflammatory molecule whose phosphorylation leads to the degranulation of neutrophils. PKCdelta is the only isotype that associates with p60TNFR within the appropriate time frame for phosphorylation to occur and is the only isozyme capable of phosphorylating p60TNFR *in vitro*, suggesting that P60TNFR is a PKCdelta substrate *in vivo* [61].

PKC Epsilon

PKCepsilon is expressed throughout the body. The substrates and binding partners for PKC-epsilon have been recently reviewed in detail [62]. PKCepsilon phosphorylates a variety of substrates which fall into a few key classes – including ion channels such as the **GABA-A receptor**, **cytoskeletal proteins**, and other intracellular signaling molecules such as **Protein Kinase B** and **STAT3**.

PKC Eta

PKC eta is highly expressed in epithelial tissue and there is evidence that it phosphorylates the tight-junction protein **occludin** [63] in cultured cells. Inhibition of PKC-eta mediated occludin phosphorylation alters the distribution of occludin in tight junctions and compromises the epithelial barrier. Conversely, constitutively active PKCeta elevates levels of phosphorylated occludin and strengthens tight junctions. This phosphorylation is thought to occur on Thr 403 and Thr 404. A Thr403/404A mutation results into the inability to localize to the tight junction complex whereas a Thr 403/404D mutation alleviates the effects PKCeta inhibition has on tight junction assembly [64].

PKC Theta

PKC theta is predominantly expressed in lymphocytes, skeletal muscle, and platelets. [62, 65, 66]. The best described role for PKC-theta is in the activation of T-cells, where it participates in a number of cell signaling pathways which ultimately result in the activation of transcriptional changes leading to T-cell activation (recently reviewed in [67, 68]).

PKC Iota

Much of the attention paid recently to the biology of PKC iota has focused on its identification as a human oncogene and thus its role in cancer [68]. A number of putative substrates have been identified, including **interleukin receptor-associated kinase (IRAK)**. It's been previously shown that IRAK is critical for NGF induced activation of NF-kappa B, and thus necessary for cell survival [69]. NGF signaling results in the formation of an IRAK-PKCiota complex that is recruited to the p75 neurotrophin receptor. The putative phosphorylation site is Thr66. Mutation of this threonine to alanine reduces the IRAK-PKCiota association [70]. Another well-described role for the aPKCs (iota and lambda) is in the regulation of cell polarity, achieved through interaction with proteins in the **PAR complex** [71, 72].

PKC Zeta

Protein kinase C zeta is implicated in the regulation of a wide variety of intracellular signaling mechanisms [73], some of which are summarized below.

Vascular endothelial growth factor (VEGF) is a cytokine that promotes angiogenesis and vascular permeability. VEGF also activates **eNOS**, producing nitric oxide (NO) to augment its effects on the vasculature. Angiopoietin-1 (Ang-1)

antagonizes VEGF by interrupting its signaling to eNOS, thus stabilizing vessels and preventing plasma leakage. Ang-1 appears to stimulate PKCzeta-mediated phosphorylation of eNOS at Thr497. Furthermore, following PKCzeta knockdown, Ang-1 is unable to inhibit the actions of VEGF and NO [74]. **Insulin-responsive aminopeptidase (IRAP)** and the type 4 glucose transport (GLUT4) are the two major constituents of the GLUT4 storage vesicle and are recruited to the plasma membrane in response to insulin [75]. Experiments with rat adipocytes suggest that IRAP is a direct substrate of PKCzeta with Ser80 as the most likely phosphorylation site [76]. **P47phox**. P47 is a component of the multi-protein NADPH oxidase complex. PKCzeta is expressed abundantly in neutrophils, a cell type in which NADPH oxidase plays a major role. *In vitro* incubation of recombinant p47phox and PKCzeta increases the phosphorylation of p47phox that is dependent on both time and concentration. Treatment with synthetic chemoattractants like fMLP stimulates translocation of PKCzeta and p47phox to the plasma membrane. Inhibition of PKCzeta prevents the translocation and phosphorylation of p47phox and results in a reduction in oxidant production. Mutagenesis studies suggest that ser 303/304 and ser 315 may be the phosphorylated residues [77].

Strategies for Developing PKC Inhibitors

Given the wide variety of aforementioned substrates, it is unsurprising that the PKC family has been the target of medications development efforts – see [78] and [40] for recent reviews on this topic. There are several aspects of PKC biology which could be targets for pharmacological intervention. These include (1) The ATP and substrate binding domains (2) effector binding domains (3) scaffold mimics that activate or inhibit the binding of PKC to RACKs and (4) the 3′UTR of PKC mRNA.

Many of the first PKC inhibitors identified, such as staurosporine and bisindolylmalemides, act at the catalytic domain. It has subsequently been discovered that the catalytic domain is highly conserved across many different kinase families and thus selectivity is a significant concern for this class of inhibitors (e.g. see [79]). Concerns over selectivity and potency result in a narrow therapeutic window and thus catalytic-site inhibitors are currently most useful as research tools rather than therapeutic agents. Inhibitors targeting the substrate binding site, as well as the C1 and C2 domains, have been developed. The majority of peptide-based substrate site inhibitors mimic the substrate recognition sequence of PKC isoforms, with the exception of an alanine at the target site, thereby making them non phosphorylatable. Limited isoform selectivity is a significant concern with this class of inhibitors. Specificity is also an issue for these small molecule substrate site inhibitors, such as the alkaloid chelerythrine [80].

Inhibition of PKC can also occur at the C1a/b domain. Examples of this type of inhibitor are bryostatin [81] and Calphostin C [82]. Calphostin C binds to C1 domains, competing with DAG and phorbol esters for this site. Bryostatin also binds to C1 domains and has actions similar to those of phorbol esters.

A third way to inhibit PKC is by preventing scaffolding proteins, which are necessary for the continuation of downstream signal transduction, from binding to the C2 domain. In the closed/inactive conformer of PKC, C2 is bound to a sequence called pseudoRACK [38]. This knowledge has also been exploited to design PKC activators by locking PKC into the open configuration by an activator that disengages the intramolecular interactions between C2 and pseudoRACK. Work by Ponting and Stallings-Mann [83, 84] and Regala [85] on PKC-iota has demonstrated that the PB1 domain may also be targeted for PKC inhibition.

Antisense oligonucleotides can be generated to recognize the 3′UTR of PKC mRNA, and target it for degradation. Antisense ogligonucleotides against PKCalpha have been particularly used in research on treatments for different types of cancer [86–88].

PKC as a Therapeutic Target

PKCs are found in all eukaryotes and in a very wide variety of cell types and anatomical locations. Multiple disease states have been identified where PKCs play a role. Here we review some of these.

Addiction

Multiple PKC isozymes have been identified as playing a role in the development and maintenance of addictive behaviour in animal models. Perhaps the best described of these is PKCepsilon, deletion of which causes an increase in sensitivity to morphine [89], cannabinoids [90] and allosteric GABA-A receptor modulators such as ethanol and benzodiazepines [91–93]. Follow up studies have shown that ethanol-drinking behaviour in mice is reduced by a selective reduction of PKCepsilon levels in the amygdala [94] and that the GABA-A receptor is a substrate for PKCepsilon [95]. Biological responses to ethanol are also regulated by PKC gamma [96–99] and PKC delta [100] and both of these effects also appear to be correlated with, at least in part, the regulation of GABA-A receptors by these isozymes.

The role of PKC isozymes in mediating biological responses to drugs of abuse and the therapeutic implications of these effects have been recently reviewed [101].

Neurodegenerative Diseases

PKC activators have potent neurotrophic and neuroprotective effects in animals, making them candidates for the treatment of neurodegenerative diseases, stroke, and traumatic brain injury. PKC activators can induce synaptic maturation, inhibit

apoptosis, increase neurotrophin levels and reduce beta-amyloid levels [102]. Beta-amyloid is a toxic peptide that's believed to be important in the progression to Alzheimer's Disease (AD) and dementia. It has been shown that overexpression of PKCepsilon reduces levels of amyloid beta in a mouse model of AD [103]. One possible mechanistic explanation for these effects comes from observations that PKC activators including phorbol esters [104], bryostatin [105], and benzolactam derivatives [106] promote the activity of alpha secretase. Alpha secretase converts the amyloid precursor protein (APP) into a non-toxic form called sAPPalpha. In fact, abnormal function in the PKC signaling cascade is one of the earliest changes in patients with AD [107].

A mechanistic theory to explain the biology of AD suggests that increased levels of Abeta suppresses PKC activity. Since PKC isozymes are important in synaptogensis, blockade of PKC activity leads to synaptic loss. And synaptic loss is one of the hallmarks of AD. However, high levels of PKC also suppress the precipitation of amyloid beta [107].

Lines of transgenic mice have been created that mimic Alzheimer's Disease by carrying specific mutations in the gene encoding for APP: APV717I and K670N/M671L (Tg2576) [105, 108]. Using APV717I transgenic mice, it has been shown that PKC activators, given over a period of several months, provide significant longevity benefits [105]. Administration of bryostatin results in increased sAPPalpha and decreased beta amyloid levels in the brain, and a concomitant increase in life expectancy [105]. Bryostatin also confers a neuroprotective effect in a different mouse model using Tg2576 mice. Administration of byrostatin restores PKC activity, which in turns reduces levels of soluble Abeta. Furthermore, bryostatin is able to prevent synaptic loss in the hippocampus and thus ablate the memory deficits that are seen in AD [108].

PKC activators can also ameliorate some of the neurological injury caused by combination of ischemia and hypoxia, a model of stroke in rats [109], suggesting they could be of therapeutic potential in the treatment of stroke. Recent studies suggest that PKCepsilon might confer protection against ischemic injury by decreasing post-ischemic cerebral blood flow [110].

Memory

PKC inhibition can reduce spatial learning [111], although PKCs activators can improve learning which is independent of protein synthesis [112, 113]. In rats trained in a spatial memory task, bryostatin increases the rate of learning and the number of mushroom spines in the hippocampus. Importantly, the effects of bryostatin can be blocked by PKC inhibitors; supporting the hypothesis that bryostatin enhances learning and memory by specifically activating PKC [102].

PKMzeta is highly expressed in neuronal tissues [4] and is thought to be a key enzyme involved in mediating various aspects of synaptic plasticity, where the characteristics of various synaptic phenomena are altered in a manner which is

hypothesized to underly the molecular basis of certain types of memory. These hypotheses are supported by studies showing that inhibition of PKMzeta has profound effects on memory in animal models. The molecular biology of PKMzeta has been extensively studied within these processes, although the specific PKMzeta substrates involved have yet to be elucidated [114].

Hematological Malignancy

Much of the literature about the biology of PKCs suggests that they play a role in cancer. Much of the work to develop pharmacological reagents which manipulate PKC has thus focused on experimental models of cancer.

Curcumin [1,7-bis-(4-hydroxy- 3-methoxyphenyl)-1,6-heptadiene-3,5-dione] is a biologically active component of the spice turmeric. Both *in vitro* and animal models have demonstrated that curcumin has antiproliferative, anti-invasive and antiangiogenic effects [115, 116]. Curcumin inhibits PKC by oxidizing the vicinal thiols present within the catalytic domain. Curcumin has already been evaluated in clinical trials for the treatment of multiple myeloma's and myelodysplastic syndromes [117, 118] as well as other inflammatory and chronic diseases [119–122].

Enzastaurin (LY317615) inhibits PKC by competing with ATP for the nucleotide triphosphate-binding site. Experimental evidence has shown that Enzastaurin potently inhibits multiple PKC isozymes including PKC-beta, -alpha, delta, gamma, and epsilon [123]. Recent studies in preclinical trials show have demonstrated that Enzastaurin has anti-tumor activity [123, 124]. Enzastaurin either alone or in combination with chemotherapeutics is currently undergoing phase I and II clinical trials for use in patients suffering from for various malignancies including leukemia and non-Hodgkin's lymphoma [125].

Enzastaurin can also inhibit the survival, proliferation, and migration of multiple myeloma cell lines and primary tumor cells [126], and abolish tumor cell growth angiogenesis and survival *in vivo.* Furthermore, *in vitro* studies demonstrate that enzastaurin has a synergistic antitumor effect with drugs currently approved for the treatment of hematalogical malignancies such as rituximab and dexamethasone [127].

Promising results have also been obtained in studies using bryostatin in the treatment of treatment-resistant acute leukemias and insidious forms of lymphoma and leukemia [128–130]. Bryostatin has been studied with TNF-related apoptosis inducing ligand (TRAIL) and with anti-TRAIL receptor agonistic antibodies [131]. For example the combination of AS101, an immunomodulator that potentiates TNF-alpha function, and bryostatin prolongs the longevity of mice in a murine model of leukaemia [132].

Another drug whose actions are enhanced by the co-administration of bryostatin is rituximab. Rituximab is an agent for the treatment of non-Hodgkin's lymphoma, however only about 50% of patients respond to rituximab. Experimental studies have demonstrated that cells pretreated with bryostatin are more susceptible to the pro-apoptotic action of rituximab, suggesting that the combination of drugs may be useful in the treatment for B cell malignancies [133]. This hypothesis is currently being tested in a clinical trial [134].

PKC Isozyme-Selective Activators and Inhibitors in the Treatment of Reperfusion Injury

Patients who suffer from acute myocardial infarction or have undergone cardiac surgery can accrue damage to the heart in two ways: ischemic injury and reperfusion injury, collectively called ischemia-reperfusion (IR) injury. While the myocardium can activate anaerobic fuel catabolism during brief periods of oxygen deprivation, long term deprivation result in irreversible cell injury, and ultimately death. Upon reperfusion, the rapid generation of ATP in combination with elevated calcium concentration can result in hypercontracture and also apoptosis. This injury can spread throughout the syncytium via gap junctions [135]. Both ischemia and reperfusion need to be addressed in order to minimize cardiac damage in patients. A number of studies have identified roles for PKC isozymes in IR injury. Activation of PKCepsilon, for example using psi(e)RACK [136–138], is important for the phenomenon of ischemic preconditioning (IPC) where brief ischemic events offers protection from a subsequent and sustained ischemic insult [139]. Selective inhibition of PKCdelta with deltaV1-1 [140] reduces reperfusion damage [137], likely through inhibiting the pro-apoptotic role for PKCdelta [140]. Interestingly, it was recently shown that chronic intermittent hypoxia, which instills protection against ischemia-reperfusion injury, increases PKC delta expression [141]. PKC beta II may also play a role in the cardioprotective effects of chronic intermittent hypoxia/hypoxic preconditioning [142].

PKC theta as an Anti-inflammatory Target

As mentioned previously, PKC theta is predominantly expressed in lymphocytes, skeletal muscle, and platelets [62, 65, 66]. It is thought that inhibition of PKCtheta has anti-inflammatory potential, based upon studies using PKCtheta KO mice. Early work in these mice has demonstrated that they exhibit reduced eosinophil infiltration and lung inflammation, while T cells from these mice exhibit reduced proliferation and production of cytokines [143, 144]. This was also apparent in a model of antigen-induced arthritis, in which PKCtheta$^{-/-}$ mice develop a markedly less severe form of the disease compared to their wild type counterparts [145]. PKCtheta $^{-/-}$ mice also exhibit a delayed rejection of a cardiac allograft [146, 147], while in these mice a dose of an immunosuppressant, that would normally have been subtherapeutic, sufficiently prevents the rejection of the graft [146].

PKC and Insulin Resistance

Type-II diabetes is characterized by insulin resistance and hyperglycemia. The serious complications of type-II diabetes include large and small vessel diseases, like cardiovascular disease and atherosclerosis, and neuropathy and nephropathy [148].

Multiple isoforms of protein kinase C have been shown to play a role in the transition from healthy to hyperglycemic. For instance, phosphorylation of insulin receptor substrate-1 is linked to insulin resistance. PKCs, including alpha [149], beta [150], delta [151], and zeta [152], are involved in the phosphorylation of IRS-1 either directly or indirectly. Another protein involved in insulin resistance is 14-3-3, which is part of the IRS-1 complex and is regulated by PKC alpha [153]. MARCKS, which also play a role in insulin resistance, is regulated by PKC beta [154] and delta [154]. PKC delta has been reported to associate tightly with insulin receptors [155]. Thus PKCs form an attractive target for therapeutic intervention in acquiring diabetes and reducing hyperglycemia. Several PKC inhibitors have been tested in clinical trials already- recently reviewed in [148].

Pain

PKCgamma is a major PKC isoform expressed in the spinal cord. Its strategic distribution in the outer lamina of the dorsal horn implies its important regulatory role in the somatosensory pathways, especially in nociception [156]. PKCgamma has a well-established role in moderating the biological response to opiates (reviewed recently in [101]). The analgesic effects of mu-opioid receptor agonists are enhanced in PKCgamma knock-out mice. Deletion of PKCgamma also results in an increased binding of enkephalin to the mu-opioid receptor in spinal cord membranes from knockout mice [156]. The molecular biology of this effect is poorly understood. PKCepsilon null mice also show an increase in sensitivity to the analgesic effects of morphine, while PKCepsilon inhibitors and activators have been shown to modulate many different aspects of chronic pain in animal models [157].

Acknowledgements We would like to thank Dr. Richard van Rijn for providing helpful suggestions and thorough review of our manuscript. This chapter was supported in part by the Department of Defense PH/TBI program under award number W81XWH-08-1-0620 (to PMN) and National Institutes of Health Award DA027948 (to PMN). Views and opinions of, and endorsements by the author(s) do not reflect those of the US Army or the Department of Defense.

References

1. Johnson LN, Barford D (1993) The effects of phosphorylation on the structure and function of proteins. Annu Rev Biophys Biomol Struct 22:199–232
2. Inoue M, Kishimoto A, Takai Y, Nishizuka Y (1977) Studies on a cyclic nucleotide-independent protein kinase and its proenzyme in mammalian tissues. II. Proenzyme and its activation by calcium-dependent protease from rat brain. J Biol Chem 252:7610–7616
3. Coussens L, Rhee L, Parker PJ, Ullrich A (1987) Alternative splicing increases the diversity of the human protein kinase C family. DNA 6:389–394
4. Hernandez AI, Blace N, Crary JF, Serrano PA, Leitges M, Libien JM, Weinstein G, Tcherapanov A, Sacktor TC (2003) Protein kinase M zeta synthesis from a brain mRNA

encoding an independent protein kinase C zeta catalytic domain. Implications for the molecular mechanism of memory. J Biol Chem 278:40305–40316
5. Rozengurt E (2011) Protein kinase D signaling: multiple biological functions in health and disease. Physiology (Bethesda) 26:23–33
6. Krauss G (1999) Biochemistry of signal transduction and regulation. Wiley-VCH Verlag GmbH & Co. KgaA
7. Liu WS, Heckman CA (1998) The sevenfold way of PKC regulation. Cell Signal 10: 529–542
8. Nishizuka Y (1988) The molecular heterogeneity of protein kinase C and its implications for cellular regulation. Nature 334:661–665
9. Mochly-Rosen D, Kauvar LM (2000) Pharmacological regulation of network kinetics by protein kinase C localization. Semin Immunol 12:55–61
10. Steinberg SF (2008) Structural basis of protein kinase C isoform function. Physiol Rev 88:1341–1378
11. House C, Kemp BE (1987) Protein kinase C contains a pseudosubstrate prototope in its regulatory domain. Science 238:1726–1728
12. Colon-Gonzalez F, Kazanietz MG (2006) C1 domains exposed: from diacylglycerol binding to protein-protein interactions. Biochim Biophys Acta 1761:827–837
13. Kazanietz MG, Bustelo XR, Barbacid M, Kolch W, Mischak H, Wong G, Pettit GR, Bruns JD, Blumberg PM (1994) Zinc finger domains and phorbol ester pharmacophore. Analysis of binding to mutated form of protein kinase C zeta and the vav and c-raf proto-oncogene products. J Biol Chem 269:11590–11594
14. Pu Y, Peach ML, Garfield SH, Wincovitch S, Marquez VE, Blumberg PM (2006) Effects on ligand interaction and membrane translocation of the positively charged arginine residues situated along the C1 domain binding cleft in the atypical protein kinase C isoforms. J Biol Chem 281:33773–33788
15. Johnson JE, Giorgione J, Newton AC (2000) The C1 and C2 domains of protein kinase C are independent membrane targeting modules, with specificity for phosphatidylserine conferred by the C1 domain. Biochemistry 39:11360–11369
16. Slater SJ, Milano SK, Stagliano BA, Gergich KJ, Curry JP, Taddeo FJ, Stubbs CD (2000) Interaction of protein kinase C with filamentous actin: isozyme specificity resulting from divergent phorbol ester and calcium dependencies. Biochemistry 39:271–280
17. Giorgione JR, Lin JH, McCammon JA, Newton AC (2006) Increased membrane affinity of the C1 domain of protein kinase C delta compensates for the lack of involvement of its C2 domain in membrane recruitment. J Biol Chem 281:1660–1669
18. Newton AC (1995) Protein kinase C: structure, function, and regulation. J Biol Chem 270:28495–28498
19. Moscat J, Diaz-Meco MT, Wooten MW (2009) Of the atypical PKCs, Par-4 and p62: recent understandings of the biology and pathology of a PB1-dominated complex. Cell Death Differ 16:1426–1437
20. Quittau-Prevostel C, Delaunay N, Collazos A, Vallentin A, Joubert D (2004) Targeting of PKCalpha and epsilon in the pituitary: a highly regulated mechanism involving a GD(E)E motif of the V3 region. J Cell Sci 117:63–72
21. Mellor H, Parker PJ (1998) The extended protein kinase C superfamily. Biochem J 332:281–292
22. Newton AC (2003) Regulation of the ABC kinases by phosphorylation: protein kinase C as a paradigm. Biochem J 370:361–371
23. Parker PJ, Parkinson SJ (2001) AGC protein kinase phosphorylation and protein kinase C. Biochem Soc Trans 29:860–863
24. Keranen LM, Dutil EM, Newton AC (1995) Protein kinase C is regulated in vivo by three functionally distinct phosphorylations. Curr Biol 5:1394–1403
25. Newton AC (2001) Protein kinase C: structural and spatial regulation by phosphorylation, cofactors, and macromolecular interactions. Chem Rev 101:2353–2364
26. Dutil EM, Newton AC (2000) Dual role of pseudosubstrate in the coordinated regulation of protein kinase C by phosphorylation and diacylglycerol. J Biol Chem 275:10697–10701

27. Dutil EM, Toker A, Newton AC (1998) Regulation of conventional protein kinase C isozymes by phosphoinositide-dependent kinase 1 (PDK-1). Curr Biol 8:1366–1375
28. Le Good JA, Ziegler WH, Parekh DB, Alessi DR, Cohen P, Parker PJ (1998) Protein kinase C isotypes controlled by phosphoinositide 3-kinase through the protein kinase PDK1. Science 281:2042–2045
29. Chou MM, Hou W, Johnson J, Graham LK, Lee MH, Chen CS, Newton AC, Schaffhausen BS, Toker A (1998) Regulation of protein kinase C zeta by PI 3-kinase and PDK-1. Curr Biol 8:1069–1077
30. Balendran A, Hare GR, Kieloch A, Williams MR, Alessi DR (2000) Further evidence that 3-phosphoinositide-dependent protein kinase-1 (PDK1) is required for the stability and phosphorylation of protein kinase C (PKC) isoforms. FEBS Lett 484:217–223
31. Bornancin F, Parker PJ (1996) Phosphorylation of threonine 638 critically controls the dephosphorylation and inactivation of protein kinase Calpha. Curr Biol 6:1114–1123
32. Facchinetti V, Ouyang W, Wei H, Soto N, Lazorchak A, Gould C, Lowry C, Newton AC, Mao Y, Miao RQ, Sessa WC, Qin J, Zhang P, Su B, Jacinto E (2008) The mammalian target of rapamycin complex 2 controls folding and stability of Akt and protein kinase C. EMBO J 27:1932–1943
33. Ikenoue T, Inoki K, Yang Q, Zhou X, Guan KL (2008) Essential function of TORC2 in PKC and Akt turn motif phosphorylation, maturation and signalling. EMBO J 27:1919–1931
34. Guertin DA, Stevens DM, Thoreen CC, Burds AA, Kalaany NY, Moffat J, Brown M, Fitzgerald KJ, Sabatini DM (2006) Ablation in mice of the mTORC components raptor, rictor, or mLST8 reveals that mTORC2 is required for signaling to Akt-FOXO and PKCalpha, but not S6K1. Dev Cell 11:859–871
35. Sarbassov DD, Ali SM, Kim DH, Guertin DA, Latek RR, Erdjument-Bromage H, Tempst P, Sabatini DM (2004) Rictor, a novel binding partner of mTOR, defines a rapamycin-insensitive and raptor-independent pathway that regulates the cytoskeleton. Curr Biol 14:1296–1302
36. Edwards AS, Faux MC, Scott JD, Newton AC (1999) Carboxyl-terminal phosphorylation regulates the function and subcellular localization of protein kinase C betaII. J Biol Chem 274:6461–6468
37. Carrasco S, Merida I (2004) Diacylglycerol-dependent binding recruits PKCtheta and RasGRP1 C1 domains to specific subcellular localizations in living T lymphocytes. Mol Biol Cell 15:2932–2942
38. Ron D, Mochly-Rosen D (1995) An autoregulatory region in protein kinase C: the pseudoanchoring site. Proc Natl Acad Sci USA 92:492–496
39. Mochly-Rosen D, Gordon AS (1998) Anchoring proteins for protein kinase C: a means for isozyme selectivity. FASEB J 12:35–42
40. Churchill EN, Qvit N, Mochly-Rosen D (2009) Rationally designed peptide regulators of protein kinase C. Trends Endocrinol Metab 20:25–33
41. Nishikawa K, Toker A, Johannes FJ, Songyang Z, Cantley LC (1997) Determination of the specific substrate sequence motifs of protein kinase C isozymes. J Biol Chem 272:952–960
42. Hardie D, Hanks S (1995) The Protein kinase FactsBook, vol 2. Academic, London p 246
43. Luo B, Prescott SM, Topham MK (2003) Protein kinase C alpha phosphorylates and negatively regulates diacylglycerol kinase zeta. J Biol Chem 278:39542–39547
44. Tigges U, Koch B, Wissing J, Jockusch BM, Ziegler WH (2003) The F-actin cross-linking and focal adhesion protein filamin A is a ligand and in vivo substrate for protein kinase C alpha. J Biol Chem 278:23561–23569
45. Feng Y, Walsh CA (2004) The many faces of filamin: a versatile molecular scaffold for cell motility and signalling. Nat Cell Biol 6:1034–1038
46. Kolch W, Heidecker G, Kochs G, Hummel R, Vahidi H, Mischak H, Finkenzeller G, Marme D, Rapp UR (1993) Protein kinase C alpha activates RAF-1 by direct phosphorylation. Nature 364:249–252
47. Strack V, Krutzfeldt J, Kellerer M, Ullrich A, Lammers R, Haring HU (2002) The Protein-tyrosine-phosphatase SHP2 is phosphorylated on serine residues 576 and 591 by protein kinase C isoforms alpha, beta 1, beta 2, and eta. Biochemistry 41:603–608

48. Grossmann KS, Rosario M, Birchmeier C, Birchmeier W (2010) The tyrosine phosphatase Shp2 in development and cancer. Adv Cancer Res 106:53–89
49. Bu Y, Shi T, Meng M, Kong G, Tian Y, Chen Q, Yao X, Feng G, Chen H, Lu Z (2011) A novel screening model for the molecular drug for diabetes and obesity based on tyrosine phosphatase Shp2. Bioorg Med Chem Lett 21:874–878
50. Nguyen L, He Q, Meiri KF (2009) Regulation of GAP-43 at serine 41 acts as a switch to modulate both intrinsic and extrinsic behaviors of growing neurons, via altered membrane distribution. Mol Cell Neurosci 41:62–73
51. Sheu FS, Marais RM, Parker PJ, Bazan NG, Routtenberg A (1990) Neuron-specific protein F1/GAP-43 shows substrate specificity for the beta subtype of protein kinase C. Biochem Biophys Res Commun 171:1236–1243
52. Park HY, Perez JM, Laursen R, Hara M, Gilchrest BA (1999) Protein kinase C-beta activates tyrosinase by phosphorylating serine residues in its cytoplasmic domain. J Biol Chem 274:16470–16478
53. Becker KP, Hannun YA (2004) Isoenzyme-specific translocation of protein kinase C (PKC) betaII and not PKCbetaI to a juxtanuclear subset of recycling endosomes: involvement of phospholipase D. J Biol Chem 279:28251–28256
54. Ramakers GM, Gerendasy DD, de Graan PN (1999) Substrate phosphorylation in the protein kinase C gamma knockout mouse. J Biol Chem 274:1873–1874
55. Asai H, Hirano M, Shimada K, Kiriyama T, Furiya Y, Ikeda M, Iwamoto T, Mori T, Nishinaka K, Konishi N, Udaka F, Ueno S (2009) Protein kinase C gamma, a protein causative for dominant ataxia, negatively regulates nuclear import of recessive-ataxia-related aprataxin. Hum Mol Genet 18:3533–3543
56. Uddin S, Sassano A, Deb DK, Verma A, Majchrzak B, Rahman A, Malik AB, Fish EN, Platanias LC (2002) Protein kinase C-delta (PKC-delta) is activated by type I interferons and mediates phosphorylation of Stat1 on serine 727. J Biol Chem 277:14408–14416
57. Jain N, Zhang T, Kee WH, Li W, Cao X (1999) Protein kinase C delta associates with and phosphorylates Stat3 in an interleukin-6-dependent manner. J Biol Chem 274: 24392–24400
58. Lee YJ, Lee DH, Cho CK, Bae S, Jhon GJ, Lee SJ, Soh JW, Lee YS (2005) HSP25 inhibits protein kinase C delta-mediated cell death through direct interaction. J Biol Chem 280:18108–18119
59. Kim EH, Lee HJ, Lee DH, Bae S, Soh JW, Jeoung D, Kim J, Cho CK, Lee YJ, Lee YS (2007) Inhibition of heat shock protein 27-mediated resistance to DNA damaging agents by a novel PKC delta-V5 heptapeptide. Cancer Res 67:6333–6341
60. Bey EA, Xu B, Bhattacharjee A, Oldfield CM, Zhao X, Li Q, Subbulakshmi V, Feldman GM, Wientjes FB, Cathcart MK (2004) Protein kinase C delta is required for p47phox phosphorylation and translocation in activated human monocytes. J Immunol 173:5730–5738
61. Kilpatrick LE, Song YH, Rossi MW, Korchak HM (2000) Serine phosphorylation of p60 tumor necrosis factor receptor by PKC-delta in TNF-alpha-activated neutrophils. Am J Physiol Cell Physiol 279:C2011–C2018
62. Baier G, Telford D, Giampa L, Coggeshall KM, Baier-Bitterlich G, Isakov N, Altman A (1993) Molecular cloning and characterization of PKC theta, a novel member of the protein kinase C (PKC) gene family expressed predominantly in hematopoietic cells. J Biol Chem 268:4997–5004
63. Tsukita S, Furuse M (1999) Occludin and claudins in tight-junction strands: leading or supporting players? Trends Cell Biol 9:268–273
64. Suzuki T, Elias BC, Seth A, Shen L, Turner JR, Giorgianni F, Desiderio D, Guntaka R, Rao R (2009) PKC eta regulates occludin phosphorylation and epithelial tight junction integrity. Proc Natl Acad Sci USA 106:61–66
65. Osada S, Mizuno K, Saido TC, Suzuki K, Kuroki T, Ohno S (1992) A new member of the protein kinase C family, nPKC theta, predominantly expressed in skeletal muscle. Mol Cell Biol 12:3930–3938
66. Chang JD, Xu Y, Raychowdhury MK, Ware JA (1994) Molecular cloning and expression of a cDNA encoding a novel isoenzyme of protein kinase C (nPKC). A new member of the

nPKC family expressed in skeletal muscle, megakaryoblastic cells, and platelets. J Biol Chem 269:31322
67. Marsland BJ, Kopf M (2008) T-cell fate and function: PKC-theta and beyond. Trends Immunol 29:179–185
68. Hayashi K, Altman A (2007) Protein kinase C theta (PKCtheta): a key player in T cell life and death. Pharmacol Res 55:537–544
69. Mamidipudi V, Li X, Wooten MW (2002) Identification of interleukin 1 receptor-associated kinase as a conserved component in the p75-neurotrophin receptor activation of nuclear factor-kappa B. J Biol Chem 277:28010–28018
70. Mamidipudi V, Lin C, Seibenhener ML, Wooten MW (2004) Regulation of interleukin receptor-associated kinase (IRAK) phosphorylation and signaling by iota protein kinase C. J Biol Chem 279:4161–4165
71. Suzuki A, Akimoto K, Ohno S (2003) Protein kinase C lambda/iota (PKClambda/iota): a PKC isotype essential for the development of multicellular organisms. J Biochem 133:9–16
72. Sugiyama Y, Akimoto K, Robinson ML, Ohno S, Quinlan RA (2009) A cell polarity protein aPKClambda is required for eye lens formation and growth. Dev Biol 336:246–256
73. Hirai T, Chida K (2003) Protein kinase Czeta (PKCzeta): activation mechanisms and cellular functions. J Biochem 133:1–7
74. Oubaha M, Gratton JP (2009) Phosphorylation of endothelial nitric oxide synthase by atypical PKC zeta contributes to angiopoietin-1-dependent inhibition of VEGF-induced endothelial permeability in vitro. Blood 114:3343–3351
75. Hirata Y, Hosaka T, Iwata T, Le CT, Jambaldorj B, Teshigawara K, Harada N, Sakaue H, Sakai T, Yoshimoto K, Nakaya Y (2011) Vimentin binds IRAP and is involved in GLUT4 vesicle trafficking. Biochem Biophys Res Commun 405:96–101
76. Ryu J, Hah JS, Park JS, Lee W, Rampal AL, Jung CY (2002) Protein kinase C-zeta phosphorylates insulin-responsive aminopeptidase in vitro at Ser-80 and Ser-91. Arch Biochem Biophys 403:71–82
77. Dang PM, Fontayne A, Hakim J, El Benna J, Perianin A (2001) Protein kinase C zeta phosphorylates a subset of selective sites of the NADPH oxidase component p47phox and participates in formyl peptide-mediated neutrophil respiratory burst. J Immunol 166:1206–1213
78. Roffey J, Rosse C, Linch M, Hibbert A, McDonald NQ, Parker PJ (2009) Protein kinase C intervention: the state of play. Curr Opin Cell Biol 21:268–279
79. Alessi DR (1997) The protein kinase C inhibitors Ro 318220 and GF 109203X are equally potent inhibitors of MAPKAP kinase-1beta (Rsk-2) and p70 S6 kinase. FEBS Lett 402:121–123
80. Herbert JM, Augereau JM, Gleye J, Maffrand JP (1990) Chelerythrine is a potent and specific inhibitor of protein kinase C. Biochem Biophys Res Commun 172:993–999
81. Smith JB, Smith L, Pettit GR (1985) Bryostatins: potent, new mitogens that mimic phorbol ester tumor promoters. Biochem Biophys Res Commun 132:939–945
82. Kobayashi E, Nakano H, Morimoto M, Tamaoki T (1989) Calphostin C (UCN-1028C), a novel microbial compound, is a highly potent and specific inhibitor of protein kinase C. Biochem Biophys Res Commun 159:548–553
83. Ponting CP, Ito T, Moscat J, Diaz-Meco MT, Inagaki F, Sumimoto H (2002) OPR, PC and AID: all in the PB1 family. Trends Biochem Sci 27(1):10
84. Stallings-Mann M, Jamieson L, Regala RP, Weems C, Murray NR, Fields AP (2006) A novel small-molecule inhibitor of protein kinase Ciota blocks transformed growth of non-small-cell lung cancer cells. Cancer Res 66:1767–1774
85. Regala RP, Thompson EA, Fields AP (2008) Atypical protein kinase C iota expression and aurothiomalate sensitivity in human lung cancer cells. Cancer Res 68:5888–5895
86. Lahn MM, Sundell KL (2004) The role of protein kinase C-alpha (PKC-alpha) in melanoma. Melanoma Res 14:85–89
87. Lahn M, Sundell K, Moore S (2003) Targeting protein kinase C-alpha (PKC-alpha) in cancer with the phosphorothioate antisense oligonucleotide aprinocarsen. Ann NY Acad Sci 1002:263–270

88. Davies AM, Gandara DR, Lara PNJ, Mack PC, Lau DH, Gumerlock PH (2003) Antisense oligonucleotides in the treatment of non-small-cell lung cancer. Clin Lung Cancer 4(Suppl 2):S68–S73
89. Newton PM, Kim JA, McGeehan AJ, Paredes JP, Chu K, Wallace MJ, Roberts AJ, Hodge CW, Messing RO (2007) Increased response to morphine in mice lacking protein kinase C epsilon. Genes Brain Behav 6:329–338
90. Wallace MJ, Newton PM, McMahon T, Connolly J, Huibers A, Whistler J, Messing RO (2009) PKCepsilon regulates behavioral sensitivity, binding and tolerance to the CB1 receptor agonist WIN55,212-2. Neuropsychopharmacology 34:1733–1742
91. Wallace MJ, Newton PM, Oyasu M, McMahon T, Chou WH, Connolly J, Messing RO (2007) Acute functional tolerance to ethanol mediated by protein kinase Cepsilon. Neuropsychopharmacology 32:127–136
92. Hodge CW, Mehmert KK, Kelley SP, McMahon T, Haywood A, Olive MF, Wang D, Sanchez-Perez AM, Messing RO (1999) Supersensitivity to allosteric GABA(A) receptor modulators and alcohol in mice lacking PKCepsilon. Nat Neurosci 2:997–1002
93. Newton PM, Messing RO (2007) Increased sensitivity to the aversive effects of ethanol in PKCepsilon null mice revealed by place conditioning. Behav Neurosci 121:439–442
94. Lesscher HM, Wallace MJ, Zeng L, Wang V, Deitchman JK, McMahon T, Messing RO, Newton PM (2009) Amygdala protein kinase C epsilon controls alcohol consumption. Genes Brain Behav 8:493–499
95. Qi ZH, Song M, Wallace MJ, Wang D, Newton PM, McMahon T, Chou WH, Zhang C, Shokat KM, Messing RO (2007) Protein kinase C epsilon regulates gamma-aminobutyrate type A receptor sensitivity to ethanol and benzodiazepines through phosphorylation of gamma2 subunits. J Biol Chem 282:33052–33063
96. Bowers BJ, Owen EH, Collins AC, Abeliovich A, Tonegawa S, Wehner JM (1999) Decreased ethanol sensitivity and tolerance development in gamma-protein kinase C null mutant mice is dependent on genetic background. Alcohol Clin Exp Res 23:387–397
97. Werner DF, Kumar S, Criswell HE, Suryanarayanan A, Fetzer JA, Comerford CE, Morrow AL (2011) PKCgamma is required for ethanol-induced increases in GABA(A) receptor alpha4 subunit expression in cultured cerebral cortical neurons. J Neurochem 116:554–563
98. Kumar S, Suryanarayanan A, Boyd KN, Comerford CE, Lai MA, Ren Q, Morrow AL (2010) Ethanol reduces GABAA alpha1 subunit receptor surface expression by a protein kinase C gamma-dependent mechanism in cultured cerebral cortical neurons. Mol Pharmacol 77:793–803
99. Proctor WR, Poelchen W, Bowers BJ, Wehner JM, Messing RO, Dunwiddie TV (2003) Ethanol differentially enhances hippocampal GABA A receptor-mediated responses in protein kinase C gamma (PKC gamma) and PKC epsilon null mice. J Pharmacol Exp Ther 305:264–270
100. Choi DS, Wei W, Deitchman JK, Kharazia VN, Lesscher HM, McMahon T, Wang D, Qi ZH, Sieghart W, Zhang C, Shokat KM, Mody I, Messing RO (2008) Protein kinase Cdelta regulates ethanol intoxication and enhancement of GABA-stimulated tonic current. J Neurosci 28:11890–11899
101. Olive MF, Newton PM (2010) Protein kinase C isozymes as regulators of sensitivity to and self-administration of drugs of abuse-studies with genetically modified mice. Behav Pharmacol 21:493–499
102. Hongpaisan J, Alkon DL (2007) A structural basis for enhancement of long-term associative memory in single dendritic spines regulated by PKC. Proc Natl Acad Sci USA 104:19571–19576
103. Choi DS, Wang D, Yu GQ, Zhu G, Kharazia VN, Paredes JP, Chang WS, Deitchman JK, Mucke L, Messing RO (2006) PKCepsilon increases endothelin converting enzyme activity and reduces amyloid plaque pathology in transgenic mice. Proc Natl Acad Sci USA 103:8215–8220
104. Buxbaum JD, Liu KN, Luo Y, Slack JL, Stocking KL, Peschon JJ, Johnson RS, Castner BJ, Cerretti DP, Black RA (1998) Evidence that tumor necrosis factor alpha converting enzyme

is involved in regulated alpha-secretase cleavage of the Alzheimer amyloid protein precursor. J Biol Chem 273:27765–27767
105. Etcheberrigaray R, Tan M, Dewachter I, Kuiperi C, Van der Auwera I, Wera S, Qiao L, Bank B, Nelson TJ, Kozikowski AP, Van Leuven F, Alkon DL (2004) Therapeutic effects of PKC activators in Alzheimer's disease transgenic mice. Proc Natl Acad Sci USA 101:11141–11146
106. Yang HQ, Pan J, Ba MW, Sun ZK, Ma GZ, Lu GQ, Xiao Q, Chen SD (2007) New protein kinase C activator regulates amyloid precursor protein processing in vitro by increasing alpha-secretase activity. Eur J Neurosci 26:381–391
107. Favit A, Grimaldi M, Nelson TJ, Alkon DL (1998) Alzheimer's-specific effects of soluble beta-amyloid on protein kinase C-alpha and -gamma degradation in human fibroblasts. Proc Natl Acad Sci USA 95:5562–5567
108. Hongpaisan J, Sun MK, Alkon DL (2011) PKC epsilon activation prevents synaptic loss, Abeta elevation, and cognitive deficits in Alzheimer's disease transgenic mice. J Neurosci 31:630–643
109. Sun MK, Hongpaisan J, Nelson TJ, Alkon DL (2008) Poststroke neuronal rescue and synaptogenesis mediated in vivo by protein kinase C in adult brains. Proc Natl Acad Sci USA 105:13620–13625
110. Della-Morte D, Raval AP, Dave KR, Lin HW, Perez-Pinzon MA (2011) Post-ischemic activation of protein kinase C epsilon protects the hippocampus from cerebral ischemic injury via alterations in cerebral blood flow. Neurosci Lett 487:158–162
111. Jiang X, Tian Q, Wang Y, Zhou XW, Xie JZ, Wang JZ, Zhu LQ (2011) Acetyl-L-carnitine ameliorates spatial memory deficits induced by inhibition of phosphoinositol-3 kinase and protein kinase C. J Neurochem 118(5):864–878
112. Bonini JS, Da Silva WC, Bevilaqua LR, Medina JH, Izquierdo I, Cammarota M (2007) On the participation of hippocampal PKC in acquisition, consolidation and reconsolidation of spatial memory. Neuroscience 147:37–45
113. Alkon DL, Sun MK, Nelson TJ (2007) PKC signaling deficits: a mechanistic hypothesis for the origins of Alzheimer's disease. Trends Pharmacol Sci 28:51–60
114. Sacktor TC (2011) How does PKMzeta maintain long-term memory? Nat Rev Neurosci 12:9–15
115. Liu JY, Lin SJ, Lin JK (1993) Inhibitory effects of curcumin on protein kinase C activity induced by 12-O-tetradecanoyl-phorbol-13-acetate in NIH 3T3 cells. Carcinogenesis 14:857–861
116. Mahmmoud YA (2007) Modulation of protein kinase C by curcumin; inhibition and activation switched by calcium ions. Br J Pharmacol 150:200–208
117. Bharti AC, Donato N, Aggarwal BB (2003) Curcumin (diferuloylmethane) inhibits constitutive and IL-6-inducible STAT3 phosphorylation in human multiple myeloma cells. J Immunol 171:3863–3871
118. Bharti AC, Donato N, Singh S, Aggarwal BB (2003) Curcumin (diferuloylmethane) down-regulates the constitutive activation of nuclear factor-kappa B and IkappaBalpha kinase in human multiple myeloma cells, leading to suppression of proliferation and induction of apoptosis. Blood 101:1053–1062
119. Surh YJ (2003) Cancer chemoprevention with dietary phytochemicals. Nat Rev Cancer 3:768–780
120. Singh S, Khar A (2006) Biological effects of curcumin and its role in cancer chemoprevention and therapy. Anticancer Agents Med Chem 6:259–270
121. Sharma RA, Steward WP, Gescher AJ (2007) Pharmacokinetics and pharmacodynamics of curcumin. Adv Exp Med Biol 595:453–470
122. Joe B, Vijaykumar M, Lokesh BR (2004) Biological properties of curcumin-cellular and molecular mechanisms of action. Crit Rev Food Sci Nutr 44:97–111
123. Neri A, Marmiroli S, Tassone P, Lombardi L, Nobili L, Verdelli D, Civallero M, Cosenza M, Bertacchini J, Federico M, De Pol A, Deliliers GL, Sacchi S (2008) The oral protein-kinase

C beta inhibitor enzastaurin (LY317615) suppresses signalling through the AKT pathway, inhibits proliferation and induces apoptosis in multiple myeloma cell lines. Leuk Lymphoma 49:1374–1383
124. Green LJ, Marder P, Ray C, Cook CA, Jaken S, Musib LC, Herbst RS, Carducci M, Britten CD, Basche M, Eckhardt SG, Thornton D (2006) Development and validation of a drug activity biomarker that shows target inhibition in cancer patients receiving enzastaurin, a novel protein kinase C-beta inhibitor. Clin Cancer Res 12:3408–3415
125. Robertson MJ, Kahl BS, Vose JM, de Vos S, Laughlin M, Flynn PJ, Rowland K, Cruz JC, Goldberg SL, Musib L, Darstein C, Enas N, Kutok JL, Aster JC, Neuberg D, Savage KJ, LaCasce A, Thornton D, Slapak CA, Shipp MA (2007) Phase II study of enzastaurin, a protein kinase C beta inhibitor, in patients with relapsed or refractory diffuse large B-cell lymphoma. J Clin Oncol 25:1741–1746
126. Ghobrial IM, Munshi NC, Harris BN, Shi P, Porter NM, Schlossman RL, Laubach JP, Anderson KC, Desaiah D, Myrand SP, Wooldridge JE, Richardson PG, Abonour R (2011) A phase I safety study of enzastaurin plus bortezomib in the treatment of relapsed or refractory multiple myeloma. Am J Hematol 86:573–578
127. Moreau AS, Jia X, Ngo HT, Leleu X, O'Sullivan G, Alsayed Y, Leontovich A, Podar K, Kutok J, Daley J, Lazo-Kallanian S, Hatjiharissi E, Raab MS, Xu L, Treon SP, Hideshima T, Anderson KC, Ghobrial IM (2007) Protein kinase C inhibitor enzastaurin induces in vitro and in vivo antitumor activity in Waldenstrom macroglobulinemia. Blood 109: 4964–4972
128. Varterasian ML, Mohammad RM, Eilender DS, Hulburd K, Rodriguez DH, Pemberton PA, Pluda JM, Dan MD, Pettit GR, Chen BD, Al-Katib AM (1998) Phase I study of bryostatin 1 in patients with relapsed non-Hodgkin's lymphoma and chronic lymphocytic leukemia. J Clin Oncol 16:56–62
129. Cragg LH, Andreeff M, Feldman E, Roberts J, Murgo A, Winning M, Tombes MB, Roboz G, Kramer L, Grant S (2002) Phase I trial and correlative laboratory studies of bryostatin 1 (NSC 339555) and high-dose 1-B-D-arabinofuranosylcytosine in patients with refractory acute leukemia. Clin Cancer Res 8:2123–2133
130. Varterasian ML, Mohammad RM, Shurafa MS, Hulburd K, Pemberton PA, Rodriguez DH, Spadoni V, Eilender DS, Murgo A, Wall N, Dan M, Al-Katib AM (2000) Phase II trial of bryostatin 1 in patients with relapsed low-grade non-Hodgkin's lymphoma and chronic lymphocytic leukemia. Clin Cancer Res 6:825–828
131. Zauli G, Secchiero P (2006) The role of the TRAIL/TRAIL receptors system in hematopoiesis and endothelial cell biology. Cytokine Growth Factor Rev 17:245–257
132. Hayun M, Okun E, Hayun R, Gafter U, Albeck M, Longo DL, Sredni B (2007) Synergistic effect of AS101 and Bryostatin-1 on myeloid leukemia cell differentiation in vitro and in an animal model. Leukemia 21:1504–1513
133. Wojciechowski W, Li H, Marshall S, Dell'Agnola C, Espinoza-Delgado I (2005) Enhanced expression of CD20 in human tumor B cells is controlled through ERK-dependent mechanisms. J Immunol 174:7859–7868
134. Mischiati C, Melloni E, Corallini F, Milani D, Bergamini C, Vaccarezza M (2008) Potential role of PKC inhibitors in the treatment of hematological malignancies. Curr Pharm Des 14:2075–2084
135. Budas GR, Churchill EN, Mochly-Rosen D (2007) Cardioprotective mechanisms of PKC isozyme-selective activators and inhibitors in the treatment of ischemia-reperfusion injury. Pharmacol Res 55:523–536
136. Dorn GW 2nd, Souroujon MC, Liron T, Chen CH, Gray MO, Zhou HZ, Csukai M, Wu G, Lorenz JN, Mochly-Rosen D (1999) Sustained in vivo cardiac protection by a rationally designed peptide that causes epsilon protein kinase C translocation. Proc Natl Acad Sci USA 96:12798–12803
137. Chen L, Hahn H, Wu G, Chen CH, Liron T, Schechtman D, Cavallaro G, Banci L, Guo Y, Bolli R, Dorn GW 2nd, Mochly-Rosen D (2001) Opposing cardioprotective actions and

parallel hypertrophic effects of delta PKC and epsilon PKC. Proc Natl Acad Sci USA 98:11114–11119
138. Inagaki K, Begley R, Ikeno F, Mochly-Rosen D (2005) Cardioprotection by epsilon-protein kinase C activation from ischemia: continuous delivery and antiarrhythmic effect of an epsilon-protein kinase C-activating peptide. Circulation 111:44–50
139. Murry CE, Jennings RB, Reimer KA (1986) Preconditioning with ischemia: a delay of lethal cell injury in ischemic myocardium. Circulation 74:1124–1136
140. Inagaki K, Chen L, Ikeno F, Lee FH, Imahashi K, Bouley DM, Rezaee M, Yock PG, Murphy E, Mochly-Rosen D (2003) Inhibition of delta-protein kinase C protects against reperfusion injury of the ischemic heart in vivo. Circulation 108:2304–2307
141. Hlavackova M, Kozichova K, Neckar J, Kolar F, Musters RJ, Novak F, Novakova O (2010) Up-regulation and redistribution of protein kinase C-delta in chronically hypoxic heart. Mol Cell Biochem 345:271–282
142. Bu X, Zhang N, Yang X, Liu Y, Du J, Liang J, Xu Q, Li J (2011) Proteomic analysis of cPKCbetaII-interacting proteins involved in HPC-induced neuroprotection against cerebral ischemia of mice. J Neurochem 117:346–356
143. Salek-Ardakani S, So T, Halteman BS, Altman A, Croft M (2004) Differential regulation of Th2 and Th1 lung inflammatory responses by protein kinase C theta. J Immunol 173:6440–6447
144. Marsland BJ, Soos TJ, Spath G, Littman DR, Kopf M (2004) Protein kinase C theta is critical for the development of in vivo T helper (Th)2 cell but not Th1 cell responses. J Exp Med 200:181–189
145. Healy AM, Izmailova E, Fitzgerald M, Walker R, Hattersley M, Silva M, Siebert E, Terkelsen J, Picarella D, Pickard MD, LeClair B, Chandra S, Jaffee B (2006) PKC-theta-deficient mice are protected from Th1-dependent antigen-induced arthritis. J Immunol 177:1886–1893
146. Manicassamy S, Yin D, Zhang Z, Molinero LL, Alegre ML, Sun Z (2008) A critical role for protein kinase C-theta-mediated T cell survival in cardiac allograft rejection. J Immunol 181:513–520
147. Wang L, Xiang Z, Ma LL, Chen Z, Gao X, Sun Z, Williams P, Chari RS, Yin DP (2009) Deficiency of protein kinase C-theta facilitates tolerance induction. Transplantation 87:507–516
148. Geraldes P, King GL (2010) Activation of protein kinase C isoforms and its impact on diabetic complications. Circ Res 106:1319–1331
149. Nawaratne R, Gray A, Jorgensen CH, Downes CP, Siddle K, Sethi JK (2006) Regulation of insulin receptor substrate 1 pleckstrin homology domain by protein kinase C: role of serine 24 phosphorylation. Mol Endocrinol 20:1838–1852
150. Mima A, Ohshiro Y, Kitada M, Matsumoto M, Geraldes P, Li C, Li Q, White GS, Cahill C, Rask-Madsen C, King GL (2011) Glomerular-specific protein kinase C-beta-induced insulin receptor substrate-1 dysfunction and insulin resistance in rat models of diabetes and obesity. Kidney Int 79:883–896
151. Waraich RS, Weigert C, Kalbacher H, Hennige AM, Lutz SZ, Haring HU, Schleicher ED, Voelter W, Lehmann R (2008) Phosphorylation of Ser357 of rat insulin receptor substrate-1 mediates adverse effects of protein kinase C-delta on insulin action in skeletal muscle cells. J Biol Chem 283:11226–11233
152. Lee S, Lynn EG, Kim JA, Quon MJ (2008) Protein kinase C-zeta phosphorylates insulin receptor substrate-1, -3, and -4 but not -2: isoform specific determinants of specificity in insulin signaling. Endocrinology 149:2451–2458
153. Oriente F, Andreozzi F, Romano C, Perruolo G, Perfetti A, Fiory F, Miele C, Beguinot F, Formisano P (2005) Protein kinase C-alpha regulates insulin action and degradation by interacting with insulin receptor substrate-1 and 14-3-3 epsilon. J Biol Chem 280:40642–40649
154. Chappell DS, Patel NA, Jiang K, Li P, Watson JE, Byers DM, Cooper DR (2009) Functional involvement of protein kinase C-betaII and its substrate, myristoylated alanine-rich C-kinase substrate (MARCKS), in insulin-stimulated glucose transport in L6 rat skeletal muscle cells. Diabetologia 52:901–911

155. Jacob AI, Horovitz-Fried M, Aga-Mizrachi S, Brutman-Barazani T, Okhrimenko H, Zick Y, Brodie C, Sampson SR (2010) The regulatory domain of protein kinase C delta positively regulates insulin receptor signaling. J Mol Endocrinol 44:155–169
156. Narita M, Mizoguchi H, Suzuki T, Narita M, Dun NJ, Imai S, Yajima Y, Nagase H, Suzuki T, Tseng LF (2001) Enhanced mu-opioid responses in the spinal cord of mice lacking protein kinase C gamma isoform. J Biol Chem 276:15409–15414
157. Reichling DB, Levine JD (2009) Critical role of nociceptor plasticity in chronic pain. Trends Neurosci 32:611–618

Chapter 29
The Role of C2 Domains in PKC Signaling

Carole A. Farah and Wayne S. Sossin

Abstract More than two decades ago, the discovery of the first C2 domain in conventional Protein Kinase Cs (cPKCs) and of its role as a calcium-binding motif began to shed light on the activation mechanism of this family of Serine/Threonine kinases which are involved in several critical signal transduction pathways. In this chapter, we review the current knowledge of the structure and the function of the different C2 domains in PKCs. The C2 domain of cPKCs is a calcium sensor and its calcium-dependent binding to phospholipids is crucial for kinase activation. While the functional role of the cPKC C2 domain is better understood, phylogenetic analysis revealed that the novel C2 domain is more ancient and related to the C2 domain in the fungal PKC family, while the cPKC C2 domain is first associated with PKC in metazoans. The C2 domain of novel PKCs (nPKCs) does not contain a calcium-binding motif but still plays a critical role in nPKCs activation by regulating C1-C2 domain interactions and consequently C2 domain-mediated inhibition in both the nPKCs of the epsilon family and the nPKCs of the delta family. Moreover, the C2 domain of the nPKCs of the delta family was shown to recognize phosphotyrosines in a novel mode different from the ones observed for the Src Homology 2 (SH2) and the phosphotyrosine binding domains (PTB). By binding to phosphotyrosines, the C2 domain regulates the activation of this subclass of PKCs. The C2 domain was also shown to be involved in protein-protein interactions and binding to the receptor for activated C-kinase (RACKs) thus contributing to the subcellular localization of PKCs. In summary, the C2 domain is a critical player that can sense the activated signaling pathway in response to external stimuli to specifically regulate the different conventional and novel PKC isoforms.

C.A. Farah • W.S. Sossin (✉)
Department of Neurology and Neurosurgery, Montreal Neurological Institute,
McGill University, BT 105, 3801 University Street, Montreal, QC H3A 2B4, Canada
e-mail: carole.abifarah@mcgill.ca; wayne.sossin@mcgill.ca

M.S. Islam (ed.), *Calcium Signaling*, Advances in Experimental Medicine and Biology 740, DOI 10.1007/978-94-007-2888-2_29,

Keywords C2 domain • Protein kinase C • Calcium • Conventional • Novel • Phosphotyrosine • Phosphatidylserine • Phosphatidic acid • Diacylglycerol • C1 domain • Receptor for activated C-kinase

Introduction

Protein kinase Cs (PKCs) are a family of lipid activated Serine/Threonine kinases which are involved in several critical signal transduction pathways including cell division, differentiation, migration, apoptosis and synaptic plasticity underlying learning and memory formation [1–7]. There are four known families of PKC isoforms in vertebrates: the conventional or Ca^{2+}-activated PKCs (cPKCs) family which includes PKC α, β1, β2 and γ, the novel or Ca^{2+}-independent PKCs (nPKCs) of the epsilon family which includes PKC ε and η also referred to as novel type I, the nPKCs or Ca^{2+}-independent PKCs of the delta family which includes PKC δ and θ also referred to as novel type II and the atypical family (aPKCs) which includes PKC ζ and ι (Fig. 29.1; [2, 8]). All isoforms have a catalytic domain located at the C-terminal and a regulatory domain located at the N-terminal. In the inactive form of the kinase, the pseudosubstrate (*P* in Fig. 29.1) located in the regulatory domain is lodged in the active site located in the catalytic domain and blocks it sterically keeping the enzyme inactive. In order for PKCs to become active, a conformational change is required to move the pseudosubstrate away from the active site and allow binding of the substrate [9, 10]. Conventional PKCs contain two tandem C1 domains which can bind to diacylglycerol (DAG)/Phorbol esters in the regulatory region and a C2 domain which mediates calcium-dependent binding to the membrane lipid phosphatidylserine (PS) and to phosphoinositide-4,5-bisphosphate [PIP2] [11–13]. Novel PKCs also contain two C1 domains that coordinate binding to DAG/Phorbol esters and a C2 domain but their C2 domain is located N-terminal to the C1 domains and lacks the critical aspartic acid residues required for coordinating Ca^{2+} ions in cPKCs [14]. In the nPKCs of the delta family, the C2 domain can also bind phosphotyrosines [15]. Atypical PKCs have one C1 domain which is said to be atypical because it cannot bind DAG/Phorbol esters and do not have a C2 domain but rather a PB1 domain in the regulatory region which mediates protein-protein interactions [16–18]. In *Aplysia californica*, our model system to study memory formation, there are three nervous system specific PKC isoforms one from each major class, namely the conventional PKC Apl I, the novel PKC Apl II which is homologous to the nPKCs of the epsilon family in vertebrates and the atypical PKC Apl III [2, 19, 20]. The present chapter will focus on the role of the C2 domains in PKC signaling. Therefore, the activation mechanisms of atypical PKCs will not be discussed in this chapter.

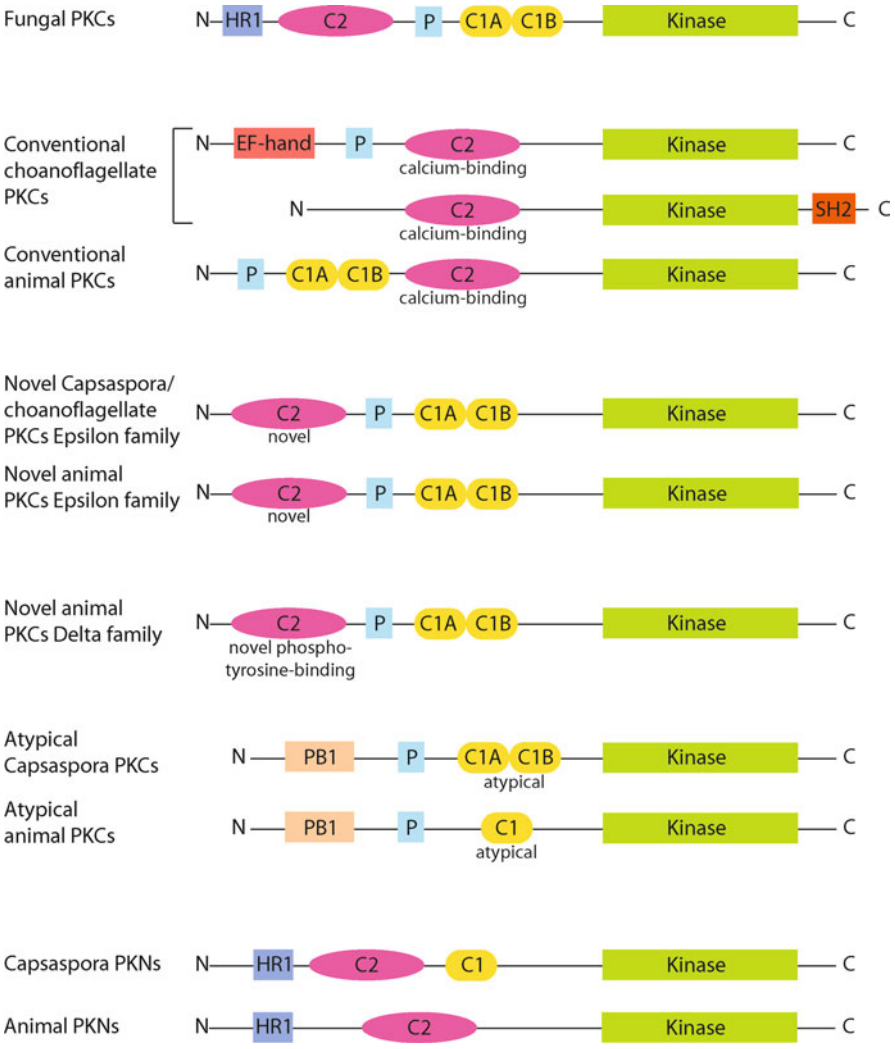

Fig. 29.1 Structure of PKC isoforms. Representative structures from each family are shown. Note that the C2 domains of nPKCs of the epsilon family and nPKCs of the delta family are located N-terminal to the C1 domains and lack the critical aspartic acid residues critical for coordinating Ca^{2+} in cPKCs. The C2 domain of nPKCs of the delta family can also bind to phosphotyrosines. Atypical PKCs don't contain a C2 domain but a PB1 domain that mediates protein-protein interactions. HR1 domains in yeast PKCs and PKNs bind to small GTP-binding proteins such as Ras and Rho. EF hands are calcium-binding domains related to the domains in calmodulin. SH2 (Src homology 2) domains are phosphotyrosine binding domains first defined in Src. *P*, pseudosubstrate

Evolution of C2 Domains

C2 domains are ancient and are found throughout eukaryotes in a wide variety of proteins [21]. In trying to understand the role of C2 domains in PKCs, it would be helpful to know whether the C2 domains in novel type I, novel type II, and conventional PKCs are directly related to each other and how the connection between the C2 domains and PKC evolved. We have previously used bioinformatics to probe the origins of the PKC family and found that (1) the four families of PKCs were already well established by the bilaterian ancestor; (2) The catalytic domains of PKCs and the related kinase protein kinase N (PKN)s are equally similar to fungal PKCs, and thus in early metazoans, the family first diverged into PKCs and PKNs; (3) atypical PKCs diverged from both conventional and novel PKCs before conventional, type I and type II PKCs diverged [2]. Since this study, the genomes of a number of primitive metazoans or species closely related to metazoans, including the choanoflagellates, Salpingoeca and Monosiga brevicollis as well as Capsaspora owczarzaki have been sequenced. We probed these organisms using Blast searches with the C2 domains from type I, type II and conventional PKCs as well as the fungal and PKN-C2 domains and examined proteins that contained C2 domains linked to a catalytic domain with strong homology to PKCs. We then used these C2 domains, as well as an assortment of other metazoan C2 domains from PKCs and PKNs as well as C2 domains from fungal PKCs to probe the evolutionary relationship of C2 domains. We used two additional well-conserved C2 domain families as reference points, the C2a domain from rabphilin, and the C2 domain from the ras GTPase-activating protein 3. These were chosen as the closest C2 domains to the novel and conventional C2 domains observed in blast searches. This analysis (Fig. 29.2) shows that C2 domains of fungal PKCs, PKNs, type I and type II PKCs form a well supported family of related C2 domains that presumably descended from a common ancestor. In contrast, the conventional PKC-C2 domain is first found associated with the catalytic domain of PKCs in choanoflagellates and is not directly related to the C2 domains in novel PKCs.

In Capsaspora owczarzaki, an organism that diverged from metazoans soon after the split between metazoans and fungi [22], there are three proteins with a catalytic domain most similar to PKCs/PKNs. One (gb/EFW44540) has the structure of a novel PKC (C2 domain N-terminal to tandem C1 domains), and the C2 domain of this protein segregates in the analysis with type I novel PKCs or epsilon-like novel PKCs (Figs. 29.1 and 29.2). Additionally, a protein is found (gb/EFW40430.1) with a PB1 domain and a kinase domain segregating with atypical PKCS (Fig. 29.1 and data not shown); notably this protein retains tandem C1 domains predicted to bind diacylglycerol, similar to yeast and animal PKCs, unlike the single atypical C1 domain found in all metazoan atypical PKCs. The third kinase has both the HR1 domains associated with mammalian PKNs and a C1 domain associated with PKCs (gb/EFW43140). The C2 domain in this protein segregates with the PKN C2 domains (Figs. 29.1 and 29.2), and thus we assume that this protein represents the PKN ancestor that had not yet completely lost its C1 domains.

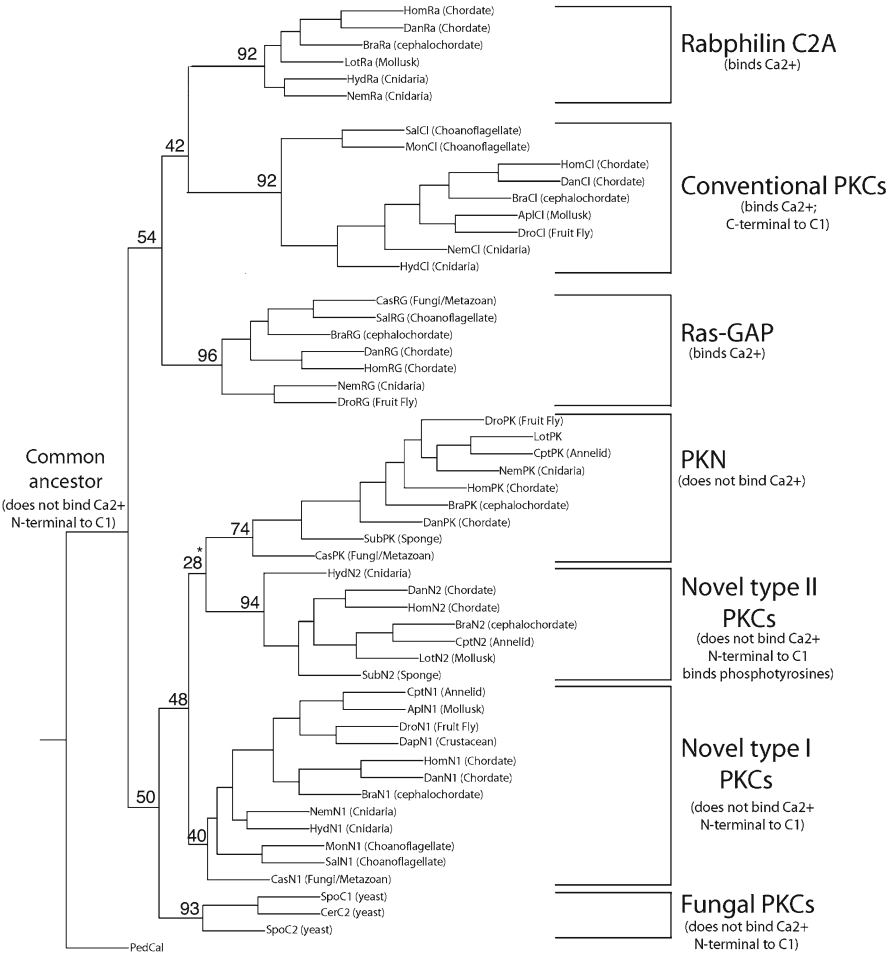

Fig. 29.2 Evolution of C2 domains. Sequences were obtained either from the NCBI site, http://blast.ncbi.nlm.nih.gov/Blast.cgi, or the JGI Genome site, http://genome.jgi-psf.org. Sequences were aligned with Clustal-W, 300 replicates were generated with the Phylip program Seqboot and then the Phylip program ProtDist was used with the Jones-Taylor-Thornton model to generate a Distance Matrix. The Phylip program Neighbor was then used to generate trees from each repetition, the program Consense to generate the consensus tree and Drawgram to make the final tree shown. Confidence numbers are given for critical nodes and represent the percentage of total trees that gave the tree shown. For more information on the workings of these programs, please see http://evolution.genetics.washington.edu/phylip/phylipweb.html. *Abbreviations* for species are: *Apl* Aplysia (Mollusk), *Bra* Brachiostoma (Lancelet, cephalochordate), *Cas* Capsaspora (Fungi/Metazoan), *Cer* S. Cervisiae (yeast), *Cpt* Capitella (Annelid), *Dan* Danio (Zebrafish; Chordate), *Dap* Daphnia (Crustacean), *Dro* Drosophila melanogaster (Fruit Fly), *Hom* Homo (Human; Chordate), *Hyd* (Hydra; Cnidaria), *Lot* Lottia (Mollusk), *Mon* Monosiga Brevicollis (Choanoflagellate), *Nem* Nemostella (Sea Anemone; Cnidaria), *Sal* Salpingoeca (Choanoflagellate), *Spo* S. Pombe (yeast), *Sub* Suberites domoncula (Sponge). The number of trees that matched the consensus tree is shown. *Other possible trees with close, but lower scores; Fungal PKCs with PKNs (20%); Type I and Type II PKCs (15%)

The choanoflagellate Salpingoeca also contains a protein with the structure of a novel PKC whose C2 domain segregates with novel type I PKCs (gb/EGD78676; Fig. 29.1). Unlike Capsaspora, it contains a kinase, EGD75514, with a C2 domain that segregates with conventional PKCs (Fig. 29.2) connected to a catalytic domain that also segregates with conventional PKCs (data not shown). However, this kinase does not contain C1 domains, but instead EF hands at the N-terminal. There is an additional protein, EGD77978 that also has a C2 domain attached to a kinase domain most similar to PKCs, although this C2 domain and kinase domain was difficult to assign to a particular group and is not included in the analysis in Fig. 29.2. This protein has a Src homology (SH2) domain at the carboxy-terminal of the kinase domain (Fig. 29.1). Similar kinases are found in the other choanoflagellate Monosiga brevicollis. We did not find a C2 domain that segregated with atypical PKCs, PKNs or type II novel PKCs in choanoflagellates.

In the Phylip analysis, the C2 domain of type II novel PKCs segregate with the PKN C2 domains, although this was not a strong association (Fig. 29.2). While it is conceivable that novel type I PKCs diverged from PKNs after the divergence of PKCs and PKNs, the previous analysis of kinase domains gave the opposite result [2]. The first appearance of two novel PKCs that are clearly related to the delta novel PKCs or type II nPKCs is in sponge and nematostella, a cnidarian. It is possible, and perhaps likely, that the divergence occurred earlier but in those genomes examined, type II PKCs were lost in the species whose genome has been sequenced. Thus, while this analysis does not determine at what point type I and type II novel PKCs diverged (either before conventional PKCs diverged or afterwards), it seems clear that the C2 domains of both of these proteins, and of PKN are ancestral, while the C2 domain of conventional PKCs became joined with the kinase domain in early metazoans. Thus, the C2 domain N-terminal to the C1 domain arrangement in novel PKCs is the ancestral arrangement, while the conventional PKCs represent a newer evolutionary event.

Recently, Zhang and Aravind [23] performed sequence-structure analysis of the C2 domain combined with phylogenetic analysis to infer the ancestral functions and subsequent diversification of C2 domains during eukaryotic evolution. They identified several novel versions of the C2 domain and their analysis shows that all families of C2 domains, except for PKC-C2 domains, lack the calcium-binding signature [23]. In agreement with our findings, they suggest that the common ancestor of all C2 domains probably did not bind calcium [23].

C2 Domain Structure

The C2 domain comprises about 130 residues and was first identified as the second of four conserved domains in the mammalian calcium-activated PKCs (Fig. 29.3; [26, 27]). The notion that this domain could act as a calcium-binding motif came from the observation that cPKCs which contained a C2 domain were regulated by calcium whereas nPKCs which were originally thought to lack a C2 domain, were

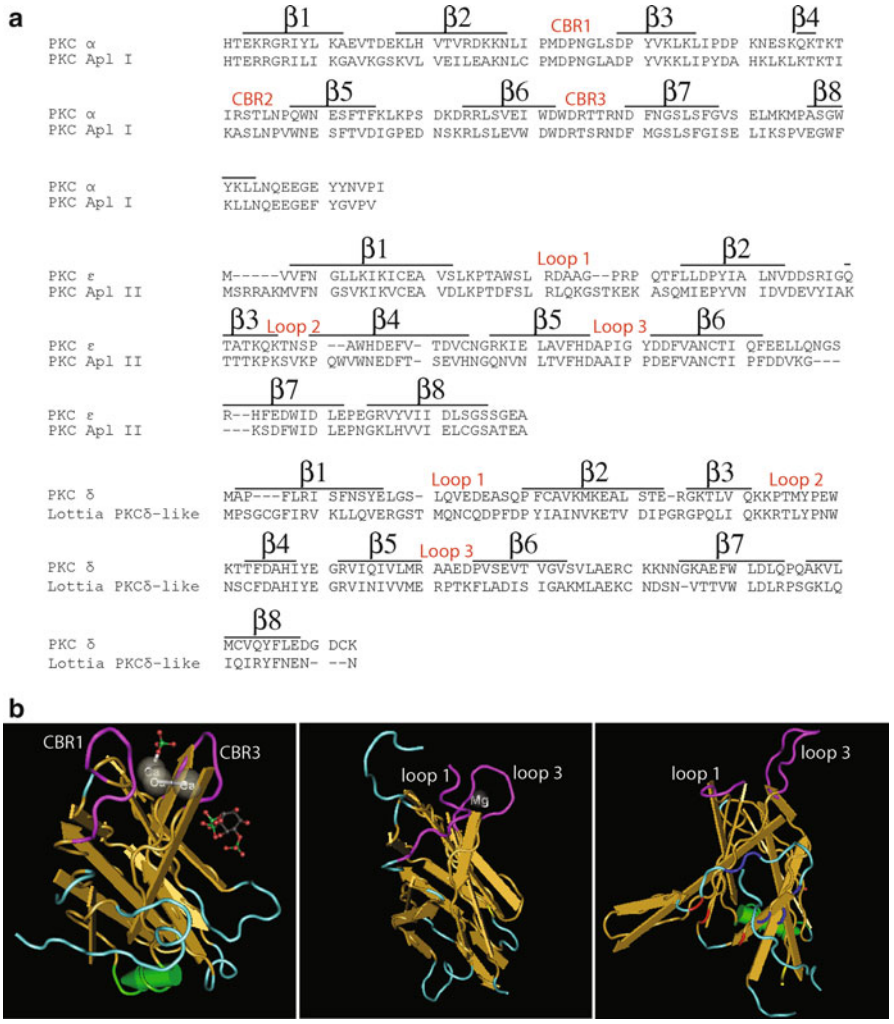

Fig. 29.3 Sequence alignment of the C2 domains and a representation of the overall structure of the C2 domains in PKCs. (**a**) Comparison of the C2 domains from vertebrate (*Mus musculus*) and invertebrate (*Aplysia californica*) conventional and novel PKCs of the epsilon family as well as from vertebrate (*Mus musculus*) and invertebrate (*Lottia*) novel PKCs of the delta family. The sequence of the conventional Ca^{2+}-dependent PKCα was aligned with that of PKC Apl I, the novel Ca^{2+}-independent type I PKCε with that of PKC Apl II and the novel Ca^{2+}-independent type II PKCδ with that of the Lottia PKCδ-like protein. *CBR*, calcium-binding region. (**b**) Three-dimensional representation of the structure of the different C2 domains based on the C2 domain of PKCα (*left panel*, [24]), the C2 domain of PKCε (*middle panel*, [25]) and the C2 domain of PKCδ (*right panel*, [15]). The structures were generated using CN3D 4.1 (produced by the National Center for Biotechnology Information; http://www.ncbi.nlm.nih.org). CBR1 and CBR3 are highlighted in *purple* in PKCα-C2 domain (*left panel*). *Loop 1* and *loop 3* are highlighted in *purple* in PKCε (*middle panel*) and PKCδ (*right panel*) C2 domains. In PKCδ-C2 domain (*right panel*), the residues that interact with the phosphates are highlighted in *red* and the residues that make contact with the peptide are highlighted in *dark blue* [15]

calcium-independent [26, 27]. We later reported that nPKCs do contain a phylogenetically conserved C2 domain that doesn't bind calcium [14, 19, 28]. The topology of the β-strands that form the C2 domains in conventional and novel PKCs is different [8]. The conventional C2 domains have a type I or a synaptotagmin-like topology whereas the novel C2 domains have a type II or phospholipase C (PLC)-like topology, consistent with their lack of common ancestry (see above). Topology I and topology II have a similar structure but differ in the orientation of the eight β-strands that form the C2 domain.

Calcium-Binding C2 Domain

The first C2 domain structure to be elucidated was that of PKCβ [29, 30]. The crystal structure of the C2 domain complexed with Ca^{2+} and o-phospho-L-serine has been determined to 2.7 Å resolution. The C2 domain of PKCβ is an antiparallel β sandwich similar in structure to the first C2 domain of synaptotagmin I with which it shares 28% amino-acid sequence identity. Each of the two sheets is composed of four antiparallel β strands. The Ca^{2+}-binding sites are located between the polypeptide loops that connect β2 to β3 and β6 to β7 and have been designated calcium-binding regions (CBRs; Fig. 29.3) I and III, respectively [31]. Three Ca^{2+}-binding subsites are arranged linearly within a broad trough lined by aspartate residues in loops β2–β3 and β6–β7 and a phosphoserine molecule binds to a lysine-rich cluster in C2. The authors suggested by model building that the C1 domain could provide carboxylate and carbonyl ligands for two of the three calcium sites and that Ca^{2+}-mediated interactions between the C1 and the C2 domains could contribute to enzyme activation as well as to the creation of a positively charged PS-binding site. Verdaguer and colleagues [32] later elucidated the three-dimensional structure of the Ca^{2+}-bound PKCα-C2 domain in the absence or presence of 1,2-dicaproyl-*sn*-phosphatidyl-L-serine (DCPS) by X-ray crystallography at 2.4 and 2.6 Å resolution respectively. The structure of PKCα-C2 domain retains most of the features found in the C2 domain of PKCβ including the organization of the calcium-binding region. However, only two calcium ions were found to bind to PKCα-C2 domain. The location corresponding to the third PKCβ-C2 calcium-binding subsite is occupied by a water molecule in PKCα-C2. In this study, a different model was suggested to explain the interaction of cPKCs with membranes. In this model, one calcium ion directly mediates the PS-specific recognition while the CBR3 might penetrate into the phospholipids bilayer [32]. Ochoa and colleagues [33] later determined the structure of PKCα-C2 domain crystallized in the presence of Ca^{2+} with either 1,2-diacetyl-sn-phosphatidyl-L-serine (DAPS) or 1,2-dicaproyl-sn-phosphatidic acid (DCPA) at 1.9 and 2.0 Å respectively. The structures showed the presence of an additional binding site for anionic phospholipids. The additional site was not located inside the calcium-binding pocket but in the vicinity of the conserved lysine-rich cluster in the concave surface of the C2 domain. In the DCPA complex, the absence of the serine headgroup and of its specific interactions seems to reduce the affinity

for the binding site inside the calcium pocket. Furthermore, in the DAPS-C2 domain complex, a third Ca^{2+}, which binds an extra phosphate group, was identified in the CBRs. In the complex with DCPA, the third Ca^{2+} might be present with partial occupancy. The third calcium ion is likely to bind with extremely low affinity in solution but might become trapped physiologically in a ternary C2 domain–membrane complex similar to what has been proposed to happen in PKCβ [34]. Finally, Guerrero-Valero and co-workers [24] determined the 3D structures of the ternary and quaternary complexes of the C2 domain of PKCα, crystallized in presence of Ca^{2+} and 1,2-diayl-*sn*-glycero-3-[phosphoinositol-4,5-bisphosphate] [PtdIns(4,5)P2] or Ca^{2+}, PtdIns(4,5)P2 and 1,2-dihexanoyl-*sn*-glycero-3-[phospho-L-serine] (PtdSer). They showed that PtdSer binds specifically to the calcium-binding region, whereas PtdIns(4,5)P2 occupies the concave surface of strands β3 and β4 allowing for the domain to be anchored to the membrane by two points. They further show that Tyr-195 and Trp-245 directly interact with the phosphate group of the inositol ring and mutating those residues impairs the ability of PKCα to localize to the plasma membrane [24].

Calcium-Independent C2 Domain

Ochoa and colleagues have determined the crystal structures of PKCε-C2 domain crystallized both in the absence and in the presence of the two acidic phospholipids, 1,2-dicaproyl-sn-phosphatidyl-L-serine (DCPS) and DCPA at 2.1, 1.7 and 2.8 Å resolution, respectively [25]. PKCε-C2 domain structure is an eight-stranded, antiparallel, β-sandwich with a type II topology similar to that of the C2 domains from PLC and from novel PKCδ (Fig. 29.3). Site-directed mutagenesis experiments and structural changes in the PKCε-C2 domain from crystals with DCPS or DCPA indicated that loops joining strands β1-β2 and β5-β6 participate in the binding to anionic membranes (Fig. 29.3; [25]). The pocket situated between loops 1 and 3 in the C2 domain of PKCε presents major differences with the corresponding pocket, the Ca^{2+}-binding pocket, defined by the CBRs in conventional PKCs. Ca^{2+} ions bind to the Ca^{2+} binding C2-domain in conventional PKCs mainly through the carboxylate groups from five conserved aspartate residues (187, 193, 246, 248 and 254 in PKCα) situated in CBR1 and CBR3. Three of the five conserved Ca^{2+} binding aspartate residues, 187, 246 and 248 in PKCα, are replaced by residues Phe36, His85 and Ala87, respectively, in PKCε. The two aspartate residues still present in PKCε, Asp39 (from loop 1) and Asp93 (from loop 3), appear to play only a structural role [25]. Furthermore, Asp86 and Asp92 in the β5-β6 loop help coordinate a magnesium (Mg^{2+}) ion one directly and one indirectly. A model for binding of PKCε-C2 domain to membranes was proposed by Ochoa and colleagues who stipulated that loop 1 would remain mostly on the surface of the membrane while loop 3 would insert into the membrane.

The crystal structure of PKCη-C2 domain was later elucidated by Littler and colleagues [35]. The structure is similar to that of PKCε-C2 domain except for

differences in the loop regions C-terminal to the two α-helices: the structure of PKCε becomes flexible for several residues immediately C-terminal to α1 following Asp-27, PKCη instead forms a loosely structured but well-defined helical turn [35]. The authors further identified two potentially phosphorylated serine residues contained within helix α1 which might regulate PKCη.

Phosphotyrosine-Binding C2 Domain

Even though PKCε-C2 and PKCδ-C2 domains share the same type II topology and diverged from a common ancestor (see above), they are considered to be representatives of different PKC subclasses. Indeed, they share only a 19% sequence identity with a number of insertions and deletions that correspond to large structural differences observed [25]. These differences include the presence in the PKCδ-C2 domain structure of a helix, between strands β6-β7, and of a protruding β hairpin with a mostly basic sequence that might define an interaction site with anionic membranes unique to PKCδ-like molecules (Fig. 29.3; [36]). Most importantly, the C2 domain of PKCδ directly binds to phosphotyrosine peptides in a sequence specific manner as shown by Benes and colleagues [15] who elucidated the crystal structure of PKCδ-C2 domain bound to a peptide containing phosphotyrosine. Prior to the Benes study, the only signaling domains known to recognize phosphotyrosine were the SH2 and the phosphotyrosine binding domains [PTB] [15, 37–39]. Benes and colleagues showed that PKCδ-C2 domain mediates the association of PKCδ with a transmembrane protein overexpressed in colon cancer, CDCP1. The activity of Src promotes this interaction by phosphorylating key residues on CDCP1, which leads to the formation of a CDCP1-Src-PKCδ complex [15]. Moreover, the crystal structure of PKCδ-C2 domain bound to a substrate peptide revealed a novel mode of phosphotyrosine recognition, different from the ones observed in SH2 and PTB domains. Indeed, the interaction with the tyrosine is maintained by stacking against a histidine residue. Overall, the structure of PKCδ-C2 domain is significantly divergent from other C2 domains only in the region where phosphotyrosine binding occurs which is situated on the opposite side of where calcium and phospholipids bind in cPKCs.

Functions of the Different C2 Domains

Calcium-Dependent Binding to Phospholipids

Conventional PKC-C2 domains clearly function as a Ca^{2+}-regulated membrane anchor. Coordination of calcium in the C2 domain causes a dramatic increase in the affinity of cPKCs to phospholipids [13, 32]. Binding to calcium is thought to be the primary step in kinase activation. First, it transiently recruits the enzyme to

the membrane where its physiological activator, DAG, resides. Second, in conjunction with the C1 domain interacting with DAG, binding of the C2 domain to PS and PIP2 provides the energy to release the autoinhibitory pseudosubstrate sequence from the substrate-binding cavity, allowing substrate phosphorylation [11–13, 24, 32, 40–43]. As such, vertebrate cPKCs as well as the cPKC Apl I from *Aplysia californica* both require calcium in association with DAG for translocation to membranes and activation [44, 45].

It is important to note that while both PS and PIP2 bind to the conventional PKC-C2 domain in a calcium-dependent manner, they bind in different ways. PS binds to the C2 domain through the Ca^{2+}-binding region with calcium acting as a bridge between the protein and the membrane lipid while in the PIP2 binding mode, Ca^{2+} is needed but does not directly mediate the phosphoinositide-domain interaction, since PIP2 binds to the lysine-rich cluster which is more distant [11, 13, 24, 32, 41, 43]. Furthermore, PS and calcium binding seems to be a prerequisite for productive phosphoinositide binding [41]. Indeed, PIP2 alone cannot drive the membrane attachment of the domain but further stabilizes the Ca^{2+}- and PS-dependent membrane binding [41].

Multiple studies have suggested that the C1 domain of cPKCs is masked in the inactive form of the kinase by the C2 domain and is inaccessible to DAG [8, 12]. This phenomenon was first described for cPKCγ, when Oancea and Meyer showed that the isolated C1 domain translocated to cellular membranes with exogenous DAG far more quickly than did the full-length PKCγ, while, in response to Ca^{2+}, the isolated C2 domain translocated to membranes with the same kinetics as the full-length protein [46]. They postulated that the region N-terminal to the C1 domain encompassing the pseudosubstrate acts as a clamp to keep the C1 domain inaccessible to DAG. The clamp is released when the C2 domain binds to membranes. Slater and co-workers later demonstrated that the complete C1 domain of PKCα was able to bind and activate the full-length enzyme in a phorbol ester/DAG-dependent manner in the absence of phospholipids. Furthermore, it was found that the C1 domain bound to a protein fragment containing the C2 domain of PKCα, and they proposed that the activating conformational change in PKCα results from the dissociation of intramolecular interactions between the C1 and C2 domains [47]. Stahelin and co-workers further performed homology modeling and a docking analysis of C1A and C2 domains of PKCα which revealed a highly complementary interface that comprised Asp55-Arg252 and Arg42-Glu282 ion pairs [48]. Mutations of these residues in the predicted C1A-C2 interface showed large effects on *in vitro* membrane binding, enzyme activity, PS selectivity and cellular membrane translocation of PKCα supporting their involvement in interdomain interactions [48]. Finally, Stensman and Larsson [49] showed that acidic residues in the C-terminal tail of PKCα bind basic residues in the C2 domain, and that this interaction maintains the kinase in a closed conformation that masks the C1a domain. The C1a domain is presumably revealed when the basic patch on the C2 domain engages PIP2 in the membrane [49]. This model is strengthened by the evidence that, while mutation of residues in either charged region to Ala residues sensitizes the enzyme to exogenous DAG, swapping the residues in the basic and acidic patches restores DAG insensitivity [49].

While the above studies are in favor of C1-C2 domain interactions and C2 domain-mediated inhibition, a recent study by Leonard and co-workers [50], who elucidated the crystal structure of PKCβII, suggested the conformation of PKCβII is best described by a single closed auto-inhibited state in which the C2 domain projects away from, and has limited contact with, the rest of the structure [50]. In their model, PKCβII translocates to the membrane upon Ca^{2+} release in the cell, where the calcium-binding regions of its C2 domain mediate bridging to PS, with an adjoining site on the C2 domain binding PIP_2 [50]. Subsequent binding of DAG to the C1A domain results in disengagement of the C1A domain, which in turn forces the removal of the pseudosubstrate from the catalytic cleft. There are a number of possible explanations for the discrepancy between this model (C2 domain as a separate module) and the earlier studies (C2 domain interacting with the C1 domains). First, since the C2 domain in the crystal was implicated in the intermolecular interactions involved in generating the crystal, its placement in the native protein may not be the same as in the crystal. Second, C1-C2 domain interactions may be isozyme specific in cPKCs. Indeed, Johnson and co-workers [51] showed that the C1 and C2 domains of PKCβII were independent membrane-targeting modules, with each, independently of the other, containing determinants for membrane recognition [51]. More crystallization studies of the different PKC isoforms will help to address this issue.

Calcium-Independent Binding to Phospholipids

While structure analysis (see above) revealed binding of the novel C2 domain to phospholipids, several studies reported a low binding affinity or no binding to phospholipids both *in vitro* and *in vivo* [48, 52–55]. As such, Jose Lopez-Andreo and colleagues reported that the C2 domain of PKCε can bind to PA but the amount of PA required to bind to the C2 domain is high compared to that for the Ca^{2+}-dependent binding of the C2 domains of cPKCs to PS [48, 55–58]. Furthermore, Giorgione and co-workers showed that C2 domain deletion in PKCε showed no effect on binding to PS/DAG containing membranes [48, 55]. However, in this study, saturating amounts of DAG were used, and this might have compensated for the lack of the C2 domain. In *Aplysia*, deleting the C2 domain in PKC Apl II did not affect translocation in response to 1,2-dioctanoyl-*sn*-glycero-3-phosphate (DiC8-PA), a cell permeable analog of PA [54].

Whereas C2 domain seems to bind poorly to lipids, Pepio and Sossin have shown that phosphorylation of PKC Apl II-C2 domain greatly increases its binding affinity to phospholipids [59]. However, a PKC Apl II with the C2 phosphomimetic mutation showed less translocation than the wild type protein in Sf9 cells and in isolated sensory neurons from *Aplysia* (Farah, CA and Sossin, WS, in preparation). It rather seemed that phosphorylation of the C2 domain was acting on C2 domain-mediated inhibition and that lipid binding to the C2 domain of PKC Apl II is dissociated from protein translocation in vivo (Farah, CA and Sossin, WS, in preparation).

In agreement with this, mutating isoleucine 89 to an asparagine in loop 3 of the vertebrate PKCε decreases translocation in response to DOG and to DiC8-PA in RBL-2H3 cells but does not affect PKCε activation by PA in an *in vitro* assay [58].

While the contribution of lipid binding to the C2 domain to protein translocation of nPKCs *in vivo* remains unclear, there seems to be a consensus that the novel C2 domain acts as an autoinhibitory module that impedes DAG binding to the C1 domains [12, 48, 53–55, 60]. Indeed, For PKC Apl II, removal of the C2 domain lowered the amount of lipid required to activate the enzyme [52, 61]. Furthermore, Pepio and Sossin showed using mixed micelle assay that the presence of the C2 domain lowers the affinity of the C1 domain to phorbol esters and this inhibition is removed by PA demonstrating that C2 domain-mediated inhibition could be regulated [53]. Farah and colleagues later confirmed that the C2 domain of PKC Apl II interacts with its C1 domain to inhibit DAG binding and that PA activates the kinase by binding to the C1b domain and removing C2 domain-mediated inhibition in live cells [54]. Binding to PA was mediated by Arg-273 in the C1b domain and this residue is conserved in the nPKCε suggesting this mechanism is conserved through evolution. In agreement with this, the C1b domain of PKCε was shown to preferentially bind to PA-containing vesicles [62].

In vertebrates, evidence for C2 domain-mediated inhibition of nPKCs came from a study by Stahelin and coworkers who reported that the deletion of the C2 domain of PKCε induced a faster membrane translocation in HEK293 cells [48]. Furthermore, the C2-deleted construct had a higher affinity (~60%) for PS/DAG membranes and a higher level of activity (<50%) than the PKCε wild type. Moreover, Melowic and colleagues reported that the deletion of the C2 domain of PKCθ greatly enhanced its affinity to PS/DAG-containing membranes. The authors proposed that the C2 domain of PKCθ is involved in keeping the enzyme in an inactive conformation, presumably by interacting with the C1a and C1b domains [60]. For PKCδ, removal of the C2 domain induces a faster response of the protein to C1 ligands [55].

Both PKCε and PKC Apl II require PA production for translocation in cells and it was shown that DAG synergizes with PA for translocation of both proteins [54, 58]. However, the model proposed for translocation of PKCε stipulates that synergism is due to PA binding to the C2 domain [58]. The main justification for this model was the *in vitro* binding of the C2 domain of PKCε to PA and the lack of translocation when residues in the C2 domain responsible for PA binding were mutated. While these mutations decreased the affinity of the C2 domain for PA, they also could have strengthened C1-C2 domain interactions, and this could be the reason for their effect on translocation. For PKC Apl II, it was suggested that PA binds first to the C1b domain to remove C2 domain-mediated inhibition and allow for DAG binding to the C1 domains [54]. One possible model that would encompass the two suggested ones is that PA would bind to the C1 domain first removing C2 domain-mediated inhibition and disengaging the C1 domains. Once C2 domain-mediated inhibition is removed, the C2 domain would bind to PA and assist in protein translocation and activation along with DAG binding to the C1 domains. In favor of this model, Farah and co-workers reported that PKC Apl II R273H, in which C2 domain-mediated inhibition is removed, translocates slightly better in response to 5HT in

isolated sensory neurons than PKC Apl II ΔC2-R273H suggesting a small positive contribution of the C2 domain once C2 domain-mediated inhibition has been removed [54].

Phosphotyrosine Binding

PKCδ can be activated by tyrosine phosphorylation independently of cleavage or production of DAG and this mechanism is specific to this class of PKCs [63, 64]. Different tyrosine residues were shown to be phosphorylated in PKCδ depending on cell stimuli [64–67]. PKCδ can be phosphorylated by various tyrosine kinases and can even associate with tyrosine kinases such as Src, Fyn, Lyn, Abl, PYK2, Lck, and growth factor receptors [64, 65, 67–76]. The mechanism of interaction of PKCδ with tyrosine kinases remained unclear until Benes and co-workers discovered that the PKCδ-C2 domain was a phosphotyrosine-binding domain [15]. Indeed, phosphorylation of PKCδ on tyrosines was facilitated by binding of activated tyrosine kinases to the C2 domain of PKCδ [15]. The effects of tyrosine phosphorylation on PKCδ activity are diverse. Indeed, the catalytic activity of PKCδ was shown to be reduced by tyrosine phosphorylation in *v-ras*-transformed keratinocytes [77], and in epidermal cell treated with epidermal growth factor [69]. However, tyrosine phosphorylation enhanced PKCδ enzymatic activity in various cell lines following stimulation with phorbol esters, growth factors and hormones [65, 68, 78–83]. In particular, phosphorylation of PKCδ at Tyr-311 located in the hinge domain led to, and was critical for, activation of the kinase in response to H_2O_2 in COS-7 cells [64]. Thus, by interacting with phosphotyrosines, PKCδ-C2 domain controls activation of the kinase and allows for cross-talk between two distinct signaling pathways. Preliminary results indicate that PKCθ, which is a member of the same family and shares 70% homology with PKCδ, also contains a phosphotyrosine binding domain and is likely to be regulated by the same mechanism [15].

Other Protein–Protein Interactions

Mochly-Rosen and co-workers discovered that translocation of PKC was associated with binding of each activated PKC isozyme to a corresponding anchoring protein, which they termed RACK, for receptor for activated C-kinase [84–86]. Examples of RACK proteins include RACK1 for PKCβ and β'cop (RACK2), which is a member of the coatomer complex COPI that binds several coatomer proteins and the small G protein ARF, for PKCε [87–92]. Mochly-Rosen and co-workers showed that RACKs bind to a site on PKC, which is only exposed when the enzyme is activated by binding to its cofactors such as DAG and PS. This is consistent with the concept that in the inactive form of the enzyme, the C2 domain interacts with the C1 domain, and the C2 domain is then released after enzyme activation. Such binding brings

PKCs closer to their cellular substrates [93, 94]. The C2 domain was shown to be critical for binding to RACKs and peptides derived from RACK-binding site were shown to act as selective inhibitors of their respective PKC isozymes [85, 95, 96]. RACK binding site was also suggested to be masked in the inactive form of the kinase by intramolecular interactions taking place with a pseudo-RACK site also located in the C2 domain which resembles and mimics a sequence in the RACKs [85, 95, 96]. Peptides derived from the pseudo-RACK site were shown to be selective activators of their respective PKC isozymes.

Schechtman and co-workers demonstrated that mutating Asp-86 to an asparagine in the pseudo-RACK domain of PKCε inhibits protein translocation [97]. They proposed a model in which Asp-86 would be involved in the intramolecular interactions between RACK and pseudo-RACK sites [97]. While this in an attractive idea, it is also possible that this mutation is acting on C1-C2 domain interactions to increase C2 domain-mediated inhibition. Studies with pharmacological peptides derived from C2-RACK and C2-pseudo-RACK domains have allowed tremendous insight into the role of the different PKC isoforms in various pathological conditions and many of those peptides are currently in clinical trials, emphasizing the important role of C2 domain in PKC regulation [95].

One issue with the model of RACK binding is the cellular localization of RACKs. RACK1 is a ribosomal protein [98] that may be more important for PKC regulation of translation [99, 100], while β'cop is involved in retrograde trafficking from Golgi to ER, and may be important for PKC regulation of Golgi trafficking [87, 101]. However, PKC translocation to different subcellular compartments, including the plasma membrane cannot be solely explained by these protein-protein interactions. It is possible that additional RACKs play important roles in PKC translocation. It is also possible that some of the actions of the peptides derived from RACK and pseudo-RACK domains are due to regulation of C1-C2 domain interactions, and not C2 domain-protein interactions.

Conclusions

In this chapter, we have described the multiple functions of the C2 domain in conventional, novel type I and novel type II PKCs. The C2 domain seems to act as a sensor of the intracellular signaling cascade activated in response to external stimuli. When calcium is produced as a second messenger, its binding to the conventional C2 domain along with DAG binding to the C1 domains will activate cPKCs. When PA is produced as a second messenger, its binding to the C1 domains of nPKCs will remove C2 domain-mediated inhibition and allow for binding of DAG to the C1 domains thus activating the kinase. Association of the C2 domain of nPKCs of the delta family with phosphotyrosines specifically regulates the activation of this subclass. Finally, protein-protein interactions involving the C2 domain were shown to be critical for kinase activation and for its subcellular localization in response to external stimuli.

It is worthwhile emphasizing that PKC can transduce signals not only in the plasma membrane but also in other subcellular compartments such as the Golgi, mitochondria and the nucleus in response to different stimuli [55, 102–104]. Interestingly, the magnitude and the duration of PKC signaling at these different compartments seems to be differentially regulated [105] and it will be interesting to determine the contribution of the C2 domain to the differential activation of PKC in those subcellular regions.

References

1. Martelli AM, Mazzotti G, Capitani S (2004) Nuclear protein kinase C isoforms and apoptosis. Eur J Histochem 48:89–94
2. Sossin WS (2007) Isoform specificity of protein kinase Cs in synaptic plasticity. Learn Mem 14:236–246
3. Oka M, Kikkawa U (2005) Protein kinase C in melanoma. Cancer Metastasis Rev 24:287–300
4. Denning MF (2004) Epidermal keratinocytes: regulation of multiple cell phenotypes by multiple protein kinase C isoforms. Int J Biochem Cell Biol 36:1141–1146
5. Gutcher I, Webb PR, Anderson NG (2003) The isoform-specific regulation of apoptosis by protein kinase C. Cell Mol Life Sci 60:1061–1070
6. Gavrielides MV, Frijhoff AF, Conti CJ, Kazanietz MG (2004) Protein kinase C and prostate carcinogenesis: targeting the cell cycle and apoptotic mechanisms. Curr Drug Targets 5:431–443
7. Farah CA, Weatherill D, Dunn TW, Sossin WS (2009) PKC differentially translocates during spaced and massed training in Aplysia. J Neurosci 29:10281–10286
8. Corbalan-Garcia S, Gomez-Fernandez JC (2006) Protein kinase C regulatory domains: the art of decoding many different signals in membranes. Biochim Biophys Acta 1761:633–654
9. House C, Kemp BE (1987) Protein kinase C contains a pseudosubstrate prototope in its regulatory domain. Science 238:1726–1728
10. Makowske M, Rosen OM (1989) Complete activation of protein kinase C by an antipeptide antibody directed against the pseudosubstrate prototope. J Biol Chem 264:16155–16159
11. Evans JH, Murray D, Leslie CC, Falke JJ (2006) Specific translocation of protein kinase Calpha to the plasma membrane requires both Ca^{2+} and PIP2 recognition by its C2 domain. Mol Biol Cell 17:56–66
12. Gallegos LL, Newton AC (2008) Spatiotemporal dynamics of lipid signaling: protein kinase C as a paradigm. IUBMB Life 60:782–789
13. Sanchez-Bautista S, Marin-Vicente C, Gomez-Fernandez JC, Corbalan-Garcia S (2006) The C2 domain of PKCalpha is a Ca^{2+}-dependent PtdIns(4,5)P2 sensing domain: a new insight into an old pathway. J Mol Biol 362:901–914
14. Sossin WS, Schwartz JH (1993) Ca^{2+}-independent protein kinase Cs contain an amino-terminal domain similar to the C2 consensus sequence. Trends Biochem Sci 18:207–208
15. Benes CH, Wu N, Elia AE, Dharia T, Cantley LC, Soltoff SP (2005) The C2 domain of PKCdelta is a phosphotyrosine binding domain. Cell 121:271–280
16. Moscat J, Diaz-Meco MT (2000) The atypical protein kinase Cs. Functional specificity mediated by specific protein adapters. EMBO Rep 1:399–403
17. Henrique D, Schweisguth F (2003) Cell polarity: the ups and downs of the Par6/aPKC complex. Curr Opin Genet Dev 13:341–350

18. Hirano Y, Yoshinaga S, Ogura K, Yokochi M, Noda Y, Sumimoto H, Inagaki F (2004) Solution structure of atypical protein kinase CPB1 domain and its mode of interaction with ZIP/p62 and MEK5. J Biol Chem 279:31883–31890
19. Sossin WS, Diaz AR, Schwartz JH (1993) Characterization of two isoforms of protein kinase C in the nervous system of Aplysia californica. J Biol Chem 268:5763–5768
20. Bougie J, Lim T, Ferraro G, Manjunath V, Scott D, Sossin WS (2006) Cloning and characterization of protein kinase C (PKC) Apl III, a homologue of atypical PKCs in Aplysia. Soc Neurosci Abstr 32:669–610
21. Nalefski EA, Falke JJ (1996) The C2 domain calcium-binding motif: structural and functional diversity. Protein Sci 5:2375–2390
22. Ruiz-Trillo I, Roger AJ, Burger G, Gray MW, Lang BF (2008) A phylogenomic investigation into the origin of metazoa. Mol Biol Evol 25:664–672
23. Zhang D, Aravind L (2010) Identification of novel families and classification of the C2 domain superfamily elucidate the origin and evolution of membrane targeting activities in eukaryotes. Gene 469:18–30
24. Guerrero-Valero M, Ferrer-Orta C, Querol-Audi J, Marin-Vicente C, Fita I, Gomez-Fernandez JC, Verdaguer N, Corbalan-Garcia S (2009) Structural and mechanistic insights into the association of PKCalpha-C2 domain to PtdIns(4,5)P2. Proc Natl Acad Sci USA 106:6603–6607
25. Ochoa WF, Garcia-Garcia J, Fita I, Corbalan-Garcia S, Verdaguer N, Gomez-Fernandez JC (2001) Structure of the C2 domain from novel protein kinase Cepsilon. A membrane binding model for Ca(2+)-independent C2 domains. J Mol Biol 311:837–849
26. Kikkawa U, Kishimoto A, Nishizuka Y (1989) The protein kinase C family: heterogeneity and its implications. Annu Rev Biochem 58:31–44
27. Nishizuka Y (1988) The molecular heterogeneity of protein kinase C and its implications for cellular regulation. Nature 334:661–665
28. Kruger KE, Sossin WS, Sacktor TC, Bergold PJ, Beushausen S, Schwartz JH (1991) Cloning and characterization of Ca(2+)-dependent and Ca(2+)-independent PKCs expressed in Aplysia sensory cells. J Neurosci 11:2303–2313
29. Sutton RB, Sprang SR (1998) Structure of the protein kinase Cbeta phospholipid-binding C2 domain complexed with Ca^{2+}. Structure 6:1395–1405
30. Shao X, Davletov BA, Sutton RB, Sudhof TC, Rizo J (1996) Bipartite Ca^{2+}-binding motif in C2 domains of synaptotagmin and protein kinase C. Science 273:248–251
31. Essen LO, Perisic O, Lynch DE, Katan M, Williams RL (1997) A ternary metal binding site in the C2 domain of phosphoinositide-specific phospholipase C-delta1. Biochemistry 36:2753–2762
32. Verdaguer N, Corbalan-Garcia S, Ochoa WF, Fita I, Gomez-Fernandez JC (1999) Ca(2+) bridges the C2 membrane-binding domain of protein kinase Calpha directly to phosphatidylserine. EMBO J 18:6329–6338
33. Ochoa WF, Corbalan-Garcia S, Eritja R, Rodriguez-Alfaro JA, Gomez-Fernandez JC, Fita I, Verdaguer N (2002) Additional binding sites for anionic phospholipids and calcium ions in the crystal structures of complexes of the C2 domain of protein kinase calpha. J Mol Biol 320:277–291
34. Nalefski EA, Newton AC (2001) Membrane binding kinetics of protein kinase C betaII mediated by the C2 domain. Biochemistry 40:13216–13229
35. Littler DR, Walker JR, She YM, Finerty PJ Jr, Newman EM, Dhe-Paganon S (2006) Structure of human protein kinase C eta (PKCeta) C2 domain and identification of phosphorylation sites. Biochem Biophys Res Commun 349:1182–1189
36. Pappa H, Murray-Rust J, Dekker LV, Parker PJ, McDonald NQ (1998) Crystal structure of the C2 domain from protein kinase C-delta. Structure 6:885–894
37. Kavanaugh WM, Williams LT (1994) An alternative to SH2 domains for binding tyrosine-phosphorylated proteins. Science 266:1862–1865
38. Sondermann H, Kuriyan J (2005) C2 can do it, too. Cell 121:158–160
39. Sadowski I, Stone JC, Pawson T (1986) A noncatalytic domain conserved among cytoplasmic protein-tyrosine kinases modifies the kinase function and transforming activity of Fujinami sarcoma virus P130gag-fps. Mol Cell Biol 6:4396–4408

40. Newton AC (2001) Protein kinase C: structural and spatial regulation by phosphorylation, cofactors, and macromolecular interactions. Chem Rev 101:2353–2364
41. Manna D, Bhardwaj N, Vora MS, Stahelin RV, Lu H, Cho W (2008) Differential roles of phosphatidylserine, PtdIns(4,5)P2, and PtdIns(3,4,5)P3 in plasma membrane targeting of C2 domains. Molecular dynamics simulation, membrane binding, and cell translocation studies of the PKCalpha C2 domain. J Biol Chem 283:26047–26058
42. Marin-Vicente C, Gomez-Fernandez JC, Corbalan-Garcia S (2005) The ATP-dependent membrane localization of protein kinase Calpha is regulated by Ca^{2+} influx and phosphatidylinositol 4,5-bisphosphate in differentiated PC12 cells. Mol Biol Cell 16:2848–2861
43. Marin-Vicente C, Nicolas FE, Gomez-Fernandez JC, Corbalan-Garcia S (2008) The PtdIns(4,5)P2 ligand itself influences the localization of PKCalpha in the plasma membrane of intact living cells. J Mol Biol 377:1038–1052
44. Zhao Y, Leal K, Abi-Farah C, Martin KC, Sossin WS, Klein M (2006) Isoform specificity of PKC translocation in living Aplysia sensory neurons and a role for Ca^{2+}-dependent PKC APL I in the induction of intermediate-term facilitation. J Neurosci 26:8847–8856
45. Codazzi F, Di Cesare A, Chiulli N, Albanese A, Meyer T, Zacchetti D, Grohovaz F (2006) Synergistic control of protein kinase C{gamma} activity by ionotropic and metabotropic glutamate receptor inputs in hippocampal neurons. J Neurosci 26:3404–3411
46. Oancea E, Meyer T (1998) Protein kinase C as a molecular machine for decoding calcium and diacylglycerol signals. Cell 95:307–318
47. Slater SJ, Seiz JL, Cook AC, Buzas CJ, Malinowski SA, Kershner JL, Stagliano BA, Stubbs CD (2002) Regulation of PKC alpha activity by C1-C2 domain interactions. J Biol Chem 277:15277–15285
48. Stahelin RV, Digman MA, Medkova M, Ananthanarayanan B, Melowic HR, Rafter JD, Cho W (2005) Diacylglycerol-induced membrane targeting and activation of protein kinase Cepsilon: mechanistic differences between protein kinases Cdelta and Cepsilon. J Biol Chem 280:19784–19793
49. Stensman H, Larsson C (2007) Identification of acidic amino acid residues in the protein kinase C alpha V5 domain that contribute to its insensitivity to diacylglycerol. J Biol Chem 282:28627–28638
50. Leonard TA, Rozycki B, Saidi LF, Hummer G, Hurley JH (2011) Crystal structure and allosteric activation of protein kinase C betaII. Cell 144:55–66
51. Johnson JE, Giorgione J, Newton AC (2000) The C1 and C2 domains of protein kinase C are independent membrane targeting modules, with specificity for phosphatidylserine conferred by the C1 domain. Biochemistry 39:11360–11369
52. Pepio AM, Fan X, Sossin WS (1998) The role of C2 domains in Ca^{2+}-activated and Ca^{2+}-independent protein kinase Cs in aplysia [published erratum appears in J Biol Chem 1998 Aug 28;273(35):22856]. J Biol Chem 273:19040–19048
53. Pepio AM, Sossin WS (1998) The C2 domain of the Ca(2+)-independent protein kinase C Apl II inhibits phorbol ester binding to the C1 domain in a phosphatidic acid-sensitive manner. Biochemistry 37:1256–1263
54. Farah CA, Nagakura I, Weatherill D, Fan X, Sossin WS (2008) Physiological role for phosphatidic acid in the translocation of the novel protein kinase C Apl II in Aplysia neurons. Mol Cell Biol 28:4719–4733
55. Giorgione JR, Lin JH, McCammon JA, Newton AC (2006) Increased membrane affinity of the C1 domain of protein kinase Cdelta compensates for the lack of involvement of its C2 domain in membrane recruitment. J Biol Chem 281:1660–1669
56. Corbalan-Garcia S, Sanchez-Carrillo S, Garcia-Garcia J, Gomez-Fernandez JC (2003) Characterization of the membrane binding mode of the C2 domain of PKC epsilon. Biochemistry 42:11661–11668
57. Medkova M, Cho W (1998) Differential membrane-binding and activation mechanisms of protein kinase C-alpha and -epsilon. Biochemistry 37:4892–4900

58. Lopez-Andreo MJ, Gomez-Fernandez JC, Corbalan-Garcia S (2003) The simultaneous production of phosphatidic acid and diacylglycerol is essential for the translocation of protein kinase Cepsilon to the plasma membrane in RBL-2H3 cells. Mol Biol Cell 14:4885–4895
59. Pepio AM, Sossin WS (2001) Membrane translocation of novel protein kinase Cs is regulated by phosphorylation of the C2 domain. J Biol Chem 276:3846–3855
60. Melowic HR, Stahelin RV, Blatner NR, Tian W, Hayashi K, Altman A, Cho W (2007) Mechanism of diacylglycerol-induced membrane targeting and activation of protein kinase Ctheta. J Biol Chem 282:21467–21476
61. Sossin WS, Fan X, Saberi F (1996) Expression and characterization of Aplysia protein kinase C: a negative regulatory role for the E region. J Neurosci 16:10–18
62. Sanchez-Bautista S, Corbalan-Garcia S, Perez-Lara A, Gomez-Fernandez JC (2009) A comparison of the membrane binding properties of C1B domains of PKCgamma, PKCdelta, and PKCepsilon. Biophys J 96:3638–3647
63. Kikkawa U, Matsuzaki H, Yamamoto T (2002) Protein kinase C delta (PKC delta): activation mechanisms and functions. J Biochem (Tokyo) 132:831–839
64. Konishi H, Yamauchi E, Taniguchi H, Yamamoto T, Matsuzaki H, Takemura Y, Ohmae K, Kikkawa U, Nishizuka Y (2001) Phosphorylation sites of protein kinase C delta in H2O2-treated cells and its activation by tyrosine kinase in vitro. Proc Natl Acad Sci USA 98:6587–6592
65. Szallasi Z, Denning MF, Chang EY, Rivera J, Yuspa SH, Lehel C, Olah Z, Anderson WB, Blumberg PM (1995) Development of a rapid approach to identification of tyrosine phosphorylation sites: application to PKC delta phosphorylated upon activation of the high affinity receptor for IgE in rat basophilic leukemia cells. Biochem Biophys Res Commun 214:888–894
66. Li W, Chen XH, Kelley CA, Alimandi M, Zhang J, Chen Q, Bottaro DP, Pierce JH (1996) Identification of tyrosine 187 as a protein kinase C-delta phosphorylation site. J Biol Chem 271:26404–26409
67. Blake RA, Garcia-Paramio P, Parker PJ, Courtneidge SA (1999) Src promotes PKCdelta degradation. Cell Growth Differ 10:231–241
68. Li W, Mischak H, Yu JC, Wang LM, Mushinski JF, Heidaran MA, Pierce JH (1994) Tyrosine phosphorylation of protein kinase C-delta in response to its activation. J Biol Chem 269:2349–2352
69. Denning MF, Dlugosz AA, Threadgill DW, Magnuson T, Yuspa SH (1996) Activation of the epidermal growth factor receptor signal transduction pathway stimulates tyrosine phosphorylation of protein kinase C delta. J Biol Chem 271:5325–5331
70. Gschwendt M, Kielbassa K, Kittstein W, Marks F (1994) Tyrosine phosphorylation and stimulation of protein kinase C delta from porcine spleen by src in vitro. Dependence on the activated state of protein kinase C delta. FEBS Lett 347:85–89
71. Shanmugam M, Krett NL, Peters CA, Maizels ET, Murad FM, Kawakatsu H, Rosen ST, Hunzicker-Dunn M (1998) Association of PKC delta and active Src in PMA-treated MCF-7 human breast cancer cells. Oncogene 16:1649–1654
72. Yuan ZM, Utsugisawa T, Ishiko T, Nakada S, Huang Y, Kharbanda S, Weichselbaum R, Kufe D (1998) Activation of protein kinase C delta by the c-Abl tyrosine kinase in response to ionizing radiation. Oncogene 16:1643–1648
73. Sun X, Wu F, Datta R, Kharbanda S, Kufe D (2000) Interaction between protein kinase C delta and the c-Abl tyrosine kinase in the cellular response to oxidative stress. J Biol Chem 275:7470–7473
74. Wrenn RW (2001) Carbachol stimulates TYR phosphorylation and association of PKCdelta and PYK2 in pancreas. Biochem Biophys Res Commun 282:882–886
75. Song JS, Swann PG, Szallasi Z, Blank U, Blumberg PM, Rivera J (1998) Tyrosine phosphorylation-dependent and -independent associations of protein kinase C-delta with Src family kinases in the RBL-2H3 mast cell line: regulation of Src family kinase activity by protein kinase C-delta. Oncogene 16:3357–3368

76. Zang Q, Lu Z, Curto M, Barile N, Shalloway D, Foster DA (1997) Association between v-Src and protein kinase C delta in v-Src-transformed fibroblasts. J Biol Chem 272:13275–13280
77. Denning MF, Dlugosz AA, Howett MK, Yuspa SH (1993) Expression of an oncogenic rasHa gene in murine keratinocytes induces tyrosine phosphorylation and reduced activity of protein kinase C delta. J Biol Chem 268:26079–26081
78. Li W, Yu JC, Michieli P, Beeler JF, Ellmore N, Heidaran MA, Pierce JH (1994) Stimulation of the platelet-derived growth factor beta receptor signaling pathway activates protein kinase C-delta. Mol Cell Biol 14:6727–6735
79. Soltoff SP, Toker A (1995) Carbachol, substance P, and phorbol ester promote the tyrosine phosphorylation of protein kinase C delta in salivary gland epithelial cells. J Biol Chem 270:13490–13495
80. Moussazadeh M, Haimovich B (1998) Protein kinase C-delta activation and tyrosine phosphorylation in platelets. FEBS Lett 438:225–230
81. Li W, Jiang YX, Zhang J, Soon L, Flechner L, Kapoor V, Pierce JH, Wang LH (1998) Protein kinase C-delta is an important signaling molecule in insulin-like growth factor I receptor-mediated cell transformation. Mol Cell Biol 18:5888–5898
82. Popoff IJ, Deans JP (1999) Activation and tyrosine phosphorylation of protein kinase C delta in response to B cell antigen receptor stimulation. Mol Immunol 36:1005–1016
83. Benes C, Soltoff SP (2001) Modulation of PKCdelta tyrosine phosphorylation and activity in salivary and PC-12 cells by Src kinases. Am J Physiol Cell Physiol 280:C1498–C1510
84. Mochly-Rosen D, Gordon AS (1998) Anchoring proteins for protein kinase C: a means for isozyme selectivity. FASEB J 12:35–42
85. Kheifets V, Mochly-Rosen D (2007) Insight into intra- and inter-molecular interactions of PKC: design of specific modulators of kinase function. Pharmacol Res 55:467–476
86. Mochly-Rosen D (1995) Localization of protein kinases by anchoring proteins: a theme in signal transduction. Science 268:247–251
87. Csukai M, Chen CH, De Matteis MA, Mochly-Rosen D (1997) The coatomer protein beta'-COP, a selective binding protein (RACK) for protein kinase Cepsilon. J Biol Chem 272:29200–29206
88. Jimenez JL, Smith GR, Contreras-Moreira B, Sgouros JG, Meunier FA, Bates PA, Schiavo G (2003) Functional recycling of C2 domains throughout evolution: a comparative study of synaptotagmin, protein kinase C and phospholipase C by sequence, structural and modelling approaches. J Mol Biol 333:621–639
89. Besson A, Wilson TL, Yong VW (2002) The anchoring protein RACK1 links protein kinase Cepsilon to integrin beta chains. Requirements for adhesion and motility. J Biol Chem 277:22073–22084
90. Stebbins EG, Mochly-Rosen D (2001) Binding specificity for RACK1 resides in the V5 region of beta II protein kinase C. J Biol Chem 276:29644–29650
91. Lopez-Bergami P, Habelhah H, Bhoumik A, Zhang W, Wang LH, Ronai Z (2005) RACK1 mediates activation of JNK by protein kinase C [corrected]. Mol Cell 19:309–320
92. Park HY, Wu H, Killoran CE, Gilchrest BA (2004) The receptor for activated C-kinase-I (RACK-I) anchors activated PKC-beta on melanosomes. J Cell Sci 117:3659–3668
93. Mochly-Rosen D, Khaner H, Lopez J (1991) Identification of intracellular receptor proteins for activated protein kinase C. Proc Natl Acad Sci USA 88:3997–4000
94. Ron D, Luo J, Mochly-Rosen D (1995) C2 region-derived peptides inhibit translocation and function of beta protein kinase C in vivo. J Biol Chem 270:24180–24187
95. Budas GR, Koyanagi T, Churchill EN, Mochly-Rosen D (2007) Competitive inhibitors and allosteric activators of protein kinase C isoenzymes: a personal account and progress report on transferring academic discoveries to the clinic. Biochem Soc Trans 35:1021–1026
96. Churchill EN, Qvit N, Mochly-Rosen D (2009) Rationally designed peptide regulators of protein kinase C. Trends Endocrinol Metab 20:25–33
97. Schechtman D, Craske ML, Kheifets V, Meyer T, Schechtman J, Mochly-Rosen D (2004) A critical intramolecular interaction for protein kinase C epsilon translocation. J Biol Chem 279(16):15831–15840

98. Rabl J, Leibundgut M, Ataide SF, Haag A, Ban N (2011) Crystal structure of the eukaryotic 40S ribosomal subunit in complex with initiation factor 1. Science 331:730–736
99. Ceci M, Gaviraghi C, Gorrini C, Sala LA, Offenhauser N, Marchisio PC, Biffo S (2003) Release of eIF6 (p27BBP) from the 60S subunit allows 80S ribosome assembly. Nature 426:579–584
100. Nilsson J, Sengupta J, Frank J, Nissen P (2004) Regulation of eukaryotic translation by the RACK1 protein: a platform for signalling molecules on the ribosome. EMBO Rep 5:1137–1141
101. Garczarczyk D, Toton E, Biedermann V, Rosivatz E, Rechfeld F, Rybczynska M, Hofmann J (2009) Signal transduction of constitutively active protein kinase C epsilon. Cell Signal 21:745–752
102. Sakai N, Sasaki K, Ikegaki N, Shirai Y, Ono Y, Saito N (1997) Direct visualization of the translocation of the gamma-subspecies of protein kinase C in living cells using fusion proteins with green fluorescent protein. J Cell Biol 139:1465–1476
103. Wang QJ, Bhattacharyya D, Garfield S, Nacro K, Marquez VE, Blumberg PM (1999) Differential localization of protein kinase C delta by phorbol esters and related compounds using a fusion protein with green fluorescent protein. J Biol Chem 274:37233–37239
104. Wang WL, Yeh SF, Chang YI, Hsiao SF, Lian WN, Lin CH, Huang CY, Lin WJ (2003) PICK1, an anchoring protein that specifically targets protein kinase Calpha to mitochondria selectively upon serum stimulation in NIH 3T3 cells. J Biol Chem 278:37705–37712
105. Gallegos LL, Kunkel MT, Newton AC (2006) Targeting protein kinase C activity reporter to discrete intracellular regions reveals spatiotemporal differences in agonist-dependent signaling. J Biol Chem 281:30947–30956

Chapter 30
Ca^{2+}/Calmodulin-Dependent Protein Kinase II (CaMKII) in the Heart

Lars S. Maier

Abstract Aim of this review is to give an overview and discuss recent findings on the role of Ca^{2+}/calmodulin-dependent protein kinase II (CaMKII) in the heart. Special attention is drawn to excitation-contraction coupling (ECC) and excitation-transcription coupling (ETC). Because CaMKII expression and activity are increased in cardiac hypertrophy, heart failure, and during arrhythmias both in animal models as well as in the human heart a clinical significance of CaMKII is implied.

Keywords Ca^{2+} • Calmodulin • Ca^{2+}/calmodulin-dependent protein kinase II (CaMKII) • Excitation-contraction coupling (ECC) • Excitation-transcription coupling (ETC) • Heart • Heart failure • Hypertrophy • Sarcoplasmic reticulum (SR) • SR Ca^{2+} leak

Introduction

Ca^{2+}/calmodulin-dependent protein kinases (CaMK) are intracellular proteins activated by Ca^{2+} bound calmodulin (Ca^{2+}/CaM). There are several CaMK which either phosphorylate specific substrates or act as multifunctional kinases (e.g. CaMKII and IV) ([1], for review see [2]). In the heart, CaMKII is the major isoform involved in excitation-contraction coupling (ECC) and excitation-transcription coupling (ETC). ECC is described by an increase in intracellular Ca^{2+} concentration ($[Ca^{2+}]_i$) during the action potential (AP), thereby activating myofilaments leading to contraction. ETC describes the process of Ca^{2+}-dependent activation of transcription

L.S. Maier, MD, FESC, FAHA (✉)
Heisenberg-Professor, Department of Cardiology and Pneumology/Heart Center, Georg-August-University Göttingen, Robert-Koch-Str. 40, 37075 Göttingen, Germany
e-mail: lmaier@med.uni-goettingen.de

M.S. Islam (ed.), *Calcium Signaling*, Advances in Experimental Medicine and Biology 740, DOI 10.1007/978-94-007-2888-2_30,

resulting in cardiac hypertrophy which often progresses towards heart failure. Initial CaMKII activation by Ca^{2+}/CaM is followed either by autophosphorylation or oxidation. Independent of the means of CaMKII activation several Ca^{2+} handling proteins are regulated by CaMKII which are centrally involved in ECC including SR Ca^{2+} release channels (ryanodine receptors, RyR2), phospholamban (PLB), L-type Ca^{2+} channels (LTCC), as well as Na^+ and K^+ channels with multiple functional consequences (for review see [3]). CaMKII activity and expression are increased in cardiac hypertrophy, heart failure, and during arrhythmias both in animal models as well as in the human heart ([4, 5], for review see [6]) implying a clinical significance of CaMKII.

CaMKII Activation

There are four CaMKII genes (α, β, γ, δ) with the δ isoform being the major, although not exclusive, isoform in the heart (for review see [2, 3]). The splice variant $CaMKII\delta_B$ is compartmentalized to the nucleus (as is CaMKIV) and $CaMKII\delta_C$ is found in the cytosol [7]. The multimeric CaMKII enzyme consists of homo- or heteromultimers of 6–12 subunits forming a wheel-like structure. Each CaMKII monomer contains an amino-terminal catalytic domain, a regulatory domain with partially overlapping autoinhibitory and CaM binding regions, and a carboxy-terminal association domain responsible for oligomerization (for review see [2, 3]). The autoinhibitory region of the regulatory domain sterically blocks access to substrates (see Fig. 30.1). When $[Ca^{2+}]_i$ increases during systole, CaM binds its four Ca^{2+} ions [8] and attaches to the regulatory domain of CaMKII. By displacing the autoinhibitory domain the enzyme is activated (half maximal activation at $[Ca^{2+}]_i$ of ~0.5–1 μM) [9]. Upon autophosphorylation of Thr-286/287 on the autoinhibitory segment CaMKII can lock itself into an activated state (for review see [2, 6]). Autophosphorylation increases the affinity of the Ca^{2+}/CaM-kinase complex thereby trapping Ca^{2+}/CaM on the autophosphorylated subunit [10]. Even when $[Ca^{2+}]_i$ declines to resting levels during diastole (i.e. ~0.1 μM), Ca^{2+}/CaM is trapped for seconds. As a result, the kinase remains fully active as long as Ca^{2+}/CaM is trapped, regardless of the $[Ca^{2+}]_i$ level. In addition, autophosphorylation disrupts autoinhibition, such that even after Ca^{2+}/CaM has dissociated from CaMKII the enzyme remains partially active [11–13]. For inactivation to occur, CaMKII must be dephosphorylated by protein phosphatases (e.g. PP1, PP2A, PP2C) (for review see [6]).

In addition to phosphorylation, CaMKII can be activated by methionine oxidation at residues 281/282 [14] e.g. during elevated levels of reactive oxygen species. This is clinically important because pro-oxidant conditions occur in heart failure, during myocardial infarction and due to increased Angiotensin II levels as in arterial hypertension. CaMKII oxidation is reversed by methionine sulfoxide reductase A. Nevertheless, initial sarcoplasmic reticulum (SR) Ca^{2+} release to activate Ca^{2+}/CaM seems to be a prerequisite for CaMKII oxidation [15].

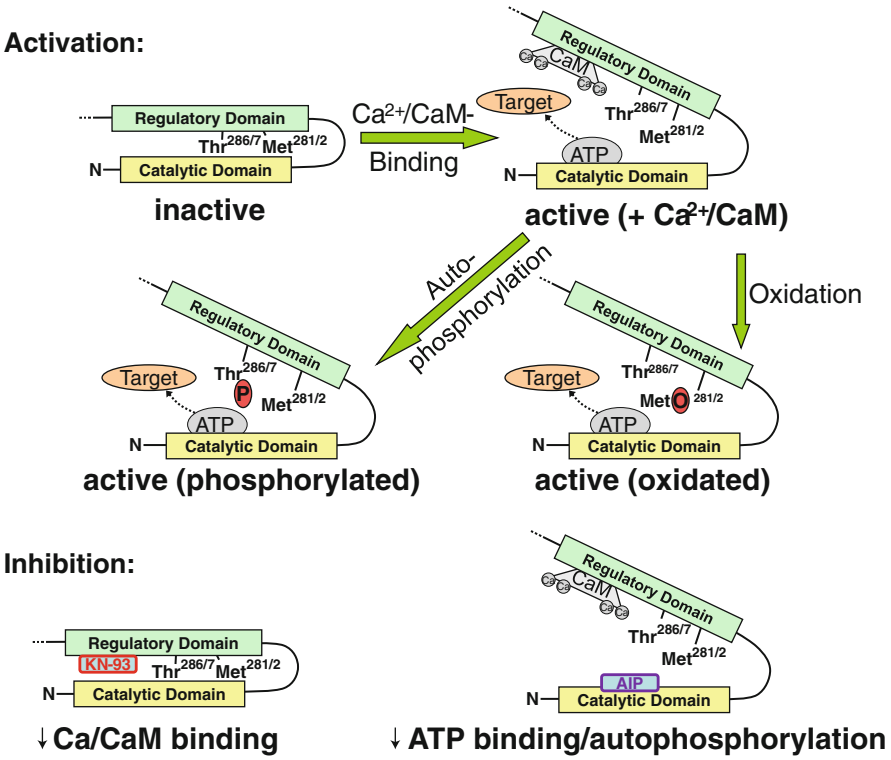

Fig. 30.1 Activation and inhibition of CaMKII (only the two main domains of the CaMKII monomer are indicated). Activation of CaMKII occurs by Ca^{2+}/CaM binding to the regulatory domain thereby opening the catalytic domain and making ATP binding possible and target protein phosphorylation. Subsequently autophosphorylation at Thr-286/7or oxidation at Met-281/2 occurs. CaMKII can be inhibited by KN-93 binding to the Ca/CaM binding site whereas AIP binding inhibits autophosphorylation (but not oxidation)

Whether there is direct ß-adrenergic activation of CaMKII was unclear. It seems likely, however, that some ß-adrenergic effects on EC coupling are mediated by CaMKII as it was shown for SR Ca^{2+} leak [16]. Recently, the guanine nucleotide exchange factor (Epac) which is activated by cyclic adenosine 3′,5′-monophosphate (cAMP) upon ß-adrenergic stimulation was shown to activate CaMKII [17–19] although the exact mechanism of activation is unknown.

Various CaMKII inhibitors exist including KN-93 (and KN-62) which competitively inhibit Ca^{2+}/CaM binding to CaMKII (for review see [2, 3, 6]). Unfortunately, these compounds have unspecific side effects on ion channels [20]. In contrast, autocamtide-2 related inhibitory peptide (AIP) and autocamtide-2 inhibitory peptide (AC3-I) are nonphosphorylatable, competitive substrates for autophosphorylation of CaMKII [21]. Potential clinically relevant CaMKII inhibitors are not available at the moment.

CaMKII in Excitation-Transcription Coupling (ETC)

Several original reports and reviews concentrated on the effects of CaMKII on transcription and hypertrophy [6, 22]. Initial studies in CaM overexpressing mice showed that cardiac hypertrophy resulted from downstream activation of CaMKII [23]. Specific activation of nuclear CaMKIIδ_B in cultured neonatal myocytes leads to hypertrophic gene expression [24] and transgenic CaMKIIδ_B mice resulted in cardiac hypertrophy [25]. CaMKIV overexpression with nuclear localization also induced hypertrophic responses in cultured cardiomyocytes and transgenic mice [26] but this mainly resulted from parallel CaMKII activation [27]. An even more severe cardiac phenotype through transgenic overexpression of cytosolic CaMKIIδ_C resulted in massive cardiac hypertrophy, dilatation, and heart failure [28]. Chronic CaMKII inhibition in a mouse model by AC3-I prevents cardiac remodeling during infarction-induced hypertrophy and heart failure [29]. Specific CaMKIIδ knockout in afterload-induced mouse models also prevents hypertrophy and heart failure [30, 31].

For the human heart, it was shown that CaMKII expression and activity are increased in end-stage heart failure [4, 5]. But even during compensated cardiac hypertrophy in patients without heart failure, CaMKII expression is increased in human myocardium [32]. More importantly, CaMKII phosphorylation seems to be stress-specific because it was shown to be increased due to increased afterload (TAC mouse model) but not when preload was increased (shunt mouse model).

But how does CaMKII induce hypertrophic signaling? CaMK has been suggested to modulate gene expression via different transcription factors including myocytes enhancer factor 2 (MEF2): Studies in crossbred mice expressing both CaMKIV and a MEF2-reporter supported the idea that MEF2 is a downstream target for CaMK [26]. Several recent studies showed that HDACs, a family of transcriptional repressors, serve as links between CaMK and MEF2 [33, 34]. Class II histone deacetylases (HDAC4, 5, 7, 9) are expressed in the heart and have a unique MEF2 binding domain. MEF2-HDAC interaction can be disrupted by phosphorylation of two HDAC serine residues, resulting in nuclear export of an HDAC/14-3-3 complex, freeing MEF2 to drive downstream gene transcription. CaMKII may be such a class II HDAC kinase (for review see [35]). Indeed, CaMKII was shown to phosphorylate HDAC4 and 5 leading to its transport from the nucleus thereby activating transcription [36]. In addition, a CaMK-independent mechanism to control class II HDAC function was suggested to exist in heart because HDAC was resistant to CaMK inhibitors [37] which may be due to a possible role of PKD for hypertrophic signaling [38]. An alternative prohypertrophic pathway may be through Epac-induced CaMKII and HDAC4 activation leading to MEF2 [39].

In the nucleus, CaMKII may be part of a local signaling complex because CaMKII associates with inositol 1,4,5-trisphosphate (IP_3) type 2 receptor in the nuclear envelope [40]. IP_3 production occurs upon activation of sarcolemmal G-protein coupled receptors, e.g. through hypertrophic neurohumoral agents such as endothelin-1 (ET-1). This causes local Ca^{2+} release from nuclear IP_3 receptors and the activation of CaMKIIδ_B within the nucleus which phosphorylates HDAC triggering its nuclear export [41].

Whether CaMKII only plays a role in pathological hypertrophy is unclear. There are a few reports that exercise training which usually leads to physiological hypertrophy also activates CaMKII but improves SR Ca^{2+} handling due to phosphorylation of PLB [42]. Also, in mice with type-2 diabetes with reduced contractile function and altered Ca^{2+} handling, exercise training resulted in reduced levels of CaMKII and improved contractile function and Ca^{2+} handling [43].

CaMKII in Excitation-Contraction Coupling (ECC)

During an AP, Ca^{2+} enters the cell through LTCC triggering subsequent Ca^{2+} release from the SR via RyR2 (Ca^{2+}-induced Ca^{2+}-release; see Fig. 30.2). The resulting increase in $[Ca^{2+}]_i$ causes Ca^{2+} binding to troponin C which activates the myofilaments leading to contraction during systole. Diastolic relaxation occurs when Ca^{2+} is removed from the cytoplasm. The SR Ca^{2+}-ATPase (SERCA2a) and the sarcolemmal Na^+/Ca^{2+}-exchanger (NCX) are the main mechanisms for Ca^{2+} removal from the cytosol (for review see [44]).

LTCC and RyR2 are co-localized forming a local SR Ca^{2+} release unit called junction or couplon. This local functional unit can be monitored by confocal microscopy measuring elementary SR Ca^{2+} release events (Ca^{2+} sparks) occurring spontaneously in cardiac myocytes and summating during normal Ca^{2+} transients in ECC. Of pathophysiological relevance is a CaMKII-dependent increased Ca^{2+} spark frequency responsible for SR Ca^{2+} leak and subsequent decreased SR Ca^{2+} load (for review see [3, 44]). This is interesting because under normal conditions Ca^{2+} spark frequency depends on SR Ca^{2+} load and follows a positive correlation (SR Ca^{2+} load-leak relation).

CaMKII can also modulate ECC by phosphorylating several important Ca^{2+} handling proteins in the heart in response to Ca^{2+} signals, including RyR2, PLB, and LTCC with significant functional consequences [45–48]. These proteins are involved in Ca^{2+} influx, SR Ca^{2+} release, and SR Ca^{2+} uptake. In addition, CaMKII-dependent regulation of Na^+ and K^+ channels occurs.

Ca^{2+} Influx and I_{Ca} Facilitation

Voltage gated LTCC ($Ca_v1.2$) are modulated by CaMKII thereby increasing Ca^{2+} current (I_{Ca}). This is most clearly seen as a positive staircase of I_{Ca} with repeated depolarizations, a process termed Ca^{2+}-dependent I_{Ca} facilitation. Several groups demonstrated that I_{Ca} facilitation is mediated by CaMKII [49–51]. CaMKII tethers to the pore forming α_{1C} subunit of the LTCC to phosphorylate the α_{1C} subunit at both amino and carboxy tails [52]. However, it was also reported that CaMKII appears to phosphorylate a site on the β_{2a}-subunit (Thr-498), which may be involved in I_{Ca} facilitation [53]. At the single channel level longer channel openings are found [54].

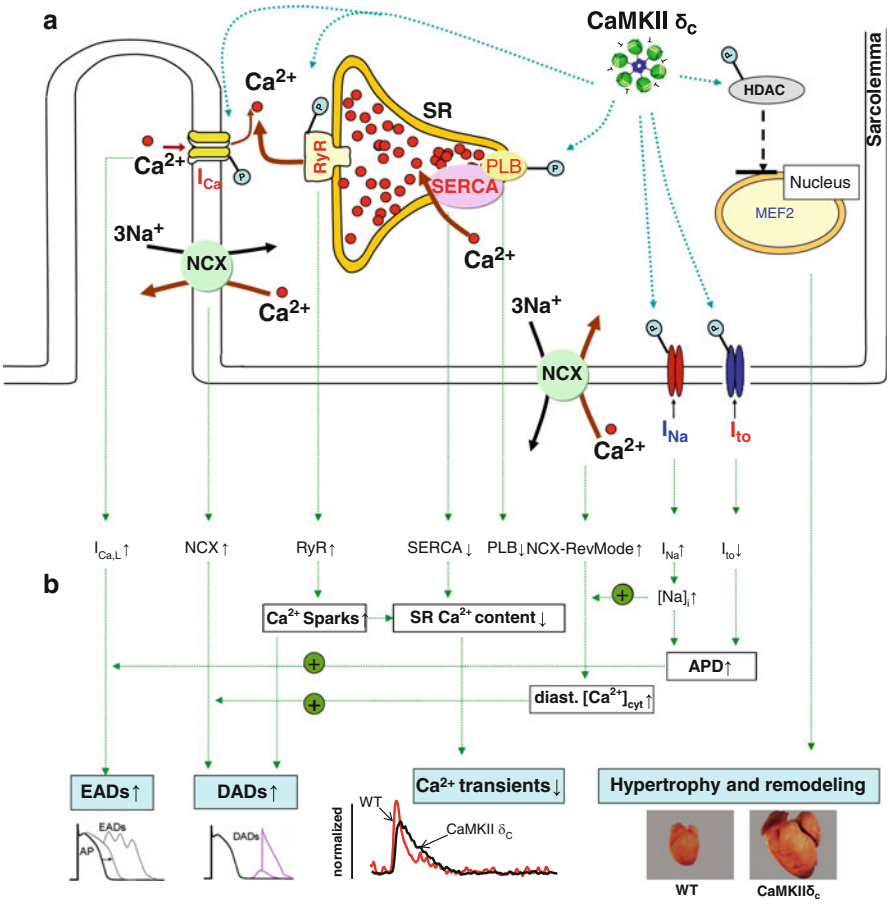

Fig. 30.2 (**a**) Effects of CaMKIIδ_C on excitation-contraction coupling (*ECC*). CaMKII phosphorylates several Ca^{2+}-handling proteins including phospholamban (*PLB*), SR Ca^{2+} release channels (*RyR*), and L-type Ca^{2+} channels responsible for Ca^{2+} influx (I_{Ca}). In addition, Na^+ channels and K^+ channels are also regulated by CaMKII. During an action potential, Ca^{2+} enters the cell via L-type Ca^{2+} channels and reverse-mode of the Na^+/Ca^{2+}-exchanger (*NCX*) thereby triggering Ca^{2+} release through RyR from the SR (filled with Ca^{2+}, *red dots*). This Ca^{2+} then activates the myofilaments during systole leading to contraction (not shown). During diastole, Ca^{2+} is taken up back into the SR by the SR Ca^{2+} ATPase (*SERCA*) and is transported outside the cells mainly by NCX, leading to relaxation. PLB inhibits SERCA when PLB is dephosphorylated. In addition, CaMKII phosphorylates HDAC activating transcription during excitation-transcription coupling (*ETC*). (**b**) Effects of CaMKIIδ_C on intracellular Ca^{2+} handling, hypertrophy development, and heart failure

By overexpressing CaMKIIδ_C I_{Ca} amplitude was increased and inactivation was slowed [55, 56]. Interestingly, enhanced open probability of LTCC due to increased CaMKII activity seems to contribute to afterdepolarizations and to the increased propensity for arrhythmias in CaMKIV transgenic mice that also showed increased CaMKII activity in parallel [27].

In line with this, it was shown that Timothy syndrome a disease of excessive cellular Ca^{2+} entry and life-threatening arrhythmias caused by a mutation in the cardiac LTCC exhibited increased CaMKII activity and a proarrhythmic phenotype that included AP prolongation, increased I_{Ca} facilitation, and afterdepolarizations. Intracellular dialysis of a CaMKII inhibitory peptide reversed I_{Ca} facilitation, normalized the AP, and prevented afterdepolarizations [57].

Interestingly, it was shown recently that CaMKII can also lead to downregulation of LTCC expression acting as a feedback mechanism enabling the heart to adjust increased I_{Ca} [58].

SR Ca^{2+} Release and SR Ca Leak

Initially, it was reported that CaMKII phosphorylates RyR2 at one site (i.e. Ser-2808 or 2809 depending on species) activating SR Ca^{2+} release [45]. However, there may be four additional CaMKII phosphorylation sites [59]. The specific effects of CaMKII on RyR2 was highly controversial. CaMKII either increased or decreased RyR2 open probability [45, 46, 60]. In intact cardiac myocytes endogenous CaMKII increased the amount of SR Ca^{2+} release for a given SR Ca^{2+} content and I_{Ca} trigger [20]. However, other studies found opposite results suggesting that CaMKII negatively regulates SR Ca^{2+} release [61, 62].

New evidence was provided in isolated myocytes showing that CaMKII is directly associated with RyR2: CaMKIIδ_C overexpression in mice increases fractional SR Ca^{2+} release during ECC and spontaneous SR Ca^{2+} release (i.e. Ca^{2+} spark frequency) for a given SR Ca^{2+} load [55, 63, 64]. These results were confirmed by CaMKIIδ_C overexpression in rabbit myocytes and direct application of activated CaMKII to permeabilized mouse myocytes [56, 65]. In contrast, AIP depresses Ca^{2+} spark frequency and ryanodine binding to RyR2, indicating that CaMKII activates RyR2 [64]. Using single channel measurements, it was shown that CaMKII increases RyR2 open probability and that CaMKII-dependent RyR2 phosphorylation occurs at Ser-2815 (or 2814 depending on species), rather than Ser-2809 [63].

In a rabbit heart failure model with increased CaMKII expression and activity more CaMKII is associated with RyR2 [66]. Moreover, the enhanced diastolic SR Ca^{2+} leak could be reversed by CaMKII inhibition [66, 67]. This CaMKII-dependent enhancement of SR Ca^{2+} leak in heart failure may contribute to both the diminished SR Ca^{2+} content characteristic of this disease, and also diastolic SR Ca^{2+} release which can activate transient inward Na^+/Ca^{2+} exchange current resulting in arrhythmias. Indeed, CaMKII inhibition increases SR Ca^{2+} content [66]. In isolated muscles from patients with heart failure it was recently shown that CaMKII inhibition is associated with positive inotropy most likely due to a reduced diastolic SR Ca^{2+} leak thus enhancing SR Ca^{2+} content [68]. In summary, CaMKII most likely enhances RyR2 activation during ECC thus influencing fractional SR Ca^{2+} release during systole but also spontaneous SR Ca^{2+} release (i.e. SR Ca^{2+} leak) during diastole, when it may unload Ca^{2+} from the SR and also contribute to arrhythmias [69] as it was recently also shown by van Oort et al. [70].

In addition, novel data suggests that CaMKII activation of mutant RyR2 promotes ectopic activity and atrial fibrillation in a transgenic mouse model [71] and in the human heart [72]. These authors also found that inhibiting CaMKII using KN-93 may prevent SR Ca^{2+} leak through RyR2 and thus atrial fibrillation.

SR Ca^{2+} Uptake and Relaxation

Upon phosphorylation of PLB, SERCA2a activity and thus SR Ca^{2+} uptake are enhanced. PLB is phosphorylated by PKA (Ser-16) and CaMKII (Thr-17). CaMKII enhances SR Ca^{2+} uptake [73, 74] and therefore CaMKII-dependent PLB phosphorylation might be responsible for the frequency-dependent acceleration of relaxation (FDAR) of twitches and SR Ca^{2+} uptake seen typically at increasing heart rates. Indeed, the level of Thr-17 phosphorylation correlates directly with the rate of relaxation [75]. However, FDAR is still prominent in PLB-KO mice [76]. Also, the time course of FDAR development is much faster during changes in frequency than that of PLB phosphorylation and in atria of transgenic mice overexpressing the CaMKII inhibition protein AC3-I no difference in FDAR was observed as compared to control mice [77, 78]. Thus, CaMKII-dependent PLB phosphorylation might contribute to FDAR but is unlikely to be the sole mechanism for FDAR. These observations are also supported by the fact that FDAR can be suppressed by CaMKII inhibitors in some reports whereas other reports could not detect FDAR inhibition [73–76, 79–81].

Na^+ Channels

CaMKII also targets cardiac Na^+ channels [82, 83]. The isoform Nav1.5 (SCN5A) of the α-subunit is the predominant isoform in the heart. However, other isoforms such as Nav1.1, Nav1.3, and Nav1.6, mainly expressed in the brain, were also found in the heart.

At resting membrane potentials (~−90 mV), cardiac Na^+ channels are in closed-available resting states. During depolarization the channels activate. Subsequent to channel activation, the channels enter inactivated states that are non-conducting for Na^+ ions. In this state, the channels are refractory to immediate depolarization, they require time for recovery at resting membrane potentials to be available for a subsequent depolarization.

A slow or late component of Na^+ current inactivation (hundreds of milliseconds) named $I_{Na,late}$ was described which seem to contribute to EADs and DADs and might even play a role for arrhythmias in heart failure [84]. Interestingly, a novel drug named ranolazine [85, 86] can be used to specifically inhibit $I_{Na,late}$.

Auxiliary β-subunits are important modulators of Na^+ channel gating and expression. The β1-subunit is widely expressed in the heart and encoded by a single gene

(SCN1B). In contrast to brain and skeletal muscle where the association of both subunits increases current density, activation and inactivation gating, the consequences of noncovalent association in the heart are controversially discussed. An α-β interaction has been suggested to be important for the maturation of Na channels from immature slow gating to mature rapid gating [87].

Most importantly, Na^+ channel activity may be regulated by CaMKII, as these channels are multiprotein regulatory complexes [88, 89]. First evidence for CaMK-dependent regulation of cardiac Na^+ channels was provided by Deschênes et al. [90] showing that the KN-93 slowed current decay, consistent with an inhibition of fast inactivation. Additionally, the steady-state voltage dependence of inactivation was shifted in the depolarizing direction resulting in an increased channel availability. Entry into the intermediate inactivated state was slowed, while the recovery from inactivation was hastened. However, KN-92 (the inactive analogue of the CaMKII inhibitor KN-93) also had effects on Na^+ channel gating, and the specific CaMKII-inhibitor AIP did not appear to affect Na^+ current. Therefore, the authors concluded that a kinase other than CaMKII might modulate Na^+ channels (suggesting CaMKIV) [91]. However, the expression levels of CaMKIV in the heart are low.

We recently examined Na^+ channel gating in rabbit myocytes overexpressing $CaMKII\delta_C$. $CaMKII\delta_C$ overexpression resulted in a leftward-shift in the steady-state voltage dependence of inactivation. The development of intermediate inactivation was enhanced and recovery from inactivation was prolonged (loss of function). All effects were reversible with CaMKII-inhibition using either KN-93 or AIP. In contrast, increased persistent I_{Na} or $I_{Na,late}$ was found (gain of function) thereby contributing to increased intracellular Na^+ accumulation and AP prolongation. These effects argue for specific CaMKII-dependent modulation of Na^+ channels. Moreover, we also found a direct association of CaMKII with the Na^+ channel and phosphorylation of Na^+ channels by CaMKII [82]. Indeed, recently Hund et al. reported a $ß_{IV}$-spectrin-dependent CaMKII-regulation of Ser571 [92].

This new evidence for additional CaMKII-dependent effects besides other well known effects on Ca^{2+}-handling proteins may be of pathophysiological importance since upregulation of CaMKII activity and expression seem to occur in patients with heart failure and animal models [4, 5, 55, 66, 93]. Altered Na^+ channel function may therefore be associated with arrhythmogenic processes.

Several human cardiac Na^+ channel mutations have been linked to either Brugada or long-QT (LQT3) syndromes with life-threatening arrhythmias [88]. One such human mutation (Asp insertion at 1795 in the C-terminus, 1795InsD), shows simultaneous LQT3-like and Brugada-like phenotypes in the same individuals [94]. Remarkably, Na^+ channels bearing this mutation expressed in mammalian cells exhibit the same phenotype that we found for CaMKII-modified normal Na^+ channel above [82, 94, 95]. At low stimulation frequencies, the prolonged inactivation and $I_{Na,late}$ can cause APD lengthening consistent with LQT3 syndrome. However, at higher heart rates, incomplete I_{Na} recovery and limited I_{Na} availability further shorten action potential duration, slow propagation and increase dispersion of repolarization similarly found for Brugada syndrome. The intriguing thing is that

CaMKII-dependent I_{Na} modulation due to upregulated CaMKII could constitute a common acquired form of arrhythmia, in otherwise normal Na^+ channels (without 1795InsD mutation). Such an acquired Na^+ channel dysfunction may contribute to arrhythmias under conditions when CaMKII effects are enhanced, as in heart failure or during atrial fibrillation [96]. In addition, recent experimental and simulated data suggests that CaMKII inhibition may be of relevance as a possible antiarrhythmic intervention [97, 98].

K^+ Channels

CaMKII regulates transient outward K^+ current (I_{to}) in myocytes from patients with atrial fibrillation [99] because CaMKII inhibition results in faster I_{to} inactivation. Further evidence for a CaMKII-dependent regulation of $I_{to,fast}$ came from human atrial myocytes showing that CaMKII inhibition accelerated $I_{to,fast}$ inactivation, whereas okadaic acid (phosphatase inhibitor) had opposite effects [100]. Similar results were obtained from rat ventricular myocytes [101] and in heterologeous expression of KV4.2/KV4.3 [101, 102]. There is even evidence suggesting that CaMKII directly phosphorylates Kv4.3 at Ser-550, thereby prolonging open-state inactivation and accelerating the rate of recovery from inactivation [102]. CaMKII-dependent regulation of I_{to} is interesting in so far that in heart failure, $I_{to,fast}$ mainly mediated by Kv4.2/3 is functionally reduced and expression of the channel proteins is lower. A recent study suggests that I_{to} channels are a functional reservoir of CaMKII and that downregulation of I_{to} results in an increase in CaMKII activity leading to hypertrophy and heart failure. In line with this, the authors found that overexpression of the I_{to} channel Kv4.3 significantly reduced the autonomous CaMKII activity without changing the total CaMKII expression [103]. Similarly, it was also shown that inhibition of CaMKII with KN93 prevented I_{to} downregulation following sustained tachycardia *in vivo* [104]. In myocytes acutely overexpressing CaMKIIδ_C, we found CaMKII-dependent enhancement of I_{to} consistent with increased Kv1.4 function, and consequent APD shortening [105]. However, it was also reported that chronic CaMKII inhibition shortens AP due to upregulation of $I_{to,fast}$ and the inward rectifier current I_{K1} [106] suggesting that CaMKII overexpression would increase APD as also shown by chronic CaMKII overexpression [55]. Indeed, further studies need to be performed to elucidate the role of CaMK-dependent K^+ channel regulation.

Role of CaMKII for Arrhythmias

Several animal models have linked increased CaMKII expression with arrhythmias *in vivo* [92, 107, 108].

Arrhythmia mechanisms *in vitro* are thought to be important as initiating mechanisms for focal arrhythmias and for initiating impulses *in vivo* that lead to arrhythmias sustained by reentrant circuits such as ventricular tachycardia in post myocardial infarction border zone scar areas. These triggers are due to increased net inward current and have been differentiated between EADs and DADs. EADs occur early relative to the completion of AP repolarization mostly during the AP plateau or during the early phases of AP resolution (so-called phase II and III) and are most often associated with repetitive LTCC openings [109] but also increased $I_{Na,late}$ [86, 96]. Signaling events that favor so-called mode 2 gating are associated with generation of EADs. Under experimental conditions EADs are independent of the release of intracellular Ca^{2+} stores [110] but it was shown that blocking SR Ca^{2+} cycling also prevents the development of EADs and arrhythmias [111]. One possible reason for the blockade of EADs and arrhythmias by inhibitors of SR Ca^{2+} cycling is that SR Ca^{2+} release is the predominant source of Ca^{2+} for CaMKII activation [112]. CaMKII inhibitory drugs or dialysis of highly specific CaMKII inhibitory peptides effectively inhibit EAD formation and arrhythmias even without shortening AP or QT intervals [69].

DADs are named because they take place during late repolarization of the AP. These afterdepolarization are mainly linked to conditions that favor SR Ca^{2+} overload. A common example of a circumstance favoring DADs occurs during digitalis toxicity where Ca^{2+} loading occurs due to poisoning of the Na^+ gradient across the cell membrane and secondary reduction in the ability of the electrogenic NCX to clear cytoplasmic Ca^{2+} to the extracellular space during its forward mode of operation. CaMKII inhibition leads to a reduction in SR Ca^{2+} content, at least in structurally normal myocardium [29] and this is one potential mechanism for CaMKII inhibition reducing DADs [113]. On the other hand, DADs can occur simultaneously with AP prolongation and EADs so that CaMKII could contribute to SR Ca^{2+} overload through enhanced cellular Ca^{2+} entry e.g. by way of LTCC during EADs [112]. These studies show that Ca^{2+} loading during a prolonged AP is capable of overloading the SR with Ca^{2+} and producing DADs. Although many inward currents have been considered candidates for generating DADs most data point to the NCX as the source of inward current for DADs [113]. Cellular arrhythmia triggers are a plausible initiating mechanism for arrhythmias, but in contrast to macro reentrant circuits, which are relatively easy to measure in an integrated preparation such as a whole heart or even a patient, it is not possible to directly measure cellular afterdepolarizations in situ. Some studies in patients have pointed to a potential role for initiation of reentrant arrhythmias by highly focal triggers that are consistent with initiation by earlier DADs. Furthermore, it is well accepted that conditions such as excessive QT interval prolongation and Ca^{2+} overload are associated with both afterdepolarizations and with enhanced susceptibility to arrhythmias in patients. In this regard, a rabbit model of excessive QT interval prolongation and Torsade de Pointes shows that CaM or CaMKII inhibitors can prevent arrhythmias, suppress prominent secondary U waves that are linked to afterdepolarizations, and prevent arrhythmias without shortening the QT interval. These same conditions suppress EADs in cellular and isolated heart studies.

Taken together, these findings show that CaMKII can facilitate EADs and DADs and plausibly link these afterdepolarizations to arrhythmias in animal models. Further studies and possibly newer "mapping" techniques applicable to patients will be necessary before afterdepolarizations are definitively linked to arrhythmias in patients. Until then, also mathematical models will help understand the role of CaMKII for ECC and arrhythmias in heart disease [97, 98, 114].

Very recently, CaMKII oxidation also was described to be involved in sinus node dysfunction upon angiotensin II infusion and CaMKII inhibition as a basis for therapy for patients with sinus node dysfunction [115].

Summary

CaMKII in the heart has gained tremendous attention over the last few years. Its involvement at multiple levels in ECC and arrhythmogenesis indicate that it is an important protein for cellular signaling and regulation in the heart. Moreover, since CaMKII expression and activation may be elevated in important pathophysiological situations (e.g. heart failure and hypertrophy), investigating CaMKII regulation in the heart will help to understand the pathophysiology of the heart and may identify new modalities of treatment for arrhythmias in heart failure.

Acknowledgements Supported by grants from the DFG through a Heisenberg-grant (MA 1982/4-1), a grant for a Clinical Research group KFO155 (MA 1982/2-1), and the Fondation Leducq Award to the Alliance for Calmodulin Kinase Signaling in Heart Disease.

References

1. Jett MF, Schworer CM, Bass M, Soderling TR (1987) Identification of membrane-bound calcium, calmodulin-dependent protein kinase II in canine heart. Arch Biochem Biophys 255:354–360
2. Braun AP, Schulman H (2005) The multifunctional calcium/calmodulin-dependent protein kinase: from form to function. Annu Rev Physiol 57:417–445
3. Maier LS, Bers DM (2007) Role of Ca^{2+}/calmodulin-dependent protein kinase (CaMK) in excitation-contraction coupling in the heart. Cardiovasc Res 73:631–640
4. Kirchhefer U, Schmitz W, Scholz H, Neumann J (1999) Activity of cAMP-dependent protein kinase and Ca^{2+}/calmodulin-dependent protein kinase in failing and nonfailing human hearts. Cardiovasc Res 42:254–261
5. Hoch B, Meyer R, Hetzer R, Krause EG, Karczewski P (1999) Identification and expression of delta-isoforms of the multifunctional Ca^{2+}/calmodulin-dependent protein kinase in failing and nonfailing human myocardium. Circ Res 84:713–721
6. Zhang T, Brown JH (2004) Role of Ca^{2+}/calmodulin-dependent protein kinase II in cardiac hypertrophy and heart failure. Cardiovasc Res 63:476–486
7. Edman CF, Schulman H (1994) Identification and characterization of δ_B-CaM kinase and δ_C-CaM kinase from rat heart, two new multifunctional Ca/calmodulin-dependent protein kinase isoforms. Biochim Biophys Acta 1221:89–101

8. Maier LS, Ziolo MT, Bossuyt J, Persechini A, Mestril R, Bers DM (2006) Dynamic changes in free Ca-calmodulin levels in adult cardiac myocytes. J Mol Cell Cardiol 41:451–458
9. Rostas JAP, Dunkley PR (1992) Multiple forms and distribution of calcium/calmodulin-stimulated protein kinase II in brain. J Neurochem 59:1191–1202
10. Meyer T, Hanson PI, Stryer L, Schulman H (1992) Calmodulin trapping by calcium-calmodulin-dependent protein kinase. Science 256:1199–1202
11. Lai Y, Nairn AC, Greengard P (1986) Autophosphorylation reversibly regulates the Ca/calmodulin-dependent protein kinase II. Proc Natl Acad Sci USA 83:4253–4257
12. Lou LL, Lloyd SJ, Schulman H (1986) Activation of the multifunctional Ca/calmodulin-dependent protein kinase by autophosphorylation: ATP modulates production of an autonomous enzyme. Proc Natl Acad Sci USA 83:9497–9501
13. Schworer CM, Colbran RJ, Soderling TR (1986) Reversible generation of a Ca-independent form of Ca (calmodulin)-dependent protein kinase II by an autophosphorylation mechanism. J Biol Chem 261:8581–8584
14. Erickson JR, Joiner ML, Guan X, Kutschke W, Yang J, Oddis CV, Bartlett RK, Lowe JS, O'Donnell SE, Aykin-Burns N, Zimmerman MC, Zimmerman K, Ham AJ, Weiss RM, Spitz DR, Shea MA, Colbran RJ, Mohler PJ, Anderson ME (2008) A dynamic pathway for calcium-independent activation of CaMKII by methionine oxidation. Cell 133:462–474
15. Wagner S, Ruff HM, Weber SL, Bellmann S, Sowa T, Schulte T, Anderson ME, Grandi E, Bers DM, Backs J, Belardinelli L, Maier LS (2011) ROS-activated Ca/calmodulin kinase IIδ is required for late I_{Na} augmentation leading to cellular Na and Ca overload. Circ Res 108:555–565
16. Curran J, Hinton MJ, Ríos E, Bers DM, Shannon TR (2007) Beta-adrenergic enhancement of sarcoplasmic reticulum calcium leak in cardiac myocytes is mediated by calcium/calmodulin-dependent protein kinase. Circ Res 100:391–398
17. Pereira L, Métrich M, Fernández-Velasco M, Lucas A, Leroy J, Perrier R, Morel E, Fischmeister R, Richard S, Bénitah JP, Lezoualc'h F, Gómez AM (2007) The cAMP binding protein Epac modulates Ca^{2+} sparks by a Ca^{2+}/calmodulin kinase signalling pathway in rat cardiac myocytes. J Physiol 583(2):685–694
18. Mangmool S, Shukla AK, Rockman HA (2010) beta-Arrestin-dependent activation of Ca^{2+}/calmodulin kinase II after $ß_1$-adrenergic receptor stimulation. J Cell Biol 189:573–587
19. Oestreich EA, Malik S, Goonasekera SA, Blaxall BC, Kelley GG, Dirksen RT, Smrcka AV (2009) Epac and phospholipase Cepsilon regulate Ca^{2+} release in the heart by activation of protein kinase Cepsilon and calcium-calmodulin kinase II. J Biol Chem 284:1514–1522
20. Li L, Satoh H, Ginsburg KS, Bers DM (1997) The effect of Ca^{2+}-calmodulin-dependent protein kinase II on cardiac excitation-contraction coupling in ferret ventricular myocytes. J Physiol 501(Pt 1):17–31
21. Ishida A, Kameshita I, Okuno S, Kitani T, Fujisawa H (1995) A novel specific and potent inhibitor of calmodulin-dependent protein kinase II. Biochem Biophys Res Commun 212:806–812
22. Anderson ME, Brown JH, Bers DM (2011) CaMKII in myocardial hypertrophy and heart failure. J Mol Cell Cardiol 51(4):468–473, Epub 2011 Jan 27
23. Colomer JM, Means AR (2000) Chronic elevation of calmodulin in the ventricles of transgenic mice increases the autonomous activity of calmodulin-dependent protein kinase II, which regulates atrial natriuretic factor gene expression. Mol Endocrinol 14:1125–1136
24. Ramirez MT, Zhao XL, Schulman H, Brown JH (1997) The nuclear δ_B isoform of Ca/calmodulin-dependent protein kinase II regulates atrial natriuretic factor gene expression in ventricular myocytes. J Biol Chem 272:31203–31208
25. Zhang T, Johnson EN, Gu Y, Morissette MR, Sah VP, Gigena MS, Belke DD, Dillmann WH, Rogers TB, Schulman H, Ross J Jr, Brown JH (2002) The cardiac-specific nuclear δ_B isoform of Ca^{2+}/calmodulin-dependent protein kinase II induces hypertrophy and dilated cardiomyopathy associated with increased protein phosphatase 2A activity. J Biol Chem 277:1261–1267
26. Passier R, Zeng H, Frey N, Naya FJ, Nicol RL, McKinsey TA, Overbeek P, Richardson JA, Grant SR, Olson EN (2000) CaM kinase signaling induces cardiac hypertrophy and activates the MEF2 transcription factor *in vivo*. J Clin Invest 105:1395–1406

27. Wu Y, Temple J, Zhang R, Dzhura I, Zhang W, Trimble R, Roden DM, Passier R, Olson EN, Colbran RJ, Anderson ME (2002) Calmodulin kinase II and arrhythmias in a mouse model of cardiac hypertrophy. Circulation 106:1288–1293
28. Zhang T, Maier LS, Dalton ND, Miyamoto S, Ross J Jr, Bers DM, Heller BJ (2003) The δ_C isoform of CaMKII is activated in cardiac hypertrophy and induces dilated cardiomyopathy and heart failure. Circ Res 92:912–919
29. Zhang R, Khoo MS, Wu Y, Yang Y, Grueter CE, Ni G, Price EE Jr, Thiel W, Guatimosim S, Song LS, Madu EC, Shah AN, Vishnivetskaya TA, Atkinson JB, Gurevich VV, Salama G, Lederer WJ, Colbran RJ, Anderson ME (2005) Calmodulin kinase II inhibition protects against structural heart disease. Nat Med 11:409–417
30. Ling H, Zhang T, Pereira L, Means CK, Cheng H, Gu Y, Dalton ND, Peterson KL, Chen J, Bers D, Brown JH (2009) Requirement for Ca^{2+}/calmodulin-dependent kinase II in the transition from pressure overload-induced cardiac hypertrophy to heart failure in mice. J Clin Invest 119(5):1230–1240
31. Backs J, Backs T, Neef S, Kreusser MM, Lehmann LH, Patrick DM, Grueter CE, Qi X, Richardson JA, Hill JA, Katus HA, Bassel-Duby R, Maier LS, Olson EN (2009) The δ isoform of CaM kinase II is required for pathological cardiac hypertrophy and remodeling after pressure overload. Proc Natl Acad Sci USA 106:2342–2347
32. Toischer K, Rokita AG, Unsöld B, Zhu W, Kararigas G, Sossalla S, Reuter SP, Becker A, Teucher N, Seidler T, Grebe C, Preuß L, Gupta SN, Schmidt K, Lehnart SE, Krüger M, Linke WA, Backs J, Regitz-Zagrosek V, Schäfer K, Field LJ, Maier LS, Hasenfuss G (2010) Differential cardiac remodeling in preload versus afterload. Circulation 122:993–1003
33. Lu J, McKinsey TA, Nicol RL, Olson EN (2000) Signal-dependent activation of the MEF2 transcription factor by dissociation from histone deacetylases. Proc Natl Acad Sci USA 97:4070–4075
34. Sparrow DB, Miska EA, Langley E, Reynaud-Deonauth S, Kotecha S, Towers N, Spohr G, Kouzarides T, Mohun TJ (1999) MEF-2 function is modified by a novel co-repressor, MITR. EMBO J 18:5085–5098
35. Frey N, McKinsey TA, Olson EN (2000) Decoding calcium signals involved in cardiac growth and function. Nat Med 6:1221–1227
36. Zhang T, Kohlhaas M, Backs J, Phillips W, Mishra S, Dybkova N, Chang S, Bers DM, Maier LS, Olson EN, Brown JH (2007) Cytoplasmic and nuclear isoforms of CaMKII differentially affect calcium handling but similarly regulate HDAC/MEF2 transcriptional response. J Biol Chem 282:35078–35087
37. Zhang CL, McKinsey TA, Chang S, Antos CL, Hill JA, Olson EN (2002) Class II histone deacetylases act as signal-responsive repressors of cardiac hypertrophy. Cell 110:479–488
38. Bossuyt J, Helmstadter K, Wu X, Clements-Jewery H, Haworth RS, Avkiran M, Martin JL, Pogwizd SM, Bers DM (2008) Ca^{2+}/calmodulin-dependent protein kinase IIdelta and protein kinase D overexpression reinforce the histone deacetylase 5 redistribution in heart failure. Circ Res 102:695–702
39. Métrich M, Laurent AC, Breckler M, Duquesnes N, Hmitou I, Courillau D, Blondeau JP, Crozatier B, Lezoualc'h F, Morel E (2010) Epac activation induces histone deacetylase nuclear export via a Ras-dependent signalling pathway. Cell Signal 22:1459–1468
40. Bare DJ, Kettlun CS, Liang M, Bers DM, Mignery GA (2005) Cardiac type 2 inositol 1,4,5-trisphosphate receptor: interaction and modulation by calcium/calmodulin-dependent protein kinase II. J Biol Chem 280:15912–15920
41. Wu X, Zhang T, Bossuyt J, Li X, McKinsey TA, Dedman JR, Olson EN, Chen J, Brown JH, Bers DM (2006) Local InsP3-dependent perinuclear Ca^{2+} signaling in cardiac myocyte excitation-transcription coupling. J Clin Invest 116:675–682
42. Kemi OJ, Ellingsen O, Ceci M, Grimaldi S, Smith GL, Condorelli G, Wisloff U (2007) Aerobic interval training enhances cardiomyocyte contractility and Ca^{2+} cycling by phosphorylation of CaMKII and Thr-17 of phospholamban. J Mol Cell Cardiol 43:354–361
43. Stolen TO, Hoydal MA, Kemi OJ, Catalucci D, Ceci M, Aasum E, Larsen T, Rolim N, Condorelli G, Smith GL, Wisloff U (2009) Interval training normalizes cardiomyocyte function, diastolic Ca2? control, and SR Ca^{2+} release synchronicity in a mouse model of diabetic cardiomyopathy. Circ Res 105:527–536

44. Bers DM (2002) Cardiac excitation-contraction coupling. Nature 415:198–205
45. Witcher DR, Kovacs RJ, Schulman H, Cefali DC, Jones LR (1991) Unique phosphorylation site on the cardiac ryanodine receptor regulates calcium channel activity. J Biol Chem 266: 11144–11152
46. Hain J, Onoue H, Mayrleitner M, Fleischer S, Schindler H (1995) Phosphorylation modulates the function of the calcium release channel of sarcoplasmic reticulum from cardiac muscle. J Biol Chem 270:2074–2081
47. Davis BA, Schwartz A, Samaha FJ, Kranias EG (1983) Regulation of cardiac sarcoplasmic reticulum calcium transport by calcium-calmodulin-dependent phosphorylation. J Biol Chem 258:13587–13591
48. Simmerman HKB, Collins JH, Theibert JL, Wegener AD, Jones LR (1986) Sequence analysis of PLB: Identification of phosphorylation sites and two major structural domains. J Biol Chem 261:13333–13341
49. Anderson ME, Braun AP, Schulman H, Premack BA (1994) Multifunctional Ca/calmodulin-dependent protein kinase mediates Ca-induced enhancement of the L-type Ca current in rabbit ventricular myocytes. Circ Res 75:854–861
50. Xiao RP, Cheng H, Lederer WJ, Suzuki T, Lakatta EG (1994) Dual regulation of Ca/calmodulin kinase II activity by membrane voltage and by calcium influx. Proc Natl Acad Sci USA 91:9659–9663
51. Yuan W, Bers DM (1994) Ca-dependent facilitation of cardiac Ca current is due to Ca-calmodulin dependent protein kinase. Am J Physiol 267:H982–H993
52. Hudmon A, Schulman H, Kim J, Maltez JM, Tsien RW, Pitt GS (2005) CaMKII tethers to L-type Ca^{2+} channels, establishing a local and dedicated integrator of Ca^{2+} signals for facilitation. J Cell Biol 171:537–547
53. Grueter CE, Abiria SA, Dzhura I, Wu Y, Ham AJL, Mohler PJ, Anderson ME, Colbran RJ (2006) L-type Ca^{2+} channel facilitation mediated by phosphorylation of the ß subunit by CaMKII. Mol Cell 23:641–650
54. Dzhura I, Wu Y, Colbran RJ, Balser JR, Anderson ME (2000) Calmodulin kinase determines calcium-dependent facilitation of L-type calcium channels. Nat Cell Biol 2:173–177
55. Maier LS, Zhang T, Chen L, DeSantiago J, Heller Brown J, Bers DM (2003) Transgenic $CaMKII\delta_C$ overexpression uniquely alters cardiac myocyte Ca^{2+} handling: reduced SR Ca^{2+} load and activated SR Ca^{2+} release. Circ Res 92:904–911
56. Kohlhaas M, Zhang T, Seidler T, Zibrova D, Dybkova N, Steen A, Wagner S, Chen L, Heller Brown J, Bers DM, Maier LS (2006) Increased sarcoplasmic reticulum calcium leak but unaltered contractility by acute CaMKII overexpression in isolated rabbit cardiac myocytes. Circ Res 98:235–244
57. Thiel WH, Chen B, Hund TJ, Koval OM, Purohit A, Song LS, Mohler PJ, Anderson ME (2008) Proarrhythmic defects in Timothy Syndrome require calmodulin kinase II. Circulation 118:2225–2234
58. Ronkainen JJ, Hänninen SL, Korhonen T, Koivumäki JT, Skoumal R, Rautio S, Ronkainen VP, Tavi P (2011) Ca^{2+}-calmodulin-dependent protein kinase II represses cardiac transcription of the L-type calcium channel 1C-subunit gene (Cacna1c) by DREAM translocation. J Physiol 589(Pt 11):2669–2686
59. Rodriguez P, Bhogal MS, Coyler J (2003) Stoichiometric phosphorylation of cardiac ryanodine receptor on serine-2809 by calmodulin-dependent kinase II and protein kinase A. J Biol Chem 278:38593–38600
60. Lokuta AJ, Rogers TB, Lederer WJ, Valdivia HH (1997) Modulation of cardiac ryanodine receptors of swine and rabbit by a phosphorylation-dephosphorylation mechanism. J Physiol (Lond) 487:609–622
61. Wu Y, Colbran RJ, Anderson ME (2001) Calmodulin kinase is a molecular switch for cardiac excitation-contraction coupling. Proc Natl Acad Sci USA 98:2877–2881
62. Yang D, Zhu WZ, Xiao B, Brochet DX, Chen SR, Lakatta EG, Xiao RP, Cheng H (2007) Ca^{2+}/calmodulin kinase II-dependent phosphorylation of ryanodine receptors suppresses Ca^{2+} sparks and Ca^{2+} waves in cardiac myocytes. Circ Res 100:399–407

63. Wehrens XH, Lehnart SE, Reiken SR, Marks AR (2004) Ca^{2+}/calmodulin-dependent protein kinase II phosphorylation regulates the cardiac ryanodine receptor. Circ Res 94:e61–e70
64. Currie S, Loughrey CM, Craig MA, Smith GL (2004) Calcium/calmodulin-dependent protein kinase IIδ associates with the ryanodine receptor complex and regulates channel function in rabbit heart. Biochem J 377:357–366
65. Guo T, Zhang T, Mestril R, Bers DM (2006) Ca/calmodulin-dependent protein kinase II phosphorylation of ryanodine receptor does affect calcium sparks in mouse ventricular myocytes. Circ Res 99:398–406
66. Ai X, Curran JW, Shannon TR, Bers DM, Pogwizd SM (2005) Ca^{2+}-calmodulin-dependent protein kinase modulates RyR2 phosphorylation and SR Ca^{2+} leak in a rabbit heart failure. Circ Res 97:1314–1322
67. Shannon TR, Pogwizd SM, Bers DM (2003) Elevated sarcoplasmic reticulum Ca leak in intact ventricular myocytes from rabbits in heart failure. Circ Res 93:592–594
68. Sossalla S, Fluschnik N, Schotola H, Ort K, Neef S, Schulte T, Wittköpper K, Renner A, Schmitto JD, Gummert J, El-Armouche A, Hasenfuss G, Maier LS (2010) Inhibition of elevated Ca^{2+}/calmodulin-dependent protein kinase II (CaMKII) improves contractility in human failing myocardium. Circ Res 107:1150–1161
69. Sag CM, Wadsack DP, Khabbazzadeh S, Abesser M, Grefe C, Neef S, Maier SKG, Maier LS (2009) CaMKII contributes to cardiac arrhythmogenesis in transgenic CaMKIIδ_C mice having heart failure. Circ Heart Fail 2:664–675
70. van Oort RJ, McCauley MD, Dixit SS, Pereira L, Yang Y, Respress JL, Wang Q, De Almeida AC, Skapura DG, Anderson ME, Bers DM, Wehrens XH (2010) Ryanodine receptor phosphorylation by calcium/calmodulin-dependent protein kinase II promotes life-threatening ventricular arrhythmias in mice with heart failure. Circulation 122:2669–2679
71. Chelu MG, Sarma S, Sood S, Wang S, van Oort RJ, Skapura DG, Li N, Santonastasi M, Müller FU, Schmitz W, Schotten U, Anderson ME, Valderrábano M, Dobrev D, Wehrens XH (2009) Calmodulin kinase II-mediated sarcoplasmic reticulum Ca^{2+} leak promotes atrial fibrillation in mice. J Clin Invest 119:1940–1951
72. Neef S, Dybkova N, Sossalla S, Ort KR, Fluschnik N, Neumann K, Seipelt R, Schöndube FA, Hasenfuss G, Maier LS (2010) CaMKII dependent diastolic SR Ca^{2+} leak and elevated diastolic Ca^{2+} levels in right atrial myocardium of patients with atrial fibrillation. Circ Res 106:1134–1144
73. Bassani RA, Mattiazzi A, Bers DM (1995) CaMKII is responsible for activity-dependent acceleration of relaxation in rat ventricular myocytes. Am J Physiol 268:H703–H712
74. DeSantiago J, Maier LS, Bers DM (2004) Phospholamban is required for CaMKII-dependent recovery of Ca transients and SR Ca reuptake during acidosis in cardiac myocytes. J Mol Cell Cardiol 36:67–74
75. Hagemann D, Kuschel M, Kuramochi T, Zhu W, Cheng H, Xiao RP (2000) Frequency-encoding Thr17 phospholamban phosphorylation is independent of Ser16 phosphorylation in cardiac myocytes. J Biol Chem 275:22532–22536
76. DeSantiago J, Maier LS, Bers DM (2002) Frequency-dependent acceleration of relaxation in the heart depends on CaMKII, but not phospholamban. J Mol Cell Cardiol 34:975–984
77. Huke S, Bers DM (2007) Temporal dissociation of frequency-dependent acceleration of relaxation and protein phosphorylation by CaMKII. J Mol Cell Cardiol 42:590–599
78. Grimm M, El-Armouche A, Zhang R, Anderson ME, Eschenhagen T (2007) Reduced contractile response to alpha1-adrenergic stimulation in atria from mice with chronic cardiac calmodulin kinase II inhibition. J Mol Cell Cardiol 42:643–652
79. Li L, Chu G, Kranias EG, Bers DM (1998) Cardiac myocyte calcium transport in phospholamban knockout mouse: relaxation and endogenous CaMKII effects. Am J Physiol 274:H1335–H1347
80. Hussain M, Drago GA, Colyer J, Orchard CH (1997) Rate-dependent abbreviation of Ca^{2+} transient in rat heart is independent of phospholamban phosphorylation. Am J Physiol 273:H695–H706
81. Kassiri Z, Myers R, Kaprielian R, Banijamali HS, Backx PH (2000) Rate-dependent changes of twitch force duration in rat cardiac trabeculae: a property of the contractile system. J Physiol 524:221–231

82. Wagner S, Dybkova N, Rasenack ECL, Jacobshagen C, Fabritz L, Kirchhof P, Maier SK, Zhang T, Hasenfuss G, Heller Brown J, Bers DM, Maier LS (2006) Ca/calmodulin-dependent protein kinase II regulates cardiac Na channels. J Clin Invest 116:3127–3138
83. Maltsev VA, Reznikov V, Undrovinas NA, Sabbah HN, Undrovinas A (2008) Modulation of late sodium current by Ca^{2+}, calmodulin, and CaMKII in normal and failing dog cardiomyocytes: similarities and differences. Am J Physiol Heart Circ Physiol 294:H1597–H1608
84. Maltsev VA, Sabbah HN, Higgins RSD, Silverman N, Lesch M, Undrovinas AI (1998) Novel, ultraslow inactivating sodium current in human ventricular cardiomyocytes. Circulation 98: 2545–2552
85. Sossalla SR, Rasenack ECL, Wagner S, Ruff H, Hasenfuss G, Belardinelli L, Maier LS (2008) Inhibition of late sodium current by ranolazine reduces diastolic dysfunction in human heart failure. J Mol Cell Cardiol 45:32–43
86. Song Y, Shryock JC, Wagner S, Maier LS, Belardinelli L (2006) Blocking late sodium current reduces hydrogen peroxide-induced arrhythmogenic activity and contractile dysfunction. J Pharmacol Exp Ther 318:214–222
87. Kupershmidt S, Yang T, Roden DM (1998) Modulation of cardiac Na^+ current phenotype by ß1-subunit expression. Circ Res 83:441–447
88. Viswanathan PC, Balser JR (2004) Inherited sodium channelopathies a continuum of channel dysfunction. Trends Cardiovasc Med 14:28–35
89. Abriel H, Kass RS (2005) Regulation of the voltage-gated cardiac sodium channel $Nav_{1.5}$ by interacting proteins. Trends Cardiovasc Med 15:35–40
90. Deschênes I, Neyroud N, DiSilvestre D, Marbán E, Yue DT, Tomaselli GF (2002) Isoform-specific modulation of voltage-gated Na^+ channels by calmodulin. Circ Res 90:e49–e57
91. Colomer JM, Mao L, Rockman HA, Means AR (2003) Pressure overload selectively up-regulates Ca^{2+}/calmodulin-dependent protein kinase II *in vivo*. Mol Endocrinol 17:183–192
92. Hund TJ, Koval OM, Li J, Wright PJ, Qian L, Snyder JS, Gudmundsson H, Kline CF, Davidson NP, Cardona N, Rasband MN, Anderson ME, Mohler PJ (2010) A βIV-spectrin/CaMKII signaling complex is essential for membrane excitability in mice. J Clin Invest 120:3508–3519
93. Currie S, Smith GL (1999) Calcium/calmodulin-dependent protein kinase II activity is increased in sarcoplasmic reticulum from coronary artery ligated rabbit hearts. FEBS Lett 459:244–248
94. Veldkamp MW, Viswanathan PC, Bezzina C, Baartscheer A, Wilde AAM, Balser JR (2000) Two distinct congenital arrhythmias evoked by a multidysfunctional Na^+ channel. Circ Res 86:e91–e97
95. Bezzina C, Veldkamp MW, van Den Berg MP, Postma AV, Rook MB, Viersma JW, van Langen IM, Tan-Sindhunata G, Bink-Boelkens MT, van Der Hout AH, Mannens MM, Wilde AA (1999) A single Na^+ channel mutation causing both long-QT and Brugada syndromes. Circ Res 85:1206–1213
96. Sossalla S, Kallmeyer B, Wagner S, Mazur M, Maurer U, Toischer K, Schmitto JD, Seipelt R, Schöndube F, Hasenfuss G, Belardinelli L, Maier LS (2010) Altered Na^+ currents in atrial fibrillation: effects of ranolazine on arrhythmias and contractility in human atrial myocardium. J Am Coll Cardiol 55:2330–2342
97. Livshitz LM, Rudy Y (2007) Regulation of Ca^{2+} and electrical alternans in cardiac myocytes: role of CaMKII and repolarizing currents. Am J Physiol Heart Circ Physiol 292: H2854–H2866
98. Grandi E, Puglisi JL, Wagner S, Maier LS, Severi S, Bers DM (2007) Simulation of Ca/calmodulin-dependent protein kinase II on rabbit ventricular myocyte ion currents and action potentials. Biophys J 93:3835–3847
99. Tessier S, Karczewski P, Krause EG, Pansard Y, Acar C, Lang-Lazdunski M, Mercadier JJ, Hatem SN (1999) Regulation of the transient outward K^+ current by Ca^{2+}/calmodulin-dependent protein kinases II in human atrial myocytes. Circ Res 85:810–819
100. Tessier S, Godreau D, Vranckx R, Lang-Lazdunski L, Mercadier JJ, Hatem SN (2001) Cumulative inactivation of the outward potassium current: a likely mechanism underlying electrical memory in human atrial myocytes. J Mol Cell Cardiol 33:755–767

101. Colinas O, Gallego M, Setien R, Lopez-Lopez JR, Perez-Garcia MT, Casis O (2006) Differential modulation of KV4.2 and KV4.3 channels by calmodulin-dependent protein kinase II in rat cardiac myocytes. Am J Physiol Heart Circ Physiol 291:H1978–H1987
102. Sergeant GP, Ohya S, Reihill JA, Perrino BA, Amberg GC, Imaizumi Y, Horowitz B, Sanders KM, Koh SD (2005) Regulation of Kv4.3 currents by Ca^{2+}/calmodulin-dependent protein kinase II. Am J Physiol Cell Physiol 288:C304–C313
103. Keskanokwong T, Lim HJ, Zhang P, Cheng J, Xu L, Lai D, Wang Y (2011) Dynamic Kv4.3-CaMKII unit in heart: an intrinsic negative regulator for CaMKII activation. Eur Heart J 32:305–315
104. Xiao L, Coutu P, Villeneuve LR, Tadevosyan A, Maguy A, Le Bouter S, Allen BG, Nattel S (2008) Mechanisms underlying rate-dependent remodeling of transient outward potassium current in canine ventricular myocytes. Circ Res 103:733–742
105. Wagner S, Hacker E, Grandi E, Weber SL, Dybkova N, Sossalla S, Sowa T, Bers DM, Maier LS (2009) Ca/calmodulin kinase II differentially modulates potassium currents. Circ Arrhythm Electrophysiol 2:285–294
106. Li J, Marionneau C, Zhang R, Shah V, Hell JW, Nerbonne JM, Anderson ME (2006) Calmodulin kinase II inhibition shortens action potential duration by upregulation of K^+ currents. Circ Res 99:1092–1099
107. Khoo MS, Li J, Singh MV, Yang Y, Kannankeril P, Wu Y, Grueter CE, Guan X, Oddis CV, Zhang R, Mendes L, Ni G, Madu EC, Yang J, Bass M, Gomez RJ, Wadzinski BE, Olson EN, Colbran RJ, Anderson ME (2006) Death, cardiac dysfunction, and arrhythmias are increased by calmodulin kinase II in calcineurin cardiomyopathy. Circulation 114:1352–1359
108. Dybkova N, Sedej S, Napolitano C, Neef S, Rokita AG, Hünlich M, Brown JH, Kockskämper J, Priori SG, Pieske B, Maier LS (2011) Overexpression of CaMKIIδc in $RyR2^{R4496C}$ knock-in mice leads to altered intracellular Ca^{2+} handling and increased mortality. J Am Coll Cardiol 57:469–479
109. January CT, Riddle JM (1989) Early afterdepolarizations: Mechanism of induction and block. A role for L-type Ca^{2+} current. Circ Res 64:977–990
110. Marban E, Robinson SW, Wier WG (1987) Mechanisms of arrhythmogenic delayed and early afterdepolarizations in ferret ventricular muscle. J Clin Invest 78:1185–1192
111. Carlsson L, Drews L, Duker G (1996) Rhythm anomalies related to delayed repolarization in vivo: influence of sarcolemmal Ca^{++} entry and intracellular Ca^{++} overload. J Pharmacol Exp Ther 279:231–239
112. Wu Y, Kimbrough JT, Colbran RJ, Anderson ME (2004) Calmodulin kinase is functionally targeted to the action potential plateau for regulation of L-type Ca^{2+} current in rabbit cardiomyocytes. J Physiol 554:145–155
113. Wu Y, Roden DM, Anderson ME (1999) Calmodulin kinase inhibition prevents development of the arrhythmogenic transient inward current. Circ Res 84:906–912
114. Hund TJ, Decker KF, Kanter E, Mohler PJ, Boyden PA, Schuessler RB, Yamada KA, Rudy Y (2008) Role of activated CaMKII in abnormal calcium homeostasis and I_{Na} remodeling after myocardial infarction: insights from mathematical modeling. J Mol Cell Cardiol 45: 420–428
115. Swaminathan PD, Purohit A, Soni S, Voigt N, Singh MV, Glukhov AV, Gao Z, He BJ, Luczak ED, Joiner ML, Kutschke W, Yang J, Donahue JK, Weiss RM, Grumbach IM, Ogawa M, Chen PS, Efimov I, Dobrev D, Mohler PJ, Hund TJ, Anderson ME (2011) Oxidized CaMKII causes cardiac sinus node dysfunction in mice. J Clin Invest. doi:10.1172/JCI57833

Chapter 31
The Role of Molecular Regulation and Targeting in Regulating Calcium/Calmodulin Stimulated Protein Kinases

Kathryn A. Skelding and John A.P. Rostas

Abstract Calcium/calmodulin-stimulated protein kinases can be classified as one of two types – restricted or multifunctional. This family of kinases contains several structural similarities: all possess a calmodulin binding motif and an autoinhibitory region. In addition, all of the calcium/calmodulin-stimulated protein kinases examined in this chapter are regulated by phosphorylation, which either activates or inhibits their kinase activity. However, as the multifunctional calcium/calmodulin-stimulated protein kinases are ubiquitously expressed, yet regulate a broad range of cellular functions, additional levels of regulation that control these cell-specific functions must exist. These additional layers of control include gene expression, signaling pathways, and expression of binding proteins and molecular targeting. All of the multifunctional calcium/calmodulin-stimulated protein kinases examined in this chapter appear to be regulated by these additional layers of control, however, this does not appear to be the case for the restricted kinases.

Keywords Phosphorylase kinase • eEF2K • Myosin light chain kinase • CaMKK • CaMKI • CaMKII • CaMKIV • Casein kinase I • Targeting

Abbreviations

α-KAP	αCaMKII anchoring protein
aa	Amino acid
ADP	Adenosine-5′-diphosphate

K.A. Skelding • J.A.P. Rostas (✉)
School of Biomedical Sciences and Pharmacy and Hunter Medical Research Institute, Faculty of Health, The University of Newcastle, University Drive, Callaghan, NSW 2308, Australia
e-mail: John.Rostas@newcastle.edu.au

M.S. Islam (ed.), *Calcium Signaling*, Advances in Experimental Medicine and Biology 740, DOI 10.1007/978-94-007-2888-2_31,

AMPK	AMP-activated protein kinase
APC	Adenomatous polyposis coli-associated protein
ATP	Adenosine triphosphate
Ca^{2+}	Calcium ions
CaM	Calmodulin
CaMK	Calcium/calmodulin stimulated protein kinases
CaMKI	Calcium/calmodulin stimulated protein kinase I
CaMKII	Calcium/calmodulin stimulated protein kinase II
CaMKIII	Calcium/calmodulin stimulated protein kinase III
CaMKIV	Calcium/calmodulin stimulated protein kinase IV
CaMKK	Calcium/calmodulin stimulated protein kinase kinase
CK1	Casein kinase 1
CLK2	CDC-like kinase 2
eEF2K	Elongation factor 2 kinase
G	Glycine
GSK-3	Glycogen synthase kinase 3
HSF1	Heat shock factor 1
kDa	Kilodalton
MAPKAP-K2/K3	Mitogen-activated protein kinase-activated protein kinase 2/ kinase 3
MDa	Megadalton
Mg^{2+}	Magnesium ions
MLCK	Myosin light chain kinase
mRNA	Messenger ribonucleic acid
PhK	Phosphorylase kinase
PKA	cAMP-dependent protein kinase
PKB	Protein kinase B; Akt
PP2A	Protein phosphatase 2A
PSD	Post-synaptic density
RLC	Regulatory light chain
RSK	Ribosomal S6 kinase
S	Serine
S6K1	Ribosomal protein S6 kinase-1
SAPK4	Stress activated protein kinase 4
T	Threonine

Introduction

Calcium is a major second messenger in all cells, and is integral in many important signaling pathways. Changes in intracellular Ca^{2+} regulate many biological processes, including neurotransmitter release, gene expression, and the cell cycle. Though free Ca^{2+} can activate a number of proteins directly (for example myosin, phospholipase A_2, and protein kinase C), it regulates the activity of many enzymes

indirectly via a number of low molecular weight Ca^{2+} binding proteins, the most abundant of which is calmodulin (CaM). CaM consists of two globular lobes, each of which contain two Ca^{2+}-binding sites. Binding of Ca^{2+} dramatically changes the conformation of CaM, allowing Ca^{2+}/CaM to interact with a variety of other proteins, including several classes of protein kinases.

Many proteins that bind Ca^{2+}/CaM contain an α-helix region consisting of approximately 20 amino acids, which contain positively charged amino acids among hydrophobic residues. There are two types of CaM binding motif classes [1]. The ***IQ motif*** (IQXXXRGXXXR) indicates the binding of CaM in the absence of Ca^{2+}. The majority, if not all, of the proteins that contain this motif are not enzymes, and appear to limit the concentration of diffusible CaM during periods of low intracellular Ca $^{2+}$. The second class of motifs are related to each other, and indicate CaM binding in the presence of Ca^{2+}. These motifs include ***1-12***, ***1-14***, ***1-5-10***, and ***1-8-14*** (named based on the conserved hydrophobic residues within these motifs). However, several identified/putative CaM binding sites have sequence motifs that are called ***unclassified*** because they do not conform to either of the preceding sequence motifs.

Ca^{2+}/CaM stimulated protein kinases are classified based on their specificity, and there are two main types: ***restricted*** kinases, which only phosphorylate one, or a small number, of substrates, and ***multifunctional*** kinases, which have broad substrate specificity (Table 31.1). A number of these kinases share several structural and regulatory features, including an autoinhibitory pseudosubstrate domain. This domain, as its name implies, acts like a substrate and binds to the active site of the kinase, thereby inhibiting the kinase until activation displaces the domain. In the case of the Ca^{2+}/CaM stimulated protein kinases discussed in this chapter, it is the binding of Ca^{2+}/CaM that causes the displacement of the autoinhibitory pseudosubstrate domain and activates the kinase.

There are multiple levels of control that regulate the functions of Ca^{2+}/CaM stimulated protein kinases. The most coarse method of controlling kinase function is via the regulation of Ca^{2+} dynamics, specifically the frequency, amplitude and duration of oscillations in the intracellular concentration of Ca^{2+}. This is most commonly controlled by ion channels and many kinases can be directly regulated by intracellular Ca^{2+} fluxes. For example, the multifunctional Ca^{2+}/CaM-stimulated protein kinase II (CaMKII) can decode the frequency of Ca^{2+} spikes into distinct amounts of kinase activity [2]. However, several additional mechanisms exist that produce extra forms of control of kinase activity. Modulation of the response to changes in Ca^{2+} can be controlled by phosphorylation and/or splicing of the kinase, or by the kinase becoming autonomously active (i.e. no longer require Ca^{2+}/CaM for activity) [3–5]. Another level of control has also been identified that provides both temporal and site-specific control of kinase function. This mechanism is termed "targeting", and involves the interactions between kinases and specific binding proteins. This chapter will examine how Ca^{2+}/CaM stimulated protein kinases are regulated, with a particular focus on the role of molecular regulation and targeting in controlling the function of Ca^{2+}/CaM stimulated protein kinases (Table 31.1).

Table 31.1 Comparison of structure and regulation of Ca^{2+}/calmodulin stimulated protein kinases

	Restricted Ca^{2+}/CaM-stimulated kinases			Multifunctional Ca^{2+}/CaM-stimulated kinases				
	Phosphorylase kinase	eEF2K	MLCK	CaMKK	CaMKI	CaMKII	CaMKIV	CK1
Genes	5 (*PHKA1, PHKA2, PHKB, PHKG2, PHKG2*)	1 (*EEF2K*)	2 (*mylk1, mylk2*)	2 (*CAMKK1, CaMKK2*)	4 (*CAMK1A, CAMK1B, CAMK1G, CAMK1D*)	4 (*CAMK2A, CAMK2B, CAMK2G, CAMK2D*)	1 (*CAMK4*)	7 (α, β, γ1, γ2, γ3, δ, ε)
Splice variants	Multiple	?	Multiple	Multiple	Multiple	Multiple	1 (CaMKIVβ)	Multiple
Subunit (kDa)	138 (α), 125 (β), 44, (γ), 17 (δ)	95–103	65–220	54–68	38–53	50–60	65–75	37–51
Structure	Tetramer	Monomer	Mixture of multimer, dimer and monomer	Monomer	Monomer	Multimer	Monomer	Monomer
CaM binding motif	1-12 motif	Unclassified	Unclassified	Unclassified	1-14 motif	1-5-10 motif	1-8-14 motif	Unclassified
Contains an autoinhibitory region?	Yes (proposed)	Yes (putative)	Yes	Yes	Yes	Yes	Yes	Yes (proposed)
Expression	Ubiquitous	Ubiquitous	Ubiquitous	Neuronal, immune, testis	Ubiquitous	α/β neuronal; γ/δ ubiquitous	Neuronal, immune, testis	Ubiquitous
Requirement for activation	Ca^{2+}/CaM	Ca^{2+}/CaM	Ca^{2+}/CaM	Ca^{2+}/CaM	Ca^{2+}/CaM	Ca^{2+}/CaM	Ca^{2+}/CaM, phosphorylation	Constitutively active
Capable of autonomous activity?	No	Yes	No	Yes	No	Yes	Yes	Yes
Number of phosphorylation sites	Multiple	Multiple	Multiple	Multiple	1 (T174–180)	Multiple	1 (T196–200)	Multiple
Regulation by phosphorylation	Autophosphorylation and Phosphorylated by PKA	Autophosphorylation (inhibitory and activating)	Phosphorylated by PKA, PKC, CaMKII	Autophosphorylation (inhibitory)	Phosphorylated by CaMKK	Autophosphorylation (inhibitory and activating)	Phosphorylated by CaMKK	Autophosphorylation (inhibitory)
Regulated by targeting?	No	No	?	?	Yes	Yes	Yes	Yes

? indicates the role of targeting in this enzyme has not been examined

Restricted Calcium/Calmodulin Stimulated Protein Kinases

Phosphorylase Kinase (PhK)

Phosphorylase kinase (PhK) is a 1.3 MDa hexadecamer, and is encoded by five genes (PHKA1, PHKA2, PHKB, PHKG1, PHKG2). PhK was the first protein kinase to have its function identified [6], and is a key enzyme in the control of glycogenolysis, as PhK phosphorylates inactive glycogen phosphorylase b, thereby converting it to active phosphorylase a. PhK is expressed in many tissues [7], and multiple tissue-specific isoforms exist in muscle and liver [8].

Structure

PhK is one of the largest and most complex protein kinases. Four copies of four different subunits (α, β, γ, δ) are arranged as a dimer of $(\alpha\beta\gamma\delta)_2$ octamers [8]. However, αγδ heterotrimers and γδ heterodimeric subcomplexes have also been identified [9]. Based on electron microscopy images, the structure of the PhK complex is a pseudo-tetrahedron, consisting of two lobes interconnected by central bridges [10–14] and resembling a butterfly.

The α (138.4 kDa) and β (125.2 kDa) subunits are regulatory inhibitory subunits (Fig. 31.1). Little is known about the structure of the α and β subunits. Sequence comparisons with known proteins suggest that aa 1–436 (α subunit) and aa 40–477 (β subunit) share sequence similarities with 15 glycosyl hydrolases [15]. In addition, residues 1,066–1,237 (α subunit) and aa 918–1,093 (β subunit) share similarities with the calcineurin B-like proteins [16]. Several autoinhibitory domains have also been proposed, including one on the β subunit (aa 420–436) that has homology to glycogen phosphorylase [17]. The γ subunit (44.7 kDa) is the catalytic subunit, and contains a catalytic domain (aa 20–276) and a CaM-binding and autoinhibitory domain (aa 298–396) (Fig. 31.1). The δ subunit (16.7 kDa) is an endogenous molecule of CaM, which binds to PhK, even in the absence of Ca^{2+} (Fig. 31.1). When isolated as a single γ subunit, the kinase domain is constitutively active. Therefore, the role of the α and β subunits is to inhibit the activity of the kinase.

Regulation

The activation of PhK is complex, and several layers of control exist. PhK can also be activated *in vitro* by increases in pH [18], autophosphorylation, limited proteolysis and adenosine-5′-diphosphate (ADP) [19]. Phosphorylation by PKA increases the activity of PhK, however, PhK remains Ca^{2+}-dependent. PKA phosphorylates PhK on at least two sites, and one well-characterised site has been observed on each of the α (S1018) and β (S27) subunits [8]. PKA phosphorylation of the β subunit increases the activity of PhK. Phosphorylation of the α subunit amplifies this affect,

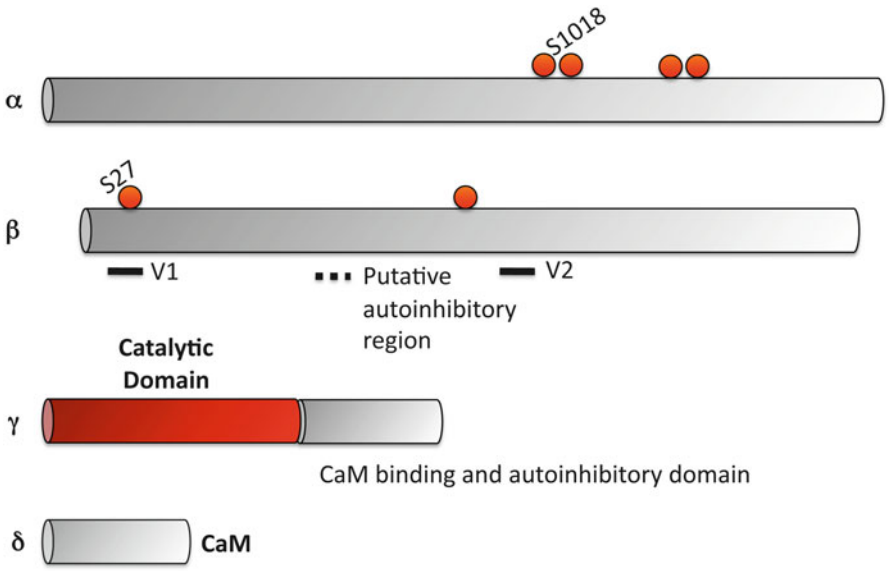

Fig. 31.1 Schematic diagram of the domain structure of Phosphorylase Kinase (PhK) subunits. PhK is one of the largest and most complex protein kinases currently known. Four different subunits (α, β, γ, δ) are arranged as a dimer of octamers. The α and β subunits are regulatory inhibitory subunits, and little is known about their structure. Both the α and β subunits contain multiple phosphorylation sites, and the β subunits also contains two variable regions (*V1* and *V2*). The γ subunit contains an N-terminal catalytic domain (*red*), and a C-terminal calmodulin (*CaM*) binding and autoinhibitory domain. The δ subunit is an endogenous molecule of CaM

but does not directly activate PhK [20, 21]. Autophosphorylation of PhK also increases activity *in vitro* [22]. However, the correlation between phosphorylation of specific sites and activation has not been examined. The activity of unactivated PhK can be increased via interacting with exogenous CaM (also called δ′) or troponin C, both of which bind to PhK in a Ca^{2+}-dependent manner [8]. In addition, there is evidence to suggest that troponin C is able to compete with CaM for binding to the γ-subunit [23]. However, interaction with exogenous CaM has no effect on PhK activity once PhK is phosphorylated [8].

The role of targeting in regulating PhK function has not been examined. However, no evidence exists to indicate that interactions with binding proteins or subcellular location influence PhK function. It is therefore unlikely that targeting plays a significant role in regulating PhK *in vivo*.

Elongation Factor 2 Kinase (eEF2K)

Elongation factor 2 kinase (eEF2K) is also known as Ca^{2+}/CaM stimulated protein kinase III (CaMKIII) [24], and is a novel kinase that is unrelated to other Ca^{2+}/CaM

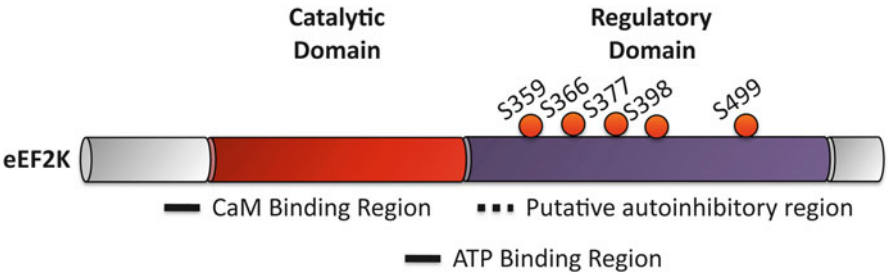

Fig. 31.2 Schematic diagram of the domain structure of Elongation Factor 2 Kinase (eEF2K). The structure of eEF2K is unrelated to other serine/threonine protein kinases. The N-terminal catalytic domain (*red*) contains none of the conserved subdomains usually present in serine/threonine protein kinases. A C-terminal regulatory domain (*purple*) contains multiple phosphorylation sites, and a putative autoinhibitory domain. A calmodulin (*CaM*) binding region has also been identified N-terminal to the catalytic domain

stimulated protein kinases [25]. It is a monomer with an apparent molecular weight of 95–103 kDa [26]. eEF2K is ubiquitously expressed in eukaryotic cells, however, tissue specific isoforms have been identified [27]. eEF2K negatively regulates eukaryotic messenger ribonucleic acid (mRNA) translation, by phosphorylating and inactivating elongation factor 2 (eEF2), which is the only known substrate of eEF2K [28]. eEF2 mediates the translocation step in which the ribosome moves along mRNA during translation.

Structure

The structure of eEF2K is unrelated to that of other serine (S)/threonine (T) kinases (Fig. 31.2). The only kinase that possesses any homology with eEF2K is *Dictyostelium* myosin heavy chain kinase, which is not Ca^{2+}/CaM dependent [29]. The catalytic domain lies in the N-terminal half of eEF2K, and it possesses none of the conserved catalytic subdomains usually present in serine/threonine kinases, apart from a GXGXXG motif that may be involved in binding Mg^{2+}/adenosine triphosphate (ATP) [30]. A putative pseudosubstrate and autoinhibitory domain are present C-terminal to the catalytic domain [25] and the CaM binding region is immediately N-terminal to the catalytic domain (aa 77–99) [31].

Regulation

eEF2K is activated by binding Ca^{2+}/CaM, resulting in partial Ca^{2+}/CaM independence of the kinase [24, 26]. The subsequent regulation of eEF2K is primarily by phosphorylation at a number of sites by a number of kinases. cAMP-dependent protein kinase (PKA) and AMP-activated protein kinase (AMPK) phosphorylate eEF2K at S499 [32] and S398 [33, 34] respectively, thereby activating eEF2K and,

in the case of S366 and S499, making it partially autonomous [35]. By contrast, phosphorylation at S377 by mitogen-activated protein kinase-activated protein kinase 2/kinase 3 (MAPKAP-K2/K3) [36, 37], S359 by stress activated protein kinase 4 (SAPK4; also called p38δ), or S366 by ribosomal protein S6 kinase-1 (S6K1) or ribosomal S6 kinase (RSK) [38], inhibits eEF2K activity. Molecular regulation of eEF2K by these kinases alters physiological outcomes. For example, AMPK is activated in anoxic hepatocytes. Under these anoxic conditions, eEF2K is activated by AMPK, which results in the phosphorylation and inactivation of eEF2 thereby inhibiting protein synthesis [33].

The role of targeting in regulating eEF2K function has not been examined. However, no evidence exists to suggest that interactions with binding proteins or subcellular location influence eEF2K function. Therefore, it is unlikely that targeting plays a role in regulating its function.

Myosin Light Chain Kinase (MLCK)

Myosin light chain kinase (MLCK) is an ubiquitously expressed protein kinase that is found in virtually all eukaryotic cells. Molecular and biochemical studies have characterised MLCKs from a variety of species, including rat [39], rabbit [40], chicken [41], and human [42]. It is encoded by at least two genes (*mylk1* and *mylk2*) [43–45], which yield both muscle and non-muscle isoforms that range from 69 to 220 kDa in size, depending on the species and isoform. *Mylk2* encodes an isoform expressed exclusively in skeletal muscle [46], whereas *mylk1* products are ubiquitously expressed [47, 48]. MLCK phosphorylates the regulatory light chain (RLC) of myosin II in the presence of Ca^{2+}/CaM and no other substrates have been identified.

Structure

Inactive (non-CaM bound) MLCK exists as a mixture of oligomeric (hexamer; 2% of MLCK in solution), dimeric (53%), and monomeric (45%) suprastructures [49]. The vertebrate MLCKs are all structurally similar (Fig. 31.3), with a catalytic domain that binds Mg^{2+}, ATP and the RLC, and a regulatory domain that contains autoinhibitory and CaM binding domains. Interestingly, the autoinhibitory domain was first suggested to act as a pseudosubstrate in MLCK [50]. This was due to the fact that the autoinhibitory region lies, in the absence of Ca^{2+}/CaM, in the substrate binding region. The majority of the Ca^{2+}/CaM stimulated protein kinases possess such a pseudosubstrate/autoinhibitory domain. The C-terminal 150 amino acid residues of the smooth muscle MLCK isoform is also expressed as an independent protein, termed telokin [51]. Telokin inhibits MLCK activity towards MLCK substrates, and activates myosin light chain phosphatase, and can thereby modulate the contractile properties of smooth muscle [52]. The different isoforms are encoded by mRNAs arising from promoters within different introns of the *mlck* gene [45, 51].

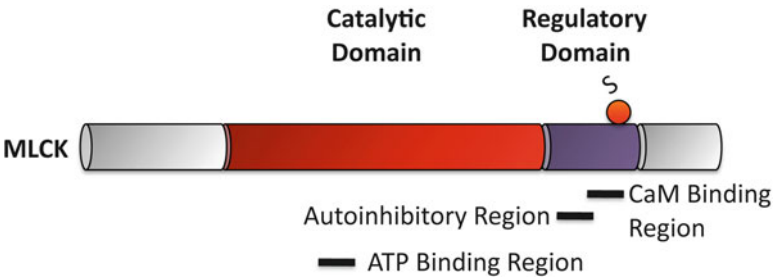

Fig. 31.3 Schematic diagram of the domain structure of Myosin Light Chain Kinase (MLCK). The vertebrate MLCKs are structurally similar. The catalytic domain (*red*) binds ATP, magnesium ions, and the regulatory light chain (*RLC*) of myosin II. The regulatory domain (*purple*) contains a phosphorylation site, and autoinhibitory and calmodulin (*CaM*) binding domains

Regulation

Vertebrate forms of MLCK are completely dependent on Ca^{2+}/CaM for activity. Several studies [50, 53–55] indicate that MLCK is inhibited by a pseudosubstrate domain that has a sequence highly homologous to the phosphorylation site of RLC (aa 1–19). Furthermore, the CaM binding site overlaps with this autoinhibitory domain. Therefore, upon binding to CaM, the autoinhibitory domain is displaced, and MLCK becomes activated.

In the absence of CaM, phosphorylation of MLCK occurs on a serine at the C-terminus of the CaM binding domain. PKA [56], protein kinase C (PKC) [57] and CaMKII [58] can phosphorylate MLCK on this serine site. Phosphorylation at this site increases the K_{CAM} (the concentration at which the rate of the enzyme reaction is half the maximal rate) approximately tenfold. This decreases the activity of MLCK [56]. However, when CaM is associated with MLCK, phosphorylation at this site is blocked [59]. Additional phosphorylation sites have been identified on MLCK *in vivo* [60]. However, the kinases involved and the potential physiological functions associated with these phosphorylation events have not been identified.

Whilst the role of targeting in regulating MLCK function has not been examined, different expression patterns have been noticed for the small (130 kDa) and large (220 kDa) forms of MLCK. For example, the large and small MLCKs are differentially distributed during cytokinesis [61]. In addition, while the small and large MLCKs have identical biochemical properties *in vitro*, their subcellular localisation and expression patterns *in vivo* are distinct [62]. This suggests that the small and large forms of MLCK are targeted to different intracellular locations by binding to different proteins and may elicit different cellular functions *in vivo*. However, whether these different forms of MLCK are regulated differently is yet to be identified.

Multifunctional Calcium/Calmodulin Stimulated Protein Kinases

Calcium/Calmodulin Stimulated Protein Kinase Kinase (CaMKK)

Calcium/calmodulin stimulated protein kinase kinase (CaMKK) is a multifunctional protein kinase that is encoded by two genes (CAMKK1 and CAMKK2) that produce CaMKKα and CaMKKβ, respectively. The CAMKK2 gene also generates several splice isoforms [63], which are between 54 and 68 kDa in size. CaMKK is primarily expressed in the brain, but is also present in the thymus, spleen, and testis [64–67]. The expression pattern of CaMKKβ appears to parallel that of CaMKIV [68]. CaMKK phosphorylates Ca^{2+}/CaM stimulated protein kinase I (CaMKI) and Ca^{2+}/CaM stimulated protein kinase IV (CaMKIV), but can also phoshorylate other proteins, such as AMP activated protein kinase (AMPK) [69] and protein kinase B (PKB; also known as Akt).

CaMKK, CaMKI and CaMKIV have been shown to form a signaling pathway termed the Ca^{2+}/CaM-dependent kinase cascade, which has been implicated in several cellular processes, including normal neuronal function [70], the cell cycle [71], and normal immune cell function [72]. An unusual aspect of this cascade is that binding of Ca^{2+}/CaM to both CaMKK and its substrates (CaMKI and CaMKIV) is required for phosphorylation of their activation loops [73]. Whilst unusual, this mechanism has been noted in other signaling pathways, including the AMP-kinase cascade [74].

Structure

The domain structure of CaMKK, CaMKI, and CaMKIV are similar [75] (Fig. 31.4), with all possessing a C-terminal regulatory domain that contains an autoinhibitory region, which keeps the kinase inactive until Ca^{2+}/CaM binds, and a conserved CaM binding region. All family members also have an N terminal catalytic domain.

Regulation

CaMKK require Ca^{2+}/CaM for maximal activity [73]. However, CaMKKβ exhibits partially autonomous activity in the absence of Ca^{2+}/CaM (50–70% Ca^{2+}/CaM-independent activity), whereas CaMKKα is completely dependent on the binding of Ca^{2+}/CaM for activity [68, 76]. CaMKK can autophosphorylate at S74 in the presence of Ca^{2+}/CaM, however, it is very slow, substochiometric, and does not appear to effect catalytic activity [68, 77].

CaMKKα can be phosphorylated at both activating and inhibitory sites. PKA can phosphorylate S52, S74, T108, S458, and S475 on CaMKKα [78], however,

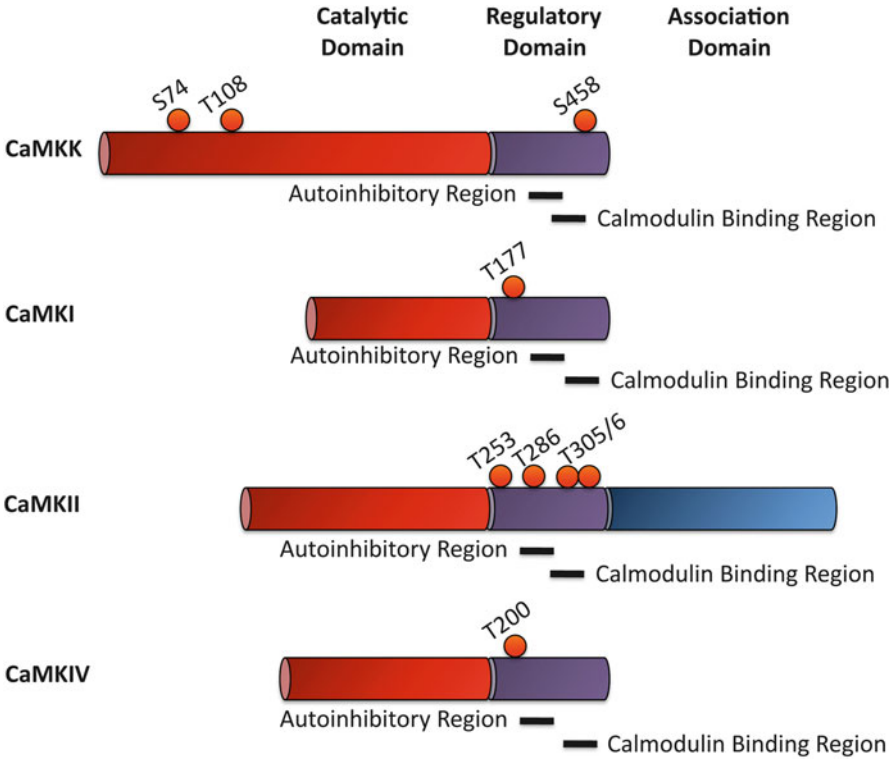

Fig. 31.4 Schematic diagram of the domain structure of the multifunctional Ca^{2+}/CaM stimulated protein kinase (CaMK) family. All of the CaMKs, except CaMKII, have similar overall domain structures. CaMKK, CaMKI, CaMKII, and CaMKIV possess an N-terminal catalytic domain (*red*), and a regulatory domain (*purple*), which is comprised of autoinhibitory and calmodulin (*CaM*) binding domains. CaMKII has an additional C-terminal association domain (*blue*). In each instance, phosphorylation sites are number according to the α isoform

phosphorylation of CaMKKβ by PKA has not been reported [79]. However, binding of Ca^{2+}/CaM blocks phosphorylation at S52, S74, T108, and S458, but enhances phosphorylation at S475 [78]. CaMKKα activity is negatively regulated by phosphorylation on S74, T108 and S458 [80–82]. In addition, cyclin dependent kinase 5 (CDK5) phosphorylates CaMKKβ at S137, therefore priming CaMKKβ for phosphorylation by glycogen synthase kinase 3β (GSK-3β) at S129 and S133 [79]. Phosphorylation at these sites decreases the autonomous activity of CaMKKβ, and regulates its half-life. In addition, phosphorylation of CaMKKβ by GSK-3β and CDK5 is critical for its role in neurite development [79].

Evidence suggests that targeting may play a role in regulating CaMKK function, as CaMKKα is known to translocate to the nucleus [83]. Furthermore, inhibition of this translocation prevents type-II monocytic cells from being activated [83]. However, whether this is regulated by phosphorylation has not been identified.

Calcium/Calmodulin Stimulated Protein Kinase I (CaMKI)

CaMKI is encoded by four genes (α, β, γ, and δ), with each gene producing at least one splice variant. All members of this family are monomeric and are between 38 and 42 kDa in size, except for CaMKIγ, which is 53 kDa. The various isoforms of CaMKI are expressed in the brain and other tissues, with CaMKIα being found in most mammalian cells [84]. CaMKI has been implicated in a variety of cellular functions, including the control of synapsin in nerve terminals [85], growth cone motility and axon outgrowth [86], aldosterone synthase expression [87], and the cell cycle [88–90].

Structure

CaMKI is monomeric, and is structurally similar to CaMKK and CaMKIV. CaMKI subunits are comprised of a regulatory domain, which contains autoinhibitory and CaM binding regions, and a N-terminal catalytic domain [75]. In addition, the crystal structure of CaMKI in its autoinhibited form has been elucidated [91]. The C-terminal regulatory domain forms a helix-loop-helix segment, which functions as an autoinhibitory domain.

Regulation

Phosphorylation of the conserved T (T174 to T180, depending on the isoform) in the activation loop by CaMKK is required for maximal CaMKI activity [92], although this depends on the substrate [93], suggesting that targeting may also be involved in the regulation of CaMKI. Various isoforms of CaMKI have been shown to translocate to the nucleus. For example, the translocation of CaMKIα to the nucleus (mediated by interacting with a CRM1 complex) is enhanced by Ca^{2+}/CaM, suggesting that nuclear export may be enhanced by activation of the kinase [94]. Furthermore, nuclear translocation of CaMKIδ is triggered by stimuli that produce an influx of intracellular calcium (potassium depolarisation or glutamate stimulation) [95]. The mechanisms and functions involved, however, remain to be determined.

Calcium/Calmodulin Stimulated Protein Kinase II (CaMKII)

Ca^{2+}/CaM stimulated protein kinase II (CaMKII) is encoded by four genes (α, β, γ, and δ) [96], which produce over 30 isoforms ranging in size from 50 to 60 kDa. One or more members of this family are found in virtually every tissue, and mediate diverse physiological functions. CaMKII is expressed most abundantly in neurons, and is involved in regulating many aspects of neuronal function, including neurotransmitter synthesis and release, cellular morphology and neurite extension,

long-term plasticity, learning, memory consolidation, and memory erasure following retrieval [97–102]. Non-neuronal CaMKII has been implicated in the regulation of other biological processes, such as fertilisation [103], osteogenic differentiation [104], the maintenance of vascular tone [105], normal cardiac function and heart failure [106], and cell proliferation [107].

Structure

Each isoform of CaMKII can be divided into three domains (Fig. 31.4): a C-terminal association domain, a N-terminal catalytic domain, and a regulatory domain in between. An autoinhibitory domain at aa 282–300 (numbered according to the α isoform) within the regulatory domain has been identified that interacts with the catalytic domain to block the ATP binding site, thereby inhibiting the kinase activity of the enzyme [108, 109]. The amino acid sequence 293–310 binds Ca^{2+}/CaM and partially overlaps with the autoinhibitory domain [110]. There are four main variable regions (V1–4) through which alternative splicing produces more than 30 isoforms. The V1 region, located between the regulatory and association domains, is the primary site for divergence among the four CaMKII genes [111].

The three-dimensional structure of CaMKII is in fact highly unusual [112]. The CaMKIIα crystal is an asymmetric unit that consists of two autoinhibited catalytic domains in a symmetric dimer held together by interactions between anti-parallel coiled-coil structures formed by the regulatory domains. The regulatory domains are joined by a hinge to the C-terminus of the catalytic domain. The regulatory domain functions like a gate (with T286 as its hinge), so that it is positioned to block the protein substrate and ATP binding sites when CaMKII is autoinhibited, and is "open" when CaMKII is autophosphorylated at T286. Therefore, CaMKII is comprised of six mutually inhibited dimers. Homomers of α, β, γ, and ∂ all exhibit the same basic structure. Whilst heteromultimers are known to exist [113], their structures are unknown.

Regulation

The biological properties of CaMKII are regulated by multi-site phosphorylation and targeting to specific subcellular locations through interactions with other proteins. These two control mechanisms can also influence one another, as the interaction between CaMKII and some binding partners can be modified by the phosphorylation state of the kinase, as well as by phosphorylation of the binding partner [3, 107].

Purified CaMKII requires the presence of Ca^{2+}/CaM for initial enzyme activity. Binding of two CaM molecules to two adjacent subunits within a holoenzyme allows autophosphorylation of one or both of these subunits to occur at T286 [114]. Autophosphorylation of T286 in CaMKIIα (T287 in CaMKIIβ, γ, and ∂) occurs quickly and produces changes in the affinity for Ca^{2+}/CaM, enzyme activity, and targeting to specific subcellular sites. CaMKII phosphorylation at T286 allows the

enzyme to remain active even after CaM has dissociated from it (autonomous activity), and can also regulate the function of the enzyme by increasing the binding of CaMKII to specific subcellular sites [115–117]. However, phosphorylation of T286 is not required for kinase activity.

Once the kinase activity of CaMKII is Ca^{2+}-independent (autonomous), and Ca^{2+}/CaM is no longer bound to the kinase, secondary sites that are within the CaM-binding site can be phosphorylated (T305/306 in CaMKIIα, and T306/307 in CaMKIIβ, γ, and ∂) [118, 119]. Once these sites are phosphorylated, CaM can no longer bind so CaMKII becomes insensitive to changes in Ca^{2+}/CaM [120].

Recently, a new phosphorylation site on CaMKII at T253 was identified *in vivo* [121]. T253 has previously been overlooked as a phosphorylation site of interest as it has no direct effect on the kinase activity of CaMKII *in vitro*. However, T253 phosphorylation has marked effects on CaMKII targeting [107, 121]. Furthermore, the overall stoichiometry of T253 phosphorylation is relatively low in the cell as a whole because it occurs only in a subpopulation of CaMKII molecules at particular cellular locations [121].

Other sites, such as S279 and S314, are phosphorylated both *in vitro* [122–124] and *in vivo* [125–127], but the stoichiometry of phosphorylation is relatively low and phosphorylation does not affect CaMKII activity *in vitro*. Although these sites have not been investigated for their effects on targeting, it is possible that, along with T253, they may belong to a new class of phosphorylation site that has its major functional role in regulating targeting rather than directly modifying enzyme activity.

There are two lines of evidence that led to the recognition of the importance of targeting in the regulation of CaMKII in cells: the differences in kinase properties between splice isoforms, and the phenomenon of subcellular translocation.

All four CaMKII genes undergo alternative splicing in their variable regions [128], which produces some variability in the kinase properties *in vitro*. However, the number of splice variants is much greater than the differences observed in enzyme activity and the splicing occurs in parts of the molecule well away from the catalytic and regulatory domains suggesting that the primary function of many of the isoforms is not to alter enzyme activity. The αCaMKII-anchoring protein (αKAP), provides an unusual example of targeting. RNA splicing of CaMKIIα produces αKAP as a truncated, enzymatically inactive protein, which is mostly comprised of the association domain of CaMKIIα, and an N-terminal lipid tail. αKAP is found in skeletal muscle and the heart, and is expressed at low levels in the lung, kidney, and testis [129]. αKAP can form heteromultimers with full length CaMKII, thereby targeting the active kinase subunits to the sarcoplasmic reticulum membrane in rat skeletal muscle [130].

A small number of splice variants of CaMKII contain a consensus nuclear localisation sequence and others contain specific binding sites for individual proteins (for example, the binding sequence for actin is specific to the CaMKIIβ isoform [131]). The fact that the association domain contains all the main sequence variations between isoforms of CaMKII suggests that most of the binding sites for other molecules are contained in this region.

A constitutively active 30 kDa fragment of CaMKII is generated by limited proteolysis following autophosphorylation [132]. This fragment is completely Ca^{2+}/CaM-independent, however, autophosphorylation sites (e.g. T286) are not contained in this fragment. This fragment exhibits a tenfold increase in V_{max} (the maximal rate of the enzyme reaction) and a 50% decrease in the K_M for synthetic peptide substrates, when compared to full length CaMKII [132]. A slightly larger fragment (32 kDa) is generated when limited proteolysis occurs prior to autophosphorylation. This fragment, however, is inactive [132]. These fragments have been identified *in vivo*, however, specific physiological functions have not been attributed to these fragments.

CaMKII translocation to the post-synaptic density (PSD) in neurons has been well characterised (reviewed in [133, 134]), and CaMKII phosphorylated at different sites (T253, T286, and T305/306) alters the amount of CaMKII that is bound to the PSD. This translocation to the PSD can occur rapidly in response to hypoxia or post-mortem delay and may involve self-assembly of CaMKII [117, 135, 136]. Phosphorylation of T305/306 decreases the amount of CaMKII bound to the PSD, stimulating translocation from the PSD to the cytosol [137]. By contrast, phosphorylation of either T286 or T253 enhances binding to the PSD, stimulating translocation from the cytosol to the PSD and the effects appear to be through independent binding proteins since phosphorylation at both sites results in an additive effect [121].

Calcium/Calmodulin Stimulated Protein Kinase IV (CaMKIV)

CaMKIV is encoded by one gene (α), which produces at least one splice variant (β). All splice variants are monomeric and are between 65 and 67 kDa in size. CaMKIV is primarily expressed in the brain, but is also present in immune cells and the testis/ovary [64–67]. As mentioned previously, the CaMKIV expression pattern is similar to that of CaMKKβ. The *CAMK4* gene also encodes calspermin, a Ca^{2+}/CaM binding protein of unknown function that is expressed exclusively in spermatids in the testes [67]. CaMKIV has been implicated in the regulation of cyclic AMP element binding protein (CREB) [138], neurite outgrowth [139], immune and inflammatory responses [140], and cell cycle control [88, 90].

Structure

The subunits of all CaMKI, CaMKIV, and CaMKK are similar (Fig. 31.4). CaMKIV subunits consist of a regulatory domain, which contains autoinhibitory and CaM binding regions, and a N-terminal catalytic domain [75]. Truncation experiments have demonstrated that the autoinhibitory region of CaMKIV encompases aa 305–317 [141, 142]. Residues 319–325 have been identified as the CaM-binding domain, which is highly homologous to other characterised CaM binding sites.

In addition, phosphorylation of S332 within the CaM binding region prevents CaM binding [143]. The two protein isoforms, CaMKIVα and CaMKIVβ, are identical, except CaMKIVβ contains a 28 aa N-terminal extension, of unknown function.

Regulation

CaMKIV requires Ca^{2+}/CaM to become active, as well as phosphorylation of the conserved T in the activation loop (T200 in human CaMKIV) by CaMKK [5]. This phosphorylation generates an autonomously active kinase. Phosphorylation at this site (T196 in CaMKIVα) enhances glucokinase promoter activity [144], suggesting that CaMKIV phosphorylation can regulate insulin secretion and glucose homeostasis. CaMKIV can translocate between the cytoplasm and nucleus, and catalytic activity is required for this translocation, as catalytically inactive CaMKIV remains in the cytoplasm [145]. This suggests that targeting also plays a role in regulating CaMKIV function, however this requires further investigation.

Casein Kinase 1 (CK1)

The casein kinase 1 (CK1) family of multifunctional serine/threonine protein kinases are abundantly expressed in all eukaryotic organisms [146], and in a variety of tissues [147]. All organisms contain several isoforms [148], and seven isoforms have been identified in vertebrates (α, β, γ1, γ2, γ3, δ, ε), some of which exhibit specific physiological functions [149–151]. In addition, several splice variants exhibiting different biochemical and cellular properties also exist [152]. The molecular weight of mammalian isoforms varies between 37 and 51 kDa. CK1 phosphorylates a variety of proteins that are involved in many cellular processes, including cell division, differentiation, circadian rhythms and metabolism [153].

CK1 phosphorylates a wide range of substrates bearing either canonical or non-canonical consensus sequences [154–159]. In addition, CK1 shows a strong preference for "primed" pre-phosphorylated substrates at N-3 (e.g. pS/T-X-X-S/T). However, CK1 can also phosphorylate unprimed substrates that contain a cluster of acidic amino acids in the N-3 position. Furthermore, CK1 purified from erythrocytes and Xenopus oocytes is able to phosphorylate tyrosine residues *in vitro* [160, 161], though it has not been determined whether this activity occurs *in vivo*.

Structure

The different isoforms/variants of CK1 are highly conserved within their catalytic domains, but vary significantly in the length and structure of their regulatory domains [162–164] (Fig. 31.5). The catalytic domain of CK1 is similar to other kinases, with a smaller N-terminal lobe, a large C-terminal lobe, and an

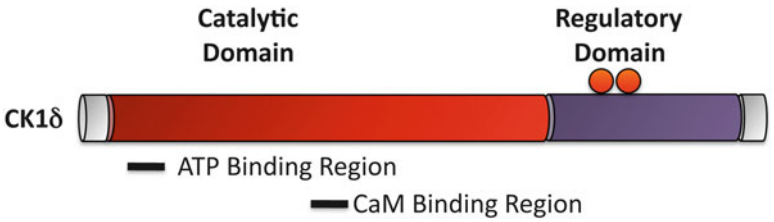

Fig. 31.5 Schematic diagram of the domain structure of casein kinase I (CK1). The different isoforms of CK1 are highly conserved within their catalytic domains (*red*), but vary considerably in the length and structure of their regulatory domains (*purple*), which contain multiple phosphorylation sites. CK1δ is represented in this diagram

intermediate catalytic cleft where ATP and substrates bind. CK1δ, ε, and γ3 have large C-terminal domains, which have been suggested to function as pseudosubstrates [162, 165, 166]. The CK1 family of kinases have been described as monomeric, constitutively active enzymes. However, CK1δ has been suggested to form dimers [166], with this dimerisation potentially inhibiting its activity. This hypothesis has yet to be proven.

Regulation

The precise mechanisms involved in regulating CK1 function are unclear, and have only recently begun to be identified. CK1 was initially identified as being stimulated by Ca^{2+}/CaM [167, 168]. However, unlike many other kinases, CK1 activity does not depend on an activation mechanism controlled by second messengers. The function of CK1 is regulated via a combination of phosphorylation and targeting to specific subcellular locations and via interactions with specific binding proteins. In addition, CK1ε can undergo limited proteolysis, which produces a protease-resistant core kinase with increased activity [163].

CK1 does not require phosphorylation on its activation loop for activity. CK1 can be autophosphorylated, or phosphorylated by PKA, PKB/Akt, CLK2 (CDC-like kinase 2) and PKC. However, phosphorylation by these kinases decreases CK1δ phosphorylation efficiency [169]. Although CK1 can autophosphorylate *in vivo*, it is actively maintained in its dephosphorylated, active state by protein phosphatases [170, 171]. Inhibitory autophosphorylation occurs most commonly in the C-terminal domain of CK1 [151, 165, 172–174], however, phosphorylation in the catalytic domain has also been noted [164].

Similarly to CaMKII, there is a large body of evidence demonstrating that targeting is an important regulatory mechanism for controlling CK1 function *in vivo*. Studies in yeast [175–177], and more recently in higher organisms [178, 179], have demonstrated that the function of constitutively active CK1 is regulated by its subcellular localisation. For example, CK1α exhibits a cell cycle dependent subcellular distribution, interacting with cytosolic vesicles and nuclear structures during

interphase, and the mitotic spindle during mitosis [180–182], with this localisation being controlled by the activity of CK1 [178]. In addition, domain swapping experiments performed with yeast CK1 demonstrate the interaction between CK1 and its substrates is controlled by subcellular distribution. Yeast encode four homologues of CK1, three of which localise to the plasma membrane, with the fourth being located at the nucleus [176, 183]. However, these homologues functionally complement each other when the localisation signals are switched [176], strongly supporting a role for subcellular targeting in regulating the function of CK1. Furthermore, alternative splicing of isoforms influences substrate binding and subcellular location [152, 184–186] highlighting another layer of complexity in the regulation of CK1.

In addition, the function of CK1 varies depending on the proteins with which it is associated. For example, CK1 can only phosphorylate β-catenin when it is associated with axin. Furthermore, CK1ε only phosphorylates CRY when both proteins are bound to PGR [187]. The phosphorylation state of CK1 can also affect its ability to interact with proteins. For example, the interaction between CK1α and 14-3-3 is dependent upon phosphorylation of CK1α [188]. By contrast, dephosphorylation of CK1ε increases activity towards the SV40 large T antigen, IκB and Ets-1 [163]. These examples highlight the importance of molecular targeting in mediating cell and tissue specific CK1 function *in vivo*.

Conclusions

Ca^{2+}/CaM stimulated protein kinases are one of the most abundant classes of enzymes in cells. They can be broadly classified as one of two types: restricted (phosphorylate only one or a few substrates) or multifunctional (phosphorylate many substrates). Multifunctional Ca^{2+}/CaM stimulated protein kinases are ubiquitously expressed, and regulate a broad range of physiological functions. This therefore raises the question of how ubiquitously expressed kinases can elicit cell and stimulus-specific functions. The answer lies in how these kinases are regulated.

All Ca^{2+}/CaM stimulated protein kinases are regulated by phosphorylation (either autophosphorylation, or phosphorylation by other kinases), and these phosphorylation events in some instances, can make the kinases autonomously active. However, with multifunctional kinases that are able to phosphorylate a number of substrates in a variety of cell types, other layers of regulation exist to control which substrate the kinase will interact with in different tissues and subcellular compartments. A number of levels of control exist that can elicit these tissue or location specific responses, including molecular regulation and targeting. Whilst the multifunctional kinases outlined in this chapter all appear to be regulated by targeting, this is not true for restricted Ca^{2+}/CaM stimulated protein kinases.

It is well established that the protein with which a kinase is associated can influence its function *in vivo*. As different cells express different complements of binding proteins, the microenvironment in which the kinase is located will affect

its functional outcome. Understanding molecular targeting will allow us to better comprehend complex signaling pathways and biological processes, and hence provide a better understanding of molecular mechanisms underlying normal and pathological cellular events. In addition, if cell specific mechanisms controlling kinase function can be identified, then drugs can be designed that will selectively disrupt interactions between kinases and substrates only in specific tissues.

References

1. Rhoads AR, Friedberg F (1997) Sequence motifs for calmodulin recognition. FASEB J 11:331–340
2. De Koninck P, Schulman H (1998) Sensitivity of CaM kinase II to the frequency of Ca^{2+} oscillations. Science 279:227–230
3. Skelding KA, Rostas JAP (2009) Regulation of CaMKII in vivo: the importance of targeting and the intracellular microenvironment. Neurochem Res 34:1792–1804
4. Hughes K, Nikolakaki E, Plyte SE, Totty NF, Woodgett JR (1993) Modulation of the glycogen synthase kinase-3 family by tyrosine phosphorylation. EMBO J 12:803–808
5. Selbert MA, Anderson KA, Huang QH, Goldstein EG, Means AR, Edelman AM (1995) Phosphorylation and activation of Ca(2+)-calmodulin-dependent protein kinase IV by Ca(2+)-calmodulin-dependent protein kinase Ia kinase Phosphorylatino of threonine 196 is essential for activation. J Biol Chem 270:17616–17621
6. Fischer EH, Krebs EG (1955) Conversion of phosphorylase b to phosphorylase a in muscle extracts. J Biol Chem 216:121–132
7. Winchester JS, Rouchka EC, Rowland NS, Rice NA (2007) In silico characterization of phosphorylase kinase: evidence for an alternate intronic polyadenylation site in PHKG1. Mol Genet Metab 92:234–242
8. Brushia RJ, Walsh DA (1999) Phosphorylase kinase: the complexity of its regulation is reflected in the complexity of its structure. Front Biosci 4:d618–d641
9. Kumar P, Brushia RJ, Hoye E, Walsh DA (2004) Baculovirus-mediated overexpression of the phosphorylase b kinase holoenzyme and alphagammadelta and gammadelta complexes. Biochemistry 43:10247–10254
10. Venien-Bryan C, Jonic S, Skamnaki V, Brown N, Bischler N, Oikonomakos NG, Boisset N, Johnson LN (2009) The structure of phosphorylase kinase holoenzyme at 9.9 angstroms resolution and location of the catalytic subunit and the substrate glycogen phosphorylase. Structure 17:117–127
11. Nadeau OW, Gogol EP, Carlson GM (2005) Cryoelectron microscopy reveals new features in the three-dimensional structure of phosphorylase kinase. Protein Sci 14:914–920
12. Norcum MT, Wilkinson DA, Carlson MC, Hainfeld JF, Carlson GM (1994) Structure of phosphorylase kinase. A three-dimensional model derived from stained and unstained electron micrographs. J Mol Biol 241:94–102
13. Nadeau OW, Carlson GM, Gogol EP (2002) A Ca(2+)-dependent global conformational change in the 3D structure of phosphorylase kinase obtained from electron microscopy. Structure 10:23–32
14. Venien-Bryan C, Lowe EM, Boisset N, Traxler KW, Johnson LN, Carlson GM (2002) Three-dimensional structure of phosphorylase kinase at 22 A resolution and its complex with glycogen phosphorylase b. Structure 10:33–41
15. Pallen MJ (2003) Glucoamylase-like domains in the alpha- and beta-subunits of phosphorylase kinase. Protein Sci 12:1804–1807
16. Carriere C, Mornon J-P, Venien-Bryan C, Boisset N, Callebaut I (2008) Calcineurin B-like domains in the large regulatory alpha/beta subunits of phosphorylase kinase. Proteins 71:1597–1606

17. Sanchez VE, Carlson GM (1993) Isolation of an autoinhibitory region from the regulatory beta-subunit of phosphorylase kinase. J Biol Chem 268:17889–17895
18. Liu W, Priddy TS, Carlson GM (2008) Physicochemical changes in phosphorylase kinase associated with its activation. Protein Sci 17:2111–2119
19. Cheng A, Fitzgerald TJ, Carlson GM (1985) Adenosine 5′-diphosphate as an allosteric effector of phosphorylase kinase from rabbit skeletal muscle. J Biol Chem 260:2535–2542
20. Ramachandran C, Goris J, Waelkens E, Merlevede W, Walsh DA (1987) The interrelationship between cAMP-dependent alpha and beta subunit phosphorylation in the regulation of phosphorylase kinase activity. Studies using subunit specific phosphatases. J Biol Chem 262: 3210–3218
21. Pickett-Gies CA, Walsh DA (1985) Subunit phosphorylation and activation of skeletal muscle phosphorylase kinase by the cAMP-dependent protein kinase. Divalent metal ion, ATP, and protein concentration dependence. J Biol Chem 260:2046–2056
22. Hallenbeck PC, Walsh DA (1983) Autophosphorylation of phosphorylase kinase. Divalent metal cation and nucleotide dependency. J Biol Chem 258:13493–13501
23. Paudel HK, Carlson GM (1990) Functional and structural similarities between the inhibitory region of troponin I coded by exon VII and the calmodulin-binding regulatory region of the catalytic subunit of phosphorylase kinase. Proc Natl Acad Sci USA 87:7285–7289
24. Mitsui K, Brady M, Palfrey HC, Nairn AC (1993) Purification and characterization of calmodulin-dependent protein kinase II from rabbit reticulocytes and rat pancreas. J Biol Chem 268:13422–13433
25. Redpath NT, Price NT, Proud CG (1996) Cloning and expression of cDNA encoding protein synthesis elongation factor-2 kinase. J Biol Chem 271:17547–17554
26. Redpath NT, Proud CG (1993) Purification and phosphorylation of elongation factor-2 kinase from rabbit reticulocytes. Eur J Biochem 12:511–520
27. Hait WN, Ward MD, Trakht IN, Ryazanov AG (1996) Elongation factor-2 kinase: immunological evidence for the existence of tissue-specific isoforms. FEBS Lett 397:55–60
28. Nairn AC, Palfrey HC (1987) Identification of the major Mr 100,000 substrate for calmodulin-dependent protein kinase III in mammalian cells as elongation factor-2. J Biol Chem 262: 17299–17303
29. Diggle TA, Seehra CK, Hase S, Redpath NT (1999) Analysis of the domain structure of elongation factor-2 kinase by mutagenesis. FEBS Lett 457:189–192
30. Ryazanov AG, Ward MD, Mendola CE, Pavur KS, Dorovkov MV, Wiedmann M, Erdjument-Bromage H, Tempst P, Parmer TG, Prostko CR, Germino FJ, Hait WN (1997) Identification of a new class of protein kinases represented by eukaryotic elongation factor-2 kinase. Proc Natl Acad Sci USA 94:4884–4889
31. Pavur KS, Petrov AN, Ryazanov AG (2000) Mapping the functional domains of elongation factor-2 kinase. Biochemistry 39:12216–12224
32. Diggle TA, Subkhankulova T, Lilley KS, Shikotra N, Willis AE, Redpath NT (2001) Phosphorylation of elongation factor-e kinase on serine 499 by cAMP-dependent protein kinase induces Ca^{2+}/calmodulin-independent activity. Biochem J 353:621–626
33. Horman S, Browne GJ, Krause U, Patel JV, Vertommen D, Bertrand L, Lavoinne A, Hue L, Proud CG, Rider MH (2002) Activation of AMP-activated protein kinase leads to the phosphorylation of elongation factor 2 and an inhibition of protein synthesis. Curr Biol 12:1419–1423
34. Browne GJ, Finn SG, Proud CG (2004) Stimulation of the AMP-activated protein kinase leads to activation of eukaryotic elongation factor 2 kinase and to its phosphorylation at a novel site, serine 398. J Biol Chem 279:12220–12231
35. Redpath NT, Proud CG (1993) Cyclic AMP-dependent protein kinase phosphorylates rabbit reticulocyte elongation factor-2 kinase and induces calcium-independent activity. Biochem J 293:31–34
36. Knebel A, Haydon CE, Morrice N, Cohen P (2002) Stress-induced regulation of eukaryotic elongation factor 2 kinase by SB 203580-sensitive and -insensitive pathways. Biochem J 367:525–532

37. Knebel A, Morrice N, Cohen P (2001) A novel method to identify protein kinase substrates: eEF2 kinase is phosphorylated and inhibited by SAPK4/p38delta. EMBO J 20:4360–4369
38. Wang X, Li W, Williams M, Terada N, Alessi DR, Proud CG (2001) Regulation of elongation factor 2 kinase by p90(RSK1) and p70 S6 kinase. EMBO J 20:4370–4379
39. Roush CL, Kennelly PJ, Glaccum MB, Helfman DM, Scott JD, Krebs EG (1988) Isolation of the cDNA encoding rat skeletal muscle myosin light chain kinase. Sequence and tissue distribution. J Biol Chem 263:10510–10516
40. Takio K, Blumenthal DK, Edelman AM, Walsh KA, Krebs EG, Titani K (1985) Amino acid sequence of an active fragment of rabbit skeletal muscle myosin light chain kinase. Biochemistry 24:6028–6037
41. Leachman SA, Gallagher PJ, Herring BP, McPhaul MJ, Stull JT (1992) Biochemical properties of chimeric skeletal and smooth muscle myosin light chain kinases. J Biol Chem 267:4930–4938
42. Potier MC, Chelot E, Pekarsky Y, Gardiner K, Rossier J, Turnell WG (1995) The human myosin light chain kinase (MLCK) from hippocampus: cloning, sequencing, expression, and localization to 3qcen-q21. Genomics 29:562–570
43. Giorgi D, Ferraz C, Mattei MG, Demaille J, Rouquier S (2001) The myosin light chain kinase gene is not duplicated in mouse: partial structure and chromosomal localization of Mylk. Genomics 75:49–56
44. Lazar V, Garcia JG (1999) A single human myosin light chain kinase gene (MLCK; MYLK). Genomics 57:256–267
45. Yin F, Hoggatt AM, Zhou J, Herring BP (2006) 130-kDa smooth muscle myosin light chain kinase is transcribed from a CArG-dependent, internal promoter within the mouse mylk gene. Am J Physiol Cell Physiol 290:C1599–C1609
46. Zhi G, Ryder JW, Huang J, Ding P, Chen Y, Zhao Y, Kamm KE, Stull JT (2005) Myosin light chain kinase and myosin phosphorylation effect frequency-dependent potentiation of skeletal muscle contraction. Proc Natl Acad Sci USA 102:17519–17524
47. Gallagher PJ, Herring BP, Griffin SA, Stull JT (1991) Molecular characterization of a mammalian smooth muscle myosin light chain kinase. J Biol Chem 266:23936–23944
48. Herring BP, Dixon S, Gallagher PJ (2000) Smooth muscle myosin light chain kinase expression in cardiac and skeletal muscle. Am J Physiol Cell Physiol 279:C1656–C1664
49. Filenko AM, Danilova VM, Sobieszek A (1997) Smooth muscle myosin light chain kinase, supramolecular organization, modulation of activity, and related conformational changes. Biophys J 73:1593–1606
50. Kemp BE, Pearson RB, Guerriero VJ, Bagchi IC, Means AR (1987) The calmodulin binding domain of chicken smooth muscle myosin light chain kinase contains a pseudosubstrate sequence. J Biol Chem 262:2542–2548
51. Gallagher PJ, Herring BP (1991) The carboxyl terminus of the smooth muscle myosin light chain kinase is expressed as an independent protein, telokin. J Biol Chem 266:23945–23952
52. Herring BP, El-Mounayri O, Gallagher PJ, Yin F, Zhou J (2006) Regulation of myosin light chain kinase and telokin expression in smooth muscle tissues. Am J Physiol Cell Physiol 291:C817–C827
53. Ito M, Guerriero VJ, Chen XM, Hartshorne DJ (1991) Definition of the inhibitory domain of smooth muscle myosin light chain kinase by site-directed mutagenesis. Biochemistry 30: 3498–3503
54. Pearson RB, Ito M, Morrice NA, Smith AJ, Condron R, Wettenhall RE, Kemp BE, Hartshorne DJ (1991) Proteolytic cleavage sites in smooth muscle myosin-light-chain kinase and their relation to structural and regulatory domains. Eur J Biochem 200:723–730
55. Pearson RB, Wettenhall RE, Means AR, Hartshorne DJ, Kemp BE (1988) Autoregulation of enzymes by pseudosubstrate prototopes: myosin light chain kinase. Science 241:970–973
56. Conti MA, Adelstein RS (1981) The relationship between calmodulin binding and phosphorylation of smooth muscle myosin kinase by the catalytic subunit of 3′:5′ cAMP-dependent protein kinase. J Biol Chem 256:3178–3181

57. Nishikawa M, Hidaka H, Adelstein RS (1983) Phosphorylation of smooth muscle heavy meromyosin by calcium-activated, phospholipid-dependent protein kinase. The effect of actin-activated MgATPase activity. J Biol Chem 258:14069–14072
58. Hashimoto Y, Soderling TR (1990) Phosphorylation of smooth muscle myosin light chain kinase by Ca^{2+}/calmodulin-dependent protein kinase II: comparative study of the phosphorylation sites. Arch Biochem Biophys 278:41–45
59. Gallagher PJ, Herring BP, Stull JT (1997) Myosin light chain kinases. J Muscle Res Cell Motil 18:1–16
60. Stull JT, Hsu LC, Tansey MG, Kamm KE (1990) Myosin light chain kinase phosphorylation in tracheal smooth muscle. J Biol Chem 265:16683–16690
61. Poperechnaya A, Varlamova O, Lin PJ, Stull JT, Bresnick AR (2000) Localization and activity of myosin light chain kinase isoforms during the cell cycle. J Cell Biol 151:697–708
62. Blue EK, Goeckeler ZM, Jin Y, Hou L, Dixon SA, Herring BP, Wysolmerski RB, Gallagher PJ (2002) 220- and 130-kDa MLCKs have distinct tissue distributions and intracellular localization patterns. Am J Physiol Cell Physiol 282:C451–C460
63. Hsu LS, Chen GD, Lee LS, Chi CW, Cheng JF, Chen JY (2001) Human Ca^{2+}/calmodulin-dependent protein kinase kinase beta gene encodes multiple isoforms that display distinct kinase activity. J Biol Chem 276:31113–31123
64. Kitsos CM, Sankar U, Illario M, Colomer-Font JM, Duncan AW, Ribar TJ, Reya T, Means AR (2005) Calmodulin-dependent protein kinase IV regulates hematopoietic stem cell maintenance. J Biol Chem 280:33101–33108
65. Ohmstede CA, Jensen KF, Sahyoun NE (1989) Ca^{2+}/calmodulin-dependent protein kinase enriched in cerebellar granule cells. Identification of a novel neuronal calmodulin-dependent protein kinase. J Biol Chem 264:5866–5875
66. Wu JY, Gonzalez-Robayana IJ, Richards JS, Means AR (2000) Female fertility is reduced in mice lacking Ca^{2+}/calmodulin-dependent protein kinase IV. Endocrinology 141:4777–4783
67. Wu JY, Means AR (2000) Ca(2+)/calmodulin-dependent protein kinase IV is expressed in spermatids and targeted to chromatin and the nuclear matrix. J Biol Chem 275:7994–7999
68. Anderson KA, Means RL, Huang QH, Kemp BE, Goldstein EG, Selbert MA, Edelman AM, Fremeau RT, Means AR (1998) Components of a calmodulin-dependent protein kinase cascade. Molecular cloning, functional characterization and cellular localization of Ca^{2+}/calmodulin-dependent protein kinase kinase beta. J Biol Chem 273:31880–31889
69. Hawley SA, Selbert MA, Goldstein EG, Edelman AM, Carling D, Hardie DG (1995) 5′-AMP activates the AMP-activated protein kinase cascade, and Ca^{2+}/calmodulin activates the calmodulin-dependent protein kinase I cascade, via three independent mechanims. J Biol Chem 270:27186–27191
70. Neal AP, Molina-Campos E, Marrero-Rosado B, Bradford AB, Fox SM, Kovalova N, Hannon HE (2010) CaMKK-CaMKI signaling pathways differentially control axon and dendrite elongation in cortical neurons. J Neurosci 30:2807–2809
71. Kahl CR, Means AR (2004) Regulation of cyclin D1/cdk4 complexes by calcium/calmodulin-dependent protein kinase I. J Biol Chem 279:15411–15419
72. Anderson KA, Means AR (2002) Defective signaling in a subpopulation of CD4(+) T cells in the absence of Ca(2+)/calmodulin-dependent protein kinase IV. Mol Cell Biol 22:23–29
73. Tokumitsu H, Soderling TR (1996) Requirements for calcium and calmodulin in the calmodulin kinase activation cascade. J Biol Chem 271:5617–5622
74. Hawley SA, Davison M, Woods A, Davies SP, Beri RK, Carling D, Hardie DG (1996) Characterization of the AMP-activated protein kinase kinase from rat liver and identification of threonine 172 as the major site at which it phosphorylates AMP-activated protein kinase. J Biol Chem 271:27879–27887
75. Wayman GA, Lee Y-S, Tokumitsu H, Silva AJ, Silva A, Soderling TR (2008) Calmodulin-kinases: modulators of neuronal development and plasticity. Neuron 59:914–931
76. Edelman AM, Mitchelhill KI, Selbert MA, Anderson KA, Hook SS, Stapleton D, Goldstein EG, Means AR, Kemp BE (1996) Multiple Ca(2+)-calmodulin-dependent protein kinase kinases from rat brain. Purification, regulation by Ca(2+)-calmodulin, and partial amino acid sequence. J Biol Chem 271:10806–10810

77. Tokumitsu H, Takahashi N, Eto K, Yano S, Soderling TR, Muramatsu M (1999) Substrate recognition by Ca^{2+}/calmodulin-dependent protein kinase kinase. Role of the arg-pro-rich insert domain. J Biol Chem 274:15803–15810
78. Okuno S, Kitani T, Fujisawa H (2001) Regulation of Ca(2+)/calmodulin-dependent protein kinase kinase alpha by cAMP-dependent protein kinase: I. Biochemical analysis. J Biochem 130:503–513
79. Green MF, Scott JW, Steel R, Oakhill JS, Kemp BE, Means AR (2011) Ca^{2+}/calmodulin-dependent protein kinase kinase beta is regulated by multisite phosphorylation. J Biol Chem 286:28066–28079
80. Davare MA, Saneyoshi T, Guire ES, Nygaard SC, Soderling TR (2004) Inhibition of calcium/calmodulin-dependent protein kinase kinase by protein 14-3-3. J Biol Chem 279: 52191–52199
81. Wayman GA, Tokumitsu H, Soderling TR (1997) Inhibitory cross-talk by cAMP kinase on the calmodulin-dependent protein kinase cascade. J Biol Chem 272:16073–16076
82. Matsushita M, Nairn AC (1999) Inhibition of the Ca^{2+}/calmodulin-dependent protein kinase I cascade by cAMP-dependent protein kinase. J Biol Chem 274:10086–10093
83. Guest CB, Deszo EL, Hartman ME, York JM, Kelley KW, Freund GG (2008) Ca^{2+}/calmodulin-dependent kinase kinase alpha is expressed by monocytic cells and regulates the activation profile. PLoS One 3:e1606
84. Picciotto MR, Zoli M, Bertuzzi G, Nairn AC (1995) Immunochemical localization of calcium/calmodulin-dependent protein kinase I. Synapse 20:75–84
85. Nairn AC, Greengard P (1987) Purification and characterization of Ca^{2+}/calmodulin-dependent protein kinase I from bovine brain. J Biol Chem 262:7273–7281
86. Wayman GA, Kaech S, Grant WF, Davare M, Impey S, Tokumitsu H, Nozaki N, Banker G, Soderling TR (2004) Regulation of axonal extension and growth cone motility by calmodulin-dependent protein kinase I. J Neurosci 24:3786–3794
87. Condon JC, Pezzi V, Drummond BM, Yin S, Rainey WE (2002) Calmodulin-dependent kinase I regulates adrenal cell expression of aldosterone synthase. Endocrinology 143: 3651–3657
88. Joseph JD, Means AR (2000) Identification and characterization of two Ca^{2+}/CaM-dependent protein kinases required for normal nuclear division in Aspergillus nidulans. J Biol Chem 275:38230–38238
89. Rasmussen CD (2000) Cloning of a calmodulin kinase I homologue from *Schizosaccharomyces pombe*. J Biol Chem 275:685–690
90. Skelding KA, Rostas JA, Verrills NM (2011) Controlling the cell cycle: the role of calcium/calmodulin-stimulated protein kinases I and II. Cell Cycle 10:631–639
91. Goldberg J, Nairn AC, Kuriyan J (1996) Structural basis for the autoinhibition of calcium/calmodulin-dependent protein kinase I. Cell 84:875–887
92. Haribabu B, Hook SS, Selbert MA, Goldstein EG, Tomhave ED, Edelman AM, Snyderman R, Means AR (1995) Human calcium-calmodulin dependent protein kinase I: cDNA cloning, domain structure and activation by phosphorylation at threonine-177 by calcium-calmodulin dependent protein kinase I kinase. EMBO J 14:3679–3686
93. Hook SS, Kemp BE, Means AR (1999) Peptide specificity determinants at P-7 and P-6 enhance the catalytic efficiency of Ca^{2+}/calmodulin-dependent protein kinase I in the absence of activation loop phosphorylation. J Biol Chem 274:20215–20222
94. Stedman DR, Uboha NV, Stedman TT, Nairn AC, Picciotto MR (2004) Cytoplasmic localization of calcium/calmodulin-dependent protein kinase I-alpha depends on a nuclear export signal in its regulatory domain. FEBS Lett 566:275–280
95. Sakagami H, Kamata A, Nishimura H, Kasahara J, Owada Y, Takeuchi Y, Watanabe M, Fukunaga K, Kondo H (2005) Prominent expression and activity-dependent nuclear translocation of Ca^{2+}/calmodulin-dependent protein kinase I delta in hippocampal neurons. Eur J Neurosci 22:2697–2707
96. Miller SG, Kennedy MB (1985) Distinct forebrain and cerebellar isozymes of type II Ca^{2+}/calmodulin-dependent protein kinase associate differentially with the postsynaptic density fraction. J Biol Chem 260:9039–9046

97. Giese KP, Fedorov NB, Filipkowski RK, Silva AJ (1998) Autophosphorylation of Thr286 of the alpha calcium-calmodulin kinase II in LTP and learning. Science 279:870–873
98. Miller S, Yasuda M, Coats SK, Jones Y, Martine ME, Mayford M (2002) Disruption of dendritic translation of CaMKIIalpha impairs stabilization of synaptic plasticity and memory consolidation. Neuron 36:507–519
99. Soderling TR, Derkach VA (2000) Postsynaptic protein phosphorylation and LTP. Trends Neurosci 23:75–80
100. Taha S, Hanover SL, Silva AJ, Stryker MP (2002) Autophosphorylation of alphaCaMKII is required for ocular dominance plasticity. Neuron 36:483–491
101. Cao X, Wang H, Mei B, An S, Yin L, Wang LP, Tsien JZ (2008) Inducible and selective erasure of memories in the mouse brain via chemical-genetic manipulation. Neuron 60: 353–366
102. von Hertzen LSJ, Giese KP (2005) Alpha-isoform of Ca^{2+}/calmodulin-dependent kinase II autophosphorylation is required for memory consolidation-specific transcription. Neuroreport 16:1411–1414
103. Jones KT (2007) Intracellular calcium in the fertilization and development of mammalian eggs. Clin Exp Pharmacol Physiol 34:1084–1089
104. Shin MK, Kim MK, Bae YS, Jo I, Lee SJ, Chung CP, Park YJ, Min do S (2008) A novel collagen-binding peptide promotes osteogenic differentiation via Ca^{2+}/calmodulin-dependent protein kinase II/ERK/AP-1 signaling pathway in human bone marrow-derived mesenchymal stem cells. Cell Signal 20:613–624
105. Munevar S, Gangopadhyay SS, Gallant C, Colombo B, Sellke FW, Morgan KG (2008) CaMKIIT287 and T305 regulate history-dependent increases in alpha agonist-induced vascular tone. J Cell Mol Med 12:219–226
106. Maier LS, Bers DM (2007) Role of Ca^{2+}/calmodulin-dependent protein kinase (CaMK) in excitation-contraction coupling in the heart. Cardiovasc Res 73:631–640
107. Skelding KA, Suzuki T, Gordon SL, Xue J, Verrills NM, Dickson PW, Rostas JAP (2010) Regulation of CaMKII by phospho-Thr253 or phospho-Thr286 sensitive targeting alters cellular function. Cell Signal 22:759–769
108. Colbran RJ, Smith MK, Schworer CM, Fong Y-L, Soderling TR (1989) Regulatory domain of calcium/calmodulin-dependent protein kinase II. Mechanism of inhibition and regulation by phosphorylation. J Biol Chem 264:4800–4804
109. Smith MK, Colbran RJ, Brickey DA, Soderling TR (1992) Functional determinants in the autoinhibitory domain of calcium-calmodulin dependent protein kinase II. J Biol Chem 267:1761–1768
110. Payne ME, Fong Y-L, Ono T, Colbran RJ, Kemp BE, Soderling TR, Means AR (1988) Calcium/calmodulin-dependent protein kinase II. Characterization of distinct calmodulin binding and inhibitory domains. J Biol Chem 263:7190–7195
111. Braun AP, Schulman H (1995) The multifunctional calcium/calmodulin-dependent protein kinase: from form to function. Annu Rev Physiol 57:417–445
112. Rosenberg OS, Deindl S, Sung RJ, Nairn AC, Kuriyan J (2005) Structure of the autoinhibited kinase domain of CaMKII and SAXS analysis of the holoenzyme. Cell 123:849–860
113. Kolb SJ, Hudmon A, Ginsberg TR, Waxham MN (1998) Identification of domains essential for the assembly of calcium/calmodulin-dependent protein kinase II holoenzymes. J Biol Chem 273:31555–31564
114. Hanson PI, Meyer T, Stryer L, Schulman H (1994) Dual role of calmodulin in autophosphorylation of multifunctional CaM kinase may underlie decoding of calcium signals. Neuron 12:943–956
115. Meyer T, Hanson PI, Stryer L, Schulman H (1992) Calmodulin trapping by calcium-calmodulin-dependent protein kinase. Science 256:1199–1202
116. Strack S, Colbran RJ (1998) Autophosphorylation-dependent targeting of calcium/calmodulin-dependent protein kinase II by the NR2B subunit of the N-methyl-D-aspartate receptor. J Biol Chem 273:20689–20692

117. Strack S, Choi S, Lovinger DM, Colbran RJ (1997) Translocation of autophosphorylated calcium/calmodulin-dependent protein kinase II to the postsynaptic density. J Biol Chem 272:13467–13470
118. Hanson PI, Schulman H (1992) Inhibitor autophosphorylation of multifunctional Ca^{2+}/calmodulin-dependent protein kinase analyzed by site-directed mutagenesis. J Biol Chem 267:17216–17224
119. Patton BL, Miller SG, Kennedy MB (1990) Activation of type II calcium/calmodulin-dependent protein kinase by Ca^{2+}/calmodulin is inhibited by autophosphorylation of threonine within the calmodulin-binding domain. J Biol Chem 265:11204–11212
120. Meador WE, Means AR, Quicho FA (1993) Modulation of calmodulin plasticity in molecular recognition of CaMKII by scaffold-dependent autophosphorylation. Science 262: 1718–1721
121. Migues PV, Lehmann IT, Fluechter L, Cammarota M, Gurd JW, Sim ATR, Dickson PW, Rostas JAP (2006) Phosphorylation of CaMKII at Thr253 occurs in vivo and enhances binding to isolated postsynaptic densities. J Neurochem 98:289–299
122. Hanson PI, Kapiloff MS, Lou LL, Rosenfeld MG, Schulman H (1989) Expression of a multifunctional Ca^{2+}/calmodulin-dependent protein kinase and mutational analysis of its autoregulation. Neuron 3:59–70
123. Lengyel I, Fieuw-Makaroff S, Hall AL, Sim AT, Rostas JA, Dunkley PR (2000) Modulation of the phosphorylation and activity of calcium/calmodulin-dependent by protein kinase II by zinc. J Neurochem 75:594–605
124. Colbran RJ, Soderling TR (1990) Calcium/calmodulin-independent autophosphorylation sites of calcium/calmodulin-dependent protein kinase II. Studies on the effect of phosphorylation of threonine 305/306 and serine 314 on calmodulin binding using synthetic peptides. J Biol Chem 265:11213–11219
125. Jaffe H, Vinade L, Dosemeci A (2004) Identification of novel phosphorylation sites on postsynaptic density proteins. Biochem Biophys Res Commun 321:210–218
126. Molloy SS, Kennedy MB (1991) Autophosphorylation of type II Ca^{2+}/calmodulin-dependent protein kinase in cultures of postnatal rat hippocampal slices. Proc Natl Acad Sci USA 88:4756–4760
127. Collins MO, Yu L, Coba MP, Hsui H, Campuzano I, Blackstock WP, Choudhary JS, Grant SG (2005) Proteomic analysis of in vivo phosphorylated synaptic proteins. J Biol Chem 280:5972–5982
128. Hudmon A, Schulman H (2002) Structure-function of the multifunctional Ca^{2+}/calmodulin-dependent protein kinase II. Biochem J 364:593–611
129. Sugai R, Takeuchi M, Okuno S, Fujisawa H (1996) Molecular cloning of a novel protein containing the association domain of calmodulin-dependent protein kinase II. J Biochem 120:773–779
130. Bayer KU, Harbers K, Schulman H (1998) alphaKAP is an anchoring protein for a novel CaM kinase II isoform in skeletal muscle. EMBO J 17:5598–5605
131. O'Leary H, Lasada E, Bayer KU (2006) CaMKIIbeta association with the actin cytoskeleton is regulated by alternative splicing. Mol Biol Cell 17:4656–4665
132. Yamagata Y, Czernik AJ, Greengard P (1991) Active catalytic fragment of Ca^{2+}/Calmodulin-dependent protein kinase II. J Biol Chem 266:15391–15397
133. Schulman H (2004) Activity-dependent regulation of calcium/calmodulin-dependent protein kinase II localization. J Neurosci 24:8399–8403
134. Colbran RJ (2004) Targeting of calcium/calmodulin-dependent protein kinase II. Biochem J 378:1–16
135. Kolb SJ, Hudmon A, Waxham MN (1995) Ca^{2+}/calmodulin kinase II translocates in a hippocampal slice model of ischemia. J Neurochem 64:2147–2156
136. Suzuki T, Okumura-Noji K, Tanaka R, Tada T (1994) Rapid translocation of cytosolic Ca^{2+}/calmodulin-dependent protein kinase II into postsynaptic density after decapitation. J Neurochem 63:1529–1537

137. Elgersma Y, Fedorov NB, Ikonen S, Choi ES, Elgersma M, Carvalho OM, Giese KP, Silva AJ (2002) Inhibitory autophosphorylation of CaMKII controls PSD association, plasticity, and learning. Neuron 36:493–505
138. Kimura Y, Corcoran EE, Eto K, Gengyo-Ando K, Muramatsu M-A, Kobayashi R, Freedman JH, Mitani S, Hagiwara M, Means AR, Tokumitsu H (2002) A CaMK cascade activates CRE-mediated transcription in neurons of *Caenorhabditis elegans*. EMBO Rep 3:962–966
139. Takemura M, Mishima T, Wang Y, Kasahara J, Fukunaga K, Ohashi K, Mizuno K (2009) Ca^{2+}/calmodulin-dependent protein kinase IV-mediated LIM kinase activation is critical for calcium signal-induced neurite outgrowth. J Biol Chem 284:28554–28562
140. Racioppi L, Means AR (2008) Calcium/calmodulin-dependent kinase IV in immune and inflammatory responses: novel routes for an ancient traveller. Trends Immunol 29:600–607
141. Tokumitsu H, Brickey DA, Glod J, Hidaka H, Sikela J, Soderling TR (1994) Activation mechanisms for Ca^{2+}/calmodulin-dependent protein kinase IV. Identification of a brain CaM-kinase IV kinase. J Biol Chem 269:28640–28647
142. Cruzalegui FH, Means AR (1993) Biochemical characterization of the multifunctional Ca^{2+}/calmodulin-dependent protein kinase type IV expressed in insect cells. J Biol Chem 268: 26171–26178
143. Watanabe K, Yamaguchi Y (1996) Molecular identification of a putative human hyaluronan synthase. J Biol Chem 271:22945–22948
144. Murao K, Li J, Imachi H, Muraoka T, Masugata H, Zhang GX, Kobayashi R, Ishida T, Tokumitsu H (2009) Exendin-4 regulates glucokinase expression by CaMKK/CaMKIV pathway in pancreatic beta-cell line. Diabetes Obes Metab 11:939–946
145. Lemrow SM, Anderson KA, Joseph JD, Ribar TJ, Noeldner PK, Means AR (2004) Catalytic activity is required for calcium/calmodulin-dependent protein kinase IV to enter the nucleus. J Biol Chem 279:11664–11671
146. Tuazon PT, Traugh JA (1991) Casein kinase I and II – multipotential serine protein kinases: structure, funciton, and regulation. Adv Second Messenger Phosphoprotein Res 23:123–164
147. Nakajo S, Hagiwara T, Nakaya K, Nakamura Y (1987) Tissue distribution of casein kinases. Biochem Int 14:701–707
148. Manning G, Whyte DB, Martinez R, Hunter T, Sudarsanam S (2002) The protein kinase complement of the human genome. Science 298:1912–1934
149. Rowles J, Slaughter C, Moomaw C, Hsu J, Cobb MH (1991) Purification of casein kinase I and isolation of cDNAs encoding multiple casein kinase I-like enzymes. Proc Natl Acad Sci USA 88:9548–9552
150. Tapia C, Featherstone T, Gomez C, Taillon-Miller P, Allende CC, Allende JE (1994) Cloning and chromosomal localization of the gene coding for human protein kinase CK1. FEBS Lett 349:307–312
151. Fish KJ, Cegielska A, Getman ME, Landes GM, Virshup DM (1995) Isolation and characterization of human casein kinase I epsilon (CK1), a novel member of the CK1 gene family. J Biol Chem 270:14875–14883
152. Burzio V, Antonelli M, Allende CC, Allende JE (2002) Biochemical and cellular characteristics of the four splice variants of protein kinase CK1alpha from zebrafish (*Danio rerio*). J Cell Biochem 86:805–814
153. Vielhaber E, Virshup DM (2001) Casein kinase I: from obscurity to center stage. IUBMB Life 51:73–78
154. Pulgar V, Marin O, Meggio F, Allende CC, Allende JE, Pinna LA (1999) Optimal sequences for non-phosphate-directed phosphorylation by protein kinase CK1 (casein kinase-1) – a re-evaluation. Eur J Biochem 260:520–526
155. Marin O, Bustos VH, Cesaro L, Meggio F, Pagano MA, Antonelli M, Allende CC, Pinna LA, Allende JE (2003) A noncanonical sequences phosphorylated by casein kinase 1 in beta-catenin may play a role in casein kinase 1 targeting of important signaling proteins. Proc Natl Acad Sci USA 100:10193–10200
156. Flowtow H, Graves PR, Wang AQ, Fiol CJ, Roeske RW, Roach PJ (1990) Phosphate groups as substrate determinants for casein kinase I action. J Biol Chem 265:14264–14269

157. Flowtow H, Roach PJ (1991) Role of acidic residues as substrate determinants for casein kinase I. J Biol Chem 266:3724–3727
158. Meggio F, Perich JW, Reynolds EC, Pinna LA (1991) A synthetic beta-casein phosphopeptide and analogues as model substrates for casein kinase-1, a ubiquitous, phosphate directed protein kinase. FEBS Lett 283:303–306
159. Bustos VH, Marin O, Meggio F, Cesaro L, Allende CC, Allende JE, Pinna LA (2005) Generation of protein kinase CK1alpha mutants which discriminate between canonical and non-canonical substrates. Biochem J 391:417–424
160. Pulgar V, Tapia C, Vignolo P, Santos J, Sunkel CE, Allende CC, Allende JE (1996) The recombinant alpha isoform of protein kinase CK1 from *Xenopus laevis* can phosphorylate tyrosine in synthetic substrates. Eur J Biochem 242:519–528
161. Braun S, Raymond WE, Racker E (1984) Synthetic tyrosine polymers as substrates and inhibitors of tyrosine-specific protein kinases. J Biol Chem 259:2051–2054
162. Graves PR, Roach PJ (1995) Role of COOH-terminal phosphorylation in the regulation of casein kinase I delta. J Biol Chem 270:21689–21694
163. Cegielska A, Gietzen KF, Rivers A, Virshup DM (1998) Autoinhibition of casein kinase I epsilon (CK1 epsilon) is relieved by protein phosphatases and limited proteolysis. J Biol Chem 273:1357–1364
164. Gietzen KF, Virshup DM (1999) Identification of inhibitory autophosphorylation sites in casein kinase I epsilon. J Biol Chem 274:32063–32070
165. Zhai L, Graves PR, Robinson LC, Italiano M, Culbertson MR, Rowles J, Cobb MH, DePaoli-Roach AA, Roach PJ (1995) Casein kinase I gamma subfamily. Molecular cloning, expression, and characterization of three mammalian isoforms and complementation of defects in the Saccharomyces cerevisiae YCK genes. J Biol Chem 270:12717–12724
166. Longenecker KL, Roach PJ, Hurley TD (1998) Crystallographic studies of casein kinase I delta toward a structural understanding of auto-inhibition. Acta Crystallogr D Biol Crystallogr 54:473–475
167. Kuret J, Schulman H (1984) Purification and characterization of a Ca^{2+}/calmodulin-dependent protein kinase from rat brain. Biochemistry 23:5495–5504
168. Brooks CL, Landt M (1984) Calcium-ion and calmodulin-dependent kappa-casein kinase in rat mammary acini. Biochem J 224:195–200
169. Giamas G, Hirner H, Shoshiashvili L, Grothey A, Gessert S, Kuhl M, Henne-Bruns D, Vorgias CE, Knippschild U (2007) Phosphorylation of CK1delta: identification of Ser370 as the major phosphorylation site targeted by PKA in vitro and in vivo. Biochem J 406: 389–398
170. Rivers A, Gietzen KF, Vielhaber E, Virshup DM (1998) Regulation of casein kinase I epsilon and casein kinase I delta by an in vivo futile phosphorylation cycle. J Biol Chem 273:15980–15984
171. Swiatek W, Tsai IC, Klimowski L, Pepler A, Barnette J, Yost HJ, Virshup DM (2004) Regulation of casein kinase I epsilon activity by Wnt signaling. J Biol Chem 279: 13011–13017
172. DeMaggio AJ, Lindberg RA, Hunter T, Hoekstra MF (1992) The budding yeast HRR25 gene product is a casein kinase I isoform. Proc Natl Acad Sci USA 89:7008–7012
173. Graves PR, Haas DW, Hagedorn CH, DePaoli-Roach AA, Roach PJ (1993) Molecular cloning, expression, and characterization of a 49-kilodalton casein kinase I isoform from rat testis. J Biol Chem 268:6394–6401
174. Carmel G, Leichus B, Cheng X, Patterson SD, Mirza U, Chait BT, Kuret J (1994) Expression, purification, crystallization, and preliminary x-ray analysis of casein kinase-1 from *Schizosaccharomyces pombe*. J Biol Chem 269:7304–7309
175. Wang PC, Vancura A, Mitcheson TG, Kuret J (1992) Two genes in *Saccharomyces cerevisiae* encode a membrane-bound form of casein kinase-1. Mol Cell Biol 3:275–286
176. Vancura A, Sessler A, Leichus B, Kuret J (1994) A prenylation motif is required for plasma membrane localization and biochemical function of casein kinase I in budding yeast. J Biol Chem 269:19271–19278

177. Ho Y, Mason S, Kobayashi R, Hoekstra M, Andrews B (1997) Role of the casein kinase I isoform, Hrr25, and the cell cycle-regulatory transcription factor, SBF, in the transcriptional response to DNA damage in *Saccharomyces cerevisiae*. Proc Natl Acad Sci USA 94:581–586
178. Milne DM, Looby P, Meek DW (2001) Catalytic activity of protein kinase CK1 delta (casein kinase 1delta) is essential for its normal subcellular localization. Exp Cell Res 263:43–54
179. Yin H, Laguna KA, Li G, Kuret J (2006) Dysbinding structural homologue CK1BP is an isoform-selective binding partner of human casein kinase 1. Biochemistry 45:5297–5308
180. Gross SD, Hoffman DP, Fisette PL, Baas P, Anderson RA (1995) A phosphatidylinositol 4,5-bisphosphate-sensitive casein kinase I alpha associates with synaptic vesicles and phosphorylates a subset of vesicle proteins. J Cell Biol 130:711–724
181. Gross SD, Simerly C, Schatten G, Anderson RA (1997) A casein kinase I isoform is required for proper cell cycle progression in the fertilized mouse oocyte. J Cell Sci 110:3083–3090
182. Brockman JL, Gross SD, Sussman MR, Anderson RA (1992) Cell cycle dependent localization of casein kinase I to mitotic spindles. Proc Natl Acad Sci USA 89:9454–9458
183. Wang X, Hoekstra MF, DeMaggio AJ, Dhillon N, Vancura A, Kuret J, Johnston GC, Singer RA (1996) Prenylated isoforms of yeast casein kinase I, including the novel Yck3p, suppress the gcs1 blockage of cell proliferation from stationary phase. Mol Cell Biol 16:5375–5385
184. Zhang J, Gross SD, Schroeder MD, Anderson RA (1996) Casein kinase I alpha and alpha L: alternative splicing-generated kinases exhibit different catalytic properties. Biochemistry 35:16319–16327
185. Takano A, Hoe HS, Isojima Y, Nagai K (2004) Analysis of the expression, localization and activity of rat casein kinase 1epsilon-3. Neuroreport 15:1461–1464
186. Kannanayakal TJ, Tao H, Vandre DD, Kuret J (2006) Casein kinase-1 isoforms differentially associate with neurofibrillary and granulovacuolar degeneration lesions. Acta Neuropathol 111:413–421
187. Eide EJ, Vielhaber EL, Hinz WA, Virshup DM (2002) The circadian regulatory protein BMAL1 and cryptochromes are substrates of casein kinase Iepsilon. J Biol Chem 277: 17248–17254
188. Clokie S, Falconer H, Mackie S, Dubois T, Aitken A (2009) The interaction between casein kinase 1alpha and 14-3-3 is phosphorylation dependent. FEBS J 276:6971–6984

Chapter 32
Calcium Sensing in Exocytosis

Natalia Gustavsson, Bingbing Wu, and Weiping Han

Abstract Neurotransmitters, neuropeptides and hormones are released through regulated exocytosis of synaptic vesicles and large dense core vesicles. This complex and highly regulated process is orchestrated by SNAREs and their associated proteins. The triggering signal for regulated exocytosis is usually an increase in intracellular calcium levels. Besides the triggering role, calcium signaling modulates the precise amount and kinetics of vesicle release. Thus, it is a central question to understand the molecular machineries responsible for calcium sensing in exocytosis. Here we provide an overview of our current understanding of calcium sensing in neurotransmitter release and hormone secretion.

Keywords Calcium sensor • Hormone secretion • Large dense core vesicle • Neuropeptide • Neurotransmitter • Regulated exocytosis • Secretory granule • Synaptic vesicle • Synaptotagmin

N. Gustavsson (✉)
Laboratory of Metabolic Medicine, Singapore Bioimaging Consortium,
Agency for Science, Technology and Research, #02-02 Helios, 11 Biopolis Way,
138667 Singapore, Singapore

Hubrecht Institute, Developmental Biology and Stem Cell Research,
A0.47, Uppsalalaan 8, 3584 CT, Utrecht, The Netherlands
e-mail: natalia.neth@gmail.com

B. Wu • W. Han
Laboratory of Metabolic Medicine, Singapore Bioimaging Consortium,
Agency for Science, Technology and Research, #02-02 Helios, 11 Biopolis Way,
138667 Singapore, Singapore
e-mail: weiping_han@sbic.a-star.edu.sg

M.S. Islam (ed.), *Calcium Signaling*, Advances in Experimental Medicine and Biology 740, DOI 10.1007/978-94-007-2888-2_32,

Exocytosis and Calcium Signal

Exocytosis is a process by which a cell releases the contents of secretory vesicles out of the plasma membrane. The contents in these membrane bound vesicles differ significantly from one type of vesicles to the next, and from cells to cells. In addition to various concentrations of salts, secretory vesicles store high concentrations of enzymes (e.g. zymogen granules in exocrine pancreas), neurotransmitters (e.g. synaptic vesicles in neurons), and/or polypeptide hormones (e.g. glucagon- and insulin-granules in pancreatic α- and β-cells). For the contents to be released into extracellular space, the vesicle membrane must fuse with the plasma membrane. As such, the word "exocytosis" sometimes is used in a narrower sense to refer to the final fusion step.

Exocytosis, a conserved function of all eukaryotic cells, includes constitutive and regulated forms. The two forms of exocytosis have distinct physiological roles and characteristics (Table 32.1). In neurons and neuroendocrine/endocrine cells, tight regulation of stimulated release is necessary to achieve coordinated action and to avoid unwanted and possibly deadly consequences. The trigger for regulated exocytosis is usually an increase in cytoplasmic calcium concentrations, a phenomenon that was first discovered by Bernard Katz and colleagues in 1952. In these landmark studies, Katz and colleagues established the quantum nature of neurotransmitter release and the pivotal role of calcium in regulating the probability of a given quantum being released [1–3]. These fundamental findings, particularly the calcium function in exocytosis, were later extended and confirmed in neuroendocrine and endocrine systems [4–7]. As it was discovered later, the role of calcium is not limited to triggering exocytosis. Calcium signaling also controls the precise amount and speed of vesicle release, *i.e.* cells sense increases in calcium concentration and respond by exocytosis of a certain number of vesicles at a certain rate. It remains one of the most fundamental biology questions to understand the molecular machineries responsible for sensing calcium changes and executing exocytosis.

In neurons and neuroendocrine cells, calcium enters the cells through voltage-gated calcium channels on the plasma membrane upon membrane depolarization. The elevated calcium levels induce vesicle fusion, which is mediated by a complex

Table 32.1 Comparison of regulated and constitutive exocytosis

Categories	Regulated exocytosis	Constitutive exocytosis
Cargo	Neurotransmitters, neuropeptides and hormones	Plasma membrane proteins, extracellular matrix proteins
Production	Via Golgi and re-uptake	Via Golgi
Carrier	Synaptic vesicles and secretory granules	Microvesicles
Triggering signal	Yes	No
Control	Membrane trafficking and exocytotic machinery	GTP-binding proteins
Speed	Microseconds to tens of seconds after stimulation	Continuous, in the absence of a stimulus

of proteins on vesicles and the plasma membrane. These proteins, which are highly conserved throughout evolution from yeast to man, include synaptobrevin, syntaxin and SNAP-25 (synaptosomal-associated protein of 25 KDa) and are collectively named SNAREs (soluble N-ethylmaleimide sensitive factor attachment protein receptors) [8–14]. Although the precise mechanisms as to how SNAREs execute the fusion process remain under intense investigations, it is well established that SNAREs are the minimal machinery responsible for the final fusion step. However, SNAREs cannot act directly as calcium receptors in exocytosis [15]. So which proteins function as calcium sensors in exocytosis in neurons and endocrine cells?

For many years since the work that defined calcium's role in neurotransmission by Katz and colleagues, the identities of proteins that sense calcium changes in the cytoplasm and transduce that to exocytotic machineries and the mechanisms of their action have been a topic of immense interest in cell biology and neuroscience. To be a suitable candidate as a calcium sensor, a protein must be able to bind calcium at the appropriate calcium concentrations at which exocytosis is triggered, to be located near or on the secretory vesicles or the plasma membrane, and to bind the membrane to initiate or facilitate exocytosis. Two groups of proteins fit these criteria: (1) proteins that contain calcium-binding C_2 domain, such as synaptotagmins, Doc2s (double C_2-domains), and ferlins; and (2) EF-hand proteins, such as calmodulin (Table 32.2). Some of these proteins have been shown to be important in regulated and non-regulated exocytosis. Among these proteins, synaptotagmins appear to be the most probable candidates and their role in regulated exocytosis is most extensively studied for neurotransmitter and hormone release [8, 16–20].

In this chapter, we will discuss calcium sensing in neurotransmitter release and hormone secretion, with a particular focus on several C_2-domain containing proteins that have been shown to regulate neuronal and endocrine exocytosis in biochemical and genetic studies.

Neurotransmitter Release

Regulated exocytosis is crucial for survival and advanced functions in animals, and thus requires tight control and coordination of highly specialized machineries. Neurons represent the most sophisticated example of such a system. Neurotransmitter (NT) is stored in synaptic vesicles (~40 nm in diameter) that are located near their release sites of the pre-synaptic membrane, called active zones. Neurons form chemical synapses where, upon arrival of an electrical impulse, neurotransmitter is released from pre-synaptic membrane of an axon terminal into the synaptic cleft and then binds to specific receptors on post-synaptic membrane of a target neuron. Neurotransmitter release is comprised of at least two kinetically distinct components: a major synchronous component and a delayed asynchronous component [21–23]. As neurotransmitter release and synaptic transmission constitute the most fundamental function of the nervous system, considerable efforts have been devoted to studies on mechanisms governing synaptic vesicle exocytosis including calcium sensing in neurons.

Table 32.2 List of calcium binding proteins that may function as calcium sensors in exocytosis

Protein name	Gene name	Accession #	AA length	References
Proteins with multiple C2-domains that contain a transmembrane domain				
Synaptotagmin-1	Synaptotagmin I	NM_009306	421	[36, 38, 47, 48, 58, 66, 68, 154]
Synaptotagmin-2	Synaptotagmin II	NM_009307	422	[33, 36, 55, 56, 58, 155]
Synaptotagmin-3	Synaptotagmin III	NM_016663	587	[36, 45, 46, 89, 97, 101, 102]
Synaptotagmin-5	Synaptotagmin IX [1]	NM_021889	491	[36, 45, 46, 89]
Synaptotagmin-6	Synaptotagmin VI	NM_018800	511	[36, 45, 89]
Synaptotagmin-7	Synaptotagmin VII [3]	NM_018801	403	[36, 88, 89, 96, 97, 111, 119, 156, 157]
Synaptotagmin-9	Synaptotagmin V [2]	NM_016908	386	[36, 58, 89, 99, 100, 103]
Synaptotagmin-10	Synaptotagmin X	NM_018803	523	[36, 45, 153]
E-Syt1	Fam62a	NM_011843	1,092	[148]
E-Syt2	Fam62b	NM_028731	845	[148]
E-Syt3	Fam62c	NM_177775	891	[148]
Dysferlin	dysferlin	Q9ESD7	2,090	[151]
Otoferlin	otoferlin	Q9ESF1	1,997	[158, 159]
Myoferlin	myoferlin	Q69ZN7	2,048	[160, 161]
MCTP1	mctp1	NM_030174	694	[152]
MCTP2	mctp2	NM_001024703	878	[152]
Proteins with multiple C2-domains that lack a transmembrane domain				
Rabphillin-3A	Rph3A	NM_011286	681	[140, 162–166]
Doc2α	Doc2a	NM_010069	405	[69, 167–170]
Doc2β	Doc2b	NM_007873	412	[65, 73, 144–147]
SLP-1	Sytl1	NM_031393	568	[171–173]
SLP-2	Sytl2	NM_001040085	934	[171, 173–175]
SLP-3	Sytl3	NM_031395	607	[171, 176]
SLP-4	Sytl4	NM_013757	673	[177–179]
SLP-5	Sytl5	NM_177704	753	[180]
Munc 13-1	Unc13a	NM_001029873	1,712	[168, 181–183]
Copine 6	Cpne6	NM_001136057	557	[150, 184]

Proteins that contain EF-hand domains				
Calmodulin 1	Calm1	NM_009790	149	[185]
Calmodulin 2	Calm2	NM_007589	149	[185]
Calmodulin 3	Calm3	NM_007590	149	[185]
Calmodulin 4	Calm4	NM_020036	148	[185]

Calcium binding proteins that may function as calcium sensors in exocytosis, their gene names and NCBI accession numbers are listed along with their amino acid residue numbers. Note that [1] gene name for synaptotagmin-5 is *synaptotagmin IX* and [2] gene name for synaptotagmin-9 is *synaptotagmin V*. Only [3] short form of synaptotagmin-7 is listed in the table. Synaptotagmin-7 is expressed in multiple splicing variants, ranging from 122 amino acids for truncated form to 687 amino acids for the long form [186]

Synchronous Neurotransmitter Release

Synchronous neurotransmitter release coincides with the arrival of an action potential at the synapse, which results in membrane depolarization, opening of voltage-sensitive calcium channels on the membrane and consequently, calcium influx into the cell. During the exocytotic process, the vesicular SNARE, synaptobrevin-2 and target SNAREs, SNAP-25 and syntaxin-1 form a tertiary complex to merge the apposing membrane bilayers of vesicle and plasma membrane. Besides the three SNARE proteins that form the core machinery, a number of other proteins interact with the SNARE proteins, participate and regulate the fusion process. For example, Munc-18, an SM (Sec1/Munc18) protein that interacts with syntaxin, is an indispensible protein for vesicle exocytosis in neurons [24–26]. The exocytotic machinery in neurons is extremely efficient, making neurotransmitter release the fastest process in cell biology. The shortest time that has been recorded in some synapses is only 60 microseconds, during which time thousands of vesicles are released [27].

Because of the extreme fast speed of neurotransmitter release and the buffering properties of the cytoplasm, it is difficult to accurately measure the calcium response within the first few 100 microseconds using a fluorescent calcium indicator. Sakmann and colleagues developed a technique by combining calcium uncaging by photolysis and rapid fluorometry to determine calcium concentrations at the synapse [28]. They show that in neurons, the time course and magnitude of neurotransmitter release are dependent on the duration of the calcium transient, and the calcium sensor is equilibrating, supralinearly amplifying the local $[Ca^{2+}]_i$ transient [28]. Furthermore, synchronous NT release requires calcium concentrations in the range of 10–40 μM with a cooperativity of ~5 as determined by photolysis of caged calcium in giant synapse of Calyx of Held, the best and most extensively analyzed system to date [18, 28–34]. The derived calcium concentration and calcium cooperativity represent the best estimate of the properties of a calcium sensor in synchronous neurotransmitter release.

Among the calcium binding proteins, synaptotagmin-1, the most prominent member of the synaptotagmin family, is one of the few that satisfy these requirements, and the best candidate as the calcium sensor for synchronous neurotransmitter release based on biochemical and structural studies [35, 36]. Synaptotagmin-1 was first described as p65, a secretory vesicle-specific membrane protein, in an antibody-binding study [37]. The molecular structure of synaptotagmin-1 suggests its potential as a calcium-sensor in mediating membrane fusion: an N-terminal transmembrane region and two functional calcium-binding C_2 domains: C_2A and C_2B (Fig. 32.1) [35, 36]. Protein structure and nuclear magnetic resonance (NMR) studies showed that C_2 domains of synaptotagmin-1, homologous to the regulatory C_2-domain of protein kinase C, bind to calcium [38]. Subsequent atomic structure analysis of synaptotagmin-1 at 1.9 Å resolution indicated that its C_2 domains are composed of a stable eight-stranded β-sandwich with flexible loops emerging from the top and bottom [39, 40]. NMR studies of synaptotagmin-1 revealed that calcium binds exclusively to the top loops, and the binding pockets are coordinated by five conserved aspartate residues: three calcium ions bind to C_2A via D172, D178,

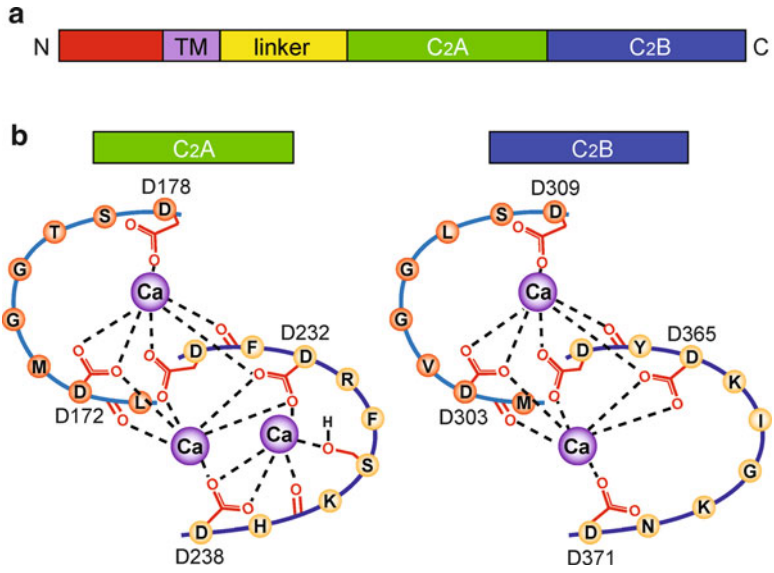

Fig. 32.1 Domain structure of synaptotagmins and top loops of synaptotagmin-1 C_2-domains. (**a**) Schematic diagram of domain structures of synaptotagmins. (**b**) Calcium-binding loops in synaptotagmin-1 C_2A and C_2B domains. Three calcium ions bind to C_2A domain via five conserved aspartate residues (D172, D178, D230, D232 and D238) and 1 serine residue (S235), while two calcium ions bind to C_2B domain via five conserved aspartate residues (D303, D309, D363, D365 and D371)

D230, D232, S235 and D238, and two calcium ions bind to C_2B via D303, D309, D363, D365 and D371 (Fig. 32.1) [41–43]. The structures flanking the calcium-coordinating amino acid residues and sequences differ in C_2 domains of individual synaptotagmins, which give rise to diverse calcium affinities in different synaptotagmins, i.e. calcium binding at either low or high calcium concentration (Fig. 32.2) [16, 36]. In fact, out of the 16 synaptotagmins, only eight have functional calcium-binding C_2 domains: synaptotagmin-1, -2, -3, -5, -6, -7, -9 and -10, while the other eight synaptotagmins do not bind to calcium [16, 36]. The diverse calcium affinity among the calcium-binding synaptotagmins enables them to cover the full range of calcium concentrations required in regulated exocytosis in a wide range of cell types [16, 36, 44–46].

Although biochemical and structural analyses support that synaptotagmin-1 functions as a calcium sensor in neurotransmission, direct evidence for an essential role of synaptotagmin-1 in neurotransmission came only later from a series of elegant studies that combined genetics and electrophysiological characterizations [16, 47–53]. In particular, deletion of synaptotagmin-1 in mice results in complete loss of the major synchronous component of neurotransmitter release in hippocampal neurons [18, 47, 48], and a mutation in the synaptotagmin-1 C_2A domain that alters the overall calcium affinity of synaptotagmin-1 produces an identical shift in synaptic vesicle exocytotic response to calcium [53]. Moreover, re-introduction of synaptotagmin-1 into synaptotagmin-1-deficent neurons

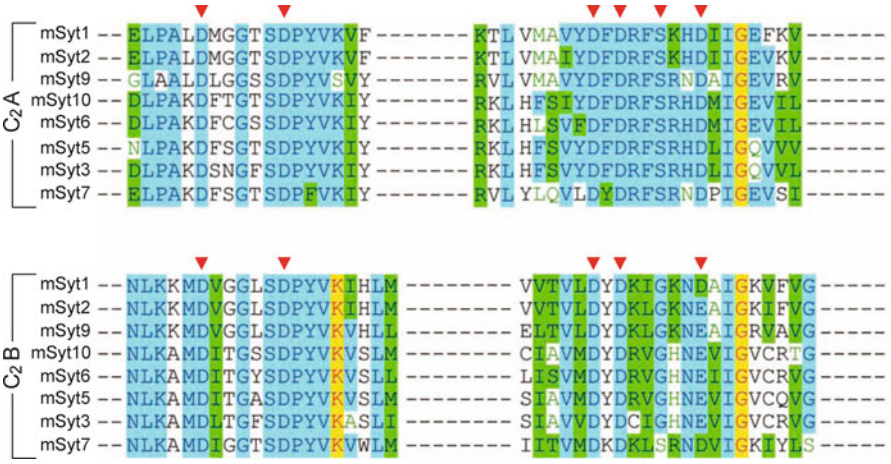

Fig. 32.2 Sequence alignments of C_2-domains of calcium-binding synaptotagmins. Sequence alignment showing amino acid residues coordinating calcium binding (*inverted red triangles*) and flanking residues in C_2A and C_2B domains

restores the exocytotic ability [54]. These studies establish synaptotagmin-1 as the calcium sensor for synchronous neurotransmitter release.

Synaptotagmin-1 expression is mostly limited to neurons in rostral brain regions, and functions specifically in synchronous neurotransmitter release. These findings prompted intense research efforts to identify calcium sensors for synchronous neurotransmitter release in other brain regions, and for other forms of neurotransmitter release. Through mouse genetic and electrophysiological studies, synaptotagmin-2 was found to be the principal calcium sensor for synchronous release in neurons of caudal brain regions, and synaptotagmin-9 appeared to act in a similar fashion in neurons in the limbic system [16, 55, 56]. In the central nervous system, synaptotagmin-1, -2 and -9 function as low affinity calcium sensors for synchronous neurotransmitter release in respective brain regions with distinct properties: synaptotagmin-2 triggers release much faster than synaptotagmin-1, and operates in synapses relying on fast signaling, such as the calyx of Held synapse or the neuromuscular junction [57]. In contrast, synaptotagmin-9 triggers release with a significantly slower time course than either synaptotagmin-1 or -2, and was found to be primarily expressed in dopaminergic neurons of the reward pathway, part of the mesolimbic pathway [58].

Asynchronous Neurotransmitter Release

In addition to tightly regulated synchronous exocytosis, neurons also release neurotransmitters in a slower asynchronous way. Asynchronous release remains to be calcium-dependent, and refers to synaptic vesicle exocytosis that is not in sync

with action potentials [33, 57]. Cultured hippocampal neurons show a greater degree of asynchronous release than excitatory synapses in neurons recorded *in situ*. As a result, cultured hippocampal neurons are used as a model to study the mechanisms of asynchronous release [21, 59]. Asynchronous release is thought to be sustained by residual Ca^{2+} in the presynaptic terminal after the synchronous phase. It is elevated during repetitive stimulations and therefore likely to significantly contribute to synaptic transmission *in vivo* where neuronal activity mostly occurs in trains [59]. The precise physiological role of this type of exocytosis is not known.

The calcium requirement for the asynchronous neurotransmitter release is estimated to be in the range of several μM to several tens of μM and a cooperativity of 2–3 [16, 18, 33]. The wide range of calcium affinity and low cooperativity, coupled with the fact that asynchronous neurotransmitter release is not abolished in neurons lacking synaptotagmin-1, -2 or -9, suggests that asynchronous release is mediated by calcium sensors other than synaptotagmin-1, -2 and -9 [47, 55, 56, 58]. Based on the working calcium concentrations and predicted calcium-binding properties, synaptotagmin-3, -5, -6 and -10 have the appropriate affinity for calcium during asynchronous release; however, these synaptotagmins, similar to synaptotagmin-1, have calcium cooperativity of 5, much higher than the required cooperativity of 2–3 [16, 36, 46]. Several proteins have been proposed as calcium sensors in asynchronous release, but so far very little, if any, definitive evidence is available for any of these proteins [60, 61].

At least in the Calyx of Held synapse, both synchronous and asynchronous release operate on the same vesicle pool [33]. So then what determines whether a particular vesicle undergoes synchronous or asynchronous release? One hypothesis is the so-called “dual sensor model”. According to this model, calcium sensors for synchronous and asynchronous release operate in competition with each other. The slower asynchronous sensor binds to calcium at lower concentrations and cooperativity, whereas the faster synchronous sensor binds at higher concentrations and cooperativity [33, 62, 63], and may inhibit the asynchronous calcium sensor [57].

Spontaneous Neurotransmitter Release

Spontaneous neurotransmitter release is a calcium-dependent process, although it occurs at low calcium concentrations and in the absence of neuronal stimulation [2, 64]. Postsynaptic currents resulting from fusion of single synaptic vesicles during spontaneous neurotransmitter release are referred to as miniature excitatory or inhibitory postsynaptic currents or “minis”. Spontaneous release has been described in cultured neurons and its role *in vivo* is yet to be determined. *In vitro* data suggest that dendritic spine maintenance may be supported by spontaneous glutamate release [64]. Because of the small amplitude, spontaneous release does not affect large, principal neurons, but it appears to modulate the processing of

synaptic inputs in small interneurons and their ability to fire action potentials [64]. Although the calcium-dependence of spontaneous release has been established, exact calcium concentrations during spontaneous neurotransmitter release have not been determined.

Two proteins, synaptotagmin-1 and Doc2b, have been suggested to function as calcium sensors for spontaneous release [65, 66]. In addition to the complete loss of synchronous neurotransmitter release [47, 51, 52], deletion of synaptotagmin-1 is associated with increases in spontaneous release in the same neurons [47–50]. Furthermore, calcium binding to synaptotagmin-1 is required for >95% of spontaneous neurotransmitter release in murine cortical neurons, and synaptotagmin-1 mutants with differing calcium affinities cause altered spontaneous and evoked release correspondingly [66]. These results support that synaptotagmin-1 mediates the spontaneous release, possibly as a calcium sensor, and at the same time, as an inhibitor of a second, unknown calcium sensor [51, 66–68]. That second calcium sensor was recently suggested to be Doc2b [65, 69]. Doc2a and Doc2b are soluble proteins that contain C_2 domains with high similarity to that of synaptotagmins [70]. Doc2s are expressed in nerve terminals and interact with exocytotic proteins [39, 71, 72]. Unlike synaptotagmins, Doc2b is not associated with synaptic vesicles and has a calcium affinity of less than 1 μM. It is possible that Doc2b competes with synaptotagmin-1 for SNARE complex binding and trigger spontaneous neurotransmitter release upon small Ca^{2+} increases. However, the view that Doc2b functions as a calcium sensor for spontaneous release is challenged by a recent study. In this study, although spontaneous release is reduced by Doc2 knockdown, the reduction is fully reversed by mutant Doc2b lacking calcium-binding sites, thus suggesting Doc2s regulate spontaneous neurotransmission by a calcium-independent mechanism [73]. Future studies are needed to define the identities of calcium sensors for spontaneous release.

Calcium Sensing in Neuropeptide and Hormone Secretion

Neuropeptide and hormone secretion from neuroendocrine and endocrine cells is fundamentally similar to neurotransmitter release in neurons (Table 32.3) [16]. For example, like neurons, neuroendocrine and endocrine cells are electrically excitable, and express voltage-gated calcium channels, which allow calcium influx upon membrane depolarization. Another key common feature is that secretory vesicle fusion in these cells is also triggered by calcium, and mediated by SNARE proteins [16]. However, there are several important differences between neuroendocrine/endocrine cells and neurons: (1) Neuropeptides and hormones are stored in large dense core vesicles, which are also referred to as secretory granules; (2) Only a small fraction of secretory granules is close to the plasma membrane and ready to be released during stimulation, whereas synaptic vesicles are located close to the active zone; (3) The release kinetics is much slower in neuroendocrine and endocrine cells. It may take several seconds after stimulation for released

Table 32.3 Comparison of neuronal and endocrine secretion

Categories	Neurotransmitter release	Peptide/hormone release
Cargo	Neurotransmitters	Peptides/hormones
Storage and trafficking	Synaptic vesicles	LDCVs or secretory granules
Vesicle size	Small (40–50 nm)	Large (200–350 nm)
Recycling pathway	Locally or through endosomal pathway	Via Golgi complex
Speed	Fast (~60 μs to 6 ms)	Slow (up to tens of s)
Release site	Synaptic active zone	Plasma membrane
Action site	Postsynaptic receptors	May be far from release site
Duration of action	Short	Long
Calcium requirement	Tens of μM	Lower (several to tens of μM)

contents to be detected, and the release process may last for tens of seconds in neuroendocrine/endocrine cells. In contrast, neurotransmitter release occurs within as short as tens of microseconds after stimulation, and lasts only a second or two; (4) Intracellular calcium concentrations at the peak of stimulation are generally lower in neuroendocrine/endocrine cells than in neurons, usually at low micromolar levels [74–76]. Compared to Ca^{2+} levels during neurotransmitter release, calcium levels that trigger insulin release in pancreatic β-cells and their derived cell lines are much lower [77, 78]. The differences between exocytosis requirements in neurons and endocrine cells suggest differences in exocytotic machinery and calcium sensing. The existence of plasmalemmal microdomains with very high calcium concentration in endocrine cells suggests that a fast calcium sensor(s) (synaptotagmin-1, -2 or -9) may participate in hormone release [79]. However, a "slow" sensor, acting at lower calcium concentrations likely mediates the majority of release.

Among synaptotagmins, synaptotagmin-3, -5, -6, -7, and -10 have higher calcium affinities and may function as slow sensors [16, 36, 46]. Of these isoforms, synaptotagmin-7 has the highest calcium-affinity in phospholipid binding in the low micromolar range [46], and has been shown to be a principal regulator of peptide hormone release in several endocrine systems, making it the most significant calcium sensor in endocrine secretion. Interestingly, synaptotagmin-7 is ubiquitously expressed during early stages of development, but becomes restricted to secretory cells after birth [54].

Catecholamine Secretion

Adrenal chromaffin cells resemble neurons in secreted compound and rate of release. This, along with the general availability of catecholamine-secreting cell lines and primary adrenal chromaffin cells makes catecholamine release an attractive cellular model to study neuronal release. Therefore, more studies have been done on calcium sensing in adrenal chromaffin cells than in any other endocrine cells [80–83].

Similar to neurotransmitter release, catecholamine release from adrenal chromaffin cells is composed of rapid and delayed phases [84–86]. Calcium concentration can reach 10 μM, which is comparable to neurons. These features of exocytosis and calcium signal suggest that both high- and low-affinity calcium sensors operate in chromaffin cells. Indeed, the first genetic study on calcium sensing in adrenal chromaffin cells showed that calcium sensing in fast burst of exocytosis is regulated by synaptotagmin-1 [87]. The other two calcium sensors that regulate neurotransmitter release, synaptotagmin-2 and -9, are not detected in adrenal chromaffin cells [58, 88]. In contrast, synaptotagmin-7 is present and its deletion resulted in ~50% reduction of calcium-dependent catecholamine release in mice [88]. Although synaptotagmin-7 shares the same domain structure with synaptotagmin-1, synaptotagmin-7 has higher calcium affinity and slower calcium binding kinetics (Fig. 32.1) [46, 88]. Deletion of synaptotagmin-1 or -7 in chromaffin cells impairs the fast or slow phase of LDCV exocytosis, respectively, and deletion of both synaptotagmin-1 and -7 inhibits both phases, suggesting that the two synaptotagmins mediate different phases of catecholamine release [88]. Furthermore, in chromaffin cells from synaptotagmin-7 knockin mice, which express normal levels of a mutant synaptotagmin-7 whose C_2B domain does not bind calcium, secretory granule exocytosis was reduced in both fast and slow phases, reminiscent of the findings in synaptotagmin-7 KO mice [88]. The findings that the secretory defects in synaptotagmin-7 KO mice can be largely reproduced when synaptotagmin-7 is unable to bind to calcium provide clear and convincing evidence in support of synaptotagmin-7's function as a major calcium sensor for chromaffin granule exocytosis.

Insulin Secretion

Because of the great importance of insulin secretion in normal physiology and pathophysiology such as diabetes, pancreatic β-cells are the most extensively studied system in understanding stimulus-secretion coupling [89–91]. Insulin release is a complex and highly regulated process (Fig. 32.3). Glucose, the main stimulus of insulin secretion, initiates a cascade of metabolic events resulting in increased ATP/ADP ratio. This leads to K_{ATP} channel closure and membrane depolarization, which opens voltage-gated calcium channels and increases the cytoplasmic calcium concentration [90]. Cytoplasmic calcium concentration in β-cells can reach low micromolar levels at peak of stimulation [74–76, 92]. Insulin secretion has a rapid first phase and sustained second phase, which has an oscillatory pattern [93]. It is generally believed that the first phase of insulin secretion requires a rapid calcium rise of high amplitude, while the second phase requires amplifying signals from glucose metabolism in addition to increase in intracellular calcium [94]. The exocytotic machinery in insulin secretion includes SNARE proteins, similar to neurotransmitter release [4, 8, 95]. Many other exocytotic proteins have been found in β-cells and functions of some of these proteins are beginning to emerge [16, 89, 95].

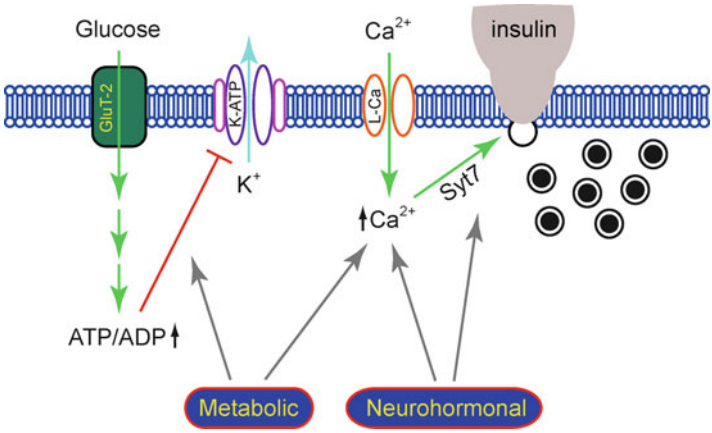

Fig. 32.3 Cellular and molecular regulation of insulin secretion. The cellular events leading to insulin secretion start with a rise in blood glucose level, which quickly leads to glucose uptake into pancreatic β-cells. Glucose in the cells then undergoes glycolysis and TCA cycle to produce ATP, resulting in an increased ATP/ADP ratio, and consequent closure of K_{ATP}-channels. Membrane depolarization from K_{ATP}-channel closure opens L-type calcium channels, allowing calcium influx into the cells and the rise in intracellular calcium levels. Calcium, mediated at least in part by synaptotagmin-7, then triggers insulin granule exocytosis and the release of insulin into blood. Many of the steps leading to insulin secretion are regulated by metabolic and neurohormonal signals. *GluT-2* glucose transporter 2, *TCA* tricarboxylic acid cycle, *Syt7* synaptotagmin-7, *K-ATP* ATP-sensitive potassium channel, *L-Ca* L-type calcium channel

Of all the synaptotagmin isoforms, synaptotagmin-7 has the highest transcript levels in pancreatic β-cells and is located to insulin granules [96]. Several studies have shown that synaptotagmin-7 regulates insulin secretion in insulin-secreting cell lines [97, 98] and in mouse islets [96]. In mice, deletion of synaptotagmin-7 results in impaired glucose tolerance and acute insulin response *in vivo*, as well as reduced glucose-stimulated insulin secretion from isolated islets [96]. The secretory defect is present only at a late exocytotic step as insulin synthesis, metabolic and calcium responses to glucose stimulation are normal, consistent with the notion that synaptotagmin-7 functions as a high-affinity calcium sensor in insulin secretion (Fig. 32.3) [96].

Similar to adrenal chromaffin cells, deletion of synaptotagmin-7 only reduces insulin secretion by 40–50% in β-cells [96]. So which protein(s) function as calcium sensors regulating the remainder of stimulated insulin secretion? While it is established that catecholamine release in chromaffin cells is also regulated by synaptotagmin-1, this isoform is not present in β-cells [88, 96]. Synaptotagmin-9 is expressed at comparable level as synaptotagmin-7 in mouse and rat islets. Although the calcium affinity of synaptotagmin-9 is rather low (10–30 μM), knockdown of synaptotagmin-9 impairs insulin secretion from rat islets and INS-1 cells [89, 99]. On the other hand, a study on pancreas-specific synaptotagmin-9 KO mice showed that the KO mice have no defects in insulin secretion [100]. Furthermore, double KO of synaptotagmin-7 and -9 does not result in further impairment of insulin

secretion than deletion of synaptotagmin-7 alone [100]. It is therefore likely that proteins other than synaptotagmin-9 serve as calcium sensors to regulate the final step in insulin secretion. The molecular structures of synaptotagmin-3, -5, -6 and -10 suggest similar calcium-and SNARE-binding properties to synaptotagmin-1, -2, -7 and -9. These synaptotagmins thus represent the best candidates as calcium sensors in regulating insulin granule exocytosis. Although some cell line studies suggest a role for some of these synaptotagmins in insulin secretion regulation, no definitive *in vivo* evidence supporting their role as calcium sensors in insulin secretion has been described for synaptotagmin-3, -5, -6 or -10 [97, 98, 101–103].

Glucagon Secretion

Glucagon is another important hormone regulating glucose homeostasis. Glucagon is produced by islet α-cells and stored in large dense core vesicles. However, unlike insulin secretion, the precise mechanisms of glucagon secretion are less well studied [5]. Some recent studies highlight the importance of glucagon secretion regulation in diabetes development, re-affirming that diabetes is a bi-hormonal disease [104–106]. Although stimulus-secretion coupling in glucagon secretion is not fully defined, it is clear that glucose and other secretagogues can directly modulate glucagon secretion [5, 107]. Furthermore, pancreatic α-cells receive inhibitory paracrine influence from neighboring β- and δ-cells, to reduce glucagon secretion and prevent the excessive action of glucagon on the liver. Among the substances released by β-cells, insulin, GABA and zinc have been shown to reduce glucagon release from α-cells [5, 108]. In addition, other circulating hormones and the autonomic nervous system regulate glucagon secretion as well [5].

Although both insulin and glucagon secretion is triggered by an increase of cytoplasmic calcium levels, calcium-influx is mediated by N-type calcium channels in α-cells, and L-type calcium channels in β-cells [107, 109, 110]. So far, only one study has been reported on calcium sensing in glucagon secretion [111]. Pancreatic α-cells contain high levels of synaptotagmin-7, and deletion of synaptotagmin-7 in mice led to nearly abolished hypoglycemia- or depolarization-induced glucagon secretion [111]. As glucagon synthesis, glucagon granule distribution, α-cell electrical activity and calcium channel currents are not affected in synaptotagmin-7 KO mice, the glucagon secretion results from the KO mice establish that synaptotagmin-7 is the principal calcium sensor for glucagon secretion [111].

GLP-1 Secretion

GLP-1 (Glucagon-like peptide-1) is a polypeptide hormone secreted by enteroendocrine L-cells in intestinal mucosa of mainly ileum and colon [112]. GLP-1 belongs

to a group of hormones called incretins, which also includes GIP (glucose-dependent insulinotropic peptide) released from K-cells in duodenum and jejunum of the gastric-intestine tract [112]. The incretins are potent stimulators of insulin secretion and effective suppressors of glucagon secretion, making them an ideal target for type 2 diabetes therapies [113]. In addition to their effect on insulin and glucagon secretion, the incretins inhibit gastric emptying and reduce appetite [112, 113].

The release of GLP-1 is stimulated by nutrients, such as glucose, fats and amino acids from intestinal lumen [114]. Intestinal L-cells also receive neuronal and paracrine input [112]. There are several subpopulations of L-cells. Some L-cells secrete only GLP-1, and some secrete both GLP-1 and peptide YY or GLP-1 and cholecystokinin [115]. Furthermore, these cells are scattered among other enterocytes and have similar morphology to neighboring cells. As such, it is a challenging task to obtain a pure culture of L-cells to study molecular control of GLP-1 secretion. Most of the previous studies on L-cell physiology and the regulation of GLP-1 secretion have been done on GLP-1 producing cell lines, such as the widely distributed GLUTag cells developed in Daniel Drucker's laboratory [116]. Recently, a transgenic mouse line with expression of a fluorescent protein in L-cells was generated, and thus allowing examination of these questions in primary cells [117]. Considering that GLP-1 secretion is regulated by the activity of sodium-glucose co-transporter 1 and ATP-sensitive K^+-channels, and requires membrane depolarization and calcium entry through L-type calcium channels, it is tempting to propose that GLP-1 secretion may be regulated in a similar fashion as insulin secretion from pancreatic β-cells: both insulin and GLP-1 secretion is stimulated by glucose, requires a glucose transporter and glucose metabolism, ATP-sensitive K^+-channels, as well as membrane depolarizations and Ca^{2+} entry through L-type Ca^{2+}-channels [117, 118]. To date, the only study on calcium sensing in L-cells was done very recently to test the role of synaptotagmin-7 *in vivo* and in GLUTag cells [119]. Synaptotagmin-7 is expressed in GLP-1 granules of intestinal L-cells and in GLUTag cells. Deletion of synaptotagmin-7 in mice and lentiviral silencing of synaptotagmin-7 in GLUTag cells result in reduced, but not abolished stimulated GLP-1 secretion without affecting calcium signals [119]. These findings demonstrate that in L-cells, like in islet β-cells and adrenal chromaffin cells, synaptotagmin-7 is a major calcium sensor, and additional proteins are also involved in regulating GLP-1 release. In addition to synaptotagmin-7, several other synaptotagmins are also expressed in GLUTag cells (unpublished observations). However, it is not clear whether the other identified synaptotagmins are involved in GLP-1 secretion in these cells.

Regulation of Synaptotagmin Activity

Although many of the players involved in the regulation and execution of neurotransmitter and peptide hormone release have been identified and a number of plausible models have been proposed [8, 57, 120, 121], there remain numerous

details as to how these proteins work together to orchestrate the very finely controlled exocytotic process, for example, (1) how many SNARE complexes are needed and whether different number of SNAREs are involved in synchronous and asynchronous neurotransmitter release and hormone secretion? (2) How do synaptotagmins trigger the membrane fusion upon receiving the calcium signal? (3) Are non-calcium binding synaptotagmins involved in regulating asynchronous neurotransmitter release, possibly by collaborating with calcium-binding synaptotagmins?

To add to the complexity of exocytosis regulation, some of the SNAREs and associated proteins, including synaptotagmins, have been shown to undergo post-translational modifications. How do these various modifications fine-tune, or even control the exocytosis process? This is a largely unexplored area, and likely will be a major excitement in exocytosis research, especially after a consensus on exocytotic mechanism is reached. In addition to the well-known and omnipresent phosphorylation, other post-translational modifications, such as acetylation, palmitoylation [122–126], sumoylation/ubiquitination [127], and glycosylation [54, 128–130] may have significant effects on their target proteins' subcellular localization, and interaction with other proteins. Several in vitro studies indicate that synaptotagmins are phosphorylated by various protein kinases with diverse consequences [131–135], for example, phosphorylation of synaptotagmin-2 and -9 affects their subcellular localization [131, 136], leads to changes in calcium-binding properties [136] and interactions with SNARE proteins [137]. In contrast, phosphorylation of synaptotagmin-1 and -2 in mouse chromaffin cells had no effect on exocytosis [138]. Palmitoylation has been described for synaptotagmin-1 and -7, which may be important for its intracellular sorting into correct vesicles and protein-protein interactions [122, 124, 139].

Other Calcium-Binding Proteins

In addition to the eight calcium-binding synaptotagmins, a number of other proteins are shown to have calcium-binding properties and, therefore, calcium-sensing potential (Table 32.2). There are several other families of membrane proteins with sequence and structure similarities to synaptotagmins. Two other protein families, rabphilin and Doc2 (double C_2 proteins), also contain two C-terminal C_2 domains but lack transmembrane regions [140–143]. The involvement of rabphilin in calcium sensing has not been established, while Doc2b may function as a calcium sensor in spontaneous neurotransmitter release [65]. Doc2b may also have a role in chromaffin cells [144], pancreatic β-cells [145, 146] and adipocytes [145, 147], although these remain to be confirmed by genetic studies. E-Syts (extended synaptotagmin-like proteins) contain an N-terminal transmembrane region, but more than two C_2 domains [148, 149]. Copines are soluble double C_2-domain proteins that can

also bind to phospholipids [150]. No functional data on E-Syts and copines have been reported.

Ferlins contain six C_2 domains and a C-terminal TMR [151], and MCTPs (multiple C_2 domain proteins with two transmembrane regions) contain three C_2 domains and two transmembrane regions (Table 32.2) [152]. Little information is available regarding precise tissue distribution, cellular localization and functions of the Ferlins and MCTPs, although certain Ferlins are linked to muscular dystrophy, possibly a result of impaired membrane fusion and consequent defects in plasma membrane repair [148, 151, 152].

Summary

Over the past 20 years, significant progress has been made in understanding the molecular mechanisms of calcium sensing in the regulation of neurotransmission and hormone secretion. It is clear now that calcium sensing is mediated by calcium-binding proteins with a unique property to bind phospholipids at a defined range of calcium concentrations. These proteins function together with SNARE proteins and promote vesicle fusion upon Ca^{2+} rise in the cytoplasm. A number of these calcium-binding proteins have been characterized and their functions in vesicle exocytosis in neurons and endocrine cells have been defined in biochemical, structural and genetic studies. Among these proteins, synaptotagmins appear to be the principal calcium sensors in neurotransmitter and peptide hormone release (Table 32.4). Synaptotagmins have distinct properties, including a wide range of calcium affinities that meet the requirements as calcium sensors in individual exocytotic systems. So far, synaptotagmin-1, -2 and -9 have been established as calcium sensors in synchronous neurotransmitter release in brain and neuromuscular junctions, synaptotagmin-7 as the calcium regulator for chromaffin, islet β-and α-cells, and intestinal L-cells, and synaptotagmin-10 as the calcium sensor for IGF-1 release in olfactory bulb neurons [153]. These findings support the synaptotagmin-calcium-sensor paradigm, which states that synaptotagmins serve as individually acting calcium sensors in neurotransmitter and peptide hormone release [16].

As we begin to piece together the puzzle in understanding the molecular mechanisms of calcium regulation in neurotransmission and hormone secretion, and in exocytosis in general, much remains to be done in identifying the players involved in calcium-dependent vesicle exocytosis, and in understanding the intricate details of how calcium signal is translated into the precise pattern of exocytosis. Calcium sensors for many types of release and cell types need to be identified. Interaction and cooperation of different calcium sensors in mediating exocytosis are not understood. Last but not least, how these calcium sensors are regulated in response to different environment cues remain largely unknown. Post-translational modifications on exocytotic proteins, including calcium sensors are potential mechanisms that well deserve further investigations.

Table 32.4 Identified calcium sensors in exocytosis

Type of release	Cell types	Triggering $[Ca^{2+}]_i$	Identified sensors	Experimental evidence
Synchronous neurotransmitter release	Brain	10–40 μM	Synaptotagmin-1	Model organisms [47, 48, 53–56, 58, 68]
	Neuromuscular junctions		Synaptotagmin-2	
			Synaptotagmin-9	
			Synaptotagmin-1	
Asynchronous neurotransmitter release	All neurons	1–10 μM	Unknown	
Spontaneous neurotransmitter release	All neurons	~1 μM	Synaptotagmin-1	KO mouse [66]
			Doc2B	KO mouse [65, 73]
Catecholamine release	Adrenal chromaffin cells	1–10 μM	Synaptotagmin-1 and -7	Model organisms [87, 88]
Insulin release	Pancreatic β-cell	1–10 μM	Synaptotagmin-7 and additional unknown proteins	Cell lines [97, 98, 101–103]
				Model organisms [96]
Glucagon release	Pancreatic α-cell	Sub- to low μM	Synaptotagmin-7	Model organisms [111]
GLP-1 release	Intestinal L-cells	Sub- to low μM	Synaptotagmin-7 and additional unknown proteins	Cell lines [119]
				Model organisms [119]

Acknowledgements Ongoing research studies in the Laboratory of Metabolic Medicine are supported by an intramural program of A*STAR (Agency for Science, Technology and Research) Biomedical Research Council in Singapore (WH).

References

1. Del Castillo J, Katz B (1954) Quantal components of the end-plate potential. J Physiol 124:560–573
2. Fatt P, Katz B (1952) Spontaneous subthreshold activity at motor nerve endings. J Physiol 117:109–128
3. Katz B (1969) The release of neural transmitter substances. Thomas, Springfield
4. Grodsky GM, Bennett LL (1966) Cation requirements for insulin secretion in the isolated perfused pancreas. Diabetes 15:910–913
5. Gromada J, Franklin I, Wollheim CB (2007) Alpha-cells of the endocrine pancreas: 35 years of research but the enigma remains. Endocr Rev 28:84–116. doi:er.2006-0007 [pii] 10.1210/er.2006-0007
6. Johansson H, Gylfe E, Hellman B (1987) The actions of arginine and glucose on glucagon secretion are mediated by opposite effects on cytoplasmic Ca2+. Biochem Biophys Res Commun 147:309–314. doi:S0006-291X(87)80122-5 [pii]
7. Rubin RP (1970) The role of calcium in the release of neurotransmitter substances and hormones. Pharmacol Rev 22:389–428
8. Jahn R, Lang T, Sudhof TC (2003) Membrane fusion. Cell 112:519–533. doi:S009286740 3001120 [pii]
9. Oyler GA et al (1989) The identification of a novel synaptosomal-associated protein, SNAP-25, differentially expressed by neuronal subpopulations. J Cell Biol 109:3039–3052
10. Baumert M, Maycox PR, Navone F, De Camilli P, Jahn R (1989) Synaptobrevin: an integral membrane protein of 18,000 daltons present in small synaptic vesicles of rat brain. EMBO J 8:379–384
11. Bennett MK, Calakos N, Scheller RH (1992) Syntaxin: a synaptic protein implicated in docking of synaptic vesicles at presynaptic active zones. Science 257:255–259
12. Weber T et al (1998) SNAREpins: minimal machinery for membrane fusion. Cell 92:759–772. doi:S0092-8674(00)81404-X [pii]
13. Pevsner J et al (1994) Specificity and regulation of a synaptic vesicle docking complex. Neuron 13:353–361. doi:0896-6273(94)90352-2 [pii]
14. Sudhof TC, Baumert M, Perin MS, Jahn RA (1989) synaptic vesicle membrane protein is conserved from mammals to Drosophila. Neuron 2:1475–1481. doi:0896-6273(89)90193-1 [pii]
15. Chen X, Tang J, Sudhof TC, Rizo J (2005) Are neuronal SNARE proteins Ca2+ sensors? J Mol Biol 347:145–158. doi:S0022-2836(05)00046-X [pii] 10.1016/j.jmb.2005.01.024
16. Gustavsson N, Han W (2009) Calcium-sensing beyond neurotransmitters: functions of synaptotagmins in neuroendocrine and endocrine secretion. Biosci Rep 29:245–259. doi:BSR20090031 [pii] 10.1042/BSR20090031
17. Sudhof TC (1995) The synaptic vesicle cycle: a cascade of protein-protein interactions. Nature 375:645–653. doi:10.1038/375645a0
18. Sudhof TC (2004) The synaptic vesicle cycle. Annu Rev Neurosci 27:509–547. doi:10.1146/annurev.neuro.26.041002.131412
19. Sudhof TC (2008) Neurotransmitter release. Handb Exp Pharmacol 184:1–21. doi:10.1007/978-3-540-74805-2_1
20. Sugita S (2008) Mechanisms of exocytosis. Acta Physiol (Oxf) 192:185–193. doi:APS1803 [pii] 10.1111/j.1748-1716.2007.01803.x
21. Goda Y, Stevens CF (1994) Two components of transmitter release at a central synapse. Proc Natl Acad Sci USA 91:12942–12946

22. Tokuoka H, Goda Y (2003) Synaptotagmin in Ca2+ -dependent exocytosis: dynamic action in a flash. Neuron 38:521–524. doi:S0896627303002903 [pii]
23. Xu-Friedman MA, Regehr WG (2000) Probing fundamental aspects of synaptic transmission with strontium. J Neurosci 20:4414–4422. doi:20/12/4414 [pii]
24. Pevsner J, Hsu SC, Scheller RH (1994) n-Sec1: a neural-specific syntaxin-binding protein. Proc Natl Acad Sci USA 91:1445–1449
25. Hata Y, Slaughter CA, Sudhof TC (1993) Synaptic vesicle fusion complex contains unc-18 homologue bound to syntaxin. Nature 366:347–351. doi:10.1038/366347a0
26. Verhage M et al (2000) Synaptic assembly of the brain in the absence of neurotransmitter secretion. Science 287:864–869. doi:8244 [pii]
27. Sabatini BL, Regehr WG (1996) Timing of neurotransmission at fast synapses in the mammalian brain. Nature 384:170–172. doi:10.1038/384170a0
28. Bollmann JH, Sakmann B, Borst JG (2000) Calcium sensitivity of glutamate release in a calyx-type terminal. Science 289:953–957. doi:8741 [pii]
29. Bollmann JH, Sakmann B (2005) Control of synaptic strength and timing by the release-site Ca2+ signal. Nat Neurosci 8:426–434. doi:nn1417 [pii] 10.1038/nn1417
30. Meinrenken CJ, Borst JG, Sakmann B (2003) Local routes revisited: the space and time dependence of the Ca2+ signal for phasic transmitter release at the rat calyx of Held. J Physiol 547:665–689. doi:10.1113/jphysiol.2002.032714 2002.032714 [pii]
31. Schneggenburger R, Neher E (2000) Intracellular calcium dependence of transmitter release rates at a fast central synapse. Nature 406:889–893. doi:10.1038/35022702
32. Schneggenburger R, Meyer AC, Neher E (1999) Released fraction and total size of a pool of immediately available transmitter quanta at a calyx synapse. Neuron 23:399–409. doi:S0896-6273(00)80789-8 [pii]
33. Sun J et al (2007) A dual-Ca2+-sensor model for neurotransmitter release in a central synapse. Nature 450:676–682. doi:nature06308 [pii] 10.1038/nature06308
34. Kochubey O, Lou X, Schneggenburger R (2011) Regulation of transmitter release by Ca(2+) and synaptotagmin: insights from a large CNS synapse. Trends Neurosci 34:237–246. doi:10.1016/j.tins.2011.02.006
35. Perin MS, Brose N, Jahn R, Sudhof TC (1991) Domain structure of synaptotagmin (p65). J Biol Chem 266:623–629
36. Sudhof TC (2002) Synaptotagmins: why so many? J Biol Chem 277:7629–7632. doi: 10.1074/jbc.R100052200 R100052200 [pii]
37. Matthew WD, Tsavaler L, Reichardt LF (1981) Identification of a synaptic vesicle-specific membrane protein with a wide distribution in neuronal and neurosecretory tissue. J Cell Biol 91:257–269
38. Perin MS, Fried VA, Mignery GA, Jahn R, Sudhof TC (1990) Phospholipid binding by a synaptic vesicle protein homologous to the regulatory region of protein kinase C. Nature 345:260–263. doi:10.1038/345260a0
39. Rizo J, Sudhof TC (1998) C2-domains, structure and function of a universal Ca2+-binding domain. J Biol Chem 273:15879–15882
40. Sutton RB, Davletov BA, Berghuis AM, Sudhof TC (1995) Structure of the first C2 domain of synaptotagmin I: a novel Ca2+/phospholipid-binding fold. Cell 80:929–938. doi: 0092-8674(95)90296-1 [pii]
41. Fernandez I et al (2001) Three-dimensional structure of the synaptotagmin 1 C2B-domain: synaptotagmin 1 as a phospholipid binding machine. Neuron 32:1057–1069. doi: S0896-6273(01)00548-7 [pii]
42. Shao X, Fernandez I, Sudhof TC, Rizo J (1998) Solution structures of the Ca2+-free and Ca2+-bound C2A domain of synaptotagmin I: does Ca2+ induce a conformational change? Biochemistry 37:16106–16115. doi:10.1021/bi981789h bi981789h [pii]
43. Ubach J, Zhang X, Shao X, Sudhof TC, Rizo J (1998) Ca2+ binding to synaptotagmin: how many Ca2+ ions bind to the tip of a C2-domain? EMBO J 17:3921–3930. doi:10.1093/emboj/17.14.3921

44. Li C, Davletov BA, Sudhof TC (1995) Distinct Ca2+ and Sr2+ binding properties of synaptotagmins. Definition of candidate Ca2+ sensors for the fast and slow components of neurotransmitter release. J Biol Chem 270:24898–24902
45. Li C et al (1995) Ca(2+)-dependent and -independent activities of neural and non-neural synaptotagmins. Nature 375:594–599. doi:10.1038/375594a0
46. Sugita S, Shin OH, Han W, Lao Y, Südhof TC (2002) Synaptotagmins form a hierarchy of exocytotic Ca(2+) sensors with distinct Ca(2+) affinities. EMBO J 21:270–280. doi:10.1093/emboj/21.3.270
47. Geppert M et al (1994) Synaptotagmin I: a major Ca2+ sensor for transmitter release at a central synapse. Cell 79:717–727. doi:0092-8674(94)90556-8 [pii]
48. Maximov A, Sudhof TC (2005) Autonomous function of synaptotagmin 1 in triggering synchronous release independent of asynchronous release. Neuron 48:547–554. doi:S0896-6273(05)00772-5 [pii] 10.1016/j.neuron.2005.09.006
49. Broadie K, Bellen HJ, DiAntonio A, Littleton JT, Schwarz TL (1994) Absence of synaptotagmin disrupts excitation-secretion coupling during synaptic transmission. Proc Natl Acad Sci USA 91:10727–10731
50. DiAntonio A, Parfitt KD, Schwarz TL (1993) Synaptic transmission persists in synaptotagmin mutants of Drosophila. Cell 73:1281–1290. doi:0092-8674(93)90356-U [pii]
51. Littleton JT, Stern M, Schulze K, Perin M, Bellen HJ (1993) Mutational analysis of Drosophila synaptotagmin demonstrates its essential role in Ca(2+)-activated neurotransmitter release. Cell 74:1125–1134. doi:0092-8674(93)90733-7 [pii]
52. Nonet ML, Grundahl K, Meyer BJ, Rand JB (1993) Synaptic function is impaired but not eliminated in C. elegans mutants lacking synaptotagmin. Cell 73:1291–1305. doi:0092-8674(93)90357-V [pii]
53. Fernandez-Chacon R et al (2001) Synaptotagmin I functions as a calcium regulator of release probability. Nature 410:41–49. doi:10.1038/35065004 35065004 [pii]
54. Han W et al (2004) N-glycosylation is essential for vesicular targeting of synaptotagmin 1. Neuron 41:85–99
55. Pang ZP et al (2006) Synaptotagmin-2 is essential for survival and contributes to Ca2+ triggering of neurotransmitter release in central and neuromuscular synapses. J Neurosci 26:13493–13504. doi:26/52/13493 [pii] 10.1523/JNEUROSCI.3519-06.2006
56. Pang ZP, Sun J, Rizo J, Maximov A, Sudhof TC (2006) Genetic analysis of synaptotagmin 2 in spontaneous and Ca2+-triggered neurotransmitter release. EMBO J 25:2039–2050. doi:7601103 [pii] 10.1038/sj.emboj.7601103
57. Pang ZP, Sudhof TC (2010) Cell biology of Ca2+-triggered exocytosis. Curr Opin Cell Biol 22:496–505. doi:S0955-0674(10)00064-5 [pii] 10.1016/j.ceb.2010.05.001
58. Xu J, Mashimo T, Sudhof TC (2007) Synaptotagmin-1, -2, and -9: Ca(2+) sensors for fast release that specify distinct presynaptic properties in subsets of neurons. Neuron 54:567–581. doi:S0896-6273(07)00338-8 [pii] 10.1016/j.neuron.2007.05.004
59. Hagler DJ Jr, Goda Y (2001) Properties of synchronous and asynchronous release during pulse train depression in cultured hippocampal neurons. J Neurophysiol 85:2324–2334
60. Hui E et al (2005) Three distinct kinetic groupings of the synaptotagmin family: candidate sensors for rapid and delayed exocytosis. Proc Natl Acad Sci USA 102:5210–5214. doi:0500941102 [pii] 10.1073/pnas.0500941102
61. Saraswati S, Adolfsen B, Littleton JT (2007) Characterization of the role of the Synaptotagmin family as calcium sensors in facilitation and asynchronous neurotransmitter release. Proc Natl Acad Sci USA 104:14122–14127. doi:0706711104 [pii] 10.1073/pnas.0706711104
62. Nishiki T, Augustine GJ (2004) Dual roles of the C2B domain of synaptotagmin I in synchronizing Ca2+-dependent neurotransmitter release. J Neurosci 24:8542–8550. doi:10.1523/JNEUROSCI.2545-04.2004 24/39/8542 [pii]
63. Nishiki T, Augustine GJ (2004) Synaptotagmin I synchronizes transmitter release in mouse hippocampal neurons. J Neurosci 24:6127–6132. doi:10.1523/JNEUROSCI.1563-04.2004 24/27/6127 [pii]

64. Glitsch MD (2008) Spontaneous neurotransmitter release and Ca2+–how spontaneous is spontaneous neurotransmitter release? Cell Calcium 43:9–15. doi:S0143-4160(07)00044-9 [pii] 10.1016/j.ceca.2007.02.008
65. Groffen AJ et al (2010) Doc2b is a high-affinity Ca2+ sensor for spontaneous neurotransmitter release. Science 327:1614–1618. doi:science.1183765 [pii] 10.1126/science.1183765
66. Xu J, Pang ZP, Shin OH, Sudhof TC (2009) Synaptotagmin-1 functions as a Ca2+ sensor for spontaneous release. Nat Neurosci 12:759–766. doi:10.1038/nn.2320
67. Chicka MC, Hui E, Liu H, Chapman ER (2008) Synaptotagmin arrests the SNARE complex before triggering fast, efficient membrane fusion in response to Ca2+. Nat Struct Mol Biol 15:827–835. doi:nsmb.1463 [pii] 10.1038/nsmb.1463
68. Pang ZP, Shin OH, Meyer AC, Rosenmund C, Sudhof TC (2006) A gain-of-function mutation in synaptotagmin-1 reveals a critical role of Ca2+-dependent soluble N-ethylmaleimide-sensitive factor attachment protein receptor complex binding in synaptic exocytosis. J Neurosci 26:12556–12565. doi:26/48/12556 [pii] 10.1523/JNEUROSCI.3804-06.2006
69. Groffen AJ, Friedrich R, Brian EC, Ashery U, Verhage M (2006) DOC2A and DOC2B are sensors for neuronal activity with unique calcium-dependent and kinetic properties. J Neurochem 97:818–833. doi:JNC3755 [pii] 10.1111/j.1471-4159.2006.03755.x
70. Sudhof TC, Rizo J (1996) Synaptotagmins: C2-domain proteins that regulate membrane traffic. Neuron 17:379–388. doi:S0896-6273(00)80171-3 [pii]
71. Bai J, Chapman ER (2004) The C2 domains of synaptotagmin–partners in exocytosis. Trends Biochem Sci 29:143–151. doi:10.1016/j.tibs.2004.01.008 S0968000404000258 [pii]
72. Friedrich R, Yeheskel A, Ashery U (2010) DOC2B, C2 domains, and calcium: a tale of intricate interactions. Mol Neurobiol 41:42–51. doi:10.1007/s12035-009-8094-8
73. Pang ZP et al (2011) Doc2 supports spontaneous synaptic transmission by a Ca(2+)-independent mechanism. Neuron 70:244–251. doi:10.1016/j.neuron.2011.03.011
74. Takahashi N, Kadowaki T, Yazaki Y, Miyashita Y, Kasai H (1997) Multiple exocytotic pathways in pancreatic beta cells. J Cell Biol 138:55–64
75. Barg S et al (2001) Fast exocytosis with few Ca(2+) channels in insulin-secreting mouse pancreatic B cells. Biophys J 81:3308–3323. doi:S0006-3495(01)75964-4 [pii] 10.1016/S0006-3495(01)75964-4
76. Proks P, Eliasson L, Ammala C, Rorsman P, Ashcroft FM (1996) Ca(2+)- and GTP-dependent exocytosis in mouse pancreatic beta-cells involves both common and distinct steps. J Physiol 496(Pt 1):255–264
77. Theler JM et al (1992) Video imaging of cytosolic Ca2+ in pancreatic beta-cells stimulated by glucose, carbachol, and ATP. J Biol Chem 267:18110–18117
78. Bokvist K, Eliasson L, Ammala C, Renstrom E, Rorsman P (1995) Co-localization of L-type Ca2+ channels and insulin-containing secretory granules and its significance for the initiation of exocytosis in mouse pancreatic B-cells. EMBO J 14:50–57
79. Rutter GA, Tsuboi T, Ravier MA (2006) Ca2+ microdomains and the control of insulin secretion. Cell Calcium 40:539–551. doi:S0143-4160(06)00180-1 [pii] 10.1016/j.ceca.2006.08.015
80. Burgoyne RD et al (1996) SNAPs and SNAREs in exocytosis in chromaffin cells. Biochem Soc Trans 24:653–657
81. Neher EA (2006) A comparison between exocytic control mechanisms in adrenal chromaffin cells and a glutamatergic synapse. Pflugers Arch 453:261–268. doi:10.1007/s00424-006-0143-9
82. Burgoyne RD, Morgan A (1998) Analysis of regulated exocytosis in adrenal chromaffin cells: insights into NSF/SNAP/SNARE function. Bioessays 20:328–335. doi:10.1002/(SICI)1521-1878(199804)20:4<328::AID-BIES9>3.0.CO;2-L [pii] 10.1002/(SICI)1521-1878(199804)20:4<328::AID-BIES9>3.0.CO;2-L
83. Burgoyne RD, Morgan A, Robinson I, Pender N, Cheek TR (1993) Exocytosis in adrenal chromaffin cells. J Anat 183(Pt 2):309–314
84. Heinemann C, Chow RH, Neher E, Zucker RS (1994) Kinetics of the secretory response in bovine chromaffin cells following flash photolysis of caged Ca2+. Biophys J 67:2546–2557. doi:S0006-3495(94)80744-1 [pii] 10.1016/S0006-3495(94)80744-1

85. Xu T, Binz T, Niemann H, Neher E (1998) Multiple kinetic components of exocytosis distinguished by neurotoxin sensitivity. Nat Neurosci 1:192–200. doi:10.1038/642 642 [pii]
86. Xu T et al (1999) Inhibition of SNARE complex assembly differentially affects kinetic components of exocytosis. Cell 99:713–722. doi:S0092-8674(00)81669-4 [pii]
87. Voets T et al (2001) Intracellular calcium dependence of large dense-core vesicle exocytosis in the absence of synaptotagmin I. Proc Natl Acad Sci USA 98:11680–11685. doi:10.1073/pnas.201398798 201398798 [pii]
88. Schonn JS, Maximov A, Lao Y, Sudhof TC, Sorensen JB (2008) Synaptotagmin-1 and -7 are functionally overlapping Ca2+ sensors for exocytosis in adrenal chromaffin cells. Proc Natl Acad Sci USA 105:3998–4003. doi:0712373105 [pii] 10.1073/pnas.0712373105
89. Gauthier BR, Wollheim CB (2008) Synaptotagmins bind calcium to release insulin. Am J Physiol Endocrinol Metab 295:E1279–E1286. doi:90568.2008 [pii] 10.1152/ajpendo.90568.2008
90. Ashcroft FM et al (1994) Stimulus-secretion coupling in pancreatic beta cells. J Cell Biochem 55(Suppl):54–65
91. Eliasson L et al (2008) Novel aspects of the molecular mechanisms controlling insulin secretion. J Physiol 586:3313–3324. doi:jphysiol.2008.155317 [pii] 10.1113/jphysiol.2008.155317
92. Barg S, Rorsman P (2004) Insulin secretion: a high-affinity Ca2+ sensor after all? J Gen Physiol 124:623–625. doi:jgp. 200409206 [pii] 10.1085/jgp.200409206
93. Rorsman P, Renstrom E (2003) Insulin granule dynamics in pancreatic beta cells. Diabetologia 46:1029–1045. doi:10.1007/s00125-003-1153-1
94. Henquin JC, Ishiyama N, Nenquin M, Ravier MA, Jonas JC (2002) Signals and pools underlying biphasic insulin secretion. Diabetes 51(Suppl 1):S60–S67
95. Gerber SH, Südhof TC (2002) Molecular determinants of regulated exocytosis. Diabetes 51(Suppl 1):S3–S11
96. Gustavsson N et al (2008) Impaired insulin secretion and glucose intolerance in synaptotagmin-7 null mutant mice. Proc Natl Acad Sci USA 105:3992–3997. doi:0711700105 [pii] 10.1073/pnas.0711700105
97. Gao Z, Reavey-Cantwell J, Young RA, Jegier P, Wolf BA (2000) Synaptotagmin III/VII isoforms mediate Ca2+-induced insulin secretion in pancreatic islet beta -cells. J Biol Chem 275:36079–36085. doi:10.1074/jbc.M004284200 M004284200 [pii]
98. Gut A et al (2001) Expression and localisation of synaptotagmin isoforms in endocrine beta-cells: their function in insulin exocytosis. J Cell Sci 114:1709–1716
99. Iezzi M, Eliasson L, Fukuda M, Wollheim CB (2005) Adenovirus-mediated silencing of synaptotagmin 9 inhibits Ca2+-dependent insulin secretion in islets. FEBS Lett 579:5241–5246. doi:S0014-5793(05)01049-5 [pii] 10.1016/j.febslet.2005.08.047
100. Gustavsson N et al (2010) Neuronal calcium sensor synaptotagmin-9 is not involved in the regulation of glucose homeostasis or insulin secretion. PLoS One 5:e15414. doi:10.1371/journal.pone.0015414
101. Brown H et al (2000) Synaptotagmin III isoform is compartmentalized in pancreatic beta-cells and has a functional role in exocytosis. Diabetes 49:383–391
102. Mizuta M et al (1997) Localization and functional role of synaptotagmin III in insulin secretory vesicles in pancreatic beta-cells. Diabetes 46:2002–2006
103. Iezzi M, Kouri G, Fukuda M, Wollheim CB (2004) Synaptotagmin V and IX isoforms control Ca2+ -dependent insulin exocytosis. J Cell Sci 117:3119–3127. doi:10.1242/jcs.01179 jcs.01179 [pii]
104. Lee Y, Wang MY, Du XQ, Charron MJ, Unger RH (2011) Glucagon receptor knockout prevents insulin-deficient type 1 diabetes in mice. Diabetes 60:391–397. doi:10.2337/db10-0426
105. Gustavsson N et al (2011) Delayed onset of hyperglycaemia in a mouse model with impaired glucagon secretion demonstrates that dysregulated glucagon secretion promotes hyperglycaemia and type 2 diabetes. Diabetologia 54:415–422. doi:10.1007/s00125-010-1950-2
106. Unger RH, Orci L (1975) The essential role of glucagon in the pathogenesis of diabetes mellitus. Lancet 1:14–16

107. MacDonald PE et al (2007) A K ATP channel-dependent pathway within alpha cells regulates glucagon release from both rodent and human islets of Langerhans. PLoS Biol 5:e143. doi:06-PLBI-RA-1371R2 [pii] 10.1371/journal.pbio.0050143
108. Ishihara H, Maechler P, Gjinovci A, Herrera PL, Wollheim CB (2003) Islet beta-cell secretion determines glucagon release from neighbouring alpha-cells. Nat Cell Biol 5:330–335. doi:10.1038/ncb951 ncb951 [pii]
109. Gopel S et al (2004) Capacitance measurements of exocytosis in mouse pancreatic alpha-, beta- and delta-cells within intact islets of Langerhans. J Physiol 556:711–726. doi:10.1113/jphysiol.2003.059675 jphysiol.2003.059675 [pii]
110. Pereverzev A et al (2005) The ablation of the Ca(v)2.3/E-type voltage-gated Ca2+ channel causes a mild phenotype despite an altered glucose induced glucagon response in isolated islets of Langerhans. Eur J Pharmacol 511:65–72. doi:S0014-2999(05)00152-4 [pii] 10.1016/j.ejphar.2005.01.044
111. Gustavsson N et al (2009) Synaptotagmin-7 is a principal Ca2+-sensor for Ca2+-induced glucagon exocytosis in pancreas. J Physiol. doi:jphysiol.2008.168005 [pii] 10.1113/jphysiol.2008.168005
112. Drucker DJ (2006) The biology of incretin hormones. Cell Metab 3:153–165. doi:S1550-4131(06)00028-3 [pii] 10.1016/j.cmet.2006.01.004
113. Lovshin JA, Drucker DJ (2009) Incretin-based therapies for type 2 diabetes mellitus. Nat Rev Endocrinol 5:262–269. doi:nrendo.2009.48 [pii] 10.1038/nrendo.2009.48
114. Tolhurst G, Reimann F, Gribble FM (2009) Nutritional regulation of glucagon-like peptide-1 secretion. J Physiol 587:27–32. doi:jphysiol.2008.164012 [pii] 10.1113/jphysiol.2008.164012
115. Solcia E et al (1985) Glucagon- and PP-related peptides of intestinal L cells and pancreatic/gastric A or PP cells. Possible interrelationships of peptides and cells during evolution, fetal development and tumor growth. Peptides 6(Suppl 3):223–229
116. Drucker DJ, Jin T, Asa SL, Young TA, Brubaker PL (1994) Activation of proglucagon gene transcription by protein kinase-A in a novel mouse enteroendocrine cell line. Mol Endocrinol 8:1646–1655
117. Reimann F et al (2008) Glucose sensing in L cells: a primary cell study. Cell Metab 8:532–539. doi:S1550-4131(08)00354-9 [pii] 10.1016/j.cmet.2008.11.002
118. Reimann F et al (2005) Characterization and functional role of voltage gated cation conductances in the glucagon-like peptide-1 secreting GLUTag cell line. J Physiol 563:161–175. doi:jphysiol.2004.076414 [pii] 10.1113/jphysiol.2004.076414
119. Gustavsson N et al (2011) Synaptotagmin-7 as a positive regulator of glucose-induced glucagon-like peptide-1 secretion in mice. Diabetologia. doi:10.1007/s00125-011-2119-3
120. Chapman ER (2008) How does synaptotagmin trigger neurotransmitter release? Annu Rev Biochem 77:615–641. doi:10.1146/annurev.biochem.77.062005.101135
121. Martens S, McMahon HT (2008) Mechanisms of membrane fusion: disparate players and common principles. Nat Rev Mol Cell Biol 9:543–556. doi:nrm2417 [pii] 10.1038/nrm2417
122. Flannery AR, Czibener C, Andrews NW (2010) Palmitoylation-dependent association with CD63 targets the Ca2+ sensor synaptotagmin VII to lysosomes. J Cell Biol 191:599–613. doi:jcb.201003021 [pii] 10.1083/jcb.201003021
123. Heindel U, Schmidt MF, Veit M (2003) Palmitoylation sites and processing of synaptotagmin I, the putative calcium sensor for neurosecretion. FEBS Lett 544:57–62. doi:S0014579303004496 [pii]
124. Kang R et al (2004) Presynaptic trafficking of synaptotagmin I is regulated by protein palmitoylation. J Biol Chem 279:50524–50536. doi:10.1074/jbc.M404981200 M404981200 [pii]
125. Veit M, Becher A, Ahnert-Hilger G (2000) Synaptobrevin 2 is palmitoylated in synaptic vesicles prepared from adult, but not from embryonic brain. Mol Cell Neurosci 15:408–416. doi:S1044-7431(99)90830-8 [pii] 10.1006/mcne.1999.0830
126. Veit M, Sollner TH, Rothman JE (1996) Multiple palmitoylation of synaptotagmin and the t-SNARE SNAP-25. FEBS Lett 385:119–123. doi:0014-5793(96)00362-6 [pii]

127. Dai XQ et al (2011) SUMOylation regulates insulin exocytosis downstream of secretory granule docking in rodents and humans. Diabetes 60:838–847. doi:db10-0440 [pii] 10.2337/db10-0440
128. Atiya-Nasagi Y, Cohen H, Medalia O, Fukudan M, Sagi-Eisenberg R (2005) O-glycosylation is essential for intracellular targeting of synaptotagmins I and II in non-neuronal specialized secretory cells. J Cell Sci 118:1363–1372. doi:jcs.01710 [pii] 10.1242/jcs.01710
129. Fukuda M (2002) Vesicle-associated membrane protein-2/synaptobrevin binding to synaptotagmin I promotes O-glycosylation of synaptotagmin I. J Biol Chem 277:30351–30358. doi:10.1074/jbc.M204056200 M204056200 [pii]
130. Kanno E, Fukuda M (2008) Increased plasma membrane localization of O-glycosylation-deficient mutant of synaptotagmin I in PC12 cells. J Neurosci Res 86:1036–1043. doi:10.1002/jnr.21568
131. Haberman Y, Ziv I, Gorzalczany Y, Fukuda M, Sagi-Eisenberg R (2005) Classical protein kinase C(s) regulates targeting of synaptotagmin IX to the endocytic recycling compartment. J Cell Sci 118:1641–1649. doi:jcs.02276 [pii] 10.1242/jcs.02276
132. Maximov A, Shin OH, Liu X, Sudhof TC (2007) Synaptotagmin-12, a synaptic vesicle phosphoprotein that modulates spontaneous neurotransmitter release. J Cell Biol 176:113–124. doi:jcb.200607021 [pii] 10.1083/jcb.200607021
133. Bennett MK, Miller KG, Scheller RH (1993) Casein kinase II phosphorylates the synaptic vesicle protein p65. J Neurosci 13:1701–1707
134. Davletov B et al (1993) Phosphorylation of synaptotagmin I by casein kinase II. J Biol Chem 268:6816–6822
135. Popoli M (1993) Synaptotagmin is endogenously phosphorylated by Ca2+/calmodulin protein kinase II in synaptic vesicles. FEBS Lett 317:85–88. doi:0014-5793(93)81496-M [pii]
136. Lee BH et al (2004) WNK1 phosphorylates synaptotagmin 2 and modulates its membrane binding. Mol Cell 15:741–751. doi:10.1016/j.molcel.2004.07.018 S109727650400440X [pii]
137. Verona M, Zanotti S, Schafer T, Racagni G, Popoli M (2000) Changes of synaptotagmin interaction with t-SNARE proteins in vitro after calcium/calmodulin-dependent phosphorylation. J Neurochem 74:209–221
138. Nagy G et al (2006) Different effects on fast exocytosis induced by synaptotagmin 1 and 2 isoforms and abundance but not by phosphorylation. J Neurosci 26:632–643. doi:26/2/632 [pii] 10.1523/JNEUROSCI.2589-05.2006
139. Huang K et al (2004) Huntingtin-interacting protein HIP14 is a palmitoyl transferase involved in palmitoylation and trafficking of multiple neuronal proteins. Neuron 44:977–986. doi:S0896627304007500 [pii] 10.1016/j.neuron.2004.11.027
140. Li C et al (1994) Synaptic targeting of rabphilin-3A, a synaptic vesicle Ca2+/phospholipid-binding protein, depends on rab3A/3 C. Neuron 13:885–898. doi:0896-6273(94)90254-2 [pii]
141. Duncan RR, Shipston MJ, Chow RH (2000) Double C2 protein. A review. Biochimie 82:421–426. doi:S0300-9084(00)00214-5 [pii]
142. Orita S et al (1995) Doc2: a novel brain protein having two repeated C2-like domains. Biochem Biophys Res Commun 206:439–448. doi:S0006-291X(85)71062-5 [pii] 10.1006/bbrc.1995.1062
143. Sakaguchi G, Orita S, Maeda M, Igarashi H, Takai Y (1995) Molecular cloning of an isoform of Doc2 having two C2-like domains. Biochem Biophys Res Commun 217:1053–1061. doi:S0006291X85728768 [pii]
144. Friedrich R et al (2008) DOC2B acts as a calcium switch and enhances vesicle fusion. J Neurosci 28:6794–6806. doi:28/27/6794 [pii] 10.1523/JNEUROSCI.0538-08.2008
145. Ke B, Oh E, Thurmond DC (2007) Doc2beta is a novel Munc18c-interacting partner and positive effector of syntaxin 4-mediated exocytosis. J Biol Chem 282:21786–21797. doi:M701661200 [pii] 10.1074/jbc.M701661200
146. Miyazaki M et al (2009) DOC2b is a SNARE regulator of glucose-stimulated delayed insulin secretion. Biochem Biophys Res Commun 384:461–465. doi:S0006-291X(09)00869-9 [pii] 10.1016/j.bbrc.2009.04.133

147. Fukuda N et al (2009) DOC2B: a novel syntaxin-4 binding protein mediating insulin-regulated GLUT4 vesicle fusion in adipocytes. Diabetes 58:377–384. doi:db08-0303 [pii] 10.2337/db08-0303
148. Min SW, Chang WP, Sudhof TC (2007) E-Syts, a family of membranous Ca2 + -sensor proteins with multiple C2 domains. Proc Natl Acad Sci USA 104:3823–3828. doi:0611725104 [pii] 10.1073/pnas.0611725104
149. Morris NJ, Ross SA, Neveu JM, Lane WS, Lienhard GE (1999) Cloning and characterization of a 22 kDa protein from rat adipocytes: a new member of the reticulon family. Biochim Biophys Acta 1450:68–76. doi:S0167-4889(99)00033-6 [pii]
150. Tomsig JL, Creutz CE (2002) Copines: a ubiquitous family of Ca(2+)-dependent phospholipid-binding proteins. Cell Mol Life Sci 59:1467–1477
151. Bansal D, Campbell KP (2004) Dysferlin and the plasma membrane repair in muscular dystrophy. Trends Cell Biol 14:206–213. doi:10.1016/j.tcb.2004.03.001 S0962892404000546 [pii]
152. Shin OH, Han W, Wang Y, Sudhof TC (2005) Evolutionarily conserved multiple C2 domain proteins with two transmembrane regions (MCTPs) and unusual Ca2+ binding properties. J Biol Chem 280:1641–1651. doi:M407305200 [pii] 10.1074/jbc.M407305200
153. Cao P, Maximov A, Sudhof TC (2011) Activity-dependent IGF-1 exocytosis is controlled by the Ca(2+)-sensor synaptotagmin-10. Cell 145:300–311. doi:10.1016/j.cell.2011.03.034
154. Shin OH, Xu J, Rizo J, Sudhof TC (2009) Differential but convergent functions of Ca2+ binding to synaptotagmin-1 C2 domains mediate neurotransmitter release. Proc Natl Acad Sci USA 106:16469–16474. doi:0908798106 [pii] 10.1073/pnas.0908798106
155. Melicoff E et al (2009) Synaptotagmin-2 controls regulated exocytosis but not other secretory responses of mast cells. J Biol Chem 284:19445–19451. doi:M109.002550 [pii] 10.1074/jbc.M109.002550
156. Li Y et al (2007) Regulation of insulin secretion and GLUT4 trafficking by the calcium sensor synaptotagmin VII. Biochem Biophys Res Commun 362:658–664. doi:S0006-291X(07)01732-9 [pii] 10.1016/j.bbrc.2007.08.023
157. Gauthier BR et al (2008) Synaptotagmin VII splice variants alpha, beta, and delta are expressed in pancreatic beta-cells and regulate insulin exocytosis. FASEB J 22:194–206. doi:fj.07-8333com [pii] 10.1096/fj.07-8333com
158. Roux I et al (2006) Otoferlin, defective in a human deafness form, is essential for exocytosis at the auditory ribbon synapse. Cell 127:277–289. doi:S0092-8674(06)01218-9 [pii] 10.1016/j.cell.2006.08.040
159. Johnson CP, Chapman ER (2010) Otoferlin is a calcium sensor that directly regulates SNARE-mediated membrane fusion. J Cell Biol 191:187–197. doi:jcb.201002089 [pii] 10.1083/jcb.201002089
160. Davis DB, Doherty KR, Delmonte AJ, McNally EM (2002) Calcium-sensitive phospholipid binding properties of normal and mutant ferlin C2 domains. J Biol Chem 277:22883–22888. doi:10.1074/jbc.M201858200 M201858200 [pii]
161. Doherty KR et al (2005) Normal myoblast fusion requires myoferlin. Development 132:5565–5575. doi:dev.02155 [pii] 10.1242/dev.02155
162. Arribas M, Regazzi R, Garcia E, Wollheim CB, De Camilli P (1997) The stimulatory effect of rabphilin 3a on regulated exocytosis from insulin-secreting cells does not require an association-dissociation cycle with membranes mediated by Rab 3. Eur J Cell Biol 74:209–216
163. Biadene M, Montaville P, Sheldrick GM, Becker S (2006) Structure of the C2A domain of rabphilin-3A. Acta Crystallogr D Biol Crystallogr 62:793–799. doi:S0907444906017537 [pii] 10.1107/S0907444906017537
164. Fukuda M, Kanno E, Yamamoto A (2004) Rabphilin and Noc2 are recruited to dense-core vesicles through specific interaction with Rab27A in PC12 cells. J Biol Chem 279:13065–13075. doi:10.1074/jbc.M306812200 M306812200 [pii]
165. Deak F et al (2006) Rabphilin regulates SNARE-dependent re-priming of synaptic vesicles for fusion. EMBO J 25:2856–2866. doi:7601165 [pii] 10.1038/sj.emboj.7601165

166. Schluter OM, Schmitz F, Jahn R, Rosenmund C, Sudhof TC (2004) A complete genetic analysis of neuronal Rab3 function. J Neurosci 24:6629–6637. doi:10.1523/JNEUROSCI.1610-04.2004 24/29/6629 [pii]
167. Higashio H et al (2008) Doc2 alpha and Munc13-4 regulate Ca(2+) -dependent secretory lysosome exocytosis in mast cells. J Immunol 180:4774–4784. doi:180/7/4774 [pii]
168. Mochida S, Orita S, Sakaguchi G, Sasaki T, Takai Y (1998) Role of the Doc2 alpha-Munc13-1 interaction in the neurotransmitter release process. Proc Natl Acad Sci USA 95:11418–11422
169. Orita S et al (1996) Doc2 enhances Ca2+-dependent exocytosis from PC12 cells. J Biol Chem 271:7257–7260
170. Orita S, Sasaki T, Takai Y (2001) Doc2 alpha as modulator of Ca(2+)-dependent exocytosis. Methods Enzymol 329:83–90
171. Fukuda M, Mikoshiba K (2001) Synaptotagmin-like protein 1-3: a novel family of C-terminal-type tandem C2 proteins. Biochem Biophys Res Commun 281:1226–1233. doi:10.1006/bbrc.2001.4512 S0006-291X(01)94512-7 [pii]
172. Mueller AM et al (2008) Novel role for SLPI in MOG-induced EAE revealed by spinal cord expression analysis. J Neuroinflammation 5:20. doi:1742-2094-5-20 [pii] 10.1186/1742-2094-5-20
173. Holt O et al (2008) Slp1 and Slp2-a localize to the plasma membrane of CTL and contribute to secretion from the immunological synapse. Traffic 9:446–457. doi:TRA714 [pii] 10.1111/j.1600-0854.2008.00714.x
174. Kuroda TS, Fukuda M (2004) Rab27A-binding protein Slp2-a is required for peripheral melanosome distribution and elongated cell shape in melanocytes. Nat Cell Biol 6:1195–1203. doi:ncb1197 [pii] 10.1038/ncb1197
175. Yu M et al (2007) Exophilin4/Slp2-a targets glucagon granules to the plasma membrane through unique Ca2+-inhibitory phospholipid-binding activity of the C2A domain. Mol Biol Cell 18:688–696. doi:E06-10-0914 [pii] 10.1091/mbc.E06-10-0914
176. Fukuda M (2002) The C2A domain of synaptotagmin-like protein 3 (Slp3) is an atypical calcium-dependent phospholipid-binding machine: comparison with the C2A domain of synaptotagmin I. Biochem J 366:681–687. doi:10.1042/BJ20020484 BJ20020484 [pii]
177. Fukuda M (2003) Slp4-a/granuphilin-a inhibits dense-core vesicle exocytosis through interaction with the GDP-bound form of Rab27A in PC12 cells. J Biol Chem 278:15390–15396
178. Fukuda M, Kanno E, Saegusa C, Ogata Y, Kuroda TS (2002) Slp4-a/granuphilin-a regulates dense-core vesicle exocytosis in PC12 cells. J Biol Chem 277:39673–39678. doi:10.1074/jbc.M205349200 M205349200 [pii]
179. Tsuboi T, Fukuda M (2006) The Slp4-a linker domain controls exocytosis through interaction with Munc18-1.syntaxin-1a complex. Mol Biol Cell 17:2101–2112. doi:E05-11-1047 [pii] 10.1091/mbc.E05-11-1047
180. Kuroda TS, Fukuda M, Ariga H, Mikoshiba K (2002) Synaptotagmin-like protein 5: a novel Rab27A effector with C-terminal tandem C2 domains. Biochem Biophys Res Commun 293:899–906. doi:10.1016/S0006-291X(02)00320-0 S0006-291X(02)00320-0 [pii]
181. Augustin I, Rosenmund C, Sudhof TC, Brose N (1999) Munc13-1 is essential for fusion competence of glutamatergic synaptic vesicles. Nature 400:457–461. doi:10.1038/22768
182. Kwan EP, Xie L, Sheu L, Ohtsuka T, Gaisano HY (2007) Interaction between Munc13-1 and RIM is critical for glucagon-like peptide-1 mediated rescue of exocytotic defects in Munc13-1 deficient pancreatic beta-cells. Diabetes 56:2579–2588. doi:db06-1207 [pii] 10.2337/db06-1207
183. Orita S et al (1997) Physical and functional interactions of Doc2 and Munc13 in Ca2+-dependent exocytotic machinery. J Biol Chem 272:16081–16084
184. Nakayama T, Yaoi T, Kuwajima G (1999) Localization and subcellular distribution of N-copine in mouse brain. J Neurochem 72:373–379
185. Pang ZP, Cao P, Xu W, Sudhof TC (2010) Calmodulin controls synaptic strength via presynaptic activation of calmodulin kinase II. J Neurosci 30:4132–4142. doi:30/11/4132 [pii] 10.1523/JNEUROSCI.3129-09
186. Sugita S (2001) Synaptotagmin VII as a plasma membrane Ca(2+) sensor in exocytosis. Neuron 30:459–473. doi:S0896-6273(01)00290-2 [pii]

Chapter 33
Regulation of Voltage-Gated Calcium Channels by Synaptic Proteins

Norbert Weiss and Gerald W. Zamponi

Abstract Calcium entry through neuronal voltage-gated calcium channels into presynaptic nerve terminal is a key step in synaptic exocytosis. In order to receive the calcium signal and trigger fast, efficient and spatially delimited neurotransmitter release, the vesicle-docking/release machinery must be located near the calcium source. In many cases, this close localization is achieved by a direct interaction of several members of the vesicle release machinery with the calcium channels. In turn, the binding of synaptic proteins to presynaptic calcium channels modulates channel activity to provide fine control over calcium entry, and thus modulates synaptic strength. In this chapter we summarize our present knowledge of the molecular mechanisms by which synaptic proteins regulate presynaptic calcium channel activity.

Keywords Calcium channel • Cav2.1 channel • Cav2.2 channel • Cav2.3 channel • SNARE • Syntaxin • SNAP25 • Neuron • Exocytosis • Neurotransmitter • Synaptic transmission

General Overview

Depolarization-evoked neurotransmitter release relies on the Ca^{2+}-regulated release of quantal packets of neurotransmitters following the fusion of presynaptic vesicles with the plasma membrane [1]. It is well known that neuronal voltage-gated Ca^{2+} channels play a key role in the first steps of this process by supporting a transient Ca^{2+} microdomain of high (10–50 μM) concentration [2] within the active zone of the synapse that is essential for synaptic exocytosis [3–5]. To date, ten distinct voltage-gated Ca^{2+} channel isoforms have been described in mammals (not including

N. Weiss (✉) • G.W. Zamponi
Department of Physiology and Pharmacology, Hotchkiss Brain Institute, University of Calgary, 3330 Hospital Dr. NW, T2N 4N1, Calgary, AB, Canada
e-mail: norbert.weiss@yahoo.fr; zamponi@ucalgary.ca

M.S. Islam (ed.), *Calcium Signaling*, Advances in Experimental Medicine and Biology 740, DOI 10.1007/978-94-007-2888-2_33,

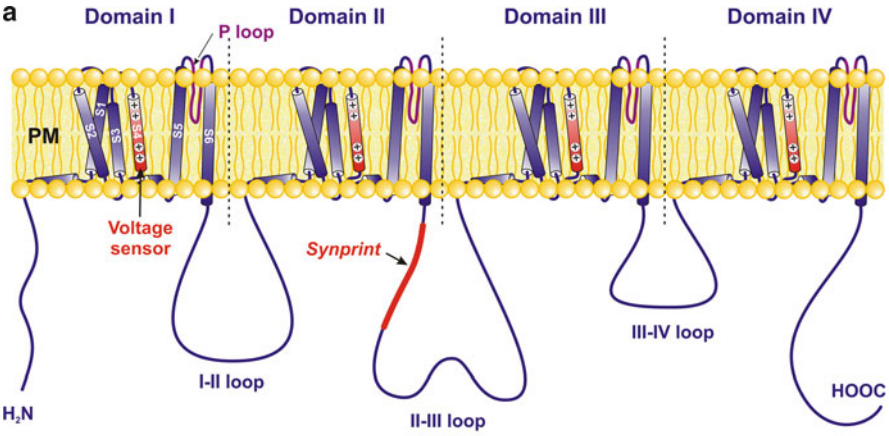

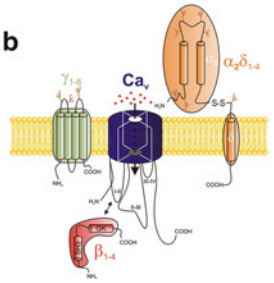

c

	Ca_v subunit	Curant	Localization
HVA	$Ca_v1.1$	L-type	Skeletal muscle
	$Ca_v1.2$		Cardiac muscle, smooth muscle, neuron, endocrine cell
	$Ca_v1.3$		Neuron, skeletal muscle, endocrine cell
	$Ca_v1.4$		Retina
	$Ca_v2.1$	P/Q-type	Neuron, β-pancreatic cell
	$Ca_v2.2$	N-type	Neuron
	$Ca_v2.3$	R-type	Neuron, endocrine cell
LVA	$Ca_v3.1$	T-type	Neuron, cardiac/smooth muscle, endocrine cell
	$Ca_v3.2$		Neuron, cardiac/smooth muscle, endocrine cell, liver
	$Ca_v3.3$		Neuron, spermatogenic cell

Fig. 33.1 Structural organization and diversity of voltage-gated calcium channels. Voltage-gated Ca^{2+} channels are composed of a Ca_v pore-forming α1 subunit, surrounded by auxiliary subunits (β, $\alpha_2\delta$ and in some cases γ) which modulate channel trafficking and gating. (**a**) Putative membrane topology of the Ca_v subunit according to the recent structure of a voltage-gated sodium channel [153]. It consists of four repeat homologous domains (I to IV), each composed of six transmembrane segments (S1 to S6). Whereas the S4 segments presumably constitute the voltage-sensor, the P loops between segments S5 and S6 form the divalent cation selectivity filter. Furthermore, the $Ca_v\alpha1$ subunit presents large intracellular loops linking the different transmembrane domains (loop I-II to III-IV) and two intracellular amino and carboxy terminal domains important for channel modulation. Specifically, binding of synaptic proteins to the $Ca_v\alpha1$ subunit occurs at the *syn*aptic *pro*tein *inte*raction site (*synprint*) located within the intracellular loop linking domains II and III (loop II-III). (**b**) Schematic representation of the voltage-gated Ca^{2+} channel macromolecular complex in association with the auxiliary subunits. (**c**) Overview of the diversity and localization of the various voltage-gated Ca^{2+} channels

splice variants) and first classified based on their voltage-dependence properties of activation into high voltage-activated (HVA) and low voltage-activated (LVA) channels, and then subdivided according to their pharmacological properties into specific subtypes [6]. Hence, the HVA family is comprised of the Ca_v1 channels ($Ca_v1.1$ through $Ca_v1.4$, all of which conduct L-type currents) and Ca_v2 channels ($Ca_v2.1$ through $Ca_v2.3$, which respectively conduct P/Q-, N- and R-type currents), whereas the LVA family is comprised of the Ca_v3 channels ($Ca_v3.1$ through $Ca_v3.3$ which conduct T-type currents) (diversity and structural organization of voltage-gated Ca^{2+} channels is presented in Fig. 33.1). Immunohistochemical characterization

of the subcellular distribution of the various voltage-gated Ca^{2+} channels [7–11] combined with pharmacological studies using selective Ca^{2+} channel antagonists [12–14] have identified $Ca_v2.1$ and $Ca_v2.2$ channels as the predominant Ca^{2+} channels involved in synaptic transmission. Whereas $Ca_v2.1$ channels play the major role at excitatory synapses of the central nervous system, $Ca_v2.2$ channels are mainly involved at the peripheral synapses, and in some inhibitory synapses where they work together with $Ca_v2.1$ channels to cause the release of GABA [15]. Immunohistochemical studies have also revealed a presynaptic localization of $Ca_v2.3$ channels in central neurons [11, 16] where they contribute in some extent to the Ca^{2+} influx into presynaptic terminals [17, 18] to mediate neurotransmitter release [19–21]. However, $Ca_v2.3$ channels trigger neurotransmission less efficiently than $Ca_v2.1$ channels, possibly because of the distant localization of these channels from the release sites [22, 23]. Moreover, the presynaptic localization of $Ca_v2.3$ channels exhibits developmental changes (e.g. in the calyx of Held $Ca_v2.3$ channels are replaced by $Ca_v2.1$ channels during postnatal development [24, 25]), suggesting that $Ca_v2.3$ channels may contribute to synaptic transmission predominantly in immature terminals. Finally, although a specific synaptic distribution has not yet been established, there is increasing evidence that low voltage-activated Ca_v3 channels can trigger fast and low-threshold exocytosis [26–29].

Considering the limited diffusion of free Ca^{2+} ions due to the high Ca^{2+} buffering capacity of neurons [30], the vesicle-docking/release machinery must be located near the source of Ca^{2+} in order to efficiently receive the Ca^{2+} signal. In mammalian synapses, this close association is mainly achieved by direct interaction of the Ca^{2+} channels with several member of the vesicle release machinery which is essential for fast (within 200 μs after the arrival of the action potential) and spatially delimited neurotransmitter release [31, 32]. In turn, the vesicle release machinery modulates Ca^{2+} channel activity to fine tune Ca^{2+} entry and thus modulating synaptic strength. Although it is beyond the scope of this review, interested readers may refer to the works of Atlas et al., for a discussion of other possible role of biochemical coupling of voltage-gated Ca^{2+} channels and synaptic proteins [33–40].

Interaction of Voltage-Gated Ca^{2+} Channels with SNARE Proteins

SNARE proteins (soluble NSF (*N*-ethylmaleimide-sensitive fusion protein) attachment protein receptor) are a key component of the vesicle release machinery [41, 42]. They encompass a family of proteins essential for membrane fusion and are classified according to the crystal structure of the heterotrimeric synaptic fusion complex into Q-SNAREs and R-SNAREs based on the amino-acids (glutamine (Q) or arginine (R)) involved in the formation of the macromolecular SNARE protein complex [43, 44]. The neuronal Q-SNARE family is comprised of syntaxin-1 (syntaxin-1A and -1B isoforms) and SNAP-25 (synaptosomal-associated protein of 25 kDa), and the R-SNARE family includes synaptobrevin-2. Consistent with their key implication in synaptic transmission, $Ca_v2.1$ and $Ca_v2.2$ channels colocalize with syntaxin-1A

at the presynaptic nerves terminal [7, 8, 45] and can be isolated in a complex with SNARE proteins [46–48]. This interaction relies to the specific binding of syntaxin-1A and SNAP-25 (but not synaptobrevin-2) to a *syn*aptic *pr*otein *in*teraction site (*synprint*) located within the intracellular loop between domains II and III of the $Ca_v2.1$ [49] and $Ca_v2.2$ [50] channels. Biochemical studies have mapped two separate microdomains separate by a flexible linker within the *synprint* site that each binds independently syntaxin-1A and SNAP-25 [49, 51]. Hence, disruption of the Ca^{2+} channel-SNARE coupling by peptides derived from the *synprint* domain, or by direct deletion of the *synprint* site, alters synaptic transmission [52–55].

Modulation of Voltage-Gated Ca^{2+} Channels by SNARE Proteins

Besides linking the vesicle release machinery to presynaptic voltage-gated Ca^{2+} channels, SNARE proteins also modulate channel gating, thus fine tuning the amount of Ca^{2+} that enters the synaptic terminal.

Modulation by Syntaxin-1

Electrophysiological studies using heterologous expression systems have shown that binding of syntaxin-1A to $Ca_v2.1$ or $Ca_v2.2$ channels reduces channel availability by shifting the voltage-dependence of inactivation toward more hyperpolarized membrane potentials [56–59], thus reducing Ca^{2+} entry into synaptic terminals. Additional evidence of a syntaxin-1A-dependent inhibition of voltage-gated Ca^{2+} channels comes from recordings on chick ciliary ganglion neurons and isolated mammalian nerve terminals (synaptosomes) where application of the botulinium neurotoxin C1 (which cleaves syntaxin-1A from its membrane anchoring domain) shifts the voltage-dependence of inactivation of the channel toward depolarized potentials, [60, 61]. Although it remains unclear how syntaxin-1A modulates channel gating, the transmembrane region of syntaxin-1A and a short region within the H3 helical cytoplasmic domain are critical for channel modulation but not for the biochemical association with the *synprint* site [62, 63]. Structure-function studies have identified two cysteines (C271 and C272) in the transmembrane domain of syntaxin-1A (and absent in syntaxin-2 which is unable to inhibit Ca^{2+} channel) as critical for channel modulation [64]. A recent study also identified the 10 amino-terminal residues of syntaxin-1A as being involved in the binding to the synprint site of Cav2.2 and as potentially important for syntaxin-1A mediated inhibition of the channel [65]. These results indicate that syntaxin-1A is engaged in two different kinds of interactions, an anchoring interaction via the *synprint* site and a modulatory interaction possibly involving additional yet unknown channel molecular determinants. In addition, syntaxin-1A exists in *open* and *closed* conformational states, with different abilities to modulate Ca^{2+} channel gating. In isolation or when interacting with munc18, syntaxin-1A adopts a *closed* conformation, whereas an *open*

conformation is preferentially adopted upon binding of SNAP-25 or synaptobrevin-2 [66, 67]. While coexpression of *closed* syntaxin-1A with $Ca_v2.2$ channels strongly modulates channel gating, coexpression of an *open* syntaxin-1A (permanently locked by introducing two point mutations [66]) has no significant effect [63]. Given that syntaxin-1A undergoes a conformational switch from a *closed* to an *open* conformation during the vesicle release cycle [66, 68, 69], this suggests that syntaxin-1A may be able to dynamically regulate Ca^{2+} channel availability during various stages of exocytosis. Interestingly, a familial hemiplegic migraine mutation (A454T) located in the intracellular loop between domains I and II of the $Ca_v2.1$ channel prevents syntaxin-1A modulation and exocytosis [70], suggesting that the I-II loop could play an important role in mediating syntaxin-1A modulation of channel gating. Although $Ca_v2.3$ channels lack a *synprint* site, several reports indicate that a similar functional regulation must occur. Hence, coexpression of syntaxin-1A with $Ca_v2.3$ channels decreases Ca^{2+} current amplitude [71, 72] whereas treatment of synaptosomes with the botulinium neurotoxin C1 promotes Ca^{2+} entry through $Ca_v2.3$ channels [61], suggesting a functional regulation that occurs independently of a direct binding of syntaxin-1A on the conventional *synprint* site.

Modulation by SNAP-25

Like syntaxin-1A, when coexpressed with $Ca_v2.1$ or $Ca_v2.2$ channels SNAP-25 decreases channel availability by shifting the voltage-dependence of inactivation toward more hyperpolarized membrane potentials [57, 58]. SNAP-25-dependent inhibitory activity of Ca^{2+} channels was recently confirmed in glutamatergic neurons where silencing of SNAP-25 leads to an increase of Ca^{2+} currents carried by $Ca_v2.1$ channels due to a depolarizing shift of the voltage-dependence of inactivation [73, 74]. Interestingly, in expression systemsSNAP-25 prevents syntaxin-1A-dependent inhibition of $Ca_v2.1$ and $Ca_v2.2$ channels [57, 58, 75], suggesting that formation of a stable syntaxin-1A-SNAP-25 complex during the vesicle release cycle may favor Ca^{2+} influx into nerve terminal, thus increasing the release probability of docked vesicles [76]. Interestingly, recent genetic studies revealed that mutations in the gene encoding SNAP-25 which alter the structure or expression of the protein lead to various neuropsychiatric and neurological disorders, possibly by altering SNAP-25-dependent regulation of presynaptic voltage-gated Ca^{2+} channels [77].

Modulation of Calcium Channels by Non SNARE Proteins

Modulation by Synaptotagmin-1

The vesicle-associated synaptotagmin-1 is not as critical as syntaxin-1A or SNAP-25 for synaptic exocytosis [78], but several studies have proposed that synaptotagmin-1 may be the Ca^{2+} sensor for fast and synchronous neurotransmitter release,

linking Ca^{2+} influx to vesicle fusion [78–85]. Synaptotagmin-1 has two rich negatively charged domains (C2A and C2B), each capable of binding Ca^{2+}. Whereas Ca^{2+} binding on the C2A domain allows insertion of synaptotagmin-1 into the plasma membrane [83], the C2B domain binds to the *synprint* site of $Ca_v2.1$ and $Ca_v2.2$ channels [86]. Although the binding of synaptotagmin-1 has no major influence on channel gating, it reduces syntaxin-1A-dependent inhibition of $Ca_v2.2$ channels [87, 88]. Reversal of syntaxin-1A inhibition by synaptotagmin-1 may be due to competition for the *synprint* site in a Ca^{2+}-dependent manner [89]. Hence, at low Ca^{2+} levels, syntaxin-1A preferentially binds to the *synprint* site whereas increasing Ca^{2+} concentration favor its interaction with synaptotagmin-1. This Ca^{2+}-dependent switch may provide an important regulatory mechanism of synaptic activity, such that at low Ca^{2+} concentration syntaxin-1A prevents channel activity, whereas at higher Ca^{2+} concentration when vesicles are docked to the plasma membrane this inhibition is relieved thus allowing Ca^{2+} influx for final steps of vesicle release. Moreover, it was also shown that synaptotagmin-1 can directly interact with the $Ca_v\beta_{4a}$ auxiliary-subunit of voltage-gated Ca^{2+} channels in a Ca^{2+} dependent manner (this interaction being more effective at low Ca^{2+} concentrations) [90] suggesting that interaction of synaptotagmin-1 with the $Ca_v\beta$ could create another dynamic interaction linking voltage-gated Ca^{2+} channels to the vesicle release machinery [91].

Modulation by Cysteine String Proteins (CSP)

Cysteine String Proteins (CSP) are vesicle-associated protein with a key chaperone role at the synapse [92]. It was proposed that CSP may serve as a link between $Ca_v2.2$ channels and presynaptic vesicles [93]. Indeed, CSP interacts with the *synprint* motif of $Ca_v2.1$ [94–96] and $Ca_v2.2$ channels [96]. Moreover, it was shown that CSP promotes presynaptic Ca^{2+} influx by recruiting dormant Ca^{2+} channels [97]. Considering that CSP interacts with syntaxin-1A [98, 99], it is tempting to propose that CSP-dependent increases in presynaptic Ca^{2+} current are due to its competition with syntaxin-1A for binding to the channel. Like synaptotagmin-1, CSP may act as a molecular switch in channel activity between undocked and docked vesicles release, thus timely controlling Ca^{2+} influx.

Modulation by Munc-18

Munc-18 plays a critical role in the assembly/disassembly of the exocytotic machinery [100, 101] and knockout of the protein in mouse leads to a complete loss of synaptic transmission [102]. Munc-18 directly interacts with the intracellular loop between domains II and III of the $Ca_v2.2$ channel [103], but coexpression of munc-18

with $Ca_v2.2$ channels has no influence on channel gating [104], indicating the munc-18 by itself is not a direct modulator of channel activity. However, as previously mentioned, munc-18 plays a critical role in the conformational switch of syntaxin-1A during the vesicle release cycle [66, 67]. Hence, in interaction with munc-18, syntaxin-1A adopts a *closed* conformation, incompatible with an interaction with the proteins of the vesicle core complex but highly favorable for Ca^{2+} channel inhibition [63]. In contrast, an *open* conformation of syntaxin-1A, favorable for an interaction with SNAP-25 or synaptobrevin-2, is unable to bind munc-18 and incapable of modulating $Ca_v2.2$ channel activity [63]. Hence, munc-18 may play an important role in regulating Ca^{2+} influx into nerve terminals by stabilizing syntaxin-1A in a *closed* state to inhibit channel activity in the absence of docked vesicle.

Modulation by Rim-1

Rim (Rab-3 interacting molecule) is part of a family of vesicle-associated proteins whose members share C2 domains (C2A and C2B) at their C-termini. It forms a protein scaffold in presynaptic nerve terminals by interacting with numerous other protein components of the active zone and participates in the docking and fusion of secretory vesicles [105–110]. Rim proteins were found to be essential for short- and long-term synaptic plasticity by affecting the readily releasable pool of vesicles [108, 111–114]. Moreover, Rim proteins were found to be required for Ca^{2+} channel targeting to presynaptic active zones [113] and normal Ca^{2+}-triggering of exocytosis [115]. It was shown that Rim Binding Proteins directly interact with $Ca_v2.2$ channels (and possibly with $Ca_v2.1$ channels), suggesting a molecular link between voltage-gated Ca^{2+} channels and Rim proteins [116]. Whereas biochemical studies using synapstosome membranes failed to demonstrate the existence of a $Ca_v2.2$/Rim complex [117], *in vitro* studies indicate a direct interaction of Rim-1 with the *synprint* site of $Ca_v2.2$ channels [109] as well as with SNAP-25 and synaptotagmin-1 via the C2 domains in a Ca^{2+}-dependent manner. At low Ca^{2+} concentrations Rim-1 thus preferentially binds SNAP-25 whereas an increase in Ca^{2+} concentration (>75 μM) favors its interaction with synaptotagmin-1 [109]. Moreover, Rim-1 also interacts with the β-subunit of voltage-gated Ca^{2+} channels, slowing $Ca_v2.1$, $Ca_v2.2$ and $Ca_v2.3$ channel inactivation when coexpressed in heterologous systems, thereby increasing Ca^{2+} influx during trains of action potentials [118]. A mutation in Rim-1 (R655H) associated with an autosomal dominant cone-rod dystrophy was found to alter Rim-1-mediated regulation of $Ca_v2.1$ channels [119] and shown to lead to a progressive loss of photoreceptors along with retinal degeneration [120, 121]. This then suggests that Rim-1-dependent regulation of Ca^{2+} channel activity may be critical for normal Ca^{2+} homeostasis at the nerve terminals. However, it remains unknown if binding of Rim-1 to SNAP-25 or synaptotagmin-1 affects Rim-1-dependent or syntaxin-1A-dependent regulation of Ca^{2+} channel activity.

Crosstalk Between SNARE Modulation and Other Signaling Pathways

G-Protein Regulation

Presynaptic voltage-gated Ca^{2+} channels are also regulated by second messenger pathways which add to the direct regulation by the vesicle release machinery [122]. The release of neurotransmitters initiates a feedback regulation of voltage-gated Ca^{2+} channel activity mediated by activation of specific G-protein coupled receptors that inhibits Ca^{2+} influx and hence terminates neurotransmitter release [123]. This spatially delimited regulation [124] relies on the direct binding of free G-protein βγ dimers [125, 126] to specific cytoplasmic regions of the channel [127–130]. Based on the observation that cleavage of syntaxin-1A by the botulinium neurotoxin C1 in chick calyx synapses prevents G-protein-dependent inhibition of Ca^{2+} currents, it was initially proposed that syntaxin-1A is required for G-protein regulation of presynaptic voltage-gated Ca^{2+} channels [131, 132]. Further studies have then revealed that syntaxin-1A is not critical but facilitates G-protein regulation of $Ca_v2.2$ channels by interacting with G-protein βγ dimers [75, 133, 134] while binding of CSP to Gβγ potentiates tonic G-protein inhibition of $Ca_v2.2$ channels [96]. Besides interacting with syntaxin-1A, Gβγ also interacts with SNAP-25 and it was proposed that binding of Gβγ to the carboxy-terminal domain of SNAP-25 mediates presynaptic inhibition [135]. Furthermore, Gβγ and synaptotagmin-1 compete for binding to the core SNARE complex in a Ca^{2+}-dependent manner such that at high Ca^{2+} concentration synaptotagmin-1 can displace Gβγ binding [136]. Hence, an increase in presynaptic Ca^{2+} concentrations may prevent Gβγ-dependent inhibition of exocytosis perhaps by Ca^{2+}-dependent competition between Gβγ and synaptotagmin-1 for SNARE binding [136]. Finally, it was recently reported that Rim-1 prevents direct G-protein inhibition of $Ca_v2.2$ channels [137]. These results clearly highlight an interplay between direct G-protein signaling pathway and the proteins of the exocytotic machinery, providing a second level of complexity in the regulation of presynaptic voltage-gated Ca^{2+} channels.

Phosphorylation

Biochemical studies have evidenced that the protein kinase C (PKC) and the Ca^{2+}-calmodulin-dependent kinase II (CaM-KII) phosphorylate the *synprint* site of $Ca_v2.2$ channels [51, 138]. Interestingly, phosphorylation of the *synprint* peptide by PKC or CaM-KII strongly inhibits binding of recombinant syntaxin-1A and SNAP-25 [138]. Hence, PKC phosphorylation of $Ca_v2.2$ channels antagonizes the syntaxin-1-mediated hyperpolarized shift in the voltage dependence of inactivation of the channel [75]. In contrast, phosphorylation of syntaxin-1A and SNAP-25 by

PKC or CaM-KII does not alter interaction with the *synprint* site [138], indicating that phosphorylation-dependent modulation of SNARE protein interaction with $Ca_v2.2$ channels is an intrinsic feature of the *synprint* site.

Hence, PKC- and CaM-KII-dependent phosphorylation of the *synprint* site may serve as a biochemical switch for interaction/modulation of voltage-gated Ca^{2+} channels with SNARE protein complexes. However, it was demonstrated that phosphorylation of SNAP-25 by PKC is required for SNAP-25-dependent inhibition of voltage-gated Ca^{2+} channels [139], suggesting that like syntaxin-1A, SNAP-25-dependent modulation of channel activity may involve molecular determinants other than the *synprint* site. Besides PKC and CaM-KII, it was also shown that phosphorylation of the *synprint* site of $Ca_v2.1$ channels by the glycogen synthase kinase-3 (GSK-3) prevents interaction of syntaxin-1A, SNAP-25 and synaptotagmin-1 with the channel and inhibits presynaptic vesicle exocytosis possibly by interfering with SNARE-dependent regulation of channel activity [140].

Huntingtin

Huntingtin, extensively studied for its key implication in Huntington's disease [141] has been found to interact directly with at least 20 proteins involved in various cellular functions such as transcription, transport or cell signaling. Interestingly, huntingtin also directly interacts with the *synprint* region of $Ca_v2.2$ channels via its amino-terminal domain [142]. Whereas coexpression of huntingtin with $Ca_v2.2$ channels has no effect on channel activity, it prevents syntaxin-1A-mediated inhibition of Ca^{2+} current [142], most likely by displacing syntaxin-1A binding from the channel [143]. Although it remains unclear if huntingtin is permanently present in the active zones of the synapse or if it could be targeted under particular physiological or pathological conditions, it may influence synaptic activity by modulating Ca^{2+} influx into presynaptic nerve terminals.

Concluding Remarks

Besides localizing the exocytosis machinery close to the Ca^{2+} source, interactions of presynaptic voltage-gated Ca^{2+} channels with various synaptic proteins provide an important regulatory feedback onto channel activity and thus neurotransmitter release. This regulation appears highly complex, with intricate interplay between different types of synaptic proteins and second messenger signaling pathways (Fig. 33.2). To further add to this complexity, Ca^{2+} entry through $Ca_v2.1$ channels induces Ca^{2+}-dependent gene transcription of synaptic proteins such as syntaxin-1A [144] providing another degree of regulation of synaptic activity. However, although much effort has been invested in studying the functional regulation of voltage-gated

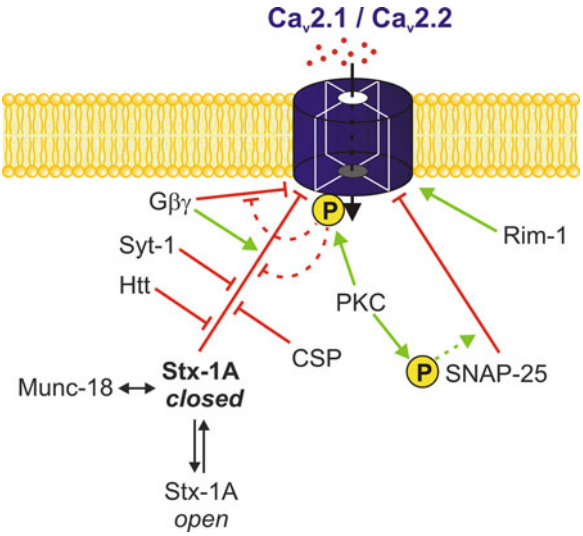

Fig. 33.2 Functional interactions between presynaptic voltage-gated Ca^{2+} channels, synaptic proteins and second messengers. Individually, syntaxin-1A (in its closed conformational state), SNAP-25 and Gβγ inhibit Ca^{2+} channels. Channel phosphorylation by PKC on different residues (including the *synprint* site) prevents syntaxin-1A and Gβγ-dependent inhibition, while phosphorylation of SNAP-25 favors its inhibitory effect. Furthermore, synaptotagmin-1, CSP and huntingtin prevent syntaxin-1A-dependent inhibition of the channel while Rim-1 potentiates Ca^{2+} influx. Abbreviations: *Stx1A* syntaxin-1A, *Syt-1* synaptotagmin-1, *Rim-1* Rab-3 interacting molecule-1, *CSP* Cysteine String Proteins, *Htt* huntingtin, *PKC* protein kinase C. *Arrow* in *red* indicates an inhibitory regulation whereas *arrow* in *green* indicates a potentiation

Ca^{2+} channels by synaptic proteins, an integrated view of the structural organization and dynamic regulation still remains to be established. Moreover, the molecular mechanisms involved in the regulation of voltage-gated Ca^{2+} channels by synaptic proteins remain largely to be explored. Previous studies have demonstrated the existence of various intramolecular interactions within the intracellular loops of the Ca_v2 channels, and that these interactions alter channel gating [145–152]. Considering that the functional regulation of voltage-gated Ca^{2+} channels by SNARE proteins likely involves modulatory channel determinants other than the anchoring *synprint* interaction site, channel remodeling upon SNARE protein interaction may represent an exciting concept by which synaptic proteins modulate Ca^{2+} channel activity.

Acknowledgments Norbert Weiss is supported by fellowships from Alberta Heritage Foundation for Medical Research (AHFMR) and from Hotchkiss Brain Institute. Gerald W. Zamponi is funded by the Canadian Institutes of Health Research, is a Canada Research Chair and Scientist of the Alberta Heritage Foundation for Medical Research.

References

1. Edwards RH (2007) The neurotransmitter cycle and quantal size. Neuron 55:835–858
2. Schneggenburger R, Neher E (2005) Presynaptic calcium and control of vesicle fusion. Curr Opin Neurobiol 15:266–274
3. Llinas R, Sugimori M, Silver RB (1992) Microdomains of high calcium concentration in a presynaptic terminal. Science 256:677–679
4. Neher E, Sakaba T (2008) Multiple roles of calcium ions in the regulation of neurotransmitter release. Neuron 59:861–872
5. Weber AM, Wong FK, Tufford AR, Schlichter LC, Matveev V, Stanley EF (2010) N-type Ca^{2+} channels carry the largest current: implications for nanodomains and transmitter release. Nat Neurosci 13:1348–1350
6. Ertel EA, Campbell KP, Harpold MM et al (2000) Nomenclature of voltage-gated calcium channels. Neuron 25:533–535
7. Westenbroek RE, Hell JW, Warner C, Dubel SJ, Snutch TP, Catterall WA (1992) Biochemical properties and subcellular distribution of an N-type calcium channel alpha 1 subunit. Neuron 9:1099–1115
8. Westenbroek RE, Sakurai T, Elliott EM et al (1995) Immunochemical identification and subcellular distribution of the alpha 1A subunits of brain calcium channels. J Neurosci 15:6403–6418
9. Westenbroek RE, Hoskins L, Catterall WA (1998) Localization of Ca^{2+} channel subtypes on rat spinal motor neurons, interneurons, and nerve terminals. J Neurosci 18:6319–6330
10. Timmermann DB, Westenbroek RE, Schousboe A, Catterall WA (2002) Distribution of high-voltage-activated calcium channels in cultured gamma-aminobutyric acidergic neurons from mouse cerebral cortex. J Neurosci Res 67:48–61
11. Day NC, Shaw PJ, McCormack AL et al (1996) Distribution of alpha 1A, alpha 1B and alpha 1E voltage-dependent calcium channel subunits in the human hippocampus and parahippocampal gyrus. Neuroscience 71:1013–1024
12. Wheeler DB, Randall A, Tsien RW (1994) Roles of N-type and Q-type Ca^{2+} channels in supporting hippocampal synaptic transmission. Science 264:107–111
13. Olivera BM, Miljanich GP, Ramachandran J, Adams ME (1994) Calcium channel diversity and neurotransmitter release: the omega-conotoxins and omega-agatoxins. Annu Rev Biochem 63:823–867
14. Dunlap K, Luebke JI, Turner TJ (1995) Exocytotic Ca^{2+} channels in mammalian central neurons. Trends Neurosci 18:89–98
15. Poncer JC, McKinney RA, Gahwiler BH, Thompson SM (1997) Either N- or P-type calcium channels mediate GABA release at distinct hippocampal inhibitory synapses. Neuron 18:463–472
16. Hanson JE, Smith Y (2002) Subcellular distribution of high-voltage-activated calcium channel subtypes in rat globus pallidus neurons. J Comp Neurol 442:89–98
17. Breustedt J, Vogt KE, Miller RJ, Nicoll RA, Schmitz D (2003) Alpha1E-containing Ca^{2+} channels are involved in synaptic plasticity. Proc Natl Acad Sci USA 100:12450–12455
18. Dietrich D, Kirschstein T, Kukley M et al (2003) Functional specialization of presynaptic Cav2.3 Ca^{2+} channels. Neuron 39:483–496
19. Wu LG, Borst JG, Sakmann B (1998) R-type Ca^{2+} currents evoke transmitter release at a rat central synapse. Proc Natl Acad Sci USA 95:4720–4725
20. Kamp MA, Krieger A, Henry M, Hescheler J, Weiergraber M, Schneider T (2005) Presynaptic 'Ca2.3-containing' E-type Ca channels share dual roles during neurotransmitter release. Eur J Neurosci 21:1617–1625
21. Gasparini S, Kasyanov AM, Pietrobon D, Voronin LL, Cherubini E (2001) Presynaptic R-type calcium channels contribute to fast excitatory synaptic transmission in the rat hippocampus. J Neurosci 21:8715–8721

22. Wu LG, Westenbroek RE, Borst JG, Catterall WA, Sakmann B (1999) Calcium channel types with distinct presynaptic localization couple differentially to transmitter release in single calyx-type synapses. J Neurosci 19:726–736
23. Brenowitz SD, Regehr WG (2003) "Resistant" channels reluctantly reveal their roles. Neuron 39:391–394
24. Iwasaki S, Momiyama A, Uchitel OD, Takahashi T (2000) Developmental changes in calcium channel types mediating central synaptic transmission. J Neurosci 20:59–65
25. Iwasaki S, Takahashi T (1998) Developmental changes in calcium channel types mediating synaptic transmission in rat auditory brainstem. J Physiol 509(Pt 2):419–423
26. Carabelli V, Marcantoni A, Comunanza V et al (2007) Chronic hypoxia up-regulates alpha1H T-type channels and low-threshold catecholamine secretion in rat chromaffin cells. J Physiol 584:149–165
27. Ivanov AI, Calabrese RL (2000) Intracellular Ca^{2+} dynamics during spontaneous and evoked activity of leech heart interneurons: low-threshold Ca currents and graded synaptic transmission. J Neurosci 20:4930–4943
28. Pan ZH, Hu HJ, Perring P, Andrade R (2001) T-type Ca(2+) channels mediate neurotransmitter release in retinal bipolar cells. Neuron 32:89–98
29. Egger V, Svoboda K, Mainen ZF (2003) Mechanisms of lateral inhibition in the olfactory bulb: efficiency and modulation of spike-evoked calcium influx into granule cells. J Neurosci 23:7551–7558
30. Foehring RC, Zhang XF, Lee JC, Callaway JC (2009) Endogenous calcium buffering capacity of substantia nigral dopamine neurons. J Neurophysiol 102:2326–2333
31. Wadel K, Neher E, Sakaba T (2007) The coupling between synaptic vesicles and Ca^{2+} channels determines fast neurotransmitter release. Neuron 53:563–575
32. Sabatini BL, Regehr WG (1996) Timing of neurotransmission at fast synapses in the mammalian brain. Nature 384:170–172
33. Atlas D, Wiser O, Trus M (2001) The voltage-gated Ca^{2+} channel is the Ca^{2+} sensor of fast neurotransmitter release. Cell Mol Neurobiol 21:717–731
34. Lerner I, Trus M, Cohen R, Yizhar O, Nussinovitch I, Atlas D (2006) Ion interaction at the pore of Lc-type Ca^{2+} channel is sufficient to mediate depolarization-induced exocytosis. J Neurochem 97:116–127
35. Marom M, Sebag A, Atlas D (2007) Cations residing at the selectivity filter of the voltage-gated Ca2+−channel modify fusion-pore kinetics. Channels (Austin) 1:377–386
36. Hagalili Y, Bachnoff N, Atlas D (2008) The voltage-gated Ca(2+) channel is the Ca(2+) sensor protein of secretion. Biochemistry 47:13822–13830
37. Cohen-Kutner M, Nachmanni D, Atlas D (2010) CaV2.1 (P/Q channel) interaction with synaptic proteins is essential for depolarization-evoked release. Channels (Austin) 4:266–277
38. Atlas D (2010) Signaling role of the voltage-gated calcium channel as the molecular on/off-switch of secretion. Cell Signal 22:1597–1603
39. Marom M, Hagalili Y, Sebag A, Tzvier L, Atlas D (2010) Conformational changes induced in voltage-gated calcium channel Cav1.2 by BayK 8644 or FPL64176 modify the kinetics of secretion independently of Ca^{2+} influx. J Biol Chem 285:6996–7005
40. Weiss N (2010) Control of depolarization-evoked presynaptic neurotransmitter release by Cav2.1 calcium channel: old story, new insights. Channels (Austin) 4:431–433
41. Hanson PI, Heuser JE, Jahn R (1997) Neurotransmitter release - four years of SNARE complexes. Curr Opin Neurobiol 7:310–315
42. Otto H, Hanson PI, Jahn R (1997) Assembly and disassembly of a ternary complex of synaptobrevin, syntaxin, and SNAP-25 in the membrane of synaptic vesicles. Proc Natl Acad Sci USA 94:6197–6201
43. Fasshauer D, Sutton RB, Brunger AT, Jahn R (1998) Conserved structural features of the synaptic fusion complex: SNARE proteins reclassified as Q- and R-SNAREs. Proc Natl Acad Sci USA 95:15781–15786
44. Sutton RB, Fasshauer D, Jahn R, Brunger AT (1998) Crystal structure of a SNARE complex involved in synaptic exocytosis at 2.4 A resolution. Nature 395:347–353

45. Cohen MW, Jones OT, Angelides KJ (1991) Distribution of Ca^{2+} channels on frog motor nerve terminals revealed by fluorescent omega-conotoxin. J Neurosci 11:1032–1039
46. Bennett MK, Calakos N, Scheller RH (1992) Syntaxin: a synaptic protein implicated in docking of synaptic vesicles at presynaptic active zones. Science 257:255–259
47. Leveque C, el Far O, Martin-Moutot N et al (1994) Purification of the N-type calcium channel associated with syntaxin and synaptotagmin. A complex implicated in synaptic vesicle exocytosis. J Biol Chem 269:6306–6312
48. Yoshida A, Oho C, Omori A, Kuwahara R, Ito T, Takahashi M (1992) HPC-1 is associated with synaptotagmin and omega-conotoxin receptor. J Biol Chem 267:24925–24928
49. Rettig J, Sheng ZH, Kim DK, Hodson CD, Snutch TP, Catterall WA (1996) Isoform-specific interaction of the alpha1A subunits of brain Ca^{2+} channels with the presynaptic proteins syntaxin and SNAP-25. Proc Natl Acad Sci USA 93:7363–7368
50. Sheng ZH, Rettig J, Takahashi M, Catterall WA (1994) Identification of a syntaxin-binding site on N-type calcium channels. Neuron 13:1303–1313
51. Yokoyama CT, Myers SJ, Fu J, Mockus SM, Scheuer T, Catterall WA (2005) Mechanism of SNARE protein binding and regulation of Cav2 channels by phosphorylation of the synaptic protein interaction site. Mol Cell Neurosci 28:1–17
52. Mochida S, Sheng ZH, Baker C, Kobayashi H, Catterall WA (1996) Inhibition of neurotransmission by peptides containing the synaptic protein interaction site of N-type Ca^{2+} channels. Neuron 17:781–788
53. Rettig J, Heinemann C, Ashery U et al (1997) Alteration of Ca^{2+} dependence of neurotransmitter release by disruption of Ca^{2+} channel/syntaxin interaction. J Neurosci 17:6647–6656
54. Harkins AB, Cahill AL, Powers JF, Tischler AS, Fox AP (2004) Deletion of the synaptic protein interaction site of the N-type (CaV2.2) calcium channel inhibits secretion in mouse pheochromocytoma cells. Proc Natl Acad Sci USA 101:15219–15224
55. Keith RK, Poage RE, Yokoyama CT, Catterall WA, Meriney SD (2007) Bidirectional modulation of transmitter release by calcium channel/syntaxin interactions in vivo. J Neurosci 27:265–269
56. Bezprozvanny I, Scheller RH, Tsien RW (1995) Functional impact of syntaxin on gating of N-type and Q-type calcium channels. Nature 378:623–626
57. Wiser O, Bennett MK, Atlas D (1996) Functional interaction of syntaxin and SNAP-25 with voltage-sensitive L- and N-type Ca^{2+} channels. EMBO J 15:4100–4110
58. Zhong H, Yokoyama CT, Scheuer T, Catterall WA (1999) Reciprocal regulation of P/Q-type Ca^{2+} channels by SNAP-25, syntaxin and synaptotagmin. Nat Neurosci 2:939–941
59. Degtiar VE, Scheller RH, Tsien RW (2000) Syntaxin modulation of slow inactivation of N-type calcium channels. J Neurosci 20:4355–4367
60. Stanley EF (2003) Syntaxin I modulation of presynaptic calcium channel inactivation revealed by botulinum toxin C1. Eur J Neurosci 17:1303–1305
61. Bergsman JB, Tsien RW (2000) Syntaxin modulation of calcium channels in cortical synaptosomes as revealed by botulinum toxin C1. J Neurosci 20:4368–4378
62. Bezprozvanny I, Zhong P, Scheller RH, Tsien RW (2000) Molecular determinants of the functional interaction between syntaxin and N-type Ca^{2+} channel gating. Proc Natl Acad Sci USA 97:13943–13948
63. Jarvis SE, Barr W, Feng ZP, Hamid J, Zamponi GW (2002) Molecular determinants of syntaxin 1 modulation of N-type calcium channels. J Biol Chem 277:44399–44407
64. Trus M, Wiser O, Goodnough MC, Atlas D (2001) The transmembrane domain of syntaxin 1A negatively regulates voltage-sensitive Ca(2+) channels. Neuroscience 104:599–607
65. Davies JN, Jarvis SE, Zamponi GW (2011) Bipartite syntaxin 1A interactions mediate Ca(V)2.2 calcium channel regulation. Biochem Biophys Res Commun 411:562–568
66. Dulubova I, Sugita S, Hill S et al (1999) A conformational switch in syntaxin during exocytosis: role of munc18. EMBO J 18:4372–4382
67. Brunger AT (2001) Structure of proteins involved in synaptic vesicle fusion in neurons. Annu Rev Biophys Biomol Struct 30:157–171

68. Fiebig KM, Rice LM, Pollock E, Brunger AT (1999) Folding intermediates of SNARE complex assembly. Nat Struct Biol 6:117–123
69. Richmond JE, Weimer RM, Jorgensen EM (2001) An open form of syntaxin bypasses the requirement for UNC-13 in vesicle priming. Nature 412:338–341
70. Serra SA, Cuenca-Leon E, Llobet A et al (2010) A mutation in the first intracellular loop of CACNA1A prevents P/Q channel modulation by SNARE proteins and lowers exocytosis. Proc Natl Acad Sci USA 107:1672–1677
71. Wiser O, Cohen R, Atlas D (2002) Ionic dependence of Ca^{2+} channel modulation by syntaxin 1A. Proc Natl Acad Sci USA 99:3968–3973
72. Cohen R, Atlas D (2004) R-type voltage-gated Ca(2+) channel interacts with synaptic proteins and recruits synaptotagmin to the plasma membrane of Xenopus oocytes. Neuroscience 128:831–841
73. Condliffe SB, Corradini I, Pozzi D, Verderio C, Matteoli M (2010) Endogenous SNAP-25 regulates native voltage-gated calcium channels in glutamatergic neurons. J Biol Chem 285:24968–24976
74. Condliffe SB, Matteoli M (2011) Inactivation kinetics of voltage-gated calcium channels in glutamatergic neurons are influenced by SNAP-25. Channels (Austin) 5:304–307
75. Jarvis SE, Zamponi GW (2001) Distinct molecular determinants govern syntaxin 1A-mediated inactivation and G-protein inhibition of N-type calcium channels. J Neurosci 21:2939–2948
76. Sudhof TC (2004) The synaptic vesicle cycle. Annu Rev Neurosci 27:509–547
77. Corradini I, Verderio C, Sala M, Wilson MC, Matteoli M (2009) SNAP-25 in neuropsychiatric disorders. Ann N Y Acad Sci 1152:93–99
78. Tucker WC, Chapman ER (2002) Role of synaptotagmin in Ca2+−triggered exocytosis. Biochem J 366:1–13
79. Koh TW, Bellen HJ (2003) Synaptotagmin I, a Ca^{2+} sensor for neurotransmitter release. Trends Neurosci 26:413–422
80. DeBello WM, Betz H, Augustine GJ (1993) Synaptotagmin and neurotransmitter release. Cell 74:947–950
81. Nishiki TI, Augustine GJ (2001) Calcium-dependent neurotransmitter release: synaptotagmin to the rescue. J Comp Neurol 436:1–3
82. Augustine GJ (2001) How does calcium trigger neurotransmitter release? Curr Opin Neurobiol 11:320–326
83. Fernandez-Chacon R, Konigstorfer A, Gerber SH et al (2001) Synaptotagmin I functions as a calcium regulator of release probability. Nature 410:41–49
84. Geppert M, Goda Y, Hammer RE et al (1994) Synaptotagmin I: a major Ca^{2+} sensor for transmitter release at a central synapse. Cell 79:717–727
85. Xu J, Mashimo T, Sudhof TC (2007) Synaptotagmin-1, -2, and −9: Ca(2+) sensors for fast release that specify distinct presynaptic properties in subsets of neurons. Neuron 54:567–581
86. Sheng ZH, Yokoyama CT, Catterall WA (1997) Interaction of the synprint site of N-type Ca^{2+} channels with the C2B domain of synaptotagmin I. Proc Natl Acad Sci USA 94:5405–5410
87. Wiser O, Tobi D, Trus M, Atlas D (1997) Synaptotagmin restores kinetic properties of a syntaxin-associated N-type voltage sensitive calcium channel. FEBS Lett 404:203–207
88. Atlas D (2001) Functional and physical coupling of voltage-sensitive calcium channels with exocytotic proteins: ramifications for the secretion mechanism. J Neurochem 77:972–985
89. Sheng ZH, Rettig J, Cook T, Catterall WA (1996) Calcium-dependent interaction of N-type calcium channels with the synaptic core complex. Nature 379:451–454
90. Vendel AC, Terry MD, Striegel AR et al (2006) Alternative splicing of the voltage-gated Ca^{2+} channel beta4 subunit creates a uniquely folded N-terminal protein binding domain with cell-specific expression in the cerebellar cortex. J Neurosci 26:2635–2644

91. Weiss N (2006) The calcium channel beta4a subunit: a scaffolding protein between voltage-gated calcium channel and presynaptic vesicle-release machinery? J Neurosci 26:6117–6118
92. Chamberlain LH, Burgoyne RD (2000) Cysteine-string protein: the chaperone at the synapse. J Neurochem 74:1781–1789
93. Mastrogiacomo A, Parsons SM, Zampighi GA, Jenden DJ, Umbach JA, Gundersen CB (1994) Cysteine string proteins: a potential link between synaptic vesicles and presynaptic Ca^{2+} channels. Science 263:981–982
94. Leveque C, Pupier S, Marqueze B et al (1998) Interaction of cysteine string proteins with the alpha1A subunit of the P/Q-type calcium channel. J Biol Chem 273:13488–13492
95. Seagar M, Leveque C, Charvin N et al (1999) Interactions between proteins implicated in exocytosis and voltage-gated calcium channels. Philos Trans R Soc Lond B Biol Sci 354:289–297
96. Magga JM, Jarvis SE, Arnot MI, Zamponi GW, Braun JE (2000) Cysteine string protein regulates G protein modulation of N-type calcium channels. Neuron 28:195–204
97. Chen S, Zheng X, Schulze KL, Morris T, Bellen H, Stanley EF (2002) Enhancement of presynaptic calcium current by cysteine string protein. J Physiol 538:383–389
98. Nie Z, Ranjan R, Wenniger JJ, Hong SN, Bronk P, Zinsmaier KE (1999) Overexpression of cysteine-string proteins in Drosophila reveals interactions with syntaxin. J Neurosci 19:10270–10279
99. Wu MN, Fergestad T, Lloyd TE, He Y, Broadie K, Bellen HJ (1999) Syntaxin 1A interacts with multiple exocytic proteins to regulate neurotransmitter release in vivo. Neuron 23:593–605
100. Toonen RF, Verhage M (2007) Munc18-1 in secretion: lonely Munc joins SNARE team and takes control. Trends Neurosci 30:564–572
101. Gulyas-Kovacs A, de Wit H, Milosevic I et al (2007) Munc18-1: sequential interactions with the fusion machinery stimulate vesicle docking and priming. J Neurosci 27:8676–8686
102. Verhage M, Maia AS, Plomp JJ et al (2000) Synaptic assembly of the brain in the absence of neurotransmitter secretion. Science 287:864–869
103. Chan AW, Khanna R, Li Q, Stanley EF (2007) Munc18: a presynaptic transmitter release site N type (CaV2.2) calcium channel interacting protein. Channels (Austin) 1:11–20
104. Gladycheva SE, Ho CS, Lee YY, Stuenkel EL (2004) Regulation of syntaxin1A-munc18 complex for SNARE pairing in HEK293 cells. J Physiol 558:857–871
105. Wang Y, Sugita S, Sudhof TC (2000) The RIM/NIM family of neuronal C2 domain proteins. Interactions with Rab3 and a new class of Src homology 3 domain proteins. J Biol Chem 275:20033–20044
106. Betz A, Thakur P, Junge HJ et al (2001) Functional interaction of the active zone proteins Munc13-1 and RIM1 in synaptic vesicle priming. Neuron 30:183–196
107. Ohtsuka T, Takao-Rikitsu E, Inoue E et al (2002) Cast: a novel protein of the cytomatrix at the active zone of synapses that forms a ternary complex with RIM1 and munc13-1. J Cell Biol 158:577–590
108. Schoch S, Castillo PE, Jo T et al (2002) RIM1alpha forms a protein scaffold for regulating neurotransmitter release at the active zone. Nature 415:321–326
109. Coppola T, Magnin-Luthi S, Perret-Menoud V, Gattesco S, Schiavo G, Regazzi R (2001) Direct interaction of the Rab3 effector RIM with Ca^{2+} channels, SNAP-25, and synaptotagmin. J Biol Chem 276:32756–32762
110. Kaeser PS, Deng L, Wang Y et al (2011) RIM proteins tether Ca^{2+} channels to presynaptic active zones via a direct PDZ-domain interaction. Cell 144:282–295
111. Castillo PE, Schoch S, Schmitz F, Sudhof TC, Malenka RC (2002) RIM1alpha is required for presynaptic long-term potentiation. Nature 415:327–330
112. Blundell J, Kaeser PS, Sudhof TC, Powell CM (2010) RIM1alpha and interacting proteins involved in presynaptic plasticity mediate prepulse inhibition and additional behaviors linked to schizophrenia. J Neurosci 30:5326–5333
113. Han Y, Kaeser PS, Sudhof TC, Schneggenburger R (2011) RIM determines Ca(2)+channel density and vesicle docking at the presynaptic active zone. Neuron 69:304–316

114. Deng L, Kaeser PS, Xu W, Sudhof TC (2011) RIM proteins activate vesicle priming by reversing autoinhibitory homodimerization of Munc13. Neuron 69:317–331
115. Schoch S, Mittelstaedt T, Kaeser PS et al (2006) Redundant functions of RIM1alpha and RIM2alpha in Ca(2+)-triggered neurotransmitter release. EMBO J 25:5852–5863
116. Hibino H, Pironkova R, Onwumere O, Vologodskaia M, Hudspeth AJ, Lesage F (2002) RIM binding proteins (RBPs) couple Rab3-interacting molecules (RIMs) to voltage-gated Ca(2+) channels. Neuron 34:411–423
117. Wong FK, Stanley EF (2010) Rab3a interacting molecule (RIM) and the tethering of presynaptic transmitter release site-associated CaV2.2 calcium channels. J Neurochem 112:463–473
118. Kiyonaka S, Wakamori M, Miki T et al (2007) RIM1 cEonfers sustained activity and neurotransmitter vesicle anchoring to presynaptic Ca^{2+} channels. Nat Neurosci 10:691–701
119. Miki T, Kiyonaka S, Uriu Y et al (2007) Mutation associated with an autosomal dominant cone-rod dystrophy CORD7 modifies RIM1-mediated modulation of voltage-dependent Ca^{2+} channels. Channels (Austin) 1:144–147
120. Barragan I, Marcos I, Borrego S, Antinolo G (2005) Molecular analysis of RIM1 in autosomal recessive Retinitis pigmentosa. Ophthalmic Res 37:89–93
121. Michaelides M, Holder GE, Hunt DM, Fitzke FW, Bird AC, Moore AT (2005) A detailed study of the phenotype of an autosomal dominant cone-rod dystrophy (CORD7) associated with mutation in the gene for RIM1. Br J Ophthalmol 89:198–206
122. Jarvis SE, Zamponi GW (2001) Interactions between presynaptic Ca^{2+} channels, cytoplasmic messengers and proteins of the synaptic vesicle release complex. Trends Pharmacol Sci 22:519–525
123. Brown DA, Sihra TS (2008) Presynaptic signaling by heterotrimeric G-proteins. Handb Exp Pharmacol 184:207–260
124. Forscher P, Oxford GS, Schulz D (1986) Noradrenaline modulates calcium channels in avian dorsal root ganglion cells through tight receptor-channel coupling. J Physiol 379:131–144
125. Ikeda SR (1996) Voltage-dependent modulation of N-type calcium channels by G-protein beta gamma subunits. Nature 380:255–258
126. Herlitze S, Garcia DE, Mackie K, Hille B, Scheuer T, Catterall WA (1996) Modulation of Ca^{2+} channels by G-protein beta gamma subunits. Nature 380:258–262
127. De Waard M, Liu H, Walker D, Scott VE, Gurnett CA, Campbell KP (1997) Direct binding of G-protein betagamma complex to voltage-dependent calcium channels. Nature 385:446–450
128. Zamponi GW, Bourinet E, Nelson D, Nargeot J, Snutch TP (1997) Crosstalk between G proteins and protein kinase C mediated by the calcium channel alpha1 subunit. Nature 385:442–446
129. Tedford HW, Zamponi GW (2006) Direct G protein modulation of Cav2 calcium channels. Pharmacol Rev 58:837–862
130. De Waard M, Hering J, Weiss N, Feltz A (2005) How do G proteins directly control neuronal Ca(2+) channel function? Trends Pharmacol Sci 26:427–436
131. Stanley EF, Mirotznik RR (1997) Cleavage of syntaxin prevents G-protein regulation of presynaptic calcium channels. Nature 385:340–343
132. Silinsky EM (2005) Modulation of calcium currents is eliminated after cleavage of a strategic component of the mammalian secretory apparatus. J Physiol 566:681–688
133. Jarvis SE, Magga JM, Beedle AM, Braun JE, Zamponi GW (2000) G protein modulation of N-type calcium channels is facilitated by physical interactions between syntaxin 1A and Gbetagamma. J Biol Chem 275:6388–6394
134. Lu Q, AtKisson MS, Jarvis SE, Feng ZP, Zamponi GW, Dunlap K (2001) Syntaxin 1A supports voltage-dependent inhibition of alpha1B Ca^{2+} channels by Gbetagamma in chick sensory neurons. J Neurosci 21:2949–2957
135. Gerachshenko T, Blackmer T, Yoon EJ, Bartleson C, Hamm HE, Alford S (2005) Gbetagamma acts at the C terminus of SNAP-25 to mediate presynaptic inhibition. Nat Neurosci 8:597–605

136. Yoon EJ, Gerachshenko T, Spiegelberg BD, Alford S, Hamm HE (2007) Gbetagamma interferes with Ca2+−dependent binding of synaptotagmin to the soluble N-ethylmaleimide-sensitive factor attachment protein receptor (SNARE) complex. Mol Pharmacol 72:1210–1219
137. Weiss N, Sandoval A, Kyonaka S, Felix R, Mori Y, De Waard M (2011) Rim1 modulates direct G-protein regulation of Ca(v)2.2 channels. Pflugers Arch 461:447–459
138. Yokoyama CT, Sheng ZH, Catterall WA (1997) Phosphorylation of the synaptic protein interaction site on N-type calcium channels inhibits interactions with SNARE proteins. J Neurosci 17:6929–6938
139. Pozzi D, Condliffe S, Bozzi Y et al (2008) Activity-dependent phosphorylation of Ser187 is required for SNAP-25-negative modulation of neuronal voltage-gated calcium channels. Proc Natl Acad Sci USA 105:323–328
140. Zhu LQ, Liu D, Hu J et al (2010) GSK-3 beta inhibits presynaptic vesicle exocytosis by phosphorylating P/Q-type calcium channel and interrupting SNARE complex formation. J Neurosci 30:3624–3633
141. Ross CA, Tabrizi SJ (2011) Huntington's disease: from molecular pathogenesis to clinical treatment. Lancet Neurol 10:83–98
142. Swayne LA, Chen L, Hameed S et al (2005) Crosstalk between huntingtin and syntaxin 1A regulates N-type calcium channels. Mol Cell Neurosci 30:339–351
143. Swayne LA, Beck KE, Braun JE (2006) The cysteine string protein multimeric complex. Biochem Biophys Res Commun 348:83–91
144. Sutton KG, McRory JE, Guthrie H, Murphy TH, Snutch TP (1999) P/Q-type calcium channels mediate the activity-dependent feedback of syntaxin-1A. Nature 401:800–804
145. Restituito S, Cens T, Barrere C et al (2000) The [beta]2a subunit is a molecular groom for the Ca^{2+} channel inactivation gate. J Neurosci 20:9046–9052
146. Geib S, Sandoz G, Cornet V et al (2002) The interaction between the I-II loop and the III-IV loop of Cav2.1 contributes to voltage-dependent inactivation in a beta -dependent manner. J Biol Chem 277:10003–10013
147. Sandoz G, Lopez-Gonzalez I, Stamboulian S, Weiss N, Arnoult C, De Waard M (2004) Repositioning of charged I-II loop amino acid residues within the electric field by beta subunit as a novel working hypothesis for the control of fast P/Q calcium channel inactivation. Eur J Neurosci 19:1759–1772
148. Agler HL, Evans J, Tay LH, Anderson MJ, Colecraft HM, Yue DT (2005) G protein-gated inhibitory module of N-type (ca(v)2.2) Ca^{2+} channels. Neuron 46:891–904
149. Raghib A, Bertaso F, Davies A et al (2001) Dominant-negative synthesis suppression of voltage-gated calcium channel Cav2.2 induced by truncated constructs. J Neurosci 21:8495–8504
150. Page KM, Heblich F, Davies A et al (2004) Dominant-negative calcium channel suppression by truncated constructs involves a kinase implicated in the unfolded protein response. J Neurosci 24:5400–5409
151. Page KM, Heblich F, Margas W et al (2010) N terminus is key to the dominant negative suppression of Ca(V)2 calcium channels: implications for episodic ataxia type 2. J Biol Chem 285:835–844
152. Bucci G, Mochida S, Stephens GJ (2011) Inhibition of synaptic transmission and G protein modulation by synthetic CaV2.2 Ca^{2+} channel peptides. J Physiol 589:3085–3101
153. Payandeh J, Scheuer T, Zheng N, Catterall WA (2011) The crystal structure of a voltage-gated sodium channel. Nature 475:353–358

Chapter 34
Regulation of Intercellular Calcium Signaling Through Calcium Interactions with Connexin-Based Channels

Juan A. Orellana, Helmuth A. Sánchez, Kurt A. Schalper, Vania Figueroa, and Juan C. Sáez

Abstract The synchronization of numerous cellular events requires complex electric and metabolic cell-cell interactions. Connexins are a family of membrane proteins that constitute the molecular basis of two kinds of channels: gap junction channels (GJCs), which allow direct cytoplasm-cytoplasm communication, and hemichannels (HCs) that provide a pathway for exchanges between the intra and extra-cellular milieu. Both kind of connexin-based channels support intercellular communication via intercellular propagation of calcium waves. Here, we review evidence supporting the role of Ca^{2+} in the regulation of GJCs and HCs formed by connexins. Also it is speculated how these connexin-based channels could contribute to the propagation of intercellular Ca^{2+} signals.

J.A. Orellana (✉)
Departamento de Neurología, Facultad de Medicina, Pontificia Universidad Católica de Chile, Marcoleta 391, 8330024 Santiago, Chile
e-mail: jaorella@uc.cl

K.A. Schalper
Servicio de Anatomía Patológica, Clínica Alemana de Santiago, Facultad de Medicina Clínica Alemana-Universidad del Desarrollo., Av. Vitacura 5951, Vitacura, Chile
e-mail: kschalper@alemana.cl

V. Figueroa
Departamento de Fisiología, Pontificia Universidad Católica de Chile, Alameda 340, 6513677 Santiago, Chile

H.A. Sánchez
Department of Neuroscience, Albert Einstein College of Medicine, Bronx, NY, USA

J.C. Sáez
Departamento de Fisiología, Pontificia Universidad Católica de Chile, Alameda 340, 6513677 Santiago, Chile

Department of Neuroscience, Albert Einstein College of Medicine, Bronx, NY, USA

M.S. Islam (ed.), *Calcium Signaling*, Advances in Experimental Medicine and Biology 740, DOI 10.1007/978-94-007-2888-2_34,

Keyword Hemichannels • Gap junctions • Connexons • Calcium waves • Dye coupling • Calmodulin

Introduction

The synchronization of numerous cellular events requires complex electric and metabolic cell-cell interactions. In vertebrates, these cellular interactions are in part mediated by low-resistance intercellular channels that most frequently are located at gap junctions. The latter are plasma membrane specializations formed by the aggregation of tens to thousands intercellular channels (gap junction channels, GJCs), which are believed to provide direct but selective cytoplasmic continuity between communicating cells. Each GJC span the appositional plasma membranes of contacting cells and is formed by the serial docking of two hemichannels (HCs) (Fig. 34.1). Each HC is composed of six protein subunits termed connexins, a family of highly conserved proteins encoded by at least 21 different genes in humans [1]. Connexins are named after their predicted molecular mass expressed in kDa, so that Cx43 has a molecular mass of ~43 kDa. GJCs allow the intercellular exchange of metabolites, such as ATP, ADP, glucose, glutamate and glutathione, and second messengers including cAMP and inositol 1,4,5-trisphosphate [2–7]. In addition, these channels permit the intercellular spread of electrotonic potentials in excitable and non-excitable tissues [8–10].

In the last decade, a new pathway for exchange of ions and molecules between the intra and extracellular milieu constituted by connexin HCs has received progressive attention [11]. For a long time, the HC docking in apposed membranes to form intercellular GJCs was the only function assigned to HCs (Fig. 34.1). However, diverse evidence obtained in mammalian cells during the last decade indicate that nonjunctional HCs can open at the unapposed cell surface, forming aqueous conduits permeable to ions and small molecules (e.g., ATP, glutamate, NAD^+ and PGE_2) that allow diffusional exchange between the intra and extracellular compartments constituting a route for autocrine/paracrine cellular communication [11]. Pioneering findings by Paul et al. [12] identified the first nonjunctional currents mediated by connexin HCs in an exogenous expression system and supported the rational that opening of these channels was incompatible with cellular life. Nevertheless, recent evidence indicate that HCs are involved in several physiological cell and tissue functions and/or responses, including cellular proliferation [13–16], regulation of aqueous humor outflow [17], ischemic tolerance [18, 19], and adhesive cell-cell interactions [20]. More recently, another gene family encoding a set of three membrane proteins, named pannexins, has been identified [21] (Fig. 34.1). So far, the absence of ultrastructural evidences for gap junction formation in mammalian cells suggests that the main function of pannexin-based channels is paracrine/autocrine communication acting predominantly in the form of HCs [22].

Changes in GJC and HC open probability can result from changes in covalent modifications of connexin subunits (e.g., phosphorylation, nitrosylation and S-glutathionylation) or variations in transmembrane physicochemical conditions (e.g.,

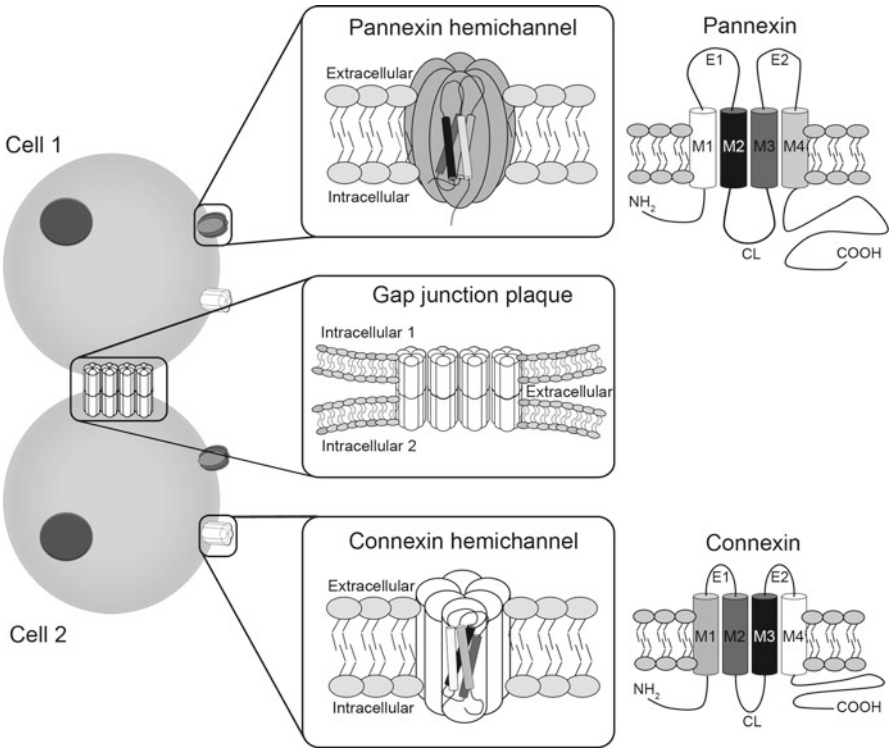

Fig. 34.1 Scheme showing the membrane topology of pannexins, connexins, hemichannels and gap junction channels. *Top and bottom right* correspond to pannexin and connexin proteins in the cell membrane, respectively. Both protein types have four transmembrane domains (*M1-4*) with amino (−*NH2*) and carboxy (−*COOH*) termini in the cytoplasmic side, two extracellular loops (*E1* and *E2*) and one cytoplasmic loop (*CL*). *Top and bottom centers* show hemichannels formed by six pannexin or connexin subunits each. The *middle center* shows an aggregate of connexin GJCs, namely a section through a gap junction "plaque", at a close contact between cells 1 and 2 as shown in the *left*. Each gap junction channel is formed by two hemichannels docked in the same plane (and rotated 30º with respect to one another). Each adjoining cell contributes with one of the hemichannels

transmembrane voltage, pH and concentration of cations) that affect the pore forming proteins. Here, we review the evidence supporting the role of Ca^{2+} in the regulation of GJCs and HCs formed by connexins. Also, it is speculated how these connexin-based channels could contribute to the propagation of intercellular Ca^{2+} signals.

Gating of Connexin-Based Channels by Ca^{2+}

Gap Junction Channels

Closure of GJCs presumably via a "gating mechanism" mediated by Ca^{2+} is a conserved mechanism in several connexin-based GJCs. Usually, an increase in

intracellular free Ca^{2+} concentration ($[Ca^{2+}]_i$) induces closure or drastic reduction gap junctional communication. The $[Ca^{2+}]_i$ that triggers this response in cell-cell communication via gap junction vary from nanomolar to micromolar range [23], and could occur by direct binding to connexins or indirectly, activating modulatory proteins.

Possible Direct Ca^{2+} Gating

Under physiological conditions, the $[Ca^{2+}]_i$ is tightly regulated by several mechanism. Thus, if Ca^{2+} directly affects connexin GJCs, a localized increase in $[Ca^{2+}]_i$ is likely to occur [23]. Once the increase in $[Ca^{2+}]_i$ is confined to a specific area, Ca^{2+} could bind directly to connexins that form GJCs. However, up to now there is no evidence of "calcium sparks" close to gap junctions. Moreover, Ca^{2+} binding sites usually consist of acidic residues contributed by carboxylate oxygen [24]. However, the variability of different connexins makes hard to indentify a potential conserved binding site. Therefore, due to the reasons mentioned above and the absence of crystal structures of different connexin-based GJCs the identification of a direct Ca^{2+} binding site at the cytoplasmic side of GJCs has been difficult [23].

A proposed mechanism for direct Ca^{2+}-dependent gating of GJCs involves the action of calmodulin (reviewed by [23, 25]). Calmodulin contains specialized domains in the N- and C-lobes that follow the $-NH_2$ terminus and Ca^{2+} binds to these domains, inducing conformational changes in the protein, enabling its interaction with several receptors. Such interaction has been observed with Cxs 38 [26], 32 [27], 37 [28], 43 [28], 44 [29], and 50 [30]. Moreover, a calmodulin mutant with high Ca^{2+}-sensitivity drastically increases the Ca^{2+} gating sensitivity of Cx32 GJCs and decreases their Vj sensitivity [28]. This was observed only when calmodulin is expressed before Cx32, suggesting that it interacts with Cx32 before gap junction formation [28]. Moreover, constructs of calmodulin and Cx32 tagged with fluorescent proteins show co-localization of both proteins when expressed in HeLa cells [28]. Similar results obtained in HeLa cells transfected with Cx50 were reported by Zhang and Qi [31]. They proposed the involvement of a Ca^{2+}-independent interaction between C-terminal and cytoplasmatic loop regions as mediator of a Ca^{2+}-dependent binding of calmodulin to Cx50 that induces closure of GJCs. In addition, Cx32 has two calmodulin interaction sites, one in the N-terminus and the other close to the C-terminal domain [32], while Cx43 has only one site in its N-terminus [23]. Moreover, the Cx32 HC activity induced by EGF is inhibited by W7, a calmodulin antagonist [33], suggesting that calmodulin could bind to Cx32 HCs, and potentially to GJCs.

Possible Indirect Ca^{2+} Gating

Indirect gating of connexin GJCs by Ca^{2+} might occur through activation of kinases, phosphatases or generation of metabolites/second messengers that modulate these

channels. Several connexins contain phosphorylation sites for more than one protein kinase, many of them with Ca^{2+}-dependent activity. These consensus sites vary between connexins and have been preferentially identified in their C-terminal domain [34]. The functional consequence could be an increase or decrease of junctional communication, response that depends on the connexin type and cell condition.

Calcineurin, a Ca^{2+} activated phosphatase highly localized in the central nervous system, is vulnerable to ischemic and traumatic insults particularly in neurons, and it is believed to play important roles in neuron-specific functions [35]. Rat astrocytes, normally expressing phosphorylated forms of Cx43, present a reduced a reduced gap junctional communication and increased Cx43 dephosphorylation when exposed to chemical hypoxia [36]. This condition rapidly increases the $[Ca^{2+}]_i$ [37], and while calcineurin inhibition with cyclosporin A or FK506 reduces the dephosphorylation of Cx43, okadaic acid or calyculin A, inhibitors of protein phosphatases 1 and 2A, had little effect. These results suggest that phosphorylated Cx43 GJCs might be substrates of calcineurin under conditions of cell stress, but perhaps not in normal astrocyte cultures, where calcineurin inhibitors had no effect on the phosphorylation state of Cx43 [13]. This would be consistent with the calmodulin-dependent activation of calcineurin [38, 39], suggesting that a calmodulin-dependent signaling systems play a relevant role in regulating GJCs.

Elevated $[Ca^{2+}]_i$ can lead to activation of calmodulin-dependent protein kinase II (CAM kinase II) that can phosphorylate Cx36 [40] and activation of CAM kinase II is associated to increase in electrical synapsis mediated by the Cx35 (ortholog of mammalian Cx36) in Mauthner neurons of the goldfish subjected to repetitive electrical stimulation that induces long term potentiation [41]. However, it remains unknown whether the increase in electrical coupling is due to a gating mechanism that activates more GJCs already present at the cell-cell interface or increase in number of GJCs due to reduced degradation and/or increased recruitment.

Ca^{2+} can induce the generation of arachidonic acid (AA), which, in turn, promotes closure of GJCs. AA is generated by activation of Ca^{2+}-dependent lipases during hypoxia-reoxygenation events and blocks intercellular coupling via GJCs in astrocytes [42] and in mouse hepatocytes expressing connexins 26 and 32 [43]. Blocking metabolization of AA with cyclooxygenase and lipoxygenase inhibitors preserve the GJC activity in astrocytes treated with AA, suggesting that downstream metabolic products of AA induce rapid channel closure or removal of Cx43 GJCs [42].

Hemichannels

A distinctive functional feature of connexin HCs is their sensitivity to variations in both extra and intracellular concentrations of divalent cations. In particular, homomeric HCs formed by all studied connexins are rapidly activated by reduction or removal of extracellular Ca^{2+} and Mg^{2+}, and their open probability is markedly reduced upon exposure to extracellular divalent cations [44]. However, the blocking effect of extracellular Mg^{2+} is less pronounced and possibly less functionally relevant

than that of Ca^{2+} [45–49]. Conversely, HCs formed by some connexins (e.g., Cxs 43 and 45) but not others (e.g. Cx26) increase the cell membrane permeability to dyes upon rises in $[Ca^{2+}]_i$ and this has been associated to increased level of HCs present at the cell surface [15]. The molecular mechanisms and functional implications of the complex/dual effect of Ca^{2+} on connexin HCs are not completely understood, but they are believed to be involved in both physiological and pathological regulation of HCs [50–53].

The first observation on connexin HC activation by reduction of extracellular Ca^{2+} concentration ($[Ca^{2+}]_e$) came from studies by DeVries and Schwartz [54]. In their seminal article using electrophysiological recordings and Lucifer yellow uptake by solitary horizontal cells of the catfish retina, they recognized undocked HCs working as single units by showing their increasing activation upon progressive reduction in $[Ca^{2+}]_e$ from 2 mM to <10 μM [54]. Afterwards and using diverse experimental models including mammalian cells with endogenous connexin expression and exogenous expression systems, HCs formed by diverse connexins were shown to be functionally modulated by variations in the $[Ca^{2+}]_e$, including HCs formed by Cxs 23 [55] [56], 26 [15, 37, 57–60], 30 [61], 30.2 [62], 31.9 [62], 32 [33, 37, 47], 35 [63], 37 [48], 38 [64–66], 43 [15, 67–75], 45 [15, 76, 77], 45.6 [78], 46 [45, 46, 79–82], 50 [83]; 52.6 [84] and 56 [85].

Homomeric HCs formed by Cxs 26 or 43 rapidly and reversibly increase their internal pore diameter upon extracellular Ca^{2+} removal [variation from 0.5 to 1.3 nm [86] and 1.8 to 2.5 nm [87], respectively] as measured by high-resolution atomic force microscopy. The latter findings support a prominent structural change of connexin-based hexamers induced by $[Ca^{2+}]_e$ variations.

Although the mechanism of HC blockade induced by extracellular Ca^{2+} is not completely understood, it is unlikely to occur solely as a consequence of conformational changes but rather involves direct polyvalent cation binding to the mouth of the HC pore. Indeed, extracellular Ca^{2+} and voltage sensitivities of Cx32 HCs in *Xenopus* oocytes are modified by substitution of two aspartate residues (D169 or D178) located at the second extracellular loop by uncharged asparagines [47]. In homomeric Cx32 HCs, these residues are believed to form a 12 aspartate ring located at the external vestibule of the pore. Binding of Ca^{2+} to these negatively charged aspartate residues could explain the blocking effect of Ca^{2+} through reduction of the effective pore diameter or stabilization of the close configuration of HCs as it has been reported for other ion channels [88, 89]. Interestingly, one naturally occurring mutation due to substitution of the aspartate residue located in position 178 by a neutral tyrosine residue (D178Y) of human Cx32 is associated to a complex human genetic disease termed X-linked Charcot-Marie-Tooth [90]. However and despite the high sequence homology of extracellular E1 and E2 loops among connexins subunits, only HCs formed by few connexins [e.g. human Cxs 30, 32, 43; rat Cxs 32, 43 and 46; mouse Cx30 [47]] share this 12 aspartate extracellular ring but those connexins lacking it are still Ca^{2+} sensitive. In addition, while mutations of the positioned E2 aspartates (D169 and D178) alter the Ca^{2+}-sensitivity of Cx32 HCs, they do not abolished the Ca^{2+} block entirely, indicating the involvement of additional molecular mechanisms. Alternatively, the presence of other negatively

charged amino acid residue such as glutamate or variations in the Ca^{2+} binding sites around or close the pore edge could account for the extracellular Ca^{2+} blockade of HCs formed by connexins lacking the anionic gate. In this regard, homomeric HCs formed by human Cx37 [lacking the anionic pore ring [47]] expressed in *Xenopus* oocytes are blocked by extracellular Ca^{2+} going through the pore (open by membrane depolarization) and reaching binding sites located at the cytoplasmic side, presumably acidic residues located in the N- and C-termini of the subunits [48]. In addition, single recordings of homomeric rat Cx46 HCs [possessing the 12 aspartate anionic pore ring [47]] expressed in Xenopus oocyte showed that divalent cations do not block directly, but rather modify the intrinsic electric gating though conformational stabilization of fully closed HCs [49]. Using excised patches, divalent cations are only effective from the extracellular side, implying that the binding sites are extracellular. Unfortunately, all available studies aimed to address the mechanism of extracellular Ca^{2+} blockade have been performed using electrophysiological measurements of HCs exogenously expressed in *Xenopus* oocytes and using membrane depolarization as activating stimulus. Several intra/extracellular molecules (e.g. ions, protons, nucleotides and cytokines), intracellular proteins (e.g. protein kinases and phosphatases) and binding partners (e.g., tight junction associated proteins and cytoskeleton proteins) have been shown to affect connexin HC structure and function [11] and may additionally be involved in the extracellular Ca^{2+} sensitivity and blocking effect. In addition, multiple gating mechanisms (e.g. chemical gating) have been identified for GJCs [91] and HCs might show similar functional complexity. In this regard, it was shown that replacement of extracellular Na^+ by K^+ (and other monovalent cations) modulates the extracellular Ca^{2+} sensitivity of homomeric Cx46 and Cx50 HCs, an effect residing in the cytoplasmic N-terminal domain of connexins [92]. In addition, diverse stimuli have been recently shown to overcome the extracellular Ca^{2+} blockade of connexin HCs even at resting negative transmembrane potentials (e.g. chemicals, mechanical stimulation, ischemia-like conditions, cytokines and growth factors) [15, 36, 93–97].

Augments in $[Ca^{2+}]_i$ increase connexin HC activation in the presence of physiological concentrations of extracellular divalent cations, possibly acting in an indirect fashion. In particular, cells expressing homomeric HCs formed by Cxs 32 or 43 increase their membrane permeability to cationic dyes and the HC-mediated ATP release in response to higher $[Ca^{2+}]_i$ and buffering the intracellular Ca^{2+} with chelating agents prevents HC activation in diverse experimental models [15, 33, 37, 74, 98]. In cells expressing Cx32 HCs, the intracellular Ca^{2+} activating concentration lies at ~500 nM and the HCs response is abolished by a selective calmodulin inhibitor [33]. Moreover, Cx32 HC activation induced my metabolic inhibition is partially prevented by a p38 MAP kinase inhibitor, totally prevented by intracellular Ca^{2+} chelators and mimicked by a Ca^{2+} ionophore in HeLa cells [37]. In HeLa cells expressing Cx43, increase HC activation induced by rising the $[Ca^{2+}]_i$ with FGF-1 or a Ca^{2+} ionophore is associated with higher surface HC levels, increased HC open probability and requires p38 MAP kinase activation [15]. Moreover, Cx43 HC activation is also triggered by intracellular concentration of ~500 nM Ca^{2+} and involves activation of complex intracellular signaling cascades including calmodulin,

calmodulin-dependent kinase II, p38 MAP kinase, phospholipase A_2, arachidonic acid, lipoxygenases, cyclooxygenases, reactive oxygen species, nitric oxide and membrane depolarization [97]. Finally, release of ATP and proliferation of the retinal pigment epithelial cells also requires Cx43 HC activation induced by increased $[Ca^{2+}]_i$ [74].

Interestingly, preventing the intracellular Ca^{2+} mobilization with BAPTA-AM or thapsigargin in cultured astrocytes does not inhibit glutamate release after exposure to a divalent cation free solution [73], indicating interdependence of the HC responses induced by extra and intracellular Ca^{2+}. However, the fact that at least some HCs are Ca^{2+} permeable [37, 99, 100], suggest possible activating loops and complex regulation of the HC responses by this cation.

Permeation of Calcium Ions Through Connexin-Based Channels

Gap Junction Channels

Up to now, only a couple of studies indicate that GJCs are permeable to Ca^{2+} [4, 101], meanly because it is difficult to rule out the involvement of cytoplasmic Ca^{2+}-mobilizing second messengers such as inositol (1,4,5)-trisphosphate (IP_3) and cyclic-ADP-ribose (cADPR) [102]. Moreover, another puzzle piece is that high $[Ca^{2+}]_i$ has been shown to reduce GJC activity in several cell types [103–105]. Nevertheless, the $[Ca^{2+}]_i$ required to block GJCs appears to be well above 1 μM [106], far higher than normal resting $[Ca^{2+}]_i$ that is between 50 and 100 nM. Therefore, it is expected that low Ca^{2+} concentrations could permeate GJCs. In fact, it has been reported that Ca^{2+} microinjected into individual hepatocytes or smooth muscle cells immediately increase the $[Ca^{2+}]_i$ in the injected cell [4, 101]. Importantly, the $[Ca^{2+}]_i$ increased within seconds in the contacting cells, while the initial rise in the $[Ca^{2+}]_i$ induced by IP_3 microinjection occur in discrete regions of the cytoplasm, which is inconsistent with simple diffusion of Ca^{2+}. The abovementioned studies indicate that IP_3 diffuses between cells to cause localized Ca^{2+} release from intracellular stores. Whereas changes in $[Ca^{2+}]_i$ seen in adjacent cells after Ca^{2+} microinjection in cells bathed in Ca^{2+} free solution are due to transjunctional Ca^{2+} diffusion from the injected cell and not to uptake from the extracellular solution [4, 101]. Accordingly, computational modeling of intercellular Ca^{2+} wave propagation support that both IP_3 and Ca^{2+} diffusion occur through GJCs [107–110].

Hemichannels

Most connexin HCs are highly sensitive to fluctuations in $[Ca^{2+}]_e$ and their open probability decreases in the presence of increasing concentrations of this cation [11]. Thus, HCs have been considered as Ca^{2+} sensors implicated in the mechanism by

which the $[Ca^{2+}]_e$ modulates the intracellular signaling [111]. Diverse studies have shown that ATP released via HCs increases the $[Ca^{2+}]_i$ via P2 receptor activation [14, 60, 74, 112–114] and thus, excluding the HC contribution as route for Ca^{2+} influx to the cytoplasm. The first experimental evidence suggesting Ca^{2+} influx through HCs was observed in cardiomyocytes subjected to metabolic inhibition. Under this treatment, cardiomyocytes exhibit an increase in intracellular free Ca^{2+} and Na^+ concentration, which are partially reduced by halothane or 1-heptanol, two HC and GJC blockers [73, 115]. However, voltage-operated Ca^{2+} and Na^+ channel blockers also reduce the intracellular increase of both cations, suggesting that HCs, as well as Ca^{2+} and Na^+ channels contribute to this phenomenon [115]. In support to the relevance of HCs in this response, the increase in $[Ca^{2+}]_i$ of cardiomyocytes subjected to ischemia is inhibited by Gap26 [116], a connexin mimetic peptide that blocks Cx43 HCs. Most experiments designed to elucidate the role of connexin HCs in Ca^{2+} influx induced by pathological or physiological conditions have been conducted in HeLa cells transfected with connexins [117, 118], since they possess all the cellular machinery required for Ca^{2+} signaling [119]. In fact, HeLa cells transfected with connexins 26, 32 or 43 exhibit Ca^{2+} waves in response to mechanical stimulation or extracellular ATP application that differ from those observed in parental HeLa cells [120]. Recent studies in HeLa cells transfected with mouse Cx43 and loaded with Fluo 4 used as calcium indicator, show that extracellular alkalinization increases the $[Ca^{2+}]_i$ in an $[Ca^{2+}]_e$-dependent way [100]. More relevant to this point, the alkalinization-induced rise in $[Ca^{2+}]_i$, was closely related to the level of Cx43 HCs present at the cell surface, suggesting that Ca^{2+} mobilization from the extracellular milieu is mediated by Cx43 HCs [100]. To demonstrate directly that Cx43 HCs are permeable to Ca^{2+}, purified Cx43 HCs were reconstituted into unilamelar liposomes loaded with Green-2 as Ca^{2+} indicator. When the $[Ca^{2+}]_e$ was increased from 5 to 20 μM the fluorescence of Green-2 increased almost twofolds. In contrast, liposomes without Cx43 HCs did not exhibit changes in $[Ca^{2+}]$ in their interior, indicating that Cx43 HCs are permeable to Ca^{2+} [100].

Cx43 HCs are not the only HCs permeable to Ca^{2+}. Cx32 HeLa transfectants subjected to metabolic inhibition show elevated $[Ca^{2+}]_i$, which does not occur within the same time course in parental cells, suggesting that Ca^{2+} influx could occur through Cx32 HCs [37]. Recently, Sánchez et al. [37] showed that activation of an endogenous Ca^{2+}-activated chloride channel in *Xenopus* oocytes occurs when Cx26 HCs are activated upon depolarization, suggesting that they allow the influx of Ca^{2+}, which further activates the chloride currents. Interestingly, a mutation positioned near TM1/E1 domain of Cx26 (G45E) associated with the Keratitis Ichthyosis Deafness syndrome (KID) leads to formation of HCs with increased Ca^{2+} permeability reflected by a robust chloride channel activation compared HC formed by with wild Cx26 [99]. Mutations in genes of Cxs 26, 32 and 43 have been associated with several human diseases, and some of them form HCs with aberrant conductances in exogenous expression systems. In light of the abovementioned findings, it is possible that altered permeability to Ca^{2+} occurs as a common mechanism for the development of these diseases [47, 99, 121]. Relevant to the lack of demonstration of this possibility are the experimental limitations of each approach used to demonstrate

Ca^{2+} influx via HCs. Reconstitution in liposomes might be a good approach since it discard other possible routes of Ca^{2+} influx that might be present in endogenous and exogenous expression systems and also eliminate all intracellular elements that regulate the functional state of HCs (e.g., kinases, phosphatase and scaffolding proteins) [44, 122]. An experimental strategy used to sense the direct passage of Ca^{2+} through GJCs has been the use of connexin-aequorin chimeras. However, in these studies it was found that some connexin-aequorin chimeras do not form functional GJCs, and remains to be demonstrate if they form functional HCs [123]. Therefore, this experimental strategy must be reviewed and its usefulness in studying the HC permeability to Ca^{2+} needs to be reevaluated.

Do Gap Junction Channels and Hemichannels Play a Role in the Propagation of Intercellular Calcium Waves?

Up to now, two mechanisms for intercellular calcium wave propagation have received more attention. One of them occurs between contacting cells and involves the diffusion through GJCs of cytoplasmic Ca^{2+}-mobilizing second messengers such as inositol (1,4,5)-trisphosphate (IP_3) [4, 124], cDAPR [125] and Ca^{2+} [4, 101] (Fig. 34.2). The another one is related to the activation of P2 purinergic receptors in neighbor cells by extracellular ATP released through vesicles [126] and/or HCs [112] (Fig. 34.2). Evidence supporting the first mechanism includes that the waves are: (i) gap junction dependent; (ii) not blocked upon ATP hydrolysis; (iii) not blocked by purine-receptor antagonists and (iv) do not jump a gap between cells [127, 128]. Whereas facts sustaining the second mechanism comprise: (i) hemichannel blockers prevent the waves; (ii) ATP is released by the initiator cell, and the calcium waves extend as far as the ATP diffuses; (iii) the waves are blocked by extracellular apyrase and by inhibitors of P2 receptors; (iv) the waves jump cell-free gaps and are deflected by flow of medium [129–132]. It is possible that these mechanisms coexist under physiological conditions. In support to this possibility, an organotypic model of mice cochlea show propagation of intercellular calcium waves at long distances through ATP released via Cx30 and Cx26 HCs, whereas GJCs composed by the same Cxs allow the simultaneous diffusion of IP_3 across coupled cells [133]. Importantly, both mechanisms occur in response to activation of P2Y/PLC/IP_3/Ca^{2+} signaling cascade and are propagated normally in cultures lacking either $P2X_7$ receptors or Panx1, indicating that the phenomena is not related to Panx1 based channels [133]. Moreover, intercellular Ca^{2+} waves induced by mechanical stimulation depend of GJCs and paracrine ATP-mediated signaling in human urothelial cells [134]. Similar calcium wave propagation has been proposed to occur in osteocytes [135]; ciliated tracheal epithelial cells [136] and astrocytes [137]. An alternative mechanism proposed for propagation of intercellular calcium waves is through the release of NAD^+ via HCs [138]. Most of cells, express CD38, an ectoenzyme that cycles NAD^+ to form cADPR, then cADPR cross the cell membrane to reach ryanodine receptors in the endoplasmic reticulum (ER), triggering release of

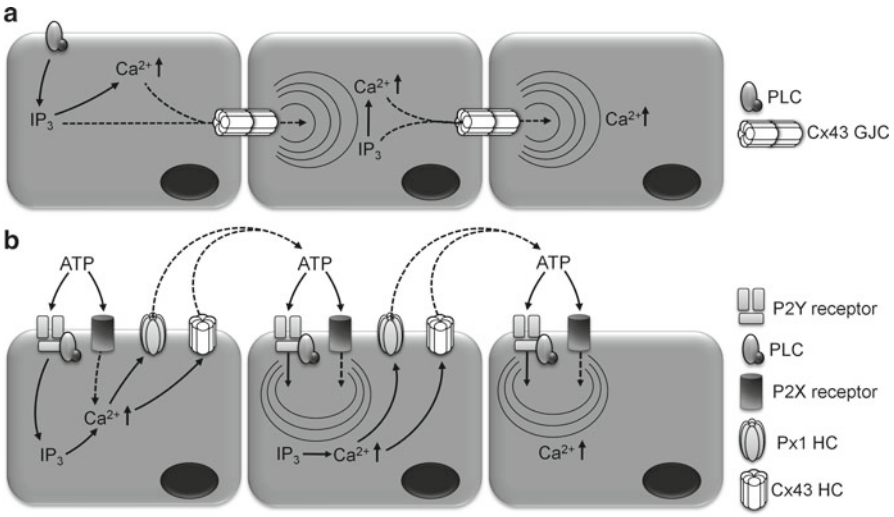

Fig. 34.2 Two models for conduction of Ca^{2+} waves in astrocytes. (**a**) Upstream receptor stimulation leads to activation of phospholipase C (*PLC*) and formation of cytoplasmic inositol (1,4,5)-trisphosphate (*IP*$_3$), which promote the release of Ca^{2+} stored in the endoplasmic reticulum. Both IP_3 and Ca^{2+} diffuse to neighboring cells through gap junction channels generating waves of rises in intracellular Ca^{2+} concentration $[Ca^{2+}]_i$. (**b**) ATP released from vesicles and/or ion channels diffuses through the extracellular space and activates membrane purinergic (P2) receptors. Stimulation of metabotropic P2Y receptors leads to activation of phospholipase C (*PLC*) and formation of IP_3. Whereas, activation of ionotropic P2X receptors leads to Ca^{2+} influx. The increase in free $[Ca^{2+}]_i$ induced by IP_3 and P2X receptor opening could promote ATP release through Cx43 and Panx1 hemichannels, extending the Ca^{2+} wave to neighboring cells

Ca^{2+} into the cytoplasm. Afterwards, subsequent release of NAD^+ via HCs and/or cADPR diffusion through GJCs [125] would propagate a calcium wave.

It is interesting that $[Ca^{2+}]_i$ at ~500 μM induces opening of HCs and closing of GJCs. This finding could have pathophysiological implications. For example, astrocytes subjected to ischemic-like conditions exhibit an increase in Cx43 HCs activity and decrease in intercellular gap junctional communication [36]. During these conditions a fast increase in $[Ca^{2+}]_i$ has been documented [37], while exposure to Ca^{2+} ionophore induces rapid closure of Cx43 GJCs [130]. A recent work from the group of Li and co-workers [139, 140] has elegantly demonstrated that only capacitative Ca^{2+} entry via store-operated channels is effective in blocking gap junctional communication, while Ca^{2+} ionophores were without effect. How $[Ca^{2+}]_i$ changes are linked to HC opening and GJC closure is currently unknown, but could depend on differential distribution of intracellular regulatory proteins in different microdomains, which may also vary in different cell types and physiological or pathophysiological states. Opening of HCs could be necessary to release toxic metabolites to the extracellular medium, and accelerate the intake of energetic metabolites. At the same time, closing GJCs might help to avoid the spreading of death signals from damaged to healthy cells, as occurs during propagation of spreading depression in nerve tissue.

Acknowledgements This work was partially supported by the CONICYT 79090028 (to JAO); FONDECYT 1111033 (to JCS); FONDEF DO7I1086 (to JCS); and ANILLO ACT-71 (to JCS) grants.

References

1. Willecke K, Eiberger J, Degen J, Eckardt D, Romualdi A, Guldenagel M, Deutsch U, Sohl G (2002) Structural and functional diversity of connexin genes in the mouse and human genome. Biol Chem 383:725–737
2. Lawrence TS, Beers WH, Gilula NB (1978) Transmission of hormonal stimulation by cell-to-cell communication. Nature 272:501–506
3. Qu Y, Dahl G (2002) Function of the voltage gate of gap junction channels: selective exclusion of molecules. Proc Natl Acad Sci USA 99:697–702
4. Sáez JC, Gregory WA, Watanabe T, Dermietzel R, Hertzberg EL, Reid L, Bennett MV, Spray DC (1989) cAMP delays disappearance of gap junctions between pairs of rat hepatocytes in primary culture. Am J Physiol 257:C1–C11
5. Niessen H, Harz H, Bedner P, Kramer K, Willecke K (2000) Selective permeability of different connexin channels to the second messenger inositol 1,4,5-trisphosphate. J Cell Sci 113:1365–1372
6. Kam Y, Kim DY, Koo SK, Joe CO (1998) Transfer of second messengers through gap junction connexin 43 channels reconstituted in liposomes. Biochim Biophys Acta 1372:384–388
7. Goldberg GS, Lampe PD, Nicholson BJ (1999) Selective transfer of endogenous metabolites through gap junctions composed of different connexins. Nat Cell Biol 1:457–459
8. Connors BW, Long MA (2004) Electrical synapses in the mammalian brain. Annu Rev Neurosci 27:393–418
9. Lee SM, Clemens MG (1992) Subacinar distribution of hepatocyte membrane potential response to stimulation of gluconeogenesis. Am J Physiol 263:G319–G326
10. Rohr S (2004) Role of gap junctions in the propagation of the cardiac action potential. Cardiovasc Res 62:309–322
11. Sáez JC, Schalper KA, Retamal MA, Orellana JA, Shoji KF, Bennett MV (2010) Cell membrane permeabilization via connexin hemichannels in living and dying cells. Exp Cell Res 316:2377–2389
12. Paul DL, Ebihara L, Takemoto LJ, Swenson KI, Goodenough DA (1991) Connexin46, a novel lens gap junction protein, induces voltage-gated currents in nonjunctional plasma membrane of Xenopus oocytes. J Cell Biol 115:1077–1089
13. Fruscione F, Scarfi S, Ferraris C, Bruzzone S, Benvenuto F, Guida L, Uccelli A, Salis A, Usai C, Jacchetti E, Ilengo C, Scaglione S, Quarto R, Zocchi E, De Flora A (2011) Regulation of human mesenchymal stem cell functions by an autocrine loop involving NAD(+) release and P2Y11-mediated signaling. Stem Cells Dev 20:1183–1198
14. Song D, Liu X, Liu R, Yang L, Zuo J, Liu W (2010) Connexin 43 hemichannel regulates H9c2 cell proliferation by modulating intracellular ATP and [Ca^{2+}]. Acta Biochim Biophys Sin (Shanghai) 42:472–482
15. Schalper KA, Palacios-Prado N, Retamal MA, Shoji KF, Martinéz AD, Sáez JC (2008) Connexin hemichannel composition determines the FGF-1-induced membrane permeability and free [Ca^{2+}]i responses. Mol Biol Cell 19:3501–3513
16. Burra S, Jiang JX (2009) Connexin 43 hemichannel opening associated with Prostaglandin E(2) release is adaptively regulated by mechanical stimulation. Commun Integr Biol 2:239–240
17. Li A, Leung CT, Peterson-Yantorno K, Mitchell CH, Civan MM (2010) Pathways for ATP release by bovine ciliary epithelial cells, the initial step in purinergic regulation of aqueous humor inflow. Am J Physiol Cell Physiol 299:C1308–C1317

18. Lin JH, Lou N, Kang N, Takano T, Hu F, Han X, Xu Q, Lovatt D, Torres A, Willecke K, Yang J, Kang J, Nedergaard M (2008) A central role of connexin 43 in hypoxic preconditioning. J Neurosci 28:681–695
19. Schock SC, Leblanc D, Hakim AM, Thompson CS (2008) ATP release by way of connexin 36 hemichannels mediates ischemic tolerance in vitro. Biochem Biophys Res Commun 368:138–144
20. Cotrina ML, Lin JH, Nedergaard M (2008) Adhesive properties of connexin hemichannels. Glia 56:1791–1798
21. Bruzzone R, Hormuzdi SG, Barbe MT, Herb A, Monyer H (2003) Pannexins, a family of gap junction proteins expressed in brain. Proc Natl Acad Sci USA 100:13644–13649
22. Locovei S, Bao L, Dahl G (2006) Pannexin 1 in erythrocytes: function without a gap. Proc Natl Acad Sci USA 103:7655–7659
23. Peracchia C (2004) Chemical gating of gap junction channels; roles of calcium, pH and calmodulin. Biochim Biophys Acta 1662:61–80
24. Elinder F, Arhem P (2003) Metal ion effects on ion channel gating. Q Rev Biophys 36:373–427
25. Rackauskas M, Neverauskas V, Skeberdis VA (2010) Diversity and properties of connexin gap junction channels. Medicina (Kaunas) 46:1–12
26. Peracchia C, Wang X, Li L, Peracchia LL (1996) Inhibition of calmodulin expression prevents low-pH-induced gap junction uncoupling in Xenopus oocytes. Pflugers Arch 431:379–387
27. Peracchia C, Sotkis A, Wang XG, Peracchia LL, Persechini A (2000) Calmodulin directly gates gap junction channels. J Biol Chem 275:26220–26224
28. Sotkis A, Wang XG, Yasumura T, Peracchia LL, Persechini A, Rash JE, Peracchia C (2001) Calmodulin colocalizes with connexins and plays a direct role in gap junction channel gating. Cell Commun Adhes 8:277–281
29. Zhou Y, Yang W, Lurtz MM, Chen Y, Jiang J, Huang Y, Louis CF, Yang JJ (2009) Calmodulin mediates the Ca^{2+}–dependent regulation of Cx44 gap junctions. Biophys J 96:2832–2848
30. Zhang X, Zou T, Liu Y, Qi Y (2006) The gating effect of calmodulin and calcium on the connexin50 hemichannel. Biol Chem 387:595–601
31. Zhang X, Qi Y (2005) Role of intramolecular interaction in connexin50: mediating the Ca^{2+}–dependent binding of calmodulin to gap junction. Arch Biochem Biophys 440:111–117
32. Torok K, Stauffer K, Evans WH (1997) Connexin 32 of gap junctions contains two cytoplasmic calmodulin-binding domains. Biochem J 326(Pt 2):479–483
33. De Vuyst E, Decrock E, Cabooter L, Dubyak GR, Naus CC, Evans WH, Leybaert L (2006) Intracellular calcium changes trigger connexin 32 hemichannel opening. EMBO J 25:34–44
34. Sáez JC, Martinéz AD, Brañes MC, Gonzalez HE (1998) Regulation of gap junctions by protein phosphorylation. Braz J Med Biol Res 31:593–600
35. Morioka M, Hamada J, Ushio Y, Miyamoto E (1999) Potential role of calcineurin for brain ischemia and traumatic injury. Prog Neurobiol 58:1–30
36. Contreras JE, Sánchez HA, Eugenín EA, Speidel D, Theis M, Willecke K, Bukauskas FF, Bennett MV, Sáez JC (2002) Metabolic inhibition induces opening of unapposed connexin 43 gap junction hemichannels and reduces gap junctional communication in cortical astrocytes in culture. Proc Natl Acad Sci USA 99:495–500
37. Sánchez HA, Orellana JA, Verselis VK, Sáez JC (2009) Metabolic inhibition increases activity of connexin-32 hemichannels permeable to Ca^{2+} in transfected HeLa cells. Am J Physiol Cell Physiol 297:C665–C678
38. Toyama J, Sugiura H, Kamiya K, Kodama I, Terasawa M, Hidaka H (1994) Ca^{2+}-calmodulin mediated modulation of the electrical coupling of ventricular myocytes isolated from guinea pig heart. J Mol Cell Cardiol 26:1007–1015
39. Jansen LA, de Vrije T, Jongen WM (1996) Differences in the calcium-mediated regulation of gap junctional intercellular communication between a cell line consisting of initiated cells and a carcinoma-derived cell line. Carcinogenesis 17:2311–2319

40. Alev C, Urschel S, Sonntag S, Zoidl G, Fort AG, Hoher T, Matsubara M, Willecke K, Spray DC, Dermietzel R (2008) The neuronal connexin36 interacts with and is phosphorylated by CaMKII in a way similar to CaMKII interaction with glutamate receptors. Proc Natl Acad Sci USA 105:20964–20969
41. Pereda AE, Rash JE, Nagy JI, Bennett MV (2004) Dynamics of electrical transmission at club endings on the Mauthner cells. Brain Res Brain Res Rev 47:227–244
42. Martinéz AD, Sáez JC (1999) Arachidonic acid-induced dye uncoupling in rat cortical astrocytes is mediated by arachidonic acid byproducts. Brain Res 816:411–423
43. Polonchuk LO, Frolov VA, Yuskovich AK, Dunina-Barkovskaya A (1997) The effect of arachidonic acid on junctional conductance in isolated murine hepatocytes. Membr Cell Biol 11:225–242
44. Sáez JC, Retamal MA, Basilio D, Bukauskas FF, Bennett MV (2005) Connexin-based gap junction hemichannels: gating mechanisms. Biochim Biophys Acta 1711:215–224
45. Ebihara L, Steiner E (1993) Properties of a nonjunctional current expressed from a rat connexin46 cDNA in Xenopus oocytes. J Gen Physiol 102:59–74
46. Ebihara L, Liu X, Pal JD (2003) Effect of external magnesium and calcium on human connexin46 hemichannels. Biophys J 84:277–286
47. Gomez-Hernandez JM, de Miguel M, Larrosa B, Gonzalez D, Barrio LC (2003) Molecular basis of calcium regulation in connexin-32 hemichannels. Proc Natl Acad Sci USA 100:16030–16035
48. Puljung MC, Berthoud VM, Beyer EC, Hanck DA (2004) Polyvalent cations constitute the voltage gating particle in human connexin37 hemichannels. J Gen Physiol 124:587–603
49. Verselis VK, Srinivas M (2008) Divalent cations regulate connexin hemichannels by modulating intrinsic voltage-dependent gating. J Gen Physiol 132:315–327
50. Evans WH, De Vuyst E, Leybaert L (2006) The gap junction cellular internet: connexin hemichannels enter the signalling limelight. Biochem J 397:1–14
51. Retamal MA, Schalper KA, Shoji KF, Orellana JA, Bennett MV, Sáez JC (2007) Possible involvement of different connexin43 domains in plasma membrane permeabilization induced by ischemia-reperfusion. J Membr Biol 218:49–63
52. Orellana JA, Sáez PJ, Shoji KF, Schalper KA, Palacios-Prado N, Velarde V, Giaume C, Bennett MV, Sáez JC (2009) Modulation of brain hemichannels and gap junction channels by pro-inflammatory agents and their possible role in neurodegeneration. Antioxid Redox Signal 11:369–399
53. Schalper KA, Orellana JA, Berthoud VM, Sáez JC (2009) Dysfunctions of the diffusional membrane pathways mediated by hemichannels in inherited and acquired human diseases. Curr Vasc Pharmacol 7:486–505
54. DeVries SH, Schwartz EA (1992) Hemi-gap-junction channels in solitary horizontal cells of the catfish retina. J Physiol 445:201–230
55. Iovine MK, Gumpert AM, Falk MM, Mendelson TC (2008) Cx23, a connexin with only four extracellular-loop cysteines, forms functional gap junction channels and hemichannels. FEBS Lett 582:165–170
56. Sonntag S, Sohl G, Dobrowolski R, Zhang J, Theis M, Winterhager E, Bukauskas FF, Willecke K (2009) Mouse lens connexin23 (Gje1) does not form functional gap junction channels but causes enhanced ATP release from HeLa cells. Eur J Cell Biol 88:65–77
57. Ripps H, Qian H, Zakevicius J (2004) Properties of connexin26 hemichannels expressed in Xenopus oocytes. Cell Mol Neurobiol 24:647–665
58. Gerido DA, DeRosa AM, Richard G, White TW (2007) Aberrant hemichannel properties of Cx26 mutations causing skin disease and deafness. Am J Physiol Cell Physiol 293:C337–C345
59. Stong BC, Chang Q, Ahmad S, Lin X (2006) A novel mechanism for connexin 26 mutation linked deafness: cell death caused by leaky gap junction hemichannels. Laryngoscope 116:2205–2210
60. Zhao HB, Yu N, Fleming CR (2005) Gap junctional hemichannel-mediated ATP release and hearing controls in the inner ear. Proc Natl Acad Sci USA 102:18724–18729

61. Valiunas V, Weingart R (2000) Electrical properties of gap junction hemichannels identified in transfected HeLa cells. Pflugers Arch 440:366–379
62. Bukauskas FF, Kreuzberg MM, Rackauskas M, Bukauskiene A, Bennett MV, Verselis VK, Willecke K (2006) Properties of mouse connexin 30.2 and human connexin 31.9 hemichannels: implications for atrioventricular conduction in the heart. Proc Natl Acad Sci USA 103:9726–9731
63. Valiunas V, Mui R, McLachlan E, Valdimarsson G, Brink PR, White TW (2004) Biophysical characterization of zebrafish connexin35 hemichannels. Am J Physiol Cell Physiol 287:C1596–C1604
64. Ebihara L (1996) Xenopus connexin38 forms hemi-gap-junctional channels in the nonjunctional plasma membrane of Xenopus oocytes. Biophys J 71:742–748
65. Ripps H, Qian H, Zakevicius J (2002) Pharmacological enhancement of hemi-gap-junctional currents in Xenopus oocytes. J Neurosci Methods 121:81–92
66. Bahima L, Aleu J, Elias M, Martin-Satue M, Muhaisen A, Blasi J, Marsal J, Solsona C (2006) Endogenous hemichannels play a role in the release of ATP from Xenopus oocytes. J Cell Physiol 206:95–102
67. Li H, Liu TF, Lazrak A, Peracchia C, Goldberg GS, Lampe PD, Johnson RG (1996) Properties and regulation of gap junctional hemichannels in the plasma membranes of cultured cells. J Cell Biol 134:1019–1030
68. Hofer A, Dermietzel R (1998) Visualization and functional blocking of gap junction hemichannels (connexons) with antibodies against external loop domains in astrocytes. Glia 24:141–154
69. John SA, Kondo R, Wang SY, Goldhaber JI, Weiss JN (1999) Connexin-43 hemichannels opened by metabolic inhibition. J Biol Chem 274:236–240
70. Kondo RP, Wang SY, John SA, Weiss JN, Goldhaber JI (2000) Metabolic inhibition activates a non-selective current through connexin hemichannels in isolated ventricular myocytes. J Mol Cell Cardiol 32:1859–1872
71. Romanello M, Pani B, Bicego M, D'Andrea P (2001) Mechanically induced ATP release from human osteoblastic cells. Biochem Biophys Res Commun 289:1275–1281
72. Stout C, Charles A (2003) Modulation of intercellular calcium signaling in astrocytes by extracellular calcium and magnesium. Glia 43:265–273
73. Ye ZC, Wyeth MS, Baltan-Tekkok S, Ransom BR (2003) Functional hemichannels in astrocytes: a novel mechanism of glutamate release. J Neurosci 23:3588–3596
74. Pearson RA, Dale N, Llaudet E, Mobbs P (2005) ATP released via gap junction hemichannels from the pigment epithelium regulates neural retinal progenitor proliferation. Neuron 46:731–744
75. De Vuyst E, Decrock E, De Bock M, Yamasaki H, Naus CC, Evans WH, Leybaert L (2007) Connexin hemichannels and gap junction channels are differentially influenced by lipopolysaccharide and basic fibroblast growth factor. Mol Biol Cell 18:34–46
76. Valiunas V (2002) Biophysical properties of connexin-45 gap junction hemichannels studied in vertebrate cells. J Gen Physiol 119:147–164
77. Bader P, Weingart R (2004) Conductive and kinetic properties of connexin45 hemichannels expressed in transfected HeLa cells. J Membr Biol 199:143–154
78. Tong JJ, Ebihara L (2006) Structural determinants for the differences in voltage gating of chicken Cx56 and Cx45.6 gap-junctional hemichannels. Biophys J 91:2142–2154
79. Trexler EB, Bennett MV, Bargiello TA, Verselis VK (1996) Voltage gating and permeation in a gap junction hemichannel. Proc Natl Acad Sci USA 93:5836–5841
80. Pfahnl A, Dahl G (1998) Localization of a voltage gate in connexin46 gap junction hemichannels. Biophys J 75:2323–2331
81. Jedamzik B, Marten I, Ngezahayo A, Ernst A, Kolb HA (2000) Regulation of lens rCx46-formed hemichannels by activation of protein kinase C, external Ca^{2+} and protons. J Membr Biol 173:39–46
82. Eskandari S, Zampighi GA, Leung DW, Wright EM, Loo DD (2002) Inhibition of gap junction hemichannels by chloride channel blockers. J Membr Biol 185:93–102

83. Zampighi GA, Loo DD, Kreman M, Eskandari S, Wright EM (1999) Functional and morphological correlates of connexin50 expressed in Xenopus laevis oocytes. J Gen Physiol 113:507–524
84. Zoidl G, Bruzzone R, Weickert S, Kremer M, Zoidl C, Mitropoulou G, Srinivas M, Spray DC, Dermietzel R (2004) Molecular cloning and functional expression of zfCx52.6: a novel connexin with hemichannel-forming properties expressed in horizontal cells of the zebrafish retina. J Biol Chem 279:2913–2921
85. Ebihara L, Berthoud VM, Beyer EC (1995) Distinct behavior of connexin56 and connexin46 gap junctional channels can be predicted from the behavior of their hemi-gap-junctional channels. Biophys J 68:1796–1803
86. Muller DJ, Hand GM, Engel A, Sosinsky GE (2002) Conformational changes in surface structures of isolated connexin 26 gap junctions. EMBO J 21:3598–3607
87. Thimm J, Mechler A, Lin H, Rhee S, Lal R (2005) Calcium-dependent open/closed conformations and interfacial energy maps of reconstituted hemichannels. J Biol Chem 280:10646–10654
88. Nilius B, Vennekens R, Prenen J, Hoenderop JG, Droogmans G, Bindels RJ (2001) The single pore residue Asp542 determines Ca^{2+} permeation and Mg^{2+} block of the epithelial Ca^{2+} channel. J Biol Chem 276:1020–1025
89. Nakazawa K, Sawa H, Ojima H, Ishii-Nozawa R, Takeuchi K, Ohno Y (2002) Size of side-chain at channel pore mouth affects Ca^{2+} block of P2X(2) receptor. Eur J Pharmacol 449:207–211
90. Bone LJ, Deschenes SM, Balice-Gordon RJ, Fischbeck KH, Scherer SS (1997) Connexin32 and X-linked Charcot-Marie-tooth disease. Neurobiol Dis 4:221–230
91. Bukauskas FF, Verselis VK (2004) Gap junction channel gating. Biochim Biophys Acta 1662:42–60
92. Srinivas M, Calderon DP, Kronengold J, Verselis VK (2006) Regulation of connexin hemichannels by monovalent cations. J Gen Physiol 127:67–75
93. Retamal MA, Froger N, Palacios-Prado N, Ezan P, Sáez PJ, Sáez JC, Giaume C (2007) Cx43 hemichannels and gap junction channels in astrocytes are regulated oppositely by proinflammatory cytokines released from activated microglia. J Neurosci 27:13781–13792
94. Orellana JA, Hernandez DE, Ezan P, Velarde V, Bennett MV, Giaume C, Sáez JC (2010) Hypoxia in high glucose followed by reoxygenation in normal glucose reduces the viability of cortical astrocytes through increased permeability of connexin 43 hemichannels. Glia 58:329–343
95. Orellana JA, Shoji KF, Abudara V, Ezan P, Amigou E, Sáez PJ, Jiang JX, Naus CC, Sáez JC, Giaume C (2011) Amyloid {beta}-induced death in neurons involves glial and neuronal hemichannels. J Neurosci 31:4962–4977
96. Garre JM, Retamal MA, Cassina P, Barbeito L, Bukauskas FF, Sáez JC, Bennett MV, Abudara V (2010) FGF-1 induces ATP release from spinal astrocytes in culture and opens pannexin and connexin hemichannels. Proc Natl Acad Sci USA 107:22659–22664
97. De Vuyst E, Wang N, Decrock E, De Bock M, Vinken M, Van Moorhem M, Lai C, Culot M, Rogiers V, Cecchelli R, Naus CC, Evans WH, Leybaert L (2009) Ca^{2+} regulation of connexin 43 hemichannels in C6 glioma and glial cells. Cell Calcium 46:176–187
98. Braet K, Vandamme W, Martin PE, Evans WH, Leybaert L (2003) Photoliberating inositol-1,4,5-trisphosphate triggers ATP release that is blocked by the connexin mimetic peptide gap 26. Cell Calcium 33:37–48
99. Sánchez HA, Mese G, Srinivas M, White TW, Verselis VK (2010) Differentially altered Ca^{2+} regulation and Ca^{2+} permeability in Cx26 hemichannels formed by the A40V and G45E mutations that cause keratitis ichthyosis deafness syndrome. J Gen Physiol 136:47–62
100. Schalper KA, Sánchez HA, Lee SC, Altenberg GA, Nathanson MH, Sáez JC (2010) Connexin 43 hemichannels mediate the Ca^{2+} influx induced by extracellular alkalinization. Am J Physiol Cell Physiol 299:C1504–C1515
101. Christ GJ, Moreno AP, Melman A, Spray DC (1992) Gap junction-mediated intercellular diffusion of Ca^{2+} in cultured human corporal smooth muscle cells. Am J Physiol 263:C373–C383

102. Harris AL (2007) Connexin channel permeability to cytoplasmic molecules. Prog Biophys Mol Biol 94:120–143
103. Rose B, Loewenstein WR (1975) Permeability of cell junction depends on local cytoplasmic calcium activity. Nature 254:250–252
104. De Mello WC (1975) Effect of intracellular injection of calcium and strontium on cell communication in heart. J Physiol 250:231–245
105. Dahl G, Isenberg G (1980) Decoupling of heart muscle cells: correlation with increased cytoplasmic calcium activity and with changes of nexus ultrastructure. J Membr Biol 53:63–75
106. Spray DC, Bennett MV (1985) Physiology and pharmacology of gap junctions. Annu Rev Physiol 47:281–303
107. Sneyd J, Charles AC, Sanderson MJ (1994) A model for the propagation of intercellular calcium waves. Am J Physiol 266:C293–C302
108. Hofer T (1999) Model of intercellular calcium oscillations in hepatocytes: synchronization of heterogeneous cells. Biophys J 77:1244–1256
109. Hofer T, Politi A, Heinrich R (2001) Intercellular Ca^{2+} wave propagation through gap-junctional Ca^{2+} diffusion: a theoretical study. Biophys J 80:75–87
110. Iacobas DA, Suadicani SO, Spray DC, Scemes E (2006) A stochastic two-dimensional model of intercellular Ca^{2+} wave spread in glia. Biophys J 90:24–41
111. Hofer AM (2005) Another dimension to calcium signaling: a look at extracellular calcium. J Cell Sci 118:855–862
112. Stout CE, Costantin JL, Naus CC, Charles AC (2002) Intercellular calcium signaling in astrocytes via ATP release through connexin hemichannels. J Biol Chem 277:10482–10488
113. Gomes P, Srinivas SP, Van Driessche W, Vereecke J, Himpens B (2005) ATP release through connexin hemichannels in corneal endothelial cells. Invest Ophthalmol Vis Sci 46:1208–1218
114. Gossman DG, Zhao HB (2008) Hemichannel-mediated inositol 1,4,5-trisphosphate (IP3) release in the cochlea: a novel mechanism of IP3 intercellular signaling. Cell Commun Adhes 15:305–315
115. Li F, Sugishita K, Su Z, Ueda I, Barry WH (2001) Activation of connexin-43 hemichannels can elevate $[Ca^{2+}]i$ and $[Na^{+}]i$ in rabbit ventricular myocytes during metabolic inhibition. J Mol Cell Cardiol 33:2145–2155
116. Shintani-Ishida K, Uemura K, Yoshida K (2007) Hemichannels in cardiomyocytes open transiently during ischemia and contribute to reperfusion injury following brief ischemia. Am J Physiol Heart Circ Physiol 293:H1714–H1720
117. Elfgang C, Eckert R, Lichtenberg-Frate H, Butterweck A, Traub O, Klein RA, Hulser DF, Willecke K (1995) Specific permeability and selective formation of gap junction channels in connexin-transfected HeLa cells. J Cell Biol 129:805–817
118. Cao F, Eckert R, Elfgang C, Nitsche JM, Snyder SA, Hu DF, Willecke K, Nicholson BJ (1998) A quantitative analysis of connexin-specific permeability differences of gap junctions expressed in HeLa transfectants and Xenopus oocytes. J Cell Sci 111:31–43
119. Bootman MD, Berridge MJ, Taylor CW (1992) All-or-nothing Ca^{2+} mobilization from the intracellular stores of single histamine-stimulated HeLa cells. J Physiol 450:163–178
120. Paemeleire K (2002) Calcium signaling in and between brain astrocytes and endothelial cells. Acta Neurol Belg 102:137–140
121. Dobrowolski R, Sommershof A, Willecke K (2007) Some oculodentodigital dysplasia-associated Cx43 mutations cause increased hemichannel activity in addition to deficient gap junction channels. J Membr Biol 219:9–17
122. Herve JC (2007) Gap junction channels: from protein genes to diseases. Prog Biophys Mol Biol 94:1–4
123. George CH, Kendall JM, Campbell AK, Evans WH (1998) Connexin-aequorin chimerae report cytoplasmic calcium environments along trafficking pathways leading to gap junction biogenesis in living COS-7 cells. J Biol Chem 273:29822–29829

124. Brehm P, Lechleiter J, Smith S, Dunlap K (1989) Intercellular signaling as visualized by endogenous calcium-dependent bioluminescence. Neuron 3:191–198
125. Churchill GC, Louis CF (1998) Roles of Ca^{2+}, inositol trisphosphate and cyclic ADP-ribose in mediating intercellular Ca^{2+} signaling in sheep lens cells. J Cell Sci 111(Pt 9): 1217–1225
126. Montana V, Malarkey EB, Verderio C, Matteoli M, Parpura V (2006) Vesicular transmitter release from astrocytes. Glia 54:700–715
127. Leybaert L, Paemeleire K, Strahonja A, Sanderson MJ (1998) Inositol-trisphosphate-dependent intercellular calcium signaling in and between astrocytes and endothelial cells. Glia 24:398–407
128. Paemeleire K, Martin PE, Coleman SL, Fogarty KE, Carrington WA, Leybaert L, Tuft RA, Evans WH, Sanderson MJ (2000) Intercellular calcium waves in HeLa cells expressing GFP-labeled connexin 43, 32, or 26. Mol Biol Cell 11:1815–1827
129. Suadicani SO, Cherkas PS, Zuckerman J, Smith DN, Spray DC, Hanani M (2010) Bidirectional calcium signaling between satellite glial cells and neurons in cultured mouse trigeminal ganglia. Neuron Glia Biol 6:43–51
130. Cotrina ML, Lin JH, Alves-Rodrigues A, Liu S, Li J, Azmi-Ghadimi H, Kang J, Naus CC, Nedergaard M (1998) Connexins regulate calcium signaling by controlling ATP release. Proc Natl Acad Sci USA 95:15735–15740
131. Arcuino G, Lin JH, Takano T, Liu C, Jiang L, Gao Q, Kang J, Nedergaard M (2002) Intercellular calcium signaling mediated by point-source burst release of ATP. Proc Natl Acad Sci USA 99:9840–9845
132. Schipke CG, Boucsein C, Ohlemeyer C, Kirchhoff F, Kettenmann H (2002) Astrocyte Ca^{2+} waves trigger responses in microglial cells in brain slices. FASEB J 16:255–257
133. Anselmi F, Hernandez VH, Crispino G, Seydel A, Ortolano S, Roper SD, Kessaris N, Richardson W, Rickheit G, Filippov MA, Monyer H, Mammano F (2008) ATP release through connexin hemichannels and gap junction transfer of second messengers propagate Ca^{2+} signals across the inner ear. Proc Natl Acad Sci USA 105:18770–18775
134. Leinonen P, Aaltonen V, Koskela S, Lehenkari P, Korkiamaki T, Peltonen J (2007) Impaired gap junction formation and intercellular calcium signaling in urinary bladder cancer cells can be improved by Go6976. Cell Commun Adhes 14:125–136
135. Jiang JX, Siller-Jackson AJ, Burra S (2007) Roles of gap junctions and hemichannels in bone cell functions and in signal transmission of mechanical stress. Front Biosci 12:1450–1462
136. Isakson BE, Olsen CE, Boitano S (2006) Laminin-332 alters connexin profile, dye coupling and intercellular Ca^{2+} waves in ciliated tracheal epithelial cells. Respir Res 7:105
137. Orellana JA, Figueroa XF, Sánchez HA, Contreras-Duarte S, Velarde V, Sáez JC (2011) Hemichannels in the neurovascular unit and white matter under normal and inflamed conditions. CNS Neurol Disord Drug Targets 10:404–414
138. Bruzzone S, Guida L, Zocchi E, Franco L, De Flora A (2001) Connexin 43 hemi channels mediate Ca2+−regulated transmembrane NAD+ fluxes in intact cells. FASEB J 15:10–12
139. Dakin K, Zhao Y, Li WH (2005) LAMP, a new imaging assay of gap junctional communication unveils that Ca^{2+} influx inhibits cell coupling. Nat Methods 2:55–62
140. Dakin K, Li WH (2006) Local Ca^{2+} rise near store operated Ca^{2+} channels inhibits cell coupling during capacitative Ca^{2+} influx. Cell Commun Adhes 13:29–39

Chapter 35
Calcium Signaling in Vascular Smooth Muscle Cells: From Physiology to Pathology

Alexandre Marchand, Aniella Abi-Gerges, Youakim Saliba, Elise Merlet, and Anne-Marie Lompré

Abstract Cyclic variations in calcium (Ca^{2+}) concentrations, through a process called excitation-contraction coupling, allow regulation of vascular smooth muscle cells contractility and thus modulation of vascular tone and blood pressure. As a second messenger, Ca^{2+} also activates signaling cascades leading to transcription factors activation in a process called excitation-transcription coupling. Furthermore, recent evidences indicate an interaction between post-transcriptional regulation by microRNAs (miRNAs) and Ca^{2+} signaling. All these actors, which are frequently altered in vascular diseases, will be reviewed here.

Keywords Calcium signaling • Excitation-contraction • Excitation-transcription • microRNA • Physiopathology • Vascular smooth muscle

Introduction

The arterial vascular smooth muscle cells (VSMCs) provide structural integrity to the vessel and regulate vascular tone and blood pressure. Normal arteries VSMCs have a contractile/quiescent phenotype whereas VSMCs switch to a proliferative/synthetic phenotype leading to vessel remodeling in diseases such as atherosclerosis, systemic or pulmonary artery hypertension (PAH) and injury-induced restenosis. This phenotypic modulation is accompanied by multiple alterations in calcium (Ca^{2+}) cycling that may precede changes in phenotype and may contribute to vascular remodeling.

A. Marchand • A. Abi-Gerges • Y. Saliba • E. Merlet • A.-M. Lompré (✉)
Inserm UMRS 956/ Université Pierre et Marie Curie Paris6,
91 boulevard de l'hôpital, 75013 Paris, France
e-mail: alexandre.marchand@upmc.fr; aniella.abi_gerges@upmc.fr;
youakim.saliba@etu.upmc.fr; elise.merlet@etu.upmc.fr; anne-marie.lompre@upmc.fr

M.S. Islam (ed.), *Calcium Signaling*, Advances in Experimental Medicine and Biology 740, DOI 10.1007/978-94-007-2888-2_35,

One important role of Ca^{2+} in VSMCs is to participate to the excitation-contraction (EC) coupling. There are two types of smooth muscles differing by their contraction: some have a phasic contraction, mainly dependent on Ca^{2+} through Ca^{2+}/calmodulin activation of the myosin light chain kinase (MLCK), such as cerebral arteries. Others, like the large arteries, are characterized by a slow rise in Ca^{2+} and a sustained tonic contraction mainly dependent on phosphorylation/dephosphorylation processes [1]. In addition to its effect in the EC coupling, Ca^{2+} is also involved in modulation of gene expression in a process now called excitation-transcription (ET) coupling. Finally, few studies have begun to emphasize the link between post-transcriptional regulation by microRNA (miRNA) and Ca^{2+}, frequently showing regulatory loop between a Ca^{2+} activated transcription factor and a miRNA. These different aspects of Ca^{2+} signaling will be reviewed.

Excitation-Contraction Coupling

In vivo, VSMCs are partially constricted with resting Ca^{2+} concentrations around 100–300 nM [2]. Increasing intraluminal pressure causes gradual depolarization of arterial smooth muscle. It is suggested that the transient receptor potential (TRP) channels play a crucial role in translating the luminal pressure increase into a depolarization of VSMCs via Na^+ entry. This activates the voltage-gated, dihydropyridine-sensitive L-type calcium channels (LTCCs), $Cav_{1.2}$, located at the sarcolemma [3, 4]. Global rise in intracellular Ca^{2+} leads to the initiation of the contractile response through activation of Ca^{2+}/calmodulin-dependent myosin light chain kinase (MLCK). On the other hand, Ca^{2+} activates the ryanodine receptors (RyR) leading to Ca^{2+} release from the sarcoplasmic reticulum (SR), a phenomenon known as the calcium-induced calcium release (CICR). Paradoxically, the small release of Ca^{2+} through the RyR, called Ca^{2+} sparks, negatively regulates contraction by activating the plasma membrane Ca^{2+}-sensitive potassium channels (K_{Ca} channels). The transient outward K^+ current generated, referred as STOC (Spontaneous Transient Outward Current) [5], hyperpolarizes the membrane closing LTCCs hence decreasing voltage-dependent Ca^{2+} entry. Afterwards, Ca^{2+} store depletion may induce an increase in Ca^{2+} entry through non voltage-dependent channels which display a large inward rectification. Reduced Ca^{2+} levels are also achieved through extrusion of cytoplasmic Ca^{2+} by the plasma membrane Ca^{2+} ATPase (PMCA) and the Na^+/Ca^{2+} exchanger (NCX) and the re-uptake by the sarco/endoplasmic reticulum Ca^{2+} ATPase (SERCA).

Voltage-Dependent Ca^{2+} Entry Through L-Type Calcium Channels

LTCCs are composed of pore-forming α_1-subunits and four additional accessory subunits (α_2, β, γ, δ) [6]. $Cav_{1.2}$ is the predominant isoform of LTCCs in arterial smooth muscle [7–9]. These channels are broadly expressed throughout the sarcolemma. However, application of novel imaging approaches revealed single or small

clusters of LTCCs operating in a high probability mode that creates sites of nearly continual Ca^{2+} influx within specific regions of the arterial myocytes' sarcolemma [8, 10–12]. These persistent Ca^{2+} sparklets, mainly regulated by $Cav_{1.2}$ channels, contribute to steady state local and global calcium in arterial SMCs under physiological conditions [11]. It is proposed that regional variations in Ca^{2+} sparklets activity are due to local targeting of protein kinase C alpha (PKCα) by the scaffolding protein AKAP150 (the rodent ortholog of human AKAP79) to specific regions of the surface membrane of arterial myocytes [13] thus allowing to phosphorylate nearby LTCCs [12, 14]. The effects of PKCα on Ca^{2+} sparklets activity are counterbalanced by the Ca^{2+}-sensitive protein phosphatase calcineurin. Hence, the level of Ca^{2+} sparklets activity varies regionally depending on the relative activities of PKCα and calcineurin [11].

Ca^{2+} sparks frequency and STOCs are modulated by protein kinases in cerebral and coronary vascular smooth muscle. cAMP-dependent protein kinase (PKA) and cGMP-dependent protein kinase (PKG) increase STOC frequency via an increase in Ca^{2+} sparks frequency while an increase in STOC amplitude appears to occur via a direct activation of plasmalemmal K_{Ca} channels by PKA and PKG [15, 16].

Voltage–Gated T-Type Calcium Channels

T-type calcium channels (TTCCs) are low voltage-activated, fast-activating and fast-inactivating channels characterized by their small unitary conductance, and relative insensitivity to agents that block L-type and other high voltage-activated Ca^{2+} channels [17]. There are three types of TTCCs: $Cav_{3.1}$ and $Cav_{3.2}$, mainly expressed in the cardiovascular system, and $Cav_{3.3}$ which are more commonly found in cerebral VSMCs [18]. The functional role of this specialized class of Ca^{2+} channels in VSM is still unclear. However, it is generally accepted that TTCCs are not involved in vasoconstriction, with the possible exception of the renal microcirculation, but appear to be important for local electromechanical coupling in VSMCs. TTCCs are also present in some veins that display spontaneous contractile activity, where they likely generate pacemaker activity. $Cav_{3.1}$ and $Cav_{3.2}$ −/− mice have unchanged blood pressure [19, 20]. In addition, coronary arteries isolated from $Cav_{3.2}$−/− mice showed normal contractile response but reduced relaxation. This could be due to a functional coupling between TTCCs and the large-conductance Ca^{2+}-activated K^+ (BK_{Ca}) channel [21]. Thus Ca^{2+} influx through TTCC seems essential for relaxation in coronary arteries. TTCC expression has also been associated with pathological proliferation of VSMCs as well as cellular growth.

Non-voltage Gated Calcium Entry

Store-operated Ca^{2+} entry (SOCE) is the pathway by which the depletion of intracellular Ca^{2+} stores activates extracellular Ca^{2+} entry to subsequently refill the emptied Ca^{2+} stores. It is an ubiquitous agonist-evoked Ca^{2+} entry pathway firstly named

capacitative Ca^{2+} entry (CCE) [22]. SOCE is activated by the actual fall of the Ca^{2+} concentration within the lumen of the sarco/endoplasmic reticulum (SR/ER) through the activation of the inositol 1,4,5 trisphosphate (IP_3) receptor (IP_3R). Upon agonist stimulation (such as angiotensin II, endothelin-1), Ca^{2+} entering through the Gq/Gi phospholipase C (PLC)-activated channels is referred to as receptor-operated Ca^{2+} entry (ROCE). The relative contribution of SOCE to EC coupling depends on the smooth muscle type and appears to be greatest in tonic smooth muscle [23]. Both SOCE and ROCE participate in hyperplasia, remodeling, arterial blood pressure regulation, blood vessel integrity and myogenic tone [24]. ROCE identity and role in VSMCs are still debated due to their plasticity and variability according to the SMC types [25].

STIM1/ORAIs/TRPCs/ARCs

A major breakthrough in SOCE understanding has been the discovery of STIM1 (stromal interaction molecule 1) as a Ca^{2+} sensor in the ER [26, 27]. Although SOCE has been long described in VSMCs, the molecular identity and role of SOCE in VSMC function remain highly contentious issues. Orai proteins (Orai1-3) are the principal candidates. Silencing Orai1 inhibits SOCE whereas silencing Orai2 and Orai3 has no effect [28, 29]. However, ectopic expression studies showed that, not only Orai1, but also Orai2 together with STIM1 enhanced SOC entry in HEK293 but not in RBL 2H3 cells, suggesting that the capability of Orai2 to form CRAC channels depends on the cell background [30, 31]. Furthermore, Orai1 knockout mice showed alteration of CRAC currents in mast cells but not in T cells, suggesting that SOC entry appears to be fulfilled by Orai2 which is more highly expressed than Orai1 and Orai3 in these cells [32]. STIM1 also heteromultimerizes with canonical TRP (TRPC) channels to determine their function as store-operated channels (SOC) [33]. TRPCs are non voltage-gated, Ca^{2+} permeable and non selective cation channels. TRPCs implications in SOCE and ROCE still need to be clarified. TRPC 1/4/5 are suggested as candidates for SOCE [34] but VSMCs from TRPC1-deficient mice have normal contractility and intact SOCE [35]. Furthermore, contradicting results were obtained using knock-down strategy. Whereas silencing TRPC1, TRPC4 and TRPC6 had no effect on SOCE [29], other studies reported that TRPC1 or TRPC6 knock-down attenuates SOCE [29, 36, 37]. Differences in the cell type (rat aorta *vs* human pulmonary artery), the silencing method (siRNA *vs* antisens oligonucleotides) and the level of silencing might be at the origin of the discrepancy. Liao suggested that a TRPC/Orai complex mediates SOCE and ROCE [38] whereas others found that TRPCs function independently of STIM1 and Orai1 [39]. The reverse mode of the NCX is another source of cytoplasmic Ca^{2+} influx. Na^+ entry, mediated by SOC, influences Na^+ pump activity and Na^+/Ca^{2+} exchange and has unexpectedly large effects on cell-wide Ca^{2+} signaling [40]. Local coupling of NCX with TRPC and Orai1 could account for agonist-induced Ca^{2+} influx in VSMCs [28, 41]. Two recent studies also reported that STIM1 directly suppresses depolarization-induced opening of $Cav_{1.2}$ while activating Orai channels [42, 43]. In addition STIM1

regulates the arachidonic acid dependent and store depletion independent Ca^{2+} selective (ARC) channels [44, 45]; ARC channels being hetero-pentameric assemblies of three Orai1 and two Orai3 subunits [46]. This arachidonic acid mediated non-capacitative Ca^{2+} entry has been reported in DDT1 MF2 and A7r5 smooth muscle cells, where it is closely related to the capacitative one [47, 48].

Other Ca^{2+} Selective and Non Selective Channels: TRPVs/TRPMs/TRPP

They are also implicated in VSMCs Ca^{2+} homeostasis [49]. TRPM4 (melastatin) and TRPV1 (vanilloid) are activated after intra-luminal pressure elevation, and contribute to the control of cerebral and mesenteric arteries myogenic tone [3]. TRPV2 is a swelling-activated channel in mouse aortic SMCs, while TRPV4 forms a signaling complex with RyR and the large-conductance Ca^{2+}-activated K^+ (BK_{Ca}) channel causing membrane hyper-polarization and dilation of cerebral arteries [50, 51]. Polycystins (TRPP1, 2) also play a pivotal role in the maintenance of vascular integrity and resistance to hemodynamic stress [52].

Sarcoplasmic Reticulum Ca^{2+} Cycling – Extrusion Through the Membrane

The SERCA pump is encoded by a family of three genes SERCA1-3. Quiescent SMC express two splice variants of the SERCA2 pre-mRNA: 2a and 2b [53]. The two SR Ca^{2+}-release channels, the RyR and the IP_3R, are expressed in VSMC. Three RyR genes (RyR 1–3), and splicing variants of each have been described. RyR 2 is widely expressed in VSMC but some studies also reported the presence of RyR1 and RyR3. The IP_3R is also encoded by three genes giving rise to more isoforms by alternative splicing of pre-messengers.

Intracellular Ca^{2+} is extruded to the extracellular space by PMCA and NCX with a respective contribution of 70% and 30%. PMCA is a high-affinity Ca^{2+} pump regulated by calmodulin, kinases and other signaling proteins. In mammals, 4 genes encode PMCA isoforms 1–4 which are expressed in medial SMC. PMCA1 seems to be involved in the repression of VSMC proliferation [54]. PMCA regulates Ca^{2+} locally thus leading to specific cellular responses. Indeed, calcineurin is recruited in a low Ca^{2+} environment by PMCA4b to prevent NFAT activation [55].

NCX is a bidirectional transporter of Na^+ and Ca^{2+} depending on the electrochemical gradient of the substrate ions. Three NCX genes (NCX1-3) have been identified: NCX1, which is ubiquitously expressed, is the only isoform expressed in VSMC. NCX expression is restricted to plasma membrane microdomains that overlie junctional ER thus controlling Ca^{2+} concentration in specialized cellular regions. NCX is involved in controlling vasoconstriction of smooth muscle and blood pressure [56, 57].

Excitation-Transcription Coupling

Recent evidences show a regulation of transcription factors by calcium in VSMC. This phenomenon known as E-T coupling involves in particular CREB, NFAT and NFkB.

cAMP Response Element Binding Protein (CREB)

CREB is highly expressed and active in quiescent smooth muscle cells. It promotes smooth muscle gene expression program and decreases proliferation by modulating the expression of multiple cell cycle regulatory genes, as well as genes encoding growth factors, growth factor receptors, and cytokines [58]. cAMP/PKA pathway, MAPK pathway and calcium/calmodulin (CaM) kinases pathway promote phosphorylation of CREB at Ser133 leading to its activation [59]. Activation of LTCCs increases cytoplasmic Ca^{2+} which activates calmodulin translocation to the nucleus. The Ca^{2+}/calmodulin complex activates the calmodulin kinase II (CaMKII), which in turn phosphorylates CREB and activates its transcriptional activity [60, 61]. On the contrary, Ca^{2+} sparks were shown to have an inhibitory effect on CREB [62]. This may be due to the activation of BK_{Ca} and their hyperpolarizing effect.

Nuclear Factor of Activated T Cells (NFAT) and Nuclear Factor-kappa B (NFκB)

The NFAT transcription factor family consists of five members NFATc1, NFATc2, NFATc3, NFATc4 and NFAT5. Only NFATc1-4 are regulated by Ca^{2+} signaling and among them NFATc3 is the most abundant in native SMC [63]. In resting cells, NFAT is phosphorylated by various kinases and remains in the cytoplasm. When VSMCs are stimulated by different stresses and growth factors, Ca^{2+} influx activates calcineurin, a calcium/calmodulin dependent phosphatase, which dephosphorylates NFAT allowing its translocation to the nucleus. NFAT then activates proliferation and inflammatory cytokines [64]. NFκB is important in mediating stress and inflammatory-induced signals which also participate to VSMC proliferation.

These transcription factors were shown to be optimally activated in response to different patterns of Ca^{2+} oscillations. Transient high Ca^{2+} spikes induce activation of NFκB while NFAT is activated by prolonged low increase in intracellular Ca^{2+} concentration [65].

The balance between Ca^{2+}-regulated and other transcription factors (for example serum response factor, SRF, myocardin- Histone deacetylase, HDAC – myocyte enhancer factor 2, MEF2 – hypoxia-inducible factor, HIF) in VSMCs can lead to differentiation or proliferation depending on their expression and activity levels. The interactions between all these different factors could allow a fine-tuning of the VMSCs phenotype but still remain to be clarified.

Post-transcriptional Regulation by microRNAs (miRNA)

miRNA are endogenous 18–24 nucleotides-long non coding RNA that have been studied in mammals since a decade. They are implicated in gene silencing by targeting mRNAs with complementary sequences in their 3′untranslated regions (UTR). This post-transcriptional regulation of gene expression is conserved among species ranging from plants to mammals and miRNA appear to be an important way of regulation in many physiological and pathological situations [66]. About 1,000 different miRNA are predicted in humans and could regulate more than 30% of all genes. Bioinformatic and basic studies have revealed that a single miRNA can regulate many genes and that one gene can be modulated by different miRNAs [67] leading to specific regulations of biological processes [68]. miRNAs seem to be critical modulators of many vascular cell functions like cell differentiation, migration, proliferation and apoptosis [69]. miR-143 and miR-145 are highly expressed in normal vascular walls. Their expression is sufficient to induce differentiation, repression of VSMCs proliferation and migration [70–72]. Since Ca^{2+}-calmodulin dependent protein kinase II delta (CamkIIδ) is directly inhibited by miR-145, this could explain the effects of this miRNA in VSMCs [70]. Presently, cardiac studies show evidences for interactions between several miRNAs and Ca^{2+} signaling contributing to pathological development, but these regulations are likely to be conserved in the vascular system.

Alteration of Ca^{2+} Signaling in Vascular Diseases

Alteration in E-C Coupling

Vascular proliferative diseases are characterized by VSMCs proliferation accompanied by loss of the major actors of the contractile phenotype [73]. The importance of LTCCs in maintaining the vascular tone is reduced in proliferative VSMCs whereas TTCCs become prevalent and control progression through the cell cycle [74, 75] possibly through the activation of calcineurin/NFAT pathway. Indeed, $Cav_{3.2}$−/− mice are protected from cardiac hypertrophy and NFAT activation in pressure-overload model [19]. Persistent Ca^{2+} sparklets appear during VSMCs proliferation and control calcineurin as well as NFATc3 activation during hypertension [76].

Furthermore, arterial SMC proliferation is associated with enhanced SOCE [77, 78]. This is consistent with data showing that STIM1 and Orai1 are up-regulated during VSMCs proliferation *in vitro* and *in vivo* [29, 78–80]. STIM1-silencing prevents VSMCs migration and proliferation as well as injury-induced restenosis [78–80]. In agreement with the increased SOCE, TRPC1, 4 and 5 are also up-regulated during VSMCs migration and proliferation [24, 81–85]. TRPC3 and TRPC6 are up-regulated in systemic and idiopathic pulmonary hypertension where angiotensin II and endothelin-1, respectively, are essential agonists [86, 87]. NCX1 is up-regulated in arteries from hypertensive rats and in human PAH [88]. Since NCX interacts with

Orai, these results point towards the increase in SOCE during vascular proliferative disease [28].

Proliferation of aortic SMC is associated with loss of the contractile isoform of SERCA, SERCA2a [53, 89, 90]. Restoring its expression inactivates calcineurin and NFAT, thus inhibiting VSMCs proliferation and migration *in vitro* [89, 91]. Besides, restoring SERCA2a in proliferating SMC *in vitro* modifies agonist-induced IP_3R Ca^{2+} release from steady-state to oscillatory mode and suppresses SOCE by preventing interactions between STIM1 and the pore forming unit Orai1 [91]. SERCA2a overexpression also inhibits neointimal formation in a model of restenosis *in vivo* [89]. RyR2 expression also disappears progressively in proliferating VSMCs whereas expression of RyR3 and IP_3R is increased [53, 81, 90, 92]. PMCA1 and PMCA4 expression is decreased during proliferation [54].

In conclusion, it seems that in quiescent/contractile VSMCs, most of the Ca^{2+} is devoted to the contractile function. On the contrary, when cells proliferate Ca^{2+} is more implicated in transcription modulations.

Alteration in E-T Coupling

In agreement with its activation by LTCCs, and the reduced importance of LTCCs during proliferation, CREB was shown to be down-regulated in different vascular diseases [58, 93]. However, CREB activation was sometimes associated with proliferation and migration and activated in the neointima after balloon injury [94–96]. CREB inhibition was accompanied by an increase in apoptosis and suppressed neointimal formation [96]. This suggests that CREB plays a role in the balance between survival and proliferation. A different pattern of expression of its co-regulator CREB Binding Protein (CBP), which is essential for proliferation [97], may explain the apparent contradictory results.

In addition to NFATc3, NFATc1 and NFATc2 are induced by different activators of SMC proliferation [98]. These proteins are activated by Ca^{2+} entry through SOCs. Indeed, silencing STIM1 [79] or overexpressing SERCA2a inhibits NFAT activity [89] by suppressing SOCE [91]. In arterial SMCs, Ca^{2+} sparklets are not sufficient to induce NFAT nuclear translocation but in hypertension their activity are persistent leading to calcineurin and NFATc3 activation [76].

Inhibition of calcineurin/NFAT interaction completely abolished NFAT nuclear translocation and thus VSMC proliferation or injury-induced neointima formation [89, 99, 100].

miRNA and Ca^{2+} Signaling Interactions

Vascular miR-143 and miR-145 expression is strongly decreased during VSMCs proliferation. In accordance with this, CAMKII delta isoform which is a direct target of miR-145 is specifically induced in proliferative cells [101]. On the contrary,

other miRNAs like miR-21 [102], miR-221/miR-222 [103] and miR-146a [104] are considered as pro-proliferative. Their expression increases during neointimal hyperplasia. Preventing these up-regulations inhibits neointima formation. Some miRNAs seem to be protective against pathological deregulations by interacting with Ca^{2+} signaling. miR-1 plays an anti-hypertrophic role in cardiac myocytes by targeting calmodulin and Mef2a genes [105]. MiR-133 and calcineurin repress each other expression in a balance leading to progressive hypertrophy [106]. NFATc4 is also a direct target of miR-133 in cardiac myocytes [107]. Other miRNAs induced by Ca^{2+} signaling are implicated in disease progression: miR-199b targets the nuclear kinase Dyrk1a (which normally phosphorylates and inactivates NFAT) in an auto-amplification loop promoting calcineurin/NFAT signaling [108]. miR-23a is also a downstream target of NFATc3 and inhibits the anti-hypertrophic protein MuRF1 [109]. As many signaling pathways are conserved between cardiac myocytes and VSMCs, the same process may be at play in vascular tissues: miR-1 and miR-23a for example are expressed in vascular cells. However, the precise Ca^{2+} signaling pathways involved in miRNA regulation have not yet been studied.

Conclusion

Figure 35.1 summarizes our current view of the alteration in Ca^{2+} signaling which occurs during VSMC proliferation. In quiescent VSMC, Ca^{2+} entry through LTCCs activates the CICR and contraction. Relaxation occurs by activation of SERCA, extrusion of Ca^{2+} by the NCX and the PCMA. In addition, Ca^{2+} sparks activate the BK_{Ca} channels thus hyperpolarizing the VSMC and inactivating LTCC. Ca^{2+} entry through LTCCs induces CaM translocation to the nucleus which then activates CaMKII, CREB phosphorylation and the activation of the contractile phenotype.

In proliferating VSMC, the Ca^{2+} actors of contraction: LTCC, RyR2, SERCA2a and PMCA are down-regulated. Furthermore, the activation of the PLC/IP3 pathway and the down-regulation of SERCA2a results in depletion of SR/ER Ca^{2+} leading to activation of STIM1. In addition, expression of TTCC, STIM1, Orais and TRPCs is up-regulated leading to an increase in Ca^{2+} entry by SOCE and ROCE. The reverse mode of the NCX may also contribute to Ca^{2+} entry. Calcineurin, normally restricted to a region of low Ca^{2+} due the proximity with PMCA4b, becomes activated and induces NFAT dephosphorylation and translocation to the nucleus where it activates proliferative genes and expression of new miRNAs such as miR-23a. miR-145 downregulation allow upregulation of one of its main targets CaMKIIδ, contributing to the proliferative phenotype.

To sum-up, it is now clear that small alterations in Ca^{2+} in VSMCs activate, either spatially or temporally, signaling pathways leading to gene expression regulation. These mechanisms are particularly important for pathological proliferation as inhibition of SERCA2a and activation of STIM1 increases cytosolic Ca^{2+} which activates NFAT transcription factor. Controlling Ca^{2+} signaling to prevent vascular disease is therefore an interesting strategy for therapeutic applications. More studies

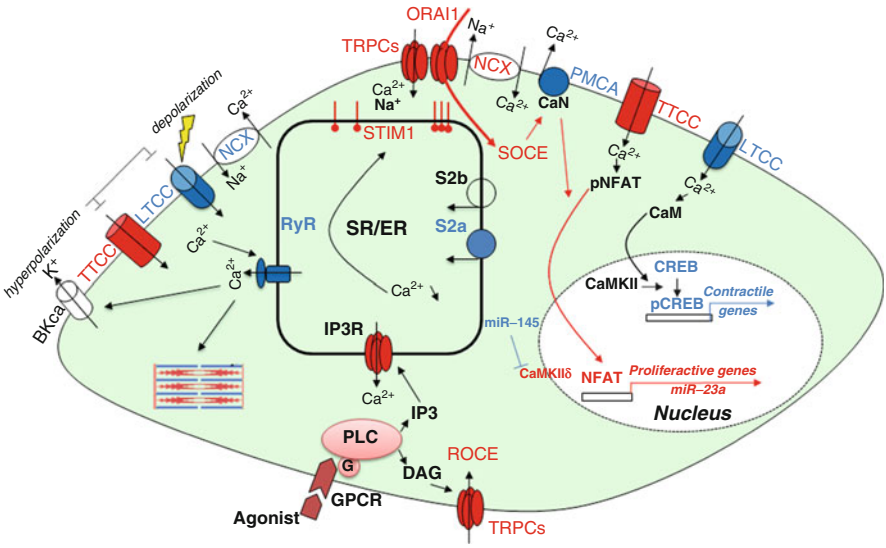

Fig. 35.1 Ca^{2+} signaling in VSMC and its alterations during proliferation. In *blue* are down-regulated or inactivated mechanisms and in *red* are up-regulated or activated mechanisms in proliferation. BK_{Ca} Large-conductance calcium (Ca^{2+}) activated potassium channel, *CaM* calmodulin, *CaMK* Ca^{2+}/calmodulin-dependent protein kinase, *CaN* calcineurin, *CREB* cAMP response element-binding protein, *pCREB* phosphorylated CREB, *DAG* diacylglycerol, *G* G protein, *GPCR* G protein-coupled receptor, *IP3* inositol 1,4,5 trisphosphate, *IP3R* IP3 receptor, *LTCC* L-type Ca^{2+} channel, *NCX* sodium (Na^+) Ca^{2+} exchanger, *NFAT* nuclear factor of activated T-cells, *pNFAT* phosphorylated NFAT, *PLC* phospholipase C, *PMCA* plasma membrane Ca^{2+} ATPase, *ROCE* receptor operated Ca^{2+} entry, *RyR* ryanodine receptor, *S2a/S2b* sarcoplasmic reticulum Ca^{2+} ATPase isoforms a and b, *SOCE* store operated Ca^{2+} entry, *SR/ER* sarco/endo-plasmic reticulum, *STIM1* stromal interaction molecule 1, *TRPC* canonical transient receptor channel, *TTCC* T-type Ca^{2+} channel

are needed to identify all components (proteins-transcription factors-miRNAs-epigenetic modifications) implicated in Ca^{2+} regulations in VSMC and how they interact with each-others. Combinatorial modulations should be an interesting strategy for future therapeutic assays.

References

1. Somlyo AP, Somlyo AV (2003) Ca^{2+} sensitivity of smooth muscle and nonmuscle myosin II: modulated by G proteins, kinases, and myosin phosphatase. Physiol Rev 83:1325–1358
2. House SJ, Potier M, Bisaillon J, Singer HA, Trebak M (2008) The non-excitable smooth muscle: calcium signaling and phenotypic switching during vascular disease. Pflugers Arch 456:769–785
3. Earley S, Straub SV, Brayden JE (2007) Protein kinase C regulates vascular myogenic tone through activation of TRPM4. Am J Physiol Heart Circ Physiol 292:H2613–H2622

4. Welsh DG, Morielli AD, Nelson MT, Brayden JE (2002) Transient receptor potential channels regulate myogenic tone of resistance arteries. Circ Res 90:248–250
5. Benham CD, Bolton TB (1986) Spontaneous transient outward currents in single visceral and vascular smooth muscle cells of the rabbit. J Physiol 381:385–406
6. Catterall WA (1995) Structure and function of voltage-gated ion channels. Annu Rev Biochem 64:493–531
7. Koch WJ, Ellinor PT, Schwartz A (1990) cDNA cloning of a dihydropyridine-sensitive calcium channel from rat aorta. Evidence for the existence of alternatively spliced forms. J Biol Chem 265:17786–17791
8. Navedo MF, Amberg GC, Westenbroek RE, Sinnegger-Brauns MJ, Catterall WA, Striessnig J, Santana LF (2007) Ca(v)1.3 channels produce persistent calcium sparklets, but Ca(v)1.2 channels are responsible for sparklets in mouse arterial smooth muscle. Am J Physiol Heart Circ Physiol 293:H1359–H1370
9. Zhang J, Berra-Romani R, Sinnegger-Brauns MJ, Striessnig J, Blaustein MP, Matteson DR (2007) Role of Cav1.2 L-type Ca^{2+} channels in vascular tone: effects of nifedipine and Mg2+. Am J Physiol Heart Circ Physiol 292:H415–H425
10. Amberg GC, Navedo MF, Nieves-Cintron M, Molkentin JD, Santana LF (2007) Calcium sparklets regulate local and global calcium in murine arterial smooth muscle. J Physiol 579: 187–201
11. Navedo MF, Amberg GC, Nieves M, Molkentin JD, Santana LF (2006) Mechanisms underlying heterogeneous Ca^{2+} sparklet activity in arterial smooth muscle. J Gen Physiol 127:611–622
12. Navedo MF, Amberg GC, Votaw VS, Santana LF (2005) Constitutively active L-type Ca^{2+} channels. Proc Natl Acad Sci USA 102:11112–11117
13. Navedo MF, Nieves-Cintron M, Amberg GC, Yuan C, Votaw VS, Lederer WJ, McKnight GS, Santana LF (2008) AKAP150 is required for stuttering persistent Ca^{2+} sparklets and angiotensin II-induced hypertension. Circ Res 102:e1–e11
14. Rubart M, Patlak JB, Nelson MT (1996) Ca^{2+} currents in cerebral artery smooth muscle cells of rat at physiological Ca^{2+} concentrations. J Gen Physiol 107:459–472
15. Robertson BE, Schubert R, Hescheler J, Nelson MT (1993) cGMP-dependent protein kinase activates Ca-activated K channels in cerebral artery smooth muscle cells. Am J Physiol 265:C299–C303
16. Taguchi H, Heistad DD, Kitazono T, Faraci FM (1995) Dilatation of cerebral arterioles in response to activation of adenylate cyclase is dependent on activation of Ca(2+)-dependent K+channels. Circ Res 76:1057–1062
17. Perez-Reyes E (2003) Molecular physiology of low-voltage-activated t-type calcium channels. Physiol Rev 83:117–161
18. Perez-Reyes E, Cribbs LL, Daud A, Lacerda AE, Barclay J, Williamson MP, Fox M, Rees M, Lee JH (1998) Molecular characterization of a neuronal low-voltage-activated T-type calcium channel. Nature 391:896–900
19. Chiang CS, Huang CH, Chieng H, Chang YT, Chang D, Chen JJ, Chen YC, Chen YH, Shin HS, Campbell KP, Chen CC (2009) The Ca(v)3.2 T-type Ca(2+) channel is required for pressure overload-induced cardiac hypertrophy in mice. Circ Res 104:522–530
20. Mangoni ME, Traboulsie A, Leoni AL, Couette B, Marger L, Le Quang K, Kupfer E, Cohen-Solal A, Vilar J, Shin HS, Escande D, Charpentier F, Nargeot J, Lory P (2006) Bradycardia and slowing of the atrioventricular conduction in mice lacking CaV3.1/alpha1G T-type calcium channels. Circ Res 98:1422–1430
21. Chen CC, Lamping KG, Nuno DW, Barresi R, Prouty SJ, Lavoie JL, Cribbs LL, England SK, Sigmund CD, Weiss RM, Williamson RA, Hill JA, Campbell KP (2003) Abnormal coronary function in mice deficient in alpha1H T-type Ca^{2+} channels. Science 302:1416–1418
22. Bitar KN, Bradford P, Putney JW Jr, Makhlouf GM (1986) Cytosolic calcium during contraction of isolated mammalian gastric muscle cells. Science 232:1143–1145
23. Leung FP, Yung LM, Yao X, Laher I, Huang Y (2008) Store-operated calcium entry in vascular smooth muscle. Br J Pharmacol 153:846–857

24. Kumar B, Dreja K, Shah SS, Cheong A, Xu SZ, Sukumar P, Naylor J, Forte A, Cipollaro M, McHugh D, Kingston PA, Heagerty AM, Munsch CM, Bergdahl A, Hultgardh-Nilsson A, Gomez MF, Porter KE, Hellstrand P, Beech DJ (2006) Upregulated TRPC1 channel in vascular injury in vivo and its role in human neointimal hyperplasia. Circ Res 98:557–563
25. Large WA (2002) Receptor-operated Ca2(+)-permeable nonselective cation channels in vascular smooth muscle: a physiologic perspective. J Cardiovasc Electrophysiol 13:493–501
26. Roos J, DiGregorio PJ, Yeromin AV, Ohlsen K, Lioudyno M, Zhang S, Safrina O, Kozak JA, Wagner SL, Cahalan MD, Velicelebi G, Stauderman KA (2005) STIM1, an essential and conserved component of store-operated Ca2+ channel function. J Cell Biol 169:435–445
27. Zhang SL, Yu Y, Roos J, Kozak JA, Deerinck TJ, Ellisman MH, Stauderman KA, Cahalan MD (2005) STIM1 is a Ca^{2+} sensor that activates CRAC channels and migrates from the Ca^{2+} store to the plasma membrane. Nature 437:902–905
28. Baryshnikov SG, Pulina MV, Zulian A, Linde CI, Golovina VA (2009) Orai1, a critical component of store-operated Ca^{2+} entry, is functionally associated with Na^{+}/Ca^{2+} exchanger and plasma membrane Ca^{2+} pump in proliferating human arterial myocytes. Am J Physiol Cell Physiol 297:C1103–C1112
29. Potier M, Gonzalez JC, Motiani RK, Abdullaev IF, Bisaillon JM, Singer HA, Trebak M (2009) Evidence for STIM1- and Orai1-dependent store-operated calcium influx through ICRAC in vascular smooth muscle cells: role in proliferation and migration. FASEB J 23:2425–2437
30. Mercer JC, Dehaven WI, Smyth JT, Wedel B, Boyles RR, Bird GS, Putney JW Jr (2006) Large store-operated calcium selective currents due to co-expression of Orai1 or Orai2 with the intracellular calcium sensor, Stim1. J Biol Chem 281:24979–24990
31. Gross SA, Wissenbach U, Philipp SE, Freichel M, Cavalie A, Flockerzi V (2007) Murine ORAI2 splice variants form functional Ca^{2+} release-activated Ca^{2+} (CRAC) channels. J Biol Chem 282:19375–19384
32. Vig M, DeHaven WI, Bird GS, Billingsley JM, Wang H, Rao PE, Hutchings AB, Jouvin MH, Putney JW, Kinet JP (2008) Defective mast cell effector functions in mice lacking the CRACM1 pore subunit of store-operated calcium release-activated calcium channels. Nat Immunol 9:89–96
33. Yuan JP, Zeng W, Huang GN, Worley PF, Muallem S (2007) STIM1 heteromultimerizes TRPC channels to determine their function as store-operated channels. Nat Cell Biol 9:636–645
34. Parekh AB, Putney JW Jr (2005) Store-operated calcium channels. Physiol Rev 85:757–810
35. Dietrich A, Kalwa H, Fuchs B, Grimminger F, Weissmann N, Gudermann T (2007) In vivo TRPC functions in the cardiopulmonary vasculature. Cell Calcium 42:233–244
36. Yu Y, Sweeney M, Zhang S, Platoshyn O, Landsberg J, Rothman A, Yuan JX (2003) PDGF stimulates pulmonary vascular smooth muscle cell proliferation by upregulating TRPC6 expression. Am J Physiol Cell Physiol 284:C316–C330
37. Sweeney M, Yu Y, Platoshyn O, Zhang S, McDaniel SS, Yuan JX (2002) Inhibition of endogenous TRP1 decreases capacitative Ca^{2+} entry and attenuates pulmonary artery smooth muscle cell proliferation. Am J Physiol Lung Cell Mol Physiol 283:L144–L155
38. Liao Y, Plummer NW, George MD, Abramowitz J, Zhu MX, Birnbaumer L (2009) A role for Orai in TRPC-mediated Ca^{2+} entry suggests that a TRPC:Orai complex may mediate store and receptor operated Ca^{2+} entry. Proc Natl Acad Sci USA 106:3202–3206
39. DeHaven WI, Jones BF, Petranka JG, Smyth JT, Tomita T, Bird GS, Putney JW Jr (2009) TRPC channels function independently of STIM1 and Orai1. J Physiol 587:2275–2298
40. Arnon A, Hamlyn JM, Blaustein MP (2000) Na(+) entry via store-operated channels modulates Ca(2+) signaling in arterial myocytes. Am J Physiol Cell Physiol 278:C163–C173
41. Dai J, Lee CH, Poburko D, Szado T, Kuo KH, van Breemen C (2007) Endothelin-1-mediated wave-like $[Ca^{2+}]_i$ oscillations in intact rabbit inferior vena cava. J Vasc Res 44:495–503
42. Wang Y, Deng X, Mancarella S, Hendron E, Eguchi S, Soboloff J, Tang XD, Gill DL (2010) The calcium store sensor, STIM1, reciprocally controls Orai and CaV1.2 channels. Science 330:105–109

43. Park CY, Shcheglovitov A, Dolmetsch R (2010) The CRAC channel activator STIM1 binds and inhibits L-type voltage-gated calcium channels. Science 330:101–105
44. Mignen O, Shuttleworth TJ (2000) I(ARC), a novel arachidonate-regulated, noncapacitative Ca(2+) entry channel. J Biol Chem 275:9114–9119
45. Mignen O, Thompson JL, Shuttleworth TJ (2007) STIM1 regulates Ca^{2+} entry via arachidonate-regulated Ca^{2+}–selective (ARC) channels without store depletion or translocation to the plasma membrane. J Physiol 579:703–715
46. Mignen O, Thompson JL, Shuttleworth TJ (2009) The molecular architecture of the arachidonate-regulated Ca^{2+}–selective ARC channel is a pentameric assembly of Orai1 and Orai3 subunits. J Physiol 587:4181–4197
47. Demuth DG, Gkoumassi E, Droge MJ, Dekkers BG, Esselink HJ, van Ree RM, Parsons ME, Zaagsma J, Molleman A, Nelemans SA (2005) Arachidonic acid mediates non-capacitative calcium entry evoked by CB1-cannabinoid receptor activation in DDT1 MF-2 smooth muscle cells. J Cell Physiol 205:58–67
48. Taylor CW, Moneer Z (2004) Regulation of capacitative and non-capacitative Ca^{2+} entry in A7r5 vascular smooth muscle cells. Biol Res 37:641–645
49. Trebak M (2011) Review of transient receptor potential channels. Channels (Austin) 5:188–190
50. Earley S, Heppner TJ, Nelson MT, Brayden JE (2005) TRPV4 forms a novel Ca^{2+} signaling complex with ryanodine receptors and BKCa channels. Circ Res 97:1270–1279
51. Muraki K, Iwata Y, Katanosaka Y, Ito T, Ohya S, Shigekawa M, Imaizumi Y (2003) TRPV2 is a component of osmotically sensitive cation channels in murine aortic myocytes. Circ Res 93:829–838
52. Sharif-Naeini R, Folgering JH, Bichet D, Duprat F, Lauritzen I, Arhatte M, Jodar M, Dedman A, Chatelain FC, Schulte U, Retailleau K, Loufrani L, Patel A, Sachs F, Delmas P, Peters DJ, Honore E (2009) Polycystin-1 and –2 dosage regulates pressure sensing. Cell 139:587–596
53. Vallot O, Combettes L, Jourdon P, Inamo J, Marty I, Claret M, Lompre AM (2000) Intracellular Ca(2+) handling in vascular smooth muscle cells is affected by proliferation. Arterioscler Thromb Vasc Biol 20:1225–1235
54. Husain M, Jiang L, See V, Bein K, Simons M, Alper SL, Rosenberg RD (1997) Regulation of vascular smooth muscle cell proliferation by plasma membrane Ca(2+)-ATPase. Am J Physiol 272:C1947–C1959
55. Buch MH, Pickard A, Rodriguez A, Gillies S, Maass AH, Emerson M, Cartwright EJ, Williams JC, Oceandy D, Redondo JM, Neyses L, Armesilla AL (2005) The sarcolemmal calcium pump inhibits the calcineurin/nuclear factor of activated T-cell pathway via interaction with the calcineurin A catalytic subunit. J Biol Chem 280:29479–29487
56. Blaustein MP, Golovina VA, Song H, Choate J, Lencesova L, Robinson SW, Wier WG (2002) Organization of Ca^{2+} stores in vascular smooth muscle: functional implications. Novartis Found Symp 246:125–137, discussion 137–141, 221–127
57. Zhang J, Ren C, Chen L, Navedo MF, Antos LK, Kinsey SP, Iwamoto T, Philipson KD, Kotlikoff MI, Santana LF, Wier WG, Matteson DR, Blaustein MP (2010) Knockout of Na^+/Ca^{2+} exchanger in smooth muscle attenuates vasoconstriction and L-type Ca^{2+} channel current and lowers blood pressure. Am J Physiol Heart Circ Physiol 298:H1472–H1483
58. Klemm DJ, Watson PA, Frid MG, Dempsey EC, Schaack J, Colton LA, Nesterova A, Stenmark KR, Reusch JE (2001) cAMP response element-binding protein content is a molecular determinant of smooth muscle cell proliferation and migration. J Biol Chem 276:46132–46141
59. Kamiya K, Sakakibara K, Ryer EJ, Hom RP, Leof EB, Kent KC, Liu B (2007) Phosphorylation of the cyclic AMP response element binding protein mediates transforming growth factor beta-induced downregulation of cyclin A in vascular smooth muscle cells. Mol Cell Biol 27:3489–3498
60. Deisseroth K, Heist EK, Tsien RW (1998) Translocation of calmodulin to the nucleus supports CREB phosphorylation in hippocampal neurons. Nature 392:198–202

61. Dolmetsch RE, Pajvani U, Fife K, Spotts JM, Greenberg ME (2001) Signaling to the nucleus by an L-type calcium channel-calmodulin complex through the MAP kinase pathway. Science 294:333–339
62. Cartin L, Lounsbury KM, Nelson MT (2000) Coupling of Ca(2+) to CREB activation and gene expression in intact cerebral arteries from mouse: roles of ryanodine receptors and voltage-dependent Ca(2+) channels. Circ Res 86:760–767
63. Stevenson AS, Gomez MF, Hill-Eubanks DC, Nelson MT (2001) NFAT4 movement in native smooth muscle. A role for differential Ca(2+) signaling. J Biol Chem 276:15018–15024
64. Gwack Y, Feske S, Srikanth S, Hogan PG, Rao A (2007) Signalling to transcription: store-operated Ca^{2+} entry and NFAT activation in lymphocytes. Cell Calcium 42:145–156
65. Dolmetsch RE, Lewis RS, Goodnow CC, Healy JI (1997) Differential activation of transcription factors induced by Ca^{2+} response amplitude and duration. Nature 386:855–858
66. Ambros V (2004) The functions of animal microRNAs. Nature 431:350–355
67. Bartel DP (2004) MicroRNAs: genomics, biogenesis, mechanism, and function. Cell 116:281–297
68. Small EM, Olson EN (2011) Pervasive roles of microRNAs in cardiovascular biology. Nature 469:336–342
69. Song Z, Li G (2010) Role of specific microRNAs in regulation of vascular smooth muscle cell differentiation and the response to injury. J Cardiovasc Transl Res 3:246–250
70. Cordes KR, Sheehy NT, White MP, Berry EC, Morton SU, Muth AN, Lee TH, Miano JM, Ivey KN, Srivastava D (2009) miR-145 and miR-143 regulate smooth muscle cell fate and plasticity. Nature 460:705–710
71. Quintavalle M, Elia L, Condorelli G, Courtneidge SA (2010) MicroRNA control of podosome formation in vascular smooth muscle cells in vivo and in vitro. J Cell Biol 189:13–22
72. Wang X, Hu G, Zhou J (2010) Repression of versican expression by microRNA-143. J Biol Chem 285:23241–23250
73. Owens GK, Kumar MS, Wamhoff BR (2004) Molecular regulation of vascular smooth muscle cell differentiation in development and disease. Physiol Rev 84:767–801
74. Kuga T, Kobayashi S, Hirakawa Y, Kanaide H, Takeshita A (1996) Cell cycle–dependent expression of L- and T-type Ca^{2+} currents in rat aortic smooth muscle cells in primary culture. Circ Res 79:14–19
75. Quignard JF, Harricane MC, Menard C, Lory P, Nargeot J, Capron L, Mornet D, Richard S (2001) Transient down-regulation of L-type Ca(2+) channel and dystrophin expression after balloon injury in rat aortic cells. Cardiovasc Res 49:177–188
76. Nieves-Cintron M, Amberg GC, Navedo MF, Molkentin JD, Santana LF (2008) The control of Ca^{2+} influx and NFATc3 signaling in arterial smooth muscle during hypertension. Proc Natl Acad Sci USA 105:15623–15628
77. Golovina VA (1999) Cell proliferation is associated with enhanced capacitative Ca(2+) entry in human arterial myocytes. Am J Physiol 277:C343–C349
78. Bisaillon JM, Motiani RK, Gonzalez-Cobos JC, Potier M, Halligan KE, Alzawahra WF, Barroso M, Singer HA, Jourd'heuil D, Trebak M (2010) Essential role for STIM1/Orai1-mediated calcium influx in PDGF-induced smooth muscle migration. Am J Physiol Cell Physiol 298:C993–C1005
79. Aubart FC, Sassi Y, Coulombe A, Mougenot N, Vrignaud C, Leprince P, Lechat P, Lompre AM, Hulot JS (2009) RNA interference targeting STIM1 suppresses vascular smooth muscle cell proliferation and neointima formation in the rat. Mol Ther 17:455–462
80. Guo RW, Wang H, Gao P, Li MQ, Zeng CY, Yu Y, Chen JF, Song MB, Shi YK, Huang L (2009) An essential role for stromal interaction molecule 1 in neointima formation following arterial injury. Cardiovasc Res 81:660–668
81. Berra-Romani R, Mazzocco-Spezzia A, Pulina MV, Golovina VA (2008) Ca^{2+} handling is altered when arterial myocytes progress from a contractile to a proliferative phenotype in culture. Am J Physiol Cell Physiol 295:C779–C790
82. Kunichika N, Yu Y, Remillard CV, Platoshyn O, Zhang S, Yuan JX (2004) Overexpression of TRPC1 enhances pulmonary vasoconstriction induced by capacitative Ca^{2+} entry. Am J Physiol Lung Cell Mol Physiol 287:L962–L969

83. Sweeney M, McDaniel SS, Platoshyn O, Zhang S, Yu Y, Lapp BR, Zhao Y, Thistlethwaite PA, Yuan JX (2002) Role of capacitative Ca^{2+} entry in bronchial contraction and remodeling. J Appl Physiol 92:1594–1602
84. Xu SZ, Muraki K, Zeng F, Li J, Sukumar P, Shah S, Dedman AM, Flemming PK, McHugh D, Naylor J, Cheong A, Bateson AN, Munsch CM, Porter KE, Beech DJ (2006) A sphingosine-1-phosphate-activated calcium channel controlling vascular smooth muscle cell motility. Circ Res 98:1381–1389
85. Zhang S, Remillard CV, Fantozzi I, Yuan JX (2004) ATP-induced mitogenesis is mediated by cyclic AMP response element-binding protein-enhanced TRPC4 expression and activity in human pulmonary artery smooth muscle cells. Am J Physiol Cell Physiol 287:C1192–C1201
86. Lin MJ, Leung GP, Zhang WM, Yang XR, Yip KP, Tse CM, Sham JS (2004) Chronic hypoxia-induced upregulation of store-operated and receptor-operated Ca^{2+} channels in pulmonary arterial smooth muscle cells: a novel mechanism of hypoxic pulmonary hypertension. Circ Res 95:496–505
87. Liu D, Yang D, He H, Chen X, Cao T, Feng X, Ma L, Luo Z, Wang L, Yan Z, Zhu Z, Tepel M (2009) Increased transient receptor potential canonical type 3 channels in vasculature from hypertensive rats. Hypertension 53:70–76
88. Pulina MV, Zulian A, Berra-Romani R, Beskina O, Mazzocco-Spezzia A, Baryshnikov SG, Papparella I, Hamlyn JM, Blaustein MP, Golovina VA (2010) Upregulation of Na^{+} and Ca^{2+} transporters in arterial smooth muscle from ouabain-induced hypertensive rats. Am J Physiol Heart Circ Physiol 298:H263–H274
89. Lipskaia L, del Monte F, Capiod T, Yacoubi S, Hadri L, Hours M, Hajjar RJ, Lompre AM (2005) Sarco/endoplasmic reticulum Ca^{2+}–ATPase gene transfer reduces vascular smooth muscle cell proliferation and neointima formation in the rat. Circ Res 97:488–495
90. Lipskaia L, Pourci ML, Delomenie C, Combettes L, Goudouneche D, Paul JL, Capiod T, Lompre AM (2003) Phosphatidylinositol 3-kinase and calcium-activated transcription pathways are required for VLDL-induced smooth muscle cell proliferation. Circ Res 92:1115–1122
91. Bobe R, Hadri L, Lopez JJ, Sassi Y, Atassi F, Karakikes I, Liang L, Limon I, Lompre AM, Hatem SN, Hajjar RJ, Lipskaia L (2011) SERCA2a controls the mode of agonist-induced intracellular Ca(2+) signal, transcription factor NFAT and proliferation in human vascular smooth muscle cells. J Mol Cell Cardiol 50:621–633
92. Massaeli H, Austria JA, Pierce GN (2000) Lesions in ryanodine channels in smooth muscle cells exposed to oxidized low density lipoprotein. Arterioscler Thromb Vasc Biol 20:328–334
93. Schauer IE, Knaub LA, Lloyd M, Watson PA, Gliwa C, Lewis KE, Chait A, Klemm DJ, Gunter JM, Bouchard R, McDonald TO, O'Brien KD, Reusch JE (2010) CREB downregulation in vascular disease: a common response to cardiovascular risk. Arterioscler Thromb Vasc Biol 30:733–741
94. Chava KR, Karpurapu M, Wang D, Bhanoori M, Kundumani-Sridharan V, Zhang Q, Ichiki T, Glasgow WC, Rao GN (2009) CREB-mediated IL-6 expression is required for 15(S)-hydroxyeicosatetraenoic acid-induced vascular smooth muscle cell migration. Arterioscler Thromb Vasc Biol 29:809–815
95. Ono H, Ichiki T, Fukuyama K, Iino N, Masuda S, Egashira K, Takeshita A (2004) cAMP-response element-binding protein mediates tumor necrosis factor-alpha-induced vascular smooth muscle cell migration. Arterioscler Thromb Vasc Biol 24:1634–1639
96. Tokunou T, Shibata R, Kai H, Ichiki T, Morisaki T, Fukuyama K, Ono H, Iino N, Masuda S, Shimokawa H, Egashira K, Imaizumi T, Takeshita A (2003) Apoptosis induced by inhibition of cyclic AMP response element-binding protein in vascular smooth muscle cells. Circulation 108:1246–1252
97. Chen J, Jiang H, Xu L, Zhu LH, Wang L, Wen HZ, Hu XR (2008) Dysregulation of CREB binding protein triggers thrombin-induced proliferation of vascular smooth muscle cells. Mol Cell Biochem 315:123–130
98. Yellaturu CR, Ghosh SK, Rao RK, Jennings LK, Hassid A, Rao GN (2002) A potential role for nuclear factor of activated T-cells in receptor tyrosine kinase and G-protein-coupled receptor agonist-induced cell proliferation. Biochem J 368:183–190

99. Liu Z, Zhang C, Dronadula N, Li Q, Rao GN (2005) Blockade of nuclear factor of activated T cells activation signaling suppresses balloon injury-induced neointima formation in a rat carotid artery model. J Biol Chem 280:14700–14708
100. Karpurapu M, Wang D, Van Quyen D, Kim TK, Kundumani-Sridharan V, Pulusani S, Rao GN (2010) Cyclin D1 is a bona fide target gene of NFATc1 and is sufficient in the mediation of injury-induced vascular wall remodeling. J Biol Chem 285:3510–3523
101. House SJ, Ginnan RG, Armstrong SE, Singer HA (2007) Calcium/calmodulin-dependent protein kinase II-delta isoform regulation of vascular smooth muscle cell proliferation. Am J Physiol Cell Physiol 292:C2276–C2287
102. Ji R, Cheng Y, Yue J, Yang J, Liu X, Chen H, Dean DB, Zhang C (2007) MicroRNA expression signature and antisense-mediated depletion reveal an essential role of MicroRNA in vascular neointimal lesion formation. Circ Res 100:1579–1588
103. Liu X, Cheng Y, Zhang S, Lin Y, Yang J, Zhang C (2009) A necessary role of miR-221 and miR-222 in vascular smooth muscle cell proliferation and neointimal hyperplasia. Circ Res 104:476–487
104. Sun SG, Zheng B, Han M, Fang XM, Li HX, Miao SB, Su M, Han Y, Shi HJ, Wen JK (2011) miR-146a and Kruppel-like factor 4 form a feedback loop to participate in vascular smooth muscle cell proliferation. EMBO Rep 12:56–62
105. Ikeda S, He A, Kong SW, Lu J, Bejar R, Bodyak N, Lee KH, Ma Q, Kang PM, Golub TR, Pu WT (2009) MicroRNA-1 negatively regulates expression of the hypertrophy-associated calmodulin and Mef2a genes. Mol Cell Biol 29:2193–2204
106. Dong DL, Chen C, Huo R, Wang N, Li Z, Tu YJ, Hu JT, Chu X, Huang W, Yang BF (2010) Reciprocal repression between microRNA-133 and calcineurin regulates cardiac hypertrophy: a novel mechanism for progressive cardiac hypertrophy. Hypertension 55:946–952
107. Li Q, Lin X, Yang X, Chang J (2010) NFATc4 is negatively regulated in miR-133a-mediated cardiomyocyte hypertrophic repression. Am J Physiol Heart Circ Physiol 298:H1340–H1347
108. da Costa Martins PA, Salic K, Gladka MM, Armand AS, Leptidis S, el Azzouzi H, Hansen A, Coenen-de Roo CJ, Bierhuizen MF, van der Nagel R, van Kuik J, de Weger R, de Bruin A, Condorelli G, Arbones ML, Eschenhagen T, De Windt LJ (2010) MicroRNA-199b targets the nuclear kinase Dyrk1a in an auto-amplification loop promoting calcineurin/NFAT signalling. Nat Cell Biol 12:1220–1227
109. Lin Z, Murtaza I, Wang K, Jiao J, Gao J, Li PF (2009) miR-23a functions downstream of NFATc3 to regulate cardiac hypertrophy. Proc Natl Acad Sci USA 106:12103–12108

Chapter 36
Calcium and Endothelium-Mediated Vasodilator Signaling

Shaun L. Sandow, Sevvandi Senadheera, T. Hilton Grayson, Don G. Welsh, and Timothy V. Murphy

Abstract Vascular tone refers to the balance between arterial constrictor and dilator activity. The mechanisms that underlie tone are critical for the control of haemodynamics and matching circulatory needs with metabolism, and thus alterations in tone are a primary factor for vascular disease etiology. The dynamic spatiotemporal control of intracellular Ca^{2+} levels in arterial endothelial and smooth muscle cells facilitates the modulation of multiple vascular signaling pathways. Thus, control of Ca^{2+} levels in these cells is integral for the maintenance of tone and blood flow, and intimately associated with both physiological and pathophysiological states. Hence, understanding the mechanisms that underlie the modulation of vascular Ca^{2+} activity is critical for both fundamental knowledge of artery function, and for the development of targeted therapies. This brief review highlights the role of Ca^{2+} signaling in vascular endothelial function, with a focus on contact-mediated vasodilator mechanisms associated with endothelium-derived hyperpolarization and the longitudinal conduction of responses over distance.

Keywords Artery • Endothelium • Calcium-activated potassium channel • Smooth muscle • Vasodilation

S.L. Sandow (✉) • S. Senadheera • T.H. Grayson
Department of Physiology, School of Medical Sciences, University of New South Wales, 2052 Sydney, NSW, Australia

Department of Pharmacology, School of Medical Sciences, University of New South Wales, 2052 Sydney, NSW, Australia
e-mail: Shaun.Sandow@unsw.edu.au

D.G. Welsh
Smooth Muscle Research Group and Physiology and Biophysics, University of Calgary, Calgary, AB, Canada

T.V. Murphy
Department of Physiology, School of Medical Sciences, University of New South Wales, 2052 Sydney, NSW, Australia

M.S. Islam (ed.), *Calcium Signaling*, Advances in Experimental Medicine and Biology 740, DOI 10.1007/978-94-007-2888-2_36,

Introduction

Anatomy and General Function

The vascular endothelium consists of a single layer of squamous cells lining the vessel lumen, with their long axis running (1) parallel with the longitudinal arterial axis and (2) perpendicular to the alignment of the smooth muscle cell layer/s (Fig. 36.1). Vascular endothelium is a semi-permeable barrier between the blood and smooth muscle and is separated from the blood column on the luminal surface by the glycocalyx, a layer of proteoglycans and glycoproteins. Blood travels up the centre of the luminal glycocalyx-lined column (*in vivo*) and is not in direct contact with the endothelial surface [2–4]. The abluminal endothelial surface is separated from the medial smooth muscle cells by the internal elastic lamina (IEL), a 'continuous' or intermittent layer of microfibrils and insoluble elastin [5], whose thickness is generally proportional to vessel size. The IEL is 'continuous' in larger diameter vessels, and intermittent to absent in small diameter arterioles. The IEL has intermittent holes or 'fenestrae', of a size and density that may be related to vessel function in health and disease [6, 7]. Further, such IEL holes represent potential low resistance pathways for the diffusion of vasoactive substances that influence endothelial and smooth muscle activity, whereas the dense elastin of the IEL is a likely significant barrier to such processes [6, 8–12].

In many resistance and larger conduit arteries, a proportion of IEL holes encompass projections from endothelial- and smooth muscle cells that form myoendothelial contact sites, where localized signaling between the two cell layers occurs ([13, 14]; Fig. 36.2). Such contact sites can retain gap junction intercellular channels that consist of connexin (Cx) proteins (Figs. 36.1, 36.2 and 36.3) and facilitate electrical coupling between the two cell layers; with the density of these myoendothelial gap junctions showing variability between vascular beds [6, 14]. In general, gap junctions between adjacent endothelial cells are large, whilst those between adjacent smooth muscle cells are small; with the implication of size being proportional to the

Fig. 36.1 (continued) smooth muscle cell layer/s (*left panel*, *red*; *right panel*, lucifer *yellow* filled smooth muscle bundle in whole mount) of the vessel wall (**a**); *left panel*; from Sandow and Hill [1]. In cross section through the vessel wall, endothelial cells line the vessel lumen ((**b**); *left panel*, *green*; *right panel*, low magnification electron microscope image), with the internal elastic lamina acting as a semi-permeable barrier from the adjacent smooth muscle layer/s ((**b**); *left panel*, *red*; *right panel*, low magnification electron microscope image). Endothelium-dependent pathways (**c**) associated with vessel dilation include nitric oxide (*NO*), prostacyclin (PGI_2) and non-NO/PGI_2 endothelium-derived hyperpolarization (*EDH*) whilst those associated with arterial constriction include endothelin (*ET*), superoxide, thromboxane (TxA_2) and prostaglandins (PGH_2). Endothelium-derived hyperpolarization (*EDH*) activity results from agonist-induced release of intracellular calcium, which activates endothelial small and/or intermediate conductance calcium-activated potassium channels (SI/IK_{Ca}), with the net effect being smooth muscle relaxation and vasodilation (**c**)

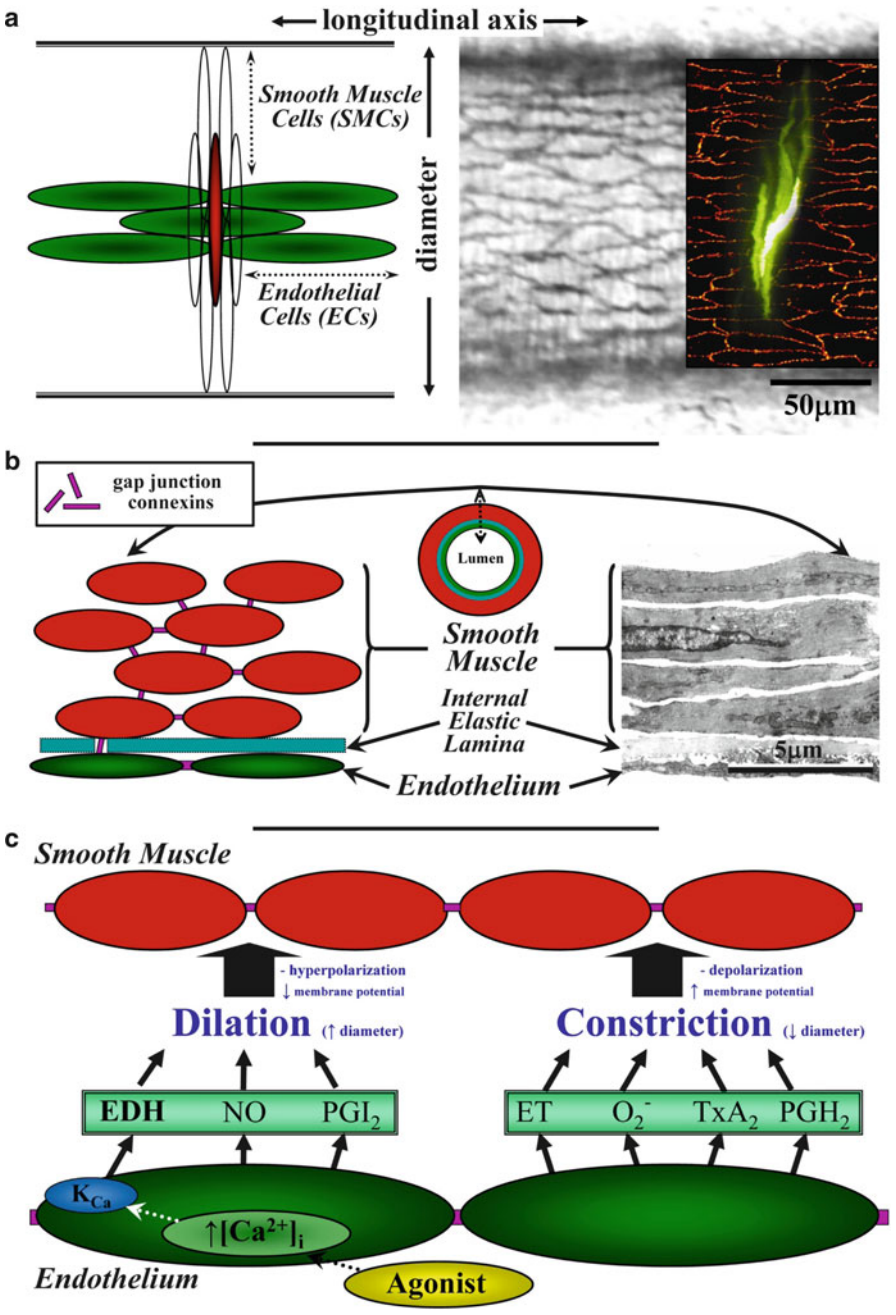

Fig. 36.1 Artery morphology and mechanisms of endothelium-dependent dilation and constriction. The long axis of endothelial cells ((**a**); *left panel*, *green*; *right panel*, *silver* stained artery and far *right*, Cx-fluorophore labelled endothelial cell gap junctions in whole mount) is aligned parallel to the longitudinal vessel axis and at ~90° perpendicular to the alignment of the primary

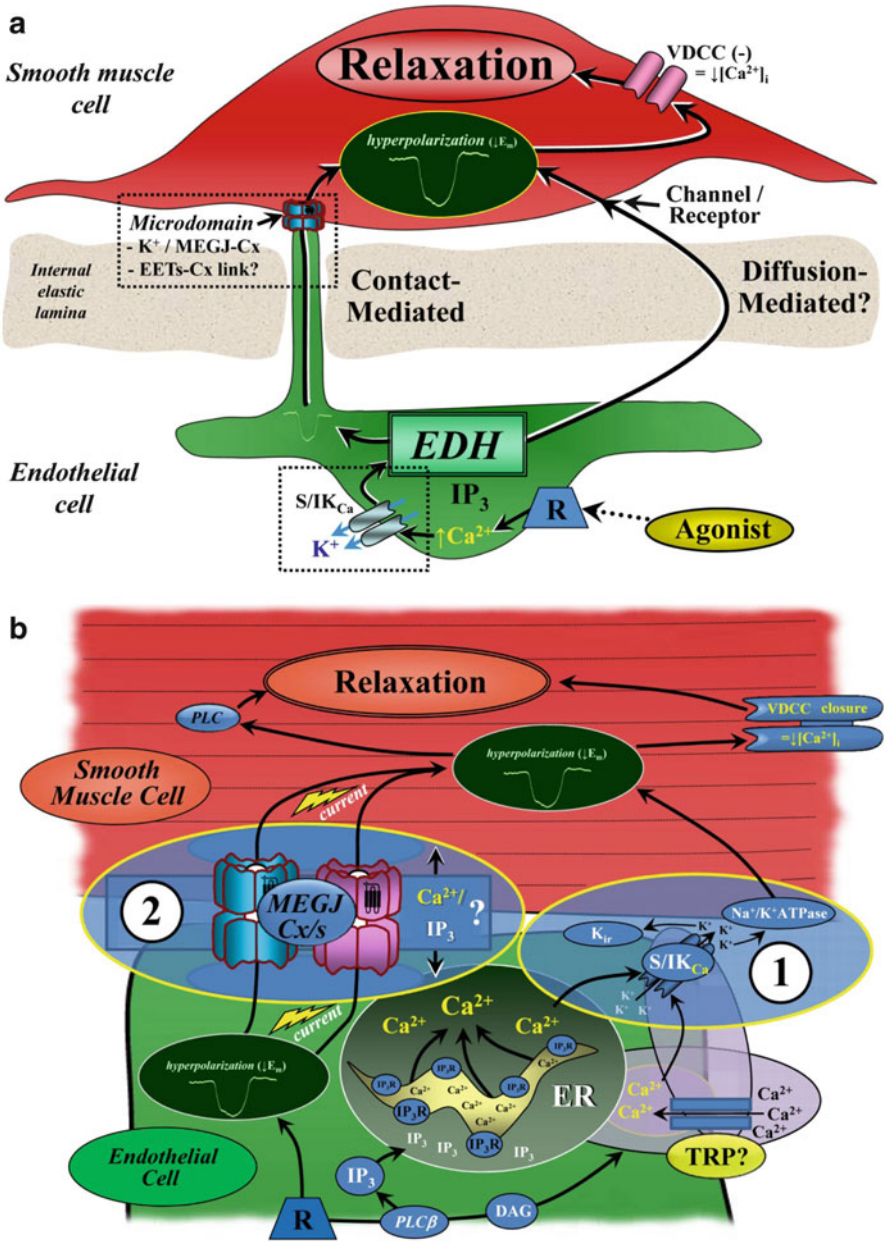

Fig. 36.2 Mechanism of endothelium-derived hyperpolarization (EDH). The mechanism/s that underlie EDH involve contact- and/or diffusion-mediated pathways (**a**, **b**). The specific contribution of components of the individual and respective pathways can differ between vascular beds, species, animal strains and during development, ageing and disease. For contact-mediated EDH, myoendothelial contact sites of different vessels can have a differential mix of spatially localized gap junction connexins (*Cx/s*), intermediate- (and perhaps small)-conductance Ca^{2+}-activated

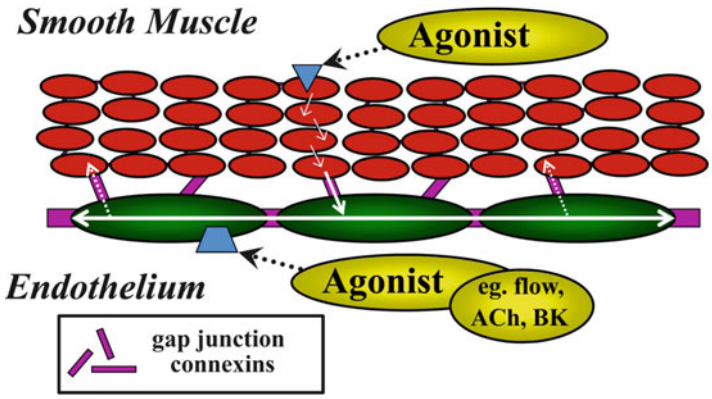

Fig. 36.3 Endothelium-mediated conduction of vasomotor responses. Vasomotor responses could, in theory, conduct along the endothelial (*green*, *horizontal arrow*) or smooth muscle cell layers (*red*, *dashed arrows*). However, as the long axis of endothelial cells aligns with the long axis of a vessel (Fig. 36.1a), and these cells are exceedingly well coupled, the primary pathway for conduction over considerable distance is the endothelium. In this scenario agonist-induced hyperpolarization of the endothelium (Fig. 36.2b) initiates a dilation that spreads along the vessel wall via the endothelium

degree of coupling. Indeed, the size, location and the expression of specific Cx subtypes [17–20] vary significantly within and between vascular beds, species, development, ageing and disease [21–24].

The arterial endothelium consists of a phenotypically diverse cell population, with characteristics that differ within and between vascular beds, species, animal strains and during development, ageing and disease [25–27]. Endothelial cells are involved in a diverse range of functions including, but not limited to, the production of antithrombotic, pro-coagulant, matrix products, inflammatory mediators and growth factors, as well as an involvement in lipid metabolism. In addition, the endothelium plays a critical role in the control of vasomotor tone, via the initiation of mechanisms that contribute to the balance of vasoconstrictor and vasodilator activity [28, 29]. Such mechanisms thus play a role in the control of blood flow and pressure in health and disease.

Fig. 36.2 (continued) potassium channels (S/IK_{Ca}), endoplasmic reticulum (*ER*) 1,4,5-triphosphate receptors (IP_3R), Na^+/K^+-ATPase and inward rectifying potassium channels (K_{ir}), and likely transient receptor potential (*TRP*) channels that in part underlie ER calcium store refilling. Such myo-endothelial microdomain sites can facilitate localized S/IK_{Ca}-mediated K^+ efflux to activate smooth muscle cell Na^+/K^+-ATPase, and/or enable transfer of an EDH current to the adjacent smooth muscle cell layer/s. The net effect is smooth muscle hyperpolarization, closure of voltage-dependent Ca^{2+} channels (*VDCCs*) and inhibition of phospholipase C (*PLC*), and subsequent smooth muscle relaxation and vessel dilation. In theory, the S/IK_{Ca}-IP_3R-TRP complex and the gap junction Cx components can operate separately or synergistically and confer significant potential for plasticity and heterogeneity in the signaling mechanism that underlies EDH. *DAG* diacylglycerol, *MEGJ* myoendothelial gap junction, *PLCβ* phospholipase C-beta (modified from Sandow and Tare [15] and Sandow et al. [16])

Endothelium-dependent pathways associated with arterial constriction include endothelin, thromboxane and superoxide [28]; whilst those associated with vessel dilation include nitric oxide (NO), prostacyclin (PGI_2) and non-NO/PGI_2 endothelium-derived hyperpolarization (EDH; [15, 30]; Figs. 36.1 and 36.2). The specific mechanisms that underlie vasoconstrictor and vasodilator activity, including that associated with EDH, vary within and between vascular beds and in disease and thus represent potential targets for therapy [28, 30–32].

The control of cellular Ca^{2+} levels in arterial endothelial and smooth muscle cells is integral for control of vascular tone, including for endothelium-dependent vasodilator activity. Mechanisms of initiating endothelium-dependent vasodilator responses, including EDH and conduction of signals over distance, involve the activation of endothelial small and intermediate conductance Ca^{2+}-activated potassium (SK_{Ca} and IK_{Ca}) channels. Subsequent hyperpolarization of the endothelium spreads to the adjacent smooth muscle layers via myoendothelial coupling, resulting in vessel dilation by limiting smooth muscle Ca^{2+} influx through voltage-dependent Ca^{2+} channels (VDCCs; Figs. 36.1c and 36.2).

This brief review highlights the role of the endothelium and myoendothelial microdomains in facilitating EDH at a local level and the conduction of responses over distance. Further, the primary experimental and physiological pathways that activate these two properties of the endothelium are emphasized.

Physiological and Experimental Agonist-Induced Mechanisms

The vascular endothelium responds to a wide variety of neural, humoral and physical stimuli, with blood flow through shear stress being of primary functional importance *in vivo* [21, 25, 33]. However, whilst agonists such as acetylcholine (ACh), bradykinin (BK) and ATP are useful for examining vascular endothelial vasodilator function in experimental settings, knowledge of their *in vivo* physiological role in such activity is limited. Indeed, although variable between vessels, the signal transduction pathways for agonist-induced activity involving substances such as ACh, BK and ATP are clearly present in the endothelium. Thus, a key question in vascular biology relates to what might be the physiological role, if any, of such substances in endothelial function?

Flow

Arguably the most important physiological stimulus of the endothelium is flowing blood [25, 33]. Increased blood flow within vessels and the resulting increase in the frictional, shearing force or stress on the endothelial cells causes an endothelium-dependent vasodilation [34, 35]. Flow-induced increases in endothelial cell [Ca^{2+}] have been shown *in vitro* (i.e. in cell culture [35–37]); and in endothelial cells *in situ* (within functioning blood vessels [38–40]). Compared with agonist-induced

Ca^{2+} signaling, relatively little is known regarding the mechanisms that underlie flow-induced increases in endothelial cell [Ca^{2+}]. The increase is dependent upon extracellular Ca^{2+} entry and may be enhanced by depletion of the intracellular Ca^{2+} store [38, 39], suggesting a store-operated component. The identity of the channel(s) responsible and their mechanism of action is not clear. Flow-induced Ca^{2+} entry may be blocked by La^{+}, Ni^{+} and other metal ions, suggesting a possible role for transient receptor potential (TRP) channels, and at least ten TRP channel subtypes are sensitive to mechanical stimuli including shear stress [41]. Recent studies suggest TRPV4 partly mediates flow-induced Ca^{2+} entry in endothelial cells of the mouse mesenteric [40] and coronary artery [42]. Kwan and colleagues [17] maintain that the channel(s) underlying this effect is sensitive to cyclic GMP and/or cGMP-activated protein kinase. Some studies suggest that flow-induced increases in endothelial cell [Ca^{2+}] are mediated by localized release of ATP or other adenine nucleotides (i.e. purinergic receptor agonists; see section "ATP", below), from the endothelial cells [43, 44]. Burnstock and colleagues took this idea further [18] and suggested that ATP, ACh, substance P and 5-HT could all be released from endothelial cells and act as 'paracrine' mediators of flow-induced vasodilation and, presumably, via a Ca^{2+}-dependent signaling mechanism in endothelial cells, although to date evidence is strongest for ATP acting in this manner, and specific data on the role of ACh in this process is limited [45]. Furthermore, in some circumstances flow-induced vasodilation may occur without an increase in endothelial cell [Ca^{2+}]; for example, in rabbit coronary arterioles the Ca^{2+} chelator BAPTA inhibited endothelium-dependent vasodilation caused by ACh and substance P, but did not alter flow-induced dilation [46]. Shear stress may activate numerous signaling pathways in endothelial cells [33, 35], such as NOS being activated through the PI3-kinase/Akt pathway, without an increase in cell [Ca^{2+}] [19, 47].

Agonist-Stimulated Ca^{2+} Signaling

A large variety of substances increase endothelial cell [Ca^{2+}] through interaction with specific receptors. The most commonly utilized and investigated include ACh, ATP and related purinergic receptor agonists, histamine, BK, substance P, thrombin and other protease-activated receptor ligands, ACh, 5-hydroxytryptamine, adrenaline and noradrenaline. For a number of these endothelium-dependent vasodilator agonists, such as ACh, their physiological role *in vivo* has not been definitively demonstrated. However, given that the mechanisms for production, receptor activation and degradation (as per ACh in many vascular beds; e.g. choline acetyltransferase (ChAt), vesicular acetylcholine transporter (vACht), muscarinic and nicotinic ACh receptors (m/nAChR), and acetylcholinesterase (AChE)) are generally present in intact artery endothelium, it follows that such agents likely have a physiologically relevant role in intact artery endothelial function; albeit a role that needs to be clarified.

In general, these substances act through $G_{q/11}$-protein coupled receptors and bring about increased endothelial cell [Ca^{2+}] through activation of phospholipase C (PLC),

subsequent IP_3-mediated release of intracellular Ca^{2+} stores and extracellular Ca^{2+} entry. Extracellular Ca^{2+} entry is not through VDCC as vascular endothelial cells typically do not express them. Ca^{2+} entry is sensitive to the electrochemical gradient across the membrane, such that Ca^{2+} entry is enhanced by hyperpolarization and reduced by depolarization of endothelial cells; thus agents which increase endothelial cell [Ca^{2+}] and activate K_{Ca} may further increase intracellular [Ca^{2+}] through the resulting hyperpolarization of the cell.

For most of these receptor-coupled stimuli, extracellular Ca^{2+} entry consists of a capacitative store-operated component (store-operated Ca^{2+} entry or SOCE) and/or entry through receptor-operated channels [20]. The mechanism of SOCE into vascular endothelial cells is not fully understood and is somewhat controversial [48]. TRP channels have been identified as being involved in the process, in particular TRPC1, C3 and C4 [49–52]. Recent studies have suggested the proteins crucial for operation of the Ca^{2+} release-activated current (I_{CRAC}), as the Ca^{2+} sensor STIM-1, and the Orai-1 channel, are involved in SOCE in vascular endothelial cells [53, 54], whilst in human endothelial cells a combination of TRP channel and STIM-1-mediated mechanisms is apparently required [55]. A receptor-operated channel mechanism is also involved and is also primarily associated with the activity of various TRPC and TRPV subtypes [20]. TRPC and TRPV may be activated by diacylglycerol, produced as a result of PLC activation and hydrolysis of phosphatidylinositol 4,5-bisphosphate.

Evidence linking particular endothelium-mediated vasodilator signaling mechanisms to specific channel and receptor activity is discussed in more detail below. Indeed, studies demonstrate significant variation between vascular beds in the mechanisms that underlie the local regulation of intracellular calcium ($[Ca^{2+}]_i$) which are reflected by significant variation in the distribution of ion channels, receptors and associated Ca^{2+} stores expressed in the endothelium and the mechanisms of Ca^{2+} signaling (see [56–59]). Thus, care should be taken to characterize these factors for a given tissue or cell culture system before concluding which vasodilator signaling pathways are of physiological relevance in a given tissue (see [56–59]).

The mechanisms of agonist-induced activity discussed below are a non-exhaustive list, and includes those that are most commonly used to stimulate Ca^{2+} responses in the vascular endothelium.

Acetylcholine (ACh)

The agonist or agent most commonly used to stimulate endothelium-dependent vasodilation is ACh. The muscarinic receptor subtypes M_1, M_3 and M_5 are coupled to $PLC\beta_1$ and subsequently generate inositol-1,4,5-trisphosphate (IP_3), which in turn results in endoplasmic reticulum (ER)-mediated intracellular Ca^{2+} release. The M_3 subtype mediates ACh-induced endothelium-dependent vasodilation in most vascular preparations studied, although there is evidence implicating a role for M_1 and M_5 receptors in some vascular beds [60]. Interestingly, M_5 receptors have been

shown to mediate ACh-induced responses in cerebral arteries of humans, cattle and mice [61, 62], suggesting regional heterogeneity in the distribution of endothelial cell muscarinic receptor subtypes [60]. Acetylcholine is infrequently used to stimulate endothelial cells in culture as M_3 receptor expression declines rapidly with successive passages [63]. Acetylcholine causes a typically biphasic increase in $[Ca^{2+}]$ in vascular endothelial cells *in situ* (ie. in whole vessel preparations [64–67]), consisting of intracellular Ca^{2+} release and extracellular Ca^{2+} entry; this latter component featured both SOCE and a receptor-mediated component, with recent evidence suggesting a role for TRPV4 channels in mouse mesenteric and carotid arteries [68, 69]; although it was noted that TRPV4 could not account for the entire extracellular Ca^{2+} influx. Acetylcholine-induced Ca^{2+} entry into aortic endothelial cells was also impaired in a TRPC4 knockout mouse model [49].

ATP

ATP and related compounds (adenine nucleotides) act upon various purinergic P2Y or P2X receptor subtypes on endothelial cells, depending upon the vascular bed under study [70–73]. P2X receptors are ligand-gated ion channels and thus increase intracellular $[Ca^{2+}]$ through extracellular Ca^{2+} influx, sensitive to membrane potential. $P2X_4$, $P2X_5$ and $P2X_7$ are expressed in endothelial cells including those derived from human tissue [70, 73] with the strongest evidence for $P2X_4$ as a physiological mediator of endothelial cell $[Ca^{2+}]$ [44]. P2Y-induced increases in intracellular $[Ca^{2+}]$ involve both IP_3-mediated intracellular Ca^{2+} release and a delayed or secondary influx of extracellular Ca^{2+} in vascular endothelial cells [74–76]. The Ca^{2+} influx consists primarily of SOCE [75], although the channel(s) involved in this process are not clear. Some studies have demonstrated a role for TRPC1 [77] and TRPC3 channel activation in this process [78], while ATP-induced SOCE was abolished in endothelial cells from the aorta of TRPC4 knockout mice [49]. Metabolically active smooth muscle cells or clotting erythrocytes may release ATP and as discussed above, shear stress may release ATP from endothelial cells which mediates subsequent flow-induced increases in endothelial cell $[Ca^{2+}]$, suggesting a prominent physiological role for ATP in activating the endothelium.

Bradykinin (BK)

Bradykinin stimulates endothelial cell Ca^{2+} signaling through the activation of the B2 receptor [79–81] and also features intracellular Ca^{2+} release and SOCE components [82]. The SOCE component has not been studied extensively, although BK was shown to activate TRPC3 secondary to PLC activation in endothelial cells derived from bovine pulmonary artery [78]. In vascular endothelial cells non-selective TRP channel inhibition using Ni^+ or SKF96365 reduced extracellular Ca^{2+} entry stimulated by BK [83].

Substance P

Substance P may have a physiological role in stimulating the endothelium due to its function as a neurotransmitter. Activation of the tachykinin receptor NK1 by substance P or other agonists brings about an increase in endothelial cell [Ca^{2+}] through both intracellular release and extracellular Ca^{2+} influx [46, 84–86], with the extracellular influx containing a significant element of SOCE [84]. Substance P evokes strong endothelial cell hyperpolarization in several preparations, suggesting the Ca^{2+} influx is closely linked to K_{Ca} channel activation. In the mouse aorta, ATP- and ACh-evoked significantly greater increases in endothelial cell [Ca^{2+}], in a greater proportion of cells, than substance P or BK [58]; yet in endothelial cells in primary culture derived from the pig coronary artery, substance P evoked a twofold increase in [Ca^{2+}], whereas ACh had no effect [57], emphasizing the importance of characterizing specific signaling pathways in different experimental models.

Thrombin

Thrombin has been used extensively to investigate Ca^{2+} signaling associated with endothelial vasodilator activity. Thrombin stimulates endothelial cell proteinase-activated receptor type-1 (PAR1) and possibly PAR3 [87], as receptors involved in the vascular component of inflammatory responses [88]. Thrombin also stimulates a biphasic increase in intracellular [Ca^{2+}], with intracellular release and subsequent extracellular influx components. In terms of TRP channel involvement in extracellular Ca^{2+} entry, thrombin was shown to stimulate TRPC1 activity through protein kinase-Cα [89, 90], while over-expression of TRPC1 enhanced thrombin-induced SOCE in various human-derived endothelial cell lines [50]. Thrombin was also shown to activate TRPC6 in human pulmonary artery endothelial cells [91] and the intracellular SOCE protein STIM-1 in porcine aortic endothelial cells [54], supporting the idea that TRP channels and STIM-1 may combine in forming a SOCE-complex [20].

Localized Myoendothelial Microdomain Signaling

The primary channels and receptors involved in the modulation of endothelial cell Ca^{2+} associated with EDH are S/IK_{Ca}, ER inositol-1,4,5-trisphosphate receptors (IP_3R), Na^+/K^+-ATPase and inward rectifying potassium channels (K_{ir}), and likely specific subtypes of the TRP channel family; that may facilitate ER Ca^{2+} store refilling (Fig. 36.2).

In many vascular beds, mechanisms associated with EDH activity occur at specialized myoendothelial microdomain contact sites [16, 92–94]. The presence of such close contact sites between the arterial endothelium and smooth muscle confers

significant potential for functional plasticity and heterogeneity. Myoendothelial gap junction Cxs and/or potassium release at localized sites facilitate the transfer of endothelial hyperpolarization to initiate smooth muscle relaxation and vessel dilation, with activity at such sites underlying vasodilation via contact-mediated EDH (Fig. 36.2).

Calcium Dependence of the Endothelium-Derived Hyperpolarization (EDH) Mechanism

Potassium release via SK_{Ca} and IK_{Ca} activation is a ubiquitous step in the generation of an EDH, and subsequent vasodilation. The likely primary source of Ca^{2+} for endothelial SK_{Ca} and IK_{Ca} activation is via ER-IP_3R-mediated stores, as suggested by the spatial localization of these channels and stores with the S/IK_{Ca} channels ([16]; Fig. 36.2); as well as via functional observations of IP_3R-mediated ER Ca^{2+} release and its association with SK_{Ca} and IK_{Ca}-mediated EDH [64, 95]. The mechanisms that underlie the refilling of such localized ER-Ca^{2+} stores are a current area of investigation and may involve spatial localization and activity of specific TRP channels with the S/IK_{Ca}-ER-IP_3R complex (Fig. 36.2). Differential expression and distribution of key components of the above channel, receptor and Ca^{2+} store with their associated differential functional activity provide significant potential for plasticity and heterogeneity in function, consistent with differential EDH activity in different vascular beds in health and disease.

The original mechanism of EDH was suggested to be due to diffusion-mediated processes; with the primary pathway reported to involve endothelial potassium ion release into the so-called IEL space, which would then diffuse through the dense elastin of the IEL to form a 'potassium cloud' around the adjacent smooth muscle [96, 97]. Such studies were consistent with an additional role for myoendothelial gap junction Cxs in EDH activity [98]. A role for diffusible epoxyeicosatrienoic acids (EETs) is implicated in EDH activity in several vascular beds [99]; perhaps being related to the regulation of myoendothelial gap junction Cx activity [100]. However, with gap junction Cx activity, contact-mediated mechanisms involving highly localized potassium release represent a more conceivable pathway to underlie EDH activity than the 'cloud' scenario [13, 14, 16, 23, 94]. This latter process primarily involves potassium release at discrete IEL hole and close myoendothelial contact sites where myoendothelial microdomain signaling sites are present (Fig. 36.2; [16, 93, 94]). In this scenario, SK_{Ca} and IK_{Ca} are present at a low level on the endothelial cell membrane, with a higher localization at a proportion of IEL hole sites, including some as myoendothelial contact sites [94, 101–103].

Myoendothelial gap junction Cxs facilitate the transfer of an endothelium-derived hyperpolarizing current to the smooth muscle (Fig. 36.2; [16, 23, 104]), as the primary contact-mediated EDH mechanism. In addition, potassium release from endothelial SK_{Ca} and/or IK_{Ca} results in the subsequent activation of smooth muscle Na^+-K^+-ATPase [102, 105]. Further, the SK_{Ca}/IK_{Ca}-mediated K^+ outflow

activates closely associated inward rectifying potassium channels (K_{ir}) located on the endothelial projection (Fig. 36.2; [94, 102]), with some activity also potentially occurring at K_{ir} diffusely distributed on the endothelial cell membrane, as well as with smooth muscle K_{ir} in some vessels. The overall result of myoendothelial Cx and potassium-mediated signaling is hyperpolarization of the adjacent smooth muscle, closure of smooth muscle VDCC, inhibition of PLC [106], and smooth muscle dilation and vessel relaxation.

In theory, there is potential for three basic types of myoendothelial microdomain signaling sites (Fig. 36.2), as myoendothelial gap junction/Cx based sites facilitating current transfer; as IK_{Ca}-ER-IP_3R and/or SK_{Ca}-ER-IP_3R based sites facilitating K^+-mediated signaling, or as a synergistic combination of the two mechanisms (Fig. 36.2; [16, 102, 105]). Indeed, as such sites maintain the ability to sustain their contribution to vascular reactivity, the involvement of a regenerative mechanism for refilling the localized ER Ca^{2+} store is implicated, with this latter mechanism likely being associated with TRP channel activity.

TRP Channels – A Mechanism for Ca^{2+} Entry Directed to Store Re-filling?

Transient receptor potential channels are a group of generally non-selective cation channels that play a significant role in cellular Ca^{2+} homeostasis [107–109]. Such channels are activated and regulated by a wide variety of stimuli, and a role for several TRP channel subtypes in vascular EDH-type function has been suggested. These include canonical type 3 (C3; [110, 111]), TRP vanilloid type 3 (V3; [112]), TRPV4 [40, 113, 114], and TRP ankyrin type 1 (A1; [112, 115]).

The potential role of TRPC3 in myoendothelial microdomain signaling comes primarily from the observations of Isakson and Duling [106]. At sites of close myoendothelial association in co-cultured mouse aortic endothelial and smooth muscle cells (which are notably absent in the intact aorta of non-diseased adult mouse; [6]), TRPC3 is in close proximity to IP_3R [110]. Such an arrangement has the potential to facilitate TRPC3 and IP_3R interaction, where localized TRPC3-mediated Ca^{2+} entry likely refills the nearby IP_3R-mediated ER stores. When subsequently activated these closely localized stores provide the necessary Ca^{2+} to facilitate endothelial S/IK_{Ca} activity (Fig. 36.2; [16]).

In rat cerebral artery, TRPV3 appears to facilitate endothelial cell Ca^{2+} influx for EDH-type vasodilator activity [112], whilst Ca^{2+} entry through endothelial TRPV4 are reported to underlie an NO-dependent relaxation in carotid artery from rat, and EDH- and NO-type relaxation in arterioles of rat gracilis muscle [114]. A role for TRPV4 in EDH-type relaxation has also been suggested in cerebral artery from rat [113]; with a further role for TRPV4 being suggested in NO- and EDH-type relaxation in the mesenteric artery of the mouse [40]. However, in the above TRPV3 and V4 studies, an unequivocal relationship to myoendothelial S/IK_{Ca}-ER-IP_3R microdomain activity was not clarified.

Of interest, an interaction of IP_3R and TRPC3 has been observed in endothelial cells of the uterine artery of sheep [111]; although a localization to microdomain sites was not examined. Further, a potential spatial association and functional link between IP_3R-K_{Ca} and TRPC3 has been observed in a number of cell systems, such as cultured endothelial cells from bovine pulmonary artery [78] and in transfected HEK cells [116]; as well as in the smooth muscle of rat cerebral and rabbit coronary artery [117, 118]. Functional interaction large conductance (B) K_{Ca} and IP_3R has also been demonstrated in smooth muscle cells of the rat basilar artery [119]; and an association of IK_{Ca} and IP_3R also being found in smooth muscle cells of the guinea pig antrum [120]. Thus, a relationship between the functional activation of K_{Ca}-IP_3R and TRPC3 and their spatial association exists in selected systems, and supports the proposition of a role for a similar complex in EDH activity in the control of vasodilator activity and vascular tone.

The Endothelium and the Conduction of Vasomotor Responses

The preceding sections highlight key endothelial properties and how they contribute to arterial vasodilation. The focus of these was on the ability of agonists (e.g. section "Physiological and Experimental Agonist-Induced Mechanisms", above) to increase the intracellular endothelial cell [Ca^{2+}], and the role of myoendothelial signaling microdomains in initiating and transferring the endothelial hyperpolarization to the smooth muscle layers; a response that dilates resistance arteries by limiting Ca^{2+} influx through VDCC (Fig. 36.2). While radial charge movement to the smooth muscle layer has garnered considerable attention in the vascular literature, charge spread along the long axis of an artery is equally important from a functional perspective ([121–123]; Fig. 36.3). Such movement enables vasomotor responses to be coordinated among multiple vessel segments. Coordination is an essential element for the optimization of blood flow dynamics, a principal demonstrated by Segal and Jacobs [121]. In particular, by selectively damaging specific cell layers, these investigators showed that by discretely compromising longitudinal communication to important resistive elements, such as external feed arteries, hyperemic responses in contracting skeletal muscle could be reduced by as much as 50%.

The ability of vasomotor responses to longitudinally conduct along an arterial wall was first described in detail by Segal and Duling [122] using a hamster cheek pouch preparation. Generally speaking, the stimulus for conducted responses under experimental conditions is initiated by applying endothelial-selective agents to a small portion of an artery such that they induce a range of Ca^{2+} events such as pulsars, waves and oscillations [124–126]. Through discrete targeting, these events selectively augment the activity of SK_{Ca} and IK_{Ca} channels in a manner that results in a localized hyperpolarization [127, 128]. Once initiated, this hyperpolarizing response preferentially conducts along the endothelium and subsequently spreads to the overlying layer(s) of smooth muscle via myoendothelial gap junctions ([129–131]; Figs. 36.1, 36.2 and 36.3); although, of note, additional pathways have

been proposed [23], and to some extent, likely reflect apparent agonist-specific activity, and potentially methodology [130].

The preferential spread of charge along the endothelium reflects the low resistivity of this layer due to robust gap junctional expression of the longitudinal orientation of endothelial cells with the arterial wall ([129, 131–133]; Fig. 36.3). As conducted responses are non-regenerative, they decrease in magnitude as they longitudinally spread, due to charge loss through endothelial ion channels and myoendothelial gap junctions [129, 131, 134]. This characteristically sets the extent of electrical decay. Studies performed over the last two decades indicate that conduction decay varies among vessel classes, with arteries from the mesentery and cheek pouch displaying greater decrement to those isolated from skeletal muscle [126, 128, 135, 136]. Functional work has also noted that conduction decay can be altered by changing the ion channel conductance or the coupling resistance among endothelial cells or between the two cell layers [134, 137, 138]. With respect to ion channels, the work of Jantzi et al. [135] is of particular note as it was the first to highlight that a specified conductance (i.e. inwardly rectifying K^+ channels) could 'facilitate' the conduction of hyperpolarization and dilation. With regard to gap junction resistivity, the use of genetically modified mice has been insightful with Cx40 knockout mice displaying an attenuated conducted response ([138]; Fig. 36.3). While investigators recognize that electrical responses originating in the endothelium can conduct several millimeters along an arterial wall, there is, at present, little evidence that Ca^{2+} responses spread in an equally robust manner [127, 139]. Indeed, findings indicate that robust endothelial Ca^{2+} responses extensively decay as they spread to neighboring cells such that they are unmeasurable at sites 200 μm distal to the point of agent application [127, 139].

Since the inception of work on the conducted vasomotor response, experimental efforts have steadily advanced from basic characterization to mechanistic biophysical examinations. While foundational knowledge has progressively increased, investigators have only begun to apply this knowledge and address whether this biological response is altered by the onset of vascular disease. Genetic models of hypertension have received some attention with existing work noting that the conduction of ACh-induced responses is modestly attenuated during the early stages of hypertension [140]. In theory, this attenuation could reflect increased gap junctional resistivity among endothelial cells. This perspective is consistent with biochemical observations from large conduit arteries which show that gap junctional expression is reduced in the hypertensive state [141]. While the preceding work illustrates that longitudinal conduction is potentially susceptible to dysfunction, it would be imprudent to suggest that any disease processes, retaining a significant vascular element, will equally effect on this key biological response. Indeed, as mouse models of severe hypercholesterolemia highlight, endothelial-initiated conduction remains largely unaffected [142].

Concluding Remarks

The primary channels and receptors involved in the modulation of vascular endothelial cell Ca^{2+} and vasodilator function are likely associated with the formation of microdomain signaling complexes. Alterations in the specific expression, distribution and function of the channels, receptors and associated calcium stores in such complexes are likely a key factor underlying the significant plasticity and heterogeneity in myoendothelial signaling mechanisms associated with vasodilator activity and the control of vascular tone. Determining the specific properties of these signaling pathways and how they might be altered in disease is an avenue for research to identify novel therapeutic targets for the control of specific artery function.

References

1. Sandow SL, Hill CE (2000) The incidence of myoendothelial gap junctions in the proximal and distal mesenteric arteries of the rat is suggestive of a role in EDHF-mediated responses. Circ Res 86:341–346
2. Becker BF, Chappell D, Jacob M (2010) Endothelial glycocalyx and coronary vascular permeability: the fringe benefit. Basic Res Cardiol 105:687–701
3. Potter DR, Damiano ER (2008) The hydrodynamically relevant endothelial cell glycocalyx observed in vivo is absent in vitro. Circ Res 102:770–776
4. Reitsma S, Slaaf DW, Vink H, van Zandvoort MA, oude Egbrink MG (2007) The endothelial glycocalyx: composition, functions, and visualization. Pflugers Arch 454:345–359
5. Wise SG, Weiss AS (2009) Tropoelastin. Int J Biochem Cell Biol 41:494–497
6. Sandow SL, Gzik DJ, Lee RMKW (2009) Arterial internal elastic lamina holes: relationship to function? J Anat 214:258–266
7. Aiello VD, Gutierrez PS, Chaves MJ, Lopes AA, Higuchi ML, Ramires JA (2003) Morphology of the internal elastic lamina in arteries from pulmonary hypertensive patients: a confocal laser microscopy study. Mod Pathol 16:411–416
8. Hassler O (1962) The windows of the internal elastic lamella of the cerebral arteries. Virchows Arch Pathol Anat Physiol Klin Med 335:127–132
9. Smith EB, Staples EM (1980) Distribution of plasma proteins across the human aortic wall–barrier functions of endothelium and internal elastic lamina. Atherosclerosis 37:579–590
10. Svendsen E, Tindall AR (1988) The internal elastic membrane and intimal folds in arteries: important but neglected structures? Acta Physiol Scand 133(S572):1–71
11. Sims FH (1989) The internal elastic lamina in normal and abnormal human arteries. A barrier to the diffusion of macromolecules from the lumen. Artery 16:159–173
12. Tada S, Tarbell JM (2004) Internal elastic lamina affects the distribution of macromolecules in the arterial wall: a computational study. Am J Physiol 287:H905–H913
13. Griffith TM (2004) Endothelium-dependent smooth muscle hyperpolarization: do gap junctions provide a unifying hypothesis? Br J Pharmacol 141:881–903
14. Sandow SL (2004) Factors, fiction and endothelium-derived hyperpolarizing factor. Clin Exp Pharmacol Physiol 31:563–570
15. Sandow SL, Tare M (2007) C-type natriuretic peptide: a new endothelium-derived hyperpolarizing factor? Trends Pharmacol Sci 28:61–67
16. Sandow SL, Haddock RE, Hill CE, Chadha PE, Kerr PM, Welsh DG, Plane F (2009) What's where and why at a vascular myoendothelial microdomain signaling complex? Clin Exp Pharmacol Physiol 36:67–76

17. Kwan HY, Huang Y, Yao X (2007) Cyclic nucleotides and Ca^{2+} influx pathways in vascular endothelial cells. Clin Hemorheol Microcirc 37:63–70
18. Burnstock G (1990) Local mechanisms of blood flow control by perivascular nerves and endothelium. J Hypertens 8:S95–S106
19. Fisslthaler B, Dimmeler S, Hermann C, Busse R, Fleming I (2000) Phosphorylation and activation of the endothelial nitric oxide synthase by fluid shear stress. Acta Physiol Scand 168:81–88
20. Dietrich A, Kalwa H, Gudermann T (2010) TRPC channels in vascular cell function. Thromb Haemost 103:262–270
21. Hill CE, Phillips JK, Sandow SL (2001) Heterogeneous control of blood flow amongst different vascular beds. Med Res Rev 21:1–60
22. Severs NJ (1999) Cardiovascular disease. Novartis Found Symp 219:188–211
23. de Wit C, Griffith TM (2010) Connexins and gap junctions in the EDHF phenomenon and conducted vasomotor responses. Pflugers Arch 459:897–914
24. Johnstone S, Isakson B, Locke D (2009) Biological and biophysical properties of vascular connexin channels. Int Rev Cell Mol Biol 278:69–118
25. Aird WC (2006) Mechanisms of endothelial cell heterogeneity in health and disease. Circ Res 98:159–162
26. Aird WC (2007) Phenotypic heterogeneity of the endothelium: II Representative vascular beds. Circ Res 100:174–190
27. Aird WC (2007) Phenotypic heterogeneity of the endothelium: I. Structure, function, and mechanisms. Circ Res 100:158–173
28. Shimokawa H (1999) A novel therapeutic target Primary endothelial dysfunction: atherosclerosis. J Mol Cell Cardiol 31:23–37
29. McGuire JJ, Ding H, Triggle CR (2001) Endothelium-derived relaxing factors: a focus on endothelium-derived hyperpolarizing factor(s). Can J Physiol Pharmacol 79:443–470
30. Feletou M, Kohler R, Vanhoutte PM (2010) Endothelium-derived vasoactive factors and hypertension: possible roles in pathogenesis and as treatment targets. Curr Hypertens Rep 12:267–275
31. Triggle CR, Ding H (2011) The endothelium in compliance and resistance vessels. Front Biosci 3:730–744
32. Boegehold MA (2010) Endothelium-dependent control of vascular tone during early postnatal and juvenile growth. Microcirculation 17:394–406
33. Davies PF (2009) Hemodynamic shear stress and the endothelium in cardiovascular pathophysiology. Nat Clin Pract Cardiovasc Med 6:16–26
34. Kuo L, Davis MJ, Chilian WM (1990) Endothelium-dependent, flow-induced dilation of isolated coronary arterioles. Am J Physiol 259:H1063–H1070
35. Davies PF (1995) Flow-mediated endothelial mechanotransduction. Physiol Rev 75:519–560
36. Ando J, Ohtsuka A, Korenaga R, Kawamura T, Kamiya A (1993) Wall shear stress rather than shear rate regulates cytoplasmic Ca^{2+} responses to flow in vascular endothelial cells. Biochem Biophys Res Commun 190:716–723
37. Ando J, Komatsuda T, Kamiya A (1988) Cytoplasmic calcium response to fluid shear stress in cultured vascular endothelial cells. In Vitro Cell Dev Biol 24:871–877
38. Kwan HY, Leung PC, Huang Y, Yao X (2003) Depletion of intracellular Ca^{2+} stores sensitizes the flow-induced Ca^{2+} influx in rat endothelial cells. Circ Res 92:286–292
39. Liu C, Ngai CY, Huang Y, Ko WH, Wu M, He GW, Garland CJ, Dora KA, Yao X (2006) Depletion of intracellular Ca^{2+} stores enhances flow-induced vascular dilatation in rat small mesenteric artery. Br J Pharmacol 147:506–515
40. Mendoza SA, Fang J, Gutterman DD, Wilcox DA, Bubolz AH, Li R, Suzuki M, Zhang DX (2010) TRPV4-mediated endothelial Ca^{2+} influx and vasodilation in response to shear stress. Am J Physiol 298:H466–H476
41. Inoue R, Jian Z, Kawarabayashi Y (2009) Mechanosensitive TRP channels in cardiovascular pathophysiology. Pharmacol Ther 123:371–385

42. Hartmannsgruber V, Heyken WT, Kacik M, Kaistha A, Grgic I, Harteneck C, Liedtke W, Hoyer J, Kohler R (2007) Arterial response to shear stress critically depends on endothelial TRPV4 expression. PLoS One 2:e827
43. Koyama T, Oike M, Ito Y (2001) Involvement of Rho-kinase and tyrosine kinase in hypotonic stress-induced ATP release in bovine aortic endothelial cells. J Physiol 532:759–769
44. Yamamoto K, Sokabe T, Matsumoto T, Yoshimura K, Shibata M, Ohura N, Fukuda T, Sato T, Sekine K, Kato S, Isshiki M, Fujita T, Kobayashi M, Kawamura K, Masuda H, Kamiya A, Ando J (2006) Impaired flow-dependent control of vascular tone and remodeling in $P2X_4$-deficient mice. Nat Med 12:133–137
45. Parnavelas JG, Kelly W, Burnstock G (1985) Ultrastructural localization of choline acetyltransferase in vascular endothelial cells in rat brain. Nature 316:724–725
46. Muller JM, Davis MJ, Kuo L, Chilian WM (1999) Changes in coronary endothelial cell Ca^{2+} concentration during shear stress- and agonist-induced vasodilation. Am J Physiol 276:H1706–H1714
47. Fleming I, Busse R (2003) Molecular mechanisms involved in the regulation of the endothelial nitric oxide synthase. Am J Physiol 284:R1–R12
48. Beech DJ (2009) Harmony and discord in endothelial calcium entry. Circ Res 104:e22–e23
49. Freichel M, Suh SH, Pfeifer A, Schweig U, Trost C, Weissgerber P, Biel M, Philipp S, Freise D, Droogmans G, Hofmann F, Flockerzi V, Nilius B (2001) Lack of an endothelial store-operated Ca^{2+} current impairs agonist-dependent vasorelaxation in TRP4−/− mice. Nat Cell Biol 3:121–127
50. Paria BC, Vogel SM, Ahmmed GU, Alamgir S, Shroff J, Malik AB, Tiruppathi C (2004) Tumor necrosis factor-alpha-induced TRPC1 expression amplifies store-operated Ca^{2+} influx and endothelial permeability. Am J Physiol 287:L1303–L1313
51. Cioffi DL, Wu S, Alexeyev M, Goodman SR, Zhu MX, Stevens T (2005) Activation of the endothelial store-operated ISOC Ca2+ channel requires interaction of protein 4.1 with TRPC4. Circ Res 97:1164–1172
52. Antoniotti S, Fiorio Pla A, Barral S, Scalabrino O, Munaron L, Lovisolo D (2006) Interaction between TRPC channel subunits in endothelial cells. J Recept Signal Transduct Res 26:225–240
53. Abdullaev IF, Bisaillon JM, Potier M, Gonzalez JC, Motiani RK, Trebak M (2008) STIM1 and Orai1 mediate CRAC currents and store-operated calcium entry important for endothelial cell proliferation. Circ Res 103:1289–1299
54. Hirano K, Hirano M, Hanada A (2009) Involvement of STIM1 in the proteinase-activated receptor 1-mediated Ca^{2+} influx in vascular endothelial cells. J Cell Biochem 108:499–507
55. Antigny F, Jousset H, Konig S, Frieden M (2011) Thapsigargin activates Ca^{2+} entry both by store-dependent, STIM1/Orai1-mediated, and store-independent, TRPC3/PLC/PKC-mediated pathways in human endothelial cells. Cell Calcium 49:115–127
56. Mizuno O, Kobayashi S, Hirano K, Nishimura J, Kubo C, Kanaide H (2000) Stimulus-specific alteration of the relationship between cytosolic Ca^{2+} transients and nitric oxide production in endothelial cells ex vivo. Br J Pharmacol 130:1140–1146
57. Budel S, Schuster A, Stergiopoulos N, Meister JJ, Beny JL (2001) Role of smooth muscle cells on endothelial cell cytosolic free calcium in porcine coronary arteries. Am J Physiol 281:H1156–H1162
58. Marie I, Beny JL (2002) Calcium imaging of murine thoracic aorta endothelium by confocal microscopy reveals inhomogeneous distribution of endothelial cells responding to vasodilator agents. J Vasc Res 39:260–267
59. Sandow SL, Grayson TH (2009) Limits of isolation and culture: intact vascular endothelium and BK_{Ca}. Am J Physiol H 297:H1–H7
60. Gericke A, Sniatecki JJ, Mayer VG, Goloborodko E, Patzak A, Wess J, Pfeiffer N (2011) Role of M_1, M_3, and M_5 muscarinic acetylcholine receptors in cholinergic dilation of small arteries studied with gene-targeted mice. Am J Physiol 300:H1602–H1608
61. Elhusseiny A, Hamel E (2000) Muscarinic- but not nicotinic- acetylcholine receptors mediate a nitric oxide-dependent dilation in brain cortical arterioles: a possible role for the M_5 receptor subtype. J Cereb Blood Flow Metab 20:298–305

62. Yamada M, Lamping KG, Duttaroy A, Zhang W, Cui Y, Bymaster FP, McKinzie DL, Felder CC, Deng CX, Faraci FM, Wess J (2001) Cholinergic dilation of cerebral blood vessels is abolished in M_5 muscarinic acetylcholine receptor knockout mice. Proc Natl Acad Sci 98:14096–14101
63. Tracey WR, Peach MJ (1992) Differential muscarinic receptor mRNA expression by freshly isolated and cultured bovine aortic endothelial cells. Circ Res 70:234–240
64. Fukao M, Hattori Y, Kanno M, Sakuma I, Kitabatake A (1997) Sources of Ca^{2+} in relation to generation of acetylcholine-induced endothelium-dependent hyperpolarization in rat mesenteric artery. Br J Pharmacol 120:1328–1334
65. Fukuta H, Hashitani H, Yamamoto Y, Suzuki H (1999) Calcium responses induced by acetylcholine in submucosal arterioles of the guinea-pig small intestine. J Physiol 515:489–499
66. Burger NZ, Kuzina OY, Osol G, Gokina NI (2009) Estrogen replacement enhances EDHF-mediated vasodilation of mesenteric and uterine resistance arteries: role of endothelial cell Ca^{2+}. Am J Physiol 296:E503–E512
67. Mumtaz S, Burdyga G, Borisova L, Wray S, Burdyga T (2011) The mechanism of agonist induced Ca^{2+} signalling in intact endothelial cells studied confocally in in situ arteries. Cell Calcium 49:66–77
68. Earley S, Pauyo T, Drapp R, Tavares MJ, Liedtke W, Brayden JE (2009) TRPV4-dependent dilation of peripheral resistance arteries influences arterial pressure. Am J Physiol 297:H1096–H1102
69. Zhang DX, Mendoza SA, Bubolz AH, Mizuno A, Ge ZD, Li R, Warltier DC, Suzuki M, Gutterman DD (2009) Transient receptor potential vanilloid type 4-deficient mice exhibit impaired endothelium-dependent relaxation induced by acetylcholine *in vitro* and *in vivo*. Hypertension 53:532–538
70. Wang L, Karlsson L, Moses S, Hultgardh-Nilsson A, Andersson M, Borna C, Gudbjartsson T, Jern S, Erlinge D (2002) P2 Receptor expression profiles in human vascular smooth muscle and endothelial cells. J Cardiovasc Pharmacol 40:841–853
71. Chi JT, Chang HY, Haraldsen G, Jahnsen FL, Troyanskaya OG, Chang DS, Wang Z, Rockson SG, van de Rijn M, Botstein D, Brown PO (2003) Endothelial cell diversity revealed by global expression profiling. Proc Natl Acad Sci 100:10623–10628
72. Burnstock G (2007) Purine and pyrimidine receptors. Cell Mol Life Sci 64:1471–1483
73. Lyubchenko T, Woodward H, Veo KD, Burns N, Nijmeh H, Liubchenko GA, Stenmark KR, Gerasimovskaya EV (2011) $P2Y_1$ and $P2Y_{13}$ purinergic receptors mediate Ca^{2+} signaling and proliferative responses in pulmonary artery vasa vasorum endothelial cells. Am J Physiol 300:C266–C275
74. Lynch M, Gillespie JI, Greenwell JR, Johnson C (1992) Intracellular calcium 'signatures' evoked by different agonists in isolated bovine aortic endothelial cells. Cell Calcium 13:227–233
75. Bishara NB, Murphy TV, Hill MA (2002) Capacitative Ca^{2+} entry in vascular endothelial cells is mediated via pathways sensitive to 2 aminoethoxydiphenyl borate and xestospongin C. Br J Pharmacol 135:119–128
76. Kwan HY, Cheng KT, Ma Y, Huang Y, Tang NL, Yu S, Yao X (2010) CNGA2 contributes to ATP-induced noncapacitative Ca^{2+} influx in vascular endothelial cells. J Vasc Res 47:148–156
77. Brough GH, Wu S, Cioffi D, Moore TM, Li M, Dean N, Stevens T (2001) Contribution of endogenously expressed Trp1 to a Ca^{2+}-selective, store-operated Ca^{2+} entry pathway. FASEB J 15:1727–1738
78. Kamouchi M, Philipp S, Flockerzi V, Wissenbach U, Mamin A, Raeymaekers L, Eggermont J, Droogmans G, Nilius B (1999) Properties of heterologously expressed hTRP3 channels in bovine pulmonary artery endothelial cells. J Physiol 518:345–358
79. Morgan-Boyd R, Stewart JM, Vavrek RJ, Hassid A (1987) Effects of bradykinin and angiotensin II on intracellular Ca^{2+} dynamics in endothelial cells. Am J Physiol 253:C588–C598
80. Stewart DE, Kirby ML, Aronstam RS (1986) Regulation of beta-adrenergic density in the non-innervated and denervated embryonic chick heart. J Mol Cell Cardiol 18:469–475
81. Bovenzi V, Savard M, Morin J, Cuerrier CM, Grandbois M, Gobeil F Jr (2010) Bradykinin protects against brain microvascular endothelial cell death induced by pathophysiological stimuli. J Cell Physiol 222:168–176

82. Paltauf-Doburzynska J, Frieden M, Graier WF (1999) Mechanisms of Ca^{2+} store depletion in single endothelial cells in a Ca^{2+}-free environment. Cell Calcium 25:345–353
83. Ihara E, Derkach DN, Hirano K, Nishimura J, Nawata H, Kanaide H (2001) Ca^{2+} influx in the endothelial cells is required for the bradykinin-induced endothelium-dependent contraction in the porcine interlobar renal artery. J Physiol 534:701–711
84. Sharma NR, Davis MJ (1995) Substance P-induced calcium entry in endothelial cells is secondary to depletion of intracellular stores. Am J Physiol 268:H962–H973
85. Frieden M, Sollini M, Beny J (1999) Substance P and bradykinin activate different types of K_{Ca} currents to hyperpolarize cultured porcine coronary artery endothelial cells. J Physiol 519:361–371
86. Uchida H, Tanaka Y, Ishii K, Nakayama K (1999) L-type Ca^{2+} channels are not involved in coronary endothelial Ca^{2+} influx mechanism responsible for endothelium-dependent relaxation. Res Commun Mol Pathol Pharmacol 104:127–144
87. Bartha K, Domotor E, Lanza F, Adam-Vizi V, Machovich R (2000) Identification of thrombin receptors in rat brain capillary endothelial cells. J Cereb Blood Flow Metab 20:175–182
88. Hirano K (2007) The roles of proteinase-activated receptors in the vascular physiology and pathophysiology. Arterioscler Thromb Vasc Biol 27:27–36
89. Ahmmed GU, Mehta D, Vogel S, Holinstat M, Paria BC, Tiruppathi C, Malik AB (2004) Protein kinase Calpha phosphorylates the TRPC1 channel and regulates store-operated Ca2+ entry in endothelial cells. J Biol Chem 279:20941–20949
90. Kwiatek AM, Minshall RD, Cool DR, Skidgel RA, Malik AB, Tiruppathi C (2006) Caveolin-1 regulates store-operated Ca^{2+} influx by binding of its scaffolding domain to transient receptor potential channel-1 in endothelial cells. Mol Pharmacol 70:1174–1183
91. Singh I, Knezevic N, Ahmmed GU, Kini V, Malik AB, Mehta D (2007) Galphaq-TRPC6-mediated Ca^{2+} entry induces RhoA activation and resultant endothelial cell shape change in response to thrombin. J Biol Chem 282:7833–7843
92. Sandow SL, Tare M, Coleman HA, Hill CE, Parkington HC (2002) Involvement of myoendothelial gap junctions in the actions of endothelium-derived hyperpolarizing factor. Circ Res 90:1108–1113
93. Mather S, Dora KA, Sandow SL, Winter P, Garland CJ (2005) Rapid endothelial cell-selective loading of connexin 40 antibody blocks endothelium-derived hyperpolarizing factor dilation in rat small mesenteric arteries. Circ Res 97:399–407
94. Dora KA, Gallagher NT, McNeish A, Garland CJ (2008) Modulation of endothelial cell KCa3.1 channels during endothelium-derived hyperpolarizing factor signaling in mesenteric resistance arteries. Circ Res 102:1247–1255
95. Cao YX, Zheng JP, He JY, Li J, Xu CB, Edvinsson L (2005) Induces vasodilatation of rat mesenteric artery in vitro mainly by inhibiting receptor-mediated Ca^{2+}-influx and Ca^{2+}-release. Arch Pharm Res 28:709–715
96. Weston AH, Absi M, Harno E, Geraghty AR, Ward DT, Ruat M, Dodd RH, Dauban P, Edwards G (2008) The expression and function of Ca^{2+}-sensing receptors in rat mesenteric artery; comparative studies using a model of type II diabetes. Br J Pharmacol 154:652–662
97. Weston AH, Richards GR, Burnham MP, Feletou M, Vanhoutte PM, Edwards G (2002) K^+-induced hyperpolarization in rat mesenteric artery: identification, localization and role of Na^+/K^+-ATPases. Br J Pharmacol 136:918–926
98. Busse R, Edwards G, Feletou M, Fleming I, Vanhoutte PM, Weston AH (2002) EDHF: bringing the concepts together. Trends Pharmacol Sci 23:374–380
99. Campbell WB, Gauthier KM (2002) What is new in endothelium-derived hyperpolarizing factors? Curr Opin Nephrol Hypertens Res 11:177–183
100. Popp R, Brandes RP, Ott G, Busse R, Fleming I (2002) Dynamic modulation of interendothelial gap junctional communication by 11,12-epoxyeicosatrienoic acid. Circ Res 90:800–806
101. Sandow SL, Neylon CB, Chen MX, Garland CJ (2006) Spatial separation of endothelial small- and intermediate-conductance calcium-activated potassium channels (K_{Ca}) and connexins: possible relationship to vasodilator function? J Anat 209:689–698
102. Haddock RE, Grayson TH, Morris MJ, Howitt L, Chadha PS, Sandow SL (2011) Diet-induced obesity impairs endothelium-derived hyperpolarization via altered potassium channel signaling mechanisms. PLoS One 6:e16423

103. Chadha PS, Haddock RE, Howitt L, Morris MJ, Murphy TV, Grayson TH, Sandow SL (2010) Obesity upregulates IK_{Ca} and myoendothelial gap junctions to maintain endothelial vasodilator function. J Pharmacol Exp Ther 335:284–293
104. Feletou M (2009) Calcium-activated potassium channels and endothelial dysfunction: therapeutic options? Br J Pharmacol 156:545–562
105. Chadha PS, Lu L, Rikard-Bell M, Senadheera S, Howitt L, Bertrand RL, Grayson TH, Murphy TV, Sandow SL (2011) Endothelium-dependent vasodilation in human mesenteric artery is primarily mediated by myoendothelial gap junctions, IK_{Ca} and NO. J Pharmacol Exp Ther 336:701–708
106. Itoh T, Seki N, Suzuki S, Ito S, Kajikuri J, Kuriyama H (1992) Membrane hyperpolarization inhibits agonist-induced synthesis of inositol 1,4,5-trisphosphate in rabbit mesenteric artery. J Physiol 451:307–328
107. Abramowitz J, Birnbaumer L (2009) Physiology and pathophysiology of canonical transient receptor potential channels. FASEB J 23:297–328
108. Earley S, Brayden JE (2010) Transient receptor potential channels and vascular function. Clin Sci 119:19–36
109. Wong CO, Yao X (2011) TRP channels in vascular endothelial cells. Adv Exp Med Biol 704:759–780
110. Isakson BE, Duling BR (2006) Organization of IP_3-R1 and TRPC3 at the myoendothelial junction may influence polarized calcium signaling. Exp Biol (Late Breaking Abstracts) 786.783
111. Gifford SM, Yi FX, Bird IM (2006) Pregnancy-enhanced store-operated Ca^{2+} channel function in uterine artery endothelial cells is associated with enhanced agonist-specific transient receptor potential channel 3-inositol 1,4,5-trisphosphate receptor 2 interaction. J Endocrinol 190:385–395
112. Earley S, Gonzales AL, Garcia ZI (2010) A dietary agonist of TRPV3 elicits endothelium-dependent vasodilation. Mol Pharmacol 77:612–620
113. Marrelli SP, O'Neil RG, Brown RC, Bryan RM Jr (2007) PLA2 and TRPV4 channels regulate endothelial calcium in cerebral arteries. Am J Physiol 292:H1390–H1397
114. Kohler R, Heyken WT, Heinau P, Schubert R, Si H, Kacik M, Busch C, Grgic I, Maier T, Hoyer J (2006) Evidence for a functional role of endothelial transient receptor potential V4 in shear stress-induced vasodilatation. Arterioscler Thromb Vasc Biol 26:1495–1502
115. Earley S, Gonzales AL, Crnich R (2009) Endothelium-dependent cerebral artery dilation mediated by TRPA1 and Ca^{2+}-Activated K^+ channels. Circ Res 104:987–994
116. Boulay G, Brown DM, Qin N, Jiang M, Dietrich A, Zhu MX, Chen Z, Birnbaumer M, Mikoshiba K, Birnbaumer L (1999) Modulation of Ca^{2+} entry by polypeptides of the inositol 1,4, 5-trisphosphate receptor (IP_3R) that bind transient receptor potential (TRP): evidence for roles of TRP and IP3R in store depletion-activated Ca^{2+} entry. Proc Natl Acad Sci 96:14955–14960
117. Adebiyi A, Zhao G, Narayanan D, Thomas CM, Bannister JP, Jaggar JH (2010) Isoform-selective physical coupling of TRPC3 channels to IP_3 receptors in smooth muscle cells regulates arterial contractility. Circ Res 106:1603–1612
118. Peppiatt-Wildman CM, Albert AP, Saleh SN, Large WA (2007) Endothelin-1 activates a Ca2+−permeable cation channel with TRPC3 and TRPC7 properties in rabbit coronary artery myocytes. J Physiol 580:755–764
119. Kim CJ, Weir BK, Macdonald RL, Zhang H (1998) Erythrocyte lysate releases Ca^{2+} from IP_3-sensitive stores and activates Ca^{2+}-dependent K^+ channels in rat basilar smooth muscle cells. Neurol Res 20:23–30
120. Yang M, Li XL, Xu HY, Sun JB, Mei B, Zheng HF, Piao LH, Xing DG, Li ZL, Xu WX (2005) Role of arachidonic acid in hyposmotic membrane stretch-induced increase in calcium-activated potassium currents in gastric myocytes. Acta Pharmacol Sin 26:1233–1242
121. Segal SS, Jacobs TL (2001) Role for endothelial cell conduction in ascending vasodilatation and exercise hyperaemia in hamster skeletal muscle. J Physiol 536:937–946

122. Segal SS, Duling BR (1987) Propagation of vasodilation in resistance vessels of the hamster: development and review of working hypothesis. Circ Res 50:260–287
123. Segal SS, Duling BR (1986) Flow control among microvessels coordinated by intercellular conduction. Science 234:868–870
124. Ledoux J, Taylor MS, Bonev AD, Hannah RM, Solodushko V, Shui B, Tallini Y, Kotlikoff MI, Nelson MT (2008) Functional architecture of inositol 1,4,5-trisphosphate signaling in restricted spaces of myoendothelial projections. Proc Natl Acad Sci 105:9627–9632
125. McSherry IN, Spitaler MM, Takano H, Dora KA (2005) Endothelial cell Ca2+ increases are independent of membrane potential in pressurized rat mesenteric arteries. Cell Calcium 38:23–33
126. Segal SS, Welsh DG, Kurjiaka DT (1999) Spread of vasodilatation and vasoconstriction along feed arteries and arterioles of hamster skeletal muscle. J Physiol 516:283–291
127. Dora KA, Xia J, Duling BR (2003) Endothelial cell signaling during conducted vasomotor responses. Am J Physiol 285:H119–H126
128. Welsh DG, Segal SS (1998) Endothelial and smooth muscle cell conduction in arterioles controlling blood flow. Am J Physiol 274:H178–H186
129. Diep HK, Vigmond EJ, Segal SS, Welsh DG (2005) Defining electrical communication in skeletal muscle resistance arteries: a computational approach. J Physiol 568:267–281
130. Emerson GG, Segal SS (2000) Endothelial cell pathway for conduction of hyperpolarization and vasodilation along hamster feed arteries. Circ Res 86:94–100
131. Tran CH, Vigmond EJ, Plane F, Welsh DG (2009) Mechanistic basis of differential conduction in skeletal muscle arteries. J Physiol 587:1301–1318
132. Sandow SL, Looft-Wilson RC, Grayson TH, Segal SS, Hill CE (2003) Expression of homocellular and heterocellular gap junctions in hamster arterioles and feed arteries. Cardiovasc Res 60:643–653
133. Sandow SL, Goto K, Rummery N, Hill CE (2004) Developmental changes in myoendothelial gap junction mediated vasodilator activity in the rat saphenous artery. J Physiol 556:875–886
134. Wolfle SE, Chaston DJ, Goto K, Sandow SL, Edwards FR, Hill CE (2011) Non-linear relationship between hyperpolarisation and relaxation enables long distance propagation of vasodilatation. J Physiol 589:2607–2623
135. Xia J, Duling BR (1998) Patterns of excitation-contraction coupling in arterioles: dependence on time and concentration. Am J Physiol 274:323–330
136. Xia J, Little TL, Duling BR (1995) Cellular pathways of the conducted electrical response in arterioles of hamster cheek pouch in vitro. Am J Physiol 269:H2031–H2038
137. Jantzi MC, Brett SE, Jackson WF, Corteling R, Vigmond EJ, Welsh DG (2006) Inward rectifying potassium channels facilitate cell-to-cell communication in hamster retractor muscle feed arteries. Am J Physiol 291:H1319–H1328
138. de Wit C, Roos F, Bolz SS, Kirchhoff S, Kruger O, Willecke K, Pohl U (2000) Impaired conduction of vasodilation along arterioles in connexin40-deficient mice. Circ Res 86:649–655
139. Tallini YN, Brekke JF, Shui B, Doran R, Hwang SM, Nakai J, Salama G, Segal SS, Kotlikoff MI (2007) Propagated endothelial Ca^{2+} waves and arteriolar dilation *in vivo*: measurements in Cx40BAC GCaMP2 transgenic mice. Circ Res 101:1300–1309
140. Kurjiaka DT, Bender SB, Nye DD, Wiehler WB, Welsh DG (2005) Hypertension attenuates cell-to-cell communication in hamster retractor muscle feed arteries. Am J Physiol 288:H861–H870
141. Figueroa XF, Isakson BE, Duling BR (2006) Vascular gap junctions in hypertension. Hypertension 48:804–811
142. Wolfle SE, de Wit C (2005) Intact endothelium-dependent dilation and conducted responses in resistance vessels of hypercholesterolemic mice *in vivo*. J Vasc Res 42:475–482

Chapter 37
Calcium Signaling in Cerebral Vasoregulation

Shantanu Ghosh and Amrita Basu

Abstract The tight coupling of regional neurometabolic activity with synaptic activity and regional cerebral blood perfusion constitutes a single functional unit, described generally as a neurovascular unit. This is central to any discussion of haemodynamic response linked to any neuronal activation. In normal as well as in pathologic conditions, neurons, astrocytes and endothelial cells of the vasculature interact to generate the complex activity-induced cerebral haemodynamic responses, with astrocytes not only partaking in the signaling but actually controlling it in many cases. Neurons and astrocytes have highly integrated signaling mechanisms, yet they form two separate networks. Bidirectional neuron-astrocyte interactions are crucial for the function and survival of the central nervous system. The primary purpose of such regulation is the homeostasis of the brain's microenvironment. In the maintenance of such homeostasis, astrocytic calcium response is a crucial variable in determining neurovascular control. Future work will be directed towards resolving the nature and extent of astrocytic calcium-mediated mechanisms for gene transcription, in modelling neurovascular control, and in determining calcium sensitive imaging assays that can capture disease variables.

Keywords Arteriole • Astrocyte • Calcium signaling • Cerebral vasoregulation • Cyclooxygenase • dHb • Functional hyperemia • Functional magnetic resonance imaging • G protein coupled receptor (GPCR) • Gliotransmitter • Glutamate • Inositol (1,4,5) triphosphate (IP3) • Metabotropic glutamate receptor (mGluR) • Neurovascular control • Nitric oxide • Regional cerebral blood flow (rCBF) • Voltage gated calcium channel (VGCC) • Vascular smooth muscle cell (VSMC)

S. Ghosh (✉)
Cognitive Science Lab, Indian Institute of Technology Delhi, 110 016 New Delhi, India
e-mail: sghosh@hss.iitd.ac.in; sghosh.neu@gmail.com

A. Basu
School of Cognitive Science, Jadavpur University, 700 032 Kolkata, India
e-mail: amrita8@gmail.com

M.S. Islam (ed.), *Calcium Signaling*, Advances in Experimental Medicine and Biology 740, DOI 10.1007/978-94-007-2888-2_37,

Introduction

Cerebral arterioles in the brain are surrounded by foot processes that originate mostly from astrocytes and to some extent, from the pericytes and macrophages [1–4]. Such astrocytic foot-processes also extend to hundreds of synapses [5] and other cellular elements in the brain including oligodendricytes, NG^{2+} cells, and microglia. The resulting dual contact with neurons and cerebral vasculature provides astrocytes with the unique architectural advantage for sensing neuronal activity, integrating electrochemical information and communicating with arterioles in the parenchyma [6]. This advantage is apparently a restatement of Cajal's idea of complex structure-function relationship between astrocytes and vascular cells [4] that extends to physiological domain as well and helps transduce signals from the source i.e., activated neurons to the cerebral microcirculation. In response to the electrochemical stimulation the foot-processes in astrocytes release vasoactive factors, thus leading to vasodilation in the vascular cells. Such a structural-functional-blend is called "neurovascular coupling," and its components (i.e., neuron, astrocyte, and vascular cells) are referred to as the "neurovascular unit" [7–9] (see Fig. 37.1 where the components of the neurovascular unit exhibit a direct relationship between local perfusion and corresponding local neuronal requirements).

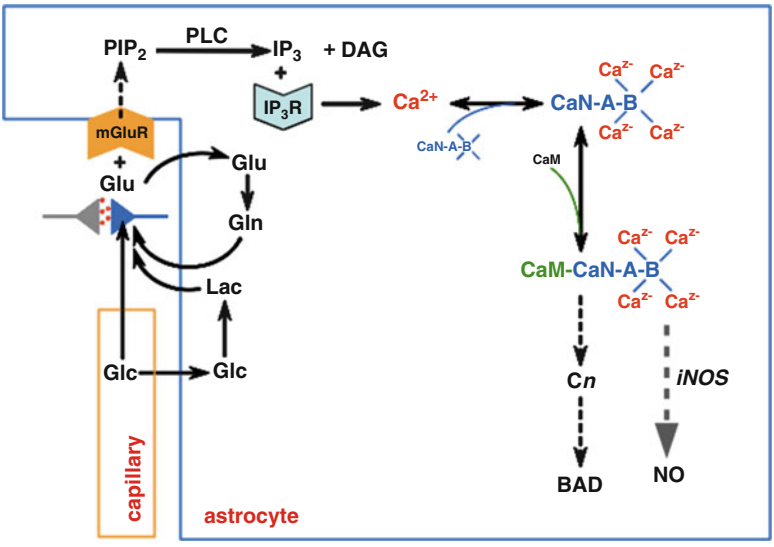

Fig. 37.1 Schematic diagram of the neuron-astrocyte-capillary system used to describe the three-compartment "neurovascular unit" (*grey neuron* = postsynaptic); *CaM* calmodulin, *CaN* calcineurin, BAD products are related to the apoptotic pathway

Cerebral circulation also exhibits a unique multi-segmental architecture of the arteriolar system. In the cerebral cortex, the parenchymal arterioles arise from surface (pial) arterioles as two separate segments, linked by penetrating arterioles. A thick layer of astrocytic processes termed the *glia limitans* isolates pial arterioles anatomically from the neurons below, barring any direct transmission of neuronal signals to the pial vasculature. However, pial arterioles have been shown to dilate in association with a variety of neuronal activation models [9] and respond to various shear-related factors [10]. Thus, intercellular conduction between the segments is essential for supporting upstream dilation in the pial arterioles, with vascular endothelium and astrocytes as the potential signaling conduits [11]. To achieve an effective communication in such a multi-segmental system, cerebrovascular processes need a common messenger in these signaling conduits that allows both short range and a long range crosstalk to achieve effective vasoregulation.

Calcium (Ca^{2+}) is the ubiquitous second messenger that plays a crucial role in cerebrovascular processes i.e., the neurons, astrocytes and blood vessels in the brain [12–15] that can regulate different cellular functions and intercellular crosstalk. Neurons have a host of Ca^{2+} modulators in the plasma membrane, endoplasmic reticulum (ER) and mitochondria that regulate the intracellular calcium concentration [16–21]. Similarly both astrocytes and cerebrovascular processes have an independent Ca^{2+} modulating mechanism as well [18, 22–27]. In addition, extracellular Ca^{2+} modulation has also been indicated [28–30] that alters the neuronal response or triggers vasoregulation. The multi-layer Ca^{2+} signaling is augmented by the presence of astrocytes and their foot-processes in the cerebral cortex. A sufficiently large increase in Ca^{2+} in an astrocyte may introduce a spreading wave of increased Ca^{2+} in adjacent astrocytes [31] (short-range communication) depending on the localized burst release of ATP [32], which further acts on purinergic receptors on adjacent astrocytes proximal to gap junctions [33]. *In vitro*, these Ca^{2+} waves show an ability to spread rapidly (in time frame of a few seconds) over hundreds of micrometers aiding in long-range communication. This multi-dimensional intercellular communication i.e., neuron-astrocyte-astrocyte and neuron-astrocyte-vascular cell, provides a basis for astrocytes to act as syncytium for possibly modulating neuronal and vascular function. In the present review, we look at the role of Ca^{2+} signaling in such a multi-dimensional vasoregulatory system; more specifically, neuronal effects on vascular cells and astrocytic effects on vascular cells via Ca^{2+} induced mediators.

Involvement of Ca^{2+} Signaling Pathway in Vasoregulation

The evidence of a possible involvement of Ca^{2+} in vasodilation comes from a series of pathbreaking studies [34–36]. Two of these studies merit special mention here. With electrical stimulation of cortical slices, Zonta et al. [34] demonstrated that the elevations in intracellular Ca^{2+} in astrocyte cell bodies and in astrocyte foot processes situated on blood vessels was followed temporarily by an increase in the

diameter of the arterioles. Astrocytes are known to express metabotropic glutamate receptors (mGluRs) of the subtypes that mediate an increase in Ca^{2+} through coupling to PLC and increased inositol (1,4,5) triphosphate (IP3). Administration of mGluR agonists reduced both the evoked increase in the Ca^{2+} and the arteriolar dilation seen with electrical activation. Further, direct stimulation of perivascular astrocytes during membrane patching also resulted in vasodilation in the adjacent blood vessels. Another study has temporally linked the increase of Ca^{2+} in astrocyte cell body and astrocyte foot-processes with subsequent suppression of spontaneous periodic Ca^{2+} waves in the neighbouring arterioles with thromboxane analog U-46619 [37]. It also indicated that there might be more than one mechanism of increasing cytosolic Ca^{2+} in astrocyes apart from mGluR-induced increase of Ca^{2+}. Further, the study demonstrates an important influence of increased Ca^{2+} in astrocytes during activation on dynamic Ca^{2+} transients in parenchymal arterioles. In both these studies, tetrodotoxin induced removal of vascular responses to electrical field stimulations showed that the neuronal action potentials play a crucial role in making the stimulus effective. However, flash photolysis of caged Ca^{2+} in green florescent protein (GFP)-labelled astrocytes to increase Ca^{2+} in individual astrocytes in brain slices demonstrated a direct role of Ca^{2+} in vasodilation when both electrical stimulation of neurons and pharmacological activation of the astrocytes were absent [37].

Ca^{2+} Signaling Pathways in the Neuron-Astrocyte Cell System

It is well known that communication through Ca^{2+} between neurons and astrocytes occur in brain slices and *in vitro*, e.g., Dani and co-workers [31] described astrocytic calcium changes in response to neuronal activity in cultured brain slices. Ca^{2+} communication from astrocytes to neurons has also been demonstrated in co-cultures [35, 38, 39]. Gap junctions though initially thought to aid in astrocyte-neuron Ca^{2+} signaling [39] have evolved as a controversial area of astrocyte-neuron signaling debate [40]. Further studies show that the bidirectional communication system is mainly carried by the extracellular messengers released from astrocytes or neurons. Various mediators such as glutamate, acetylcholine, GABA, ATP or NO, released by neurons through calcium-dependent exocytosis in cortical astrocytes [36], in hippocampal astrocytes [41, 42] and in Bregmann glia [43]. In addition, Ca^{2+} dependent glutamate and ATP release from the astrocytes also trigger changes in neurons in mixed cortical cultures [35], hippocampal cultures [44, 45], and in hippocampal or cortical slices [36, 46]. Such a bidirectional flow has led to propositions that a feedback system via the astrocytic glutamate release exists that modulate the synaptic transmission [36, 47]. Clearly Ca^{2+} signal transduction mechanisms are of crucial importance between neuron-astrocyte communications.

Astrocytes express a large number of GPCRs that mobilise Ca^{2+} from caged internal stores, most of them Gq-coupled GPCRs (Gq GPCRs) that respond to exogenous

agonists [40, 48] and neurotransmitters [42, 49, 50] alike. Astrocytic excitability from neurotransmitters demonstrates the existence of neuron-astrocyte interactions [2, 16], with the Gq GPCRs being the putative link between neuronal activity and astrocytic Ca^{2+} levels [3, 9, 10, 13]. Reciprocal effect of conditioned media released by astrocytes containing neuroactive molecules (or "gliotransmitters") elicited elevations in Ca^{2+} in neurons and a simultaneous increase in lactate levels assayed with 1H-NMR [51]. The release of these gliotransmitters is also mediated by Gq GPCRs and is Ca^{2+}-dependent, which correlated to changes of neuronal ionotropic glutamate receptor (iGluR) activity [36]. In addition, elevated Ca^{2+} levels under certain conditions *in situ* can result in the release of gliotransmitters, including glutamate, ATP, and D-serine, which can bind to receptors in pre- and/or post-synaptic terminals of synaptic boutons to modulate synaptic transmission and NMDAR-mediated neuronal activity [52, 53]. This has led to the proposal of the astrocyte being a functional component of the synapse in addition to pre- and post-synaptic compartments, thus leading to a "tripartite synapse" [52, 54] (see Fig. 37.1 for schematics).

However, astrocytic Ca^{2+} elevations are by itself insufficient to produce glutamatergic modulation of neuronal iGluR-mediated synaptic activity during *in situ* experiments involving brain slices from transgenic mice that express Gq GPCR only in astrocytes [55]. Widespread Ca^{2+} elevations in stratum radiatum astrocytes in such acute hippocampal slices do not increase neuronal Ca^{2+} [5, 55], thus contradicting the emerging consensus that Ca^{2+} elevations in astrocytes modulates synaptic activity *in situ*.

Ca^{2+} Signaling Pathways in the Astrocyte-Vascular Cell System

The search for Ca^{2+} signaling pathways in astrocyte-vascular communication started with the question whether astrocytes further propagate the signal communicated between neurons and astrocytes to the cerebral blood vessels. The question is the next logical step as astrocytes circumscribe the smooth muscle cells of arterioles which determine the diameter and thus the blood flow, and endothelial cells of the capillary vessels which form the blood brain barrier. Recent research has established several Ca^{2+} signaling pathways for astrocyte to vascular cell and endothelium transport that are reviewed in the subsequent sections.

Glutamate Induced $(Ca^{2+})_i$ Increase as Mediator for $K_{Ca}{}^{2+}$ Release

Glutamate receptor systems expressed in astrocytes are linked to calcium regulation and remain stable *in vitro* for several weeks even in the absence of neurons [56]. Astrocytes produce Ca^{2+} spikes at glutamate concentrations of 100 nM or higher, with 50% of the cells in a culture responding at 300 nM [57]. Further, glutamate concentrations also influence presence of oscillations, the frequency of oscillations and occurrence of intracellular and intercellular Ca^{2+} waves [57]. The average period

of oscillation has been shown to decrease with increasing agonist concentrations. However, coupling between oscillations in neighbouring cells has not been established, and oscillations within individual astrocytes demonstrate either constant or monotonically decreasing frequency [57, 58].

In addition, the pattern of intracellular Ca^{2+} $(Ca^{2+})_i$ signaling has been shown to be dependent upon the concentration of extracellular glutamate. For example, at concentrations of glutamate less than 1 mM small regions of the astrocyte cytoplasm flicker asynchronously, with propagation of the intracellular Ca^{2+} wave occurring in contained areas of the cytoplasm. If the extracellular glutamate concentrations are increased to between 1 and 10 mM, propagation of Ca^{2+} in waves is more common, and these waves travel throughout the cell, often propagating into neighbouring cells [57]. The locus of origin and the regions of calcium spikes with the highest amplitude remained invariant during the propagation of successive intracellular calcium waves [59]. Calcium waves have also been shown to be initiated at discrete regions of the cells where the calcium concentrations were highest, and they were propagated in a saltatory manner through the cytoplasm to other loci, where the rising calcium from the approaching wave front provoked a large Ca^{2+} increase. Models of intracellular wave propagation indicated that the propagation was dependent upon a Ca^{2+}-sensitive autocatalytic step [60, 61]. Glutamate was shown to stimulate the release of Ca^{2+} from intracellular stores in astrocytes [62] (Box 37.1).

Box 37.1 Hungry Neurons and the Supply of Nutrients

It is likely that the canonical PLC/IP3 pathway is critically involved in the astrocytes providing metabolic support to active neurons even before the vasculature can deliver nutrients to the neuronal tissue. Three major metabolic cycles take part in this support mechanism: (1) the malate-aspartate cycle, (2) the glutamate-glutamine cycle, and (3) the lactate shuttle. Among these, the lactate shuttle is particularly important as it transfers lactate from astrocytes to the energy-hungry neurons (also known as "astrocyte-neuron lactate shuttle," ANLS) [67] in a Ca^{2+}-dependent manner. A part of the glutamate released during synaptic activity binds to metabotropic glutamate receptors (mGluR5) residing on the astrocytic cell surface causing an upregulation of IP3. This causes the Gq GPCR activation, which leads to increases in astrocytic Ca^{2+} at specific sites within astrocytic processes and then are spread to other regions of the astrocytes [55]. This helps in the propagation of Ca^{2+} waves along organised clusters of IP3Rs residing on the ER surface, causing a unique Ca^{2+} "fingerprint" following Gq GPCR activation during high synaptic activity. It has been proposed that glutamate, released from neurons during such intense synaptic activity, is taken up by astrocytes in a sodium-coupled process, and the ensuing sodium-dependent activation of the Na^+/K^+-ATPase trigger glucose uptake, resulting in the rapid formation and release of lactate from astrocytes.

(continued)

Box 37.1 (continued)

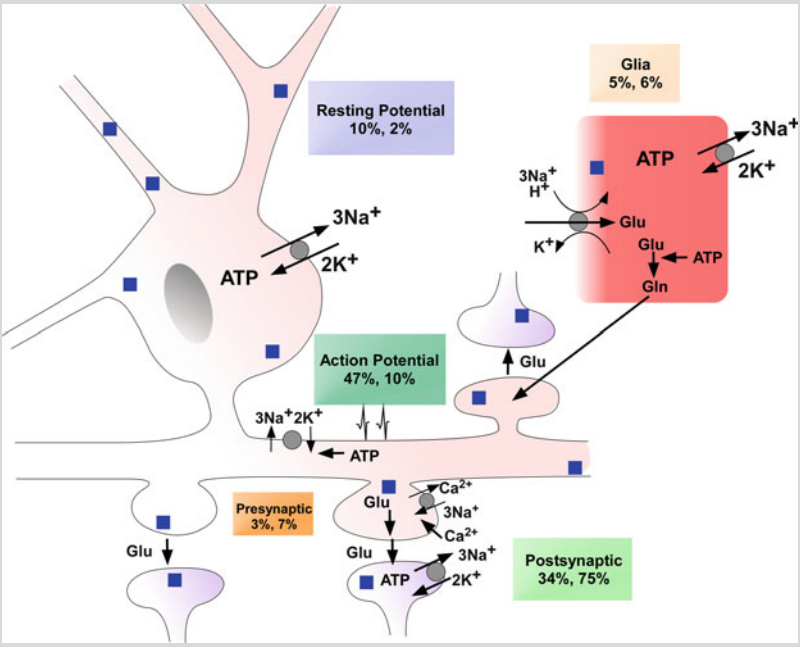

Fig. 37.2 Energy budget of neurons (Figure courtesy: Soumya Iyengar)

The primary purpose of such regulation is the homeostasis of the brain's microenvironment, and is central to the understanding of the haemodynamic response due to neuronal activation. The ANLS hypothesis also predicts that the rates of astrocytic glutamate cycling should be equal to the rate at which the metabolised glucose enters the neuronal tricarboxylic acid (TCA) cycle. This is because of a 1:1 stoichiometric relationship that exists between oxidative glucose metabolism and glutamate recycling [68]. However, it still did not conclusively prove that anaerobic glucose metabolism in astrocytes accounts for most of the lactate supplied to the neurons, as neither the site nor the mode of glucose uptake was determined. Consequently, the complex mechanisms that link energy metabolism (see Fig. 37.2) to neuron-astrocyte signaling are poorly understood. Hence, the ANLS hypothesis has remained controversial [69].

An important constituent of the lactate shuttle is the enzyme lactate dehydrogenase (LDH), which links pyruvate and lactate fluxes. Lactate concentrations are dependent on LDH buffers, and are characterized by metabolic competition for pyruvate among its various isoenzymes. The "metabolic signature" of any tissue will therefore vary with relative intracellular expression levels of the LDH isoenzyme subtypes, which may range from lower for LDH1 (adapted to functioning in an aerobic cell such as cardiac tissue) to

(continued)

Box 37.1 (continued)

higher for LDH5 (adapted to functioning in an anaerobic cell such as muscle tissue). Therefore, a higher LDH1/LDH5 ratio in any tissue indicates that it may be under anaerobic stress, which may lead to increased lactate production. Changes in mRNA subtype expressions of LDH isoenzymes in astrocytes can thus lead to differential lactic acid metabolism. This difference has important consequences for cellular physiology. In humans, for instance, LDH1 mRNA subtype is exclusively found in neurons, while both LDH1 and LDH5 and their respective mRNA subtypes may be present in astrocytes [70, 71]. Computer simulations of the IP3-mediated pathway of calcium signaling reveal that in the event of the astrocytes not being connected through gap junctions, intracellular Ca^{2+} concentration $(Ca^{2+})_i$ in individual astrocytes continue to oscillate. Delayed coupling of astrocytes tends to damp these astrocytic Ca^{2+} oscillations, eventually reducing the amplitude of $(Ca^{2+})_i$ to zero [51, 72]. A similar oscillatory response has been suggested for NADH (which reflects mitochondrial activity, the key variable for understanding the relationship between Ca^{2+} oscillations and brain activation) [67], and has been also established experimentally in mouse hippocampal brain slices [73]. In prepared brain slices or *in situ*, the sudden increase in the demand for energy imposed on the neuronal tissue as a result of synaptic signaling (measured by evoked-field excitatory post-synaptic potentials, fEPSP) causes elevation of astrocytic Ca^{2+} in a PLC-dependent manner, and probably also results in an increase of CBF owing to the resulting oxygen and glucose deficits. However, CBF increases evoked by neuronal activity may originate from synaptic neurotransmitter-based signaling, but could easily be caused by neuronal metabolic demands. Because cytosolic $NADH/NAD^+$ ratio can act as a sensor for the coupling of CBF to the redox state of astrocytes (through lactate-pyruvate cycling in astrocytic mitochondria as a consequence of astrocytic TCA cycle), the $NADH/NAD^+$ ratio can indicate the astrocytic energy metabolism. Specifically, monitoring the NADH fluorescence (indicative of the astrocyte's oxidative metabolism) in regions of intense neuronal activation, will provide the link between astrocytic metabolism and neuronal activity. In sum, elevations in extracellular lactate concentrations may occur due to anaerobic glycolysis, and serves as an indicator of increased astrocyte-mediated neurotransmission rather than energy compensation for neurons, since ATP generation is much less efficient through non-oxidative glycolysis. Under anaerobic conditions, therefore, the neuronal energy demand can still be met through oxidative metabolism at different levels of neuronal activities despite the significant observed elevation of (Lac); however, lactate is also reported to decrease at the onset of neural activity. Hence lactate concentration levels in astrocytes can act as a possible metabolic "sensor" linked to biphasic NOS levels, determining the polarity of astrocyte response [74] and may become the basis of functional biomarkers in different pathologies.

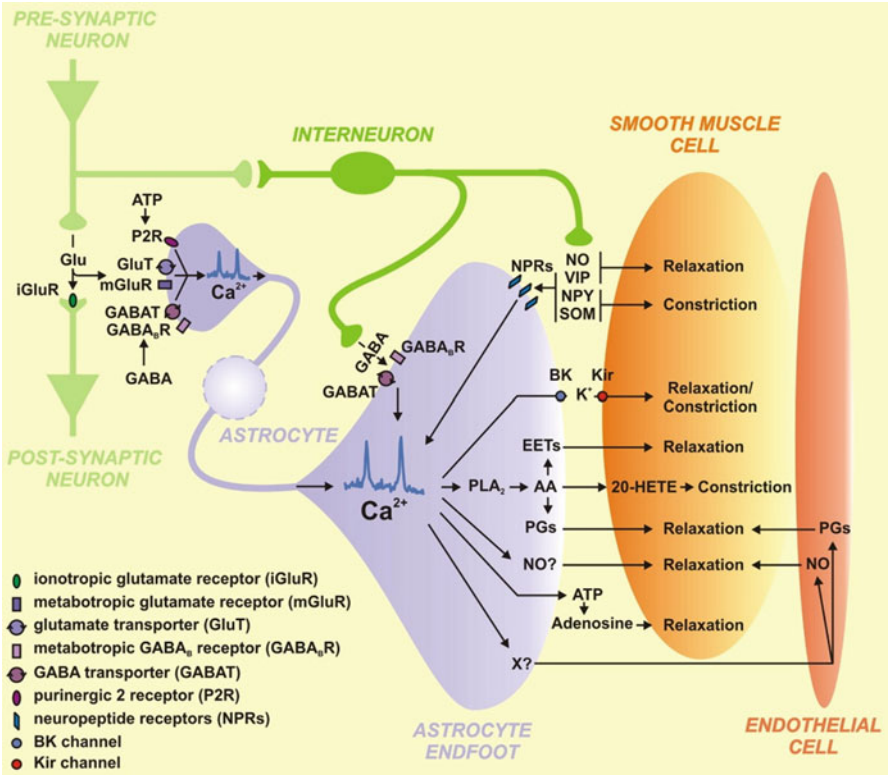

Fig. 37.3 The neurovascular unit and the role of Ca^{2+} signaling from Carmignoto and Gómez-Gonzalo [66] (Used with permission from Elsevier)

Further, Mulligan and MacVicar [63] also showed that with the increase in laser intensity induced Ca^{2+} wave spreading to the astrocyte end-feet, arteriolar constriction occurred and degree of constriction increased with astrocyte Ca^{2+} concentration. Application of norepinephrine to the culture produced increases in astrocyte Ca^{2+} which led to vasoconstriction within 1–2 s depending on the time of transmission of Ca^{2+} wave to the end feet. As a confirmatory test to vasoregulation, the study blocked the uncaging of Ca^{2+} by phospholipase A_2 (PLA_2) inhibitor and 20-hydrooxyeicosatetraenoic acid (20-HETE) (a known constrictor in smooth muscle cells that acts by blocking the calcium-sensitive K channels (K_{ca})) [64, 65]. The study therefore led the authors to believe that Ca^{2+} waves propagating to the end-feet activate PLA_2 and mobilise arachidonic acid (AA), which then is transported to the smooth muscle of the blood vessels to act as a substrate for CYP ω-hydroxylase formation of 20-HETE (see Fig. 37.3).

EET Induced Ca^{2+} Release

Conversion of arachidonic acid to EETs has been described in cultured astrocytes and in brain parenchyma [75–77]. Further, expression of CYP 2C11 in rat brain colocalizes with glial fibrillary acidic protein-positive astrocytes, including perivascular astrocytes [78]. EETs are stored in the phospholipid membrane, including astrocyte membranes, and thus do not require any *de novo* synthesis before mobilization [79]. Within astrocytes, release of Ca^{2+} from internal stores induced by thapsigargin causes arachidonic acid to be mobilized followed by formation of EETs and Ca^{2+} influx [80]. Moreover, EETs can promote the opening of iberiotoxin-insensitive K_{Ca} channels [81]. The resultant efflux of K^+ is expected to partially offset the influx of Ca^{2+} and maintain a hyperpolarized membrane for sustaining Ca^{2+} entry [82]. Addition of glutamate to cultured astrocytes causes release of EETs into the media [83]. The release of EETs evoked by a mGluR agonist is reduced by an inhibitor of K_{Ca} channels, suggesting a link between hyperpolarization induced by K_{Ca} channel opening, sustained Ca^{2+} influx, and release of EETs by astrocytes [82].

In vascular smooth muscle, EETs cause hyperpolarization by opening of K_{Ca} channels [75, 84, 85] and dilation of cerebral arteries [84, 86, 87]. Thus it has been proposed that EETs might serve as an astrocyte-derived vasodilator [85]. In support of this hypothesis, increases in CBF elicited by topical glutamate application to the brain surface or by dialysis of NMDA into striatal tissue are markedly reduced by inhibitors of epoxygenase activity [83, 88]. Furthermore, epoxygenase inhibitors applied to the cortical surface reduced the CBF response to whisker stimulation [89] and to electrical stimulation of the forepaw [78]. Therefore, an astrocyte-based epoxygenase pathway appears to be critical in the coupling of CBF to neuronal activation in cortex.

Prostaglandins are released due to Ca^{2+} dependent breakdown of arachidonic acid (AA) and are proposed to induce vasodilation in the vascular cells. The changes in astrocytic Ca^{2+} are crucial for regulating synthesis and/or release of AA by the Ca^{2+}-mediated stimulation of phospholipase A2 (PLA2). Calcium dependent AA elevations trigger different metabolic cascades that synthesises vasoactive agents acting on the neurovasculature. In mice, for instance, cytochrome oxidase 1 (COX-1) oxidises AA to prostanoid precursor PGH2, which is then acted upon by specific prostanoid synthases within astrocytic endfeet. [3, 90, 91] Other isoforms of COX, viz., the highly inducible COX-2, and COX-3 (alternative splice variant of the *COX-1* gene), also exist in the cerebral cortex of humans. But although the role of COX-3 in NVC is not very well known, all COX isoforms catalyse the conversion of AA to PGH2, which can be further converted to vasoactive products: (1) Vasodilatory AA metabolites that dilate VSMC by opening Ca^{2+} sensitive K^+ channels (K_{Ca}) in the VSMC membrane [92]. Glutamate triggered vasodilation also releases prostaglandin E2 (PGE2) from the astrocyte that might further mediate K_{Ca} opening [93], following the switch from oxidative to glycolytic metabolism to overcome tissue oxidative stress as a coping strategy, which has been proposed to be the basis of neurovascular coupling, because the lactate produced by glycolysis inhibits reuptake

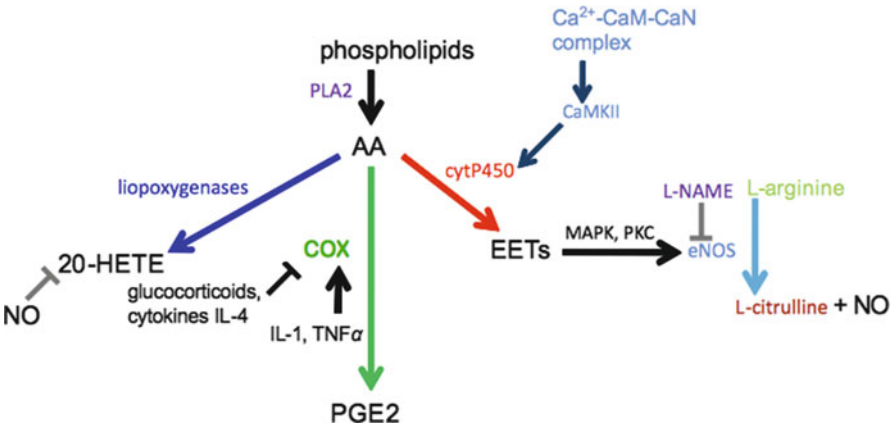

Fig. 37.4 Calcium activity and metabolism of arachidonic acid (*AA*) through the cytP450 pathway that releases NO through the production of eNOS

of PGE2 from extracellular medium into astrocytes [74], (2) Vasodilatory prostacyclin and prostaglandin I causes relaxation of cerebral arterioles by signaling cascades involving cAMP and NO formation along with K^+ regulation, (3) vasoconstrictive factors thromboxane A2 (TXA2) and prostaglandin F2α [46, 93]. Alternative pathways can convert AA into (4) vasodilatory epoxyeicosatrienoic acids (EETs) by cytochrome P450 2C11, or AA can diffuse into the VSMC from astrocytic endfeet where cytochrome P450 4A (ω-hydroxylase), thus generating 20-hydroxyeicosatetraenoic acid (20-HETE) that is vasoconstrictive by effecting the closure of K_{Ca} in VSMC [63, 74] (see Fig. 37.4).

Extracellular ATPs as Mediators in Ca^{2+} Signaling

ATP is now emerging as the extracellular signaling element that drives astrocytic Ca^{2+} waves. They can proceed via an extracellular pathway as shown by continuous propagation of Ca^{2+} waves between astrocytes in cultures [94] and they are known to cross cell-free gaps. Additionally they are affected by the direction and strength of a perfusion bath [94]. Guthrie et al. [95] demonstrated that subsequent calcium waves are produced if naïve cells are exposed to the medium collected from the cultures that previously supported a propagating wave, thus providing a compelling evidence of the existence of an extracellular mediator for calcium wave propagation. Subsequent chemiluminescence and Fluo3M calcium imaging studies [96] at millisecond temporal resolution demonstrated extracellular ATP mediated intracellular calcium wave propagation. The purinergic receptors (P2Y) function as G-protein coupled Ca^{2+} mobilizing ATP receptors operating via the stimulation of phospholipase C (PLC) and formation of IP3 and diacylglycerol (DAG). IP3 induces

release of Ca^{2+} from intracellular stores of calcium. P2X-type receptors act as ligand-gated ion channels and P2Z receptors are involved in ATP-induced pore formation [97]. Astrocytes demonstrate an ability to both release ATP (paracrine behaviour) and respond to ATP (autocrine behaviour) and have two potential pathways from the cell i.e., either a passage through anion channels formed by connexin hemichannels [98–100] or Ca^{2+}-dependent and quantal release of vesicularly stored ATP [101].

The release of vesicular ATP has also been demonstrated by Coco et al. [101] from primary cultures of hippocampal rat astrocytes. This study reported that apart from the usual cytosolic release of the Ca^{2+} which is enhanced during Ca^{2+} depletion there is a gap junction-independent, Ca^{2+}-dependent release of ATP. This release is inhibited by bafilomycin, an inhibitor of ATP uptake into secretory granules. Furthermore, astrocytic Ca^{2+} elevations can lead to secretion of other [102] vasodilatory substances from perivascular endfeet, such as adenosine and nitric oxide (NO) synthesised by neuronal or endothelial nitric oxide synthase (nNOS, eNOS), resulting in inhibition of 20-HETE, thus increasing local blood flow. This mechanism also permits EET-dependent vasodilation [103]. Regulation of localised extracellular K^+ concentrations also plays a role in neurovascular coupling [104, 105]. Several neuropeptides have been shown to exert vasoactive effects, for example, neuropeptide Y, somatostatin (both vasoconstrictive), and vasoactive intestine peptide (vasodilatory). Thus, astrocytes by releasing vasoactive molecules and gliotransmitters mediate the neuron-astrocyte-endothelial signaling pathway and play a profound role in coupling blood flow to neuronal activity (see Fig. 37.4).

Ca^{2+} Signaling Pathways in the Astrocyte-Astrocyte Cell System

Synaptically released neurotransmitters regulate astrocytic calcium levels, thus making astrocytes sensitive to neuronal signals [106]. Ca^{2+} signals in response to these signals travels in astrocytes as waves where increases in free cytosolic $(Ca^{2+})_i$ spreads from initially stimulated cell across an astrocytic syncytium [107]. A wide array of studies in cultured and *in situ* astrocytes has pointed to the canonical phospholipase C (PLC)/IP3 pathway as the widely accepted mechanism for astrocytic Ca^{2+} signaling [108]. Following Gq GPCR activation, PLC-mediated hydrolysis of phosphatidylinositol 4,5-bisphosphate yields diacylglycerol (DAG) and IP3. The latter binds to IP3Rs, and also releases Ca^{2+} inside the astrocyte from the ER. The activity of IP3Rs could be influenced by several factors: (1) the astrocyte's cytoplasmic Ca^{2+} elevations themselves that activate IP3Rs due to the coagonistic action of Ca^{2+} on these receptors, (2) the continuous metabolism of IP3 through the Ca^{2+}-dependent activation of PLC, and (3) the phosphorylation and consequent potentiation of IP3Rs following ATP binding to its receptor [109]. In addition, the DAG/protein kinase C (PKC) pathway may be involved in the termination of astrocytic Ca^{2+} transients [110, 111] (Fig. 37.1).

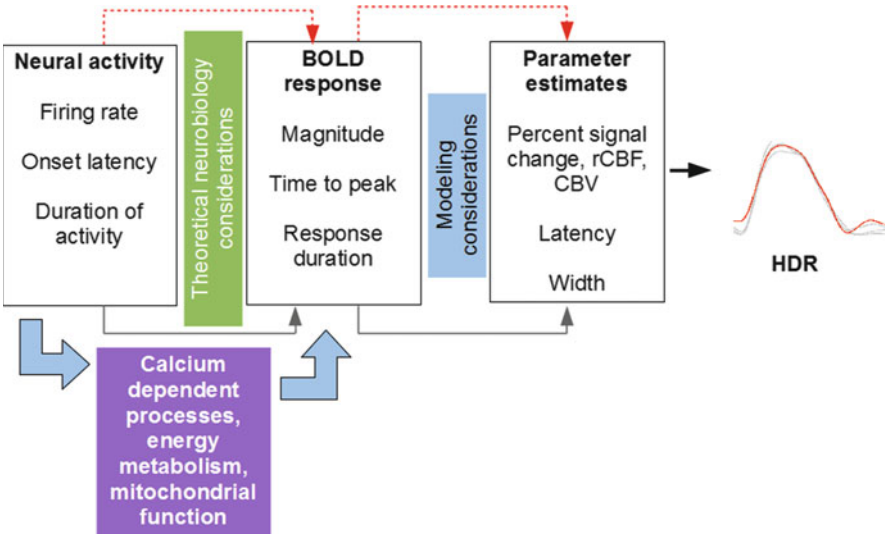

Fig. 37.5 Relationship between neuronal activity, calcium dynamics, evoked changes in haemodynamic response, and the estimated BOLD, CBF and other parameters. *Solid lines* are expected relationships, and *dotted lines* are confounding variables that complicate the interpretation of HDR. The relationship between activity-dependent responses and BOLD responses are determinants of theoretical limits that lead to interpretation of the parameter estimates. The interplay of calcium-dependent mechanisms introduces additional theoretical constraints on the interpretability of parameter estimates

Role of ER and Mitochondria in Calcium Signaling

In neurons, ER is a continuous membrane system extending from the nucleus in the cell soma to the dendrites and synapses [13] and acts both as a major source and sink for Ca^{2+} in neurons [112, 113], acting to buffer Ca^{2+} signals by rapidly pumping Ca^{2+} into the ER lumen. The existence of such a reservoir has a significant effect in shaping neuronal signals [114] allowing localized increase or decrease in concentration of Ca^{2+} or global calcium waves. The Ca^{2+} is modulated by a set of ER receptors such as IP3R and RyR channels by initiating Ca^{2+} release into the cytosol, SERCA Ca^{2+} pump initiating Ca^{2+} uptake into the ER lumen. Recently, presenilins (PS) have also been shown to form passive Ca^{2+} leak channels in the ER membrane.

ER as a Source of Ca^{2+} Release

The phosphoinositide system is well developed in the neurons [13] and IP3Rs show relatively wide distribution in the brain, particularly in cerebral Purkinje cells, hippocampal CA1 pyramidal cells and pyramidal cell bodies and proximal dendrites of

the cortex [115]. When activated, IP3Rs allow release of Ca^{2+} in the cytosol from the ER lumen down the electrochemical gradient [116]. IP3, the physiological ligand for IP3R, is produced in the cytoplasm. Apart from IP3R, many different receptors trigger IP3 mediated release of Ca^{2+} from the IP3R receptors [13]. However for an effective activation of IP3R, Ca^{2+} and IP3 have to be present together suggesting a possible role of coincidence detector [116] and a trigger for increasing Ca^{2+} sensitivity of IP3R [117]. Ryanodine receptors (RyRs), large calcium release channels in the membrane of ER, are very sensitive to both extracellular or receptor mediated Ca^{2+} influx [118]. Multiple isoforms of the receptor exist, with the RyR3 type (OMIM 180903) expressed most widely in the brain. The Ca^{2+} entering though either VGCCs or receptor mediated channels (RMCs) serves a trigger for Ca^{2+} release from the ER lumen, often known as Ca^{2+} induced Ca^{2+} release (CICR) [119]. The CICR amplifies the Ca^{2+} signals in response to action potentials or neurotransmitters in neurons [13]. In a RyR cluster, the rise in calcium levels establishes a positive feedback loop resulting in a spatio-temporally restricted CICR known as a "calcium spark". All three isoforms for the RyRs are expressed in dentate gyrus, CA3/4 areas of the hippocampus, and long thin apical dendrites of cortical pyramidal cells [119] suggesting distinct roles of IP3R and RyR Ca^{2+} pools in neuronal processes. Several endogenous modulators of RyR activity are also present such as ions (e.g., Ca^{2+}, Mg^{2+}, H^{+}, Fe^{2+}, and inorganic phosphate), adenine neucleotide, calmodulin, cyclic adenine diphosphate ribose and protein kinase dependent phosphorylation and redox state of the cell [120]. Presenilin (PS) Ca^{2+} leak channels (PSCL) result due to the formation of low- conductance cations permeable ion channels in planar lipid bilayers [121]. PSCL acts as a passive Ca^{2+} leak channel on the ER membrane as the knockout of PS in MEF cells results in the overload of Ca^{2+} stores in the ER [121].

ER as a Sink Triggering Ca^{2+} Uptake

Sarco/Endoplasmic reticulum Ca^{2+} ATPases (SERCA) can boost Ca^{2+} uptake into the lumen rapidly against an electrochemical gradient from the cytoplasm (2 Ca^{2+} ions to 1 ATP hydrolysed) [122]. For example, in the neocortical pyramidal neurons, a large proportion of the Ca^{2+} entering the dendrites during back-propagating action potential are pumped into the ER [123] thus acting as a major buffering system [124]. By soaking up and storing the brief pulses of Ca^{2+} associated with each action potential, the ER may keep track of the brief neuronal bursts of localized Ca^{2+} pulses and relay regenerative global signals to the nucleus via periodic Ca^{2+} bursts generated as a result of prolonged firing of the neurons [13]. Apart from these, the L-Type ER voltage-gated calcium channels (VGCCs) bind with Ca^{2+} binding protein calmodulin (CaM) to trigger a signaling cascade from the plasma membrane to the nucleus as shown by the depolarization-induced phosphorylation of the cAMP response element binding protein (CREB) [125].

Ca^{2+} Modulators in Mitochondria

Mitochondria are the primary generators of energy and are found widely distributed in the brain, particularly concentrated in the areas where the neurons have high metabolic demands such as nodes of Ranvier, and the myelination/demyelination interfaces [23]. Apart from the role of ATP generators, they also contribute significantly to the neuronal Ca^{2+} signaling. They can modulate the amplitude of Ca^{2+} signals through rapid influx of cytosolic Ca^{2+} into the mitochondrial lumen [126]. Interestingly, mitochondria do not require large global Ca^{2+} signals, but in fact produce highly spatially restricted increases in Ca^{2+} due to increased Ca^{2+} uptake in these regions, possibly using CICR as the mechanism of choice [127]. Several channels such as voltage dependent anion selective channel (VDAC), Mitochondrial Ca^{2+} uniporter (mUP), mitochondrial Na^{2+}/Ca^{2+} exchanger (mNCX), mitochondrial permeability transition pore (mPTP), cytosolic Ca^{2+} binding proteins, and ER Ca^{2+} binding proteins are all involved in Ca^{2+} modulation in mitochondria. VDAC transports the Ca^{2+} from the cytoplasm across the outer mitochondrial membrane. Given its small size Ca^{2+} pass through the VDAC during both the closed and open conditions [128]. mUP is selectively Ca^{2+} transporter that sequesters Ca^{2+} to pass through the inner mitochondrial membrane to the lumen [129]. If blocked, they may induce CBF changes *in vivo* [130]. The mUP requires an electrochemical gradient (at ~500 nM of cytoplasmic Ca^{2+} in the vicinity of mitochondria) to allow Ca^{2+} influx into the mitochondrial lumen [131] and serves as mitochondrial Ca^{2+} sink. Mitochondrial Na^{2+}/Ca^{2+} exchanger (mNCX) may also be present as studies have shown efflux of Ca^{2+} ions in exchange for Ca^{2+} ions [132–134]. There is also evidence for the existence of a H^{+}/Ca^{2+} exchanger (mHCX) that mobilizes protons into the mitochondrial lumen in exchange for Ca^{2+} ions. Mitochondrial Permeability Transition Pore (MPTP) is another non-specific pore in the connecting junctions of the outer and inner mitochondrial membrane that allows efflux of Ca^{2+} ions out of the mitochondrial lumen with increased concentration of Ca^{2+} (~1–3 μM) [135]. Apart from these, cytosolic ER Ca^{2+} binding proteins (such as parvabumin and calbindin-D28K in the cytoplasm) also participate in the modulation of amplitude and duration of Ca^{2+} signals by binding to the rapidly incoming Ca^{2+} ions [29, 136, 137].

Contribution of Neuronal Signals in Vasoregulation in Pial Arteries

Several key indications about the nature of propagation of neuronal signals in the pial arterioles leading to vasodilation have arisen in recent studies [11] using activation models. Some of them are elicitation of consistent, reversible and repeatable pial arteriolar dilations and neuronal activity dependent dilations. It has also been

shown that selective injury to the *glia limitans* prevents neural activation induced pial arteriolar dilation. The role of astrocytes seems to be crucial here, with the participation of a diffusible mediator like NO [66]. The role of Ca^{2+}, though not established so far, cannot be ruled out [11]. In neocortical and hippocampal tissue slices too, glutamate has also been found to have a significant vasodilatory effect. In addition, exogenous glutamate application or selective GluR agonists dilate pial arterioles and precapillary microvessels [138].

Modelling Vasoregulation

Brain imaging technique like functional magnetic resonance imaging (fMRI) relies heavily on the fact that vasoregulatory effects seen after focal stimulation of brain areas contain information on neuronal activity. It has now become clear that in the event of any brain region activating, it consumes oxygen and energy, which must be delivered by fresh oxygenated blood supply. The initial consumption of oxygen leads to an initial increase in deoxyhaemoglobin (dHb), which is more than compensated for by the rush of oxygenated (HbO2) blood about 2–3 s later. This sequence of events forms the basis of the blood-oxygenation level dependent (BOLD) signal, changes of which give rise to the signal dephasing of protons captured by fMRI. Again, it is an advantageous fact of biophysics that dHb is paramagnetic as compared to HbO2, leading to generation of blood vessel contrast in the two conditions. Ogawa and Lee [139, 140] first took advantage of this fact to generate images of neuronal activation localised to a particular brain region based on the oxygenation contrast. The primary physiological variables that are responsible for neuronal activity-dependent blood oxygenation changes are the fraction of oxygen extracted (OEF) due to increase in metabolic demand (cerebral metabolic rate of oxygen consumption, CMRO2), and increased regional cerebral blood flow (rCBF) that also transports HbO2 to the needy tissue. The interplay of these counteracting forces determines local BOLD signal amplitude as a surrogate of neuronal activity via concomitant dHb concentration level changes.

Quantitative modelling of the BOLD phenomenon has been successful to a large extent using windkessel models [141, 142], models using optical imaging to construct pseudo-Bayesian statistics, [143] and linear time invariant dynamic state space models of dilation-constriction interactions [144]. However, interpretations of, and comparisons between, these modelling results are difficult since many basic questions regarding the origin of these signals remain unanswered. In this review we have seen how the complex calcium-dependent signaling pathways can modulate the contributory parameters to influence neurovascular coupling by controlling the production of vasoactive molecules in astrocytes. On the other hand, interneurons of the neocortex directly contact vascular processes and can directly provoke dilatory or Ca^{2+} constrictory effects on the adjacent blood vessels *in vitro*, showing that they may also be players in the signaling orchestra. A recent report [70] showed that fMRI (illustrating neurometabolic coupling) reflects synaptic rather than

spiking activity. It has also been shown recently that blood flow changes in parts of the cortex, e.g. the visual cortex *in vivo,* reflect changes in astrocyte activation closely tuned, or sometimes better tuned, the local neuronal activity they surround [145]. These facts raise several interesting questions regarding which aspects of neuronal or astrocytic activity (presynaptic, postsynaptic, spiking, maintaining local field potentials, excitatory, inhibitory, modulatory, metabolic etc.) are more closely related on a spatio-temporal scale to calcium-dependent vasoregulation. The precise tuning of the astrocytes [145] with respect to orientation preference demonstrates that astrocytes located tens of micrometers apart can have different behaviours, calling into question broadly interconnected astrocytic networks. It remains to be seen whether groups of closely located astrocytes form local synctia that interact only with a small number of neurons surrounded by it. Understanding astrocytic calcium responses will be the crucial step in understanding micro-level cerebral haemodynamic regulation, as captured in BOLD functional magnetic resonance imaging.

In sum, the research highlighted in this review confirms the complex nature of the astrocyte's interactions with neurons and VSMCs in normal and pathological states. It reveals that astrocytes respond rapidly to their environment with Ca^{2+} transients, affecting functional hyperemia, as well as synchronous somato-dendritic activity of the neurons. Future research will thus be directed towards examining the precise location and timing of synaptic activity concurrent with changes in CBF patterns by multiphoton imaging and functional neurovascular coupling (esfMRI) that maps spontaneous cortical activity with Ca^{2+} reporters in fMRI in health and disease highlighted in the next section.

Outstanding Issues and Future Directions

Five major areas of research beg immediate attention:

1. While the **molecular target(s) of MAPK/PKC phosphorylation** in the vasoregulatory mechanism remain undetermined, the two most likely candidates are either Gq GPCRs or the IP3R itself. Furthermore, the role of Ca^{2+} in lending such signaling support within the astrocyte is also not fully known, and new investigations will be needed to unravel the **full range of signaling repertoire** available to astrocytes and neurons. The **role of GABAergic interneurons in neurovascular coupling** has also been highlighted in the past, but has not been explored in great detail so far. As more functions of interneurons in different areas of the brain get elucidated, combining electron microscopy with superresolution microscopy using multiphoton excitation and Ca^{2+} reporters, can provide relevant data about correlations between brain microstructure and cellular function. This will go a long way in defining the **functional brain connectome**.
2. **Neuronal activity dependent on astrocytic calcium signal gives dendritic metabolic readout.**

   Functional hyperemia is linked to metabolic adaptations and adjustments that take place in the brain in normal tissue and neurodegenerative diseases like

Alzheimer's Disease (AD) and ischaemia, tumours and/or traumatic brain injuries (TBI), or during increased astrogliosis following viral infection, followed by upregulation of glutamate transporter proteins GLT-1 and GLAST. Such changes are accompanied by the enhanced ability of astrocytes to detoxify glutamate, inactivate free radical and produce neurotrophic factors that are involved in neuroprotection. The neuroimaging community is currently looking for physiological evidence of the involvement of calcium-dependent synaptic mitochondrial pathways to determine whether the functional signal is a surrogate of **metabolic readout and indicative of the state of tissue excitability and thus (possibly) linked to tissue health, and whether this information could be useful for monitoring metabolism-linked diseases such as diabetes, or even inflammatory responses in neurodegeneration**. On the other hand, the expression levels of VGCC in the dendritic membrane also provide direct molecular readout of electrical excitability. In particular, **dendritic calcium signals** activated by back-propagating action potentials reliably encode the level of axonal spike firing in apical dendrites of pyramidal neurons. This measure therefore provides an indirect "frequency code" where firing rate, which could be interpreted either as a readout of dendritic biochemical signal, or as a surrogate of synaptic information processing [146], and needs to be thoroughly investigated. This readout can also have nonlinear frequency dependence if it involves activation of **dendritic calcium spikes**. The **calcium signal** can in turn activate voltage-gated potassium currents, thus acting as a feedback regulator of excitability, which changes the input–output gain of the neuron, which might be affected in brain pathology. A similar readout of dendritic excitability can be provided by dendritic Na^+ signals in intracellular environments, in turn regulating axonal excitability via activation of Na^+-activated K^+ channels. Alternatively, the biochemical intracellular signaling pathways in dendrites may themselves contribute to the metabolic state detection in unique ways. For example, the IP3R is cooperatively activated by both Ca^{2+} and IP3, which allows for detection of Ca^{2+} and IP3 delivered by different sources, such as action potentials and synaptic mGluR activation. The proposal that processing by intracellular networks can implement a second layer of dendritic signaling coupled to, but semi-independent from, the electrical signaling in the cell membrane is promising, but has not received much attention. However, some recent reports of neuronal excitability being sensed and modulated by astrocytic Ca^{2+} could provoke renewed interest, since such a Ca^{2+} metabolic sensor, combined with NADH and lactate readouts could have enormous disease detection/identification power through techniques available already (e.g. MRS, fMRI). This approach will lead to brain tissue metabolism based assays that might be helpful in understanding functional recovery after stroke/TBI or even state of cognitive or motor decline in AD/PD patients. Clinical correlations with such novel procedures may be helpful in disease monitoring and prediction of neurodegeneration among at-risk populations.

3. Do calcium signaling pathways regulating **membrane-to-nucleus signaling** offer a mechanism for VGCCs to interact with Ca^{2+}/CaM in novel ways? For example, Ca^{2+} entry via P/Q-type VGCCs might affect the transcription of a

unique set of genes. Given that human genome sequencing has identified numerous calcium-related proteins associated with neuronal structure, function and development [147], many of them with undertemined activity, a large number of potential associations between Ca^{2+} and VGCC-related gene transcription is open to investigation. Molecular differences could be correlated with phenotypic differences to reveal cellular and developmental processes unique to individuals and unique to different brain pathologies, which will provide ways to targeted treatments. The need of the hour is to determine how these factors modulate cerebral vasoregulatory mechanisms to establish the ground truth.

4. **Imaging Genetics/Genomics** approach [148, 149] (the use of fMRI, MRS, VBM, PET techniques to determine (potentially) imbalanced NVC mechanisms for therapeutics, disease prediction and monitoring) opens up the possibility of exploring, selecting and **evaluating gene variants of interest that affect neurovascular coupling**. Functional haemodynamic phenotyping may thus be of clinical interest in many diseases assayed by neuroimaging, especially using allelic variations and frequencies as covariates. For instance, a single nucleotide polymorphism (SNP) related to the popular antipsychotic drug olanzapine was identified in the drug metabolizing enzyme cytochrome P450 3A43 (CYP3A43; rs472660), which accounts for racial variations in olanzapine response [150]. Further, since cytochrome P450 is involved in the metabolism of EETs, it is possible that SNPs and allelic variations may modulate Ca^{2+} signaling in astrocytes, and such effects on neuronal signaling may influence the CBF in various disease pathologies. These variations could be mapped in different ways using calcium weighted functional neuroimaging (next subsection). This will be a completely different way to look at a disease, and is an hence an exciting research possibility.
5. **Neuroimaging approaches with molecular probes** (contrast agents) sensitive to aspects of neurophysiological changes is the next big thing in fMRI research. These bioactive, responsive or "smart" contrast agents (SCA) are able to produce signals that are directly linked to neuronal processing, for example, specific gadolinium based tissue level markers responsive to the fast physiological Ca^{2+} fluctuations have been designed, e.g. calcium sensitive contrast agent for T2* relaxation - superparamagentic iron oxide nanoparticles (SPIO) that deliver better contrast-to-noise ratio (CNR) of haemodynamic response (HDR) from EPI data as seen from relaxometric Ca^{2+} titrations of $Gd_2 L^1$ and $Gd_2 L^2$ [151]. The field of fMRI research will benefit from future research directed towards the design, synthesis, and the *in vitro* and *in vivo* characterization of such novel molecules.

To conclude our review, it is our understanding that the role of calcium in neurovascular coupling will benefit immensely from attempts to calibrate the BOLD signal using marker proteins, in order for the latter to reflect as closely as possible the actual energy metabolism in neuronal tissue using novel reporter assays. These proposed techniques will be able to unravel novel roles of calcium-dependent processes involved in the complex neurovascular and flow-metabolsim coupling.

Acknowledgement This work was supported by Department of Science and Technology, Government of India grant SERC/LS-0434/2008 (to S.G.). A.B. is supported by the Ministry of Communications and Information Technology, Government of India.

References

1. Rama Rao KV, Chen M, Simrad JM, Norenberg MD (2003) Increased aquaporin-4 expression in ammonia-treated cultured astrocytes. Neuroreport 14:2379–2382
2. Haydon PG, Carmignoto G (2006) Astrocyte control of synaptic transmission and neurovascular coupling. Physiol Rev 86:1009–1031
3. Takano T, Tian GF, Peng W, Lou N, Libionka W, Han X, Nedergaard M (2006) Astrocyte-mediated control of cerebral blood flow. Nat Neurosci 9:260–267
4. Simard M, Arcuino G, Takano T, Liu QS, Nedergaard M (2003) Signalling at the gliovascular interface. J Neurosci 23:9254–9262
5. Bushong EA, Martone ME, Jones YZ, Ellisman MH (2002) Protoplasmic astrocytes in CA1 stratum radiatum occupy separate anatomical domains. J Neurosci 22:183–192
6. Paspalas CD, Papadopoulous GC (1998) Ultrastructural evidence for combined action of noradrenaline and vasoactive intestinal polpeptide upon neurons, astrocytes, and blood vessels of rat cerebral cortex. Brain Res Bull 45:247–259
7. Anderson CM, Nedergaard M (2003) Astrocyte-mediated control of cerebral microcirculation. Trends Neurosci 26:340–344
8. Hamel E (2006) Perivascular nerves and the regulation of cerebrovascular tone. J Appl Physiol 100:1059–1064
9. Koehler RC, Gebremedhin D, Harder DR (2006) Role of astrocytes in cerebrovascular regulation. J Appl Physiol 100:307–317
10. Andresen J, Shafi NI, Bryan RM Jr (2006) Endothelial influences on cerebrovascular tone. J Appl Physiol 100:318–327
11. Xu HL, Mao L, Ye S, Paisansathan C, Vetri F, Pelligrino DA (2008) Astrocytes are a key conduit for upstream signaling of vasodilation during cerebral cortical neuronal activation *in vivo*. Am J Physiol Heart Circ Physiol 294:H622–H632. doi:10.1152/ajpheart.00530.2007
12. Bernardi P (1999) Mitochondrial transport of cations: channels, exchangers, and permeability transition. Physiol Rev 79:1127–1155
13. Berridge MJ (1998) Neuronal calcium signalling. Neuron 21:13–26
14. Bradley J (2006) Splice variants of the NR1 subunit differentially induce NMDA receptor-dependent gene expression. J Neurosci 26:1065–1076
15. Brandl CJ (1987) Adult forms of the Ca^{2+}ATPase of sarcoplasmic reticulum: expression in developing skeletal muscle. J Biol Chem 262:3768–3774
16. Ghosh A et al (1995) Calcium signalling in neurons: molecular mechanisms and cellular consequences. Science 268:239–247. doi:10.1126/science.7716515
17. Ryglewski S, Pflueger HJ, Duch C (2007) Expanding the Neuron's calcium signalling repertoire: intracellular calcium release via voltage-induced PLC and IP3R activation. PLoS Biol 5:e66. doi:10.1371/journal.pbio.0050066
18. Brustovetsky N (2002) Calcium-induced cytochrome c release from CNS mitochondria is associated with the permeability transition and rupture of the outer membrane. J Neurochem 80:207–228
19. Carafoli E (1991) Calcium pump of the plasma membrane. Physiol Rev 71:129–153
20. Carafoli E (1974) The release of calcium from heart mitochondria by sodium. J Mol Cell Cardiol 6:361–371
21. Catterall WA (2005) International Union of Pharmacology. XLVIII. Nomenclature and structure-function relationships of voltage-gated calcium channels. Pharmacol Rev 57:411–425
22. Celio MR (1990) Calbindin D-28k and parvalbumin in the rat nervous system. Neuroscience 35(2):p375–p475

23. Chang DT, Reynolds IJ (2006) Mitochondrial trafficking and morphology in healthy and injured neurons. Prog Neurobiol 80:241–268
24. Crompton M (1999) The mitochondrial permeability transition pore and its role in cell death. Biochem J 2:233–249
25. Cull-candy S, Kelly L, Farrant M (2006) Regulation of Ca^{2+}-permeable AMPA receptors: synaptic plasticity and beyond. Curr Opin Neurobiol 16:288–297
26. Dolphin AC (2003) Beta subunits of voltage-gated calcium channels. J Bioenerg Biomembr 35:599–620
27. Dubel SJ, Altier C, Chaumont S, Lory P, Bourinet E, Nargeot J (2004) Plasma membrane expression of T-type calcium channel alpha(1) subunits is modulated by high voltage-activated auxiliary subunits. J Biol Chem 279:29263–29269
28. Finch EA, Turner TJ, Goldin SM (1991) Calcium as a coagonist of inositol 1,4,5-trisphosphate-induced calcium release. Science 252:443–446
29. Gelebart P, Opas M, Michalak M (2005) Calreticulin. A Ca^{2+}-binding chaperone of the endoplasmic reticulum. Int J Biochem Cell Biol 37:260–266
30. Gincel D, Zaid H, Shoshan-barmatz V (2001) Calcium binding and translocation by the voltage-dependent anion channel: a possible regulatory mechanism in mitochondrial function. Biochem J 1:147–155
31. Dani JW, Chernjavsky A, Smith SJ (1992) Neuronal activity triggers calcium waves in hippocampal astrocyte networks. Neuron 8:429–440
32. Arcuino G, Lin JH, Takano T, Liu C, Jiang L, Gao Q, Kang J, Nedergaard M (2002) Intercellular calcium signaling mediated by point-source burst release of ATP. Proc Natl Acad Sci USA 99:9840–9845
33. Haydon PG (2001) Glia: listening and talking to the synapse. Nat Rev Neurosci 2:185–193
34. Zonta M, Angulo MC, Gobbo S, Rosengarten B, Hossmann KA, Pozzan T, Carmignoto G (2003) Neuron-to-astrocyte signaling is central to the dynamic control of brain microcirculation. Nat Neurosci 6:43–50
35. Parpura V, Basarsky TA, Liu F, Jeftinija K, Jeftinija S, Haydon PG (1994) Glutamate-mediated astrocyte-neuron signalling. Nature 369:744–747
36. Pasti L, Volterra A, Pozzan T, Carmignoto G (1997) Intracellular calcium oscillations in astrocytes: a highly plastic, bidirectional form of communication between neurons and astrocytes in situ. J Neurosci 17:7817–7830
37. Filosa JA, Bonev AD, Nelson MT (2004) Calcium dynamics in cortical astrocytes and arterioles during neurovascular coupling. Circ Res 95:e73–e81
38. Charles AC (1994) Glia-neuron intercellular calcium signaling. Dev Neurosci 16:196–206
39. Nedergaard M (1994) Direct signaling from astrocytes to neurons in cultures of mammalian brain cells. Science 263:1768–1771
40. Schmitz D, Schuchmann S, Fisahn A, Draguhn A, Buhl EH, Petrasch-Parwez E, Dermietzel R, Heinemann U, Traub RD (2001) Axoaxonal coupling. a novel mechanism for ultrafast neuronal communication. Neuron 31:831–840
41. Porter JT, McCarthy KD (1996) Hippocampal astrocytes in situ respond to glutamate released from synaptic terminals. J Neurosci 16:5073–5081
42. Araque A, Martin ED, Perea G, Arellano JI, Buno W (2002) Synaptically released acetylcholine evokes Ca^{2+} elevations in astrocytes in hippocampal slices. J Neurosci 22:2443–2450
43. Matyash V, Filippov V, Mohrhagen K, Kettenmann H (2001) Nitric oxide signals parallel fiber activity to Bergmann glial cells in the mouse cerebellar slice. Mol Cell Neurosci 18:664–670
44. Hassinger TD, Atkinson PB, Strecker GJ, Whalen LR, Dudek FE, Kossel AH, Kater SB (1995) Evidence for glutamate-mediated activation of hippocampal neurons by glial calcium waves. J Neurobiol 28:159–170
45. Araque A, Li N, Doyle RT, Haydon PG (2000) SNARE proteindependent glutamate release from astrocytes. J Neurosci 20:666–673
46. Bezzi P, Carmignoto G, Pasti L, Vesce S, Rossi D, Rizzini BL, Pozzan T, Volterra A (1998) Prostaglandins stimulate calciumdependent glutamate release in astrocytes. Nature 391:281–285

47. Newman EA, Zahs KR (1998) Modulation of neuronal activity by glial cells in the retina. J Neurosci 18:4022–4028
48. Porter JT, McCarthy KD (1995) GFAP-positive hippocampal astrocytes in situ respond to glutamatergic neuroligands with increases in (Ca^{2+})i. Glia 13:101–112
49. Navarrete M, Araque A (2008) Endocannabinoids mediate neuron-astrocyte communication. Neuron 57:883–893
50. Perea G, Araque A (2005) Properties of synaptically evoked astrocyte calcium signal reveal synaptic information processing by astrocytes. J Neurosci 25:2192–2203
51. Ghosh S, Kaushik DK, Gomes J, Nayeem S, Deep S, Basu A (2010) Changes in cytosolic Ca($^{2+}$) levels correspond to fluctuations of lactate levels in crosstalk of astrocyte-neuron cell lines. Indian J Exp Biol 48:529–537
52. Agulhon C, Petravicz J, McMullen AB, Sweger EJ, Minton SK et al (2008) What is the role of astrocyte calcium in neurophysiology? Neuron 59:932–946
53. Parri HR et al (2001) Spontaneous astrocytic Ca^{2+} oscillations in situ drive NMDAR-mediated neuronal excitation. Nat Neurosci 4:803–812
54. Perea G, Navarrete M, Araque A (2009) Tripartite synapses: astrocytes process and control synaptic information. Trends Neurosci 32:421–431
55. Fiacco TA, Agulhon C, Taves SR, Petravicz J, Casper KB et al (2007) Selective stimulation of astrocyte calcium in situ does not affect neuronal excitatory synaptic activity. Neuron 54:611–626
56. McCarthy KD, Salm AK (1991) Pharmacologically distinct subsets of astroglia can be identified by their calcium response to neuroligands. Neuroscience 41:325–333
57. Cornell-Bell AH, Finkbeiner SM, Cooper MS, Smith SJ (1990) Glutamate induces calcium wavs in cultured astrocytes: long-range glial signaling. Science 247:470–473
58. Cornell-Bell A, Finkbeiner SM (1991) Ca^{2+} waves in astrocytes. Cell Calcium 12:185–204
59. Yagodin SV, Holtzclaw LA, Sheppard CA, Russell JT (1994) Nonlinear propagation of agonist-induced cytoplasmic calcium waves in single astrocytes. J Neurobiol 25:265–280
60. Berridge MJ (1993) Inositol trisphosphate and calcium signaling. Nature 361:315–325
61. Meyer T, Stryer L (1991) Calcium spiking. Annu Rev Biophys Biophys Chem 20:153–174
62. Ahmed Z, Lewis CA, Faber DS (1990) Glutamate stimulates release of Ca^{2+} from internal stores in astroglia. Brain Res 516:165–169
63. Mulligan SJ, MacVicar BA (2004) Calcium transients in astrocyte endfeet cause cerebrovascular constrictions. Nature 431:195–199
64. Alonso-Galicia M, Hudetz AG, Shen H, Harder DR, Roman RJ (1999) Contribution of 20-HETE to vasodilator actions of nitric oxide in the cerebral microcirculation. Stroke 30:2727–2734
65. Sun CW, Falck JR, Okamoto H, Harder DR, Roman RJ (2000) Role of cGMP versus 20-HETE in the vasodilator response to nitric oxide in rat cerebral arteries. Am J Physiol Heart Circ Physiol 279:H339–H350
66. Carmignoto G, Gómez-Gonzalo M (2008) The contribution of astrocyte signalling to neurovascular coupling. Brain Res Rev 63:138–148. doi:10.1016/j.brainresrev.2009.11.007
67. Pellerin L, Magistretti P (1994) Glutamate uptake in astrocytes stimulates aerobic glycolysis: a mechanism coupling neuronal activity to glucose utilization. Proc Natl Acad Sci USA 91:47881–47889
68. Gjedde A (2001) Brain energy metabolism and the hemodynamic response. In: Jezzard P, Matthews PM, Smith SM (eds) Functional MRI: an introduction to methods. OUP, Oxford, pp 37–65
69. Bittar PG, Charnay Y, Pellerin L, Bouras C, Magistretti P (1996) Selective distribution of lactate dehydrogenase isoenzymes in neurones and astrocytes of human brain. J Cereb Blood Flow Metab 16:1079–1089
70. Viswanathan A, Freeman RD (2008) Neurometabolic coupling in cerebral cortex reflects synaptic more than spiking activity. Nat Neurosci 10:1308–1312. doi:10.1038/nn1977
71. Laughton JD et al (2000) Differential messenger RNA distribution of lactate dehydrogenase LDH-1 and LDH-5 isoforms in the rat brain. Neuroscience 96:619–625

72. Ullah G, Jung P, Cornell-Bell AH (2006) Anti-phase Calcium oscillations in astrocytes via inositol (1,4,5)-triphosphate regeneration. Cell Calcium 39:197–211
73. Serres S, Raffard G, Franconi J-F, Merle M (2008) Close coupling between astrocytic and neuronal metabolism to fulfill anaplerotic and energy needs in the rat brain. J Cereb Blood Flow Metab 28:712–724. doi:10.1038/sj.jcbfm.9600568
74. Gordon GRJ, Choi HB, Rungta RL, Ellis-Davies GCR, MacVicar BA (2008) Brain metabolism dictates the polarity of astrocyte control over arterioles. Nature 456:745–749. doi:10.1038/nature07525
75. Alkayed NJ, Narayanan J, Gebremedhin D, Medhora M, Roman RJ, Harder DR (1996) Molecular characterization of an arachidonic acid epoxygenase in rat brain astrocytes. Stroke 27:971–979
76. Amruthesh SC, Boerschel MF, McKinney JS, Willoughby KA, Ellis EF (1993) Metabolism of arachidonic acid to epoxyeicosatrienoic acids, hydroxyeicosatetraenoic acids, and prostaglandins in cultured rat hippocampal astrocytes. J Neurochem 61:150–159
77. Amruthesh SC, Falck JR, Ellis EF (1992) Brain synthesis and cerebrovascular action of epoxygenase metabolites of arachidonic acid. J Neurochem 58:503–510
78. Peng X, Zhang C, Alkayed NJ, Harder DR, Koehler RC (2004) Dependency of cortical functional hyperemia to forepaw stimulation on epoxygenase and nitric oxide synthase activities in rats. J Cereb Blood Flow Metab 24:509–517
79. Shivachar AC, Willoughby KA, Ellis EF (1995) Effect of protein kinase C modulators on 14,15-epoxyeicosatrienoic acid incorporation into astroglial phospholipids. J Neurochem 65:338–346
80. Rzigalinski BA, Willoughby KA, Hoffman SW, Falck JR, Ellis EF (1999) Calcium influx factor, further evidence it is 5,6-epoxyeicosatrienoic acid. J Biol Chem 274:175–182
81. Gebremedhin D, Yamaura K, Zhang C, Bylund J, Koehler RC, Harder DR (2003) Metabotropic glutamate receptor activation enhances the activities of two types of Ca^{2+}-activated K+ channels in rat hippocampal astrocytes. J Neurosci 23:1678–1687
82. Gebremedhin D, Narayanan J, Harder DR (2005) Role of astrocytic KCa channel openings in the glutamate receptor mediated release of EETs from rat brain astrocytes (Abstract). FASEB J 19:A1257
83. Alkayed NJ, Birks EK, Narayanan J, Petrie KA, Kohler-Cabot AE, Harder DR (1997) Role of P-450 arachidonic acid epoxygenase in the response of cerebral blood flow to glutamate in rats. Stroke 28:1066–1072
84. Gebremedhin D, Ma YH, Falck JR, Roman RJ, VanRollins M, Harder DR (1992) Mechanism of action of cerebral epoxyeicosatrienoic acids on cerebral arterial smooth muscle. Am J Physiol Heart Circ Physiol 263:H519–H525
85. Harder DR, Alkayed NJ, Lange AR, Gebremedhin D, Roman RJ (1998) Functional hyperemia in the brain. Hypothesis for astrocyte-derived vasodilator metabolites. Stroke 28: 229–234
86. Ellis EF, Police RJ, Yancey L, McKinney JS, Amruthesh SC (1990) Dilation of cerebral arterioles by cytochrome P-450 metabolites of arachidonic acid. Am J Physiol Heart Circ Physiol 259:H1171–H1177
87. Leffler CW, Fedinec AL (1997) Newborn piglet cerebral microvascular responses to epoxyeicosatrienoic acids. Am J Physiol Heart Circ Physiol 273:H333–H338
88. Bhardwaj A, Northington FJ, Carhuapoma JR, Falck JR, Harder DR, Traystman RJ, Koehler RC (2000) P-450 epoxygenase and NO synthase inhibitors reduce cerebral blood flow response to N-methyl-Daspartate. Am J Physiol Heart Circ Physiol 279:H1616–H1624
89. Peng X, Carhuapoma JR, Bhardwaj A, Alkayed NJ, Falck JR, Harder DR, Traystman RJ, Koehler RC (2002) Suppression of cortical functional hyperemia to vibrissal stimulation in the rat by epoxygenase inhibitors. Am J Physiol Heart Circ Physiol 283:H2029–H2037
90. Simmons DL, Botting RM, Hla T (2004) Cyclooxygenase isozymes: the biology of prostaglandin synthesis and inhibition. Pharmacol Rev 56:387–437
91. Stefanovic B, Bosetti F, Silva AC (2006) Modulatory role of cyclooxygenase-2 in cerebrovascular coupling. Neuroimage 32:23–32

92. Tanioka T, Nakatani Y, Semmyo N, Murakami M, Kudo L (2000) Molecular identification of cytosolic prostaglandin E2 synthase that is functionally coupled with cyclooxygenase-1 in immediate prostaglanding E2 biosynthesis. J Biol Chem 275:32775–32782
93. Blanco VM, Stern JE, Filosa JA (2008) Tone-dependent vascular responses to astrocyte-derived signals. Am J Physiol Heart Circ Physiol 294:H2855–H2863
94. Hassinger TD, Guthrie PB, Atkinson PB, Bennett MV, Kater SB (1996) An extracellular signaling component in propagation of astrocytic calcium waves. Proc Natl Acad Sci USA 93:13268–13273
95. Guthrie PB, Knappenberger J, Segal M, Bennett MV, Charles AC, Kater SB (1999) ATP released from astrocytes mediates glial calcium waves. J Neurosci 19:520–528
96. Wang Z, Haydon PG, Yeung ES (2000) Direct observation of calciumindependent intercellular ATP signaling in astrocytes. Anal Chem 72:2001–2007
97. Dubyak GR, el-Moatassim C (1993) Signal transduction via P2-purinergic receptors for extracellular ATP and other nucleotides. Am J Physiol 265:C577–C606
98. Cotrina ML, Lin JH, Alves-Rodrigues A, Liu S, Li J et al (1998) Connexins regulate calcium signaling by controlling ATP release. Proc Natl Acad Sci 95:15735–15740
99. Cotrina ML, Lin JHC, Nedergaard M (1998) Cytoskeletal assembly and ATP release regulate astrocytic calcium signalling. J Neurosci 18:8704–8804
100. Stout CE, Costantin JL, Naus CC, Charles AC (2002) Intercellular calcium signaling in astrocytes via ATP release through connexin hemichannels. J Biol Chem 277:10482–10488
101. Coco S, Calegari F, Pravettoni E, Pozzi D, Taverna E, Rosa P, Matteoli M, Verderio C (2003) Storageand release of ATP from astrocytes in culture. J Biol Chem 278:1354–1362
102. Cauli B, Tong XK, Rancillac A, Serluca N, Lambolez B, Rossier J, Hamel E (2004) Cortical GABA interneurons in neurovascular coupling: relays for subcortical vasoactive pathways. J Neurosci 24:8940–8949
103. Liu X, Li C, Falck JR, Roman RJ, Harder DR, Koehler RC (2008) Interaction of nitric oxide, 20-HETE, and EETs during functional hyperemia in whisker barrel cortex. Am J Physiol Heart Circ Physiol 295:H619–H631
104. Filosa JA, Blanco VM (2007) Neurovascular coupling in the mammalian brain. Exp Physiol 92:641–646
105. Girouard H, Bonev AD, Hannah RM, Meredith A, Aldrich RW, Nelson MT (2010) Astrocytic endfoot Ca^{2+} and BK channels determine both arteriolar dilation and constriction. Proc Natl Acad Sci USA 107:3811–3816
106. Smith SJ (1994) Neural signalling. Neuromodulatory astrocytes. Curr Biol 4:807–810
107. Cornell-Bell AH, Jung P, Trinkaus-Randall V (2004) Decoding calcium wave signaling. Adv Mol Cell Biol 31:661–687
108. Scemes E, Giaume C (2006) Astrocyte calcium waves: what they are and what they do. Glia 54:716–725
109. Foskett JK, White C, Cheung KH, Mak DO (2007) Inositol triphosphate receptor Ca^{2+} release channels. Physiol Rev 87:593–658
110. Codazzi F, Teruel MN, Meyer T (2001) Control of astrocyte $Ca(^{2+})$ oscillations and waves by oscillating translocation and activation of protein kinase C. Curr Biol 11:1089–1097
111. Parri HR, Crunelli V (2003) The role of Ca^{2+} in the generation of spontaneous astrocytic Ca^{2+} oscillations. Neuroscience 120:979–992
112. Simpson PB, Challis RAJ, Nahorski SR (1995) Neuronal Ca^{2+} stores: activation and function. Trends Neurosci 18:299–306
113. Miller RJ (1991) The control of neuronal Ca^{2+} homeostasis. Prog Neurobiol 37:255–285
114. Garaschuk O, Yaari Y, Konnerth A (1997) Release and sequestration of calcium by ryanodine-sensitive stores in rat hippocampal neurons. J Physiol (Lond) 502:13–30
115. Sharp AH et al (1993) Differential immunohistochemical localization of inositol 1,4,5-trisphosphate- and ryanodine-sensitive Ca^{2+} release channels in rat brain. J Neurosci 13:3051–3063
116. Parys JB et al (2000) Regulation of inositol 1,4,5-triphosphate-induced Ca^{2+} release by Ca^{2+}. In: Pochet R (ed) Calcium: the molecular basis of calcium action in biology and medicine. Kluwer Academic Publishers, Dordrecht, pp 179–190

117. Miller LDP, Petrozzino JJ, Golarai G, Connor JA (1996) Ca^{2+} release from intracellular stores induced by afferent stimulation of CA3 pyramidal neurons in hippocampal slices. J Neurophysiol 76:554–562
118. Berridge MJ (1997) Elementary and global aspects of calcium. J Physiol 499:291–306
119. Zucchi R, Ronca-Testoni S (1997) The sarcoplasmic reticulum Ca^{2+} channel/ryanodine receptor: modulation by endogenous effectors, drugs and disease states. Pharmacol Rev 49:1–51
120. Rossi D et al (2000) Ryanodine-sensitive calcium release channels. In: Pochet R (ed) Calcium: the molecular basis of calcium action in biology and medicine. Kluwer Academic Publishers, Dordrecht, pp 205–219
121. Tu H et al (2006) Presenilins form ER Ca^{2+} leak channels, a function disrupted by familial Alzheimer's disease-linked mutations. Cell 126:981–993
122. Misquitta CM, Mack DP, Grover AK (1999) Sarco/endoplasmic reticulum Ca^{2+} (SERCA)-pumps: link to heart beats and calcium waves. Cell Calcium 25:277–290
123. Markram H, Helm PJ, Sakmann B (1995) Dendritic calcium transients evoked by single back-propagating action-potentials in rat neocortical pyramidal neurons. J Physiol 485:1–20
124. Lipscombe D, Madison DV, Peonie M, Reuter H, Tsien RW, Tsien RY (1998) Imaging of cytosolic C21 transients arising from Ca21 stores and Ca21 channels in sympathetic neurons. Neuron 1:355–365
125. Ikeda SR (2001) Calcium channels- link locally, act globally. Science 294:318–319. doi:10.1126/science.1066160
126. Nicholls DG et al (2003) Interactions between mitochondrial bioenergetics and cytoplasmic calcium in cultured cerebellar granule cells. Cell Calcium 34:407–424
127. Rizzuto R, Pozzan T (2006) Microdomains of intracellular Ca^{2+}: molecular determinants and functional consequences. Physiol Rev 86:369–408
128. Lemasters JJ, Holmuhamedov E (2006) Voltage-dependent anion channel (VDAC) as mitochondrial governator–thinking outside the box. Biochim Biophys Acta 1762:181–190
129. Kirichok Y, Krapivinsky G, Clapham DE (2004) The mitochondrial calcium uniporter is a highly selective ion channel. Nature 427:360–364
130. Kannurpatti SS, Biswal BB (2008) Mitochondrial Ca^{2+} uniporter blockers influence activation-induced CBF response in the rat somatosensory cortex. J Cereb Blood Flow Metab 28:772–785. doi:10.1038/sj.jcbfm.9600574
131. Hajnoczky G et al (2006) Mitochondrial calcium signalling and cell death: approaches for assessing the role of mitochondrial Ca^{2+} uptake in apoptosis. Cell Calcium 40:553–560
132. Kim B, Matsuoka S (2007) Mitochondrial Ca^{2+} flux through Na+/Ca^{2+} exchange. Ann N Y Acad Sci 1099:507–511
133. Carafoli E et al (1974) The release of calcium from heart mitochondria by sodium. J Mol Cell Cardiol 6:361–371
134. Wingrove DE, Gunter TE (1986) Kinetics of mitochondrial calcium transport. I. Characteristics of the sodium-independent calcium efflux mechanism of liver mitochondria. J Biol Chem 261:15159–15165
135. Brustovetsky N et al (2002) Calcium-induced cytochrome c release from CNS mitochondria is associated with the permeability transition and rupture of the outer membrane. J Neurochem 80:207–218
136. Schmidt H et al (2003) Mutational analysis of dendritic Ca^{2+} kinetics in rodent Purkinje cells: role of parvalbumin and calbindin D28k. J Physiol 551(Pt 1):13–32
137. Celio MR (1990) Calbindin D-28k and parvalbumin in the rat nervous system. Neuroscience 35:375–475
138. Iadecola C (2004) Neurovascular regulation in the normal brain and in Alzheimer's Disease. Nat Rev Neurosci 5:347–360. doi:10.1038/nrn1387
139. Ogawa S, Lee TM (1990) Magnetic resonance imaging of blood vessels at high fields: in vivo and in vitro measurements and image simulations. Magn Reson Med 16:9–18
140. Ogawa S, Lee TM, Kay AR, Tank DW (1990) Brain magnetic resonance imaging with contrast dependent on blood oxygenation. Proc Natl Acad Sci USA 87:9868–9872
141. Buxton RB, Frank LR (1997) A model for the coupling between cerebral blood flow and oxygen metabolism during neural stimulation. J Cereb Blood Flow Metab 17:64–72

142. Buxton RB, Uludag K, Dubowitz DJ, Liu TT (2004) Neuroimage 23(Suppl 1):S220–S233
143. Huppert TJ, Allen MS, Benav H, Jones PB, Boas DA (2007) A multicompartment vascular model for inferring baseline and functional changes in cerebral oxygen metabolism and arterial dilation. J Cereb Blood Flow Metab 27:1262–1279
144. Zheng Y, Pan Y, Harris S, Billings S, Coca D, Berwick J et al (2010) A dynamic model of neurovascular coupling: Implications for blood vessel dilation and constriction. Neuroimage 52:1135–1147
145. Schummers JR, Yu H, Sur M (2008) Tuned responses of astrocytes and their influence on haemodynamic signals in the visual cortex. Science 320:1638–1643
146. Araque A (2008) Astrocytes process synaptic information. Neuron Glia Biol 4:3–10
147. Venter JC et al (2001) The sequence of the human genome. Science 291:1304–1351
148. Bigos KL, Weinberger DR (2010) Imaging genetics - days of future past. Neuroimage 53:804–809
149. Thompson PM, Martin NG, Wright M (2010) Imaging genomics. Curr Opin Neurol 23:368–373. doi:10.1097/WCO.0b013e32833b764c
150. Bigos KL, Bies RR, Pollock BG, Lowy JJ, Zhang F, Weinberger DR (2011) Genetic variation in CYP3A43 explains racial difference in olanzapine clearance. Mol Psychiatry 16:620–625. doi:10.1038/mp.2011.38
151. Angelovski G, Fouskova P, Mamedov I, Canals S, Toth E, Logothetis NK (2008) Smart magnetic resonance imaging agents that sense extracellular calcium fluctuations. Chembiochem 9:1729–1734

Chapter 38
Ca^{2+} Signaling Mechanisms in Bovine Adrenal Chromaffin Cells

Jamie L. Weiss

Abstract Calcium (Ca^{2+}) is a crucial intracellular messenger in physiological aspects of cell signaling. Adrenal chromaffin cells are the secretory cells from the adrenal gland medulla that secrete catecholamines, which include epinephrine and norepinephrine important in the 'fight or flight' response. Bovine adrenal chromaffin cells have long been used as an important model for secretion (exocytosis) not only due to their importance in the short-term stress response, but also as a neuroendocrine model of neurotransmtter release, as they have all the same exocytotic proteins as neurons but are easier to prepare, culture and use in functional assays. The components of the Ca^{2+} signal transduction cascade and it role in secretion has been extensively characterized in bovine adrenal chromaffin cells. The Ca^{2+} sources, signaling molecules and how this relates to the short-term stress response are reviewed in this book chapter in an endeavor to generally overview these mechanisms in a concise and uncomplicated manner.

Keywords Bovine adrenal chromaffin cells • Calcium • Ca^{2+} • Ca^{2+} signaling • Neuronal calcium sensor-1 • NCS-1 • Ca^{2+} microdomains • Ca^{2+} transients • Ca^{2+} stores • Intracellular signaling • Splanchnic nerves

Overview

Bovine adrenal chromaffin cells are a classical well-established model for the study of neuroendocrine physiology. They are the cells made even more famous by Nobel prize laureates Erwin Neher and Bert Sakmann, as they used bovine adrenal chromaffin

J.L. Weiss (✉)
Department of Biology, William Paterson University, 300 Pompton Road, Wayne, NJ 07470, USA
e-mail: weissj7@wpunj.edu

M.S. Islam (ed.), *Calcium Signaling*, Advances in Experimental Medicine and Biology 740, DOI 10.1007/978-94-007-2888-2_38,

cells to help develop the patch-clamp technique [1–3]. Adrenal chromaffin cells are an extensively characterized model system for secretory cells [4, 5]. These cells, which are found in the adrenal medulla, are derived embryonically from the neural crest that contain the same precursor cells that give rise to sympathetic neurons. Chromaffin cells are used as neuronal cell models because they contain many of the same proteins that are involved in neuronal function and share common mechanisms for regulated exocytosis [6]. They are used as a model for exocytosis or neurotransmission and Ca^{2+}-signaling and are relatively easy to isolate, culture and manipulate [7] as compared to neurons. Although neurons are very highly specialized cells, with each type of neuron having signaling mechanisms specifically targeted to its neuronal network in its region of the CNS or PNS, they do share common Ca^{2+}-signaling mechanisms [8]. Therefore it is highly likely that if a novel mechanism is found in a chromaffin cell it can also be found in one or more specific neuronal cells. For example Neuronal Ca^{2+} Sensor-1 (NCS-1) was first shown to modulate exocytosis and regulate Ca^{2+} channels in bovine adrenal chromaffin cells [9–11]. NCS-1 was later shown to have the same role in neurons and other animal models having important roles in neurotransmission and synaptic plasticity [12]. Bovine adrenal chromaffin cells are also used as models for toxicological studies [13] and are also a terrific cell type to use for the 'three Rs' in animal research-reduction, refinement, and replacement [14] as they come from the same animals that are slaughtered for meat. These bovine adrenal glands are often discarded after the skirt meat has been removed. Therefore not only are using these bovine adrenal chromaffin cells thought to be more humane as compared to primary cells obtained from other sources, they also keep biomedical research costs down as they avoid the additional funds necessary for the upkeep of laboratory animals.

In this chapter an attempt has been made to not only succinctly generally review Ca^{2+}-signaling mechanisms by way of Ca^{2+} stores and sources as well as the signaling proteins channels and receptors that are important cellular tools for Ca^{2+}-signaling mechanisms but also to relate this to the physiology of the cell type and how this translates to overall animal/Human physiology of the stress response [15–17]. Chromaffin cells secrete epinephrine and norepinephrine that are very important for the 'fight or flight' and the stress response. This chapter will not cover Ca^{2+}-evoked-exocytosis in bovine adrenal chromaffin cells in detail as this has been extensively reviewed elsewhere [18, 19]. These cells are also useful because they have neuronal lineages having come from the same precursors sympathetic neurons they can be treated with neurotrophic factors such as Nerve Growth Factor (NGF) or high K^+ to emit neurites [12, 20, 21]. They are currently being used for regeneration studies in animals in vivo or in culture with the right factors and environment to facilitate neural progenitor cell survival [22]. Chromaffin cells can be thought of in some ways as stem cells to help the survival of neurons that are lost in spinal cord injury or neurological disorders such as Alzheimer's and Parkinson's [22–24].

There are different Ca^{2+} stores or sources that have been characterized in many cell types especially in neuronal cells, the most famous classical Ca^{2+} store being the Endoplasmic Reticulum or ER [8, 25]. Mitochondria are also another important

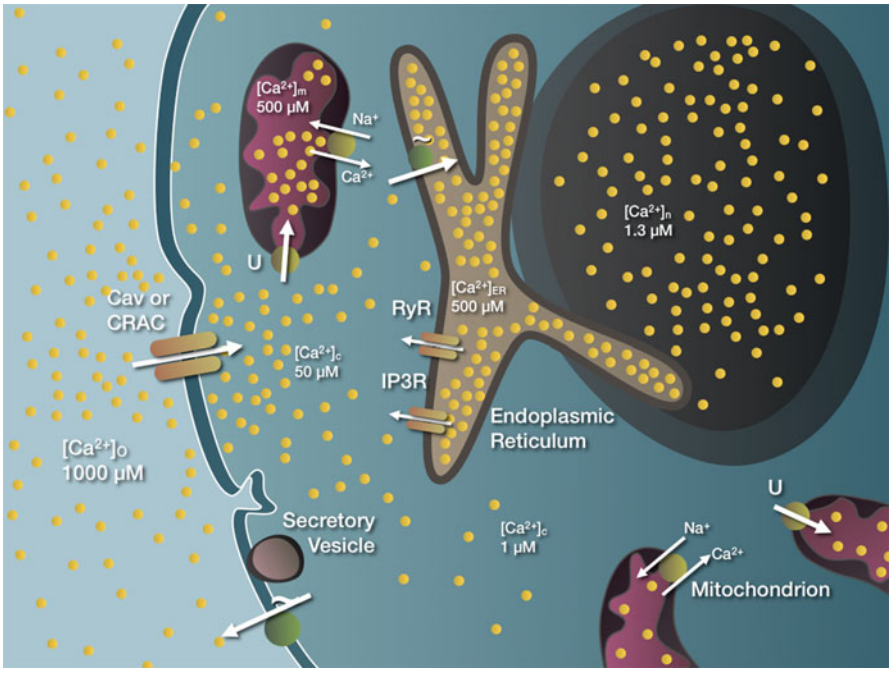

Fig. 38.1 Ca^{2+} stores/sources that have been identified in bovine adrenal chromaffin cells. The relative Ca^{2+} concentration has been listed to give an idea of how the Ca^{2+} sources maintain Ca^{2+} transients that contribute to Ca^{2+} signaling and physiological functions of chromaffin cells such as exocytosis of catecholamines. Organelles sizes are not meant to be an accurate representation of relative size. Figure based on Montero et al. [27] and Garcia et al. [18]. Cav – voltage-gated Ca^{2+} channels, CRAC – Ca^{2+} Release Activated Channels. $[Ca^{2+}]o$ – relative Ca^{2+}concentration outside the cell. $[Ca^{2+}]m$ – relative Ca^{2+} concentration in mitochondria. $[Ca^{2+}]ER$ – relative Ca^{2+} concentration endoplasmic reticulum. $[Ca^{2+}]n$ – relative Ca^{2+} concentration in the nucleus

Ca^{2+} store/source [26, 27] important for exocytosis in chromaffin cells as well as Ca^{2+} buffering [28]. The nucleus has a nuclear envelope that has nuclear pores through which Ca^{2+} can enter [29]. When the Ca^{2+} concentration levels become high enough Ca^{2+} can enter and get into these pores. There is evidence that these Ca^{2+} sources (mitochondria and nucleus) may help to maintain and Ca^{2+} transients and waves that are crucial to Ca^{2+} signaling in many cell types including bovine adrenal chromaffin cells [30–33]. In addition to the ER, the nucleus, mitochondria [32] and even the Golgi-apparatus [34] are considered to be important Ca^{2+} sources for maintaining Ca^{2+} microdomains (Fig. 38.1). These Ca^{2+}-microdomains [35] are vital for activating and regulating a variety of signaling proteins, receptors and channels ([36]; Fig. 38.2). This then leads to changes in response to environmental signals important in adrenal chromaffin cell physiology such as exocytosis and endocrine release crucial in the stress response ([15, 18]; Fig. 38.3).

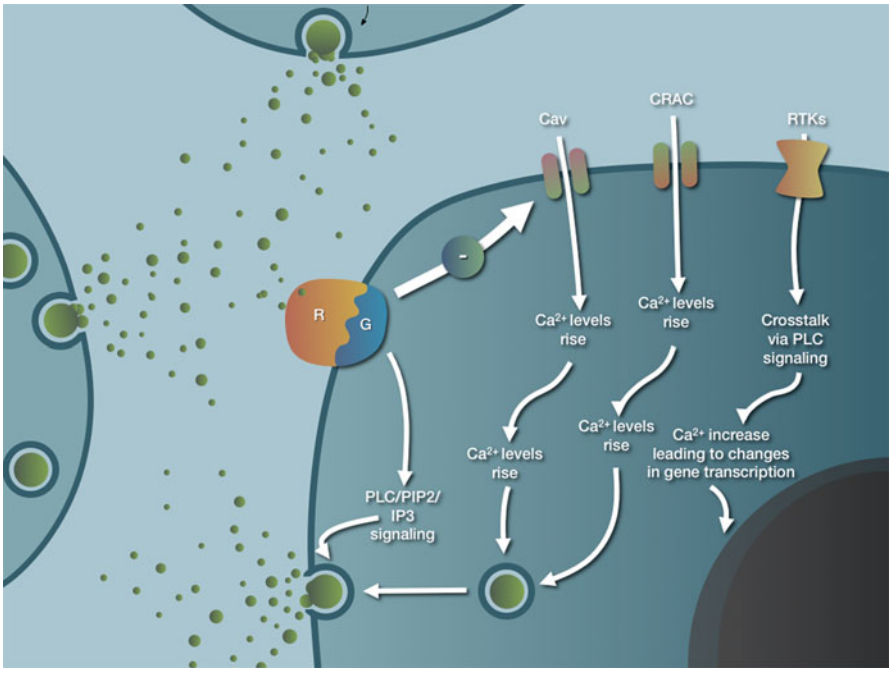

Fig. 38.2 The best-characterized Ca^{2+} signal transduction pathways in bovine adrenal chromaffin cells, which control both paracrine and autocrine signaling. Chromaffin cells in culture and in the adrenal medullar signal to each other via catecholamines and ATP. These act on G-Protein-Coupled Receptor (*GPCR*) s, which in turn act on and/or crosstalk with voltage-gated Ca^{2+} channels (*Cavs*), Ca^{2+}-release activated channels (*CRAC*) and Receptor Tyrosine Kinases (*RTKs*). Ca^{2+} sensors/ binding proteins such as Calmodulin (*CaM*), NCS-1, Calneuron, CaBP-1 and buffers such as Calbindin further mediate these Ca^{2+} signaling pathways. Which in turn provide feedback to the membrane receptors/channels and secretion

The Ca^{2+} Signaling Cellular Apparatus

Ca^{2+} Stores, Sources and Transients

Evidence in many cell types including bovine adrenal chromaffin cells suggests that cellular organelles stores or sources of Ca^{2+} contribute to shaping Ca^{2+} signals and exocytosis [8, 18, 25, 35, 37]. Ca^{2+} transients are localized increases in Ca^{2+} concentration that are crucial for cellular physiological processes in spatial- temporal aspects of cellular signaling [37]. The main source Ca^{2+} entry into chromaffin cells and neuroendocrine cells is Ca^{2+} entry through voltage-gated Ca^{2+} channels (Cavs; [38]). Large amounts of Ca^{2+} coming through Cav channels are crucial to supporting the Ca^{2+} needed for ER Ca^{2+} store and Ca^{2+} sources in organelles such as mitochondria [18, 32, 38, 39]. Cytosolic Ca^{2+} transients, buffering and diffusion in bovine

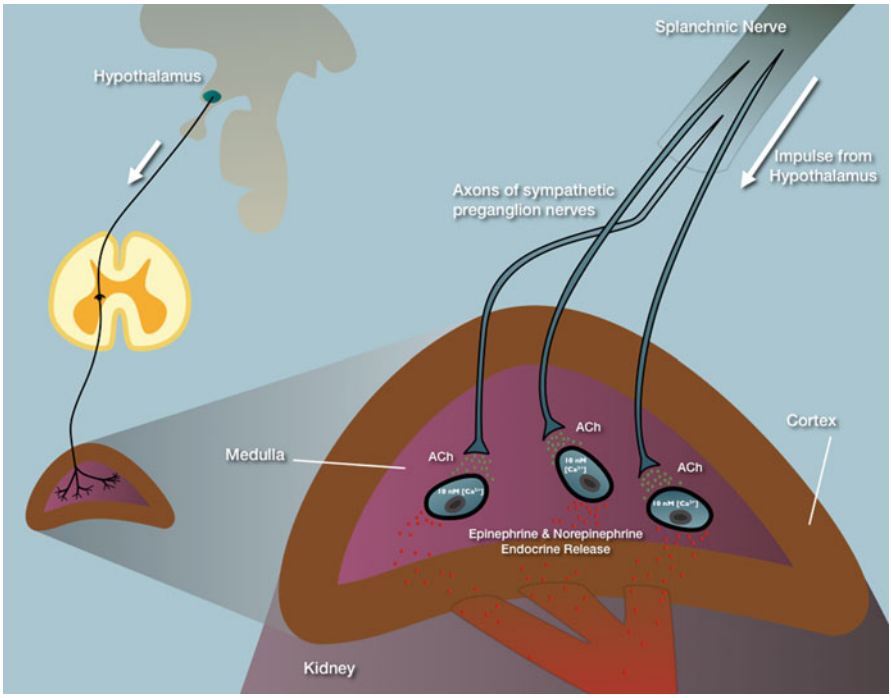

Fig. 38.3 Bovine adrenal chromaffin cells physiological responses to sympathetic innervation of the adrenal medulla. The splanchnic nerve–chromaffin cell synapse, which is cholinergic, is depicted in the adrenal medulla showing the location of the adrenal gland anatomically as it sits on top of the kidney. Nerve impulses from the hypothalamus travel to splanchnic nerve terminals (sympathetic preganglionic axons) innervating the adrenal medulla and the subsequent action potentials cause release of acetylcholine (*Ach*). Functionally adrenal chromaffin cells are postsynaptic to sympathetic preganglionic axon terminals. The adrenal chromaffin cell membrane becomes depolarized in response to prolonged release of Ach or other stimulatory chemicals. This causes activation of Cavs and the Ca^{2+} signaling pathways shown in Fig. 38.2. This leads to secretion of catecholamines including epinephrine and norepinephrine that are crucial to the 'fight or flight' response

adrenal chromaffin cells Ca^{2+} dependence of exocytosis has also been examined [40, 41] and continues to been an important active area of study [18].

In Fig. 38.1 a stereotypical chromaffin cell is depicted. The approximate Ca^{2+} concentrations are shown the outside of the cell at approximately 1000 μM and the approximate Ca^{2+} concentration in organelles are also depicted such as ER, mitochondria and nucleus. Ca^{2+} release channels such as Ryanodine (RyR) and IP3 receptors located the ER membrane are shown. In Fig. 38.1 the Ca^{2+} stores that are detected in bovine adrenal chromaffin cells are depicted. These include the ER, mitochondria and nucleus. When Ca^{2+} enters through channels the mitochondrial Ca^{2+} concentration can be as high as 500 μM. It is thought that the ER and nucleus are in close proximity to each other. There is no known Ca^{2+} pump to bring Ca^{2+} into

the nucleus as there is in the ER (Sarco/Endoplasmic Reticulum Ca^{2+}-ATPase; SERCA) as such, however this close proximity of the ER to the nucleus may help Ca^{2+} to enter the nucleus by through pores in the nuclear membrane or nuclear envelope. Research by Villalobos et al. [30], using bovine adrenal chromaffin cell and Ca^{2+} imaging examined the ER the uptake of Ca^{2+} mitochondria and nucleus in response to depolarizing stimulation. Neher and colleagues first described the idea that transient opening of Cavs during action potentials generate high Ca^{2+} transient microdomains near Cav channel pores [41]. These Ca^{2+} microdomains are focal to Ca^{2+} signaling being regulated both spatially and temporally as the Ca^{2+} rapidly diffuses to be adjacent cytosol. However due to Ca^{2+} entry into organelles such as mitochondria and their role to act as a delay barrier to buffer the Ca^{2+} waves, the Ca^{2+} transients can longer lasting. There are also Ca^{2+} binding proteins and buffers such as Calbindin that restrict Ca^{2+} transients [42].

It has been found in chromaffin cells, which rely very fast catecholamine release, that there is a very tightly controlled infrastructure of spatial-temporal organization of these Ca^{2+} transients so that the sustained Ca^{2+} entry via Cav channels can allow highly concentrated cytosolic Ca^{2+} microdomains that are high enough to trigger exocytosis. This complex and tightly controlled Ca^{2+} wave network expedites reactions to physiological changes. There is also evidence that these Ca^{2+} microdomains are essential in the interplay between these Ca^{2+} stores and sources in the organelles that is especially important for the chromaffin cell reserve pool of exocytotic vesicles [33] in order to respond quickly to physiological stimuli such as in the 'fight or flight' response [18, 30, 32].

Ca^{2+} Channels and Receptors

Voltage-gated Ca^{2+} channel (Cav)s are crucial components of excitable cells [43, 44]. The channel complexes have 3–4 subunits made up of pore forming α subunits, with auxiliary subunits β, $\alpha 2\delta$ and sometimes γ [38, 45]. The L, N and P/Q-subtypes of Cavs are subject to various forms of modulation including inhibition via G-Protein-Coupled Receptor (GPCR) signaling pathways [46]. The best studied is direct binding of G-proteins to Cav channels rendering them reluctant to open. This type of GPCR inhibition is relieved by applying a large depolarizing prepluse (i.e. +90 mV) and as such is called voltage-dependent inhibition [46, 47]. GPCR mediated Cav inhibition can also be relieved by affecting component(s) of the signaling pathway and there is a subsequent increase in the Ca^{2+} channel current. For example, application of antagonists to GPCRs at the top of this pathway will yield a Cav current increase [18, 48]. These GPCR pathways for Cav regulation are extensively studied in both neurons and neuroendocrine cells such as bovine adrenal chromaffin Cells [49–51]. Several types of Cavs, including L, N and P/Q-types, have been well characterized in bovine adrenal chromaffin cells [18, 39].

In chromaffin cells GPCR inhibition is controlled by an autocrine/paracrine feedback loop where cells undergoing exocytosis co-release ATP and opioids along

with catecholamines [18]. The ATP and opioids act on P2Y purinergic and μ- and δ-opioid receptors, which activate the GPCR pathway and inhibit N- and P/Q-type Cav channels. This voltage-independent inhibition [18, 52] of Ca^{2+} influx exerts a tonic regulation of neurotransmitter release that is insensitive to neuronal firing or depolarization. The voltage-independent pathway is dependent on Ca^{2+} as it is blocked by Ca^{2+} ion chelators [53]. The Ca^{2+} sensor NCS-1 has been shown to play a role in the voltage-independent inhibitory GPCR mediated-pathway in bovine adrenal chromaffin Cells [10, 12, 54, 55].

There is evidence that Ca^{2+} from intracellular stores and Ca^{2+} release activated currents (CRAC) have an important role in exocytosis in bovine adrenal chromaffin [56, 57] and are also key players in intracellular Ca^{2+} signaling [36].

Ca^{2+} Binding Proteins and/or Sensors

There are many Ca^{2+}-binding proteins that have been characterized in different cell types including bovine adrenal chromaffin cells [12, 58]. There is an important difference between Ca^{2+} binding proteins and Ca^{2+} sensing proteins. Some Ca^{2+} binding proteins bind Ca^{2+} but do not pass the signal on. They are mainly present to act as biological buffers [42] to control Ca^{2+} transients and microdomains [35]. In contrast to buffers, Ca^{2+} sensing proteins will bind Ca^{2+} and then undergo a conformational change to pass the signal on [59]. In this manner Ca^{2+} sensing proteins are signal transducers. For example when there is resting levels of Ca^{2+}, at approximately 100 μM, the Ca^{2+} sensing proteins would not have its Ca^{2+} binding domains fully bound to Ca^{2+} and would interact with a number of different signaling proteins. However when the Ca^{2+} levels increase, the Ca^{2+} sensor binds Ca^{2+} fully then undergoes a confirmation change, which can change its protein-protein interactions to some binding partners when the Ca^{2+} concentration is low as compared to different binding partners when Ca^{2+} is fully bound [10, 12, 60]. This could inhibit or enhance an activity depending on the concentration level of Ca^{2+}. The way Ca^{2+} sensing proteins respond when they bind Ca^{2+} is more complex than the Ca^{2+} buffers for example in the Neuronal Ca^{2+} sensor family, which is a subfamily of the CaM superfamily of EF-hand Ca^{2+} binding proteins, there is a Ca^{2+}-myristoyl-switch that occurs [61, 62]. Evidence for cooperative binding of to the EF-hands of the NCS family members involving the myristoyl group has been described and is especially interesting in regard to Ca^{2+} regulation of NCS-1 activity and how this influences its Ca^{2+}-dependent interactions with other signaling proteins [61, 63].

Recent studies have demonstrated that Calmodulin and other EF-hand Ca^{2+}-sensing proteins are involved in Cav modulation [55, 61]. NCS-1, a member of a family of myristoylated, EF-hand Ca^{2+} sensing proteins [62] plays an essential role in the tonic inhibition of P/Q channels in bovine adrenal chromaffin cells specifically in the voltage-independent pathway [10]. This pathway for autocrine inhibition requires exocytosis and relies on the activity of a Src-like kinase [54]. Calmodulin (CaM) has been shown to be important for the regulation of N-type

channels in bovine adrenal chromaffin cells. It was shown that there is differential regulation of Cav subtypes by CaM and that this impacts on the ability of these channels to regulate neurotransmitter release in chromaffin cells [64]. Ca^{2+} binding protein-1 (CaBP-1) has been shown to inhibit Cav channels and exocytosis in bovine adrenal chromaffin cells [65]. In addition Calneuron I has been show to also inhibit bovine N-type Cavs in chromaffin cells and its subcellular localization is important for this regulation [66].

Signaling Molecules

There are many signal transduction pathways that are activated with elevated Ca^{2+} levels. These Ca^{2+} activated signal transduction pathways can cross talk with each other and other signaling pathways. The main Ca^{2+} signal transduction pathways are: Phosphatidyl Inositol (PI)s, PhosphoLipase C (PLC), Inositol Triphosphate (IP3) pathway, Protein Kinase C (PKC) pathway, and Calmodulin(CaM)/Calmodulin Kinase II pathway. These signaling pathways can also crosstalk with GPCR signaling pathways such as Protein kinase A pathways and with Receptor Tyrosine Kinase (RTK) pathways [36].

Activation of GPCRs and their downstream signaling pathways can lead to activation of PLC, which cleaves DAG into PIP2 and IP3. IP3 can bind to receptors on the ER store and release internal Ca^{2+} into the surrounding area. PI signaling is important in exocytosis in bovine adrenal chromaffin cells [57, 67]. PIP2 itself is also a critical signaling molecule and has been shown to be vital not only to exocytosis in chromaffin cells [11] but also for the stability of Cav channels in the plasma membrane [12]. There are several IP3 receptor isoforms characterized in bovine adrenal chormaffin cells [68]. There is also some data that Store Operated Channels (SOC) or Ca^{2+} Activated Release Channels (CRAC) can also contribute to Ca^{2+} signals in bovine adrenal chromaffin cells [56]. IP3 receptors in chromaffin cells have been localized to the ER, nucleus and secretory granules. However the highest percentage of IP3 receptors are found on the secretory granules themselves (58–69%; [68]). Therefore there are two main sources of Ca^{2+} for Ca^{2+} signals in bovine adrenal chromaffin cells, (1) Entry of external Ca^{2+} via Ca^{2+} channels (Cavs or CRACs) and (2) internal Ca^{2+} release by the IP3 receptors located in the ER store and secretory granules. Since NCS-1 has been shown to regulate or interact with TRPC1/5 channels [12, 69] and is also a regulator of PIP2 levels there is ample opportunity for crosstalk between these signaling pathways in response to Ca^{2+} levels [12, 69].

Evidence for Ryanodine receptors and caffeine sensitive stores has also been found in both PC12 [21] and chromaffin [70, 71] cells. In Fig. 38.2 the main signaling pathways that are activated by Ca^{2+} or that use Ca^{2+} as an intracellular messenger are depicted (E.g. GPCR Signaling, PI/IP3 Signaling, PKC Signaling and crosstalk with RTKs). Only the main pathways are shown and the main receptors and channels types. GPCRs can regulate Cavs and activate Ca^{2+} release activated pathways

with IP3. These in turn stimulate SOC or CRAC channels. These pathways can converge with RTKs [8, 36]. Ca^{2+} sensors and buffers can regulate all of these pathways and link them to Ca^{2+} signaling pathways [42, 59].

Cellular Physiology of Ca^{2+} Signaling in Chromaffin Cells

Control of Neurite Outgrowth

Chromaffin cells like their cell line counter part PC12 cells can be treated with NGF or high K^+ to emit neurites [12, 20, 21, 69]. PC12 cells also have similar Ca^{2+} signaling mechanisms [72]. There is evidence in bovine adrenal chromaffin cells that Cavs are located in neurites and that exocytosis is important to the outgrowth process [20].

We have shown that a Ca^{2+} deficient mutant of NCS-1 NCS-1(E120Q) [10] is observed to translocate into the filopodia and lamellipodia region of both PC12 and bovine adrenal chromaffin cells when overexpressed with DNTRPC5 [69]. It is not apparently an overexpression effect as neither the overexpressed wild-type NCS-1/DNTRPC5 nor NCS-1 (E120Q)/wild- type TRPC5 combinations yielded the same staining pattern. To explain this phenomenon, we hypothesize that Ca^{2+} entry through TRPC5 channels is required when inhibition of neurite elongation is needed. When enhanced neurite outgrowth occurs due to DNTRPC5, more TRPC5 channels are required to insert into the growth cone filopodia and lamellipodia regions. Therefore the NCS-1(E120Q) bound to the TRPC5 channels are enriched in the same locations. In the experimental groups where wild-type NCS-1 was co-expressed with DNTRPC5 or NCS-1 (E120Q) with TRPC5 are co-expressed, the neurite elongation effect was rescued and therefore, there was no translocation for the NCS-1-TRPC5 complex. Similar results were obtained in transfected chromaffin cells differentiated by NGF or K^+ depolarization [12]. We also speculate that TRPC and Cavs signaling may crosstalk in order to help regulate neurite outgrowth [12].

Control of Secretion

Exocytosis and its control by Ca^{2+} has been and still is a controversial and extensively studied subject in neurons and in chromaffin cells [18, 19]. The SNARE complex forms the directly exocytotic machinery, which is brought into close proximity to Cav channels and sources of Ca^{2+} entry in order to tightly control exocytotic vesicle fusion with the plasma membrane [18]. The cell cytoskeletal network is thought to play a crucial role in this process [73] and is essential for vesicle docking [74].

There is much debate over the existence and Ca^{2+}–dependence of different exocytotic vesicle pools and this continues to be an extremely active area of study [75]. Which Ca^{2+}-sensors and proteins contained within and outside the SNARE complex that regulate this exocytotic vesicle docking is not well understood [76, 77]. Nevertheless Sec1/Munc18 proteins are thought to have an important role in this process [78]. Detailed mechanisms of Ca^{2+} evoked release in bovine adrenal chromaffin cells have been well reviewed elsewhere [18, 73].

Role in the Stress Response

Corticosteroids have many roles in physiology including the regulation of sex hormones, ion balance, and the long-term stress response. There are three main stages of stress after a stress-inducing situation, real or perceived, is encountered. (1) Activation of the 'fight or flight' response for the short-term stress response, (2) Circulating levels of corticosteroids inhibit the immune system in the long-term stress response and (3) Homeostatic mechanisms attempt to restore the body back to the pre-stress state. The long-term stress response is activated by Adrenocorticotropic hormone (ACTH) coming from the anterior pituitary gland (via hypothalamic control) and is mediated by glucocorticoids released by the adrenal cortex [79].

This chapter focuses on the adrenal medulla chromaffin cells, which secrete epinephrine and norepinephrine that mediate the short-term stress response. Epinephrine and noreepinephrine mediate the short-term stress response via endocrine release by binding to receptors located in cells in many target organs of the body. This allows many simultaneous physiological responses to occur by speeding up metabolism, increasing mental alertness, to quickly make a decision to 'fight or flight', both breathing and heart rate increase and there is a dilation of blood vessels. The continued release of catecholamines sustain this sympathetic nervous system response [15, 79].

The role of Cavs and their regulation in the 'fight or flight' response has been reviewed elsewhere [17]. This chapter will focus on the role of acetylcholine (Ach) release onto chromaffin cell of the adrenal medulla and Ca^{2+} entry into chromaffin cells and subsequent secretion of catecholamines crucial to the stress response (Fig. 38.3).

Ach Secretion and Ca^{2+}

Ach is released at the splanchnic nerve terminal-chromaffin cell synapses due to the incoming action potentials arising from the nerve impulses initiated in the hypothalamus ([15, 79]; Fig. 38.3). Ach released from the splanchnic nerve, which terminates (axons of preganglion nerves) with chromaffin cells in the adrenal medulla, acts on act on both nicotinic and muscarinic Ach receptors. Activation of nicotinic

Ach receptors in bovine adrenal chromaffin cells leads to an increase from resting levels of Ca^{2+} at approximately 100 μM to as high as 10,000 μM while activation of muscarinc Ach receptors leads to a doubling of resting Ca^{2+} levels ([16, 67, 80]; Figs. 38.1 and 38.3). There is also some evidence that there may be differential expression of nicotinic and muscarinic Ach receptors on adrenal chromaffin cells and that this is linked to epinerphrine versus norepinephrine secreting chromaffin cells [81]. Action potentials are elcited in chromaffin cells via Ach acting on its receptors and this is thought to cause depolarizations which open Cav channels [15]. There are elevated Ca^{2+} levels via this Ca^{2+} entry through Cavs, which increase concentration near the mouth of the channel up to 10,000 μM. This rise in Ca^{2+} stimulates exocytotic vesicles to fuse and dock with the plasma membrane to secrete epinephrine and norepinephrine, which then go into the blood stream to 'rev-up' the sympathetic nervous system [15] to prepare to 'fight or flight'.

Summary and Conclusions

Bovine adrenal chromaffin cells are excellent models for signaling and exocytosis-giving clues to mechanisms of neurotransmitter release in neurons and helping us to further understand the cellular physiology of the short-term stress response. However more physiologically relevant studies may be achieved by comparing their cellular mechanisms of cultured chromaffin cells to adrenal gland slices [15].

Acknowledgements This author is very grateful to Chris North for his help with the figures.

References

1. Hamill OP, Marty A, Neher E, Sakmann B, Sigworth FJ (1981) Improved patch-clamp techniques for high-resolution current recording from cells and cell-free membrane patches. Pflugers Arch 391:85–8100
2. Sakmann B, Neher E (1984) Patch clamp techniques for studying ionic channels in excitable membranes. Annu Rev Physiol 46:455–472
3. Neher E, Sakmann B (1992) The patch clamp technique. Sci Am 266:44–51
4. Carmichael SW, Winkler H (1985) The adrenal chromaffin cell. Sci Am 253:40–49
5. Burgoyne RD (1991) Control of exocytosis in adrenal chromaffin cells. Biochim Biophys Acta 1071:174–202
6. Morgan A, Burgoyne RD (1997) Common mechanisms for regulated exocytosis in the chromaffin cell and the synapse. Semin Cell Dev Biol 8:141–149
7. O'Connor DT, Mahata SK, Mahata M, Jiang Q, Hook VY, Taupenot L (2007) Primary culture of bovine chromaffin cells. Nat Protoc 2:1248–1253
8. Berridge MJ, Lipp P, Bootman MD (2000) The versatility and universality of calcium signalling. Nat Rev Mol Cell Biol 1:11–21
9. McFerran BW, Graham ME, Burgoyne RD (1998) Neuronal Ca2+ sensor 1, the mammalian homologue of frequenin, is expressed in chromaffin and PC12 cells and regulates neurosecretion from dense-core granules. J Biol Chem 273:22768–22772

10. Weiss JL, Archer DA, Burgoyne RD (2000) Neuronal Ca2+ sensor-1/frequenin functions in an autocrine pathway regulating Ca2+ channels in bovine adrenal chromaffin cells. J Biol Chem 275:40082–40087
11. Pan C-Y, Jeromin A, Lundstrom K, Yoo SH, Roder J, Fox AP (2002) Alterations in exocytosis induced by neuronal Ca2+ sensor-1 in bovine chromaffin cells. J Neurosci 22:2427–2433
12. Weiss JL, Hui H, Burgoyne RD (2010) Neuronal calcium sensor-1 regulation of calcium channels, secretion, and neuronal outgrowth. Cell Mol Neurobiol 30:1283–1292
13. Quesada E, Sogorb MA, Vilanova E, Carrera V (2004) Bovine chromaffin cell cultures as model to study organophosporus neurotoxicity. Toxicol Lett 151:163–170
14. Goldberg AM, Zurlo J, Rudacille D (1996) The three Rs and biomedical research. Science 272:1403
15. de Diego AM, Gandia L, Garcia AG (2008) A physiological view of the central and peripheral mechanisms that regulate the release of catecholamines at the adrenal medulla. Acta Physiol (Oxf) 192:287–301
16. de Diego AM (2010) Electrophysiological and morphological features underlying neurotransmission efficacy at the splanchnic nerve-chromaffin cell synapse of bovine adrenal medulla. Am J Physiol Cell Physiol 298:C397–C405
17. Fuller MD, Emrick MA, Sadilek M, Scheuer T, Catterall WA (2010) Molecular mechanism of calcium channel regulation in the fight-or-flight response. Sci Signal 3:ra70
18. Garcia AG, Garcia-De-Diego AM, Gandia L, Borges R, Garcia-Sancho J (2006) Calcium signaling and exocytosis in adrenal chromaffin cells. Physiol Rev 86:1093–1131
19. Mustafa T (2010) Secretion mechanisms. Cell Mol Neurobiol 30:1293–1294
20. Gil A, Viniegra S, Neco P, Gutierrez LM (2001) Co-localization of vesicles and P/Q Ca2+−channels explains the preferential distribution of exocytotic active zones in neurites emitted by bovine chromaffin cells. Eur J Cell Biol 80:358–365
21. Greene LA, Tischler AS (1976) Establishment of a noradrenergic clonal line of rat adrenal pheochromocytoma cells which respond to nerve growth factor. Proc Natl Acad Sci USA 73:2424–2428
22. Schumm MA, Castellanos DA, Frydel BR, Sagen J (2004) Improved neural progenitor cell survival when cografted with chromaffin cells in the rat striatum. Exp Neurol 185:133–142
23. Hanke M, Farkas LM, Jakob M, Ries R, Pohl J, Sullivan AM (2004) Heparin-binding epidermal growth factor-like growth factor: a component in chromaffin granules which promotes the survival of nigrostriatal dopaminergic neurones in vitro and in vivo. Neuroscience 124:757–766
24. Ehrhart-Bornstein M, Vukicevic V, Chung K-F, Ahmad M, Bornstein SR (2010) Chromaffin progenitor cells from the adrenal medulla. Cell Mol Neurobiol 30:1417–1423
25. Berridge MJ (1998) Neuronal calcium signaling. Neuron 21:13–26
26. Giovannucci DR, Hlubek MD, Stuenkel EL (1999) Mitochondria regulate the Ca(2+)-exocytosis relationship of bovine adrenal chromaffin cells. J Neurosci 19:9261–9270
27. Montero M, Alonso MT, Carnicero E, Cuchillo-Ibanez I, Albillos A, Garcia AG, Garcia-Sancho J, Alvarez J (2000) Chromaffin-cell stimulation triggers fast millimolar mitochondrial Ca2+ transients that modulate secretion. Nat Cell Biol 2:57–61
28. Hernandez-Guijo JM, Maneu-Flores VE, Ruiz-Nuno A, Villarroya M, Garcia AG, Gandia L (2001) Calcium-dependent inhibition of L, N, and P/Q Ca2+ channels in chromaffin cells: role of mitochondria. J Neurosci 21:2553–2560
29. Echevarria W, Leite MF, Guerra MT, Zipfel WR, Nathanson MH (2003) Regulation of calcium signals in the nucleus by a nucleoplasmic reticulum. Nat Cell Biol 5:440–446
30. Villalobos C, Nunez L, Montero M, Garcia AG, Alonso MT, Chamero P, Alvarez J, Garcia-Sancho J (2002) Redistribution of Ca2+ among cytosol and organella during stimulation of bovine chromaffin cells. FASEB J 16:343–353
31. Gerasimenko O, Gerasimenko J (2004) New aspects of nuclear calcium signalling. J Cell Sci 117:3087–3094
32. Alonso MT, Villalobos C, Chamero P, Alvarez J, Garcia-Sancho J (2006) Calcium microdomains in mitochondria and nucleus. Cell Calcium 40:513–525

33. Garcia-Sancho J, Verkhratsky A (2008) Cytoplasmic organelles determine complexity and specificity of calcium signalling in adrenal chromaffin cells. Acta Physiol (Oxf) 192:263–271
34. Dolman NJ, Tepikin AV (2006) Calcium gradients and the Golgi. Cell Calcium 40:505–512
35. Berridge MJ (2006) Calcium microdomains: organization and function. Cell Calcium 40:405–412
36. Nowycky MC, Thomas AP (2002) Intracellular calcium signaling. J Cell Sci 115:3715–3716
37. Cheek TR (1989) Spatial aspects of calcium signalling. J Cell Sci 93(Pt 2):211–216
38. Catterall WA (2011) Voltage-gated calcium channels. Cold Spring Harb Perspect Biol 3:a003947
39. Fox AP, Cahill AL, Currie KPM, Grabner C, Harkins AB, Herring B, Hurley JH, Xie Z (2008) N- and P/Q-type Ca2+ channels in adrenal chromaffin cells. Acta Physiol (Oxf) 192:247–261
40. Augustine GJ, Neher E (1992) Calcium requirements for secretion in bovine chromaffin cells. J Physiol 450:247–271
41. Neher E, Augustine GJ (1992) Calcium gradients and buffers in bovine chromaffin cells. J Physiol 450:273–301
42. Schwaller B (2010) Cytosolic Ca2+ buffers. Cold Spring Harb Perspect Biol 2:a004051
43. Minor DL Jr, Findeisen F (2010) Progress in the structural understanding of voltage-gated calcium channel (CaV) function and modulation. Channels (Austin) 4:459–474
44. Nakao A, Takada Y, Mori Y (2011) Calcium channels regulate neuronal function, gene expression, and development. Brain Nerve 63:657–667
45. Dolphin AC (2009) Calcium channel diversity: multiple roles of calcium channel subunits. Curr Opin Neurobiol 19:237–244
46. Dolphin AC (2003) G protein modulation of voltage-gated calcium channels. Pharmacol Rev 55:607–627
47. Zhang Y, Chen YH, Bangaru SD, He L, Abele K, Tanabe S, Kozasa T, Yang J (2008) Origin of the voltage dependence of G-protein regulation of P/Q-type Ca2+ channels. J Neurosci 28:14176–14188
48. Dolphin AC (1998) Mechanisms of modulation of voltage-dependent calcium channels by G proteins. J Physiol 506(Pt 1):3–11
49. Currie KP (2010) Inhibition of Ca2+ channels and adrenal catecholamine release by G protein coupled receptors. Cell Mol Neurobiol 30:1201–1208
50. Currie KP (2010) G protein modulation of CaV2 voltage-gated calcium channels. Channels (Austin) 4:497–509
51. Currie KP, Fox AP (2000) Voltage-dependent, pertussis toxin insensitive inhibition of calcium currents by histamine in bovine adrenal chromaffin cells. J Neurophysiol 83:1435–1442
52. Currie KP, Fox AP (1997) Comparison of N- and P/Q-type voltage-gated calcium channel current inhibition. J Neurosci 17:4570–4579
53. Beech DJ, Bernheim L, Mathie A, Hille B (1991) Intracellular Ca2+ buffers disrupt muscarinic suppression of Ca2+ current and M current in rat sympathetic neurons. Proc Natl Acad Sci USA 88:652–656
54. Weiss JL, Burgoyne RD (2001) Voltage-independent inhibition of P/Q-type Ca2+ channels in adrenal chromaffin cells via a neuronal Ca2+ sensor-1-dependent pathway involves Src family tyrosine kinase. J Biol Chem 276:44804–44811
55. Weiss JL, Burgoyne RD (2002) Sense and sensibility in the regulation of voltage-gated Ca(2+) channels. Trends Neurosci 25:489–491
56. Fomina AF, Nowycky MC (1999) A current activated on depletion of intracellular Ca2+ stores can regulate exocytosis in adrenal chromaffin cells. J Neurosci 19:3711–3722
57. Pan CY, Fox AP (2000) Rundown of secretion after depletion of intracellular calcium stores in bovine adrenal chromaffin cells. J Neurochem 75:1132–1139
58. McCue HV, Haynes LP, Burgoyne RD (2010) The diversity of calcium sensor proteins in the regulation of neuronal function. Cold Spring Harb Perspect Biol 2:1–20
59. Krebs J, Heizmann CW (2007) Calcium-binding proteins and the EF-hand principle. pp 51–93, in Calcium: a matter of life or death, edited by Joachim Krebs, Marek Michalak. 1st ed. Amsterdam ; Oxford : Elsevier, 2007. (Series: New comprehensive biochemistry; v. 41)

60. McFerran BW, Weiss JL, Burgoyne RD (1999) Neuronal Ca(2+) sensor 1. Characterization of the myristoylated protein, its cellular effects in permeabilized adrenal chromaffin cells, Ca(2+)-independent membrane association, and interaction with binding proteins, suggesting a role in rapid Ca(2+) signal transduction. J Biol Chem 274:30258–30265
61. Burgoyne RD (2007) Neuronal calcium sensor proteins: generating diversity in neuronal Ca2+ signalling. Nat Rev Neurosci 8:182–193
62. Burgoyne RD, Weiss JL (2001) The neuronal calcium sensor family of Ca2+–binding proteins. Biochem J 353:1–12
63. Lim S, Strahl T, Thorner J, Ames JB (2011) Structure of a Ca2+–myristoyl switch protein that controls activation of a phosphatidylinositol 4-kinase in fission yeast. J Biol Chem 286:12565–12577
64. Wykes RCE, Bauer CS, Khan SU, Weiss JL, Seward EP (2007) Differential regulation of endogenous N- and P/Q-type Ca2+ channel inactivation by Ca2+/calmodulin impacts on their ability to support exocytosis in chromaffin cells. J Neurosci 27:5236–5248
65. Chen M-L, Chen Y-C, Peng IW, Kang R-L, Wu M-P, Cheng P-W, Shih P-Y, Lu L-L, Yang C-C, Pan C-Y (2008) Ca2+ binding protein-1 inhibits Ca2+ currents and exocytosis in bovine chromaffin cells. J Biomed Sci 15:169–181
66. Shih P-Y, Lin C-L, Cheng P-W, Liao J-H, Pan C-Y (2009) Calneuron I inhibits Ca(2+) channel activity in bovine chromaffin cells. Biochem Biophys Res Commun 388:549–553
67. Forsberg EJ, Rojas E, Pollard HB (1986) Muscarinic receptor enhancement of nicotine-induced catecholamine secretion may be mediated by phosphoinositide metabolism in bovine adrenal chromaffin cells. J Biol Chem 261:4915–4920
68. Huh YH, Yoo JA, Bahk SJ, Yoo SH (2005) Distribution profile of inositol 1,4,5-trisphosphate receptor isoforms in adrenal chromaffin cells. FEBS Lett 579:2597–2603
69. Hui H, McHugh D, Hannan M, Zeng F, Xu S-Z, Khan S-U-H, Levenson R, Beech DJ, Weiss JL (2006) Calcium-sensing mechanism in TRPC5 channels contributing to retardation of neurite outgrowth. J Physiol 572:165–172
70. Bennett DL, Bootman MD, Berridge MJ, Cheek TR (1998) Ca2+ entry into PC12 cells initiated by ryanodine receptors or inositol 1,4,5-trisphosphate receptors. Biochem J 329(Pt 2): 349–357
71. Santodomingo J, Vay L, Camacho M, Hernandez-Sanmiguel E, Fonteriz RI, Lobaton CD, Montero M, Moreno A, Alvarez J (2008) Calcium dynamics in bovine adrenal medulla chromaffin cell secretory granules. Eur J Neurosci 28:1265–1274
72. Duman JG, Chen L, Hille B (2008) Calcium transport mechanisms of PC12 cells. J Gen Physiol 131:307–323
73. Torregrosa-Hetland CJ, Villanueva J, Lopez-Font I, Garcia-Martinez V, Gil A, Gonzalez-Velez V, Segura J, Viniegra S, Gutierrez LM (2010) Association of SNAREs and calcium channels with the borders of cytoskeletal cages organizes the secretory machinery in chromaffin cells. Cell Mol Neurobiol 30:1315–1319
74. de Wit H (2010) Molecular mechanism of secretory vesicle docking. Biochem Soc Trans 38:192–198
75. Alvarez YD, Marengo FD (2011) The immediately releasable vesicle pool: highly coupled secretion in chromaffin and other neuroendocrine cells. J Neurochem 116:155–163
76. Burgoyne RD, Morgan A (1998) Calcium sensors in regulated exocytosis. Cell Calcium 24:367–376
77. Burgoyne RD, Morgan A (2003) Secretory granule exocytosis. Physiol Rev 83:581–632
78. Burgoyne RD, Morgan A (2007) Membrane trafficking: three steps to fusion. Curr Biol 17:255–258
79. Tortora GJ, Derrickson BH (2009) Principles of Anatomy and Physiology. 12th Edition, John Wiley and Sons, Hoboken, New Jersey
80. Kao LS, Schneider AS (1986) Calcium mobilization and catecholamine secretion in adrenal chromaffin cells. A Quin-2 fluorescence study. J Biol Chem 261:4881–4888
81. Zaika OL, Pochynyuk OM, Kostyuk PG, Yavorskaya EN, Lukyanetz EA (2004) Acetylcholine-induced calcium signalling in adrenaline- and noradrenaline-containing adrenal chromaffin cells. Arch Biochem Biophys 424:23–32

Chapter 39
Calcium Stores in Vertebrate Photoreceptors

David Križaj

Abstract This review lays out the emerging evidence for the fundamental role of Ca^{2+} stores and store-operated channels in the Ca^{2+} homeostasis of rods and cones. Calcium-induced calcium release (CICR) is a major contributor to steady-state and light-evoked photoreceptor Ca^{2+} homeostasis in the darkness whereas store-operated Ca^{2+} channels play a more significant role under sustained illumination conditions. The homeostatic response includes dynamic interactions between the plasma membrane, endoplasmic reticulum (ER), mitochondria and/or outer segment disk organelles which dynamically sequester, accumulate and release Ca^{2+}. Coordinated activation of SERCA transporters, ryanodine receptors (RyR), inositol triphosphate receptors (IP3Rs) and TRPC channels amplifies cytosolic voltage-operated signals but also provides a memory trace of previous exposures to light. Store-operated channels, activated by the STIM1 sensor, prevent pathological decrease in $[Ca^{2+}]i$ mediated by excessive activation of PMCA transporters in saturating light. CICR and SOCE may also modulate the transmission of afferent and efferent signals in the outer retina. Thus, Ca^{2+} stores provide additional complexity, adaptability, tuneability and speed to photoreceptor signaling.

Keywords Calcium store • Light • Photoreceptor • Retina • Ryanodine receptor

Introduction

Visual behavior in diurnal vertebrates is guided by two classes of retinal photoreceptor. Rods subserve highly sensitive black-and-white vision at starlight and moonlight whereas daytime vision is mediated by cones which provide color vision and

D. Križaj (✉)
Department of Ophthalmology and Visual Sciences, John A. Moran Eye Center, University of Utah School of Medicine, Salt Lake City, UT 84132, USA
e-mail: david.krizaj@hsc.utah.edu

M.S. Islam (ed.), *Calcium Signaling*, Advances in Experimental Medicine and Biology 740, DOI 10.1007/978-94-007-2888-2_39,

spatial resolution. As is the case with all primary sensory neurons, both photoreceptor cell types are compartmentalized into input (outer segment, OS) and output domains that are distinct in terms of anatomy, physiology, molecular composition and ion homeostasis. The distinguishing characteristic of photoreceptor signaling is that release of the neurotransmitter glutamate occurs in the absence of external input (light) whereas absorption of photons in the OS elicits an intensity-dependent decrease in exocytosis. Signaling mechanisms that affect photoreceptor $[Ca^{2+}]i$ levels inevitably modulate retinal output and perception of light by regulating light adaptation, gene expression, metabolic function and transmitter release in rods and cones. In particular, Ca^{2+} release from internal stores has been shown in recent years to modulate tonic signaling at photoreceptor synapses in a manner that is unparalleled in the CNS (reviewed in [32, 53, 96]). Ca^{2+} release from ER stores has a profound and non-redundant role in sustaining neurotransmitter release in darkness [52, 90] whereas light causes closure of voltage-operated Ca channels, resulting in depletion of Ca^{2+} stores in the endoplasmic reticulum (ER). The resultant influx of Ca^{2+} through store-operated channels (SOCs) replenishes the stores but may also modulate synaptic transmission [94]. By dynamically regulating release and sequestration of Ca^{2+} and activation of SOCs, Ca^{2+} stores control the amplitude, response speed and sensitivity of photoreceptor signals [12, 90, 95]. Critical for photoreceptor cell health, ER and mitochondrial stores also maintain proper basal calcium levels within photoreceptor cytosol [4, 5, 92]. This essay reviews the current information regarding how Ca^{2+}stores participate in and maintain Ca^{2+} homeostasis, cellular adaptation and synaptic function.

Photoreceptor Ultrastructure Is Designed for Local Ca^{2+} Store Signaling

The ultrastructure of rod and cone photoreceptors follows the general design of primary sensory neurons. A vertebrate photoreceptor cell is constructed of two separate anatomical/functional compartments that process signal input and output, respectively (Fig. 39.1). An “outer segment” (OS) is uniquely designed to carry out transduction of the photon energy into an electrical signal, whereas the downstream “inner” regions host transcriptional, translational, metabolic and synaptic functions. Rod OSs differ from cone OSs in that they are tightly packed with hundreds of membrane sacs (“disks”), rather mysterious organelles spaced at ~0.3 nm that contain a high density of the visual pigment opsin ([8, 70]; Fig. 39.1a). The inner photoreceptor region consist of ellipsoid, subellipsoid and cell body domains connected to a synaptic terminal through a short but thick axon (Fig. 39.1). Unless otherwise indicated, the cell compartment downstream from the outer segment will be referred to as the “inner segment (IS)”.

The OS and IS compartments are separated by a thin nonmotile cilium which represents a bottleneck for diffusion of ions and molecules but also supports

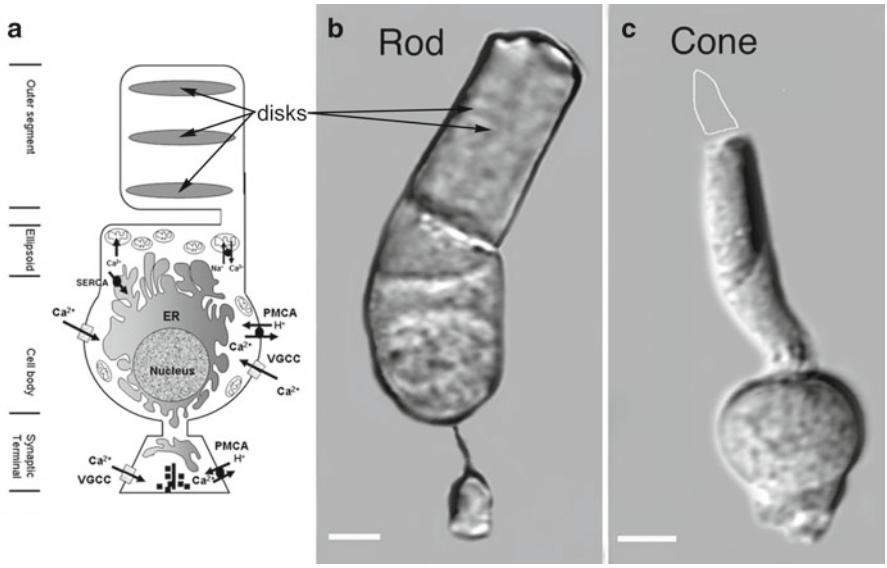

Fig. 39.1 (**a**) Schematized generic rod photoreceptor. The outer segment (OS) is filled with stacked disk organelles (*arrows*) containing the visual pigment rhodopsin. The inner segment (IS) downstream from the OS is formed by three anatomically distinct domains: (i) ellipsoid, which contains most of cell's mitochondria; (ii) the cell body, which contains the cell nucleus, nuclear envelope formed by the ER cisternae and (iii) the synaptic terminal, packed with synaptic vesicles and cisternae of smooth ER. (**b**) Dissociated salamander rod and (**c**) Salamander cone photoreceptor. Abbreviations: *PMCA* plasma membrane Ca^{2+}ATP-ase, *CaBP4* calcium binding protein isoform 4, *IP3R* IP3 receptor, *RyR* ryanodine receptor, *SERCA* sarcoplasmic-endoplasmic reticulum Ca^{2+} ATPase, *VGCC* voltage-gated channel, *ER* endoplasmic reticulum, Ca^{2+} sequestration and release from the mitochondria occurs via Ca^{2+} uniporter channels and Na^{+}/Ca^{2+} transporters, respectively. Scale bars = 5 mm

continuous translocation of proteins and lipids into the OS via specialized dynein/kinesin motors and Ca^{2+} buffers such as centrin, calmodulin, kinesin II, unc117 and myosin VII (e.g., [61, 106]). The ellipsoid region represents the cell's powerhouse with up to 80% of its overall volume filled with mitochondria [34, 70, 76]. In some species (such as mouse), mitochondria are also found in synaptic terminals where they may occupy up to 25% of the volume [42]. The subellipsoid region near the perikaryon contains rough ER sacs and tubules which extend into the smooth ER that spans the entire IS (including the synaptic terminal) but does not enter the OS [66]. Transitional smooth ER, localized close to the Golgi apparatus in the subellipsoid space, regulates the incessant trafficking of proteins into the OS. Proximal to the inner segment is the perikaryon composed of the nucleus surrounded by ER-like membranes. The synaptic region also contains copious smooth ER tubules and sacs [66], which may play a role in the presynaptic synthesis of proteins (e.g., [29]) and transmitter release (see below).

Brief Overview of Ca Homeostasis in Photoreceptors

Calcium regulation lies at the heart of photoreceptor signaling. The spatiotemporal properties of Ca^{2+} signals in rods and cones are specific to each subcellular location and are markedly influenced by light/dark adaptation and metabolic status of the cell. In turn, changes in $[Ca^{2+}]i$ spanning ~10–25-fold dynamic range play a key role in the biological regulation of these processes that include phototransduction, energy metabolism, cytoskeletal dynamics and transmitter release (reviewed in [23, 32, 93, 96]). The peculiar feature of photoreceptor signaling is that "resting" $[Ca^{2+}]i$ levels are high in darkness (estimated at ~300–700 nM) whereas the encoding of light is associated with a decrease in $[Ca^{2+}]i$ (to ~5–50 nM; [81]). The functional separation between input and output regions is mirrored by molecular separation between different types of plasma membrane and intracellular store transporters and ion channels (Križaj and Copenhagen, 1998; 2002). These impart domain-specific amplitude and frequency modulation of light-evoked $[Ca^{2+}]i$ levels with voltage-sensitivity, Ca^{2+} affinities, transport and modulation properties particular to each segment. The quasi-independent regulation of Ca influx and clearance allows for specific tuning a wide array of Ca^{2+} signaling systems that use sensors with differing affinities (Križaj and Copenhagen, 1998; [93]).

The Outer Segment

The sole function of the outer segment is to intercept photons and transduce photon energy into graded changes in the membrane potential. The OS possesses a single plasma membrane Ca^{2+} entry pathway (the cGMP-gated [CNG] channel) and one Ca^{2+} clearance pathway, the Na, K^+-Ca^{2+} exchanger [NKCX] driven by combined Na^+ and K^+ gradients (NCKX1 in rods; NCKX2 in cones) [45, 69, 73]. In darkness, $[Ca^{2+}]i$ is high due to sustained cation influx through CNG channels which are regulated by the dynamic equilibrium between cGMP synthesis and hydrolysis. Because both cation influx through CNG channels and cGMP synthesis are directly suppressed by Ca^{2+}, light-regulated $[Ca^{2+}]i$ levels in the OS are essential for the ability of rods and cones to adapt to ambient light levels [23, 45, 102].

Using suction electrodes, Matthews and Fain [63] observed that the outer segment Ca^{2+} concentration in salamander rods was strictly proportional to the Ca^{2+} flux across the OS plasma membrane. There was no evidence of contributions from IP3-sensitive stores, leading them to conclude that intracellular compartments (i.e., disks) do not contribute to light-evoked changes in $[Ca^{2+}]_{OS}$. Despite the negative findings obtained through mostly electrophysiological means [41, 63], the exclusivity of the CNGC/NKCX mechanism has been challenged by biochemical and molecular data accumulated over the past 30 years. ROS disks were suggested to be close to impermeable in the darkness [109]. Early studies showed that disks are capable of accumulating significant amounts of Ca^{2+} [21, 44, 84] which was released in response to light. More recently, light was shown to *increase* cytosolic

$[Ca^{2+}]_{OS}$ in rods and cones by releasing as much as 10–50 μM Ca^{2+} per liter tissue volume from some type of still uncharacterized buffer or store [10, 62, 63]. This phenomenon was sensitive to BAPTA and depletion of Ca^{2+} from intracellular storage sites. Although the intensity of light required to induce it was too strong to regulate physiological rod $[Ca^{2+}]_{OS}$, the mechanism could be more physiologically relevant for cones as it occurs at intensities that bleach only a few percent of the cone photopigment [10, 15]. Its independence of photochannel-mediated influx and cone phototransduction argues for the presence of a new signaling mechanism that could be associated with a new buffer site or store but is also likely to involve Ca^{2+} diffusion from mitochondrial stores within the adjacent ellipsoid.

Schnetkamp [84] estimated that the intradiskal $[Ca^{2+}]$i is ~3 orders of magnitude higher than in the cytosol (15–25 μM) with a capacity of 8–9 Ca^{2+} binding sites per rhodopsin molecule. This was confirmed by the Koutalos group which used fluorescent Ca^{2+} and pH dyes to measure $[Ca^{2+}]$i and pH within the intradiskal space. They found that concentrations of these two ions differ markedly from cytosolic and extracellular $[Ca^{2+}]$ and pH values with high intradiskal $[Ca^{2+}]$ at an acidic pH of 6.5 [13, 56]. Thus, with respect to Ca^{2+} and proton regulation, disks may not act as passive sacs but rather comprise an active cellular organelle. While the molecular identity of putative disk Ca^{2+} sequestration and release mechanisms has not been determined, circumstantial evidence has implicated ryanodine receptor, IP3 receptor and/or SERCA mechanisms ([20, 86, 87, 101]; but see [15, 41, 63]). Biochemical studies have suggested that Ca^{2+} fluxes into the disks might be driven by a SERCA-like Ca^{2+} pump [18, 75, 87]. Conversely, cADPR, a known physiological activator of ryanodine receptor (RyR) channels, evoked Ca^{2+} release from suspensions of osmotically intact disks prepared from bovine ROS; ADPR cyclase activity was detected in disk, but not cytosolic ROS fraction [20]. Finally, isolated disks contain a protein with high molecular weight similar to RyRs (~520 kDa; [119]) whereas RyR1 was localized to the disk rim using antibody staining and electron microscopy [87]. Taken together, these findings suggest that rod disks express the typical ER-like Ca^{2+} signaling arrangement possibly associated with SERCA3 and RyR1 [51, 87].

Another unresolved issue pertains to the role of phospholipase C (PLC) signaling in the OS. Phospholipase C plays a key role in Ca signaling through its hydrolysis of the membrane phospholipid phosphatidylinositol 4,5-biphosphate (PIP_2) to inositol 1,4,5-triphosphate (IP3; an agonist of IP3 receptors) and diacylglycerol (DAG; an activator of protein kinase C and TRPC3/6/7 channels). The enzyme has been localized to OSs membranes with molecular, biochemical, physiological and genetic approaches. PLCβ4 and/or PLCγ1 activity was observed in rod disks and the plasma membrane ([27, 28]; Gehm et al., 1992), apparently under control of light ([31]; [118]; [28]), visual pigment [11] and Ca^{2+} [25]. Activation of PLCβ4 triggered Ca^{2+} release from bovine OS membranes [44, 84]. PLCβ4 was proposed to colocalize with $G_{\alpha q11}$ [74]. Consistent with such an arrangement, PLC function in light-activated ROS was suppressed by addition of GTPγS [114]. While a number of studies suggested that light activates PLC in parallel to transducin activation and cGMP hydrolysis ([26]; 1985; [108] 1987; [43]; [118]; [48]), the physiological function of such a mechanism in the OS is completely unknown. A potential clue may originate in

measurements of light responses from PLCβ4 knockout mice which showed that the a-wave component of the ERG (thought to reflect the compound light response of retinal photoreceptors) is four times smaller in knockout eyes than in wild type eyes [40]. Taken together, biochemical studies seem to argue that rod OSs are capable of sequestering and releasing Ca^{2+}, however, this process may only be detected under appropriate experimental conditions that preclude dialysis of cytosol with patch pipettes (e.g., [41]).

The Cilium and the Ellipsoid

From the viewpoint of Ca^{2+} and pHi regulation, the outer and inner segment compartments are separated by a ciliary barrier that limits diffusion of H^+, Ca^{2+} and cGMP [46]. A patch pipette filled with cGMP, when applied to the inner segment, is not very effective in increasing the concentration of cGMP and the photocurrent in the outer segment, in contrast to patched OSs when whole cell mode can sustain cGMP-induced currents of >1 nA for up top 30 min [112]. Likewise, linescan confocal imaging showed that large-scale Ca^{2+} release from internal stores in the rod IS does not affect Ca^{2+} signals in the OS [54]. It remains to be seen whether diffusion diffusion of Ca^{2+} across the cilium plays a greater role in intact tissue undergoing light–dark transitions.

The gatekeeper for Ca^{2+} diffusion across the cilium are the ellipsoid mitochondria. These organelles, which generate ATP required to drive the circulating dark current, possess a remarkable capacity for Ca^{2+} sequestration [92] which serves to protect the gain control mechanisms in the OS from interference by Ca^{2+} fluxes in the IS. On the other hand, it is not inconceivable that these mitochondria represent a releasable Ca^{2+} store that liberates Ca^{2+} in response to light (e.g., [15]).

ER Ca^{2+} Stores in the IS

Photoreceptor ER is a continuous, dynamic, constantly rearranging network of smooth cisternae that extend from the synaptic terminal to the subellipsoid space. This multifunctional organelle represents the site of synthesis and proper folding of newly synthesized proteins, phospholipids and glucosylphosphatidylinositols as well as a graveyard for unwanted molecules and toxins ([35, 64]; [121]). In addition, ER cisternae contain the highest intracellular Ca^{2+} content in photoreceptor cells [89, 98, 99], consistent with their function as a cellular Ca^{2+} reservoir that represents the second line of defense, after the cytosolic buffer proteins, against pathologically high or low $[Ca^{2+}]i$ [93].

ATP-dependent Ca^{2+} uptake into IS ER [99] is mediated by the SERCA (sarco-endoplasmic reticulum calcium ATPase) family mostly represented by the SERCA isoform 2 [2, 50, 51]. SERCA2 (Kd ~ 0.7 μM) shares Ca^{2+} clearance from

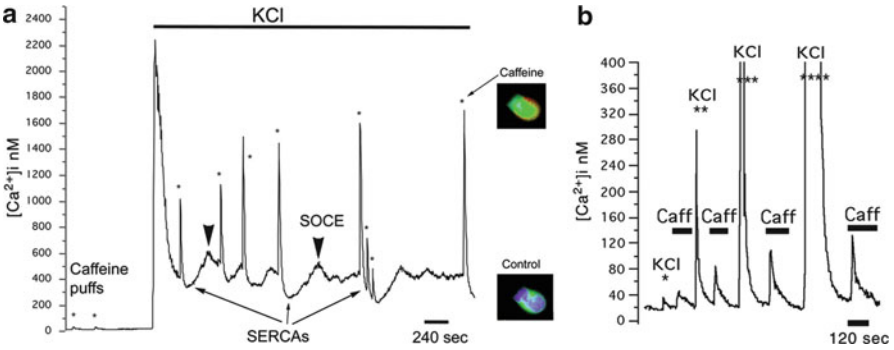

Fig. 39.2 CICR in rod photoreceptor under hyperpolarized and depolarized conditions. The fura-2-loaded cell was stimulated with puffs of 10 mM caffeine to stimulate ryanodine receptors. Sustained superfusion with 20 mM KCl activated voltage-operated Ca^{2+} entry, resulting in a transient increase in $[Ca^{2+}]i$ followed by a gradual decline to a stable plateau due to Ca^{2+}-dependent VOCC inactivation. Caffeine puffs evoked substantially lager $[Ca^{2+}]i$ transients under depolarized conditions. Each transient response was followed by an undershoot caused by SERCA activation (*arrows*), and a transient overshoot resulting from the activation of store-operated Ca^{2+} entry (*arrowhead*). (**b**) The magnitude of caffeine-evoked Ca^{2+} release depends on the magnitude of the conditioning depolarization. Rod photoreceptor inner segment. Conditioning steps of high K^+ were followed by superfusion with 10 mM caffeine. Each *star* represents a single 128 ms KCl puff; bars denote superfusion. Increase in the duration of conditioning $[Ca^{2+}]i$ steps caused a subsequent increase in the magnitude of caffeine-evoked $[Ca^{2+}]i$ responses. These occurred after $[Ca^{2+}]i$ returned to the baseline, implying a form of intracellular "memory"

the cytosol with high-affinity PMCA1 and PMCA2 pumps (Kd ~ 0.2 μM) [54, 94]. Under light-saturated conditions, Ca^{2+} sequestration into the ER lowers the steady-state $[Ca^{2+}]_{IS}$ by ~25–40 nM; that is, SERCAs contribute ~50% to baseline $[Ca^{2+}]i$ [54, 94]. SERCA contribution is considerably higher in depolarized cells where it can reach hundreds of nM (Fig. 39.2a). Episodes of darkness reload ER stores and consequently the ER reverts from a sink to source (e.g., [36]). The amount of releasable Ca^{2+} reflects the magnitude of the depolarizing stimulus and the amplitude of $[Ca^{2+}]i$. ([52, 54]; Fig 39.2b). CICR contributes to steady-state $[Ca^{2+}]i$, as suggested by ~20–50% reduction in the magnitude of depolarization-evoked $[Ca^{2+}]i$ elevations in rod and cone perikarya following SERCA blockade [2, 54, 92].

Amphibian and mammalian photoreceptors express RyR1 and RyR2 isoforms (detailed descriptions of expression profiles, biophysical activation properties, mechanisms of activation and function of the 3 known RyRs are provided elsewhere; e.g., [58]). As in most brain regions, RyR2 are the dominant isoform in photoreceptors [51, 55] which may express a new retina-specific variant of RyR2 that includes a 21 bp deletion from exon 4 [87]. Physiological studies showed that CICR in the IS was a smoothly graded function of Ca^{2+} influx [52], a characteristic typical of RyR2 [88]. RT-PCR, in situ hybridization and antibody staining suggest mammalian photoreceptors might also express the skeletal RyR1 isoform ([86, 87]; [113]). RyR1s are typically Ca^{2+} -independent but can also participate in

CICR, when in the "uncoupled mode" ([110]; [71]). The retina also expresses RyR3 mRNA and protein ([86]; [113]), a developmentally regulated isoform that can be co-expressed with RyR2 [64]. Surprisingly, developing avian photoreceptors were reported to express a thapsigargin-sensitive pool that does not contain RyRs or IP3Rs ([17]; but see [39]).

In contrast to voltage-operated entry that is characterized by rapid, local Ca^{2+} influx at the active zone [3, 65, 96], release from ER stores mediated by RyRs and possibly IP3Rs participates in slower, longer-range Ca^{2+} signaling. Under strong illumination when the resident L-type voltage-operated channels are closed and $[Ca^{2+}]i$ is low, RyRs are likely to be constitutively active at a random frequency within the range of homeostatic fluctuation of the hyperpolarized membrane potential (~−60 to −70 mV; e.g.; [7]) whereas in the darkness, sustained Ca^{2+} release from ryanodine stores represents a significant additional source of cytosolic $[Ca^{2+}]i$ [52, 54]. Release from ryanodine stores may contribute to the membrane potential either as positive or negative feedback, depending on the pattern of activation of Ca^{2+}-dependent K^+ and Cl^- conductances, and Ca^{2+}-induced inactivation of voltage-operated L-type channels [2, 52]. Given that CICR acts as an amplification device, its contribution is most pronounced in depolarized rods responding to flashes that evoke small changes in presynaptic voltage [90]. Parenthetically, the majority of studies that focused on photoreceptor CICR used pharmacological agents such as caffeine, ryanodine, Ruthenium Red, 2-APB and/or SERCA antagonists. These non-physiological modulators are often non-specific and/or have multiple targets. There is a pressing need to determine the function of physiological modulators such as $NAAD^+$; cADP ribose and/or β-NAD^+.

CICR signals are far more prominent in rods than in cones. Stimulation with caffeine produced small $[Ca^{2+}]i$ elevations in a tiny subset of amphibian cones whereas the majority of cells evinced no response whatsoever [54]. Consistent with this observation, the time course of depolarization-induced $[Ca^{2+}]i$ elevations in rods, but not cones, was strongly dependent on store release [92]. The absolute capacity of cones to sequester Ca^{2+} in intracellular compartments appears to be comparable to rods, however, because exposure to thapsigargin elicits comparable (~50%) decreases in the size of the residual intracellular Ca^{2+} pool [92]. This might suggest that the magnitude of caffeine-evoked Ca^{2+} transients in cones is reduced by stronger PMCA-mediated Ca^{2+} clearance (Križaj and Copenhagen, 1998), activation of K^+/Cl^- channels and/or by mitochondrial uptake through ER:mitochondrial microdomains. Consistent with this hypothesis, caffeine consistently induced significant Ca^{2+} responses in cones in the presence of PMCA or mitochondrial blockers [54].

While Ca^{2+} sequestration into ER stores plays a crucial role in IS Ca^{2+} homeostasis and tonic neurotransmitter release, depletion of ryanodine-sensitive Ca^{2+} stores empties only a fraction of total accumulated Ca^{2+} in rods [54]. This suggests that IP3 stores, mitochondrial, lysosomal and Golgi apparatus also mediate Ca^{2+} sequestration and release in rods and cones (e.g., [92]). In contrast to the clear evidence of PLC-IP3 signals in invertebrate photoreceptors [100], physiological investigations of IP3R function in vertebrate photoreceptors have been lagging behind.

The available evidence suggests that IS regions express PLC and IP3 receptors [39, 55, 74] that may be associated with metabotropic mGluR signaling [47], synaptic output [40] and circadian rhythmicity mediated by presynaptic somatostatin 2A receptors and PLC [39].

Ca Stores and Neurotransmission at Photoreceptor Synapses

Ca^{2+} release from intracellular stores was suggested to regulate the level of tonic neuronal activity at some central synapses by contributing to spontaneous neurotransmitter release that sets the frequency of mEPSCs (reviewed in [9, 16]). The role of Ca^{2+} stores is particularly prominent in sensory "ribbon" synapses of photoreceptors and hair cells [2, 12, 59, 90]. EM and X-ray diffraction analyses have identified copious intracellular storage sites in synaptic terminals of rods and cones. These are represented mainly by smooth ER cisternae that contain both RyRs and IP3Rs ([66, 99]; [120]; [2]).

The primary source of cytosolic Ca^{2+} at ribbon synapses are dihydropyridine-sensitive, L-type channels which are mainly localized at peri-ribbon sites near the active zone [65]. Within the synaptic terminal, release from Ca^{2+} stores and subsequent influx through store-operated channels act in parallel with voltage-operated Ca^{2+} entry. Wallace Thoreson's group at the University of Nebraska used paired recordings from photoreceptors and postsynaptic cells to show that high concentrations of ryanodine evince a reduction in the late component of the postsynaptic EPSC [12]. Calcium stores are located away from the active zone yet still within the diffusible distance of ~600 nm from the ribbon [2] at which they could stimulate release from the reserve pool(s) of synaptic vesicles [97]. Capacitance recordings from dissociated salamander photoreceptors showed that photolysis of caged presynaptic $[Ca^{2+}]i$ can under certain conditions evoke slow exocytosis that presumably bypasses the early releasable pool [49], offering an alternative parallel route possibly consisting of ectopic release of synaptic vesicles from non-ribbon sites (e.g., [57, 105]).

Presynaptic $[Ca^{2+}]i$ drives the exocytotic process and information transfer across the photoreceptor synapse at the astonishing rate of 100–400 vesicles/s [14, 79, 97]. The high rate of release is presumably required to support reliable transfer of presynaptic voltage changes in the order of 1 μV [22]. Indeed, the rod synapse was the first documented case where synaptic release was shown to be driven by submicromolar to low micromolar levels of average cytosolic $[Ca^{2+}]i$ [49, 79, 97] rather than hundreds of μM typically required at central synapses. In part, this is made possible by the high Ca^{2+}affinity of presynaptic SNAREs and buffering proteins (reviewed in [32]) and in part by the close proximity of L-type channels to the ribbon [65], which allows for the generation of local microdomains where $[Ca^{2+}]i$ is likely to be substantially higher. In addition to high affinity of Ca^{2+} binding, the synapse is characterized by its capacity for tonic release which is subserved by the resistance of presynaptic channels to inactivation (McRory et al., 2005) and by CICR which

boosts synaptic release when rods are maintained at physiological resting membrane potentials of ~−40 mV [12, 52, 90]. CICR is required for the maintenance of tonic release at physiological membrane potentials whereas the presynaptic potential required non-physiological depolarizations to ~−20 mV in the absence of CICR [90]. Elimination of RyR-mediated Ca^{2+} release converted a tonic synaptic signals into phasic bursts of vesicle release [90]. Hence, over most of the dynamic range, Ca^{2+} release from internal stores is likely to contribute to maintaining linear synaptic transfer of information between photoreceptors and postsynaptic horizontal/bipolar cells [97, 103].

Store-Operated Channels

Although depolarization-evoked glutamate release from rods is completely suppressed by L-type channel antagonists that inhibit voltage-dependent Ca^{2+} entry, saturating white light blocked only a fraction of total released glutamate [82, 83]. This suggests that other, voltage-independent Ca^{2+} influx pathways that are activated in light-adapted and strongly hyperpolarized cells, regulate the dynamic range of rod signaling. One such mechanism might consist of transient receptor potential (TRP) channels localized to photoreceptor terminals. Data from amphibian and mammalian rods suggest that TRP-like channels contribute to baseline $[Ca^{2+}]i$ [67, 94]. At least a subset of these channels appears to be regulated by depletion of intracellular Ca^{2+} stores through the STIM1 sensor mechanism [4, 5, 94, 95] (Fig. 39.3). While the physiological function of the SOCE is still unclear, depletion of ER cisternae in rod terminals caused an increase in presynaptic $[Ca^{2+}]i$

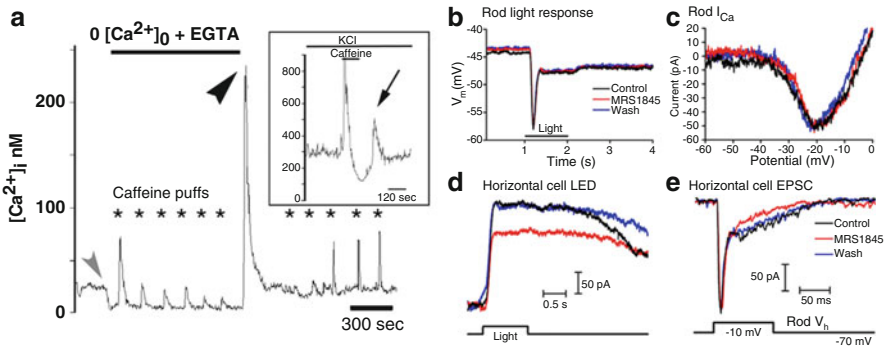

Fig. 39.3 Depletion of Ca^{2+} stores facilitates plasma membrane Ca^{2+} entry and modules synaptic transmission. (**a**) Depletion of Ca^{2+} stores evoked a $[Ca^{2+}]i$ overshoot characteristic of SOCE. The same phenomenon was observed in depolarized cells (*inset).* (**b**–**e**) Paired whole cell recordings from rod-horizontal cell pairs. The SOCE antagonist MRS-1845 has no effect on the light response (**b**) or voltage-operated Ca^{2+} current (**c**). Injection of depolarizing current in the rod, however, evokes a reduction in the amplitude of the light-evoked horizontal cell response (**d**), reflected in the smaller amplitude of the late EPSC component (**e**)

that was capable of modulating release of FM1-43 -labeled vesicles [94]. Consistent with this finding, inhibition of SOCE suppressed the slow component of the horizontal cell EPSC without having affecting voltage-operated signals [95] (Fig. 39.3e). The molecular identity of channel underlying SOCE has not been unequivocally established. Most retinal cells, including photoreceptors, appear to express multiple TRP subfamilies and isoforms [68, 80, 107]. TRPC1 isoform-specific siRNAs reduced SOCE in rods but had no effect on cone SOCE [94] whereas the TRPC3/6/7 channel antagonist diacylglycerol induces $[Ca^{2+}]i$ elevations in mammalian rods and cones.

Summary

It has become increasingly clear that photoreceptor ER and mitochondria are capable of storing remarkable amounts of Ca^{2+} in a compartment-specific manner and that calcium stores and store-operated channels play a significant role in vertebrate photoreceptors Ca^{2+} homeostasis and synaptic signaling. Photoreceptor signaling in darkness is strongly associated with CICR whereas light-induced signaling is characterized by depleted ER stores and activation of SOCE. Rod and cone cells exhibit differences both in the magnitude/kinetics of the releasable Ca^{2+} pool, interactions with plasma membrane Ca^{2+} signaling mechanisms and in the physiological manifestations of CICR and SOCE. Thus, Ca^{2+} accumulation into and release from internal stores endow photoreceptor signaling with potential for far more complex, tunable and adaptable homeostatic regulation than believed so far.

Acknowledgements The work was supported by the National Institutes of Health (EY13870, EY014800), Foundation Fighting Blindness, the Moran TIGER award and an unrestricted grant from Research to Prevent Blindness to the Moran Eye Institute at the University of Utah.

References

1. Allbritton NL, Meyer T, Stryer LF (1992) Range of messenger action of calcium ion and inositol 1,4,5-trisphosphate. Science 258:1812–1815
2. Babai N, Morgans CW, Thoreson WB (2009) Calcium-induced calcium release contributes to synaptic release from mouse rod photoreceptors. Neuroscience 165(4):1447–1456
3. Babai N, Bartoletti TM, Thoreson WB (2010) Calcium regulates vesicle replenishment at the cone ribbon synapse. J Neurosci 30(47):15866–15877
4. Barabas P, Cutler-Peck C, Križaj D (2010) Do calcium channels blockers rescue dying photoreceptors in the $Pde6b^{rd1}$ mouse? Adv Exp Med Biol 664:491–499
5. Barabas P, Huang W, Xing W, Rao A, Le YZ, Chen CKJ, Križaj D (2010) Store-operated calcium entry increases calcium levels in photoreceptor cells and affects vision in mice. IOVS Abstract, Fort Lauderdale
6. Belgum JH, Copenhagen DR (1988) Synaptic transfer of rod signals to horizontal and bipolar cells in the retina of the toad (Bufo marinus). J Physiol 396:225–245
7. Berrout J, Isokawa M (2009) Homeostatic and stimulus-induced coupling of the L-type Ca^{2+} channel to the ryanodine receptor in the hippocampal neuron in slices. Cell Calcium 46(1):30–38

8. Blaurock AE, Wilkins MH (1972) Structure of retinal photoreceptor membranes. Nature 236(5345):313–314
9. Bouchard R, Pattarini R, Geiger JD (2003) Presence and functional significance of presynaptic ryanodine receptors. Prog Neurobiol 69(6):391–418, Apr
10. Brockerhoff SE, Rieke F, Matthews HR, Taylor MR, Kennedy B, Ankoudinova I, Niemi GA, Tucker CL, Xiao M, Cilluffo MC, Fain GL, Hurley JB (2003) Light stimulates a transducin-independent increase of cytoplasmic Ca^{2+} and suppression of current in cones from the zebrafish mutant nof. J Neurosci 23(2):470–480
11. Brown JE, Blazynski C, Cohen AI (1987) Light induces a rapid and transient increase in inositol-trisphosphate in toad rod outer segments. Biochem Biophys Res Commun 146:1392–1396
12. Cadetti L, Bryson EJ, Ciccone CA, Rabl K, Thoreson WB (2006) Calcium-induced calcium release in rod photoreceptor terminals boosts synaptic transmission during maintained depolarization. Eur J Neurosci 23:2983–2990
13. Chen C, Jiang Y, Koutalos Y (2002) Dynamic behavior of rod photoreceptor disks. Biophys J 83(3):1403–1412
14. Choi SY, Borghuis BG, Rea R, Levitan ES, Sterling P, Kramer RH (2005) Encoding light intensity by the cone photoreceptor synapse. Neuron 48:555–562
15. Cilluffo MC, Matthews HR, Brockerhoff SE, Fain GL (2004) Light-induced Ca^{2+} release in the visible cones of the zebrafish. Vis Neurosci 21(4):599–609
16. Collin T, Marty A, Llano I (2005) Presynaptic calcium stores and synaptic transmission. Curr Opin Neurobiol 15(3):275–281
17. Cristóvão AJ, Capela AN, Carvalho CM (2007) Ca^{2+} stores in the chick embryo retina cells. Cell Signal 9(1):97–103
18. Davis WL, Farmer GF, Martin JH, Bridges G (1988) Electron microscopic cytochemical localization of Ca-ATPase in the rod outer segments of the toad Bufo marinus. Anat Rec 221:761–768
19. Day NS, Koutz CA, Anderson RE (1993) Inositol-1,4,5-trisphosphate receptors in the vertebrate retina. Curr Eye Res 12:981–992
20. Fabiano A, Panfoli I, Calzia D, Bruschi M, Ravera S, Bachi A, Cattaneo A, Morelli A, Candiano G (2011) Catalytic properties of the retinal rod outer segment disk ADP-ribosyl cyclase. Vis Neurosci 28(2):121–128
21. Fain GL, Schroder WH (1990) Light-induced calcium release and re-uptake in toad rods. J Neurosci 10:2238–2249
22. Fain GL, Granda AM, Maxwell JM (1977) Voltage signal of photoreceptors at visual threshold. Nature 265(5590):181–183
23. Fain GL, Matthews HR, Cornwall MC, Koutalos Y (2001) Adaptation in vertebrate photoreceptors. Physiol Rev 81(1):117–151
24. Gan J, Iuvone PM (1997) Depolarization and activation of dihydropyridine-sensitive Ca^{2+} channels stimulate inositol phosphate accumulation in photoreceptor-enriched chick retinal cell cultures. J Neurochem 68:2300–2307
25. Gehm BD, Pinke RM, Laquerre X, Chafouleas J, Schultz DA, Pepperl DJ, McConnell DG (1991) Activation of bovine rod outer segment phosphatidylinositol-4,5-bisphosphate phospholipase C by calmodulin antagonists does not depend on calmodulin. Biochemistry 30:11302–11306
26. Ghalayini A, Anderson RE (1984) Phosphatidylinositol 4,5-bisphosphate: light-mediated breakdown in the vertebrate retina. Biochem Biophys Res Commun 124:503–506
27. Ghalayini AJ, Tarver AP, Mackin AM, Koutz CA, Anderson RE (1991) Identification and immunolocalization of phospholipase C in bovine rod outer segments. J Neurochem 57:1405–1412
28. Ghalayini AJ, Weber NR, Rundle DR, Koutz CA, Lambert D, Guo XX, Anderson RE (1998) Phospholipase Cgamma1 in bovine rod outer segments: immunolocalization and light-dependent binding to membranes. J Neurochem 70(1):171–178
29. Giuditta A, Kaplan BB, van Minnen J, Alvarez J, Koenig E (2002) Axonal and presynaptic protein synthesis: new insights into the biology of the neuron. Trends Neurosci 25:400–404
30. Haeseleer F, Imanishi Y, Maeda T, Possin DE, Maeda A, Lee A, Rieke F, Palczewski K (2004) Essential role of Ca^{2+}-binding protein 4, a Cav1.4 channel regulator, in photoreceptor synaptic function. Nat Neurosci 7(10):1079–1087

31. Hayashi F, Amakawa T (1985) Light-mediated breakdown of phosphatidylinositol-4,5-bisphosphate in isolated rod outer segments of frog photoreceptor. Biochem Biophys Res Commun 128:954–959
32. Heidelberger R, Thoreson WB, Witkovsky P (2005) Synaptic transmission at retinal ribbon synapses. Prog Retin Eye Res 24:682–720
33. Henkart M (1980) Identification and function of intracellular calcium stores in axons and cell bodies of neurons. Fed Proc 10:2783–2789
34. Hoang QV, Linsenmeier RA, Chung CK, Curcio CA (2002) Photoreceptor inner segments in monkey and human retina: mitochondrial density, optics, and regional variation. Vis Neurosci 19:395–407
35. Holtzman E, Mercurio AM (1980) Membrane circulation in neurons and photoreceptors: some unresolved issues. Int Rev Cytol 67:1–67
36. Hongpaisan J, Pivovarova NB, Colegrove SL, Leapman RD, Friel DD, Andrews SB (2001) Multiple modes of calcium-induced calcium release in sympathetic neurons. A $[Ca^{2+}]_i$- and location-dependent transition from endoplasmic reticulum Ca accumulation to net Ca release. J Gen Physiol 118(1):101–112
37. Huang W, Howell GJ, John SMW, Križaj D (2010) Differential expression of genes coding for internal calcium release is phenotype-dependent. IOVS Supplement, Proceedings of ARVO, Fort Lauderdale, 2010
38. Jafri MS, Keizer J (1995) On the roles of Ca^{2+} diffusion, Ca^{2+} buffers, and the endoplasmic reticulum in IP_3-induced Ca^{2+} waves. Biophys J 69:2139–2153
39. Jian K, Barhoumi R, Ko ML, Ko GY (2009) Inhibitory effect of somatostatin-14 on L-type voltage-gated calcium channels in cultured cone photoreceptors requires intracellular calcium. J Neurophysiol 102(3):1801–1810
40. Jiang H, Lyubarsky A, Dodd R, Vardi N, Pugh E, Baylor D, Simon MI, Wu D (1996) Phospholipase C b4 is involved in modulating the visual response in mice. Proc Natl Acad Sci 93:14598–14601
41. Jindrová H, Detwiler PB (1998) Protein kinase C and IP3 in photoresponses of functionally intact rod outer segments: constraints about their role. Physiol Res 47(4):285–290
42. Johnson JE Jr, Perkins GA, Giddabasappa A, Chaney S, Xiao W, White AD, Brown JM, Waggoner J, Ellisman MH, Fox DA (2007) Spatiotemporal regulation of ATP and Ca^{2+} dynamics in vertebrate rod and cone ribbon synapses. Mol Vis 13:887–919
43. Jung HH, Remé CE, Pfeilschifter J (1993) Light evoked inositol trisphosphate release in the rat retina in vitro. Curr Eye Res 12(8):727–732
44. Kaupp UB, Schnetkamp PP, Junge W (1979) Light-induced calcium release in isolated intact cattle rod outer segments upon photoexcitation of rhodopsin. Biochim Biophys Acta 554(2):441–459
45. Korenbrot JI, Rebrik TI (2002) Tuning outer segment Ca^{2+} homeostasis to phototransduction in rods and cones. Adv Exp Med Biol 514:179–203
46. Koskelainen A, Donner K, Kalamkarov G, Hemilä S (1994) Changes in the light-sensitive current of salamander rods upon manipulation of putative pH-regulating mechanisms in the inner and outer segment. Vision Res 34(8):983–994
47. Koulen P, Kihn R, Wassle H, Brandstatter JH (1999) Modulation of the intracellular calcium concentration in photoreceptor terminals by a presynaptic metabotropic glutamate receptor. Proc Natl Acad Sci 96:9909–9914
48. Koyanagi M, Terakita A (2008) Gq-coupled rhodopsin subfamily composed of invertebrate visual pigment and melanopsin. Photochem Photobiol 84(4):1024–1030
49. Kreft M, Križaj D, Grilc S, Zorec R (2003) Properties of exocytotic response in vertebrate photoreceptors. J Neurophysiol 90:218–225
50. Križaj D (2005a) Compartmentalization of calcium entry pathways in mouse rods. Eur J Neurosci 22:3292–3296
51. Križaj D (2005b) SERCA isoform expression in the mammalian retina. Exp Eye Res 81:690–699

52. Križaj D, Bao JX, Schmitz Y, Witkovsky P, Copenhagen DR (1999) Caffeine-sensitive calcium stores regulate synaptic transmission from retinal rod photoreceptors. J Neurosci 19:7249–7261
53. Križaj D, Demarco SJ, Johnson J, Strehler EE, Copenhagen DR (2002) Cell-specific expression of plasma membrane calcium ATPase isoforms in retinal neurons. J Comp Neurol 451:1–21
54. Križaj D, Lai FA, Copenhagen DR (2003) Ryanodine stores and calcium regulation in the inner segments of salamander rods and cones. J Physiol 547:761–774
55. Križaj D, Liu X, Copenhagen DR (2004) Expression of calcium transporters in the retina of the tiger salamander (*Ambystoma tigrinum*). J Comp Neurol 475:463–480
56. Križaj D, Mercer AJ, Thoreson WB, Barabas P (2011) Intracellular pH modulates inner segment calcium homeostasis in vertebrate photoreceptors. Am J Physiol Cell Physiol 300(1):C187–C197
57. Kuromi H, Kidokoro Y (2002) Selective replenishment of two vesicle pools depends on the source of Ca^{2+} at the Drosophila synapse. Neuron 35(2):333–343
58. Lanner JT, Georgiou DK, Joshi AD, Hamilton SL (2010) Ryanodine receptors: structure, expression, molecular details, and function in calcium release. Cold Spring Harb Perspect Biol 2(11):a003996
59. Lelli A, Perin P, Martini M, Ciubotaru CD, Prigioni I, Valli P, Rossi ML, Mammano F (2003) Presynaptic calcium stores modulate afferent release in vestibular hair cells. J Neurosci 23:6894–6903
60. Leonelli M, Martins DO, Britto LR (2011) TRPV1 receptors modulate retinal development. Int J Dev Neurosci 29(4):405–413
61. Liu Q, Tan G, Levenkova N, Li T, Pugh EN Jr, Rux JJ, Speicher DW, Pierce EA (2007) The proteome of the mouse photoreceptor sensory cilium complex. Mol Cell Proteomics 6(8):1299–1317
62. Matthews HR, Fain GL (2001) A light-dependent increase in free Ca^{2+} concentration in the salamander rod outer segment. J Physiol 532:305–321
63. Matthews HR, Fain GL (2003) The effect of light on outer segment calcium in salamander rods. J Physiol 552(Pt 3):763–776
64. Meldolesi J (2001) Rapidly exchanging Ca^{2+} stores in neurons: molecular, structural and functional properties. Prog Neurobiol 65:309–338
65. Mercer AJ, Chen M, Thoreson WB (2011) Lateral mobility of presynaptic L-type calcium channels at photoreceptor ribbon synapses. J Neurosci 31(12):4397–4406
66. Mercurio AM, Holtzman E (1982) Smooth endoplasmic reticulum and other agranular reticulum in frog retinal photoreceptors. J Neurocytol 11:263–293
67. Molnar T, Barabas P, Punzo C, Križaj D (2011) Store-operated calcium entry regulates intracellular calcium levels in mouse rod photoreceptors. IOVS Abstract, Fort Lauderdale, 2011
68. Morgans CW, Brown RL, Duvoisin RM (2010) TRPM1: the endpoint of the mGluR6 signal transduction cascade in retinal ON-bipolar cells. Bioessays 32(7):609–614
69. Nakatani K, Yau KW (1988) Calcium and light adaptation in retinal rods and cones. Nature 334(6177):69–71
70. Nilsson SE (1965) The ultrastructure of the receptor outer segments in the retina of the leopard frog (rana pipiens). J Ultrastruct Res 12:207–231
71. Ouardouz M, Nikolaeva MA, Coderre E, Zamponi GW, McRory JE, Trapp BD, Yin X, Wang W, Woulfe J, Stys PK (2003) Depolarization-induced Ca^{2+} release in ischemic spinal cord white matter involves L-type Ca^{2+} channel activation of ryanodine receptors. Neuron 40:53–63
72. Ouyang K, Zheng H, Qin X, Zhang C, Yang D, Wang X, Wu C, Zhou Z, Cheng H (2005) Ca^{2+} sparks and secretion in dorsal root ganglion neurons. Proc Natl Acad Sci USA 102(34): 12259–12264
73. Paillart C, Winkfein RJ, Schnetkamp PP, Korenbrot JI (2007) Functional characterization and molecular cloning of the K^+-dependent Na^+/Ca^{2+} exchanger in intact retinal cone photoreceptors. J Gen Physiol 129(1):1–16

74. Peng YW, Rhee SG, Yu WP, Ho YK, Schoen T, Chader GJ, Yau KW (1997) Identification of components of a phosphoinositide signaling pathway in retinal rod outer segments. Proc Natl Acad Sci USA 94(5):1995–2000
75. Pepe IM, Panfoli I, Notari L, Morelli A (2000) ATP synthesis in rod outer segments of bovine retina by the reversal of the disk calcium pump. Biochem Biophys Res Commun 268:625–627
76. Perkins GA, Ellisman MH, Fox DA (2003) Three-dimensional analysis of mouse rod and cone mitochondrial cristae architecture: bioenergetic and functional implications. Mol Vis 9:60–73
77. Pozzo-Miller LD, Pivovarova NB, Connor JA, Reese TS, Andrews SB (1999) Correlated measurements of free and total intracellular calcium concentration in central nervous system neurons. Microsc Res Tech 46:370–379
78. Rentería RC, Strehler EE, Copenhagen DR, Križaj D (2005) Ontogeny of plasma membrane calcium ATPase isoforms in the neural retina of the postnatal rat. Vis Neurosci 22:263–274
79. Rieke F, Schwartz EA (1996) Asynchronous transmitter release: control of exocytosis and endocytosis at the salamander rod synapse. J Physiol 493:1–8
80. Ryskamp DA, Witkovsky P, Barabas P, Huang W, Koehler C, Akimov NP, Lee SH, Chauhan S, Xing W, Rentería RC, Liedtke W, Križaj D (2011) The polymodal ion channel transient receptor potential vanilloid 4 modulates calcium flux, spiking rate, and apoptosis of mouse retinal ganglion cells. J Neurosci 31(19):7089–7101
81. Sampath AP, Matthews HR, Cornwall MC, Bandarchi J, Fain GL (1999) Light-dependent changes in outer segment free-Ca^{2+} concentration in salamander cone photoreceptors. J Gen Physiol 113:267–277
82. Schmitz Y, Witkovsky P (1996) Glutamate release by the intact light-responsive photoreceptor layer of the Xenopus retina. J Neurosci Methods 68:55–60
83. Schmitz Y, Witkovsky P (1997) Dependence of photoreceptor glutamate release on a dihydropyridinesensitive calcium channel. Neuroscience 78:1209–1216
84. Schnetkamp PP (1979) Calcium translocation and storage of isolated intact cattle rod outer segments in darkness. Biochim Biophys Acta 554(2):441–459
85. Schnetkamp PP, Basu DK, Szerencsei RT (1989) Na^{+}-Ca^{2+} exchange in bovine rod outer segments requires and transports K^{+}. Am J Physiol 257:C153–C157
86. Shoshan-Barmatz V, Orr I, Martin C, Vardi N (2005) Novel ryanodine-binding properties in mammalian retina. Int J Biochem Cell Biol 37(8):1681–1695
87. Shoshan-Barmatz V, Zakar M, Shmuelivich F, Nahon E, Vardi N (2007) Retina expresses a novel variant of the ryanodine receptor. Eur J Neurosci 26(11):3113–3125
88. Solovyova N, Veselovsky N, Toescu EC, Verkhratsky A (2002) $Ca^{(2+)}$ dynamics in the lumen of the endoplasmic reticulum in sensory neurons: direct visualization of $Ca^{(2+)}$-induced $Ca^{(2+)}$ release triggered by physiological $Ca^{(2+)}$ entry. EMBO J 21(4):622–630
89. Somlyo AP, Walz B (1995) Elemental distribution in Rana pipiens retinal rods: quantitative electron probe analysis. J Physiol 358:183–195
90. Suryanarayanan A, Slaughter MM (2006) Synaptic transmission mediated by internal calcium stores in rod photoreceptors. J Neurosci 26:1759–1766
91. Szikra T, Križaj D (2006) The dynamic range and domain-specific signals of intracellular calcium in photoreceptors. Neuroscience 141:143–155
92. Szikra T, Križaj D (2007) Intracellular organelles and calcium homeostasis in rods and cones. Vis Neurosci 24:733–743
93. Szikra T, Križaj D (2009) Calcium signals in inner segments of photoreceptors. In: Tombran-Tink J, Barnstable C (eds) The visual transduction cascade: basic and clinical principles. Humana Press, Totowa, pp 197–223
94. Szikra T, Cusato K, Thoreson WH, Barabas P, Bartoletti M, Križaj D (2008) Store-operated calcium channels regulate visual function. J Physiol 586:4859–4875
95. Szikra T, Barabas P, Bartoletti T, Huang H, Akopian A, Thoreson WB, Križaj D (2009) Calcium homeostasis and neurotransmission in cone photoreceptors is regulated by interactions between calcium stores and plasma membrane ion channels. PLoS One 4(8):e6723

96. Thoreson WB (2007) Kinetics of synaptic transmission at ribbon synapses of rods and cones. Mol Neurobiol 36(3):205–223
97. Thoreson WB, Rabl K, Townes-Anderson E, Heidelberger R (2004) A highly Ca^{2+}-sensitive pool of vesicles contributes to linearity at the rod photoreceptor ribbon synapse. Neuron 42:595–605
98. Ungar F, Piscopo I, Holtzman E (1981) Calcium accumulation in intracellular compartments of frog retinal rod photoreceptors. Brain Res 205:200–206
99. Ungar F, Piscopo I, Holtzman E (1984) Uptake of calcium by the endoplasmic reticulum of the frog photoreceptor. J Cell Biol 98:1645–1655
100. Walz B, Baumann O (1995) Structure and cellular physiology of Ca^{2+} stores in invertebrate photoreceptors. Cell Calcium 18:342–351
101. Wang TL, Sterling P, Vardi N (1993) Localization of type I inositol 1,4,5-triphosphate receptor in the outer segments of mammalian cones. J Neurosci 19:4221–4228
102. Weitz D, Zoche M, Müller F, Beyermann M, Körschen HG, Kaupp UB, Koch KW (1998) Calmodulin controls the rod photoreceptor CNG channel through an unconventional binding site in the N-terminus of the beta-subunit. EMBO J 17(8):2273–2284
103. Witkovsky P, Schmitz Y, Akopian A, Križaj D, Tranchina D (1997) Gain of rod to horizontal cell synaptic transfer: relation to glutamate release and a dihydropyridine-sensitive calcium current. J Neurosci 17:7297–7306
104. Woodruff ML, Lem J, Fain GL (2004) Early receptor current of wild-type and transducin knockout mice: photosensitivity and light-induced Ca^{2+} release. J Physiol 557:821–828
105. Zenisek D (2008) Vesicle association and exocytosis at ribbon and extraribbon sites in retinal bipolar cell presynaptic terminals. Proc Natl Acad Sci USA 105(12):4922–4927
106. Zhang H, Constantine R, Vorobiev S, Baehr W et al (2011) UNC119 is required for G protein trafficking in sensory neurons. Nat Neurosci 14:874–880
107. Zimov S, Yazulla S (2004) Localization of vanilloid receptor 1 (TRPV1/VR1)-like immunoreactivity in goldfish and zebrafish retinas: restriction to photoreceptor synaptic ribbons. J Neurocytol 33(4):441–452
108. Das ND, Yoshioka T, Samuelson D, Cohen RJ, Shichi H (1987) Immunochemical evidence for the light-regulated modulation of phosphatidylinositol-4,5-bisphosphate in rat photoreceptor cells. Cell Struct Funct 12(5):471–481
109. Fain GL, Schröder WH (1985) Calcium content and calcium exchange in dark-adapted toad rods. J Physiol 368:641–665
110. Fill M, Copello JA (2002) Ryanodine receptor calcium release channels. Physiol Rev 82(4):893–922
111. Gehm BD, Mc Connell DG (1990) Phosphatidylinositol-4,5-bisphosphate phospholipase C in bovine rod outer segments. Biochemistry 29(23):5447–5452
112. Hestrin S, Korenbrot JI (1987) Effects of cyclic GMP on the kinetics of the photocurrent in rods and in detached rod outer segments. J Gen Physiol 90(4):527–551
113. Huang W, Xing W, Ryskamp DA, Punzo C, Križaj D (2011) Localization and phenotype-specific expression of ryanodine calcium release channels in C57BL6 and DBA/2J mouse strains. Exp Eye Res 93(5):700–709
114. Jelsema CL (1989) Regulation of phospholipase A2 and phospholipase C in rod outer segments of bovine retina involves a common GTP-binding protein but different mechanisms of action. Ann N Y Acad Sci 559:158–177
115. Krizaj D, Copenhagen DR (1998) Compartmentalization of calcium extrusion mechanisms in the outer and inner segments of photoreceptors. Neuron 21:249–256
116. Krizaj D, Copenhagen DR (2002) Calcium regulation in photoreceptors. Frontiers in Biosciences 7:2023–2044
117. McRory JE, Hamid J, Doering CJ, Garcia E, Parker R, Hamming K, Chen L, Hildebrand M, Beedle AM, Feldcamp L, Zamponi GW, Snutch TP (2004) The CACNA1F gene encodes an L-type calcium channel with unique biophysical properties and tissue distribution. J Neurosci 24(7):1707–1718

118. Millar FA, Fisher SC, Muir CA, Edwards E, Hawthorne JN (1988) Polyphosphoinositide hydrolysis in response to light stimulation of rat and chick retina and retinal rod outer segments. Biochim Biophys Acta 970(2):205–211
119. Panfoli I, Ravera S, Fabiano A, Magrassi R, Diaspro A, Morelli A, Pepe IM (2007) Localization of the cyclic ADP-ribose-dependent calcium signaling pathway in bovine rod outer segments. Invest Ophthalmol Vis Sci 48(3):978–984
120. Peng YW, Sharp AH, Snyder SH, Yau KW (1991) Localization of the inositol 1,4,5-trisphosphate receptor in synaptic terminals in the vertebrate retina. Neuron 6(4):525–531
121. Verkhratsky A (2005) Physiology and pathophysiology of the calcium store in the endoplasmic reticulum of neurons. Physiol Rev 85(1):201–279

Chapter 40
Stem Cells and Calcium Signaling

Fernanda M.P. Tonelli, Anderson K. Santos, Dawidson A. Gomes, Saulo L. da Silva, Katia N. Gomes, Luiz O. Ladeira, and Rodrigo R. Resende

Abstract The increasing interest in stem cell research is linked to the promise of developing treatments for many lifethreatening, debilitating diseases, and for cell replacement therapies. However, performing these therapeutic innovations with safety will only be possible when an accurate knowledge about the molecular signals that promote the desired cell fate is reached. Among these signals are transient changes in intracellular Ca^{2+} concentration $[Ca^{2+}]_i$. Acting as an intracellular messenger, Ca^{2+} has a key role in cell signaling pathways in various differentiation stages of stem cells. The aim of this chapter is to present a broad overview of various moments in which Ca^{2+}-mediated signaling is essential for the maintenance of stem cells and for promoting their development and differentiation, also focusing on their therapeutic potential.

Keywords Calcium transients • Embryonic stem cells • GPCR and RTK receptors • Calcium signaling • Stem cells differentiation

F.M.P. Tonelli • A.K. Santos • K.N. Gomes • L.O. Ladeira • R.R. Resende (✉)
Nanomaterials Laboratory, Department of Physics, Institute of Exact Sciences, Federal University of Minas Gerais, 31270-901 Belo Horizonte, MG, Brazil
e-mail: rrresende@hotmail.com

D.A. Gomes
Department of Biochemistry and Immunology, Institute of Biological Sciences, Federal University of Minas Gerais, 31270-901 Belo Horizonte, MG, Brazil

S.L. da Silva
Universidade Federal de São João Del Rei Campus Alto Paraopeba, 36420-000 Ouro Branco, MG, Brazil

M.S. Islam (ed.), *Calcium Signaling*, Advances in Experimental Medicine and Biology 740, DOI 10.1007/978-94-007-2888-2_40,

Abbreviations

7TMS	7-transmembrane segment receptor
Akt	Protein kinase B
AM	Amplitude modulation
BDNF	Brain-derived neurotrophic factor
BMP	Bone morphogenetic protein
BMP4	Bone morphogenetic protein 4
CaMK	Calcium/calmodulin dependent kinase protein
CaR	Calcium sensing receptor
cAMP	Cyclic adenosine monophosphate
cGMP	Cyclic guanosine monophosphate
CREB	Binding element responsive to cAMP
DAG	Diacylglycerol
DKK1	Dickkopf 1
ECC	Embryonic carcimona cells
ECM	Extracellular matrix
ELK	Eph-related tyrosine kinase
ER	Endoplasmatic reticulum
ERK	Extracellular-signal-regulated kinase
ESC	Embryonic stem cells
ExEn	Extraembryonic endoderm
FGF	Fibroblast growth factor
FGF1	Fibroblast growth factor 1
FGF2	Fibroblast growth factor 2
FL	Fluorescein
FM	Frequency modulation
FZD	*Frizzled*
GFP	Green fluorescent protein
GPCR	G protein-coupled receptor
hESC	Human embryonic stem cell
hHSC	Human hematopoietic stem cell
hMSC	Human mesenchymal stem cell
HSC	Hematopoietic stem cell
ICM	Inner cell mass
iMEF	Mitotically inactivated embryonic fibroblast
IP3	Inositol 1,4,5-triphosphate
IP3Rs	Inositol 1,4,5-triphosphate receptors
iPSC	Induced pluripotent stem cell
IVF	*in vitro* fertilized
JAK	Janus kinase
Klf4	Gut-enriched Krüppel-like factor
LIF	Leukemia inhibitory factor
LPA	Lysophosphatidic acid

MKK3	Mitogen-activated Protein Kinase Kinase 3
MAP	Microtubule-associated protein
MAP1B	Protein association with the microtubule 1B
MAP2	Protein associated with type 2 microtubule
MAPK	Pathways of mitogen-activated protein kinases
MAPKK	MAP kinase kinase
mESC	Mouse embryonic stem cell
NAAD	Nicotinic Acid Adenine Dinucleotide
NANOG	Nanog homeobox
NFAT	Nuclear factors of activated T-cells
NFκB	Nuclear factor κBl
NSC	Neural stem cell
OAP	Oct/octamer-associated protein
OCT-4	Octamer-binding transcription factor 4
PI3K	Phosphoinositide Kinase-3
PIP2	Phosphatidylinositol 4,5-biphosphate
PKA	Protein *kinase* A
PKC	Protein kinase C
PLC	Phospholipase C
PSC	Pluripotent stem cell
Ras	Rat sarcoma similar to G protein GTPase
Rcn2	Reticulocalbin-2
RyR	Ryanodine receptors
ROC	Receptor-operated channels
RTKs	Receptors tyrosine kinase
Stk40	Serine/threonine kinase 40
SOX2	Sex determining region Y box 2
SR	Sarcoplasmatic reticulum
SOC	Store-operated channels
SSC	Somatic stem cell
STAT3	Signal transducer and activator of transcription 3
Stk40	Serine/threonine kinase 40
TBX3	T-box transcription factor
Tc	Tetracycline
TGF-β	Transforming growth factor-β
TSC	Tumor stem cell
VOCC	Voltage-operated calcium channels

Introduction

Calcium (Ca^{2+}) is a ubiquitous intracellular signal responsible for controlling numerous cellular processes such as cell differentiation, proliferation, and apoptosis. At one level, its action is simple: cells at rest have a Ca^{2+} of 100 nM but are activated

when this level rises to roughly 1,000 nM. The immediate question is how can this elevation of Ca^{2+} concentration regulate so many processes? The answer lies in the versatility of the Ca^{2+} signaling mechanism in terms of speed, amplitude and spatio-temporal patterning [1].

It is well known that Ca^{2+} is important for cell differentiation and proliferation in mammalian somatic cells. However, $[Ca^{2+}]_i$ in stem cells has not been investigated until recent years [2–5]. This research has attracted a high interest in the field because the evidence suggests that Ca^{2+} signaling is related to cell proliferation and differentiation, which are important functions of stem cells. Recent studies have shown that stem cells have functional Inositol 1,4,5-trisphosphate receptor (IP3R)-regulated intracellular Ca^{2+} stores. They are sensitive to stimulation with ATP, histamine, and platelet-derived growth factor and depend on Ca^{2+} entry through store-operated channels (SOC) entry for refilling of their intracellular Ca^{2+} stores.

The efforts of seeking a broader understanding about these cells are justified by the promising scientific advance that they are able to provide. Besides that their use is still a very controversial topic, both in therapy (due to security in its use without the promotion of carcinogenic effect), and in research (mainly due to the source of the cells to be used in research).

Through the elucidation of the molecular mechanisms in which second messengers (such as Ca^{2+}) act, the possibility of using stem cells can be improved, allowing better use of this important tool: in the repair of epithelial tissue after extensive lesions, in the treatment of degenerative diseases, in reduction on levels of immune rejection in transplantation, and even in research of mechanism of diseases, drug toxicology *screening*, among other purposes [6].

What Are Stem Cells and How to Classify Them?

Stem cells are unspecialized cells that can proliferate while remaining as stem cells, or adopt the process of differentiation: relying on signals received from their neighborhood. To conceptualize them two main properties are considered: their ability to promote their self-renewal in an unlimited way and their ability to terminally differentiate into a wide variety of specific cell types [7].

The ways to classify such cells changes according to the scientific approach adopted by each group. In order to classify stem cells different classifying systems were suggested and to opt for one or other system, divide researchers' opinion. In this chapter we present a merge of the classification existing categories.

A Classifying System Based on the Obtaining Source of Stem Cells

The classification is required to reassemble the origins of pluripotent cells populations, that can be obtained from natural (blastocyst ICM (inner cell mass), niches from adult body, populations of cancer cells) or not natural sources (using cell and molecular biology as tools) (Fig. 40.1).

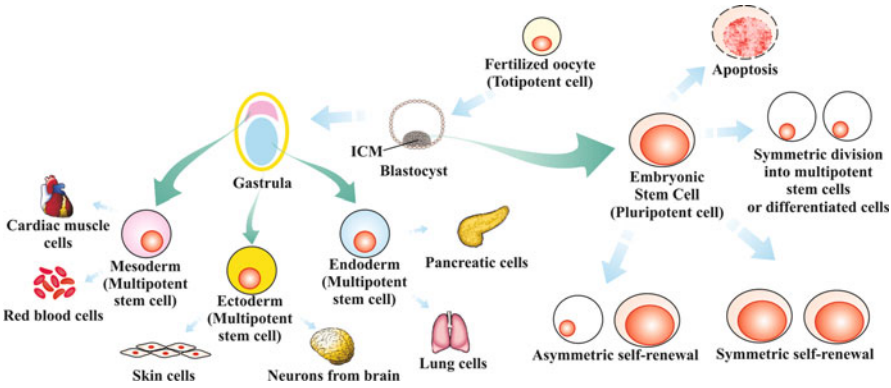

Fig. 40.1 Origin of stem cells potency, and fates. Totipotent cells exist from the fertilized oocyte until the initial morula's blastomeres during embryo development. When these cells proliferate and specialize they originate blastocyst, which has two different cell types including ICM cells. ESCs (embryonic stem cells) that are pluripotent, derive from the ICM. After the blastocyst there is the gastrula stage which has mesoderm endoderm and ectoderm cells (multipotent stem cells). These cells can be generated by ESC differentiation and can differentiate into cells from a specific tissue. So, stem cells can proliferate in symmetric self-renewal (diving into two identical daughter stem cells – increasing the stem cells pool) or asymmetric self-renewal (dividing into one differentiated daughter cell and one stem cell – maintaining the stem cell pool), differentiate through symmetric division without self-renewal (originating two differentiated daughter cells) and suffer apoptosis, besides staying quiescent

The stem cells derived from the ICM of blastocyst are said embryonic stem cells (ESC's): widely found in the developing embryo. Then, pluripotent stem cells can be obtained from *in vitro* fertilized (IVF): the ICM can be extracted from the blastocyst and cultured with a *feeder layer*.

The pluripotent stem cells that remain in niches located in specific regions of an adult body are known as adult or somatic stem cells (SSCs); they are considered remnants of the ESC's and are present in small proportions in tissues.

As will later be descript in this chapter, populations of cancer cells may include cells that dedifferentiated to a stage of stem cells, similar to the ESC's stage (the gene expression profile is similar); these are known as tumor stem cells (TSCs) [8].

There are also not natural sources to obtain stem cells through methodology that involves the transfer of nuclear contents between cells [9], cell fusion (e.g. of ESC-extract with differentiated cell) [10] or through genetic manipulation [11].

A Classifying System Based on the Potency of Stem Cells

This classification is based primarily on differences in stem cells' differentiation potential. The classes of stem cells regarding potency of cell lines are: totipotent, pluripotent, multipotent, unipotent. And some scientists also consider the omnipotent class.

Totipotent are the cells that exist from the zygote until the initial morula's blastomeres; these cells have the ability to originate any cell type. This totipotence ends before the blastocyst stage because, at this stage, it is already possible to identify two different cell types: the trophectoderm's cells and inner cell mass cells (pluripotent cells) [12]. Although omnipotent is not an universally accepted concept, there is still researchers who design this concept disagreeing with those who consider these cells totipotent. However, totipotent cells are capable of cellular self-organization (cells that have the ability to form a basic body plan through gastrulation) and omnipotent cells aren't capable of this self-organization; they are cells with the potential to generate all cell types (as well as totipotent cells), but nevertheless not necessarily these omnipotent cells must have potential for self-organization (unlike totipotent) [13].

The pluripotent ICM cells have the potential to generate many, but not all, cell types [13]. They have lost some of their differentiation potency compared to the totipotent cells.

Multipotent cells are stem cells capable of self renewal, and that can differentiate into various cell types, but these types are limited to a specific tissue, organ or system; for example, the neural multipotent stem cells can differentiate into many cell types (glial cells and neurons), but all of them belong to neural lineage of cell differentiation [13].

Unipotent cells are those capable of generating only one cell type when they adopt a differentiation route [8]. So, it is remarkable, that as the body develops from the embryonic stage of early morula to adult stage, there is a reduction in the capacity of differentiation of stem cells from an individual. That's because the genome, since the beginning of the progress of embryogenesis, becomes transcriptionally active and suffers epigenetic modifications with the passage of time; together these changes will control development since the embryonic stage until adult age.

As these changes occur, the vast majority of cells begin to originate specific transcriptomes, and differentiate into specific cell types; however, not all cells differentiate terminally. There are still somatic stem cells (SSCs) in adults and this occurs because the stem cells can undergo changes in their genomes, but not sufficient to promote total differentiation into a specific cell type; these changes in the genome can, nevertheless, promote a reduction in these cells potential for differentiation.

If stem cells do not receive signals to adopt a differentiation route it can continue as stem cells maintaining potency or adopt an alternative route: apoptosis (programmed cell death) [14].

Alterations on Stem Cell's Transcriptome

The mechanisms and signaling pathways involved in controlling growth and differentiation of stem cells, are not fully elucidated. The various types of tyrosine kinase receptors (RTKs) and G protein-coupled receptor (GPCR) in the membrane

of these cells allow a multitude of different ligands to join, specifically to their receptors, and trigger signaling pathways intracellularly. The different signaling pathways activated by these ligands, after integration of their individual messages, lead to a final cellular response: to maintain stem cells in their undifferentiated state, to conduct the cells to apoptosis, or cause them to adopt a route of cell differentiation. As an example of ligands that interact with these receptors there are several growth factors (as fibroblast grow factor 2 – FGF-2) and cytokines (as activin and leukemia inhibitory factor – LIF), among other signaling molecules [15].

In this chapter will be addressed some signal transduction pathways, activated by these molecules, that lead to changes in gene expression profile of stem cells inducing: cellular differentiation, or the maintenance of these cells' pluripotency.

The Embryonic Stem Cells

The interest to search and isolate pluripotent cells derived from blastocyst on preimplantation stage emerged from studies of tumors in mice gonads. In the 1960s was achieved isolation of undifferentiated cells with: remaining expansion capacity when in culture with mitotically inactivated embryonic fibroblasts (iMEF), and multi-lineage differentiation capacity; these were called embryonic carcinoma cells (ECC) [7].

From this first contact with these cells to the isolation of ESC in mice, it took more than 13 years [7]; the first human embryonic stem cells, in turn, were only isolated in the 1990s: in 1998 [8]. As mentioned earlier in this chapter, the embryonic stem cells are derived from ICM, the blastocyst cell population responsible for originating extra embryonic tissue and tissues of the whole body.

How to Study ESC in Culture

To establish and maintain ESCs with normal karyotype and the ability to fully differentiate into functional cells, scientists generally start by plating undifferentiated ESC with the supply of factors capable of maintaining them undifferentiated in the medium, but also capable of allow their proliferation. That's way onto a *"feeder layer*" comprised of mouse embryonic fibroblasts, in addition to supplying as-yet-unidentified support factors also supplies LIF, which prevents ESC differentiation.

In order to maintain the undifferentiated status: LIF is added to the cultivation of mESC (mouse embryonic stem cell), or if the cells are hESC (human embryonic stem cell), and the cellular propagation takes place using manual microdissection; this latter procedure involves the use of a Pasteur's pipette, for example, to dissect individual hESC's colony into small fragments and then transfer them to new containers with fresh culture [6].

Although, besides keeping the cell on non-differentiated stage, it is also important to promote the generation of specialized functional cells from the ESCs. However one of the great challenges that scientists face is to make this differentiation process be controlled and directed to a specific and unique cell type. In the following topics covered in this chapter the reader can get an overview of which are the mainly pathways that promote stem cell's differentiation into some specific cell types.

induced-Pluripotent Stem Cells (iPSCs)

The induced pluripotent stem cell (iPSC) is a kind of adult cells who suffered genetic reprogrammation to an embryonic stem cell–like state. These cells were first obtained in 2006 from mouse somatic cells [16]. In 2007, Yu et.al. reprogrammed somatic human cell nuclei to an undifferentiated state, and according to them, four factors (*OCT4*, *SOX2*, *NANOG*, and *LIN28*) are sufficient to reprogram human somatic cells to pluripotent stem cells embryonic stem cells-like [17]. Since these findings, researchers are looking for new ways to generate these cells, like using adenovirus [18], bacterial artificial cromossomes [19], and recombinant proteins [20].

The possibility of iPSCs generation from somatic cells, avoids ethical difficulties on using embryonic stem cells in studies and future therapeutical applications; that is because iPSCs also have the ability to self-renew maintaining themselves undifferentiated, and to differentiate into various different cell types [21].

Today there is a large number of studies using these cells trying to understand mechanisms and to find a treatment for degenerative and genetic diseases is huge [22]. But when it comes to the therapeutic use, iPSCs are not ready to be used; however are promising. It is expected that in a near future, iPSCs will be successfully used to treat, for example, brain tumor, neurological diseases [23], and vascular diseases [10].

Mechanistic Basis of Calcium Activity

Intracellular calcium controls many cellular processes, such as fertilization, gene transcription, muscle contraction and cell death. Changes in calcium levels may occur in microseconds or hours, and can be propagated through cells and tissues [1, 24]. In the neuronal function, calcium regulates excitability, excitotoxicity, synaptic transmission, gene expression and as well as cell death [25]. Although many growth factors and neurotrophic factors can influence neuronal differentiation, diverse lines of evidence suggest that neurotransmitters, induce variations in intracellular Ca^{2+}, which is a key regulator of differentiation. Changes in concentration of free intracellular calcium resulting from spontaneous events or from regulated cell cascades, have been shown to initiate specific courses of cell behavior in many circumstances, such as in osteo- and neuronal differentiation of mesenchymal stem cells [26, 27].

During advanced stages of development, intracellular calcium is involved in the induction of differentiation of individual cells. In contrast to the gradient of the calcium response for axial specification, rapid calcium increases induce differentiation, at least in neuronal and muscle cells [28]. In *Xenopus*, spontaneous calcium events produced by Ryanodine receptors (RYRs) during a brief period of development [29], directs differentiation of myocytes in somites. The development of neurons also is regulated by these calcium events, which control processes such as the expression of channels and specific neurotransmitters [30, 31], establishment of growth cones [32] and proper wiring of neuronal networks [33].

It should be noted, however, that the elementary events that constitute intracellular Ca^{2+} signaling – Ca^{2+} Blips or Quarks [34, 35], Puffs or Sparks [36, 37], Intracellular Waves [38] – most probably form the basis of most of all subsequent intercellular signaling events [1, 39]. It is known that Ca^{2+} has a regulatory function in the process of cell fate specification in the nervous system. For example, in spinal neurons from *Xenopus* embryos it was possible to identify two types of spontaneous calcium events which have been characterized both *in vitro* and *in vivo*: rapid increases of global $[Ca^{2+}]_i$ resembling action potentials, and small transient increases of calcium, called waves, which are generated in the growth cone. It has been demonstrated that global increases in calcium usually control the production of neurotransmitters and the maturation of potassium channels, while local calcium waves regulate neurite extension [30, 32]. Many of these effects of calcium are mediated by the regulation of phosphorylation of structural proteins [40]. Other effects, such as acquisition of a phenotype associated with the release of certain neurotransmitters probably require transcription [41–43].

Increases in $[Ca^{2+}]_i$ occur due to influx of Ca^{2+} through the plasma membrane or due to its release from intracellular stores, such as the endoplasmatic reticulum (ER) or, in muscle, from the sarcoplasmatic reticulum (SR). Calcium release from ER/SR is activated by many second messengers, among which is inositol-1,4,5-trisphosphate (IP_3) – a substance that stimulates and modulates activity of IP_3 receptor which release calcium from intracellular stores [44, 45]. When a calcium channel is opened, calcium levels increase in that region, and this micro-domain dissipates as soon as the channel is closed [45, 46].

The highly localized events of opening and rapidly closing calcium channels are referred to calcium *sparks* or *puffs*, depending on the nature and location of the channels. Calcium signals can appear for two purposes: for either activate processes in the micro-domain that has high calcium levels or to recruit other channels in the cell, thus promoting an increase of global $[Ca^{2+}]_i$. However, prolonged increases in $[Ca^{2+}]_i$ may be lethal, so cells use low amplitude calcium signals, or transient calcium signals, known as calcium oscillations. Cells can then use amplitude modulation (AM) or frequency modulation (FM) to decode the information contained in the calcium signal. In AM signaling, it is the amplitude of the calcium signal that initiates the cascade. This mode of signaling is generally considered less reliable than FM, leading to difficulties in detecting small increases in calcium slightly above noise levels, but cells have been shown to be able to respond to small increases in calcium [47]. In FM signaling, the frequency of calcium oscillations is used to

propagate information. For example, in activated T cells it is used to optimize gene expression directed by nuclear transcription factors nuclear factors of activated T-cells (NF-AT) of the Oct/octamer-associated protein (OAP) and of nuclear factor κB (NF-κB) [48, 49].

Calcium could also be propagated from one cell to their neighboring cells through intercellular calcium waves. The spread of calcium waves across progenitor cell populations from brain could be exemplified by radial glial cells. Radial glial cell gap junction coupling is greatest during mid-neurogenesis and decreases in late neurogenesis [50]. However, this decrease in overall cell coupling is accompanied by an increase in gap junction hemichannel-mediated Ca^{2+} waves. It has been shown that gap junction hemichannels mediate Ca^{2+} waves in the developing VZ through the release of ATP that binds to purinergic P2Y1 receptors on neighboring radial glia, thereby activating an IP3-mediated release of Ca^{2+} from internal stores [51, 52]. Interestingly, Ca^{2+} wave frequency, size and distance increase in late neurogenesis [52].The observation that similar levels and types of Cxs are expressed in mid- and late neurogenesis [53–55] suggests that Cx proteins are regulated at a molecular level such that they underlie the formation of gap junction-coupled clusters of cells during mid-neurogenesis and the hemichannel-mediated spread of Ca^{2+} waves during late neurogenesis.

In 2010 Resende et al. reported Ca^{2+} transients in G1 to S transition during cell cycle progression in diverse cell lines, including undifferentiated cells; on these cells the oscillations involve inositol 1,4,5-triphosphate receptors (IP3Rs) and L-type channels. This was an evidence that transients may be involved in stem cell's proliferation [56, 57]. The cell large capacity of convey a wide range of different information through a common cellular second messenger (Ca^{2+}), can consist in the fact that distinct variations in length, frequency and amplitude of oscillations in intracellular Ca^{2+} concentration, encodes for different cellular responses. Understanding the mechanisms that regulate these oscillations and the processes involved in converting its effects on cellular responses, still at large process of research and development.

Flow of cellular information requires coordinated activity of a wide network of signaling pathways. Interaction between pathways provides complex non-linear outputs for a given combination of stimuli. Examples on the density of these interactions were shown by Natarajan and his group [58]. They demonstrated that various receptors, separated or in groups are able to: mobilize calcium, initiate cyclic adenosine monophosphate (cAMP) and cytokines synthesis and also to promote phosphorylation of a variety of proteins involved in signalization. These findings suggest that different external stimuli may converge in a relatively small number of interaction mechanisms to promote signaling.

In this way growth factors, hormones and drugs elicit cellular responses in the form of Ca^{2+} oscillations, the frequencies of which are determined by the amount and type of the agent [59–62]. Patterns of spontaneous and stimulated Ca^{2+} transients drive transcription of specific genes [48, 62–64], and stimulated cAMP transients directly or through BDNF [64] also regulate gene expression [65, 66]. It was shown that only certain bursts of Ca^{2+} spikes generate a cAMP increase [67]. Which can be useful in understanding the coding of gene expression by interactions between

Ca^{2+} transients and cAMP oscillations. Higher frequencies of Ca^{2+} spikes have been shown to control gene expression more directly via Ca^{2+}-dependent kinases that are not efficiently activated by low frequencies of Ca^{2+} transients. For example, cAMP increases induced by serotonin lead to translocation of PKA catalytic subunits into the nucleus of *Aplysia* neurons and gene expression underlying long-term facilitation [66, 68]. The theoretical model combining Ca^{2+} oscillatory machinery and feedback regulation of cAMP synthesis, studied by Gorbunova and Spitzer [67] predicts the existence of low-frequency cAMP transients rather than high-frequency events [69, 70]. These results suggest that it could be fruitful to investigate interactions among other classes of second messengers, as tiers of messenger systems may be necessary to generate different patterns of transients that produce unique cellular responses to stimulation.

Some discussion and works involving the $G\alpha_{i/o}$-coupled receptors demonstrated that, activation of this signaling pathway, generating cAMP, would lead carcinoma stem cells to differentiate into neuronal cells [42, 71], and neural stem cells to regulate neurite outgrowth [72].

Expression Profile

Correlations between spatial patterns of Ca^{2+} signaling and those of developmental gene expression represent perhaps the most exciting areas of research at present. It has been known for some time, from work with cultured cells, that Ca^{2+} can activate signaling pathways in both the nucleus and cytoplasm to stimulate gene expression by different pathways [73, 74], that it can function as an inhibitor as well as an activator of gene expression [75, 76], and that the frequency as well as the amplitude of Ca^{2+} transients is important for the regulation of gene expression [48, 76–78]. We suggest that many of the features of Ca^{2+}-activated gene expression that are found in cultured cells might also be relevant to intact embryos. In T-cells, for example, oscillations enhance both the efficiency and specificity of signaling through the Ca^{2+}-dependent transcription factors nuclear factor of activated T-cells (NFAT), Oct/Oap and nuclear factor kappa B (NF kappa B) in ways that are consistent with each factor's Ca^{2+} dependence and kinetics of activation and deactivation [48]. In addition, in Xenopus embryos the expression of the early neural genes Zic3 and geminin were shown to be downregulated when Ca^{2+} transients, which occurred at the right time and in the right place to be associated with neural induction, were blocked by specific L-type Ca^{2+}-channel antagonists [79, 80].

The expression profile of differentiating cells can reveal key factors involved in the neuronal differentiation process. Observations based on the construction of networks from gene per gene analyses also suggest that hematopoietic sources activate multiple programs that compete subsequently with other programs, although the way in which this competition is resolved is not clear [81]. Comparisons of initial and late differentiation events reveal an increase in the number of genes differentially regulated in the latter [82]. This can be explained by multiple initiating cell

lines: initial cells from the differentiation still express genes that correlate with multiple lineages, but throughout later stages of differentiation programs that are not required are inactivated, while end markers of differentiation are activated. Clearly, many late functions, such as cell cycle control and constitutive machinery, will be the same for all differentiated cells [82].

In order to understand the topology and the dynamics of transcriptional regulatory networks that control biological processes, one must focus on the following issues:

1. The identity and expression levels of overlap and interaction
2. How interactions change over time
3. The phenotypic impact of interrupting key overlaping points

The complexity of the eukaryotic transcriptional regulatory machinery reflects the many responses that it controls, but it also makes the understanding of these a networks a difficult task. This issue leads to obvious questions relates to the mechanisms through which a specific transcriptional response is triggered, including how a signaling pathway activates a transcription factor, how temporal specificity is generated, and the origins of a target.

For example, it is frequently assumed that the equilibrium state of a message RNA (mRNA) (measured in a microarray) is indicative of the rate at which transcription or even translation of a protein occurs. Moreover, it is also assumed that if a transcription factor is expressed it is active, even though dimerization, post-translational modifications and cytolocalization should also be considered. Even in the absence of knowledge about the architecture of a network it is possible to use the gene expression patterns to prove that the structural state of a complex network is natural, and to extract characteristic signatures of high dimensional stable attractor. It is not evident that such stable behavior can arise from the interactions of a large number of irregularly connected elements [83], but an important result of the analysis of discrete genetic networks is that they provide the architectural characteristics of a global network. A complex network will produce spontaneously globally coherent patterns of gene activation, such as rapid deceleration of a group of relatively small stable attractors, instead of eventually visiting all the possible states [84]. The architectural characteristics of a network known to increase the regime of ordered behavior includes:

1. Few interactions [84].
2. Preferential use of certain groups of functions for regulatory interactions between genes [84].
3. A topology without scale boundaries [85].

These characteristics have been predominant in gene and protein networks. It has been verified that differentiation of embryonic P19 cells into neurons, and of HL60 cells into neutrophils [86] does not result from a simple transition state of a bi-stable state as described in the traditional model [87, 88]. Instead, cell differentiation in mammals seems to be a process of many steps in high dimension, a result which is consistent with the high connectivity of the cellular complex that sustains the

regulatory genomic network. Studies in analysis revealed that differentiation is a process of many steps consistent with a model in which many keys are coupled along many states of space and dimensions, and that originates multiple stable stated which represent high dimensional attractors in the wide regulatory genomic network [84, 89]. Such an emphasis suggests a new way of specifying the many step processes of cell differentiation in a sequence of discrete meta stable intermediaries which evade conventional analysis of elapsed time of the entire population. The existence of a multi-stable and multi-dimensional behavior during cell differentiation in mammals has important implications in the way in which differentiation is interpreted and ultimately, in how commitment of stem cells during development occurs.

Major Pathways Involved in Maintaining Pluripotency of Embryonic Stem Cells in Culture

It is known today, as a result of various studies on embryonic stem cells of mice and humans, that the Wnt/β-catenin pathway is involved in maintaining pluripotency in both human and mice stem cells. The Wnt signaling pathway can activate a cascade of intracellular reactions triggered by the binding of Wnt proteins, and palmiltolated glycoproteins, to their receptors on the cell's membrane (Fig. 40.2).

In mouse embryonic stem cells LIF/Signal Transducer and Activator of Transcription (STAT-3), bone morphogenetic protein (BMP)/Id and LIF/phosphatidylinositol 3-kinases (PI3K)-protein kinase B (Akt) pathways are also involved in maintaining cell's pluripotency and to study their influency on mESCs pluripotence, these cells can be cultured in the presence or absence of serum [90]; when serum is

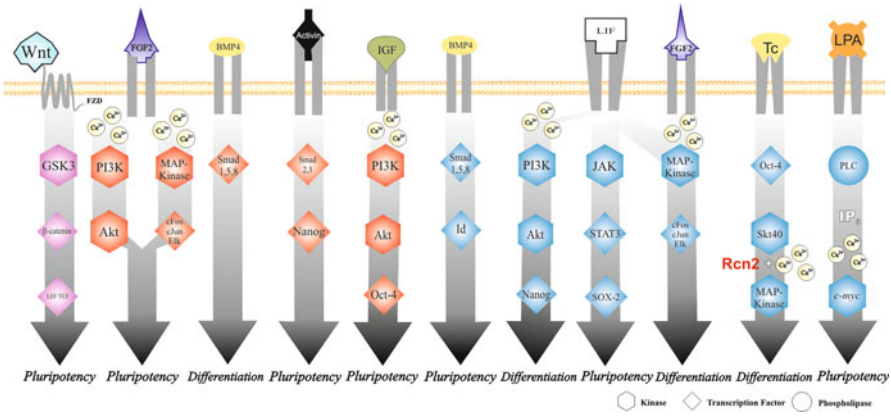

Fig. 40.2 Major pathways involved in maintaining pluripotency of embryonic stem cells, or promoting their differentiation in culture. Pathways in *blue* are from mESC; those in *red* are from hESC. In *purple* are the pathways observed in both cell types

present, the LIF (a serum derivative molecule) is responsible for triggering signaling pathways involving JAK, PI3K or mitogen-activated protein kinases (MAPK) [91]. In the first two situations, this molecule acts promoting the maintenance of cellular pluripotency, while in the latter situation, it induces their differentiation. In the absence of serum in cell culture, the pluripotency can be maintained through the combined addition of LIF and BMP4 into culture. As BMP4 join to its receptors, it leads to activation of Smad1, 5, 8, which in turns induce the activation of the transcription factor Id, thus maintaining the cell's pluripotency.

In hESC, the presence of LIF and BMP-4 in the culture medium is not sufficient to maintain pluripotency; according to results reported by Wei and colleagues, this fact is justified by differences in trancriptoma of murine and human cells. In human cells exogenous or cells' produced FGF-2, acts as an important signaling ligand for the maintenance of pluripotency [92]. This molecule can trigger the activation of MAPK and PI3K/Akt to do so [93]. Activin is also a ligand that leads to the maintenance of pluripotency through activation of Smad2, 3, which in turn lead to direct transcriptional activation of a gene for pluripotency: *Nanog* [92]. Signaling pathways that increases the expression of other genes from the transcription factors Oct4, Sox2, Klf4, cMYC and Lin28 are also relationated with promotion of pluripotency [10].

When it comes to calcium, according to Todorova et al., lysophosphatidic acid (LPA), a potent mitogen present in serum, can evoke Ca^{2+} mobilization from the endoplasmic reticulum through the phospholipase C (PLC) pathway on mESC. After binding to a G-protein coupled receptor, LPA can induce the PLC activation and IP3 production. In the endoplasmatic reticulum IP3 finally stimulates Ca^{2+} release inducing a signaling cascade which leads to the induction of *cmyc* expression. Additionally, the DNA synthesis is also increased by this ligand on these cells: it stimulates maintenance of pluripotency and the cell proliferation [94].

Wnt, Frizzled Receptors and Ca^{2+}

The Wnt family of glycoproteins are able to promote the activation of *Frizzled* (FZD) receptors, a G protein-coupled receptors [95], that are largely involved in embryonic development. The Wnt pathway, as seen earlier, is critical for maintenance of undifferentiated murine and hESC, for maintenance of large populations of these cells by stimulating their proliferation and suppressing their apoptosis.

Three possible well-characterized signaling pathways can be activated by this ligand on FZD receptors: canonical pathway-Wnt/β-catenin, FZD/planar cell polarity pathway, and FZD/Ca^{2+} pathway.

It is unclear whether the initiation of this signaling pathway involves activation of phospholipases by GPCR and/or an increase in cGMP. It is known, however, that atypical protein kinase C (aPKC, a.k.a. PKCζ) is activated in this signaling pathway in a Ca^{2+}-dependent mechanism [95].

Major Pathways Involved in Differentiation of Embryonic Stem Cells in Culture

Through the MAPK pathway signaling cascade a ligand can trigger activation of cFos, cJun or Elk, thus inducing cell differentiation, and also inhibit the activity of transcription factor TBX3. This factor is responsible for activation of *Nanog* gene: a gene of paramount importance for the maintenance of pluripotency; then, with TBX3 inhibited the pluripotency is not maintained and the cell enters into a differentiation route [8].

In human embryonic stem cells, induction of cell differentiation can occurs through signaling triggered for the association of the ligand BMP-4 to its receptor on the cell surface; this signaling pathway involves the participation of transcription factors Smad1,5,8 [8].

Recently has been shown the involvement of REX1 on the regulation of proliferation/differentiation of hMSCs through the suppression of p38 MAPK pathway. REX1 represses the expression of MKK3 (or MAPKK3 – an activator of p38 MAPK in hMSCs); so when it is present in high concentration, cell differentiation is suppressed and proliferation is stimulated. This marker also suppress Notch and STAT3 signaling [96].

Li et al. results showed that in mouse embryonic stem cell besides being an important transcription factor for the maintenance of an undifferentiated state, Oct4 is also related to Erk/MAPK pathway (that is involved on ESC differentiation). Oct4, after binding of tetracycline (Tc) on surface receptors, has serine/threonine kinase 40 (Stk40) gene as a target gene and Stk40 can activate the Erk/MAPK pathway and induce extraembryonic–endoderm (ExEn) differentiation in mESCs. Stk40 is also able to promote this kind of differentiation interacting with Rcn2 (a calcium binding protein), which activates Erk1/2 itself [97].

Somatic Stem Cells

SSCs, or adult stem cells are found in already developed tissues and they are very rare which difficult their isolation for study. They have distinct characteristics from regular body cells due to their microenvironments and the expression of specific markers of some tissues, mainly related to the extracellular matrix (ECM) [98]; these cells also have the ability to generate specialized cells of other tissues, a process also known as transdifferentiation.

There are several examples of transdifferentiation of SSCs that occur naturally. The most common occurrence is probably in cancer, resulting in different types of tumors. In this case, the patterns of gene expression result in a change of morphology and behavior, contributing to carcinogenesis. However, the mechanism by which transdifferentiation is activated is still unknown, although it is of great interest for application in cellular therapies [99].

The interaction of stem cells with specific microenvironmental factors is a key mechanism in regulating the maintenance of their self-renewal and differentiation capacity. Many of the stem cells' differentiation mechanisms are analogous to the pathways that promote tumoriogenesis, which leads scientists to consider, in some cases, that the formation of a neoplasm can occur initially from stem cells [2].

There are several types of adult stem cells such as epidermal, hematopoietic, cardiac, neuronal and mesenchymal [100]. The latter are found in the stroma of organs and is therefore also known as stromal stem cells [101, 102]. In this chapter will be discussed only the main types of stem cells and their mechanism of proliferation and differentiation, focusing on the ones related to Ca^{2+}.

Ca^{2+} Signaling in the Process of Hematopoietic Stem Cells' Differentiation

Among SSCs, the best characterized with regard to its mechanisms of differentiation are the hematopoietic stem cells (HSCs), found in bone marrow and umbilical cord blood.

The niche of HSCs is an anatomical unit located in the endosteum of the bone marrow cavity, which is composed of osteoblasts, osteoclasts and stromal fibroblasts, beyond others cells. In some studies it is evident the importance of osteoblasts to the development of HSCs [103]. These osteoblasts express high levels of Jagged-1, a ligand for Notch receptors. Activation of Notch1 has been shown to result in a greater degree of self-renewal of HSCs, probably by inducing the expression of a set of self-renewal genes, including HES1.

The conditional suppression of BMPR1 also leads to increased numbers of N-cadherin $^{+}$CD45^{-} osteoblastic. Thus, signaling by BMP type IA BMPR complex, regulates the population of HSCs and consequently the size of the niche. A subpopulation of murine LSK cells also expressed N-cadherin, which interacts and forms a complex with β-catenin [90, 104].

Wnt proteins have been used to maintain and expand mHSCs because they are potent inducers of β-catenin signaling. It is possible that under certain conditions, some metalloproteinases such as ADAM10 cause the breakdown of membrane-bound N-cadherin, thereby increasing β-catenin cytoplasmic pool, which will now be available to work in the canonical Wnt pathway (inducing expression of target genes, including cell cycle regulatory proteins). Together with β-catenin, cMYC, cMYB, JUNB, p18 and p27 are initially responsible by proliferation and differentiation of HSCs.

HSCs are sensitive to high levels of Ca^{2+}, mainly due to the GPCRs receptors expressed on their membranes [105]. This kind of receptor is required to maintain HSCs near to the endosteal surface of bone. The MUC1 protein can initiate Ca^{2+} signaling through association with its ligand ICAM-1; this suggests that MUC1 mediates cytoskeletal rearrangements to facilitate the interaction between HSC and its niches.

Once allocated and located within the niche, cytokines, and growth factors are secreted locally and direct the fate of stem cells, initiating a cascade of intracellular signals.

Transforming growth factor-β (TGF-β) is one of the few negative regulators of HSCs known. It keeps stem cells in a state of slow or idle activity partially blocking the expression of cytokine receptors on the cell surface [92]. The arrest of cell cycle regulation requires hHSCs p57. Furthermore, angiopoietin-1, produced by stromal cells, enhances HSCs capacity to become quiescent, through interaction with receptor RTKs.

FGF-1 in stem cells has the role of self-renewal and proliferation. After binding to its receptors some signaling pathways can be activated, including MAPK, STAT and PI3Ks [15]. Recent evidence indicates that members of the protein complex PCG play key role in normal hematopoiesis, and repress the expression of HOX gene in mice [106]; this HOX gene is an important regulator of differentiation pathways. However, overexpression of HOXB4 in human cells was not related to any increase in expansion or to the promotion of myeloid differentiation [107].

Cardiac Stem Cells and Dependence of Ca^{2+} Signals

Regenerative cardiovascular medicine hopes that it will be possible to use this type of stem cells for therapeutic purposes. However, although they have great chances of being employed in cardiac reparative therapies, it is necessary first to confirm its expansion *in vitro*; a clinical application may only be possible after intensive research on this expansion. The accurate control of proliferation of these cells is necessary, because their number in cardiac muscle tissue is vanishingly small [108].

In cardiac stem cells differentiation into cardiomiocytes, FGF and TGFβ factor's family are the main regulators. The activity of TAK, a protein that belongs to MAPK pathway, is stimulated by activation of TGFβ receptors. The TAK acts on the transcription factors ATF2 and CREB through the Ca^{2+} responsive MAPK pathway [109]. ATF2 can also bind to the Smads to promote the expression of transcription factors responsible for the development of cardiac phenotype. P42/P44 MAPK pathway (ERK) is activated by FGFs, through Ras protein [110] (Fig. 40.3).

Wnt11 also participates in the process, acting through activation of Ca^{2+} dependent pathway; this pathway include the participation of Ca^{2+}/calmodulin-dependent protein kinase (CaMK)-II, PKC and JNK [111].

Wnt proteins can also be repressors of cardiac differentiation and these proteins can be inhibited by antagonists such as Crescent and DKK1 (*Dickkopf*); the latter promotes differentiation into cardiomyocytes. However, *Dishevelled*, a mediator of the canonical pathway Wnt/β-catenin, which implies the β-catenin and transcription factor family TCF/LEF, has recently been used to activate CaMK pathway by PCP (planar cell polarity) [108].

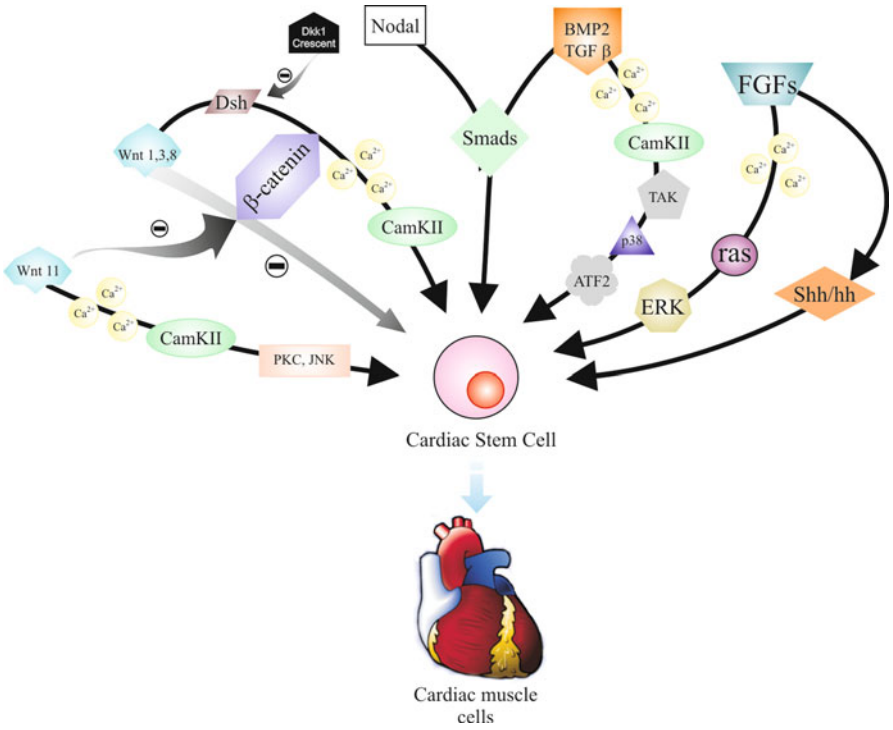

Fig. 40.3 Major pathways involved in maintaining pluripotency of cardiac stem cells, or promoting their differentiation. See text for more information

Neural Stem Cells and the Ca^{2+} Signaling

Neural stem cells (NSCs) have the ability to guarantee the proliferation of cells in the adult nervous system, also being responsible for both the formation of neuronal and glial components. The process of neuronal differentiation, after embryonic development, is restricted to specific brain regions such as the dentate gyrus of the hippocampus and the subventricular zone (where this kind of stem cell was first identified) [112].

In development of NSCs, when these cells receives an external stimulus, often by growth factor binding to their receptors, there is an suppression on the expression of genes responsible for the pluripontent phenotype (mainly components of the Wnt pathway and transcription factors), whereas the genes that confer typical neurons characteristics are now widely expressed [113]. Some factors that promote neuronal differentiation, such as NeuroD, begin to act on the cell that is now differentiating.

The NeuroD binds to specific sequences of DNA when phosphorylated by CaMK (enzyme whose modulation activity is dependent on intracellular Ca^{2+}) [114]. At the same time begin to be expressed neuronal cytoskeleton binding proteins such as proteins from MAP family, for example MA1B; protein that is sensitive to Ca^{2+}

Future Perspectives and Conclusions

The use of stem cells as an alternative to treatments for diseases will change the medicine concepts currently known. The implementation of stem cells in cell substitution therapies will require a detailed understanding of the effect of growth factors on proliferation and differentiation of these cells *in vitro* and *in vivo*, particularly when it comes to be delivery to patient.

The proposed cell substitution in new clinical approaches involving the transplantation of exogenous stem cells to sites of disease, should be viewed with caution; however this promising new form of treatment should be considered due to the large potential of bring benefits to society.

Use of linear signal transduction pathways for developmental and cell differentiation control is dictated by the current information processing paradigm in cell biology lead us to rapidly reached its limits. The base of this paradigm emerged from experiments which demonstrated that soluble hormones and neurotransmitters present functional effects on cell regulation which are mediated by their binding to cell surface signaling receptors. However, more recent studies have clarified that calcium signaling pathways induced by calcium oscillations play equally important roles in the control of the cellular phenotype [27, 115–117]. Furthermore, cell shape regulates switching between different cell fates by inducing the same gene and calcium-dependent signal protein activity profiles that are activated by cell binding to specific growth factors and oscillating patterns. These observations, which can be combined with the increasing information available, but not interconnected, the processing of information within cell signaling networks emphasizes the need to build a more comprehensive and integrated model of cell regulation.

Calcium as an attractor in stem cells and progenitor cells drive the differentiation to great diversity of specialized neuronal cells and glial cells compositing a tridimensional complex cyto-architecture called brain. A great intrinsic signaling process is activated composed by neurotransmitter receptors, CaR, ROC, RYR, SOC, VOCC, NAADP or second messengers such as – DAG, 1,4,5IP3, cAMP, PIP_2 or even by modulation of kinase proteins, ERK or MAPK and enzyme, PLC. All the process is regulated by wakes and peak of calcium localized in micro-domains or in the role cell. In addition of it there are events such as amplitude and frequencies of calcium signalization. The study of the network of signalization is complex because each part of it can be involved in different levels of organization in different nets, organized around different attractors composing regulatory genetic networks which can be helpful to try understand the role process.

We suggest that further technical advances in several key areas will add greatly to our understanding. The first will be the continued development of Ca^{2+} reporters that can be targeted to specific cell types within a developing embryo and to subcellular compartments within these cells. There have been some encouraging advances in this area [118, 119]. The second area for advancement will be the generation of targeted reporters that can be used as probes for non-invasive imaging of gene expression patterns in living embryos. Once again, advances are being made on this front.

Dorsky et al. reported the development of a technique for long-term imaging of regulated gene expression in zebrafish [120]. Such probes could potentially be expressed in embryos along with a Ca^{2+} reporter, and their activity simultaneously (or near simultaneously) imaged. The third area to be advanced will be the continuation of the development of reporters to visualize the activation of Ca^{2+}-sensitive targets that mediate the crosslinking between Ca^{2+} signals and other developmental signaling networks. Encouraging advances, such as the use of fluorescein (FL)- or green fluorescent protein (GFP)-linked calmodulin (CaM) probes [121, 122], and the development of fluorescence resonance energy transfer (FRET)-based biosensors to monitor agonist-induced phospholipase C activation [123], have been made in this area. The future, therefore, looks encouragingly bright for the continued exploration of developmental Ca^{2+} signaling.

Acknowledgements This work was supported by Instituto Nacional de Ciência e Tecnologia de Nanomateriais de Carbono, CNPq (Conselho Nacional de Desenvolvimento Científico e Tecnológico), Brazil. R.R.R, L.O.L., K.N.G., and D.A.G. are grateful for grants from CNPq (Conselho Nacional de Desenvolvimento Científico e Tecnológico), FAPEMIG (Fundação de Amparo à Pesquisa do Estado de Minas Gerais), and CAPES (Coordenação de Aperfeiçoamento de Pessoal de Nível Superior).

References

1. Berridge MJ, Lipp P, Bootman MD (2000) The versatility and universality of calcium signalling. Nat Rev Mol Cell Biol 1:11–21
2. Kawano S, Shoji S, Ichinose S, Yamagata K, Tagami M, Hiraoka M (2002) Characterization of Ca(2+) signaling pathways in human mesenchymal stem cells. Cell Calcium 32:165–174
3. Kawano S, Otsu K, Shoji S, Yamagata K, Hiraoka M (2003) Ca(2+) oscillations regulated by Na(+)-Ca(2+) exchanger and plasma membrane Ca(2+) pump induce fluctuations of membrane currents and potentials in human mesenchymal stem cells. Cell Calcium 34:145–156
4. Li GR, Sun H, Deng X, Lau CP (2005) Characterization of ionic currents in human mesenchymal stem cells from bone marrow. Stem Cells 23:371–382
5. Heubach JF, Graf EM, Leutheuser J, Bock M, Balana B, Zahanich I, Christ T, Boxberger S, Wettwer E, Ravens U (2004) Electrophysiological properties of human mesenchymal stem cells. J Physiol 554:659–672
6. Ameen C, Strehl R, Bjorquist P, Lindahl A, Hyllner J, Sartipy P (2008) Human embryonic stem cells: current technologies and emerging industrial applications. Crit Rev Oncol Hematol 65:54–80
7. Friel R, van der Sar S, Mee PJ (2005) Embryonic stem cells: understanding their history, cell biology and signalling. Adv Drug Deliv Rev 57:1894–1903
8. Callihan P, Mumaw J, Machacek DW, Stice SL, Hooks SB (2011) Regulation of stem cell pluripotency and differentiation by G protein coupled receptors. Pharmacol Ther 129:290–306
9. Wakayama T, Tabar V, Rodriguez I, Perry AC, Studer L, Mombaerts P (2001) Differentiation of embryonic stem cell lines generated from adult somatic cells by nuclear transfer. Science 292:740–743
10. Kane NM, Xiao Q, Baker AH, Luo Z, Xu Q, Emanueli C (2011) Pluripotent stem cell differentiation into vascular cells: a novel technology with promises for vascular re(generation). Pharmacol Ther 129:29–49

11. Takayama N, Nishikii H, Usui J, Tsukui H, Sawaguchi A, Hiroyama T, Eto K, Nakauchi H (2008) Generation of functional platelets from human embryonic stem cells in vitro via ES-sacs, VEGF-promoted structures that concentrate hematopoietic progenitors. Blood 111:5298–5306
12. Niwa H (2007) How is pluripotency determined and maintained? Development 134:635–646
13. Denker HW (2006) Potentiality of embryonic stem cells: an ethical problem even with alternative stem cell sources. J Med Ethics 32:665–671
14. Leandri RD, Archilla C, Bui LC, Peynot N, Liu Z, Cabau C, Chastellier A, Renard JP, Duranthon V (2009) Revealing the dynamics of gene expression during embryonic genome activation and first differentiation in the rabbit embryo with a dedicated array screening. Physiol Genomics 36:98–113
15. Suwinska A, Tarkowski AK, Ciemerych MA (2010) Pluripotency of bank vole embryonic cells depends on FGF2 and activin A signaling pathways. Int J Dev Biol 54:113–124
16. Takahashi K, Yamanaka S (2006) Induction of pluripotent stem cells from mouse embryonic and adult fibroblast cultures by defined factors. Cell 126:663–676
17. Yu J, Vodyanik MA, Smuga-Otto K, Antosiewicz-Bourget J, Frane JL, Tian S, Nie J, Jonsdottir GA, Ruotti V, Stewart R, Slukvin II, Thomson JA (2007) Induced pluripotent stem cell lines derived from human somatic cells. Science 318:1917–1920
18. Stadtfeld M, Maherali N, Breault DT, Hochedlinger K (2008) Defining molecular cornerstones during fibroblast to iPS cell reprogramming in mouse. Cell Stem Cell 2:230–240
19. Woltjen K, Michael IP, Mohseni P, Desai R, Mileikovsky M, Hamalainen R, Cowling R, Wang W, Liu P, Gertsenstein M, Kaji K, Sung HK, Nagy A (2009) piggyBac transposition reprograms fibroblasts to induced pluripotent stem cells. Nature 458:766–770
20. Kim JB, Sebastiano V, Wu G, Arauzo-Bravo MJ, Sasse P, Gentile L, Ko K, Ruau D, Ehrich M, van den Boom D, Meyer J, Hubner K, Bernemann C, Ortmeier C, Zenke M, Fleischmann BK, Zaehres H, Scholer HR (2009) Oct4-induced pluripotency in adult neural stem cells. Cell 136:411–419
21. Qin T, Miao XY (2010) Current progress and application prospects of induced pluripotent stem cells. Yi Chuan 32:1205–1214
22. Park IH, Arora N, Huo H, Maherali N, Ahfeldt T, Shimamura A, Lensch MW, Cowan C, Hochedlinger K, Daley GQ (2008) Disease-specific induced pluripotent stem cells. Cell 134:877–886
23. Emdad L, D'Souza SL, Kothari HP, Qadeer ZA, Germano IM (2011) Efficient differentiation of human embryonic and induced pluripotent stem cells into functional astrocytes. Stem Cells Dev. Not available-, ahead of print. doi:10.1089/scd.2010.0560
24. Bootman MD, Lipp P, Berridge MJ (2001) The organisation and functions of local Ca(2+) signals. J Cell Sci 114:2213–2222
25. Berridge MJ (1998) Neuronal calcium signaling. Neuron 21:13–26
26. Sun S, Liu Y, Lipsky S, Cho M (2007) Physical manipulation of calcium oscillations facilitates osteodifferentiation of human mesenchymal stem cells. FASEB J 21:1472–1480
27. Gu X, Olson EC, Spitzer NC (1994) Spontaneous neuronal calcium spikes and waves during early differentiation. J Neurosci 14:6325–6335
28. Buonanno A, Fields RD (1999) Gene regulation by patterned electrical activity during neural and skeletal muscle development. Curr Opin Neurobiol 9:110–120
29. Ferrari MB, Ribbeck K, Hagler DJ, Spitzer NC (1998) A calcium signaling cascade essential for myosin thick filament assembly in Xenopus myocytes. J Cell Biol 141:1349–1356
30. Gu X, Spitzer NC (1995) Distinct aspects of neuronal differentiation encoded by frequency of spontaneous Ca2+ transients. Nature 375:784–787
31. Carey MB, Matsumoto SG (1999) Spontaneous calcium transients are required for neuronal differentiation of murine neural crest. Dev Biol 215:298–313
32. Gomez TM, Spitzer NC (1999) In vivo regulation of axon extension and pathfinding by growth-cone calcium transients. Nature 397:350–355
33. Wong RC, Pera MF, Pebay A (2008) Role of gap junctions in embryonic and somatic stem cells. Stem Cell Rev 4:283–292

34. Bootman M, Niggli E, Berridge M, Lipp P (1997) Imaging the hierarchical Ca2+ signalling system in HeLa cells. J Physiol 499(Pt 2):307–314
35. Lipp P, Niggli E (1998) Fundamental calcium release events revealed by two-photon excitation photolysis of caged calcium in Guinea-pig cardiac myocytes. J Physiol 508(Pt 3):801–809
36. Yao Y, Choi J, Parker I (1995) Quantal puffs of intracellular Ca2+ evoked by inositol trisphosphate in Xenopus oocytes. J Physiol 482(Pt 3):533–553
37. Cheng H, Lederer WJ, Cannell MB (1993) Calcium sparks: elementary events underlying excitation-contraction coupling in heart muscle. Science 262:740–744
38. Bootman MD, Berridge MJ (1996) Subcellular Ca2+ signals underlying waves and graded responses in HeLa cells. Curr Biol 6:855–865
39. Bootman MD, Berridge MJ, Lipp P (1997) Cooking with calcium: the recipes for composing global signals from elementary events. Cell 91:367–373
40. Lautermilch NJ, Spitzer NC (2000) Regulation of calcineurin by growth cone calcium waves controls neurite extension. J Neurosci 20:315–325
41. Spitzer NC, Root CM, Borodinsky LN (2004) Orchestrating neuronal differentiation: patterns of Ca2+ spikes specify transmitter choice. Trends Neurosci 27:415–421
42. Resende RR, Alves AS, Britto LR, Ulrich H (2008) Role of acetylcholine receptors in proliferation and differentiation of P19 embryonal carcinoma cells. Exp Cell Res 314:1429–1443
43. Resende RR, Gomes KN, Adhikari A, Britto LR, Ulrich H (2008) Mechanism of acetylcholine-induced calcium signaling during neuronal differentiation of P19 embryonal carcinoma cells in vitro. Cell Calcium 43:107–121
44. Bird GS, Putney JW Jr (1996) Effect of inositol 1,3,4,5-tetrakisphosphate on inositol trisphosphate-activated Ca2+ signaling in mouse lacrimal acinar cells. J Biol Chem 271: 6766–6770
45. Tumelty J, Scholfield N, Stewart M, Curtis T, McGeown G (2007) Ca2+-sparks constitute elementary building blocks for global Ca2+-signals in myocytes of retinal arterioles. Cell Calcium 41:451–466
46. Maier LS, Zhang T, Chen L, DeSantiago J, Brown JH, Bers DM (2003) Transgenic CaMKIIdeltaC overexpression uniquely alters cardiac myocyte Ca2+ handling: reduced SR Ca2+ load and activated SR Ca2+ release. Circ Res 92:904–911
47. Dolmetsch RE, Lewis RS, Goodnow CC, Healy JI (1997) Differential activation of transcription factors induced by Ca2+ response amplitude and duration. Nature 386:855–858
48. Dolmetsch RE, Xu K, Lewis RS (1998) Calcium oscillations increase the efficiency and specificity of gene expression. Nature 392:933–936
49. Li W, Llopis J, Whitney M, Zlokarnik G, Tsien RY (1998) Cell-permeant caged InsP3 ester shows that Ca2+ spike frequency can optimize gene expression. Nature 392:936–941
50. Lo Turco JJ, Kriegstein AR (1991) Clusters of coupled neuroblasts in embryonic neocortex. Science 252:563–566
51. Weissman TA, Riquelme PA, Ivic L, Flint AC, Kriegstein AR (2004) Calcium waves propagate through radial glial cells and modulate proliferation in the developing neocortex. Neuron 43:647–661
52. Cotrina ML, Lin JH, Alves-Rodrigues A, Liu S, Li J, Azmi-Ghadimi H, Kang J, Naus CC, Nedergaard M (1998) Connexins regulate calcium signaling by controlling ATP release. Proc Natl Acad Sci USA 95:15735–15740
53. Kihara AH, Paschon V, Akamine PS, Saito KC, Leonelli M, Jiang JX, Hamassaki DE, Britto LR (2008) Differential expression of connexins during histogenesis of the chick retina. Dev Neurobiol 68:1287–1302
54. Kihara AH, Santos TO, Osuna-Melo EJ, Paschon V, Vidal KS, Akamine PS, Castro LM, Resende RR, Hamassaki DE, Britto LR (2010) Connexin-mediated communication controls cell proliferation and is essential in retinal histogenesis. Int J Dev Neurosci 28:39–52
55. Cina C, Bechberger JF, Ozog MA, Naus CC (2007) Expression of connexins in embryonic mouse neocortical development. J Comp Neurol 504:298–313

56. Resende RR, da Costa JL, Kihara AH, Adhikari A, Lorencon E (2010) Intracellular Ca2+ regulation during neuronal differentiation of murine embryonal carcinoma and mesenchymal stem cells. Stem Cells Dev 19:379–394
57. Resende RR, Adhikari A, da Costa JL, Lorencon E, Ladeira MS, Guatimosim S, Kihara AH, Ladeira LO (2010) Influence of spontaneous calcium events on cell-cycle progression in embryonal carcinoma and adult stem cells. Biochim Biophys Acta 1803:246–260
58. Natarajan K, Berk BC (2006) Crosstalk coregulation mechanisms of G protein-coupled receptors and receptor tyrosine kinases. Methods Mol Biol 332:51–77
59. Shen P, Larter R (1995) Chaos in intracellular Ca2+ oscillations in a new model for non-excitable cells. Cell Calcium 17:225–232
60. Woods NM, Cuthbertson KS, Cobbold PH (1986) Repetitive transient rises in cytoplasmic free calcium in hormone-stimulated hepatocytes. Nature 319:600–602
61. Kraus M, Wolf B (1993) Cytosolic calcium oscillators: critical discussion and stochastic modelling. Biol Signals 2:1–15
62. Haisenleder DJ, Yasin M, Marshall JC (1997) Gonadotropin subunit and gonadotropin-releasing hormone receptor gene expression are regulated by alterations in the frequency of calcium pulsatile signals. Endocrinology 138:5227–5230
63. Chang LW, Spitzer NC (2009) Spontaneous calcium spike activity in embryonic spinal neurons is regulated by developmental expression of the Na+, K+-ATPase beta3 subunit. J Neurosci 29:7877–7885
64. Kuczewski N, Porcher C, Ferrand N, Fiorentino H, Pellegrino C, Kolarow R, Lessmann V, Medina I, Gaiarsa JL (2008) Backpropagating action potentials trigger dendritic release of BDNF during spontaneous network activity. J Neurosci 28:7013–7023
65. Willoughby D, Cooper DM (2006) Ca2+ stimulation of adenylyl cyclase generates dynamic oscillations in cyclic AMP. J Cell Sci 119:828–836
66. Kaang BK, Kandel ER, Grant SGN (1993) Activation of camp-responsive genes by stimuli that produce long-term facilitation in aplysia sensory neurons. Neuron 10:427–435
67. Gorbunova YV, Spitzer NC (2002) Dynamic interactions of cyclic AMP transients and spontaneous Ca(2+) spikes. Nature 418:93–96
68. Bacskai BJ, Hochner B, Mahaut-Smith M, Adams SR, Kaang BK, Kandel ER, Tsien RY (1993) Spatially resolved dynamics of cAMP and protein kinase A subunits in Aplysia sensory neurons. Science 260:222–226
69. Cooper DM, Mons N, Karpen JW (1995) Adenylyl cyclases and the interaction between calcium and cAMP signalling. Nature 374:421–424
70. Willoughby D, Cooper DM (2007) Organization and Ca2+ regulation of adenylyl cyclases in cAMP microdomains. Physiol Rev 87:965–1010
71. Resende RR, Britto LR, Ulrich H (2008) Pharmacological properties of purinergic receptors and their effects on proliferation and induction of neuronal differentiation of P19 embryonal carcinoma cells. Int J Dev Neurosci 26:763–777
72. Ciccolini F, Collins TJ, Sudhoelter J, Lipp P, Berridge MJ, Bootman MD (2003) Local and global spontaneous calcium events regulate neurite outgrowth and onset of GABAergic phenotype during neural precursor differentiation. J Neurosci 23:103–111
73. Bading H (2000) Transcription-dependent neuronal plasticity the nuclear calcium hypothesis. Eur J Biochem 267:5280–5283
74. Hardingham GE, Chawla S, Johnson CM, Bading H (1997) Distinct functions of nuclear and cytoplasmic calcium in the control of gene expression. Nature 385:260–265
75. Studzinski DM, Callahan RE, Benjamins JA (1999) Increased intracellular calcium alters myelin gene expression in the N20.1 oligodendroglial cell line. J Neurosci Res 57: 633–642
76. Ferreira-Martins J, Rondon-Clavo C, Tugal D, Korn JA, Rizzi R, Padin-Iruegas ME, Ottolenghi S, De Angelis A, Urbanek K, Ide-Iwata N, D'Amario D, Hosoda T, Leri A, Kajstura J, Anversa P, Rota M (2009) Spontaneous calcium oscillations regulate human cardiac progenitor cell growth. Circ Res 105:764–774

77. Uhlen P, Burch PM, Zito CI, Estrada M, Ehrlich BE, Bennett AM (2006) Gain-of-function/Noonan syndrome SHP-2/Ptpn11 mutants enhance calcium oscillations and impair NFAT signaling. Proc Natl Acad Sci USA 103:2160–2165
78. Scemes E, Duval N, Meda P (2003) Reduced expression of P2Y1 receptors in connexin43-null mice alters calcium signaling and migration of neural progenitor cells. J Neurosci 23:11444–11452
79. Moreau M, Neant I, Webb SE, Miller AL, Leclerc C (2008) Calcium signalling during neural induction in Xenopus laevis embryos. Philos Trans R Soc Lond B Biol Sci 363:1371–1375
80. Leclerc C, Webb SE, Daguzan C, Moreau M, Miller AL (2000) Imaging patterns of calcium transients during neural induction in Xenopus laevis embryos. J Cell Sci 113(Pt 19):3519–3529
81. Swiers G, Patient R, Loose M (2006) Genetic regulatory networks programming hematopoietic stem cells and erythroid lineage specification. Dev Biol 294:525–540
82. Theilgaard-Monch K, Jacobsen LC, Borup R, Rasmussen T, Bjerregaard MD, Nielsen FC, Cowland JB, Borregaard N (2005) The transcriptional program of terminal granulocytic differentiation. Blood 105:1785–1796
83. May RM (1972) Will a large complex system be stable? Nature 238:413–414
84. Kauffman S (1993) The origins of order: self-organization and selection in evolution. Oxford University Press, New York
85. Aldana M, Cluzel P (2003) A natural class of robust networks. Proc Natl Acad Sci USA 100:8710–8714
86. Chang HH, Oh PY, Ingber DE, Huang S (2006) Multistable and multistep dynamics in neutrophil differentiation. BMC Cell Biol 7:11
87. Ferrell JE, Xiong W (2001) Bistability in cell signaling: how to make continuous processes discontinuous, and reversible processes irreversible. Chaos 11:227–236
88. Xiong W, Ferrell JE Jr (2003) A positive-feedback-based bistable 'memory module' that governs a cell fate decision. Nature 426:460–465
89. Huang S, Guo YP, May G, Enver T (2007) Bifurcation dynamics in lineage-commitment in bipotent progenitor cells. Dev Biol 305:695–713
90. Ying QL, Nichols J, Chambers I, Smith A (2003) BMP induction of Id proteins suppresses differentiation and sustains embryonic stem cell self-renewal in collaboration with STAT3. Cell 115:281–292
91. Niwa H, Ogawa K, Shimosato D, Adachi K (2009) A parallel circuit of LIF signalling pathways maintains pluripotency of mouse ES cells. Nature 460:118–122
92. Wei CL, Miura T, Robson P, Lim SK, Xu XQ, Lee MY, Gupta S, Stanton L, Luo Y, Schmitt J, Thies S, Wang W, Khrebtukova I, Zhou D, Liu ET, Ruan YJ, Rao M, Lim B (2005) Transcriptome profiling of human and murine ESCs identifies divergent paths required to maintain the stem cell state. Stem Cells 23:166–185
93. Dvorak P, Dvorakova D, Koskova S, Vodinska M, Najvirtova M, Krekac D, Hampl A (2005) Expression and potential role of fibroblast growth factor 2 and its receptors in human embryonic stem cells. Stem Cells 23:1200–1211
94. Todorova MG, Fuentes E, Soria B, Nadal A, Quesada I (2009) Lysophosphatidic acid induces Ca2+ mobilization and c-Myc expression in mouse embryonic stem cells via the phospholipase C pathway. Cell Signal 21:523–528
95. Schulte G, Bryja V (2007) The Frizzled family of unconventional G-protein-coupled receptors. Trends Pharmacol Sci 28:518–525
96. Bhandari DR, Seo KW, Roh KH, Jung JW, Kang SK, Kang KS (2010) REX-1 expression and p38 MAPK activation status can determine proliferation/differentiation fates in human mesenchymal stem cells. PLoS One 5:e10493
97. Li L, Sun L, Gao F, Jiang J, Yang Y, Li C, Gu J, Wei Z, Yang A, Lu R, Ma Y, Tang F, Kwon SW, Zhao Y, Li J, Jin Y (2010) Stk40 links the pluripotency factor Oct4 to the Erk/MAPK pathway and controls extraembryonic endoderm differentiation. Proc Natl Acad Sci USA 107:1402–1407

98. Jiang H, Grenley MO, Bravo MJ, Blumhagen RZ, Edgar BA (2011) EGFR/Ras/MAPK signaling mediates adult midgut epithelial homeostasis and regeneration in Drosophila. Cell Stem Cell 8:84–95
99. Batts SA, Raphael Y (2007) Transdifferentiation and its applicability for inner ear therapy. Hear Res 227:41–47
100. Dalby MJ, Gadegaard N, Tare R, Andar A, Riehle MO, Herzyk P, Wilkinson CD, Oreffo RO (2007) The control of human mesenchymal cell differentiation using nanoscale symmetry and disorder. Nat Mater 6:997–1003
101. Charbord P, Moore K (2005) Gene expression in stem cell-supporting stromal cell lines. Ann NY Acad Sci 1044:159–167
102. Dutt P, Wang JF, Groopman JE (1998) Stromal cell-derived factor-1 alpha and stem cell factor/kit ligand share signaling pathways in hemopoietic progenitors: a potential mechanism for cooperative induction of chemotaxis. J Immunol 161:3652–3658
103. de Boer J, Siddappa R, Gaspar C, van Apeldoorn A, Fodde R, van Blitterswijk C (2004) Wnt signaling inhibits osteogenic differentiation of human mesenchymal stem cells. Bone 34:818–826
104. Rizo A, Vellenga E, de Haan G, Schuringa JJ (2006) Signaling pathways in self-renewing hematopoietic and leukemic stem cells: do all stem cells need a niche? Hum Mol Genet 15(Spec No 2):R210–R219
105. Clapham DE (2007) Calcium signaling. Cell 131:1047–1058
106. Kajiume T, Ninomiya Y, Ishihara H, Kanno R, Kanno M (2004) Polycomb group gene mel-18 modulates the self-renewal activity and cell cycle status of hematopoietic stem cells. Exp Hematol 32:571–578
107. Singh V, Mueller U, Freyschmidt-Paul P, Zoller M (2011) Delayed type hypersensitivity-induced myeloid-derived suppressor cells regulate autoreactive T cells. Eur J Immunol 41:2871–2882
108. Puceat M, Jaconi M (2005) Ca2+ signalling in cardiogenesis. Cell Calcium 38:383–389
109. Park JS, Kim YS, Yoo MA (2009) The role of p38b MAPK in age-related modulation of intestinal stem cell proliferation and differentiation in Drosophila. Aging (Albany NY) 1:637–651
110. Grajales L, Garcia J, Banach K, Geenen DL (2010) Delayed enrichment of mesenchymal cells promotes cardiac lineage and calcium transient development. J Mol Cell Cardiol 48:735–745
111. Biteau B, Hochmuth CE, Jasper H (2008) JNK activity in somatic stem cells causes loss of tissue homeostasis in the aging Drosophila gut. Cell Stem Cell 3:442–455
112. Reim K, Mansour M, Varoqueaux F, McMahon HT, Sudhof TC, Brose N, Rosenmund C (2001) Complexins regulate a late step in Ca2+-dependent neurotransmitter release. Cell 104:71–81
113. Kawano S, Otsu K, Kuruma A, Shoji S, Yanagida E, Muto Y, Yoshikawa F, Hirayama Y, Mikoshiba K, Furuichi T (2006) ATP autocrine/paracrine signaling induces calcium oscillations and NFAT activation in human mesenchymal stem cells. Cell Calcium 39:313–324
114. Sauka-Spengler T, Bronner-Fraser M (2008) A gene regulatory network orchestrates neural crest formation. Nat Rev Mol Cell Biol 9:557–568
115. Winkler DA, Burden FR, Halley JD (2009) Predictive mesoscale network model of cell fate decisions during *C. elegans* embryogenesis. Artif Life 15:411–421
116. Raff MC (1992) Social controls on cell survival and cell death. Nature 356:397–400
117. Evan G, Littlewood T (1998) A matter of life and cell death. Science 281:1317–1322
118. Baubet V, Le Mouellic H, Campbell AK, Lucas-Meunier E, Fossier P, Brulet P (2000) Chimeric green fluorescent protein-aequorin as bioluminescent Ca2+ reporters at the single-cell level. Proc Natl Acad Sci USA 97:7260–7265
119. Brini M, Pinton P, Pozzan T, Rizzuto R (1999) Targeted recombinant aequorins: tools for monitoring [Ca2+] in the various compartments of a living cell. Microsc Res Tech 46:380–389

120. Dorsky RI, Sheldahl LC, Moon RT (2002) A transgenic Lef1/beta-catenin-dependent reporter is expressed in spatially restricted domains throughout zebrafish development. Dev Biol 241:229–237
121. Li CJ, Heim R, Lu P, Pu Y, Tsien RY, Chang DC (1999) Dynamic redistribution of calmodulin in HeLa cells during cell division as revealed by a GFP-calmodulin fusion protein technique. J Cell Sci 112(Pt 10):1567–1577
122. Torok K, Wilding M, Groigno L, Patel R, Whitaker M (1998) Imaging the spatial dynamics of calmodulin activation during mitosis. Curr Biol 8:692–699
123. Groth RD, Mermelstein PG (2003) Brain-derived neurotrophic factor activation of NFAT (nuclear factor of activated T-cells)-dependent transcription: a role for the transcription factor NFATc4 in neurotrophin-mediated gene expression. J Neurosci 23:8125–8134

Chapter 41
Calcium Signaling in Osteoclast Differentiation and Bone Resorption

Hiroshi Kajiya

Abstract Calcium (Ca^{2+}) signaling controls multiple cellular functions and is regulated by the release of Ca^{2+} from internal stores and its entry from the extracellular fluid. Ca^{2+} signals in osteoclasts are essential for diverse cellular functions including differentiation, bone resorption and gene transcription. Recent studies have highlighted the importance of intracellular Ca^{2+} signaling for osteoclast differentiation. Receptor activator of NF-κB ligand (RANKL) signaling induces oscillatory changes in intracellular Ca^{2+} concentrations, resulting in Ca^{2+}/calcineurin-dependent dephosphorylation and activation of nuclear factor of activated T cells c1 (NFATc1), which translocates to the nucleus and induces osteoclast-specific gene transcription to allow differentiation of osteoclasts. Recently, some reports indicated that RANKL-induced Ca^{2+} oscillation involved not only repetitive intracellular Ca^{2+} release from inositol 1, 4, 5-triphosphate channels in Ca^{2+} store sites, but also via store-operated Ca^{2+} entry and Ca^{2+} entry via transient receptor potential V channels during osteoclast differentiation. Ca^{2+}-regulatory cytokines and elevation of extracellular Ca^{2+} concentrations have been shown to increase intracellular Ca^{2+} concentrations ($[Ca^{2+}]_i$) in mature osteoclasts, regulating diverse cellular functions. RANKL-induced $[Ca^{2+}]_i$ increase has been reported to inhibit cell motility and the resorption of cytoskeletal structures in mature osteoclasts, resulting in suppression of bone-resorption activity. In conclusion, Ca^{2+} signaling activates differentiation in osteoclast precursors but suppresses resorption in mature osteoclasts. This chapter focuses on the roles of long-term Ca^{2+} oscillations in differentiation and of short-term Ca^{2+} increase in osteoclastic bone resorption activity.

H. Kajiya (✉)
Department of Physiological Science and Molecular Biology, Fukuoka Dental College, Fukuoka 814-0133, Japan
e-mail: kajiya@college.fdcnet.ac.jp

M.S. Islam (ed.), *Calcium Signaling*, Advances in Experimental Medicine and Biology 740, DOI 10.1007/978-94-007-2888-2_41,

Keywords Bone resorption • Calcium oscillation • Calcineurin • Cell motility • Differentiation • Inositol triphosphate • Nuclear factor of activated T cells c1 • Osteoclast • Receptor activator of NF-κB ligand • Store-operated calcium entry • Transient receptor potential vanilloid channels

Introduction

Maintenance of body calcium (Ca^{2+}) is of crucial importance for many physiological functions, including neuronal excitability, muscle contraction, and bone formation. Bone is the major Ca^{2+} store in the body and, together with the intestines and kidney, is responsible for regulating the whole-body balance. The principal Ca^{2+}-metabolizing hormones regulate Ca^{2+} uptake and release in the kidney, intestine and bone. Bone mineral is also modified by parathyroid hormone, vitamin D and calcitonin. In bone, adequate bone density and quality are crucial for maintaining the balance between bone formation and resorption. The cells in bone tissues control over 99% of the human body's Ca^{2+} content. Despite processing such massive quantities of Ca^{2+}, bone cells use Ca^{2+} in their homeostatic control processes. The massive movement of Ca^{2+} is carried out by specialized and regulated calcium transporters. Defects in these transporters cause diseases that can affect bone structure or function. Indeed, inborn errors have been very important in defining the calcium transport mechanisms in bone.

Calcium is a universal second messenger with a pivotal role in almost all cell types [1–3]. Ca^{2+} signaling also controls proliferation, differentiation, transcription, activation and apoptosis in bone cells such as osteoblasts, osteoclasts and osteocytes [4–6]. The consequences of Ca^{2+} signals can be classified according to whether short- or long-term functions are affected. Furthermore, short- and long-term Ca^{2+} signaling are known to affect different physiological functions. Short-term functions are generally influenced within minutes and are independent of new gene expression. They include the regulation of cell motility and the inhibition of bone resorption in mature osteoclasts. Hormonal/cytokine factors such as calcitonin, interleukin (IL)-4 and interferon-γ, and elevation of extracellular Ca^{2+} concentrations ($[Ca^{2+}]_o$) induce a quick increase in intracellular Ca^{2+} concentrations $[Ca^{2+}]_i$, which suppress the motility of osteoclasts, destruction of resorbing cytoskeletal structure, and apoptosis, resulting in suppression of bone-resorption activity. The long-term functions downstream of Ca^{2+} signaling include Ca^{2+}-dependent phosphatase (calcineurin), transcription factors (nuclear factor of activated T cells, NFATc1), and the differentiation of osteoclast precursors into mature osteoclasts. These events all need sustained oscillatory Ca^{2+} changes to maintain $[Ca^{2+}]_i$ after receptor activator of NF-κB ligand (RANKL) stimulation.

Ca^{2+} signaling is regulated by Ca^{2+} release from internal stores and entry through Ca^{2+}-permeable channels in the plasma membrane. However, the molecular basis of the relationship between Ca^{2+} signaling and intra- and extracellular Ca^{2+} transporters remains largely unidentified.

Some studies have reported the expression of Ca^{2+} transporters such as voltage-operated Ca^{2+} channels, store-operated Ca^{2+} (SOC) channels and transient receptor potential (TRP) channels in various mammalian osteoclasts [7–10]. However, the roles of short-term Ca^{2+} increase in bone-resorption activity and long-term Ca^{2+} oscillation in differentiation remain unclear.

This chapter describes intra- and extracellular calcium transporters from the standpoint of short- and long-term cellular Ca^{2+} regulation in osteoclasts, and discusses calcium-dependent cellular regulatory functions based on the framework of functional calcium transporters.

Role of Calcium Signaling in Osteoclast Differentiation

Osteoclasts are unique, multinucleated giant cells responsible for the decalcification and resorption of the bone matrix. Osteoclasts differentiate from the monocyte-macrophage lineage [11]. Their differentiation is dependent on the tumor necrosis factor-family cytokine, RANKL. RANKL induces osteoclast differentiation by activating the transcription factor NFATc1, which is required for osteoclastogenesis [12]. RANKL signaling is known to induce oscillatory changes in $[Ca^{2+}]_i$, resulting in Ca^{2+}/calcineurin-dependent dephosphorylation and activation of NFATc1, which translocates to the nucleus and induces osteoclast-specific gene transcription, allowing the differentiation of osteoclasts. RANKL-induced Ca^{2+} oscillation is initiated approximately 24 h after RANKL stimulation, when NFATc1 induction also becomes evident. Ca^{2+} oscillation is subsequently sustained thereafter until the multinucleation stage. The differential activation of transcription factors is known to depend on the pattern of Ca^{2+} signaling; NFATs are activated by a low but sustained Ca^{2+} activation [13], while Ca^{2+} oscillation reduces the effective Ca^{2+} threshold for the activation of transcription factors [14, 15]. Long-term Ca^{2+} oscillation is thus thought to maintain NFATc1 in the nucleus and ensure the long-lasting transcriptional activation of NFATc1 required for terminal differentiation during osteoclastogenesis [16]. Ca^{2+} oscillation is thus a critical feature of osteoclastogenic signaling. The change in $[Ca^{2+}]_i$ occurs through the sequential operation of two processes: Ca^{2+} release from internal Ca^{2+} store sites such as the endoplasmic reticulum (ER) and mitochondria, and Ca^{2+} entry through Ca^{2+}-permeable channels in the plasma membrane [6, 17]. However, the molecular basis of the relationship between Ca^{2+} oscillations and intra- and extracellular Ca^{2+} channels remains largely unknown.

In many non-excitable cells, inositol 1, 4, 5-triphosphate (IP_3) activates phospholipase C (PLC)-mediated Ca^{2+} signaling by binding to IP_3 receptors (IP_3Rs) [18, 19]. IP_3Rs function as major Ca^{2+} channels, allowing the release of Ca^{2+} from intracellular Ca^{2+} stores upon IP_3 binding. Three subtypes of IP_3Rs are expressed in tissue- and development-specific manners, and the Ca^{2+} signaling patterns depend on the differential expression of these IP_3R subtypes. IP_3R2 is the most sensitive to IP_3 and is required for long-lasting Ca^{2+} oscillation [20]. RANKL stimulates PLCγ, resulting

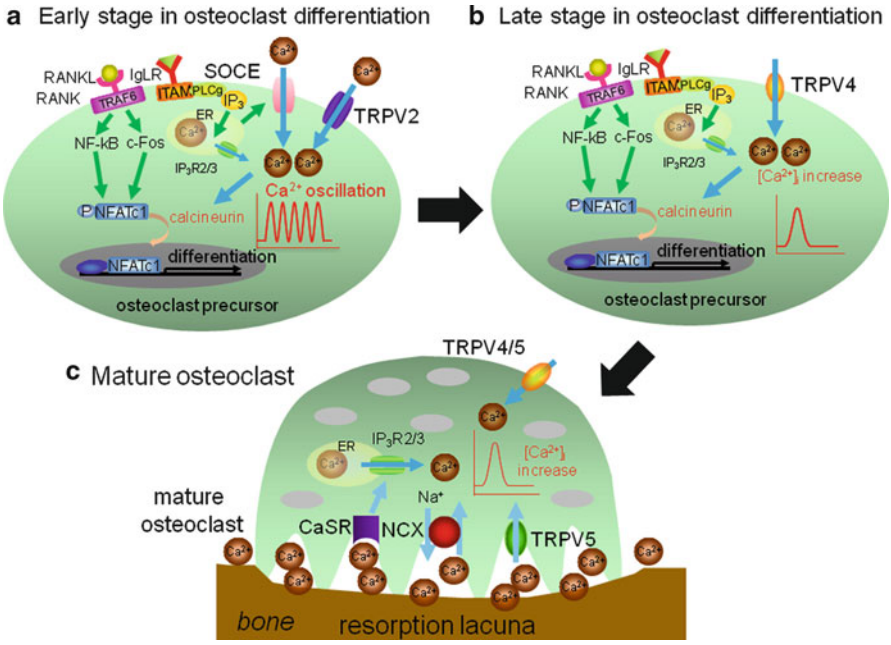

Fig. 41.1 Molecular Ca^{2+} signaling mechanism in osteoclastic differentiation/bone resorption. (**a**) The oscillatory changes in intracellular Ca^{2+} concentration (Ca^{2+} oscillation) necessary for *NFATc1* activation during the early stage of osteoclast differentiation. *RANK* and immunoreceptor tyrosine-based activation motif (*ITAM*)-associated immunoglobulin-like receptor (*IgLR*) signals cooperate to activate *PLCγ*. *PLCγ* produces IP_3, which evokes Ca^{2+} release from the ER and subsequently generates Ca^{2+} oscillation. *SOC* entry and *TRPV2* are suggested to be involved in the activation of Ca^{2+} oscillation. The Ca^{2+} oscillations induce Ca^{2+}/calcineurin-dependent dephosphorylation, resulting in activation of *NFATc1*. (**b**) The transition of Ca^{2+} signaling pattern during osteoclast differentiation. Ca^{2+} oscillation gradually disappears during differentiation, and influx of extracellular Ca^{2+} via *TRPV4* becomes necessary for sustained Ca^{2+} signaling during the later stages. The channels do not contribute to Ca^{2+} oscillation during the early stage of osteoclastogenesis. (**c**) During bone resorption, *TRPV5* and *NCX* are expressed on the ruffled border membrane and probably contribute to cytoplasmic Ca^{2+} transcytosis. *TRPV4* and *TRPV5* channels in the basolateral membrane may be necessary for the regulation of osteoclastic bone resorption. Termination of bone resorption occurs through sensing an increase in $[Ca^{2+}]_o$. CaSRs are expressed on the plasma membrane of osteoclasts and are involved in the inhibition of bone resorption in response to the increase in $[Ca^{2+}]_o$. These receptors mediate $[Ca^{2+}]_o$-induced $[Ca^{2+}]_i$ increase through modulating *PLCγ* activation, which leads to Ca^{2+} release via IP_3 production

in Ca^{2+} oscillations during the early stage of osteoclastogenesis (Fig. 41.1). IP_3R2 has been reported to be predominantly expressed in mouse osteoclasts, and RANKL-induced Ca^{2+} oscillations were abolished in bone marrow macrophages derived from IP_3R2 and -3 knockout mice. The physiological role of IP_3-mediated signals in the osteoclast lineage has been investigated, and Ca^{2+} oscillations were impaired in osteoclast precursors derived from IP_3R2 and $IP_3R2/3$-deficient mice, resulting in inhibition of osteoclastogenesis [21]. However, the differentiation of $IP_3R2/3$-deficient

osteoclast precursors into mature osteoclasts was largely unaffected in co-culture with osteoblasts. Bone mass and osteoclast number were normal in $IP_3R2/3$-deficient mice, suggesting that either IP_3-mediated Ca^{2+} signaling is dispensable for osteoclastogenesis or that $IP_3R2/3$ are dispensable for transmitting IP_3-mediated Ca^{2+} signals [21]. However, PLCγ-mediated IP_3 production and subsequent activation of Ca^{2+} release from Ca^{2+} store sites play significant roles, because bone mass was increased in PLCγ-deficient mice [22]. IP_3-mediated Ca^{2+} signaling might occur via a compensatory mechanism. It is possible that IP_3-independent Ca^{2+} release is upregulated by an as yet unknown mechanism. It has emerged that IP_3 production does not always correlate with the magnitude of $[Ca^{2+}]_i$ increase, implying that other Ca^{2+} channels may be involved. Ca^{2+} release from Ca^{2+} store sites is also induced in an IP_3-independent manner through the ryanodine receptor (RyR) and/or nicotinic acid adenine dinucleotide phosphate receptors [23, 24]. Although Ca^{2+} oscillation is likely to induce repetitive Ca^{2+} release from Ca^{2+} store sites, IP_3-mediated Ca^{2+} release occurs in parallel with Ca^{2+} entry through Ca^{2+}-permeable channels in most cells [25], and the way in which Ca^{2+} enters osteoclasts through plasma membrane channels during osteoclast differentiation is therefore also important.

In hematopoietic cells, SOC channels represent the major means of Ca^{2+} entry [1, 26]. Further, the type IA transmembrane protein Stim1 and the plasma membrane Ca^{2+} channel Orai1 [1, 27, 28] have been defined as the molecular mediators of SOC channel activity. On Ca^{2+} store depletion, Stim1colocalizes with the Orai1 Ca^{2+}-permeable channels [27, 29, 30]. Genetic deletion of Orai1 in mice abolishes SOC entry in some, but not all hematopoietic cells [31]. The silencing of Orai1 has been reported to abrogate osteoclast differentiation from human monocytes through suppression of multinucleation [32]. Furthermore, RANKL activates a reactive oxygen-species pathway through PLCγ, and induces Ca^{2+} oscillations via Stim1 [33]. Stim1 and Orai1 have also been reported to be transiently upregulated 24 h after RANKL in mouse osteoclast precursors. The silencing of Stim1 or Orai1 suppressed RANKL-induced Ca^{2+} oscillations, suggesting partial involvement of SOC channels in Ca^{2+} oscillation during the early stage of osteoclastogenesis [7]. However, the mechanisms whereby SOC channels influence osteoclast differentiation remains unclear, and better understanding of the significance of SOC channels in Ca^{2+} oscillation-dependent osteoclastogenesis may provide a more complete molecular picture of the mechanisms underlying Ca^{2+} signaling in bone. Several recent studies have focused on TRP channels as candidates for the channels underlying Ca^{2+} entry in RANKL-induced Ca^{2+} oscillations. The TRP superfamily consists of seven subfamilies, namely TRPC, TRPV, TRPM, TRPA, TRPP, TRPN and TRPML. However, the Ca^{2+}-permeable channels involved in controlling Ca^{2+} signaling during osteoclast differentiation remain elusive. Among the TRP vanilloid (TRPV) members, TRPV5 [10, 34], TRPV4 [8, 35] and TRPV2 [7] have been reported to be involved in osteoclast differentiation. Transepithelial Ca^{2+}-transport roles for TRPV5 and TRPV6 have been well documented, and these channels mediate the apical entry of Ca^{2+} that is then extruded basolaterally by sodium-Ca^{2+} exchangers and Ca^{2+}-ATPases [36]. TRPV5 channels are apparently expressed in human and murine bone samples and in cultured osteoclasts [10]. TRPV5 is localized to the ruffled border

membrane of osteoclasts, suggesting it plays a critical role in osteoclastic bone resorption *in vitro*. TRPV5 mediates Ca^{2+} entry into the cytoplasm where it can be transiently stored prior to basolateral extrusion. TRPV5 may therefore contribute to cytoplasmic Ca^{2+} transcytosis, but have little involvement in Ca^{2+} oscillation during osteoclastogenesis. TRPV4 channels have also been suggested to play a role in bone. No bone abnormalities have been reported in TRPV4-deficient mice under normal conditions, but they show a blunted effect of mechanical unloading [35] correlated with a lack of increase in osteoclast numbers in the unloaded bones, indicating a differentiation defect. In contrast, osteoclasts in TRPV4-knockout mice show impaired bone-resorption activity, resulting in an increase in bone mass [8]. Although osteoblast phenotypes were unaffected in TRPV4-knockout mice, the expression of NFATc1 mRNA was attenuated in cultured TRPV4-knockout osteoclasts, suggesting that TRPV4 contributes solely to the differentiation and function of osteoclasts. However, TRPV4 deficiency led to an impairment of mature osteoclast differentiation despite normal Ca^{2+} oscillation in these cells during the early stage of osteoclastogenesis, suggesting that TRPV4 is not required for the induction of Ca^{2+} oscillation. This study showed that the Ca^{2+} oscillation gradually disappeared during differentiation. TRPV4-mediated Ca^{2+} entry has been suggested to regulate terminal differentiation in osteoclasts after the disappearance of Ca^{2+} oscillation. It is noteworthy that TRPV4-deficient mice exhibited increased bone mass due to impaired bone resorption despite the increased number and size of osteoclasts *in vivo*, suggesting the importance of Ca^{2+} entry for resorption activity in mature osteoclasts [10]. These results suggest that other Ca^{2+}-permeable channels and linked Ca^{2+} oscillation may underlie Ca^{2+} entry during the early stages of osteoclast differentiation. Whole-cell patch clamp and Ca^{2+} imaging methods have demonstrated that murine osteoclast precursors and mature osteoclasts do not possess functional voltage-dependent Ca^{2+} channels, but use alternative Ca^{2+} permeable entry pathways [7]. TRPV2 was recently reported to be highly expressed in RANKL-treated osteoclast precursors using DNA microarray analysis. Although RANKL dominantly evokes Ca^{2+} oscillation during osteoclastogenesis, inhibition or silencing of TRPV2 suppresses Ca^{2+} oscillations, resulting in reduced NFATc1 expression, its nuclear translocation, and osteoclastogenesis. These results suggest that RANKL-induced Ca^{2+} oscillation involves not only repetitive Ca^{2+} release from intracellular Ca^{2+} store sites, but also Ca^{2+} entry through TRPV2 channels during the early stage of osteoclast differentiation.

Calcineurin/NFATc1 Activation in Osteoclasts

The transcription factor NFAT has been identified in the context of T-cell activation [37] and is known to be involved in the function and development of diverse cells in the cardiovascular and muscular systems [4]. NFATc1 is most potently induced by RANKL and is regulated by the serine/threonine phosphatase calcineurin, which is in turn activated by increased $[Ca^{2+}]_i$. Dephosphorylation of the serine residues in

NFAT by calcineurin leads to exposure of the nuclear-localization signal and subsequent translocation into the nucleus. During osteoclast differentiation, NFATc1 undergoes nuclear translocation in response to RANKL stimulation, suggesting the activation of Ca^{2+}-calcineurin signals [38].

Furthermore, signaling by the second messenger Ca^{2+} is mediated by Ca^{2+}-binding proteins during osteoclastogenesis. A calcium-binding protein molecule A8/calgranulin A (S100A8) is reported to be upregulated during osteoclastogenesis [39]. Calmodulin is major Ca^{2+}-binding protein that contains four Ca^{2+}-binding EF hands arranged in pairs at both its N- and C-termini, linked by a helix. Ca^{2+} interacts with the four Ca^{2+} binding EF hands in response to transient increases in $[Ca^{2+}]_i$, inducing a dramatic conformational shift. This Ca^{2+}-dependent conformational change induces activation of its downstream effector proteins, the Ca^{2+}/calmodulin-dependent protein kinases (CaMKs), as well as the phosphatase calcineurin. Inhibition of CaMK results in inhibition of osteoclastogenesis through the reduced phosphorylation of cAMP-responsive element binding protein (CREB)-targeted CaMK. CaMK IV, a member of the CaMK family, was recently reported to be critically involved in osteoclast differentiation and function [40]. The report suggested that the Ca^{2+}-CaMK-CREB pathway was important during the early stage of osteoclast differentiation. Furthermore, the CaMK-CREB pathway also regulates the expression of osteoclast-specific genes in cooperation with NFATc1. The two Ca^{2+}-regulated pathways were mediated by CaMK and calcineurin converge on the transcriptional control of osteoclast-specific genes.

RANKL-induced Ca^{2+} oscillation is initiated approximately 24 h after RANKL stimulation, when NFATc1 induction also becomes evident. Ca^{2+} oscillation is subsequently sustained until the multinucleation stage. Differential activation of transcription factors is known to be contingent on the pattern of Ca^{2+} signaling; NFATs are activated by low but sustained Ca^{2+} activation [41], while Ca^{2+} oscillations reduce the effective Ca^{2+} threshold for the activation of transcription factors [14, 15]. Long-term Ca^{2+} oscillation is therefore thought to maintain NFATc1 in the nucleus and ensure the long-lasting transcriptional activation of NFATc1 required for terminal differentiation, such as osteoclastogenesis [16]. However, although there is scant genetic evidence of the need for Ca^{2+} oscillation in osteoclastogenesis, this process is impaired in virtually all cases where Ca^{2+} oscillation is not induced [42, 43]. This suggests that Ca^{2+} oscillation is essential for the NFATc1 induction required for osteoclastogenesis.

Role of Ca^{2+} Signaling in Resorption and Motility of Mature Osteoclasts

Mature osteoclasts reorganize the actin cytoskeletal ring to form an osteoclast-specific structure, which enables cells to adhere to the bone surface via integrin receptors and to generate a specific microenvironment for bone resorption called Howship's lacunae. Morphologically, these are characterized by ruffled borders and

a clear zone with a highly polarized cytoplasmic organization. After cytoskeleton formation, osteoclasts actively degrade the bone matrix proteins and decalcify the inorganic bone components through the release of proteolytic enzymes (such as cathepsin K and matrix metalloproteinases) and hydrochloric acid, respectively [44, 45]. Osteoclasts secrete protons and chloride ions to the resorption lacunae via V-ATPase and Cl^- transporters, especially Clcn7. Finally, osteoclasts complete the resorption and settle on a new surface area of the bone.

Hydrochloric acid and proteolytic enzymes solubilize large amounts of Ca^{2+} (up to 40 mM) and organic breakdown products [46]. During bone resorption, osteoclasts dissolve the mineral components of the bone matrix, resulting in Ca^{2+} accumulation in the resorption lacunae. It is believed that much of these inorganic and organic components are transported through the osteoclast to the basolateral side of the cell by transcytosis [46, 47]. Although cellular collagen trafficking only occurs after several hours [48], it is unlikely that Ca^{2+} and phosphate ions are completely prevented from entering the resorbing osteoclast. Thus, the plasma membrane Ca^{2+}-permeable channels characterized in osteoclasts are mainly involved in transporting extracellular Ca^{2+} released during bone resorption during the process of transcytosis. As expected, many of these Ca^{2+} transporters are localized at the apical side of resorbing osteoclasts. Several Ca^{2+}-transporting membrane proteins have been detected in osteoclasts using electrophysiology and calcium imaging techniques [49, 50]. In addition, as in other cells types, changes in $[Ca^{2+}]_i$ are also thought to act as an important second messenger regulating a number of functions, including cell motility and bone resorption in mature osteoclasts [9, 49, 51–54].

Many different stimuli have been shown to regulate Ca^{2+} concentrations in mature osteoclasts. Application of ATP triggers a transient increase in $[Ca^{2+}]_i$ in rabbit osteoclasts [55]. Mechanical perturbation of osteoclasts induces a Ca^{2+}-mobilization response, the amplitude and duration of which depend on the $[Ca^{2+}]_o$ concentration [56, 57]. Some hormonal/cytokine factors such as calcitonin and IL-4 also increase $[Ca^{2+}]_i$ in osteoclasts [58, 59]. High levels of $[Ca^{2+}]_o$ or potassium have also been reported to increase $[Ca^{2+}]_i$, indicating the importance of cell membrane potential in Ca^{2+} entry. Membrane depolarization has been reported to increase $[Ca^{2+}]_i$ by increasing Ca^{2+} entry via a dihydropyridine (DHP)-sensitive pathway [9, 58]. In contrast, no DHP-sensitive Ca^{2+} channels were detected in rodent osteoclasts, but a lanthanum-sensitive Ca^{2+}-entry pathway suggested the presence of Ca^{2+} permeable channels [53, 60]. Although the presence of voltage-activated Ca^{2+} channels in osteoclasts remains unresolved, plasma membrane Ca^{2+}-entry pathways must exist in mature osteoclasts during resorption. However, the molecular basis of the relationship between Ca^{2+} entry and transcytosis and/or intracellular Ca^{2+} change in mature osteoclasts remains unclear. Osteoclasts express several other Ca^{2+} transporter proteins, including a Ca^{2+} ATPase [61] and Ca^{2+}-permeable TRPV channels [7, 8, 10], which are involved in Ca^{2+} transportation and may undertake significant cytoplasmic calcium transcytosis.

In line with this finding, loss of TRPV5 led to reduced resorption and doubling of osteoclast numbers both *in vitro and in vivo*, with increased multinuclearity compared with controls [10]. TRPV5 has been reported to reside in the ruffled

membrane of resorbing osteoclasts, and could therefore mediate the entry of Ca^{2+} into the cytoplasm. This Ca^{2+} could then be transiently stored in the ER before being extruded basolaterally. It is therefore not clear how far elevated osteoclast numbers mirror increased survival or just increased osteoclast formation. However, TRPV5-knockout animals have severe renal Ca^{2+} wasting and high vitamin D levels, with a bone phenotype characterized by reduced trabecular and cortical thickness of long bones [34]. Furthermore, impaired osteoclast activity seems at variance with the observed bone phenotype in TRPV5 knockout mice. In contrast, although TRPV5 knockout does not cause osteopetrosis, rickets and hyperparathyroidism do occur [62].

Silencing of TRPV5 using TRPV5-targeted siRNA also leads to inhibition of the RANKL-induced Ca^{2+} influx in human osteoclasts, suggesting that TRPV5 is a major player in the RANKL-induced $[Ca^{2+}]_i$ increment in human osteoclasts [63]. However, despite the apparent role of TRPV5 in RANKL-induced Ca^{2+} signaling in osteoclasts, silencing of TRPV5 has been shown to promote bone resorption, suggesting that TRPV5 may function as a negative regulator of bone homeostasis [63]. In addition, osteoclasts are exposed to very high $[Ca^{2+}]_o$, which regulates diverse cellular functions. Elevation of $[Ca^{2+}]_o$ concentration has been shown to increase $[Ca^{2+}]_i$ in mature osteoclasts. Sensitivity of this response to the non-selective Ca^{2+} channel blockers nickel and lanthanum [9, 64] suggests that the $[Ca^{2+}]_o$-induced $[Ca^{2+}]_i$ arises, at least in part, through channel-mediated influx of Ca^{2+}. These observations led to the proposal that a low-affinity receptor for external Ca^{2+} exists on the osteoclast membrane, and that receptor occupancy is linked to activation of a Ca^{2+} channel and release of Ca^{2+} from internal stores.

To complete Ca^{2+} transport, the high Ca^{2+} solution at the osteoclast attachment [65] must be moved to and diluted in the extracellular space. Some Ca^{2+} may be released when the osteoclast detaches, which occurs roughly once a day under normal circumstances, but the volume of solubilized bone producing Ca^{2+} and phosphate is too great for this to be the sole mechanism. Studies using confocal imaging and labeled matrix showed that the transport of Ca^{2+} and other degraded membrane components through the osteoclast by vacuolar transcytosis plays a role in this process [47].

The massive Ca^{2+} movement involved in bone resorption requires the osteoclast to have a mechanism for protecting cytoplasmic and organellar Ca^{2+} content, even if the transport is vesicular. Understanding the parallel contributions of transcytosis and cytoplasmic transport will thus require a quantitative analysis of their relative contributions. $[Ca^{2+}]_o$ must be maintained within a very narrow range (1.1–1.3 mM). The maintenance of $[Ca^{2+}]_o$ in bone largely controls bone remodeling, while $[Ca^{2+}]_o$ controls bone remodeling through the regulation of osteoclasts and osteoblasts. Osteoclastic bone resorption results in increased $[Ca^{2+}]_o$ in resorption lacunae (>40 mM), which in turn triggers a rapid increase in $[Ca^{2+}]_i$, leading to the inhibition of bone resorption through osteoclast dysfunction and apoptosis [49, 66]. The elevated $[Ca^{2+}]_o$ subsequently stimulates migration, proliferation, and differentiation of osteoblasts for bone formation [67]. Thus, the Ca^{2+} release caused by bone resorption may play an important role not only in the feedback inhibition of osteoclast activity, but also in the formal coupling of bone resorption to bone formation.

The calcium-sensing receptor (CaSR), which is a G-coupled receptor, is abundantly expressed in the parathyroid gland and kidney, and controls systemic Ca^{2+} homeostasis through sensing changes in $[Ca^{2+}]_o$. CaSR is also expressed in osteoclasts and negatively regulates osteoclast differentiation and bone resorption in response to increased $[Ca^{2+}]_o$ [68, 69]. A study using CaSR-deficient cells showed that Ca^{2+} influx in osteoclasts was mediated by the type II RyR (RyR2) at the plasma membrane, and the RyR2 was therefore proposed to be involved in the $[Ca^{2+}]_o$-induced $[Ca^{2+}]_i$ increase via Ca^{2+} release from internal stores. However, it has reported that $[Ca^{2+}]_i$ stimulated by high $[Ca^{2+}]_o$ does not require Ca^{2+} release from stores, and that TRP may support store-independent Ca^{2+} entry [70]. Further studies are needed to elucidate the detailed molecular mechanisms underlying Ca^{2+} sensing in osteoclasts throughout the entire differentiation process.

In addition to the Ca^{2+} transporters described above, the expression of a Na^+/Ca^{2+} exchanger contributes to the functional bone-resorbing activity in isolated murine osteoclasts [71, 72]. Na^+/Ca^{2+} exchanger variants NCX1.3, 1.41 and 3.2 have been reported to be expressed in mouse osteoclasts, and the inhibition of osteoclastic bone resorption by NCX inhibitors and siRNAs was therefore deemed to be due to reduced Ca^{2+} influx. NCX is therefore an interesting candidate for the disposal of Ca^{2+} from the osteoclastic resorption lacunae. Osteoclasts change their morphological and functional properties between the resorbing and non-resorbing/motile states of the resorption cycle [73, 74]. Resorbing osteoclasts exhibiting a so-called actin ring have a resting membrane potential of −10 to approximately −20 mV [60, 75], while non-resorbing/motile osteoclasts exhibiting pseudopodia have a resting membrane potential of −50 to approximately −70 mV. The reversal potential of NCX was calculated according to published equations [76, 77]; if NCX protein is located on the ruffled border of the osteoclast, the high Ca^{2+} concentration (40 mM) in the resorption lacunae means that the calculated reversal potential of NCX would be as low as −70 to about −150 mV, which is far lower than the cell membrane potential. It can therefore be predicted that NCX on the ruffled border operates in the Ca^{2+} influx mode in resorbing osteoclasts, suggesting that it could play a very important role in the regulation of Ca^{2+} transcytosis.

Role of Ca^{2+} Signaling in Bone Resorption and Cell Motility

Several studies have shown that changes in $[Ca^{2+}]_i$ in mature osteoclasts results in inhibition of osteoclastic bone-resorption activities, such as cell motility [78], inhibition of enzyme release [79, 80], and inhibition of pit formation [81, 82].

Osteoclasts change their morphological and functional properties between the resorbing and non-resorbing/motile states of the resorption cycle [73, 74, 83]. Resorbing osteoclasts exhibit actin rings without pseudopodia, whereas non-resorbing/motile osteoclasts have pseudopodia but not actin rings. In the resorbing state, osteoclasts recognize bone matrix proteins, adhere to the bone surface through integrin receptors, and exhibit a ring formation of F-actin microfilaments with ruffled

borders and clear zones [84, 85]. Actin-ring formation correlates with bone-resorption activity, and disruption of actin rings results in suppression of pit-forming activity in osteoclasts [84–86]. Actin-ring formation in osteoclasts is regulated by signaling pathways mediated by protein kinase A [87, 88], protein kinase C [89], phosphatidylinositol 3-kinase [84], and $[Ca^{2+}]_i$ [53, 90, 91]. $[Ca^{2+}]_i$ increase in mature osteoclasts induces disruption of actin-ring formation and subsequent inhibition of bone-resorbing activity. However, the effects of changes of $[Ca^{2+}]_i$ on osteoclast function vary, possibly because of differences in the origins and differentiation states of the osteoclasts investigated and the experimental setups.

Resorbing activity in osteoclasts gradually declines and the osteoclasts turn into non-resorbing/motile osteoclasts with pseudopodia, rather than actin rings, and they migrate and settle on a new surface area of the bone. RANKL-induced $[Ca^{2+}]_i$ changes have been reported to regulate chemotactic migration and motility of osteoclasts: hepatocyte growth factor was reported to increase $[Ca^{2+}]_i$ and stimulate chemotactic migration in osteoclast-like cells obtained from human giant cell tumors [92]. The soluble laminin-2 (merosin), which is expressed in basement membranes and binds integrin receptors, increases $[Ca^{2+}]_i$ and stimulates the chemotactic migration of human osteoclast-like cells [93]. Resorbing osteoclasts with flat, round morphology mostly had low basal $[Ca^{2+}]_i$ (around 50 nM), while non-resorbing/motile osteoclasts with serrated edges had high basal $[Ca^{2+}]_i$ (around 100 nM) [60]. Membrane depolarization induced a decrease in $[Ca^{2+}]_i$, which contributed to the suppression of cell motility. Furthermore, the reduction of cytosolic Ca^{2+} has also been reported to facilitate actin-ring formation in avian osteoclasts [9]. In non-resorbing/motile osteoclasts, higher basal $[Ca^{2+}]_i$ maintained a high level of motile activity, while $[Ca^{2+}]_i$ reduction induced by depolarization suppressed motility and promoted anchoring of the cells onto the bone surface and their conversion to resorbing osteoclasts with actin rings [60].

In conclusion, changes in $[Ca^{2+}]_i$ in mature osteoclasts contribute to the regulation of motility in non-resorbing/motile osteoclasts and bone resorption in resorbing osteoclasts through the control of Ca^{2+}-entry pathways.

Concluding Remarks

Ca^{2+} has a unique function in living systems because of its dominant role in intracellular signaling. Its regulation in bone cells, which need to handle massive amounts of this mineral, is therefore of particular importance. Ca^{2+} signaling pathways play an important role in regulating osteoclast differentiation and bone resorption. Ca^{2+} signaling targets calcineurin/NFATc1 during differentiation and cytoskeletal structure during resorption. Ca^2 has a dynamic and direct effect on functional activities such as differentiation, motility and bone resorption. The discovery of RANKL/RANK signaling has brought about a major breakthrough in the understanding of the regulatory mechanisms behind osteoclast differentiation. In particular, the identification of NFATc1 as the master transcription factor in osteoclastogenesis led to

realization of the importance of Ca^{2+} signaling in osteoclast differentiation. However, much remains to be learned regarding the functions of Ca^{2+} signaling, and further progress in understanding the significance of SOC entry and Orai channels in calcineurin/NFATc1-dependent osteoclast differentiation may provide a more complete molecular picture of the mechanisms underlying Ca^{2+} signaling in bone. Further studies will thus not only improve our understanding of osteoclast differentiation and function, but also provide an important molecular basis for the development of novel therapeutic strategies for bone disorders.

Acknowledgments This work was supported by Grants-in-Aid for Scientific Research from the Ministry of Education, Culture, Sports, Science and Technology of Japan (20390475) and the Strategic Study Base Formation Support Business (S1001059).

References

1. Feske S (2007) Calcium signaling in lymphocyte activation and disease. Nat Rev Immunol 7:690–702
2. Lewis RS (2001) Calcium signaling mechanisms in T lymphocytes. Annu Rev Immunol 19:497–521
3. Scharenberg AM, Humphries LA, Rawlings DJ (2007) Calcium signaling and cell-fate choice in B cells. Nat Rev Immunol 7:778–789
4. Hogan PG, Chen L, Nardone J, Rao A (2003) Transcriptional regulation by calcium, calcineurin, and NFAT. Genes Dev 17:2205–2232
5. Hogan PG, Rao A, Dissecting I (2007) CRAC, a store-operated calcium current. Trends Biochem Sci 32:235–245
6. Lewis RS (2007) The molecular choreography of a store-operated calcium channel. Nature 446:284–287
7. Kajiya H, Okamoto F, Nemoto T, Kimachi K, Goto-T K, Nakayama S, Okabe K (2010) RANKL-induced TRPV2 expression regulates osteoclastogenesis via calcium oscillations. Cell Calcium 48:260–269
8. Masuyama R, Vriens J, Voets T, Karashima Y, Owsianik G, Vennekens R, Lieben L, Torrekens S, Moermans K, Bosch AV, Bouillon R, Nillius B, Carmeliet G (2008) TRPV4-mediated calcium influx regulates terminal differentiation of osteoclasts. Cell Metab 8:257–265
9. Miyauchi A, Hruska KA, Greenfield EM, Duncan R, Alvarez J, Barattolo R, Colucci S, Zambonin-Zallone A, Teitelbaum SL, Teti A (1990) Osteoclast cytosolic calcium, regulated by voltage-gated calcium channels and extracellular calcium, controls podosome assembly and bone resorption. J Cell Biol 111:2543–2552
10. van der Eerden BC, Hoenderop JG, de Vries TJ, Schoenmaker T, Buurman CJ, Uitterlinden AG, Pols HA, Bindels RJ, van Leeuwen JP (2005) The epithelial Ca^{2+} channel TRPV5 is essential for proper osteoclastic bone resorption. Proc Natl Acad Sci USA 102:17507–17512
11. Boyle WJ, Simonet WS, Lacey DL (2003) Osteoclast differentiation and activation. Nature 423:337–342
12. Takayanagi H, Kim S, Koga T, Nishina H, Isshiki M, Yoshida H, Saiura A, Isobe M, Yokochi T, Inoue J, Wagner EF, Mak TW, Kodama T, Taniguchi T (2002) Induction and activation of the transcription factor NFATc1 (NFAT2) integrate RANKL signaling in terminal differentiation of osteoclasts. Dev Cell 3:889–901
13. Dolmetsch RE, Dolmetsch RE, Lewis RS, Goodnow CC, Healy JI (1997) Differential activation of transcription factors induced by Ca^{2+} response amplitude and duration. Nature 386:855–858

14. Dolmetsch RE, Xu K, Lewis RS (1998) Calcium oscillations increase the efficiency and specificity of gene expression. Nature 392:933–936
15. Tomida T, Hirose K, Takizawa A, Shibasaki F, Iino M (2003) NFAT functions as a working memory of Ca^{2+} signals in decoding Ca^{2+} oscillation. EMBO J 22:3825–3832
16. Koga T, Matsui Y, Asagiri M, Kodama T, de Crombrugghe B, Nakashima K, Takayanagi H (2005) NFAT and Osterix cooperatively regulate bone formation. Nat Med 11:880–885
17. Berridge MJ, Bootman MD, Roderick HL (2003) Calcium signaling: dynamics, homeostasis and remodeling. Nat Rev Mol Cell Biol 4:517–529
18. Bootman MD (1995) The elemental principles of calcium signaling. Cell 83:675–678
19. Clapham DE (2007) Calcium signaling. Cell 131:1047–1058
20. Miyakawa T, Maeda A, Yamazawa T, Hirose K, Kurosaki T, Iino M (1999) Encoding of Ca^{2+} signals by differential expression of IP_3 receptor subtypes. EMBO J 18:1303–1308
21. Kuroda Y (2008) Osteoblasts induce Ca^{2+} oscillation-independent NFATc1 activation during osteoclastogenesis. Proc Natl Acad Sci USA 105:8643–8648
22. Yang S, Li YP (2007) RGS12 is essential for RANKL-evoked signaling for terminal differentiation of osteoclasts in vitro. J Bone Miner Res 22:45–54
23. Grafton G (2001) Calcium channels in lymphocytes. Immunology 104:119–126
24. House SJM, Potier M, Bisaillon J, Singer HA, Trebak M (2008) The non-excitable smooth muscle: calcium signaling and phenotypic switching during vascular disease. Pflugers Arch 456:769–785
25. Schmidt U, Schmidt U, Boucheron N, Unger B, Ellmeier W (2004) The role of Tec family kinases in myeloid cells. Int Arch Allergy Immunol 134:65–78
26. Deng X, Wang Y, Soboloff J, Gill DL (2009) Stim and Orai: dynamic intermembrane coupling to control cellular calcium signals. J Biol Chem 284:22501–22505
27. Liou J, Kim ML, Heo WD, Jones JT, Myers JW, Ferrell JE Jr, Meyer T (2005) STIM is a Ca^{2+} sensor essential for Ca^{2+}-store-depletion-triggered Ca^{2+} influx. Curr Biol 15:1235–1241
28. Roos DI, Gregorio PJ, Yeromin AV, Ohlsen K, Lioudyno M, Zhang S, Safrina O, Kozak JA, Wagner SL, Cahalan MD, Veliçelebi G, Stauderman KA (2005) STIM1, an essential and conserved component of store-operated Ca^{2+} channel function. J Cell Biol 169:435–445
29. Stathopulos PB, Zheng L, Li GY, Plevin MJ, Ikura M (2008) Structural and mechanistic insights into STIM1-mediated initiation of store-operated calcium entry. Cell 135:110–122
30. Wu MM, Buchanan J, Luik RM, Lewis RS (2006) Ca^{2+} store depletion causes STIM1 to accumulate in ER regions closely associated with the plasma membrane. J Cell Biol 174:803–813
31. Vig M, Peinelt C, Beck A, Koomoa DL, Rabah D, Koblan-Huberson M, Kraft S, Turner H, Fleig A, Penner R, Kinet JP (2006) CRACM1 is a plasma membrane protein essential for store-operated Ca^{2+} entry. Science 312:1220–1223
32. Zhou Y, Lewis TL, Robinson LJ, Brundage KM, Schafer R, Martin KH, Blair HC, Soboloff J, Barnett JB (2011) The role of calcium release activated calcium channels in osteoclast differentiation. J Cell Physiol 226:1082–1089
33. Kim MS, Yang YM, Son A, Tian YS, Lee SI, Kang SW, Muallem S, Shin DM (2010) RANKL-mediated reactive oxygen species pathway that induces long lasting Ca^{2+} oscillations essential for osteoclastogenesis. J Biol Chem 285:6913–6921
34. Hoenderop JG, van Leeuwen JP, van der Eerden BC, Kersten FF, van der Kemp AW, Mérillat AM, Waarsing JH, Rossier BC, Vallon V, Hummler E, Bindels RJ (2003) Renal Ca^{2+} wasting, hyperabsorption, and reduced bone thickness in mice lacking TRPV5. J Clin Invest 112:1906–1914
35. Mizoguchi F, Mizuno A, Hayata T, Nakashima K, Heller S, Ushida T, Sokabe M, Miyasaka N, Suzuki M, Ezura Y, Noda M (2008) Transient receptor potential vanilloid 4 deficiency suppresses unloading-induced bone loss. J Cell Physiol 216:47–53
36. Nillius B (2007) Transient receptor potential (TRP) cation channels: rewarding unique proteins. Bull Mem Acad R Med Belg 162:244–253
37. Shaw JP, Utz PJ, Durand DB, Toole JJ, Emmel EA, Crabtree GR (1988) Identification of a putative regulator of early T cell activation genes. Science 241:202–205

38. Takayanagi H (2007) The role of NFAT in osteoclast formation. Ann N Y Acad Sci 1116:227–237
39. Sambandam Y, Blanchard JJ, Daughtridge G, Kolb RJ, Shanmugarajan S, Pandruvada SN, Bateman TA, Reddy SV (2010) Microarray profile of gene expression during osteoclast differentiation in modelled microgravity. J Cell Biochem 111:1179–1187
40. Sato K, Suematsu A, Nakashima T, Takemoto-Kimura S, Aoki K, Morishita Y, Asahara H, Ohya K, Yamaguchi A, Takai T, Kodama T, Chatila TA, Bito H, Takayanagi H (2006) Regulation of osteoclast differentiation and function by the CaMK-CREB pathway. Nat Med 12:1410–1416
41. Dolmetsch RE, Lewis RS, Goodnow CC, Healy JI (1997) Differential activation of transcription factors induced by Ca^{2+} response amplitude and duration. Nature 386:855–858
42. Koga T, Inui M, Inoue K, Kim S, Suematsu A, Kobayashi E, Iwata T, Ohnishi H, Matozaki T, Kodama T, Taniguchi T, Takayanagi H, Takai T (2004) Costimulatory signals mediated by the ITAM motif cooperate with RANKL for bone homeostasis. Nature 428:758–763
43. Yang S, Li YP (2007) RGS10-null mutation impairs osteoclast differentiation resulting from the loss of $[Ca^{2+}]_i$ oscillation regulation. Genes Dev 21:1803–1816
44. Blair HC, Teitelbaum SL, Ghiselli R, Gluck S (1989) Osteoclastic bone resorption by a polarized vacuolar proton pump. Science 245:855–857
45. Kornak U, Kasper D, Bösl MR, Kaiser E, Schweizer M, Schulz A, Friedrich W, Delling G, Jentsch TJ (2001) Loss of the ClC-7 chloride channel leads to osteopetrosis in mice and man. Cell 104:205–215
46. Salo J, Lehenkari P, Mulari M, Metsikkö K, Väänänen HK (1997) Removal of osteoclast bone resorption products by transcytosis. Science 276:270–273
47. Nesbitt SA, Horton MA (1997) Trafficking of matrix collagens through bone-resorbing osteoclasts. Science 276:266–269
48. Datta HK, Horrocks BR (2003) Mechanisms of calcium disposal from osteoclastic resorption hemivacuole. J Endocrinol 176:1–5
49. Datta HK, MacIntyre I, Zaidi M (1989) The effect of extracellular calcium elevation on morphology and function of isolated rat osteoclasts. Biosci Rep 9:747–751
50. Zaidi M, Moonga BS, Adebanjo OA (2002) Novel mechanisms of calcium handling by the osteoclast: a review-hypothesis. Proc Assoc Am Physicians 111:319–327
51. Bax CM, Shankar VS, Moonga BS, Huang CL, Zaidi M (1992) Is the osteoclast calcium "receptor" a receptor-operated calcium channel? Biochem Biophys Res Commun 183:619–625
52. Bennett BD, Alvarez U, Hruska KA (2001) Receptor-operated osteoclast calcium sensing. Endocrinology 142:1968–1974
53. Kajiya H, Okabe K, Okamoto F, Tsuzuki T, Soeda H (2000) Protein tyrosine kinase inhibitors increase cytosolic calcium and inhibit actin organization as resorbing activity in rat osteoclasts. J Cell Physiol 183:83–90
54. Lakkakorpi PT, Lehenkari PP, Rautiala TJ, Väänänen HK (1996) Different calcium sensitivity in osteoclasts on glass and on bone and maintenance of cytoskeletal structures on bone in the presence of high extracellular calcium. J Cell Physiol 168:668–677
55. Yu H, Ferrier J (1993) ATP induces an intracellular calcium pulse in osteoclasts. Biochem Biophys Res Commun 191:357–363
56. Radding W, Radding W, Jordan SE, Hester RB, Blair HC (1999) Intracellular calcium puffs in osteoclasts. Exp Cell Res 253:689–696
57. Xia SL, Ferrier J (1995) Calcium signal induced by mechanical perturbation of osteoclasts. J Cell Physiol 163:493–501
58. Bizzarri C, Shioi A, Teitelbaum SL, Ohara J, Harwalkar VA, Erdmann JM, Lacey DL, Civitelli R (1994) Interleukin-4 inhibits bone resorption and acutely increases cytosolic Ca^{2+} in murine osteoclasts. J Biol Chem 269:13817–13824
59. Moonga BS, Alam AS, Bevis PJ, Avaldi F, Soncini R, Huang CL, Zaidi M (1992) Regulation of cytosolic free calcium in isolated rat osteoclasts by calcitonin. J Endocrinol 132:241–249

60. Kajiya H, Okamoto F, Fukushima H, Takada K, Okabe K (2003) Mechanism and role of high-potassium-induced reduction of intracellular Ca^{2+} concentration in rat osteoclasts. Am J Physiol Cell Physiol 285:C457–C466
61. Bekker PJ, Gay CV (1990) Biochemical characterization of an electrogenic vacuolar proton pump in purified chicken osteoclast plasma membrane vesicles. J Bone Miner Res 5:569–579
62. Renkema KY, Nijenhuis T, van der Eerden BC, van der Kemp AW, Weinans H, van Leeuwen JP, Bindels RJ, Hoenderop JG (2005) Hypervitaminosis D mediates compensatory Ca^{2+} hyperabsorption in TRPV5 knockout mice. J Am Soc Nephrol 16:3188–3195
63. Chamoux E, Bisson M, Payet MD, Roux S (2010) TRPV-5 mediates a receptor activator of NF-kappa B (RANK) ligand-induced increase in cytosolic Ca^{2+} in human osteoclasts and down-regulates bone resorption. J Biol Chem 285:25354–253562
64. Zaidi M, Shankar VS, Towhidul Alam AS, Moonga BS, Pazianas M, Huang CL (1992) Evidence that a ryanodine receptor triggers signal transduction in the osteoclast. Biochem Biophys Res Commun 188:1332–1336
65. Silver IA, Murrills RJ, Etherington DJ (1988) Microelectrode studies on the acid microenvironment beneath adherent macrophages and osteoclasts. Exp Cell Res 175:266–276
66. Lorget F, Kamel S, Mentaverri R, Wattel A, Naassila M, Maamer M, Brazier M (2000) High extracellular calcium concentrations directly stimulate osteoclast apoptosis. Biochem Biophys Res Commun 268:899–903
67. Yamaguchi T (2008) The calcium-sensing receptor in bone. J Bone Miner Metab 26:301–311
68. Kameda T, Mano H, Yamada Y, Takai H, Amizuka N, Kobori M, Izumi N, Kawashima H, Ozawa H, Ikeda K, Kameda A, Hakeda Y, Kumegawa M (1998) Calcium-sensing receptor in mature osteoclasts, which are bone resorbing cells. Biochem Biophys Res Commun 245:419–422
69. Kanatani M, Sugimoto T, Kanzawa M, Yano S, Chihara K (1999) High extracellular calcium inhibits osteoclast-like cell formation by directly acting on the calcium-sensing receptor existing in osteoclast precursor cells. Biochem Biophys Res Commun 261:144–148
70. Bennet BD, Alvarez U, Hruska KA (2001) Receptor-operated osteoclast calcium sensing. Endocrinology 142:1968–1974
71. Moonga BS, Davidson R, Sun L, Adebanjo OA, Moser J, Abedin M, Zaidi N, Huang CL, Zaidi M (2001) Identification and characterization of a sodium/calcium exchanger, NCX-1, in osteoclasts and its role in bone resorption. Biochem Biophys Res Commun 283:770–775
72. Li JP, Kajiya H, Okamoto F, Nakao A, Iwamoto T, Okabe K (2007) Three Na^{+}/Ca^{2+} exchanger (NCX) variants are expressed in mouse osteoclasts and mediate calcium transport during bone resorption. Endocrinology 148:2116–2125
73. Arkett SA, Dixon SJ (1992) Sims SM Substrate influences rat osteoclast morphology and expression of potassium conductances. J Physiol 458:633–653
74. Kanehisa J, Yamanaka T, Doi S, Turksen K, Heersche JN, Aubin JE, Takeuchi H (1990) A band of F-actin containing podosomes is involved in bone resorption by osteoclasts. Bone 11:287–293
75. Sims SM, Dixon SJ (1989) Inwardly rectifying K^{+} current in osteoclasts. Am J Physiol 256:C1277–C1282
76. Dong H, Dunn J, Lytton J (2002) Electrophysiological studies of the cloned rat cardiac NCX1.1 in transfected HEK cells: a focus on the stoichiometry. Ann NY Acad Sci 976:159–165
77. Sokolow S, Manto M, Gailly P, Molgo J, Vandebrouck C, Vanderwinden JM, Herchuelz A, Schurmans S (2004) Impaired neuromuscular transmission and skeletal muscle fiber necrosis in mice lacking Na/Ca exchanger 3. J Clin Invest 113:265–273
78. Zaidi M, Datta HK, Moonga B, MacIntyre I (1990) Evidence that the action of calcitonin on the osteoclast is mediated by two G proteins acting via separate post-receptor pathways. J Endocrinol 125:437–481
79. Chambers TJ, Fuller K, Darby JA (1987) Hormonal regulation of acid phosphatase release by osteoclasts disaggregated from neonatal rat bone. J Cell Physiol 132:92–96
80. Moonga BS, Moss DW, Patchell A, Zaidi M (1990) Intracellular regulation of enzyme secretion from rat osteoclasts and evidence for functional role in bone resorption. J Physiol 490:29–46

81. Malgaroli A, Meldolesi J, Zambonin-Zallone A, Teti A (1987) Control of cytosolic free calcium in rat and chicken osteoclasts the role of extracellular calcium and calcitonin. J Biol Chem 264:14342–14347
82. Zaidi M, Chambers TJ, Bevis PJR, Beacham JL, Gaines D, MacIntyre I (1988) Effects of the peptides from the calcitonin gene on bone and bone cells. Q J Exp Physiol 73:471–485
83. Lakkakorpi PT, Väänänen HK (1991) Kinetics of the osteoclasts cytoskeleton during the resorption cycle in vitro. J Bone Miner Res 6:817–826
84. Nakamura I, Takahashi N, Sasaki T, Tanaka S, Udagawa N, Murakami H, Kimura K, Kabuyama Y, Kurokawa T, Suda T, Fukui Y (1995) Wortmannin, a specific inhibitor of phosphatidylinositol-3 kinase, blocks osteoclastic bone resorption. FEBS Lett 361:79–84
85. Zhang D, Udagawa N, Nakamura I, Murakami H, Saito S, Yamasaki K, Shibasaki Y, Morii N, Narumiya S, Takahashi N, Suda T (1995) The small GTP-binding protein, rho p21, is involved in bone resorption by regulating cytoskeletal organization in osteoclasts. J Cell Sci 108:2285–2292
86. Teti A, Blair HC, Schlesinger P, Grano M, Zambonin-Zallone A, Kahn AJ, Teitelbaum SL, Hruska A (1989) Extracellular protons acidify osteoclasts, reduce cytosolic calcium, and promote expression cell matrix attachment structures. J Clin Invest 84:773–780
87. Lakkakorpi PT, Väänänen HK (1990) Calcitonin, prostaglandin E2 and dibutyryl cyclic adenosine 3, 5-monophospahte disperse the specific microfilament structure in resorbing osteoclasts. J Histochem Cytochem 38:1487–1493
88. Suzuki H, Nakamura I, Takahashi N, Ikuhara T, Matsuzaki K, Isogai Y, Hori M, Suda T (1996) Calcitonin-induced changes in the cytoskeleton are mediated by a signal pathway associated with protein kinase A in osteoclast. Endocrinology 137:4685–4690
89. Teti A, Colucci S, Grano M, Argentino L, Zambonin-Zallone A (1992) Protein kinase C affects microfilaments, bone resorption, and $[Ca^{2+}]_o$ sensing in cultured osteoclasts. Am J Physiol 263:C130–C139
90. Miyauchi A, Alvarez J, Greenfield EM, Teti A, Grano M, Colucci S, Zambonin-Zallone A, Ross FP, Teitelbaum SL, Cheresh D, Hruska KA (1991) Recognition of osteopontin and related peptides by an $\alpha v\beta 3$ integrin stimulated immediate cell signals in osteoclasts. J Biol Chem 266:20369–20374
91. Zallone A (1992) Protein kinase C affects microfilaments, bone resorption, and $[Ca^{2+}]_o$ sensing in cultured osteoclasts. Am J Physiol Cell Physiol 263:C130–C139
92. Grano M, Galimi F, Zambonin G, Colucci S, Cottone E, Zallone-Zambonin A (1996) Hepatocyte growth factor is a coupling factor for osteoclasts and osteoblasts in vitro. Proc Natl Acad Sci USA 93:7644–7648
93. Colucci S, Giannelli G, Grano M, Faccio R, Quaranta V, Zallone-Zambonin A (1996) Human osteoclast-like cells selectively recognize laminin isoforms, an event that induces migration and activates Ca^{2+} mediated signals. J Cell Sci 109:1527–1535

Chapter 42
Calcium Signaling in Renal Tubular Cells

Milica Bozic and Jose M. Valdivielso

Abstract The kidney handles calcium by filtration and reabsorption. About 60% of the plasma calcium is filterable, and 99% is reabsorbed in the tubule. In the proximal tubule, the reabsorption is passive and paracellular, but in the distal tubule is active and transcellular. Thus, renal tubular cells are exposed to very high concentrations of calcium in both, the extracellular and the intracellular compartments. Extracellular calcium signaling is transmitted by the calcium sensing receptor, located both in the luminal and basolateral sides of tubular cells. This receptor is able to control levels of extracellular calcium and acts in consequence to maintain calcium homeostasis. Furthermore, renal tubular cells possess several calcium channels that regulate some of the cell functions. Among those, voltage gated calcium channels, transient receptor potential channels and N-methyl-D-aspartate receptor channels have been reported to control several functions. Those functions include survival, apoptosis, differentiation, epithelial-mesenchymal transition, and active vitamin D and renin synthesis.

Keywords Voltage gated calcium channels • TRP • NMDAR • Calcium sensing receptor

Introduction

Kidneys are essential excretory organs of the body that are responsible for preserving the internal environment of the organism. Alongside with bone and intestine, kidneys represent vital organs for the maintenance of overall calcium (Ca^{2+}) homeostasis.

M. Bozic • J.M. Valdivielso (✉)
Nephrology Research Laboratory, IRB Lleida, University Hospital Arnau de Vilanova, Rovira Roure 80, Planta 1, 25198 Lleida, Spain
e-mail: milicabozic@yahoo.com; valdivielso@medicina.udl.cat

M.S. Islam (ed.), *Calcium Signaling*, Advances in Experimental Medicine and Biology 740, DOI 10.1007/978-94-007-2888-2_42,

Glomerular filtration, tubular reabsorption, and tubular excretion are the three mechanisms by which kidneys accomplish the homeostasis of the internal environment. The basic structural and functional unit of the kidney, the nephron, takes the responsibility of nearly all of the kidney's functions, especially functions concerning reabsorption and secretion of different soluble substances. In order to maintain Ca^{2+} balance, >98% of the Ca^{2+} filtered at the glomerulus must be reabsorbed along the nephron [1, 2]. This review will focus on the renal tubule, the part of the kidney nephron into which the glomerular filtrate passes after reaching the Bowman's capsule. The renal tubule starts with proximal convoluted tubule (PCT), continues as the loop of Henle and through the ascending branch connects to the distal convoluted tubule (DCT). Many DCT converge into a single collecting duct leading to the renal pelvis. The main part of the calcium reabsorption takes place along the proximal tubule and thick ascending loop of Henle through a passive paracellular pathway [2]. The remaining calcium reabsorption occurs in the distal part of the nephron such as DCT, connecting tubules and the initial portion of the cortical collecting duct, where approximately 10–15% of the total Ca^{2+} is reabsorbed [1, 2]. Distal convoluted tubule (DCT) is the major site of hormone- and diuretic-regulated calcium transport in the kidney [3].

A multitude of cellular responses such as sensory transduction, cell activation, degranulation and ion secretion, regulation of cell contraction, cell proliferation, and apoptosis [4] are regulated by changes in intracellular free calcium levels, making this ion a universal intracellular mediator [5]. Ca^{2+} ions participate in a large variety of structural and functional processes in the kidney and the influx of extracellular calcium is required for signal transduction in various renal tubular epithelial cells [6]. Entrance of calcium ions into the cell can be achieved through channel-mediated Ca^{2+} influx and/or receptor-induced Ca^{2+} release from intracellular stores [4]. Generally, calcium enters a cell by passing through a calcium channel that opens in response to different stimuli [7]. Membrane depolarization, ligand binding and release of intracellular stores are all capable of causing plasma membrane calcium channels to open [7, 8]. Calcium channels in the kidney play important roles in maintaining the total body calcium homeostasis. Impairment of function of calcium channels in the kidney may be associated with several human diseases such as hypercalciuric nephrolithiasis, certain forms of osteoporosis, Gitelman's disease and Bartter's syndrome [9], as well as with certain genetic disorders such as autosomal dominant polycystic kidney disease (ADPKD) [4, 10–12]. Therefore, it is of vital importance understanding the mechanisms that control entry of calcium into renal tubular cells, as well as how tubular cell distinguishes between different Ca^{2+} signaling pathways.

Calcium Channels in Renal Tubular Cells

Voltage-Gated Ca^{2+} Channels

Voltage-gated calcium channels comprise a large group of transmembrane multiprotein complexes that couple membrane depolarization to cellular calcium entry [13]. Voltage-gated Ca^{2+} channels form a complex of different subunits: α_1, $\alpha_2\delta$, β_{1-4}

and γ, where α_1 subunit form a central pore and contains the voltage sensor and drug receptor [6]. A large body of evidence implicates that voltage-gated Ca^{2+} channels, including L-type, T-type, N-type, and P/Q-type, are present within renal tubular tissues and the blockade of these Ca^{2+} channels produces different effects on renal microcirculation. The unique distribution of the mRNA for each calcium channel isoform in the kidney suggests that each calcium channel subunit isoform is probably coupled to unique calcium signaling pathways that in turn affect epithelial function [14].

It has been demonstrated that the α_{1C} subunit of the L-type Ca^{2+} channel was expressed in the whole rat kidney as well as in the proximal and distal tubules. In the proximal tubule α_{1C} subunit was found to be localized mainly in the intercellular compartments [14]. According to channel blocker studies, calcium influx via L-type Ca^{2+} channels could be a necessary component of the volume regulatory machinery [14]. Furthermore, overactivation of the L-type calcium channels seems to be involved in ischemia-reperfusion injury in tubular cells, because inhibition of the pore attenuated the damage to the cells both, *in vitro* and *in vivo* [15, 16]. Additionally, α_{1C} subunit was found to be highly expressed in both outer and inner medullary collecting ducts [14]. α_{1G} subunit of T-type Ca^{2+} channel was found in the inner medullary collecting ducts, distal collecting ducts and connecting tubules, particularly on the apical site. Brunette et al. [17] reported a dual kinetics of Ca^{2+} transport by the luminal membrane of the distal tubule. Using several different calcium channel blockers they inhibited Ca^{2+} transport through the membrane confirming the role for L-type, P/Q-type and L-type Ca^{2+} channels in the distal tubule of the kidney [17]. Another subtype of voltage-gated Ca^{2+} channels, T-type channels (TCC), have been found to be present in renal tubules as well [18]. It has been suggested that TCCs participate in the release of renin and aldosterone, and conversely the effect of aldosterone on renal arterioles is mediated by TCCs [18]. Inhibition of T-type Ca^{2+} channels prevented the formation of nuclear factor-κB (NF-κB) and suppressed Rho-kinase, which subsequently ameliorated the inflammatory process in the glomerulus and the interstitium [18], showing beneficial effect of Ca^{2+} channel blockade. Although those effects were described to be secondary to a hemodynamic effect, studies by Sugano et al. [19] demonstrated also a direct effect decreasing epithelial-mesenchymal transition (EMT) in tubular cells. Barry et al. [3] showed the presence of the α_{1C} and β_3 subunits of L-type channels in mouse distal convoluted tubule (DCT) cells and demonstrated importance of α_{1C} subunit in the diuretic-mediated calcium influx and β3 subunit in both parathyroid hormone (PTH)- and drug-induced Ca^{2+} uptake [3].

Transient Receptor Potential (TRP) Channels

Transient receptor potential (TRP) channels belong to a superfamily of multifunctional cation channels [10] that are present in a variety of organs, being kidney one of them. The TRP superfamily consists of seven families: TRPC (Canonical), TRPV

(Vanilloid), TRPM (Melastatin), TRPN (Nompc), TRPA (Ankyrin-like with transmembrane domain 1), TRPML (Mucolipin), TRPP (Polycystin) (reviewed by Giamarchi et al. [10]). TRP proteins are nonselective cation channels with permeability to diverse cations, including high permeability for Ca^{2+} ions [4, 20]. TRPP1 or polycystin-1 (PC1) and TRPP2 or polycystin-2 (PC2) are members of the TRPP family of transient receptor potential superfamily of cation channels. TRPP1 has been found in the renal tubular epithelia, predominantly associated with the plasma membrane [21], as well as on the lateral membrane [22], at cell-to-cell junctions [23] and in the primary cilia of mouse collecting duct cells [24]. TRPP2 is expressed in the tubules throughout the kidney, with highest expression levels in the medullary thick ascending limb and distal convoluted tubules [4, 23, 25]. Markowitz et al. [25] reported strong expression of TRPP2 in the maturing distal tubules and to a lesser degree in the proximal tubules of the elongating nephron and suggested a specific developmental role for TRPP2 in the mouse kidney, as well as in the maintenance of differentiated tubular architecture in the mature kidney. It has been shown that TRPP2 is important in the regulation of different physiological processes in the body, including renal tubular differentiation [10, 25]. TRPP1 and TRPP2 together make an obligatory functional channel complex implicated in the regulation of ion transport and cell signaling, activation of kinase cascades, as well as transduction of environmental signals into cellular events, renal epithelial cell growth and normal tubular morphogenesis (reviewed by Cantiello [4]). It has been shown that mutations of either PKD1 (gene coding TRPP1) or PKD2 (gene coding TRPP2) [10, 12] or disruption of stable heterodimeric complex of TRPP1 and TRPP2 [22] could be the main causes of different cases of autosomal dominant polycystic kidney disease (ADPKD), a syndrome characterized by extensive formation of renal cysts and progressive renal failure [26]. Loss of TRPP1-TRPP2 heterodimeric complex results in impairment of Ca^{2+} signaling that regulates renal epithelial cell growth and promotes normal tubular morphogenesis and function [27]. Stable over-expression of polycystin-1 in MDCK cells slowed their growth, protected them from apoptosis and induced spontaneous formation of branching tubules [28]. On the other hand, loss of polycystin-2 expression led to a loss of tubular epithelial phenotype and formation of renal cyst in mouse mutant model [29].

The molecular identity of the apical Ca^{2+} entry pathway in tubular cells remained elusive until the epithelial Ca^{2+} channels TRPV5 and TRPV6 were identified [30, 31]. These channels convey the rate-limiting step in active Ca^{2+} transport and play, therefore, a pivotal role in Ca^{2+} homeostasis. Alterations in channel expression and function are responsible for many human conditions, mainly related to defective Ca^{2+} handling. Thus, Vitamin D-deficiency rickets type I and type II (autosomal recessive diseases characterized by low or undetectable levels of $1,25(OH)_2D_3$ and mutations in the vitamin D receptor respectively) are related with lower expression of TRPV5 and 6 in tubular cells, which causes the characteristic hypocalcemia in the patients [32]. In addition TRPV5 and TRPV6 can be involved in calcium-related disturbances associated with sex. Thus, estrogen has a stimulatory effect on the expression of TRPV5 in the kidney [33, 34], which may account for the protection shown by premenopausal women against Ca^{2+} nephrolithiasis by increasing Ca^{2+}

reabsorption. Conversely, decreased active Ca^{2+} transport through TRPV5 and TRPV6, as a result of estrogen deficiency, would be in line with increased Ca^{2+} wasting and Ca^{2+} malabsorption in postmenopausal women.

Calcium Sensing Receptor (CaSR)

Calcium sensing receptor (CaSR) is a member of the family of G protein-coupled receptors that binds calcium ions [35]. The extracellular Ca^{2+}-sensing receptor plays an essential role in extracellular Ca^{2+} homeostasis. It is located in key tissues regulating extracellular calcium levels (parathyroid gland, kidney, thyroid, intestine and bone) and senses variations of extracellular calcium, thus regulating the function of those tissues aiming to correct the calcium imbalance. For instance, activation of the receptor by low calcium levels suppresses secretion of parathyroid hormone (PTH). It also regulates the rate of renal tubular calcium reabsorption in the kidney [36, 37], the production of calcitonin in thyroid C cells [38] and the reabsorption of bone by osteoclasts [39]. Binding of extracellular calcium or other CaR agonists to the extracellular domain of the receptor triggers a number of intracellular signaling pathways, including PLC, PLA2, MAPK and protein kinases [35]. In the kidney, the CaSR is localized on the basolateral cell surface in the cortical thick ascending limb, as well as in the proximal and distal tubular segments [40, 41]. In the proximal tubule, CaSR protein is expressed on the apical membrane while in the distal convoluted tubule it is localized on the basolateral membrane [40]. Thus, this unique distribution pattern suggests that the receptor is capable of detecting changes occurring both within the urinary space and in the interstitium. Potential roles for the CaSR in proximal tubule function have been proposed and include modulation of 1-hydroxylation of 25-hydroxyvitamin D_3 and PTH stimulated second messenger production [42, 43]. The apical localization of the CaSR in proximal tubule also suggests potential roles for luminal divalent minerals and/or polyvalent cations in regulating solute reabsorption processes including bicarbonate or phosphate [44], urine concentration [45] and acidification [46]. Furthermore, a role of CaSR in regulating renin release has also been proposed [47].

N-Methyl-D-Aspartate Receptor (NMDAR)

N-methyl-D-aspartate receptor (NMDAR) is a cation channel which belongs to a large family of excitatory ionotropic glutamate receptors (iGluRs) that has been extensively studied in the nervous system. NMDAR is characterized by a specific molecular composition and unique pharmacological and functional properties [48, 49]. An essential feature of the NMDAR is that its activation and subsequent influx of calcium ions could trigger a series of Ca^{2+}-mediated intracellular events and via this Ca^{2+} entry NMDAR performs its important physiological functions. NMDAR is a heteromeric

protein complex composed of different subunits from two separate protein families, termed as NMDAR1 (NR1; zeta 1 for mice) and NMDAR2 (NR2; epsilon for mice) protein family [50, 51]. The channel properties are highly dependable on the subunit composition of the receptor [52]. Functional NMDARs usually require members from each family and probably exist as a tetramer [51] that most often comprises of two NR1 and two NR2 subunits of the same or different subtypes [48, 53, 54].

The NR1 subunit is the main subunit of the NMDAR and it is essential for channel activity [55–57], whereas the NR2 subunits have modulatory properties [58]. The NR2 subunit family is composed of four members (NR2A, 2B, 2C and 2D) produced from separate, but related genes [59–61]. Within recent years, a novel subunit of the NMDAR family has been cloned and characterized [8, 62]. This subunit, termed as NR3, is found in the form of NR3A and NR3B and has been demonstrated to be developmentally and spatially regulated, as all other NMDAR subunits [63]. It has been shown that NR3A subunit, when forming the NMDAR complex together with NR1 and NR2 subunits, has the ability to decrease NMDA-evoked current [64] and Ca^{2+} permeability of the NMDAR in heterologous cells [65, 66].

The NMDAR is a ligand-gated ion channel that requires simultaneous binding of two agonists, glutamate and glycine, for the proper channel activation and its opening [48, 67]. Magnesium (Mg^{2+}) acts as a voltage-dependent antagonist of the NMDAR and depolarization of the membrane will relieve this block. Therefore, the full activation and opening of the NMDAR requires three distinct events – binding of two agonists and membrane depolarization [8].

In addition to NMDAR's broad distribution in neurons, it has become evident that functional NMDAR is also expressed in a variety of non-neuronal cells and tissues, where numerous function have been ascribed to this receptor such as proliferation [68, 69], apoptosis [68, 70], cell adhesion and migration [68, 69, 71], actin rearrangement [72, 73], cell growth and differentiation [69] and regulation of hormone secretion [74]. Leung et al. [58] demonstrated presence of NR1 in total rat kidney, cortex and medulla, while of other subunits of NMDAR, only NR2C was detectable in the rat kidney [58]. Both NR1 and NR2C are present in Madin-Darby canine kidney, opossum kidney and LLC-PK1 cells [58]. Importance of NMDAR in peripheral tissues, such as kidney, and its functional role has emerged as an interesting research topic. It has been shown that the abundance of an essential NR1 subunit of the NMDAR increases with kidney development [58]. Results from Deng et al. [75] showed the presence of NR1 subunit of NMDAR in the basolateral proximal tubules of the rat kidney where it plays an important role in regulation of the normal kidney function [76]. Functional NMDAR was found present in human [77] and mouse [77, 78] podocytes, where glutamatergic signaling driven by these visceral epithelial cells contributes to the integrity of the glomerular filtration barrier [78]. Recently, this group demonstrated that renal NMDARs independently stimulate proximal tubular reabsorption and glomerular filtration [76]. Sproul et al. [79] showed high expression of NMDAR subunits NR3A and NR3B in the neonatal kidney and suggested that there is continued expression of NR3A in the renal medulla and papilla of the adult mouse. These authors showed specific presence of NR3A in basolateral membrane of collecting duct cells where this subunit may play an important reno-protective role [79]. Recent data from Anderson et al. [77]

suggested that, as in the brain, basal activation of NMDAR may be essential for normal podocyte and kidney function, but excessive activation may trigger a number of pathophysiological processes [77].

Recent results from our group pointed to an indispensable role of NMDAR in the preservation of normal epithelial phenotype of proximal tubular cells and in the modulation of important steps of tubular EMT [80]. Thus, knockdown of an essential NR1 subunit of the NMDAR induced remarkable changes in epithelial phenotype of HK-2 cells, evident as a decrease of E-cadherin and an increase of α-SMA, alongside with the changes in cell morphology. Furthermore, *in vitro*, HK-2 cells exposed to TGF-β1 demonstrated downregulation of E-cadherin and membrane-associated β-catenin, F-actin reorganization, *de novo* expression of mesenchymal markers such as α-SMA and vimentin, upregulation of Snail1 and elevated cell migration. Co-treatment with NMDA attenuated all described signs of EMT induced by TGF-β1. Additionally, TGF-β1 increased cell velocity on collagen and fibronectin matrices, which was inhibited by co-treatment with NMDA. *The mechanism behind the effect of NMDA on TGF-β1-induced tubular EMT seems to be related with the inhibition of the Ras-MEK pathway*. In an *in vivo* study, administration of NMDA significantly inhibited expression of α-SMA in the obstructed mouse kidneys at 5 and 15 days after UUO. Collagen I expression was significantly diminished in obstructed kidneys of NMDA-treated mice at day 15 after UUO. Furthermore, administration of NMDA blunted the downregulation of E-cadherin and an increase of FSP1 induced by UUO, pointing to a paramount role of NMDAR in the preservation of normal epithelial phenotype of proximal tubular cells and in the modulation of important steps of tubular EMT.

Furthermore, NMDAR activation in renal proximal tubular cells also influenced the synthesis of the active form of vitamin D and provoked hyperparathyroidism. Thus, treatment during 4 days caused downregulation of 1α-hydroxylase expression in proximal tubular cells, both *in vivo* and *in vitro* [81]. This downregulation resulted in a drop in $1,25(OH)_2D_3$ synthesis and in the blood levels of $1,25(OH)_2D_3$. It is well known that low levels of $1,25(OH)_2D_3$ strongly affect the parathyroid gland stimulating the synthesis and release of PTH. Thus, the lack of inhibitory effect of vitamin D on the parathyroid gland in sustained treatments provoked an increase of PTH levels. Indeed when we treated animals with both, NMDA and $1,25(OH)_2D_3$, PTH levels did not rise, confirming that a decrease in circulating $1,25(OH)_2D_3$ levels is, at least in part, responsible for the increase in PTH induced by NMDA treatment. Furthermore, glutamate levels were increased in kidneys of animals with chronic kidney disease, pointing to glutamate and an overactivation of tubular NMDAR to a possible cause for the onset of secondary hyperparathyroidism.

Summary

Renal tubular cells are one of the main cell types regulating Ca^{2+} homeostasis in the body. This specific function make them exposed to high Ca^{2+}, because are responsible for absorption of the most of the Ca^{2+} filtered in the glomerulus.

Most of the Ca^{2+} is reabsorbed by paracellular ways in the proximal tubule, where extracellular CaSR acts. However, in the distal part of the nephron, transcellular absorption of calcium is the main pathway, making cells more exposed to high intracellular calcium concentrations. Thus, the control of calcium signaling in renal tubular cells is a complicated issue that is not completely understood. Further research in this direction is needed to fully identify the complex actions of calcium in renal tubular cells.

References

1. Friedman PA, Gesek FA (1995) Cellular calcium transport in renal epithelia: measurement, mechanisms, and regulation. Physiol Rev 75:429–471
2. Hoenderop JG, Willems PH, Bindels RJ (2000) Toward a comprehensive molecular model of active calcium reabsorption. Am J Physiol Renal Physiol 278:F352–F360
3. Barry EL, Gesek FA, Yu AS, Lytton J, Friedman PA (1998) Distinct calcium channel isoforms mediate parathyroid hormone and chlorothiazide-stimulated calcium entry in transporting epithelial cells. J Membr Biol 161:55–64
4. Cantiello HF (2004) Regulation of calcium signaling by polycystin-2. Am J Physiol Renal Physiol 286:F1012–F1029
5. Leung FP, Yung LM, Yao X, Laher I, Huang Y (2008) Store-operated calcium entry in vascular smooth muscle. Br J Pharmacol 153:846–857
6. Andreasen D, Jensen BL, Hansen PB, Kwon TH, Nielsen S, Skott O (2000) The alpha(1G)-subunit of a voltage-dependent Ca(2+) channel is localized in rat distal nephron and collecting duct. Am J Physiol Renal Physiol 279:F997–F1005
7. Tykocki NR, Watts SW (2010) The interdependence of endothelin-1 and calcium: a review. Clin Sci (Lond) 119:361–372
8. Lynch DR, Guttmann RP (2001) NMDA receptor pharmacology: perspectives from molecular biology. Curr Drug Targets 2:215–231
9. Peng JB, Hediger MA (2002) A family of calcium-permeable channels in the kidney: distinct roles in renal calcium handling. Curr Opin Nephrol Hypertens 11:555–561
10. Giamarchi A, Padilla F, Coste B, Raoux M, Crest M, Honore E, Delmas P (2006) The versatile nature of the calcium-permeable cation channel TRPP2. EMBO Rep 7:787–793
11. Igarashi P, Somlo S (2002) Genetics and pathogenesis of polycystic kidney disease. J Am Soc Nephrol 13:2384–2398
12. Fu X, Wang Y, Schetle N, Gao H, Putz M, von Gersdorff G, Walz G, Kramer-Zucker AG (2008) The subcellular localization of TRPP2 modulates its function. J Am Soc Nephrol 19:1342–1351
13. Minor DL Jr, Findeisen F (2010) Progress in the structural understanding of voltage-gated calcium channel (CaV) function and modulation. Channels (Austin) 4:459–474
14. Zhao PL, Wang XT, Zhang XM, Cebotaru V, Cebotaru L, Guo G, Morales M, Guggino SE (2002) Tubular and cellular localization of the cardiac L-type calcium channel in rat kidney. Kidney Int 61:1393–1406
15. Tanaka T, Nangaku M, Miyata T, Inagi R, Ohse T, Ingelfinger JR, Fujita T (2004) Blockade of calcium influx through L-type calcium channels attenuates mitochondrial injury and apoptosis in hypoxic renal tubular cells. J Am Soc Nephrol 15:2320–2333
16. Wu D, Chen X, Ding R, Qiao X, Shi S, Xie Y, Hong Q, Feng Z (2008) Ischemia/reperfusion induce renal tubule apoptosis by inositol 1,4,5-trisphosphate receptor and L-type Ca2+ channel opening. Am J Nephrol 28:487–499
17. Brunette MG, Leclerc M, Couchourel D, Mailloux J, Bourgeois Y (2004) Characterization of three types of calcium channel in the luminal membrane of the distal nephron. Can J Physiol Pharmacol 82:30–37

18. Hayashi K, Wakino S, Sugano N, Ozawa Y, Homma K, Saruta T (2007) Ca2+ channel subtypes and pharmacology in the kidney. Circ Res 100:342–353
19. Sugano N, Wakino S, Kanda T, Tatematsu S, Homma K, Yoshioka K, Hasegawa K, Hara Y, Suetsugu Y, Yoshizawa T, Hara Y, Utsunomiya Y, Tokudome G, Hosoya T, Saruta T, Hayashi K (2008) T-type calcium channel blockade as a therapeutic strategy against renal injury in rats with subtotal nephrectomy. Kidney Int 73:826–834
20. Minke B, Cook B (2002) TRP channel proteins and signal transduction. Physiol Rev 82:429–472
21. Geng L, Segal Y, Peissel B, Deng N, Pei Y, Carone F, Rennke HG, Glucksmann-Kuis AM, Schneider MC, Ericsson M, Reeders ST, Zhou J (1996) Identification and localization of polycystin, the PKD1 gene product. J Clin Invest 98:2674–2682
22. Newby LJ, Streets AJ, Zhao Y, Harris PC, Ward CJ, Ong AC (2002) Identification, characterization, and localization of a novel kidney polycystin-1-polycystin-2 complex. J Biol Chem 277:20763–20773
23. Foggensteiner L, Bevan AP, Thomas R, Coleman N, Boulter C, Bradley J, Ibraghimov-Beskrovnaya O, Klinger K, Sandford R (2000) Cellular and subcellular distribution of polycystin-2, the protein product of the PKD2 gene. J Am Soc Nephrol 11:814–827
24. Yoder BK, Hou X, Guay-Woodford LM (2002) The polycystic kidney disease proteins, polycystin-1, polycystin-2, polaris, and cystin, are co-localized in renal cilia. J Am Soc Nephrol 13:2508–2516
25. Markowitz GS, Cai Y, Li L, Wu G, Ward LC, Somlo S, D'Agati VD (1999) Polycystin-2 expression is developmentally regulated. Am J Physiol 277:F17–F25
26. Nickel C, Benzing T, Sellin L, Gerke P, Karihaloo A, Liu ZX, Cantley LG, Walz G (2002) The polycystin-1 C-terminal fragment triggers branching morphogenesis and migration of tubular kidney epithelial cells. J Clin Invest 109:481–489
27. Hanaoka K, Qian F, Boletta A, Bhunia AK, Piontek K, Tsiokas L, Sukhatme VP, Guggino WB, Germino GG (2000) Co-assembly of polycystin-1 and -2 produces unique cation-permeable currents. Nature 408:990–994
28. Boletta A, Qian F, Onuchic LF, Bhunia AK, Phakdeekitcharoen B, Hanaoka K, Guggino W, Monaco L, Germino GG (2000) Polycystin-1, the gene product of PKD1, induces resistance to apoptosis and spontaneous tubulogenesis in MDCK cells. Mol Cell 6:1267–1273
29. Wu G, D'Agati V, Cai Y, Markowitz G, Park JH, Reynolds DM, Maeda Y, Le TC, Hou H Jr, Kucherlapati R, Edelmann W, Somlo S (1998) Somatic inactivation of Pkd2 results in polycystic kidney disease. Cell 93:177–188
30. Montell C, Birnbaumer L, Flockerzi V, Bindels RJ, Bruford EA, Caterina MJ, Clapham DE, Harteneck C, Heller S, Julius D, Kojima I, Mori Y, Penner R, Prawitt D, Scharenberg AM, Schultz G, Shimizu N, Zhu MX (2002) A unified nomenclature for the superfamily of TRP cation channels. Mol Cell 9:229–231
31. Peng JB, Chen XZ, Berger UV, Vassilev PM, Tsukaguchi H, Brown EM, Hediger MA (1999) Molecular cloning and characterization of a channel-like transporter mediating intestinal calcium absorption. J Biol Chem 274:22739–22746
32. van Abel M, Hoenderop JG, Bindels RJ (2005) The epithelial calcium channels TRPV5 and TRPV6: regulation and implications for disease. Naunyn Schmiedebergs Arch Pharmacol 371:295–306
33. van Abel M, Hoenderop JG, Dardenne O, St Arnaud R, Van Os CH, Van Leeuwen HJ, Bindels RJ (2002) 1,25-dihydroxyvitamin D(3)-independent stimulatory effect of estrogen on the expression of ECaC1 in the kidney. J Am Soc Nephrol 13:2102–2109
34. van Abel M, Hoenderop JG, van der Kemp AW, van Leeuwen JP, Bindels RJ (2003) Regulation of the epithelial Ca2+ channels in small intestine as studied by quantitative mRNA detection. Am J Physiol Gastrointest Liver Physiol 285:G78–G85
35. Brown EM, MacLeod RJ (2001) Extracellular calcium sensing and extracellular calcium signaling. Physiol Rev 81:239–297
36. Fudge NJ, Kovacs CS (2004) Physiological studies in heterozygous calcium sensing receptor (CaSR) gene-ablated mice confirm that the CaSR regulates calcitonin release in vivo. BMC Physiol 4:5

37. Vargas-Poussou R, Huang C, Hulin P, Houillier P, Jeunemaitre X, Paillard M, Planelles G, Dechaux M, Miller RT, Antignac C (2002) Functional characterization of a calcium-sensing receptor mutation in severe autosomal dominant hypocalcemia with a Bartter-like syndrome. J Am Soc Nephrol 13:2259–2266
38. Garrett JE, Tamir H, Kifor O, Simin RT, Rogers KV, Mithal A, Gagel RF, Brown EM (1995) Calcitonin-secreting cells of the thyroid express an extracellular calcium receptor gene. Endocrinology 136:5202–5211
39. Yamaguchi T, Chattopadhyay N, Kifor O, Brown EM (1998) Extracellular calcium (Ca2+(o))-sensing receptor in a murine bone marrow-derived stromal cell line (ST2): potential mediator of the actions of Ca2+(o) on the function of ST2 cells. Endocrinology 139:3561–3568
40. Riccardi D, Hall AE, Chattopadhyay N, Xu JZ, Brown EM, Hebert SC (1998) Localization of the extracellular Ca2+/polyvalent cation-sensing protein in rat kidney. Am J Physiol 274: F611–F622
41. Riccardi D, Lee WS, Lee K, Segre GV, Brown EM, Hebert SC (1996) Localization of the extracellular Ca(2+)-sensing receptor and PTH/PTHrP receptor in rat kidney. Am J Physiol 271:F951–F956
42. Egbuna O, Quinn S, Kantham L, Butters R, Pang J, Pollak M, Goltzman D, Brown E (2009) The full-length calcium-sensing receptor dampens the calcemic response to 1alpha,25(OH)2 vitamin D3 in vivo independently of parathyroid hormone. Am J Physiol Renal Physiol 297:F720–F728
43. Maiti A, Beckman MJ (2007) Extracellular calcium is a direct effecter of VDR levels in proximal tubule epithelial cells that counter-balances effects of PTH on renal Vitamin D metabolism. J Steroid Biochem Mol Biol 103:504–508
44. Riccardi D, Brown EM (2010) Physiology and pathophysiology of the calcium-sensing receptor in the kidney. Am J Physiol Renal Physiol 298:F485–F499
45. Sands JM, Naruse M, Baum M, Jo I, Hebert SC, Brown EM, Harris HW (1997) Apical extracellular calcium/polyvalent cation-sensing receptor regulates vasopressin-elicited water permeability in rat kidney inner medullary collecting duct. J Clin Invest 99:1399–1405
46. Renkema KY, Velic A, Dijkman HB, Verkaart S, van der Kemp AW, Nowik M, Timmermans K, Doucet A, Wagner CA, Bindels RJ, Hoenderop JG (2009) The calcium-sensing receptor promotes urinary acidification to prevent nephrolithiasis. J Am Soc Nephrol 20:1705–1713
47. Maillard MP, Tedjani A, Perregaux C, Burnier M (2009) Calcium-sensing receptors modulate renin release in vivo and in vitro in the rat. J Hypertens 27:1980–1987
48. Dingledine R, Borges K, Bowie D, Traynelis SF (1999) The glutamate receptor ion channels. Pharmacol Rev 51:7–61
49. Cull-Candy SG, Brickley SG, Misra C, Feldmeyer D, Momiyama A, Farrant M (1998) NMDA receptor diversity in the cerebellum: identification of subunits contributing to functional receptors. Neuropharmacology 37:1369–1380
50. Magnusson KR (1998) The aging of the NMDA receptor complex. Front Biosci 3:e70–e80
51. Guttmann RP, Sokol S, Baker DL, Simpkins KL, Dong Y, Lynch DR (2002) Proteolysis of the N-methyl-d-aspartate receptor by calpain in situ. J Pharmacol Exp Ther 302:1023–1030
52. Bellone C, Nicoll RA (2007) Rapid bidirectional switching of synaptic NMDA receptors. Neuron 55:779–785
53. Paoletti P, Neyton J (2007) NMDA receptor subunits: function and pharmacology. Curr Opin Pharmacol 7:39–47
54. Rebola N, Srikumar BN, Mulle C (2010) Activity-dependent synaptic plasticity of NMDA receptors. J Physiol 588:93–99
55. Luo J, Wang Y, Yasuda RP, Dunah AW, Wolfe BB (1997) The majority of N-methyl-D-aspartate receptor complexes in adult rat cerebral cortex contain at least three different subunits (NR1/NR2A/NR2B). Mol Pharmacol 51:79–86
56. Haddad JJ (2005) N-methyl-D-aspartate (NMDA) and the regulation of mitogen-activated protein kinase (MAPK) signaling pathways: a revolving neurochemical axis for therapeutic intervention? Prog Neurobiol 77:252–282

57. Chazot PL (2004) The NMDA receptor NR2B subunit: a valid therapeutic target for multiple CNS pathologies. Curr Med Chem 11:389–396
58. Leung JC, Travis BR, Verlander JW, Sandhu SK, Yang SG, Zea AH, Weiner ID, Silverstein DM (2002) Expression and developmental regulation of the NMDA receptor subunits in the kidney and cardiovascular system. Am J Physiol Regul Integr Comp Physiol 283:R964–R971
59. Ishii T, Moriyoshi K, Sugihara H, Sakurada K, Kadotani H, Yokoi M, Akazawa C, Shigemoto R, Mizuno N, Masu M (1993) Molecular characterization of the family of the N-methyl-D-aspartate receptor subunits. J Biol Chem 268:2836–2843
60. Meguro H, Mori H, Araki K, Kushiya E, Kutsuwada T, Yamazaki M, Kumanishi T, Arakawa M, Sakimura K, Mishina M (1992) Functional characterization of a heteromeric NMDA receptor channel expressed from cloned cDNAs. Nature 357:70–74
61. Nakanishi S (1992) Molecular diversity of glutamate receptors and implications for brain function. Science 258:597–603
62. Ciabarra AM, Sullivan JM, Gahn LG, Pecht G, Heinemann S, Sevarino KA (1995) Cloning and characterization of chi-1: a developmentally regulated member of a novel class of the ionotropic glutamate receptor family. J Neurosci 15:6498–6508
63. Das S, Sasaki YF, Rothe T, Premkumar LS, Takasu M, Crandall JE, Dikkes P, Conner DA, Rayudu PV, Cheung W, Chen HS, Lipton SA, Nakanishi N (1998) Increased NMDA current and spine density in mice lacking the NMDA receptor subunit NR3A. Nature 393:377–381
64. Nishi M, Hinds H, Lu HP, Kawata M, Hayashi Y (2001) Motoneuron-specific expression of NR3B, a novel NMDA-type glutamate receptor subunit that works in a dominant-negative manner. J Neurosci 21:RC185
65. Matsuda K, Fletcher M, Kamiya Y, Yuzaki M (2003) Specific assembly with the NMDA receptor 3B subunit controls surface expression and calcium permeability of NMDA receptors. J Neurosci 23:10064–10073
66. Perez-Otano I, Ehlers MD (2004) Learning from NMDA receptor trafficking: clues to the development and maturation of glutamatergic synapses. Neurosignals 13:175–189
67. Lynch DR, Guttmann RP (2002) Excitotoxicity: perspectives based on N-methyl-D-aspartate receptor subtypes. J Pharmacol Exp Ther 300:717–723
68. Miglio G, Dianzani C, Fallarini S, Fantozzi R, Lombardi G (2007) Stimulation of N-methyl-D-aspartate receptors modulates Jurkat T cell growth and adhesion to fibronectin. Biochem Biophys Res Commun 361:404–409
69. Nahm WK, Philpot BD, Adams MM, Badiavas EV, Zhou LH, Butmarc J, Bear MF, Falanga V (2004) Significance of N-methyl-D-aspartate (NMDA) receptor-mediated signaling in human keratinocytes. J Cell Physiol 200:309–317
70. Mentaverri R, Kamel S, Wattel A, Prouillet C, Sevenet N, Petit JP, Tordjmann T, Brazier M (2003) Regulation of bone resorption and osteoclast survival by nitric oxide: possible involvement of NMDA-receptor. J Cell Biochem 88:1145–1156
71. Rakic P, Komuro H (1995) The role of receptor/channel activity in neuronal cell migration. J Neurobiol 26:299–315
72. Shorte SL (1997) N-methyl-D-aspartate evokes rapid net depolymerization of filamentous actin in cultured rat cerebellar granule cells. J Neurophysiol 78:1135–1143
73. Itzstein C, Espinosa L, Delmas PD, Chenu C (2000) Specific antagonists of NMDA receptors prevent osteoclast sealing zone formation required for bone resorption. Biochem Biophys Res Commun 268:201–209
74. Parisi E, Almaden Y, Ibarz M, Panizo S, Cardus A, Rodriguez M, Fernandez E, Valdivielso JM (2009) N-methyl-D-aspartate receptors are expressed in rat parathyroid gland and regulate PTH secretion. Am J Physiol Renal Physiol 296:F1291–F1296
75. Deng A, Valdivielso JM, Munger KA, Blantz RC, Thomson SC (2002) Vasodilatory N-methyl-D-aspartate receptors are constitutively expressed in rat kidney. J Am Soc Nephrol 13: 1381–1384
76. Deng A, Thomson SC (2009) Renal NMDA receptors independently stimulate proximal reabsorption and glomerular filtration. Am J Physiol Renal Physiol 296:F976–F982

77. Anderson M, Suh JM, Kim EY, Dryer SE (2011) Functional NMDA receptors with atypical properties are expressed in podocytes. Am J Physiol Cell Physiol 300:C22–C32
78. Giardino L, Armelloni S, Corbelli A, Mattinzoli D, Zennaro C, Guerrot D, Tourrel F, Ikehata M, Li M, Berra S, Carraro M, Messa P, Rastaldi MP (2009) Podocyte glutamatergic signaling contributes to the function of the glomerular filtration barrier. J Am Soc Nephrol 20:1929–1940
79. Sproul AD, Steele SL, Thai TL, Yu SP, Klein JD, Sands JM, Bell PD (2011) N-methyl-D-aspartate receptor subunit NR3a expression and function in principal cells of the collecting duct. Am J Physiol Renal Physiol 301(1):F44–F54. doi:10.1152/ajprenal.00666.2010
80. Bozic M, de Rooij J, Parisi E, Ortega MR, Fernandez E, Valdivielso JM (2011) Glutamatergic signaling maintains the epithelial phenotype of proximal tubular cells. J Am Soc Nephrol 22:1099–1111
81. Parisi E, Bozic M, Ibarz M, Panizo S, Valcheva P, Coll B, Fernandez E, Valdivielso JM (2010) Sustained activation of renal N-methyl-D-aspartate receptors decreases vitamin D synthesis: a possible role for glutamate on the onset of secondary HPT. Am J Physiol Endocrinol Metab 299:E825–E831

Chapter 43
Calcium in Epidermis

Martin J. Behne and Jens-Michael Jensen

Introduction

Calcium is the ubiquitous second messenger system in cell biology (e.g., [1, 2]), as shown in great detail in this volume. In contrast, calcium has been implicated in a host of functions in skin, which have seen only partial clarification to date. Within this chapter, we will present an overview of known physiologic and pathophysiologic aspects to give a perspective of the overall role of calcium, in skin focusing on epidermis.

Global Calcium Distribution in Epidermis

The key event calcium controls in epidermis is epidermal barrier homeostasis and repair [3]. From a dermatologist's point of view, barrier function is the occasionally overlooked key function of skin, or as it has been put pointedly before:

> The mechanisms whereby nutrients, electrolytes, and water are transferred from the environment across the epithelia into the organism have been defined in varying detail for most epithelia and in a number of animal species. However, physiologists have paid less attention

M.J. Behne, MD (✉)
University Medical Center Hamburg-Eppendorf, Department of Dermatology and Venerology, Martinistr. 52, 20246 Hamburg, Germany

Hautarztpraxis Schleswig, Stadtweg 26, 24837 Schleswig, Germany
e-mail: m.behne@uke.de

J.-M. Jensen, MD (✉)
Department of Dermatology, Venerology and Allergology, University Hospitals of Schleswig-Holstein, Campus Kiel, University of Kiel, 24105 Kiel, Schittenhelmstr. 7

Hautarztpraxis Schleswig, Stadtweg 26, 24837 Schleswig, Germany
e-mail: mjensen@dermatology.uni-kiel.de

M.S. Islam (ed.), *Calcium Signaling*, Advances in Experimental Medicine and Biology 740, DOI 10.1007/978-94-007-2888-2_43,

> to the other major function of epithelia: their ability to serve as barriers between the outside world and the internal milieu of the organism. No doubt this is because the epithelial properties that allow the frog skin to absorb sodium from concentrations as low as 1 mM in pond water or the rabbit urinary bladder "to prevent loss of Na+ from the body during Na+ depletion" are the same properties that allow these epithelia to keep the pond out of the frog and the urine out of the rabbit [4].

The viable epidermis is at the intersection of both these aspects: it does not contain a vascular network and keratinocytes obtain their nutrients by passive diffusion from the underlying dermal compartment, with the compacted, enucleated Stratum corneum (SC) as the outward "seal" (for a historic overview refer to [5]). This manifests itself in a calcium gradient in the epidermis with a relatively low calcium concentration in the basal epidermis, and possibly even lower concentration in the spinous layers, while the highest calcium concentrations are found in the granular layers. Calcium in the SC is very low for a possible conserving strategy [6], and because the relatively dry and lipophilic SC may not able to solve the highly polar ions [7–9].

The physiologic role of this gradient has been established for keratinocyte differentiation [10–13] on a cellular level, and in neonatal barrier establishment [14] for the whole organ. Its function becomes more obvious when the permeability barrier is disrupted: After disruption there is influx of water into the SC and the ion gradient is lost. This depletion of calcium initiates barrier repair which comprises differentiation from underlying epidermal layers including protein- and lipid synthesis, packaging of lipids into lamellar bodies for subsequent exocytosis [3, 15–19] and replacement of cells in the SG which terminally differentiate to substitute cells lost at the surface [20]. Experimentally, this has been proven as occlusive therapy normalizes barrier function and the calcium-gradient [21], and the transglutaminases necessary for crosslinking of the cornified envelope are calcium dependent [11, 22, 23].

A change in calcium distribution has been shown to be connected to a host of pathologic states [24], and a disruption of the gradient is among the features of a range of conditions: while the calcium gradient appears to be typical for young epidermis, in aged epidermis it is largely lost, with calcium distributed more evenly throughout the epidermis [25]. Altered calcium-distribution is a hallmark of two frequent dermatologic conditions: in Psoriasis, both global [9, 21, 26] and intracellular levels [26] are altered; in Atopic Eczema, both a global alteration and influence of external calcium have been demonstrated [27, 28]. In both conditions, treatment affects calcium and/or uses pathways involving calcium [29]. Finally, in patients undergoing dialysis, a condition which may affect ionic balance globally, a number of calcium-related problems arise, such as pruritus [30, 31] and calcinosis/calciphylaxis [32, 33].

Calcium and Enzyme-Activity

A dysregulation in lipid processing has been credited with part of the barrier-abnormality in Atopic Eczema. Although unclear at this time, the defective barrier and concomitant change in calcium levels in SC could differentially lower the activity of certain sphingomyelinases [34, 35] and matrix metalloproteinases [36], while

increasing other activities such as expression of antimicrobial proteins [37]. The latter is further compounded through their varying and multiple roles, and their proper regulations [38, 39]. Similarly, a host of proteases has been shown to be present in SC, although they have been mostly incompletely characterized to date. The role of transglutaminases in cornification has been mentioned above, while the predominant role of proteases is presumed to lie at the other functional endpoint, i.e. in SC desquamation and its regulation. Factors that depend on the actual environment and thus suggest varying degrees of proteolytic activity are differing calcium-requirements, pH, hydration state, and in case of a disrupted barrier also a rise in calcium, which may contribute to disease severity (e.g. [40–42]). Although activation or regulation of proteolytic activity through calcium is a generally accepted principle [43, 44], it has not been assessed in its entirety for epidermis and SC, most likely due to the numerous enzyme families, the processes that regulate them, and their interconnectivity [42]. Lastly, such processes also may form an important factor in the above mentioned clinical challenges of pruritus and calciphylaxis.

Measurement Methodology

Despite the detailed knowledge about calcium distribution and its cellular regulation, tissue- and cellular Ca^{2+} concentrations in physiologic and diseased conditions are only partially known. This can be attributed to the very barrier properties of skin, which make it poorly accessible to conventional measurement procedures. Recent reviews on the topic point to an apparent lack of experimental options [45, 46]. In cell culture experiments regulation of proliferation and differentiation through calcium levels is standard procedure (e.g., [47–49]), and intracellular concentration ranges are therefore established. Reports about Ca^{2+}-concentrations in skin are somewhat divergent, hardly comparable qualitative ultrastructural methods (histochemical calcium-precipitation followed by transmission electron microscopy [3, 9]) and quantitative PIXE-experiments (proton-induced x-ray emission; this method has rendered the detailed view about the epidermal calcium-gradient) [7–9, 16, 50]. Together, these findings have defined the view of calcium's role in skin. By contrast, our recent work has focused on a novel method where close to in-vivo we map dynamic changes of calcium in skin [6, 51, 52]. Currently, observation in-vivo/in-situ is only beginning, as specifically a close differentiation of intracellular changes compared to changes in the extracellular/interstitial compartment are lacking (Fig. 43.1).

Intracellular Calcium

While the conditions listed above entail rather global changes in calcium-distribution, the main constituent cells of epidermis, keratinocytes, are known to posses the full complement of metabolic pathways regulating calcium. E.g., locally produced 1,25- dihydroxyvitamin D3 (1,25(OH)2D3) and extracellular calcium act jointly as

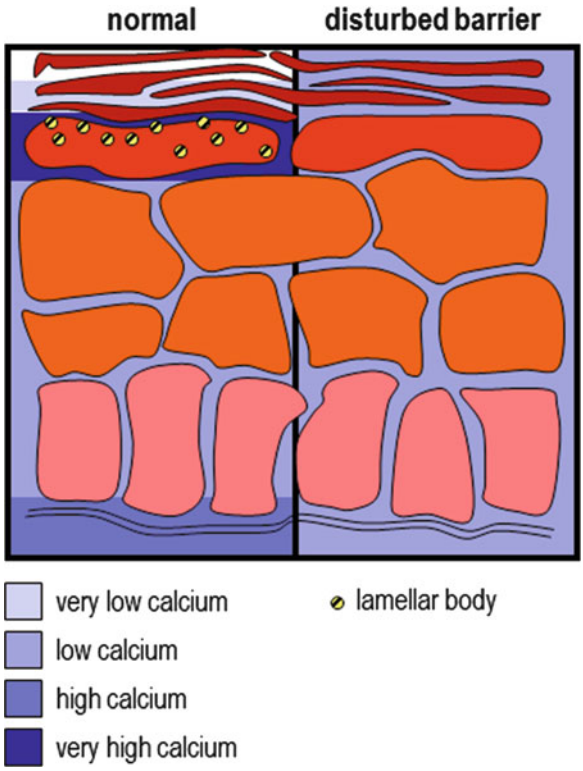

Fig. 43.1 Changes in the calcium gradient after barrier disruption regulate lamellar body secretion and epidermal differentiation. This figure depicts the established, global calcium-distribution in epidermis (e.g., [16]), with the caveat that recent advances [6, 52] may alter this view, specifically differentiating intracellular and interstitial compartments

key regulators of cellular proliferation [53], and while moderate expression of the VDR is found in nearly all tissues, highest expression is found, among others, in skin [54], where it is involved in epidermis-specific Sphingolipid production essential for permeability barrier function [55]. Consequently, the 1α,25(OH)2D3-dependent balance between proliferation and differentiation of keratinocytes may be a basis for prevention and treatment of skin cancer [20, 56–59].

Implications from Hailey-Hailey and Darier's Disease

A closer view on intracellular dysregulation and how intracellular calcium is controlled by more than one mechanism has come through investigation of two distinct hereditary diseases, Hailey-Hailey disease (HHD) and Darier's disease (DD), and their characteristic effects on skin. Hailey-Hailey disease (OMIM 169600) is an autosomal dominant blistering disease, traditionally termed familial benign chronic pemphigus; it was first described in 1939 [60]. The disorder usually presents in adulthood and is typically characterized by rather superficial vesicles and crusted erosions, as a result of impaired cell-to-cell adhesion (acantholysis), causing an

intercellular split among the suprabasal keratinocytes in the epidermis. In clinical/histologic diagnosis, internalization of desmosomal components is the other typical finding in HHD, whereas adherens junctions and gap junctions are preserved [61–63]. In normal keratinocytes in vitro, calcium stimulates the complexing of desmosomal components including E-cadherin, α-, β-, and γ-catenin, and actin polymerization, causing the formation of "adhesion zippers" [64]. Skin specimens from patients with HHD reveal deficient actin reorganization with abnormal stress fibers [63] and abnormal localization of actin filaments [65], a feature that we could reproduce in vitro with calcium-induced cell-differentiation [66]. HHD is caused by mutations in ATP2C1 (in haploinsufficiency), which encodes an intracellular calcium pump [8, 67] localized to the Golgi [68]. This is consistent with the location of its homolog in yeast, PMR1 [69], while studies in Caenorhabditis elegans demonstrate that this class of ATPases transports calcium from the cytosol into intracellular stores [70]. As a consequence of the Golgi being an inositol 1,4,5-trisphosphate-sensitive calcium store (IP3) [71], cytosolic calcium was abnormally high with lower Golgi-calcium-concentrations in keratinocytes cultured from HHD patients, and no calcium-induced calcium release (CICR) [8, 68].

Disturbed regulation of calcium metabolism and increased TEWL occur in Darier's disease [72], a similar blistering skin disease which is also characterized by a loss of adhesion between suprabasal epidermal cells, but additionally shows abnormal keratinization. The gene for Darier's disease (ATP2A2, OMIM 124200) encodes a calcium transport ATPase of the sarco (endo)plasmic reticulum (SERCA2) [73–75]. Endoplasmic reticulum calcium stores also are present in keratinocytes, and pharmacologic blockade of the calcium ATPase ATP2A2 with thapsigargin prevents calcium-induced redistribution of E-cadherin to the cell periphery [49].

Raised extracellular calcium acts through a well-defined cascade of signaling events, including binding to a plasma membrane calcium receptor, generation of IP3, release of intracellular calcium (CICR), and subsequent influx through plasma membrane channels and (re)filling or rather maintenance of intracellular stores. On the other hand, through findings in both HHD and DD, consequences of intracellular calcium-dysregulation through defective intracellular stores are somewhat defined at the cellular level. Yet, just how this leads to the eventual disease-phenotype is less evident. A recent report has begun to unravel the complexity of mechanisms involved in HHD: an alteration of Notch and p63 signaling based on the calcium-dysregulation compounded with oxidative stress led to the clinical phenotype in this subset of HHD patients [76].

Conclusion

This chapter can but point out some of the multitudinous roles of calcium in skin, more specifically in epidermis. There are many excellent reviews on facets we barely touched upon; we recommend these reviews to the inclined reader, rather than to duplicate such efforts. Also, the comments on HHD and DD may help to

illustrate that despite the level of detail in knowledge in certain areas, we are far from understanding the entire complexity which governs calcium in skin, and by which it is governed. To truly explore this field, an entire volume rather than a chapter would be needed, especially if it were to be extended to skin as a whole.

References

1. Dupont G, Combettes L, Leybaert L (2007) Calcium dynamics: spatio-temporal organization from the subcellular to the organ level. Int Rev Cytol 261:193–245
2. Parekh AB (2003) Store-operated Ca^{2+} entry: dynamic interplay between endoplasmic reticulum, mitochondria and plasma membrane. J Physiol 547:333–348
3. Menon GK, Elias PM, Lee SH, Feingold KR (1992) Localization of calcium in murine epidermis following disruption and repair of the permeability barrier. Cell Tissue Res 270:503–512
4. Powell DW (1981) Barrier function of epithelia. Am J Physiol 241:G275–G288
5. Scheuplein RJ (1976) Percutaneous absorption after twenty-five years: or "old wine in new wineskins". J Invest Dermatol 67:31–38
6. Behne MJ, Sanchez S, Barry NP, Kirschner N, Meyer W, Mauro TM, Moll I, Gratton E (2011) Major translocation of calcium upon epidermal barrier insult: imaging and quantification via FLIM/Fourier vector analysis. Arch Dermatol Res 303:103–115
7. Forslind B, Werner-Linde Y, Lindberg M, Pallon J (1999) Elemental analysis mirrors epidermal differentiation. Acta Derm Venereol 79:12–17
8. Hu Z, Bonifas JM, Beech J, Bench G, Shigihara T, Ogawa H, Ikeda S, Mauro T, Epstein EH Jr (2000) Mutations in ATP2C1, encoding a calcium pump, cause Hailey-Hailey disease. Nat Genet 24:61–65
9. Menon GK, Elias PM (1991) Ultrastructural localization of calcium in psoriatic and normal human epidermis. Arch Dermatol 127:57–63
10. Jamora C, Fuchs E (2002) Intercellular adhesion, signalling and the cytoskeleton. Nat Cell Biol 4:E101–E108
11. Segre J (2003) Complex redundancy to build a simple epidermal permeability barrier. Curr Opin Cell Biol 15:776–782
12. Yuspa SH, Kilkenny AE, Steinert PM, Roop DR (1989) Expression of murine epidermal differentiation markers is tightly regulated by restricted extracellular calcium concentrations in vitro. J Cell Biol 109:1207–1217
13. Tu CL, Oda Y, Komuves L, Bikle DD (2004) The role of the calcium-sensing receptor in epidermal differentiation. Cell Calcium 35:265–273
14. Elias PM, Nau P, Hanley K, Cullander C, Crumrine D, Bench G, Sideras-Haddad E, Mauro T, Williams ML, Feingold KR (1998) Formation of the epidermal calcium gradient coincides with key milestones of barrier ontogenesis in the rodent. J Invest Dermatol 110:399–404
15. Lee SH, Elias PM, Proksch E, Menon GK, Mao-Quiang M, Feingold KR (1992) Calcium and potassium are important regulators of barrier homeostasis in murine epidermis. J Clin Invest 89:530–538
16. Mauro T, Bench G, Sidderas-Haddad E, Feingold K, Elias P, Cullander C (1998) Acute barrier perturbation abolishes the Ca^{2+} and K^{+} gradients in murine epidermis: quantitative measurement using PIXE. J Invest Dermatol 111:1198–1201
17. Menon GK, Price LF, Bommannan B, Elias PM, Feingold KR (1994) Selective obliteration of the epidermal calcium gradient leads to enhanced lamellar body secretion. J Invest Dermatol 102:789–795
18. Lee SH, Elias PM, Feingold KR, Mauro T (1994) A role for ions in barrier recovery after acute perturbation. J Invest Dermatol 102:976–979

19. Elias P, Ahn S, Brown B, Crumrine D, Feingold KR (2002) Origin of the epidermal calcium gradient: regulation by barrier status and role of active vs passive mechanisms. J Invest Dermatol 119:1269–1274
20. Elias PM, Ahn SK, Denda M, Brown BE, Crumrine D, Kimutai LK, Komuves L, Lee SH, Feingold KR (2002) Modulations in epidermal calcium regulate the expression of differentiation-specific markers. J Invest Dermatol 119:1128–1136
21. Hwang SM, Ahn SK, Menon GK, Choi EH, Lee SH (2001) Basis of occlusive therapy in psoriasis: correcting defects in permeability barrier and calcium gradient. Int J Dermatol 40:223–231
22. Fuchs E (1990) Epidermal differentiation: the bare essentials. J Cell Biol 111:2807–2814
23. Kalinin AE, Kajava AV, Steinert PM (2002) Epithelial barrier function: assembly and structural features of the cornified cell envelope. Bioessays 24:789–800
24. Missiaen L, Robberecht W, van den Bosch L, Callewaert G, Parys JB, Wuytack F, Raeymaekers L, Nilius B, Eggermont J, De Smedt H (2000) Abnormal intracellular ca(2+) homeostasis and disease. Cell Calcium 28:1–21
25. Denda M, Tomitaka A, Akamatsu H, Matsunaga K (2003) Altered distribution of calcium in facial epidermis of aged adults. J Invest Dermatol 121:1557–1558
26. Karvonen SL, Korkiamaki T, Yla-Outinen H, Nissinen M, Teerikangas H, Pummi K, Karvonen J, Peltonen J (2000) Psoriasis and altered calcium metabolism: downregulated capacitative calcium influx and defective calcium-mediated cell signaling in cultured psoriatic keratinocytes. J Invest Dermatol 114:693–700
27. McNally NJ, Williams HC, Phillips DR, Smallman-Raynor M, Lewis S, Venn A, Britton J (1998) Atopic eczema and domestic water hardness. Lancet 352:527–531
28. Pallon J, Malmqvist KG, Werner-Linde Y, Forslind B (1996) Pixe analysis of pathological skin with special reference to psoriasis and atopic dry skin. Cell Mol Biol (Noisy-le-Grand) 42:111–118
29. Li M, Hener P, Zhang Z, Kato S, Metzger D, Chambon P (2006) Topical vitamin D3 and low-calcemic analogs induce thymic stromal lymphopoietin in mouse keratinocytes and trigger an atopic dermatitis. Proc Natl Acad Sci USA 103:11736–11741
30. Momose A, Kudo S, Sato M, Saito H, Nagai K, Katabira Y, Funyu T (2004) Calcium ions are abnormally distributed in the skin of haemodialysis patients with uraemic pruritus. Nephrol Dial Transplant 19:2061–2066
31. Manenti L, Tansinda P, Vaglio A (2009) Uraemic pruritus: clinical characteristics, pathophysiology and treatment. Drugs 69:251–263
32. Reiter N, El-Shabrawi L, Leinweber B, Berghold A, Aberer E (2011) Calcinosis cutis Part II. Treatment options. J Am Acad Dermatol 65:15–22
33. Reiter N, El-Shabrawi L, Leinweber B, Berghold A, Aberer E (2011) Calcinosis cutis Part I. Diagnostic pathway. J Am Acad Dermatol 65:1–12
34. Imokawa G (2009) A possible mechanism underlying the ceramide deficiency in atopic dermatitis: expression of a deacylase enzyme that cleaves the N-acyl linkage of sphingomyelin and glucosylceramide. J Dermatol Sci 55:1–9
35. Jensen JM, Folster-Holst R, Baranowsky A, Schunck M, Winoto-Morbach S, Neumann C, Schutze S, Proksch E (2004) Impaired sphingomyelinase activity and epidermal differentiation in atopic dermatitis. J Invest Dermatol 122:1423–1431
36. Sudbeck BD, Pilcher BK, Pentland AP, Parks WC (1997) Modulation of intracellular calcium levels inhibits secretion of collagenase 1 by migrating keratinocytes. Mol Biol Cell 8:811–824
37. Glaser R, Meyer-Hoffert U, Harder J, Cordes J, Wittersheim M, Kobliakova J, Folster-Holst R, Proksch E, Schroder JM, Schwarz T (2009) The antimicrobial protein psoriasin (S100A7) is upregulated in atopic dermatitis and after experimental skin barrier disruption. J Invest Dermatol 129:641–649
38. Morizane S, Yamasaki K, Kabigting FD, Gallo RL (2010) Kallikrein expression and cathelicidin processing are independently controlled in keratinocytes by calcium, vitamin D(3), and retinoic acid. J Invest Dermatol 130:1297–1306

39. Yamasaki K, Kanada K, Macleod DT, Borkowski AW, Morizane S, Nakatsuji T, Cogen AL, Gallo RL (2011) TLR2 expression is increased in rosacea and stimulates enhanced serine protease production by keratinocytes. J Invest Dermatol 131:688–697
40. Calugaru SV, Swanson R, Olson ST (2001) The pH dependence of serpin-proteinase complex dissociation reveals a mechanism of complex stabilization involving inactive and active conformational states of the proteinase which are perturbable by calcium. J Biol Chem 276: 32446–32455
41. Bissett DL, McBride JF, Patrick LF (1987) Role of protein and calcium in stratum corneum cell cohesion. Arch Dermatol Res 279:184–189
42. Eissa A, Amodeo V, Smith CR, Diamandis EP (2011) Kallikrein-related peptidase-8 (KLK8) is an active serine protease in human epidermis and sweat and is involved in a skin barrier proteolytic cascade. J Biol Chem 286:687–706
43. Huntington JA, Read RJ, Carrell RW (2000) Structure of a serpin-protease complex shows inhibition by deformation. Nature 407:923–926
44. Twining SS (1994) Regulation of proteolytic activity in tissues. Crit Rev Biochem Mol Biol 29:315–383
45. Brini M, Carafoli E (2000) Calcium signalling: a historical account, recent developments and future perspectives. Cell Mol Life Sci 57:354–370
46. Rudolf R, Mongillo M, Rizzuto R, Pozzan T (2003) Looking forward to seeing calcium. Nat Rev Mol Cell Biol 4:579–586
47. Hennings H, Holbrook KA, Yuspa SH (1983) Factors influencing calcium-induced terminal differentiation in cultured mouse epidermal cells. J Cell Physiol 116:265–281
48. Bikle DD, Ratnam A, Mauro T, Harris J, Pillai S (1996) Changes in calcium responsiveness and handling during keratinocyte differentiation. Potential role of the calcium receptor. J Clin Invest 97:1085–1093
49. Li L, Tucker RW, Hennings H, Yuspa SH (1995) Chelation of intracellular Ca^{2+} inhibits murine keratinocyte differentiation in vitro. J Cell Physiol 163:105–114
50. Grundin TG, Roomans GM, Forslind B, Lindberg M, Werner Y (1985) X-ray microanalysis of psoriatic skin. J Invest Dermatol 85:378–380
51. Celli A, Mackenzie DS, Crumrine DS, Tu CL, Hupe M, Bikle DD, Elias PM, Mauro TM (2011) Endoplasmic reticulum Ca(2+) depletion activates XBP1 and controls terminal differentiation in keratinocytes and epidermis. Br J Dermatol 164(1):16–25
52. Celli A, Sanchez S, Behne M, Hazlett T, Gratton E, Mauro T (2010) The epidermal Ca(2+) gradient: measurement using the phasor representation of fluorescent lifetime imaging. Biophys J 98:911–921
53. Reichrath J, Kamradt J, Zhu XH, Kong XF, Tilgen W, Holick MF (1999) Analysis of 1,25-dihydroxyvitamin D(3) receptors (VDR) in basal cell carcinomas. Am J Pathol 155:583–589
54. Bookout AL, Jeong Y, Downes M, Yu RT, Evans RM, Mangelsdorf DJ (2006) Anatomical profiling of nuclear receptor expression reveals a hierarchical transcriptional network. Cell 126:789–799
55. Oda Y, Uchida Y, Moradian S, Crumrine D, Elias PM, Bikle DD (2009) Vitamin D receptor and coactivators SRC2 and 3 regulate epidermis-specific sphingolipid production and permeability barrier formation. J Invest Dermatol 129:1367–1378
56. Oda Y, Sihlbom C, Chalkley RJ, Huang L, Rachez C, Chang CP, Burlingame AL, Freedman LP, Bikle DD (2003) Two distinct coactivators, DRIP/mediator and SRC/p160, are differentially involved in vitamin D receptor transactivation during keratinocyte differentiation. Mol Endocrinol 17:2329–2339
57. Bikle DD (2004) Vitamin D and skin cancer. J Nutr 134:3472S–3478S
58. Tu CL, Chang W, Xie Z, Bikle DD (2008) Inactivation of the calcium sensing receptor inhibits E-cadherin-mediated cell-cell adhesion and calcium-induced differentiation in human epidermal keratinocytes. J Biol Chem 283:3519–3528
59. Tu CL, Chang W, Bikle DD (2007) The role of the calcium sensing receptor in regulating intracellular calcium handling in human epidermal keratinocytes. J Invest Dermatol 127: 1074–1083

60. Hailey H, Hailey H (1939) Familial benign chronic pemphigus. Arch Dermatol Syphilol 39:679–685
61. Harada M, Hashimoto K, Fujiwara K (1994) Immunohistochemical distribution of CD44 and desmoplakin I & II in Hailey-Hailey's disease and Darier's disease. J Dermatol 21:389–393
62. Hashimoto K, Fujiwara K, Harada M, Setoyama M, Eto H (1995) Junctional proteins of keratinocytes in Grover's disease. Hailey-Hailey's disease and Darier's disease. J Dermatol 22:159–170
63. Metze D, Hamm H, Schorat A, Luger T (1996) Involvement of the adherens junction-actin filament system in acantholytic dyskeratosis of Hailey-Hailey disease. A histological, ultrastructural, and histochemical study of lesional and non-lesional skin. J Cutan Pathol 23:211–222
64. Vasioukhin V, Bauer C, Yin M, Fuchs E (2000) Directed actin polymerization is the driving force for epithelial cell-cell adhesion. Cell 100:209–219
65. Inohara S, Tatsumi Y, Tanaka Y, Sagami S (1990) Immunohistochemical localization of desmosomal and cytoskeletal proteins in the epidermis of healthy individuals and patients with Hailey-Hailey's disease. Acta Derm Venereol 70:239–241
66. Aronchik I, Behne MJ, Leypoldt L, Crumrine D, Epstein E, Ikeda S, Mizoguchi M, Bench G, Pozzan T, Mauro T (2003) Actin reorganization is abnormal and cellular ATP is decreased in Hailey-Hailey keratinocytes. J Invest Dermatol 121:681–687
67. Sudbrak R, Brown J, Dobson-Stone C, Carter S, Ramser J, White J, Healy E, Dissanayake M, Larregue M, Perrussel M, Lehrach H, Munro CS, Strachan T, Burge S, Hovnanian A, Monaco AP (2000) Hailey-Hailey disease is caused by mutations in ATP2C1 encoding a novel Ca(2+) pump. Hum Mol Genet 9:1131–1140
68. Behne MJ, Tu CL, Aronchik I, Epstein E, Bench G, Bikle DD, Pozzan T, Mauro TM (2003) Human keratinocyte ATP2C1 localizes to the Golgi and controls Golgi Ca^{2+} stores. J Invest Dermatol 121:688–694
69. Antebi A, Fink GR (1992) The yeast Ca(2+)-ATPase homologue, PMR1, is required for normal Golgi function and localizes in a novel Golgi-like distribution. Mol Biol Cell 3:633–654
70. Van Baelen K, Vanoevelen J, Missiaen L, Raeymaekers L, Wuytack F (2001) The Golgi PMR1 P-type ATPase of Caenorhabditis elegans. Identification of the gene and demonstration of calcium and manganese transport. J Biol Chem 276:10683–10691
71. Pinton P, Pozzan T, Rizzuto R (1998) The Golgi apparatus is an inositol 1,4,5-trisphosphate-sensitive Ca^{2+} store, with functional properties distinct from those of the endoplasmic reticulum. EMBO J 17:5298–5308
72. Lavrijsen AP, Oestmann E, Hermans J, Bodde HE, Vermeer BJ, Ponec M (1993) Barrier function parameters in various keratinization disorders: transepidermal water loss and vascular response to hexyl nicotinate. Br J Dermatol 129:547–553
73. Foggia L, Hovnanian A (2004) Calcium pump disorders of the skin. Am J Med Genet C Semin Med Genet 131C:20–31
74. Sakuntabhai A, Ruiz-Perez V, Carter S, Jacobsen N, Burge S, Monk S, Smith M, Munro CS, O'Donovan M, Craddock N, Kucherlapati R, Rees JL, Owen M, Lathrop GM, Monaco AP, Strachan T, Hovnanian A (1999) Mutations in ATP2A2, encoding a Ca^{2+} pump, cause Darier disease. Nat Genet 21:271–277
75. Verboomen H, Wuytack F, De Smedt H, Himpens B, Casteels R (1992) Functional difference between SERCA2a and SERCA2b Ca^{2+} pumps and their modulation by phospholamban. Biochem J 286(Pt 2):591–595
76. Cialfi S, Oliviero C, Ceccarelli S, Marchese C, Barbieri L, Biolcati G, Uccelletti D, Palleschi C, Barboni L, De Bernardo C, Grammatico P, Magrelli A, Salvatore M, Taruscio D, Frati L, Gulino A, Screpanti I, Talora C (2010) Complex multipathways alterations and oxidative stress are associated with Hailey-Hailey disease. Br J Dermatol 162:518–526

Chapter 44
Calcium Signaling in Mast Cells: Focusing on L-Type Calcium Channels

Yoshihiro Suzuki, Toshio Inoue, and Chisei Ra

Abstract Mast cells play central roles in adaptive and innate immunity. IgE-dependent stimulation of the high-affinity IgE receptor (FcεRI) results in rapid secretion of various proinflammatory chemical mediators and cytokines. All of the outputs depend to certain degrees on an increase in the intracellular Ca^{2+} concentration, and influx of Ca^{2+} from the extracellular space is often required for their full activation. There is strong evidence that FcεRI stimulation induces two different modes of Ca^{2+} influx, store-operated Ca^{2+} entry (SOCE) and non-SOCE, which are activated in response to endoplasmic reticulum Ca^{2+} store depletion and independently of Ca^{2+} store depletion, respectively, in mast cells. Although Ca^{2+} release-activated Ca^{2+} channels are the major route of SOCE, recent evidence indicates that they are not the only Ca^{2+} channels activated by Ca^{2+} store depletion. The recent data suggest that L-type Ca^{2+} channels, which were thought to be a characteristic feature of excitable cells, exist in mast cells to mediate non-SOCE, which is critical for protecting mast cells against activation-induced mitochondrial cell death. In this chapter, we provide an overview of recent advances in our understanding of Ca^{2+} signaling in mast cells with a special attention to the emerging role for the L-type Ca^{2+} channels as a regulator of mast cell survival.

Keywords Ca^{2+} signaling • Mast cell • CRAC channel • L-type Ca^{2+} channel

Y. Suzuki (✉) • T. Inoue • C. Ra
Division of Molecular Cell Immunology and Allergology,
Nihon University Graduate School of Medical Science,
30-1 Oyaguchikami-cho Itabashi-ku, Tokyo 173-8610, Japan
e-mail: suzuki.yoshihiro@nihon-u.ac.jp

M.S. Islam (ed.), *Calcium Signaling*, Advances in Experimental Medicine and Biology 740, DOI 10.1007/978-94-007-2888-2_44,

Introduction

Mast Cells and Ca^{2+}

Mast cells play central roles in adaptive and innate immunity. Upon stimulation of the high-affinity IgE receptor (FcεRI), mast cells have remarkably diverse functional outputs. These outputs include degranulation (secretion of pre-formed chemical mediators stored in granules such as histamine and serotonin), synthesis and secretion of arachidonate-derived mediators such as leukotrienes (LTs) and prostaglandins (PGs), and the production of cytokines and chemokines. These mediators cause various pathophysiological events, including vasodilation, vascular hyperpermeability, and recruitment and activation of other inflammatory cells, thereby contributing to acute and chronic allergic responses and diseases (1) (Fig. 44.1). All these outputs depend to certain degrees on an increase in the intracellular Ca^{2+} concentration ($[Ca^{2+}]_i$). In most cell types, including mast cells, the cytosolic Ca^{2+} concentration is maintained at low levels (50–150 nM) in resting cells. However, agonists including hormones, growth factors and antigens induce an increase in

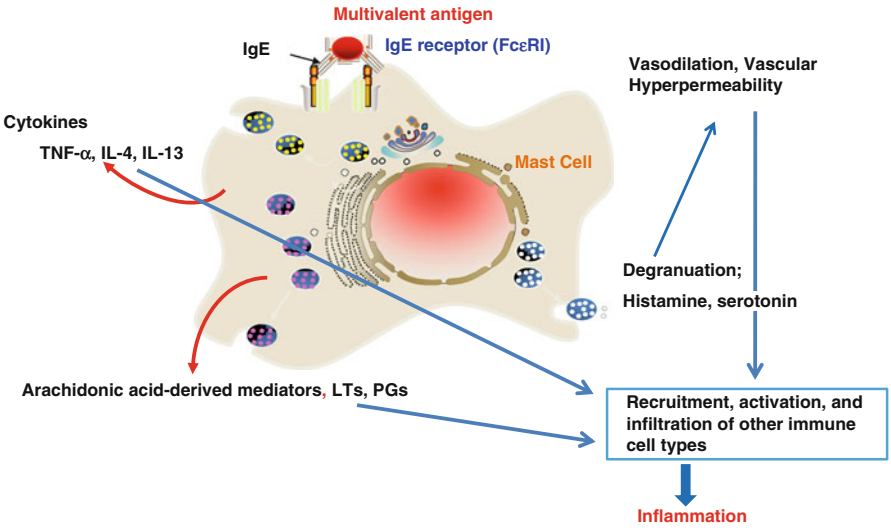

Fig. 44.1 IgE-dependent activation of mast cells. Cross-linking of the high-affinity IgE receptor (FcεRI) by IgE plus a multivalent antigen results in mast cell activation pathways that lead to remarkably diverse functional outputs. These outputs include degranulation (i.e., the secretion of pre-formed chemical mediators stored in granules such as histamine and serotonin), the synthesis and secretion of arachidonic acid-derived mediators such as leukotrienes (*LTs*) and prostaglandins (*PGs*) and the production of cytokines, such as tumor necrosis factor (*TNF*)-α, interleukin (*IL*)-4 and IL-13, and chemokines. These mediators cause various pathophysiological events, including vasodilation, vascular hyperpermeability, and recruitment, activation and infiltration of other inflammatory cells, thereby contributing to acute and chronic allergic responses and diseases

$[Ca^{2+}]_i$ of up to 1 μM by stimulating the mobilization of Ca^{2+} from intracellular stores such as the endoplasmic reticulum (ER) and mitochondria as well as the extracellular space. However, sustained influx of external Ca^{2+} is considered to be mainly responsible for the elevation in $[Ca^{2+}]_i$ and secretory responses in rodent mast cells [1]. Similarly, influx of Ca^{2+} from the extracellular fluid is required for histamine release from human lung mast cells [2]. Therefore, the channels involved in Ca^{2+} signaling are of great interest as novel targets for the development of anti-allergic drugs. Mast cell degranulation involves the steps of translocation, docking and fusion of granules with the plasma membrane, and Ca^{2+} is thought to play essential or important roles in these processes. It has been noted that degranulation is at least partly, similar to presynaptic Ca^{2+}-triggered exocytosis [3]. Certain Ca^{2+}-sensing proteins such as synaptotagmins are involved in membrane fusion, and increases in $[Ca^{2+}]_i$ may activate or amplify this process [4]. Secretion of cysteinyl-LTs requires their *de novo* synthesis and secretion, which involve complicated biochemical processes including cytosolic phospholipase A_2 ($cPLA_2$)-mediated arachidonic acid (AA) release from the plasma membrane followed by oxidation by 5-lipoxygenase (5-LOX). Ca^{2+} is a key physiological regulator of LTC_4 synthesis, since Ca^{2+} binds to the N-terminal C2 domain of $cPLA_2$, thereby promoting its translocation and activation [5]. Moreover, in rat basophilic leukemia (RBL) mast cell line activated with thapsigargin or agonists, the recruitment of protein kinase C and components of the extracellular signal-regulated protein kinase (ERK)/PLA_2/5-LOX pathway is strictly dependent on a Ca^{2+} influx [6, 7]. Ca^{2+} also plays important roles in the production of cytokines via the Ca^{2+}/calcineurin/NFAT pathway [1]. Figure 44.2 shows the possible Ca^{2+} dependence of biochemical processes in mast cell outputs.

FcεRI is a member of the immunoglobulin superfamily of antigen receptors, which also includes T and B cell receptors, and the signal transduction pathways present in mast cells have many similarities with those in T and B cells. FcεRI is a tetramer consisting of an α-chain, a β-chain and a γ-chain homodimer, among which the α-chain binds to IgE, and the β- and γ-chains contain immunoreceptor tyrosine-based activation motifs (ITAMs), which are critical for cell activation through cell surface receptors [1] (Fig. 44.3).

Regulatory Mechanisms of Intracellular Ca^{2+} in Eukaryotic Cells

A variety of different Ca^{2+}-permeable channels are known to coexist in the plasma membrane and to play major roles in the entry of extracellular Ca^{2+} into eukaryotic cells (Fig. 44.4). These channels include voltage-operated Ca^{2+} (VOC) channels, receptor-operated Ca^{2+} (ROC) channels, second messenger-operated Ca^{2+} (SMOC) channels and store-operated Ca^{2+} (SOC) channels such as Ca^{2+} release-activated Ca^{2+} (CRAC) channels. On the other hand, Ca^{2+} is extruded through two molecular machineries, Na^+-Ca^{2+} exchangers (NCX) and plasma membrane Ca^{2+}-ATPase (PMCA). The release of Ca^{2+} from intracellular stores, mainly the ER, and clearance

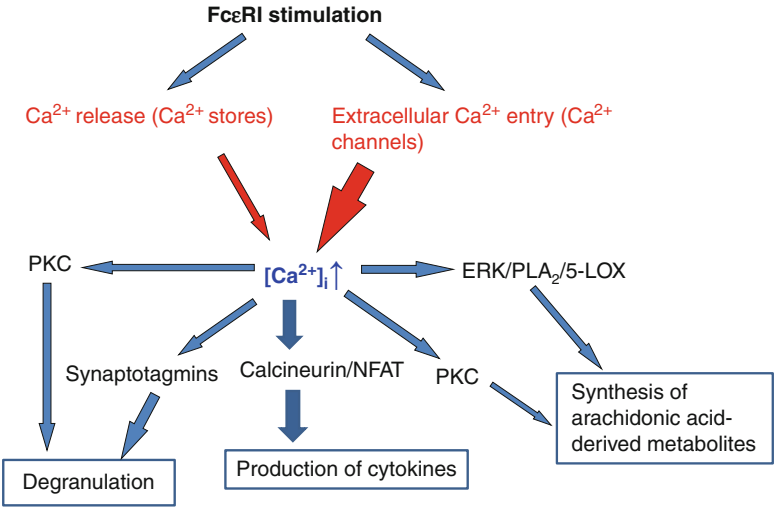

Fig. 44.2 Ca^{2+} entry from the extracellular space is essential for full mast cell activation. FcεRI stimulation results in an increase in $[Ca^{2+}]_i$ by stimulating Ca^{2+} mobilization from intracellular stores and the extracellular space, but sustained influx of external Ca^{2+} is usually required for full activation of the outputs. Ca^{2+} can activate protein kinase C (*PKC*), an important player in mast cell signaling. Ca^{2+} is also thought to play essential or important roles in each step of the translocation, docking and fusion of granules with the plasma membrane during degranulation. Degranulation is similar to presynaptic Ca^{2+}-triggered exocytosis. Certain Ca^{2+}-sensing proteins such as synaptotagmins are involved in the membrane fusion and increases in $[Ca^{2+}]_i$ may activate or amplify this process. During *de novo* synthesis and secretion of cysteinyl-LTs, Ca^{2+} mainly plays key roles in two different processes. Ca^{2+} binds to the N-terminal C2 domain of $cPLA_2$, thereby promoting its translocation and activation. Also the recruitment of PKC and components of the ERK/PLA_2/5-LOX pathway are strictly dependent on Ca^{2+} influx. Ca^{2+} also plays a critical role in the production of cytokines via the Ca^{2+}/calcineurin/NFAT pathway

of Ca^{2+} from the cytosol by resequestration into organelles such as the ER and mitochondria are also important in the regulation of $[Ca^{2+}]_i$ [8]. VOC channels or voltage-gated Ca^{2+} (Ca_v) channels are found in electrically excitable cells like nerve and muscle cells, become activated by membrane depolarization, and serve as the principal routes of Ca^{2+} entry into these cells. ROC channels open rapidly upon binding of external ligands such as neurotransmitters and are predominantly found in excitable cells. SMOC channels are found in some excitable and nonexcitable cells, and are activated by any of a number of small second messenger molecules, typically inositol phosphates, cyclic nucleotides and lipid-derived messengers such as diacylglycerol and AA and its metabolites. In addition to its Ca^{2+}-mobilizing activity from the ER, nicotinic acid adenine dinucleotide phosphate (NAADP) has been shown to evoke Ca^{2+} entry in some cell types, although the localization and nature of its specific receptors, referred as to NAADP receptors (NAADPRs), are poorly understood [9, 10]. It is widely accepted that the ER plays a central role in the regulation of Ca^{2+} influx in eukaryotic cells and the second messenger inositol-1,4,

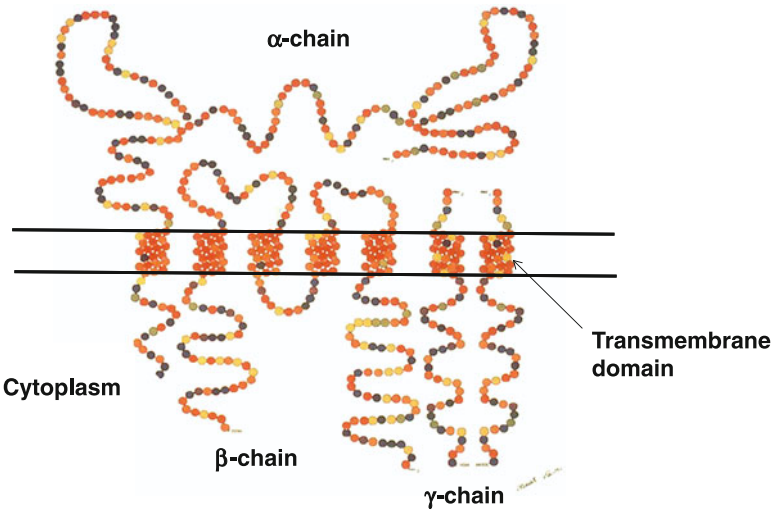

Fig. 44.3 Membrane topology and structure of FcεRI. FcεRI is a member of the immunoglobulin superfamily of antigen receptors, which also includes T and B cell receptors, and the signal transduction pathways present in mast cells have many similarities with those in T and B cells. FcεRI is a tetramer consisting of an α-chain, a β-chain and a γ-chain homodimer of which the α-chain binds to IgE and the β- and γ-chains contain immunoreceptor tyrosine-based activation motifs, which are critical for cell activation through cell surface receptors

5-triphosphate (IP_3) generated by surface receptor-mediated activation of phospholipase C (PLC) is an essential component of this regulation [11]. IP_3 binds to IP_3 receptors located on the surface of the ER and activates the release of Ca^{2+}. In addition to IP_3, two other intracellular Ca^{2+} mobilizing agents, cyclic ADP ribose and NAADP are involved in the release of Ca^{2+} from intracellular stores, by binding to ryanodine receptors and NAADPRs, respectively [12–14] (Fig. 44.4). Depletion of Ca^{2+} stores in the ER results in store-operated Ca^{2+} entry (SOCE) through the activation of SOC channels on the plasma membrane. These channels appear to be widespread, and apparently exist in all eukaryotes from yeasts [15] to humans [16]. Such channels are also activated by pharmacological emptying of intracellular Ca^{2+} stores via the actions of pharmacological agents, such as the sarco/endoplasmic reticulum Ca^{2+}-ATPase (SERCA) inhibitor thapsigargin (Tg) [17]. It is widely accepted that SOCE is the main mode of Ca^{2+} influx in electrically non-excitable cells, including mast cells, and that CRAC channels are the major SOC channels [18]. A growing body of evidence suggests that store depletion also leads to the activation of other channels that are relatively non-selective for Ca^{2+} but contribute to SOCE in several cell types, and transient receptor potential canonical (TRPC) channels are typical of this channel type. It has been shown that SOCE is not the only mode of Ca^{2+} entry into mast cells. Recent evidence indicates that Ca^{2+} entry into mast cells also occurs independently of Ca^{2+} store depletion (non-SOCE) and that L-type Ca^{2+} (LTCCs),

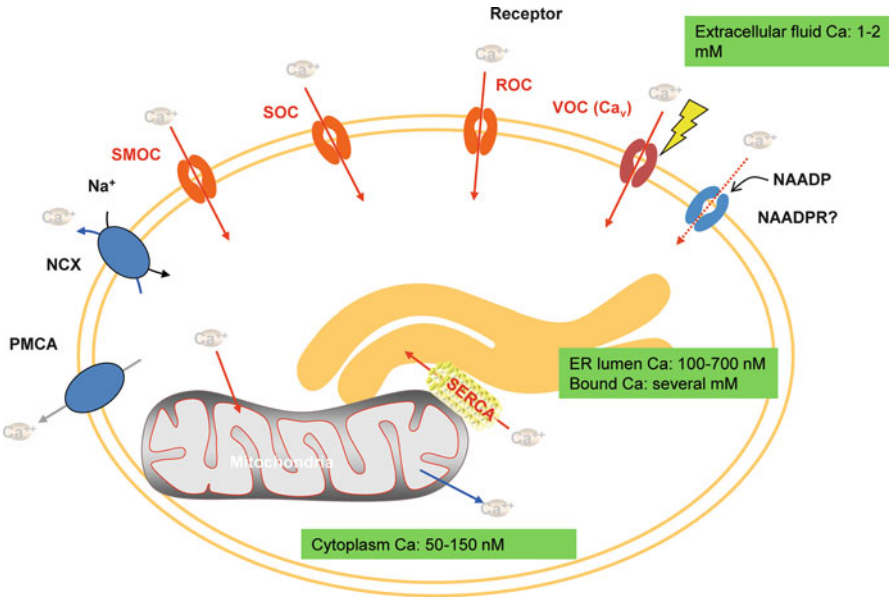

Fig. 44.4 Ca^{2+} influxes and effluxes through the plasma membrane in a eukaryotic cell. $[Ca^{2+}]_c$ levels are controlled by the balance between Ca^{2+} entry into the cell and Ca^{2+} extrusion from the cell. Ca^{2+} enters the cell through voltage-operated Ca^{2+} (*VOC*) channels, receptor-operated Ca^{2+} (*ROC*) channels, second messenger-operated Ca^{2+} (*SMOC*) channels and store-operated Ca^{2+} (*SOC*) channels in the plasma membrane. It should be noted that these Ca^{2+} channels are not necessarily expressed and do not always operate in a given cell. On the other hand, Ca^{2+} is extruded through two molecular machineries, Na^+-Ca^{2+} exchangers (*NCX*) and plasma membrane Ca^{2+}-ATPase (*PMCA*). Release of Ca^{2+} from intracellular stores such as the endoplasmic reticulum (*ER*) and mitochondria and clearance of Ca^{2+} from the cytosol by resequestration into these organelles are also important in the regulation of $[Ca^{2+}]_c$

which were thought to be a characteristic feature of excitable cells, mediate this mode of Ca^{2+} influx. TRPC channels have also been proposed to be involved in not only SOCE, but also non-SOCE. We briefly introduce recent developments in this field of research with a special focus on CRAC channels and LTCCs in the following section, since there is evidence that the two types of channels are coordinately rather than independently regulated. Readers who are interested in more detailed information about CRAC channels and TRPC channels should refer to two excellent recent reviews [19, 20].

CRAC Channels

The best-characterized SOC channels, CRAC channels were originally identified in a study on the currents passing through the channels, I_{CRAC} in RBL mast cells and display high Ca^{2+} selectivity [21]. It is now well established that CRAC channels

account for the SOCE and cell function in T lymphocytes, mast cells, platelets and some types of smooth muscle and endothelial cells [22, 23]. It has recently been shown that the mammalian protein stromal interaction molecule 1 (STIM1) acts as a molecular sensor for Ca^{2+} store emptying [24–26]. STIM1 senses the status of the Ca^{2+} stores in the ER via a luminal N-terminal Ca^{2+}-binding EF-hand domain, and dissociation of Ca^{2+} from this domain induces the oligomerization of STIM1 to the ER regions that are close to the plasma membrane, thereby regulating the CRAC channel activity. On the other hand, Orai1 is a pore-forming subunit of the CRAC channels [27–30]. On the assumption that Orai1 and STIM1 play specific roles in CRAC channel function, the effects of their defects on cell function were analyzed using mast cells derived from Orai1- and STIM1-knockout mice. Mast cells lacking either STIM1 or Orai1 exhibited considerable defects in degranulation, while FcεRI-mediated in vivo anaphylaxis was strongly inhibited in Orai1-knockout mice and to a lesser extent in STIM1-knockout mice [31, 32]. Similar levels of Ca^{2+} release from the ER stores were observed in the wild-type and Orai1-knockout mice, suggesting that Ca^{2+} influx through the Orai1 channel is critical for degranulation. LT secretion is also strongly inhibited in Orai1-knockout mice [32], consistent with a previous report that CRAC channels play key roles in LTC_4 secretion in RBL cells [6]. Increased $[Ca^{2+}]_i$ activates NFAT and NF-κB, which regulate the transcription of genes encoding cytokines. Therefore, the overall cytokine production was also expected to be affected in Orai1- or STIM1-knockout mice. However, the results revealed that individual cytokines were affected to different extents. For example, tumor necrosis factor (TNF)-α secretion was much lower in Orai1- or STIM1-knockout mice while interleukin (IL)-6 secretion was minimally affected [31, 32], suggesting that the Ca^{2+} influx pathways involved in the regulation of cytokine gene expression may be more complicated than previously thought. Collectively, the effects of the Orai1 and STIM1 defects were not necessarily identical, thereby arguing against the view that both molecules are specific components of CRAC channels. In fact, the emerging view is that neither Orai1 nor STIM1 is specific for CRAC channels. A growing body of evidence suggests that TRPC proteins can also act as channel-forming molecules in CRAC channels (Fig. 44.5). There is also an increasing body of evidence that CRAC channels can exist in multimeric structures, and the molecular entities of the CRAC channels therefore remain a matter of debate [33]. On the other hand, STIM1 was shown to be a far more universal regulator of Ca^{2+} entry pathways than previously thought. Strikingly, STIM1 was also shown to also regulate non-SOCE. AA-regulated Ca^{2+}-selective (ARC) channels are a widely expressed mode of agonist-activated Ca^{2+} entry in non-excitable cells and are activated completely independently of Ca^{2+} store depletion [34]. Although agonists can activate both CRAC channel and ARC channel activities, activation of ARC channels specifically occurs at low agonist concentrations that are typically associated with oscillatory Ca^{2+} signals [35]. In addition, the two types of channels are distinguishable in terms of their sensitivities to 2-aminoethoxydiphenyl borate (2-APB) and Gd^{3+}, since the currents through ARC channels, I_{ARC}, but not I_{CRAC} were strongly blocked by Gd^{3+} while the CRAC channel inhibitor 2-APB had no effect on I_{ARC} [36]. As mentioned above, the sensing of Ca^{2+} store depletion by its Ca^{2+}-binding EF-hand

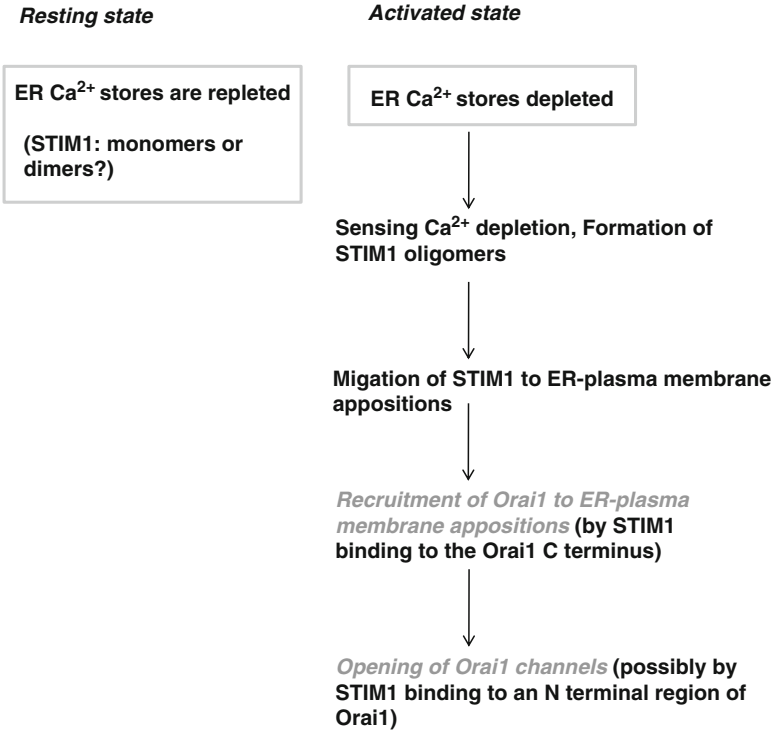

Fig. 44.5 Regulation of Ca^{2+} release-activated Ca^{2+} (*CRAC*) channels by STIM1 and Orai1 in response to endoplasmic reticulum Ca^{2+} stores depletion. The mammalian proteins stromal interaction molecule 1 (*STIM1*) is a Ca^{2+} sensor in the endoplasmic reticulum (*ER*), while Orai1 is a pore-forming subunit of *CRAC* channels. In resting state, *ER* Ca^{2+} stores are replete and *STIM1* exists as monomer of dimers. When *ER* Ca^{2+} stores are depleted in response to receptor activation, *STIM1* senses the depletion via its a luminal N-terminal Ca^{2+}-binding EF-hand domain and forms oligomers. *STIM1* oligomers migrate to ER-plasma membrane appositions and recruit Orai1 channels to the ER-plasma membrane appositions by binding to the Orai1 C-terminus. The *STIM1* oligomers may open the Orai1 channels possibly by binding to an N-terminal region of Orai1

domain and its translocation to the plasma membrane are critical in the current models for the action of STIM1 on Ca^{2+} entry. On the contrary, STIM1 regulation of ARC channels was shown to be independent of all these machineries and events [37]. Evidence suggests that there is a pool of STIM1 that constitutively resides in the plasma membrane and regulates the ARC channel activity through its extracellular N-terminal domain, since antibodies against this domain and mutations in STIM1 that prevent its constitutive expression specifically inhibited the ARC channel activity without affecting the CRAC channel activity [37]. Interestingly, I_{ARC} was successfully detected in RBL mast cells [36]. Moreover, our recent data showed that stimulation with antigen as well as AA evoked a robust Ca^{2+} influx in RBL-2H3 cells, which was blocked by Gd^{3+}, but not by 2-APB. Collectively, these

observations suggest that ARC channels may be activated in response to FcεRI stimulation to regulate Ca^{2+} influx in the cells, although further studies are needed to elucidate the role of ARC channels in mast cell Ca^{2+} responses. Better understanding of the functions of the two Ca^{2+}-selective Ca^{2+} channels may clarify whether the aforementioned data from the STIM1-knockout mice can indeed be attributed to be dysfunction of CRAC channels alone rather than to dysfunction of multiple STIM1-regulated Ca^{2+} entry pathways, including ARC channels.

LTCCs

Molecular Entities of LTCCs

There is some evidence that mast cells also utilize non-SOCE, as another mode of Ca^{2+} entry, in the regulation of their Ca^{2+} responses. Several Ca^{2+} channels [38–40] and non-selective cation channels [41] have been shown to be activated to allow Ca^{2+} influx independently of Ca^{2+} store depletion. In particular, phosphatidylinositol-3,4,5- trisphosphate-sensitive Ca^{2+} channels were reported to be activated independently of Ca^{2+} store depletion and PLC activation in RBL-2H3 cells [38]. Although the molecular entities of the channels remain unclear, they are distinguishable from SOC channels and TRPC channels in terms of their activation manner. Nonetheless, little attention has been paid to the roles for non-SOCE in mast cell Ca^{2+} signaling, probably because it has conventionally been thought that FcεRI stimulation and pharmacological Ca^{2+} store depletion (e.g. by SERCA inhibitors such as Tg) induce similar modes of Ca^{2+} influx (i.e. SOCE). However, it was revealed that FcεRI stimulation, but not Tg, induces robust non-SOCE [42]. This non-SOCE is minimally affected by 2-APB and SK&F96365 applied at concentrations that block SOCE, indicating that the Ca^{2+} channels responsible for non-SOCE are distinct from CRAC channels and TRPC channels. Instead, non-SOCE is strongly blocked by the dihydropyridine receptor (DHPR) antagonist nifedipine, and is remarkably augmented by its agonist (S)-BayK8644 [42]. The DHPR was originally well known as the α_1-subunit of LTCCs in excitable cells [43]. LTCCs in neurons and myocytes are heterotetrameric polypeptide complexes consisting of a channel-forming α_1-subunit, including four subtypes of α_{1S} ($Ca_v1.1$), α_{1C} ($Ca_v1.2$), α_{1D} ($Ca_v1.3$) and α_{1F} ($Ca_v1.4$), and at least three auxiliary subunits (α_2/δ, γ and β) that specifically modulate the activity and allow depolarization-induced Ca^{2+} influx into the cytosol [43]. The predicted topology of the α_1-subunit has four repeated motifs (I-IV) and an inward-dipping loop between the S5 and S6 transmembrane segments that forms the channel pore, while the S4 transmembrane segment contains conserved positively charged amino acids that are voltage sensors and move outward upon membrane depolarization to open the Ca^{2+} channel by analogy with the voltage-gated K^+ channel [44]. The spectrum of DHP derivatives, which specifically bind with high affinities to the α_1 subunits of LTCCs and regulate their functional state

from closing to opening or vice versa, allows both the identification and functional analyses of this class of molecules.

Given that DHPR was originally identified as the α_1 subunit of LTCCs in excitable cells, the modulation of non-SOCE by DHPR antagonists/agonists implies that LTCCs or their analogous molecules may exist in mast cells. In fact, RT-PCR analyses revealed that substantial amounts of the α_{1C} subunit ($Ca_v1.2$) and to a lesser extent the α_{1D} subunit ($Ca_v1.3$) are expressed in RBL-2H3 cells and bone marrow-derived mast cells (BMMCs) [45] as well as the human mast cell line, LAD-2. In addition, the α_{1C} subunit with DHP binding capacity was shown to be expressed on the cell surface [45]. Thus, $Ca_v1.2$ LTCCs appear to be ubiquitously and mainly expressed in various mast cell populations. Consistent with a role for $Ca_v1.2$ LTCCs in non-SOCE, different LTCC-selective antagonists, diltiazem and verapamil block non-SOCE [45]. Gene silencing using small-interfering RNAs enabled us to prepare RBL-2H3 cells in which $Ca_v1.2$ LTCC gene expression was downregulated at both mRNA and protein levels. In the $Ca_v1.2$-knockdown cells, expression of the α_{1C} subunit with DHP binding capacity on the cell surface was completely abolished. The downregulation of $Ca_v1.2$ LTCCs abolished non-SOCE, with minimal effects on thapsigargin-induced SOCE [45] (Fig. 44.5). Taken together, these observations show that $Ca_v1.2$ LTCCs are mainly responsible for FcεRI-mediated non-SOCE in mast cells. It has recently been shown that a variety of hematopoietic cells, including B cells, T cells, neutrophils, dendritic cells and natural killer cells, express LTCCs or LTCC-like channels. Thus, the emerging view is that LTCCs comprise a general Ca^{2+} entry mechanism in immune cells [46, 47].

Activation Mechanisms of LTCCs

Role of FcεRIβ

The molecular basis of LTCC activation in immune cells upon antigen receptor stimulation is poorly understood to date. However, there is evidence that FcεRIβ is crucial for LTCC activation in mast cells upon FcεRI stimulation. Lyn is a major Src family kinase (SFK) found in mast cells. This kinase loosely binds to the FcεRIβ even in resting cells and is immediately activated upon FcεRI stimulation to bind to FcεRIβ tightly and transduce downstream signals. It is established that the FcεRIβ ITAM is an important site of interaction with Lyn for signal transduction [48]. Tg cannot evoke tyrosine phosphorylation of FcεRIβ and LTCC activation [49] BMMCs expressing wild-type (YYY) FcεRIβ or FcεRIβ mutant in which all the tyrosine residues within the ITAM are replaced by phenylalanine (FFF mutant) were prepared. The FFF mutant lacked the FcεRIβ-Lyn interaction via the ITAM [50] (Fig. 44.6). Analyses using these cells revealed that the FcεRIβ-Lyn interaction via the ITAM is essential for full activation of IgE-dependent Ca^{2+} influx, but not Tg-induced Ca^{2+} influx. Subsequently, it was revealed that the FcεRIβ-Lyn interaction via the ITAM is essential for IgE-dependent activation of

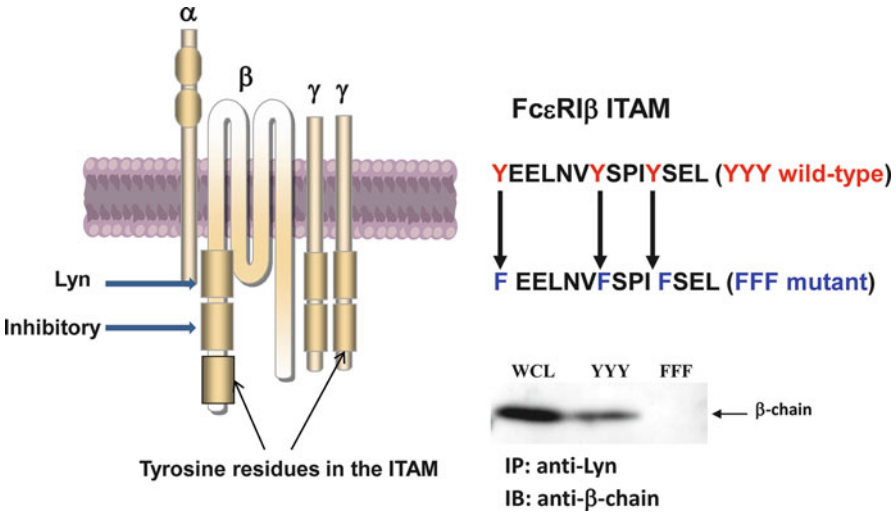

Fig. 44.6 Structure of the FcεRIβ chain and its ITAM. The FcεRIβ- and γ-chains contain immunoreceptor tyrosine-based activation motif (ITAM), a conserved feature of many antigen receptors. The ITAM consensus sequence is (D/E)*XXYXXL*X_{7-11}–Y*XX*L(L/I), where the tyrosine residues are phosphoacceptor sites for the action of receptor-associated protein tyrosine kinases such as Lyn and Syk. Phospho-ITAMs provide a docking site for cytoplasmic proteins that contain the Src-homology domain. Among the three tyrosine residues in the wild-type (YYY) β-chain ITAM, the canonical tyrosine residues are thought to serve a docking site for Lyn and positively regulate cell activation, while the non-canonical residue (middle tyrosine residue) mediates an inhibitory signal for cell activation. In the FFF mutant, all three tyrosine residues are replaced by phenylalanine *(right, upper panel).* Immunoprecipitation with an anti-Lyn antibody followed by western blot analysis with an anti-β-chain antibody reveals that the FcεRIβ-Lyn interaction via the ITAM is completely abolished in the FFF mutant *(right, lower panel). WCL* whole cell lysate used as a control

LTCCs, but not CRAC channels [42]. Moreover, phosphatidylinositol-3-kinase (PI3K) is also essential for LTCC activation, and it appears to negatively regulate CRAC channel activation, since the PI3K-selective inhibitors wortmannin and LY294002 inhibit the former but enhance the latter [42].

Role of Nitric Oxide (NO)

Another critical factor involved in LTCC activation is NO. NO is a potent radical with diverse roles in biological processes, including vasodilatation, platelet aggregation and neuronal transmission. It also regulates the functions, death and survival of various cell types, including cells involved in immunity and inflammation, depending on the cell type and concentration [51, 52]. NO also suppresses mast cell activation and the subsequent features of inflammation as well as IgE-dependent

degranulation, LT secretion and cytokine expression and secretion in mast cells [53, 54]. The emerging view is that mast cells themselves are NO producers in response to physiological stimuli. Mast cells can produce robust NO upon FcεRI stimulation in RBL-2H3 cells and BMMCs [55]. This NO production is attributed to nitric oxide synthase (NOS) activated in a Ca^{2+}-dependent manner (i.e. constitutively expressed NOS isoform). Moreover, the NO production is accompanied by increased phosphorylation of endothelial NOS (eNOS) at Ser-1177 and Akt at Ser-473, which are considered to comprise an important mechanism for increasing eNOS activity [56, 57]. Subsequent studies revealed that mast cells express eNOS but not neuronal NOS mRNA and that gene silencing of eNOS completely abolishes IgE-dependent NO production [58]. In an expansion of the pharmacological data, downregulation of eNOS gene expression was found to completely abolish $Ca_v1.2$ LTCC activation [58]. These observations strongly suggest that eNOS is essential for IgE-dependent $Ca_v1.2$ LTCC activation. To date, the mechanisms by which NO stimulates $Ca_v1.2$ LTCC activation are unclear. However, our recent data showed that eNOS can regulate cell membrane depolarization in mast cells (Suzuki et al., unpublished data). As described in the next section, an increasing body of evidence suggests that $Ca_v1.2$ LTCCs can be activated in a voltage-gated manner in nonexcitable cells. In addition, eNOS is activated in a manner that is dependent on PI3K activity [55], which is thought to be activated via the FcεRIβ-Lyn interaction. Collectively, it is possible that upon FcεRI stimulation, the FcεRIβ-Lyn interaction triggers endogenous NO production by the PI3K-Akt-eNOS pathway, which activates $Ca_v1.2$ LTCCs via cell membrane depolarization.

The Gating Mode of LTCCs: Voltage-Gated or Not?

Analyses using cell membrane potential-sensitive dyes showed that FcεRI stimulation results in immediate membrane depolarization, which reaches its maximum within 1 min, followed by repolarization but not hyperpolarization. On the contrary, Tg causes sustained hyperpolarization but does not evoke any membrane depolarization [45]. Thus, FcεRI stimulation specifically induces cell membrane depolarization, although FcεRI stimulation and Tg commonly activate CRAC channel activity. It was shown that T cells express both regulatory β and pore-forming α_1 subunits of LTCCs found in excitable cells. T cell receptor stimulation also results in similar patterns of cell membrane depolarization and LTCC activation [52]. Therefore, by analogy to LTCCs expressed in excitable cells, LTCCs expressed in mast cells and T cells are expected to be activated in a voltage-gated manner. Nevertheless, the issue of whether these channels open in a voltage-gated manner has been a matter of much debate, since K^+-mediated depolarization causes a minimal increase in $[Ca^{2+}]_i$ in these cells [45, 59]. However, K^+-mediated depolarization was found to be capable of evoking robust Ca^{2+} entry into mitochondria [45]. Moreover, a substantial increase in $[Ca^{2+}]_i$ was observed in response to depolarization when CRAC channel activity was impaired. These Ca^{2+} responses are blocked

by LTCC antagonists and downregulation of $Ca_v1.2$ LTCCs, and are enhanced by LTCC agonists. Collectively, these data show that in mast cells, $Ca_v1.2$ LTCCs can be activated by membrane depolarization to allow Ca^{2+} entry into the cytosol or mitochondria depending on the activation status of CRAC channels. Recent work has provided evidence that $Ca_v1.2$ LTCCs can be activated by membrane depolarization in nonexcitable cells [60, 61]. It is therefore, possible that LTCCs in mast cells are activated in a voltage-gated manner in response to cell membrane depolarization upon FcεRI stimulation. However, the term "voltage-gated channels" truly means those that are directly activated by membrane depolarization beyond a threshold voltage. Hence, further studies are needed to confirm that $Ca_v1.2$ LTCCs in nonexcitable cells are identical to those in excitable cells at the molecular level. Cell membrane polarization is a driving force of Ca^{2+} entry through CRAC channels and may hamper the activation of $Ca_v1.2$ LTCC activity. Moreover, it may stimulate the gating of $Ca_v1.2$ LTCCs, but inhibit Ca^{2+} entry through CRAC channels. Consequently, the activities of the two channels may be coordinately rather than independently controlled. Indeed, it was recently shown that the activities of $Ca_v1.2$ LTCCs and CRAC channels are reciprocally regulated by one another [60, 61]. This interesting issue will be discussed in more detail in section "Coordinated regulation of CRAC channels and $Ca_v1.2$ LTCCs".

Role for LTCCs in Mast Cell Function

Analyses using pharmacological LTCC modulators and $Ca_v1.2$-knockdown cells have revealed unique roles of $Ca_v1.2$ LTCCs in mast cell function. The channels negatively regulate mast cell degranulation and positively control LTC_4 and cytokine production [45, 62]. It is of special interest that $Ca_v1.2$ LTCCs regulate the production of cytokines such as IL-13 and TNF-α, since LTCCs have been shown to play roles in the regulation of NFAT and cytokine production in TCR-activated T cells [59, 63]. Moreover, the DHPR, as the α subunit of LTCCs, was shown to be a selective marker of Th2 cells and to be involved in Ca^{2+} responses, IL-4, IL-5 and IL-10 productions and Th2-mediated pathologies [64]. Collectively, it is possible that in mast cells and T cells, LTCCs are involved in the regulation of antigen receptor-mediated Ca^{2+} signaling and cytokine production, thereby contributing to Th2-cytokine secretion and Th2-mediated pathologies. Consistent with the roles of LTCCs in Th2-dependent pathologies, LTCC antagonists were shown to effectively prevent or revert airway inflammation, remodeling and hyperresponsiveness in experimental models of Th2-driven asthma [65].

Roles of LTCCs in Mast Cell Survival

Mast cells are described as being long-lived cells that are maintained at relatively constant numbers in tissues under physiological conditions. Anti-apoptotic mechanisms

limit the initiation of programmed cell death, thereby contributing to the multiple pathological conditions that involve mast cell activation. Although CRAC channels were shown to play a critical role in regulating mast cell function, they appear to play minor roles in mast cell differentiation and survival, since the development and survival of mast cells derived from Orai1- and STIM1-knockout mice are normal [31, 32]. Despite their importance, there is little information regarding Ca^{2+} channels regulating mast cell survival. In this regard, it should be noted that $Ca_v1.2$ LTCCs have an anti-apoptotic function. $Ca_v1.2$ LTCCs were shown to protect mast cells against activation-induced cell death (AICD) following FcεRI stimulation [66]. Tg induces considerable apoptosis of RBL-2H3 cells, while FcεRI stimulation alone has minimal effects on their survival. However, when the $Ca_v1.2$ LTCC activity is downregulated by LTCC antagonists or by $Ca_v1.2$ gene silencing, RBL-2H3 cells undergo substantial apoptosis after FcεRI stimulation. On the contrary, activation of $Ca_v1.2$ LTCC activity by extracellular K^+ and (S)-BayK8644 protects the cells against Tg-induced apoptosis. Similar results were obtained for BMMCs [66]. These data strongly suggest that $Ca_v1.2$ LTCCs are essential for the survival of activated mast cells. The anti-apoptotic function involves prevention of the intrinsic mitochondrial cell death pathway. Besides their well-known role as the power plants in eukaryotic cells, mitochondria are now recognized as central gateway controllers in the cell death pathway. Permeabilization of the outer mitochondrial membrane (OMM) by proapoptotic Bcl-2 family proteins promotes the release of a number of apoptosis-inducing proteins such as cytochrome c from the inner mitochondrial membrane (IMM) space into the cytosol. Cytochrome c interacts with the apoptotic peptidase activating factor 1, leading to the formation of the multimeric apoptosome in the presence of ATP/dATP [67, 68]. The apoptosome then activates the initiator caspase, caspase-9, which subsequently cleaves and activates effector caspases such as caspases-3 and caspase-7. A cytochrome c-independent apoptosis pathway has also been defined, and this pathway requires proteins such as endonuclease G and apoptosis-inducing factor to carry out apoptosis. Hence, in this paradigm, mitochondrial integrity disruption and downstream apoptogenic protein release and caspase activation play pivotal roles. Although the molecular mechanisms underlying the OMM permeabilization are poorly understood, there is strong evidence that the mitochondrial permeability transition (MPT) plays a key role. The MPT was originally defined as a sudden increase in the IMM permeability to solutes with molecular masses of ~1,500 Da. It is now believed that opening of a putative megachannel referred as to the mitochondrial permeability transition complex (PTPC) is responsible for the MPT [69, 70]. The PTPC is a high-conductance non-specific pore in the IMM that is composed of proteins that link the IMM and OMM. Several mitochondrial proteins localized in the IMM and OMM, such as voltage-dependent anion channels, adenine nucleotide translocase, hexokinase, peripheral benzodiazepine receptors and cyclophilin-D, are thought to constitute the PTPC, but the role of some components are a matter of debate. Under physiological conditions, the proteins in the OMM and IMM that constitute the PTPC are believed in close proximity to one another and in a closed or low conductance formation, although the PTPC has not been isolated and the components of this complex remain controversial [69–71]. When the PTPC changes to an open conformation, water and solutes with

molecular masses of up to 1,500 Da enter the mitochondrial matrix, resulting in osmotic swelling of the mitochondrion. It has been believed that when multiple PTPCs open concurrently and extensive mitochondrial swelling takes place, physical disorganization of the OMM occurs and mitochondrial apoptogenic proteins are released, thereby triggering apoptosis [72]. There is some evidence indicating that PTPC opening and the downstream caspase cascade are critical for FcεRI-mediated apoptosis of mast cells. In accordance with the requirement of NO for the survival of mast cells after FcεRI stimulation [55], substantial FcεRI-mediated apoptosis occurs in eNOS-knockdown cells [58]. The apoptosis is accompanied by altered mitochondrial integrity, including increased cytochrome c release from mitochondria and dissipation of the mitochondrial membrane potential (mitochondrial depolarization) and caspase-3/7 activation. Moreover, the apoptosis is completely prevented by the PTPC antagonist bongkrekic acid (BKA) and caspase-3/7-specific inhibitor, z-DEVD-fmk, and is enhanced by the PTPC agonist atractyloside [55, 58]. In addition, BKA and z-DEVD-fmk prevent the apoptosis even under conditions where eNOS gene expression is downregulated [58]. Taken together with the essential role of eNOS in $Ca_v1.2$ LTCC activation, these observations suggest that $Ca_v1.2$ LTCCs regulate the open/-closed state of the PTPC and the downstream caspase cascade, thereby controlling cell survival.

Roles of LTCCs in the Regulation of the Mitochondrial Ca^{2+} Concentration ($[Ca^{2+}]_m$)

The next question to be addressed is how $Ca_v1.2$ LTCCs regulate the open-close state of the PTPC. One biochemical change that has been associated with the induction of apoptosis in several cell types is deregulation of the intracellular Ca^{2+} concentrations. Excessive intracellular Ca^{2+} levels, such as those induced by Ca^{2+} ionophores have been shown to induce apoptosis [73]. Moreover, apoptosis appears to involve a Ca^{2+}-dependent endonuclease [74], and intracellular Ca^{2+} increases have been linked to apoptosis of both activated T cell hybridomas [75] and immature thymocytes upon T cell antigen stimulation [76]. In addition to its pro-apoptotic effects, Ca^{2+} has also been shown to act as an anti-apoptotic factor. IL-3-dependent primary cultured mast cells and cell lines can be protected against growth factor withdrawal-mediated apoptosis by the addition of Ca^{2+} ionophores [77], and programmed neuronal death is suppressed by an increase in intracellular Ca^{2+} [78]. Collectively, Ca^{2+} appears to be necessary for both inducing and protecting against cell death, and the roles of Ca^{2+} in regulating cell death therefore appear to be more complex than initially thought. There is no general model that can depict the dual effects of Ca^{2+}. However, mitochondrial Ca^{2+} handling seems to play a role in the dual effects. It is widely accepted that mitochondria play a key role in the deregulation of intracellular Ca^{2+} concentrations. It is quite likely that an appropriate elevation in the mitochondrial Ca^{2+} concentration ($[Ca^{2+}]_m$) supports energy metabolism, cell activation and cell survival, while $[Ca^{2+}]_m$ overload causes increased cell death. $[Ca^{2+}]_m$ overload can damage mitochondrial integrity, thereby inducing PTPC opening

and resulting in the release of apoptogenic proteins [79, 80]. Therefore, $[Ca^{2+}]_m$ appears to be necessary for both cell death and survival, although the precise mechanisms underlying the dual effects are currently unclear. It is noteworthy that a non-apoptotic stimulus (FcεRI stimulation) and an apoptotic stimulus (Tg) exert different effects on $[Ca^{2+}]_m$ in mast cells [55]. Although both stimuli induce a substantial increase in $[Ca^{2+}]_m$, their modes are different. The $[Ca^{2+}]_m$ increase in response to FcεRI stimulation is observed immediately, and is subsequently maintained at a higher level or gradually declines. Tg also induces an immediate and robust increase in $[Ca^{2+}]_m$ but the increase is less persistent and $[Ca^{2+}]_m$ returned to the resting levels within a few minute even in the persistent presence of Tg. Taking our recent data together with previous findings [55], $Ca_v1.2$ LTCCs are involved in the $[Ca^{2+}]_m$ increase induced by FcεRI stimulation, but not by Tg. Moreover, in the presence of K^+ or (S)-BayK8644, a more sustained $[Ca^{2+}]_m$ increase is observed after Tg treatment, similar to the case for FcεRI stimulation. In addition, downregulation of $Ca_v1.2$ LTCCs by gene silencing reduces the FcεRI- or K^+-mediated $[Ca^{2+}]_m$ increase. Taken together, these findings show that $Ca_v1.2$ LTCCs activated by cell membrane depolarization are necessary for the maintenance of $[Ca^{2+}]_m$ in mast cells. In this regard, it should be noted that maintenance of $[Ca^{2+}]_m$ homeostasis is essential for cell survival, and that loss of $[Ca^{2+}]_m$ is closely correlated with cell death in cultured cells [81]. In addition, it was recently revealed that $[Ca^{2+}]_m$ efflux through the mitochondrial Na^+/Ca^{2+}-exchanger (mtNCX) plays a pro-apoptotic role and that activation of $Ca_v1.2$ LTCCs prevents the $[Ca^{2+}]_m$ efflux. The extrusion of Ca^{2+} from mitochondria is mediated by mtNCX, which is thought to allow continuous recycling of Ca^{2+} across the mitochondrial membrane, resulting in reciprocal changes in its concentrations in the mitochondria and cytosol. Enhanced mtNCX activity results in reduced $[Ca^{2+}]_m$ and cell survival as well as the pathological defects typically observed in human mitochondrial type I deficiency [82]. Collectively, these findings raises the intriguing possibility that $Ca_v1.2$ LTCCs act as key players in the maintenance of $[Ca^{2+}]_m$ homeostasis in conjunction with mtNCX. It should be noted that $Ca_v1.2$ LTCCs are necessary for the survival of activated but not resting mast cells [66], suggesting that they may be essential for preventing an excessive $[Ca^{2+}]_m$ efflux by mtNCX upon cell activation. Since the absence of $Ca_v1.2$ LTCCs is significantly compensated for by blocking PTPC opening or inhibiting the downstream caspase cascade pathway, this type of Ca^{2+} channel may prevent extensive PTPC opening, thereby playing a key role in the maintenance of mitochondrial integrity. Further studies are required to clarify the mechanisms underlying LTCC-mediated maintenance of $[Ca^{2+}]_m$ and cell survival.

Coordinated Regulation of CRAC Channels and $Ca_v1.2$ LTCCs

It was recently reported that CRAC channels and $Ca_v1.2$ LTCCs are reciprocally regulated by STIM1. STIM1 activation by Ca^{2+} store depletion or mutational modifications strongly suppresses voltage-operated $Ca_v1.2$ LTCCs while activating

Table 44.1 Activation of CRAC channels and $Ca_v1.2$ LTCCs and the survival of activated mast cells

	CRAC	$Ca_v1.2$	Survival/death	References
FcεRI	Activated	Activated	Survival	[66]
FcεRI/nifedipine	Activated	Inactivated	Death	[66]
FcεRI/$Ca_v1.2$-KD	Activated	Inactivated	Death	[66]
FcεRI/NOS inhibitors	Activated	Inactivated	Death	[55]
FcεRI/eNOS-KD	Activated	Inactivated	Death	[58]
Tg	Activated	Inactivated	Death	[66]
Tg/K^+	Activated	Activated	Survival	Unpublished
Tg/(S)-BayK8644	Activated	Activated	Survival	[66]
K^+	Inactivated	Activated	Death	Unpublished

store-operated CRAC channels [60]. Both actions are mediated by the short STIM-Orai activating region of STIM1 and STIM1 appears to interact with $Ca_v1.2$ LTCCs within the ER membrane junctions. Consequently, STIM1 knockdown enables K^+-mediated plasma membrane depolarization to induce a robust Ca^{2+} influx through $Ca_v1.2$ LTCCs. Another group reported that STIM1 can bind to the C-terminus of $Ca_v1.2$ LTCCs through the CRAC activation domain and inhibits gating of the channels through its long-term internalization [61]. Taken together, these data suggest a physical and functional association between CRAC channels and $Ca_v1.2$ LTCCs. This enables coordinated control of the two types of Ca^{2+} channels, which may be critical for the fine-tuning of Ca^{2+} signals and Ca^{2+}-dependent cellular outputs. Our findings that $Ca_v1.2$ LTCCs and CRAC channels reciprocally regulate mast cell degranulation while cooperatively controlling LTC_4 and cytokine production [45] may be an example of such coordinated regulation of mast cell functions by CRAC channels and $Ca_v1.2$ LTCCs. Table 44.1 summarizes the survival and death of mast cells stimulated under various conditions. There is a tendency that the cells survive after activation under conditions in which both CRAC channels and $Ca_v1.2$ LTCCs are activated, while they undergo cell death when biased activation of either channel is induced. Therefore, it is possible that the balanced activation of the two types of Ca^{2+} channels is essential for maintaining the appropriate $[Ca^{2+}]_i$ required for cell survival.

A growing body of evidence suggests a close functional coupling between reactive oxygen species (ROS) and Ca^{2+} channels in mast cells. FcεRI stimulation results in the generation of intracellular ROS, which are involved in the regulation of Ca^{2+} signals, mast cell degranulation, LT secretion and cytokine production and survival [83, 84]. Moreover, it was revealed that discrete generations of superoxide (O_2^-) and hydrogen peroxide (H_2O_2) occur in mast cells following FcεRI stimulation [85]. These findings are similar to previous observations in T cells after TCR stimulation [86], suggesting the involvement of similar mechanisms in the generations of the two oxidants between mast cells and T cells. The two oxidants appear to be generated by separate intracellular signaling pathways, since the H_2O_2 generation is dependent on the SFK and PI3K activities, but independent of extracellular Ca^{2+}, and the FcεRIβ ITAM plays an essential role. On the other hand, the O_2^- generation

is strictly dependent on extracellular Ca^{2+} but is negatively regulated by the SFK and PI3K activities and is independent of the FcεRIβ ITAM [85]. In this regard, it is noteworthy that Ca^{2+} influx through SOC channels, most likely CRAC channels results in the generation of O_2^- within mitochondria in mast cells. Collectively, the most likely source of the PI3K-independent O_2^- generation is mitochondria. Although the molecular entity of the source for H_2O_2 remains unclear, a NOX family enzyme is a possible candidate, since the generation is strongly blocked by the NOX inhibitors diphenyleneiodonium and apocynin [49]. Analyses using Tg revealed that O_2^- and H_2O_2 may mediate different outputs. Tg can evoke mitochondrial O_2^- generation but not PI3K-dependent H_2O_2 generation, and can induce mast cell degranulation and LTC_4 secretion more strongly than FcεRI stimulation [49]. However, Tg is much less effective than FcεRI stimulation for evoking TNF-α and IL-13 production. Regardless of the stimulus applied, mast cell degranulation and LTC_4 and cytokine production are strictly dependent on extracellular Ca^{2+}. Therefore, the PI3K-independent O_2^- generation rather than the PI3K-dependent H_2O_2 generation is important for mediating the Ca^{2+} influx required for mast cell degranulation. This is consistent with the finding that selective scavenging of H_2O_2 by ebselen has minimal effects on mast cell degranulation [83]. On the other hand, the PI3K-dependent H_2O_2 generation appears to be critical for the Ca^{2+} influx that leads to cytokine production. Further analyses revealed that the two oxidants regulate different Ca^{2+} influx pathways. H_2O_2 appears to be necessary for store-independent Ca^{2+} influx but not Ca^{2+} influx through SOC channels while O_2^- is required for SOC channel activation [85]. As mentioned above, Ca^{2+} influx through SOC channels may result in the generation of O_2^- within mitochondria, suggesting the possible existence of a feed-forward loop between the O_2^- generation and SOC channels activation. $Ca_v1.2$ LTCCs are activated via the FcεRIβ ITAM in a store-independent manner and are required for LTC_4 and cytokine production, but not degranulation [45]. Moreover, the $Ca_v1.2$ LTCC activity is inhibited by ebselen. Therefore, $Ca_v1.2$ LTCCs are the most likely targets of H_2O_2 in mediating LTC_4 and cytokine production. It should be noted that the signaling pathways involved in the generation of H_2O_2 such as SFK and PI3K activation negatively regulate the generation of O_2^- and SOC channels (most likely CRAC channel) activity [85]. Recent experiments have revealed that O_2^- generation and SOC channel activity are significantly increased in $Ca_v1.2$ LTCC-knockdown cells compared with control cells (Suzuki et al., unpublished data). These findings suggest that ROS may play an important role in the coordinated regulation of the two modes of Ca^{2+} influx pathways, which may be essential for the fine-tuning of Ca^{2+} signals and diverse outputs.

Conclusions

Recent progress in the identification of the molecular entities of the two CRAC channel components STIM1 and Orai1 were initially expected to provide a molecular basis for studying and manipulating their functions. However, it is becoming

increasingly evident that their functions are more complicated than previously thought. Both molecules can act as regulators in a wide range of Ca^{2+} channels, including TRPC channels and ARC channels, rather than being specific for CRAC channels. The unanticipated discovery of the occurrence of functional $Ca_v1.2$ LTCCs in nonexcitable mast cells opens a novel field of research regarding Ca^{2+} signaling in mast cells, especially the regulatory mechanisms for cell survival. Since CRAC channels and $Ca_v1.2$ LTCCs operate in mutually regulated manners, rather than independently, it is possible that their balance and interplay are key determinants of the amplitude, timing and duration of Ca^{2+} signals, thereby contributing to the fate decision of a given cell after cell activation. Thus, the two types of Ca^{2+} channels may play more comprehensive roles in regulating Ca^{2+} responses in eukaryotic cells. Therefore, clarification of their interplay may afford novel insights into the spatiotemporal regulation of Ca^{2+} signaling and Ca^{2+} regulation of physiological cell functions and pathological abnormalities.

Acknowledgments The authors thank Drs. T. Yoshimaru, S. Nunomura, K. Mizuno, K. Togo, K. Hayama and T. Ochiai for their collaborations and/or technical assistance. This work was partially supported by a Grant-in-Aid for the High-Tech Research Center Project (2003–2007) for Private Universities and a matching fund subsidy for Private Universities (2007–2009) from the Ministry of Education, Culture, Sports, Science and Technology, Japan and Grants-in-Aid from Nihon University

References

1. Galli SJ, Kalesnikoff J, Grimbaldeston MA, Piliponsky AM, Williams CM, Tsai M (2005) Mast cells as “tunable” effector and immunoregulatory cells: recent advances. Annu Rev Immunol 23:749–786
2. Church MK, Pao GJ, Holgate ST (1982) Characterization of histamine secretion from mechanically dispersed human lung mast cells: effects of anti-IgE, calcium ionophore A23187, compound 48/80, and basic polypeptides. J Immunol 129:2116–2121
3. Baram D, Mekori YA, Sagi-Eisenberg R (2001) Synaptotagmin regulates mast cell functions. Immunol Rev 179:25–34
4. Blank U, Cyprien B, Martin-Verdeaux S, Paumet F, Pombo I, Rivera J, Roa M, Varin-Blank N (2002) SNAREs and associated regulators in the control of exocytosis in the RBL-2H3 mast cell line. Mol Immunol 38:1341–1345
5. Gijón MA, Spencer DM, Kaiser AL, Leslie CC (1999) Role of phosphorylation sites and the C2 domain in regulation of cytosolic phospholipase A_2. J Cell Biol 145:1219–1232
6. Chang WC, Nelson C, Parekh AB (2006) Ca^{2+} influx through CRAC channels activates cytosolic phospholipase A_2, leukotriene C_4 secretion, and expression of c-fos through ERK-dependent and -independent pathways in mast cells. FASEB J 20:2381–2383
7. Chang WC, Di Capite J, Nelson C, Parekh AB (2007) All-or-none activation of CRAC channels by agonist elicits graded responses in populations of mast cells. J Immunol 179: 5255–5263
8. Pozzan T, Rizzuto R, Volpe P, Meldolesi J (1994) Molecular and cellular physiology of intracellular calcium stores. Physiol Rev 74:595–636
9. Masgrau R, Churchill GC, Morgan AJ, Ashcroft SJ, Galione A (2003) NAADP: a new second messenger for glucose-induced Ca^{2+} responses in clonal pancreatic β cells. Curr Biol 13:247–251

10. Guse AH (2003) Regulation of calcium signaling by the second messenger cyclic adenosine diphosphoribose (cADPR). Curr Mol Med 4:239–248
11. Putney JW Jr (1987) Formation and actions of calcium-mobilizing messenger, inositol 1,4,5-trisphosphate. Am J Physiol 252:G149–G157
12. Malavasi F, Deaglio S, Funaro A, Ferrero E, Horenstein AL, Ortolan E, Vaisitti T, Aydin S (2008) Evolution and function of the ADP ribosyl cyclase/CD38 gene family in physiology and pathology. Physiol Rev 88:841–886
13. Grafton G, Thwaite L (2001) Calcium channels in lymphocytes. Immunology 104:119–126
14. Fliegert R, Gasser A, Guse AH (2007) Regulation of calcium signalling by adenine-based second messengers. Biochem Soc Trans 35:109–114
15. Locke EG, Bonilla M, Liang L, Takita Y, Cunningham KW (2000) A homolog of voltage-gated Ca^{2+} channels stimulated by depletion of secretory Ca^{2+} in yeast. Mol Cell Biol 20:6686–6694
16. Partiseti M, Le Deist F, Hivroz C, Fischer A, Korn H, Choquet D (1994) The calcium current activated by T cell receptor and store depletion in human lymphocytes is absent in a primary immunodeficiency. J Biol Chem 269:32327–32335
17. Montero M, Alvarez J, Garcia-Sancho J (1991) Agonist-induced Ca^{2+} influx in human neutrophils is secondary to the emptying of intracellular calcium stores. Biochem J 277:73–79
18. Parekh AB, Putney JW Jr (2005) Store-operated calcium channels. Physiol Rev 85:757–810
19. Ma HT, Beaven MA (2009) Regulation of Ca^{2+} signaling with particular focus on mast cells. Crit Rev Immunol 29:155–186
20. Di Capite JL, Bates GJ, Parekh AB (2011) Mast cell CRAC channel as a novel therapeutic target in allergy. Curr Opin Allergy Clin Immunol 11:33–38
21. Hoth M, Penner R (1992) Depletion of intracellular calcium stores activates a calcium current in mast cells. Nature 355:353–356
22. Parekh AB (2010) Store-operated CRAC channels: function in health and disease. Nat Rev Drug Discov 9:399–410
23. Feske S (2010) CRAC channelopathies. Pflugers Arch 460:417–435
24. Liou J, Kim ML, Heo WD, Jones JT, Myers JW, Ferrell JE Jr, Meyer T (2005) STIM is a Ca^{2+} sensor essential for Ca^{2+}-store-depletion-triggered Ca^{2+} influx. Curr Biol 15:1235–1241
25. Roos J, DiGregorio PJ, Yeromin AV, Ohlsen K, Lioudyno M, Zhang S, Safrina O, Kozak JA, Wagner SL, Cahalan MD, Veliçelebi G, Stauderman KA (2005) STIM1, an essential and conserved component of store-operated Ca^{2+} channel function. J Cell Biol 169:435–445
26. Feske S, Gwack Y, Prakriya M, Srikanth S, Puppel SH, Tanasa B, Hogan PG, Lewis RS, Daly M, Rao A (2006) A mutation in Orai1 causes immune deficiency by abrogating CRAC channel function. Nature 441:179–185
27. Vig M, Beck A, Billingsley JM, Lis A, Parvez S, Peinelt C, Koomoa DL, Soboloff J, Gill DL, Fleig A, Kinet JP, Penner R (2006) CRACM1 multimers form the ion-selective pore of the CRAC channel. Curr Biol 16:2073–2079
28. Prakriya M, Feske S, Gwack Y, Srikanth S, Rao A, Hogan PG (2006) Orai1 is an essential pore subunit of the CRAC channel. Nature 443:230–233
29. Yeromin AV, Zhang SL, Jiang W, Yu Y, Safrina O, Cahalan MD (2006) Molecular identification of the CRAC channel by altered ion selectivity in a mutant of Orai. Nature 443:226–229
30. Feske S (2007) Calcium signalling in lymphocyte activation and disease. Nat Rev Immunol 7:690–702
31. Baba Y, Nishida K, Fujii Y, Hirano T, Hikida M, Kurosaki T (2008) Essential function for the calcium sensor STIM1 in mast cell activation and anaphylactic responses. Nat Immunol 9:81–88
32. Vig M, DeHaven WI, Bird GS, Billingsley JM, Wang H, Rao PE, Hutchings AB, Jouvin MH, Putney JW, Kinet JP (2008) Defective mast cell effector functions in mice lacking the CRACM1 pore subunit of store-operated calcium release-activated calcium channels. Nat Immunol 9:89–96
33. Smyth JT, Dehaven WI, Jones BF, Mercer JC, Trebak M, Vazquez GJ, Putney JW Jr (2006) Emerging perspectives in store-operated Ca^{2+} entry: roles of Orai, Stim and TRP. Biochim Biophys Acta 1763:1147–1160

34. Shuttleworth TJ, Thompson JL, Mignen O (2007) STIM1 and the noncapacitative ARC channels. Cell Calcium 42:183–191
35. Mignen O, Thompson JL, Shuttleworth TJ (2001) Reciprocal regulation of capacitative and arachidonate-regulated noncapacitative Ca^{2+} entry pathways. J Biol Chem 276:35676–35683
36. Mignen O, Thompson JL, Shuttleworth TJ (2003) Ca^{2+} selectivity and fatty acid specificity of the noncapacitative, arachidonate-regulated Ca^{2+} (ARC) channels. J Biol Chem 278:10174–10181
37. Mignen O, Thompson JL, Shuttleworth TJ (2007) STIM1 regulates Ca^{2+} entry via arachidonate-regulated Ca^{2+}-selective (ARC) channels without store depletion or translocation to the plasma membrane. J Physiol 579:703–715
38. Ching TT, Hsu AL, Johnson AJ, Chen CS (2001) Phosphoinositide 3-kinase facilitates antigen-stimulated Ca^{2+} influx in RBL-2H3 mast cells via a phosphatidylinositol 3,4,5-trisphosphate-sensitive Ca^{2+} entry mechanism. J Biol Chem 276:14814–14820
39. Bradding P, Okayama Y, Kambe N, Saito H (2003) Ion channel gene expression in human lung, skin, and cord blood-derived mast cells. J Leukoc Biol 73:614–620
40. Kahr H, Schindl R, Fritsch R, Heinze B, Hofbauer M, Hack ME, Mörtelmaier MA, Groschner K, Peng JB, Takanaga H, Hediger MA, Romanin C (2004) CaT1 knock-down strategies fail to affect CRAC channels in mucosal-type mast cells. J Physiol 557:121–132
41. Fasolato C, Hoth M, Matthews G, Penner R (1993) Ca^{2+} and Mn^{2+} influx through receptor-mediated activation of nonspecific cation channels in mast cells. Proc Natl Acad Sci USA 90:3068–3072
42. Suzuki Y, Yoshimaru T, Inoue T, Nunomura S, Ra C (2008) The high-affinity immunoglobulin E receptor (FcεRI) regulates mitochondrial calcium uptake and a dihydropyridine receptor-mediated calcium influx in mast cells: role of the FcεRIβ chain immunoreceptor tyrosine-based activation motif. Biochem Pharmacol 75:1492–1503
43. Bodi I, Mikala G, Koch SE, Akhter SA, Schwartz A (2005) The L-type calcium channel in the heart: the beat goes on. J Clin Invest 115:3306–3317
44. Jiang Y, Ruta V, Chen J, Lee A, MacKinnon R (2003) The principle of gating charge movement in a voltage-dependent K^+ channel. Nature 423:42–48
45. Yoshimaru T, Suzuki Y, Inoue T, Ra C (2009) L-type Ca^{2+} channels in mast cells: activation by membrane depolarization and distinct roles in regulating mediator release from store-operated Ca^{2+} channels. Mol Immunol 46:1267–1277
46. Kotturi MF, Hunt SV, Jefferies WA (2006) Roles of CRAC and Cav-like channels in T cells: more than one gatekeeper? Trends Pharmacol Sci 27:360–367
47. Suzuki Y, Inoue T, Ra C (2010) L-type Ca^{2+} channels: a new player in the regulation of Ca^{2+} signaling, cell activation and cell survival in immune cells. Mol Immunol 47:640–648
48. Rivera J (2002) Molecular adapters in FcεRI signaling and the allergic response. Curr Opin Immunol 14:688–693
49. Inoue T, Suzuki Y, Yoshimaru T, Ra C (2008) Reactive oxygen species produced up- or downstream of calcium influx regulate proinflammatory mediator release from mast cells: role of NADPH oxidase and mitochondria. Biochim Biophys Acta 1783:789–802
50. Furumoto Y, Nunomura S, Terada T, Rivera J, Ra C (2004) The FcεRIβ immunoreceptor tyrosine-based activation motif exerts inhibitory control on MAPK and IκB kinase phosphorylation and mast cell cytokine production. J Biol Chem 279:49177–49187
51. Grisham MB, Jourd'Heuil D, Wink DA (1999) Nitric oxide. I. Physiological chemistry of nitric oxide and its metabolites: implications in inflammation. Am J Physiol 276:G315–G321
52. Coleman JW (2002) Nitric oxide: a regulator of mast cell activation and mast cell-mediated inflammation. Clin Exp Immunol 129:4–10
53. Eastmond NC, Banks EM, Coleman JW (1997) Nitric oxide inhibits IgE-mediated degranulation of mast cells and is the principal intermediate in IFN-γ-induced suppression of exocytosis. J Immunol 159:1444–1450
54. Davis BJ, Flanagan BF, Gilfillan AM, Metcalfe DD, Coleman JW (2004) Nitric oxide inhibits IgE-dependent cytokine production and Fos and Jun activation in mast cells. J Immunol 173:6914–6920

55. Inoue T, Suzuki Y, Yoshimaru T, Ra C (2008) Nitric oxide protects mast cells from activation-induced cell death: the role of the phosphatidylinositol-3-kinase-Akt-endothelial nitric oxide synthase pathway. J Leukoc Biol 83:1218–1229
56. Gallis B, Corthals GL, Goodlett DR, Ueba H, Kim F, Presnell SR, Figeys D, Harrison DG, Berk BC, Aebersold R, Corson MA (1999) Identification of flow-dependent endothelial nitric-oxide synthase phosphorylation sites by mass spectrometry and regulation of phosphorylation and nitric oxide production by the phosphatidylinositol 3-kinase inhibitor LY294002. J Biol Chem 274:30101–30108
57. McCabe TJ, Fulton D, Roman LJ, Sessa WC (2000) Enhanced electron flux and reduced calmodulin dissociation may explain "calcium-independent" eNOS activation by phosphorylation. J Biol Chem 275:6123–6128
58. Suzuki Y, Inoue T, Ra C (2010) Endothelial nitric oxide synthase is essential for nitric oxide generation, L-type Ca^{2+} channel activation and survival in RBL-2H3 mast cells. Biochim Biophys Acta 1803:372–385
59. Badou A, Jha MK, Matza D, Mehal WZ, Freichel M, Flockerzi V, Flavell RA (2006) Critical role for the β regulatory subunits of Cav channels in T lymphocyte function. Proc Natl Acad Sci USA 103:15529–15534
60. Wang Y, Deng X, Mancarella S, Hendron E, Eguchi S, Soboloff J, Tang XD, Gill DL (2010) The calcium store sensor, STIM1, reciprocally controls Orai and $Ca_V1.2$ channels. Science 330:105–109
61. Park CY, Shcheglovitov A, Dolmetsch R (2010) The CRAC channel activator STIM1 binds and inhibits L-type voltage-gated calcium channels. Science 330:101–105
62. Togo K, Suzuki Y, Yoshimaru T, Inoue T, Terui T, Ochiai T, Ra C (2009) Aspirin and salicylates modulate IgE-mediated leukotriene secretion in mast cells through a dihydropyridine receptor-mediated Ca^{2+} influx. Clin Immunol 131:145–156
63. Matza D, Badou A, Kobayashi KS, Goldsmith-Pestana K, Masuda Y, Komuro A, McMahon-Pratt D, Marchesi VT, Flavell RA (2008) A scaffold protein, AHNAK1, is required for calcium signaling during T cell activation. Immunity 28:64–74
64. Savignac M, Gomes B, Gallard A, Narbonnet S, Moreau M, Leclerc C, Paulet P, Mariamé B, Druet P, Saoudi A, Fournié GJ, Guéry JC, Pelletier L (2004) Dihydropyridine receptors are selective markers of Th2 cells and can be targeted to prevent Th2-dependent immunopathological disorders. J Immunol 172:5206–5212
65. Pelletier L, Guéry JC (2008) Dihydropyridine receptor blockade in the treatment of asthma. Recent Pat Inflamm Allergy Drug Discov 2:109–116
66. Suzuki Y, Yoshimaru T, Inoue T, Ra C (2009) $Ca_V1.2$ L-type Ca^{2+} channel protects mast cells against activation-induced cell death by preventing mitochondrial integrity disruption. Mol Immunol 46:2370–2380
67. Danial NN, Korsmeyer SJ (2004) Cell death: critical control points. Cell 116:205–219
68. Yan N, Shi Y (2005) Mechanisms of apoptosis through structural biology. Annu Rev Cell Dev Biol 21:35–56
69. Lemasters JJ, Theruvath TP, Zhong Z, Nieminen AL (2009) Mitochondrial calcium and the permeability transition in cell death. Biochim Biophys Acta 1787:1395–1401
70. Halestrap AP, Brennerb C (2003) The adenine nucleotide translocase: a central component of the mitochondrial permeability transition pore and key player in cell death. Curr Med Chem 10:1507–1525
71. Zhivotovsky B, Galluzzi L, Kepp O, Kroemer G (2009) Adenine nucleotide translocase: a component of the phylogenetically conserved cell death machinery. Cell Death Differ 16:1419–1425
72. Hail N Jr (2005) Mitochondria: a novel target for the chemoprevention of cancer. Apoptosis 10:687–705
73. Tadakuma T, Kizaki H, Odaka C, Kubota R, Ishimura Y, Yagita H, Okumura K (1990) $CD4^+CD8^+$ thymocytes are susceptible to DNA fragmentation induced by phorbol ester, calcium ionophore and anti-CD3 antibody. Eur J Immunol 20:779–784

74. Ribeiro JM, Carson DA (1993) Ca^{2+}/Mg^{2+}-dependent endonuclease from human spleen: purification, properties, and role in apoptosis. Biochemistry 32:9129–9136
75. Merćep M, Noguchi PD, Ashwell JD (1989) The cell cycle block and lysis of an activated T cell hybridoma are distinct processes with different Ca^{2+} requirements and sensitivity to cyclosporine A. J Immunol 142:4085–4092
76. McConkey DJ, Hartzell P, Amador-Perez FJ, Orrenius S, Jondal M (1989) Calcium-dependent killing of immature thymocytes by stimulation via the CD3/T cell receptor complex. J Immunol 143:1801–1806
77. Rodriguez-Tarduchy G, Prupti M, Lopez-Rivas A, Collins MKL (1992) Inhibition of apoptosis by calcium ionophores in IL-3-dependent bone marrow cells is dependent upon production of IL-4. J Immunol 148:1416–1422
78. Lampe PA, Cornbrooks EB, Juhasz A, Johnson EJ, Franklin JL (1995) Suppression of programmed neuronal death by a thapsigargin-induced Ca^{2+} influx. J Neurobiol 26:205–212
79. Green DR, Reed JC (1998) Mitochondria and apoptosis. Science 281:1309–1312
80. Zhu LP, Yu XD, Ling S, Brown RA, Kuo TH (2000) Mitochondrial Ca^{2+} homeostasis in the regulation of apoptotic and necrotic cell deaths. Cell Calcium 28:107–117
81. Kuo TH, Zhu L, Golden K, Marsh JD, Bhattacharya SK, Liu BF (2002) Altered Ca^{2+} homeostasis and impaired mitochondrial function in cardiomyopathy. Mol Cell Biochem 272:187–199
82. Visch HJ, Rutter GA, Koopman WJ, Koenderink JB, Verkaart S, de Groot T, Varadi A, Mitchell KJ, van den Heuvel LP, Smeitink JA, Willems PH (2004) Inhibition of mitochondrial Na^{+}-Ca^{2+} exchange restores agonist-induced ATP production and Ca^{2+} handling in human complex I deficiency. J Biol Chem 279:40328–40336
83. Suzuki Y, Yoshimaru T, Matsui T, Inoue T, Niide O, Nunomura S, Ra C (2003) FcεRI signaling of mast cells activates intracellular production of hydrogen peroxide: role in the regulation of calcium signals. J Immunol 171:6119–6127
84. Suzuki Y, Yoshimaru T, Inoue T, Niide O, Ra C (2005) Role of oxidants in mast cell activation. Chem Immunol Allergy 87:32–42
85. Suzuki Y, Yoshimaru T, Inoue T, Ra C (2009) Discrete generations of intracellular hydrogen peroxide and superoxide in antigen-stimulated mast cells: reciprocal regulation of store-operated Ca^{2+} channel activity. Mol Immunol 46:2200–2209
86. Devadas S, Zaritskaya L, Rhee SG, Oberley L, Williams MS (2002) Discrete generation of superoxide and hydrogen peroxide by T cell receptor stimulation: selective regulation of mitogen-activated protein kinase activation and fas ligand expression. J Exp Med 195:59–70

Chapter 45
Proteinase-Activated Receptors (PARs) and Calcium Signaling in Cancer

Roland Kaufmann and Morley D. Hollenberg

Abstract Proteinase activated receptors (PARs), a small subfamily of G protein-coupled receptors with four members, PAR_1, PAR_2, PAR_3 and PAR_4, are expressed in various tumours from epithelial origin and can play an important role in tumour progression and metastasis. Within the complex intracellular PAR signaling networks triggered by PARs, an elevation in intracellular free calcium ion concentrations represents a key second messenger system. In this review, we summarize current information about the mechanisms whereby PARs can signal via intracellular calcium in the setting of cancer and we discuss possibilities for using the PAR-$[Ca^{2+}]_i$ signaling pathway as a target for the therapy of epithelial cancer.

Keywords Proteinase activated receptors • PARs • Thrombin receptor • PAR_1 • PAR_2 • PAR_3 • PAR_4 • Signal transduction • Calcium signaling • Intracellular free calcium ion • Carcinogenesis • Cancer progression

R. Kaufmann (✉)
Experimental Transplantation Surgery, Department of General, Visceral and Vascular Surgery, Jena University Hospital, Erlanger Allee 101, D-07747, Jena, Germany
e-mail: roland.kaufmann@med.uni-jena.de

M.D. Hollenberg
Inflammation Research Network, Department of Physiology & Pharmacology and Department of Medicine, Faculty of Medicine, University of Calgary, Calgary, Canada, T2N 4N1
e-mail: mhollenb@ucalgary.ca

M.S. Islam (ed.), *Calcium Signaling*, Advances in Experimental Medicine and Biology 740, DOI 10.1007/978-94-007-2888-2_45,

Proteinase Activated Receptors: A Specialized Subfamily of G Protein Coupled Receptors with Complex Intracellular Signal Transduction Pathways

Proteinase activated receptors (PARs) comprise a unique subfamily of G protein-coupled receptors (GPCRs) with four subtypes, PAR_1, PAR_2, PAR_3 and PAR_4 [for reviews see: [1–4]]. Although PARs share basic structural features of all GPCRs, including seven putative hydrophobic transmembrane-spanning alpha helices, they exhibit a novel mechanism of activation that distinguishes them from all other GPCRs. While most GPCRs are activated reversibly by small hydrophilic molecules to elicit cellular responses [5], PAR activation occurs through an irreversible proteolytic mechanism that involves the recognition and cleavage of the receptor by a proteinase at a specific 'cleavage-activation' site located at the extracellular amino-terminus (Fig. 45.1).

This cleavage exposes a cryptic N-terminal domain that acts as a 'tethered ligand' that binds to the receptor extracellular domains to trigger receptor signaling [3, 6–8]. Remarkably, short synthetic peptides modelled on the sequences of the proteolytically-exposed tethered ligand sequences are capable of binding to PARs 1, 2 and 4, mimicking the actions of agonist proteinases [right-hand portion, Fig. 45.1; [9, 10]]. However, the proteolytically exposed N-terminal sequence of PAR_3 and its corresponding synthetic peptides appear to be incapable of causing PAR_3 signaling and instead are able to activate PAR_1 and PAR_2 [11, 12]. As an alternative, a proteinase may cleave a PAR downstream of the 'tethered ligand sequence' (e.g. red arrow,

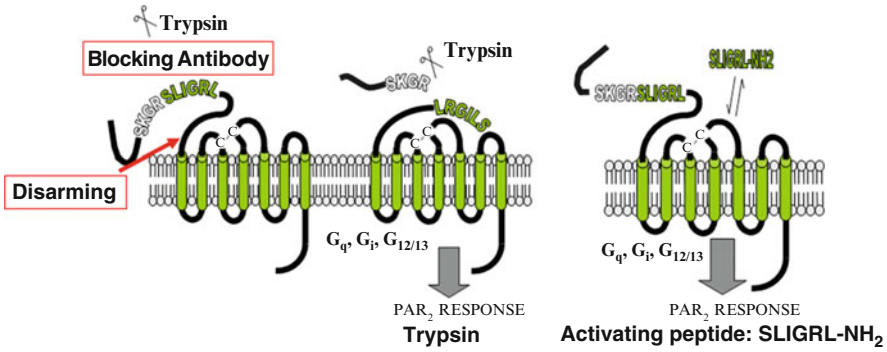

Fig. 45.1 Model for activation and dis-arming of PAR_2. The scheme illustrates activation of the intact receptor (*left-hand panel*) by two distinct mechanisms: either (I) by proteolysis and unmasking of the tethered ligand sequence (*middle Panel*: green sequence, SLIGRL, also seen in the intact receptor) or (II) by a receptor-derived peptide (SLIGRL-NH_2: *right-hand panel*) that activates signaling without the need for receptor proteolysis. The scheme also shows the 'disarming' site for the receptor, where cleavage removes the tethered ligand sequence and the 'cleavage-activation' site', where a 'blocking antibody' can prevent proteolytic activation of the receptor (Redrawn from Hollenberg and Compton, Ref. [6])

left-hand portion, Fig. 45.1), to as to 'dis-arm' and prevent activation of the PAR by an enzyme that would otherwise expose the tethered ligand. Thus, PARs have a variety of both endogenous 'tethered ligand-exposing' proteinase agonists as well as a number of endogenous proteolytic 'antagonists' that can 'silence' receptor activation by other proteinases. Therefore, in the setting of a tumour, both tumour-derived and non-tumour-derived proteinases in the microenvironment can play roles as either PAR agonists or antagonists.

During the last few years it has become evident that PARs, which are triggered by endogenous serine proteinases, mediate hormone-like cellular responses. PAR_1 [9, 13], PAR_3 [14] and PAR_4 [15, 16] are targeted not only by the coagulation cascade proteinases including thrombin, factor Xa and activated protein C, but also by other proteinases including cathepsin and matrix metalloproteinase-I [17–19]. PAR_2 [20] can be activated by trypsin, mast cell tryptase, neutrophil proteinase 3, tissue factor/factor VIIa/factor Xa, human kallikrein-related peptidases, membrane-tethered serine proteinase-1/matriptase 1 and by parasite cysteine proteinases, but not by thrombin [2, 3, 21, 22].

The PAR family is able to stimulate a variety of intracellular signaling pathways which can be either overlapping or distinct for the different PARs, depending on the PAR subtype and the phenotype or stage of differentiation of its specific cellular 'host' [e.g. platelets vs. hepatocytes: for reviews see: [4, 22–28]]. Like other 'GPCRs', the PARs signal via a variety of heterotrimeric guanyl nucleotide-binding proteins (G proteins), including G_q, G_i, $G_{12/13}$ but not directly via G_s [7, 29]. In addition, PAR_2 and possibly the other PARs are able to signal via a non-G-protein mechanism that involves the beta-arrestin-mediated internalization of a PAR_2-beta-arrestin signaling scaffold [30–35]. The coupling of the PARs to either the G-proteins or arrestins is driven by ligand-triggered changes of receptor conformation that for other GPCRs is thought to involve the putative transmembrane helices 3 and 6 of the receptor [36, 37]. Of importance, different agonists are in principle capable of driving different conformational changes in the receptor to result in selective interactions with different downstream 'effectors'. This principle was outlined by the 'floating' or 'mobile' receptor paradigm some time ago [38, 39]. More recently, the concept has evolved to encompass the concept of 'biased receptor signaling' or 'functional selectivity' as outlined in detail elsewhere [40]. For G-protein-mediated signaling, the receptor acts as a ligand-triggered guanine nucleotide exchange factor (GEF), stimulating the exchange of GTP for GDP in the G_α subunit of the heterotrimeric G-protein oligomer. This exchange enables the 'release' of the G_α subunit from its tight binding to the $G_{\beta\gamma}$ dimer subunit. Each of the G-protein moieties (G_α-GTP and $G_{\beta\gamma}$) is then independently able to interact with other select downstream signaling effectors like ion channels ($G_{\beta\gamma}$) or phospholipase C-β (G_q). This 'dual effector' signaling resulting in principle from the same PAR-activated G-protein heterotrimer (e.g. G_q $G_{\beta\gamma}$) can converge for complex downstream signaling, for instance leading to NF-κB activation and ICAM-1 transcription by the engagement of parallel G_q/PKC- and G_i/PI3-kinase pathways that converge [41, 42]. Alternatively, via a 'biased signaling' process, PARs can be activated to affect selec-

tively, MAPKinase signaling via a $G_{12/13}$-triggered process, without causing a G_q-mediated calcium signaling event [31]. This kind of selective signaling can depend not only on the agonist per se [e.g. thrombin or activated protein-C (APC)] but also upon the membrane environment in which a PAR is localized. For instance, triggering of PAR_1 localized in the caveolae by APC can signal via a distinct set of downstream effectors that differ from those regulated when thrombin activates PAR_1 in a non-caveolar environment [29]. The PAR_1 signal pathways activated in these distinct membrane environments lead to a diametrically opposed set of responses that either increase or decrease endothelial barrier integrity. Thus in principle, it is possible to activate and/or inhibit selectively one or other of the downstream signaling pathways activated by PARs (e.g. calcium vs. MAPKinase signals).

PARs Are Involved in Cancer Progression

Local and systemic coagulation is a hallmark of cancer [review: [43]]. In this complicated scenario, tissue factor (TF) induces the formation of the complex TF-VIIa. Both the complex TF-VIIa-Xa and thrombin (factor IIa) can activate proteinase activated receptors. Thrombin can activate PAR_1 and PAR_4 [44], whereas the binary TF-VIIa enzyme complex is able to activate PAR_2 but not PAR_1 [45, 46]. However, as a TF-VIIa-Xa complex, factor Xa efficiently cleaves PAR_2 as well as PAR_1 [47, 48]. In addition, a variety of other proteinases may also be important in the tumour microenvironment, where both stromal and tumour-derived cells can produce PAR-regulating proteinases. Such enzymes can either, like tumour-derived tissue kallikreins [49–51], activate PAR_2, or alternatively proteinases of tissue origin can 'dis-arm' a PAR, by cleaving downstream of the 'tethered ligand' domain (Fig. 45.1, left), thereby silencing a PAR from activation by its target proteinase (e.g. disarmed PAR_1 can no longer respond to thrombin). Moreover tumour-derived proteinases like matrix metalloproteinase-I can cleave the N-terminal domain of a PAR to unmask a 'non-canonical' tethered activating sequence different from the one revealed by serine proteinases [19, 52]. The ability of thrombin to act via PARs was highlighted by the demonstration of the ability of PAR_1 to stimulate tumour invasion [53, 54] by its expression in carcinosarcoma and melanoma cells [55]. The extensive work in this field related to tumour tissue done over the past decade has therefore focused primarily on PAR_1 for which the expression and signaling at the cellular level have been characterized in tumour cells from different tumour entities including cancers of the larynx [56], pancreas [57], glioma [58, 59], glioblastoma [60, 61], meningioma [62], prostate [63] and colon [64]. In addition, PAR_1 activation has been observed to cause (I) increased tumour cell adhesion to the endothelium, extracellular matrix and platelets, (II) enhanced metastatic capacity of tumour cells, (III) activated cell growth and (IV) increased angiogenesis [65–67]. In breast and pancreatic carcinoma cells, the level of PAR_1 expression has been correlated with the degree of invasiveness [54, 68]. Furthermore, transfection of B16F10 melanoma cells with PAR_1, compared with non-transfected cells, leads to a 2.5-fold

enhanced thrombin-induced tumour cell adhesion to fibronectin and a 39-fold increase in pulmonary metastasis [69]. At present there is substantial evidence that thrombin acting via PAR_1 contributes to the metastatic process of certain epithelial tumours including breast [53, 54, 70], colon [64], kidney [71] and liver [72]. However, PAR_1 is not the only functional receptor for thrombin in tumour cells since several reports have demonstrated that PAR_1 can cooperate with the other thrombin target, PAR_4, to act as a 'dual receptor system' in human astrocytoma cells [73] and in cells from liver cancer [72]. In addition to PAR_1, PAR_2 is also known to be expressed in a variety of epithelial tumour cells from different origins [32, 74–82] and to act as an upstream activator of promigratory signaling pathways [34, 75, 80, 83] resulting in an enhancement of tumour progression.

Multiple Effects of PAR Activation on Cancer Cells

Studies dealing with a variety of tumour-related cells have observed important effects of PAR activation, several examples of which will be outlined in this paragraph. Seminal work from the Bar-Shavit laboratory has demonstrated the key role that PAR_1 may exhibit in breast cancer cell invasion [53, 54, 70] and recently Gonda et al. provided impressive data showing movements of breast cancer cells and PAR_1 during metastasis *in vivo* using a highly sophisticated nano-imaging technique [84]. In breast carcinoma cells PAR_1 mediates both migratory and invasive effects [85]. These PAR_1-mediated actions occur in cooperation with alpha-vbeta 5 integrin [53] and with the involvement of increases in intracellular calcium [86]. In 1321N1 astrocytoma cells, Blum and colleagues demonstrated that PAR_1-stimulated ATP release is Ca^{2+}-dependent and that concurrent Rho signaling markedly potentiates this effect [87]. In keratinocyte-related HaCaT cells, PAR_2 activation by matriptase, a membrane-tethered serine proteinase released from the cell surface, has been shown to induce intracellular calcium mobilization and to inhibit proliferation. Based on this information, a role for PAR_2 signaling in skin cancer has been suggested [82]. A substantial amount of data also exist pointing to a role for PARs in colon cancer. In cells from this tumour entity, PAR_1 and PAR_2 have been demonstrated to signal via $[Ca^{2+}]_i$ and to induce migratory and proliferative effects that also involve both activation of p42/p44-MAPKinase and trans-activation of the receptor for epidermal growth factor (EGFR) [64, 74, 88, 89]. In addition, PAR_4 has recently surfaced as a new important player in the regulation of colon tumour-derived cells. In colon carcinoma cells activation of PAR_4 has been found to be involved in stimulating mitogenesis. This stimulation is observed to occur in the setting of PAR_4-induced increases intracellular calcium and activation of p42/p44 MAPKinase along with trans-activation of ErbB-2, a member of the epidermal growth factor receptor B-2 receptor family, but not via trans-activation of the EGF-Erb-B1 homodimer receptor itself [90]. Since PAR_4 does not mediate an increase in cytoplasmic free Ca^{2+} in hepatocellular carcinoma cells [72], but does so in colon carcinoma cells, the ability of PAR_4 to stimulate increases in intracellular calcium appears to be dependent

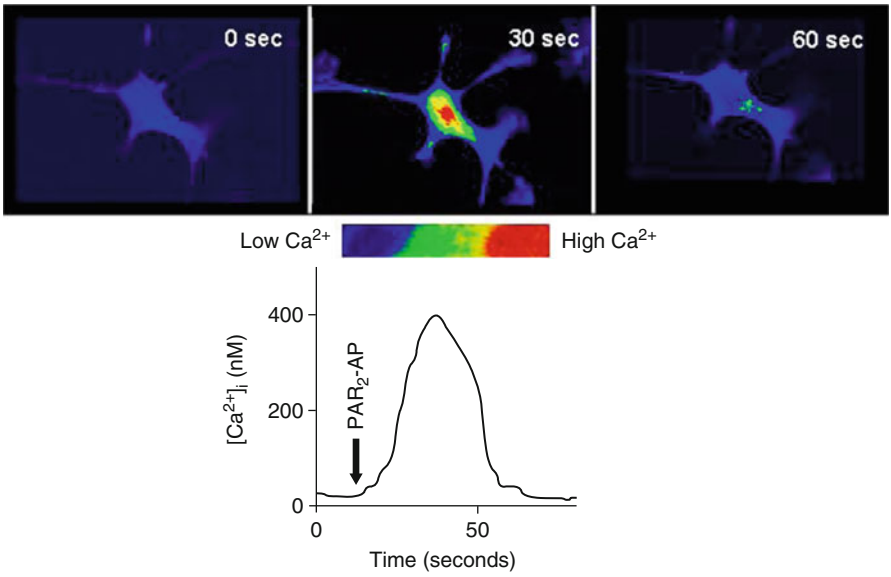

Fig. 45.2 PAR_2 mediates $[Ca^{2+}]_i$ increase in LX-2 hepatic stellate cells. LX-2 cells grown on Lab Tek chambered borosilicate coverglass were loaded with fluo-4-AM (0.5 μM). For calcium measurements, an inverted confocal laser scanning microscope LSM 510 was used. Fluorescence was monitored at 488 nm. *Upper part:* Fluorescence images, in pseudocolor, from an individual LX-2 cell preloaded with fluo-4-AM dye and stimulated with the PAR_2-activating peptide, 2-furoyl-LIGRLO-NH_2 (10 μM). The time sequence of three panels shows a transient fluorescence increase 30 s after PAR_2-AP addition (0 s: time of addition of PAR_2-AP), with a return to baseline fluorescence at 1 min. *Lower part:* Time course of calcium response induced by the PAR_2-activating peptide, 2-furoyl-LIGRLO-NH_2 (10 μM). The intracellular calcium concentration was calculated using the equation $[Ca^{2+}]_i = 345\ (F–F_{min})/(F_{max}–F)$ [104]. The Ca^{2+} affinity of fluo-4 (Kd) is 345 nM [105]. Fmax was obtained by addition of 10 μM ionomycin (+6 mM $CaCl_2$), Fmin by addition of 10 mM ethylene glycol-bis(2-aminoethylether)-N,N,N′,N′-tetraacetic acid (EGTA). Data represent the mean ± SE from calcium measurements in 20 single cells. (LX-2 cells were a gift from Prof. Scott L. Friedman, Division of Liver Diseases, Mount Sinai School of Medicine, New York)

upon the cellular context in which the receptor is expressed. Thus, different tumours with their unique expression of GPCR-regulated effectors have the potential to respond to PAR activation in a unique way that may or may not depend on calcium signaling.

PARs Are Relevant in Different Cells from the Tumour Microenvironment

Relatively recently, oncologists have begun to focus on the tumour microenvironment as a major contributing factor to the development of cancer. Thus, in the setting of a tumour, both the resident non-tumour cells as well as the tumour cells can

engage in signaling cross-talk (tumour cell to stromal cell and back) that changes the phenotype of the stromal cells and alters the growth and metastatic potential of the tumour cell [91–93]. This cross-talk communication between tumour and stromal cells is mediated by a variety of hormone-like regulators, including secreted growth factors and proteinases [94–96]. PAR expression and function in different cell types found in the stromal elements of the tumour microenvironment, including fibroblasts, inflammatory leukocytes, platelets, macrophages, endothelial cells and smooth muscle cells has been documented in other contexts [reviewed: [1–4]]. Thus, the potential function of PARs in these stromal bystander cells is directly relevant to the malignant process and is currently under close scrutiny [97–102]. For example, in the setting of hepatocellular carcinoma (HCC), one of the leading malignancies worldwide, recently published data suggest that activated stromal hepatic stellate cells (HSCs) in the tumour microenvironment may contribute to the promotion of HCC tumorigenicity [103]. As illustrated in Fig. 45.2 PAR_2 mediates calcium signaling in HSCs that could readily occur in the setting of a hepatic tumour.

Intracellular Calcium – A Key Secondary Messenger in Cancer and a Potential Target for Therapy

Ca^{2+} is a ubiquitous intracellular signaling molecule that is involved in the regulation of almost all cellular functions including gene transcription, metabolism, proliferation and apoptosis [reviewed: [106–110]]. Since cancer growth is based on increased proliferation, decreased differentiation and decreased apoptosis, all of which processes involve a regulation of intracellular calcium concentrations, Ca^{2+}-homeostasis has become an important topic in current cancer research. Apart from the 'calcium-sensing receptor' [111, 112], G-protein-coupled receptor mechanisms involving G_q-stimulated phospholipase C_β and growth factor receptor mechanisms that trigger phospholipase C_γ represent key receptor mechanisms that regulate intracellular calcium. These mechanisms are in addition to the voltage-regulated and other ion channel mechanisms that regulate the entry of calcium from the extracellular environment. The current knowledge in this area is well documented by several detailed and comprehensive review articles that are cited in the following text. Here, only a brief overview is provided that is relevant for understanding the rationale for targeting PAR-mediated Ca^{2+} signaling as a possible therapeutic option for the treatment of cancer.

It is well known that an elevation of cytoplasmic $[Ca^{2+}]_i$ can result either from Ca^{2+}-influx from the extracellular space through a variety of plasma membrane ion channels or from Ca^{2+}-release from intracellular stores. More specifically, voltage- and ligand-gated Ca^{2+} channels in the plasma membrane, along with intracellular ryanodine receptors and inositol (1,4,5)-triphosphate ($InsP_3$) receptors in the endoplasmic reticulum as well as mitochondrial voltage-dependent anion channels and calcium ion exchangers provide fluxes of Ca^{2+} to the cytoplasm [106–108].

It has become evident that during the multistage process of carcinogenesis, the transformation of a normal cell into the malignant state is associated with a major change in the organization and expression of Ca^{2+} pumps, Na/Ca exchangers and Ca^{2+} channels. These changes occur in a setting that leads to the enhanced proliferation and impaired ability of the cancer cell to die [109]. In addition, work in this area done over the past decade has shown that altered intracellular Ca^{2+} signaling stimulated by G-protein coupled receptors via G_q [113–115] and involving tumour-associated changes in calcium release depots like the ryanodine receptor [116] can play a role in various tumourigenic pathways [117–120]. Thus, modulation of $[Ca^{2+}]_i$ signaling is a potential therapeutic option in cancer. In this regard, strategies can include specific blockade of membrane-localized calcium channels and targeting calcium release mechanisms via the $InsP_3$ and ryanodine receptors. Since many of these targets are expressed in a large number of cell types and organs where they may have essential functions, targeting specific Ca^{2+} channels or pumps with restricted tissue distribution, altered expression in cancer and/or a role in the regulation of tumourigenic pathways are a potential way to specifically disrupt intracellular Ca^{2+} homeostasis in cancer cells wherein different pharmacological strategies are possible [117–120]. One approach makes use of a bystander enzyme mechanism that results in the metabolic conversion of a pro-drug to an active moiety specifically at a site of restricted expression of that enzyme. For instance, since the human kallikrein-related serine peptidase-3 (KLK3, also known as 'prostate-specific antigen') is highly restricted in its expression to prostate tissue, it has proved possible to target the conversion of a thapsigargin 'prodrug' for activation in prostate cancer tissue, where the released thapsigargin can block the sarcoplasmic/endoplasmic Ca^{2+} pump. This 'smart-bomb' targeting method has the ability to induce cell death in prostate cancer cells [121]. A second pharmacological approach involves the direct targeting of specific isoforms of Ca^{2+} channels or pumps associated with a specific cancer type. There is yet another aspect in Ca^{2+} signaling that makes Ca^{2+} channels and pumps highly attractive as therapeutic targets in cancer. While the Ca^{2+} signal in differentiated non malignant cells is spatially and temporally highly regulated [106–110], in tumour cells there is a shift to a more global elevation of intracellular calcium with a sustained elevation of intracellular calcium. Therefore, cancer cells and their calcium-regulated signaling pathways may be more susceptible than normal cells to modulation of their Ca^{2+} channels and pumps [117–120]. Taken together the information obtained over the past decade, including quite recent data [122–124] suggest that the intracellular calcium-regulating machinery may represent a promising target for cancer therapy.

$[Ca^{2+}]_i$ Is Involved in PAR Signaling in Cancer

As outlined above, one of the main cell signaling pathways triggered by activation of distinct PARs is the $G_{q/11}$–mediated activation of phospholipase C_β. This activation, leads to the formation of inositol (1,4,5)-triphosphate and diacylglycerol that

in turn cause the elevation of intracellular Ca^{2+} (illustrated for LX-2 hepatic stellate cells in Fig. 45.2) and activation of protein kinase C. Indeed, the ability of the PAR_1 receptor for thrombin to mobilize intracellular calcium was instrumental in its cloning via an oocyte expression system [9].

This $G_{q/11}$ calcium signaling pathway activated by PARs has been observed in a variety of cancer cell types as seen by the activation of calcium signaling by thrombin in glioma cells ostensibly via PAR_1 [125]. The documentation of PAR-mediated calcium signaling in cancer-derived cells was greatly facilitated by the use of PAR subtype selective peptide agonists based on the sequences of the revealed PAR tethered ligands and PAR_1-targeted antagonists (see Table 45.1 for PAR-selective agonists and antagonists).

The presence of a specific PAR in a target cancer cell and its ability to increase intracellular calcium can be established using a receptor cross-desensitization protocol with PAR-selective agonists and appropriate PAR-inactive 'control' peptides [126]. This approach that uses fluorimetric methods to monitor calcium transients with different calcium sensitive fluorescence dyes has documented PAR-mediated increases in $[Ca^{2+}]_i$ in cells from various malignancies including those from brain [53, 56, 57, 109], colon [64, 74], pancreas [127], kidney[128], breast [19], larynx [56], prostate [112] and liver [72]. Although all of PARs 1, 2 and 4 can couple with G_q to elevate intracellular calcium in all PAR-expressing cells so far examined, the precise downstream consequences of elevated calcium *per se* have not been established in any detail. Further, as already mentioned, upon enzyme or peptide agonist activation the PARs can activate multiple G-proteins leading not only to elevations of intracellular calcium but also to (I) a G_i-mediated inhibition of adenylyl cyclase, (II) activation of MAPKinase [both G_i-dependent as well as G-protein independent *via* beta-arrestin interactions: review: [35]] and (III) a $G_{12/13}$-mediated activation of Rho and its downstream targets. Thus, singling out the PAR-triggered signal pathways that are uniquely calcium-mediated represents a considerable challenge.

$Ca^{2\pm}$ and PAR_2-Triggered p42/p44 MAPKinase Signaling

Increases in intracellular calcium result in a complex signaling network that includes p42/p44 MAPKinases as an intracellular effector system critically related to cell growth and transcriptional regulation [129, 130]. For prostate cancer PC3 cells it has been shown that kallikrein related peptidase 4 (KLK4), one of the 15 members of the human KLK family and a trypsin-like prostate cancer-associated serine protease, initiates Ca^{2+} signaling via PAR_1 and PAR_2. Stimulation of PAR_2 by KLK4 also results in p42/p44 MAPKinase activation [131]. Very recently, for hepatocellular carcinoma where altered Ca^{2+} signaling contributes to cancer development and progression [132], a PAR_2 dependent calcium-p42/p44 MAPKinase signaling axis was defined [133]. Since p42/p44 MAPKinases are established key players in HCC progression and invasive growth [134–137], and more specifically, since they contribute to a PAR_2-mediated effect on HCC cell invasion, the results

Table 45.1 PAR tethered ligand sequences, activating peptides, control inactive peptides and antagonists

IUPHAR recommended name	PAR_1	PAR_2	PAR_3	PAR_4
PAR tethered ligand sequences	SFLLRN (h), SFFLRN (m,r) PAR_1 AP, activates PAR_1 and PAR_2	SLIGKV (h), SLIGRL (m,r) PAR_2 AP only activates PAR_2	TFRGAP (h) PAR_3 AP only activates PARs 1 and 2	GYPGQV (h) GYPGKF (m) PAR_4 APs don't activate other PARs
PAR activating peptides	TFLLRN-NH_2, selective for PAR_1	SLIGRL-NH_2 2-furoyl-LIGRLO-NH_2		AYPGKF-NH_2
Control PAR-inactive peptides	RLLFT-NH_2 FTLLR-NH_2	LRGILS-NH_2 LSIGRL-NH_2 2-furoyl-LRGILS-NH_2		YAPGKF-NH_2
PAR antagonists	Trans-cinnamoyl-parafluoro-Phe-paraguanidino-Phe-Leu-Arg-Arg-NH_2 Mercaptopropionyl-Phe-Cha-Arg-Lys-Pro-Lys-Pro-Asn-Asp-Lys-NH_2 Non-peptide antagonists: RWJ56110 and RWJ58259 SCH 530348	Non-peptide antagonist: ENMD 1068 (N1-Methylbutyryl-N4-6-aminohexanoyl-piperazine) Peptide antagonist: K-14585 Palmitoyl-RSSAMDENSEKKRKSAIK (P2pal-18S)		Trans-cinnamoyl-YPGKF-NH_2

suggest a role for both Ca^{2+} and p42/p44 MAPKinase-driven signaling as an invasive axis in HCC cells. What is difficult to sort out is the signaling route whereby MAPKinase is activated in the HCC cells. Activation of p42/p44 MAPKinase could be (I) directly downstream of Ca^{2+} signaling as a consequence of the activation of protein kinase C, (II) independent of $G_{q/11}$ Ca^{2+} signaling, via a $G_{12/13}$-Rho kinase mechanism or (III) via a G-protein-independent mechanism triggered by a beta-arrestin-internalized signal scaffold [35]. In principle, all three mechanisms could result in the activation of MAPKinase signaling pathways in cancer cells. However, it is likely that the downstream effects of MAPKinase activation by these three distinct mechanisms will be found to differ (e.g. increase in transcription vs. activation of cytosolic phospholipase-A2 or changes in cell motility). Thus, identifying those events that result uniquely from elevations in intracellular calcium will be of much interest in the setting of tumour cell behaviour. To sum up, although Ca^{2+} plays a central role in regulating cancer cell behaviour, it has not yet proved possible to single out the impact on tumourigenesis of blocking Ca^{2+} signaling selectively, without affecting other PAR-triggered signaling events.

PAR-Mediated Increases in Cytoplasmic Free $Ca^{2\pm}$: Involvement of Both Extracellular and Intracellular Calcium

For numerous GPCRs it has been shown, as outlined above, that receptor-triggered increases in free intracellular calcium ion concentration can result from both influx of Ca^{2+} across the plasma membrane and the release of Ca^{2+} from intracellular stores [106, 138]. For PAR_2 this dual mechanism has been suggested for hepatocellular carcinoma cells, where PAR_2-stimulated increases in intracellular calcium can be reduced either by removing extracellular Ca^{2+} with the use of EGTA or by depletion of internal Ca^{2+} stores with thapsigargin [133]. This ‘dual mechanism’ for calcium signaling very likely also occurs for PARs 1 and 4. Thus, to block calcium signaling completely in cancer cells, it may be necessary to inhibit not only the G_q-triggered calcium signal that involves intracellular stores but also the receptor-mediated calcium entry process that occurs via receptor-regulated channels.

Intracellular Calcium Oscillations in Cancer-Derived Cells

Most of the knowledge about the effects of receptor agonists on $[Ca^{2+}]_i$ has come from studies on cell suspensions. In such experiments, the estimated $[Ca^{2+}]_i$ value represents the average value of $[Ca^{2+}]_i$ in all cells in the sample being explored. That response is represented by a peak of intracellular calcium that occurs within a minute of cell activation and a return to baseline calcium concentrations over a 2–5-min time frame, as calcium is first released and then rapidly taken back up into intracellular stores. However, at the single cell level, agonists can also trigger persistent

oscillations in intracellular calcium ion concentrations that wax and wane with time. Agonist-induced oscillations in intracellular calcium concentrations have been observed in many excitable and non-excitable cells, wherein a number of mechanisms have been proposed [for reviews see e.g.:[107, 138–140]]. As an example, such oscillations have been observed in response to PAR_1 activation in glioblastoma cells. The oscillatory response was observed after treatment with either thrombin or by the dual PAR_{1-2} activating peptide, SFLLRN-NH_2 [60]. The relevance of these oscillating intracellular calcium concentrations to tumour cell behaviour has yet to be determined.

Can PAR-Mediated Calcium Signaling Be Selectively Blocked?

Given that PAR-triggered calcium signaling can be of importance for the oncogenic process, an important question to deal with is: Can PAR-mediated calcium signaling be selectively blocked? Studies with human PAR_2 have identified a C-terminal domain that is directly involved in the ability of this receptor to stimulate elevations in intracellular calcium [141]. Thus, when activated by trypsin, a mutant PAR_2 missing a key C-terminal domain was able to stimulate MAPKinase and JNK, but not an elevation in intracellular calcium. In principle, this region of PAR_2 can thus be targeted as a 'calcium regulating domain' for the development of receptor-selective antagonists that will potentially affect calcium transients only in PAR_2-expressing tumour cells. A similar situation was found for the activation of PAR_1. It has been shown that the C-terminal part of PAR_1 is a critical site for receptor coupling to phospholipase C activation and thus for Ca^{2+}-signaling, while the third intracellular loop of PAR_1 is implicated in PAR_1 coupling to MAPkinase activation. Therefore, a strategy specifically targeting Ca^{2+} signaling might be possible not only for PAR_2 but also for the other PAR subtypes [142].

One may readily ask: How might such signal-selective antagonists be developed? The answer lies in making use of (I) the concept of 'biased' signaling and (II) cell-penetrating peptides. For instance, the PAR_2 antagonist, K-14585 can block PAR_2-stimulated elevations of intracellular calcium and a concurrent activation of p42/44 MAPKinase, but cannot block increases in p38 MAPKinase activation [143]. This compound therefore exhibits 'biased' antagonism for PAR_2. In principle more potent antagonists of this kind can be developed to block calcium signaling selectively. The concurrent blockade of both MAPkinase and calcium signaling may be particularly attractive in terms of targeting cancer cells.

"Pepducins" are cell-penetrating palmitoylated peptides based on sequences of the intracellular loops of G protein-coupled receptors. Due to the ability of their lipid moiety to anchor to the lipid bilayer of the plasma membrane these lipopeptides are thought to act by being internalized and then targeting the receptor-G protein interface [144, 145]. "Pepducins" based on the third intracellular loop of proteinase activated receptors have been successfully used for inhibition of PAR-mediated effects on signaling and cellular level [146–149]. The 'pepducin GPCR

antagonist' approach provides an excellent platform technology for the design of a variety of other PAR inhibiting cell-penetrating peptide variants corresponding to sequences of the intracellular receptor domains that are important for G protein coupling of GPCRs [150, 151]. It is known that for GPCRs, the C-terminus appears to be only of modest relevance for interacting with some G proteins [152–154]. However, as outlined above, a sequence in the C-terminus of PAR_2 has been shown to be important for calcium signaling [141]. This C-terminal domain can be a target for palmitoylation that results in a potential '8th helix' and a 'fourth intracellular loop' in G-protein-coupled receptors. Of particular note, a synthetic pepducin, termed jF5, targeted to this domain of GPCRs, including PAR_1 and the alpha-2A adrenoceptor, can selectively block GPCR-triggered calcium signaling, but not signaling via $G_{\alpha 12}$ [155]. It can be predicted that jF5 would also affect PAR_2 calcium signaling, which is dependent on a homologous sequence that can be a target for palmitoylation [141]. Finally, this 'lipopeptide concept' could also be expanded in principle to target PAR sequences within the transmembrane helical domains 3 and 6 that are also known to regulate GPCR G-protein coupling [36, 37].

Possible Impact of PAR-Triggered Calcium Signaling in Cancer Therapy

Data describing the PAR-induced effects in cancer published over the last 15 years clearly highlight PARs as possible targets in cancer treatment [156]. Given that PAR_1 is an attractive therapeutic target for thromboembolic disease, a number of receptor-targeted antagonists have been developed. Two PAR_1-targeted antagonists, SCH 530348 and E5555 or Atopaxar are currently in Phase III clinical trials for treating acute coronary syndrome [157–159]. Whether these antagonists will prove of value in the clinic for cardiovascular disease is yet to be determined. The compounds may, however be considered for use in the prevention of cancer metastasis and invasion. In addition, novel PAR_2 antagonists containing nonpeptidic moieties have been developed very recently [160]. Their therapeutic potential should also be tested for epithelial carcinoma. Since PAR stimulation does activate calcium signaling and because calcium signaling *per se* can affect cancer cell migration and invasion, agents that also target intracellular Ca^{2+}-signaling like those used in cardiovascular disease [for reviews see e.g.: [161–164]] may prove of value in the setting of cancer along with PAR antagonists. This possibility has yet to be considered.

Over the past decade there has been substantial success in targeting signal transduction pathways for treating cancer [165–167]. Impressive success can be seen in the use of the Abl-kinase-targeted imatinib-like inhibitors and their analogues, and a 'multitarget drug' that affects a number of signal pathways, sorafenib (BAY-43-9006), a bis-aryl urea-type inhibitor that blocks several kinases involved in tumour proliferation and angiogenesis. This inhibitor can affect Raf, vascular endothelial growth factor receptor (VEGFR) and platelet derived growth factor receptor (PDGFR) signaling [168]. Data from several patient studies indicate that sorafenib

seems to be a promising drug for the treatment of various epithelial cancers including those from breast, colon, kidney and liver [for review see e.g.: [169]]. Since targeting multiple signal pathways rather than a single enzyme may be advantageous in treating cancer, it can be suggested that in combination with other therapeutic agents, the selective blockade of PAR-mediated calcium signaling may be worthy of consideration for dealing with epithelial carcinoma.

Acknowledgements Work in the author's laboratories is supported by grants from German Cancer Aid (RK) and German Research Foundation (RK), the Canadian Institutes for Health Research (MDH) and the Heart & Stroke Foundation of Alberta and Nunavut (MDH). We are grateful for the referee's comments which have helped with the writing of this article.

References

1. Ossovskaya V, Bunnett N (2004) Protease-activated receptors: contribution to physiology and disease. Physiol Rev 84:579–621
2. Ramachandran R, Hollenberg M (2008) Proteinases and signalling: pathophysiological and therapeutic implications via PARs and more. Br J Pharmacol 153(Suppl 1):S263–S282
3. Steinhoff M, Buddenkotte J, Shpacovitch V, Rattenholl A, Moormann C, Vergnolle N, Luger T, Hollenberg M (2005) Proteinase-activated receptors: transducers of proteinase-mediated signaling in inflammation and immune response. Endocr Rev 26:1–43
4. Adams MN, Ramachandran R, Yau MK, Suen JY, Fairlie DP, Hollenberg MD, Hooper JD (2011) Structure, function and pathophysiology of protease activated receptors. Pharmacol Ther 130(3):248–282
5. Wettschureck N, Offermanns S (2005) Mammalian G proteins and their cell type specific functions. Physiol Rev 85:1159–1204
6. Hollenberg M, Compton S (2002) International Union of Pharmacology. XXVIII. Proteinase-activated receptors. Pharmacol Rev 54:203–217
7. Coughlin SR (2005) Protease-activated receptors in hemostasis, thrombosis and vascular biology. J Thromb Haemost 3:1800–1814
8. Gandhi PS, Chen Z, Di Cera E (2010) Crystal structure of thrombin bound to the uncleaved extracellular fragment of PAR1. J Biol Chem 285:15393–15398
9. Vu T, Hung D, Wheaton V, Coughlin S (1991) Molecular cloning of a functional thrombin receptor reveals a novel proteolytic mechanism of receptor activation. Cell 64:1057–1068
10. Scarborough RM, Naughton MA, Teng W, Hung DT, Rose J, Vu TK, Wheaton VI, Turck CW, Coughlin SR (1992) Tethered ligand agonist peptides. Structural requirements for thrombin receptor activation reveal mechanism of proteolytic unmasking of agonist function. J Biol Chem 267:13146–13149
11. Hansen KK, Saifeddine M, Hollenberg MD (2004) Tethered ligand-derived peptides of proteinase-activated receptor 3 (PAR3) activate PAR1 and PAR2 in Jurkat T cells. Immunology 112:183–190
12. Kaufmann R, Schulze B, Krause G, Mayr LM, Settmacher U, Henklein P (2005) Proteinase-activated receptors (PARs)–the PAR3 Neo-N-terminal peptide TFRGAP interacts with PAR1. Regul Pept 125:61–66
13. Rasmussen UB, Vouret-Craviari V, Jallat S, Schlesinger Y, Pagès G, Pavirani A, Lecocq JP, Pouysségur J, Van Obberghen-Schilling E (1991) cDNA cloning and expression of a hamster alpha-thrombin receptor coupled to Ca2+ mobilization. FEBS Lett 288:123–128
14. Ishihara H, Connolly A, Zeng D, Kahn M, Zheng Y, Timmons C, Tram T, Coughlin S (1997) Protease-activated receptor 3 is a second thrombin receptor in humans. Nature 386:502–506

15. Xu WF, Andersen H, Whitmore TE, Presnell SR, Yee DP, Ching A, Gilbert T, Davie EW, Foster DC (1998) Cloning and characterization of human protease-activated receptor 4. Proc Natl Acad Sci USA 95:6642–6646
16. Kahn ML, Zheng YW, Huang W, Bigornia V, Zeng D, Moff S, Farese RV, Tam C, Coughlin SR (1998) A dual thrombin receptor system for platelet activation. Nature 394:690–694
17. Sambrano GR, Huang W, Faruqi T, Mahrus S, Craik C, Coughlin SR (2000) Cathepsin G activates protease-activated receptor-4 in human platelets. J Biol Chem 275:6819–6823
18. Schuepbach RA, Riewald M (2010) Coagulation factor Xa cleaves protease-activated receptor-1 and mediates signaling dependent on binding to the endothelial protein C receptor. J Thromb Haemost 8:379–388
19. Boire A, Covic L, Agarwal A, Jacques S, Sherifi S, Kuliopulos A (2005) PAR1 is a matrix metalloprotease-1 receptor that promotes invasion and tumorigenesis of breast cancer cells. Cell 120:303–313
20. Nystedt S, Emilsson K, Wahlestedt C, Sundelin J (1994) Molecular cloning of a potential proteinase activated receptor. Proc Natl Acad Sci USA 91:9208–9212
21. Grab D, Garcia-Garcia J, Nikolskaia O, Kim Y, Brown A, Pardo C, Zhang Y, Becker K, Wilson B, de Lima A, Scharfstein J, Dumler J (2009) Protease activated receptor signaling is required for African trypanosome traversal of human brain microvascular endothelial cells. PLoS Negl Trop Dis 3:e479
22. McCoy KL, Traynelis SF, Hepler JR (2010) PAR1 and PAR2 couple to overlapping and distinct sets of G proteins and linked signaling pathways to differentially regulate cell physiology. Mol Pharmacol 77:1005–1015
23. Sekiguchi F, Takaoka K, Kawabata A (2007) Proteinase-activated receptors in the gastrointestinal system: a functional linkage to prostanoids. Inflammopharmacology 15:246–251
24. Macfarlane S, Plevin R (2003) Intracellular signalling by the G-protein coupled proteinase-activated receptor (PAR) family. Drug Dev Res 59:367–374
25. Coelho A, Ossovskaya V, Bunnett N (2003) Proteinase-activated receptor-2: physiological and pathophysiological roles. Curr Med Chem Cardiovasc Hematol Agents 1:61–72
26. Kawabata A, Kawao N (2005) Physiology and pathophysiology of proteinase-activated receptors (PARs): PARs in the respiratory system: cellular signaling and physiological/pathological roles. J Pharmacol Sci 97:20–24
27. Soh UJ, Dores MR, Chen B, Trejo J (2010) Signal transduction by protease-activated receptors. Br J Pharmacol 160:191–203
28. Hollenberg MD (2005) Physiology and pathophysiology of proteinase-activated receptors (PARs): proteinases as hormone-like signal messengers: PARs and more. J Pharmacol Sci 97:8–13
29. Russo A, Soh UJ, Trejo J (2009) Proteases display biased agonism at protease-activated receptors: location matters! Mol Interv 9:87–96
30. Chen CH, Paing MM, Trejo J (2004) Termination of protease-activated receptor-1 signaling by beta-arrestins is independent of receptor phosphorylation. J Biol Chem 279:10020–10031
31. Ramachandran R, Mihara K, Mathur M, Rochdi MD, Bouvier M, Defea K, Hollenberg MD (2009) Agonist-biased signaling via proteinase activated receptor-2: differential activation of calcium and mitogen-activated protein kinase pathways. Mol Pharmacol 76:791–801
32. Ge L, Shenoy SK, Lefkowitz RJ, DeFea K (2004) Constitutive protease-activated receptor-2-mediated migration of MDA MB-231 breast cancer cells requires both beta-arrestin-1 and -2. J Biol Chem 279:55419–55424
33. Wang P, Jiang Y, Wang Y, Shyy JY, DeFea KA (2010) Beta-arrestin inhibits CAMKKbeta-dependent AMPK activation downstream of protease-activated-receptor-2. BMC Biochem 11:36
34. Zoudilova M, Kumar P, Ge L, Wang P, Bokoch GM, DeFea KA (2007) Beta-arrestin-dependent regulation of the cofilin pathway downstream of protease-activated receptor-2. J Biol Chem 282:20634–20646
35. Defea K (2008) Beta-arrestins and heterotrimeric G-proteins: collaborators and competitors in signal transduction. Br J Pharmacol 153(Suppl 1):S298–S309

36. Weis WI, Kobilka BK (2008) Structural insights into G-protein-coupled receptor activation. Curr Opin Struct Biol 18:734–740
37. Gether U, Kobilka BK (1998) G protein-coupled receptors. II. Mechanism of agonist activation. J Biol Chem 273:17979–17982
38. de Haën C (1976) The non-stoichiometric floating receptor model for hormone sensitive adenylyl cyclase. J Theor Biol 58:383–400
39. Jacobs S, Cuatrecasas P (1976) The mobile receptor hypothesis and "cooperativity" of hormone binding. Application to insulin. Biochim Biophys Acta 433:482–495
40. Kenakin T, Miller LJ (2010) Seven transmembrane receptors as shapeshifting proteins: the impact of allosteric modulation and functional selectivity on new drug discovery. Pharmacol Rev 62:265–304
41. Hung DT, Wong YH, Vu TK, Coughlin SR (1992) The cloned platelet thrombin receptor couples to at least two distinct effectors to stimulate phosphoinositide hydrolysis and inhibit adenylyl cyclase. J Biol Chem 267:20831–20834
42. Rahman A, True AL, Anwar KN, Ye RD, Voyno-Yasenetskaya TA, Malik AB (2002) Galpha(q) and Gbetagamma regulate PAR-1 signaling of thrombin-induced NF-kappaB activation and ICAM-1 transcription in endothelial cells. Circ Res 91:398–405
43. ten Cate H, Falanga A (2008) Overview of the postulated mechanisms linking cancer and thrombosis. Pathophysiol Haemost Thromb 36:122–130
44. Coughlin SR (2000) Thrombin signalling and protease-activated receptors. Nature 407: 258–264
45. Rao LV, Pendurthi UR (2005) Tissue factor-factor VIIa signaling. Arterioscler Thromb Vasc Biol 25:47–56
46. Belting M, Ahamed J, Ruf W (2005) Signaling of the tissue factor coagulation pathway in angiogenesis and cancer. Arterioscler Thromb Vasc Biol 25:1545–1550
47. Riewald M, Ruf W (2001) Mechanistic coupling of protease signaling and initiation of coagulation by tissue factor. Proc Natl Acad Sci USA 98:7742–7747
48. Schaffner F, Ruf W (2009) Tissue factor and PAR2 signaling in the tumor microenvironment. Arterioscler Thromb Vasc Biol 29:1999–2004
49. Borgoño CA, Diamandis EP (2004) The emerging roles of human tissue kallikreins in cancer. Nat Rev Cancer 4:876–890
50. Oikonomopoulou K, Diamandis EP, Hollenberg MD (2010) Kallikrein-related peptidases: proteolysis and signaling in cancer, the new frontier. Biol Chem 391:299–310
51. Oikonomopoulou K, Hansen KK, Saifeddine M, Tea I, Blaber M, Blaber SI, Scarisbrick I, Andrade-Gordon P, Cottrell GS, Bunnett NW, Diamandis EP, Hollenberg MD (2006) Proteinase-activated receptors, targets for kallikrein signaling. J Biol Chem 281:32095–32112
52. Trivedi V, Boire A, Tchernychev B, Kaneider NC, Leger AJ, O'Callaghan K, Covic L, Kuliopulos A (2009) Platelet matrix metalloprotease-1 mediates thrombogenesis by activating PAR1 at a cryptic ligand site. Cell 137:332–343
53. Even-Ram SC, Maoz M, Pokroy E, Reich R, Katz BZ, Gutwein P, Altevogt P, Bar-Shavit R (2001) Tumor cell invasion is promoted by activation of protease activated receptor-1 in cooperation with the alpha vbeta 5 integrin. J Biol Chem 276:10952–10962
54. Even-Ram S, Uziely B, Cohen P, Grisaru-Granovsky S, Maoz M, Ginzburg Y, Reich R, Vlodavsky I, Bar-Shavit R (1998) Thrombin receptor overexpression in malignant and physiological invasion processes. Nat Med 4:909–914
55. Wojtukiewicz MZ, Tang DG, Ben-Josef E, Renaud C, Walz DA, Honn KV (1995) Solid tumor cells express functional "tethered ligand" thrombin receptor. Cancer Res 55:698–704
56. Kaufmann R, Schafberg H, Rudroff C, Nowak G (1997) Thrombin receptor activation results in calcium signaling and protein kinase C-dependent stimulation of DNA synthesis in HEp-2g laryngeal carcinoma cells. Cancer 80:2068–2074
57. Rudroff C, Schafberg H, Nowak G, Weinel R, Scheele J, Kaufmann R (1998) Characterization of functional thrombin receptors in human pancreatic tumor cells (MIA PACA-2). Pancreas 16:189–194

58. Kaufmann R, Lindschau C, Höer A, Henklein P, Adomeit A, Haller H, Liebmann C, Oberdisse E, Nowak G (1996) Signaling effects of alpha-thrombin and SFLLRN in rat glioma C6 cells. J Neurosci Res 46:641–651
59. Schafberg H, Nowak G, Kaufmann R (1997) Thrombin has a bimodal effect on glioma cell growth. Br J Cancer 76:1592–1595
60. Kaufmann R, Patt S, Schafberg H, Kalff R, Neupert G, Nowak G (1998) Functional thrombin receptor PAR1 in primary cultures of human glioblastoma cells. Neuroreport 9:709–712
61. Zieger M, Tausch S, Henklein P, Nowak G, Kaufmann R (2001) A novel PAR-1-type thrombin receptor signaling pathway: cyclic AMP-independent activation of PKA in SNB-19 glioblastoma cells. Biochem Biophys Res Commun 282:952–957
62. Kaufmann R, Patt S, Kraft R, Zieger M, Henklein P, Neupert G, Nowak G (1999) PAR 1-type thrombin receptors are involved in thrombin-induced calcium signaling in human meningioma cells. J Neurooncol 42:131–136
63. Chay CH, Cooper CR, Gendernalik JD, Dhanasekaran SM, Chinnaiyan AM, Rubin MA, Schmaier AH, Pienta KJ (2002) A functional thrombin receptor (PAR1) is expressed on bone-derived prostate cancer cell lines. Urology 60:760–765
64. Darmoul D, Gratio V, Devaud H, Lehy T, Laburthe M (2003) Aberrant expression and activation of the thrombin receptor protease-activated receptor-1 induces cell proliferation and motility in human colon cancer cells. Am J Pathol 162:1503–1513
65. Nierodzik ML, Bain RM, Liu LX, Shivji M, Takeshita K, Karpatkin S (1996) Presence of the seven transmembrane thrombin receptor on human tumour cells: effect of activation on tumour adhesion to platelets and tumor tyrosine phosphorylation. Br J Haematol 92:452–457
66. Helland IB, Klementsen B, Jørgensen L (1997) Addition of both platelets and thrombin in combination accelerates tumor cells to adhere to endothelial cells in vitro. In Vitro Cell Dev Biol Anim 33:182–186
67. Klementsen B, Jørgensen L (1997) Distribution of adhesion molecules on HeLa cells, platelets and endothelium in an in vitro model mimicking the early phase of metastasis. An immunogold electron microscopic study. APMIS 105:546–558
68. Rudroff C, Seibold S, Kaufmann R, Zetina CC, Reise K, Schäfer U, Schneider A, Brockmann M, Scheele J, Neugebauer EA (2002) Expression of the thrombin receptor PAR-1 correlates with tumour cell differentiation of pancreatic adenocarcinoma in vitro. Clin Exp Metastasis 19:181–189
69. Nierodzik ML, Chen K, Takeshita K, Li JJ, Huang YQ, Feng XS, D'Andrea MR, Andrade-Gordon P, Karpatkin S (1998) Protease-activated receptor 1 (PAR-1) is required and rate-limiting for thrombin-enhanced experimental pulmonary metastasis. Blood 92:3694–3700
70. Henrikson KP, Salazar SL, Fenton JW, Pentecost BT (1999) Role of thrombin receptor in breast cancer invasiveness. Br J Cancer 79:401–406
71. Bergmann S, Junker K, Henklein P, Hollenberg MD, Settmacher U, Kaufmann R (2006) PAR-type thrombin receptors in renal carcinoma cells: PAR1-mediated EGFR activation promotes cell migration. Oncol Rep 15:889–893
72. Kaufmann R, Rahn S, Pollrich K, Hertel J, Dittmar Y, Hommann M, Henklein P, Biskup C, Westermann M, Hollenberg M, Settmacher U (2007) Thrombin-mediated hepatocellular carcinoma cell migration: cooperative action via proteinase-activated receptors 1 and 4. J Cell Physiol 211:699–707
73. Kaufmann R, Patt S, Zieger M, Kraft R, Tausch S, Henklein P, Nowak G (2000) The two-receptor system PAR-1/PAR-4 mediates alpha-thrombin-induced [Ca(2+)](i) mobilization in human astrocytoma cells. J Cancer Res Clin Oncol 126:91–94
74. Darmoul D, Gratio V, Devaud H, Laburthe M (2004) Protease-activated receptor 2 in colon cancer: trypsin-induced MAPK phosphorylation and cell proliferation are mediated by epidermal growth factor receptor transactivation. J Biol Chem 279:20927–20934
75. Hjortoe GM, Petersen LC, Albrektsen T, Sorensen BB, Norby PL, Mandal SK, Rao L (2004) Tissue factor-factor VIIa-specific up-regulation of IL-8 expression in MDA-MB-231 cells is mediated by PAR-2 and results in increased cell migration. Blood 103:3029–3037

76. Jikuhara A, Yoshii M, Iwagaki H, Mori S, Nishibori M, Tanaka N (2003) MAP kinase-mediated proliferation of DLD-1 carcinoma by the stimulation of protease-activated receptor 2. Life Sci 73:2817–2829
77. Shi X, Gangadharan B, Brass L, Ruf W, Mueller B (2004) Protease-activated receptors (PAR1 and PAR2) contribute to tumor cell motility and metastasis. Mol Cancer Res 2:395–402
78. Shimamoto R, Sawada T, Uchima Y, Inoue M, Kimura K, Yamashita Y, Yamada N, Nishihara T, Ohira M, Hirakawa K (2004) A role for protease-activated receptor-2 in pancreatic cancer cell proliferation. Int J Oncol 24:1401–1406
79. Rattenholl A, Seeliger S, Buddenkotte J, Schön M, Schön M, Ständer S, Vergnolle N, Steinhoff M (2007) Proteinase-activated receptor-2 (PAR2): a tumor suppressor in skin carcinogenesis. J Invest Dermatol 127:2245–2252
80. Morris DR, Ding Y, Ricks TK, Gullapalli A, Wolfe BL, Trejo J (2006) Protease-activated receptor-2 is essential for factor VIIa and Xa-induced signaling, migration, and invasion of breast cancer cells. Cancer Res 66:307–314
81. Versteeg H, Schaffner F, Kerver M, Petersen H, Ahamed J, Felding-Habermann B, Takada Y, Mueller B, Ruf W (2008) Inhibition of tissue factor signaling suppresses tumor growth. Blood 111:190–199
82. Bocheva G, Rattenholl A, Kempkes C, Goerge T, Lin C, D'Andrea M, Ständer S, Steinhoff M (2009) Role of matriptase and proteinase-activated receptor-2 in nonmelanoma skin cancer. J Invest Dermatol 129:1816–1823
83. Kaufmann R, Oettel C, Horn A, Halbhuber KJ, Eitner A, Krieg R, Katenkamp K, Henklein P, Westermann M, Bohmer FD, Ramachandran R, Saifeddine M, Hollenberg MD, Settmacher U (2009) Met receptor tyrosine kinase transactivation is involved in proteinase-activated receptor-2-mediated hepatocellular carcinoma cell invasion. Carcinogenesis 30:1487–1496
84. Gonda K, Watanabe TM, Ohuchi N, Higuchi H (2010) In vivo nano-imaging of membrane dynamics in metastatic tumor cells using quantum dots. J Biol Chem 285:2750–2757
85. Su S, Li Y, Luo Y, Sheng Y, Su Y, Padia RN, Pan ZK, Dong Z, Huang S (2009) Proteinase-activated receptor 2 expression in breast cancer and its role in breast cancer cell migration. Oncogene 28:3047–3057
86. Kamath L, Meydani A, Foss F, Kuliopulos A (2001) Signaling from protease-activated receptor-1 inhibits migration and invasion of breast cancer cells. Cancer Res 61:5933–5940
87. Blum AE, Joseph SM, Przybylski RJ, Dubyak GR (2008) Rho-family GTPases modulate Ca(2+) -dependent ATP release from astrocytes. Am J Physiol Cell Physiol 295:C231–C241
88. Darmoul D, Marie JC, Devaud H, Gratio V, Laburthe M (2001) Initiation of human colon cancer cell proliferation by trypsin acting at protease-activated receptor-2. Br J Cancer 85:772–779
89. Darmoul D, Gratio V, Devaud H, Peiretti F, Laburthe M (2004) Activation of proteinase-activated receptor 1 promotes human colon cancer cell proliferation through epidermal growth factor receptor transactivation. Mol Cancer Res 2:514–522
90. Gratio V, Walker F, Lehy T, Laburthe M, Darmoul D (2009) Aberrant expression of proteinase-activated receptor 4 promotes colon cancer cell proliferation through a persistent signaling that involves Src and ErbB-2 kinase. Int J Cancer 124:1517–1525
91. De Wever O, Mareel M (2003) Role of tissue stroma in cancer cell invasion. J Pathol 200:429–447
92. Micke P, Ostman A (2004) Tumour-stroma interaction: cancer-associated fibroblasts as novel targets in anti-cancer therapy? Lung Cancer 45(Suppl 2):S163–S175
93. Ostman A, Augsten M (2009) Cancer-associated fibroblasts and tumor growth–bystanders turning into key players. Curr Opin Genet Dev 19:67–73
94. Fukumura D, Xavier R, Sugiura T, Chen Y, Park EC, Lu N, Selig M, Nielsen G, Taksir T, Jain RK, Seed B (1998) Tumor induction of VEGF promoter activity in stromal cells. Cell 94:715–725
95. Vitolo D, Ciocci L, Cicerone E, Rossi C, Tiboni F, Ferrauti P, Gallo A, Baroni CD (2001) Laminin alpha2 chain (merosin M chain) distribution and VEGF, FGF(2), and TGFbeta1 gene expression in angiogenesis of supraglottic, lung, and breast carcinomas. J Pathol 195:197–208

96. Tuxhorn JA, McAlhany SJ, Dang TD, Ayala GE, Rowley DR (2002) Stromal cells promote angiogenesis and growth of human prostate tumors in a differential reactive stroma (DRS) xenograft model. Cancer Res 62:3298–3307
97. D'Andrea MR, Derian CK, Santulli RJ, Andrade-Gordon P (2001) Differential expression of protease-activated receptors-1 and -2 in stromal fibroblasts of normal, benign, and malignant human tissues. Am J Pathol 158:2031–2041
98. Blackburn JS, Brinckerhoff CE (2008) Matrix metalloproteinase-1 and thrombin differentially activate gene expression in endothelial cells via PAR-1 and promote angiogenesis. Am J Pathol 173:1736–1746
99. Wang W, Zhang X, Mize G, Takayama T (2008) Protease-activated receptor-I upregulates fibroblast growth factor 7 in stroma of benign prostatic hyperplasia. Prostate 68:1064–1075
100. Al-Ani B, Hewett P, Cudmore M, Fujisawa T, Saifeddine M, Williams H, Ramma W, Sissaoui S, Jayaraman P, Ohba M, Ahmad S, Hollenberg M, Ahmed A (2010) Activation of proteinase-activated receptor 2 stimulates soluble vascular endothelial growth factor receptor 1 release via epidermal growth factor receptor transactivation in endothelial cells. Hypertension 55(3): 689–697
101. Nakanuma S, Tajima H, Okamoto K, Hayashi H, Nakagawara H, Onishi I, Takamura H, Kitagawa H, Fushida S, Tani T, Fujimura T, Kayahara M, Ohta T, Wakayama T, Iseki S, Harada S (2010) Tumor-derived trypsin enhances proliferation of intrahepatic cholangiocarcinoma cells by activating protease-activated receptor-2. Int J Oncol 36:793–800
102. Zhang X, Wang W, True L, Vessella R, Takayama T (2009) Protease-activated receptor-1 is upregulated in reactive stroma of primary prostate cancer and bone metastasis. Prostate 69:727–736
103. Amann T, Bataille F, Spruss T, Mühlbauer M, Gäbele E, Schölmerich J, Kiefer P, Bosserhoff A, Hellerbrand C (2009) Activated hepatic stellate cells promote tumorigenicity of hepatocellular carcinoma. Cancer Sci 100:646–653
104. Grynkiewicz G, Poenie M, Tsien R (1985) A new generation of Ca2+ indicators with greatly improved fluorescence properties. J Biol Chem 260:3440–3450
105. Gee K, Brown K, Chen W, Bishop-Stewart J, Gray D, Johnson I (2000) Chemical and physiological characterization of fluo-4 Ca(2+)-indicator dyes. Cell Calcium 27:97–106
106. Bootman M, Collins T, Peppiatt C, Prothero L, MacKenzie L, De Smet P, Travers M, Tovey S, Seo J, Berridge M, Ciccolini F, Lipp P (2001) Calcium signalling–an overview. Semin Cell Dev Biol 12:3–10
107. Berridge M, Bootman M, Roderick H (2003) Calcium signalling: dynamics, homeostasis and remodelling. Nat Rev Mol Cell Biol 4:517–529
108. Clapham D (2007) Calcium signaling. Cell 131:1047–1058
109. Carafoli E (2002) Calcium signaling: a tale for all seasons. Proc Natl Acad Sci USA 99:1115–1122
110. Rizzuto R, Pozzan T (2006) Microdomains of intracellular Ca2+: molecular determinants and functional consequences. Physiol Rev 86:369–408
111. Brown EM, Pollak M, Hebert SC (1998) The extracellular calcium-sensing receptor: its role in health and disease. Annu Rev Med 49:15–29
112. Brown EM, Pollak M, Chou YH, Seidman CE, Seidman JG, Hebert SC (1995) Cloning and functional characterization of extracellular Ca(2+)-sensing receptors from parathyroid and kidney. Bone 17:7S–11S
113. Gutkind JS (1998) Cell growth control by G protein-coupled receptors: from signal transduction to signal integration. Oncogene 17:1331–1342
114. Cabrera-Vera TM, Vanhauwe J, Thomas TO, Medkova M, Preininger A, Mazzoni MR, Hamm HE (2003) Insights into G protein structure, function, and regulation. Endocr Rev 24:765–781
115. Spiegelberg BD, Hamm HE (2007) Roles of G-protein-coupled receptor signaling in cancer biology and gene transcription. Curr Opin Genet Dev 17:40–44
116. Abdul M, Ramlal S, Hoosein N (2008) Ryanodine receptor expression correlates with tumor grade in breast cancer. Pathol Oncol Res 14:157–160

117. Jaffe LF (2005) A calcium-based theory of carcinogenesis. Adv Cancer Res 94:231–263
118. Monteith GR, McAndrew D, Faddy HM, Roberts-Thomson SJ (2007) Calcium and cancer: targeting Ca2+ transport. Nat Rev Cancer 7:519–530
119. Capiod T, Shuba Y, Skryma R, Prevarskaya N (2007) Calcium signalling and cancer cell growth. Subcell Biochem 45:405–427
120. Roderick HL, Cook SJ (2008) Ca2+ signalling checkpoints in cancer: remodelling Ca2+ for cancer cell proliferation and survival. Nat Rev Cancer 8:361–375
121. Denmeade SR, Isaacs JT (2005) The SERCA pump as a therapeutic target: making a "smart bomb" for prostate cancer. Cancer Biol Ther 4:14–22
122. Kaddour-Djebbar I, Choudhary V, Brooks C, Ghazaly T, Lakshmikanthan V, Dong Z, Kumar MV (2010) Specific mitochondrial calcium overload induces mitochondrial fission in prostate cancer cells. Int J Oncol 36:1437–1444
123. McCubrey JA, Abrams SL, Stadelman K, Chappell WH, Lahair M, Ferland RA, Steelman LS (2010) Targeting signal transduction pathways to eliminate chemotherapeutic drug resistance and cancer stem cells. Adv Enzyme Regul 50:285–307
124. Lin J, Denmeade S, Carducci MA (2009) HIF-1alpha and calcium signaling as targets for treatment of prostate cancer by cardiac glycosides. Curr Cancer Drug Targets 9:881–887
125. Turner JS, Redpath GT, Humphries JE, Gonias SL, Vandenberg SR (1994) Plasmin modulates the thrombin-evoked calcium response in C6 glioma cells. Biochem J 297(Pt 1): 175–179
126. Kawabata A, Saifeddine M, Al-Ani B, Leblond L, Hollenberg MD (1999) Evaluation of proteinase-activated receptor-1 (PAR1) agonists and antagonists using a cultured cell receptor desensitization assay: activation of PAR2 by PAR1-targeted ligands. J Pharmacol Exp Ther 288:358–370
127. Kaufmann R, Schafberg H, Nowak G (1998) Proteinase-activated receptor-2-mediated signaling and inhibition of DNA synthesis in human pancreatic cancer cells. Int J Pancreatol 24:97–102
128. Kaufmann R, Junker U, Nuske K, Westermann M, Henklein P, Scheele J, Junker K (2002) PAR-1- and PAR-3-type thrombin receptor expression in primary cultures of human renal cell carcinoma cells. Int J Oncol 20:177–180
129. Kanno H, Horikawa Y, Hodges R, Zoukhri D, Shatos M, Rios J, Dartt D (2003) Cholinergic agonists transactivate EGFR and stimulate MAPK to induce goblet cell secretion. Am J Physiol Cell Physiol 284:C988–C998
130. Hodges R, Horikawa Y, Rios J, Shatos M, Dartt D (2007) Effect of protein kinase C and Ca(2+) on p42/p44 MAPK, Pyk2, and Src activation in rat conjunctival goblet cells. Exp Eye Res 85:836–844
131. Ramsay AJ, Dong Y, Hunt ML, Linn M, Samaratunga H, Clements JA, Hooper JD (2008) Kallikrein-related peptidase 4 (KLK4) initiates intracellular signaling via protease-activated receptors (PARs). KLK4 and PAR-2 are co-expressed during prostate cancer progression. J Biol Chem 283:12293–12304
132. Gearhart T, Bouchard M (2010) The hepatitis B virus X protein modulates hepatocyte proliferation pathways to stimulate viral replication. J Virol 84:2675–2686
133. Kaufmann R, Mußbach F, Henklein P, Settmacher U (2011) Proteinase-activated receptor 2-mediated calcium signaling in hepatocellular carcinoma cells. J Cancer Res Clin Oncol 137(6):965–973
134. Huynh H, Nguyen T, Chow K, Tan P, Soo K, Tran E (2003) Over-expression of the mitogen-activated protein kinase (MAPK) kinase (MEK)-MAPK in hepatocellular carcinoma: its role in tumor progression and apoptosis. BMC Gastroenterol 3:19
135. Tsuboi Y, Ichida T, Sugitani S, Genda T, Inayoshi J, Takamura M, Matsuda Y, Nomoto M, Aoyagi Y (2004) Overexpression of extracellular signal-regulated protein kinase and its correlation with proliferation in human hepatocellular carcinoma. Liver Int 24:432–436
136. Klein P, Schmidt C, Wiesenauer C, Choi J, Gage E, Yip-Schneider M, Wiebke E, Wang Y, Omer C, Sebolt-Leopold J (2006) The effects of a novel MEK inhibitor PD184161 on MEK-ERK signaling and growth in human liver cancer. Neoplasia 8:1–8

137. Calvisi D, Pascale R, Feo F (2007) Dissection of signal transduction pathways as a tool for the development of targeted therapies of hepatocellular carcinoma. Rev Recent Clin Trials 2:217–236
138. Berridge MJ, Irvine RF (1989) Inositol phosphates and cell signalling. Nature 341:197–205
139. Berridge MJ, Rapp PE (1979) A comparative survey of the function, mechanism and control of cellular oscillators. J Exp Biol 81:217–279
140. Berridge MJ (2007) Inositol trisphosphate and calcium oscillations. Biochem Soc Symp 74:1–7
141. Seatter MJ, Drummond R, Kanke T, Macfarlane SR, Hollenberg MD, Plevin R (2004) The role of the C-terminal tail in protease-activated receptor-2-mediated Ca2+ signalling, proline-rich tyrosine kinase-2 activation, and mitogen-activated protein kinase activity. Cell Signal 16:21–29
142. Chen X, Berrou J, Vigneau C, Rondeau E (2001) Role of the third intracellular loop and of the cytoplasmic tail in the mitogenic signaling of the protease-activated receptor 1. Int J Mol Med 8:309–314
143. Goh FG, Ng PY, Nilsson M, Kanke T, Plevin R (2009) Dual effect of the novel peptide antagonist K-14585 on proteinase-activated receptor-2-mediated signalling. Br J Pharmacol 158:1695–1704
144. Covic L, Gresser AL, Talavera J, Swift S, Kuliopulos A (2002) Activation and inhibition of G protein-coupled receptors by cell-penetrating membrane-tethered peptides. Proc Natl Acad Sci USA 99:643–648
145. Tressel SL, Koukos G, Tchernychev B, Jacques SL, Covic L, Kuliopulos A (2011) Pharmacology, biodistribution, and efficacy of GPCR-based pepducins in disease models. Methods Mol Biol 683:259–275
146. Yang E, Boire A, Agarwal A, Nguyen N, O'Callaghan K, Tu P, Kuliopulos A, Covic L (2009) Blockade of PAR1 signaling with cell-penetrating pepducins inhibits Akt survival pathways in breast cancer cells and suppresses tumor survival and metastasis. Cancer Res 69:6223–6231
147. Covic L, Misra M, Badar J, Singh C, Kuliopulos A (2002) Pepducin-based intervention of thrombin-receptor signaling and systemic platelet activation. Nat Med 8:1161–1165
148. Agarwal A, Covic L, Sevigny LM, Kaneider NC, Lazarides K, Azabdaftari G, Sharifi S, Kuliopulos A (2008) Targeting a metalloprotease-PAR1 signaling system with cell-penetrating pepducins inhibits angiogenesis, ascites, and progression of ovarian cancer. Mol Cancer Ther 7:2746–2757
149. Sevigny LM, Zhang P, Bohm A, Lazarides K, Perides G, Covic L, Kuliopulos A (2011) Interdicting protease-activated receptor-2-driven inflammation with cell-penetrating pepducins. Proc Natl Acad Sci USA 108(20):8491–8496
150. Iida-Klein A, Guo J, Takemura M, Drake MT, Potts JT, Abou-Samra A, Bringhurst FR, Segre GV (1997) Mutations in the second cytoplasmic loop of the rat parathyroid hormone (PTH)/PTH-related protein receptor result in selective loss of PTH-stimulated phospholipase C activity. J Biol Chem 272:6882–6889
151. Cotecchia S, Ostrowski J, Kjelsberg MA, Caron MG, Lefkowitz RJ (1992) Discrete amino acid sequences of the alpha 1-adrenergic receptor determine the selectivity of coupling to phosphatidylinositol hydrolysis. J Biol Chem 267:1633–1639
152. Estall JL, Koehler JA, Yusta B, Drucker DJ (2005) The glucagon-like peptide-2 receptor C terminus modulates beta-arrestin-2 association but is dispensable for ligand-induced desensitization, endocytosis, and G-protein-dependent effector activation. J Biol Chem 280:22124–22134
153. Budd DC, McDonald J, Emsley N, Cain K, Tobin AB (2003) The C-terminal tail of the M3-muscarinic receptor possesses anti-apoptotic properties. J Biol Chem 278:19565–19573
154. Wess J, Bonner TI, Brann MR (1990) Chimeric m2/m3 muscarinic receptors: role of carboxyl terminal receptor domains in selectivity of ligand binding and coupling to phosphoinositide hydrolysis. Mol Pharmacol 38:872–877
155. Dowal L, Sim DS, Dilks JR, Blair P, Beaudry S, Denker BM, Koukos G, Kuliopulos A, Flaumenhaft R (2011) Identification of an antithrombotic allosteric modulator that acts through helix 8 of PAR1. Proc Natl Acad Sci USA 108:2951–2956

156. García-López MT, Gutiérrez-Rodríguez M, Herranz R (2010) Thrombin-activated receptors: promising targets for cancer therapy? Curr Med Chem 17:109–128
157. O'Donoghue ML, Bhatt DL, Wiviott SD, Goodman SG, Fitzgerald DJ, Angiolillo DJ, Goto S, Montalescot G, Zeymer U, Aylward PE, Guetta V, Dudek D, Ziecina R, Contant CF, Flather MD, Investigators obotLA (2011) Safety and tolerability of atopaxar in the treatment of patients with acute coronary syndromes: the lessons from antagonizing the cellular effects of thrombin-acute coronary syndromes trial. Circulation 123(17):1843–1853
158. Leonardi S, Tricoci P, Mahaffey KW (2012) Promises of PAR-1 inhibition in acute coronary syndrome. Curr Cardiol Rep 14(1):32–39
159. Wiviott SD, Flather MD, O'Donoghue ML, Goto S, Fitzgerald DJ, Cura F, Aylward P, Guetta V, Dudek D, Contant CF, Angiolillo DJ, Bhatt DL, Investigators obotLC (2011) Randomized trial of atopaxar in the treatment of patients with coronary artery disease: the lessons from antagonizing the cellular effect of thrombin-coronary artery disease trial. Circulation 123(17): 1854–1863
160. Barry GD, Suen JY, Le GT, Cotterell A, Reid RC, Fairlie DP (2010) Novel agonists and antagonists for human protease activated receptor 2. J Med Chem 53:7428–7440
161. Ghali J, Smith W, Torre-Amione G, Haynos W, Rayburn B, Amato A, Zhang D, Cowart D, Valentini G, Carminati P, Gheorghiade M (2007) A phase 1–2 dose-escalating study evaluating the safety and tolerability of istaroxime and specific effects on electrocardiographic and hemodynamic parameters in patients with chronic heart failure with reduced systolic function. Am J Cardiol 99:47A–56A
162. Triposkiadis F, Parissis JT, Starling RC, Skoularigis J, Louridas G (2009) Current drugs and medical treatment algorithms in the management of acute decompensated heart failure. Expert Opin Investig Drugs 18:695–707
163. Talukder MA, Zweier JL, Periasamy M (2009) Targeting calcium transport in ischaemic heart disease. Cardiovasc Res 84:345–352
164. Duncan RS, Goad DL, Grillo MA, Kaja S, Payne AJ, Koulen P (2010) Control of intracellular calcium signaling as a neuroprotective strategy. Molecules 15:1168–1195
165. Roberts L, Gores G (2005) Hepatocellular carcinoma: molecular pathways and new therapeutic targets. Semin Liver Dis 25:212–225
166. Beeram M, Patnaik A (2002) Targeting intracellular signal transduction. A new paradigm for a brave new world of molecularly targeted therapeutics. Hematol Oncol Clin North Am 16:1089–1100
167. Levitzki A, Klein S (2010) Signal transduction therapy of cancer. Mol Aspects Med 31: 287–329
168. Wilhelm S, Chien DS (2002) BAY 43-9006: preclinical data. Curr Pharm Des 8:2255–2257
169. Sharma PS, Sharma R, Tyagi T (2011) VEGF/VEGFR pathway inhibitors as anti-angiogenic agents: present and future. Curr Cancer Drug Targets 11(5):624–653

Chapter 46
Mechanosensory Calcium Signaling

Thomas J. Jones and Surya M. Nauli

Abstract Mechanotransduction describes the cellular process by which mechanical stimuli are translated into intracellular adaptive responses through biochemical signals. Current research has begun to focus on the once-forgotten organelle, the primary cilia, in this mechanotransduction process. Primary cilia are found on almost every cell type, with a functional role in transducing mechanical and extracellular signals towards intracellular responses through the ciliary extension into the extracellular space. In this regard, the modulation of intracellular calcium signaling by various mechanical stimuli has generated an assortment of attractive models to understand this mechanotransduction process.

Keywords Cardiovascular • Polycystic kidney disease • Primary cilia • Sensory cilium

Introduction

Abnormal cellular responses to stress, whether mechanical, chemical, gravitational, temperature or radiation, have the ability to contribute to pathology. Much work has been done in recent years to address the physiological and pathological signaling involved in these transduction pathways, with the goal contributing to innovative therapeutic approaches. In particular, work focusing on mechanotransduction has contributed to an understanding of various disease etiologies including

T.J. Jones • S.M. Nauli, Ph.D. (✉)
Department of Pharmacology, The University of Toledo, Health Science Campus; HEB 274, 3000 Arlington Ave.; MS 1015, Toledo, OH 43614, USA

Departments of Pharmaceutical Sciences, Northeastern Ohio Universities Colleges of Medicine and Pharmacy, Rootstown, OH 44272, USA
e-mail: Surya.Nauli@UToledo.Edu

M.S. Islam (ed.), *Calcium Signaling*, Advances in Experimental Medicine and Biology 740, DOI 10.1007/978-94-007-2888-2_46,

cardiovascular disease, diabetes, the encompassing metabolic syndrome. Mechanical forces have been found to be an important and at times critical regulator of various cellular and molecular processes that can contribute to disease development. Here we discuss the role of calcium as a signal transduction ion involved in many of these physiological responses.

Calcium Signaling

Calcium signaling regulates a large number of signaling pathways and can be considered a multipurpose intracellular signaling molecule. Calcium signaling is important for gene expression, neurotransmitter release, synaptic transmission, muscle contraction, metabolism, proliferation, fertilization, and many other processes. Cytosolic calcium is buffered by the intraorganellar store and the extracellular content (Fig. 46.1). Within the intraorganellar store, there are two calcium release channels that predominantly coordinate intracellular calcium signaling

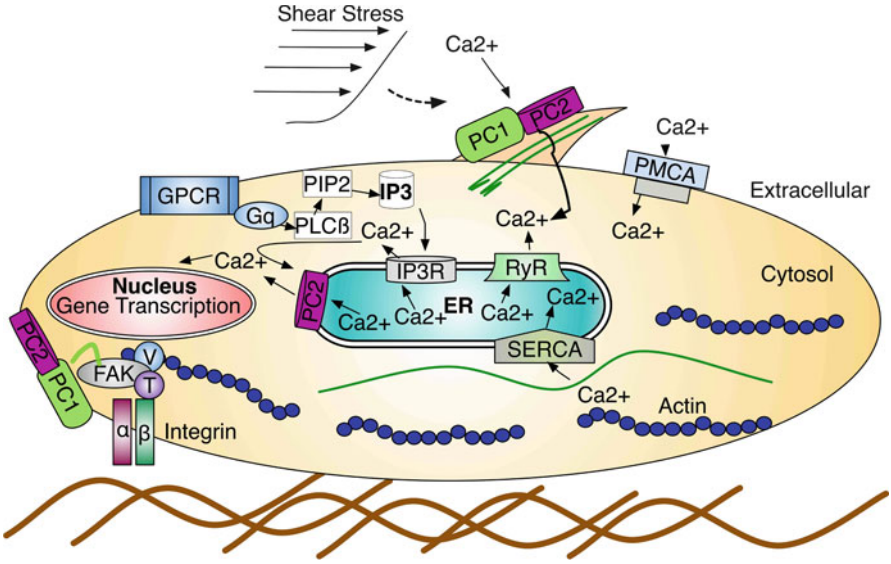

Fig. 46.1 Schematic diagram of mechanotransduction-induced Ca^{2+} signaling in the cell. Shown on the apical membrane are the plasma membrane Ca^{2+}-ATPase (*PMCA*), G-coupled protein receptor (*GPCR*), and primary cilium. On the ciliary membrane, polycystin-1 (*PC1*) and polycystin-2 (*PC2*) interact through their coiled-coil domains. When the cilium senses flow, polycystin-1 is activated which opens polycystin-2 channel, allowing entry of Ca^{2+} from extracellular space into the cytosol. This initial Ca^{2+} entry can activate the ryanodine receptor (*RyR*) via Ca^{2+}-induced Ca^{2+} release mechanism. When membrane bound *GPCRs* are activated, they activate Gq which stimulates phospholipase C beta (*PLCβ*) to break down phosphatidylinositol-4,5-bisphosphate (*PIP2*) into inositol 1,4,5-trisphosphate (IP_3) and diacylglycerol (*DAG*). IP_3 can then bind the IP_3 receptor (*IP3R*) and release Ca^{2+} from the endoplasmic reticulum (*ER*) into the cytosol. Ca^{2+} release through the *IP3R* can further activate polycystin-2 to potentiate Ca^{2+} release from the *ER* stores

with regard to mechanosensing [1]. These receptor ion channels include inositol 1,4,5-trisphosphate (IP3R) and ryanodine (RyR) receptors. In response to mechanical forces, both channels are associated with or regulated by mTOR [2], polycystin-1 [3], polycystin-2 [4], and purinergic receptors [5].

Movement of calcium into the cell from extracellular spaces can occur in response to stimulation by stretch or shear stress. Additionally, these mechanical stimulations have the ability to trigger and activate the IP3Rs and RyRs, stimulating the release of calcium from intracellular endoplasmic reticulum stores [6–8]. Overall cytosolic concentration is determined by extracellular calcium entry and intraorganellar calcium release [1].

The endothelial influx of the extracellular calcium in response to mechanical stimuli is considered to be one of the fastest transitions to occur. When stimulated (Fig. 46.1), the plasma membrane allows the entry of calcium through three different types of calcium channels: stretch-activated, store-operated, or voltage-operated [9, 10]. The calcium channels most closely associated with the endothelium are the transient receptor potential (TRP) channels along with the P2X4 purinoceptors. Additionally, intracellular calcium levels can be boosted by calcium release from intracellular stores. The endoplasmic reticulum stores the vast majority of intracellular calcium, with the mitochondria also capable of functioning as high-capacity calcium store [11].

The release of intracellular calcium can occur in response to mechanical stress-induced activation of the IP3R and RyR [12]. IP3Rs are stimulated by inositol 1,4,5-trisphosphate (IP3), which triggers the rapid release of stored calcium. IP3 itself, is produced through the activation of G protein-coupled receptors (GPCRs), activated PLC-beta, or receptor tyrosine kinases (RTK's) signaling to PLC-gamma [13–19]. Intercellular calcium levels are buffered through the movement of intracellular calcium to the extracellular space by the calcium ATPase Na^{+}/Ca^{2+} exchanger and/or through sarcoplasmic reticulum Ca^{+2}-ATPase (SERCA) pump mediated redistribution into the intraorganellar stores (Fig. 46.1).

The endothelial actions of shear and mechanical stimuli on extracellular and intracellular calcium flux provides us an opportunity to look at mechanotransduction and calcium signaling [18]. The Endothelium lining the lumen of vasculature is a focal point of shear and mechanical stress. Its response to shear mediating calcium fluxes through both ligand-independent and -dependent pathways.

Mechanotransduction by Primary Cilia

Mechanotransduction describes the process of converting physical forces into biological signals. Mechanotransduction is diverse and includes osteoblast proliferation and cartilage synthesis in response to exercise [18, 20], feeding induced shear stimulating gut mucosal proliferation [21], and mechanical stress in cardiac tissue leading to myocyte hypertrophy [22]. The primary cilium has been considered a key signaling organelle capable of responding to both chemical and mechanical stimuli [23].

The structural component responsible for this characteristic is cilia length [24], which is responsive to shear [25, 26]. Additionally, these mechanosensitve responses can be impeded by the absence of or abnormal incidence of stress. An example of this is seen in the primary cilium disassembly that has been observed [27] under conditions of high or disturbed oscillatory flow which can contribute to the developing atherosclerotic lesions [28, 29]. This phenomenon parallels the clinical observations of cardiovascular dysfunction and increased risk of hypertension in patients with polycystic kidney disease [30].

The endothelial primary cilia form a direct connection to the extracellular environment in addition to an indirect connection through their association with the glycocalyx or outermost boundary of the cell [31, 32]. Primary cilia directly connected to the cytoskeleton through the basal body and interact with integrins and the extracellular matrix [33, 34]. This cytoskeletal interaction provides an uninterrupted link between the extracellular environment and cellular remodeling [35, 36]. The most studied ciliary signaling components revolve around their ability to flex or bend. This mechanical movement induces responses in various signaling pathways including mTOR [37], PDGF receptor α (PDGFRα) [38], and the purinergic receptor family [39]. The eventual outcome of these signaling pathways can be the initiation of calcium transients [40, 41].

Polycystin in Calcium Signaling

Calcium signaling through the primary cilia has been studied robustly in polycystic kidney disease and can be reviewed in the work performed by Surya Nauli, in conjunction with Donald Ingber and Jing Zhou [42, 43]. Their work demonstrated polycystin-1 and -2 signaling does contribute to PKD, in addition to some of its associated cardiovascular abnormalities.

The observed changes in intracellular calcium are dependent on the localization of polycystin-1 and -2 to the primary cilia [44, 45]. The mechanosensing ability of primary cilia is important in the onset and development of a wide collection of disease states, termed “ciliopathies” [46]. These diseases range from the dominant and recessive forms of polycystic kidney disease (PKD) to Bardet–Biedl syndrome (BBS). Ciliopathies themselves tend to involve multisystem pathology with polycystic kidney and liver disease being a commonality between them. One of the most studied ciliopathies is BBS, which involves obesity, Type 2 diabetes, hypertension, and cardiovascular disease. This global involvement of systems makes it a good candidate for understanding metabolic syndrome. The cystic kidney phenotype, on the other hand, is detected in all ciliopathies, although defects in polycystin-1 and/or -2 are most commonly seen in the dominant form of PKD. The commonality in phenotypes of cilia defects demonstrates the importance of this organelle in the progression and development of the ciliopathy family of diseases.

Polycystin-1 and polycystin-2 constitute a mechanosensitive heterodimeric calcium channel [47–49]. Mechanical bending or fluid flow-induced stimulation of

the primary cilium initiates the influx of extracellular calcium (Fig. 46.1), with the signal dispersion to adjacent cells through paracrine signaling [50]. However, polycystin-2 is also found in multiple intracellular compartments, with its highest concentration in the endoplasmic reticulum [51]. The C-terminal domain of polycystin-2 contains an endoplasmic reticulum retention sequence that prevents membrane trafficking in the absence of polycystin-1 [47, 48, 52]. In the intracellular compartments, polycystin-2 acts as a calcium release channel that can intensify calcium transients and mediate the calcium-induced calcium release seen in the IP3 and ryanodine receptors [47, 53]. However, when polycystin-2 is located on the cell surface, the increase in intracellular calcium results from the influx of extracellular calcium [54].

Mechanotransduction by Calcium

The transient receptor potential (TRP) superfamily of proteins can regulate calcium entry and activity and is grouped into seven categories based on sequence homology and multimeric state. Dimerization, however, is the most common and harbors a predisposition to enhance channel activity [55]. TRPP2 (or polycystin-2) is one of these channels. It has the ability to dimerize and interact, through its COOH terminals, with polycystin-1 forming the primary cilia mechanosensitive calcium channel complex [47, 49, 56]. Polycystin-2 itself, has substantial homology with the TRPC transient receptor potential (TRP) channels [57].

The polycystin-1 and -2 heterodimeric calcium channel is opened by the mechanical bending of the cilia initiating extracellular calcium entry and calcium-induced calcium release from ryanodine-regulated intracellular stores [42]. The physiological effect of endothelial calcium changes is seen in the augmentation of various cellular responses. The endothelium however, can also mediate calcium influx through ligand-dependent pathways, such as GPCR signaling of bradykinin 2 (BK-2) [58]. Stress can induce the ligand-dependent activation of BK-2, which in turn releases calcium from intracellular stores by the activation of PLC and the production of DAG. The consequence of the depletion in calcium stores is the influx of extracellular calcium by store-operated calcium channels [59] or from store-independent channels like bradykinin [60]. Alternatively, calcium can enter the cell through the actions of various mechanical sensitivity cell surface proteins [61, 62].

Integrin Signaling

The extracellular matrix (ECM) is an important component in cellular mechanotransduction. In response to shear-induced increases in cytosolic calcium the ECM interacts with the integrin family of proteins. This interaction contributes to the

number of cellular adhesions to the substrate and diffuses the magnitude of the stress throughout the cell [35]. An example of this can be seen in coronary arteries where shear stress provokes an integrin-matrix interaction that, through focal adhesions, elicits coronary vasodilation [63].

The integrin family comprises a linage of transmembrane proteins containing alpha and beta subunits. Their extracellular domains bind to multiple components on the matrix including fibronectin, vitronectin, and collagen. Their cytoplasmic domains can interact with multiple signaling molecules including focal adhesion kinase (FAK), c-Src of focal adhesions (FA), and the cytoskeletal proteins talin and alpha actinin [61]. The ability of integrins to connect the extracellular space to intracellular compartments allows for an uninterrupted passage of extracellular mechanical signals to the cytoskeleton and contributing to gene expression. Integrins also stabilize cells against various mechanical stresses through the formation of focal adhesions [22, 35, 64].

Integrins can mediate the endothelial response to mechanical forces by augmenting cell membrane permeability and proliferation, in addition to cellular alignment and migration [61, 65]. Co-localization studies have demonstrated that alpha2beta1 integrins interact with polycystin-1 [66] in addition to members of the focal adhesion complex [67]. The focal adhesions regulate the cellular adaptive response through cytoskeletal-dependent actions and are the site of ECM-actin cytoskeleton contact [68]. Cellular calcium levels play a role in this response by contributing to the association of the mechanosensitive polycystin-1 protein and integrins. As calcium levels increase, the association of polycystin-1 with E-cadherin and beta-catenin also increases. This association of polycystin-1 with E-cadherin and beta-catenin predominantly occurs during development and migration, while polycystin-1 and FAK association occurs mostly in adult tissue [67].

Cytoskeleton

A key to regulating cytoskeletal proteins is intracellular calcium signaling. The cytoskeletal protein, α-actinin, is a mechanosensory protein that is strongly influenced by calcium. This family of proteins links transmembrane proteins to the cytoskeleton, enabling them to function as a signaling conduit connecting the cytoskeleton to various signaling pathways [69]. Another calcium-regulated cytoskeletal protein is gelsolin. It is involved in actin growth, remodeling, and cell apoptosis. Gelsolin functions to regulate cytoskeletal remodeling by severing the actin filaments and controlling filament elongation though its capping function. Gelsolin's activity is regulated by calcium and phosphatidylinositol 4,5-bisphosphate [70]. Cell adhesions and contractility are also highly regulated by intracellular calcium [71]. Cells' adhesion to other cells and to the substrate determines not only the shape of the cell but also its ability to move. The ability of a cell to migrate in a specific direction is determined by the concentration of calcium at the cell's leading migratory edge [72]. Additionally, the turning ability of that cell in response to stimuli is controlled in part by calcium.

The highest microdomain concentration of calcium is located at a cell's leading edge and directs the ability to turn [73].

Cell morphology is likewise influenced by calcium. Generally, cells maintained under normal, static conditions adopt a consistent cobblestone cellular morphology [74]. However, in response to flow-shear stress, substantial remodeling and adaptations occur, usually in the direction of the flow [75]. The goal of these changes is to adapt capacity of cells to respond to the stressful environments. An example of this can be seen when cells are exposed to mechanical stress. The induction of force upon the cell induces a time-dependent alignment and promotes a change in cell shape from "polygonal to ellipsoidal" [76]. These changes compelled by the restructuring and adaptation of the cytoskeleton. The cytoskeleton, under conditions of mechanical stress, functions to redistribute the localized mechanical forces throughout the entire cell by rearranging the intermediate filament network. Cytoskeletal changes are then communicated to adjacent cells though tight junctions. The formation of tight junctions generates a focal point for mechanical stresses, like flow, to induce cellular realignment and initiate a cellular tension that is propagated through the monolayer [77, 78]. Cytoskeletal changes are not limited to tight junction but can also be seen in reorganization of actin filaments and their attachment to and formation of focal adhesions [79, 80]. The response of the actin cytoskeleton is typically to reorient and form stress fibers in the direction of the mechanical force.

Mechanical forces imposed upon a cellular network tend to initiate change in the levels of intracellular calcium. Endothelial cells, which have tight junctions oriented in the direction of flow, have a reduced intracellular calcium response compared to cells with tight junctions oriented in the opposite direction [81]. This demonstrates a preconditioned response of "oriented" cells to flow. This orientation-dependent calcium response directly exposes a connection between cells' mechanotransduction ability and tight junctions of the cytoskeleton. It further shows that a cells structural adaptability to shear stress results in a reduction in mechanosensitivity. This observation is consistent with the clinical model in which atherosclerotic lesions tend to develop in areas of disturbed flow and are rarely seen in regions of consistent laminar flow [82]. This postulates that the cellular adaptability to mechanical shear invokes a protective effect upon the cell and tissues, which has been termed atheroprotective [83]. In areas of disturbed flow, the inefficiency in a cell's adaptability increased the mitogenic and pathologic potential of the cell [84]. Consistent with this view, primary cilia are found to be located at the atherosclerotic predilection sites, where flow is disturbed [29].

The modification of cellular shape in response to mechanical forces through calcium is of great importance in the field of vascular biology. Changes in cell shape are an adaptive response to long-term shear stress [85, 86]. The primary cilium contributes to this response by amplifying mechanical cues, at least in endothelial cells. Poelmann et al. suggested that this adaptive signaling is a two-step process [87, 88]; the immediate response involves primary cilium signaling and polycystin complex-mediating calcium signaling, and the long-term response is associated with cellular adaptation and cytoskeletal changes. In response to shear stress, vasoactive gene expression is modified with the aim of alleviating the stress.

An example of this is seen with Kruppel-like factor-2 (*KLF2/LKLF*). KLF2 expression is enhanced under mechano-induced stress and modulates the expression of endothelin-1 [89, 90]. Endotehlin-1 is down-regulated in the areas of high and pulsatile flow, while eNOS expression is up-regulated [91]. When KLF2 expression is down-regulated, in those areas of oscillatory or disturbed flow, there is a tendency toward the development of atherosclerosis [92]. Consistent with this, the expression of primary cilia is down-regulated in these areas of disturbed flow, with an increase also in the inflammatory response that contributes to plaque formation. However, in areas of extreme shear stress cells tend to disassemble their cilia [27].

Nucleus

Mechanical stress can also influence the structural component of the nucleus [93]. Cells exposed to various mechanical stresses tend to increase their cell rigidity as a form of cellular adaptation [94, 95]. This change in cellular stiffness is also seen in the nucleus. The nucleus does adapt and change in response to mechanical forces. It spreads and elongates in response to flow [96]. Nuclear changes also alter chromosome assembly [97] and gene expression [98]. Changes in cellular chromosome structure and gene expression also extended to changes in cell growth and differentiation [99]. Maniotis et al. explains the continuity in the cellular, cytoskeletal, and nuclear changes by pointing out that the ECM, the actin cytoskeleton, and the nuclear compartment are connected [100]. This "connection" facilitates the ability for ECM strain to transmit any tension imposed upon it throughout the cell and nucleus [95, 100, 101]. However, this continuity of whole-cell stress signaling is not the only accepted model and suggest that the fluid and membranes external to the nucleus form a mechanoprotective layer or buffer [102].

Cell Motility

The regulation and contribution of cell motility to vascular remodeling, angiogenesis, and wound healing cannot be understated. Cellular mobility or mechanotaxis occurs in response to numerous cues, including mechanical, to which the endothelium is constantly exposed. It involves the reorganization of the through changes in various signal transduction pathways and focal adhesions. The process encompasses the creation of adhesions at the leading edge of the moving cell, followed by cell contraction and the dissolution of the adhesion from the trailing edge [103, 104].

Endothelial migration can be described with the conception of a cellular leading edge and a rear or trailing edge (Fig. 46.2). Under conditions of shear, the leading edge is formed in the direction of the flow by the production of lamellipodia with the retraction of the rear edge allowing for migration and movement [105]. This is regulated through the signaling of Rac and Rho [106], in conjunction with phosphatidylinositol 3-kinase (PI3K) and ERK [107, 108]. Migration can be described

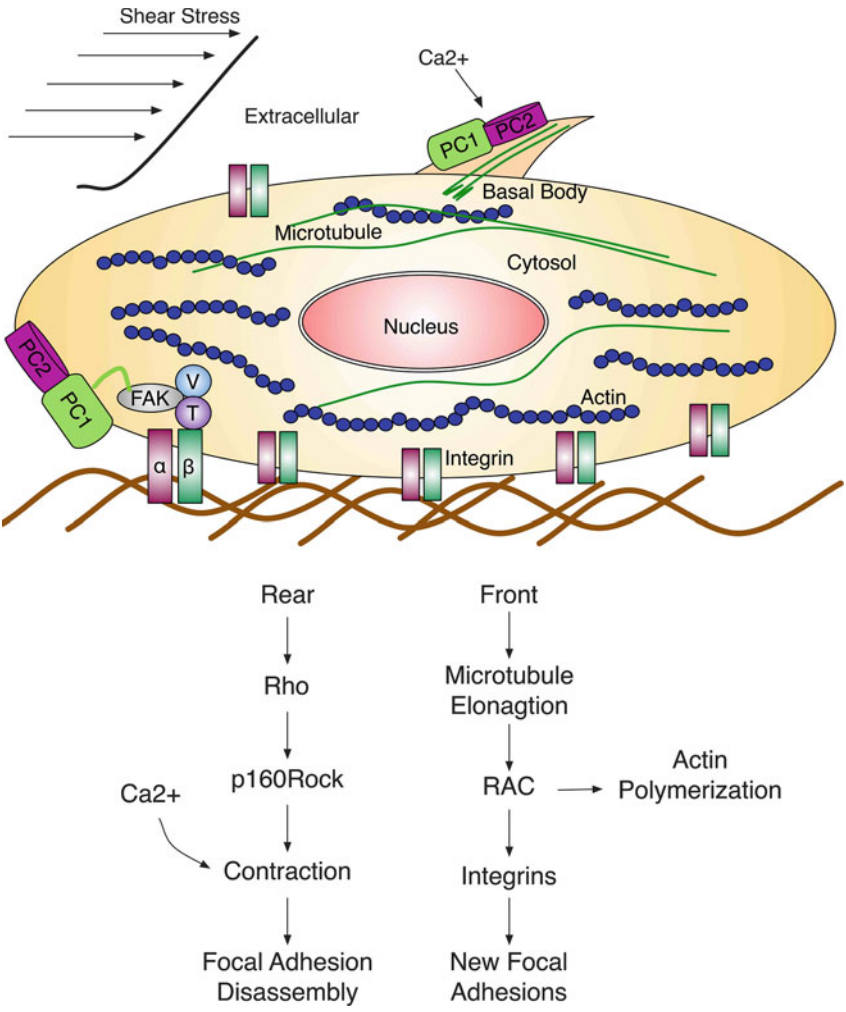

Fig. 46.2 A Schematic representation of the mechanotransduction process during endothelial cell migration. The application of mechanical shear can be sensed by cell membrane and primary cilia. This mechanical force is transmitted throughout the cell to its adhesions and the underlying structure. Shear can induce directional migration of endothelial cells by the protrusion and the formation of focal adhesions at the front edge of the cell, in the direction flow. At the rear edge, disassembly of focal adhesion occurs. These changes contribute to directional migration through multiple signaling molecules and structural components including microtubules, RAC, actin and integrin complex. Microtubule elongation occurs at the front activating RAC to induce actin polymerization and projection of the cell forward. In addition, it recruits and activates in integrins forming new focal adhesions. At the rear, the microtubules shorten and activate the Rho-p160ROCK pathway inducing contraction to detach the focal adhesions. In addition, a shear induced Ca^{2+} wave can be initiated to enhance the function of p160ROCK and the contraction. The polycystin heterocomplex is a mechanosensitive channel activation located in primary cilia and in adherens junctions. The mechanical force of shear induces conformational change in the microtubule-polycystins complex, activating the polycystin-2 calcium channel and inducing an inward Ca^{2+} gradient that may regulate the cells response. The polycystin complex is also found on the plasma membrane, can interact with the adherens junction proteins α-, β-catenin and E-cadherin and may contribute to cellular focal adhesions. *V* vinculin, *FAK* focal adhesion kinase, E-cadherin, *α* α-catenin, *β* ß-catenin, *PC1* polycystin-1, *PC2* polycystin-2

in three-steps. The initial step involves formation of a protruding edge with new adhesions, followed by a second step of cell contraction and finally the release of the adhesions in the trailing edge [103, 104]. Additionally, intracellular calcium concentration is an integral part of this process [109–111].

Conclusions

Mechanoregulation is not limited to one cell or tissue type but is a systemic mechanism that can regulate and coordinate structural and molecular changes throughout the body. Consequently, forces applied to an individual cell or tissue could be translated and transmitted throughout the body or system. Most cells contain stress-sensitive ion channels or organelles that can respond to mechanical and chemical cues to modulate ion flux. The hope is that through future research, we can better understand how the mechanical cues that the cell interprets are translated into biochemical and physiological responses. In this regard, a mechanosensitive organelle, the primary cilium, has gained considerable interest in recent years. This organelle has been shown to respond to mechanical and chemical cues with an ability to modulate calcium ion channel in response to stress, mediating a cell's adaptation and cytoskeletal changes. There is no doubt that we are on the verge of understanding this unique organelle, and its mechanosensory roles in cell cycle [112] with endothelial-to-mesenchymal transition [113] a future topic of discussion.

Acknowledgments Due to restricted space, we apologize to those whose work is not described in this review. Works from our laboratory that are cited in this review have been supported by grants from the National Institutes of Health (DK080640), and the NIH Recovery Act Funds. Authors are grateful to Charisse Montgomery for her editorial support.

References

1. Nauli SM, Williams JM, Akopov SE, Zhang L, Pearce WJ (2001) Developmental changes in ryanodine- and IP(3)-sensitive Ca(2+) pools in ovine basilar artery. Am J Physiol Cell Physiol 281:C1785–C1796
2. Fregeau MO, Regimbald-Dumas Y, Guillemette G (2011) Positive regulation of inositol 1,4,5-trisphosphate-induced Ca^{2+} release by mammalian target of rapamycin (mTOR) in RINm5F cells. J Cell Biochem 112:723–733
3. Puri S, Magenheimer BS, Maser RL, Ryan EM, Zien CA, Walker DD, Wallace DP, Hempson SJ, Calvet JP (2004) Polycystin-1 activates the calcineurin/NFAT (nuclear factor of activated T-cells) signaling pathway. J Biol Chem 279:55455–55464
4. Wegierski T, Steffl D, Kopp C, Tauber R, Buchholz B, Nitschke R, Kuehn EW, Walz G, Kottgen M (2009) TRPP2 channels regulate apoptosis through the Ca^{2+} concentration in the endoplasmic reticulum. EMBO J 28:490–499
5. Mo M, Eskin SG, Schilling WP (1991) Flow-induced changes in Ca^{2+} signaling of vascular endothelial cells: effect of shear stress and ATP. Am J Physiol 260:H1698–H1707
6. AbouAlaiwi WA, Lo ST, Nauli SM (2009) Primary cilia: highly sophisticated biological sensors. Sensors 9:7003–7020

7. Kolb RJ, Nauli SM (2008) Ciliary dysfunction in polycystic kidney disease: an emerging model with polarizing potential. Front Biosci 13:4451–4466
8. Nauli SM, Zhou J (2004) Polycystins and mechanosensation in renal and nodal cilia. Bioessays 26:844–856
9. Liu B, Lu S, Zheng S, Jiang Z, Wang Y (2011) Two distinct phases of calcium signalling under flow. Cardiovasc Res 91(1):124–133
10. Sharma R, Yellowley CE, Civelek M, Ainslie K, Hodgson L, Tarbell JM, Donahue HJ (2002) Intracellular calcium changes in rat aortic smooth muscle cells in response to fluid flow. Ann Biomed Eng 30:371–378
11. Camello-Almaraz C, Gomez-Pinilla PJ, Pozo MJ, Camello PJ (2006) Mitochondrial reactive oxygen species and Ca^{2+} signaling. Am J Physiol Cell Physiol 291:C1082–C1088
12. Borisova L, Wray S, Eisner DA, Burdyga T (2009) How structure, Ca signals, and cellular communications underlie function in precapillary arterioles. Circ Res 105:803–810
13. Berridge MJ, Lipp P, Bootman MD (2000) The versatility and universality of calcium signalling. Nat Rev Mol Cell Biol 1:11–21
14. Rebecchi MJ, Pentyala SN (2000) Structure, function, and control of phosphoinositide-specific phospholipase C. Physiol Rev 80:1291–1335
15. Rhee SG (2001) Regulation of phosphoinositide-specific phospholipase C. Annu Rev Biochem 70:281–312
16. Kwan HY, Leung PC, Huang Y, Yao X (2003) Depletion of intracellular Ca^{2+} stores sensitizes the flow-induced Ca^{2+} influx in rat endothelial cells. Circ Res 92:286–292
17. Schwarz G, Callewaert G, Droogmans G, Nilius B (1992) Shear stress-induced calcium transients in endothelial cells from human umbilical cord veins. J Physiol 458:527–538
18. Nilius B, Droogmans G (2001) Ion channels and their functional role in vascular endothelium. Physiol Rev 81:1415–1459
19. Oike M, Droogmans G, Nilius B (1994) Mechanosensitive Ca^{2+} transients in endothelial cells from human umbilical vein. Proc Natl Acad Sci USA 91:2940–2944
20. Deschner J, Hofman CR, Piesco NP, Agarwal S (2003) Signal transduction by mechanical strain in chondrocytes. Curr Opin Clin Nutr Metab Care 6:289–293
21. Basson MD (2003) Paradigms for mechanical signal transduction in the intestinal epithelium. Category: molecular, cell, and developmental biology. Digestion 68:217–225
22. Ruwhof C, van der Laarse A (2000) Mechanical stress-induced cardiac hypertrophy: mechanisms and signal transduction pathways. Cardiovasc Res 47:23–37
23. Nauli SM, Haymour HS, AbouAlaiwi WA, Lo ST, Nauli AM (2011) Primary cilia are mechanosensory organelles in vestibular tissues. In: Mechanosensitivity and Mechanotransduction.. ISBN 978-990-481-9880-9881
24. Resnick A, Hopfer U (2007) Force-response considerations in ciliary mechanosensation. Biophys J 93:1380–1390
25. AbouAlaiwi WA, Takahashi M, Mell BR, Jones TJ, Ratnam S, Kolb RJ, Nauli SM (2009) Ciliary polycystin-2 is a mechanosensitive calcium channel involved in nitric oxide signaling cascades. Circ Res 104:860–869
26. Nauli SM, Kawanabe Y, Kaminski JJ, Pearce WJ, Ingber DE, Zhou J (2008) Endothelial cilia are fluid shear sensors that regulate calcium signaling and nitric oxide production through polycystin-1. Circulation 117:1161–1171
27. Iomini C, Tejada K, Mo W, Vaananen H, Piperno G (2004) Primary cilia of human endothelial cells disassemble under laminar shear stress. J Cell Biol 164:811–817
28. Van der Heiden K, Groenendijk BC, Hierck BP, Hogers B, Koerten HK, Mommaas AM, Gittenberger-de Groot AC, Poelmann RE (2006) Monocilia on chicken embryonic endocardium in low shear stress areas. Dev Dyn 235:19–28
29. Van der Heiden K, Hierck BP, Krams R, de Crom R, Cheng C, Baiker M, Pourquie MJ, Alkemade FE, DeRuiter MC, Gittenberger-de Groot AC, Poelmann RE (2008) Endothelial primary cilia in areas of disturbed flow are at the base of atherosclerosis. Atherosclerosis 196:542–550
30. Ratnam S, Nauli SM (2010) Hypertension in autosomal dominant polycystic kidney disease: a clinical and basic science perspective. Int J Nephrol Urol 2:294–308

31. Weinbaum S, Tarbell JM, Damiano ER (2007) The structure and function of the endothelial glycocalyx layer. Annu Rev Biomed Eng 9:121–167
32. Yao Y, Rabodzey A, Dewey CF Jr (2007) Glycocalyx modulates the motility and proliferative response of vascular endothelium to fluid shear stress. Am J Physiol Heart Circ Physiol 293:H1023–H1030
33. Jensen CG, Poole CA, McGlashan SR, Marko M, Issa ZI, Vujcich KV, Bowser SS (2004) Ultrastructural, tomographic and confocal imaging of the chondrocyte primary cilium in situ. Cell Biol Int 28:101–110
34. Poole CA, Flint MH, Beaumont BW (1985) Analysis of the morphology and function of primary cilia in connective tissues: a cellular cybernetic probe? Cell Motil 5:175–193
35. Alenghat FJ, Nauli SM, Kolb R, Zhou J, Ingber DE (2004) Global cytoskeletal control of mechanotransduction in kidney epithelial cells. Exp Cell Res 301:23–30
36. Resnick A (2010) Use of optical tweezers to probe epithelial mechanosensation. J Biomed Opt 15:015005
37. Boehlke C, Kotsis F, Patel V, Braeg S, Voelker H, Bredt S, Beyer T, Janusch H, Hamann C, Godel M, Muller K, Herbst M, Hornung M, Doerken M, Kottgen M, Nitschke R, Igarashi P, Walz G, Kuehn EW (2010) Primary cilia regulate mTORC1 activity and cell size through Lkb1. Nat Cell Biol 12:1115–1122
38. Schneider L, Clement CA, Teilmann SC, Pazour GJ, Hoffmann EK, Satir P, Christensen ST (2005) PDGFRalphaalpha signaling is regulated through the primary cilium in fibroblasts. Curr Biol 15:1861–1866
39. Knight MM, McGlashan SR, Garcia M, Jensen CG, Poole CA (2009) Articular chondrocytes express connexin 43 hemichannels and P2 receptors – a putative mechanoreceptor complex involving the primary cilium? J Anat 214:275–283
40. Praetorius HA, Spring KR (2001) Bending the MDCK cell primary cilium increases intracellular calcium. J Membr Biol 184:71–79
41. Schwartz EA, Leonard ML, Bizios R, Bowser SS (1997) Analysis and modeling of the primary cilium bending response to fluid shear. Am J Physiol 272:F132–F138
42. Nauli SM, Alenghat FJ, Luo Y, Williams E, Vassilev P, Li X, Elia AE, Lu W, Brown EM, Quinn SJ, Ingber DE, Zhou J (2003) Polycystins 1 and 2 mediate mechanosensation in the primary cilium of kidney cells. Nat Genet 33:129–137
43. Nauli SM, Rossetti S, Kolb RJ, Alenghat FJ, Consugar MB, Harris PC, Ingber DE, Loghman-Adham M, Zhou J (2006) Loss of polycystin-1 in human cyst-lining epithelia leads to ciliary dysfunction. J Am Soc Nephrol 17:1015–1025
44. Abdul-Majeed S, Nauli SM (2011) Calcium-mediated mechanisms of cystic expansion. Biochim Biophys Acta 1812(10):1281–1290
45. Yoder BK, Hou X, Guay-Woodford LM (2002) The polycystic kidney disease proteins, polycystin-1, polycystin-2, polaris, and cystin, are co-localized in renal cilia. J Am Soc Nephrol 13:2508–2516
46. Badano JL, Mitsuma N, Beales PL, Katsanis N (2006) The ciliopathies: an emerging class of human genetic disorders. Annu Rev Genomics Hum Genet 7:125–148
47. Hanaoka K, Qian F, Boletta A, Bhunia AK, Piontek K, Tsiokas L, Sukhatme VP, Guggino WB, Germino GG (2000) Co-assembly of polycystin-1 and -2 produces unique cation-permeable currents. Nature 408:990–994
48. Newby LJ, Streets AJ, Zhao Y, Harris PC, Ward CJ, Ong AC (2002) Identification, characterization, and localization of a novel kidney polycystin-1-polycystin-2 complex. J Biol Chem 277:20763–20773
49. Tsiokas L, Kim E, Arnould T, Sukhatme VP, Walz G (1997) Homo- and heterodimeric interactions between the gene products of PKD1 and PKD2. Proc Natl Acad Sci USA 94:6965–6970
50. Xu C, Shmukler BE, Nishimura K, Kaczmarek E, Rossetti S, Harris PC, Wandinger-Ness A, Bacallao RL, Alper SL (2009) Attenuated, flow-induced ATP release contributes to absence of flow-sensitive, purinergic Cai2+ signaling in human ADPKD cyst epithelial cells. Am J Physiol Renal Physiol 296:F1464–F1476

51. Cai Y, Maeda Y, Cedzich A, Torres VE, Wu G, Hayashi T, Mochizuki T, Park JH, Witzgall R, Somlo S (1999) Identification and characterization of polycystin-2, the PKD2 gene product. J Biol Chem 274:28557–28565
52. Chen XZ, Segal Y, Basora N, Guo L, Peng JB, Babakhanlou H, Vassilev PM, Brown EM, Hediger MA, Zhou J (2001) Transport function of the naturally occurring pathogenic polycystin-2 mutant, R742X. Biochem Biophys Res Commun 282:1251–1256
53. Koulen P, Cai Y, Geng L, Maeda Y, Nishimura S, Witzgall R, Ehrlich BE, Somlo S (2002) Polycystin-2 is an intracellular calcium release channel. Nat Cell Biol 4:191–197
54. O'Toole CM, Arnoult C, Darszon A, Steinhardt RA, Florman HM (2000) Ca(2+) entry through store-operated channels in mouse sperm is initiated by egg ZP3 and drives the acrosome reaction. Mol Biol Cell 11:1571–1584
55. Tsiokas L (2009) Function and regulation of TRPP2 at the plasma membrane. Am J Physiol Renal Physiol 297:F1–F9
56. Qian F, Germino FJ, Cai Y, Zhang X, Somlo S, Germino GG (1997) PKD1 interacts with PKD2 through a probable coiled-coil domain. Nat Genet 16:179–183
57. Tsiokas L, Arnould T, Zhu C, Kim E, Walz G, Sukhatme VP (1999) Specific association of the gene product of PKD2 with the TRPC1 channel. Proc Natl Acad Sci USA 96:3934–3939
58. Chachisvilis M, Zhang YL, Frangos JA (2006) G protein-coupled receptors sense fluid shear stress in endothelial cells. Proc Natl Acad Sci USA 103:15463–15468
59. Putney JW Jr (1990) Receptor-regulated calcium entry. Pharmacol Ther 48:427–434
60. Leung PC, Cheng KT, Liu C, Cheung WT, Kwan HY, Lau KL, Huang Y, Yao X (2006) Mechanism of non-capacitative Ca^{2+} influx in response to bradykinin in vascular endothelial cells. J Vasc Res 43:367–376
61. Li YS, Haga JH, Chien S (2005) Molecular basis of the effects of shear stress on vascular endothelial cells. J Biomech 38:1949–1971
62. Praetorius HA, Spring KR (2003) The renal cell primary cilium functions as a flow sensor. Curr Opin Nephrol Hypertens 12:517–520
63. Muller JM, Chilian WM, Davis MJ (1997) Integrin signaling transduces shear stress – dependent vasodilation of coronary arterioles. Circ Res 80:320–326
64. Lelievre S, Weaver VM, Bissell MJ (1996) Extracellular matrix signaling from the cellular membrane skeleton to the nuclear skeleton: a model of gene regulation. Recent Prog Horm Res 51: 417–432
65. Thodeti CK, Matthews B, Ravi A, Mammoto A, Ghosh K, Bracha AL, Ingber DE (2009) TRPV4 channels mediate cyclic strain-induced endothelial cell reorientation through integrin-to-integrin signaling. Circ Res 104:1123–1130
66. Wilson PD, Geng L, Li X, Burrow CR (1999) The PKD1 gene product, "polycystin-1," is a tyrosine-phosphorylated protein that colocalizes with alpha2beta1-integrin in focal clusters in adherent renal epithelia. Lab Invest 79:1311–1323
67. Geng L, Burrow CR, Li HP, Wilson PD (2000) Modification of the composition of polycystin-1 multiprotein complexes by calcium and tyrosine phosphorylation. Biochim Biophys Acta 1535:21–35
68. Gilmore AP, Romer LH (1996) Inhibition of focal adhesion kinase (FAK) signaling in focal adhesions decreases cell motility and proliferation. Mol Biol Cell 7:1209–1224
69. Otey CA, Carpen O (2004) Alpha-actinin revisited: a fresh look at an old player. Cell Motil Cytoskeleton 58:104–111
70. Sun HQ, Yamamoto M, Mejillano M, Yin HL (1999) Gelsolin, a multifunctional actin regulatory protein. J Biol Chem 274:33179–33182
71. Doyle AD, Lee J (2005) Cyclic changes in keratocyte speed and traction stress arise from Ca^{2+}-dependent regulation of cell adhesiveness. J Cell Sci 118:369–379
72. Brundage RA, Fogarty KE, Tuft RA, Fay FS (1991) Calcium gradients underlying polarization and chemotaxis of eosinophils. Science 254:703–706
73. Wei C, Wang X, Chen M, Ouyang K, Song LS, Cheng H (2009) Calcium flickers steer cell migration. Nature 457:901–905

74. Langille BL, Adamson SL (1981) Relationship between blood flow direction and endothelial cell orientation at arterial branch sites in rabbits and mice. Circ Res 48:481–488
75. Barbee KA, Mundel T, Lal R, Davies PF (1995) Subcellular distribution of shear stress at the surface of flow-aligned and nonaligned endothelial monolayers. Am J Physiol 268:H1765–H1772
76. Dewey CF Jr, Bussolari SR, Gimbrone MA Jr, Davies PF (1981) The dynamic response of vascular endothelial cells to fluid shear stress. J Biomech Eng 103:177–185
77. Fung YC, Liu SQ (1993) Elementary mechanics of the endothelium of blood vessels. J Biomech Eng 115:1–12
78. Liu SQ, Yen M, Fung YC (1994) On measuring the third dimension of cultured endothelial cells in shear flow. Proc Natl Acad Sci USA 91:8782–8786
79. McCue S, Noria S, Langille BL (2004) Shear-induced reorganization of endothelial cell cytoskeleton and adhesion complexes. Trends Cardiovasc Med 14:143–151
80. Noria S, Xu F, McCue S, Jones M, Gotlieb AI, Langille BL (2004) Assembly and reorientation of stress fibers drives morphological changes to endothelial cells exposed to shear stress. Am J Pathol 164:1211–1223
81. Melchior B, Frangos JA (2010) Shear-induced endothelial cell-cell junction inclination. Am J Physiol Cell Physiol 299:C621–C629
82. Brooks AR, Lelkes PI, Rubanyi GM (2004) Gene expression profiling of vascular endothelial cells exposed to fluid mechanical forces: relevance for focal susceptibility to atherosclerosis. Endothelium 11:45–57
83. Cunningham KS, Gotlieb AI (2005) The role of shear stress in the pathogenesis of atherosclerosis. Lab Invest 85:9–23
84. DePaola N, Gimbrone MA Jr, Davies PF, Dewey CF Jr (1992) Vascular endothelium responds to fluid shear stress gradients. Arterioscler Thromb 12:1254–1257
85. Tzima E (2006) Role of small GTPases in endothelial cytoskeletal dynamics and the shear stress response. Circ Res 98:176–185
86. Tzima E, Irani-Tehrani M, Kiosses WB, Dejana E, Schultz DA, Engelhardt B, Cao G, DeLisser H, Schwartz MA (2005) A mechanosensory complex that mediates the endothelial cell response to fluid shear stress. Nature 437:426–431
87. Hierck BP, Van der Heiden K, Alkemade FE, Van de Pas S, Van Thienen JV, Groenendijk BC, Bax WH, Van der Laarse A, Deruiter MC, Horrevoets AJ, Poelmann RE (2008) Primary cilia sensitize endothelial cells for fluid shear stress. Dev Dyn 237:725–735
88. Poelmann RE, Van der Heiden K, Gittenberger-de Groot AC, Hierck BP (2008) Deciphering the endothelial shear stress sensor. Circulation 117:1124–1126
89. Dekker RJ, van Soest S, Fontijn RD, Salamanca S, de Groot PG, VanBavel E, Pannekoek H, Horrevoets AJ (2002) Prolonged fluid shear stress induces a distinct set of endothelial cell genes, most specifically lung Kruppel-like factor (KLF2). Blood 100:1689–1698
90. Dekker RJ, van Thienen JV, Rohlena J, de Jager SC, Elderkamp YW, Seppen J, de Vries CJ, Biessen EA, van Berkel TJ, Pannekoek H, Horrevoets AJ (2005) Endothelial KLF2 links local arterial shear stress levels to the expression of vascular tone-regulating genes. Am J Pathol 167:609–618
91. Wang N, Miao H, Li YS, Zhang P, Haga JH, Hu Y, Young A, Yuan S, Nguyen P, Wu CC, Chien S (2006) Shear stress regulation of Kruppel-like factor 2 expression is flow pattern-specific. Biochem Biophys Res Commun 341:1244–1251
92. Dai G, Kaazempur-Mofrad MR, Natarajan S, Zhang Y, Vaughn S, Blackman BR, Kamm RD, Garcia-Cardena G, Gimbrone MA Jr (2004) Distinct endothelial phenotypes evoked by arterial waveforms derived from atherosclerosis-susceptible and -resistant regions of human vasculature. Proc Natl Acad Sci USA 101:14871–14876
93. Caille N, Thoumine O, Tardy Y, Meister JJ (2002) Contribution of the nucleus to the mechanical properties of endothelial cells. J Biomech 35:177–187
94. Sato M, Levesque MJ, Nerem RM (1987) Micropipette aspiration of cultured bovine aortic endothelial cells exposed to shear stress. Arteriosclerosis 7:276–286
95. Wang N, Butler JP, Ingber DE (1993) Mechanotransduction across the cell surface and through the cytoskeleton. Science 260:1124–1127

96. Galbraith CG, Skalak R, Chien S (1998) Shear stress induces spatial reorganization of the endothelial cell cytoskeleton. Cell Motil Cytoskeleton 40:317–330
97. Maniotis AJ, Bojanowski K, Ingber DE (1997) Mechanical continuity and reversible chromosome disassembly within intact genomes removed from living cells. J Cell Biochem 65:114–130
98. Gimbrone MA Jr, Resnick N, Nagel T, Khachigian LM, Collins T, Topper JN (1997) Hemodynamics, endothelial gene expression, and atherogenesis. Ann N Y Acad Sci 811: 1–10, discussion 10–11
99. Ingber DE, Folkman J (1989) Mechanochemical switching between growth and differentiation during fibroblast growth factor-stimulated angiogenesis in vitro: role of extracellular matrix. J Cell Biol 109:317–330
100. Maniotis AJ, Chen CS, Ingber DE (1997) Demonstration of mechanical connections between integrins, cytoskeletal filaments, and nucleoplasm that stabilize nuclear structure. Proc Natl Acad Sci USA 94:849–854
101. Ingber DE (1993) Cellular tensegrity: defining new rules of biological design that govern the cytoskeleton. J Cell Sci 104(Pt 3):613–627
102. Evans E, Yeung A (1989) Apparent viscosity and cortical tension of blood granulocytes determined by micropipet aspiration. Biophys J 56:151–160
103. Lauffenburger DA, Horwitz AF (1996) Cell migration: a physically integrated molecular process. Cell 84:359–369
104. Sheetz MP, Felsenfeld DP, Galbraith CG (1998) Cell migration: regulation of force on extracellular-matrix-integrin complexes. Trends Cell Biol 8:51–54
105. Li S, Butler P, Wang Y, Hu Y, Han DC, Usami S, Guan JL, Chien S (2002) The role of the dynamics of focal adhesion kinase in the mechanotaxis of endothelial cells. Proc Natl Acad Sci USA 99:3546–3551
106. Li S, Huang NF, Hsu S (2005) Mechanotransduction in endothelial cell migration. J Cell Biochem 96:1110–1126
107. Go YM, Park H, Maland MC, Darley-Usmar VM, Stoyanov B, Wetzker R, Jo H (1998) Phosphatidylinositol 3-kinase gamma mediates shear stress-dependent activation of JNK in endothelial cells. Am J Physiol 275:H1898–H1904
108. Urbich C, Dernbach E, Reissner A, Vasa M, Zeiher AM, Dimmeler S (2002) Shear stress-induced endothelial cell migration involves integrin signaling via the fibronectin receptor subunits alpha(5) and beta(1). Arterioscler Thromb Vasc Biol 22:69–75
109. Malek AM, Izumo S (1996) Mechanism of endothelial cell shape change and cytoskeletal remodeling in response to fluid shear stress. J Cell Sci 109(Pt 4):713–726
110. Miyazaki T, Ohata H, Yamamoto M, Momose K (2001) Spontaneous and flow-induced Ca^{2+} transients in retracted regions in endothelial cells. Biochem Biophys Res Commun 281:172–179
111. Yoshikawa N, Ariyoshi H, Ikeda M, Sakon M, Kawasaki T, Monden M (1997) Shear-stress causes polarized change in cytoplasmic calcium concentration in human umbilical vein endothelial cells (HUVECs). Cell Calcium 22:189–194
112. AbouAlaiwi WA, Ratnam S, Booth RL, Shah JV, Nauli SM (2011) Endothelial cells from humans and mice with polycystic kidney disease are characterized by polyploidy and chromosome segregation defects through survivin down-regulation. Hum Mol Genet 20:354–367
113. Egorova AD, Khedoe PP, Goumans MJ, Yoder BK, Nauli SM, Ten Dijke P, Poelmann RE, Hierck BP (2011) Lack of primary cilia primes shear-induced endothelial-to-mesenchymal transition. Circ Res 108(9):1093–1101

Chapter 47
Role Ca^{2+} in Mechanisms of the Red Blood Cells Microrheological Changes

Alexei Muravyov and Irina Tikhomirova

Abstract To assess the physiological role of intracellular Ca^{2+} in the changes of microrheological red blood cell (RBC) properties (RBC deformability and aggregation), we employed several types of chemicals that can increase and decrease of the intracellular Ca^{2+} concentration. The rise of Ca^{2+} influx, stimulated by mechanical loading, A23187, thrombin, prostaglandin $F_2\alpha$ was accompanied by a moderate red cell deformability lowering and an increase of their aggregation. In contrast, Ca^{2+} entry blocking into the red cells by verapamil led to a significant RBC aggregation decrease and deformability rise. Similar microrheological changes were observed in the red blood cells treated with phosphodiesterase inhibitors IBMX, vinpocetine, rolipram, pentoxifylline. When forskolin (10 μM), an AC stimulator was added to RBC suspension, the RBC deformability was increased ($p < 0.05$). Somewhat more significant deformability rise appeared after RBC incubation with dB-AMP. Red cell aggregation was significantly decreased under these conditions ($p < 0.01$). On the whole the total data clearly show that the red cell aggregation and deformation changes were connected with an activation of both intracellular signaling pathways: Ca^{2+} regulatory mechanism and Gs-protein/adenylyl-cyclase-cAMP system. And the final red cell microrheological regulatory effect is connected with the crosstalk between these systems.

Keywords Adenylyl cyclase • Ca^{2+}- control mechanism • Red blood cell deformability and aggregation

A. Muravyov (✉) • I. Tikhomirova
Department of Medicine and Biology, State Pedagogical University, Yaroslavl, Russia
e-mail: alexei.47@mail.ru

M.S. Islam (ed.), *Calcium Signaling*, Advances in Experimental Medicine and Biology 740, DOI 10.1007/978-94-007-2888-2_47,

Introduction

In order to understand blood circulation, knowledge of the rheological properties of blood is required. One of the blood rheological properties is the deformability of erythrocytes. Erythrocyte deformability is an important determinant of red cell life span and depends on at least three key factors: shape, internal viscosity and membrane mechanical properties [1, 2]. In the microcirculation, where cells must deform to pass through narrow capillaries (Fig. 47.1), cellular rheology (i.e. the deformability of individual cells) is a major determinant of resistance to flow.

An unusual combination of membrane properties allows the RBC to undergo extensive deformation without cell fragmentation, enabling it to effectively perform its function of oxygen delivery during its long life span in circulation [3]. Another microrheological property of red blood cells (RBCs) is their ability to form aggregates under the low flow conditions, mainly in form of rouleaux (Fig. 47.2) [4, 5].

Previous rotational viscometric studies showed that the apparent viscosity of blood increased at low shear rates and that this rise is primarily due to red blood cell aggregation. As this effect occurs in the physiological range of shear rates in venous vessels, it was believed that red blood cell aggregation is an important determinant of venous resistance [6].

RBCs have traditionally been viewed as simple conduits for oxygen transport; however, these cells contain a broad range of signaling molecules [7–10]. Some of the most well-studied signaling pathways in RBCs are mediated by the second messengers cyclic adenosine monophosphate (cAMP), generated by the conversion of adenosine triphosphate (ATP) to cAMP via membrane-associated adenylyl cyclase and Ca^{2+}-Calmodulin [11, 12]. In recent years calcium has become recognized as an important "second messenger", in that an increase in free intracellular calcium ion concentration is involved in many aspects of cellular activation. In excitable cells such as smooth muscle or cardiac tissue an influx of extracellular calcium ions through voltage sensitive calcium channels plays a major role in increasing the cytoplasmic free calcium concentration. It is now known that the activity of these calcium channels may be inhibited or stimulated by a range of ions, toxins and drugs [13]. The source of the Ca^{2+} for the former mechanism is mainly extracellular [14]. Intracellular calcium regulates a number of membrane functions in the erythrocyte, including control of shape, membrane lipid composition and cation permeability [13]. Measurement of total red cell calcium has yielded values between 5 and 15 nM/ml cells, and these low values in part reflect the absence of Ca^{2+}-containing organelles. Most intracellular Ca^{2+} is bound and the low cell ionized

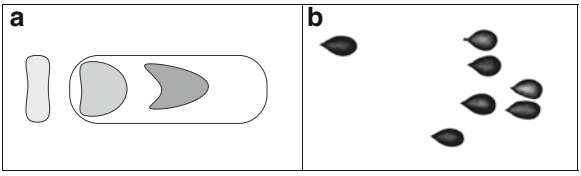

Fig. 47.1 (**a**) Scheme of red blood cell shape change in blood flow, (**b**) the deformed red blood cell in the flow microchamber (personal data)

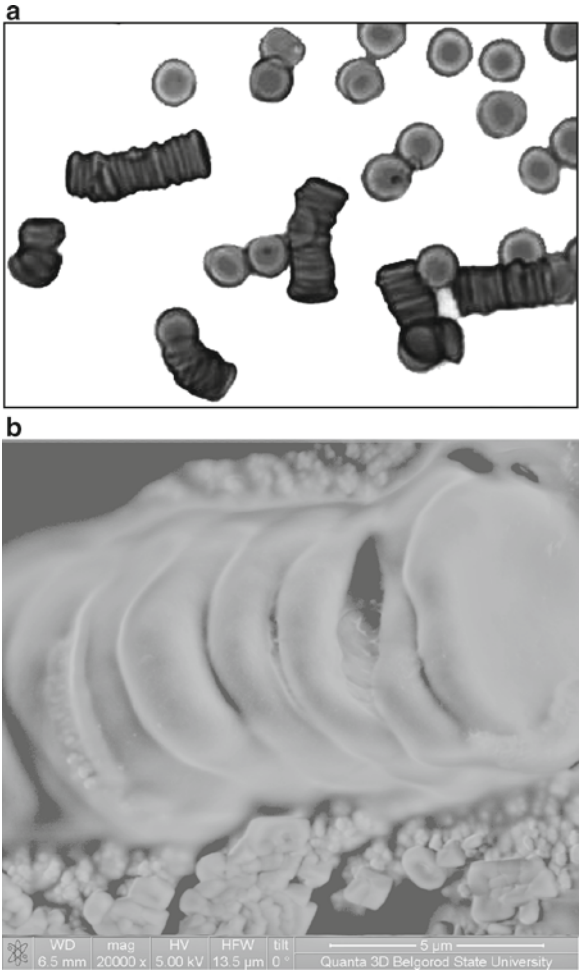

Fig. 47.2 Red blood cell aggregation, mainly in form of rouleaux: (**a**) light microscopy (MC20, MICROS, Austria; objective 40, digital eyepiece, DCM-500); (**b**) Electronic microscopy (Electronic microscope Quanta 200, FEI Company, USA; Magnification – 20,000×)

Ca^{2+} concentration (approximately 0.2 μM) is maintained by a combination of low membrane permeability and a powerful Ca^{2+}-pump. This pump has been identified with a (Ca^{2+} + Mg^{2+})-stimulated ATPase, and both Ca^{2+} transport and ATP splitting are stimulated by calmodulin, a low molecular weight protein which binds Ca^{2+} avidly and activates many Ca^{2+}-dependent enzymes [10, 11, 13].

Thus, in addition to a plethora of hormone receptors, mature RBCs contain substantial numbers of cyclases, phospholipases, kinases, phosphatases, and both ligand-gated and mechanically activated ion channels [15]. Although the responsiveness of RBCs to regulators of circulatory health and homeostasis is becoming more apparent, the signaling pathways that mediate the changes in RBC properties remain unresolved. One of the more common intermediates implicated in regulating RBC behavior is an influx of extracellular calcium and adenylyl cyclase activation [11].

The present study was designed to explore the adenylyl cyclase signaling pathway and Ca^{2+} regulatory mechanism of RBCs together with their microrheological changes.

Alterations of Red Blood Cell Deformability

Methods. Blood samples for rheological measurements (10 ml) were drawn via sterile venipuncture using heparin (5 IU/ml) as the anticoagulant and used within 4 h; all preparations and measurements were carried out at room temperature (20 ± 1°C). RBC were washed three times in PBS; following the third wash, the RBC were resuspended in the final medium (autologous plasma) at hematocrit of 40.0 ± 0.3% for aggregation and red cell suspension viscosity measurements.

Red cell suspension viscosity (Hct = 40%) was measured with capillary viscometer under 6 shear rates. The reproducibility of the capillary viscometer system was ranged between 0.8% and 1.0% as indexed by the coefficient of variation for several repeated measurements of the same sample.

To estimate the deformability of RBCs they were placed into a flow microchamber [16]. The cells were attached to the bottom part of the chamber with "one point" and then were deformed by shear flow (Fig. 47.3), under constant shear stress (τ). At a given volume flow rate Q (determined by weighing the amount of saline which flows through the flow channel in a given time period) the shear stress at the surface τ_s, is given by:

$$\tau_s = 6\eta Q / wh^2,$$

where η is the viscosity of the perfusate, and w is the width and h is the height of the flow passageway. In our experiments, $\eta = 1.07$ mPa.s, $w = 0.90$ cm, $h = 0.01$ cm.The length (L) and width (W) of each of about hundred cells were measured and elongation index (EI) as an index of red cell deformability was calculated according to: EI = (L−W)/(L+W).

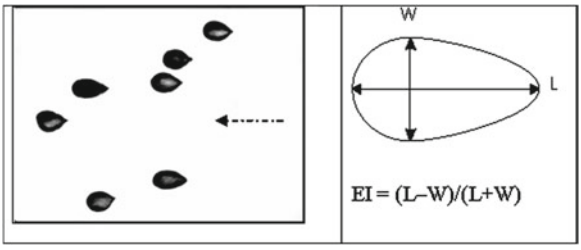

Fig. 47.3 Red blood cells (*RBCs*) under shear flow in the microchamber (**a**); RBC elongation index calculation (**b**); the *arrow* (Fig. 47.1a) shows flow direction

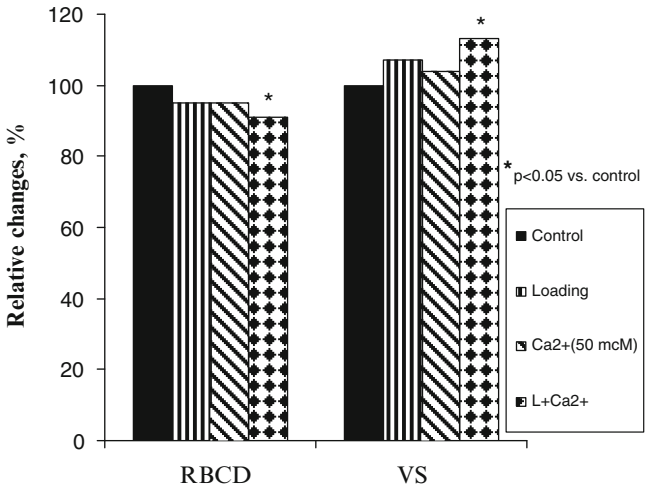

Fig. 47.4 The red blood cell deformability (*RBCD*) and viscosity of suspension (*VS*) changes (in % vs. control) after the mechanically cell loading, cell incubation with Ca^{2+} (50 μM) and under combination of cell loading and Ca^{2+} incubation (L + Ca^{2+})

The Change of Red Cell Deformability Under a Rise in Extracellular Ca^{2+} Concentration

It is known that the mechanical stress of the cell membrane is accompanied by an influx of Ca^{2+} into cells [11, 17]. We have found that after mechanical loading of red blood cells (RBCs) their deformability was decreased slightly (Fig. 47.4).

There was the lowering of red blood cell deformability (RBCD) after both cell mechanically loading and their incubation with Ca^{2+} (50 μM). However these changes were also not significant. While combined influence upon cells: the mechanical loading and Ca^{2+} (100 μM) was accompanied by a marked red cell deformability lowering (by 13%, $p < 0.05$, Fig. 47.4).

We have measured Ca^{2+} concentration in RBCs (confocal microscopy, Calcium-green, the laser wave length – 488 nM) and have found its increase by 11% ($p < 0.05$) after combined influence (the mechanical loading and calcium) on the cells (Fig. 47.5).

Using atomic force microscopy (AFM) it has been found that a rise in intracellular Ca^{2+} concentration was accompanied by the red cell membrane rigidity increase. The increase of cell rigidity was in dose-dependant manner and the membrane rigidity index was higher by 18% as comparison with control. Maximum effect was reached under Ca^{2+} 200 μM in incubation medium (Fig. 47.6). Y. Takakuwa et al. suppose [18] that membrane deformability decreased only at Ca^{2+} concentrations greater than 100 μM.

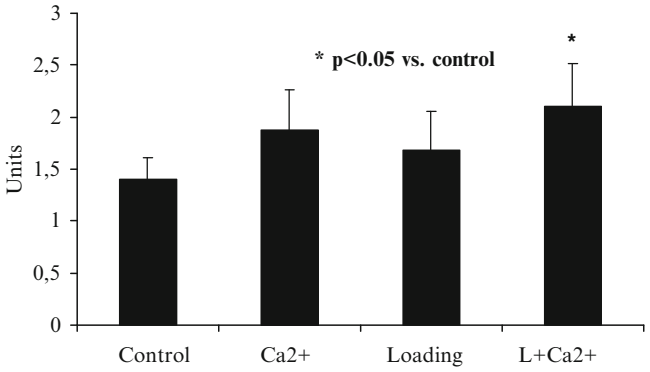

Fig. 47.5 The change in intracellular Ca^{2+} concentration of red blood cell under the calcium incubation (50 μM), mechanical loading and their combination of cell loading and Ca^{2+} (L+Ca^{2+}) vs. control

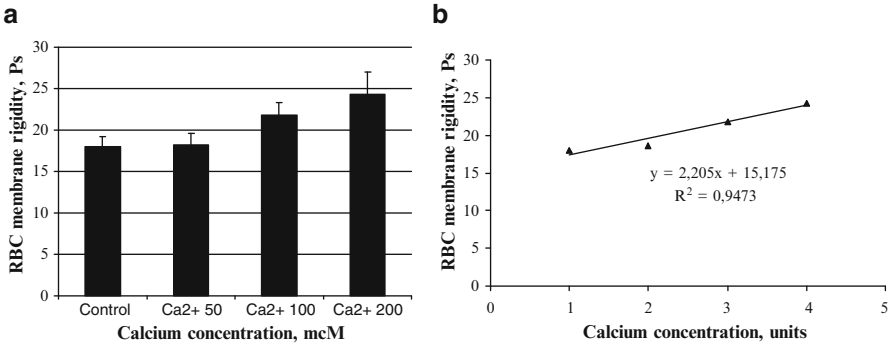

Fig. 47.6 The change of red cell membrane rigidity (atomic force microscopy) under an increase of Ca^{2+} concentration in incubation media (**a**) and linear regression dependence of these alterations (**b**), vs. control. *Abbreviations*: *Ca^{2+} 50* 50 μM calcium in media (*2*), *Ca^{2+} 100* 100 μM calcium in media (*3*), *Ca^{2+} 200* 200 μM calcium in media (*4*)

The Change of Red Cell Deformability Under Ca^{2+} Influx Stimulation

It has been found that a rise in intracellular Ca^{2+} concentration, stimulated by A23187 [19] was accompanied by a decrease of RBCD, whereas red cell suspension viscosity was changed insignificantly (Table 47.1). Contrasting with it a Ca^{2+} chelator – EGTA changed RBC viscosity and their deformability significantly (Table 47.1).

The activation of membrane-bound, Ca^{2+} stimulating PKC by phorbol 12-myristate 13-acetate (PMA, 3 μM) did not bring to the change of red cell deformability (Fig. 47.7). However PKC could down-modulate the activity of native Ca^{2+} activated

Table 47.1 Effect of Ca^{2+} entry by ionophore (A23187) and EGTA on RBC microrheology (M ± m)

Parameters	Control	A23187	EGTA
SV, mPa s	3.40 ± 0.05	3.45 ± 0.08	3.12 ± 0.06*
EI	0.196 ± 0.003	0.182 ± 0.004*	0.268 ± 0.006**

Abbreviations: *SV* suspension viscosity of red blood cells under high shear rate, *EI* elongation index – a showing of red cell deformability
*it means $p < 0.05$; **it means $p < 0.01$

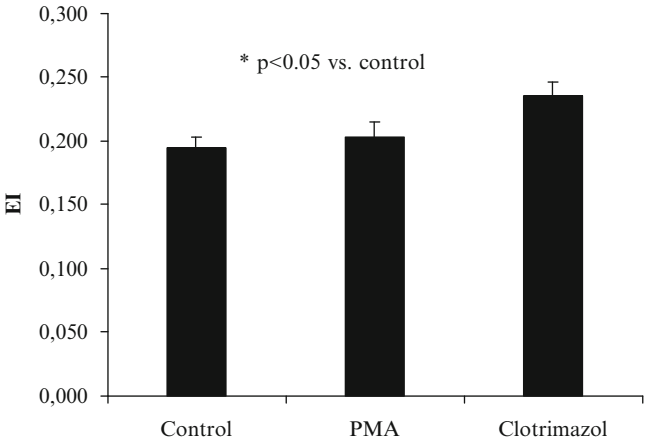

Fig. 47.7 The red blood cell deformability (*RBCD*) changes after the cell incubation with Phorbol 12-myristate 13-acetate (*PMA*, 3.0 μM) and Clotrimazol (50 μM) vs. control

K^+ channels of human erythrocytes [20]. It has been confirmed by the observation that clotrimazol (50 μM) as a blocker of these type of RBC membrane channels [21] raised the red cell deformability by 20% ($p < 0.05$; Fig. 47.7).

The similar microrheological effect was found when we incubated the native RBCs and their resealed ghosts with Ca^{2+} sensitive K^+ (Gardos) channel inhibitor clotrimazol (Fig. 47.8).

Although PMA did not alter RBCD significantly both compounds – bisindolylmaleimide (BIM) and PMA increased red cell deformability by 10% (Fig. 47.9).

Small effect of PKC on red cell deformability might be connected with the different time course in the phosphorylation of 4.1R. Using antibodies raised against phosphopeptides of 4.1R and adducin, it was documented significant differences in the time course of phosphorylation of adducin and 4.1R by PKC [22].

Prostaglandin $F_{2\alpha}$ ($PGF_{2\alpha}$) also is known as a calcium cell entry stimulator [23]. Under the $PGF_{2\alpha}$ erythrocyte incubation RBCD was decreased by 10% ($p < 0.05$).

Taken together our data for the first time demonstrate that that the changes of Ca^{2+} concentration in cell environment and calcium influx rise into cells lead to the

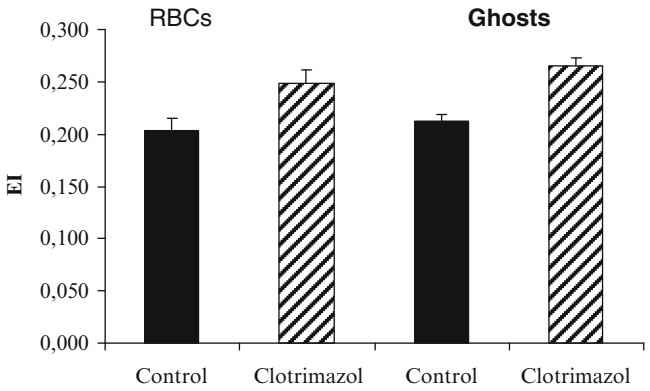

Fig. 47.8 The change of the red blood cell deformability the native human red blood cells (*RBCs*) and their resealed ghosts after incubation with Ca^{2+} sensitive K^+ (Gardos) channel inhibitor clotrimazol (25.0 μM) vs. control

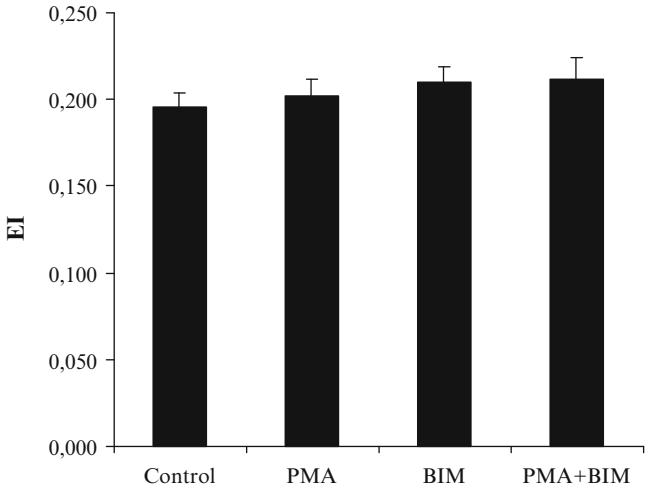

Fig. 47.9 The red blood cell deformability (*RBCD*) changes after the cell incubation with Phorbol 12-myristate 13-acetate (*PMA*, 3.0 μM), bisindolylmaleimide (*BIM*, 3.0 μM) and *PMA* and *BIM* combination (*PMA* + *BIM*) vs. control

moderate cell deformability decrease. A probable change mechanism may be connected with the protein phosphate activation and dephosphorylation of the key proteins of membrane skeleton that is responsible for the cell elasticity on the whole [22]. The spectrin skeleton thus forms a point of convergence between kinase/phosphatase and Ca^{2+}-mediated signaling cascades [24]. On the other hand beta-spectrin phosphorylation by casein kinase-I has been shown to decrease membrane mechanical stability [22].

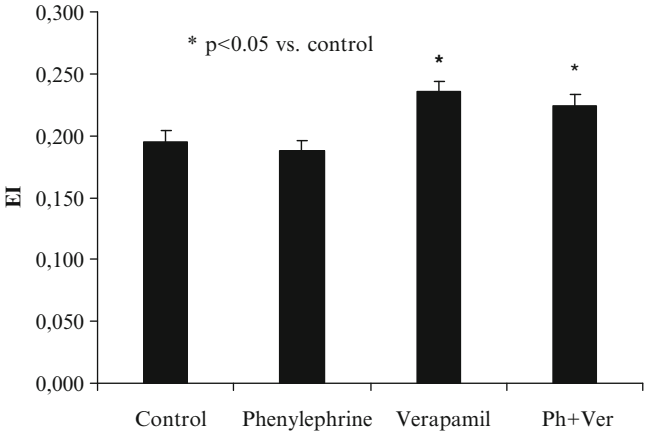

Fig. 47.10 The red blood cell deformability (*RBCD*) changes after the cell Incubation with phenylephrine (1.0 μM), verapamil (10.0 μM) and their combination. *Abbreviations: Ph* phenylephrine, *Ver* verapamil vs. control

Table 47.2 Effect of Ca^{2+} independent protein kinase (PKA) activation by Forskolin, Db-cAMP and IBMX on RBC microrheology (M ± m)

Parameters	Control	Forskolin	Db-cAMP	IBMX
SV, mPa s	3.40 ± 0.05	2.60 ± 0.02	2.86 ± 0.12	3.18 ± 0.06
EI	0.196 ± 0.005	0.246 ± 0.005	0.242 ± 0.004	0.223 ± 0.005

For abbreviations, see Table 47.1

Role Ca^{2+} Influx Stimulation on the Change of Red Cell Deformability

A Ca^{2+} entering into cells can be intensifying under some membrane receptor activation, for example, α_1- adrenergic receptors. This subtype of adrenergic receptor is coupled with Ca^{2+} channel [25]. The red cell membranes contain both α_1- and β-adrenergic receptors [26] and under the heightened sensibility of α_1-receptors adrenalin can activate them [27, 28]. It lead to the rise of Ca^{2+} influx into red cells and a change of red cell microrheology [11, 16].

Ca^{2+} entry blocking into the red cells by verapamil [29] led to the red cell deformability rise (Fig. 47.12). Indeed the preincubation of RBCs with verapamil removed a small negative effect of α_1- adrenergic receptor agonist – phenylephrine on red cell deformability. Not only verapamil alone but their combination with phenylephrine increased RBCD markedly (Fig. 47.10).

The adrenergic receptors are associated with stimulation of Gs-protein/adenylyl cyclase (AC) activity. In our experimental model a direct stimulation of adenylyl cyclase (AC) by forskolin and an increase of the intracellular cAMP level, by using its stable analog – dB-cAMP led to red cell deformability increase (Table 47.2).

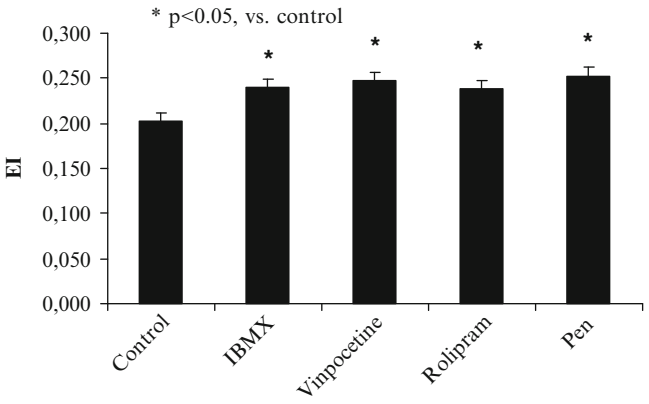

Fig. 47.11 Red blood cell deformability change (vs. control) under incubation with: IBMX (100 μM), vinpocetine (10 μM); rolipram (10 μM), pentoxifylline (10 μM)

Taken together these data and the results of the study of PDE inhibition support that the beta-adrenergic receptor – G-protein – AC complex is involved in the RBC microrheological control mechanisms. Since epinephrine can activate not only α-adrenergic receptors but also β-ones it is quite possible that its positive red cell deformability effect is connected with red cell membrane β-receptor activation. On the other hand, elevation of the cAMP leads to cytosolic Ca^{2+} decrease via inhibition of its entry into cells [30]. An increase in intracellular Ca^{2+} concentration could be removed, if it was added to incubation medium preliminary phosphodiesterase inhibitor or a permeable cAMP analog [31]. It was found that all four PDE inhibitors: isobutyl-methyl-xanthine (IBMX) – nonselective PDE inhibitor, vinpocetine, rolipram, pentoxifylline increased RBCD significantly [16, 28]. All drugs having PDE activity increased red cell deformability in the similar mode (Fig. 47.11).

Na-vanadate is a commonly used Ca^{2+} pump blocker, exerting a substantial effect on Ca^{2+} extrusion at millimolar concentrations in human red cells. At such levels, Na-vanadate also seems to open an L type-like Ca^{2+} channel in these cells [32]. We inhibited red cell tyrosine phosphatase activity by Na-vanadate and activated Lyn protein tyrosine kinase of Src family by cisplatin [33]. After that a significant red cell deformability rise was observed (Fig. 47.12).

These chemicals induce protein tyrosine phosphorylation of a number of cellular proteins, which suggests involvement of protein tyrosine kinases in the activation process of red cell membrane [34]. The latter is expected to lead to a dissociation of ternary complex (band 3 – band 4.1R – spectrin) and to an increase of red cell membrane plasticity [22]. In addition it was also observed that Ca^{2+}/calmodulin and calmodulin-dependent kinases are involved in the regulation of cisplatin-induced Lyn expression and activation in erythrocytes [33].

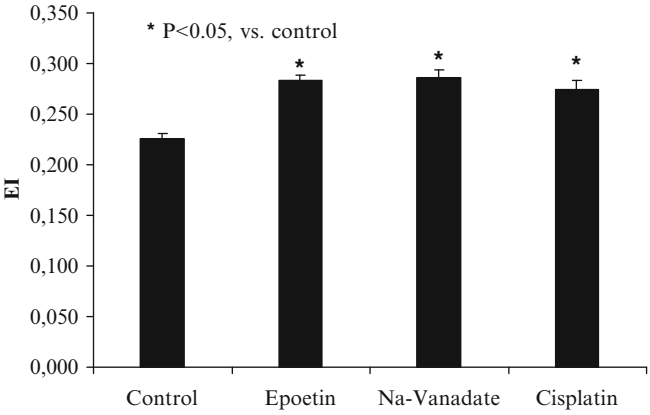

Fig. 47.12 Red cell deformability (*RBCD*) change under cell incubation with Epoetin (10.0 I.E./ml) Na-vanadate (100 μM) and Cisplatin (0.10 μM)

Alterations in Human Red Blood Cell Aggregation

Methods. Red blood cell aggregation (RBCA) in native plasma was assessed by two methods [16, 28]: (1) direct microscopic method with computer image analysis. This method gives two indexes of red cell aggregation: (1) ratio of the number of aggregates to the number nonaggregated red blood cells; (2) a number red blood cell per one aggregate.

The second one was the use of the Myrenne Aggregometer (Germany) which provides an index of RBC aggregation facilitated by low shear. In brief, the suspension was subjected to a short period of high shear to disrupt pre-existing aggregates, following which the shear was abruptly reduced to 3 s^{-1} and light transmission through the suspension that was integrated for 10 s; the resulting index, termed "M1" by the manufacturer and "ARBC" herein, increased with enhanced RBC aggregation. There was a positive correlation between microscopic aggregation index and Myrenne aggregometer one (e.g. one of M indexes; $r=0.860$)

The role of ionized calcium in intercellular interactions is well known, because any cellular contacts fail in the absence of calcium ions. Red blood cell aggregation is a special type of intercellular interactions, the mechanism and physiological importance of which are not clearly understood now, so this phenomena needs further investigations.

Human erythrocytes join forming linear or branched aggregates when they are suspended in blood plasma or solutions containing macromolecular polymers (Fig. 47.13). The linear aggregates are often termed "rouleaux" since they resemble a stack of coins [35]. In vivo red blood cell aggregation occurs at low shear stress or stasis and is a major determinant of low shear blood viscosity and thus in vivo flow dynamics [36, 37]. Red blood cell aggregation in contrast to erythrocyte agglutination

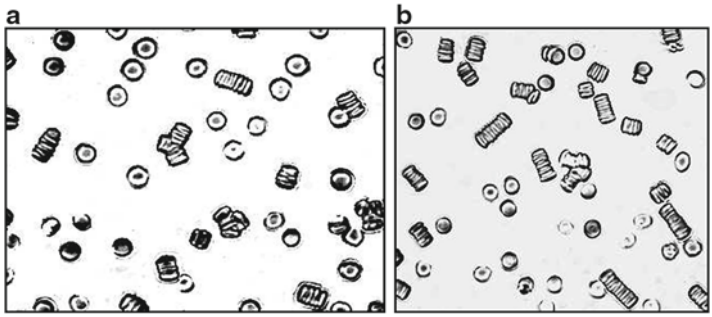

Fig. 47.13 Normal erythrocyte aggregation in human blood (**a**); enhanced erythrocyte aggregation (**b**)

or blood coagulation is reversible process: aggregates may be dispersed by external (fluid flow) forces and then reform when forces are removed.

Enhanced aggregation is found in many clinical and pathophysiological states, such as acute myocardial infarction [38], angina [39], cerebral ischemia [40], chronic renal failure [41], diabetes [42], subarachnoid hemorrhage [43], HIV infection [44], cardiac syndrome X [45].

The specific mechanisms determining the process of erythrocyte aggregation have not yet been elucidated, and thus the relation between pathology and red blood cell aggregation is not fully understood. In past most reports dealt primarily with the ability of plasma proteins (mainly fibrinogen) and higher macromolecular polymers to promote aggregation. Studies specifically focused on cellular factors and mechanisms in RBC aggregation began in the late 1980s [46].

The non-nucleated red cell is unique among human cell type in that the plasma membrane, its only structural component, accounts for all of its diverse antigenic, transport, and mechanical characteristics [47]. RBC's have been traditionally considered as rather reduced ("dead") cells because mature erythrocytes are devoid of a nucleus, mitochondria and other internal organelles and regarded as simple reservoirs for oxygen transportation ("bag of hemoglobin") [48]. But are they dead? Recently, it has become increasingly clear that, in addition to passively carrying and delivering oxygen, the erythrocyte participates in the regulation of its own distribution within the microcirculation. ATP released from erythrocytes can be thought of as a component of a local hormonal signaling system whose purpose is to regulate the distribution of blood perfusion to precisely meet local tissue oxygen need [49].

In addition it has been determined that red blood cells have a significant number of signaling molecules [15, 50, 51]. It has been proven experimentally that RBC membrane contains α- и β-adrenoreceptors [26, 52, 53], insulin receptors [54, 55], ceruloplasmin receptors [56], endothelin-1 receptors [57], cholinergic muscarinic receptors [58] etc. These findings suggest that RBC's participate in regulatory processes, which integrate body functions.

Blood is a liquid tissue, where erythrocytes are dispersed in plasma, so that the extracellular calcium could play the significant part in RBC aggregation process. About one a half of total blood plasma calcium is free so that it is physiologically active.

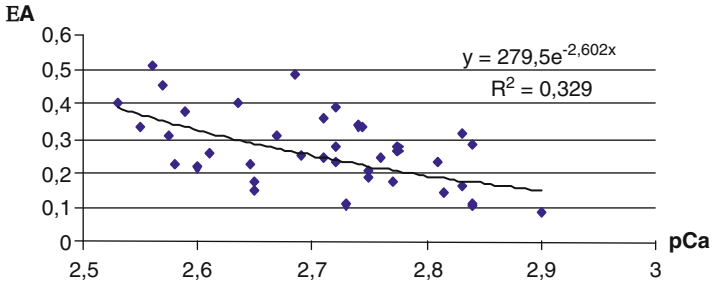

Fig. 47.14 Relation between the extent of erythrocyte aggregation (*EA*) and free plasma calcium content (*pCa*)

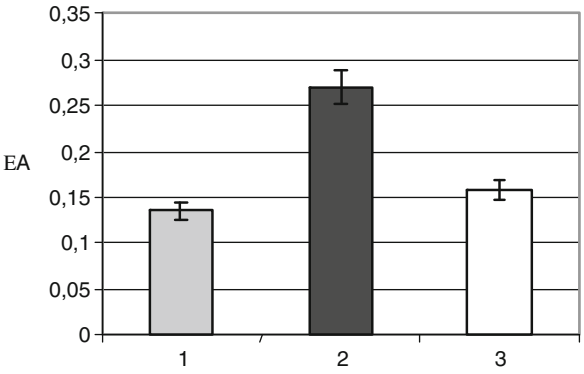

Fig. 47.15 Extent of red blood cell aggregation: *1* in autoplasma, *2* in plasma with addition of 1.0 mM $CaCl_2$, *3* in autoplasma with addition of 1 mM $CaCl_2$ in presence of 1 mM EGTA

Our experimental data indicated that even moderate elevation of the ionized calcium level in human blood plasma (up to 20.6%) caused significant increase of red blood cell aggregability (by 80.4%, $p<0.01$). It was shown that this Ca^{2+}-induced growth of erythrocyte aggregability is dose dependent and the exponential relation between the extent of aggregation (EA) and pCa (–log [Ca^{2+}]) was revealed in physiological area of plasma calcium content (Fig. 47.14).

The Ca^{2+}-induced increase of red blood cell aggregability was markedly inhibited in presence of EGTA (Fig. 47.15).

Elevation of ionized calcium content in plasma leads to an increase of erythrocyte membrane-bound quantity of calcium. Calcium is capable to bind to cell membrane anions, mainly to carboxyl groups of proteins and acid phospholipids. It is known that EGTA treatment almost fully (up to 90%) removes the membrane-bound calcium which is localized at the outer side of cell surface. Thus the inhibition of Ca^{2+}-induced growth of erythrocyte aggregability in presence of EGTA let us to suppose that membrane-bound calcium plays a major role in RBC aggregation process.

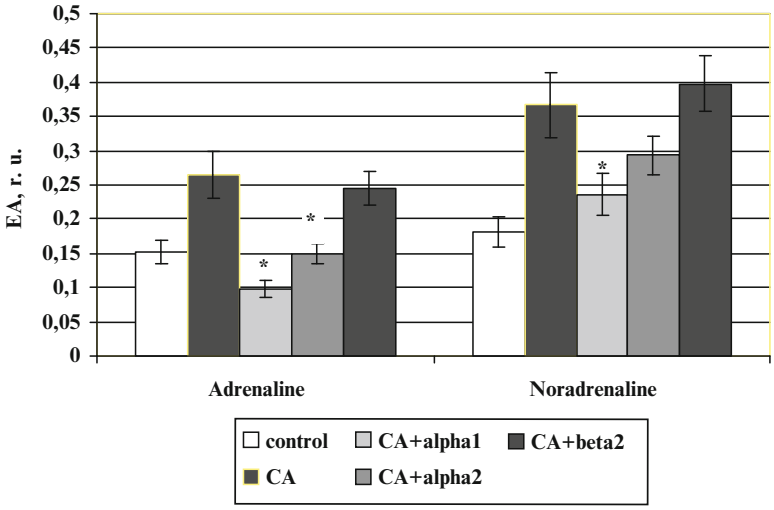

Fig. 47.16 Extent of red blood cell aggregation (*EA*) under catecholamine (*CA*) action in presence of *α1 blocker* corynanthine, *α2 blocker* yohimbine and *β2 blocker* propranolol

Membrane-bound calcium is capable to change substantially not only the cell surface charge, but also it has influence on the structure and properties of cell membrane and can facilitate calcium influx. Intracellular calcium regulates a number of membrane functions of erythrocytes, including maintenance of normal discoid shape, control of membrane lipid composition and permeability.

Measurement of total red cell calcium concentration has yielded values between 5 and 50 nM [59], while only a few percent of total red cell calcium is in ionized form. Most intracellular Ca^{2+} is bound and the low cell ionized Ca^{2+} concentration is maintained by a combination of low membrane permeability and a powerful Ca^{2+}-pump. This pump has been identified with a (Ca^{2+} + Mg^{2+})-stimulated ATPase, and both Ca^{2+} transport and ATP splitting are stimulated by calmodulin [60].

An elevation in intracellular Ca^{2+} concentration accompanied by an increase of erythrocyte aggregability is fixed in a number of pathological states and under red blood cell ageing or depletion [61–63].

There is an established functional connection between calcium influx and apoptosis-like events in mature erythrocytes (so called “eryptosis”) [64].

When we studied the effect of catecholamines (adreanaline and noradrenaline) on erythrocyte aggregation, the significant increase of red blood cell aggregability was registered in the presence of both substances (10^{-6} M) (Figs. 47.16 and 47.17). This promoting action of adrenaline and noradrenaline was markedly inhibited by α1 blocker corynanthine, it led us to suppose that this proaggregative effect of catecholamines was mediated by the activation of α1 adrenoceptors.

Alpha1 adrenoceptor activation is followed by the cascade of reactions with involvement of Ca^{2+} and protein kinase C. Staurosporine aglycone is considered as nonselective PKC inhibitor and it inhibits calcium influx into erythrocytes [65].

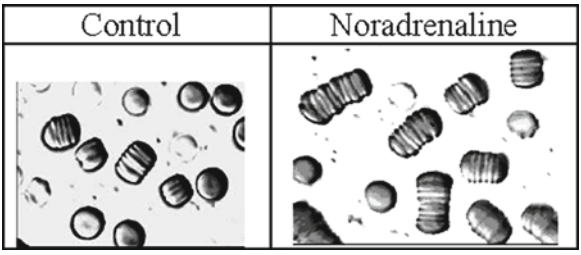

Fig. 47.17 Red blood cell aggregation changes under incubation with noradrenaline (10^{-6} M, 15 min, at 37°C)

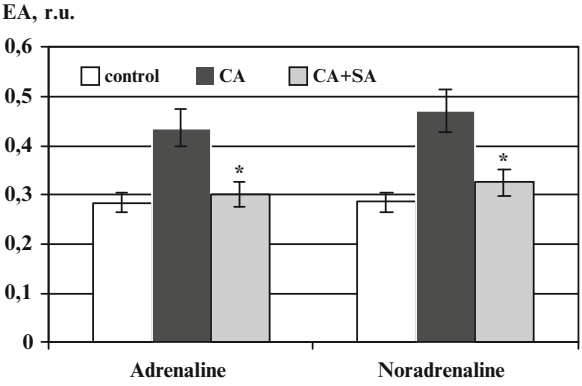

Fig. 47.18 Extent of red blood cell aggregation (*EA*) under catecholamine (*CA*) action in presence of proteinkinase C inhibitor staurosporin aglycone (*SA*)

In presence of staurosporin aglycone (2 nM) the stimulative effect of catecholamines on erythrocyte aggregation was neglected (Fig. 47.18), provided the conclusion that PKC and Ca^{2+} play significant role in this process.

Any rise in intracellular Ca^{2+} in erythrocytes activates a specific K^+ channel ("Gardos" channel) which normally makes little contribution to K^+ fluxes [66, 67]. To determine whether proaggregative effect of catecholamines is followed by the activation of Gardos channel, we added to blood plasma $BaCl_2$ (up to 2.5 mM) which prevented the Gardos effect. Again, the stimulating effect of catecholamines was neglected (Fig. 47.19).

Finally, the effect of controlled increase of intracellular calcium on red blood cell aggregability was studied in two cases: (1) under elevation of Ca^{2+} influx caused the erythrocyte treatment by calcimycin A23187 1.0 μM, thrombin 0.05 U/ml or sodium fluoride 1.0 mM and (2) under Ca-ATPase inhibition by sodium vanadate 0.1 mM, trifluoperazine 10 μM or staurosporine aglycone 0.1 μM. Specific Ca-ATPase inhibitor is unknown, but it is known that this enzyme in erythrocytes is activated by calmodulin and PKC, so that we used inhibitors of these proteins – trifluoperazine and staurosporine aglycone. Vanadate is a commonly used Ca^{2+} pump blocker [32].

Red blood cell treatment by stimulators of Ca^{2+} influx as well as inhibition of calcium efflux resulted in markedly increased erythrocyte aggregation (Figs. 47.20 and 47.21).

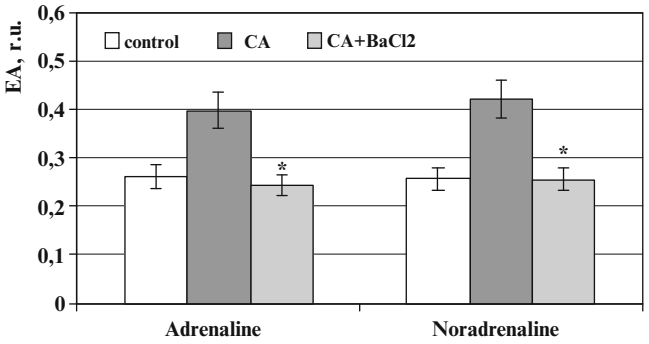

Fig. 47.19 Extent of red blood cell aggregation (*EA*) under catecholamine (*CA*) action in presence of Gardos effect inhibitor $BaCl_2$

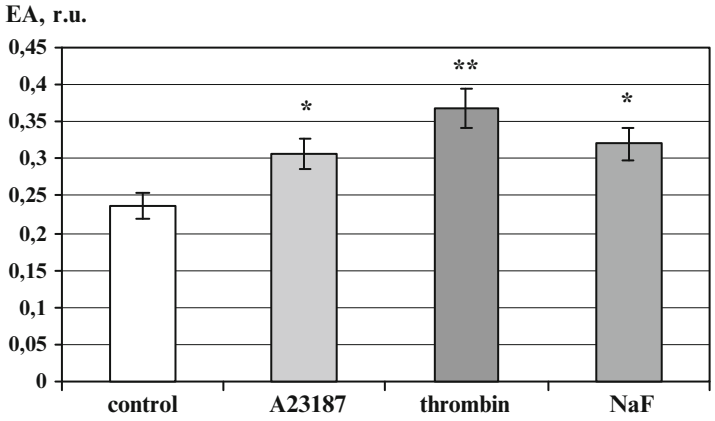

Fig. 47.20 Red blood cell extent of aggregation (*EA*) under stimulation of Ca influx

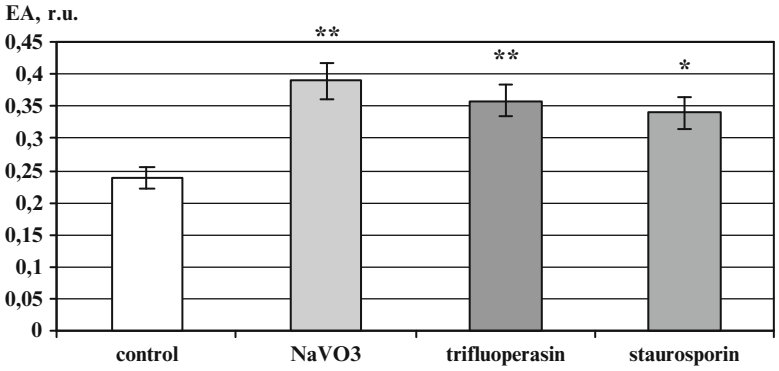

Fig. 47.21 Red blood cell extent of aggregation (*EA*) under inhibition of Ca efflux

Conclusion

The mechanical properties of human erythrocyte membrane are largely regulated by submembranous protein skeleton whose principal components are alpha- and beta-spectrin, actin, protein 4.1, adducin, and dematin. All of these proteins, except for actin, are phosphorylated by various kinases present in the erythrocyte [22].

Our data for the first time demonstrate that an increase of cytosolic Ca^{2+} lead to the cell deformability lowering (Fig. 47.22). On the contrary the Ca^{2+} cell entry blocking is accompanied by an improvement of red cell mechanical properties.

Thus the control of the main red cell microrheological properties are connected with oxygen transport efficiency might be realized under an activation of the molecular signaling pathways. The increase Ca^{2+} entry into cells was accompanied by a significant RBCA rise and some deformability lowering. RBCs have already been reported to contain nonspecific, voltage-gated cation channels that favors monovalent cations, but can transport Ca^{2+} as well [68]. The blocking Ca^{2+} influx with verapamil leads to a decrease of RBCA. On the other hand there were positive changes of red cell microrheology after Ca^{2+} entry blocking or under adenylyl cyclase activation. There is a particularly rich source of potential sites of crosstalk between the cAMP and the Ca^{2+} signaling pathways. Potential sites of cross-talk between the Ca^{2+} and cAMP signaling systems in red blood cells may be PDEs. For example, under basal conditions, the constitutive type 4 phosphodiesterase activity rapidly hydrolyzes cAMP so that the Ca^{2+} inhibition of AC_6 is difficult to resolve, indicating that high phosphodiesterase activity works coordinately with AC_6 to regulate membrane-delimited cAMP concentrations, which is important for control of cell-cell apposition [69]. Moreover there are data that clearly indicate that an activation of AC and cAMP increase lead to the Ca^{2+} influx decrease

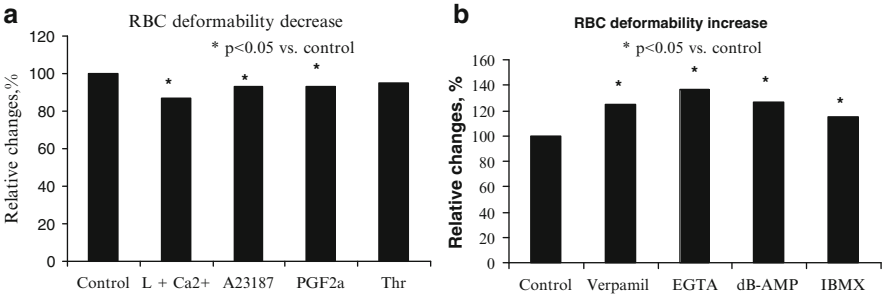

Fig. 47.22 The red blood cell deformability changes under increase of intracellular Ca^{2+} concentration (**a**) and under its decrease one (**b**) *Abbreviations*: $L + Ca^{2+}$ combined effect of mechanical loading (L) and calcium (Ca^{2+}), *A23187* calcium ionophore, *PGF2a* prostaglandin $F_{2\alpha}$, *Thr* thrombin

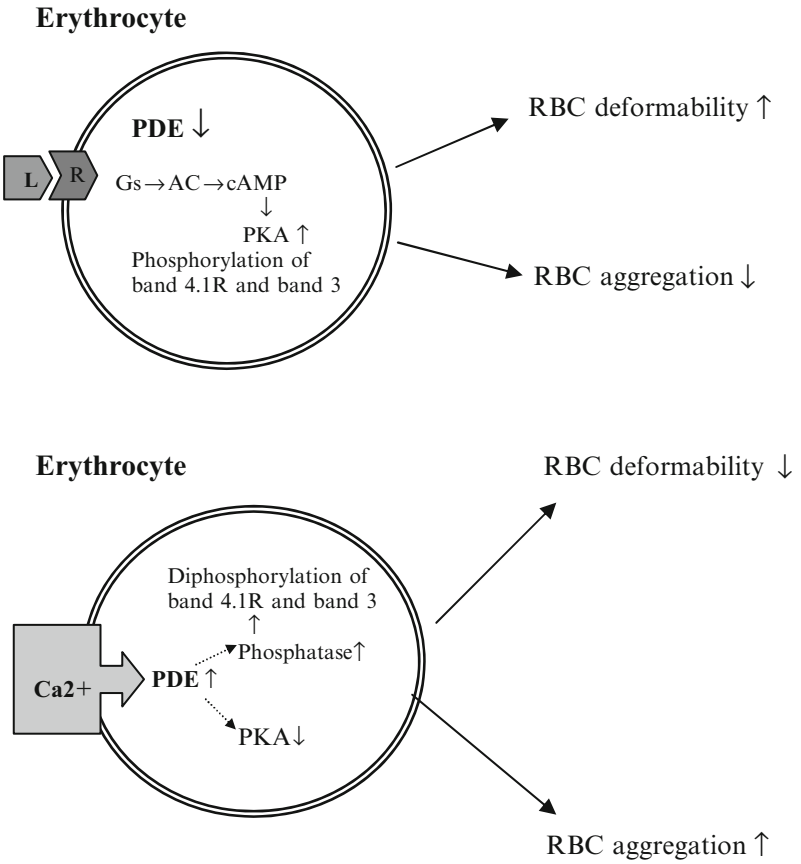

Fig. 47.23 Signaling pathway probably activated under red cell deformation increase and aggregation lowering. *Abbreviations*: *L* ligand, *R* membrane receptor, *PDE* phosphodiesterase, *Gs* G- protein, *AC* adenylyl cyclase, *PKA* protein kinase A

[70]. In our experiments it is accompanied by red cell aggregation lowering and deformability rise. The similar results were found under the blocking Ca^{2+} entry into cell or PDE activity inhibition.

A probable molecular signaling pathway under a positive RBC microrheology response may include: the membrane receptor coupled with Gs-protein (e.g. β-adrenergic receptor), AC, cAMP, PKA, band 4.1R (Fig. 47.23).

Erythrocyte membrane mechanical function is regulated by the spectrin-based membrane skeleton composed of alpha- and beta-spectrin, actin, protein 4.1R (4.1R), and adducin [70]. It has been showed that the phosphorylation of 4.1R by PKC results in its decreased ability to form a ternary complex with spectrin and actin as well as dissociation of glycophorin C from the membrane skeleton. Results show that phosphorylation of band 4.1 by cAMP-dependent kinase may be central

to the regulation of red cell cytoskeletal organization and membrane mechanical properties [71, 72].

A rise in intracellular Ca^{2+} concentration of the erythrocytes may stimulate of PDE activity and PKA inhibition. It was accompanied by dephosphorylation band 4.1R and formation of a ternary complex. It leads to membrane stability increase and red cell deformation lowering [22].

Our data suggest that a simulation of red cell AC-cAMP-signaling system leads to change RBC microrheological properties. Spotlighting these important molecular loci at which cAMP and Ca^{2+} signaling pathways converge in non-excitable cells should help us further understand and appreciate the complexity and specificity of stimulus-response coupling in these cells. These processes will also be highlighted in an attempt to focus attention on important new directions for future research.

Thus Ca^{2+} entry blocking into the red cells by verapamil or its chelating in medium by EGTA led to significant RBCA decrease and deformability rise ($p < 0.05$).

On the whole the total data clearly show that the red cell aggregation and deformation changes were connected with an activation of the intracellular signaling pathways.

It seems reasonable to suppose that RBCA increase was mainly associated with activation of Ca^{2+} control mechanisms, while the red cell deformability was closely associated of the adenylyl-cyclase-cAMP system.

Acknowledgments Work was supported by FSP "Research and educational personnel of innovative Russia for 2009–2013 years" and by grant of RFBR No. 09-04-00436-a

References

1. Berga L, Dolz J, Vives-Corrons JL, Feliu E, Rozman C (1984) Viscometric methods for assessing red cell deformability and fragmentation. Biorheology Suppl 1:297–301
2. Nash GB, Meiselman HJ (1985) Alteration of red cell membrane viscoelasticity by heat treatment: effect on cell deformability and suspension viscosity. Biorheology 22(1):73–84
3. Mohandas N, Chasis JA (1993) Red blood cell deformability, membrane material properties and shape: regulation by transmembrane, skeletal and cytosolic proteins and lipids. Semin Hematol 30(3):171–192
4. Zhang J, Johnson PC, Popel AS (2008) Red blood cell aggregation and dissociation in shear flows simulated by lattice Boltzmann method. J Biomech 41:47–55
5. Kaliviotis E, Ivanov I, Antonova N, Yianneskis M (2010) Erythrocyte aggregation at non-steady flow conditions: a comparison of characteristics measured with electrorheology and image analysis. Clin Hemorheol Microcirc 44:43–54
6. Bishop JJ, Nance PR, Popel AS, Intaglietta M, Johnson PC (2001) Effect of erythrocyte aggregation on velocity profiles in venules. Am J Physiol Heart Circ Physiol 280:H222–H236
7. Minetti G, Low PS (1997) Erythrocyte signal transduction pathways and their possible functions. Curr Opin Hematol 4:116–121
8. Hilario S, Saldanha C, Martin-a-Silva J (1999) The effect of adrenaline upon human erythrocyte properties sex-related differences? (abstract). Biorheology 36(1–2):124

9. De Oliveira S, Silva-Herdade A, Saldanha C (2008) Modulation of erythrocyte deformability by PKC activity. Clin Hemorheol Microcirc 39:363–373
10. De Oliveira S, Saldanha C (2010) An overview about erythrocyte membrane. Clin Hemorheol Microcirc 44:63–74
11. Oonishi T, Sakashita K, Uyesaka N (1997) Regulation of red blood cell filterability by Ca^{2+} influx and cAMP-mediated signaling pathways. Am J Physiol 273:C1828–C1834
12. Tuvia S, Moses A, Gulayev N, Levin S, Korenstein R (1999) Beta-adrenergic agonists regulate cell membrane fluctuations of human erythrocytes. J Physiol 516:781–792
13. Towart R, Schramm M (1985) Calcium channel modulators and calcium channels. Biochem Soc Symp 50:81–95
14. Hallett MB, Campbell AK (1984) Is intracellular Ca^{2+} the trigger for oxygen radical production by polymorphonuclear leucocytes? Cell Calcium 5(1):1–19
15. Minetti G, Ciana A, Balduini C (2004) Differential sorting of tyrosine kinases and phosphotyrosine phosphatases acting on band 3 during vesiculation of human erythrocytes. Biochem J 377:489–497
16. Muravyov AV, Tikhomirova IA, Maimistova AA, Bulaeva SV (2010) Crosstalk between adenylyl cyclase signaling pathway and Ca^{2+} regulatory mechanism under red blood cell microrheological changes. Clin Hemorheol Microcirc 45:337–345
17. Sauer H, Hescheler J, Wartenberg M (2000) Mechanical strain-induced Ca^{2+} waves are propagated via ATP release and purinergic receptor activation. Am J Physiol Cell Physiol 279:C295–C307
18. Takakuwa Y, Mohandas N, Ishibashi T (1990) Regulation of red cell membrane deformability and stability by skeletal protein network. Biorheology 27(3–4):357–365
19. Thiel M, Bardenheuer H (1992) Regulation of oxygen radical production of human polymorphonuclear leukocytes by adenosine: the role of calcium. Pflugers Arch 420(5–6):522–528
20. Del Carlo B, Pellegrini M, Pellegrino M (2003) Modulation of Ca^{2+}-activated K^+ channels of human erythrocytes by endogenous protein kinase C. Biochim Biophys Acta 1612(1):107–116
21. Lang F, Birka C, Myssina S, Lang KS, Lang PA, Tanneur V, Duranton C, Wieder T, Huber SM (2004) Erythrocyte ion channels in regulation of apoptosis. Adv Exp Med Biol 559:211–217
22. Manno S, Takakuwa Y, Mohandas N (2005) Modulation of erythrocyte membrane mechanical function by protein 4.1 phosphorylation. J Biol Chem 280(9):7581–7587
23. Pitter JG, Szanda G, Duchen MR et al (2005) Prostaglandin $F_{2\alpha}$ potentiates the calcium dependent activation of mitochondrial metabolism in luteal cells. Cell Calcium 37:35–44
24. Nedrelow JH, Cianci CD, Morrow JS (2003) c-Src binds alpha II spectrin's Src homology 3 (SH3) domain and blocks calpain susceptibility by phosphorylating Tyr1176. J Biol Chem 278(9):7735–7741
25. Tepperman J, Tepperman H (1987) Metabolic and endocrine physiology and introductory text. Year Book Publishers, Inc., Chicago/London
26. Sundquist J, Bias DS, Hogan JE (1992) The α_1-adrenergic receptor in human erythrocyte membranes mediates interaction in vitro of epinephrine and thyroid hormone at the membrane Ca^{2+}-ATPase. Cell Signal 4:795–799
27. Horga JF, Gisbert JJ, De Agustin C (2000) A beta-2-adrenergic receptor activates adenylate cyclase in human erythrocyte membranes at physiological calcium plasma concentrations. Blood Cells Mol Dis 26:223–228
28. Muravyov AV, Yakusevich VV, Maimistova AA, Chuchkanov FA, Bulaeva SV (2007) Hemorheological efficiency of drugs, targeting on intracellular phosphodiesterase activity: in vitro study. Clin Hemorheol Microcirc 24:19–23
29. Laszlo R, Winkler C, Wöhrl S, Laszlo S, Eick C, Schreieck J, Bosch RF (2007) Influence of verapamil on tachycardia-induced alterations of PP1 and PP2A in rabbit atrium. Exp Clin Cardiol 12(4):175–178
30. Cooper DM, Brooker G (1993) Ca^{2+}-inhibited adenylate cyclase in cardiac tissue. Trends Pharmacol Sci 14:34–35
31. Phillips PG, Long Lu, Wilkins MR, Morrell NW (2005) cAMP phosphodiesterase inhibitors potentiate effects of prostacyclin analogs in hypoxic pulmonary vascular remodeling. Am J Physiol Lung Cell Mol Physiol 288:L103–L115

32. Romero PJ, Romero EA (2003) New vanadate-induced Ca^{2+} pathway in human red cells. Cell Biol Int 27(11):903–912
33. Singh RA, Sodhi A (1998) Expression and activation of lyn in macrophages treated in vitro with cisplatin: regulation by kinases, phosphatases and Ca^{2+}/calmodulin. Biochim Biophys Acta 21:171–179
34. Tong W, Zhang J, Lodish HF (2005) Lnk inhibits erythropoiesis and Epo-dependent JAK2 activation and downstream signaling pathways. Blood 15:4604–4612
35. Neu B, Meiselman HJ (2007) Red blood cell aggregation. In: Baskurt OK, Hardeman MR, Rampling MW, Meiselman HJ (eds) Handbook of hemorheology and hemodynamics. Ios Press, Amsterdam/Berlin/Tokyo/Washington, DC, pp 114–136
36. Kim S, Popel AS, Intaglietta M, Johnson PC (2005) Aggregate formation of erythrocytes in postcapillary venules. Am J Physiol Heart Circ Physiol 288:H584–H590
37. Baskurt OK, Meiselman HJ (2007) Hemodynamic effects of red blood cell aggregation. Indian J Exp Biol 45:25–31
38. Toth K, Bogar L, Juricskay I, Kelti M et al (1997) The effect of RheothRx Injection on the hemorheological parameters in patients with acute myocardial infarction. Clin Hemorheol Microcirc 17:117–125
39. Rainer C, Norris S, Haywood LJ, Meiselman HJ (1989) Blood rheology and RBC aggregation in patients with angina pectoris and a prior history of myocardial infarction. Clin Hemorheol 9:923–934
40. Fisher M, Meiselman HJ (1991) Hemorheological factors in cerebral ischemia. Stroke 22:1164–1169
41. Hein HJ, Bauersachs RM, Feinstein E, Meiselman HJ (1988) Hemorheological abnormalities in chronic renal failure. Clin Hemorheol 8:425–431
42. Chong-Martinez B, Buchanan TA, Wenby RB, Meiselman HJ (2003) Decreased red blood cell aggregation subsequent to improved glycemic control in type 2 diabetes mellitus. Diabet Med 20:301–306
43. Fisher M, Giannotta S, Meiselman HJ (1987) Hemorheological alterations in patients with subarachnoid hemorrhage. Clin Hemorheol 7:611–618
44. Kim A, Dadgostar H, Holland GN, Wenby R et al (2006) Hemorheologic abnormalities associated with HIV infection: altered erythrocyte aggregation and deformability. Invest Ophthalmol Vis Sci 47:3927–3932
45. Lee BK, Durairaj A, Mehra A, Wenby RB et al (2008) Microcirculatory dysfunction in cardiac syndrome X: role of abnormal blood rheology. Microcirculation 15:451–460
46. Meiselman HJ (2009) RBC aggregation: 45 years being curious. Biorheology 46:1–19
47. Mohandas N, Gallagher P (2008) Red cell membrane: past, present, and future. Blood 112(10):3939–3948
48. Sprague RS, Stephenson AH, Ellsworth ML (2007) Red not dead: signaling in and from. Trends Endocrinol Metab 18(9):350–355
49. Ellsworth ML, Ellis CG, Goldman D, Stephenson AH, Dietrich HH, Sprague RS (2009) Erythrocytes: oxygen sensors and modulators of vascular tone. Physiology 24:107–116
50. An X, Debnath G, Guo X et al (2005) Identification and functional characterization of protein 4.1R and actin-binding sites in erythrocyte beta spectrin: regulation of the interactions by phosphatidylinositol-4,5-bisphosphate. Biochemistry 44:10681–10688
51. Hines PS, Zen Q, Burney SN et al (2003) Novel epinephrine and cyclic cAMP – mediated action on BCAM/Lu – dependent sickle (SS) RBC adhesion. Blood 101(8):3281–3287
52. Bree F, Gault I P, d'Athis and Tillement JP (1984) Beta adrenoceptors of human red cells, determination of their subtypes. Biochem. Pharmacol 33:4045–4050
53. Sager G, Jacobsen S (1985) Effect of plasma on human erythrocyte beta-adrenergic receptors. Biochem Pharmacol 34:3767–3771
54. Bhattacharya S, Chakaborty PS, Basu RS et al (2001) Purification and properties of insulin-activated nitric oxide synthase from human erythrocyte membranes. Arch Physiol Biochem 109:441–449

55. Zancan P, Sola-Penna M (2005) Calcium influx: a possible role for insulin modulation of intracellular distribution and activity of 6-phosphofructo-1-kinase in human erythrocytes. Mol Genet Metab 86(3):392–400
56. Saenko EL, Yaropolov AI (1990) Studies on receptor interaction of ceruloplasmin with human red blood cells. Biochem Int 20(2):215–225
57. Sakashita K, Oonishi T, Ishioka N, Uyesaka N (1999) Endothelin-1 improves the impaired filterability of red blood cells through the activation of protein kinase C. Jpn J Physiol 49:113–120
58. Tang LC, Schoomaker E, Wiesmann WP (1984) Cholinergic agonists stimulate calcium uptake and cGMP formation in human erythrocytes. Biochim Biophys Acta 772:235–238
59. Engelmann B (1991) Calcium homeostasis of human erythrocytes and its pathophysiological implications. Klin Wochenschr 69(4):137–142
60. Wiley JS, McCulloch KE (1982) Calcium ions, drug action and the red cell membrane. Pharmacol Ther 18(2):271–292
61. Romero PJ, Romero EA (1999) The role of calcium metabolism in human red blood cell ageing: a proposal. Blood Cells Mol Dis 25(1):9–19
62. Cicco G, Carbonara M, Stingi G, Pirrelli A (2001) Cytosolic calcium and hemorheological patterns during arterial hypertension. Clin Hemorheol 24:25–31
63. Ohnishi ST, Ohnishi T, Ogunmola GB (2001) Green tea extract and aged garlic extract inhibit anion transport and sickle cell dehydration in vitro. Blood Cells Mol Dis 27(1):148–157
64. Antonelou M, Kriebardis A, Papassideri I (2010) Aging and death signalling in mature red cells: from basic science to transfusion practice. Blood Transfus 8(3):39–47
65. Klarl BA, Lang PA, Kempe DS et al (2006) Protein kinase C mediates erythrocyte "programmed cell death" following glucose depletion. Am J Physiol Cell Physiol 290:C244–C253
66. Kaiserova K, Lakatos B, Peterajova E, Orlicky J, Varecka L (2002) Investigation of properties of the Ca^{2+} influx and of the Ca^{2+}-activated K^+ efflux (Gardos effect) in vanadate-treated and ATP-depleted human red blood cells. Gen Physiol Biophys 21(4):429–442
67. Hoffman JF, Joiner W, Nehrke K et al (2003) The hSK4 (KCNN4) isoform is the Ca^{2+}-activated K^+ channel (Gardos channel) in human red blood cells. Proc Natl Acad Sci USA 100:7366–7371
68. Christophersen P, Bennekou P (1991) Evidence for a voltage-gated, non-selective cation channel in the human red cell membrane. Biochim Biophys Acta 1065:103–106
69. Creighton JR, Cooper DMN, Stevens T (2003) Coordinate regulation of membrane cAMP by Ca^{2+}-inhibited adenylyl cyclase and phosphodiesterase activities. Am J Physiol (Lung Cell Mol Physiol) 284:L100–L107
70. Herzog M, Scherer EQ, Albrecht B, Rorabaugh B, Scofield MA (2002) CGRP receptors in the gerbil spiral modiolar artery mediate a sustained vasodilatation via a transient cAMP-mediated Ca^{2+}-decreased. J Membr Biol 189:225–236
71. Ling E, Danilov YN, Cohen CM (1988) Modulation of red cell band 4.1 function by cAMP-dependent kinase and protein kinase C phosphorylation. J Biol Chem 15:2209–2216
72. Nunomura W, Takakuwa Y (2006) Regulation of protein 4.1R interactions with membrane proteins by Ca^{2+} and calmodulin. Front Biosci 1(11):1522–1539

Chapter 48
Calcium Imaging in the Zebrafish

Petronella Kettunen

Abstract The zebrafish (*Danio rerio*) has emerged as a new model system during the last three decades. The fact that the zebrafish larva is transparent enables sophisticated *in vivo* imaging. While being the vertebrate, the reduced complexity of its nervous system and small size make it possible to follow large-scale activity in the whole brain. Its genome is sequenced and many genetic and molecular tools have been developed that simplify the study of gene function. Since the mid 1990s, the embryonic development and neuronal function of the larval, and later, adult zebrafish have been studied using calcium imaging methods. The choice of calcium indicator depends on the desired number of cells to study and cell accessibility. Dextran indicators have been used to label cells in the developing embryo from dye injection into the one-cell stage. Dextrans have also been useful for retrograde labeling of spinal cord neurons and cells in the olfactory system. Acetoxymethyl (AM) esters permit labeling of larger areas of tissue such as the tectum, a region responsible for visual processing. Genetically encoded calcium indicators have been expressed in various tissues by the use of cell-specific promoters. These studies have contributed greatly to our understanding of basic biological principles during development and adulthood, and of the function of disease-related genes in a vertebrate system.

Keywords Calcium • Development • Genetically encoded calcium indicator • Transgenic • Zebrafish

P. Kettunen, Ph.D. (✉)
Institute of Neuroscience and Physiology, Sahlgrenska Academy at the University of Gothenburg

Klinisk kemi, Bruna stråket 16, 41345 Gothenburg, Sweden
e-mail: petronella.kettunen@neuro.gu.se

M.S. Islam (ed.), *Calcium Signaling*, Advances in Experimental Medicine and Biology 740, DOI 10.1007/978-94-007-2888-2_48,

Introduction

The zebrafish (*Danio rerio*) (Fig. 48.1) has emerged as a new model system during the last three decades. Its attractiveness as an experimental system stems from a number of factors that are pushing the zebrafish to the forefront as a model system for biomedical research. The fact that the zebrafish larva is transparent during its first days, and can stay transparent longer with chemical treatment or as non-pigmented strains (Fig. 48.1b) [2] enables sophisticated *in vivo* imaging. While being a vertebrate, the reduced complexity of its nervous system and small size make it possible to follow large-scale activity in the whole brain. Its genome is sequenced and many genetic and molecular tools have been developed that simplify the study of gene function. For example, a variety of mutants strains have been isolated in large mutagenesis screens. The identification of cell-specific enhancers and promoters has been used for the development of transgenic animals. Moreover, proteins can be easily overexpressed transiently or in stable lines using DNA injection into the fertilized egg. Similarly, proteins can be down-regulated during the first 5 days by the use of morpholino oligonucleotides [3].

Due to its external and fast embryonic development, the zebrafish initially attracted developmental scientists. With time, the zebrafish has showed usefulness in different areas, including cardiovascular research [4], neurodegenerative diseases [5], psychiatry [6] and cancer research [7]. One quickly growing field using the zebrafish is high-throughput chemical and toxicological screening benefitting from the small size and simplicity of drug delivery through the skin [8, 9]. Also, various techniques such as electrophysiological recordings, calcium imaging and behavioral tests have demonstrated the convenience of the zebrafish as a model system. Particularly, the combination of *in vivo* physiological and behavioral techniques in wild-type, mutated or transgenic zebrafish has made it possible to perform studies that would be hard or impossible in other preparations.

The aim of this chapter is to give a broad summary of the indicator dyes and labeling techniques used to record intracellular calcium in various zebrafish preparations and a review of findings from projects using calcium imaging in the zebrafish.

Fig. 48.1 The zebrafish can be studied at various ages. (**a**) Photo of wild type zebrafish embryos, ~24 h post-fertilization (Reprinted from Kaufman et al. [1] by permission from Macmillan Publishers Ltd. Copyright 2009). (**b**) Zebrafish *nacre* mutant larva, ~72 h post-fertilization (Photo: Todd O. Anderson). (**c**) Adult male zebrafish (Photo: Todd O. Anderson)

Calcium Indicators

The main advantages of using the zebrafish for calcium imaging are the variety of labeling methods and the small size, enabling *in vivo* imaging of many different structures in either anesthetized or awake animals. Since the mid 1990s, the embryonic development and neuronal function of the larval, and later, adult zebrafish have been studied using calcium imaging methods. Calcium indicators can be divided according to their chemical structure, optical properties and means of delivery [10]. Dextran-conjugated indicators, membrane-permeable acetoxymethyl (AM) ester dyes and genetically encoded calcium sensors have all been used in the zebrafish, studying phenomena ranging from the fertilization of the oocyte to following neuronal activity in the adult animal. The choice of calcium indicator depends on the desired number of cells to study and cell accessibility. For example, dextran indicators can restrict their labeling to a limited number of cells, or label cells in a cell lineage during development [11]. In contrast to dextrans, the perfusion of AM esters permits labeling of larger areas of tissue using multi-cell bolus loading [12] or can be used to label isolated organs or cells in culture [13]. Genetically encoded indicators can give precise labeling of identified cell types by the use of cell-specific gene enhancers or promoters, either limited to a couple of specific neurons or labeling the whole brain or organ with a general promoter, such as the neuronal *HuC* promoter [14].

Dextrans

The water-soluble dextran-conjugated calcium indicators have a wide variety of applications, ranging from injection into developing eggs, dialysis into cells or injection into axonal pathways which leads to local dye uptake with subsequent anterograde and retrograde transport over hours and days. Dextran dyes can fill structures far away meaning that imaging can be done at a distance from the injection site where the tissue might be damaged and unspecifically stained, increasing the background fluorescence. In comparison with the AM ester dyes they show no compartmentalization and have low toxicity.

Calcium Green-1 dextran is the most common visible light–excitable calcium imaging dye used in the larval zebrafish [15]. Injected into the axonal tracts of the spinal cord of larval zebrafish it can backfill neurons in the spinal cord, hindbrain and midbrain [16]. Injections of Calcium Green-1 dextran into eggs at the one-cell stage have helped showing calcium fluctuations during fertilization, cleavage and blastula period. If injected embryos are let to develop, dye is retained in developing cells becoming for example neurons, which can then be optically recorded from. Calcium Green-1 dextran injections into the olfactory bulb in adult zebrafish have contributed to knowledge about processing in olfactory sensory neurons [17]. Dissociated muscle cells from zebrafish can also be dialyzed with Calcium Green-1 dextran for imaging [18].

The related dye Oregon Green 488 BAPTA-1 has low calcium-binding affinity, high fluorescence yield and great resistance to photobleaching. It has been used similarly to retrograde label neurons and to stain cells following egg injections. It has been used together with Texas Red dextran for ratiometric calcium measurements during gastrulation [19]. Similarly, Fluo-4 dextran has been used to monitor calcium events in the zebrafish blastula [20] and in muscle fibers after egg injections [21]. The ratiometric dextran-conjugated calcium indicators in the UV spectra, Fura-2 and Bis-Fura-2, have been used to image somitogenesis [22].

AM Esters

Cell-permeable AM esters diffuse into cells where endogenous esterases will cleave the ester groups, trapping the indicators inside the cells. AM esters can simultaneously and nonselectively label numerous cells. On the other hand, AM esters serve as a faster means of labeling cells (30 min) than dextran dye backfilling (12–24 h) [23]. AM esters are often mixed with pluronic acid, increasing the solubilization of water-insoluble dyes.

The first attempt to label larger portions of the larval zebrafish spinal cord was done by Brustein and colleagues in 2003, using bolus injections of AM ester calcium dyes [23]. However, this method to label the spinal cord failed to gain any success, perhaps due to the development of genetically encoded calcium indicators blooming around the same time. However, this technique has been useful when labeling structures in the tectum with Oregon Green 488 BAPTA-1 AM [24]. Embryonic hearts have been labeled with Fluo-4 and Calcium Orange AM esters before imaging [25, 26]. In the red spectra, rhod-2 AM labels the larval [27] and adult [28] zebrafish olfactory bulb.

Genetically Encoded Calcium Indicators (GECIs)

Bioluminescent Aequorins

Protein-based calcium indicators can be divided into being fluorescent or bioluminescent, i.e. either emitting light when excited by light, or emitting visible light following a chemical reaction in a living organism. The first bioluminescent calcium sensitive photoprotein used in the zebrafish was aequorin derived from the jellyfish *Aequorea Victoria* [29, 30]. The binding of calcium ions to the photoprotein starts an enzymatic reaction leading to an emission of blue light. In contrast with fluorescent reporters, aequorin has no background light emission at basal calcium levels and does not require excitation light. Since no input of radiation energy is required, problems with photobleaching, phototoxicity and autofluorescence are avoided.

Recombinant aequorin has been directly injected into the zebrafish egg before fertilization to study calcium patterns during the whole embryogenesis up to ~24 h

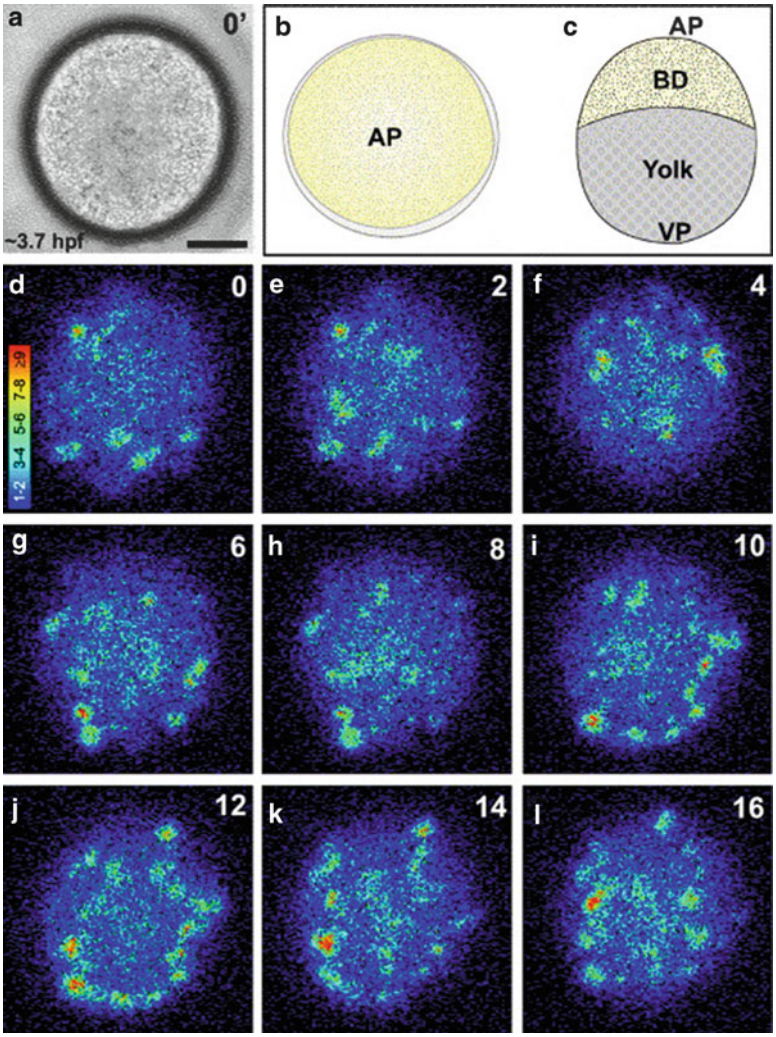

Fig. 48.2 Localized calcium signaling events occur during the blastula period of zebrafish development. (**a**) A bright-field image of a blastula stage embryo (3.7 h) viewed from the animal pole. Scale bar is 200 μm. (**b**, **c**) Schematics of the embryo from animal pole (*AP*) views (**b**) and lateral views (**c**) to show the morphology of the blastula stage embryo more clearly. *BD* and *VP* are blastoderm and vegetal pole, respectively. (**d**–**m**) The patterns of aequorin-generated light that are emitted by groups of interconnected enveloping layer cells within the blastoderm of the embryo shown in *panel A*. Each panel represents 240 s of accumulated luminescence with a 120 s gap between each image. Color scale indicates luminescence flux in photons/pixel (Reprinted from Webb and Miller [31]. Copyright 2006, with permission from Elsevier)

(Figs. 48.2 and 48.3), from fertilization to the formation of somites [33, 34]. To allow calcium imaging at later stages, mRNA coding for the native apoaequorin has been injected into the fertilized egg, expressing the fluorescent protein in somites and the trunk as late as 48 h [35].

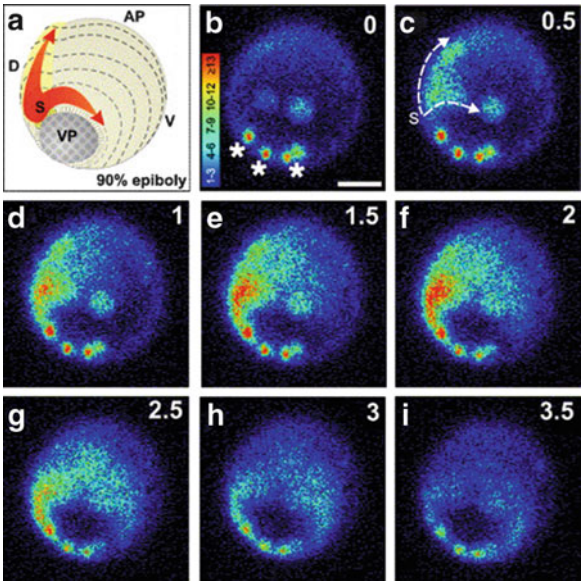

Fig. 48.3 Non-propagating localized domains of calcium and pan-embryonic intercellular calcium waves occur during the gastrula period of zebrafish development. (**a**) Schematic representation of the embryo illustrated in *panels B–I*, to show its orientation and the direction of propagation of the calcium waves more clearly. *AP, VP, D, V* and *S* are animal pole, vegetal pole, dorsal, ventral and shield, respectively. (**b–i**) A representative example of two pan-embryonic intercellular calcium waves at ~90% epiboly, recorded using aequorin. These waves are initiated at the embryonic shield, marked with an "*S*" in *panel C*, and propagates both around the blastoderm margin and along the embryonic axis in an anterior direction. Examples of non-propagating localized domains of elevated calcium are marked with asterisks in *panel B*. Each panel represents 120 s of accumulated luminescence with a 30 s gap between each image. Color scale indicates luminescence flux in photons/pixel. Scale bar is 200 μm (Reprinted from Webb and Miller [32]. Copyright 2006, with permission from Elsevier)

Despite a good signal to noise ratio, the low quantum yield of aequorin has limited its use. However, aequorin naturally exists in complex with green fluorescent protein (GFP), and energy from the chemical reaction of aequorin is transferred to GFP, leading to an emission of green light. This association with GFP is increasing the efficiency of calcium-dependent photoemission from aequorin from 10% to 90%, which inspired the development of a GFP-aequorin fusion protein [36]. Injection of chimeric GFP-aequorin mRNA gives protein expression as early as blastula stage [37] until at least 48 h post-fertilization (hpf) [35]. Zebrafish with GFP-apoaequorin expression driven by the *neuro-β-tubulin* promoter in hypocretin neurons as late as 7 days post-fertilization (dpf) have been used to study neuronal activity during natural behaviors [38].

GFP-Derived Fluorescent Indicators

Cameleon

A majority of the fluorescent GECIs are derivatives of GFP [39]. One of the first genetically encoded calcium indicators to be developed was cameleon, a hybrid protein in which cyan fluorescent protein (CFP) and yellow fluorescent protein (YFP) are linked by calmodulin and a calmodulin-binding peptide of myosin light-chain kinase (M13) [40]. When calcium levels are increasing, calcium binds to calmodulin, resulting in fluorescence resonance energy transfer (FRET) from CFP to YFP [41]. When excited by a wavelength appropriate for CFP excitation, an increase in calcium concentration causes an increase in the YFP/CFP fluorescence intensity ratio. Thus cameleon serves as a ratiometric calcium indicator.

Yellow cameleon 2.1 (YC2.1) has been generally expressed in the zebrafish brain using the *HuC* promoter, and specifically in spinal neurons using the *Islet-1* promoter [42]. Injection of YC2.12 mRNA into the fertilized egg gives YC expression between 3 and 48 h and has helped researchers to follow calcium changes during gastrulation [41].

The most recent YC indicators, the YC-Nano group of sensors, have an increased calcium affinity and large signal change. Initial tests in the zebrafish where purified YC-Nano proteins were injected in fertilized egg show calcium fluctuations from spontaneous muscle contractions in embryonic fish [43].

Pericams

Pericams [44] are based on a circular permutated GFP mutant. In pericams, calcium binding opens and closes a structure in the molecule, causing large changes in fluorescence [45]. Three types of pericams were generated with distinct spectral properties: probes whose fluorescence increases with calcium (flash pericam), decrease with calcium (inverse pericam) or undergoes a shift in excitation wavelength in a calcium-dependent manner (ratiometric pericam). Inverse pericam has been used to study calcium signaling in the olfactory bulb in both larval and adult zebrafish [46].

GCaMP

In 2001, Nakai and coworkers developed a calcium probe based on a single GFP molecule with high calcium affinity named GCaMP [47]. GCaMP expressed in larval hearts have illustrated muscle contractions *in vivo* [48] and the versions GCaMP1.6 and GCaMP3 have been expressed in the zebrafish tectum, a brain area responsible for visual processing [49]. The latest addition of GCaMP probes is the GCaMP-HS (GCaMP-*h*yper *s*ensitive) [50] which is brighter at the resting level

and more sensitive to the change of intracellular calcium concentrations than the previous version. It has been used to record spontaneous activity in motoneurons in larval zebrafish [50].

SyGCaMP2, is a fusion of GCaMP2 to the cytoplasmic side of synaptophysin, a transmembrane protein in synaptic vesicles [51]. By imaging zebrafish *in vivo*, it has been demonstrated that SyGCaMP2 can be used to monitor visual activity in synapses of spiking neurons in the optic tectum and neurons in the retina, sampling hundreds of terminals simultaneously (Fig. 48.10) [51].

In conclusion, depending on the cell-specificity and temporal resolution required, calcium photoproteins can be delivered and used in different ways. Injecting a purified photoprotein enables detection of calcium signals already at fertilization, while injection of mRNA delays the time when the photoprotein is available, but gives a prolonged window of protein expression. DNA injections of the photoprotein gene driven by cell-specific promoters give a precise spatiotemporal pattern. Due to the external development of the zebrafish embryo, the ease of genetic manipulations and possible *in vivo* imaging, the zebrafish has been a valuable model system for the development of new calcium probes.

Calcium Imaging Studies in the Zebrafish

Development

The popularity of the zebrafish initially started among the developmental biologists, hence leading to the fact that the first zebrafish calcium imaging experiments were studying calcium signaling in the zebrafish egg and early embryo [52]. Embryological studies of the zebrafish are particularly rewarding since the developmental process is done *ex utero*. Fertilized eggs are collected from breeding couples in the morning and can then be studied throughout the day, reaching the segmentation period within the first 24 h. The early development of the zebrafish embryo is comparably fast, and the speed of development can be manipulated by increasing or decreasing the temperature of the eggs/embryos. The precise developmental periods have been described by Kimmel and colleagues [53]. When incubated at 28.5°C the times for the developmental stages are the following: zygote (0–0.75 h), cleavage period (0.75–2.25 h), blastula period (2.25–5.25 h), gastrula period (5.25–10.33 h), segmentation period (10.33–24 h), pharyngula period (24–48 h) and hatching period (48–72 h).

Calcium signaling has been studied throughout the whole development of the zebrafish embryo [34, 54, 55]. The zygote and cleavage periods are dominated by intracellular calcium signals, but as the embryonic cell number increases, there is an appearance of localized intercellular signals along with the intracellular ones [56]. This transition proceeds through the blastula and early gastrula periods. Then, as global patterning processes starts during the rest of the gastrula period, pan-embryonic intercellular signals associated with the dramatic morphological events

of gastrulation can be observed [20]. Once the germ layers and major body axes are established, there is a return to localized intercellular signals associated with the generation of specific structures, for example somite formation, brain partitioning, eye development, and heart formation [33].

Fluctuations in intracellular calcium during **fertilization** and later developmental periods have been studied using injections of recombinant aequorin [34, 57] and Calcium Green-1 dextran, 10 kDa, [58]. Oocytes are held in place using an egg injection chamber [57] when carefully injected with the calcium indicator without affecting the normal development of the oocyte. In the zebrafish oocyte, the blastodisc (animal pole) is located on top of the yolk cell (vegetal pole). Activation and fertilization of the oocyte are then done under the confocal microscope to monitor the fluorescence during these processes. The unfertilized zebrafish oocyte exhibits little evidence of calcium signaling, however both activation with water and fertilization trigger rapid increases in intracellular calcium in the oocyte cortex. This fluorescence continues to increase during the first 12–15 min post-insemination (mpi), particularly at the animal pole [58]. The initial transient is followed by a more prolonged transient reaching a higher amplitude with a maximum at 8–10 mpi [58]. These two initial transients are followed by later calcium oscillations (30–60 mpi) associated with blastodisc expansion and cytokinesis [34, 57, 59].

The zebrafish **cleavage period** is represented by six rapid and synchronical cell cleavages, with one blastomere division approximately every 15 min. The zebrafish embryo undergoes discoidal cleavage, meaning that the blastodisc is located at the animal pole and is divided with cleavage furrows that do not penetrate or divide the yolk. The cells remain interconnected by cytoplasmic bridges. Elevation of intracellular calcium can be seen at the cleavage furrow before the first cell cleavage, i.e. the furrow positioning signal, then during the furrow formation and deepening of the furrow [60]. Next, calcium elevations can be observed along the equators of the dividing cells, where the second cleavage furrow emerges. Thus, it appears that there is a close spatial correlation between elevated calcium and the formation of a cell cleavage furrow [59, 61]. The calcium signals at cleavage furrows [62] and subsequent cell divisions [59] have indeed been prevented by injection of the calcium chelator BAPTA into the embryo, indicating the importance of calcium for cell division [63].

At the 256-cell stage, the **blastula period** begins with the start of asynchronous cell divisions and zygotic gene transcription. During this period, the yolk syncytial layer (YSL) forms, and epiboly begins. This means spreading and flattening of the blastula to finally cover the whole yolk at the end of epiboly. During this period, there is a transition from intracellular signals to intercellular signals within the blastula. Using 70 kDa Calcium Green-1 dextran, Reinhard and others [34, 56] demonstrated that localized elevations of calcium, so called calcium spikes, are generated in individual cells or small groups of cells in the blastoderm (Fig. 48.2). These signals are restricted to the enveloping layer (EVL) cells and appear to propagate as calcium waves [56].

During the **gastrula period**, each germ layer (endoderm, mesoderm, ectoderm) is spatially organized so that organs and tissues can form in the correct locations.

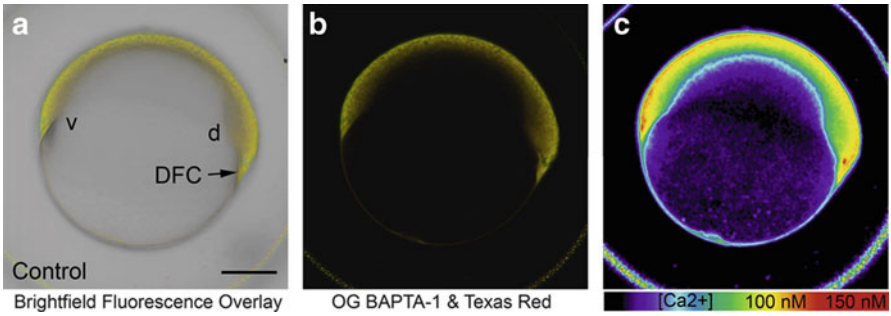

Fig. 48.4 Ratiometric imaging of cytosolic calcium patterns during gastrulation. (**a**) Overlay of bright field (*grey-scale*), the calcium indicator Oregon Green BAPTA-1 dextran (*green*), and the calcium-insensitive control Texas Red dextran (*red*) images of a 6-h-old embryo. *DFC* dorsal forerunner cells. (**b**) Overlay of Oregon Green BAPTA-1 dextran and Texas Red dextran. (**c**) Pseudocolored ratiometric image (*green/red*). Scale bar is 200 μm (Reprinted from Kreilig et al. [19]. Copyright 2008, with permission from Elsevier)

The morphogenetic movements of involution, convergence, and extension form the epiblast, hypoblast, and embryonic axis through the end of epiboly [19]. The level of intracellular calcium reaches a maximum during early gastrulation (6.5 h), when epiboly resumes and the embryonic shield starts to extend towards the animal pole [34]. Fast intracellular calcium waves have been observed around the blastoderm margin during late epiboly, moving up the trunk in an anterior direction (Fig. 48.3) [20, 54]. The function of these axial waves are unknown but are thought to contribute to the calcium waves that underlie the large-scale migrations of cells during this period.

Other calcium release events that are seen during gastrulation are aperiodic transient fluxes found mainly in the EVL and dorsal forerunner cells becoming the Kuppfer's vesicle, a structure implicated in laterality [64]. Kreilig et al. [19] used ratiometric calcium measurements using Oregon Green 488 BAPTA-1 dextran and the calcium-insensitive control Texas Red dextran to investigate the role of calcium for lateralization during gastrulation (Fig. 48.4). They found that gastrula stage embryos maintain a distinct pattern of cytosolic calcium along the dorsal-ventral axis, with higher calcium concentrations in the ventral margin and lower calcium concentrations in the dorsal margin and dorsal forerunner cells. Suppression of the endoplasmic reticulum calcium pump with thapsigargin elevates cytosolic calcium in all embryonic regions, induces a randomization of laterality in the heart and brain and malformation of the Kupffer's vesicle.

Following the dramatic global rearrangements during gastrulation, the embryo now undergoes a series of more localized morphogenetic movements that make up the **segmentation period**. Somites and the neural cord develop during this period, as well as the primary organs. The earliest body movements can be seen at this time. At 10–11 h of development, distinct calcium patterns can be recognized along the antero-posterior axis of the embryo [34]. High calcium levels can be observed in the

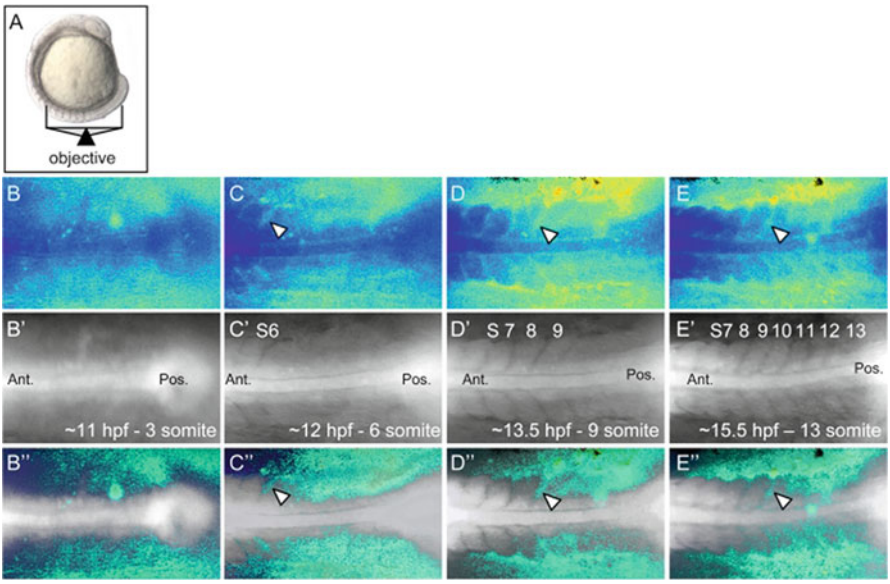

Fig. 48.5 Calcium dynamics during zebrafish somitogenesis. (**a**) Illustration of the position of a 10 somite stage (14 h post-fertilization) zebrafish embryo relative to the objective during calcium imaging. The embryo is labeled with injections of the ratiometric dye Fura-2 at the one-cell stage and imaged on an epifluorescent microscope. (**b**–**e**) Representative ratio images, pseudocolored with low ratio (*low calcium*) represented by *blue* and high ratio (*high calcium*) represented by *yellow/red*, of 3, 6, 9 and 13 somite stage embryos. (B'–E') The forming somites and notochord can be identified by the grey-scale fluorescence images. (B"–E") Overlay of grey-scale and ratio images illustrate the regions of calcium release activity relative to morphology. Arrowheads indicate areas of sustained calcium activity between forming somites. *Ant.* Anterior, *Pos.* Posterior, *S* somite number (Reprinted from Freisinger et al. [22])

presumptive mid- and forebrain in contrast to low calcium in the presumptive hindbrain. This specific calcium pattern in the brain remains clearly visible for several hours and precedes morphological patterning of the brain [34]. Apart from the calcium patterns in the head, various calcium waves, gradients, and spikes were observed in the trunk and tail region (Fig. 48.5). The most pronounced is an ultraslow calcium wave moving posteriorly along with the formation of the somites and neural keel at 10–14 h [34].

Freisinger et al. [22] used the ratiometric dextran-conjugated calcium indicators Fura-2 and Bis-Fura-2, injected into the developing oocyte to monitor calcium changes during somitogenesis (Fig. 48.5). They combined these recordings with down-regulation of specific genes using morpholinos to investigate their involvement during segmentaton. Experiments showed that *rgs3* and *wnt5b* gene function are required for appropriate frequency and amplitude of calcium release activity in the embryo during segmentation [22].

The zebrafish embryo enters the **pharyngula period** at 24 h when the body axis begins to straighten. The circulation system develops and the heart starts to beat.

The brain has now five distinct lobes and the pharyngula shows tactile sensitivity and uncoordinated movement. The **hatching** embryo (48–72 h) continues to form the primary organ systems and the sensory systems are complemented by hair cells and olfactory placodes [53]. The zebrafish is considered a **larva** from 72 h to 30 days (Fig. 48.1b) when it grows in size to become an adult animal (Fig. 48.1c). Pigmentation of the zebrafish skin starts around 24 h which requires 1-phenyl-2-thiourea treatment to keep embryos transparent, or the use of non-pigmented strains like *nacre* [2]. Calcium imaging of different parts of the nervous system and muscle cells during these later stages will be described in the next section of this chapter.

The Hindbrain and Reticulospinal Neurons

At the time when developmental biologists started to monitor calcium signaling events during development, physiologists started to inject dextran-conjugated Calcium Green-1 into the spinal cord to investigate firing properties of neurons in the spinal circuits and hindbrain [15, 65]. Since then, calcium imaging has been an important noninvasive tool in larval zebrafish to study neuronal activity and connectivity, simultaneously from a population of neurons.

The Mauthner cell network is one of the first circuits in the zebrafish brain that was studied using calcium imaging [15, 65]. The Mauthner cell is a large reticulospinal neuron located in the hindbrain (Fig. 48.6b, c) and responsible for the startle response, elicited by various sensory stimuli such as touch, sound, and visual input. It has two prominent dendrites and its axon crosses over to the contralateral side where it activates motoneurons, contracting the muscles to propel the fish trough the water. Two homologous reticulospinal neurons, MiD2cm and MiD3cm, are located in adjacent segments (Fig. 48.6c) and can elicit a startle response if the Mauthner cell is deleted [66].

In the first experiments labeling Mauthner cells by Fetcho and O'Malley, 10 kDa Calcium Green-1 dextran was injected into the spinal cord of anesthetized larvae [15, 65]. Animals of a few days up to 2 weeks were used. Due to the severing of axons, the water-soluble dye can enter and fill the Mauthner cell bodies even at a far distance. Using a 50% dye solutions, injections produced intensely labeled Mauthner cells that could be imaged within 12 h (Fig. 48.6a, b). Neuronal activity corresponding to an escape response was elicited in the imaged neurons by tapping the head of the fish with a small glass probe attached to a piezoelectric crystal. These initial confocal recordings showed that calcium responses in the Mauthner cell only occurred when an escape response was produced. Calcium transients in the Mauthner cell were elicited from both head and tail stimulations, while the homologs only responded to head taps. Using the same preparation, Gathan et al. discovered that a substantial majority of the ~220 descending neurons, spanning the rostral-caudal extent of the brain stem, are signaling during the startle response (Fig. 48.7) [16].

A later confocal imaging study used Oregon Green 488 BAPTA-1 dextran-labeled Mauthner cells and homologs to investigate potential differences in their

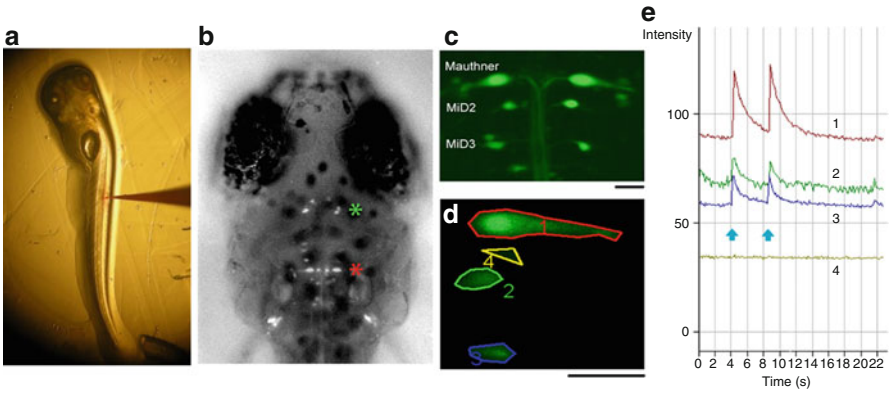

Fig. 48.6 Labeling of reticulospinal neurons in the larval zebrafish and recording of changes in intracellular calcium during the startle response. (**a**) Injection of a dextran dye (here calcium-insensitive rhodamine dextran) into the spinal cord of a larval zebrafish. (**b**) Descending projection neurons labeled with Calcium Green-1 dextran (10 kDa) in a wild type larva with normal pigmentation 24 h after injection. The pair of Mauthner cells is marked with a *red* asterisk and the midbrain neurons with a *green* asterisk. (**c**) Confocal microscopy image showing Mauthner cells and its homologs labeled with Calcium Green-1 dextran in a 5-day-old larva. Scale bar is 25 μm. (**d**) The region of interest (ROI) 1 marks the Mauthner cell, ROI 2 the closest segmental homolog, MiD2cm, and ROI 3 the homolog MiD3cm. Background activity from non-labeled cells is recorded from ROI 4. Scale bar is 25 μm. (**e**) Graph of the changes in intracellular calcium levels from ROI1-4 during weak electrical stimulation of the skin. The X-axis indicates time. Two skin shocks to the head were delivered to the fish at the time points indicated by the blue arrows. The Y-axis indicates the fluorescence intensity in arbitrary units. 0 represents no fluorescence; the value of maximal fluorescence is 256. The numbers and colors of the traces correspond to those for the ROIs in (**d**). Thus, trace 1 depicts the calcium response in ROI 1, trace 2 the calcium response in ROI 2, etc. The two skin shocks produced two fast peaks in intracellular calcium in the Mauthner cell and the segmental homologs. Each of the calcium transient lasted about 5 s

responsiveness to various sensory inputs [67]. The authors showed that auditory or vestibular inputs lead to a Mauthner cell-mediated fast escape with short latency. In contrast to previous work by O'Malley et al. [65], Kohashi et al. showed that a water pulse directed to the head did not induce Mauthner cell firing, but the homolog MiD3cm was more active than in the short-latency escape [67].

Our knowledge of the structure and function of reticulospinal neurons has grown during the last two decades. The fact that these neurons are large and their morphology easily distinguishable and their activation lead to a distinct response makes this system very useful to functional investigations of genetic modifications. With the discovery of a variety of mutant strains, generated in large-scale genetic screens, the possibilities to learn about the formation and function of the nervous system are unlimited. For example, in one large-scale screen for behavioral locomotive defects, over 150 motility mutants were identified [68]. Interestingly, many of these mutants, including *orbiter*, *mercury* and *gemini*, lack the ability to startle to vibrational stimuli, mediated by mechanosensory hair cells to the reticulospinal neurons.

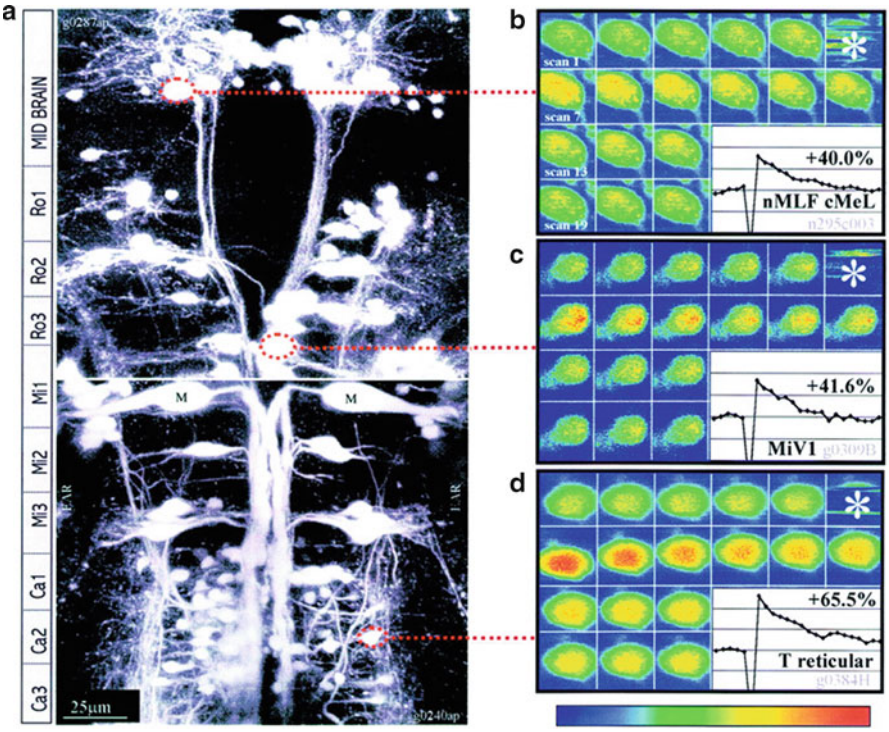

Fig. 48.7 Examples of calcium-responsive neurons in the zebrafish hindbrain and midbrain. (**a**) A composite of two confocal image stacks, showing the rostral-caudal extent of neurons that project from the brain into the spinal cord, labeled with Oregon Green 488 BAPTA-1 dextran. The segmental arrangement of the neurons is indicated alongside the image. (**b–d**) Examples of calcium responses from three neurons located in midbrain or hindbrain. Each neuron shows a robust calcium response (plotted in the inset) in response to a tap to the head (during the frame marked by an asterisk). Frames were acquired at 450-ms intervals and are plotted from left to right in consecutive rows. Fluorescence plots are background subtracted and normalized to the preceding baseline. Relative fluorescence intensity is indicated by the color scale at the bottom. *nMLF* nucleus of the medial longitudinal fasciculus, *cMeL* medial-lateral cell, *MiV1* reticulospinal neuron in rhombomere 4, *T reticular* T reticular interneurons (Reprinted from Gahtan et al. [16] with permission from the American Physiological Society)

Using fluorescent microscopy, the hindbrain activity of 5-day-old mutants labeled with egg injections of Calcium Green-1 dextran, was recorded [69]. By comparing the responsiveness of hindbrain neurons to either vibrational or acoustical stimuli, it was possible to distinguish between defects in hair cell function and events downstream of mechanotransduction.

Another mutant line, found in the large-scale screens, was the zebrafish *deadly seven/notch1a* (*des*) mutant resulting in supernumerary Mauthner cells [70]. Labeling of all these Mauthner cells with Calcium Green-1 dextran and subsequent confocal imaging revealed that they are all active during an escape response [71].

Similarly, overexpressing the *hoxb1b* gene via injection of *hoxb1b* mRNA into the one-cell stage resulted in ectopic Mauthner cells in rhombomere 2 in addition to the Mauthner cells in rhombomere 4 [72]. Ratiometric calcium imaging comparing the fluorescence from Calcium Green-1 dextran with the calcium insensitive Texas Red dextran in these animals showed that the ectopic Mauthner cells also responded to head taps. These two studies show how calcium imaging is a useful tool to investigate how network properties are adjusted when the number of homologous cells changes during evolution.

Soon, the field of reticulospinal cell imaging expanded to involve networks feeding into the Mauthner cell, regulating its function. For example, investigations were made of the three different inhibitory connections of the Mauthner cell network; recurrent inhibition mediated by an ipsilateral collateral of the Mauthner cell axon, feed-forward inhibition driven by sensory afferents, and reciprocal inhibition between bilaterally opposed Mauthner cells [73]. This inhibition could be confirmed by confocal recordings of calcium signals in Mauthner cells when these inhibitory connections where stimulated.

With time, calcium imaging studies in the larval zebrafish have started to involve even larger networks around the Mauthner cell, aiming at explaining the complex mechanisms of sensory regulation [74, 75]. Orger et al. [74] investigated which neurons control specific motor patterns by measuring calcium responses from the whole population of descending projection neurons during visually induced locomotor patterns, including swimming and turns. First, the specific visual patterns that evoked turns in freely swimming larval zebrafish were determined. Then, the same patterns were presented to Calcium Green-1 dextran-injected fish, identifying the neurons responding to the turn-evoking visual stimuli. To confirm their involvement in turning, two-photon laser ablation of labeled neurons were done prior to behavioral testing. It was found that stimuli that drive distinct behaviors activated distinct subsets of projection neurons, consisting, in some cases, of just a few cells. This stands in contrast to the distributed activation seen for more complex behaviors [76].

One group of neurons that showed an optomotor response in the study by Orger et al. was the nucleus of the medial longitudinal fasciculus (nMLF), the most rostral of the descending projecting neurons (Fig. 48.8a). They had previously been implicated in escape, swimming and prey capture behaviors [16, 77]. Sankrithi and O'Malley performed calcium imaging in Oregon Green 488 BAPTA-1-labeled 3–5 day-old-animals [75]. Calcium responses were monitored simultaneously with recording swimming, turning and struggling movements, elicited by head taps and abrupt illumination (Fig. 48.8b, c). This type of preparation shows the advantage of using the transparent zebrafish larvae to study which cells are active during certain behaviors, which would be more complicated in other vertebrate systems.

Spinal Cord Neurons

In parallel with recording activity in reticulospinal neurons, recordings in the downstream spinal cord neurons started. Spinal cord neurons were labeled in the same

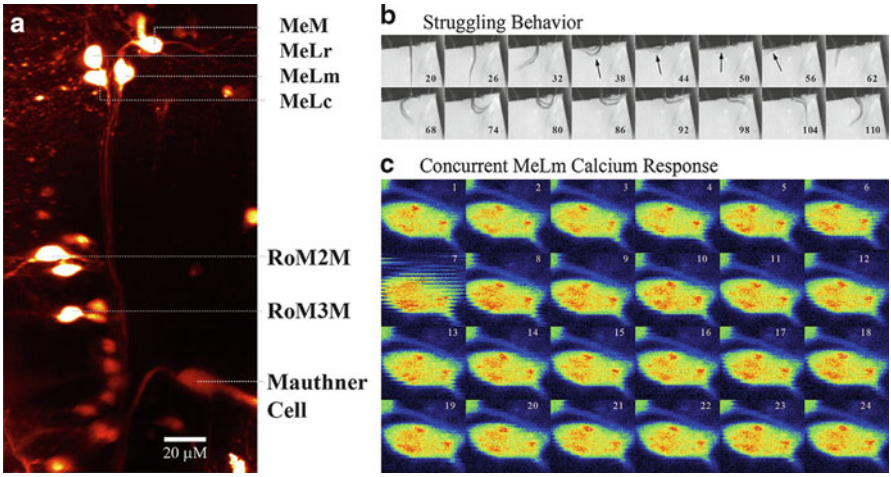

Fig. 48.8 Midbrain neurons are activated during struggling behavior. (**a**) Micrograph showing *in vivo* labeling of neurons in the nucleus of the medial longitudinal fasciculus (*nMLF*) and the hindbrain (Mauthner cell and *RoM2M*, *RoM3M* rhombomere-2 and rhombomere-3 Medial-Medial cells, respectively) using Oregon Green 488 BAPTA-1 dextran. The nMLF contains several clusters of small neurons that can be individually identified as *MeM* (medial-medial) and *MeL* (medial-lateral) cells: MeLr, MeLc, and MeLm. They are readily distinguished in this larva with unilateral labeling. The large MeL cells have extensive lateral and ventral dendrites and project ipsilaterally. (**b**) A sequence of trunk movements characteristic of a larval struggle is shown. Every third frame is shown from a representative struggling behavior recorded at 500 frames/s (time after the head-tap stimulus is shown in ms). The arrows point to where the trunk is pressed flat against the agar. (**c**) In a concurrent calcium recording, this MeLm neuron shows a modest fluorescence response during the struggling. The frames were collected at 440 ms/frame. The behavior occurred during the seventh confocal frame when a movement artifact can be observed (Reprinted from Sankrithi and O'Malley [75]. Copyright 2010, with permission from Elsevier)

way as described previously for the Mauthner cells (Fig. 48.6) [15]. The labeling depend on the injection site; muscle injections label only motoneurons and sensory Rohon-Beard cells, while spinal injections also label spinal interneurons. Head-taps lead to a calcium increase in the primary motoneurons downstream of the Mauthner cell. Similarly, the activation of interneurons can be followed during the elicited escape response and swimming, revealing that different interneuron classes are responsible for the two behaviors [78].

Further improvement of this imaging method involved ratiometric imaging of Calcium Green-1 and Alexa Fluor 647 dextrans, which prevents fluorescence fluctuations due to movements. Using low magnification, Bhatt et al. were able to monitor up to six body segments for simultaneous imaging [79]. From these recordings, it was possible to conclude that a group of identified excitatory spinal CiD interneurons is recruited differently depending of the location of the stimuli, i.e. the head or the tail. Head stimuli, which evoke stronger movements, involve activation of every CiD interneuron. Tail stimuli also massively recruit nearly the entire interneuronal

pool, but with a lesser activation of the individual neurons. These findings show that CiD interneurons do not follow the general principle to increase strength in movements by the gradual recruitment of inactive motoneurons with larger motor units and by increased firing of active cells [80]. In CiD interneurons, no difference in size was distinguished between recruited neurons and firing frequency, corresponding to higher calcium indicator ratios [79].

The development of spinal cord networks is partly regulated by spontaneous activity. This activity can be studied during the pharyngula period following injection of dextran dyes into a single blastomere between the 32- and 128-cell stage [81]. This randomly labels cells in all regions of the developing embryo, such as spinal cord, muscle and skin. At this stage, the neurons have few processes making it difficult to label them with dextran dye injection directly into the spinal cord. The activity in spinal cord neurons has been followed using confocal microscopy between 16 and 24 h, showing spontaneous calcium oscillations in precursor cells in the spinal cord [81, 82]. Also, increased calcium levels from muscle contractions during the escape response could be distinguished at this early stage [81].

To shorten the fairly long labeling time using dextran dyes that could harm the early development by chelating intracellular calcium [82], Brustein et al. developed a method for bolus injections of AM ester calcium indicators in 4–60 day-old-animals [23]. Dye was directly injected into the spinal cord at multiple sites using low pressure. Calcium recordings using a two-photon laser-scanning microscope could be started 30–60 min after dye injection. To elicit calcium spikes in spinal neurons, iontophoretic application of glutamate, GABA and glycine were given to the cells, and air puffs to the skin elicited a startle response. Moreover, long-term recordings revealed spontaneous calcium transients in individual spinal neurons. However, the use of this technique in the spinal cord since Brustein et al. has not been common. A possible reason could be that the dense labeling makes a morphological identification of single neurons more difficult, than the relatively more sparse labeling following injection of dextran dyes.

The obvious direction after using synthetic dyes has been the use of GECIs to study spinal cord physiology. In the first study of GECI used in the zebrafish, yellow cameleon 2.1(YC2.1) constructs were injected in zebrafish eggs at the one-cell stage, using different promoters to drive the expression in specific cells [42]. Sensory Rohon-Beard neurons in the spinal cord were labeled using the *Islet-1* promoter [83], motoneurons and interneurons using the *α-tubulin* promoter and stable transgenic lines expressed YC2.1 in all neurons using the *HuC* promoter [14]. Confocal imaging at 2–3 days of development showed that Rohon-Beard neurons responded with calcium elevations to electrical skin stimulations. Similarly, primary motoneurons and CiD interneurons responded to a head tap.

Recently, a new and brighter GECI, GCaMP-hyper sensitive, was expressed in a subset of spinal neurons, including the caudal primary motoneurons [50]. Similar to the fish labeled with synthetic dyes, spontaneous activity from the motoneurons could be detected in the developing spinal cord using a high-sensitivity cooled CCD camera.

Tectum and the Visual System

The zebrafish retinotectal system is responsible for converting moving visual inputs to the appropriate motor output, thus analogous to the mammalian superior colliculus [84]. The tectum is located just beneath the transparent skin and is therefore easily accessible to imaging and manipulations. The topographic map of the visual field present in the retina is conveyed into the tectum. Each retinal ganglion cell axon is targeted to a single lamina and arborizes exclusively in this lamina. Information flows primarily from the superficial to the deeper layers in the tectum. In the deeper neuropil layers, information is transmitted from the axons of interneurons to tectal projection neurons reaching premotor areas in the midbrain and hindbrain [85].

The first recordings of calcium activity in the larval zebrafish tectum (Fig. 48.9) were done after bolus labeling of Oregon Green 488 BAPTA-1 AM into the tectal neuropil at 60 hpf to 9 dpf (Fig. 48.9c) [24]. Visual stimuli of vertically moving dots were presented using a miniature LCD screen (Fig. 48.9a). Larvae were not anesthetized during imaging, as the agarose was sufficient to restrain them and prevent eye movements. A two-photon microscope collected images of visually evoked calcium fluctuation in tectal neurons, showing that zebrafish receptive field properties could be determined, such as visual topography, receptive field width, and direction and size selectivity (Fig. 48.9d–f) [24].

The function of the tectum is to localize and track moving prey [86–88]. To reveal the size filtering required to detect small objects, the response of tectal neurons to different visual stimuli has been tested [89]. Cell-specific promoters expressed GCaMP1.6 and GCaMP3 in tectal neuropil, in superficial layers or in neurons projecting to premotor regions. Imaging of 6–8 dpf animals showed that small visual stimuli activated the deep layers and the dendrites of single tectal neurons. This size filtering relies on inhibitory interneurons that are located in the superficial input layer and respond only to large visual stimuli. Photoablation of these cells eliminated the size tuning of deeper layers and prevented prey capture.

The zebrafish retinotectal system is a useful network to study the neuronal wiring mechanisms that result in vision. Although the zebrafish tectum only receives monocular information from the contralateral retina, Ramyda and Engert [90] were able to induce functional binocular projections in developing larvae. To induce a rewiring from the ipsilateral eye, one tectal lobe was surgical removed at 2 dpf. Two-photon calcium imaging using Oregon Green 488 BAPTA-1 AM ester in the rewired tectum confirmed that ipsilateral tectal activity could be stimulated. When the eye was activated with a moving dot, directed waves of activity moving across the tectum could be observed. This implies that the functional topography of the rewired tectum was conserved.

In recent years, methods to study learning and memory in the larval zebrafish have emerged. Sumbre and coauthors [91] presented a new preparation to investigate a possible zebrafish correlate of working memory. In 3–15 dpf embryos loaded with Oregon Green 488 BAPTA-1 AM, calcium fluctuations in the tectum were monitored by confocal or two-photon imaging upon visual stimulation. The fish was

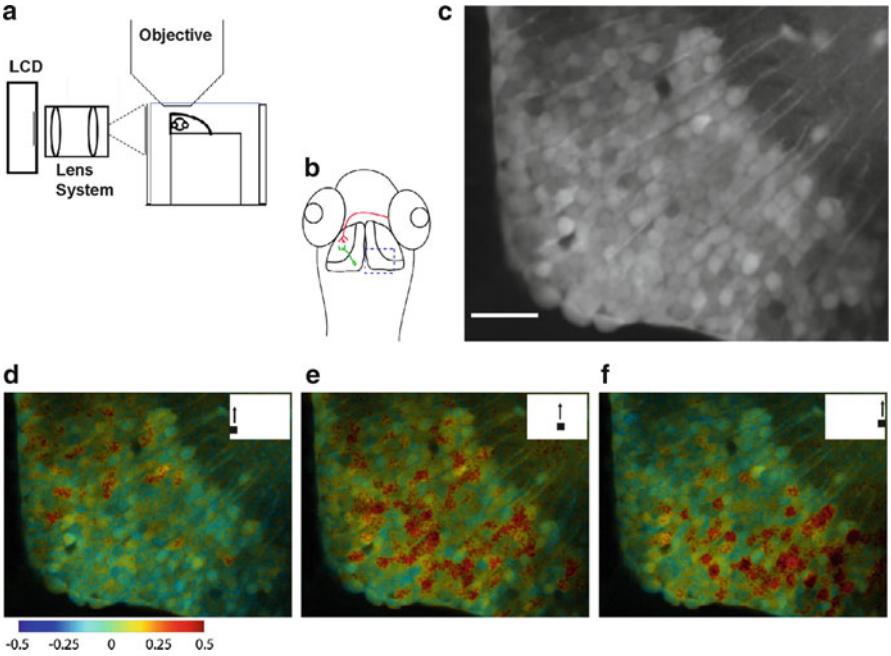

Fig. 48.9 Imaging calcium responses to visual stimuli from the tectum. (**a**) Schematic diagram of configuration to provide visual stimuli from a miniature LCD screen while performing two-photon imaging. (**b**) Drawing of the zebrafish visual system, showing a retinal ganglion cell axon (*red*) and a tectal cell dendrite (*green*) projecting into the tectal neuropil. *Blue* box shows the region imaged in (**c**–**f**). (**c**) Fluorescence image of one tectal hemisphere loaded with Oregon Green 488 BAPTA-1 AM. The periventricular cell body layer is located centrally, and the neuropil is on the upper right. Scale bar is 15 μm. (**d**–**f**) Fluorescence changes upon presentation of visual stimulus. Upper right-hand corner illustrates the stimulus being provided to the contralateral eye. Vertically moving spots at different anterior-posterior regions of the visual space activate different groups of neurons from rostral to caudal. Pseudocolor scale shows fractional change in fluorescence intensity relative to an average baseline image (Reprinted from Niell and Smith [24]. Copyright 2005, with permission from Elsevier)

given a repetitive visual conditioning stimulation of a moving light bar that the tectal cells responded to rhythmically. After the end of visual stimulation, continued rhythmic activity up to three cycles could be observed in the tectal cells, corresponding to the activity during the visual stimulation.

Apart from the tectal recordings, very few other calcium imaging experiments have been done in the zebrafish visual system. For example, calcium signals have been recorded from dissociated retinal ganglion cells from adult animals, incubated with Fluo-3 AM ester [92]. However, the recent development of GEICs means new ways to detect calcium signals from the cells in the visual system. SyGCaMP2 [51], the genetically encoded reporter of synaptic activity has been used to investigate synaptic events in the larval retina and tectum [93]. SyGCaMP2 constructs with the *ribeye* promoter for ribbon synapse cells and *α-tubulin* for tectal cells were injected

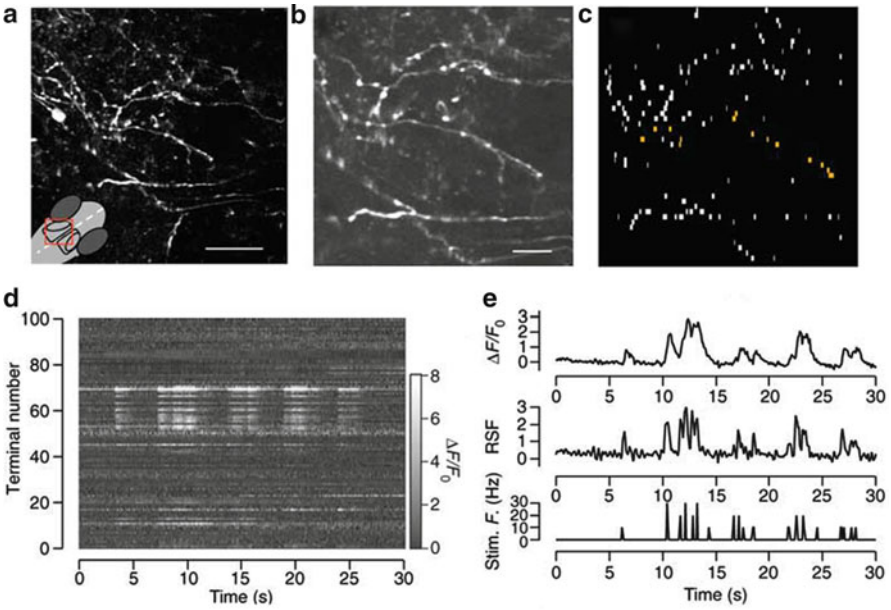

Fig. 48.10 Monitoring synaptic activity in the optic tectum of zebrafish using a genetically encoded calcium indicator. (**a**) Fluorescence image of an optic tectum of a 9-day-old zebrafish transiently expressing SyGCaMP2 under the *α-tubulin* promoter. The red box in the schematic (*bottom left*) indicates the area imaged in the head. Scale bar is 50 μm. (**b**) Magnified fluorescence image of the optic tectum shown in (**a**). Scale bar is 20 μm. (**c**) Regions of interest corresponding to single synapses in (**b**). Terminals responding to light are in amber. (**d**) Raster plots showing fluorescence responses from 100 terminals marked in (**c**), elicited by an electric field (*E top*) SyGCaMP2 signals averaged from 12 terminals (from different areas of the tectum, same fish). (*E middle*). Relative spike frequency (*RSF*) calculated by deconvolution using the minimum impulse response (rising and decay time constants of 50 and 350 ms). (*E bottom*) Pattern of field stimulation (*bottom*) (Reprinted from Dreosti et al. [51] by permission from Macmillan Publishers Ltd. Copyright 2009)

into the fertilized egg [51]. Animals of 8–9 days of age were immobilized in agarose and synaptic calcium signals were detected with a two-photon microscope upon light stimulation. By simultaneously recording activity across tens of bipolar cell terminals distributed throughout the inner plexiform layer of the retina, it was possible to make a functional map of the ON and OFF signaling cells. Synaptic activity could also be detected from tectal neurons when stimulated with light and electric field (Fig. 48.10).

Olfaction

One of the few neural systems that has involved calcium imaging of adult zebrafish is the olfactory system, due to the small size, transparent nature, and accessibility of

the adult olfactory bulb for labeling, imaging and stimulation. In the nasal cavity, olfactory receptor neurons (ORNs) are stimulated by odors, and send a single unbranched axon to the first relay station in central nervous system, the olfactory bulb (OB). ORN axons synapse onto mitral cells (MCs) and local interneurons in the olfactory glomeruli [94]. Each glomerulus receives convergent input from sensory neurons expressing the same odorant receptor [95]. MC axons exit the OB and project to several higher brain areas, most of which are telencephalic [96].

To stain the adult olfactory bulb, a solution of 12% Calcium Green-1-dextran, 10 kDa, is injected into the nasal cavities and washed out after 4–6 min [97]. Within ~8 h after injection, the dye distributes throughout ORN axons. The OB can then be imaged using a cooled CCD camera [97]. For odorant stimulation, all structures caudal to the telencephalon and ventral from the OB and the telencephalon are removed to give an intact preparation of the olfactory system. Alternatively, an explant of the intact zebrafish brain and nose is prepared [98] and can be analyzed using a two-photon microscope [99]. Olfactory stimuli such as amino acids (AAs) and bile acids are applied to the naris of one olfactory epithelium. In this preparation, it is possible to monitor patterns of presynaptic activity in glomeruli induced by repeated applications in the same animal. In preparations where the telencephalon is spared [99], it is possible to record odor-generated activity in the telencephalic targets, e.g. the fish homolog of the olfactory cortex.

Calcium imaging from the zebrafish OB has shown that AAs and bile acids stimulate different parts of the OB. AAs induce complex patterns of active glomerular modules that are unique for different stimuli and concentrations. Interestingly, the similarity of odorant-induced activity patterns is the highest for AAs that are chemically close [97]. Using the same preparation, Fuss and Korsching described the specific chemical structure of odorants that activate AA-responsive receptors [100]. The activity patterns measured from the OB induced by a homolog series of AAs became more similar to each other at higher concentrations. At intermediate concentrations, patterns were unique across substances and across concentrations.

To investigate the neuronal representation of mixtures, mixtures of AAs and food extracts were given during calcium imaging of afferents to olfactory glomeruli in the OB and electrophysiological recordings from MCs [17]. These recordings showed that the patterns of afferent glomerular activity evoked by binary odor mixtures were similar to the patterns of the individual odors. In MCs however, the firing patterns were different for mixtures. Responses to mixtures of AAs were often dominated by one of the component responses, while those of food extracts were more distinct from both component responses.

Yellow cameleon [41] expressed under the control of the *HuC* promoter selectively labels MCs in the zebrafish OB, but leaves interneurons (INS) transmitting γ-aminobutyric acid (GABA) unlabeled with YC. Odor-stimulated calcium activity in MCs and INs can be recorded using two-photon microscopy, to follow the formation of topological response patterns throughout the time of odor application [28]. Since the OB explant is fairly permeable, pharmacological treatment can be done during the calcium imaging recordings. In this way, Tabor et al. [101] recorded odor-evoked activity from ORN terminals before and after application of GABA

antagonists, and concluded that inhibitory connections are important for regulating OB output activity and odor-encoding activity patterns.

The formation of the olfactory system has also been studied in zebrafish [46]. To label the developing OB, rhod-2 AM ester is carefully perfused in the larval OB. Alternatively, GECIs such as inverse pericam (IP) can be used. As in the adult fish, the neuronal *HuC* promoter labels mainly MCs. Odor responses from AAs and bile acids can evoke calcium responses in the larval OB between 2.5 and 4 dpf depending on the stimulus. Because the two-photon imaging procedure is noninvasive, the same larva can be analyzed repeatedly at later stages of development. At 3 dpf, clear regional differences in the distribution of activity evoked by different stimuli could be observed. Food extracts containing many different compounds evoked stronger and more widespread signals than AAs and bile acids. Already at this age, a coarse spatial organization of odor response patterns corresponding to activity patterns in the adult OB is present. Since the IP expression in adult zebrafish is sufficient to monitor odor-elicited calcium responses using a CCD camera, comparison between larvae and adult animals can be made [46].

To be able to follow IN development in the OB, constructs expressing GFP under the control of promoter of homeobox genes *dlx4* and *dlx6* [102] have be used [46]. This allows for the identification of GFP-labeled INs when the whole OB is stained with the red-spectrum rhod-2 AM ester dye (Fig. 48.11). Animals of 3–6 days of age were investigated using two-photon calcium imaging [27] and their odor-evoked response patterns indicated that the number of INs and their responses in larval fish are sparser than in the adult animal.

Muscle

So far, the use of the zebrafish to study muscle physiology *in vivo* has been restricted to a handful of cases despite the fact that the larval zebrafish muscle is easily imaged beneath a transparent skin layer. Créton et al. [34] reported calcium transients from embryonic muscle during development, using injections of recombinant aequorin into the fertilized oocyte. Apart from calcium imaging recordings of somitogenesis [103], the studies of calcium fluctuations later in development have been sparse.

In 2005, Brennan et al. recorded calcium transients in muscles between 16 and 22 h, when the first functional neuromuscular synapses are established in the zebrafish [21]. Muscle fibers were labeled via egg injections with the high affinity calcium indicator Oregon Green 488 BAPTA-1 dextran or the low affinity calcium indicator Fluo-4 dextran, both together with the calcium-insensitive tetramethylrhodamine dextran (all 10 kDa) for ratiometric analyses. Using confocal microscopy the authors characterized the dynamics of nerve-generated calcium signals in single muscle cells during the initial stages of slow muscle development. The earliest calcium transients were observed at 17.25 hpf when the first muscle contractions could be distinguished. During the development, the frequency of calcium signals increased, peaking at 19 h and the duration of peaks decreased throughout the test period (Fig. 48.12).

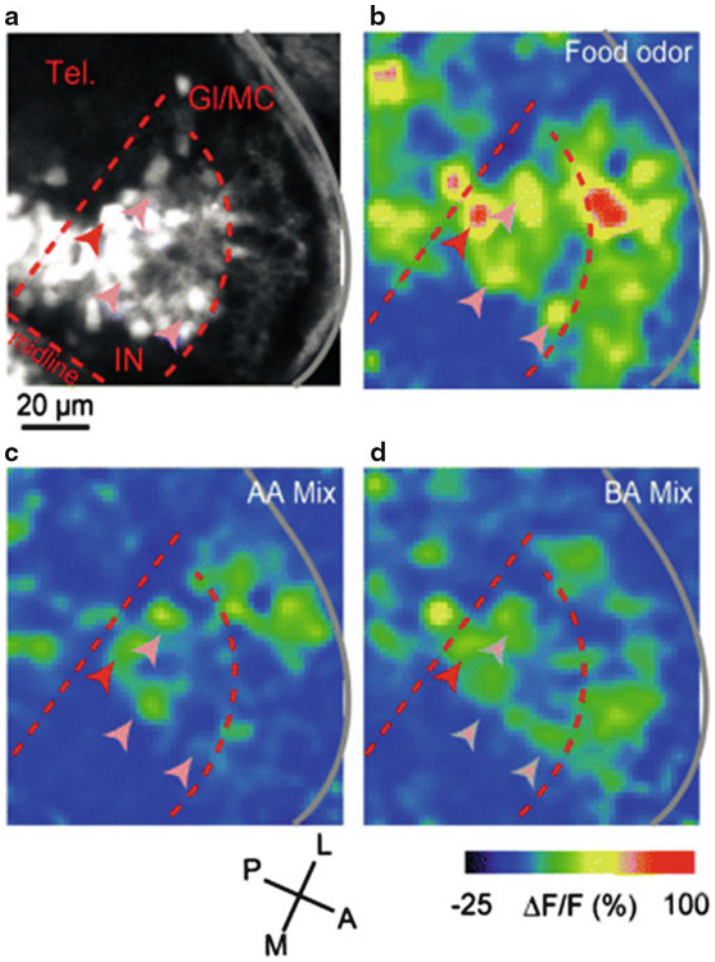

Fig. 48.11 Development of interneuron responses in the larval olfactory bulb. (**a**) The *dlx4/6::GFP* transgenic line, expressing GFP under the control of promotor regions of the homeobox genes *dlx4* and *dlx6* marks interneurons (*IN*) in the olfactory bulb (*OB*) at 5 days post-fertilization. The *grey line* outlines the border of the forebrain. The *red curved line* delineates the border between the IN and glomerular/mitral cell (*Gl/MC*) layers. The *straight lines* demarcate the borders between the OB and telencephalon (*Tel.*) and the midline. The *red arrowhead* marks a dlx4/6::GFP-positive soma that corresponds to a focal calcium signal evoked by stimulation with food odor (**b**) and the bile acid mixture (**d**). *Pink arrowheads* depict examples of calcium signals that do not correspond to dlx4/6::GFP-positive somata. (**b**) Pattern of calcium signals in response to food odor stimulation in the same view as in *A*, measured by two-photon imaging of rhod-2. (**c**, **d**) Response patterns evoked by mixtures of amino acids (*AA Mix*) and bile acids (*BA Mix*) in the same optical section. *A* anterior, *P* posterior, *L* lateral, *M* medial (Reprinted from Mack-Bucher et al. [27]. Copyright 2007, with permission from John Wiley and Sons, Inc)

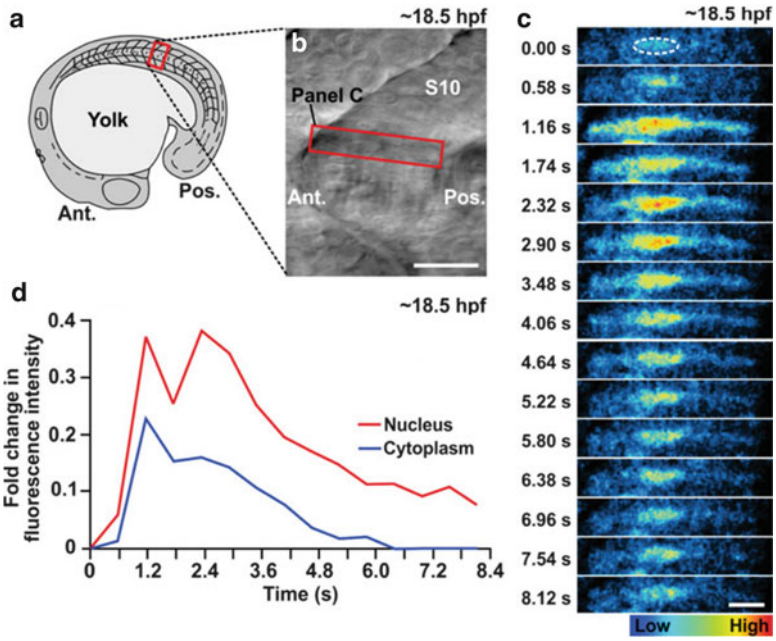

Fig. 48.12 Calcium imaging from zebrafish muscle cells. (**a**) Schematic diagram showing the position of somite 10 (*red box*) in the at ~18.5-h-old zebrafish embryo where the calcium signal was recorded. (**b**) Bright-field image of somite 10 with the position of the imaged cell indicated (see *red box*). Scale bar is 25 μm (**c**) Single confocal sections to show the calcium signal generated in the imaged cell over a period of ~8 s. Embryo was loaded with Calcium Green-1 dextran at the one-cell stage and images were acquired via confocal microscopy. The images were acquired every ~0.58 s. The nucleus is outlined with a *white dashed line* in the first panel. The color scale represents the level of intracellular calcium, where *red* indicates a high level and *blue* indicates a low level. *Ant.* and *Pos*. are anterior and posterior, respectively. Scale bar is 10 μm. (**d**) Temporal profiles of the fold change in fluorescence intensity in the nucleus and cytoplasm in this muscle cell for the duration of the calcium signal (Reprinted from Cheung et al. [104] with permission from The International Journal of Developmental Biology)

To confirm that the calcium transients were produced by acetylcholine-transmitting nerve terminals, embryos were incubated in the acetylcholine receptor blocker α-bungarotoxin, with their tails slit to enable the spread of the drug. In animals treated with the blocker, the calcium transients normally seen in the slow muscles were abolished.

Recently, the development of slow muscles was studied using the co-expression bioluminescent apoaequorin and enhanced GFP, driven by the muscle specific *α-actin* promoter (Fig. 48.12) [104]. Stable transgenic lines were made and used for the confocal imaging studies. Using these embryos, Cheung et al. could confirm that the previously reported duration of calcium signals decreased with age, and that the frequency maxima was observed around 19 hpf [21]. To check that the calcium signals did indeed originate from developing slow muscle cells, embryos were

treated with cyclopamine and forskolin, known to inhibit slow muscle formation [105, 106]. Chemically blocking the calcium release from intracellular stores affected the calcium transients, suggesting that these stores contributed to the calcium spikes.

Calcium imaging from zebrafish muscles have been used for the characterization of mutant strains expressing muscle phenotypes. The *slow-muscle-omitted* (*smo*) gene encodes the zebrafish smoothened protein, which is required for the development of the slow muscle cells [107]. In homozygous $smo^{-/-}$ embryos injected with aequorin mRNA, the calcium transients normally observed at ~17.5–19.5 hpf were completely absent [104].

The *accordion* mutant was found in a large-scale screen [68] and it was determined that it carried a mutation in the *SERCA* gene, encoding a protein that is responsible for translocation and uptake of cytosolic calcium during muscle contractions [108]. The typical phenotype shows contracted muscles. A prolonged decay of intracellular calcium was confirmed by recordings from isolated muscle fibers from 4 dpf *accordion* mutants dialyzed with Calcium Green-1 dextran. The same result was achieved *in vivo*, when calcium signals were recorded from muscle fibers in 24 hpf animals injected with Calcium Green-1 dextran at one-cell stage [109].

Finally, the *relatively relaxed* (*ryr*) mutant was identified due to its slow swimming due to weak muscle contractions [110]. *Ryr* has a mutation in the gene encoding for the ryanodine receptor 1 that normally allows release of intracellular calcium to activate muscle contractions in fast muscle cells. To investigate the calcium signals from stimulated muscles, Calcium Green-1 dextran was injected into 8- to 16- cell-stage progeny of *ryr* carriers. At 48 hpf animals were restrained and immobilized with a muscle myosin inhibitor. Water jets to the tail of the fish stimulated calcium transients in the muscle fibers without contractions due to the immobilization. Confocal imaging experiments confirmed that the *ryr* animals lacked calcium transients in the fast muscle fibers, while the slow muscle fibers signaled normally.

Heart

The development of the heart and cardiovascular system has been extensively studied in the zebrafish [48, 111]. Despite these efforts, there is not much known about the intracellular calcium handling in the zebrafish heart. One thorough study investigating the cardiac conduction system in the zebrafish was done by Chi et al. [48]. The authors had developed a cardiac-specific GECI zebrafish transgenic line, *Tg(cmlc2:gCaMP)*^{s878}, that was used for *in vivo* calcium imaging (Figs. 48.13 and 48.14). In this line, GCaMP is driven by the heart-specific *cmlc2* promoter [92]. Apart from describing the development of the cardiac conduction, authors also screened for a number of conduction specific mutations.

Two of the first studies using calcium imaging to study heart function published back to back in 2005 [26, 32]. They were analyses of the zebrafish *tremblor* (*tre*) mutant suffering embryonic lethal cardiac arrhythmia. The *tre* locus encodes the

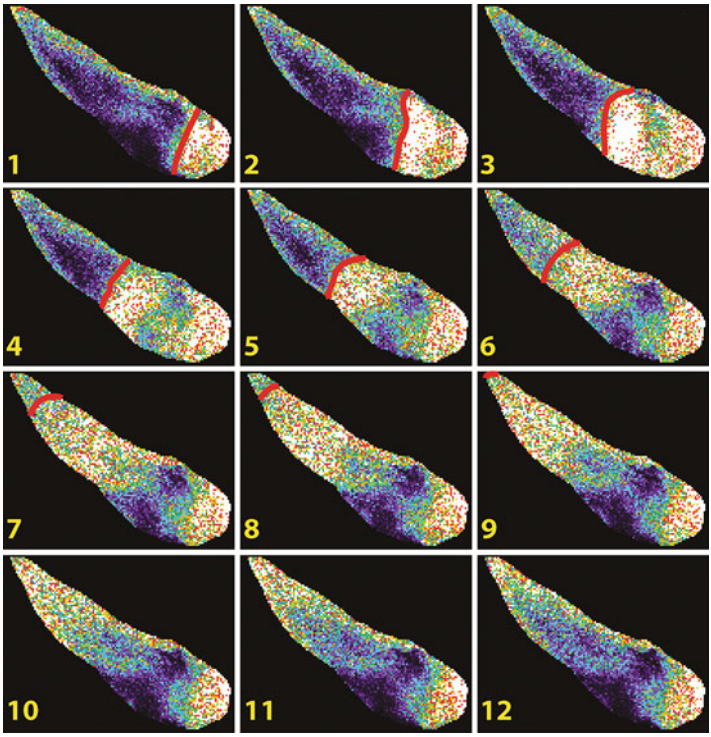

Fig. 48.13 Recording calcium signals from a larval zebrafish heart using the genetically encoded calcium indicator GCaMP. Sequential calcium activation images (one every 60 ms) of a 24 h post-fertilization zebrafish heart expressing *Tg(cmlc2:gCaMP)*^{s878}. These experiments revealed that conduction travels unidirectionally in a relatively slow and linear pattern without significant pauses from the sinus venosus (*right lower corner*) to the outflow tracts (*left top corner*) (Reprinted from Chi et al. [48])

zebrafish cardiac-specific sodium-calcium exchanger required for maintaining rhythmicity and calcium transients in the embryonic zebrafish heart [32]. Ebert et al. injected Calcium Orange AM into the pericardium of the larval heart and recorded calcium fluctuations *in vivo* using a CCD camera [26]. The normal calcium wave that is seen sweeping across the heart during a contraction in 48 hpf animals was absent in mutated animals. Instead, calcium levels appeared elevated in the ventricle. *tre* animals of the same age that had been injected with Calcium Green-1 dextran at the one-cell stage showed a similar lack of contractile calcium signals when studied with confocal imaging [32].

Another mutant showing a heart phenotype, *dco*^{s226}, was isolated in the large-scale screen previously mentioned [48]. These animals showed dysynchronous ventricular contractions leading to hear failure, caused by a mutation in the *connexin48.5* gene. *dco*^{s226} animals carrying the *Tg(cmlc2:gCaMP)*^{s878} reporter in the ventricle were

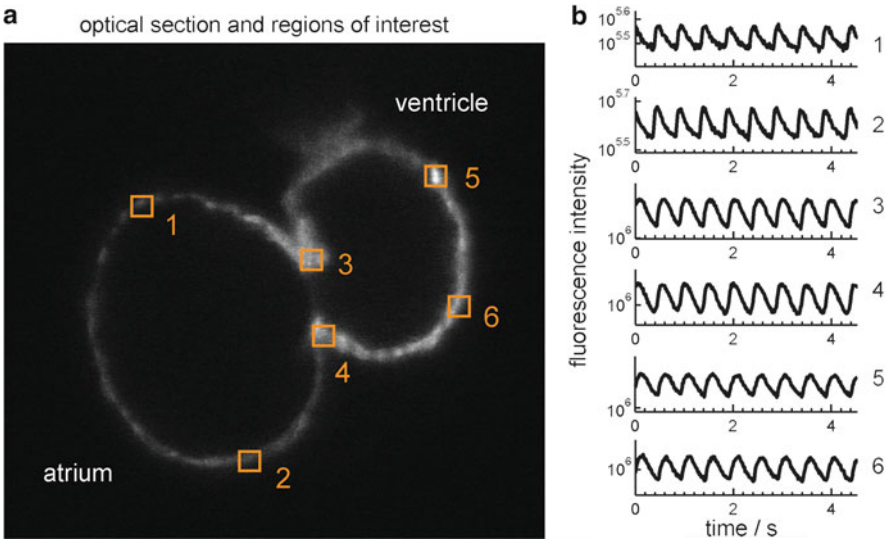

Fig. 48.14 Recording calcium transients from the atrium and ventricle myocardium from a zebrafish larva expressing GCaMP in its heart. (**a**) Optical section of a heart in a 48-h-old *Tg(cmlc2:gCaMP)*^{s878} animal. Numbers represent areas where calcium transients for the atrium, ventricle, and atrioventricular canal were recorded. (**b**) Fluorescence intensity of a single pixel from each region was recorded to obtain calcium transients and plotted over time in seconds. All plots are semilogarithmic and identically scaled (Reprinted from Chi et al. [48])

used to investigate how this mutation affects cardiac conduction. Selective plane illumination microscopy [89] of 60 dpf larvae revealed abnormal conduction through the ventricle. Additionally, *dco* cardiomyocytes carrying a dsRed marker were transplanted into wild type hearts, where they disrupted the electrical conduction [112].

Preparations monitoring isolating zebrafish hearts have also been used to study the conduction properties. Jou et al. [25] were interested in testing whether blebbestatin, a drug that uncouple cardiac contractions, could be used to prevent heart contractions without eliminating calcium signals. Isolated hearts from 48 hpf larvae were incubated in Fluo-4 AM and blebbestatin with subsequent wash. Using confocal microscopy, it was possible to record simultaneous calcium signals from both the atrium and ventricle. The authors concluded that blebbistatin is a useful drug to remove motion artifacts during imaging.

Finally, enzymatically isolated zebrafish myocytes from adult animals have been used to study the cellular properties underlying excitation-contraction coupling [18]. Together with patch-clamp recordings and measurements of cell shortening changes in the cytosolic calcium were visualized with a resonance scanning confocal microscope. While patching the myocytes they were perfused with Fluo-4 through the patch pipette. By parallel electrical stimulation and calcium imaging it was possible to elucidate the relationship between electrical depolarization and intracellular calcium signals.

Conclusion

The described preparations and experiments show the diversity of studies that have benefitted from calcium imaging in zebrafish cells, tissues and intact animals. These studies have contributed greatly to our understanding of basic biological principles during development and adulthood and the function of disease-related genes in a vertebrate system. However, it is evident that we still lack knowledge in certain biomedical areas, where new preparations of the zebrafish would be valuable. Nevertheless, the technical advances in biomedical research promise exciting possibilities. For example, the discovery of new cell-specific promoters in combination with GECIs will undoubtedly be important for future analyses of neuronal cell types and regions that so far have been unreachable by conventional labeling methods. Also, the combination of optogenetics with calcium imaging within the brain will mean valuable dissections of network function and connectivity. The development of new microscopy techniques with increased resolution, speed and imaging depth will also be critical for the advancements of calcium imaging in the zebrafish, allowing the monitoring of processes in older animals and larger brain areas. New large-scale imaging methods [38, 91, 113] and sophisticated analysis of activity from neuronal ensembles will bring our understanding of neuronal processing even further. The emerging use of the zebrafish as a model system for diseases, e.g. in the field of psychiatry, will mean exciting findings in the years to come. My hope is that this chapter will serve as an inspiration to continue the development of the zebrafish as a model organism to study the physiological processes and the complex biomedical mechanisms that are vital for biological beings.

References

1. Kaufman CK, White RM, Zon L (2009) Chemical genetic screening in the zebrafish embryo. Nat Protoc 4:1422–1432
2. Lister JA, Robertson CP, Lepage T, Johnson SL, Raible DW (1999) nacre encodes a zebrafish microphthalmia-related protein that regulates neural-crest-derived pigment cell fate. Development 126:3757–3767
3. Nasevicius A, Ekker SC (2000) Effective targeted gene 'knockdown' in zebrafish. Nat Genet 26:216–220
4. Dahme T, Katus HA, Rottbauer W (2009) Fishing for the genetic basis of cardiovascular disease. Dis Model Mech 2:18–22
5. Sager JJ, Bai Q, Burton EA (2010) Transgenic zebrafish models of neurodegenerative diseases. Brain Struct Funct 214:285–302
6. Panula P, Chen YC, Priyadarshini M, Kudo H, Semenova S, Sundvik M, Sallinen V (2010) The comparative neuroanatomy and neurochemistry of zebrafish CNS systems of relevance to human neuropsychiatric diseases. Neurobiol Dis 40:46–57
7. Liu S, Leach SD (2011) Zebrafish models for cancer. Annu Rev Pathol 6:71–93
8. Yang L, Ho NY, Alshut R, Legradi J, Weiss C, Reischl M, Mikut R, Liebel U, Muller F, Strahle U (2009) Zebrafish embryos as models for embryotoxic and teratological effects of chemicals. Reprod Toxicol 28:245–253

9. Peal DS, Peterson RT, Milan D (2010) Small molecule screening in zebrafish. J Cardiovasc Transl Res 3:454–460
10. Gobel W, Helmchen F (2007) In vivo calcium imaging of neural network function. Physiology (Bethesda) 22:358–365
11. O'Donovan MJ, Ho S, Sholomenko G, Yee W (1993) Real-time imaging of neurons retrogradely and anterogradely labelled with calcium-sensitive dyes. J Neurosci Methods 46:91–106
12. Stosiek C, Garaschuk O, Holthoff K, Konnerth A (2003) In vivo two-photon calcium imaging of neuronal networks. Proc Natl Acad Sci USA 100:7319–7324
13. Tsien RY (1981) A non-disruptive technique for loading calcium buffers and indicators into cells. Nature 290:527–528
14. Park HC, Kim CH, Bae YK, Yeo SY, Kim SH, Hong SK, Shin J, Yoo KW, Hibi M, Hirano T, Miki N, Chitnis AB, Huh TL (2000) Analysis of upstream elements in the HuC promoter leads to the establishment of transgenic zebrafish with fluorescent neurons. Dev Biol 227:279–293
15. Fetcho JR, O'Malley DM (1995) Visualization of active neural circuitry in the spinal cord of intact zebrafish. J Neurophysiol 73:399–406
16. Gahtan E, Sankrithi N, Campos JB, O'Malley DM (2002) Evidence for a widespread brain stem escape network in larval zebrafish. J Neurophysiol 87:608–614
17. Tabor R, Yaksi E, Weislogel JM, Friedrich RW (2004) Processing of odor mixtures in the zebrafish olfactory bulb. J Neurosci 24:6611–6620
18. Zhang PC, Llach A, Sheng XY, Hove-Madsen L, Tibbits GF (2011) Calcium handling in zebrafish ventricular myocytes. Am J Physiol Regul Integr Comp Physiol 300:R56–R66
19. Kreiling JA, Balantac ZL, Crawford AR, Ren Y, Toure J, Zchut S, Kochilas L, Creton R (2008) Suppression of the endoplasmic reticulum calcium pump during zebrafish gastrulation affects left-right asymmetry of the heart and brain. Mech Dev 125:396–410
20. Gilland E, Miller AL, Karplus E, Baker R, Webb SE (1999) Imaging of multicellular large-scale rhythmic calcium waves during zebrafish gastrulation. Proc Natl Acad Sci USA 96:157–161
21. Brennan C, Mangoli M, Dyer CE, Ashworth R (2005) Acetylcholine and calcium signalling regulates muscle fibre formation in the zebrafish embryo. J Cell Sci 118:5181–5190
22. Freisinger CM, Fisher RA, Slusarski DC (2010) Regulator of g protein signaling 3 modulates wnt5b calcium dynamics and somite patterning. PLoS Genet 6:e1001020
23. Brustein E, Marandi N, Kovalchuk Y, Drapeau P, Konnerth A (2003) "In vivo" monitoring of neuronal network activity in zebrafish by two-photon Ca(2+) imaging. Pflugers Arch 446:766–773
24. Niell CM, Smith SJ (2005) Functional imaging reveals rapid development of visual response properties in the zebrafish tectum. Neuron 45:941–951
25. Jou CJ, Spitzer KW, Tristani-Firouzi M (2010) Blebbistatin effectively uncouples the excitation-contraction process in zebrafish embryonic heart. Cell Physiol Biochem 25:419–424
26. Ebert AM, Hume GL, Warren KS, Cook NP, Burns CG, Mohideen MA, Siegal G, Yelon D, Fishman MC, Garrity DM (2005) Calcium extrusion is critical for cardiac morphogenesis and rhythm in embryonic zebrafish hearts. Proc Natl Acad Sci USA 102:17705–17710
27. Mack-Bucher JA, Li J, Friedrich RW (2007) Early functional development of interneurons in the zebrafish olfactory bulb. Eur J Neurosci 25:460–470
28. Yaksi E, Judkewitz B, Friedrich RW (2007) Topological reorganization of odor representations in the olfactory bulb. PLoS Biol 5:e178
29. Shimomura O, Johnson FH, Saiga Y (1962) Extraction, purification and properties of aequorin, a bioluminescent protein from the luminous hydromedusan, Aequorea. J Cell Comp Physiol 59:223–239
30. Chiesa A, Rapizzi E, Tosello V, Pinton P, de Virgilio M, Fogarty KE, Rizzuto R (2001) Recombinant aequorin and green fluorescent protein as valuable tools in the study of cell signalling. Biochem J 355:1–12
31. Webb SE, Miller AL (2006) Ca^{2+} signaling and early embryonic patterning during the blastula and gastrula periods of zebrafish and Xenopus development. Biochim Biophys Acta 1763:1192–1208

32. Langenbacher AD, Dong Y, Shu X, Choi J, Nicoll DA, Goldhaber JI, Philipson KD, Chen JN (2005) Mutation in sodium-calcium exchanger 1 (NCX1) causes cardiac fibrillation in zebrafish. Proc Natl Acad Sci USA 102:17699–17704
33. Webb SE, Miller AL (2000) Calcium signalling during zebrafish embryonic development. Bioessays 22:113–123
34. Creton R, Speksnijder JE, Jaffe LF (1998) Patterns of free calcium in zebrafish embryos. J Cell Sci 111(Pt 12):1613–1622
35. Cheung CY, Webb SE, Meng A, Miller AL (2006) Transient expression of apoaequorin in zebrafish embryos: extending the ability to image calcium transients during later stages of development. Int J Dev Biol 50:561–569
36. Baubet V, Le Mouellic H, Campbell AK, Lucas-Meunier E, Fossier P, Brulet P (2000) Chimeric green fluorescent protein-aequorin as bioluminescent Ca^{2+} reporters at the single-cell level. Proc Natl Acad Sci USA 97:7260–7265
37. Ashworth R, Brennan C (2005) Use of transgenic zebrafish reporter lines to study calcium signalling in development. Brief Funct Genomic Proteomic 4:186–193
38. Naumann EA, Kampff AR, Prober DA, Schier AF, Engert F (2010) Monitoring neural activity with bioluminescence during natural behavior. Nat Neurosci 13:513–520
39. Pologruto TA, Yasuda R, Svoboda K (2004) Monitoring neural activity and [Ca2+] with genetically encoded Ca^{2+} indicators. J Neurosci 24:9572–9579
40. Miyawaki A, Llopis J, Heim R, McCaffery JM, Adams JA, Ikura M, Tsien RY (1997) Fluorescent indicators for Ca^{2+} based on green fluorescent proteins and calmodulin. Nature 388:882–887
41. Tsuruwaka Y, Konishi T, Miyawaki A, Takagi M (2007) Real-time monitoring of dynamic intracellular Ca(2+) movement during early embryogenesis through expression of yellow cameleon. Zebrafish 4:253–260
42. Higashijima S, Masino MA, Mandel G, Fetcho JR (2003) Imaging neuronal activity during zebrafish behavior with a genetically encoded calcium indicator. J Neurophysiol 90:3986–3997
43. Horikawa K, Yamada Y, Matsuda T, Kobayashi K, Hashimoto M, Matsu-ura T, Miyawaki A, Michikawa T, Mikoshiba K, Nagai T (2010) Spontaneous network activity visualized by ultrasensitive Ca(2+) indicators, yellow Cameleon-Nano. Nat Methods 7:729–732
44. Nagai T, Sawano A, Park ES, Miyawaki A (2001) Circularly permuted green fluorescent proteins engineered to sense Ca^{2+}. Proc Natl Acad Sci USA 98:3197–3202
45. Demaurex N (2005) Calcium measurements in organelles with Ca^{2+}-sensitive fluorescent proteins. Cell Calcium 38:213–222
46. Li J, Mack JA, Souren M, Yaksi E, Higashijima S, Mione M, Fetcho JR, Friedrich RW (2005) Early development of functional spatial maps in the zebrafish olfactory bulb. J Neurosci 25:5784–5795
47. Nakai J, Ohkura M, Imoto K (2001) A high signal-to-noise Ca(2+) probe composed of a single green fluorescent protein. Nat Biotechnol 19:137–141
48. Chi NC, Shaw RM, Jungblut B, Huisken J, Ferrer T, Arnaout R, Scott I, Beis D, Xiao T, Baier H, Jan LY, Tristani-Firouzi M, Stainier DY (2008) Genetic and physiologic dissection of the vertebrate cardiac conduction system. PLoS Biol 6:e109
49. Del Bene F, Wyart C, Robles E, Tran A, Looger L, Scott EK, Isacoff EY, Baier H (2010) Filtering of visual information in the tectum by an identified neural circuit. Science 330:669–673
50. Muto A, Ohkura M, Kotani T, Higashijima S, Nakai J, Kawakami K (2011) Genetic visualization with an improved GCaMP calcium indicator reveals spatiotemporal activation of the spinal motor neurons in zebrafish. Proc Natl Acad Sci USA 108:5425–5430
51. Dreosti E, Odermatt B, Dorostkar MM, Lagnado L (2009) A genetically encoded reporter of synaptic activity in vivo. Nat Methods 6:883–889
52. Meng CL, Chang DC (1994) Study of calcium signaling in cell cleavage using confocal microscopy. Biol Bull 187:234–235
53. Kimmel CB, Ballard WW, Kimmel SR, Ullmann B, Schilling TF (1995) Stages of embryonic development of the zebrafish. Dev Dyn 203:253–310

54. Webb SE, Miller AL (2003) Imaging intercellular calcium waves during late epiboly in intact zebrafish embryos. Zygote 11:175–182
55. Webb SE, Fluck RA, Miller AL (2011) Calcium signaling during the early development of medaka and zebrafish. Biochimie 93(12):2112–2125
56. Reinhard E, Yokoe H, Niebling KR, Allbritton NL, Kuhn MA, Meyer T (1995) Localized calcium signals in early zebrafish development. Dev Biol 170:50–61
57. Lee KW, Webb SE, Miller AL (1999) A wave of free cytosolic calcium traverses zebrafish eggs on activation. Dev Biol 214:168–180
58. Sharma D, Kinsey WH (2008) Regionalized calcium signaling in zebrafish fertilization. Int J Dev Biol 52:561–570
59. Chang DC, Meng C (1995) A localized elevation of cytosolic free calcium is associated with cytokinesis in the zebrafish embryo. J Cell Biol 131:1539–1545
60. Chang DC, Lu P (2000) Multiple types of calcium signals are associated with cell division in zebrafish embryo. Microsc Res Tech 49:111–122
61. Webb SE, Lee KW, Karplus E, Miller AL (1997) Localized calcium transients accompany furrow positioning, propagation, and deepening during the early cleavage period of zebrafish embryos. Dev Biol 192:78–92
62. Leung CF, Webb SE, Miller AL (1998) Calcium transients accompany ooplasmic segregation in zebrafish embryos. Dev Growth Differ 40:313–326
63. Webb SE, Li WM, Miller AL (2008) Calcium signalling during the cleavage period of zebrafish development. Philos Trans R Soc Lond B Biol Sci 363:1363–1369
64. Schneider I, Houston DW, Rebagliati MR, Slusarski DC (2008) Calcium fluxes in dorsal forerunner cells antagonize beta-catenin and alter left-right patterning. Development 135: 75–84
65. O'Malley DM, Kao YH, Fetcho JR (1996) Imaging the functional organization of zebrafish hindbrain segments during escape behaviors. Neuron 17:1145–1155
66. Liu KS, Fetcho JR (1999) Laser ablations reveal functional relationships of segmental hindbrain neurons in zebrafish. Neuron 23:325–335
67. Kohashi T, Oda Y (2008) Initiation of Mauthner- or non-Mauthner-mediated fast escape evoked by different modes of sensory input. J Neurosci 28:10641–10653
68. Granato M, van Eeden FJ, Schach U, Trowe T, Brand M, Furutani-Seiki M, Haffter P, Hammerschmidt M, Heisenberg CP, Jiang YJ, Kane DA, Kelsh RN, Mullins MC, Odenthal J, Nusslein-Volhard C (1996) Genes controlling and mediating locomotion behavior of the zebrafish embryo and larva. Development 123:399–413
69. Nicolson T, Rusch A, Friedrich RW, Granato M, Ruppersberg JP, Nusslein-Volhard C (1998) Genetic analysis of vertebrate sensory hair cell mechanosensation: the zebrafish circler mutants. Neuron 20:271–283
70. van Eeden FJ, Granato M, Schach U, Brand M, Furutani-Seiki M, Haffter P, Hammerschmidt M, Heisenberg CP, Jiang YJ, Kane DA, Kelsh RN, Mullins MC, Odenthal J, Warga RM, Allende ML, Weinberg ES, Nusslein-Volhard C (1996) Mutations affecting somite formation and patterning in the zebrafish, Danio rerio. Development 123:153–164
71. Liu KS, Gray M, Otto SJ, Fetcho JR, Beattie CE (2003) Mutations in deadly seven/notch1a reveal developmental plasticity in the escape response circuit. J Neurosci 23:8159–8166
72. Hale ME, Kheirbek MA, Schriefer JE, Prince VE (2004) Hox gene misexpression and cell-specific lesions reveal functionality of homeotically transformed neurons. J Neurosci 24: 3070–3076
73. Takahashi M, Narushima M, Oda Y (2002) In vivo imaging of functional inhibitory networks on the mauthner cell of larval zebrafish. J Neurosci 22:3929–3938
74. Orger MB, Kampff AR, Severi KE, Bollmann JH, Engert F (2008) Control of visually guided behavior by distinct populations of spinal projection neurons. Nat Neurosci 11:327–333
75. Sankrithi NS, O'Malley DM (2010) Activation of a multisensory, multifunctional nucleus in the zebrafish midbrain during diverse locomotor behaviors. Neuroscience 166:970–993
76. Bizzi E, D'Avella A, Saltiel P, Tresch M (2002) Modular organization of spinal motor systems. Neuroscientist 8:437–442

77. O'Malley DM, Sankrithi NS, Borla MA, Parker S, Banden S, Gahtan E, Detrich HW 3rd (2004) Optical physiology and locomotor behaviors of wild-type and nacre zebrafish. Methods Cell Biol 76:261–284
78. Ritter DA, Bhatt DH, Fetcho JR (2001) In vivo imaging of zebrafish reveals differences in the spinal networks for escape and swimming movements. J Neurosci 21:8956–8965
79. Bhatt DH, McLean DL, Hale ME, Fetcho JR (2007) Grading movement strength by changes in firing intensity versus recruitment of spinal interneurons. Neuron 53:91–102
80. Henneman E (1957) Relation between size of neurons and their susceptibility to discharge. Science 126:1345–1347
81. Zimprich F, Ashworth R, Bolsover S (1998) Real-time measurements of calcium dynamics in neurons developing in situ within zebrafish embryos. Pflugers Arch 436:489–493
82. Ashworth R, Zimprich F, Bolsover SR (2001) Buffering intracellular calcium disrupts motoneuron development in intact zebrafish embryos. Brain Res Dev Brain Res 129:169–179
83. Higashijima S, Hotta Y, Okamoto H (2000) Visualization of cranial motor neurons in live transgenic zebrafish expressing green fluorescent protein under the control of the islet-1 promoter/enhancer. J Neurosci 20:206–218
84. Fraser SE (1992) Patterning of retinotectal connections in the vertebrate visual system. Curr Opin Neurobiol 2:83–87
85. Nevin LM, Robles E, Baier H, Scott EK (2010) Focusing on optic tectum circuitry through the lens of genetics. BMC Biol 8:126
86. Gahtan E, Tanger P, Baier H (2005) Visual prey capture in larval zebrafish is controlled by identified reticulospinal neurons downstream of the tectum. J Neurosci 25:9294–9303
87. Borla MA, Palecek B, Budick S, O'Malley DM (2002) Prey capture by larval zebrafish: evidence for fine axial motor control. Brain Behav Evol 60:207–229
88. McElligott MB, O'Malley DM (2005) Prey tracking by larval zebrafish: axial kinematics and visual control. Brain Behav Evol 66:177–196
89. Huisken J, Swoger J, Del Bene F, Wittbrodt J, Stelzer EH (2004) Optical sectioning deep inside live embryos by selective plane illumination microscopy. Science 305:1007–1009
90. Ramdya P, Engert F (2008) Emergence of binocular functional properties in a monocular neural circuit. Nat Neurosci 11:1083–1090
91. Sumbre G, Muto A, Baier H, Poo MM (2008) Entrained rhythmic activities of neuronal ensembles as perceptual memory of time interval. Nature 456:102–106
92. Huang L, Maaswinkel H, Li L (2005) Olfactoretinal centrifugal input modulates zebrafish retinal ganglion cell activity: a possible role for dopamine-mediated Ca^{2+} signalling pathways. J Physiol 569:939–948
93. Dorostkar MM, Dreosti E, Odermatt B, Lagnado L (2010) Computational processing of optical measurements of neuronal and synaptic activity in networks. J Neurosci Methods 188: 141–150
94. Shepherd GM (1993) Principles of specificity and redundancy underlying the organization of the olfactory system. Microsc Res Tech 24:106–112
95. Mombaerts P (2001) How smell develops. Nat Neurosci 4(Suppl):1192–1198
96. Shipley MT, Ennis M (1996) Functional organization of olfactory system. J Neurobiol 30:123–176
97. Friedrich RW, Korsching SI (1997) Combinatorial and chemotopic odorant coding in the zebrafish olfactory bulb visualized by optical imaging. Neuron 18:737–752
98. Friedrich RW, Laurent G (2001) Dynamic optimization of odor representations by slow temporal patterning of mitral cell activity. Science 291:889–894
99. Yaksi E, von Saint Paul F, Niessing J, Bundschuh ST, Friedrich RW (2009) Transformation of odor representations in target areas of the olfactory bulb. Nat Neurosci 12:474–482
100. Fuss SH, Korsching SI (2001) Odorant feature detection: activity mapping of structure response relationships in the zebrafish olfactory bulb. J Neurosci 21:8396–8407
101. Tabor R, Yaksi E, Friedrich RW (2008) Multiple functions of GABA A and GABA B receptors during pattern processing in the zebrafish olfactory bulb. Eur J Neurosci 28:117–127

102. Ghanem N, Jarinova O, Amores A, Long Q, Hatch G, Park BK, Rubenstein JL, Ekker M (2003) Regulatory roles of conserved intergenic domains in vertebrate Dlx bigene clusters. Genome Res 13:533–543
103. Ashworth R (2004) Approaches to measuring calcium in zebrafish: focus on neuronal development. Cell Calcium 35:393–402
104. Cheung CY, Webb SE, Love DR, Miller AL (2011) Visualization, characterization and modulation of calcium signaling during the development of slow muscle cells in intact zebrafish embryos. Int J Dev Biol 55(2):153–174
105. Chen JK, Taipale J, Cooper MK, Beachy PA (2002) Inhibition of Hedgehog signaling by direct binding of cyclopamine to Smoothened. Genes Dev 16:2743–2748
106. Barresi MJ, D'Angelo JA, Hernandez LP, Devoto SH (2001) Distinct mechanisms regulate slow-muscle development. Curr Biol 11:1432–1438
107. Barresi MJ, Stickney HL, Devoto SH (2000) The zebrafish slow-muscle-omitted gene product is required for Hedgehog signal transduction and the development of slow muscle identity. Development 127:2189–2199
108. Gleason MR, Armisen R, Verdecia MA, Sirotkin H, Brehm P, Mandel G (2004) A mutation in serca underlies motility dysfunction in accordion zebrafish. Dev Biol 276:441–451
109. Hirata H, Saint-Amant L, Waterbury J, Cui W, Zhou W, Li Q, Goldman D, Granato M, Kuwada JY (2004) accordion, a zebrafish behavioral mutant, has a muscle relaxation defect due to a mutation in the ATPase Ca^{2+} pump SERCA1. Development 131:5457–5468
110. Hirata H, Watanabe T, Hatakeyama J, Sprague SM, Saint-Amant L, Nagashima A, Cui WW, Zhou W, Kuwada JY (2007) Zebrafish relatively relaxed mutants have a ryanodine receptor defect, show slow swimming and provide a model of multi-minicore disease. Development 134:2771–2781
111. Stainier DY (2001) Zebrafish genetics and vertebrate heart formation. Nat Rev Genet 2:39–48
112. Chi NC, Bussen M, Brand-Arzamendi K, Ding C, Olgin JE, Shaw RM, Martin GR, Stainier DY (2010) Cardiac conduction is required to preserve cardiac chamber morphology. Proc Natl Acad Sci USA 107:14662–14667
113. Miri A, Daie K, Burdine RD, Aksay E, Tank DW (2011) Regression-based identification of behavior-encoding neurons during large-scale optical imaging of neural activity at cellular resolution. J Neurophysiol 105:964–980

Chapter 49
Calcium Signaling in *Xenopus oocyte*

Matthieu Marin

Abstract Knowledge about calcium signaling had increased thanks to the development and manipulation of various cell models. Among all of these prototypes, *Xenopus laevis* oocyte appears to be one of the most relevant. The understanding of the role of calcium during oocyte oogenesis, maturation and fertilization is facilitated by the big size of the cell but also by using imaging and electrophysiological approaches. So, this chapter presents how recordings of calcium-activated chloride channels and Store-Operated Calcium Channels activities lead to demonstrate the implication of the MPF in the uncoupling between intracellular calcium releasing and capacitative calcium entry. Moreover, it will help us to understand the several reorganizations happening consequently to the pH variations of maturation or just at the moment of fertilization.

Keywords Xenopus laevis • Oocyte • Calcium signaling • Maturation • pH • Electrophysiology • Double electrode • Microinjection • Calcium-activated chloride channels • Cell cycle • Meiosis • Germinal vesicle break down • G2/M transition • MPF • Calcium entry • Calcium release • Store Operated Calcium Entry • IP3 • Fertilization

Abbreviations

CaCC	Calcium-Activated Chloride Channels
CRAC	Calcium Release-Activated Channels
GVBD	Germinal Vesicle BreakDown

M. Marin (✉)
Laboratoire de Regulation des Signaux de Division, EA 4479, IFR 147,
Université Lille1, Sciences et Technologies, Cité Scientifique,
59655, Villeneuve d'Ascq, France
e-mail: matthieu.marin@univ-lille1.fr

M.S. Islam (ed.), *Calcium Signaling*, Advances in Experimental Medicine and Biology 740, DOI 10.1007/978-94-007-2888-2_49,

ICl	Calcium-activated chloride currents measured with the triple step protocol
IClCa	Calcium-dependent chloride currents
InsP3 & Ins(1, 4, 5)P3	Inositol 1,4,5-triphosphate
IP3R	IP3 Receptor
I_{SOCE}	SOCE Current
MAPK	Mitogen Activated Protein Kinase
MPF	M-phase promoting factor
pHe	Extracellular pH
pHi	Intracellular pH
PMCA	Plasma Membrane Calcium ATPase
RyR	Ryanodine Receptor
SERCA	Sarcoplasmic Endoplasmic Reticulum Calcium ATPase
SOCC	Store-Operated Calcium Channels
SOCE	Store-Operated Calcium Entry
VDCC	Voltage-Dependent Chloride Channels

This review is focused on the *Xenopus laevis,* a famous frog from South Africa, which proved, and still is, useful in many lines of researches. Especially, its oocytes are considered as a model of interest to investigate the role of calcium during the physiological events associated with the cell cycle regulation during meiotic progression and early development using biochemical and electrophysiological approaches.

The crucial cellular responses to both environmental and individual modifications are the result of numerous interacting and interconnecting signaling cascades. Among the second messengers known all over the animal kingdom, the intracellular ionic calcium seems to be one of the most widespread and may be the most important one. Intracellular calcium signals are found from bacteria to human and have been implicated in many physiological and pathological cellular processes, encompassing gene expression, T-cell activation, cell cycle deregulation, pain signaling, muscle contraction, synaptic transmission or even oocyte maturation and fertilization [1]. Here is presented in a first section the model and its advantages for studying calcium signaling; the second section considers oocyte maturation, focusing on store-operated calcium entry and on the complex relationships between calcium and intracellular pH, and the third section presents the first events of fertilization, that is to say the beginning of a long way towards organogenesis.

The *Xenopus oocyte*, a Great Research Model for Calcium Signaling

Forty years ago, Dumont described *Xenopus laevis* oogenesis (Fig. 49.1). During this period, oocytes undergo morphological and biochemical modifications in order to be ready for maturation and fertilization. Ovary can be surgically collected

a

Stage	I	II	III	IV	V	VI
Diameter (μM)	50-300	300-450	450-600	600-1000	1000-1200	1200-1300
outward show	translucent	white	brownish	Individualization of 2 poles	Animal and vegetal poles clearly defined	Equatorial area without pigment

b

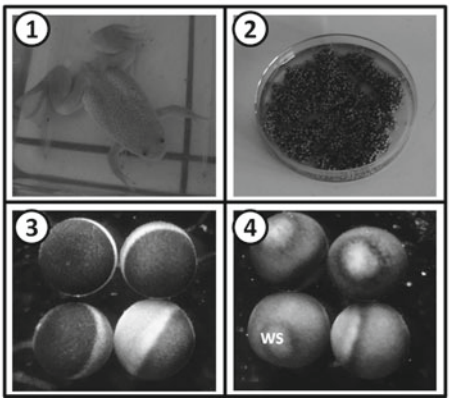

Fig. 49.1 *Xenopus laevis* and its oocytes. (**a**) typical features of oocyte in terms of stage, diameter and appearance according to (*2*). (**b**) the frog, *Xenopus laevis* (*1*), *stages I to VI* oocytes in the ovary (*2*), defolliculated *stage VI* – immature – oocytes (*3*), and mature oocytes – eggs –after progesterone treatment (*4*). Eggs are characterized by a white spot (*WS*) at the top of the animal pole

and hundreds of oocytes individualized and denuded easily by enzymatic and mechanic treatment [2].

These cells were classified in six stages, from I to VI (Fig. 49.1a). Stage V or VI have a diameter ranging from 1 to 1.3 mm with a highly folded plasma membrane with an area of about 20 mm^2. Stage VI oocytes are blocked at prophase of meiosis I (in a G2-like arrest), and are considered as "immature oocytes". This meiotic arrest could be released in response to the natural hormonal inducer, progesterone (metaphase/anaphase or G2/M transition) [3, 4]. Then, "immature oocytes" could continue meiosis until a second block in metaphase of meiosis II, waiting for fertilization. Such oocytes are called "mature oocytes" or "eggs" (Fig. 49.1b) and could be identified by a "white spot" at the top of the animal pole which corresponds to the germinal vesicle breakdown (GVBD) (Fig. 49.1b). The egg is ready for fertilization that is the final trigger that allows the completion of meiosis.

Many characteristics specific to the *Xenopus* oocyte make it an excellent experimental system. The large size makes the oocyte easy to dissect manually as well as to carry out various assays within single oocytes [5, 6].

The *Xenopus laevis* oocyte is an important model for the study of the huge diversity of calcium signaling, ranging from "hot spots" to calcium oscillations and waves that sweep across the whole cytosol. Calcium oscillations could be induced in *Xenopus* oocytes under various conditions, including injection of Ins(1, 4, 5)P3

or Ins(l,4,5)P3-analogs [7]. Typically, calcium waves – travelling from animal to vegetal pole of the oocyte – are observed at fertilization or after stimulation of receptors linked to the inositol phosphate pathway or again directly after injection of Ins(1, 4, 5)P3 and analogs [8–10]. Moreover, in most cell models, calcium itself, ionomycin, thapsigargin, caffeine, or ryanodine were able to induce calcium waves. What is striking and interesting with *Xenopus laevis* oocyte is the fact that the study of the elementary events of calcium signaling is facilitated by the lack of ER calcium-release channels (e.g., ryanodine receptors (RyRs) and cADP-ribose receptors) other than IP3Rs [11, 12] even if RyRs have been implicated in oocyte maturation and/or activation/fertilization in other species (starfish and pig for example) and very recently in *Bufo arenarum*, another amphibian [13]. Moreover, in another species of *Xenopus*, *Xenopus tropicalis*, genomic sequences have released about RyR-like receptors [14]. This should provide molecular tools to look further for the expression of such receptors in *Xenopus laevis* oocytes. In addition, *Xenopus oocyte* is favourable to understand store-operated calcium entry (SOCE) regulation because it was observed and demonstrated a decoupling between calcium release from intracellular stores and calcium entry via SOCE channels (see "SOCE and maturation" section for details).

The large size of the oocyte facilitates microinjection of either DNA into the nucleus or mRNA into the cytoplasm (the estimated volume of the oocyte is appreciatively equivalent to 50,000 somatic cells). The oocyte contains large amounts of the components required for gene expression including RNA polymerases, ribonucleotide triphosphates, transcription factors, histones, and ribosomes. Finally, the equipment required for *Xenopus* oocytes isolation, culture, manipulation and microinjection is relatively simple and inexpensive. Various protocols, outlining oocyte manipulation, microinjection and other techniques, like electrophysiological approach or imaging techniques, have been published [6, 15, 16]. Moreover, in good accordance with the literature, neither somatic cells nor *in vitro* systems offer a similar facility as *Xenopus* oocytes for *in vivo* studies of the mechanisms that control cell cycle and orchestrate cell reorganization at M-Phase. That is the reason why a lot of studies were carried out with the *Xenopus laevis* oocyte to decipher the function of calcium in the pathways of the cell cycle. Indeed, in addition to their high capacity of protein synthesis and their physiological synchronization, *Xenopus* oocyte is also valuable to analyze the MAPK cascade in the morphological events of M-phase [17].

Electrophysiological Features

Among the methods using *Xenopus* oocyte, electrophysiological approaches are of particular interest, since the oocyte is increasingly used in physiological, pharmacological and neuro-physiological research. In that way, studies typically used a conventional two-electrode voltage-clamp technique. On the contrary to the whole-cell patch-clamp approach, the two-electrode method preserves intact the intracellular

Table 49.1 Concatenation of the electrophysiological features of stage VI *Xenopus* oocyte

A	Ion	Concentration (mM)	References
Intracellular concentrations of main ions, according to the literature	Na^+	4 to 23	[23–25]
	K^+	76 to 48	[23, 25, 26]
	Cl^-	24 to 62	[23–26]
	Ca^{2+}	0.003 to 0.4	[27, 28]
	Mg^{2+}	>0.5	[28]
B	Ion	E_{ion} (mV)	References
Various reversal potentials measured in different studies	E_{Na+}	46 to 61	[23, 29]
	E_{K+}	−95 to −108	[30]
	E_{Cl-}	−14 to −28	[23, 29, 31]
C		E_m	References
Membrane potential of *X. laevis* oocytes		−27 mV	[23]
		−50 mV	[32]
		−59 mV	[33]

medium and organelles during long recordings [18–22]. Healthy cells survive electrode insertion and allow recordings lasting for tens of minutes without appreciable deterioration. The electrical parameters of the oocytes (membrane resistance, membrane potential and membrane currents) are essential factors that are a reliable indicator of oocytes quality (Table 49.1). Of importance is the notion of the intrinsic diversity of the cells. Indeed, these various parameters differ from one oocyte to another within one batch coming from a single female and differences could be even larger in oocytes from different donors or at different seasons. In order to run experiments, homogeneity is desirable and the choice of oocytes is thus crucial. In general, electrical membrane resistance of the oocyte is relatively high (ranging from 100 kOhms to 2 MOhms) and oocytes exhibiting significantly lower resistance should not be used for microinjection and electrophysiological experiments. Furthermore, the literature indicated large differences in the membrane potential of the oocytes ranging from −27 to −90 mV, when determined in physiological Ringer solution [5, 30, 34] (Table 49.1C). Finally, intracellular ion concentrations are very important for the investigation of passive or active transport systems since the rate and/or the direction of the respective transports are determined by the electrochemical gradients [5] (Table 49.1A).

Often, *Xenopus* oocytes were and are always used as a heterologous expression system for the study of cloned ion channels. This appears to be essential in order to understand the structure and the function of ion channels and or receptors [35], like potassium channels Kcv [36], G-protein coupled receptors [37] or transient receptor potential channels [38] for example.

In order to analyze calcium signaling pathways in *Xenopus* oocyte itself, it appears important to describe some useful endogenously membrane transport systems. In the middle of the 1980s, Dascal and colleagues [39] used the oocyte as a heterologous expression system for calcium expression. They first described different endogenous voltage-dependent calcium channels (VDCC). This was performed

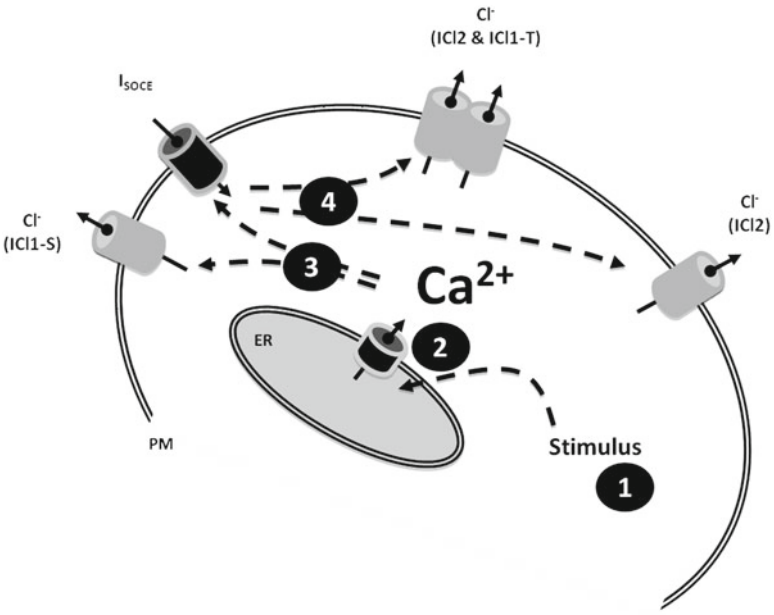

Fig. 49.2 Calcium fluxes in *Xenopus* oocyte. Stimulation (*1*) of IP3R is responsible for calcium stores depletion from endoplasmic reticulum (*2*). This efflux activates ICl1-S and elicits calcium influx – I_{SOCE} – (*3*) which in turns activates ICl2 and ICl1-T (*4*)

while abolishing (or simply decreasing) other conductances, in particular calcium-activated chloride channels, that masked the calcium currents since studies showed that VDCC currents are usually rather small ranging from 10 to 100 nA. Endogenous VDCC are classically stimulated by InsP3, cAMP and are sensitive to Mn^{2+}. They belong to L-type, T-type and N-type calcium channels .

Another major class of calcium channels largely studied in the *Xenopus* oocyte is Store-Operated Calcium Channels (SOCC) (Fig. 49.2). Initially identified in somatic cells, these channels are activated by the depletion of intracellular calcium stores (notably the endoplasmic reticulum but also the mitochondria) evoked by InsP3. Calcium release results in an increase in intracellular calcium concentration which in turn modulates InsP3 production, contributing to the often durable and/or oscillatory nature of many calcium signals. Consequently, these sustained responses necessitate the refilling of the empty stores, which is performed by calcium entry from extracellular medium, an entry itself activated by store-depletion through an obviously complex and still undeciphered mechanism. This neat auto-regulatory system is called Store-Operated Calcium Entry (SOCE) and mobilizes the SOCC. In 1997, Yao & Tsien showed that capacitative calcium entry *via* SOCC in the *Xenopus* oocyte behaves like CRAC in mast cells [22]. Nevertheless, even if this phenomenon is well described (in particular with the identification of Stim1 and Orai1), in *Xenopus* oocyte the regulation of SOCC the coupling machinery involved and the role of calcium during meiosis are still a matter of debate (see section "Calcium and Maturation").

Originally, calcium fluxes were indirectly measured by recording calcium-dependent chloride currents (also called calcium-activated chloride channels, CaCC). This could be done by using the triple step protocol developed by Parekh in 1995 and modified by Kuruma & Hartzell in 1999 [40, 41] (Fig. 49.2). This protocol allows the discrimination of the source of calcium mobilized, between intracellular calcium stores and/or SOCE [31, 41–43]. It was shown that ICl-1 and ICl-2 channels were asymmetrically distributed in *Xenopus* oocytes. In fact, (i) ICl1 density was found about five times higher in the animal hemisphere than in the vegetal pole, and (ii) ICl-2 was "only" threefold. The difference in density of the currents in the two poles could in part be due to differences in the amplitude of the calcium signal in the two hemispheres: the levels of calcium release from endoplasmic stores and calcium entry from the extracellular medium in the animal hemisphere were about twofold higher in the animal versus the vegetal hemispheres. These data could account, at least partly, for the five- and threefold difference observed for ICl-1 and ICl-2 [40, 42, 44–46]. Since *Xenopus* oocyte is a popular model system for studying calcium signaling, these observations provide additional information about spatial features of the calcium pathways in oocytes and highlight the question of how calcium release from reticular stores and calcium influx from extracellular medium could differentially regulate two different chloride channels (ICl-1 and ICl-2 respectively). Another obvious question that is raised by these studies is about the physiological role(s) of these calcium-activated chloride channels. It is renowned that fertilization results in a calcium transient (activating CaCC) [11] which triggers exocytosis of cortical granules and which participates to the block of polyspermy [47]. However, the role of these calcium activated chloride channels is not clearly defined yet [42, 48].

In addition, the sole plasma membrane calcium fluxes can also be directly measured by recording store-operated calcium entry currents [22, 49, 50], but this necessitates slightly less physiological conditions. Store-Operated Calcium currents (Fig. 49.2) have been described in *Xenopus* oocyte by using the advantageous voltage-clamp technique [19, 21]. Since it is well-known that calcium-activated chloride currents are of large amplitude in this oocyte and mask calcium currents, I_{SOCE} was isolated thanks to the inhibition of CaCC currents (microinjection of a calcium chelator like BAPTA or EGTA for example) and by rising extracellular calcium concentration [22].

Calcium and Maturation

In a lot of animal models, calcium signals have been convincingly shown to play a role and being profoundly modified during mitosis, meiosis and egg activation at fertilization. Indeed, during mitosis, calcium signals are involved in nuclear envelope breakdown, anaphase onset and cell cleavage [51, 52]. This is the reason why the role of calcium signaling and its subsequent modifications have been of wide interest in *Xenopus laevis* oocyte as well (Tables 49.2 and 49.3). A variety of genetic and biochemical evidence supports a role for calcium and its downstream effectors calmodulin and CAMK2 in mitosis and following fertilization [64–67]. By contrast, the role of calcium signals during mammals' oocyte meiosis remains contentious

Table 49.2 Diversity of the methods used to elicit calcium variations and/or maturation in *Xenopus* oocyte

Method	Results	Maturation	References
A23187 + high $[Ca^{2+}]_e$	Rise of $[Ca^{2+}]_i$	Spontaneous maturation without H	[53]
Ionophoresis	Rise of $[Ca^{2+}]_i$	Spontaneous maturation without H	[54]
TMB-8	No calcium release	NTR	[55]
Extracellular EGTA	Decrease of $[Ca^{2+}]_e$	Delayed maturation	[56]
Extracellular EGTA	Decrease of $[Ca^{2+}]_e$	No maturation	[57]
O-$[Ca^{2+}]_e$ and extracellular EGTA or BAPTA	Decrease of $[Ca^{2+}]_e$	NTR	[58]
EGTA injection and O-$[Ca^{2+}]_e$	Decrease of $[Ca^{2+}]_e$ and $[Ca^{2+}]_i$	Delayed maturation	[58]
IP3R antisens	No calcium release	Delayed maturation	[59]
IP3 injection before maturation stimulation (H)	Rise of $[Ca^{2+}]_e$	Accelerated maturation	[60]
Intracellular acidification (NH_4Cl)	Calcium release and calcium entry	Delayed maturation	[31]
Intracellular alkalyzation (increase of pHe)	Calcium release and calcium entry	Accelerated maturation	[61]
IP3R inhibition (antisens)	SOCE inhibition	Delayed maturation	[59]
IP3R inhibition (antisens) AND RyR surexpression	Calcium release with caffeine	Comparable maturation	[59]

NTR nothing to report, *H* hormonal stimulation (progesterone)

Table 49.3 Intracellular calcium concentration variations detections during oocyte maturation, are dependent upon technical approach (^{45}Ca, Aequorin or microelectrode)

Ca variation during oocyte maturation	Methods	References
NTR	$^{45}Ca^{2+}$	[27]
Transient rise	$^{45}Ca^{2+}$	[62]
Transient rise	$^{45}Ca^{2+}$	[58]
NTR	Calcium imaging (Aequorin)	[63]
Transient rise	Calcium imaging (Aequorin)	[54]
NTR	Ion selective microelectrode	[64]

NTR nothing to report

(Tables 49.2 and 49.3). In *Xenopus*, early reports argued that a calcium rise is sufficient to induce oocyte maturation, and injection of calcium buffers block maturation. However, even the activation of calcium signals downstream of progesterone is also controversial. These conflicting reports clearly indicate that in *Xenopus laevis* oocytes the relationship between calcium and oocyte maturation is complex. Studies regarding the role of calcium during mammalian oocyte maturation also produced conflicting results [68]. Does calcium play any role in releasing oocytes meiotic arrest? The preponderance of the evidence argues that this is not the case

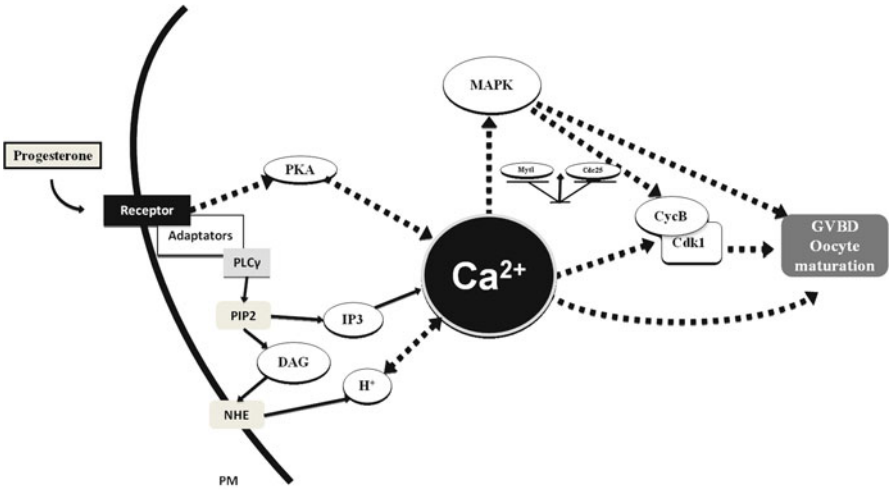

Fig. 49.3 Molecular and signaling pathways during oocyte maturation. The meiotic arrest is released by the binding of progesterone to its membrane receptor. This activates various pathways responsible for intracellular calcium modifications. Calcium has a central role and could interact with the intracellular pH (H^+), the *MAPK* cascade and the *MPF* (Cyclin B-Cdk1 complex) pathway. All these ionic and biochemical pathways play a role in the G2/M transition

and that release from meiotic arrest occurs independently from a calcium signal. However, there are also compelling reports arguing for a potential role of calcium signals in the initiation of oocyte maturation. Incubation of oocytes in high calcium concentrations in the presence of ionophore was reported to induce oocyte maturation [53]. Similarly, calcium electroporation was also effective at inducing oocyte maturation [54] (Table 49.2). If indeed calcium is important for the release from meiotic arrest, then one would expect calcium transient to be associated with oocyte maturation. Such calcium transients were reported following the induction of oocyte maturation in *Xenopus* by some groups [27, 62, 69], but could not be confirmed by others [55, 64]. In addition, injection of IP3 into the oocyte, which empties calcium from intracellular stores, did not release meiotic arrest.

Cellular and developmental decisions are the result of often competing and/or dialoguing signaling processes that include crosstalk, feedback activating and inhibiting mechanisms, allowing flexible regulation of critical differentiation pathways. As stated before, while oocytes develop in the ovary to prepare for fertilization, they remain arrested at prophase of meiosis I in a G2-like state of the cell cycle with a visible nucleus (called germinal vesicle) and a potentially active transcription state.

In *Xenopus*, meiotic arrest is released in response to progesterone (Figs. 49.1 and 49.3). Ensuing, cell cycle proceeding is characterized by morphological, biochemical and physiological changes, which include calcium signaling pathways remodelling [61]. Other signal can trigger cell cycle resuming and all induce a complex kinase cascade that, *in fine*, activates MPF (M-phase promoting factor)

and commits the oocyte to maturation [70, 71]. The details of this cascade are best defined in *Xenopus* oocyte with close parallels in mammals (Fig. 49.3). In *Xenopus* oocyte, the activation of a progesterone cell surface serpentine G-protein coupled receptor leads to the accumulation of the oocyte specific MAPKK, Mos. Induction of the MAPK cascade culminates in activation of p90Rsk, which inhibits Myt1, a kinase that phosphorylates and inhibits MPF [72, 73]. A parallel pathway to the MAPK cascade is also activated leading to the induction of Cdc25, which dephosphorylates and activates MPF. Combined Cdc25 activation and inhibition of Myt1 lead to a dramatic rise in MPF activity [50, 74]. What is MPF? It is a member of the cyclin-dependent kinase family or cell cycle regulators. Cyclin-dependent kinases are master regulators of entry and progression through both mitosis and meiosis [75]. In that capacity, MPF controls various cellular processes crucial for meiotic progression. For example, MPF induces GVBD and stabilizes Mos kinase, which is a component of CSF [76]. If MPF is necessary for cell cycle resumption – and the transformation of the oocyte in an egg apt to sustain egg activation – CSF is also necessary for the subsequent cell cycle arrest in metaphase II arrest until fertilization [77].

Furthermore, injection of calcium chelators at high concentrations effectively blocked oocyte maturation [54, 58]. However, this inhibition is apparently not due to calcium chelation, but rather to chelation of transition metals, specifically zinc [78]. This is plausible since calcium chelators such as BAPTA are also powerful chelators of transition metals [79, 80]. Indeed, it was shown that these chelators when injected into the oocyte inhibit the activation of Cdc25, and hence MPF and commitment to meiosis [78]. Cdc25 directly binds zinc, and this is important for Cdc25 substrate recognition and dephosphorylation and activation of MPF. Additional support against a role for calcium signals in releasing meiotic arrest comes from a study where oocytes were completely deprived of calcium signals by emptying calcium stores and incubating the cells in nominally calcium-free media. Under these conditions, oocytes entered meiosis in response to progesterone and underwent GVBD, with the associated activation of the kinase cascade that drives oocyte maturation [81]. However, in the absence of calcium signals such oocytes were not able to complete meiosis I because formation of the bipolar spindle and hence polar body extrusion was defective [81]. Similar results were obtained in mouse oocytes [82]. Together these data argue that calcium signals are not required for the release of meiotic arrest. This is especially the case when one evaluates the consistent effects of interfering with calcium signaling on fertilization in different species as compared to release of oocyte meiotic arrest [66].

SOCE and Maturation

Oocyte maturation entails a complex series of biochemical and morphological modifications that transform immature oocytes into fertilization-competent eggs, able to support embryonic development. Early electron microscopy studies have described morphological changes that occur concomitantly with *Xenopus* oocyte maturation

(for review see [83]). Furthermore, extensive studies have characterized biochemical cascades that drive oocyte maturation [84]. There remains much to be learned about how these signal transduction cascades regulate physiologically relevant pathways during oocyte maturation. That is why the relationships between the Mos–MAPK–MPF kinase cascade and SOCE have been envisaged.

In the early 2000s, the oocyte maturation was considered as a new physiological context to revisit the issue of calcium influx during the M phase of the cell cycle. As well as during mitosis, it was shown, during *Xenopus* oocytes meiosis that SOCE inactivates completely. This inhibition is central in the overall calcium signaling remodelling that allows the fully mature oocyte the capacity to produce specialized calcium transient required at fertilization [66]. SOCE inactivates specifically at the GVBD stage of *Xenopus* oocyte maturation (Fig. 49.5, personal data) [65]. Hence, inactivation of SOCE current (I_{SOCE}) at the GVBD stage, just after the entry into meiosis, might be assimilated to a protection to prevent early egg activation before fertilization. Such inactivation were described for others ionic channels/currents in various models [85–88]; this demonstrates that such events are conserved and fundamental.

On the opposite, the level of calcium-activated chloride current does not decrease during maturation [65]. Therefore, during oocyte maturation, there is a specific regulation of membrane proteins, not limited to *Xenopus* oocytes. So, SOCE has been shown to inactivate during mitosis of HeLa cells [89], and membrane trafficking in general is inhibited during mammalian cell mitosis [90]. Hence, determining the molecular mechanisms controlling SOCE inactivation during *Xenopus* oocyte maturation provides valuable insights into the regulation of plasma membrane protein levels during M phase.

Intracellular calcium concentration has been shown to negatively regulate SOCE current by inducing channel inactivation either directly or through store refilling [18, 91, 92]; nevertheless, intracellular calcium rise is not required for SOCE activation [93].

In addition, in 2003, Machaca and colleagues showed that intracellular calcium could have a potentiating effect on SOCE. This is probably due to the result of CaMKII activation. Indeed, inhibition of CaMKII activity and expression of CaMKIIca is sufficient to potentiate I_{SOCE}, in a manner independent of intracellular calcium [94]. Nevertheless, it is important to note that this activation needs stores depletion. These findings about the effect of CaMKII are consistent with others in various cell types and argue that CaMKII modulation of I_{SOCE} is a widespread mechanism that is not cell type-specific. Taken together, these data show that SOCE can be added to the catalog of cellular functions/pathways modulated by CaMKII [95, 96].

MPF Activation Leads to Uncoupling Store Depletion from SOCE

The differentiation of calcium signaling pathways is an important element of *Xenopus laevis* oocyte maturation. It could also play a much larger role since, 10 years ago, MPF has been shown to regulate calcium oscillations at fertilization in ascidians' eggs [97].

During progesterone induced maturation, I_{SOCE} inactivation at GVBD coincides with MPF activation (Figs. 49.3 and 49.5). Furthermore, regardless of the method by which we induced oocyte maturation (progesterone, cyclin B1, or Mos injection), every cell in which I_{SOCE} was inactivated had high MPF activity. In addition, cells with low MPF activity always activated I_{SOCE} in response to store depletion. Specifically blocking MPF activation under these conditions with Wee1, reversed I_{SOCE} inactivation. This demonstrates that MPF activation during oocyte maturation is necessary for I_{SOCE} inactivation. Moreover, Machaca and collaborators showed that (i) MPF activation is paralleled to SOCE current inhibition, (ii) on the contrary, any correlation between SOCE current density and MAPK/ Mos levels were found, and (iii) activation of MPF after SOCE activation was unable to block I_{SOCE} [66]. Taken together, these studies allow concluding that MPF is sufficient and necessary to uncouple store depletion from SOCE.

Calcium and pH

In addition to the classical benefits of the *Xenopus* oocyte (see the first section), it is also a useful model for pH manipulation. Actually, intracellular pH in *Xenopus* oocyte could be easily modulated by changing extracellular pH which consequently modifies pHi [98]. Another mean to modulate intracellular pH is the use of various compounds. In that goal, in *Xenopus* oocyte, weak bases are the more used mean found to trigger a slow pHi acidification associated with a large membrane resistance decrease and an acidification [99–102]. For example, both NH_4Cl and procaine, in the same way, are able to induce intracellular acidification (0.2–0.4 pH units) in few minutes with instantaneous electrophysiological modifications [23, 31, 103, 104]. Studies showed that acidification activated a calcium-dependent chloride current, which can be recorded using the triple step protocol (see *electrophysiological features*; [40]) but also, that the intracellular pH decrease is responsible for intracellular calcium stores depletion and subsequent extracellular calcium entry, *i.e.* SOCE (Figs. 49.4 and 49.5). Such conclusions were confirmed with calcium imaging approaches and in others cellular models [102, 105–107]. Finally, it was shown that intracellular calcium concentration could regulate the MAPK-MPF cascade, as well as intracellular acidification [61] by mobilizing various calcium sources [31]. These concomitant events are associated to crucial events in *Xenopus* oocyte maturation and mitosis during early embryogenesis [108, 109] and seem to be connected to cyclic activity like MPF one [110]. Finally, calcium pathways activated by intracellular acidification could be hypothesized to be relevant in cell adjustment to variable environmental conditions [44].

It is well known that all the phases of the cell cycle are characterized by changes in intracellular pH (pHi) and intracellular calcium mobilization [111, 112]. More precisely, these ionic actors contribute to crucial events allowing transition between the phases of the cell cycle, particularly during G2/M transition, that is to say during M-phase entry [113]. What is true during mitosis is also the case for meiosis.

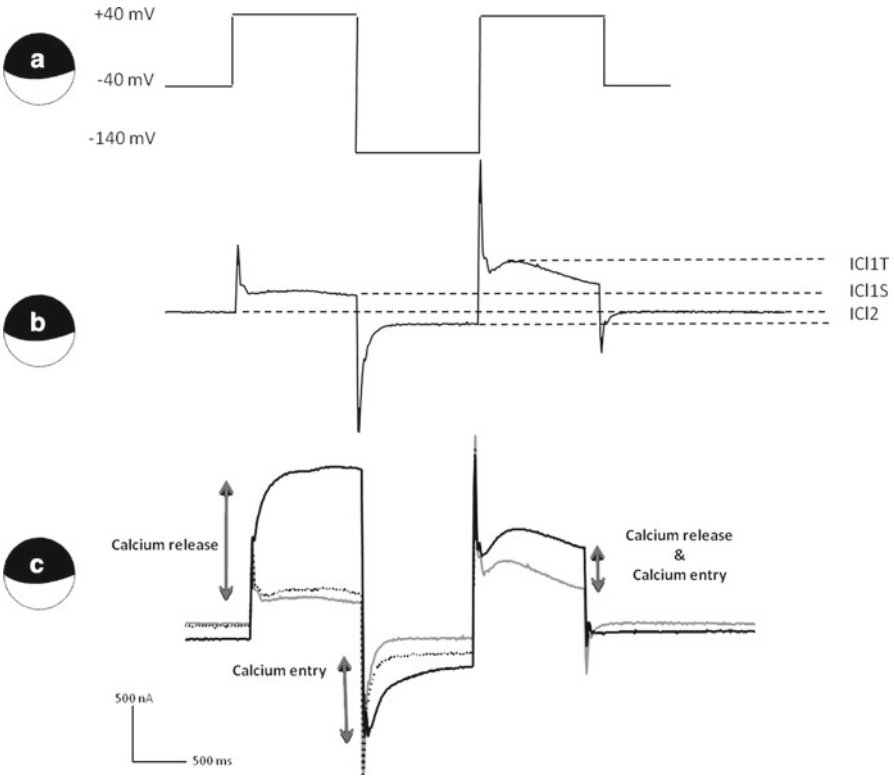

Fig. 49.4 Effect of intracellular calcium stores depletion on calcium-activated chloride currents (ICl). (**a**) typical triple step protocols. Oocytes were held at −40 mV and stepped to +40 mV for 1 s, to −140 mV for 1 s and then back to +40 mV (modified from [40, 41]). (**b**) typical current recording after triple step stimulation. The protocol allows respectively the recording of a non-inactivating outward current (*ICl1-S*, measured at the end of the first pulse at +40 mV), a slow inward current (*ICl2*, measured at the end of the −140 mV pulse) and a transient outward current (*ICl1-T*, calculated by measuring the peak transient current during the second pulse at +40 mV and subtracting *ICl1-S*). All three components are carried by chloride [31]. (**c**) the figure depicts representative recordings before (*black dotted line*), during (*black line*) and after (*grey line*) calcium store depletion

So, Lee and collaborators first described a transient alkalization during *Xenopus* oocyte maturation [114]. This alkalization occurs before germinal vesicle breakdown (GVBD), could be mobilize in germinal vesicle migration towards animal pole and appears as a widespread mechanism since it was observed in other species like urodels or starfish [115]. Moreover, calcium signaling pathways could participate to the regulation of the MAPK-MPF cascade or to the completion of meiosis I [50, 61, 116, 117].

Even if, separately, both intracellular pH and calcium signals appeared like crucial events of the cell cycle, the mechanisms driving interplay between the two remain unclear and are largely a matter of debate. For example, it was both shown

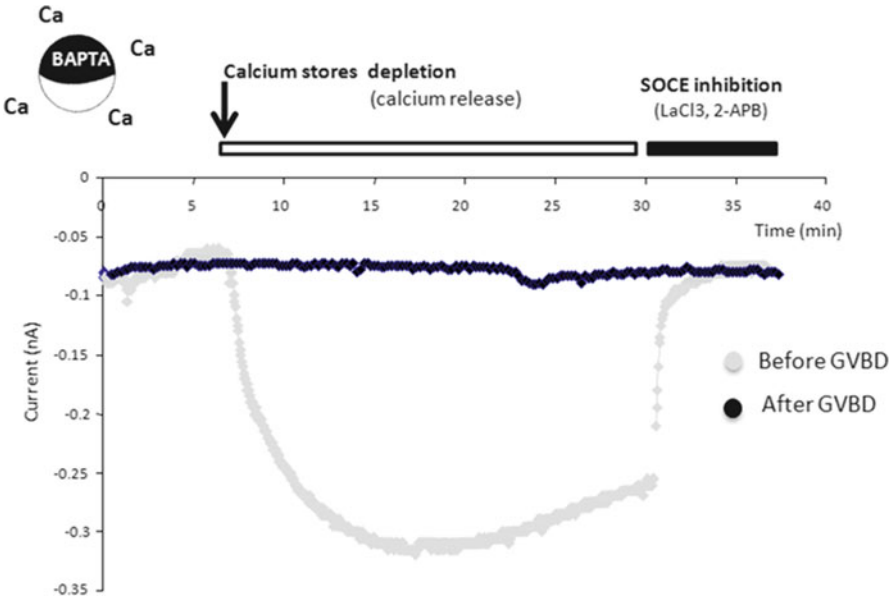

Fig. 49.5 Uncoupling between store depletion and store-operated calcium entry during oocyte maturation (personal data). I_{SOCE} were recording as described in [50]. Before Germinal Vesicle Breakdown (*GVBD*), calcium stores depletion elicits a typical SOCE current (*grey trace*), inhibited by lanthanum or 2-APB. On the contrary, after *GVBD*, calcium stores depletion is unable to activate calcium entry (*black line*)

that intracellular acidification is associated with a rise of intracellular calcium [31, 118, 119], while calcium variations are also strongly coupled to intracellular alkalization [120–123].

Readiness for Fertilization and Embryogenesis?

Oocyte maturation corresponds clearly to a cellular differentiation period that prepares the immature oocyte for fertilization. On the opposite, egg activation could rather to correspond to the first cellular events following fertilization which allows the transition from the egg to the embryo [124]. This includes the onset of the different polyspermy blocks, the completion of meiosis and the onset of embryonic mitosis [68, 124, 125].

The egg activation is mediated by a rise in intracellular calcium concentration with specialized spatial and temporal dynamics [124]. In *Xenopus* the specialized fertilization-specific calcium signal looks like a slow sweeping calcium wave followed by a high calcium plateau that lasts for several minutes [11, 49, 126] (Fig. 49.6b). As discussed in the maturation section, immature oocytes possess a

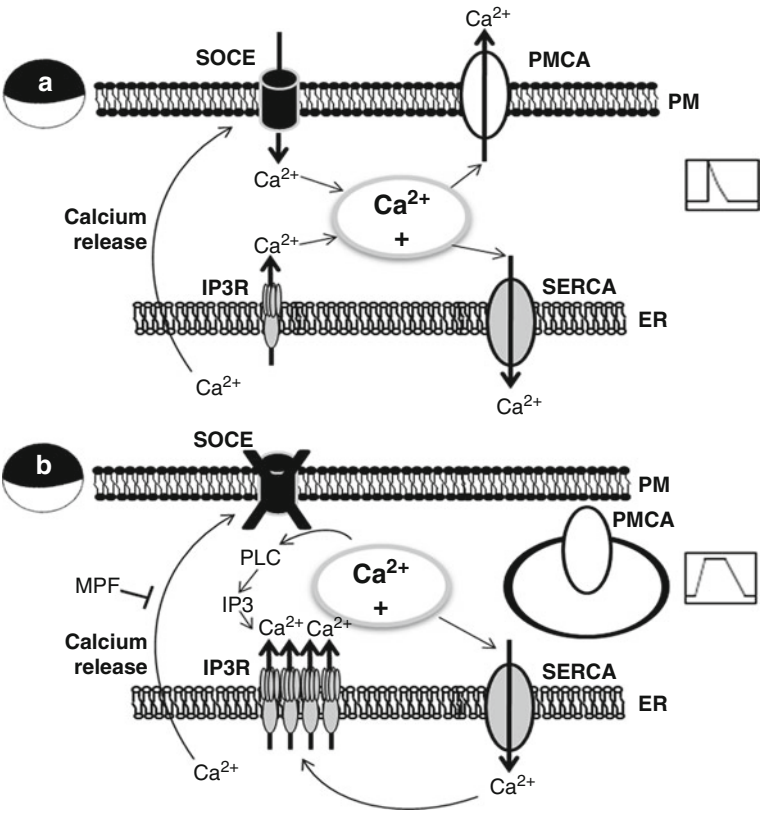

Fig. 49.6 Calcium signaling modifications after (**a**) and before (**b**) oocyte maturation. (**a**) calcium store depletion is responsible for store-operated calcium entry. The intracellular calcium concentration is regulated by the plasma membrane calcium ATPase (*PMCA*) which extruded calcium out of the cell, and by the calcium ATPase of the endoplasmic reticulum (*SERCA*) which refills calcium stores. This is why the typical calcium signal is a transient one (inset on the *right*) (**b**) during maturation, activation of MPF leads to the uncoupling of store depletion from SOCE; the PMCA is internalized and IP3 receptors are clustering at the membrane of the endoplasmic reticulum. These modifications would be central in the shift to a long lasting signal (inset on the *right*) according to the literature (see [126])

strong and well defined SOCE current, whereas in mature oocytes – arrested in metaphase II of meiosis – SOCE could not be activated any more as a consequence of MPF activation [65]. Therefore, the calcium signaling pathways associated with oocyte egg activation is generated without any contribution of SOCE channels.

So, it appears that the actors responsible for this calcium signal at fertilization are reorganized during the maturation of the oocyte. Maturation implies, among multiple phenomena, the internalization of the plasma membrane calcium ATPase (PMCA) [125, 127] (Fig. 49.6). Therefore, if PMCA is localized at the cell membrane in

immature oocytes, it is translocated in intracellular vesicles in mature eggs. Hence, calcium could be no longer extruded out of the oocyte, which is consistent with the sustained intracellular calcium rise triggered by fertilization (Fig. 49.6). PMCA is not the only transporter internalized during oocyte maturation. This is consistent with a strong decrease of membrane area could be observed during maturation. The internalization of specific ionic transporters into an intracellular vesicular pool, in addition to the membrane properties restructuration, generates a pool of membranes and membrane proteins that can be incorporate into the newly formed blastomeres during the rapid early embryonic mitotic divisions [128, 129]. Despite, the internalization of many proteins, transporters and channels, others are functionally enriched. This is the case for calcium-activated chloride channels, which are critical actors for the block of polyspermy [113, 130]. Indeed, calcium-activated chloride channels are activated and responsible for membrane depolarization which inhibits voltage-dependent sperm fusion [126]. How to block polyspermy in such a big cell, with such a large area? What a challenge! In fact, this corresponds to an electrical block, also called fertilization potential [131]. Thus, after a lot of morphological, biochemical and ionic modifications and reorganizations, the egg is now ready to undergo development. However, more considerable events await the cells (embryogenesis, organogenesis for example) in which calcium would have, again, a key role.

To conclude, it appears that the *Xenopus laevis* oocyte is a very good model to study calcium signaling. It is essential to decipher the pathways implicated in oocyte physiology in order to transpose them to other research models.

Acknowledgments I would like to thank all the members of the 'Laboratoire de Régulation des Signaux de Division, EA 4479', particularly Drs Bodart, Browaeys, Cailliau and Paul for reading this manuscript. This job was supported by the French Ministry of Research and the University of Lille1.

References

1. Clapham DE (1995) Calcium signaling. Cell 80:259–268
2. Dumont JN (1972) Oogenesis in Xenopus laevis (Daudin). I. Stages of oocyte development in laboratory maintained animals. J Morphol 136:153–179
3. Jacobelli S, Hanocq J, Baltus E, Brachet J (1974) Hormone-induced maturation of Xenopus laevis oocytes: effects of different steroids and study of the properties of a progesterone receptor. Differentiation 2:129–135
4. Brachet J, Baltus E, de Schutter A, Hanocq F, Hanocq-Quertier J, Hubert E, Iacobelli S, Steinert G (1974) Biochemical changes during progesterone-induced maturation in Xenopus laevis oocytes. Mol Cell Biochem 3:189–205
5. Weber W (1999) Ion currents of Xenopus laevis oocytes: state of the art. Biochim Biophys Acta 1421:213–233
6. Cailliau K, Browaeys-Poly E (2009) A microinjectable biological system, the Xenopus oocyte, as an approach to understanding signal transduction protein function. Methods Mol Biol 518:43–55
7. Delisle S (1991) The four dimensions of calcium signalling in Xenopus oocytes. Cell Calcium 12:217–227

8. DeLisle S, Pittet D, Potter BV, Lew PD, Welsh MJ (1992) InsP3 and Ins(1, 3–5)P4 act in synergy to stimulate influx of extracellular Ca^{2+} in Xenopus oocytes. Am J Physiol 262:C1456–C1463
9. DeLisle S, Welsh MJ (1992) Inositol trisphosphate is required for the propagation of calcium waves in Xenopus oocytes. J Biol Chem 267:7963–7966
10. Lechleiter JD, Clapham DE (1992) Molecular mechanisms of intracellular calcium excitability in X. laevis oocytes. Cell 69:283–294
11. Busa WB, Ferguson JE, Joseph SK, Williamson JR, Nuccitelli R (1985) Activation of frog (Xenopus laevis) eggs by inositol trisphosphate. I. Characterization of Ca^{2+} release from intracellular stores. J Cell Biol 101:677–682
12. DeLisle S, Krause KH, Denning G, Potter BV, Welsh MJ (1990) Effect of inositol trisphosphate and calcium on oscillating elevations of intracellular calcium in Xenopus oocytes. J Biol Chem 265:11726–11730
13. Ajmat MT, Bonilla F, Zelarayan L, Buhler MI (2011) Participation of inositol trisphosphate and ryanodine receptors in Bufo arenarum oocyte activation. Zygote 19:171–180
14. Yamasaki-Mann M, Demuro A, Parker I (2010) Modulation of endoplasmic reticulum Ca^{2+} store filling by cyclic ADP-ribose promotes inositol trisphosphate (IP3)-evoked Ca^{2+} signals. J Biol Chem 285:25053–25061
15. Dargan SL, Demuro A, Parker I (2006) Imaging Ca^{2+} signals in Xenopus oocytes. Methods Mol Biol 322:103–119
16. Heikkila JJ, Kaldis A, Morrow G, Tanguay RM (2007) The use of the Xenopus oocyte as a model system to analyze the expression and function of eukaryotic heat shock proteins. Biotechnol Adv 25:385–395
17. Bodart JF (2010) Extracellular-regulated kinase-mitogen-activated protein kinase cascade: unsolved issues. J Cell Biochem 109:850–857
18. Hoth M, Fasolato C, Penner R (1993) Ion channels and calcium signaling in mast cells. Ann NY Acad Sci 707:198–209
19. Hoth M, Penner R (1992) Depletion of intracellular calcium stores activates a calcium current in mast cells. Nature 355:353–356
20. Premack BA, Gardner P (1994) Properties of Ca currents activated by T cell receptor signaling. Adv Exp Med Biol 365:91–102
21. Lewis RS, Cahalan MD (1995) Potassium and calcium channels in lymphocytes. Annu Rev Immunol 13:623–653
22. Yao Y, Tsien RY (1997) Calcium current activated by depletion of calcium stores in Xenopus oocytes. J Gen Physiol 109:703–715
23. Cougnon M, Bouyer P, Hulin P, Anagnostopoulos T, Planelles G (1996) Further investigation of ionic diffusive properties and of NH4+ pathways in Xenopus laevis oocyte cell membrane. Pflugers Arch 431:658–667
24. Barish ME (1983) A transient calcium-dependent chloride current in the immature Xenopus oocyte. J Physiol 342:309–325
25. Kusano K, Miledi R, Stinnakre J (1982) Cholinergic and catecholaminergic receptors in the Xenopus oocyte membrane. J Physiol 328:143–170
26. Lotan I, Dascal N, Cohen S, Lass Y (1982) Adenosine-induced slow ionic currents in the Xenopus oocyte. Nature 298:572–574
27. O'Connor CM, Robinson KR, Smith LD (1977) Calcium, potassium, and sodium exchange by full-grown and maturing Xenopus laevis oocytes. Dev Biol 61:28–40
28. Wu G, McBride DW Jr, Hamill OP (1998) Mg^{2+} block and inward rectification of mechanosensitive channels in Xenopus oocytes. Pflugers Arch 435:572–574
29. Costa PF, Emilio MG, Fernandes PL, Ferreira HG, Ferreira KG (1989) Determination of ionic permeability coefficients of the plasma membrane of Xenopus laevis oocytes under voltage clamp. J Physiol 413:199–211
30. Weber WM (1999) Endogenous ion channels in oocytes of xenopus laevis: recent developments. J Membr Biol 170:1–12

31. Marin M, Sellier C, Paul-Antoine AF, Cailliau K, Browaeys-Poly E, Bodart JF, Vilain JP (2010) Calcium dynamics during physiological acidification in Xenopus oocyte. J Membr Biol 236:233–245
32. Weber WM, Liebold KM, Reifarth FW, Clauss W (1995) The Ca(2+)-induced leak current in Xenopus oocytes is indeed mediated through a Cl− channel. J Membr Biol 148:263–275
33. Milovanovic S, Frindt G, Tate SS, Windhager EE (1991) Expression of renal Na(+)-Ca^{2+} exchange activity in Xenopus laevis oocytes. Am J Physiol 261:F207–F212
34. Sasaki S, Ishibashi K, Nagai T, Marumo F (1992) Regulation mechanisms of intracellular pH of Xenopus laevis oocyte. Biochim Biophys Acta 1137:45–51
35. Dascal N (2001) Voltage clamp recordings from Xenopus oocytes. Curr Protoc Neurosci Chapter 6. 6.12.1–6.12.20
36. Abenavoli A, DiFrancesco ML, Schroeder I, Epimashko S, Gazzarrini S, Hansen UP, Thiel G, Moroni A (2009) Fast and slow gating are inherent properties of the pore module of the K^+ channel Kcv. J Gen Physiol 134:219–229
37. Hansen KB, Brauner-Osborne H (2009) Xenopus oocyte electrophysiology in GPCR drug discovery. Methods Mol Biol 552:343–357
38. Wegierski T, Steffl D, Kopp C, Tauber R, Buchholz B, Nitschke R, Kuehn EW, Walz G, Kottgen M (2009) TRPP2 channels regulate apoptosis through the Ca^{2+} concentration in the endoplasmic reticulum. EMBO J 28:490–499
39. Dascal N, Snutch TP, Lubbert H, Davidson N, Lester HA (1986) Expression and modulation of voltage-gated calcium channels after RNA injection in Xenopus oocytes. Science 231:1147–1150
40. Parekh AB (1995) Interaction between capacitative Ca^{2+} influx and Ca^{2+}-dependent Cl− currents in Xenopus oocytes. Pflugers Arch 430:954–963
41. Kuruma A, Hartzell HC (1999) Dynamics of calcium regulation of chloride currents in Xenopus oocytes. Am J Physiol 276:C161–C175
42. Machaca K, Hartzell HC (1998) Asymmetrical distribution of Ca-activated Cl channels in Xenopus oocytes. Biophys J 74:1286–1295
43. Machaca K, Hartzell HC (1999) Adenophostin A and inositol 1,4,5-trisphosphate differentially activate Cl− currents in Xenopus oocytes because of disparate Ca^{2+} release kinetics. J Biol Chem 274:4824–4831
44. Berridge MJ (1988) Inositol trisphosphate-induced membrane potential oscillations in Xenopus oocytes. J Physiol 403:589–599
45. Robinson KR (1979) Electrical currents through full-grown and maturing Xenopus oocytes. Proc Natl Acad Sci USA 76:837–841
46. Lupu-Meiri M, Shapira H, Oron Y (1988) Hemispheric asymmetry of rapid chloride responses to inositol trisphosphate and calcium in Xenopus oocytes. FEBS Lett 240:83–87
47. Machaca K, Qu Z, Kuruma A, Criss Hartzell H, McCarty N (2002) The endogenous Calcium-activate Cl channel in Xenopus oocytes: a physiological and biophysically rich model system. Curr Top Membranes 53:3–39
48. Moody WJ, Simoncini L, Coombs JL, Spruce AE, Villaz M (1991) Development of ion channels in early embryos. J Neurobiol 22:674–684
49. Machaca K (2007) Ca^{2+} signaling differentiation during oocyte maturation. J Cell Physiol 213:331–340
50. Machaca K, Haun S (2002) Induction of maturation-promoting factor during Xenopus oocyte maturation uncouples Ca(2+) store depletion from store-operated Ca(2+) entry. J Cell Biol 156:75–85
51. Oh JS, Susor A, Conti M (2011) Protein tyrosine kinase Wee1B is essential for metaphase II exit in mouse oocytes. Science 332(6028):462–465
52. Jones KT (2005) Mammalian egg activation: from Ca^{2+} spiking to cell cycle progression. Reproduction 130:813–823
53. Wasserman WJ, Masui Y (1975) Initiation of meiotic maturation in Xenopus laevis oocytes by the combination of divalent cations and ionophore A23187. J Exp Zool 193:369–375

54. Moreau M, Guerrier P, Doree M (1976) Early changes in the electric properties of the oocyte plasma membrane of Xenopus laevis during the reinitiation of meiosis induced by progesterone, para chloromercuribenzoate (PCMB) or the ionophore A 23187. C R Acad Sci Hebd Seances Acad Sci D 282:1309–1312
55. Cork RJ, Cicirelli MF, Robinson KR (1987) A rise in cytosolic calcium is not necessary for maturation of Xenopus laevis oocytes. Dev Biol 121:41–47
56. Gelerstein S, Shapira H, Dascal N, Yekuel R, Oron Y (1988) Is a decrease in cyclic AMP a necessary and sufficient signal for maturation of amphibian oocytes? Dev Biol 127:25–32
57. Han JK, Lee SK (1995) Reducing PIP2 hydrolysis, Ins(1,4,5)P3 receptor availability, or calcium gradients inhibits progesterone-stimulated Xenopus oocyte maturation. Biochem Biophys Res Commun 217:931–939
58. Duesbery NS, Masui Y (1996) The role of microtubules and inositol triphosphate induced Ca^{2+} release in the tyrosine phosphorylation of mitogen-activated protein kinase in extracts of Xenopus laevis oocytes. Zygote 4:21–30
59. Kobrinsky EM, Kirchberger MA (2001) Evidence for a role of the sarcoplasmic/endoplasmic reticulum Ca(2+)-ATPase in thapsigargin and Bcl-2 induced changes in Xenopus laevis oocyte maturation. Oncogene 20:933–941
60. Stith BJ, Maller JL (1987) Induction of meiotic maturation in Xenopus oocytes by 12-O-tetradecanoylphorbol 13-acetate. Exp Cell Res 169:514–523
61. Sellier C, Bodart JF, Flament S, Baert F, Gannon J, Vilain JP (2006) Intracellular acidification delays hormonal G2/M transition and inhibits G2/M transition triggered by thiophosphorylated MAPK in Xenopus oocytes. J Cell Biochem 98:287–300
62. Wasserman WJ, Pinto LH, O'Connor CM, Smith LD (1980) Progesterone induces a rapid increase in [Ca^{2+}]in of Xenopus laevis oocytes. Proc Natl Acad Sci USA 77:1534–1536
63. Belle R, Ozon R, Stinnakre J (1977) Free calcium in full grown Xenopus laevis oocyte following treatment with ionophore A 23187 or progesterone. Mol Cell Endocrinol 8:65–72
64. Robinson KR (1985) Maturation of Xenopus oocytes is not accompanied by electrode-detectable calcium changes. Dev Biol 109:504–508
65. Machaca K, Haun S (2000) Store-operated calcium entry inactivates at the germinal vesicle breakdown stage of Xenopus meiosis. J Biol Chem 275:38710–38715
66. Machaca K (2010) Ca(2+) signaling, genes and the cell cycle. Cell Calcium 48:243–250
67. Ozon R, Belle R, Huchon D, Mulner O (1979) Roles of cyclic AMP and calcium in maturation of Xenopus laevis oocytes. J Steroid Biochem 11:709–713
68. Sun L, Hodeify R, Haun S, Charlesworth A, MacNicol AM, Ponnappan S, Ponnappan U, Prigent C, Machaca K (2008) Ca^{2+} homeostasis regulates Xenopus oocyte maturation. Biol Reprod 78:726–735
69. Moreau M, Vilain JP, Guerrier P (1980) Free calcium changes associated with hormone action in amphibian oocytes. Dev Biol 78:201–214
70. Masui Y, Markert CL (1971) Cytoplasmic control of nuclear behavior during meiotic maturation of frog oocytes. J Exp Zool 177:129–145
71. Masui Y (2001) From oocyte maturation to the in vitro cell cycle: the history of discoveries of Maturation-Promoting Factor (MPF) and Cytostatic Factor (CSF). Differentiation 69: 1–17
72. Martinez S, Grandy R, Pasten P, Montecinos H, Montecino M, Olate J, Hinrichs MV (2006) Plasma membrane destination of the classical Xenopus laevis progesterone receptor accelerates progesterone-induced oocyte maturation. J Cell Biochem 99:853–859
73. Bagowski CP, Myers JW, Ferrell JE Jr (2001) The classical progesterone receptor associates with p42 MAPK and is involved in phosphatidylinositol 3-kinase signaling in Xenopus oocytes. J Biol Chem 276:37708–37714
74. Bodart JF, Gutierrez DV, Nebreda AR, Buckner BD, Resau JR, Duesbery NS (2002) Characterization of MPF and MAPK activities during meiotic maturation of Xenopus tropicalis oocytes. Dev Biol 245:348–361
75. Morgan DO (1997) Cyclin-dependent kinases: engines, clocks, and microprocessors. Annu Rev Cell Dev Biol 13:261–291

76. Palmer A, Nebreda AR (2000) The activation of MAP kinase and p34cdc2/cyclin B during the meiotic maturation of Xenopus oocytes. Prog Cell Cycle Res 4:131–143
77. Daar I, Paules RS, Vande Woude GF (1991) A characterization of cytostatic factor activity from Xenopus eggs and c-mos-transformed cells. J Cell Biol 114:329–335
78. Sun L, Chai Y, Hannigan R, Bhogaraju VK, Machaca K (2007) Zinc regulates the ability of Cdc25C to activate MPF/cdk1. J Cell Physiol 213:98–104
79. Tsien RY, Rink TJ (1980) Neutral carrier ion-selective microelectrodes for measurement of intracellular free calcium. Biochim Biophys Acta 599:623–638
80. Tsien RY, Pozzan T, Rink TJ (1982) Calcium homeostasis in intact lymphocytes: cytoplasmic free calcium monitored with a new, intracellularly trapped fluorescent indicator. J Cell Biol 94:325–334
81. Sun L, Machaca K (2004) Ca(2+)(cyt) negatively regulates the initiation of oocyte maturation. J Cell Biol 165:63–75
82. Tombes RM, Simerly C, Borisy GG, Schatten G (1992) Meiosis, egg activation, and nuclear envelope breakdown are differentially reliant on Ca^{2+}, whereas germinal vesicle breakdown is Ca^{2+} independent in the mouse oocyte. J Cell Biol 117:799–811
83. Bement WM, Capco DG (1990) Transformation of the amphibian oocyte into the egg: structural and biochemical events. J Electron Microsc Tech 16:202–234
84. Nebreda AR, Ferby I (2000) Regulation of the meiotic cell cycle in oocytes. Curr Opin Cell Biol 12:666–675
85. Schmalzing G, Eckard P, Kroner S, Passow H (1990) Downregulation of surface sodium pumps by endocytosis during meiotic maturation of Xenopus laevis oocytes. Am J Physiol 258:C179–C184
86. Wright EM, Hirsch JR, Loo DD, Zampighi GA (1997) Regulation of Na^+/glucose cotransporters. J Exp Biol 200:287–293
87. Yu F, Sun L, Machaca K (2010) Constitutive recycling of the store-operated Ca^{2+} channel Orai1 and its internalization during meiosis. J Cell Biol 191:523–535
88. Day ML, Pickering SJ, Johnson MH, Cook DI (1993) Cell-cycle control of a large-conductance K^+ channel in mouse early embryos. Nature 365:560–562
89. Preston SF, Sha'afi RI, Berlin RD (1991) Regulation of Ca^{2+} influx during mitosis: Ca^{2+} influx and depletion of intracellular Ca^{2+} stores are coupled in interphase but not mitosis. Cell Regul 2:915–925
90. Warren G (1993) Membrane partitioning during cell division. Annu Rev Biochem 62: 323–348
91. Zweifach A, Lewis RS (1995) Slow calcium-dependent inactivation of depletion-activated calcium current. Store-dependent and -independent mechanisms. J Biol Chem 270:14445–14451
92. Zweifach A, Lewis RS (1995) Rapid inactivation of depletion-activated calcium current (ICRAC) due to local calcium feedback. J Gen Physiol 105:209–226
93. Parekh AB, Penner R (1997) Store depletion and calcium influx. Physiol Rev 77:901–930
94. Machaca K (2003) Ca^{2+}-calmodulin-dependent protein kinase II potentiates store-operated Ca^{2+} current. J Biol Chem 278:33730–33737
95. Hook SS, Means AR (2001) Ca(2+)/CaM-dependent kinases: from activation to function. Annu Rev Pharmacol Toxicol 41:471–505
96. Hudmon A, Schulman H (2002) Structure-function of the multifunctional Ca^{2+}/calmodulin-dependent protein kinase II. Biochem J 364:593–611
97. McDougall A, Levasseur M, O'Sullivan AJ, Jones KT (2000) Cell cycle-dependent repetitive Ca(2+)waves induced by a cytosolic sperm extract in mature ascidian eggs mimic those observed at fertilization. J Cell Sci 113(Pt 19):3453–3462
98. Roos A, Boron WF (1981) Intracellular pH. Physiol Rev 61:296–434
99. Lopo A, Vacquier VD (1977) The rise and fall of intracellular pH of sea urchin eggs after fertilisation. Nature 269:590–592
100. Shen SS, Steinhardt RA (1978) Direct measurement of intracellular pH during metabolic derepression of the sea urchin egg. Nature 272:253–254

101. Burckhardt BC, Thelen P (1995) Effect of primary, secondary and tertiary amines on membrane potential and intracellular pH in Xenopus laevis oocytes. Pflugers Arch 429:306–312
102. Rodeau JL, Flament S, Browaeys E, Vilain JP (1998) Effect of procaine on membrane potential and intracellular pH in Xenopus laevis oocytes. Mol Membr Biol 15:145–151
103. Burckhardt BC, Fromter E (1992) Pathways of NH3/NH4+ permeation across Xenopus laevis oocyte cell membrane. Pflugers Arch 420:83–86
104. Boldt M, Burckhardt G, Burckhardt BC (2003) NH(4)(+) conductance in Xenopus laevis oocytes. III. Effect of NH(3). Pflugers Arch 446:652–657
105. Woodward RM, Miledi R (1992) Sensitivity of Xenopus oocytes to changes in extracellular pH: possible relevance to proposed expression of atypical mammalian GABAB receptors. Brain Res Mol Brain Res 16:204–210
106. Nagaraja TN, Brookes N (1998) Intracellular acidification induced by passive and active transport of ammonium ions in astrocytes. Am J Physiol 274:C883–C891
107. Kuruma A, Hartzell HC (2000) Bimodal control of a Ca(2+)-activated Cl(−) channel by different Ca(2+) signals. J Gen Physiol 115:59–80
108. Grandin N, Charbonneau M (1990) Cycling of intracellular pH during cell division of Xenopus embryos is a cytoplasmic activity depending on protein synthesis and phosphorylation. J Cell Biol 111:523–532
109. Webb DJ, Nuccitelli R (1981) Intracellular pH changes accompanying the activation of development in frog eggs: comparison of pH microelectrodes and 31P-NMR measurements. Kroc Found Ser 15:293–324
110. Keating TJ, Cork RJ, Robinson KR (1994) Intracellular free calcium oscillations in normal and cleavage-blocked embryos and artificially activated eggs of Xenopus laevis. J Cell Sci 107(Pt 8):2229–2237
111. Lipskaia L, Lompre AM (2004) Alteration in temporal kinetics of Ca2+ signaling and control of growth and proliferation. Biol Cell 96:55–68
112. Munaron L, Antoniotti S, Lovisolo D (2004) Intracellular calcium signals and control of cell proliferation: how many mechanisms? J Cell Mol Med 8:161–168
113. Whitaker M (2006) Calcium microdomains and cell cycle control. Cell Calcium 40: 585–592
114. Lee SC, Steinhardt RA (1981) pH changes associated with meiotic maturation in oocytes of Xenopus laevis. Dev Biol 85:358–369
115. Picard A, Cavadore JC, Lory P, Bernengo JC, Ojeda C, Doree M (1990) Microinjection of a conserved peptide sequence of p34cdc2 induces a Ca^{2+} transient in oocytes. Science 247:327–329
116. Flament S, Browaeys E, Rodeau JL, Bertout M, Vilain JP (1996) Xenopus oocyte maturation: cytoplasm alkalization is involved in germinal vesicle migration. Int J Dev Biol 40:471–476
117. Machaca K (2004) Increased sensitivity and clustering of elementary Ca^{2+} release events during oocyte maturation. Dev Biol 275:170–182
118. Siskind MS, McCoy CE, Chobanian A, Schwartz JH (1989) Regulation of intracellular calcium by cell pH in vascular smooth muscle cells. Am J Physiol 256:C234–C240
119. Wakabayashi I, Groschner K (1997) Divergent effects of extracellular and intracellular alkalosis on Ca^{2+} entry pathways in vascular endothelial cells. Biochem J 323(Pt 2):567–573
120. Dube F, Epel D (1986) The relation between intracellular pH and rate of protein synthesis in sea urchin eggs and the existence of a pH-independent event triggered by ammonia. Exp Cell Res 162:191–204
121. Kim D, Smith TW (1988) Cellular mechanisms underlying calcium-proton interactions in cultured chick ventricular cells. J Physiol 398:391–410
122. Kottgen M, Leipziger J, Fischer KG, Nitschke R, Greger R (1994) pH regulation in HT29 colon carcinoma cells. Pflugers Arch 428:179–185
123. Naccache PH, Faucher N, Caon AC, McColl SR (1988) Propionic acid-induced calcium mobilization in human neutrophils. J Cell Physiol 136:118–124
124. Stricker SA (1999) Comparative biology of calcium signaling during fertilization and egg activation in animals. Dev Biol 211:157–176

125. Ullah G, Jung P, Machaca K (2007) Modeling Ca^{2+} signaling differentiation during oocyte maturation. Cell Calcium 42:556–564
126. Busa WB, Nuccitelli R (1985) An elevated free cytosolic Ca^{2+} wave follows fertilization in eggs of the frog, Xenopus laevis. J Cell Biol 100:1325–1329
127. El-Jouni W, Jang B, Haun S, Machaca K (2005) Calcium signaling differentiation during Xenopus oocyte maturation. Dev Biol 288:514–525
128. Angres B, Muller AH, Kellermann J, Hausen P (1991) Differential expression of two cadherins in Xenopus laevis. Development 111:829–844
129. Gawantka V, Ellinger-Ziegelbauer H, Hausen P (1992) Beta 1-integrin is a maternal protein that is inserted into all newly formed plasma membranes during early Xenopus embryogenesis. Development 115:595–605
130. Muller HA (2001) Of mice, frogs and flies: generation of membrane asymmetries in early development. Dev Growth Differ 43:327–342
131. Webb DJ, Nuccitelli R (1985) Fertilization potential and electrical properties of the Xenopus laevis egg. Dev Biol 107:395–406

Chapter 50
Calcium Oscillations, Oocyte Activation, and Phospholipase C zeta

Junaid Kashir, Celine Jones, and Kevin Coward

Abstract In mammals, gamete fusion initiates a succession of oscillations in the intracellular concentration of calcium within the oocyte, prompting a series of events to occur that are collectively known as "oocyte activation". Such events are a fundamental necessity for the initiation of cell division and subsequent embryogenesis. Compelling evidence now indicates that these calcium oscillations are caused by a testis-specific phospholipase C (PLC) termed PLCzeta (PLCζ), released into the oocyte following gamete fusion. A series of recent studies indicate that abnormal expression or aberrant activity of PLCζ is linked to certain types of human male infertility, where oocyte activation ability is impaired or absent altogether. In this chapter, we discuss the critical role of calcium oscillations in the process of oocyte activation, review the role of PLCs in this fundamental biological reaction, describe how PLCζ has been formally linked to male infertility, and postulate the potential roles for PLCζ in terms of clinical diagnosis and therapy.

Keywords Sperm • Oocyte • Calcium • Phospholipase C (PLC) • Phospholipase C zeta (PLCzeta) • Fertilisation • Oocyte activation • Infertility • Assisted reproductive technology (ART) • Assisted oocyte activation (AOA)

Fertilisation and Oocyte Activation

At fertilisation, the fusion of mammalian gametes ensures the successful initiation of development. Mammalian oocytes remain arrested for most of their existence at the dictyate stage of prophase I [74]. These then undergo first meiotic division

J. Kashir • C. Jones • K. Coward (✉)
Nuffield Department of Obstetrics and Gynaecology, Level 3, Women's Centre, John Radcliffe Hospital, University of Oxford, UK
e-mail: junaid.kashir@obs-gyn.ox.ac.uk; celine.jones@obs-gyn.ox.ac.uk; kevin.coward@obs-gyn.ox.ac.uk

M.S. Islam (ed.), *Calcium Signaling*, Advances in Experimental Medicine and Biology 740, DOI 10.1007/978-94-007-2888-2_50,

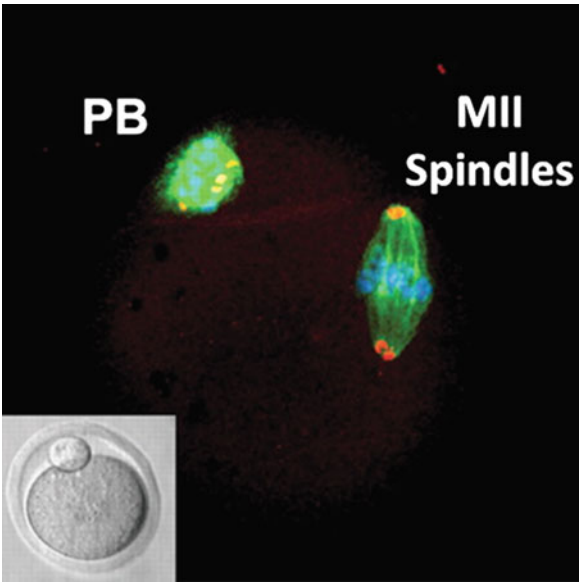

Fig. 50.1 Representative fluorescence micrograph of a normal MII arrested mouse oocyte. Inset shows brightfield image of the same oocyte. *Green*: β-tubulin (polymerized microtubules); *red*/*orange*: pericentrin (microtubule organizing centers); *blue*: chromatin. *PB* polar body (Reproduced from Swain et al. [143] with permission)

within the ovary, immediately after which, and just before ovulation, oocytes become arrested at metaphase of the second meiotic division (MII), following the exclusion of the first polar body [70, 71] (Fig. 50.1). This arrest is maintained by stabilization of the M-Phase promoting factor (MPF), the universal driver for the transition of the cell cycle from the G2- to the M-phase (G2/M transition). MPF is a heterodimer consisting of a regulatory cyclin subunit, cyclin B, and a catalytic subunit, Cdc2 kinase. Active Cdc2 drives entry into M-phase by phosphorylating substrates which lead to nuclear envelope breakdown and spindle formation [54]. Successful sperm/oocyte fusion at fertilisation must alleviate this MII arrest to proceed with embryogenesis.

Alleviation of MII arrest occurs through a series of events, collectively termed "oocyte activation". Characterized by the formation of the second polar body and the male and female pronuclei [105], oocyte activation also involves cortical granule exocytosis, progression of the cell cycle (Fig. 50.2a), and maternal mRNA recruitment, collectively resulting in cell division and embryogenesis (Fig. 50.2b) [79, 105, 123, 144, 145]. The sperm nucleus is remodelled, permitting DNA replication and fusion with the female pronucleus. The sperm nuclear envelope is removed, and sperm-specific protamines or histones are replaced by maternal histone variants [54]. Maternal mRNAs and proteins then undergo several dynamic changes, including regulated degradation, translation, or post-translational modification. The duration and initiation of these events differ between species, beginning at day 1 (2-cell stage) in the mouse. Cytoskeletal rearrangements also occur, presumably to support zygotic growth and development [54].

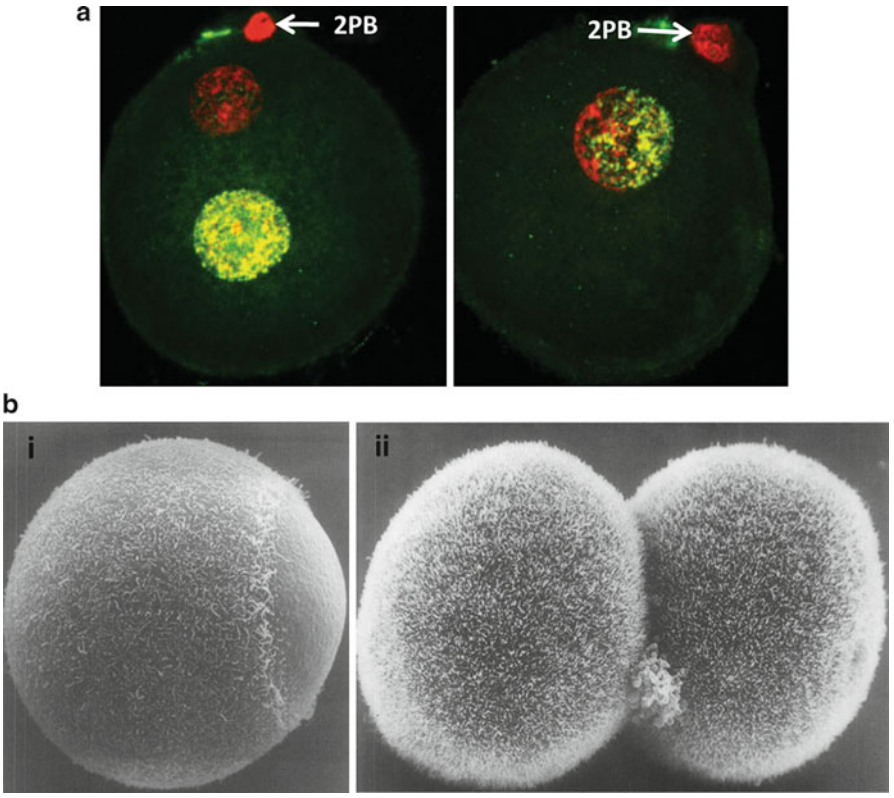

Fig. 50.2 Representative images showing key stages of oocyte activation. (**a**) Fluorescent micrograph of an activated mouse zygote with two pronuclei. *Right panel*: (*yellow*/*green*: larger male pronucleus; *red*: smaller female pronucleus). The nucleus of the second polar body (2PB) is visible above the female pronucleus. *Left panel*: A zygote with a single large pronucleus resulting from male and female pronuclei fusion. The male chromatin (*yellow*/*green*) occupies half of the pronucleus, while the other half is occupied by maternal chromatin (*red*). The nucleus of the 2PB (*red*) is apparent above the pronucleus, slightly to the *right*. (**b**) Scanning electron micrographs of (i) an unfertilised mouse oocyte, and (ii) the early mouse embryo at the 2 cell stage following removal of the zona pellucida (Reproduced from Phillips and Shalgi [121], Liu et al. [96], Krukowska and Tarkowski [83] with permission)

The Role of Calcium in Oocyte Activation

Several key experiments have established that the mechanisms underlying mammalian oocyte activation are induced by repeated oscillations in the concentration of intracellular calcium (Ca^{2+}) [79, 123], while in many non-mammalian species such as sea urchins and frogs, there is only a single Ca^{2+} transient (Fig. 50.3) [159]. Experiments involving the application of Ca^{2+}-sensitive dyes to oocytes and eggs

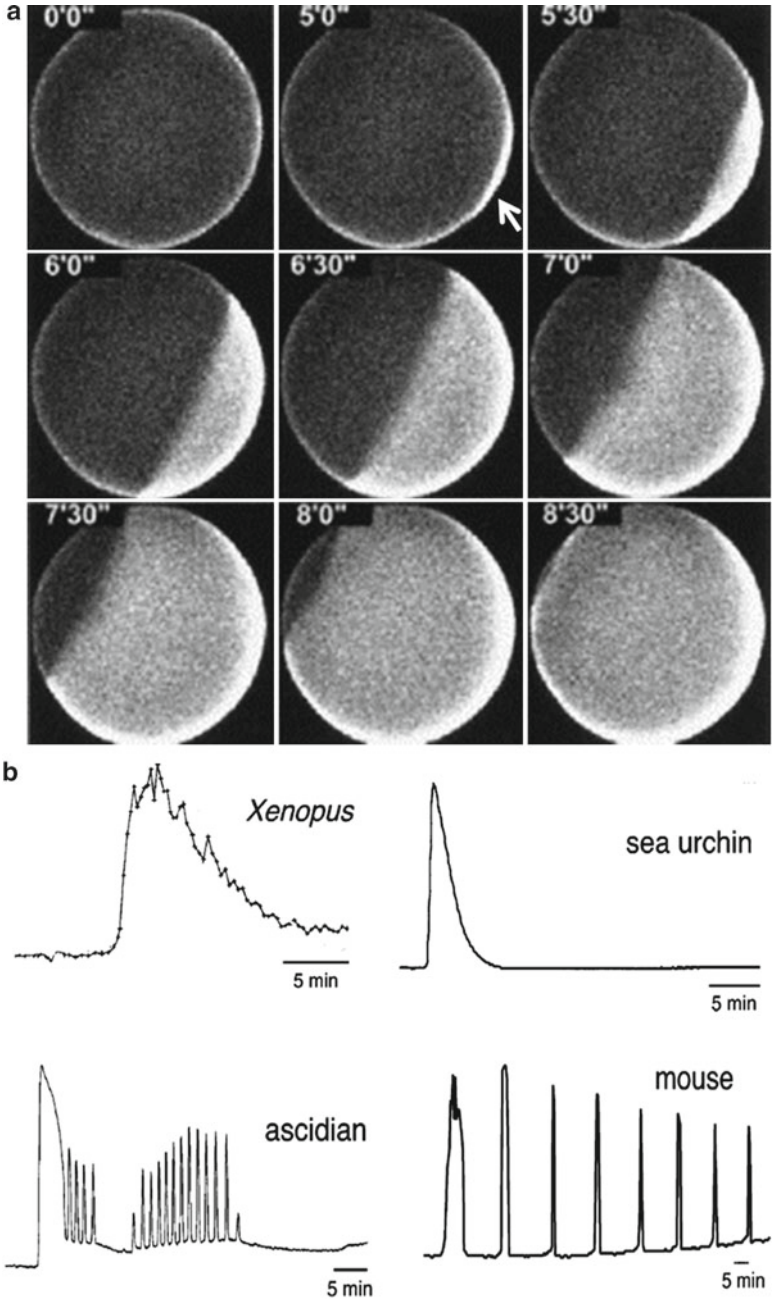

Fig. 50.3 (**a**) Calcium wave as observed using calcium-green-1-dextran in a *Xenopus* egg. Time 0 shows the egg's resting levels of calcium. The sperm-induced calcium wave was initiated by sperm entry (indicated by *white arrow*), and traversed the entire egg. (**b**) Ca^{2+} responses at fertilization in eggs and oocytes of several species (Reproduced from Fontanilla and Nuccitelli [39], Miyazaki [104], Miyazaki and Ito [105] with permission)

from a wide range of species, established the importance of Ca^{2+} transients in oocyte activation and embryogenesis [31], while the microinjection of Ca^{2+} ions alone triggered embryo development up to the blastocyst stage in mice [44, 145]. Repetitive Ca^{2+} oscillations at oocyte activation are thus necessary to alleviate MPF-mediated MII arrest, an insufficiency which may result in altered oocyte to embryo transition [30].

Ca^{2+} oscillations within the oocyte are commonly accepted to occur as a direct result of inositol triphosphate (IP_3)-mediated Ca^{2+} release [117, 119, 133, 146, 148, 159]. Blocking IP_3 receptors (IP_3Rs) within oocytes using specific antibodies [108], down-regulating IP_3Rs using adenophostin [12, 68], and reducing the expression of IP_3Rs by siRNA [164], all lead to the inhibition of Ca^{2+} oscillations. Studies have also reported cytosolic increases in the concentration of IP_3 during fertilization in mammalian oocytes [146], compounding the importance of IP_3 levels and IP3-mediated Ca^{2+} release within this process.

While the type 1 isoform of IP3Rs (IP_3R1) appears predominant in human and mouse oocytes [38, 46, 102, 120], it is thought that cells may express and redistribute ion channels. It is therefore likely that differential localization of such channels may impact upon developmental events [152, 155]. Indeed, the dynamic phosphorylation of IP_3R1 during maturation may increase IP_3R1 sensitivity, while sustained release of IP_3 during oocyte activation may lead to an overall reduction in IP3R1 number, a mechanism possibly responsible for the regulation of Ca^{2+} oscillations during oocyte activation [61, 93, 154].

Mammalian oocytes are released from MII arrest through the degradation of cyclin B1 by proteolysis, mediated by ubiquitin/proteasome activation via Ca^{2+} oscillations at fertilisation [105] (Fig. 50.4). Binding of Ca^{2+} to calmodulin activates calmodulin-dependent kinase II (CaMKII) [97, 105], a repetitive process which reoccurs coincident with each Ca^{2+} peak in fertilised mouse oocytes [100]. Cyclin B1 is then poly-ubiquitinated by the anaphase promoting complex or cyclosome (APC/C), an E3 ubiquitin ligase, resulting in degradation of cyclin B1. This process is prevented in unfertilised oocytes by cytostatic factor (CSF), which assists MPF in maintaining MII arrest [57, 69, 105]. Upon mammalian fertilisation, CaMKII is thought to inhibit CSF components Emi 1, Mad2, or Bub1 [57].

Persistent Ca^{2+} oscillations are thought to be responsible for pronucleus formation via the reduction of mitogen-associated protein kinase (MAPK) activity [30, 105]. The temporal pattern of Ca^{2+} oscillations is largely species-specific in terms of amplitude, duration, and frequency [30, 31, 72, 106]. Remarkably, oocytes appear to "count" each wave of oscillations, with early events such as cortical granule exocytosis requiring fewer oscillations than later events such as the alleviation of MII arrest [98, 140]. Indeed, the frequency and amplitude of Ca^{2+} oscillations have been reported to affect early embryo protein profiles in mice [30], and embryonic development in rabbits, playing a role in compaction, blastocyst formation, and the rate of successful transplantation of 4-cell embryo to host mothers [105, 145].

Spatial and temporal Ca^{2+} and IP_3 gradients assist in the establishment of the dorsal–ventral axis of various developing embryos [118, 158], with similar roles

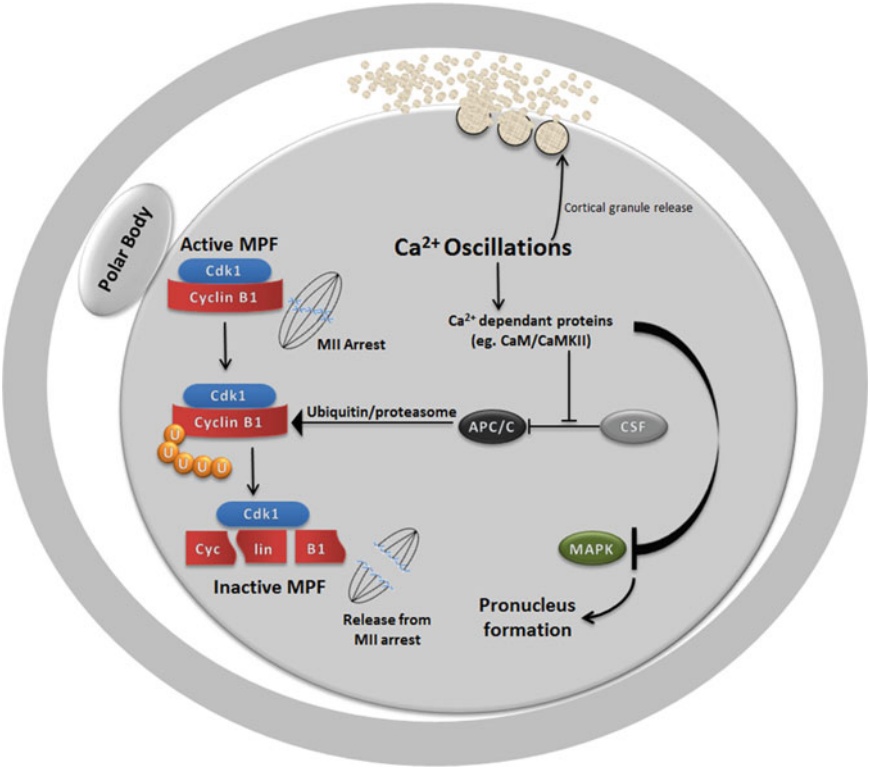

Fig. 50.4 Schematic representation of the signaling mechanism, downstream of Ca^{2+} release at fertilisation, thought to alleviate MII arrest in mammalian oocytes and leading to subsequent embryogenesis

for the velocity and duration of Ca^{2+} waves [65, 160]. Experiments inducing a variety of Ca^{2+} release profiles did not all induce good quality embryos [44, 84, 128, 153]. Ca^{2+} transients at fertilization are also responsible for the activation of Ca^{2+}-sensitive genes or proteins important in subsequent embryo development, such as CAMKII [28, 55]. Indeed, CaMKIIγ (the predominant CamKII isoform in mouse oocytes) is thought to specifically control mouse oocyte activation via cell cycle resumption [3].

Although it is well-established that Ca^{2+} oscillations are of the utmost importance for oocyte activation, the precise mechanism responsible has been the subject of intense debate, particularly in relation to the relative roles played by both gametes during gamete fusion. Three predominant models have been hypothesized: (1) the Ca^{2+} conduit model, (2) the membrane receptor model, and (3) the soluble sperm factor model [119, 133, 148].

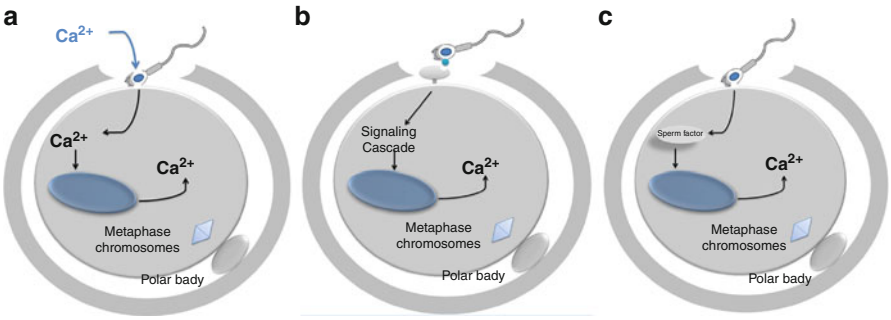

Fig. 50.5 Schematic representations of (**a**) Ca^{2+} conduit, (**b**) membrane receptor, and (**c**) sperm factor models of oocyte activation (Figure adapted from Parrington et al. [119])

The Ca^{2+} Conduit Model

This model hypothesizes the introduction of a bolus of Ca^{2+} directly into the oocyte following gamete fusion, leading to Ca^{2+}-induced Ca^{2+} release [62, 64], and was subsequently modified, based on sea urchin sperm-egg binding, to suggest that channels on the surface of the sperm membrane acted as a conduit following gamete fusion, allowing Ca^{2+} influx into the oocyte (Fig. 50.5a) [23, 24]. While an attractive model initially, particularly for sea urchin egg activation, this model did not take into account mechanisms of activation in other species such as mice or ascidicans. Experimental evidence strongly implicated that IP_3-mediated Ca^{2+} release was an integral aspect of oocyte activation. Furthermore, direct injection of Ca^{2+} into oocytes failed to induce further Ca^{2+} increase [145], whilst other studies failed to detect localised elevations in cytoplasmic concentrations of Ca^{2+} during mouse gamete fusion [72]. Furthermore, sea urchin eggs can be activated by acrosome-reacted sperm in seawater lacking Ca^{2+} [35, 159], rendering it difficult to envisage how Ca^{2+} flux through the sperm could be sustained where Ca^{2+} concentrations are lower or similar to resting concentrations within the egg [72].

The Membrane Receptor Model

This model proposed that an interaction between a ligand on the sperm surface and a corresponding receptor on the oocyte triggered activation (Fig. 50.5b), and was the dominant hypothesis for many years [36, 63, 119, 134]. Adopting one of the most fundamental features of cell signaling in somatic cells, where such surface mediated interactions are a normal feature, this model proposed that a signaling cascade triggered by sperm/egg interaction, would lead to the activation of a

phospholipase C (PLC) inside the oocyte [36, 63, 134]. At present, the proposed oocyte-sperm receptor is based on indirect evidence, arising from experiments involving the over-expression of G-protein-linked receptors in oocytes and corresponding application of ligands (Santella et al. 2004). Furthermore, sperm-induced Ca^{2+} transients were inhibited by the injection of G-protein antagonists in hamster oocytes, indicating that G-proteins may activate PLCβ in response to sperm-oocyte interaction ([103]; Santella et al. 2004), while injection of the hydrolysis-resistant GTP analogue, GTP-γS, in sea urchin and frog eggs and mammalian oocytes elicited Ca^{2+} release ([66]; Santella et al. 2004). However, while these experiments indeed demonstrated Ca^{2+} release, the transients observed were dissimilar to those observed at fertilisation, particularly in the case of mammalian oocytes. Furthermore, despite many targeted research studies, such a sperm ligand/oocyte receptor remains to be characterized [119]. Critically, the successful nature of intracytoplasmic sperm injection (whereby sperm is directly microinjected into the oocyte cytosol; ICSI) casts significant doubt over such a mechanism as this method bypasses sperm/oocyte membrane interaction completely.

The Soluble Sperm Factor Model

This model proposed that oocyte activation is triggered by a soluble factor released from the sperm into the oocyte during, or immediately following, gamete fusion (Fig. 50.5c). This was supported by the injection of sea urchin sperm extracts into eggs, which induced egg activation [26], followed by similar observations using ascidian sperm [25], suggesting that the activating stimulus was a protein or a Ca^{2+} mobilizing messenger. A series of studies, in which sperm extracts were injected into eggs of a variety of species, including marine worms, and ascidians, resulted in successful Ca^{2+} release and oocyte activation [88, 141, 144]. Sperm extracts from frogs, chickens, and tilapia fish, have also been shown to trigger Ca^{2+} oscillations in mouse oocytes [18, 29], suggesting the existence of a similar sperm-based mechanism throughout a wide spectra of species. However, the precise identity of this "sperm factor" remained a mystery for some time, although considerable research suggested that the IP_3-dependant nature of oocyte activation depended upon a PLC-mediated mechanism [119].

PLCs at Fertilisation and Oocyte Activation

Phosphoinositide metabolism is a vital intracellular signaling system involved in many cellular functions including hormone secretion, neurotransmitter transduction, growth factor signaling, membrane trafficking, cytoskeletal regulation, and have also been linked to fertilisation and embryogenesis ([15, 67, 135]; for reviews see [43, 110]). PLCs are key enzymes within this system, involved in the hydrolysis of phosphotidylinositol 4,5-bisphosphate (PIP_2) into IP_3 and diacylglycerol (DAG). DAG mediates protein kinase C (PKC) activation, and IP3 triggers Ca^{2+} from

intracellular stores [8, 43, 113]. Ca^{2+} is also a major player in many other aspects of sperm function, including chemotaxis [5, 9, 16, 32, 76, 138]. PLC and IP_3R signaling mechanisms are also involved in sperm thermotaxis, where elevated levels of Ca^{2+} may modify flagellar bending and sperm motion paths [4, 5, 10, 33, 53].

Currently, there are 13 known mammalian PLC isozymes, categorized on the basis of structure and regulatory activation mechanisms: PLC-delta (PLC-δ 1, 3, and 4), PLC beta (PLCβ 1–4), PLC gamma (PLCγ 1 and 2), PLC epsilon (PLCε), PLC zeta (PLCζ), and PLC eta (PLCη 1 and 2) [43, 56, 109, 125, 175]. PLC isozymes may contain catalytic X and Y domains as well as various regulatory domains, including the C2 domain, EF-hand motif, and pleckstrin homology (PH) domain, in various conformations, depending on the isozyme. Some isozymes also consist of subtype-specific domains, thought to contribute to towards specific regulatory mechanisms. These include the Src homology (SH) domain in PLC γ [125] and the Ras-associating and Ras-GTPase exchange factor-like domains in PLC ε [77, 137].

Sperm from PLCδ4 knockout (KO) mice induced activation of fewer oocytes following *in vitro* fertilization (IVF), failing to elicit Ca^{2+} oscillations, indicating an essential role in oocyte activation in sperm for PLCδ4 [41]. Solubilized mouse zona pellucida (a protective glycoprotein layer surrounding the oocyte; ZP) was able to induce the acrosome reaction (an essential step in fertilization involving the digestion of the ZP) in sperm from normal mice, but could not do so in PLC δ4 KO sperm. Elevations of Ca^{2+} levels were thought to have a primary role in this process [11, 27], and sperm from normal mice treated with ZP exhibited continuous elevations in Ca^{2+}, while incubation of ZP with PLCδ4 KO sperm induced only a small increase in Ca^{2+}, suggesting a role for PLCδ4 in the ZP-induced acrosome reaction [42, 43, 110].

Evidence suggests that PLCγ1, modulated by tyrosine phosphorylation, may be activated in mouse spermatozoa [37, 129, 151]. Immunostaining indicated that PLCγ-1 was localised to the sperm head, and that capacitation induced a translocation of this localisation pattern [151]. An increase in PLCγ 1 activity was observed following treatment with ZP, an observation prevented by suppressing ZP-induced acrosomal exocytosis [95, 129]. While there is no direct evidence supporting a role for PLCβ in sperm, both PLCβ1 and β3 have been identified in acrosomal regions of mouse sperm, along with Gαq/11 [41, 157]. Considering that PLCβ is activated by pertussis toxin-insensitive GTP-binding proteins Gq and G11 in somatic cells, the observation that progesterone-stimulated DAG formation was not blocked by pertussis toxin may infer a possible role for PLCβ in acrosomal exocytosis [108, 129]. Indeed, sperm from PLCβ1 KO mice exhibited lower acrosome reaction rates than their normal counterparts [14]. However, more in-depth studies are required to further elucidate the exact roles of these PLC isozymes during fertilisation [129].

Several observations suggest that there may be a role for endogenous oocyte PLCs during oocyte activation [132]. Oocytes contain significant amounts of PLC isoforms, including β, γ, and δ, which may be regulated by the Ca^{2+} oscillations at fertilisation [58]. Reduced levels of oocyte PLCβ1 decreased the amplitude of Ca^{2+} oscillations at oocyte activation, but did not change their duration or frequency.

Over-expression of PLCβ1 in oocytes prior to fertilization did not result in spontaneous Ca^{2+} oscillations, but altered the Ca^{2+} oscillation profile following fertilization, indicating a role for oocyte derived PLCs in sperm-induced oocyte activation in mammals [58]. Furthermore PLCβ1 has been implicated in nuclear translocation following meiotic resumption in mouse oocytes, apparently to perichromatin and interchromatin granules, followed by a subsequent shift to the nucleoplasm [2, 96].

In starfish eggs, the Ca^{2+} rise associated with activation requires an egg Src family kinase (SFK) that activates PLCγ via a SH2 domain-mediated mechanism involving the endoplasmic reticulum (ER) [130, 150]. It is not yet known if PLCδ, ε, or ζ are present in echinoderm oocytes. However PLCβ may be activated by heterotrimeric G protein-coupled receptors, while PLC γ may be activated by receptor and non-receptor protein tyrosine kinases (PTK), or via translocation to the plasma membrane [130, 166]. However, whether G protein-PLCβ or PTK-PLCγ plays a role during egg activation in other invertebrates, or whether these pathways function synergistically remains controversial [166].

Coward et al. [20] recently identified a novel PLCδ isoform in sea urchin gametes, termed PLCδsu, although its precise role during fertilization and early embryogenesis remains unknown. While a green fluorescent protein tagged PLCδsu PH domain was observed to localise to the plasma membrane, increasing in intensity at fertilization, recombinant PLCδsu failed to elicit Ca^{2+} signals characteristic of fertilization in mouse oocytes and sea urchin eggs, suggesting that PLCδsu may not be directly involved in egg activation, but may play a role in further downstream extracellular signals. Intriguingly, the *in vivo* expression of PLCδsu cRNA did not result in Ca^{2+} transients in either mouse or sea urchin eggs. This observation is consistent with the behaviour of recombinant PLCβ1, PLCγ1, PLCγ2, PLCδ1, PLCδ3 and PLCδ4 protein and cRNA, none of which cause Ca^{2+} release in mouse oocytes. However, the specific PLC isozyme responsible for oocyte activation itself remained a mystery until Saunders et al. [132], using mouse express sequence tag databases, identified a novel, and importantly testis-specific, PLC, termed PLCzeta (PLCζ), a protein ~74 kDa in mice and ~70 kDa in humans, which was proven to play a key role in mammalian oocyte activation.

PLCζ, the Mammalian Oocyte Activation Factor

General consensus agrees that the soluble factor which elicits Ca^{2+} release within oocytes is sperm-specific, as extracts from other tissues do not induce Ca^{2+} increase upon oocyte injection [144, 162]. Data indicated that the mammalian sperm factor was a sperm-specific PLC possessing distinct enzymatic properties compared to other known PLCs [72, 73]. Indeed, this correlated with the hypothesis that oocyte activation involved Ca^{2+} oscillations generated in an IP_3-mediated manner, supporting the notion that the soluble sperm factor was a PLC which mediated the hydrolysis of PIP_2 to IP_3 and DAG [106, 132, 146]. Expression studies in mice concluded that PLCζ mRNA was first detectable in spermatids [132].

More systematic studies of PLCζ mRNA expression during porcine spermatogenesis observed PLCζ mRNA translation in elongating spermatids [168]. Northern blot analyses of testes from post-natal hamsters showed that PLCζ mRNA was present as early as day 17 [171].

A large body of evidence supports the identity of the mammalian oocyte activation factor as PLCζ. The injection of recombinant PLCζ RNA into mouse oocytes resulted in the initiation of Ca^{2+} oscillations and supported embryonic development to the blastocyst stage [82, 132]. Immuno-depletion of PLCζ from sperm extracts suppressed their ability to release Ca^{2+} [132], while sperm fractionation studies correlated the presence of PLCζ in sperm to their ability to induce Ca^{2+} oscillations [40, 86]. Furthermore, RNA interference (RNAi) experiments yielded transgenic mice exhibiting disruption of PLCζ expression in the testis, while sperm from these mice induced Ca^{2+} oscillations that ended prematurely, with a clear reduction in litter size [80]. Data strongly suggests that PLCζ may be a universal feature of vertebrate oocyte activation. For example, sperm extracts and PLCζ cRNA from one species are able to elicit Ca^{2+} release upon microinjection in oocytes from another species [7, 22]. Furthermore, non-mammalian PLCζ homologues have been identified in the chicken [19], medaka fish [60], and quail [107].

Immunofluorescence studies [40, 169, 171] have shown that PLCζ is predominantly localized to post-acrosomal regions of the sperm head in mice, a pattern maintained following the acrosome reaction (Fig. 50.6a) [171]. Intriguingly, however, this pattern of PLCζ immunofluorescence was reported to change during capacitation [171], increasing in intensity and implying modified PLCζ structure or molecular interactions, or that PLCζ becomes more accessible to antibody following capacitation due to physiological changes within the sperm membrane [49, 156, 171]. Intriguingly a second acrosomal population of PLCζ was also identified, suggesting multiple roles for PLCζ besides oocyte activation, such as the acrosome reaction [171]. Immunoblots of porcine sperm extracts revealed a variety of isoforms [40], ranging from the expected full length 74 kDa PLCζ to fragments ranging from 27 to 50 kDa, all of which may exist in a stable complex, retaining enzymatic activity [87].

In non-capacitated human sperm, PLCζ is predominantly localized to equatorial regions of the sperm head (Fig. 50.6b) [47, 170], an ideal location for a sperm factor since the equatorial segment of the sperm remains intact following the acrosome reaction [6, 47, 161], allowing PLCζ to be one of the first sperm proteins to be released into the oocyte following gamete fusion [47]. As in mouse and hamster sperm, a second population of PLCζ was also identified in acrosomal regions of human sperm [47], while capacitation resulted in dynamic changes in localization patterns in post-acrosomal/equatorial regions [47, 171].

Studies suggest that human PLCζ may be much more potent that other isoforms at eliciting Ca^{2+} release [173]. An interesting point to consider is the fundamental requirement of a specific amount of PLCζ for the initiation of Ca^{2+} oscillations within the oocyte. Although, too little or too much PLCζ does indeed cause Ca^{2+} oscillations within the oocyte, it is clear that such oscillations are either not sufficient to activate oocytes, or cause excessive Ca^{2+} signaling, resulting in activation

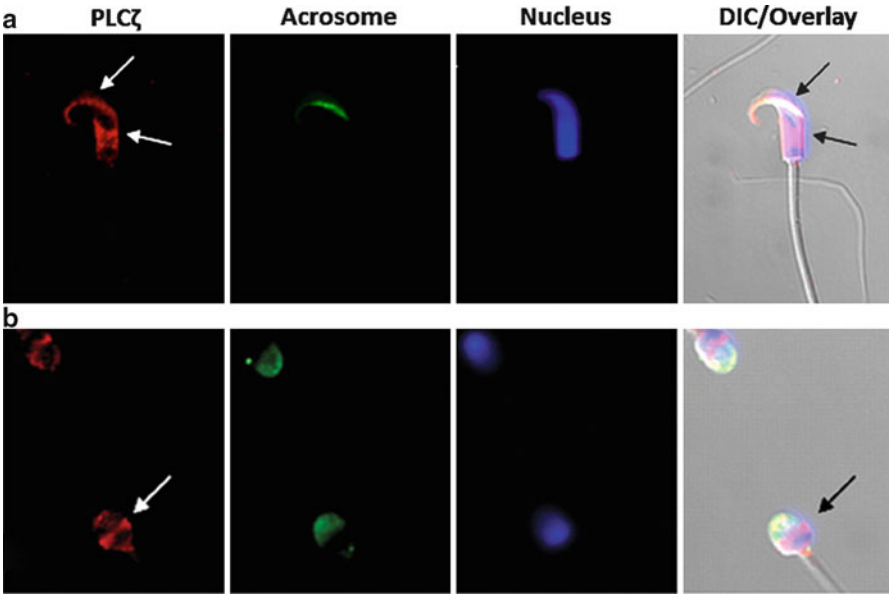

Fig. 50.6 Immunofluorescent localization of PLCζ (*red*) in hamster (**a**) and human (**b**) sperm. Fluorescein isothiocyanate-conjugated peanut agglutinin (FITC-PNA)-lectin staining (*green*) identifies the acrosome, and Hoescht-33342 staining (*blue*) identifies the nuclei. *Arrows* indicate the immunolocalization of PLCζ within the acrosome and equatorial segment of hamster and equatorial segment of human sperm (Reproduced from Young et al. [171] and Grasa et al. [47] with permission)

failure [127, 173]. Different species have been shown to possess varying amounts of PLCζ within sperm, with species delivering "fine-tuned" doses of PLCζ, with varying potencies adjusted via evolutionary processes to match the size and sensitivity of the oocyte being activated [148]. The varying solubility of PLCζ in sperm of various species may also contribute to this inference. Hamster sperm initiates Ca^{2+} oscillations within approximately 10 s of gamete fusion, whereas there is a 1–3 min delay before Ca^{2+} oscillations begin in mice [91]. It is therefore possible that PLCζ activity and concentration in mammalian species has naturally been optimised to achieve the precise Ca^{2+} oscillation profile required for normal oocyte activation and embryo development within that species [17]. Recent data also suggests that PLCζ RNA transcripts are present within sperm [89, 122], which may be transcribed during fertilization, sustaining a "long-lived" Ca^{2+} response [89], which may also explain the presence of varying PLCζ isoforms within the sperm. However, the role for PLCζ and other RNA transcripts within sperm remain elusive, and require further examination [74].

Interestingly, while all mammalian isoforms of PLCζ have been testis-specific, Coward et al. [21] identified ovarian and brain forms of PLCζ in puffer-fish. Injection of cRNA corresponding to the ovarian isoform into mouse oocytes did not result in Ca^{2+} oscillations. This is particularly interesting given the debate regarding the

mechanism responsible for oocyte activation [21, 36, 105, 119]. The discovery that PLCζ may be present in oocytes of some species raises the question of how a sperm stimulus may activate the oocyte. While the majority of scientific opinion agrees that PLCζ is the endogenous sperm factor, recent studies have demonstrated possible candidates for sperm factors apart from PLCζ, which are able to induce meiotic progression or elicit Ca^{2+} oscillations in a variety of species. Harada et al. [48] identified a new 45 kDa protein, termed citrate synthase, as the major component responsible for egg activation in the newt *Cynops pyrrhogaster*. Wu et al. [163] also reported another possible candidate for the sperm factor, which resides in the post-acrosomal sheath region of the perinuclear theca, termed post-acrosomal sheath WW domain-binding protein (PAWP), in bovine sperm and other mammalian species. However, the molecular mechanisms underlying the precise function of both PAWP and citrate synthase are currently unknown [1, 163]. It is, of course, possible that oocyte activation involves the collective action of PLCζ and other sperm factors. However, this theory remains to be established [74].

PLCζ Structure and Function

While general consensus now agrees that PLCζ is the physiological agent of mammalian oocyte activation [70, 74, 119, 148, 159], many questions remain regarding its precise mechanism of action. PLCζ is unique from other PLC isoforms in its high sensitivity to Ca^{2+} and Ca^{2+} oscillation induction [81, 124]. In all species in which PLCζ has been characterized, PLCζ ranges from 70 to 75 kDa in molecular weight [148], representing the smallest PLC isoform found to date. PLCζ exhibits typical PLC domain structure [132] with closest homology to PLCδ isoforms [75, 124], particularly PLCδ1 [148]. PLCζ possesses characteristic X and Y catalytic domains which form the active site common to all PLCs [124, 148], a C2 domain and a set of EF hands, similar to PLCδ (Fig. 50.7).

PLCζ is unique from other PLC isoforms in that it lacks a PH domain [124, 132], and it is thus unclear as to how PLCζ targets its membrane-bound substrate PIP_2. Intriguingly, experiments suggest that the PH domain is not integral to the membrane localizing ability of PLCδ4 [92], leaving the possibility open that PLCζ localizes to the plasma membrane through an alternate mechanism. It is possible that indirect interaction binds PLCζ to the membrane, or indeed that PLCζ acts upon cytosolic PIP_2 instead of membrane-bound forms. Regardless, it would seem that the target of PLCζ is membrane-bound PIP_2, since this would increase the local concentration of substrate for the enzyme to act upon, significantly increasing hydrolysis rate [78, 101, 124, 125].

PLCζ has four EF-hand motifs at the N-terminus, which are important for enzymatic activity [148], and are arranged in a similar lobed way to the Ca^{2+} binding domains of calmodulin and troponin [124, 148]. Deletion of the EF hands led to a reduction in Ca^{2+} response upon injection of cRNA into mouse oocytes [114], suggesting that the EF hands play a structural role in maintaining PLCζ activity. However, there is some conflicting data with regards to the importance of EF hands

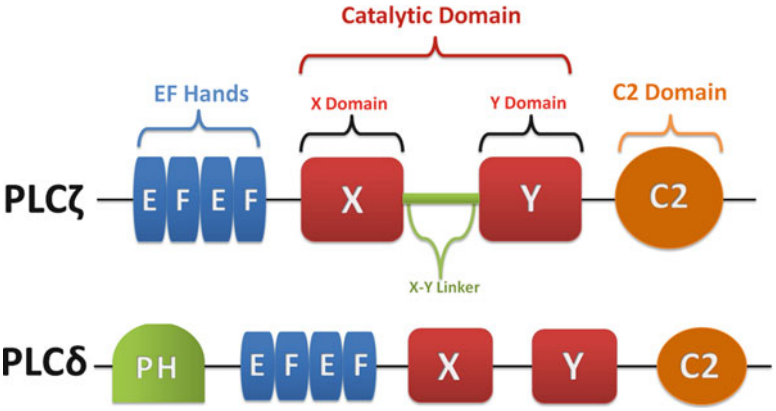

Fig. 50.7 Schematic illustrations of domain structure for PLCζ and it's closest PLC homologue, PLCδ

in the Ca^{2+} oscillation producing ability of PLCζ, where offspring were obtained following round spermatid injection (ROSI) in mouse oocytes, along with the injection of a truncated form of PLCζ [111] reportedly found in the testis where the first three EF hands are lacking [40, 81, 86, 167].

C2 domains are able to bind to phospholipid containing membranes, as is the case with PLCδ1 binding to phosphatidylserine or PLCA2 binding to phosphatidylcholine [126]. Deletion of the PLCζ C2 domain led to some loss of enzymatic activity, and only a slight reduction in Ca^{2+} sensitivity. However, the injection of PLCζ cRNA lacking the C2 domain in mouse oocytes did not induce Ca^{2+} release, implying that the C2 domain is also required for oocyte activation [114, 148].

A non-catalytic PLCζ domain possibly involved in the regulation of activity is a segment between the X and Y catalytic domains, referred to as the X-Y linker [115, 148]. This apparently unstructured cluster of residues shows greatest divergence between species, and is longest in *Macaca fascicularis*, but shortest in humans [132, 148]. It remains unclear what these differences mean in terms of biological importance, but the proximity of the X-Y linker to the active site implies potential involvement in regulating catalytic activity, or by sequestering PIP_2 in the locality of PLCζ in an electrostatic manner [115, 148]. However, unlike PLCγ, the PLCζ X-Y linker does not contain any regions of predicted secondary structure, casting doubt as to how the X-Y linker would play a role in anchoring PLCζ to PIP_2 [148]. There is also evidence to suggest that PLCζ remains functional following proteolytic cleavage at the X-Y linker, which can form complexes that retain activity [87]. Indeed, proteolytic cleavage may be required for PLCζ to be able to bind to the membrane and act upon PIP_2 [132]. Intriguingly, studies show that the X-Y linker in some, if not all, PLC isoforms play an auto-inhibitory role, the deletion of which results in elevated activity [52].

Following fertilization, Ca^{2+} oscillations in the oocyte cease after pronuclei formation [99], following which some oscillations are subsequently observed in

mouse zygotes during mitosis [13, 99]. One possible explanation of this cell-cycle dependant termination and resumption, was that PLCζ was localized to the pronuclei during interphase [13, 148], resulting in the cessation of Ca^{2+} oscillations which resume following pronuclear envelope breakdown during the oocytes entry into mitosis [148]. When pronuclear formation was inhibited, Ca^{2+} oscillations persisted for much longer than normal [60, 99]. cRNA coding for mouse PLCζ tagged with either a Venus fluorescent protein or a Myc epitope, revealed that PLCζ was associated with the nascent pronuclei [85, 90, 135, 167]. Tagged PLCζ was also observed to return to the cytoplasm during first mitosis, coinciding with the resumption of Ca^{2+} oscillations [90].

This "nuclear sequestration" activity appears to be the result of a specific signal sequence within the X-Y Linker region of PLCζ, termed the nuclear localisation signal (NLS) [85, 90, 148]. Mutational analysis of the NLS resulted in termination of PLCζ nuclear sequestration, but still induced Ca^{2+} oscillations which continued beyond pronuclear formation, suggesting that PLCζ pronuclear sequestration plays a role in regulating Ca^{2+} oscillations at fertilization [90, 148]. While a NLS has been predicted in a variety of mammalian PLCζs, located in a similar location within the PLCζ structure [148], only the mouse PLCζ NLS has been shown to be functional in oocytes [148]; further study is required for other species. Alternate explanations for the termination of Ca^{2+} oscillations have also been reported. For example, changes in the cellular distribution of IP_3Rs [46] may also be involved. Indeed, IP_3 is known to be down-regulated following fertilization [12, 68]. Alternatively, a negative feedback mechanism involving the production of DAG and subsequently protein kinase C (PKC) might affect PLCζ activity [172].

PLCζ is known to re-accumulate in blastomere nuclei [85, 135]. It is therefore possible that PLCζ may promote further cell division during embryogenesis in a Ca^{2+} dependant manner. As PLCζ targets nuclei specifically during interphase [135], there may be a role for PLCζ at this stage of the cell cycle. Indeed, PLCβ1 translocates to nuclei during G2 to M transition in immature mouse oocytes, contributing towards the breakdown of the germinal vesicle via DAG and PKC [2, 45, 142]. PLCδ1 also possesses a NLS [165], which in a manner similar to PLCζ, localises to nuclear structures at the G_1/S phase boundary of the cell cycle [139, 142]. Suppressing PLCδ1 results in increased levels of cyclin E, thus inhibiting cellular proliferation [139]. When considered with reports that concentrations of nuclear PIP_2 are significantly increased at the G_1/S boundary, and at least doubled at G_0, one can speculate that PLCδ1 may regulate certain nuclear functions [142, 174], a possibility that should be investigated for PLCζ.

The Role of PLCζ in Human Infertility

Considering the pivotal role of PLCζ in mammalian fertilisation, defective forms of PLCζ may contribute to cases of male infertility where oocyte activation is deficient (OAD) [74]. Infertility represents a major problem to a growing proportion of the global population. Consequently, worldwide investment in assisted reproductive

technology (ART) has significantly increased over recent years. ART now accounts for ~7% of all births in some developed countries [112], and over eight million ART babies have been born worldwide thus far [59]. A key technique in ART is intracytoplasmic sperm injection (ICSI), whereby a sperm is microinjected directly into the oocyte cytosol. Predominantly used to treat male factor infertility following the failure of conventional *in vitro* fertilisation (IVF), ICSI remains a highly successful technique that, on average, results in normal fertilization in 70% of cases [112]. However, a noted phenomenon associated with male infertility is the failure of some oocytes to activate, even following ICSI (for review, see [74]). Recent studies have successfully linked cases of oocyte activation failure to aberrant expression, localization and structure of PLCζ in sperm from patients diagnosed with oocyte activation deficiency, particularly in cases of globozoospermia (round headed, acrosome-less sperm) [50, 170].

Sperm from some infertile men who consistently fail IVF and ICSI are either unable to elicit Ca^{2+} oscillations upon injection into mouse oocytes, or produce oscillations uncharacteristic of fertilisation, showing reduced frequency and amplitude (Fig. 50.8a). Furthermore, immunofluorescence and immunoblots have revealed that sperm from ICSI failed infertile patients showed abnormal PLCζ expression (Fig. 50.8b) [50, 170]. Interestingly, and of crucial importance to future therapeutic options, the activating ability of ICSI failed human sperm can be rescued upon co-injection with mouse PLCζ mRNA (Fig. 50.8c) [170]. Interestingly, sperm from wobbler mice (a strain of mice which suffer from motor neuron disease caused by a naturally occurring mutation, in whom males are infertile) elicit low rates of fertilisation using ICSI, and exhibit an abnormal PLCζ localisation profile. Intriguingly, sperm from these mice produce healthy pups following ICSI and artificial oocyte activation (AOA) [51]. Taylor et al. [149] further showed that successful pregnancy and birth could be achieved using globozoospermic sperm lacking PLCζ by utilising ICSI and AOA [149] (for review on AOA see [74, 112]).

Importantly, Heytens et al. [50] identified a substitution mutation in a non-globozoospermic infertile male within the Y domain of PLCζ at position 398, resulting in a histidine to proline substitution (H398P) (Fig. 50.9a). Predictive modelling suggested that this residue change may disrupt the active site loop (Fig. 50.9b), and the ability of PLCζ to interact with PIP_2 [116]. Multiple sequence alignments confirmed that the histidine at this position is highly conserved across all mammalian [22, 132, 168, 171], chicken [19], and medaka isoforms of PLCζ [60], as well as all PLCδ isoforms [34, 132], indicating that this residue may play a critical role within the active protein [50]. Furthermore, the injection of H398P PLCζ cRNA into mouse oocytes resulted in highly abnormal Ca^{2+} release which was insufficient for oocyte activation (Fig. 50.9c) [50].

Yoon et al. [170] and Heytens et al. [50] provided the first key link between defective PLCζ and human male infertility. However, further analytical studies are needed to explore the precise functional effects of the H398P mutation identified by Heytens et al. [50]. Studies investigating larger cohorts of patients, from a range of

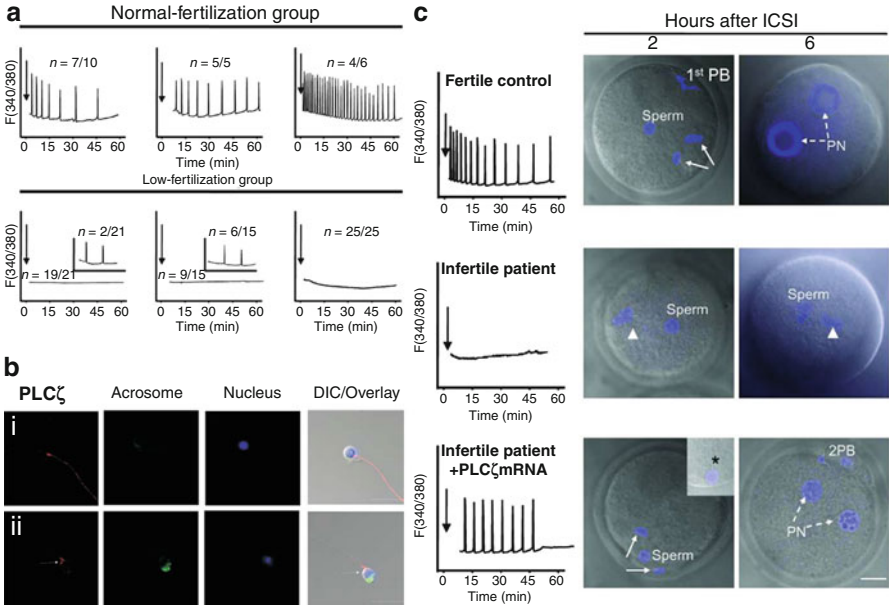

Fig. 50.8 (**a**) Ca^{2+} oscillation profiles following the injection of sperm from normal fertile humans (*top panel*) and infertile patients who had previously failed or exhibited low fertilisation rates following ICSI (*bottom panel*). *Arrows* denote time of sperm injection, and *n* indicates the number of mouse oocytes exhibiting the corresponding Ca^{2+} oscillation profile. (**b**) Reduced PLCζ immunostaining (*red*) in sperm from infertile ICSI failed patients exhibiting abnormal morphology (in this case globozoospermia; acrosome-less, round-headed sperm) (i), and normal morphology (ii). Fluorescein isothiocyanate-conjugated peanut agglutinin (FITC-PNA)-lectin staining (*green*) identifies the acrosome, and Hoescht-33342 staining (*blue*) identifies the nuclei. *Arrow* indicates reduced PLCζ immunolocalisation of within the equatorial segment. Scale bars indicate 5 μm. (**c**) (*Top panel*) Injection of a sperm from a fertile control was able to elicit Ca^{2+} oscillations and activate mouse oocytes. (*Middle panel*) Sperm from an infertile patient with a history of ICSI failure was unable to elicit Ca^{2+} oscillations, and was unable to activate mouse oocytes following injection, but was able to do so following the co-injection of PLCζ mRNA (*Bottom panel*). *Arrows* denote time of sperm injection. *1st PB* first polar body, *2PB* second polar body. TO-PRO-3 staining (*blue*) stains chromatin. *Asterisk* in inset points to the persistence of the human sperm tail in mouse oocytes. Scale bar indicates 10 μm (Reproduced from Yoon et al. [170] and Heytens et al. [50] with permission)

biogeographical regions, targeting specific male factor conditions, and utilizing high-throughput genetic screening techniques may be invaluable in discovering the prevalence of such mutations in human infertility.

Further analyses should also systematically map out specific clinical conditions in which aberrant forms or reduced expression of PLCζ may play a role, and thus provide the foundations for the development of a therapeutic version of PLCζ to aid such patients as an alternative to current AOA protocols which remain the source of

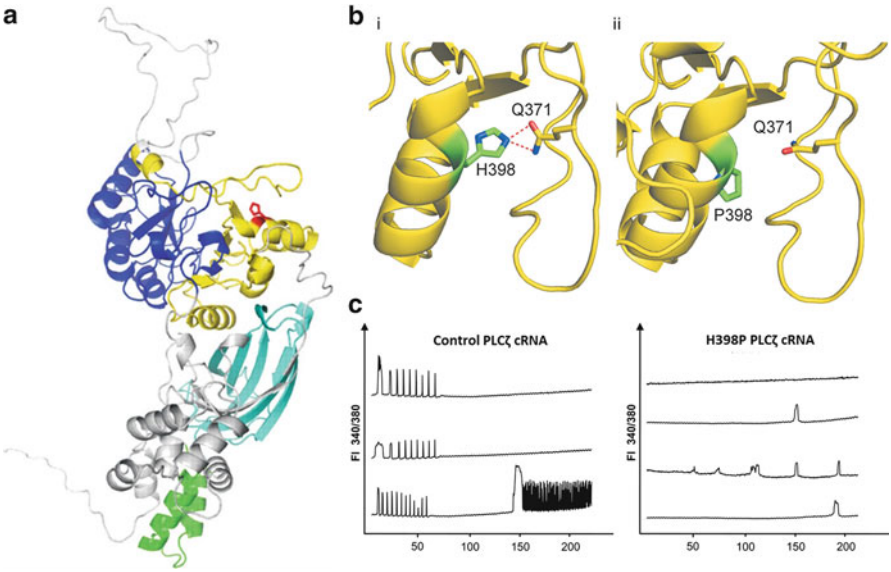

Fig. 50.9 Histidine>Proline point mutation (H398P) identified by Heytens et al. [50] in an infertile male patient diagnosed with oocyte activation deficiency. (**a**) Model of human PLCζ functional domains (*green* – EF hands, *blue* – X catalytic domain, *yellow* – Y catalytic domain and *cyan* – C2 domain). Histidine398 (H398) is shown in *red*. (**b**) Close-up of H398 showing side-chain-side-chain hydrogen bonds (bi), alongside a close-up of P398 in mutant PLCζ showing no side-chain-side-chain hydrogen bonds (bii). (**c**) Microinjection of wild type and mutant PLCζ into mouse oocytes and resulting calcium release patterns (Reproduced from Heytens et al. [50] with permission)

some concern [74]. While Yoon et al. [170] provided the first real evidence the PLCζ as a novel therapeutic, Rogers et al. [127] provided additional supportive evidence by activating aged human oocytes incapable of being activated by any other means.

Currently, we know little of the precise mechanisms of PLCζ action, the regulatory pathways involved, and the relative roles of the various localisation patterns reported in the literature. Systematic analysis of these issues represents a critical challenge in the translation of PLCζ into a routine therapeutic agent for the clinic. In addition, immunofluorescence and immunoblot analysis of PLCζ expression and localization in human sperm, combined with assays of PLCζ enzymatic activity, may have potential use as diagnostic tools with which to identify and treat men with oocyte activation deficiency. While much remains unknown with regards to PLCζ and its mode of activity within oocytes, and in particular it's potential role in embryogenesis, the utilization of PLCζ as a clinical therapeutic holds much promise for the future treatment of human infertility.

References

1. Aarabi M, Qin Z, Xu W, Mewburn J, Oko R (2010) Sperm borne protein, PAWP, initiates zygotic development in Xenopus laevis by eliciting intracellular calcium release. Mol Reprod Dev 77:249–256
2. Avazeri N, Courtot AM, Pesty A, Duguenne C, Lefèvre B (2000) Cytoplasmic and nuclear phospholipase C-beta 1 relocation: role in resumption of meiosis in the mouse oocyte. Mol Biol Cell 11:4369–4380
3. Backs J, Stein P, Backs T, Duncan FE, Grueter CE, McAnally J, Qi X, Schultz RM, Olson EN (2010) The gamma isoform of CaM kinase II controls mouse egg activation by regulating cell cycle resumption. Proc Natl Acad Sci USA 107:81–86
4. Bahat A, Eisenbach M (2006) Sperm thermotaxis. Mol Cell Endocrinol 252:115–119
5. Bahat A, Eisenbach M (2010) Human sperm thermotaxis is mediated by phospholipase C and inositol trisphosphate receptor Ca2+ channel. Biol Reprod 82:606–616
6. Bedford JM, Moore HD, Franklin LE (1979) Significance of the equatorial segment of the acrosome of the spermatozoon in eutherian mammals. Exp Cell Res 119:119–126
7. Bedford-Guaus SJ, Yoon SY, Fissore RA, Choi YH, Hinrichs K (2008) Microinjection of mouse phospholipase C zeta complementary RNA into mare oocytes induces long-lasting intracellular calcium oscillations and embryonic development. Reprod Fertil Dev 20: 875–883
8. Berridge MJ, Irvine RF (1984) Inositol trisphosphate, a novel second messenger in cellular signal transduction. Nature 312:315–321
9. Böhmer M, Van Q, Weyand I, Hagen V, Beyermann M, Matsumoto M, Hoshi M, Hildebrand E, Kaupp UB (2005) Ca2+ spikes in the flagellum control chemotactic behavior of sperm. EMBO J 24:2741–2752
10. Bootman MD, Collins TJ, Mackenzie L, Roderick HL, Berridge MJ, Peppiatt CM (2002) 2-aminoethoxydiphenyl borate (2-APB) is a reliable blocker of store-operated Ca2+ entry but an inconsistent inhibitor of InsP3-induced Ca2+ release. FASEB J 16:1145–1150
11. Breitbart H (2002) Intracellular calcium regulation in sperm capacitation and acrosomal reaction. Mol Cell Endocrinol 187:139–144
12. Brind S, Swann K, Carroll J (2000) Inositol 1,4,5-Trisphosphate receptors are downregulated in mouse oocytes in response to sperm or adenophostin a but not to increases in intracellular Ca^{2+} or egg activation. Dev Biol 223:251–265
13. Carroll J (2001) The initiation and regulation of Ca^{2+} signaling at fertilization in mammals. Semin Cell Dev Biol 12:37–43
14. Choi D, Lee E, Hwang S, Jun K, Kim D, Yoon BK, Shin HS, Lee JH (2001) The biological significance of phospholipase C beta1 gene mutation in mouse sperm in the acrosome reaction, fertilization and embryo development. J Assist Reprod Genet 18:305–310
15. Cockcroft S, Carvou N (2007) Biochemical and biological functions of class I phosphatidylinositol transfer proteins. Biochim Biophys Acta 1771:677–691
16. Cook SP, Brokaw CJ, Muller CH, Babcock DF (1994) Sperm chemotaxis: egg peptides control cytosolic calcium to regulate flagellar responses. Dev Biol 165:10–19
17. Cooney MA, Malcuit C, Cheon B, Holland MK, Fissore RA, D'Cruz NT (2010) Species-specific differences in the activity and nuclear localization of murine and bovine phospholipase C zeta 1. Biol Reprod 83:92–101
18. Coward K, Campos-Mendoza A, Larman M, Hibbitt O, McAndrew B, Bromage N, Parrington J (2003) Teleost fish spermatozoa contain a cytosolic protein factor that induces calcium release in sea urchin egg homogenates and triggers calcium oscillations when injected into mouse oocytes. Biochem Biophys Res Commun 305:299–304
19. Coward K, Ponting CP, Chang HY, Hibbitt O, Savolainen P, Jones KT, Parrington J (2005) Phospholipase Czeta, the trigger of egg activation in mammals, is present in a non-mammalian species. Reproduction 130:157–163

20. Coward K, Owen H, Tunwell R, Swann K, Parrington J (2007) Phospholipid binding properties and functional characterization of a sea urchin phospholipase Cdelta in urchin and mouse eggs. Biochem Biophys Res Commun 357:964–970
21. Coward K, Ponting CP, Zhang N, Young C, Huang CJ, Chou CM, Kashir J, Fissore RA, Parrington J (2011) Identification and functional analysis of an ovarian form of the egg activation factor phospholipase C zeta (PLCζ) in pufferfish. Mol Reprod Dev 78:48–56
22. Cox LJ, Larman MG, Saunders CM, Hashimoto K, Swann K, Lai FA (2002) Sperm phospholipase C zeta from humans and cynomolgus monkeys triggers Ca^{2+} oscillations, activation and development of mouse oocytes. Reproduction 124:611–623
23. Créton R, Jaffe LF (1995) Role of calcium influx during the latent period in sea urchin fertilization. Dev Growth Differ 37:703–709
24. Créton R, Jaffe LF (2001) Chemiluminescence microscopy as a tool in biomedical research. Biotechniques 31:1098–1100
25. Dale B (1988) Primary and secondary messengers in the activation of Ascidian eggs. Exp Cell Res 177:205–211
26. Dale B, DeFelice LJ, Ehrenstein G (1985) Injection of a soluble sperm fraction into sea-urchin eggs triggers the cortical reaction. Experientia 41:1068–1070
27. Darszon A, Beltran C, Felix R, Nishigaki T, Trevino CL (2001) Ion transport in sperm signaling. Dev Biol 240:1–14
28. De Koninck P, Schulman H (1998) Sensitivity of CaM kinase II to the frequency of Ca2+ oscillations. Science 279:227–230
29. Dong JB, Tang TS, Sun FZ (2000) Xenopus and chicken sperm contain a cytosolic soluble protein factor which can trigger calcium oscillations in mouse eggs. Biochem Biophys Res Commun 268:947–951
30. Ducibella T, Huneau D, Agelichio E, Xu Z, Schultz RM, Kopf GS et al (2002) Egg-to-embryo transition is driven by differential responses to Ca2+ oscillation number. Dev Biol 250:280–291
31. Ducibella T, Schultz RM, Ozil JP (2006) Role of calcium signals in early development. Semin Cell Dev Biol 17:324–332
32. Eisenbach M (1999) Sperm chemotaxis. Rev Reprod 4:56–66
33. Eisenbach M, Giojalas LC (2006) Sperm guidance in mammals – an unpaved road to the egg. Nat Rev Mol Cell Biol 7:276–285
34. Ellis MV, James SR, Perisic O, Downes CP, Williams RL, Katan M (1998) Catalytic domain of phosphoinositide-specific phospholipase C (PLC). Mutational analysis of residues within the active site and hydrophobic ridge of plcδ1. J Biol Chem 273:11650–11659
35. Epel D, Perry G, Schmidt T (1982) Intracellular calcium and fertilization: role of the cation and regulation of intracellular calcium levels. Prog Clin Biol Res 91:171–183
36. Evans JP, Kopf GS (1998) Molecular mechanisms of sperm-egg interactions and egg activation. Andrologia 30:297–307
37. Feng H, Sandlow JI, Sandra A (1997) Expression and function of the *c-kit* proto-oncogene protein in mouse sperm. Biol Reprod 57:194–203
38. Fissore RA, Longo FJ, Anderson E, Parys JB, Ducibella T (1999) Differential distribution of inositol trisphosphate receptor isoforms in mouse oocytes. Biol Reprod 60:49–57
39. Fontanilla RA, Nuccitelli R (1998) Characterization of the sperm-induced calcium wave in Xenopus eggs using confocal microscopy. Biophys J 75:2079–2087
40. Fujimoto S, Yoshida N, Fukui T, Amanai M, Isobe T, Itagaki C, Izumi T, Perry AC (2004) Mammalian phospholipase Czeta induces oocyte activation from the sperm perinuclear matrix. Dev Biol 274:370–383
41. Fukami K, Nakao K, Inoue T, Kataoka Y, Kurokawa M, Fissore RA, Nakamura K, Katsuki M, Mikoshiba K, Yoshida N, Takenawa T (2001) Requirement of phospholipase Cdelta4 for the zona pellucida-induced acrosome reaction. Science 292:920–923
42. Fukami K, Yoshida M, Inoue T, Kurokawa M, Fissore RA, Yoshida N, Mikoshiba K, Takenawa T (2003) Phospholipase Cdelta4 is required for Ca2+ mobilization essential for acrosome reaction in sperm. J Cell Biol 161:79–88

43. Fukami K, Inanobe S, Kanemaru K, Nakamura Y (2010) Phospholipase C is a key enzyme regulating intracellular calcium and modulating the phosphoinositide balance. Prog Lipid Res 49:429–437
44. Fulton BP, Whittingham DG (1978) Activation of mammalian oocytes by intracellular injection of calcium. Nature 273:149–151
45. Goss VL, Hocevar BA, Thompson LJ, Stratton CA, Burns DJ, Fields AP (1994) Identification of nuclear beta II protein kinase C as a mitotic lamin kinase. J Biol Chem 269:19074–19080
46. Goud PT, Goud AP, Van Oostveldt P, Dhont M (1999) Presence and dynamic redistribution of type I inositol 1,4,5-trisphosphate receptors in human oocytes and embryos during in-vitro maturation, fertilization and early cleavage divisions. Mol Hum Reprod 5:441–451
47. Grasa P, Coward K, Young C, Parrington J (2008) The pattern of localization of the putative oocyte activation factor, phospholipase C zeta, in uncapacitated, capacitated, and ionophore-treated human spermatozoa. Hum Reprod 23:2513–2522
48. Harada Y, Matsumoto T, Hirahara S, Nakashima A, Ueno S, Oda S, Miyazaki S, Iwao Y (2007) Characterization of a sperm factor for egg activation at fertilization of the newt Cynops pyrrhogaster. Dev Biol 306:797–808
49. Harrison RA, Gadella B (2005) Bicarbonate-induced membrane processing in sperm capacitation. Theriogenology 63:342–351
50. Heytens E, Parrington J, Coward K, Young C, Lambrecht S, Yoon SY, Fissore RA, Hamer R, Deane CM, Ruas M et al (2009) Reduced amounts and abnormal forms of phospholipase C zeta in spermatozoa from infertile men. Hum Reprod 24:2417–2428
51. Heytens E, Schmitt-John T, Moser JM, Jensen NM, Soleimani R, Young C, Coward K, Parrington J, De Sutter P (2010) Reduced fertilization after ICSI and abnormal phospholipase C zeta presence in spermatozoa from the wobbler mouse. Reprod Biomed Online 21:742–749
52. Hicks SN, Jezyk MR, Gershburg S, Seifert JP, Harden TK, Sondek J (2008) General and Versatile autoinhibition of PLC isozymes. Mol Cell 31:383–394
53. Hofmann SL, Majerus PW (1982) Modulation of phosphatidylinositol-specific phospholipase C activity by phospholipid interactions, diglycerides, and calcium ions. J Biol Chem 257:14359–14364
54. Horner VL, Wolfner MF (2008) Transitioning from egg to embryo: triggers and mechanisms of egg activation. Dev Dyn 237:527–544
55. Hudmon A, Schulman H (2002) Structure-function of the multifunctional Ca2+/calmodulin-dependent protein kinase II. Biochem J 364(Pt3):593–611
56. Hwang JI, Oh YS, Shin KJ, Kim H, Ryu SH, Suh PG (2005) Molecular cloning and characterization of a novel phospholipase C, PLC-eta. Biochem J 389:181–186
57. Hyslop LA, Nixon VL, Levasseur M, Chapman F, Chiba K, McDougall A (2004) Ca2+−promoted cyclin B1 degradation in mouse oocytes requires the establishment of a metaphase arrest. Dev Biol 269:206–219
58. Igarashi H, Knott JG, Schultz RM, Williams CJ (2007) Alterations of PLCbeta1 in mouse eggs change calcium oscillatory behavior following fertilization. Dev Biol 312:321–330
59. International Committee for Monitoring Assisted Reproductive Technology (ICMART), de Mouzon J, Lancaster P, Nygren KG, Sullivan E, Zegers-Hochschild F, Mansour R, Ishihara O, Adamson D (2009) World collaborative report on assisted reproductive technology, 2002. Hum Reprod 24:2310–2320
60. Ito M, Shikano T, Kuroda K, Miyazaki S (2008) Relationship between nuclear sequestration of PLCzeta and termination of PLCzeta-induced Ca^{2+} oscillations in mouse eggs. Cell Calcium 44:400–410
61. Ito J, Yoshida T, Kasai Y, Wakai T, Parys JB, Fissore RA, Kashiwazaki N (2010) Phosphorylation of inositol 1,4,5-triphosphate receptor 1 during in vitro maturation of porcine oocytes. Anim Sci J 81:34–41
62. Jaffe LF (1983) Sources of calcium in egg activation: a review and hypothesis. Dev Biol 99:265–276
63. Jaffe LA (1990) First messengers at fertilization. J Reprod Fertil Suppl 42:107–116

64. Jaffe LF (1991) The path of calcium in cytosolic calcium oscillations: a unifying hypothesis. Proc Natl Acad Sci USA 88:9883–9887
65. Jaffe LF (2008) Calcium waves. Philos Trans R Soc Lond B Biol Sci 363:1311–1316
66. Jaffe LA, Turner PR, Kline D, Kado RT, Shilling F (1988) G-proteins and egg activation. Cell Differ Dev 25(suppl):15–18
67. Janetopoulos C, Devreotes P (2006) Phosphoinositide signaling plays a key role in cytokinesis. J Cell Biol 174:485–490
68. Jellerette T, He CL, Wu H, Parys JB, Fissore RA (2000) Down-regulation of the inositol 1,4,5-trisphosphate receptor in mouse eggs following fertilization or parthenogenetic activation. Dev Biol 223:238–250
69. Jones KT (2004) Turning it on and off: M-phase promoting factor during meiotic maturation and fertilization. Mol Hum Reprod 10:1–5
70. Jones KT (2005) Mammalian egg activation: from Ca^{2+} spiking to cell cycle progression. Reproduction 130:813–823
71. Jones KT (2007) Intracellular calcium in the fertilization and development of mammalian eggs. Clin Exp Pharmacol Physiol 34:1084–1089
72. Jones KT, Soeller C, Cannell MB (1998) The passage of Ca^{2+} and fluorescent markers between the sperm and egg after fusion in the mouse. Development 125:4627–4635
73. Jones KT, Matsuda M, Parrington J, Katan M, Swann K (2000) Different Ca^{2+}-releasing abilities of sperm extracts compared with tissue extracts and phospholipase C isoforms in sea urchin egg homogenate and mouse eggs. Biochem J 346(pt3):743–749
74. Kashir J, Heindryckx B, Jones C, De Sutter P, Parrington J, Coward K (2010) Oocyte activation, phospholipase C zeta and human infertility. Hum Reprod Update 16:690–703
75. Katan M (1998) Families of phosphoinositide-specific phospholipase C: structure and function. Biochim Biophys Acta 1436:5–17
76. Kaupp UB, Solzin J, Hildebrand E, Brown JE, Helbig A, Hagen V, Beyermann M, Pampaloni F, Weyand I (2003) The signal flow and motor response controlling chemotaxis of sea urchin sperm. Nat Cell Biol 5:109–117
77. Kelley GG, Reks SE, Ondrako JM, Smrcka AV (2001) Phospholipase C(epsilon): a novel Ras effector. EMBO J 20:743–754
78. Kholodenko BN, Hoek JB, Westerhoff HV (2000) Why cytoplasmic signaling proteins should be recruited to cell membranes. Trends Cell Biol 10:173–178
79. Kline D, Kline JT (1992) Repetitive calcium transients and the role of calcium in exocytosis and cell cycle activation in the mouse egg. Dev Biol 149:80–89
80. Knott JG, Kurokawa M, Fissore RA, Schultz RM, Williams CJ (2005) Transgenic RNA interference reveals role for mouse sperm phospholipase Czeta in triggering Ca^{2+} oscillations during fertilization. Biol Reprod 72:992–996
81. Kouchi Z, Fukami K, Shikano T, Oda S, Nakamura Y, Takenawa T, Miyazaki S (2004) Recombinant phospholipase Czeta has high Ca^{2+} sensitivity and induces Ca^{2+} oscillations in mouse eggs. J Biol Chem 279:10408–10412
82. Kouchi Z, Shikano T, Nakamura Y, Shirakawa H, Fukami K, Miyazaki S (2005) The role of EF-hand domains and C2 domain in regulation of enzymatic activity of phospholipase Czeta. J Biol Chem 280:21015–21021
83. Krukowska A, Tarkowski AK (2005) Mouse zygotes with one diploid pronucleus formed as a result of ICSI can develop normally beyond birth. Mol Reprod Dev 72:346–353
84. Kubiak JZ (1989) Mouse oocytes gradually develop the capacity for activation during the metaphase II arrest. Dev Biol 136:537–545
85. Kuroda K, Ito M, Shikano T, Awaji T, Yoda A, Takeuchi H, Kinoshita K, Miyazaki S (2006) The role of X/Y linker region and N-terminal EF-hand domain in nuclear translocation and Ca^{2+} oscillation-inducing activities of phospholipase Czeta, a mammalian egg-activating factor. J Biol Chem 281:27794–27805
86. Kurokawa M, Sato K, Wu H, He C, Malcuit C, Black SJ, Fukami K, Fissore RA (2005) Functional, biochemical, and chromatographic characterization of the complete [Ca2+]i oscillation-inducing activity of porcine sperm. Dev Biol 282:376–392

87. Kurokawa M, Yoon SY, Alfandari D, Fukami K, Sato K, Fissore RA (2007) Proteolytic processing of phospholipase C zeta and $[Ca^{2+}]_i$ oscillations during mammalian fertilization. Dev Biol 312:407–418
88. Kyozuka K, Deguchi R, Mohri T, Miyazaki S (1998) Injection of sperm extract mimics spatiotemporal dynamics of Ca2+ responses and progression of meiosis at fertilization of ascidian oocytes. Development 125:4099–4105
89. Lalancette C, Miller D, Li Y, Krawetz SA (2008) Paternal contributions: new functional insights for spermatozoal RNA. J Cell Biochem 104:1570–1579
90. Larman MG, Saunders CM, Carroll J, Lai FA, Swann K (2004) Cell cycle-dependent Ca^{2+} oscillations in mouse embryos are regulated by nuclear targeting of PLCzeta. J Cell Sci 117(Pt12):2513–2521
91. Lawrence Y, Whitaker M, Swann K (1997) Sperm-egg fusion is the prelude to the initial Ca^{2+} increase at fertilization in the mouse. Development 124:233–241
92. Lee SB, Varnai P, Balla A, Jalink K, Rhee SG, Balla T (2004) The pleckstrin homology domain of phosphoinositide-specific phopholipase C delta (4) is not a critical determinant of the membrane localization of the enzyme. J Biol Chem 279:24362–24371
93. Lee B, Yoon SY, Malcuit C, Parys JB, Fissore RA (2010) Inositol 1,4,5-trisphosphate receptor 1 degradation in mouse eggs and impact on [Ca2+]i oscillations. J Cell Physiol 222:238–247
94. Lefèvre B, Pesty A, Courtot AM, Martins CV, Broca O, Denys A, Arnault E, Poirot C, Avazeri N (2007) The phosphoinositide-phospholipase C (PI-PLC) pathway in the mouse oocyte. Crit Rev Eukaryot Gene Expr 17:259–269
95. Leyton L, LeGuen P, Bunch D, Saling PM (1992) Regulation of mouse gamete interaction by a sperm tyrosine kinase. Proc Natl Acad Sci USA 89:11692–11695
96. Liu M, Sims D, Calarco P, Talbot P (2003) Biochemical heterogeneity, migration, and pre-fertilization release of mouse oocyte cortical granules. Reprod Biol Endocrinol 1:77
97. Lorca T, Cruzalegui FH, Fesquet D, Cavadore JC, Méry J, Means A, Dorée M (1993) Calmodulin-dependent kinase II mediates inactivation of MPF and CSF upon fertilization of Xenopus eggs. Nature 366:270–273
98. Malcuit C, Kurokawa M, Fissore RA (2006) Calcium oscillations and mammalian egg activation. J Cell Physiol 206:565–573
99. Marangos P, FitzHarris G, Carroll J (2003) Ca^{2+} oscillations at fertilization in mammals are regulated by the formation of pronuclei. Development 130:1461–1472
100. Markoulaki S, Matson S, Ducibella T (2004) Fertilization stimulates long-lasting oscillations of CaMKII activity in mouse eggs. Dev Biol 272:15–25
101. McLaughlin S, Wang J, Gambhir A, Murray D (2002) PIP_2 and proteins: interactions, organization, and information flow. Annu Rev Biophys Biomol Struct 31:151–175
102. Mehlmann LM, Mikoshiba K, Kline D (1996) Redistribution and increase in cortical inositol 1,4,5-trisphosphate receptors after meiotic maturation of the mouse oocyte. Dev Biol 180:489–498
103. Miyazaki S (1998) Inositol 1,4,5-trisphosphate-induced calcium release and guanine nucleotide-binding protein-mediated periodic calcium rises in golden hamster eggs. J Cell Biol 106:345–353
104. Miyazaki S (2006) Thirty years of calcium signals at fertilization. Semin Cell Dev Biol 17:233–243
105. Miyazaki S, Ito M (2006) Calcium signals for egg activation in mammals. J Pharmacol Sci 100:545–552
106. Miyazaki S, Shirakawa H, Nakada K, Honda Y (1993) Essential role of the inositol 1,4,5-trisphosphate receptor/Ca2+ release channel in Ca^{2+} waves and Ca^{2+} oscillations at fertilization of mammalian eggs. Dev Biol 158:62–78
107. Mizushima S, Takagi S, Ono T, Atsumi Y, Tsukada A, Saito N, Shimada K (2008) Developmental enhancement of intracytoplasmic sperm injection (ICSI) – Generated quail embryos by phospholipase C zeta cRNA. J Poult Sci 45:152–158
108. Murase T, Roldan ERS (1996) Progesterone and the zona pellucida activate different transducing pathways in the sequence of events leading to diacylglycerol generation during mouse sperm acrosomal exocytosis. Biochem J 320:1017–1023

109. Nakahara M, Shimozawa M, Nakamura Y, Irino Y, Morita M, Kudo Y, Fukami K (2005) A novel phospholipase C, PLC(eta)2, is a neuron-specific isozyme. J Biol Chem 280: 29128–29134
110. Nakamura Y, Fukami K (2009) Roles of phospholipase C isozymes in organogenesis and embryonic development. Physiology 24:332–341
111. Nakanishi T, Ishibashi N, Kubota H, Inoue K, Ogonuki N, Ogura A, Kashiwabara S, Baba T (2008) Birth of normal offspring from mouse eggs activated by a phospholipase C zeta protein lacking three EF-hand domains. J Reprod Dev 54:244–249
112. Nasr-Esfahani MH, Deemeh MR, Tavalaee M (2009) Artificial oocyte activation and intracytoplasmic sperm injection. Fertil Steril 94:520–526
113. Nishizuka Y (1988) The molecular heterogeneity of protein kinase C and its implications for cellular regulation. Nature 334:661–665
114. Nomikos M, Blayney LM, Larman MG, Campbell K, Rossbach A, Saunders CM, Swann K, Lai FA (2005) Role of phospholipase C-zeta domains in Ca^{2+}-dependent phosphatidylinositol 4,5-bisphosphate hydrolysis and cytoplasmic Ca^{2+} oscillations. J Biol Chem 280:31011–31018
115. Nomikos M, Mulgrew-Nesbitt A, Pallavi P, Mihalyne G, Zaitseva I, Swann K, Lai FA, Murray D, McLaughlin S (2007) Binding of phosphoinositide-specific phospholipase C-zeta (PLC-zeta) to phospholipid membranes: potential role of an unstructured cluster of basic residues. J Biol Chem 282:16644–16653
116. Nomikos M, Elgmati K, Theodoridou M, Calver B, Cumbes B, Nounesis G, Swann K, Lai FA (2011) Male infertility-linked point mutation disrupts the Ca2+ oscillation-inducing and PIP2 hydrolysis activity of sperm PLCζ. Biochem J 434:211–217
117. Ozil JP, Markoulaki S, Toth S, Matson S, Banrezes B, Knott JG, Schultz RM, Huneau D, Ducibella T (2005) Egg activation events are regulated by the duration of a sustained [Ca2+] cyt signal in the mouse. Dev Biol 282:39–54
118. Ozil JP, Banrezes B, Tóth S, Pan H, Schultz RM (2006) Ca2+ oscillatory pattern in fertilized mouse eggs affects gene expression and development to term. Dev Biol 300:534–544
119. Parrington J, Davis LC, Galione A, Wessel G (2007) Flipping the switch: how a sperm activates the egg at fertilization. Dev Dyn 236:2027–2038
120. Pesty A, Avazeri N, Lefevre B (1998) Nuclear calcium release by InsP3-receptor channels plays a role in meiosis reinitiation in the mouse oocyte. Cell Calcium 24:239–251
121. Phillips DM, Shalgi R (1980) Surface architecture of the mouse and hamster zona pellucida and oocyte. J Ultrastruct Res 72:1–12
122. Platts AE, Dix DJ, Chemes HE, Thompson KE, Goodrich R, Rockett JC, Rawe VY, Quintana S, Diamond MP, Strader LF, Krawetz SA (2007) Success and failure in human spermatogenesis as revealed by teratozoospermic RNAs. Hum Mol Genet 16:763–773
123. Publicover S, Harper CV, Barratt C (2007) $[Ca^{2+}]_i$ signalling in sperm – making the most of what you've got. Nat Cell Biol 9:235–242
124. Rebecchi MJ, Pentyala SN (2000) Structure, function, and control of phosphoinositide-specific phospholipase C. Physiol Rev 80:1291–1335
125. Rhee SG (2001) Regulation of phosphoinositide-specific phospholipase C. Annu Rev Biochem 70:281–312
126. Rizo J, Südhof TC (1998) C2-domains, structure and function of a universal Ca^{2+}-binding domain. J Biol Chem 273:15879–15882
127. Rogers NT, Hobson E, Pickering S, Lai FA, Braude P, Swann K (2004) Phospholipase Czeta causes Ca^{2+} oscillations and parthenogenetic activation of human oocytes. Reproduction 128:697–702
128. Rogers NT, Halet G, Piao Y, Carroll J, Ko MS, Swann K (2006) The absence of a Ca(2+) signal during mouse egg activation can affect parthenogenetic preimplantation development, gene expression patterns, and blastocyst quality. Reproduction 132:45–57
129. Roldan ER, Shi QX (2007) Sperm phospholipases and acrosomal exocytosis. Front Biosci 12:89–104
130. Runft LL, Carroll DJ, Gillett J, Giusti AF, O'Neill FJ, Foltz KR (2004) Identification of a starfish egg PLC-gamma that regulates Ca2+ release at fertilization. Dev Biol 269:220–236

131. Santella L, Lim D, Moccia F (2004) Calcium and fertilization: the beginning of life. Trends Biochem Sci 29:400–408
132. Saunders CM, Larman MG, Parrington J, Cox LJ, Royse J, Blayney LM, Swann K, Lai FA (2002) PLC zeta: a sperm-specific trigger of Ca(2+) oscillations in eggs and embryo development. Development 129:3533–3544
133. Saunders CM, Swann K, Lai FA (2007) PLC zeta, a sperm-specific PLC and its potential role in fertilization. Biochem Soc Symp 74:23–36
134. Schultz RM, Kopf GS (1995) Molecular basis of mammalian egg activation. Curr Top Dev Biol 30:21–62
135. Singal T, Dhalla NS, Tappia PS (2004) Phospholipase C may be involved in norepinephrine-induced cardiac hypertrophy. Biochem Biophys Res Commun 320:1015–1019
136. Sone Y, Ito M, Shirakawa H, Shikano T, Takeuchi H, Kinoshita K, Miyazaki S (2005) Nuclear translocation of phospholipase C-zeta, an egg-activating factor, during early embryonic development. Biochem Biophys Res Commun 330:690–694
137. Song C, Hu CD, Masago M, Kariyai K, Yamawaki-Kataoka Y, Shibatohge M, Wu D, Satoh T, Kataoka T (2001) Regulation of a novel human phospholipase C, PLCepsilon, through membrane targeting by Ras. J Biol Chem 276:2752–2757
138. Spehr M, Gisselmann G, Poplawski A, Riffell JA, Wetzel CH, Zimmer RK, Hatt H (2003) Identification of a testicular odorant receptor mediating human sperm chemotaxis. Science 299:2054–2058
139. Stallings JD, Zeng YX, Narvaez F, Rebecchi MJ (2008) Phospholipase C-delta1 expression is linked to proliferation, DNA synthesis, and cyclin E levels. J Biol Chem 283:13992–14001
140. Stitzel ML, Seydoux G (2007) Regulation of the oocyte-to-zygote transition. Science 316:407–408
141. Stricker SA (1999) Comparative biology of calcium signalling during fertilisation and egg activation in mammals. Dev Biol 211:157–176
142. Suh PG, Park JI, Manzoli L, Cocco L, Peak JC, Katan M, Fukami K, Kataoka T, Yun S, Ryu SH (2008) Multiple roles of phosphoinositide-specific phospholipase C isozymes. BMB Rep 41:415–434
143. Swain JE, Ding J, Wu J, Smith GD (2008) Regulation of spindle and chromatin dynamics during early and late stages of oocyte maturation by aurora kinases. Mol Hum Reprod 14:291–299
144. Swann K (1990) A cytosolic sperm factor stimulates repetitive calcium increases and mimics fertilization in hamster eggs. Development 110:1295–1302
145. Swann K, Ozil JP (1994) Dynamics of the calcium signal that triggers mammalian egg activation. Int Rev Cytol 152:183–222
146. Swann K, Yu Y (2008) The dynamics of calcium oscillations that activate mammalian eggs. Int J Dev Biol 52:585–594
147. Swann K, Larman MG, Saunders CM, Lai FA (2004) The cytosolic sperm factor that triggers Ca2+ oscillations and egg activation in mammals is a novel phospholipase C: PLCzeta. Reproduction 127:431–439
148. Swann K, Saunders CM, Rogers NT, Lai FA (2006) PLCzeta (zeta): a sperm protein that triggers Ca2+ oscillations and egg activation in mammals. Semin Cell Dev Biol 17:264–273
149. Taylor SL, Yoon SY, Morshedi MS, Lacey DR, Jellerette T, Fissore RA, Oehninger S (2010) Complete globozoospermia associated with PLCzeta deficiency treated with calcium ionophore and ICSI results in pregnancy. Reprod Biomed Online 20:559–564
150. Tokmakov AA, Sato KI, Iwasaki T, Fukami Y (2002) Src kinase induces calcium release in Xenopus egg extracts via PLCgamma and IP3-dependent mechanism. Cell Calcium 32: 11–20
151. Tomes CN, McMaster CR, Saling PM (1996) Activation of mouse sperm phosphatidylinositol-4,5 bisphosphate - phospholipase C by zona pellucida is modulated by tyrosine phosphorylation. Mol Reprod Dev 43:196–204
152. Tosti E (2010) Dynamic roles of ion currents in early development. Mol Reprod Dev 77:856–867

153. Tóth S, Huneau D, Banrezes B, Ozil JP (2006) Egg activation is the result of calcium signal summation in the mouse. Reproduction 131:27–34
154. Vanderheyden V, Wakai T, Bultynck G, De Smedt H, Parys JB, Fissore RA (2009) Regulation of inositol 1,4,5-trisphosphate receptor type 1 function during oocyte maturation by MPM-2 phosphorylation. Cell Calcium 46:56–64
155. Vermassen E, Parys JB, Mauger JP (2004) Subcellular distribution of the inositol 1,4,5-trisphosphate receptors: functional relevance and molecular determinants. Biol Cell 96:3–17
156. Visconti PE, Galantino-Homer H, Moore GD, Bailey JL, Ning X, Fornes M, Kopf GS (1998) The molecular basis of sperm capacitation. J Androl 19:242–248
157. Walensky LD, Snyder SH (1995) Inositol 1,4,5- trisphosphate receptors selectively localized to the acrosomes of mammalian sperm. J Cell Biol 130:857–869
158. Webb SE, Miller AL (2006) Ca2+ signaling and early embryonic patterning during the blastula and gastrula periods of zebrafish and Xenopus development. Biochim Biophys Acta 1763:1192–1208
159. Whitaker M (2006) Calcium at fertilization and in early development. Physiol Rev 86:25–88
160. Whitaker M (2008) Calcium signalling in early embryos. Philos Trans R Soc Lond B Biol Sci 363:1401–1418
161. Wolkowicz MJ, Shetty J, Westbrook A, Klotz K, Jayes F, Mandal A, Flickinger CJ, Herr JC (2003) Equatorial segment protein defines a discrete acrosomal subcompartment persisting throughout acrosomal biogenesis. Biol Reprod 69:735–745
162. Wu H, He CL, Fissore RA (1997) Injection of a porcine sperm factor triggers calcium oscillations in mouse oocytes and bovine eggs. Mol Reprod Dev 46:176–189
163. Wu AT, Sutovsky P, Manandhar G, Xu W, Katayama M, Day BN, Park KW, Yi YJ, Xi YW, Prather RS, Oko R (2007) PAWP, a sperm-specific WW domain-binding protein, promotes meiotic resumption and pronuclear development during fertilization. J Biol Chem 282:12164–12175
164. Xu Z, Williams CJ, Kopf GS, Schutlz RM (2003) Maturation-associated increase in IP3 receptor type 1: role in conferring increased IP3 sensitivity and Ca^{2+} oscillatory behavior in mouse eggs. Dev Biol 254:163–171
165. Yamaga M, Fujii M, Kamata H, Hirata H, Yagisawa H (1999) Phospholipase C-delta1 contains a functional nuclear export signal sequence. J Biol Chem 274:28537–28541
166. Yin X, Eckberg WR (2009) Characterization of phospholipases C beta and gamma and their possible roles in Chaetopterus egg activation. Mol Reprod Dev 76:460–470
167. Yoda A, Oda S, Shikano T, Kouchi Z, Awaji T, Shirakawa H, Kinoshita A, Miyazaki S (2004) Ca^{2+} oscillation-inducing phospholipase C zeta expressed in mouse eggs is accumulated to the pronucleus during egg activation. Dev Biol 268:245–257
168. Yoneda A, Kashima M, Yoshida S, Terada K, Nakagawa S, Sakamoto A, Hayakawa K, Suzuki K, Ueda J, Watanabe T (2006) Molecular cloning, testicular postnatal expression, and oocyte-activating potential of porcine phospholipase C zeta. Reproduction 132:393–401
169. Yoon SY, Fissore RA (2007) Release of phospholipase C zeta and $[Ca^{2+}]_i$ oscillation-inducing activity during mammalian fertilization. Reproduction 134:695–704
170. Yoon SY, Jellerette T, Salicioni AM, Lee HC, Yoo MS, Coward K, Parrington J, Grow D, Cibelli JB, Visconti PE et al (2008) Human sperm devoid of PLC, zeta 1 fail to induce Ca^{2+} release and are unable to initiate the first step of embryo development. J Clin Invest 118:3671–3681
171. Young C, Grasa P, Coward K, Davis LC, Parrington J (2009) Phospholipase C zeta undergoes dynamic changes in its pattern of localization in sperm during capacitation and the acrosome reaction. Fertil Steril 91:2230–2242
172. Yu Y, Halet G, Lai FA, Swann K (2008) Regulation of diacylglycerol production and protein kinase C stimulation during sperm- and PLCzeta-mediated mouse egg activation. Biol Cell 100:633–643
173. Yu Y, Saunders CM, Lai FA, Swann K (2008) Preimplantation development of mouse oocytes activated by different levels of human phospholipase C zeta. Hum Reprod 23:365–373

174. Zhao K, Wang W, Rando OJ, Xue Y, Swiderek K, Kuo A, Creabtree GR (1998) Rapid and phosphoinositol-dependent binding of the SWI/SNF-like BAF complex to chromatin after T lymphocyte receptor signaling. Cell 95:625–636
175. Zhou Y, Wing MR, Sondek J, Harden TK (2005) Molecular cloning and characterization of PLCeta2. Biochem J 391:667–676

Chapter 51
Nuclear Calcium Signaling and Its Involvement in Transcriptional Regulation in Plants

Benoit Ranty, Valérie Cotelle, Jean-Philippe Galaud, and Christian Mazars

Abstract Calcium is a key second messenger in signaling pathways associated with developmental and adaptive processes in plants. Stimulus-specific calcium signals, considered as calcium signatures, are translated into appropriate cellular responses through the action of various calcium-binding proteins and downstream effectors. We review here recent progress made in calcium signaling in the nucleus of plant cell. Experimental evidences show that nuclei can generate calcium signals on their own and point out the importance of calcium in the regulation of gene transcription. Future directions are given concerning the need to elucidate the mechanisms involved in the regulation of nuclear calcium homeostasis, the conversion of calcium signals into transcriptional responses or other fundamental downstream nuclear functions. Overall, a better understanding of nuclear signaling will be useful to get an integrated picture of the signaling network of the plant cell.

Keywords Nuclear calcium signaling • Aequorin • Calcium sensors • Calmodulin • Transcriptional regulation

Introduction

A chapter dealing with calcium signaling in plants could appear as an intruder in a textbook mostly dedicated to signaling in animals. However, a closer look at calcium signaling in plants reveals that generation of calcium signals and the way

B. Ranty • V. Cotelle • J.-P. Galaud • C. Mazars (✉)
Université de Toulouse, Université Paul Sabatier, UMR 5546, Laboratoire de Recherche en Sciences végétales, BP 42617, Auzeville, F-31326 Castanet-Tolosan, France

CNRS, UMR 5546, BP 42617, Auzeville, F-31326 Castanet-Tolosan, France
e-mail: ranty@lrsv.ups-tlse.fr; cotelle@lrsv.ups-tlse.fr; galaud@lrsv.ups-tlse.fr; mazars@lrsv.ups-tlse.fr

M.S. Islam (ed.), *Calcium Signaling*, Advances in Experimental Medicine and Biology 740, DOI 10.1007/978-94-007-2888-2_51,

they are shaped and decoded are roughly conserved in photosynthetic and non photosynthetic eukaryotes, thus making this chapter quite in the scope of this book. Nevertheless, plants also possess unique features that we will try to point out in this chapter. Calcium is a macronutrient with key structural and signaling roles that can act as an osmoticum in the vacuolar compartment, as a stabilizing agent in plant cell walls and of course as an ubiquitous second messenger [1]. In plants, calcium signaling studies really emerged in the late 1980s early 1990s, thanks to the cloning of the natural calcium probe aequorin from the jellyfish [2, 3] and the pioneering work performed by Anthony J. Trewavas and Marc Knight that used this calcium probe as a tool to monitor real-time calcium changes in plant cells in response to environmental cues [4, 5]. The cloning of the aequorin gene was really a breakthrough in the way to approach free calcium measurements in plants because it immediately alleviated the difficulties encountered using the first generation of fluorescent calcium probes. Indeed, according to the tissues, the type of cells and the nature of plants used, free diffusion of these calcium probes was impaired by the thick cell wall and ionic charges. As an alternative, microinjection as performed in animal cells was really a challenge due to the necessity to thwart the high cell turgor encountered with plant cells. In addition, it is well known from animal studies that reliable monitoring of free calcium changes with fluorescent chemical probes, generate problems specially in the nucleus where they appear brighter than in the cytosol. Indeed, it is known that their affinity for Ca^{2+} is dependent on their environment [6–8]. The discovery of aequorin as the first calcium probe encoded by a specific gene immediately boosted the field due to the flexibility associated with genetic methods such as molecular engineering and the great ease to perform *Agrobacterium*-mediated transformation of model plants. These advantages stimulated some researchers to design new targetable calcium probes such as cameleon [9], pericam [10], easy to express in plant cells and able to overcome some limitations of the aequorin probe in calcium imaging. Most data concerning calcium measurements in plants were obtained with these encoded calcium probes. The diversity of calcium signals observed led to the conclusion that calcium signals generated in response to biotic or abiotic stimuli could encode specificity through their spatio-temporal and amplitude parameters as previously noticed in animal cells [11, 12]. This concept of calcium fingerprint also accepted in plant field [13–15] was concomitantly accompanied by the need to answer the crucial question of how these calcium signals are decoded to achieve specificity. Key elements of the calcium toolkit as defined in animals [12] are required to shape and relay the calcium signal to the final adaptive response. Some of these tools (channels, transporters, calcium-binding proteins) were discovered upon the completion of the sequencing of plant genomes such as the one of *Arabidopsis thaliana* [16]. Indeed, such available and complete database favored the *in silico* data mining using already known Ca^{2+}-binding domains and motifs like the "EF-hand" motif [17]. This approach ended in the set up of a diversified repertoire of about 250 EF-hand proteins in *Arabidopsis*, slightly larger than in animals, including calmodulin (CaM) and calmodulin-like proteins [18, 19]. In contrast to animals where only one CaM isoform is present unexpectedly 3 CaM isoforms

and 50 CaM-like proteins are encoded by the *Arabidopsis* genome [20] and Table 51.1. Furthermore, bifunctional calcium-sensors harbouring a CaM-like domain associated with a Ser/Thr protein kinase domain on a single polypeptide and known as CDPKs (Calcium-Dependent Protein Kinase) are unique to plants [50]. Besides these plant specific calcium sensors, other calcium-regulated proteins are shared by plants and animals such as calcium-regulated transcription factors (TFs) belonging to the calmodulin binding transcription activator (CAMTA) group [51]. In this particular case, calcium studies devoted to plants have first led to the demonstration that CAMTAs function as DNA-binding proteins.

From data associated with calcium signaling in plants, two main surprising points arose: the larger diversity of EF-hand proteins able to decode the calcium signals and the surprising lack of knowledge on the diversity and structures of calcium channels, in comparison to what is known in animals. More particularly, calcium channels associated with internal calcium pools such as the endoplasmic reticulum (ER) supposed to be stimulated by inositol 1,4,5 trisphosphate (IP_3) or cyclic ADP-ribose (cADPR) are still undiscovered in plants. The large family of animal Ca^{2+}-permeable transient receptor potential (TRP) channels [52] have no counterparts in the model plant *Arabidopsis thaliana*, although some orthologous members have been found in the genome of the photosynthetic algae *Chlamydomonas* [48]. Nevertheless, a pharmacological profile similar to the animal TRPM3 channel [53] has been observed in isolated nuclei of tobacco cells [28].

Although most of available data concerning calcium signaling in plants are related to calcium signals and their decoding processes in the cytosol only, studies of nuclear calcium signaling are now gaining interest because it is admitted that each cell compartment can use its own calcium signatures as part of the signaling pathway, to drive downstream signaling events such as modification of gene transcription. Analyzing gene transcription in hippocampal neurons, Hardingham and his collaborators could demonstrate that nuclear calcium signals activate gene transcription by a mechanism that is distinct from gene regulation driven by cytoplasmic calcium signals [54]. This seminal result highlighted the role of calcium signatures and the importance of calcium compartmentalization in the mounting of cell responses. Two independent calcium signatures in two different compartments would help to explain how response specificity could be achieved in response to various environmental stimuli using the calcium ion as an ubiquitous second messenger. Due to the presumed importance of nuclear calcium signaling in regulating nuclear events associated with cell division, development, defense or programmed cell death, this facet of calcium signaling is presently gaining increasing attention in both animal and plant fields as highlighted by recent reviews [32, 55–59]. For these reasons, we propose to give here the current view of nuclear calcium signaling in plants focusing on data reporting nuclear calcium signals both in whole cells and isolated nuclei in response to environmental cues. A particular emphasis will be given to possible decoding processes in the nucleus and their consequences on transcriptional regulation.

Table 51.1 Comparative analysis of the calcium toolkit concerning calcium transport and calcium-binding proteins from *Arabidopsis thaliana* and *Homo sapiens*

		Arabidopsis thaliana			*Homo Sapiens*	
Organism		Number of homologous proteins*	Nuclear localisation	Other localisation	Number of homologous proteins*	Nuclear localisation
Transporters:						
Channels	VDCC type HVA (L)	1 (TPC1)[21]	No	Tonoplast	6+1 (TPC1)	No
	ROCC :					
	CNGC	20	3 Suspected [22]	Plasmalemma	4	No
	GluR (AMPA)	20	suspected [23]		5	Yes [24, 25]
	Ryanodine receptor	0			8	Yes [26, 27]
	IP3 receptor	0	Suspected [28]		3	Yes [29, 30]
	NAADP receptor	0	No		?	Yes [31]
	cADPR receptor	?	Suspected		?	Yes [31]
Pumps	P-Type Ca^{2+} ATPase		6 Suspected [22]			Yes [32]
	Type IIA	4[33]		Eca3 (plastid) Eca1,2 (ER)	8	
	Type IIB	10[33]		Aca1 (plastid) Aca4,11 (tonoplast) Aca8,9,10 (plasmalemma)	11	
Ca^{2+} exchangers	Ca^{2+}/H^{+}	8 and 6 [34]	?		0	Yes [35]
	Ca^{2+}/Na^{+}	0	?		3	
	$Ca^{2+}/Na^{+}/K^{+}$	5	?		5	

Calcium binding proteins	EF-hand proteins					
	CaM	7	Yes [36]	Yes (plasmalemma) [37]	7 ?	Yes [32]
	CaM-like	50	Yes [38]		0 ?	
	Centrin (caltractin)	2	Yes [39]		5	
	Calcineurin B	0			5	
	Calcineurin B-like	10	Yes [40]	Yes (tonoplast, plasmalemma) [40]	0 ?	
	CCaMK	0 but 2 in legumes	Yes in legumes [41]		6	
	CaMK	3			4	
	CDPK	34	Yes [42]	Yes (plasmalemma, peroxisome) [43]	0	
	CRK (CDPK-related)	4	?		0	
	Calcium/phospholipid binding proteins			?	19	
	Annexins	8	[44]	?	13	Yes [45]
	Phospholipase C	6	?			Yes [46, 47]
	Calcium storage protein			?	2	
	Calreticulin	5	?			

Specific cell sublocalizations have been indicated when known. * numbers indicating the number of homologous proteins are taken from the previous work of Nagata et al. [49] except for numbers bearing specific references. Additional information can also be obtained from the work of Merchant et al. [48]

Monitoring Calcium Signals in the Nuclei of Plant Cells

Different lines of evidence mainly obtained from animal systems have shown that nuclei contain calcium channels and transporters that could shape calcium signals within the nucleus [29, 30, 35, 60] and Table 51.1. The main calcium reservoir supposed to be used by these channels and transporters is the nuclear envelope (NE), a double membrane that separates the cytoplasm from the nucleoplasm. The space between the inner and the outer membrane called perinuclear space or cisternae is in continuity with the lumen of the ER that contains high concentrations of calcium. Thus, this organelle is supposed to fuel the perinuclear space with calcium ions. However, the NE is punctuated with nuclear pores complexes (NPC) of wide diameter (up to 110–120 nm in nuclei of *Xenopus* oocytes [61], allowing the translocation of large molecules (proteins, RNAs) and suggesting, that ions such as calcium can freely diffuse. This assumption led to the idea that changes in free calcium concentration measured in the nucleoplasm could be the result of the free diffusion of calcium ions from the cytosol through NPCs, providing an alternative explanation for the generation of nuclear calcium signals. During years these two views of nuclear calcium signaling had their own supporters and detractors and the source of the nuclear calcium signals remained a very controversial issue, as reported in the successive symposia on calcium signaling [60, 62, 63].

In plants, the origin of nuclear calcium may also be questioned because of the structure of the nuclear envelope which is similar to that of animal nuclei and is punctuated with one of the highest density of NPCs (40–50 *per* μm^2) found so far in eukaryotes [64]. However, much less experimental evidences are available to sustain a debate on the origin of nuclear calcium signals. As reported in the introduction, nuclear calcium studies in plants were really boosted by the emergence of aequorin constructs addressed to the nucleoplasm. Using *Nicotiana plumbaginifolia* seedlings constitutively expressing a chimera aequorin, van der Luit and collaborators reported calcium changes in the nucleus in response to either wind or cold shock [65]. This study was the first report on nuclear calcium signals in plants but also the first to suggest that transcription can be differentially regulated by nuclear calcium signals. These authors also suggested that wind-induced expression of the tobacco CaM isoform NpCaM1 is regulated by a signaling pathway depending on nuclear calcium whereas its expression in response to cold is regulated by a cytosolic-dependent calcium pathway [65].

At the same period, using protoplasts of tobacco BY-2 cells expressing a nucleoplasmin-aequorin construct, Pauly et al. showed that mastoparan was able to induce a dose-dependent calcium response in the nucleus, delayed with respect to the cytosolic calcium response [66]. The higher the concentration, the higher the delay was shortened. Using the same biological model, they further investigated the nuclear response at the whole cell level using changes in osmolarity as an easily quantifiable physical stimulus. Lowering the osmolarity of the culture medium from 250 to 100 mosmol by diluting the medium with water, induced an immediate cytosolic $[Ca^{2+}]$ change with two successive calcium peaks appearing at 15 and 60 s respectively.

The cytosolic calcium level remained elevated (0.5 μM) even after 5 min of incubation while a rapid mono-phasic increase in nuclear [Ca^{2+}] concomitant with the first cytosolic Ca^{2+} peak, was observed. This nuclear peak reached its maximum amplitude at 46 s and the nuclear calcium level went down with the same kinetics than the cytosolic calcium. In contrast, increasing the osmolarity from 250 to 400 mosmol elicited a smaller but identical biphasic response in cytosolic [Ca^{2+}] without inducing changes in nuclear [Ca^{2+}] [67]. These results pointed out that cytosolic calcium do not freely diffuse into the nucleoplasm through NPCs, even when cytosolic concentrations reached levels higher than 1 μM [67].The second conclusion drawn from these results was the ability of the plant cell to discriminate stimuli (hypo *versus* hyper osmotic shocks) and to transduce them as distinct cell calcium signatures involving either the two compartments, nucleus and cytosol, or only the cytosol. This ability of the nucleus to convert external stimuli into calcium responses was not restricted to abiotic stimuli. Using pathogen-derived elicitors such as cryptogein, a polypeptide secreted by the oomycete *Phytophthora cryptogea* able to promote defence responses in plants, it was possible to elicit calcium transients in the nucleus of tobacco cells in addition to those induced in the cytosol [68, 69]. Interestingly, nuclear Ca^{2+} variations occurred 15 min after the cytosolic Ca^{2+} peak, suggesting that increases in $[Ca^{2+}]_{nuc}$ were likely not due to a simple diffusion of cytosolic calcium through the NPCs. All together, these data obtained on tobacco cells demonstrated that changes in nuclear [Ca^{2+}] may be disconnected from cytosolic Ca^{2+} transients. Nuclear calcium responses are also observed in beneficial plant-microbe interactions. During the establishment of symbiosis between legumes and *rhizobia,* a molecular dialog takes place between the two partners. Flavonoïds are produced by the roots of the plant to attract the bacteria which in turn will produce specific lipochito-oligosaccharides signals known as nodulation factors (NFs) [70], able to activate a plethora of events in the root hair cells [71]. A crucial role of the calcium signal has been demonstrated in the establishment of this symbiosis. The calcium signal is composed of an immediate cytosolic calcium flux followed by a delayed train of calcium oscillations that are absolutely required for the formation of the root nodule which is the nitrogen-fixing organ [72, 73]. It was initially shown that NF-induced calcium spiking was taking place around the nucleus and was then diffusing through the cell [72]. Using a nucleoplasmin-cameleon fusion (Nup YC2.1) addressed specifically to the nucleus, Sieberer et al. showed that NFs trigger persistent nuclear calcium oscillations within the growing root hairs and that the initial increase in nuclear calcium originate from the nucleus periphery [74]. Similarly, occurrence of nuclear calcium signals was also observed during the arbuscular mycorrhizal symbiosis (AM) in legume and nonlegume plants. Upon contact between the hyphen and the root, an adhesion structure develops on non root hair epidermal cells referred to as atrichoblasts [75]. Using the nuclear-targeted "cameleon' calcium probe, Chabaud et al. reported sustained nuclear calcium spiking in atrichoblasts in both legume and non legume [76]. These studies showed that the nucleus can generate calcium signals in response to bacterial and AM symbiosis, but the relationship between cytosolic and nuclear calcium in this context is still an open question.

Generating Nuclear Calcium Signals Independently of Cytosolic Calcium Signals

Among the available data concerning plant nuclear calcium responses, two scenarios have been reported: either the nuclear calcium response is lacking even when cytosolic calcium transient occurs, or the nuclear calcium response is delayed from several seconds to several minutes with respect to the cytosolic calcium response. Both cases suggest that nuclear calcium does not diffuse freely through the NPCs. The autonomy of the nucleus in generating its own calcium signals was definitely confirmed in a situation where the nucleus compartment was shown to be able to generate calcium transients in the absence of any cytosolic calcium changes. Such a situation was encountered during a structure-function study using jasmonates derivatives. These compounds are considered as important hormones involved in plant development and defence [77]. A series of biologically active or synthetic derivatives of jasmonic acid were applied on tobacco cells constitutively expressing aequorin either in the cytosol or in the nucleus. The structure-activity analysis revealed that jasmonates fall into three distinct classes: (1) compounds inducing calcium changes both in the cytosol and the nucleus, (2) compounds inactive on either compartments and (3) compounds inducing calcium transients selectively in the nucleus [78]. Isoleucine conjugates only belong to the third class. Interestingly one of them, the natural compound jasmonoyl-isoleucine, was recently found to be the one able to bind the SKP1 Cullin F-box protein E3 ubiquitin ligase (SCF^{COI1}) and to promote its association with the JAsmonate ZIM-domain (JAZ1) transcriptional repressor in order to allow JAZ1 degradation through the 26S proteasome [79]. Upon proteolysis of the JAZ1 repressor, the MYC2 transcription factor enhances transcription of jasmonate-responsive genes [80]. These data unambiguously demonstrate for the first time in plants and in the context of a major signaling pathway associated with plant defense and development, that the nucleus is able to elicit its own calcium signals independently of cytosolic calcium [78].

To investigate the possibility of the full autonomy of the nucleus in regulating its own calcium homeostasis, Xiong et al. purified functional nuclei from tobacco protoplasts [28]. These nuclei were challenged with various stimuli, mechanical, chemical (Long Chain Bases or LCBs) and physical ones (T°). All these stimuli externally applied to purified nuclei induced dose-dependent calcium responses completely disconnected from the external sources of calcium, and were controlled by the pH of the incubation medium. An important property of the purified nuclei was the lack of desensitization to successive mechanical stimulations indicating that a still unknown system was able to refill the calcium reservoir. A pharmacological approach performed to characterize the possible channel activities involved in the nuclear calcium responses suggested that IP_3 receptor (IP_3R) and/or TRP-like calcium activities could be involved in response to these stimuli. However, as mentioned in the introductory part, IP_3R or TRP-like proteins have not been found in upper plants so far (Table 51.1). Finally, in a recent study devoted to understand the role of calcium compartmentalization associated with the programmed cell death

induced by dihydrosphingosine (DHS) in tobacco cells, it was possible to selectively inhibit nuclear calcium signals with blockers of ionotropic glutamate receptors without affecting the cytosolic calcium changes. Such blocking prevented programmed cell death even in the presence of an unchanged calcium response in the cytosol [23]. These data attributed a crucial role to nuclear calcium signals in promoting programmed cell death in plants.

Modeling the Nuclear Calcium Homeostasis

The control of nuclear calcium homeostasis was evaluated using a simple mathematical model to simulate the data obtained with purified nuclei from tobacco cells [28]. The model was based upon the assumption that nucleoplasmic calcium is shaped by the balance between activities of Ca^{2+} channels and Ca^{2+} transporters in a closed system, *i.e* being independent of external calcium concentration [81].

Using such a model, the authors could fit the experimental calcium traces assuming the coordinated action of calcium channels and transporters likely located on the inner membrane of the NE. To be compatible with the measured kinetics, a very slow calcium buffer system was introduced in the model in addition to the calcium transporters. Such a system explains the continuous refilling of the NE store. This refilling is absolutely required to restore the resting level necessary to support successive calcium transients observed in response to successive mechanical stimulations. The average time constant of SERCA-ATPases [82] being compatible with the time constant range observed for the calcium decrease measured in the nucleoplasm of purified nuclei suggest their involvement. The modeling suggests that the variations of resting $[Ca^{2+}]_{nuc}$ induced by the temperature or the pH can be explained by an increase of the Ca^{2+} channel kinetic constants rather than by a decrease in transport activity. In the same way, the pH-dependence of the nuclear calcium dynamics may be due to simultaneous changes of the Ca^{2+}-binding capacity and the modulation of Ca^{2+} channel activity rather than Ca^{2+} re-uptake [81]. This model could explain the observed experimental results, but the molecular supports (channels, transporters) compatible with this model still remain to be characterized.

Sensing Calcium Signals in the Nucleus

How these nuclear calcium signals evoked by various stimuli can be decoded and used to control downstream events in the nucleus remains to be investigated. However some relevant data related to calcium binding proteins found in the nucleus can help to elucidate the putative role of these nuclear signals. Several nuclear processes including DNA replication, DNA repair, DNA degradation during programmed cell death and gene transcription are known to be linked to calcium signaling in animal and plant systems. In plants, available data mainly describe the

regulation of transcription by calcium and the search for calcium-cis elements, for review see [83–85]. Thus, data on the dynamics of the spatial distribution of calcium-binding proteins in plant cells in response to various stimuli implicate diverse types of calcium sensors including calmodulin (CaM), calmodulin-like proteins (CMLs) and calcium-dependent protein kinases (CDPKs) that are supposed to take part in the recognition of nuclear calcium signals. The presence of CaM in the plant cell nucleus and the identification of nuclear-localized CaM targets suggest the importance of CaM in nuclear calcium signaling [86]. In addition to CaM, CMLs and CDPKs, which belong to large protein families essentially found in plants, exhibit diverse sub-cellular localizations including the cytosol, the nucleus and the plasma membrane [87–89] and Table 51.1. It is now clear that intracellular trafficking of CMLs and CDPKs occurs in response to diverse stimuli and allows the formation of nuclear pools of these calcium sensors when required. For example, the partitioning of the calmodulin-like protein CaM53 in petunia between the plasma membrane and the nucleus is governed by light/dark exposure and the carbon status of the cell [37] (Fig. 51.1). Under light exposure or carbon-saturated conditions, CaM53 is associated to the plasma membrane through prenylation of its C-terminal extension whereas in the dark or under carbon starvation, the protein is targeted to the nucleus. Interestingly, the ectopic expression of the wild-type CaM53 or of a nuclear-localized mutant form in transgenic plants, promotes distinct phenotypes, suggesting that CaM53 controls specific signaling pathways in each cell compartment. Nuclear translocation of several CDPKs were also reported in response to osmotic and salt stress [42, 90]. The growing list of CDPK substrates and CML-interacting proteins including DNA-binding proteins, suggests a role for these calcium sensors in the regulation of gene expression. Moreover, the co-localization of CDPKs and CMLs with their respective targets in plant cell nucleus supports their involvement in nuclear calcium signaling [38, 91].

Converting Nuclear Calcium Signals into Transcriptional Responses

Calcium-Binding Proteins as Transcription Factors

In plants, accumulating data provide evidence for calcium-modulated transcriptional regulation through processes involving calcium-dependent phosphorylation or dephosphorylation of TFs, the binding of calcium sensors to TFs or the direct interaction of calcium-binding proteins with gene promoters. As observed with DREAM, a well-characterized calcium-binding transcriptional repressor in animals [92, 93], plant proteins bearing calcium-binding EF-hand motifs were identified as transcriptional regulators. *AtNIG1*, a salt stress-responsive gene in *Arabidopsis thaliana*, encodes a nuclear protein with a single EF-hand motif and a basic helix-loop-helix domain which specifically binds the E-box DNA sequence found in the

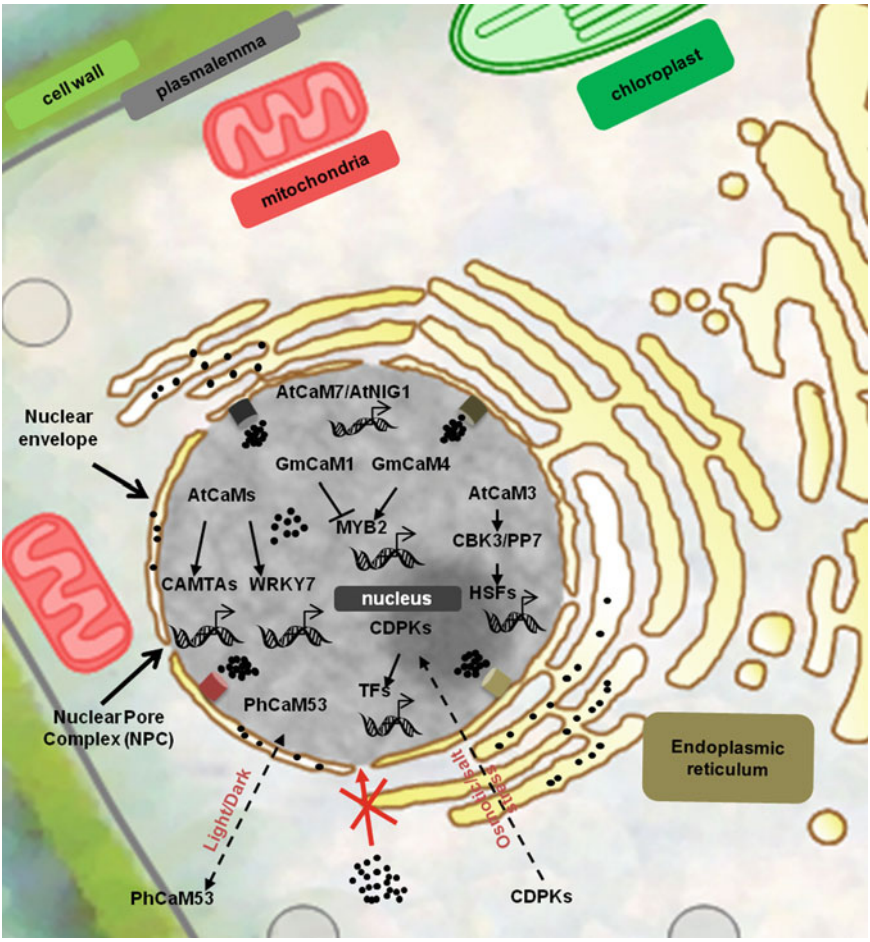

Fig. 51.1 Current view of nuclear calcium decoders able to regulate directly or indirectly gene transcription. The *cartoon* illustrates the absence of free diffusion of calcium through NPCs. *Dotted arrows* illustrate the translocation of calcium-sensing proteins. *Black dots* represent calcium ions. *Coloured cylinders* represent various putative calcium channels located on the inner membrane of the envelope. *CAMTA* Calmodulin binding transcription activator, *CBK3* calmodulin binding protein kinase 3, *CDPK* Calcium-dependent protein kinase, *GmCaM1* Glycine max calmodulin 1, *GmCaM4* Glycine max calmodulin 4, *HSF* Heat shock transcription factor, *MYB2* MYB transcription factor, *PhCaM53* Petunia hybrida calmodulin 53, *PP7* calmodulin binding protein phosphatase 7, *TF* transcription factor, *WRKY7* WRKY transcription factor 7

promoter region of many stress-responsive genes [94]. Functional analysis of this gene revealed that an *atnig1* knockout mutant show enhanced sensitivity to salt stress, suggesting a significant role for the calcium-binding protein in salt stress signaling. However, the direct role of calcium binding on the activity of AtNIG1 as a transcription factor in the expression of stress-responsive genes remains unclear (Fig. 51.1).

A recent study on the regulation of light-responsive genes led to identify AtCaM7, a typical CaM in *Arabidopsis thaliana*, as a sequence-specific DNA-binding protein [36]. AtCaM7 was found to specifically recognize the Z-box and G-box motifs, two similar regulatory elements in light-responsive promoters, whereas AtCaM3, another isoform differing from AtCaM7 by a single amino acid, is unable to bind these promoters. Chromatin immunoprecipitation experiments confirmed the *in vivo* interaction of AtCaM7 with gene promoters. Furthermore, genetic evidence showed that AtCaM7 promotes the expression of light-inducible genes and photomorphogenesis even in the dark, suggesting a role for this CaM isoform in light/dark signaling (Fig. 51.1). This unexpected finding reveals a novel mechanism of CaM action by a direct use of calcium signals to regulate gene expression. However, it is still unknown if AtCaM7 regulates gene expression by itself or associated to a transcriptional complex.

CaM-Binding Transcription Factors

In addition to CaM as a direct regulator, a group of CaM-binding transcription factors referred to as CAMTAs, have been found in plants and belongs to a family of evolutionary conserved proteins from plants to animals [51, 95]. All CAMTAs share a conserved domain organization including a C-terminal calmodulin-binding domain and a CG-1 DNA-binding domain in the N-terminal end. Plant CAMTAs participate in diverse signal transduction pathways by integrating responses to phytohormones that are critical for plant growth and stress tolerance. A recent study revealed that CAMTA3 loss-of-function results in an enhanced resistance to pathogens and increased levels of salicylic acid, an hormone playing an essential role in plant immunity [96]. Additional analysis showed that CAMTA3 repress the expression of "Enhanced Disease Susceptibility" 1 (EDS1) a positive regulator of salicylic acid synthesis, by direct binding to the EDS1 gene promoter. Importantly, genetic evidences indicate that calcium/CaM binding to CAMTA3 is required for the function of the transcription factor in plant immunity, demonstrating a direct role for calcium/CaM complex in regulating CAMTA3 activity. In the same way, recent data provided evidence for a role of CAMTAs in cold acclimation by demonstrating that members of the CAMTA family bind to regulatory elements in the promoter of *CBF2* gene, a master regulator of cold-inducible gene expression [97]. Cold induction of *CBF2* and other cold-responsive genes is reduced in the *camta3* mutant, and *camta1/camta3* double mutants are impaired in their cold acclimation and freezing tolerance. Collectively, these data indicate that direct decoding of stress-induced calcium signatures into the regulation of gene expression may occur through the calcium-dependent interaction of CaM with members of the CAMTA family (Fig. 51.1).

The function of CaM in the regulation of gene expression may involve other classes of transcription factors including MYBs, WRKYs, NAC domain containing transcription factors and GT-element-binding proteins [56, 83]. MYB proteins constitute a large family of transcription factors that contain a variable number of

adjacent repeats of the MYB DNA-binding domain. Two soybean CaM isoforms (GmCaM1 and GmCaM4) were reported to bind MYB2, a transcriptional regulator of salt- and dehydration-responsive genes [98]. The DNA-binding activity of MYB2 was found to be enhanced in a calcium-dependent manner by its interaction with GmCaM4 whereas its activity was inhibited by GmCaM1. Furthermore, the ectopic expression of GmCaM4 increases the expression of MYB2 target genes and confers salt tolerance in transgenic plants whereas GmCaM1 does not (Fig. 51.1). This suggests that a specific CaM isoform mediates salt-induced calcium signaling through the activation of a MYB transcription factor. The WRKY protein family is another large group of transcription factors that appears to be mainly implicated in the regulation of transcriptional reprogramming associated with plant immunity [99]. WRKYs preferentially bind to the W-box element found in the promoters of a large variety of defense-related genes and the WRKY genes themselves. AtWRKY7, a representative member of a subgroup IId of the Arabidopsis WRKY family, was recently reported to interact with CaM in a calcium-dependent manner through a CaM-binding domain conserved in all WRKY subgroup IId proteins [100]. Although experimental evidence supports a role for AtWRKY7 as a transcriptional repressor that enhances plant susceptibility to pathogen invasion [101], the regulation of AtWRKY7 function by CaM binding needs to be clarified .

Overall, these results clearly establish a function of calcium/CaM complex in transcriptional regulation during plant response to environmental stresses, through a direct interaction of CaM with diverse types of transcription factors. Since biotic and abiotic stresses often promote calcium pulses in the cytosol and in the nucleus, the direct regulation of nuclear-localized proteins by nuclear CaM is a likely mechanism for decoding nuclear calcium signals triggered by stress. Further investigations are required to identify the target genes of the CaM-binding transcription factors in order to better understand this direct role of CaM in transcriptional regulation.

Calcium-Dependent Post-translational Modifications of Transcription Factors

Like in animals, several studies in plants suggest that calcium participates in transcriptional regulation *via* phosphorylation/dephosphorylation of transcription factors. Phosphorylation can regulate transcription factors by modulating their DNA-binding affinity, transcriptional activity, stability and sub-cellular distribution. As previously mentioned, a major group of calcium sensors in plants is represented by the CDPK family. Typically, CDPKs combine in a single polypeptide, a kinase domain, an autoinhibitory domain and a CaM-like regulatory domain bearing 4 EF-hands. Binding of calcium to EF-hands results in the activation of the kinase by displacing the autoinhibitory domain from the active site. CDPKs are activated in response to various abiotic and biotic stimuli known to trigger calcium signals, and they have many different substrates which reflect the diversity of their functions [88, 102]. CDPKs were shown to phosphorylate basic leucine-zipper (bZIP)

transcription factors that are key regulators in stress and hormone signaling pathways [91, 103–106]. Phosphorylation of plant bZIPs can interfere with their DNA-binding activity and intracellular localization.

The calcium-dependent modification of transcription factors can also be accomplished by CaM-binding protein kinases or phosphatases. Genetic dissection of heat-shock signal transduction in *Arabidopsis* identified AtCaM3 and two CaM targets, the protein kinase AtCBK3 and the protein phosphatase AtPP7 as key components of the heat-shock response acting on the regulation of heat-shock transcription factors (HSFs) [107] (Fig. 51.1). *AtCaM3* mutants were found to exhibit a reduction in thermotolerance which correlates with a decrease in the activity of HSFs and the synthesis of heat-shock proteins. HSFs are known to be regulated by reversible phosphorylation *via* mechanisms involving multiple phosphorylation sites and distinct protein kinases/phosphatases. Interestingly, AtCBK3 and AtPP7 are nuclear-localized CaM targets that were found to interact with HSFs, and knockout mutations in *AtCBK3* and *AtPP7* genes impair thermotolerance as observed for AtCaM3 [108, 109]. Collectively, these data suggests that the calcium/CaM complex plays a major role in the heat-shock response and the synthesis of heat-shock proteins through the modulation of the phosphorylation status of HSFs.

Conclusions and Future Directions

This short review summarized by the cartoon depicted in Fig. 51.1 sustains the idea that the nucleus is an active and autonomous organelle able to generate and regulate its calcium signals in response to environmental cues. In plants, there are no clear data yet that could suggest a free diffusion of cytosolic calcium through the NPCs as observed in some animal cells [32, 110]. Available data rather support the hypothesis of a strict control of calcium exchanges between the cytosol and the nucleoplasm. However, this lack of experimental evidences does not preclude that free calcium diffusion may occur in some circumstances. On the whole, these data are in good agreement with recent results obtained in the animal field which are in favor of an independent intranuclear calcium signaling system [111]. The presence of a nucleoplasmic reticulum, a nuclear calcium store continuous with the endo/sarcoplasmic reticulum and the nuclear envelope and harboring functional IP_3R or ryanodine receptor (RyR), allows nuclear calcium to regulate cellular functions independently of the cytosolic calcium increase [111, 112]. Such structures have also been observed in plants [113] but further data are needed to demonstrate their involvement in nuclear calcium signaling.

Considering the ability of the nucleus to decode its own calcium signals, numerous calcium-binding proteins are constitutively localized in the nucleus or are able to shuttle between the cytoplasm and the nucleus during the response to environmental cues (Table 51.1). Their presence at one time in the nucleus suggest that they could be involved in the decoding of nuclear calcium signals. Genetic evidences have been obtained for the CCamK (DMI3) in the legumes and its crucial role in symbiosis

but up to date no direct demonstration of nuclear calcium requirement for its activity has been brought. The current knowledge on nuclear calcium signaling in plants, points out the occurrence of several black boxes in the regulation of nuclear calcium homeostasis. What really are the actors (channels, transporters and/or exchangers) involved in the autonomous generation of nuclear calcium signals and in the regulation of the calcium homeostasis? Based on the knowledge accumulated in the animal field, one can envision characterizing these actors by using either targeted or global approaches. Targeted strategies will focus on already known tools of the calcium toolkit whose cDNA are already available. Such a strategy has been already performed by screening the plant genome. Using BLASTX program, Nagata et al. [49] searched for sequence homologies at the amino acid level. They downloaded sequences data from NCBI's Genbank and checked the alignment pattern of the query sequences at a similarity threshold of $E < 10^{-100}$. From these data they could establish a comparative table between the calcium toolkit from *Homo sapiens and Arabidopsis thaliana* . Part of this table has been exploited in the construction of Table 51.1 of this manuscript [49]. It clearly appears from this table that some calcium tools are very specific for plants but most of them are shared and conserved during evolution from plants to human. Others nevertheless still need to be discovered in plants as proposed below. Similarly a screening of the plant *Arabidopsis* genome was performed to sort out all the channels and pumps containing the canonical bipartite Nuclear Localization Signal (NLS)-like sequences [22]. Using the INTERPRO domain database, these authors were able to fish out six P-type ATPases able to catalyze cation uptake and/or efflux, 3 out of 19 probable cyclic nucleotide gated channels and 2 out of 15 K^+ channels that could modulate calcium channels as suggested for CASTOR and POLLUX channels in *Lotus Japonicus* [114]. However this method exclude the discovery of new possible actors containing non canonical NLS or still unknown calcium channel such as InsP3R or RyR found in the nucleus of most animal cells but still having no counterparts in plants. An alternative method would be to develop a non targeted approach using purified membranes from purified nuclei and extract the inner and outer membrane of the envelope as already done by the group of Malviya using purified rat liver nuclei [29]. From these membranes, hydrophobic proteins should then be extracted and characterized through MS/MS analysis. Knowledge of these actors is completely required to study the regulation of nuclear calcium homeostasis and to design future projects devoted to investigate the role of nuclear calcium signals on nuclear downstream events.

Indeed, future work on nuclear calcium signaling in plants has to focus on the molecular mechanisms involved to shape and decode the nuclear calcium signals. This goal can be achieved by setting up new genetic screens to isolate mutants altered in the generation of nuclear calcium signals. The targets of nuclear calcium sensors need also to be investigated either by combined approaches of proteomics and cell biology in order to characterize the interactants and to visualize their interaction with the calcium sensors. Finally, all these studies should lead to a better comprehensive view of the nuclear calcium signaling integrated in the whole cell signaling network, during important steps of the plant life such as symbiotic or pathogenic plant-microbe interactions as recently reviewed [115] .

Acknowledgements Authors acknowledge the CNRS and the Université de Toulouse for research funding.

References

1. Gilliham M, Dayod M, Hocking BJ, Xu B, Conn SJ, Kaiser BN, Leigh RA, Tyerman SD (2011) Calcium delivery and storage in plant leaves: exploring the link with water flow. J Exp Bot 62:2233–2250
2. Inouye S, Noguchi M, Sakaki Y, Takagi Y, Miyata T, Iwanaga S, Miyata T, Tsuji FI (1985) Cloning and sequence analysis of cDNA for the luminescent protein aequorin. Proc Natl Acad Sci USA 82:3154–3158
3. Prasher D, McCann RO, Cormier MJ (1985) Cloning and expression of the cDNA coding for aequorin, a bioluminescent calcium-binding protein. Biochem Biophys Res Commun 126:1259–1268
4. Knight MR, Campbell AK, Smith SM, Trewavas AJ (1991) Transgenic plant aequorin reports the effects of touch and cold-shock and elicitors on cytoplasmic calcium. Nature 352:524–526
5. Johnson C, Knight M, Kondo T, Masson P, Sedbrook J, Haley A, Trewavas A (1995) Circadian oscillations of cytosolic and chloroplastic free calcium in plants. Science 269:1863–1865
6. O'Malley DM, Burbach BJ, Adams PR (1999) Fluorescent calcium indicators: subcellular behavior and use in confocal imaging. Methods Mol Biol 122:261–303
7. Perez-Terzic C, Jaconi M, Clapham DE (1997) Nuclear calcium and the regulation of the nuclear pore complex. Bioessays 19:787–792
8. Thomas D, Tovey SC, Collins TJ, Bootman MD, Berridge MJ, Lipp P (2000) A comparison of fluorescent Ca2+ indicator properties and their use in measuring elementary and global Ca2+ signals. Cell Calcium 28:213–223
9. Miyawaki A, Llopis J, Heim R, McCaffery JM, Adams JA, Ikura M, Tsien RY (1997) Fluorescent indicators for Ca2+ based on green fluorescent proteins and calmodulin. Nature 388:882–887
10. Nagai T, Sawano A, Park ES, Miyawaki A (2001) Circularly permuted green fluorescent proteins engineered to sense Ca2+. Proc Natl Acad Sci USA 98:3197–3202
11. Berridge MJ, Bootman MD, Roderick HL (2003) Calcium signalling: dynamics, homeostasis and remodelling. Nat Rev Mol Cell Biol 4:517–529
12. Berridge MJ, Lipp P, Bootman MD (2000) The versatility and universality of calcium signalling. Nat Rev Mol Cell Biol 1:11–21
13. McAinsh MR, Hetherington AM (1998) Encoding specificity in Ca^{2+} signalling systems. Trends Plant Sci 3:32–36
14. McAinsh MR, Pittman JK (2009) Shaping the calcium signature. New Phytol 181:275–294
15. Ng CK, McAinsh MR (2003) Encoding specificity in plant calcium signalling: hot-spotting the ups and downs and waves. Ann Bot (Lond) 92:477–485
16. AGI (2000) Analysis of the genome sequence of the flowering plant Arabidopsis thaliana. Nature 408:796–815
17. Kretsinger R, Moncrief N (1989) Evolution of calcium modulated proteins. Va Explor 5:7–9
18. Day IS, Reddy VS, Shad Ali G, Reddy AS (2002) Analysis of EF-hand-containing proteins in Arabidopsis. Genome Biol 3:RESEARCH0056
19. Haiech J, Moulhaye SB, Kilhoffer MC (2004) The EF-Handome: combining comparative genomic study using FamDBtool, a new bioinformatics tool, and the network of expertise of the European Calcium Society. Biochim Biophys Acta 1742:179–183
20. McCormack E, Tsai Y-C, Braam J (2005) Handling calcium signaling: Arabidopsis CaMs and CMLs. Trends Plant Sci 10:383–389

21. Peiter E, Maathuis FJ, Mills LN, Knight H, Pelloux J, Hetherington AM, Sanders D (2005) The vacuolar Ca2+-activated channel TPC1 regulates germination and stomatal movement. Nature 434:404–408
22. Matzke M, Aufsatz W, Gregor W, van Der Winden J, Papp I, Matzke AJ (2001) Ion transporters in the nucleus? Plant Physiol 127:10–13
23. Lachaud C, Da Silva D, Cotelle V, Thuleau P, Xiong TC, Jauneau A, Briere C, Graziana A, Bellec Y, Faure JD, Ranjeva R, Mazars C (2010) Nuclear calcium controls the apoptotic-like cell death induced by d-erythro-sphinganine in tobacco cells. Cell Calcium 47:92–100
24. Jong YJ, Kumar V, Kingston AE, Romano C, O'Malley KL (2005) Functional metabotropic glutamate receptors on nuclei from brain and primary cultured striatal neurons. Role of transporters in delivering ligand. J Biol Chem 280:30469–30480
25. Kumar V, Jong YJ, O'Malley KL (2008) Activated nuclear metabotropic glutamate receptor mGlu5 couples to nuclear Gq/11 proteins to generate inositol 1,4,5-trisphosphate-mediated nuclear Ca2+ release. J Biol Chem 283:14072–14083
26. Gerasimenko JV, Maruyama Y, Yano K, Dolman NJ, Tepikin AV, Petersen OH, Gerasimenko OV (2003) NAADP mobilizes Ca2+ from a thapsigargin-sensitive store in the nuclear envelope by activating ryanodine receptors. J Cell Biol 163:271–282
27. Marius P, Guerra MT, Nathanson MH, Ehrlich BE, Leite MF (2006) Calcium release from ryanodine receptors in the nucleoplasmic reticulum. Cell Calcium 39:65–73
28. Xiong TC, Jauneau A, Ranjeva R, Mazars C (2004) Isolated plant nuclei as mechanical and thermal sensors involved in calcium signalling. Plant J 40:12–21
29. Humbert JP, Matter N, Artault JC, Koppler P, Malviya AN (1996) Inositol 1,4,5-trisphosphate receptor is located to the inner nuclear membrane vindicating regulation of nuclear calcium signaling by inositol 1,4,5-trisphosphate. Discrete distribution of inositol phosphate receptors to inner and outer nuclear membranes. J Biol Chem 271:478–485
30. Malviya AN (1994) The nuclear inositol 1,4,5-trisphosphate and inositol 1,3,4,5-tetrakisphosphate receptors. Cell Calcium 16:301–313
31. Bezin S, Charpentier G, Lee HC, Baux G, Fossier P, Cancela JM (2008) Regulation of nuclear Ca2+ signaling by translocation of the Ca2+ messenger synthesizing enzyme ADP-ribosyl cyclase during neuronal depolarization. J Biol Chem 283:27859–27870
32. Bootman MD, Fearnley C, Smyrnias I, MacDonald F, Roderick HL (2009) An update on nuclear calcium signalling. J Cell Sci 122:2337–2350
33. Kudla J, Batistic O, Hashimoto K (2010) Calcium signals: the lead currency of plant information processing. Plant Cell 22:541–563
34. Dodd AN, Kudla J, Sanders D (2010) The language of calcium signaling. Annu Rev Plant Biol 61:593–620
35. Ledeen RW, Wu G (2007) Sodium-calcium exchangers in the nucleus: an unexpected locus and an unusual regulatory mechanism. Ann N Y Acad Sci 1099:494–506
36. Kushwaha R, Singh A, Chattopadhyay S (2008) Calmodulin7 plays an important role as transcriptional regulator in Arabidopsis seedling development. Plant Cell 20:1747–1759
37. Rodriguez-Concepcion M, Yalovsky S, Zik M, Fromm H, Gruissem W (1999) The prenylation status of a novel plant calmodulin directs plasma membrane or nuclear localization of the protein. EMBO J 18:1996–2007
38. Perochon A, Dieterle S, Pouzet C, Aldon D, Galaud JP, Ranty B (2010) Interaction of a plant pseudo-response regulator with a calmodulin-like protein. Biochem Biophys Res Commun 398:747–751
39. Liang L, Flury S, Kalck V, Hohn B, Molinier J (2006) CENTRIN2 interacts with the Arabidopsis homolog of the human XPC protein (AtRAD4) and contributes to efficient synthesis-dependent repair of bulky DNA lesions. Plant Mol Biol 61:345–356
40. Weinl S, Kudla J (2009) The CBL-CIPK Ca(2+)-decoding signaling network: function and perspectives. New Phytol 184:517–528
41. Levy J, Bres C, Geurts R, Chalhoub B, Kulikova O, Duc G, Journet EP, Ane JM, Lauber E, Bisseling T, Denarie J, Rosenberg C, Debelle F (2004) A putative Ca2+ and calmodulin-dependent protein kinase required for bacterial and fungal symbioses. Science 303:1361–1364

42. Chehab EW, Patharkar OR, Hegeman AD, Taybi T, Cushman JC (2004) Autophosphorylation and subcellular localization dynamics of a salt- and water deficit-induced calcium-dependent protein kinase from ice plant. Plant Physiol 135:1430–1446
43. Dammann C, Ichida A, Hong B, Romanowsky SM, Hrabak EM, Harmon AC, Pickard BG, Harper JF (2003) Subcellular targeting of nine calcium-dependent protein kinase isoforms from Arabidopsis. Plant Physiol 132:1840–1848
44. Clark GB, Dauwalder M, Roux SJ (1998) Immunological and biochemical evidence for nuclear localization of annexin in peas. Plant Physiol Biochem 36:621–627
45. Raynal P, Kuijpers G, Rojas E, Pollard HB (1996) A rise in nuclear calcium translocates annexins IV and V to the nuclear envelope. FEBS Lett 392:263–268
46. Cocco L, Faenza I, Follo MY, Billi AM, Ramazzotti G, Papa V, Martelli AM, Manzoli L (2009) Nuclear inositides: PI-PLC signaling in cell growth, differentiation and pathology. Adv Enzyme Regul 49:2–10
47. Kockskamper J, Zima AV, Roderick HL, Pieske B, Blatter LA, Bootman MD (2008) Emerging roles of inositol 1,4,5-trisphosphate signaling in cardiac myocytes. J Mol Cell Cardiol 45: 128–147
48. Merchant SS, Prochnik SE, Vallon O, Harris EH, Karpowicz SJ, Witman GB, Terry A, Salamov A, Fritz-Laylin LK, Marechal-Drouard L, Marshall WF, Qu LH, Nelson DR, Sanderfoot AA, Spalding MH, Kapitonov VV, Ren Q, Ferris P, Lindquist E, Shapiro H, Lucas SM, Grimwood J, Schmutz J, Cardol P, Cerutti H, Chanfreau G, Chen CL, Cognat V, Croft MT, Dent R, Dutcher S, Fernandez E, Fukuzawa H, Gonzalez-Ballester D, Gonzalez-Halphen D, Hallmann A, Hanikenne M, Hippler M, Inwood W, Jabbari K, Kalanon M, Kuras R, Lefebvre PA, Lemaire SD, Lobanov AV, Lohr M, Manuell A, Meier I, Mets L, Mittag M, Mittelmeier T, Moroney JV, Moseley J, Napoli C, Nedelcu AM, Niyogi K, Novoselov SV, Paulsen IT, Pazour G, Purton S, Ral JP, Riano-Pachon DM, Riekhof W, Rymarquis L, Schroda M, Stern D, Umen J, Willows R, Wilson N, Zimmer SL, Allmer J, Balk J, Bisova K, Chen CJ, Elias M, Gendler K, Hauser C, Lamb MR, Ledford H, Long JC, Minagawa J, Page MD, Pan J, Pootakham W, Roje S, Rose A, Stahlberg E, Terauchi AM, Yang P, Ball S, Bowler C, Dieckmann CL, Gladyshev VN, Green P, Jorgensen R, Mayfield S, Mueller-Roeber B, Rajamani S, Sayre RT, Brokstein P, Dubchak I, Goodstein D, Hornick L, Huang YW, Jhaveri J, Luo Y, Martinez D, Ngau WC, Otillar B, Poliakov A, Porter A, Szajkowski L, Werner G, Zhou K, Grigoriev IV, Rokhsar DS, Grossman AR (2007) The Chlamydomonas genome reveals the evolution of key animal and plant functions. Science 318:245–250
49. Nagata T, Iizumi S, Satoh K, Ooka H, Kawai J, Carninci P, Hayashizaki Y, Otomo Y, Murakami K, Matsubara K, Kikuchi S (2004) Comparative analysis of plant and animal calcium signal transduction element using plant full-length cDNA data. Mol Biol Evol 21:1855–1870
50. Harper JF, Breton G, Harmon A (2004) Decoding Ca^{2+} signals through plant protein kinases. Annu Rev Plant Biol 55:263–288
51. Bouché N, Scharlat A, Snedden W, Bouchez D, Fromm H (2002) A novel family of calmodulin-binding transcription activators in multicellular organisms. J Biol Chem 277:21851–21861
52. Clapham DE, Runnels LW, Strubing C (2001) The TRP ion channel family. Nat Rev Neurosci 2:387–396
53. Grimm C, Kraft R, Schultz G, Harteneck C (2005) Activation of the melastatin-related cation channel TRPM3 [corrected] by D-erythro-sphingosine. Mol Pharmacol 67:798–805
54. Hardingham GE, Chawla S, Johnson CM, Bading H (1997) Distinct functions of nuclear and cytoplasmic calcium in the control of gene expression. Nature 385:260–265
55. Alonso MT, Garcia-Sancho J (2011) Nuclear Ca(2+) signalling. Cell Calcium 49:280–289
56. Kim MC, Chung WS, Yun DJ, Cho MJ (2009) Calcium and calmodulin-mediated regulation of gene expression in plants. Mol Plant 2:13–21
57. Mazars C, Bourque S, Mithöfer A, Pugin A, Ranjeva R (2009) Calcium homeostasis in plant cell nuclei. New Phytol 181:261–274
58. Mazars C, Thuleau P, Lamotte O, Bourque S (2010) Cross-talk between ROS and calcium in regulation of nuclear activities. Mol Plant 4:706–718

59. Rodrigues MA, Gomes DA, Nathanson MH, Leite MF (2009) Nuclear calcium signaling: a cell within a cell. Braz J Med Biol Res 42:17–20
60. Gerasimenko OV, Gerasimenko JV, Tepikin AV, Petersen OH (1996) Calcium transport pathways in the nucleus. Pflugers Arch 432:1–6
61. Goldberg MW, Allen TD (1996) The nuclear pore complex and lamina: three-dimensional structures and interactions determined by field emission in-lens scanning electron microscopy. J Mol Biol 257:848–865
62. Carafoli E, Nicotera P, Santella L (1997) Calcium signalling in the cell nucleus. Cell Calcium 22:313–319
63. Rogue PJ, Malviya AN (1999) Calcium signals in the cell nucleus. EMBO J 18:5147–5152
64. Xu XM, Meier I (2008) The nuclear pore comes to the fore. Trends Plant Sci 13:20–27
65. van der Luit AH, Olivari C, Haley A, Knight MR, Trewavas AJ (1999) Distinct calcium signaling pathways regulate calmodulin gene expression in tobacco. Plant Physiol 121:705–714
66. Pauly N, Knight MR, Thuleau P, van der Luit AH, Moreau M, Trewavas AJ, Ranjeva R, Mazars C (2000) Cell signalling: control of free calcium in plant cell nuclei. Nature 405:754–755
67. Pauly N, Knight MR, Thuleau P, Graziana A, Muto S, Ranjeva R, Mazars C (2001) The nucleus together with the cytosol generates patterns of specific cellular calcium signatures in tobacco suspension culture cells. Cell Calcium 30:413–421
68. Lecourieux D, Lamotte O, Bourque S, Wendehenne D, Mazars C, Ranjeva R, Pugin A (2005) Proteinaceous and oligosaccharidic elicitors induce different calcium signatures in the nucleus of tobacco cells. Cell Calcium 38:527–538
69. Lecourieux D, Mazars C, Pauly N, Ranjeva R, Pugin A (2002) Analysis and effects of cytosolic free calcium increases in response to elicitors in *Nicotiana plumbaginifolia* cells. Plant Cell 14:2627–2641
70. Lerouge P, Roche P, Faucher C, Maillet F, Truchet G, Prome JC, Denarie J (1990) Symbiotic host-specificity of Rhizobium meliloti is determined by a sulphated and acylated glucosamine oligosaccharide signal. Nature 344:781–784
71. Oldroyd GED, Downie JA (2008) Coordinating nodule morphogenesis with rhizobial infection in legumes. Annu Rev Plant Biol 59:519–546
72. Miwa H, Sun J, Oldroyd GE, Downie JA (2006) Analysis of calcium spiking using a cameleon calcium sensor reveals that nodulation gene expression is regulated by calcium spike number and the developmental status of the cell. Plant J 48:883–894
73. Walker SA, Viprey V, Downie JA (2000) Dissection of nodulation signaling using pea mutants defective for calcium spiking induced by Nod factors and chitin oligomers. Proc Natl Acad Sci USA 97:13413–13418
74. Sieberer BJ, Chabaud M, Timmers AC, Monin A, Fournier J, Barker DG (2009) A nuclear-targeted cameleon demonstrates intranuclear Ca^{2+} spiking in *Medicago truncatula* root hairs in response to rhizobial nodulation factors. Plant Physiol 151:1197–1206
75. Parniske M (2008) Arbuscular mycorrhiza: the mother of plant root endosymbioses. Nat Rev Microbiol 6:763–775
76. Chabaud M, Genre A, Sieberer BJ, Faccio A, Fournier J, Novero M, Barker DG, Bonfante P (2010) Arbuscular mycorrhizal hyphopodia and germinated spore exudates trigger Ca2+ spiking in the legume and nonlegume root epidermis. New Phytol 189:347–355
77. Wasternack C (2007) Jasmonates: an update on biosynthesis, signal transduction and action in plant stress response, growth and development. Ann Bot 100:681–697
78. Walter A, Mazars C, Maitrejean M, Hopke J, Ranjeva R, Boland W, Mithöfer A (2007) Structural requirements of jasmonates and synthetic analogues as inducers of Ca^{2+} signals in the nucleus and the cytosol of plant cells. Angew Chem Int Ed 46:4783–4785
79. Thines B, Katsir L, Melotto M, Niu Y, Mandaokar A, Liu G, Nomura K, He SY, Howe GA, Browse J (2007) JAZ repressor proteins are targets of the SCF(COI1) complex during jasmonate signalling. Nature 448:661–665
80. Staswick PE (2008) JAZing up jasmonate signaling. Trends Plant Sci 13:66–71

81. Brière C, Xiong TC, Mazars C, Ranjeva R (2006) Autonomous regulation of free Ca2+ concentrations in isolated plant cell nuclei: a mathematical analysis. Cell Calcium 39:293–303
82. Zima AV, Copello JA, Blatter LA (2004) Effects of cytosolic NADH/NAD(+) levels on sarcoplasmic reticulum Ca(2+) release in permeabilized rat ventricular myocytes. J Physiol 555:727–741
83. Galon Y, Finkler A, Fromm H (2010) Calcium-regulated transcription in plants. Mol Plant 3:653–669
84. Kaplan B, Davydov O, Knight H, Galon Y, Knight MR, Fluhr R, Fromm H (2006) Rapid transcriptome changes induced by cytosolic Ca2+ transients reveal ABRE-related sequences as Ca2+-responsive cis elements in Arabidopsis. Plant Cell 18:2733–2748
85. Moscatiello R, Mariani P, Sanders D, Maathuis FJ (2006) Transcriptional analysis of calcium-dependent and calcium-independent signalling pathways induced by oligogalacturonides. J Exp Bot 57:2847–2865
86. Snedden WA, Fromm H (2001) Calmodulin as a versatile calcium signal transducer in plants. New Phytol 151:35–66
87. Boonburapong B, Buaboocha T (2007) Genome-wide identification and analyses of the rice calmodulin and related potential calcium sensor proteins. BMC Plant Biol 7:4
88. Cheng SH, Willmann MR, Chen HC, Sheen J (2002) Calcium signaling through protein kinases. The Arabidopsis calcium-dependent protein kinase gene family. Plant Physiol 129:469–485
89. McCormack E, Braam J (2003) Calmodulins and related potential calcium sensors of Arabidopsis. New Phytol 159:585–598
90. Patharkar OR, Cushman JC (2006) A novel coiled-coil protein co-localizes and interacts with a calcium-dependent protein kinase in the common ice plant during low-humidity stress. Planta 225:57–73
91. Ishida S, Yuasa T, Nakata M, Takahashi Y (2008) A tobacco calcium-dependent protein kinase, CDPK1, regulates the transcription factor REPRESSION OF SHOOT GROWTH in response to gibberellins. Plant Cell 20:3273–3288
92. Mellstrom B, Savignac M, Gomez-Villafuertes R, Naranjo JR (2008) Ca2+-operated transcriptional networks: molecular mechanisms and in vivo models. Physiol Rev 88:421–449
93. Savignac M, Mellstrom B, Naranjo JR (2007) Calcium-dependent transcription of cytokine genes in T lymphocytes. Pflugers Arch 454:523–533
94. Kim J, Kim HY (2006) Functional analysis of a calcium-binding transcription factor involved in plant salt stress signaling. FEBS Lett 580:5251–5256
95. Finkler A, Ashery-Padan R, Fromm H (2007) CAMTAs: calmodulin-binding transcription activators from plants to human. FEBS Lett 581:3893–3898
96. Du L, Ali GS, Simons KA, Hou J, Yang T, Reddy AS, Poovaiah BW (2009) Ca(2+)/calmodulin regulates salicylic-acid-mediated plant immunity. Nature 457:1154–1158
97. Doherty CJ, Van Buskirk HA, Myers SJ, Thomashow MF (2009) Roles for Arabidopsis CAMTA transcription factors in cold-regulated gene expression and freezing tolerance. Plant Cell 21:972–984
98. Yoo JH, Park CY, Kim JC, Do Heo W, Cheong MS, Park HC, Kim MC, Moon BC, Choi MS, Kang YH, Lee JH, Kim HS, Lee SM, Yoon HW, Lim CO, Yun D-J, Lee SY, Chung WS, Cho MJ (2005) Direct interaction of a divergent CaM isoform and the transcription factor, MYB2, enhances salt tolerance in Arabidopsis. J Biol Chem 280:3697–3706
99. Eulgem T, Somssich IE (2007) Networks of WRKY transcription factors in defense signaling. Curr Opin Plant Biol 10:366–371
100. Park CY, Lee JH, Yoo JH, Moon BC, Choi MS, Kang YH, Lee SM, Kim HS, Kang KY, Chung WS, Lim CO, Cho MJ (2005) WRKY group IId transcription factors interact with calmodulin. FEBS Lett 579:1545–1550
101. Kim KC, Fan B, Chen Z (2006) Pathogen-induced Arabidopsis WRKY7 is a transcriptional repressor and enhances plant susceptibility to Pseudomonas syringae. Plant Physiol 142:1180–1192

102. Klimecka M, Muszynska G (2007) Structure and functions of plant calcium-dependent protein kinases. Acta Biochim Pol 54:219–233
103. Kirchler T, Briesemeister S, Singer M, Schutze K, Keinath M, Kohlbacher O, Vicente-Carbajosa J, Teige M, Harter K, Chaban C (2010) The role of phosphorylatable serine residues in the DNA-binding domain of Arabidopsis bZIP transcription factors. Eur J Cell Biol 89:175–183
104. Meshi T, Moda I, Minami M, Okanami M, Iwabuchi M (1998) Conserved Ser residues in the basic region of the bZIP-type transcription factor HBP-1a(17): importance in DNA binding and possible targets for phosphorylation. Plant Mol Biol 36:125–136
105. Uno Y, Rodriguez Milla MA, Maher E, Cushman JC (2009) Identification of proteins that interact with catalytically active calcium-dependent protein kinases from Arabidopsis. Mol Genet Genomics 281:375–390
106. Zhu SY, Yu XC, Wang XJ, Zhao R, Li Y, Fan RC, Shang Y, Du SY, Wang XF, Wu FQ, Xu YH, Zhang XY, Zhang DP (2007) Two calcium-dependent protein kinases, CPK4 and CPK11, regulate abscisic acid signal transduction in Arabidopsis. Plant Cell 19:3019–3036
107. Zhang W, Zhou RG, Gao YJ, Zheng SZ, Xu P, Zhang SQ, Sun DY (2009) Molecular and genetic evidence for the key role of AtCaM3 in heat-shock signal transduction in Arabidopsis. Plant Physiol 149:1773–1784
108. Liu HT, Gao F, Li GL, Han JL, Liu DL, Sun DY, Zhou RG (2008) The calmodulin-binding protein kinase 3 is part of heat-shock signal transduction in Arabidopsis thaliana. Plant J 55:760–773
109. Liu HT, Li GL, Chang H, Sun DY, Zhou RG, Li B (2007) Calmodulin-binding protein phosphatase PP7 is involved in thermotolerance in Arabidopsis. Plant Cell Environ 30:156–164
110. Eder A, Bading H (2007) Calcium signals can freely cross the nuclear envelope in hippocampal neurons: somatic calcium increases generate nuclear calcium transients. BMC Neurosci 8:57
111. Leite MF, Thrower EC, Echevarria W, Koulen P, Hirata K, Bennett AM, Ehrlich BE, Nathanson MH (2003) Nuclear and cytosolic calcium are regulated independently. Proc Natl Acad Sci USA 100:2975–2980
112. Echevarria W, Leite MF, Guerra MT, Zipfel WR, Nathanson MH (2003) Regulation of calcium signals in the nucleus by a nucleoplasmic reticulum. Nat Cell Biol 5:440–446
113. Collings DA, Carter CN, Rink JC, Scott AC, Wyatt SE, Allen NS (2000) Plant nuclei can contain extensive grooves and invaginations. Plant Cell 12:2425–2440
114. Matzke M, Weiger TM, Papp I, Matzke AJ (2009) Nuclear membrane ion channels mediate root nodule development. Trends Plant Sci 14:295–298
115. Deslandes L, Rivas S (2011) The plant cell nucleus: a true arena for the fight between plants and pathogens. Plant Signal Behav 6:42–48

Chapter 52
Remodeling of Calcium Handling in Human Heart Failure

Qing Lou, Ajit Janardhan, and Igor R. Efimov

Abstract Heart failure (HF) is an increasing public health problem accelerated by a rapidly aging global population. Despite considerable progress in managing the disease, the development of new therapies for effective treatment of HF remains a challenge. To identify targets for early diagnosis and therapeutic intervention, it is essential to understand the molecular and cellular basis of calcium handling and the signaling pathways governing the functional remodeling associated with HF in humans. Calcium (Ca^{2+}) cycling is an essential mediator of cardiac contractile function, and remodeling of calcium handling is thought to be one of the major factors contributing to the mechanical and electrical dysfunction observed in HF. Active research in this field aims to bridge the gap between basic research and effective clinical treatments of HF. This chapter reviews the most relevant studies of calcium remodeling in failing human hearts and discusses their connections to current and emerging clinical therapies for HF patients.

Keywords Calcium • Remodeling • Heart failure • Human • Clinical treatment

Introduction

HF is a rising public health problem, with a prevalence of over 5.8 million in the USA, over 23 million worldwide, and continues to increase [1, 2]. The contractile dysfunction and arrhythmogenesis associated with HF is closely related to the

Q. Lou, Ph.D. • I.R. Efimov, Ph.D. (✉)
Department of Biomedical Engineering, Washington University in St. Louis,
390E Whitaker Hall, One Brookings Drive, St. Louis, MO 63130, USA
e-mail: igor@wustl.edu

A. Janardhan, M.D., Ph.D.
Department of Medicine, Division of Cardiology, Washington University
School of Medicine, St. Louis, MO 63110, USA

M.S. Islam (ed.), *Calcium Signaling*, Advances in Experimental
Medicine and Biology 740, DOI 10.1007/978-94-007-2888-2_52,

remodeling of calcium handling [3], which, in turn, is partially controlled by several signaling pathways in which Ca^{2+} has a prominent role [4]. Deriving a mechanistic understanding of alterations in calcium handling and calcium signaling is a critical step towards the development and improvement of physiology-based treatments for HF.

Overview of Cardiac Calcium Signaling

Ca^{2+} plays a central part in regulating excitation-contraction (EC) coupling and in modulating systolic and diastolic function in the heart as shown in Fig. 52.1. Ca^{2+} signal transduction in EC coupling comprises four steps [4–6]. Firstly, the trigger Ca^{2+} current (I_{Ca}) is generated by the L-type Ca^{2+} channels expressed in the transverse tubules (T-tubules) and is initiated by membrane depolarization. Secondly, the Ca^{2+} ions diffuse across the narrow junctional zone to activate ryanodine receptors (RyRs) and generate Ca^{2+} sparks, which considerably amplifies the original trigger Ca^{2+} signal. This process is known as Ca^{2+}-induced Ca^{2+} release (CICR). Thirdly, the Ca^{2+} efflux from the sarcoplasmic reticulum (SR) then diffuses in the cytoplasm to activate contraction by Ca^{2+} binding to troponin-C. Lastly, Ca^{2+} is transported back to the SR by SR Ca^{2+}-ATPases (SERCA) and out of cell via Na^{+}/Ca^{2+} exchangers (NCX). Abnormal handling of intracellular Ca^{2+} at any of these steps can cause cardiac dysfunction [7].

Intracellular Ca^{2+} homeostasis of cardiac myocytes is regulated by the phosphorylation and dephosphorylation of several key Ca^{2+}-handling proteins. One important regulatory kinase is cAMP-dependant protein kinase (PKA), which has been shown to regulate L-type Ca^{2+} channels, RyR and phospholamban (PLN). Despite the fact that global PKA activity is not changed in the failing human heart [8, 9], its activity in the RyR macromolecular signaling complex might be locally increased [10, 11].

Another important regulatory kinase is the Ca^{2+}/calmodulin-dependent protein kinase II (CaMKII) [12]. CAMKII is a protein kinase that modulates several intracellular Ca^{2+}-handling proteins such as RyR, PLN, L-type Ca^{2+} channels as well as Na^{+} channels [12]. CAMKII is associated directly with the RyR and modulates the activity of RyR [13–15]. Phosphorylation of PLN via CAMKII or PKA enhances the SR Ca^{2+} uptake via increased SERCA activity. The activity of CAMKII was shown to be significantly increased in the failing human heart and is correlated with the impaired ejection fraction [9, 16]. Both PKA and CAMKII can be activated by β-adrenergic stimulation.

Finally, multiple isoforms of protein kinase C (PKC) might also play a role in regulating the Ca^{2+} handling. PKC-α is the dominant isoform of PKC in the human heart [17] and its activity is triggered by the activation of $G_{\alpha q}$ coupled receptors (angiotensin II receptor, endothelin-1 receptor, and the α-adrenergic receptor) [18]. PKC-α can phosphorylate protein phosphatase inhibitor 1 (I-1), consequently

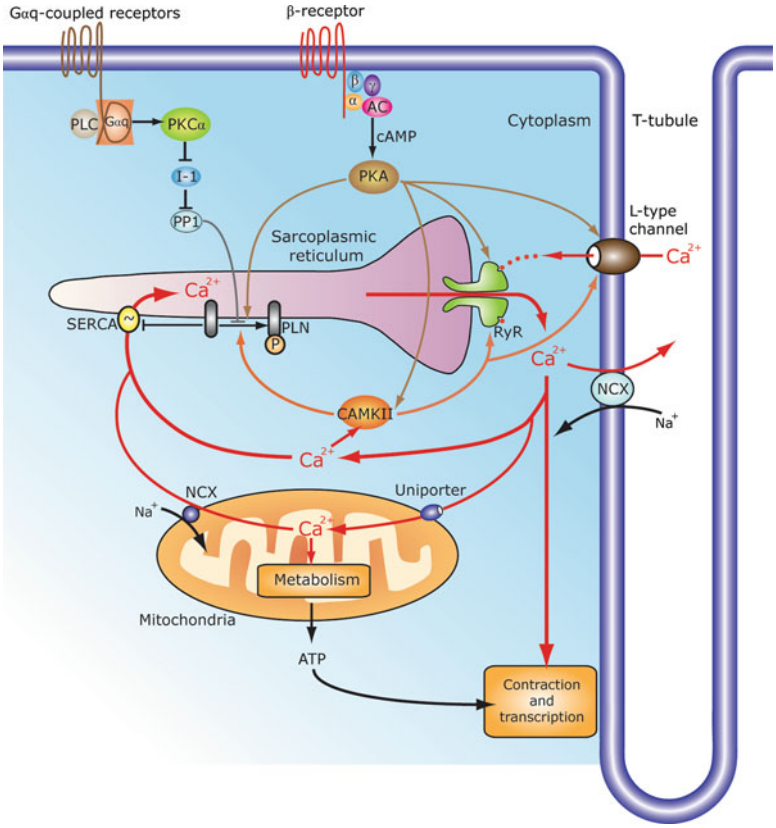

Fig. 52.1 Intracellular Ca^{2+} cycling and regulation by signaling pathways. After the activation of sarcolemma (including T-tubules), Ca^{2+} enters cytoplasm through L-type Ca^{2+} channel. The entering Ca^{2+} then induces a much larger Ca^{2+} release from the sarcoplasmic reticulum (*SR*) via the ryanodine receptor (*RyR*). The released Ca^{2+} binds with Troponin-C to activate contraction. Relaxation starts when Ca^{2+} is returned by sarcoplasmic reticulum Ca^{2+} ATPase (*SERCA*) to SR and via the Na^{+}/Ca^{2+} exchanger (*NCX*) to the extracellular domain. Some Ca^{2+} enters mitochondria to stimulate the production of ATP which is utilized for contraction and transcription. *SERCA* is inhibited by the dephosphorylated phospholamban (*PLN*). *PLN* can be phosphorylated by protein kinase A (*PKA*) and Ca^{2+}/calmodulin-dependent kinase (*CAMKII*), both of which can be activated by β-adrenergic stimulation. PLN can be dephosphorylated by phosphatase 1 (*PP1*), which can be activated through Gαq-coupled receptors (angiotensin II receptor, endothelin 1 receptor, or α-adrenergic receptor). α G-protein subunit α, β G-protein subunit β, γ G-protein subunit γ, *AC* adenylate cyclase, *cAMP* cyclic adenosine monophosphate

increasing the activity of protein phosphatase 1 (PP1), and leading to dephosphorylation of PLN and thus decreasing the activity of SERCA [19]. The level of PKC-α is increased in human HF [20–22]. The role of other isoforms of PKC in regulating calcium handling remains to be elucidated.

Alteration in Intracellular Ca^{2+} and Functional Abnormality in Failing Human Heart

Abnormal Ca^{2+} Handling and Mechanical Dysfunction in Human HF

The amount of Ca^{2+} delivered to the cytoplasm and the rate of Ca^{2+} removal from the cytoplasm are the two of the major factors determining the rate, intensity and duration of myocyte contraction [23]. Understanding of alterations in the intracellular Ca^{2+} concentration ($[Ca^{2+}]_i$) and their causal roles in contractile dysfunction in the failing human heart has been greatly advanced by the use of fluorescent $[Ca^{2+}]_i$ indicators [5, 24–32], which reflect changes in the free $[Ca^{2+}]_i$ necessary for the activation of contractile proteins [33, 34].

In isolated cells and tissues from failing human hearts, decreased amplitude of Ca^{2+} transient measured by the fluorescent intracellular Ca^{2+} indicators implies reduced Ca^{2+} release from SR [28, 30, 35]. This is correlated with decreased peak stretch amplitude, a measure of myocardial contraction [6, 36]. The reduced amplitude of Ca^{2+} transient is associated with decreased EC coupling gain [37] and decreased SR Ca^{2+} content [30, 38–42].

Moreover, the Ca^{2+} transient from failing human heart exhibits a reduced rate of Ca^{2+} removal [24, 28, 30]. The slowed rate of recovery of Ca^{2+} transient recovery is associated with a marked delay in tension relaxation in the failing human heart [24]. Finally, failing human heart exhibits increased resting intracellular Ca^{2+} level, leading to diastolic dysfunction [27, 28].

Altered $[Ca^{2+}]_i$ is frequency-dependent and most obvious at high heart rate [43]. Normally, the amplitude of the $[Ca^{2+}]_i$ transient is larger at higher stimulation frequencies [33]. In human HF, however, the amplitude of Ca^{2+} transient was decreased at faster stimulation rates, leading to reduced tension development at higher frequencies [27, 29]. Increased resting $[Ca^{2+}]_i$ and a fusion of Ca^{2+} transient at fast frequencies may also occur, leading to an increase of end-diastolic tension and a decrease of active tension generation associated with incomplete relaxation and twitch fusion [27]. The blunted or negative force frequency relationship (FFR) observed in both *in vivo* and *in vitro* studies of failing human hearts is in contrast with the positive FFR in non-failing human hearts, [27, 44–46] and is associated with altered Ca^{2+} and Na^{+} homeostasis as well as an inability to increase the SR Ca^{2+} content at increasing stimulation frequencies [39, 42].

The alteration of Ca^{2+} transient in failing human hearts is also region-dependent. We recently demonstrated the transmural hetergeneous remodeling of Ca^{2+} handing in the coronary-perfused left ventricular wedge preparations from failing and non-failing human hearts [31]. The sequence of Ca^{2+} transient relaxation is from epicardium to endocardium in both failing and non-failing human hearts at a slow heart rate (e.g., 0.67 Hz/40 BPM) during endocardial pacing, because the difference

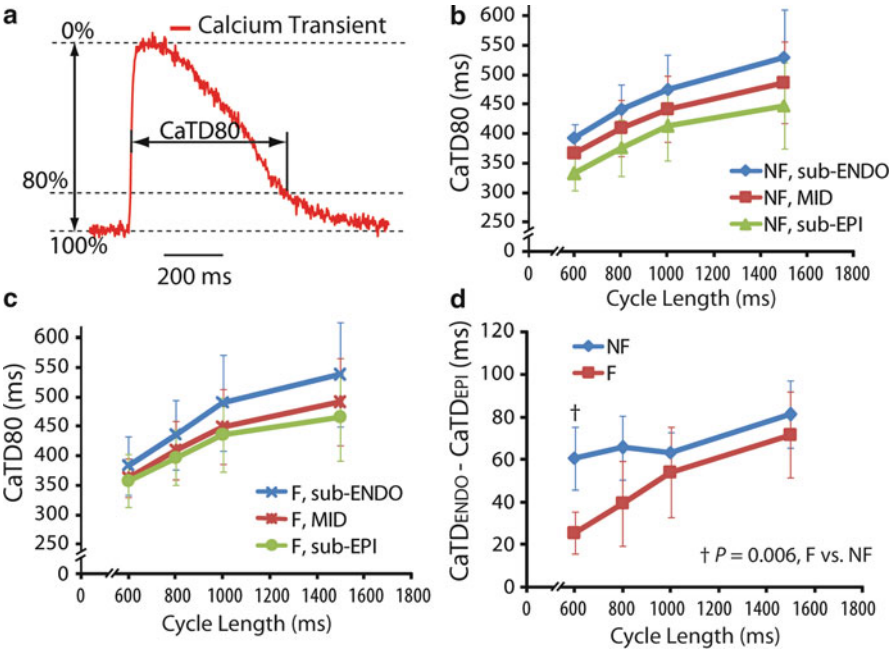

Fig. 52.2 Region-dependent and cycle-length-dependent calcium transient duration (*CaTD*) in failing human heart. (**a**) *CaTD* was quantified at 80% relaxation (*CaTD80*). (**b**) *CaTD80* at nonfailing human hearts (n = 6) at subendocardium (*sub-ENDO*), midmyocardium (*MID*), and subepicardium (*sub-EPI*). (**c**) CaTD80 at failing human hearts (n = 5). (**d**) The difference of *CaTD80* between *sub-ENDO* and *sub-EPI*. It can be seen that this difference is significantly reduced in failing heart at faster heart rate (cycle length at 600 ms) [31]. These data are obtained from Ca^{2+} transient measured using Rhod-2 AM from the coronary-perfused wedge preparations from both failing and non-failing human hearts

of Ca^{2+} transient duration between subendocardium and subepicardium (or duration difference) is larger than the conduction time from subendocardium to subepicardium (Fig. 52.2). Interestingly, this sequence is reversed at a fast heart rate (e.g., 1.67 Hz/100 BPM) in the failing human heart due to a significant decrease of this duration difference (Fig. 52.2c, d). In contrast, this sequence is not reversed in the non-failing human heart because the duration difference is not significantly changed at faster frequencies (Fig. 52.2b, d). We hypothesize that this reversed sequence of relaxation at fast heart rates could contribute to the end-systolic dysfunction [44] observed in the failing human heart. The maintenance of the normal relaxation sequence at slow heart rates in the failing hearts provides another mechanism for the beneficial effects of the heart-rate reduction in the patients with HF [47].

Abnormal Ca^{2+} Handling and Arrhythmia in Human HF

While approximately 50% HF patients die from progressive HF, the remainders die suddenly, mostly due to arrhythmias [48]. The relevance of arrhythmia to HF is evident from the significantly beneficial effects of implantable cardioveter-defibrillator (ICD) on survival of HF patients [49]. Among multiple mechanisms contributing to the development of arrhythmia in HF patients [50], changes in Ca^{2+} handling in HF could provide both trigger and substrate for the induction of arrhythmia in HF.

Alterations in the Ca^{2+} handling in HF could contribute to triggered activities arising from delayed after-depolarization (DAD) or early after-depolarization (EAD). DADs result from elevated intracellular Ca^{2+} load and spontaneous SR Ca^{2+} release, which leads to activation of transient inward current presumably carried by NCX [51]. In a rabbit model of HF, enhanced NCX in HF was found to underlie increased propensity for DADs [51]. In a dog model of HF, increased RyR-mediated SR Ca^{2+} leak was found to cause the arrhythmic DADs [52]. EAD could occur in the settings of enhanced lability of repolarization in HF [53], and could result from synergistic activation of L-type Ca^{2+} current and NCX during phase 2 and phase 3 of action potential (AP) [54]. The cellular mechanisms of triggered activity have been reviewed elsewhere by Pogwizd and Bers [55].

In contrast to the amount of work in animal models, our knowledge of triggered activity directly from human studies remains rather limited. Using three-dimensional intraoperative mapping, Pogwizd et al. [56] found that focal mechanisms maintained the arrhythmia in end-stage HF patients with idiopathic dilated cardiomyopathy. However, whether these focal activations were triggered activities was not directly demonstrated in this study. Vermeulen et al. [57] showed that both DAD and EAD were not observed when the ventricular trabeculae of failing human heart were perfused with normal Tyrodes' solution. DAD was induced only during perfusion with a modified Tyrode's solution (mimic the extracellular milieu of patients with severe HF) [57]. EAD was never observed even in the modified solution [57]. In the same study, EAD could be induced in 30% of failing rabbit trabeculae [57]. This difference between failing human heart and failing rabbit hearts asks for caution in using animal models and suggests the importance in conducting mechanistic studies directly in failing human hearts.

Abnormal Ca^{2+} handling could also produce the substrate for arrhythmia by facilitating AP duration (APD) alternans (or repolarization alternans) [58, 59], the relevance of which was implicated in the predictive power of T-wave alternans in the arrhythmic events in the HF patients [60]. Spatially discordant APD alternans increase dispersion of repolarization and promote unidirectional block and subsequent induction of arrhythmia [61]. In a dog model of HF, Wilson et al. [59] showed that HF significantly lowered heart-rate threshold for calcium transient alternans. They also demonstrated that calcium transient alternans enhancement was independent from HF-associated changes in repolarization and appeared to be responsible for the enhanced APD alternans [59]. Improvement of Ca^{2+} cycling through targeted SERCA2a gene expression was shown to retard the development of APD alternans [62]. It remains to be demonstrated how the altered Ca^{2+} cycling leads to cellular alternans in the failing human heart.

Molecular and Cellular Basis of Abnormal Calcium Handling and Signaling in Human HF

Alteration in the $[Ca^{2+}]_i$ is attributed to the abnormal calcium handling in the EC coupling process, which is operated by the sarcolemma and SR, including L-type Ca^{2+} channels, RyR, NCX and SERCA2a. Altered EC coupling in HF have been reviewed in detail elsewhere [3, 18, 43]. Here we mainly focus on reviewing the results regarding the failing human heart.

Calcium-Induced Calcium Release (CICR)

Triggering of CICR (i.e., I_{Ca}) in the failing human heart is mostly unchanged [26, 28, 30, 63], though inhibition of I_{Ca} was observed at higher frequencies [64]. Thus, the smaller Ca^{2+} transient observed in HF is mainly due to a reduced capability of I_{Ca} to trigger Ca^{2+} release from the SR (or a reduced EC coupling gain).

The reduced EC coupling gain may result from the hyperphosphorylation of RyRs in the failing human heart [10]. PKA hyperphosphorylation of RyRs leads to the dissociation of the FKBP12.6 regulatory subunit, which inhibits the coupled gating of arrays of RyR channels and thus could result in a loss of EC coupling gain [10]. This is supported by the reduced amplitude and changed properties of Ca^{2+} sparks measured from isolated ventricular myocytes from failing human hearts [65]. More discussion of RyRs can be found in the section "RyR".

Rapid activation of RyRs by I_{Ca} is facilitated by the close proximity of the L-type Ca^{2+} channels and RyRs. Reduced EC coupling gain in HF could thus also originate from the geometric derangement of RyRs and L-type Ca^{2+} channels, as suggested by the spontaneous hypertensive rat with HF (SHR-HF) [37]. Disorganization of T-tubules and a decrease in the colocalization of L-type Ca^{2+} channels and RyRs have been demonstrated in fixed ventricular samples from failing human hearts [66]. The actual loss of T-tubules in isolated myocytes from failing human heart was reported in one study [67] but not in another [68], findings that might be explained by the large spatial variations in T-tubule remodeling in human HF [66].

The ultrastructural defects in the T-tubule system were demonstrated to cause the dyssynchronous Ca^{2+} release (or defective EC coupling) by confocal line scanning techniques in the isolated ventricular myocytes from SHR-HF, with Ca^{2+} release being delayed in certain regions of a myocyte compared to the other normally coupled areas [69]. Louch and coworkers showed modest dyssynchrony of Ca^{2+} release in the isolated myocytes from failing human hearts [70]. While the local delayed SR Ca^{2+} release was confirmed in the whole heart level in SHR-HF [71], no study has been done so far to demonstrate the dyssynchronous Ca^{2+} release at the tissue level from the failing human hearts. However, the morphological changes of Ca^{2+} transient observed in our recent left ventricular wedge preparations from failing human hearts imply the potentially important role of dyssynchronous Ca^{2+} [31].

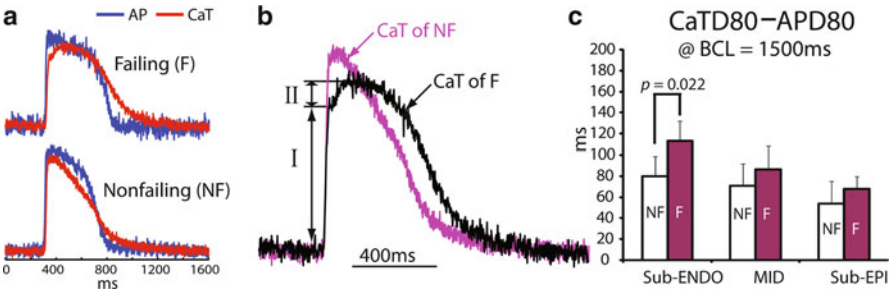

Fig. 52.3 Morphological changes of calcium transient (*CaT*) and its relation to action potential (*AP*). (**a**) Simultaneous recordings of AP and CaT at one site at subendocardium from a failing human heart (F, *top*) and a nonfailing human heart (NF, *bottom*). (**b**) The two CaTs from panel A are overlapped for easy comparison. Compared to the CaT from NF, there is a distinct second rising component (labeled by "II") in the CaT from failing human heart. Note that this second component was only observed at the sub-endocardium in 60% of the studied failing human hearts. (**c**) CaT duration at 80% relaxation (*CaTD80*) minus AP duration at 80% (*APD80*), summarized from five nonfailing hearts and five failing hearts (two ischemic cardiomyopathy and three idiopathic cardiomyopathy). It can be seen that this duration difference is significantly longer at the subendocardium in the failing human heart compared with the non-failing human heart, which is reflected in the example shown in *panel A* [31]

We observed two components in the rising portion of Ca^{2+} transient, with a slow rising component following an initial fast rising component (Fig. 52.3a, b) [31]. It is possible that the first fast-rising component corresponds to the normally triggered Ca^{2+} release and the second slow-rising component corresponds to the delayed Ca^{2+} release, which has been shown in SHR-HF [71]. Interestingly, this morphological change of Ca^{2+} was only observed at the subendocardium in 60% of the studied failing human hearts [31]. This regional difference might result from the higher susceptibility to ischemia by the endocardium compared with epicardium [72, 73], and suggests that the extrapolation of results from one region (e.g., endocardium) to another region (e.g., epicardium) in human studies should be done with caution. This delayed Ca^{2+} release might be also underlie the slower recovery of intracellular Ca^{2+} relative to the recovery of the action potential observed in our study (Fig. 52.3a, c). That is, the Ca^{2+} transient outlasts the action potential at the subendocardium of the failing human heart, which might lead to phase three early afterdepolarization [74].

The reduced EC coupling gain could also result from decreased SR Ca^{2+} content, which has been extensively demonstrated in human HF [30, 38, 39, 41, 42]. The success of molecular therapies aimed at restoring SR Ca^{2+} content further underscores the importance of SR Ca^{2+} content [75, 76]. Reduced SR Ca^{2+} content in the failing human heart could result from leaky RyRs, reduced SR Ca^{2+} uptake via SERCA2a, and increased Ca2+ extrusion via NCX, which are reviewed in the sections below ("RyR" and "SERCA2a, PLN and NCX").

RyR

Most studies showed no change in the protein expression of RyR in human HF [3, 43]. However, the characteristics of Ca^{2+} sparks are altered in isolated myocytes from failing human hearts [65]. Furthermore, RyRs in human HF are "leaky," [10] contributing to a reduction of SR Ca^{2+} content [77]. The SR Ca^{2+} leak occurred despite reduced SR Ca^{2+} loading in a canine model of HF [77].

Leaky RyR is thought to result from hyperphosphorylation of RyR by PKA or CAMKII. Increased Ca^{2+} sensitivity and higher probability of open RyR in failing human hearts was first observed by Marx and coworkers [10]. They concluded that the increased local PKA-mediated phosphorylation of RyR in HF leads to the disassociation of FKBP12.6 from RyRs, leading to higher open probability at rest [10]. They also observed decreased association of phosphatases (PP1, protein phosphatase 2A [PP2A]) to RyR, which may exacerbate PKA-mediated hyperphosphorylation of RyR [10]. The hyperphosphorylation of RyRs could also result from the deficiency of phosphodiesterase 4D (PDE4D), which resides in the RyR macromolecular signaling complex and regulates the local concentration of cAMP that activates PKA [11]. The impact of PKA phosphorylation in reducing the RyR/FKBP12.6 association remains controversial [78, 79].

Increased SR Ca^{2+} leak in isolated myocytes from failing rabbit hearts was shown to relate to the hyperphosphorylation of RyR by CAMKII [80]. Ca^{2+} leak was reduced by the inhibition of CAMKII but not altered by PKA inhibition [80], suggesting the potential role of CAMKII inhibition in improving the Ca^{2+} handling in HF. This hypothesis is further supported by a recent study by Sossalla et al. [16] who showed a significant increase in the expression the CAMKII in both left and right ventricles of the failing human heart, and observed that inhibition of CAMKII reduced the SR Ca^{2+} leak and increased the Ca^{2+} content. Importantly, they also showed that inhibition of CAMKII improved contractility in isolated ventricular trabeculae [16]. They reported that CAMKII inhibition restored the positive FFR [16]. This is in sharp contrast to the study by Kushiner et al. [81] which showed that CAMKII inhibition completely abolished the positive FFR in mouse heart. The result from the latter study is consistent with the hypothesis that CAMKII is responsible for sensing the frequency of Ca2+ oscillation [82] as well as for causing the positive FFR via increased phosphorylation of RyR and PLN at increasing frequencies [13, 83]. Kushiner and coworkers also showed that RyR phosphorylation by CAMKII was decreased in failing human hearts in despite of the global increase of CAMKII [81], and suggested that the impaired RyR phosphorylation by CAMKII plays a role in blunted FFR in human HF. Further studies are needed to resolve these areas of controversy and clarify the molecular mechanism and the promise of CAMKII inhibition in improving the Ca^{2+} handling in human HF.

While much evidence supports altered regulation and function of the RyR leading to abnormal Ca^{2+} handling in failing human heart, there are studies indicating the opposite. Recordings of currents through the RyR from failing human hearts did not reveal any significant alterations at a single channel level [84]. Jiang et al.

observed neither structural nor functional change of RyRs from the failing human heart but did report a significant reduction in SERCA2a expression, suggesting that abnormal Ca^{2+} uptake may contribute more to the altered Ca^{2+} handling in human HF [78].

SERCA2a, PLN and NCX

SR Ca^{2+} uptake was reduced in the failing human heart [30, 46, 85, 86]. This might be due to depressed protein expression of SERCA2a. Hasenfuss et al. observed downregulation of SERCA2a expression as well as a significant correlation between SERCA protein levels and SR Ca^{2+} uptake in failing human hearts [46]. Overexpression of SERCA2a has been shown to restore the Ca^{2+} handling and the contractile function with positive FFR in isolated failing human myocytes [87, 88]. While some studies observed the downregulation of protein expression of SERCA2a in the failing human heart, others did not find any changes in the protein expression of SERCA2a [89]. This inconsistency might be explained by our recent findings [31]. We observed down-regulation of SERCA2a expression in samples from the subendocardium of failing human hearts with ischemic cardiomyopathy but not in samples from epicardium or from failing hearts with dilated cardiomyopathy (Fig. 52.4a), suggesting that the alteration of SERCA2a expression might be region-dependent as well as HF etiology-dependent [31].

Besides the potential decrease in protein expression, the decreased activity of SERCA2a in HF might also result from altered regulation. This is supported by the findings that decreased SR Ca^{2+} uptake was observed in despite unchanged protein levels of SERCA2a [85, 86, 90].

SERCA2a is directly regulated by PLN which is mainly phosphorylated by PKA and CAMKII [89]. PLN inhibits SERCA2a activity when it is not phosphorylated, while its phosphorylated form disassociates from SERCA2a. In the failing human heart, majority of the studies indicate no change in the protein expression of PLN [31, 89], which is consistent with our recent study (Fig. 52.4b) [31]. However, the phosphorylation state of PLN was decreased in the failing human heart [85, 90, 91], suggesting increased inhibition of SERCA2a by PLN in the failing human heart. PLN is mainly phosphorylated by PKA at serine-16 and by CAMKII at threonine-17. Phosphorylation at threonine-17 is decreased due to increased dephosphorylation by calcineurin in failing human hearts with dilated cardiomyopathy [92]. PLN phosphorylation at serine-16 is decreased presumably due to increased level of PP1 in the failing human heart, [90, 93] which might be a result of increased PKC-α [19, 20]. Interventions to attenuate the inhibitory effect of PLN on SERCA2a have been tested in animal models. Minamisawa et al. found that knockout of PLN significantly increased SR Ca^{2+} content and completely rescued the spectrum of heart-failure phenotype in a mouse model of HF [94]. Decreased PLN expression via adenoviral gene transfer of antisense of PLN was shown to improve both contraction

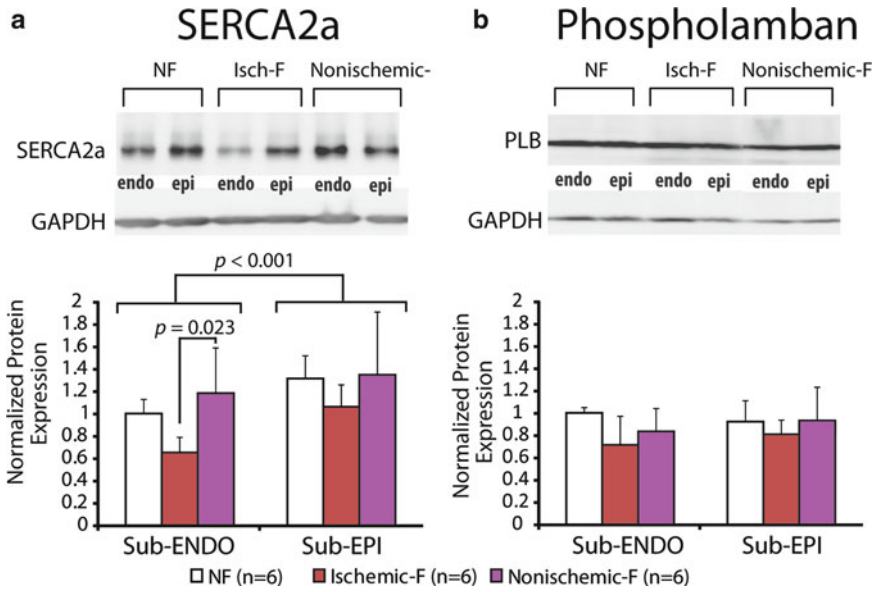

Fig. 52.4 Protein expressions of sarcoplasmic reticulum Ca^{2+} ATPase 2a (*SERCA2a*) and phospholamban (*PLN*). Representative examples of Western blots (*top*) and normalized protein expression (*bottom*) are shown for SERCA2a (**a**) and PLN (**b**). *NF (n = 6)* indicates the group of non-failing hearts, *Isch-F (n = 6)* the group of failing hearts with ischemic cardiomyopathy, Nonischemic-F (n = 6) the group of failing hearts with nonischemic/idiopathic cardiomyopathy [31]. *ENDO* indicates endocardium, *EPI* epicardium

and relaxation in isolated myocytes from failing human hearts [88]. Inhibition of PKC-α was shown to increase the SR Ca^{2+} load and protect the mouse from HF [19, 95]. The importance of PKC-α and other isoforms of PKC in the Ca^{2+} handling in human HF remains to be determined.

While protein expression of NCX was found upregulated in most animal models of HF [3], it is less consistent in the failing human heart, with most studies finding either increased or unchanged protein expression of NCX [43]. In contrast to reduced SR Ca^{2+} uptake, the NCX current density as a function of $[Ca^{2+}]$ was not changed in the failing human heart [30]. However, the contribution of NCX to the $[Ca^{2+}]_i$ relaxation was increased due to the depressed SR Ca^{2+} uptake [30]. Furthermore, the preference of NCX current direction during the action potential plateau shifted from inward direction (Ca^{2+} efflux) to outward direction (Ca^{2+} influx) due to a reduced submembrane $[Ca^{2+}]_i$ and increased $[Na^+]_i$ in the failing human heart [96]. The reversed-mode NCX during AP plateau could contribute to a slow decay of $[Ca^{2+}]_i$ transient [41, 96], which may facilitate contraction at slow heart rates but may also lead to diastolic dysfunction at faster heart rates [42].

Loss of Metabolic Capacity

Ca^{2+} handling and energy homeostasis are interdependent [97]. Ca^{2+} homeostasis relies on efficient energy-driven ionic fluxes, i.e., through SERCA2a and Na^{+}-K^{+} ATPase, while $[Ca^{2+}]_i$ in turn determines energy consumption through contraction and Ca^{2+} transport as well as energy production via the regulation of ATP generation in mitochondria [97, 98]. Disturbance of the finely tuned balance between the two could be responsible for the abnormal Ca^{2+} handling and diminished contractility that are hallmarks of HF.

HF is associated with defects in energy metabolism, with decreased energy production as well as impaired energy transfer and utilization [97]. These impaired cardiac energetics may represent the thermodynamic limit for Ca^{2+} handling [99]. Reduced local ATP/ADP ratio, due to a local lack of creatinine kinase, could affect the kinetic and thermodynamic efficiency of SERCA in HF [99], providing another mechanism for impaired SR Ca^{2+} uptake. Indeed, ATP was reported to protect SERCA2a from being denatured by hydroxyl radicals [100], implying that energy starvation might render SERCA2a unprotected from increased oxidative stress in human HF.

Improving the myocardial energetics has been shown to normalize the Ca^{2+} cycling in isolated failing human myocytes [101]. β-blockers, which decrease the energy demand and thus ameliorate the mismatch between energy production and consumption, has been shown to normalize the function and regulation of key Ca^{2+} handling proteins in failing human hearts [102]. Similarly, left ventricular assist devices (LVADs), which unload the heart and support the circulation, impart improved Ca^{2+} handling in human HF [10, 103]. Finally, hemodynamic improvement by cardiac resynchronization therapy (CRT) is correlated with improved Ca^{2+} handling in the subset of HF patients who respond to this therapy [104]. On the other hand, restoration of Ca^{2+} homeostasis may result in improved cardiac energetics [105].

Correcting Abnormal Calcium Handling in HF

While the causes of HF may differ, there is a common theme underlying the progression from normal to failing heart. An initial cardiac insult, which, in the United States is most commonly inadequate myocardial flow (myocardial infarction), prolonged pressure overload (hypertension), or abnormal flow through the heart valves (valvular stenosis or insufficiency), causes the heart to alter the shape of its principal pumping chamber, the left ventricle, and the surrounding organs to activate multiple hormonal systems in an attempt to maintain cardiac output. These compensatory changes are initially helpful in sustaining adequate cardiac output and blood pressure [106]. Over time, however, these same changes become maladaptive. The remodeled ventricle becomes increasingly dilated and hypertrophied, resulting in

suboptimal pump geometry. In parallel, continuous activation of the sympathetic nervous system and the renin-angiotensin-aldosterone (RAA) axis [107, 108] leads to increased oxygen consumption, increased metabolism and molecular changes that ultimately impair the contractile function of myocytes. In this manner, an initial cardiac insult initiates a cascade of events leading to reduced ejection fraction, reduced myocardial contractility and poor cardiac output. Current clinical therapies aim to halt or reverse these maladaptive events. Myocardial revascularization by coronary artery bypass grafting (CABG) and percutaneous coronary intervention (PCI) restores myocardial blood flow to ensure that adequate oxygen and metabolites are supplied to the myocardium. On the other hand, most medical therapies aim to block the deleterious effects of prolonged hormonal stimulation and the subsequent molecular changes that ultimately impair myocardial contractility and promote fatal cardiac arrhythmias. Importantly, reduced cardiac contractility and diminished contractile reserve are hallmarks of HF, and central to these pathologies is defective intracellular Ca^{2+} handling [39]. Current and future medical strategies to restore the function of the key calcium handling molecules are discussed below.

Molecular Changes Due to Activation of the Sympathetic Nervous System

After an initial cardiac insult, the sympathetic nervous system is activated to maintain adequate cardiac output. This stress response, also known as the "fight or flight" response, is highly conserved evolutionarily and crucial to increasing cardiac stroke volume and heart rate [109], the product of which is cardiac output. Catecholamines such as epinephrine and norepinephrine (adrenaline and noradrenaline, respectively) are released into the bloodstream where they effect changes on target organs, including the heart.

In response to sympathetic stimulation, both heart rate and myocyte contractility are increased, the latter of which is directly related to changes in Ca^{2+} handling. Epinephrine and norepinephrine bind to the β-adrenoreceptor, leading to activation of several signaling pathways that ultimately increase the amount of intracellular Ca^{2+} released by the RyR per amount of trigger Ca^{2+} entering the cell through L-type Ca^{2+} channels, thereby increasing EC coupling gain [37]. β-adrenoreceptor binding also increases contractile force and allows more rapid release and reuptake of Ca^{2+}, allowing more time for diastolic filling, increasing stroke volume and therefore increasing cardiac output [109, 110].

Downstream effectors activated through these pathways include PKA via G protein activation of adenylate cyclase [106] and increased CAMKII activity [13], while activation of both the RAA axis or β_1-adrenoreceptor leads to activation of PKC [19, 111]. PKA and CAMKII phosphorylate L-type Ca^{2+} channels, RyR and PLN. Many of these signaling events inherent to the "fight or flight" response are seen physiologically and in fact, are crucial for survival during isolated periods of

stress or exercise. However, the continuous activation of these pathways that occurs in HF ultimately leads to defective Ca^{2+} handling and diminished contractility [112, 113], and are therefore attractive targets of current and future medical therapies.

Chronic activation of G protein coupled β-adrenoreceptors by sympathetic hormones leads to several maladaptive changes including decreased expression and function of adenylate cyclase, increased expression of inhibitory proteins G protein G_i and β-adrenoreceptor kinase, and even decreased expression and coupling of the β-adrenoreceptor itself [106, 114–116]. Downstream of the β-adrenoreceptor, additional changes occur. PKA hyperphosphorylates L-type Ca^{2+} channels, RyR and NCX, while simultaneously, the protein levels of L-type Ca^{2+} channels, RyR and SERCA2a are altered [10, 41, 117, 118]. In summary, chronic β-adrenoreceptor activation induces numerous changes that alter the function of proteins critical to Ca^{2+} handling. Determining which of these changes are causal for the diminished cardiac contractility seen in HF has proven far more challenging. Nonetheless, a number of pathways and targets have been elucidated.

Combating Chronic β-adrenoreceptor Stimulation

Blockade of β-adrenoreceptors using a class of drugs known as β-blockers restores cardiac function and significantly increase the survival of patients with HF [119–123]. The effectiveness of this therapy is somewhat counterintuitive since β-blockers depress contractility and heart rate, two major determinants of cardiac output. Indeed, physicians treating acute HF often temporarily discontinue β-blockers to improve cardiac output and restore fluid balance. After the acute volume overload has been corrected, however, treatment with β-blockers is reinstituted. The reasoning behind this strategy is that chronic activation of β-adrenoreceptors is ultimately maladaptive to the heart, and leads to the progression of HF. β-blockers combat this chronic sympathetic stimulation. Mechanistically, they decrease intracellular cAMP concentration and thus decrease the activity of PKA, restoring physiologic function and expression levels of downstream effectors [102, 118, 124–128]. Treatment with β-blockers also reverses the hyperphosphorylation of RyR to improve binding of FKBP12.6, thereby restoring physiologic RyR function [102, 125, 128, 129]. Diminished SERCA2a protein levels are also restored by β-blocker therapy, allowing appropriate reuptake of Ca^{2+} to allow adequate diastolic function and filling time [129]. Thus, β-blocker therapy may halt or reverse disease progression and reduce mortality by reversing the diminished Ca^{2+} transient amplitude in systole, while simultaneously reversing increased intracellular Ca^{2+} concentration and slowed rate of Ca^{2+} transient decay in diastole [28, 130]. It is important to point out that despite numerous studies showing improvement in HF with the use of β-blockers, the precise mechanisms responsible for their well established beneficial effects remain controversial. And while effects on Ca^{2+} handling have been demonstrated, improved organ level structural changes have also been observed [106].

Inhibiting the Effect of Angiotensin II

In addition to the sympathetic nervous system, another hormonal axis is chronically elevated in patients with HF. The renin-angiotensin-aldosterone (RAA) axis is central to maintaining blood pressure. In response to low blood pressure, renin is released from the kidney and converts the pre-hormone angiotensinogen to angiotensin I. Angiotensin I is converted to Angiotensin II (ATII) in the lungs by angiotensin converting enzyme (ACE). ATII potently increase blood pressure by binding ATI receptors in the vasculature and causing constriction of blood vessels. ATI receptors are also located on myocytes, where they are acted upon by ATII. Two major categories of drugs designed to lower blood pressure by inhibiting this pathway are angiotensin converting enzyme inhibitors (ACEI), which block the conversion of ATI to ATII, and angiotensin receptor blockers (ARB), which inhibit the binding of ATII to ATI-receptors.

HF is a state of low cardiac output, which results in diminished blood pressure. However, low blood pressure is typically seen only at the last stages of HF. This is likely due to the maintenance of blood pressure by chronically elevated levels of ATII seen in HF patients [107, 108]. Importantly, the use of ACEIs and ARBs has been shown to further significantly reduce mortality and fatal cardiac arrhythmias in patients with HF [122]. Hence, in addition to β-blockers, ACEIs or ARBs are recommended first line agents for the treatment of HF [108]. ACEIs and ARBs likely reduce mortality by lowering blood pressure and reducing myocardial fibrosis in patients with HF. More recently, however, they have been shown to alter signaling cascades that are involved in Ca^{2+} handling.

ATII binding to ATI receptors on myocytes activates the G protein Gq, which has multiple downstream effectors that impact the progression of HF. One of these effectors is PLC, which, in turn, activates PKCα, the predominant cardiac PKC isoform [131]. PKC-α activates I-1, which increases the activity of PP1 to dephosphorylate PLN [19]. In a mouse model of diastolic HF, ACE was overexpressed to increase levels of ATII, resulting in dephosphorylation of PLN and diastolic HF. [132] Importantly, dephosphorylated PLN inhibits the ability of SERCA2a to pump Ca^{2+} back into the SR, which may impair heart function by increasing the Ca^{2+} transient duration and decreasing the SR Ca^{2+} content. This alteration likely exacerbates the reduced diastolic filling time, stroke volume and contractility that are seen in heart failure.

ATII mediated Gq activation also causes activation of the downstream effectors calcineurin [133, 134] and mitogen-activated protein (MAP) kinases such as extracellular signal regulated kinases 1 and 2 (ERK1/2) [118, 135], leading to pathological hypertrophic ventricular remodeling. Calcineurin, a Ca^{2+}-dependent phosphatase that regulates hypertrophic gene transcription by desphosphorylating transcription factors such as nuclear factor of activated T-cells (NFAT), has been identified as a key enzyme involved in the induction of pathological cardiac hypertrophy. NFAT activity was upregulated in mouse models of pressure overload and HF but not in mice with exercise-induced physiological hypertrophy [136]. Supporting this notion,

inhibition of calcineurin prevented cardiac hypertrophy in rodent models of cardiomyopathy and pressure overload [137]. ACEIs and ARBs may thus impart some of their beneficial effects on failing hearts by reversing maladaptive effects of ATII on Ca^{2+} handling, which, in turn, may also ameliorate ventricular remodeling via the Ca^{2+} dependent calcineurin pathway. Interestingly, all of these effects appear to occur through activation of major phosphatase, rather than kinase effectors.

Patients with HF exhibit elevated levels of reactive oxygen species (ROS) [138]. ATII has been shown to be a key player in producing destructive ROS that are involved in the progression of HF [139, 140]. ATII induces the production of ROS in the heart [141], leading to damage to cellular components that are critical to calcium handling in myocytes such as the outer and inner membranes of organelles such as the SR and protein involved in Ca^{2+} signaling and handling [142–145]. ROS alter the function of NCX, decrease L-type Ca^{2+} channel currents and depress the activity of SERCA2a [146–148]. Thus, blockade of ATII through ACEIs and ARBs provides clinicians a tool to reduce oxidative stress in failing myocytes and move closer to the goal of restoring calcium handling.

Interestingly, blocking ATII may also directly inhibit β-adrenoreceptor overstimulation. The ARB valsartan binds presynaptic ATI receptors to inhibit the release of norepinephrine while also stimulating its reuptake [149], thereby reducing the amount of norepinephrine released into the bloodstream. Whether this holds true for other ARBs is unclear.

Calcium Channel Blockade

One of the disappointments of clinicians and researchers alike is the lack of benefit and even detrimental effect of drugs that block L-type Ca^{2+} channels (dihydropyridine receptors). These drugs, used primarily to treat blood pressure, have dilatory effects on blood vessels inside and outside the heart. The vasodilatory action of Ca^{2+} channel blockers was theorized by many to improve cardiac performance and reduce myocardial ischemia. However, these theoretical advantages have not been translated into clinical benefits in controlled clinical HF trials, discussed in more detail below.

Ca^{2+} channel blocking drugs have not improved symptoms of HF or enhanced exercise tolerance, and significantly, both short- and long-term treatment with these drugs have increased the risks of worsening HF and death [150–156]. L-type Ca^{2+} channel blockade is also ineffective in mild HF [157], and non-dihydropyridine type Ca^{2+} antagonists, including T-type Ca^{2+} channel blockers, have also proven ineffective [158, 159]. Moreover, Ca^{2+} channel blockers can have life threatening interactions with β-blockers and ACEIs, by inducing severe bradycardia (low heart rate) and hypotension (low blood pressure) [160, 161]. As a result, most Ca^{2+} channel blockers are avoided in patients with HF, even when used for the treatment of chest pain or hypertension. Of available agents, only the dihydropyridine drug amlodipine has been shown not to adversely affect survival, although experience with the drug

exists largely in patients who are not taking β-blockers [162]. In fact, current clinical HF guidelines state that Ca^{2+} channel blocking drugs are contraindicated in the treatment for patients with current or prior symptoms of HF and reduced left ventricular ejection fraction [108].

Experimental Therapies Targeting Abnormal Calcium Handling

The limited medical therapies available for the treatment of HF and the significant abnormalities in Ca^{2+} handling observed in failing hearts has prompted significant interest in developing therapies that directly target and correct these altered molecular pathways. A subset of some promising therapies and strategies are discussed below.

Sensitizing β-adrenoreceptor Function

Restoring sensitization of β-adrenoreceptors via new agents represents an attractive drug therapy. The desensitization of β-adrenoreceptors is mediated in part by G-protein coupled receptor kinase (GRK, also known as β-ARK). Activation of GRK desensitizes β-adrenoreceptors in the heart [163]. In contrast, inhibition of GRK with concomitant β-blocker therapy improves survival in a mouse model of HF [164, 165]. Currently, no drug has been developed to inhibit GRK pharmacologically, but a dominant-negative GRK expressed in a mouse model of HF has been shown to prevent disease progression [165]. In the future, such a multipronged approach to combat chronic β-adrenoreceptor stimulation may provide significant further benefit in the treatment of HF.

Improving RyR Function

Hyperphosphorylation of RyR by PKA occurs due to chronic β-adrenergic stimulation and leads to Ca^{2+} leak through the RyR [10, 166], which contributes to contractile dysfunction and fatal ventricular arrhythmias [109, 167, 168]. These arrhythmias are a major cause of death in patients with advanced HF [108]. This knowledge has prompted efforts to design a small molecule that will improve RyR function. JTV519 is an experimental drug that enhances the binding of FKBP12.6 to RyR and reduces Ca^{2+} leak from the SR. Encouragingly, this agent has been shown to suppress ventricular arrhythmias in a mouse model [168] and improve contractile function in a canine model of HF [169]. Finally, Inhibition of CAMKII, which also hyperphosphorylates RyR, represents another strategy of reducing the RyR Ca^{2+} leak seen in HF. Chemical or genetic inhibition of CAMKII prevented cardiac remodeling in a murine model of isoproterenol-induced cardiomyopathy [170].

Enhancing SERCA2a Reuptake of Calcium

As discussed above, diminished Ca^{2+} reuptake in failing hearts is likely due to a combination of decreased levels of SERCA2a expression [29, 31, 43, 171] and hypophosphorylation of PLN [172, 173]. Understandably, methods to increase SERCA2a expression and PLN phosphorylation are being actively pursued by investigators.

Attempts to overexpress SERCA2a in humans with advanced HF are currently underway [76]. In this study, a SERCA2a expression vector packaged in an Adenovirus-Associated Virus (AAV) envelope is administered by direct intracoronary injection [76]. Of the 9 patients treated, 5 demonstrated improvements from baseline to month 6 across a number of parameters important in HF, including symptoms, 6-min walk test, oxygen consumption, and ejection fraction [76]. Notably, 2 patients who failed to improve had preexisting anti-AAV neutralizing antibodies, underscoring a limitation of such an approach [76].

Selectively enhancing PLN phosphorylation is another avenue being actively pursued. One such line of experiments involves the delivery of a pseudo-phosphorylated mutant of PLN into failing hearts using a viral vector. Interestingly, this mutant was demonstrated to suppress HF progression in hamsters [174] and post-myocardial infarction rats [175], and reversed HF in sheep with chronic pacing induced HF [176]. Decreasing the activity of PP1 (which dephosphorylates PLN) is another possible approach. Inhibitor-2 (INH-2) is an endogenous phosphatase that inhibits PP1 that selectively decreases SR microvesicle-associated PP1 activity. Moreover, gene delivery of INH-2 was shown to increase PLN phosphorylation and increase survival in a hamster model HF [177]. Despite these encouraging studies, no small molecules that can selectively increase PLN phosphorylation have been developed to date.

Retarding ROS Effects

Established experimental studies showing that ROS are detrimental have prompted efforts to combat oxidative damage in patients with HF. The β-blocker carvedilol has been proven effective in reducing the progression of HF, and notably, may exert some of its beneficial effects through anti-oxidant activity [119]. Xanthine oxidase (X0), an enzyme involved in the synthesis of DNA precursors, has been shown to generate ROS, and has attracted the interest of researchers as a molecule to target with inhibitors [178, 179]. Encouragingly, inhibition of XO with the drug allopurinol improved myocardial efficiency in patients with HF [180], and prompted the initiation of a large-scale clinical trial testing its safety and efficacy in patients with advanced HF [181]. While this study did not show a reduction in morbidity or mortality overall, post-hoc analysis revealed benefit in a subset of patients with elevated levels of the XO product uric acid [182]. And while it will be helpful to determine the specific changes in Ca^{2+} handling pathways that were affected in this subset of patient, this study also suggests that more robust improvements in HF may be elicited in future trials by more specifically targeting the subset of HF patients with elevated ROS activity.

Calcium Abnormalities in Human Ischemic and Nonischemic Cardiomyopathy

End-stage HF that is the result of myocardial infarction is known as ischemic cardiomyopathy (ICM). HF in patients with no history of myocardial infarction is referred to as non-ischemic cardiomyopathy (NICM). Interestingly, distinct abnormalities in calcium handling have been demonstrated depending upon the etiology of HF. For example, mRNA expression of RyR is significantly decreased in the hearts of patients with end-stage ICM, but increased (albeit nonsignificantly) in patients with NICM [183]. Similarly, ICM is associated with a decreased rate of calcium uptake into the SR, while NICM is associated with a decreased rate of calcium release from the SR [184]. The authors of the latter study concluded that abnormal SR calcium uptake may explain the contractile dysfunction seen in ICM, while abnormal SR calcium release may be the primary disruption in NICM. Thus, different insults leading to cardiomyopathy may do so by disrupting calcium handling via different mechanisms.

While different etiologies of HF exhibit different profiles of calcium handling abnormalities, there are no therapies to date that have been shown to improve calcium handling in an etiology-specific manner. Recently, Sossalla and colleagues demonstrated that inhibition of CaMKII using two different small molecules significantly increased contractility of isolated preparations of human failing heart tissue [16]. The increase in contractility was equally significant in ischemic and non-ischemic cardiomyopathy. These studies suggest that in addition to the need to use human tissue to evaluate signaling pathways and small molecules for improved calcium handling, using an etiology-specific approach is sensible.

Conclusion

It has been well recognized that abnormal Ca^{2+} handling is a key pathophysiological mechanism in human HF. However, our understanding of the underlying molecular and cellular mechanisms for the altered calcium handling in the failing human heart remains incomplete.

This is partly due to the complexity of the system, which involves the interplay between a number of signaling pathways that regulates the Ca^{2+} homeostasis at different time scales [75, 185]. That is, while interrupting or augmenting one of pathways in the cascade might lead to expected beneficial therapeutic effects, it might also produce unexpected deleterious effects [75]. Nevertheless, the overall structure of this complex system is continually being revealed by ongoing basic and clinical research, which carries the hope of facilitating the development of effective diagnostic and treatment modalities for HF. The progress is also slowed by limited data from human studies. While many mechanistic hypothesis and potential therapeutic intervention for the abnormal Ca^{2+} handling in HF are being proposed and tested in animal models of HF, the examination of these hypothesis and therapies using

functional studies of isolated cells or tissues from the failing human heart are rather limited. Basic understanding and clinical translation can be greatly facilitated by testing these hypotheses in explanted human heart and human heart tissue donated for research by patients [186].

Gaining a clearer understanding of the causative mechanisms of abnormal Ca^{2+} handling is crucial to developing promising new therapies to treat HF. Despite our best efforts, there are currently only two major medical pharmacological approaches available to the clinician for the treatment of patients with HF: blockade of the β-adrenoreceptor and inhibition of the RAA axis. These therapies are used to treat non-ischemic (the majority of which are idiopathic), ischemic and valvular cardiomyopathies, even though we recognize fundamental differences in the insults that cause these separate conditions. Such blanket approaches demonstrate the limits of our current knowledge, and the need for further observation and testing before new therapies can be delivered to the patient. Moreover, it is clear that many pathways involving Ca^{2+} handling converge on and act through a few key molecules. Thus, the complex biological processes leading to HF must be further dissected with respect to specific isoforms, subcellular locations and etiology of HF. Similarly, it is important to realize that individual drugs effects must be categorized based on the species and type of animal model used. Finally, we must recognize that the road to developing a human therapeutic agent, i.e., going from the bench to the bedside, is a time consuming and expensive one, and littered with failures. These complexities may explain why after years of research, the clinical armamentarium for reversing HF remains rather limited. Despite these drawbacks, it is encouraging that many promising new therapies to ameliorate abnormal calcium handling are visible on the horizon, based on findings in animal models of HF. Increased research on functional human heart tissue would facilitate translation of these findings to the clinic.

References

1. Lloyd-Jones D, Adams RJ, Brown TM, Carnethon M, Dai S, De Simone G, Ferguson TB, Ford E, Furie K, Gillespie C (2010) Heart disease and stroke statistics-2010 update: a report from the American Heart Association. Circulation 121(7):e46
2. Bui AL, Horwich TB, Fonarow GC (2011) Epidemiology and risk profile of heart failure. Nat Rev Cardiol 8(1):30–41
3. Bers DM (2001) Excitation-contraction coupling and cardiac contractile force. Springer, The Netherlands
4. Berridge MJ, Bootman MD, Roderick HL (2003) Calcium signalling: dynamics, homeostasis and remodelling. Nat Rev Mol Cell Biol 4(7):517–529
5. Morgan JP (1991) Abnormal intracellular modulation of calcium as a major cause of cardiac contractile dysfunction. N Engl J Med 325(9):625–632
6. Hasenfuss G, Pieske B, Holubarsch C, Alpert NR, Just H (1993) Excitation-contraction coupling and contractile protein function in failing and nonfailing human myocardium. Adv Exp Med Biol 346:91–100
7. Katz AM (1990) Cardiomyopathy of overload. A major determinant of prognosis in congestive heart failure. N Engl J Med 322(2):100–110

8. Bohm M, Reiger B, Schwinger RH, Erdmann E (1994) cAMP concentrations, cAMP dependent protein kinase activity, and phospholamban in non-failing and failing myocardium. Cardiovasc Res 28(11):1713–1719
9. Kirchhefer U, Schmitz W, Scholz H, Neumann J (1999) Activity of cAMP-dependent protein kinase and Ca^{2+}/calmodulin-dependent protein kinase in failing and nonfailing human hearts. Cardiovasc Res 42(1):254–261
10. Marx SO, Reiken S, Hisamatsu Y, Jayaraman T, Burkhoff D, Rosemblit N, Marks AR (2000) PKA phosphorylation dissociates FKBP12.6 from the calcium release channel (ryanodine receptor): defective regulation in failing hearts. Cell 101(4):365–376
11. Lehnart SE, Wehrens XH, Reiken S, Warrier S, Belevych AE, Harvey RD, Richter W, Jin SL, Conti M, Marks AR (2005) Phosphodiesterase 4D deficiency in the ryanodine-receptor complex promotes heart failure and arrhythmias. Cell 123(1):25–35
12. Maier LS, Bers DM (2007) Role of Ca^{2+}/calmodulin-dependent protein kinase (CaMK) in excitation-contraction coupling in the heart. Cardiovasc Res 73(4):631–640
13. Wehrens XH, Lehnart SE, Reiken SR, Marks AR (2004) Ca^{2+}/calmodulin-dependent protein kinase II phosphorylation regulates the cardiac ryanodine receptor. Circ Res 94(6):e61–e70
14. Hain J, Onoue H, Mayrleitner M, Fleischer S, Schindler H (1995) Phosphorylation modulates the function of the calcium release channel of sarcoplasmic reticulum from cardiac muscle. J Biol Chem 270(5):2074–2081
15. Currie S, Loughrey CM, Craig MA, Smith GL (2004) Calcium/calmodulin-dependent protein kinase IIdelta associates with the ryanodine receptor complex and regulates channel function in rabbit heart. Biochem J 377(Pt 2):357–366
16. Sossalla S, Fluschnik N, Schotola H, Ort KR, Neef S, Schulte T, Wittkopper K, Renner A, Schmitto JD, Gummert J, El-Armouche A, Hasenfuss G, Maier LS (2010) Inhibition of elevated Ca^{2+}/calmodulin-dependent protein kinase II improves contractility in human failing myocardium. Circ Res 107(9):1150–1161
17. Hambleton M, Hahn H, Pleger ST, Kuhn MC, Klevitsky R, Carr AN, Kimball TF, Hewett TE, Dorn GW 2nd, Koch WJ, Molkentin JD (2006) Pharmacological- and gene therapy-based inhibition of protein kinase Calpha/beta enhances cardiac contractility and attenuates heart failure. Circulation 114(6):574–582
18. Yano M, Ikeda Y, Matsuzaki M (2005) Altered intracellular Ca^{2+} handling in heart failure. J Clin Invest 115(3):556–564
19. Braz JC, Gregory K, Pathak A, Zhao W, Sahin B, Klevitsky R, Kimball TF, Lorenz JN, Nairn AC, Liggett SB, Bodi I, Wang S, Schwartz A, Lakatta EG, DePaoli-Roach AA, Robbins J, Hewett TE, Bibb JA, Westfall MV, Kranias EG, Molkentin JD (2004) PKC-alpha regulates cardiac contractility and propensity toward heart failure. Nat Med 10(3):248–254
20. Bowling N, Walsh RA, Song G, Estridge T, Sandusky GE, Fouts RL, Mintze K, Pickard T, Roden R, Bristow MR, Sabbah HN, Mizrahi JL, Gromo G, King GL, Vlahos CJ (1999) Increased protein kinase C activity and expression of Ca^{2+}-sensitive isoforms in the failing human heart. Circulation 99(3):384–391
21. Wang J, Liu X, Sentex E, Takeda N, Dhalla NS (2003) Increased expression of protein kinase C isoforms in heart failure due to myocardial infarction. Am J Physiol Heart Circ Physiol 284(6):H2277–H2287
22. Simonis G, Briem SK, Schoen SP, Bock M, Marquetant R, Strasser RH (2007) Protein kinase C in the human heart: differential regulation of the isoforms in aortic stenosis or dilated cardiomyopathy. Mol Cell Biochem 305(1–2):103–111
23. Yue DT, Marban E, Wier WG (1986) Relationship between force and intracellular [Ca^{2+}] in tetanized mammalian heart muscle. J Gen Physiol 87(2):223–242
24. Gwathmey JK, Copelas L, MacKinnon R, Schoen FJ, Feldman MD, Grossman W, Morgan JP (1987) Abnormal intracellular calcium handling in myocardium from patients with end-stage heart failure. Circ Res 61(1):70–76
25. Gwathmey JK, Slawsky MT, Hajjar RJ, Briggs GM, Morgan JP (1990) Role of intracellular calcium handling in force-interval relationships of human ventricular myocardium. J Clin Invest 85(5):1599–1613

26. Beuckelmann DJ, Nabauer M, Erdmann E (1991) Characteristics of calcium-current in isolated human ventricular myocytes from patients with terminal heart failure. J Mol Cell Cardiol 23(8):929–937
27. Gwathmey JK, Warren SE, Briggs GM, Copelas L, Feldman MD, Phillips PJ, Callahan M Jr, Schoen FJ, Grossman W, Morgan JP (1991) Diastolic dysfunction in hypertrophic cardiomyopathy. Effect on active force generation during systole. J Clin Invest 87(3):1023–1031
28. Beuckelmann DJ, Nabauer M, Erdmann E (1992) Intracellular calcium handling in isolated ventricular myocytes from patients with terminal heart failure. Circulation 85(3):1046–1055
29. Pieske B, Kretschmann B, Meyer M, Holubarsch C, Weirich J, Posival H, Minami K, Just H, Hasenfuss G (1995) Alterations in intracellular calcium handling associated with the inverse force-frequency relation in human dilated cardiomyopathy. Circulation 92(5):1169–1178
30. Piacentino V 3rd, Weber CR, Chen X, Weisser-Thomas J, Margulies KB, Bers DM, Houser SR (2003) Cellular basis of abnormal calcium transients of failing human ventricular myocytes. Circ Res 92(6):651–658
31. Lou Q, Fedorov VV, Glukhov AV, Moazami N, Fast VG, Efimov IR (2011) Transmural heterogeneity and remodeling of ventricular excitation-contraction coupling in human heart failure. Circulation 123:1881–1890
32. Vahl CF, Bonz A, Timek T, Hagl S (1994) Intracellular calcium transient of working human myocardium of seven patients transplanted for congestive heart failure. Circ Res 74(5):952–958
33. Allen DG, Blinks JR (1978) Calcium transients in aequorin-injected frog cardiac muscle. Nature 273(5663):509–513
34. Blinks JR, Wier WG, Hess P, Prendergast FG (1982) Measurement of Ca^{2+} concentrations in living cells. Prog Biophys Mol Biol 40(1–2):1–114
35. Kubo H, Margulies KB, Piacentino V 3rd, Gaughan JP, Houser SR (2001) Patients with end-stage congestive heart failure treated with beta-adrenergic receptor antagonists have improved ventricular myocyte calcium regulatory protein abundance. Circulation 104(9):1012–1018
36. Hasenfuss G, Mulieri LA, Leavitt BJ, Allen PD, Haeberle JR, Alpert NR (1992) Alteration of contractile function and excitation-contraction coupling in dilated cardiomyopathy. Circ Res 70(6):1225–1232
37. Gomez AM, Valdivia HH, Cheng H, Lederer MR, Santana LF, Cannell MB, McCune SA, Altschuld RA, Lederer WJ (1997) Defective excitation-contraction coupling in experimental cardiac hypertrophy and heart failure. Science 276(5313):800–806
38. Lindner M, Erdmann E, Beuckelmann DJ (1998) Calcium content of the sarcoplasmic reticulum in isolated ventricular myocytes from patients with terminal heart failure. J Mol Cell Cardiol 30(4):743–749
39. Pieske B, Maier LS, Bers DM, Hasenfuss G (1999) Ca^{2+} handling and sarcoplasmic reticulum Ca^{2+} content in isolated failing and nonfailing human myocardium. Circ Res 85(1):38–46
40. Hobai IA, O'Rourke B (2001) Decreased sarcoplasmic reticulum calcium content is responsible for defective excitation-contraction coupling in canine heart failure. Circulation 103(11):1577–1584
41. Dipla K, Mattiello JA, Margulies KB, Jeevanandam V, Houser SR (1999) The sarcoplasmic reticulum and the Na^+/Ca^{2+} exchanger both contribute to the Ca^{2+} transient of failing human ventricular myocytes. Circ Res 84(4):435–444
42. Pieske B, Maier LS, Piacentino V 3rd, Weisser J, Hasenfuss G, Houser S (2002) Rate dependence of $[Na^+]i$ and contractility in nonfailing and failing human myocardium. Circulation 106(4):447–453
43. Hasenfuss G, Pieske B (2002) Calcium cycling in congestive heart failure. J Mol Cell Cardiol 34(8):951–969
44. Feldman MD, Alderman JD, Aroesty JM, Royal HD, Ferguson JJ, Owen RM, Grossman W, McKay RG (1988) Depression of systolic and diastolic myocardial reserve during atrial pacing tachycardia in patients with dilated cardiomyopathy. J Clin Invest 82(5):1661–1669
45. Mulieri LA, Hasenfuss G, Leavitt B, Allen PD, Alpert NR (1992) Altered myocardial force-frequency relation in human heart failure. Circulation 85(5):1743–1750

46. Hasenfuss G, Reinecke H, Studer R, Meyer M, Pieske B, Holtz J, Holubarsch C, Posival H, Just H, Drexler H (1994) Relation between myocardial function and expression of sarcoplasmic reticulum Ca(2+)-ATPase in failing and nonfailing human myocardium. Circ Res 75(3):434–442
47. Swedberg K, Komajda M, Bohm M, Borer JS, Ford I, Dubost-Brama A, Lerebours G, Tavazzi L (2010) Ivabradine and outcomes in chronic heart failure (SHIFT): a randomised placebo-controlled study. Lancet 376(9744):875–885
48. Ørn S, Dickstein K (2002) How do heart failure patients die? Eur Heart J Suppl 4(suppl D):D59
49. Bardy GH, Lee KL, Mark DB, Poole JE, Packer DL, Boineau R, Domanski M, Troutman C, Anderson J, Johnson G, McNulty SE, Clapp-Channing N, Davidson-Ray LD, Fraulo ES, Fishbein DP, Luceri RM, Ip JH (2005) Amiodarone or an implantable cardioverter-defibrillator for congestive heart failure. N Engl J Med 352(3):225–237
50. Tomaselli GF, Marban E (1999) Electrophysiological remodeling in hypertrophy and heart failure. Cardiovasc Res 42(2):270–283
51. Pogwizd SM, Schlotthauer K, Li L, Yuan W, Bers DM (2001) Arrhythmogenesis and contractile dysfunction in heart failure: roles of sodium-calcium exchange, inward rectifier potassium current, and residual beta-adrenergic responsiveness. Circ Res 88(11):1159–1167
52. Belevych AE, Terentyev D, Terentyeva R, Nishijima Y, Sridhar A, Hamlin RL, Carnes CA, Gyorke S (2011) The relationship between arrhythmogenesis and impaired contractility in heart failure: role of altered ryanodine receptor function. Cardiovasc Res 90(3):493–502
53. Tomaselli GF, Beuckelmann DJ, Calkins HG, Berger RD, Kessler PD, Lawrence JH, Kass D, Feldman AM, Marban E (1994) Sudden cardiac death in heart failure. The role of abnormal repolarization. Circulation 90(5):2534–2539
54. Weiss JN, Garfinkel A, Karagueuzian HS, Chen PS, Qu Z (2010) Early afterdepolarizations and cardiac arrhythmias. Heart Rhythm 7(12):1891–1899
55. Pogwizd SM, Bers DM (2004) Cellular basis of triggered arrhythmias in heart failure. Trends Cardiovasc Med 14(2):61–66
56. Pogwizd SM, McKenzie JP, Cain ME (1998) Mechanisms underlying spontaneous and induced ventricular arrhythmias in patients with idiopathic dilated cardiomyopathy. Circulation 98(22):2404–2414
57. Vermeulen JT, McGuire MA, Opthof T, Coronel R, de Bakker JM, Klopping C, Janse MJ (1994) Triggered activity and automaticity in ventricular trabeculae of failing human and rabbit hearts. Cardiovasc Res 28(10):1547–1554
58. Pruvot EJ, Katra RP, Rosenbaum DS, Laurita KR (2004) Role of calcium cycling versus restitution in the mechanism of repolarization alternans. Circ Res 94(8):1083–1090
59. Wilson LD, Jeyaraj D, Wan X, Hoeker GS, Said TH, Gittinger M, Laurita KR, Rosenbaum DS (2009) Heart failure enhances susceptibility to arrhythmogenic cardiac alternans. Heart Rhythm 6(2):251–259
60. Klingenheben T, Zabel M, D'Agostino RB, Cohen RJ, Hohnloser SH (2000) Predictive value of T-wave alternans for arrhythmic events in patients with congestive heart failure. Lancet 356(9230):651–652
61. Pastore JM, Girouard SD, Laurita KR, Akar FG, Rosenbaum DS (1999) Mechanism linking T-wave alternans to the genesis of cardiac fibrillation. Circulation 99(10):1385–1394
62. Cutler MJ, Wan X, Laurita KR, Hajjar RJ, Rosenbaum DS (2009) Targeted SERCA2a gene expression identifies molecular mechanism and therapeutic target for arrhythmogenic cardiac alternans. Circ Arrhythm Electrophysiol 2(6):686–694
63. Mewes T, Ravens U (1994) L-type calcium currents of human myocytes from ventricle of non-failing and failing hearts and from atrium. J Mol Cell Cardiol 26(10):1307–1320
64. Sipido KR, Stankovicova T, Flameng W, Vanhaecke J, Verdonck F (1998) Frequency dependence of Ca^{2+} release from the sarcoplasmic reticulum in human ventricular myocytes from end-stage heart failure. Cardiovasc Res 37(2):478–488
65. Lindner M, Brandt MC, Sauer H, Hescheler J, Bohle T, Beuckelmann DJ (2002) Calcium sparks in human ventricular cardiomyocytes from patients with terminal heart failure. Cell Calcium 31(4):175–182

66. Crossman DJ, Ruygrok PR, Soeller C, Cannell MB (2011) Changes in the organization of excitation-contraction coupling structures in failing human heart. PLoS One 6(3):e17901
67. Lyon AR, MacLeod KT, Zhang Y, Garcia E, Kanda GK, Lab MJ, Korchev YE, Harding SE, Gorelik J (2009) Loss of T-tubules and other changes to surface topography in ventricular myocytes from failing human and rat heart. Proc Natl Acad Sci USA 106(16):6854–6859
68. Ohler A, Weisser-Thomas J, Piacentino V, Houser SR, Tomaselli GF, O'Rourke B (2009) Two-photon laser scanning microscopy of the transverse-axial tubule system in ventricular cardiomyocytes from failing and non-failing human hearts. Cardiol Res Pract 2009:802373
69. Song LS, Sobie EA, McCulle S, Lederer WJ, Balke CW, Cheng H (2006) Orphaned ryanodine receptors in the failing heart. Proc Natl Acad Sci USA 103(11):4305–4310
70. Louch WE, Bito V, Heinzel FR, Macianskiene R, Vanhaecke J, Flameng W, Mubagwa K, Sipido KR (2004) Reduced synchrony of Ca^{2+} release with loss of T-tubules-a comparison to Ca^{2+} release in human failing cardiomyocytes. Cardiovasc Res 62(1):63–73
71. Wasserstrom JA, Sharma R, Kapur S, Kelly JE, Kadish AH, Balke CW, Aistrup GL (2009) Multiple defects in intracellular calcium cycling in whole failing rat heart. Circ Heart Fail 2(3):223–232
72. Jantunen E, Collan Y (1989) Transmural differences in ischaemic heart disease: a quantitative histologic study. Appl Pathol 7(3):179–187
73. Figueredo VM, Brandes R, Weiner MW, Massie BM, Camacho SA (1993) Endocardial versus epicardial differences of intracellular free calcium under normal and ischemic conditions in perfused rat hearts. Circ Res 72(5):1082–1090
74. Burashnikov A, Antzelevitch C (2003) Reinduction of atrial fibrillation immediately after termination of the arrhythmia is mediated by late phase 3 early afterdepolarization-induced triggered activity. Circulation 107(18):2355–2360
75. Sobie EA, Guatimosim S, Song LS, Lederer WJ (2003) The challenge of molecular medicine: complexity versus Occam's razor. J Clin Invest 111(6):801–803
76. Jaski BE, Jessup ML, Mancini DM, Cappola TP, Pauly DF, Greenberg B, Borow K, Dittrich H, Zsebo KM, Hajjar RJ (2009) Calcium upregulation by percutaneous administration of gene therapy in cardiac disease (CUPID Trial), a first-in-human phase 1/2 clinical trial. J Card Fail 15(3):171–181
77. Kubalova Z, Terentyev D, Viatchenko-Karpinski S, Nishijima Y, Gyorke I, Terentyeva R, da Cunha DN, Sridhar A, Feldman DS, Hamlin RL, Carnes CA, Gyorke S (2005) Abnormal intrastore calcium signaling in chronic heart failure. Proc Natl Acad Sci USA 102(39):14104–14109
78. Jiang MT, Lokuta AJ, Farrell EF, Wolff MR, Haworth RA, Valdivia HH (2002) Abnormal Ca^{2+} release, but normal ryanodine receptors, in canine and human heart failure. Circ Res 91(11):1015–1022
79. Li Y, Kranias EG, Mignery GA, Bers DM (2002) Protein kinase A phosphorylation of the ryanodine receptor does not affect calcium sparks in mouse ventricular myocytes. Circ Res 90(3):309–316
80. Ai X, Curran JW, Shannon TR, Bers DM, Pogwizd SM (2005) Ca^{2+}/calmodulin-dependent protein kinase modulates cardiac ryanodine receptor phosphorylation and sarcoplasmic reticulum Ca^{2+} leak in heart failure. Circ Res 97(12):1314–1322
81. Kushnir A, Shan J, Betzenhauser MJ, Reiken S, Marks AR (2010) Role of CaMKIIdelta phosphorylation of the cardiac ryanodine receptor in the force frequency relationship and heart failure. Proc Natl Acad Sci USA 107(22):10274–10279
82. De Koninck P, Schulman H (1998) Sensitivity of CaM kinase II to the frequency of Ca^{2+} oscillations. Science 279(5348):227–230
83. Zhao W, Uehara Y, Chu G, Song Q, Qian J, Young K, Kranias EG (2004) Threonine-17 phosphorylation of phospholamban: a key determinant of frequency-dependent increase of cardiac contractility. J Mol Cell Cardiol 37(2):607–612
84. Holmberg SR, Williams AJ (1989) Single channel recordings from human cardiac sarcoplasmic reticulum. Circ Res 65(5):1445–1449
85. Schmidt U, Hajjar RJ, Kim CS, Lebeche D, Doye AA, Gwathmey JK (1999) Human heart failure: cAMP stimulation of SR Ca(2+)-ATPase activity and phosphorylation level of phospholamban. Am J Physiol 277(2 Pt 2):H474–H480

86. Schwinger RH, Bohm M, Schmidt U, Karczewski P, Bavendiek U, Flesch M, Krause EG, Erdmann E (1995) Unchanged protein levels of SERCA II and phospholamban but reduced Ca^{2+} uptake and Ca(2+)-ATPase activity of cardiac sarcoplasmic reticulum from dilated cardiomyopathy patients compared with patients with nonfailing hearts. Circulation 92(11):3220–3228
87. del Monte F, Harding SE, Schmidt U, Matsui T, Kang ZB, Dec GW, Gwathmey JK, Rosenzweig A, Hajjar RJ (1999) Restoration of contractile function in isolated cardiomyocytes from failing human hearts by gene transfer of SERCA2a. Circulation 100(23):2308–2311
88. del Monte F, Harding SE, Dec GW, Gwathmey JK, Hajjar RJ (2002) Targeting phospholamban by gene transfer in human heart failure. Circulation 105(8):904–907
89. Frank KF, Bolck B, Brixius K, Kranias EG, Schwinger RH (2002) Modulation of SERCA: implications for the failing human heart. Basic Res Cardiol 97(Suppl 1):I72–I78
90. Schwinger RH, Munch G, Bolck B, Karczewski P, Krause EG, Erdmann E (1999) Reduced Ca(2+)-sensitivity of SERCA 2a in failing human myocardium due to reduced serin-16 phospholamban phosphorylation. J Mol Cell Cardiol 31(3):479–491
91. Dash R, Frank KF, Carr AN, Moravec CS, Kranias EG (2001) Gender influences on sarcoplasmic reticulum Ca^{2+}-handling in failing human myocardium. J Mol Cell Cardiol 33(7): 1345–1353
92. Munch G, Bolck B, Karczewski P, Schwinger RH (2002) Evidence for calcineurin-mediated regulation of SERCA 2a activity in human myocardium. J Mol Cell Cardiol 34(3):321–334
93. Mishra S, Gupta RC, Tiwari N, Sharov VG, Sabbah HN (2002) Molecular mechanisms of reduced sarcoplasmic reticulum Ca(2+) uptake in human failing left ventricular myocardium. J Heart Lung Transplant 21(3):366–373
94. Minamisawa S, Hoshijima M, Chu G, Ward CA, Frank K, Gu Y, Martone ME, Wang Y, Ross J Jr, Kranias EG, Giles WR, Chien KR (1999) Chronic phospholamban-sarcoplasmic reticulum calcium ATPase interaction is the critical calcium cycling defect in dilated cardiomyopathy. Cell 99(3):313–322
95. Liu Q, Chen X, Macdonnell SM, Kranias EG, Lorenz JN, Leitges M, Houser SR, Molkentin JD (2009) Protein kinase C{alpha}, but not PKC{beta} or PKC{gamma}, regulates contractility and heart failure susceptibility: implications for ruboxistaurin as a novel therapeutic approach. Circ Res 105(2):194–200
96. Weber CR, Piacentino V 3rd, Houser SR, Bers DM (2003) Dynamic regulation of sodium/calcium exchange function in human heart failure. Circulation 108(18):2224–2229
97. Ventura-Clapier R, Garnier A, Veksler V (2004) Energy metabolism in heart failure. J Physiol 555(Pt 1):1–13
98. Bers DM (2008) Calcium cycling and signaling in cardiac myocytes. Annu Rev Physiol 70:23–49
99. De Sousa E, Veksler V, Minajeva A, Kaasik A, Mateo P, Mayoux E, Hoerter J, Bigard X, Serrurier B, Ventura-Clapier R (1999) Subcellular creatine kinase alterations. Implications in heart failure. Circ Res 85(1):68–76
100. Xu KY, Zweier JL, Becker LC (1997) Hydroxyl radical inhibits sarcoplasmic reticulum Ca(2+)-ATPase function by direct attack on the ATP binding site. Circ Res 80(1):76–81
101. Hasenfuss G, Maier LS, Hermann HP, Luers C, Hunlich M, Zeitz O, Janssen PM, Pieske B (2002) Influence of pyruvate on contractile performance and Ca(2+) cycling in isolated failing human myocardium. Circulation 105(2):194–199
102. Reiken S, Wehrens XH, Vest JA, Barbone A, Klotz S, Mancini D, Burkhoff D, Marks AR (2003) Beta-blockers restore calcium release channel function and improve cardiac muscle performance in human heart failure. Circulation 107(19):2459–2466
103. Chaudhary KW, Rossman EI, Piacentino V 3rd, Kenessey A, Weber C, Gaughan JP, Ojamaa K, Klein I, Bers DM, Houser SR, Margulies KB (2004) Altered myocardial Ca^{2+} cycling after left ventricular assist device support in the failing human heart. J Am Coll Cardiol 44(4):837–845
104. Vanderheyden M, Mullens W, Delrue L, Goethals M, de Bruyne B, Wijns W, Geelen P, Verstreken S, Wellens F, Bartunek J (2008) Myocardial gene expression in heart failure patients treated with cardiac resynchronization therapy responders versus nonresponders. J Am Coll Cardiol 51(2):129–136

105. del Monte F, Williams E, Lebeche D, Schmidt U, Rosenzweig A, Gwathmey JK, Lewandowski ED, Hajjar RJ (2001) Improvement in survival and cardiac metabolism after gene transfer of sarcoplasmic reticulum Ca(2+)-ATPase in a rat model of heart failure. Circulation 104(12):1424–1429
106. Rockman HA, Koch WJ, Lefkowitz RJ (2002) Seven-transmembrane-spanning receptors and heart function. Nature 415(6868):206–212
107. Cambronero F, Marin F, Roldan V, Hernandez-Romero D, Valdes M, Lip GY (2009) Biomarkers of pathophysiology in hypertrophic cardiomyopathy: implications for clinical management and prognosis. Eur Heart J 30(2):139–151
108. Hunt SA, Abraham WT, Chin MH, Feldman AM, Francis GS, Ganiats TG, Jessup M, Konstam MA, Mancini DM, Michl K, Oates JA, Rahko PS, Silver MA, Stevenson LW, Yancy CW (2009) 2009 Focused update incorporated into the ACC/AHA 2005 guidelines for the diagnosis and management of heart failure in adults a report of the American College of Cardiology Foundation/American Heart Association task force on practice guidelines developed in collaboration with the International Society for Heart and Lung Transplantation. J Am Coll Cardiol 53(15):e1–e90
109. Wehrens XH, Lehnart SE, Huang F, Vest JA, Reiken SR, Mohler PJ, Sun J, Guatimosim S, Song LS, Rosemblit N, D'Armiento JM, Napolitano C, Memmi M, Priori SG, Lederer WJ, Marks AR (2003) FKBP12.6 deficiency and defective calcium release channel (ryanodine receptor) function linked to exercise-induced sudden cardiac death. Cell 113(7):829–840
110. DeSantiago J, Maier LS, Bers DM (2002) Frequency-dependent acceleration of relaxation in the heart depends on CaMKII, but not phospholamban. J Mol Cell Cardiol 34(8):975–984
111. Sugden PH, Bogoyevitch MA (1995) Intracellular signalling through protein kinases in the heart. Cardiovasc Res 30(4):478–492
112. Kluger J, Cody RJ, Laragh JH (1982) The contributions of sympathetic tone and the renin-angiotensin system to severe chronic congestive heart failure: response to specific inhibitors (prazosin and captopril). Am J Cardiol 49(7):1667–1674
113. Cohn JN, Levine TB, Olivari MT, Garberg V, Lura D, Francis GS, Simon AB, Rector T (1984) Plasma norepinephrine as a guide to prognosis in patients with chronic congestive heart failure. N Eng J Med 311(13):819–823
114. Ungerer M, Bohm M, Elce JS, Erdmann E, Lohse MJ (1993) Altered expression of beta-adrenergic receptor kinase and beta 1-adrenergic receptors in the failing human heart. Circulation 87(2):454–463
115. Daaka Y, Luttrell LM, Lefkowitz RJ (1997) Switching of the coupling of the beta2-adrenergic receptor to different G proteins by protein kinase A. Nature 390(6655):88–91
116. Bristow MR, Minobe WA, Raynolds MV, Port JD, Rasmussen R, Ray PE, Feldman AM (1993) Reduced beta 1 receptor messenger RNA abundance in the failing human heart. J Clin Invest 92(6):2737–2745
117. Wei SK, Ruknudin A, Hanlon SU, McCurley JM, Schulze DH, Haigney MC (2003) Protein kinase A hyperphosphorylation increases basal current but decreases beta-adrenergic responsiveness of the sarcolemmal Na^{+}-Ca^{2+} exchanger in failing pig myocytes. Circ Res 92(8): 897–903
118. Beta-Blocker Evaluation of Survival Trial Investigators (2001) A trial of the beta-blocker bucindolol in patients with advanced chronic heart failure. N Eng J Med 344(22):1659–1667
119. Packer M, Bristow MR, Cohn JN, Colucci WS, Fowler MB, Gilbert EM, Shusterman NH (1996) The effect of carvedilol on morbidity and mortality in patients with chronic heart failure. U.S. Carvedilol Heart Failure Study Group. N Engl J Med 334(21):1349–1355
120. MERIT-HFTrial (1999) Effect of metoprolol CR/XL in chronic heart failure: Metoprolol CR/XL Randomised Intervention Trial in Congestive Heart Failure (MERIT-HF). Lancet 353(9169):2001–2007
121. CIBIS-IITrial (1999) The Cardiac Insufficiency Bisoprolol Study II (CIBIS-II): a randomised trial. Lancet 353(9146):9–13
122. Yancy CW (2005) Comprehensive treatment of heart failure: state-of-the-art medical therapy. Rev Cardiovasc Med 6(Suppl 2):S43–S57
123. Bristow MR (2000) beta-adrenergic receptor blockade in chronic heart failure. Circulation 101(5):558–569

124. Lowes BD, Gilbert EM, Abraham WT, Minobe WA, Larrabee P, Ferguson D, Wolfel EE, Lindenfeld J, Tsvetkova T, Robertson AD, Quaife RA, Bristow MR (2002) Myocardial gene expression in dilated cardiomyopathy treated with beta-blocking agents. N Engl J Med 346(18):1357–1365
125. Reiken S, Gaburjakova M, Gaburjakova J, He Kl KL, Prieto A, Becker E, Yi Gh GH, Wang J, Burkhoff D, Marks AR (2001) beta-adrenergic receptor blockers restore cardiac calcium release channel (ryanodine receptor) structure and function in heart failure. Circulation 104(23):2843–2848
126. Reiken S, Gaburjakova M, Guatimosim S, Gomez AM, D'Armiento J, Burkhoff D, Wang J, Vassort G, Lederer WJ, Marks AR (2003) Protein kinase A phosphorylation of the cardiac calcium release channel (ryanodine receptor) in normal and failing hearts. Role of phosphatases and response to isoproterenol. J Biol Chem 278(1):444–453
127. Yano M, Ono K, Ohkusa T, Suetsugu M, Kohno M, Hisaoka T, Kobayashi S, Hisamatsu Y, Yamamoto T, Noguchi N, Takasawa S, Okamoto H, Matsuzaki M (2000) Altered stoichiometry of FKBP12.6 versus ryanodine receptor as a cause of abnormal Ca(2+) leak through ryanodine receptor in heart failure. Circulation 102(17):2131–2136
128. Doi M, Yano M, Kobayashi S, Kohno M, Tokuhisa T, Okuda S, Suetsugu M, Hisamatsu Y, Ohkusa T, Matsuzaki M (2002) Propranolol prevents the development of heart failure by restoring FKBP12.6-mediated stabilization of ryanodine receptor. Circulation 105(11): 1374–1379
129. George I, Sabbah HN, Xu K, Wang N, Wang J (2011) {Beta}-adrenergic receptor blockade reduces endoplasmic reticulum stress and normalizes calcium handling in a coronary embolization model of heart failure in canines. Cardiovasc Res 91(3):447–455
130. Beuckelmann DJ, Nabauer M, Kruger C, Erdmann E (1995) Altered diastolic $[Ca^{2+}]_i$ handling in human ventricular myocytes from patients with terminal heart failure. Am Heart J 129(4):684–689
131. Pass JM, Gao J, Jones WK, Wead WB, Wu X, Zhang J, Baines CP, Bolli R, Zheng YT, Joshua IG, Ping P (2001) Enhanced PKC beta II translocation and PKC beta II-RACK1 interactions in PKC epsilon-induced heart failure: a role for RACK1. Am J Physiol Heart Circ Physiol 281(6):H2500–H2510
132. Silberman GA, Fan TH, Liu H, Jiao Z, Xiao HD, Lovelock JD, Boulden BM, Widder J, Fredd S, Bernstein KE, Wolska BM, Dikalov S, Harrison DG, Dudley SC Jr (2010) Uncoupled cardiac nitric oxide synthase mediates diastolic dysfunction. Circulation 121(4):519–528
133. Mende U, Kagen A, Cohen A, Aramburu J, Schoen FJ, Neer EJ (1998) Transient cardiac expression of constitutively active Galphaq leads to hypertrophy and dilated cardiomyopathy by calcineurin-dependent and independent pathways. Proc Natl Acad Sci USA 95(23): 13893–13898
134. Taigen T, De Windt LJ, Lim HW, Molkentin JD (2000) Targeted inhibition of calcineurin prevents agonist-induced cardiomyocyte hypertrophy. Proc Natl Acad Sci USA 97(3): 1196–1201
135. Thomas WG, Brandenburger Y, Autelitano DJ, Pham T, Qian H, Hannan RD (2002) Adenoviral-directed expression of the type 1A angiotensin receptor promotes cardiomyocyte hypertrophy via transactivation of the epidermal growth factor receptor. Circ Res 90(2):135–142
136. Wilkins BJ, Molkentin JD (2004) Calcium-calcineurin signaling in the regulation of cardiac hypertrophy. Biochem Biophys Res Commun 322(4):1178–1191
137. Sussman MA, Lim HW, Gude N, Taigen T, Olson EN, Robbins J, Colbert MC, Gualberto A, Wieczorek DF, Molkentin JD (1998) Prevention of cardiac hypertrophy in mice by calcineurin inhibition. Science 281(5383):1690–1693
138. Maack C, Kartes T, Kilter H, Schafers HJ, Nickenig G, Bohm M, Laufs U (2003) Oxygen free radical release in human failing myocardium is associated with increased activity of rac1-GTPase and represents a target for statin treatment. Circulation 108(13):1567–1574
139. Giordano FJ (2005) Oxygen, oxidative stress, hypoxia, and heart failure. J Clin Invest 115(3):500–508
140. Sawyer DB, Siwik DA, Xiao L, Pimentel DR, Singh K, Colucci WS (2002) Role of oxidative stress in myocardial hypertrophy and failure. J Mol Cell Cardiol 34(4):379–388

141. Seshiah PN, Weber DS, Rocic P, Valppu L, Taniyama Y, Griendling KK (2002) Angiotensin II stimulation of NAD(P)H oxidase activity: upstream mediators. Circ Res 91(5):406–413
142. Rathore N, John S, Kale M, Bhatnagar D (1998) Lipid peroxidation and antioxidant enzymes in isoproterenol induced oxidative stress in rat tissues. Pharmacol Res 38(4):297–303
143. Thollon C, Iliou JP, Cambarrat C, Robin F, Vilaine JP (1995) Nature of the cardiomyocyte injury induced by lipid hydroperoxides. Cardiovasc Res 30(5):648–655
144. Suematsu N, Tsutsui H, Wen J, Kang D, Ikeuchi M, Ide T, Hayashidani S, Shiomi T, Kubota T, Hamasaki N, Takeshita A (2003) Oxidative stress mediates tumor necrosis factor-alpha-induced mitochondrial DNA damage and dysfunction in cardiac myocytes. Circulation 107(10):1418–1423
145. Nishida M, Maruyama Y, Tanaka R, Kontani K, Nagao T, Kurose H (2000) G alpha(i) and G alpha(o) are target proteins of reactive oxygen species. Nature 408(6811):492–495
146. Guerra L, Cerbai E, Gessi S, Borea PA, Mugelli A (1996) The effect of oxygen free radicals on calcium current and dihydropyridine binding sites in guinea-pig ventricular myocytes. Br J Pharmacol 118(5):1278–1284
147. Kaplan P, Babusikova E, Lehotsky J, Dobrota D (2003) Free radical-induced protein modification and inhibition of Ca^{2+}-ATPase of cardiac sarcoplasmic reticulum. Mol Cell Biochem 248(1–2):41–47
148. Goldhaber JI (1996) Free radicals enhance Na^{+}/Ca^{2+} exchange in ventricular myocytes. Am J Physiol 271(3 Pt 2):H823–H833
149. Okuda S, Yano M, Doi M, Oda T, Tokuhisa T, Kohno M, Kobayashi S, Yamamoto T, Ohkusa T, Matsuzaki M (2004) Valsartan restores sarcoplasmic reticulum function with no appreciable effect on resting cardiac function in pacing-induced heart failure. Circulation 109(7):911–919
150. Agostoni PG, De Cesare N, Doria E, Polese A, Tamborini G, Guazzi MD (1986) Afterload reduction: a comparison of captopril and nifedipine in dilated cardiomyopathy. Br Heart J 55(4):391–399
151. Tan LB, Murray RG, Littler WA (1987) Felodipine in patients with chronic heart failure: discrepant haemodynamic and clinical effects. Br Heart J 58(2):122–128
152. Elkayam U, Amin J, Mehra A, Vasquez J, Weber L, Rahimtoola SH (1990) A prospective, randomized, double-blind, crossover study to compare the efficacy and safety of chronic nifedipine therapy with that of isosorbide dinitrate and their combination in the treatment of chronic congestive heart failure. Circulation 82(6):1954–1961
153. Cohn JN, Ziesche S, Smith R, Anand I, Dunkman WB, Loeb H, Cintron G, Boden W, Baruch L, Rochin P, Loss L (1997) Effect of the calcium antagonist felodipine as supplementary vasodilator therapy in patients with chronic heart failure treated with enalapril: V-HeFT III. Vasodilator-Heart Failure Trial (V-HeFT) Study Group. Circulation 96(3):856–863
154. Elkayam U, Parikh K, Torkan B, Weber L, Cohen JL, Rahimtoola SH (1985) Effect of diltiazem on renal clearance and serum concentration of digoxin in patients with cardiac disease. Am J Cardiol 55(11):1393–1395
155. Barjon JN, Rouleau JL, Bichet D, Juneau C, De Champlain J (1987) Chronic renal and neurohumoral effects of the calcium entry blocker nisoldipine in patients with congestive heart failure. J Am Coll Cardiol 9(3):622–630
156. Goldstein RE, Boccuzzi SJ, Cruess D, Nattel S (1991) Diltiazem increases late-onset congestive heart failure in postinfarction patients with early reduction in ejection fraction. The Adverse Experience Committee; and the Multicenter Diltiazem Postinfarction Research Group. Circulation 83(1):52–60
157. Littler WA, Sheridan DJ (1995) Placebo controlled trial of felodipine in patients with mild to moderate heart failure. UK Study Group. Br Heart J 73(5):428–433
158. Mohindra SK, Udeani GO (1989) Long-acting verapamil and heart failure. JAMA 261(7):994
159. Levine TB, Bernink PJ, Caspi A, Elkayam U, Geltman EM, Greenberg B, McKenna WJ, Ghali JK, Giles TD, Marmor A, Reisin LH, Ammon S, Lindberg E (2000) Effect of mibefradil, a T-type calcium channel blocker, on morbidity and mortality in moderate to severe congestive heart failure: the MACH-1 study. Mortality assessment in congestive heart failure trial. Circulation 101(7):758–764

160. Mullins ME, Horowitz BZ, Linden DH, Smith GW, Norton RL, Stump J (1998) Life-threatening interaction of mibefradil and beta-blockers with dihydropyridine calcium channel blockers. JAMA 280(2):157–158
161. Benatar D, Hall V, Reddy S, Gheorghiade M (1998) Clinical and neurohormonal effects of nicardipine hydrochloride in patients with severe chronic heart failure receiving angiotensin-converting enzyme inhibitor therapy. Am J Ther 5(1):25–32
162. Packer M, O'Connor CM, Ghali JK, Pressler ML, Carson PE, Belkin RN, Miller AB, Neuberg GW, Frid D, Wertheimer JH, Cropp AB, DeMets DL (1996) Effect of amlodipine on morbidity and mortality in severe chronic heart failure. Prospective randomized amlodipine survival evaluation study group. N Eng J Med 335(15):1107–1114
163. Freedman NJ, Liggett SB, Drachman DE, Pei G, Caron MG, Lefkowitz RJ (1995) Phosphorylation and desensitization of the human beta 1-adrenergic receptor. Involvement of G protein-coupled receptor kinases and cAMP-dependent protein kinase. J Biol Chem 270(30):17953–17961
164. Harding VB, Jones LR, Lefkowitz RJ, Koch WJ, Rockman HA (2001) Cardiac beta ARK1 inhibition prolongs survival and augments beta blocker therapy in a mouse model of severe heart failure. Proc Natl Acad Sci USA 98(10):5809–5814
165. Rockman HA, Chien KR, Choi DJ, Iaccarino G, Hunter JJ, Ross J Jr, Lefkowitz RJ, Koch WJ (1998) Expression of a beta-adrenergic receptor kinase 1 inhibitor prevents the development of myocardial failure in gene-targeted mice. Proc Natl Acad Sci USA 95(12):7000–7005
166. Marx SO, Reiken S, Hisamatsu Y, Gaburjakova M, Gaburjakova J, Yang YM, Rosemblit N, Marks AR (2001) Phosphorylation-dependent regulation of ryanodine receptors: a novel role for leucine/isoleucine zippers. J Cell Biol 153(4):699–708
167. Most P, Koch WJ (2003) Sealing the leak, healing the heart. Nat Med 9(8):993–994
168. Wehrens XH, Lehnart SE, Reiken SR, Deng SX, Vest JA, Cervantes D, Coromilas J, Landry DW, Marks AR (2004) Protection from cardiac arrhythmia through ryanodine receptor-stabilizing protein calstabin2. Science 304(5668):292–296
169. Yano M, Kobayashi S, Kohno M, Doi M, Tokuhisa T, Okuda S, Suetsugu M, Hisaoka T, Obayashi M, Ohkusa T, Matsuzaki M (2003) FKBP12.6-mediated stabilization of calcium-release channel (ryanodine receptor) as a novel therapeutic strategy against heart failure. Circulation 107(3):477–484
170. Zhang R, Khoo MS, Wu Y, Yang Y, Grueter CE, Ni G, Price EE Jr, Thiel W, Guatimosim S, Song LS, Madu EC, Shah AN, Vishnivetskaya TA, Atkinson JB, Gurevich VV, Salama G, Lederer WJ, Colbran RJ, Anderson ME (2005) Calmodulin kinase II inhibition protects against structural heart disease. Nat Med 11(4):409–417
171. Limas CJ, Olivari MT, Goldenberg IF, Levine TB, Benditt DG, Simon A (1987) Calcium uptake by cardiac sarcoplasmic reticulum in human dilated cardiomyopathy. Cardiovasc Res 21(8):601–605
172. Schmitt JP, Kamisago M, Asahi M, Li GH, Ahmad F, Mende U, Kranias EG, MacLennan DH, Seidman JG, Seidman CE (2003) Dilated cardiomyopathy and heart failure caused by a mutation in phospholamban. Science 299(5611):1410–1413
173. Huang B, Wang S, Qin D, Boutjdir M, El-Sherif N (1999) Diminished basal phosphorylation level of phospholamban in the postinfarction remodeled rat ventricle: role of beta-adrenergic pathway, G(i) protein, phosphodiesterase, and phosphatases. Circ Res 85(9):848–855
174. Hoshijima M, Ikeda Y, Iwanaga Y, Minamisawa S, Date MO, Gu Y, Iwatate M, Li M, Wang L, Wilson JM, Wang Y, Ross J Jr, Chien KR (2002) Chronic suppression of heart-failure progression by a pseudophosphorylated mutant of phospholamban via in vivo cardiac rAAV gene delivery. Nat Med 8(8):864–871
175. Iwanaga Y, Hoshijima M, Gu Y, Iwatate M, Dieterle T, Ikeda Y, Date MO, Chrast J, Matsuzaki M, Peterson KL, Chien KR, Ross J Jr (2004) Chronic phospholamban inhibition prevents progressive cardiac dysfunction and pathological remodeling after infarction in rats. J Clin Invest 113(5):727–736
176. Kaye DM, Preovolos A, Marshall T, Byrne M, Hoshijima M, Hajjar R, Mariani JA, Pepe S, Chien KR, Power JM (2007) Percutaneous cardiac recirculation-mediated gene transfer of an

inhibitory phospholamban peptide reverses advanced heart failure in large animals. J Am Coll Cardiol 50(3):253–260
177. Yamada M, Ikeda Y, Yano M, Yoshimura K, Nishino S, Aoyama H, Wang L, Aoki H, Matsuzaki M (2006) Inhibition of protein phosphatase 1 by inhibitor-2 gene delivery ameliorates heart failure progression in genetic cardiomyopathy. FASEB J 20(8):1197–1199
178. Dawson J, Walters M (2006) Uric acid and xanthine oxidase: future therapeutic targets in the prevention of cardiovascular disease? Br J Clin Pharmacol 62(6):633–644
179. Spector T (1988) Oxypurinol as an inhibitor of xanthine oxidase-catalyzed production of superoxide radical. Biochem Pharmacol 37(2):349–352
180. Cappola TP, Kass DA, Nelson GS, Berger RD, Rosas GO, Kobeissi ZA, Marban E, Hare JM (2001) Allopurinol improves myocardial efficiency in patients with idiopathic dilated cardiomyopathy. Circulation 104(20):2407–2411
181. Freudenberger RS, Schwarz RP Jr, Brown J, Moore A, Mann D, Givertz MM, Colucci WS, Hare JM (2004) Rationale, design and organisation of an efficacy and safety study of oxypurinol added to standard therapy in patients with NYHA class III–IV congestive heart failure. Expert Opin Investig Drugs 13(11):1509–1516
182. Hare JM, Mangal B, Brown J, Fisher C Jr, Freudenberger R, Colucci WS, Mann DL, Liu P, Givertz MM, Schwarz RP (2008) Impact of oxypurinol in patients with symptomatic heart failure. Results of the OPT-CHF study. J Am Coll Cardiol 51(24):2301–2309
183. Brillantes AM, Allen P, Takahashi T, Izumo S, Marks AR (1992) Differences in cardiac calcium release channel (ryanodine receptor) expression in myocardium from patients with end-stage heart failure caused by ischemic versus dilated cardiomyopathy. Circ Res 71(1):18–26
184. Sen L, Cui G, Fonarow GC, Laks H (2000) Differences in mechanisms of SR dysfunction in ischemic vs. idiopathic dilated cardiomyopathy. Am J Physiol Heart Circ Physiol 279(2):H709–H718
185. Houser SR (2001) Reduced abundance of transverse tubules and L-type calcium channels: another cause of defective contractility in failing ventricular myocytes. Cardiovasc Res 49(2):253–256
186. Efimov IR, Fedorov VV, Glukhov A, Lou Q, Ambrosi C, Janks D, Hucker WJ, Kurian T, Schuessler RB, Moazami N (2010) Multiscale imaging of the human heart: building the foundation for human systems physiology and translational medicine. Conf Proc IEEE Eng Med Biol Soc 2010:5177–5180

Chapter 53
Proarrhythmic Atrial Calcium Cycling in the Diseased Heart

Niels Voigt, Stanley Nattel, and Dobromir Dobrev

Abstract During the last decades Ca^{2+} has been found to play a crucial role in cardiac arrhythmias associated with heart failure and a number of congenital arrhythmia syndromes. Recent studies demonstrated that altered atrial Ca^{2+} cycling may promote the initiation and maintenance of atrial fibrillation, the most common clinical arrhythmia that contributes significantly to population morbidity and mortality. This article describes physiological Ca^{2+} cycling mechanisms in atrial cardiomyocytes and relates them to fundamental cellular proarrhythmic mechanisms involving Ca^{2+} signaling abnormalities in the atrium during atrial fibrillation.

Keywords Calcium • Atrial arrhythmias • Remodeling • Ion channels • Reentry • Triggered activity

Introduction

Atrial fibrillation (AF) is a common and clinically-problematic arrhythmia that contributes significantly to population morbidity and mortality [1]. Current treatment of AF with traditional antiarrhythmic drugs is inadequate and is associated with limited efficacy and a high risk of proarrhythmia [2]. Therefore there is a hope that novel mechanism-based approaches will offer more effective therapeutic options

N. Voigt • D. Dobrev (✉)
Division of Experimental Cardiology, Medical Faculty Mannheim, University of Heidelberg, Theodor-Kutzer-Ufer 1-3, 68167 Mannheim, Germany
e-mail: niels.voigt@medma.uni-heidelberg.de; dobromir.dobrev@medma.uni-heidelberg.de

S. Nattel
Montreal Heart Institute, University of Montreal and Research Center, 5000 Belanger Street E, Montreal, QC, Canada, H1T 1C8
e-mail: stanley.nattel@icm-mhi.org

M.S. Islam (ed.), *Calcium Signaling*, Advances in Experimental Medicine and Biology 740, DOI 10.1007/978-94-007-2888-2_53,

with improved safety profiles. AF has been traditionally considered a "re-entrant" arrhythmia due to self-reexciting impulse propagation around a functional or anatomically non-excitable obstacle. However, increasing evidence points to a central role of altered atrial Ca^{2+} cycling in the generation of focal sources of excitation that may promote AF [3–12]. The aim of this article is to describe physiological Ca^{2+} cycling mechanisms in atrial myocytes and to relate them to fundamental atrial-cellular proarrhythmic mechanisms. We focus on key changes in atrial Ca^{2+} cycling that predispose to AF induction and maintenance in the diseased heart.

Atrial Calcium Cycling and Excitation-Contraction Coupling

The cellular correlate of electrical excitation of cardiac myocytes is the "cardiac action potential" (AP), reflecting characteristic time-dependent changes in cellular membrane voltage, starting from a negative resting membrane potential (RMP, ~−70 to −80 mV in cardiac myocytes, Fig. 53.1, [13]). The upstroke of the atrial AP is mediated by the fast sodium current (I_{Na}), whereas the AP "plateau" is due to Ca^{2+} influx through L-type Ca^{2+} channels (LTCC). Repolarization is mediated by opening of a variety of K^+ channels, with some of them being atrial-specific and contributing to the maintenance of the negative RMP during diastole [14].

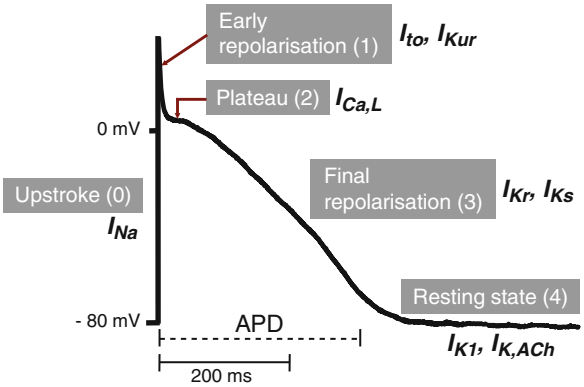

Fig. 53.1 Atrial action potential (AP) and ion currents. The AP is controlled by ions flowing through ion channels, whereby outward currents repolarize (more negative) and inward currents depolarize (more positive) the membrane potential. During diastole (phase 4, resting state) the membrane potential is mainly determined by inward rectifier K^+ channels I_{K1} and $I_{K,ACh}$. The AP upstroke (phase 0), initiating cellular excitation, results from activation of fast sodium currents (I_{Na}). The following early repolarization (phase 1) is mainly due the transient outward (I_{to}) and ultra-rapid delayed rectifier potassium currents (I_{Kur}). Subsequent Ca^{2+} entry through L-type Ca^{2+} channels ($I_{Ca,L}$) is the major depolarizing current responsible for the characteristic plateau phase (phase 2). Final repolarization (phase 3) is governed by several K^+ currents including I_{Kur}, rapid (I_{Kr}), and slow (I_{Ks}) delayed rectifier currents. APD=action potential duration

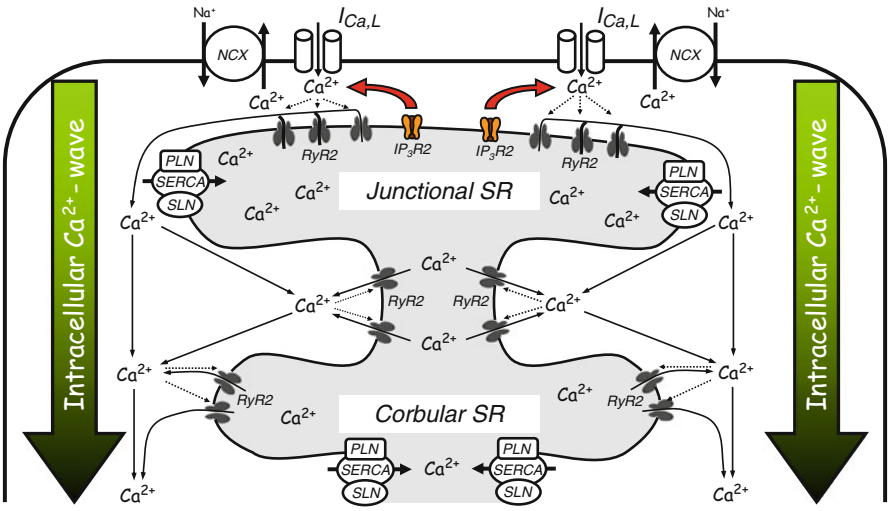

Fig. 53.2 Subcellular architecture of excitation contraction coupling in the atrium. During each action potential Ca^{2+} influx through sarcolemmal L-Typ Ca^{2+}-channels ($I_{Ca,L}$) triggers a larger ryanodine receptor (*RyR2*) mediated Ca^{2+} release from the subsarcolemmal sarcoplasmic reticulum (*junctional SR*). The released Ca^{2+} diffuses into the cell interior and activates RyR2 located in internal SR compartments (*corbular SR*), thereby creating a centripetal Ca^{2+} wave. During diastole cytosolic Ca^{2+} is extruded from the cell through Na^+-Ca^{2+} exchanger (*NCX*) or pumped back into the SR by SR-Ca^{2+}-ATPase (*SERCA*), which is regulated by phospholamban (*PLN*) and sarcolipin (*SLN*). The SR Ca^{2+} release through RyR2 is amplified by inositol 1,4,5-trisphosphate type-2 channels (IP_3R2). See text for further details

In cardiomyocytes, the L-type Ca^{2+} current ($I_{Ca,L}$) flowing through LTCC during the AP plateau triggers a much greater Ca^{2+} release from the sarcoplasmic reticulum (SR) through Ca^{2+}-release channels known as "ryanodine receptor channels" (RyRs, RyR2 = cardiac form), a process termed Ca^{2+}-induced Ca^{2+} release (CICR). The systolically released Ca^{2+} (reflected by the intracellular Ca^{2+} transient) binds to troponin–C in the myofilaments and initiates cardiomyocyte contraction (excitation-contraction [EC] coupling). During diastole the high transsarcolemmal Ca^{2+}-gradient is restored by Ca^{2+} reuptake into the SR, mediated via SR Ca^{2+}-ATPase ("SERCA", SERCA2a = cardiac form) and by Ca^{2+} extrusion into extracellular space via forward-mode Na^+-Ca^{2+} exchanger (reviewed in [15–17]), bringing 3 Na^+ ions per extruded Ca^{2+} ion into the cell. In steady state, influx and efflux of Ca^{2+} are balanced to maintain physiological levels of SR Ca^{2+} content and intracellular Ca^{2+} homeostasis [18].

Although the CICR process is in principal comparable between atrial and ventricular myocytes, there are some important differences in the subcellular architecture (Fig. 53.2). Whereas in ventricular myocytes LTCC are primarily located in T-tubules, deep invaginations of the plasmalemma allowing membrane depolarization to quickly penetrate to the interior of the myocyte, atrial myocytes have only a rudimentary T-tubule system [3, 8, 9]. In ventricular myocytes, T-tubule system allows $I_{Ca,L}$ to initiate a simultaneous and uniform increase in intracellular Ca^{2+}

($[Ca^{2+}]_i$) throughout the cardiomyocyte, whereas in atrial myocytes $I_{Ca,L}$ activation triggers SR Ca^{2+} release only through RyR2 located in the subsarcolemmal ("junctional") SR. The Ca^{2+} wave then propagates from the junctional SR to the cell center, activating with some delay central ("corbular") SR compartments [19–21]. In addition, atrial myocytes possess inositol 1,4,5-trisphosphate type-2 receptors (IP_3R2), which are located in the junctional SR in close vicinity to RyR2, amplifying CICR and facilitating Ca^{2+} wave propagation to cell centre [22–24]. Modulation of atrial IP_3R2 represents one key mechanism through which G_q protein-coupled receptors (e.g. α_1-, AT_1- and ET1-receptors) regulate atrial Ca^{2+} signaling and contractility by increasing IP_3 availability [22, 25, 26].

Homeostatic adaptation of atrial Ca^{2+} cycling to changes in extracellular milieu occurs through a variety of additional mechanisms, one of which is post-translational modification (e.g. phosphorylation) of key Ca^{2+} handling and regulatory proteins. For instance, stimulation of β-adrenoceptor signaling and the subsequent activation of protein kinase A (PKA), and to some extent of Ca^{2+}-calmodulin-dependent protein kinase II (CaMKII), phosphorylate LTCC and increase amplitude of $I_{Ca,L}$ [15]. In addition, SR Ca^{2+} release is enhanced by PKA-mediated RyR2 phosphorylation at Ser2808 (2809, depending on species) and CaMKII-induced phosphorylation at Ser2814 (Ser2815 depending on species), both of which increase open probability and thus activity of RyR2 [27]. Hence the phosphorylation of LTCC and RyR2 increases the strength of cardiomyocyte contraction. The β-adrenoceptor-mediated phosphorylation of phospholamban (PLN), an endogenous inhibitor of SERCA2a, at Ser16 (PKA-site) and at Thr17 (CaMKII-site), relieves SERCA2a inhibition, enhancing SR Ca^{2+} uptake and accelerating relaxation during diastole [28]. In addition, the phosphorylation of RyR2 (at Ser2814) and PLN (at Ser16) are further amplified by concomitant PKA-induced phosphorylation (activation) of inhibitor-1 (at Thr35), a cytosolic protein that inhibits activity of the counterbalancing type-1 protein-phosphatase (PP1) exclusively at the SR [29–31]. This effect shifts the balance between kinases and phosphatases, increasing steady-state RyR2 and PLN phosphorylation [31]. Thus, dynamic protein phosphorylation allows fine-tuning of intracellular Ca^{2+} signaling in cardiomyocytes.

Fundamental Mechanisms of Arrhythmogenesis and Role of Ca^{2+}

Abnormal atrial Ca^{2+} handling can contribute to atrial arrhythmogenesis through multiple mechanisms (Fig. 53.3). For instance, changes in Ca^{2+} cycling modify the function of cardiac ion channels and the shape and the dynamics of the AP, creating tissue properties (vulnerable "substrate") that facilitate the initiation and maintenance of reentry circuits (reviewed in [32]). In addition, Ca^{2+} handling abnormalities may promote nonphysiological impulse formation outside the sinus node (ectopic or triggered activity) by generation of abnormal oscillations of the myocyte membrane potential (afterdepolarizations) that can trigger arrhythmias. In this article we

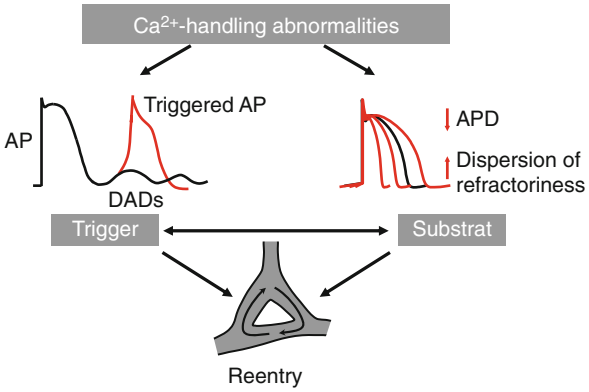

Fig. 53.3 Calcium handling abnormalities may contribute to both triggered activity and reentry. In addition to a susceptible substrate, which is characterized by shortened action potential duration (APD), reduced conduction velocity and increased dispersion of refractoriness, reentry induction requires a trigger, usually provided by an ectopic beat. Ca^{2+} handling abnormalities in AF may contribute to both Ca^{2+} dependent ion channel remodeling that underlies the inhomogeneous APD shortening, and through the increased diastolic SR Ca^{2+} leak and NCX activation to the higher incidence of delayed afterdepolarisations (DADs), which may play an important role in ectopic impulse formation. Furthermore DADs are supposed to increase the dispersion of atrial refractoriness, which in turn creates a substrate supporting AF maintenance

briefly reviewed the details of the two major AF mechanisms; for further in-depth discussion of fundamental AF mechanisms we refer the reader to excellent previous reviews [33, 34].

Ectopic Impulse Formation (Triggered Activity)

Ectopic activity is attributable to afterdepolarizations occurring during the repolarization phase of the AP (early afterdepolarizations, EADs) or after completion of a regular AP (delayed afterdepolarisations, DADs). EADs are usually associated with bradycardia or pauses and result from factors that impair repolarization. At the molecular level reduction of rapidly or slowly activating delayed rectifier potassium currents (I_{Kr} and I_{Ks}) and enhancement of late sodium current (late I_{Na}) prolong APD and increase the likelihood of $I_{Ca,L}$ or I_{Na} re-activation, thereby triggering a new AP (triggered AP, [35]). These forms of EADs are a potential mechanism for AF associated with Long-QT syndrome [36, 37]. However, their role in common AF forms remains unclear.

DADs commonly appear at rapid heart rates and usually result from abnormal diastolic SR Ca^{2+} release (SR Ca^{2+} leak), which is caused by either SR Ca^{2+} overload or RyR2 dysfunction [38]. Excess diastolic Ca^{2+} is handled by NCX, creating a depolarizing transient inward current ("I_{ti}") that can produce DADs (for details see below).

Reentry Mechanisms

Conceptually reentry describes continuous impulse propagation around functional and/or anatomical obstacles that requires a trigger (e.g. an extrasystolic beat) for induction and arrhythmogenic conditions (substrate) that support reentry maintenance [33, 34]. The time during which the excitation travels along the potential reentrant circuit needs to be long enough for the initially activated tissue zone to regain excitability so that the excitation wave can reenter the circuit. The time period, in which tissue remains inexcitable after excitation is called the "refractory period". Shortening of the refractory period increases the likelihood of reentry, because the excitation front encounters tissue with regained excitability. Thus the two major conditions favoring reentry include slow impulse conduction and/or an abbreviated refractory period [33].

At the cellular level the refractory period is largely determined by the AP duration. After initial membrane depolarization, the Na^+ channels are quickly inactivated and the cell cannot be re-fired until Na^+ channels recovered from inactivation, which normally occurs after full repolarization. Thus in normal hearts, the relatively long APD protects cardiac tissue from reentrant excitations and arrhythmias. However, disease- and AF-related remodeling of atrial ion channels abbreviates atrial APD, creating a substrate for reentry (see below).

Ca^{2+} Handling Abnormalities in Experimental AF Paradigms and AF Patients

Enhanced SR Ca^{2+} Leak and Increased NCX Facilitate DAD Development

DADs associate with rapid rhythms and are therefore likely to occur during AF. They result from spontaneous (non-synchronized) diastolic SR Ca^{2+} releases and SR Ca^{2+} leak (Fig. 53.4a). Although there is evidence for increased SR Ca^{2+} leak in AF the underlying molecular mechanisms are incompletely understood (Fig. 53.4b, [6, 7]). Mice with a gain-of-function mutation of RyR2 exhibit SR Ca^{2+} leak and increased susceptibility to pacing-induced AF, suggesting that RyR2 dysfunction may contribute to SR Ca^{2+} leak in AF [39]. Knock-out mice lacking FK-506 binding protein 12.6 kDa (FKBP12.6), a RyR2 stabilizing subunit, also exhibit increased SR Ca^{2+} leak [40] and enhanced vulnerability to pacing-induced AF. Interestingly, FKBP12.6 levels are reduced in patients with chronic AF (cAF), which may explain why RyR2 channels fail to remain closed during diastole. In addition, dogs with pacing-induced AF and patients with cAF exhibit increased RyR2 phosphorylation at Ser2808, which is suggested to enhance dissociation of FKBP12.6 from RyR2 and to enhance its open probability [41]. Moreover, PKA-overexpressing mice with

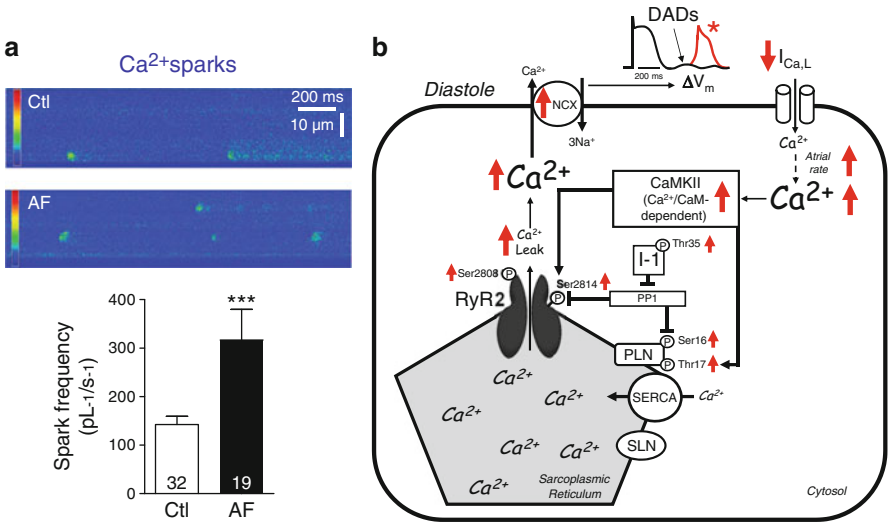

Fig. 53.4 Abnormal atrial Ca^{2+} handling and delayed afterdepolarisations. (**a**), Representative line-scan images in myocytes from patients in sinus rhythm (Ctl) or AF. The frequency of Ca^{2+} sparks, which are suggested to represent spontaneous openings of RyR2, is increased in AF. Numbers within columns represent number of myocytes. (Reproduced with permission from Neef et al. [7]). (**b**), Abnormal spontaneous sarcoplasmic reticulum Ca^{2+} release events through ryanodine receptor channels (RyR2) during diastole may activate the Na^{2+}-Ca^{2+} exchanger (NCX), which brings 3 Na^{+} ions per Ca^{2+} ion into the myocyte, thereby creating a depolarizing inward current (I_{ti}). The resulting delayed afterdepolarisations (DADs), may trigger ectopic action potentials (*) thereby facilitating induction or maintenance of atrial fibrillation. For further details see text

PKA (Ser2808)-hyperphosphorylated RyR2 develop AF, pointing to potential significance of Ser2808 hyperphosphorylation for AF promotion [42].

In atria of cAF patients, RyR2 is hyperphosphorylated at its CaMKII site (Ser2814) [7, 39] and mice with an enhanced vulnerability to pacing-induced AF due to a gain-of-function mutation of RyR2 are less susceptible to inducible AF after pharmacologic or genetic inhibition of CaMKII. In addition, RyR2-Ser2814A knock-in mice, in which CaMKII-phosphorylation of RyR2 is genetically inhibited, are resistant to carbachol-induced AF, confirming the importance of this phosphorylation site for the pathogenesis of atrial arrhythmias. The cAF associated hyperphosphorylation of RyR2 at Ser2814 may be due to increased expression and activity (autophosphorylation at Thr287) of CaMKII [39, 43, 44].

Changes in PKA- and CaMKII-dependent RyR2 phosphorylation may result not only from changed kinase activity, but also from alterations in activity of the dephosphorylating phosphatases PP1 and type-2 protein phosphatase (PP2A). Although overall cellular PP1 and PP2A activities are increased in cAF [45, 46], local PP1 and PP2A activities within the RyR2 macromolecular complex are unknown. It has been suggested that inhibitor-1, which specifically controls PP1 activity in the SR [47],

is PKA (Thr35)-hyperphosphorylated and thus maximally activated in cAF patients [45]. This should lead to strong inhibition of PP1-mediated dephosphorylation at Ser2814 of RyR2 and at Ser16 of PLN [29, 30], additionally contributing to the enhanced phosphorylation of SR-located proteins.

Diastolic RyR2 openings in cAF may result not only from RyR2 hyperphosphorylation, but also from enhanced SR Ca^{2+} releases through IP_3R2, which should increase the Ca^{2+} concentration in the RyR2-IP_3R2 microdomain, promoting spontaneous RyR2 openings and increasing SR Ca^{2+} leak [23, 24]. Consistent with this hypothesis, application of IP_3R2 agonists like adenophostin increased Ca^{2+} spark frequency and changed the spatiotemporal properties of Ca^{2+} sparks in atrial myocytes [22, 48]. Since expression of IP_3Rs is increased in AF patients [49–51] and atrial myocytes from cAF patients exhibit a significantly stronger cross-talk between IP_3Rs and RyR2 [22, 48], it is possible, but not proven, that increased IP_3Rs activity may contribute to RyR2-mediated SR Ca^{2+} leak in AF.

At the cardiomyocyte level, SR Ca^{2+} leak in AF patients appears as an increased rate of spatially localized elevations in cytoplasmic Ca^{2+} (Ca^{2+} sparks; [6, 7]), which are believed to represent synchronous Ca^{2+} release through a cluster of 50–200 RyRs forming a so-called "couplon" [52]. Although Ca^{2+} sparks are accepted as a surrogate of SR Ca^{2+} leak, recent evidence suggests that Ca^{2+} sparks may represent only a small part of the total RyR2-mediated Ca^{2+} leak and that there is a clear Ca^{2+}-spark independent component of RyR2-mediated leak [53–55]. One way to quantify total SR Ca^{2+} leak is the use of the tetracaine protocol established by Shannon et al. [56], which exploits the ability of tetracaine to reduce Ca^{2+} sensitivity and thus open probability of RyR2 and to unmask SR Ca^{2+} leak. Using this protocol in atrial myocytes from cAF patients, we showed increased total SR Ca^{2+} leak in cAF vs. sinus rhythm patients [11, 12]. At the single RyR2-channel level, open probability of RyR2 reconstituted in lipid bilayer membranes is enhanced during cAF in dogs and humans [11, 41], representing the molecular correlate of increased SR Ca^{2+} leak in cAF. Of note, discontinuous spontaneous Ca^{2+} release events representing Ca^{2+} microwaves travelling inside cells are more frequent in myocytes from cAF patients compared to sinus rhythm patients, and preliminary results suggest that these Ca^{2+} release events may cause DADs and triggered APs in myocytes from cAF patients [11].

In normal hearts, safety factors in the plasma membrane limit the ability of SR Ca^{2+} leak to cause DADs and triggered activity [57]. The size of a DAD depends amongst others on the sensitivity of membrane voltage (V_m) to $[Ca^{2+}]_i$ ($[Ca^{2+}]_i$–V_m coupling "gain"), which is determined by the amplitude of depolarizing I_{NCX} and the membrane resistance, set by background conductances like the inward rectifier potassium current I_{K1}, with enhanced I_{NCX} and/or reduced I_{K1} both promoting DAD development. Expression of NCX1 and $[Ca^{2+}]_i$-corrected I_{NCX} amplitude are greater in cAF than in sinus rhythm myocytes; however, I_{K1} is upregulated in cAF patients, suggesting that a higher incidence of spontaneous Ca^{2+} release events and increased I_{NCX}, rather than reduced I_{K1}, accounts for the stronger $[Ca^{2+}]_i$–V_m coupling "gain" in cAF myocytes. [7, 8, 12, 45, 58].

Role of SERCA2a and Phospholamban in SR Ca^{2+} Leak

Diastolic SR Ca^{2+} leak via RyR2 can only persist if a critical amount of SR Ca^{2+} load is maintained to guarantee sufficient RyR2 sensitization to intra-SR (luminal) Ca^{2+} [59]. Although SR Ca^{2+} load appears normal in cAF (Fig. 53.4a, b; [7, 8, 11, 12]), the mechanisms that ensure maintained SR Ca^{2+} load are not fully understood. In cAF patients, the hyperphosphorylation of PLN at both Ser16 (PKA-site) and Thr17 (CaMKII-site) may prevent SR Ca^{2+} depletion during AF, potentially explaining the normal SR Ca^{2+} content [7, 11, 12, 45]. In addition, it has been demonstrated that the expression levels of sarcolipin (SLN), a SERCA2a inhibitor that like PLN loses its SERCA2a-inhibitory properties when phosphorylated by CaMKII at Thr5 [60], is decreased in cAF patients [61]. Reduced SLN binding to SERCA2a together with altered PLN regulation could theoretically enhance SR Ca^{2+} reuptake, offsetting the Ca^{2+} loss due to increased SR Ca^{2+} leak.

As mentioned above, SR Ca^{2+} leak that may cause DADs and triggered activity requires either RyR2 dysfunction or SR Ca^{2+} overload. SR Ca^{2+} load represents the balance between SR Ca^{2+} release and Ca^{2+} reuptake. In dogs and goats with short term AF, SR Ca^{2+} content is reduced [9, 62], suggesting ineffective compensation of increased SR Ca^{2+} leak through defective RyR2 in early phases of AF. However, despite increased SR Ca^{2+} leak due to RyR2 dysfunction, SR Ca^{2+} load is normal in patients with cAF [6–8, 12] and sheep with persistent AF [8], pointing to the possibility that the initial reduction in SR Ca^{2+} load is offset by hyperphosphorylated (less inhibitory) PLN and decreased expression of SLN, both accelerating Serca2a mediated SR Ca^{2+} reuptake. Thus, the preserved SR Ca^{2+} content plays a permissive role in diastolic SR Ca^{2+} leak by preventing depletion of SR Ca^{2+} content.

Reduced Atrial $I_{Ca,L}$ and Increased K^+ Currents Promote Reentry

In computer simulations, reduction of $I_{Ca,L}$ or increases of K^+ currents abbreviate APD, promoting reentry that sustains AF [63]. Studies in various animal models and in patients with cAF show that decreased $I_{Ca,L}$ (reduced depolarisation power), increased inward rectifier K^+ current I_{K1} and a constitutively-active form of the acetylcholine-gated K^+-current $I_{K,ACh}$ (enhanced repolarization power) are major contributors to APD shortening [13, 64–71]. Reduced $I_{Ca,L}$ and the associated abbreviation of APD protect the myocytes from the cytotoxic effects of excessive intra-cellular Ca^{2+} load which may contribute to apoptosis and necrotic cell death found in atria from AF patients [72]. However, the protection against increased Ca^{2+} influx occurs at the expense of shorter effective refractory period which promotes AF maintenance and impairs atrial hypocontractility [9, 62, 73], one major determinant of AF-associated stroke [74]. Thus normalization of atrial cardiomyocyte Ca^{2+} influx might not be an advisable therapeutic option for AF patients. Of note, clinical AF usually occurs in context of cardiovascular diseases such as heart failure, hypertension or coronary artery disease, in which there is a complex interplay between electrical

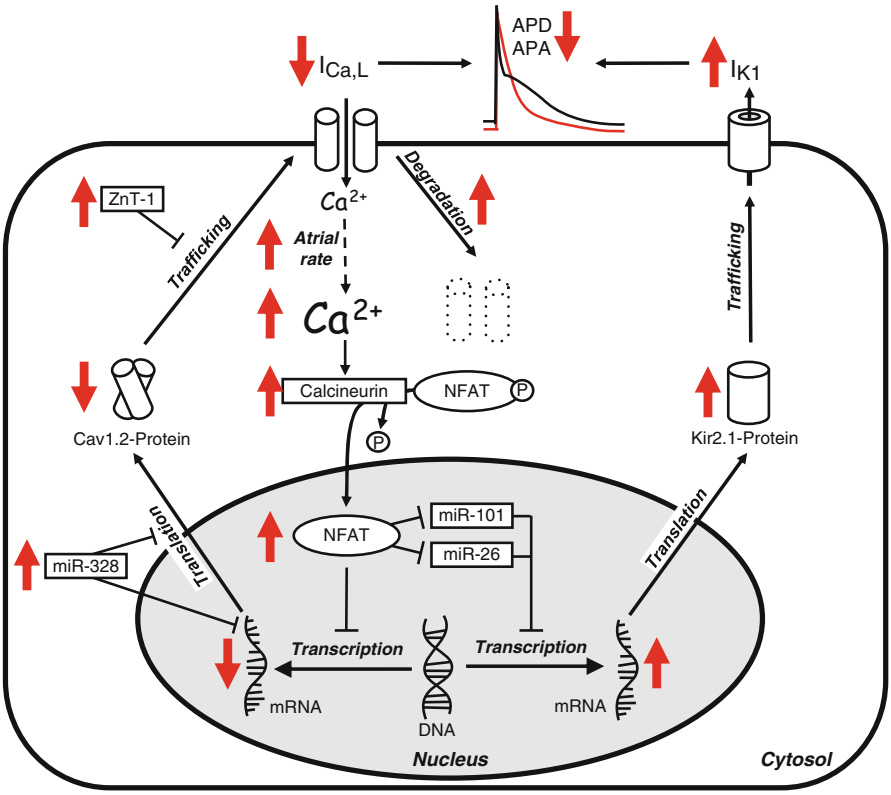

Fig. 53.5 Ca^{2+} handling abnormalities involved in remodeling of $I_{Ca,L}$ and I_{K1}. The high atrial rate in atrial fibrillation (AF) increases intracellular Ca^{2+}-load, activating the Ca^{2+} dependent phosphatase calcineurin. Calcineurin stimulates nuclear translocation of Nuclear Factor of Activated T-Lymphocytes (NFAT), reducing transcription of the principal $I_{Ca,L}$ subunit, Cav1.2. In addition, increased mRNA-degradation/impaired protein-translation of Cav1.2 and breakdown of Cav1.2 protein by calpains may also contribute to the lower Cav1.2 protein levels in AF. Increased expression of the Zinc transporter-1 (ZnT-1) may impair membrane trafficking of Cav1.2. NFAT also reduces expression of Kir2.1-inhibitory microRNAs (miR-26, miR-1) leading to a higher expression of the major I_{K1}-channel subunit Kir2.1. Both reduced $I_{Ca,L}$ and increased I_{K1} are major contributors to action potential duration (APD) shortening in AF

and structural remodeling resulting in prolonged rather then abbreviated atrial APD. Therefore in AF patients with complex atrial remodeling the reduction of APD is much weaker compared to animal models with atrial tachycardia remodeling in which AF is induced in the absence of cardiovascular diseases. For further discussion the readers are referred to a recent excellent review [34].

The molecular basis of decreased $I_{Ca,L}$ in AF is complex and multifactorial (Fig. 53.5). During AF the high atrial rate increases intracellular Ca^{2+} load, activating the Ca^{2+}-dependent phosphatase calcineurin via the Ca^{2+}/calmodulin system. Calcineurin stimulates nuclear translocation of NFAT ("Nuclear Factor of Activated

T-Lymphocytes"), which reduces transcription of Cav1.2, the major $I_{Ca,L}$-channel subunit [75–78]. In addition, increased degradation of Cav1.2 mRNA by miRNA-328 and of Cav1.2 protein by Ca^{2+}-dependent proteases like calpain are also described [79]. Increased expression of the Zinc transporter-1 (ZnT-1), an endogenous inhibitor of $I_{Ca,L}$, could impair membrane trafficking of Cav1.2 [80–82], additionally reducing Cav1.2 expression in the plasma membrane. Overall, studies at the mRNA and protein level are inconsistent, showing either reduced Cav1.2 abundance [83, 84] or preserved mRNA and protein levels of Cav1.2 in AF patients [46, 68, 85], suggesting that functional mechanisms may contribute to $I_{Ca,L}$ downregulation. Consistent with this notion, enhanced activity of PP1 and PP2A has been shown to contribute to AF-associated Ca^{2+}-channel dephosphorylation, which is expected to reduce open probability of $I_{Ca,L}$, in AF [45, 46, 68]. In addition, oxidative stress also affects $I_{Ca,L}$, because increased S-nitrosylation of Cav1.2 has been associated with the $I_{Ca,L}$ reduction in AF patients [86]. Finally, there is evidence, that reduced $I_{Ca,L}$ is at least partially caused by decreased expression of accessory β_1, β_{2a}, β_{2b}, β_3 and $\alpha_2\beta_2$ LTCC subunits [68, 83, 85, 87, 88]. Collectively, these data suggest that a variety of mechanisms participate in the reduction of $I_{Ca,L}$ in an individual AF patient and that therapeutic approaches targeting common signaling pathways may be more effective than targeting individual contributors to decreased $I_{Ca,L}$.

Ca^{2+} cycling abnormalities contribute to atrial arrhythmogenesis in AF by causing Ca^{2+}-dependent remodeling of additional ion channels. Here we describe Ca^{2+}-dependent remodeling of I_{K1} and the constitutively active $I_{K,AChc}$ ($I_{K,AChc}$) because of their established contributions to electrical remodeling in AF. For other atrial ion channels like the transient outward potassium current I_{to} and the ultra-rapid delayed inward rectifier potassium current I_{Kur} we refer the interested reader to other publications [43].

The amplitude of I_{K1} is increased in patients with cAF, contributing to the shorter APD and the more hyperpolarized RMP. The greater amplitude of I_{K1} results from increased expression of the underlying Kir2.1 subunit, although the open probability of single I_{K1} channels also increases during cAF [66]. It was recently suggested that increased nuclear NFAT translocation, resulting from the high $[Ca^{2+}]_i$ during AF (see above), reduces the amount of Kir2.1-inhibitory microRNAs (miR-26 and miR-101, Fig. 53.5; [89]). This results in increased translation or decreased degradation of Kir2.1, the principal I_{K1} channel subunit [13, 83, 90], contributing to the greater I_{K1} amplitude in AF.

There are emerging evidence to suggest that the development of constitutively active $I_{K,ACh}$ ($I_{K,AChc}$) that contributes to the larger I_{K1} in AF patients and experimental AF models [65–67, 69, 71] likely results from abnormal Ca^{2+} signaling. Recently, Makary et al. demonstrated that canine atrial myocytes develop constitutively active $I_{K,AChc}$ when paced in-vitro at 3 Hz for 24 h, which could be prevented with the cell permeable Ca^{2+} chelator BAPTA-AM (1 μM), pointing to a critical role of altered $[Ca^{2+}]_i$ also for $I_{K,AChc}$ remodeling [91]. Taken together, these data indicate that abnormal Ca^{2+}-dependent processes are critically involved in the AF-related changes of key reentry-promoting ion currents, pointing to the possibility that normalization of altered intracellular Ca^{2+} cycling might be a viable therapeutic option for AF.

Other Ca^{2+}-Dependent Mechanisms of AF

Recently Burashnikov et al. suggested an alternative mechanism as the potential basis for the premature beats that re-induce AF after successful conversion to sinus rhythm [35, 92]. According to this theory, sympathovagal imbalances during the postcardioversion period may additionally shorten the remodeled (abbreviated) AP (parasympathetic effect) in combination with increased and prolonged intracellular Ca^{2+} transients (sympathetic effect). The increased $[Ca^{2+}]_i$ during final AP repolarization at voltages negative to the equilibrium potential for I_{NCX} (−40 mV), can generate a depolarizing I_{NCX}, causing EADs and triggered activity. In contrast to DAD-induced triggered activity, these NCX-mediated EADs do not result from spontaneous (non-stimulated) SR Ca^{2+} releases. In order to distinguish these EADs from the classical forms induced by reactivation of $I_{Ca,L}$ or I_{Na}, they were termed "late phase 3" EADs. The precise role of late phase 3 EADs in AF pathophysiology needs to be established.

Conclusions

Ca^{2+} regulates a variety of key cellular cardiomyocyte functions such as EC coupling and gene transcription. Ca^{2+} cycling abnormalities may underlie atrial arrhythmogenesis through multiple mechanisms. It is well established that reduced $I_{Ca,L}$ contributes to the shorter APD in AF, a major hallmark of atrial remodeling that facilitates reentrant mechanisms. More recent work has shown that Ca^{2+} cycling abnormalities are involved in AF-associated dysregulation of I_{K1} and $I_{K,ACh}$, two other established determinants of functional reentry, and in the formation of ectopic impulses (via DADs), both contributing to AF initiation and maintenance. Since Ca^{2+} regulates the function of other atrial ion channels [43], abnormalities of Ca^{2+} signaling appear to have broader maladaptive consequences for atrial function during AF than initially appreciated. Thus, a better understanding of the precise molecular mechanisms underlying altered Ca^{2+} cycling associated with atrial arrhythmias may open new avenues for the development of novel therapeutic strategies and more efficient AF management.

Acknowledgements The author's research is supported by the Deutsche Forschungsgemeinschaft (Do769/1-1-3, to DD), the German Federal Ministry of Education and Research (BMBF; Atrial Fibrillation Competence Network [01Gi0204] and German Center of Cardiovascular Research, both to DD), the European Union through the European Network for Translational Research in Atrial Fibrillation, (EUTRAF, FP7-HEALTH-2010, large-scale integrating project, Proposal No. 261057 to DD), the Canadian Institutes of Health Research (MOP44365, to SN) and the European-North American Atrial Fibrillation Research Alliance (ENAFRA) grant of Fondation Leducq (07CVD03, to DD and SN).

References

1. Miyasaka Y, Barnes ME, Gersh BJ, Cha SS, Bailey KR, Abhayaratna WP, Seward JB, Tsang TS (2006) Secular trends in incidence of atrial fibrillation in Olmsted County, Minnesota, 1980 to 2000, and implications on the projections for future prevalence. Circulation 114:119–125
2. Dobrev D, Nattel S (2010) New antiarrhythmic drugs for treatment of atrial fibrillation. Lancet 375:1212–1223
3. Dobrev D, Teos LY, Lederer WJ (2009) Unique atrial myocyte Ca^{2+} signaling. J Mol Cell Cardiol 46:448–451
4. Nattel S, Burstein B, Dobrev D (2008) Atrial remodeling and atrial fibrillation: mechanisms and implications. Circ Arrhythm Electrophysiol 1:62–73
5. Wakili R, Voigt N, Kääb S, Dobrev D, Nattel S (2011) Recent advances in the molecular pathophysiology of atrial fibrillation. J Clin Invest 121:2955–2968
6. Hove-Madsen L, Llach A, Bayes-Genis A, Roura S, Rodriguez Font E, Aris A, Cinca J (2004) Atrial fibrillation is associated with increased spontaneous calcium release from the sarcoplasmic reticulum in human atrial myocytes. Circulation 110:1358–1363
7. Neef S, Dybkova N, Sossalla S, Ort KR, Fluschnik N, Neumann K, Seipelt R, Schondube FA, Hasenfuss G, Maier LS (2010) CaMKII-dependent diastolic SR Ca^{2+} leak and elevated diastolic Ca^{2+} levels in right atrial myocardium of patients with atrial fibrillation. Circ Res 106:1134–1144
8. Lenaerts I, Bito V, Heinzel FR, Driesen RB, Holemans P, D'Hooge J, Heidbuchel H, Sipido KR, Willems R (2009) Ultrastructural and functional remodeling of the coupling between Ca^{2+} influx and sarcoplasmic reticulum Ca^{2+} release in right atrial myocytes from experimental persistent atrial fibrillation. Circ Res 105:876–885
9. Wakili R, Yeh YH, Yan Qi X, Greiser M, Chartier D, Nishida K, Maguy A, Villeneuve LR, Boknik P, Voigt N, Krysiak J, Kaab S, Ravens U, Linke WA, Stienen GJ, Shi Y, Tardif JC, Schotten U, Dobrev D, Nattel S (2010) Multiple potential molecular contributors to atrial hypocontractility caused by atrial tachycardia remodeling in dogs. Circ Arrhythm Electrophysiol 3:530–541
10. Yeh YH, Wakili R, Qi XY, Chartier D, Boknik P, Kaab S, Ravens U, Coutu P, Dobrev D, Nattel S (2008) Calcium-handling abnormalities underlying atrial arrhythmogenesis and contractile dysfunction in dogs with congestive heart failure. Circ Arrhythm Electrophysiol 1:93–102
11. Voigt N, Trafford AW, Qiongling W, Wehrens XH, Ravens U, Dobrev D (2010) Abstract 16909: Sarcoplasmic reticulum calcium leak and enhanced NCX increase occurrence of delayed afterdepolarisations in atrial myocytes from patients with chronic atrial fibrillation. Circulation 122:A16909
12. Voigt N, Trafford AW, Ravens U, Dobrev D (2009) Abstract 2630: Cellular and molecular determinants of altered atrial Ca^{2+} signaling in patients with chronic atrial fibrillation. Circulation 120:S667–S668
13. Dobrev D, Graf E, Wettwer E, Himmel HM, Hala O, Doerfel C, Christ T, Schuler S, Ravens U (2001) Molecular basis of downregulation of G-protein-coupled inward rectifying K^+ current $I_{K,\,ACh}$ in chronic human atrial fibrillation: decrease in GIRK4 mRNA correlates with reduced $I_{K,\,ACh}$ and muscarinic receptor-mediated shortening of action potentials. Circulation 104:2551–2557
14. The Task Force of the Working Group on Arrhythmias of the European Society of Cardiology (1991) The 'Sicilian Gambit'. A new approach to the classification of antiarrhythmic drugs based on their actions on arrhythmogenic mechanisms. Eur Heart J 12:1112–1131
15. Bers DM (2002) Cardiac excitation-contraction coupling. Nature 415:198–205
16. Diaz ME, Graham HK, O'Neill SC, Trafford AW, Eisner DA (2005) The control of sarcoplasmic reticulum Ca content in cardiac muscle. Cell Calcium 38:391–396
17. Trafford AW, Diaz ME, O'Neill SC, Eisner DA (2002) Integrative analysis of calcium signalling in cardiac muscle. Front Biosci 7:d843–d852

18. Trafford AW, Diaz ME, Eisner DA (2001) Coordinated control of cell Ca^{2+} loading and triggered release from the sarcoplasmic reticulum underlies the rapid inotropic response to increased L-type Ca^{2+} current. Circ Res 88:195–201
19. Hatem SN, Benardeau A, Rucker-Martin C, Marty I, de Chamisso P, Villaz M, Mercadier JJ (1997) Different compartments of sarcoplasmic reticulum participate in the excitation-contraction coupling process in human atrial myocytes. Circ Res 80:345–353
20. Bootman MD, Higazi DR, Coombes S, Roderick HL (2006) Calcium signalling during excitation-contraction coupling in mammalian atrial myocytes. J Cell Sci 119:3915–3925
21. Tanaami T, Ishida H, Seguchi H, Hirota Y, Kadono T, Genka C, Nakazawa H, Barry WH (2005) Difference in propagation of Ca^{2+} release in atrial and ventricular myocytes. Jpn J Physiol 55:81–91
22. Zima AV, Blatter LA (2004) Inositol-1,4,5-trisphosphate-dependent Ca^{2+} signalling in cat atrial excitation-contraction coupling and arrhythmias. J Physiol 555:607–615
23. Garcia KD, Shah T, Garcia J (2004) Immunolocalization of type 2 inositol 1,4,5-trisphosphate receptors in cardiac myocytes from newborn mice. Am J Physiol Cell Physiol 287:C1048–C1057
24. Lipp P, Laine M, Tovey SC, Burrell KM, Berridge MJ, Li W, Bootman MD (2000) Functional InsP3 receptors that may modulate excitation-contraction coupling in the heart. Curr Biol 10:939–942
25. Tadevosyan A, Maguy A, Villeneuve LR, Babin J, Bonnefoy A, Allen BG, Nattel S (2010) Nuclear-delimited angiotensin receptor-mediated signaling regulates cardiomyocyte gene expression. J Biol Chem 285:22338–22349
26. Mackenzie L, Bootman MD, Laine M, Berridge MJ, Thuring J, Holmes A, Li WH, Lipp P (2002) The role of inositol 1,4,5-trisphosphate receptors in Ca^{2+} signalling and the generation of arrhythmias in rat atrial myocytes. J Physiol 541:395–409
27. Wehrens XH, Lehnart SE, Reiken SR, Marks AR (2004) Ca^{2+}/calmodulin-dependent protein kinase II phosphorylation regulates the cardiac ryanodine receptor. Circ Res 94:e61–e70
28. MacLennan DH, Kranias EG (2003) Phospholamban: a crucial regulator of cardiac contractility. Nat Rev Mol Cell Biol 4:566–577
29. El-Armouche A, Wittkopper K, Degenhardt F, Weinberger F, Didie M, Melnychenko I, Grimm M, Peeck M, Zimmermann WH, Unsold B, Hasenfuss G, Dobrev D, Eschenhagen T (2008) Phosphatase inhibitor-1-deficient mice are protected from catecholamine-induced arrhythmias and myocardial hypertrophy. Cardiovasc Res 80:396–406
30. Wittkopper K, Fabritz L, Neef S, Ort KR, Grefe C, Unsold B, Kirchhof P, Maier LS, Hasenfuss G, Dobrev D, Eschenhagen T, El-Armouche A (2010) Constitutively active phosphatase inhibitor-1 improves cardiac contractility in young mice but is deleterious after catecholaminergic stress and with aging. J Clin Invest 120:617–626
31. Wittkopper K, Dobrev D, Eschenhagen T, El-Armouche A (2011) Phosphatase-1 inhibitor-1 in physiological and pathological β-adrenoceptor signalling. Cardiovasc Res 91:392–401
32. Dobrev D, Nattel S (2008) Calcium handling abnormalities in atrial fibrillation as a target for innovative therapeutics. J Cardiovasc Pharmacol 52:293–299
33. Nattel S (2002) New ideas about atrial fibrillation 50 years on. Nature 415:219–226
34. Schotten U, Verheule S, Kirchhof P, Goette A (2011) Pathophysiological mechanisms of atrial fibrillation: a translational appraisal. Physiol Rev 91:265–325
35. Burashnikov A, Antzelevitch C (2006) Late-phase 3 EAD. A unique mechanism contributing to initiation of atrial fibrillation. Pacing Clin Electrophysiol 29:290–295
36. Johnson JN, Tester DJ, Perry J, Salisbury BA, Reed CR, Ackerman MJ (2008) Prevalence of early-onset atrial fibrillation in congenital long QT syndrome. Heart Rhythm 5:704–709
37. Zellerhoff S, Pistulli R, Monnig G, Hinterseer M, Beckmann BM, Kobe J, Steinbeck G, Kaab S, Haverkamp W, Fabritz L, Gradaus R, Breithardt G, Schulze-Bahr E, Bocker D, Kirchhof P (2009) Atrial Arrhythmias in long-QT syndrome under daily life conditions: a nested case control study. J Cardiovasc Electrophysiol 20:401–407
38. Dobrev D, Voigt N, Wehrens XH (2011) The ryanodine receptor channel as a molecular motif in atrial fibrillation: pathophysiological and therapeutic implications. Cardiovasc Res 89:734–743

39. Chelu MG, Sarma S, Sood S, Wang S, van Oort RJ, Skapura DG, Li N, Santonastasi M, Muller FU, Schmitz W, Schotten U, Anderson ME, Valderrabano M, Dobrev D, Wehrens XH (2009) Calmodulin kinase II-mediated sarcoplasmic reticulum Ca^{2+} leak promotes atrial fibrillation in mice. J Clin Invest 119:1940–1951
40. Sood S, Chelu MG, van Oort RJ, Skapura D, Santonastasi M, Dobrev D, Wehrens XH (2008) Intracellular calcium leak due to FKBP12.6 deficiency in mice facilitates the inducibility of atrial fibrillation. Heart Rhythm 5:1047–1054
41. Vest JA, Wehrens XH, Reiken SR, Lehnart SE, Dobrev D, Chandra P, Danilo P, Ravens U, Rosen MR, Marks AR (2005) Defective cardiac ryanodine receptor regulation during atrial fibrillation. Circulation 111:2025–2032
42. Antos CL, Frey N, Marx SO, Reiken S, Gaburjakova M, Richardson JA, Marks AR, Olson EN (2001) Dilated cardiomyopathy and sudden death resulting from constitutive activation of protein kinase a. Circ Res 89:997–1004
43. Tessier S, Karczewski P, Krause EG, Pansard Y, Acar C, Lang-Lazdunski M, Mercadier JJ, Hatem SN (1999) Regulation of the transient outward K^+ current by Ca^{2+}/calmodulin-dependent protein kinases II in human atrial myocytes. Circ Res 85:810–819
44. Dobrev D, Wehrens XH (2010) Calmodulin kinase II, sarcoplasmic reticulum Ca^{2+} leak, and atrial fibrillation. Trends Cardiovasc Med 20:30–34
45. El-Armouche A, Boknik P, Eschenhagen T, Carrier L, Knaut M, Ravens U, Dobrev D (2006) Molecular determinants of altered Ca^{2+} handling in human chronic atrial fibrillation. Circulation 114:670–680
46. Greiser M, Halaszovich CR, Frechen D, Boknik P, Ravens U, Dobrev D, Luckhoff A, Schotten U (2007) Pharmacological evidence for altered src kinase regulation of $I_{Ca,\,L}$ in patients with chronic atrial fibrillation. Naunyn Schmiedebergs Arch Pharmacol 375:383–392
47. Carr AN, Schmidt AG, Suzuki Y, del Monte F, Sato Y, Lanner C, Breeden K, Jing SL, Allen PB, Greengard P, Yatani A, Hoit BD, Grupp IL, Hajjar RJ, DePaoli-Roach AA, Kranias EG (2002) Type 1 phosphatase, a negative regulator of cardiac function. Mol Cell Biol 22:4124–4135
48. Liang X, Xie H, Zhu PH, Hu J, Zhao Q, Wang CS, Yang C (2009) Enhanced activity of inositol-1,4,5-trisphosphate receptors in atrial myocytes of atrial fibrillation patients. Cardiology 114:180–191
49. Guo JH, Liu YS, Zhang HC, Li XB, Xu Y, Zhang YY, Yuan L (2004) Expression and function changes of ryanodine receptors and inositol 1,4,5-triphosphate receptors of atrial myocytes during atrial fibrillation. Zhonghua Yi Xue Za Zhi 84:1196–1199
50. Zhao ZH, Zhang HC, Xu Y, Zhang P, Li XB, Liu YS, Guo JH (2007) Inositol-1,4,5-trisphosphate and ryanodine-dependent Ca^{2+} signaling in a chronic dog model of atrial fibrillation. Cardiology 107:269–276
51. Yamda J, Ohkusa T, Nao T, Ueyama T, Yano M, Kobayashi S, Hamano K, Esato K, Matsuzaki M (2001) Up-regulation of inositol 1,4,5 trisphosphate receptor expression in atrial tissue in patients with chronic atrial fibrillation. J Am Coll Cardiol 37:1111–1119
52. Franzini-Armstrong C, Protasi F, Ramesh V (1999) Shape, size, and distribution of Ca^{2+} release units and couplons in skeletal and cardiac muscles. Biophys J 77:1528–1539
53. Zima AV, Bovo E, Bers DM, Blatter LA (2010) Ca^{2+} spark-dependent and -independent sarcoplasmic reticulum Ca^{2+} leak in normal and failing rabbit ventricular myocytes. J Physiol 588:4743–4757
54. Lipp P, Niggli E (1996) Submicroscopic calcium signals as fundamental events of excitation–contraction coupling in guinea-pig cardiac myocytes. J Physiol 492(Pt 1):31–38
55. Sobie EA, Guatimosim S, Gomez-Viquez L, Song LS, Hartmann M, Saleet Jafri H, Lederer WJ (2006) The Ca^{2+} leak paradox and rogue ryanodine receptors: SR Ca^{2+} efflux theory and practice. Prog Biophys Mol Biol 90:172–185
56. Shannon TR, Ginsburg KS, Bers DM (2002) Quantitative assessment of the SR Ca^{2+} leak-load relationship. Circ Res 91:594–600
57. Schlotthauer K, Bers DM (2000) Sarcoplasmic reticulum Ca^{2+} release causes myocyte depolarization. Underlying mechanism and threshold for triggered action potentials. Circ Res 87:774–780

58. Schotten U, Greiser M, Benke D, Buerkel K, Ehrenteidt B, Stellbrink C, Vazquez-Jimenez JF, Schoendube F, Hanrath P, Allessie M (2002) Atrial fibrillation-induced atrial contractile dysfunction: a tachycardiomyopathy of a different sort. Cardiovasc Res 53:192–201
59. Venetucci LA, Trafford AW, Eisner DA (2007) Increasing ryanodine receptor open probability alone does not produce arrhythmogenic calcium waves: threshold sarcoplasmic reticulum calcium content is required. Circ Res 100:105–111
60. Bhupathy P, Babu GJ, Ito M, Periasamy M (2009) Threonine-5 at the N-terminus can modulate sarcolipin function in cardiac myocytes. J Mol Cell Cardiol 47:723–729
61. Uemura N, Ohkusa T, Hamano K, Nakagome M, Hori H, Shimizu M, Matsuzaki M, Mochizuki S, Minamisawa S, Ishikawa Y (2004) Down-regulation of sarcolipin mRNA expression in chronic atrial fibrillation. Eur J Clin Invest 34:723–730
62. Greiser M, Neuberger HR, Harks E, El-Armouche A, Boknik P, de Haan S, Verheyen F, Verheule S, Schmitz W, Ravens U, Nattel S, Allessie MA, Dobrev D, Schotten U (2009) Distinct contractile and molecular differences between two goat models of atrial dysfunction: AV block-induced atrial dilatation and atrial fibrillation. J Mol Cell Cardiol 46:385–394
63. Pandit SV, Berenfeld O, Anumonwo JM, Zaritski RM, Kneller J, Nattel S, Jalife J (2005) Ionic determinants of functional reentry in a 2-D model of human atrial cells during simulated chronic atrial fibrillation. Biophys J 88:3806–3821
64. Van Wagoner DR, Pond AL, Lamorgese M, Rossie SS, McCarthy PM, Nerbonne JM (1999) Atrial L-type Ca^{2+} currents and human atrial fibrillation. Circ Res 85:428–436
65. Voigt N, Friedrich A, Bock M, Wettwer E, Christ T, Knaut M, Strasser RH, Ravens U, Dobrev D (2007) Differential phosphorylation-dependent regulation of constitutively active and muscarinic receptor-activated $I_{K,ACh}$ channels in patients with chronic atrial fibrillation. Cardiovasc Res 74:426–437
66. Dobrev D, Friedrich A, Voigt N, Jost N, Wettwer E, Christ T, Knaut M, Ravens U (2005) The G protein-gated potassium current $I_{K,ACh}$ is constitutively active in patients with chronic atrial fibrillation. Circulation 112:3697–3706
67. Cha TJ, Ehrlich JR, Chartier D, Qi XY, Xiao L, Nattel S (2006) Kir3-based inward rectifier potassium current: potential role in atrial tachycardia remodeling effects on atrial repolarization and arrhythmias. Circulation 113:1730–1737
68. Christ T, Boknik P, Wohrl S, Wettwer E, Graf EM, Bosch RF, Knaut M, Schmitz W, Ravens U, Dobrev D (2004) L-type Ca^{2+} current downregulation in chronic human atrial fibrillation is associated with increased activity of protein phosphatases. Circulation 110:2651–2657
69. Ehrlich JR, Cha TJ, Zhang L, Chartier D, Villeneuve L, Hebert TE, Nattel S (2004) Characterization of a hyperpolarization-activated time-dependent potassium current in canine cardiomyocytes from pulmonary vein myocardial sleeves and left atrium. J Physiol 557:583–597
70. Yue L, Feng J, Gaspo R, Li GR, Wang Z, Nattel S (1997) Ionic remodeling underlying action potential changes in a canine model of atrial fibrillation. Circ Res 81:512–525
71. Voigt N, Maguy A, Yeh YH, Qi X, Ravens U, Dobrev D, Nattel S (2008) Changes in $I_{K,ACh}$ single-channel activity with atrial tachycardia remodelling in canine atrial cardiomyocytes. Cardiovasc Res 77:35–43
72. Aime-Sempe C, Folliguet T, Rucker-Martin C, Krajewska M, Krajewska S, Heimburger M, Aubier M, Mercadier JJ, Reed JC, Hatem SN (1999) Myocardial cell death in fibrillating and dilated human right atria. J Am Coll Cardiol 34:1577–1586
73. Schotten U, Ausma J, Stellbrink C, Sabatschus I, Vogel M, Frechen D, Schoendube F, Hanrath P, Allessie MA (2001) Cellular mechanisms of depressed atrial contractility in patients with chronic atrial fibrillation. Circulation 103:691–698
74. Kannel WB, Abbott RD, Savage DD, McNamara PM (1982) Epidemiologic features of chronic atrial fibrillation: the Framingham study. N Engl J Med 306:1018–1022
75. Brundel BJ, Van Gelder IC, Henning RH, Tieleman RG, Tuinenburg AE, Wietses M, Grandjean JG, Van Gilst WH, Crijns HJ (2001) Ion channel remodeling is related to intraoperative atrial effective refractory periods in patients with paroxysmal and persistent atrial fibrillation. Circulation 103:684–690

76. Qi XY, Yeh YH, Xiao L, Burstein B, Maguy A, Chartier D, Villeneuve LR, Brundel BJ, Dobrev D, Nattel S (2008) Cellular signaling underlying atrial tachycardia remodeling of L-type calcium current. Circ Res 103:845–854
77. Sun H, Chartier D, Leblanc N, Nattel S (2001) Intracellular calcium changes and tachycardia-induced contractile dysfunction in canine atrial myocytes. Cardiovasc Res 49:751–761
78. Yue L, Melnyk P, Gaspo R, Wang Z, Nattel S (1999) Molecular mechanisms underlying ionic remodeling in a dog model of atrial fibrillation. Circ Res 84:776–784
79. Brundel BJ, Ausma J, van Gelder IC, Van der Want JJ, van Gilst WH, Crijns HJ, Henning RH (2002) Activation of proteolysis by calpains and structural changes in human paroxysmal and persistent atrial fibrillation. Cardiovasc Res 54:380–389
80. Beharier O, Etzion Y, Katz A, Friedman H, Tenbosh N, Zacharish S, Bereza S, Goshen U, Moran A (2007) Crosstalk between L-type calcium channels and ZnT-1, a new player in rate-dependent cardiac electrical remodeling. Cell Calcium 42:71–82
81. Beharier O, Etzion Y, Levi S, Mor M, Dror S, Kahn J, Katz A, Moran A (2010) The involvement of ZnT-1, a new modulator of cardiac L-type calcium channels, in [corrected] atrial tachycardia remodeling. [corrected]. Ann NY Acad Sci 1188:87–95
82. Levy S, Beharier O, Etzion Y, Mor M, Buzaglo L, Shaltiel L, Gheber LA, Kahn J, Muslin AJ, Katz A, Gitler D, Moran A (2009) Molecular basis for zinc transporter 1 action as an endogenous inhibitor of L-type calcium channels. J Biol Chem 284:32434–32443
83. Gaborit N, Steenman M, Lamirault G, Le Meur N, Le Bouter S, Lande G, Leger J, Charpentier F, Christ T, Dobrev D, Escande D, Nattel S, Demolombe S (2005) Human atrial ion channel and transporter subunit gene-expression remodeling associated with valvular heart disease and atrial fibrillation. Circulation 112:471–481
84. Klein G, Schroder F, Vogler D, Schaefer A, Haverich A, Schieffer B, Korte T, Drexler H (2003) Increased open probability of single cardiac L-type calcium channels in patients with chronic atrial fibrillation. role of phosphatase 2A. Cardiovasc Res 59:37–45
85. Schotten U, Haase H, Frechen D, Greiser M, Stellbrink C, Vazquez-Jimenez JF, Morano I, Allessie MA, Hanrath P (2003) The L-type Ca^{2+} –channel subunits alpha1C and beta2 are not downregulated in atrial myocardium of patients with chronic atrial fibrillation. J Mol Cell Cardiol 35:437–443
86. Carnes CA, Janssen PM, Ruehr ML, Nakayama H, Nakayama T, Haase H, Bauer JA, Chung MK, Fearon IM, Gillinov AM, Hamlin RL, Van Wagoner DR (2007) Atrial glutathione content, calcium current, and contractility. J Biol Chem 282:28063–28073
87. Bosch RF, Scherer CR, Rub N, Wohrl S, Steinmeyer K, Haase H, Busch AE, Seipel L, Kuhlkamp V (2003) Molecular mechanisms of early electrical remodeling: transcriptional downregulation of ion channel subunits reduces $I_{Ca,\,L}$ and I_{to} in rapid atrial pacing in rabbits. J Am Coll Cardiol 41:858–869
88. Grammer JB, Zeng X, Bosch RF, Kuhlkamp V (2001) Atrial L-type Ca^{2+}–channel, beta-adrenorecptor, and 5-hydroxytryptamine type 4 receptor mRNAs in human atrial fibrillation. Basic Res Cardiol 96:82–90
89. Luo X, Pan Z, Xiao J, Zhang J, Lu Y, Yang B, Wang Z (2010) Abstract 19435: Critical role of microRNAs miR-26 and miR-101 in atrial electrical remodeling in experimental atrial fibrillation. Circulation 122:A19435
90. Voigt N, Trausch A, Knaut M, Matschke K, Varro A, Van Wagoner DR, Nattel S, Ravens U, Dobrev D (2010) Left-to-right atrial inward rectifier potassium current gradients in patients with paroxysmal versus chronic atrial fibrillation. Circ Arrhythm Electrophysiol 3:472–480
91. Makary S, Voigt N, Maguy A, Wakili R, Nishida K, Harada M, Dobrev D, Nattel S (2011) Differential protein kinase C isoform regulation and increased constitutive activity of acetylcholine-regulated potassium channels in atrial remodeling. Circ Res 109:1031–43
92. Burashnikov A, Antzelevitch C (2003) Reinduction of atrial fibrillation immediately after termination of the arrhythmia is mediated by late phase 3 early afterdepolarization-induced triggered activity. Circulation 107:2355–2360

Chapter 54
Neuronal Calcium Signaling and Alzheimer's Disease

Neha Kabra Woods and Jaya Padmanabhan

Abstract Calcium plays a major role in normal functioning of the cells. Deregulation of calcium-mediated signaling has been implicated in many neurodegenerative diseases including Alzheimer's disease. Studies in neurons and mice expressing Alzheimer's disease-associated transgenes have shown that the expression of familial Alzheimer's disease (FAD) mutants of presenilin (PS) and amyloid precursor protein (APP) alter calcium homeostasis and cause synaptic dysfunction and dendritic spine loss in neurons. Mechanistic studies have shown that FAD mutants of presenilin can affect the intracellular calcium levels by affecting the ER calcium stores. A function for presenilins as ER calcium leak channels has been established and studies show that presenilins affect ER calcium load through an effect on IP_3 receptors, ryanodine receptors, or SERCA pumps. Even in the absence of an active gamma-secretase complex, presenilins seem to affect calcium homeostasis suggesting that these two functions of presenilins are independent of each other. Studies using FAD mutants of APP have shown that unlike presenilins, FAD-APP do not affect calcium homeostasis in the absence of Aβ. Both Aβ and presenilins seem to affect calcium homeostasis at very early stages of disease development affecting the synaptic transmission and function prior to neuritic plaque development. Altered calcium signaling differentially regulates genes such as calcineurin, calmodulin kinase II, MAP kinase etc and induces protein modifications and neurite degeneration. Since functional synapses and synaptic transmission are fundamental processes in memory formation, alterations in these processes can lead to neuronal dysfunction and memory deficit as seen in Alzheimer's disease. This chapter gives an overview

N.K. Woods • J. Padmanabhan, Ph.D. (✉)
Department of Molecular Medicine, University of South Florida,
12901 Bruce B. Downs Blvd., Tampa, FL 33612, USA

Department of Molecular Medicine, USF Health Byrd Alzheimer's Institute,
University of South Florida, 4001 E. Fletcher Ave., Tampa, FL 33613, USA
e-mail: nkabra@health.usf.edu; jpadmana@health.usf.edu

M.S. Islam (ed.), *Calcium Signaling*, Advances in Experimental Medicine and Biology 740, DOI 10.1007/978-94-007-2888-2_54,

of calcium signaling in different systems, specifically neurons, the functioning of pre- and post-synaptic signaling, and how their deregulation influences pathology development in Alzheimer's disease.

Keywords NMDA receptors (NMDAR) • IP_3 • Calcineurin • Calmodulin kinase • LTP • LTD • Postsynaptic density (PSD) • IP_3 receptor (IP_3R) • Ryanodine receptor (RyR) • Presenilin • FAD (familial Alzheimer's disease) mutations • Amyloid precursor protein (APP) • Amyloid beta (Aβ) • Endoplasmic reticulum (ER) • Mitochondria

Introduction

Calcium was primarily considered a structural element until the mid-twentieth century when seminal work by Weber, Ebashi and others suggested its potential role in signaling [1–5]. Since then, the function of calcium as a second messenger in important signaling pathways in the cell has been widely investigated. Some of the fundamental questions regarding calcium signaling pertain to the understanding of the mechanism of calcium-mediated signal transduction and regulation of intracellular levels of this element which lead us to identify its role in influencing the function, localization and interaction of different proteins in a cell.

Mechanisms of maintenance of calcium levels within the cytoplasm are a widely researched subject. It is well known now that cytoplasmic calcium level is maintained at approximately 100 nM (a few thousand fold less than extracellular regions ~2 mM) and this is achieved by a constant expulsion of calcium ions from cytoplasm to the ER, mitochondria or the extracellular matrix via calcium channels and ion pumps (Fig. 54.1). The ER and mitochondria behave as the cell's internal stores for calcium. ATPase pumps constitute an important factor in maintaining low levels of calcium within the cytoplasm over a long duration. These are considered high-affinity, low-capacity channels that tirelessly pump out excess calcium that is constantly leaking into the cytoplasm from different sources within and around the cell. Sarcoendoplasmic Reticular Ca^{2+} ATPase (SERCA) pumps calcium ions into the ER from the cytoplasm while Plasma Membrane Ca^{2+} ATPase (PMCA) pumps calcium ions out of the cell. ATPase pumps are also present in the Golgi and nuclear envelope. As the name suggests, these ATPase pumps exchange calcium for protons and this process is accompanied with ATP hydrolysis [6–9].

Other calcium channels include the sodium-calcium (NCX) exchangers that are low-affinity, high capacity pumps. These pumps are either NCX wherein one Ca^{2+} ion is exchanged for three Na^+ ions or NCKX pumps which allow exchange of one K^+ ion and one Ca^{2+} ion for four Na^+ ions. The NCX channels are present on the plasma membrane along with PMCA and they serve to rapidly adjust calcium levels within the cell during signaling [10].

Perhaps the fastest calcium transporting channels are the voltage-gated channels [11]. These paddle-shaped transmembrane ion channels are normally closed but can

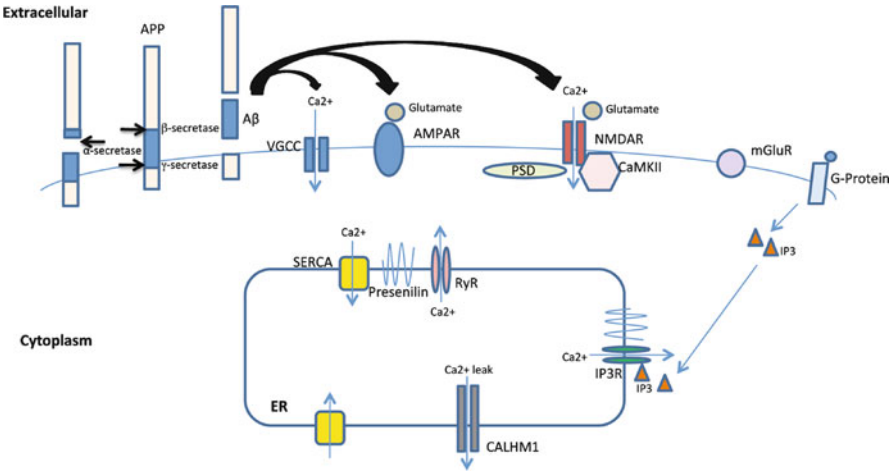

Fig. 54.1 Calcium signaling pathways and AD-associated changes: Calcium ions are maintained at low levels in the cytoplasm by the tireless activity of several calcium pumps and channels which expel ions from the cytoplasm into the *ER*, mitochondria and the extracellular matrix. Entry of calcium into the cytoplasm is a highly regulated process that occurs via cell surface receptors, such as *VGCC*, *NMDAR*, *AMPAR*, and the endoplasmic reticulum (*ER*) receptors, such as *RyR* and IP_3R. G protein-coupled receptors on the membrane surface activate phospholipase C to cleave phosphatidylinositol-4,5-bisphosphate into *DAG* and IP_3. IP_3 translocates to the *ER* and binds to IP_3R and activates it. *SERCA*, on the other hand, pumps calcium from the cytoplasm into the *ER*. Presenilins (*PS*) are associated with the *ER* membrane and mutations in *PS* are speculated to perturb the function of *RyRs*, IP_3Rs and *SERCA* pumps, thereby disrupting calcium homeostasis. As part of the gamma secretase complex, presenilins also promote the formation of $A\beta$ from *APP* cleavage at the cell surface. $A\beta$ has been shown to affect *NMDAR*, *AMPAR* and *VGCC*. Deregulated calcium entry due to the influence of $A\beta$ has been shown to affect gene expression and other signaling pathways within the cell. This includes inhibition of CAMKII phosphorylation, which in turn affects synaptic plasticity and memory formation. Expression of *CALHM1* on *ER* suggests its role as calcium leak channel similar to presenilins. *CALHM1* has also been shown to reduce *ER* calcium uptake by affecting the *SERCA* pumps

undergo a conformational change due to changes in membrane potential. This conformational change causes the channels to open and specifically allow a large number of calcium ions to flow down the ~20,000-fold gradient. These voltage channels are highly selective for calcium due to high binding affinity for calcium within the pore but upon removal of extracellular calcium, these channels can conduct sodium or potassium ions as well. These voltage-gated channels play an important role in neuron excitation and muscle contraction. Voltage-gated channels have been classified into several types on the basis of their structures, voltage range for activation and inactivation and pharmacological inhibition/activation. These are designated as L, T, P, Q, N and R-type channels [12]. Other channels and receptors such as ligand-dependent channels, ryanodine receptors and IP_3 receptors regulate levels of calcium within the cytoplasm and ensure the maintenance of appropriate levels of calcium within the ER and mitochondria.

Calcium Signaling

In simple words, calcium signaling can be defined as a series of events wherein an external stimulus can lead to specific intracellular responses via changes in cytoplasmic calcium levels. Calcium enters the cytoplasm from external sources or intracellular calcium stores. A general mode of calcium signaling involves the release of calcium from the intracellular compartments upon external activating signals. In non-excitable cells, ligand binding causes the G-protein coupled receptors (GPCRs) and receptor tyrosine kinases (RTKs) to activate phospholipase C (PLC) to cleave phosphatidylinositol 4,5 bisphosphate (PIP_2) into 1,4,5-inositol triphosphate (IP_3) and diacylglycerol (DAG). IP_3 binds to IP_3 receptor (IP_3R) on the ER and allows the diffusion of calcium from the ER into the cytoplasm such that the cytoplasmic calcium levels increase from 100 nM to ~1 μM [13] (Fig. 54.1). Increased calcium in the cytoplasm triggers a cascade of signaling pathways that involve proteins that activate upon binding to calcium and amplify the calcium signal thereby affecting important processes involved in metabolism, transcription, motility, proliferation, etc. [14]. Meanwhile, the depleted stores in ER replenish their calcium levels via a mechanism called the store-operated calcium entry [15]. A small but highly selective Ca^{2+} -release activated current (I_{CRAC}) is generated across the ER and with the help of transmembrane proteins STIM1 and Orai, the calcium reserves are replenished.

In excitable cells, calcium signaling is generally initiated by changes in membrane potential and introduction of calcium via different channels on the plasma membrane. Besides the IP_3 receptors, ER in these cells also express ryanodine receptors (RyR) [16]. These RyR are also Calcium-Induced Calcium Release (CICR) receptors. Calcium functions as the main ligand for RyR and low levels of cytoplasmic calcium open these channels to allow release of more calcium from ER/sarcoplasmic reticulum into the cytoplasm. These RyRs are transmembrane homotetrameric channels that interact with a number of different proteins in the cytoplasm such as Calmodulin, CamKII, calcineurin, PKA, etc. IP_3R can also exhibit CICR receptor behavior but usually some IP_3 is required for its activation [17]. It has been shown that small molecule cADPR (cyclic ADP Ribose) can sensitize RyR to calcium and allow for calcium release from ER via this channel [18]. Similarly, nicotinic acid adenine dinucleotide phosphate (NAADP) can sensitize IP_3 receptors and RyRs to calcium release although the mechanism by which it does so is not fully understood [19, 20].

Calcium waves and oscillations have been observed in almost every type of cell. Calcium waves are usually a result of a cascade of calcium release and diffusion. The initial release of calcium from a site activates nearby stores that are sensitive to calcium and they further release calcium which subsequently diffuses and activates additional stores [21]. The strength of the wave depends on the sensitivity of the receptors of the additional stores and their proximity to the initial calcium release site. Release of calcium from clusters of IP_3Rs is termed Ca^{2+}"puffs" while RyRs give rise to Ca^{2+}"sparks" [22]. These local calcium signals propagate to a global scale by activating calcium release from neighboring stores within the cells and

between cells. Calcium waves can be highly localized and intense if the initial calcium trigger and subsequent calcium signaling molecules (RyRs in ER/SR) are in close proximity. This phenomenon is usually observed in events such as muscle contraction or synaptic transmission. On the other hand, processes such as gene transcription, post-translational modifications and cellular migration require prolonged and global calcium signaling and in such cases calcium waves are repetitive and not strictly spatially confined [21, 22].

The remainder of this chapter is devoted to understanding the mechanism of calcium signaling in neuronal cells and its deregulation which has important implications in the pathology of Alzheimer's disease.

Neuronal Calcium Signaling

Neurons are the basic units of the nervous system and these rely heavily on calcium for maintaining their function and homeostasis. Calcium regulates the cation channels in neurons, functions as an important second messenger in signaling pathways and gene transcription and promotes neurotransmitter release at synaptic junctions.

Calcium Channels

Calcium entry in neurons can be via voltage-gated calcium channels (VGCC) or ligand-gated ion channels. As described previously, VGCCs are regulated by changes in membrane potential. Conformational change in these channels allows for the entry of calcium which activates IP_3Rs and RyRs to release more calcium from internal stores thereby increasing cytoplasmic levels and influencing important signaling pathways. The general structure of a VGCC consists of five subunits. The largest is the $\alpha 1$ subunit that forms the pore which is responsible for ion selectivity and conductance. This subunit has four domains, each with six transmembrane segments. The $\alpha 1$ subunit pore is also the binding site for agonists and antagonists. The $\alpha 1$ subunit associates variably with $\alpha 2$, β, γ and δ subunits to form the voltage-gated channel [11, 23, 24] and this leads to the recognition of three families of VGCCs, i.e., Ca_v1, Ca_v2 and Ca_v3 [25]. On the basis of sensitivity to pharmacological drugs and other biophysical criteria, the VGCCs have been classified into several subtypes. These are the L-, N-, P-, Q-, R-, T- type current conducting channels [26] and they are sensitive to different toxins. The T-type currents are low voltage activated (LVA) that are activated slowly and inactivated rapidly. The other currents are generally considered as high voltage activated (HVA) which are activated rapidly and differ in their rates of inactivation. Ca_v1 generally conducts L-type current while Ca_v2 conducts N, P, Q and R-type currents. Ca_v3 conducts T-type current. The Ca_v2 family of channels is most prominent in neurons and neuroendocrine cells. These channels are responsible for the release of neurotransmitters at

synaptic junctions, hormones and neuropeptides. As is understood, these channels are activated by membrane depolarization and this facilitates Ca^{2+} currents. It has been shown that activated G-protein can regulate these channels by associating with them and slowing the rate of activation upon depolarization [27, 28]. In presynaptic nerve terminals, calcium can regulate these calcium channels as well. Initial entry of calcium into the cell allows for the binding of calcium/calmodulin to these channels which enhances Ca^{2+} dependent facilitation of calcium current as well as voltage-dependent inactivation of these channels [29, 30]. At pre-synaptic terminals, voltage-gated calcium channels are the primary source of calcium entry that facilitate neurotransmitter release. Protein and lipid components that are involved in exocytosis and synaptic vesicles are organized in a region called the active zone [31]. Synaptogamins and SNARE protein complex composed of SNARE-25, syntaxin and synaptobrevin are all present in this active zone. It has been reported that synaptogamins bind to the calcium channels either directly [32] or via the SNARE complex [33, 34]. Synaptogamins function as calcium sensors that bind lipids in a calcium-dependent fashion and allow for exocytosis and subsequent neurotransmitter release from the synaptic vesicles [35].

Calcium entry into neuronal cells can also be achieved by a different type of calcium channel, namely, the N-methyl D-aspartate receptor (NMDAR) (Fig. 54.1). NMDAR is a voltage as well as ligand-gated channel. The activation of this channel requires membrane depolarization as well as binding of the neurotransmitter glutamate [36]. At resting potential, the channel is blocked by Mg^{2+} and upon membrane depolarization, the block is released to allow entry of calcium as well as sodium ions [37]. The NMDA receptors have transmembrane segments and intracellular domains that can be modified by phosphorylation by enzymes such as protein kinase C (PKC) [38]. These channels can also be regulated by tyrosine phosphorylation which plays an important role in intracellular signaling pathways [39]. NMDARs play an important role in LTP and LTD.

Besides VGCC and NMDAR, neuronal cells also contain other calcium channels such as the neuronal acetylcholine receptor (nAChR), type 3 serotonin receptor ($5HT_3R$) and the AMPA receptor.

Calcium Release from Intracellular Stores and Capacitative Calcium Entry

Cytoplasmic calcium levels are regulated by extracellular calcium entry as well as calcium release from internal calcium stores. As mentioned earlier, ER and mitochondria serve as the major intracellular calcium stores and they express channels/receptors that allow for calcium release into the cytoplasm upon activation. Two major channels for calcium transport on ER include the ryanodine receptor and the IP_3 receptor [40, 41]. Interestingly, IP_3R is most efficiently activated to release calcium in the presence of both IP_3 and Ca^{2+} and this mechanism of autoactivation is called Calcium Induced Calcium Release (CICR). CICR is the major mechanism

of activation for RyRs. In this case, calcium that enters the cytoplasm from external sources due to membrane depolarization sensitizes RyRs to release more calcium from the ER. However, cytoplasmic calcium concentrations above 10 μM inhibit the receptor to prevent further release of calcium from the stores. CICR are therefore responsible for regenerative calcium waves within the cell. Within the neurons, second messenger cyclic ADP ribose (cADPr) has been shown to increase the calcium sensitivity of RyRs such that they release more calcium upon depolarization [42]. Caffeine has also been shown to increase the sensitivity of RyRs to calcium. The extent of calcium release from ER upon membrane depolarization also depends on the calcium content within the ER. Through the SERCA pumps, calcium is constantly pumped back from the cytoplasm into the ER and this allows ER to behave as a large calcium sink. Hence, ER is capable of releasing calcium in response to periodic pulses of action potential thereby transmitting global calcium waves to promote signal transduction and gene transcription.

Discharge of calcium from internal stores causes ER to signal the cell membrane to allow calcium entry from extracellular space in order to replenish the stores. This form of regulated calcium entry is called 'capacitative calcium entry' [43]. It was thought to occur only in non-excitable cells until recently when it was also discovered in neurons and neuroendocrine cells [44]. The mechanism by which the ER communicates with plasma membrane regarding its depleted stores is not fully understood. It is speculated that either the communication occurs by a diffusible signal or via physical protein-protein interaction [45, 46]. A few mechanisms have been proposed to explain this phenomenon. The earliest explanation involved the presence of a calcium influx factor (CIF) that increased calcium entry in several cell types although how CIF was activated in response to calcium depletion was unknown [46]. Next, an exocytosis model was proposed wherein channels might be inserted into the membrane by vesicle fusion in response to depletion of internal calcium stores [47]. At present, the conformational coupling theory is being widely studied which suggests that the IP_3-liganded IP_3 receptor undergoes a conformational change upon calcium depletion in the ER and this transmits information to the plasma membrane by protein-protein interaction [48, 49].

Presynaptic and Postsynaptic Calcium Signaling

Neurotransmitter Release

Calcium influx has been implicated in neurotransmitter release from presynaptic terminals. Depolarization allows calcium to enter the cell via VGCCs and this stimulates RyRs and IP_3 receptors to release calcium from the internal stores. The sparks and puffs that result from multiple activated RyRs and IP_3Rs greatly increase localized calcium levels which triggers exocytosis of synaptic vesicles to release neurotransmitters [50]. The efficiency of this mode of regulation depends on the proximity of the internal stores to the plasma membrane and synaptic vesicles.

Hence, it has been observed that ER is very closely associated with the plasma membrane and the secretory vesicles in the synaptic regions [50]. cADPr has been shown to enhance vesicular exocytosis by promoting calcium release from the ryanodine receptors [51]. Certain synaptic proteins have been demonstrated to help localize the synaptic vesicle to the active zone of the presynaptic terminals. These include the synaptogamins and proteins of the SNARE complex (syntaxin1 and SNAP-25). These proteins bind to the α1 subunit of the N-type and P/Q-type calcium channels at the synprint site [52, 53]. Synaptogamins behave as calcium sensors and disruption of synaptogamin binding can alter the properties of the calcium channels and inhibit neurotransmitter release [54].

Postsynaptic Calcium Signaling

Calcium functions as an important signaling molecule in postsynaptic processes and it can enter dendrites through voltage-gated channels as well as transmitter-gated channels. The neurotransmitter glutamate plays a crucial role in synaptic transmission as well as calcium signaling. Two major receptors that transduce the glutamate signal include the AMPA (α amino-3-hydroxy-5-methyl-4-isoxazolepropionic acid) receptor and the NMDA (N-methyl-D-aspartate) receptor (Fig. 54.1). The AMPA receptor is activated upon glutamate binding while the NMDAR, which is a calcium permeable receptor, is activated upon glutamate stimulation as well as membrane depolarization [37, 55]. Dendritic calcium signaling has been classified into several types depending on the spatial range of the signals. Calcium action potential arises from regenerative activation of VGCCs. Generation of action potential requires activation of multiple synapses to achieve a threshold value. Action potentials can either be localized to the dendrites or can spread to the entire cell body [56]. Calcium waves result from intracellular calcium release that follows repetitive activation of metabotropic glutamate receptors (mGluRs). Activation of mGluRs induces the production of IP_3 that bind and activate IP_3 receptors thereby releasing calcium from internal stores and propagating the wave. Regional calcium signaling is generally non-propagating and localized within the dendritic spines and the dendrite from which they arise. Spine calcium signals are tightly restricted within the individual spine and these signals arise due to influx of calcium via VGCCs, NMDA receptors and internal stores [57]. The postsynaptic density (PSD) is a postsynaptic membrane associated concentration of proteins which extends into the cytoplasm. Within the PSD, a large number of proteins bind to important calcium and transmitter receptors such as the NMDAR, AMPA and mGluR [58, 59]. These include a number of calcium binding proteins and calcium activated proteins that propagate important signaling pathways.

Synaptic plasticity is considered to be the basis for memory and learning. It is defined as changes in the strength and efficiency of synaptic transmission. Long-term potentiation (LTP) and long-term depression (LTD) are the two forms of synaptic plasticity [60] and NMDA receptors play an important role in regulating these. LTP can be generated rapidly, is prolonged and found to be associated with memory formation. Initiation of LTP requires activation of NMDAR. When the cell is

sufficiently depolarized, the Mg2+ block dissociates from NMDAR and this allows the entry of sodium and calcium ions into the dendritic spine. Resulting burst of calcium levels within the cytoplasm triggers LTP. LTP can be classified into Early LTP (E-LTP) which occurs immediately in response to elevated calcium levels and lasts for an hour and Late LTP (L-LTP) which lasts much longer than an hour and involves gene transcription and protein expression [50]. Interestingly, NMDA receptor activation is also responsible for triggering LTD. It is believed that the spatial and temporal changes in calcium concentration and signaling can induce LTP or LTD [61]. Rapid and large influxes of calcium into the cytoplasm trigger LTP while prolonged and low influxes of calcium give rise to LTD.

NMDA receptors consist of four subunits: two are the NR1 subunits and the other two are regulatory subunits that can be NR2A to D or NR3A to D. Different combinations of the subunits alter the function of the NMDA receptor [62]. Synaptic and extrasynaptic NMDAR have been shown to activate different signaling pathways that affects initiation of LTP or LTD but these findings are controversial [63, 64]. It has been suggested that extrasynaptic NMDAR is composed of NR2B subunit while NR2A is a subunit of synaptic NMDAR [65, 66] but this subject is also controversial [67]. Several studies have suggested that NR2B-containing NMDAR mediates LTP because important LTP signaling molecule CAMKII preferentially binds to NR2B [68]. Other studies have indicated that NR2A-subunit containing NMDAR mediates LTP [69]. Further research will hopefully solve these discrepancies. Finally, it has been speculated that higher ratios of NR2A/NR2B might favor LTD induction although this would still require that the above controversies regarding NMDA subunit functions be first resolved [70].

Besides NMDA, the AMPA receptors also play a key role in initiating LTP and LTD. During basal synaptic transmission, glutamate acts on both the AMPA and NMDAR. Sodium ions flow through AMPA but not through NMDAR due to the Mg^{2+} block. Upon membrane depolarization, the Mg^{2+} block is released and NMDAR can transport sodium as well as calcium ions into the cytoplasm. These events trigger LTP. Biochemical studies show that there is an increase in miniature electrophysiologic synaptic current (EPSC) in the postsynaptic cell in response to neurotransmitter release during LTP and this is an indicator of increase in number or function of postsynaptic receptors. The AMPA receptor subunit GluR1 is phosphorylated by CaMKII and this increases its channel conductance thereby contributing to the manifestation of LTP [71–73]. AMPA receptors can be inserted into the postsynaptic membrane during LTP and this is facilitated by activation of Ras and CaMKII by NMDAR. Removal of AMPA from the synaptic plasma membrane by endocytosis is characteristic of LTD and this is brought about by activation of Rap [74–76].

Calmodulin Kinase II (CaMKII) is a key molecule in LTP associated signal transduction. It is autophosphorylated at several threonine residues which regulates its activity and sub-cellular localization [77]. Other important proteins are PKC and PKA. On the other hand, it has been suggested that protein phosphatases are preferentially activated during LTD. This includes activation of calcium/calmodulin-dependent phosphatase, calcineurin (or PP2B) and protein phosphatase 1 (PP1) [78]. PP1 is inhibited by phosphorylated inhibitor1. Activated calcineurin can

dephosphorylate inhibitor1 and release PP1 such that it can manifest the effects of LTD by promoting AMPA endocytosis at the postsynaptic terminals [55, 79]. PP2B has higher affinity for calmodulin as compared to CaMKII. Hence, it can get activated by small increases in intracellular calcium levels to further activate PP1. However, a large increase in cellular calcium concentrations activates CaMKII as well as PKA which are associated with LTP. Increases in PKA activity leads to phosphorylation of inhibitor1 which inactivates PP1 and therefore inhibits LTD [78, 80].

PSD Components and Signaling

The postsynaptic density (PSD) is a dynamic structure that reorganizes its signal transduction components during calcium signaling. The PSD contains receptors, scaffolding proteins and calcium binding and mobilizing proteins [55, 59].

NMDAR is a key receptor in postsynaptic calcium signaling. The C-terminus of NMDAR associates with scaffolding protein PSD-95, cytoskeletal proteins and calmodulin and this allows it to remain integrated in the PSD [81] (Fig. 54.1). Calcium-CaM-dependent kinase II (CaMKII) is an essential protein that mediates NMDAR-dependent LTP. The enzyme has an autoinhibitory domain that keeps the catalytic domain inactive [82]. Calcium ions entering PSD via NMDAR bind to calmodulin which in turn binds to CaMKII and releases the autoinhibition. Activated CaMKII is phosphorylated at Thr286/287 which makes it functional despite fall in calcium/clamodulin levels [83, 84]. CaMKII has been shown to enhance channel conductance of AMPAR by phosphorylating the AMPAR subunit GluR1 [73]. In response to LTP, CaMKII induces insertion of AMPAR to the postsynaptic membrane surface by stimulating exocytosis of AMPAR containing vesicles by an undetermined mechanism [83]. PP1 has been shown to dephosphorylate CaMKII in PSD while PP2A is unable to do so [85]. Some research suggests that PP1 inhibits CaMKII activation because overexpression of inhibitor1 seemed to suppress PP1 and enhance autophosphorylation of CaMKII, AMPAR and CREB [86]. PP1, calcineurin and PKA are localized within the PSD via interaction with anchoring proteins such as AKAP79 [87, 88].

PSD-95 is a key scaffolding protein in the postsynaptic density and it plays an important role in anchoring different proteins with the NMDAR-associated complex. It is also referred to as SAP-90 and contains five protein binding domains (three PDZ domains followed by SH3 and a GuK domain). The first two PDZ domains bind to the C-terminus of NMDAR while the other domains interact with different signaling molecules [89]. Other proteins that bind to PSD-95 include nNOS, neuroligin and SynGAP [90, 91]. SynGAP is synaptic RasGAP. It enhances the GTPase activity of Ras which in turn regulates the MAPkinase pathway. SynGAP activity can be inhibited by phosphorylation by CaMKII upon stimulation of NMDAR thereby activating the MAPkinase pathway [92]. Calcium influx through NMDAR has been shown to activate Ras-GRF (guanine releasing factor) which stimulates Ras activity [93] which subsequently promotes the insertion of AMPAR into the postsynaptic membrane [75]. The different components of the MAPkinase

pathway are present within the PSD as part of NMDAR complex [94] and upon activation, they propagate signals generated by LTP.

Besides interacting with different PSD proteins, PSD-95 also associates with another set of scaffolding protein called Shank via guanylate kinase-associated protein or GKAP [95]. Shank can multimerize and associate with Homer which facilitates the important interaction of mGluR with IP_3 receptors [22]. Homer ensures the localization of IP_3R in the spines and close to PSD such that calcium entry from mGluR and other receptors can trigger the formation of IP_3 and stimulate IP_3R to release calcium from internal stores. This activates the calcium sensors within the PSD to promote calcium signaling. Thus, Shank-Homer complexes can successfully link the NMDAR, mGluR and IP_3R in the PSD for efficient calcium influx and signaling.

Calcium Signaling and Gene Expression

Calcium entry and signaling initiated at the postsynaptic membrane finally results in regulation of gene transcription in the nucleus for long-term effects of neurotransmission. Central to the regulation of gene expression from calcium-dependent signaling is the posttranslational modification of the transcription factor CREB (cyclic AMP response element binding) protein. Phosphorylation of CREB in the nucleus affects multiple transcription events. CREB is generally bound to the cyclic AMP response element (CRE) on the promoters of target genes. Upon calcium influx and stimulation of adenylate cyclase, cyclic AMP levels increase which drive the phosphorylation of CREB at Ser133 [96, 97]. Subsequently, CREB recruits CBP (CREB binding protein) which is a transcriptional co-activator and it acetylates the histones at the target promoters as well as recruits RNA polymerase II to facilitate transcription of the gene [98, 99].

Calcium influx triggers at least four different signaling pathways to phosphorylate CREB at Ser133 in order to activate it. Calcium enters through voltage or ligand-gated channels and binds to calmodulin to activate CaM kinases. CaMKII and CaMKIV can translocate to the nucleus and phosphorylate CREB at Ser133 [100]. Interestingly, CREB has been found to be phosphorylated at Ser142 as well but this phosphorylation inhibits its transcriptional activating function by disrupting the association of CREB with CBP [101]. This inhibitory phosphorylation appears to be mediated by CaMKII although it is less effective at modulating the function of CREB as compared to the activating phosphorylation at Ser133 by CaMKIV [102]. It has also been shown that after phosphorylation at Ser133, CREB can be phosphorylated at Ser129 by GSK3 (glycogen synthetase kinase 3). Phosphorylation at this site contributes to the activation of CREB [39]. The other important pathway that is activated upon calcium entry at PSD is the Ras/MAPK pathway. Activation of Ras stimulates the activation of subsequent downstream members of the pathway such as Raf, MEK, ERK1/2 and RSK kinase. RSK then translocates to the nucleus where it phosphorylates CREB at Ser133 to activate it [103]. It has been suggested that the Ras/MAPK pathway and CaMK pathway are activated simultaneously but CaMK

brings about rapid phosphorylation of CREB while phosphorylation by the Ras pathway is slower and effective after a long time post-stimulation [104].

Another pathway that leads to phosphorylation of CREB is the cAMP-PKA pathway. Calcium influx influences levels of cAMP by activation of adenylate cyclase (AC). Increase in cAMP levels activates PKA which enters the nucleus and phosphorylates CREB to switch on its transcriptional activity [37, 105]. Additionally, calcium dependent calcium release from the internal stores such as ER also contributes to cellular calcium that diffuses into the nucleus and promotes gene transcription by associating with calcium binding transcription factors. The net result of phosphorylation and activation of CREB is the expression of important proteins such as BDNF (brain derived neurotrophic factor). BDNF binds to its receptor tyrosine kinase and neurotrophin receptor p75 to activate signaling pathways that promote survival of the neurons and modulate synaptic activity [106, 107]. Several studies have shown that the route of calcium entry affects the transcription of neuronal genes such as BDNF. Calcium entry into the cytosol can be either through the ion channels such as NMDAR and AMPAR, the voltage-dependent calcium channels or from receptors that release calcium from internal stores [108]. While the NMDA glutamate receptor is responsible for the major fraction of calcium entry that initiates LTP and transcription of immediate-early genes, it is not the major driver of BDNF transcription. Calcium influx through the VGCC (L-type) induces CREB phosphorylation and BDNF transcription [109]. Calcium entering from both types of channels is capable of phosphorylating CREB at Ser133 but it has been speculated that NMDAR-mediated calcium influx could either phosphorylate CREB at the inhibitory site of Ser142 or fail to phosphorylate at the positive regulatory site Ser129 and this could explain the differential expression of BDNF in response to different channel stimulation [37]. It has also been observed that embryonic neurons that were cultured for 7 days *in vitro* were able to initiate CREB phosphorylation from calcium influx via NMDAR but by day 14 this calcium influx could not sustain CREB phosphorylation. It was suggested that while L-type VGCC can induce sustained phosphorylation of CREB, calcium entry from NMDAR was unable to do so because this mode of entry activates PP1 that dephosphorylates CREB at Ser133 [110]. Such mechanisms of differential gene regulation by the same calcium ion result in diverse outcomes that affect many aspects of the biology of neuronal cells.

Following sections in this chapter will address the deregulation of several points in the calcium signaling pathway and their effect in the manifestation of neurodegenerative diseases particularly, Alzheimer's disease.

Deregulation of Calcium Signaling in Alzheimer's Disease

The major pathological hallmarks of Alzheimer's Disease are the presence of neuritic plaques and neurofibrillary tangles (NFTs) in the affected areas of the brain [111–117]. The plaques are formed by the aggregation of a proteolytic fragment of

amyloid precursor protein (APP) known as amyloid beta (Aβ), and NFTs are formed from the hyperphosphorylated microtubule associated protein, tau. Majority of the cases of AD are of late onset or sporadic in nature and the cause or mechanisms involved in the disease development are not clearly understood.

Approximately 5–10% of the total reported cases of AD are associated with mutations in the APP or presenilin (PS) genes. Aβ is generated by sequential cleavage of APP by beta and gamma-secretases [116, 118] (Fig. 54.1). Gamma-secretase is a complex of four different proteins, Aph1, Pen2, Disastrin, and presenilin (PS) [119, 120]. PS is essential for gamma-secretase activity and mutations in PS and APP have been associated with increased generation of Aβ and early onset of AD (familial AD or FAD) [118].

Calcium deregulation has been implicated in AD for quite some time and several laboratories are examining the mechanism by which the deregulation affects pathology development [118–121]. It has been proposed that mutations in PS that cause autosomal dominant early onset AD (FAD) can induce perturbations in Ca^{2+} homeostasis in cells [122, 123]. This perturbation in calcium homeostasis can further induce Aβ generation [124], that can negatively affect synaptic plasticity and therefore neuronal function.

The long term effect of calcium deregulation is brought about by modulations in gene transcription and function. Studies by Wu and Colleagues [125] have shown that Aβ oligomers can activate the calcium-dependent phosphatase, CaN (PP2B), which in turn can induce the NFAT (nuclear factor of activated T cells) signaling pathway. Even in the absence of Aβ, activation of NFAT pathway can induce defects in neuronal activity by inducing neurite degeneration and dendritic spine loss, analogous to that brought about by Aβ. Inhibition of calcineurin ameliorates the morphological and functional deficits in neurons suggesting that calcium overload may affect calcineurin activation and downstream signaling events that can cause neurodegeneration [125, 126]

Presenilins and Ca^{2+} Homeostasis

In addition to the generation of higher levels of Aβ, FAD mutations in PS (FAD-PS) can cause Ca^{2+} signaling defects [122, 127–133]. FAD-PS have been shown to deregulate Ca^{2+} homeostasis by affecting IP_3-mediated Ca^{2+} release from ER stores, through perturbation of the store-operated Ca^{2+} channels and by affecting Ca^{2+} entry from extracellular regions. In addition to the interaction of PS with IP_3 receptor, it also interacts with ryanodine receptor (RyR) and enhances ER calcium release [122, 134–137] (Fig. 54.1). A role for presenilin as a passive ER calcium leak channel has been shown by Wu and colleagues [138]. Their studies in PS1 and PS2 double knockout (DKO) mouse embryonic fibroblasts (MEFs) showed that PS is essential for ER calcium homeostasis and deletion or mutation can lead to aberrant levels of ER Ca^{2+} load. Calcium deregulation in DKO cells could be prevented

by expression of presenilin holoproteins confirming that presenilins are essential for normal functioning and maintenance of ER calcium stores. Some of the presenilin FAD mutations (PS1-M146V) failed to rescue the Ca^{2+} defects suggesting that these mutations may prevent the presenelins from functioning as a Ca^{2+} leak channel on ER membrane. Co-expression of mutant PS (PS1-M146V or PS2-N141I) with WT PS did not rescue the defective calcium signaling, suggesting a dominant effect of this mutation over the WT presenilin gene. This validates that just one copy of the mutated gene is sufficient to cause the deregulation in calcium and demonstrates why FAD patients, with just one copy of mutated presenilin gene, are not spared from getting the disease. Not all the mutations in PS are associated with an increase in ER calcium load. Expression of PS1-dE9 (PS1 exon 9 deletion) mutant shows an increase in ER Ca^{2+} leak channel activity, which encompasses that of WT-PS1, suggesting that the PS1-dE9 is a 'gain of function' mutation [138]. The gamma-secretase activity of presenilins did not seem to be necessary for its functioning as a passive ER Ca^{2+} leak channel but the fact that Aβ can also induce calcium deregulation suggests that these two may act synergistically to induce calcium deregulation in FAD patients.

In addition to its role as a passive Ca^{2+} leak channel, PS can also affect calcium homeostasis through its association with SERCA (sarcoplasmic/endoplasmic reticulum calcium ATPase) pump (Fig. 54.1). Studies by Green and colleagues [139] showed that presenilins are required for proper functioning and activity of SERCA pumps. Presenilins physically associate with SERCA and modulate its function. Isoform specific knockdown of SERCA2b brought about similar disruption of Ca^{2+} dynamics as the presenilin-null cells suggesting that presenilins are necessary for the normal functioning of the SERCA. Similarly, studies using PS2 FAD mutations have shown a partial depletion of intracellular calcium stores due to reduced SERCA activity and increased calcium leak [140, 141]. This is also another example of a presenilin mutation that affects the ER calcium homeostasis by enhanced release and not accumulation of calcium in ER.

The activity of SERCA seems to affect generation of Aβ, with higher activity inducing and lower activity reducing the levels of Aβ. Thus, presenilin, independently or through its association with other Ca^{2+} operating pumps or through its functioning as a gamma-secretase, contributes significantly to the regulation of Ca^{2+} in cells. A recent study suggested that presenilins can also affect neurotransmitter release through low level ionic calcium influx into presynaptic axon terminals [142]. This calcium influx did not depend on activation of voltage gated calcium channels, NMDA receptors or the intracellular stores of calcium suggesting a novel role for presnilin in calcium-dependent synaptic function.

Whether FAD mutations in APP affect calcium homeostasis similar to presenilins is not clearly understood. Although there are several studies that suggest that APP may directly affect calcium homeostasis independently of Aβ production [143–145], a recent study suggests that unlike presenilins, FAD mutations in APP do not affect the intracellular Ca^{2+} levels independent of Aβ [146].

Polymorphisms in CALHM1 Gene and Alzheimer's Disease

Analysis of genes located at AD linkage region has shown an association between polymorphisms in calcium homeostasis modulator 1 (CALHM1) and development of sporadic AD (SAD). The correlation was mainly observed in healthy adults and not in the AD patients. Comparison of CSF samples from AD patients and healthy young individuals showed that while there was no association between CSF Aβ and AD, CALHM1 polymorphism in normal adults was associated with increased levels of Aβ 42 and 40 in CSF and increased risk for AD [147]. Analysis of cellular distribution of CALHM1 in brains and cells of neuronal lineage showed that CALHM1 is mainly expressed in ER and plasma membrane. Ca^{2+} influx through CALHM1 was shown to lower Aβ generation by increasing sAPP-alpha secretion. Downregulation of CALHM1 led to an increase in Aβ generation suggesting that it may affect the secretases that cleave APP. Since the majority of CALHM1 is expressed in ER, it is possible that it functions as an ER calcium leak channel similar to presenilins (Fig. 54.1). A recent study showed that, in addition to an increase in the calcium leak from ER, CALHM1 reduces ER calcium uptake by reducing the transport capacity and the calcium affinity of the SERCA pump [148]. This led to a drastic reduction in the ER calcium concentration and increased ER stress leading to upregulation in expression of ER stress-related proteins. Thus, CALHM1 seems to play a central role in mediating calcium deregulation, ER stress, and cellular damage observed in Alzheimer's disease.

Calcium Channels and Receptor Mediated Calcium Influx in AD Pathology Development

NMDA receptor-mediated calcium influx has been shown to affect the ryanodine receptor activation and ER calcium perturbation in dendritic processes, spine heads, and soma of pyramidal neurons in AD transgenic mice [149]. These mice also showed higher calcium response with synaptic or NMDAR stimulation suggesting an abnormal CICR effect within the spine and dendrites. This study proposes that presenilin associated disruptions in RyR signaling and the NMDAR-mediated calcium influx and CICR effect may induce synaptic dysfunction that serves as a causative factor for the early synaptic changes observed in AD. The exact mechanism by which RyR and NMDAR communicate with each other is not clear.

As we discussed earlier in the chapter, calcium influx requires repetitive activation of mGluRs which produce the second messenger IP_3 that binds to IP_3Rs on ER. This leads to release of the ER pool of calcium into the cytosol which plays an important role in triggering LTD. Most of the intracellular calcium required for the manifestation of LTP and LTD is generated by its influx through the NMDA receptors on the postsynaptic spines [57]. Strong activation of NMDA receptors leads to LTP and weak and sustained activation leads to LTD. Several studies suggest that Aβ can

perturb calcium signaling and affect NMDAR and the L-type voltage gated calcium channel at the dendritic spines thereby influencing LTP. Deregulated calcium entry has been shown to affect gene expression as well as activation or inhibition of different downstream signaling cascades such as MAP kinases, calcineurin, CaMKII, CREB etc. Some of these signaling pathways influence tau hyperphosphorylation and cytoskeletal defects leading to generation of dystrophic neurites and synaptic dysfunction in AD [150]. Activation of CamKII is essential for LTP generation through its effect on AMPA receptor, and activation of calcineurin has been shown to inhibit CaMKII [115, 151]. High levels of Aβ can induce calcineurin and inhibit phosphorylation of CaMKII thereby causing a deficit in synaptic plasticity and memory formation [152] (Fig. 54.1). Similarly, studies in AD transgenic mice have shown that calcineurin-dependent dephosphorylation of the CREB-regulated transcription factor CRTC1 is disrupted by reduced calcium flux which was reversed by expression of an active CRTC1 S151A or mutants of calcineurin [153]. CRTC1 has been shown to regulate the expression of genes such as BDNF which play a role in memory formation and this suggests that Aβ-mediated calcium deregulation couples synaptic dysfunction to gene transcription required for hippocampus-dependent memory.

Studies in SH-SY5Y cells have shown that aggregated Aβ can induce NMDAR activation which could be inhibited by neutralizing antibodies to beta-1 integrin and src inhibitor [154]. This suggests that Aβ aggregates may bind the beta-1 integrin and induce src kinases dependent phosphorylation and activation of NMDAR. Aβ oligomers have also been shown to affect spontaneous synaptic activity by inhibiting P/Q-type calcium currents [155]. This is contributed by a reduction in vesicular release of GABAergic and glutamatergic synapses. In addition, a channel forming function for Aβ has been suggested by Jang and colleagues [156] where they showed that Aβ forms dynamic cationic channels in the bilayer with strong affinity for calcium ions. Aβ has been shown to induce cytosolic levels of calcium even after depleting the intracellular calcium stores suggesting a role for this in calcium deregulation and membrane disruption [123].

Examination of young triple transgenic mice (3x-Tg-AD) have shown a significant increase in ryanodine receptor (RyR)-evoked Ca^{2+} release in synaptic-dense CA1 regions [137]. Presence of excess intracellular calcium affects the synaptic plasticity in these young mice and contributes to the development of extensive pathology and cognitive deficits in the older AD mice. It has been shown that the NMDA receptor (NR2A) accumulates in the pre and post-synaptic sites in hippocampal CA1 with a concomitant decrease in the non-synaptic sites suggesting that the trapped NMDARs may contribute to the diminished synaptic plasticity at a very early age [157].

Mitochondria and Calcium Signaling in AD

Mitochondria play a major role in buffering of cytosolic calcium and in determining cell fate by facilitating or inhibiting cell death [158]. Calcium entry into the mitochondria is mediated by the inwardly rectifying ion channel, mitochondrial

calcium uniporter (mCU) and through the Ca2+ influx pathway [159, 160]. Under apoptotic conditions, excessive calcium accumulation in mitochondria leads to formation of permeability transition pores and secretion of proapoptotic factors into the cytoplasm of the cells. Mitochondrial dysfunction has been reported in many neurodegenerative diseases including Alzheimer's disease [108, 161–164]. Studies in mouse models of AD have shown that synaptic mitochondria show age-dependent accumulation of Aβ which occurs prior to mitochondrial alterations such as upregulation of mitochondrial permeability transition pore, cytochrome C release, and oxidative stress [158]. Studies conducted in rat cortical neurons have shown that Aβ oligomers can induce inward current and increase intracellular calcium levels through NMDA and AMPA receptor-mediated pathway. Excess calcium accumulates in mitochondria and affects mitochondrial function leading to oxidative stress, and mitochondrial membrane depolarization [165]. Prolonged treatment with even nanomolar concentrations of Aβ induces the activation of NMDA and AMPA receptor activation and associated cell death supporting a role for calcium deregulation and receptor activation in mitochondrial dysfunction and neurotoxicity.

It is not clear how the FAD mutations in PS lead to the accumulation of calcium in mitochondria. We discussed above that mutations in presenilin can affect the ER calcium homeostasis by affecting the calcium leak channel. Expression of presenilins has been shown to be high in domains of ER that preferentially interact with mitochondria. This may allow the accumulated calcium in ER to get transferred to the mitochondria through ER-mitochondria cross-talk leading to mitochondrial accumulation of calcium and mitochondrial dysfunction [166]. Studies conducted in SY5Y and neuronal cells agree with this notion and show that overexpression or downregulation of PS2 results in calcium shuttling between ER and mitochondria with the FAD mutants favoring the calcium transfer [167]. This calcium increase is caused by a physical interaction between ER and mitochondria.

In summary, it is clear that calcium homeostasis is important for normal functioning of neurons. Alterations in the intracellular and synaptic calcium levels caused by mutations in APP or presenilin can induce synaptic defects at a very early age and development of neurodegeneration and Alzheimer's pathology later in life. Maintenance of calcium homeostasis is central for normal functioning of neurons and drugs that are effective in protecting calcium homeostasis may prove to be beneficial for prevention and treatment of synaptic dysfunction and neurodegeneration observed in AD. Significant research is being done in this field and some drugs have been developed that have shown promising results in the treatment of AD. Memantine, for example, is a non-competitive antagonist of NMDA receptor and is currently in clinical trials [168]. Other NMDA receptor antagonists include APV and MK-801 [169]. MEM-1003, an L-type VGCC inhibitor has also shown beneficial effects in AD clinical trials [168]. Other potential targets for AD include the intracellular channels on the ER and SERCA pumps. Much work is needed to resolve the complex pathways that are deregulated in AD and targeting multiple points in the calcium signaling network will hopefully provide us with a better means of managing this disease.

Acknowledgements The work in JP's laboratory is supported by grants from NIH-NIA (1R21AG031429-01A2), Alzheimer's Association (IIRG-08-90842), Small Research Pilot Grant from Signature Interdisciplinary Program in Neuroscience at University of South Florida, and startup funds from the Byrd Alzheimer's Institute and Department of Molecular Medicine.

References

1. Weber A (1959) On the role of calcium in the activity of adenosine 5′-triphosphate hydrolysis by actomyosin. J Biol Chem 234:2764–2769
2. Ebashi F (1961) Does EDTA bind to actomyosin? J Biochem 50:77–78
3. Hasselbach W, Makinose M (1961) The calcium pump of the "relaxing granules" of muscle and its dependence on ATP-splitting. Biochem Z 333:518–528
4. Ebashi S, Lipmann F (1962) Adenosine triphosphate-linked concentration of calcium ions in a particulate fraction of rabbit muscle. J Cell Biol 14:389–400
5. Ebashi F, Ebashi S (1962) Removal of calcium and relaxation in actomyosin systems. Nature 194:378–379
6. Carafoli E (1991) Calcium pump of the plasma membrane. Physiol Rev 71:129–153
7. Carafoli E (1991) The calcium pumping ATPase of the plasma membrane. Annu Rev Physiol 53:531–547
8. Strehler EE, Heim R, Carafoli E (1991) Molecular characterization of plasma membrane calcium pump isoforms. Adv Exp Med Biol 307:251–261
9. Strehler EE, Treiman M (2004) Calcium pumps of plasma membrane and cell interior. Curr Mol Med 4:323–335
10. Schnetkamp PP (2004) The SLC24 Na+/Ca2+–K+ exchanger family: vision and beyond. Pflugers Arch 447:683–688
11. Catterall WA (1995) Structure and function of voltage-gated ion channels. Annu Rev Biochem 64:493–531
12. Perez-Reyes E, Schneider T (1995) Molecular biology of calcium channels. Kidney Int 48:1111–1124
13. Bezprozvanny I, Ehrlich BE (1995) The inositol 1,4,5-trisphosphate (InsP3) receptor. J Membr Biol 145:205–216
14. Carafoli E, Santella L, Branca D, Brini M (2001) Generation, control, and processing of cellular calcium signals. Crit Rev Biochem Mol Biol 36:107–260
15. Parekh AB, Penner R (1997) Store depletion and calcium influx. Physiol Rev 77:901–930
16. Ehrlich BE, Bezprozvanny I (1994) Intracellular calcium release channels. Chin J Physiol 37:1–7
17. Bootman MD, Berridge MJ, Roderick HL (2002) Calcium signalling: more messengers, more channels, more complexity. Curr Biol 12:R563–R565
18. Lee HC (2001) Physiological functions of cyclic ADP-ribose and NAADP as calcium messengers. Annu Rev Pharmacol Toxicol 41:317–345
19. Yamasaki M, Churchill GC, Galione A (2005) Calcium signalling by nicotinic acid adenine dinucleotide phosphate (NAADP). FEBS J 272:4598–4606
20. Lee HC (2005) Nicotinic acid adenine dinucleotide phosphate (NAADP)-mediated calcium signaling. J Biol Chem 280:33693–33696
21. Berridge MJ, Dupont G (1994) Spatial and temporal signalling by calcium. Curr Opin Cell Biol 6:267–274
22. Berridge M, Lipp P, Bootman M (1999) Calcium signalling. Curr Biol 9:R157–R159
23. De Waard M, Gurnett CA, Campbell KP (1996) Structural and functional diversity of voltage-activated calcium channels. Ion Channels 4:41–87
24. Lacinova L (2005) Voltage-dependent calcium channels. Gen Physiol Biophys 24(Suppl 1):1–78

25. Ertel EA, Campbell KP, Harpold MM, Hofmann F, Mori Y, Perez-Reyes E, Schwartz A, Snutch TP, Tanabe T, Birnbaumer L, Tsien RW, Catterall WA (2000) Nomenclature of voltage-gated calcium channels. Neuron 25:533–535
26. Catterall WA (2000) Structure and regulation of voltage-gated Ca2+ channels. Annu Rev Cell Dev Biol 16:521–555
27. Patil PG, de Leon M, Reed RR, Dubel S, Snutch TP, Yue DT (1996) Elementary events underlying voltage-dependent G-protein inhibition of N-type calcium channels. Biophys J 71:2509–2521
28. Ikeda SR, Dunlap K (1999) Voltage-dependent modulation of N-type calcium channels: role of G protein subunits. Adv Second Messenger Phosphoprotein Res 33:131–151
29. Lee A, Wong ST, Gallagher D, Li B, Storm DR, Scheuer T, Catterall WA (1999) Ca2+/calmodulin binds to and modulates P/Q-type calcium channels. Nature 399:155–159
30. Lee A, Scheuer T, Catterall WA (2000) Ca2+/calmodulin-dependent facilitation and inactivation of P/Q-type Ca2+ channels. J Neurosci 20:6830–6838
31. Burns ME, Augustine GJ (1995) Synaptic structure and function: dynamic organization yields architectural precision. Cell 83:187–194
32. Charvin N, L'Eveque C, Walker D, Berton F, Raymond C, Kataoka M, Shoji-Kasai Y, Takahashi M, De Waard M, Seagar MJ (1997) Direct interaction of the calcium sensor protein synaptotagmin I with a cytoplasmic domain of the alpha1A subunit of the P/Q-type calcium channel. EMBO J 16:4591–4596
33. Bajjalieh SM, Scheller RH (1995) The biochemistry of neurotransmitter secretion. J Biol Chem 270:1971–1974
34. Catterall WA (1999) Interactions of presynaptic Ca2+ channels and snare proteins in neurotransmitter release. Ann N Y Acad Sci 868:144–159
35. Chapman ER, Jahn R (1994) Calcium-dependent interaction of the cytoplasmic region of synaptotagmin with membranes. Autonomous function of a single C2-homologous domain. J Biol Chem 269:5735–5741
36. Collingridge GL, Randall AD, Davies CH, Alford S (1992) The synaptic activation of NMDA receptors and Ca2+ signalling in neurons. Ciba Found Symp 164:162–171; discussion 172–165
37. Ghosh A, Greenberg ME (1995) Calcium signaling in neurons: molecular mechanisms and cellular consequences. Science 268:239–247
38. Ben-Ari Y, Aniksztejn L, Bregestovski P (1992) Protein kinase C modulation of NMDA currents: an important link for LTP induction. Trends Neurosci 15:333–339
39. Fiol CJ, Williams JS, Chou CH, Wang QM, Roach PJ, Andrisani OM (1994) A secondary phosphorylation of CREB341 at Ser129 is required for the cAMP-mediated control of gene expression. A role for glycogen synthase kinase-3 in the control of gene expression. J Biol Chem 269:32187–32193
40. Henzi V, MacDermott AB (1992) Characteristics and function of Ca(2+)- and inositol 1,4,5-trisphosphate-releasable stores of Ca2+ in neurons. Neuroscience 46:251–273
41. Berridge MJ (1993) Cell signalling. A tale of two messengers. Nature 365:388–389
42. Hua SY, Tokimasa T, Takasawa S, Furuya Y, Nohmi M, Okamoto H, Kuba K (1994) Cyclic ADP-ribose modulates Ca2+ release channels for activation by physiological Ca2+ entry in bullfrog sympathetic neurons. Neuron 12:1073–1079
43. Putney JW Jr (1986) A model for receptor-regulated calcium entry. Cell Calcium 7:1–12
44. Putney JW Jr (2003) Capacitative calcium entry in the nervous system. Cell Calcium 34:339–344
45. Putney JW Jr (1994) Bird GS: calcium mobilization by inositol phosphates and other intracellular messengers. Trends Endocrinol Metab 5:256–260
46. Randriamampita C, Tsien RY (1995) Degradation of a calcium influx factor (CIF) can be blocked by phosphatase inhibitors or chelation of Ca2+. J Biol Chem 270:29–32
47. Fasolato C, Hoth M, Penner R (1993) A GTP-dependent step in the activation mechanism of capacitative calcium influx. J Biol Chem 268:20737–20740
48. Irvine RF (1990) 'Quantal' Ca2+ release and the control of Ca2+ entry by inositol phosphates–a possible mechanism. FEBS Lett 263:5–9

49. Berridge MJ (1995) Capacitative calcium entry. Biochem J 312(Pt 1):1–11
50. Berridge MJ (1998) Neuronal calcium signaling. Neuron 21:13–26
51. Mothet JP, Fossier P, Meunier FM, Stinnakre J, Tauc L, Baux G (1998) Cyclic ADP-ribose and calcium-induced calcium release regulate neurotransmitter release at a cholinergic synapse of Aplysia. J Physiol 507(Pt 2):405–414
52. Leveque C, el Far O, Martin-Moutot N, Sato K, Kato R, Takahashi M, Seagar MJ (1994) Purification of the N-type calcium channel associated with syntaxin and synaptotagmin. A complex implicated in synaptic vesicle exocytosis. J Biol Chem 269:6306–6312
53. Sheng ZH, Rettig J, Cook T, Catterall WA (1996) Calcium-dependent interaction of N-type calcium channels with the synaptic core complex. Nature 379:451–454
54. Augustine GJ (2001) How does calcium trigger neurotransmitter release? Curr Opin Neurobiol 11:320–326
55. Sheng M, Kim MJ (2002) Postsynaptic signaling and plasticity mechanisms. Science 298:776–780
56. Schiller J, Helmchen F, Sakmann B (1995) Spatial profile of dendritic calcium transients evoked by action potentials in rat neocortical pyramidal neurones. J Physiol 487(Pt 3): 583–600
57. Sabatini BL, Maravall M, Svoboda K (2001) Ca(2+) signaling in dendritic spines. Curr Opin Neurobiol 11:349–356
58. Franks KM, Sejnowski TJ (2002) Complexity of calcium signaling in synaptic spines. Bioessays 24:1130–1144
59. Kennedy MB (2000) Signal-processing machines at the postsynaptic density. Science 290:750–754
60. Bear MF, Malenka RC (1994) Synaptic plasticity: LTP and LTD. Curr Opin Neurobiol 4:389–399
61. Cummings JA, Mulkey RM, Nicoll RA, Malenka RC (1996) Ca2+ signaling requirements for long-term depression in the hippocampus. Neuron 16:825–833
62. Cull-Candy S, Brickley S, Farrant M (2001) NMDA receptor subunits: diversity, development and disease. Curr Opin Neurobiol 11:327–335
63. Hardingham GE, Fukunaga Y, Bading H (2002) Extrasynaptic NMDARs oppose synaptic NMDARs by triggering CREB shut-off and cell death pathways. Nat Neurosci 5:405–414
64. Ivanov A, Pellegrino C, Rama S, Dumalska I, Salyha Y, Ben-Ari Y, Medina I (2006) Opposing role of synaptic and extrasynaptic NMDA receptors in regulation of the extracellular signal-regulated kinases (ERK) activity in cultured rat hippocampal neurons. J Physiol 572:789–798
65. Scimemi A, Fine A, Kullmann DM, Rusakov DA (2004) NR2B-containing receptors mediate cross talk among hippocampal synapses. J Neurosci 24:4767–4777
66. Stocca G, Vicini S (1998) Increased contribution of NR2A subunit to synaptic NMDA receptors in developing rat cortical neurons. J Physiol 507(Pt 1):13–24
67. Thomas CG, Miller AJ, Westbrook GL (2006) Synaptic and extrasynaptic NMDA receptor NR2 subunits in cultured hippocampal neurons. J Neurophysiol 95:1727–1734
68. Zhou Y, Takahashi E, Li W, Halt A, Wiltgen B, Ehninger D, Li GD, Hell JW, Kennedy MB, Silva AJ (2007) Interactions between the NR2B receptor and CaMKII modulate synaptic plasticity and spatial learning. J Neurosci 27:13843–13853
69. Liu L, Wong TP, Pozza MF, Lingenhoehl K, Wang Y, Sheng M, Auberson YP, Wang YT (2004) Role of NMDA receptor subtypes in governing the direction of hippocampal synaptic plasticity. Science 304:1021–1024
70. Yashiro K, Philpot BD (2008) Regulation of NMDA receptor subunit expression and its implications for LTD, LTP, and metaplasticity. Neuropharmacology 55:1081–1094
71. Barria A, Derkach V, Soderling T (1997) Identification of the Ca2+/calmodulin-dependent protein kinase II regulatory phosphorylation site in the alpha-amino-3-hydroxyl-5-methyl-4-isoxazole-propionate-type glutamate receptor. J Biol Chem 272:32727–32730
72. Derkach V, Barria A, Soderling TR (1999) Ca2+/calmodulin-kinase II enhances channel conductance of alpha-amino-3-hydroxy-5-methyl-4-isoxazolepropionate type glutamate receptors. Proc Natl Acad Sci USA 96:3269–3274

73. Benke TA, Luthi A, Isaac JT, Collingridge GL (1998) Modulation of AMPA receptor unitary conductance by synaptic activity. Nature 393:793–797
74. Hayashi Y, Shi SH, Esteban JA, Piccini A, Poncer JC, Malinow R (2000) Driving AMPA receptors into synapses by LTP and CaMKII: requirement for GluR1 and PDZ domain interaction. Science 287:2262–2267
75. Zhu JJ, Qin Y, Zhao M, Van Aelst L, Malinow R (2002) Ras and Rap control AMPA receptor trafficking during synaptic plasticity. Cell 110:443–455
76. Luscher C, Xia H, Beattie EC, Carroll RC, von Zastrow M, Malenka RC, Nicoll RA (1999) Role of AMPA receptor cycling in synaptic transmission and plasticity. Neuron 24:649–658
77. Schulman H (2004) Activity-dependent regulation of calcium/calmodulin-dependent protein kinase II localization. J Neurosci 24:8399–8403
78. Mulkey RM, Endo S, Shenolikar S, Malenka RC (1994) Involvement of a calcineurin/inhibitor-1 phosphatase cascade in hippocampal long-term depression. Nature 369:486–488
79. Ehlers MD (2000) Reinsertion or degradation of AMPA receptors determined by activity-dependent endocytic sorting. Neuron 28:511–525
80. Mulkey RM, Herron CE, Malenka RC (1993) An essential role for protein phosphatases in hippocampal long-term depression. Science 261:1051–1055
81. Garner CC, Nash J, Huganir RL (2000) PDZ domains in synapse assembly and signalling. Trends Cell Biol 10:274–280
82. Kelly PT, Weinberger RP, Waxham MN (1988) Active site-directed inhibition of Ca2+/calmodulin-dependent protein kinase type II by a bifunctional calmodulin-binding peptide. Proc Natl Acad Sci USA 85:4991–4995
83. Lisman J, Schulman H, Cline H (2002) The molecular basis of CaMKII function in synaptic and behavioural memory. Nat Rev Neurosci 3:175–190
84. Miller SG, Kennedy MB (1986) Regulation of brain type II Ca2+/calmodulin-dependent protein kinase by autophosphorylation: a Ca2+–triggered molecular switch. Cell 44:861–870
85. Strack S, Barban MA, Wadzinski BE, Colbran RJ (1997) Differential inactivation of postsynaptic density-associated and soluble Ca2+/calmodulin-dependent protein kinase II by protein phosphatases 1 and 2A. J Neurochem 68:2119–2128
86. Genoux D, Haditsch U, Knobloch M, Michalon A, Storm D, Mansuy IM (2002) Protein phosphatase 1 is a molecular constraint on learning and memory. Nature 418:970–975
87. Westphal RS, Tavalin SJ, Lin JW, Alto NM, Fraser ID, Langeberg LK, Sheng M, Scott JD (1999) Regulation of NMDA receptors by an associated phosphatase-kinase signaling complex. Science 285:93–96
88. Colledge M, Dean RA, Scott GK, Langeberg LK, Huganir RL, Scott JD (2000) Targeting of PKA to glutamate receptors through a MAGUK-AKAP complex. Neuron 27:107–119
89. Kornau HC, Schenker LT, Kennedy MB, Seeburg PH (1995) Domain interaction between NMDA receptor subunits and the postsynaptic density protein PSD-95. Science 269:1737–1740
90. Kim JH, Liao D, Lau LF, Huganir RL (1998) SynGAP: a synaptic RasGAP that associates with the PSD-95/SAP90 protein family. Neuron 20:683–691
91. Scannevin RH, Huganir RL (2000) Postsynaptic organization and regulation of excitatory synapses. Nat Rev Neurosci 1:133–141
92. Chen HJ, Rojas-Soto M, Oguni A, Kennedy MB (1998) A synaptic Ras-GTPase activating protein (p135 SynGAP) inhibited by CaM kinase II. Neuron 20:895–904
93. Cullen PJ, Lockyer PJ (2002) Integration of calcium and Ras signalling. Nat Rev Mol Cell Biol 3:339–348
94. Husi H, Ward MA, Choudhary JS, Blackstock WP, Grant SG (2000) Proteomic analysis of NMDA receptor-adhesion protein signaling complexes. Nat Neurosci 3:661–669
95. Naisbitt S, Kim E, Tu JC, Xiao B, Sala C, Valtschanoff J, Weinberg RJ, Worley PF, Sheng M (1999) Shank, a novel family of postsynaptic density proteins that binds to the NMDA receptor/PSD-95/GKAP complex and cortactin. Neuron 23:569–582
96. Sheng M, Thompson MA, Greenberg ME (1991) CREB: a Ca(2+)-regulated transcription factor phosphorylated by calmodulin-dependent kinases. Science 252:1427–1430

97. Ginty DD, Bonni A, Greenberg ME (1994) Nerve growth factor activates a Ras-dependent protein kinase that stimulates c-fos transcription via phosphorylation of CREB. Cell 77:713–725
98. Cardinaux JR, Notis JC, Zhang Q, Vo N, Craig JC, Fass DM, Brennan RG, Goodman RH (2000) Recruitment of CREB binding protein is sufficient for CREB-mediated gene activation. Mol Cell Biol 20:1546–1552
99. Kwok RP, Lundblad JR, Chrivia JC, Richards JP, Bachinger HP, Brennan RG, Roberts SG, Green MR, Goodman RH (1994) Nuclear protein CBP is a coactivator for the transcription factor CREB. Nature 370:223–226
100. Dash PK, Karl KA, Colicos MA, Prywes R, Kandel ER (1991) CAMP response element-binding protein is activated by Ca2+/calmodulin- as well as cAMP-dependent protein kinase. Proc Natl Acad Sci USA 88:5061–5065
101. Parker D, Jhala US, Radhakrishnan I, Yaffe MB, Reyes C, Shulman AI, Cantley LC, Wright PE, Montminy M (1998) Analysis of an activator: coactivator complex reveals an essential role for secondary structure in transcriptional activation. Mol Cell 2:353–359
102. Sun P, Enslen H, Myung PS, Maurer RA (1994) Differential activation of CREB by Ca2+/calmodulin-dependent protein kinases type II and type IV involves phosphorylation of a site that negatively regulates activity. Genes Dev 8:2527–2539
103. Xing J, Ginty DD, Greenberg ME (1996) Coupling of the RAS-MAPK pathway to gene activation by RSK2, a growth factor-regulated CREB kinase. Science 273:959–963
104. Wu GY, Deisseroth K, Tsien RW (2001) Activity-dependent CREB phosphorylation: convergence of a fast, sensitive calmodulin kinase pathway and a slow, less sensitive mitogen-activated protein kinase pathway. Proc Natl Acad Sci USA 98:2808–2813
105. Cooper DM, Mons N, Karpen JW (1995) Adenylyl cyclases and the interaction between calcium and cAMP signalling. Nature 374:421–424
106. Jones KR, Farinas I, Backus C, Reichardt LF (1994) Targeted disruption of the BDNF gene perturbs brain and sensory neuron development but not motor neuron development. Cell 76:989–999
107. Schwartz PM, Borghesani PR, Levy RL, Pomeroy SL, Segal RA (1997) Abnormal cerebellar development and foliation in BDNF−/− mice reveals a role for neurotrophins in CNS patterning. Neuron 19:269–281
108. Hirai K, Aliev G, Nunomura A, Fujioka H, Russell RL, Atwood CS, Johnson AB, Kress Y, Vinters HV, Tabaton M, Shimohama S, Cash AD, Siedlak SL, Harris PL, Jones PK, Petersen RB, Perry G, Smith MA (2001) Mitochondrial abnormalities in Alzheimer's disease. J Neurosci 21:3017–3023
109. Ghosh A, Carnahan J, Greenberg ME (1994) Requirement for BDNF in activity-dependent survival of cortical neurons. Science 263:1618–1623
110. Sala C, Rudolph-Correia S, Sheng M (2000) Developmentally regulated NMDA receptor-dependent dephosphorylation of cAMP response element-binding protein (CREB) in hippocampal neurons. J Neurosci 20:3529–3536
111. Hardy J, Allsop D (1991) Amyloid deposition as the central event in the aetiology of Alzheimer's disease. Trends Pharmacol Sci 12:383–388
112. Selkoe DJ (1986) Altered structural proteins in plaques and tangles: what do they tell us about the biology of Alzheimer's disease? Neurobiol Aging 7:425–432
113. Selkoe DJ (1989) The deposition of amyloid proteins in the aging mammalian brain: implications for Alzheimer's disease. Ann Med 21:73–76
114. Henderson VW, Finch CE (1989) The neurobiology of Alzheimer's disease. J Neurosurg 70:335–353
115. Silva AJ, Paylor R, Wehner JM, Tonegawa S (1992) Impaired spatial learning in alpha-calcium-calmodulin kinase II mutant mice. Science 257:206–211
116. Shoji M, Golde TE, Ghiso J, Cheung TT, Estus S, Shaffer LM, Cai XD, McKay DM, Tintner R, Frangione B et al (1992) Production of the Alzheimer amyloid beta protein by normal proteolytic processing. Science 258:126–129

117. Masters CL, Multhaup G, Simms G, Pottgiesser J, Martins RN, Beyreuther K (1985) Neuronal origin of a cerebral amyloid: neurofibrillary tangles of Alzheimer's disease contain the same protein as the amyloid of plaque cores and blood vessels. EMBO J 4:2757–2763
118. Abraham CR, Selkoe DJ, Potter H (1988) Immunochemical identification of the serine protease inhibitor alpha 1-antichymotrypsin in the brain amyloid deposits of Alzheimer's disease. Cell 52:487–501
119. McGeer PL, Schulzer M, McGeer EG (1996) Arthritis and anti-inflammatory agents as possible protective factors for Alzheimer's disease: a review of 17 epidemiologic studies. Neurology 47:425–432
120. Rogers J, Webster S, Lue LF, Brachova L, Civin WH, Emmerling M, Shivers B, Walker D, McGeer P (1996) Inflammation and Alzheimer's disease pathogenesis. Neurobiol Aging 17:681–686
121. Smith MA, Perry G, Richey PL, Sayre LM, Anderson VE, Beal MF, Kowall N (1996) Oxidative damage in Alzheimer's. Nature 382:120–121
122. LaFerla FM (2002) Calcium dyshomeostasis and intracellular signalling in Alzheimer's disease. Nat Rev Neurosci 3:862–872
123. Demuro A, Mina E, Kayed R, Milton SC, Parker I, Glabe CG (2005) Calcium dysregulation and membrane disruption as a ubiquitous neurotoxic mechanism of soluble amyloid oligomers. J Biol Chem 280:17294–17300
124. Querfurth HW, Selkoe DJ (1994) Calcium ionophore increases amyloid beta peptide production by cultured cells. Biochemistry 33:4550–4561
125. Wu HY, Hudry E, Hashimoto T, Kuchibhotla K, Rozkalne A, Fan Z, Spires-Jones T, Xie H, Arbel-Ornath M, Grosskreutz CL, Bacskai BJ, Hyman BT (2010) Amyloid beta induces the morphological neurodegenerative triad of spine loss, dendritic simplification, and neuritic dystrophies through calcineurin activation. J Neurosci 30:2636–2649
126. Kuchibhotla KV, Lattarulo CR, Hyman BT, Bacskai BJ (2009) Synchronous hyperactivity and intercellular calcium waves in astrocytes in Alzheimer mice. Science 323:1211–1215
127. De Strooper B, Saftig P, Craessaerts K, Vanderstichele H, Guhde G, Annaert W, Von Figura K, Van Leuven F (1998) Deficiency of presenilin-1 inhibits the normal cleavage of amyloid precursor protein. Nature 391:387–390
128. Wolfe MS, Xia W, Ostaszewski BL, Diehl TS, Kimberly WT, Selkoe DJ (1999) Two transmembrane aspartates in presenilin-1 required for presenilin endoproteolysis and gamma-secretase activity. Nature 398:513–517
129. Yoo AS, Cheng I, Chung S, Grenfell TZ, Lee H, Pack-Chung E, Handler M, Shen J, Xia W, Tesco G, Saunders AJ, Ding K, Frosch MP, Tanzi RE, Kim TW (2000) Presenilin-mediated modulation of capacitative calcium entry. Neuron 27:561–572
130. Herms J, Schneider I, Dewachter I, Caluwaerts N, Kretzschmar H, Van Leuven F (2003) Capacitive calcium entry is directly attenuated by mutant presenilin-1, independent of the expression of the amyloid precursor protein. J Biol Chem 278:2484–2489
131. Smith IF, Hitt B, Green KN, Oddo S, LaFerla FM (2005) Enhanced caffeine-induced Ca2+ release in the 3xTg-AD mouse model of Alzheimer's disease. J Neurochem 94:1711–1718
132. Ris L, Dewachter I, Reverse D, Godaux E, Van Leuven F (2003) Capacitative calcium entry induces hippocampal long term potentiation in the absence of presenilin-1. J Biol Chem 278:44393–44399
133. Takeda T, Asahi M, Yamaguchi O, Hikoso S, Nakayama H, Kusakari Y, Kawai M, Hongo K, Higuchi Y, Kashiwase K, Watanabe T, Taniike M, Nakai A, Nishida K, Kurihara S, Donoviel DB, Bernstein A, Tomita T, Iwatsubo T, Hori M, Otsu K (2005) Presenilin 2 regulates the systolic function of heart by modulating Ca2+ signaling. FASEB J 19:2069–2071
134. Bezprozvanny I, Mattson MP (2008) Neuronal calcium mishandling and the pathogenesis of Alzheimer's disease. Trends Neurosci 31:454–463
135. Leissring MA, Paul BA, Parker I, Cotman CW, LaFerla FM (1999) Alzheimer's presenilin-1 mutation potentiates inositol 1,4,5-trisphosphate-mediated calcium signaling in Xenopus oocytes. J Neurochem 72:1061–1068

136. Stutzmann GE, Smith I, Caccamo A, Oddo S, Parker I, Laferla F (2007) Enhanced ryanodine-mediated calcium release in mutant PS1-expressing Alzheimer's mouse models. Ann N Y Acad Sci 1097:265–277
137. Chakroborty S, Goussakov I, Miller MB, Stutzmann GE (2009) Deviant ryanodine receptor-mediated calcium release resets synaptic homeostasis in presymptomatic 3xTg-AD mice. J Neurosci 29:9458–9470
138. Isaacs AM, Senn DB, Yuan M, Shine JP, Yankner BA (2006) Acceleration of amyloid beta-peptide aggregation by physiological concentrations of calcium. J Biol Chem 281:27916–27923
139. Green KN, Demuro A, Akbari Y, Hitt BD, Smith IF, Parker I, LaFerla FM (2008) SERCA pump activity is physiologically regulated by presenilin and regulates amyloid beta production. J Cell Biol 181:1107–1116
140. Brunello L, Zampese E, Florean C, Pozzan T, Pizzo P, Fasolato C (2009) Presenilin-2 dampens intracellular Ca2+ stores by increasing Ca2+ leakage and reducing Ca2+ uptake. J Cell Mol Med 13:3358–3369
141. Zatti G, Burgo A, Giacomello M, Barbiero L, Ghidoni R, Sinigaglia G, Florean C, Bagnoli S, Binetti G, Sorbi S, Pizzo P, Fasolato C (2006) Presenilin mutations linked to familial Alzheimer's disease reduce endoplasmic reticulum and Golgi apparatus calcium levels. Cell Calcium 39:539–550
142. Pratt KG, Zhu P, Watari H, Cook DG, Sullivan JM (2011) A novel role for {gamma}-secretase: selective regulation of spontaneous neurotransmitter release from hippocampal neurons. J Neurosci Off J Soc Neurosci 31:899–906
143. Rojas G, Cardenas AM, Fernandez-Olivares P, Shimahara T, Segura-Aguilar J, Caviedes R, Caviedes P (2008) Effect of the knockdown of amyloid precursor protein on intracellular calcium increases in a neuronal cell line derived from the cerebral cortex of a trisomy 16 mouse. Exp Neurol 209:234–242
144. Lopez JR, Lyckman A, Oddo S, Laferla FM, Querfurth HW, Shtifman A (2008) Increased intraneuronal resting [Ca2+] in adult Alzheimer's disease mice. J Neurochem 105:262–271
145. Leissring MA, Murphy MP, Mead TR, Akbari Y, Sugarman MC, Jannatipour M, Anliker B, Muller U, Saftig P, De Strooper B, Wolfe MS, Golde TE, LaFerla FM (2002) A physiologic signaling role for the gamma -secretase-derived intracellular fragment of APP. Proc Natl Acad Sci USA 99:4697–4702
146. Stieren E, Werchan WP, El Ayadi A, Li F, Boehning D (2010) FAD mutations in amyloid precursor protein do not directly perturb intracellular calcium homeostasis. PLoS One 5:e11992
147. Dreses-Werringloer U, Lambert JC, Vingtdeux V, Zhao H, Vais H, Siebert A, Jain A, Koppel J, Rovelet-Lecrux A, Hannequin D, Pasquier F, Galimberti D, Scarpini E, Mann D, Lendon C, Campion D, Amouyel P, Davies P, Foskett JK, Campagne F, Marambaud P (2008) A polymorphism in CALHM1 influences Ca2+ homeostasis, Abeta levels, and Alzheimer's disease risk. Cell 133:1149–1161
148. Gallego-Sandin S, Alonso MT, Garcia-Sancho J (2011) Calcium homeostasis modulator 1 (CALHM1) reduces the calcium content of the endoplasmic reticulum (ER) and triggers ER stress. Biochem J 437(3):469–475
149. Goussakov I, Miller MB, Stutzmann GE (2010) NMDA-mediated Ca(2+) influx drives aberrant ryanodine receptor activation in dendrites of young Alzheimer's disease mice. J Neurosci 30:12128–12137
150. Impey S, Obrietan K, Storm DR (1999) Making new connections: role of ERK/MAP kinase signaling in neuronal plasticity. Neuron 23:11–14
151. Malinow R, Schulman H, Tsien RW (1989) Inhibition of postsynaptic PKC or CaMKII blocks induction but not expression of LTP. Science 245:862–866
152. Zhao D, Watson JB, Xie CW (2004) Amyloid beta prevents activation of calcium/calmodulin-dependent protein kinase II and AMPA receptor phosphorylation during hippocampal long-term potentiation. J Neurophysiol 92:2853–2858

153. Espana J, Valero J, Minano-Molina AJ, Masgrau R, Martin E, Guardia-Laguarta C, Lleo A, Gimenez-Llort L, Rodriguez-Alvarez J, Saura CA (2010) Beta-amyloid disrupts activity-dependent gene transcription required for memory through the CREB coactivator CRTC1. J Neurosci Off J Soc Neurosci 30:9402–9410
154. Uhasz GJ, Barkoczi B, Vass G, Datki Z, Hunya A, Fulop L, Budai D, Penke B, Szegedi V (2010) Fibrillar Abeta (1–42) enhances NMDA receptor sensitivity via the integrin signaling pathway. J Alzheimers Dis 19:1055–1067
155. Nimmrich V, Grimm C, Draguhn A, Barghorn S, Lehmann A, Schoemaker H, Hillen H, Gross G, Ebert U, Bruehl C (2008) Amyloid beta oligomers (a beta(1–42) globulomer) suppress spontaneous synaptic activity by inhibition of P/Q-type calcium currents. J Neurosci Off J Soc Neurosci 28:788–797
156. Jang H, Zheng J, Nussinov R (2007) Models of beta-amyloid ion channels in the membrane suggest that channel formation in the bilayer is a dynamic process. Biophys J 93:1938–1949
157. Aoki C, Lee J, Nedelescu H, Ahmed T, Ho A, Shen J (2009) Increased levels of NMDA receptor NR2A subunits at pre- and postsynaptic sites of the hippocampal CA1: an early response to conditional double knockout of presenilin 1 and 2. J Comp Neurol 517:512–523
158. Contreras L, Drago I, Zampese E, Pozzan T (2010) Mitochondria: the calcium connection. Biochim Biophys Acta 1797:607–618
159. Kirichok Y, Krapivinsky G, Clapham DE (2004) The mitochondrial calcium uniporter is a highly selective ion channel. Nature 427:360–364
160. Jiang D, Zhao L, Clapham DE (2009) Genome-wide RNAi screen identifies Letm1 as a mitochondrial Ca2+/H+ antiporter. Science 326:144–147
161. Du H, Guo L, Yan S, Sosunov AA, McKhann GM, Yan SS (2010) Early deficits in synaptic mitochondria in an Alzheimer's disease mouse model. Proc Natl Acad Sci USA 107:18670–18675
162. Moreira PI, Cardoso SM, Pereira CM, Santos MS, Oliveira CR (2009) Mitochondria as a therapeutic target in Alzheimer's disease and diabetes. CNS Neurol Disord Drug Targets 8:492–511
163. Swerdlow RH, Khan SM (2009) The Alzheimer's disease mitochondrial cascade hypothesis: an update. Exp Neurol 218:308–315
164. Su B, Wang X, Zheng L, Perry G, Smith MA, Zhu X (2010) Abnormal mitochondrial dynamics and neurodegenerative diseases. Biochim Biophys Acta 1802:135–142
165. Alberdi E, Sanchez-Gomez MV, Cavaliere F, Perez-Samartin A, Zugaza JL, Trullas R, Domercq M, Matute C (2010) Amyloid beta oligomers induce Ca2+ dysregulation and neuronal death through activation of ionotropic glutamate receptors. Cell Calcium 47:264–272
166. Giacomello M, Drago I, Pizzo P, Pozzan T (2007) Mitochondrial Ca2+ as a key regulator of cell life and death. Cell Death Differ 14:1267–1274
167. Zampese E, Fasolato C, Kipanyula MJ, Bortolozzi M, Pozzan T, Pizzo P (2011) Presenilin 2 modulates endoplasmic reticulum (ER)-mitochondria interactions and Ca2+ cross-talk. Proc Natl Acad Sci USA 108:2777–2782
168. Bezprozvanny I (2009) Calcium signaling and neurodegenerative diseases. Trends Mol Med 15:89–100
169. Texido L, Martin-Satue M, Alberdi E, Solsona C, Matute C (2011) Amyloid beta peptide oligomers directly activate NMDA receptors. Cell Calcium 49:184–190

Chapter 55
Voltage-Gated Ca^{2+} Channel Mediated Ca^{2+} Influx in Epileptogenesis

Magdalena Siwek, Christina Henseler, Karl Broich, Anna Papazoglou, and Marco Weiergräber

Abstract Voltage- and ligand-gated ion channels are key elements in the etiopathogenesis of various forms of epilepsy. In this chapter, we present an overview of the functional implications of voltage-gated Ca^{2+} channels in modulating internal Ca^{2+} level fluctuations and generating ictiform/epileptiform cellular electrophysiological activity. A specific focus will be on the fascinating and evolving field of high-voltage activated (HVA) Non-L-type $Ca_v2.3$ R-type channels and low-voltage activated (LVA) $Ca_v3.1$–3.3 T-type Ca^{2+} channels in the genesis of plateau potentials and excessive rebound bursting. Plateau potentials have been characterised in the hippocampus and were shown to be triggered by $Ca_v2.3$ which subsequently activate CNG channels that mediate long-lasting plateaus. In the thalamocortical network, a complex ion channel armamentarium is involved in regulating a complex balance of burst and tonic mode activity. Recent findings point to an outstanding role of R- and T-type channels in both thalamocortical eurhythmia and pathophysiological aberrations. Thus, pharmacological modulation of voltage-gated Ca^{2+}-channels might prove more and more important in treatment of neurological and psychiatric disorder such as schizophrenia, mania, dementia and epilepsy.

Keywords Epilepsy • Hippocampus • Plateau potentials • Rebound burst firing • Voltage-gated Ca^{2+} channels

M. Siwek, MS • C. Henseler • K. Broich, MD • A. Papazoglou, Ph.D. • M. Weiergräber, MD, Ph.D. (✉)
Federal Institute for Drugs and Medical Devices (Bundesinstitut für Arzneimittel und Medizinprodukte, BfArM), Kurt-Georg-Kiesinger-Allee 3, 53175 Bonn, Germany
e-mail: magdalena.siwek@bfarm.de; christina.henseler@bfarm.de; karl.broich@bfarm.de; anna.papazoglou@bfarm.de; marco.weiergraber@bfarm.de

M.S. Islam (ed.), *Calcium Signaling*, Advances in Experimental Medicine and Biology 740, DOI 10.1007/978-94-007-2888-2_55,

Abbreviations

5-HT	Serotonin
AED	Antiepileptic drug
AHP	Afterhyperpolarisation
CNS	Central nervous system
DAG	Diacyl glycerol
GAERS	Genetic absence epilepsy rat from Strasbourg
HCN	Hyperpolarization and cyclic-nucleotide gated non-specific cation
HVA	High voltage activated
IC	Inferior colliculus
IGEs	Idiopathic generalized epilepsies
IP3	Inositoltrisphosphat
lh	Lethargic
LVA	Low voltage activated
M	Muscarinic receptor
PKA	Protein kinase A
PKC	Protein kinase C
PLC	Phospholipase C
RTN	Reticular thalamic nucleus
sAHP	Slow afterhyperpolarisation
SRS	Spontaneous recurrent seizures
stg	Stargazer
SWD	Spike-wave discharge
SWS	Slow-wave sleep
tg	Tottering mouse model
VGCCS	Voltage-gated calcium channels
WAG/RiJ	Wistar Albino Glaxo rats

Neuronal Calcium Channelopathies in Animal Models of Epilepsy and Human Disorders – Functional Role of Voltage-Gated Ca^{2+} Channels

The frequency, importance and sociocultural effects of epilepsy in contemporary society can hardly be overestimated. While manifest epilepsy affects around 0.5–1% of the population in North America and Europe [1], almost 5% of the population perceive a single seizure in their lifetime and about 10% display increased seizure susceptibility. Epilepsy is characterized by a strong heterogeneity regarding etiology, age of onset, seizure classification, responsiveness to pharmacological treatment, short- and long-term prognosis and occurrence of further disorders. Principally, epileptic disorders can be differentiated into primary, idiopathic forms and secondary forms, e.g. due cerebral ischemia or brain macro-, micro-dysgenesis or neoplasm.

Regardless of this ethiopathogenetic heterogeneity, the fundamental electrophysiological basis for hyperexcitability associated with ictogenesis/epileptogenesis are paroxysmal depolarization shifts in neuronal cell populations. Within the last decade a number of epileptic disorders originally termed idiopathic turned out to be due to ion channel dysfunctions, i.e. channelopathies triggering depolarization shifts. These ion channel entities comprise both voltage-gated Na^+-, K^+-, Ca^{2+}-, Cl^{-1}-channels and ligand-gated ion channels, e.g. GABA, glutamate, glycine and acetylcholine receptors [2]. It has been shown that voltage gated Ca^{2+} channels (VGCCs) significantly contribute to the etiology and pathogenesis of epilepsies, such as absence epilepsy or juvenile myoclonic epilepsy [3]. Besides mutations in neuropeptides, vesicle docking complex proteins, transporters, signal transduction molecules and extracellular matrix proteins were also reported to be linked to an epileptic phenotype [4]. Physiologically VGCCs mediate and modulate Ca^{2+} influx into living cells triggering a number of cellular processes, such as excitation–contraction-coupling [5], excitation–secretion-coupling [6], neurotransmitter/hormonal release [7] and regulation of gene expression [8, 9]. Ten different pore-forming α_1-subunits of VGCCs have been cloned so far which can be differentiated based on electrophysiological and pharmacological properties into high-voltage activated (HVA) L-type ($Ca_v1.1$–1.4) and HVA Non-L-Type ($Ca_v2.1$–2.3) Ca^{2+} channels, and LVA T-type channels ($Ca_v3.1$–3.3) [10, 11]. In addition, a number of auxiliary subunits (β_{1-4}, $\alpha_2\delta_{1-4}$, γ_{1-8}) are associated with the ion-conducting Ca_v-α_1-subunit capable of modulating fundamental electrophysiological and pharmacological properties of the Ca^{2+} channel complex [12]. Recent studies point to an increasing number of mutations in both, ion-conducting and auxiliary subunits, i.e. calcium channelopathies resulting in various neurological, cardiovascular and muscular diseases not only in animal models but particularly in humans [13]. So far, neuronal calcium channelopathies in humans are primarily restricted to the $Ca_v2.1$ and $Ca_v3.2$ VGCCs resulting in absence of epilepsy-like activity, episodic ataxia type 2, spinocerebellar ataxia type six or familial hemiplegic migraine [13] in $Ca_v2.1$ or absence epilepsy in patients with $Ca_v3.2$ mutations [14]. Furthermore, autoantibodies against $Ca_v2.1$ and $Ca_v2.2$ are associated with Lambert-Eaton myasthenic syndrome [15] and may also be of significance in sporadic amyotrophic lateral sclerosis [16]. In the retina, which ontogenetically originates from the diencephalon, mutations in the $Ca_v1.4$ VGCC are reported to cause congenital stationary night blindness in humans [17]. In addition, a gain-of-function missense mutation (G406R) of $Ca_v1.2$ was recently described to cause Timothy syndrome, a multisystem disorder in humans including complex neuropsychatric symptoms such as autism (60%), autism spectrum disorders (80%), mental retardation (25%) and seizures (21%) [18]. Several animal models with a complex neurological phenotype, including cerebellar ataxia, paroxysmal dyskinesia and absence epilepsy, have been described in the past based on mutations either in the pore-forming $Ca_v\alpha_1$- subunit or auxiliary subunits. Most mutations are again restricted to the HVA Non-L-type $Ca_v2.1$ VGCC, e.g. the tottering (tg) [19], tottering leaner [19], rolling Nagoya [20] and rocker [21] mouse model, whereas others are related to mutations in accessory subunits, e.g. the β_4-subunit mutation in lethargic (lh) mice [22], the γ_2-subunit

mutation in stargazer (stg) mice [23], and the $\alpha_2\delta_2$-subunit mutations associated with the ducky and entla phenotype [24–27]. This apparently limited number of VGCC entities being affected is an astonishing observation, particularly as other VGCCs are also widely distributed throughout the brain, e.g. the $Ca_v2.3$ E/R-type channel which is present in most basal ganglia regions, the thalamus, hypothalamus, amygdala, hippocampus and cortex [28]. The HVA L-type Ca^{2+} channels $Ca_v1.1$–1.4 are not reported to be directly associated with primary or secondary forms of epilepsy despite incidental occurrence of seizures in Timothy patients. In addition, no seizure phenotype has been associated with mutations in the $Ca_v2.2$ and $Ca_v2.3$ VGCCs so far. Nevertheless, both HVA and LVA Ca^{2+} channels represent potent targets for antiepileptic drugs (AEDs). Blockade of these channels can inhibit the release of neurotransmitter or modulate neuronal firing patterns such as burst activity or intrinsic oscillations [29]. Pharmacodynamically some newer AEDs directly target the pore-forming Ca_v-α_1-subunit of Ca^{2+} channel complexes, e.g. levetiracetam, felbamate, lamotrigine and topiramate for HVA channels and ethosuximide or zonisamide for LVA T-type Ca^{2+} channels [29–31]. However, other AEDs were reported to interact with auxiliary subunits, e.g. gabapentin and pregabalin that interfere with the $\alpha_2\delta$ subunit of VGCCs [32]. Constrictively, one has to state that most of these AEDs are broad-spectrum pharmacons that also exert complex effects on other voltage- and ligand-gated ion channels. In this chapter we will focus on new interesting findings on the functional relevance of the HVA Non-L-type $Ca_v2.3$ VGCC as well as LVA T-type $Ca_v3.1$–3.3. Ca^{2+} channels in etiology and pathogenesis of seizures with a specific emphasis on non-convulsive absence seizures. Based on biochemical, molecular, electrophysiological and pharmacological analysis given, we will develop an integrative view of how $Ca_v2.3$ and $Ca_v3.1$–3.3 channels are capable of triggering epileptiform activity and why these channels are getting more and more important as a novel target in AED treatment in humans.

Distribution and Functional Characteristics of the HVA $Ca_v2.3$ E/R-Type VGCC

The $Ca_v2.3$ VGCC is widely distributed throughout the organism, not only in the peripheral and central nervous system (CNS), but also the endocrine [33, 34], cardiovascular [35, 36], reproductive [37] and gastrointestinal system [38]. Four groups independently generated mice lacking the $Ca_v2.3$ VGCC. In the last few years, these knock-out mouse models provided detailed insight into the functional relevance of this intractable channel. Within the CNS, $Ca_v2.3$ plays an important role in neurotransmitter release and presynaptic plasticity [39, 40]. Furthermore, $Ca_v2.3$ was reported to be involved in the physiology of fear [41], control of pain behaviour [42] and myelinogenesis [43]. In addition, the channel is likely to exert a protective role in ischemic neuronal injury [44] and to be involved in vasospasms following subarachnoid hemorrhage in humans [45]. The $Ca_v2.3$ VGCC exhibits a dominant presynaptic expression, e.g. in mossy fibers of the hippocampus [46]

and the pallidal globe [47], besides $Ca_v2.1$ [48] and $Ca_v2.2$ [49]. It can also be detected at the neuromuscular junction [50]. Presynaptically a smaller fraction of $Ca_v2.3$ is restricted to the active zone of the vesicle fusion machinery and thus involved in neurotransmission [48]. Furthermore, a larger fraction of $Ca_v2.3$ is localized more distant in the synapse responsible for synaptic plasticity, e.g. long-term potentiation (LTP) [40, 51]. E/R-type Ca^{2+} channels also exhibit a dominant expression on the soma and dendrites. Localization experiments revealed that $Ca_v2.3$ is preferentially distributed homogeneously on the cell soma and the dendritic arbor. The dendritic expression appears to be the most complex and only specific CNS nuclei and certain cell types display positive staining in dendrites, e.g. CA1 neurons, which will be discussed in more detail below. Depending on the cell type a distribution in proximal or distal dendrites is preferred. This is an observation that differs from other HVA Ca^{2+} channels pointing out the highly organized spatial distribution of $Ca_v2.3$ [52]. Thus, $Ca_v2.3$ was found to be involved in the generation of Ca^{2+}-mediated action potentials that are conducted along the length of the dendritic arbor which is an important site of Ca^{2+} entry and electrogenesis in neurons [53]. This somatic and dendritic role of $Ca_v2.3$ is of special interest and likely to contribute to a number of electrical phenomena characteristic for ictiform/epileptiform activity which will be discussed later.

Novel Mechanisms of $Ca_v2.3$ and $Ca_v3.2$ Ca^{2+}-Sensitivity

A number of splice variants of the $Ca_v2.3$ Ca^{2+} subunit have been described in the past [54]. This diversity could potentially be further amplified by partnering with the various isoforms of the $\alpha_2\delta$, β, and γ Ca^{2+} channel auxiliary subunits. On the biochemical level $Ca_v2.3$ is subject to complex regulatory mechanisms, including phosphorylation and dephosphorylation. Such mechanisms are of particular importance as they may alter basic electrophysiological properties of a channel and induce epileptiform burst activity in neurons [31]. Interestingly, Ca^{2+} influx through $Ca_v2.3$ E/R-type Ca^{2+} channels has opposite effects on the channel activity itself. At lower cytosolic Ca^{2+} concentrations, a positive feedback mechanism, which includes activation through protein kinase C (PKC) slows down inactivation and speeds up recovery from short-term inactivation [55, 56]. This positive feedback mechanism is dependent on the presence of the exon 19 encoded arginine rich insert 1 in the cytosolic II–III loop [54]. $Ca_v2.3e$ E/R-type Ca^{2+} channels lacking exon 19 encoded insert 1 demonstrate a minor but still significant phorbol ester mediated stimulation. We interpreted this as a reduced affinity for scaffolding proteins, which bind PKC to the II–III loop of the $Ca_v2.3d$ splice variant containing insert 1 [57]. This model is supported by the observation that co-expression of PKCα with $Ca_v2.3e$ leads to similar kinetics of inactivation and recovery as recorded for the full length II–III loop splice variant $Ca_v2.3$. Consequently, the pattern of $Ca_v2.3$ splice variants in different brain regions is likely to be of tremendous importance in neuroprotection, icto-/epileptogenesis and seizure propagation [58]. It's noteworthy that besides

$Ca_v2.3$, a Ca^{2+}-mediated positive feedback mechanism was also reported for HVA L-type Ca^{2+} channels which are mediated through Ca^{2+}/calmodulin kinase II [59]. However, at elevated cytosolic Ca^{2+} concentrations, a prominent Ca^{2+}-dependent inactivation renders the channel activity to further increase [60]. PKC-mediated phosphorylation is of substantial physiological relevance, mediating hormonal effects and those of intracellular messengers. VGCCs are effectors in various regulatory neurotransmitter and hormonal pathways initiated by G-proteins. Principally, this G-protein dependent regulation of VGCCs can either be indirect via second messengers and/or protein kinases or direct via physical interaction between G-protein subunits and the Ca_v-α_1 subunit. Functional studies elicited that G-protein interaction reversibly inhibits neuronal non-L-type Ca^{2+}-channels. Peak current amplitude is reduced and activation kinetics are slowed. The effects of the heterotrimeric G-proteins on VGCC are well described for the $G_{\beta\gamma}$ dimer [61, 62], whereas the role of G_α is yet not well understood. There is evidence that $G_{\beta\gamma}$ directly interacts with the I–II linker of the Ca_v α_1-subunit [63, 64]. In addition, the N-terminus of Ca_v2-α_1 subunits also seems to be involved in G-protein coupled channel modulation [65] including $Ca_v2.3$ channel. The $G_{\beta\gamma}$ interaction site within the I–II linker partially overlaps the AID (α_1-interacting domain) where β-subunits bind suggesting a physical competition between the agonistic β-subunits [65] and the antagonistic effects of $G_{\beta\gamma}$ ([66]). Interestingly, $G_{\beta\gamma}$ seems to exert inhibitory effects on LVA T-type Ca^{2+}- channels via interaction with the II–III-loop [67]. Besides, there are hints of a complex interdependence between PKC and G-protein pathways as activation of PKC antagonizes adjacent receptor-mediated G-protein inhibition of VGCC [64, 68]. Thus, accumulation of internal Ca^{2+} at low concentrations leads to tonic activation of $Ca_v2.3$d resulting in augmented responses, slowed inactivation and accelerated recovery from inactivation [55]. According to Dietrich et al. [40], $Ca_v2.3$ contributes selectively to the so-called residual $[Ca^{2+}]_i$ which also underlies various forms of synaptic plasticity but contributes less to neurotransmitter release. However, this residual internal background Ca^{2+} reaches concentration of up to 0.5 mM [69] and is in the same range as has been shown to facilitate Ca^{2+} currents through $Ca_v2.3$d channels [55]. Initial positive feedback mechanisms based on PKC activity might later be attenuated by negative feedback loops involving N-lobe calmodulin-dependent modulation as described previously by Liang et al.[60] and therefore help to maintain physiological $[Ca^{2+}]_i$ concentrations.

Functional Characteristics of $Ca_v3.2$ Ca^{2+} Channels

L-type channels T-type VGCCs are also play a critical role in epilepsy. Thereby, it can be demonstrated that high cellular Ca^{2+} currents of T-type channels occurring in increased intrinsic burst firing result from a selective or transient up-regulation of $Ca_v3.2$ subunits on protein and mRNA level after status epilepticus [70]. Furthermore, a huge range of G protein coupled receptors such as corticotropin releasing factor (CRF) receptor 1, muscarinic (M_1) or serotonin (5-HT)-receptors

leading to the activation of different intracellular second messenger pathways are involved in the regulation of T-type channels. However, it has to be pointed out that by taking into consideration the different tissue types expressing T-type channels for the investigation of current properties of $Ca_v3.2$ T-type channel currents, protein kinase A (PKA) regulation effects seem to be variable.

Taking a look at serine/threonine kinases, CamKs and tyrosine kinases it became obvious that CamKII, for example, causes a hyperpolarising shift in the activation curve of $Ca_v3.2$ channels being due to a stronger availability for opening of the channel pore [71]. In this regard, the domain II–III linker region serves as a key structure being involved in CamKII regulation [67]. Facilitation of the $Ca_v3.2$ channel activation properties can either be managed by PKC effects being possibly linked to the domain II–III linker region of the channel [72] or by the activation of PKA. Within the domain II–III linker region clusters of threonines and serines have been identified as target sites for the action of Rho kinase mediating a reversible inhibition and furthermore a shift towards more depolarized potential of the $Ca_v3.2$ activation and inactivation curves [73]. Therefore, the domain II–III linker region plays an important role in regulation of the T-type channel functions and may provide clinical relevance in the genesis of epilepsy.

Another possibility for regulation of $Ca_v3.2$ channels is the redox modulation by endogenous amino acid L-cysteine, resulting in an upregulation of T-type currents in nociceptive neurons [74] as well as in reticular thalamic neurons [75]. The effects of redox modulation stress the important role of $Ca_v3.2$ T-type channel being involved in pathophysiological neuronal states like epilepsy and pain. Regulation of $Ca_v3.2$ channels can also be managed by selectively inhibition of the channel itself via CRF receptors [76]. Thereby, inhibition demonstrated by a decrease in size of the current window and reduced opening availability is dependent on $G_{\beta\gamma}$ subunits activated by a cholera toxin sensitive G_{α} pathway. However, the effects of CRF differs depending on the T-type channel splice isoform. Recent investigations show that inhibition of T-type channels expressed in MN9D cells was also dependent on the activation of PKC activity. Therefore, cellular environment interferes with both CRF receptors and PKC mediated pathways [70].

Internal Cell Calcium and Regulation of Neuronal Excitability

Numerous cell functions are regulated by the free cytosolic Ca^{2+} concentration. Calcium ions can enter the cell through the plasma membrane or from internal stores via different types of Ca^{2+} channels, the Na^+/Ca^{2+} exchanger, and through release channels from internal Ca^{2+} stores (Inositoltrisphosphat (IP_3)-receptor, Ryanodine receptor). The resulting cytosolic Ca^{2+} signal is highly organized in space and time, i.e. frequency and amplitude because the localization and the integrated free cytosolic Ca^{2+} concentration over time codes for specific information [16]. Action potentials mediate Ca^{2+} entry through HVA Ca^{2+} channels in pyramidal cells [77]. Until cellular buffering mechanisms restore resting Ca^{2+} levels [78], cytosolic free Ca^{2+}

regulates critical cellular functions, including gene transcription, neurotransmitter release and channel modulation. Cytoplasmic Ca^{2+} may also provide the cell with an index of recent spiking activity [77]. The calcium hypothesis of epileptogenesis implies that alterations in internal Ca^{2+} play a tremendous role in the etiopathogenesis of epilepsy [79–81]. Consequently, the extracellular Ca^{2+} concentrations decrease during epileptiform activity [82]. Although numerous studies provide clear evidence for increased neuronal Ca^{2+} influx during epileptiform activity, direct visualizations and measurements of the underlying $[Ca^{2+}]_i$ are rare and the molecular and structural basis of Ca^{2+} influx is only partially known. HVA Ca^{2+} channels are likely to be predominant candidates for $[Ca^{2+}]_i$ elevation during epileptiform activity [79, 83], mediating both seizure initialization and propagation. In hippocampal tissue for example, Ca^{2+} current density was reported to be upregulated during epileptogenesis [84] and blockade of these channels also depressed epileptiform activity [85]. Recently, transcriptional up-regulation of $Ca_v3.2$ T-type Ca^{2+} channels was related to a rat model of pilocarpine induced chronic hippocampal seizures [84]. In addition, Berg et al. [86] proved that seizure activity induced by kainate, e.g. in the hippocampus is strongly based on internal Ca^{2+} which also plays a critical role in seizure-related excitotoxicity. Consequently, various AEDs were reported to exert neuroprotective effects in different animal models by inhibiting components of the excitotoxic cascade [87]. Besides HVA L-type and LVA T-type Ca^{2+} channels, internal Ca^{2+}-levels were further shown to be regulated by $Ca_v2.3$ R-type channels which are modulated by Ca^{2+}/calmodulin and PKC [76]. $Ca_v2.3$ Ca^{2+} channels turned out to be key regulators in neuronal excitability triggering epileptiform activity, as discussed later for CA1 neurons.

The $Ca_v2.3$ and $Ca_v3.2$ VGCC in Neuronal Epileptiform Activity

Voltage-Gated Ca^{2+} Channels in Plateau Potential Generation

Epilepsy marks a disorder in which disruption of normal neuronal activity pattern are common. As a combination of both, abnormal brain wiring and an imbalance of nerve signaling, epilepsy can result in the development of seizures being promoted by increased excitability of neurons as being previously described. Nowadays for a closer and better understanding of such distinct abnormalities, it is necessary to take a look at intrinsic properties on a molecular cell level. In this case VGCCs play a critical role in regard to regulation of oscillatory activity and transmitter release, influencing membrane currents that redound to hyperexcitability [88]. Hence, VGCCs contribute to the pathogenesis of various forms of epilepsies. Extracellular epileptiform/ictiform field potentials can be based on various cellular epileptiform/ictiform voltage changes, including plateau potentials, afterdepolarizations and excessive rebound bursting.

Abnormal burst activity is a characteristic feature of epileptiform, neuronal activity. Each cellular burst is sustained by a slow, persistent depolarization,

the so-called plateau potential [89], which is initiated at the beginning of the burst and lasts for several hundred milliseconds to seconds [90]. The plateau is spike dependent and regenerative and is triggered by the summation of depolarising action potentials [91]. The depolarising action potentials that follow two or more closely spaced spikes sum up to a much larger afterpotential, and the resulting depolarization can take the cell above spike threshold. Additionally, a concomitant increase in internal Ca^{2+} after multiple spikes further supports this process by inhibiting $I_{K\text{-}leak}$ and so more strongly depolarizes the cell. If the resulting summed depolarising action potentials are then sufficient to carry the cell above spike threshold, the resulting action potential brings in more Ca^{2+} eliciting further depolarising action potentials via a positive feedback mechanism. Consequently, recurrence of the process results in a sustained plateau potential which supports repetitive spiking [89]. After several seconds of activity, but long before termination, $[Ca^{2+}]_i$ attains a plateau that is typically >200 nM above rest. However, the plateau potential quickly collapses, once the electrical activity has ceased and the membrane repolarises again [91]. The cause of plateau potential termination has not yet been fully established, although an accumulation of $[Ca^{2+}]_i$ and the subsequent activation of a hyperpolarising Ca^{2+}-dependent K^+- mediated afterhyperpolarisation (AHP) has been proposed [92, 93]. A shift from Ca^{2+}-dependent facilitation to Ca^{2+} dependent inactivation of VGCCs at elevated $[Ca^{2+}]_i$ might also play a role. In neocortical pyramidal cells, [94] have shown that there is a linear relationship between plateau $[Ca^{2+}]_i$ and firing frequency in soma and proximal dendrites. The rise in $[Ca^{2+}]_i$ finally activates K^+ channels underlying the AHP, consisting of two Ca^{2+}-dependent components, medium and slow AHP. Principally, plateau potentials as outlined above, but also afterdepolarisations are a common feature of different neuronal cell types in various brain regions, e.g. spinal and brainstem motoneurons, spinal interneurons, dorsal horn neurons, subthalamic nucleus neurons, suprachiasmatic neurons, striatal cholinergic neurons, hippocampal pyramidal cells, subicular and entorhinal cortical cells [95]. Though a common phenomenon within the CNS, plateau potentials and afterdepolarisations still harbor a plethora of secrets as the underlying ion channel entities are still not fully described. However, recent studies more and more point to the fact that $Ca_v2.3$ indeed is a potent player in plateau potential and afterdepolarisation generation. In lumbar spinal cord motor neurons, plateau potentials were originally reported to be driven by L-type Ca^{2+} channels in dendrites [96]. Li and Bennett [97] have argued that a TTX-sensitive persistent sodium and L-type Ca^{2+} current are responsible for plateau potentials in these cells. Both Cd^{2+} (400 μM), a non-specific Ca^{2+} channel blocker, and nimodipine (10–20 μM), a specific L-type Ca^{2+} channel blocker, completely abolished this TTX-resistant plateau and therefore Li and Bennett [97] concluded that it was mediated by L-type Ca^{2+} channels. However, the nimodipine- sensitive Ca^{2+} current in this preparation was LVA (−50 mV) and concluded to be associated with the $Ca_v1.3$ Ca^{2+} channel with low-voltage behaviour. This L-type current was usually fully activated at <−40 mV. Additionally, the authors clearly ruled out that other HVA Ca^{2+} channels, i.e. $Ca_v2.1$ and $Ca_v2.2$ are related to the persistent low-threshold inward Ca^{2+} current by using various Ca^{2+} channel blockers, e.g. ω-conotoxin GVIA (2 μM)

and ω-conotoxin MVIIC (1 μM). Although L-type Ca^{2+} channels are conventionally considered as HVA channels, Li and Bennett [97] demonstrated that the threshold of L-type Ca^{2+} channels in their preparation is around the firing threshold of the motoneurons, which is similar to the lowthreshold obtained in other studies of plateaus in neurons (i.e., −45 to −55 mV) [98–102]. Interestingly, other studies further elicited that these L-type like Ca^{2+} channels involved in generation of plateau potentials require a higher concentration of dihydropyridines, e.g. 10 μM nimodipine [97], 15 μM nifedipine [98] 10 μM nifedipine [101] or 50 μM nifedipine [99] to be completely blocked than actually do conventional L-type Ca^{2+} channels (1 mM) [103, 104]. However, one has to consider that these data were obtained from different tissue preparations from various species and that dihydropyridine action on VGCCs is further influenced by experimental conditions, such as cell membrane potential or penetration depth of these drugs in CNS slices. Similar studies were carried out [105] in striatal medium spiny neurons of the rat. Again, L-type Ca^{2+} channels were reported to be necessary for promoting the generation of plateau potentials from relatively depolarized holding potentials if elicited from the soma (−60 to −55 mV) [106, 107] The application of the L-type Ca^{2+} channel antagonist nitrendipine (5 μM) reduced plateau potentials in these and other cells tested [105]. A central question remains: what's the nature of this low-dihydropyridine sensitive, L-type like Ca^{2+} current? Fascinatingly, not only neurological but also cardiovascular studies suggest that $Ca_v1.3$ is a possible candidate for a low-threshold and low-dihydropyridine sensitive L-type Ca^{2+} current component [108, 109] and thus is likely to promote generation of plateau potentials in different studies on neuronal cell types. Whereas the characteristics of a LVA behaviour of $Ca_v1.3$ have recently been described [108, 110], $Ca_v2.3$ has already been reported to conduct transient Ca^{2+} currents with both activation and steady-state inactivation occurring at relatively negative membrane potentials, thus sometimes called a low- to mid-voltage activated channel [111]. To determine, whether $Ca_v2.3$ might be indeed a possible candidate for a low dihydropyridine sensitive VGCC, we recently performed dose–response analyses of isradipine effects on two $Ca_v2.3$ splice variants, $Ca_v2.3d$ and $Ca_v2.3e$ yielding IC_{50} values of 9.1 and 14.6 μM, respectively [35]. Furthermore, when $Ca_v2.3$ was co-expressed with $\alpha_2\delta$ and β_{1b} in COS-7 cells the dihydropyridine nicardipine was reported to exert a 51 ± 7% inhibition of Ca^{2+} influx at 1 μM [112]. In contrast, other studies failed to show an inhibitory effect of nifedipine or isradipine on $Ca_v2.3$ VGCCs expressed in Xenopus oocytes [28, 111, 113] indicating that the expression system, splice variants and subunit distribution might be of central importance for dihydropyridine-sensitivity. Nevertheless, it is highly questionable whether low micromolar concentrations of dihydropyridines should be regarded as diagnostic for L-type Ca^{2+} channels. Considering, that $Ca_v1.3$ and $Ca_v2.3$ are coexpressed in most regions capable of exhibiting neuronal plateau potentials, it becomes obvious, that $Ca_v2.3$ is likely to contribute significantly to plateau potential and afterdepolarisation generation. In 2005, Pierson et al. [95], further corroborated this hypothesis by demonstrating that E/R-type Ca^{2+} channels are likely to play a major role in the genesis of plateau potentials in hypothalamic suprachiasmatic neurons from rat. In contrast to most other studies carried out before, the authors used low

doses of isradipine (2 mM) which clearly failed to prevent or reduce Ca^{2+}- dependent plateau potentials, whereas ω-conotoxin GVIA (1 μM) and ω-agatoxin IVA (200 nM) caused only a slight reduction in plateau potential duration. Based on this observation Pierson et al. [95] concluded that E/R-type Ca^{2+} channels significantly contribute to plateau potential generation, particularly, as suprachiasmatic neurons seem to express large E/R-type Ca^{2+} currents of up to 50% [114]. Thus, by contributing to sustained plateau potentials, E/R-type Ca^{2+} channels might enhance neuronal excitability and contribute to epileptogenic processes. Moreover, two recent publications directly proved that $Ca_v2.3$ is involved in generation of plateau potentials and afterdepolarisations and contributes to epileptiform burst activity in CA1 neurons of the hippocampus [115, 116]. Early studies by Fraser and MacVicar [117] and Fraser et al. [118] already elicited that cholinergic stimulation of hippocampal CA1 neurons using carbachol results in slow afterdepolarisation and longlasting plateau potentials resembling epileptiform activity. Principally, triggering the cholinergic system is one wellknown mechanism to induce limbic seizure activity in vitro and in vivo [119, 120] and plateau potentials are supposed to play an important role in this field by Ca^{2+} entry through VGCCs as well as muscarinic receptor-mediated activation of guanylate cyclase activity and subsequent increase in cGMP [121]. It is further known that E/R-type Ca^{2+} channels are primarily responsible for the Ca^{2+} influx in dendrites and spines of CA1 neurons [122] and therefore reduction of E/R-type Ca^{2+} current results in reduction of postsynaptic Ca^{2+} accumulation, especially during repetitive synaptic activation [123, 124]. The role of $Ca_v2.3$ seems to be particularly important during cholinergic stimulation, as in the absence of carbachol large plateau Ca^{2+} spikes are based on L-, N-, and P/Q-type Ca^{2+} channels, with E/R-type Ca^{2+} channels exhibiting only minor contribution [125, 126]. However, when carbachol is present, L-, N-, and P/Q-type VGCCs are depressed [127, 128] whereas E/R-type-dependent spiking is unmasked and dramatically enhanced. In 2000 Palmieri et al., reported that topiramate can depress carbachol-induced plateau potentials in subicular bursting cells [129]. Whereas the authors did not further investigate the ionic background of plateau potentials, [115] directly proved that topiramate inhibits generation of plateau potentials by depressing E/R-type VGCCs. Topiramate itself is a newer AED, used in treatment of partial seizures, primary generalized tonic-clonic seizures and seizures associated with Lennox-Gastaut-syndrome [130]. On the molecular level, topiramate is supposed to interfere with different systems, e.g. block of voltage-gated sodium channels, VGCCs, AMPA/kainite receptors or GABA(A) receptors, although there are also contradictory reports [131]. Using $Ca_v2.3$ expressing tsA-201 cells co-transfected with β_{1b} and $\alpha_2\delta$ subunits, Kuzmiski et al. [115] revealed that topiramate is capable of inhibiting $Ca_v2.3$ mediated Ca^{2+} currents at therapeutically relevant concentrations ($IC_{50} = 50.9$ μM) and, in addition shifts the steady-state inactivation curve to more negative potentials supporting transition of the channel into the inactivated state. Interestingly, topiramate had no effect on Ca^{2+} spikes under control conditions, but it reduced Ca^{2+} spikes after cholinergic receptor stimulation which is in accordance with increased E/R-type activity after carbachol application. Carbachol-induced plateau potentials in CA1 neurons were completely depressed by topiramate at

therapeutically relevant concentrations (50 μM). Calcium spikes elicited in this study were high-threshold activated, transient Ca^{2+}-dependent action potentials. Using a cocktail of TTX and various VGCC blockers (i.e. nifedipine 10 μM) the remaining Ca^{2+} spike was E/R-type based and shown to be increased by carbachol. In addition, an increase in spike frequency and a decrease in threshold for $Ca_v2.3$-mediated spiking was observed upon carbachol administration. Again, topiramate resulted in a highly significant reduction of E/R-type Ca^{2+} spike amplitude. Although Kuzmiski et al. [115] did not try to block this E/R-type Ca^{2+} current component by SNX-482, a selective blocker of E/R-type Ca^{2+} channels [132], it is known that $Ca_v2.3$ contributes at around 80% to the blocker-resistant E/R-type Ca^{2+} current in CA1 neurons [133] and in addition the E/R-type component turned out to be sensitive to low concentrations of Ni^{2+} (50 μM). Considering the fact that 10 μM nifedipine is likely to exert inhibitory effects on $Ca_v2.3$ [35, 112] one could imagine that the real $Ca_v2.3$-mediated topiramate effect on carbachol-induced Ca^{2+} spikes is even more dramatic. Studies by Melliti et al. [134] and Bannister et al. [135] have provided first detailed information how $Ca_v2.3$ is actually regulated by M_1, M_3 and M_5 muscarinergic receptors, e.g. via carbachol. All three muscarinic receptors were proven to exert various effects on $Ca_v2.3$ VGCCs. The $G_{\beta\gamma}$ subunit was reported to mediate inhibition of $Ca_v2.3$ whereas the stimulation of $Ca_v2.3$ involves a pertussis toxin-insensitive $G_{\alpha q/11}$ subunit, Phospholipase C (PLC_β), diacyl glycerol (DAG) and a Ca^{2+} independent PKC mechanism. This PKC mediated stimulation might also have severe pharmacological implications regarding topiramate effects on $Ca_v2.3$ [136]. It is also possible that VGCCs, e.g. $Ca_v2.3$ trigger further intracellular cascades that effect other channel and receptor systems. In rats deep dorsal horn interneurons, it has been described that after initiation of plateau potentials, activation of a Ca^{2+}-activated non-selective cation current can prolong existing plateau potentials [100]. Recently, muscarinic activation via M_1/M_3-cholinergic receptors was shown to enhance R-type, but not T-type, Ca^{2+} currents in rat hippocampal CA1 pyramidal neurons after N-, P/Q-, and L-type Ca^{2+} currents were selectively blocked [137]. This muscarinic stimulation, e.g. using carbachol is capable of inducing sADP and PP on the cellular level but also bursts in extracellular recordings from the CA1 region. Hippocampal pyramidal neurons express high levels of postsynaptic M_1 and M_3 receptors [138] which are $G_{\alpha q/11}$ coupled. Their activation results in the generation of DAG and IP3 following PLC activation. Subsequently, DAG activates Ca^{2+}-independent group II PKCs, most probably PKCδ [137]. In the presence of PKC inhibitors R-type Ca^{2+}-currents were inhibited by muscarinic stimulation in CA1 neurons probably mediated by activation of pertussis toxin-sensitive G-protein-coupled M_2/M_4 receptors and $G_{\beta\gamma}$ [135, 139]. The functional epileptogenic capacity of $Ca_v2.3$ in triggering hippocampal seizure activity is further supported by the observation that M_1 receptor knock-out mice exhibit decreased seizure susceptibility to pilocarpine-induced seizures [140]. To provide a global view of $Ca_v2.3$ involvement in epileptogenesis one also has to consider secondary effects of VGCCs. In the rat hippocampus for example, the establishment of a focus of epileptiform activity was reported to lead to enhanced voltage-dependent Ca^{2+} conductance of CA1 pyramidal neurones [141]. Hendriksen et al. [142] induced epileptogenesis by

application of electrical tetanic stimulation of the Schaffer collateral/commissural fibre pathway in the hippocampus. Interestingly, during the initial stages of epileptogenesis, $Ca_v2.1$, $Ca_v1.3$- and particularly, $Ca_v2.3$ subunit mRNA levels were significantly increased in the different hippocampal subareas compared to levels in control animals. Similar results were obtained from the hippocampus of seizure-prone gerbils [143]. It becomes obvious that the complex regulation of the $Ca_v2.3$ VGCC by muscarinic receptors, including PKC mediated and Ca^{2+}-dependent channel activation, harbours a potent and outstanding epileptogenic mechanism that will also enable pharmacological interference in the future. In total, VGCCs represent important molecular targets for multiple AEDs [29, 31] and many AEDs described in the past were reported to inhibit LVA or HVA Ca^{2+} channels.

Voltage-Gated Ca^{2+} Channels in Excessive Rebound Burst Firing – The Ethiopathogenesis of Absence Epilepsy

Typical absence epilepsy is characterized by a paroxysmal loss of consciousness of sudden onset and termination that is normally accompanied by bilateral synchronous spike-wave discharge (SWD) activity of species specific frequency [144]. Absence seizures are based on abnormal hypersynchronous activity in the thalamocortical-corticothalamic circuitry. This neuronal circuitry mainly consists of thalamic relay cells of the ventroposterolateral and ventroposteromedial thalamic region that exert glutamatergic projections on cortical pyramidal neurons, predominantly in layer III and IV. Pyramidal neurons within these layers either project directly or via GABAergic interneurons to pyramidal neurons in layer V and VI of the cortex and the latter finally re-innervate the ventrobasal thalamus using glutamate as neurotransmitter. At the lateral edge of the thalamic region the shell-shaped reticular thalamic nucleus (RTN) is localized and functionally integrated into the thalamocortical circuitry. Being exclusively composed of GABAergic interneurons, the RTN receives glutamatergic collateral projections from both cortical pyramidal and thalamic relay neurons. In addition, RTN neurons synapse onto each other resulting in lateral inhibition [145], and most importantly, RTN cells also innervate thalamic relay neurons. Not only GABA but also somatostatin, acetylcholine, and cholecystokinin can found in RTN neurons serving as neurotransmitters [146]. Furthermore, RTN neurons are morphologically diverse, classified as round, small fusiform or large fusiform neurons [146]. RTN neurons, in general, exhibit complex dendritic ramification allowing interaction between each other via both chemical and electrical dendrodendritic synapses [147–149].

Importantly, the thalamocortical circuitry is not structurally and functionally isolated. Various extrathalamocortical structures, such as the nucleus basalis Meynert, raphe nuclei, pedunculopontine and laterodorsal tegmental nuclei, and the cerebellum are known to project to and modify the activity of the thalamocortical circuitry via neuromodulators, such as noradrenalin, histamine, 5-HT and acetylcholine [144, 145]. Some brain structures like the hippocampus or cerebellum

classically not known to be involved in the production of absence SWDs, could in fact participate in the development of this phenotype [150].

Both thalamocortical relay neurons as well as RTN cells harbour the capability to switch between different functional modes; tonic, intermediate and burst modes of action. At slightly depolarized membrane potentials, e.g. −55 mV, neurons exhibit tonic activity in which the cells serve as a sensory gate to the cortex processing peripheral receptive information encoded as action potential firing to the cortex [151]. The depolarisation of thalamic relay cells, at least in part, is due to the activating input of deeper brainstem structures, as the reticular formation, and disinhibition of RTN neurons that project to ventrobasal thalamic cells. The tonic firing mode is characteristic of stages of high vigilance. With decreasing activity from deeper activating brain regions, thalamic relay cells tend to re- and hyperpolarize passing through the intermediate mode finally reaching the so called rebound burst firing mode of action. This mode exhibits typical features of neuronal pacemaker activity and the underlying voltage- and ligand-gated ion channel armamentarium including T-type Ca^{2+} channels, hyperpolarization and cyclic-nucleotide gated, non-specific cation (HCN) channels etc. clearly resembles the situation observed in cardiac pacemaker cells [152]. Beginning with a strong hyperpolarization, an oscillatory cycle starts with activation of HCN channels (HCN2 and HCN4), which in turn results in a slow, ramp-like depolarization. This next activates LVA $Ca_v3.1$–3.3 T-type Ca^{2+} channels, resulting in so called low-threshold calcium spikes with superimposed bursts of conventional Na^+/K^+ action potentials (sodium spikes) in both thalamic relay and RTN cells. The cycle is completed by the inactivation of Na^+ and Ca^{2+} channels and the opening of various K^+ channels, both voltage and Ca^{2+}-activated, resulting in the pronounced hyperpolarization initiating the next cycle. The underlying current entities are known as I_A and $I_{K(Ca2+)}$ whereas the molecular ion channel entities still have to be determined.

T-type Ca^{2+} channels thus play a pivotal role in this oscillatory burst pattern. They can be activated only from rather hyperpolarized membrane potentials, since negative potentials will allow them to undergo conformational changes from the inactivated state, after having been activated, to the resting state, a process known as *de-inactivation* or *repriming* [152]. The rebound burst firing mode leads to characteristic phenomena within the thalamocortical circuitry and is typical for low stages of vigilance, such as slow-wave sleep (SWS). At that stage, the electroencephalography is characterized by low-frequency, high amplitude theta- and delta-wave activity. Enhanced oscillatory discharges resulting in rebound burst firing of thalamic relay neurons and RTN cells has been clearly implicated to play a crucial role in the etiopathogenesis of absence epilepsy [153]. Under these condition, RTN neurons were reported to generate spontaneous oscillations, such as rhythmic spike-burst activities [154, 155] which strongly inhibit ventrobasal relay neurons serving as a major driving force for rebound burst firing due to the hyperpolarization processes. Interestingly, absence epilepsy turned out to be the pathophysiological correlate of SWS as thalamocortical hyperoscillation results in hypersynchrony and SWD generation which can finally be recorded from the brain surface. Epicortical SWDs can indeed be interpreted as a pathophysiological aberration of physiological sleep-spindles typical of stage C/2 of regular SWS.

VGCCs channels turned out to be of major relevance in the pathogenesis of absence epilepsy due to their unique electrophysiological properties and cellular distribution [11, 153, 156, 157]. In thalamic relay neurons, $Ca_v3.1$ (α_1G) T-type Ca^{2+} channels are expressed, whereas in the RTN cells, $Ca_v3.2$ and $Ca_v3.3$ can be found [158, 159]. In accordance with its selective expression in the ventrobasal thalamus, $Ca_v3.1$ ablation resulted in resistance to γ-hydroxybutyrolactone (GBL)- or baclofen induced SWDs [160] and both reduction of SWS and alteration of sleep architecture [161]. In addition, crossbreeding of $Ca_v3.1^{-/-}$ mice with various $Ca_v2.1$ mouse mutants, e.g. tg, lh, stg or $Ca_v2.1^{-/-}$ mice that display spontaneous SWD activity, resulted in offspring that were either free from absence seizures or exhibited significant reduction in SWD severity [162]. Conversely, Ernst et al. [163] reported that overexpression of Cacna1g gene for $Ca_v3.1$ (α_1G) T-type Ca^{2+} channels in two mouse lines resulted in bilateral cortical SWDs with behavioural arrest typical of pure absence epilepsy. This mouse model was the first to show that selective overexpression of a thalamic T-type Ca^{2+} channel by itself can result in pure absence epilepsy not being associated with additional neurological deficits typical for $Ca_v2.1^{-/-}$ mice and $Ca_v2.1$ mouse mutants. Recently, Powell et al. [164] described a single-nucleotide missense mutation in the $Ca_v3.2$ T-type Ca^{2+} channel gene (Cacna1h) in Genetic absence epilepsy rats from Strasbourg (GAERS) localized within the III–IV linker of the channel. This mutation is supposed to facilitate the expression of a $Ca_v3.2$ splice variant containing exon 25 which finally results in significantly faster recovery from channel inactivation and greater charge transfer during high-frequency bursts.

In GAERS, an increase of T-type Ca^{2+} current in the RTN has been described by Tsakiridou et al. [165]. Furthermore, in this animal model $Ca_v3.1$ and $Ca_v3.2$ transcripts were also shown to be increased in the relay neurons and RTN cells, respectively. In Wistar Albino Glaxo (WAG/Rij) rats, another rat model of absence epilepsy, multiple alterations in VGCCs have been described, including enhanced thalamic T-type Ca^{2+} current [166], increased $Ca_v2.1$ expression in the RTN and a lack of $Ca_v2.3$ expression levels in the RTN at the time of seizure onset, i.e. three months of age [167].

Thus, absence seizure activity can be substantially driven not only by the ventrobasal thalamus but also the RTN with latter turning out to be one of the critical factors in absence epileptogenesis. Gene ablation studies on $Ca_v3.2$ and $Ca_v3.3$ T-type Ca^{2+} channels in thalamocortical rhythmicity have not yet been published, but preliminary results indicate that $Ca_v3.2$ VGCCs can essentially contribute to thalamocortical hyperoscillation induced by baclofen [153]. In humans, various gain-of-function missence mutations for $Ca_v3.2$ have been described so far, which are associated with childhood absence epilepsy [153, 168, 169].

The exact role of the high-voltage activated (HVA) $Ca_v2.1$ Ca^{2+} channel in absence epileptogenesis still remains to be determined. In some $Ca_v2.1$ mutants, thalamic T-type current was reported to be secondarily increased, which is likely to serve as a pro-absence factor in these animals [162]. However, as $Ca_v2.1^{-/-}$ X $Ca_v3.1^{+/-}$ mice still exhibit absence seizures despite a 25% reduction in thalamic T-type Ca^{2+} current compared to controls, the absence or impairment of $Ca_v2.1$ itself should additionally contribute to their phenotype probably due to impaired excitatory neurotransmission in cortex or thalamus [13, 145].

In summary, the enhancement of LVA T-type Ca^{2+} current in RTN neurons plays an essential role in absence epileptogenesis and inhibition of this phenomenon displays an effective anti-absence strategy. Thus it is obviously to conclude that the question of *to burst or not to burst* is based on the relation of LVA T-type – to HVA L/Non-L-type Ca^{2+} currents. L-type Ca^{2+} channels activate at more depolarized potentials and, more importantly, inactivate much more slowly resulting in pushing neurons into an overall more depolarized state for extended periods of time. Therefore, an alternative to pharmacological blockade of LVA T-type Ca^{2+} current in order to prevent hyperoscillation, is facilitation of HVA Ca^{2+} currents on the thalamic level. This approach represents an alternative strategy to shift the functional balance to the more depolarized state, thus favouring the tonic mode of action. This potential SWD suppressing effect of HVA Ca^{2+} channel activation has been reported in GAERS, a rat model of absence epilepsy, in which SWDs are effectively diminished by administration of BayK-8644, an L-type Ca^{2+} channel agonist, but enhanced by L-type Ca^{2+} channel blockers, e.g. dihydropyridines [170]. Thus, clinical use of HVA Ca^{2+} channel blockers that can penetrate the blood-brain barrier in patients suffering from absence epilepsy should be avoided or carefully monitored. On the other hand, selective HVA Ca^{2+} channel augmentation in the thalamocortical loop could serve as an alternative pharmacological strategy to control hyperbursting activity.

Recent studies demonstrate that the HVA non-L-type $Ca_v2.3$ Ca^{2+} channel is likely to play an important role in thalamocortical rhythmicity as well. The $Ca_v2.3$ Ca^{2+} channel is expressed in GABAergic interneurons of the cortex and the RTN [156, 171]. Interestingly, de Borman et al. [172] and Lakaye et al. [150] detected a significant reduction of $Ca_v2.3$ transcript levels in both cerebellum and medulla of GAERS, two extrathalamocortical brain structures, the brainstem and cerebellum which project to the thalamocortical circuitry, capable of modifying its oscillatory behaviour [173, 174]. On the other hand, the WAG/Rij rat model of absence epilepsy was also reported to exhibit altered VGCC expression. Development of spike-wave discharges in these rats is concomitant with an increased expression of $Ca_v2.1$ in the RTN. Furthermore, van de Bovenkamp-Janssen et al. [167] demonstrated that normal control rats exhibit an increase of $Ca_v2.3$ expression within the RTN during development (from 3 to 6 months of age) whereas WAG/Rij rats were lacking this $Ca_v2.3$ increase concomitant with the establishment of SWDs. These observations clearly point to a functional role of $Ca_v2.3$ in etiology and pathogenesis of absence epilepsy like activity and, in addition might be related to sleep disorders. Pharmacological studies further support this observation. Lamotrigine for example, which exerts inhibitory actions on $Ca_v2.3$ VGCCs [175] was proven to be effective in suppressing spike-wave discharges in both GAERS and WAG/Rij rats [144, 176] and thalamocortical burst complexes in rat brain slices [177]. Analysis of absence seizure susceptibility in $Ca_v2.3^{-/-}$ and control animals revealed first hints that $Ca_v2.3$ deficient mice exhibit altered thalamocortical rhythmicity and seizure susceptibility [171]. The role of $Ca_v2.3$ Ca^{2+} channels in thalamocortical rhythmicity was further elaborated in more detail on both the thalamic [178] and cortical level [179]. In addition, mutations in EFHC1, a C-terminal interaction partner of $Ca_v2.3$ are functionally related to juvenile myoclonic epilepsy in humans [180]. An extensive

characterisation of $Ca_v2.3$ in thalamocortical rhythmicity was carried out by Zaman et al. [181] using a combination of in vitro and in vivo methods. Injection of a hyperpolarising current in a brain slice approach was capable of triggering a low-threshold Ca^{2+} spike with superimposed sodium bursts in RTN neurons from $Ca_v2.3^{-/-}$ mice. Interestingly, subsequent oscillatory burst charges were strongly suppressed and slow afterhyperpolarisations (sAHP) reduced. About 51% of HVA Ca^{2+} current in RTN neurons was SNX-482 sensitive and could be dedicated to $Ca_v2.3$ VGCCs. Furthermore, $Ca_v2.3$ mediated Ca^{2+} influx was shown to interfere with voltage-insensitive SK2 channels that contribute to the generation of Ca^{2+}-dependent sAHP. Zaman et al. [181] argue that T-type Ca^{2+} channels per se are not sufficient to maintain Ca^{2+} levels to trigger sAHP, which are a prerequisite for re-priming T-type Ca^{2+} channels and thus sustained rebound bursting. Consequently, $Ca_v2.3^{-/-}$ RTN neurons display reduced oscillatory activity and reduced absence seizure susceptibility. Contemporaneously, Astori et al. [182] analyzed the effects of $Ca_v3.3$ VGCCs on the oscillatory activity of RTN neurons. $Ca_v3.3$ channels turned out to be indispensible for RTN function and sleep spindles. Similar to $Ca_v2.3$, $Ca_v3.3$ ablation prevented oscillatory bursting as the remaining Ca^{2+} influx obviously was not sufficient to trigger small conductance-type 2 (SK2) K^+ channels, which are important for facilitating burst activity.

Another important class of ion channels involved in the regulation of tonic and burst firing are the HCN channels, with HCN2 and HCN4 being predominantly expressed in the thalamus exhibiting pacemaker activity. When HCN2 is experimentally ablated in mice, animals exhibit increased absence seizure susceptibility [183]. This is based on a marked hyperpolarization shift of the resting membrane potential and strong repriming of the crucial T-type Ca^{2+} channel fraction [183, 184]. In WAG/Rij rats, Bude et al. [185] observed increased HCN1 expression in the epileptic thalamus, associated with a decrease in cAMP responsiveness of I_h current in thalamocortical neurons and subsequent impairment to control the shift from burst to tonic firing. Thus, burst activity is prolonged after recruitment of I_h during absence seizures. The HCN4 channel effect in thalamocortical rhythmicity is still unclear as HCN4 channel knock-outs are lethal at the embryonic stage. Pharmacological interference with the HCN system to manage absence epilepsy in humans has not been established yet. Usage of newly developed HCN blockers, such as ivabradine, might be critical in patients suffering from absence epilepsy or exhibiting increased absence seizure susceptibility.

Future Perspectives

Within the recent years, studies on the involvement of VGCCs in etiology and pathogenesis of epilepsies have mainly focused on the non-L-type $Ca_v2.1$ and the T-type $Ca_v3.2$ VGCCs. Given the significance of VGCCs, it is not surprising that acquired channelopathies can arise from transcriptional changes concerning different VGCCs isoforms [164]. Hereby, the expression of VGCCs can be perturbed by

transcriptional upregulation of functionally different classes of channels and furthermore causing inhibitory and excitatory imbalance [186].

Recent biochemical, molecular and electrophysiological findings on cellular and whole animal level together with pharmacological analyses point the outstanding role of the $Ca_v2.3$ E/R-type Ca^{2+} channel in epileptogenesis and seizure propagation. In addition, the number of $Ca_v2.3$ splice variants and their distribution throughout the brain in combination with their biochemical regulation via muscarinic receptors, PKC and Ca^{2+}-dependent activation and inactivation processes make Ca^{2+} channels key players. It is therefore plausible that mutations in $Ca_v2.3$ will turn out to be responsible for different forms of epilepsies in humans in the future. Thus, generation of new AEDs specifically targeting $Ca_v2.3$ becomes absolutely indispensable. Animal models of acquired epilepsy serve as excellent tools to study drug targeting.

Acquired channelopathies can be related to the basis of an enhancement of VGCCs or a reduced expression of ion channels extenuating electrophysiological activity of neurons [186]. Based on the pathological conditions of epilepsy, low-threshold transient (T-type) Ca^{2+} channels as one example of VGCCs can be seen as key generators which provide normal and balanced neuronal rhythms [186]. Given the special properties of these channel type to remove inactivation by hyperpolarising the cell membrane, its exceptional position in epileptogenesis becomes clearly obvious. From recent studies it is well known that these channels will be abnormally up-regulated in CA1 region of hippocampal dendrites during chronic SRS after an injection of pilocarpine. Hence, increased bursting rates in CA1 dendrites of the hippocampus as well as enhanced gene expression of $Ca_v3.2$ genes contribute to status epilepticus.

Actually, it has to be taken into account that the hippocampus is not the only region being involved in epileptogenesis. Recent studies show that limbic as well as subcortical connections, as an extended neuronal network, have to be taken into consideration contributing to altered voltage-gated properties of $Ca_v3.2$ channels. In this case, decreased appearance of Ca^{2+}-dependent burst activity during latent period of SRS on the one hand or increased one during chronic SRS stadium on the other hand could by experimentally explored. The latter at this was distinguished in the reuniens nucleus of the thalamus. Consequently gene expression of $Ca_v3.2$ channels and its effects on hyperexcitability has to be seen against the background of a global SRS generating network [186].

In terms of such a good global functioning network of distinct brain regions, the rapidly activating A-type K^+ channels shape up as another essential target concerning the occurrence of seizures. $K_v4.2$ channels promote the regulation of backpropagation from the soma of CA1 neurons to the dendrites. Thereby, increased sensitivity of pyramidal neurons causes hyperexcitability of the membrane too. By taking a closer look at the $K_v4.2$ channel itself, it becomes obvious that because of its Ca^{2+} binding domains dendritic Ca^{2+} influx can be modulated. Increased Ca^{2+} influx, as being evaluated in $K_v4.2$ knockout mice, leads to seizure [186].

Together with $Ca_v3.2$ and $Ca_v3.3$ Ca^{2+} channel isoforms, K_v4 channels form a signaling complex modulating the inactivation voltage of $K_v4.2$ and furthermore

influencing the subthreshold membrane potential range. In this way firing properties of neurons can be regulated, exhibiting the importance of Ca_v3-K_v4 signaling complex in regard to cell latency and electrical properties [187]. Calcium channels and their contribution to epilepsy cannot only be examined on the transcriptional level, including upregulation, [188] but also on an elementary molecular level itself. It is surely out of question, that for investigating the genetic determinants of idiopathic generalized epilepsies (IGEs), mutations in channel genes provide better insights to resolve the origins of this type of disorder. Studies using GAERS as a model of IGEs, clearly figure out that different splice variants leading to measureable functional changes of T-type Ca^{2+} channels. T-type channels themselves are responsible for the low-threshold spikes contributing to oscillatory thalamocortical rhythms as well as burst firing and tonic patterns. Given the regulatory importance of these channels, altered electrophysiological properties occur if mutations in the channel gene (Cacna1h) of the IGEs rat model are confirmed [164]. $Ca_v3.2$ mutations (gcm) include substitution in exon 24 of the channel gene. Admittedly, it could be demonstrated that gcm codominantly segregating with the number of neuronal seizures, presume exon 25 to be existent for the development of seizures. In the presence of exon 25, T-type Ca^{2+} channel splice variants cause an epileptic status based on the fact that hyperexcitability of neurons results in a faster recovery channel inactivation. Moreover, higher charge transference according to high-frequency bursts is given leading to functional disarrangement of Ca^{2+} channels too [88, 186]. Depending on the splicing variations even missense mutations, having no greater direct impact on functional properties of $Ca_v3.2$ channels, may interfere with regulatory sequences and therefore implicate an epileptic phenotype [188]. However, it has to be pointed out that even if the implications for IGEs is given, normal neurological functioning can be still preserved. In summary the gain-of-function mutation of the T-type Ca^{2+} channel gene provides new insights into the genetic origin of absence epilepsy. By understanding and more accurate identification of exonic splicing mechanism as well as its functional consequences, novel targets of pharmacological treatment could be developed. To verify seizure initiation in different neuroanatomical areas like the inferior colliculus (IC), the animal model of the genetically epilepsy-prone rat can be taken into consideration. Therefore, seizure initiation results in the enhancement of high voltage-activated Ca^{2+} channels in IC neuronal cells, which markedly elevate enhanced Ca^{2+} current density in turn. In comparison to control animals, the altered properties are changes in the pore-forming α_1D (L-type) and the α_1E (R-type) subunit of calcium channels. This mechanism of up-regulation in protein levels of Ca^{2+} regulatory subunits contribute to the genetics of epilepsy and their seizure susceptibility [189].

Taken the biochemical and molecular approaches together, we are now a step closer in comprehending the mechanisms of protein regulatory processes being involved in expression of Ca^{2+} channels. Therefore, we can better understand the background of different forms of Epilepsy as well as its symptomatic outcome step by step.

References

1. Forsgren L, Beghi E, Oun A, Sillanpaa M (2005) The epidemiology of epilepsy in Europe – a systematic review. Eur J Neurol 12:245–253
2. Mulley JC, Scheffer IE, Harkin LA, Berkovic SF, Dibbens LM (2005) Susceptibility genes for complex epilepsy. Hum Mol Genet 14:R243–R249
3. Turnbull J, Lohi H, Kearney JA, Rouleau GA, Delgado-Escueta AV, Meisler MH, Cossette P, Minassian BA (2005) Sacred disease secrets revealed: the genetics of human epilepsy. Hum Mol Genet 14(2):2491–2500
4. Puranam RS, McNamara JO (1999) Seizure disorders in mutant mice: relevance to human epilepsies. Curr Opin Neurobiol 9:281–287
5. Bers DM (2002) Cardiac excitation-contraction coupling. Nature 415:198–205
6. Yang SN, Berggren PO (2005) beta-cell Ca-V channel regulation in physiology and pathophysiology. Am J Physiol Endocrinol Metab 288:E16–E28
7. Catterall WA (1999) Interactions of presynaptic Ca^{2+} channels and snare proteins in neurotransmitter release. Ann NY Acad Sci 868:144–159
8. Bito H, Deisseroth K, Tsien RW (1997) Ca^{2+}-dependent regulation in neuronal gene expression. Curr Opin Neurobiol 7:419–429
9. Hofmann F, Lacinová L, Klugbauer N (1999) Voltage-dependent calcium channels: from structure to function. Rev Physiol Biochem Pharmacol 139:33–87
10. Catterall WA (2000) Structure and regulation of voltage-gated Ca^{2+} channels. Annu Rev Cell Dev Biol 16:521–555
11. Perez-Reyes E (2003) Molecular physiology of low-voltage-activated T-type calcium channels. Physiol Rev 83:117–161
12. Lacinova L (2005) Voltage-dependent calcium channels. Gen Physiol Biophys 24(Suppl 1): 1–78
13. Pietrobon D (2005) Function and dysfunction of synaptic calcium channels: insights from mouse models. Curr Opin Neurobiol 15:257–265
14. Chen Y, Lu J, Pan H, Zhang Y, Wu H, Xu K, Liu X, Jiang Y, Bao X, Yao Z, Ding K, Lo WH, Qiang B, Chan P, Shen Y, Wu X (2003) Association between genetic variation of CACNA1H and childhood absence epilepsy. Ann Neurol 54:239–243
15. Pinto A, Moss F, Lang B, Boot J, Brust P, Williams M, Stauderman K, Harpold M, Newsom-Davis J (1998) Differential effect of Lambert-Eaton myasthenic syndrome immunoglobulin on cloned neuronal voltage-gated calcium channels. Ann NY Acad Sci 841:687–690
16. Missiaen L, Robberecht W, Van Den Bosch L, Callewaert G, Parys JB, Wuytack F, Raeymaekers L, Nilius B, Eggermont J, De Smedt H (2000) Abnormal intracellular Ca^{2+} homeostasis and disease. Cell Calcium 28:1–21
17. Bech-Hansen NT, Naylor MJ, Maybaum TA, Pearce WG, Koop B, Fishman GA, Mets M, Musarella MA, Cott KM (1998) Loss-of-function mutations in a calcium-channel α1-subunit gene in Xp11.23 cause incomplete X-linked congenital stationary night blindness. Nat Genet 19:264–267
18. Splawski I, Timothy KW, Sharpe LM, Decher N, Kumar P, Bloise R, Napolitano C, Schwartz PJ, Joseph RM, Condouris K, Tager-Flusberg H, Priori SG, Sanguinetti MC, Keating MT (2004) Ca(V)1.2 calcium channel dysfunction causes a multisystem disorder including arrhythmia and autism. Cell 119:19–31
19. Fletcher CF, Lutz CM, O'Sullivan TN, Shaughnessy JD Jr, Hawkes R, Frankel WN, Copeland NG, Jenkins NA (1996) Absence epilepsy in tottering mutant mice is associated with calcium channel defects. Cell 87:607–617
20. Mori Y, Wakamori M, Oda S, Fletcher CF, Sekiguchi N, Mori E, Copeland NG, Jenkins NA, Matsushita K, Matsuyama Z, Imoto K (2000) Reduced voltage sensitivity of activation of P/Q-type Ca^{2+} channels is associated with the ataxic mouse mutation rolling nagoya (tg^{rol}). J Neurosci 20:5654–5662

21. Zwingman TA, Neumann PE, Noebels JL, Herrup K (2001) Rocker is a new variant of the voltage-dependent calcium channel gene Cacna1a. J Neurosci 21:1169–1178
22. Burgess DL, Jones JM, Meisler MH, Noebels JL (1997) Mutation of the Ca^{2+} channel beta subunit gene Cchb4 is associated with ataxia and seizures in the lethargic (lh) mouse. Cell 88:385–392
23. Letts VA, Felix R, Biddlecome GH, Arikkath J, Mahaffey CL, Valenzuela A, Bartlett FS II, Mori Y, Campbell KP, Frankel WN (1998) The mouse stargazer gene encodes a neuronal Ca^{2+}-channel gamma subunit. Nat Genet 19:340–347
24. Burgess DL, Noebels JL (1999) Voltage-dependent calcium channel mutations in neurological disease. Ann NY Acad Sci 868:199–212
25. Gao BN, Sekido Y, Maximov A, Saad M, Forgacs E, Latif F, Wei MH, Lerman M, Lee JH, Perez-Reyes E, Bezprozvanny I, Minna JD (2000) Functional properties of a new voltage-dependent calcium channel $\alpha_2\delta$ auxiliary subunit gene (CACNA2D2). J Biol Chem 275:12237–12242
26. Barclay J, Balaguero N, Mione M, Ackerman SL, Letts VA, Brodbeck J, Canti C, Meir A, Page KM, Kusumi K, Perez-Reyes E, Lander ES, Frankel WN, Gardiner RM, Dolphin AC, Rees M (2001) Ducky mouse phenotype of epilepsy and ataxia is associated with mutations in the *Cacna2d2* gene and decreased calcium channel current in cerebellar Purkinje cells. J Neurosci 21:6095–6104
27. Brill J, Klocke R, Paul D, Boison D, Gouder N, Klugbauer N, Hofmann F, Becker CM, Becker K (2004) Entla: a novel epileptic and ataxic Cacna2d2 mutant of the mouse. J Biol Chem 279(8):7322–7330
28. Williams ME, Marubio LM, Deal CR, Hans M, Brust PF, Philipson LH, Miller RJ, Johnson EC, Harpold MM, Ellis SB (1994) Structure and functional characterization of neuronal α_{1E} calcium channel subtypes. J Biol Chem 269:22347–22357
29. Rogawski MA, Loscher W (2004) The neurobiology of antiepileptic drugs. Nat Rev Neurosci 5:553–564
30. Gomora JC, Daud AN, Weiergraber M, Perez-Reyes E (2001) Block of cloned human T-type calcium channels by succinimide antiepileptic drugs. Mol Pharmacol 60:1121–1132
31. Remy S, Beck H (2006) Molecular and cellular mechanisms of pharmacoresistance in epilepsy. Brain 129:18–35
32. Sills GJ (2006) The mechanisms of action of gabapentin and pregabalin. Curr Opin Pharmacol 6:108–113
33. Jing X, Li DQ, Olofsson CS, Salehi A, Surve VV, Caballero J, Ivarsson R, Lundquist I, Pereverzev A, Schneider T, Rorsman P, Renstrom E (2005) Ca(V)2.3 calcium channels control second-phase insulin release. J Clin Invest 115:146–154
34. Pereverzev A, Salehi A, Mikhna M, Renstrom E, Hescheler J, Weiergraber M, Smyth N, Schneider T (2005) The ablation of the $Ca_v2.3$/E-type voltage-gated Ca^{2+} channel causes a mild phenotype despite an altered glucose induced glucagon response in isolated islets of Langerhans. Eur J Pharmacol 511:65–72
35. Lu Z-L, Pereverzev A, Liu H-L, Weiergraber M, Henry M, Krieger A, Smyth N, Hescheler J, Schneider T (2004) Arrhythmia in isolated prenatal hearts after ablation of the $Ca_v2.3$ (α_1E) subunit of voltage-gated Ca^{2+} channels. Cell Physiol Biochem 14:11–22
36. Weiergräber M, Henry M, Südkamp M, De Vivie ER, Hescheler J, Schneider T (2005) Ablation of $Ca_v2.3$/E-type voltage-gated calcium channel results in cardiac arrhythmia and altered autonomic control within the murine cardiovascular system. Basic Res Cardiol 100:1–13
37. Sakata Y, Saegusa H, Zong SQ, Osanai M, Murakoshi T, Shimizu Y, Noda T, Aso T, Tanabe T (2002) $Ca_v2.3$ (α_{1E}) Ca^{2+} channel participates in the control of sperm function. FEBS Lett 516:229–233
38. Grabsch H, Pereverzev A, Weiergräber M, Schramm M, Henry M, Vajna R, Beattie RE, Volsen SG, Klöckner U, Hescheler J, Schneider T (1999) Immunohistochemical detection of α1E voltage-gated Ca^{2+} channel isoforms in cerebellum, INS-1 cells, and neuroendocrine cells of the digestive system. J Histochem Cytochem 47:981–993

39. Breustedt J, Vogt KE, Miller RJ, Nicoll RA, Schmitz D (2003) Alpha1E-containing Ca2+ channels are involved in synaptic plasticity. Proc Natl Acad Sci USA 100:12450–12455
40. Dietrich D, Kirschstein T, Kukley M, Pereverzev A, von der Brelie C, Schneider T, Beck H (2003) Functional specialization of presynaptic $Ca_v2.3$ Ca^{2+} channels. Neuron 39:483–496
41. Lee SC, Choi S, Lee T, Kim HL, Chin H, Shin HS (2002) Molecular basis of R-type calcium channels in central amygdala neurons of the mouse. Proc Natl Acad Sci USA 99:3276–3281
42. Saegusa H, Kurihara T, Zong SQ, Minowa O, Kazuno AA, Han WH, Matsuda Y, Yamanaka H, Osanai M, Noda T, Tanabe T (2000) Altered pain responses in mice lacking α_{1E} subunit of the voltage-dependent Ca^{2+} channel. Proc Natl Acad Sci USA 97:6132–6137
43. Chen S, Ren YQ, Bing RJ, Hillman DE (2000) Alpha 1E subunit of the R-type calcium channel is associated with myelinogenesis. J Neurocytol 29:719–728
44. Toriyama H, Wang L, Saegusa H, Zong S, Osanai M, Murakoshi T, Noda T, Ohno K, Tanabe T (2002) Role of $Ca_v2.3$ (alpha1E) Ca^{2+} channel in ischemic neuronal injury. Neuroreport 13:261–265
45. Ishiguro M, Wellman TL, Honda A, Russell SR, Tranmer BI, Wellman GC (2005) Emergence of a R-type Ca^{2+} channel ($Ca_v2.3$) contributes to cerebral artery constriction after subarachnoid hemorrhage. Circ Res 96:419–426
46. Day NC, McCormack AL, Ince PG, Shaw PJ, Craig PJ, Smith W, Beattie RE, Ellis SB, Harpold MM, Lodge D, Volsen SG (1996) Distribution of voltage-dependent calcium channel (VDCC) beta subunits in the human hippocampus. Neuropathol Appl Neurobiol 22:458
47. Hanson JE, Smith Y (2002) Subcellular distribution of high-voltage-activated calcium channel subtypes in rat globus pallidus neurons. J Comp Neurol 442:89–98
48. Wu LG, Westenbroek RE, Borst JGG, Catterall WA, Sakmann B (1999) Calcium channel types with distinct presynaptic localization couple differentially to transmitter release in single calyx-type synapses. J Neurosci 19:726–736
49. Westenbroek RE, Hell JW, Warner C, Dubel SJ, Snutch TP, Catterall WA (1992) Biochemical properties and subcellular distribution of an N-type calcium channel $\alpha1$ subunit. Neuron 9:1099–1115
50. Day NC, Wood SJ, Ince PG, Volsen SG, Smith W, Slater CR, Shaw PJ (1997) Differential localization of voltage-dependent calcium channel α_1 subunits at the human and rat neuromuscular junction. J Neurosci 17:6226–6235
51. Kamp MA, Krieger A, Henry M, Hescheler J, Weiergraber M, Schneider T (2005) Presynaptic 'Ca2.3-containing' E-type Ca channels share dual roles during neurotransmitter release. Eur J Neurosci 21:1617–1625
52. Westenbroek RE, Sakurai T, Elliott EM, Hell JW, Starr TVB, Snutch TP, Catterall WA (1995) Immunochemical identification and subcellular distribution XX of the α_{1A} subunits of brain calcium channels. J Neurosci 15:6403–6418
53. Tank DW, Sugimori M, Connor JA, Llinas RR (1988) Spatially resolved calcium dynamics of mammalian Purkinje cells in cerebellar slice. Science 242:773–777
54. Pereverzev A, Leroy J, Krieger A, Malecot CO, Hescheler J, Pfitzer G, Klockner U, Schneider T (2002) Alternate splicing in the cytosolic II–III loop and the carboxy terminus of human E-type voltage-gated Ca^{2+} channels: electrophysiological characterization of isoforms. Mol Cell Neurosci 21:352–365
55. Leroy J, Pereverzev A, Vajna R, Qin N, Pfitzer G, Hescheler J, Malécot CO, Schneider T, Klöckner U (2003) Ca^{2+}-sensitive regulation of E-type Ca^{2+} channel activity depends on an arginine rich region in the cytosolic II–III loop. Eur J Neurosci 18:841–855
56. Klöckner U, Pereverzev A, Leroy J, Krieger A, Vajna R, Hescheler J, Pfitzer G, Malecot CO, Schneider T (2004) The cytosolic II–III loop of $Ca_v2.3$ provides an essential determinant for the phorbol ester-mediated stimulation of E-type Ca^{2+} channel activity. Eur J Neurosci 19:2659–2668
57. Krieger A, Radhakrishnan K, Pereverzev A, Siapich SA, Banat M, Kamp MA, Leroy J, Klockner U, Hescheler J, Weiergraber M, Schneider T (2006) The molecular chaperone hsp70 interacts with the cytosolic II–III loop of the $Ca_v2.3$ E-type voltagegated Ca^{2+} channel. Cell Physiol Biochem 17:97–110

58. Weiergraber M, Henry M, Krieger A, Kamp M, Radhakrishnan K, Hescheler J, Schneider T (2006) Altered seizure susceptibility in mice lacking the $Ca_v2.3$ E-type Ca^{2+} channel. Epilepsia 47:839–850
59. Dzhura I, Wu Y, Colbran RJ, Balser JR, Anderson ME (2000) Calmodulin kinase determines calcium-dependent facilitation of L-type calcium channels. Nat Cell Biol 2:173–177
60. Liang H, DeMaria CD, Erickson MG, Mori MX, Alseikhan BA, Yue DT (2003) Unified mechanisms of Ca^{2+} regulation across the Ca^{2+} channel family. Neuron 39:951–960
61. Herlitze S, Garcia DE, Mackie K, Hille B, Scheuer T, Catterall WA (1996) Modulation of Ca^{2+} channels by G-protein βgamma subunits. Nature 380:258–262
62. Ikeda SR (1996) Voltage-dependent modulation of N-type calcium channels by G-proteins βτ subunits. Nature 380:255–258
63. De Waard M, Liu H, Walker D, Scott VES, Gurnett CA, Campbell KP (1997) Direct binding of G-protein βgamma complex to voltage-dependent calcium channels. Nature 385:446–450
64. Zamponi GW, Bourinet E, Nelson D, Nargeot J, Snutch TP (1997) Crosstalk between G proteins and protein kinase C mediated by the calcium channel α1 subunit. Nature 385:442–446
65. Dolphin AC (2003) Beta subunits of voltage-gated calcium channels. J Bioenerg Biomembr 35:599–620
66. Sandoz G, Lopez-Gonzalez I, Grunwald D, Bichet D, Altafaj X, Weiss N, Ronjat M, Dupuis A, De WM (2004) Cavbeta-subunit displacement is a key step to induce the reluctant state of P/Q calcium channels by direct G protein regulation. Proc Natl Acad Sci USA 101:6267–6272
67. Wolfe JT, Wang H, Howard J, Garrison JC, Barrett PQ (2003) T-type calcium channel regulation by specific G-protein betagamma subunits. Nature 424:209–213
68. Doering CJ, Kisilevsky AE, Feng ZP, Arnot MI, Peloquin J, Hamid J, Barr W, Nirdosh A, Simms B, Winkfein RJ, Zamponi GW (2004) A single Gbeta subunit locus controls cross-talk between protein kinase C and G protein regulation of N-type calcium channels 5. J Biol Chem 279:29709–29717
69. Brenowitz SD, Regehr WG (2003) "Resistant" channels reluctantly reveal their roles. Neuron 39:391–394
70. Kim Y, Park MK, Uhm DY, Chung S (2007) Modulation of T-type Ca2+ channels by corticotropin-releasing factor through protein kinase C pathway in MN9D dopaminergic cells. Biochem Biophys Res Commun 358:796–801
71. Yao J, Davies LA, Howard JD, Adney SK, Welsby PJ, Howell N, Carey RM, Colbran RJ, Barrett PQ (2006) Molecular basis for the modulation of native T-type Ca2+ channels in vivo by Ca^{2+}/calmodulin-dependent protein kinase II. J Clin Invest 116:2403–2412
72. Park JY, Kang HW, Moon HJ, Huh SU, Jeong SW, Soldatov NM, Lee JH (2006) Activation of protein kinase C augments T-type Ca^{2+} channel activity without changing channel surface density. J Physiol 577:513–523
73. Iftinca M, McKay BE, Snutch TP, McRory JE, Turner RW, Zamponi GW (2006) Temperature dependence of T-type calcium channel gating. Neuroscience 142:1031–1042
74. Inoue M, Rashid MH, Fujita R, Contos JJ, Chun J, Ueda H (2004) Initiation of neuropathic pain requires lysophosphatidic acid receptor signaling. Nat Med 10:712–718
75. Nelson MT, Joksovic PM, Su P, Kang HW, Van DA, Baumgart JP, David LS, Snutch TP, Barrett PQ, Lee JH, Zorumski CF, Perez-Reyes E, Todorovic SM (2007) Molecular mechanisms of subtype-specific inhibition of neuronal T-type calcium channels by ascorbate. J Neurosci 27:12577–12583
76. Tao J, Hildebrand ME, Liao P, Liang MC, Tan G, Li S, Snutch TP, Soong TW (2008) Activation of corticotropin-releasing factor receptor 1 selectively inhibits $Ca_v3.2$ T-type calcium channels. Mol Pharmacol 73:1596–1609
77. Helmchen F, Svoboda K, Denk W, Tank DW (1999) In vivo dendritic calcium dynamics in deep-layer cortical pyramidal neurons. Nat Neurosci 2:989–996
78. Gibney GT, Zhang JH, Douglas RM, Haddad GG, Xia Y (2002) Na^+/Ca^{2+} exchanger expression in the developing rat cortex. Neuroscience 112:65–73
79. Albowitz B, Konig P, Kuhnt U (1997) Spatiotemporal distribution of intracellular calcium transients during epileptiform activity in guinea pig hippocampal slices. J Neurophysiol 77:491–501

80. DeLorenzo RJ, Pal S, Sombati S (1998) Prolonged activation of the N-methyl-D-aspartate receptor-Ca2+ transduction pathway causes spontaneous recurrent epileptiform discharges in hippocampal neurons in culture. Proc Natl Acad Sci USA 95:14482–14487
81. Sun DA, Sombati S, Blair RE, DeLorenzo RJ (2002) Calcium-dependent epileptogenesis in an in vitro model of stroke-induced "epilepsy". Epilepsia 43:1296–1305
82. Heinemann U, Hamon B (1986) Calcium and epileptogenesis. Exp Brain Res 65:1–10
83. Pisani A, Bonsi P, Martella G, De Persis C, Costa C, Pisani F, Bernardi G, Calabresi P (2004) Intracellular calcium increase in epileptiform activity: modulation by levetiracetam and lamotrigine. Epilepsia 45:719–728
84. Beck H, Steffens R, Elger CE, Heinemann U (1998) Voltage-dependent Ca^{2+} currents in epilepsy. Epilepsy Res 32:321–332
85. Straub H, Speckmann EJ, Bingmann D, Walden J (1990) Paroxysmal depolarization shifts induced by bicuculline in CA3 neurons of hippocampal slices: suppression by the organic calcium antagonist verapamil. Neurosci Lett 111:99–101
86. Berg M, Bruhn T, Frandsen A, Schousboe A, Diemer NH (1995) Kainic acid-induced seizures and brain damage in the rat: role of calcium homeostasis. J Neurosci Res 40:641–646
87. Sullivan PG (2005) Interventions with neuroprotective agents: novel targets and opportunities. Epilepsy Behav 7(Suppl 3):S12–S17
88. Benarroch EE (2010) Neuronal voltage-gated calcium channels: brief overview of their function and clinical implications in neurology. Neurology 74:1310–1315
89. Andrew RD, Dudek FE (1983) Burst discharge in mammalian neuroendocrine cells involves an intrinsic regenerative mechanism. Science 221:1050–1052
90. Andrew RD (1987) Endogenous bursting by rat supraoptic neuroendocrine cells is calcium dependent. J Physiol 384:451–465
91. Andrew RD, Dudek FE (1984) Analysis of intracellularly recorded phasic bursting by mammalian neuroendocrine cells. J Neurophysiol 51:552–566
92. Hlubek MD, Cobbett P (2000) Differential effects of K^+ channel blockers on frequency-dependent action potential broadening in supraoptic neurons. Brain Res Bull 53:203–209
93. Roper P, Callaway J, Shevchenko T, Teruyama R, Armstrong W (2003) AHP's, HAP's and DAP's: how potassium currents regulate the excitability of rat supraoptic neurones. J Comput Neurosci 15:367–389
94. Abel HJ, Lee JC, Callaway JC, Foehring RC (2004) Relationships between intracellular calcium and afterhyperpolarizations in neocortical pyramidal neurons. J Neurophysiol 91:324–335
95. Pierson PM, Liu X, Raggenbass M (2005) Suppression of potassium channels elicits calcium-dependent plateau potentials in suprachiasmatic neurons of the rat. Brain Res 1036:50–59
96. Simon M, Perrier JF, Hounsgaard J (2003) Subcellular distribution of L-type Ca^{2+} channels responsible for plateau potentials in motoneurons from the lumbar spinal cord of the turtle. Eur J Neurosci 18:258–266
97. Li Y, Bennett DJ (2003) Persistent sodium and calcium currents cause plateau potentials in motoneurons of chronic spinal rats. J Neurophysiol 90:857–869
98. Hounsgaard J, Kiehn O (1989) Serotonin-induced bistability of turtle motoneurones caused by a nifedipine-sensitive calcium plateau potential. J Physiol 414:265–282
99. Mills JD, Pitman RM (1997) Electrical properties of a cockroach motor neuron soma depend on different characteristics of individual Ca components. J Neurophysiol 78:2455–2466
100. Morisset V, Nagy F (1999) Ionic basis for plateau potentials in deep dorsal horn neurons of the rat spinal cord. J Neurosci 19:7309–7316
101. Voisin DL, Nagy F (2001) Sustained L-type calcium currents in dissociated deep dorsal horn neurons of the rat: characteristics and modulation. Neuroscience 102:461–472
102. Zhang B, Harris-Warrick RM (1995) Calcium-dependent plateau potentials in a crab stomatogastric ganglion motor neuron. I. Calcium current and its modulation by serotonin. J Neurophysiol 74:1929–1937
103. Fanelli RJ, McCarthy RT, Chisholm J (1994) Neuropharmacology of nimodipine: from single channels to behavior. Ann NY Acad Sci 747:336–350

104. McCarthy RT, TanPiengco PE (1992) Multiple types of high-threshold calcium channels in rabbit sensory neurons: high-affinity block of neuronal L-type by nimodipine. J Neurosci 12:2225–2234
105. Vergara R, Rick C, Hernandez-Lopez S, Laville JA, Guzman JN, Galarraga E, Surmeier DJ, Bargas J (2003) Spontaneous voltage oscillations in striatal projection neurons in a rat corticostriatal slice. J Physiol 553:169–182
106. Hernandez-Lopez S, Bargas J, Surmeier DJ, Reyes A, Galarraga E (1997) D1 receptor activation enhances evoked discharge in neostriatal medium spiny neurons by modulating an L-type Ca^{2+} conductance. J Neurosci 17:3334–3342
107. Hernandez-Lopez S, Tkatch T, Perez-Garci E, Galarraga E, Bargas J, Hamm H, Surmeier DJ (2000) D2 dopamine receptors in striatal medium spiny neurons reduce L-type Ca^{2+} currents and excitability via a novel $PLC_{\beta 1}$-IP3-calcineurin-signaling cascade. J Neurosci 20: 8987–8995
108. Koschak A, Reimer D, Huber I, Grabner M, Glossmann H, Engel J, Striessnig J (2001) α1D (Ca_v1.3) subunits can form L-type Ca^{2+} channels activating at negative voltages. J Biol Chem 276:22100–22106
109. Xu WF, Lipscombe D (2001) Neuronal $Ca_v1.3\alpha_1$ L-type channels activate at relatively hyperpolarized membrane potentials and are incompletely inhibited by dihydropyridines. J Neurosci 21:5944–5951
110. Michna M, Knirsch M, Hoda JC, Muenkner S, Langer P, Platzer J, Striessnig J, Engel J (2003) Ca_v1.3 (alpha1D) Ca^{2+} currents in neonatal outer hair cells of mice. J Physiol 553: 747–758
111. Soong TW, Stea A, Hodson CD, Dubel SJ, Vincent SR, Snutch TP (1993) Structure and functional expression of a member of the low voltage-activated calcium channel family. Science 260:1133–1136
112. Stephens GJ, Page KM, Burley JR, Berrow NS, Dolphin AC (1997) Functional expression of rat brain cloned alpha1E calcium channels in COS-7 cells. Pflugers Arch 433:523–532
113. Wakamori M, Niidome T, Rufutama D, Furuichi T, Mikoshiba K, Fujita Y, Tanaka I, Katayama K, Yatani A, Schwartz A, Mori Y (1994) Distinctive functional properties of the neuronal BII (class E) calcium channel. Receptors Channels 2:303–314
114. Cloues RK, Sather WA (2003) Afterhyperpolarization regulates firing rate in neurons of the suprachiasmatic nucleus. J Neurosci 23:1593–1604
115. Kuzmiski JB, Barr W, Zamponi GW, MacVicar BA (2005) Topiramate inhibits the initiation of plateau potentials in CA1 neurons by depressing R-type calcium channels. Epilepsia 46:481–489
116. Metz AE, Jarsky T, Martina M, Spruston N (2005) R-type calcium channels contribute to afterdepolarization and bursting in hippocampal CA1 pyramidal neurons. J Neurosci 25:5763–5773
117. Fraser DD, MacVicar BA (1996) Cholinergic-dependent plateau potential in hippocampal CA1 pyramidal neurons. J Neurosci 16:4113–4128
118. Fraser DD, Doll D, MacVicar BA (2001) Serine/threonine protein phosphatases and synaptic inhibition regulate the expression of cholinergic-dependent plateau potentials. J Neurophysiol 85:1197–1205
119. Lothman EW, Bertram EH III, Stringer JL (1991) Functional anatomy of hippocampal seizures. Prog Neurobiol 37:1–82
120. Wasterlain CG, Fujikawa DG, Penix L, Sankar R (1993) Pathophysiological mechanisms of brain damage from status epilepticus. Epilepsia 34(Suppl 1):S37–S53
121. Kuzmiski JB, MacVicar BA (2001) Cyclic nucleotide-gated channels contribute to the cholinergic plateau potential in hippocampal CA1 pyramidal neurons. J Neurosci 21: 8707–8714
122. Yasuda R, Sabatini BL, Svoboda K (2003) Plasticity of calcium channels in dendritic spines. Nat Neurosci 6:948–955
123. Qian J, Noebels JL (2001) Presynaptic Ca^{2+} channels and neurotransmitter release at the terminal of a mouse cortical neuron. J Neurosci 21:3721–3728

124. Qian J, Noebels JL (2003) Topiramate alters excitatory synaptic transmission in mouse hippocampus. Epilepsy Res 55:225–233
125. Magee JC, Johnston D (1995) Synaptic activation of voltage-gated channels in the dendrites of hippocampal pyramidal neurons. Science 268:301–304
126. Westenbroek RE, Ahlijanian MK, Catterall WA (1990) Clustering of L-type Ca^{2+} channels at the base of major dendrites in hippocampal pyramidal neurons. Nature 347:281–284
127. Gahwiler BH, Brown DA (1987) Muscarine affects calcium-currents in rat hippocampal pyramidal cells in vitro. Neurosci Lett 76:301–306
128. Toselli M, Lang J, Costa T, Lux HD (1989) Direct modulation of voltage-dependent calcium channels by muscarinic activation of a pertussis toxin-sensitive G-protein in hippocampal neurons. Pflugers Arch 415:255–261
129. Palmieri C, Kawasaki H, Avoli M (2000) Topiramate depresses carbachol-induced plateau potentials in subicular bursting cells. Neuroreport 11:75–78
130. LaRoche SM, Helmers SL (2004) The new antiepileptic drugs: scientific review. JAMA 291:605–614
131. Waugh J, Goa KL (2003) Topiramate: as monotherapy in newly diagnosed epilepsy. CNS Drugs 17:985–992
132. Newcomb R, Szoke B, Palma A, Wang G, Chen XH, Hopkins W, Cong R, Miller J, Urge L, Tarczy-Hornoch K, Loo JA, Dooley DJ, Nadasdi L, Tsien RW, Lemos J, Miljanich G (1998) Selective peptide antagonist of the class E calcium channel from the venom of the tarantula *Hysterocrates gigas*. Biochemistry 37:15353–15362
133. Sochivko D, Pereverzev A, Smyth N, Gissel C, Schneider T, Beck H (2002) The α1E calcium channel subunit underlies R-type calcium current in hippocampal and cortical pyramidal neurons. J Physiol 542:699–710
134. Melliti K, Meza U, Adams B (2000) Muscarinic stimulation of α_1E Ca channels is selectively blocked by the effector antagonist function of RGS2 and phsopholipase C-β1. J Neurosci 20:7167–7173
135. Bannister RA, Melliti K, Adams BA (2004) Differential modulation of $Ca_v2.3$ Ca^{2+} channels by G{alpha}q/11-coupled muscarinic receptors. Mol Pharmacol 65:381–388
136. Curia G, Aracri P, Sancini G, Mantegazza M, Avanzini G, Franceschetti S (2004) Protein-kinase C-dependent phosphorylation inhibits the effect of the antiepileptic drug topiramate on the persistent fraction of sodium currents. Neuroscience 127:63–68
137. Tai C, Kuzmiski JB, MacVicar BA (2006) Muscarinic enhancement of R-type calcium currents in hippocampal CA1 pyramidal neurons. J Neurosci 26:6249–6258
138. Levey AI, Edmunds SM, Koliatsos V, Wiley RG, Heilman CJ (1995) Expression of m1-m4 muscarinic acetylcholine receptor proteins in rat hippocampus and regulation by cholinergic innervation. J Neurosci 15:4077–4092
139. Meza U, Bannister R, Melliti K, Adams B (1999) Biphasic, opposing modulation of cloned neuronal α_1E Ca channels by distinct signaling pathways coupled to M2 muscarinic acetylcholine receptors. J Neurosci 19:6806–6817
140. Hamilton SE, Loose MD, Qi M, Levey AI, Hille B, McKnight GS, Idzerda RL, Nathanson NM (1997) Disruption of the m1 receptor gene ablates muscarinic receptor- dependent M current regulation and seizure activity in mice. Proc Natl Acad Sci USA 94:13311–13316
141. Vreugdenhil M, Wadman WJ (1994) Kindling-induced long-lasting enhancement of calcium current in hippocampal CA1 area of the rat: relation to calcium-dependent inactivation. Neuroscience 59:105–114
142. Hendriksen H, Kamphuis W, da Silva FHL (1997) Changes in voltage-dependent calcium channel alpha1-subunit mRNA levels in the kindling model of epileptogenesis. Mol Brain Res 50:257–266
143. Kang TC, Kim DS, Yoo KY, Hwang IK, Kwak SE, Kim JE, Jung JY, Won MH, Suh JG, Oh YS (2004) Elevated voltage-gated Ca^{2+} channel immunoreactivities in the hippocampus of seizure-prone gerbil. Brain Res 1029:168–178
144. Manning JP, Richards DA, Bowery NG (2003) Pharmacology of absence epilepsy. Trends Pharmacol Sci 24:542–549

145. Khosravani H, Zamponi GW (2006) Voltage-gated calcium channels and idiopathic generalized epilepsies. Physiol Rev 86:941–966
146. Nagaeva DV, Akhmadeev AV (2006) Structural organization, neurochemical characteristics, and connections of the reticular nucleus of the thalamus. Neurosci Behav Physiol 36:987–995
147. Mulle C, Madariaga A, Deschenes M (1986) Morphology and electrophysiological properties of reticularis thalami neurons in cat: in vivo study of a thalamic pacemaker. J Neurosci 6:2134–2145
148. Fuentealba P, Steriade M (2005) The reticular nucleus revisited: intrinsic and network properties of a thalamic pacemaker. Prog Neurobiol 75:125–141
149. Destexhe A, Contreras D, Steriade M, Sejnowski TJ, Huguenard JR (1996) In vivo, in vitro, and computational analysis of dendritic calcium currents in thalamic reticular neurons. J Neurosci 16:169–185
150. Lakaye B, Thomas E, Minet A, Grisar T (2002) The genetic absence epilepsy rat from Strasbourg (GAERS), a rat model of absence epilepsy: computer modeling and differential gene expression. Epilepsia 43(Suppl 5):123–129
151. Contreras D (2006) The role of T-channels in the generation of thalamocortical rhythms. CNS Neurol Disord Drug Targets 5:571–585
152. Llinas RR, Steriade M (2006) Bursting of thalamic neurons and states of vigilance. J Neurophysiol 95:3297–3308
153. Shin HS (2006) T-type Ca^{2+} channels and absence epilepsy. Cell Calcium 40:191–196
154. Von Krosigk M, Bal T, McCormick DA (1993) Cellular mechanisms of a synchronized oscillation in the thalamus. Science 261:361–364
155. Kim U, Bal T, McCormick DA (1995) Spindle waves are propagating synchronized oscillations in the ferret LGNd in vitro. J Neurophysiol 74:1301–1323
156. Weiergraber M, Kamp MA, Radhakrishnan K, Hescheler J, Schneider T (2006) The Cav2.3 voltage-gated calcium channel in epileptogenesis – shedding new light on an enigmatic channel. Neurosci Biobehav Rev 30:1122–1144
157. Shin HS, Lee J, Song I (2006) Genetic studies on the role of T-type Ca^{2+} channels in sleep and absence epilepsy. CNS Neurol Disord Drug Targets 5:629–638
158. Talley EM, Cribbs LL, Lee JH, Daud A, Perez-Reyes E, Bayliss DA (1999) Differential distribution of three members of a gene family encoding low voltage-activated (T-type) calcium channels. J Neurosci 19:1895–1911
159. Talley EM, Solórzano G, Depaulis A, Perez-Reyes E, Bayliss DA (2000) Low-voltage-activated calcium channel subunit expression in a genetic model of absence epilepsy in the rat. Mol Brain Res 75:159–165
160. Kim D, Song I, Keum S, Lee T, Jeong MJ, Kim SS, McEnery MW, Shin HS (2001) Lack of the burst firing of thalamocortical relay neurons and resistance to absence seizures in mice lacking α_{1G} T-type Ca^{2+} channels. Neuron 31:35–45
161. Lee J, Kim D, Shin HS (2004) Lack of delta waves and sleep disturbances during non-rapid eye movement sleep in mice lacking alpha1G-subunit of T-type calcium channels. Proc Natl Acad Sci USA 101:18195–18199
162. Song I, Kim D, Choi S, Sun M, Kim Y, Shin HS (2004) Role of the alpha1G T-type calcium channel in spontaneous absence seizures in mutant mice. J Neurosci 24:5249–5257
163. Ernst WL, Zhang Y, Yoo JW, Ernst SJ, Noebels JL (2009) Genetic enhancement of thalamocortical network activity by elevating alpha 1g-mediated low-voltage-activated calcium current induces pure absence epilepsy. J Neurosci 29:1615–1625
164. Powell KL, Cain SM, Ng C, Sirdesai S, David LS, Kyi M, Garcia E, Tyson JR, Reid CA, Bahlo M, Foote SJ, Snutch TP, O'Brien TJ (2009) A $Ca_v3.2$ T-type calcium channel point mutation has splice-variant-specific effects on function and segregates with seizure expression in a polygenic rat model of absence epilepsy. J Neurosci 29:371–380
165. Tsakiridou E, Bertollini L, de Curtis M, Avanzini G, Pape HC (1995) Selective increase in T-type calcium conductance of reticular thalamic neurons in a rat model of absence epilepsy. J Neurosci 15:3110–3117

166. Broicher T, Kanyshkova T, Meuth P, Pape HC, Budde T (2008) Correlation of T-channel coding gene expression, IT, and the low threshold Ca^{2+} spike in the thalamus of a rat model of absence epilepsy. Mol Cell Neurosci 39:384–399
167. van de Bovenkamp-Janssen M, Scheenen WJ, Kuijpers-Kwant FJ, Kozicz T, Veening JG, van Luijtelaar EL, McEnery MW, Roubos EW (2004) Differential expression of high voltage-activated Ca^{2+} channel types in the rostral reticular thalamic nucleus of the absence epileptic WAG/Rij rat. J Neurobiol 58:467–478
168. Khosravani H, Altier C, Simms B, Hamming KS, Snutch TP, Mezeyova J, McRory JE, Zamponi GW (2004) Gating effects of mutations in the $Ca_v3.2$ T-type calcium channel associated with childhood absence epilepsy. J Biol Chem 279:9681–9684
169. Khosravani H, Bladen C, Parker DB, Snutch TP, McRory JE, Zamponi GW (2005) Effects of Cav3.2 channel mutations linked to idiopathic generalized epilepsy. Ann Neurol 57:745–749
170. van Luijtelaar G, Wiaderna D, Elants C, Scheenen W (2000) Opposite effects of T- and L-type Ca^{2+} channels blockers in generalized absence epilepsy. Eur J Pharmacol 406:381–389
171. Weiergraber M, Henry M, Ho MS, Struck H, Hescheler J, Schneider T (2008) Altered thalamocortical rhythmicity in $Ca_v2.3$-deficient mice. Mol Cell Neurosci 39:605–618
172. De Borman B, Lakaye B, Minet A, Zorzi W, Vergnes M, Marescaux C, Grisar T (1999) Expression of mRNA encoding α_1E and α1G subunit in the brain of a rat model of absence epilepsy. Neuroreport 10:569–574
173. Filakovszky J, Gerber K, Bagdy G (1999) A serotonin-1A receptor agonist and an N-methyl-D-aspartate receptor antagonist oppose each others effects in a genetic rat epilepsy model. Neurosci Lett 261:89–92
174. Deransart C, Landwehrmeyer GB, Feuerstein TJ, Lucking CH (2001) Up-regulation of D3 dopaminergic receptor mRNA in the core of the nucleus accumbens accompanies the development of seizures in a genetic model of absence-epilepsy in the rat. Brain Res Mol Brain Res 94:166–177
175. Hainsworth AH, McNaughton NC, Pereverzev A, Schneider T, Randall AD (2003) Actions of sipatrigine, 202W92 and lamotrigine on R-type and T-type Ca^{2+} channel currents. Eur J Pharmacol 467:77–80
176. van Luijtelaar EL, Drinkenburg WH, van Rijn CM, Coenen AM (2002) Rat models of genetic absence epilepsy: what do EEG spike-wave discharges tell us about drug effects? Methods Find Exp Clin Pharmacol 24(Suppl D):65–70
177. Gibbs JW III, Zhang YF, Ahmed HS, Coulter DA (2002) Anticonvulsant actions of lamotrigine on spontaneous thalamocortical rhythms. Epilepsia 43:342–349
178. Joksovic PM, Weiergraber M, Lee W, Struck H, Schneider T, Todorovic SM (2009) Isoflurane-sensitive presynaptic R-type calcium channels contribute to inhibitory synaptic transmission in the rat thalamus. J Neurosci 29:1434–1445
179. Long P, Mercer A, Begum R, Stephens GJ, Sihra TS, Jovanovic JN (2009) Nerve terminal GABAA receptors activate Ca^{2+}/calmodulin-dependent signalling to inhibit voltage-gated Ca2+ influx and glutamate release. J Biol Chem 284(13):8726–8737
180. Suzuki T, Delgado-Escueta AV, Aguan K, Alonso ME, Shi J, Hara Y, Nishida M, Numata T, Medina MT, Takeuchi T, Morita R, Bai D, Ganesh S, Sugimoto Y, Inazawa J, Bailey JN, Ochoa A, Jara-Prado A, Rasmussen A, Ramos-Peek J, Cordova S, Rubio-Donnadieu F, Inoue Y, Osawa M, Kaneko S, Oguni H, Mori Y, Yamakawa K (2004) Mutations in EFHC1 cause juvenile myoclonic epilepsy. Nat Genet 36:842–849
181. Zaman T, Lee K, Park C, Paydar A, Choi JH, Cheong E, Lee CJ, Shin HS (2011) $Ca_v2.3$ channels are critical for oscillatory burst discharges in the reticular thalamus and absence epilepsy. Neuron 70:95–108
182. Astori S, Wimmer RD, Prosser HM, Corti C, Corsi M, Liaudet N, Volterra A, Franken P, Adelman JP, Luthi A (2011) The $Ca_v3.3$ calcium channel is the major sleep spindle pacemaker in thalamus. Proc Natl Acad Sci USA 108:13823–13828
183. Ludwig A, Budde T, Stieber J, Moosmang S, Wahl C, Holthoff K, Langebartels A, Wotjak C, Munsch T, Zong X, Feil S, Feil R, Lancel M, Chien KR, Konnerth A, Pape HC, Biel M,

Hofmann F (2003) Absence epilepsy and sinus dysrhythmia in mice lacking the pacemaker channel HCN2. EMBO J 22:216–224
184. Herrmann S, Stieber J, Ludwig A (2007) Pathophysiology of HCN channels. Pflugers Arch 454:517–522
185. Budde T, Caputi L, Kanyshkova T, Staak R, Abrahamczik C, Munsch T, Pape HC (2005) Impaired regulation of thalamic pacemaker channels through an imbalance of subunit expression in absence epilepsy. J Neurosci 25:9871–9882
186. Graef JD, Godwin DW (2010) Intrinsic plasticity in acquired epilepsy: too much of a good thing? Neuroscientist 16:487–495
187. Anderson D, Rehak R, Hameed S, Mehaffey WH, Zamponi GW, Turner RW (2010) Regulation of the $K_v4.2$ complex by $Ca_v3.1$ calcium channels. Channels (Austin) 4:163–167
188. Zamponi GW, Lory P, Perez-Reyes E (2010) Role of voltage-gated calcium channels in epilepsy. Pflugers Arch 460:395–403
189. N'Gouemo P, Faingold CL, Morad M (2009) Calcium channel dysfunction in inferior colliculus neurons of the genetically epilepsy-prone rat. Neuropharmacology 56:665–675

Index

M.S. Islam (ed.), *Calcium Signaling*, Advances in Experimental Medicine and Biology 740, DOI 10.1007/978-94-007-2888-2,

D

N

T